Springer Mineralogy

Nikita V. Chukanov
Alexandr D. Chervonnyi

Infrared Spectroscopy of Minerals and Related Compounds

Springer

Springer Mineralogy

More information about this series at http://www.springer.com/series/13488

Nikita V. Chukanov
Alexandr D. Chervonnyi

Infrared Spectroscopy of Minerals and Related Compounds

Springer

Nikita V. Chukanov
The Institute of Problems of Chemical Physics of the Russian Academy of Sciences
Chernogolovka
Russia

and

The Lomonosov Moscow State University
Moscow
Russia

Alexandr D. Chervonnyi
The Institute of Problems of Chemical Physics of the Russian Academy of Sciences
Chernogolovka
Russia

and

The Lomonosov Moscow State University
Moscow
Russia

ISSN 2366-1585 ISSN 2366-1593 (electronic)
Springer Mineralogy
ISBN 978-3-319-25347-3 ISBN 978-3-319-25349-7 (eBook)
DOI 10.1007/978-3-319-25349-7

Library of Congress Control Number: 2015955385

Springer Cham Heidelberg New York Dordrecht London

Printed on acid-free paper

Springer International Publishing AG Switzerland is part of Springer Science+Business Media (www.springer.com)

The index of the book contained some errors. The term "Orthophosphate" was appearing instead of "Niobate". The index has been corrected and show the correct terms.

Preface

Until recently, the infrared spectroscopy had no broad application as a method of identification of minerals. The main reason for this was the lack of sufficiently complete reference books and databases in this area. To fill this gap, a handbook (Chukanov 2014) containing more than three thousands spectra of about two thousands minerals obtained by the author was published by Springer. However, these data were still incomplete, and it was the main reason for the publication of this book, which is the most complete compilation, with a critical review, of the most reliable data on more than 1300 IR spectra of minerals and related compounds published during last sixty years. In addition, this book contains about three hundreds IR spectra of minerals which were obtained by the authors and have never been published earlier. Along with the spectra, the book contains various supporting data on the localities, general appearance, mineral associations, crystallographic characteristics, chemical composition, and some properties of reference samples, as well as kind of sample preparation and methods of spectra registration.

In Chap. 1, the most important methodological aspects and some modern trends in the IR spectroscopy of minerals are overviewed. Chapter 2 contains IR spectra of minerals accompanied by authors' comments and characteristics of reference samples.

This work was carried out with assistance of numerous colleagues. The working partnership with Prof. I.V. Pekov was most significant. Reference samples and valuable analytical data were kindly granted by G.A. Sidorenko, A.E. Zadov, E.V. Belogub, R. Scholz, D. Atencio, I.S. Lykova, S.I. Konovalenko, S.A. Ananyev, E. Jonssen, S. Jančev, M.M. Moiseev, S. Encheva, P. Petrov, A.N. Sapozhnikov, and many other mineralogists, as well as mineral collectors, of which the contribution of G. Möhn, R. Kristiansen, W. Schüller, B. Ternes, G. Blass, A.V. Kasatkin, C. Schäfer, R. Allori, and A.B. Loskutov was most important. Collaboration with the crystallographers R.K. Rastsvetaeva, S.M. Aksenov, S.V. Krivovichev, N.V. Zubkova, D.I. Pushcharovsky, S. Merlino, S.N. Britvin, O.I. Siidra, O.V. Yakubovich, K.A. Rozenberg, and F. Nestola, as well as with specialists in different areas of geosciences and analytical methods (P. Voudouris, A. Magganas, A. Katerinopoulos, J. Göttlicher, K.V. Van, D.A. Varlamov, D.I. Belakovskiy, L.A. Korshunova, V.O. Yapaskurt, L.C.A. de Oliveira, A.I. Bakhtin, A.G. Nikolaev, R. Gainov, F.G. Vagizov, J.V. Bychkova, L.A. Pautov, S.A.

Vozchikova, V.S. Rusakov, G. Klingelhöfer, M. Blumers, A.A. Baeva, O.N. Lopatin, T.S. Nebera) was especially fruitful. All of them are kindly appreciated.

The work was supported by the Russian Science Foundation, Grant no. 14-17-00048 (in part of the mineralogical studies of numerous reference samples carried out by the authors of this book in the Lomonosov Moscow State University).

Contents

Some General Aspects of the Application of IR Spectroscopy to the Investigation of Minerals

1

1.1 Sources of Errors and Artifacts in IR Spectroscopy of Minerals

When using infrared spectroscopy for the study of minerals, researchers often face a number of specific difficulties. This may be due to various factors, including lack of available substance, small sizes of monomineral grains and aggregates, the presence of structural impurities and mechanical inclusions, instability of some minerals, scattering effects, atmospheric disturbance, background noice, anomalous dispersion, interference, etc. One can distinguish three kinds of sources of errors and artifacts in IR spectroscopy of minerals, which are connected with experimental procedures, data proceeding and data interpretation.

1.1.1 Experimental Procedures

IR spectra of minerals can be obtained in the reflection, the transmission, or the absorption mode.

Reflectance techniques, including internal reflection (attenuated total reflection, ATR), specular external reflection from polished flat surfaces, and diffuse external reflection from rough surfaces are used for samples that cannot be analyzed by the conventional transmittance method. Compared to the transmission spectrum, substantial differences (band distortion, band broadening and strong changes of relative band intensities) may be seen in an ATR spectrum due to the dependency of the penetration depth on wavelength and dispersion effects.

Specular external reflection is used in IR spectroscopy of minerals when only small monomineral grains included in rock are available. In such cases IR spectra are obtained from polished sections using IR microscope. When using specular external reflection, both the dependency of the penetration depth on wavelength and the dependency of band intensities on the orientation of single-crystal grains are the potential sources of distortions and irreproducibility of IR spectra. According to the Kramers-Krönig relationship, the wavelength dependence of the real part of the refractive index is related to the extinction coefficient. This phenomenon is known as anomalous dispersion (see Fig. 1.1).

In diffuse reflectance spectroscopy (DRS, DRIFTS) reproducibility strongly depends on particle sizes and the kind of sample preparation (packing density, the character of sample surface, etc.). Applying Kubelka-Munk function (Kubelka and Munk 1931; Boroumand et al. 1992) to a diffuse reflectance spectrum produces a corrected spectrum that nearly approximates the transmission spectrum.

It is important to note that reflectance mode IR spectra, IR spectra obtained without immersion medium, as well as IR spectra of single crystals,

N.V. Chukanov and A.D. Chervonnyi, *Infrared Spectroscopy of Minerals and Related Compounds*, Springer Mineralogy, DOI 10.1007/978-3-319-25349-7_1

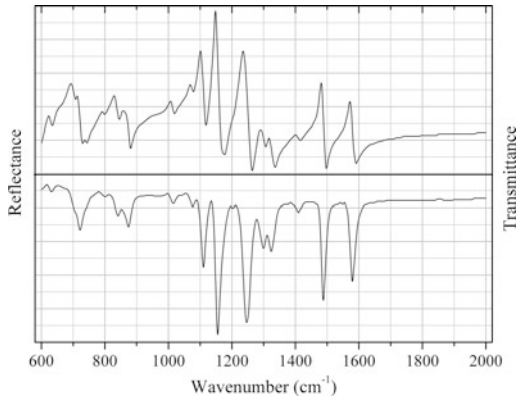

Fig. 1.1 Reflection IR spectrum recorded from the surface of a thick molding of PES, and corresponding transmission spectrum calculated using the Kramers-Kronig relationship. The picture is drawn based on data from Chalmers (2006)

coarse-grained or textured aggregates cannot be considered as reproducible and reliable diagnostic characteristics of mineral species due to specific effects induced by orientation, polarization (see Fig. 1.2), scattering, dispersion, and reflection conditions. Taking into account the above considerations, transmittance or absorbance IR spectroscopy using pulverized samples dispersed in an immersion medium should be considered as the preferred and reliable way to obtain reproducible data. However this technique is not devoid of drawbacks.

Most frequently, milling and pressing with alkali halides (KBr, more rarely CsI or RbI) to form a disk is used to obtain a transmittance-mode IR spectrum. This method exploits the property that alkali halides become plastic when subjected to pressure. KBr and CsI may be used to measure the infrared spectra in the regions above 360 and 250 cm^{-1}, respectively. It should be noted that alkali halides are hygroscopic, and their fine powders absorb much humidity from the air. This leads to an increased background in the ranges 1600–1700 and 3000–3900 cm^{-1} (Fig. 1.3). Grinding in a box filled with dry nitrogen or argon minimizes the contribution of adsorbed water to the spectrum.

In addition to water and grease, typical impurities in KBr discs are SO_4^{2-} (see Fig. 1.4) and NO_3^-. In particular, a narrow band at ~1383–1384 cm^{-1} indicates the presence of NO_3^-. These impurities may initially be kept in KBr or arise as a result of exposure to acid vapors.

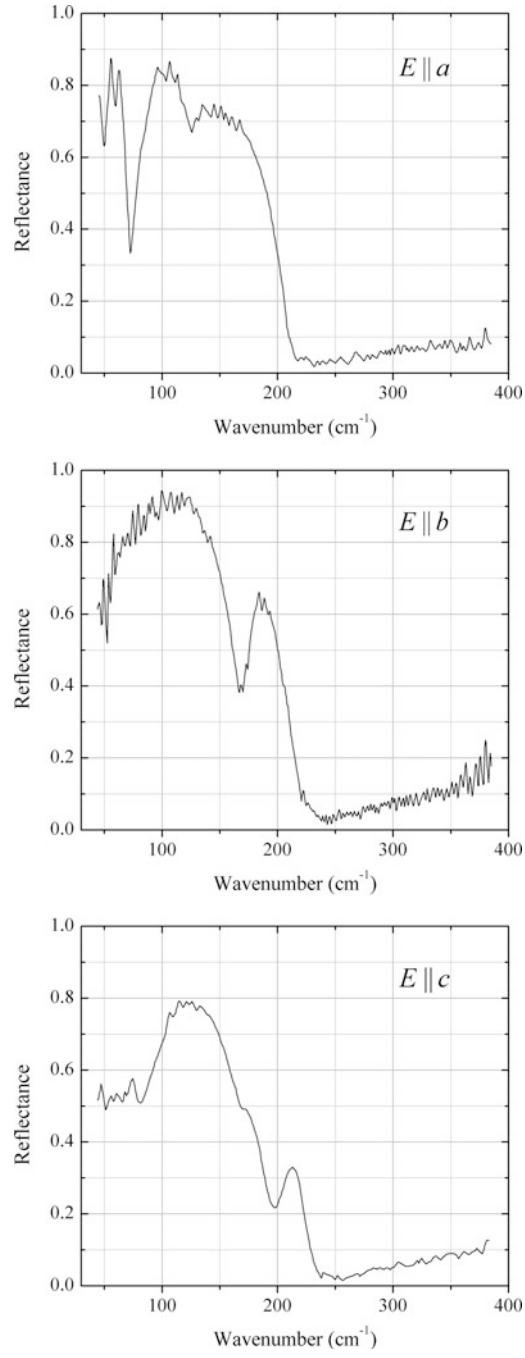

Fig. 1.2 Reflection spectra of $PbCl_2$ single crystal (space group *Pnma*) obtained by light polarized parallel to *a*, *b* and *c* (drawn using data from Hiraishi et al. 1979)

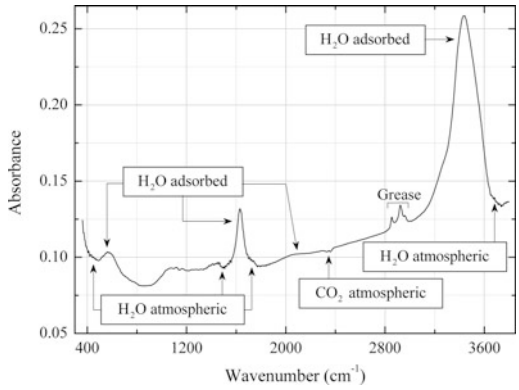

Fig. 1.3 IR spectrum of KBr disc with typical impurities (adsorbed water and grease). The IR spectrum of atmospheric air (containing enhanced amounts of H_2O and CO_2) is subtracted. The spectrum was obtained by N.V. Chukanov

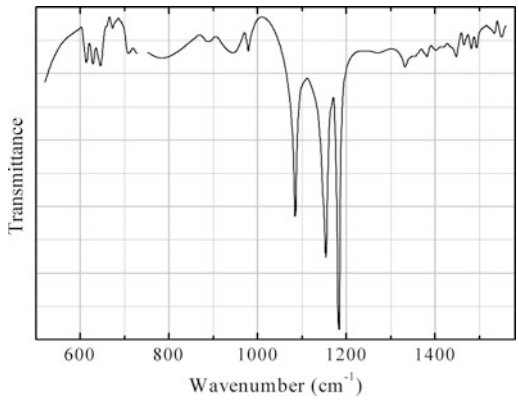

Fig. 1.4 IR spectrum of SO_4^{2-} in KBr crystal grown from commercial pure-grade KBr. The picture is drawn using data from Goriletsky et al. (2001)

As noted by Chalmers (2006), "to many readers, contamination may seem too obvious …, but sources that are obvious to many are still novel to some, and indeed have been overlooked in research publications by experts". In the cited paper, IR spectra of KBr discs with typical impurities (NO_3^-, phthalate plasticizer, silicone vacuum grease) are given.

Another kind of imperfections in any IR spectrum are absorption bands arising from the presence of atmospheric H_2O and CO_2 in the path of the IR beam between the source and the detector (Fig. 1.5). These bands may be observed either with positive or negative intensities, depending on their relative contents in the sample and background spectra.

Application of the method of pelletizing with alkali halides is limited because of possible mechanochemical reactions of a sample with immersion medium, as well as hydration, dehydration, oxidation, amorphization or phase transitions that can take place when milling and pressing. In particular, solid-state ion-exchange reactions are possible between KBr and hydrous sulfates of Cd, Cu, Zn, and Mg, as well as water-soluble nitrates and chlorides (Meloche and Kalbus 1958; Fernández-Bertrán and Reguera 1997). Ion-exchange reactions between water-soluble salts (sulfates, carbonates, phosphates, nitrates and halides) with CsCl and CsI matrices are reported by Yariv and Shoval (1985). When water-soluble Na salts are milled with CsCl, the formation of NaCl and the corresponding Cs salt takes place.

The presence of moisture in the KBr or its absorption from the atmosphere during the milling and pressing, as well as intensive trituration accelerate the ion-exchange processes. For example, slightly milled mixture of chalcanthite $CuSO_4 \cdot 5H_2O$ and KBr contains copper predominantly in the form $CuK_2(SO_4)_4$, whereas after strong milling the bromide analogue of chlorothionite, $CuK_2(SO_4)Br_2$ is formed (Fernández et al. 1993).

Reduction of potassium ferricyanide to ferrocyanide (kafehydrocyanite, $K_4Fe^{2+}(CN)_6 \cdot 3H_2O$) on prolonged grinding is reported by Fernández-Bertrán and Reguera (1997). We observed change of colour of ferrosaponite pressed in KBr disc from green to brown (as a result of oxidation of Fe^{2+} to Fe^{3+}) during one day.

As noted by Fernández-Bertrán and Reguera (1997), under the effect of pressure (during preparation of a KBr disc), some crystalline compounds can undergo phase transformations. After the KBr disc is decompressed, reverse phase transition may require considerable time. This phenomenon is most typical for crystals of organic compounds with weak van der Waals intermolecular interactions. As a rule, phase transitions in ionic compounds occur at greater

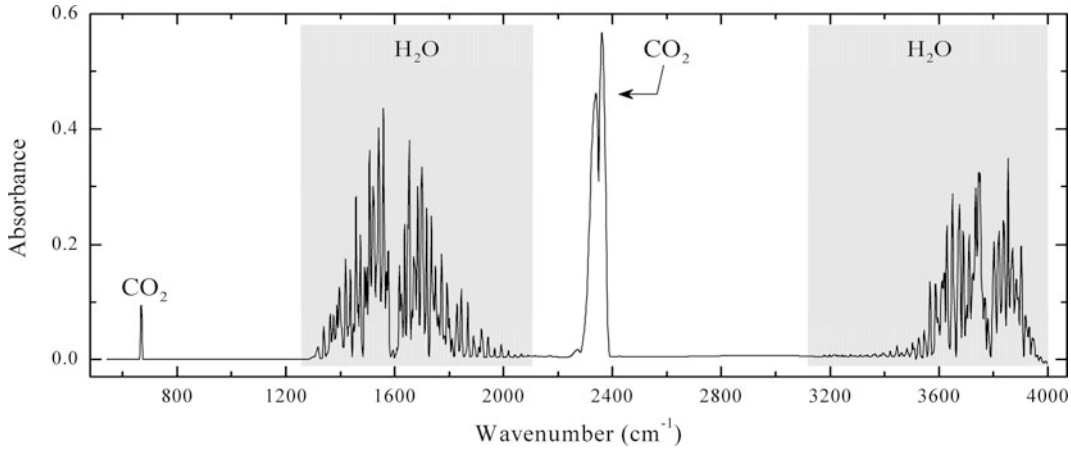

Fig. 1.5 IR spectrum of atmospheric air obtained with the resolution of 4 cm^{-1} and showing absorption bands of H_2O and CO_2. The spectrum was obtained by N.V. Chukanov

pressures than those used for the preparation of KBr discs.

In cases when the possibility of chemical reactions or polymorphic transformations is intended, the IR spectra obtained by the disk technique are to be compared with ones recorded for samples dispersed as suspension in an inert liquid (e.g. Nujol). Nujol, or paraffin oil, is chemically inert and nonhygroscopic, but its IR spectrum contains relatively strong bands between 2950–2800, 1465–1450, and 1380–1370 cm^{-1}, as well a weaker band at $\sim$720 cm^{-1} and several very weak absorptions in the range from 800 to 1300 cm^{-1}. In order to obtain a transmittance-mode IR spectrum of mineral, its mull (a very thick suspension) in Nujol is placed between IR-transparent plates. In the range from 1360 to 4000 cm^{-1} Fluorolube (i.e. fluorinated hydrocarbon) can be used instead of Nujol because in this range Fluprolube is non-absorbing, except a weak band around 2322 cm^{-1}.

Polyethylene (PE) is another chemically inert and non-hygroscopic material. PE discs are regularly used to obtain transmission IR spectra of minerals in the far IR region. The PE discs are prepared at rather high temperatures (150–200 °C). In order to verify the optical homogeneity of the disc, different temperatures of the hot plate (150, 175, 180, 200, 225 °C) have been tested by Kendix et al. (2009). According to their data, at 180 °C and

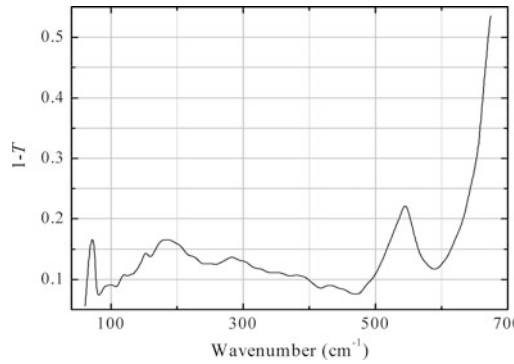

Fig. 1.6 IR spectrum of a pure PE disc (*ca* 1 mm thick) produced at 180 °C (T = transmittance). The picture is drawn using data from Kendix et al. (2009)

for higher temperatures, the produced PE disc is fully homogenous and visually transparent. The IR spectrum of pure PE disc is given in Fig. 1.6.

1.1.2 Data Proceeding

The most widely used **pre-processing** techniques in IR spectroscopy can be divided into two categories: baseline correction methods and spectral derivatives. The baseline of the transmission spectrum is usually curved. This is caused by scattering of the infrared light at the sample surface or interior, and this effect is greater for the shorter wavelengths.

Two kinds of algorithms are used for **baseline correction**. One of them permits the drawing of curves in a manner that allows full control of the line curvatures by the user. Corresponding algorithms can be based on polynomial methods using least-squares fitted lines or the method of Bezier (Koch and Weber 1998). As opposed to this, a fast automatic algorithm was proposed for baseline correction of IR spectral signals by Lan et al. (2007). The latter method is based on iterative curve fitting where orthogonal polynomials are used; the algorithm can process the spectra automatically, without human intervention.

The scattering curve depends in a complex way on size distribution of absorbing particles, their shapes and spatial distribution, as well as on refraction indices of absorbing particles and immersion medium (KBr, Nujol, etc.). In case of elastic (Rayleigh) scattering, the intensity of light scattered by any one of the small spheres of diameter d and refractive index n is proportional to the value $d^6(n^2 - 1)^2(n^2 + 2)^{-2}\nu^4$, where ν is light frequency. In more complex cases the intensity of light scattering can be approximated by the expression $\Sigma k_n \nu^{2n}$, where $n = 0, 1, 2, 3 \ldots$ and k_n are coefficients which can be determined from the root-mean-square approximation of the spectrum in the region free of strong absorption.

A review of the most common pre-processing techniques, including scatter-correction methods and spectral derivatives for near-infrared spectra is given by Rinnan et al. (2009).

Band component analysis is the most important source of errors and artifacts during data processing because of low correctness of inverse problems: small errors in experimental data lead to strong uncertainty of the final result. Additional uncertainty is connected with arbitrary choice of the band shape (Gauss, Lorentz, Voigt, or Lorentz-Gauss cross-product function), the number of components and the acceptable values of the correlation coefficient R (e.g. 0.99, 0.995, or 0.999). Most software packages enable specific parameters to be fixed or varied, and that leads to even greater uncertainty of the fitting. Let us consider several illustrating examples.

The results of band component analysis for the IR spectrum of gmelinite-K in the region of Si–O-stretching vibrations carried out with different starting parameters, without base line correction are presented in Fig. 1.7 and in Table 1.1. In both cases fitting using four Gaussian components, without base line correction was used. As can be seen from these data, both options give a good approximation accuracy (in both cases $R^2 \approx 0.9995$), but lead to substantially different results.

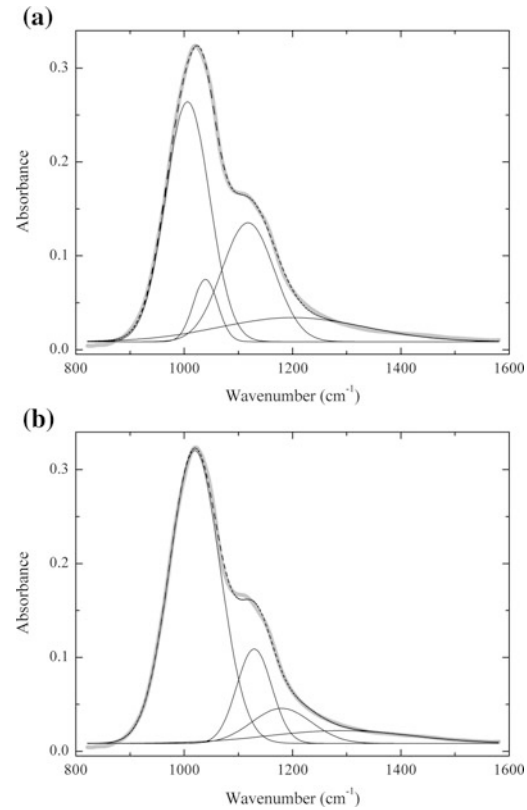

Fig. 1.7 The results of band component analysis for the IR spectrum of gmelinite-K in the region of Si–O-stretching vibrations carried out with different starting parameters. In both cases experimental curve (*grey lines*) was approximated by a superposition of four Gaussian components (*dashed lines*)

Table 1.1 The results of band component analysis for the IR spectrum of gmelinite-K in the region of Si–O-stretching vibrations carried out with different starting parameters (see Fig. 1.7)

Component	Center (cm^{-1})	Maximal height (absorbance units)	Area
	Fitting 1 (Fig. 1.7a), R^2 = 0.99951		
Gaussian 1	1006.2	0.2557	26.12
Gaussian 2	1039.2	0.0665	3.78
Gaussian 3	1117.9	0.1268	15.33
Gaussian 4	1200.4	0.0257	8.71
	Fitting 2 (Fig. 1.7b), R^2 = 0.99947		
Gaussian 1	1019.5	0.3121	36.35
Gaussian 2	1129.3	0.1007	8.15
Gaussian 3	1179.8	0.0373	5.17
Gaussian 4	1288.7	0.0135	4.48

As another example, let us consider the IR spectrum of another zeolite, montesommaite, in the region of Si–O-stretching vibrations. The band component analysis was carried out with different number of Gaussian components and different starting parameters. The results are presented in Fig. 1.8 and in Table 1.2. In all cases a procedure of base line correction was used. As in case of gmelinite-K, a good fitting (with the standard error of approximation below the experimental error), was obtained using different sets of Gaussian components. Note that in the case of the approximation of the spectrum with six Gaussian components there are numerous alternatives. There are no objective criteria to prefer one of the options to another one. Application of the second derivative method in this case is also unproductive because of strong noise (see Fig. 1.9). Preference to a particular variant of fitting may be given only on the basis of physical criteria. Unfortunately, researchers rarely resort to such an analysis.

1.1.3 Data Interpretation

Incorrect **band assignment** is one of the most frequent mistakes in the interpretation of IR spectra of minerals. The limits of frequencies for characteristic bands of most important anionic groups (CO_3^{2-}, NO_3^-, BO_3^{3-}, SO_4^{2-}, PO_4^{3-}, BO_4^{5-}, SiO_4^{4-}, CrO_4^{2-}, AsO_4^{3-}, VO_4^{3-}, SeO_4^{2-}, MoO_4^{2-}, WO_4^{2-}, IO_3^-, SeO_3^{2-}, TeO_3^{2-}) in IR spectra of minerals are published by Povarennykh (1978). For each of these groups, regions of specific vibrations overlap with those of one or more other groups. The least characteristic area is that between 800 and 900 cm^{-1}, where strong bands of SiO_4^{4-}, CrO_4^{2-}, AsO_4^{3-}, VO_4^{3-}, SeO_4^{2-}, MoO_4^{2-} and WO_4^{2-} can be present.

Some spectral intervals are often tentatively considered as characteristic of certain types of chemical groups. For example, bands in the range 2000–3800 cm^{-1} are usually ascribed to O–H-stretching vibrations of isolated OH^- anions or O–H bonds belonging to H_2O, H_3O^+, $B(OH)_3$, HPO_4^{2-} and other complex ions and molecules. But it should be kept in mind that the region 2500–3500 cm^{-1} is characteristic of N–H-stretching vibrations too. The bands in the interval from 1600 to 1700 cm^{-1} are regularly ascribed to bending vibrations of H_2O molecules, but IR spectra of some organic compounds also contain bands in this region. In most cases, bands in the range from 1360 to 1500 cm^{-1} indicate the presence of carbonate groups. However bands of non-covalent-bonded H^+ and NH_3^+ may be observed in this interval too.

The **factor group method** is regularly used for calculation of the symmetry properties and selection rules for vibrational modes of crystals with known structures (see review DeAngelis

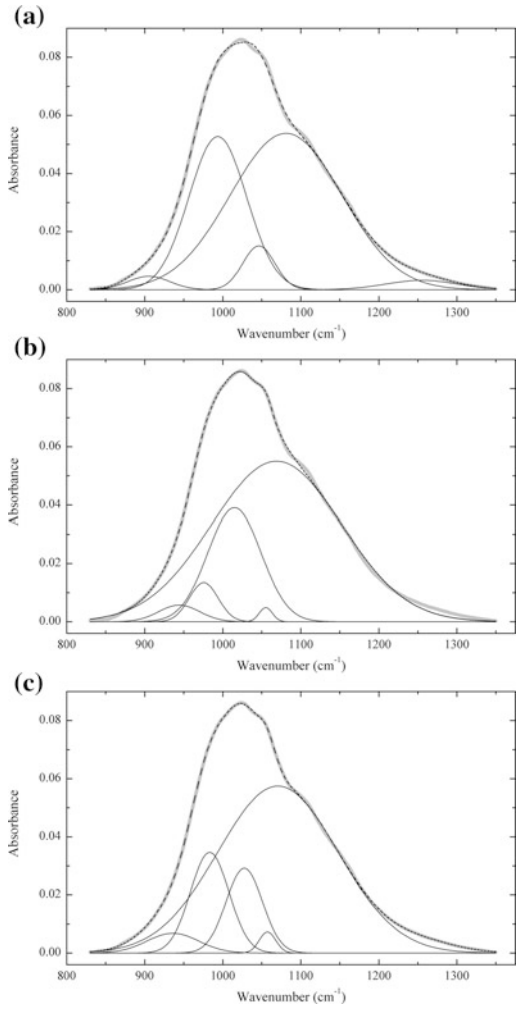

Fig. 1.8 The results of band component analysis for the IR spectrum of montesommaite in the region of Si–O-stretching vibrations carried out with different starting parameters, as a superposition of five (**a**, **b**) and six (**c**) Gaussian components

et al. 1972). However this method is effective only to IR spectra of minerals having the simplest structures. In most cases, the determination of the number of active modes in IR spectra of minerals is impossible due to the overlapping of spectral bands, resonance splitting and different factors distorting translational symmetry of real crystals (solid solutions involving different complex anions, alteration of different kinds of stacking of layers, local defects, etc. – see Chukanov 2014a).

1.2 Characteristic Bands in IR Spectra of Minerals

Absorption bands observed in the IR spectrum of a crystalline compound are the result of the resonant interaction of radiation with collective vibrations of a large number of atoms. However, with a certain degree of approximation IR bands in different frequency ranges can be associated with vibrations of appropriate groups of atoms. One of the first attempts of this kind applied to minerals has been undertaken by Povarennykh (1978) who suggested the following formula for the calculation of the frequency ν of cation-anion stretching vibrations:

$$v = AkV_cV_aZ^{-1}d^{-1}M^{-1/2} \qquad (1.1)$$

where A is a proportionality coefficient that depends on the cation valence; k is coefficient of relative bond strength which varies from 1 to 2 according to the degree of covalency of the bond; V_c and V_a are valences of the cation and the anion; Z is coordination number of the cation; d is the interatomic cation-anion distance; M is the reduced mass of the cation, equal to the sum of atomic weights of the cation and of all anions that coordinate it. However in practice, the use of the relation (1.1) is complicated due to the fact that the exact values of a number of its constituent parameters are unknown. Empirical approach, when ranges of the characteristic bands are determined from IR spectra of compounds with known crystal structures, remains the most common. The article by Povarennykh (1978) presents such data for some particular cases (Fig. 1.10).

Table 1.3 lists the ranges of wavenumbers of characteristic bands corresponding to stretching vibrations of some other groups and coordination polyhedra that are known in minerals and related compounds. In most cases, the assignments have been made based on the data from Miller and Wilkins (1952), Povarennykh (1978), Potter and Rossman (1979b), Nakamoto (2008, 2009), Rastsvetaeva et al. (2012), and Chukanov (2014a). In some particular cases additional references are given.

Table 1.2 The results of band component analysis for the IR spectrum of montesommaite in the region of Si–O-stretching vibrations carried out with different starting parameters and different number of Gaussian components (see Fig. 1.8)

Component	Center (cm^{-1})	Maximal height (absorbance units)	Area
	Fitting 1 (Fig. 1.8a), R^2 = 0.99976		
Gaussian 1	905.3	0.00464	0.3126
Gaussian 2	993.6	0.05272	4.8885
Gaussian 3	1046.2	0.01510	0.7752
Gaussian 4	1081.0	0.05381	9.6418
Gaussian 5	1255.0	0.00324	0.3687
	Fitting 2 (Fig. 1.8b), R^2 = 0.99929		
Gaussian 1	944.1	0.00572	0.377
Gaussian 2	975.6	0.01345	0.626
Gaussian 3	1015.0	0.03908	3.345
Gaussian 4	1055.2	0.00484	0.103
Gaussian 5	1068.9	0.05502	11.464
	Fitting 3 (Fig. 1.8c), R^2 = 0.99992		
Gaussian 1	936.0	0.00681	0.567
Gaussian 2	983.2	0.03465	2.147
Gaussian 3	1027.5	0.02922	1.709
Gaussian 4	1057.3	0.00728	0.194
Gaussian 5	1070.7	0.05748	11.069
Gaussian 6	1259.3	0.00278	0.307

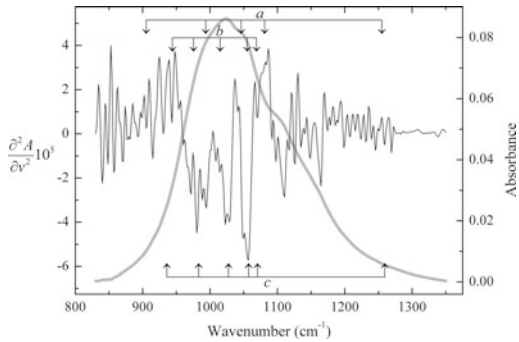

Fig. 1.9 IR spectrum of montesommaite in the region of Si–O-stretching vibrations (*grey line*) and its second derivative (*black line*). The positions of Gaussian components for different variants of fitting are shown with *arrows*

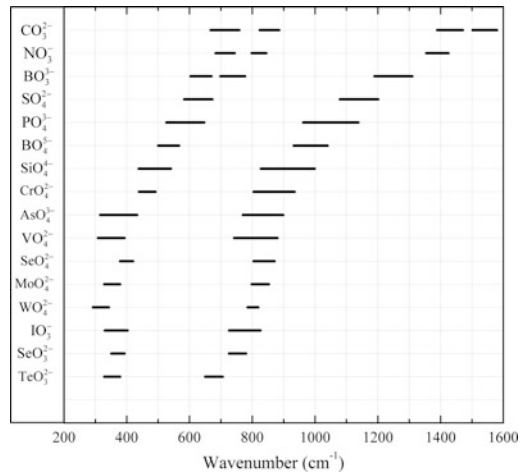

Fig. 1.10 The limits of frequencies of characteristic vibrations of some isolated groups with covalent bonds in IR spectra of minerals. The diagram is drawn using data from Povarennykh (1978)

Table 1.3 The ranges of strongest stretching bands for some isolated groups and coordination polyhedra

Bond	Range, cm^{-1}	Comment
Hg–Hg	130–140	In $(Hg_2)_3(AsO_4)_2$ (Baran et al. 1999b)
$^{VI}Mn^{2+}$–O	~310	Octahedra with 8 edges shared per MnO_6 octahedron
^{IX}Y–F	~380	Trigonal prism (in waimirite)
$^{VI}Mn^{2+}$–O	400–440	Isolated octahedron
$^{VI}Fe^{2+}$–O	410–440	Isolated octahedron
^{VI}Mg–O	430–460	Isolated octahedron
$^{VI}Mn^{4+}$–O	430–500	Octahedra with 5 edges shared per MnO_6 octahedron
$^{VI}Fe^{3+}$–O	450–500	Octahedron
$^{III}Sb^{3+}$–O	460–560	Valentinite
$^{VI}Mn^{4+}$–O	470–480	Octahedra with 6 edges shared per MnO_6 octahedron
$^{VI}Mn^{4+}$–O	480–530	Octahedra with 4 edges shared per MnO_6 octahedron
^{IV}Li–O	490–610?	Tetrahedron
^{VI}Al–O	500–560	Octahedron
$^{III}As^{3+}$–O	500–610	AsO_3^{3-}
^{VI}Sn–O	500–670	Octahedra with 2 edges shared per SnO_6 octahedron (cassiterite)
$^{VI}Te^{6+}$–O	500–730	Octahedron. Usually the band is split into several components.
^{VII}Zr–O	~510	Baddeleyite
^{VI}(Ti, Nb)–O	510–600	Octahedral framework
$^{III}As^{3+}$–O	510–600	$HAsO_3^{2-}$
$^{V}(Mn^{2+}, Fe^{2+})$–O	518–529	Tetragonal pyramid
$^{V}Fe^{3+}$–O	529–533	Tetragonal pyramid
^{IV}Zr–O	530–531	Flat square
^{VI}Sn–O	530–534	The octahedron $Sn(OH)_6^{2-}$. Additional bands are present in the ranges 1150–1175 and 3125 – 3260 cm^{-1}
^{IV}Zn–O	530–580	Octahedron
^{IV}Ta–O	534	Flat square
$^{IV}Fe^{2+}$–O	540–544	Flat square
^{VI}Ti–O	540–570	Isolated octahedron
^{V}Ti–O	549–627	Tetragonal pyramid (lamprophyllite-group minerals, fresnoite, natisite, paranatisite)
^{VI}Al–O	550–630	Octahedron $Al(OH)_6$ in ettringite-group minerals. Additionally, the band of O–Al–O bending vibrations at ~410–420 cm^{-1} is present
^{VI}Al–O	550–640	$[Al(OH)_6]^{3-}$
^{IV}Nb–O	551–555	Flat square
$^{VI}Sb^{5+}$–O	590–605	The octahedron $Sb(OH)_6^-$. Additional bands are present in the ranges 1030–1070 and 3320–3360 cm^{-1}
$^{VI}Mn^{4+}$–O	600–650	Octahedra with 2 edges shared per MnO_6 octahedron
^{V}Al–O	600–715	In augelite, andalusite and vyuntspakhkite-(Y)
^{VI}Zr–O	610–620	Isolated octahedron
$^{IV}Fe^{3+}$–O	610–660	Tetrahedron
$^{VI}W^{6+}$–O	615–815	Octahedron

(continued)

Table 1.3 (continued)

Bond	Range, cm^{-1}	Comment
^{VI}(Ti, Nb)–O	660–700	Chain of vertex-sharing octahedra
^{VI}Si–O	670–890	Octahedra with 2 edges shared per SiO_6 octahedron (stishovite)
$^{VI}Sb^{5+}$–O	680–740	Octahedron
^{IV}Be–O	700–805	Tetrahedron
^{VI}Si–O	720–760	Octahedron $Si(OH)_6$ in ettringite-group minerals. Additionally, the band of O–Si–O bending vibrations at ~500 cm^{-1} is present
^{IV}Al–O	720–860	Tetrahedron. The frequency depends on the degree of polymerization of the tetrahedra
$^{III}Sb^{3+}$–O	~730	Sb_2O_6 cluster (sénarmontite)
U^{6+}=O	850–1000	Uranyl group, UO_2^{2+}
^{IV}P–O	860–1170	Acid orthophosphates. Numerous bands in this region. Additional bands are present in the range 1800–2900 cm^{-1}
^{IV}P–O	900–1350	Polyphosphates. Numerous bands in this region
$^{III}S^{4+}$–O	930–990	SO_3^{2-} (often a doublet)
V^{5+}–O	950–985	$V^{5+}{}_{10}O_{28}{}^{6-}$
^{IV}B–O	950–1000	$B(OH)_4^-$
V^{5+}–O	960–1000	$V^{5+}{}_6O_{16}{}^{2-}$. Additional very strong bands are present in the range 530–575 cm^{-1}
^{III}B–O	1190	$BO_{2.25}$ (orthoborate group with oxygen vacancies: Belokoneva et al. 2002b)
^{III}B–O	1190–1360	Isolated BO_3^{3-} anion
C–O	1300–1700	Acid carbonates. Numerous bands in this region. Additional bands are present in the range 1800–3000 cm^{-1}
C–O	1310–1370, 1620–1720	Symmetric and antisymmetric stretching vibrations of carboxylate groups COO^- in oxalate anions
C–O	1310–1450, 1600–1650	Symmetric and antisymmetric stretching vibrations of carboxylate groups COO^- in formate and acetate anions
C–O	1340–1370	Carbonate anions in hydrotalcite-group minerals and related compounds
C=O	1680–1780	Carbonyl and carboxyl groups in organic compounds
O–H	1700–3000	Acid groups C–OH, P–OH, S–OH, Si–OH, V–OH, As–OH, etc. Multiple, rather broad bands
O–H	2500–3750	OH^- anions and H_2O molecules. In case of H_2O molecules, additional band(s) of the H–O–H bending vibrations are present in the range 1500–1700 cm^{-1}
N–H	2800–3400	NH_4^+ cations and amine groups. In case of NH_4^+ cations, additional band(s) of the H–O–H bending vibrations are present in the range 1400–1440 cm^{-1}
C–H	2820–2980	Aliphatic hydrocarbonic groups $(CH_2)_n$, CH_3. Additional band(s) of bending vibrations are present in the range 1340–1480 cm^{-1}
C–H	3000–3100	Aromatic hydrocarbonic groups. Additional bands are present in the range 1400–1620 cm^{-1}
O–H	3125–3260	The octahedron $Sn(OH)_6{}^{2-}$. Additional bands are present in the ranges 530–534 and 1150–1175 cm^{-1}
N–H	3240–3330	NH_3 as ligand in ammine complexes. Additional bands of bending vibrations are present in the ranges 1240–1270 and 1590–1630 cm^{-1} (Bojar et al. 2010; Chukanov et al. 2015b)

(continued)

Table 1.3 (continued)

Bond	Range, cm^{-1}	Comment
O–H	3320–3360	The octahedron $Sb(OH)_6^-$. Additional bands are present in the ranges 590–605 and 1030–1070 cm^{-1}
N–H	3420–3500	Tetrammine copper (II) cation $[Cu(NH_3)_4]^{2+}$ (e.g. in shilovite), $[Cu(NH_3)_4](NO_3)_2$. Additional strong bands of bending vibrations are present in the range 1110–1170 cm^{-1}

The coordination numbers are indicated with Roman numerals

1.3 Hydrogen in Nominally Hydrogen-Free Minerals

Hydrogen-bearing groups commonly occur in trace to minor amounts in nominally hydrogen-free minerals (NHFMs), i.e. minerals whose idealized chemical formulae are written without hydrogen (Beran and Zemann 1969, 1971; Beran 1970a, b, 1971a, b; Beran and Gotzinger 1987; Beran et al. 1989; Beran and Rossman 1989). Usually, hydrogen is present in NHFMs in the form of OH groups. Such hydroxyl is colloquially known in the petrologic literature as "water" (Walker et al. 2007), and the term "nominally anhydrous minerals" (NAMs) is commonly used. We will use a more exact term, "nominally hydrogen-free minerals" (NHFMs). Trivial cases of homovalent substitutions (e.g. when OH^- anions partly replace F^- or Cl^-), are out of a subject of this section.

The early interest in OH groups in NHFMs came from the study of inorganic industrial materials (Kats and Haven 1960; Brunner et al. 1961; Kats 1962; Belt 1967; Beran 1991; Rossman 2006). Over a period of last decades, NHFMs have been discussed from the viewpoint of mechanisms of water storage capacity of olivine and other minerals in the upper mantle (Martin and Donnay 1972; Winkler et al. 1989; Bell and Rossman 1992; Cynn and Hofmeister 1994; Kohlstedt et al. 1996; Skogby 1999; Ingrin and Skogby 2000; Bolfan-Casanova et al. 2000; Bolfan-Casanova et al. 2006; Rossman 2006).

IR spectroscopy is one of the most sensitive methods to detect and analyze OH groups and H_2O molecules in minerals and glasses, but for quantitative determination of these components a calibration based on independent methods of analysis (e.g. ^1H NMR, mass-spectrometry or thermogravimetry) are required. Based on the data for synthetic hydrous ringwoodite, wadsleyite and forsterite, it was proposed that within a polymorphic mineral series of the same composition the absorption coefficient of O–H-stretching vibrations positively correlates with the density (Koch-Müller and Rhede 2010). However this hypothesis is to be proved involving more representative data.

Three kinds of H-bearing components of NHFMs can be distinguished. Components of the first type are H-bearing groups occupying fixed positions in the crystal structures, mainly crystallographically oriented OH groups. These groups can be detected using polarized infrared radiation. This approach, that can be also used for the determination of the orientation of O–H bonds, may be misleading in case of the presence of included oriented pseudomorphs of H-bearing phases after H-free minerals (e.g. homoaxial pseudomorphs of amphiboles or micas after pyroxenes). H-bearing components of the second type are present in inclusions of a fluid from which crystals of an H-free mineral were grown. H-bearing components of the third type are present in inclusions of secondary OH-bearing or hydrous compounds substituting primary minerals (the typical examples are randomly oriented individuals of serpentines and chlorites present in crystals of pyroxenes and olivines as products of their low-temperature alteration along cracks, dislocations and interblock borders).

H-bearing components of the first type can be subdivided into two subtypes: those present in structural channels (typically, H_2O molecules) and those substituting O atoms in common sites.

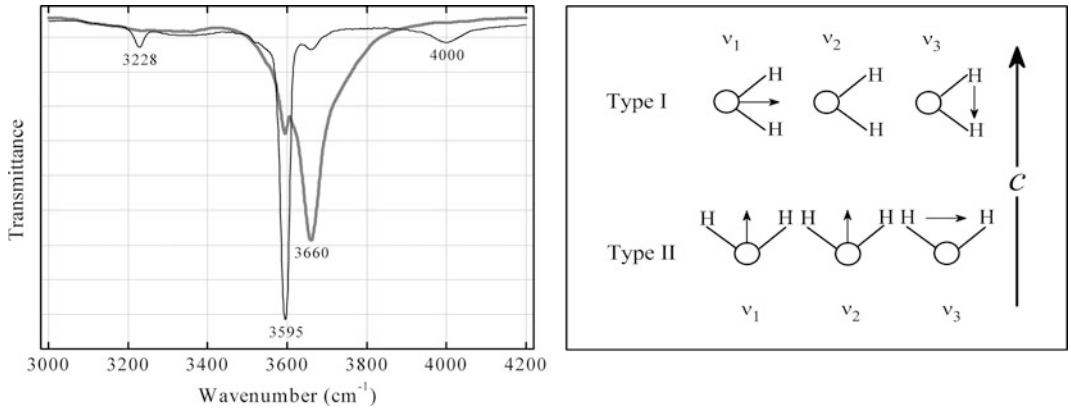

Fig. 1.11 Polarized spectra of stoppaniite collected with the electric vector $E \perp c$ (*grey line*) and $E \parallel c$ (*black line*) (*left*) and schematic representation of the dipole moment vectors of the fundamental modes of type I and type II water in beryl (*right*). The pictures are drawn using data from Della Ventura et al. (2007b) and Charoy et al. (1996)

The examples of minerals containing H_2O in channels are the members of the beryl and cordierite groups (Sugitani et al. 1966; Wood and Nassau 1967; Charoy et al. 1996; Farrell and Newnham 1967; Zolotarev and Dufour 1995; Łodziński et al. 2005). Among **beryl-group** minerals, only in stoppaniite, ideally $Fe^{3+}{}_3MgNa(Be_6Si_{12}O_{36})\cdot 2H_2O$ (Della Ventura et al. 2007b), H_2O is present as a species-defining component, but in beryl, that are considered as a NHFM, minor amounts of water molecules in two independent crystallographic orientations have been also detected in *c*-axis channels (Fig. 1.11).

In the IR spectrum of alkaline beryl $Cs_{0.08}Na_{0.42}(H_2O)_{0.18}[Al_2(Be_{2.35}Li_{0.65})Si_6O_{18}]$ from Mokrusha pegmatite, Murzinka, Middle Urals (Yakubovich et al. 2009; see Fig. 1.12) distinct bands of water are observed at 3660, 3590 and 1626 cm^{-1} (respectively, antisymmetric stretching, symmetric stretching and bending vibrations of H_2O molecules which do not form strong hydrogen bonds). These bands are related to water molecules whose O atom coordinates an alkaline cation, and the vector H–H is perpendicular to *c*. In the IR spectrum of low-alkaline beryl from Lipovka, Urals the doublet 3660 + 3590 cm^{-1} is not observed (Fig. 1.12).

Calcinaksite is the only **litidionite-group** mineral containing water as a species-defining component present in channels. The other members of this group, namely, **fenaksite** $KNaFe^{2+}(Si_4O_{10})$, **manaksite** $KNaMn^{2+}(Si_4O_{10})$ and **litidionite** $KNaCu^{2+}(Si_4O_{10})$ have been described as anhydrous minerals (Dorfman et al. 1959; Martin Pozas et al. 1975; Khomyakov

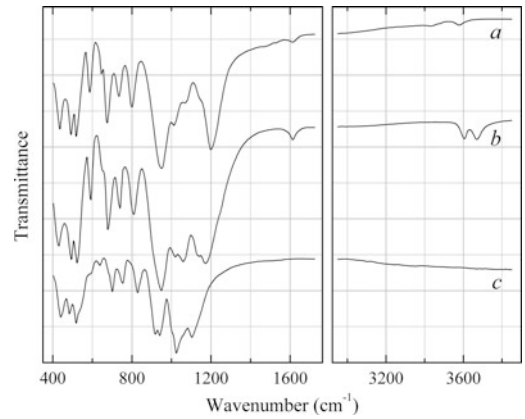

Fig. 1.12 IR spectra of (*a*) low-alkaline beryl $(Na_{0.06}Cs_{0.01}Rb_{0.01})Be_3(Al_{1.88}Fe_{0.09}Mg_{0.03})(Si_{5.95}Al_{0.05}O_{18})\cdot xH_2O$ ($x \ll 1$) from Lipovka, Urals, (*b*) alkaline beryl $Cs_{0.08}Na_{0.42}(H_2O)_{0.18}[Al_2(Be_{2.35}Li_{0.65})Si_6O_{18}]$ from Mokrusha, Urals, and (*c*) pezzottaite (ideally, $CsBe_2LiAl_2Si_6O_{18}$). The IR spectra were obtained by N.V. Chukanov

et al. 1992). However recent data (Aksenov et al. 2014; Chukanov et al. 2015a) show that, at least, fenaksite and manaksite contain water in trace amounts.

In calcinaksite, $KNaCa(Si_4O_{10})\cdot H_2O$, water molecules are situated in the heteropolyhedral channel and occupy a site at the vertex of the Ca-centered octahedron $CaO_5(H_2O)$. There are three short distances between the water molecule and oxygen atoms, $O_w\cdots O4$ [2.834(5) Å], $O_w\cdots O9$ [2.745(5) Å] and $O_w\cdots O_w$ [2.861(9) Å] (Aksenov et al. 2014). These distances may correspond to three hydrogen bonds detected by IR data (the bands at 3340, 3170 and 3540 cm^{-1} respectively; see Fig. 1.13). Thus one of two H atoms of the H_2O molecule is disordered between two acceptors, O9 and O_w. One can suppose that in fenaksite and manaksite water preferably occupies unit cells in which Fe or Mn are substituted with calcium that is present in these minerals in minor amounts.

In **feldspars** hydrogen-bearing groups can be present as structural defects (Hofmeister and Rossman 1985; Beran 1986; Beran 1987). A feldspar in which alkali cations are almost completely substituted by protons was prepared and characterized by powder and single-crystal X-ray diffraction data (Müller 1988; Paulus and Müller 1988; Deubener et al. 1991).

Hydrogen in H-bearing feldspar with an average H_2O content of 3.55 wt% was obtained by annealing Na-exchanged feldspars twice for 3 days at 310 °C in H_2SO_4 and studied by single crystal IR microspectroscopy (Behrens and Müller 1995; see Fig. 1.14). The strongest absorption bands are observed at 3000 and 2485 cm^{-1}. The largest absorbance of polarized radiation in (010) was observed at these wavenumbers, if the *E*-vector of IR radiation vibrates approximately parallel to the *a*-axis. The shoulder at 3500 cm^{-1} which showed no significant dependence on the orientation of the crystal was assigned to an amorphous phase. The bands at 3000 and 2485 cm^{-1} are shifted to lower wavenumbers (2440 and 1840 cm^{-1}, respectively) in the IR spectrum of the deuterated analogue of H-feldspar. Low frequencies of these bands indicate their acid character. Possibly, they correspond to H_3O^+ cations or, less probably, to silanol groups Si–OH formed as a result of the reaction $Si–O–Si + H_2O \rightarrow Si–OH + HO–Si$. The presence of acid groups in hydrogen feldspar may be a result of its preparation in high-acidic medium. Another hypothetical explanation for the low frequency band, based on the assumption that the hydrogen is bound to the bridging oxygen (Behrens and Müller 1995), is less

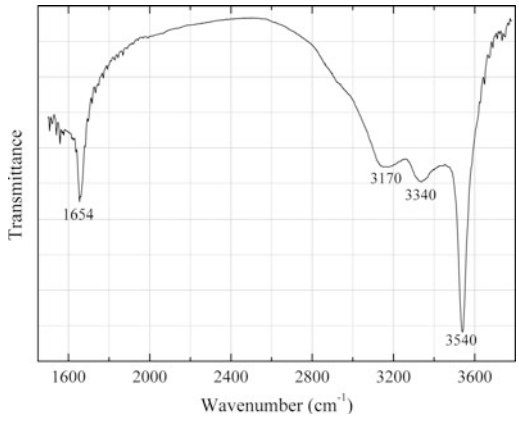

Fig. 1.13 Powder IR spectrum of calcinaksite in the region of stretching and bending vibrations of water molecules. The IR spectrum was obtained by N.V. Chukanov

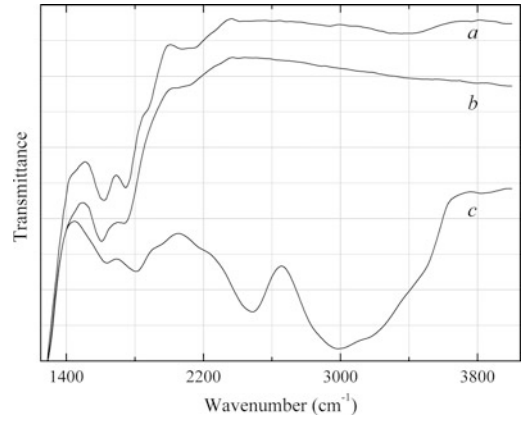

Fig. 1.14 IR spectra of (*a*) sanidine, (*b*) Na-feldspar, and (*c*) H-feldspar taken from fragments flattened on (010) (thickness: *ca.* 50 μm) using a partially polarized beam with an *E*-vector predominantly oriented parallel to the *a*-axis. The picture is drawn using data from Behrens and Müller (1995)

convincing taking into account local charge balance requirements.

Natural metasomatic sanidine from Volkesfeld, Eifel Mts., Germany contains only traces of structurally bound hydrogen. The band at 2470 cm^{-1} in its IR spectrum exists with maximum absorbance of polarized radiation for the same orientation as for the band at 3050 cm^{-1} (Behrens and Müller 1995).

Another kind of hydrogen incorporation takes place in hydrothermally synthesized Rb-feldspar (rubicline), $Rb_{0.811}Al_{1.059}Si_{3.003}O_8$ (Kyono and Kimata 2001a). As noted by the authors of this paper, deficite of Rb at the *M*-site of this compound favours the structural incorporation of the H_2O molecule. As a result, a broad band at 3450 cm^{-1} is observed in the single-crystal IR spectrum. However the formula of this sample recalculated under this assumption on 4 framework atoms, i.e. $(H_2O)_xRb_{0.799}[Al_{1.043}Si_{2.957}O_8]$ (with the framework composition given in square brackets), isn't electrically neutral. This fact indicates that, most probably, at least a part of hydrogen is present in this sample not as H_2O, but in a cationic form.

Pyroxenes which contain significant amounts of hydrogen (up to 0.1 wt% H_2O) may be an important concentrator of hydrogen in the Earth's upper mantle. IR spectra of clinopyroxenes are characterized by four pleochroic OH stretching bands, I, II, III and IV, centered at 3630–3650, 3530–3540, 3450–3470 and 3350–3360 cm^{-1} (Libowitzky and Beran 2006; Fig. 1.15). The band I which is strongly polarized in the direction of the projection of long diagonal of the unit cell onto [010] was assigned to OH groups in the O2 site coordinated by 1 Mg, 1 Ca and 1 Si or (in case of vacant *M*1 site) by 1 Ca and 1 Si. The doublet III + IV was assigned to OH groups nearly parallel to the [010] projection of the short diagonal of the unit cell; these OH groups coordinated by 1 Mg (or Fe) and 1 Si (or Al) are generated by a partial replacement of O2 oxygen atoms with an orientation pointing strongly above the Ca vacancy site (Libowitzky and Beran 2006).

In IR spectra of amphiboles, bands in the region from 3630 to 3650 cm^{-1} have been assigned to the configurations $(MgR^{2+}R^{2+})$–OH–□ and $(MgMgR^{3+})$–OH–□ where R = Fe or Mn (Ishida and Hawthorne 2001). Consequently, taking into account that uniaxial (epitaxial and syntaxial) intergrowths of amphiboles and pyroxenes are wide spread in nature, the band I could be also assigned to the amphibole modules which may occur as a defect part in pyroxene crystals. Additionally, a band at 3615 cm^{-1} can be present in the IR spectrum of mantle clynopyroxenes due to the admixture of exsolved phengite (Sakamaki and Ogasawara 2013).

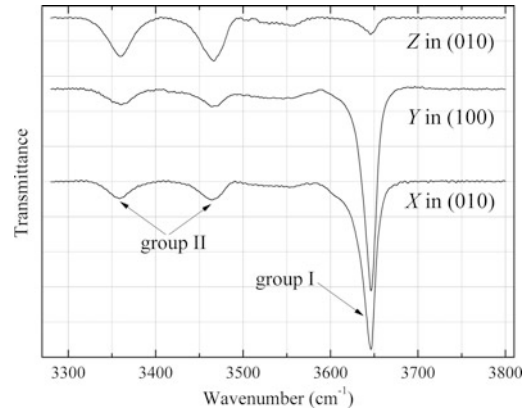

Fig. 1.15 *X*-, *Y*- and *Z*-polarized OH absorption spectra of diopside from Rotkopf, Zillertal, Tyrol, Austria, measured on (100) and (010) plates (*X*, *Y* and *Z* are optical axes). The picture is drawn using data from Andrut et al. (2003) and Libowitzky and Beran (2006)

Ilmenite-type and perovskite-type high-pressure polymorphs of enstatite, $(Mg,Fe)SiO_3$, are hypothetical mineral phases of the Earth's lower mantle. Five types of OH groups in synthetic ilmenite-type $MgSiO_3$ (akimotoite) correspond to five pleochroic IR bands located at 3390, 3320, 3300, 3260 and 3050 cm^{-1} (Bolfan-Casanova et al. 2002; Libowitzky and Beran 2006). The bands at 3320 and 3300 cm^{-1} are polarized perpendicular to the *c* axis and are oriented nearly parallel to the plane of the shared face between two SiO_6 octahedra. The band at 3390 cm^{-1} polarized parallel to the *c* axis was assigned to OH groups pointing into a tetrahedral cavity. Unpolarized IR spectrum of akimotoite synthesized at 22 GPa and 1500 °C contains additional bands at 3410 and 3345 cm^{-1} which

indicate another mechanism of OH incorporation in the akimotoite structure (Ye et al. 2013).

It is to be noted that analogies between the IR spectra of ilmenite-type and perovskite-type $M^{2+}SiO_3$ compounds and those of corundum Al_2O_3 and perovskite $CaTiO_3$, respectively (Libowitzky and Beran 2006) are rather speculative because of strong crystal-chemical differences between the pairs of cations Mg and Al, Ca and Mg, Ti and Si.

A series of experiments showed that the solubility of H_2O in olivine at 12 GPa increases with temperature to 8900 ppm by weight (ppmw) at 1250 °C and decreases at higher temperature with the onset of melting (Smyth et al. 2006). Sample characterization by infrared spectroscopy indicates that the primary hydration mechanism is the substitution of $2H^+$ for Mg^{2+}. According to (Litasov et al. 2007), the hydrogen content of olivine (Fo_{90}–Fo_{95}) coexisting with enstatite and hydrous melt increases from about 4600 ppmw at 1100 °C to a maximum of 6250 ppmw at 1200 °C. Above 1400 °C, the hydrogen content of olivine decreases non-linearly, reaching 160–240 ppmw in the 1800–2000 °C range where there is a high melt fraction and no enstatite. Numerous data for mantle olivine from kimberlite derived from IR spectroscopic data, calibrated using MMR, show that mean H_2O content in natural samples varies from 50 to 239 ppmw (Beran and Libowitzky 2006). These data show that olivine may be a very important concentrator of hydrogen in the upper mantle.

Available data on the nature of OH groups in olivine are ambiguous. Pleochroic absorption bands at ~3590, 3570, 3520, and 3230 cm^{-1} in gem-quality crystals of hydrothermal origin from Zabargad, Egypt have been assigned to $(OH,O)_4$ tetrahedra substituting SiO_4 groups (Beran and Putnis 1983).

OH-defect types in mantle-related olivines from different localities are reviewed by Beran and Libowitzky (2006). In polarized IR absorption spectra of the near-endmember forsterite from a skarn deposit in Pamir, Tadzikistan pleochroic band doublets centered at 3674/3624, 3647/3598 and 3640/3592 cm^{-1} are oriented parallel to [100], and an OH band doublet at 3570/3535 cm^{-1} shows both, a strong absorption parallel to [100] and a strong component parallel to [001]. These bands are supposed to be related to vacant Si and Mg sites (Libowitzky and Beran 1995; Beran and Libowitzky 2006). A similar conclusion was drawn on the basis of polarized FTIR spectroscopic study of synthetic pure forsterite (Lemaire et al. 2004): the bands at (3613, 3580, 3566, 3555, 3480), (3160), and (3600, 3220) cm^{-1} are supposed to be related to Si, *M*1 and *M*2 vacancies, respectively. It should be noted that the band at 3674 cm^{-1} observed in the IR spectra of forsterite from Pamir is close to the strongest bands of O–H-stretching vibrations of some magnesium serpentines and talc. One cannot exclude that this band corresponds to oriented inclusions of a phyllosilicate in forsterite crystals.

Bands at 3571, 3524, and 3402 cm^{-1} in olivine from a kimberlite were assigned to OH-bearing layers like those present in humite-group minerals (Kitamura et al. 1987). This conclusion was confirmed by TEM observations.

According to (Kovács et al. 2010), there are four ways by which OH groups commonly substitutes O atoms in olivine, namely those associated with Si vacancies, Mg vacancies, Ti or trivalent cations (correspondingly, the defects of the types I, II, III and IV).

In the defect of the type I, four H atoms charge-balance a Si vacancy in a tetrahedral site by being bound to O atoms at the apices of the tetrahedron. This mechanism produces a series of O-H absorption peaks, the strongest of which are at 3613, 3580, 3567, and 3480 cm^{-1}. This assignment was confirmed by polarization IR spectroscopy.

In the defect of the type II, two H^+ substitute for divalent cations in the octahedral sites. This mechanism results in IR absorption peaks between 3300–3100 cm^{-1} including two strong bands at 3220 and 3160 cm^{-1}. Low wavenumbers of these bands indicate that they may correspond to silanol groups Si–OH.

The presence of Ti in olivine promotes the formation of a "titanoclinohumite-like point-defect", $MgTiH_2O_4$ (the defect of the type III).

In this mechanism, Ti^{4+} is charge-balanced by a substitution of Si^{4+} by two protons on a neighboring tetrahedral site. This mechanism produces two prominent absorption peaks at 3572 and 3525 cm^{-1}, the most common and intense infrared hydroxyl stretching bands observed in spinel peridotite mantle olivines (Berry et al. 2005; Berry et al. 2007b; Walker et al. 2007; Kovács et al. 2010).

The incorporation of trivalent cations into octahedral sites of olivine produces the absorption peaks between 3400 and 3300 cm^{-1} (Berry et al. 2007a).

The high-pressure orthorhombic forsterite polymorph **wadsleyite**, β-Mg_2SiO_4, is supposed to be the most abundant mineral in the upper part of the mantle transition zone (McMillan et al. 1991). In some cases IR spectra of wadsleyite show only two or three peaks around 3340 and 3600 cm^{-1} (McMillan et al. 1991; Mernagh and Liu 1996; Kudoh et al. 1996; Kleppe et al. 2001), whereas some others show more complex spectra. The investigation of wadsleyite synthesized at 1300 °C and 15 GPa by means of ^1H MAS NMR and FTIR spectroscopy (Kohn et al. 2002) demonstrated that in high-hydrated samples containing 0.8–1.5 wt% H_2O hydroxyl anions occupy at least 14 of the 17 possible O-H···O environments, including some with strong hydrogen bonding, but the strongest absorption is observed in the narrow interval from 3330 to 3360 cm^{-1}. At lower water concentrations (<0.4 wt%) the most abundant are three environments involving protonation of O1 and, probably, one environment involving O2-H···O2. The differences in IR spectra of wadsleyite may be due to differences in Fe concentration and oxidation state, water concentration, symmetry or the presence of impurity phases (Kohn et al. 2002).

Another high-pressure polymorph of forsterite, **ringwoodite** (cubic γ-Mg_2SiO_4 with spinel-type structure), possibly plays an important role in the lower transition zone of the Earth's mantle as a concentrator of hydrogen (Bolfan-Casanova 2005; Ohtani 2005). This mineral can incorporate up to 1.5–2 wt% H_2O (Thomas et al. 2015). Unpolarized IR spectra of ringwoodite in the O–H-stretching region show broad absorption features with band maxima ranging from ~3130 to 3174, from ~3531 to 3568, and from ~3656 to 3675 cm^{-1}, with the strongest and broad band at ~ 3130 cm^{-1}. These features indicate the predominant role of silanol groups Si–OH related to vacancies in octahedral sites. Relatively weak bands above 3500 cm^{-1} are related to tetrahedral defects of either the hydrogarnet-type substitution (see below) or Mg replacing Si atoms.

The main way of the incorporation of OH groups in **garnets** is the replacement of SiO_4 groups with $(OH)_4$ tetrahedra (the hydrogarnet substitution). The IR absorption patterns of synthetic garnets belonging to the **grossular-katoite** solid-solution series, $Ca_3Al_2[SiO_4,(OH)_4]_3$, change remarkably with OH contents (Kobayashi and Shoji 1983). In the IR spectrum of a sample with a low OH content, three weak bands are observed at 3700, 3670 and 3620 cm^{-1}. These bands gradually shift with the enhancement of the OH: (Si + 4OH) ratio (up to 3750, 3660 and 3610 cm^{-1}, respectively, for end-member katoite). According to Rossman and Aines (1991), the IR spectroscopic characteristics of hydrogrossulars with more than 5 wt% H_2O are two overlapping absorption bands centered around 3600 and 3660 cm^{-1}. However, these spectroscopic characteristics were generally not observed in grossular containing less than 0.3 wt% H_2O, in which OH defects apparently exist in multiple other environments (Beran and Libowitzky 2006). Optically isotropic behavior of garnets is considered as a factor preventing from the assignment of O–H-stretching IR absorption bands to possible sites of hydrogen incorporation (Beran and Libowitzky 2006). However it is important to note that even in cubic garnets different crystallographic directions are non-equivalent, and polarization IR spectra of oriented plates could be used to obtain some information on the orientation of O–H bonds.

Another problem seems to be more serious. In numerous publications on polarized spectra of OH-bearing nesosilicates, it is implied that each O–H-stretching band corresponds to local vibrations of a single OH group. Really, in case of the

short distances between OH groups, one can expect the existence of normal modes involving more than one OH group and, consequently, polarized differently than every individual O–H bond. Apparently, this matter needs a more detailed investigation.

Band doublets at 3559/3540, 3572/3565, and 3595/3588 cm^{-1}, as well as a single band at 3618 cm^{-1} in natural anisotropic garnets close to the uvarovite-grossular binary are assigned to the hydrogarnet substitution, whereas the band doublet at 3652/3602 cm^{-1} and the single band at 3640 cm^{-1}, are explained by the presence of silanol groups Si–OH compensating vacancies in cationic sites (Andrut et al. 2002).

In the IR spectrum of natural Fe^{3+}-bearing gem-quality grossular ("hessonite") from Tanzania, numerous additional weak bands are present in the range from 3500 to 3680 cm^{-1}, along with a strong triplet in the range from 3620 to 3700 cm^{-1} (Maldener et al. 2003; see Fig. 1.16).

Andradite samples from different geological environments, as well as synthetic hydroandradite samples were studied by Amthauer and Rossman (1998) by means of IR spectroscopy. The complexity of the spectra of natural samples is due to the complexity of their composition and, possibly, additional types of OH incorporation. It was concluded that the most intense peak near 3560 cm^{-1} may be assigned to the hydrogarnet substitution.

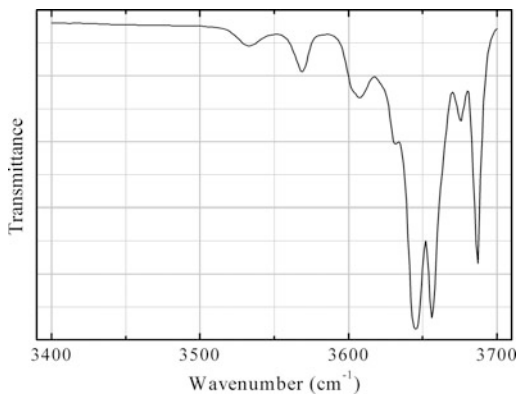

Fig. 1.16 Single-crystal IR spectrum of "hessonite" (grossular with ~11 and ~2 % of andraditic and uvarovitic components, respectively) in the region of O–H-stretching vibrations drawn using data from Maldener et al. (2003)

OH band positions in IR spectra of mantle garnets enriched in the **pyrope component** are different in different samples. In particular, the bands at 3645–3660 (sometimes split into 3641 + 3651 + 3661), 3630, 3602, 3560–3590 and 3512–3525 cm^{-1} are observed in garnets of this type (Beran and Libowitzky 2006). The assignment of these bands is ambiguous. By analogy with synthetic pyropes (Ackermann et al. 1983; Geiger et al. 1991), one can suppose that the bands at 3602 and 3630 cm^{-1} may correspond to the hydrogarnet substitution. The band in the range from 3512 to 3525 cm^{-1} is related to Ti defects.

Based on the data on polarization IR spectra of mantle **kyanite**, it was concluded that the bands at (3386 + 3410 + 3440) and (3260 + 3275) cm^{-1} are related to two different O sites, not bound to Si (Beran 1971a; Wieczorek et al. 2004; Beran and Libowitzky 2006).

Polarization IR spectra of a mantle **zircon** $Zr(SiO_4)$ from Kimberley, South Africa demonstrate the presence of two kinds of differently polarized OH groups. The bands at 3420 and 3380 cm^{-1} have the polarization parallel and perpendicular to *c* respectively (Bell and Rossman 1992; Nasdala et al. 2001).

The IR spectrum of mantle titanite $CaTi(SiO_4)O$ shows a strong absorption band at 3485 cm^{-1} (Sakamaki and Ogasawara 2013). Most probably, this band corresponds to OH groups substituting O atoms that are not bonded to Si, e.g. according to the schemes of heterovalent isomorphic substitution like $Fe^{3+} + OH^- \rightarrow Ti^{4+} + O^{2-}$, or $Na^+ + OH^- \rightarrow Ca^{2+} + O^{2-}$.

IR spectra of some other mantle-related accessory minerals in the O–H-stretching region are reviewed by Beran and Libowitzky (2006).

1.4 Stretching Modes of OH Groups in IR Spectra of Amphiboles

The general crystal-chemical formula of amphiboles is $AB_2C_5(T_8O_{22})W_2$, where $A = \square$, Na, K, Ca, Pb; B = Na, Ca, Mn^{2+}, Fe^{2+}, Mg, Li; C = Mg,

Fe^{2+}, Mn^{2+}, Al, Cr^{3+}, Fe^{3+}, Mn^{3+}, Ti^{4+}, Li; T = Si, Al, Ti^{4+}, Be; W = OH, F, Cl, O. Here C denotes the group of octahedral sites $M1 + M2 + M3$. In the accepted nomenclature of amphibole-supergroup minerals (Hawthorne et al. 2012b), the amphibole supergroup is divided into two groups according to the dominant W species, ^{W}(OH,F,Cl)-dominant amphiboles and ^{W}O-dominant amphiboles (oxo-amphiboles). Amphiboles with OH, F, or Cl dominant at W are divided into eight subgroups according to the dominant charge-arrangements and type of B-group cations. In an amphibole with an empty A site, hydroxyl completes the octahedral coordination of the M(l) and M(3) sites by forming the apex of a flat pseudotrigonal pyramid, the base of which consists of two M(l) sites and one M(3) site (Mottana and Griffin 1986).

In numerous publications the assignment of O–H-stretching bands in IR spectra of amphiboles to different configurations around OH groups has been carried out based on compositional data, powder and single-crystal X-ray diffraction and Mössbauer spectra.

1.4.1 Monoclinic (*C*2/*m*) Amphiboles

As it was concluded by Burns and Strens (1966), when all the cation sites are occupied by Mg, the cluster around OH has the configuration (MgMgMg)–OH–A, and the IR spectrum consists of a single, strong and sharp peak at 3673 cm^{-1} (peak A of Burns and Strens). When cations other than Mg occupy M(1) and/or M(3), a frequency shift takes place that depends upon the change in the energy of the M–OH bond, in turn affected by the electronegativity of the cation (Strens 1974). Therefore the cluster having the configuration ($Fe^{2+}Fe^{2+}Fe^{2+}$)–OH–A has a characteristic frequency at 3625 cm^{-1} (peak D of Burns and Strens), and it is not only shifted to lower energy, but is also weaker than the 3673 cm^{-1} peak. Other clusters, having different types of segregation such as ($MgMgFe^{2+}$)–OH–□ and ($MgFe^{2+}Fe^{2+}$)–OH–□, generate independent peaks at 3660 and 3648 cm^{-1} (peaks C and D of Burns and Strens).

Subsequent investigations demonstrated that this assignment of O–H-stretching bands in IR spectra of amphiboles is not universal. For example, for potassium-fluor-richterite and K-rich richterites the band of stretching vibrations of OH groups belonging to the cluster MgMgMg–OH–(K) is observed in the range from 3694 to 3730 cm^{-1} (Della Ventura et al. 1992, 1998; Gottschalk and Andrut 1998). In the IR spectrum of synthetic end-member potassium richterite this band is observed at 3734 cm^{-1} (Hawthorne 1995).

In the IR spectra of synthetic pargasites and hastingsites, the bands A and B (at ~3710 and ~3680 cm^{-1}) have been assigned to MgMgMg–OH–(Na) and MgMgAl–OH–(Na), respectively (Robert et al. 1996; see also Semet 1973; Raudsepp et al. 1987b; Welch et al. 1994; Della Ventura et al. 1998b, 1999a). The minor A* band, which has been assigned to the MgMgMg–OH–□ configuration (Raudsepp et al. 1987b; Della Ventura et al. 1999a), suggests that nominal end-member pargasite departs slightly from its ideal composition toward magnesiohornblende. In the spectra of pargasite of intermediate OH and/or F contents, each of these two bands is replaced by the new bands (A′ and B′) at lower wavenumbers, 3692–3693 and 3656–3661 cm^{-1}, respectively. In particular, in fluoro-pargasite the band of MgMgAl–OH–(Na) shifts towards ~3658 cm^{-1} (Robert et al. 1996). Based on IR spectroscopic data, it was also shown that trivalent cations (namely, Al, Cr^{3+}, V^{3+} and Ga) occur in these amphiboles at more than one of the M(1, 2, 3) sites (Semet 1973; Raudsepp et al. 1987a, b, 1991).

The presence of F which replaces OH at the O(3) site across the A cavity occupied with Na results in the shift of the band of O–H-stretching vibrations. Based on the IR spectroscopic and X-ray diffraction data of five natural samples of fluoro-edenite and fluoro-pargasite, a detailed assignment of O–H-stretching bands was suggested by Della Ventura et al. (2014) (see Table 1.4). It was concluded that in local environments involving empty A sites the OH–OH and OH–F configurations cannot be distinguished. The spectra show that in the

Table 1.4 Band assignments for fluoro-edenite and fluoro-pargasite according to Della Ventura et al. (2014)

M(1)*M*(1)*M*(3)	*A*	*T*(1)*T*(1)	O(3)–O(3)	Wavenumber, cm^{-1}	Band
MgMgMg	Na	SiAl	OH–OH	3710	A, A′
MgMgMg	Na	SiAl	OH–F	3692	A*
MgMgAl	Na	SiAl	OH–OH	3678	B
MgMgAl	Na	SiAl	OH–F	3660	B*
MgMgMg	□	SiSi	OH–OH	3671	T
MgMgMg	□	SiAl	OH–OH	3642	G
MgMgAl	□	SiAl	OH–OH	3622	H

fluoro-edenite/pargasite structure, the *T* cations, Si and Al, are ordered in such a way that Si–O(7)–Si linkages regularly alternate with Si–O(7)–Al linkages along the double chain.

Some minor and trace elements such as Zn, Ni, Co, V, Co, Ni, Cu, Sc, Zr, Ga, Ge have been found (mainly as C cations) in natural amphiboles (Hawthorne et al. 2012b; Mason and Allen 1973). In (Raudsepp et al. 1987b) bands in the region of O–H-stretching vibrations in the IR-spectra of synthetic pargasite and its analogues with M^{3+} = Cr, Ga, Sc, and In are assigned based on Rietveld structure refinement and NMR spectroscopy. The bands at 3710, 3659, and 3674 (shoulder) cm^{-1} in the IR spectrum of synthetic chromio-pargasite were assigned to the configurations MgMgMg–OH–(Na), MgMgCr–OH–(Na), and MgMgAl–OH–(Na), respectively. In the IR-spectrum of gallium and scandium pargasite analogues, the bands at 3665 and 3673 cm^{-1} were assigned to MgMgGa–OH–(Na) and MgMgSc–OH–(Na), respectively. IR spectra of synthetic Ni- and Co-substitutedrichterites with Ni:(Mg + Ni) and Co:(Mg + Co) varying from 0 to 1 are discussed by Della Ventura et al. (1997) (see Table 1.5).

Lithium amphiboles $\square Li_2(Mg,Fe^{2+})_3Fe^{3+}{}_2(Si_8O_{22})(OH)_2$ belonging to the series clino-ferri-holmquistite – clino-ferro-ferri-holmquistite have been synthesized hydrothermally (Iezzi et al. 2005). The infrared spectra of intermediate compositions in the O–H-stretching region showed fine structure caused by ordering of Mg and Fe^{2+} over the *M*1 and *M*3 sites. This fine structure consists of four main bands (at 3662, 3647, 3631 and 3614 cm^{-1}) assigned to the four local combinations of (Mg,Fe^{2+}) at *M*(1,3). The presence of four weak components in the range from 3610 to 3670 cm^{-1} are assigned to minor (Fe^{2+},Mg) at *M*(4).

In amphiboles with vacant *A*-site, the OH-stretching bands can be divided into two regions. The lower-frequency bands between 3680 and 3600 cm^{-1} are ascribed to OH groups adjacent to a vacant *A*-site, [*M*(1)*M*(1)*M*(3)]–OH–□, and the higher-frequency bands above 3680 cm^{-1} are ascribed to OH groups adjacent to a filled *A*-site, [*M*(1)*M*(1)*M*(3)]–OH–*A*, where *A* is occupied with Na or K (Ishida and Hawthorne 2001; see Table 1.6).

As a result of annealing of Mn-bearing arfvedsonite in air, the OH stretching band, A*, of the (MgMgMg)–OH–A–OH configuration shifts downward from 3730 to near 3700 cm^{-1} with formation of the (MgMgMg)–OH–A–O configuration due to dehydrogenation of OH at the O3 site (Ishida and Hawthorne 2001). Another assignment of the band in the range from 3711 to 3714 cm^{-1} in IR spectra of richterites was suggested by Robert et al. (1999): When F replaces OH at the O3 site, a new band appears in the spectrum at 3714 or 3711 cm^{-1}, respectively, for $^{(A)}K$ or $^{(A)}Na$ (Fig. 1.17). This behaviour indicates the existence of two distinct configurations in the structure, and these must be assigned to local arrangements involving OH and F, as this is the only variable in the system.

Exact positions of the bands listed in Table 1.6 depend on the nature of the C cation. For example, in amphiboles belonging to the tremolite-richterite series the configuration $^{M(1)}Mg^{M(1)}Mg^{M(3)}Mg$–OH–$^{A}\square$ corresponds to

Table 1.5 Band assignments for Ni- and Co-substituted richterites according to Della Ventura et al. (1997)

Band	Configuration	Wavenumber (cm^{-1})
A	MgMgMg–(OH)–Na	3731
B	NiMgMg–(OH)–Na CoMgMg–(OH)–Na	3714–3715 3711
C	NiMgNi–(OH)–Na CoMgCo–(OH)–Na	3697–3699 3692–3693
D	NiNiNi–(OH)–Na CoCoCo–(OH)–Na	3677.5–3679 3671–3672
A*	MgMgMg–(OH)–□	3675
B*	NiMgMg–(OH)–□ CoMgMg–(OH)–□	3660–3662 3656–3658
C*	NiMgNi–(OH)–□ CoMgCo–(OH)–□	3644–3645 3641–3642
D*	NiNiNi–(OH)–□ CoCoCo–(OH)–□	3625 3622–3623

Table 1.6 Assignments of OH-stretching bands for richteritic amphiboles (R = Fe or Mn) according to Ishida and Hawthorne (2001)

Band	Configuration	Wavenumber (cm^{-1})
H-bands (higher-frequency region)		
A*	(MgMgMg)–OH–A–OH	3730–3710
B*	(MgMgR^{2+})–OH–A–OH	3715–3710
C*	(Mg$R^{2+}R^{2+}$)–OH–A–OH	3697–3696
E*	(MgMgR^{3+})–OH–A	3795 (?)
A**	(MgMgMg)–OH–K–O	3709
A**	(MgMgMg)–OH–Na–O	3700–3696
A**	(MgMgMg)–OH–Na–F	3705–3696
A**	(MgMgMg)–OH–Na–Cl	3700–3696 (?)
L-bands (lower-frequency region)		
A	(MgMgMg)–OH–□	3670–3666
B	(MgMgR^{2+})–OH–□	3657–3655
C	(Mg$R^{2+}R^{2+}$)–OH–□	3644–3640
E	(MgMgR^{3+})–OH–□	3643

Note The substitution of ^{A}Na for ^{A}K results in the enhancement of the wavenumber of A* band on 6–7 cm^{-1} (Hawthorne 1995)

the wavenumbers ranging from 3670 to 3675 cm^{-1} (Hawthorne and Della Ventura 2007; Iezzi et al. 2003b). The substitution of Si for Al at the T sites results in the lowering of O–H-stretching frequencies (see Table 1.7).

The influence of ^{B}Na–^{B}Li substitution on IR spectra of synthetic A-site-vacant amphiboles belonging to the clino-ferro-ferri-holmquistite – riebeckite solid-solution series has been analyzed by Iezzi et al. (2003a). The reference bands in this system located at 3614 and 3618 cm^{-1} were assigned to the $^{M1}Fe^{2+M1}Fe^{2+M3}Fe^{2+}$–OH–^{A}□–^{B}Li and $^{M1}Fe^{2+M1}Fe^{2+M3}Fe^{2+}$–OH–^{A}□–^{B}Na configurations. The broad band at ~3672 cm^{-1} was confidently assigned to the configurations $^{M1}Fe^{2+M1}Fe^{2+M3}Fe^{2+}$–OH–^{A}Na–^{B}(Li,Na). The minor bands at 3646 and 3633 cm^{-1} are shifted 30 and 19 cm^{-1} toward

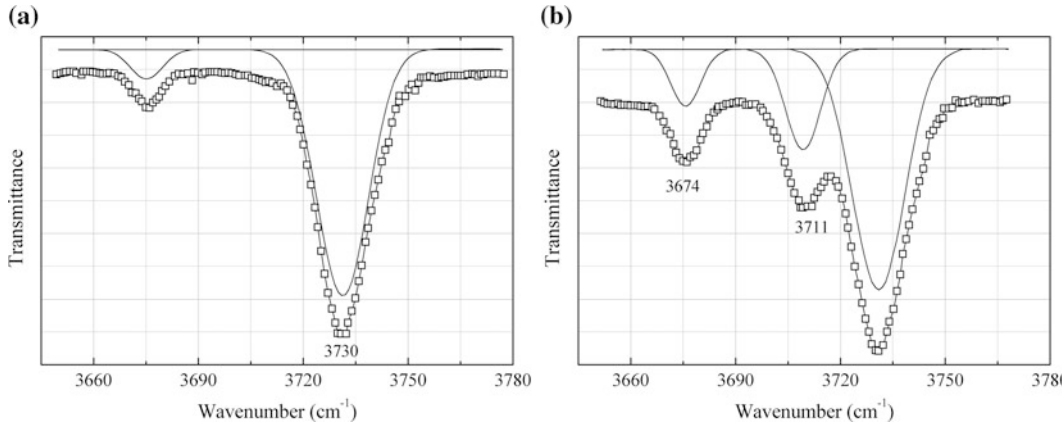

Fig. 1.17 Peak fits to the IR spectra of synthetic end-member richterite (**a**) and fluororichterite (**b**) with nominal F = 1.2 apfu drawn using data from Robert et al. (1999)

Table 1.7 Assignments of OH-stretching bands for parvo-mangano-edenite according to Oberti et al. (2006)

Band	Configuration	Wavenumber (cm^{-1})
A	SiSi–(MgMgMg)–OH–^{A}Na	3725
B	AlSi–(MgMgMg)–OH–^{A}Na	3711
B*	SiSi–(MgMgMn)–OH–^{A}Na	3709
C	AlSi–(MgMgMn)–OH–^{A}Na	3692
C*	SiSi–(MgMgMn)–OH–^{A}Na	3693
D	SiSi–(MgMgMg)–OH–$^{A}\square$	3672
D*	SiSi–(MnMnMn)–OH–^{A}Na	3677
E	SiSi–(MgMgMn)–OH–$^{A}\square$	3659
F	SiSi–(MgMnMn)–OH–$^{A}\square$	3641
G	SiSi–(MnMnMn)–OH–$^{A}\square$	3621
H	SiSi–(MgMgM^{3+})–OH–$^{A}\square$	3603

See also Hawthorne and Della Ventura (2007)

higher frequency with respect to the main band at 3614 cm^{-1}; therefore, they were assigned to the configurations $^{M1}Fe^{2+M1}Fe^{2+M3}$Li–OH–$^{A}\square$ and $^{M1}Fe^{2+M1}Fe^{3+M3}$Li–OH–$^{A}\square$, respectively. The latter assignment was made taking into account that the presence of a trivalent cation (Al) at the OH-coordinated sites produces a negative shift of ~15 cm^{-1} (see e.g. Della Ventura et al. 1998b).

Based on numerous publications, the differences in OH-stretching frequency (in cm^{-1}) for different arrangements of cations, relative to the OH-stretching frequency and cation arrangements in tremolite, are as follows (Hawthorne and Della Ventura 2007): +55 for ^{A}Na, +60 for ^{A}K and ^{A}Rb, +50 for ^{A}Li, −13 to −23 for $^{T(2)}$Ti, −20 for $^{T(1)}$Al, −15 to −18 for $^{M(1,3)}$(Ni,Co,Fe^{2+}), −15 for $^{M(1,3)}$(Mn^{2+}), −33 for $^{M(1,3)}$(Al), −40 for $^{M(1,3)}$(Sc), −45 for $^{M(1,3)}$(Ga^{3+}), −50 for $^{M(1,3)}$(Cr^{3+}, Fe^{3+}), −8 for $^{M(4)}$(Mg); +2 for $^{M(4)}$(Sr), −4 for $^{M(4)}$(Li), −15 to −20 for $^{O(3)}$F, and −23 for $^{O(3)}O^{2-}$.

Bands with the wavenumbers ~3604–3619, ~3624–3636, ~3647–3652, and ~3662–3667 cm^{-1} in the IR spectra of clino-ferri-holmquistite, clino-ferro-ferri-holmquistite and magnesioriebeckite have been assigned to $^{M(1)}Fe^{2+M(1)}Fe^{2+M(3)}Fe^{2+}$–OH–$^{A}\square$, $^{M(1)}Mg^{M(1)}Fe^{2+M(3)}Fe^{2+}$–OH–$^{A}\square$, $^{M(1)}Mg^{M(1)}Mg^{M(3)}Fe^{2+}$–OH–$^{A}\square$, and $^{M(1)}Mg^{M(1)}Mg^{M(3)}Mg$–OH–$^{A}\square$, respectively (Iezzi et al. 2003a, 2004a; Della Ventura et al. 2005b). In the IR spectra of amphiboles belonging

to the glaucophane-riebeckite solid-solution series these configurations correspond to the bands at ~3617, ~3632, ~3646, and ~3662 cm^{-1}, respectively; a minor band A′ at 3690 cm^{-1} was ascribed to hydroxyl groups in the cell whose *A* site is occupied by alkaline cations (Ishida 1990) . In the infrared spectra of amphiboles along the clino-ferri-holmquistite – magnesioriebeckite join (except clino-ferri- holmquistite endmember) corresponding bands D*, C*, B* and A* for configurations with occupied *A*-site are located at 3689–3690, 3701, 3713–3714, and 3726–3728 cm^{-1}, respectively (Della Ventura et al. 2005b). Based on these assignments, it was concluded that analogous four local situations correspond to the bands at 3613, 3630, 3646, and 3667 cm^{-1} present in the IR spectrum of ferro-pedrizite (Fig. 1.18) having the crystal-chemical formula $^{A}(Na_{0.60}K_{0.02})^{M(4)}(Li_{1.89}Na_{0.07}Ca_{0.04})^{C}[^{M(1)}(Mg_{0.90}Fe^{2+}{}_{0.75}Fe^{3+}{}_{0.35})^{M(2)}(Al_{1.88}Fe^{3+}{}_{0.12})^{M(3)}(Li_{0.65}Fe^{2+}{}_{0.28}Mn_{0.07})]^{T}[Si_{7.79}Al_{0.21}O_{22}]^{W}[(OH)_{1.36}F_{0.49}O_{0.15})]$ (Konovalenko et al. 2015). The bands observed at 3688 and 3707 cm^{-1}, which are to be assigned to the local configurations *M*(1)*M*(1)*M*(3)–OH–^{A}Na, are weak. Despite extinction coefficients of O–H stretching bands of OH groups coordinated by Na seem to be lower than that of OH groups attached to vacancy, this observation may indicate that Na^{+} cations are predominantly coordinated by F^{-} anions, and only a minor part of $^{A(m)}$Na is involved in the local configuration of the OH.

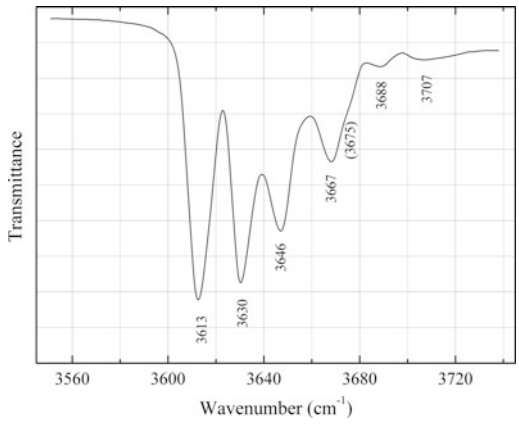

Fig. 1.18 Powder IR absorption spectrum of ferro-pedrizite in the region of O–H-stretching vibrations. The IR spectrum was obtained by N.V. Chukanov

1.4.2 Orthorhombic (*Pnma*) and Monoclinic ($P2_1/m$) Amphiboles

As well as in case of monoclinic ($C2/m$) amphiboles, the principal OH-stretching bands in IR spectra of orthorhombic (Mg, Fe, Mn, Li) amphiboles of the holmquistite and the anthophyllite – gedrite series show fine structure (Law 1981, 1982; Law and Whittaker 1981; Ishida and Hawthorne 2003). Four main bands labelled A, B, C, and D and assigned to local configurations C_3–OH–*A* where A = □ or Na, and C_3 = MgMgMg, MgMgFe, MgFeFe and FeFeFe for A, B, C and D, respectively. The two *M*(1) *M*(2)*M*(3) configurations, MgMgFe and Mg FeMg, are slightly different in terms of the way in which they affect the OH stretching frequency. As a result, the B band is split into two components.

Additional splitting of O–H-stretching bands (Fig. 1.19 right) is due to the occurrence of two symmetrically distinct OH groups in the crystal structure. In monoclinic amphiboles this splitting absent (Fig. 1.19 left), and for holmquistite it is smaller than for the members of the anthophyllite–gedrite series (Table 1.8).

These data seem to be in contradiction with IR spectra of holmquistite published earlier (Ishida 1999) that does not show any obvious additional splitting of the bands A, B, C and D (see Fig. 1.20).

A well-defined splitting of the absorption band corresponding to the configuration SiSi–(MgMgMg)–OH–^{A}Na was observed also in the IR spectrum of synthetic monoclinic ($P2_1/m$) amphibole $Na(NaMg)Mg_5(Si_8O_{22})(OH)_2$ into the bands at 3742 and 3715 cm^{-1} due to the presence of two independent anion sites [O(3A) and O (3B)] in its crystal structure (Iezzi 2004b). In synthetic amphiboles $^{A}Na^{B}(Na_xLi_{1-x}Mg)^{C}Mg_5(Si_8O_{22})(OH)_2$ the two most intense absorption bands O–H-stretching vibrations (at 3741 and 3716 cm^{-1}) are assigned to two non-equivalent O–H dipoles in the $P2_1/m$ structure, bonded to the same local environment [*M*(1)*M*(3)*M*(3)]–OH–^{A}Na, and pointing toward two differently linked tetrahedral rings. These bands

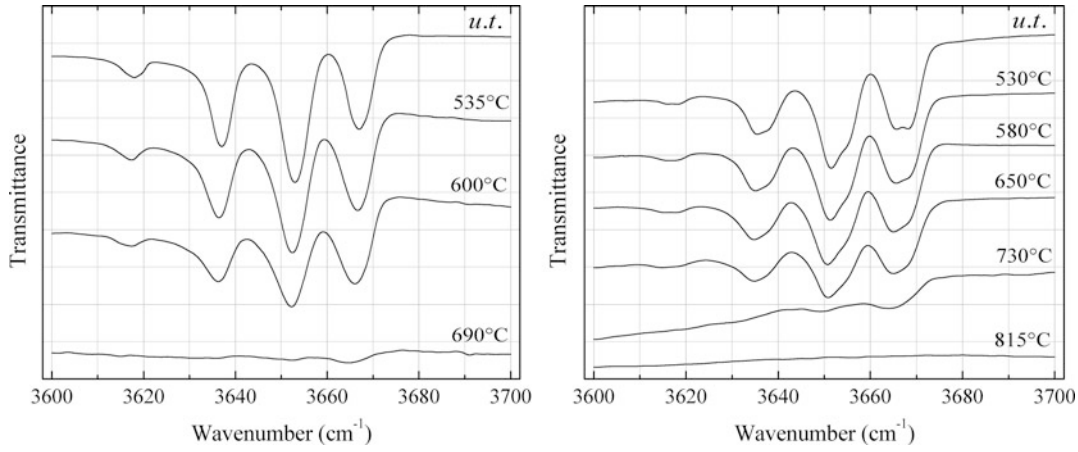

Fig. 1.19 IR spectra (in the region of O–H-stretching vibrations) of amphiboles heat-treated in air. *Left* cummingtonite from Nagano-Toge, Maebaru, Fukuoka Pref., Japan. *Right* anthophyllite from Kisco, Finland. The spectra are drawn using data from Ishida and Hawthorne (2003)

Table 1.8 Positions of the bands in the infrared O–H-stretching spectra of some monoclinic *C*2/*m* and orthorhombic *Pnma* amphiboles. After Ishida and Hawthorne (2003)

	A or A_A/A_B	B or B_A/B_B	C or C_A/C_B	D or D_A/D_B
Cummingtonite – manganocummingtonite	3667–3668	3653–3655	3637–3640	3618–3621
Holmquistite	3661–3662/ 3658–3659	3647–3648/ 3643–3644	3629/3629	3613–3613.5/ 3610.5–3612
Anthophyllite-gedrite	3669–3670/ 3665–3666	3655–3656/ 3650–3652	3638–3639/ 3635–3636	3619/3616

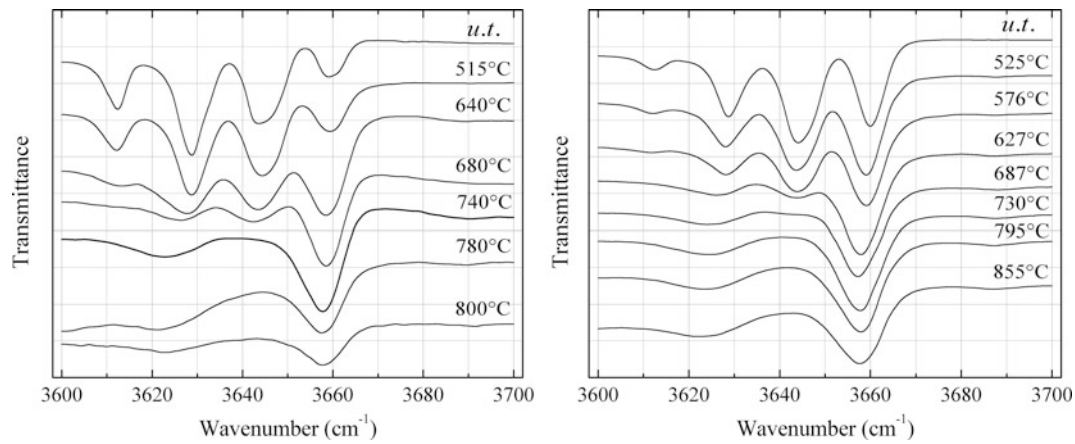

Fig. 1.20 IR spectra (in the region of O–H-stretching vibrations) of holmquistite heat-treated in air. The spectra are drawn using data from Ishida and Hawthorne, 2003 (*left*) and Ishida, 1999 (*right*)

progressively merge to give a unique symmetrical absorption with increasing pressure, suggesting a change in symmetry from $P2_1/m$ to $C2/m$ (Iezzi et al. 2009).

1.5 Hydroxyl Groups in Rock-Forming Phyllosilicates

Various phyllosilicates (micas, chlorites, smectites, members of the kaolinite-serpentine group, talc, vermiculite, mixed-layer minerals) are important components of different sedimentary, metamorphic, metasomatic and igneous rocks, as well as soils (Farmer and Palmieri 1975). Quite often these minerals are components of fine-grained polymictic aggregates. IR spectroscopy in the region of O–H-stretching vibrations is one of the most reliable methods of identification of phyllosilicates in polymineral mixtures. One of the earliest compilations of characteristic O–H-stretching bands of clay minerals was made by Farmer and Russell (1964) (see Table 1.9).

In most cases, O–H-stretching bands of OH groups coordinating octahedral cations and interlayer water molecules are located above 3500 cm^{-1} and below 3450 cm^{-1}, respectively. However the bands of OH groups forming strong hydrogen bonds may shift towards lower frequencies (the typical examples are chlorites and Al- or Fe^{3+}-bearing members of the serpentine group). In ammonium-bearing minerals, broad N–H-stretching bands are typically present in the range from 3000 to 3400 cm^{-1}. The presence of H_2O molecules and NH_4^+ cations can be detected by the bands of H–O–H and H–N–H bending vibrations in the ranges from 1550 to 1700 and from 1350 to 1450 cm^{-1}, respectively.

In **micas**, three kinds of O–H-stretching bands can be distinguished from the viewpoint of local environments of OH groups: 3 M^{2+} (M = Mg or Fe) for N-bands, 2 M^{2+} + M^{3+} (M^{3+} = Fe^{3+} or Al) for I-bands, and 2(M^{3+},M^{2+}) + □ for V-bands (Vedder 1964). The following empirical correlations have been obtained for the wavenumbers of O–H-stretching bands of **dioctahedral and trioctahedral micas** belonging to the solid-solution system K_2O–MgO–Al_2O_3–SiO_2–H_2O (Robert and Kodama 1988):

$$\nu_N = -11.20\ Al_T + 3735\ cm^{-1} \text{ for } Al_T \leq 1;$$
$$\nu_N = -22.56\ Al_T + 3748\ cm^{-1} \text{ for } Al_T > 1;$$
$$\nu_I = -37.30\ Al_T + 3732\ cm^{-1};$$
$$\nu_V = -11.45\ Al_T + 3592\ cm^{-1},$$

where Al_T is the total amount of Al atoms in octahedral and tetrahedral sites per formula unit $K(Al,Mg)_{2\text{-}3}[(Si,Al)_4O_{10}](OH)_2$. The Al_T value can vary from 0 for the synthetic OH-analogue of yangzhumingite, $K(Mg_{2.5}□_{0.5})(Si_4O_{10})(OH)_2$, to 3 for the members of the solid-solution series muscovite $KAl_2(Si_3AlO_{10})(OH)_2$ – eastonite $K(Mg_2Al)(Si_2Al_2O_{10})(OH)_2$.

Vedder (1964) supposed that the O–H-stretching frequency depends on the O–H bond strength and the reduced mass of the vibration system. However later it was shown that there are other factors that control the band position for each given cation pair bonded to OH groups.

A simple analytical dependence between the OH frequencies and the mass and valency of cations bonded to OH groups in **dioctahedral micas** has been found by Besson and Drits (1997b). Quantitatively, the dependence between the OH stretching frequencies (ν_{OH}) and the atomic weight and valency of the cations bonded to OH groups can be expressed as follows:

$$\nu_{OH}(M_2{-}M_{2'}) = 15[V_2 + V_{2'} + n(1+\mu)^{-1} - 4] - 1.237(m_2 + m_{2'}) + 3643\ cm^{-1},$$

where M_2 and $M_{2'}$ are the cations (Al, Mg, Fe^{2+} and Fe^{3+}) bonded to OH groups; m_2, V_2 and $m_{2'}$, $V_{2'}$ are atomic masses and valences of M_2 and $M_{2'}$ cations, respectively; $\mu = m_2/m_{Al}$; n is an integer equal to the number of A1 cations bonded to OH groups (n = 0, 1, or 2).

Based on the analogy with talc, it was supposed (Wilkins 1967) that the replacement of each Mg^{2+} by Fe^{2+} in the triad of adjacent

Table 1.9 Wavenumbers of characteristic stretching bands of OH groups in IR spectra of some randomly oriented phyllosilicates (the range 3500–3750 cm^{-1})

Mineral	Wavenumbers
Kaolinite	**3697**, 3669w, 3652w, 3620
Dickite	3704, 3654, **3622**
Nacrite	3703, **3647**, 3629
Talc	**3676**, 3660w
Pyrophyllite	**3675**, 3647w
Muscovite or paragonite	**3636**, 3624 (shoulder)
Phlogopite	**3704**, 3665
Biotite	**3700**, 3663–3668w, **3596-3622**, 3570–3600
Celadonite	3601w, **3557**, 3534
Margarite	**3632**b
Rectorite	**3627**b
Beidellite	**3660**b
Montmorillonite	**3620–3632**b
Nontronite	**3564**b
Saponite	3710w, **3676**
Hectorite	**3676**

After Farmer and Russell (1964)
Note The strongest bands are given in bold type; "*b*" denotes broad bands; "*w*" denotes relatively weak bands

octahedral ions in **trioctahedral Mg,Fe-micas** (i.e. **biotites**) leads to a ~ 16 cm^{-1} decrease in the hydroxyl-ion vibration frequency for both N- and I-bands. Corresponding assignment of O–H-stretching bands is given in Table 1.10. Generally, this assignment is confirmed by experimental data, but O–H-stretching bands in IR spectra of natural biotites are rather broad and poor-resolved.

Additionally, it was shown that the high frequency O–H-stretching absorption bands (i.e. N- and I-bands) in single-crystal IR spectra of **K depleted (hydrated) biotites**is the sum of two absorptions: the first corresponds to the initial mica spectrum, the second corresponds to the hydrated phase in which wavenumbers of corresponding bands are ~ 36 cm^{-1} lower than in initial samples (Chaussidon 1972). These results show that natural weathering of biotite which is accompanied by K depletion, oxidation of Fe^{2+}, and hydration, results in the formation of minerals whose O–H-stretching bands are poor-resolved and shifted towards low frequencies.

The intensity of the OH-band, centered in the spectral range 3674–3678 cm^{-1}, in the IR spectra of synthetic solid solutions of phlogopite with its Cs- and Rb-analogues and with kinoshitalite is correlated with the deficiency of interlayer cations (Wunder and Melze 2002). This phenomenon was explained by the presence of the talc component $Mg_3(Si_4O_{10})(OH)_2$.

IR spectra of synthetic Mg-free **annites**, ideally $K(Fe,Al)_3[(Si,Al)_4O_{10}](OH)_2$, obtained from various gels at 600 °C show partial dioctahedral character which increases with increasing oxygen fugacity (Boukili et al. 2002). In particular, the V bands in the range 3540–3580 cm^{-1} and at 3530 cm^{-1} (Fig. 1.21) were assigned to OH groups bonded to $Fe^{2+}(Fe^{3+},Al)\square$ and $Fe^{3+}Fe^{3+}\square$, respectively. These values are much lower than those predicted by Vedder (1964) (see Table 1.10).

In the frequency range 3670–3640 cm^{-1}, IR spectra of synthetic **annites** contain two

Table 1.10 The assignment of O–H-stretching bands in IR spectra of powdered biotites

Band notation	Local environment of the OH group	Wavenumber, cm^{-1}
N_A	$Mg^{2+}Mg^{2+}Mg^{2+}$	3712
N_B	$Mg^{2+}Mg^{2+}Fe^{2+}$	3696
N_C	$Mg^{2+}Fe^{2+}Fe^{2+}$	3680
N_D	$Fe^{2+}Fe^{2+}Fe^{2+}$	3664
I_A	$Mg^{2+}Mg^{2+}R^{3+}$	3668
I_B	$Mg^{2+}Fe^{2+}R^{3+}$	3652
I_C	$Fe^{2+}Fe^{2+}R^{3+}$	3636
V_A	$R^{2+}R^{2+}\square$	~3625
V_B	$R^{2+}R^{3+}\square$	~3600
V_C	$R^{3+}R^{3+}\square$	~3560

After Vedder (1964), Wilkins (1967) and Chaussidon (1972)

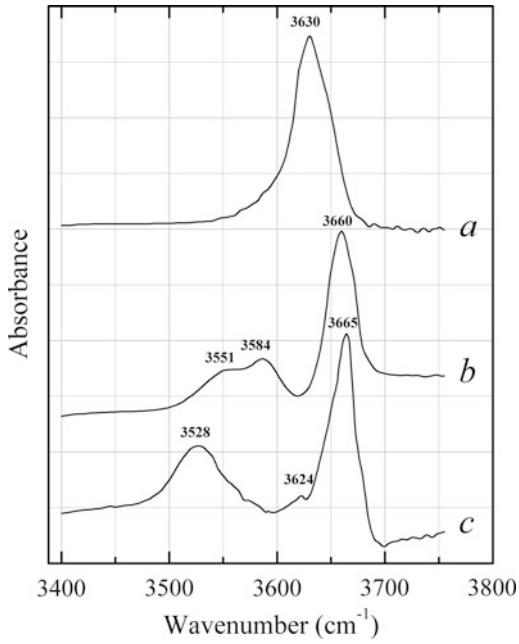

Fig. 1.21 Representative IR spectra in the O–H-stretching region of (*a*) siderophyllite, (*b*) Al-rich biotite and (*c*) annite synthesized in the presence of Ni-NiO buffer. The spectra (drawn using data from Boukili et al. 2003) have been offset for comparison

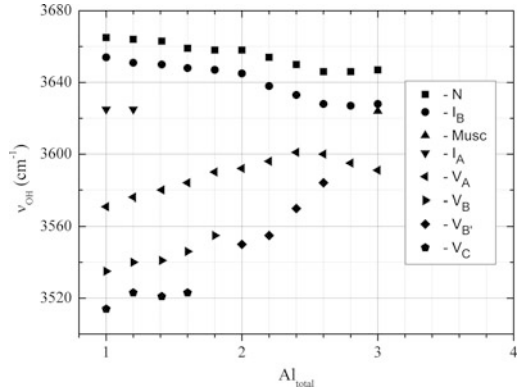

Fig. 1.22 Evolution of the OH-stretching wavenumbers (in cm^{-1}) of N, I and V-bands as a function of Al_{total} from decomposed spectra of micas of the annite-siderophyllite join synthesized at 600 °C and 1 kbar in the presence of Ni-NiO buffer and muscovite (Musc). The diagram is drawn using data from Boukili et al. (2003)

overlapping bands located around 3666 and 3650 cm^{-1} (Boukili et al. 2003). The former band shifts towards lower wavenumbers (Fig. 1.22), and the latter band becomes stronger with the enhancement of the total Al content. These bands are assigned to OH groups having local environment $Fe^{2+}Fe^{2+}Fe^{2+}$ and $Fe^{2+}Fe^{2+}Al^{3+}$ and are therefore an N_D-type band and an I_B-type band, respectively. These values are also much lower than those indicated in Table 1.10 for V bands.

The assignment of O–H-stretching bands in the IR spectra of **celadonite**, $K(Mg,Fe^{2+})(Fe^{3+},Al)(Si_{4.00}O_{10})(OH)_2$ is proposed by Slonimskaya et al. (1986) and Besson and Drits (1997a); see Table 1.11. According to these data, the replacement of Fe^{3+} with Fe^{2+} results in the lowering of the O–H-stretching frequency. This fact is inconsistent with the data of other authors for micas (see e.g. Table 1.10), as well as with general trends for other mineral groups (see e.g.

Table 1.11 The assignment of O–H-stretching bands in IR spectra of celadonite

Band notation	Pairs of cations bonded to OH groups	Wavenumber, cm^{-1} (after Slonimskaya et al. 1986)	Wavenumber, cm^{-1} (after Besson and Drits 1997a)
V_A	MgMg	3505[a]	3580–3585
V_A	$MgFe^{2+}$	No data	3542–3545
V_A	$Fe^{2+}Fe^{2+}$	3494	3503–3507
V_B	MgAl	3605	3601–3604
V_B	$MgFe^{3+}$	3560	No data
V_B	$Fe^{2+}Al$	3580	3556–3560
V_B	$Fe^{2+}Fe^{3+}$	3531[b]	3520–3526
V_C	AlAl	3620-3640	3621
V_C	$AlFe^{3+}$	No data	3571–3575
V_C	$Fe^{3+}Fe^{3+}$	3531[b]	3533–3537

[a]Obviously, an error: the correct value should be 3585 cm^{-1}
[b]Unresolved doublet

the sections "O–H Stretching Modes in Amphiboles" and "Hydroxyl Groups in Tourmalines" in this book). Consequently, the major (V_B) bands at ~3600–3605, ~3580–3585, ~3555–3560, and ~3530–3535 cm^{-1} in the IR spectra of Mg, Fe, Al-based celadonite-type minerals, $K(R^{2+}, R^{3+})(R^{3+},R^{2+})(Si_{4.00}O_{10})(OH)_2$ (see Figs. 1.23 and 1.24) can be assigned to OH groups coordinated to MgAl□, Fe^{2+}Al□, $MgFe^{3+}$□ and $Fe^{2+}Fe^{3+}$□, respectively, whereas the assignment of subordinate V_A and V_C bands (Table 1.11) is to be corrected. It is to be noted that in most cases weak bands V_A and V_C in IR spectra of celadonite-type minerals can be determined only with a rather low accuracy, as a result of the decomposition of the overall spectrum into individual Voigt components.

The bands V_B and V_C in IR spectra of celadonite-type micas and Cr, V-analogues of phengite are observed at 3605, 3580, 3560, 3535 cm^{-1} (MgAl□, Fe^{2+}Al□, $MgFe^{3+}$□ and $Fe^{2+}Fe^{3+}$□, respectively) for hydrated celadonite $K_{0.91}(Mg_{0.55}Fe_{0.45})(Fe_{0.54}Al_{0.46})(Si_{3.88}Al_{0.12}O_{10})(OH)_2 \cdot nH_2O$ from Srednyaya Padma, Karelia, Russia; at 3600 and 3635 (shoulder) cm^{-1} (MgAl□ and AlAl□, respectively) for Mg-poor aluminoceladonite $K_{0.93}Na_{0.02}(Al_{1.41}Mg_{0.59})(Si_{3.60}Al_{0.40}O_{10})(OH)_2$ from Dora Maira massif, Italy; at 3515 and 3552 cm^{-1} (CrR^{3+}□ and MgCr□, respectively) for holotype chromceladonite sample $(K_{0.94}Na_{0.02})(Cr_{0.95}V_{0.10}Al_{0.05}Fe^{3+}{}_{0.03}Ti_{0.01})(Mg_{0.83}Fe^{2+}{}_{0.04}Li_{0.04}Zn_{0.01}Mn_{0.01})(Si_{3.78}Al_{0.22}O_{10})(OH)_{1.60}F_{0.13}O_{0.13}$ from Srednyaya Padma; at 3517 and 3565 cm^{-1} ($R^{3+}R^{3+}$□ and MgR^{3+}□, respectively) for "chromphengite" $(K_{0.94}Na_{0.01})(Cr_{0.75}Mg_{0.69}Fe_{0.31}V_{0.18}Ti_{0.02}Li_x)(Si_{3.44}Al_{0.56}O_{10})(OH)_{1.9}F_{0.1}$ from Srednyaya

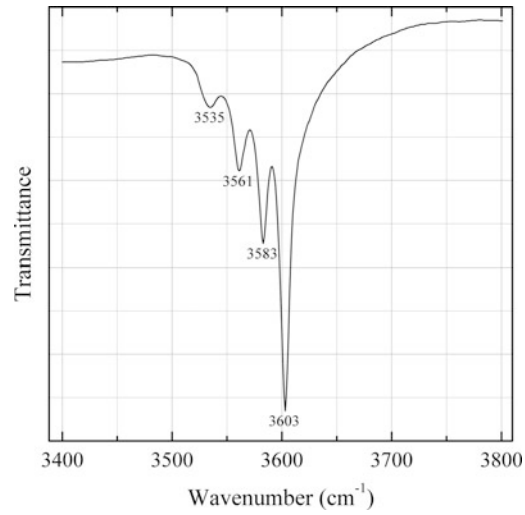

Fig. 1.23 IR spectrum of aluminoceladonite ("leucophyllite") $K_{0.72}Na_{0.01}(Mg_{0.59}Fe^{2+}{}_{0.21}Fe^{3+}{}_{0.17}Al_{1.05})(Si_{4.00}O_{10})(OH)_2$ in the O–H-stretching region drawn using data from Besson and Drits (1997a). The bands at 3603, 3583, 3561, 3536 cm^{-1} correspond to the local environments of the OH group MgAl□, Fe^{2+}Al□, $MgFe^{3+}$□, and $Fe^{2+}Fe^{3+}$□, respectively

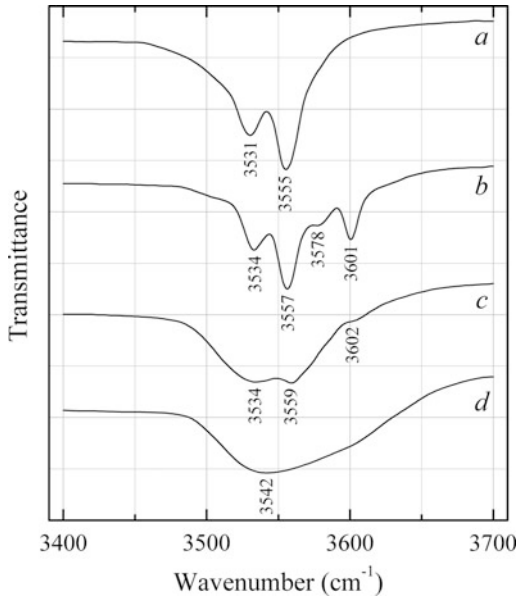

Fig. 1.24 Typical IR spectra of celadonites (*a*, *b*) and glauconites (*c*, *d*) drawn using data from Buckley et al. (1978). Spectra have been offset for comparison

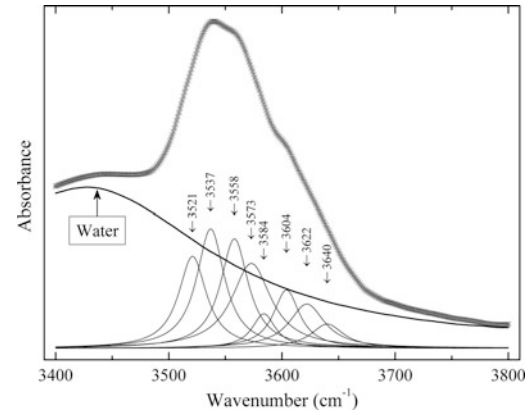

Fig. 1.25 Decomposition of the IR spectrum of glauconite with the empirical formula $K_{0.80}(Fe^{3+}_{0.89}Al_{0.55}Mg_{0.39}Fe^{2+}_{0.18})(Si_{3.78}Al_{0.22}O_{10})(OH)_2$. The picture is drawn using data from Besson and Drits (1997a)

Padma; at 3518 and 3550 (shoulder) cm^{-1} ($R^{3+}R^{3+}\square$ and $MgR^{3+}\square$, respectively) for "vanadiophengite" $(K_{0.90}Na_{0.02})(V_{0.80}Mg_{0.79}Al_{0.26}Fe_{0.22}Cr_{0.05}Ti_{0.01}Zn_{0.01})(Si_{3.42}Al_{0.58}O_{10})(OH)_{1.8}F_{0.2}$ from Srednyaya Padma; around 3540 cm^{-1} (unresolved doublet corresponding to $(Fe^{2+},Mg)Fe^{3+}\square$) for $K_{1.01}Fe_{1.00}(Fe_{0.59}Mg_{0.41})(Si_{3.86}Al_{0.10}Fe_{0.04}O_{10})(OH)_2$ from Mikhailovskii mine, Zheleznogorsk, Russia (Chukanov 2014a).

IR spectra of glauconite $K_{1-x}[(Fe^{3+},Al)_{4/3}(Mg,Fe^{2+})_{2/3}][(Si,Al)_4O_{10}](OH)_2$, as compared to those of celadonite-type micas, typically contain more broad and poor-resolved bands in the O–H-stretching region (Buckley et al. 1978; Slonimskaya et al. 1986; see Fig. 1.4), which is due to the overlapping of numerous V_B- and V_C-bands (Fig. 1.25), as well as to the usual presence of interlayering with hydrous phyllosilicates (Chukhrov 1992b).

As compared to micas, **smectites** contain interlayer water molecules and are characterized by more disordered crystal structures. In the IR spectra of trioctahedral smectites $(Ca,Na,K)_x(Mg,Fe^{2+},Fe^{3+},Al,Zn,Li)_3[(Si,Al)_4O_{10}](OH)_2\cdot nH_2O$ ($x < 0.5$), O–H-stretching bands broaden and shift towards lower wavenumbers with the enhancement of the contents of trivalent cations and, to a less extent, Fe^{2+} and Zn in octahedral sites. In the IR spectra of **saponite** samples close to the magnesium end-member, the strongest O–H-stretching band is located around 3690 cm^{-1} (Chukhrov 1992b). This band shifts towards 3635–3650 and 3500–3525 cm^{-1} in samples containing 0.33–0.35 ^{VI}Al and 1.14–1.20 $^{VI}Fe^{3+}$ atoms pfu, respectively (Chukanov 2014a). Usually, all (or almost all) iron in saponite is trivalent because of rapid oxidation of Fe^{2+} by atmospheric oxygen. O–H-stretching band of fresh **ferrosaponite** (holotype sample forming aggregates included into crystals of Iceland spar) with the formula $Ca_{0.31}Na_{0.04}K_{0.01}(Fe^{2+}_{1.56}Mg_{0.87}Fe^{3+}_{0.52})_{\Sigma 2.95}[(Si_{2.91}Al_{1.03}Fe^{3+}_{0.06})_{\Sigma 4}O_{10}](OH)_2\cdot 4.24H_2O$ is observed as a shoulder at 3510 cm^{-1} (Chukanov et al. 2003). As compared to saponite, its Li- and F-bearing analogue **hectorite** shows in the IR spectrum an additional weaker but broader band at 3610 cm^{-1} (Chukhrov 1992b).

In IR spectra of Zn-dominant smectites, sauconite and zincsilite, this band is observed in the range from 3610 to 3645 cm^{-1} (Yokoyama et al. 2006; Chukhrov 1992b). This band shifts towards lower wavenumbers with the enhancement of the contents of trivalent cations.

IR spectra of dioctahedral smectites contain stronger O–H-stretching bands whose positions

vary from 3600–3635 cm^{-1} for Al-dominant members (**montmorillonite** and **beidellite**) to 3536–3560 cm^{-1} for **nontronite** (Russell 1979; Chukhrov 1992b; Chukanov 2014a).

Kaolinite, **dickite** and **nacrite** are phyllosilicates which have the same chemical formula $Al_2(Si_2O_5)(OH)_4$, but are different in the manner of stacking of layers. These minerals are dioctahedral members of the kaolinite-serpentine group whose structures consist of a tetrahedral sheet with silicon filling the tetrahedral sites and an octahedral sheet with aluminum filling two thirds of the octahedral sites. In all these minerals, one the four hydroxyls in the formula is in the plane shared by the two sheets, and other three OH groups form the outer surface of the octahedral sheet (Drits and Kashaev 1960; Zvyagin 1967; Newnham 1961; Blount et al. 1969). The polymorphs of $Al_2(Si_2O_5)(OH)_4$ are characterized by different distances between O atoms of OH groups and O atoms that are acceptors of weak hydrogen bonds: 2.89, 2.90 and 3.02 Å in kaolinite; 2.92, 2.97 and 3.10 Å in dickite; 2.97, 2.98 and 3.06 in nacrite. In structural models involving H atoms (Giese and Datta 1973), four sites of H atoms are distinguished for each polymorph. Accordingly, the positions of O–H-stretching bands in IR spectra of these minerals are different (see Fig. 1.26).

Three distances between OH groups and H-bond acceptor indicated by for each $Al_2(Si_2O_5)(OH)_4$ polymorph (Zvyagin 1967; Newnham 1961; Blount et al. 1969) should correspond to three bands of O–H-stretching vibrations. However the number of observed IR absorption bands in the range from 3600 to 3680 cm^{-1} corresponding to weak hydrogen bonds in kaolinite, dickite and nacrite is often more than 3, and total number of O–H-stretching bonds may be more than 4. The number of these bands increases with lowering of temperature, despite no phase change occurs (Prost et al. 1989; see Fig. 1.27). This phenomenon can be explained by a combination of different factors, including changes of donor-acceptor distances with temperature, phase inhomogeneity, the presence of local configurations of different

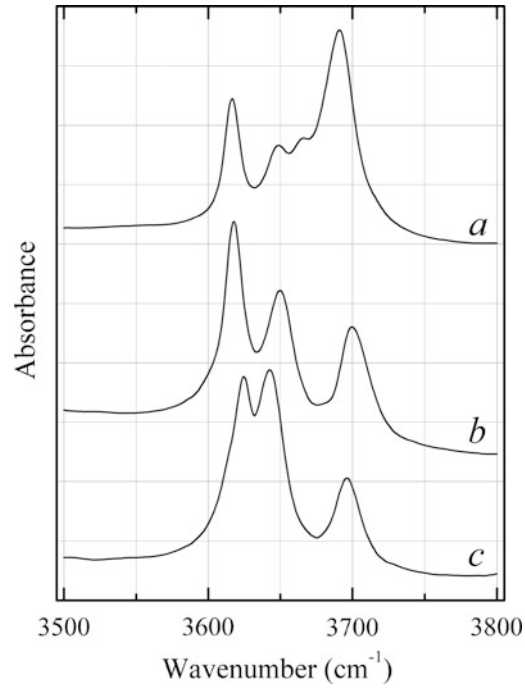

Fig. 1.26 Infrared absorption spectra in the O–H-stretching region of (*a*) kaolinite, (*b*) dickite, and (*c*) nacrite drawn using data from Prost et al. (1989). Spectra have been offset for comparison

polymorphs and polytypes of dioctahedral aluminum members of the kaolinite-serpentine group (which are not detectable by X-ray powder diffraction), as well as partial substitution of Al for Fe.

The strongest band of O–H-stretching vibrations in the IR spectra of magnesium serpentines is located at 3673–3685 cm^{-1} (antigorite), 3687–3697 cm^{-1} (chrysotile) or 3685–3693 cm^{-1} (lizardite) (Chukanov 2014a). The exact position of this band corresponding to OH groups coordinating three Mg cations is different for various polytypes and samples with different degree of crystallinity. Weaker bands in the range from 3600 to 3700 cm^{-1} correspond to OH groups having other local environments and forming hydrogen bonds of different strengths. For example, the strongest O–H-stretching bands are observed at 3635–3650 cm^{-1} for pecoraite $Ni_3(Si_2O_5)(OH)_4$, 3620 cm^{-1} for greenalite $(Fe^{2+}, Fe^{3+})_{3-x}(Si_2O_5)(OH)_4$, 3620 and 3370 cm^{-1}

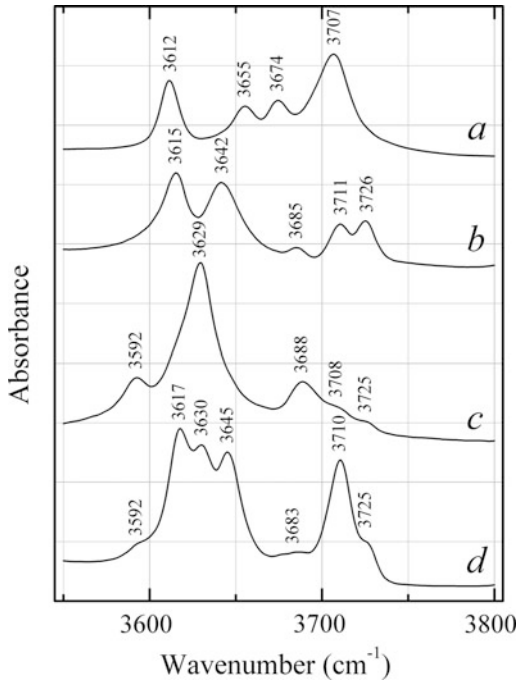

Fig. 1.27 IR spectra of (*a*) kaolinite, (*b*) dickite, (*c*) nacrite, and (*d*) poorly crystallized kaolinite obtained at 5 K for samples pressed in KBr discs. The picture is drawn using data from Prost et al. (1989). Spectra have been offset for comparison

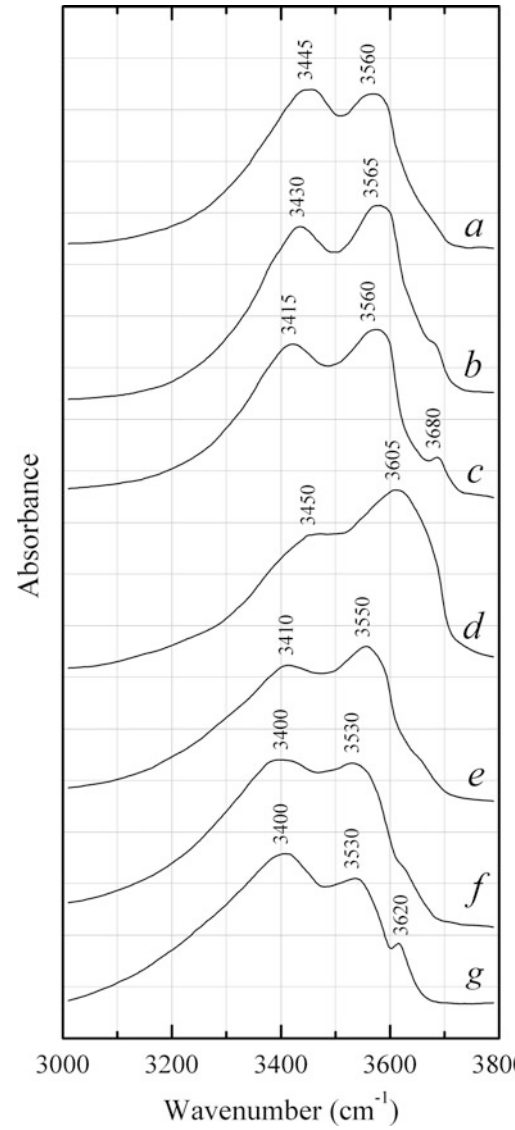

Fig. 1.28 IR spectra of trioctahedral chlorites: (*a*) Al-rich Mg-leptochlorite, (*b*) Mg-lepto-chlorite, (*c*) Mg-orthochlorite, (*d*) Al-poor Mg-orthochlorite, (*e*) FeMg-orthochlorite, (*f*) Fe-orthochlorite, and (*g*) Fe-orthochlorite drawn using data from Shirozu (1980). Spectra have been offset for comparison

for berthierine $(Fe^{2+},Al)_3[(Si,Al)_2O_5](OH)_4$, 3625 and 3420 cm^{-1} for kellyite $(Mn^{2+},Al)_3[(Si,Al)_2O_5](OH)_4$, 3410 cm^{-1} for amesite $Mg_2Al(SiAlO_5)(OH)_4$, 3420 cm^{-1} for fraipontite $(Zn,Al)_3[(Si,Al)_2O_5](OH)_4$, 3420 cm^{-1} for cronstedtite $Fe^{2+}{}_2Fe^{3+}(SiFe^{3+}O_5)(OH)_4$, etc. (Chukanov 2014a, Chukhrov 1992a). The substitution of bivalent octahedral cations with trivalent ones (and related substitution of Si for Al and, especially, Fe^{3+} in tetrahedral sites) results in the formation of relatively strong hydrogen bonds and, as a result, in the broadening of O–H-stretching bands and their shifts towards lower frequencies.

The IR spectra of **chlorite-group minerals** are very diverse (see e.g. Figs. 1.28 and 1.29) due to the existence of various polytypes (Brown and Bailey 1962; Eggleton and Bailey 1967; Walker 1989), wide variations in the chemical composition of the octahedral and tetrahedral layers and interlayering with serpentines, micas, smectites, vermiculite and other phyllosilicates (Chukhrov 1992b).

As compared with magnesium serpentines, O–H-stretching bands of chlorites are broadened and partly shifted towards low-frequency region due to the formation of rather strong hydrogen bonds. Three regions of O–H-stretching

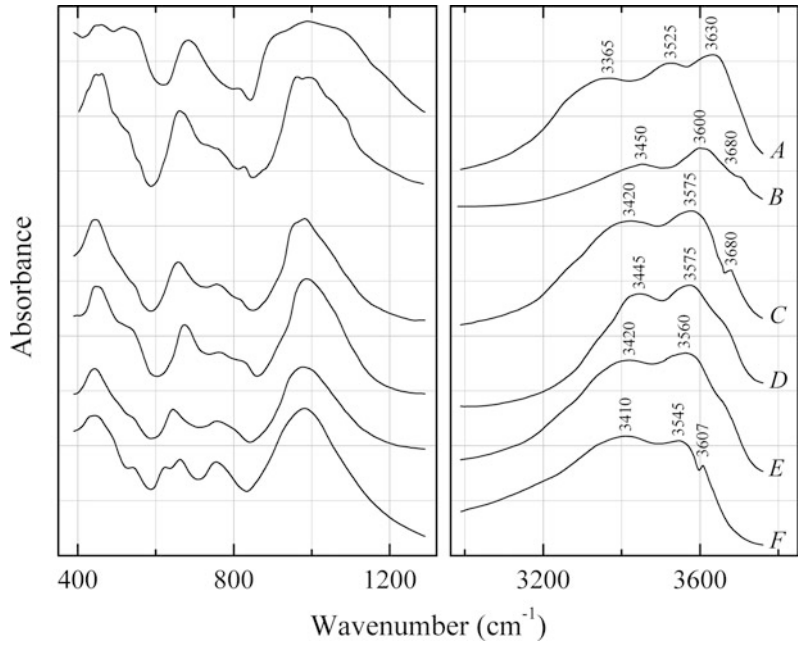

Fig. 1.29 IR spectra of 14 Å chlorites having different compositions, drawn using data from Oinuma and Hayashi (1968) and Chukanov (2014a). Spectra have been offset for comparison. *A*, $(Ca_{0.11}Mg_{1.18}Fe^{2+}_{0.03}Fe^{3+}_{0.35}Al_{3.02})(Si_{3.26}Al_{0.74}O_{10})(OH)_8$; *B*, $(Mg_{4.80}Fe_{0.11}Al_{1.09})(Si_{2.91}Al_{1.09})O_{10}(OH)_8$; *C*, $(Mg_{4.74}Mn_{0.05}Fe^{3+}_{0.07}Al_{1.16})(Si_{2.73}Al_{1.27}O_{10})(OH)_8$; *D*, $(Ca_{0.09}Mg_{3.35}Fe^{2+}_{0.03}Fe^{3+}_{0.09}Al_{2.10})(Si_{2.67}Al_{1.33}O_{10})(OH)_8$; *E*, $(Mg_{2.86}Mn_{0.04}Fe^{2+}_{1.85}Fe^{3+}_{0.14}Al_{1.13})(Si_{2.69}Al_{1.31}O_{10})(OH)_8$; *F*, $(Mg_{0.79}Mn_{0.59}Fe^{2+}_{2.82}Fe^{3+}_{0.12}Al_{1.45})(Si_{2.87}Al_{1.13}O_{10})(OH)_8$

vibrations can be distinguished in the IR spectra of Mg, Fe, Al-chlorites: 3615–3683, 3520–3586, and 3340–3436 cm^{-1} (Chukhrov 1992b). Bands in the region 3615–3618 cm^{-1} are related to OH groups of the 2:1 module; these bands are most distinct in Al-rich chlorites and disappear on heating to 690–820 °C. Bands in the regions 3520–3586 and 3340–3436 cm^{-1} correspond to OH groups of the intermodular octahedral layer; the substitution of Mg with Al and (to a lesser extent) with Fe^{2+} results in the shifts of these bands towards lower wavenumbers. In Al-poor trioctahedral and Al-rich dioctahedral chlorites, absorption maximum of the third group of bands is located above and below 3380 cm^{-1}, respectively. Bands in the range 730–850 cm^{-1} correspond to libration modes of OH groups forming hydrogen bonds, $(RR'R'')O–H\cdots O(Si,Al)_2$, where *R, R′*, and *R″* are octahedral cations.

FTIR spectra of natural trioctahedral chlorites of polytype IIb were obtained for a series of samples characterized by Fe/(Fe + Mg) ratio ranging from 0.04 to 0.94 and Si/Al ratio ranging from 5.18 to 1.86 (Prieto et al. 1991). The wavenumber of the weak O–H-stretching band from the 2:l layer (in the range 3610–3683 cm^{-1}) decreases with an increase of iron content at constant ^{IV}Al content. Bands in the range from 3400 to 3600 cm^{-1} correspond to OH groups forming hydrogen bonds, directed ⊥ (001), with oxygen of the tetrahedral layer; these bands shift towards lower frequencies with the enhancement of ^{IV}Al and ^{VI}Fe contents. In addition, the enhancement of ^{IV}Al content results in the intensity growth at ~3600 cm^{-1} and in the broadening of the band near 3500 cm^{-1}, which indicates the strengthening of hydrogen bonds.

The **talc group** of minerals includes trioctahedral $(Mg,Ni,Fe^{2+})_3(Si_4O_{10})(OH)_2$ and dioctahedral $(Al,Fe^{3+})_2(Si_4O_{10})(OH)_2$ members, with OH groups coordinating three and two octahedral cations, respectively. IR spectra of intermediate

members of talc-**willemseite** and talc-**minnesotaite** solid solutions, as well as synthetic talc-type compounds with Mg partially substituted with Ni, Fe^{2+}, Co^{2+}, Zn, Mn, or Cu, contain numerous narrow and well-resolved O–H-stretching bands corresponding to different local environments of the OH group (De Waal 1970; Wilkins and Ito 1967; Ferrage et al. 2003; Nkoumbou et al. 2008; Ersoy et al. 2013; Chukhrov 1992b; see Table 1.12).

The bands at ~3675, ~3645, and ~3620 cm^{-1} in IR spectra of dioctahedral talc group members, Fe^{3+}-bearing **pyrophyllites** (Al, $Fe^{3+})_2(Si_4O_{10})(OH)_2$, have been assigned to (AlAl□)–OH, (AlFe^{3+}□)–OH and ($Fe^{3+}Fe^{3+}$□)–OH, respectively (Lantenois et al. 2007). However this assignment disagrees with the data on IR spectra of synthetic ferripyrophyllite $Fe^{3+}{}_2(Si_4O_{10})(OH)_2$, in which the only ($Fe^{3+}$ Fe^{3+}□)–OH band at 3595 cm^{-1} is observed in the O–H-stretching region (Grauby 1993). In natural ferripyrophyllite samples the strongest O–H-stretching band is located in the region from 3568 to 3590 cm^{-1} (Chukhrov et al. 1979; Chukanov 2014a). These discrepancies show that the origin of the bands at ~3645 and ~3620 cm^{-1} in IR spectra of Fe^{3+}-bearing pyrophyllites needs further investigation.

According to Lantenois et al. (2007), the additional band at 3668 cm^{-1}, which is present in IR spectra of some pyrophyllite samples, corresponds to (AlAl□)–OH groups of *cis*-vacant layers, whereas the band at 3675 cm^{-1} is characteristic of (AlAl□)–OH groups belonging to *trans*-vacant layers.

1.6 Hydroxyl Groups in Tourmalines

The tourmaline supergroup includes trigonal and, rarely, pseudo-trigonal minerals with the general formula $XY_3Z_6(Si,Al,B)_6O_{18}(BO_3)_3V_3W$ (Hawthorne and Henry 1999; Henry et al. 2011), where X = Na, Ca, K, □; Y = Li, Mg, Fe^{2+}, Mn^{2+}, Al, Cr^{3+}, V^{3+}, Fe^{3+}, Ti; Z = Al, Cr^{3+}, V^{3+}, Mg, Fe^{2+}; V = OH^-, O^{2-}; W = OH^-, F^-, O^{2-}. The octahedral Z-sites are smaller than the octahedral Y-sites. Consequently, in most samples these sites are predominantly occupied by trivalent and bivalent cations, respectively. F^- is exclusively contained in the W site, and O^{2-} tends to be preferentially contained in this site (Grice and Ercit 1993). The OH groups can occupy two different positions: at the center of hexagonal rings (W) or at the border of brucite-like fragments (V). The V [O(3)] site is coordinated by one Y cation and two Z cations. The local situation around the W [O(1)] site involves three Y cations. In Li-free tourmalines, the stable local short-range Y-site cation configurations for OH^- at the W site are $3R^{2+}$ or $R^{3+} + 2R^{2+}$; in Li-rich tourmalines these configurations are $2Al^{3+} + Li^+$ or $Al^{3+} + 2Li^+$ (Henry et al. 2011).

The occurence of O^{2-} at the W site controls the Y site occupation due to local bond-valence and bond-length requirements. For example, in oxy-dravite cation arrangements around O1 are associated with $3Y = 3Al^{3+}$ or $2Al^{3+} + Mg^{2+}$ (de Oliveira et al. 2002).

Three regions of O–H-stretching vibrations in the IR spectra of tourmalines can be distinguished

Table 1.12 Wavenumbers (cm^{-1}) of O–H-stretching bands for OH groups having different local environments in IR spectra of trioctahedral talc-group minerals and related synthetic compounds

R	Local environments of OH groups			
	MgMgMg	$MgMgR^{2+}$	$MgR^{2+}R^{2+}$	$R^{2+}R^{2+}R^{2+}$
Ni	3676–3680	3662–3663	3645–3647	3624–3627
Co	3676–3680	3661	3643	3622
Zn	3676–3680	3664–3665	3650–3652	3635
Fe	3676–3680	3661–3663.5	3643–3646	3624
Mn	3676–3680	3664	3650	No data
Cu	3676–3680	3670	3664	3656

(Gonzalez-Carreño et al. 1988; see Fig. 1.30). The strongest bands observed in the range from 3400 to 3600 cm^{-1} are assigned to OH groups at the *V* site. This part of the IR spectrum depends mainly on the composition of the octahedral sites; individual bands in this region correspond to the groups of surrounding cations, e.g. AlAlLi, A1A1R^{2+} (R = Mg, Mn or Fe) or AlAlAl. Exact positions of these bands depend on the occupancy of the *X* site (Na, Ca, or vacancy).

In the ranges 3630–3750 and 3200–3400 cm^{-1}, weaker bands (narrow and broad, respectively) are present. The former region is assigned to OH groups in the *W* site located at the center of hexagonal rings and coordinated to $R^{2+}R^{2+}R^{2+}$ (from 3633 for $Fe^{2+}Fe^{2+}Fe^{2+}$ to 3738 cm^{-1} for MgMgMg in the IR spectra of the members of the schorl-dravite solid-solution series), AlAlLi (3650–3690 cm^{-1} for elbaite) and AlR^{2+}Li (3692 and 3670 cm^{-1} for Fe- and Mn-rich elbaites, respectively) (Gonzalez-Carreño et al. 1988).

In Fe^{3+}-bearing Mg-poor schorl from the Limoeiro mine, Murta, Minas Gerais, Brazil, the band of OH groups in the *W* site coordinated to $Fe^{2+}Fe^{2+}Fe^{2+}$ is observed at 3628 cm^{-1} (de Oliveira et al. 2002). The bands at 3380, 3483, and 3550 cm^{-1} in the IR spectrum of this sample can be presumably assigned to OH groups in the *V* site coordinated to $AlAlFe^{3+}$, AlAlAl, and $AlAlFe^{2+}$, respectively.

Infrared and polarized Raman spectra of different tourmaline species in the spectral range associated with the hydroxyl vibration modes have been analyzed by Fantini et al. (2014). The profiles of IR absorption bands of the hydroxyl groups (Fig. 1.31) are in good agreement with the Raman results. The assignments of O–H-stretching bands for OH groups based on the data on polarized Raman spectra are given in Table 1.13. These vibrational modes are oriented along the crystal *c*-axis.

Based on chemical data and polarized FTIR absorption spectra in the OH-stretching frequency

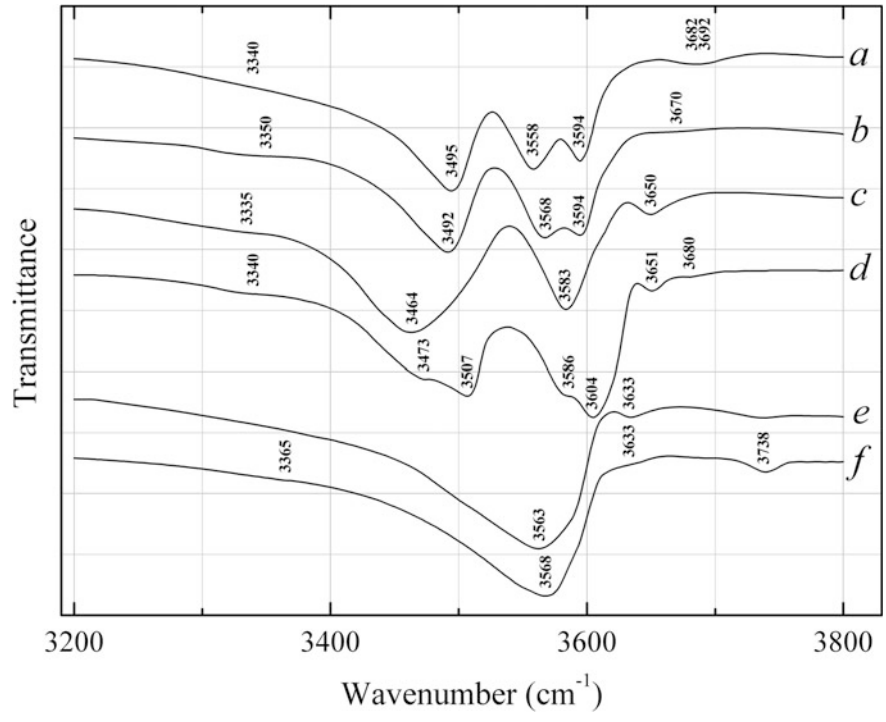

Fig. 1.30 Hydroxyl stretching region of the IR spectra of (*a*) Fe-rich elbaite, (*b*) Mn-rich elbaite, (*c*) elbaite, (*d*) Ca-bearing elbaite, (*e*) Mn-rich schorl, and (*f*) dravite. The picture is drawn using data from Gonzalez-Carreño et al. (1988)

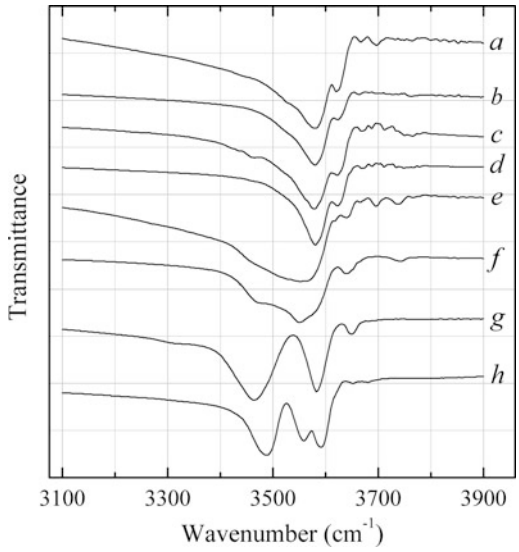

Fig. 1.31 IR spectra in the O–H-stretching range of different samples of uvite (*a*, *b*), fluor-uvite (*c*, *d*), dravite (*e*), magnesio-foitite (*f*), and elbaite (*g*, *h*) drawn using data from Fantini et al. (2014)

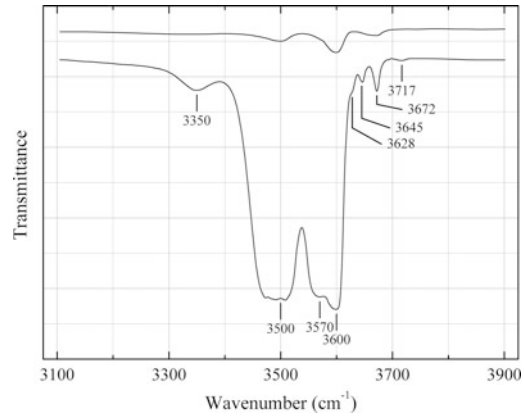

Fig. 1.32 Polarized FTIR absorption spectra in the O–H-stretching region of tsilaisite (*upper curve E* ∥ *a*, *lower curve E* ∥ *c*) drawn using data from Bosi et al. (2012b)

region (Fig. 1.32) of holotype tsilaisite from island of Elba, Italy, containing $[Mn^{2+}_{1.34}Al_{1.14}Li_{0.54}Ti_{0.04}]$ at the *Y* site, the following assignment of O–H-stretching bands was suggested (Bosi et al. 2012b): ~3717 cm^{-1}—^{Y}(LiMnMn)–O1 or ^{Y}(LiLiAl)–O1; ~3672 cm^{-1}—^{Y}(LiMnAl)–O1; ~3645 cm^{-1}—^{Y}(MnMnAl)–O1, ^{Y}(LiAlAl)–O1 or ^{Y}(MnMnMn)–O1; ~3628 cm^{-1}—^{Y}(MnMnAl)–O1 or ^{Y}(LiAlAl)–O1; ~3600 cm^{-1}—(^{Y}Li ^{Z}Al^{Z}Al)–O3; ~3570 cm^{-1}—(^{Y}Mn^{Z}Al^{Z}Al)–O3; ~3500 cm^{-1}—(^{Y}Al^{Z}Al^{Z}Al)–O3; 3350 cm^{-1}—O3–H···O5 (hydrogen bond).

Based on comparative crystal-chemical data for Li-bearing tourmalines (solid solutions of elbaite, tsilaisite and schorl), the following assignment of O–H-stretching bands to triads of cations coordinating OH group was suggested by

Table 1.13 Raman frequencies (cm^{-1}) of O–H-stretching modes for OH groups with different local environments in some tourmaline-supergroup minerals

Site	Local environment	Mineral				
		Uvite	Fluor-uvite	Magnesio-foitite	Na-deficient dravite	Na-deficient elbaite
V	^{Y}Al^{Z}Al^{Z}Al	–	–	3482	3485	3471–3481
V	^{Y}Mg^{Z}Mg^{Z}Mg	3518–3528	3539–3547	3516	–	–
V	^{Y}Fe^{Z}Al^{Z}Al	–	–	–	3518	3491
V	^{Y}Mg^{Z}Al^{Z}Mg	3554–3560	–	–	–	–
?	?	–	–	3552[a]	3548[a]	3564–3566[a]
V	^{Y}Mg^{Z}Al^{Z}Al	3592–3593	3584–3589	3587	3577	3591–3591
W	^{X}Ca^{Y}(3 Mg)	3635–3636	3627–3630	–	–	–
?	?	–	–	3646[b] 3676[b]	3645[b] 3744[b]	3655–3660[b]

The wavenumbers are indicated in accordance with Fantini et al. (2014)
[a]Bands associated with Na in *X*. [b]Bands associated with vacancy in *X*

Bosi et al. (2015): 3628–3630 cm^{-1} – ($R^{2+}R^{2+}$Al); 3643–3645 cm^{-1} – ($R^{2+}R^{2+}R^{2+}$); 3672 cm^{-1} – (LiR^{2+}Al); 3717 cm^{-1} – ($LiR^{2+}R^{2+}$) or (LiLiAl).

The polarization infrared spectra of chromo-alumino-povondraite from the Sludyanka crystalline complex, Southern Baikal region, Russia, containing $[Cr^{3+}_{1.94}Mg_{0.93}Al_{0.07}Ti_{0.06}]$ at the *Y* site, $[Al_{3.74}Mg_{1.43}Fe^{3+}_{0.32}V^{3+}_{0.19}Cr^{3+}_{0.16}Fe^{2+}_{0.15}]$ at the *Z* site and $[O_{0.69}F_{0.23}(OH)_{0.08}]$ at the *W* site (Bosi et al. 2013) are strongly dominated by a broad absorption band centered at 3530 cm^{-1}, which is predominantly polarized in the *c* direction (Fig. 1.33) and is considered to result from overlapping peaks related to a large set of different local arrangements around the OH group at the O3 site. Sharper and weaker bands at 3763, 3732, and 3716 cm^{-1}, also polarized in the *c*-axis direction, have been assigned to the local arrangements ^{Y}(3Mg)–^{W}(OH) and ^{Y}(R^{3+}+ 2Mg)–^{W}(OH). However, taking into account low content of Al in the Y site, the assignment of these bands to ^{Y}(3Mg)–^{W}(OH), ^{Y}(Cr^{3+}+2Mg)–^{W}(OH) and ^{Y}($2Cr^{3+}$+ Mg)–^{W}(OH) seems to be more reliable. The comparatively low intensity of the bands with wavenumbers above 3700 cm^{-1} reflects the reduced contents of OH groups at the *W* site. In the IR spectrum of holotype chromo-alumino-povondraite with $[O_{0.73}F_{0.25}(OH)_{0.02}]$ at the *W* site these bands are even weaker (Reznitskii et al. 2014).

Similar data have been obtained for vanadio-oxy-dravite from the same locality (Bosi et al. 2014a; see Fig. 1.34). This sample contains $[V^{3+}_{1.39}Mg_{1.16}Al_{0.35}Ti_{0.04}Fe^{2+}_{0.02}]$ at the *Y* site, $[Al_{3.74}Mg_{1.28}V^{3+}_{0.78}Cr^{3+}_{0.20}]$ at the *Z* site and $[O_{0.74}(OH)_{0.26}]$ at the *W* site. The main band in its IR spectrum located around 3550 cm^{-1} may be related to the local arrangement ($^{Y}V^{3+Z}R^{Z}$R)–O3, i.e., to the occurrence of (OH) at the V position. The two weaker bands at 3732 and 3761 cm^{-1} are consistent with the minor concentrations of OH groups at the W position and may be related to the local arrangements ^{Y}(MgMgR^{3+}) and ^{Y}(MgMgMg).

For the IR spectra of tourmalines in the O–H-stretching region (including overtones of O–H-stretching bands) see also the papers by Novák et al. (2013), Bosi et al. (2012a, 2014b), and Reddy et al. (2007).

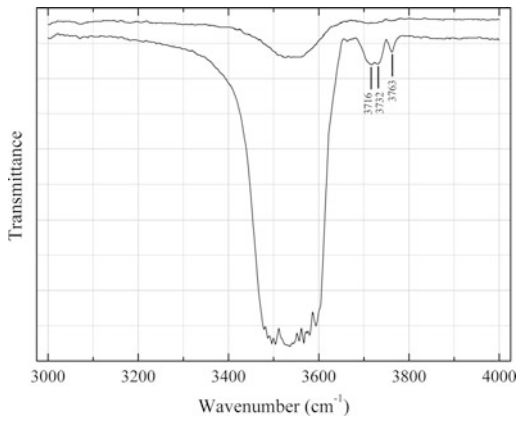

Fig. 1.33 Polarized FTIR absorption spectra of Fe-bearing chromo-alumino-povondraite (*upper curve E ∥ a*, *lower curve E ∥ c*) drawn using data from Bosi et al. (2013)

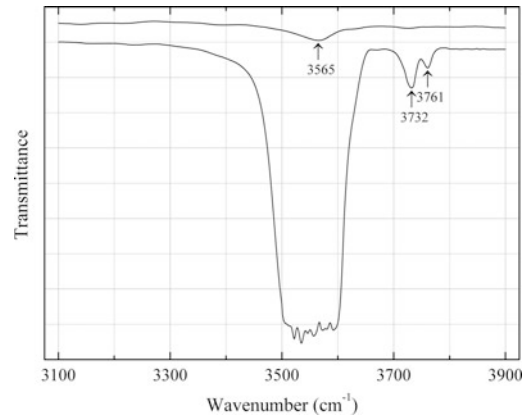

Fig. 1.34 Polarized FTIR absorption spectra in the O–H-stretching region of vanadio-oxy-dravite (*upper curve E ∥ a*, *lower curve E ∥ c*) drawn using data from Bosi et al. (2014a). The main band around 3550 cm^{-1} is truncated along ordinate due to excessive absorption

1.7 Acid OH Groups in Minerals

The hydrogen atom contains only one electron, which in different compounds is involved in the formation of a binding orbital. As a result, for OH groups in which O and H atoms form covalent bond, only the determination of the position of the electron pair (but not of the H atom itself) is possible by means of structural methods based on X-ray diffraction. As a result, the lengths of covalent O–H bonds determined from X-ray diffraction data are, on the average, 0.2 Å less than their real values (Baur 1972). Moreover, isolated H^+ cation cannot be detected by X-ray diffraction methods because it does not contain electrons. Crystals of minerals suitable for single-crystal structural investigations by means of diffraction of neutrons are often not available. For these reasons, IR spectroscopy is considered as one the most informative methods of the investigation of the nature of acid hydroxyl groups.

Generally, a low force constant of the O–H bond indicates a high acid strength of the OH group and is reflected by a low wavenumber of the O–H-stretching band in the vibrational spectrum. IR spectra of acid salts (silicates, carbonates, phosphates etc.) possess a number of specific features including the presence of numerous bands of acid OH groups in the range ~1150–3000 cm^{-1}, splittings and shifts of the bands of stretching vibrations of anionic groups like $HSiO_4^{3-}$, $H_2SiO_4^{2-}$, HCO_3^-, HPO_4^{2-}, $H_2PO_4^-$, $HAsO_4^-$ et al. (Nyquist and Kagel 1971; Chukanov and Pekov 2012; Chukanov 2014a, b). Some examples of IR spectra of acid phosphates and arsenates are given in Figs. 1.35 and 1.36. Multiple bands in the range from 1150 to 3000 cm^{-1} were observed also in the IR spectra of synthetic acid selenites of divalent metals (Unterderweide et al. 1994), magnesium acid vanadate $Mg_{13.4}(OH)_6(HVO_4)_2(H_{0.2}VO_4)_6$ (Đorđević et al. 2008), barium acid arsenate $Ba(HAsO_4)$ (Đorđević and Karanović 2010), synthetic ammonium vanadyl phosphate $(NH_4)_2(VO)(HPO_4)_2 \cdot H_2O$ (Liu et al. 1999b), etc.

Relatively narrow bands present in the IR spectra of some acid oxysalts in the range from 1150 to 1500 cm^{-1} are due to vibrations of H^+ cations formed as a result of reversible heterolytic dissociation of acid OH-groups. In particular, in case of silanol groups of pectolite and some related acid inosilicates (sérandite,

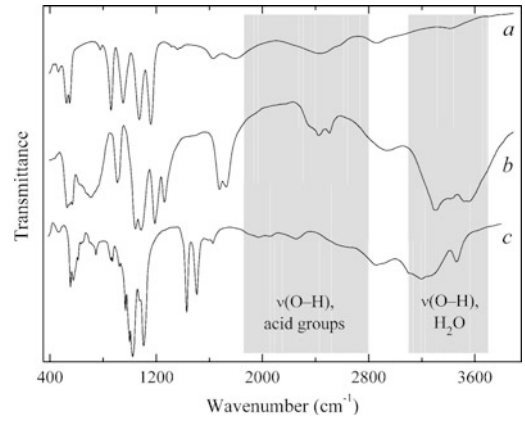

Fig. 1.35 Powder IR spectra of acid phosphates: nahpoite $Na_2(HPO_4)$ from peralkaline pegmatite of the Lovozero massif (*a*), newberyite $Mg(HPO_4) \cdot 3H_2O$ from guano of the Guañape island, Peru (*b*), and girvasite $NaCa_2Mg_3(PO_4)_2(H_2PO_4)(CO_3)(OH)_2 \cdot 4H_2O$ from dolomite carbonatite of the Kovdor massif (*c*). The spectra were obtained by N.V. Chukanov. Spectra have been offset for comparison

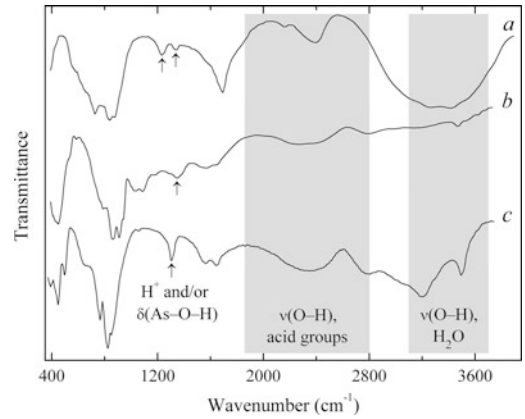

Fig. 1.36 Powder IR spectra of acid arsenates: rösslerite $Mg(HAsO_4) \cdot 7H_2O$ from the Belorechenskoe uranium deposit, Northern Caucasus (*a*), weilite $Ca(HAsO_4)$ from the oxidation zone of the Sainte Marie aux Mines deposit, France (*b*), and koritnigite $Zn(HAsO_4) \cdot H_2O$ from the oxidation zone of the Jáchymov deposit, Czech Republic (*c*). The spectra were obtained by N.V. Chukanov. Spectra have been offset for comparison

marshallsussmanite, babingtonite, manganobabingtonite, nambulite, natronambulite, marsturite, lithiomarsturite, and some other) the dynamic equilibrium ≡SiO–H ↔ ≡SiO + H^+ is strongly shifted to the right, i.e. towards the formation of non-covalent bonded H^+ cation. In other words, in these minerals hydrogen is predominantly present in the form of the isolated cation H^+ vibrating in a weak and strongly anharmonic force field. Weak and broad bands above 1400 cm^{-1} are related to overtones and combination modes involving vibrations of H^+ (Chukanov and Pekov 2012; see Fig. 1.37).

In mozartite, $CaMn^{3+}O(SiO_3OH)$, the acid-base equilibrium is strongly shifted to the left, and narrow bands in the range from 1150 to 1500 cm^{-1}, characteristic of isolated H^+ cations, are absent in the IR spectrum. Instead, two very strong bands, both polarized parallel to [010], are observed in the ranges ~1100–2000 and ~2300–3000 cm^{-1} (Fig. 1.38). The tetrahedron SiO_4 in the mozartite structure is distorted, with one bond length (Si–O2) equal to 1.647 Å and three other bonds ranging from 1.631 to 1.636 Å. Due to the Jahn-Teller distortion of the $Mn^{3+}O_6$ octahedron, one bond (Mn–O5) is shortened as compared with other Mn–O bonds and has the length of 1.860 Å. As a result, O5 acts as an acceptor of very strong hydrogen bond: the distance O2···O5 is close to 2.5 Å, and the O2 valence sum is equal to 1.365 v.u. (Nyfeler et al. 1997). The weak but sharp absorption band at 3557 cm^{-1}, also polarized ∥ [010], was assigned to structural defects. However this band may correspond to OH groups formed as a result of proton transfer to O5 and the formation of OH^- anion coordinating Mn^{3+}:

$$\mathrm{Si{-}O2{-}H\cdots O5\cdots Mn^{3+}} \rightarrow \mathrm{Si{-}O2 + H{-}O5\cdots Mn^{3+}}.$$

For the localization of H in mozartite, a procedure based on physically reasonable bond distances and angles was used (Nyfeler et al. 1997). The presence of only one site of hydrogen in the crystal structure found using this procedure seems to be in contradiction with the presence of two identically polarized (i.e. related to O–H-**stretching** vibrations) strong and broad absorption bands in the ranges ~2300–3000 and ~1100–2000 cm^{-1}. The most probable explanation of this phenomenon is the existence of two local long-living states of hydrogen between O2 and O5. Transitions between these states would occur due to thermally induced predissociation of the O–H bond. Relatively high values of the anisotropic displacement parameters U_{11} and U_{33} for the atom O2 (0.013 and 0.0092, respectively)

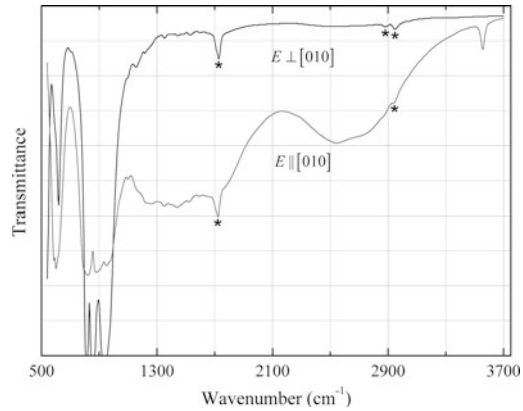

Fig. 1.38 Polarized single-crystal FTIR spectra of mozartite drawn using data from Nyfeler et al. (1997). Bands marked with asterisk correspond to epoxy impurity

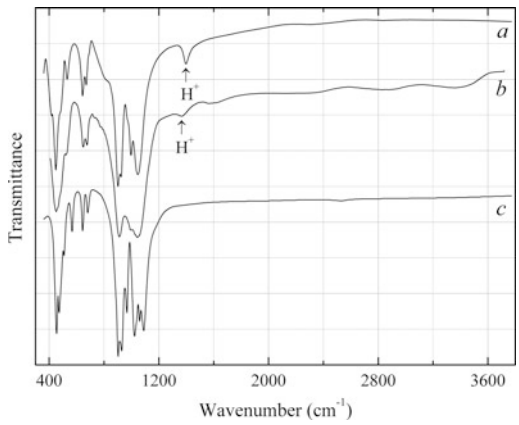

Fig. 1.37 Powder IR spectra of pectolite-1*A* from the Kovdor alkaline-ultrabasic massif (*a*), sérandite from Kedykverpakhk Mt., Lovozero alkaline complex, Kola peninsula, Murmansk region, Russia (*b*), and wollastonite from the Akchatau deposit, Kazakhstan (*c*). The spectra were obtained by N.V. Chukanov. Spectra have been offset for comparison

confirm this assumption. Consequently, the complete hypothetical scheme of acid-base equilibria in mozartite is:

$$\begin{aligned} &\mathrm{Si{-}O2{-}H\cdots O5\cdots Mn^{3+}} \\ &\quad\leftrightarrow \mathrm{Si{-}O2\cdots H\cdots O5\cdots Mn^{3+}} \\ &\quad\leftrightarrow \mathrm{Si{-}O2 + H{-}O5\cdots Mn^{3+}}. \end{aligned}$$

Powder IR spectra of some other acid silicates containing isolated groups of SiO_4 tetrahedra are given in Fig. 1.39. All of them contain numerous bands in the range from 1600 to 3000 cm^{-1}.

Another example of acid salts is the synthetic acid phosphate $K_4Mn_3(HPO_4)_4(H_2PO_4)_2$ (Feng et al. 2009; see Fig. 1.40). The IR bands of this compound observed in the range from 1500 to 3000 cm^{-1} are related to stretching vibrations of acid OH groups forming very strong hydrogen bonds with the distances O···O equal to 2.449, 2.469, 2.562, and 2.612 Å. Narrower bands in the range from 1200 to 1300 cm^{-1} may correspond to vibrations of free H^+ cation formed as a result of dissociation of acid phosphate groups.

Similar features shows IR spectrum synthetic barium acid arsenate $Ba(HAsO_4)$ (Đorđević and Karanović 2010). It contains numerous very broad bands of stretching vibrations of weakened O–H-bonds (in the range from 1500 to 3000 cm^{-1}) and narrower bands in the range from 1110 to 1400 cm^{-1} assigned to As–O–H bending vibrations. However the latter bands (at least, a part of them) may be related to the vibrations of the H^+ cation.

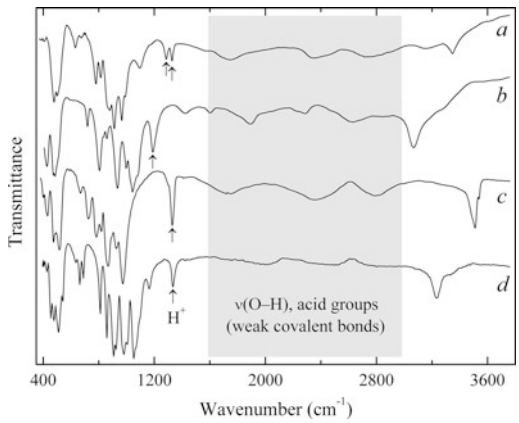

Fig. 1.39 Powder IR spectra of ortho-, diortho-, and triorthosilicates containing silanol groups Si–OH: afwillite $Ca_3(H_2SiO_4)(SiO_4)\cdot 2H_2O$ (*a*) and suolunite $Ca_2[Si_2O_5(OH)_2]\cdot H_2O$ (*b*) (both from the Yoko-Dovyren massif, Northern Baikal area), olmiite $CaMn(HSiO_4)(OH)$ from N'Chwaning II mine, Kalahari manganese fields, South Africa (*c*), and rosenhahnite $Ca_3(H_2Si_3O_{10})$ from Russian River basin, California, USA (*d*). The spectra were obtained by N.V. Chukanov. Spectra have been offset for comparison

As one can see from the above examples, broad bands in the range 1200–3000 cm^{-1} corresponding to stretching vibrations of OH groups with low force constants of covalent O–H bonds are typical for acid salts. In most cases, such bands are absent in IR spectra of neutral and basic salts, including crystalline hydrates. However there are numerous exceptions to this rule (several examples are given in Figs. 1.41 and 1.42). This phenomenon is nontrivial and needs explanation. Indeed, the wavenumber 2000 cm^{-1} corresponds to a force constant of the O–H bond that is more than three times less than that of free (non-H-bonded) covalent O–H bond. Broad bands between 1250 and 1900 cm^{-1} correspond to stretching vibrations of even weaker O–H bonds (4–9 times weaker than those of free OH groups).

In the crystal structure of bakhchisaraitsevite (Yakubovich et al. 2000) the tetrahedra PO_4 are distorted: in three of four independent orthophosphate anions variation of the bond lengths P–O is about 0.03 Å; mean valence sums at O atoms forming long (1.549–1.559 Å) and short (1.521–1.522 Å) P–O bonds are equal to 1.948 and 1.993 v.u., respectively. As a rule, protonation of an O atom of the orthophosphate anion results in the elongation of corresponding P–O bond (Rouff et al. 2009), although exceptions to this rule are known (Escobal et al. 2000). Consequently, one can suppose that the presence of absorption bands of acid groups in the IR spectrum of bakhchisaraitsevite results from a partial protonation of PO_4^{3-} groups by H_2O molecules forming strong hydrogen bonds with O atoms of these groups.

Another possible explanation of the anomalous specific features of the bakhchisaraitsevite IR spectrum is based on the assumption of possible presence of hydrated proton like hydronium,

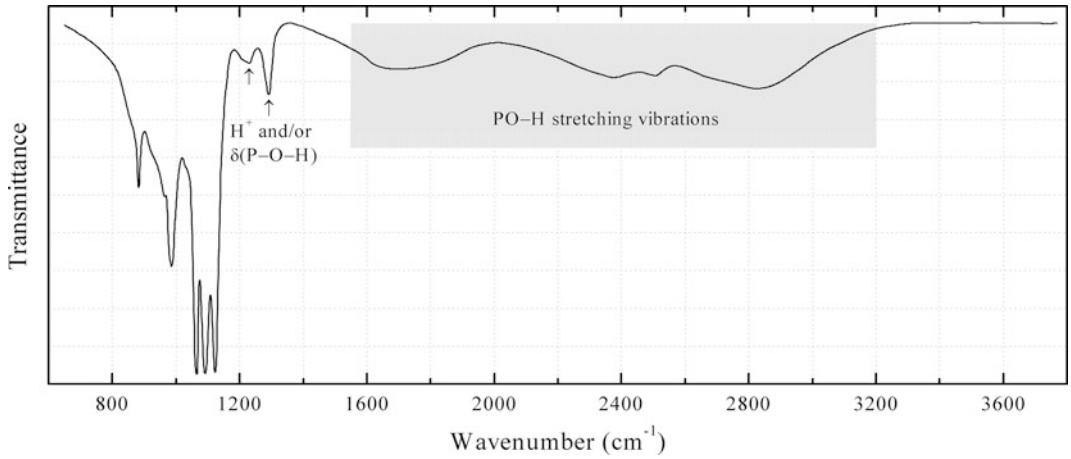

Fig. 1.40 FTIR spectrum of $K_4Mn_3(HPO_4)_4(H_2PO_4)_2$ drawn using data from Feng et al. (2009)

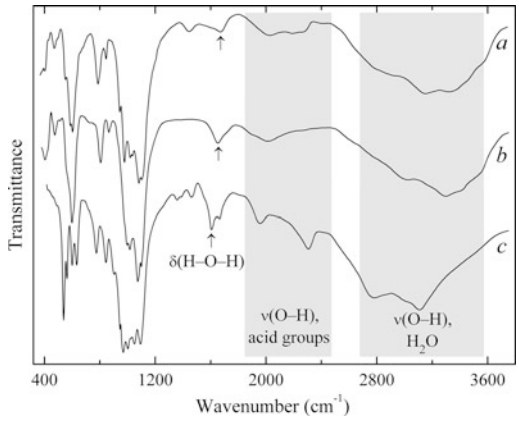

Fig. 1.41 IR spectra of nominally neutral phosphates: bakhchisaraitsevite $Na_2Mg_5(PO_4)_4{\cdot}7H_2O$ (*a*), rimkorolgite $Mg_5Ba(PO_4)_4{\cdot}8H_2O$ (*b*) (both from dolomite carbonatite of the Kovdor massif), and anapaite $Ca_2Fe^{2+}(PO_4)_2{\cdot}$from the Kerch iron-ore basin (*c*). The spectra were obtained by N.V. Chukanov. Spectra have been offset for comparison

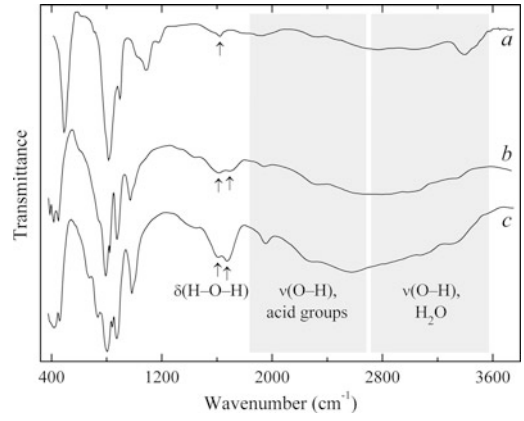

Fig. 1.42 IR spectra of a basic and nominally neutral arsenates: gartrellite $PbCuFe^{3+}(AsO_4)_2(OH){\cdot}H_2O$ from the oxidation zone of the Anticline deposit, Australia (*a*), brandtite $Ca_2Mn(AsO_4)_2{\cdot}2H_2O$ from skarn (Harstigen mine, Sweden) (*b*), and roselite $Ca_2Co(AsO_4)_2{\cdot}2H_2O$ from the oxidation zone of the Bou-Azzer deposit, Morocco (*c*). The spectra were obtained by N.V. Chukanov. Spectra have been offset for comparison

Zundel or Eigen cations (Chukanov 2014b). In the structure of this mineral water molecules form hydrogen bonds with each other and with phosphate anions. The site W7 is split into two subsites W7a and W7b at a separation of 0.913(7) Å, which are considered to be occupied by H_2O molecules with a probability of occupancy of 43 and 57 %, respectively (Yakubovich et al. 2000, see Fig. 1.43). Note that the atoms H15 and H16 were not localized in the cited paper: their positions were postulated to be fixed at the distance of 0.85 Å from O atoms. The atom O_{w7} that is an acceptor of hydrogen bond with disordered water molecule W7, has three short distances to H atoms. Such configuration resembles that of hydronium cation.

The distortion of phosphate groups in bakhchisaraitsevite is relatively small. However it is to be taken into account that the crystal structure of this mineral was solved for a crystal at the temperature of 193 K. It is known that pH

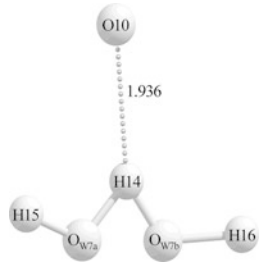

Fig. 1.43 Scheme of disordering of the W7 water position in the bakhchisaraitsevite structure drawn using data from Yakubovich et al. (2000)

of a buffer solution decreases with temperature lowering (Mohan 2003). Consequently, as a result of temperature lowering, the acid-base equilibrium $PO_4^{3-} + H_2O \leftrightarrow HPO_4^{2-} + OH^-$ shifts to the left, and it is possible that HPO_4^{2-} are present in low concentrations and cannot be identified by means of X-ray structural analysis.

The latter assumption is indirectly confirmed by the structural characteristics of rimkorolgite, a mineral whose crystal structure is related to that of bakhchisaraitsevite: both structures are based on the octahedral-tetrahedral sheets of the same type. The crystal structure of rimkorolgite was solved from single-crystal X-ray diffraction data obtained at room temperature (Krivovichev et al. 2002). Four independent PO_4 tetrahedra are present in rimkorolgite, and two of them are strongly distorted: the atoms O17 and O21 form elongated P–O bonds (1.554 and 1.559 Å, respectively). Valence sums at these O atoms are equal to 1.15 and 1.13 v.u., respectively. The atom O20 belonging to a phosphate group is also characterized by the lowered valence sum of 1.66 v.u. In calculating these values the contribution of hydrogen bonds with water molecules $H_2O(2)$, $H_2O(19)$ and $H_2O(22)$ was not taken into account. On the other hand, such strong hydrogen bonds may facilitate the shift of the dynamic equilibrium $PO_4^{3-} + H_2O \leftrightarrow HPO_4^{2-} + OH^-$ to the right. In this reference it is important to note that the valence sums at the water molecules $H_2O(19)$ and $H_2O(2)$ are rather high (0.53 and 0.60, respectively). The valence sum at the water molecule $H_2O(22)$ is not given; this molecule is characterized by anomalously high values of anisotropic displacement parameters.

Thus the presence of the bands of acid OH groups in the IR spectra of bakhchisaraitsevite and rimkorolgite (in the range from 1900 to 2300 cm^{-1}) may be explained by a partial protonation of phosphate groups, which is promoted by very strong hydrogen bonds with water molecules. However, the available data do not allow us to determine the degree of protonation. A rough estimation based on the comparison with IR spectra of acid phosphates results in the values of the ratios $[HPO_4^{2-}]$: $[HPO_4^{2-} + PO_4^{3-}]$ for bakhchisaraitsevite and rimkorolgite in the limits from 0.1 to 0.3.

A similar mechanism of partial protonation of phosphate anions may be expected in anapaite $Ca_2Fe^{2+}(PO_4)_2 \cdot 4H_2O$: as noted in (Catti et al. 1979), this mineral contains "one of the strongest hydrogen bonded water molecules ever found in crystal structures", with the distances O_W–O equal to 2.597 and 2.600 Å.

Apparently, a similar mechanism of protonation of tetrahedral anionic groups is implemented in some **hydrous nominally neutral and basic arsenates and vanadates** (e.g. members of the tsumcorite and roselitegroups), whose IR spectra contain bands indicative of acid OH groups. In the structures of these minerals tetrahedral anionic groups are usually distorted and form strong hydrogen bonds with water molecules (see Krause et al. 1998a; Herwig and Hawthorne 2006).

Acid groups in **nominally anhydrous basic salts** (mainly, phosphates, arsenates, and vanadates) are a special case. Arsenate bayldonite [nominally, $PbCu_3(AsO_4)_2(OH)_2$] and related vanadate vésigniéite [nominally, $BaCu_3(VO_4)_2(OH)_2$] are examples of such minerals. In the IR spectra of these minerals (Fig. 1.44) there are bands of acid OH groups (in the range from 1250 to 3000 cm^{-1}), whereas bands of As–O- and V–O-stretching vibrations are strongly split, which is also characteristic of acid arsenates and vanadates. For this reason, and taking into account the data of thermal analysis, the formula $Cu_3PbO(HOAsO_3)_2(OH)_2$ was proposed for bayldonite by de Portilla et al. (1981). The authors of this work wrote that the crystal structure of bayldonite is unknown. However, the results of a study of the crystal structure of bayldonite published two years earlier (Ghose

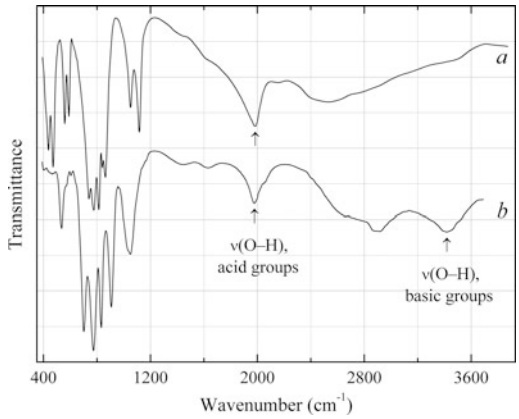

Fig. 1.44 IR spectra of bayldonite from the Tsumeb deposit, Namibia (*a*) and vésigniéite from the Kara-Chagyr deposit, Kyrgyzstan (*b*). The spectra were obtained by N.V. Chukanov. Spectra have been offset for comparison

and Wan 1979) have shown that in fact the formula of this mineral should contain 10, but not 11 oxygen atoms, and H atom appears to be disordered between the OH group and a highly charge-deficient O atom, which is bonded to the Pb atom, in addition to the As atom. Ghose and Wan (1979) write the formula of bayldonite as $PbCu_3(AsO_4)_2(OH)_2$. Taking into account the data of IR spectroscopy, it would be more correct to speak about the dynamic acid-base equilibrium $PbCu_3(AsO_4)_2(OH)_2 \leftrightarrow PbCu_3(HAsO_4)_2O_2$, which is strongly shifted to the right, because integral intensities of the bands of O–H-stretching vibrations of basic OH-groups (above 3000 cm^{-1}) is significantly lower than the total integral intensity of the bands of acid OH-groups (in the range 1250–3000 cm^{-1}).

In vésigniéite acid OH-groups also dominate over basic ones, however, the relative fraction of the virtual basic structure $BaCu_3(VO_4)_2(OH)_2$ in this mineral is somewhat higher than for bayldonite. Strongly hydrogen bonded OH groups are present also in the nominally basic vanadates brackebuschite $Pb_2Mn^{3+}(VO_4)_2(OH)$ and gamagarite $Ba_2Fe^{3+}(VO_4)_2(OH)$. Along with strong and broad bands at 2750–3000 cm^{-1}, IR spectra of these minerals contain shoulders in the range 2000–2600 cm^{-1}, which are similar to the bands in the IR spectra of acid salts (Harlow et al. 1984). The authors of the cited paper concluded: "…with a reevaluation of previously published structure data, our interpretation prefers the brackebuschite-type structure as a partially acid vanadate (arsenate and phosphate) containing HVO_4^{2-} type units".

Bands of acid OH groups are also typical of reddingite-group phosphates. The simplified general formula of these minerals is usually written as $M(1)M(2)_2(PO_4)_2(OH,H_2O)_3$, where *M*(1) and *M*(2) are octahedral cations. Mineral species belonging to the reddingite group are listed in Table 1.14. The bands at 2530, 2033, and 1890 cm^{-1} in the IR spectrum of correianevesite (Fig. 1.45, curve *a*) indicate the presence

Table 1.14 Dominant components in cationic sites of reddingite-group minerals

Mineral	M(1)	M(2)
Reddingite	Mn^{2+}	Mn^{2+}
Phosphoferrite	Fe^{2+}	Fe^{2+}
Landesite	Fe^{3+}	Mn^{2+}
Kryzhanovskite	Fe^{3+}	Fe^{3+}
Garyansellite	Mg	Fe^{3+}
Correianevesite	Fe^{2+}	Mn^{2+}

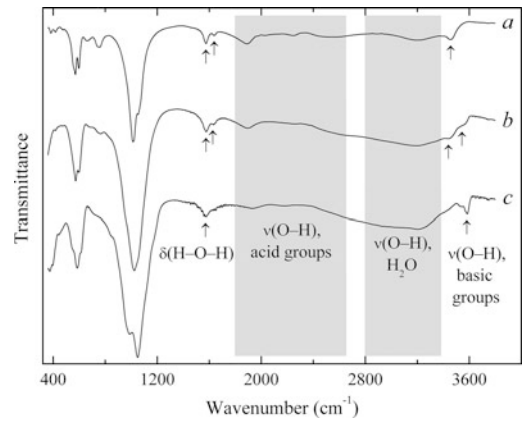

Fig. 1.45 IR spectra of reddingite-group minerals correianevesite [nominally, $Fe^{2+}Mn^{2+}{}_2(PO_4)_2 \cdot 3H_2O$] from Cigana mine, Brazil (*a*), landesite [nominally, $Fe^{3+}Mn^{2+}{}_2(PO_4)_2(OH)\cdot$] from Bull Moose mine, South Dakota, USA (*b*), and garyansellite [nominally, $Mg_2Fe^{3+}(PO_4)(OH)\cdot 2H_2O$] from Rapid Creek area, Yukon Territory, Canada (*c*). The spectra were obtained by N.V. Chukanov. Spectra have been offset for comparison

of the groups P–OH. The most probable mechanism of the formation of the HPO_4^{2-} group is proton transfer between H_2O molecule and O1 atom forming strong hydrogen bond with the distance O_w–O1 equal to 2.538 Å (Chukanov et al. 2014c). Note that earlier for the same sample of correianevesite, described under the name "reddingite", strong band of symmetric stretching vibrations of the HPO_4^{2-} ion at 1007 cm^{-1}, as well as a number of weaker bands of asymmetric vibrations of this ion have been detected in the Raman spectrum (Frost et al. 2012). The formula of the virtual acid form of correianevesite can be written as follows: $Fe^{2+}Mn^{2+}_2(HPO_4)_2(OH)\cdot H_2O$.

In reddingite-group minerals containing trivalent cations, which are nominally basic salts, bands of acid OH groups are less distinct (Fig. 1.45, curves *b* and *c*). Similar, but usually weaker bands of stretching vibrations of acid OH-groups are present in the IR spectra of many other phosphates, arsenates, and vanadates, which usually are not referred to acid salts. The frequency ν of these vibrations is related to the force constant of the O–H bond according to the formula $\nu = (f/\mu)^{1/2}$, where $\mu \approx 1.06$ amu is effective reduced mass of the O–H-stretching vibrations. The typical wavenumber of O–H-stretching vibrations of a covalent O–H bond, not involved in hydrogen bonds, is around 3700 cm^{-1}, which corresponds approximately to the force constant $f°_{O–H} = 8.5$ mdyne/Å. Typical acid bands in the range 1900–2400 cm^{-1} correspond to the effective force constants $f = (0.25–0.42)f°_{O–H}$. Such a significant weakening of the covalent O–H bond is a precondition for its heterolytic dissociation and dynamic equilibrium between acid and neutral forms of an oxysalt.

Absorption bands of acid OH groups are present in the IR spectra of a number of phosphates (namely, rimkorolgite, bakhchisaraitsevite, collinsite, goyazite, girvasite) from dolomitic carbonatites of the Kovdor alkaline-ultrabasic complex, Kola peninsula, although only in girvasite acid phosphate groups have been localized by X-ray structure analysis. The presence of acid groups in the minerals formed in the basic environment may seem paradoxical. *Ex facte*, even more unusual appears the formation of acid salts (nahcolite $NaHCO_3$, wegscheiderite $Na_5(CO_3)(HCO_3)_3$, barentsite $Na_7Al(CO_3)_2(HCO_3)_2F_4$, nahpoite Na_2HPO_4, dorfmanite $Na_2HPO_4\cdot 2H_2O$) in peralkaline agpaitic pegmatites of the Khibiny-Lovozero alkaline complex. However, it should be noted that the pH values of aqueous solutions of $NaHCO_3$ and Na_2HPO_4 are above 7.

The appearance of **hydronium groups** H_3O^+ in the IR spectra of solids still remains a debatable matter. The available data discussed in (Chukanov 2014a) are rather controversial. In most cases IR spectra of hydronium minerals contain bands (at least weak ones or shoulders) in the range from 1700 to 1800 cm^{-1}. For trögerite ["hydrogen uranospinite", $(H_3O)(UO_2)(AsO_4)\cdot 3H_2O$], the IR absorption band at 1740 cm^{-1} was indicated by Wilkins et al. (1974). Similar bands are present in the IR spectra of chernikovite $(H_3O)(UO_2)(PO_4)\cdot 3H_2O$ (Fig. 1.46). Unlike synthetic analogue of chernikovite, natural sample gives in the IR spectrum an additional weak but distinct band at 1402 cm^{-1} which indicates possible partial dissociation of hydronium anions to form solvated proton.

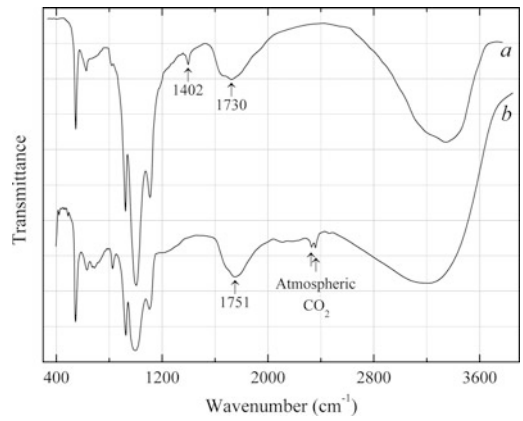

Fig. 1.46 The IR spectra of chernikovite $(H_3O)_xCa_{0.12}Na_{0.08}(UO_2)_{1.15}[(PO_4)_{0.97}(AsO_4)_{0.03}]\cdot nH_2O$ from the uranium deposit Djedeli, Kazakhstan (*a*) and synthetic analogue of chernikovite drawn using data from van Haverbeke et al. (1996) (*b*). The spectrum of chernikovite was obtained by N.V. Chukanov. Spectra have been offset for comparison

Hydrated protons in liquid water reveal a quasi-continuum absorption, which makes the assignment of IR specific bands to these cations difficult. The band around 1740 cm^{-1} is indicative of the monohydrated H_3O^+ cation (i.e. Zundel cation, $H_5O_2^+$), but not of the Eigen cation, $H^+(H_2O)_4$. Experimental vibrational frequencies 1741 and 1725 cm^{-1} in the infrared multiphoton dissociation spectra have been tentatively assigned to equatorial bending vibrations of H_3O^+ in gas-phase Zundel and Eigen cations, respectively (Kulig and Agmon 2014, Kaposta 2005). The calculated vibrational spectra for $H_5O_2^+ \cdot Ar$ are in good agreement with the experimental infrared spectra showing the characteristic Zundel frequency at $\sim$1770 cm^{-1} (Park et al. 2007). Consequently, bands in the range from 1700 to 1800 cm^{-1} can be considered as an indicator of hydronium cation and other forms of hydrated proton in minerals.

In a natural hydroniumjarosite sample with the empirical formula $(H_3O)^+_{0.77}(Na_{0.20}K_{0.02})S_{0.22}(Fe_{2.95}Al_{0.03})[(SO_4)_{1.97}(SiO_4)_{0.03}](OH)_{6.12}$, a local environment of the O4 atom, which could correspond to two alternating orientations of the H_3O^+ cations, was documented in difference Fourier maps (Plášil et al. 2014), although the same configuration could correspond to water molecules disordered between 6 orientations. For this sample, the authors indicate the presence of a band at 1715 cm^{-1} in the IR spectrum. However, the figure of the IR spectrum from the cited paper does not show the presence of a peak or a shoulder at this frequency. IR spectrum of hydroniumjarosite from Morro Mejillones, Chile (the spectrum **S320** in this book) shows an asymmetric band at the frequency 1653 cm^{-1}, which is typical for bending vibrations of H_2O molecules, but does not show distinct features in the range from 1700 to 1800 cm^{-1}. The empirical formula of this sample could be written as follows: $Na_{0.02}Fe_{3.03}(SO_4)_2(OH,H_2O)_n$. Note that the single-crystal X-ray study of a synthetic analogue of hydroniumjarosite did not reveal the position of the H atoms in the H_3O^+ group: these H atoms were not evident in difference-Fourier maps (Majzlan et al. 2004). The IR spectrum of this sample contains a band at 1637 cm^{-1} and a weaker band at somewhat lower frequency, which can correspond to the presence of water molecules of two types. Consequently, hypothetically, the correct idealized formula of hydroniumjarosite may be $(H_2O)Fe^{3+}_3(SO_4)_2(OH)_5 \cdot H_2O$. However, this matter needs further investigation.

1.8 Isolated Molecules (CO_2, CO, NH_3, $B(OH)_3$, and Hydrocarbons) in Crystal Structures of Minerals

Most minerals occur as ionic compounds, but many of them (almost a third of all known mineral species) contain water of hydration, i.e. water molecules that are a part of the crystalline structure. H_2O is the most common neutral molecule in minerals. Among water-bearing solids, one can distinguish stoichiometric crystalline hydrates, compounds with layered structures containing variable amounts of interlayer H_2O molecules (e.g. smectites and some other clay minerals, heterophyllosilicates (Ferraris and Gula 2005), autunite-group members etc.) and compounds with zeolite water in structural channels and cages (zeolites *s.s.*, zeolite-like minerals with heteropolyhedral frameworks (Chukanov and Pekov 2005), cancrinite-group minerals etc.). Crystal chemistry, hydrogen bonding and IR spectroscopic characteristics of water in minerals and synthetic solids are discussed in numerous publications, and these subjects aren't discussed in this section.

The molecules NH_3, N_2, CH_4, and BO_3 are known as major and species-defining components in some minerals, whereas CO_2, CO, H_2 and some other small molecules are may be present as minor components entrapped in channels and structural cavities of minerals with microporous and framework structures. However, as a rule, diatomic molecules N_2, H_2 and O_2 cannot be detected by means of IR spectroscopy because their stretching modes are practically IR inactive. The forbidden 2328.2 cm^{-1} N_2 stretching fundamental is only seen in ices because interactions of N_2 with neighboring

molecules leads to polarization and symmetry breaking. The strength of the N≡N-stretching band near 2328 cm^{-1} is moderately enhanced in the presence of NH_3, strongly enhanced in the presence of H_2O and very strongly enhanced (by over a factor of 1000) in the presence of CO_2 (Bernstein and Sandford 1999).

In this section we will consider IR spectroscopic characteristics of some isolated small molecules (other than H_2O, N_2, H_2 and O_2) in minerals.

Minerals belonging to the **cordierite-sekaninaite** solid-solution series, $(Mg,Fe)_2(Al_4Si_5O_{18})$, are able to trap significant amounts of molecular H_2O, carbon oxides and nitrogen (Goldman et al. 1977; Armbruster et al. 1982; Armbruster and Bloss 1982; Armbruster 1985; Vry et al. 1990; Della Ventura et al. 2006; Hervig et al. 2014). For this reason, cordierite-group minerals are considered as a useful tool to characterize volatile components in mineral-forming media. The content of CO_2 in cordierite varies in a wide range, from amounts undetectable by means of IR spectroscopy (Aines and Rossman 1984) to 2.4 wt% (Khomenko and Langer 2005).

Narrow IR absorption bands in the range from 2100 to 2400 cm^{-1} in single-crystal polarized IR spectra of cordierite from Allumiere, Latium, Italy have been assigned to C = O-stretching vibrations of CO_2 and CO molecules oriented ‖ *a* (Della Ventura et al. 2006). In particular, it was shown that the bands corresponding to $^{12}C^{16}O_2$, $^{13}C^{16}O_2$, $^{12}C^{16}O^{18}O$ and $^{12}C^{16}O$ (at 2348, 2282, 2330 and 2135 cm^{-1}, respectively) can be distinguished (Fig. 1.47).

Similar results have been obtained also by Khomenko and Langer (2005) for cordierite and sekaninaite samples from different localities. In the IR spectra of synthetic well-ordered cordierites with CO_2 introduced experimentally into structural channels, two strong bands at 2348 and 2353 cm^{-1} are related to two different types of CO_2 molecules (Le Breton 1989). The band at 2353 cm^{-1} appears at 2.6 wt% CO_2 and becomes stronger than the band at 2348 cm^{-1} in a sample containing 4.6 wt% CO_2.

FTIR investigations of hexagonal high-temperature polymorphs of cordierite and sekaninaite, i.e. indialite and ferroindialite, respectively, show the absence of the bands corresponding to volatile components CO_2, CO and H_2O (Balassone et al. 2004; Chukanov et al. 2014a). However in beryl, which is isostructural with indialite, the channels can host CO_2 molecules, which are oriented perpendicular to *c* (Wood and Nassau 1967).

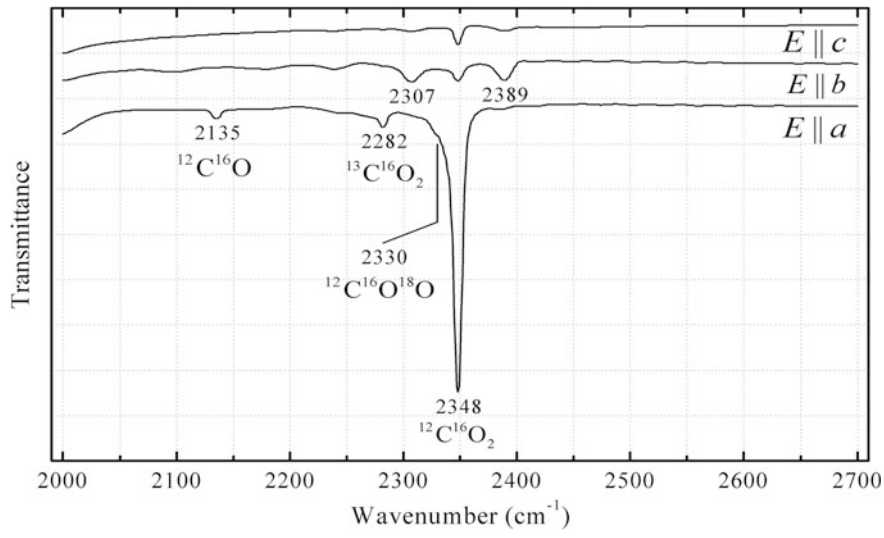

Fig. 1.47 IR absorption spectra of cordierite from Allumiere, Latium, Italy in the region of C = O-stretching vibrations collected with the electric vector polarized along the three optical directions. The picture is drawn using data from Della Ventura et al. (2006)

Feldspathoids of the **cancrinite group** (Bonaccorsi and Merlino 2005) are hexagonal and trigonal tecto-aluminosilicates with frameworks consisting of layers containing six-membered rings of Si- and Al-centered tetrahedra perpendicular to the *c* axis. The rings centered by 6-fold or 3-fold axes [1/3 2/3 *z*], [2/3 1/3 *z*] and [0 0 *z*] are usually denoted by the letters *A*, *B,* and *C*, respectively. Rings of each type form layers (levels). Every ring is linked to three rings of the preceding layer and to three rings of the succeeding layer. The stacking of the *A*, *B*, *C* layers along the *c* axis determines the type of the framework that contains zeolitic cavities forming channels running along [001]. The channels host extra-framework cations (major: Na^+, Ca^{2+}, K^+), anions (species-defining: CO_3^{2-}, SO_4^{2-}, Cl^-, OH^-, S^{2-}, $C_2O_4^{2-}$, PO_4^{3-}), and, in many cases, H_2O molecules. Carbon dioxide is a minor, but a typical constituent present in channels of cancrinite-group minerals.

Polarized-light FTIR spectra of a single crystal of the cancrinite-group mineral **pitiglianoite** $K_2Na_6(Si_6Al_6O_{24})(SO_4)\cdot 2H_2O$ from Monte Cavalluccio, Sacrofano, Rome, Italy show a sharp band at 2351 cm^{-1} having maximum absorption with $E \perp c$, suggesting that the linear CO_2 molecules are oriented perpendicular to the crystallographic *c* axis, as in beryl or cordierite (Della Ventura et al. 2005a). Similar bands at 2351 and 2352 cm^{-1} are observed in the IR spectra of **vishnevite**, $(Na,K)_2Na_6(Si_6Al_6O_{24})(SO_4)\cdot 2H_2O$, a mineral closely related to pitiglianoite, and the 14-1ayer cancrinite-group mineral **farneseite**, $(Na,K)_{46}Ca_{10}(Si_{42}Al_{42}O_{168})(SO_4)_{12}\cdot 3H_2O$, respectively (Della Ventura et al. 2007a; Cámara et al. 2005; Fig. 1.48). In the IR spectrum of the 33-1ayer cancrinite-group mineral **fantappièite**, ideally $[(Na,K)_{99}Ca_{33}](Si_{99}Al_{99}O_{396})(SO_4)_{33}\cdot 6H_2O$, the band of antisymmetric vibrations of CO_2 molecules is observed at 2338 cm^{-1} (Cámara et al. 2010). Channels of both minerals, farneseite and fantappièite, contain liottite, sodalite, and cancrinite cages, alternating along *c*. Consequently, one can suppose that different positions of the bands of CO_2 molecules of these minerals may be due to different local surroundings of CO_2. The band of antisymmetric vibrations of CO_2 molecules of the 36-layer cancrinite-group mineral **kircherite**, $Na_{90}K_{18}Ca_{36}(Si_{108}Al_{108}O_{432})(SO_4)_{36}\cdot 6H_2O$, whose channel contains alternating cancrinite, sodalite, and losod cages, is observed at the same frequency 2338 cm^{-1}, as in case of fantappièite, whereas for marinellite, $(Na,K)_{42}Ca_6(Si_{36}Al_{36}O_{144})(SO_4)_8Cl_2\cdot 3H_2O$, containing cancrinite, sodalite and liottite cages, this band is observed at 2352 cm^{-1}, i.e. practically at the same frequency as for pitiglianoite and farneseite (Cámara et al. 2012). These data show that CO_2 molecules in cancrinite-group minerals can be present in two distinct kinds of locally different states, but each sample contains only one type of CO_2.

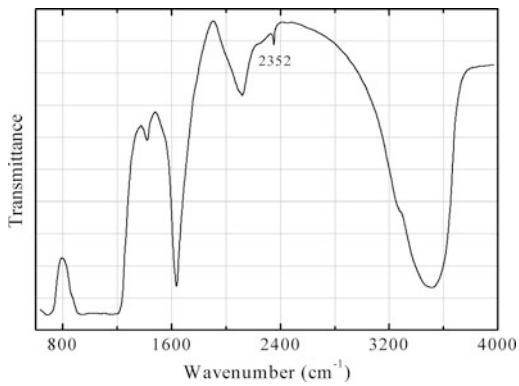

Fig. 1.48 Unpolarised single-crystal FTIR spectrum of farneseite drawn using data from Cámara et al. (2005)

Single-crystal FTIR spectroscopy shows that haüyne and nosean typically contain enclathrated CO_2 molecules, in addition to H_2O and minor carbonate, while sodalite is virtually CO_2-free (Bellatreccia et al. 2009b). The band at 2338 cm^{-1} observed in IR spectra of some cancrinite-group minerals, is close to the band at 2340 cm^{-1}, assigned to $^{12}CO_2$ in the IR spectrum of a sodalite-group mineral from the Somma-Vesuvius volcanic complex, Italy, with the empirical formula $(Ca_{0.98}Na_{6.02}K_{0.56}Mg_{0.02}Sr_{0.01}Fe_{0.01})(Si_{5.94}Al_{6.07}O_{24})(SO_4)_{1.27}Cl_{0.40}F_{0.02}\cdot nH_2O$, described as "sulfatic sodalite" (Balassone et al. 2012; see Fig. 1.49). In the strict sense, this mineral is not sodalite, but a Cl-bearing member of the haüyne-nosean solid-solution series. A very weak but well resolved band at 2274 cm^{-1} in the IR

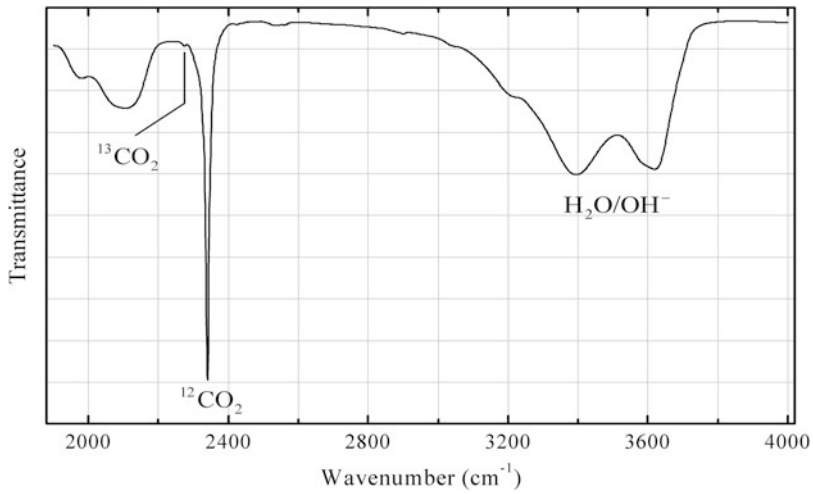

Fig. 1.49 Single crystal, unpolarized FTIR spectrum of a Cl-bearing member of the solid-solution series haüyne-nosean from a K-feldspar-rich syenitic rock of the Somma-Vesuvius volcanic complex. The picture is drawn using data from Balassone et al. (2012)

spectrum of this sample was assigned to the antisymmetric stretching absorption of $^{13}CO_2$. In the IR spectrum of sodalite *s.s.* from the same locality bands of CO_2 are absent.

Based on the above data for the minerals belonging to the cancrinite and the sodalite groups, one can suppose that the band observed at 2338–2340 cm^{-1} may correspond to CO_2 molecules in sodalite cavities of samples enriched in SO_4^{2-}.

The crystal structure of **capranicaite**, $KCaNaAl_4B_4Si_2O_{18}$, is based on a bi-dimensional tetrahedral network characterized by large channels (Callegari et al. 2011). A weak but sharp band at 2341 cm^{-1} observed in the IR spectrum of capranicaite (Fig. 1.50) was assigned to CO_2 molecules which could be located in cavities incompletely occupied by K and minor Cs. Estimated CO_2 content is in the order of hundreds of ppm.

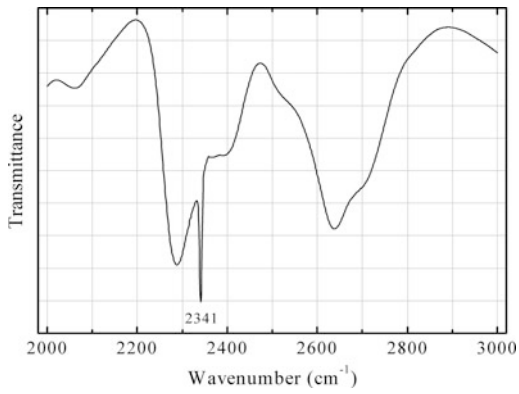

Fig. 1.50 Single-crystal, unpolarized FTIR spectrum of capranicaite drawn using data from Callegari et al. (2011). Broad bands correspond to overtones of B–O-stretching vibrations

A relatively weak but extremely sharp peak at 2348 cm^{-1} in the single-crystal FTIR spectrum of **pollucite** from Maine, USA shows that this mineral also contains CO_2 molecules in structural cavities (Bellatreccia et al. 2012).

Melanophlogite is a clathrate compound which consists of a 3-dimensional host framework of SiO_4 tetrahedra and guest molecules N_2, CO_2, and CH_4 entrapped within the cages of the host structure (Gies 1983; Nakagawa et al. 2001; Kolesov and Geiger 2000). Among known mineral species, melanophlogite is most enriched in carbon dioxide: it contains about 3 wt% CO_2. The molecules of carbon dioxide located in the $[5^{12}6^2]$ cages can rotate and are statistically distributed between 12 possible equivalent orientations. The IR spectrum of melanophlogite from Rio Fortullino, Lovorno province, Tuscany, Italy contains a strong band at 2330-2336 cm^{-1} (see Fig. 1.51a). A weaker peak at ~2375 cm^{-1} present it IR spectra of some melanophlogite samples

from this locality (Chukanov 2014a) may be due to rotational splitting or correspond to a minor amount of CO_2 molecules in the $[5^{12}]$ cages, which are predominantly occupied by CH_4.

About 20 mineral species are organic compounds forming molecular crystals, i.e. crystals consisting of neutral molecules. Among them, there are 9 unsaturated hydrocarbons, one saturated hydrocarbon (evenkite) and about 10 O- and N-bearing organic compounds. Molecules of hydrocarbons can occur also in ionic and covalent crystals. Melanophlogite and chibaite are the examples of such minerals.

In melanophlogite from Mt. Hamilton, California, USA the occupancy factor of the CH_4 site in the $[5^{12}]$ cage is about 90 % (Gies 1983). The bands at 2900 and 2909 cm^{-1} in the single-crystal Raman spectrum of melanophlogite from this locality have been assigned to asymmetric stretching modes of CH_4 located in the $[5^{12}]$ and $[5^{12}6^2]$ cages, respectively (Kolesov and Geiger 2003). However powder IR spectra of melanophlogite from other localities do not show any presence of methane molecules. In the frequency range from 2800 to 3000 cm^{-1}, a sample from Chvaletice, Bohemia shows the presence of three overlapping, relatively broad bands indicative of the contamination by a polyatomic aliphatic hydrocarbon, most probably grease (Žák 1972). Similar, but much weaker bands are present in the IR spectrum of melanophlogite from Fortullino, Italy (Fig. 1.51b), but no characteristic bands of methane are observed in this spectrum too. Instead, weak bands of O–H-stretching vibrations are observed at 3598 and 3702 cm^{-1}. Apparently, this matter needs clarification.

For **chibaite**, $Na_x(Si_{136-x}Al_x)O_{272}\cdot(CH_4, C_2H_6, C_3H_8, C_4H_{10})_{24-x}$, only Raman spectrum is published (Momma et al. 2011). It contains characteristic bands of methane and several higher aliphatic hydrocarbons (Fig. 1.52).

Until recently, coordination compounds containing ammonia molecules were unknown in nature. Zinc ammine complex $ZnCl_2(NH_3)_2$ was described as technogenetic compound from burned dumps of the Chelyabinsk coal basin, South Urals, Russia under the name "**amminite**" (Chesnokov et al. 1991). Not long ago, a copper analogue of "amminite", **ammineite** $CuCl_2(NH_3)_2$ was discovered in the guano deposit on the Mt. Pabellón de Pica, Iquique Province, Tarapacá Region, Chile (Bojar et al. 2010). Now four valid minerals with neutral ammonia molecule NH_3 as a species-defining component are

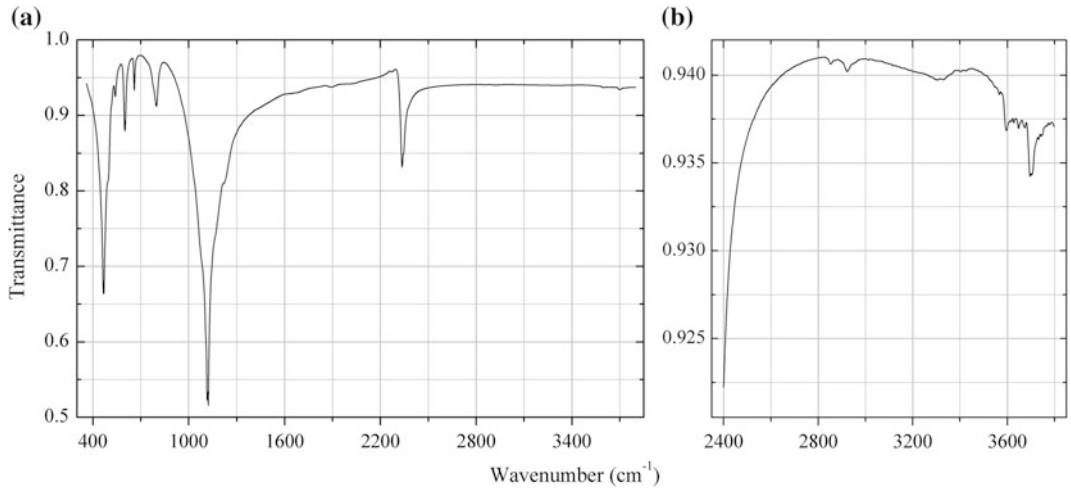

Fig. 1.51 Powder IR spectrum of melanophlogite from Fortullino, Italy (**a**) and an enlarged fragment of this spectrum in the range 2400–3800 cm^{-1} (**b**). The spectrum was obtained by N.V. Chukanov

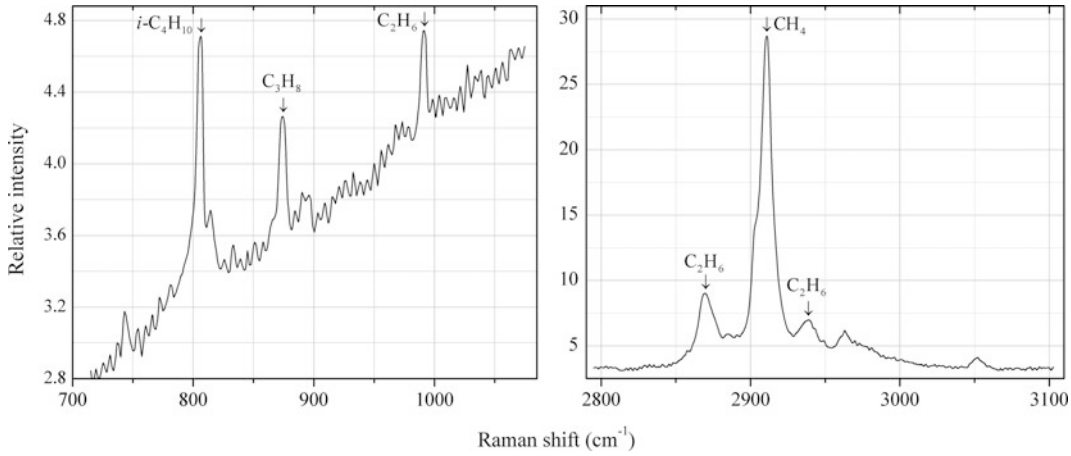

Fig. 1.52 Raman spectra of hydrocarbons in chibaite drawn using data from Momma et al. (2011)

known: ammineite, $CuCl_2(NH_3)_2$, **joanneumite**, $Cu(C_3N_3O_3H_2)_2(NH_3)_2$ (Bojar and Walter 2012), **chanabayaite**, $Cu_4(N_3C_2H_2)_4(NH_3)_4Cl_2(Cl,OH)_2 \cdot H_2O$ (Chukanov et al. 2015b) and **shilovite**, $Cu(NH_3)_4(NO_3)_2$ (Chukanov et al. 2014b, 2015c). All these minerals have been discovered at Pabellón de Pica, and in all these minerals ammonia molecules coordinate Cu^{2+}. Isocyanurate and triazolate anions occur as additional ligands in joanneumite and chanabayaite, respectively. In shilovite Cu^{2+} cation coordinated by four ammonia molecules forms complex copper(II) tetrammine cation $[Cu(NH_3)_4]^{2+}$. Characteristic bands of NH_3 molecules in these compounds are given in Table 1.15. The band of symmetric bending vibrations of NH_3 is very sensitive to the strengths of hydrogen bonds NH···A. This results in a strong splitting of this band in the IR spectra of shilovite and chanabayaite.

Sassolite (crystalline boric acid) consists of layers of $B(OH)_3$ molecules held together by hydrogen bonds (Greenwood and Earnshaw 1997). The wavenumbers (cm^{-1}) of the strongest bands in the IR spectrum of sassolite (Chukanov 2014a) correspond to the following vibrations:

Table 1.15 Assignment of characteristic bands of NH_3 molecules in minerals and "amminite"

Assignment of the bands	"Amminite"	Ammineite	Shilovite	Joanneumite	Chanabayaite
	Wavenumbers, cm^{-1}				
N–H-stretching	3330, 3253, 3195, 3160	3316, 3241, 3157	3472	3415, 3268, 3186	3430[a], 3369[a], 3310, 3253, 3233, 3173
Degenerate bending	1605	1594	1650	1634, 1610	1646[a], 1636[a], 1620[a]
Symmetric bending	1247	1245	1361, 1159	1254	1299, 1269, 1198, 1173
Libration	688, 667, 638	716, 661	639, 624	692	667
M–N-stretching	460, (413)	480	485, 463	455, 432	(470)
Source	Chukanov (2014a)	Bojar et al. (2010)	This book	Chukanov (2014a)	This book

[a]The bands possibly overlapping with those of H_2O molecules

3214 (O–H-stretching), 1456 (asymmetric B–O stretching), 1195 (B–O–H in-plane bending), 807 (B–O–H out-of-plane bending), 648, 548 (O–B–O bending) (see Peak et al. 2003). A weaker band at 884 cm^{-1} corresponds to symmetric B–O stretching vibrations.

The molecules $B(OH)_3$ occur, along with the anions $B(OH)_4^-$, in some boron-bearing ettringite-group minerals. For example, the crystal-chemical formula of sturmanite from the Black Rock mine, Kuruman District, South Africa, determined from its crystal structure refinement, is $Ca_6[Fe_{0.6}Al_{0.2}Mn^{2+}_{0.2}]_2(SO_4)_{2.6}[B(OH)_3]_{0.6}[B(OH)_4]_{0.4}(OH)_{12}\cdot 23.1H_2O$ (Pushcharovsky et al. 2004). Unfortunately, most bands of boron-bearing groups overlap with strong bands of ettringite-group minerals. The presence of the groups $B(OH)_3$ and $B(OH)_4^-$ can be reliably detected only by the bands in the ranges 1200–1250 and 950–1000 cm^{-1}, respectively. IR spectra of boron-free ettringite-group minerals don't contain these bands. Usually the band between 1200 and 1250 cm^{-1} is observed as a shoulder. The strongest band in this region (with the absorption maximum at 1232 cm^{-1}) is present in the IR spectrum of buryatite, $Ca_3(Si,Fe^{3+},Al)(SO_4)[B(OH)_4,B(OH)_3](OH)_5O\cdot 12H_2O$ (Fig. 1.53).

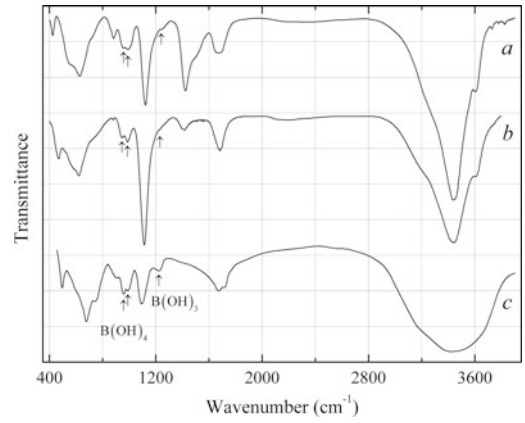

Fig. 1.53 IR spectra of (*a*) CO_3-rich charlesite (drawn using data from Kumarathasan et al. 1989), (*b*) sturmanite from the Black Rock mine, South Africa (the spectrum obtained by N.V. Chukanov) and (*c*) buryatite from the Fuka mine, Japan (drawn using data from Chukanov 2014a)

IR Spectra of Minerals and Related Compounds, and Reference Samples' Data

2

This chapter contains IR spectra of mineral species and varieties, most of which was not included in the preceding reference book (Chukanov 2014a). Along with spectra obtained by us, we provide the most reliable data on the infrared spectra of minerals published elsewhere during the last 60 years. Each spectrum is accompanied with analytical data on the reference sample, its occurrence and general appearance, associated minerals, as well as kind of sample preparation and/or method of registration of the spectrum. In addition, we provide IR spectra of some synthetic compounds which are chemically or structurally related to any known minerals or may be hypothetically considered as synthetic analogs of potentially new mineral species.

Sections 2.1, 2.2, 2.3, etc. are arranged in ascending order of the atomic number Z_a of the main species-defining element for a given class of minerals: first for borate minerals (with $Z_a = 5$ for boron), than for carbon, carbides, carbonates, and organic substances (with $Z_a = 6$ for carbon), for nitrates (with $Z_a = 7$ for nitrogen), for oxides and hydroxides (with $Z_a = 8$ for oxygen) and so on.

About 300 spectra presented in this chapter have been obtained by one of the authors (NVC). In order to obtain absorption infrared spectra, powdered mineral samples have been mixed with anhydrous KBr, pelletized, and analysed using ALPHA FT IR spectrometer (Bruker Optics, Ettlingen, Germany) with a resolution of 4 cm^{-1} and 16 scans. IR spectrum of an analogous disc of pure KBr was used as a reference. It is important to note that reflectance mode IR spectra, IR spectra obtained without immersion medium (e.g. KBr), as well as IR spectra of single crystals, coarse-grained or textured aggregates cannot be considered as stable and reliable diagnostic characteristics of mineral species due to specific effects induced by orientation, polarization, scattering, and reflection conditions. For example, in case of a single crystal, bands corresponding to normal vibrations with polarization vector parallel to the direction of propagation of IR radiation are absent in the spectrum. However these bands can be observed at another orientation of the crystal. In more detail these aspects were considered above (see section Sources of Errors and Artifacts in IR Spectroscopy of Minerals in this book). For the above reasons, **only transmittance or absorbance IR spectrum of a pulverized sample dispersed in an immersion medium is a stable characteristic of a mineral and can be used as a diagnostic tool**.

Additional information includes general appearance, associated minerals, methods of the mineral species identification, and the list of wavenumbers of absorption bands with the indication of strong bands, weak bands and shoulders. IR spectroscopy itself can be considered as an adequate identification method if IR spectrum is unique for a given mineral and coincides with IR spectrum of a well-investigated sample. For most synthetic samples the method of synthesis is shortly characterized.

N.V. Chukanov and A.D. Chervonnyi, *Infrared Spectroscopy of Minerals and Related Compounds*, Springer Mineralogy, DOI 10.1007/978-3-319-25349-7_2

For 603 samples empirical formulae are given. For more than 400 samples (mainly holotypes of mineral species), a more detailed information is given including unit-cell dimensions, symmetry, strongest reflections of the powder X-ray diffraction pattern, empirical formula, optical data, density, etc.

The following **abbreviations** are used in this chapter:

Mt.	Mountain
Co.	County
IR	Infrared
D	Density
D_{meas}	Measured density
D_{calc}	Calculated density
apfu	Atoms per formula unit
Z	The number of formula units per unit cell
α, β, γ	Refractive indices for biaxial minerals
ω, ε	Refractive indices for uniaxial minerals
n	Refractive index for isotropic minerals
$2V$	Angle between optic axes
d	Interplanar spacing
I	Relative intensity of a line in the powder X-ray diffraction pattern
REE	Rare-earth elements
Ln	Lanthanides
s	Strong band
w	Weak band
sh	Shoulder
□	Vacancy

In most cases the terms "strong band" and "weak band" mean band having transmittance minimum below and above any conventional values, respectively. As a rule, "shoulder" means inflection point of the spectral curve. For the convenience of visual perception, the positions of all peaks and shoulders in the figures are indicated by arrows.

For the numeration of samples, double letter-figure symbols are used. The same numeration is used in this chapter for figure captions. The meaning of letter parts of the symbols is explained in Table 2.1. Note that these designations are conventional and not unambiguous. For example, zirsilite-(Ce), $Na_{12-x}(Ce,Na)_3Ca_6Mn_3Zr_3NbSi_{25}O_{73}(OH)_3(CO_3)\cdot H_2O$, can be classified as cyclosilicate, as zirconosilicate or as carbonatosilicate.

Table 2.1 The meaning of letter symbols used in the numbering of reference samples

Symbol	Meaning of the symbol	Symbol	Meaning of the symbol
Bo	Borates with isolated orthogroups BO_3	CSi	Carbonato-silicates
B	Other borates	PSi	Phosphato-silicates
BC	Carbonatoborates	SSi	Sulfato-silicates
BAs	Arsenatoborates	TiSi	Titanosilicates and related zircono-, niobo- and stannosilicates (except heterophyllosilicates and minerals belongitg to the labuntsovite and the eudialyte groups)
C	Carbon and carbonates	AsSi	Arsenato-silicates
Org	Organic compounds and salts of organic acids	USi	Silicates with uranyl groups UO_2^{2+} (except nesosilicates)
N	Nitrides and nitrates	P	Phosphides and phosphates
O	Oxides and hydroxides	S	Sulfates
F	Fluorides	SC	Carbonato-sulfates
FCl	Chloridofluorides	SP	Phosphato-sulfates
Sio	Nesosilicates (i.e. silicates with orthogroups SiO_4)	SMo	Sulfatomolybdates
Sid	Sorosilicates (i.e. silicates with diorthogroups Si_2O_7 or $SiAlO_7$)	Cl	Chlorides and hydroxychlorides

(continued)

Table 2.1 (continued)

Symbol	Meaning of the symbol	Symbol	Meaning of the symbol
Siod	Silicates containing both orthogroups SiO_4 and diorthogroups Si_2O_7	V	Vanadates, V oxides, and hydroxides
Sit	Triorthosilicates with groups Si_3O_{10}	Cr	Chromates
Siot	Ortho-triorthosilicates	Ge	Germanates
Sir	Cyclosilicates ("r" means "ring")	As	Arsenic, arsenides, arsenites, arsenates, and sulfato-arsenates
Sic	Inosilicates with chains formed by SiO_4 and AlO_4 tetrahedra	UAs	Uranyl arsenates
Sib	Inosilicates with bands formed by SiO_4 and AlO_4 tetrahedra	AsS	Sulfato-arsenates
Sil	Phyllosilicates with layers formed by SiO_4 and AlO_4 tetrahedra	Sb	Antimonides and antimonates
Sif	Tectosilicates (aluminosilicates with 3d frameworks formed by SiO_4 and AlO_4 tetrahedra), except zeolites	Br	Bromides and bromates
Sif_Z	Zeolites	Se	Selenium, selenides, and selenites
Si	Silicon, silicides, and silicates with unknown or complex structures	Mo	Molybdates, and Mo-beariung oxides
Sia	Amorphous silicates	Te	Tellurides, tellurites, and tellurates
BeSi	Beryllosilicates	I	Iodides, iodites, and iodates
BSi	Borosilicates and borato-silicates	W	Tungstates and W-bearing oxides

2.1 Borates, Including Arsenatoborates and Carbonatoborates

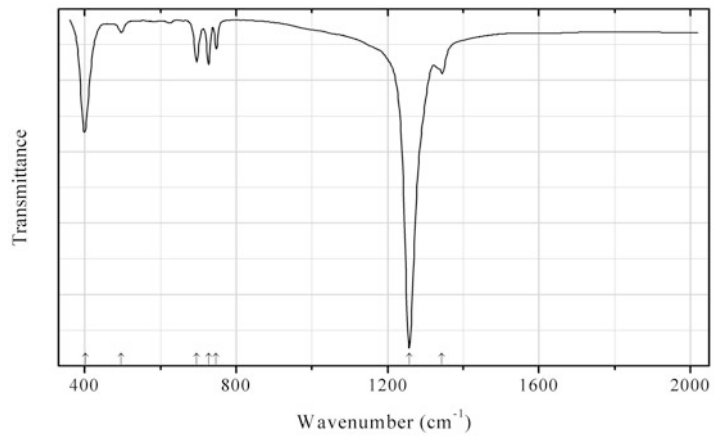

Fig. 2.1 IR spectrum of chubarovite obtained by N.V. Chukanov

Bo32 Chubarovite $KZn_2(BO_3)Cl_2$ (Fig. 2.1)
Locality: Arsenatnaya fumarole, Second scoria cone of the Northern Breakthrough of the Great Tolbachik Fissure Eruption, Tolbachik volcano, Kamchatka peninsula, Russia (type locality).

Description: Colourless crystals from the association with hematite, tenorite, fluoborite, krasheninnikovite, sylvite, steklite, langbeinite, calciolangbeinite, palmierite, wulffite, alumoklyuchevskite, ericlaxmanite, kozyrevskite, popovite, etc. Holotype sample. Trigonal, space group *R*32, a = 4.9431 (4), c = 26.3461(19) Å, V = 557.50(8) Å^3, Z = 3. D_{meas} = 2.68(2) g/cm^3, D_{calc} = 2.716 g/cm^3. Optically uniaxial (−), ω = 1.541(2), ε = 1.539(2). The empirical formula is $(K_{1.05}Rb_{0.01})Zn_{2.00}B_{0.95}O_{2.92}Cl_{2.08}$. The strongest lines of the powder X-ray diffraction pattern [*d*, Å (*I*, %) (*hkl*)] are: 8.79 (100) (003), 4.394 (43) (006), 4.225 (25) (101), 4.074 (91) (012), 3.590 (90) (104), 3.324 (30) (015), 2.470 (67) (110), 2.245 (25) (1.0.10).
Kind of sample preparation and/or method of registration of the spectrum: KBr disc. Absorption.
Wavenumbers (cm^{-1}): 1344, 1257s, 747, 727, 695, 496w, 402s.

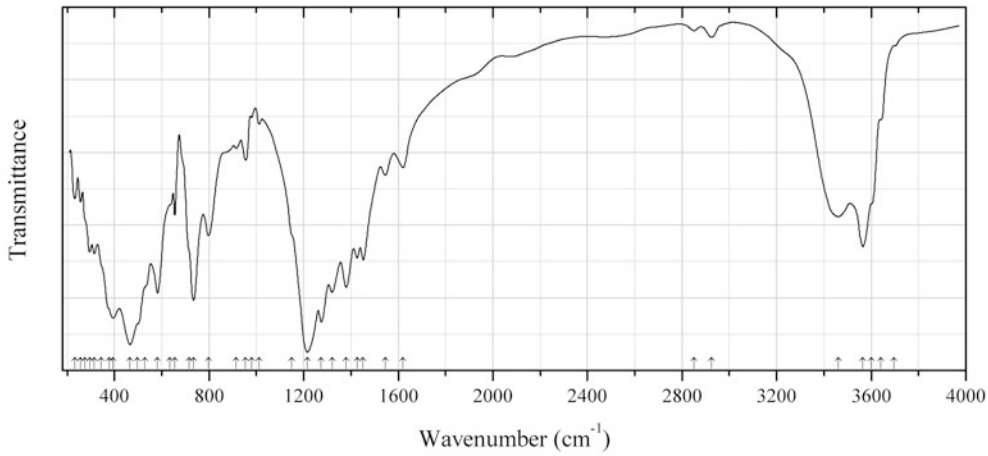

Fig. 2.2 IR spectrum of karlite drawn using data from Franz et al. (1981)

Bo33 Karlite $(Mg,Al)_7(BO_3)_3(OH,Cl,O)_5$ (Fig. 2.2)
Locality: Schlegeistal, Zillertaler Alps, Austria (type locality).
Description: Light green aggregates of acicular crystals. Holotype sample. Orthorhombic, space group $P2_12_12_1$, a = 17.929(5), b = 17.600(5), c = 3.102(1) Å, Z = 4. D_{meas} = 2.80–2.85 g/cm^3, D_{calc} = 3.02 g/cm^3. Optically biaxial (−), α = 1.589, β = 1.632, γ = 1.634, $2V$ = 24°. The empirical formula is $(Mg_{6.60}Al_{0.26}Fe^{2+}_{0.14}Mn_{0.01}Ca_{0.01})(BO_3)_{2.97}[(OH)_{4.37}Cl_{0.42}O_{0.26}F_{0.04}]$.
Kind of sample preparation and/or method of registration of the spectrum: Transmission. Kind of sample preparation is not indicated.
Source: Franz et al. (1981).
Wavenumbers (cm^{-1}): 3695sh, 3640sh, 3600sh, 3565, 3460, 2925w, 2850w, 1620w, 1545, 1452, 1426, 1380, 1320, 1275s, 1215s, 1150sh, 1012w, 980w, 955w, 915w, 798, 735s, 715sh, 655, 635sh, 582, 530sh, 498sh, 466s, 395s, 377sh, 345sh, 315, 295, 274sh, 256, 232w.
Note: The wavenumbers were partly determined by us based on spectral curve analysis of the published spectrum. The band positions denoted by Franz et al. (1981) as 3640, 3665 and 1112 cm^{-1} were determined by us at 3460, 3565 and 1012 cm^{-1}, respectively. Weak bands in the range 2800–3000 cm^{-1} correspond to the admixture of an organic substance. The band at 1620 cm^{-1} indicates the presence of H_2O molecules.

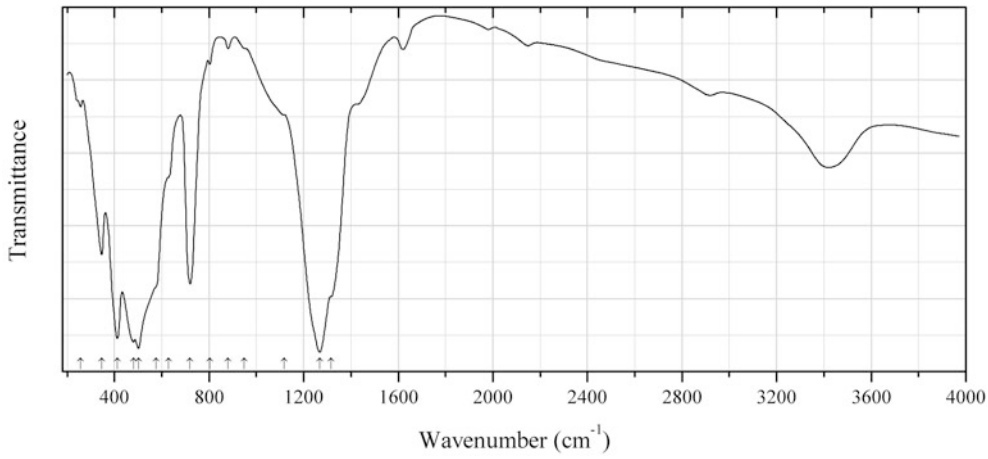

Fig. 2.3 IR spectrum of ludwigite Mg-rich drawn using data from Franz et al. (1981)

Bo34 Ludwigite Mg-rich $Mg_2Fe^{3+}(BO_3)O_2$ (Fig. 2.3)
Locality: Schlegeistal, Zillertaler Alps, Austria.
Description: Grains from the association with karlite. The content of MgO is 38.20 wt%.
Kind of sample preparation and/or method of registration of the spectrum: Transmission. Kind of sample preparation is not indicated.
Source: Franz et al. (1981).
Wavenumbers (cm^{-1}): 1315sh, 1268s, 1118sh, 950sh, 880w, 803w, 720s, 630sh, 575sh, 502s, 480s, 412s, 346, 257w.
Note: Bands with wavenumbers above 1400 cm^{-1} correspond to impurities.

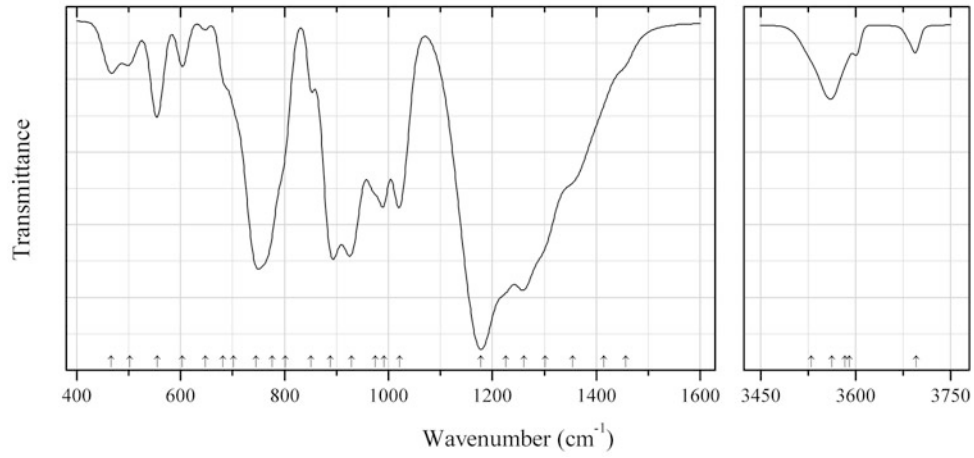

Fig. 2.4 IR spectrum of pertsevite-(OH) drawn using data from Galuskina et al. (2010)

Bo35 Pertsevite-(OH) $Mg_2(BO_3)(OH)$ (Fig. 2.4)
Locality: Snezhnoye boron deposit, Sakha-Yakutia Republic, Russia (type locality).
Description: Light brown (almost colourless) grains in a ludwigite-kotoite magnesian skarn. Holotype sample. Orthorhombic, space group *Pnma*, $a = 20.499(1)$, $b = 11.900(1)$, $c = 4.589(1)$ Å, $V = 1119.4(3)$

Å^3. D_{calc} = 3.156 g/cm^3. Optically biaxial (+), α = 1.611(1), β = 1.623(1), γ = 1.644(1), 2 V = 55–65°. The crystal-chemical formula is $(Mg_{1.95}Fe_{0.04}Mn_{0.01})(BO_3)_{0.75}(SiO_4)_{0.25}[(OH)_{0.45}F_{0.30}]$. The strongest lines of the powder X-ray diffraction pattern [d, Å (I, %) (hkl)] are: 2.7480 (61) (331), 2.4788 (42) (141), 2.4197 (35) (711), 2.2455 (86) (441), 2.2408 (45) (801), 1.7124 (100) (442), 1.7074 (47) (802), 1.4817 (51) (12.4.0).

Kind of sample preparation and/or method of registration of the spectrum: KBr disc. Absorption.

Source: Galuskina et al. (2010).

Wavenumbers (cm^{-1}): 3696, 3583sh, 3404, 3590sh, 3562, 3530sh, 1457sh, 1414sh, 1354sh, 1302sh, 1261s, 1226sh, 1178s, 1022, 992, 975sh, 929s, 888s, 851w, 802sh, 777sh, 745s, 702sh, 682sh, 648w, 604w, 555, 502w, 466w.

Note: Wavenumbers are indicated for the maxima of individual bands obtained as a result of the spectral curve analysis (in accordance with data from the cited paper).

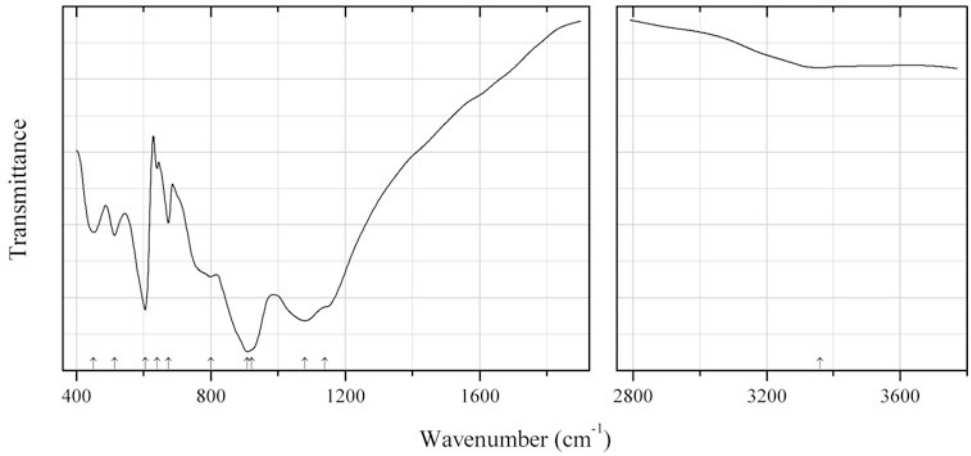

Fig. 2.5 IR spectrum of rhodizite obtained by N.V. Chukanov

B66 Rhodizite $(K,□,H_2O)Al_4(Be,Li,Al)_4(B,Be)_{12}O_{28}$ (Fig. 2.5)

Locality: Sahutany pegmatite field, Madagascar.

Description: Yellowish semitransparent well-shaped, octahedral crystals with subordinate {110} faces from the massive aggregate of potassic feldspar, albite, and quartz. Investigated by I.V. Pekov. The empirical formula is $(K_{0.67}Cs_{0.11}Rb_{0.10}Na_{0.02})Al_{4.35}B_{11.62}Be_{3.53}Li_{0.05}O_{27.94}F_{0.06}\cdot nH_2O$. Confirmed by powder X-ray diffraction data.

Kind of sample preparation and/or method of registration of the spectrum: KBr disc. Absorption.

Wavenumbers (cm^{-1}): 3360w, 1140sh, 1080s, 921sh, 909s, 800, 674, 640w, 605s, 514, 452.

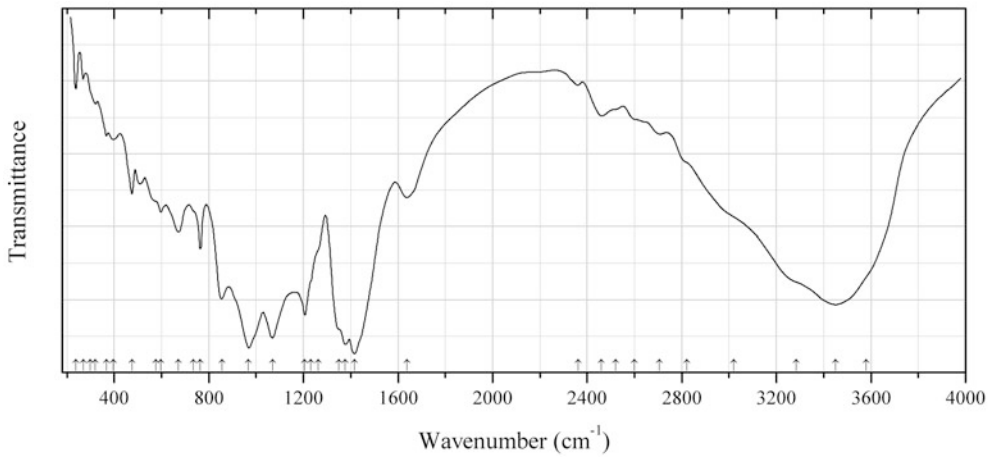

Fig. 2.6 IR spectrum of alfredstelznerite drawn using data from Galliski et al. (2010)

B120 Alfredstelznerite $Ca_4[B_4O_4(OH)_6]_4 \cdot 19H_2O$ (Fig. 2.6)
Locality: Sijes borate deposit, Salta, NW Argentina (type locality).
Description: White aggregates of acicular crystals from the association with colemanite, hydroboracite, ulexite, inyoite, gypsum, anhydrite, meyerhofferite, nobleite, gowerite, inderborite, inderite, orpiment, and realgar. Orthorhombic, space group $Pca2_1$, a = 12.161(2), b = 40.477(8), c = 10.1843(17) Å, V = 5013(3) Å^3, Z = 4. D_{meas} = 1.77(1) g/cm^3, D_{calc} = 1.775 g/cm^3. Optically biaxial (+), α = 1.476(3), β = 1.478(3), γ = 1.494(3). The strongest lines of the powder X-ray diffraction pattern [*d*, Å (*I*, %) (*hkl*)] are: 10.501 (10) (120), 5.226 (7) (201), 3.837 (7) (222), 3.118 (7b) (322), 2.612 (6) (402), 2.538 (6) (004).
Kind of sample preparation and/or method of registration of the spectrum: KBr disc. Transmission.
Source: Galliski et al. (2010).
Wavenumbers (cm^{-1}): 3580 sh, 3450s, 3285sh, 3020sh, 2823sh, 2706, 2600sh, 2520sh, 2460, 2361, 1639w, 1416, 1378, 1350sh, 1262sh, 1232sh, 1206, 1069, 968, 855, 764, 735sh, 672, 598, 575sh, 475, 396, 367, 321, 300sh, 269, 238.
Note: The wavenumbers were determined by us based on spectral curve analysis of the published spectrum.

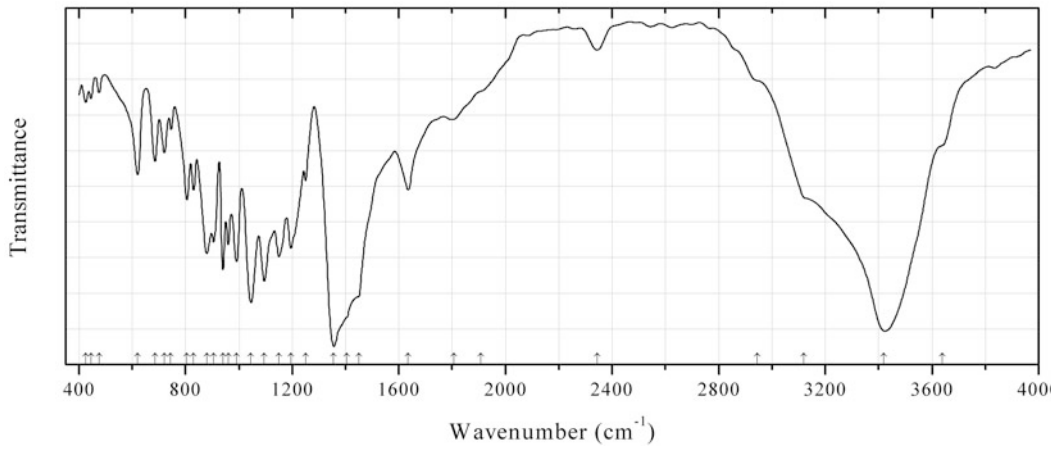

Fig. 2.7 IR spectrum of aristarainite drawn using data from Hurlbut and Erd (1974)

B121 Aristarainite $Na_2Mg[(B_6O_8(OH)_4]_2 \cdot 4H_2O$ (Fig. 2.7)
Locality: Tincalayu borax deposit, Salar del Hombre Muerto, Salta province, Argentina (type locality).
Description: Colourless crystals from the association with borax, kernite, and tincalconite. Holotype sample. Monoclinic, space group $P2_1/a$, a = 18.869(2), b = 7.531(1), c = 7.810(1) Å, β = 98.73(1)°, V = 1099.8(2) Å^3. D_{meas} = 2.027(5) g/cm^3, D_{calc} = 2.102 g/cm^3. Optically biaxial (−), α = 1.484(1), β = 1.498(1), γ = 1.523(1), 2 V = 70°. The strongest lines of the powder X-ray diffraction pattern [d, Å (I, %) (hkl)] are: 7.74 (100) (001), 5.40 (11) (011), 3.869 (12) (002), 3.037 (13) (−601), 2.579 (19) (003), 2.400 (10) (620, −403).
Kind of sample preparation and/or method of registration of the spectrum: Transmission.
Source: Hurlbut and Erd (1974).
Wavenumbers (cm^{-1}): 3640, 3420s, 3120, 2945sh, 2344w, 1908sh, 1806w, 1635, 1450sh, 1405sh, 1355s, 1250w, 1195, 1150, 1095, 1045s, 990, 960, 940, 905, 880, 830, 805, 745, 720, 685, 620, 475w, 445w, 425w.
Note: The wavenumbers were partly determined by us based on spectral curve analysis of the published spectrum.

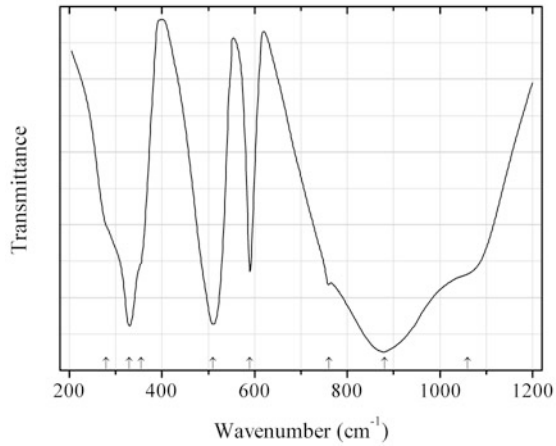

Fig. 2.8 IR spectrum of behierite drawn using data from Blasse and van den Heuvel (1973)

B122 Behierite $Ta(BO_4)$ (Fig. 2.8)
Locality: Synthetic.
Description: Identified by powder X-ray diffraction data.
Kind of sample preparation and/or method of registration of the spectrum: KBr disc. Transmission.
Source: Blasse and van den Heuvel (1973).
Wavenumbers (cm^{-1}): 1060, 880s, 760, 590, 510s, 355sh, 330s, 280sh.
Note: For the IR spectrum of behierite see also Ross (1972).

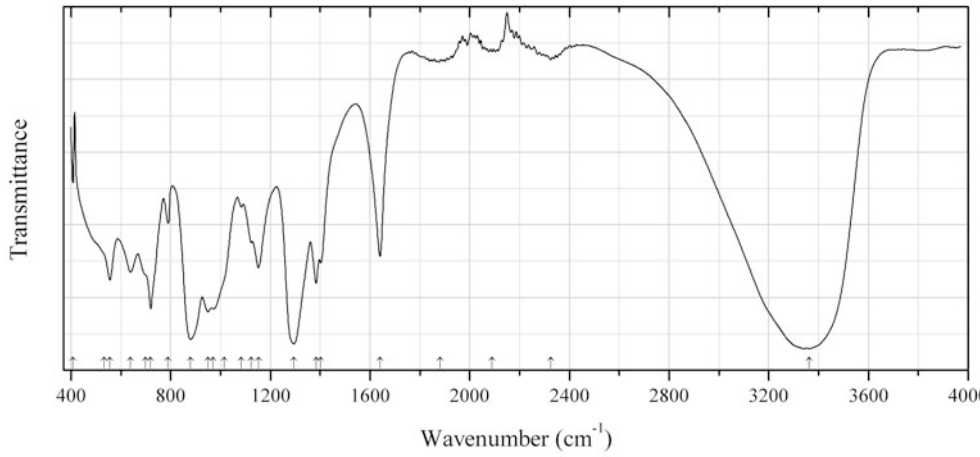

Fig. 2.9 IR spectrum of brianroulstonite drawn using data from Grice et al. (1997a)

B123 Brianroulstonite $Ca_3[B_5O_6(OH)_6](OH)Cl_2 \cdot 8H_2O$ (Fig. 2.9)
Locality: Potash Corporation of Saskarchewan (New Brunswick Division) mine, near Penobsquis, Kings Co., New Brunswick, Canada (type locality).
Description: White massive from the association with halite, hilgardite, pringleite, trembathite, sellaite, fluorite, hematite, muscovite, penobsquisite, and a clay mineral. Holotype sample. Triclinic, space group *Pa*, $a = 17.42(4)$, $b = 8.077(5)$, $c = 8.665(6)$ Å, $\beta = 121.48(7)°$, $V = 1040(2)$ Å^3, $Z = 2$. $D_{meas} = 1.97(3)$ g/cm^3, $D_{calc} = 1.93$ g/cm^3. Optically biaxial (−), $\alpha = 1.506(2)$, $\beta = 1.527(2)$, $\gamma = 1.532(2)$, $2V = 56(1)°$. The empirical formula is $(Ca_{3.00}K_{0.01})[B_5O_6(OH)_6](OH)Cl_{1.99} \cdot 8H_2O$. The strongest lines of the powder X-ray diffraction pattern [*d*, Å (*I*, %) (*hkl*)] are: 8.10 (100) (010), 4.04 (40) (020), 3.56 (20) (221), 2.834 (20) (601, 203), 2.535 (20) (230, 031), 2.276 (20) (231).
Kind of sample preparation and/or method of registration of the spectrum: Diamond-anvil cell microsampling. Transmission.
Source: Grice et al. (1997a).
Wavenumbers (cm^{-1}): 3363s, 2325w, 2090w, 1880w, 1640, 1403, 1384, 1295s, 1153, 1123, 1084, 1015sh, 971, 950, 879, 790, 720, 700sh, 638, 556, 533sh, (408).
Note: The wavenumbers were partly determined by us based on spectral curve analysis of the published spectrum. The band position denoted by Grice et al. (1997a) as 920 cm^{-1} was determined by us at 950 cm^{-1}.

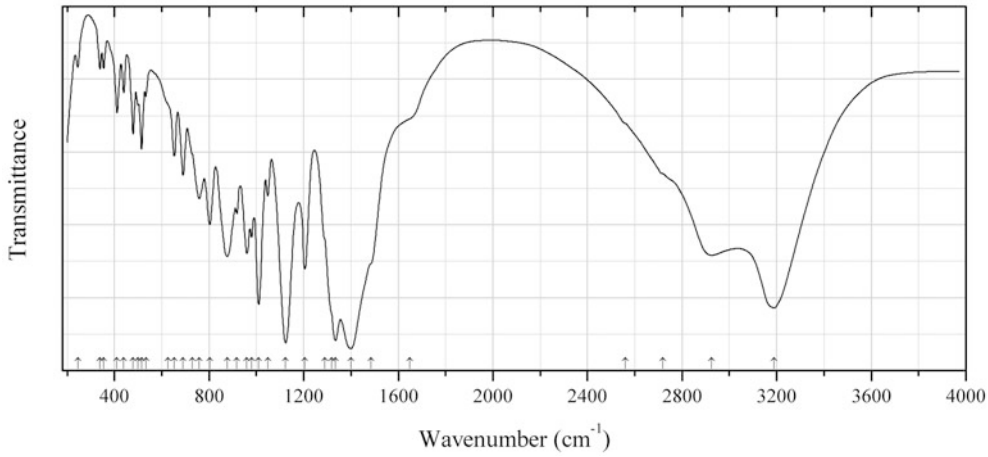

Fig. 2.10 IR spectrum of clinometaborite drawn using data from Bertoluzza et al. (1980)

B124 Clinometaborite HBO_2 (Fig. 2.10)
Locality: Synthetic.
Description: Synthesized by dehydrating of orthoboric acid at 140 °C during 78 h.
Kind of sample preparation and/or method of registration of the spectrum: Suspension in mineral oil. Transmission.
Source: Bertoluzza et al. (1980).
Wavenumbers (cm^{-1}): 3190s, 2925, (2720sh), (2560sh), 1650sh, 1485sh, 1400s, 1335s, 1318sh, 1290sh, 1205s, 1124s, 1048w, 1010s, 980w, 960, 918w, 877s, 803, 758, 730sh, 690, 653, 627sh, 533, 515, 500, 479, 439, 411, 354, 339, 245.
Note: The wavenumbers were partly determined by us based on spectral curve analysis of the published spectrum. For the IR spectrum of orthorhombic HBO_2 polymorph see Parsons (1960), Bertoluzza et al. (1980).

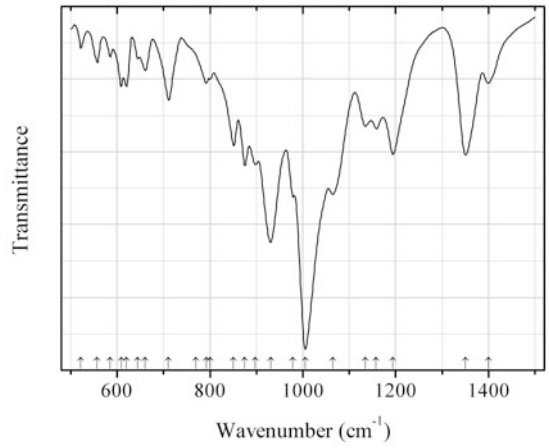

Fig. 2.11 IR spectrum of congolite drawn using data from Burns and Carpenter (1997)

B125 Congolite $Fe^{2+}{}_3B_7O_{13}Cl$ (Fig. 2.11)
Locality: Kłodawa salt dome, Mid-Polish Trough, central Poland.

Description: Euhedral crystals from the association with halite, anhydrite, quartz, calcite, hematite, chlorite, and hydromica. Confirmed by electron microprobe analysis and X-ray diffraction data. The empirical formula is $(Fe_{2.22}Mg_{0.73}Mn_{0.05})B_7O_{13}Cl$.
Kind of sample preparation and/or method of registration of the spectrum: KBr disc. Absorption.
Source: Burns and Carpenter (1997).
Wavenumbers (cm^{-1}): 1400, 1350, 1194, 1158, 1135, 1065s, 1005s, 979, 931s, 898, 875, 851, 800, 792, 770, 711, 661, 644w, 620, 609, 585w, 557w, 522w.
Note: The wavenumbers were determined by us based on spectral curve analysis of the published spectrum.

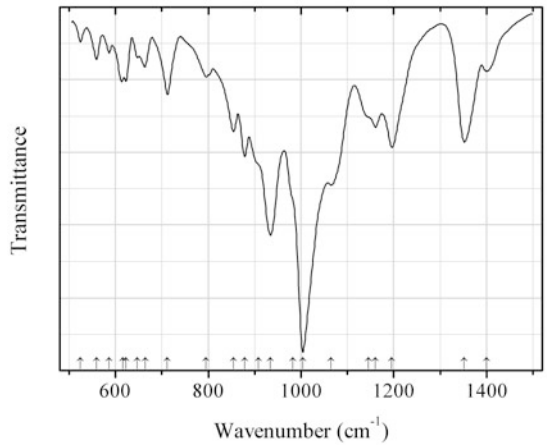

Fig. 2.12 IR spectrum of trembathite drawn using data from Burns and Carpenter (1997)

B126 Trembathite $Mg_3B_7O_{13}Cl$ (Fig. 2.12)
Locality: Salt Springs potash deposit, Sussex, New Brunswick, Canada (type locality).
Description: Crystals from the association with halite, hilgardite, hydroboracite, and boracite-group minerals. Confirmed by electron microprobe analysis and X-ray diffraction data. The empirical formula is $(Mg_{1.51}Fe_{1.47}Mn_{0.02})B_7O_{13}Cl$.
Kind of sample preparation and/or method of registration of the spectrum: KBr disc. Absorption.
Source: Burns and Carpenter (1997).
Wavenumbers (cm^{-1}): 1400w, 1352, 1196, 1160, 1145sh, 1064, 1004s, 982sh, 934, 908sh, 879, 854, 795w, 712, 664w, 647w, 623, 616, 587w, 559w, 524w.
Note: The wavenumbers were determined by us based on spectral curve analysis of the published spectrum.

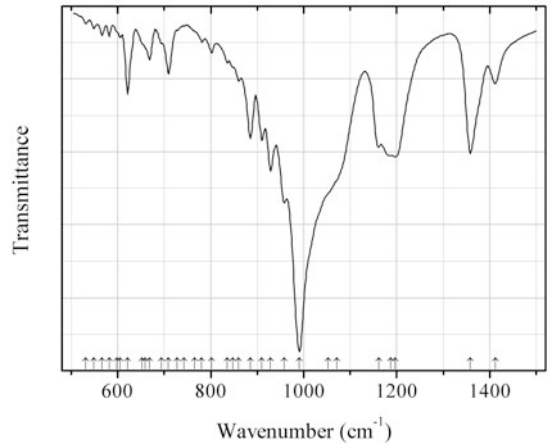

Fig. 2.13 IR spectrum of trembathite orthorhombic polymorph drawn using data from Burns and Carpenter (1997)

B127 Trembathite orthorhombic polymorph $Mg_3B_7O_{13}Cl$ (Fig. 2.13)
Locality: Salt Springs potash deposit, Sussex, New Brunswick, Canada (type locality).
Description: Crystals from the association with halite, hilgardite, hydroboracite, and boracite-group minerals. Confirmed by electron microprobe analysis and X-ray diffraction data. The empirical formula is $(Mg_{2.83}Fe_{0.17})B_7O_{13}Cl$.
Kind of sample preparation and/or method of registration of the spectrum: KBr disc. Absorption.
Source: Burns and Carpenter (1997).
Wavenumbers (cm^{-1}): 1412, 1358, 1197, 1187sh, 1161, 1071sh, 1052sh, 991s, 958, 929, 910, 885, 860, 848, 836, 802, 781w, 765sh, 743, 728, 709, 694, 669, 659sh, 653sh, 621, 605w, 599sh, 582w, 566w, 549w, 531w.
Note: The wavenumbers were determined by us based on spectral curve analysis of the published spectrum.

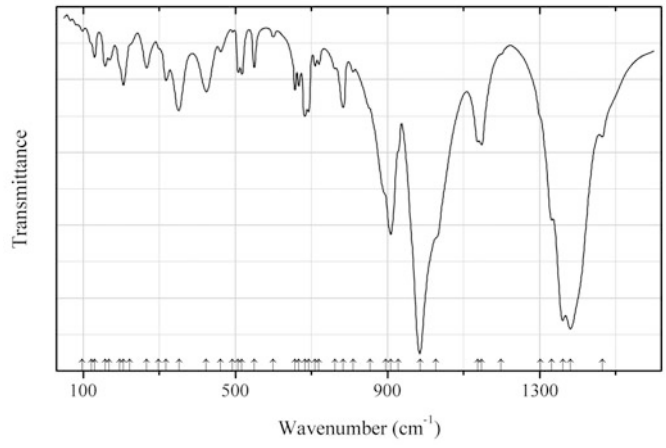

Fig. 2.14 IR spectrum of diomignite drawn using data from Zhigadlo et al. (2001)

B128 Diomignite $Li_2B_4O_7$ (Fig. 2.14)

Locality: Synthetic.
Description: Crystals grown in the [100] and [001] directions by the Czochralski method in air from a stoichiometric melt. Confirmed by powder X-ray diffraction data.
Kind of sample preparation and/or method of registration of the spectrum: Absorption. KBr disc (for the range from 500 to 1600 cm^{-1}), CsI disc (for the range from 200 to 700 cm^{-1}), polyethylene disc (for the range from 50 to 300 cm^{-1}).
Source: Zhigadlo et al. (2001).
Wavenumbers (cm^{-1}): 1465, 1381s, 1361s, 1332, 1302sh, 1198sh, 1148, 1137, 1028sh, 986s, 929sh, 909, 895sh, 854sh, 810w, 784, 762w, 720w, 710w, 693, 683, 667, 657, 600w, 550, 518, 508, 493w, 462, 424, 352, 318, 298sh, 267, 223sh, 206, 196sh, 169, 158, 130, 122, 98w.

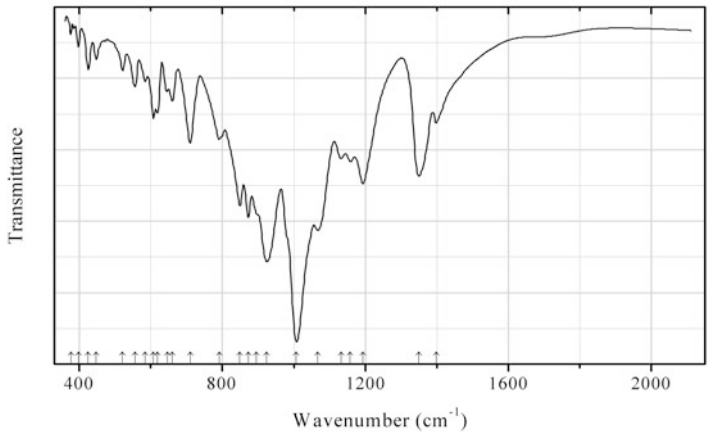

Fig. 2.15 IR spectrum of chambersite obtained by N.V. Chukanov

B129 Chambersite $Mn_3B_7O_{13}Cl$ (Fig. 2.15)
Locality: Verkhnekamskoe K deposit, Solikamsk, Perm Territory, Middle Urals, Russia.
Description: Tetrahedral crystal from the association with halite, sylvite, and a clay mineral. Investigated by I.V. Pekov. The empirical formula is $(Mn_{1.5}Fe_{0.9}Mg_{0.6})B_7O_{13}Cl_{0.8}$.
Kind of sample preparation and/or method of registration of the spectrum: KBr disc. Absorption.
Wavenumbers (cm^{-1}): 1398, 1349s, 1193s, 1158, 1133, 1066s, 1007s, 924s, 895sh, 872s, 849s, 791, 710, 660, 647, 618, 607, 584w, 556, 521w, 447w, 425w, 398w, 378w.

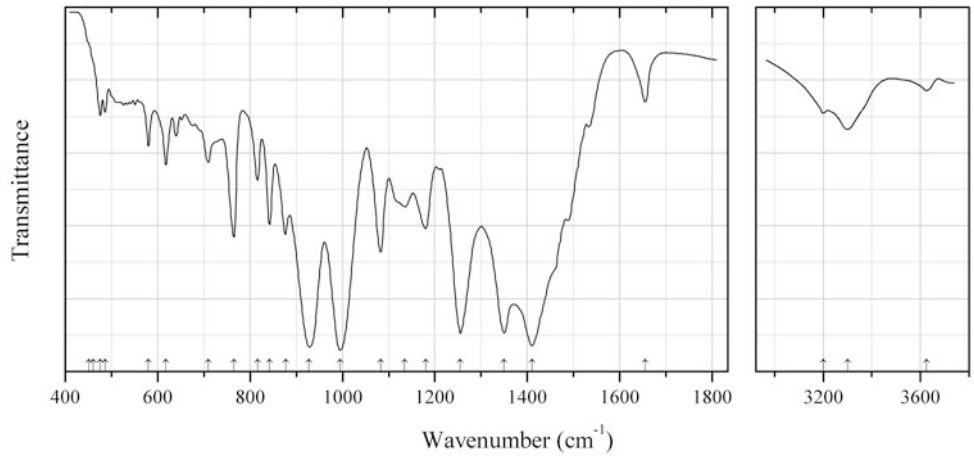

Fig. 2.16 IR spectrum of calcium pentaborate drawn using data from Yamnova et al. (2003)

B130 Calcium pentaborate $Ca[(B_5O_8(OH)]\cdot H_2O$ (Fig. 2.16)
Locality: Synthetic.
Description: Synthesized under hydrothermal conditions in the $CaCl_2$–Na_2CO_3–B_2O_3 system. The crystal structure is solved. Monolinic, space group $P2_1/c$, a = 6.5303(9), b = 19.613(3), c = 6.5303(9) Å, β = 119.207(2)°, V = 2513(2) Å^3, Z = 2. D_{calc} = 2.74 g/cm^3. The Ca layers are located between loose B–O networks composed of $\{^{[4]}B_2^{[3]}B_3O_8(OH)\}^{2-}$ pentaborate groups. Somewhat related to volkovskite and veatchite.
Kind of sample preparation and/or method of registration of the spectrum: KBr disc. Transmission.
Source: Yamnova et al. (2003).
Wavenumbers (cm^{-1}): 3625w, 3300, 3200, 1655, 1533, 1487, 1454sh, 1410s, 1350s, 1255s, 1209, 1180, 1135, 1123sh, 1083, 995s, 928s, 877, 842, 816, 765, 710w, 694sh, 676, 652, 640, 618w, 580w, 486, 476, 461sh, 451sh.
Note: The wavenumbers were partly determined by us based on spectral curve analysis of the published spectrum. The band position denoted by Yamnova et al. (2003) as 867 cm^{-1} was determined by us at 877 cm^{-1}.

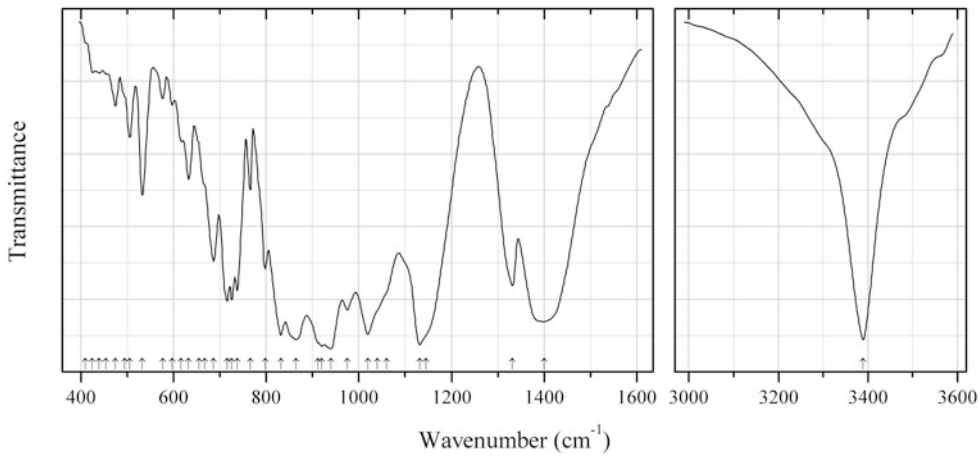

Fig. 2.17 IR spectrum of fabianite drawn using data from Kühn and Moenke (1963)

B131 Fabianite $CaB_3O_5(OH)$ (Fig. 2.17)
Locality: Borehole (depth 2381.9 m) in the natural gas deposit Rehden, near Deapholz, Lower Saxony, Germany (type locality).
Description: Colourless crystals from the association with howlite, szaibélyite, halite, and anhydrite.
Kind of sample preparation and/or method of registration of the spectrum: KBr disc. Transmission.
Source: Kühn and Moenke (1963).
Wavenumbers (cm^{-1}): 3390s, 1400s, 1332, 1146sh, 1132s, 1060sh, 1040sh, 1020s, 975s, 940s, 920s, 912sh, 865s, 832, 798, 766, 738, 726, 716, 687, 667, 655, 633, 616, 597, 577, 533, 506, (495), 475, (455), 440w, 425w, 410w.
Note: In the figure given by Kühn and Moenke (1963), the band quantified at 677 cm^{-1} is really present at 687 cm^{-1}.

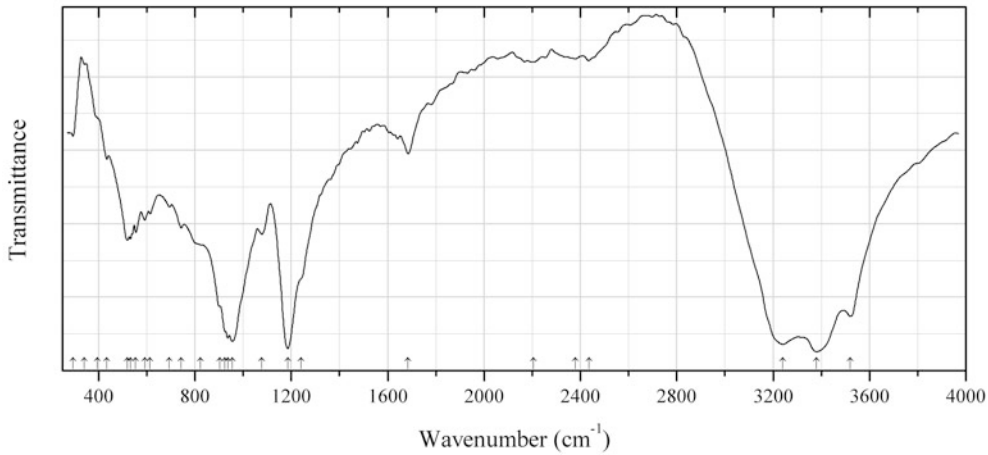

Fig. 2.18 IR spectrum of hexahydroborite drawn using data from Kusachi et al. (1999)

B132 Hexahydroborite $Ca[B(OH)_4]_2 \cdot 2H_2O$ (Fig. 2.18)
Locality: Fuka mine, Bicchu-cho, near Takahashi city, Okayama prefecture, Honshu Island, Japan.
Description: Aggregate of colourless pyramidal crystals from the association with olshanskite and calcite. Monoclinic, $a = 16.011(2)$, $b = 6.688(1)$, $c = 7.954(2)$ Å, $\beta = 103.81(1)°$. $D_{meas} = 1.84$ g/cm^3. Optically biaxial (+), $\alpha = 1.502(2)$, $\beta = 1.505(2)$, $\gamma = 1.509(2)$. The empirical formula is (wet analysis and ICP MS): $Ca_{1.001}B_{2.102}O_{4.154} \cdot 5.846H_2O$. The strongest lines of the powder X-ray diffraction pattern [*d*, Å (*I*, %) (*hkl*)] are: 7.78 (100) (200), 6.15 (22) (110), 3.368 (22) (311), 2.821 (18) (510), 2.525 (20) (22–2), 1.944 (18) (800).
Kind of sample preparation and/or method of registration of the spectrum: KBr disc. Transmission.
Source: Kusachi et al. (1999).
Wavenumbers (cm^{-1}): 3520s, 3380s, 3240s, 2435w, 2378w, 2205w, 1685, 1240sh, 1185s, 1078, 955s, 936s, 925, 903sh, 823sh, 743w, 694w, 614, 592, 553, 532, 520, 435, 395sh, 342w, 293w.
Note: The wavenumbers were partly determined by us based on spectral curve analysis of the published spectrum.

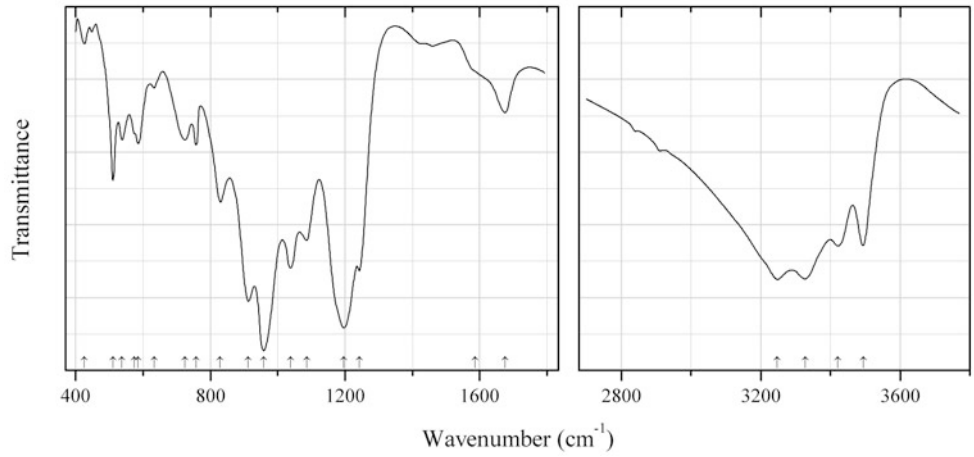

Fig. 2.19 IR spectrum of hexahydroborite drawn using data from Yamnova et al. (2011)

B133 Hexahydroborite $Ca[B(OH)_4]_2 \cdot 2H_2O$ (Fig. 2.19)
Locality: Synthetic.
Description: Obtained in the experiments on the recrystallization of calciborite at T = 250 °C and P = 70–80 atm. Identified by the powder X-ray diffraction pattern. The crystal structure is solved. Monoclinic, space group $P2/c$, = 7.9941(3), b = 6.6321(2), c = 7.9871(3) Å, β = 104.166(4)°, V = 410.58(3) Å^3, Z = 2. D_{calc} = 1.891 g/cm^3.
Kind of sample preparation and/or method of registration of the spectrum: Transmission. Kind of sample preparation is not indicated.
Source: Yamnova et al. (2011).
Wavenumbers (cm^{-1}): 3494, 3422, 3328s, 3247s, 1676, 1586sh, 1242s, 1196s, 1086, 1038, 959s, 912s, 829, 758, 725, 633w, 586, 575sh, 538, 511, 426w.
Note: Weak bands in the range 1400–1500 cm^{-1} correspond to the admixture of a carbonate.

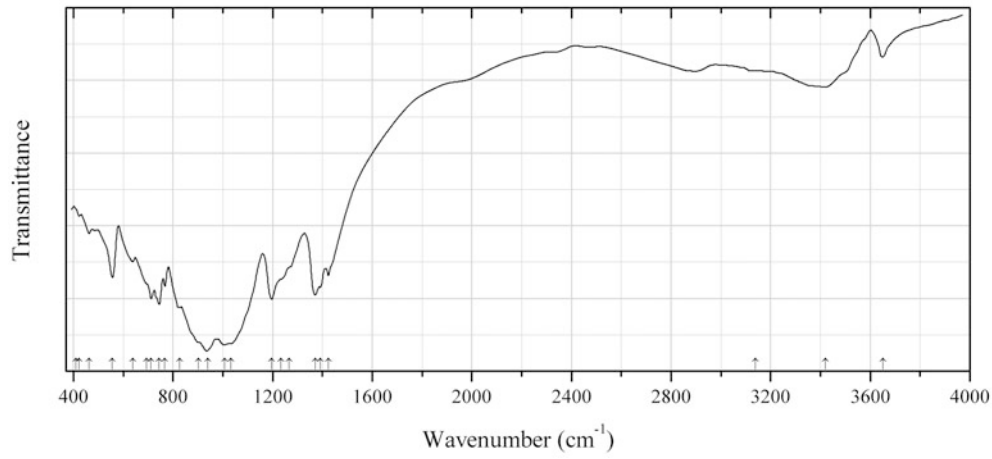

Fig. 2.20 IR spectrum of barium hydroxyborate B134 drawn using data from Heyward et al. (2012)

B134 Barium hydroxyborate B134 $Ba_3B_6O_{11}(OH)_2$ (Fig. 2.20)

Locality: Synthetic.
Description: Synthesized from $K_2B_4O_7 \cdot 4H_2O$, H_3BO_3, and $Ba(OH)_2 \cdot H_2O$ under hydrothermal conditions, in the presence of NaOH. Monoclinic, space group *Pc*, a = 6.958(14), b = 7.024(14), c = 11.346(2) Å, β = 90.10(3)°, V = 554.51(15) Å^3, Z = 2. D_{calc} = 4.114 g/cm^3. The crystal structure contains bicyclic building block $[B_6O_{11}(OH)_2]^{6-}$ with boron having both 3- and 4-fold coordination.
Kind of sample preparation and/or method of registration of the spectrum: KBr disc. Transmission.
Source: Heyward et al. (2012).
Wavenumbers (cm^{-1}): 3650, 3420, 3140, 1425, 1392, 1371, 1267, 1234sh, 1197, 1033s, 1007s, 940s, 903sh, 826, 767, 745, 712, 695sh, 638, 557, 463w, 422w, 409sh.
Note: The wavenumbers were determined by us based on spectral curve analysis of the published spectrum.

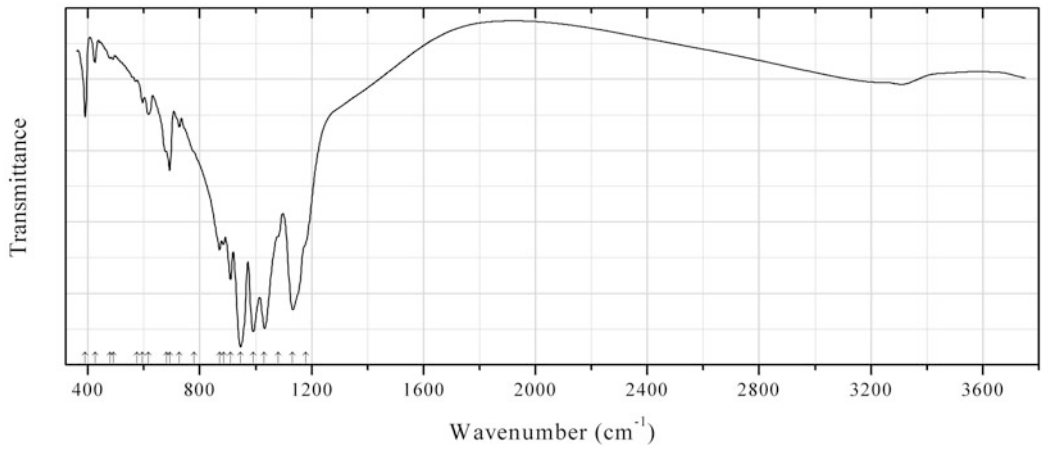

Fig. 2.21 IR spectrum of santarosaite obtained by N.V. Chukanov

B135 Santarosaite CuB_2O_4 (Fig. 2.21)
Locality: Santa Rosa mine, Iquique, I Region, Atacama desert, Chile (type locality).
Description: Blue crust from the association with anhydrite, malachite, and an atacamite-group mineral. Confirmed by the IR spectrum.
Kind of sample preparation and/or method of registration of the spectrum: KBr disc. Absorption.
Wavenumbers (cm^{-1}): 1180sh, 1132s, 1080sh, 1031s, 991s, 946s, 910, 886, 870, 780sh, 727, 692, 680sh, 616, 595w, 575w, 490w, 480w, 425w, 390.
Note: For the IR spectrum of the synthetic analogue of santarosaite see Petrakovskii et al. (2005). The IR spectrum of the santarosaite holotype sample is published by Schlüter et al. (2008).

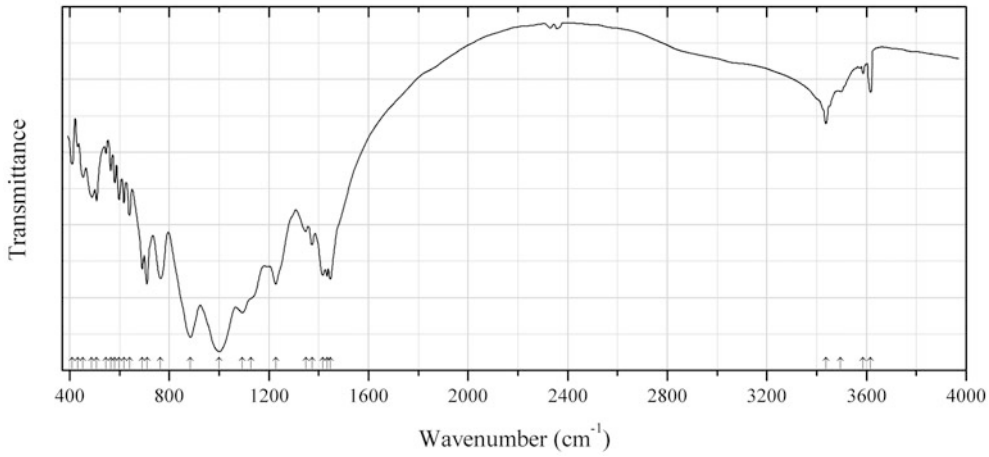

Fig. 2.22 IR spectrum of strontium hydroxyborate B136 drawn using data from Heyward et al. (2012)

B136 Strontium hydroxyborate B136 $Sr_3B_6O_{11}(OH)_2$ (Fig. 2.22)
Locality: Synthetic.
Description: Synthesized by a hydrothermal method. The crystal structure is solved. Triclinic, space group *P*-1, a = 6.6275(13) Å, b = 6.6706(13) Å, c = 11.393(2) Å, α = 91.06(3)°, β = 94.50(3)°, γ = 93.12(3)°, V = 501.26(17) Å^3, Z = 2. D_{calc} = 3.563 g/cm^3. The crystal structure consists of three crystallographically distinct strontium atoms and bicyclic building block $[B_6O_{11}(OH)_2]^{6-}$ with boron having both 3- and 4-fold coordination.
Kind of sample preparation and/or method of registration of the spectrum: KBr disc. Transmission.
Source: Heyward et al. (2012).
Wavenumbers (cm^{-1}): 3617, 3587w, 3495, 3437, 1447, 1434, 1416,1374, 1348, 1228, 1127sh, 1093s, 1001s, 885s, 765, 711, 692, 640, 599, 618, 581, 565, 546w, 508, 489, 454, 432w, 410.
Note: The wavenumbers were partly determined by us based on spectral curve analysis of the published spectrum.

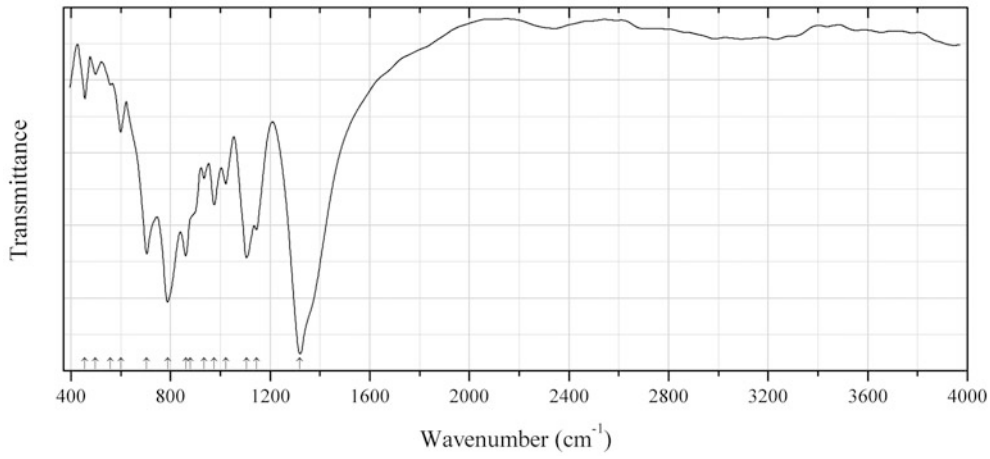

Fig. 2.23 IR spectrum of calciborite drawn using data from Kobayashi et al. (2014)

B137 Calciborite CaB_2O_4 (Fig. 2.23)
Locality: Fuka mine, Bicchu-cho, near Takahashi city, Okayama prefecture, Honshu Island, Japan.
Description: Massive aggregate forming veinlet in crystalline limestone. Associated minerals are shimazakiite, fluorite, bornite, and calcite. Orthorhombic, $a = 8.373(2)$, $b = 13.811(8)$, $c = 5.012(4)$ Å. $D_{meas} = 2.88(2)$ g/cm^3, $D_{calc} = 2.881$ g/cm^3. Optically biaxial (−), $\alpha = 1.594(2)$, $\beta = 1.654(2)$, $\gamma = 1.672(2)$. The empirical formula is $Ca_{0.999}Mn_{0.001}Co_{0.001}B_{1.999}O_4$. The strongest lines of the powder X-ray diffraction pattern [*d*, Å (*I*, %) (*hkl*)] are: 7.17 (19) (110), 4.04 (16) (130), 3.581 (24) (220), 3.458 (100) (040), 2.665 (21) (240).
Kind of sample preparation and/or method of registration of the spectrum: KBr disc. Transmission.
Source: Kobayashi et al. (2014).
Wavenumbers (cm^{-1}): 1320s, 1145, 1105s, 1022, 975, 935, 880sh, 861s, 788s, 705s, 600, 558w, 499w, 456.
Note: The wavenumbers were partly determined by us based on spectral curve analysis of the published spectrum.

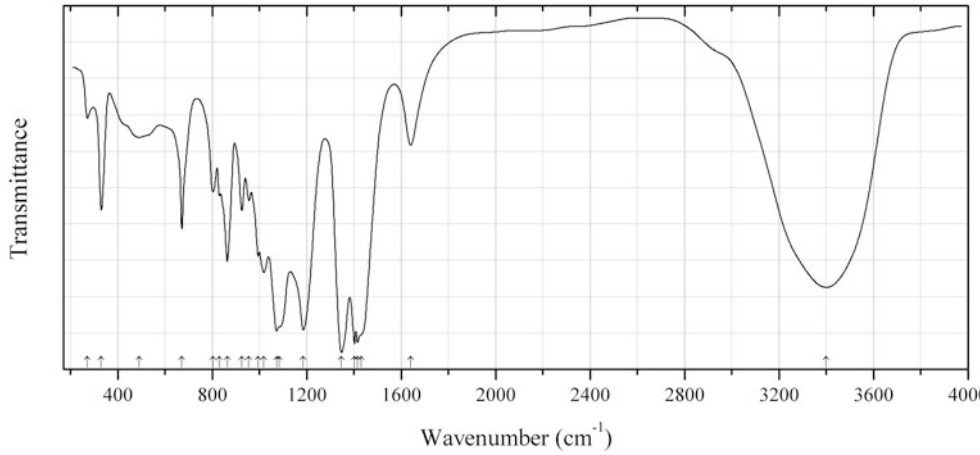

Fig. 2.24 IR spectrum of iquiqueite drawn using data from Ericksen et al. (1986)

B138 Iquiqueite $K_3Na_4Mg(CrO_4)B_{24}O_{39}(OH)\cdot 12H_2O$ (Fig. 2.24)
Locality: Iquiqui, about 100 km from Zapiga, Tarapacá province, Chile (type locality).
Description: Yellow thin hexagonal platelets from the association with nitratite, halite, niter, darapskite, blödite, glauberite, dietzeite, brüggenite, ulexite, and gypsum. Holotype sample. Hexagonal, space group $P31c$, $a = 11.6369(14)$, $c = 30.158(7)$ Å, $Z = 3$. $D_{meas} = 2.05(9)$ g/cm^3. Optically uniaxial (−), $\varepsilon = 1.447(2)$, $\omega = 1.502(2)$. The strongest lines of the powder X-ray diffraction pattern [*d*, Å (*I*, %) (*hkl*)] are: 10.11 (85) (100), 6.04 (85) (104), 3.28 (85) (207), 3.22 (85) (215), 3.02 (100) (208), 2.856 (100) (222).
Kind of sample preparation and/or method of registration of the spectrum: KBr disc. Transmission.
Source: Ericksen et al. (1986).
Wavenumbers (cm^{-1}): 3400s, 1640, 1430sh, 1415s, 1402s, 1347s, 1185s, 1085sh, 1072s, 1018, 994, 955, 925, 863, 830, 803, 671, 490, 330, 271w.
Note: The wavenumbers were partly determined by us based on spectral curve analysis of the published spectrum.

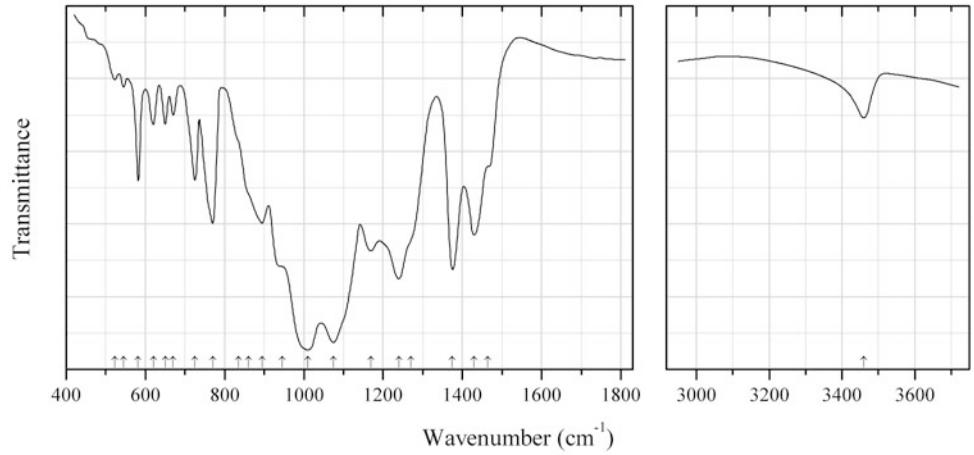

Fig. 2.25 IR spectrum of korzhinskite drawn using data from Dimitrova et al. (2004)

B139 Korzhinskite $CaB_2O_4 \cdot nH_2O$ ($n < 1$) (Fig. 2.25)
Locality: Synthetic.
Description: The strongest lines of the powder X-ray diffraction pattern [*d*, Å (*I*, %)] are: 3.271 (19), 3.171 (47), 3.132 (96), 2.802 (100), 2.716 (51), 2.180 (20), 2.177 (19), 2.039 (63), 1.912 (31).
Kind of sample preparation and/or method of registration of the spectrum: Polycrystalline film deposited on a KBr plate. Transmission.
Source: Dimitrova et al. (2004).
Wavenumbers (cm^{-1}): 3460, 1465, 1430, 1375s, 1271sh, 1240s, 1170, 1075s, 1010s, 945, 895, 860sh, 835sh, 770, 725, 670w, 650w, 620w, 582, 545w, 523w.
Note: The wavenumbers were partly determined by us based on spectral curve analysis of the published spectrum. The band position denoted by Dimitrova et al. (2004) as 545 cm^{-1} was determined by us at 582 cm^{-1}.

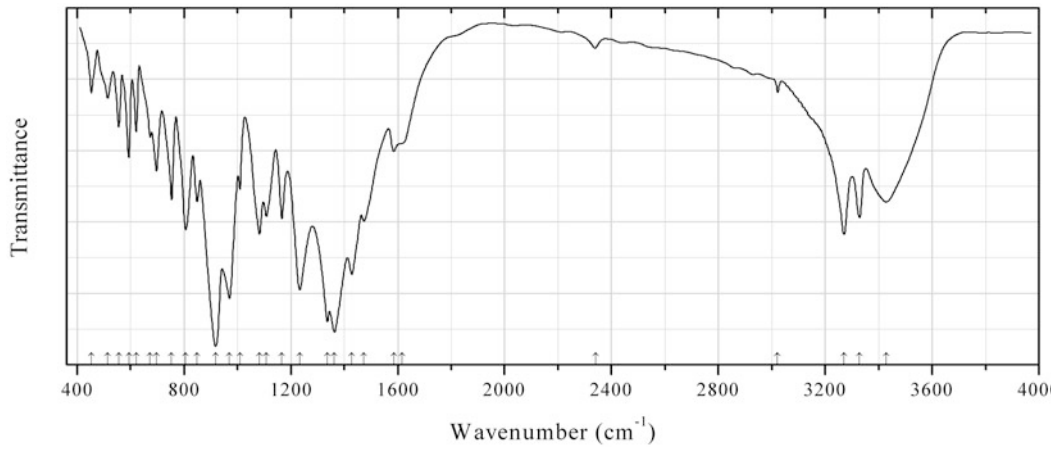

Fig. 2.26 IR spectrum of lead pentaborate hydrate drawn using data from Chen et al. (2006)

B140 Lead pentaborate hydrate $Pb[B_5O_8(OH)] \cdot 1.5H_2O$ (Fig. 2.26)
Locality: Synthetic.

Description: Synthesized in a hydrothermal reaction between $Na_2B_4O_7 \cdot 10H_2O$ and $PbBiBO_4$ at 170 °C. A layered compound containing double ring $[B_5O_8(OH)]^{2-}$ building units. Triclinic, space group *P*-1, $a = 6.656(2)$, $b = 6.714(2)$, $c = 10.701(2)$ Å, $\alpha = 99.07(2)°$, $\beta = 93.67(2)°$, $\gamma = 118.87(1)°$, $V = 571.6(3)$ Å^3, $Z = 2$.
Kind of sample preparation and/or method of registration of the spectrum: KBr disc. Transmission.
Source: Chen et al. (2006).
Wavenumbers (cm^{-1}): 3428, 3329, 3270, 3022w, 2340w, 1615sh, 1585, 1473, 1428s, 1363s, 1336s, 1233s, 1166, 1108, 1082, 1009, 970s, 918s, 849, 806, 753, 697, 673, 621, 593, 556, 514, 453.
Note: The wavenumbers were partly determined by us based on spectral curve analysis of the published spectrum.

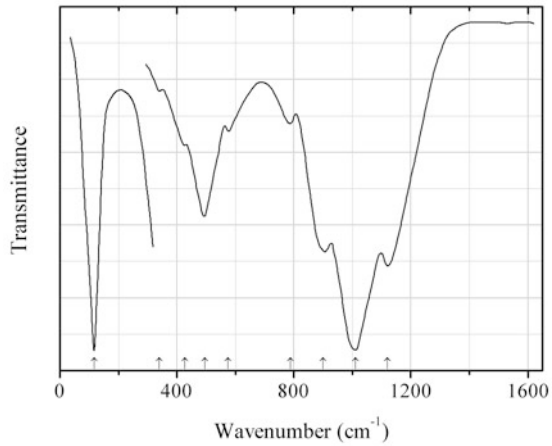

Fig. 2.27 IR spectrum of lisitsynite drawn using data from Rulmont and Tarte (1987)

B141 Lisitsynite $K(BSi_2O_6)$ (Fig. 2.27)
Locality: Synthetic.
Description: Synthesized by a solid-state technique. Structurally related to pollucite.
Kind of sample preparation and/or method of registration of the spectrum: KBr disc (above 300 cm^{-1}); polyethylene disc (below 300 cm^{-1}). Transmission.
Source: Rulmont and Tarte (1987).
Wavenumbers (cm^{-1}): 1120s, 1010s, 900s, 788, 575, 495, 427, 340w, 117s.
B142 Nobleite $CaB_6O_9(OH)_2 \cdot 3H_2O$
Locality: Not indicated.
Description: No data.
Kind of sample preparation and/or method of registration of the spectrum: Perfluorokerosene mull. Transmission.
Source: Weir (1966).
Wavenumbers (cm^{-1}): 3540, 3380s, 3200s, 2400s, 1675, 1385sh, 1322s, 1300sh, 1180, 1160, 1125, 1107, 1033sh, 965s, 930, 880s, 827, 805s, 737, 705, 670, 602, 570w, 460w, 425w.

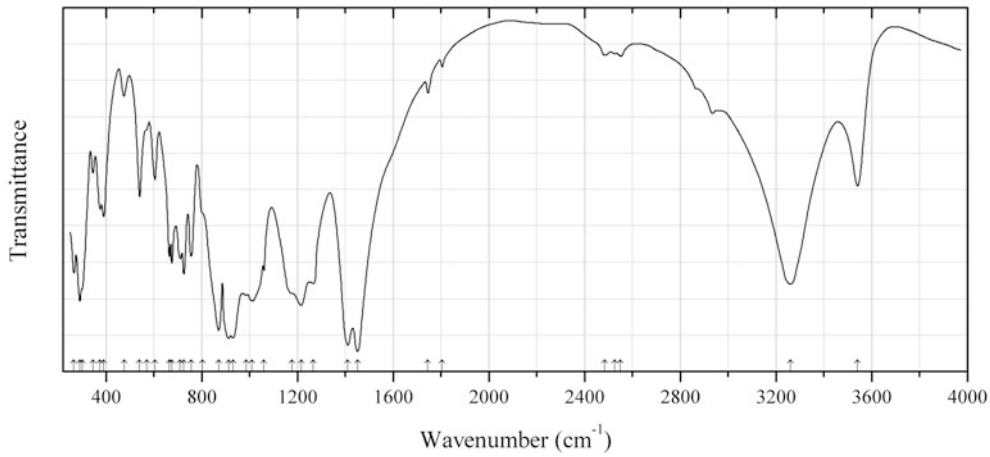

Fig. 2.28 IR spectrum of numanoite drawn using data from Ohnishi et al. (2007b)

B143 Numanoite $Ca_4CuB_4O_6(OH)_6(CO_3)_2$ (Fig. 2.28)
Locality: Fuka mine, Bicchu-cho, near Takahashi city, Okayama prefecture, Honshu Island, Japan (type locality).
Description: Blue-green zones in borcarite crystals from the association with nifontovite, bultfonteinite, calcite, and an unidentified magnesium silicate mineral. Holotype sample. Monoclinic, space group *C*2/*m*, $a = 17.794(2)$, $b = 8.381(1)$, $c = 4.4494(7)$ Å, $\beta = 102.42(2)°$, $Z = 2$. $D_{meas} = 2.96$ (2) g/cm^3, $D_{calc} = 2.93$ g/cm^3. Optically biaxial (−), $\alpha = 1.618(2)$, $\beta = 1.658(2)$, $\gamma = 1.672(2)$, $2V = 60°$. The empirical formula is $Ca_{3.99}(Cu_{0.74}Mg_{0.15}Zn_{0.04})B_{3.97}O_{5.615}(OH)_{6.21}(CO_3)_{2.06}$. The strongest lines of the powder X-ray diffraction pattern [*d*, Å (*I*, %) (*hkl*)] are: 7.57 (100) (110), 2.671 (84) (−421), 2.727 (68) (221), 1.887 (52) (041, 440), 2.272(48) (−331), 2.899 (44) (600), 1.698 (34) (640).
Kind of sample preparation and/or method of registration of the spectrum: KBr disc. Transmission.
Source: Ohnishi et al. (2007b).
Wavenumbers (cm^{-1}): 3540, 3260, 2550w, 2525w, 2485w, 1805w, 1745w, 1450s, 1410s, 1265, 1215s, 1177sh, 1060, 1010s, 985, 930s, 912s, 870s, 802sh, 755, 725, 710, 675, 665, 605, 570sh, 540, 475w, 390, 375, 345, 300sh, 290, 265.
Note: The wavenumbers were partly determined by us based on spectral curve analysis of the published spectrum. Weak bands in the range 2800–3000 cm^{-1} correspond to the admixture of an organic substance.

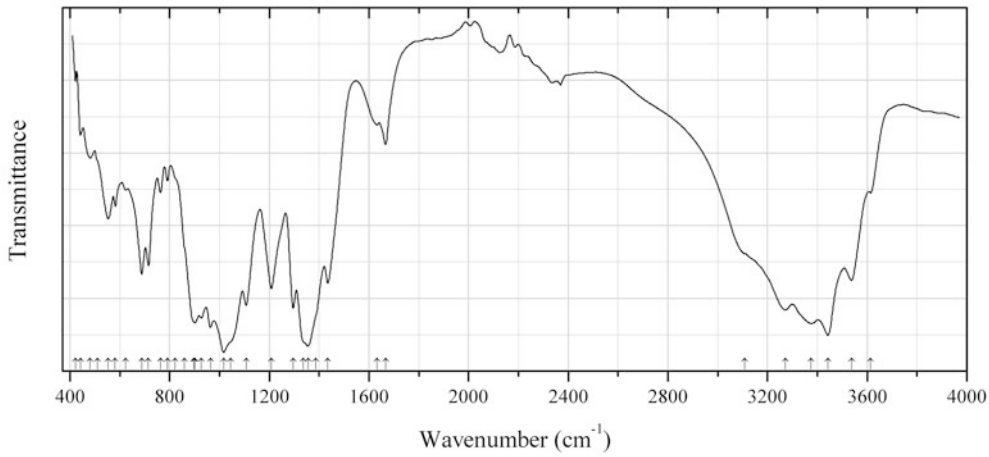

Fig. 2.29 IR spectrum of penobsquisite drawn using data from Grice et al. (1996)

B144 Penobsquisite $Ca_2Fe^{2+}[B_9O_{13}(OH)_6]Cl{\cdot}4H_2O$ (Fig. 2.29)
Locality: Potash Corporation of Saskatchewan (New Brunswick Division) mine, Penobsquis, Kings Co., New Brunswick, Canada (type locality).
Description: Pale yellow, vitreous crystals from the association with halite, boracite, hilgardite, pringleite, trembathite, sellaite, fluorite, hematite, and malachite. Holotype sample. Monoclinic, space group $P2_1$, a = 11.63(4), b = 9.38(1), c = 8.735(9) Å, β = 98.40(7)°, V = 942.7(1) Å^3, Z = 2. D_{meas} = 2.36(3) g/cm^3, D_{calc} = 2.27 g/cm^3. Optically biaxial (+), α = 1.550(2), β = 1.554(2), γ = 1.592 (2), 2 V = 33(2)°. The empirical formula is $Ca_{1.99}(Fe_{0.67}Mg_{0.29}Mn_{0.02})[B_9O_{12.95}(OH)_{5.99}]Cl_{1.05}{\cdot}4.01H_2O$. The strongest lines of the powder X-ray diffraction pattern [d, Å (I, %) (hkl)] are: 8.65 (30) (001), 7.29 (100) (110), 5.32 (20) (111), 4.50 (20) (211), 2.958 (30) (320, 312, 031), 2.744 (20) (013, 203), 2.113 (30) (114).
Kind of sample preparation and/or method of registration of the spectrum: Diamond-anvil cell microsampling.
Source: Grice et al. (1996).
Wavenumbers (cm^{-1}): 3614, 3537, 3442s, 3376s, 3272s, 3110sh, 1667, 1632w, 1435, 1387sh, 1356s, 1337sh, 1296s, 1208, 1107, 1045sh, 1017s, 964s, 928s, 902s, 897sh, 860sh, 823sh, 791w, 763w, 715, 688, 623w, 582, 553, 510sh, 481, 442w, 422w.
Note: The wavenumbers were determined by us based on spectral curve analysis of the published spectrum.

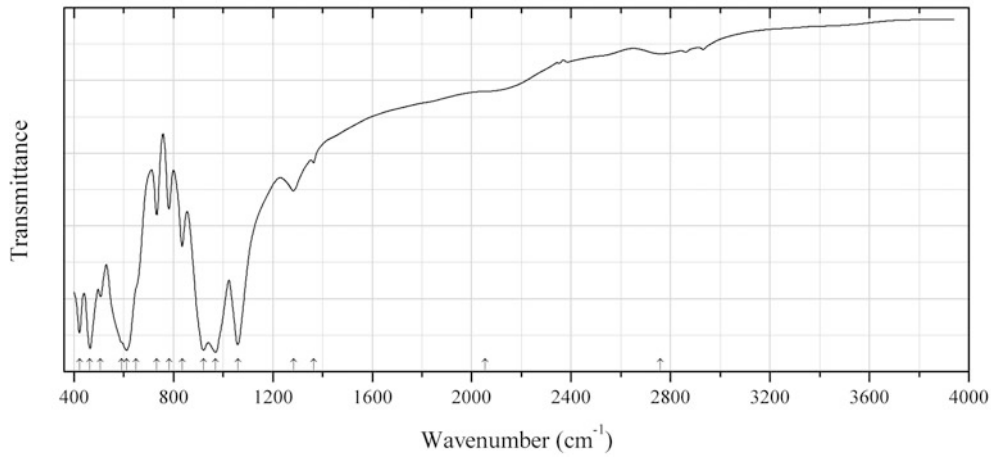

Fig. 2.30 IR spectrum of pseudosinhalite drawn using data from Daniels et al. (1997)

B145 Pseudosinhalite $Mg_2Al_3(BO_4)_2O(OH)$ (Fig. 2.30)
Locality: Synthetic.
Description: Prepared from gels of MgO and Al_2O_3 and H_3BO_3 at 949 °C. The crystal structure is solved. Monoclinic, space group $P2_1/c$, a = 7.455(1), b = 4.330(1), c = 9.825(2) Å, β = 110.68(1)°. The strongest lines of the powder X-ray diffraction pattern [d, Å (I, %) (hkl)] are: 2.606 (34) (−113), 2.3846 (36) (−213), 2.1360 (100) (−312, −114), 2.0995 (48) (212), 1.6232 (70) (−322, −124), 1.6071 (33) (222).
Kind of sample preparation and/or method of registration of the spectrum: RbI disc. Transmission.
Source: Daniels et al. (1997).
Wavenumbers (cm^{-1}): 2760w, 2055sh, 1364w, 1283w, 1059s, 969s, 921s, 835, 782, 732, 650sh, 611s, 592sh, 507, 464s, 422s.
Note: The wavenumbers were determined by us based on spectral curve analysis of the published spectrum. The absence of absorption bands above 3000 cm^{-1} indicates possible acid nature of OH groups. Weak bands in the range 2800–3000 cm^{-1} correspond to the admixture of an organic substance.

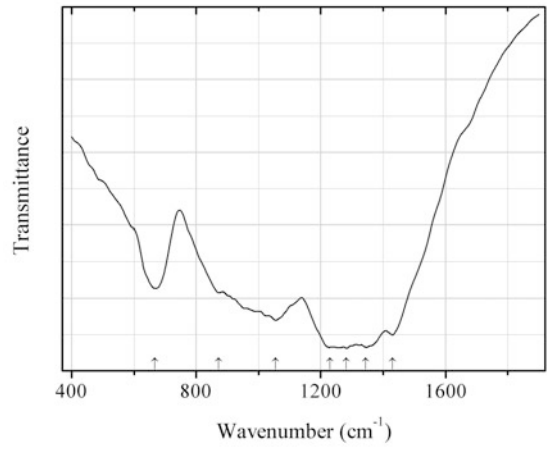

Fig. 2.31 IR spectrum of santarosaite amorphous dimorph drawn using data from Petrakovskii et al. (2005)

B146 Santarosaite amorphous dimorph CuB_2O_4 (Fig. 2.31)
Locality: Synthetic.
Description: Produced by fast pouring of the melt on a metal substrate. Confirmed by powder X-ray diffraction data.
Kind of sample preparation and/or method of registration of the spectrum: KBr disc. Absorption.
Source: Petrakovskii et al. (2005).
Wavenumbers (cm^{-1}): 1431s, 1343s, 1282s, 1230s, 1055, 872, 668.
Note: The wavenumbers were determined by us based on spectral curve analysis of the published spectrum.

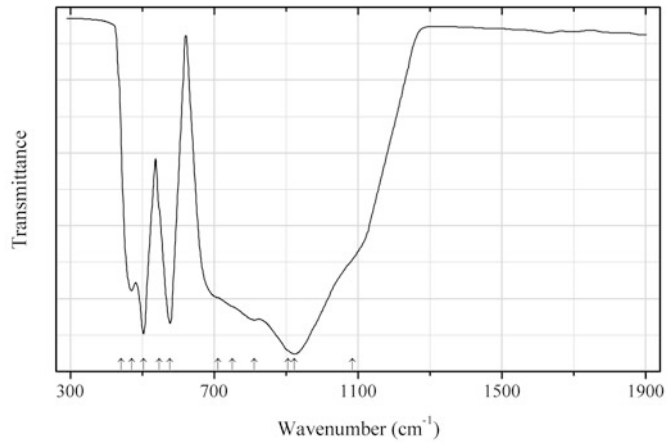

Fig. 2.32 IR spectrum of schiavinatoite drawn using data from Heyns et al. (1990)

B147 Schiavinatoite $Nb(BO_4)$ (Fig. 2.32)
Locality: Synthetic.
Description: Prepared at a high pressure. Contains only the ^{10}B isotope of boron.
Kind of sample preparation and/or method of registration of the spectrum: KBr disc. Transmission.
Source: Heyns et al. (1990).
Wavenumbers (cm^{-1}): 1085sh, 922s, 905sh, 812, 750sh, 710sh, 577s, 547sh, 503s, 470, 440.
Note: The wavenumbers were partly determined by us based on spectral curve analysis of the published spectrum. The band position calculated by Heyns et al. (1990) as 828 cm^{-1} was determined by us at 812 cm^{-1}.

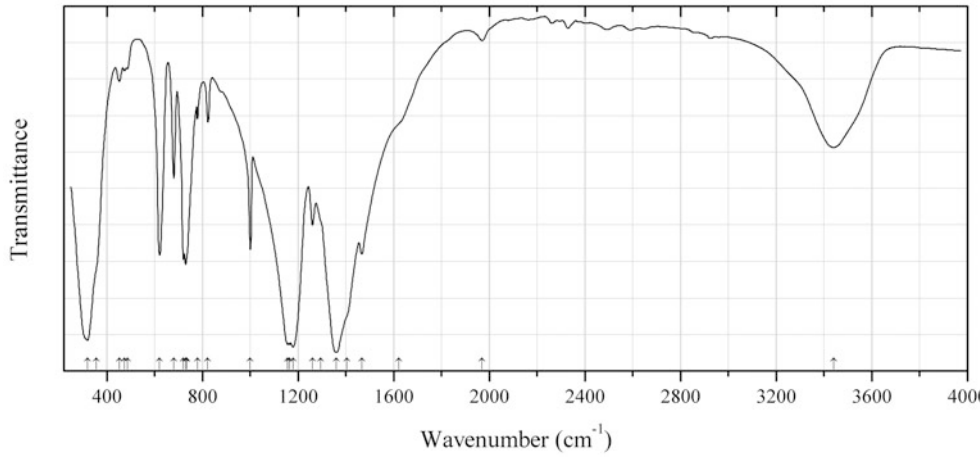

Fig. 2.33 IR spectrum of shimazakiite-4*M* drawn using data from Kusachi et al. (2013)

B148 Shimazakiite-4*M* $Ca_2B_2O_5$ (Fig. 2.33)
Locality: Fuka mine, Bicchu-cho, near Takahashi city, Okayama prefecture, Honshu Island, Japan (type locality).
Description: Greyish white aggregate from the association with takedaite, sibirskite, olshanskyite, parasibirskite, nifontovite, calcite, etc. Holotype sample. Monoclinic, space group $P2_1/c$, a = 3.5485 (12), b = 6.352(2), c = 19.254(6) Å, β = 92.393(13)°, V = 433.6(3) Å^3. D_{calc} = 2.78 g/cm^3. Optically biaxial (−), α = 1.586(2), β = 1.650(2), γ = 1.667(2). The empirical formula is $Ca_2B_{1.92}O_{4.76}(OH)_{0.24}$. The strongest lines of the powder X-ray diffraction pattern [d, Å (I, %) (hkl)] are: 3.02 (84) (022), 2.92 (100) (10–4), 2.81 (56) (104), 2.76 (32) (113), 1.880 (32) (11–8, 12–6, 126, 118).
Kind of sample preparation and/or method of registration of the spectrum: KBr disc. Transmission.
Source: Kusachi et al. (2013).
Wavenumbers (cm^{-1}): 3440, 1970w, 1622sh, 1467, 1405sh, 1360s, 1295sh, 1260w, 1179s, 1164s, 1156s, 1000, 821, 779, 735sh, 730, 720, 680, 620, 486w, 474w, 452w, 355sh, 320s.
Note: The bands at 3440 and 1622 cm^{-1} indicate the presence of H_2O (adsorbed water or a H_2O-bearing impurity). The wavenumbers were partly determined by us based on spectral curve analysis of the published spectrum. The band position denoted by Kusachi et al. (2013) as 1170 cm^{-1} was determined by us as a triplet (1179, 1164 and 1156 cm^{-1}).

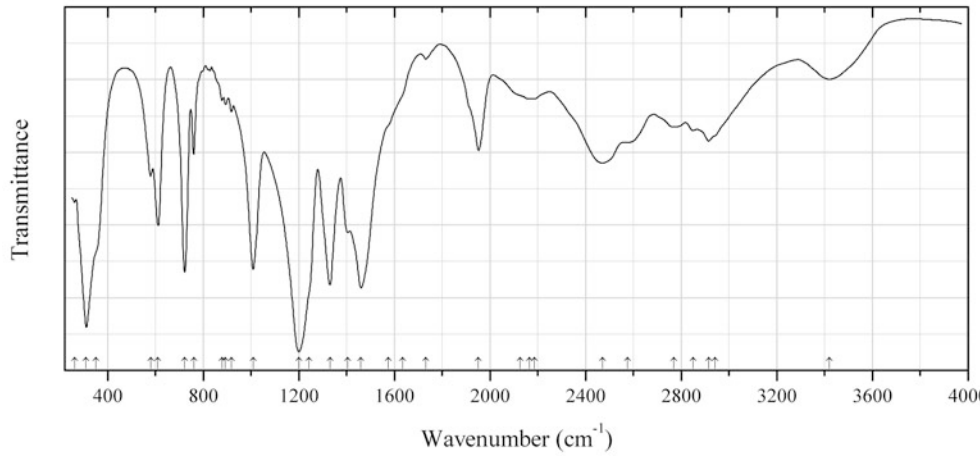

Fig. 2.34 IR spectrum of sibirskite drawn using data from Kusachi et al. (1997a)

B149 Sibirskite $CaH(BO_3)$ (Fig. 2.34)
Locality: Fuka mine, Bicchu-cho, near Takahashi city, Okayama prefecture, Honshu Island, Japan.
Description: Aggregates of prismatic crystals from the association with takedaite, frolovite, and calcite. Monoclinic, space group $P2_1/a$, a = 8.643(6), b = 9.523(2), c = 3.567(3) Å, β = 119.23(3)°, Z = 4. D_{meas} = 2.58(3) g/cm^3, D_{calc} = 2.59 g/cm^3. Optically biaxial (−), α = 1.554(2), β = 1.638(2), γ = 1.652(2). The empirical formula is $Ca_{1.004}H_{1.071}B_{0.974}O_3$. The strongest lines of the powder X-ray diffraction pattern [d, Å (I, %) (hkl)] are: 4.77 (33) (020), 3.329 (32) (11–1, 20–1), 2.955 (100) (011, 220), 2.927 (21) (130), 2.603 (94) (021, 31–1), 1.891 (20) (041).
Kind of sample preparation and/or method of registration of the spectrum: KBr disc. Transmission.
Source: Kusachi et al. (1997a).
Wavenumbers (cm^{-1}): 3420, 2940sh, 2914, 2850, 2770, 2575sh, 2470, 2186, 2164, 2125sh, 1950, 1732w, 1633sh, 1573sh, 1460s, 1405, 1330s, 1242sh, 1200s, 1010s, 917w, 893w, 879w, 760, 722s, 610, 580, 350sh, 310s, 261w.
Note: The wavenumbers were partly determined by us based on spectral curve analysis of the published spectrum. Bands in the range 1900–3000 cm^{-1} indicate the presence of acid OH groups. In the cited paper the wavenumber 1330 cm^{-1} is erroneously indicated as 1350 cm^{-1}.

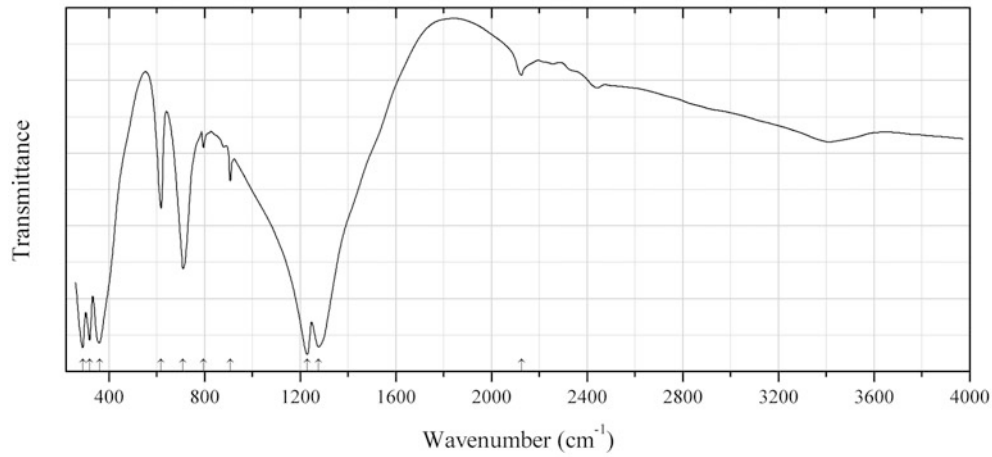

Fig. 2.35 IR spectrum of takedaite drawn using data from Kusachi et al. (1995)

B150 Takedaite $Ca_3B_2O_6$ (Fig. 2.35)
Locality: Fuka mine, Bicchu-cho, near Takahashi city, Okayama prefecture, Honshu Island, Japan (type locality).
Description: White to pale grey granular aggregates from the association with nifontovite, olshanskyite, pentahydroborite, frolovite, sibirskite, and calcite. Holotype sample. Trigonal, space group R-3c, a = 8.638(1), c = 11.850(2) Å, Z = 6. D_{meas} = 3.10(2) g/cm^3, D_{calc} = 3.11 g/cm^3. Optically uniaxial (−), ω = 1.726, ε = 1.630. The empirical formula is $Ca_{3.053}B_{1.965}O_6$. The strongest lines of the powder X-ray diffraction pattern [d, Å (I, %) (hkl)] are: 2.915 (100) (113), 1.895 (75) (223), 2.756 (61) (104), 2.493 (44) (300), 2.044 (21) (214, 131), 2.160 (19) (220), 1.976 (18) (006), 1.549 (12) (306).
Kind of sample preparation and/or method of registration of the spectrum: KBr disc. Transmission.
Source: Kusachi et al. (1995).
Wavenumbers (cm^{-1}): 2430w, 2125w, 1275s, 1230s, 907w, 795w, 710, 618, 360s, 320s, 290s.

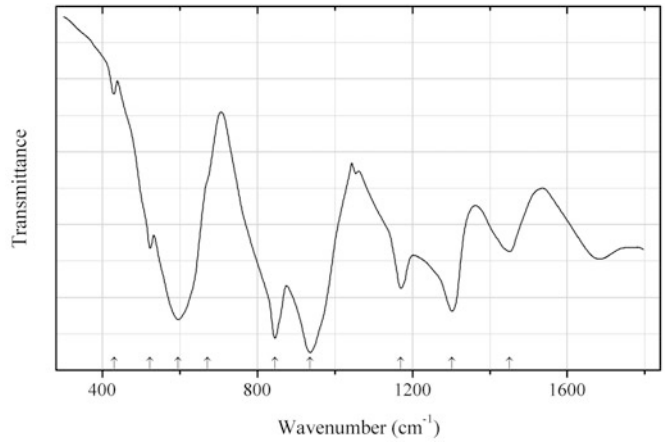

Fig. 2.36 IR spectrum of teepleite drawn using data from Weir (1966)

B151 Teepleite $Na_2[B(OH)_4]Cl$ (Fig. 2.36)
Locality: Borax Lake, Lake Co., California, USA (type locality).
Description: Specimen No. 102798 from the mineral collection of the Smithsonian Institution.
Kind of sample preparation and/or method of registration of the spectrum: Thin powdery film deposited on CsBr plate. Transmission.
Source: Weir (1966).
Wavenumbers (cm^{-1}): 3530s, 3400–2500s (broad), 1450, 1302, 1170, 935s, 845s, 670sh, 595s, 522, 430w.
Note: The band at 1680 cm^{-1} may correspond a H_2O-bearing impurity. For the IR spectrum of teepleite see also Klee (1966).

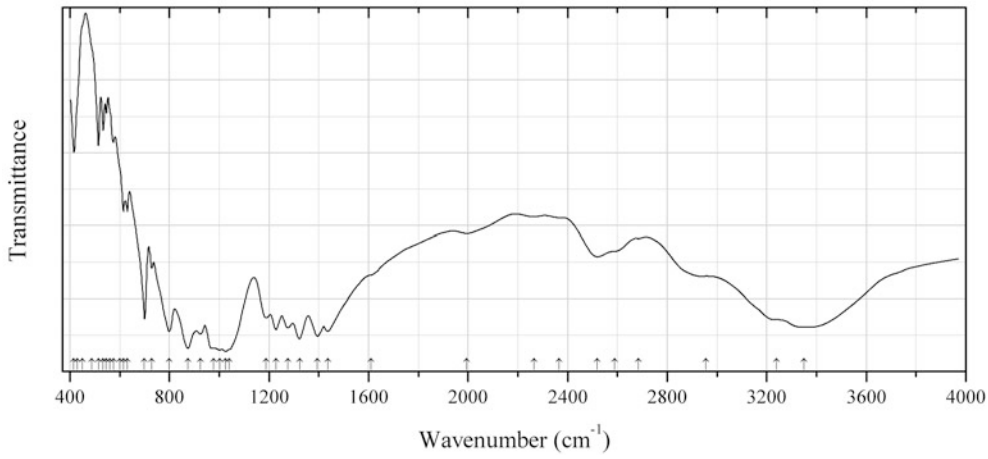

Fig. 2.37 IR spectrum of trisodium triborate B152 drawn using data from Andrieux et al. (2010)

B152 Trisodium triborate B152 $Na_3[B_3O_4(OH)_4]$ (Fig. 2.37)
Locality: Synthetic.
Description: The crystal structure is solved. Monoclinic, space group *Cc*, $a = 12.8274(6)$, $b = 7.7276(4)$, $c = 6.9690(3)$ Å, $\beta = 98.161(3)°$, $Z = 2$. The polyanions $[B_3O_4(OH)_4]^{3-}$ are based on

B-O-containing rings with two tetracoordinated boron atoms and one tricoordinated boron atom in the fragments $BO_2(OH)_2$ and BO_3, respectively.
Kind of sample preparation and/or method of registration of the spectrum: KBr disc. Transmission.
Source: Andrieux et al. (2010).
Wavenumbers (cm^{-1}): 3350, 3240sh, 2955sh, 2685, 2590sh, 2520, 2365w, 2265w, 1995, 1611sh, 1437, 1395s, 1323s, 1276, 1228, 1188, 1040sh, 1025s, 1002s, 978sh, 924, 874s, 799, 729, 700, 631, 615, 600sh, 575w, 562sh, 546w, 534w, 515w, 489sh, 450sh, 431sh, 416w.
Note: The wavenumbers were determined by us based on spectral curve analysis of the published spectrum.

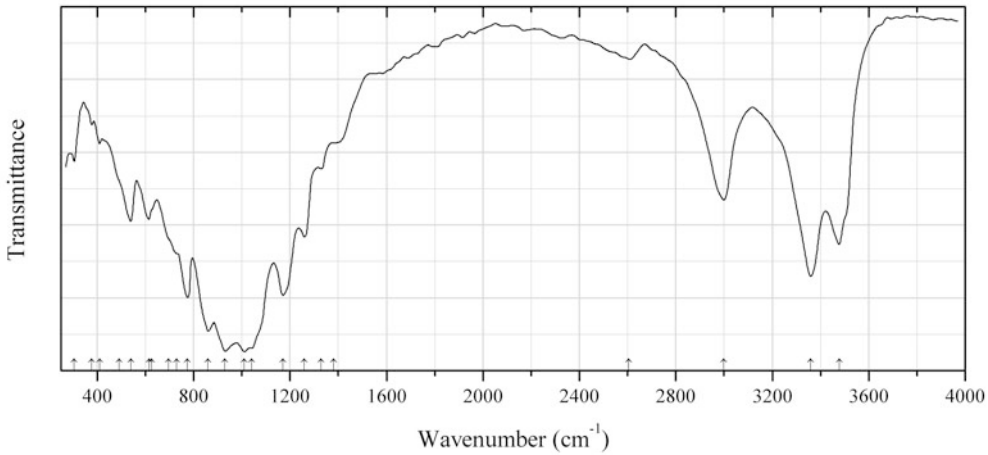

Fig. 2.38 IR spectrum of uralborite drawn using data from Kusachi et al. (2000)

B153 Uralborite $CaB_2O_2(OH)_4$ (Fig. 2.38)
Locality: Fuka mine, Bicchu-cho, near Takahashi city, Okayama prefecture, Honshu Island, Japan.
Description: Aggregates of white fibrous crystals from the association with sibirskite, borcarite, fluorite, and calcite. Monoclinic, a = 6.923(1), b = 12.326(1), c = 9.831(1) Å, β = 97.09(1)°. D_{meas} = 2.58(2) g/cm^3. Optically biaxial (+), α = 1.605(2), β = 1.611(2), γ = 1.618(2). The empirical formula is $Ca_{1.006}B_{2.019}O_{2.069}(OH)_{3.931}$.
Kind of sample preparation and/or method of registration of the spectrum: KBr disc. Transmission.
Source: Kusachi et al. (2000).
Wavenumbers (cm^{-1}): 3480, 3360, 3000, 2605w, 1382sh, 1330w, 1260, 1170s, 1042s, 1010s, 930s, 860s, 775s, 731sh, 697sh, 627sh, 615, 540, 491sh, 410w, 377w, 305w.
Note: The wavenumbers were partly determined by us based on spectral curve analysis of the published spectrum.

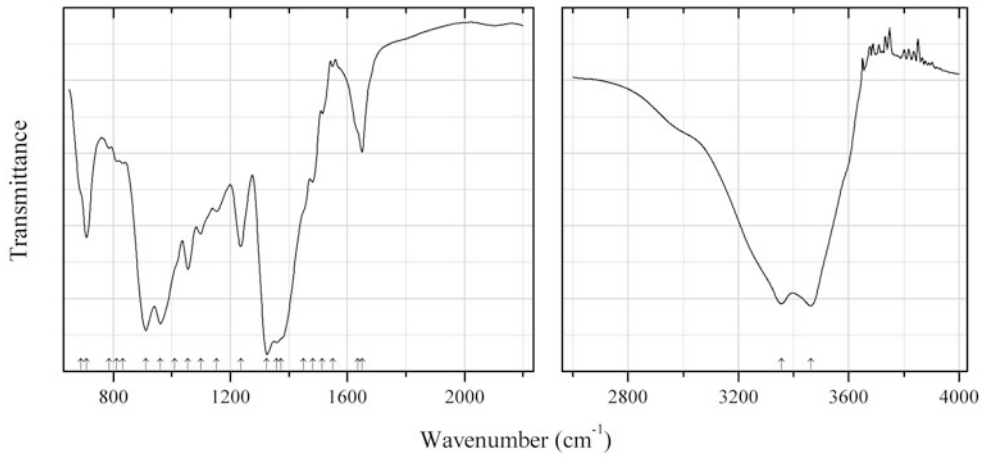

Fig. 2.39 IR spectrum of walkerite drawn using data from Grice et al. (2002)

B154 Walkerite $Ca_{16}(\square,Mg,Li,Fe)_2[B_{13}O_{17}(OH)_{12}]_4Cl_6{\cdot}28H_2O$ (Fig. 2.39)
Locality: Potash Corporation of Saskatchewan (New Brunswick Division) mine, Penobsquis, near Sussex, Kings Co., New Brunswick, Canada (type locality).
Description: Colourless to white, fibrous to acicular crystals from the association with halite, hydroboracite, hilgardite, volkovskite, boracite, szaibelyite, a mica-group mineral, and anhydrite. Holotype sample. The crystal structure is solved. Orthorhombic, space group *Pba*2, a = 15.52(1), b = 22.74(1), c = 8.761(4) Å, V = 3091(2) Å^3, Z = 1. D_{calc} = 2.05 g/cm^3. Optically biaxial (+), α = 1.516(2), β = 1.532(2), γ = 1.554(2), 2V = 82(3)°. The empirical formula is $(Ca_{15.60}Na_{0.16}K_{0.06})(\square_{0.97}Mg_{0.55}Li_{0.31}Fe_{0.17})B_{51.43}O_{68}(OH)_{48}[Cl_{5.26}(OH)_{0.74}]H_{2.53}{\cdot}28H_2O$. The strongest lines of the powder X-ray diffraction pattern [d, Å (I, %) (hkl)] are: 12.820 (100) (110), 7.785 (80) (200), 6.319 (40) (121), 5.649 (30) (211), 3.176 (30) (170), 2.570 (30) (461, 550).
Kind of sample preparation and/or method of registration of the spectrum: Microsampling using a diamond-anvil cell. Transmission.
Source: Grice et al. (2002).
Wavenumbers (cm^{-1}): 3463s, 3356s, 1650, 1635sh, 1550w, 1515w, 1481, 1451sh, 1374sh, 1359s, 1325s, 1236, 1153, 1100, 1056, 1011sh, 962s, 912s, 833w, 812w, 785w, 709, 690sh.
Note: The wavenumbers were partly determined by us based on spectral curve analysis of the published spectrum.

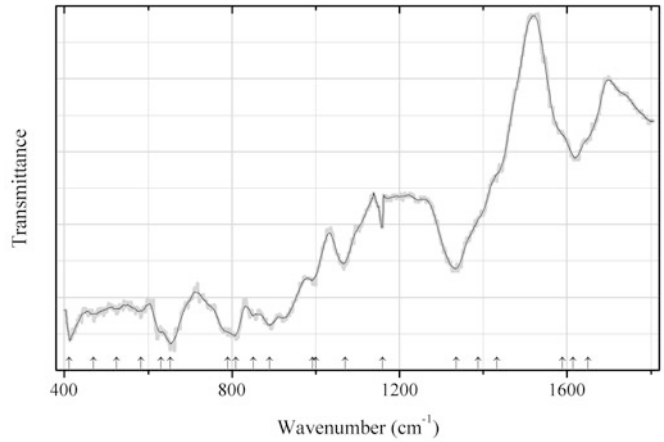

Fig. 2.40 IR spectrum of wardsmithite drawn using data from Erd et al. (1970)

B155 Wardsmithite $Ca_5Mg(B_4O_7)_6{\cdot}30H_2O$ (Fig. 2.40)
Locality: Hard Scramble claim, Ryan, Black Mts., Furnace Creek district, Death Valley region, Inyo Co., California, USA (type locality).
Description: Colourless crystals from the association with gowerite, ulexite, and colemanite. Holotype sample. Optically uniaxial (−), ω = 1.490(2), ε = 1.476(2). The strongest lines of the powder X-ray diffraction pattern [*d*, Å (*I*, %)] are: 13.5 (100), 12.3 (62), 6.12 (55), 3.358 (51), 4.721 (42), 2.744 (26).
Kind of sample preparation and/or method of registration of the spectrum: Transmission. Kind of sample preparation is not indicated.
Source: Erd et al. (1970).
Wavenumbers (cm^{-1}): 1650sh, 1615, 1589sh, 1433sh, 1388sh, 1335s, 1160, 1070, 1000, 992, 890, 851, 810, 790sh, 653, 630sh, 582, 524, 470, 412.
Note: The wavenumbers were partly determined by us based on spectral curve analysis of the published spectrum.

B156 Ericaite $Fe^{2+}{}_3B_7O_{13}Cl$
Locality: Thomas Müntzer pit, Bischofferode, near Ohmberg, Thuringia, Germany.
Kind of sample preparation and/or method of registration of the spectrum: KBr disc. Absorption.
Source: Moenke (1962).
Wavenumbers (cm^{-1}): (1630w), 1405, 1357, 1200, 1162, 1135, 1070, 1010s, 982sh, 930s, 900sh, 878, 852, 794, 710, 662, 648, 625sh, 610, 586, 555, 522, 448, 426sh.

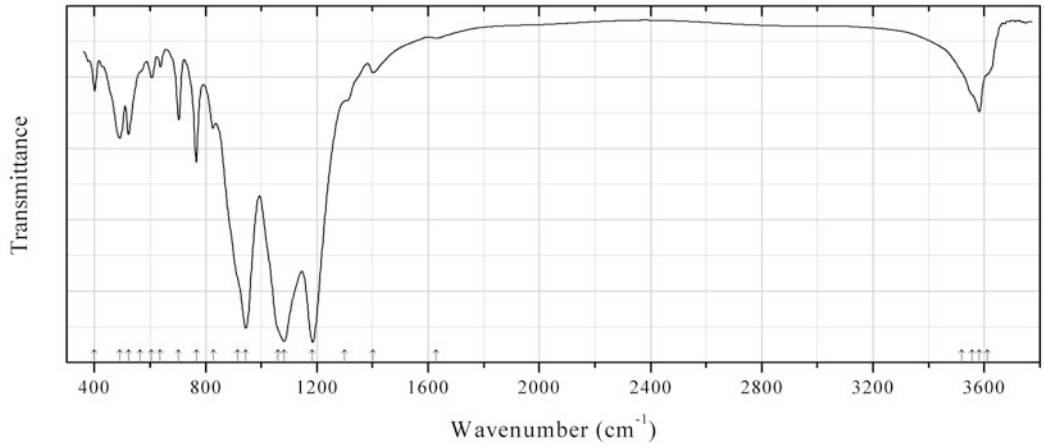

Fig. 2.41 IR spectrum of braitschite-(Ce) obtained by N.V. Chukanov

B157 Braitschite-(Ce) $(Ca,Na)_7(Ce,REE)_2[B_6O_7(OH,O)_6]_4 \cdot H_2O$ (Fig. 2.41)
Locality: Moab, Paradox basin, Grand Co., Utah, USA (type locality).
Description: Pink nests from the association with anhydrite, dolomite, and halite. The empirical formula is (electron microprobe): $(Ca_{6.9}Na_{0.1})(Ce_{0.8}La_{0.5}Nd_{0.3}Y_{0.4})B_x(O,OH)_yCl_{1.0} \cdot nH_2O$.
Kind of sample preparation and/or method of registration of the spectrum: KBr disc. Absorption.
Wavenumbers (cm^{-1}): 3610sh, 3581, 3555sh, 3520sh, 1630w, 1401w, 1300sh, 1184s, 1082s, 1060sh, 944s, 915sh, 827, 766, 703, 637w, 605w, 565sh, 522, 491, 400.

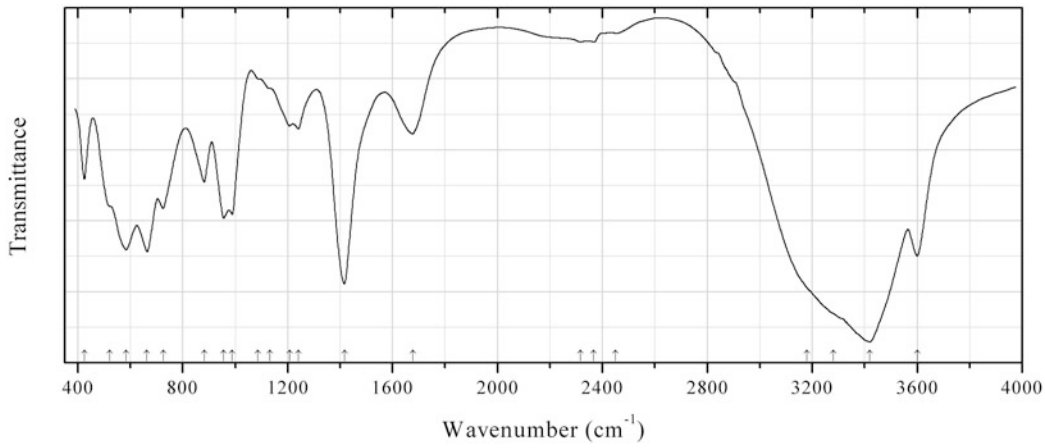

Fig. 2.42 IR spectrum of imayoshiite drawn using data from Nishio-Hamane et al. (2015)

B158 Imayoshiite $Ca_3Al(CO_3)[B(OH)_4](OH)_6 \cdot 12H_2O$ (Fig. 2.42)
Locality: Suisho-dani valley, near Ise City, Mie Prefecture, Japan (type locality).
Description: White fibrous aggregates from gabbro xenolith hosted by dunite. Associated minerals are oyelite, hydrogarnet, xonotlite, tobermorite, bultfonteinite, apophyllite, and prehnite. Holotype sample. Hexagonal, space group $P6_3$, a = 11.04592(2), c = 10.61502(19) Å, V = 1121.65(4) Å^3,

$Z = 2$. $D_{calc} = 1.790$ g/cm^3. Optically biaxial (−), $\omega = 1.497(2)$, $\varepsilon = 1.470(2)$. The empirical formula is $Ca_3Al_{0.889}Si_{0.116}(CO_3)_{1.015}[B(OH)_4]_{0.937}(SO_4)_{0.063}[(OH)_{5.961}O_{0.039}]\cdot 11.709H_2O$. The strongest lines of the powder X-ray diffraction pattern [*d*, Å (*I*, %) (*hkl*)] are: 9.5434 (100) (100), 4.6364 (40) (102), 3.8217 (33) (112), 3.7293 (31) (302), 2.5253 (69) (213, 123), 2.1739 (30) (223), 2.1198 (23) (313, 133), 1.7677 (28) (006).

Kind of sample preparation and/or method of registration of the spectrum: KBr disc. Transmission.

Source: Nishio-Hamane et al. (2015).

Wavenumbers (cm^{-1}): 3600s, 3420s, 3280sh, 3180sh, 2450w, (2368w), (2317w), 1678, 1417s, 1241, 1207, 1132sh, 1086sh, 989, 957, 882, 725, 664s, 585s, 522sh, 425.

Note: The wavenumbers were partly determined by us based on spectral curve analysis of the published spectrum. The weak bands at 2368 and 2368 cm^{-1} may correspond to atmospheric CO_2.

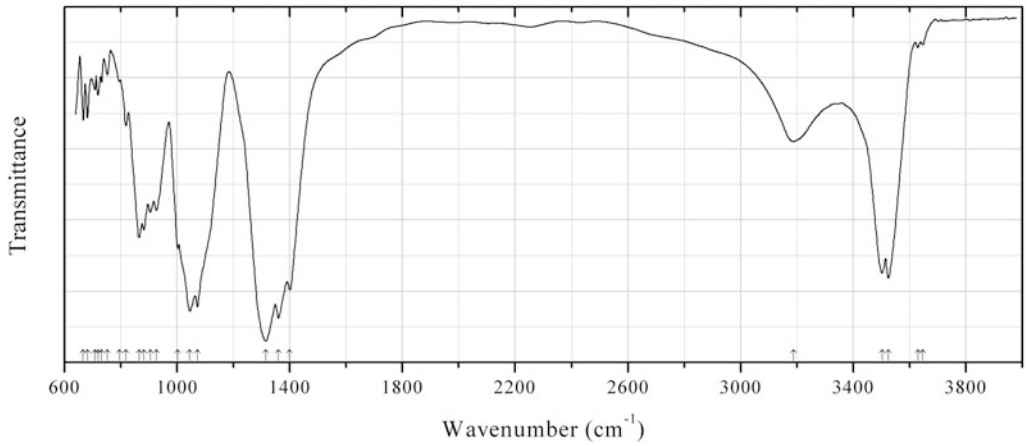

Fig. 2.43 IR spectrum of roweite drawn using data from Ando et al. (2015)

B159 Roweite $Ca_2Mn_2B_4O_7(OH)_6$ (Fig. 2.43)

Locality: Fuka mine, Bicchu-cho, near Takahashi city, Okayama prefecture, Honshu Island, Japan.

Description: Brown crystals from the association with uralborite, shimazakiite, frolovite, bultfonteinite, fluorite, and calcite. Orthorhombic, $a = 9.057(2)$, $b = 13.335(3)$, $c = 8.284(3)$. $D_{calc} = 2.92$ g/cm^3. The empirical formula is $Ca_{2.006}(Mn_{1.410}Fe_{0.333}Mg_{0.181}Zn_{0.036}Co_{0.004})B_{4.017}O_{6.989}(OH)_{6.011}$. The strongest lines of the powder X-ray diffraction pattern [*d*, Å (*I*, %) (*hkl*)] are: 5.39 (25) (120), 3.98 (99) (201), 3.06 (24) (202), 2.60 (100) (042), 2.19 (31) (401, 152), 2.13 (40) (043), 1.706 (27) (442), 1.637 (24) (081).

Kind of sample preparation and/or method of registration of the spectrum: Transmission. Kind of sample preparation is not indicated.

Source: Ando et al. (2015).

Wavenumbers (cm^{-1}): 3647w, 3630w, 3525s, 3503s, 3188, 1400s, 1360s, 1315s, 1072s, 1045s, 1002, 927, 905, 882, 865, 819, 794w, 752w, 732w, 720w, 708w, 682, 667.

Note: The wavenumbers were partly determined by us based on spectral curve analysis of the published spectrum.

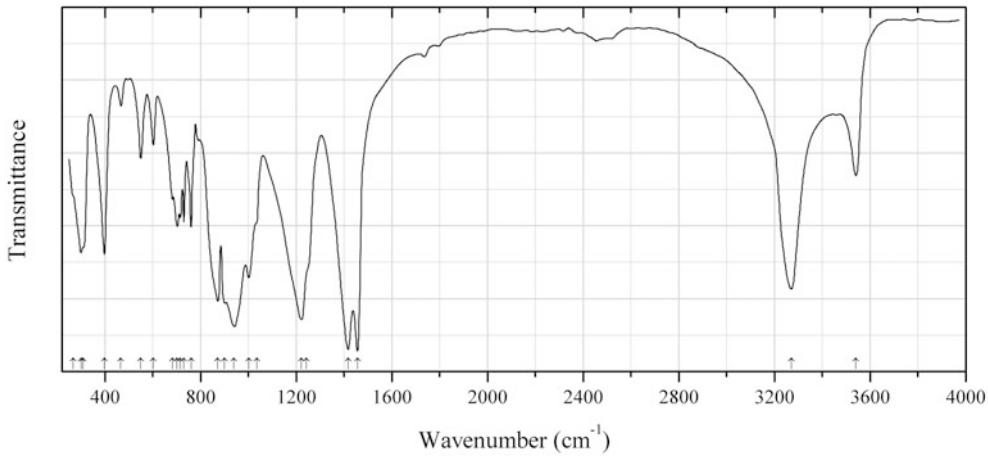

Fig. 2.44 IR spectrum of borcarite drawn using data from Kusachi et al. (1997b)

BC8 Borcarite $Ca_4MgB_4O_6(CO_3)_2(OH)_6$ (Fig. 2.44)
Locality: Fuka mine, Bicchu-cho, near Takahashi city, Okayama prefecture, Honshu Island, Japan.
Description: Light bluish green crystals from the association with olshanskyite, bultfonteinite, and calcite. Monoclinic, a = 17.82(1), b = 8.382(4), c = 4.452(3) Å, β = 101.95(4)°. D_{meas} = 2.56 g/cm^3. Optically biaxial (−), α = 1.592, β = 1.653, γ = 1.655. The empirical formula is $Ca_{3.944}(Mg_{0.815}Fe_{0.089})B_{3.981}O_{5.705})(OH)_{6.097}(CO_3)_{2.066}$. The strongest lines of the powder X-ray diffraction pattern [d, Å (I, %) (hkl)] are: 7.58 (100) (110), 2.912 (43) (600), 2.735 (39) (221), 2.671 (58) (−421), 2.271 (32) (−331), 1.887 (30) (440, 041, 910).
Kind of sample preparation and/or method of registration of the spectrum: KBr disc. Transmission.
Source: Kusachi et al. (1997b).
Wavenumbers (cm^{-1}): 3540, 3270s, 1456s, 1416s, 1242sh, 1222s, 1035sh, 1001, 940s, 900s, 872s, 760, 730, 715, 702, 682, 602, 550, 467w, 398, 308sh, 300, 268sh.
Note: The wavenumbers were partly determined by us based on spectral curve analysis of the published spectrum.

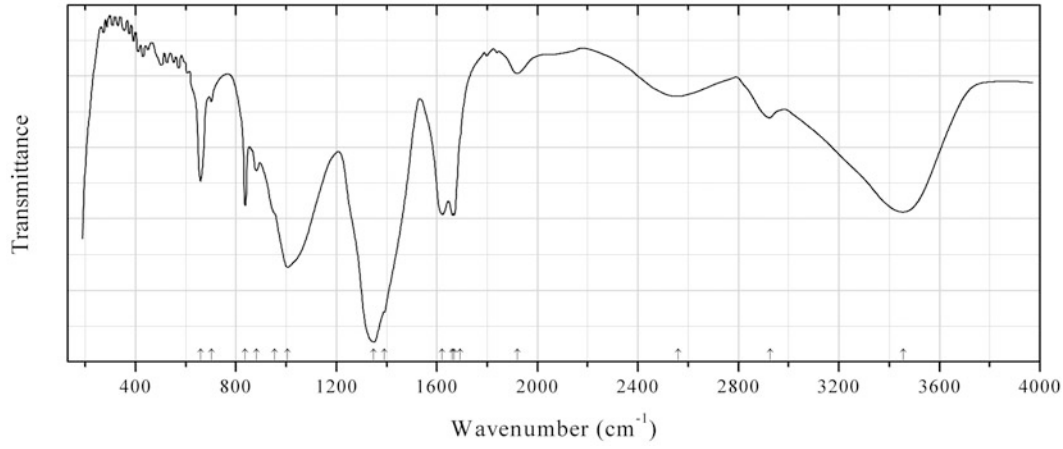

Fig. 2.45 IR spectrum of qilianshanite drawn using data from Luo et al. (1993)

BC9 Qilianshanite $Na(HCO_3)(H_3BO_3)\cdot 2H_2O$ (Fig. 2.45)
Locality: Juhongtu boron deposit, Qilian Mts., Qinghai province, China (type locality).
Description: Massive aggregates of colourless individuals from the association with quartz, calcite, tincalconite, and nahcolite. Holotype sample. Monoclinic, space group $C2$, a = 16.119(8), b = 6.928 (4), c = 6.730(3) Å, β = 100.46(4)°, V = 739.0(7) Å^3, Z = 4. D_{meas} = 1.706 g/cm^3. Optically biaxial (−), α = 1.351 (calculated), β = 1.459(2), γ = 1.486(2), 2 V = 50°. The empirical formula is $Na_{1.07}Ca_{0.01}H_{8.86}C_{0.71}B_{1.06}O_{8.00}$. The strongest lines of the powder X-ray diffraction pattern [d, Å (I, %) (hkl)] are: 6.36 (25) (110), 3.464 (100) (020), 3.173 (59) (220), 1.731 (19) (040).
Kind of sample preparation and/or method of registration of the spectrum: Transmission.
Source: Luo et al. (1993).
Wavenumbers (cm^{-1}): 3457s, 2927, 2559, 1920w, 1692sh, 1669, 1662, 1622, 1391sh, 1349s, 1006s, 955sh, 882, 837, 702w, 659.
Note: The wavenumbers were partly determined by us based on spectral curve analysis of the published spectrum.

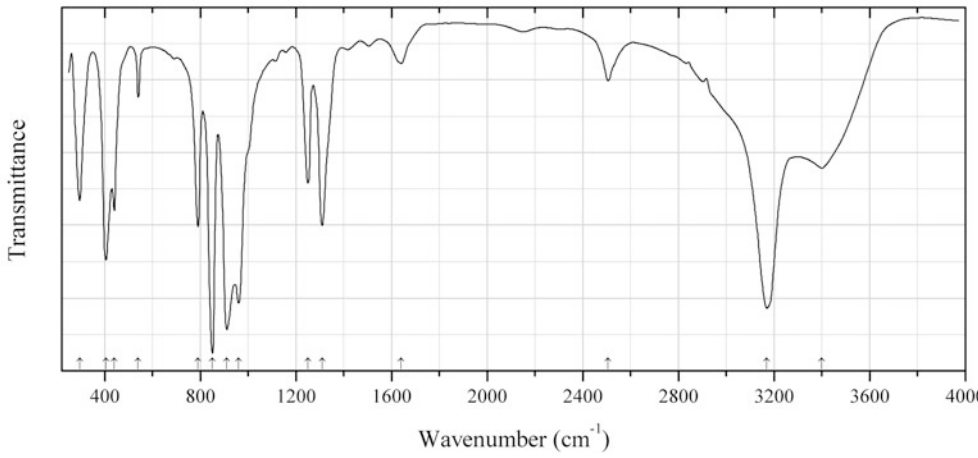

Fig. 2.46 IR spectrum of cahnite drawn using data from Shiraga et al. (2002)

BAs3 Cahnite $Ca_2B(AsO_4)(OH)_4$ (Fig. 2.46)
Locality: Fuka mine, Bicchu-cho, near Takahashi city, Okayama prefecture, Honshu Island, Japan.
Description: Aggregate of pseudotetrahedral crystals from the association with calcite, johnbaumite, andradite, arsenopyrite, and löllingite. Tetragonal, a = 7.101(1), c = 6.192(1) Å. D_{meas} = 3.13(2) g/cm^3. Optically uniaxial (−), ω = 1.658(1), ε = 1.657(1). The empirical formula is $Ca_{2.09}B_{0.95}As_{0.93}Si_{0.06}O_{3.92}(OH)_{4.08}$. The strongest lines of the powder X-ray diffraction pattern [d, Å (I, %) (hkl)] are: 5.04 (16) (110), 4.68 (10) (101), 3.56 (100) (200), 2.827 (10) (211), 2.636 (16) (112), 2.247 (12) (310), 1.817 (18) (312).
Kind of sample preparation and/or method of registration of the spectrum: KBr disc. Transmission.
Source: Shiraga et al. (2002).
Wavenumbers (cm^{-1}): 3400, 3170s, 2505w, 1640w, 1310, 1250, 960s, 910s, 850s, 790, 540w, 440, 405s, 295.
Note: The bands at 3400 and 1640 cm^{-1} may correspond to adsorbed water.

2.2 Carbon and Carbonates

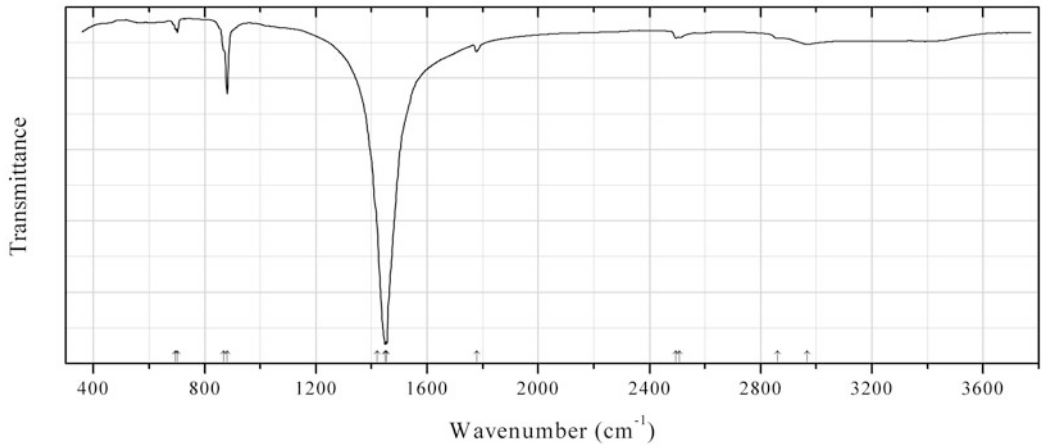

Fig. 2.47 IR spectrum of natrite obtained by N.V. Chukanov

C225 Natrite $Na_2(CO_3)$ (Fig. 2.47)
Locality: Oleniy Stream apatite deposit, Khibiny alkaline complex, Kola peninsula, Murmansk region, Russia.
Description: White granular aggregate from peralkaline pegmatite. Investigated by I.V. Pekov.
Kind of sample preparation and/or method of registration of the spectrum: KBr disc. Absorption.
Wavenumbers (cm^{-1}): 2968w, 2862w, 2507w, 2495w, 1778w, 1455s, 1449s, 1420sh, 880, 870sh, 702w, 695sh.

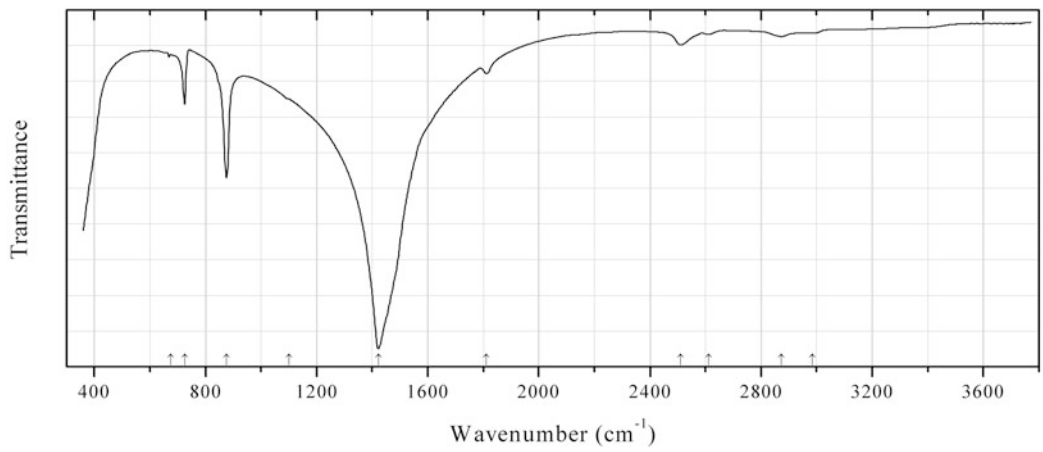

Fig. 2.48 IR spectrum of ankerite obtained by N.V. Chukanov

C226 Ankerite $Ca(Fe^{2+},Mg)(CO_3)_2$ (Fig. 2.48)
Locality: Smallcleugh mine, Nenthead, Alston Moor district, Cumbria, England, UK.

Description: Brownish-yellow split rhombohedral crystals. The empirical formula is $Ca_{1.00}(Fe_{0.48}Mg_{0.35}Ca_{0.09}Mn_{0.08})(CO_3)_2$.
Kind of sample preparation and/or method of registration of the spectrum: KBr disc. Absorption.
Wavenumbers (cm^{-1}): 2985w, 2873w, 2612w, 2510w, 1811w, 1422s, 1100sh, 875s, 725, 675w.

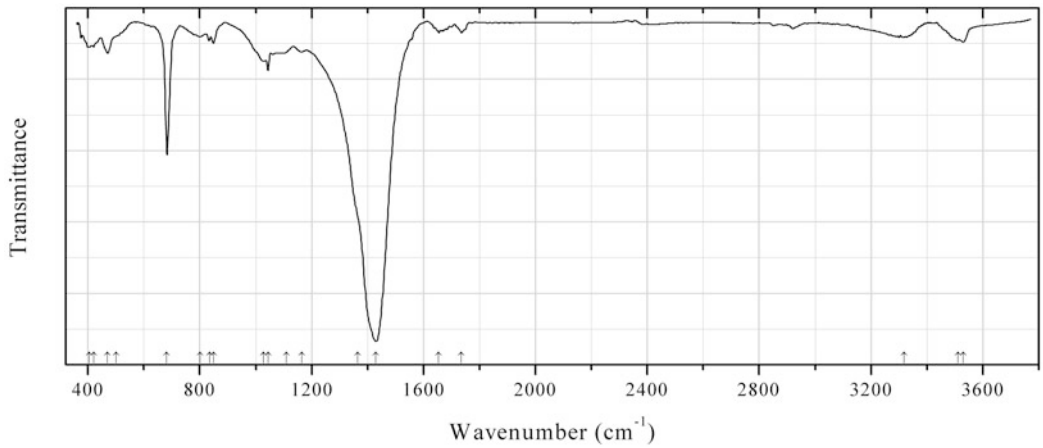

Fig. 2.49 IR spectrum of hydrocerussite obtained by N.V. Chukanov

C227 Hydrocerussite $Pb_3(CO_3)_2(OH)_2$ (Fig. 2.49)
Locality: Passa Limani, near Lavrion, Attiki Prefecture, Greece.
Description: Colourless platy crystals from ancient slag. Confirmed by the single-crystal X-ray diffraction pattern.
Kind of sample preparation and/or method of registration of the spectrum: KBr disc. Absorption.
Wavenumbers (cm^{-1}): 3530, 3510sh, (3318), 1735w, (1654), 1430s, 1365sh, 1165, 1110, 1044, 1027, 849, 834, 802w, 682s, 500sh, 470, 420, 404.

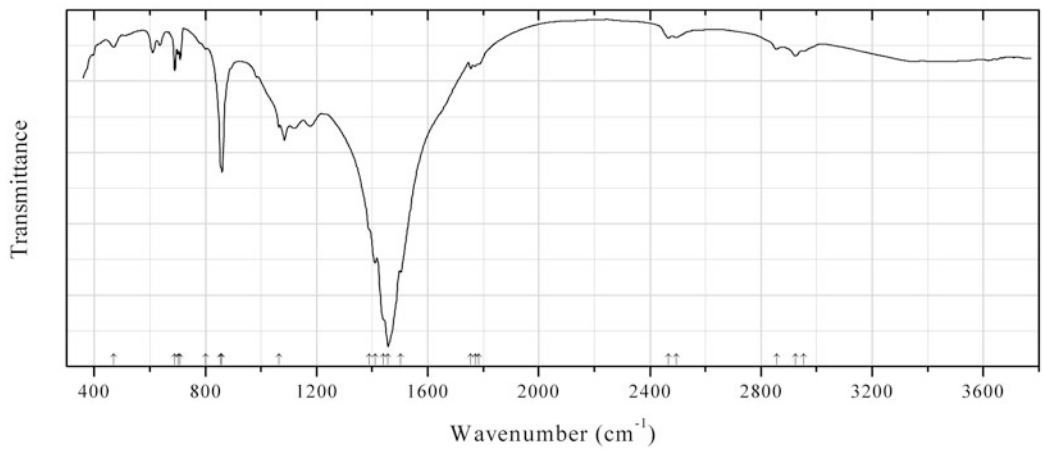

Fig. 2.50 IR spectrum of paralstonite obtained by N.V. Chukanov

C228 Paralstonite $BaCa(CO_3)_2$ (Fig. 2.50)

Locality: Minerva No. 1 mine, Ozark-Mahoning Group, Cave-in-Rock, Hardin Co., Illinois, USA (type locality).
Description: White crystals from the association with barite.
Kind of sample preparation and/or method of registration of the spectrum: KBr disc. Absorption.
Wavenumbers (cm^{-1}): 2953w, 2923w, 2855w, 2495w, 2466w, 1783w, 1771w, 1755w, 1503s, 1457s, 1440sh, 1410s, 1390sh, 1065, 860s, 855sh, 802w, 709, 701w, 690, 470w.
Note: Additional bands at 1177, 1122, 1084, 985, 635, and 610 cm^{-1} correspond to the admixture of barite.

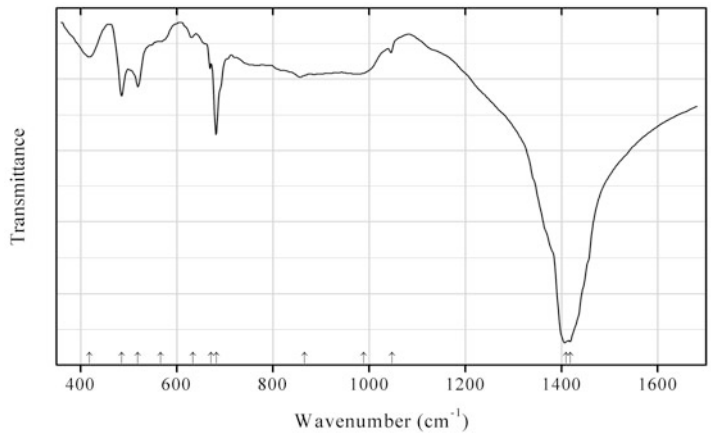

Fig. 2.51 IR spectrum of hydrocerussite obtained by N.V. Chukanov

C229 Hydrocerussite $Pb_3(CO_3)_2(OH)_2$ (Fig. 2.51)
Locality: Nyorkpakhk Mt., Khibiny alkaline complex, Kola peninsula, Murmansk region, Russia.
Description: White pseudomorph after galena. The associated minerals are malachite, hemimorphite, fraipontite, natrolite, bornite, sphalerite, and potassium feldspar. The strongest lines of the powder X-ray diffraction pattern [*d*, Å (*I*, %)] are: 4.464 (50), 4.242 (49), 3.604 (84), 3.281 (100), 2.622 (94), 2.231 (25). Confirmed by qualitative electron microprobe analysis.
Kind of sample preparation and/or method of registration of the spectrum: KBr disc. Absorption.
Wavenumbers (cm^{-1}): 1418s, 1409s, 1047w, 989, 865sh, 682, 672w, 634w, 566w, 519, 486, 419.

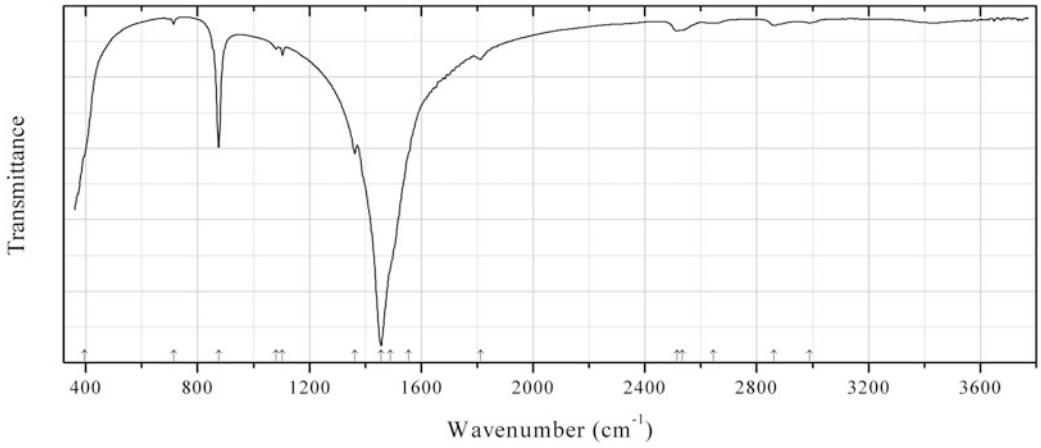

Fig. 2.52 IR spectrum of eitelite obtained by N.V. Chukanov

C230 Eitelite $Na_2Mg(CO_3)_2$ (Fig. 2.52)
Locality: Westvaco mine, Green River formation, Sweetwater Co., Wyoming, USA.
Description: Wax-yellow columnar aggregate. Confirmed by semiquantitative electron microprobe analysis.
Kind of sample preparation and/or method of registration of the spectrum: KBr disc. Absorption.
Wavenumbers (cm^{-1}): 2990w, 2862w, 2645w, 2535sh, 2514w, 1811w, 1555sh, 1490sh, 1456s, 1362, 1103w, 1081w, 875, 714w, 395sh.

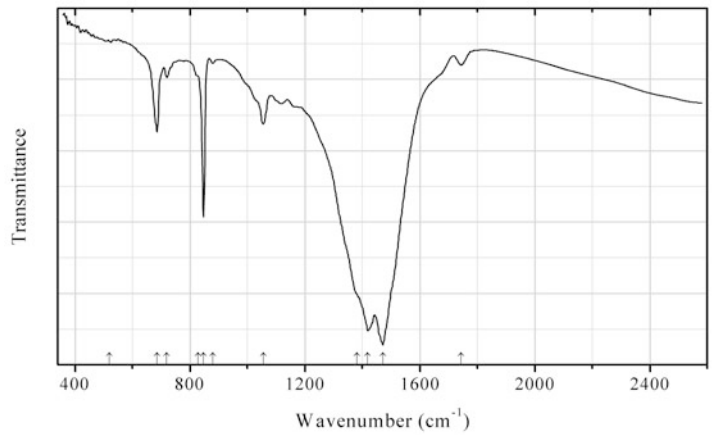

Fig. 2.53 IR spectrum of sanrománite obtained by N.V. Chukanov

C231 Sanrománite $Na_2CaPb_3(CO_3)_5$ (Fig. 2.53)
Locality: Santa Rosa mine, Iquique, I Region, Atacama desert, Chile (type locality).
Description: Clusters of light yellow crystals from the association with chalconatronite. Confirmed by qualitative electron microprobe analysis.
Kind of sample preparation and/or method of registration of the spectrum: KBr disc. Absorption.
Wavenumbers (cm^{-1}): 1744w, 1472s, 1419s, 1380sh, 1055, 880w, 847s, 830sh, 720w, 686, 520w.

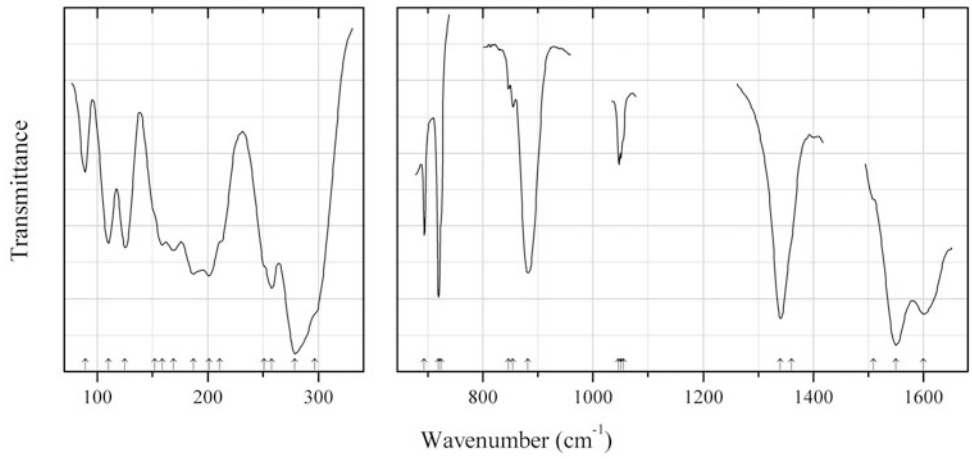

Fig. 2.54 IR spectrum of agricolaite drawn using data from Anderson et al. (1980)

C232 Agricolaite $K_4(UO_2)(CO_3)_3$ (Fig. 2.54)
Locality: Synthetic.
Description: Pale yellow crystals. The crystal structure is solved. Monoclinic, space group *C*2/*c*, a = 10.247(3), b = 9.202(2), c = 12.226(3) Å, β = 95.22(2)°, V = 1148.2(6) Å^3, Z = 4.
Kind of sample preparation and/or method of registration of the spectrum: Transmittance. Kind of sample preparation is unknown.
Source: Anderson et al. (1980).
Wavenumbers (cm^{-1}): 1600s, 1550s, 1509sh, 1360sh, 1340s, 1055, 1050.5, 1046.5, 882s, 855w, 847w, 724sh, 720s, 694 (mid IR region); 297sh, 279s, 258, 251sh, 211sh, 201, 187, 169, 159, 152sh, 125, 110, 89.

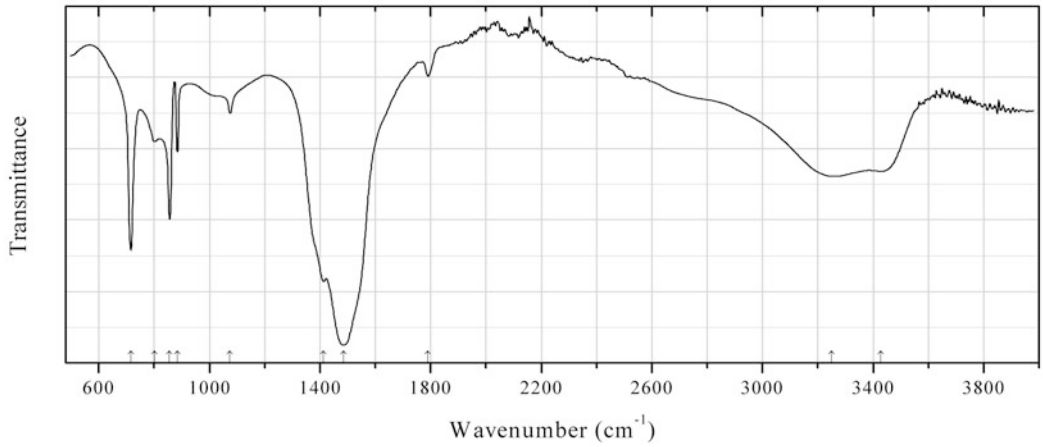

Fig. 2.55 IR spectrum of arisite-(Ce) drawn using data from Piilonen et al. (2010)

C233 Arisite-(Ce) $NaCe_2(CO_3)_2[F_{2x}(CO_3)_{1-x}]F$ (Fig. 2.55)
Locality: Ariskop Quarry, Aris, near Windhoek, Windhoek district, Khomas Region, Namibia (type locality).

Description: Vitreous, transparent, beige, hexagonal plates from miarolitic cavities in phonolite. Holotype sample. The crystal structure is solved. Hexagonal, space group *P*-6*m*2, a = 5.1109(2), c = 8.6713(4) Å, V = 196.16(6) Å^3, Z = 1. D_{calc} = 4.126 g/cm^3. The empirical formula is $(Na_{0.97}Ca_{0.03})(Ce_{0.92}La_{0.80}Nd_{0.11}Pr_{0.04}Sm_{0.01}Ca_{0.09})(CO_3)_2[(CO_3)_{0.7}F_{0.59}]F$. The strongest lines of the powder X-ray diffraction pattern [*d*, Å (*I*, %) (*hkl*)] are: 4.439 (100) (100), 4.352 (52) (002), 3.103 (87) (102), 2.561 (38) (110), 2.212 (43) (200), 1.9748 (42) (202).
Kind of sample preparation and/or method of registration of the spectrum: Transmission. A crystal was positioned in a Spectra-Tech low-pressure diamond-anvil cell and pressed into a thin film.
Source: Piilonen et al. (2010).
Wavenumbers (cm^{-1}): 3427, 3251, 1790w, 1485s, 1413s, 1075, 884, 856s, 802, 716s.

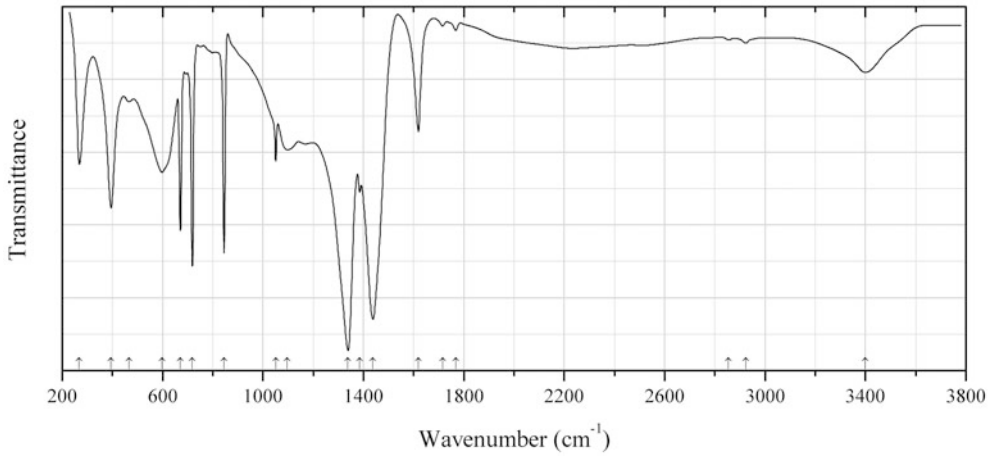

Fig. 2.56 IR spectrum of barstowite drawn using data from Stanley et al. (1991)

C234 Barstowite $Pb_4(CO_3)Cl_6 \cdot H_2O$ (Fig. 2.56)
Locality: Bounds Cliff, St. Endellion, Cornwall, UK (type locality).
Description: Colourless crystals from the association with quartz, dolomite, phosgenite, cerussite, sphalerite, pyrite, chalcopyrite, galena, and jamesonite. Holotype sample. Monoclinic, space group $P2_1/m$, a = 4.218(2), b = 9.180(2), c = 16.673(4) Å, β = 91.49(3)°, V = 645.38 Å^3, Z = 2. D_{meas} = 5.71 g/cm^3. The empirical formula is $Pb_{4.02}Cl_{5.82}C_{1.03}H_{1.97}O_{4.16}$. The strongest lines of the powder X-ray diffraction pattern [*d*, Å (*I*, %) (*hkl*)] are: 4.02 (100) (022), 2.296 (80) (040, 12–5, 106), 2.377 (60) (007, 026), 4.160 (50) 004), 2.108 (40) (200), 3.790 (30) (014).
Kind of sample preparation and/or method of registration of the spectrum: KBr disc. Transmission.
Source: Stanley et al. (1991).
Wavenumbers (cm^{-1}): 3400, (2924w), (2855w), 1768w, 1716w, 1619, 1438s, (1385w), 1339s, 1096w, 1051w, 845s, 719s, 671s, 598, 467w, 394s, 268.
Note: The weak bands at 2924 and 2855 cm^{-1} correspond to the impurity of grease. The small peak at 1385 cm^{-1} may be due to the impurity of a nitrate in the KBr medium. For the IR spectrum of barstowite see also Jones and Jackson (1993).
C235 Bastnäsite-(La) $La(CO_3)F$
Locality: Bastnäs, Riddarhyttan, Västmanland, Sweden.

Description: La:Ce:Nd ≈ 5:4:1.
Kind of sample preparation and/or method of registration of the spectrum: KBr disc. Transmission.
Source: Jones and Jackson (1993).
Wavenumbers (cm^{-1}): 3747w, 3608w, 3581w, 3494, 3440, 2842, 2582w, 2500, 1822, 1760, 1443s, 1087, 880s, 868s, 842, 789w, 749, 728, 720, 664w, 360s, 266s.

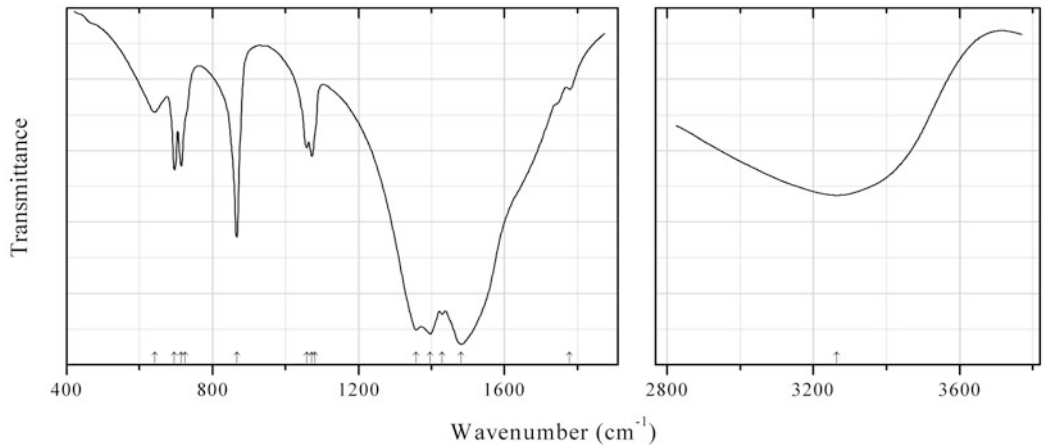

Fig. 2.57 IR spectrum of ewaldite drawn using data from Voloshin et al. (1992b)

C236 Ewaldite $Ba(Na,Ca,Y,REE,K)(CO_3)_2 \cdot nH_2O$ (n = 2–3) (Fig. 2.57)
Locality: Vuoriyarvi alkaline-ultramafic pluton, Northern Karelia, Russia.
Description: Disc-like crystals from the association with fluorite, calcite, zhonghuacerite-(Ce), mckelveyite-(Y), donnayite-(Y), ancylite-(Ce), pectolite, vinogradovite, a labuntsovite-group mineral, and pyrite. The crystal structure is solved. Hexagonal, space group $P6_3mc$, a = 5.318(2), c = 12.837 (7) Å, Z = 2. D_{meas} = 3.47 g/cm^3. The strongest lines of the powder X-ray diffraction pattern [d, Å (I, %) (hkl)] are: 4.34 (70) (101), 3.135 (100) (103), 2.655 (80) (110), 2.626 (80) (104), 2.044 (90) (114), 1.024 (90) (203).
Kind of sample preparation and/or method of registration of the spectrum: KBr disc. Absorption.
Source: Voloshin et al. (1992b).
Wavenumbers (cm^{-1}): 3264, 1779w, 1482s, 1429, 1397s, 1358s, 1080sh, 1072, 1058, 866s, 725sh, 714, 696, 641.
Note: The wavenumbers were partly determined by us based on spectral curve analysis of the published spectrum.

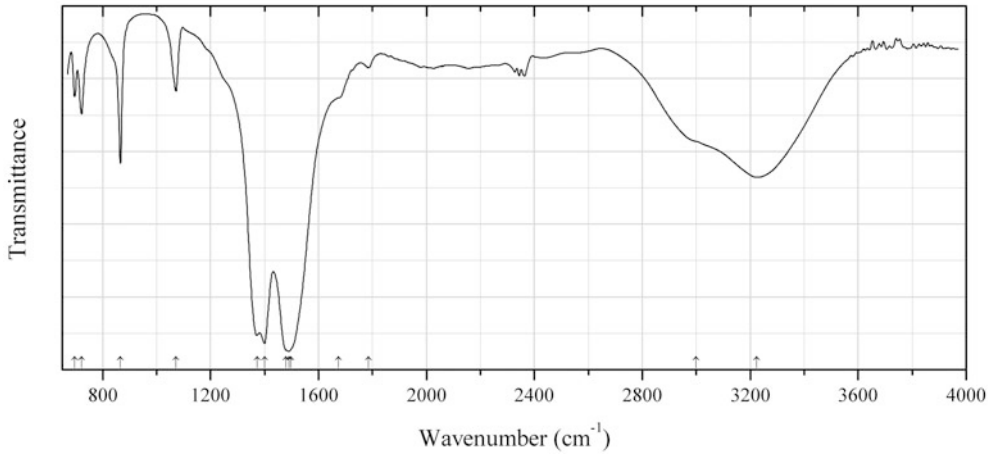

Fig. 2.58 IR spectrum of ewaldite drawn using data from Petersen et al. (2003)

C237 Ewaldite $Ba(Na,Ca,Y,REE,K)(CO_3)_2 \cdot nH_2O$ (n = 2–3) (Fig. 2.58)
Locality: Narssârssuq pegmatite, Igaliko alkaline complex, South Greenland.
Description: Colourless to white crystals with epitaxy of donnayite-(Y) from the association with calcite, ashcroftine-(Y), ancylite-(Ce), fluorite, aegirine, elpidite, orthoclase, graphite, and polylithionite. Hexagonal, presumed space group $P6_3mc$, a = 5.294(2), c = 12.666(4) Å. Uniaxial (−), ε = 1.552, ω = 1.653. The empirical formula is $(Ba_{2.37}Sr_{0.60})(Na_{1.06}Ca_{0.89}(Y_{0.38}Ce_{0.24}Nd_{0.18}La_{0.08}Dy_{0.06}Pr_{0.06}Sm_{0.04}Er_{0.03})(CO_3)_6 \cdot 3H_2O$.
Kind of sample preparation and/or method of registration of the spectrum: Diamond anvil-cell sampling.
Source: Petersen et al. (2003).
Wavenumbers (cm^{-1}): 3225, 3000sh, 1785w, 1675sh, 1498sh, 1490s, 1479sh, 1400s, 1372s, 1072, 866, 722, 696.
Note: The wavenumbers were partly determined by us based on spectral curve analysis of the published spectrum.

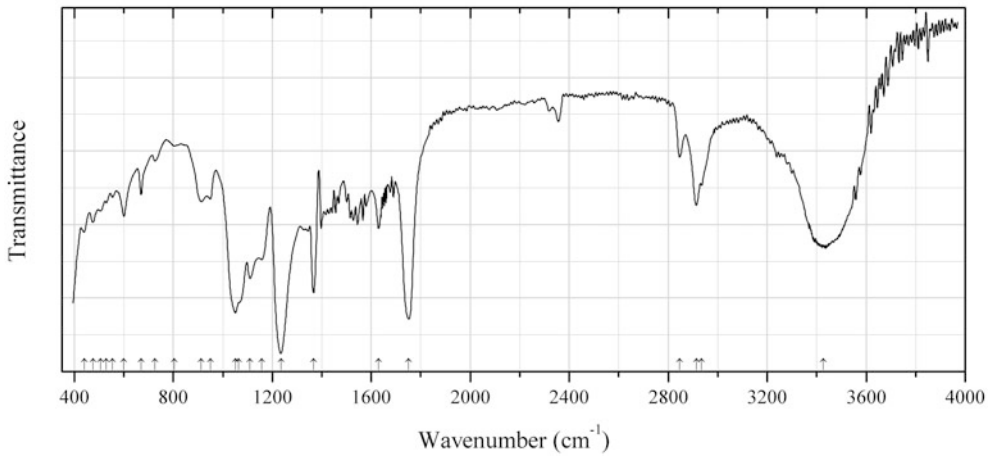

Fig. 2.59 IR spectrum of blatonite drawn using data from Vochten and Deliens (1998)

C238 Blatonite $(UO_2)(CO_3)\cdot H_2O$ (Fig. 2.59)
Locality: Jomac mine, Brown's Rim, San Juan Co., Utah, USA (type locality).
Description: Canary yellow acicular crystals from the association with boltwoodite, coconinoite, metazeunerite, rutherfordine, azurite, brochantite, carbonate-cyanotrichite, malachite, and gypsum. Holotype sample. Hexagonal or trigonal, a = 15.79(1), c = 23.93(3) Å, V = 5167(9) Å^3, Z = 36. D_{meas} = 4.05(2) g/cm^3, D_{calc} = 4.02 g/cm^3. Optically biaxial (+), ω = 1.588(2), ε = 1.612(2). The empirical formula is $0.988UO_2\cdot 1.004CO_2\cdot 1.029H_2O$. The strongest lines of the powder X-ray diffraction pattern [d, Å (I, %) (hkl)] are: 7.86 (47) (110), 6.91 (55) (103), 6.56 (77) (201), 4.76 (40) (114), 4.34 (36) (213), 3.06 (100) (207).
Kind of sample preparation and/or method of registration of the spectrum: KBr disc. Transmission.
Source: Vochten and Deliens (1998).
Wavenumbers (cm^{-1}): 3426s, 2935, 2914, 2846, 1750s, 1630, 1367, 1235s, 1159, 1110, 1064sh, 1051s, 950, 914, 805w, 727w, 670w, 600, 555w, 530w, 506w, 475w, 440w.
Note: The crystal structure of blatonite is not investigated. The wavenumbers were partly determined by us based on spectral curve analysis of the published spectrum. The bands at 2935, 2914, 1750, 1367, and 1235 cm^{-1} indicate that blatonite is perhaps an organic mineral, or the sample used is strongly contaminated with an organic matter. Weak bands in the region 2300–2400 cm^{-1} correspond to atmospheric CO_2.

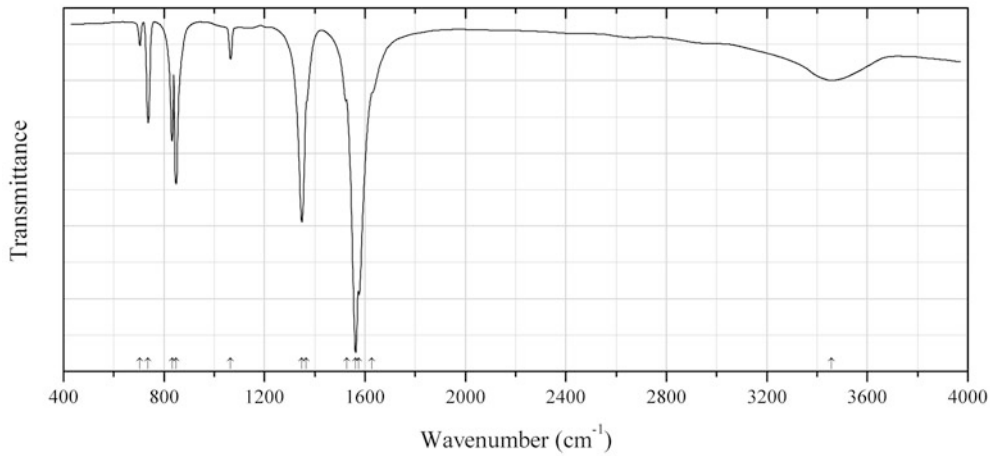

Fig. 2.60 IR spectrum of čejkaite drawn using data from Ondruš et al. (2003)

C239 Čejkaite $Na_4(UO_2)(CO_3)_3$ (Fig. 2.60)
Locality: Svornost shaft, Jáchymov, Krušné Hory Mts. (Ore Mts.), Czech Republic (type locality).
Description: Yellow earthy aggregates from the association with andersonite and schröckingerite. Holotype sample. Triclinic, space group $P1$ or P-1, a = 9.291(2), b = 9.292(2), c = 12.895(2) Å, α = 90.73 (2)°, β = 90.82(2)°, γ = 120.00(1)°, V = 963.7(4) Å^3, Z = 4. D_{meas} = 3.67(1) g/cm^3, D_{calc} = 3.766 g/cm^3. The calculated mean refractive index is 1.5825. The empirical formula is $(Na_{3.77}Fe_{0.04}Mg_{0.02})(UO_2)_{1.03}(CO_3)_{2.98}$. The strongest lines of the powder X-ray diffraction pattern [d, Å (I, %) (hkl)] are: 8.022 (92) (1–10, 010, 100), 5.080 (57) (−102, 0–12), 5.024 (60) (−112, 1–12), 4.967 (68) (012, 102), 4.639 (100) (1–20, 2–10, 110), 3.221 (63) (004), 2.681 (60) (3–30, −114, 030, 300).
Kind of sample preparation and/or method of registration of the spectrum: KBr disc. Absorption.

Source: Ondruš et al. (2003).
Wavenumbers (cm^{-1}): 3457, 1627sh, 1576s, 1563s, 1527sh, 1366sh, 1349s, 1065, 848, 832, 737, 704w.
Note: The bands at 3457 and 1627 cm^{-1} correspond to H_2O molecules.

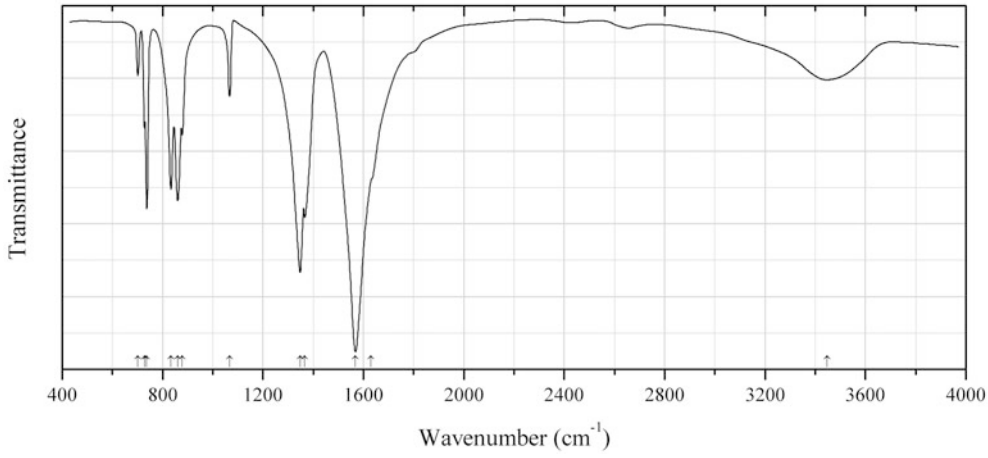

Fig. 2.61 IR spectrum of čejkaite polymorph drawn using data from Ondruš et al. (2003)

C240 Čejkaite polymorph $Na_4(UO_2)(CO_3)_3$ (Fig. 2.61)
Locality: Synthetic.
Description: Confirmed by powder X-ray diffraction data. Trigonal, space group *P*-3*c*1, a = 9.3380 (2), c = 12.8170(3) Å.
Kind of sample preparation and/or method of registration of the spectrum: KBr disc. Absorption.
Source: Ondruš et al. (2003).
Wavenumbers (cm^{-1}): 3447, 1630sh, 1568s, 1366, 1348s, 1067, 878, 860, 833, 737, 728, 701.
Note: The bands at 3447 and 1630 cm^{-1} correspond to H_2O molecules. For the IR spectrum of trigonal polymorph of čejkaite see also Chernorukov et al. (2003).

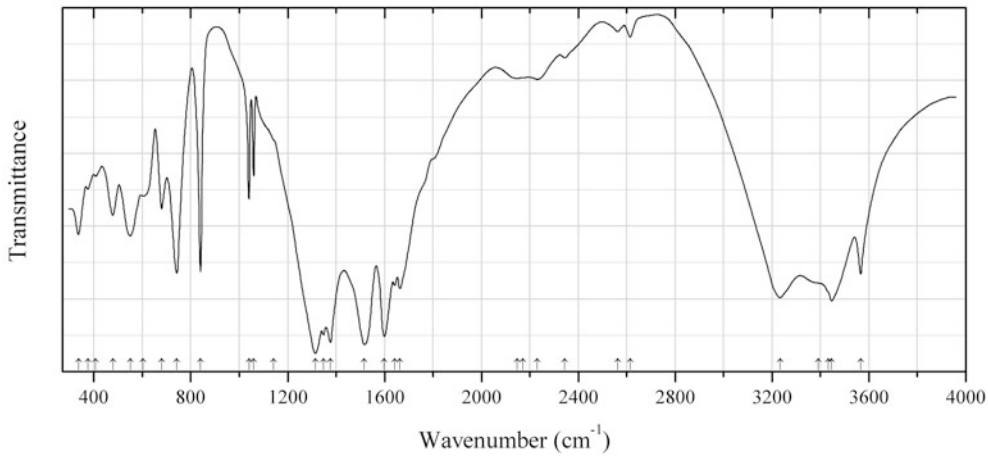

Fig. 2.62 IR spectrum of chalconatronite drawn using data from Pollard et al. (1991)

C241 Chalconatronite $Na_2Cu(CO_3)_2 \cdot 3H_2O$ (Fig. 2.62)
Locality: Synthetic.
Description: Confirmed by powder X-ray diffraction data.
Kind of sample preparation and/or method of registration of the spectrum: KBr disc. Absorption.
Source: Polland et al. (1991).
Wavenumbers (cm^{-1}): 3566, 3446s, 3432sh, 3390sh, 3233s, 2614w, 2563w, 2345w, 2230, 2170sh, 2148, 1664, 1642, 1598s, 1517s, 1377s, 1348s, 1314s, 1143sh, 1060, 1040, 840, 742, 680, 603, 551, 478, 407w, 375w, 336.
Note: The wavenumbers were determined by us based on spectral curve analysis of the published spectrum.

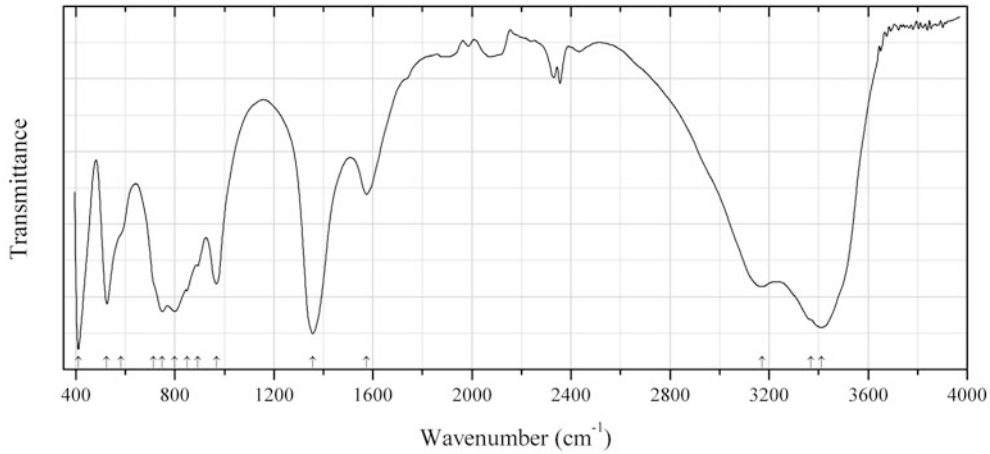

Fig. 2.63 IR spectrum of charmarite-2*H* drawn using data from Chao and Gault (1997)

C242 Charmarite-2*H* $Mn_4Al_2(OH)_{12}(CO_3) \cdot 3H_2O$ (Fig. 2.63)
Locality: Poudrette (Demix) quarry, Mont Saint-Hilaire, Rouville RCM (Rouville Co.), Montérégie, Québec, Canada (type locality).
Description: Orange-brown tabular crystals from the association with analcime, natrolite, microcline, aegirine, astrophyllite, gonnardite, catapleiite, calcite, siderite, rhodochrosite, burbankite, and kutnohorite. Holotype sample. Hexagonal, space group $P6_322$, a = 10.985(5), c = 15.10(2) Å, V = 1578 (3) $Å^3$, Z = 4. D_{meas} = 2.47(1) g/cm^3, D_{calc} = 2.50 g/cm^3. Optically uniaxial (−), ω = 1.587(1), ε = 1.547(1). The empirical formula is $(Mn_{3.99}Mg_{0.01}Fe_{0.05})Al_{2.03}[(OH)_{12.04}F_{0.03}](CO_3)_{1.09} \cdot nH_2O$. The strongest lines of the powder X-ray diffraction pattern [d, Å (I, %) (hkl)] are: 7.53 (100) (002), 3.768 (60) (004), 2.578 (50) (222), 2.221 (40) (224), 1.856 (40) (226), 1.552 (40) (602).
Kind of sample preparation and/or method of registration of the spectrum: Diamond-anvil cell microsampling. Transmission.
Source: Chao and Gault (1997).
Wavenumbers (cm^{-1}): 3411s, 3368sh, 3172, 1575, 1357s, 968, 892, 849, 800s, 750s, 714sh, 582sh, 525s, 410s.
Note: The wavenumbers were determined by us based on spectral curve analysis of the published spectrum. Bands in the range from 2300 to 2400 cm^{-1} correspond to atmospheric CO_2.

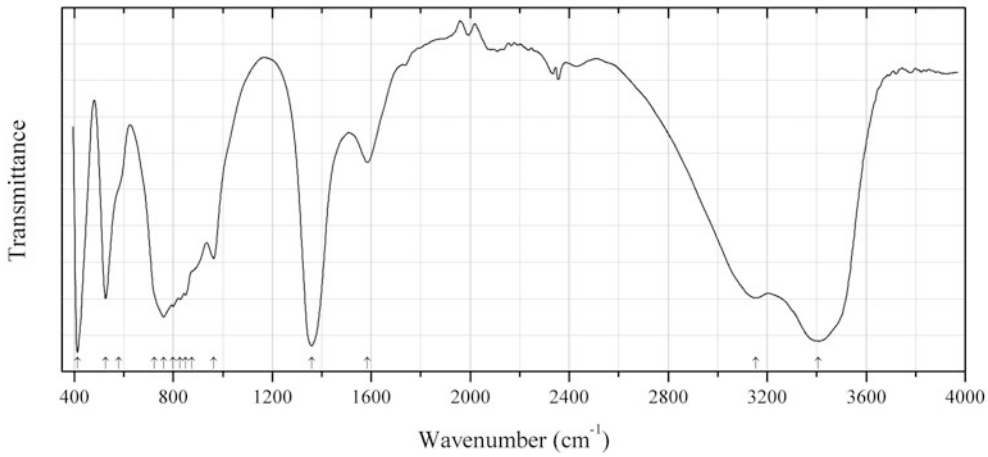

Fig. 2.64 IR spectrum of charmarite-3*T* drawn using data from Chao and Gault (1997)

C243 Charmarite-3*T* $Mn_4Al_2(OH)_{12}(CO_3)\cdot 3H_2O$ (Fig. 2.64)
Locality: Poudrette (Demix) quarry, Mont Saint-Hilaire, Rouville RCM (Rouville Co.), Montérégie, Québec, Canada (type locality).
Description: Orange-brown platy crystals from the association with analcime, natrolite, microcline, aegirine, astrophyllite, gonnardite, catapleiite, calcite, siderite, rhodochrosite, burbankite, and kutnohorite. Holotype sample. Trigonal, space group $P3_112$ or $P3_212$, a = 10.985(3), c = 22.63(3) Å, V = 2366(4) Å^3, Z = 6. D_{meas} = 2.48(1) g/cm^3, D_{calc} = 2.50 g/cm^3. Optically uniaxial (−), ω = 1.587 (1), ε undetermined. The empirical formula is $Mn_{4.01}(Al_{1.98}Fe_{0.02})Al_{2.03}(OH)_{12.02}(CO_3)\cdot nH_2O$. The strongest lines of the powder X-ray diffraction pattern [*d*, Å (*I*, %) (*hkl*)] are: 7.55 (100) (003), 3.770 (90) (006), 2.670 (70) (222), 2.346 (70) (225), 1.973 (60) (228), 1.586 (30) (600), 1.562 (30) (603).
Kind of sample preparation and/or method of registration of the spectrum: Diamond-anvil cell microsampling. Transmission.
Source: Chao and Gault (1997).
Wavenumbers (cm^{-1}): 3407s, 3154, 1584, 1359s, 964, 875sh, 850, 827, 800, 761s, 724sh, 580sh, 527, 412s.
Note: The wavenumbers were determined by us based on spectral curve analysis of the published spectrum. Bands in the range from 2300 to 2400 cm^{-1} correspond to atmospheric CO_2.

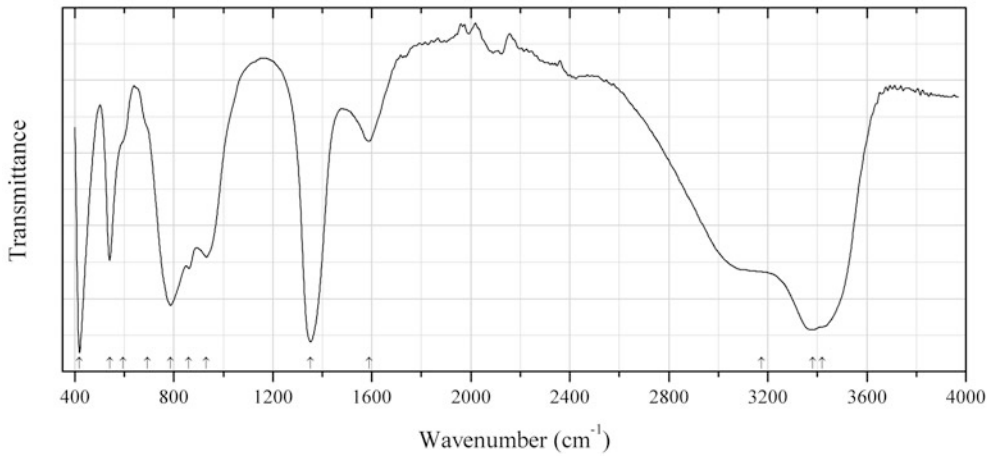

Fig. 2.65 IR spectrum of caresite-3*T* drawn using data from Chao and Gault (1997)

C244 Caresite-3*T* $Fe_4Al_2(OH)_{12}(CO_3)\cdot 3H_2O$ (Fig. 2.65)
Locality: Poudrette (Demix) quarry, Mont Saint-Hilaire, Rouville RCM (Rouville Co.), Montérégie, Québec, Canada (type locality).
Description: Greenish-black crystals from the association with smectite and chamosite. Holotype sample. Trigonal, space group $P3_112$ or $P3_212$, $a = 10.805(3)$, $c = 22.48(3)$ Å, $V = 2373(4)$ Å^3, $Z = 6$. $D_{meas} = 2.59(1)$ g/cm^3, $D_{calc} = 2.59$ g/cm^3. Optically uniaxial (−), $\omega = 1.599(1)$, $\varepsilon = 1.570(1)$. The empirical formula is $(Fe_{3.56}Mg_{0.21}Mn_{0.21})Al_{2.06}(OH)_{12.14}(CO_3)\cdot nH_2O$. The strongest lines of the powder X-ray diffraction pattern [*d*, Å (*I*, %) (*hkl*)] are: 7.49 (100) (003), 3.746 (50) (006), 2.625 (40) (222), 2.314 (50) (225), 1.948 (40) (228), 1.526 (20) (603).
Kind of sample preparation and/or method of registration of the spectrum: Diamond-anvil cell microsampling. Transmission.
Source: Chao and Gault (1997).
Wavenumbers (cm^{-1}): 3420sh, 3381s, 3175sh, 1589, 1353s, 931, 860, 787s, 693sh, 594sh, 541, 419s.
Note: The wavenumbers were determined by us based on spectral curve analysis of the published spectrum.

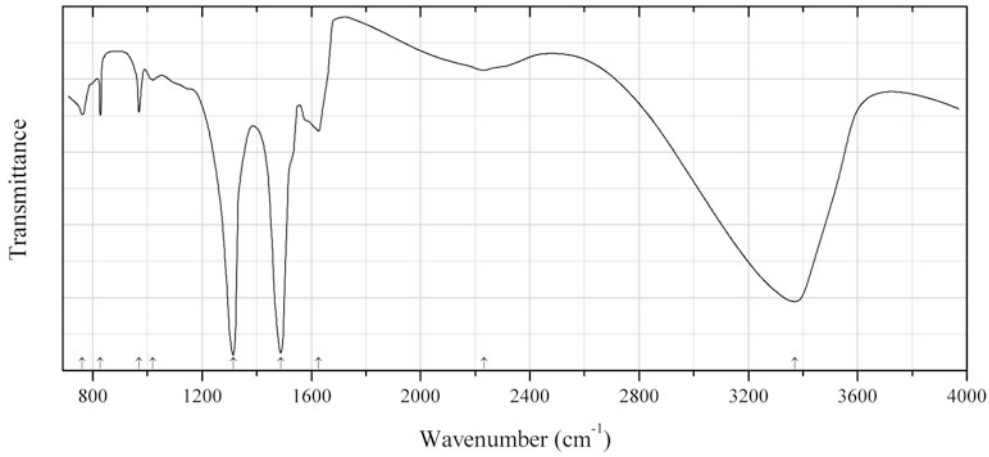

Fig. 2.66 IR spectrum of clearcreekite drawn using data from Roberts et al. (2001b)

C245 Clearcreekite $Hg^{+}_{3}(CO_3)(OH)\cdot 2H_2O$ (Fig. 2.66)
Locality: Clear Creek mercury mine, New Idria district, San Benito Co., California, USA (type locality).
Description: Pale greenish yellow cluster of crystals from the association with cinnabar and edoylerite. Holotype sample. Monoclinic, space group $P2_1/c$, a = 6.760(4), b = 9.580(4), c = 10.931(4) Å, β = 105.53(5)°, V = 682.1(6) Å^3, Z = 4. D_{calc} = 6.96 g/cm^3. The empirical formula is $Hg^{+}_{2.92}(C_{1.01}O_{2.98})(OH)_{1.04}\cdot 2H_2O$. The strongest lines of the powder X-ray diffraction pattern [d, Å (I, %) (hkl)] are: 7.09 (70) (011), 5.32 (40) (−111), 4.62 (90) (012), 2.831 (100) (023), 2.767 (100) (211, −221), 2.391 (40) (040, −204).
Kind of sample preparation and/or method of registration of the spectrum: Transmission. For the kind of sample preparation see Roberts et al. (1995a).
Source: Roberts et al. (2001b).
Wavenumbers (cm^{-1}): 3370s, 2233, 1627, 1488s, 1314s, 1020w, 969, 828, 762.
Note: The band position denoted by Roberts et al. (2001b) as 726 cm^{-1} was determined by us at 762 cm^{-1} based on spectral curve analysis of the published spectrum.

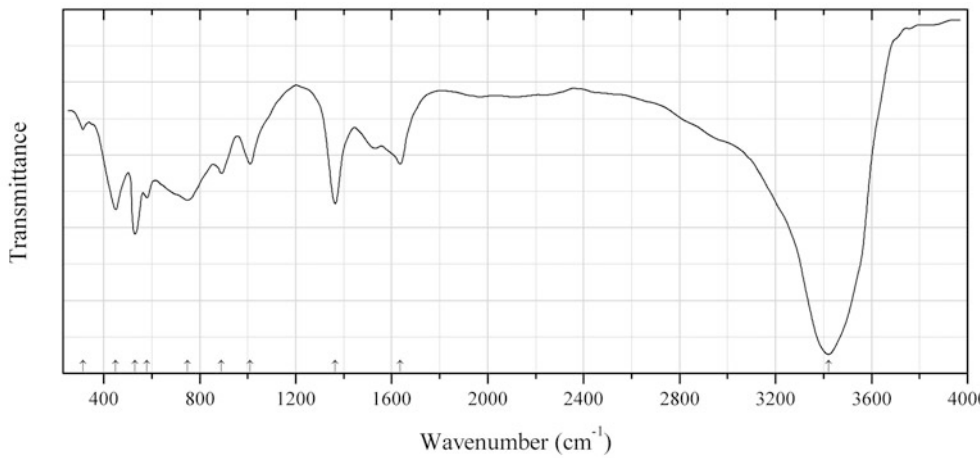

Fig. 2.67 IR spectrum of comblainite drawn using data from Piret and Deliens (1980)

C246 Comblainite $Ni_4Co^{3+}{}_2(CO_3)(OH)_{12}\cdot 3H_2O$ (Fig. 2.67)
Locality: Shinkolobwe, Katanga (Shaba), Democratic Republic of Congo (type locality).
Description: Turquoise blue cryptocrystalline crust from the association with rutherfordine and becquerelite. Holotype sample. Trigonal, a = 3.038, c = 22.79 Å. Measured refractive indices are from 1.684 to 1.690. The contents of NiO and Co_2O_3 are about 44 and 23 wt%, respectively. The strongest lines of the powder X-ray diffraction pattern [d, Å (I, %) (hkl)] are: 7.64 (100) (003), 3.808 (50) (006), 2.567 (70) (012), 2.278 (50) (015), 1.934 (40) (018), 1.489 (30) (113).
Kind of sample preparation and/or method of registration of the spectrum: Absorption. Kind of sample preparation is not indicated.
Source: Piret and Deliens (1980).
Wavenumbers (cm^{-1}): 3420s (broad), 1635, 1365, 1010, 890, 750 (broad), 580, 530, 450, 313w.
Note: The wavenumbers were partly determined by us based on spectral curve analysis of the published spectrum.

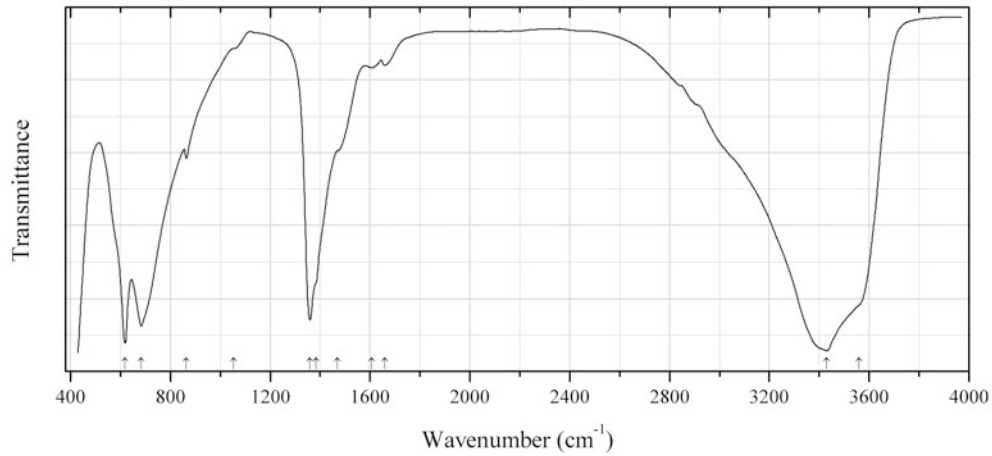

Fig. 2.68 IR spectrum of desautelsite drawn using data from Hansen and Taylor (1991)

C247 Desautelsite $Mg_6Mn^{3+}{}_2(CO_3)(OH)_{16}\cdot 4H_2O$ (Fig. 2.68)
Locality: Synthetic.
Description: Synthesized by aerial oxidation of $MnCO_3$ in $Mg(NO_3)_2$ solution at pH 9 and temperature of 35 °C. Identified by chemical analyses and powder X-ray diffraction data.
Kind of sample preparation and/or method of registration of the spectrum: KBr disc. Absorption.
Source: Hansen and Taylor (1991).
Wavenumbers (cm^{-1}): 3560sh, 3430s, 1660w, 1606w, 1468sh, 1383, 1360s, 1053sh, 864, 684s, 619s.
Note: The bands at 1383 and 864 cm^{-1} are due to residual nitrate and $MnCO_3$, respectively.

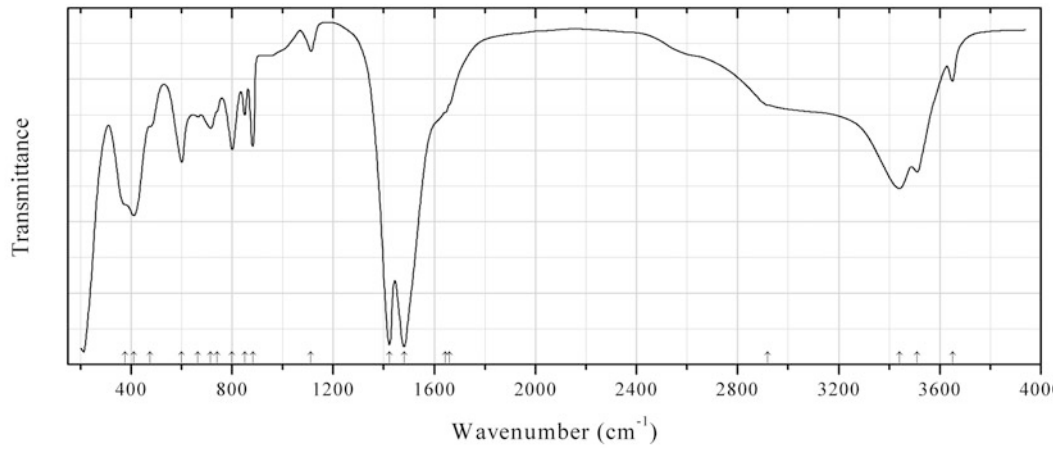

Fig. 2.69 IR spectrum of dypingite drawn using data from Canterford et al. (1984)

C248 Dypingite $Mg_5(CO_3)_4(OH)_2 \cdot 5H_2O$ (Fig. 2.69)
Locality: Synthetic.
Description: Aggregate of microscopic platy crystals from a material obtained during the production of high purity magnesia by the calcination/ CO_2-leaching process. Confirmed by powder X-ray diffraction data and thermal analysis. The strongest lines of the powder X-ray diffraction pattern [*d*, Å (*I*, %)] are: 31.00 (40), 15.62 (40), 10.40 (100), 6.34 (20), 5.86 (30), 2.928 (17), 2.847 (18).
Kind of sample preparation and/or method of registration of the spectrum: KBr disc. Transmission.
Source: Canterford et al. (1984).
Wavenumbers (cm^{-1}): 3650w, 3510, 3440s, 2920sh, 1660sh, 1645sh, 1480s, 1422s, 1112w, 881, 850, 800, 740sh, 715, 665, 600, 475sh, 410s, 375sh.
Note: For the IR spectrum of dypingite see also Raade (1970), Jones and Jackson (1993).

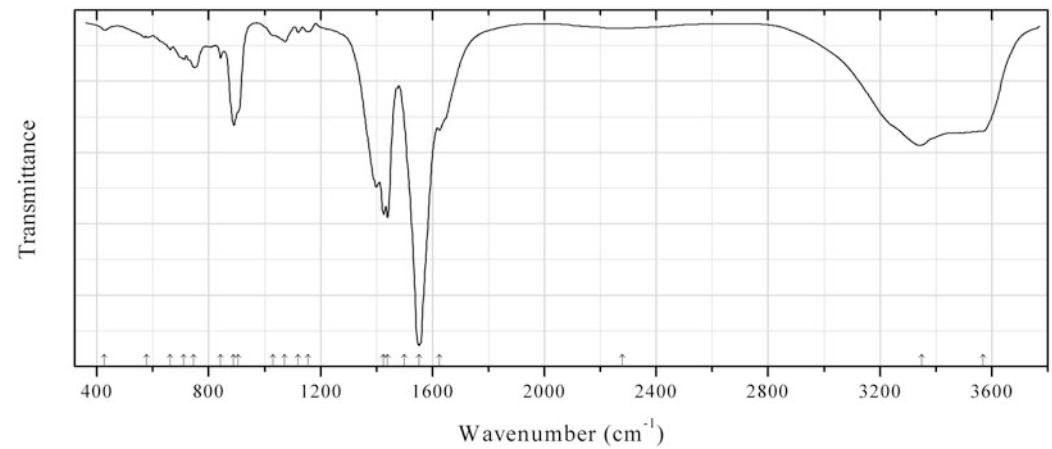

Fig. 2.70 IR spectrum of rabbittite obtained by N.V. Chukanov

C249 Rabbittite $Ca_3Mg_3(UO_2)_2(CO_3)_6(F,Cl)_4 \cdot 18H_2O$ (Fig. 2.70)
Locality: Belorechenskoe deposit, 70 km S. from Maikop, Adygea (Adygeya) Republic, Northern Caucasus, Russia.

Description: Yellow crystals from the association with calcite, dolomite, nickeline, gersdorffite, uraninite, and schrökingerite. Investigated by I.V. Pekov. The empirical formula is (electron microprobe): $Ca_{3.1}Mg_{2.8}(UO_2)_{2.1}(CO_3)_6F_{3.3}Cl_{0.7}\cdot nH_2O$. The strongest lines of the powder X-ray diffraction pattern [*d*, Å (*I*, %)] are: 19.3 (57), 11.2 (37), 8.26 (100), 6.48 (44), 5.79 (48), 4.35 (52).
Kind of sample preparation and/or method of registration of the spectrum: KBr disc. Absorption.
Wavenumbers (cm^{-1}): 3568, 3350, (2280w), 1625sh, 1552s, 1439s, 1425s, 1499s, 1154w, 1120w, 1072, 1030sh, 905sh, 889, 842, 747, 711, 661, 577w, 426w.

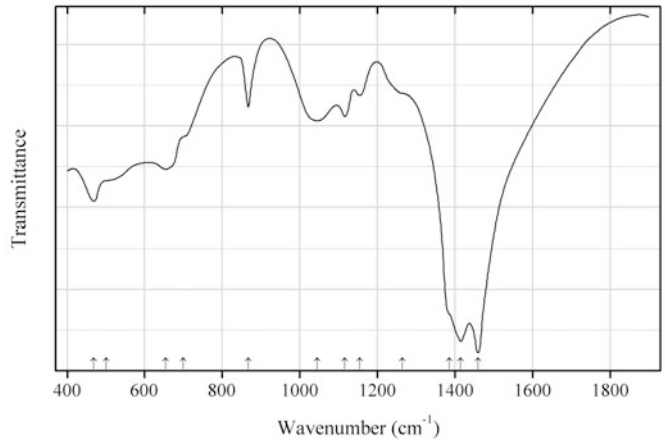

Fig. 2.71 IR spectrum of fairchildite drawn using data from Pertlik (1981)

C250 Fairchildite $K_2Ca(CO_3)_2$ (Fig. 2.71)
Locality: Synthetic.
Description: The crystal structure is solved. Hexagonal, space group $P6_3/mmc$, a = 5.294(1), c = 13.355(2) Å.
Kind of sample preparation and/or method of registration of the spectrum: KBr disc. Transmission.
Source: Pertlik (1981).
Wavenumbers (cm^{-1}): 1460s, 1415s, 1385sh, 1265sh, 1155, 1116, 1045, 867, 700sh, 654, 500sh, 469.
Note: The wavenumbers were partly determined by us based on spectral curve analysis of the published spectrum.

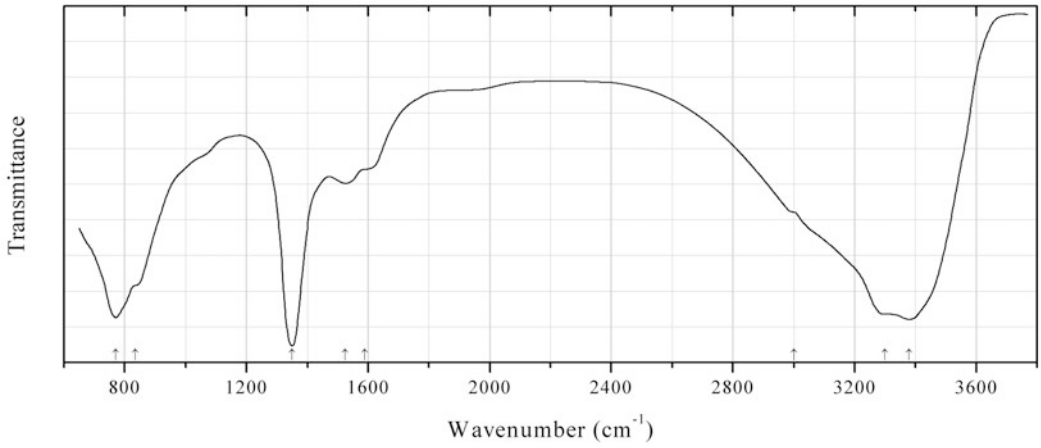

Fig. 2.72 IR spectrum of fougèrite drawn using data from Taylor (1980)

C251 Fougèrite $Fe^{2+}{}_4Fe^{3+}{}_2(OH)_{12}(CO_3)\cdot 4H_2O$ (Fig. 2.72)
Locality: Synthetic.
Description: Green powder. Prepared by precipitation of Fe(II) with Fe(III) from carbonate solution around neutral pH value. Confirmed by powder X-ray diffraction pattern.
Kind of sample preparation and/or method of registration of the spectrum: KBr disc. Transmission.
Source: Taylor (1980).
Wavenumbers (cm^{-1}): 3380s, 3300sh, 3000sh, 1590sh, 1525, 1350s, 835sh, 770s.

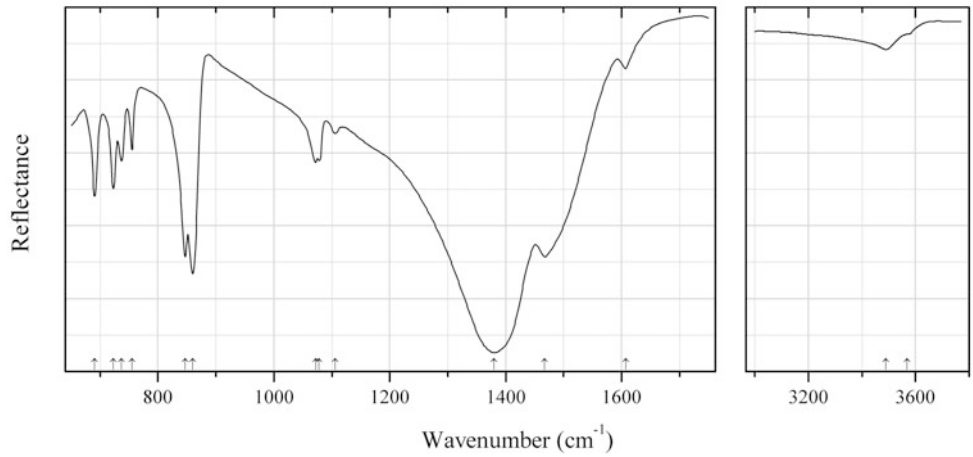

Fig. 2.73 IR spectrum of galgenbergite-(Ce) drawn using data from Walter et al. (2013)

C252 Galgenbergite-(Ce) $CaCe_2(CO_3)_4\cdot H_2O$ (Fig. 2.73)
Locality: The railroad tunnel Galgenberg between Leoben and St. Michael, Styria, Austria (type locality).
Description: Rosette-shaped aggregates from the association with albite, chlorite, siderite, ancylite-(Ce), pyrite, and calcite. The crystal structure is solved. Triclinic, space group *P*-1, $a = 6.3916(5)$, $b = 6.4005(4)$, $c = 12.3898(9)$ Å, $\alpha = 100.884(4)°$, $\beta = 96.525(4)°$, $\gamma = 100.492(4)°$, $V = 483.64(6)$ Å^3,

$Z = 2$. $D_{calc} = 4.97$ g/cm^3. The empirical formula is $Ca_{1.00}(Ce_{1.04}La_{0.42}Nd_{0.42}Pr_{0.12})(CO_3)_4 \cdot H_2O$. The strongest lines of the powder X-ray diffraction pattern [*d*, Å (*I*, %) (*hkl*)] are: 5.899 (59) (−101), 5.052 (100) (011), 4.694 (38) (−102), 3.900 (51) (1–12), 3.125 (46) (−201), 3.011 (70) (0–22), 3.006 (66) (004), 2.526 (42) (022).

Kind of sample preparation and/or method of registration of the spectrum: Attenuated total reflection of powdered mineral. No ATR correction was performed.

Source: Walter et al. (2013).

Wavenumbers (cm^{-1}): 3569sh, 3489, 1607w, 1467s, 1380s, 1106w, 1078, 1072, 860s, 847s, 755, 737, 723, 691.

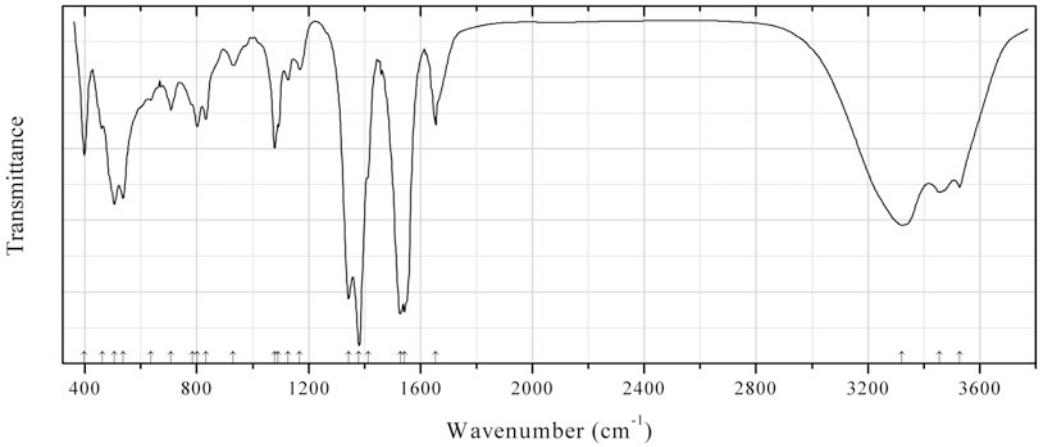

Fig. 2.74 IR spectrum of putnisite obtained by N.V. Chukanov

C253 Putnisite $SrCa_4Cr^{3+}{}_8(CO_3)_8(SO_4)(OH)_{16} \cdot 25H_2O$ (Fig. 2.74)

Locality: Armstrong mine, Widgiemooltha, Coolgardie Shire, Western Australia, Australia.

Description: Deep violet isometric crystals. The empirical formula is (electron microprobe): $Sr_{1.14}Ca_{3.88}Na_{0.07}(Cr_{7.60}Fe_{0.11}Mg_{0.05}Ti_{0.04}Al_{0.02})(SO_4)_{1.02}(CO_3)_x(OH)_y \cdot nH_2O$.

Kind of sample preparation and/or method of registration of the spectrum: KBr disc. Absorption.

Wavenumbers (cm^{-1}): 3528, 3457, 3321s, 1654, 1542s, 1527s, 1412sh, 1380s, 1342s, 1168w, 1126w, 1090, 1078, 930w, 832, 801, 785sh, 707, 635w, 536s, 505s, 462, 398.

Note: For the IR spectrum of putnisite from its type locality see Elliott et al. (2014b).

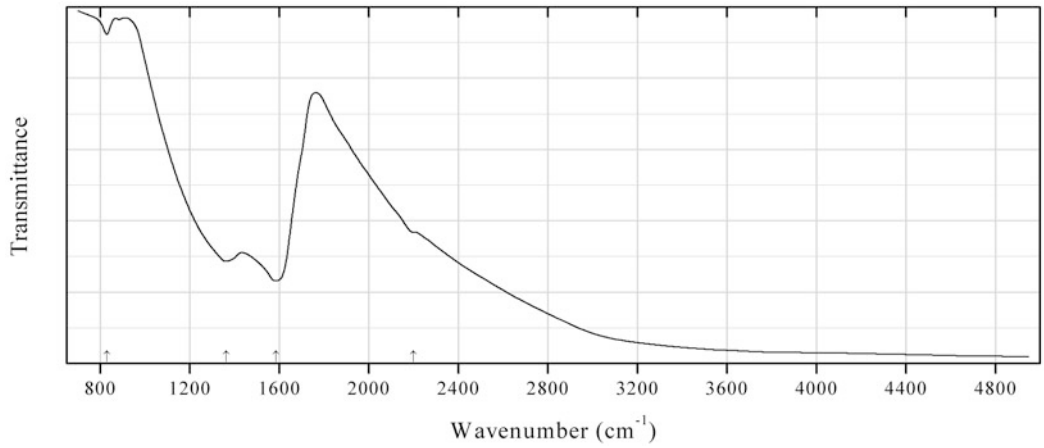

Fig. 2.75 IR spectrum of graphite drawn using data from Friedel and Carlson (1971)

C254 Graphite C (Fig. 2.75)
Locality: Unknown.
Description: Powder obtained after intensive grinding of initial graphite during 120 h.
Kind of sample preparation and/or method of registration of the spectrum: KBr disc. Transmission.
Source: Friedel and Carlson (1971).
Wavenumbers (cm^{-1}): 2200w, 1587s, 1362s, 830w.

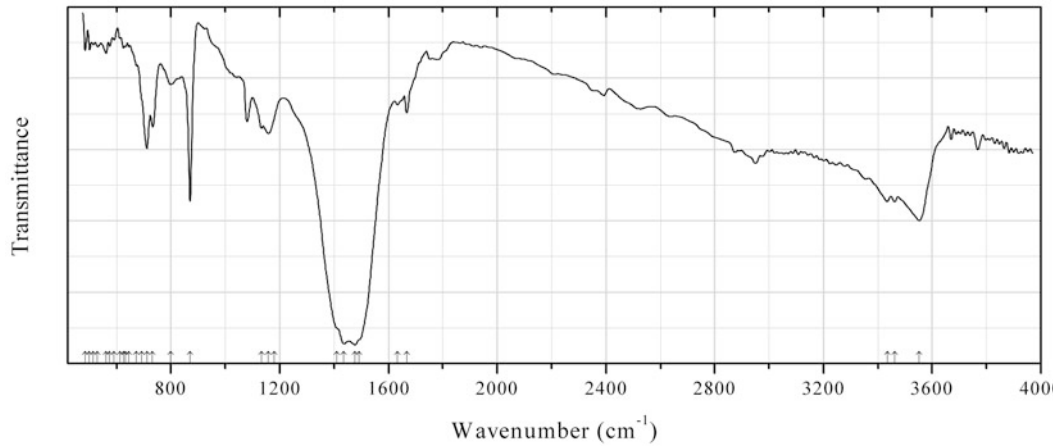

Fig. 2.76 IR spectrum of gysinite-(Nd) drawn using data from Olmi and Sabelli (1991)

C255 Gysinite-(Nd) $PbNd(CO_3)_2(OH)\cdot H_2O$ (Fig. 2.76)
Locality: Sa Duchessa mine, Oridda, Domusnovas, Carbonia-Iglesias province, Sardinia, Italy.
Description: Pink grains from the association with quartz, chrysocolla, agardite-(Y), philipsburgite, and theisite. Orthorhombic, space group *Pcnm*, a = 5.039(1), b = 8.600(2), c = 7.290(2) Å. The empirical formula is $Pb_{1.33}(Nd_{1.00}La_{0.87}Pr_{0.44}Sm_{0.18}Gd_{0.10}Eu_{0.08})(CO_3)_{4.27}(OH)_{2.13}\cdot 1.36H_2O$. The strongest lines of the powder X-ray diffraction pattern [d, Å (I, %) (hkl)] are: 5.57 (35) (011), 4.35 (100) (110), 3.74 (46) (111), 3.71 (31) (021), 2.957 (44) (102), 2.519 (49) (200), 2.084 (32) (221).

Kind of sample preparation and/or method of registration of the spectrum: KBr disc. Transmission.
Source: Olmi and Sabelli (1991).
Wavenumbers (cm^{-1}): 3552s, 3462, 3435, 1667, 1633, 1493sh, 1476s, 1436s, 1410sh, 1158, 1132, 1180, 870s, 798, 732w, 711w, 692sh, 673w, 645w, 632w, 625w, 612w, 590w, 574w, 561w, 530w, 514w, 500w, 484w.
Note: The wavenumbers were determined by us based on spectral curve analysis of the published spectrum.

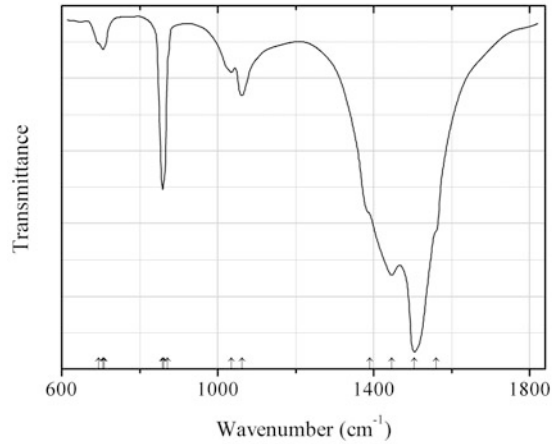

Fig. 2.77 IR spectrum of khanneshite obtained by N.V. Chukanov

C256 Khanneshite $(Na,Ca)_3(Ba,Sr,REE)_3(CO_3)_5$ (Fig. 2.77)
Locality: Tulilukht gulf, the eastern part of the Khibiny alkaline massif, Kola peninsula, Russia.
Description: Red grains. Investigated by I.V. Pekov.
Kind of sample preparation and/or method of registration of the spectrum: KBr disc. Absorption.
Wavenumbers (cm^{-1}): 1560sh, 1505s, 1446s, 1390sh, 1062, 1035, 872sh, 862sh, 859, 710sh, 706, 695sh.

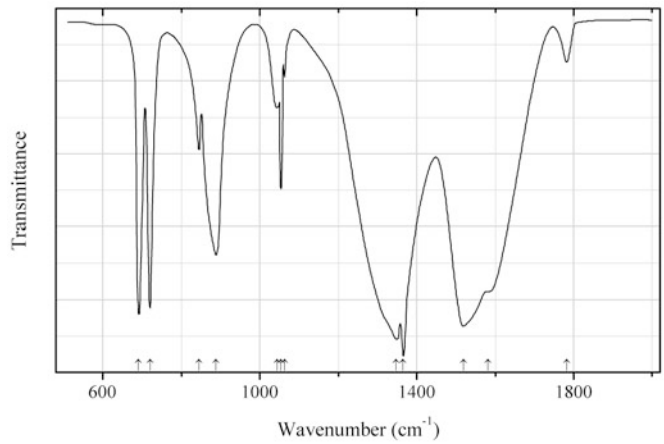

Fig. 2.78 IR spectrum of ammonium uranyl carbonate C257 drawn using data from Chernorukov et al. (2003)

C257 Ammonium uranyl carbonate C257 $(NH_4)_4(UO_2)(CO_3)_3$ (Fig. 2.78)
Locality: Synthetic.
Description: Prepared from a solution of uranyl nitrate and ammonium carbonate. Monoclinic, $a = 10.68(1)$, $b = 9.38(1)$, $c = 12.85(1)$ Å, $\beta = 96.5(1)°$, $V = 1279(1)$ Å^3, $Z = 4$. The strongest lines of the powder X-ray diffraction pattern [*d*, Å (*I*, %) (*hkl*)] are: 6.360 (100) (−111), 5.972 (53) (111), 5.218 (48) (102), 3.873 (35) (202), 3.022 (46) (014).
Kind of sample preparation and/or method of registration of the spectrum: KBr disc. Transmission.
Source: Chernorukov et al. (2003).
Wavenumbers (cm^{-1}): 3191s, 1782w, 1581s, 1519s, 1365s, 1348s, 1063w, 1054, 1044, 888, 845, 720s, 691s.

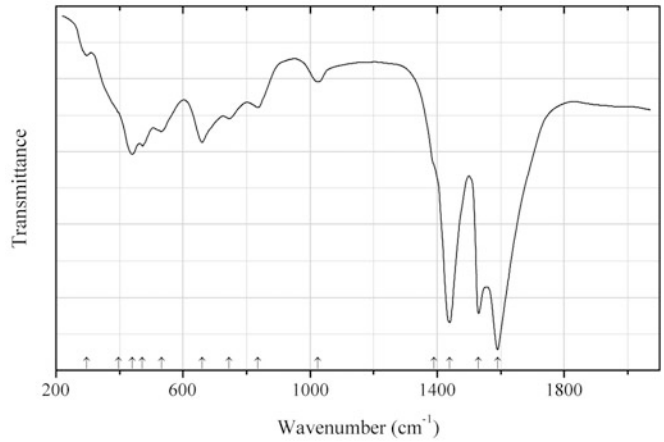

Fig. 2.79 IR spectrum of artinite dimorph drawn using data from Livingstone (1987)

C258 Artinite dimorph (?) $Mg_2(CO_3)(OH)_2 \cdot 3H_2O$ (Fig. 2.79)
Locality: Swinna Ness, Unst, Shetland, UK.
Description: Soft porous aggregate from the association with brucite. Characterized by thermal and chemical analytical data. Monoclinic, $a = 11.45$, $b = 24.17$, $c = 7.54$ Å, $\beta = 105.21°$. The strongest lines of the powder X-ray diffraction pattern [*d*, Å (*I*, %) (*hkl*)] are: 11.60 (100) (020), 6.40 (90) (130), 4.92 (30) (121), 4.81 (30) (050). 3.97 (80) (15–1), 2.95 (60) (311, 35–1), 2.718 (30) 360, 212), 2.598 (30) (28–1, 271), 2.528 (40) (41–2, 37–1).
Kind of sample preparation and/or method of registration of the spectrum: KBr disc. Transmission.
Source: Livingstone (1987).
Wavenumbers (cm^{-1}): 1590s, 1530s, 1440s, 1390sh, 1025w, 835, 745, 660, 471, 532, 440, 396sh, 297w.
Note: The wavenumbers were partly determined by us based on spectral curve analysis of the published spectrum.

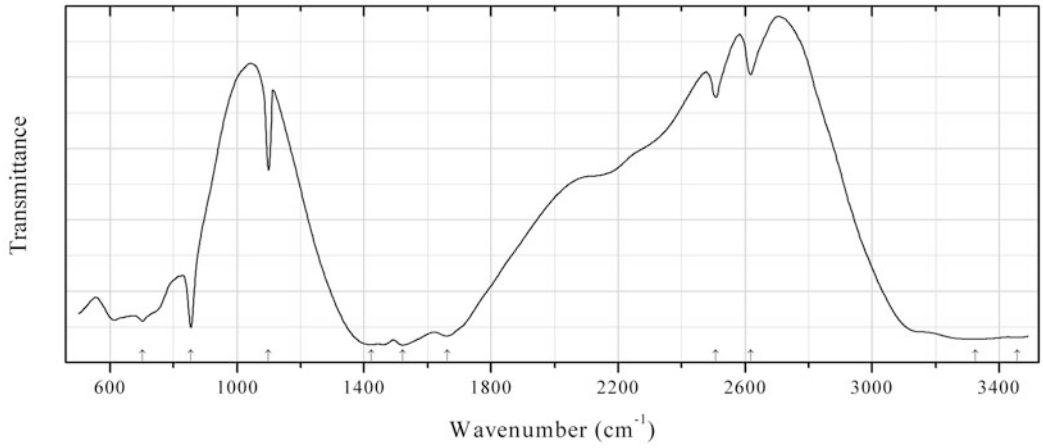

Fig. 2.80 IR spectrum of baylissite NH_4-analogue drawn using data from Fischer (2007)

C259 Baylissite NH_4-analogue $(NH_4)_2Mg(CO_3)_2 \cdot 4H_2O$ (Fig. 2.80)
Locality: Synthetic.
Description: The crystal structure is solved. Monoclinic, space group $P2_1/n$, $a = 6.321(2)$, $b = 12.437(3)$, $c = 6.676(2)$ Å, $\beta = 95.59(2)°$, $V = 522.3(2)$ Å^3.
Kind of sample preparation and/or method of registration of the spectrum: Transmission. Kind of sample preparation is not indicated.
Source: Fischer (2007).
Wavenumbers (cm^{-1}): 3457s, 3325s, 2617w, 2508w, 1661, 1522s, 1423s, 1099, 855s, 702.
Note: The wavenumbers were partly determined by us based on spectral curve analysis of the published spectrum.

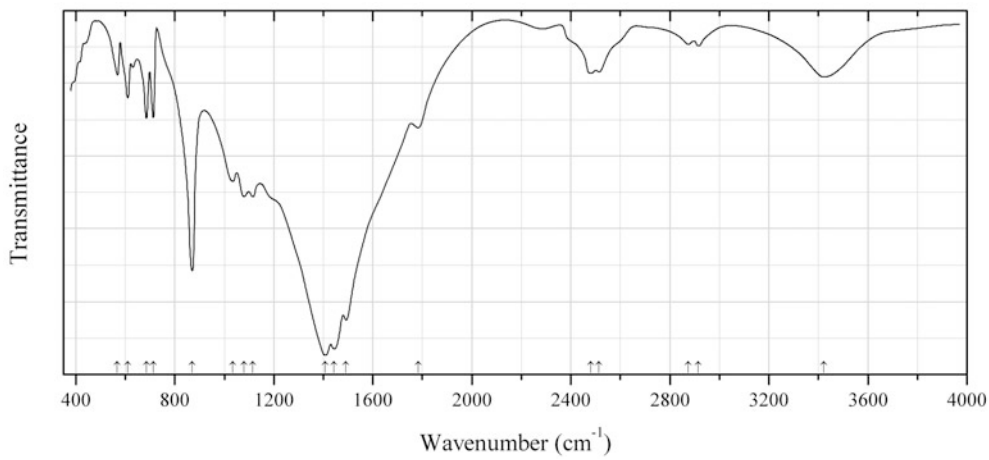

Fig. 2.81 IR spectrum of benstonite Mg-deficient analogue drawn using data from Konev et al. (2004)

C260 Benstonite Mg-deficient analogue $(Ba,Sr)_6Ca_6(Ca,Mg)(CO_3)_{13}$ (Fig. 2.81)
Locality: Biraya carbonatite dyke (at 56°52' N, 116°45' E), the basin of the river Biraya, Irkutsk region, Siberia, Russia.

Description: Anhedral grains from the association with calcite, dolomite, norsethite, strontianite, barytocalcite, carbocernaite, cordilite-(Ce), kukharenkoite-(Ce), and other *REE* minerals. Trigonal, $a = 18.21(1)$, $c = 8.67(1)$ Å. $D_{meas} = 3.56(1)$ g/cm^3. Optically biaxial (−), $\omega = 1.687(1)$, $\varepsilon = 1.526(5)$. The empirical formula is $(Ba_{3.25}Sr_{2.75})(Ca_{5.42}Sr_{0.36}La_{0.13}Ce_{0.07}Pr_{0.01}Nd_{0.01})(Ca_{0.50}Mg_{0.33}Fe_{0.05}Mn_{0.02})(CO_3)_{13}O$. The strongest lines of the powder X-ray diffraction pattern [*d*, Å (*I*, %) (*hkl*)] are: 3.89 (10) (131), 3.17 (12) (050), 3.08 (100) (312), 3.03 (20) (330), 2.53 (10) (250), 2.12 (12) (621).
Kind of sample preparation and/or method of registration of the spectrum: KBr disc. Transmission.
Source: Konev et al. (2004).
Wavenumbers (cm^{-1}): 3423, 2915w, 2875w, 2514, 2481, 1785, 1491s, 1443s, 1407s, 1116, 1080, 1034, 870s, 713, 685, 610, 568.
Note: The band at 3423 cm^{-1} corresponds to adsorbed water molecules.

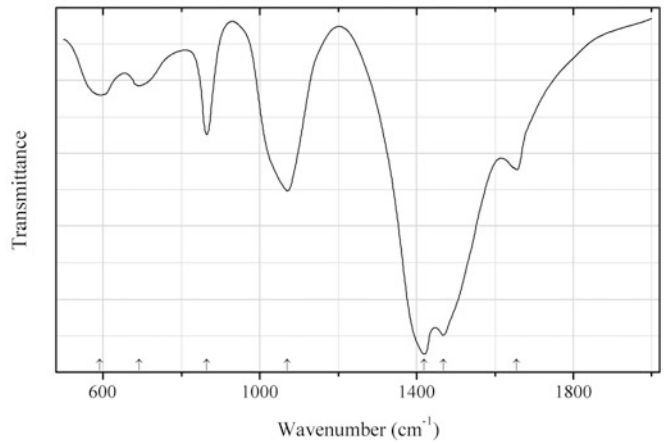

Fig. 2.82 IR spectrum of calcium carbonate (amorphous) drawn using data from Raz et al. (2002)

C261 Calcium carbonate (amorphous) $CaCO_3$ (?) (Fig. 2.82)
Locality: Calcium storage product from the terrestrial crustacean *Orchestia cavimana*.
Description: Aggregate of spheruliths intergrown with calcite. X-ray amorphous. Confirmed by electron microprobe analysis.
Kind of sample preparation and/or method of registration of the spectrum: KBr disc. Absorption.
Source: Raz et al. (2002).
Wavenumbers (cm^{-1}): 1655, 1468s, 1419s, 1070, 864, 692, 592.
Note: The band at 1655 cm^{-1} indicates the presence of H_2O molecules.

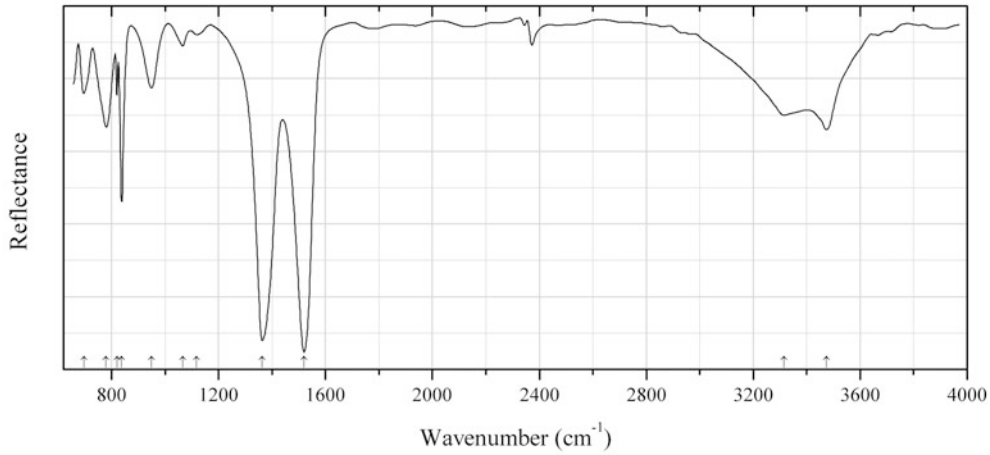

Fig. 2.83 IR spectrum of chukanovite drawn using data from Rémazeilles and Refait (2009)

C262 Chukanovite $Fe_2(CO_3)(OH)_2$ (Fig. 2.83)
Locality: Glinet, France.
Description: Product of alteration of archaeological (16th century) iron nail. Chukanovite forms inner corrosion layer. Outer layers consist of siderite, goethite, etc.
Kind of sample preparation and/or method of registration of the spectrum: Attenuated total reflection of powdered mineral.
Source: Rémazeilles and Refait (2009).
Wavenumbers (cm^{-1}): 3473, 3316, 1520s, 1364s, 1118w, 1066, 950, 838s, 820, 780, 696.
Note: The wavenumbers were partly determined by us based on spectral curve analysis of the published spectrum.

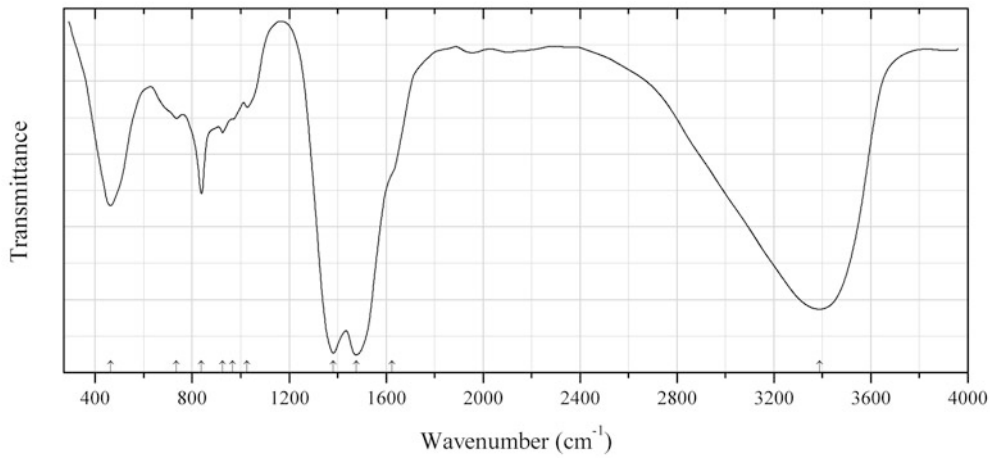

Fig. 2.84 IR spectrum of georgeite drawn using data from Pollard et al. (1991)

C263 Georgeite $Cu_5(CO_3)_3(OH)_4 \cdot 6H_2O$ (Fig. 2.84)
Locality: Synthetic.
Description: Synthesized in a rapid reaction from $CuCl_2 \cdot 2H_2O$ and Na_2CO_3 at 20 °C. Amorphous. Confirmed by chemical analyses.

Kind of sample preparation and/or method of registration of the spectrum: KBr disc. Transmission.
Source: Pollard et al. (1991).
Wavenumbers (cm^{-1}): 3388s, 1625sh, 1476s, 1381s, 1027, 967sh, 925, 838, 735, 463.
Note: The wavenumbers were determined by us based on spectral curve analysis of the published spectrum.

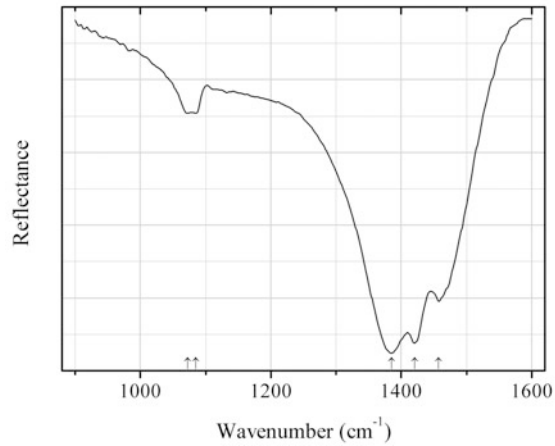

Fig. 2.85 IR spectrum of huanghoite-(Ce) drawn using data from Frost et al. (2013a)

C264 Huanghoite-(Ce) $BaCe(CO_3)_2F$ (Fig. 2.85)
Locality: Bayan-Obo, Inner Mongolia, China (type locality).
Description: Specimen SAB-116 from the collection of the Geology Department of the Federal University of Ouro Preto, Minas Gerais, Brazil. Confirmed by semiquantitative electron microprobe analysis.
Kind of sample preparation and/or method of registration of the spectrum: Attenuated total reflection of powdered mineral.
Source: Frost et al. (2013a).
Wavenumbers (cm^{-1}): 1457s, 1421s, 1385s, 1085w, 1073w.
Note: Huanghoite-(Ce) and cebaite-(Ce) could not be distinguished by semi-quantitative electron microprobe analysis. The wavenumbers are given according to drawing. In the cited paper, the wavenumbers are indicated for the maxima of individual bands obtained as a result of the spectral curve analysis. Details of this analysis are not described. The wavenumbers were determined by us based on spectral curve analysis of the published spectrum.

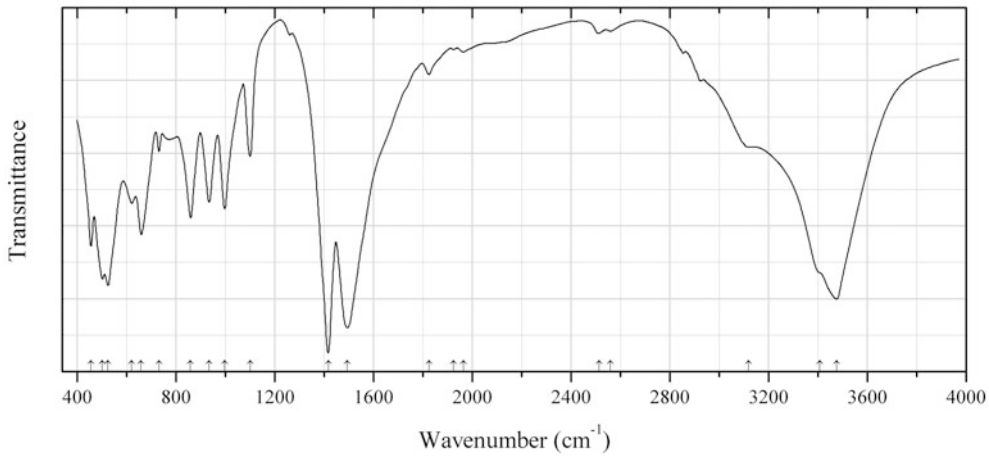

Fig. 2.86 IR spectrum of dawsonite K,H_2O-analogue drawn using data from Fernández-Carrasco and Rius (2006)

C265 Dawsonite K,H_2O-analogue $KAl(CO_3)(OH)_2 \cdot H_2O$ (Fig. 2.86)
Locality: Synthetic.
Description: Synthesised by adding metal aluminium powder to a 2 M potassium carbonate solution at 25 °C. Orthorhombic, space group $Pna2_1$, $a = 8.3312(4)$, $b = 11.2670(5)$, $c = 5.661(2)$ Å, $V = 531.3(2)$ Å^3. Structurally related to dawsonite. The strongest lines of the powder X-ray diffraction pattern [*d*, Å (*I*, %) (*hkl*)] are: 6.699 (100) (110), 4.166 (30) (200), 3.350 (54) (201, 220), 3.215 (60) (211), 2.883 (40) (221), 2.341 (25) (202).
Kind of sample preparation and/or method of registration of the spectrum: KBr disc. Transmission.
Source: Fernández-Carrasco and Rius (2006).
Wavenumbers (cm^{-1}): 3475s, 3407sh, 3119, 2560w, 2513w, 1965w, 1925w, 1825w, 1494s, 1417s, 1101, 998, 935, 860, 732, 660, 622, 525s, 503s, 457.
Note: The wavenumbers were partly determined by us based on spectral curve analysis of the published spectrum.

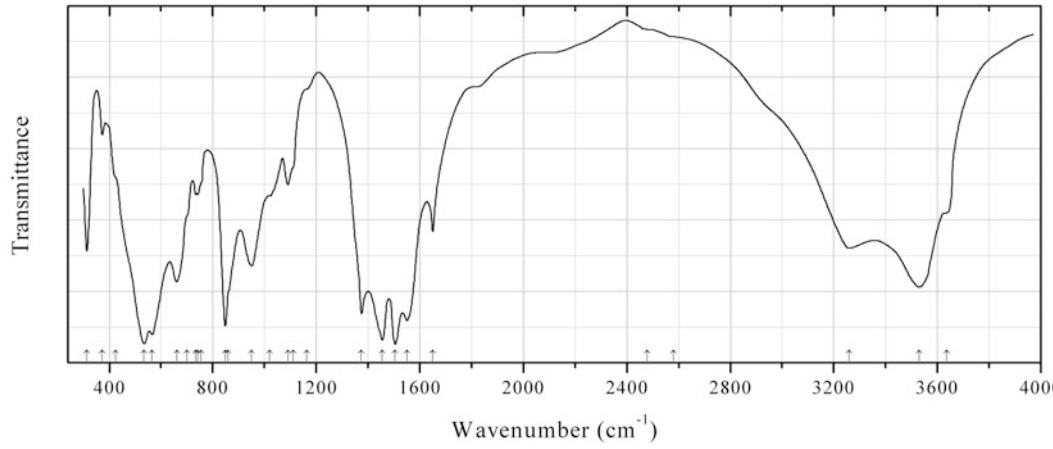

Fig. 2.87 IR spectrum of hydrodresserite drawn using data from Farrell (1977)

C266 Hydrodresserite $BaAl_2(CO_3)_2(OH)_4 \cdot 3H_2O$ (Fig. 2.87)
Locality: Francon quarry, Saint-Michel, Montréal, Québec, Canada (type locality).
Kind of sample preparation and/or method of registration of the spectrum: KBr disc. Transmission.
Source: Farrell (1977).
Wavenumbers (cm^{-1}): 3635sh, 3530s, 3260, 2580sh, 2480sh, 1650, 1550s, 1505s, 1455s, 1375s, 1162sh, 1110sh, 1090, 1020sh, 950, 860sh, 848s, 755sh, 741, 734, 700sh, 660, 565s, 535s, 425sh, 373w, 313.
Note: The wavenumbers were partly determined by us based on spectral curve analysis of the published spectrum.

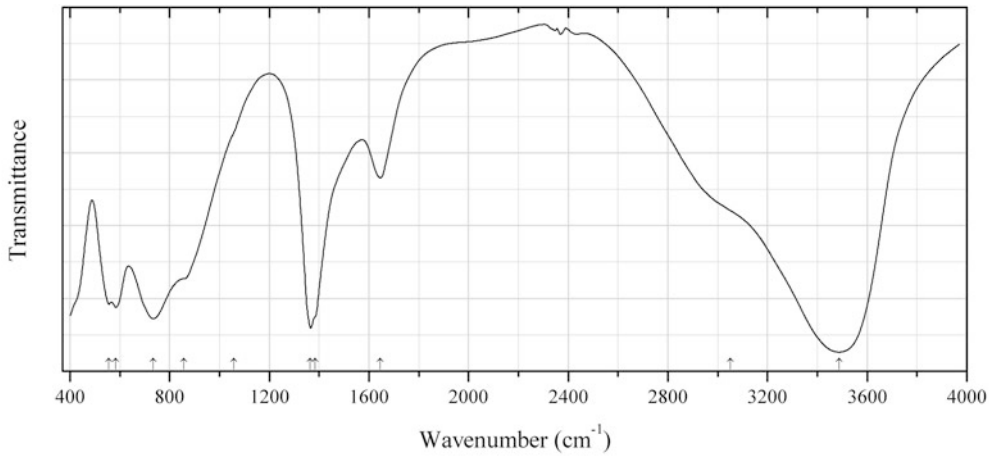

Fig. 2.88 IR spectrum of hydrotalcite Co^{2+} analogue drawn using data from Kloprogge and Frost (1999)

C267 Hydrotalcite Co^{2+}analogue $Co_6Al_2(CO_3)(OH)_{16} \cdot nH_2O$ (Fig. 2.88)
Locality: Synthetic.
Description: Synthesized from aluminum nitrate and cobalt chloride solution in the presence of NaOH and Na_2CO_3, at pH > 10. Confirmed by the powder X-ray diffraction pattern. Trigonal, a = 3.065(6), c = 23.17(4) Å.
Kind of sample preparation and/or method of registration of the spectrum: KBr disc. Transmission.
Source: Kloprogge and Frost (1999).
Wavenumbers (cm^{-1}): 3487s, 3050sh, 1646, 1384sh, 1365s, 1058sh, 856sh, 734, 584, 556.
Note: The wavenumbers are given according to drawing. In the cited paper, the wavenumbers are indicated only for the maxima of individual bands obtained as a result of the spectral curve analysis.

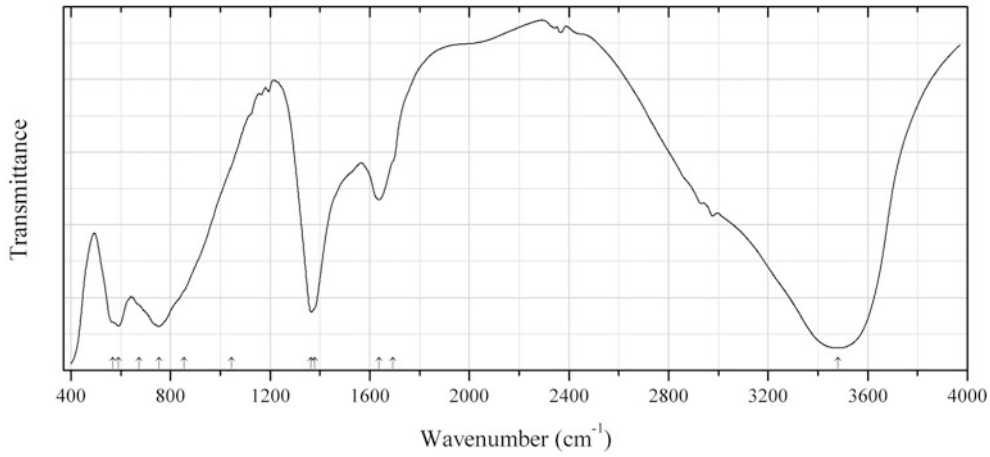

Fig. 2.89 IR spectrum of takovite drawn using data from Kloprogge and Frost (1999)

C268 Takovite $Ni_6Al_2(CO_3)(OH)_{16}{\cdot}nH_2O$ (Fig. 2.89)
Locality: Synthetic.
Description: Hydrotalcite Ni analogue. Synthesized from aluminum nitrate and nickel chloride solution in the presence of NaOH and Na_2CO_3, at pH > 10. Confirmed by the powder X-ray diffraction pattern. Trigonal, a = 3.024(5), c = 23.48(5) Å.
Kind of sample preparation and/or method of registration of the spectrum: KBr disc. Transmission.
Source: Kloprogge and Frost (1999).
Wavenumbers (cm^{-1}): 3480s, 1693sh, 1637, 1379sh, 1365s, 1046sh, 854sh, 753s, 673sh, 590s, 568sh.
Note: The wavenumbers are given according to drawing. In the cited paper, the wavenumbers are indicated only for the maxima of individual bands obtained as a result of the spectral curve analysis.

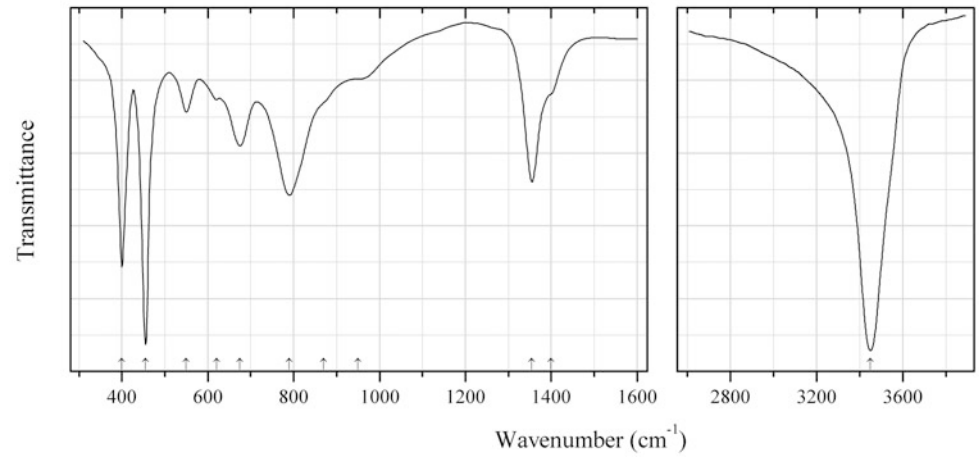

Fig. 2.90 IR spectrum of quintinite drawn using data from Hernandez-Moreno et al. (1985)

C269 Quintinite $Mg_4Al_2(OH)_{12}(CO_3){\cdot}nH_2O$ (Fig. 2.90)

Locality: Synthetic.
Description: Synthesized by slow addition of NaOH (1.2 M) to mixed Mg/Al chloride solution with molar ratio 2/1 until a final pH 9–10 was achieved. The gel obtained was hydrothermally treated at about 130 °C for several days to improve crystallinity. Confirmed by chemical analysis and powder X-ray diffraction data.
Kind of sample preparation and/or method of registration of the spectrum: KBr disc. Absorption.
Source: Hernandez-Moreno et al. (1985).
Wavenumbers (cm^{-1}): 3450s, 1400sh, 1355s, 950sh, 870sh, 790s, 675, 620w, 550, 455s, 400.

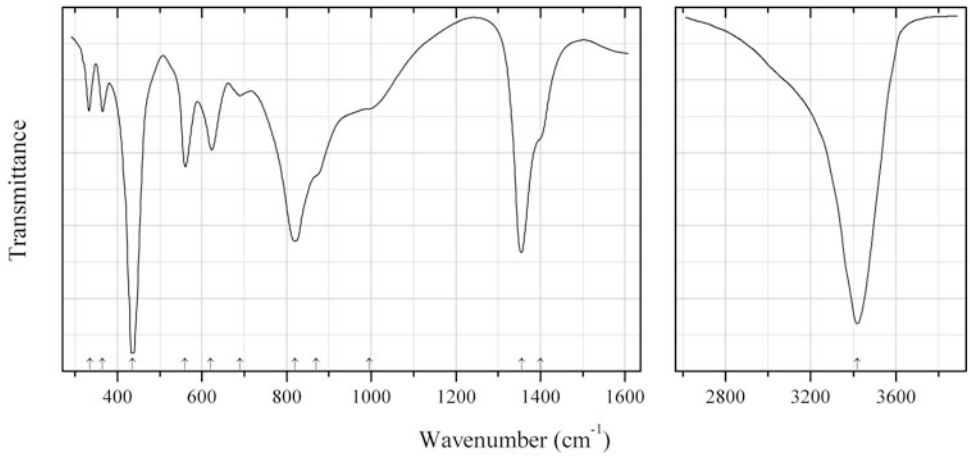

Fig. 2.91 IR spectrum of quintinite Ni analogue drawn using data from Hernandez-Moreno et al. (1985)

C270 Quintinite Ni analogue $Ni_6Al_2(CO_3)(OH)_{16}{\cdot}nH_2O$ (Fig. 2.91)
Locality: Synthetic.
Description: Synthesized by slow addition of NaOH (1.2 M) to mixed Ni/Al chloride solution with molar ratio 2/1 until a final pH 9–10 was achieved. The gel obtained was hydrothermally treated at about 130 °C for several days to improve crystallinity. Confirmed by chemical analysis and powder X-ray diffraction data.
Kind of sample preparation and/or method of registration of the spectrum: KBr disc. Absorption.
Source: Hernandez-Moreno et al. (1985).
Wavenumbers (cm^{-1}): 3420s, 1400sh, 1355s, 995sh, 870sh, 820s, 690w, 620, 560, 435s, 365, 335.

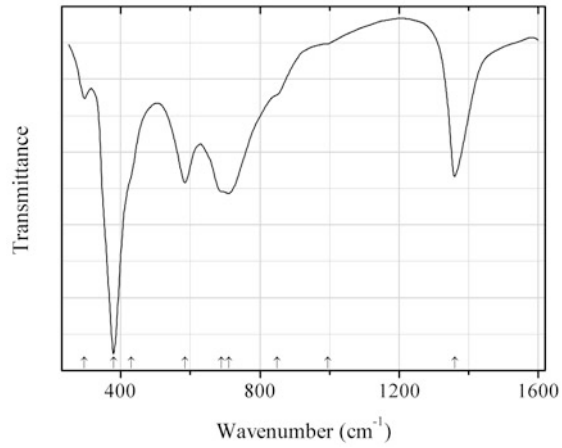

Fig. 2.92 IR spectrum of quintinite Fe^{3+} analogue drawn using data from Hernandez-Moreno et al. (1985)

C271 Quintinite Fe^{3+} analogue $Mg_4Fe^{3+}{}_2(OH)_{12}(CO_3)\cdot nH_2O$ (Fig. 2.92)
Locality: Synthetic.
Description: Synthesized by slow addition of NaOH (1.2 M) to mixed Mg/Fe^{3+} chloride solution with molar ratio 2/1 until a final pH 9–10 was achieved. The gel obtained was hydrothermally treated at about 130 °C for several days to improve crystallinity. Confirmed by chemical analysis and powder X-ray diffraction data.
Kind of sample preparation and/or method of registration of the spectrum: KBr disc. Absorption.
Source: Hernandez-Moreno et al. (1985).
Wavenumbers (cm^{-1}): 1360, 995sh, 850sh, 710s, 690sh, 585, 430sh, 380s, 295w.

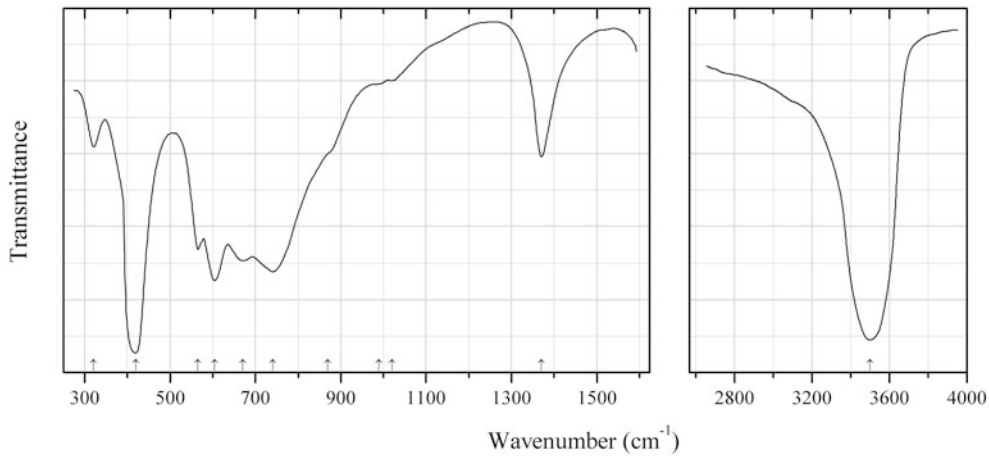

Fig. 2.93 IR spectrum of takovite drawn using data from Hernandez-Moreno et al. (1985)

C272 Takovite $Ni_6Al_2(OH)_{16}(CO_3)\cdot nH_2O$ (Fig. 2.93)
Locality: Synthetic.
Description: Synthesized by slow addition of NaOH (1.2 M) to mixed Mg/Fe^{3+} chloride solution with molar ratio 3/1 until a final pH 9–10 was achieved. The gel obtained was hydrothermally treated

at about 130 °C for several days to improve crystallinity. Confirmed by chemical analysis and powder X-ray diffraction data.
Kind of sample preparation and/or method of registration of the spectrum: KBr disc. Absorption.
Source: Hernandez-Moreno et al. (1985).
Wavenumbers (cm^{-1}): 3500s, 1370, 1020w, 990sh, 870sh, 740s, 670, 605s, 565, 420s, 320.

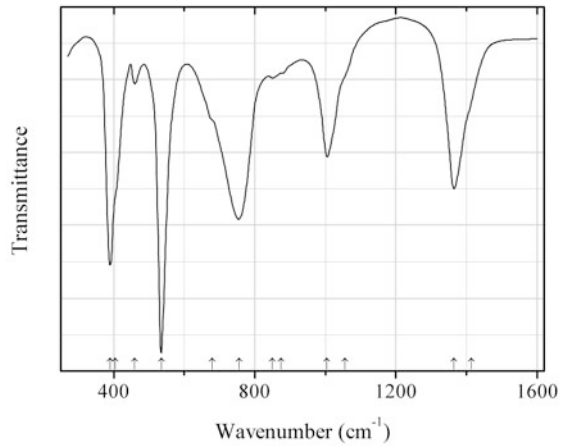

Fig. 2.94 IR spectrum of quintinite Al,Li-analogue drawn using data from Hernandez-Moreno et al. (1985)

C273 Quintinite Al, Li-analogue $LiAl_2(OH)_6(CO_3)_{0.5}\cdot nH_2O$ (?) (Fig. 2.94)
Locality: Synthetic.
Description: Confirmed by chemical analysis and powder X-ray diffraction data.
Kind of sample preparation and/or method of registration of the spectrum: KBr disc. Absorption.
Source: Hernandez-Moreno et al. (1985).
Wavenumbers (cm^{-1}): 1415sh, 1365s, 1055sh, 1005, 875sh, 850w, 755s, 680sh, 535s, 460w, 405sh, 390s.
Note: In the cited paper, the formula $Al_2Li(OH)_6(CO_3)\cdot nH_2O$ is given which is none charge-balanced.

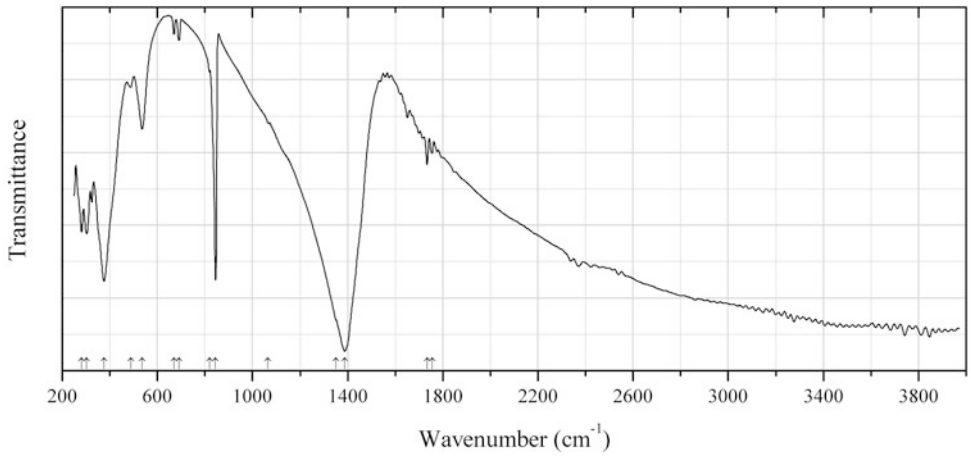

Fig. 2.95 IR spectrum of bismutite drawn using data from Taylor et al. (1984)

C274 Bismutite $(BiO)_2(CO_3)$ (Fig. 2.95)
Locality: Synthetic.
Description: Confirmed by powder X-ray diffraction data.
Kind of sample preparation and/or method of registration of the spectrum: KBr disc. Absorption.
Source: Taylor et al. (1984).
Wavenumbers (cm^{-1}): 1755w, 1734w, 1389s, 1351sh, 1065w, 845s, 819w, 691w, 671w, 536, 488w, 377s, 303, 282.
Note: The wavenumbers were partly determined by us based on spectral curve analysis of the published spectrum.

C275 Ikaite $Ca(CO_3)\cdot 6H_2O$
Locality: Barrow, Alaska, USA.
Description: Brown, translucent, bipyramidal isolated crystals.
Kind of sample preparation and/or method of registration of the spectrum: KBr disc. Transmission.
Source: Jones and Jackson (1993).
Wavenumbers (cm^{-1}): 3467s, 2515w, 2387w, 2258w, 1797w, 1641s, 1421s, 1082w, 877s, 710, 680, 614, 571, 316s.
Note: Ikaite is unstable at room temperature. The specimen may be partially decomposed to calcite and water. IR spectrum of ikaite given by Goleyshaw et al. (2003) does not contain characteristic strong bands of CO_3^{2-} groups in the range from 1300 to 1550 cm^{-1} (only weak bands at 1425 and 1411 cm^{-1} are indicated).

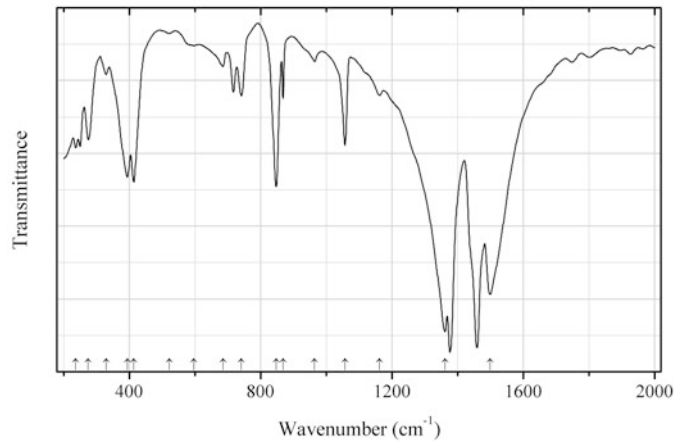

Fig. 2.96 IR spectrum of juangodoyite drawn using data from Healy and White (1972)

C276 Juangodoyite $Na_2Cu(CO_3)_2$ (Fig. 2.96)
Locality: Synthetic.
Description: Blue crystals. The crystal structure is solved. Monoclinic, space group $P2_1/a$, a = 6.18 (2), b = 8.19(2), c = 5.64(2) Å, β = 116.2(2)°, V = 256 $Å^3$, Z = 2. D_{meas} = 3.1(1) g/cm^3, D_{calc} = 2.98 g/cm^3.
Kind of sample preparation and/or method of registration of the spectrum: Nujol mull. Transmission.
Source: Healy and White (1972).

Wavenumbers (cm^{-1}): 1500s, 1362s, 1163w, 1058, 965w, 869, 848, 742, 686, 598w, 522w, 415, 395, 330, 276, 238.
Note: Additional bands at 1460, 1378, and 718 cm^{-1} are ascribable to Nujol. The wavenumbers were partly determined by us based on spectral curve analysis of the published spectrum.

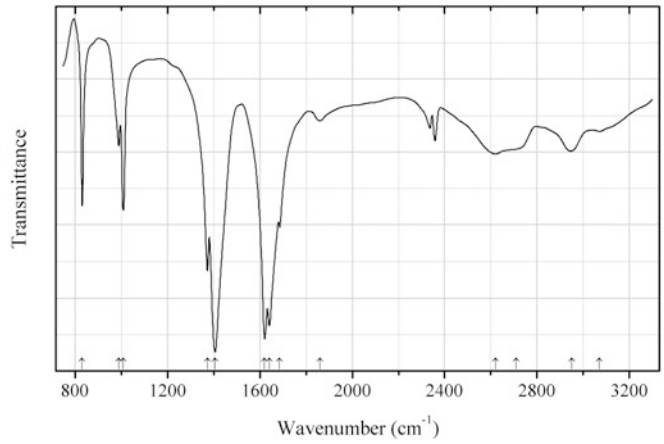

Fig. 2.97 IR spectrum of kalicinite drawn using data from Kagi et al. (2003)

C277 Kalicinite $K(HCO_3)$ (Fig. 2.97)
Locality: Synthetic.
Description: Prepared by bubbling CO_2 gas through 50 wt% potassium carbonate solution at room temperature.
Kind of sample preparation and/or method of registration of the spectrum: CsI disc. Absorption.
Source: Kagi et al. (2003).
Wavenumbers (cm^{-1}): 3070w, 2950, 2710sh, 2620, 1860w, 1685, 1640s, 1620s, 1405s, 1372, 1008, 988, 830.
Note: The wavenumbers were partly determined by us based on spectral curve analysis of the published spectrum. Bands in the region 2300–2400 cm^{-1} correspond to atmospheric CO_2.

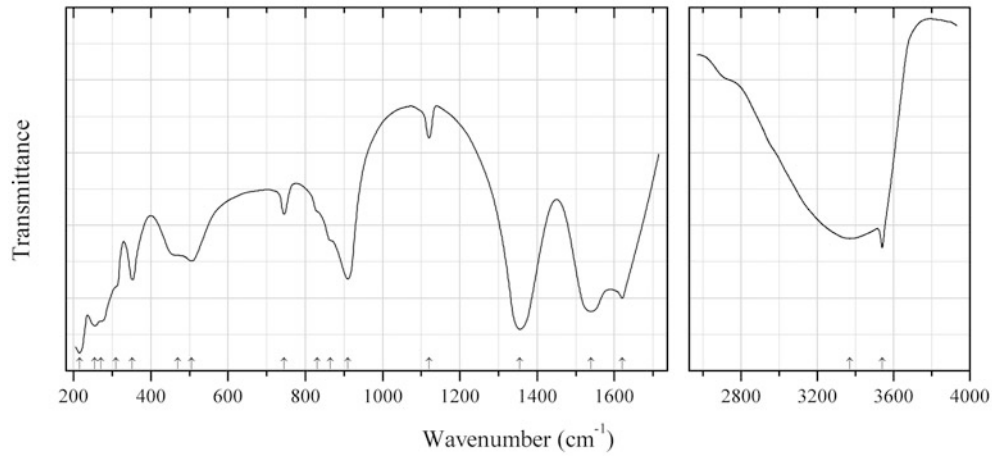

Fig. 2.98 IR spectrum of kamotoite-(Y) drawn using data from Botto et al. (1989b)

C278 Kamotoite-(Y) $Y_2(UO_2)_4(CO_3)_3O_4 \cdot 14H_2O$ (Fig. 2.98)
Locality: Kamoto, Souther Shaba, Zaire (type locality).
Description: Bright yellow elongate blades on uraninite. Confirmed by electron microprobe analysis.
Kind of sample preparation and/or method of registration of the spectrum: KBr disc. Transmission.
Source: Botto et al. (1989b).
Wavenumbers (cm^{-1}): 3540, 3370s, 1620s, 1540s, 1355s, 1120w, 910s, 865sh, 830sh, 745, 505, 470sh, 352, 310sh, 270sh, 255s, 215.
Note: According to Jones and Jackson (1993), the wavenumbers of the bands in the IR spectrum of kamotoite-(Y) are 3423, 2929, 2857, 2457, 1865, 1731, 1606, 1537, 1364, 1195, 1151, 1122, 911, 742, 660, 509, 366, and 280 cm^{-1}.

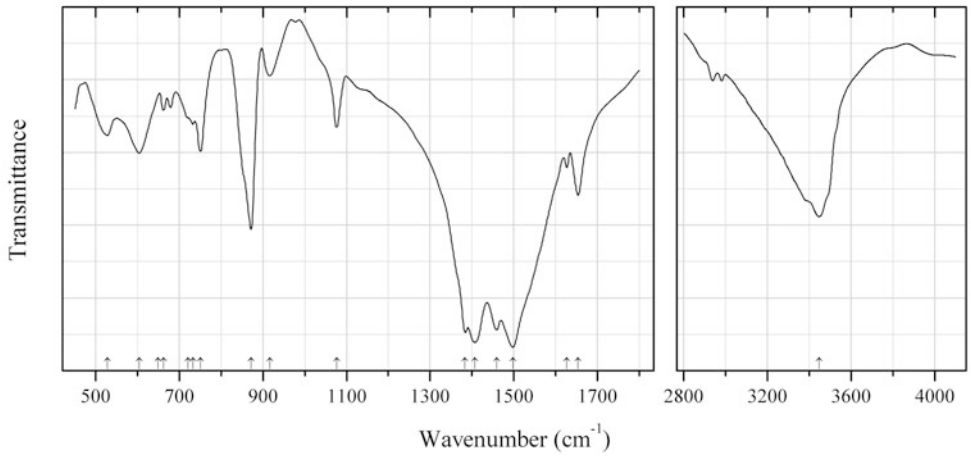

Fig. 2.99 IR spectrum of kamphaugite-(Y) drawn using data from Verwoerd (2008)

C279 Kamphaugite-(Y) $CaY(CO_3)_2(OH) \cdot H_2O$ (Fig. 2.99)
Locality: Goudini volcanic carbonatite complex, South Africa.
Description: White spheroids in cavities of a quartz-barite vein. Tetragonal, $a = 7.402(3)$, $c = 21.778(1)$ Å. $D_{meas} = 3.18(1)$ g/cm^3. The empirical formula is $Ca_{1.84}Y_{1.46}REE_{0.54}(CO_3)_4(OH)_{1.65} \cdot 2H_2O$. The strongest lines of the powder X-ray diffraction pattern [*d*, Å (*I*, %) (*hkl*)] are: 6.07 (100) (102), 4.40 (80) (104), 3.517 (60) (202), 2.888 (70) (107), 2.628 (70) (220), 1.885 (100) (228, 2.0.10).
Kind of sample preparation and/or method of registration of the spectrum: KBr disc. Transmission.
Source: Verwoerd (2008).
Wavenumbers (cm^{-1}): 3448s, 1654, 1627, 1498s, 1459s, 1407s, 1384s, 1076, 916w, 872s, 750, 732, 721sh, 649w, 662w, 604, 527.
Note: The wavenumbers were partly determined by us based on spectral curve analysis of the published spectrum. Weak bands in the range from 2800 to 3000 cm^{-1} are due to an organic impurity.

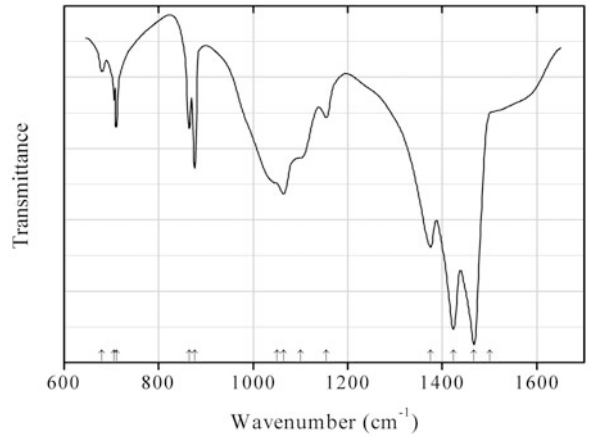

Fig. 2.100 IR spectrum of kukharenkoite-(La) drawn using data from Pekov et al. (2003)

C280 Kukharenkoite-(La) $Ba_2La(CO_3)_3F$ (Fig. 2.100)
Locality: Kirovskii Mine, Kukisvumchorr Mt., Khibiny alkaline massif, Kola peninsula, Russia (type locality).
Description: Colourless flattened-prismatic to needle-shaped crystals from the association with microcline, albite, calcite, nenadkevichite, hilairite, catapleiite, strontianite, donnayite-(Y), synchysite-(Ce), pyrite, etc. Holotype sample. Monoclinic, space group $P2_1/m$, a = 13.396(4), b = 5.111(1), c = 6.672(2) Å, β = 106.628(4)°, V = 437.7(3) Å^3, Z = 2. D_{calc} ≈ 4.64 g/cm^3. Optically biaxial (−), α = 1.581(3), β ≈ γ = 1.715(5), 2 V = 5(3)°. The empirical formula is: $(Ba_{1.78}Sr_{.14}K_{.04})(La_{0.43}Th_{0.22}Ce_{0.20}Ca_{0.11}Na_{0.05}Pr_{0.03}Nd_{0.03})(CO_3)_3F_{1.10}$. The strongest lines of the powder X-ray diffraction pattern [d, Å (I, %) (hkl)] are: 4.01 (100) (11–1, 201), 3.27 (100) (310, 40–1, 20–2), 2.54 (50) (020, 112), 2.14 (80) (221, 51–2, 600), 1.998 (80) (42–1, 22–2, 511, 31–3).
Kind of sample preparation and/or method of registration of the spectrum: KBr disc. Absorption.
Source: Pekov et al. (2003).
Wavenumbers (cm^{-1}): (1500sh), 1467s, 1423s, 1375s, 1154, 1100sh, 1064, 1050sh, 876, 865, 711, 705, 680w.

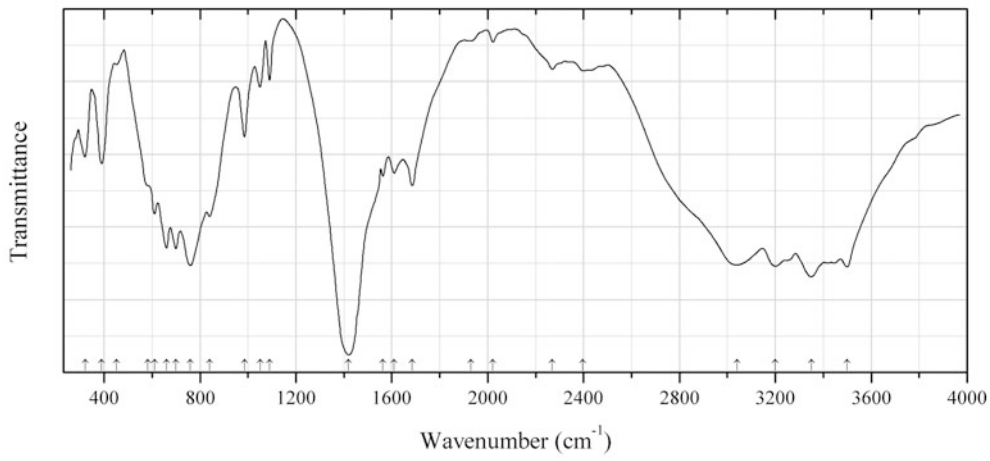

Fig. 2.101 IR spectrum of lansfordite drawn using data from Hill et al. (1982)

C281 Lansfordite $Mg(CO_3)\cdot 5H_2O$ (Fig. 2.101)
Locality: Not indicated.
Description: No data.
Kind of sample preparation and/or method of registration of the spectrum: KBr disc. Transmission.
Source: Hill et al. (1982).
Wavenumbers (cm^{-1}): 3500s, 3350s, 3200s, 3040s, 2397w, 2269w, 2022w, 1929w, 1685, 1610w, 1563w, 1420s, 1090w, 1050w, 985, 840, 760s, 700s, 660s, 610, 582sh, 451w, 390, 320.
Note: The wavenumbers were partly determined by us based on spectral curve analysis of the published spectrum.

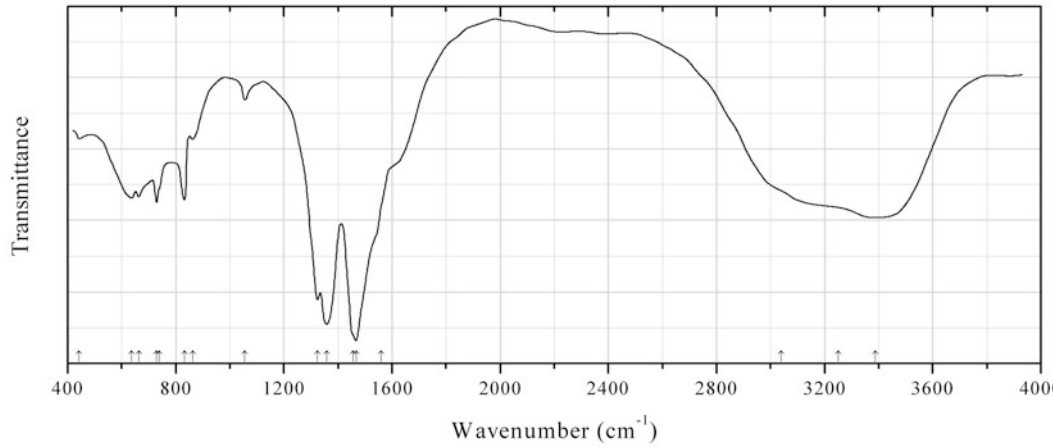

Fig. 2.102 IR spectrum of lanthanite-(Ce) drawn using data from Liu et al. (1999a)

C282 Lanthanite-(Ce) $Ce_2(CO_3)_3\cdot 8H_2O$ (Fig. 2.102)
Locality: Synthetic.
Description: Prepared from cerous chloride and ammonium bicarbonate. Confirmed by chemical and TG analyses.
Kind of sample preparation and/or method of registration of the spectrum: KBr disc. Transmission.
Source: Liu et al. (1999a).
Wavenumbers (cm^{-1}): 3387s, 3250sh, 3040sh, 1559sh, 1559sh, 1468s, 1456sh, 1358s, 1324, 1056w, 862, 832, 739sh, 729, 663, 637, 443.
Note: The wavenumbers were determined by us based on spectral curve analysis of the published spectrum.

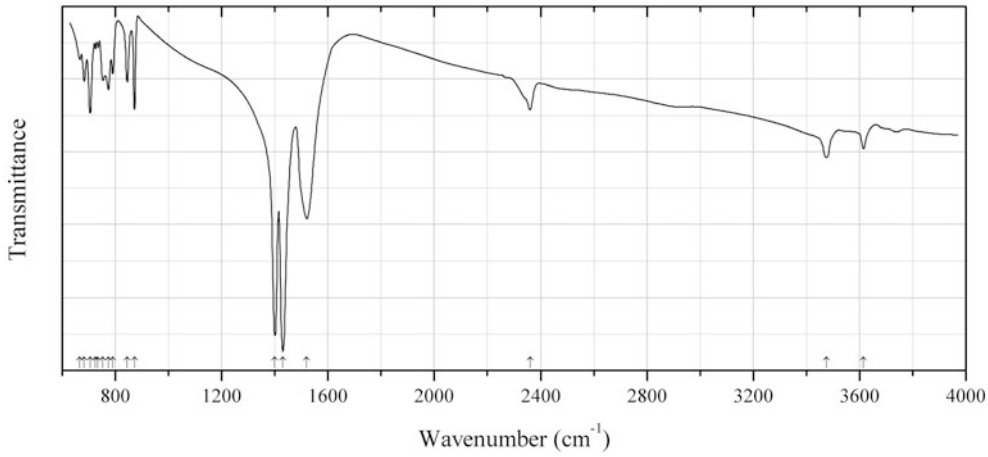

Fig. 2.103 IR spectrum of lanthanum hydroxycarbonate drawn using data from Pol et al. (2009)

C283 Lanthanum hydroxycarbonate $La(CO_3)(OH)$ (Fig. 2.103)
Locality: Synthetic.
Description: Synthesized by a solvent-free, one-pot reaction under autogenic pressure at elevated temperature process. Hexagonal. Confirmed by the powder X-ray diffraction pattern.
Kind of sample preparation and/or method of registration of the spectrum: KBr disc. Absorption.
Source: Pol et al. (2009).
Wavenumbers (cm^{-1}): 3615w, 3475w, 2360w, 1520s, 1430s, 1400s, 872, 845, 790, 774, 754, 735w, 725w, 705, 683, 667w.
Note: The wavenumbers were partly determined by us based on spectral curve analysis of the published spectrum.

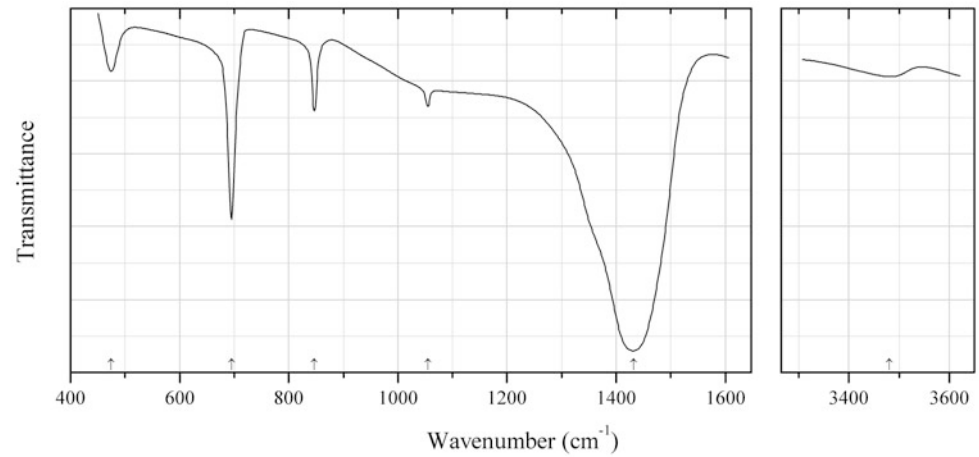

Fig. 2.104 IR spectrum of lead sodium hydroxycarbonate drawn using data from Belokoneva et al. (2002a)

C284 Lead sodium hydroxycarbonate $Pb_2Na(CO_3)_2(OH)$ (Fig. 2.104)
Locality: Synthetic.
Description: Prepared by hydrothermal synthesis. The crystal structure is solved. Trigonal, space group $P31c$, a = 5.268(4), c = 13.48(1) Å, V = 324.0(7) $Å^3$, Z = 2. D_{calc} = 5.877(9) g/cm^3.

Kind of sample preparation and/or method of registration of the spectrum: Thin film between KBr supporting plates. Transmission.
Source: Belokoneva et al. (2002a).
Wavenumbers (cm^{-1}): 3480w, 1432s, 1055w, 847, 695s, 475.

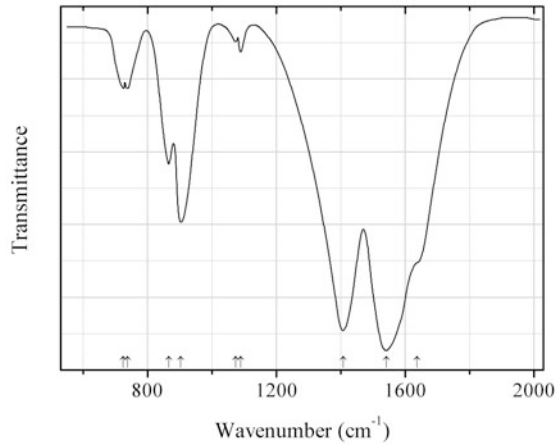

Fig. 2.105 IR spectrum of lithium uranyl carbonate hydrate drawn using data from Chernorukov et al. (2003)

C285 Lithium uranyl carbonate hydrate $Li_4(UO_2)(CO_3)_3 \cdot 1.5H_2O$ (Fig. 2.105)
Locality: Synthetic.
Description: Prepared by the reaction of $(UO_2)(CO_3)$ with the lithium carbonate. Holotype sample. Monoclinic, a = 7.496(3), b = 5.865(3), c = 8.833(3) Å, β = 95.5(1)°, V = 386.5(5) $Å^3$, Z = 2. The strongest lines of the powder X-ray diffraction pattern [d, Å (I, %) (hkl)] are: 4.732 (20) (011), 4.396 (100) (002), 3.986 (40) (111), 2.585 (25) (121), 2.212 (15) (203), 2.166 (20) (−104).
Kind of sample preparation and/or method of registration of the spectrum: KBr disc. Transmission.
Source: Chernorukov et al. (2003).
Wavenumbers (cm^{-1}): 3572s, 3453s, 3204, 1637sh, 1542s, 1408s, 1089w, 1074w, 904s, 866, 737, 725.

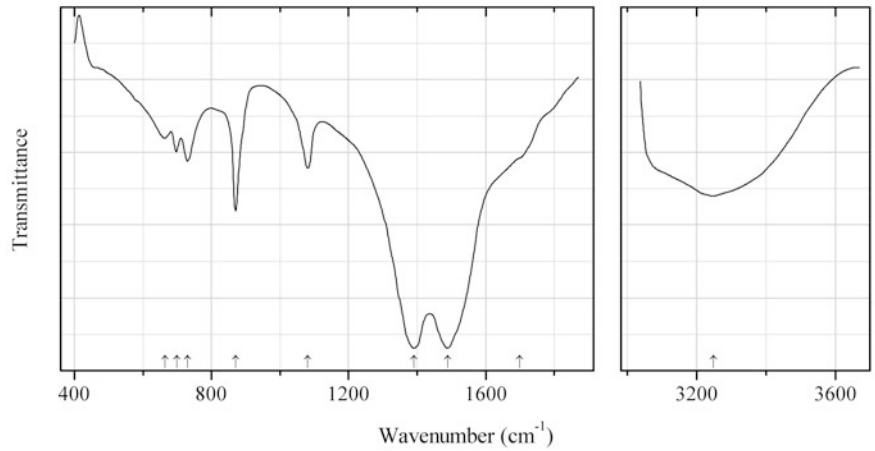

Fig. 2.106 IR spectrum of mckelveyite-(Y) drawn using data from Voloshin et al. (1990)

C286 Mckelveyite-(Y) $Na(Ba,Sr)_3Ca(Y,REE)(CO_3)_6 \cdot 3H_2O$ (Fig. 2.106)
Locality: Not indicated. Probably, Vuoriyarvi alkaline-ultramafic pluton, Northern Karelia, Russia.
Description: Confirmed by chemical and powder X-ray diffraction data.
Kind of sample preparation and/or method of registration of the spectrum: KBr disc. Absorption.
Source: Voloshin et al. (1990).
Wavenumbers (cm^{-1}): 3250, 1700sh, 1490s, 1390s, 1080, 870, 730, 700, 665.

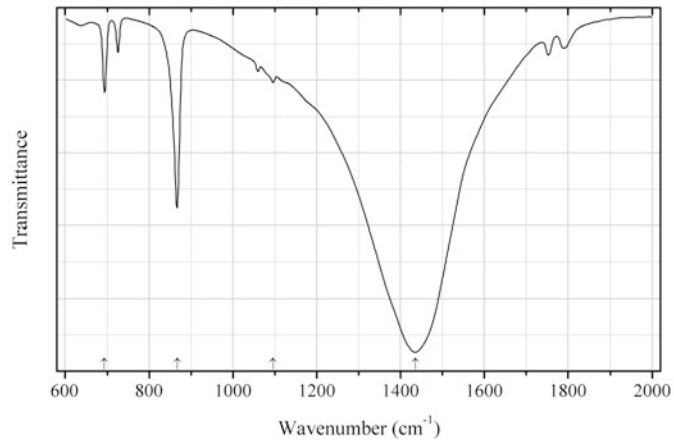

Fig. 2.107 IR spectrum of norsethite Mn analogue drawn using data from Schmidt et al. (2013)

C287 Norsethite Mn analogue $BaMn(CO_3)_2$ (Fig. 2.107)
Locality: Synthetic.
Description: Synthesized from a 1:1 molar mixture of $BaCO_3$ and $MnCO_3$ at 15 kbar and 510 °C. Confirmed by the powder X-ray diffraction pattern. Contains rhodochrosite and witherite impurities.
Kind of sample preparation and/or method of registration of the spectrum: KBr disc. Transmission.
Source: Schmidt et al. (2013).
Wavenumbers (cm^{-1}): 1435s, 1096w, 867.5s, 694.
Note: Other bands correspond to impurities.

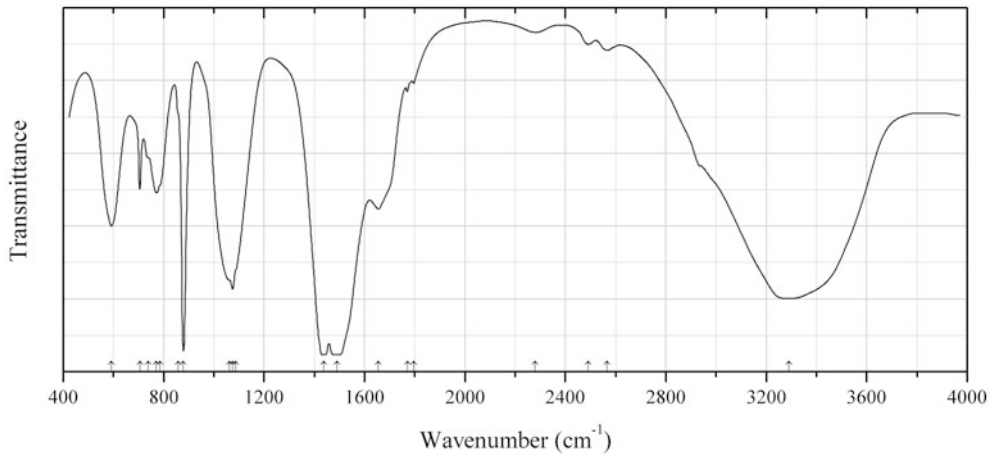

Fig. 2.108 IR spectrum of monohydrocalcite drawn using data from Skinner et al. (1977)

C288 Monohydrocalcite $Ca(CO_3)\cdot H_2O$ (Fig. 2.108)
Locality: Biogenetic.
Description: The guinea pig bladder stone (a whitish-tan concretion about 1 cm in diameter). Hexagonal or trigonal, a = 10.602, b = 7.548. D_{meas} = 2.39(3) g/cm^3, D_{calc} = 2.391 g/cm^3. Optically uniaxial, ε = 1.548, ω = 1.594. Contaminated with Mg^{2+} and SO_4^{2-}. The strongest lines of the powder X-ray diffraction pattern are observed 4.34, 3.08, and 1.935 Å.
Kind of sample preparation and/or method of registration of the spectrum: Transmission.
Source: Skinner et al. (1977).
Wavenumbers (cm^{-1}): 3290s, 2567w, 2492, 2280, 1796w, 1771w, 1655, 1490s, 1437s, 1088sh, 1074s, 1063sh, 879s, 858sh, 785sh, 772, 738sh, 705, 592.
Note: The wavenumbers were determined by us based on spectral curve analysis of the published spectrum.

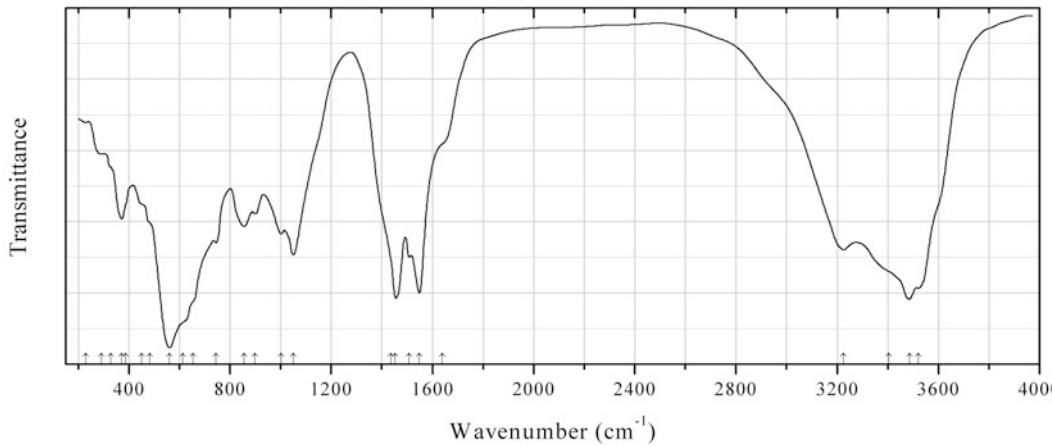

Fig. 2.109 IR spectrum of montroyalite drawn using data from Roberts et al. (1986)

C289 Montroyalite $Sr_4Al_8(CO_3)_3(OH)_{26}\cdot 10H_2O$ (?) (Fig. 2.109)
Locality: Francon quarry, Saint-Michel, Montréal, Québec, Canada (type locality).
Description: White l-mm-sized hemispheres in cavities in a silicocarbonatite sill. The associated minerals are albite, quartz, strontiodresserite, calcite, dawsonite, ankerite, and fluorite. Holotype sample. Triclinic (?). D_{meas} = 2.677 g/cm^3. Optically biaxial (−), α = 1.515(5), β = 1.530(5), γ = 1.545 (5), 2 V = 80(10)°. The empirical formula is $(Sr_{3.78}Ca_{0.28})Al_8(CO_3)_{2.96}[(OH)_{17.63}F_{8.57}]\cdot 10.52H_2O$. The strongest lines of the powder X-ray diffraction pattern [d, Å (I, %)] are: 6.57 (100), 4.00 (50), 3.283 (55), 3.190 (50), 2.862 (40), 2.551 (40), 2.481 (40), 2.356 (45).
Kind of sample preparation and/or method of registration of the spectrum: Transmission. Kind of sample preparation is not indicated.
Source: Roberts et al. (1986).
Wavenumbers (cm^{-1}): 3522s, 3485s, 3403sh, 3226s, 1638sh, 1548s, 1508, 1453s, 1437sh, 1049, 1002, 899, 855, 745, 652sh, 612sh, 560s, 483sh, 451sh, 388sh, 371, 329sh, 291w, 230w.
Note: The wavenumbers were determined by us based on spectral curve analysis of the published spectrum.

C290 Mroseite $CaTe^{4+}(CO_3)O_2$
Locality: No data.
Description: No data.
Kind of sample preparation and/or method of registration of the spectrum: KBr disc. Absorption.
Source: Povarennykh (1981a).
Wavenumbers (cm^{-1}): 1470s, 1360s, 840, 770.

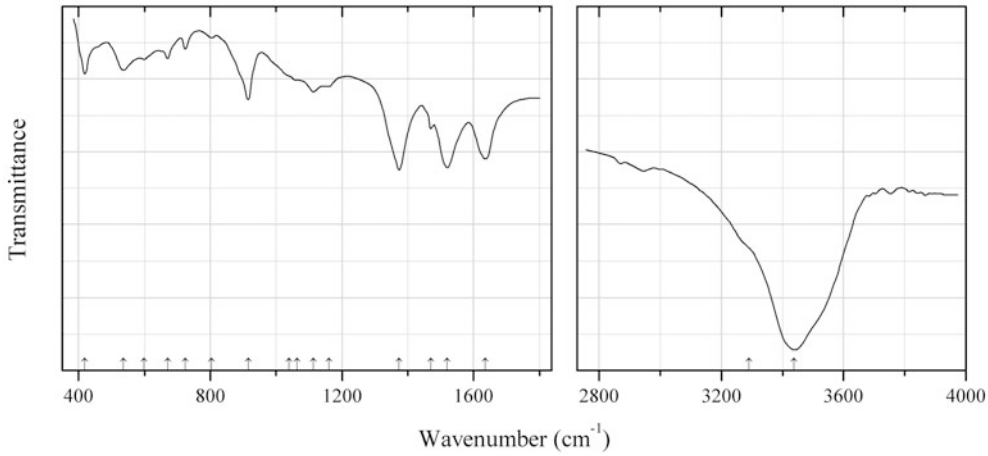

Fig. 2.110 IR spectrum of oswaldpeetersite drawn using data from Vochten et al. (2001)

C291 Oswaldpeetersite $(UO_2)_2(CO_3)(OH)_2 \cdot 4H_2O$ (Fig. 2.110)
Locality: Jomac uranium mine, Brown's Rim, San Juan Co., Utah, USA (type locality).
Description: Aggregates of canary yellow prismatic crystals from the association with gypsum, cuprite, antlerite, goethite, lepidocrocite, mbobomkulite, hydrombobomkulite, sklodowskite, etc. Holotype sample. Monoclinic, space group $P2_1/c$, $a = 4.1425(6)$, $b = 14.098(3)$, $c = 18.374(5)$ Å, $\beta = 103.62(1)°$, $V = 1042.8(3)$ $Å^3$, $Z = 4$. $D_{calc} = 4.54$ g/cm^3. Optically biaxial (−), $\alpha = 1.583(2)$, $\beta = 1.669(2)$, $\gamma = 1.712(2)$, $2V = 67.4(2)°$. The empirical formula is $(UO_2)_{2.03}(CO_3)_{1.01}(OH)_{2.05} \cdot 3.85H_2O$. The strongest lines of the powder X-ray diffraction pattern [*d*, Å (*I*, %) (*hkl*)] are: 8.95 (65) (002), 7.54 (63) (012), 4.55 (96) (031), 4.26 (60) (014), 3.46 (62) (015), 3.32 (100) (−114), 3.029 (85) (043), 2.273 (62) (062).
Kind of sample preparation and/or method of registration of the spectrum: KBr disc. Transmission.
Source: Vochten et al. (2001).
Wavenumbers (cm^{-1}): 3437s, 3290sh, 1636s, 1520s, 1470, 1374s, 1160, 1114, 1063sh, 1039sh, 915, 804w, 724w, 670, 598w, 537, 419.
Note: The wavenumbers were partly determined by us based on spectral curve analysis of the published spectrum.

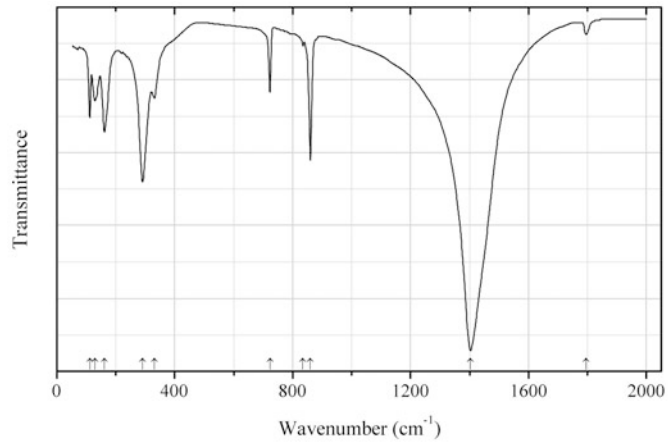

Fig. 2.111 IR spectrum of otavite drawn using data from Bromiley et al. (2007)

C292 Otavite $Cd(CO_3)$ (Fig. 2.111)
Locality: Synthetic.
Description: Pure $Cd(CO_3)$ synthesized at 800 °C and 1 GPa for 1 h. Trigonal, space group *P*-3*c*.
Kind of sample preparation and/or method of registration of the spectrum: KBr and polyethylene discs. Absorption.
Source: Bromiley et al. (2007).
Wavenumbers (cm^{-1}): 1796w, 1403s, 860, 835w, 723, 331, 290s, 162, 129, 112.
Note: The wavenumbers were determined by us based on spectral curve analysis of the published spectrum.

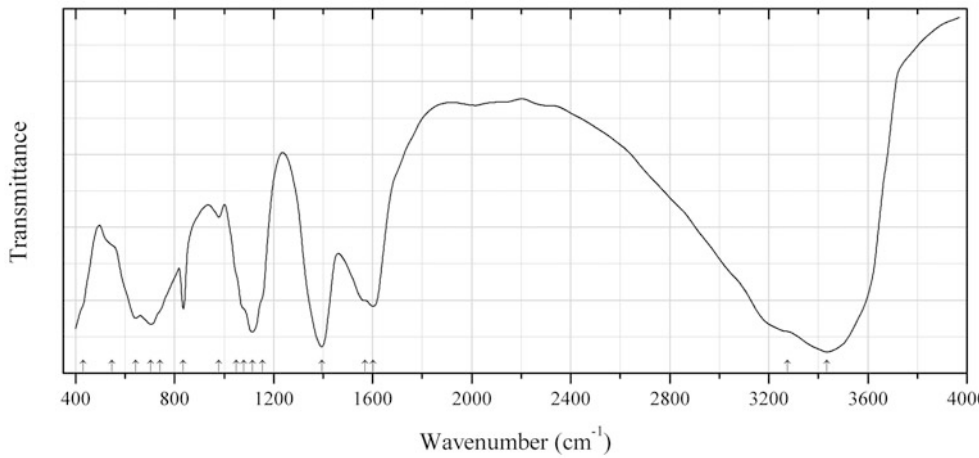

Fig. 2.112 IR spectrum of otwayite drawn using data from Henry and Birch (1992)

C293 Otwayite $Ni_2(CO_3)(OH)_2 \cdot 2H_2O$ (Fig. 2.112)
Locality: Lord Brassey mine, near Heaslewood, Tasmania.
Description: Bright green clay-like coating on serpentine. The empirical formula is $Ni_2(CO_3)_{0.84}(SO_4)_{0.16}(OH)_2 \cdot nH_2O$. Confirmed by powder X-ray diffraction data.
Kind of sample preparation and/or method of registration of the spectrum: KBr disc. Transmission.
Source: Henry and Birch (1992).

Wavenumbers (cm^{-1}): 3435s, 3275sh, 1601s, 1568sh, 1394s, 1154sh, 1115s, 1079sh, 1048sh, 979w, 835, 740sh, 703s, 642, 547sh, 430sh.
Note: The wavenumbers were determined by us based on spectral curve analysis of the published spectrum.

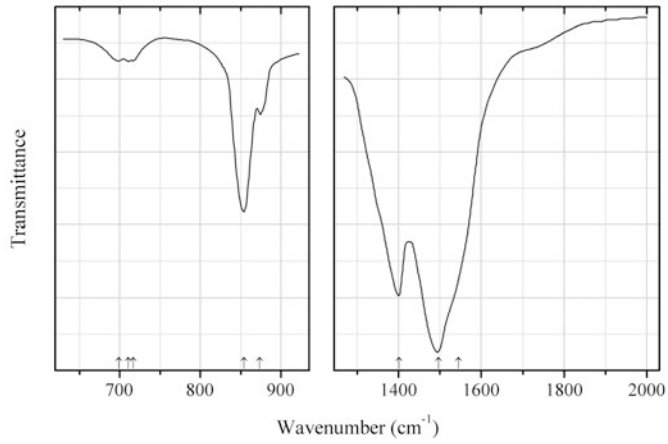

Fig. 2.113 IR spectrum of petersenite-(Ce) drawn using data from Pekov et al. (1998)

C294 Petersenite-(Ce) $Na_4Ce_2(CO_3)_5$ (Fig. 2.113)
Locality: Koashva Mt., Khibiny alkaline complex, Kola peninsula, Murmansk region, Russia.
Description: Yellow-broen granular aggregates from peralkaline pegmatite, from the association with vitusite, nacaphite, pectolite, thermonatrite, aegirine, lomonosovite, etc. Monoclinic, a = 20.89, b = 6.338, c = 10.60 Å, β = 120.8°. The empirical formula is (electron microprobe): $(Na_{3.70}Ca_{0.30})(Ce_{0.71}La_{0.48}Ca_{0.34}Sr_{0.25}Nd_{0.20}Pr_{0.06}Th_{0.02}Ba_{0.02}Sm_{0.01})(CO_3)_5$. The strongest lines of the powder X-ray diffraction pattern are observed at 9.20, 5.19, 4.65, 3.72, 3.03, 2.601, and 1.919 Å.
Kind of sample preparation and/or method of registration of the spectrum: KBr disc. Absorption.
Source: Pekov et al. (1998).
Wavenumbers (cm^{-1}): 1545sh, 1496s, 1401s, 873, 854s, 717w, 711w, 699w.

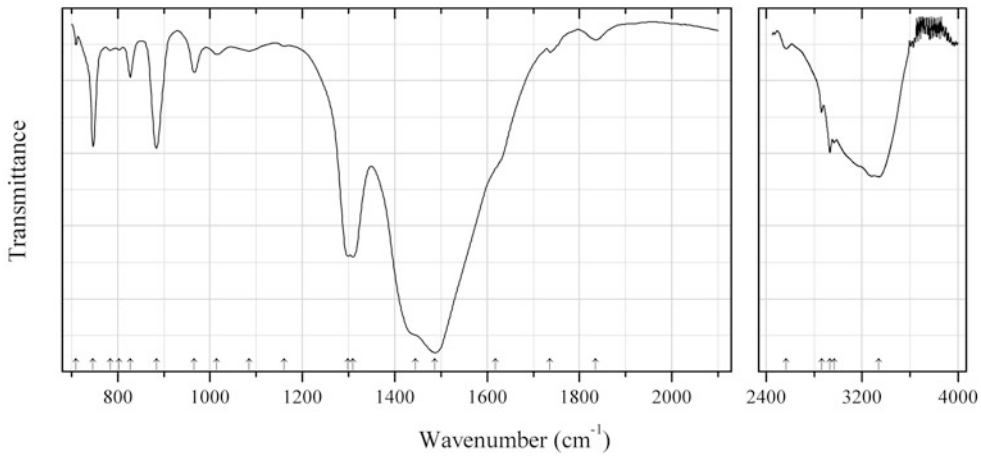

Fig. 2.114 IR spectrum of peterbaylissite drawn using data from Roberts et al. (1995a)

C295 Peterbaylissite $Hg_3(CO_3)(OH)\cdot 2H_2O$ (Fig. 2.114)
Locality: Abandoned Clear Creek mercury mine, New Idria district, San Benito Co., California, USA (type locality).
Description: Black to very dark red-brown crystals from the association with magnesite, quartz, cinnabar, metacinnabar, and native mercury. Holotype sample. The crystal structure is solved. Orthorhombic, pseudo-tetragonal, space group *Pcab*, a = 11.130(2), b = 11.139(3), c = 10.725(3) Å, V = 1330(1) Å^3, Z = 8. D_{calc} = 7.14 g/cm^3. The strongest lines of the powder X-ray diffraction pattern [d, Å (I, %) (hkl)] are: 4.84 (50) (012), 2.969 (70) (231), 2.786 (70) (040, 400), 2.648 (100) (223), 2.419 (60) (241, 024, 412), 1.580 (50) (623).
Kind of sample preparation and/or method of registration of the spectrum: Transmittance of a sample crushed in a diamond anvil microsample cell.
Source: Roberts et al. (1995a).
Wavenumbers (cm^{-1}): 3340, 2966, 2931, 2862, 2565w, 1835w, 1736w, 1618sh, 1487s, 1445sh, 1309s, 1299s, 1161w, 1085w, 1015w, 966, 884, 827, 803w, 784w, 747, 710w.
Note: The wavenumbers were partly determined by us based on spectral curve analysis of the published spectrum.

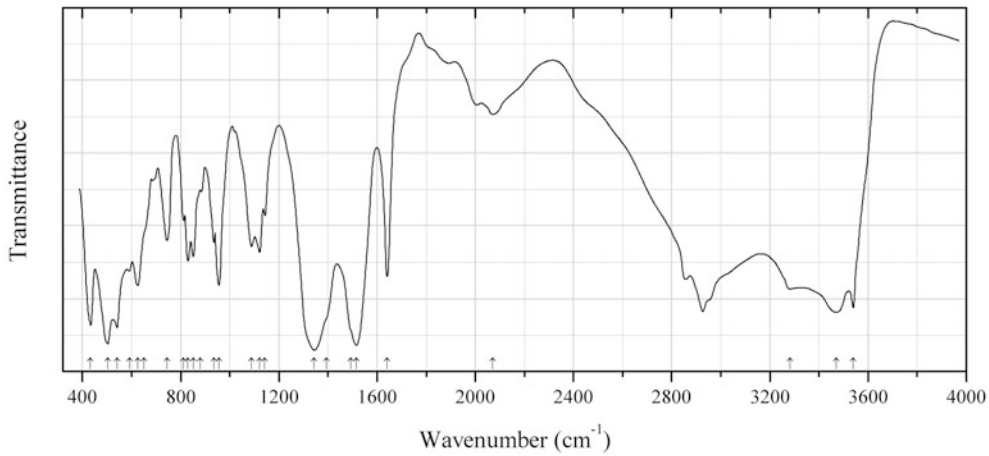

Fig. 2.115 IR spectrum of petterdite drawn using data from Birch et al. (2000)

C296 Petterdite $PbCr_2(CO_3)_2(OH)_4\cdot H_2O$ (Fig. 2.115)
Locality: Dundas mineral field, Zeehan district, northwestern Tasmania, Australia (type locality).
Description: Crusts made up of tiny platy crystals from the association with crocoite, cerussite, bindheimite, pyromorphite, and relict galena. Holotype sample. Orthorhombic, space group *Pbnm*, a = 9.079(3), b = 16.321(9), c = 5.786(7) Å, V = 857(1) Å^3, Z = 4. D_{calc} = 3.95 g/cm^3. Optically biaxial (−), α = 1.704(5), β ≈ 1.802, γ = 1.842(5). The empirical formula is $(Pb_{0.99}Sr_{0.07})(Cr^{3+}_{1.52}Al_{0.36}Sb_{0.02})(CO_3)_{2.12}(OH)_{3.62}\cdot 1.02H_2O$. The strongest lines of the powder X-ray diffraction pattern [d, Å (I, %) (hkl)] are: 7.937 (100) (110), 4.686 (50) (021, 111), 3.633 (70) (131), 3.270 (40) (221), 2.718 (40) (022, 060), 2.690 (40) (241, 301).
Kind of sample preparation and/or method of registration of the spectrum: KBr disc. Transmission.
Source: Birch et al. (2000).
Wavenumbers (cm^{-1}): 3540s, 3470s, 3282, 2072w, 1641, 1516s, 1493sh, 1394sh, 1343s, 1143, 1122, 1089, 956, 935, 881sh, 852, 830, 812, 744, 650sh, 626, 592, 541s, 504s, 433s.
Note: The bands in the range from 2800 to 3000 cm^{-1} are supposed to be due to the admixture of an organic substance.

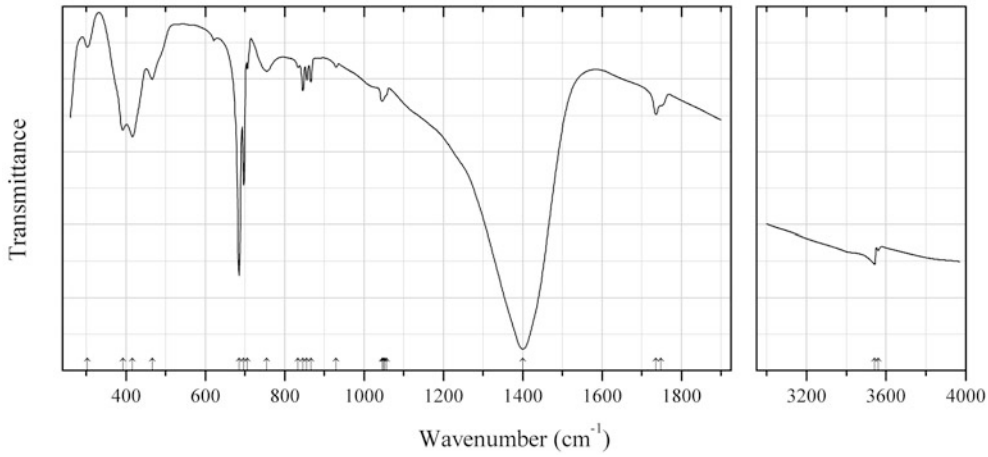

Fig. 2.116 IR spectrum of plumbonacrite drawn using data from Brooker et al. (1983)

C297 Plumbonacrite $Pb_5(CO_3)_3O(OH)_2$ (Fig. 2.116)
Locality: Synthetic.
Description: Prepared by refluxing synthetic hydrocerussite in a 0.1 mol/l solution of K_2CO_3, with the pH adjusted to 13. Confirmed by powder X-ray diffraction data.
Kind of sample preparation and/or method of registration of the spectrum: KBr disc. Transmission.
Source: Brooker et al. (1983).
Wavenumbers (cm^{-1}): 3560w, 3542w, 1748sh, 1736w, 1400s, 1057w, 1053w, 1049w, 1046w, 930w, 866w, 856w, 846w, 834w, 755w, 706w, 697s, 685s, 466, 416s, 392, 303w.

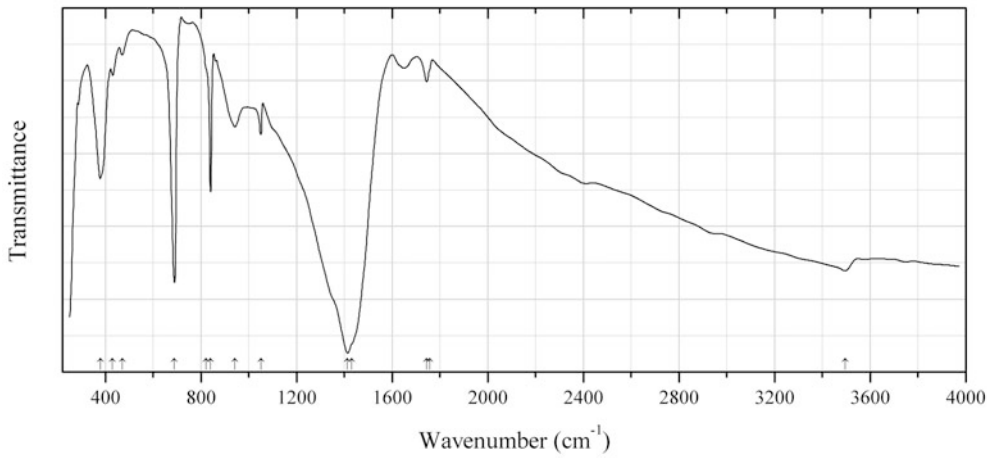

Fig. 2.117 IR spectrum of potassium basic lead carbonate drawn using data from Brooker et al. (1983)

C298 Potassium basic lead carbonate $KPb_2(CO_3)_2(OH)$ (Fig. 2.117)
Locality: Synthetic.
Description: Prepared by refluxing cerussite or hydrocerussite at 100 °C in K_2CO_3 solution (5 mol/l) for 1–2 days. Hexagonal, a = 5.348(2), c = 13.990(5) Å. The strongest lines of the powder X-ray

diffraction pattern [*d*, Å (*I*, %)] are: 4.631 (25), 4.396 (23), 3.288 (100), 2.673 (35), 2.075 (37), 1.7573 (23).

Kind of sample preparation and/or method of registration of the spectrum: KBr disc. Transmission.

Source: Brooker et al. (1983).

Wavenumbers (cm^{-1}): 3495w, 1756w, 1744w, 1430sh, 1413s, 1050, 942, 840s, 822w, 689s, 470w, 430w, 379s.

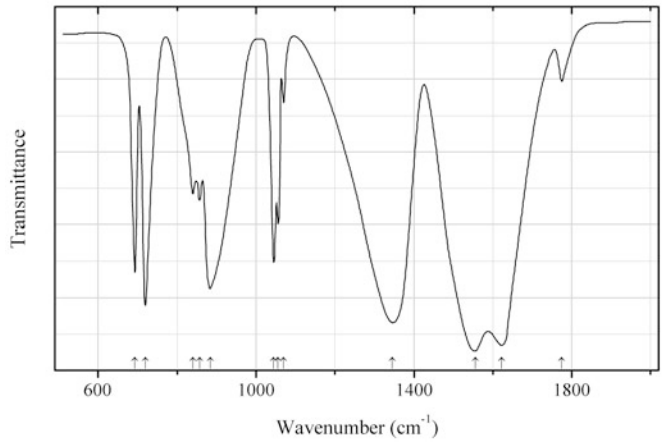

Fig. 2.118 IR spectrum of potassium uranyl carbonate drawn using data from Chernorukov et al. (2003)

C299 Potassium uranyl carbonate $K_4(UO_2)(CO_3)_3$ (Fig. 2.118)

Locality: Synthetic.

Description: Prepared by the reaction of UO_2CO_3 with aqueous solution containing stoichiometric amount of potassium carbonate with subsequent evaporation of water at 100 °C. Monoclinic, a = 10.247(3), b = 9.202(2), c = 12.226(3) Å, β = 95.1(1)°, V = 1148(1) $Å^3$, Z = 4. D_{meas} = 2.39(3) g/cm^3, D_{calc} = 2.391 g/cm^3. The strongest lines of the powder X-ray diffraction pattern [*d*, Å (*I*, %) (*hkl*)] are: 6.834 (100) (110), 6.117 (86) (−111), 5.446 (25) (−102), 5.036 (32) (102), 4.094 (28) (−202), 3.671 (26) (022), 3.026 (64) (311).

Kind of sample preparation and/or method of registration of the spectrum: KBr disc. Transmission.

Source: Chernorukov et al. (2003).

Wavenumbers (cm^{-1}): 1775, 1623s, 1556s, 1346s, 1069w, 1056, 1045s, 884s, 857w, 840w, 719s, 693s.

Note: The band positions denoted by Chernorukov et al. (2003) a s 1049, 851, and 848 cm^{-1} were determined by us at 1069, 857, and 840 cm^{-1}, respectively, based on spectral curve analysis of the published spectrum.

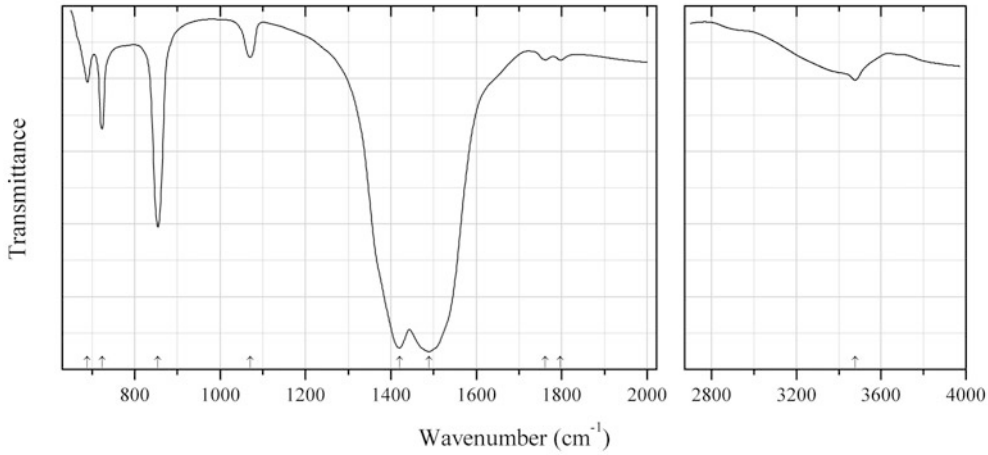

Fig. 2.119 IR spectrum of qaqarssukite-(Ce) drawn using data from Grice et al. (2006)

C300 Qaqarssukite-(Ce) $BaCe(CO_3)_2F$ (Fig. 2.119)
Locality: Qaqarssuk carbonatite complex, southern West Greenland (type locality).
Description: Yellow-brown to brown crystals and aggregates from the association with calcite, dolomite, strontianite, phlogopite, and pyrite. Holotype sample. Trigonal, space group *P*-3*c*1, a = 7.2036(9), c 18.172(3) Å, V = 816.6(2) Å^3, Z = 6. D_{calc} = 4.64 g/cm^3. Optically uniaxial (+), ω = 1.672(3), ε = 1.751(5). The empirical formula is (electron microprobe, CO_3 calculated): $(Ba_{0.68}Ca_{0.19}Sr_{0.14})(Ce_{0.47}La_{0.21}Nd_{0.15}Pr_{0.04}Sm_{0.01})Ti_{0.07}(CO_3)_2F_{1.01}$. The strongest lines of the powder X-ray diffraction pattern [*d*, Å (*I*, %) (*hkl*)] are: 5.14 (28) (102), 4.55 (43) (004), 3.671 (32) (104), 3.534 (41) (111), 3.348 (100) (112), 3.093 (40) (113), 2.569 (35) (204), 2.078 (60) (300).
Kind of sample preparation and/or method of registration of the spectrum: Transmittance of a powdered sample using a diamond anvil microsample cell.
Source: Grice et al. (2006).
Wavenumbers (cm^{-1}): 3478, 1797w, 1762w, 1489s, 1420s, 1070, 854s, 723, 689.
Note: The band at 3478 cm^{-1} indicates the presence of OH groups.

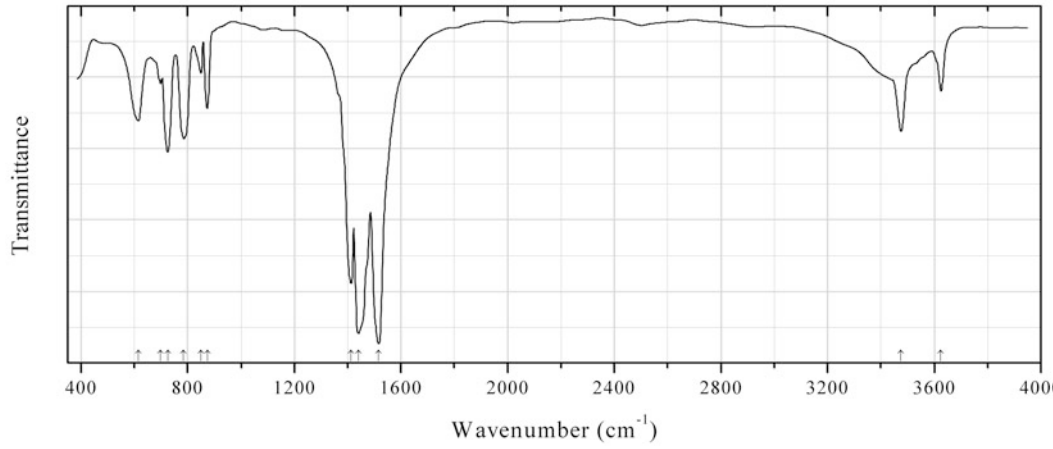

Fig. 2.120 IR spectrum of hydroxylbastnäsite-(Nd) drawn using data from Shang et al. (2009)

C301 Hydroxylbastnäsite-(Nd) $Nd(CO_3)(OH)$ (Fig. 2.120)
Locality: Synthetic.
Description: Prepared under hydrothermal conditions, by the reaction of neodymium nitrate and ammonium hydrogen carbonate. Hexagonal, a = 12.32, c = 9.880 Å, Confirmed by powder X-ray diffraction data.
Kind of sample preparation and/or method of registration of the spectrum: Transmission. Kind of sample preparation is not indicated.
Source: Shang et al. (2009).
Wavenumbers (cm^{-1}): 3625, 3475, 1517s, 1441s, 1413s, 875, 850w, 785, 725, 698w, 615.
Note: The wavenumbers were partly determined by us based on spectral curve analysis of the published spectrum.

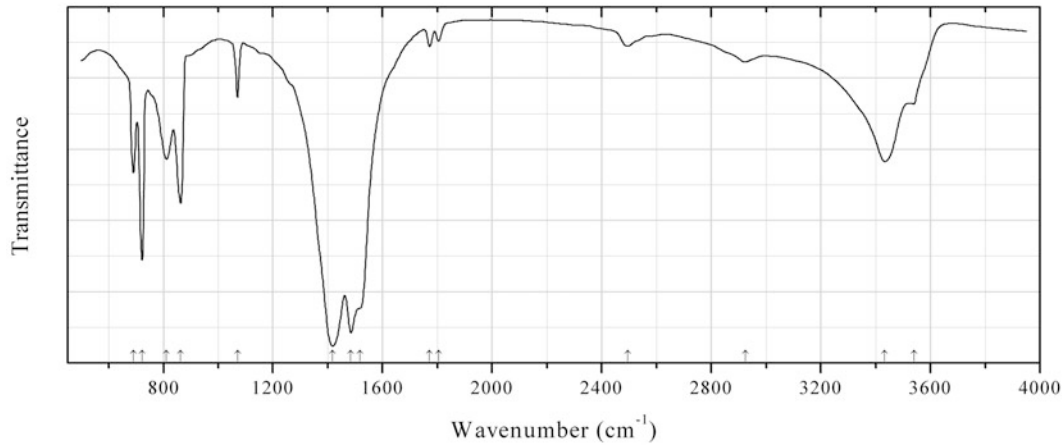

Fig. 2.121 IR spectrum of kozoite-(La) drawn using data from Li et al. (2010)

C302 Kozoite-(La) $La(CO_3)(OH)$ (Fig. 2.121)
Locality: Synthetic.
Description: Synthesized via a facile homogeneous precipitation route under mild conditions. Orthorhombic. Confirmed by the powder X-ray diffraction pattern.
Kind of sample preparation and/or method of registration of the spectrum: KBr disc. Transmission.
Source: Li et al. (2010).
Wavenumbers (cm^{-1}): 3540, 3433, 2924w, 2494w, 1804w, 1772w, 1518sh, 1484s, 1418s, 1070, 863, 812, 722s, 690.
Note: The wavenumbers were partly determined by us based on spectral curve analysis of the published spectrum.

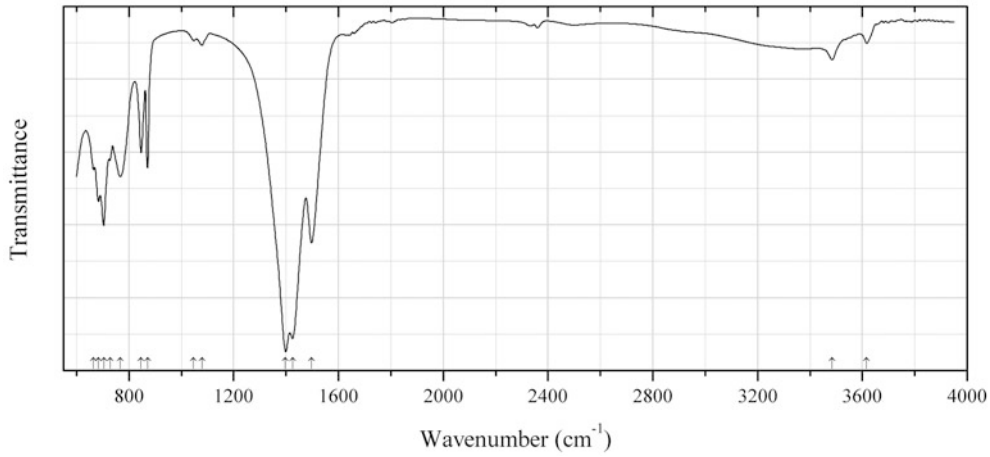

Fig. 2.122 IR spectrum of hydroxylbastnäsite-(La) drawn using data from Lee and Jung (2013)

C303 Hydroxylbastnäsite-(La) $La(CO_3)(OH)$ (Fig. 2.122)
Locality: Synthetic.
Description: Hexagonal polymorph of $La(CO_3)(OH)$ prepared by a hydrothermal reaction under ambient pressure and characterized by thermogravimetry and powder X-ray diffraction.
Kind of sample preparation and/or method of registration of the spectrum: Powdered sample. Transmission.
Source: Lee and Jung (2013).
Wavenumbers (cm^{-1}): 3617w, 3485w, 1497s, 1425s, 1398s, 1079w, 1047w, 871, 846, 766, 728, 704, 683, 665.
Note: The wavenumbers were partly determined by us based on spectral curve analysis of the published spectrum.

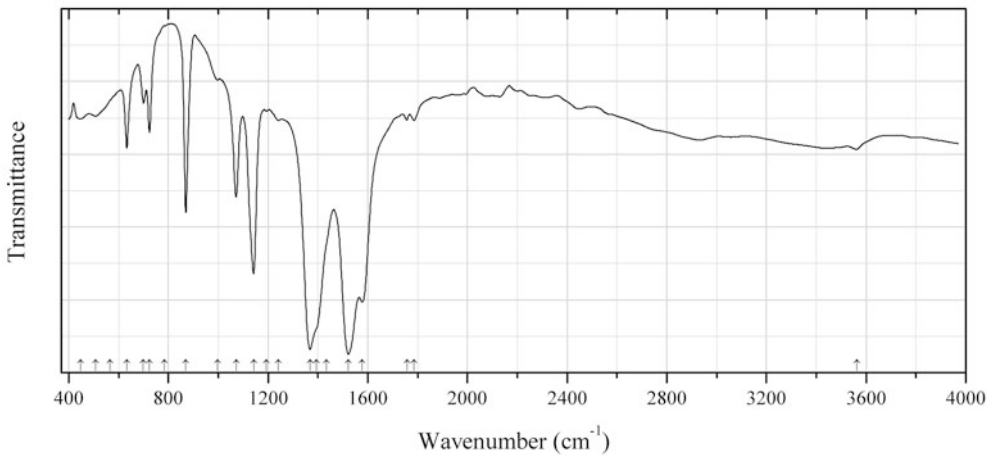

Fig. 2.123 IR spectrum of reederite-(Y) drawn using data from Grice et al. (1995)

C304 Reederite-(Y) $(Na,Mn)_{15}Y_2(CO_3)_9(SO_3F)Cl$ (Fig. 2.123)
Locality: Poudrette (Demix) quarry, Mont Saint-Hilaire, Rouville RCM (Rouville Co.), Montérégie, Québec, Canada (type locality).

Description: Yellow to orange-brown grains from the association with trona, shortite, petersenite-(Ce), catapleiite, analcime, and manganotychite. Holotype sample. Hexagonal, space group *P*-6, a = 8.773(1), c = 10.746(2) Å, Z = 1. D_{meas} = 2.91(3) g/cm^3, D_{calc} = 2.85 g/cm^3. Optically uniaxial (−), ω = 1.548(1), ε = 1.537(1). The empirical formula is (electron microprobe, CO_3 by structural data): $(Na_{13.63}Al_{0.32}Mn_{0.22}Ca_{0.16}Fe_{0.07})(Y_{1.13}Ce_{0.27}Nd_{0.15}La_{0.11}Dy_{0.09}Er_{0.08}Gd_{0.06}Sm_{0.04}Pr_{0.03}Yb_{0.02})(CO_3)_9(SO_3F)_{0.79}(Cl_{0.72}F_{0.43})O_{1.14}$. The strongest lines of the powder X-ray diffraction pattern [*d*, Å (*I*, %) (*hkl*)] are: 2.532 (100) (212), 4.39 (80) (102) 2.774, (80) (113), 2.240 (80) (213), 6.20 (40) (101), 1.657 (40) (116, 314, 322, 410), 2.067 (30) (105, 303).

Kind of sample preparation and/or method of registration of the spectrum: The spectrum was obtained using a diamond-anvil cell microsampling device.

Source: Grice et al. (1995).

Wavenumbers (cm^{-1}): 3562w, 1786w, 1757w, 1577s, 1523s, 1434sh, 1395sh, 1368s, 1242w, 1193w, 1142s, 1072, 997w, 870, 785, 724, 700, 633, 565, 508, 447.

Note: The wavenumbers were partly determined by us based on spectral curve analysis of the published spectrum. According to Grice et al. (1995), "the absence of a peak in the 3560 cm^{-1} region, the O–H stretching frequency, is significant because it indicates a lack of either OH^- anions or H_2O molecules". However a weak band is present in this region (exactly at 3562 cm^{-1}). Moreover, a weak broad band centered between 2800 and 3000 cm^{-1} may correspond to acid HSO_4^- groups. The presence of these groups could explain distortion of S-centered tetrahedra.

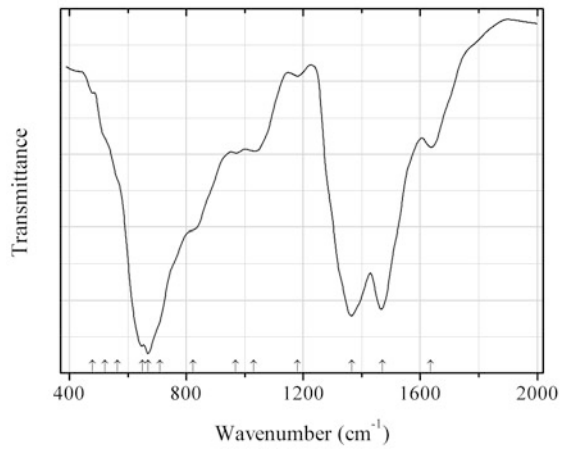

Fig. 2.124 IR spectrum of reevesite Co-analogue drawn using data from Song and Moon (1998)

C305 Reevesite Co-analogue $Ni_6Co_2(CO_3)(OH)_{16}\cdot 4H_2O$ (Fig. 2.124)

Locality: Synthetic.

Description: Obtained by coprecipitation of corresponding hydroxides in alkaline solution in the presence of Na_2CO_3. Confirmed by chemical analyses and powder X-ray diffraction data.

Kind of sample preparation and/or method of registration of the spectrum: KBr disc. Transmission.

Source: Song and Moon (1998).

Wavenumbers (cm^{-1}): 1635, 1470s, 1365s, 1181w, 1030, 969, 823sh, 710sh, 670s, 649s, 565sh, 521sh, 480w.

Note: The wavenumbers were partly determined by us based on spectral curve analysis of the published spectrum. The band at 1470 cm^{-1} is non-typical for carbonate hydrotalcite-group minerals and their synthetic analogues (see Hernandez-Moreno et al. 1985; Kloprogge and Frost 1999; Chukanov 2014a). Possibly, its presence is due to the contamination by another (amorphous?) carbonate.

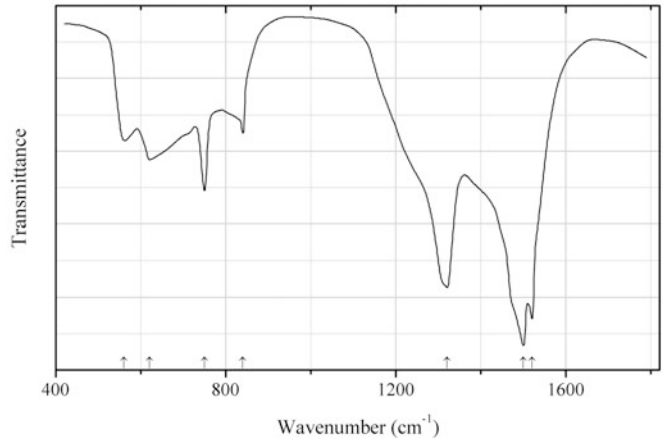

Fig. 2.125 IR spectrum of phosgenite Br analogue drawn using data from Al'Ama et al. (2006)

C306 Phosgenite Br analogue $Pb_2(CO_3)Br_2$ (Fig. 2.125)
Locality: Synthetic.
Description: Synthesized hydrothermally in the KBr–$PbCO_3$–B_2O_3–H_2O system at 270–280 °C. The crystal structure is solved. Tetragonal, space group *P*4/*mbm*, a = 8.353(4), c = 9.077(3) Å, V = 633.3 (8) Å^3, Z = 4. D_{calc} = 6.651 g/cm^3.
Kind of sample preparation and/or method of registration of the spectrum: A thin layer of powdered sample on a KBr plate. Transmission.
Source: Al'Ama et al. (2006).
Wavenumbers (cm^{-1}): 1520s, 1500s, 1320s, 840, 750, 620, 560.

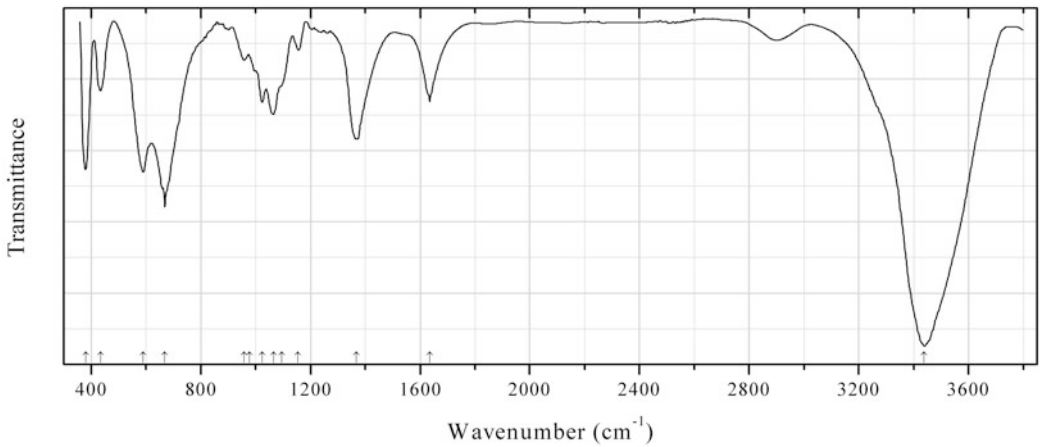

Fig. 2.126 IR spectrum of brugnatellite obtained by N.V. Chukanov

C307 Brugnatellite $Mg_6Fe^{3+}(CO_3)(OH)_{13}\cdot 4H_2O$ (Fig. 2.126)
Locality: Borehole No. 31, Tolovskiy ultrabasite massif, near Miass, South Urals, Russia.
Description: Silvery-white scaly aggregate from the association with serpentine and brucite. Investigated by V.A. Popov and V.I. Popova. Optically uniaxial (−), ω = 1.543–1.546. The empirical formula is

(electron microprobe): $Mg_{5.3}Fe_{1.7}(CO_3,SO_4)_x(OH)_{13}\cdot nH_2O$. The strongest lines of the powder X-ray diffraction pattern [*d*, Å (*I*, %)] are: 7.82 (100), 4.74 (30), 3.90 (70), 3.64 (20), and 2.59 (20).
Kind of sample preparation and/or method of registration of the spectrum: KBr disc. Absorption.
Wavenumbers (cm^{-1}): 3438s, 1635, 1368, 1155w, 1095sh, 1065, 1024, 977sh, 959w, 669s, 590, 434, 380.
Note: For the IR spectrum of brugnatellite see also Jones and Jackson (1993).

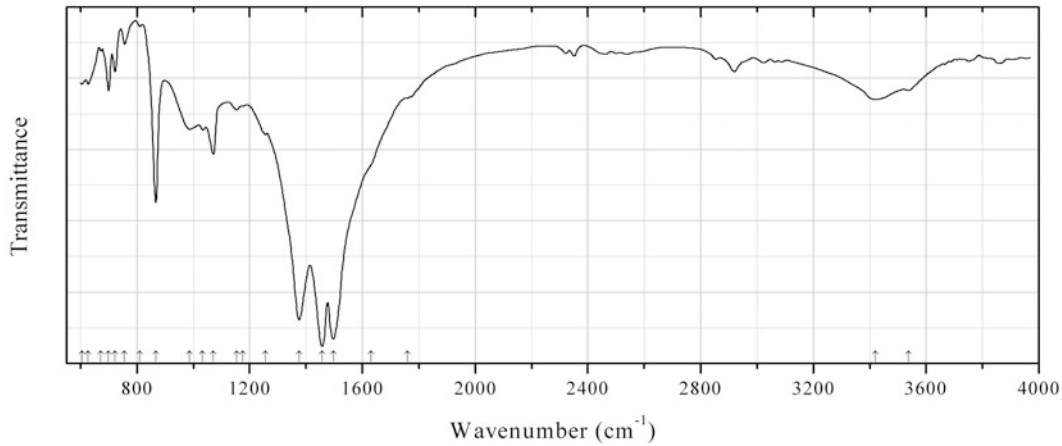

Fig. 2.127 IR spectrum of rouvilleite drawn using data from McDonald et al. (1991)

C308 Rouvilleite $Na_3CaMn^{2+}(CO_3)_3F$ (Fig. 2.127)
Locality: Poudrette quarry, Mont St. Hilaire, Rouville Co., Québec, Canada (type locality).
Description: Prismatic crystals from the association with villiaumite, shortite, aegirine, microcline, cancrinite, analcime, vuonnemite, cryolite, kogarkoite, etc. Holotype sample. Monoclinic, a = 8.04 {4), b = 15.812(5), c = 7.030(3) Å, β = 101.16(3)°, V = 877.1(4) $Å^3$, Z = 4. D_{meas} = 2.67(2) g/cm^3, D_{calc} = 2.69 g/cm^3. Optically biaxial (−), α = 1.472(1), β = 1.562(1), γ = 1.569(1), 2 V = 25(1)°. The empirical formula is $Na_{2.97}(Ca_{1.67}Mn_{0.34}Fe_{0.02})(CO_3)_3F_{1.06}$. The strongest lines of the powder X-ray diffraction pattern [*d*, Å (*I*, %) (*hkl*)] are: 7.081 (80) (110), 2.937 (70) (150), 2.895 (100) (20–2), 2.711 (90) (22–2), 2.039 (70) (242), 1.869 (75) (35–2).
Kind of sample preparation and/or method of registration of the spectrum: KBr disc. Transmission.
Source: McDonald et al. (1991).
Wavenumbers (cm^{-1}): 3537, 3420, 1760sh, 1630sh, 1497s, 1457s, 1376s, 1256w, 1176w, 1153w, 1071, 1033w, 987w, 867s, 810w, 756w, 722, 699, 672, 627, 605w.
Note: The wavenumbers were partly determined by us based on spectral curve analysis of the published spectrum. The bands in the range from 2800 to 3000 cm^{-1} are due to the admixture of an organic substance.

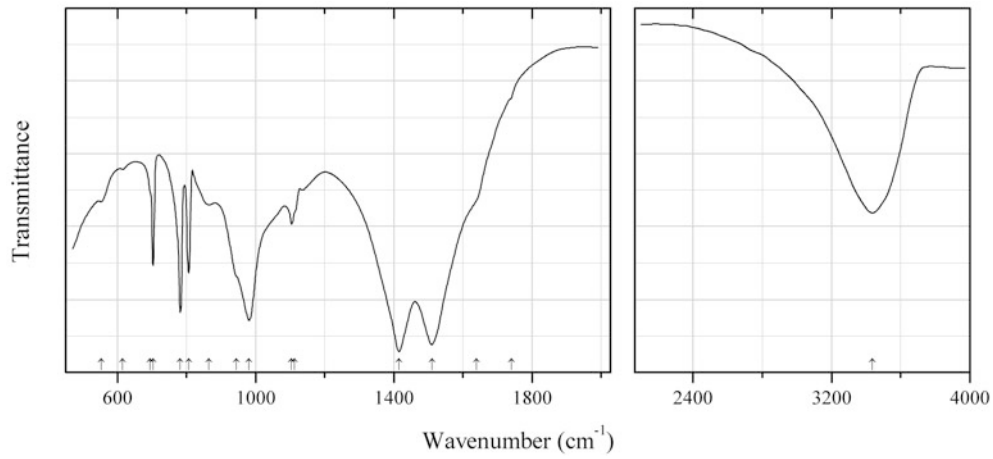

Fig. 2.128 IR spectrum of rutherfordine drawn using data from Urbanec and Čejka (1979b)

C309 Rutherfordine $(UO_2)(CO_3)$ (Fig. 2.128)
Locality: Shinkolobwe, Katanga (Shaba), Democratic Republic of Congo.
Description: Confirmed by powder X-ray diffraction data.
Kind of sample preparation and/or method of registration of the spectrum: KBr disc. Transmission.
Source: Urbanec and Čejka (1979b).
Wavenumbers (cm^{-1}): 3435s, (1740), 1640sh, 1510s, 1415s, 1112sh, 1104, 981s, 945sh, 865w, 806, 782s, 703, 695sh, 615w, 554w.
Note: The bands at 3435 and 1640 cm^{-1} correspond to H_2O molecules (interlayer or adsorbed ones).

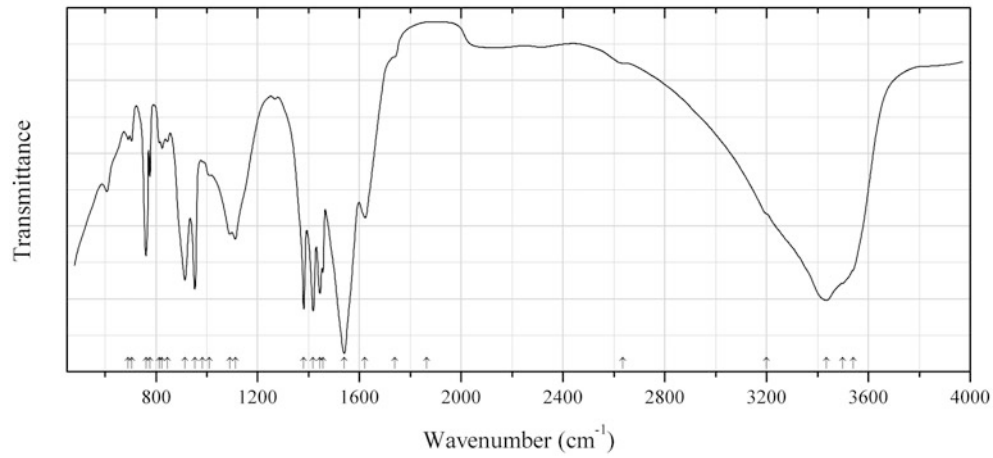

Fig. 2.129 IR spectrum of sharpite drawn using data from Urbanec and Čejka (1979b)

C310 Sharpite $Ca(UO_2)_6(CO_3)_5(OH)_4 \cdot 6H_2O$ (Fig. 2.129)
Locality: Shinkolobwe, Katanga (Shaba), Democratic Republic of Congo (type locality).
Description: Specimen No. 115318 from the National Museum of the Smithsonian Institution, Washington, USA. Confirmed by powder X-ray diffraction data.
Kind of sample preparation and/or method of registration of the spectrum: KBr disc. Transmission.

Source: Urbanec and Čejka (1979b).
Wavenumbers (cm^{-1}): 3540sh, 3500sh, 3435s, 3200sh, 2635w, 1863w, 1740sh, 1622, 1540s, 1456, 1445s, 1418s, 1381s, 1112, 1090, 1010w, 982sh, 953s, 914s, 845w, 824w, 813w, 776w, 761, 705, 691w.
Note: For the IR spectrum of sharpite see also Jones and Jackson (1993).

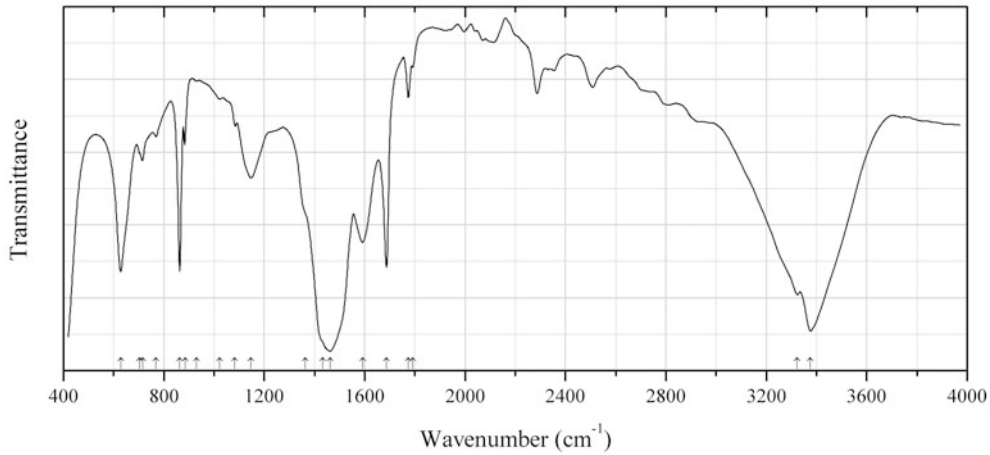

Fig. 2.130 IR spectrum of sheldrickite drawn using data from Grice et al. (1997b)

C311 Sheldrickite $NaCa_3(CO_3)_2F_3 \cdot H_2O$ (Fig. 2.130)
Locality: Mont Saint-Hilaire, Rouville Co., Québec, Canada (type locality).
Description: Aggregate of blocky, colorless to white crystals from the association with pectolite, shortite, microcline, polylithionite, arfvedsonite, and minor molybdenite. Holotype sample. Trigonal, space group $P3_2$, a = 6.718(3), c = 15.050(4) Å, V = 588.3(3) Å^3, Z = 3. D_{meas} = 2.86(4) g/cm^3, D_{calc} = 2.86 g/cm^3. Optically biaxial (+), ω = 1.538(2), ε = 1.563(4). The empirical formula is $Na_{1.01}Ca_{2.97}Sr_{0.01}(CO_3)_2[F_{2.9}(OH)_{0.07}] \cdot H_2O$. The strongest lines of the powder X-ray diffraction pattern [d, Å (I, %) (hkl)] are: 5.809 (30) (100), 5.010 (30) (003), 3.358 (30) (110), 2.791 (50) (113), 2.508 (40) (006), 2.010 (100) (116), 1.939 (40) (300).
Kind of sample preparation and/or method of registration of the spectrum: Microsampling using a diamond-anvil cell. Transmission.
Source: Grice et al. (1997b).
Wavenumbers (cm^{-1}): 3376s, 3324s, 1791, 1774, 1687s, 1592, 1464s, 1433sh, 1364sh, 1148, 1083, 1023w, 930w, 885w, 863s, 769, 715, 704sh, 628s.
Note: The wavenumbers were partly determined by us based on spectral curve analysis of the published spectrum.

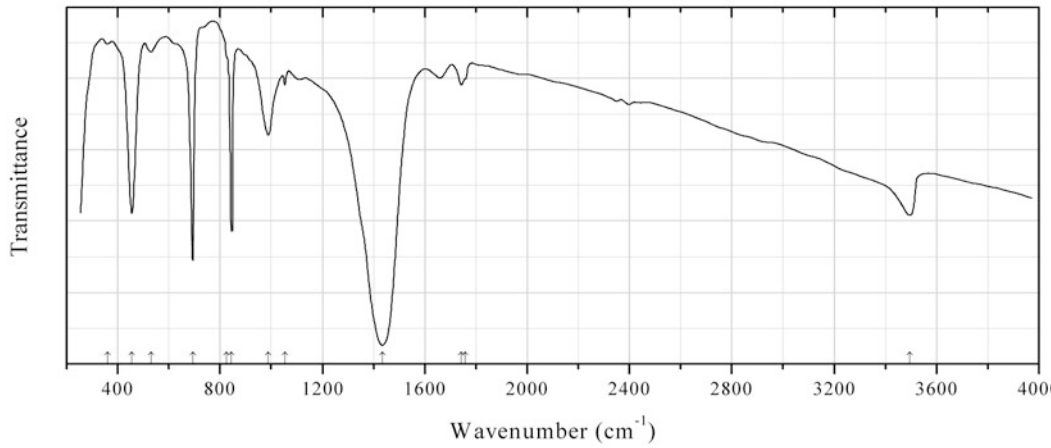

Fig. 2.131 IR spectrum of sodium lead basic carbonate drawn using data from Brooker et al. (1983)

C312 Sodium lead basic carbonate $NaPb_2(CO_3)_2(OH)$ (Fig. 2.131)
Locality: Synthetic.
Description: Hexagonal, a = 5.273(2), c = 13.448(5) Å.
Kind of sample preparation and/or method of registration of the spectrum: KBr disc. Transmission.
Source: Brooker et al. (1983).
Wavenumbers (cm^{-1}): 3495, 1758sh, 1743w, 1435s, 1053w, 988, 843s, 825w, 693s, 530w, 455s, 360w.

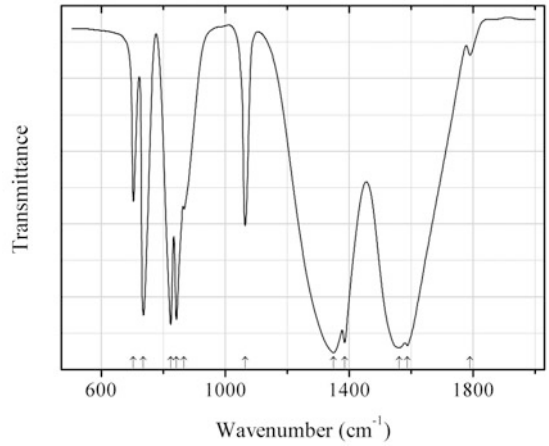

Fig. 2.132 IR spectrum of čejkaite polymorph drawn using data from Chernorukov et al. (2003)

C313 Čejkaite polymorph $Na_4(UO_2)(CO_3)_3$ (Fig. 2.132)
Locality: Synthetic.
Description: Prepared by the reaction between $(UO_2)(CO_3)$ and aqueous solution of sodium carbonate with subsequent evaporation to dryness at 100 °C. Hexagonal, a = 9.313(1), c = 12.883(4) Å, V = 967.6(4) $Å^3$, Z = 4. The strongest lines of the powder X-ray diffraction pattern [d, Å (I, %)] are: 5.030 (64), 4.660 (100), 4.032 (28), 2.756 (29), 2.688 (61), 2.329 (50), 1.756 (31).
Kind of sample preparation and/or method of registration of the spectrum: KBr disc. Transmission.

Source: Chernorukov et al. (2003).
Wavenumbers (cm^{-1}): 1790w, 1588s, 1561s, 1385s, 1349s, 1064, 867, 841.5s, 823s, 735s, 703.
Note: The wavenumbers were partly determined by us based on spectral curve analysis of the published spectrum.

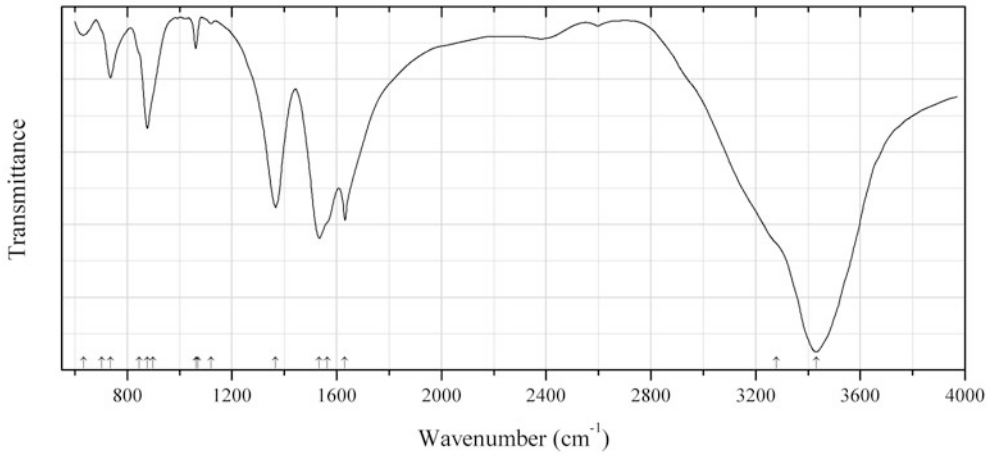

Fig. 2.133 IR spectrum of swartzite drawn using data from Amayri et al. (2004)

C314 Swartzite $CaMg(UO_2)(CO_3)_3 \cdot 12H_2O$ (Fig. 2.133)
Locality: Synthetic.
Description: Synthesized by slowly adding of an aqueous solution of calcium nitrate to an aqueous solution containing synthetic bayleyite with subsequent ageing for 24 h. Identified by the powder X-ray diffraction pattern.
Kind of sample preparation and/or method of registration of the spectrum: KBr disc. Absorption.
Source: Amayri et al. (2004).
Wavenumbers (cm^{-1}): 3431s, 3280sh, 1632s, 1563sh, 1534s, 1367s, 1121w, 1070sh, 1063w, 898sh, 877, 846sh, 737, 702sh, 633w.
Note: The wavenumbers were partly determined by us based on spectral curve analysis of the published spectrum.

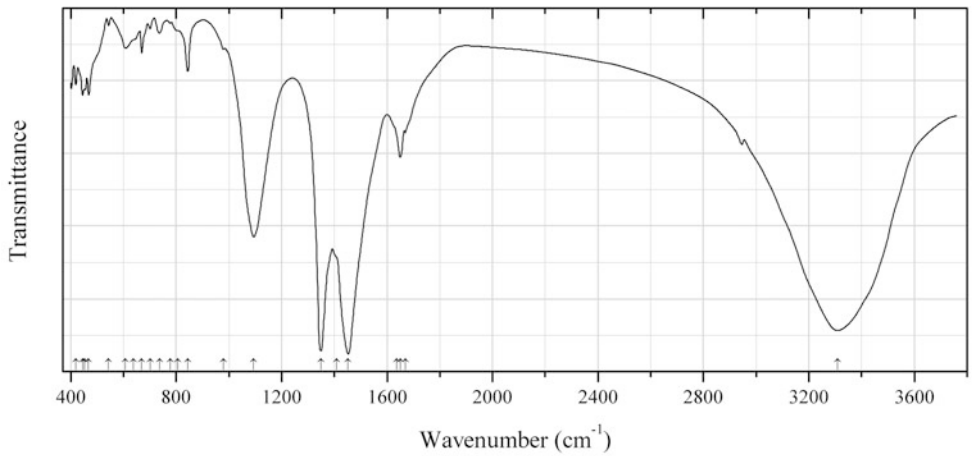

Fig. 2.134 IR spectrum of szymańskiite drawn using data from Roberts et al. (1990b)

C315 Szymańskiite $(H_3O)_8Hg^+_{16}Ni_6(CO_3)_{12}(OH)_{12}\cdot 3H_2O$ (Fig. 2.134)
Locality: Clear Creek mercury mine, New Idria district, San Benito Co., California, USA (type locality).
Description: Light blue-grey radial aggregates from the association with cinnabar, montroydite, native mercury, edgarbaileyite, and millerite. Holotype sample. The crystal structure is solved. Hexagonal, space group $P6_3$, a = 17.415(5), c = 6.011(4) Å, V = 1579(2) Å^3. D_{calc} = 4.85 g/cm^3. Optically uniaxial (−), ω = 1.795(3), ε = 1.786(3). The empirical formula is $(H_3O)_8Hg_{16}^+(Ni_{4.08}Mg_{1.92})(CO_3)_{12}(OH)_{12}\cdot 3H_2O$. The strongest lines of the powder X-ray diffraction pattern [d, Å (I, %) (hkl)] are: 14.9 (100) (100), 5.60 (100) (101), 3.299 (80) (410), 3.201 (50) (401), 2.704 (60) (510, 501), 2.665 (60) (212), 2.476 (50) (222), 1.751 (50) (702, 532).
Kind of sample preparation and/or method of registration of the spectrum: Thin film prepared by a diamond micro compression cell. Transmission.
Source: Roberts et al. (1990b).
Wavenumbers (cm^{-1}): 3308s, 1669, 1650, 1637sh, 1452s, 1410sh, 1350s, 1094s, 979w, 844, 806sh, 777w, 737w, 702w, 669w, 638sh, 608w, 544w, 468w, 454, 445, 419.
Note: The wavenumbers were partly determined by us based on spectral curve analysis of the published spectrum.

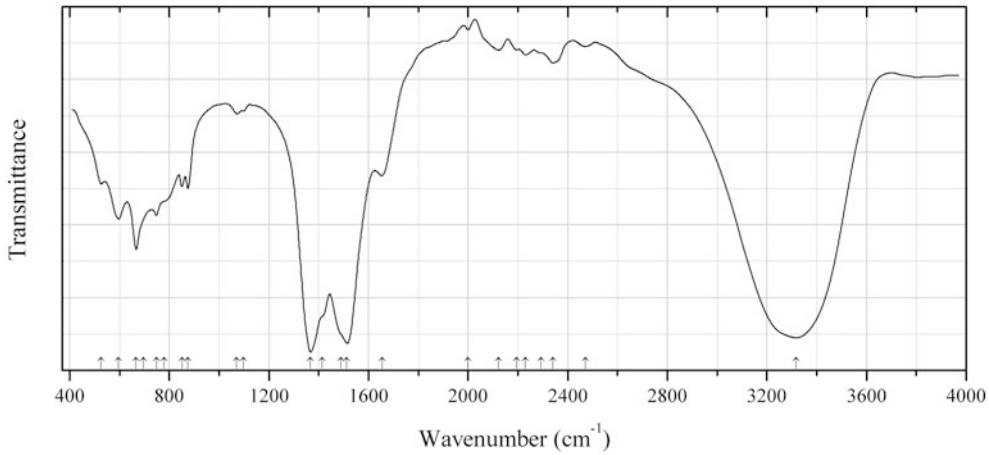

Fig. 2.135 IR spectrum of thomasclarkite-(Y) drawn using data from Grice and Gault (1998)

C316 Thomasclarkite-(Y) $NaY(HCO_3)(OH)_3\cdot 4H_2O$ (Fig. 2.135)
Locality: Mont Saint-Hilaire, Rouville RCM (Rouville Co.), Montérégie, Québec, Canada (type locality).
Description: Blocky crystals from peralkaline pegmatite. Monoclinic, space group $P2$, a = 4.556(1), b = 13.018(6), c = 4.556(2) Å, β = 90.15(3)°, V = 270.2(2) Å^3, Z = 1. D_{meas} = 2.30(2) g/cm^3, D_{calc} = 2.34 g/cm^3. Optically pseudo-uniaxial (−), ω = 1.540(4), ε = 1.40(2). The empirical formula is $(Na_{0.80}Ce_{0.18}Ca_{0.02})(Y_{0.48}Ce_{0.21}La_{0.20}Nd_{0.12}Dy_{0.04}Er_{0.04}Pr_{0.04}Sm_{0.03}Gd_{0.03}Yb_{0.03})(HCO_3)(O_{6.97}F_{0.03})H_{9.93}$. The strongest lines of the powder X-ray diffraction pattern [d, Å (I, %) (hkl)] are: 12.97 (100) (010), 6.52 (30) (020), 4.57 (30) (100, 001), 4.32 (50) (110, 011), 3.223 (30) (−101, 101), 3.133 (50) (−111, 111), 2.593 (30) (−131, 131), 2.035 (30) (201, 102), 2.016 (40) (230, 032), 1.844 (30) (231, 132).
Kind of sample preparation and/or method of registration of the spectrum: Thin film prepared by a diamond micro compression cell. Transmission.

Source: Grice and Gault (1998).
Wavenumbers (cm^{-1}): 3316s, 2470, 2340, 2292sh, 2230, 2195, 2123, 2000w, 1905w, 1655, 1512s, 1490sh, 1415sh, 1367s, 1097w, 1070w, 875, 851, 780sh, 748, 667, 697, 595, 526.
Note: The wavenumbers were partly determined by us based on spectral curve analysis of the published spectrum. In the cited paper the wavenumber 1367 cm^{-1} is erroneously indicated as 1376 cm^{-1}.

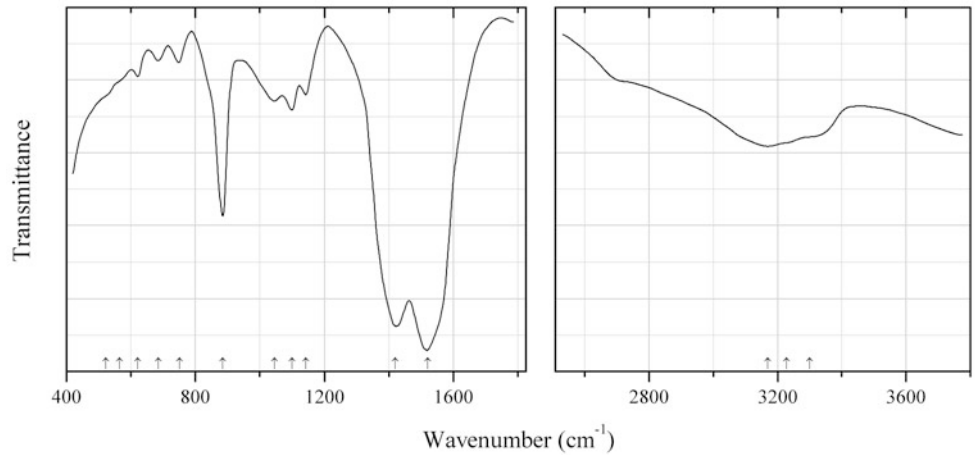

Fig. 2.136 IR spectrum of thorbastnäsite drawn using data from Akhmanova and Orlova (1966)

C317 Thorbastnäsite $ThCa(CO_3)_2F_2 \cdot 3H_2O$ (Fig. 2.136)
Locality: Pichekhol' massif, Sangilenskoye upland, Tuva republic, Russia (type locality).
Description: Type material (see Pavlenko et al. 1965).
Kind of sample preparation and/or method of registration of the spectrum: KBr disc. Transmission.
Source: Akhmanova and Orlova (1966).
Wavenumbers (cm^{-1}): 3300sh, 3227sh, 3170, 1520s, 1420s, 1142, 1045, 1100, 885s, 750, 685, 621, 565sh, 522sh.
Note: The wavenumbers were partly determined by us based on spectral curve analysis of the published spectrum.

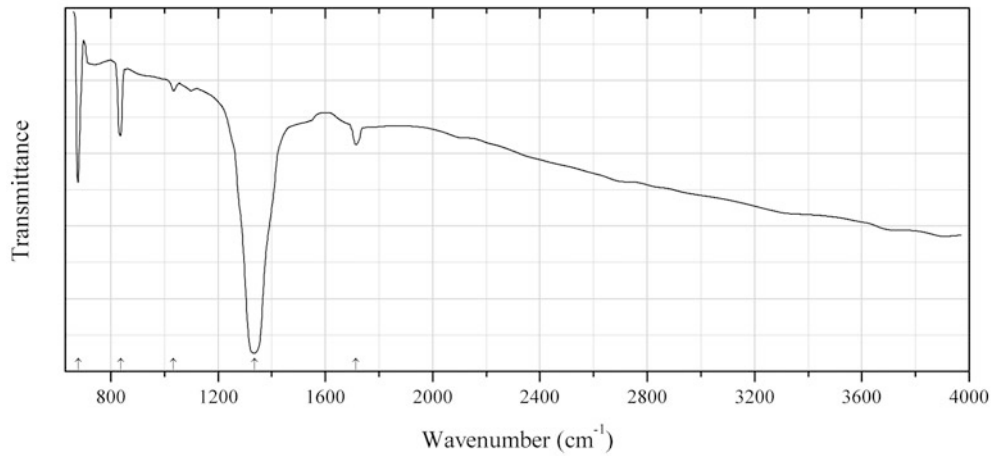

Fig. 2.137 IR spectrum of vasilyevite drawn using data from Roberts et al. (2003c)

C318 Vasilyevite $Hg^{2+}{}_{10}O_6I_3Br_2Cl(CO_3)$ (Fig. 2.137)
Locality: Clear Creek Claim, New Idria district, San Benito Co., California, USA (type locality).
Description: Anhedral cryptocrystalline masses from the association with native mercury, eglestonite, montroydite, cinnabar, etc. in a host rock principally composed of quartz and ferroan magnesite. Holotype sample. Triclinic, space group *P*-1, a = 9.344(2), b = 10.653(2), c = 18.265(4) Å, α = 93.262(5)°, β = 90.548(4)°, γ = 115.422(4)°, V = 1638.3(9) Å^3, Z = 2. D_{calc} = 9.57 g/cm^3. The empirical formula is $Hg_{20.82}O_{6.85}I_{2.69}(Br_{1.52}Cl_{0.82})[(CO_3)_{0.89}S^{2-}{}_{0.15}]$. The strongest lines of the powder X-ray diffraction pattern [*d*, Å (*I*, %) (*hkl*)] are: 7.645 (60) (−11–1), 4.205 (80) (01–4), 3.296 (50) (−115, 105), 3.132 (90) (12–3, −13–3), 2.894 (100) (−312, −32–2), 2.722 (80) (124), 2.629 (50) (130, −140).
Kind of sample preparation and/or method of registration of the spectrum: Transmission. Kind of sample preparation is not indicated.
Source: Roberts et al. (2003c).
Wavenumbers (cm^{-1}): 1714, 1336s, 1034w, 837, 678s.

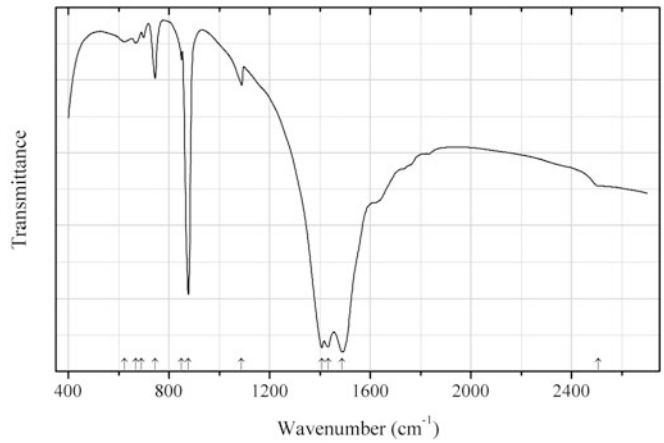

Fig. 2.138 IR spectrum of vaterite drawn using data from Nebel and Epple (2008)

C319 Vaterite $Ca(CO_3)$ (Fig. 2.138)
Locality: Synthetic.
Description: Prepared from the aqueous solution containing 2 M $CaCl_2$ and 0.05 M Na_2CO_3 at 1 °C. Confirmed by powder X-ray diffraction data.
Kind of sample preparation and/or method of registration of the spectrum: KBr disc. Transmission.
Source: Nebel and Epple (2008).
Wavenumbers (cm^{-1}): 2507w, 1489s, 1432s, 1408s, 1089, 877s, 850, 745, 690w, 668w, 623w.
Note: The wavenumbers were determined by us based on spectral curve analysis of the published spectrum. The band at 699 cm^{-1} in the spectrum arises from the admixture of aragonite. For the IR spectra of vaterite see also Sato and Matsuda (1969), Xyla and Koutsoukos (1989), Jones and Jackson (1993).

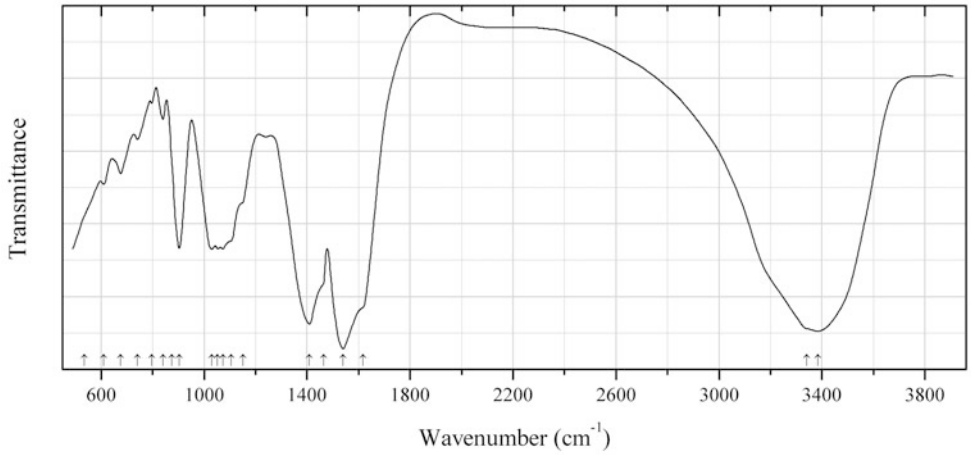

Fig. 2.139 IR spectrum of voglite drawn using data from Urbanec and Čejka (1979a)

C320 Voglite $Ca_2Cu(UO_2)(CO_3)_4 \cdot 6H_2O$ (Fig. 2.139)
Locality: Jáchymov uranium deposit, Krušné Hory (Ore Mts.), Western Bohemia, Czech Republic (type locality).
Description: Specimen No. 15699 from the collection of the National Museum in Prague. Confirmed by powder X-ray diffraction data.
Kind of sample preparation and/or method of registration of the spectrum: KBr microdisc. Transmission.
Source: Urbanec and Čejka (1979a).
Wavenumbers (cm^{-1}): 3385s, 3340sh, 1618sh, 1540s, 1465sh, 1410s, 1151sh, 1105sh, 1073, 1053, 1030, 903, 875sh, 841w, 796w, 741w, 676w, 610w, 535sh.
Note: For the IR spectrum of voglite see also Jones and Jackson (1993).

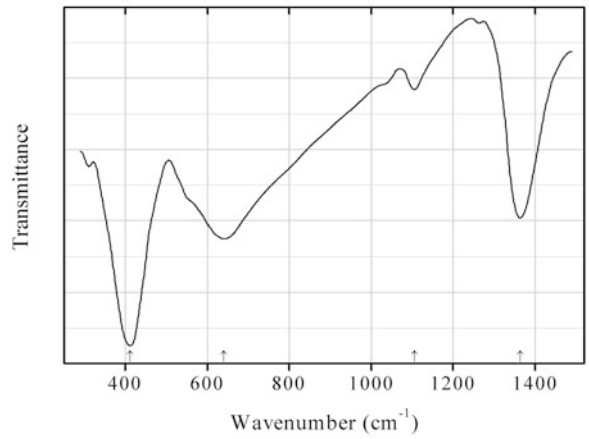

Fig. 2.140 IR spectrum of wermlandite CO_3^{2-} analogue drawn using data from Rius and Allmann (1984)

C321 Wermlandite CO_3^{2-} analogue$CaMg_7Al_2(OH)_{18}(CO_3,SO_4)_2 \cdot 12H_2O$ (?) (Fig. 2.140)
Locality: Långban deposit, Bergslagen ore region, Filipstad district, Värmland, Sweden (type locality).

Description: The crystal structure is solved. Trigonal, space group *P*-3*c*1, $a = 9.303(3)$, $c = 22.57(1)$ Å, $Z = 2$. $D_{calc} = 1.96$ g/cm^3.
Kind of sample preparation and/or method of registration of the spectrum: KBr disc. Transmission.
Source: Rius and Allmann (1984).
Wavenumbers (cm^{-1}): 1363s, 1105, 640s, 411s.
Note: In spite of the statement of the authors that "the CO_3^{2-} bands are missing", the band at 1363 cm^{-1} definitely indicates the presence of carbonate groups like those in hydrotalcite-group minerals. Moreover, the intensities of the bands at 1363 and 1105 cm^{-1} indicate the prevalence of CO_3^{2-} over SO_4^{2-}.

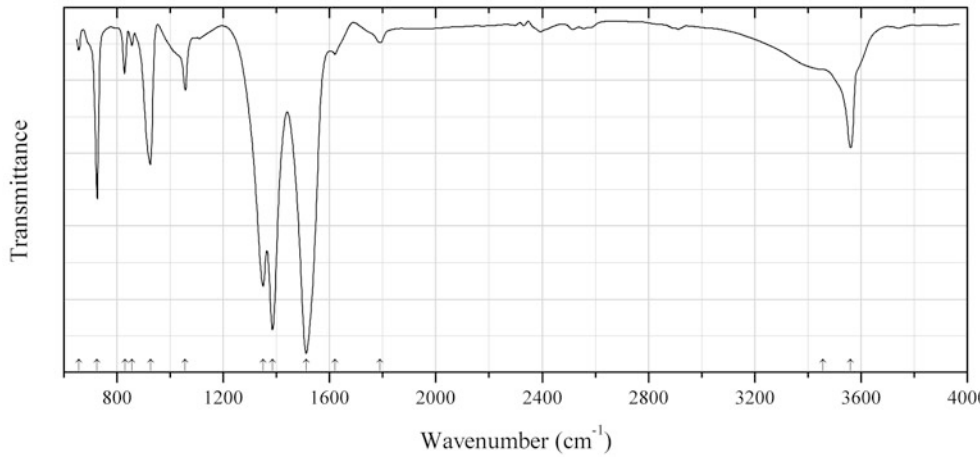

Fig. 2.141 IR spectrum of widenmannite drawn using data from Elton and Hooper (1995)

C322 Widenmannite $Pb_2(UO_2)(CO_3)_3$ (Fig. 2.141)
Locality: Loe Warren Zawn area, St Just district, West Penwith, Cornwall, UK.
Description: Aggregates of colourless to pale greenish yellow, lath-like crystals from the association with dewindtite, intermediate members of the torbernite-zeunerite series, kasolite, cerussite, malachite, etc. Orthorhombic, $a = 8.971(3)$, $b = 9.381(3)$, $c = 5.002(2)$ Å, $V = 421.0$ Å^3. The strongest lines of the powder X-ray diffraction pattern [*d*, Å (*I*, %) (*hkl*)] are: 4.16 (84) (120), 4.05 (10) (210), 3.235 (33) (220), 2.989 (14) (300), 2.409 (14) (102), 2.345 (100) (040).
Kind of sample preparation and/or method of registration of the spectrum: KBr disc. Transmission.
Source: Elton and Hooper (1995).
Wavenumbers (cm^{-1}): 3561, 3457sh, 1790w, 1620w, 1512s, 1385s, 1350s, 1057, 926, 856.5w, 829.5, 725s, 656w.
Note: For the DRIFT spectrum of widenmannite see Plášil et al. (2010).

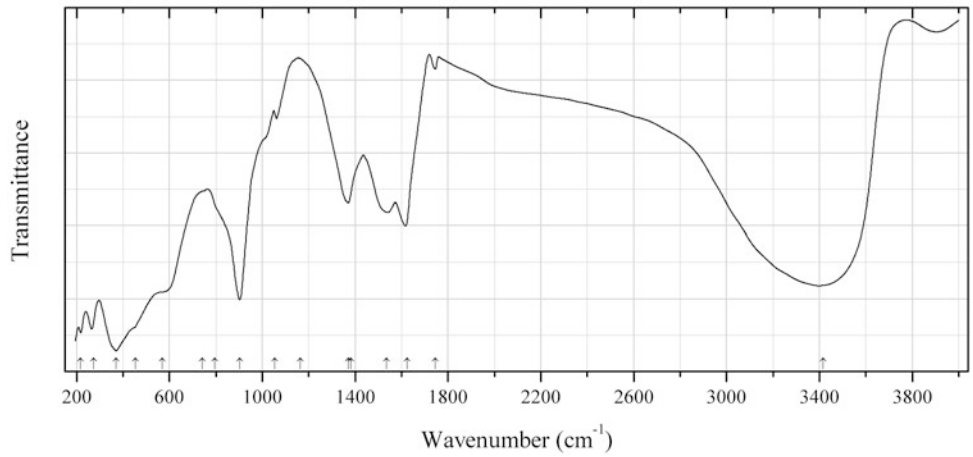

Fig. 2.142 IR spectrum of wyartite drawn using data from Čejka and Urbanec (1990)

C323 Wyartite $CaU^{5+}(UO_2)_2(CO_3)O_4(OH)\cdot 7H_2O$ (Fig. 2.142)
Locality: No data.
Description: No data.
Kind of sample preparation and/or method of registration of the spectrum: KBr disc. Transmission.
Source: Čejka and Urbanec (1990).
Wavenumbers (cm^{-1}): 3399s, 1745w, 1617, 1540, 1369, 1061, 1012sh, 903s, 801sh, 745sh, 570sh, 445sh, 371s, 265, 218.
Note: The wavenumbers were determined by us based on spectral curve analysis of the published spectrum. According to Jones and Jackson (1993), wavenumbers of absorption bands in the IR spectrum of wyartite from its type locality (Shinkolobwe, Katanga Democratic Republic of Congo) are: 3417s, 1745, 1623s, 1535s, 1381sh, 1372, 1165w, 1054w, 902s, 795w, 742w, 571sh, 453s, 371s, 274.

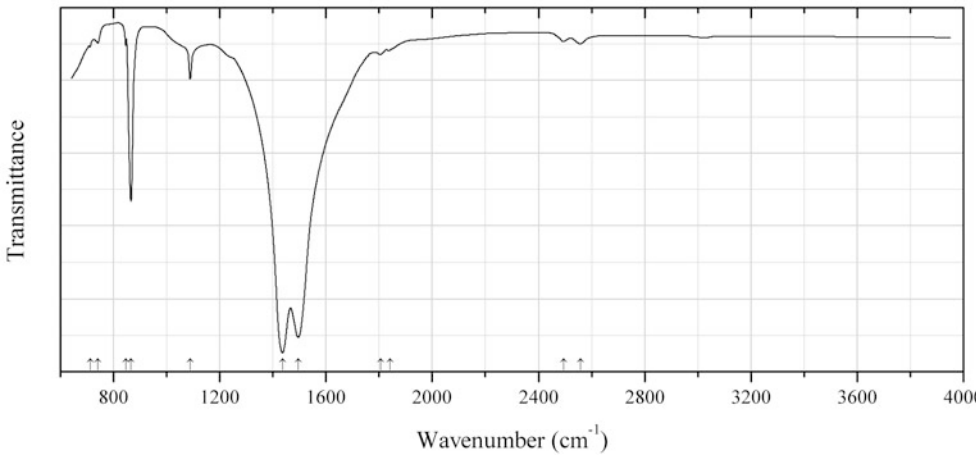

Fig. 2.143 IR spectrum of zabuyelite drawn using data from Buijs and Schutte (1961)

C324 Zabuyelite $Li_2(CO_3)$ (Fig. 2.143)

Locality: Synthetic.
Description: Commercial reactant.
Kind of sample preparation and/or method of registration of the spectrum: Thin film on a NaCl plate.
Source: Buijs and Schutte (1961).
Wavenumbers (cm^{-1}): 2558w, 2494w, 1842w, 1806w, 1495s, 1437s, 1088, 866s, 846w, 741w, 712w.
Note: For the IR spectra of synthetic $Li_2(CO_3)$ and natural zabuyelite see also Brooker and Bates (1971), Anderson et al. (2001).

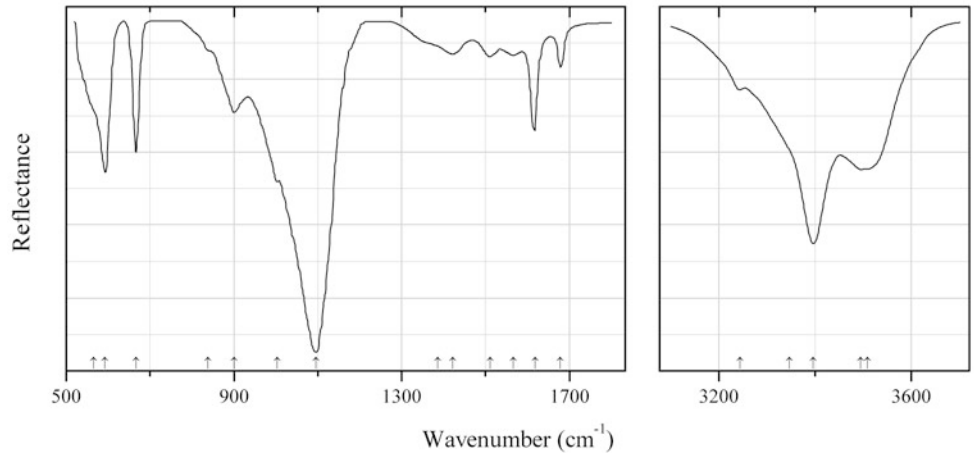

Fig. 2.144 IR spectrum of zellerite drawn using data from Frost et al. (2008b)

C325 Zellerite $Ca(UO_2)(CO_3)_2 \cdot 5H_2O$ (Fig. 2.144)
Locality: White Canyon No. 1 Mine, Frey Point, Utah, USA.
Description: No data.
Kind of sample preparation and/or method of registration of the spectrum: Attenuated total reflection of powdered mineral.
Source: Frost et al. (2008b).
Wavenumbers (cm^{-1}): 3508, 3495, 3396s, 3346sh, 3244w, 1679, 1618, 1567w, 1511w, 1422w, 1387sh, 1096s, 1004sh, 901, 838sh, 667, 593s, 565sh.
Note: The wavenumbers were determined by us based on spectral curve analysis of the published spectrum. The data are highly questionable because the intensities of the bands of C–O stretching vibrations (in the range from 1400 to 1600 cm^{-1}) are too low for a carbonate mineral. In the cited paper, the wavenumbers are indicated only for the maxima of individual bands obtained as a result of the spectral curve analysis. There is no evidence that the fitting used is the only possible or the best one. Observed absorption maxima are not indicated. For more reliable data on the IR spectrum of zellerite see Jones and Jackson (1993).

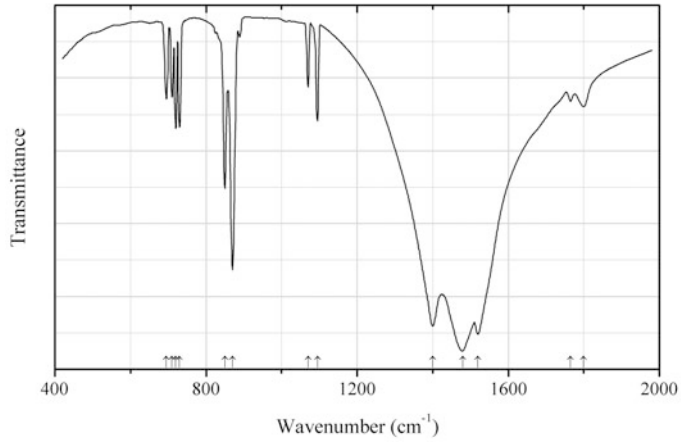

Fig. 2.145 IR spectrum of zemkorite drawn using data from Parthasarathy et al. (2002)

C326 Zemkorite $Na_2Ca(CO_3)_2$ (Fig. 2.145)
Locality: Venkatampalle, Wajrakarur Kimberlite Province, Andhra Pradesh, India.
Description: Friable aggregates of microscopic lamellar crystals from kimberlite. Hexagonal, $a = 10.038(5)$, $c = 12.726(5)$. The empirical formula is $(Na_{1.765}K_{0.294})Ca_{1.076}C_{1.947}O_{5.992}$. The strongest lines of the powder X-ray diffraction pattern [*d*, Å (*I*, %) (*hkl*)] are: 6.363 (90) (002), 4.347 (100) (200), 3.036 (100) (203), 2.510 (100) (220), 2.173 (70) (400), 2.058 (100) (402, 106), 1.795 (80) (404).
Kind of sample preparation and/or method of registration of the spectrum: KBr disc. Transmission.
Source: Parthasarathy et al. (2002).
Wavenumbers (cm^{-1}): 1800w, 1765w, 1520s, 1480s, 1400s, 1095, 1070, 870s, 850, 730, 720, 710, 695.
Note: The spectrum is very close to that of shortite.

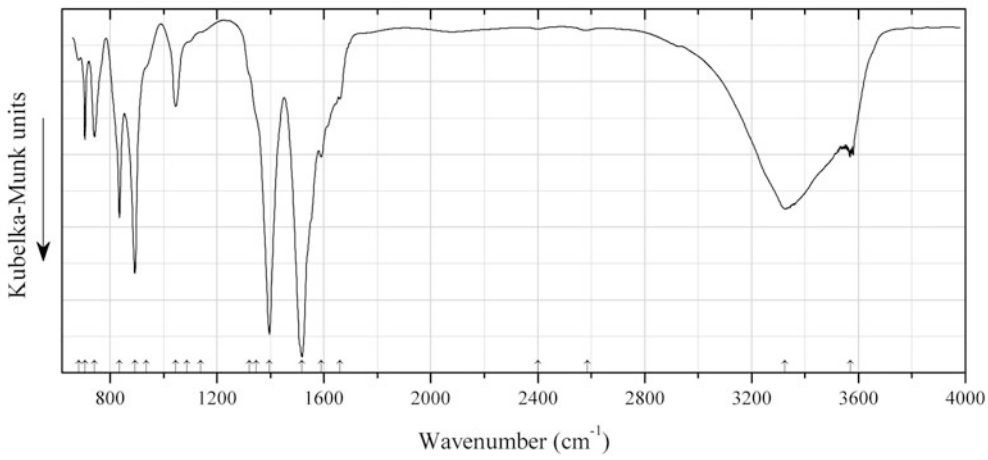

Fig. 2.146 IR spectrum of znucalite drawn using data from Plášil et al. (2008)

C327 Znucalite $CaZn_{11}(UO_2)(CO_3)_3(OH)_{20}·4H_2O$ (Fig. 2.146)

Locality: Háje, near Příbram, Příbram uranium district, Central Bohemia region, Czech Republic (type locality).
Description: Characterized by powder X-ray diffraction data.
Kind of sample preparation and/or method of registration of the spectrum: Diffuse reflectance of a powdered sample.
Source: Plášil et al. (2008).
Wavenumbers (cm^{-1}): 3570, 3325s, 2585w, 2400w, 1660, 1590, 1518s, 1396s, 1348sh, 1321sh, 1139sh, 1087sh, 1046, 935sh, 893s, 835, 742, 706, 682w.
Note: The wavenumbers were determined by us based on spectral curve analysis of the published spectrum. For the IR spectrum of znucalite see also Jones and Jackson (1993).

C328 Bayleyite $Mg_2(UO_2)(CO_3)_3 \cdot 18H_2O$
Locality: Homestake mine, Ambrosia Lakes, McKinley County, New Mexico, USA.
Description: Bright yellow prismatic crystals on sandstone with anderstonite.
Kind of sample preparation and/or method of registration of the spectrum: KBr disc. Transmission.
Source: Jones and Jackson (1993).
Wavenumbers (cm^{-1}): 3547s, 3406s, 2233w, 2116w, 1619s, 1553s, 1387s, 1144s, 1116s, 903s, 849w, 795, 775, 731, 693, 668, 604, 510, 465, 426, 396, 374, 285.

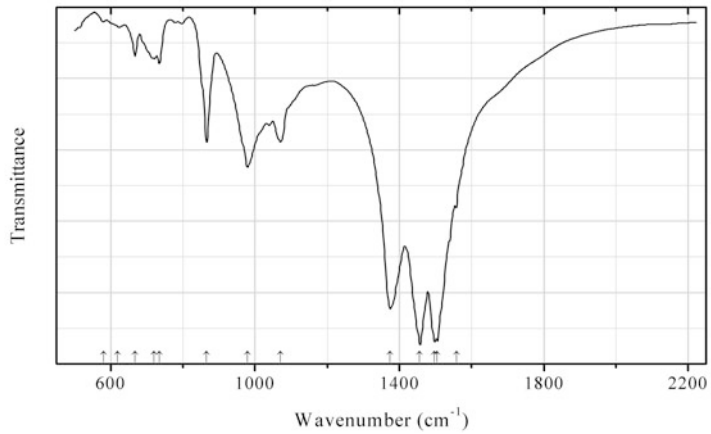

Fig. 2.147 IR spectrum of rouvilleite obtained by N.V. Chukanov

C329 Rouvilleite $Na_3(Ca,Mn^{2+})_2(CO_3)_3F$ (Fig. 2.147)
Locality: Poudrette (Demix) quarry, Mont Saint-Hilaire, Rouville RCM (Rouville Co.), Montérégie, Québec, Canada (type locality).
Description: Pale cream-coloured grains in peralkaline pegmatite. Confirmed by the IR spectrum.
Kind of sample preparation and/or method of registration of the spectrum: KBr disc. Absorption.
Wavenumbers (cm^{-1}): (1558), 1505s, 1498s, 1457s, 1375s, 1071, (979), 866, 735, 720, 668, 620w, 581w.
Note: The band at 979 cm^{-1} may be due to the admixture of a silicate mineral.

C330 Kambaldaite $NaNi_4(CO_3)_3(OH)_3 \cdot 3H_2O$

Locality: Kambalda, Coolgardie Shire, Western Australia, Australia (type locality).
Description: Confirmed by powder X-ray diffraction data.
Kind of sample preparation and/or method of registration of the spectrum: KBr disc. Transmission.
Source: Jones and Jackson (1993).
Wavenumbers (cm^{-1}): 3519s, 3483s, 2927w, 2545w, 2499w, 2457w, 2169w, 1806w, 1619, 1471s, 1395s, 1086, 968, 872, 856, 739, 721, 508s, 412, 368s, 340, 285.

C331 Roubaultite $Cu_2(UO_2)_3(CO_3)_2O_2(OH)_2 \cdot 4H_2O$
Locality: Kamoto-Olivera-Virgule mine, Shaba, Zaïre.
Description: Pale green fibrous. Confirmed by powder X-ray diffraction data.
Kind of sample preparation and/or method of registration of the spectrum: KBr disc. Transmission.
Source: Jones and Jackson (1993).
Wavenumbers (cm^{-1}): 3522, 3397s, 3306, 3196, 2646w, 2615w, 2516w, 2339w, 2025w, 1859w, 1836w, 1733, 1638, 1504s, 1399s, 1148w, 1015, 894s, 824, 791, 755, 733, 708, 524, 469, 421s, 318, 279, 246 (?).

C332 Stenonite $Sr_2Al(CO_3)F_5$
Locality: Ivigtut cryolite deposit, Ivittuut municipality, Arsuk Firth, Westgreenland province, Greenland (type locality).
Description: White to colourless massive from the association with pyrite, sphalerite, etc. Confirmed by powder X-ray diffraction data and semiquantitative analysis of chemical composition.
Kind of sample preparation and/or method of registration of the spectrum: KBr disc. Transmission.
Source: Jones and Jackson (1993).
Wavenumbers (cm^{-1}): 3341w, 2935w, 2857w, 2572w, 2539w, 1846w, 1807w, 1486s, 1432s, 1098, 1027sh, 870s, 843w, 799, 751, 710, 702, 606s, 551, 496s, 429, 404, 339, 299, (246).

C333 Synchysite-(Y) $CaY(CO_3)_2F$
Locality: Poudrette (Demix) quarry, Mont Saint-Hilaire, Rouville RCM (Rouville Co.), Montérégie, Québec, Canada.
Description: Confirmed by powder X-ray diffraction data.
Kind of sample preparation and/or method of registration of the spectrum: KBr disc. Transmission.
Source: Jones and Jackson (1993).
Wavenumbers (cm^{-1}): 3687w, 3440, 2500w, 2349w, 1816w, 1744w, 1464s, 1482s, 1079, 871s, 741, 602, 352s, 287s.

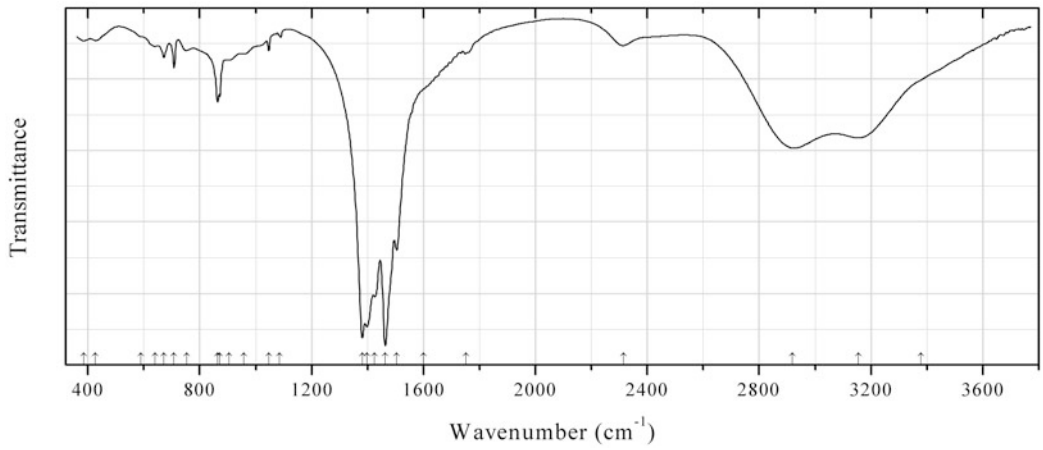

Fig. 2.148 IR spectrum of alexkhomyakovite obtained by N.V. Chukanov

C334 Alexkhomyakovite $K_6(Ca_2Na)(CO_3)_5Cl{\cdot}6H_2O$ (Fig. 2.148)
Locality: Koashva open pit of the Vostochnyi (Eastern) apatite mine, Mt. Koashva, Khibiny massif, Kola peninsula, Russia (type locality).
Description: White grains from the association with villiaumite, natrite, potassic feldspar, pectolite, sodalite, biotite, lamprophyllite, titanite. Holotype sample. Hexagonal, space group $P6_3/mcm$, 9.2691 (2), c = 15.8419(4) Å, V = 1178.72(5) Å^3, Z = 2. D_{meas} = 2.25(1) g/cm^3, D_{calc} = 2.20 g/cm^3. Optically uniaxial (−), ω = 1.543(2), ε = 1.476(2). The empirical formula is $K_{5.90}Ca_{2.07}Na_{1.03}(CO_3)_5(SO_4^{-})_{0.01}O_{0.05}Cl_{0.95}{\cdot}6H_2O$. The strongest lines of the powder X-ray diffraction pattern [*d*, Å (*I*, %) (*hkl*)] are: 7.96 (27) (002), 3.486 (35) (113), 3.011 (100) (114), 2.977 (32) (211), 2.676 (36) (300), 2.626 (42) (006, 213, 115), 2.206 (26) (206, 311), 1.982 (17) (008).
Kind of sample preparation and/or method of registration of the spectrum: KBr disc. Absorption.
Wavenumbers (cm^{-1}): 3380sh, 3156, 2920s, 2314, 1752w, 1600sh, 1504s, 1463s, 1425s, 1398s, 1381s, 1086w, 1047w, 957w, 906w, 870, 863, 754w, 708, 672, 639w, 590w, 427w, 384w.

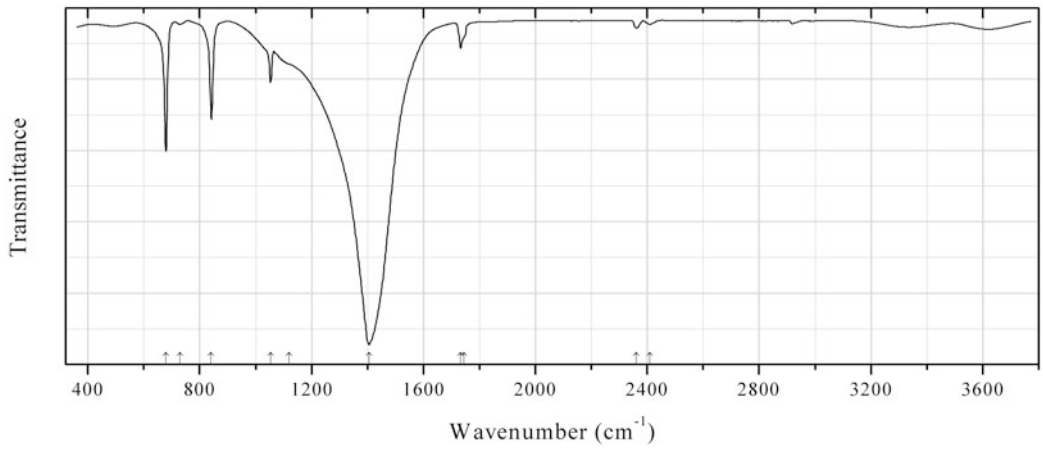

Fig. 2.149 IR spectrum of cerussite Ca-bearing obtained by N.V. Chukanov

C335 Cerussite Ca-bearing $(Pb,Ca)(CO_3)$ (Fig. 2.149)

Locality: Kombat mine, Kombat, Grootfontein district, Otjozondjupa region, Namibia.
Description: Light gray massive. The empirical formula is (electron microprobe): $(Pb_{0.88}Ca_{0.08}Ba_{0.03}Sr_{0.01})(CO_3)$. Confirmed by powder X-ray diffraction data.
Kind of sample preparation and/or method of registration of the spectrum: KBr disc. Absorption.
Wavenumbers (cm^{-1}): 2408w, 2361w, 1745sh, 1733, 1405s, 1120sh, 1053, 841, (728w), 679s.

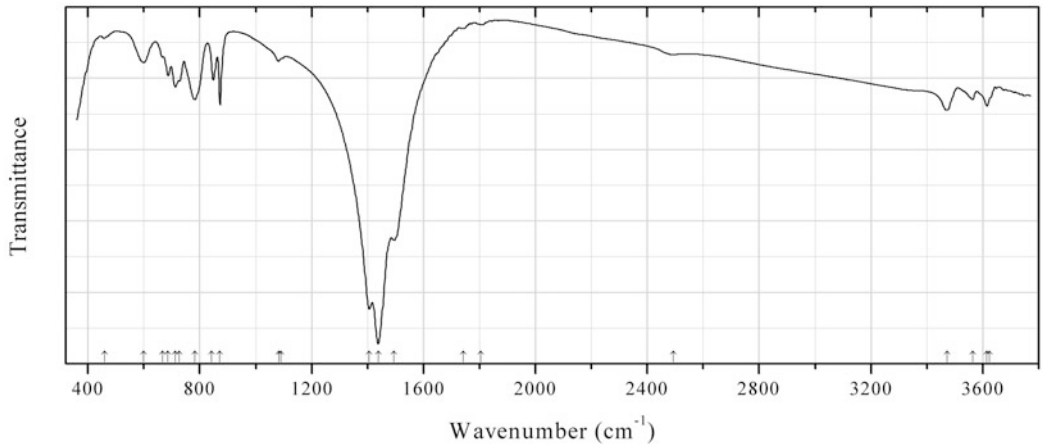

Fig. 2.150 IR spectrum of hydroxylbastnäsite-(La) obtained by N.V. Chukanov

C336 Hydroxylbastnäsite-(La) $La(CO_3)(OH)$ (Fig. 2.150)
Locality: Vuoriyarvi alkaline-ultramafic pluton, Northern Karelia, Russia.
Description: Brown crystals from the association with calcite, dolomite, ancylite-(Ce), barite, strontianite, etc. Investigated by I.V. Pekov. The empirical formula is (electron microprobe, OH calculated): $(La_{0.50}Ce_{0.41}Nd_{0.05}Pr_{0.02}Sr_{0.015}Ca_{0.015})(CO_3)(OH)_{0.58}F_{0.42}$. Confirmed by single-crystal X-ray diffraction data.
Kind of sample preparation and/or method of registration of the spectrum: KBr disc. Absorption.
Wavenumbers (cm^{-1}): 3625sh, 3615, 3563, 3472, 2493w, 1806w, 1742w, 1495s, 1438s, 1406s, (1091), 1082, 872, 843, 781, 726, 712, 687, 667w, 599, 459w.

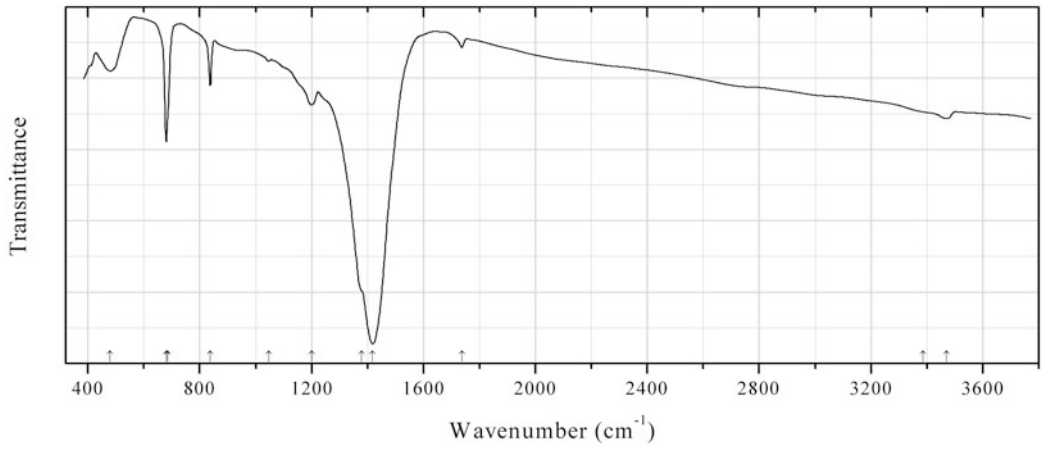

Fig. 2.151 IR spectrum of grootfonteinite obtained by N.V. Chukanov

C337 Grootfonteinite $Pb_3O(CO_3)_2$ (Fig. 2.151)
Locality: Kombat mine, Grootfontein district, Otjozondjupa region, northern Namibia (type locality).
Description: Colourless platy grains from the association with jacobsite, cerussite, dolomite, clinochlore, hausmannite, melanotekite, sahlinite, rhodochrosite, barite. Holotype sample. The cryatal structure is solved. Hexagonal, space group $P6_3mc$, $a = 5.3028(10)$, $c = 13.7705(25)$ Å, $V = 335.34(1)$ Å^3, $Z = 2$. $D_{calc} = 6.856$ g/cm^3. The empirical formula is $H_{0.20}Na_{0.28}Ca_{0.04}Pb_{2.64}C_{2.04}O_7$. The strongest lines of the powder X-ray diffraction pattern [*d*, Å (*I*, %) (*hkl*)] are: 4.353 (9) (011), 3.441 (8) (004), 3.244 (100) (013), 2.652 (30) (110), 2.294 (21) (020), 2.053 (39) (023).
Kind of sample preparation and/or method of registration of the spectrum: KBr disc. Absorption.
Wavenumbers (cm^{-1}): 3470w, 3386w, 1738, 1418s, 1380sh, 1200, 1046, 837, 685sh, 680s, ~480.

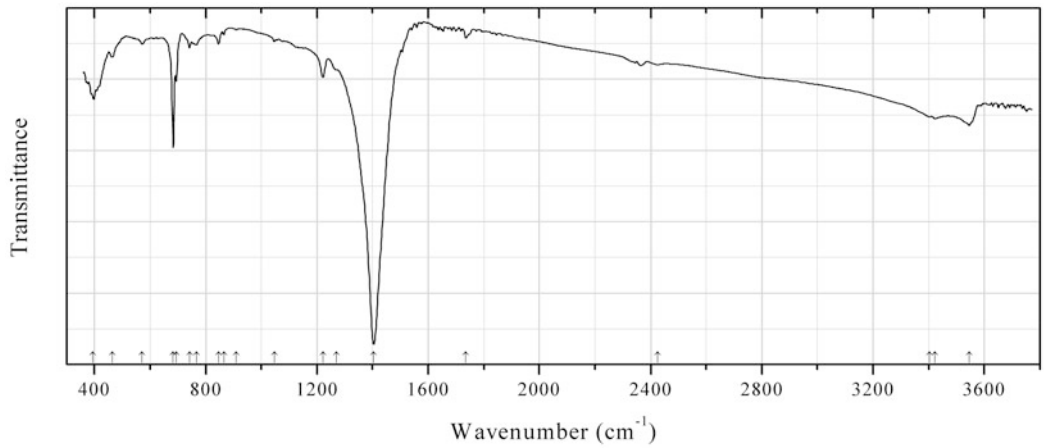

Fig. 2.152 IR spectrum of plumbonacrite obtained by N.V. Chukanov

C338 Plumbonacrite $Pb_5(CO_3)_3O(OH)_2$ (Fig. 2.152)
Locality: Långban deposit, Bergslagen ore region, Filipstad district, Värmland, Sweden (type locality).
Description: White aggregates of platy crystals. Investigated by O.I. Siidra. Identified by the single-crystal X-ray diffraction pattern. Space group $P\text{-}3c1$, $a = 9.0891(5)$, $c = 24.832(1)$ Å, $V = 1776.6(1)$ Å^3, $Z = 6$.
Kind of sample preparation and/or method of registration of the spectrum: KBr disc. Absorption.
Wavenumbers (cm^{-1}): 3546, 3423, 3403, 2424w, 1736w, 1404s, 1270, 1221, 1049w, 910w, 866w, 846, 766, 742, 694, 683s, 572, 464, 395s.

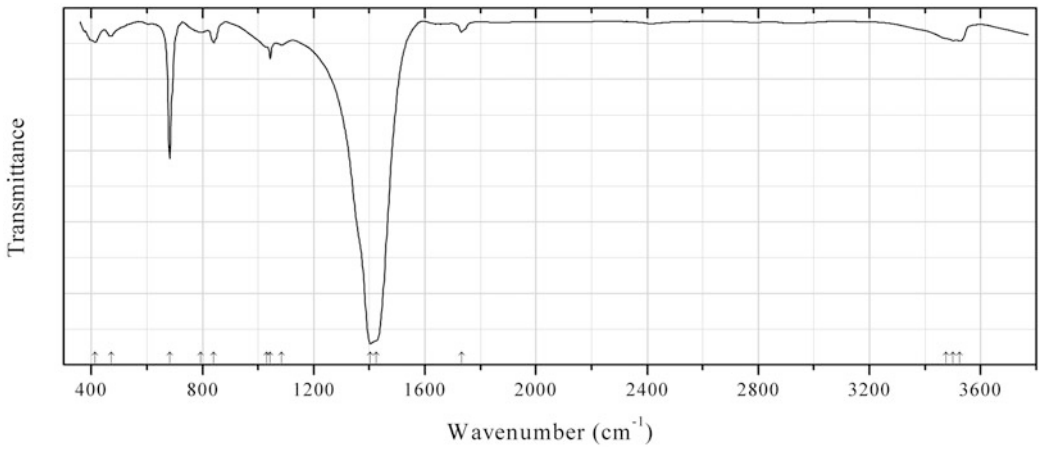

Fig. 2.153 IR spectrum of hydrocerussite obtained by N.V. Chukanov

C339 Hydrocerussite $Pb_3(CO_3)_2(OH)_2$ (Fig. 2.153)
Locality: Legrena (Legraina), Attiki Prefecture, Greece.
Description: Colourless platy crystals from ancient slag. Confirmed by single-crystal X-ray diffraction data.
Kind of sample preparation and/or method of registration of the spectrum: KBr disc. Absorption.
Wavenumbers (cm^{-1}): 3525, 3500, 3475sh, 1732w, 1425sh, 1404s, 1085, 1044, 1030sh, 840, 794w, 682s, 471w, 413.

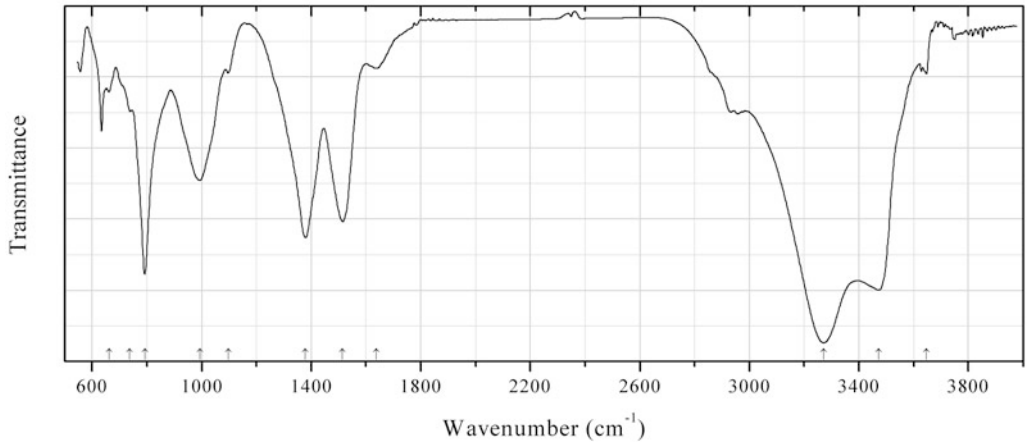

Fig. 2.154 IR spectrum of parádsasvárite drawn using data from Fehér et al. (2015)

C340 Parádsasvárite $Zn_2(CO_3)(OH)_2$ (Fig. 2.154)
Locality: Nagy-Lápafő area, Parádsasvár, Mátra Mts., Hungary (type locality).
Description: Pale beige, globular aggregates from the association with calcite, smithsonite, hemimorphite, hydrozincite, aurichalcite, and rosasite. Holotype sample. Monoclinic, space group $P2_1/a$, a = 12.92(1), b = 9.372(7), c = 3.159(4) Å, β = 110.4(1)°, V = 358.5(5) $Å^3$, Z = 4. D_{calc} = 4.175 g/cm^3. The empirical formula is $(Zn_{0.62}Cu_{0.36}Pb_{0.01})Zn_{1.00}(CO_3)(OH)_2$. The strongest

lines of the powder X-ray diffraction pattern [*d*, Å (*I*, %) (*hkl*)] are: 6.054 (67) (200), 5.085 (100) (210), 3.703 (87) (310, 220), 3.021 (25) (400, 130), 2.971 (25) (−211 and 001), 2.603 (62) (−221), 2.539 (36) (420).

Kind of sample preparation and/or method of registration of the spectrum: Attenuated total reflection of powdered mineral. A diamond ATR cell was used.

Source: Fehér et al. (2015).

Wavenumbers (cm^{-1}): 3647w, 3473s, 3272s, 1637w, 1514s, 1379s, 1097w, 993, 792s, 738w, 661w.

Note: Sharp peak near 634 cm^{-1} is an artifact.

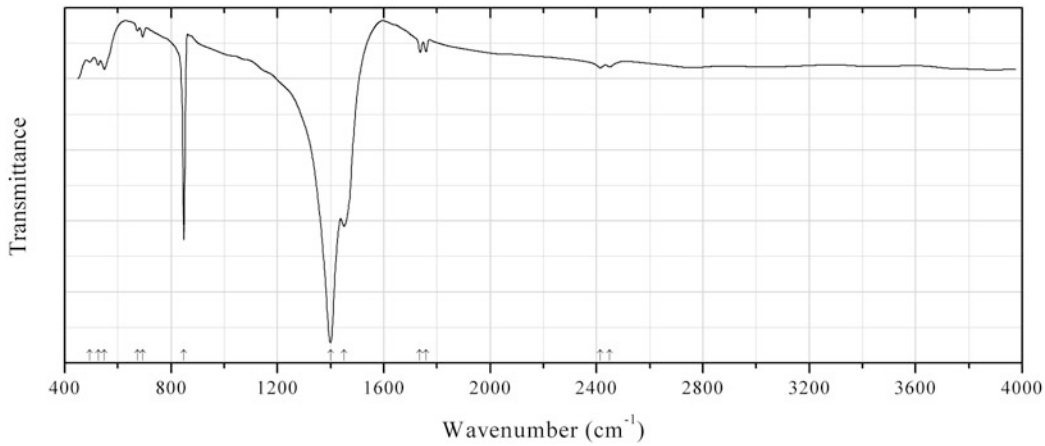

Fig. 2.155 IR spectrum of bismutite drawn using data from Huang et al. (2014)

C341 Bismutite $Bi_2O_2(CO_3)$ (Fig. 2.155)

Locality: Synthetic.

Description: Synthesized hydrothermally from $Bi(NO_3)_3{\cdot}5H_2O$ and urea. Confirmed by powder X-ray diffraction data. Tetragonal, a = 3.8658(5), c = 13.6757(5) Å.

Kind of sample preparation and/or method of registration of the spectrum: KBr disc. Transmission.

Source: Huang et al. (2014).

Wavenumbers (cm^{-1}): 2450w, 2414w, 1760w, 1734w, 1450s, 1400s, 848s, 694w, 674w, 550, 526, 494.

Note: The wavenumbers were partly determined by us based on spectral curve analysis of the published spectrum.

2.3 Organic Compounds and Salts of Organic Acids

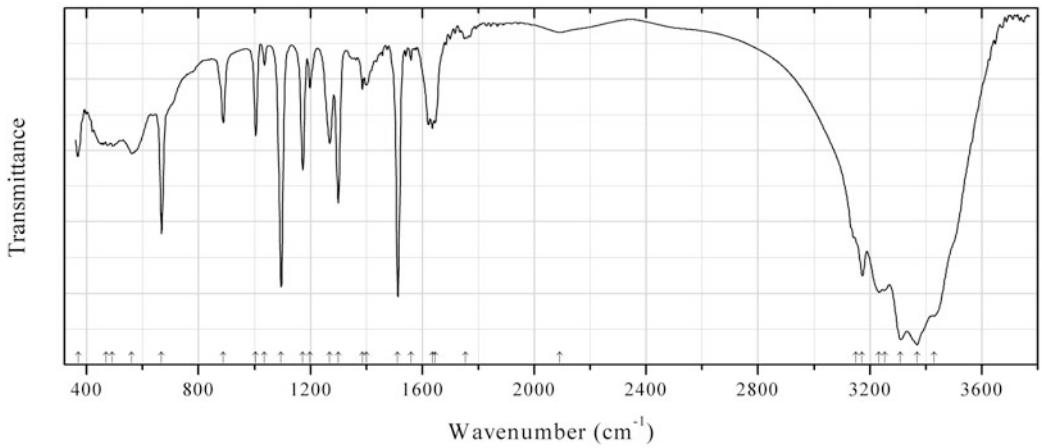

Fig. 2.156 IR spectrum of chanabayaite obtained by N.V. Chukanov

Org37 Chanabayaite $Cu_4(N_3C_2H_2)_4(NH_3)_4Cl_2(Cl,OH)_2 \cdot H_2O$ (Fig. 2.156)
Locality: Pabellón de Pica Mountain, near Chanabaya village, Iquique Province, Tarapacá Region, Chile (type locality).
Description: Radial aggregate of blue prismatic crystals from the association with salammoniac, halite, joanneumite, nitratine, and earlier chalcopyrite. Holotype sample. The crystal structure is solved. Orthorhombic, space group *Imma*, a = 19.484(3), b = 7.2136(10), c = 11.999(4) Å, V = 1686.5(7) Å^3, Z = 2. In chanabayaite, chains of the corner-sharing Cu(1)-centered octahedra and single Cu(2)-centred octahedra are connected via 1,2,4-triazolate anions $C_2N_3H_2^-$. NH_3 and Cl^- are additional ligands coordinating Cu^{2+}. D_{meas} = 1.48(2) g/cm^3, D_{calc} = 1.464 g/cm^3. Optically biaxial (−), α = 1.561(2), β = 1.615(3), γ = 1.620(2), 2 V = 25(10)°. The empirical formula is (Z = 4): $Cu_{1.92}Fe_{0.08}Cl_{1.72}N_{8.09}C_{3.85}H_{11.66}O_{0.81}$. The strongest lines of the powder X-ray diffraction pattern [d, Å (I, %) (hkl)] are: 10.19 (100) (101), 6.189 (40) (011), 5.729 (23) (301), 5.216 (75) (211, 202), 4.964 (20) (400), 2.830 (20) (602, 413, 503), 2.611 (24) (123, 422, 404).
Kind of sample preparation and/or method of registration of the spectrum: KBr disc. Absorption.
Wavenumbers (cm^{-1}): 3430s, 3369s, 3310s, 3253s, 3233s, 3173s, 3150sh, 2091w, 1755w, 1646, 1636, 162, 1559w, 1512s, 1400, 1385, 1299s, 1269, 1198, 1173, 1095s, 1035w, 1004, 888, 667s, 561, 492, (470), 370.

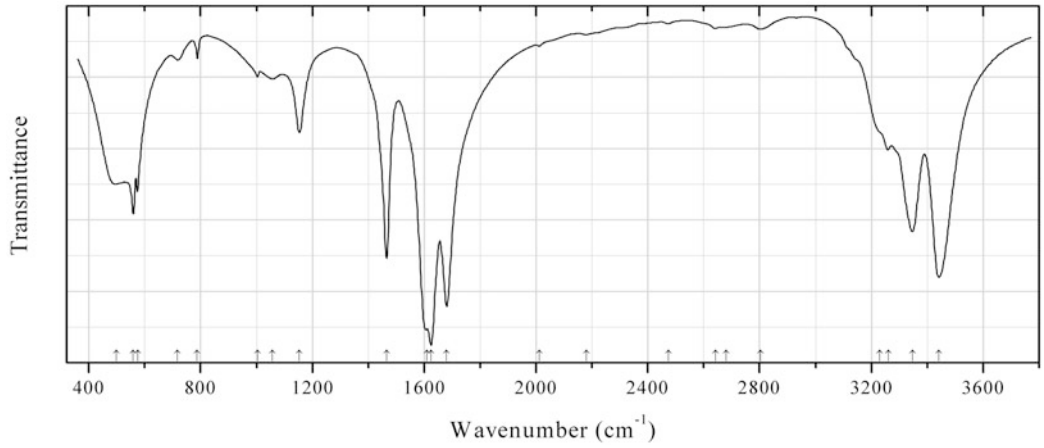

Fig. 2.157 IR spectrum of urea obtained by N.V. Chukanov

Org38 Urea $CO(NH_2)_2$ (Fig. 2.157)
Locality: Atacama desert, Chile (artificial?).
Description: Aggregate of colourless acicular crystals. Confirmed by the IR spectrum.
Kind of sample preparation and/or method of registration of the spectrum: KBr disc. Absorption.
Wavenumbers (cm^{-1}): 3441s, 3347s, 3262, 3230sh, 2803w, 2680sh, 2643w, 2475w, 2180w, 2013w, 1680s, 1624s, 1610s, 1465s, 1153, 1057, 1003, 788w, 718w, 574, 559s, 497.

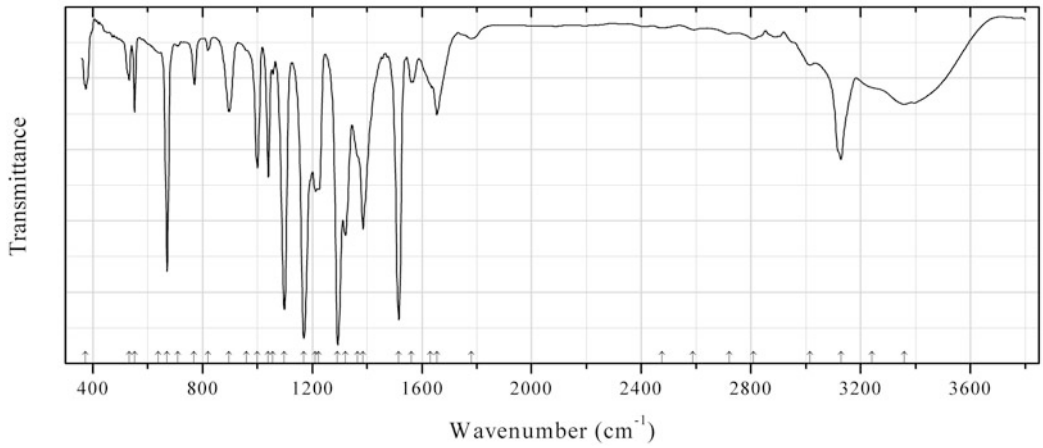

Fig. 2.158 IR spectrum of chanabayaite obtained by N.V. Chukanov

Org39 Chanabayaite $Cu_4(N_3C_2H_2)_4(NH_3)_4Cl_2(Cl,OH)_2 \cdot H_2O$ (Fig. 2.158)
Locality: Pabellón de Pica Mountain, near Chanabaya village, Iquique Province, Tarapacá Region, Chile (type locality).
Description: Dark blue fine-grained aggregate from the association with salammoniac, halite, joanneumite, nitratine, and earlier chalcopyrite. A SO_4-rich and NH_3-poor variety. The empirical formula is (electron microprobe for Cu, Fe, S, and Cl; a deficiency of NH_3 follows from the IR spectrum): $Cu_{0.95–0.98}Fe_{0.04–0.05}[Cl_{0.24–0.40}(SO_4)_{0.22–0.25}(OH)_x](N_3C_2H_2)(NH_3)_y \cdot nH_2O$

Kind of sample preparation and/or method of registration of the spectrum: KBr disc. Absorption.
Wavenumbers (cm^{-1}): 3360, 3240w, 3128, 3015w, 2808w, 2720w, 2588w, 2475w, 1780w, 1654, 1630sh, 1561w, 1516s, 1385, 1365sh, 1321, 1293s, 1222, 1212, 1169s, 1098s, 1057w, 1040, 1000, 960sh, 897, 820w, 770, 710w, 671s, 640sh, 552, 533, 374.

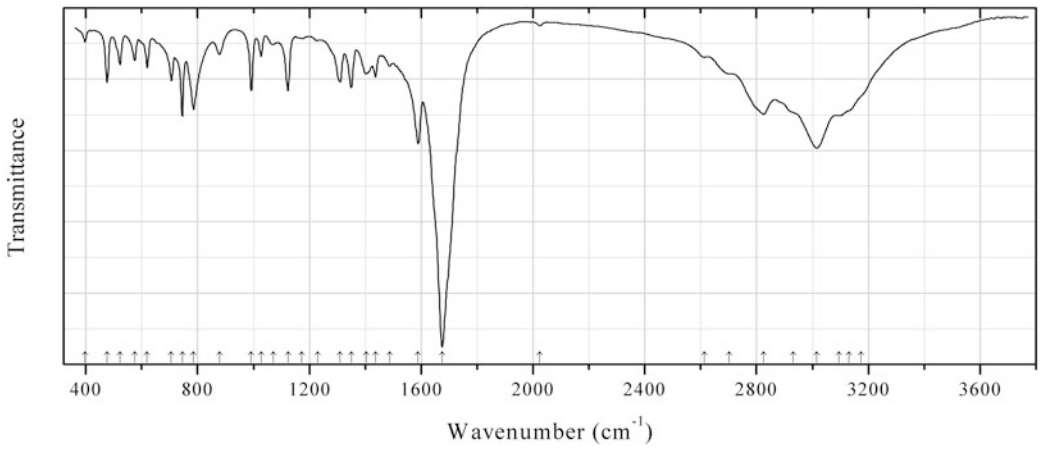

Fig. 2.159 IR spectrum of uricite obtained by N.V. Chukanov

Org40 Uricite $C_5H_4N_4O_3$ (uric acid) (Fig. 2.159)
Locality: Burned dump of the Chelyabinsk coal basin, Kopeisk, South Urals, Russia.
Description: Yellowish powdery aggregate. A product of the reaction of hot gases from a burning coal dump with excrement from European falcon. Identified by the IR spectrum.
Kind of sample preparation and/or method of registration of the spectrum: KBr disc. Absorption.
Wavenumbers (cm^{-1}): 3175sh, 3130sh, 3096, 3015s, 2930sh, 2825s, 2703, 2613, 2025w, 1675s, 1589s, 1487w, 1436, 1402, 1349, 1310, 1229w, 1173w, 1123, 1070w, 1027, 992, 878, 785s, 745s, 706, 619, 574, 522, 476, 396w.

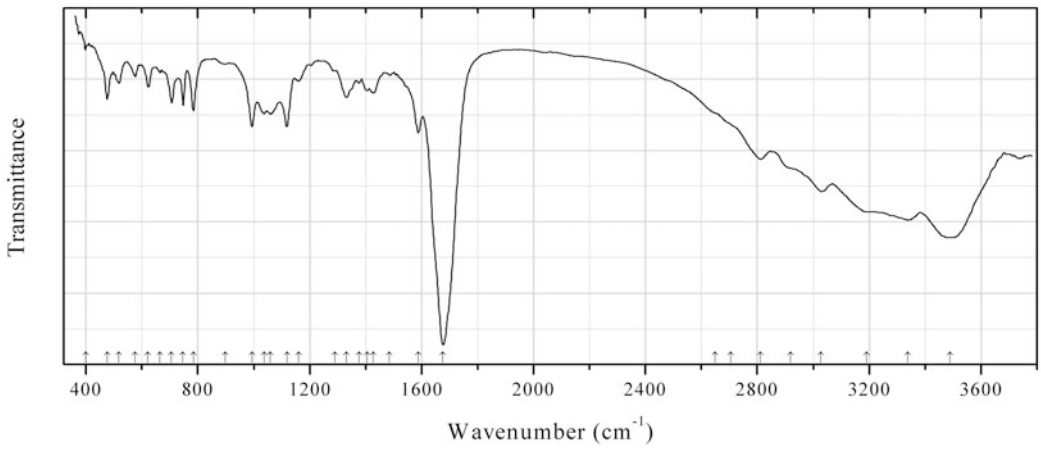

Fig. 2.160 IR spectrum of tinnunculite obtained by N.V. Chukanov

Org41 Tinnunculite $C_5H_4N_4O_3 \cdot 2H_2O$ (uric acid dihydrate) (Fig. 2.160)

Locality: Rasvumchorr Mt., Khibiny alkaline complex, Kola peninsula, Murmansk region, Russia.
Description: Yellow crystals on the surface of peralkaline rock mainly consisting of potassic feldspar, aegirine, and nepheline. A product of supergene alteration of bird guano. Monoclinic, space group $P2_1/c$, a = 7.261(9), b = 6.365(7), c = 17.48(3) Å, β = 91.0(1)°, V = 808(3) Å^3, Z = 4. D_{calc} = 1.68 g/cm^3. Optically biaxial (−), α = 1.503(3), β = 1.712(3), γ = 1.74(1), 2 V = 40(10)°. The strongest lines of the powder X-ray diffraction pattern [d, Å (I, %) (hkl)] are: 8.82 (84) (002), 5.97 (15) (011), 5.63 (24) (10–2, 102), 4.22 (22) (11–2, 112), 3.240 (27) (11–4, 114), 3.180 (100) (020, 210), 3.116 (44) (21–1, 211), 2.576 (14) (024).
Wavenumbers (cm^{-1}): 3489s, 3338s, 3190, 3028, 2920sh, 2811, 2705sh, 2650sh, 1676s, 1588, 1486w, 1427, 1405, 1377w, 1331, 1289w, 1160w, 1118, 1060, 1037, 994, 898w, 784, 747, 706, 663w, 622, 576, 518, 476, 399w.

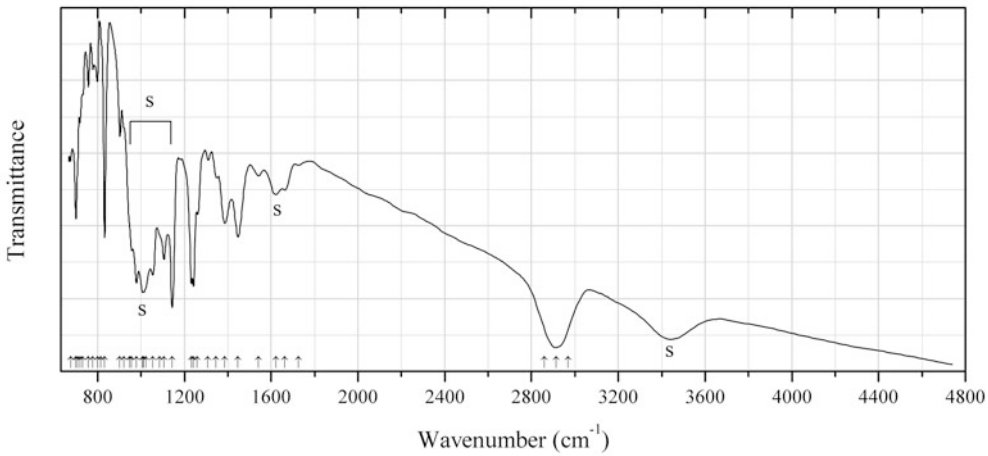

Fig. 2.161 IR spectrum of abelsonite drawn using data from Milton et al. (1978)

Org42 Abelsonite $NiC_{31}H_{32}N_4$ (nickel porphyrin) (Fig. 2.161)
Locality: Mahogany Zone oil shale, Green River formation, near Dragon, Uintah Co., Utah, USA (type locality).
Description: Aggregate of reddish platy crystals from the association with orthoclase, pyrite, quartz, dolomite, analcime, and a K-Fe micaceous mineral. Holotype sample. Triclinic, a = 8.44, b = 11.12, c = 7.28 Å, α = 90° 53′, β = 113° 45′, γ = 79° 34′, V = 613.8 Å^3, Z = 1. The strongest lines of the powder X-ray difraction pattern [d, Å (I, %) (hkl)] are: 10.9 (100) (010), 7.63 (50) (100), 5.79 (40) (1–10), 3.77 (80) (1–11), 3.14 (40) (01–2). The bands at 3430, 1635, 995, and 440 cm^{-1} correspond to the admixture of a hydrous silicate (designated as S).
Kind of sample preparation and/or method of registration of the spectrum: CsI microdisc, transmission.
Source: Milton et al. (1978).
Wavenumbers (cm^{-1}): 2970sh, 2915s, 2860sh, 1727w, 1662, 1622, 1542w, 1446, 1385, 1346, 1309w, 1260, 1242s, 1232s, 1143s, 1106, 1085sh, 1054, 1022sh, 1012sh, 1007, 978, 956, 946sh, 921sh, 902w, 832s, 816sh, 799w, 778w, 757w, 730sh, 718, 708sh, 700, 675, 620w, 602w, 535w, 512w, 441s, 392w.
Note: The wavenumbers were partly determined by us based on spectral curve analysis of the published spectrum.

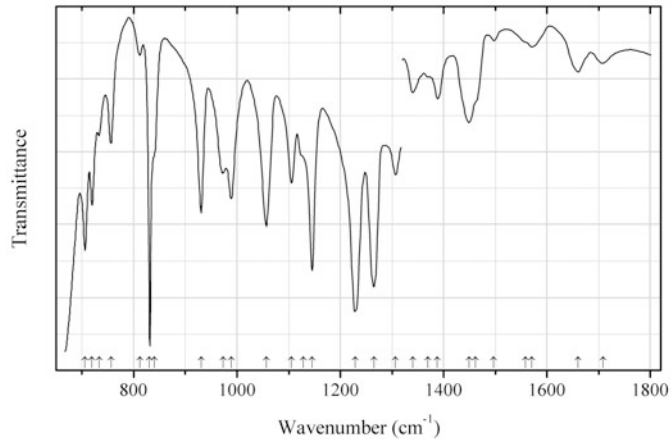

Fig. 2.162 IR spectrum of abelsonite drawn using data from Milton et al. (1978)

Org43 Abelsonite $NiC_{31}H_{32}N_4$ (nickel porphyrin) (Fig. 2.162)
Locality: Synthetic.
Description: Nickel 8-desmethyldeoxophylloerthyroetioporphyrin (presumably identical with abelsonite).
Kind of sample preparation: Nujol and fluorolub mulls, transmission.
Source: Milton et al. (1978).
Wavenumbers: **(cm^{-1})**: 1708, 1660, 1570, 1558sh, 1497w, 1461sh, 1449, 1388, 1369, 1340, 1307, 1265s, 1229s, 1145s, 1128sh, 1105, 1057, 989, 973, 931, 840sh, 831s, 812w, 756, 733, 719, 706s.
Note: The wavenumbers were determined by us based on spectral curve analysis of the published spectrum.

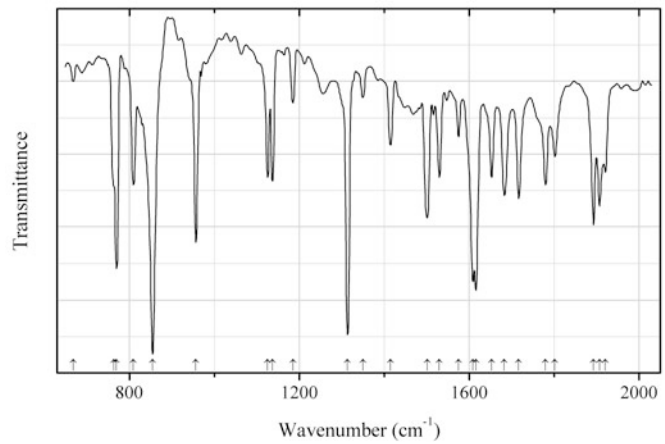

Fig. 2.163 IR spectrum of carpathite drawn using data from Echigo et al. (2007)

Org44 Carpathite $C_{24}H_{12}$ (Fig. 2.163)
Locality: Picacho Peak Area, San Benito Co., California, USA.
Description: Euhedral crystals from the association with cinnabar, magnesite, and quartz. The crystal structure is solved. Monoclinic, space group $P2_1/a$, a = 16.094(9), b = 4.690(3), c = 10.049(8) Å, β = 110.79(2)°, V = 709.9(8) Å^3, Z = 2.

Kind of sample preparation and/or method of registration of the spectrum: Single crystal. Transmission.
Source: Echigo et al. (2007).
Wavenumbers (cm^{-1}; weak peaks are not indicated): 1921, 1907, 1893s, 1802, 1780, 1717, 1683, 1653, 1616s, 1609s, 1575, 1530, 1501s, 1415, 1350w, 1314s, 1185, 1137, 1126, 957s, 855s, 810, 770s, 764, 668.

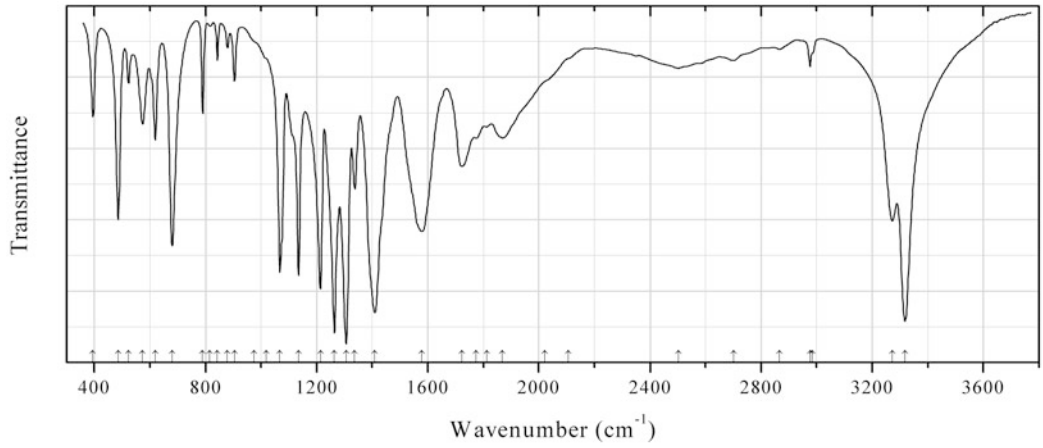

Fig. 2.164 IR spectrum of wine stone (acid potassium tartrate) obtained by N.V. Chukanov

Org45 Wine stone (acid potassium tartrate) $HK(C_4O_6H_4)\cdot nH_2O$ (Fig. 2.164)
Locality: Byproduct of wine industry. Beaujolais nouveau, France, harvest of 2012.
Description: Red rosettes from the intergrowths with colourless crystals of calcium wine stone. Identified by IR spectrum (as a tartrate) and by electron microprobe analysis (as a K salt). Contains about 40 wt% K_2O.
Wavenumbers (cm^{-1}): 3318s, 3272, 2985sh, 2976w, 2866w, 2700w, 2502, 2105sh, 2020sh, 1869, 1813, 1775, 1723, 1578, 1409s, 1337, 1306s, 1264s, 1214s, 1135s, 1068s, 1020sh, 975sh, 904, 879w, 843, 816w, 790, 680, 619, 574, 523, 486, 395.

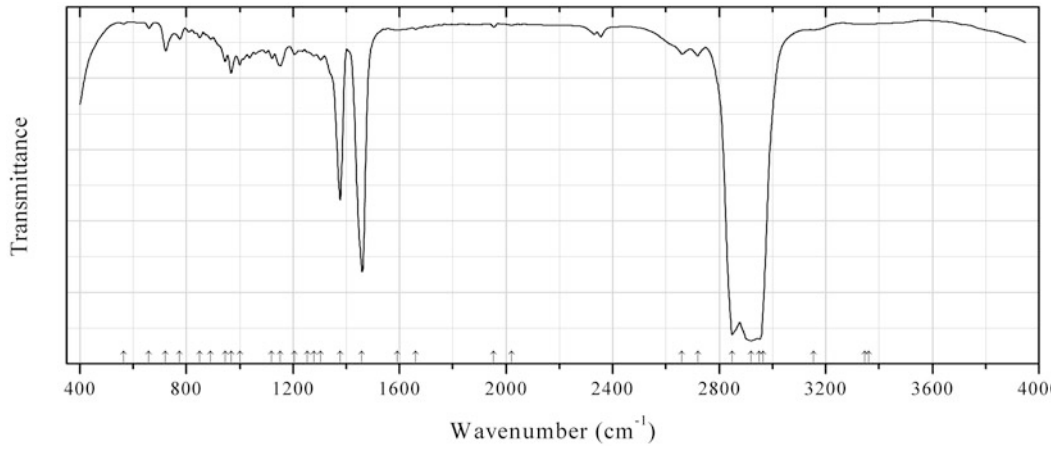

Fig. 2.165 IR spectrum of dinite solution drawn using data from Franzini et al. (1991)

Org46 Dinite solution $C_{20}H_{36}$ (Fig. 2.165)
Locality: Castelnuovo Garfagnana, Garfagnana, Lucca province, Tuscany, Italy (type locality).
Description: Pale yellow massive from bituminous wood. The crystal structure is solved. Dinite is an alicyclic saturated hydrocarbon with three condensed cycles in the formula unit. Orthorhombic, space group $P2_12_12_1$, a = 12.356(4), b = 12.762(4), c = 11.427(3) Å, α = 99.773(5)°, β = 91.141(6)°, γ = 115.58(5)°, V = 571.6(3) Å^3, Z = 2. D_{meas} = 1.01(1) g/cm^3, D_{calc} = 1.02 g/cm^3. The empirical formula is $C_{20}H_{36.91}$. The strongest lines of the powder X-ray diffraction pattern are observed at 8.92, 8.32, 7.00, 5.53, 5.06, and 4.02 Å.
Kind of sample preparation and/or method of registration of the spectrum: Solution in mineral oil (Nujol).
Source: Franzini et al. (1991).
Wavenumbers (cm^{-1}): 3362w, 3346sh, 3155w, 2965sh, 2951, 2919, 2849, 2719, 2660, 2020, 1953, 1660, 1591, 1459s, 1377s, 1303, 1278, 1253, 1205, 1152, 1121, 1000, 968, 945, 891, 850, 775, 722, 659, 565.
Note: The wavenumbers were determined by us based on spectral curve analysis of the published spectrum. The spectrum is a superposition of the spectra of different saturated hydrocarbons, including components of Nujol.

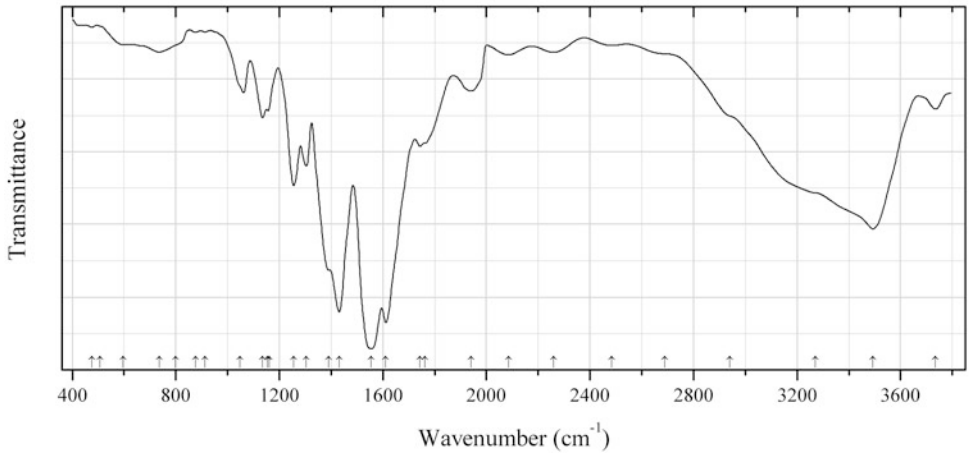

Fig. 2.166 IR spectrum of earlandite drawn using data from Fox et al. (1967)

Org47 Earlandite $Ca_3(C_6H_5O_7)_2{\cdot}4H_2O$ (Fig. 2.166)
Locality: Artificial.
Description: Granules isolated from evaporated milk stored at 21 °C for 10 months. Identified by the IR spectrum.
Kind of sample preparation and/or method of registration of the spectrum: KBr disc. Transmission.
Source: Fox et al. (1967).
Wavenumbers (cm^{-1}): 3735, 3493s, 3270sh, 2940, 2690sh, 2484w, 2260w, 2085w, 1940, 1763, 1744, 1611s, 1554s, 1431s, 1390s, 1304, 1255, 1155, 1135, 1161, 1049sh, 913w, 876w, 800sh, 736w, 597sh, 507sh, 475w.
Note: The wavenumbers were determined by us based on spectral curve analysis of the published spectrum.

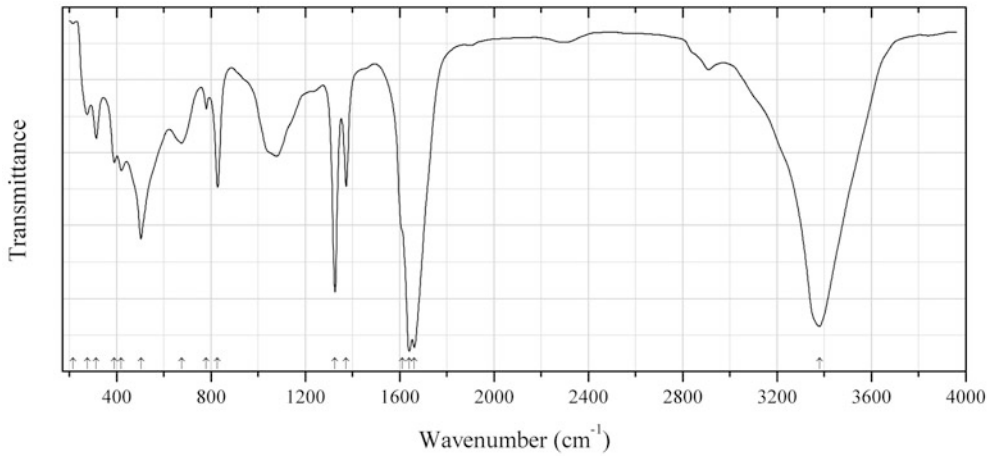

Fig. 2.167 IR spectrum of glushinskite drawn using data from Wilson et al. (1980)

Org48 Glushinskite $Mg(C_2O_4)\cdot 2H_2O$ (Fig. 2.167)
Locality: Mill of Johnston, near Insch, north-east Scotland, UK.
Description: Creamy white layer on serpentine intermingled with the hyphae of the lichen fungus. Confirmed by chemical analyses and powder X-ray diffraction data.
Kind of sample preparation and/or method of registration of the spectrum: KBr disc. Absorption.
Source: Wilson et al. (1980).
Wavenumbers (cm^{-1}): 3380s, 1662s, 1640s, 1610sh, 1373, 1326s, 828, 780w, 675, 503s, 420, 390, 314, 275, 214w.
Note: Weak bands in the range from 2800 to 3000 cm^{-1} correspond to the admixture of an organic substance containing C–H bonds. Broad band between 950 and 1200 cm^{-1} indicates a small amount of cellular polysaccharide from fungal hyphae and a trace of silicate.

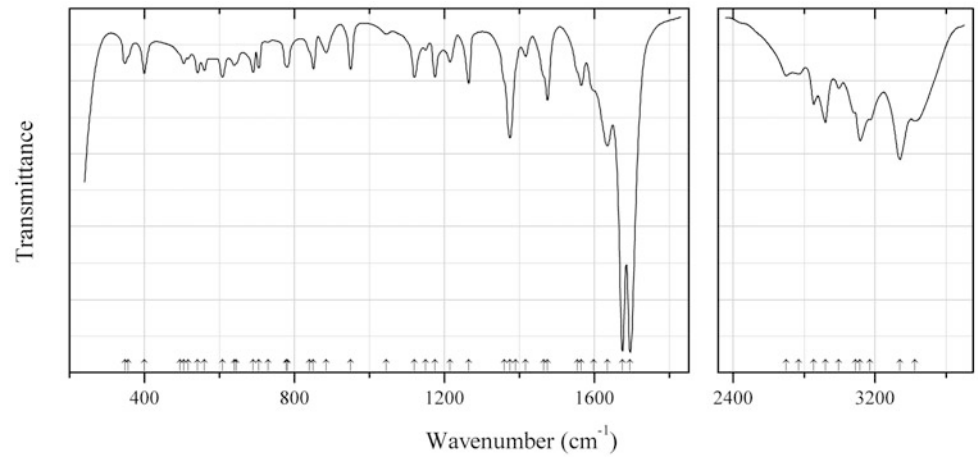

Fig. 2.168 IR spectrum of guanine drawn using data from Szczepaniak and Szczesniak (1987)

Org49 Guanine $C_5H_3(NH_2)N_4O$ (Fig. 2.168)
Locality: Synthetic.

Kind of sample preparation and/or method of registration of the spectrum: KBr disc. Absorption.
Source: Szczepaniak and Szczesniak (1987).
Wavenumbers (cm^{-1}): 3422, 3340s, 3170sh, 3115s, 3090sh, 2996, 2920, 2855, 2770w, 2700w, 1695s, 1675s, 1635s, 1598sh, 1565, 1555sh, 1475, 1465sh, 1417w, 1390sh, 1375s, 1360sh, 1265, 1215, 1175, 1150, 1120, 1045w, 950, 885, 850, 840sh, 781, 778sh, 730, 705, 690, 645sh, 640, 608, 560, 542, 516, 505, 495sh, 400, 356sh, 348.
Note: The wavenumbers were partly determined by us based on spectral curve analysis of the published spectrum.

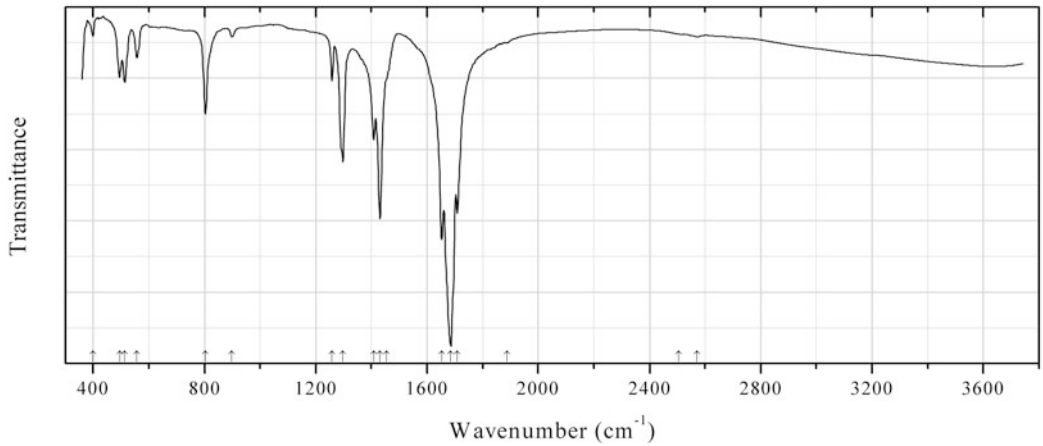

Fig. 2.169 IR spectrum of antipinite obtained by N.V. Chukanov

Org50 Antipinite $KNa_3Cu_2(C_2O_4)_4$ (Fig. 2.169)
Locality: Pabellón de Pica Mt., 1.5 km south of Chanabaya village, Iquique Province, Tarapacá Region, Chile (type locality).
Description: Light blue prismatic crystals from the association with halite, salammoniac, chanabayaite, joanneumite, and clay minerals. Holotype sample. The crystal structure is solved. Triclinic, space group *P*-1, $a = 7.1574(5)$, $b = 10.7099(8)$, $c = 11.1320(8)$ Å, $\alpha = 113.093(1)°$, $\beta = 101.294(1)°$, $\gamma = 90.335(1)°$, $V = 766.51(3)$ Å^3, $Z = 2$. $D_{meas} = 2.53(3)$ g/cm^3, $D_{calc} = 2.549$ g/cm^3. Optically biaxial (+), $\alpha = 1.432(3)$, $\beta = 1.530(1)$, $\gamma = 1.698(5)$, $2V = 75(10)°$. The empirical formula is $K_{0.96}Na_{3.04}Cu_{2.03}(C_{2.00}O_4)_4$. The strongest lines of the powder X-ray diffraction pattern [*d*, Å (*I*, %) (*hkl*)] are: 5.22 (40) (1–11), 3.47 (100) (0–32), 3.39 (80) (−210), 3.01 (30) (0–33, 220), 2.543 (40) (122, 0–34, −104), 2.481 (30) (−213), 2.315 (30) (1–43, −310), 1.629 (30) (1–46, −4–14, −243, −160).
Kind of sample preparation and/or method of registration of the spectrum: KBr disc. Absorption.
Wavenumbers (cm^{-1}): 2570w, 2505w, 1888w, 1709s, 1685s, 1653s, 1455sh, 1431s, 1408, 1298, 1258, 898w, 804, 557, 513, 495, 399w.

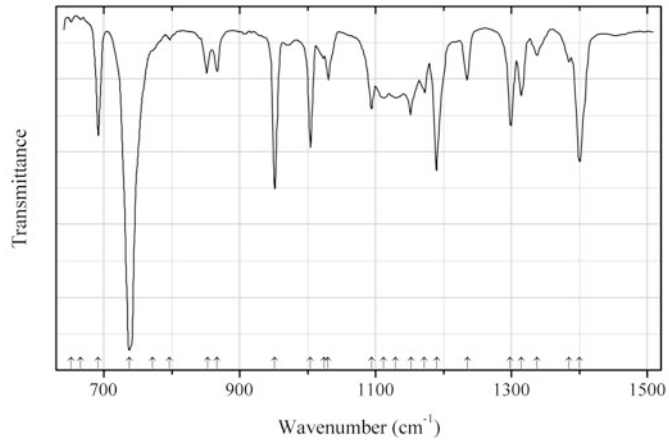

Fig. 2.170 IR spectrum of fluorene drawn using data from Scherf and Brown (1960)

Org51 Fluorene $(C_6H_4)CH_2(C_6H_4)$ (Fig. 2.170)
Kratochvilite-related compound
Locality: Synthetic.
Kind of sample preparation and/or method of registration of the spectrum: Transmission. Kind of sample preparation is not indicated.
Source: Scherf and Brown (1960).
Wavenumbers (cm^{-1}): 2930, 1400s, 1385w, 1338, 1315, 1298, 1235, 1190s, 1172, 1152, 1129, 1112, 1094, 1030, 1024, 1004s, 952s, 867, 853, 797, 772, 738s, 692s, 666w, 652w.
Note: The wavenumbers were partly determined by us based on spectral curve analysis of the published spectrum.

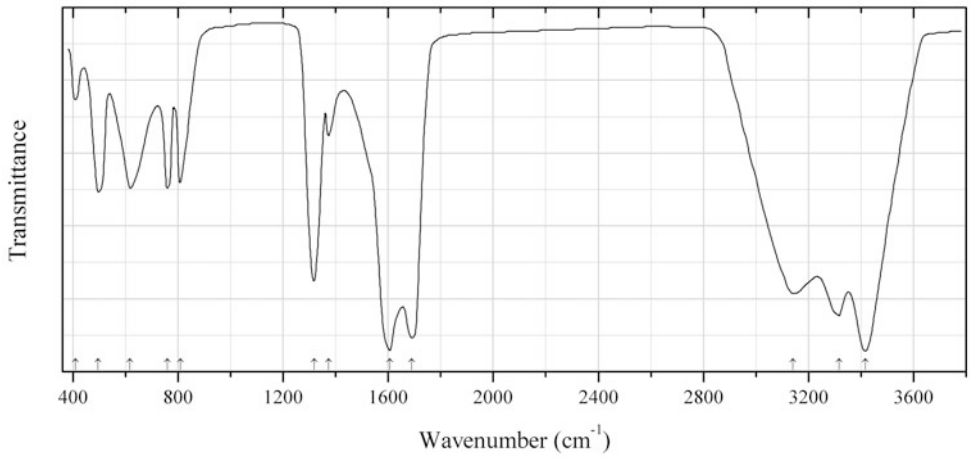

Fig. 2.171 IR spectrum of falottaite drawn using data from Gyrdasova et al. (2009)

Org52 Falottaite $Mn(C_2O_4)\cdot 3H_2O$ (Fig. 2.171)
Locality: Synthetic.
Description: Synthesized by addition of a stoichiometric amount of a cooled solution of manganese (II) sulfate to a cooled solution of oxalic acid with continuous stirring. Confirmed by thermal and powder X-ray diffraction data.

Kind of sample preparation and/or method of registration of the spectrum: Transmission. Kind of sample preparation is not indicated.
Source: Gyrdasova et al. (2009).
Wavenumbers (cm^{-1}): 3417s, 3317s, 3141s, 1689s, 1607s, 1373w, 1318s, 809, 759, 618, 496, 410w.

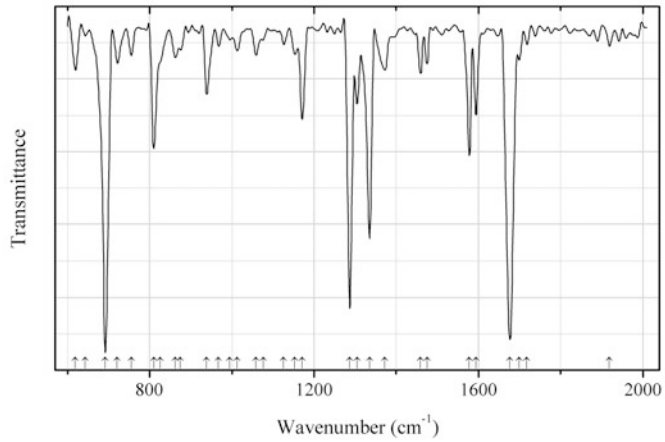

Fig. 2.172 IR spectrum of hoelite drawn using data from Kang et al. (1998)

Org53 Hoelite $C_{14}H_8O_2$ (9,10-anthraquinone) (Fig. 2.172)
Locality: Synthetic.
Description: Commercial reactant.
Kind of sample preparation and/or method of registration of the spectrum: KBr disc. Absorption.
Source: Kang et al. (1998).
Wavenumbers (cm^{-1}): 1919w, 1718w, 1699, 1677s, 1594, 1578s, 1475, 1459, 1372, 1335s, 1305, 1287s, 1171, 1153, 1126, 1076w, 1058w, 1013, 995w, 967w, 939, 875w, 862, 825sh, 810s, 755, 721, 692s, 643w, 619.
Note: The wavenumbers were partly determined by us based on spectral curve analysis of the published spectrum.

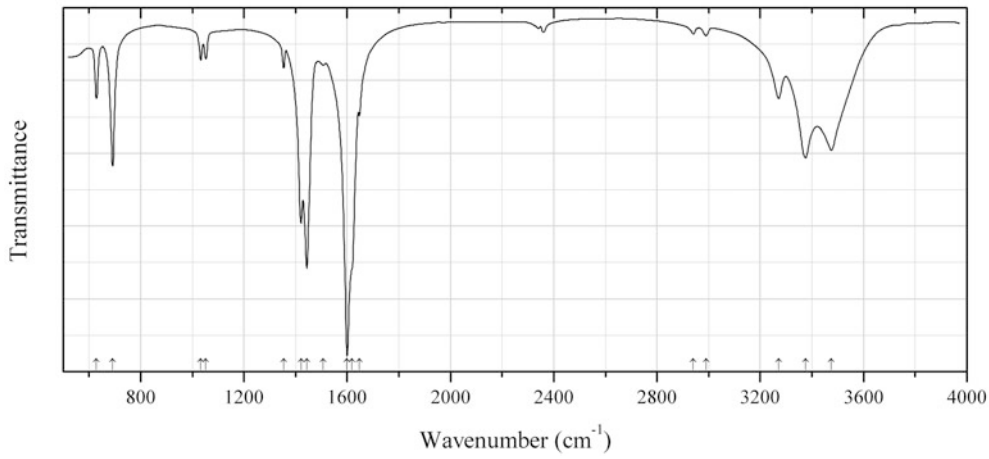

Fig. 2.173 IR spectrum of hoganite drawn using data from Salvadó et al. (2013)

Org54 Hoganite $Cu(CH_3COO)_2 \cdot H_2O$ (Fig. 2.173)
Locality: Synthetic.
Description: Prepared from copper (II) hydroxide and acetic acid. Confirmed by powder X-ray diffraction data.
Kind of sample preparation and/or method of registration of the spectrum: Transmittance a of powdered sample.
Source: Salvadó et al. (2013).
Wavenumbers (cm^{-1}): 3475s, 3375s, 3271, 2990w, 2941w, 1647w, 1618sh, 1600s, 1508w, 1444s, 1421s, 1354w, 1053w, 1033w, 692s, 629.
Note: Weak bands in the range from 2300 to 2400 cm^{-1} may correspond to atmospheric CO_2.

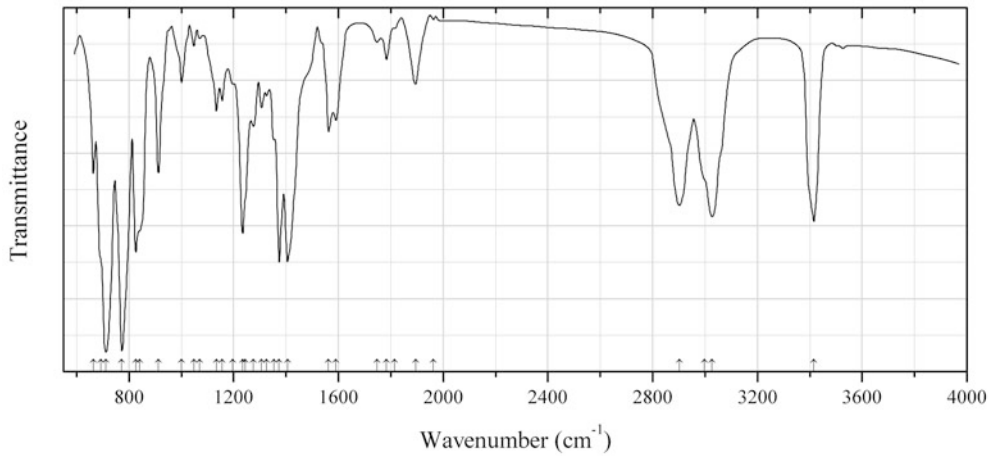

Fig. 2.174 IR spectrum of idrialite drawn using data from Echigo et al. (2009)

Org55 Idrialite $C_{22}H_{14}$ (Fig. 2.174)
Locality: Skaggs Springs, Sonoma Co., California, USA.
Description: Yellow lamellae embedded in a brown amorphous organic matter. The associated minerals are metacinnabar, opal, and siderite. Confirmed by the powder X-ray diffraction pattern.
Kind of sample preparation and/or method of registration of the spectrum: Small particles deposited on a KBr plate. Transmission.
Source: Echigo et al. (2009).
Wavenumbers (cm^{-1}): 3416s, 3027s, 2999sh, 2902s, 1963w, 1895, 1814sh, 1784, 1747w, 1591, 1562, 1406s, 1374s, 1355sh, 1326w, 1307, 1276, 1245sh, 1234s, 1197sh, 1157, 1134, 1070w, 1048w, 1001, 913, 840sh, 826s, 773s, 712s, 692sh, 664.
Note: The wavenumbers were determined by us based on spectral curve analysis of the published spectrum.

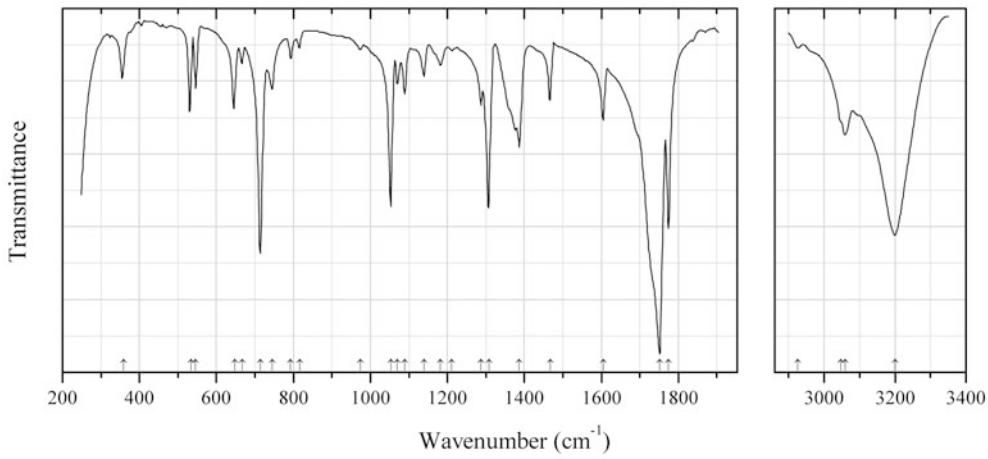

Fig. 2.175 IR spectrum of kladnoite drawn using data from Moroz et al. (2004)

Org56 Kladnoite $C_6H_4(CO)_2NH$ (phthalimide) (Fig. 2.175)
Locality: Burned dump of the Chelyabinsk coal basin, Kopeisk, South Urals, Russia.
Description: Aggregate of lamellar crystals. Investigated by B.V. Chesnokov and E.P. Shcherbakova. Monoclinic. D_{meas} = 1.43–1.50 g/cm^3. Optically biaxial (+), α = 1.48, β = 1.55, γ = 1.76–1.77. The strongest lines of the powder X-ray diffraction pattern [*d*, Å (*I*, %) (*hkl*)] are: 6.46 (100) (210), 5.70 (40) (400), 3.79 (90) (600, 020), 3.41 (50) (011), 3.30 (100) (21–1), 3.16 (60) (420), 2.43 (40) (701), 2.13 (40) (920).
Kind of sample preparation and/or method of registration of the spectrum: Absorption. Kind of sample preparation is not indicated.
Source: Moroz et al. (2004), Chesnokov and Shcherbakova (1991).
Wavenumbers (cm^{-1}): 3200s, 2926, 3059, 3048sh, 1774s, 1751s, 1605, 1468, 1387, 1308s, 1287, 1211w, 1182, 1139, 1089, 1070, 1053s, 975w, 816w, 792w, 745, 714s, 667, 546, 648, 534, 359.
Note: The wavenumbers were partly determined by us based on spectral curve analysis of the published spectrum.

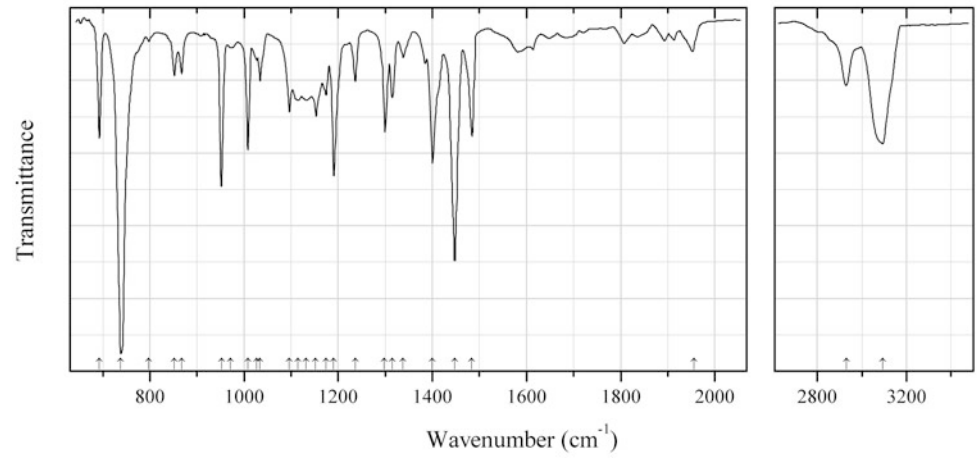

Fig. 2.176 IR spectrum of kratochvílite solution drawn using data from Scherf and Brown (1960)

Org57 Kratochvílite solution $C_{13}H_{10}$ (Fig. 2.176)
Locality: Synthetic.
Description: Fluorene (commercial reactant: Eastman Kodak, 98 % practical grade).
Kind of sample preparation and/or method of registration of the spectrum: Solutions in CS_2 and CCl_4.
Source: Scherf and Brown (1960).
Wavenumbers (cm^{-1}): 3093, 2930, 1956, 1484, 1448s, 1400s, 1338, 1315, 1298, 1236, 1190s, 1174, 1152, 1132, 1115, 1096, 1034, 1027, 1008s, 971w, 952s, 868, 852, 797w, 738s, 692.
Note: The wavenumbers were partly determined by us based on spectral curve analysis of the published spectrum.

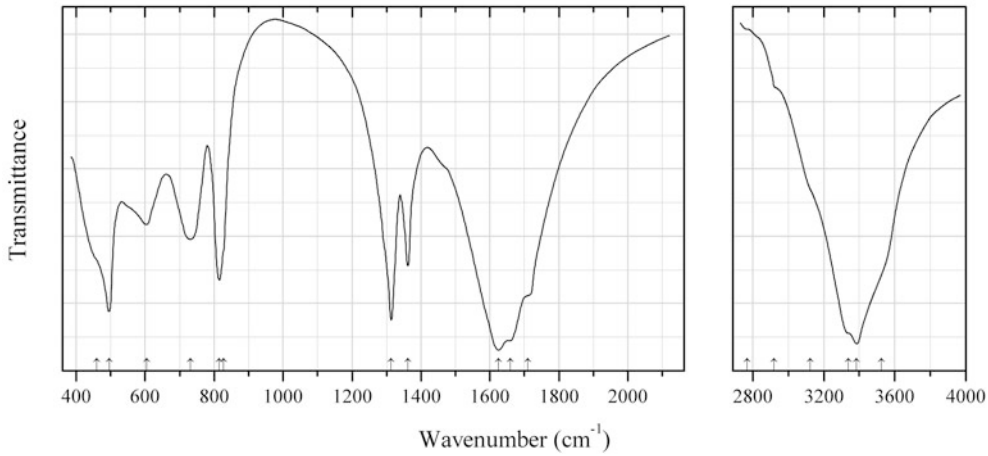

Fig. 2.177 IR spectrum of lindbergite drawn using data from Mancilla et al. (2009)

Org58 Lindbergite $Mn(C_2O_4)\cdot 2H_2O$ (Fig. 2.177)
Locality: Synthetic.
Description: Monoclinic polymorph, space group *C*2/*c*. Obtained at room temperature by slow addition of a diluted manganese(II) acetate solution over another one containing the stoichiometric amount of oxalic acid.
Kind of sample preparation and/or method of registration of the spectrum: KBr disc. Transmission.
Source: Mancilla et al. (2009).
Wavenumbers (cm^{-1}): 3525sh, 3386s, 3340sh, 3125sh, 2920sh, (2770sh), 1710sh, 1660sh, 1625s, 1362, 1314s, 827sh, 815s, 731, 604, 495s, 460sh.
Note: The wavenumbers were partly determined by us based on spectral curve analysis of the published spectrum.

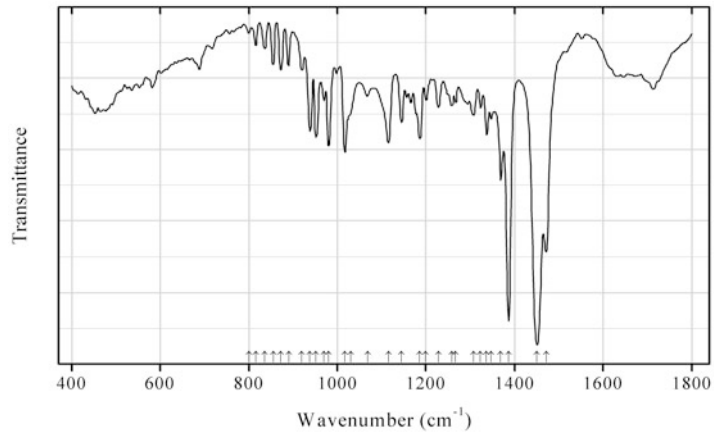

Fig. 2.178 IR spectrum of fichtelite drawn using data from Moenke (1961)

Org59 Fichtelite $C_{19}H_{34}$ (Fig. 2.178)
Locality: Wampen, Thiersheim, Marktredwitz, Fichtelgebirge, Franconia, Bavaria, Germany (type locality).
Description: No data.
Kind of sample preparation and/or method of registration of the spectrum: KBr disc. Transmission.
Source: Moenke (1961).
Wavenumbers (cm^{-1}): 3003, 2990, 2980, 2966, 2950, 2940, 2925, 2895, 2870, 2850, 2845, 2840, 1472s, 1450s, 1386s, 1369s, 1347, 1337, 1323, 1307, 1267, 1258, 1228, 1200, 1186, 1145, 1115, 1068, 1030, 1017, 980, 970w, 952, 938, 920w, 890, 872w, 855w, 836w, 816w, 800w.
Note: The wavenumbers were partly determined by us based on spectral curve analysis of the published spectrum. Intensities of the bands observed above 2800 cm^{-1} are not indicated.

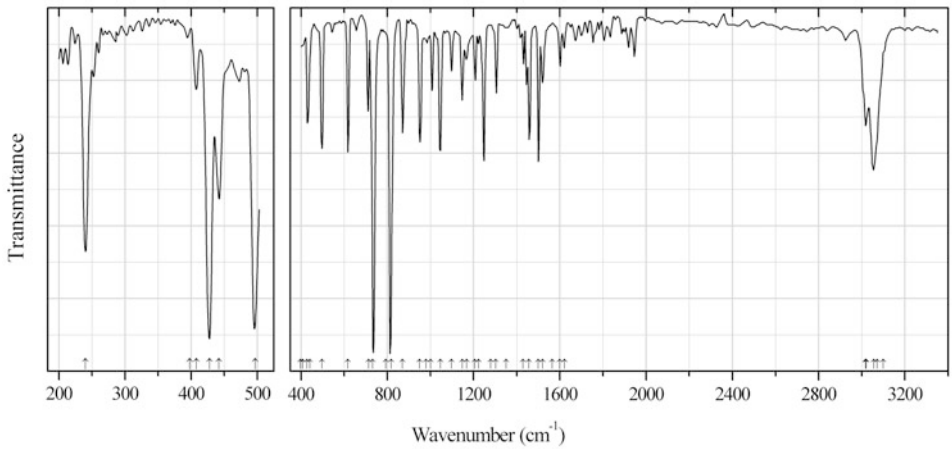

Fig. 2.179 IR spectrum of ravatite drawn using data from Witt and Mecke (1967)

Org60 Ravatite $C_{14}H_{10}$ (Fig. 2.179)
Locality: Synthetic.
Description: Commercial phenanthrene.
Kind of sample preparation and/or method of registration of the spectrum: Crystalline layer.
Source: Witt and Mecke (1967).

Wavenumbers (cm^{-1}): 3100sh, 3071, 3056, 3020sh, 1622, 1600, 1565, 1521, 1500, 1457, 1430, 1352, 1303, 1280, (1223), (1206), 1168, 1148, 1098, 1046, 1001, (980), 950, 870, 818s, 793, 733s, 714, 618, 497, 442, 428, 408, (398), 240.
Note: The wavenumbers were partly determined by us based on spectral curve analysis of the published spectrum.

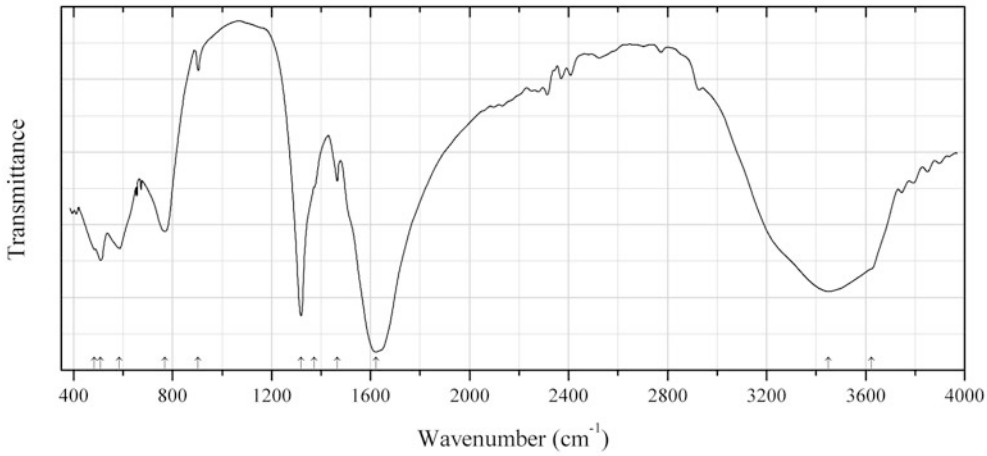

Fig. 2.180 IR spectrum of strontium oxalate dihydrate drawn using data from D'Antonio et al. (2015)

Org61 Strontium oxalate dihydrate $Sr(C_2O_4)\cdot 2H_2O$ (Fig. 2.180)
Locality: Synthetic.
Description: Obtained by dropwise addition of a 0.5 M aqueous solution of $H_2C_2O_4\cdot 2H_2O$ to a 0.5 M aqueous solution of strontium nitrate, in equimolecular proportions, with subsequent precipitation at room temperature. The purity was confirmed by powder X-ray diffractometry, as well as by elemental chemical analysis.
Kind of sample preparation and/or method of registration of the spectrum: KBr disc. Transmission.
Source: D'Antonio et al. (2015).
Wavenumbers (cm^{-1}): 3625sh, 3450s, 1621s, 1465w, 1372sh, 1320s, 904w, 769, 586, 510, 485sh.

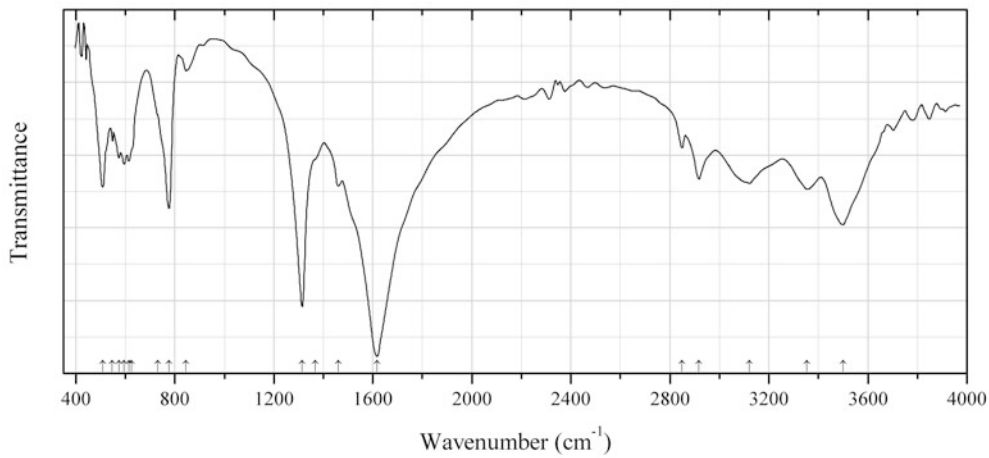

Fig. 2.181 IR spectrum of strontium oxalate monohydrate drawn using data from D'Antonio et al. (2015)

Org62 Strontium oxalate monohydrate $Sr(C_2O_4)\cdot H_2O$ (Fig. 2.181)
Locality: Synthetic.
Description: Obtained by dropwise addition of a 0.5 M aqueous solution of $H_2C_2O_4\cdot 2H_2O$ to a 0.5 M aqueous solution of strontium nitrate, in equimolecular proportions, with subsequent precipitation from a boiling solution. The purity was confirmed by powder X-ray diffractometry, as well as by elemental chemical analysis.
Kind of sample preparation and/or method of registration of the spectrum: KBr disc. Transmission.
Source: D'Antonio et al. (2015).
Wavenumbers (cm^{-1}): 3500s, 3354, 3122, 2918, 2850w, 1616s, 1460w, 1366sh, 1315s, 845w, 777s, 730sh, 626sh, (614), 595, (574), (548), 509s.

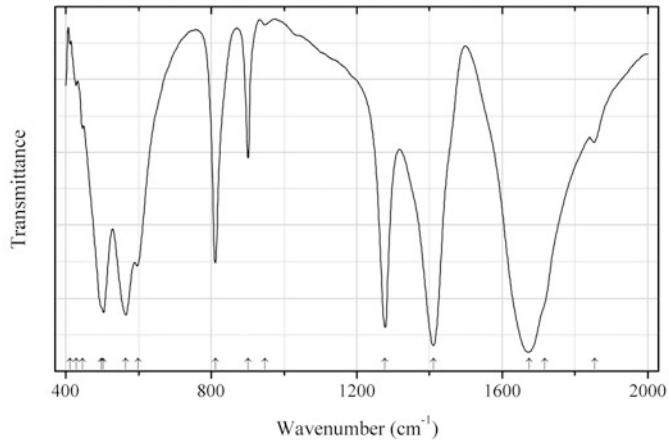

Fig. 2.182 IR spectrum of wheatleyite drawn using data from Palacios et al. (2011)

Org64 Wheatleyite $Na_2Cu(C_2O_4)_2\cdot 2H_2O$ (Fig. 2.182)
Locality: Synthetic.
Description: Prepared by slow evaporation of an aqueous solution containing stoichiometric amounts of copper and sodium oxalates. Characterized by powder X-ray diffractometry and chemical analysis.
Kind of sample preparation and/or method of registration of the spectrum: KBr disc. Transmission.
Source: Palacios et al. (2011).
Wavenumbers (cm^{-1}): 3536s, 3447s, 3313sh, 3236w, 1855w, 1717sh, 1674s, 1412s, 1278s, 948w, 901, 811, 598sh, 565s, 503s, 498sh, 445w, 428w, 411w.
Note: The wavenumbers were partly determined by us based on spectral curve analysis of the published spectrum.

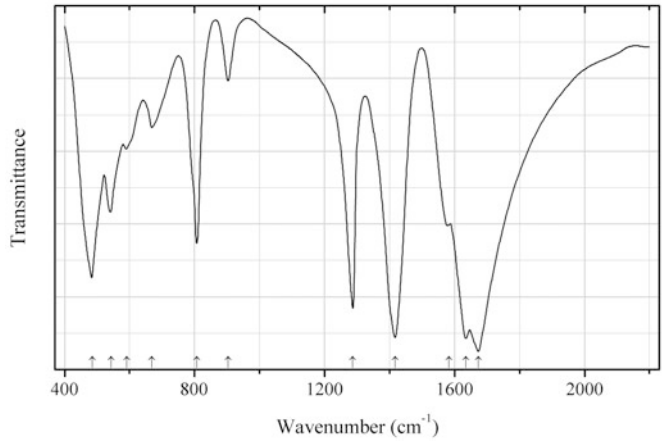

Fig. 2.183 IR spectrum of wheatleyite K analogue drawn using data from Palacios et al. (2011)

Org65 Wheatleyite K analogue $K_2Cu(C_2O_4)_2 \cdot 2H_2O$ (Fig. 2.183)
Locality: Synthetic.
Description: Prepared by slow evaporation of an aqueous solution containing stoichiometric amounts of copper and potassium oxalates. Characterized by powder X-ray diffractometry and chemical analysis.
Kind of sample preparation and/or method of registration of the spectrum: KBr disc. Transmission.
Source: Palacios et al. (2011).
Wavenumbers (cm^{-1}): 3502, 3401s, 2921w, 2841w, 1673s, 1635s, 1583, 1417s, 1287s, 903, 807s, 669, 591, 543, 485s.

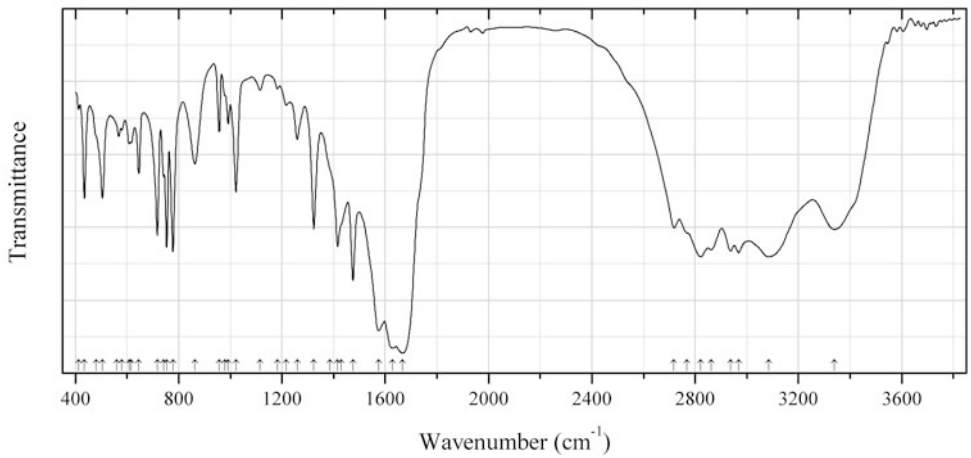

Fig. 2.184 IR spectrum of uric acid monohydrate drawn using data from Schubert et al. (2005)

Org66 Uric acid monohydrate $C_5H_4N_4O_3 \cdot H_2O$ (Fig. 2.184)
Locality: Urinary calculus.
Description: Characterized by powder X-ray diffraction. Monoclinic, space group $P2_1/c$, a = 4.786 (4), b = 16.812(6), c = 8.598(5) Å, β = 90.13(7)°, V = 691.7(8) $Å^3$, Z = 4. D_{calc} = 1.787 g/cm^3.
Kind of sample preparation and/or method of registration of the spectrum: KBr disc. Transmission.

Source: Schubert et al. (2005).
Wavenumbers (cm^{-1}): 3340s, 3084s, 2968s, 2862s, 2937s, 2821s, 2768sh, 2718, 1667s, 1629s, 1574s, 1475s, 1430sh, 1416s, 1386sh, 1323, 1259, 1216w, 1182w, 1116w, 1022, 992, 980sh, 957, 863, 778, 754, 742, 717, 646, 616, 608, 581, 561, 505, 481sh, 435, 412w.

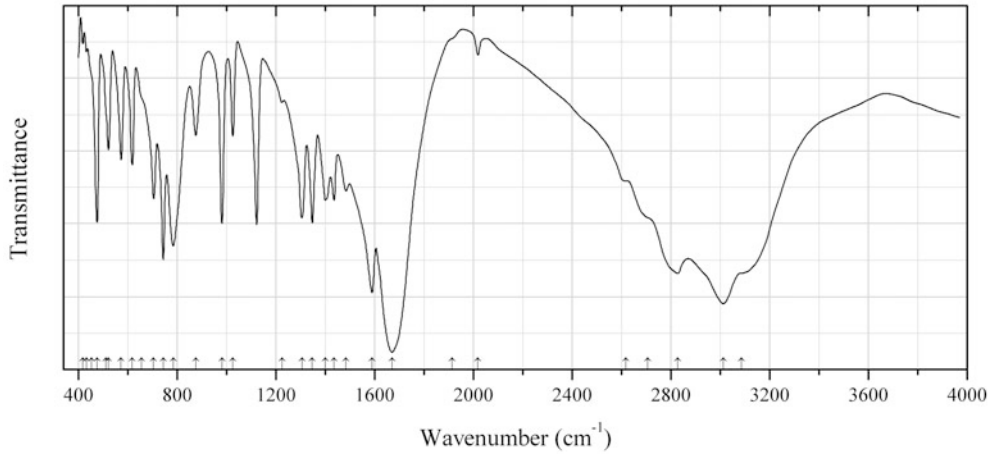

Fig. 2.185 IR spectrum of uricite drawn using data from Benramdane et al. (2008)

Org67 Uricite $C_5H_4N_4O_3$ (Fig. 2.185)
Locality:
Description:
Kind of sample preparation and/or method of registration of the spectrum:
Source: Benramdane et al. (2008).
Wavenumbers (cm^{-1}): 3085sh, 3012s, 2828s, 2706sh, 2618sh, 2019w, 1915sh, 1671s, 1590s, 1485, 1436, 1401, 1348, 1306, 1225w, 1026, 982, 876, 785s, 744s, 705, 657sh, 619, 574, 522, 512sh, 476, 455sh, 433w, 419w.
Note: The wavenumbers were partly determined by us based on spectral curve analysis of the published spectrum.

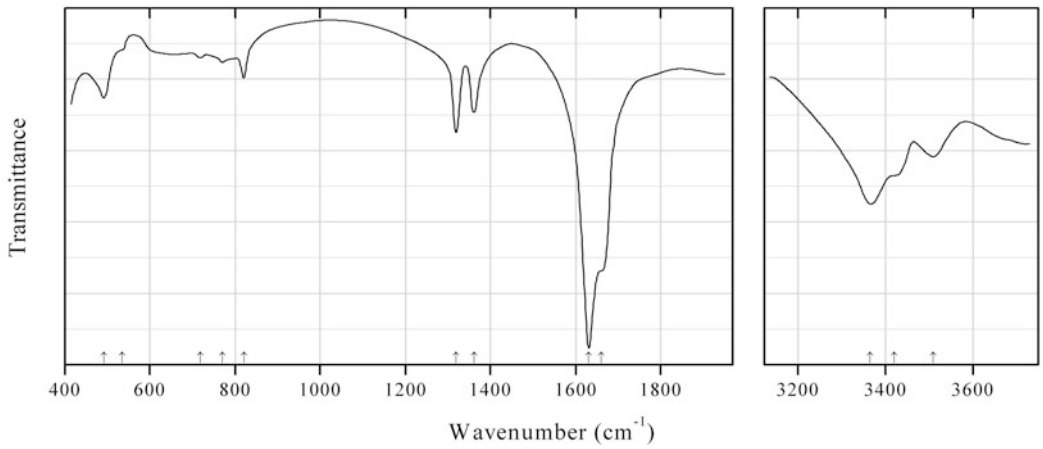

Fig. 2.186 IR spectrum of nickel oxalate dihydrate obtained by N.V. Chukanov

Org68 Nickel oxalate dihydrate $Ni(C_2O_4)\cdot 2H_2O$ (Fig. 2.186)
Locality: Lipovka Ni mine, Rezh district, Middle Urals, Russia.
Description: Yellow-green crust on millerite. Isostructural with humboldtine. Identified by qualitative electron microprobe analyses and powder X-ray diffraction data.
Kind of sample preparation and/or method of registration of the spectrum: KBr disc. Absorbtion.
Wavenumbers (cm^{-1}): 3510, 3420sh, 3365s, 1660sh, 1631s, 1361, 1319, 820, 770w, 718w, 535sh, 491.

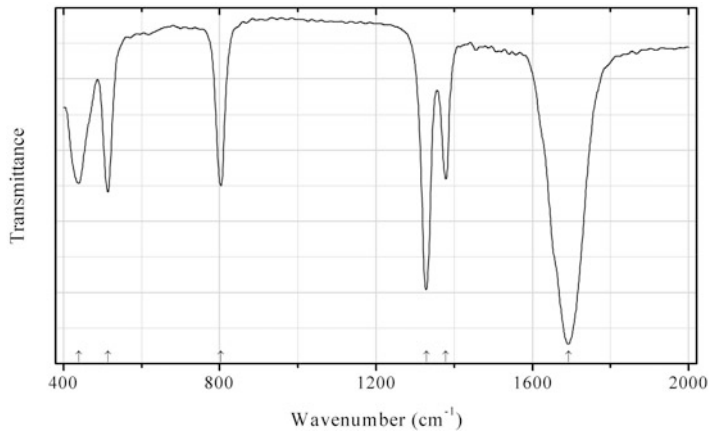

Fig. 2.187 IR spectrum of magnesium oxalate drawn using data from D'Antonio et al. (2010)

Org69 Magnesium oxalate $Mg(C_2O_4)$ (Fig. 2.187)
Locality: Synthetic.
Description: Obtained by isothermal dehydration of α-$MgC_2O_4\cdot 2H_2O$ at 200 °C during 48 h. Monoclinic.
Kind of sample preparation and/or method of registration of the spectrum: KBr disc. Transmission.
Source: D'Antonio et al. (2010).
Wavenumbers (cm^{-1}): 1692s, 1379, 1329s, 803, 514, 439.

2.4 Nitrides and Nitrates

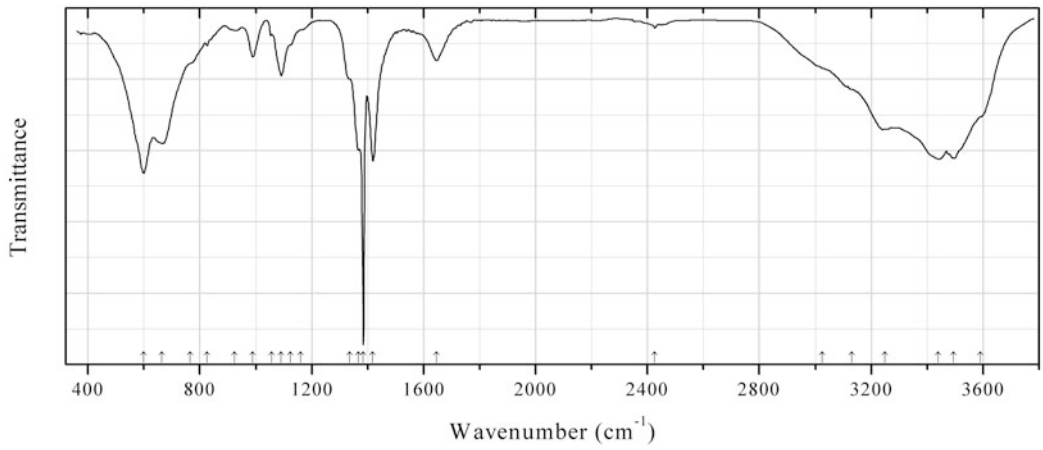

Fig. 2.188 IR spectrum of sveite obtained by N.V. Chukanov

N12 Sveite $KAl_7(NO_3)_4(OH)_{16}Cl_2 \cdot 8H_2O$ (Fig. 2.188)
Locality: Autana cave, Amazonas, Venezuela (type locality).
Description: White flakes from the association with chalcedony.
Kind of sample preparation and/or method of registration of the spectrum: KBr disc. Absorption.
Wavenumbers (cm^{-1}): 3590sh, 3495s, 3440s, 3250, 3130sh, 3025sh, 2427w, 1645, 1418s, (1384s), 1368s, 1335sh, 1160sh, 1125sh, 1091, 1057w, 989, 925w, (825w), 765sh, 665s, 599s.
Note: The bands at 1384 and 825 cm^{-1} correspond to the admixture of KNO_3.

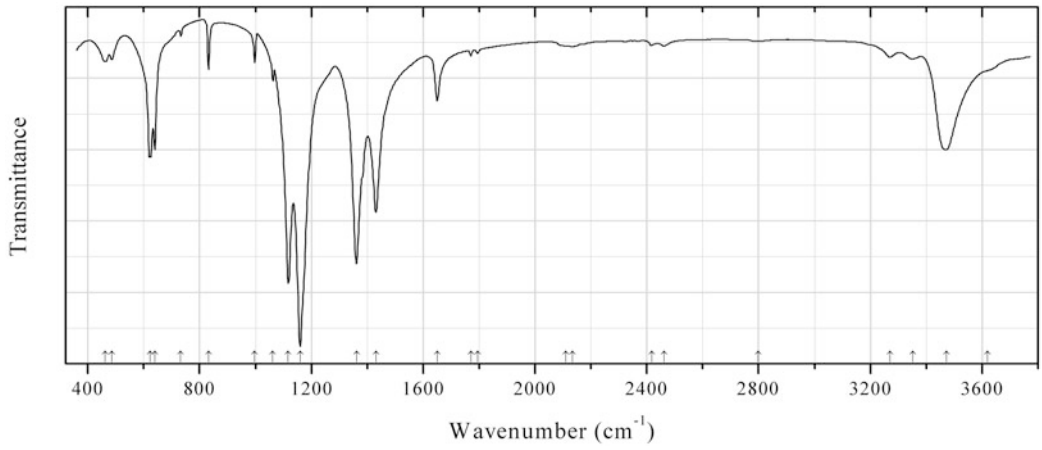

Fig. 2.189 IR spectrum of shilovite obtained by N.V. Chukanov

N13 Shilovite $Cu(NH_3)_4(NO_3)_2$ (Fig. 2.189)
Locality: Pabellón de Pica Mountain, 1.5 km south of Chanabaya, Iquique Province, Tarapacá Region, Chile (type locality).
Description: Deep violet blue thick tabular to equant crystals from the association with halite, ammineite, atacamite, and thenardite. Holotype sample. Orthorhombic, space group *Pnn*2, a = 23.6585(9), b = 10.8238(4), c = 6.9054(3) Å, V = 1768.3(1) $Å^3$, Z = 8. D_{calc} = 1.92 g/cm^3.

Optically biaxial (+), α = 1.527(2), β = 1.545(5), γ = 1.610(2). The empirical formula is $H_{12.56}(Cu_{1.09}Fe_{0.01})N_{5.87}O_{6.00}$. The strongest lines of the powder X-ray diffraction pattern [*d*, Å (*I*, %) (*hkl*)] are: 5.931 (41) (400), 5.841 (100) (011), 5.208 (47) (410), 4.162 (88) (411), 4.005 (62) (002, 710), 3.207 (32) (031).

Kind of sample preparation and/or method of registration of the spectrum: KBr disc. Absorption.

Wavenumbers (cm^{-1}): 3620sh, 3472, 3352w, 3271w, 2798w, 2461w, 2418w, 2134w,2110sh, 1796w, 1770w, 1650, 1431s, 1361s, 1159s, 1117s, 1062, 997, 832, 732w, 639s, 624s, 485, 463.

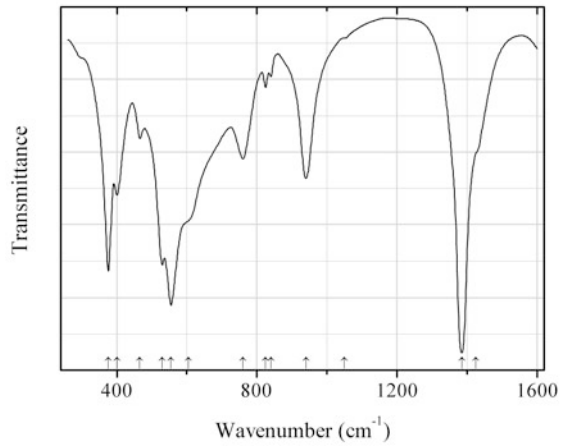

Fig. 2.190 IR spectrum of quintinite Al,Li,NO_3-analogue drawn using data from Hernandez-Moreno et al. (1985)

N14 Quintinite Al,Li,NO_3-analogue $LiAl_2(OH)_6(NO_3)\cdot nH_2O$ (?) (Fig. 2.190)

Locality: Synthetic.

Description: Confirmed by chemical analysis and powder X-ray diffraction data.

Kind of sample preparation and/or method of registration of the spectrum: KBr disc. Absorption.

Source: Hernandez-Moreno et al. (1985).

Wavenumbers (cm^{-1}): 1425sh, 1385s, 1050sh, 940, 840w, 825w, 760, 605sh, 555s, 530s, 465, 400, 375s.

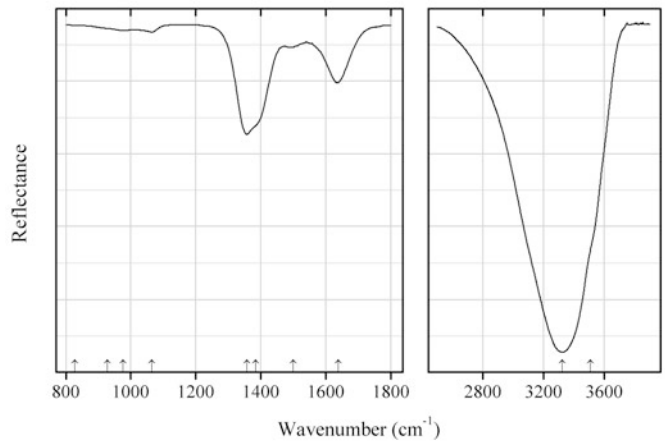

Fig. 2.191 IR spectrum of hydrotalcite NO_3-analogue drawn using data from Frost et al. (2005a)

N15 Hydrotalcite NO_3-analogue $Ni_6Al_2(NO_3)_2(OH)_{16}\cdot 4H_2O$ (?) (Fig. 2.191)

Locality: Synthetic.
Description: Synthesised by the co-precipitation of NaOH, $NaNO_3$, and $Ni(NO_3)_2$. No data on the product are given.
Kind of sample preparation and/or method of registration of the spectrum: Not indicated. Possibly, attenuated total reflection of powdered sample.
Source: Frost et al. (2005a).
Wavenumbers (cm^{-1}): 3507sh, 3324s, 1638, 1500w, 1384sh, 1357s, 1065w, 977w, 928sh, 828w.
Note: The wavenumbers are given according to drawing. In the cited paper, wavenumbers are indicated for the maxima of individual bands obtained as a result of the spectral curve analysis. The idealized formula $Ni_6Al_2(NO_3)(OH)_{16}{\cdot}4H_2O$ given by Frost et al. (2005a) is not charge-balanced.

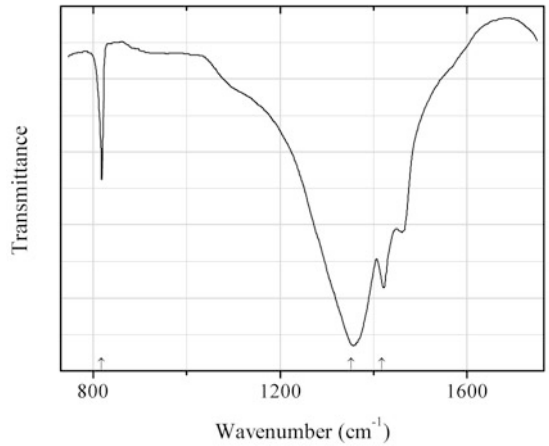

Fig. 2.192 IR spectrum of nitrobarite drawn using data from Miller and Wilkins (1952)

N16 Nitrobarite $Ba(NO_3)_2$ (Fig. 2.192)
Locality: Synthetic.
Description: Commercial product.
Kind of sample preparation and/or method of registration of the spectrum: Nujol mull. Transmission.
Source: Miller and Wilkins (1952).
Wavenumbers (cm^{-1}): 1418, 1352s, 817.
Note: bands with wavenumbers above 1430 cm^{-1} correspond to Nujol.

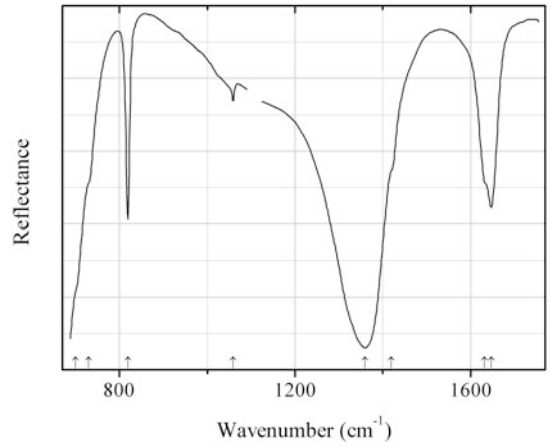

Fig. 2.193 IR spectrum of nitromagnesite drawn using data from Chang and Irish (1973)

N17 Nitromagnesite $Mg(NO_3)_2 \cdot 6H_2O$ (Fig. 2.193)
Locality: Synthetic.
Description: Obtained by twice recrystallizing the magnesium nitrate provided by Fisher Scienific Co.
Kind of sample preparation and/or method of registration of the spectrum: Multiple internal reflectance of powdered sample.
Source: Chang and Irish (1973).
Wavenumbers (cm^{-1}): 3580sh, 3520sh, 3352, 3242w, 1647, 1632sh, 1420sh, 1360s, 1059w, 819s, 730w, 700sh, ~630, ~550.

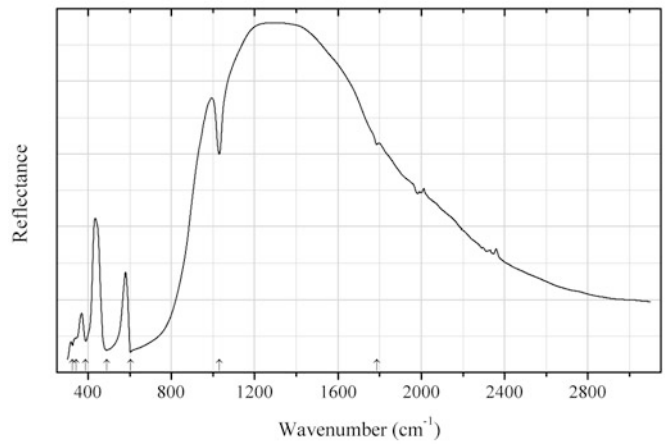

Fig. 2.194 IR spectrum of nierite dimorph drawn using data from Lorenzzi (2007)

N18 Nierite dimorph β-Si_3N_4 (Fig. 2.194)
Locality: Synthetic.
Description: Polycrystalline aggregate. Hexagonal, space group $P6_3/m$, $a \approx 7.595$, $c \approx 2.902$ Å. Confirmed by powder X-ray diffraction data. The sample contains an insignificant admixture of α-Si_3N_4 and yttrium dissolved at grain boundaries.

Kind of sample preparation and/or method of registration of the spectrum: Attenuated total reflection of a powdered sample.
Source: Lorenzzi (2007).
Wavenumbers (cm^{-1}): 1786w, 1031, 604s, 490s, 389, 344sh, 325.
Note: The wavenumbers were partly determined by us based on spectral curve analysis of the published spectrum.

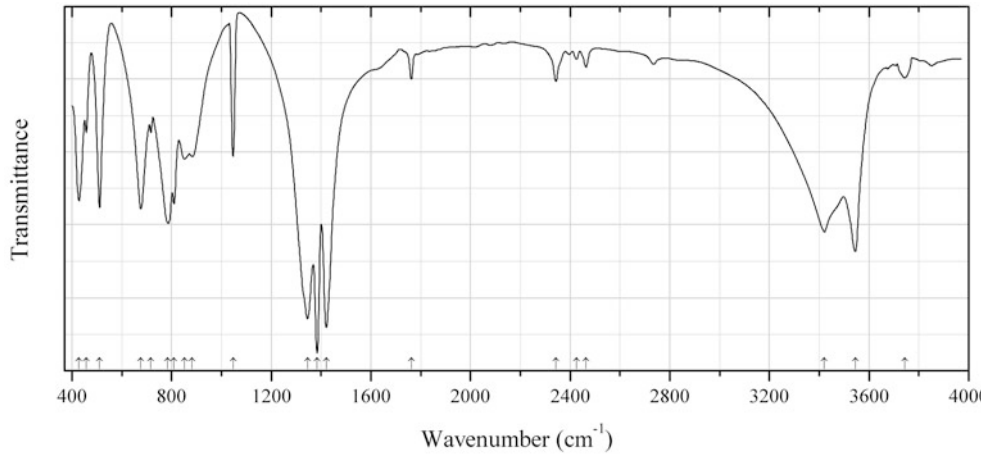

Fig. 2.195 IR spectrum of rouaite drawn using data from Nytko et al. (2009)

N19 Rouaite $Cu_2(NO_3)(OH)_3$ (Fig. 2.195)
Locality: Synthetic.
Description: Blue-green powder. Synthesized in the reaction between aqueous solutions of $Cu(NO_3)_2 \cdot 2.5\ H_2O$ and NaOH. Confirmed by powder X-ray diffraction data.
Kind of sample preparation and/or method of registration of the spectrum: KBr disc. Transmission.
Source: Nytko et al. (2009).
Wavenumbers (cm^{-1}): 3743w, 3545s, 3421s, 2464w, 2426w, 2343w, 1763w, 1421s, 1384s, 1346s, 1047, 883, 852, 810, 785s, 717w, 677, 511, 457w, 428.

2.5 Oxides and Hydroxides

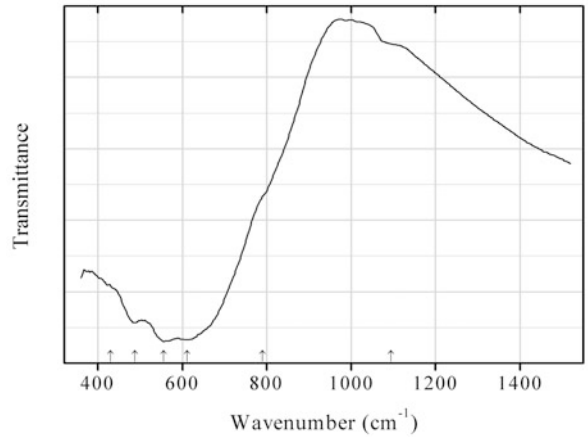

Fig. 2.196 IR spectrum of titanowodginite obtained by N.V. Chukanov

O245 Titanowodginite $Mn^{2+}TiTa_2O_8$ (Fig. 2.196)
Locality: Tanco pegmatite, Tanco mine, Bernik lake, Lac-du-Bonnet area, Manitoba, Canada (type locality).
Description: Black crystals from the association with microlite, manganocolumbite, albite, quartz, muscovite, etc. The empirical formula is (electron microprobe): $(Mn_{0.77}Fe_{0.19}Ca_{0.03}Mg_{0.01})(Ti_{0.51}Sn_{0.35}Fe_{0.10}Nb_{0.04})(Ta_{1.62}Nb_{0.38})O_8$.
Kind of sample preparation and/or method of registration of the spectrum: KBr disc. Absorption.
Wavenumbers (cm^{-1}): 1095sh, 790sh, 612s, 556s, 488, 430sh.

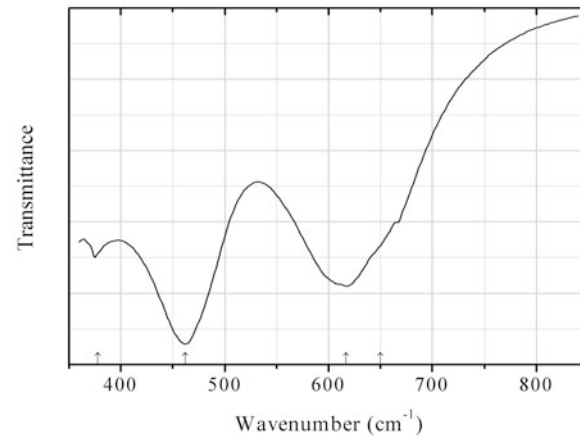

Fig. 2.197 IR spectrum of nežilovite obtained by N.V. Chukanov

O246 Nežilovite $PbZn_2Mn^{4+}{}_2Fe^{3+}{}_8O_{19}$ (Fig. 2.197)
Locality: "Mixed series" metamorphic complex, near the Nežilovo village, 40 km SW of Veles, Pelagonian massif, Macedonia (type locality).

Description: Black lamellar crystals from the association with Zn-bearing phlogopite, Zn,Cu-bearing braunite, gahnite, dolomite, and barite. The empirical formula is (electron microprobe): $Pb_{1.01}Zn_{1.97}(Mn^{4+}_{1.31}Ti_{0.54}Sb_{0.15})(Fe^{3+}_{5.72}Mn^{3+}_{0.97}Al_{1.31})O_{19}$.
Kind of sample preparation and/or method of registration of the spectrum: KBr disc. Absorption.
Wavenumbers (cm^{-1}): 650sh, 617s, 462s, 378.

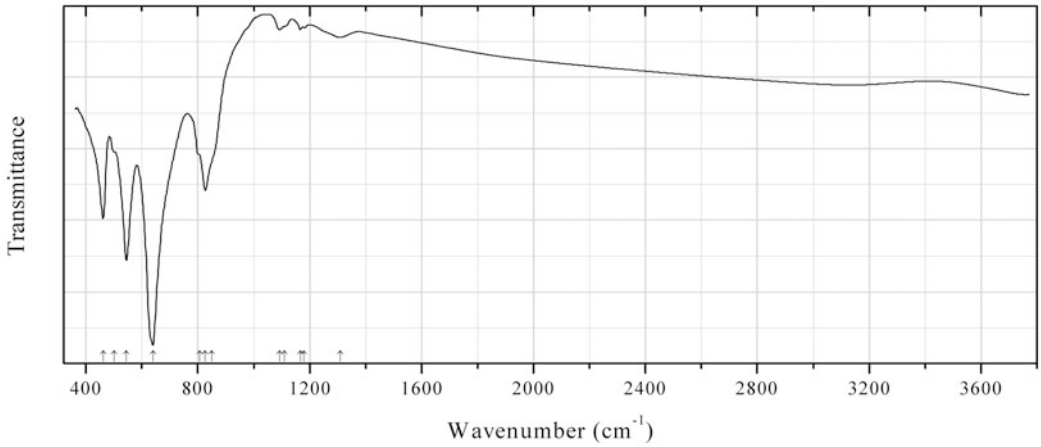

Fig. 2.198 IR spectrum of claudetite obtained by N.V. Chukanov

O247 Claudetite As_2O_3 (Fig. 2.198)
Locality: Freiberg, Germany.
Description: Technogenetic. Colourless tabular crystals. Investigated by I.V. Pekov. Confirmed by single-crystal X-ray diffraction data.
Kind of sample preparation and/or method of registration of the spectrum: KBr disc. Absorption.
Wavenumbers (cm^{-1}): 1310w, 1180w, 1166w, 1110sh, 1092w, 850sh, 826, 805sh, 639s, 544s, 500sh, 461.

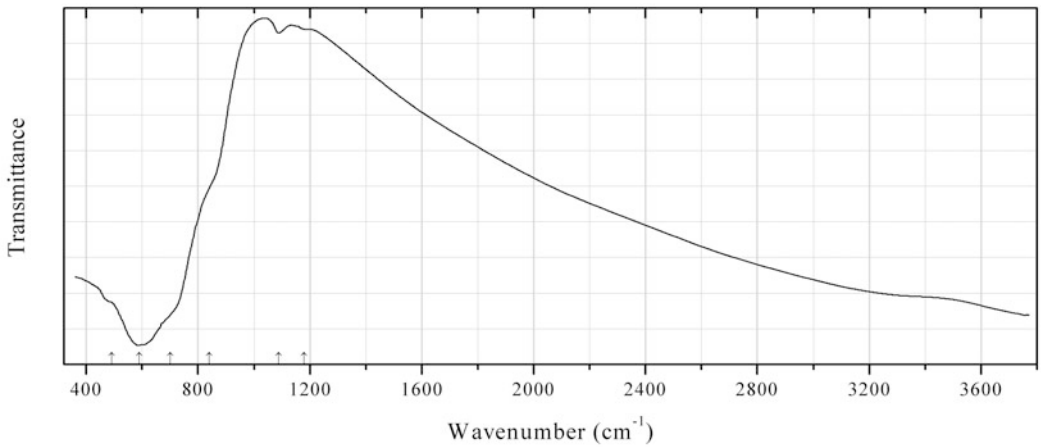

Fig. 2.199 IR spectrum of fersmite obtained by N.V. Chukanov

O248 Fersmite $(Ca,Ce,Na)(Nb,Ta,Ti)_2(O,OH,F)_6$ (Fig. 2.199)

Locality: Vishnevye (Vishnyovye) Mts., Chelyabinsk region, South Urals, Russia (type locality).
Description: Black partial pseudomorph after a pyrochlore-group mineral from alkaline pegmatite. Amorphous, metamict. Investigated by I.V. Pekov.
Kind of sample preparation and/or method of registration of the spectrum: KBr disc. Absorption.
Wavenumbers (cm^{-1}): 1180w, 1088w, 840sh, 700sh, 589s, 490sh.

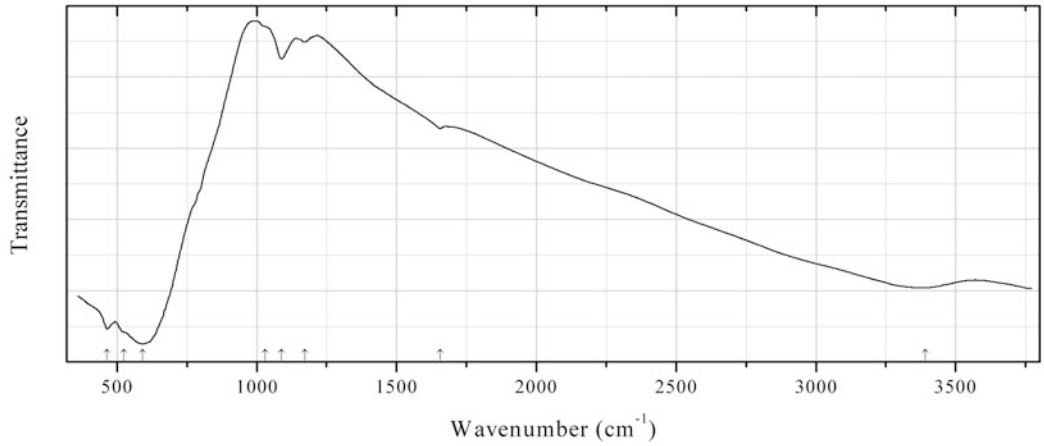

Fig. 2.200 IR spectrum of aeschynite-(Ce) obtained by N.V. Chukanov

O249 Aeschynite-(Ce) (Ce,*REE*,Ca,Th)(Ti,Nb)$_2$(O,OH)$_6$ (Fig. 2.200)
Locality: Ilmeny (Il'menskie) Mts., South Urals, Russia (type locality).
Description: Black crystal from miaskite pegmatite. Amorphous, metamict. The empirical formula is (electron microprobe): $[(Ce_{0.27}La_{0.11}Nd_{0.10}Pr_{0.03}Sm_{0.03})Th_{0.31}Y_{0.10}Ca_{0.08}Na_{0.08}](Ti_{1.04}Nb_{0.85}Fe_{0.11})(O,OH)_6 \cdot nH_2O$.
Kind of sample preparation and/or method of registration of the spectrum: KBr disc. Absorption.
Wavenumbers (cm^{-1}): 3390, 1655w, 1172w, 1088, 1030sh, 591s, 525sh, 464.

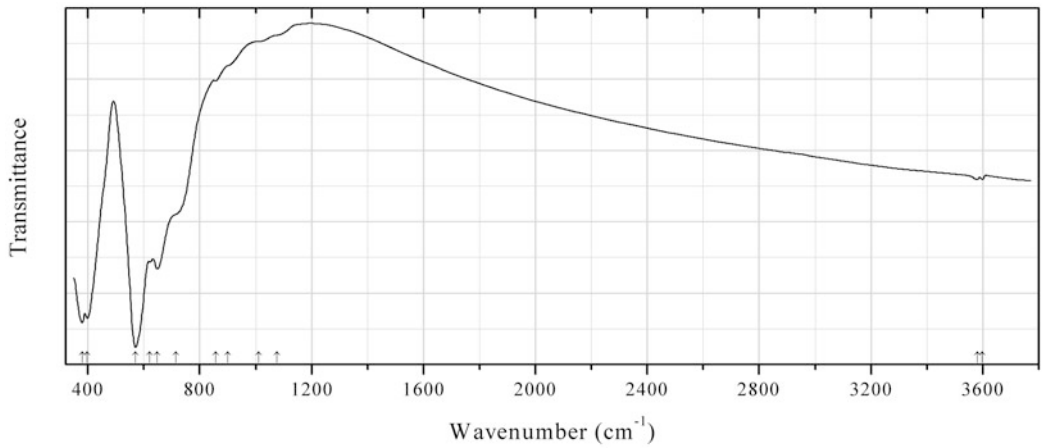

Fig. 2.201 IR spectrum of hydroxycalciomicrolite obtained by N.V. Chukanov

O250 Hydroxycalciomicrolite $Ca_{1.5}Ta_2O_6(OH)$ (Fig. 2.201)
Locality: Volta Grande pegmatite, Nazareno, Minas Gerais, Brazil (type locality).

Description: Yellow octahedral crystal from the association with albite, apatite, beryl, cassiterite, epidote, fluorcalciomicrolite, fluorite, garnet, gahnite, hydrokenomicrolite, etc. Holotype sample. Cubic, space group $P4_332$, $a = 10.4211(8)$, $V = 1131.72(15)$ Å^3, $Z = 8$. $D_{calc} = 6.141$ g/cm^3. Optically isotropic, $n_{calc.} = 2.010$. The empirical formula is: $(Ca_{1.44}Na_{0.07}Mn_{0.01})_{\Sigma 1.52}(Ta_{1.86}Nb_{0.12}Sn_{0.02})_{\Sigma 2.00}O_6[(OH)_{0.65}F_{0.31}]$. The strongest lines of the powder X-ray diffraction pattern [*d*, Å (*I*, %) (*hkl*)] are: 6.025 (100) (111), 3.145 (15) (311), 3.010 (73) (111), 2.606 (7) (400), 2.006 (7) (511, 333), 1.843 (8) (440).
Kind of sample preparation and/or method of registration of the spectrum: KBr disc. Absorption.
Wavenumbers (cm^{-1}): 3599w, 3580w, 1075sh, 1010sh, 900sh, 856w, 715sh, 648, 622, 570s, 398s, 379s.

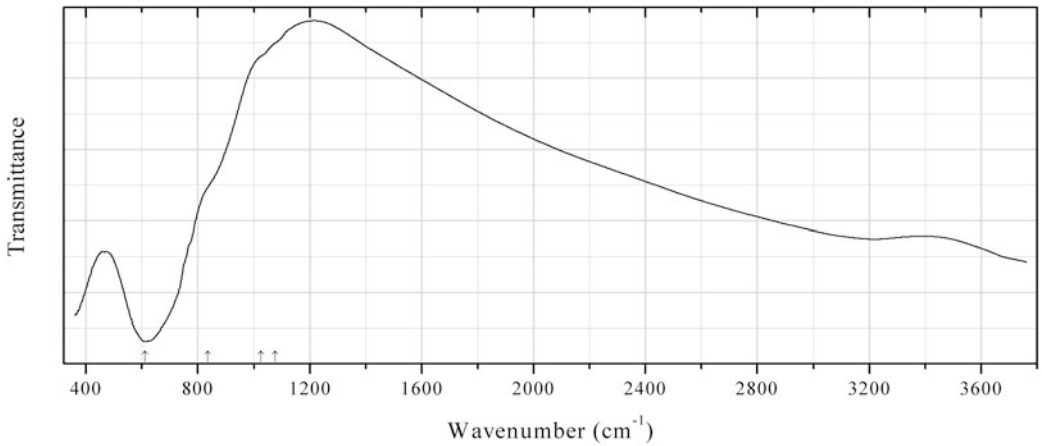

Fig. 2.202 IR spectrum of fluornatromicrolite obtained by N.V. Chukanov

O251 Fluornatromicrolite $(Na,Ca,Bi)_2(Ta,Nb)_2O_6(F,OH)$ (Fig. 2.202)
Locality: Vasin-Myl'k Mt., Voron'i Tundras, Kola peninsula, Murmansk region, Russia.
Description: Light brown crystal from the association with albite and trilithionite. The empirical formula is (electron microprobe): $Na_{1.06}Ca_{0.95}(Ta_{1.77}Nb_{0.16}W_{0.05}Sn_{0.02})O_6F_{0.93}(OH)_{0.06}$.
Kind of sample preparation and/or method of registration of the spectrum: KBr disc. Absorption.
Wavenumbers (cm^{-1}): 1075sh, 1025sh, 835sh, 611s.

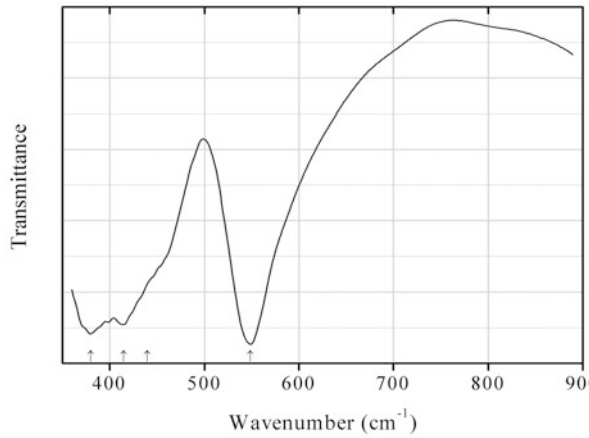

Fig. 2.203 IR spectrum of magnetoplumbite obtained by N.V. Chukanov

O252 Magnetoplumbite $PbFe^{3+}{}_{12}O_{19}$ (Fig. 2.203)
Locality: Långban deposit, Bergslagen ore region, Filipstad district, Värmland, Sweden (type locality).
Description: Black veinlet in phlogopite-calcite aggregate. A Mn-rich variety. Confirmed by qualitative electron microprobe analysis.
Kind of sample preparation and/or method of registration of the spectrum: KBr disc. Absorption.
Wavenumbers (cm^{-1}): 549s, 440sh, 415, 380.

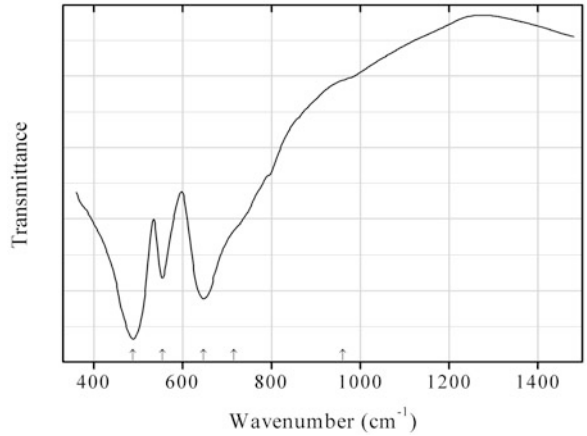

Fig. 2.204 IR spectrum of hercynite obtained by N.V. Chukanov

O254 Herzynite $Fe^{2+}Al_2O_4$ (Fig. 2.204)
Locality: Rischorr Mt., Khibiny alkaline complex, Kola peninsula, Murmansk region, Russia.
Description: Black octahedral crystal from the association with corundum, biotite, and feldspar. The empirical formula is (electron microprobe): $(Fe_{0.86}Mn_{0.08}Mg_{0.06})(Al_{1.91}Fe_{0.07}Ti_{0.02})O_4$.
Kind of sample preparation and/or method of registration of the spectrum: KBr disc. Absorption.
Wavenumbers (cm^{-1}): 960sh, 715sh, 646s, 554, 488s.

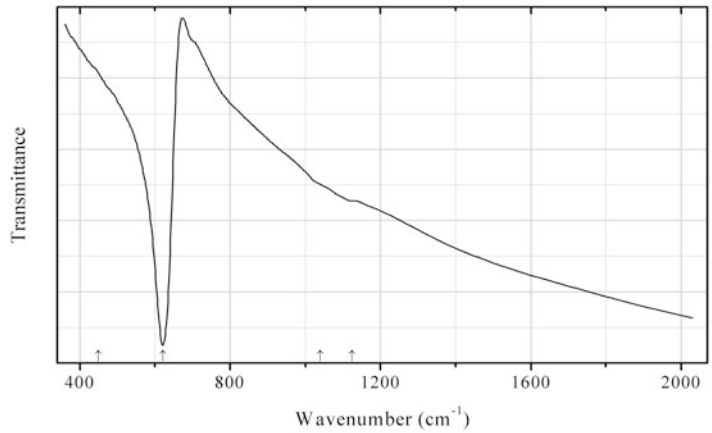

Fig. 2.205 IR spectrum of cuprite obtained by N.V. Chukanov

O255 Cuprite Cu_2O (Fig. 2.205)

Locality: Rubtsovskoe base-metal deposit, Rubtsovsk ore district, northwestern Altai Mts., Siberia, Russia.
Description: Deep red octahedral crystals from the association with copper, silver, and miersite.
Kind of sample preparation and/or method of registration of the spectrum: KBr disc. Absorption.
Wavenumbers (cm^{-1}): 1125w, 1040sh, 621s, 450sh.
Note: Far infrared spectrum of synthetic Cu_2O contains strong band at 147–154 cm^{-1} (McDevitt and Davidson 1965; Taylor and Weichman 1971).

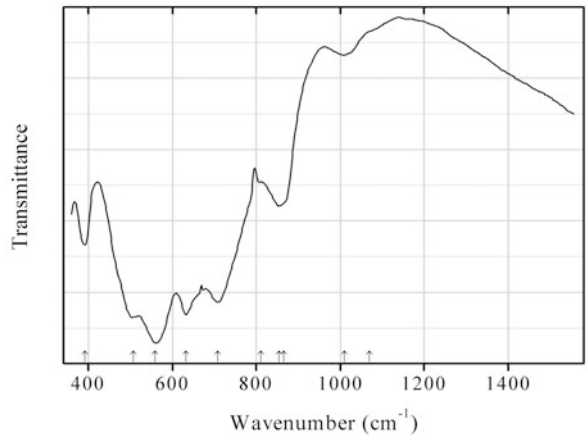

Fig. 2.206 IR spectrum of tantalite-(Mg) obtained by N.V. Chukanov

O256 Tantalite-(Mg) $MgTa_2O_6$ (Fig. 2.206)
Locality: Lipovka mine, Lipovka pegmatite field, Rezh district, Middle Urals, Russia.
Description: Dark brown grain with brown streak from the association with U-rich microlite, tantalite-(Mg) (relics), plagioclase, calcite, tourmaline of the dravite-uvite series, chrysoberyl, phenakite, clinochlore, and Be-rich cordierite. Investigated by I.V. Pekov. A Fe-rich variety. The empirical formula is (electron microprobe): $(Mg_{0.45–0.53}Fe_{0.42–0.49}Mn_{0.03–0.06})(Ta_{1.14–1.19}Nb_{0.78–0.85}Ti_{0.02})O_6$.
Kind of sample preparation and/or method of registration of the spectrum: KBr disc. Absorption.
Wavenumbers (cm^{-1}): 1070sh, 1009w, 865sh, 854, 810sh, 708s, 632s, 559s, 507s, 392.

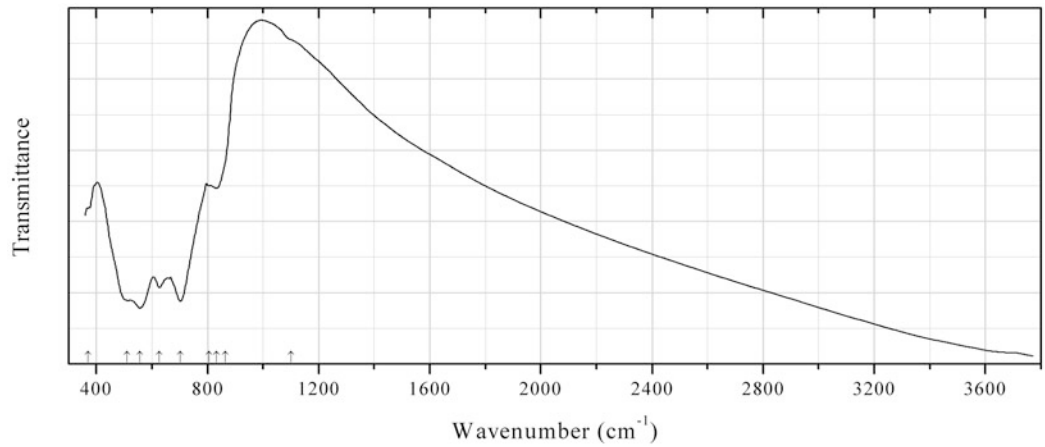

Fig. 2.207 IR spectrum of columbite-(Mn) obtained by N.V. Chukanov

O257 Columbite-(Mn) $MnNb_2O_6$ (Fig. 2.207)
Locality: Ploskaya Mt., Keivy massif, Kola peninsula, Murmansk region, Russia.
Description: Black crystal from the association with fergusonite-(Y), oxyplumbopyrochlore, and cerussite.
Kind of sample preparation and/or method of registration of the spectrum: KBr disc. Absorption.
Wavenumbers (cm^{-1}): 1100sh, 865sh, 833, 805, 702s, 627s, 557s, 511s, 370sh.

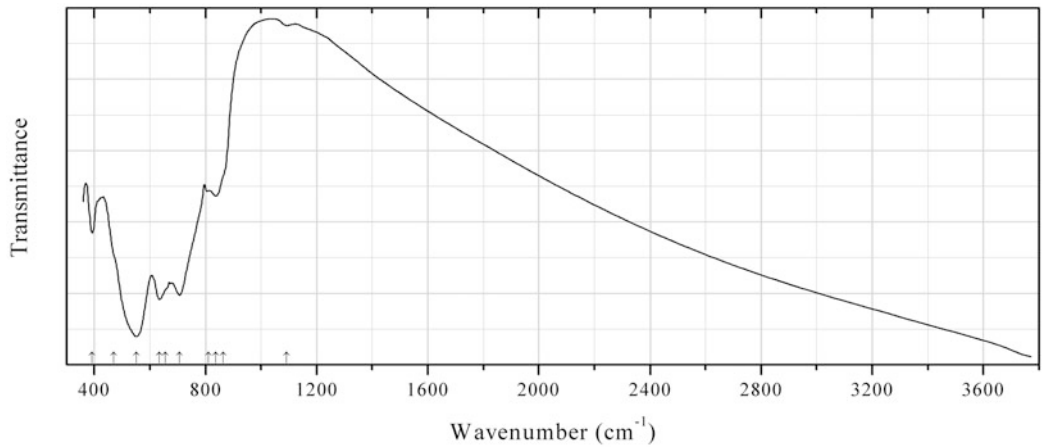

Fig. 2.208 IR spectrum of columbite-(Mg) obtained by N.V. Chukanov

O258 Columbite-(Mg) $MgNb_2O_6$ (Fig. 2.208)
Locality: Muzeinaya vein, Kukh-i Lal gem spinel deposit, Pyandzh River valley, Pamir Mts., Tajikistan (type locality).
Description: Black crystal with reddish-brown streak from the association with dravite and ilmenorutile.
Kind of sample preparation and/or method of registration of the spectrum: KBr disc. Absorption.
Wavenumbers (cm^{-1}): 1092w, 865sh, 838, 810, 707s, 655sh, 634s, 551s, 470sh, 393.

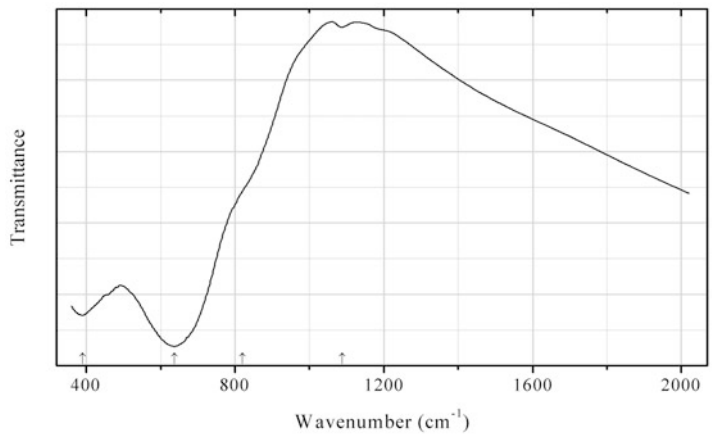

Fig. 2.209 IR spectrum of fergusonite-(Y) obtained by N.V. Chukanov

O259 Fergusonite-(Y) $YNbO_4$ (Fig. 2.209)
Locality: Rov Mt., Western Keivy massif, Kola peninsula, Murmansk region, Russia.
Description: Dark brown prismatic crystals in quartz. The empirical formula is (electron microprobe): $[(Y_{0.65}Yb_{0.09}Er_{0.04}Dy_{0.04})Ca_{0.08}U_{0.04}Fe_{0.03}Th_{0.01}]Nb_{0.99}Ta_{0.01}O_4$.
Kind of sample preparation and/or method of registration of the spectrum: KBr disc. Absorption.
Wavenumbers (cm^{-1}): 1088w, 820sh, 637s, 390s.

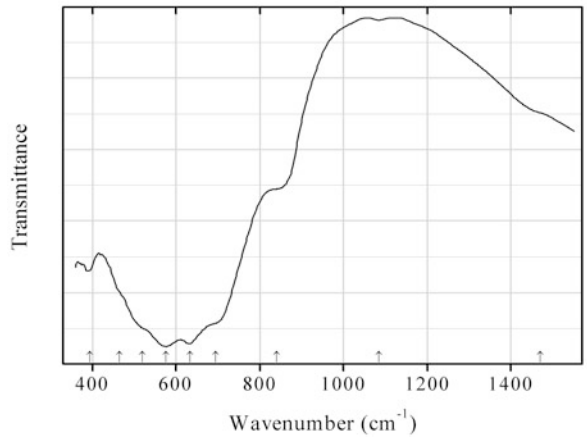

Fig. 2.210 IR spectrum of tantalite-(Fe) obtained by N.V. Chukanov

O260 Tantalite-(Fe) $Fe^{2+}Ta_2O_6$ (Fig. 2.210)
Locality: Lipovka mine, Lipovka pegmatite field, Rezh district, Middle Urals, Russia.
Description: Black grain with brown streak from the association with U-rich microlite, columbite-(Fe), andesine, calcite, dravite, magnesio-hornblende, and chrysoberyl. Investigated by I.V. Pekov. A Mg- and Nb-rich variety. The empirical formula is (electron microprobe): $(Fe_{0.53}Mg_{0.45}Mn_{0.03})(Ta_{1.16}Nb_{0.83}Ti_{0.01})O_6$.
Kind of sample preparation and/or method of registration of the spectrum: KBr disc. Absorption.
Wavenumbers (cm^{-1}): 1470sh, 1085w, 840sh, 695sh, 633s, 576s, 520sh, 465sh, 394.

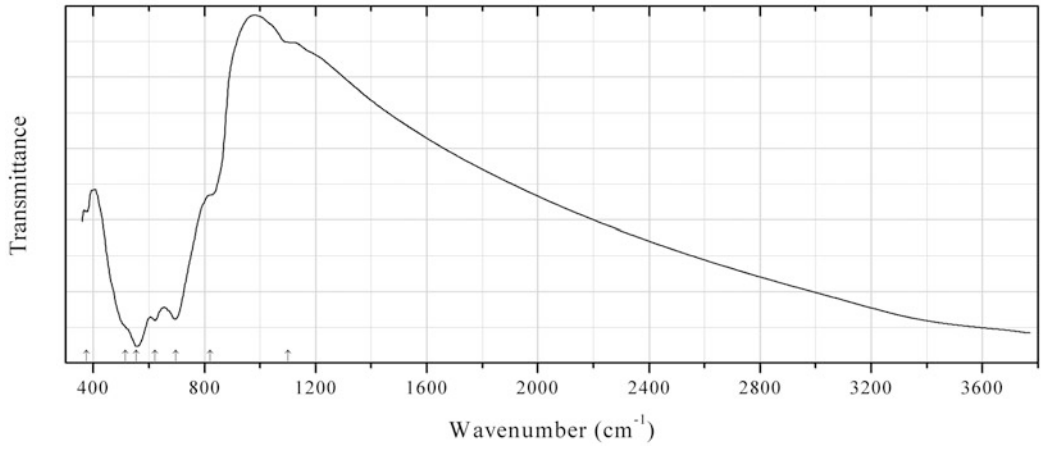

Fig. 2.211 IR spectrum of columbite-(Fe) obtained by N.V. Chukanov

O261 Columbite-(Fe) $Fe^{2+}Nb_2O_6$ (Fig. 2.211)
Locality: São José da Safira, Minas Gerais, Brazil.
Description: Black crystal with dark reddish-brown streak. The empirical formula is $(Fe_{0.76}Mn_{0.22}Mg_{0.02})(Nb_{1.65}Ta_{0.24}W_{0.04}Ti_{0.03}Fe_{0.03}Sn_{0.01})O_6$.
Kind of sample preparation and/or method of registration of the spectrum: KBr disc. Absorption.
Wavenumbers (cm^{-1}): 1100w, 820, 696s, 622s, 555s, 515sh, 375.

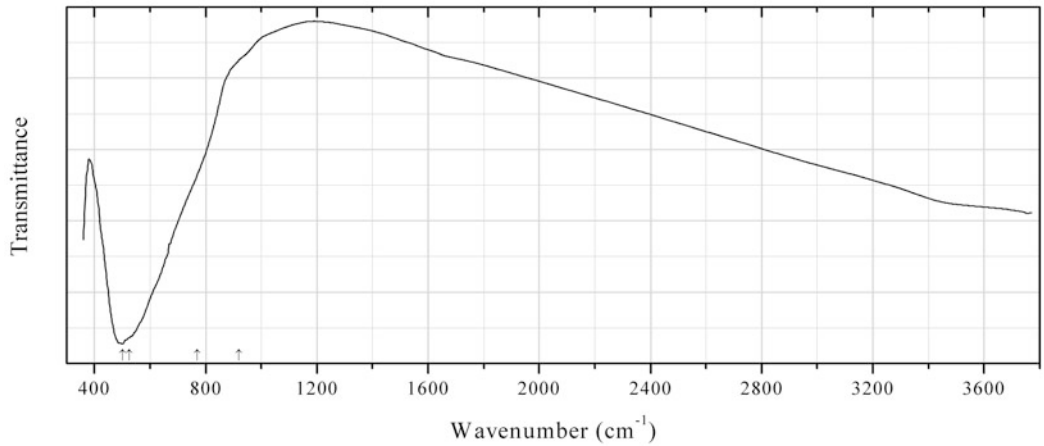

Fig. 2.212 IR spectrum of anatase obtained by N.V. Chukanov

O262 Anatase TiO_2 (Fig. 2.212)
Locality: Mogok, Myanmar.
Description: Dark blue pseudo-cubic crystal from a placer. The empirical formula is $Ti_{0.98}V_{0.01}Nb_{0.01}O_2$.
Kind of sample preparation and/or method of registration of the spectrum: KBr disc. Absorption.
Wavenumbers (cm^{-1}): 920sh, 770sh, 525sh, 501s.

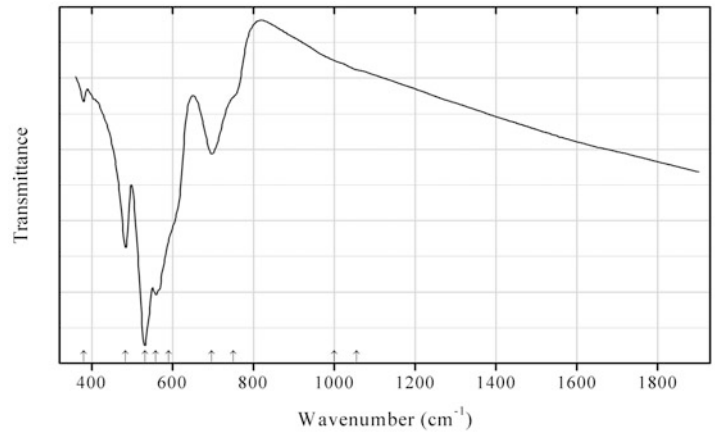

Fig. 2.213 IR spectrum of ramsdellite obtained by N.V. Chukanov

O263 Ramsdellite MnO_2 (Fig. 2.213)

Locality: Nesugata Mt., Shimoda, Sizuoka, Japan.
Description: Aggregate of black prismatic crystals filling a crack in rhyolite. Confirmed by the IR spectrum.
Kind of sample preparation and/or method of registration of the spectrum: KBr disc. Absorption.
Wavenumbers (cm^{-1}): (3330w), 1055sh, 1000sh, 750sh, 697, 590sh, 559s, 531s, 484, 380.

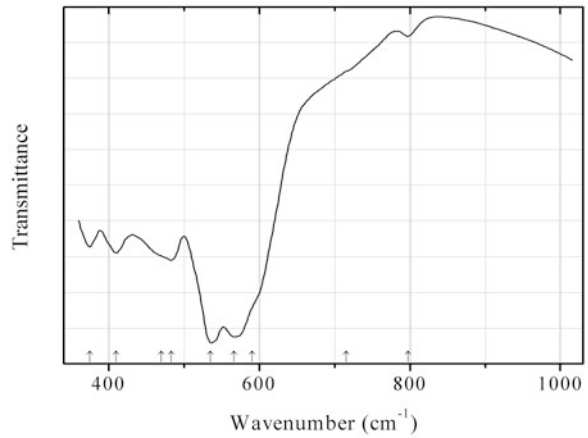

Fig. 2.214 IR spectrum of strontiomelane obtained by N.V. Chukanov

O264 Strontiomelane $SrMn^{3+}{}_2Mn^{4+}{}_6O_{16}$ (Fig. 2.214)
Locality: Kangan Kunde Hill, Zomba, Malawi.
Description: Black (with dark brown streak) massive from the association with carbonates. The empirical formula is (electron microprobe): $(Sr_{0.51}Ba_{0.42}K_{0.18})(Mn_{7.54}Fe_{0.26}Mg_{0.12}Al_{0.08})O_{16}$.
Kind of sample preparation and/or method of registration of the spectrum: KBr disc. Absorption.
Wavenumbers (cm^{-1}): 798w, (715sh), 590sh, 566s, 535s, 483, 470sh, 410, 375.

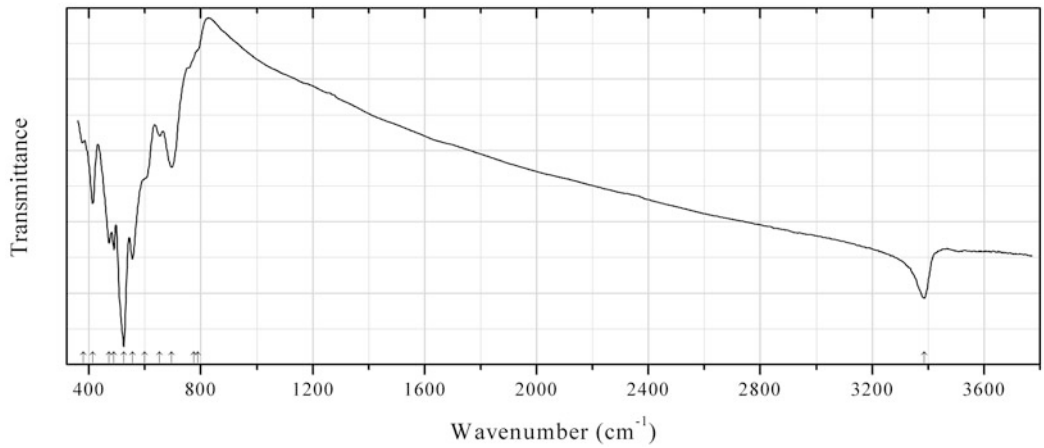

Fig. 2.215 IR spectrum of "groutellite" obtained by N.V. Chukanov

O266 "Groutellite" $Mn^{3+}{}_{0.5}Mn^{4+}{}_{0.5}O_{1.5}(OH)_{0.5}$ (Fig. 2.215)
Locality: El'vor (El'vorskoe) deposit, Göygöl (Hanlar) district, Azerbaijan.

Description: Black (with black streak) radial aggregate. Intermediate member of the series groutite–ramsdellite. Confirmed by powder X-ray diffraction data and IR spectrum.
Kind of sample preparation and/or method of registration of the spectrum: KBr disc. Absorption.
Wavenumbers (cm^{-1}): 3387, 790sh, 775sh, 695, 653w, 600sh, 555s, 524s, 489s, 472s, 413, 379w.

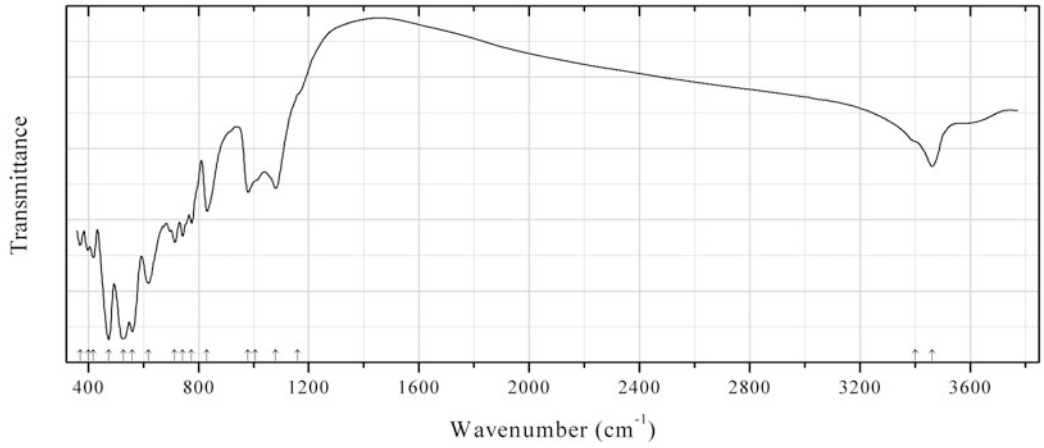

Fig. 2.216 IR spectrum of zinconigerite-2*N*1S obtained by N.V. Chukanov

O267 Zinconigerite-2*N*1*S* $(Al,Zn,Fe)_2(Al,Sn)_6O_{11}(OH)$ (Fig. 2.216)
Locality: Uis, Erongo region, Usakos district, Namibia.
Description: Yellowish brown tabular crystal from the association with quartz, feldspar, and muscovite. The empirical formula is (electron microprobe): $(Al_{0.8}Zn_{0.7}Fe_{0.5})(Al_{5.0}Sn_{0.95}Ti_{0.05})(O,OH)_{12}$.
Kind of sample preparation and/or method of registration of the spectrum: KBr disc. Absorption.
Wavenumbers (cm^{-1}): 3463, 3400sh, 1160sh, 1080, 1005sh, 979, 831, 775, 742, 714, 619, 560s, 528s, 474s, 418, 401, 372.

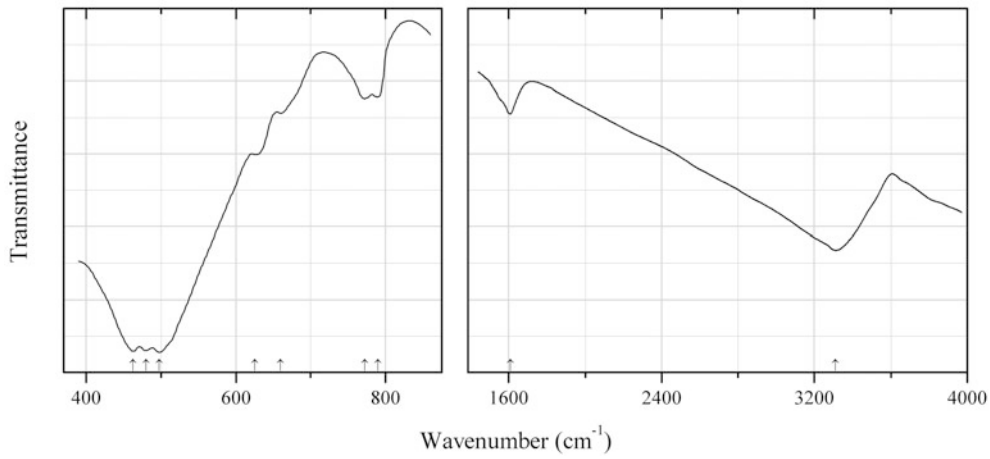

Fig. 2.217 IR spectrum of asbolane obtained by N.V. Chukanov

O268 Asbolane $(Co,Ni,Mg,Ca)_xMn^{4+}O_2(OH)_{2x}\cdot nH_2O$ (Fig. 2.217)

Locality: Lipovka mine, Lipovka pegmatite field, Rezh district, Middle Urals, Russia.
Description: The ratio NiO:CoO:CaO:MnO_2 is 11.42:6.91:1.60:46.91.
Kind of sample preparation and/or method of registration of the spectrum: KBr disc. Absorption.
Wavenumbers (cm^{-1}): 3310, 1608, (790), (772), 660sh, 625sh, 498s, 480s, 463s.
Note: For the IR spectrum of asbolane see also Chukhrov et al. (1980).

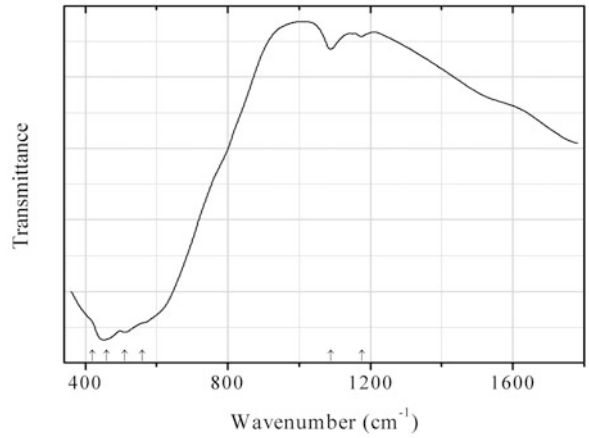

Fig. 2.218 IR spectrum of zirconolite obtained by N.V. Chukanov

O269 Zirconolite (Ca,Y,*REE*)Zr(Ti,Fe,Nb)$_2O_7$ (Fig. 2.218)
Locality: Håkestad quarry, Håkestad, Tjølling, Larvik, Vestfold, Norway.
Description: Dark brown long-prismatic crystal from the association with feldspar, hastingsite, biotite, apatite, zircon, and ilmenite. Amorphous, metamict. The empirical formula is (electron microprobe): $(Ca_{1.1}Ce_{0.4}Nd_{0.2}La_{0.1}Th_{0.2})Zr_{2.0}(Ti_{1.7}Fe_{1.2}Nb_{1.0}Mg_{0.1})$.
Kind of sample preparation and/or method of registration of the spectrum: KBr disc. Absorption.
Wavenumbers (cm^{-1}): 1175w, 1088w, 560sh, 510s, 459s, 420sh.

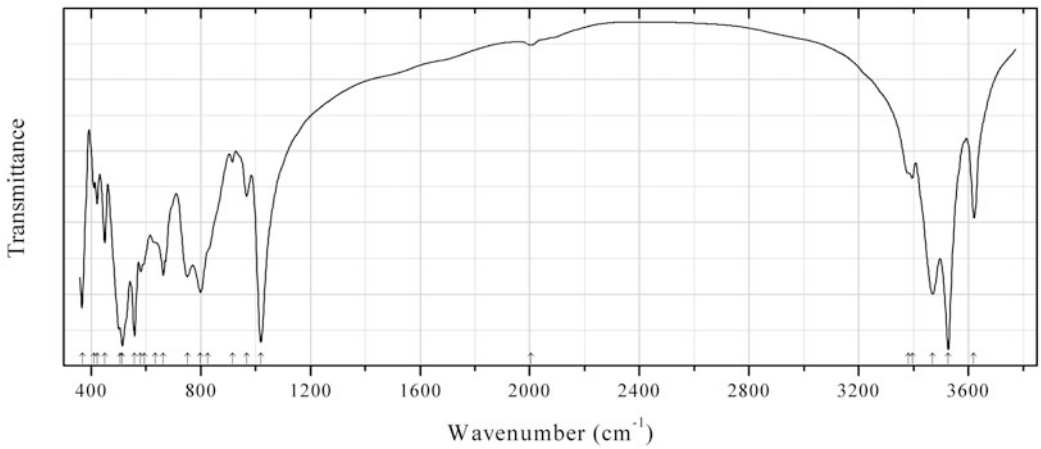

Fig. 2.219 IR spectrum of gibbsite obtained by N.V. Chukanov

O270 Gibbsite $Al(OH)_3$ (Fig. 2.219)

Locality: Marchenko peak, Kukisvumchorr Mt., Khibiny alkaline complex, Kola peninsula, Murmansk region, Russia.
Description: Colourless platy crystals with perfect cleavage from the association with pitiglianoite and amicite. Identified by IR spectrum.
Kind of sample preparation and/or method of registration of the spectrum: KBr disc. Absorption.
Wavenumbers (cm^{-1}): 3620, 3526s, 3470s, 3395, 3380, 2005w, 1019s, 967, 915w, 825sh, 799s, 751, 664, 635sh, 595sh, 581, 558s, 514s, 505sh, 450, 422, 410w, 368s.

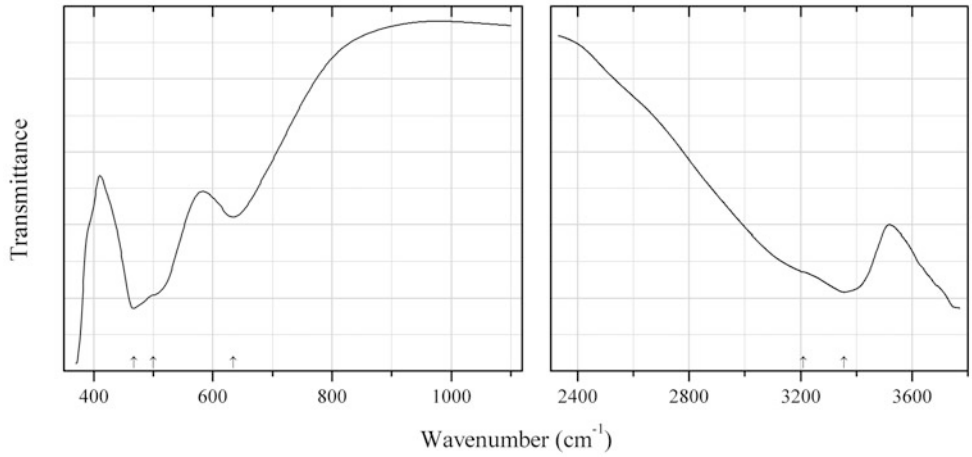

Fig. 2.220 IR spectrum of corvusite obtained by N.V. Chukanov

O271 Corvusite $(Na,Ca,K)_{1-x}(V^{5+},V^{4+},Fe)_8O_{20}\cdot 4H_2O$ (Fig. 2.220)
Locality: U deposit Srednyaya Padma, Zaonezhskii peninsula, Onega sea, Karelia, Russia.
Description: Black crust on chromceladonite-dolomite aggregate.
Kind of sample preparation and/or method of registration of the spectrum: KBr disc. Absorption.
Wavenumbers (cm^{-1}): 3356s, 3210sh, 634, 500sh, 467s.

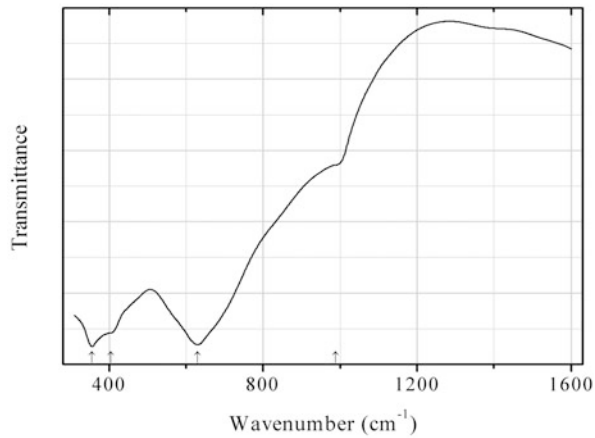

Fig. 2.221 IR spectrum of yttrotantalite-(Y) obtained by N.V. Chukanov

O272 Yttrotantalite-(Y) $YTaO_4$ (Fig. 2.221)

Locality: Ytterby, Resarö, Vaxholm, Uppland, Sweden (type locality).
Description: Brownish black anhedral grains. Amorphous, metamict. The empirical formula is (electron microprobe): $[(Y_{0.67}Yb_{0.06}Dy_{0.02}Er_{0.02}Sm_{0.01}Gd_{0.01})Ca_{0.21}Sr_{0.05}U_{0.02}](Ta_{0.56}Nb_{0.32}Fe_{0.03}Ti_{0.02}Mg_{0.02})(O,OH)_4$.
Kind of sample preparation and/or method of registration of the spectrum: KBr disc. Absorption.
Wavenumbers (cm^{-1}): 989sh, 630s, 405sh, 355s.

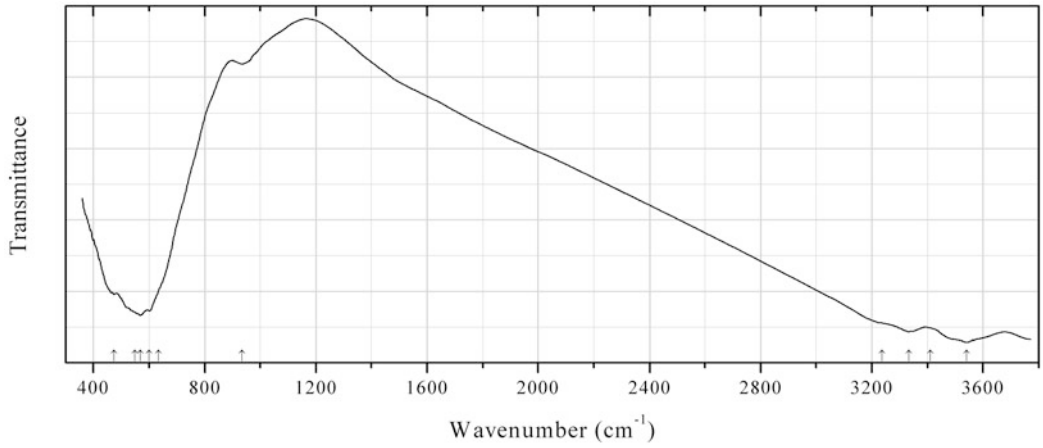

Fig. 2.222 IR spectrum of lucasite-(Ce) obtained by N.V. Chukanov

O273 Lucasite-(Ce) $CeTi_2O_5(OH)$ (Fig. 2.222)
Locality: Koashva Mt., Khibiny alkaline complex, Kola peninsula, Murmansk region, Russia.
Description: Brown spherulites from the association with pyrophanite, ivanyukite-K, lamprophyllite, aegirine, and microcline. Investigated by I.V. Pekov. The empirical formula is (electron microprobe): $(Ce_{0.36}Ca_{0.25}La_{0.14}Nd_{0.11}Mn_{0.08}Th_{0.03}Pr_{0.02})(Ti_{1.87}Nb_{0.15}Fe_{0.06})O_5(OH)$. The strongest lines of the powder X-ray diffraction pattern [*d*, Å (*I*, %)] are: 3.37 (100), 3.26 (70). 3.19 (100), 2.78 (40), 2.57 (30), 2.21 (30).
Kind of sample preparation and/or method of registration of the spectrum: KBr disc. Absorption.
Wavenumbers (cm^{-1}): 3540, 3410sh, 3332, 3235sh, 935w, 635sh, 601s, 568s, 550sh, 475s.

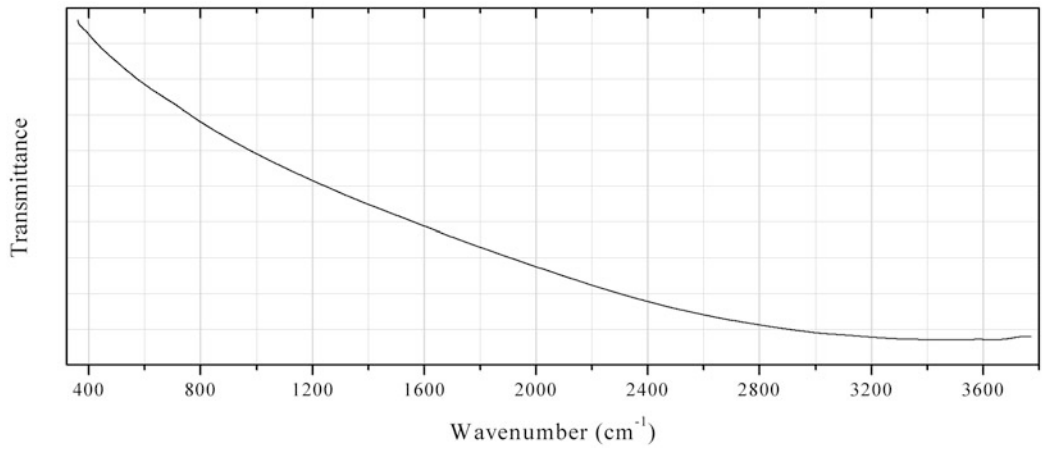

Fig. 2.223 IR spectrum of plattnerite obtained by N.V. Chukanov

O274 Plattnerite PbO_2 (Fig. 2.223)
Locality: Mina Ojuela (Ojuela mine), Mapimi, Durango, Mexico.
Description: Black tabular crystals.
Kind of sample preparation and/or method of registration of the spectrum: KBr disc. Absorption.
Wavenumbers (cm^{-1}): No absorption bands are observed in the range from 360 to 4000 cm^{-1}.

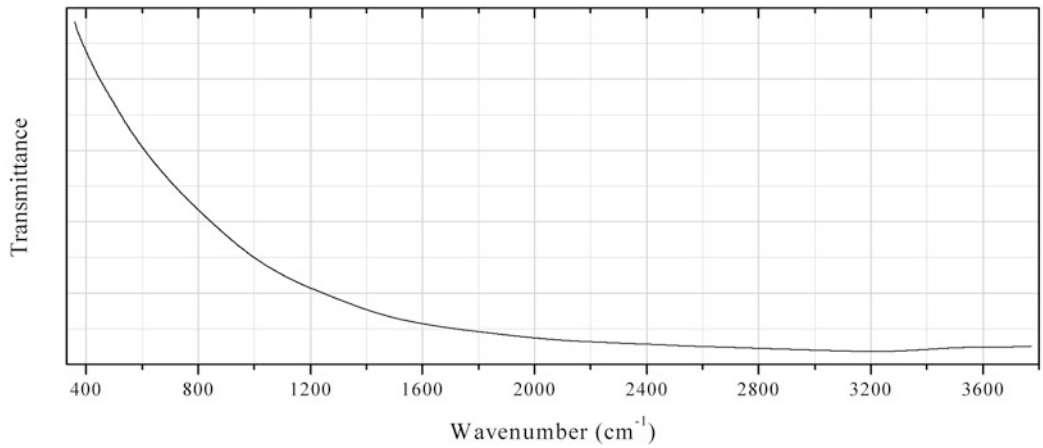

Fig. 2.224 IR spectrum of murdochite obtained by N.V. Chukanov

O275 Murdochite $Cu_{12}Pb_2(O_{15}\square_3)Cl_2$ (Fig. 2.224)
Locality: Mammoth mine, Tiger, Pinal Co., Arizona, USA (type locality).
Description: Black cubic crystals. The empirical formula is (electron microprobe): $Cu_{11.70}Al_{0.26}Fe_{0.14}Pb_{1.88}O_{18-x}Cl_{2.02}$.
Kind of sample preparation and/or method of registration of the spectrum: KBr disc. Absorption.
Wavenumbers (cm^{-1}): No bands are observed above 360 cm^{-1}.

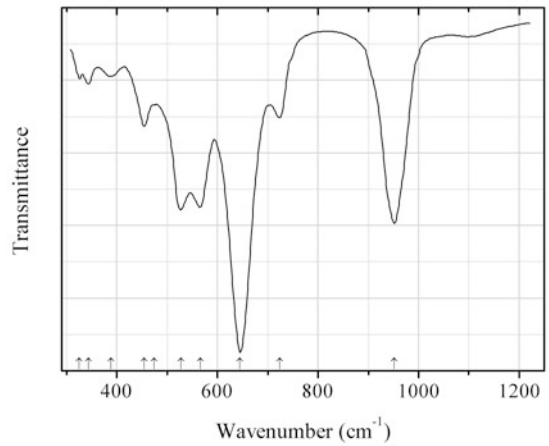

Fig. 2.225 IR spectrum of abswurmbachite drawn using data from Reinecke et al. (1991)

O276 Abswurmbachite $Cu^{2+}Mn^{3+}{}_6O_8(SiO_4)$ (Fig. 2.225)
Locality: Synthetic.

Description: Tetragonal, a = 9.409(1), c = 18.552(1) Å. The empirical formula is: $Cu_{0.98}Mn_{6.02}O_8(SiO_4)$. The strongest lines of the powder X-ray diffraction pattern [d, Å (I, %) (hkl)] are: 3.475 (9) (123), 2.702 (100) (224), 2.350 (15) (040), 2.133 (15) (235), 1.6627 (10) (440), 1.6507 (30) (048), 1.4159 (14) (264), 1.4016 (11) (2.2.12).
Kind of sample preparation and/or method of registration of the spectrum: RbI disc, absorption.
Source: Reinecke et al. (1991).
Wavenumbers (cm^{-1}): (only those indicated by Reinecke et al. 1991): 952s, 724, 645s, 566s, 527s, 474w, 454, 388w, 344w, 325w.

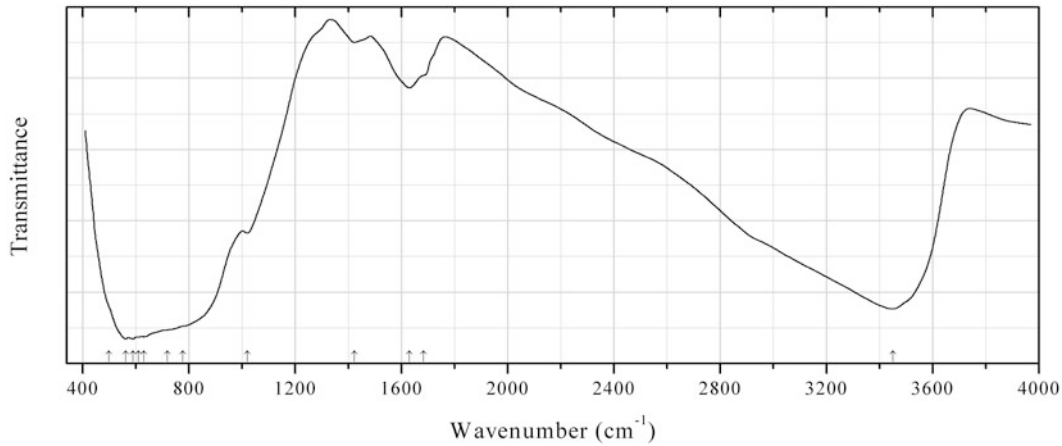

Fig. 2.226 IR spectrum of "tohdite" drawn using data from Tilley and Eggleton (1996)

O277 "Tohdite" $5Al_2O_3 \cdot H_2O$ (Fig. 2.226)
Locality: Weipa, Cape York peninsula, Northern Australia.
Description: Soft pisolith from bauxite, from the association with gibbsite, boehmite, quartz, hematite, kaolinite, and anatase. Analogue of synthetic "tohdite". Possibly related to akdalaite. Hexagonal, a = 5.555, c = 8.968 Å. The strongest lines of the powder X-ray difraction pattern [d, Å (I, %) (hkl)] are: 3.33 (50) (102), 2.82 (40) (110), 2.53 (60) (103), 2.37 (65) (200, 112, 201), 2.12 (75) (202), 1.89 (40) (203), 1.41 (55) (205), 1.39 (100) (220).
Kind of sample preparation and/or method of registration of the spectrum: Transmission.
Source: Tilley and Eggleton (1996).
Wavenumbers (cm^{-1}): 3450s, 1685sh, 1630, 1424w, 1020, 778sh, 719sh, 630s, 610s, 590s, 563s, 500sh.
Note: The wavenumbers were partly determined by us based on spectral curve analysis of the published spectrum.

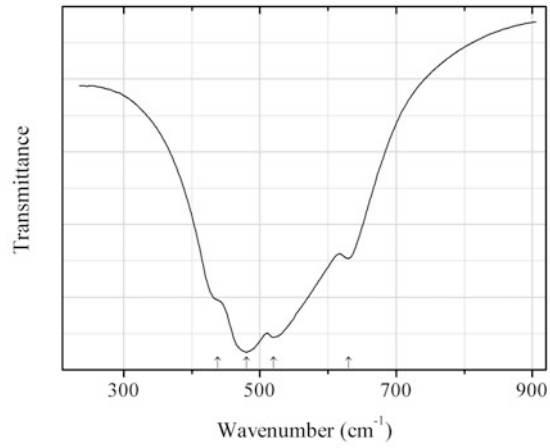

Fig. 2.227 IR spectrum of allendeite drawn using data from Lopato et al. (1992)

O278 Allendeite $Sc_4Zr_3O_{12}$ (Fig. 2.227)
Locality: Synthetic.
Description: Confirmed by powder X-ray diffraction data.
Kind of sample preparation and/or method of registration of the spectrum: Suspension in mineral oil. Absorption.
Source: Lopato et al. (1992).
Wavenumbers (cm^{-1}): 630, 520s, 480s, 438.

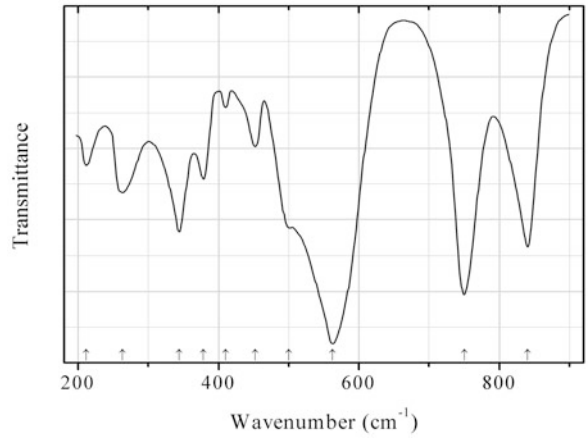

Fig. 2.228 IR spectrum of alumotantite drawn using data from Povarennykh (1981b)

O279 Alumotantite $AlTaO_4$ (Fig. 2.228)
Locality: Synthetic.
Description: No data.
Kind of sample preparation and/or method of registration of the spectrum: KBr disc. Absorption.
Source: Povarennykh (1981b).
Wavenumbers (cm^{-1}): 984, 840s, 750s, 562s, 500, 452, 410w, 378, 344, 263, 212.

Note: In the paper cited (Povarennykh 1981b) the band at 984 cm^{-1} is not shown in the figure of the spectrum. It is given only in tabulated data.

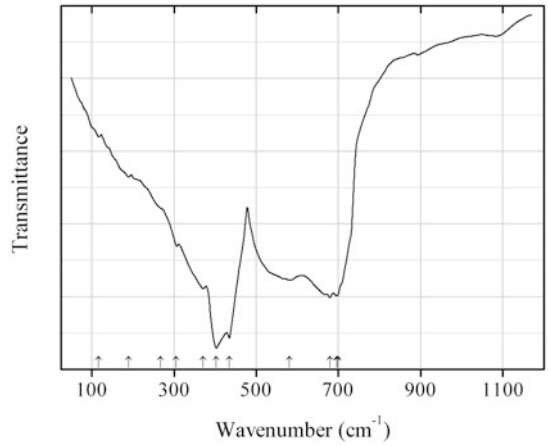

Fig. 2.229 IR spectrum of argutite drawn using data from Madon et al. (1991)

O280 Argutite GeO_2 (Fig. 2.229)
Locality: Synthetic.
Description: Confirmed by powder X-ray diffraction pattern.
Kind of sample preparation and/or method of registration of the spectrum: CsI disc (mid IR region) and suspension in paraffin (far IR region). Absorption.
Source: Madon et al. (1991).
Wavenumbers (cm^{-1}): 700sh, 696, 679, 580, 435s, 403s, 371, 305, 267sh, 190w, 117w.
Note: The wavenumbers were partly determined by us based on spectral curve analysis of the published spectrum.

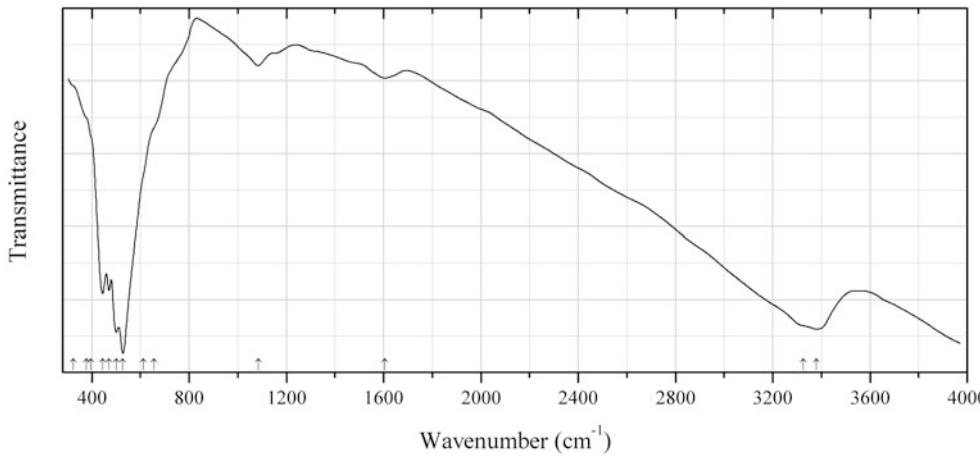

Fig. 2.230 IR spectrum of aurorite drawn using data from Potter and Rossman (1979a)

O281 Aurorite $(Mn^{2+},Ag,Ca)Mn^{4+}{}_3O_7 \cdot 3H_2O$ (Fig. 2.230)

Locality: 56 km south of San Felipe, Baja California, Mexico.
Description: The strongest lines of the powder X-ray diffraction pattern [*d*, Å (*I*, %)] are: 6.94 (100), 4.06 (50), 3.46 (70), 2.54 (50), 2.23 (50), 1.56 (50), 1.43 (50).
Kind of sample preparation and/or method of registration of the spectrum: Absorption. Kind of sample preparation is not indicated.
Source: Potter and Rossman (1979a).
Wavenumbers (cm^{-1}): 3380, 3325sh, 1605, 1085, 656sh, 612sh, 528s, 500s, 471s, 444s, 397sh, 378sh, 324sh.
Note: The wavenumbers were determined by us based on spectral curve analysis of the published spectrum.

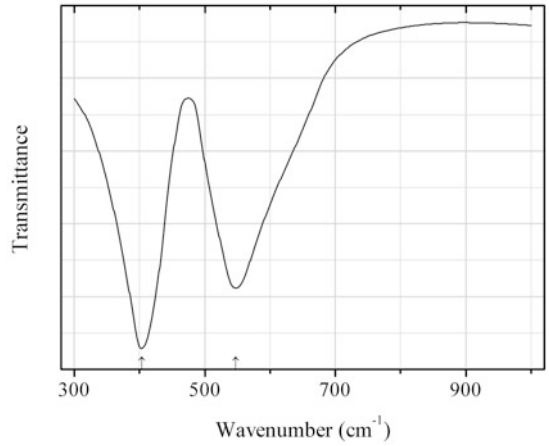

Fig. 2.231 IR spectrum of barioperovskite drawn using data from Last (1957)

O282 Barioperovskite $BaTiO_3$ (Fig. 2.231)
Locality: Synthetic.
Description: Presumably tetragonal or pseudotetrahonal orthorhombic.
Kind of sample preparation and/or method of registration of the spectrum: KBr disc. Transmission.
Source: Last (1957).
Wavenumbers (cm^{-1}): 547, 404s.
Note: The wavenumbers were determined by us based on spectral curve analysis of the published spectrum. IR spectra of different $BaTiO_3$ polymorphs in the range of wavenumbers from 450 to 800 cm^{-1} and in the temperature interval from −190 to 130 °C are also given by Last (1957).

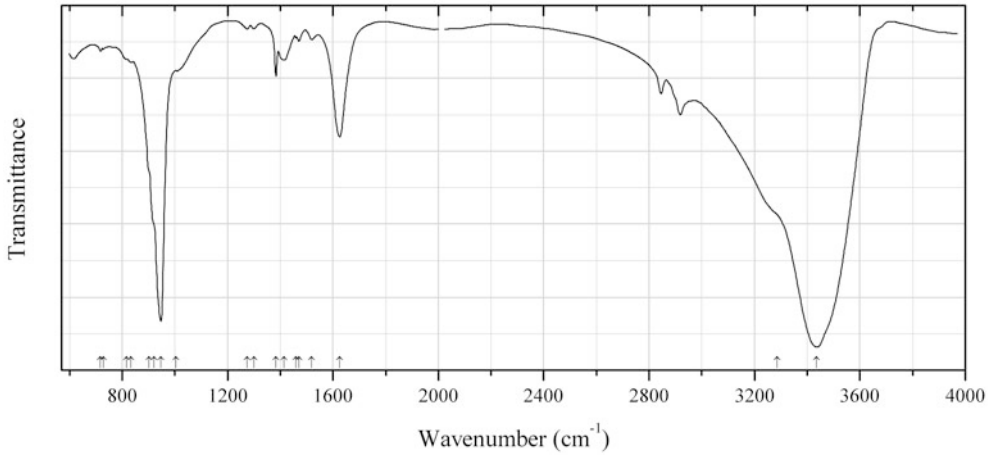

Fig. 2.232 IR spectrum of becquerelite drawn using data from Amayri et al. (2004)

O284 Becquerelite $Ca(UO_2)_6O_4(OH)_6 \cdot 8H_2O$ (Fig. 2.232)
Locality: Synthetic.
Description: Yellow powder. Synthesized by stoichiometric mixing of uranyl nitrate solution and calcium nitrate solution at room temperature. Identified by powder X-ray diffraction data.
Kind of sample preparation and/or method of registration of the spectrum: KBr disc. Transmission.
Source: Amayri et al. (2004).
Wavenumbers (cm^{-1}): 3436s, 3285sh, 1626, 1520, 1471, 1459, 1415w, 1384w, 1300w, 1275w, 1004sh, 946s, 920sh, 902sh, 834, (817), 728, 717.
Note: The wavenumbers were partly determined by us based on spectral curve analysis of the published spectrum. Weak bands in the range from 2800 to 3000 cm^{-1} correspond to the impurity of grease. The small peak at 1384 cm^{-1} may be due to the impurity of a nitrate in the KBr medium. For IR spectrum of becquerelite see also Čejka and Urbanec (1990).

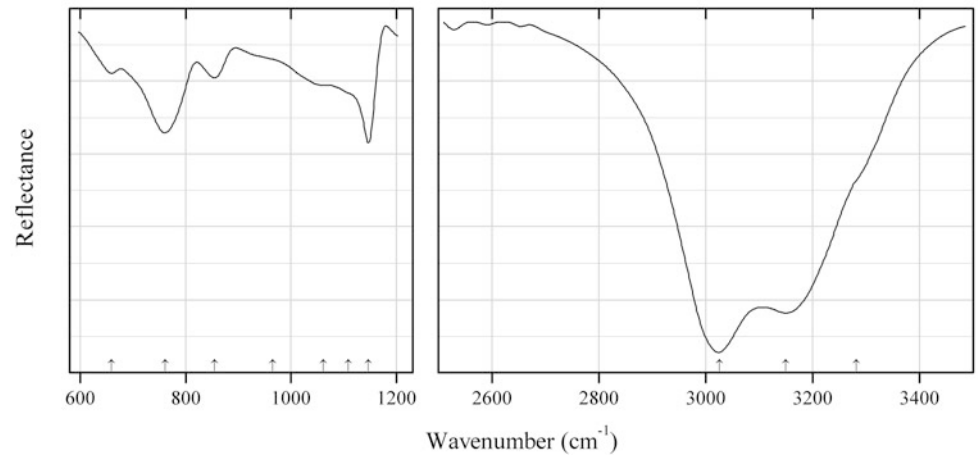

Fig. 2.233 IR spectrum of bernalite drawn using data from McCammon et al. (1995)

O285 Bernalite $Fe(OH)_3$ (Fig. 2.233)

Locality: Broken Hill deposit, Yancowinna Co., New South Wales, Australia (type locality).
Description: Polysynthetically twinned crystals from the association with goethite and coronadite. Cotype sample.
Kind of sample preparation and/or method of registration of the spectrum: Thin section. Reflection.
Source: McCammon et al. (1995).
Wavenumbers (cm^{-1}): 3281sh, 3150s, 3026s, 1147, 1109sh, 1062, 965sh, 855, 761, 660.
Note: The wavenumbers were partly determined by us based on spectral curve analysis of the published spectrum.

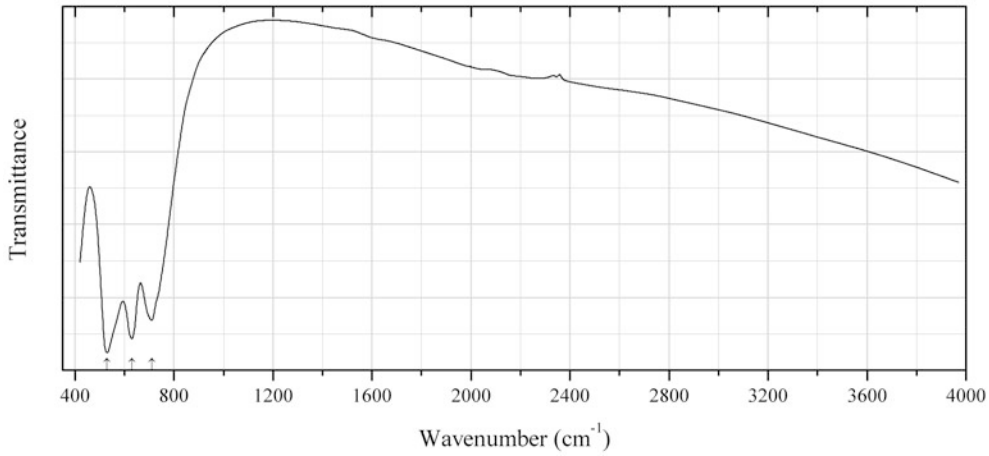

Fig. 2.234 IR spectrum of billwiseite drawn using data from Hawthorne et al. (2012a)

O286 Billwiseite $Sb^{3+}{}_5Nb_3WO_{18}$ (Fig. 2.234)
Locality: Stak Dala pegmatite, Nanga Parbat–Haramosh massif, near Stak Nala, 70 km east of Gilgit, Pakistan (type locality).
Description: Pale yellow crystals from the association with albite, quartz, potassic feldspar, tourmaline, mica, topaz, and fluorite. Holotype sample. Monoclinic, space group $C2/c$, a = 54.116(5), b = 4.9143(5), c = 5.5482(5) Å, β = 90.425(2)°, V = 1475.5(2) $Å^3$, Z = 4. D_{calc} = 6.330 g/cm^3. Optically biaxial, 2 V = 76(2)°. The empirical formula is $Sb^{3+}{}_{4.87}(Nb_{1.33}Ta_{1.28}Ti_{0.18})W_{1.26}O_{18}$. The strongest lines of the powder X-ray diffraction pattern [d, Å (I, %)] are: 3.147 (100), 3.500 (55), 1.662 (53), 3.017 (48), 1.906 (47), 1.735 (30), 1.762 (25).
Kind of sample preparation and/or method of registration of the spectrum: Not indicated.
Source: Hawthorne et al. (2012a).
Wavenumbers (cm^{-1}): 710, 630s, 530s.

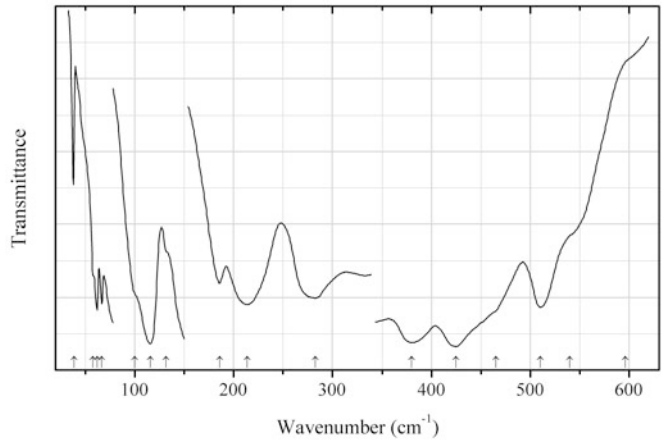

Fig. 2.235 IR spectrum of bismite drawn using data from Betsch and White (1978)

O287 Bismite Bi_2O_3 (Fig. 2.235)
Locality: Synthetic.
Kind of sample preparation and/or method of registration of the spectrum: Suspension in mineral oil (Nujol) deposited on polyethylene slab. Transmission.
Source: Betsch and White (1978).
Wavenumbers (cm^{-1}): 596sh, 540sh, 510, 465sh, 425s, 380s, 283, 214, 186, 132sh, 116, 100sh, 67, 62, 58, 39.
Note: For the IR spectrum of bismite see also Narang et al. (1994).

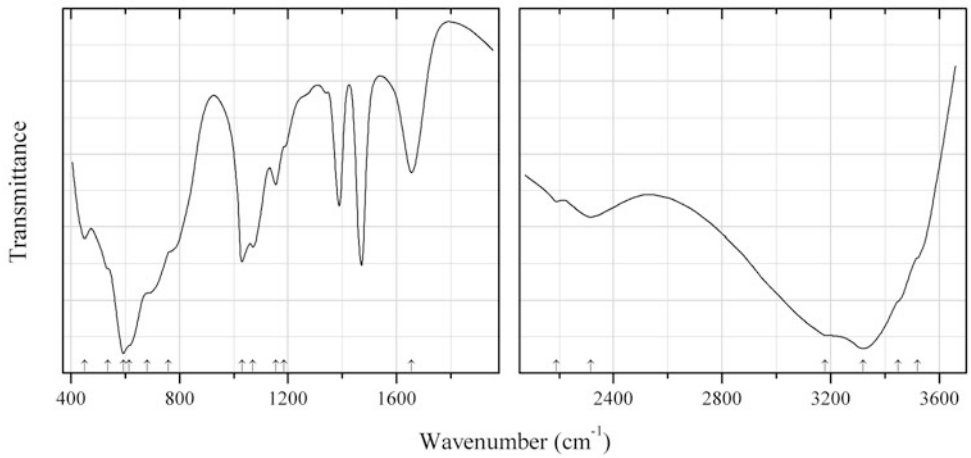

Fig. 2.236 IR spectrum of brandholzite drawn using data from Balicheva and Roi (1971)

O288 Brandholzite $MgSb_2(OH)_{12}\cdot 6H_2O$ (Fig. 2.236)
Locality: Synthetic.
Description: Confirmed by chemical analysis and thermogravimetric data.
Kind of sample preparation and/or method of registration of the spectrum: Suspensions in mineral oil (below 2000 cm^{-1}) and in fluorinated mineral oil (above 2000 cm^{-1}). Absorption.

Source: Balicheva and Roi (1971).
Wavenumbers (cm^{-1}): 3520sh, 3450sh, 3320s, 3180sh, 2315w, 2190w, 1655, 1185sh, 1155, 1070, 1030, 760sh, 680, 615sh, 593s, 535sh, 450.
Note: Stong bands in the range from 1300 to 1500 cm^{-1} correspond to mineral oil.

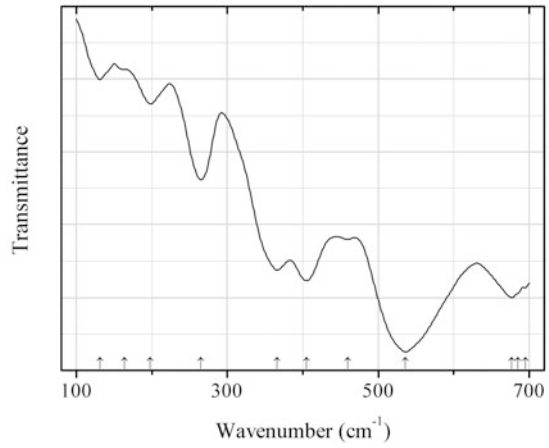

Fig. 2.237 IR spectrum of thorutite drawn using data from Zhang et al. (2011a)

O289 Thorutite $ThTi_2O_6$ (Fig. 2.237)
Locality: Synthetic.
Description: Confirmed by powder X-ray diffraction data. Monoclinic, a = 9.646(5), b = 3.785(2), c = 6.951(3) Å, β = 118.18(3)°.
Kind of sample preparation and/or method of registration of the spectrum: Suspension in mineral oil. Absorption.
Source: Zhang et al. (2011a).
Wavenumbers (cm^{-1}): 695w, 685sh, 677s, 536s, 460, 405s, 366, 265, 198, 164sh, 131w.
Note: The wavenumbers were determined by us based on spectral curve analysis of the published spectrum.

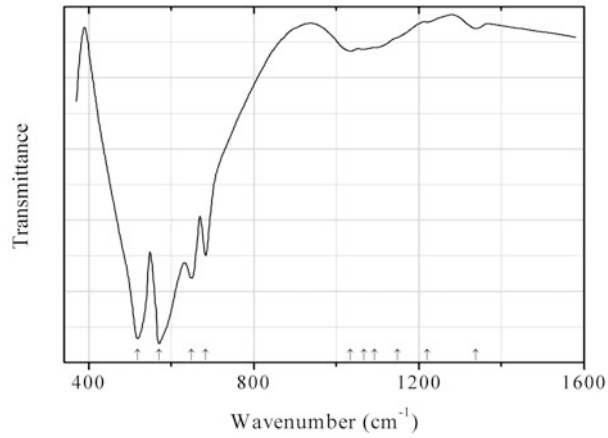

Fig. 2.238 IR spectrum of brizziite drawn using data from Olmi and Sabelli (1994)

O290 Brizziite $NaSbO_3$ (Fig. 2.238)
Locality: Le Cetine mine, Chiusdino, Siena province, Tuscany, Italy (type locality).
Description: White aggregates of platy crystals from the association with stibiconite and mopungite. Holotype sample. The crystal structure is solved. Hexagonal, space group *R*-3, a = 5.301(1), c = 15.932(4) Å, Z = 6. D_{meas} = 4.8(2) g/cm^3, D_{calc} = 4.95 g/cm^3. Optically uniaxial (−), ε = 1.631(1), ω ≈ 1.84. Electron microprobe analyses give Na_2O 15.98 and Sb_2O_5 83.28 wt%, corresponding to the formula $NaSbO_3$. The strongest lines of the powder X-ray diffraction pattern [*d*, Å (*I*, %) (*hkl*)] are: 5.30 (53) (003), 3.00 (55) (104), 2.650 (67) (006, 110), 2.365 (69) (113), 1.874 (100) (116), 1.471 (69) (119, 303).
Kind of sample preparation and/or method of registration of the spectrum: KBr microdisc. Transmission.
Source: Olmi and Sabelli (1994).
Wavenumbers (cm^{-1}): 1338, 1220, 1148sh, 1092sh, 1066, 1034, 683, 648, 570s, 518s.
Note: The wavenumbers were partly determined by us based on spectral curve analysis of the published spectrum.

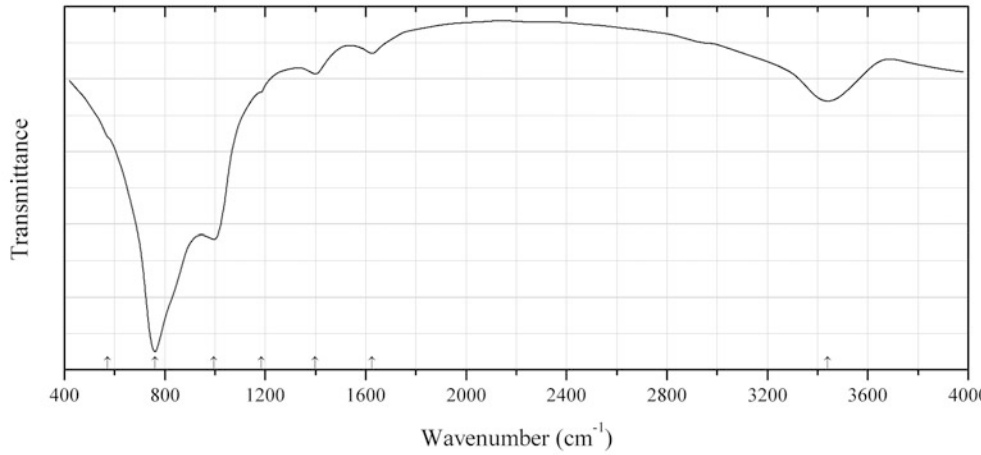

Fig. 2.239 IR spectrum of bromellite drawn using data from Larsen et al. (1987)

O291 Bromellite BeO (Fig. 2.239)
Locality: Saga larvikite quarry, Mørje, Porsgrunn, southern Oslo region, Norway.
Description: White platy crystals from the association with natrolite, diaspore, and chamosite. Hexagonal, space group $P6_3mc$, a = 2.697(4), c = 4.372(4) Å, V = 27.54(6) Å^3. A chemical analysis gave (in wt%): SiO_2 0.7, B_2O_3 1.4, Al_2O_3 1.2, Fe_2O_3 0.1, BeO 93.2, CaO 0.1, H_2O 3.4, total 100.1.
Kind of sample preparation and/or method of registration of the spectrum: KBr disc. Transmission.
Source: Larsen et al. (1987).
Wavenumbers (cm^{-1}): 3440, 1625w, 1398w, 1184sh, 995s, 761s, 573sh.
Note: For IR spectrum of bromellite see also Hofmeister et al. (1987).

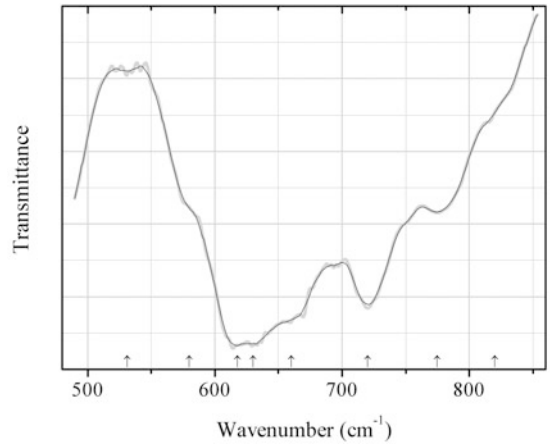

Fig. 2.240 IR spectrum of brownmillerite drawn using data from Puertas et al. (1990)

O292 Brownmillerite $Ca_2(Al,Fe^{3+})_2O_5$ (Fig. 2.240)
Locality: Synthetic.
Description: The empirical formula is $Ca_4(Al_{2.00}Fe_{1.71}Mn_{0.29})O_{10}$. Confirmed by powder X-ray diffraction data.
Kind of sample preparation and/or method of registration of the spectrum: Transmission. Kind of sample preparation is not indicated.
Source: Puertas et al. (1990).
Wavenumbers (cm^{-1}): 820sh, 775, 720s, 660sh, 630sh, 618s, 580sh, 531w.
Note: The wavenumbers were determined by us based on spectral curve analysis of the published spectrum.

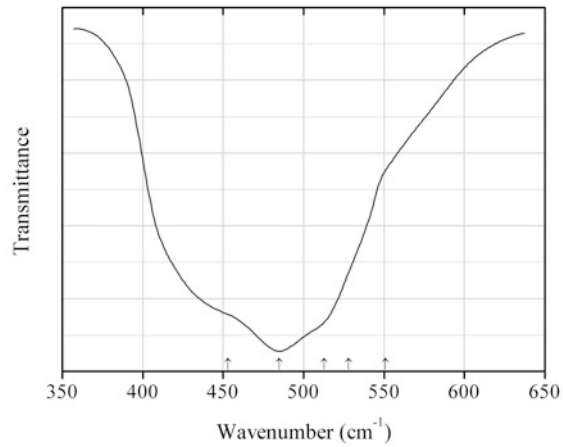

Fig. 2.241 IR spectrum of bunsenite drawn using data from Hunt et al. (1973)

O293 Bunsenite NiO (Fig. 2.241)
Locality: Synthetic.
Description: Nanocrystalline aggregate.

Kind of sample preparation and/or method of registration of the spectrum: Powder dispersed in polyethylene. Absorption.
Source: Hunt et al. (1973).
Wavenumbers (cm^{-1}): 551sh, 528sh, 513sh, 485s, 453sh.
Note: The wavenumbers were partly determined by us based on spectral curve analysis of the published spectrum. According to Peng and Liu, 1982, wavenumbers of IR absorption bands for bunsenite are: 560sh, 445s, 390sh.

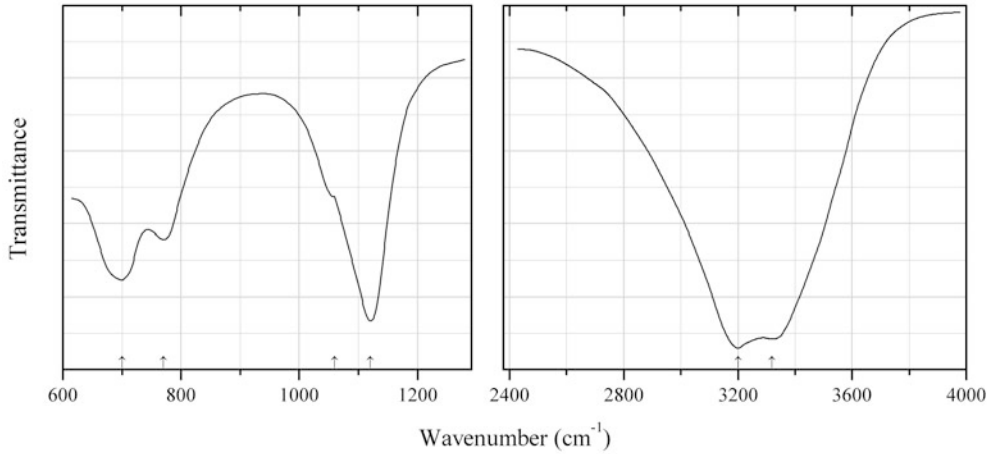

Fig. 2.242 IR spectrum of burtite drawn using data from Cohen-Addad (1968)

O294 Burtite $CaSn^{4+}(OH)_6$ (Fig. 2.242)
Locality: Synthetic.
Description: The crystal structure is solved.
Kind of sample preparation and/or method of registration of the spectrum: KBr disc. Transmission.
Source: Cohen-Addad (1968).
Wavenumbers (cm^{-1}): 3320s, 3200s, 1120s, 1060sh, 770, 700.

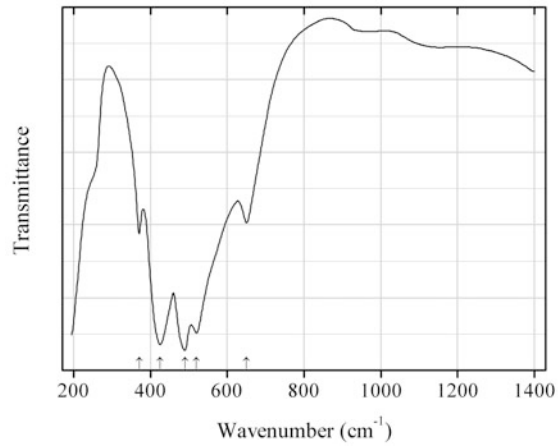

Fig. 2.243 IR spectrum of buserite drawn using data from Bilinski et al. (2002)

O295 Buserite $Na_4Mn_{14}O_{27}\cdot 21H_2O$ (?) (Fig. 2.243)
Locality: Synthetic.
Description: Confirmed by powder X-ray diffraction data.
Kind of sample preparation and/or method of registration of the spectrum: KBr disc. Absorption.
Source: Bilinski et al. (2002).
Wavenumbers (cm^{-1}): 3400s, 650, 520s, 490s, 425s, 370.
Note: For the IR spectrum of buserite see also Potter and Rossman (1979b).

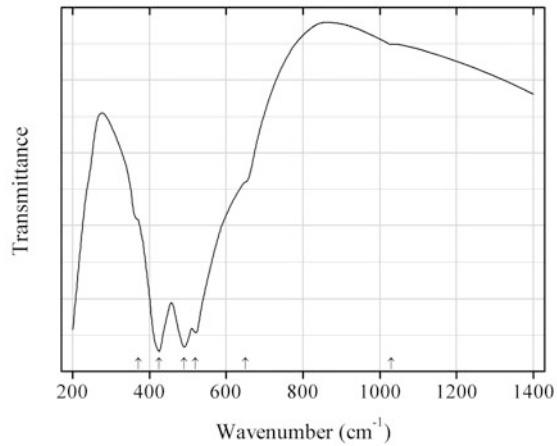

Fig. 2.244 IR spectrum of buserite Ca-analogue drawn using data from Bilinski et al. (2002)

O296 Buserite Ca-analogue $Ca_2Mn_{14}O_{27}\cdot 21H_2O$ (?) (Fig. 2.244)
Locality: Synthetic.
Description: Confirmed by electron microprobe analysis and powder X-ray diffraction data.
Kind of sample preparation and/or method of registration of the spectrum: KBr disc. Absorption.
Source: Bilinski et al. (2002).
Wavenumbers (cm^{-1}): 3400s, 1030, 650, 520s, 490s, 425s, 370sh.

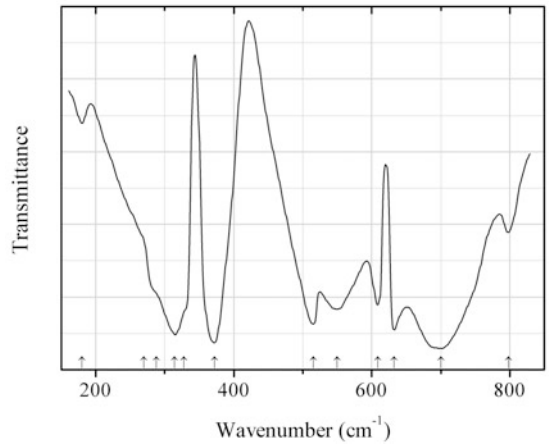

Fig. 2.245 IR spectrum of byströmite drawn using data from Husson et al. (1979)

O297 Byströmite $MgSb^{5+}{}_2O_6$ (Fig. 2.245)
Locality: Synthetic.
Description: Synthesized in the reaction of Sb_2O_3 with MgO at 1050 °C during 50 h in air.
Kind of sample preparation and/or method of registration of the spectrum: Transmission. Kind of sample preparation is not indicated.
Source: Husson et al. (1979).
Wavenumbers (cm^{-1}): 798, 700s, 632s, 609, 550s, 515s, 372s, 328sh, 314s, 288sh, 270sh, 180w.
Note: For IR spectrum of byströmite see also White (1967).

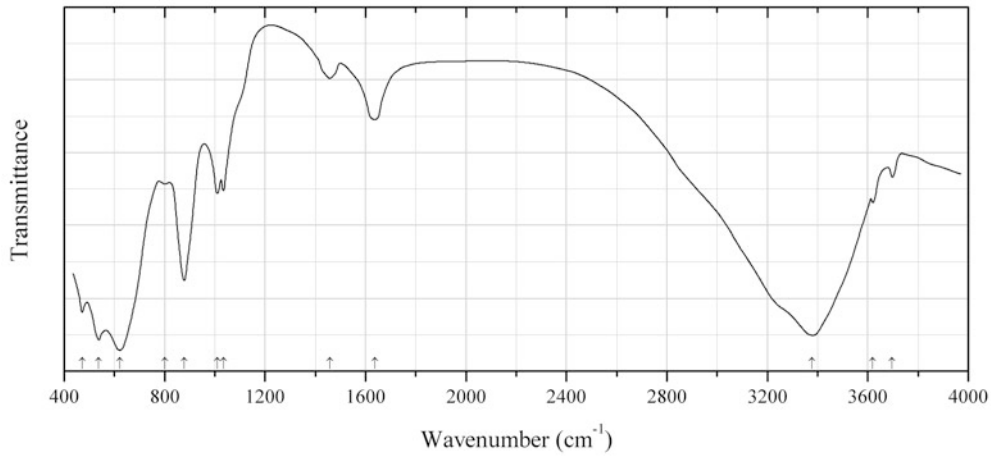

Fig. 2.246 IR spectrum of carlosbarbosaite drawn using data from Atencio et al. (2012)

O298 Carlosbarbosaite $(UO_2)_2Nb_2O_6(OH)_2 \cdot 2H_2O$ (Fig. 2.246)
Locality: Jaguaraçu pegmatite, Jaguaraçu municipality, Minas Gerais, Brazil (type locality).
Description: Yellow aggregate of flattened lath-like crystals from the association with quartz, orthoclase, microcline, albite, muscovite, beryl, elbaite, schorl, spodumene, etc. Holotype sample. The crystal structure is solved. Orthorhombic, space group *Cmcm*, a = 14.150(6), b = 10.395(4), c = 7.529(3) Å, V = 1107(1) $Å^3$, Z = 4. Optically biaxial (+), α = 1.760(5), β = 1.775(5), γ = 1.795(5), 2 V = 70(1)°. The strongest lines of the powder X-ray diffraction pattern [d, Å (I, %) (hkl)] are: 8.405 (80) (110), 7.081 (100) (200), 4.201 (90) (220), 3.333 (60) (202), 3.053 (80) (022), 2.931 (70) (420), 2.803 (60) (222), 2.589 (50) (040, 402).
Kind of sample preparation and/or method of registration of the spectrum: Not indicated.
Source: Atencio et al. (2012).
Wavenumbers (cm^{-1}): 3697w, 3620w, 3377s, 1638, 1458w, 1034, 1010, 878, 802w, 621s, 538s, 471s.
Note: The band position denoted by Atencio et al. (2012) as 1004 cm^{-1} was determined by us at 1034 cm^{-1} based on spectral curve analysis of the published spectrum. The bands at 3697, 3620, 538, and 471 cm^{-1} may correspond to the admixture of kaolinite.

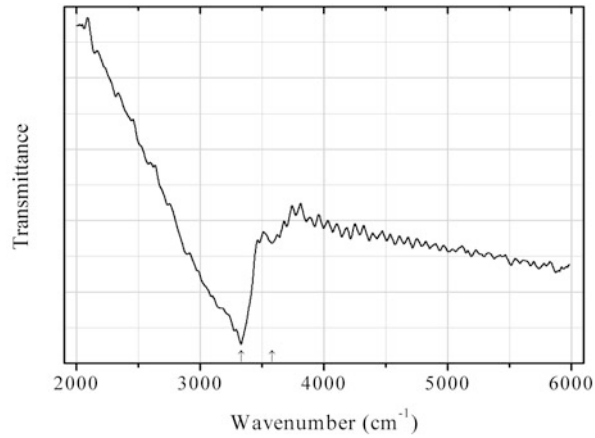

Fig. 2.247 IR spectrum of carmichaelite drawn using data from Wang et al. (2000)

O299 Carmichaelite $(Ti,Cr,Fe)(O,OH)_2$ (Fig. 2.247)
Locality: Garnet ridge, Navajo volcanic field, Colorado plateau, Arizona, USA (type locality).
Description: Cinnamon-brown platy inclusions in mantle-derived pyrope crystals from the association with rutile, srilankite, ilmenite, minerals of the crichtonite group, spinel, and olivine. Holotype sample. The crystal structure is solved. Monoclinic, space group $P2_1/c$, a = 7.706(1), b = 4.5583(6), c = 20.187(3) Å, β = 92.334(2)°, V = 708.5(3) Å^3, Z = 22. D_{calc} = 4.13 g/cm^3. The empirical formula is $Ti_{0.62}Cr_{0.19}Fe_{0.09}Mg_{0.06}Al_{0.03}V_{0.01}O_{1.5}(OH)_{0.5}$. The strongest lines of the powder X-ray diffraction pattern [d, Å (I, %) (hkl)] are: 2.842 (100) (−115), 3.773 (94) (013), 2.664 (70) (213), 1.688 (54) (−322), 1.679 (44, 226), 1.661 (44) (−128), 1.648 (34) (1.1.11).
Kind of sample preparation and/or method of registration of the spectrum: Single-crystal grain. Absorption.
Source: Wang et al. (2000).
Wavenumbers (cm^{-1}): 3580w, 3330.

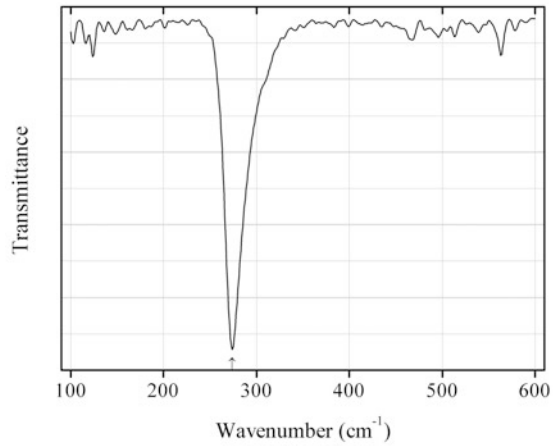

Fig. 2.248 IR spectrum of cerianite-(Ce) drawn using data from Kidchob et al. (2009)

O300 Cerianite-(Ce) CeO_2 (Fig. 2.248)

Locality: Synthetic.
Description: Ceria films after annealing at 800 °C showing the typical diffraction pattern of cubic cerianite with the peaks (111), (200), (220), (311), (222), and a calculated lattice parameter of 5.4 Å.
Kind of sample preparation and/or method of registration of the spectrum: Compact film. Absorption.
Source: Kidchob et al. (2009).
Wavenumbers (cm^{-1}): 274.
Note: Peng and Liu (1982) give the following wavenumbers for cerianite-(Ce): 700sh, 400s.

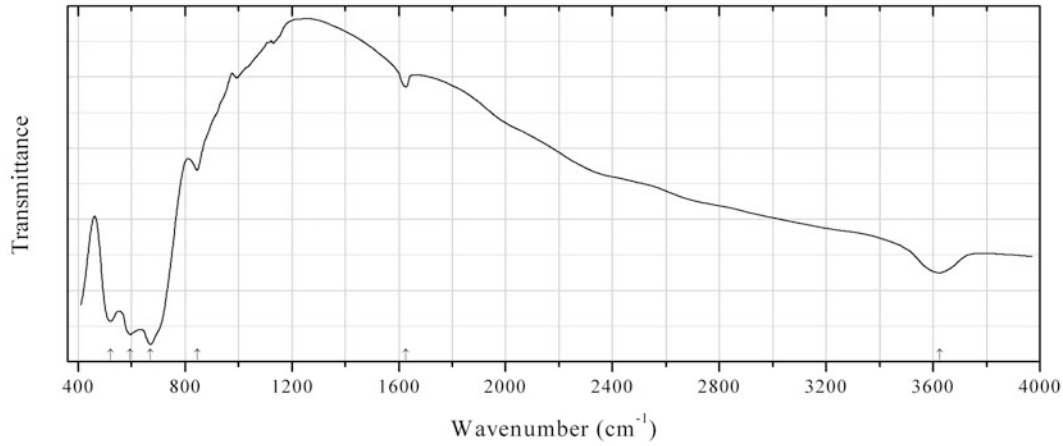

Fig. 2.249 IR spectrum of cesstibtantite drawn using data from Voloshin et al. (1981)

O301 Cesstibtantite $Cs_x(Sb,Na)Ta_2(O,OH)_7 \cdot nH_2O$ (Fig. 2.249)
Locality: Vasin-Myl'k Mt., Voron'i Tundras, Kola peninsula, Murmansk region, Russia (type locality).
Description: Light gray grain from granite pegmatite. The empirical formula is $Cs_{0.30}(Sb_{0.54}Na_{0.24}Pb_{0.04}Bi_{0.02}Ca_{0.01})(Ta_{1.90}Nb_{0.10})(O,OH)_7 \cdot nH_2O$. The strongest lines of the powder X-ray diffraction pattern [*d*, Å (*I*, %)] are: 3.17 (90), 3.04 (100), 2.024 (80), 1.860 (100), 1.587 (100), 1.474 (80), 1.370 (90), 1.208 (80).
Kind of sample preparation and/or method of registration of the spectrum: KBr disc. Absorbande.
Source: Voloshin et al. (1981).
Wavenumbers (cm^{-1}): 3625, 1625, 845, 670s, 595s, 520s.
Note: According to the approved nomenclature of the pyrochlore supergroup of minerals (Atencio et al. 2010), cesstibtantite is considered as a variety of hydroxykenomicrolite.

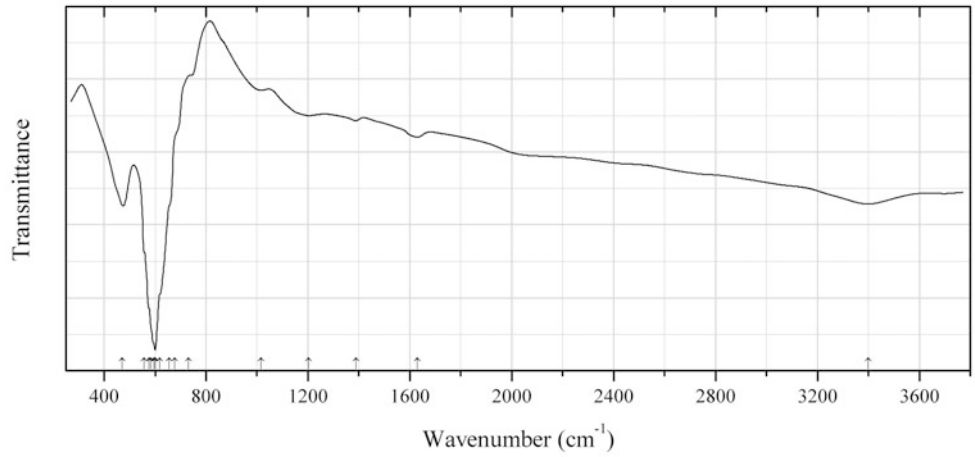

Fig. 2.250 IR spectrum of cetineite drawn using data from Sabelli and Vezzalini (1987)

O302 Cetineite $(K,Na)_{3+x}(Sb_2O_3)_3(SbS_3)(OH)_x \cdot 2–3H_2O$ (Fig. 2.250)
Locality: Cetine mine, Tuscany, Italy (type locality).
Description: Orange-red acicular crystals from the association with mopungite and senarmontite. Holotype sample. Hexagonal, space group $P6_3$, a = 14.230(2), c = 5.579(1) Å, Z = 2. D_{calc} = 4.21 g/cm^3. Optically uniaxial (+), α = 1.554(1), β = 1.558(1), γ = 1.566(1), 2 V = 70(5)°. The empirical formula is $(K_{1.78}Na_{1.57})(Sb_2O_3)_{3.03}(SbS_3)_{0.94}(OH)_{0.53} \cdot 2.64H_2O$. The strongest lines of the powder X-ray diffraction pattern [d, Å (I, %) (hkl)] are: 12.41 (80) (100), 4.67 (54) (120), 4.11 (55) (300), 2.916 (100) (131), 2.690 (61) (410).
Kind of sample preparation and/or method of registration of the spectrum: KBr disc. Transmission.
Source: Sabelli and Vezzalini (1987).
Wavenumbers (cm^{-1}): 3400w, 1630w, 1390w, 1203w, 1015w, 732sh, 678sh, 655sh, 618sh, 600s, 595sh, 584sh, 577sh, 558sh, 470.
Note: The wavenumbers were partly determined by us based on spectral curve analysis of the published spectrum.

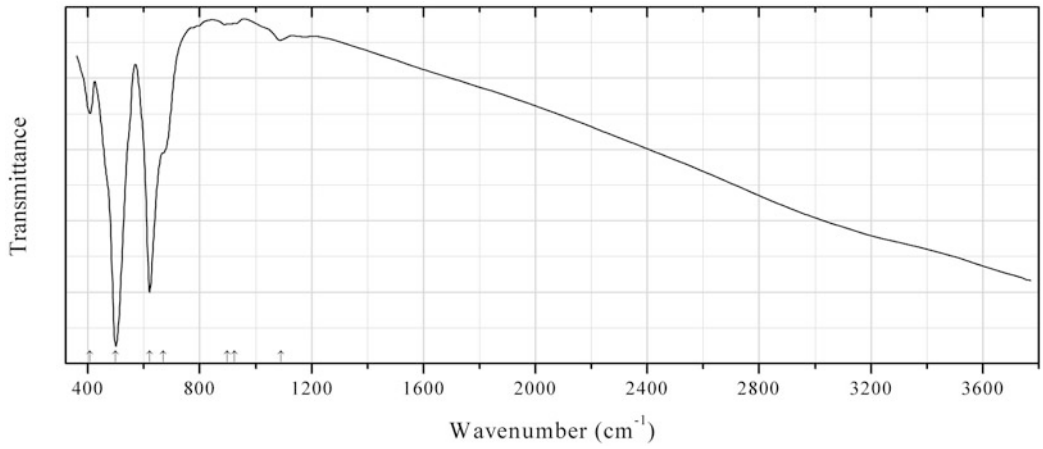

Fig. 2.251 IR spectrum of chromite obtained by N.V. Chukanov

O303 Chromite $Fe^{2+}Cr_2O_4$ (Fig. 2.251)
Locality: Seymchan (Seimchan) meteorite, Magadanskaya Oblast' (Magadan region), Far-Eastern area, Russia.
Description: Black grains from the association with kamacite, troilite, and forsterite. The empirical formula is $(Fe_{0.58}Mg_{0.40}Mn_{0.02})(Cr_{1.93}Al_{0.05}V_{0.02})O_4$.
Kind of sample preparation and/or method of registration of the spectrum: KBr disc. Absorption.
Wavenumbers (cm^{-1}): (1089w), 925w, 898w, 670sh, 620s, 499s, 407.

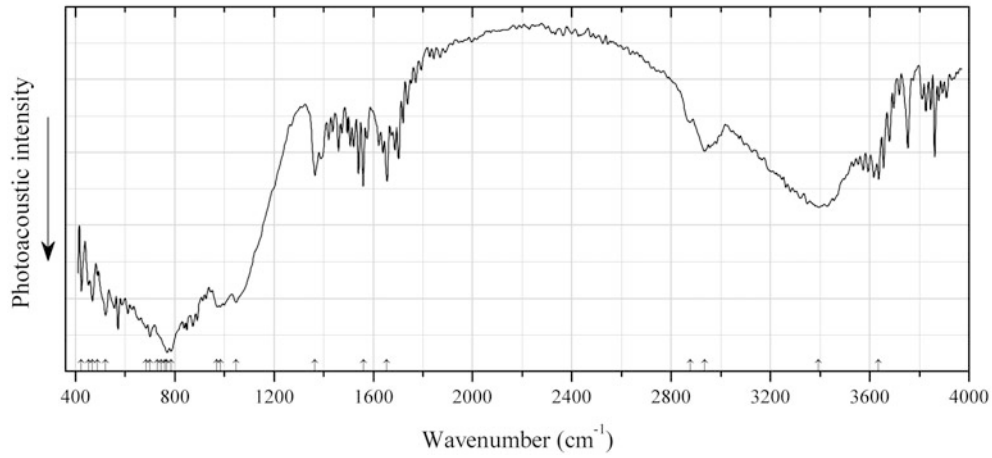

Fig. 2.252 IR spectrum of cleusonite drawn using data from Wülser et al. (2005)

O304 Cleusonite $Pb(U^{4+},U^{6+})(Fe^{2+},Zn)_2(Ti,Fe)_{18}(O,OH)_{38}$ (Fig. 2.252)
Locality: Cleuson valley, upper Val de Nendaz, Valais, Switzerland (type locality).
Description: Black tabular crystal from the association with quartz, chlorite, calcite, albite, microcline, tourmaline, fluorapatite, zircon, ilmenite, hematite, titanite, pyrite, chalcopyrite, tennantite, rutile, crichtonite, monazite-(Ce), and gold. Holotype sample. Trigonal, space group *R*-3, a = 10.573 (3), c = 21.325(5) Å. Partly metamict. The calculated density varies from 5.02(6) (untreated) to 5.27 (5) (heat-treated crystal). The empirical formula is $(Pb_{0.89}Sr_{0.12})(U^{4+}_{0.79}U^{6+}_{0.30})(Fe^{2+}_{1.91}Zn_{0.09})(Ti_{11.80}Fe^{2+}_{3.44}Fe^{3+}_{2.33}V^{5+}_{0.19}Mn_{0.08}Al_{0.07})[O_{35.37}(OH)_{2.63}]$.
Kind of sample preparation and/or method of registration of the spectrum: KBr disc. Photoacoustic method of registration.
Source: Wülser et al. (2005).
Wavenumbers (cm^{-1}): 3636, 3394, 2935, 2877, 1655, 1560, 1365, 1047, 984, 970, 786s, 769s, 759sh, 745sh, 729sh, 701, 684, 521, 489, 468, 452, 424.
Note: The wavenumbers were partly determined by us based on spectral curve analysis of the published spectrum.

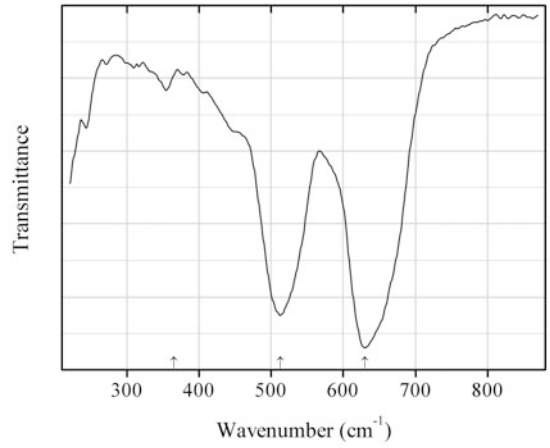

Fig. 2.253 IR spectrum of cochromite drawn using data from Allen and Paul (1995)

O305 Cochromite $CoCr_2O_4$ (Fig. 2.253)
Locality: Synthetic.
Description: Prepared in solid-state reaction at 950 °C. The empirical formula is $CoCr_{1.5}Fe^{3+}{}_{0.5}O_4$.
Kind of sample preparation and/or method of registration of the spectrum: KBr disc. Absorption.
Source: Allen and Paul (1995).
Wavenumbers (cm^{-1}): 630s, 513s, 365w.
Note: The band position denoted by Allen and Paul (1995) as 365 cm^{-1} was determined by us at 355 cm^{-1} based on spectral curve analysis of the published spectrum.

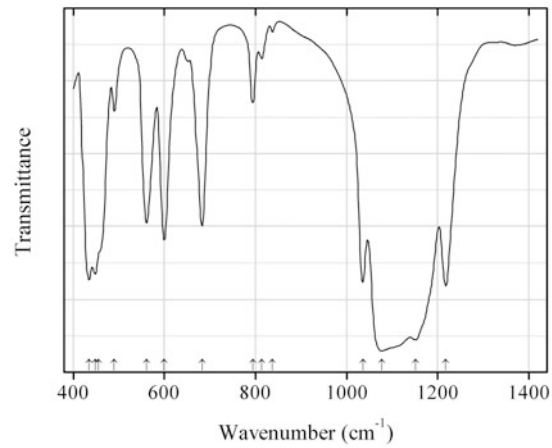

Fig. 2.254 IR spectrum of coesite drawn using data from Lyon and Burns (1963)

O306 Coesite SiO_2 (Fig. 2.254)
Locality: Synthetic.
Kind of sample preparation and/or method of registration of the spectrum: KBr disc. Absorption.
Source: Lyon and Burns (1963).

Wavenumbers (cm^{-1}): 1218s, 1152s, 1077s, 1036s, 837w, 814w, 794, 683w, 600, 561, 490, 455sh, 448s, 435s.
Note: For IR spectrum of coesite see also Kieffer (1979), Williams et al. (1993).

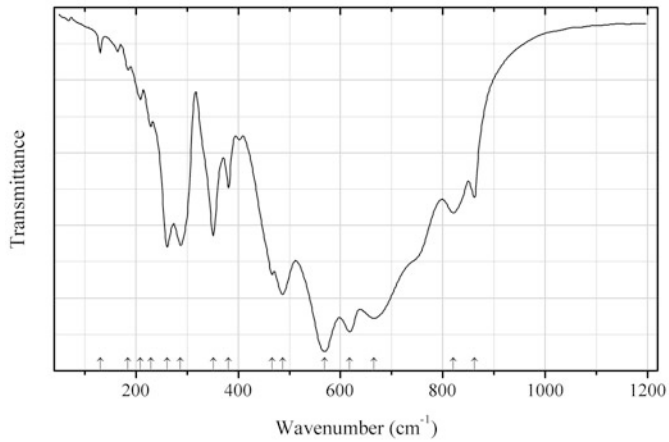

Fig. 2.255 IR spectrum of columbite-(Fe) drawn using data from Tarantino et al. (2005)

O307 Columbite-(Fe) $Fe^{2+}Nb_2O_6$ (Fig. 2.255)
Locality: Synthetic.
Description: Synthesised by solid-state reaction, starting from stoichiometric amounts of Nb_2O_5, Fe, and Fe_2O_3 at 950 °C for a total time of at least 3 weeks in evacuated silica vial. Confirmed by electron microprobe analysis and powder X-ray diffraction data. Mössbauer investigation confirmed that Fe is divalent.
Kind of sample preparation and/or method of registration of the spectrum: Polyethylene disc (for the range 50–500 cm^{-1}). CsI disc (for the range 400–1500 cm^{-1}).
Source: Tarantino et al. (2005).
Wavenumbers (cm^{-1}): 862, 821, 666s, 618s, 569s, 487s, 466, 381, 351, 287, 261, 229w, 209w, 184w, 130w.

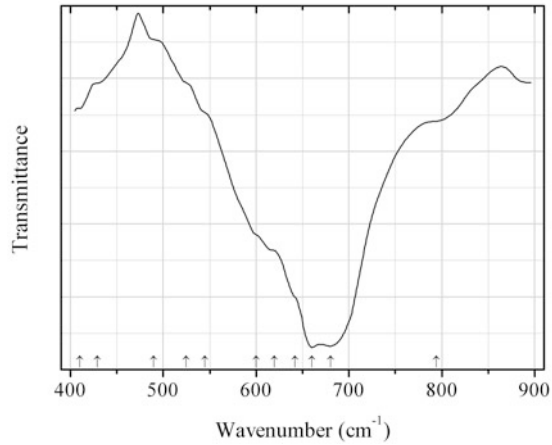

Fig. 2.256 IR spectrum of crednerite drawn using data from Bessekhouad et al. (2007)

O308 Crednerite $CuMnO_2$ (Fig. 2.256)
Locality: Synthetic.
Description: Brown powder. Synthesized by solid-state exchange reaction: $CuCl + LiMnO_2 \rightarrow CuMnO_2 + LiCl$ 520 °C for 5 days. Confirmed by powder X-ray diffraction data.
Kind of sample preparation and/or method of registration of the spectrum: Transmission. Kind of sample preparation is not indicated.
Source: Bessekhouad et al. (2007).
Wavenumbers (cm^{-1}): 794sh, 680s, 660s, 642sh, 620sh, 600sh, 545sh, 525sh, 490sh, 429sh, 410w.
Note: Bands with wavenumbers > 900 cm^{-1} in the spectrum given by Bessekhouad et al. (2007) presumably correspond to impurities.
Note: The wavenumbers were partly determined by us based on spectral curve analysis of the published spectrum.

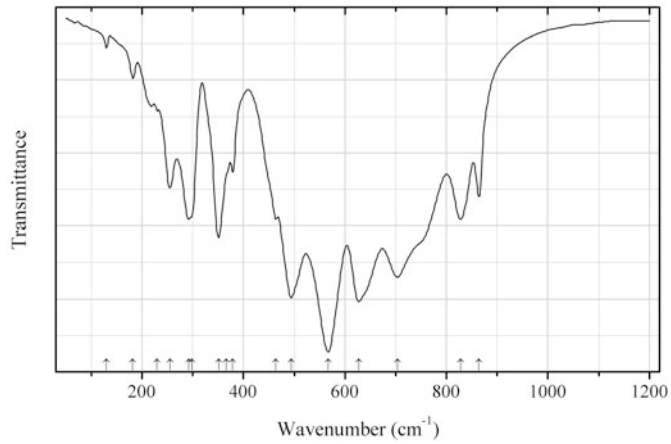

Fig. 2.257 IR spectrum of columbite O310 drawn using data from Tarantino et al. (2005)

O310 Columbite O310 $Fe^{2+}_{0.5}Mn^{2+}_{0.5}Nb_2O_6$ (Fig. 2.257)
Locality: Synthetic.
Description: Synthesised by solid-state reaction, starting from stoichiometric amounts of Nb_2O_5, MnO, Fe, and Fe_2O_3 at 950 °C for a total time of at least 3 weeks in evacuated silica vial. Confirmed by electron microprobe analysis and powder X-ray diffraction data. Mössbauer and XANES investigations confirmed that both Mn and Fe are divalent.
Kind of sample preparation and/or method of registration of the spectrum: Polyethylene disc (for the range 50–500 cm^{-1}). CsI disc (for the range 400–1500 cm^{-1}).
Source: Tarantino et al. (2005).
Wavenumbers (cm^{-1}): 864, 828, 704s, 627s, 567s, 494s, 464, 379, 366, 351, 298, 292, 255, 230w, 182w, 130w.

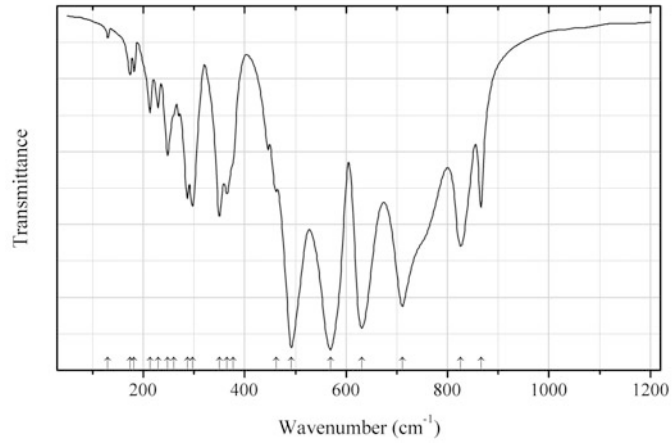

Fig. 2.258 IR spectrum of columbite-(Mn) drawn using data from Tarantino et al. (2005)

O311 Columbite-(Mn) $Mn^{2+}Nb_2O_6$ (Fig. 2.258)
Locality: Synthetic.
Description: Synthesised by solid-state reaction, starting from stoichiometric amounts of Nb_2O_5 and MnO at 950 °C for a total time of at least 3 weeks in evacuated silica vial. Confirmed by electron microprobe analysis and powder X-ray diffraction data. XANES investigation confirmed that Mn is divalent.
Kind of sample preparation and/or method of registration of the spectrum: Polyethylene disc (for the range 50–500 cm^{-1}). CsI disc (for the range 400–1500 cm^{-1}).
Source: Tarantino et al. (2005).
Wavenumbers (cm^{-1}): 866, 826, 711s, 631s, 569s, 492s, 462, 377sh, 365, 350, 297, 287, 260w, 248, 229w, 213w, 182w, 174w, 130w.

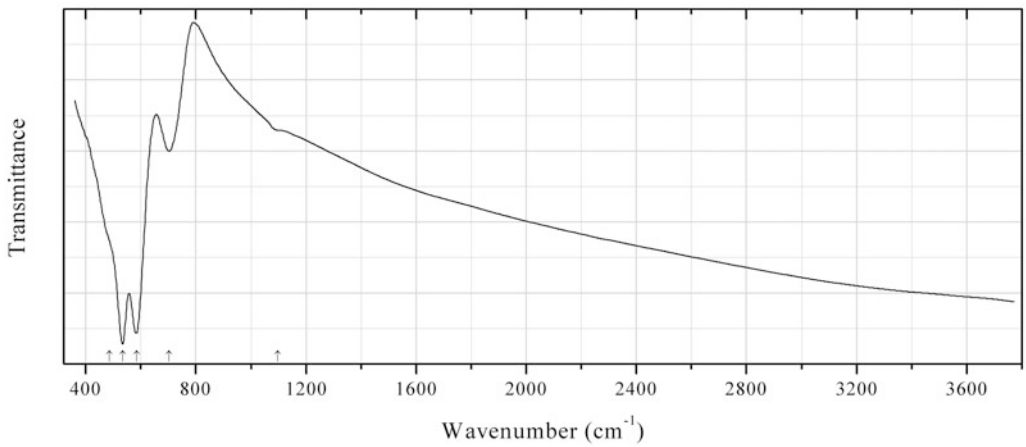

Fig. 2.259 IR spectrum of cryptomelane obtained by N.V. Chukanov

O312 Cryptomelane $K(Mn^{4+}{}_7Mn^{3+})O_{16}$ (Fig. 2.259)
Locality: Kent granite massif, Karagandy province, Central Kazakhstan.
Description: Black kidney-like aggregate. The empirical formula is (semiquantitative electron microprobe analysis): $K_{0.6}Na_{0.15}Ba_{0.05}(Mn_{7.9}Al_{0.1})O_{16}$.

Kind of sample preparation and/or method of registration of the spectrum: KBr disc. Absorption.
Wavenumbers (cm^{-1}): 1097w, 702, 585s, 534s, 485sh.
Note: For the IR spectrum of cryptomelane see also Potter and Rossman (1979b).

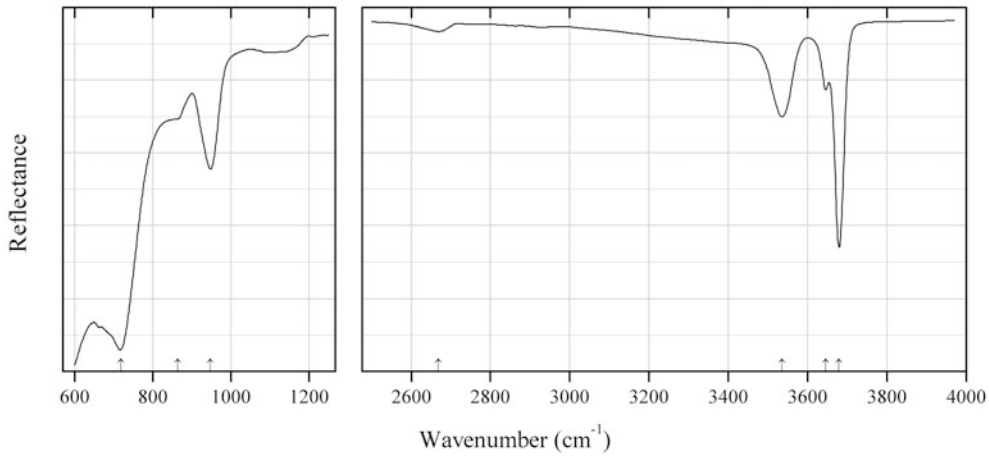

Fig. 2.260 IR spectrum of magnesium hydroxide fluoride drawn using data from Crichton et al. (2012)

O313 Magnesium hydroxide fluoride Mg(OH)F (Fig. 2.260)
Locality: Synthetic.
Description: Synthesized by a subcritical hydrothermal route from a 1:1 molar mixture of brucite, $Mg(OH)_2$, and sellaite, MgF_2 with a rutile type structure, in excess water. The topology of the structure is intermediate between those of the OH and F endmembers. Orthorhombic, space group *Pnma*, $a = 10.116(3)$, $b = 4.6888(10)$, $c = 3.0794(7)$ Å. The strongest lines of the powder X-ray diffraction pattern [*d*, Å (*I*, %) (*hkl*)] are: 4.253 (70) (101), 2.291 (100) (211), 2.229 (60) (401), 1.747 (70) (212), 1.480 (40) (610).
Kind of sample preparation and/or method of registration of the spectrum: Attenuated total reflection of powdered sample.
Source: Crichton et al. (2012).
Wavenumbers (cm^{-1}): 3679s, 3645w, 3535, 2669w, 948, 865sh, 719s.

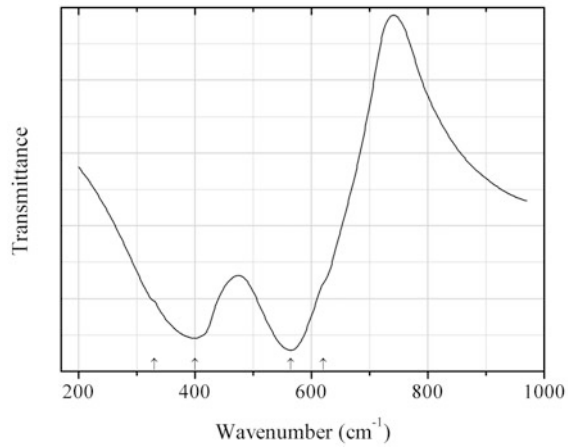

Fig. 2.261 IR spectrum of cuprospinel drawn using data from Srinivasan et al. (1984)

O314 Cuprospinel $Cu^{2+}Fe^{3+}{}_2O_4$ (Fig. 2.261)
Locality: Synthetic.
Description: Monophase ceramic. Confirmed by powder X-ray diffraction data.
Kind of sample preparation and/or method of registration of the spectrum: KBr disc. Transmission.
Source: Srinivasan et al. (1984).
Wavenumbers (cm^{-1}): 620sh, 565s, 400s, 330sh.
Note: For the IR spectrum of synthetic cuprospinel see also Mazen et al. (1992).

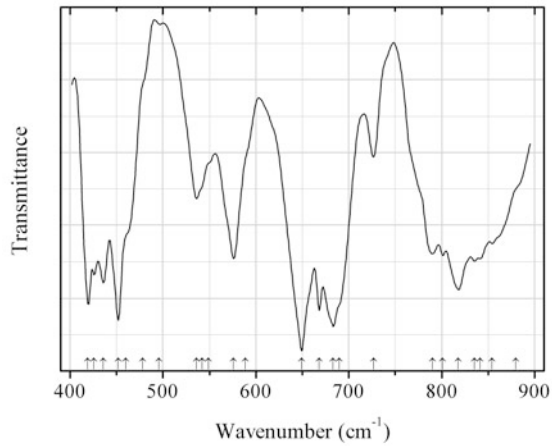

Fig. 2.262 IR spectrum of calcium aluminate O315 drawn using data from Janáková et al. (2007)

O315 Calcium aluminate O315 $CaAl_2O_4$ (Fig. 2.262)
Locality: Synthetic.
Description: Metastable polymorph of dmitryivanovite and krotite prepared by thermal treatment of stoichiometric xerogel at 850 °C in air for 4 h. Hexahonal, a = 8.7402(2), c = 8.0904(2) Å. Identified by powder X-ray diffraction data.
Kind of sample preparation and/or method of registration of the spectrum: KBr disc. Absorption.
Source: Janáková et al. (2007).
Wavenumbers (cm^{-1}): 880sh, 854, 841, 835, 818s, 801, 790sh, 727, 690sh, 683s, 668s, 649s, 589sh, 576, 549sh, 542sh, 536, 496w, 478sh, 460sh, 452s, 436, 426, 419s.
Note: The wavenumbers were determined by us based on spectral curve analysis of the published spectrum.

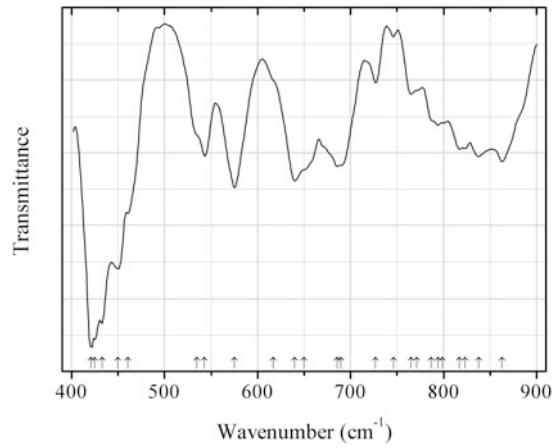

Fig. 2.263 IR spectrum of krotite drawn using data from Janáková et al. (2007)

O316 Krotite $CaAl_2O_4$ (Fig. 2.263)
Locality: Synthetic.
Description: Prepared by thermal treatment of stoichiometric xerogel at 1200 °C in air for 6 h. Monoclinic. Identified by powder X-ray diffraction data.
Kind of sample preparation and/or method of registration of the spectrum: KBr disc. Absorption.
Source: Janáková et al. (2007).
Wavenumbers (cm^{-1}): 863, 838, 823, 817, 799sh, 794, 787sh, 771sh, 765, 746w, 727, 690sh, 686, 650sh, 640, 617sh, 575s, 543, 535sh, 461s, 450s, 433s, 425s, 421s.
Note: The wavenumbers were determined by us based on spectral curve analysis of the published spectrum.

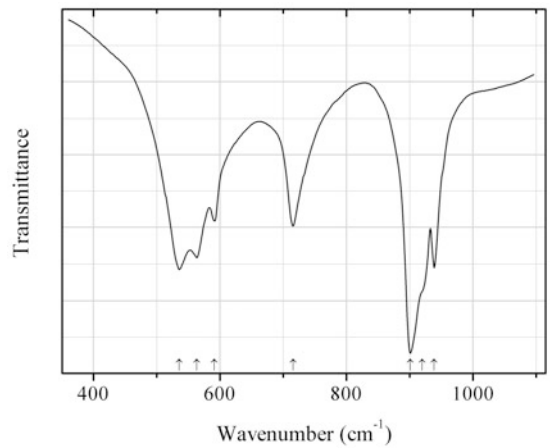

Fig. 2.264 IR spectrum of downeyite drawn using data from Giguère and Falk (1960)

O317 Downeyite SeO_2 (Fig. 2.264)
Locality: Synthetic.
Description: Solid film obtained by dehydration of H_2SeO_3 at room temperature.

Kind of sample preparation and/or method of registration of the spectrum: Film on a polished AgCl disc. Transmission.
Source: Giguère and Falk (1960).
Wavenumbers (cm^{-1}): 939s, 920sh, 901s, 716, 591, 563s, 535s.
Note: For the IR spectrum of vapour deposited thin film of SeO_2 see Burley (1968).

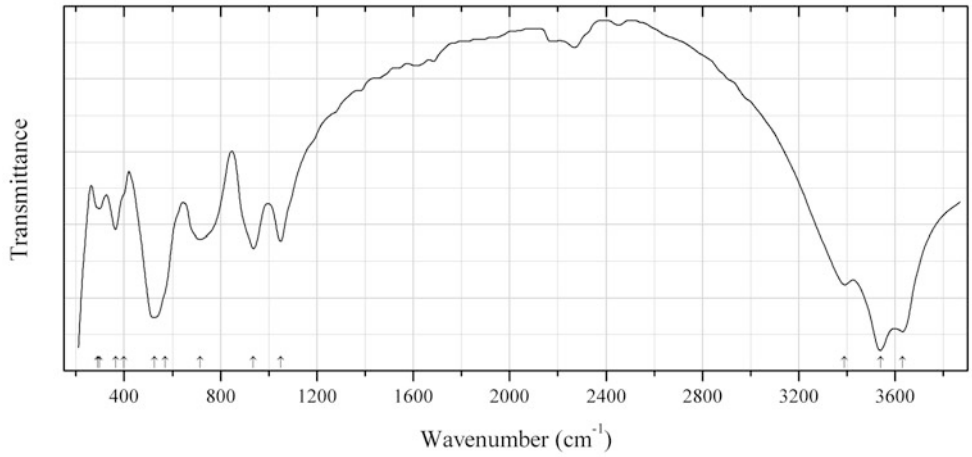

Fig. 2.265 IR spectrum of doyleite drawn using data from Chao et al. (1985)

O318 Doyleite $Al(OH)_3$ (Fig. 2.265)
Locality: Francon quarry, Mont Saint-Hilaire, Rouville RCM (Rouville Co.), Montérégie, Québec, Canada (type locality).
Description: White tabular crystals from the association with weloganite, cryolite, calcite, quartz, etc. Holotype sample. Triclinic, space group *P*-1, a = 5.002(1), b = 5.175(1), c = 4.980(2) Å, α = 97.50 (1)°, β = 118.60(1)°, γ = 104.74(1)°, V = 104.32(5) $Å^3$, Z = 2. D_{meas} = 2.48(1) g/cm^3, D_{calc} = 2.482 g/cm^3. Optically biaxial (+), α = 1.545(1), β = 1.553(1), γ = 1.566(1), 2 V = 77°. The empirical formula is $Al_{0.99}Ca_{0.01}(OH)_3$. The strongest lines of the powder X-ray diffraction pattern [*d*, Å (*I*, %) (*hkl*)] are: 4.794 (100) (010), 2.360 (40) (101), 1.972 (30) (−221), 1.857 (30) (111), 1.842 (30) (−122).
Kind of sample preparation and/or method of registration of the spectrum: Transmission. Kind of sample preparation is not indicated.
Source: Chao et al. (1985).
Wavenumbers (cm^{-1}): 3630s, 3540s, 3390s, 1050, 935, 715, 570sh, 525s, 400sh, 364, 298, 290sh.
Note: The wavenumbers were partly determined by us based on spectral curve analysis of the published spectrum.

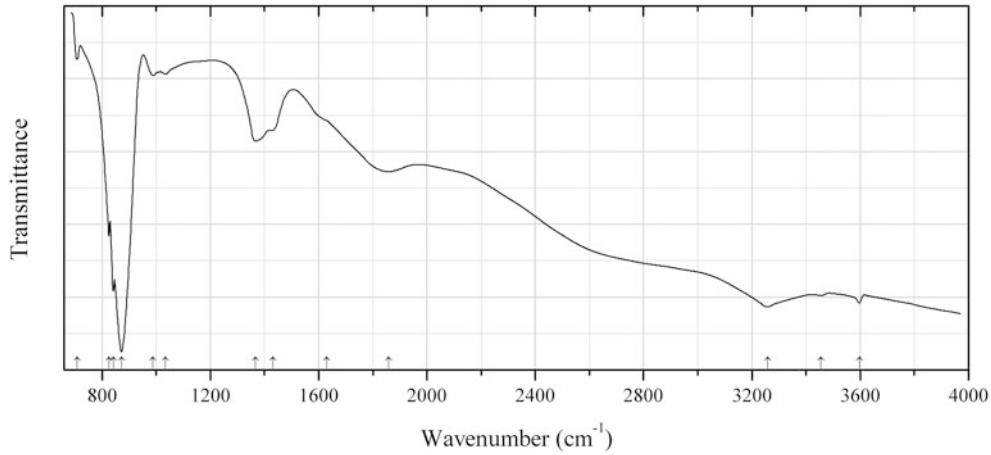

Fig. 2.266 IR spectrum of dukeite drawn using data from Burns et al. (2000)

O319 Dukeite $Bi^{3+}{}_{24}Cr^{6+}{}_{8}O_{57}(OH)_6 \cdot 3H_2O$ (Fig. 2.266)
Locality: São José mine, Brejaúba, Minas Gerais, Brazil (type locality).
Description: Aggregate of yellow acicular crystals from the association with pucherite, schumacherite, bismutite, and hechtsbergite. Holotype sample. Trigonal, space group $P31c$, $a = 15.067(3)$, $c = 15.293(4)$, $V = 3007(1)$ Å^3, $Z = 2$. $D_{calc} = 7.171$ g/cm^3. Optically biaxial (+), $\alpha = 1.554(1)$, $\beta = 1.558(1)$, $\gamma = 1.566(1)$, $2V = 70(5)°$. The empirical formula is $Bi_{23.95}(Cr_{7.64}V_{0.43})O_{56.84}(OH)_{6.16} \cdot 3.01H_2O$. The strongest lines of the powder X-ray diffraction pattern [*d*, Å (*I*, %) (*hkl*)] are: 7.650 (50) (002), 3.812 (40) (004), 3.382 (100) (222), 2.681 (70) (224), 2.175 (40) (600), 2.106 (40) (226), 1.701 (50) (228).
Kind of sample preparation and/or method of registration of the spectrum: Transmittance of a powdered sample.
Source: Burns et al. (2000).
Wavenumbers (cm^{-1}): 3597w, 3455w, 3258, 1858, 1631sh, 1431sh, 1367, 1034w, 989w, 872s, 842s, 826, 708w.
Note: The wavenumbers were partly determined by us based on spectral curve analysis of the published spectrum. Absorptions in the range from 1700 to 3000 cm^{-1} indicate the presence of acid groups.

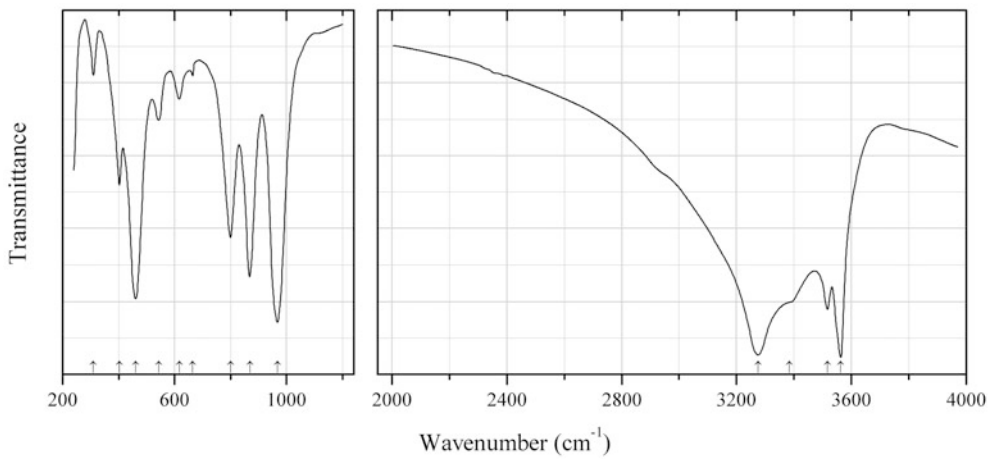

Fig. 2.267 IR spectrum of duttonite drawn using data from Ferrer and Baran (1994)

O320 Duttonite $V^{4+}O(OH)_2$ (Fig. 2.267)
Locality: Synthetic.
Description: Confirmed by the powder X-ray diffraction data.
Kind of sample preparation and/or method of registration of the spectrum: KBr disc. Transmission.
Source: Ferrer and Baran (1994).
Wavenumbers (cm^{-1}): 3563s, 3517s, 3384sh, 3275s, 968s, 870s, 800, 665w, 617w, 543, 461s, 403, 310w.
Note: The wavenumbers were partly determined by us based on spectral curve analysis of the published spectrum.

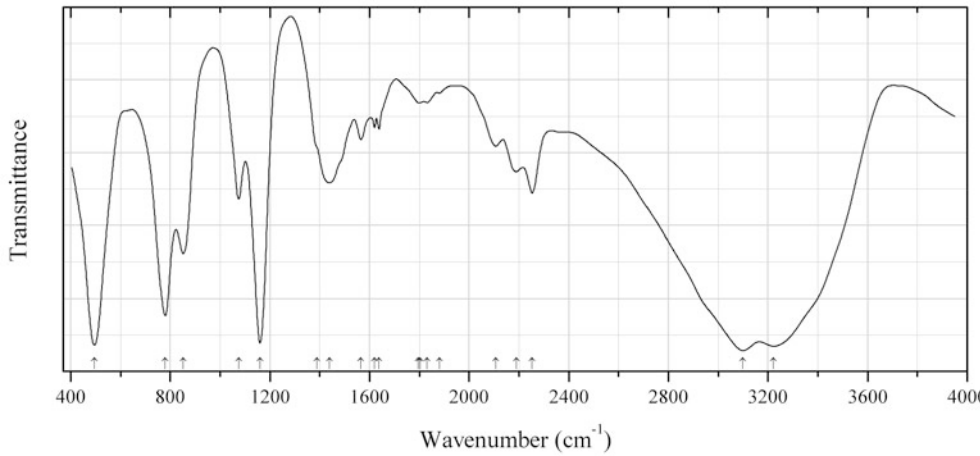

Fig. 2.268 IR spectrum of dzhalindite drawn using data from Dai et al. (2013)

O321 Dzhalindite $In(OH)_3$ (Fig. 2.268)
Locality: Synthetic.
Description: Aggregate of cubic crystals. Commercial reagent (99 %, Aldrich). Confirmed by powder X-ray diffraction data.
Kind of sample preparation and/or method of registration of the spectrum: Transmission. Kind of sample preparation is not indicated.
Source: Dai et al. (2013).
Wavenumbers (cm^{-1}): 3222s, 3100s, 2253, 2189, 2107, 1880w, 1832w, 1804w, 1795w, 1638, 1620, 1565, 1439, 1388sh, 1160s, 1075, 852, 780s, 496s.
Note: The wavenumbers were partly determined by us based on spectral curve analysis of the published spectrum. The band positions denoted by Dai et al. (2013) as 1100 and 531 cm^{-1} were determined by us at 1075 and 496 cm^{-1}, respectively.

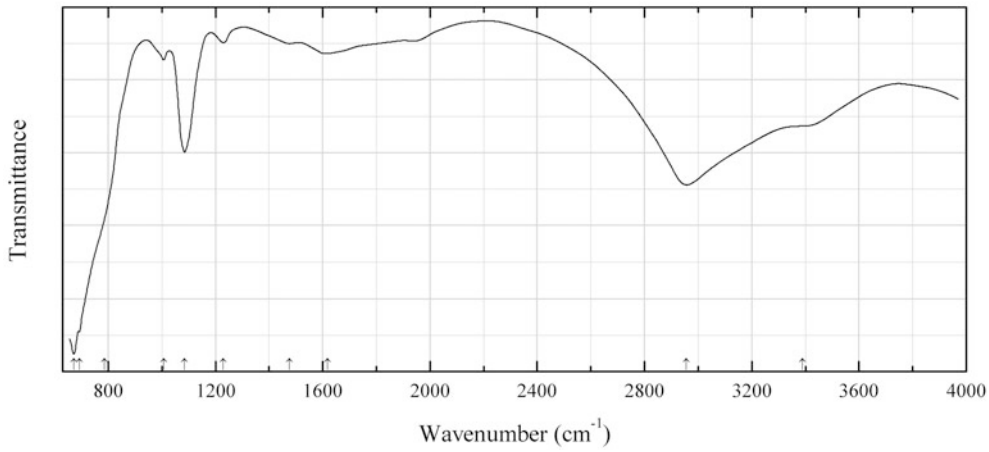

Fig. 2.269 IR spectrum of eyselite drawn using data from Roberts et al. (2004)

O322 Eyselite $Fe^{3+}Ge_3O_7(OH)$ (Fig. 2.269)
Locality: Tsumeb mine, Tsumeb, Namibia (type locality).
Description: Brown-yellow fine-grained aggregate from a vug in massive renierite-germanite-tennantite ore. Holotype sample. Orthorhombic with a *P* lattice, $a = 8.302(4)$, $b = 9.718(4)$, $c = 4.527(2)$ Å, $V = 365.2(3)$ Å^3, $Z = 2$. $D_{calc} = 3.639$ g/cm^3. Optically biaxial (+). The empirical formula is $(Fe^{3+}_{0.93}Ga^{3+}_{0.04})Ge_{2.98}O_{6.90}(OH)_{1.17}$. The strongest lines of the powder X-ray diffraction pattern [*d*, Å (*I*, %) (*hkl*)] are: 4.105 (40) (011), 3.681 (100) (111), 3.121 (60b) (220, 121), 2.921 (100) (211), 2.512 (40) (131), 2.403 (90) (320), 1.646 (80) (322), 1.624 (50) (142).
Kind of sample preparation and/or method of registration of the spectrum: Transmission.
Source: Roberts et al. (2004).
Wavenumbers (cm^{-1}): 3389sh, 2957s, 1617w, 1475w, 1230w, 1085, 1007w, 785sh, 692s, 672s.
Note: The wavenumbers were partly determined by us based on spectral curve analysis of the published spectrum.

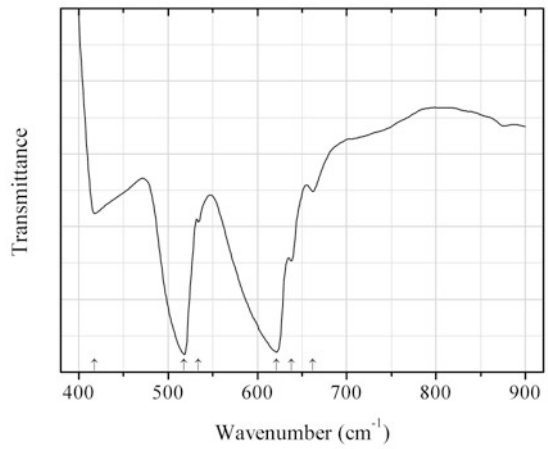

Fig. 2.270 IR spectrum of feitknechtite drawn using data from Peng and Ichinose (2011)

O323 Feitknechtite $Mn^{3+}O(OH)$ (Fig. 2.270)

Locality: Synthetic.
Description: Nanofibers. Tetragonal. Confirmed by powder X-ray diffraction pattern.
Kind of sample preparation and/or method of registration of the spectrum: KBr disc. Transmission.
Source: Peng and Ichinose (2011).
Wavenumbers (cm^{-1}): 662w, 638, 621s, 534w, 518s, 418.
Note: The band position denoted by Peng and Ichinose (2011) as 630 cm^{-1} was determined by us at 638 cm^{-1} based on spectral curve analysis of the published spectrum.

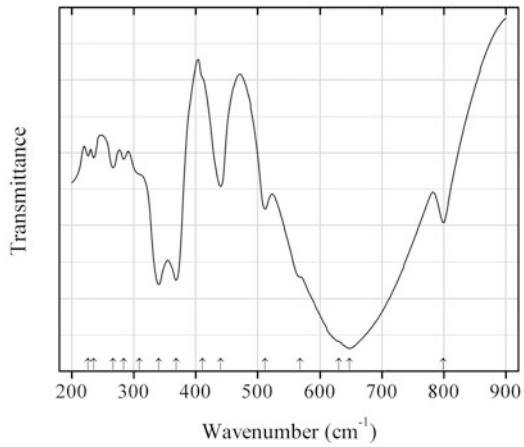

Fig. 2.271 IR spectrum of fergusonite-(Ce)-β drawn using data from Pradhan and Choudhary (1987)

O324 Fergusonite-(Ce)-β $CeNbO_4$ (Fig. 2.271)
Locality: Synthetic.
Description: Synthesized in solid-state reaction between fine powders of Ce_2O_3 and Nb_2O_5 compacted at 4.5×10^4 kg/cm^3, fired at 1623 K in air for 5 h and quenched. Confirmed by powder X-ray diffraction data.
Kind of sample preparation and/or method of registration of the spectrum: CsI disc. Transmission.
Source: Pradhan and Choudhary (1987).
Wavenumbers (cm^{-1}): 799s, 648s, 631sh, 568sh, 512, 440s, 411sh, 369s, 340s, 309sh, 284w, 267w, 235w, 226w.
Note: The wavenumbers were partly determined by us based on spectral curve analysis of the published spectrum.

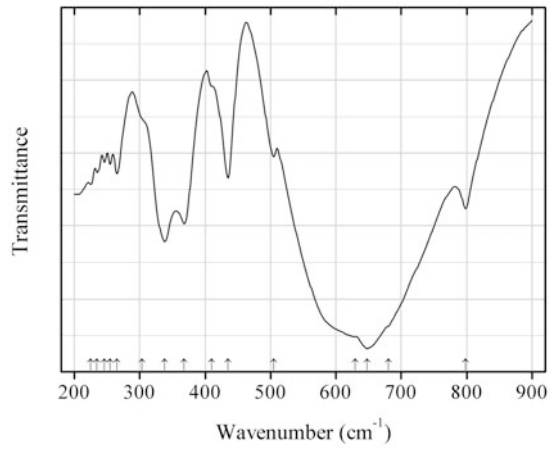

Fig. 2.272 IR spectrum of fergusonite-(La)-β drawn using data from Pradhan and Choudhary (1987)

O325 Fergusonite-(La)-β $LaNbO_4$ (Fig. 2.272)
Locality: Synthetic.
Description: Synthesized in solid-state reaction between fine powders of La_2O_3 and Nb_2O_5 compacted at 4.5×10^4 kg/cm^3, fired at 1623 K in air for 5 h and quenched. Confirmed by powder X-ray diffraction data.
Kind of sample preparation and/or method of registration of the spectrum: CsI disc. Transmission.
Source: Pradhan and Choudhary (1987).
Wavenumbers (cm^{-1}): 798s, 680sh, 648, 630, 505w, 435s, 410w, 368s, 338s, 304sh, 265w, 255w, 246w, 235w, 225w.
Note: The wavenumbers were partly determined by us based on spectral curve analysis of the published spectrum. The band position denoted by Pradhan and Choudhary (1987) as 404 cm^{-1} was not determined by us after spectral curve analysis.

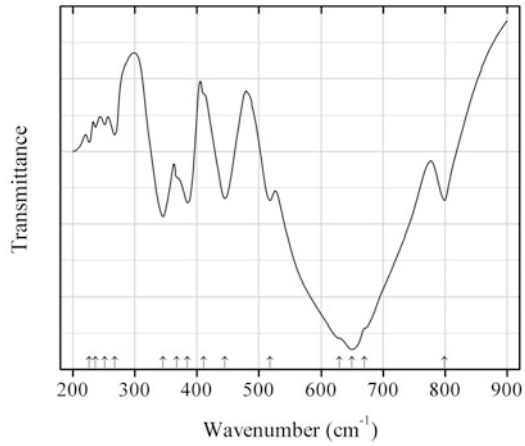

Fig. 2.273 IR spectrum of fergusonite-(Nd)-β drawn using data from Pradhan and Choudhary (1987)

O326 Fergusonite-(Nd)-β $NdNbO_4$ (Fig. 2.273)
Locality: Synthetic.

Description: Synthesized in solid-state reaction between fine powders of Nd_2O_3 and Nb_2O_5 compacted at $4.5 \cdot 10^4$ kg/cm^3, fired at 1623 K in air for 5 h and quenched. Confirmed by powder X-ray diffraction data.
Kind of sample preparation and/or method of registration of the spectrum: CsI disc. Transmission.
Source: Pradhan and Choudhary (1987).
Wavenumbers (cm^{-1}): 799s, 670sh, 650s, 630sh, 518, 445, 411sh, 385, 368sh, 345s, 268w, 252w, 236w, 226w.
Note: The wavenumbers were partly determined by us based on spectral curve analysis of the published spectrum.

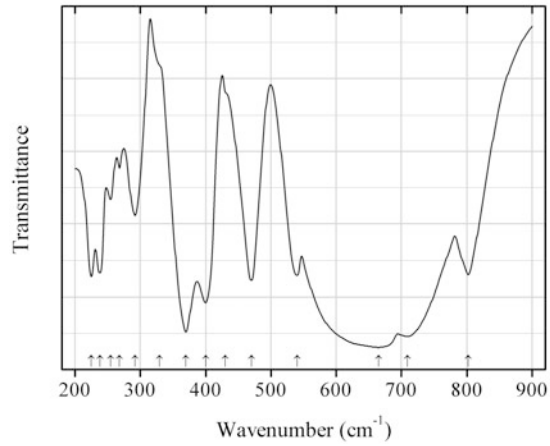

Fig. 2.274 IR spectrum of fergusonite-(Y)-β drawn using data from Pradhan and Choudhary (1987)

O327 Fergusonite-(Y)-β $YNbO_4$ (Fig. 2.274)
Locality: Synthetic.
Description: Synthesized in solid-state reaction between fine powders of Y_2O_3 and Nb_2O_5 compacted at 4.5×10^4 kg/cm^3, fired at 1623 K in air for 5 h and quenched. Confirmed by powder X-ray diffraction data.
Kind of sample preparation and/or method of registration of the spectrum: CsI disc. Transmission.
Source: Pradhan and Choudhary (1987).
Wavenumbers (cm^{-1}): 802s, 709s, 665s, 540, 470s, 430sh, 400s, 370s, 330sh, 292, 268w, 255w, 238, 225.
Note: The wavenumbers were partly determined by us based on spectral curve analysis of the published spectrum.

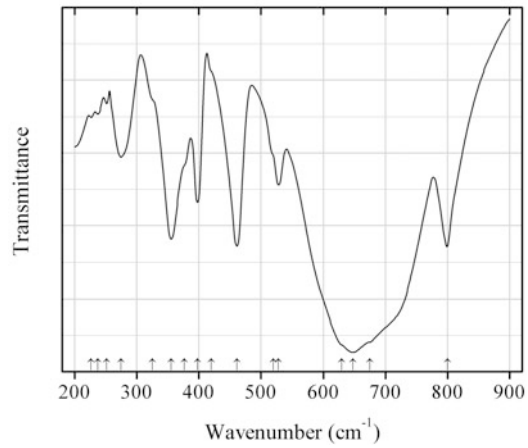

Fig. 2.275 IR spectrum of fergusonite-(Gd)-β drawn using data from Pradhan and Choudhary (1987)

O328 Fergusonite-(Gd)-β $GdNbO_4$ (Fig. 2.275)
Locality: Synthetic.
Description: Synthesized in solid-state reaction between fine powders of Gd_2O_3 and Nb_2O_5 compacted at 4.5×10^4 kg/cm^3, fired at 1623 K in air for 5 h and quenched. Confirmed by powder X-ray diffraction data.
Kind of sample preparation and/or method of registration of the spectrum: CsI disc. Transmission.
Source: Pradhan and Choudhary (1987).
Wavenumbers (cm^{-1}): 800s, 675sh, 648s, 630sh, 528, 520sh, 461s, 420sh, 398s, 377sh, 355s, 325sh, 275, 252w, 237w, 226w.
Note: The wavenumbers were partly determined by us based on spectral curve analysis of the published spectrum. The band position denoted by Pradhan and Choudhary (1987) as 665 cm^{-1} was determined by us at 648 cm^{-1}.

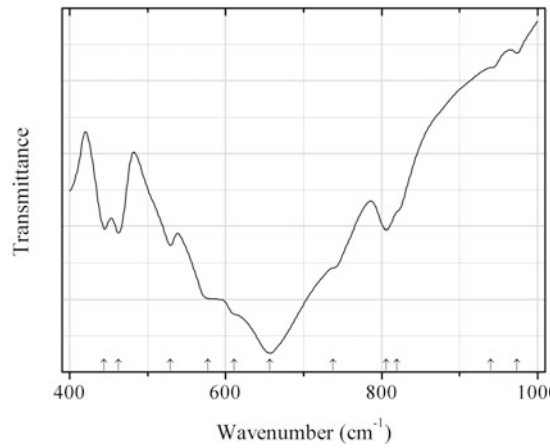

Fig. 2.276 IR spectrum of fergusonite-(Sm)-β drawn using data from Meireles (2011)

O329 Fergusonite-(Sm)-β $SmNbO_4$ (Fig. 2.276)
Locality: Synthetic.

Description: Synthesized on heating of $SmNbO_4$ nanocrystalline powder above 800 °C. Confirmed by powder X-ray diffraction data. Monoclinic, a = 5.421, b = 11.170, c = 5.120 Å, β = 94.7°.
Kind of sample preparation and/or method of registration of the spectrum: KBr disc. Transmission.
Source: Meireles (2011).
Wavenumbers (cm^{-1}): 974w, 940sh, 820sh, 806, 738sh, 657s, 611sh, 577s, 529, 462, 444.

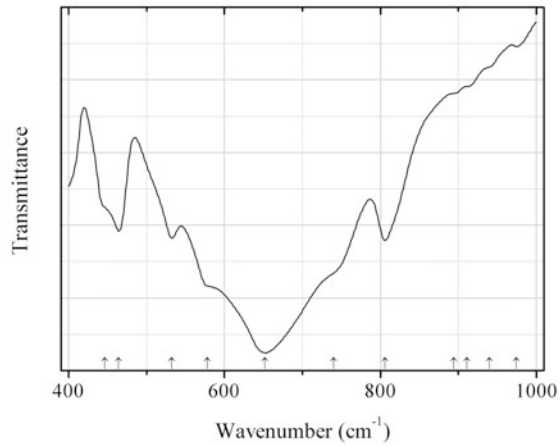

Fig. 2.277 IR spectrum of fergusonite-(Eu)-β drawn using data from Meireles (2011)

O330 Fergusonite-(Eu)-β $EuNbO_4$ (Fig. 2.277)
Locality: Synthetic.
Description: Synthesized on heating of $EuNbO_4$ nanocrystalline powder above 800 °C. Confirmed by powder X-ray diffraction data. Monoclinic, a = 5.393, b = 11.130, c = 5.112 Å, β = 94.7°.
Kind of sample preparation and/or method of registration of the spectrum: KBr disc. Transmission.
Source: Meireles (2011).
Wavenumbers (cm^{-1}): 975w, 940sh, 911w, 894w, 806, 740sh, 652s, 578sh, 532, 464, 446sh.

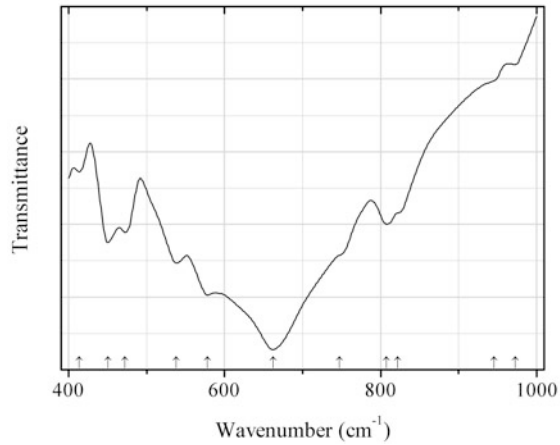

Fig. 2.278 IR spectrum of fergusonite-(Dy)-β drawn using data from Meireles (2011)

O331 Fergusonite-(Dy)-β $DyNbO_4$ (Fig. 2.278)
Locality: Synthetic.
Description: Synthesized on heating of $DyNbO_4$ nanocrystalline powder above 800 °C. Confirmed by powder X-ray diffraction data. Monoclinic, a = 5.321, b = 10.986, c = 5.090 Å, β = 94.5°.
Kind of sample preparation and/or method of registration of the spectrum: KBr disc. Transmission.
Source: Meireles (2011).
Wavenumbers (cm^{-1}): 973w, 946sh, 822sh, 808, 747sh, 662s, 578sh, 538, 472, 450, 413sh.

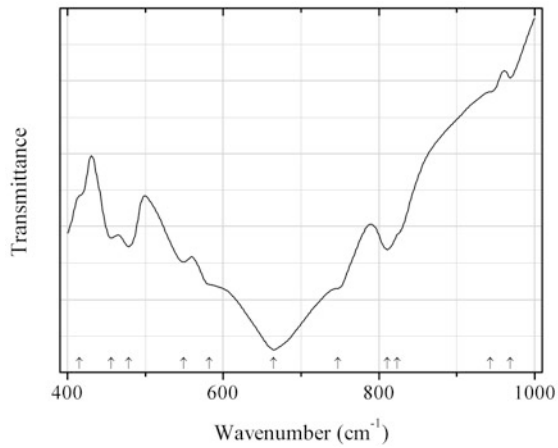

Fig. 2.279 IR spectrum of fergusonite-(Er)-β drawn using data from Meireles (2011)

O332 Fergusonite-(Er)-β $ErNbO_4$ (Fig. 2.279)
Locality: Synthetic.
Description: Synthesized on heating of $ErNbO_4$ nanocrystalline powder above 800 °C. Confirmed by powder X-ray diffraction data. Monoclinic, a = 5.278, b = 10.915, c = 5.055 Å, β = 94.5°.
Kind of sample preparation and/or method of registration of the spectrum: KBr disc. Transmission.
Source: Meireles (2011).
Wavenumbers (cm^{-1}): 969w, 943sh, 824sh, 811, 747sh, 665s, 582sh, 549, 478, 456, 415sh.

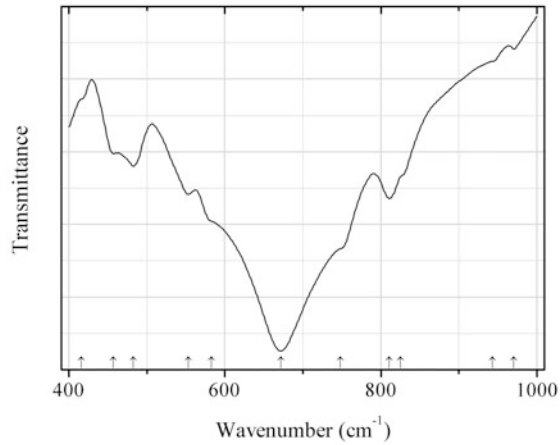

Fig. 2.280 IR spectrum of fergusonite-(Tm)-β drawn using data from Meireles (2011)

O333 Fergusonite-(Tm)-β $TmNbO_4$ (Fig. 2.280)
Locality: Synthetic.
Description: Synthesized on heating of $TmNbO_4$ nanocrystalline powder above 800 °C. Confirmed by powder X-ray diffraction data. Monoclinic, a = 5.258, b = 10.870, c = 5.044 Å, β = 94.6°.
Kind of sample preparation and/or method of registration of the spectrum: KBr disc. Transmission.
Source: Meireles (2011).
Wavenumbers (cm^{-1}): 971w, 943w, 825sh, 811, 748sh, 672s, 583sh, 553, 482, 457, 416sh.
Note: The band position denoted by Meireles (2011) as 563, 487, and 434 cm^{-1} were determined by us at 553, 457, and 416 cm^{-1}, respectively, based on spectral curve analysis of the published spectrum.

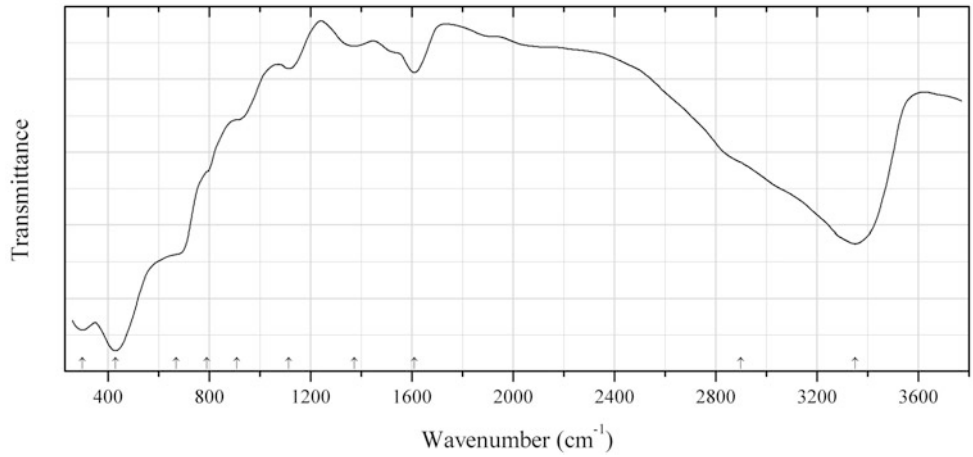

Fig. 2.281 IR spectrum of feroxyhyte drawn using data from Carlson and Schwertmann (1980)

O334 Feroxyhyte $Fe^{3+}O(OH)$ (Fig. 2.281)
Locality: Synthetic.
Description: Brown powder. Synthesized by oxidizing $FeCl_2$ solution with H_2O_2 at pH 8. The strongest lines of the powder X-ray diffraction pattern are observed at 2.563, 2.231, 1.70, and 1.477 Å.
Kind of sample preparation and/or method of registration of the spectrum: KBr disc. Transmission.
Source: Carlson and Schwertmann (1980).
Wavenumbers (cm^{-1}): 3350, 2900sh, 1610, 1372w, 1115w, 910, 790sh, 670sh, 430s, 300s.
Note: The wavenumbers were partly determined by us based on spectral curve analysis of the published spectrum. For IR spectrum of feroxyhyte see also Cornell and Schwertmann (2003).

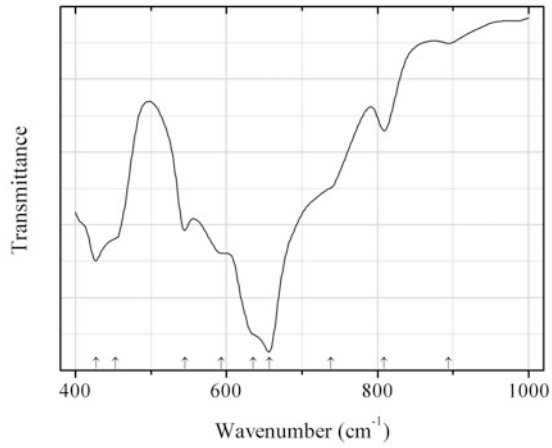

Fig. 2.282 IR spectrum of formanite-(Y) drawn using data from Popovici et al. (2010)

O335 Formanite-(Y) $YTaO_4$ (Fig. 2.282)
Locality: Synthetic.
Description: Prepared by solid-state reaction from the mixture of fine powders of Y_2O_3 and Ta_2O_5 at 1200 °C for 4 h. Confirmed by powder X-ray diffraction data.
Kind of sample preparation and/or method of registration of the spectrum: KBr disc. Absorption.
Source: Popovici et al. (2010).
Wavenumbers (cm^{-1}): 894w, 809w, 738sh, 657s, 635sh, 593sh, 545, 453sh, 427s.

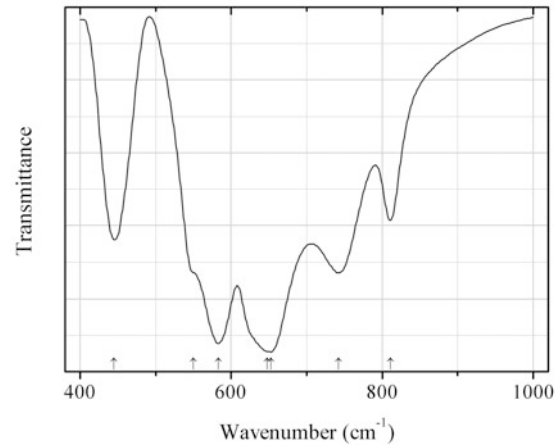

Fig. 2.283 IR spectrum of formanite-(Y) drawn using data from Nazarov and Nazarov (2009)

O336 Formanite-(Y) $YTaO_4$ (Fig. 2.283)
Locality: Synthetic.
Description: Prepared by solid-state reaction from the mixture of fine powders of Y_2O_3 and Ta_2O_5 at 1200 °C for 4 h. Confirmed by powder X-ray diffraction pattern.
Kind of sample preparation and/or method of registration of the spectrum: Absorption. Kind of sample preparation is not indicated.
Source: Nazarov and Nazarov (2009).

Wavenumbers (cm^{-1}): 811, 742, 653s, 648sh, 583s, 550sh, 445.
Note: The wavenumbers were determined by us based on spectral curve analysis of the published spectrum.

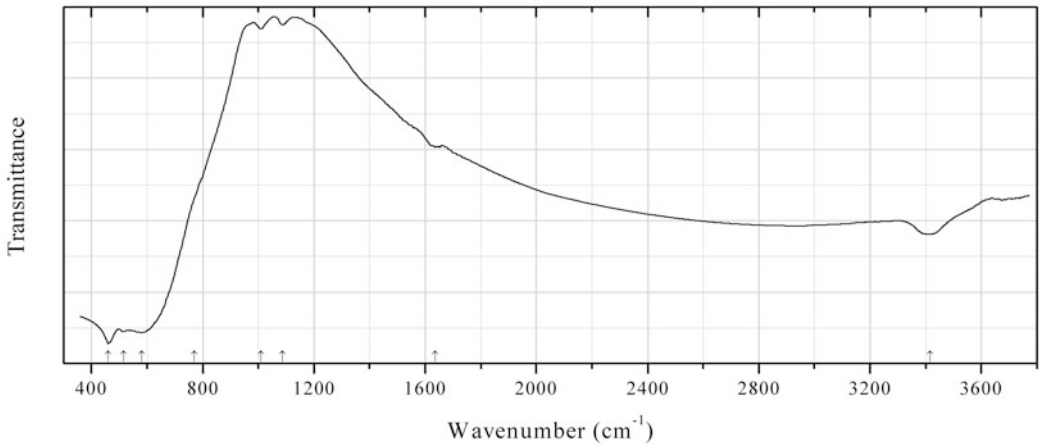

Fig. 2.284 IR spectrum of nioboaeschynite-(Ce) obtained by N.V. Chukanov

O337 Nioboaeschynite-(Ce) $(Ce,Ca)(Nb,Ti)_2(O,OH)_6$ (Fig. 2.284)
Locality: Pit No. 255, Ilmeny (Il'menskie) Mts., South Urals, Russia.
Description: Black grains with conchoidal fracture from the association with fergusonite-(Ce), fergusonite-(Y), phlogopite, calcite, and fluoro-richterite. Amorphous, metamict. Investigated by I.V. Pekov. The empirical formula is (electron microprobe): $(Ce_{0.25}Nd_{0.1}La_{0.1}Ca_{0.3}Th_{0.2})(Nb_{1.25}Ti_{0.75})(O,OH)_6 \cdot nH_2O$.
Kind of sample preparation and/or method of registration of the spectrum: KBr disc. Absorption.
Wavenumbers (cm^{-1}): 3414, 1636w, 1087w, 1009w, 770sh, 580s, 515s, 460s.

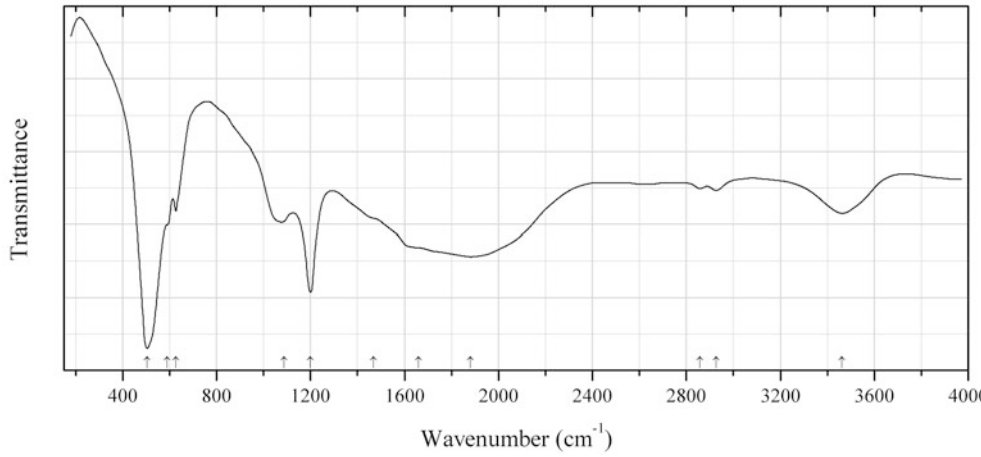

Fig. 2.285 IR spectrum of grimaldiite drawn using data from Livingstone et al. (1984)

O338 Grimaldiite CrO(OH) (Fig. 2.285)

Locality: Hiaca mine, 30 km ENE of Colquechaka, Bolivia.
Description: Pinkish-brown crusts from the association with penroseite and baryte. Confirmed by electron microprobe analyses, TG and powder X-ray diffraction data. Al-bearing variety (the content of Al_2O_3 is from 6.8 to 9.2 wt%).
Kind of sample preparation and/or method of registration of the spectrum: Transmission. Kind of sample preparation is not indicated.
Source: Livingstone et al. (1984).
Wavenumbers (cm^{-1}): 3463, 2927w, 2858w, 1880, 1660sh, 1468sh, 1200s, 1087, 627w, 590sh, 505s.
Note: The wavenumbers were partly determined by us based on spectral curve analysis of the published spectrum.

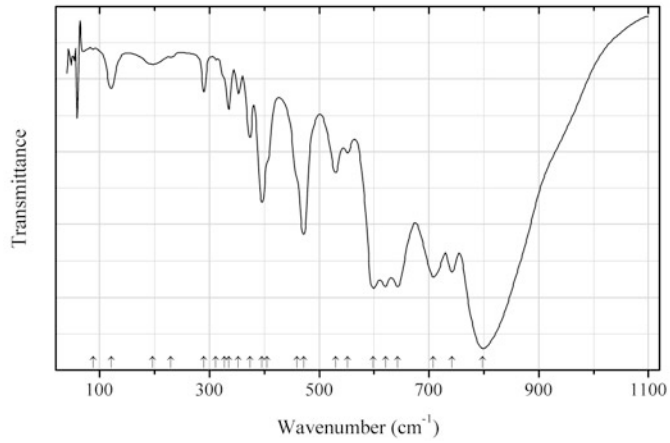

Fig. 2.286 IR spectrum of hibonite drawn using data from Hofmeister et al. (2004)

O339 Hibonite $CaAl_{12}O_{19}$ (Fig. 2.286)
Locality: Synthetic.
Description: Synthesized at high temperature from a stoichiometric mixture of oxides. Confirmed by the powder X-ray diffraction pattern.
Kind of sample preparation and/or method of registration of the spectrum: Powder infrared-absorption spectrum was obtained using a diamond-anvil microsample cell.
Source: Hofmeister et al. (2004).
Wavenumbers (cm^{-1}): 788s, 742s, 708s, 643s, 621s, 599s, 552, 530, 472s, 460sh, 405sh, 396, 374, 353, 335, 327sh, ~312w, 290, ~230w, 197w, 121w, ~88w.
Note: The band position denoted by Hofmeister et al. (2004) as 788 cm^{-1} was determined by us at 798 cm^{-1} based on spectral curve analysis of the published spectrum. Unlike natural hibonite containing impurities (Chukanov 2014a), synthetic pure $CaAl_{12}O_{19}$ gives in the IR spectrum multiple well-resolved peaks.

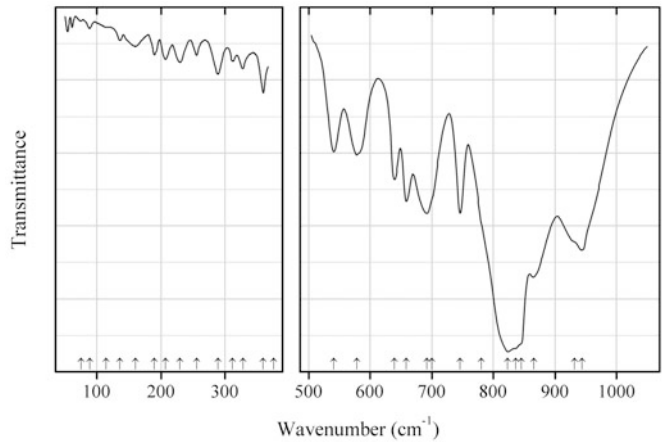

Fig. 2.287 IR spectrum of grossite drawn using data from Hofmeister et al. (2004)

O340 Grossite $CaAl_4O_7$ (Fig. 2.287)
Locality: Synthetic.
Description: Synthesized at high temperature from a stoichiometric mixture of oxides. Confirmed by powder X-ray diffraction data.
Kind of sample preparation and/or method of registration of the spectrum: Powder infrared-absorption spectrum was obtained using a diamond-anvil microsample cell.
Source: Hofmeister et al. (2004).
Wavenumbers (cm^{-1}): 944s, 932sh, 866s, 846sh, 836sh, 823s, 781sh, 746, 700sh, 692, 659, 639, 578, 541, 445, 425w, 376w, 360w, 328w, 312w, 289, 256w, 230w, 207w, 190w, 160w, 136w, 114w, 89w, 75w.
Note: The band positions denoted by Hofmeister et al. (2004) as 942, 872, 813, and 682 cm^{-1} were determined by us at 932, 866, 823, and 692 cm^{-1}, respectively, based on spectral curve analysis of the published spectrum. For the IR spectrum of synthetic grossite see also Taş (1988).

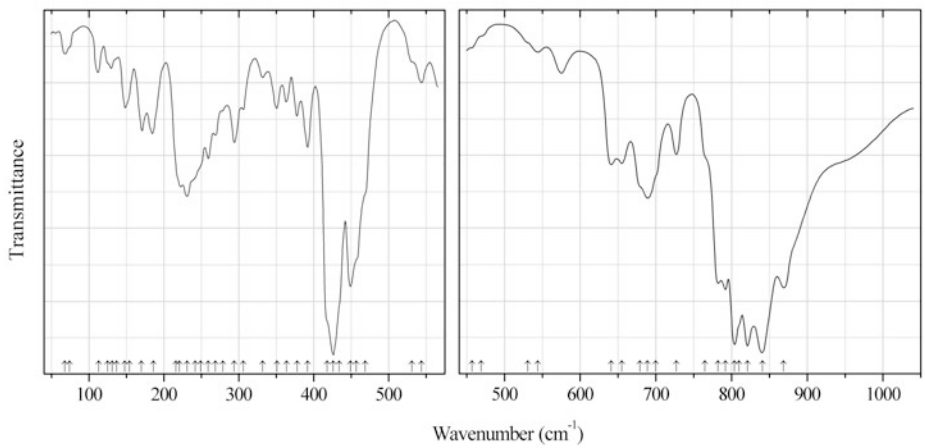

Fig. 2.288 IR spectrum of calcium monoaluminate drawn using data from Hofmeister et al. (2004)

O341 Calcium monoaluminate $CaAl_2O_4$ (Fig. 2.288)

Locality: Synthetic.
Description: Synthesized at high temperature from a stoichiometric mixture of oxides. Confirmed by the powder X-ray diffraction pattern.
Kind of sample preparation and/or method of registration of the spectrum: Powder infrared-absorption spectrum was obtained using a diamond-anvil microsample cell.
Source: Hofmeister et al. (2004).
Wavenumbers (cm^{-1}): 869s, 841s, 821s, 810sh, 804s, 792s, 782s, 765sh, 727, 700sh, 689, 679sh, 655, 641, 575w, 544w, 531sh, 469sh, 457sh, 449s, 434s, 426s, 418s, 392, 378, 364, 351, 332w, 306, 294, 279sh, 269, 259, 249sh, 242sh, 231, 221, 216sh, 186, 170, 154sh, 148, 137sh, 131w, 125sh, 113w, 74sh, 68w.

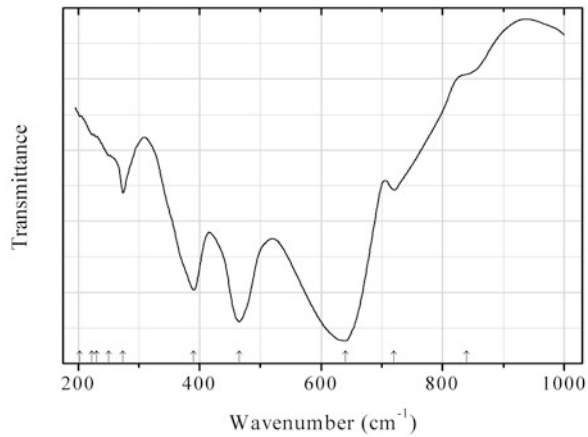

Fig. 2.289 IR spectrum of aeschynite-(Ce) end-member drawn using data from Shabalin (1982)

O342 Aeschynite-(Ce) end-member $CeTiNbO_6$ (Fig. 2.289)
Locality: Synthetic.
Description: Synthesized by means of annealing of a stoichiometric mixture of components.
Kind of sample preparation and/or method of registration of the spectrum: CsI disc. Absorption.
Source: Shabalin (1982).
Wavenumbers (cm^{-1}): 840sh, 720, 640s, 465s, 390s, 274, 250w, 230w, 223w, 203w.

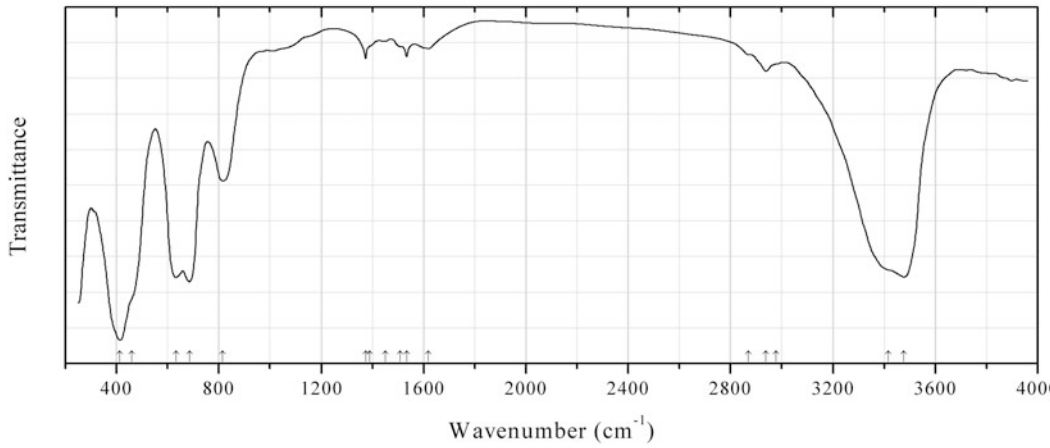

Fig. 2.290 IR spectrum of akaganeite drawn using data from Murad (1979)

O343 Akaganeite $(Fe^{3+},Fe^{2+})(OH,O)_2Cl_x$ (Fig. 2.290)
Locality: Synthetic.
Description: Prepared by slow hydrolysis of $FeCl_3$ solution. Tetragonal or pseudotetragonal, $a = 10.535$, $c = 3.030$ Å. The strongest lines of the powder X-ray diffraction pattern [*d*, Å (*I*, %) (*hkl*)] are: 7.467 (40) (110), 5.276 (30) (200), 3.333 (100) (310), 2.5502 (55) (211), 2.2952 (35) (301), 1.6434 (35) (521).
Kind of sample preparation and/or method of registration of the spectrum: KBr disc. Absorption.
Source: Murad (1979).
Wavenumbers (cm^{-1}): 3477s, 3416sh, 2978sh, 2938w, 2871w, 1620w, 1534sh, 1510sh, 1452w, 1390sh, 1374w, 816, 685s, 633s, 460sh, 414s.
Note: The wavenumbers were determined by us based on spectral curve analysis of the published spectrum. The weak bands in the range from 2800 to 3000 cm^{-1} may correspond to the admixture of an organic substance.

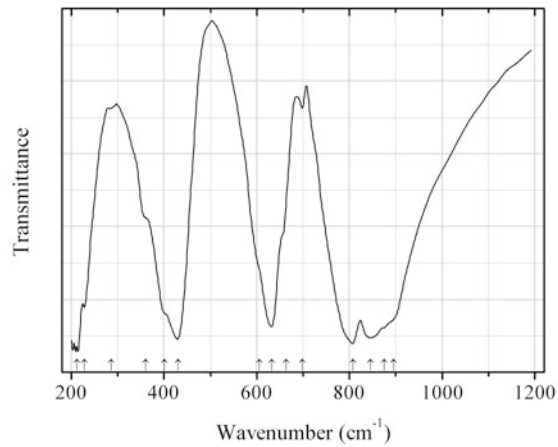

Fig. 2.291 IR spectrum of barium monoaluminate drawn using data from Henderson and Taylor (1982)

O344 Barium monoaluminate $BaAl_2O_4$ (Fig. 2.291)

Locality: Synthetic.
Description: Prepared by mixing of $BaCO_3$ with $Al(NO_3)_3 \cdot 9H_2O$ and heating at 1400 °C for 4 h. Hexagonal, a = 5.22, c = 8.79 Å, V = 207.7 Å^3.
Kind of sample preparation and/or method of registration of the spectrum: KBr disc. Transmission.
Source: Henderson and Taylor (1982).
Wavenumbers (cm^{-1}): 895sh, 875sh, 845s, 808s, 698w, 663sh, 632s, 606sh, 401sh, 430s, 360sh, 286w, 228, 212.
Note: The wavenumbers were partly determined by us based on spectral curve analysis of the published spectrum.

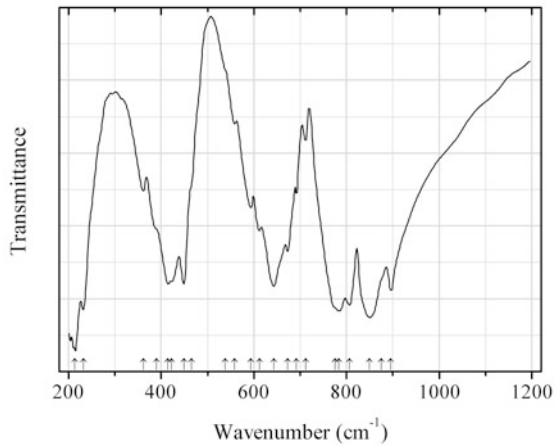

Fig. 2.292 IR spectrum of strontium monoaluminate drawn using data from Henderson and Taylor (1982)

O345 Strontium monoaluminate $SrAl_2O_4$ (Fig. 2.292)
Locality: Synthetic.
Description: Prepared by mixing of $SrCO_3$ with $Al(NO_3)_3 \cdot 9H_2O$ and heating at 1400 °C for 4 h. Monoclinic, a = 5.15, b = 8.83, c = 8.44 Å, β = 93.4° V = 383.0 Å^3.
Kind of sample preparation and/or method of registration of the spectrum: KBr disc. Transmission.
Source: Henderson and Taylor (1982).
Wavenumbers (cm^{-1}): 896s, 875sh, 850s, 807s, 784s, 775sh, 712, 692w, 673, 643s, 612, 593, 559, 538sh, 465sh, 449s, 423s, 415s, 390, 362, 232s, 214s.
Note: The wavenumbers were partly determined by us based on spectral curve analysis of the published spectrum.

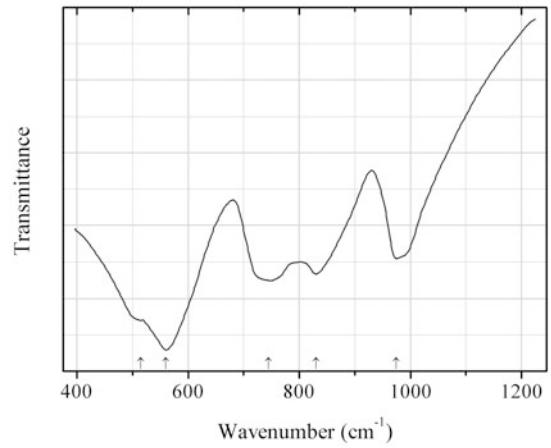

Fig. 2.293 IR spectrum of alumotantite drawn using data from Yamaguchi et al. (1987)

O346 Alumotantite $AlTaO_4$ (Fig. 2.293)
Locality: Synthetic.
Description: Orthorhombic. The strongest lines of the powder X-ray diffraction pattern [*d*, Å (*I*, %) (*hkl*)] are: 5.03 (55) (101), 3.69 (45) (020), 3.57 (100) (102), 3.07 (60) (200), 2.685 (65) (211).
Kind of sample preparation and/or method of registration of the spectrum: KBr disc. Transmission.
Source: Yamaguchi et al. (1987).
Wavenumbers (cm^{-1}): 975, 830, 745, 560s, 515s.

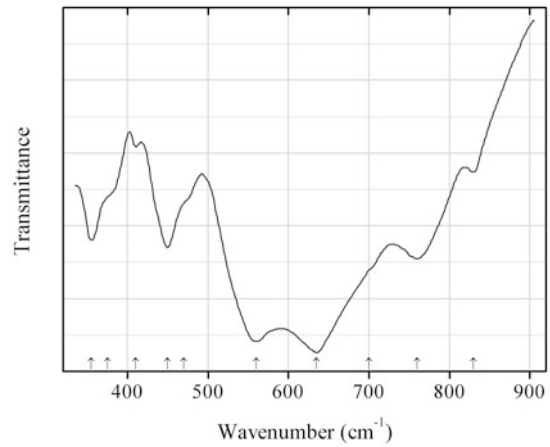

Fig. 2.294 IR spectrum of barium niobate O347 drawn using data from Repelin et al. (1979)

O347 Barium niobate O347 $BaNb_2O_6$ (Fig. 2.294)
Locality: Synthetic.
Description: No data.
Kind of sample preparation and/or method of registration of the spectrum: Transmission. Kind of sample preparation is not indicated.

Source: Repelin et al. (1979).
Wavenumbers (cm^{-1}): 830w, 760, 700sh, 635s, 560s, 470sh, 450, 410w, 375sh, 355.

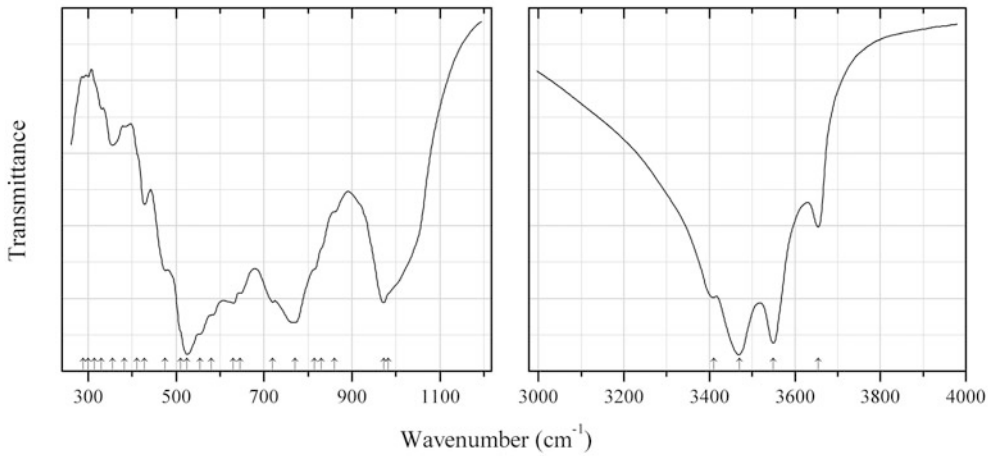

Fig. 2.295 IR spectrum of bayerite drawn using data from Elderfield and Hem (1973)

O348 Bayerite $Al(OH)_3$ (Fig. 2.295)
Locality: Synthetic.
Kind of sample preparation and/or method of registration of the spectrum: KBr disc. Transmission.
Source: Elderfield and Hem (1973).
Wavenumbers (cm^{-1}): 3655, 3550s, 3470s, 3410, 982sh, 972, 860, 830sh, 815sh, 770s, 720, 646sh, 630, 580s, 555s, 525s, 510sh, 475, 428, 410sh, 382w, 355w, 330w, 314sh, 300w, 289w.
Note: The wavenumbers were partly determined by us based on spectral curve analysis of the published spectrum.

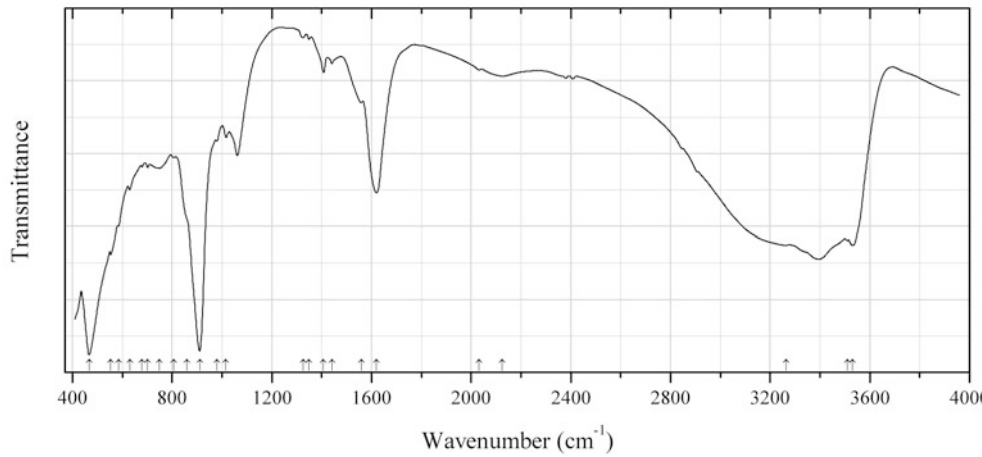

Fig. 2.296 IR spectrum of billietite drawn using data from Čejka et al. (1998)

O349 Billietite $Ba(UO_2)_6O_4(OH)_6 \cdot 8H_2O$ (Fig. 2.296)

Locality: Synthetic.
Description: Synthesized in the reaction between $Ba(NO_3)_2$ and $(UO_2)(CH_3COO)_2$ in aqueous solution, at the ratio Ba:U = 1:10. Confirmed by thermal analysis and powder X-ray diffraction data. Orthorhombic, space group $Pna2_1$; a = 30.191(6), b = 12.077(3), c = 7.142(2) Å. The strongest lines of the powder X-ray diffraction pattern [d, Å (I, %) (hkl)] are: 7.55 (100) (400), 3.769 (27) (800), 3.506 (23) (031), 3.227 (29) (402), 3.180 (35) (431), 2.0471 (37) (12.0.2).
Kind of sample preparation and/or method of registration of the spectrum: Diffusion reflectance. Suspension in Nujol (in the range from 50 to 600 cm^{-1}) and KBr disc.
Source: Čejka et al. (1998).
Wavenumbers (cm^{-1}): 3531s, 3510s, 3265s, 2124w, 2033w, 1621s, 1560sh, 1441w, 1408w, 1349w, 1326w, 1016, 980, 911s, 860sh, (807), 750, (702), (680), (630), (585), (554), 467s, 407, 357s, 329sh, 299, 268, 245.
Note: The wavenumbers were partly determined by us based on spectral curve analysis of the published spectrum. Weak bands in the range from 2800 to 3000 cm^{-1} may correspond to the admixture of an organic substance.

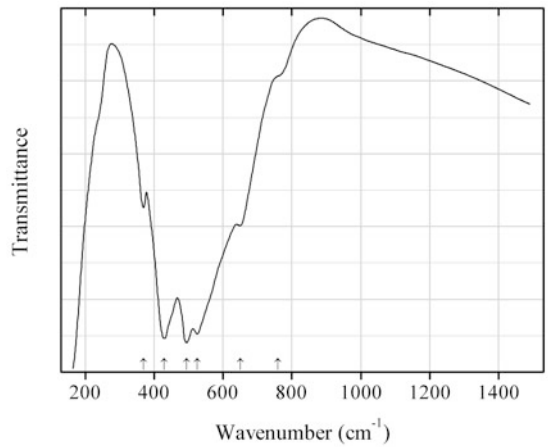

Fig. 2.297 IR spectrum of birnessite drawn using data from Bilinski et al. (2002)

O350 Birnessite $(Na,Ca,K)_{0.5–1}(Mn^{4+},Mn^{3+})_2O_4 \cdot nH_2O$ ($n \approx 1.5$) (Fig. 2.297)
Locality: Synthetic.
Description: Confirmed by electron microprobe analysis and powder X-ray diffraction data.
Kind of sample preparation and/or method of registration of the spectrum: KBr disc. Absorption.
Source: Bilinski et al. (2002).
Wavenumbers (cm^{-1}): 760sh, 650, 525s, 494s, 430s, 370.
Note: The wavenumbers were partly determined by us based on spectral curve analysis of the published spectrum.

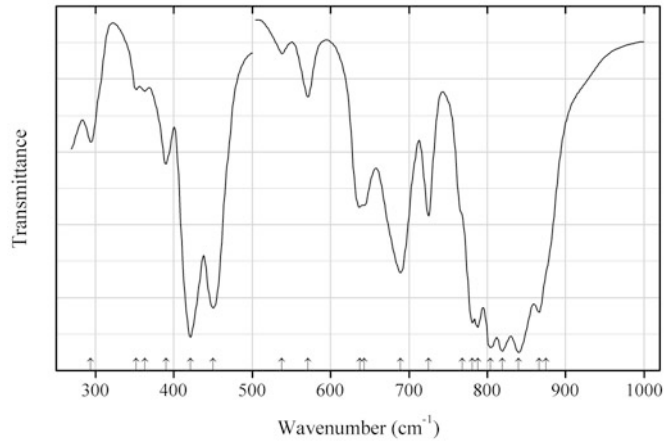

Fig. 2.298 IR spectrum of calcium monoaluminate drawn using data from Tarte (1967)

O351 Calcium monoaluminate $CaAl_2O_4$ (Fig. 2.298)
Locality: Synthetic.
Description: Synthesized by solid state reaction between $Al(OH)_3$ and CaO or $CaCO_3$.
Kind of sample preparation and/or method of registration of the spectrum: KBr and KI discs. Transmission.
Source: Tarte (1967).
Wavenumbers (cm^{-1}): 875sh, 866s, 840s, 819s, 804s, 788s, 781s, 768sh, 725, 689, 643, 637, 571, 538w, 450s, 421s, 390, 363w, 352w, 294.
Note: The wavenumbers were determined by us based on spectral curve analysis of the published spectrum.

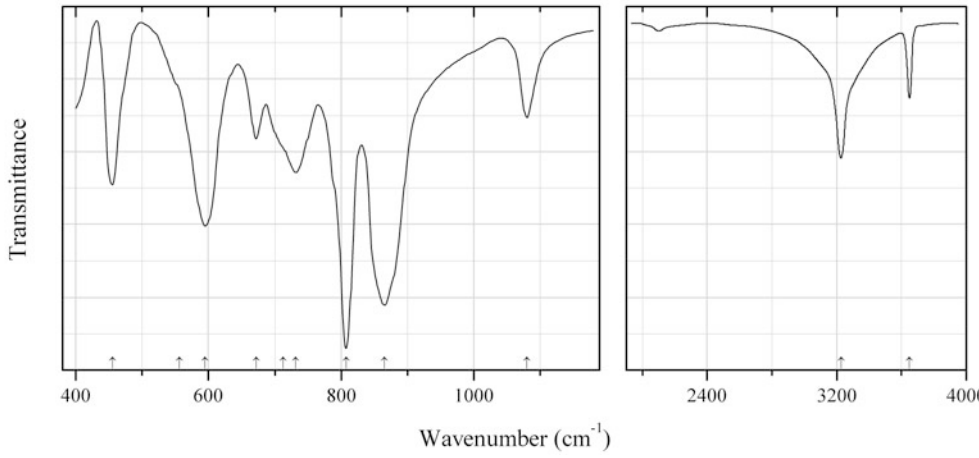

Fig. 2.299 IR spectrum of calcium aluminate O352 drawn using data from Peters et al. (2012)

O352 Calcium aluminate O352 $Ca_4Al_6O_{13}\cdot 3H_2O$ (Fig. 2.299)
Locality: Synthetic.
Description: Synthesized by means of hydrothermal treatment. Orthorhombic, space group *Aema*, $a \approx 12.43$, $b \approx 12.81$, $c \approx 8.87$ Å (Portland cement phase $C_4A_3H_3$).

Kind of sample preparation and/or method of registration of the spectrum: KBr disc. Absorption.
Source: Peters et al. (2012).
Wavenumbers (cm^{-1}): 3649, 3227, 1080, 865s, 808s, 732, 713sh, 672, 595s, 556sh, 455.
Note: The wavenumbers were partly determined by us based on spectral curve analysis of the published spectrum.

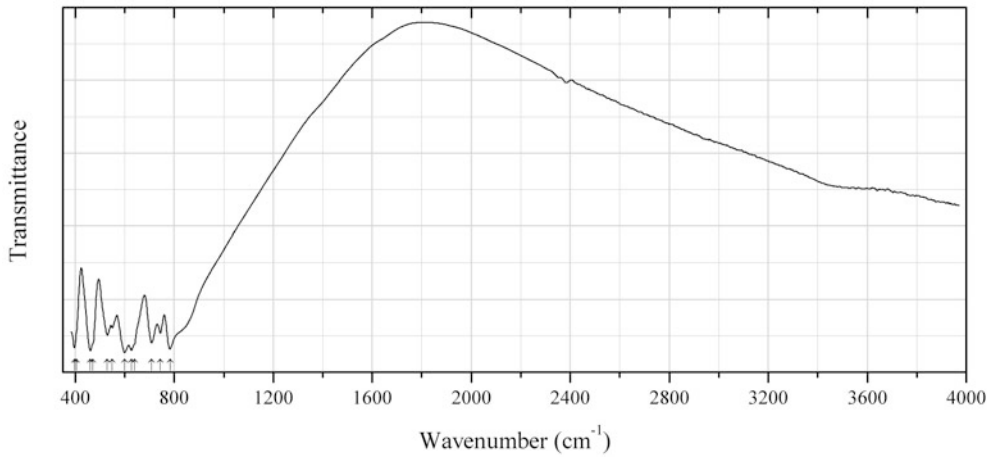

Fig. 2.300 IR spectrum of hibonite drawn using data from Taş (1998)

O354 Hibonite $CaAl_{12}O_{19}$ (Fig. 2.300)
Locality: Synthetic.
Description: Calcium hexaaluminate (hybonite end-member). Synthesized as high-compound-purity ceramic powder by using the self-propagating combustion synthesis method. Confirmed by powder X-ray diffraction data.
Kind of sample preparation and/or method of registration of the spectrum: KBr disc. Transmission.
Source: Taş (1998).
Wavenumbers (cm^{-1}): 783s, 745, 708, 640sh, 627s, 600s, 530, 550, 472sh, 461s, 405sh, 397s.
Note: The wavenumbers were determined by us based on spectral curve analysis of the published spectrum.

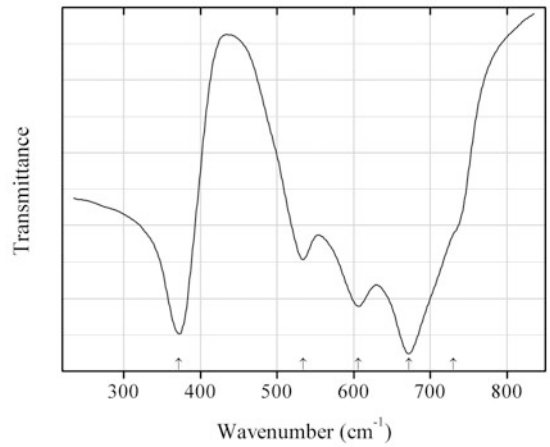

Fig. 2.301 IR spectrum of cesstibtantite drawn using data from Povarennykh (1981b)

O355 Cesstibtantite $Cs_x(Sb,Na)Ta_2(O,OH)_7 \cdot nH_2O$ (Fig. 2.301)
Locality: Not indicated.
Kind of sample preparation and/or method of registration of the spectrum: KBr disc. Absorption.
Source: Povarennykh (1981b).
Wavenumbers (cm^{-1}): 730sh, 672s, 606, 534, 372s.
Note: According to the approved nomenclature of the pyrochlore supergroup of minerals (Atencio et al. 2010), cesstibtantite is considered as a variety of hydroxykenomicrolite.

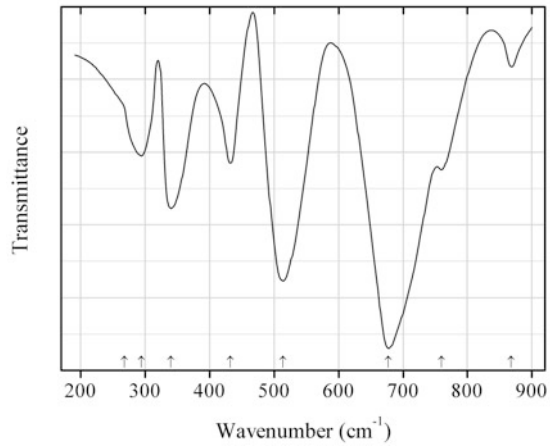

Fig. 2.302 IR spectrum of changbaiite drawn using data from Povarennykh (1981b)

O356 Changbaiite $PbNb_2O_6$ (Fig. 2.302)
Locality: Synthetic.
Kind of sample preparation and/or method of registration of the spectrum: KBr disc. Transmission.
Source: Povarennykh (1981b).
Wavenumbers (cm^{-1}): 868w, 760, 677s, 514s, 432, 340, 294, 268sh.

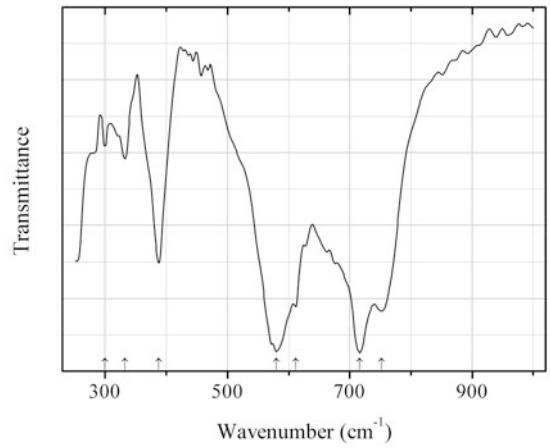

Fig. 2.303 IR spectrum of chromium antimonate drawn using data from Filipek et al. (2000)

O357 Chromium antimonate $CrSbO_4$ (Fig. 2.303)
Tripuhyite Cr analogue

Locality: Synthetic.
Description: Obtained by heating an equimolar Sb_2O_3/Cr_2O_3 mixture in air at 1473 K for 3 days. Isostructural with tripuhyite. Confirmed by powder X-ray diffraction data.
Kind of sample preparation and/or method of registration of the spectrum: KBr disc. Transmission.
Source: Filipek et al. (2000).
Wavenumbers (cm^{-1}): 752, 716s, 612sh, 580s, 388, 332w, 300w.

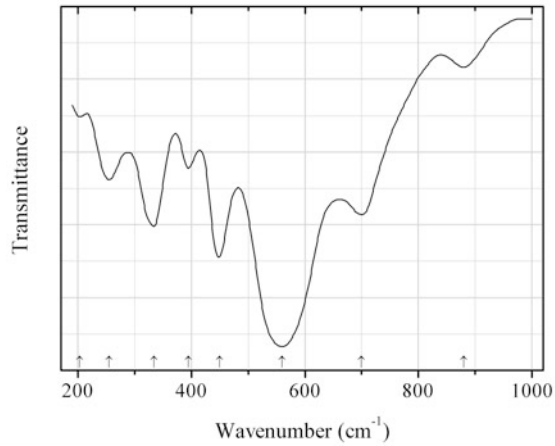

Fig. 2.304 IR spectrum of ecandrewsite drawn using data from Shabalin (1982)

O358 Ecandrewsite $ZnTiO_3$ (Fig. 2.304)
Locality: Synthetic.
Description: Synthesized from oxides in a solid-state reaction. Confirmed by means of chemical analysis and powder X-ray diffraction.
Kind of sample preparation and/or method of registration of the spectrum: CsI disc. Transmission.
Source: Shabalin (1982).
Wavenumbers (cm^{-1}): 880w, 700, 560s, 450s, 395w, 334, 255, 203w.

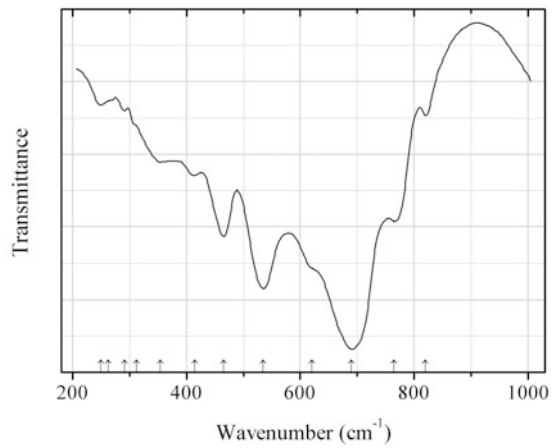

Fig. 2.305 IR spectrum of euxenite-(Y) drawn using data from Shabalin (1982)

O359 Euxenite-(Y) $(Y,Ca,Ce,U,Th)(Nb,Ta,Ti)_2O_6$ (Fig. 2.305)
Locality: Synthetic.
Description: A compound with the formula $YNbTiO_6$ corresponding to the euxenite end-member. Synthesized in a solid-state reaction. Confirmed by the powder X-ray diffraction pattern.
Kind of sample preparation and/or method of registration of the spectrum: CsI disc. Transmission.
Source: Shabalin (1982).
Wavenumbers (cm^{-1}): 820w, 765, 690s, 620sh, 535s, 465, 414, 354w, 312sh, 291w, 263sh, 249w.

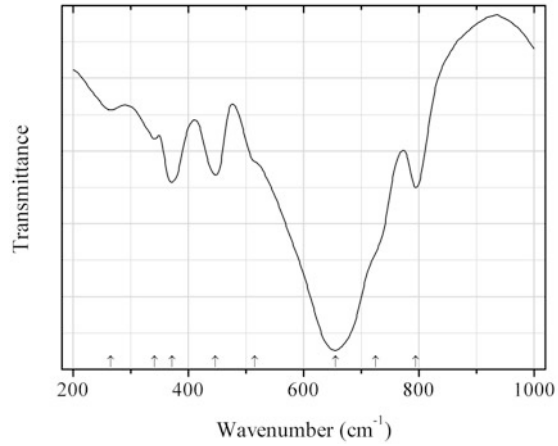

Fig. 2.306 IR spectrum of fergusonite-(Ce) drawn using data from Shabalin (1982)

O360 Fergusonite-(Ce) $CeNbO_4$ (Fig. 2.306)
Locality: Synthetic.
Description: Synthesized in solid-state reaction. Confirmed by powder X-ray diffraction data.
Kind of sample preparation and/or method of registration of the spectrum: CsI disc. Transmission.
Source: Shabalin (1982).
Wavenumbers (cm^{-1}): 795, 725sh, 655s, 515sh, 447, 371, 341, 265w.

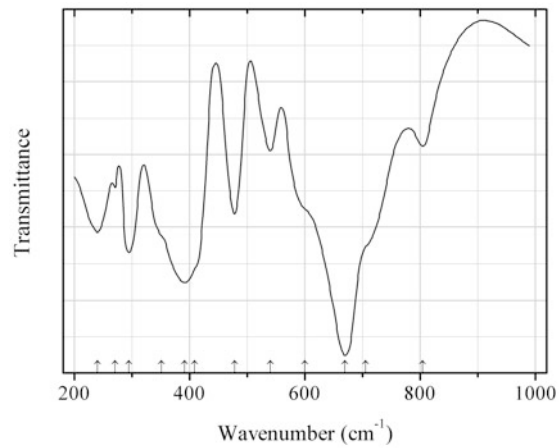

Fig. 2.307 IR spectrum of fergusonite-(Y)-β drawn using data from Shabalin (1982)

O361 Fergusonite-(Y)-β $YNbO_4$ (Fig. 2.307)

β-Fergusonite-(Y)
Locality: Synthetic.
Description: Synthesized in solid-state reaction. Confirmed by powder X-ray diffraction data.
Kind of sample preparation and/or method of registration of the spectrum: CsI disc. Transmission.
Source: Shabalin (1982).
Wavenumbers (cm^{-1}): 805w, 706sh, 670s, 600sh, 540w, 478, 408sh, 391s, 351sh, 294, 270w, 240.

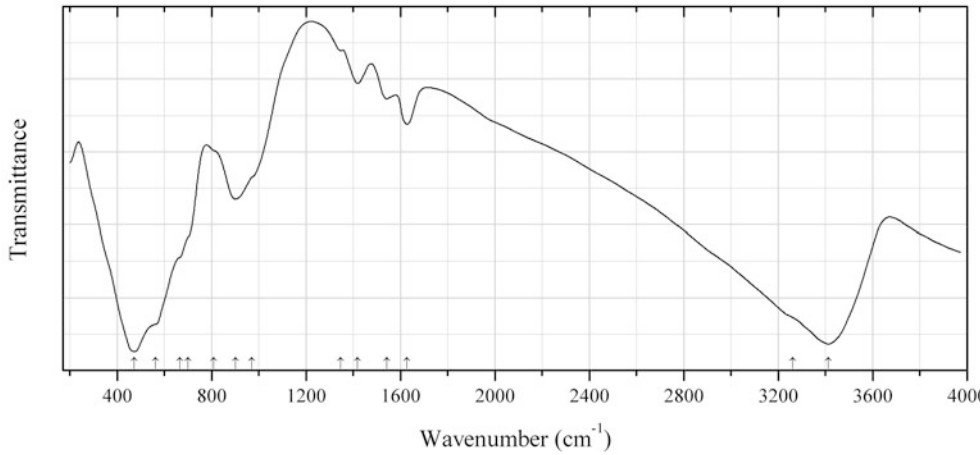

Fig. 2.308 IR spectrum of ferrihydrite drawn using data from Wilson and Russell (1983)

O362 Ferrihydrite $Fe^{3+}_{5-x}(O,OH)_8$ (Fig. 2.308)
Locality: Mineral Hill, Middleton, Delaware Co., Pennsylvania, USA.
Description: Specimen No. 66908 from the British Museum of Natural History. Shiny black massive. A Si-bearing variety, with 7.42 wt% SiO_2 ("melanosiderite"). The strongest lines of the powder X-ray diffraction pattern [*d*, Å (*I*, %)] are: 4.26 (40), 2.55 (75), 2.45 (20), 2.24 (100), 1.980 (30), 1.719 (30), 1.512 (40), 1.471 (60).
Kind of sample preparation and/or method of registration of the spectrum: KBr disc. Transmission.
Source: Wilson and Russell (1983).
Wavenumbers (cm^{-1}): 3412s, 3260sh, 1627, 1542w, 1418w, 1346w, 970sh, 900, 809sh, 700sh, 665sh, 563sh, 472s.
Note: The wavenumbers were partly determined by us based on spectral curve analysis of the published spectrum.

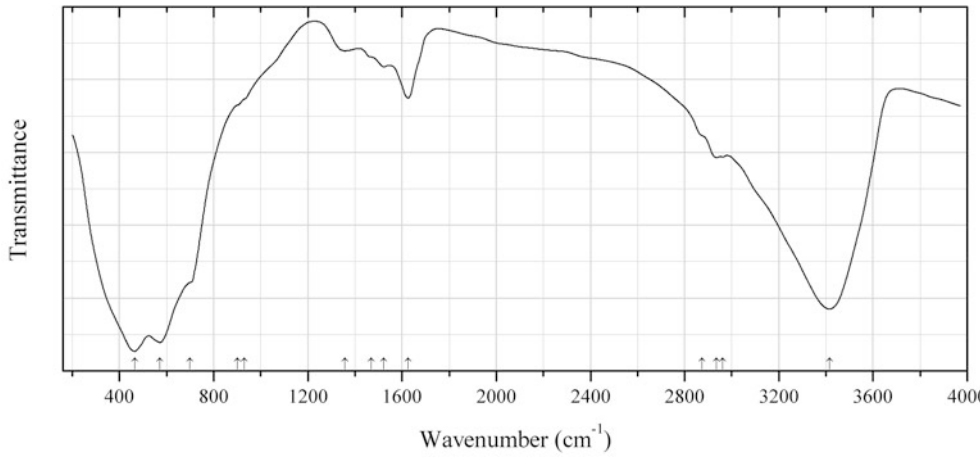

Fig. 2.309 IR spectrum of ferrihydrite drawn using data from Wilson and Russell (1983)

O363 Ferrihydrite $Fe^{3+}_{5-x}(O,OH)_8$ (Fig. 2.309)
Locality: Synthetic.
Description: No data.
Kind of sample preparation and/or method of registration of the spectrum: KBr disc. Transmission.
Source: Wilson and Russell (1983).
Wavenumbers (cm^{-1}): 3415s, 2962, 2935, 2875sh, 1626, 1523w, 1468w, 1357w, 931sh, 900sh, 700sh, 572s, 465s.
Note: The wavenumbers were partly determined by us based on spectral curve analysis of the published spectrum. The bands in the range from 2800 to 3000 cm^{-1} may correspond to the admixture of an organic substance.

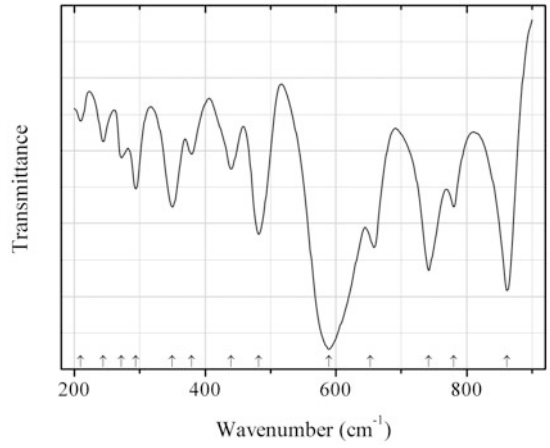

Fig. 2.310 IR spectrum of fersmite drawn using data from Povarennykh (1981b)

O364 Fersmite (Ca,*REE*,Na)(Nb,Ta,Ti)$_2$(O,OH,F)$_6$ (Fig. 2.310)

Locality: Synthetic.
Description: Pure $CaNb_2O_6$.
Kind of sample preparation and/or method of registration of the spectrum: KBr disc. Transmission.
Source: Povarennykh et al. (1981b).
Wavenumbers (cm^{-1}): 862s, 780, 742s, 653, 589s, 482, 440, 379, 350, 294s, 272, 244, 210w.

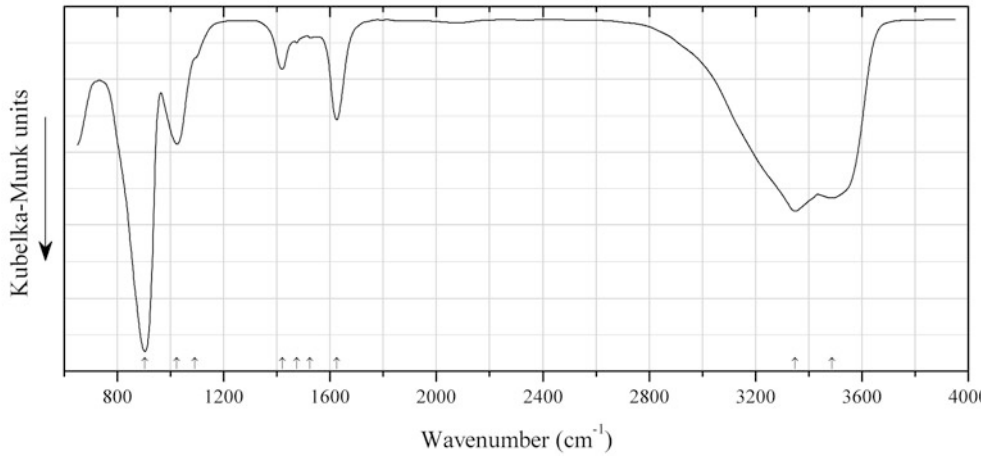

Fig. 2.311 IR spectrum of fourmarierite drawn using data from Plášil et al. (2008)

O365 Fourmarierite $Pb(UO_2)_4O_3(OH)_4 \cdot 4H_2O$ (Fig. 2.311)
Locality: Háje, near Přibram, Central Bohemia region, Czech Republic.
Description: Identified by powder X-ray diffraction data.
Kind of sample preparation and/or method of registration of the spectrum: Diffuse reflectance of a powdered sample.
Source: Plášil et al. (2008).
Wavenumbers (cm^{-1}): 3487s, 3348s, 1625s, 1525w, 1474w, 1420, 1092sh, 1024, 903s.
Note: The wavenumbers were determined by us based on spectral curve analysis of the published spectrum.

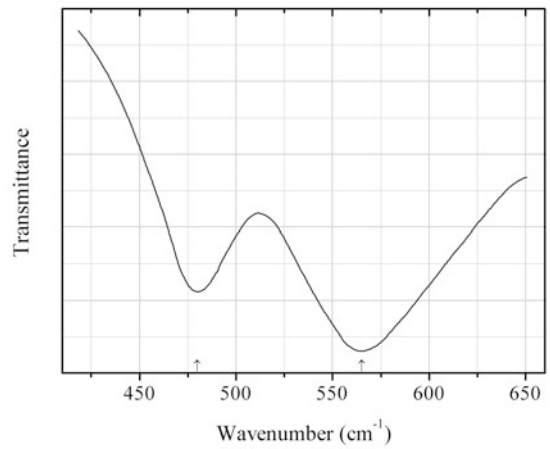

Fig. 2.312 IR spectrum of geikielite drawn using data from Bushueva et al. (1983)

O366 Geikielite $MgTiO_3$ (Fig. 2.312)
Locality: Synthetic.
Description: Synthesized from TiO_2 and magnesium oxalate at 750 °C and partial pressure of water 1.01×10^8 Pa during 7 days. Confirmed by the powder X-ray diffraction pattern.
Kind of sample preparation and/or method of registration of the spectrum: Nujol mull. Absorption.
Source: Bushueva et al. (1983).
Wavenumbers (cm^{-1}): 565s, 480s.
Note: In the solid-solution series $FeTiO_3$–$MgTiO_3$ gradual shifts of the bands from 530 to 565 and from 438 to 480 cm^{-1} is observed.

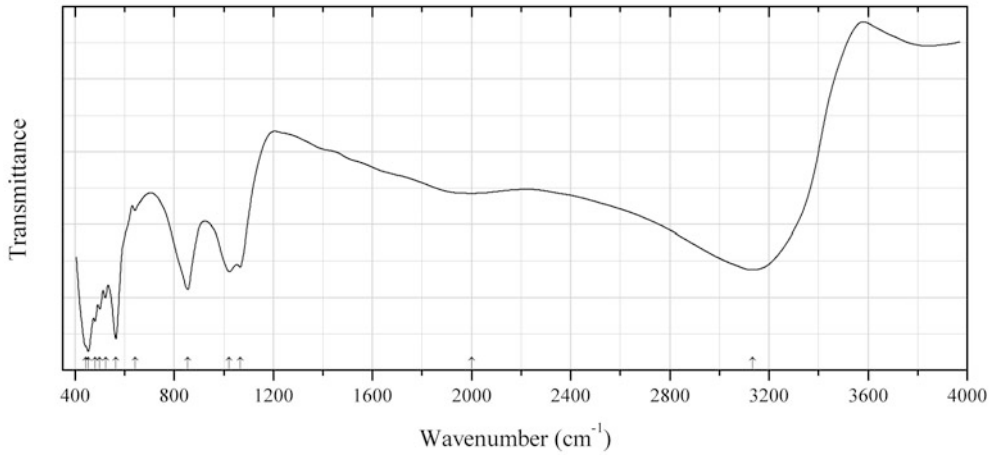

Fig. 2.313 IR spectrum of claringbullite drawn using data from Nytko (2008)

O367 Claringbullite $Cu^{2+}{}_4Cl(OH)_7$ (Fig. 2.313)
Locality: Synthetic.
Description: Synthesized in the reaction between $Cu_2(OH)_2CO_3$, NaCl, and HBF_4 under hydrothermal conditions. The empirical formula is $Cu_4(OH)_{6.73}Cl_{1.27}$. The crystal structure is solved.
Kind of sample preparation and/or method of registration of the spectrum: KBr disc. Transmission.
Source: Nytko (2008).
Wavenumbers (cm^{-1}): 3133s, 2001, 1067, 1022, 855, 642w, 565s, 523, 500, 480, 453s, 444sh.
Note: The wavenumbers were partly determined by us based on spectral curve analysis of the published spectrum.

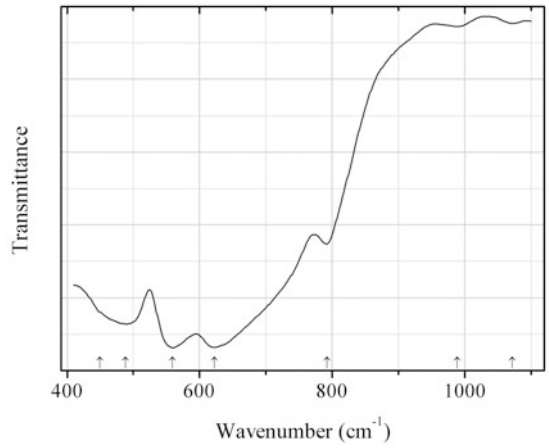

Fig. 2.314 IR spectrum of heftetjernite drawn using data from Arkhipova et al. (2006)

O368 Heftetjernite $ScTaO_4$ (Fig. 2.314)
Locality: Synthetic.
Description: Prepared by multi-stage annealing of a mixture of oxides in air at temperatures from 600 to 1400 °C with intermediate grinding of the charge. Isostructural with wolframite. The empirical formula is $ScTa_{0.92}Nb_{0.08}O_4$. Confirmed by powder X-ray diffraction data.
Kind of sample preparation and/or method of registration of the spectrum: Suspension in mineral oil. Transmission.
Source: Arkhipova et al. (2006).
Wavenumbers (cm^{-1}): 1072w, 989w, 792, 622s, 559s, 488s, 450sh.
Note: The wavenumbers were partly determined by us based on spectral curve analysis of the published spectrum.

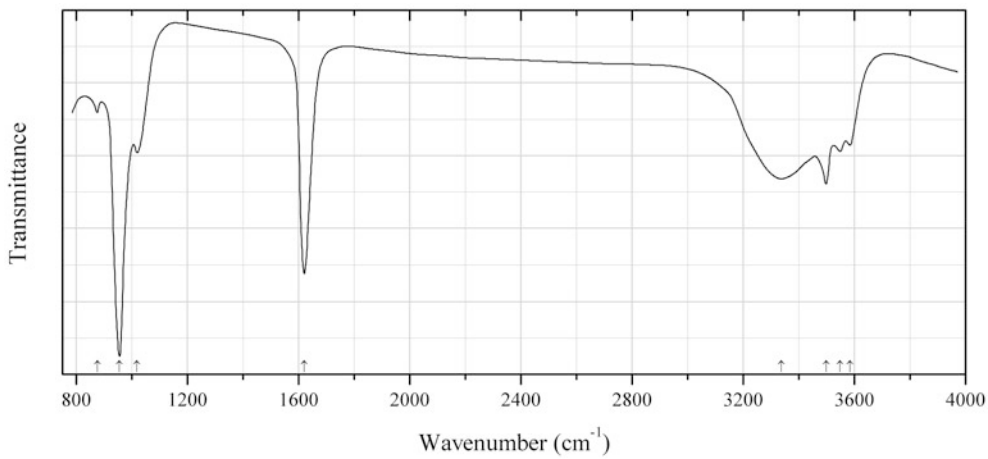

Fig. 2.315 IR spectrum of heisenbergite drawn using data from Price and Stuart (1973)

O369 Heisenbergite $(UO_2)(OH)_2 \cdot H_2O$ (Fig. 2.315)
Locality: Synthetic.

Description: Obtained from UO_3 by exposure to water vapour for 3 days at room temperature. Confirmed by thermal and chemical analyses.
Kind of sample preparation and/or method of registration of the spectrum: Nujol mull. Transmission.
Source: Price and Stuart (1973).
Wavenumbers (cm^{-1}): 3584, 3548, 3498, 3338, 1620s, 1018w, 955s, 875w.
Note: The wavenumbers were partly determined by us based on spectral curve analysis of the published spectrum.

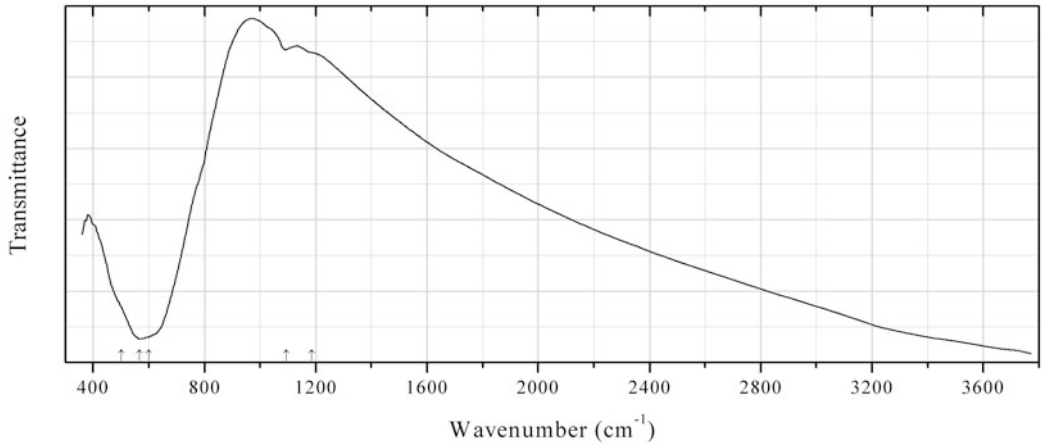

Fig. 2.316 IR spectrum of rossovskyite obtained by N.V. Chukanov

O370 Rossovskyite (Fe,Ta)(Nb,Ti)O_4 (Fig. 2.316)
Locality: Bulgut pegmatite occurrence, Altai Mountains, Mongolia (type locality).
Description: Black imperfect crystal from the association with microcline, albite, muscovite, and triplite. Holotype sample. Monolinic, space group: *P*2/*c*, a = 4.668(1), b = 5.659(1), c = 5.061(1) Å, β = 90.21(1)°, V = 133.69(4) $Å^3$, Z = 2. D_{meas} = 6.06(10) g/cm^3, D_{calc} = 6.032 g/cm^3. The empirical formula is $Mn^{2+}_{0.06}Fe^{2+}_{0.21}Fe^{3+}_{0.47}Ti_{0.25}Nb_{0.51}Ta_{0.43}W_{0.06}O_4$. The strongest lines of the powder X-ray diffraction pattern [*d*, Å (*I*, %) (*hkl*)] are: 3.604 (49) (110), 2.938 (100) (−1–11), 2.534 (23) (021), 2.476 (29) (021), 2.337 (27) (200), 1.718 (26) (−202, 202), 1.698 (31) (−2–21), 1.440 (21) (−311, −132).
Kind of sample preparation and/or method of registration of the spectrum: KBr disc. Absorption.
Wavenumbers (cm^{-1}): 1185sh, 1093w, 600sh, 567s, 500sh.

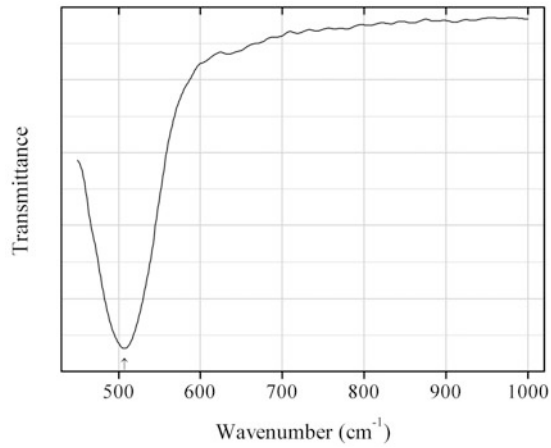

Fig. 2.317 IR spectrum of heterogenite-*2H* drawn using data from Tang et al. (2008)

O371 Heterogenite-2*H* $Co^{3+}O(OH)$ (Fig. 2.317)
Locality: Synthetic.
Description: Prepared by precipitation-oxidation from cobalt nitrate aqueous solution (through a precipitation with sodium hydroxide and an oxidation by hydrogen peroxide) and subsequent calcination. Confirmed by powder X-ray diffraction data.
Kind of sample preparation and/or method of registration of the spectrum: KBr disc. Absorption.
Source: Tang et al. (2008).
Wavenumbers (cm^{-1}): 507s.

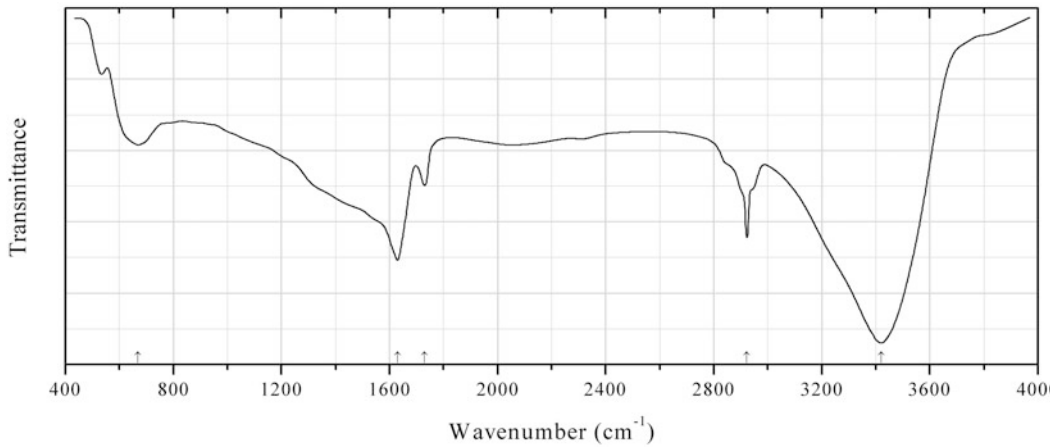

Fig. 2.318 IR spectrum of heterogenite orthorhombic polymorph drawn using data from Jagadale et al. (2012)

O372 Heterogenite orthorhombic polymorph $Co^{3+}O(OH)$ (Fig. 2.318)
Locality: Synthetic.
Description: Thin film electrodeposited on to the stainless steel substrate using potentiodynamic mode of electrodeposition from an alkaline solution of 0.1 M $CoCl_2$ at room temperature. Orthorhombic. The powder X-ray diffraction pattern is in good agreement with the standard JCPDS card No. 26-0480.

Kind of sample preparation and/or method of registration of the spectrum: No data.
Source: Jagadale et al. (2012).
Wavenumbers (cm^{-1}): 3420s, 2923, 1730, 1630, 670.
Note: The band at 1630 cm^{-1} corresponds to bending vibrations of H_2O molecules (adsorbed water?). In the paper by Jagadale et al. (2012) this band is erroneously assigned to Co–O.

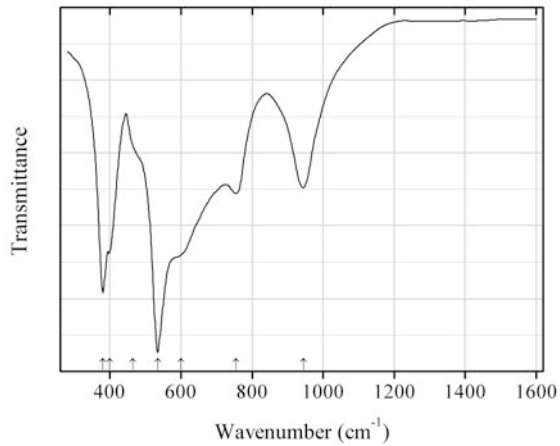

Fig. 2.319 IR spectrum of quintinite Al,Li,Cl-analogue drawn using data from Hernandez-Moreno et al. (1985)

O373 Quintinite Al,Li,Cl-analogue $LiAl_2(OH)_6Cl{\cdot}nH_2O$ (Fig. 2.319)
Locality: Synthetic.
Description: Confirmed by chemical analysis and powder X-ray diffraction data.
Kind of sample preparation and/or method of registration of the spectrum: KBr disc. Absorption.
Source: Hernandez-Moreno et al. (1985).
Wavenumbers (cm^{-1}): 945, 755, 600sh, 535s, 465sh, 400, 380s.

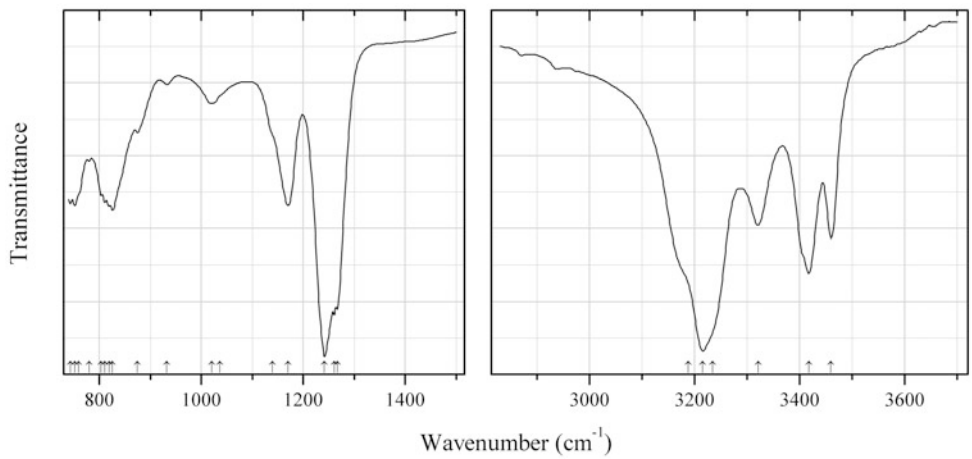

Fig. 2.320 IR spectrum of Mg,Si-hydroxide O374 drawn using data from Wunder et al. (2012)

O374 Mg,Si-hydroxide O374 $MgSi(OH)_6$ (Fig. 2.320)
Locality: Synthetic.

Description: High-pressure phase with both Mg and Si having 6-fold coordination. Monoclinic, space group $P2_1$, a = 5.1131(3), b = 5.1898(3), c = 7.3303(4) Å, β = 90.03(1)°, V = 194.52(2) Å^3, Z = 2. D_{calc} = 2.637 g/cm^3.
Kind of sample preparation and/or method of registration of the spectrum: Thin film. Absorption.
Source: Wunder et al. (2012).
Wavenumbers (cm^{-1}): 3460, 3418s, 3321, 3235sh, 3216s, 3188sh, 1267s, 1261s, 1242s, 1171, 1140sh, 1037sh, 1021, 933w, 875, 826, 819, 811, 804, 780, 760sh, 752, 743.
Note: The wavenumbers were partly determined by us based on spectral curve analysis of the published spectrum.

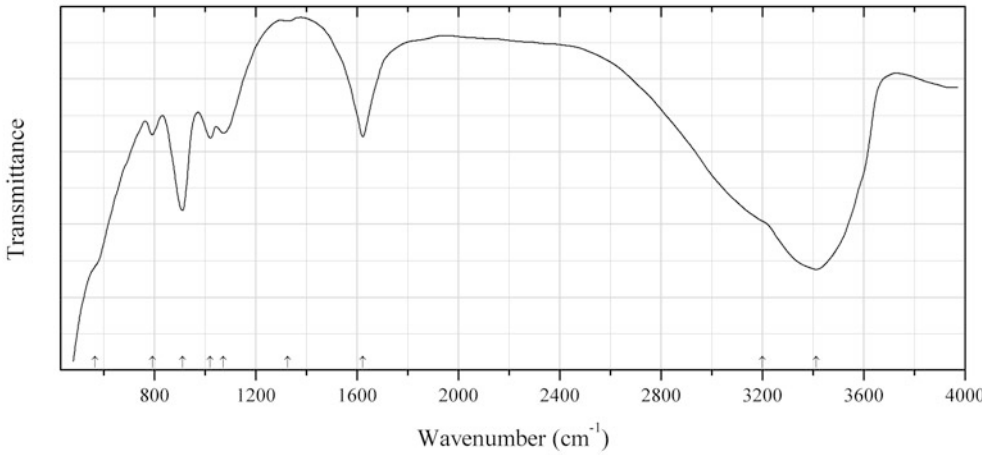

Fig. 2.321 IR spectrum of ianthinite drawn using data from Čejka and Urbanec (1990)

O375 Ianthinite $U^{4+}{}_2(UO_2)_4O_3(OH)_4 \cdot 9H_2O$ (Fig. 2.321)
Locality: Not indicated.
Kind of sample preparation and/or method of registration of the spectrum: KBr microdisc. Transmission.
Source: Čejka and Urbanec (1990).
Wavenumbers (cm^{-1}): 3412s, 3200sh, 1623, 1326w, 1073, 1021, 911s, 792, 567sh
Note: The wavenumbers were determined by us based on spectral curve analysis of the published spectrum.

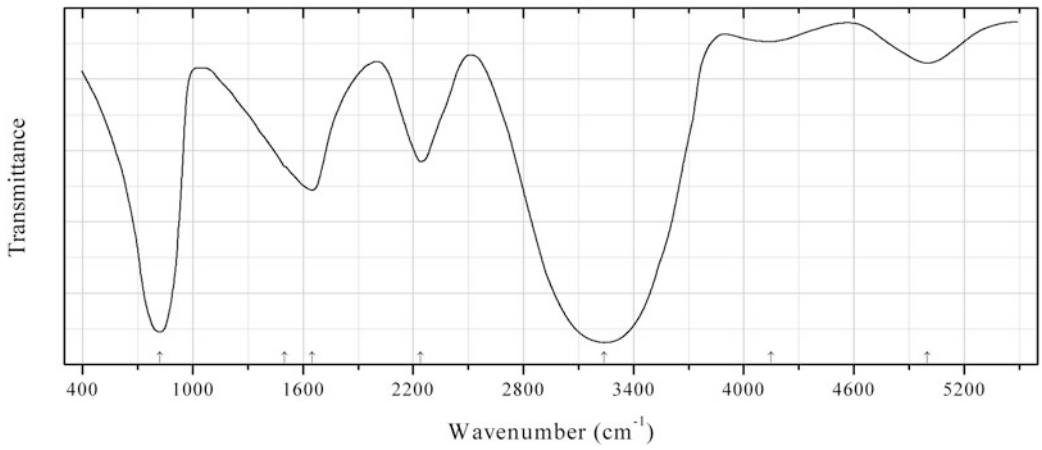

Fig. 2.322 IR spectrum of ice drawn using data from Giguére and Harvey (1956)

O376 Ice H_2O (Fig. 2.322)
Locality: Artificial.
Description: Thin film condensed on a plate at −55 °C.
Kind of sample preparation and/or method of registration of the spectrum: Absorption.
Source: Giguére and Harvey (1956).
Wavenumbers (cm^{-1}): 5000, 4150w, 3240s, 2240, 1650, 1500sh, 820s.

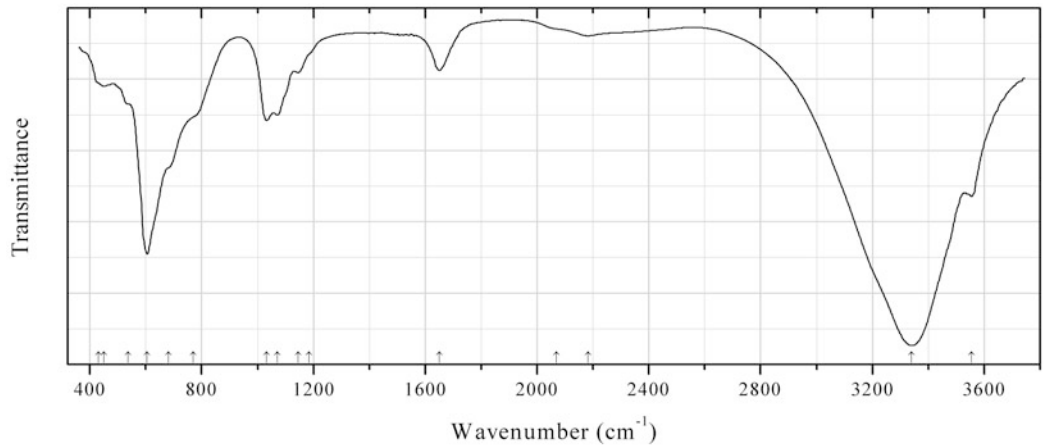

Fig. 2.323 IR spectrum of brandholzite obtained by N.V. Chukanov

O377 Brandholzite $MgSb_2(OH)_{12}·6H_2O$ (Fig. 2.323)
Locality: Krížnica deposit, near Pernek, Malé Karpaty Mountains, Slovakia.
Description: Colourless platy crystals from the association with roméite-group minerals, sulfur, aragonite, gypsum, and sénarmontite. Confirmed by IR spectrum.
Kind of sample preparation and/or method of registration of the spectrum: KBr disc. Absorption.
Wavenumbers (cm^{-1}): 3554s, 3340s, 2183w, 2070sh, 1652, 1185sh, 1146w, 1070, 1032, 770sh, 680sh, 605s, 536, 450, 430sh.

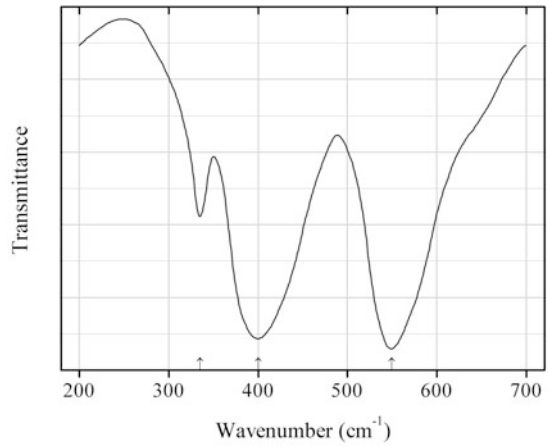

Fig. 2.324 IR spectrum of jacobsite drawn using data from Brabers and Klerk (1974)

O378 Jacobsite $Mn^{2+}Fe^{3+}{}_2O_4$ (Fig. 2.324)
Locality: Synthetic.
Description: Syntesized as a single crystal by means of the floating zone technique. Confirmed by powder X-ray diffraction data.
Kind of sample preparation and/or method of registration of the spectrum: KBr disc. Transmission.
Source: Brabers and Klerk (1974).
Wavenumbers (cm^{-1}): 549s, 400s, 335
Note: The wavenumbers were partly determined by us based on spectral curve analysis of the published spectrum.

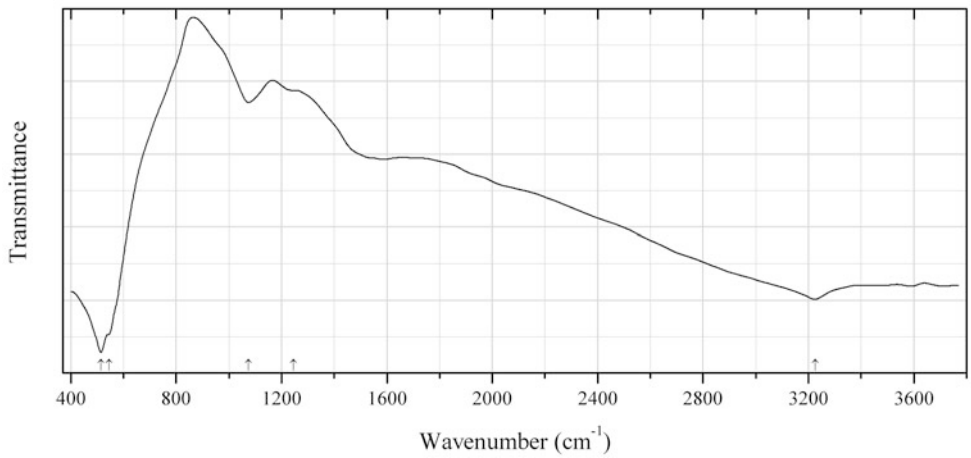

Fig. 2.325 IR spectrum of janggunite drawn using data from Kim (1977)

O379 Janggunite $Mn^{2+}Mn^{4+}{}_5O_8(OH)_6$ (Fig. 2.325)
Locality: Janggun mine, Bonghwa-gun, Gyeongsangbuk-do, South Korea (type locality).
Description: Black aggregates of flakes from the cementation zone of the supergene manganese oxide deposit. Holotype sample. Orthorhombic, a = 9.324, b = 14.05, c = 7.956 Å, Z = 4. D_{meas} = 3.59 g/cm^3, D_{calc} = 3.58 g/cm^3. The empirical formula is $Mn^{4+}_{4.85}Mn^{2+}_{0.90}Fe^{3+}_{0.30}O_{8.09}(OH)_{5.91}$.

The strongest lines of the powder X-ray diffraction pattern are observed at 9.34, 7.09, 4.62, 4.17, 3.547, 3.101, 2.469, 1.525, and 1.405 Å.
Kind of sample preparation and/or method of registration of the spectrum: KBr disc. Transmission.
Source: Kim (1977).
Wavenumbers (cm^{-1}): 3225, 1246w, 1075, 545sh, 515s.
Note: The wavenumbers were partly determined by us based on spectral curve analysis of the published spectrum.

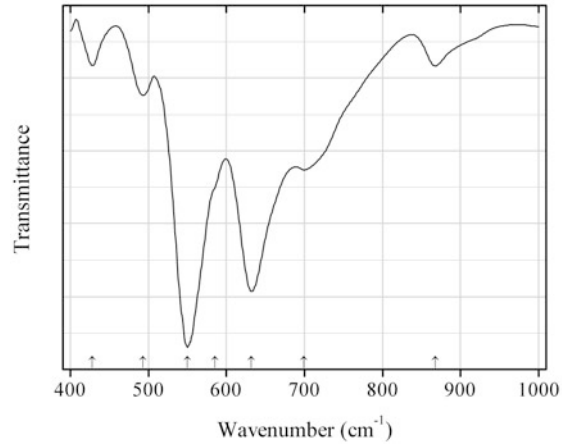

Fig. 2.326 IR spectrum of "kalitantite" drawn using data from Babaryk et al. (2013)

O380 "**Kalitantite**" $K_2Ta_4O_{11}$ (Fig. 2.326)
Locality: Synthetic.
Description: Synthesized from the mixture of K_2CO_3, Ta_2O_5, and $K_2Mo_2O_7$ taken in a molar ratio of 3.0/5.4/7.0 by the flux method. The K-analogue of natrotantite. The crystal structure is solved. Trigonal, space group *R*-3*c*, $a = 6.2732(2)$, $c = 36.8575(13)$ Å, $V = 1256.11(7)$ $Å^3$, $Z = 6$. $D_{calc} = 7.758$ g/cm^3.
Kind of sample preparation and/or method of registration of the spectrum: KBr disc. Absorption.
Source: Babaryk et al. (2013).
Wavenumbers (cm^{-1}): 868w, 699, 632s, 585sh, 550s, 493, 428w.

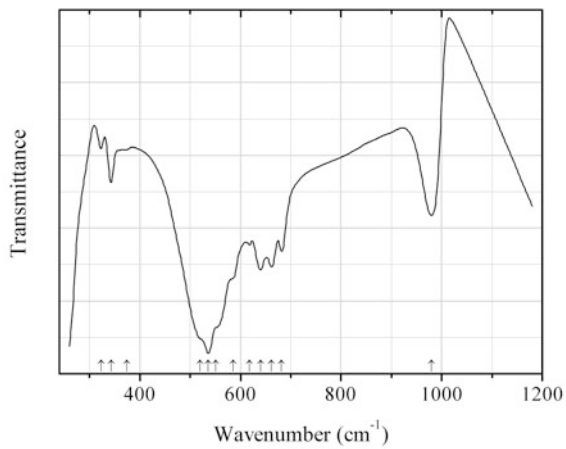

Fig. 2.327 IR spectrum of karelianite drawn using data from Botto et al. (1997b)

O381 Karelianite V_2O_3 (Fig. 2.327)
Locality: Synthetic.
Description: Confirmed by the powder X-ray diffraction pattern.
Kind of sample preparation and/or method of registration of the spectrum: KBr disc. Transmission.
Source: Botto et al. (1997b).
Wavenumbers (cm^{-1}): 980, 682, 662, 641, 618, 586sh, 551sh, 536s, 520sh, 374sh, 343, 323w.
Note: The band at 980 cm^{-1} corresponds to an impurity.

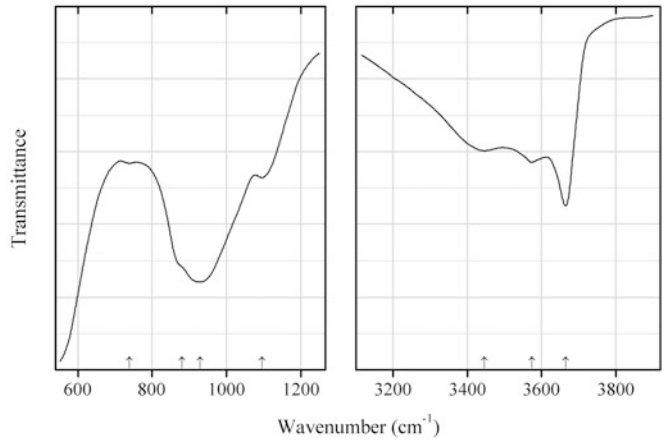

Fig. 2.328 IR spectrum of katoite drawn using data from Passaglia and Rinaldi (1984)

O382 Katoite $Ca_3Al_2(OH)_{12}$ (Fig. 2.328)
Locality: Pietramassa, near Montalto di Castro, Viterbo, Italy (type locality).
Description: White rounded microcrystals from the association with calcium silicates and aluminates. Holotype sample. Cubic, space group *Ia3d*, a = 12.358(2). Optically isotropic, n = 1.632(1). The empirical formula is $Ca_{2.96}(Al_{1.85}Mg_{0.01})(Si_{0.69}S_{0.11})O_{2.93}(OH)_{9.07}$.
Kind of sample preparation and/or method of registration of the spectrum: KBr disc. Transmission.
Source: Passaglia and Rinaldi (1984).
Wavenumbers (cm^{-1}): 3666s, 3575, 3446, 1096, 929s, 880sh, 739w.
Note: The wavenumbers were determined by us based on spectral curve analysis of the published spectrum.

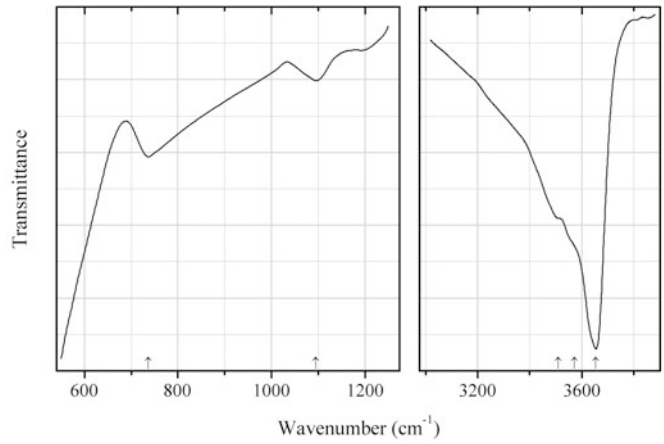

Fig. 2.329 IR spectrum of katoite drawn using data from Passaglia and Rinaldi (1984)

O383 Katoite $Ca_3Al_2(OH)_{12}$ (Fig. 2.329)
Locality: Synthetic.
Kind of sample preparation and/or method of registration of the spectrum: KBr disc. Transmission.
Source: Passaglia and Rinaldi (1984) (reproduced from Żabiński 1966).
Wavenumbers (cm^{-1}): 3654s, 3571sh, 3510sh, 1095, 737.
Note: The wavenumbers were determined by us based on spectral curve analysis of the published spectrum.

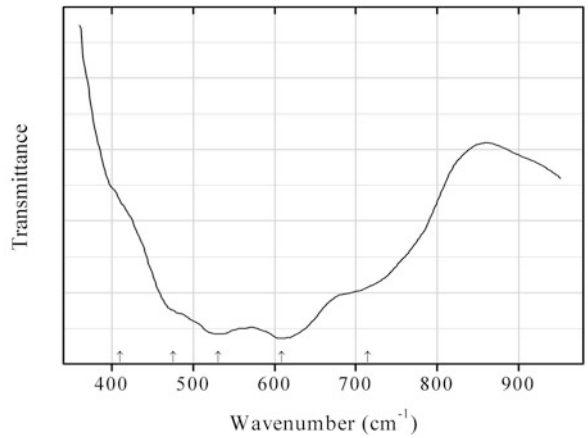

Fig. 2.330 IR spectrum of senaite obtained by N.V. Chukanov

O384 Senaite $Pb(Mn,Y)(Fe,Zn)_2(Ti,Fe)_{18}O_{36}(O,OH)_2$ (Fig. 2.330)
Locality: La Fée, Les deux Alpes, Isère, France.
Description: Black tabular crystals from the association with quartz. The empirical formula is (electron microprobe): $(Pb_{0.49}Sr_{0.38}Na_{0.11})(Mn_{0.49}Y_{0.35}Fe_{0.16})(Fe_{1.58}Zn_{0.42})(Ti_{13.75}Fe_{3.92}V_{0.21}Al_{0.12})O_{36}(O,OH)_2$.
Kind of sample preparation and/or method of registration of the spectrum: KBr disc. Absorption.
Wavenumbers (cm^{-1}): 715sh, 609s, 531s, 475sh, 410sh.

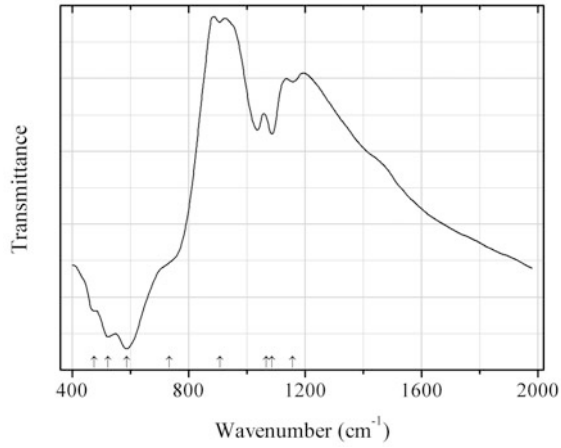

Fig. 2.331 IR spectrum of kyzylkumite drawn using data from Smyslova et al. (1981)

O385 Kyzylkumite $V^{3+}Ti_2O_5(OH)$ (Fig. 2.331)
Locality: Koscheka U deposit, Auminzatau Mts., Central Kyzylkum (Qyzylqum) region, Kyzylkum desert, Uzbekistan (type locality).
Description: Black subhedral prismatic crystals from the association with chlorite, pyrite, and rutile. Holotype sample. Monoclinic, space group $P2_1/c$, a = 33.80, b = 4.578, c = 19.99 Å, β = 93.40°. D_{meas} = 3.75 g/cm^3.
Kind of sample preparation and/or method of registration of the spectrum: Transmission. Kind of sample preparation is not indicated.
Source: Smyslova et al. (1981).
Wavenumbers (cm^{-1}): 1158w, 1087, 1067, 908w, 735sh, 588s, 523s, 476s.
Note: The wavenumbers were determined by us based on spectral curve analysis of the published spectrum.

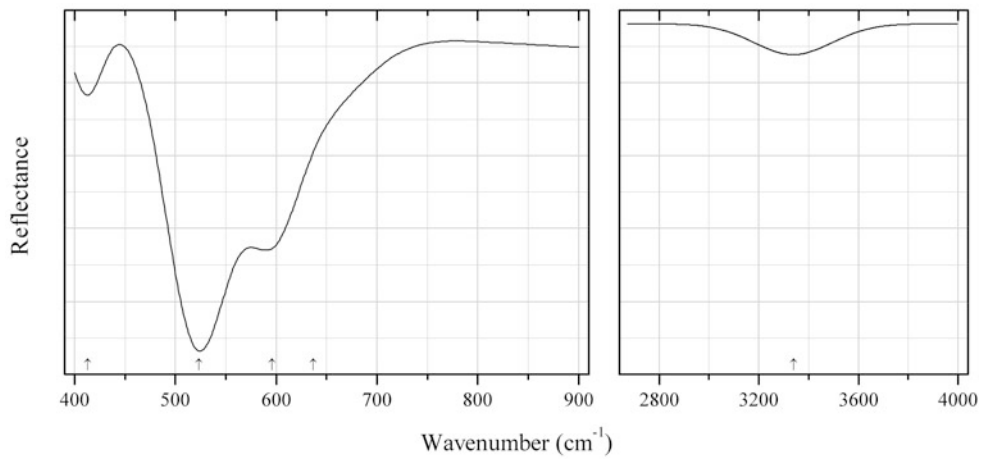

Fig. 2.332 IR spectrum of lakargiite drawn using data from Galuskin et al. (2008)

O386 Lakargiite $CaZrO_3$ (Fig. 2.332)

Locality: Lakargi Mt., Upper Chegem caldera, Kabardino-Balkarian Republic, Northern Caucasus, Russia (type locality).
Description: Pseudo-cubic crystals from the association with spurrite, larnite, calcio-olivine, calcite, cuspidine, rondorfite, reinhardbraunsite, wadalite, perovskite, and minerals of the ellestadite group. Holotype sample. Orthorhombic, space group *Pbnm*, $a = 5.556(1)$, $b = 5.715(1)$, $c = 7.960(1)$ Å, $V = 252.7(1)$ Å^3, $Z = 4$. Optically biaxial (+), $\alpha \approx \beta \approx \gamma = 2.1(1)$. The strongest lines of the powder X-ray diffraction pattern [*d*, Å (*I*, %) (*hkl*)] are: 3.970 (28) (110), 2.850 (25) (020), 2.807 (100) (112), 2.771 (22) (200), 1.988 (34) (220), 1.610 (36) (312).
Kind of sample preparation and/or method of registration of the spectrum: Attenuated total reflection of a pressed sample.
Source: Galuskin et al. (2008).
Wavenumbers (cm^{-1}): 3340w, (637sh), 596, 523s, 413.
Note: The wavenumbers are indicated for the maxima of individual bands obtained as a result of the spectral curve analysis.

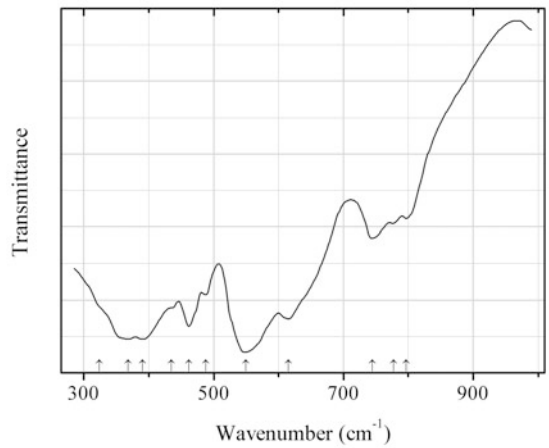

Fig. 2.333 IR spectrum of lanthanum titanate drawn using data from Knop et al. (1969)

O387 Lanthanum titanate $La_2Ti_2O_7$ (Fig. 2.333)
Locality: Synthetic.
Kind of sample preparation and/or method of registration of the spectrum: KBr disc. Transmission.
Source: Knop et al. (1969).
Wavenumbers (cm^{-1}): 797, 777, 745, 615s, 550s, 488, 462s, 435sh, 390s, 368s, 324sh.
Note: The wavenumbers were partly determined by us based on spectral curve analysis of the published spectrum. The powder X-ray diffraction pattern of $La_2Ti_2O_7$ differs from those of pyrochlore-type compounds $REE_2Ti_2O_7$ with *REE* = Sm, Gd, Er or Lu.

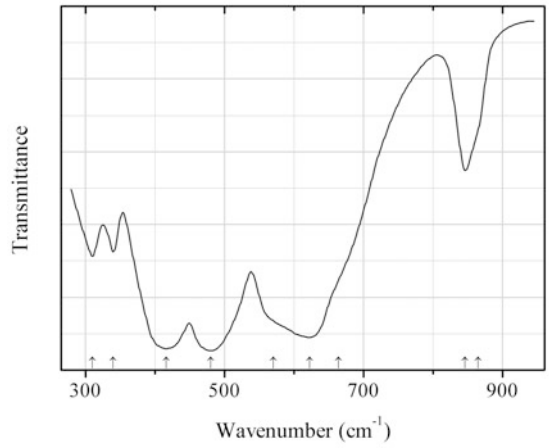

Fig. 2.334 IR spectrum of yttrium titanate drawn using data from Tarte et al. (1990)

O388 Yttrium titanate Y_2TiO_5 (Fig. 2.334)
Locality: Synthetic.
Description: No data.
Kind of sample preparation and/or method of registration of the spectrum: No data.
Source: Tarte et al. (1990).
Wavenumbers (cm^{-1}): 865sh, 846, 664sh, 622s, 570sh, 480s, 416s, 340, 310.
Note: The wavenumbers were determined by us based on spectral curve analysis of the published spectrum.

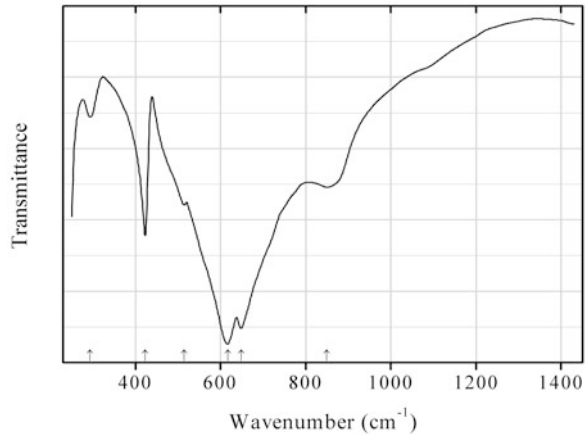

Fig. 2.335 IR spectrum of ilmenite Zn,Si-analogue drawn using data from Leinenweber et al. (1989)

O389 Ilmenite Zn,Si-analogue $ZnSiO_3$ (Fig. 2.335)
Locality: Synthetic.
Description: Synthesized at high pressure. Confirmed by powder X-ray diffraction data. Trigonal, a = 4.7469(2), c = 13.7536(8) Å, V = 268.39 Å^3.
Kind of sample preparation and/or method of registration of the spectrum: KBr disc. Absorption.
Source: Leinenweber et al. (1989).
Wavenumbers (cm^{-1}): 850, 648s, 617s, 515, 423, 294w.

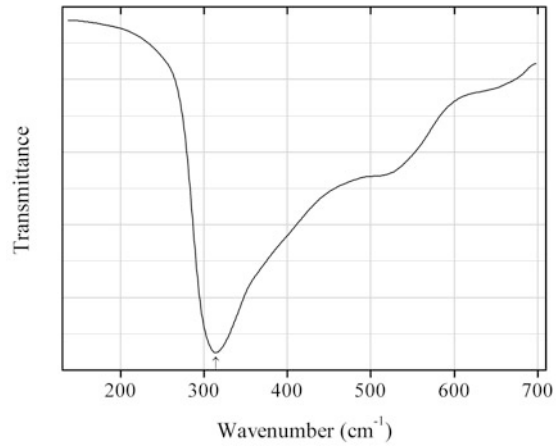

Fig. 2.336 IR spectrum of lime drawn using data from Hofmeister et al. (2003)

O390 Lime CaO (Fig. 2.336)
Locality: Synthetic.
Description: Commercial reactant heated in N_2 at 800 K for 4 days.
Kind of sample preparation and/or method of registration of the spectrum: Thin film. Absorption.
Source: Hofmeister et al. (2003).
Wavenumbers (cm^{-1}): 314.
Note: The shoulders are interference fringes.

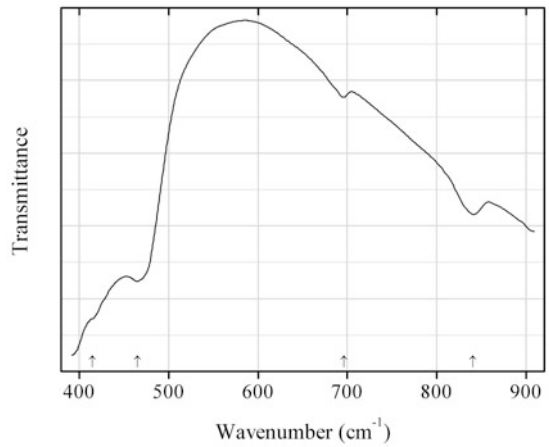

Fig. 2.337 IR spectrum of litharge drawn using data from White et al. (1961)

O391 Litharge PbO (Fig. 2.337)
Locality: Synthetic.
Description: Synthesized hydrothermally. Confirmed by the powder X-ray diffraction pattern.
Kind of sample preparation and/or method of registration of the spectrum: Transmission. Kind of sample preparation is not indicated.
Source: White et al. (1961).
Wavenumbers (cm^{-1}): 840, 696w, 465s, 415sh.
Note: The wavenumbers were determined by us based on spectral curve analysis of the published spectrum.

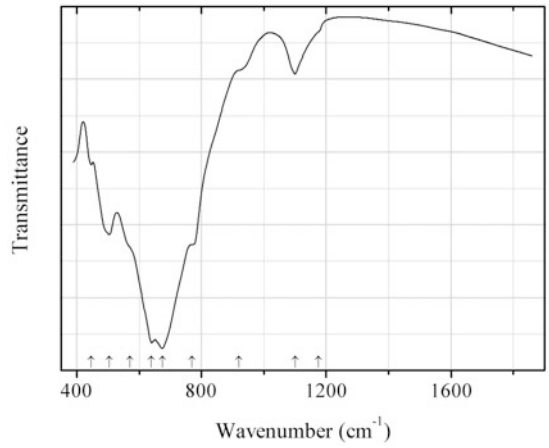

Fig. 2.338 IR spectrum of lithiotantite drawn using data from Voloshin et al. (1983b)

O392 Lithiotantite $LiTa_3O_8$ (Fig. 2.338)
Locality: Ognevka (Ognyovka) Ta deposit, Ralba range, Eastern Kazakhstan (type locality).
Description: Pseudomorph after thoreaulite from the association with cassiterite and rankamaite. Holotype sample. Monoclinic, space group $P2_1/c$, a = 7.444, b = 5.044, c = 15.255 Å, β = 107.18°. D_{meas} = 7.0 g/cm^3, D_{calc} = 7.08 g/cm^3. The empirical formula is $Li_{0.92}Ta_{1.90}Nb_{1.10}Sn_{0.02}O_8$. The strongest lines of the powder X-ray diffraction pattern [d, Å (I, %) (hkl)] are: 4.13 (50) (012, 110), 2.96 (100) (−212, 014), 2.490 (50) (021), 1.900 (50) (222), 1.772 (60) (206), 1.722 (80) (−226), 1.715 (50) (018), 1.526 (50) (323, 034), 1.451 (80) (232, 226).
Kind of sample preparation and/or method of registration of the spectrum: KBr disc. Absorption.
Source: Voloshin et al. (1983b).
Wavenumbers (cm^{-1}): 1175sh, 1100w, 920sh, 770, 675s, 640s, 570sh, 505, 447w.
Note: The spectrum is obtained with a systematic shift on several cm^{-1} towards the short-wave region. The bands at 1175, 1100, and 570 cm^{-1} may be due to the admixture of quartz.

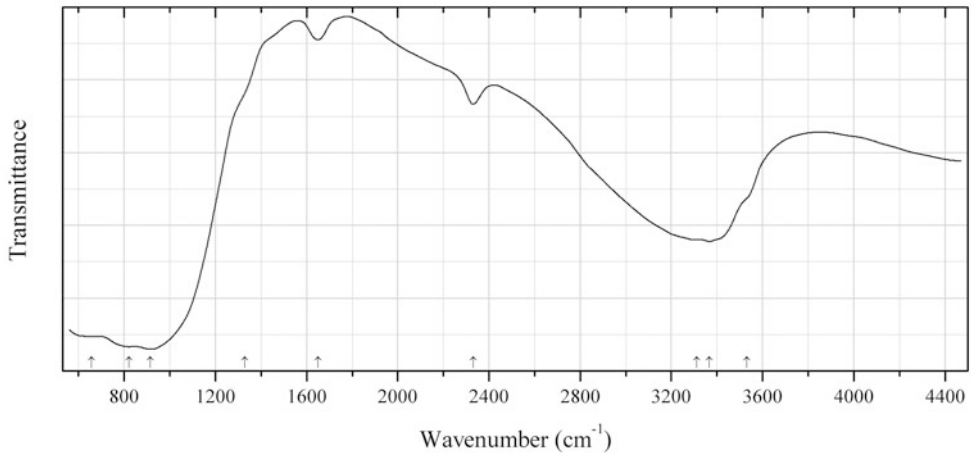

Fig. 2.339 IR spectrum of loparite Th-rich variety drawn using data from Mitchell and Chakhmouradian (1998)

O393 Loparite Th-rich variety (Na,*REE*,Th)(Ti,Nb)O_3 (Fig. 2.339)
Locality: Eveslogchorr Mt., Khibiny alkaline complex, Kola peninsula, Murmansk region, Russia.
Description: Th-enriched rims of zoned crystals from the association with aegirine, astrophyllite, eudialyte, lorenzenite, lamprophyllite, magnesio-arfvedsonite, and gerasimovskite. Amorphous, metamict. After annealing gives a powder X-ray diffraction pattern corresponding to cubic unit cell with a = 3.867(2) Å. The most Th-rich composition corresponds to the empirical formula $(Na_{0.39}LREE_{0.19}Th_{0.12}Ca_{0.05}Sr_{0.02})(Ti_{0.76}Nb_{0.27})O_3$.
Kind of sample preparation and/or method of registration of the spectrum: The spectrum was obtained with an IR microscope on 0.2–0.3 mm thick unfractured slabs of the mineral.
Source: Mitchell and Chakhmouradian (1998).
Wavenumbers (cm^{-1}): 3530sh, 3366, 3300–3320, 2330w, 1650w, 1330sh, 915s, 821s, 655sh.
Note: The wavenumbers were partly determined by us based on spectral curve analysis of the published spectrum.

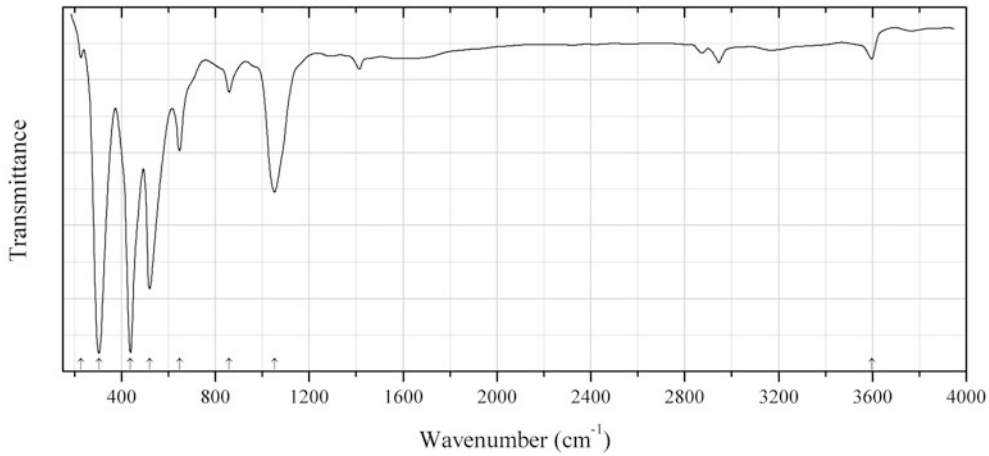

Fig. 2.340 IR spectrum of macaulayite drawn using data from Wilson et al. (1984)

O394 Macaulayite $Fe^{3+}{}_{24}Si_4O_{43}(OH)_2$ (Fig. 2.340)
Locality: Inverurie, Aberdeenshire, Scotland, UK (type locality).
Description: Red fine-grained aggregates from deeply weathered granite. A mixture with kaolinite and illite. Holotype sample. Monoclinic, a = 5.038, b = 8.726, c = 36.342 Å, β = 92°. D_{calc} = 4.41 g/cm^3. The empirical formula is $(Fe^{3+}{}_{44.75}Al_{3.38})Si_{7.95}O_{86}(OH)_4$. The strongest lines of the powder X-ray diffraction pattern [d, Å (I,)] are: 36.6 (vs), 18.16 (vs), 3.700 (25), 2.720 (35), 2.533 (100), 2.214 (20), 1.420 (35).
Kind of sample preparation and/or method of registration of the spectrum: The spectrum is obtained as a computer-generated difference spectrum between the magnetic concentrate and the clay. Kind of sample preparation is not indicated.
Source: Wilson et al. (1984).
Wavenumbers (cm^{-1}): 3597w, 1052, 858w, 647, 520s, 438s, 304s, 227w.

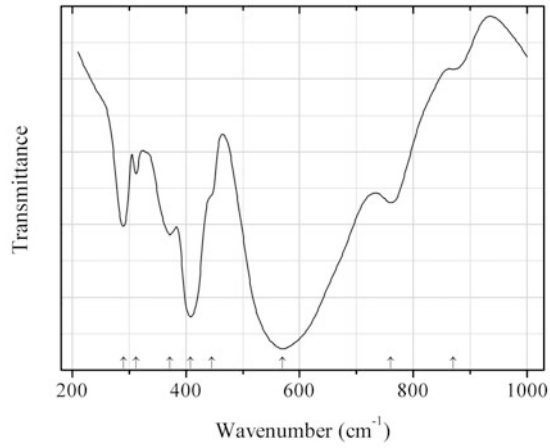

Fig. 2.341 IR spectrum of macedonite drawn using data from Shabalin (1982)

O395 Macedonite $PbTiO_3$ (Fig. 2.341)
Locality: Synthetic.
Description: Obtained in a solid-state reaction.
Kind of sample preparation and/or method of registration of the spectrum: CsI disc. Transmission.
Source: Shabalin (1982).
Wavenumbers (cm^{-1}): 870w, 760, 570s, 445sh, 408s, 372, 312, 290.

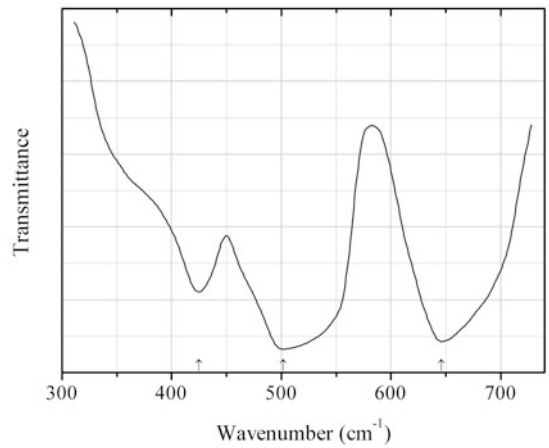

Fig. 2.342 IR spectrum of magnesiochromite drawn using data from Basak and Ghose (1994)

O396 Magnesiochromite $MgCr_2O_4$ (Fig. 2.342)
Locality: Synthetic.
Description: Prepared by the usual ceramic technique. Confirmed by powder X-ray diffraction data.
Kind of sample preparation and/or method of registration of the spectrum: KBr disc. Transmission.
Source: Basak and Ghose (1994).
Wavenumbers (cm^{-1}): 646s, 502s, 425.
Note: The wavenumbers were determined by us based on spectral curve analysis of the published spectrum.

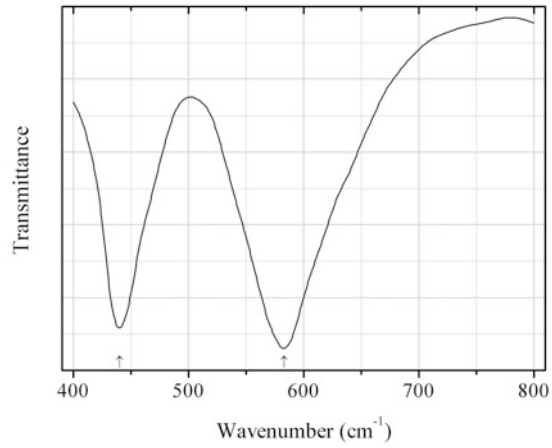

Fig. 2.343 IR spectrum of magnetoplumbite drawn using data from Yang et al. (2007)

O398 Magnetoplumbite $PbFe^{3+}{}_{12}O_{19}$ (Fig. 2.343)
Locality: Synthetic.
Description: Obtained in the reaction of lead citrate, lead nitrate, and iron citrate in aqueous solution with subsequent dehydration and heating at 900 °C during 2 h. Confirmed by the powder X-ray diffraction pattern.
Kind of sample preparation and/or method of registration of the spectrum: KBr disc. Absorption.
Source: Nan Yang et al. (2007).
Wavenumbers (cm^{-1}): 583s, 440s.

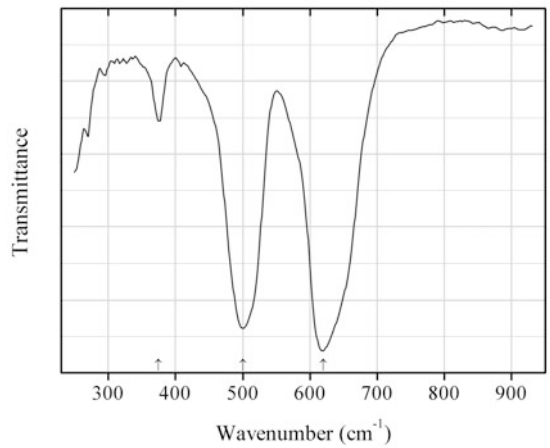

Fig. 2.344 IR spectrum of manganochromite drawn using data from Allen and Paul (1995)

O399 Manganochromite $Mn^{2+}Cr_2O_4$ (Fig. 2.344)
Locality: Synthetic.
Description: Prepared by a solid-state reaction from oxides at 950 °C in atmosphere of CO_2.
Kind of sample preparation and/or method of registration of the spectrum: KBr disc. Transmission.
Source: Allen and Paul (1995).
Wavenumbers (cm^{-1}): 620s, 500s, 375.

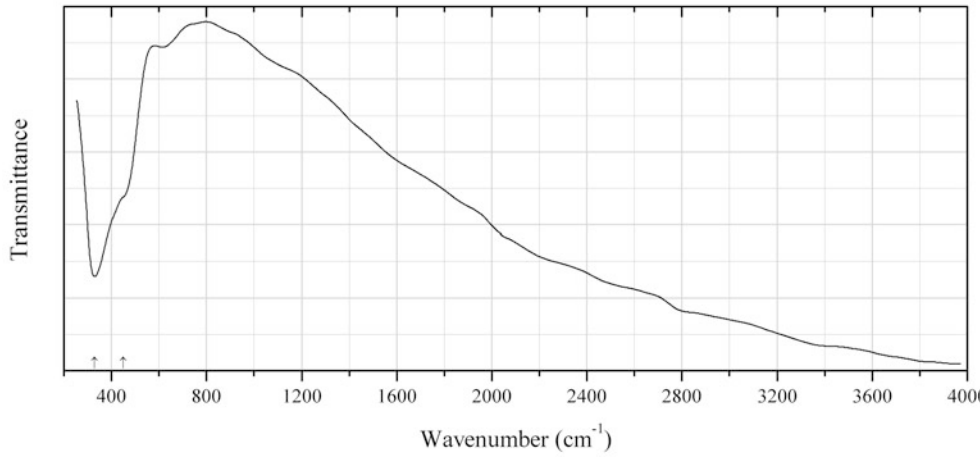

Fig. 2.345 IR spectrum of manganosite drawn using data from Mendelovici et al. (1994)

O400 Manganosite MnO (Fig. 2.345)
Locality: Synthetic.
Description: Commercial reactant with mean particle size of 16 μm. D_{meas} = 5.34. Confirmed by powder X-ray diffraction data.
Kind of sample preparation and/or method of registration of the spectrum: CsI disc. Transmission.
Source: Mendelovici et al. (1994).
Wavenumbers (cm^{-1}): 450sh, 330s.

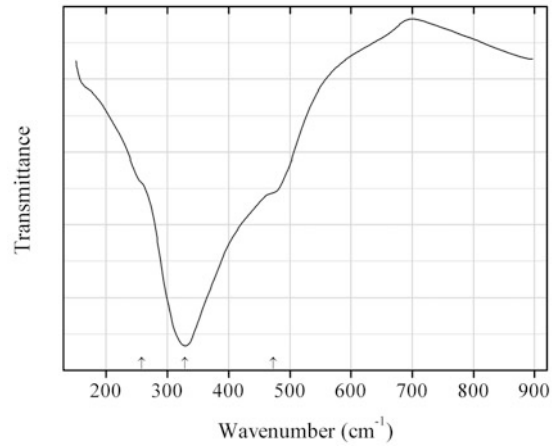

Fig. 2.346 IR spectrum of manganosite drawn using data from Julien et al. (2004)

O401 Manganosite MnO (Fig. 2.346)
Locality: Synthetic.
Description: Commercial reactant. Confirmed by the powder X-ray diffraction pattern. Cubic, a = 4.44 Å.
Kind of sample preparation and/or method of registration of the spectrum: CsI disc. Absorption.
Source: Julien et al. (2004).
Wavenumbers (cm^{-1}): 473sh, 329s, 258sh.

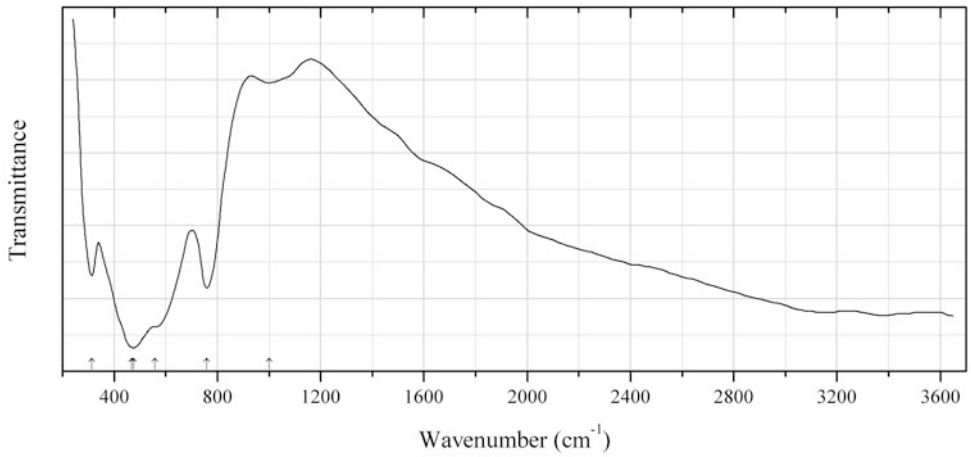

Fig. 2.347 IR spectrum of mannardite drawn using data from Ming et al. (1989)

O402 Mannardite $Ba(Ti_6V^{3+}{}_2)O_{16}$ (Fig. 2.347)
Locality: Shiti mine, Hanbin district, Ankang prefecture, Shaanxi province, China.
Description: Black prismatic crystals from the association with quartz, barite, barytocalcite, Ba-bearing roscoelite, diopside, etc. Tetragonal, $a = 10.118(1)$, $c = 2.956(3)$ Å, $V = 302.62$ Å^3, $Z = 1$. $D_{meas} = 4.44$ g/cm^3, $D_{calc} = 4.389$ g/cm^3. The empirical formula is $Ba_{1.09}(Ti_{5.48}V_{2.41}Cr_{0.22})O_{16}$. The strongest lines of the powder X-ray diffraction pattern [*d*, Å (*I*, %) (*hkl*)] are: 3.580 (50) (220), 3.202 (100) (310), 2.476 (70) (211), 2.264 (40) (420), 2.233 (50) (301), 1.892 (50) (411), 1.685 (50) (600), 1.589 (70) (521, 620), 1.397 (50) (640, 541).
Kind of sample preparation and/or method of registration of the spectrum: KBr disc. Transmission.
Source: Ming et al. (1989).
Wavenumbers (cm^{-1}): 1000, 760, 558sh, 475s, (468sh), 314.
Note: This sample was described as a new mineral ankangite. The mineral name ankangite was discredited in 2012 (IMA 11-F) because "ankangite" is a H_2O-free variety of mannardite. The wavenumbers were partly determined by us based on spectral curve analysis of the published spectrum.

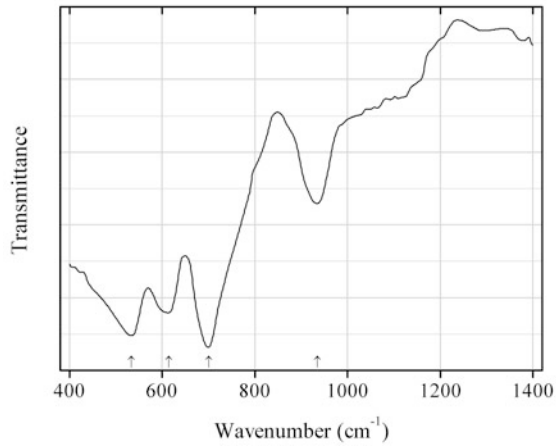

Fig. 2.348 IR spectrum of mariinskite drawn using data from Pautov et al. (2012)

O403 Mariinskite $BeCr_2O_4$ (Fig. 2.348)
Locality: Mariinsky (Malyshevo) deposit, the Ural Emerald Mines, Middle Urals, Russia (type locality).
Description: Dark green anhedral grains from the association with chromite, fluorphlogopite, Cr-bearing muscovite, eskolaite, and tourmaline. Holotype sample. Isostructural with chrysoberyl. Orthorhombic, space group *Pnma*, $a = 9.727(3)$, $b = 5.619(1)$, $c = 4.499(1)$ Å, $V = 245.9(3)$ Å^3, $Z = 4$. D_{meas} = 4.25(2) g/cm^3, D_{calc} = 4.25 g/cm^3. The empirical formula is $Be_{1.03}(Cr_{1.22}Al_{0.74}Ti_{0.01}Fe_{0.01}V_{0.01})O_4$. The strongest lines of the powder X-ray diffraction pattern [*d*, Å (*I*, %) (*hkl*)] are: 4.08 (40) (101), 3.31 (90) (111), 2.629 (50) (301), 2.434 (50) (220), 2.381 (40) (311), 2.139 (60) (221), 1.651 (100) (222).
Kind of sample preparation and/or method of registration of the spectrum: KBr disc. Transmission.
Source: Pautov et al. (2012).
Wavenumbers (cm^{-1}): 935, 700s, 614s, 534s.

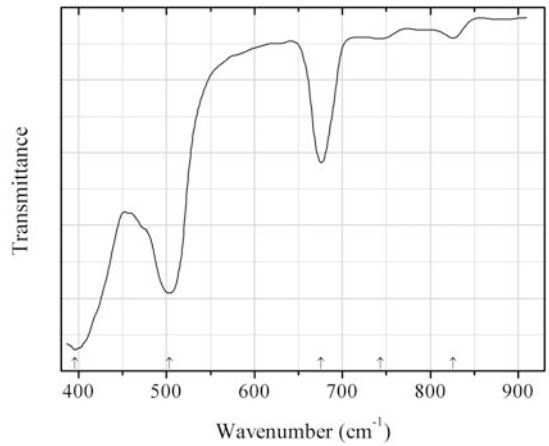

Fig. 2.349 IR spectrum of massicot drawn using data from White et al. (1961)

O404 Massicot PbO (Fig. 2.349)
Locality: Synthetic.
Description: A yellow orthorhombic modification of PbO. Confirmed by the powder X-ray diffraction pattern.
Kind of sample preparation and/or method of registration of the spectrum: Transmission. Kind of sample preparation is not indicated.
Source: White et al. (1961).
Wavenumbers (cm^{-1}): 826w, 743w, 676, 503s, 396s.
Note: The wavenumbers were determined by us based on spectral curve analysis of the published spectrum.

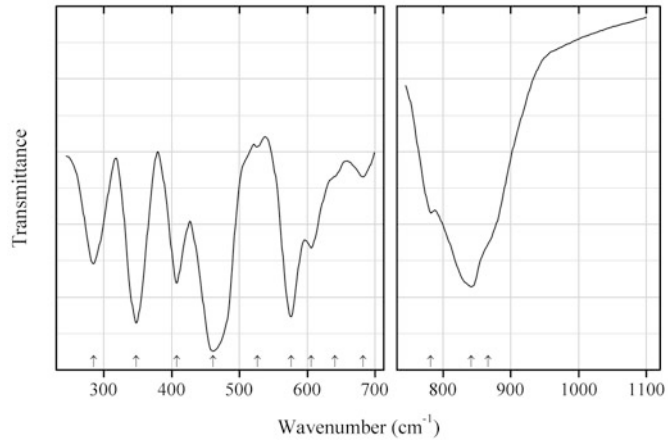

Fig. 2.350 IR spectrum of mayenite drawn using data from Tarte (1967)

O405 Mayenite $Ca_{12}Al_{14}O_{33}$ (Fig. 2.350)
Locality: Synthetic.
Description: Synthesized by solid state reaction between $Al(OH)_3$ and CaO.
Kind of sample preparation and/or method of registration of the spectrum: KBr or KI disc. Transmission.
Source: Tarte (1967).
Wavenumbers (cm^{-1}): 867sh, 842s, 782, 682w, 641sh, 606, 576s, 527w, 461s, 408, 348s, 285.
Note: The wavenumbers were determined by us based on spectral curve analysis of the published spectrum.

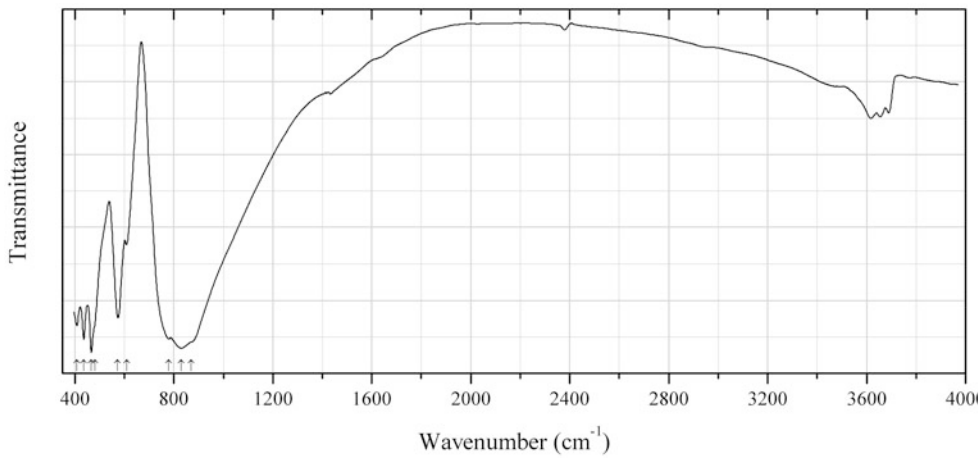

Fig. 2.351 IR spectrum of mayenite drawn using data from Taş (1998)

O406 Mayenite $Ca_{12}Al_{14}O_{33}$ (Fig. 2.351)
Locality: Synthetic.
Description: Synthesized from Al and Ca nitrates at 510 °C with subsequent calcination in air at 1100 °C. by solid state reaction between $Al(OH)_3$ and CaO. Confirmed by powder X-ray diffraction data. Cubic, a = 11.971 Å.

Kind of sample preparation and/or method of registration of the spectrum: KBr disc. Transmission.
Source: Taş (1998).
Wavenumbers (cm^{-1}): 870sh, 830s, 780s, 609, 573, 480sh, 466s, 436s, 408.
Note: The wavenumbers were determined by us based on spectral curve analysis of the published spectrum. Weak bands above 1200 cm^{-1} may correspond to OH groups partly substituting O atoms or to a secondary OH- and/or H_2O-bearing product formed as a result of the contact with air.

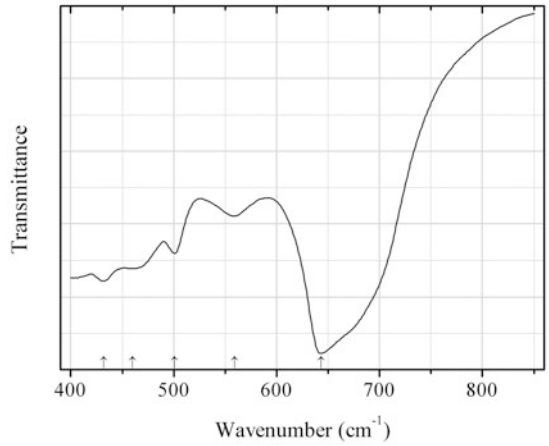

Fig. 2.352 IR spectrum of megawite drawn using data from Zheng et al. (2012)

O407 Megawite $CaSnO_3$ (Fig. 2.352)
Locality: Synthetic.
Description: Nanofibers synthesized by using an electrospinning technique. Characterized by X-ray diffraction and scanning electron microscopy. The sample is contaminated with calcite.
Kind of sample preparation and/or method of registration of the spectrum: No data.
Source: Zheng et al. (2012).
Wavenumbers (cm^{-1}): 643s, 559, 501, 460, 432.
Note: The wavenumbers were partly determined by us based on spectral curve analysis of the published spectrum.

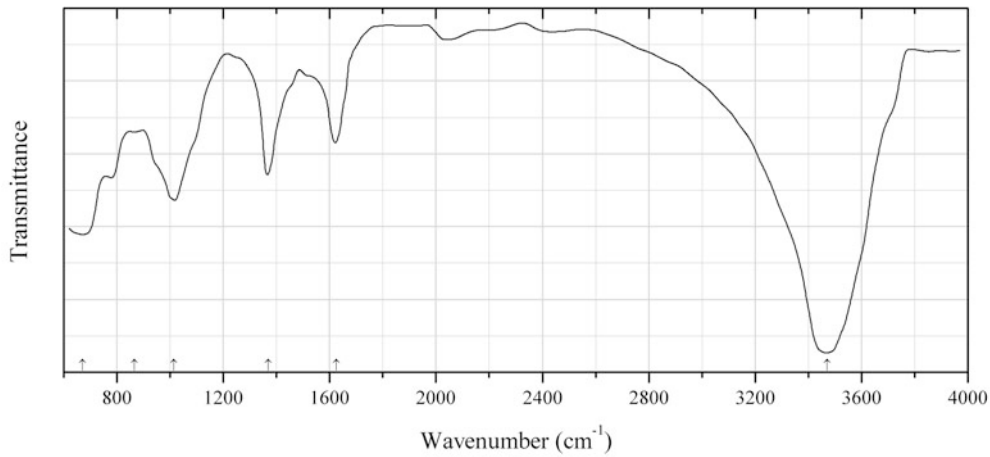

Fig. 2.353 IR spectrum of meixnerite drawn using data from Koritnig and Süsse (1975)

O408 Meixnerite $Mg_6Al_2(OH)_{18}\cdot 4H_2O$ (Fig. 2.353)
Locality: Yspertal, Ybbs-Persenbeug, Lower Austria (type locality).
Description: Colourless tabular crystals from the association with serpentine, pyrope, talc, and aragonite. Holotype sample. Trigonal, space group *R*-3 *m*, a = 3.0463(15), c = 22.93(2) Å, Z = 3/8. D_{meas} = 1.9(1) g/cm^3, D_{calc} = 1.95 g/cm^3. Optically biaxial (−), ω = 1.517. The chemical composition is (electron microprobe, wt%): MgO 36.5, Al_2O_3 15.0, Fe_2O_3 0.55.
Kind of sample preparation and/or method of registration of the spectrum: KBr disc. Transmission.
Source: Koritnig and Süsse (1975).
Wavenumbers (cm^{-1}): 3470s, 1625, 1370, 1015, 865w, 670s.
Note: Despite no gas evolution in HCl was observed, the band at 1370 cm^{-1} definitely indicates a high content of CO_3^{2-} groups. Taking into account low concentration of CO_2 in air, rapid carbonatization during pressing of a KBr disc supposed by the authors is hardly possible.

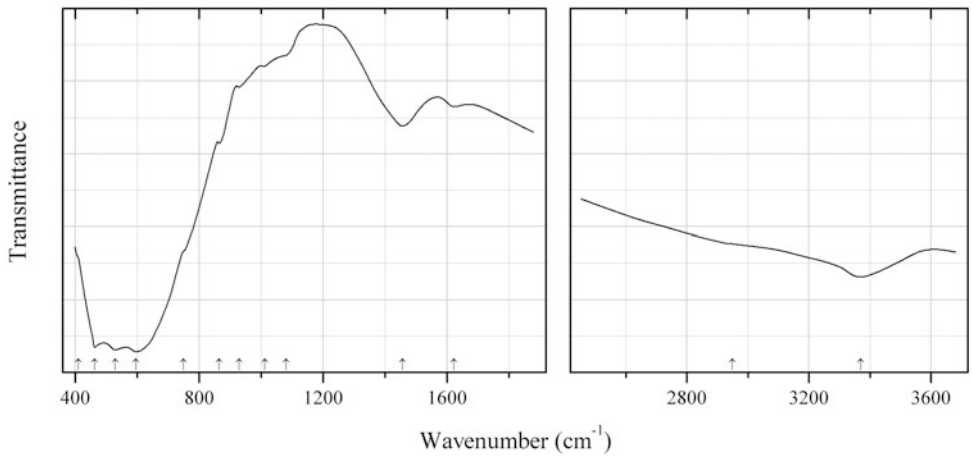

Fig. 2.354 IR spectrum of "metaloparite" drawn using data from Chakhmouradian et al. (1999)

O409 "Metaloparite" *REE*Ti_2O_{6-x} $(OH,F)_x\cdot nH_2O$ (Fig. 2.354)
Locality: Burpala alkaline complex, North Baikal area, Siberia, Russia.
Description: Pseudomorphs after loparite crystals. Amorphous, metamict.
Kind of sample preparation and/or method of registration of the spectrum: KBr disc. Transmission.
Source: Chakhmouradian et al. (1999).
Wavenumbers (cm^{-1}): 3370, 2950sh, 1623w, 1457, 1081w, 1012w, 930sh, 865, 750sh, 597s, 530s, 464s, 410sh.

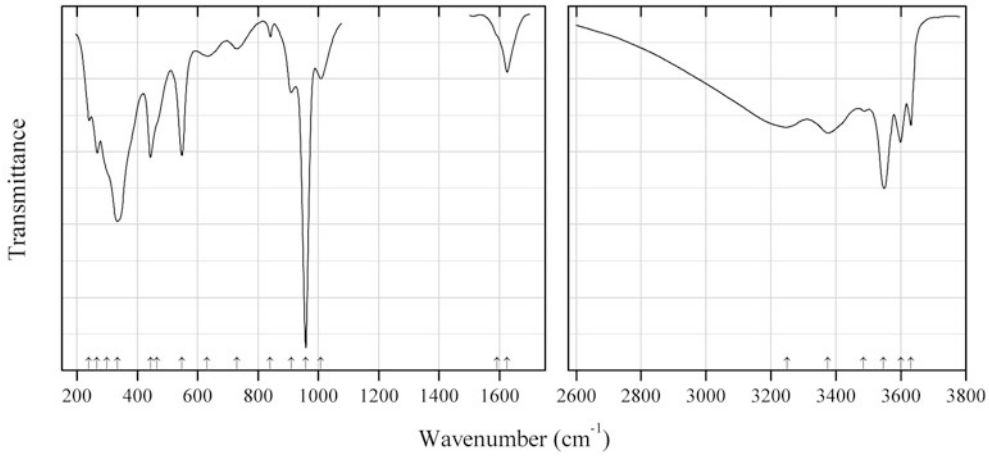

Fig. 2.355 IR spectrum of metaschoepite drawn using data from Hoekstra and Siegel (1973)

O410 Metaschoepite $(UO_2)_8O_2(OH)_{12}\cdot 10H_2O$ or $UO_3\cdot 1–2H_2O$ (Fig. 2.355)
Locality: Synthetic.
Description: Confirmed by the powder X-ray diffraction pattern. Orthorhombic, space group *Pbna*, a = 13.977(4)(3), b = 16.696(4), c = 14.672(4) Å.
Kind of sample preparation and/or method of registration of the spectrum: Nujol mull (in the range from 200 to 500 cm^{-1}); KBr disc (above 500 cm^{-1}). Absorption.
Source: Hoekstra and Siegel (1973).
Wavenumbers (cm^{-1}): 3630, 3600, 3545s, 3485, 3375, 3250, 1625, 1591sh, 1008, 958s, 910, 840w, 730w, 630w, 547, 465sh, 445, 335s, 300sh, 265, 240.

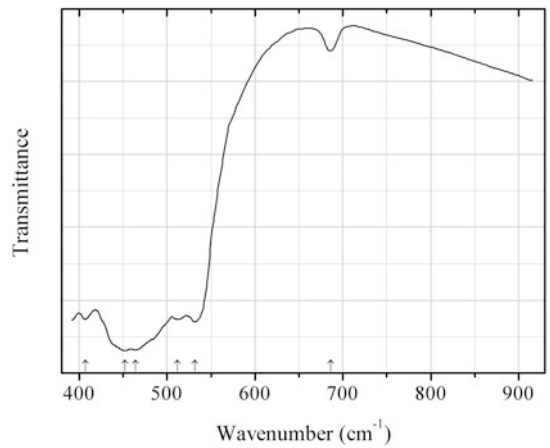

Fig. 2.356 IR spectrum of minium drawn using data from White et al. (1961)

O411 Minium $Pb^{2+}{}_2Pb^{4+}O_4$ (Fig. 2.356)
Locality: Synthetic.
Description: Bright-scarlet material. Obtained hydrothermally. Tetragonal, space group $P4_2/mbc$.
Kind of sample preparation and/or method of registration of the spectrum: Transmission. Kind of sample preparation is not indicated.

Source: White et al. (1961).
Wavenumbers (cm^{-1}): 686w, 532, 512, 464s, 452s, 407.
Note: The wavenumbers were determined by us based on spectral curve analysis of the published spectrum.

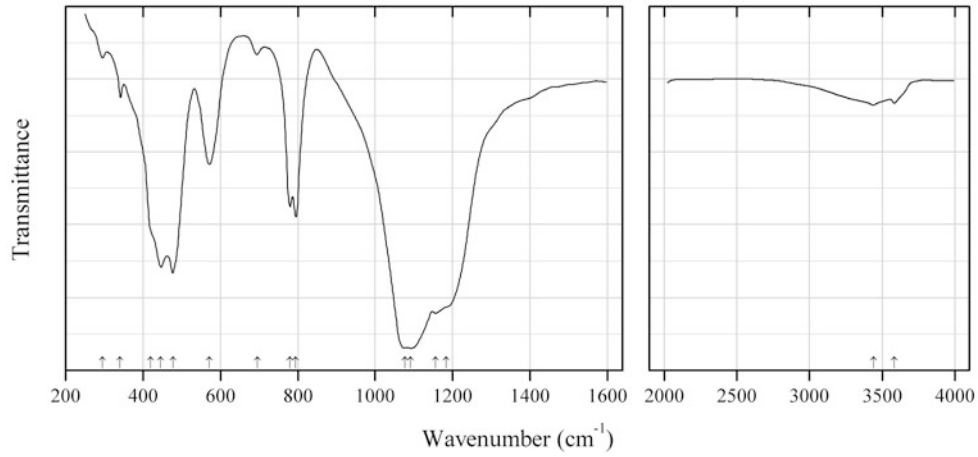

Fig. 2.357 IR spectrum of mogánite drawn using data from Miehe and Graetsch (1992)

O412 Mogánite $SiO_2 \cdot nH_2O$ (Fig. 2.357)
Locality: Mogán formation, Gran Canaria (type locality).
Description: Microcrystalline fillings of cavities. Monoclinic, a = 8.758(2), b = 4.876(1), c = 10.715 (2) Å, β = 90.08(3)°. D_{calc} = 2.617 g/cm^3.
Kind of sample preparation and/or method of registration of the spectrum: KBr disc. Transmission.
Source: Miehe and Graetsch (1992).
Wavenumbers (cm^{-1}): 3585w, 3440w, 1183sh, 1156s, 1092s, 1076s, 795, 780, 695w, 572, 477 h, 445 h, 420sh, 341, 295w.
Note: The wavenumbers were partly determined by us based on spectral curve analysis of the published spectrum. For the IR spectrum of moganite see also Zhang and Moxon (2014).

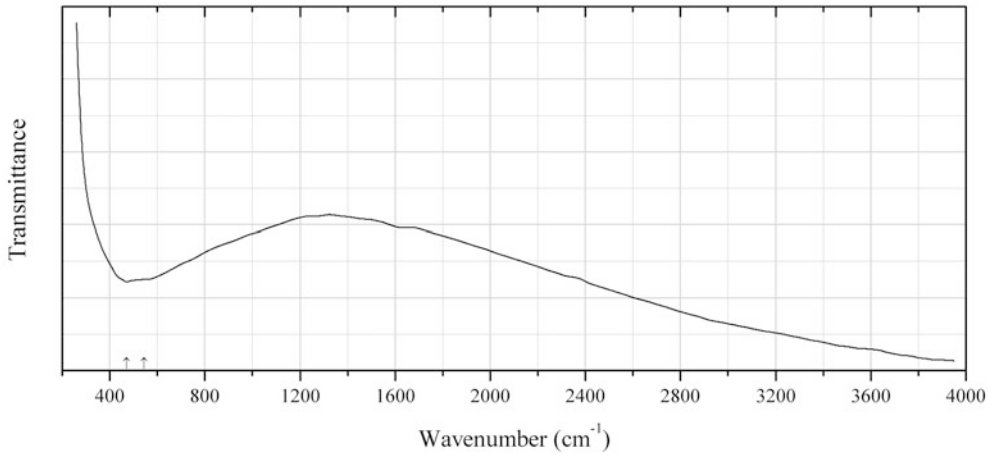

Fig. 2.358 IR spectrum of monteponite drawn using data from Ristić et al. (2004)

O413 Monteponite CdO (Fig. 2.358)
Locality: Synthetic.
Description: Obtained by autoclaving the $Cd(OH)_2$ suspension at 220 °C. Confirmed by powder X-ray diffraction data.
Kind of sample preparation and/or method of registration of the spectrum: KBr disc. Transmission.
Source: Ristić et al. (2004).
Wavenumbers (cm^{-1}): 543sh, 471s.

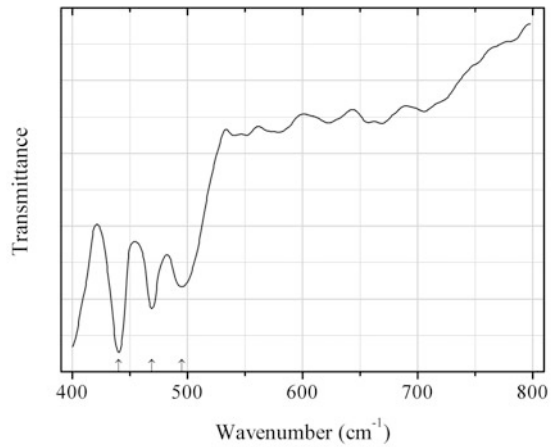

Fig. 2.359 IR spectrum of montroydite polymorph drawn using data from Refat and Elsabawy (2011)

O414 Montroydite polymorph HgO (Fig. 2.359)
Locality: Synthetic.
Description: Obtained in the reaction of acetamide aqueous solutions with $HgCl_2$ at 90 °C. Orthorhombic, space group *Imm*2, a = 3.3113, b = 3.5288, c = 3.688 Å.
Kind of sample preparation and/or method of registration of the spectrum: KBr disc. Transmission.
Source: Refat and Elsabawy (2011).
Wavenumbers (cm^{-1}): 495, 469, 440s.

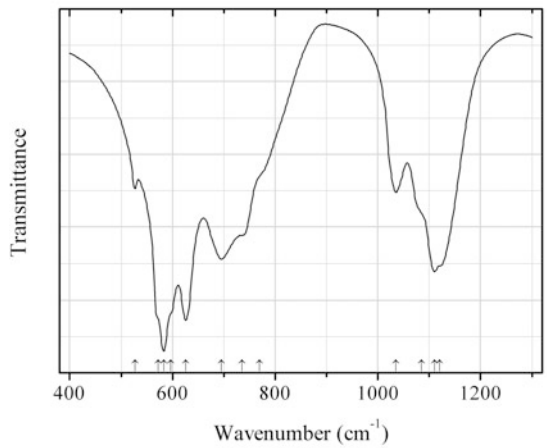

Fig. 2.360 IR spectrum of mopungite drawn using data from Balicheva and Roi (1971)

O415 Mopungite $NaSb^{5+}(OH)_6$ (Fig. 2.360)
Locality: Synthetic.
Description: Confirmed by powder X-ray diffraction data. Tetragonal space group $P4_2/n$, a = 8.01, c = 7.88 Å.
Kind of sample preparation and/or method of registration of the spectrum: Suspension in mineral oil.
Source: Balicheva and Roi (1971).
Wavenumbers (cm^{-1}): 1120sh, 1110s, 1085sh, 1035, 770sh, 735sh, 695s, 626s, 597sh, 583s, 572sh, 527w.

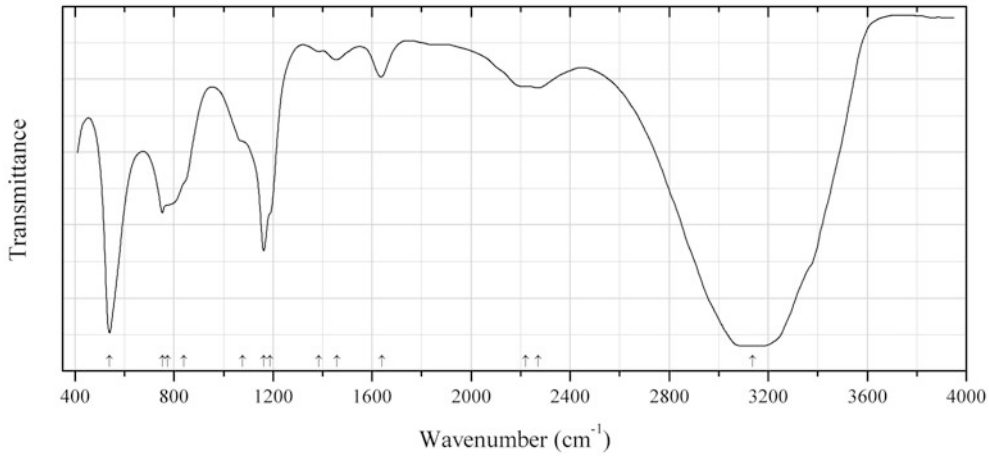

Fig. 2.361 IR spectrum of mushistonite dimorph drawn using data from Zhong et al. (2011)

O416 Mushistonite dimorph $Cu^{2+}Sn^{4+}(OH)_6$ (Fig. 2.361)
Locality: Synthetic.
Description: Submicrospheres with diameters of 400–900 nm obtained by successive addition of the solutions of ammonia and Na_2SnO_3 to the solution of $CuSO_3$ at room temperature. Tetragonal, $a \approx 7.6$, $c \approx 8.1$ Å. Confirmed by powder X-ray diffraction data.
Kind of sample preparation and/or method of registration of the spectrum: Transmission. Kind of sample preparation is not indicated.
Source: Zhong et al. (2011).
Wavenumbers (cm^{-1}): 3137s, 2270, 2220, 1639, 1457w, 1385w, 1188sh, 1162s, 1077sh, 840sh, 775sh, 753, 540s.
Note: The wavenumbers were partly determined by us based on spectral curve analysis of the published spectrum. The band at 1639 cm^{-1} indicates the presence of H_2O molecules.

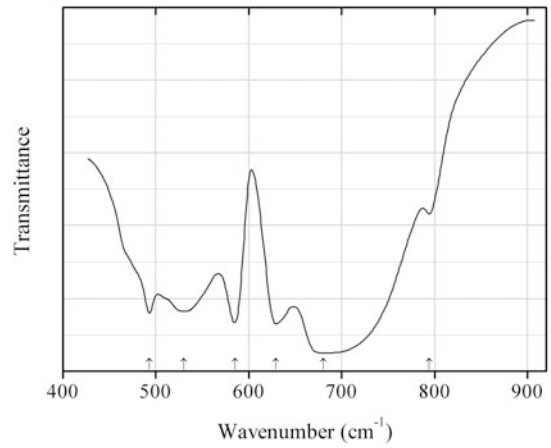

Fig. 2.362 IR spectrum of ordoñezite drawn using data from White (1967)

O417 Ordoñezite $ZnSb^{5+}{}_2O_6$ (Fig. 2.362)
Locality: Synthetic.
Description: Prepared by heating pressed discs of the proper ratio of component oxides in air at 950 °C for 48 h. Tetragonal, with a trirutile-type unit cell. Confirmed by the powder X-ray diffraction pattern.
Kind of sample preparation and/or method of registration of the spectrum: KBr disc. Transmission.
Source: White (1967).
Wavenumbers (cm^{-1}): 794w, 680s, 629, 585, 530, 493.

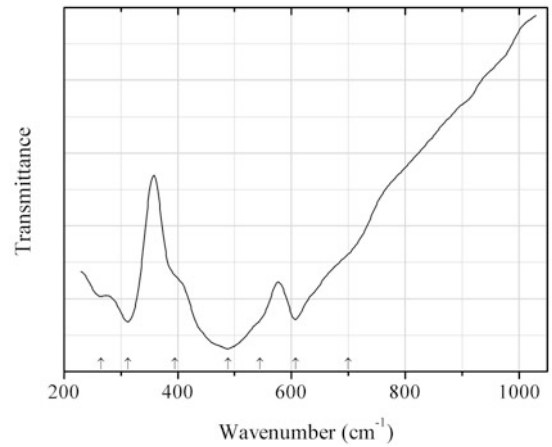

Fig. 2.363 IR spectrum of oxy-yttrobetafite-(Yb) drawn using data from Shcherbakova et al. (1979)

O418 Oxy-yttrobetafite-(Yb) $Yb_2Ti_2O_7$ (Fig. 2.363)
Locality: Synthetic.
Description: Obtained by a solid-state reaction method.
Kind of sample preparation and/or method of registration of the spectrum: Transmission. Kind of sample preparation is not indicated.
Source: Shcherbakova et al. (1979).

Wavenumbers (cm^{-1}): 700sh, 607s, 545sh, 488s, 395sh, 312s, 265.
Note: The wavenumbers were determined by us based on spectral curve analysis of the published spectrum.

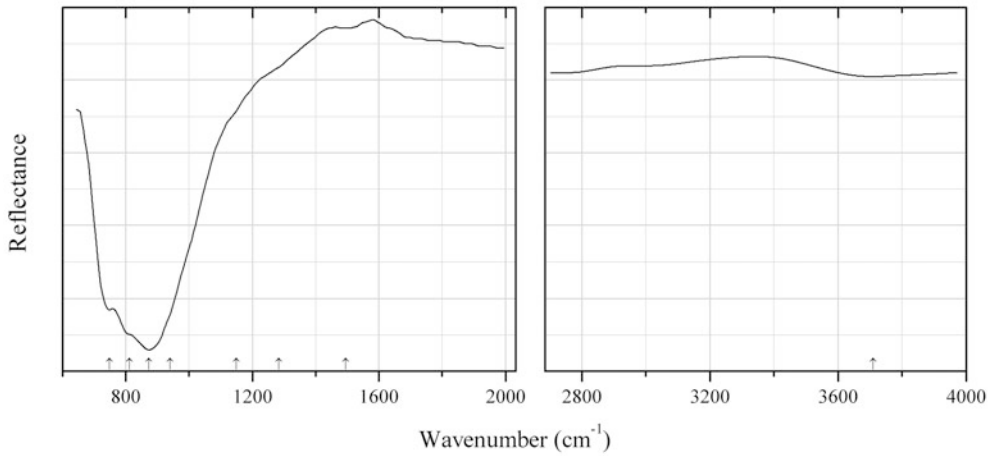

Fig. 2.364 IR spectrum of oxycalcioroméite drawn using data from Biagioni et al. (2013)

O419 Oxycalcioroméite $Ca_2Sb^{5+}{}_2O_7$ (Fig. 2.364)
Locality: Buca della Vena mine, Apuan Alps, Tuscany, Italy (type locality).
Description: Reddish-brown octahedral crystals embedded in dolostone lenses. The associated minerals are barite, pyrite, and iron oxides. Holotype sample. Cubic, space group *Fd*-3*m*, a = 10.3042(7) Å, V = 1094.06(13) $Å^3$, Z = 8. D_{calc} = 5.393 g/cm^3. Optically isotropic, n_{calc} = 1.950. The empirical formula is $(Ca_{1.07}Fe^{2+}{}_{0.34}Sb^{3+}{}_{0.33}Na_{0.12}Pb_{0.01}Mn_{0.01})(Sb^{5+}{}_{1.73}Ti_{0.19}V_{0.04}Al_{0.02}Sn_{0.01})(O_{6.68}F_{0.28})$.
Kind of sample preparation and/or method of registration of the spectrum: A single crystal. Reflection.
Source: Biagioni et al. (2013).
Wavenumbers (cm^{-1}): 3710w, 1494w, 1283sh, 1150sh, 940sh, 873s, 812sh, 749s.
Note: The wavenumbers were partly determined by us based on spectral curve analysis of the published spectrum.

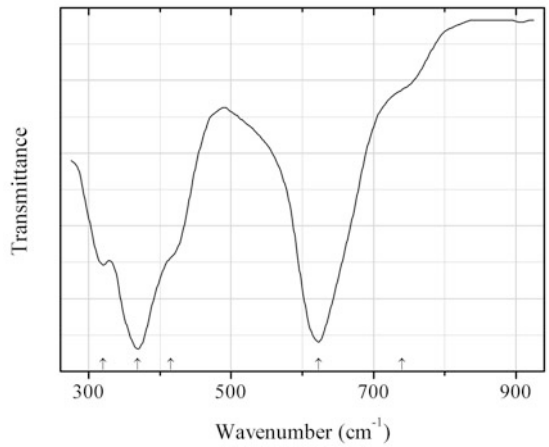

Fig. 2.365 IR spectrum of oxyplumboroméite drawn using data from Brisse et al. (1972)

O420 Oxyplumboroméite $Pb_2Sb_2O_7$ (Fig. 2.365)
Locality: Synthetic.
Description: Synthesized hydrothermally from PbO_2 and Sb_2O_3 at 350 °C for 24 h. Cubic, with a pyrochlore-type structure.
Kind of sample preparation and/or method of registration of the spectrum: Absorption.
Source: Brisse et al. (1972).
Wavenumbers (cm^{-1}): 740sh, 623s, 415sh, 368s, 320.
Note: The wavenumbers were determined by us based on spectral curve analysis of the published spectrum.

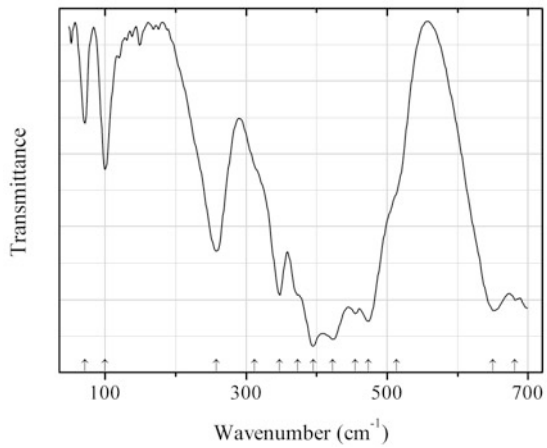

Fig. 2.366 IR spectrum of oxyplumboroméite drawn using data from Kendix et al. (2008)

O421 Oxyplumboroméite $Pb_2Sb_2O_7$ (Fig. 2.366)
Locality: Synthetic.
Description: The pigment Naples yellow obtained from Kremer (ID no. 43130). Cubic, with the pyrochlore-type structure.
Kind of sample preparation and/or method of registration of the spectrum: Polyethylene disc. Transmission.
Source: Kendix et al. (2008).
Wavenumbers (cm^{-1}): 681, 650s, 513sh, 473s, 455s, 423s, 395s, 373sh, 347, 312sh, 258, 100, 71.
Note: The wavenumbers were partly determined by us based on spectral curve analysis of the published spectrum.

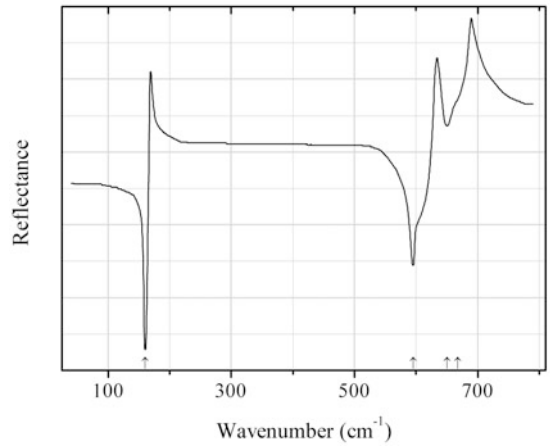

Fig. 2.367 IR spectrum of palladinite drawn using data from Kliche (1985b)

O422 Palladinite PdO (Fig. 2.367)
Locality: Synthetic.
Description: Greenish polycrystalline aggregate obtained by heating Pd powder in an atmosphere of pure O_2 at 973 K.
Kind of sample preparation and/or method of registration of the spectrum: Pressed and polished disc. Reflection.
Source: Kliche (1985b).
Wavenumbers (cm^{-1}): 668sh, 650, 595, 160s.
Note: The wavenumbers were partly determined by us based on spectral curve analysis of the published spectrum.

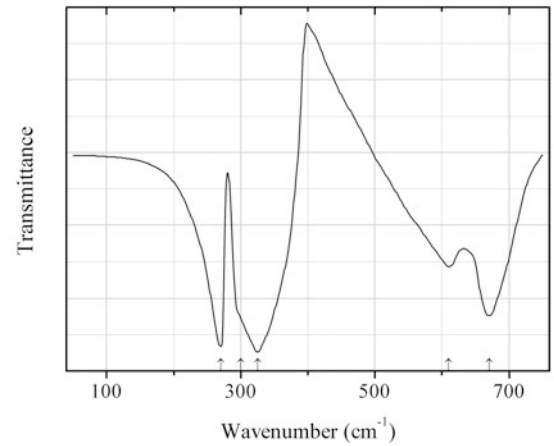

Fig. 2.368 IR spectrum of cassiterite drawn using data from Luxon and Summitt (1969)

O423 Cassiterite SnO_2 (Fig. 2.368)
Locality: Synthetic.
Description: Powder of tetragonal SnO_2 crystals.

Kind of sample preparation and/or method of registration of the spectrum: Transmission. Kind of sample preparation is not indicated.
Source: Luxon and Summitt (1969).
Wavenumbers (cm^{-1}): 670s, 610, 325s, 300sh, 270s.

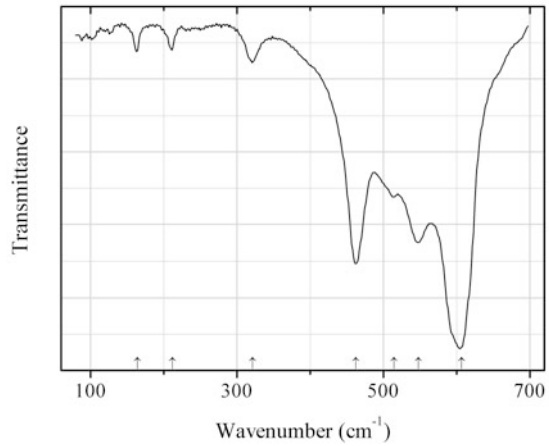

Fig. 2.369 IR spectrum of paramelaconite drawn using data from Debbichi et al. (2012)

O424 Paramelaconite $Cu^{+}_{2}Cu^{2+}_{2}O_3$ (Fig. 2.369)
Locality: Synthetic.
Description: Confirmed by powder X-ray diffraction data. Tetragonal, a = 5.595, c = 9.650 Å.
Kind of sample preparation and/or method of registration of the spectrum: A film deposited on a Si substrate. Transmission.
Source: Debbichi et al. (2012).
Wavenumbers (cm^{-1}): 607s, 548, 515, 463s, 322w, 212w, 164w.
Note: The wavenumbers were partly determined by us based on spectral curve analysis of the published spectrum.

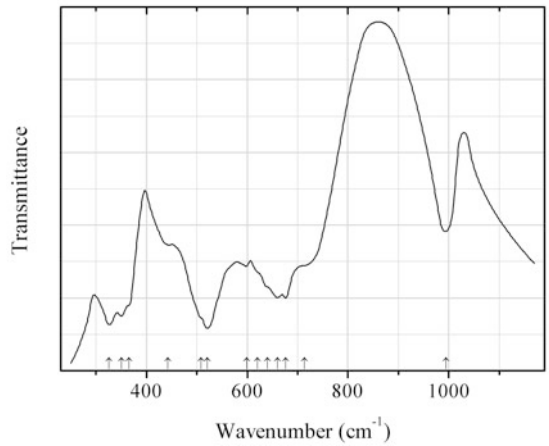

Fig. 2.370 IR spectrum of paramontroseite dimorph drawn using data from Botto et al. (1997b)

O425 Paramontroseite dimorph VO_2 (Fig. 2.370)

Locality: Synthetic.
Description: Obtained by temperature-programmed reduction of V_2O_5 under low H_2 pressure. A high-temperature tetragonal modification of VO_2. Confirmed by powder X-ray diffraction data.
Kind of sample preparation and/or method of registration of the spectrum: KBr disc. Transmission.
Source: Botto et al. (1997b).
Wavenumbers (cm^{-1}): 995, 714sh, 677s, 660s, 640sh, 620sh, 599w, 521s, 508sh, 443, 365sh, 350s, 326s.

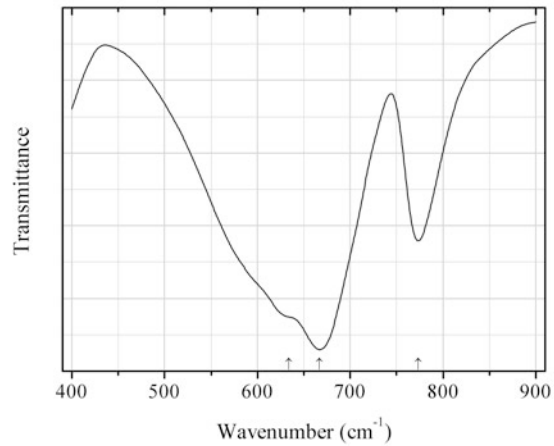

Fig. 2.371 IR spectrum of paratellurite drawn using data from Noguera et al. (2003)

O426 Paratellurite α-TeO_2 (Fig. 2.371)
Locality: Synthetic.
Kind of sample preparation and/or method of registration of the spectrum: KBr disc. Absorption.
Source: Noguera et al. (2003).
Wavenumbers (cm^{-1}): 773, 667, 634sh.
Note: The wavenumbers were determined by us based on spectral curve analysis of the published spectrum.

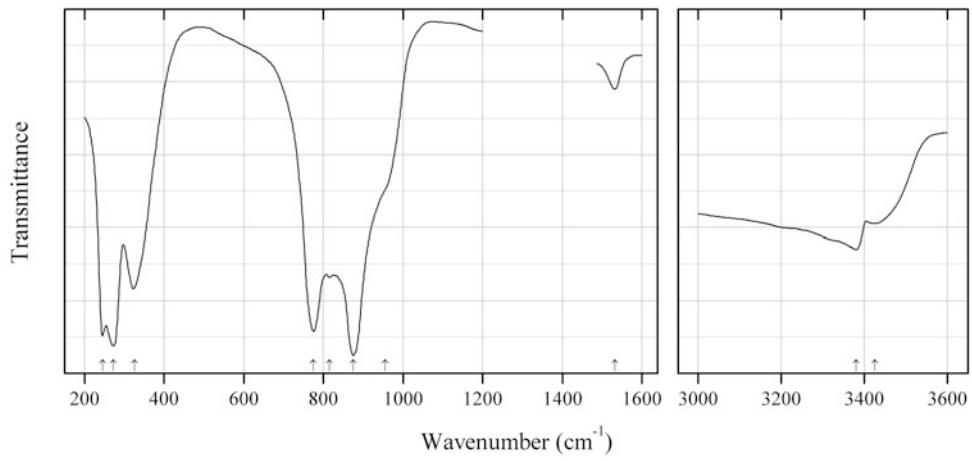

Fig. 2.372 IR spectrum of paulscherrerite drawn using data from Hoekstra and Siegel (1973)

O427 Paulscherrerite $(UO_2)(OH)_2$ (Fig. 2.372)
Locality: Synthetic.
Description: Confirmed by powder X-ray diffraction data.
Kind of sample preparation and/or method of registration of the spectrum: KBr disc. Absorption.
Source: Hoekstra and Siegel (1973).
Wavenumbers (cm^{-1}): 3425, 3380, 1532w, 815, 775s, 955sh, 875s, 325, 272s, 245s.

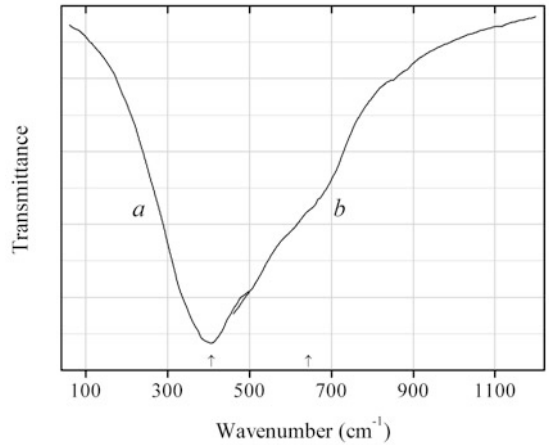

Fig. 2.373 IR spectrum of periclase drawn using data from Busca (1996)

O428 Periclase MgO (Fig. 2.373)
Locality: Synthetic.
Kind of sample preparation and/or method of registration of the spectrum: Polyethylene (curve *a*) and KBr (curve *b*) discs. Absorption.
Source: Busca (1996).
Wavenumbers (cm^{-1}): 643sh, 407s.

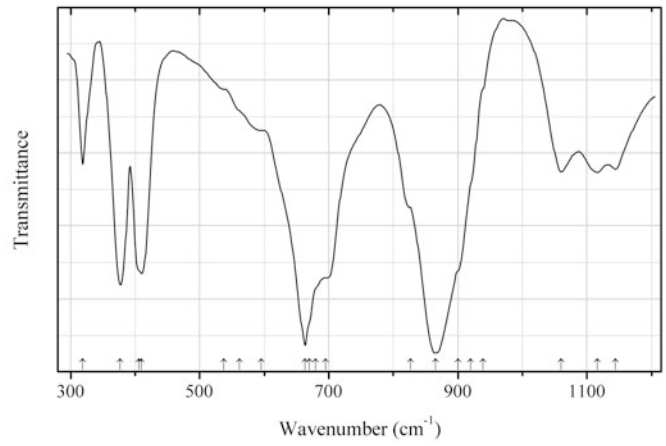

Fig. 2.374 IR spectrum of downeyite drawn using data from Oppermann et al. (2001)

O429 Downeyite SeO_2 (Fig. 2.374)

Locality: Synthetic.
Description: Powdery sample purified by sublimation. Confirmed by powder X-ray diffraction data.
Kind of sample preparation and/or method of registration of the spectrum: Transmission. Kind of sample preparation is not indicated.
Source: Oppermann et al. (2001).
Wavenumbers (cm^{-1}):1144, 1116, 1060, 920sh, 939sh, 900sh, 866s, 827sh, 695sh, 680sh, 670sh, 663s, 596w, 562sh, 537w, 410s, 406sh, 377s, 319.
Note: The wavenumbers were determined by us based on spectral curve analysis of the published spectrum.

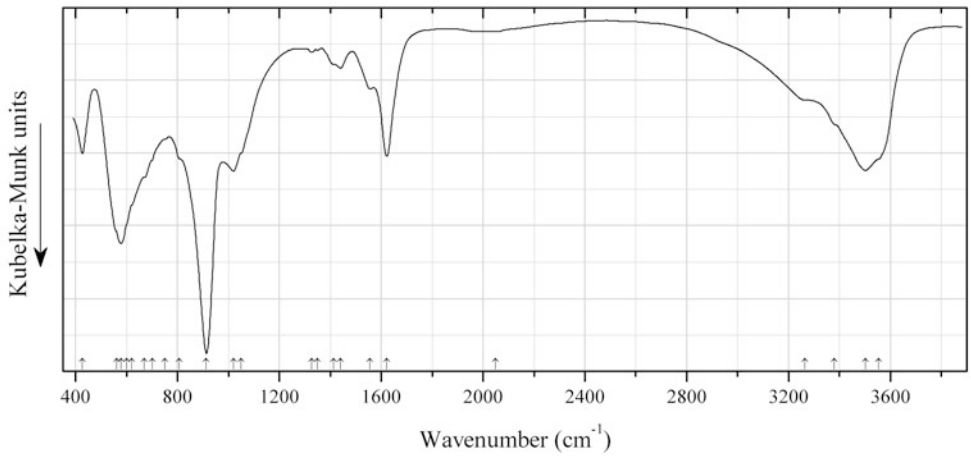

Fig. 2.375 IR spectrum of protasite drawn using data from Čejka et al. (1998)

O430 Protasite $Ba(UO_2)_3O_3(OH)_2{\cdot}3H_2O$ (Fig. 2.375)
Locality: Synthetic.
Description: Monoclinic, space group *Pn*, a = 12.173(2), b = 7.338(2), c = 7.030(1) Å, β = 89.980(1)°, V = 628.0(4) $Å^3$. The strongest lines of the powder X-ray diffraction pattern [*d*, Å (*I*, %)] are: 7.33 (100), 3.659 (34), 3.166 (68), 2.534 (32), 2.2983 (30), 2.2221 (30), 2.0046 (44), 1.9547 (41), 1.7568 (30).
Kind of sample preparation and/or method of registration of the spectrum: Diffuse reflectance of powdered sample.
Source: Čejka et al. (1998).
Wavenumbers (cm^{-1}): 3553sh, 3503s, 3380sh, 3265sh, 2050w, 1622, 1556, 1440w, 1413sh, 1349w, 1326w, 1050sh, 1020, 913s, 807sh, 750sh, 700sh, 670sh, 620sh, 600sh, 578s, 560sh, 426.
Note: Weak bands in the range from 2800 to 3000 cm^{-1} correspond to the admixture of an organic substance.

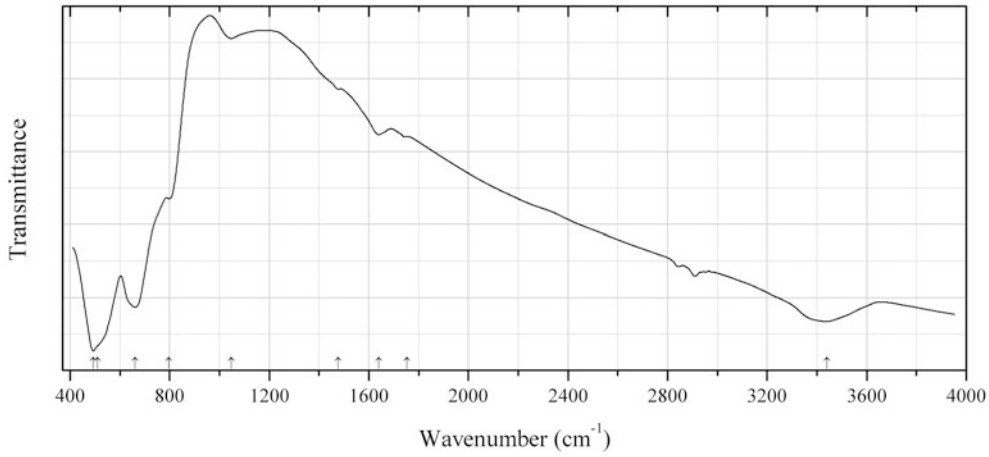

Fig. 2.376 IR spectrum of pseudobrookite drawn using data from Enhessari et al. (2012)

O431 Pseudobrookite $Fe^{3+}{}_2TiO_5$ (Fig. 2.376)
Locality: Synthetic.
Description: Nanopowder calcinated at 900 °C. Confirmed by the powder X-ray diffraction pattern.
Kind of sample preparation and/or method of registration of the spectrum: KBr disc. Transmission.
Source: Enhessari et al. (2012).
Wavenumbers (cm^{-1}): 3439, 1754sh, 1640w, 1478w, 1047w, 798, 660s, 510sh, 493s.
Note: The wavenumbers were partly determined by us based on spectral curve analysis of the published spectrum. Weak bands in the range from 2800 to 3000 cm^{-1} correspond to the admixture of an organic substance. Other bands with wavenumbers above 1500 cm^{-1} correspond to adsorbed water.

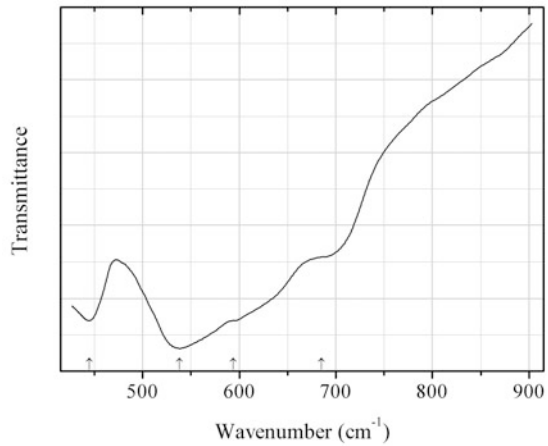

Fig. 2.377 IR spectrum of pyrophanite drawn using data from White (1967)

O432 Pyrophanite $Mn^{2+}TiO_3$ (Fig. 2.377)
Locality: Synthetic.
Description: Prepared by heating pelletized equimolar mixture of MnO_2 and TiO_2 powders in vacuum at 970 °C, then regrinding and heating at 990 °C. Confirmed by powder X-ray diffraction data.

Kind of sample preparation and/or method of registration of the spectrum: KBr disc. Transmission.
Source: White (1967).
Wavenumbers (cm^{-1}): 685, 594, 538s, 445s.
Note: The wavenumbers were partly determined by us based on spectral curve analysis of the published spectrum.

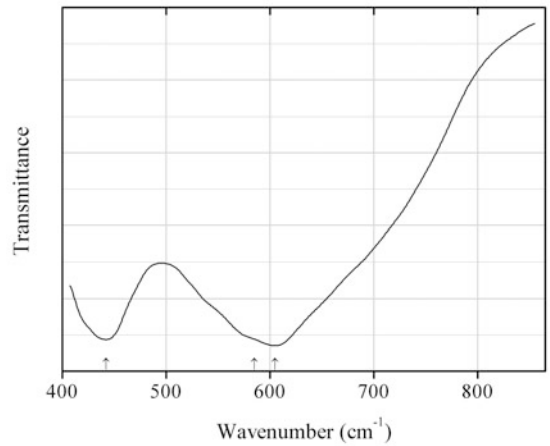

Fig. 2.378 IR spectrum of qandilite drawn using data from Oktyabrsky et al. (1992)

O433 Qandilite $(Mg,Fe^{3+},Fe^{2+})_2(Ti,Fe^{3+},Al)O_4$ (Fig. 2.378)
Locality: Northern part of the exocontact zone of the Kondyor massif, Aldan Shield, Siberia, Russia.
Description: Characterized by chemical analyses and powder X-ray diffraction data.
Kind of sample preparation and/or method of registration of the spectrum: Absorption. Kind of sample preparation is not indicated.
Source: Oktyabrsky et al. (1992).
Wavenumbers (cm^{-1}): 605s, 585sh, 442s.
Note: The wavenumbers were determined by us based on spectral curve analysis of the published spectrum.

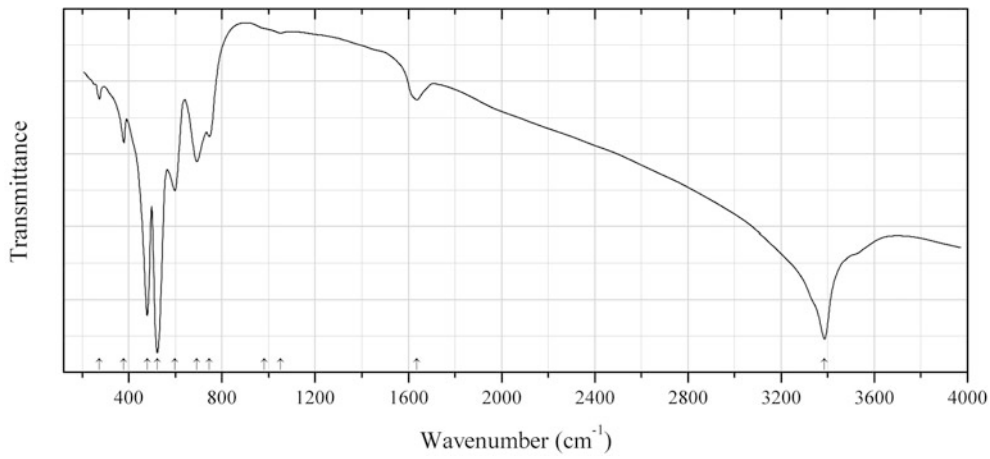

Fig. 2.379 IR spectrum of ramsdellite drawn using data from Potter and Rossman (1979b)

O435 Ramsdellite MnO_2 (Fig. 2.379)
Locality: Chihuahua, Mexico.
Description: Confirmed by powder X-ray diffraction data.
Kind of sample preparation and/or method of registration of the spectrum: TlBr or KBr disc. Absorption.
Source: Potter and Rossman (1979b).
Wavenumbers (cm^{-1}): 3386s, 1637w, 1051w, 982sh, 745, 692, 598, 522s, 479s, 378, 274w.
Note: The wavenumbers were determined by us based on spectral curve analysis of the published spectrum. The bands with wavenumbers above 1500 cm^{-1} indicate the presence of water.

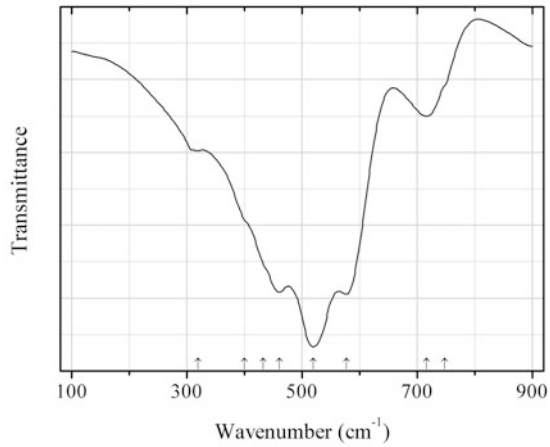

Fig. 2.380 IR spectrum of romanèchite drawn using data from Julien et al. (2004)

O436 Romanèchite $(Ba,H_2O)_2(Mn^{4+},Mn^{3+})_5O_{10}$ (Fig. 2.380)
Locality: Romanèche, France (type locality).
Description: Characterized by powder X-ray diffraction data.
Kind of sample preparation and/or method of registration of the spectrum: CsI disc. Absorbtance.
Source: Julien et al. (2004).
Wavenumbers (cm^{-1}): 748sh, 716, 577s, 520s, 461s, (432sh), (400sh), 319.

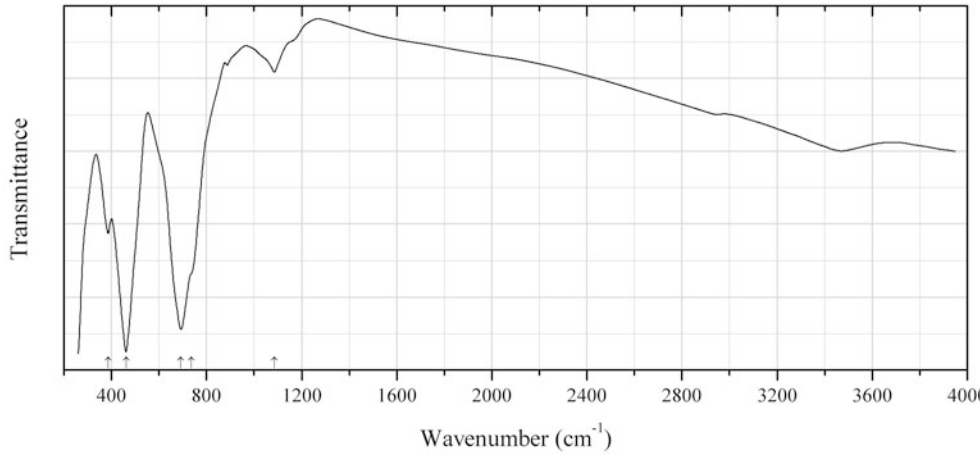

Fig. 2.381 IR spectrum of fluorcalcioroméite drawn using data from Brugger et al. (1997)

O437 Fluorcalcioroméite $(Ca,Na)_2(Sb^{5+},Ti^{4+})_2O_6(F,O,OH)$ (Fig. 2.381)
Locality: Fianel, Val Ferrera, Switzerland.
Description: Crystals from quartz veinlets, from the association with hematite and carbonates. Confirmed by electron microprobe analyses and powder X-ray diffraction data.
Kind of sample preparation and/or method of registration of the spectrum: KBr disc. Transmission.
Source: Brugger et al. (1997).
Wavenumbers (cm^{-1}): 1085w, 736sh, 692s, 462s, 387.
Note: The band at 1085 cm^{-1} corresponds to the admixture of quartz.

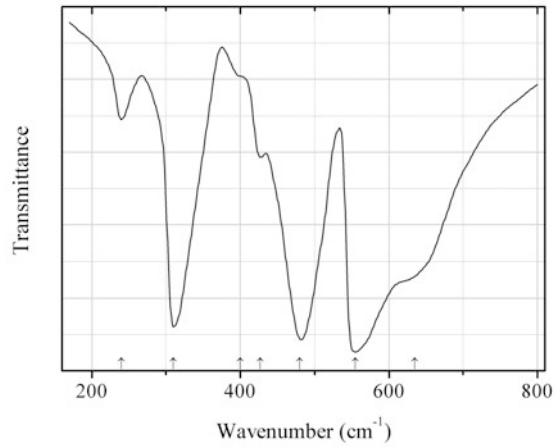

Fig. 2.382 IR spectrum of rosiaite drawn using data from Vandenborre et al. (1980)

O438 Rosiaite $PbSb_2O_6$ (Fig. 2.382)
Locality: Synthetic.
Description: Obtained in a solid-state reaction between Sb_2O_3 and lead carbonate. Confirmed by powder X-ray diffraction data. Trigonal, a = 5.287, c = 5.364 Å.

Kind of sample preparation and/or method of registration of the spectrum: CsI disc. Transmission.
Source: Vandenborre et al. (1980).
Wavenumbers (cm^{-1}): 635sh, 555s, 480s, 427, 400sh, 310s, 240.
Note: The wavenumbers were partly determined by us based on spectral curve analysis of the published spectrum.

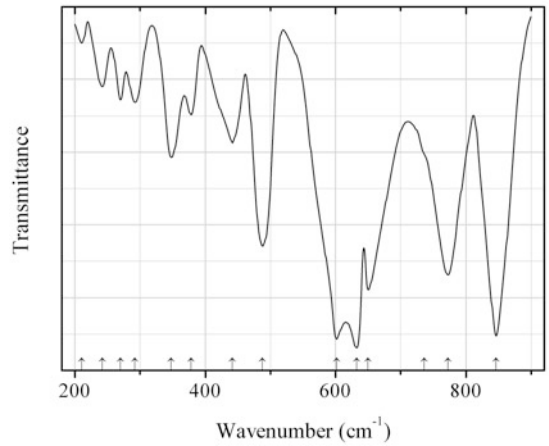

Fig. 2.383 IR spectrum of rynersonite drawn using data from Povarennykh (1981b)

O439 Rynersonite $CaTa_2O_6$ (Fig. 2.383)
Locality: Synthetic.
Description: No data are given in the cited paper.
Kind of sample preparation and/or method of registration of the spectrum: KBr disc. Absorption.
Source: Povarennykh (1981b).
Wavenumbers (cm^{-1}): 846s, 772s, 736sh, 650s, 632s, 602s, 488s, 442, 378, 348, 292, 270, 242, 211w.

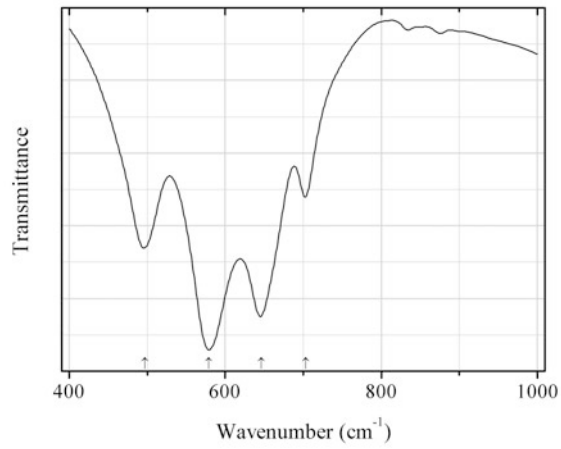

Fig. 2.384 IR spectrum of schafarzikite drawn using data from Sejkora et al. (2007)

O440 Schafarzikite $Fe^{2+}Sb^{3+}{}_2O_4$ (Fig. 2.384)
Locality: Pernek, Malé Karpaty Mountains, Slovakia (type locality).
Description: Dark brown prismatic crystals from the association with ankerite, berthierite, stibnite, valentinite, kermesite, senarmontite, and gypsum. Tetragonal, a = 8.6073(2), c = 5.9093(3) Å, V = 437.80(2) Å^3. The empirical formula is (electron microprobe): $Fe_{0.97}(Sb_{1.99}As_{0.02})O_4$. The strongest lines of the powder X-ray diffraction pattern [d, Å (I, %) (hkl)] are: 4.302 (38) (200), 3.224 (100) (211), 3.042 (65) (220), 2.721 (76) (310), 2.029 (43) (330), 1.9682 (87) (411).
Kind of sample preparation and/or method of registration of the spectrum: KBr disc. Absorption.
Source: Sejkora et al. (2007).
Wavenumbers (cm^{-1}): 703, 646s, 579s, 497.

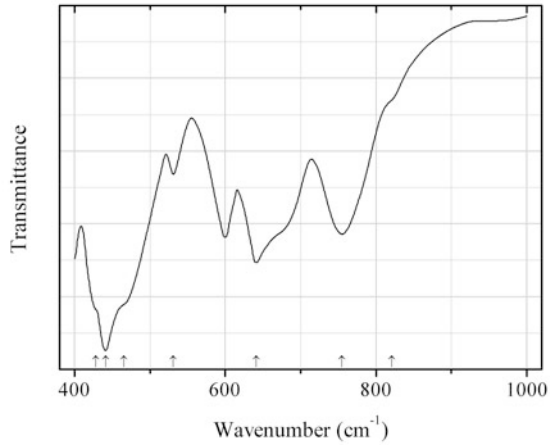

Fig. 2.385 IR spectrum of cervantite drawn using data from Costa et al. (1990)

O441 Cervantite $Sb^{3+}Sb^{5+}O_4$ (Fig. 2.385)
Locality: Synthetic.
Description: Prepared by heating sénarmontite to 650 °C in air. Confirmed by powder X-ray diffraction data.
Kind of sample preparation and/or method of registration of the spectrum: KBr disc. Transmission.
Source: Costa et al. (1990).
Wavenumbers (cm^{-1}): 821sh, 755, 641s, 531, 465sh, 441s, 428sh.
Note: Additionally, a wand with the wavenumber of 599 cm^{-1} was determined by us based on spectral curve analysis of the published spectrum.

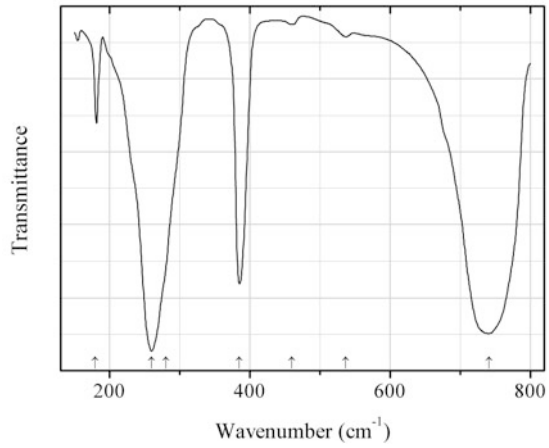

Fig. 2.386 IR spectrum of sénarmontite drawn using data from Voit et al. (2009)

O443 Sénarmontite Sb_2O_3 (Fig. 2.386)
Locality: Synthetic.
Description: Commercial reactant. Cubic modification of Sb_2O_3 produced by Merck (chemically pure).
Kind of sample preparation and/or method of registration of the spectrum: Suspension in vaseline oil. Absorption.
Source: Voit et al. (2009).
Wavenumbers (cm^{-1}): 741s, 537w, 460w, 385s, 280sh, 260s, 179.
Note: For the IR spectra of sénarmontite see also Brisse et al. (1972), Costa et al. (1990).

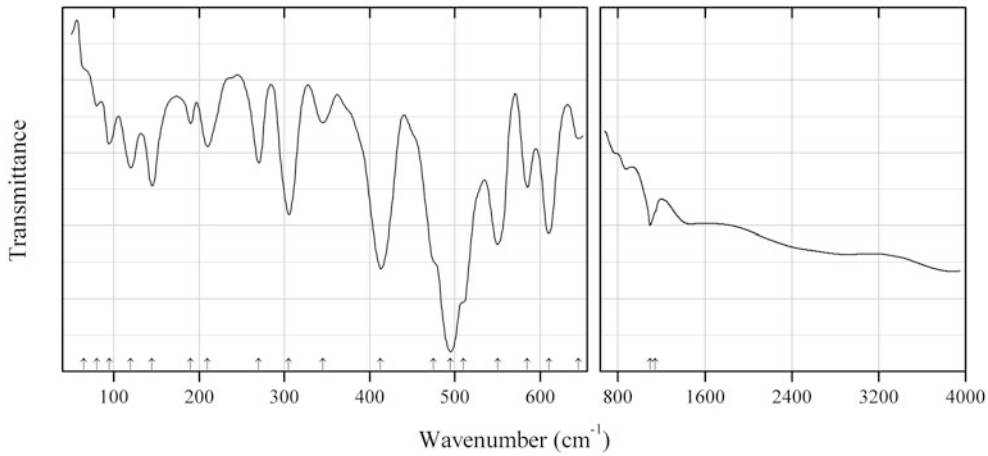

Fig. 2.387 IR spectrum of shakhovite drawn using data from Kovaleva and Vasiliev (1987)

O444 Shakhovite $Hg^{+}_{4}Sb^{5+}O_3(OH)_3$ (Fig. 2.387)
Locality: Kelyana Hg deposit, Buryatia, Transbaikal territory, Siberia, Russia (type locality).
Kind of sample preparation and/or method of registration of the spectrum: Suspension in perfluorinated mineral oil (in the range from 1400 to 4000 cm^{-1}); KBr disc (in the range from 600 to 1400 cm^{-1}); suspension in vaseline oil (in the range from 50 to 650 cm^{-1}). Transmission.

Source: Kovaleva and Vasiliev (1987).
Wavenumbers (cm^{-1}): 1145sh, 1095, 645w, 610s, 585, 550s, 510sh, 495s, 475sh, 413s, 345, 305, 270, 210, 190w, 145, 120, 95, 80w, 65sh.
Note: Diffuse absorption in the range from 2000 to 3000 cm^{-1} may correspond to OH groups forming strong hydrogen bonds.

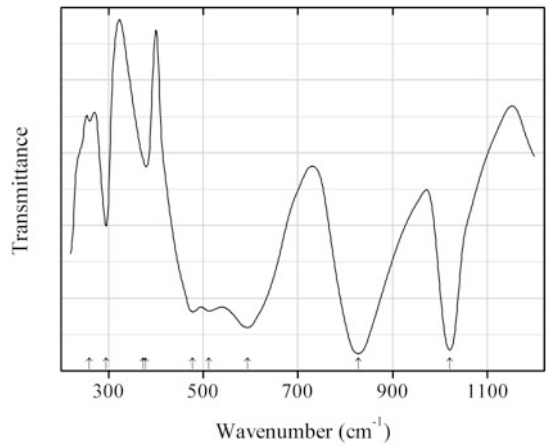

Fig. 2.388 IR spectrum of shcherbinaite drawn using data from Botto et al. (1997b)

O445 Shcherbinaite V_2O_5 (Fig. 2.388)
Locality: Synthetic.
Description: Obtained on thermal treatment of NH_4VO_3 at 500 °C. Identified by powder X-ray diffraction data.
Kind of sample preparation and/or method of registration of the spectrum: KBr disc. Transmission.
Source: Botto et al. (1997b).
Wavenumbers (cm^{-1}): 1020s, 828s, 594s, 512, 478, 379, 373sh, 295, 260w.

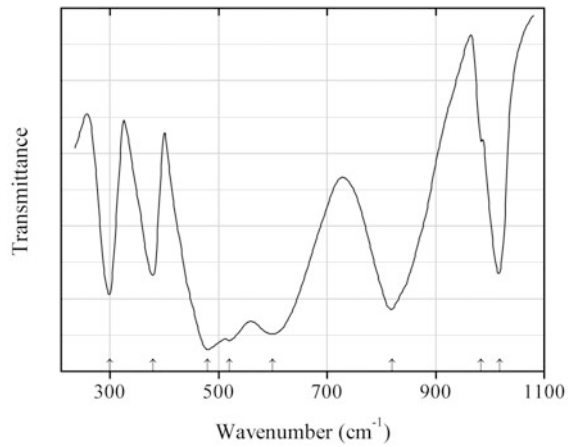

Fig. 2.389 IR spectrum of shcherbinaite drawn using data from Sanchez et al. (1982)

O446 Shcherbinaite V_2O_5 (Fig. 2.389)

Locality: Synthetic.
Description: Commercial reactant. Identified by powder X-ray diffraction data.
Kind of sample preparation and/or method of registration of the spectrum: Nujol mull. Transmission.
Source: Sanchez et al. (1982).
Wavenumbers (cm^{-1}): 1018, (983w), 820, 600s, 520s, 480s, 380, 300.
Note: For the IR spectrum of synthetic V_2O_5 see also Menezes et al. (2009).

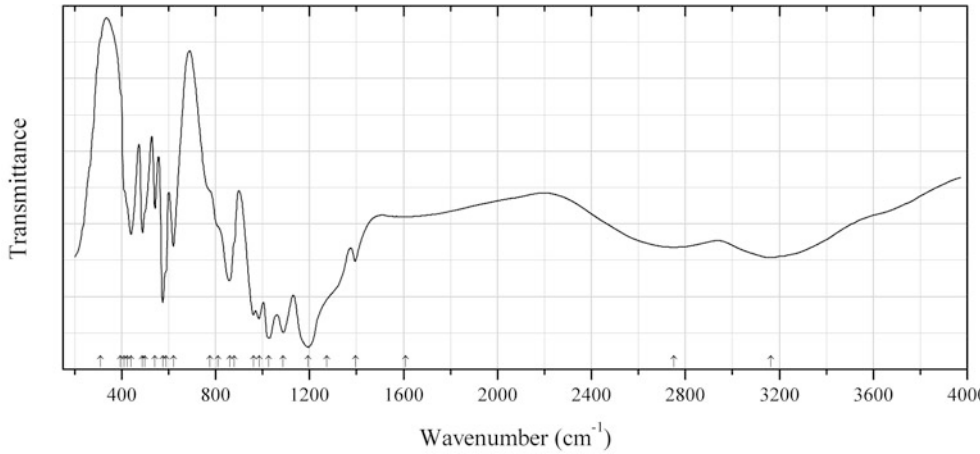

Fig. 2.390 IR spectrum of sidwillite drawn using data from Philip et al. (1988)

O447 Sidwillite $MoO_3 \cdot 2H_2O$ (Fig. 2.390)
Locality: Synthetic.
Kind of sample preparation and/or method of registration of the spectrum: KBr disc. Transmission.
Source: Philip et al. (1988).
Wavenumbers (cm^{-1}): 3163 (broad), 2750 (broad), 1610w, 1395, 1273sh, 1195s, 1088s, 1027s, 985s, 961s, 879sh, 860, 810sh, 776sh, 620, 590sh, 575s, 542, 500sh, 489, 440, 425sh, 410sh, 395sh, 310sh.
Note: The wavenumbers were partly determined by us based on spectral curve analysis of the published spectrum. For the IR spectrum of synthetic $MoO_3 \cdot 2H_2O$ see also Seguin et al. (1995).

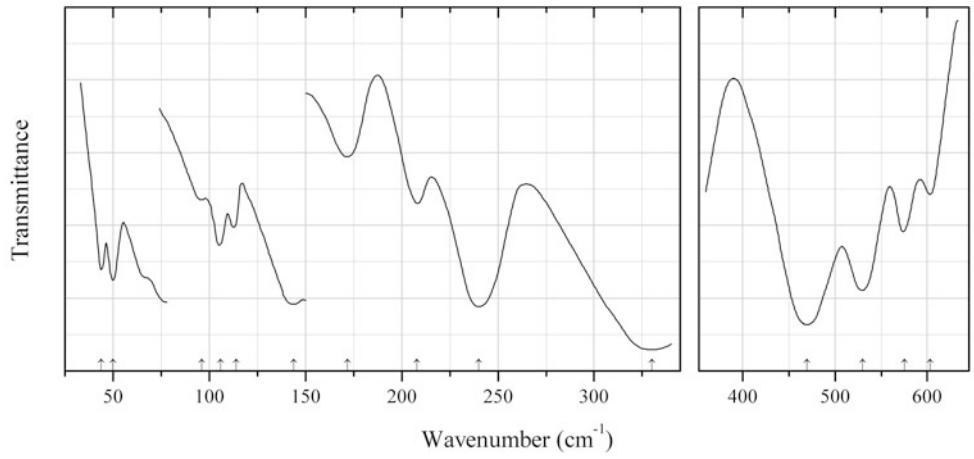

Fig. 2.391 IR spectrum of sillénite drawn using data from Betsch and White (1978)

O448 Sillénite $Bi_{12}SiO_{20}$ (Fig. 2.391)
Locality: Synthetic.
Description: Synthesized from the stoichiometric mixture of oxides at 700 °C for 48 h. Cubic, space group *I*23.
Kind of sample preparation and/or method of registration of the spectrum: KBr disc (above 300 cm^{-1}) and Nujol mull (in the range from 33 to 700 cm^{-1}). Transmission.
Source: Betsch and White (1978).
Wavenumbers (cm^{-1}): 603, 575, 530s, 470s, 330s, 240s, 208, 172, 144, 114, 106, 96, 50, 44.

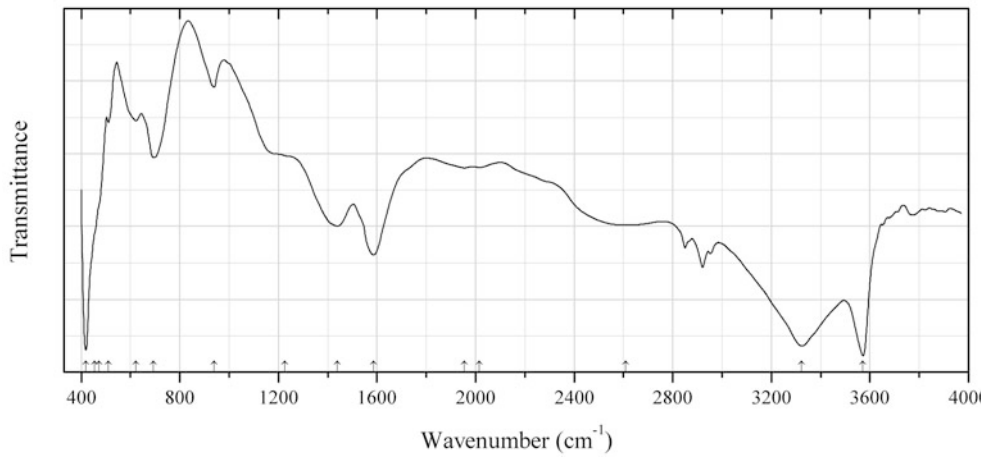

Fig. 2.392 IR spectrum of spertiniite drawn using data from Paterakis (2003)

O449 Spertiniite $Cu(OH)_2$ (Fig. 2.392)
Locality: Technogenetic.
Description: The product of corrosion of copper alloy.
Kind of sample preparation and/or method of registration of the spectrum: A diamond-anvil cell were used.

Source: Paterakis (2003).
Wavenumbers (cm^{-1}): 3572s, 3323s, 2610 (broad), 2014, 1954, 1586s, 1440, 1225sh, 939w, 694, 622w, 510w, 473sh, 455sh, 420s.
Note: The wavenumbers were partly determined by us based on spectral curve analysis of the published spectrum. Weak bands in the range from 2800 to 3000 cm^{-1} correspond to the admixture of an organic substance.

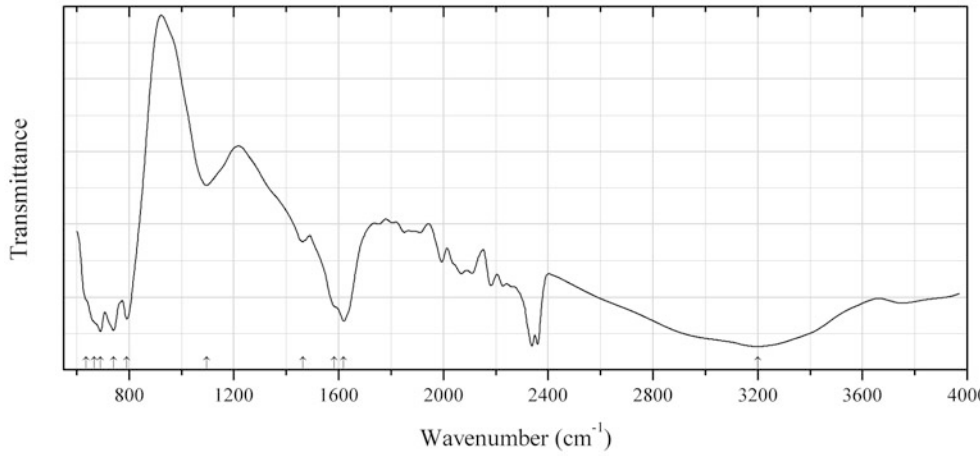

Fig. 2.393 IR spectrum of spriggite drawn using data from Brugger et al. (2004)

O450 Spriggite $Pb_3(UO_2)_6O_8(OH)_2 \cdot 3H_2O$ (Fig. 2.393)
Locality: Mt. Painter, Arkaroola, Northern Flinders Ranges, South Australia, Australia (type locality).
Description: Orange prismatic crystals from the association with uranophane-β, soddyite, kasolite, françoisite-(Nd), metatorbernite, billietite, boltwoodite, schoepite, metaschoepite, and weeksite. Holotype sample. The crystal structure is solved. Monoclinic, space group *C*2/*c*, a = 28.355(9), b = 11.990(4), c = 13.998(4) Å, β = 104.248(5)°, V = 4613(3) $Å^3$, Z = 8. D_{calc} = 7.64 g/cm^3. Optically biaxial, n_{min} = 1.807, n_{max} = 1.891. The empirical formula is (electron microprobe): $(Pb_{2.77}Ca_{0.06}Ba_{0.04})U_{6.00}O_{19.9}(OH)_2 \cdot 3H_2O$. The strongest lines of the powder X-ray diffraction pattern [*d*, Å (*I*, %) (*hkl*)] are: 6.92 (60) (400), 6.02 (30) (11–2, 020), 3.46 (80) (800), 3.10 (100) (204, −604, 3–32, −532), 2.74 (30) (−440), 2.01 (30) (33–6), 1.918 (60) (10.0.–4, 14.0.–4, 11.–3.2, −1.−3.31), 1.738 (30) (5–36, −1.–1.36).
Kind of sample preparation and/or method of registration of the spectrum: A diamond-anvil cell was used.
Source: Brugger et al. (2004).
Wavenumbers (cm^{-1}): 3200s (very broad), 1620s, 1584sh, 1463, 1096, 792s, 740s, 691s, 667sh, 637sh.
Note: The wavenumbers were partly determined by us based on spectral curve analysis of the published spectrum. The doublet in the range from 2300 to 2400 cm^{-1} may correspond to atmospheric CO_2.

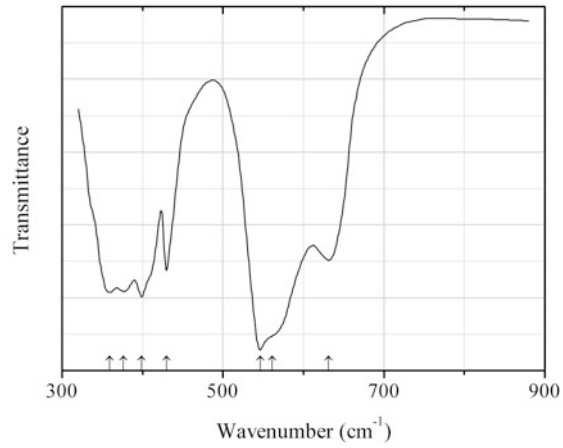

Fig. 2.394 IR spectrum of srebrodolskite drawn using data from Tarte (1967)

O451 Srebrodolskite $Ca_2Fe^{3+}{}_2O_5$ (Fig. 2.394)
Locality: Synthetic.
Description: No data.
Kind of sample preparation and/or method of registration of the spectrum: KBr or KI disc. Transmission.
Source: Tarte (1967).
Wavenumbers (cm^{-1}): 631, 561sh, 546s, 430, 399s, 376s, 359s.
Note: The wavenumbers were determined by us based on spectral curve analysis of the published spectrum.

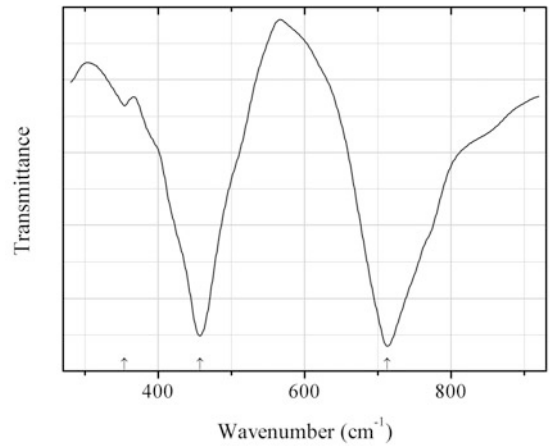

Fig. 2.395 IR spectrum of stibiconite drawn using data from Brisse et al. (1972)

O452 Stibiconite $Sb^{3+}Sb^{5+}{}_2O_6(OH)$ (Fig. 2.395)
Locality: San Luis, Potosi, Mexico.
Description: Characterized by Mössbauer spectrum: both Sb^{3+} and Sb^{5+} are present.
Kind of sample preparation and/or method of registration of the spectrum: KBr disc. Transmission.

Source: Brisse et al. (1972).
Wavenumbers (cm^{-1}): 713s, 457s, 354w.
Note: Stibiconite is considered as a questional mineral species. According to the current nomenclature of the pyrochlore supergroup, it should be named hydroxystibioroméite. The wavenumbers were determined by us based on spectral curve analysis of the published spectrum.

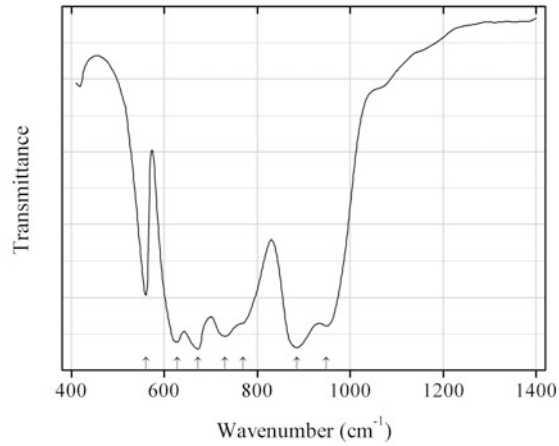

Fig. 2.396 IR spectrum of stishovite drawn using data from Lyon and Burns (1963)

O453 Stishovite SiO_2 (Fig. 2.396)
Locality: Meteor Crater (Barringer Crater), Winslow, Coconino Co., Arizona, USA (type locality).
Description: Residue from HF leaching of impacted Coconino sandstone.
Kind of sample preparation and/or method of registration of the spectrum: KBr disc. Transmission.
Source: Lyon and Burns (1963).
Wavenumbers (cm^{-1}): 949, 885s, 769sh, 730s, 672s, 628s, 560.
Note: For the IR spectra of stishovite see also Kieffe (1979), Plyusnina et al. (1970).

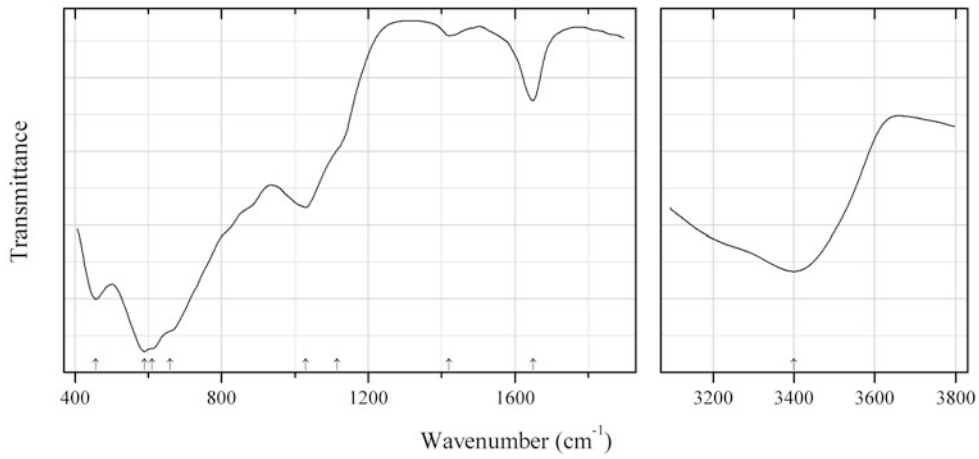

Fig. 2.397 IR spectrum of "strontiopyrochlore" drawn using data from Voloshin et al. (1989)

O454 "Strontiopyrochlore" $(H_2O,\square,Sr)_2Nb_2O_6(H_2O)$ (?) (Fig. 2.397)

Locality: Vavnbed Mt., Lovozero alkaline complex, Kola peninsula, Murmansk region, Russia.
Description: Red crystals from the association with albite, aegirine, ilmenite, and zircon. Characterized by electron microprobe analyses and powder X-ray diffraction data. The content of Sr is from 0.4 to 0.6 atoms per formula unit.
Kind of sample preparation and/or method of registration of the spectrum: KBr disc. Transmission.
Source: Voloshin et al. (1989).
Wavenumbers (cm^{-1}): 3400, 1650, 1420w, 1115sh, 1030, 660sh, 610sh, 590s, 457s.
Note: The wavenumbers were partly determined by us based on spectral curve analysis of the published spectrum. Strontiopyrochlore by Voloshin et al. was discredited as a valid mineral species (see Atencio et al. 2010).

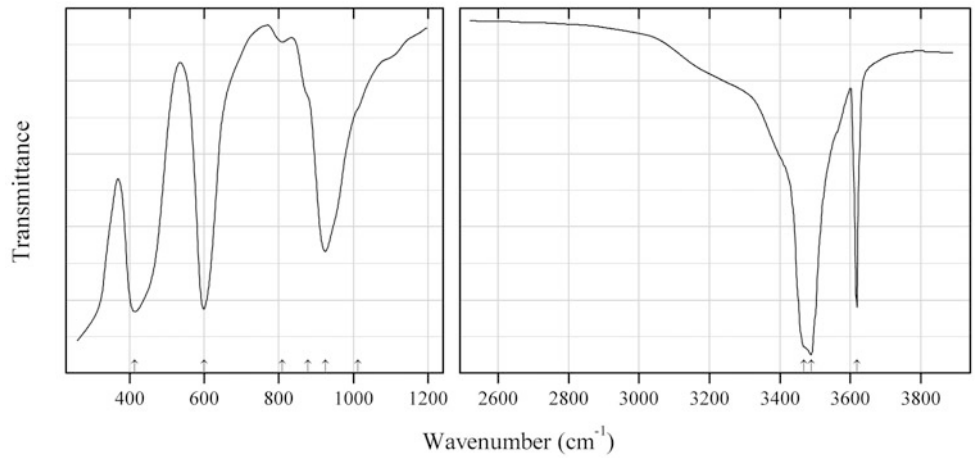

Fig. 2.398 IR spectrum of strontium hydroxide drawn using data from Lutz et al. (1981)

O455 Strontium hydroxide $Sr(OH)_2$ (Fig. 2.398)
Locality: Synthetic.
Description: No data.
Kind of sample preparation and/or method of registration of the spectrum: Transmission. Kind of sample preparation is not indicated.
Source: Lutz et al. (1981).
Wavenumbers (cm^{-1}): 3618s, 3490s, 3468sh, 1012sh, 925, 878sh, 810w, 600s, 415s.
Note: The wavenumbers were partly determined by us based on spectral curve analysis of the published spectrum.

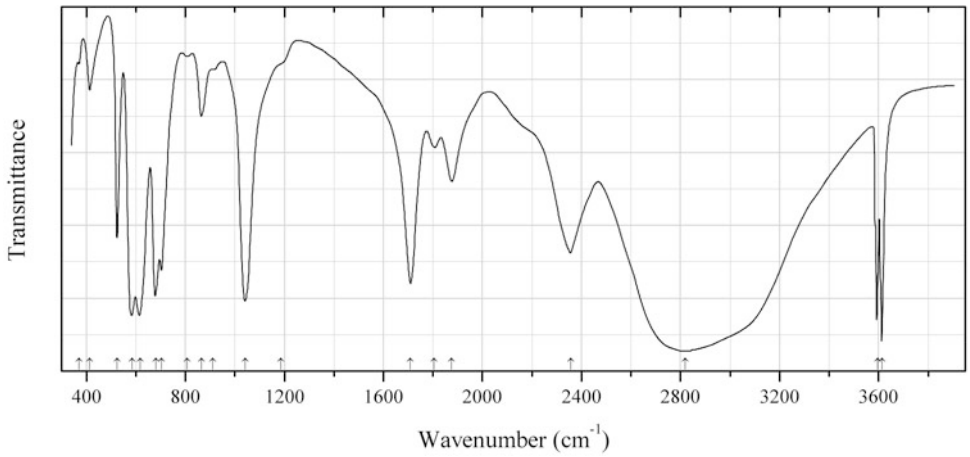

Fig. 2.399 IR spectrum of strontium hydroxide monohydrate drawn using data from Lutz et al. (1981)

O456 Strontium hydroxide monohydrate $Sr(OH)_2 \cdot H_2O$ (Fig. 2.399)
Locality: Synthetic.
Description: No data.
Kind of sample preparation and/or method of registration of the spectrum: Transmission. Kind of sample preparation is not indicated.
Source: Lutz et al. (1981).
Wavenumbers (cm^{-1}): 3614s, 3596s, 2820s, 2356, 1875, 1805, 1709, 1185sh, 911sh, 1043s, 866, 808w, 705, 680s, 618s, 585s, 524, 413, 371w.
Note: The wavenumbers were partly determined by us based on spectral curve analysis of the published spectrum.

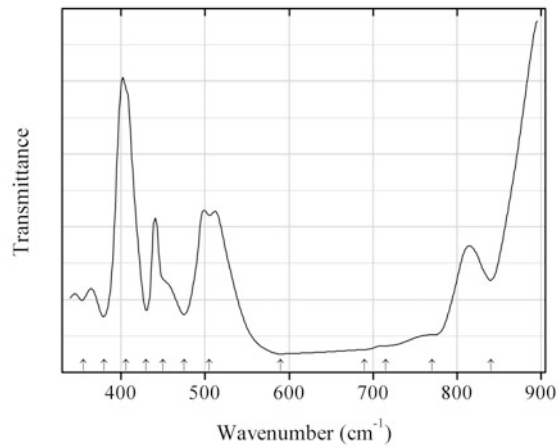

Fig. 2.400 IR spectrum of strontium niobate drawn using data from Repelin et al. (1979)

O457 Strontium niobate $SrNb_2O_6$ (Fig. 2.400)
Locality: Synthetic.
Description: Orthorhombic.

Kind of sample preparation and/or method of registration of the spectrum: Transmission. Kind of sample preparation is not indicated.
Source: Repelin et al. (1979).
Wavenumbers (cm^{-1}): 840, 770sh, 715sh, 690sh, 590s (broad), 505w, 475s, 450sh, 430s, 406sh, 380s, 355.

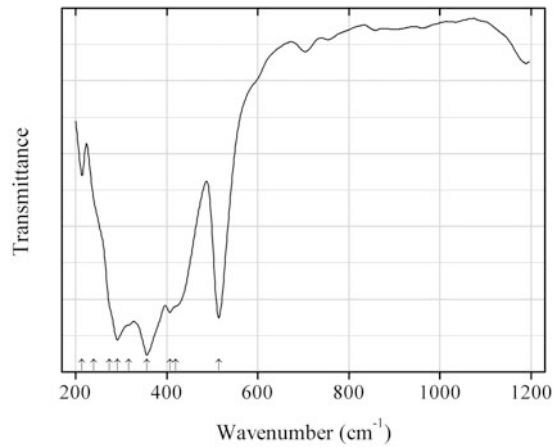

Fig. 2.401 IR spectrum of strontium lead(IV) oxide O458 drawn using data from Keester and White (1970)

O458 Strontium lead(IV) oxide O458 $Sr_2Pb^{4+}O_4$ (Fig. 2.401)
Locality: Synthetic.
Description: Orthorhombic, space group *Pbam* or *Pba*2, $a = 6.162(1)$, $b = 10.079(1)$, $c = 3.505(1)$ Å, $Z = 2$. $D_{calc} = 6.810$ g/cm^3. The strongest lines of the powder X-ray diffraction pattern [*d*, Å (*I*, %) (*hkl*)] are: 5.26 (36) (110), 3.08 (31) (200), 2.95 (92) (130), 2.917 (100) (111), 2.879 (46) (021), 2.1034 (55) (221), 1.6808 (46) (151).
Kind of sample preparation and/or method of registration of the spectrum: CsI disc. Transmission.
Source: Keester and White (1970).
Wavenumbers (cm^{-1}): 515s, 420sh, 407, 357s, 317sh, 292s, 275sh, 240sh, 214.
Note: The wavenumbers were partly determined by us based on spectral curve analysis of the published spectrum. In the cited paper the wavenumber 292 cm^{-1} is erroneously indicated as 240 cm^{-1}.

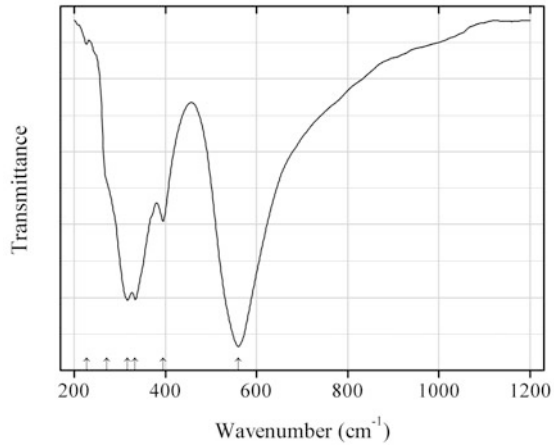

Fig. 2.402 IR spectrum of strontium lead(IV) oxide O459 drawn using data from Keester and White (1970)

O459 Strontium lead(IV) oxide O459 $SrPb^{4+}O_3$ (Fig. 2.402)
Locality: Synthetic.
Description: Orthorhombic, with distorted perovskite-type structure. Space group *Pnma* or $Pna2_1$, a = 5.860(1), b = 5.958(1), c = 8.331(1) Å. D_{calc} = 7.827 g/cm^3. The strongest lines of the powder X-ray diffraction pattern [d, Å (I, %) (hkl)] are: 4.177 (24) (002), 2.980 (33) (020), 2.951 (100) (112), 2.932 (24) (200), 2.089 (33) (220), 1.715 (26) (132), 1.697 (40) (312).
Kind of sample preparation and/or method of registration of the spectrum: CsI disc. Transmission.
Source: Keester and White (1970).
Wavenumbers (cm^{-1}): 560s, 395, 334s, 317s, 271sh, 227w.
Note: The wavenumbers were partly determined by us based on spectral curve analysis of the published spectrum.

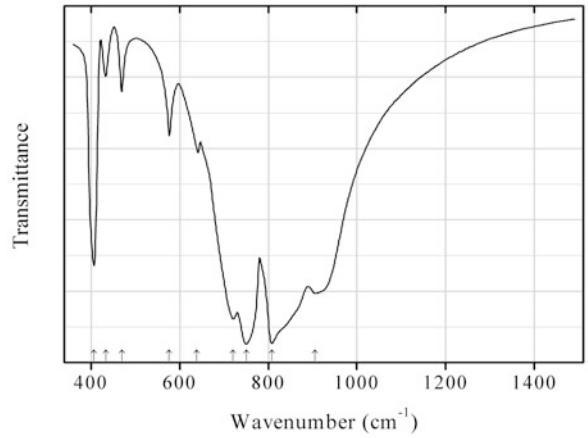

Fig. 2.403 IR spectrum of swedenborgite drawn using data from Povarennykh et al. (1982)

O460 Swedenborgite $NaBe_4Sb^{5+}O_7$ (Fig. 2.403)
Locality: Långban deposit, Bergslagen ore region, Filipstad district, Värmland, Sweden (type locality).
Description: Confirmed by optical methods and spectrographic analysis of chemical composition.

Kind of sample preparation and/or method of registration of the spectrum: KBr disc. Transmission.
Source: Povarennykh et al. (1982).
Wavenumbers (cm^{-1}): 906, 808s, 750s, 720s, 638, 576, 470, 434w, 407.

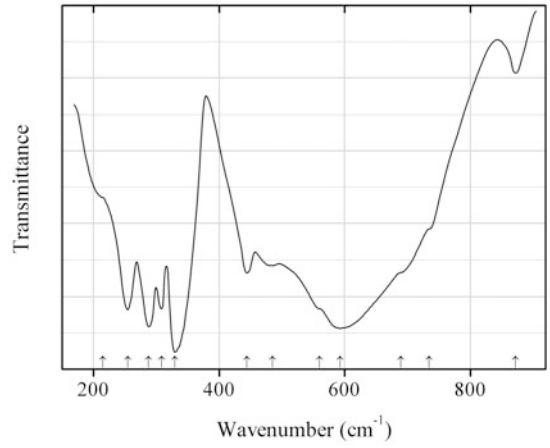

Fig. 2.404 IR spectrum of tantalite-(Mg) drawn using data from Husson et al. (1979)

O461 Tantalite-(Mg) $MgTa_2O_6$ (Fig. 2.404)
Locality: Synthetic.
Description: Synthesized in a solid-state reaction between Ta_2O_5 and MgO at 1050° for 50 h. Confirmed by powder X-ray diffraction data.
Kind of sample preparation and/or method of registration of the spectrum: Absorption. Kind of sample preparation is not indicated.
Source: Husson et al. (1979).
Wavenumbers (cm^{-1}): 872w, 734sh, 690sh, 593s, 560sh, 485, 444, 330s, 309, 288s, 255, 215sh.

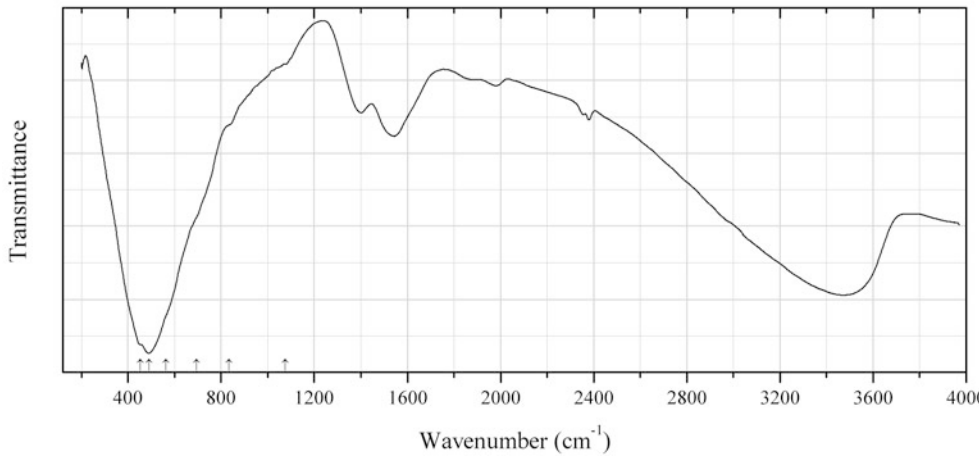

Fig. 2.405 IR spectrum of tazheranite drawn using data from Phillippi and Mazdiyasni (1971)

O462 Tazheranite $(Zr,Ti,Ca)(O,\square)_2$ (Fig. 2.405)

Locality: Synthetic.
Description: Metastable cubic ZrO_2.
Kind of sample preparation and/or method of registration of the spectrum: CsI disc. Transmission.
Source: Phillippi and Mazdiyasni (1971).
Wavenumbers (cm^{-1}): 1076sh, 834sh, 695sh, 564sh, 490s, 453s.
Note: The wavenumbers were determined by us based on spectral curve analysis of the published spectrum. The bands above 1300 cm^{-1} correspond to H_2O molecules (adsorbed water?). For the infrared absorption spectrum of Ca-stabilized cubic zirconia see McDevitt and Baun (1964).

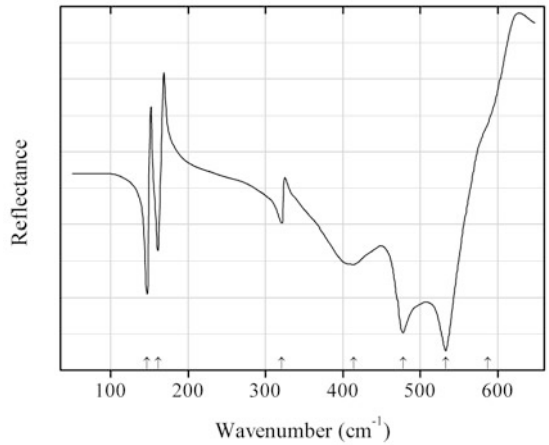

Fig. 2.406 IR spectrum of tenorite drawn using data from Kliche and Popovic (1990)

O463 Tenorite CuO (Fig. 2.406)
Locality: Synthetic.
Description: Polycrystalline sample prepared by oxidation of high-purity copper powder in air at 700 °C. Confirmed by powder X-ray diffraction data.
Kind of sample preparation and/or method of registration of the spectrum: Pressed disc. Reflection.
Source: Kliche and Popovic (1990).
Wavenumbers (cm^{-1}): 587sh, 533s, 478s, 414, 321w, 161, 147.

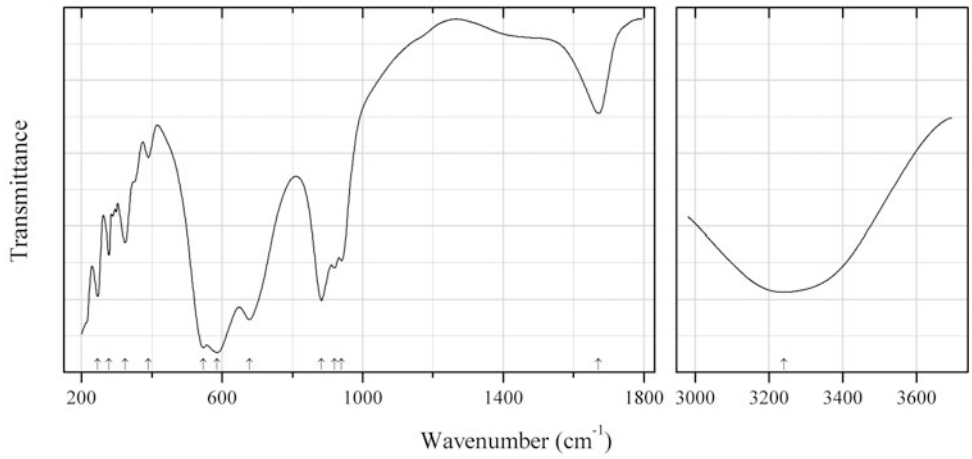

Fig. 2.407 IR spectrum of ternovite drawn using data from Subbotin et al. (1997)

O464 Ternovite $MgNb_4O_{11}\cdot 8–12H_2O$ (Fig. 2.407)
Locality: Vuoriyarvi alkaline-ultrabasic massif, Northern Karelia, Russia (type locality).
Description: White radial fibrous aggregates from the association with calcite, dolomite, magnetite, phlogopite, apatite, serpentine, zircon, pyrochlore, belkovite, etc. Holotype sample. Monoclinic, $a = 20.656(6)$, $b = 13.062(5)$, $c = 6.338(3)$ Å, $\beta = 91.90(8)°$, $V = 1709.1(5)$ Å^3, $Z = 4$. $D_{meas} = 2.95(2)$ g/cm^3, $D_{calc} = 2.99$ g/cm^3. Optically biaxial (−), $\alpha = 1.725(3)$, $\beta = 1.830(5)$, $\gamma = 1.845(5)$, $2V = 39.5(1)°$. The empirical formula is $(Mg_{0.73}Ca_{0.21}Ba_{0.06}Sr_{0.01})(Nb_{3.98}Fe_{0.02}Ti_{0.01})O_{11}\cdot 10.1H_2O$. The strongest lines of the powder X-ray diffraction pattern [*d*, Å (*I*, %) (*hkl*)] are: 10.33 (100) (200), 5.16 (7) (400), 4.56 (8) (021), 3.15 (17) (10–2), 3.12 (15) (102), 3.06 (7) (20–2, 11–2).
Kind of sample preparation and/or method of registration of the spectrum: KBr disc. Transmission.
Source: Subbotin et al. (1997).
Wavenumbers (cm^{-1}): 3240s, 1670, 940, 920, 882s, 678s, 585s, 547s, 390w, 324, 278, 246s.

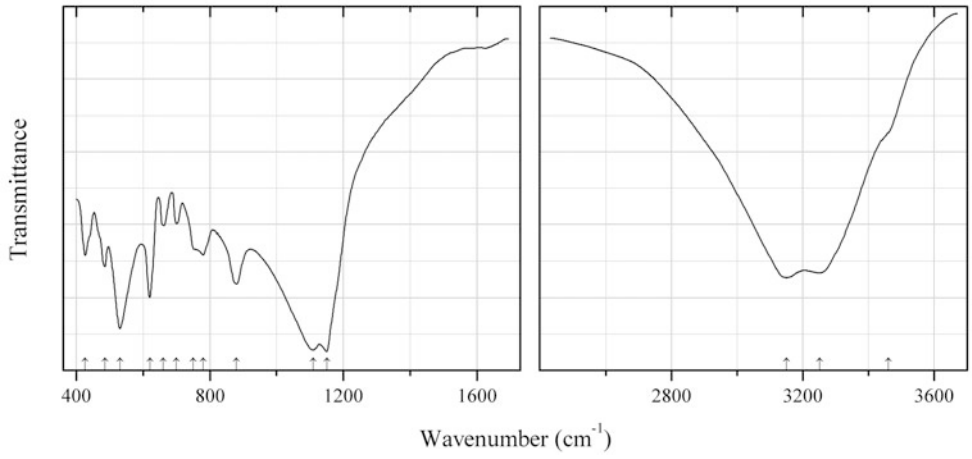

Fig. 2.408 IR spectrum of tetrawickmanite drawn using data from Konovalenko et al. (1984)

O465 Tetrawickmanite $Mn^{2+}[Sn^{4+}(OH)_6]$ (Fig. 2.408)

Locality: Southwestern Pamirs.
Description: Orange-yellow to honey-yellow dipyramidal crystals from the association with quartz, orthoclase, tourmaline, zircon, columbite, microlite, and hambergite. Tetragonal, a = 7.866, c = 7.804 Å. Optically uniaxial (−), ω = 1.705, ε = 1.704. The crystals are heterogeneous in composition. The empirical formula is (electron microprobe, ranges of formula coefficients are given): $(Mn_{0.65–0.90}Fe_{0.10–0.31})(Sn_{1.00–1.02}W_{0–0.01})(OH)_6$.
Kind of sample preparation and/or method of registration of the spectrum: Transmission. Kind of sample preparation is not indicated.
Source: Konovalenko et al. (1984).
Wavenumbers (cm^{-1}): 3460sh, 3250s, 3150s, 1150s, 1110s, 880s, 780, 750sh, 700, 660, 620s, 530s, 485, 425.

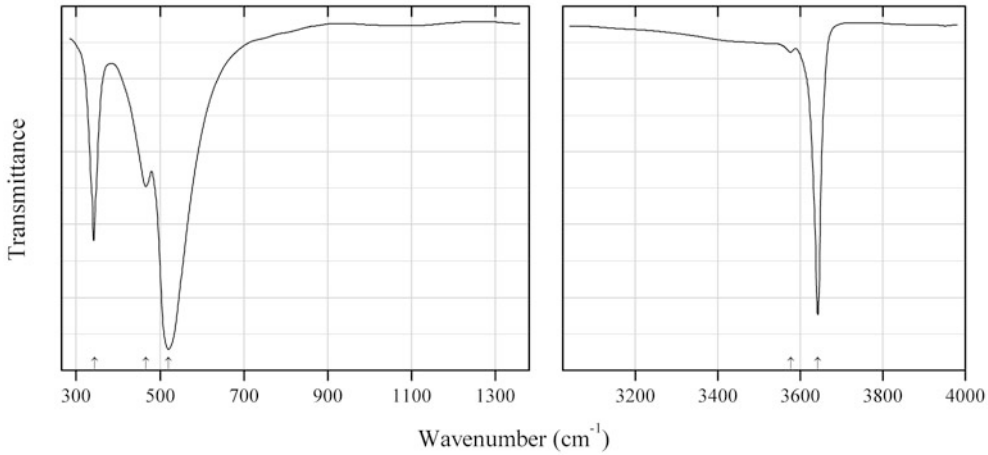

Fig. 2.409 IR spectrum of theophrastite drawn using data from Kermarec et al. (1994)

O466 Theophrastite $Ni(OH)_2$ (Fig. 2.409)
Locality: Synthetic.
Description: Prepared by adding 40 mL of a 1 M ammoniacal solution to 50 mL of a 0.4 M $Ni(NO_3)_2$ solution with subsequent hydrothermal treatment at 190 °C during 15 days.
Kind of sample preparation and/or method of registration of the spectrum: KBr disc. Absorption.
Source: Kermarec et al. (1994).
Wavenumbers (cm^{-1}): 3642s, 3577w, 520s, 466, 344s.

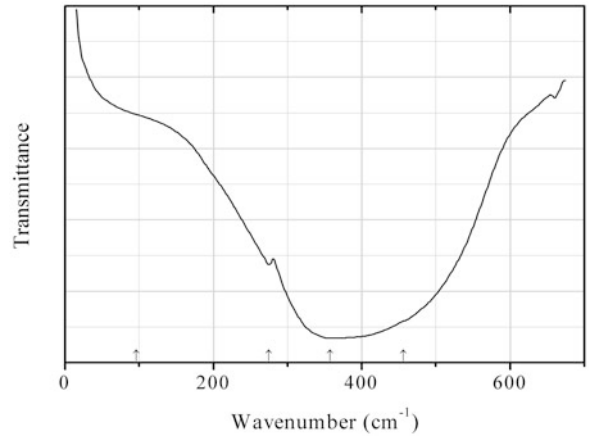

Fig. 2.410 IR spectrum of thorianite drawn using data from Hubert and Thouvenot (1992)

O467 Thorianite ThO_2 (Fig. 2.410)
Locality: Synthetic.
Description: No data.
Kind of sample preparation and/or method of registration of the spectrum: Transmission. Kind of sample preparation is not indicated.
Source: Hubert and Thouvenot (1992).
Wavenumbers (cm^{-1}): 456sh, 357s, 275, 96sh.

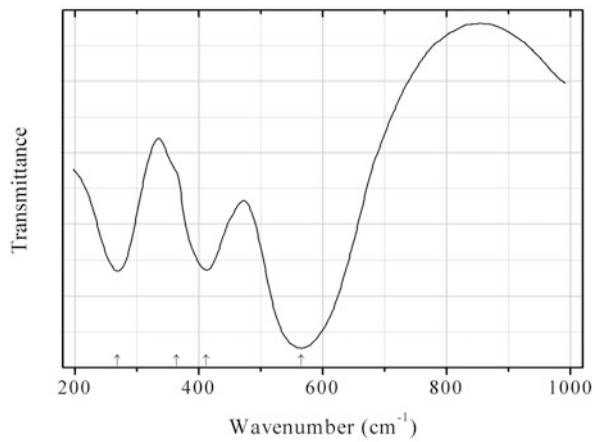

Fig. 2.411 IR spectrum of thorutite drawn using data from Shabalin (1982)

O468 Thorutite $(Th,U,Ca)Ti_2(O,OH)_6$ (Fig. 2.411)
Locality: Synthetic.
Description: Thorutite end-member $ThTi_2O_6$ obtained in solid-state reaction in coprecipitate of Th- and Ti-bearing precursors. Monoclinic, space group *C*2/*m*, $a = 9.82$, $b = 3.82$, $c = 7.04$ Å, $\beta = 118.8°$.
Kind of sample preparation and/or method of registration of the spectrum: CsI disc. Transmission.
Source: Shabalin (1982).
Wavenumbers (cm^{-1}): 565s, 412, 364sh, 268.

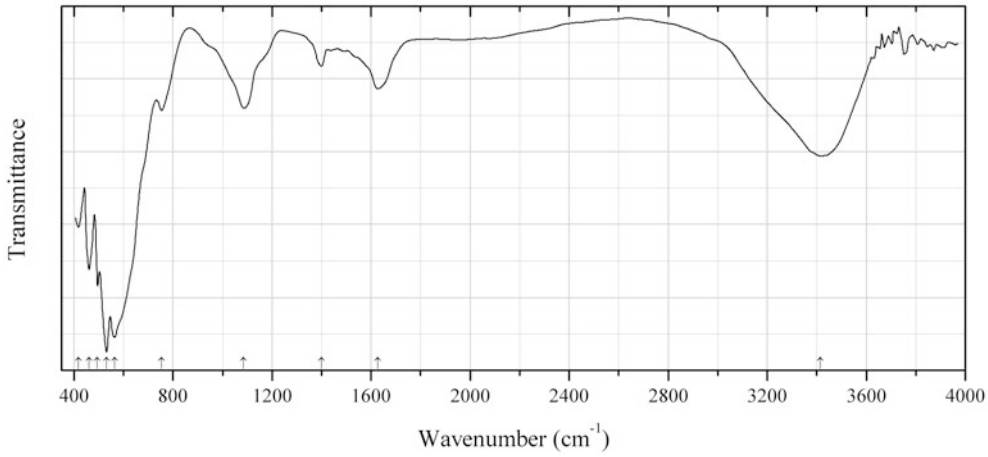

Fig. 2.412 IR spectrum of todorokite Ba-rich variety drawn using data from Gómez-Caballero et al. (2010)

O469 Todorokite Ba-rich variety $(Ca,Ba,Na)_{1-x}(Mn,Mg,Al)_6O_{12}\cdot nH_2O$ (Fig. 2.412)
Locality: San Miguel Tenango area, northern part of the State of Puebla, Mexico.
Description: Brown micro-fibrous aggregate. The content of BaO varies from 2.6 to 4.95 wt%. Characterized by powder X-ray diffraction data.
Kind of sample preparation and/or method of registration of the spectrum: Transmission. Kind of sample preparation is not indicated.
Source: Gómez-Caballero et al. (2010).
Wavenumbers (cm^{-1}): 3414, 1627, 1400w, 1085, 754, 565s, 532s, 495, 461, 419.

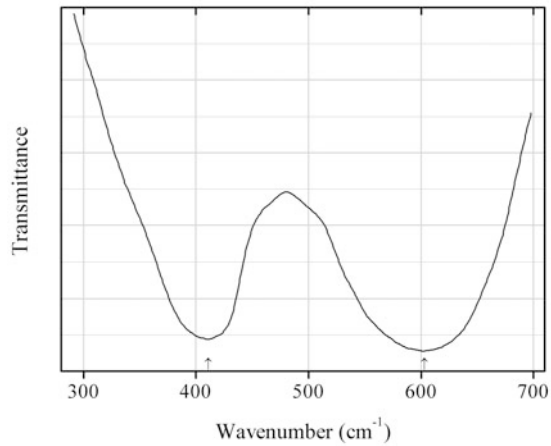

Fig. 2.413 IR spectrum of trevorite drawn using data from Gotić et al. (1998)

O470 Trevorite $NiFe^{3+}{}_2O_4$ (Fig. 2.413)
Locality: Synthetic.
Description: Nanocrystalline sample synthesized by heating of the stoichiometric coprecipitate of Fe $(OH)_3$ and $Ni(OH)_2$ at 773 K. Characterized by Mössbauer spectroscopy and powder X-ray diffraction data.

Kind of sample preparation and/or method of registration of the spectrum: KBr disc. Transmission.
Source: Gotić et al. (1998).
Wavenumbers (cm^{-1}): 603s, 411s.

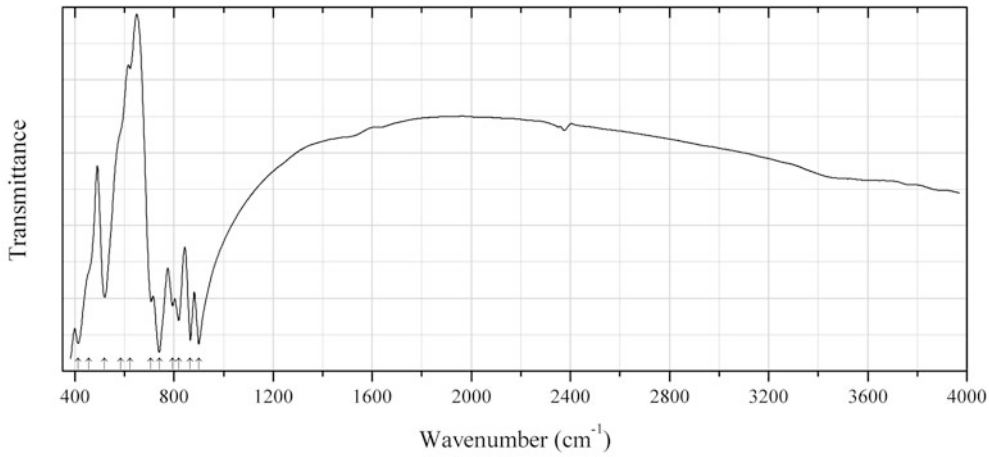

Fig. 2.414 IR spectrum of tricalcium aluminate drawn using data from Taş (1998)

O471 Tricalcium aluminate $Ca_3Al_2O_6$ (Fig. 2.414)
Locality: Synthetic.
Description: Synthesized as high-compound-purity powders by using the selfpropagating combustion synthesis method. Characterized by powder X-ray diffraction data.
Kind of sample preparation and/or method of registration of the spectrum: KBr disc. Transmission.
Source: Taş (1998).
Wavenumbers (cm^{-1}): 900s, 866s, 819, 794, 740s, 707, 623, 585sh, 520, 457sh, 413s.
Note: The wavenumbers were determined by us based on spectral curve analysis of the published spectrum.

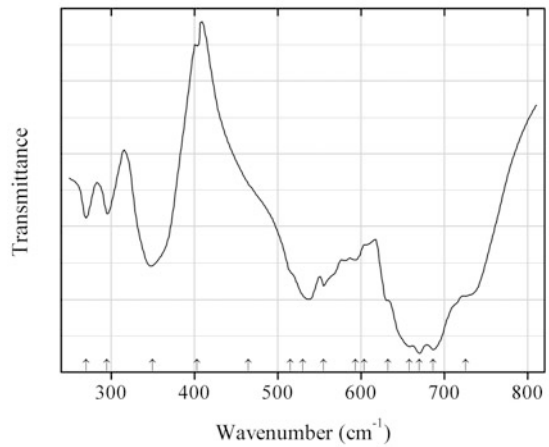

Fig. 2.415 IR spectrum of tripuhyite drawn using data from Walczak et al. (1997)

O472 Tripuhyite $Fe^{3+}Sb^{5+}O_4$ (Fig. 2.415)
Locality: Synthetic.
Description: Synthesized from the stoichiometric mixture of oxides on heating up to 900 °C. Characterized by powder X-ray diffraction data.
Kind of sample preparation and/or method of registration of the spectrum: KBr disc. Transmission.
Source: Walczak et al. (1997).
Wavenumbers (cm^{-1}): 725sh, 686s, 670s, 658s, 632sh, 604sh, 593, 555, 530s, 515sh, 465sh, 403w, 350, 295, 270.
Note: The wavenumbers were partly determined by us based on spectral curve analysis of the published spectrum.

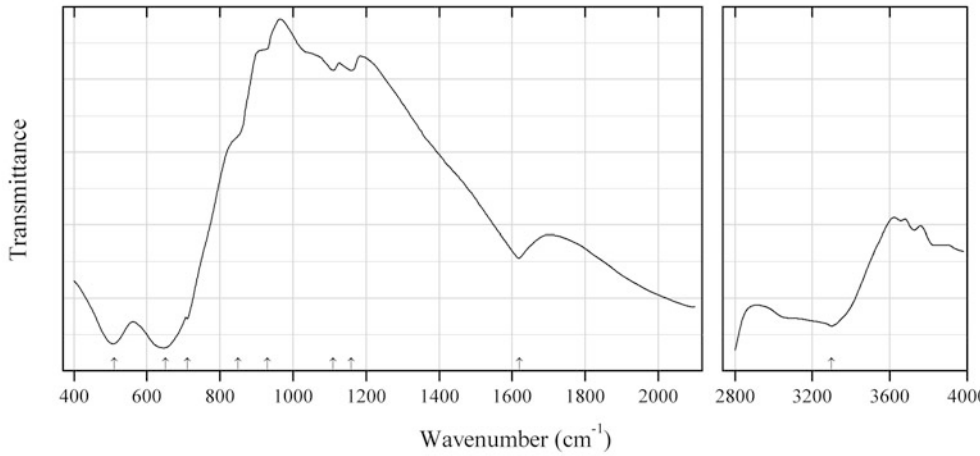

Fig. 2.416 IR spectrum of tripuhyite drawn using data from Sergeev et al. (1997)

O473 Tripuhyite $Fe^{3+}Sb^{5+}O_4$ (Fig. 2.416)
Locality: Olimpiadinskiy mine, Krasnoyarsk Krai, Siberia, Russia.
Description: Botryoidal aggregates from the association with other secondary Sb minerals. Tetragonal, pseudo-cell parameters are: a = 4.64–4.67, c = 3.05 Å. D_{meas} = 4.01(1) g/cm^3. The empirical formula is $Fe_{0.8–0.9}Sb_{0.8–0.9}W_{0.1–0.4}As_{<0.1}\cdot nH_2O$.
Kind of sample preparation and/or method of registration of the spectrum: Transmission. Kind of sample preparation is not indicated.
Source: Sergeev et al. (1997).
Wavenumbers (cm^{-1}): 3300, 1620, 1160w, 1110w, 930sh, 850sh, 710sh, 650s, 510s.
Note: The bands at 3300 and 1620 cm^{-1} correspond to H_2O molecules (adsorbed water?).

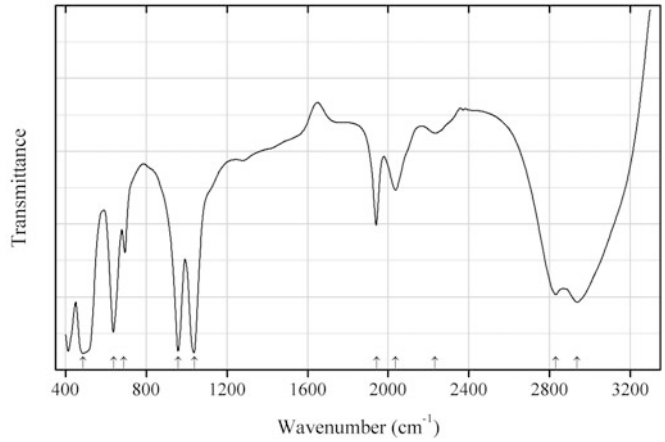

Fig. 2.417 IR spectrum of tsumgallite drawn using data from Zhan et al. (2009)

O474 Tsumgallite GaO(OH) (Fig. 2.417)
Locality: Synthetic.
Description: Nanocrystals synthesized hydrothermally from a solution containing $Ga(NO_3)_3$ and NaN_3. Orthorhombic, space group *Pbnm*, a = 4.510, b = 9.750, c = 2.965 Å.
Kind of sample preparation and/or method of registration of the spectrum: KBr disc. Transmission.
Source: Zhan et al. (2009).
Wavenumbers (cm^{-1}): 2938s, 2832s, 2233w, 2036, 1942, 1038s, 960s, 688, 640s, 486s.

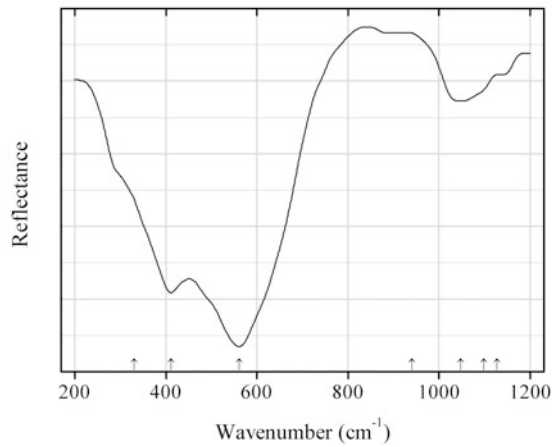

Fig. 2.418 IR spectrum of ulvöspinel drawn using data from Estep et al. (1972)

O475 Ulvöspinel $Fe^{2+}{}_2TiO_4$ (Fig. 2.418)
Locality: Lunar Apollo 14 sample.
Description: Anhedral grain from the association with pyroxene, olivine, and ilmenite.
Kind of sample preparation and/or method of registration of the spectrum: CsI microdisc. Reflection.

Source: Estep et al. (1972).
Wavenumbers (cm^{-1}): 1127sh, 1098sh, 1047, 940sh, 561s, 412s, 330sh.
Note: The wavenumbers were determined by us based on spectral curve analysis of the published spectrum.

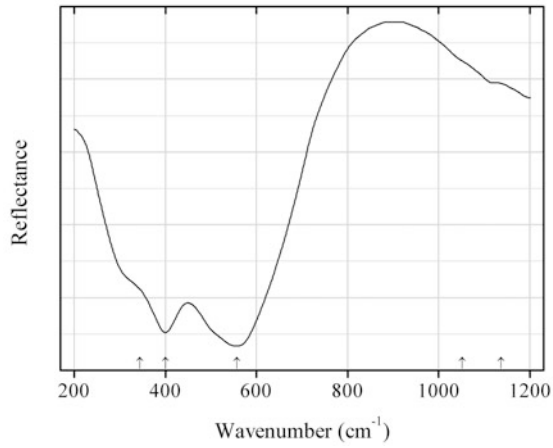

Fig. 2.419 IR spectrum of ulvöspinel drawn using data from Estep et al. (1972)

O476 Ulvöspinel $Fe^{2+}{}_2TiO_4$ (Fig. 2.419)
Locality: Synthetic.
Description: Pure $Fe^{2+}{}_2TiO_4$.
Kind of sample preparation and/or method of registration of the spectrum: CsI microdisc. Reflection.
Source: Estep et al. (1972).
Wavenumbers (cm^{-1}): 1136sh, 1052sh, 557s, 400s, 344sh.
Note: The wavenumbers were determined by us based on spectral curve analysis of the published spectrum.

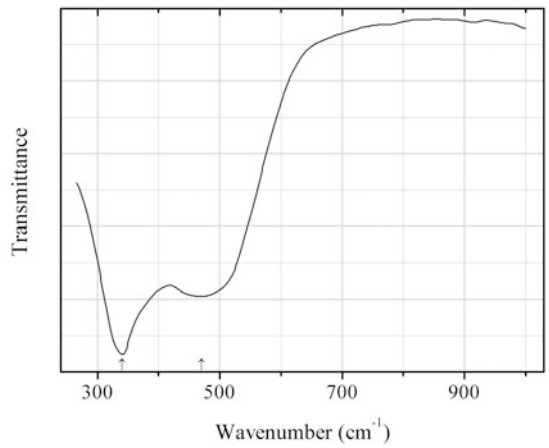

Fig. 2.420 IR spectrum of uraninite drawn using data from Allen et al. (1976)

O477 Uraninite UO_2 (Fig. 2.420)
Locality: Synthetic.
Description: A sample of commercial UO_2, was outgassed at 1073 K for 2 h. A 10:1 mixture of CO: CO_2 was then passed over the sample with the temperature maintained at 1073 K to reduce the $UO_{2.18}$ to pure UO_2. Confirmed by powder X-ray diffraction data.
Kind of sample preparation and/or method of registration of the spectrum: No data.
Source: Allen et al. (1976).
Wavenumbers (cm^{-1}): 470, 340s.

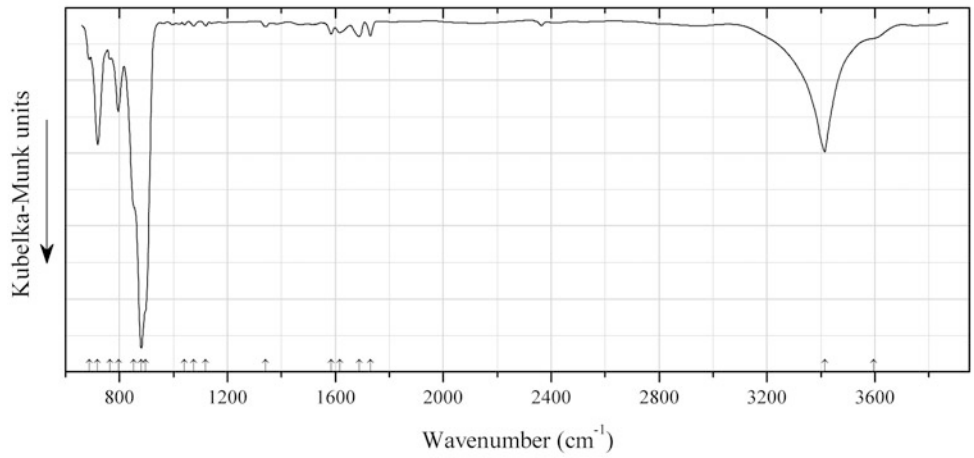

Fig. 2.421 IR spectrum of uranosphaerite drawn using data from Sejkora et al. (2008)

O478 Uranosphaerite $Bi(UO_2)O_2(OH)$ (Fig. 2.421)
Locality: Horní Halže, near Měděnec, Krušné Hory (Ore Mts.), Czech Republic.
Description: Dark orange to yellowish-brown crystalline aggregates from a quartz gangue. Monoclinic, a = 7.558(1), b = 7.824(1), c = 7.699(1) Å, β = 92.90(1)°, V = 454.7(1) $Å^3$. The empirical formula is (electron microprobe): $Bi_{1.02}(UO_2)_{0.99}O_{2.02}(OH)$. The strongest lines of the powder X-ray diffraction pattern [d, Å (I, %) (hkl)] are: 5.263 (100) (101), 4.367 (19) (111), 3.913 (20) (020), 3.193 (19) (11–2), 3.163 (38) (21–1), 3.139 (27) (121), 3.087 (27) (112), 3.059 (32) (211).
Kind of sample preparation and/or method of registration of the spectrum: Powder mixed with KBr. Diffuse reflection.
Source: Sejkora et al. (2008).
Wavenumbers (cm^{-1}): 3596sh, 3414s, 1730w, 1688w, 1616w, 1585w, 1341w, 1120w, 1074w, 1041w, 896sh, 881s, 853sh, 796s, 764w, 719s, 687w.

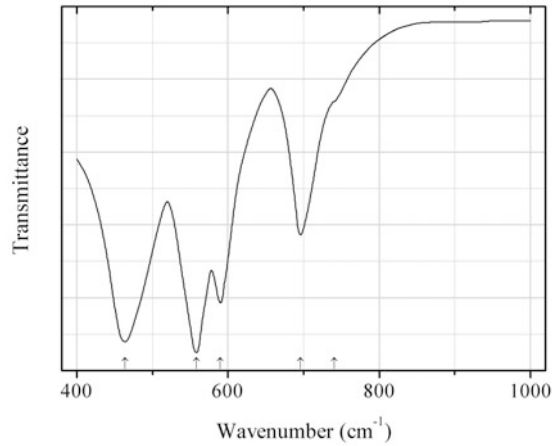

Fig. 2.422 IR spectrum of valentinite drawn using data from Costa et al. (1990)

O479 Valentinite Sb_2O_3 (Fig. 2.422)
Locality: Synthetic.
Description: Commercial reactant. Confirmed by powder X-ray diffraction data.
Kind of sample preparation and/or method of registration of the spectrum: KBr disc. Absorption.
Source: Costa et al. (1990).
Wavenumbers (cm^{-1}): 741sh, 696, 590, 558s, 464s.

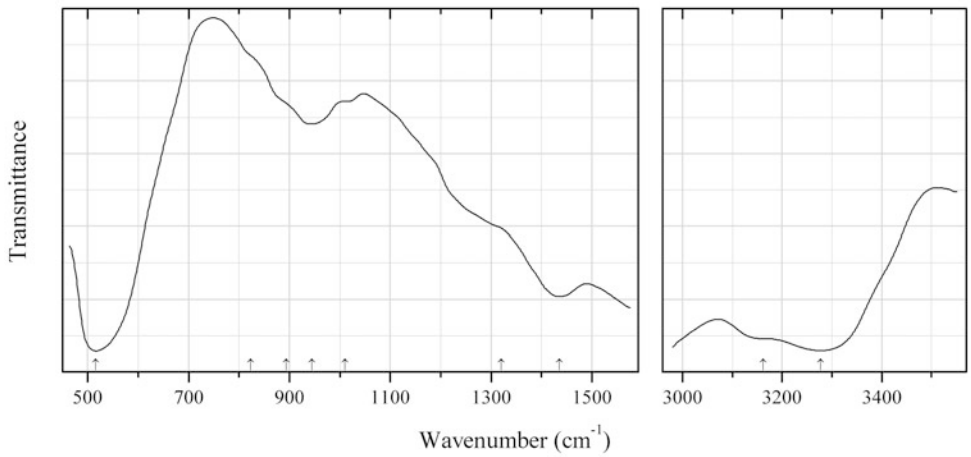

Fig. 2.423 IR spectrum of vernadite drawn using data from Chukhrov et al. (1978)

O480 Vernadite $(Mn,Fe,Ca,Na)(O,OH)_2 \cdot nH_2O$ (Fig. 2.423)
Locality: The bottom of the Pacific Ocean.
Description: Fine-grained aggregate consisting of microscopic scales from a Fe–Mn nodule. Characterized by electron microdiffraction.
Kind of sample preparation and/or method of registration of the spectrum: No data.
Source: Chukhrov et al. (1978).
Wavenumbers (cm^{-1}): 3277s, 3162sh, 1435s, 1320sh, 1010sh, 944, 894sh, 823sh, 516s.
Note: The wavenumbers were determined by us based on spectral curve analysis of the published spectrum.

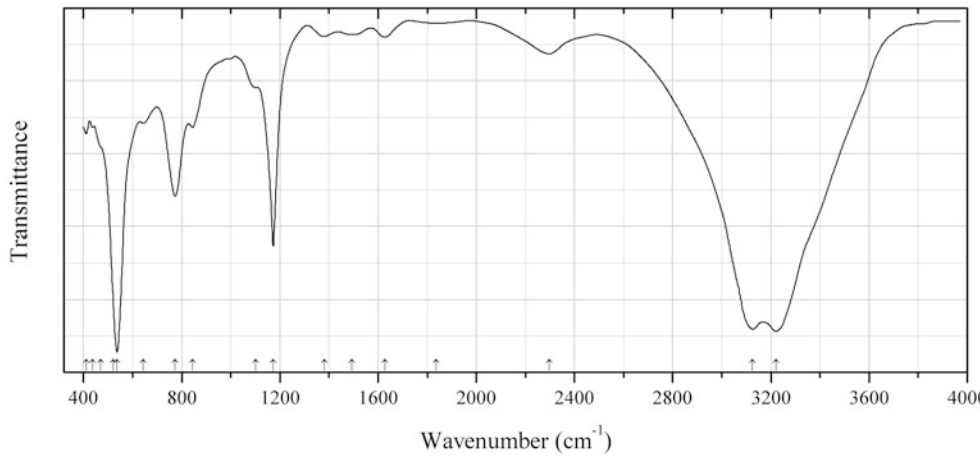

Fig. 2.424 IR spectrum of vismirnovite drawn using data from Kramer et al. (2009)

O481 Vismirnovite $ZnSn(OH)_6$ (Fig. 2.424)
Locality: Synthetic.
Description: Synthesized by a simple solid state metathesis approach, assisted by microwave energy. Characterized by powder X-ray diffraction data and thermogravimetric analysis.
Kind of sample preparation and/or method of registration of the spectrum: KBr disc. Transmission.
Source: Kramer et al. (2009).
Wavenumbers (cm^{-1}): 3220s, 3125s, 2298w, 1837w, 1628w, 1494w, 1382w, 1173s, 1102sh, 845, 773, 643w, 537s, 521sh, 470sh, 437w, 411w.
Note: The wavenumbers were determined by us based on spectral curve analysis of the published spectrum.

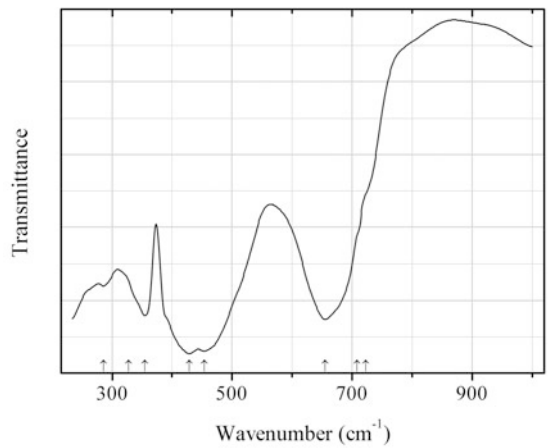

Fig. 2.425 IR spectrum of vorlanite dimorph drawn using data from Carnall et al. (1965)

O482 Vorlanite dimorph $CaUO_4$ (Fig. 2.425)
Locality: Synthetic.
Description: Rhombohedral, a = 3.86, c = 17.50 Å.

Kind of sample preparation and/or method of registration of the spectrum: KBr disc. Absorption.
Source: Carnall et al. (1965).
Wavenumbers (cm^{-1}): 723sh, 708sh, 655s, 454s, 429s, 355, 328sh, 286 m, 165w, ~75.
Note: The wavenumbers were partly determined by us based on spectral curve analysis of the published spectrum.

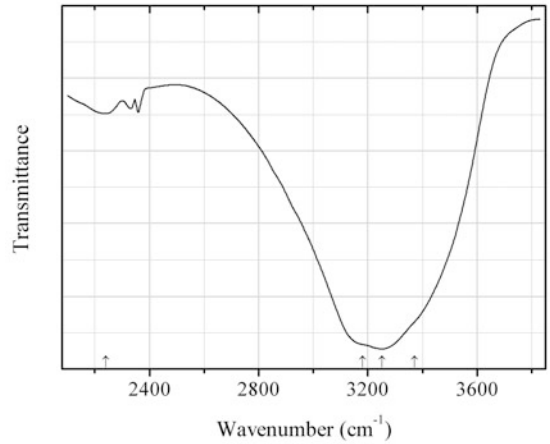

Fig. 2.426 IR spectrum of wickmanite drawn using data from Jena et al. (2004)

O483 Wickmanite $Mn^{2+}Sn^{4+}(OH)_6$ (Fig. 2.426)
Locality: Synthetic.
Description: Characterized by powder X-ray diffraction data. Cubic, a = 7.846(2) Å.
Kind of sample preparation and/or method of registration of the spectrum: KBr or KCl disc. Transmission.
Source: Jena et al. (2004).
Wavenumbers (cm^{-1}): 3370sh, 3252s, 3180sh, 2240w.
Note: The wavenumbers were determined by us based on spectral curve analysis of the published spectrum. Weak bands in the range from 2300 to 2400 cm^{-1} correspond to atmospheric CO_2.

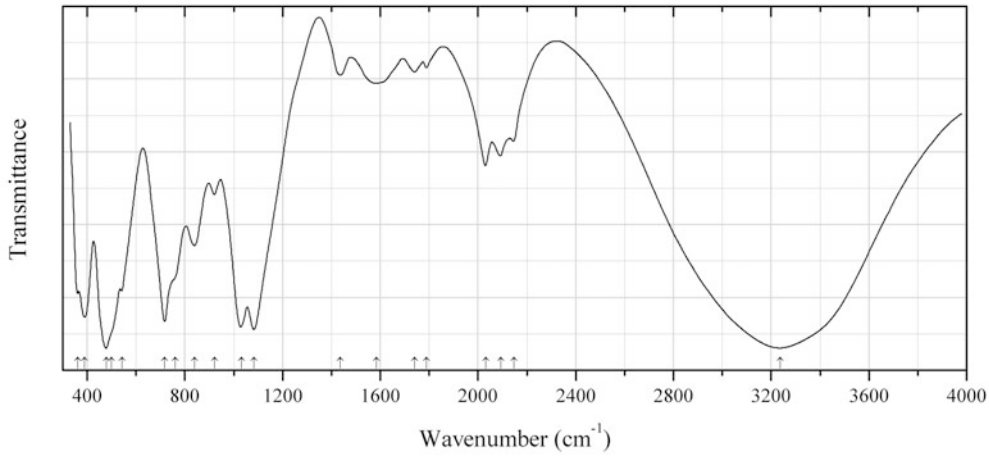

Fig. 2.427 IR spectrum of wülfingite drawn using data from Lutz et al. (1998)

O484 Wülfingite ε-$Zn(OH)_2$ (Fig. 2.427)
Locality: Synthetic.
Description: Obtained as a result of recrystallization (on the Zn surface) of microcrystalline product of the reaction between aqueous solutions of annonia and zinc nitrate.
Kind of sample preparation and/or method of registration of the spectrum: KBr disc. Transmission.
Source: Lutz et al. (1998).
Wavenumbers (cm^{-1}): 3238s, 2147sh, 2093, 2033, 1788w, 1741w, 1584w, 1436w, 1083s, 1032s, 923, 840, 760sh, 717s, 543sh, 500, 479s, 390, 361.
Note: The wavenumbers were partly determined by us based on spectral curve analysis of the published spectrum. For the IR spectrum of ε-$Zn(OH)_2$ see also Ghotbi (2010).

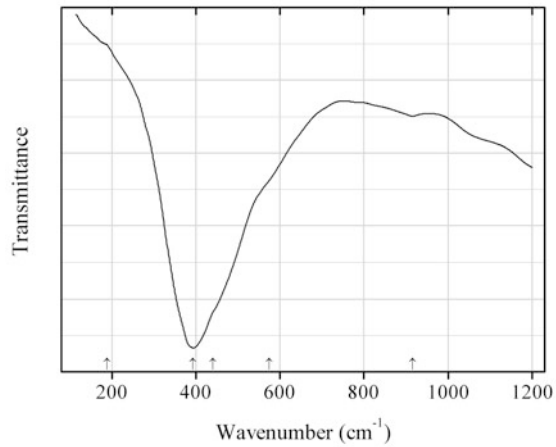

Fig. 2.428 IR spectrum of wüstite drawn using data from Hofmeister et al. (2003)

O485 Wüstite FeO (Fig. 2.428)
Locality: Synthetic.
Description: Commercial reactant.
Kind of sample preparation and/or method of registration of the spectrum: Powdery film prepared using a diamond-anvil cell. Absorption.
Source: Hofmeister et al. (2003).
Wavenumbers (cm^{-1}): 915w, 575sh, 440sh, 393s, 189sh.
Note: The wavenumbers were determined by us based on spectral curve analysis of the published spectrum.

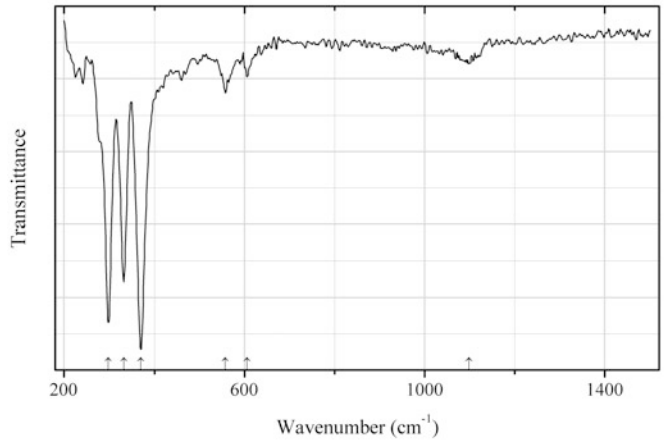

Fig. 2.429 IR spectrum of yttriaite-(Y) drawn using data from Bakovets et al. (2002)

O486 Yttriaite-(Y) Y_2O_3 (Fig. 2.429)
Locality: Synthetic.
Description: Thin film deposited on polished (100) Si wafer via thermal decomposition of yttrium tris (2,2,6,6-tetramethyl-3,5-heptanedionate) vapor at a substrate temperature of 590 °C. Characterized by the powder X-ray diffraction pattern. Cubic, a = 10.6041 Å.
Kind of sample preparation and/or method of registration of the spectrum: Compact film. Absorption.
Source: Bakovets et al. (2002).
Wavenumbers (cm^{-1}): 1098w, 606w, 558w, 370s, 332s, 298s.
Note: The band position denoted by Bakovets et al. (2002) as 322 cm^{-1} was determined by us at 332 cm^{-1} based on spectral curve analysis of the published spectrum. Weak bands at 1098 and 558 cm^{-1} may correspond to SiO_2.

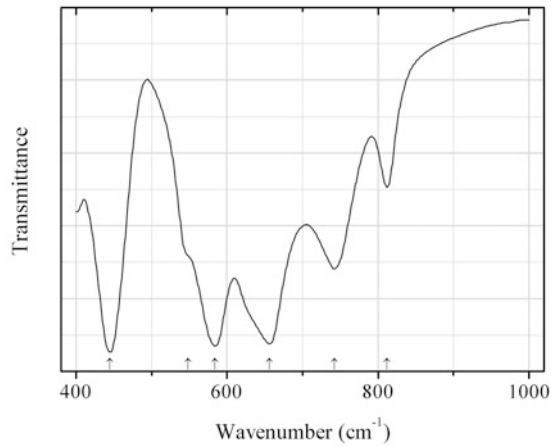

Fig. 2.430 IR spectrum of iwashiroite-(Y) drawn using data from Popovici et al. (2008)

O487 Iwashiroite-(Y) $YTaO_4$ (Fig. 2.430)
Locality: Synthetic.

Description: Prepared at 1200° by solid state reaction, from homogeneous mixture consisting of Y_2O_3, and Na_2SO_4 as flux. Monoclinic. Characterized by the powder X-ray diffraction pattern.
Kind of sample preparation and/or method of registration of the spectrum: KBr disc. Absorption.
Source: Popovici et al. (2008).
Wavenumbers (cm^{-1}): 812, 742, 656s, 584s, 548sh, 445s.

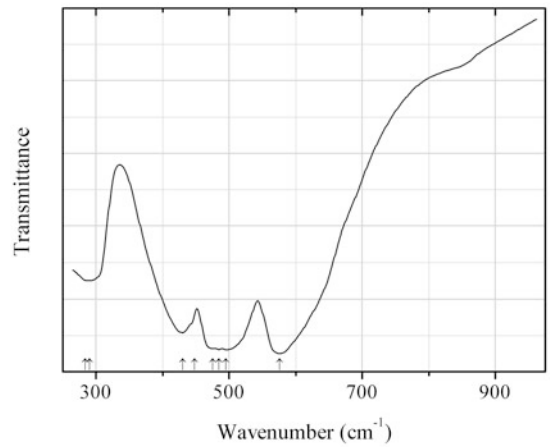

Fig. 2.431 IR spectrum of "oxy-yttrobetafite-(Y)" drawn using data from Knop et al. (1969)

O488 "Oxy-yttrobetafite-(Y)" $Y_2Ti_2O_7$ (Fig. 2.431)
Locality: Synthetic.
Description: Cubic, with pyrochlore-type structure. Characterized by powder X-ray diffraction data.
Kind of sample preparation and/or method of registration of the spectrum: KBr disc. Transmission.
Source: Knop et al. (1969).
Wavenumbers (cm^{-1}): 576s, 495s, 485s, 475s, 448sh, 430s, 290, 284sh.
Note: The wavenumbers were partly determined by us based on spectral curve analysis of the published spectrum.

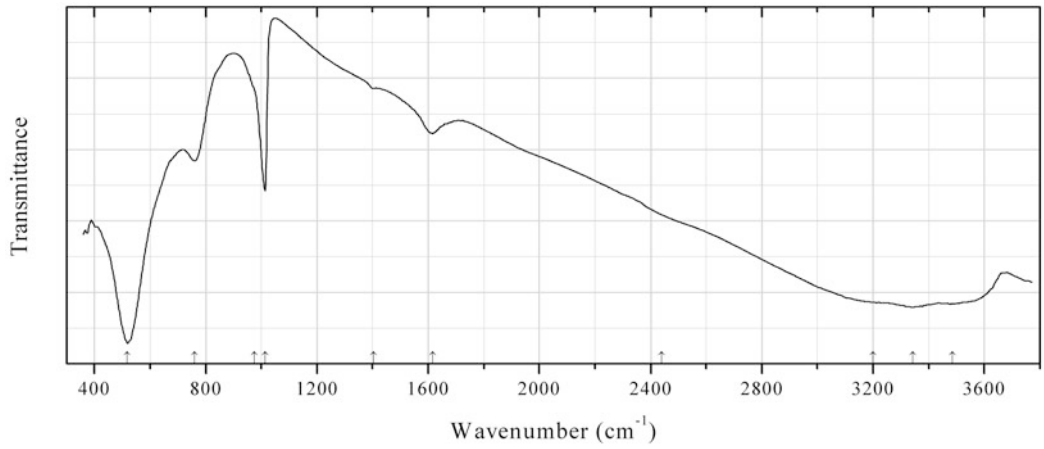

Fig. 2.432 IR spectrum of bariandite obtained by N.V. Chukanov

O489 Bariandite $Al_{0.6}(V^{5+},V^{4+})_8O_{20}\cdot 9H_2O$ (?) (Fig. 2.432)
Locality: Mounana (Mouana) mine, Franceville, Haut-Ogooué province, Gabon (type locality).
Description: Black bladed radiating aggregates with greenish black streak.
Kind of sample preparation and/or method of registration of the spectrum: KBr disc. Absorption.
Wavenumbers (cm^{-1}): 3485s, 3342s, 3200sh, 2440sh, 1616, 1404w, 1013s, 975sh, 759, 519s.

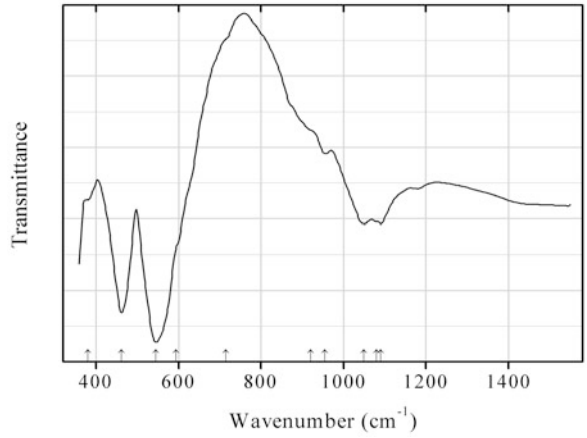

Fig. 2.433 IR spectrum of iwakiite obtained by N.V. Chukanov

O490 Iwakiite $Mn^{2+}Fe^{3+}{}_2O_4$ (Fig. 2.433)
Locality: Gozaisho mine, Iwaki city, Fukushima prefecture, Japan (type locality).
Description: Black fine-grained aggregate. The empirical formula is (electron microprobe): $(Mn^{2+}{}_{0.89}Mg_{0.08}Cu_{0.02}Ca_{0.01})(Fe^{3+}{}_{1.77}Mn^{3+}{}_{0.21}Al_{0.02})O_4$.
Kind of sample preparation and/or method of registration of the spectrum: KBr disc. Absorption.
Wavenumbers (cm^{-1}): 1091, 1080, 1049, 955w, 920sh, 715sh, 595sh, 546s, 462s, 380w.

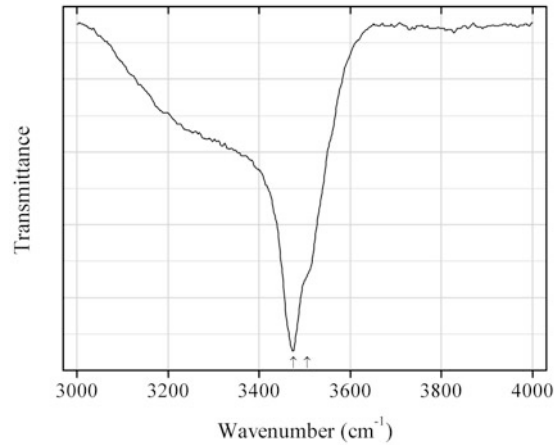

Fig. 2.434 IR spectrum of anzaite-(Ce) drawn using data presented by A.R. Chakhmouradian

O491 Anzaite-(Ce) $Ce_4Fe^{2+}Ti_6O_{18}(OH)_2$ (Fig. 2.434)

Locality: Afrikanda intrusive complex, ~4 km WSW of Afrikanda railway station, Kola peninsula, Murmansk Region, Russia (type locality).
Description: Grayish black anhedral to subhedral crystals from calcite-amphibole-clinopyroxene silicocarbonatite. Holotype sample. Monoclinic, space group *C*2/*m*, a = 5.293(1), b = 14.586(3), c = 5.233(1) Å, β = 97.30(2)°, V = 400.7(2) Å^3, Z = 1. D_{calc} = 5.054 g/cm^3. The empirical formula is (electron microprobe): $(Ce_{2.18}Nd_{0.85}La_{0.41}Pr_{0.26}Sm_{0.08}Ca_{0.36}Th_{0.01})Fe_{0.97}(Ti_{5.68}Nb_{0.22}Si_{0.04})O_{18}(OH)_2$. The strongest lines of the powder X-ray diffraction pattern [*d*, Å (*I*, %) (*hkl*)] are: 2.596 (100) (002), 1.935 (18) (170), 1.506 (14) (133), 1.286 (13) (1.11.0), 2.046 (12) (−241), 1.730 (12) (003), 1.272 (12) (0.10.2), 3.814 (11) (−111).
Kind of sample preparation and/or method of registration of the spectrum: A single crystal. Absorbance using IR microscope.
Source: Chakhmouradian et al. (2013), personal communication of A.R. Chakhmouradian.
Wavenumbers (cm^{-1}): 3505sh, 3475.

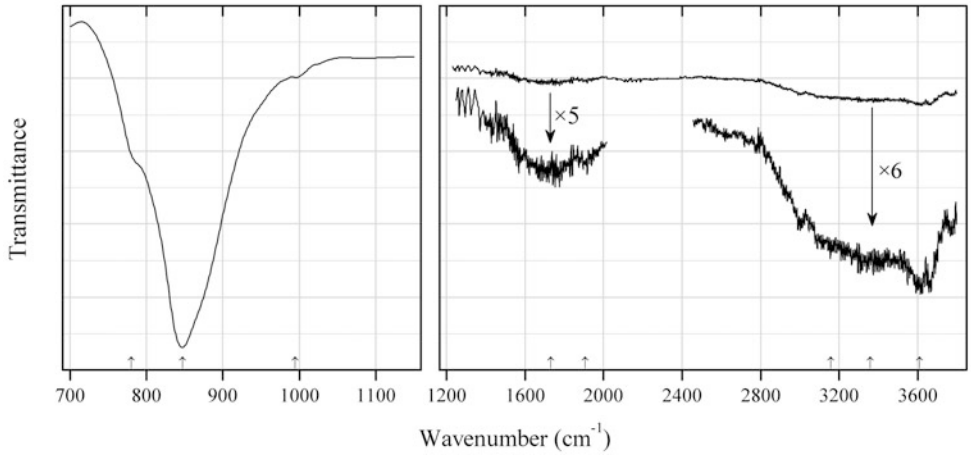

Fig. 2.435 IR spectrum of chlorkyuygenite drawn using data from Galuskin et al. (2015)

O492 Chlorkyuygenite $Ca_{12}Al_{14}O_{32}[(H_2O)_4Cl_2]$ (Fig. 2.435)
Locality: Upper Chegem Caldera, Northern Caucasus, Kabardino-Balkaria, Russia (type locality).
Description: Colourless rounded grains and crystals from the association with chegemite, reinhardbraunsite, and srebrodolskite. Holotype sample. The crystal structure is solved. Cubic, space group *I*-43*d*, a = 12.0285(1) Å, V = 1740.34(3) Å^3, Z = 2. D_{calc} = 2.941 g/cm^3. Optically isotropic, n = 1.672(1). The crystal-chemical formula is $Ca_{11.98}(Al_{12.99}Fe^{3+}_{0.82}Si_{0.18}Ti_{0.03})O_{32}[(H_2O)_{3.77}Cl_{2.23}]$.
Kind of sample preparation and/or method of registration of the spectrum: Reflection spectrum obtained using IR microscope was converted to absorption spectrum using Fourier and Kramers-Krönig transformations.
Source: Galuskin et al. (2015).
Wavenumbers (cm^{-1}): 3610, 3360, 3160sh, 1905, 1730, 995w, 847s, 780sh.
Note: The wavenumbers were partly determined by us based on spectral curve analysis of the published spectrum. Taking into account the position and abnormally large width of the (very weak) band at 1730 cm^{-1}, it hardly can be assigned to bending vibrations of H_2O molecules. Raman spectrum of chlorkyuygenite does not contain bands in the range from 1500 to 1700 cm^{-1} that could correspond to bending vibrations of H_2O molecules. Moreover, no data on the bond-valence calculations for the *W* site

(presumably containing water molecules) are given in the cited paper. Consequently, the presence of H_2O in chlorkyuygenite is questionable. This mineral needs further, more detailed investigations.

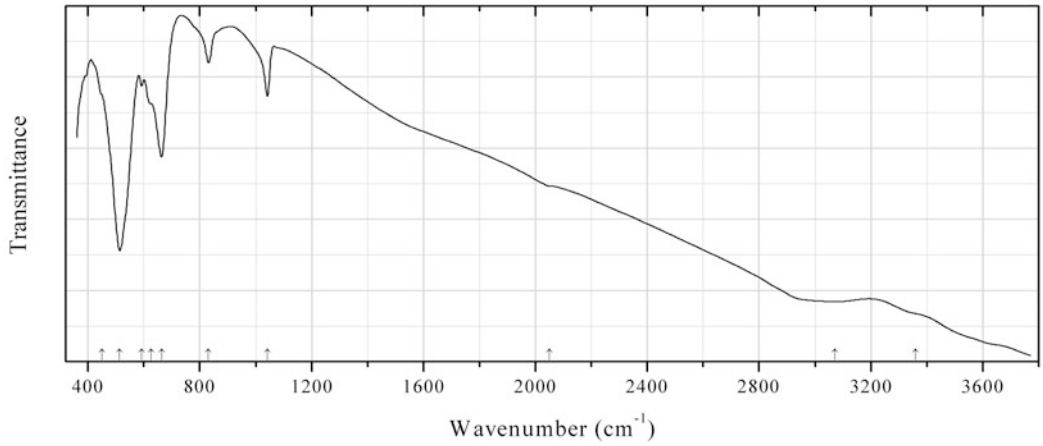

Fig. 2.436 IR spectrum of quenselite obtained by N.V. Chukanov

O493 Quenselite $PbMn^{3+}O_2(OH)$ (Fig. 2.436)
Locality: Långban deposit, Bergslagen ore region, Filipstad district, Värmland, Sweden (type locality).
Description: Dark brown prismatic crystals from the association with hausmannite and braunite. The empirical formula is (electron microprobe): $Pb_{0.98}Mn_{0.98}Fe_{0.04}O_2(OH)$.
Kind of sample preparation and/or method of registration of the spectrum: KBr disc. Absorption.
Wavenumbers (cm^{-1}): 3360sh, 3070, 2050w, 1041, 831, 663s, 625sh, 591, 513s, 450sh.

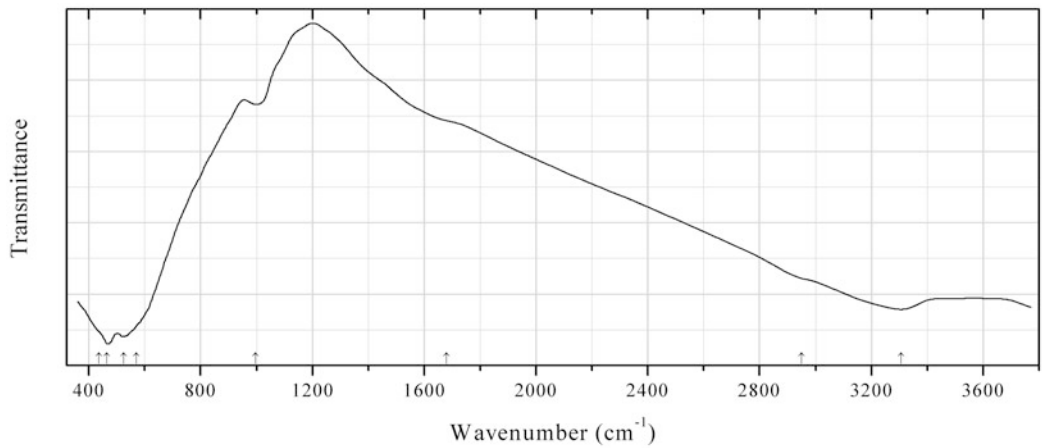

Fig. 2.437 IR spectrum of kobeite-(Y) obtained by N.V. Chukanov

O494 Kobeite-(Y) $(Y,U)(Ti,Nb)_2(O,OH)_6$ (?) (Fig. 2.437)
Locality: Shiraishi-yama (Shiroishi Mt.), Kobe, Kyoto prefecture, Japan (type locality).
Description: Brown prismatic crystals from granite pegmatite. Amorphous, metamict. The empirical formula is (electron microprobe): $(Y_{0.6}Yb_{0.1}Ce_{0.1}U_{0.1}Ca_{0.1})(Zr_{0.4}Sc_{0.25}Nb_{0.2}Ti_{0.1})(Ti_{1.3}Fe_{0.6}Mn_{0.1})(O,OH)_7 \cdot nH_2O$.

Kind of sample preparation and/or method of registration of the spectrum: KBr disc. Absorption.
Wavenumbers (cm^{-1}): 3307, 2950sh, 1680sh, 996w, 570sh, 525s, 465s, 435sh.

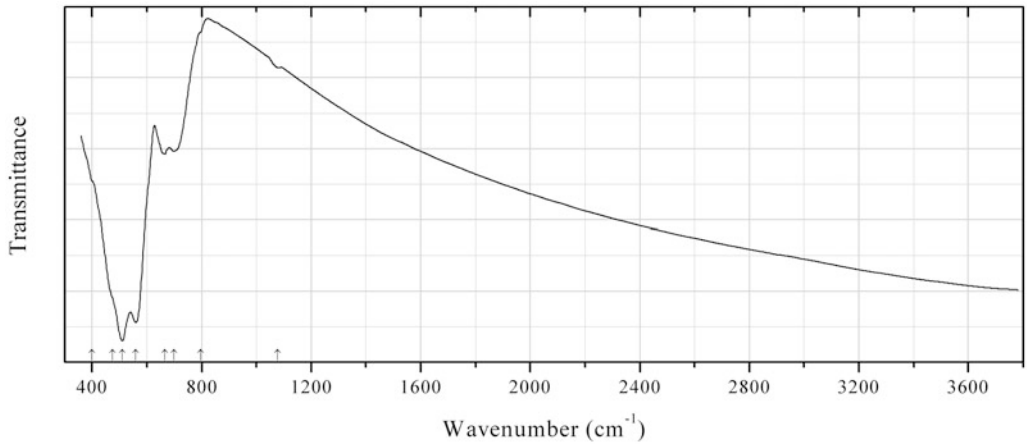

Fig. 2.438 IR spectrum of ferricoronadite obtained by N.V. Chukanov

O495 Ferricoronadite $Pb(Mn^{4+}{}_6Fe^{3+}{}_2)O_{16}$ (Fig. 2.438)
Locality: "Mixed Series" formation, Babuna valley, 40 km SW of Veles, near Nežilovo village, Jacupica Mountains, Macedonia (type locality).
Description: Black veinlet. Associated minerals are gahnite, franklinite, barite, and Zn-bearing talc. Holotype sample. Tetragonal, space group *I*4/*m*, $a = 9.9043(7)$, $c = 2.8986(9)$ Å, $V = 284.34$ (5) $Å^3$, $Z = 1$. The empirical formula is: $(Pb_{1.03}Ba_{0.32})(Mn^{4+}{}_{4.85}Fe^{3+}{}_{1.35}Mn^{3+}{}_{1.18}Ti_{0.49}Al_{0.09}Zn_{0.04})O_{16}$. According to Mössbauer spectroscopic data, all iron is trivalent. The strongest lines of the powder X-ray diffraction pattern [*d*, Å (*I*, %)] are: 3.50 (30), 3.13 (87), 2.87 (69), 2.53 (22), 2.45 (100), 2.428 (45), 2.213 (22), 2.181 (21), 1.656 (24), 1.568 (35), 1.557 (28), 1.440 (29), 1.367 (31).
Kind of sample preparation and/or method of registration of the spectrum: KBr disc. Absorption.
Wavenumbers (cm^{-1}): 1078w, 795sh, 700, 665, 560s, 510s, 475sh, 400sh.

2.6 Fluorides

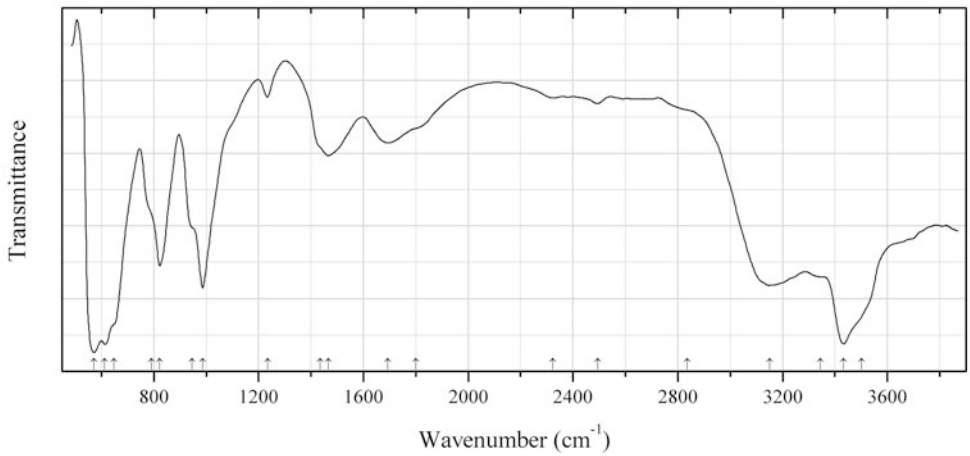

Fig. 2.439 IR spectrum of acuminite drawn using data from Pauly and Petersen (1987)

F40 Acuminite $SrAlF_4(OH)\cdot H_2O$ (Fig. 2.439)
Locality: Ivigtut cryolite deposit, Ivittuut municipality, Arsuk Firth, Westgreenland province, Greenland (type locality).
Description: Aggregate of colourless spear-shaped crystals from the association with celestite, fluorite, jarlite, thomsenolite, pachnolite, ralstonite, and gearksutite. Holotype sample. Monoclinic, space group *C*2/*c* or *Cc*, $a = 13.223(1)$, $b = 14.251(1)$, $c = 14.251(1)$ Å, $\beta = 111.61(1)°$, $V = 906.8$ Å^3, $Z = 8$. $D_{calc} = 3.305$ g/cm^3. Optically biaxial (+), $\alpha = 1.451$, $\beta = 1.453$, $\gamma = 1.463$. The empirical formula is: $Sr_{0.98}Al_{1.02}F_{4.07}(OH)_{0.93}\cdot H_2O$. The strongest lines of the powder X-ray diffraction pattern [*d*, Å (*I*, %) (*hkl*)] are: 4.7674 (100) (110), 4.7058 (100) (11–1), 3.5049 (100) (20–4, 11–3), 3.3530 (100) (31–1), 3.3124 (80) (004), 3.2857 (80) (40–2, 31–2), 2.0748 (90) (51–5), 2.0319 (80) (314).
Kind of sample preparation and/or method of registration of the spectrum: Not indicated.
Source: Pauly and Petersen (1987).
Wavenumbers (cm^{-1}): 3501sh, 3433s, 3345sh, 3152, 2835sh, 2495w, 2323w, 1800, 1694, 1466, 1435sh, 1234w, 987, 947sh, 823, 790sh, 647sh, 613s, 572s.
Note: The wavenumbers were partly determined by us based on spectral curve analysis of the published spectrum.

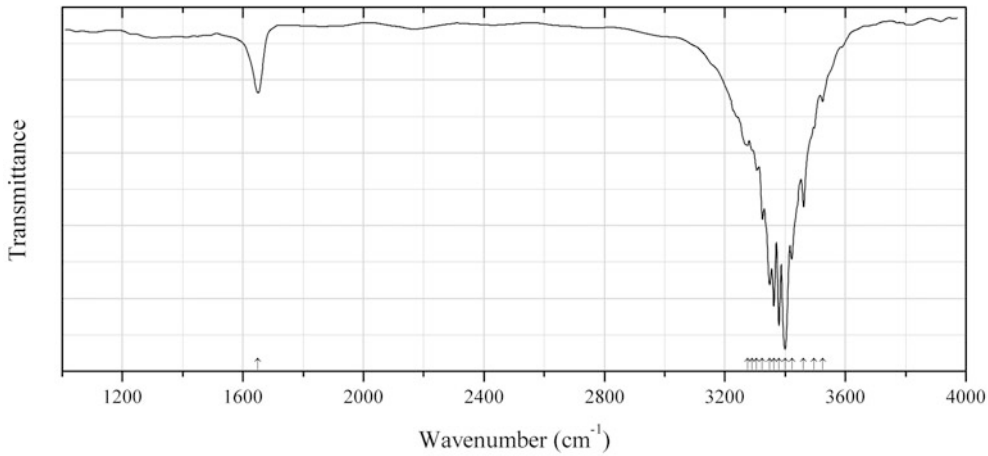

Fig. 2.440 IR spectrum of aravaipaite drawn using data from Kampf et al. (1989)

F41 Aravaipaite $Pb_3AlF_9 \cdot H_2O$ (Fig. 2.440)
Locality: Grand Reef (Aravaipa) mine, Laurel canyon, Grand Reef Mt., Klondyke, Santa Teresa Mts., Aravaipa district, Graham Co., Arizona, USA (type locality).
Description: Colourless platy crystals from the association with grandreefite, pseudograndreefite, laurelite, quartz, fluorite, and galena. Holotype sample. Triclinic, space group *P*1 or *P*-1, $a = 5.842(2)$, $b = 25.20(5)$, $c = 2.652(2)$ Å, $\alpha = 93.84(4)°$, $\beta = 90.14(4)°$, $\gamma = 85.28(4)°$, $V = 827(2)$ Å^3, $Z = 4$. $D_{calc} = 6.37$ g/cm^3. Optically biaxial (−), $\alpha = 1.678(2)$, $\beta = 1.690(2)$, $\gamma = 1.694(2)$, $2V = 70(3)°$. The empirical formula is $Pb_{2.90}Al_{1.09}F_{9.00} \cdot 1.36H_2O$. The strongest lines of the powder X-ray diffraction pattern [*d*, Å (*I*, %) (*hkl*)] are: 11.089 (100) (001), 3.540 (81) (0–13, −1–12), 5.484 (79) (002, 101), 2.918 (60) (−122), 3.089 (33) (−113, 201), 4.022 (30) (102, −112), 6.826 (23) (010).
Kind of sample preparation and/or method of registration of the spectrum: Single-crystal plate. Absorption.
Source: Kampf et al. (1989).
Wavenumbers (cm^{-1}): 3524w, 3496, 3461, 3424, 3400s, 3380s, 3363s, 3349s, 3324, 3306, 3290, 3275w, 1650.
Note: The wavenumbers were partly determined by us based on spectral curve analysis of the published spectrum. Water content was determined by single-crystal infrared spectroscopy method which is unsuitable due to crucial dependence of the extinction coefficient on the O–H bond polarization and the crystal orientation.

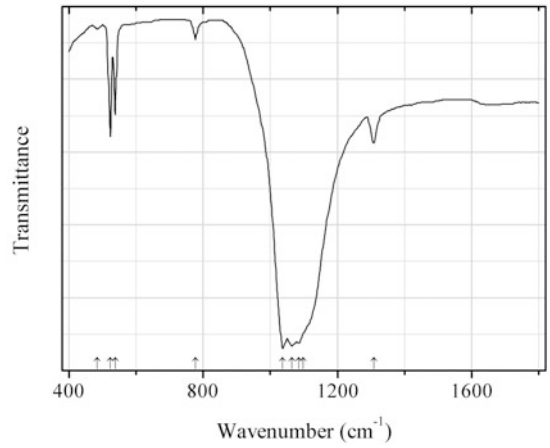

Fig. 2.441 IR spectrum of avogadrite drawn using data from Il'inchik (2008)

F42 Avogadrite KBF_4 (Fig. 2.441)
Locality: Synthetic.
Description: Commercial reagent, at least 98 % pure.
Kind of sample preparation and/or method of registration of the spectrum: KBr disc. Absorption.
Source: Il'inchik (2008).
Wavenumbers (cm^{-1}): 1308w, 1098sh, 1085s, 1064s, 1036s, 777w, 538, 524, 485.
Note: The wavenumbers were determined by us based on spectral curve analysis of the published spectrum. For IR spectra of synthetic analogue of avogadrite see also Bonadeo and Silberman (1970), Bates and Quist (1974), Zavorotynska et al. (2011).

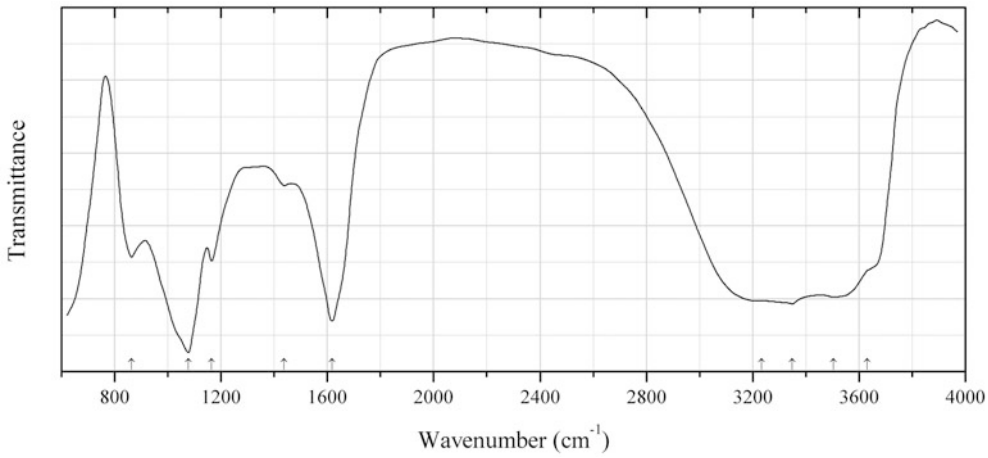

Fig. 2.442 IR spectrum of chukhrovite-(Ca) drawn using data from Vignola et al. (2012)

F43 Chukhrovite-(Ca) $Ca_3Ca_{1.5}Al_2(SO_4)F_{13}\cdot 12H_2O$ (Fig. 2.442)
Locality: Val Cavallizza Pb–Zn–Ag mine, Cuasso al Monte, Varese province, Italy (type locality).
Description: Colourless crystals from the association with marcasite, gypsum, and hydrated Fe oxides. Holotype sample. Cubic, space group *Fd*-3, a = 16.749(1) Å, Z = 8. D_{calc} = 2.23 g/cm^3.

Optically isotropic, n = 1.432(1). The empirical formula is $(Ca_{4.33}Na_{0.11}Fe_{0.03})Al_{2.10}(S_{0.90}O_{3.72})F_{13.10}\cdot nH_2O$. The strongest lines of the powder X-ray diffraction pattern [d, Å (I, %) (hkl)] are: 9.665 (100) (111), 5.921 (31) (022), 5.053 (16) (113), 4.190 (10) (004), 3.226 (15) (333, 115), 2.556 (10) (533), 2.182 (12) (355, 137), 1.915 (17) (626).

Kind of sample preparation and/or method of registration of the spectrum: Transmission. Kind of sample preparation is not indicated.

Source: Vignola et al. (2012).

Wavenumbers (cm^{-1}): 3631sh, 3504s, 3349s, 3233sh, 1618s, 1438sh, 1165, 1077s, 864.

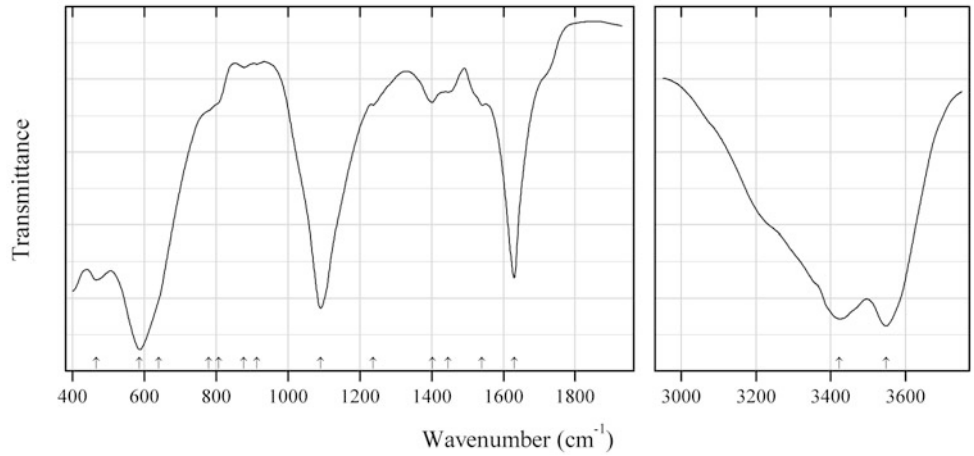

Fig. 2.443 IR spectrum of chukhrovite-(Nd) drawn using data from Pautov et al. (2005)

F44 Chukhrovite-(Nd) $Ca_3NdAl_2(SO_4)F_{13}\cdot 12H_2O$ (Fig. 2.443)

Locality: Kara-Oba W deposit, Betpakdala desert, Karagandy region, Kazakhstan (type locality).

Description: Colourless grains crystals from the association with quartz, fluorite, halloysite, chukhrovite-(Y), anglesite, gearksutite, creedite, and jarosite-group minerals. Holotype sample. Cubic, space group $Fd3$, a = 16.759(3) Å, Z = 8. D_{meas} = 2.42(3) g/cm^3, D_{calc} = 2.42 g/cm^3. Optically isotropic, n = 1.443(2). The empirical formula is $Ca_{3.06}(Nd_{0.32}Y_{0.15}La_{0.12}Sm_{0.09}Ce_{0.07}Pr_{0.07}Gd_{0.05}Dy_{0.02}Ho_{0.01})Al_{2.03}S_{1.01}O_{3.96}F_{13.06}\cdot 11.87H_2O$. The strongest lines of the powder X-ray diffraction pattern [d, Å (I, %) (hkl)] are: 9.7 (100) (111), 5.92 (70) (220), 3.22 (80) (511), 2.555 (70) (533), 2.240 (50) (642), 2.180 (60) (731), 1.827 (50) (842).

Kind of sample preparation and/or method of registration of the spectrum: KBr disc. Absorption.

Source: Pautov et al. (2005).

Wavenumbers (cm^{-1}): 3548s, 3423s, 1630s, 1539w, 1446w, 1402w, 1237w, 1090s, 913w, 877w, 807sh, 779sh, 639sh, 586s, 465.

Note: The wavenumbers were partly determined by us based on spectral curve analysis of the published spectrum.

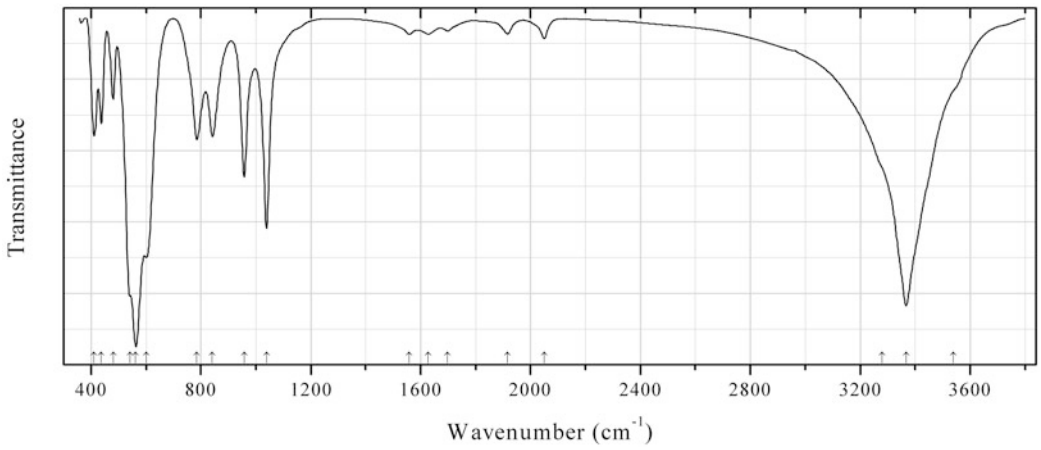

Fig. 2.444 IR spectrum of artroeite obtained by N.V. Chukanov

F45 Artroeite $PbAlF_3(OH)_2$ (Fig. 2.444)
Locality: Vesuvius Mt., Monte Somma-Vesuvius complex, Naples province, Campania, Italy.
Description: Clusters of colourless prismatic crystals. The empirical formula is $Pb_{0.98}Al_{1.00}Fe_{0.01}F_{2.88}(OH)_{2.12}$.
Kind of sample preparation and/or method of registration of the spectrum: KBr disc. Absorption.
Wavenumbers (cm^{-1}): 3540sh, 3367s, 3280sh, 2050w, 1916w, 1697w, 1627w, 1558w, 1039s, 958, 842, 785, 601s, 563s, 543sh, 480, 437, 411.

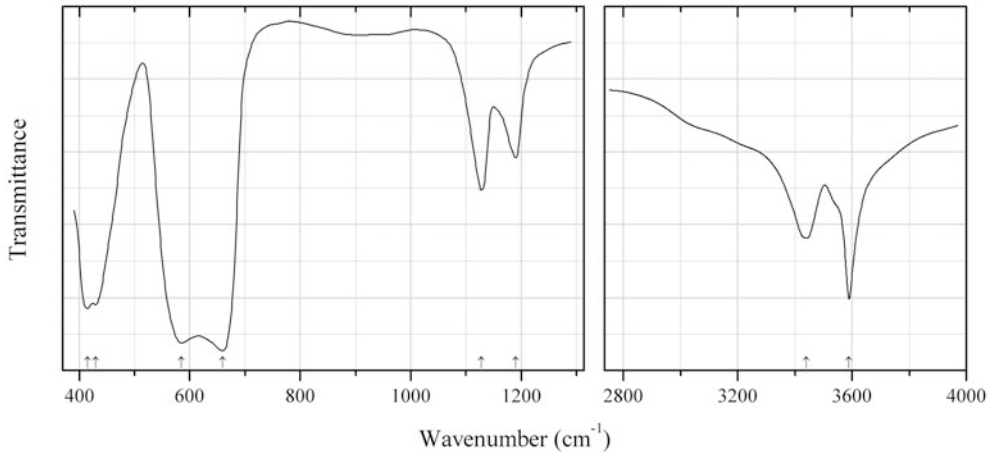

Fig. 2.445 IR spectrum of calcjarlite drawn using data from Povarennykh (1973)

F46 Calcjarlite $Na_2(Ca,Sr,Na,\square)_{14}Al_{12}Mg_2(F,OH)_{64}(OH)_4$ (Fig. 2.445)
Locality: The upper course of the river Pravaya Noiba, Yenisei Mts., Siberia, Russia (type locality).
Description: White tabular crystals from the association with fluorite, thorite, usovite, chamosite, phillipsite, erionite, micas, and halloysite. Holotype sample. D_{meas} = 3.34 g/cm^3. Optically biaxial (+), α = 1.425(1), β = 1.428(1), γ = 1.432(1), 2 V = 72°. The melting point is 730 °C. The empirical formula is $Na_{3.48}K_{0.44}Ca_{7.00}Sr_{2.44}Ba_{0.64}Al_{11.76}Mg_{2.32}F_{56.24}(OH)_{7.76}$. The strongest lines of the

powder X-ray diffraction pattern [*d*, Å (*I*, %)] are: 3.51 (50), 3.44 (30), 3.16 (60), 3.04 (70), 2.96 (100), 2.23 (40), 2.15 (40).
Kind of sample preparation and/or method of registration of the spectrum: KBr disc. Absorption.
Source: Povarennykh (1973).
Wavenumbers (cm^{-1}): 3590s, 3440, 1190, 1128, 660s, 585s, 430s, 415s.

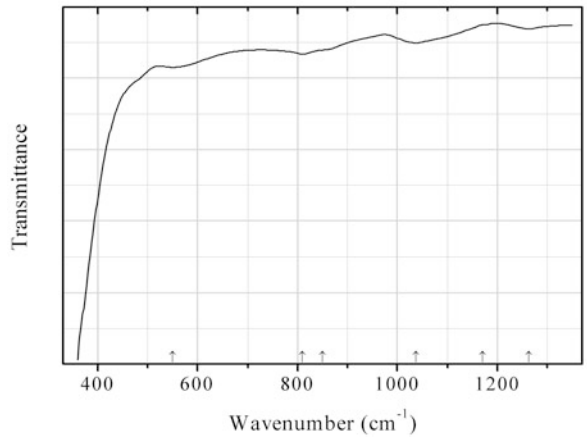

Fig. 2.446 IR spectrum of polezhaevaite-(Ce) obtained by N.V. Chukanov

F47 Polezhaevaite-(Ce) $NaSrCeF_6$ (Fig. 2.446)
Locality: Koashva Mt., Khibiny alkaline complex, Kola peninsula, Murmansk region, Russia (type locality).
Description: White fibrous aggregate from the association with strontiofluorite. Confirmed by qualitative electron microprobe analysis.
Kind of sample preparation and/or method of registration of the spectrum: KBr disc. Absorption.
Wavenumbers (cm^{-1}): 1264w, 1170sh, 1037w, 850sh, 810w, 550w.

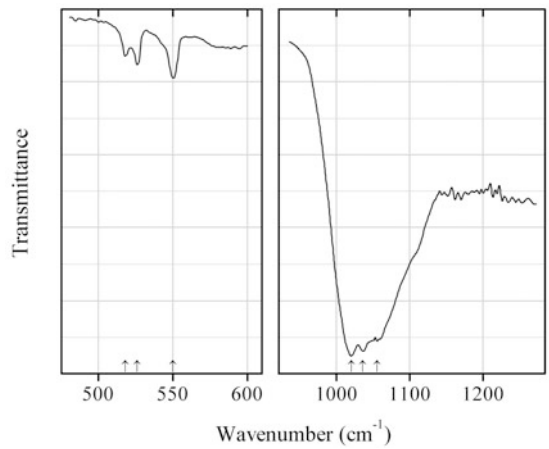

Fig. 2.447 IR spectrum of ferruccite drawn using data from Bates et al. (1971)

F48 Ferruccite $NaBF_4$ (Fig. 2.447)

Locality: Synthetic.
Description: Polycrystalline sample.
Kind of sample preparation and/or method of registration of the spectrum: Film of powdered $NaBF_4$ pressed onto the surface of a polyethylene window. Transmission.
Source: Bates et al. (1971).
Wavenumbers (cm^{-1}): 1055s, 1036s, 1020s, 550, 526, 518, 353w.
Note: The wavenumbers were partly determined by us based on spectral curve analysis of the published spectrum.

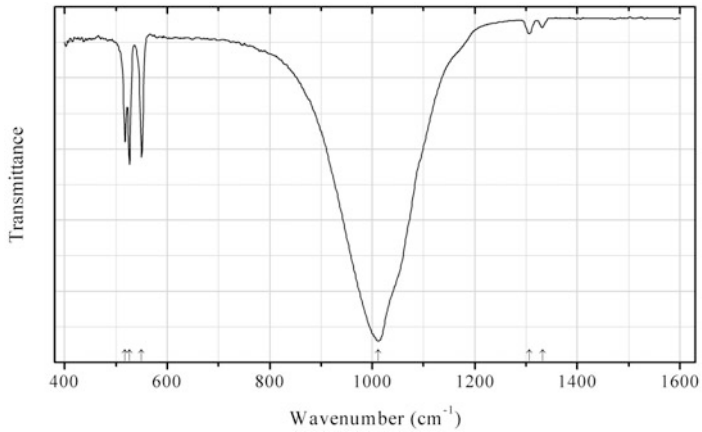

Fig. 2.448 IR spectrum of ferruccite drawn using data from Zavorotynska et al. (2011)

F49 Ferruccite $NaBF_4$ (Fig. 2.448)
Locality: Synthetic.
Description: Commercial reactant of > 98 % purity. Confirmed by powder X-ray diffraction data.
Kind of sample preparation and/or method of registration of the spectrum: Attenuated total reflection of powdered sample.
Source: Zavorotynska et al. (2011).
Wavenumbers (cm^{-1}): 1332w, 1306w, 1012s, 550, 526, 517.
Note: The wavenumbers were determined by us based on spectral curve analysis of the published spectrum.

F50 Fluocerite-(Ce) CeF_3
Locality: No data.
Kind of sample preparation and/or method of registration of the spectrum: KBr disc. Transmission.
Source: Peng and Liu (1982).
Wavenumbers (cm^{-1}): 395sh, 355s.

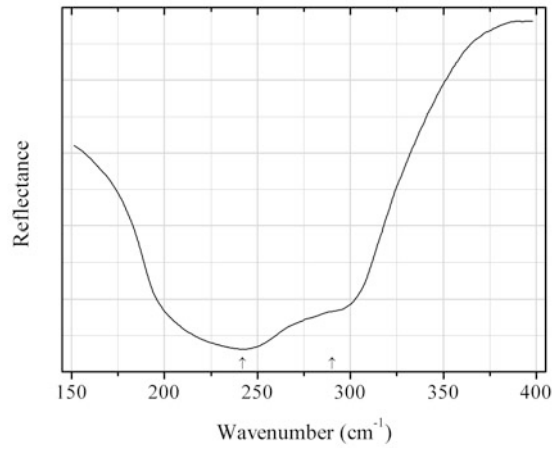

Fig. 2.449 IR spectrum of frankdicksonite drawn using data from Denham et al. (1970)

F51 Frankdicksonite BaF_2 (Fig. 2.449)
Locality: Synthetic.
Description: Single crystal.
Kind of sample preparation and/or method of registration of the spectrum: Reflectance spectrum of a polished crystal.
Source: Denham et al. (1970).
Wavenumbers (cm^{-1}): 290sh, 242.
Note: The wavenumbers were determined by us based on spectral curve analysis of the published spectrum.

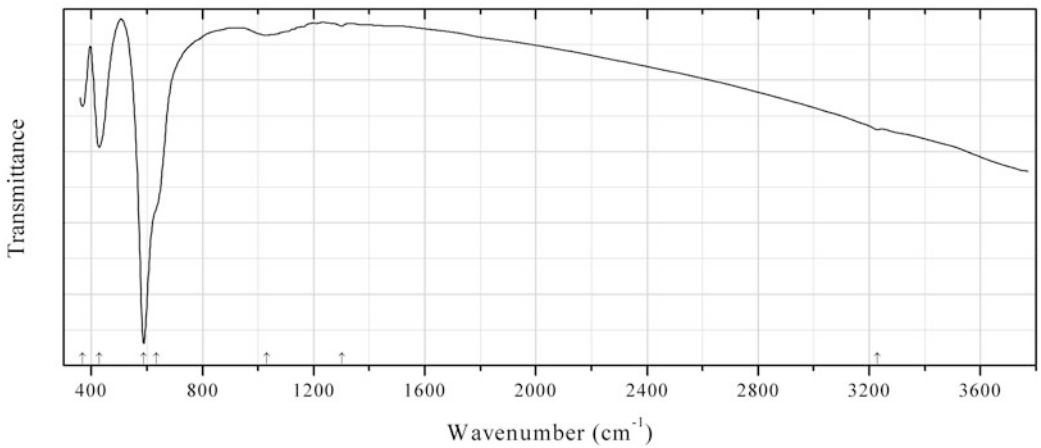

Fig. 2.450 IR spectrum of colquiriite obtained by N.V. Chukanov

F52 Colquiriite $CaLiAlF_6$ (Fig. 2.450)
Locality: Serra Branca mine, Pedra Lavreda, Paraiba, Brazil.
Description: Colourless grains from the association with carlhinzeite, phosphosiderite, triphylite, and triplite. Investigated by I.V. Pekov. Confirmed by single-crystal X-ray diffraction data. Hexagonal, a = 5.005(12), c = 9.636(20) Å, V = 209.0(8) $Å^3$.

Kind of sample preparation and/or method of registration of the spectrum: KBr disc. Absorption.
Wavenumbers (cm^{-1}): 3228w, 1301w, 1030w, 635sh, 588s, 428s, 368.

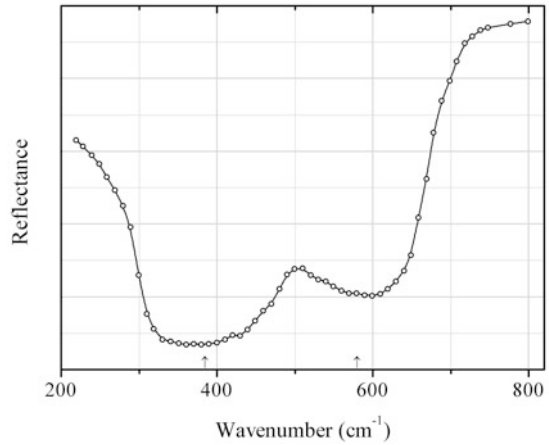

Fig. 2.451 IR spectrum of griceite drawn using data from Jasperse et al. (1966)

F53 Griceite LiF (Fig. 2.451)
Locality: Synthetic.
Description: Single crystal
Kind of sample preparation and/or method of registration of the spectrum: Reflectance from the polished surface of a single crystal at 85 K.
Source: Jasperse et al. (1966).
Wavenumbers (cm^{-1}): 580, 385s.
Note: The wavenumbers were determined by us based on spectral curve analysis of the published spectrum.

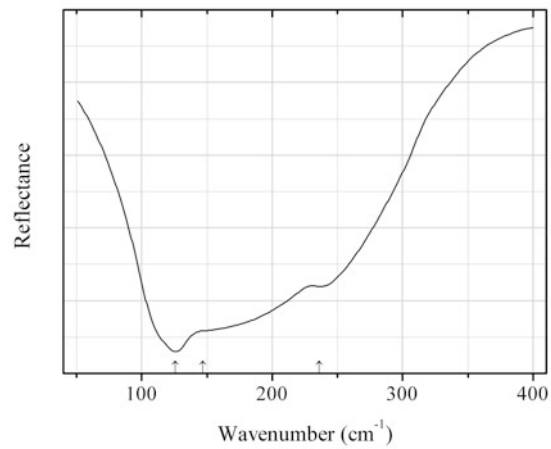

Fig. 2.452 IR spectrum of fluorocronite drawn using data from Denham et al. (1970)

F54 Fluorocronite PbF_2 (Fig. 2.452)
Locality: Synthetic.

Description: Single crystal.
Kind of sample preparation and/or method of registration of the spectrum: Reflectance spectrum of a polished crystal.
Source: Denham et al. (1970).
Wavenumbers (cm^{-1}): 236, 147sh, 126s.
Note: The wavenumbers were determined by us based on spectral curve analysis of the published spectrum.

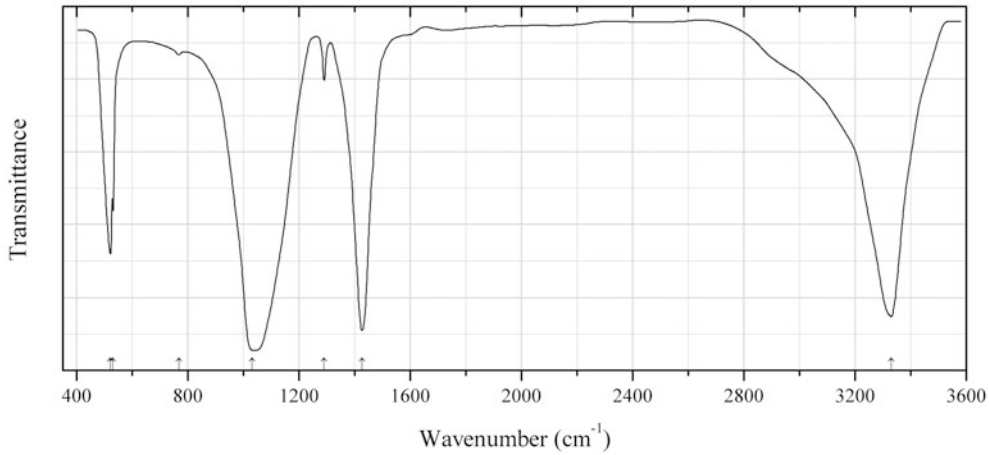

Fig. 2.453 IR spectrum of barberiite drawn using data from Schutte and Van Rensburg (1971)

F55 Barberiite $(NH_4)(BF_4)$ (Fig. 2.453)
Locality: Synthetic.
Kind of sample preparation and/or method of registration of the spectrum: Nujol or fluorolube mull. Transmission.
Source: Schutte and van Rensburg (1971).
Wavenumbers (cm^{-1}): 3330s, 1426s, 1290w, 1030s, 767w, 530, 521.
Note: In the book by Chukanov (2014a) instead of the IR spectrum of barberiite, IR spectrum of associated sassolite was erroneously given.

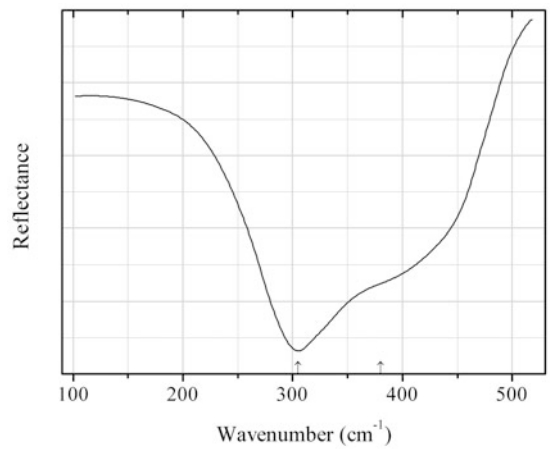

Fig. 2.454 IR spectrum of fluorite drawn using data from Denham et al. (1970)

F56 Fluorite CaF_2 (Fig. 2.454)
Locality: Synthetic.
Kind of sample preparation and/or method of registration of the spectrum: Reflection.
Source: Denham et al. (1970).
Wavenumbers (cm^{-1}): 380sh, 305s.
Note: The wavenumbers were determined by us based on spectral curve analysis of the published spectrum.

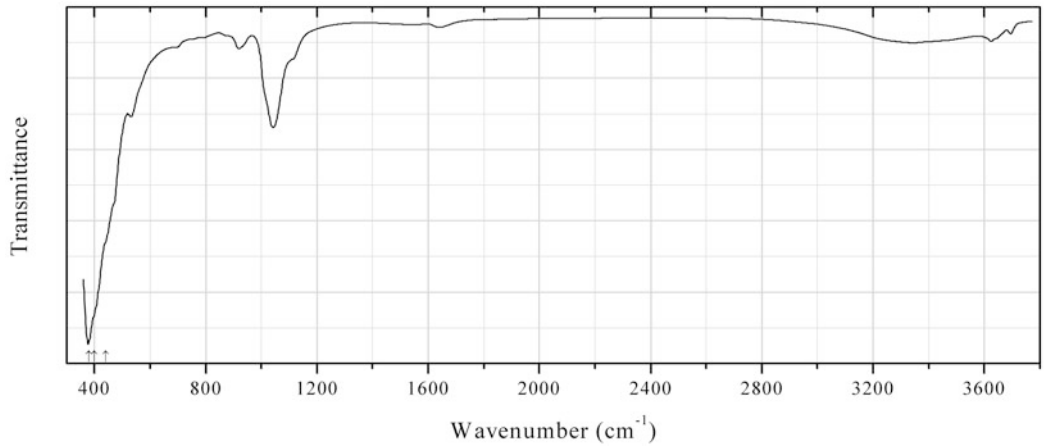

Fig. 2.455 IR spectrum of waimirite-(Y) obtained by N.V. Chukanov

F57 Waimirite-(Y) YF_3 (Fig. 2.455)
Locality: Pitinga mine, Presidente Figueiredo Co., Amazonas State, Brazil (type locality).
Description: Pale pink massive aggregate from the association with potassium feldspar, albite, quartz, riebeckite, micas, cryolite, fluorite, zircon, pyrochlore-group minerals, thorite, xenotime-(Y), gagarinite-(Y), fluocerite-(Ce), halloysite, etc. Holotype sample. Orthorhombic, space group *Pnma*, a = 6.386(1), b = 6.877(1), c = 4.401(1) Å, V = 193.28(7) $Å^3$, Z = 4. D_{calc} = 5.586 g/cm^3. The empirical formula is (electron microprobe): $(Y_{0.69}Dy_{0.08}Er_{0.06}Yb_{0.05}Ca_{0.03}Gd_{0.02}Ho_{0.02}Nd_{0.01}Sm_{0.01}Tb_{0.01}Tm_{0.01}Lu_{0.01})[F_{2.54}\square_{0.25}O_{0.21}]$. The strongest lines of the powder X-ray diffraction pattern [d, Å (I, %) (hkl)] are: 3.707 (26) (011), 3.623 (78) (101), 3.438 (99) (020), 3.205 (100) (111), 2.894 (59) (210), 1.937 (33) (131), 1.916 (24) (301), 1.862 (27) (230).
Kind of sample preparation and/or method of registration of the spectrum: KBr disc. Absorption.
Wavenumbers (cm^{-1}): 440sh, 400sh, 380s.
Note: All bands present above 440 cm^{-1} correspond to the admixture of halloysite.

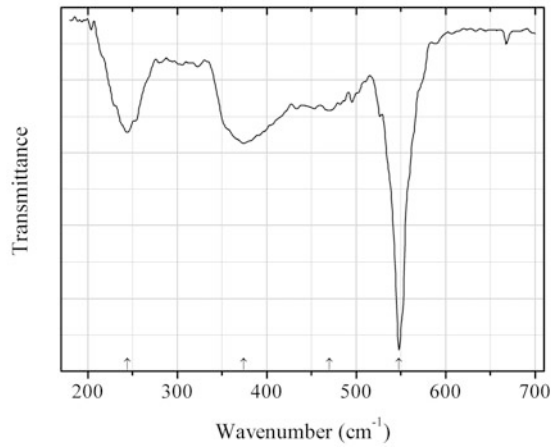

Fig. 2.456 IR spectrum of lanthanum oxyfluoride (trigonal) drawn using data from Hölsä et al. (1993)

F58 Lanthanum oxyfluoride (trigonal) LaOF (Fig. 2.456)
Håleniusite-(La) rhombohedral polymorph
Locality: Synthetic.
Description: Synthesized in the solid state reaction between La_2O_3 and NH_4F at 950 °C for 2 h. Confirmed by powder X-ray diffraction data.
Kind of sample preparation and/or method of registration of the spectrum: CsI disc. Absorption.
Source: Hölsä et al. (1993).
Wavenumbers (cm^{-1}): 548s, 470, 374, 244.

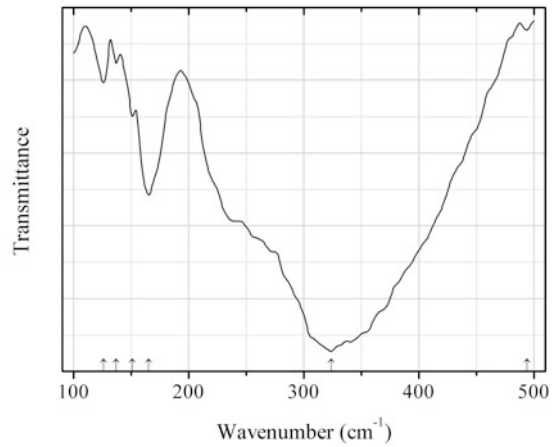

Fig. 2.457 IR spectrum of lanthanum oxyfluoride (tetragonal) drawn using data from Hölsä et al. (1997)

F59 Lanthanum oxyfluoride (tetragonal) LaOF (Fig. 2.457)
Håleniusite-(La) tetragonal polymorph
Locality: Synthetic.
Description: Synthesized in the solid state reaction between La_2O_3 and NH_4F at the ratio NH_4F/La_2O_3 from 2.00 to 2.75, the temperature 1050 °C, for 1.5 h. Confirmed by thermal and powder X-ray diffraction data. Tetragonal, $a \approx 4.09$, $c \approx 5.83$ Å. The empirical formula is $LaO_{0.89}F_{1.22}$.

Kind of sample preparation and/or method of registration of the spectrum: Polyethylene disc. Absorption.
Source: Hölsä et al. (1997).
Wavenumbers (cm^{-1}): 494w, 324s, 165, 151, 137w, 126.
Note: The wavenumbers were determined by us based on spectral curve analysis of the published spectrum.

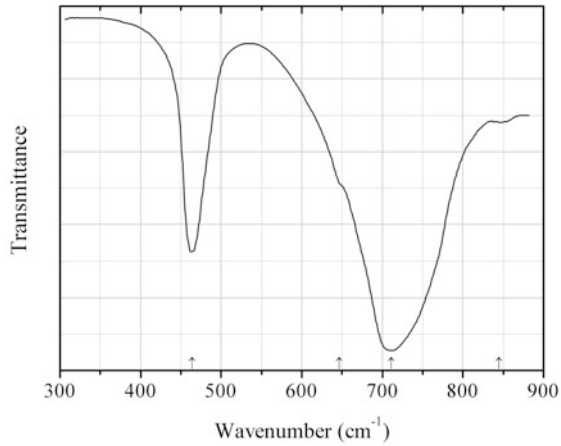

Fig. 2.458 IR spectrum of heklaite drawn using data from Antonkhina et al. (1992)

F60 Heklaite $KNaSiF_6$ (Fig. 2.458)
Locality: Synthetic.
Description: Obtained by acidifying a 1:1 aqueous solution of K_2SiF_6 and Na_2SiF_6 with HCl, followed by evaporation of the solution. Orthorhombic, $a = 5.59$, $b = 9.95$, $c = 9.21$ Å, $V = 512.3$ Å^3, $Z = 4$. $D_{meas} = 2.70$ g/cm^3, $D_{calc} = 2.65$ g/cm^3. Confirmed by chemical analyses and powder X-ray diffraction data.
Kind of sample preparation and/or method of registration of the spectrum: Transmission. Kind of sample preparation is not indicated.
Source: Antonkhina et al. (1992).
Wavenumbers (cm^{-1}): 845w, 711s, 647sh, 464.

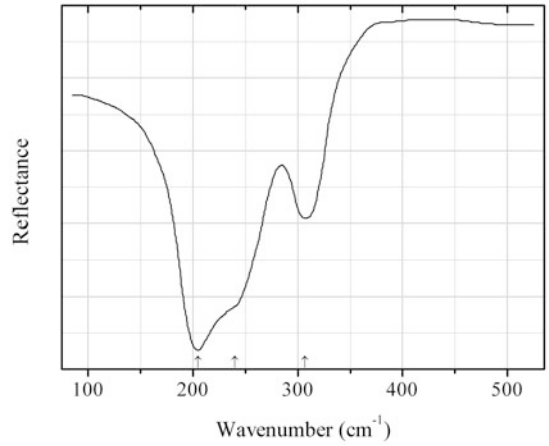

Fig. 2.459 IR spectrum of carobbiite drawn using data from Hass (1963)

F61 Carobbiite KF (Fig. 2.459)
Locality: Synthetic.
Kind of sample preparation and/or method of registration of the spectrum: Reflection.
Source: Hass (1963).
Wavenumbers (cm^{-1}): 307, 240sh, 205s.
Note: The wavenumbers were determined by us based on spectral curve analysis of the published spectrum.

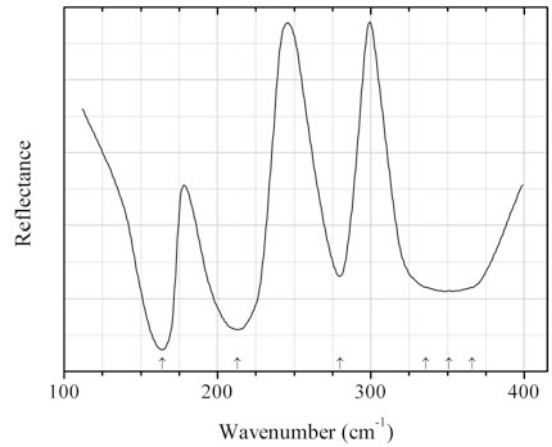

Fig. 2.460 IR spectrum of fluocerite-(La) drawn using data from Bauman and Porto (1967)

F62 Fluocerite-(La) LaF_3 (Fig. 2.460)
Locality: Synthetic.
Kind of sample preparation and/or method of registration of the spectrum: Reflectance, with electric vector parallel to a crystal axis.
Source: Bauman and Porto (1967).
Wavenumbers (cm^{-1}): 366sh, 351, 336sh, 280, 213, 164.
Note: The wavenumbers were determined by us based on spectral curve analysis of the published spectrum.

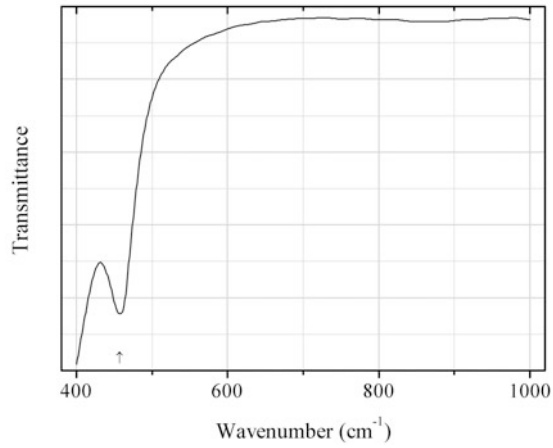

Fig. 2.461 IR spectrum of gananite orthorhombic polymorph drawn using data from Bervas et al. (2006)

F63 Gananite orthorhombic polymorph BiF_3 (Fig. 2.461)
Locality: Synthetic.
Description: Orthorhombic, space group *Pnma*. Confirmed by the powder X-ray diffraction pattern.
Kind of sample preparation and/or method of registration of the spectrum: KBr disc. Transmission.
Source: Bervas et al. (2006).
Wavenumbers (cm^{-1}): 457.

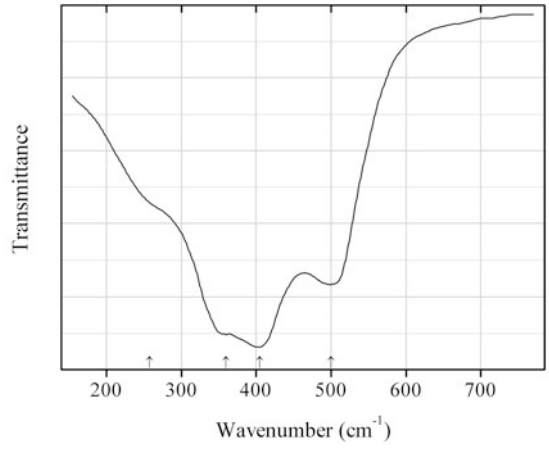

Fig. 2.462 IR spectrum of håleniusite-(La) drawn using data from Kustova et al. (1968)

F64 Håleniusite-(La) LaOF (Fig. 2.462)
Locality: Synthetic.
Description: Cubic modification of LaOF. Prepared by sintering of equimolar mixture of LaF_3 and La_2O_3. Identified by chemical analysis and powder X-ray diffraction data.
Kind of sample preparation and/or method of registration of the spectrum: KBr or CsI disc. Absorption.
Source: Kustova et al. (1968).

Wavenumbers (cm^{-1}): 500, 405s, 360s, 268sh.
Note: Additional absorption maximum is present in the figure at 402 cm^{-1}, but its wavenumber is not indicated in the cited paper.

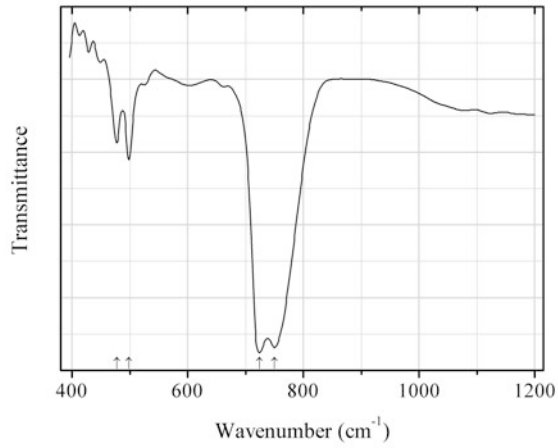

Fig. 2.463 IR spectrum of malladrite drawn using data from Du et al. (2011)

F65 Malladrite Na_2SiF_6 (Fig. 2.463)
Locality: Synthetic.
Description: Nanowires synthesized by a reaction between NaF and Na_2SiO_3 in the presence of polyacrylic acid and ethylene glycol at 120 °C. Hexagonal, a = 8.866, c = 5.043 Å.
Kind of sample preparation and/or method of registration of the spectrum: Transmission. Kind of sample preparation is not indicated.
Source: Du et al. (2011).
Wavenumbers (cm^{-1}): 750s, 724s, 498, 477.
Note: For the IR spectrum of Na_2SiF_6 see also Badachhape et al. (1966).

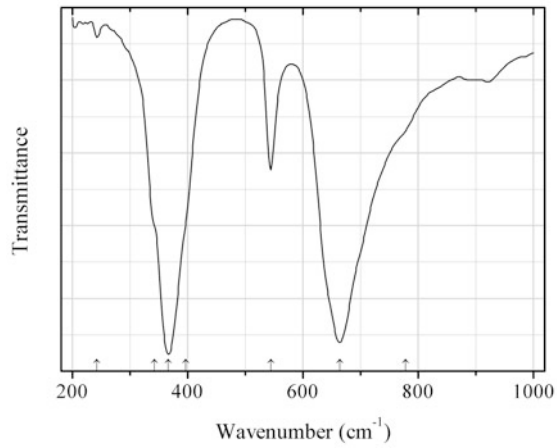

Fig. 2.464 IR spectrum of oskarssonite drawn using data from König et al. (2010)

F67 Oskarssonite α-AlF_3 (Fig. 2.464)

Locality: Synthetic.
Description: Rhombohedral polymorph, space group *R*-3*c*. Confirmed by the elemental analysis and powder X-ray diffraction data.
Kind of sample preparation and/or method of registration of the spectrum: KBr or CsI disc. Transmission.
Source: König et al. (2010).
Wavenumbers (cm^{-1}): 778sh, 664s, 544, 397sh, 366s, 342sh, 242w.
Note: The wavenumbers were determined by us based on spectral curve analysis of the published spectrum.

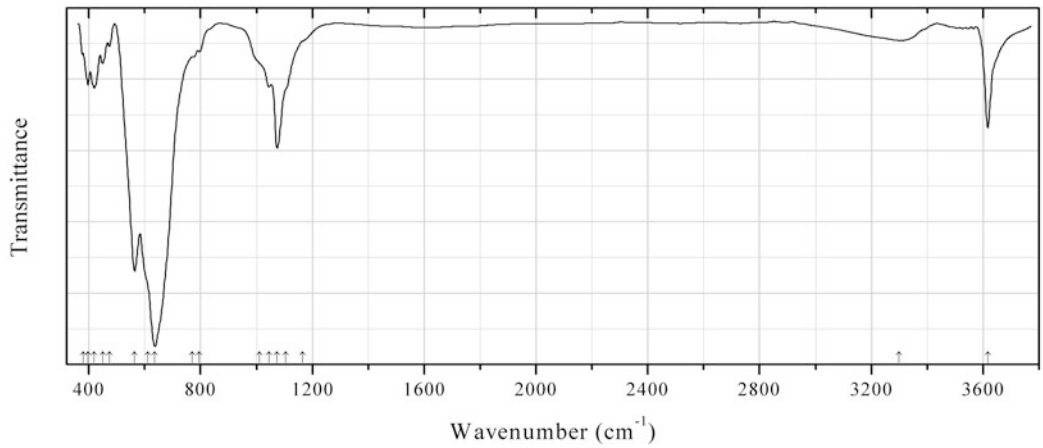

Fig. 2.465 IR spectrum of jørgensenite obtained by N.V. Chukanov

F68 Jørgensenite $Na_2Sr_{14}Na_2Al_{12}F_{64}(OH)_4$ (Fig. 2.465)
Locality: Ivigtut cryolite deposit, Ivittuut municipality, Arsuk Firth, Westgreenland province, Greenland (type locality).
Description: Colourless crystals from the association with cryolite and thomsenolite. The empirical formula is (electron microprobe): $Na_{4.00}Sr_{13.60}Al_{12.59}F_{64.00}(OH,O)_4$.
Kind of sample preparation and/or method of registration of the spectrum: KBr disc. Absorption.
Wavenumbers (cm^{-1}): 3617, (3300w), 1165sh, 1105sh, 1073, 1045, 1010sh, 794w, 770w, 636s, 610sh, 564s, 475w, 449, 419, 398, 379w.

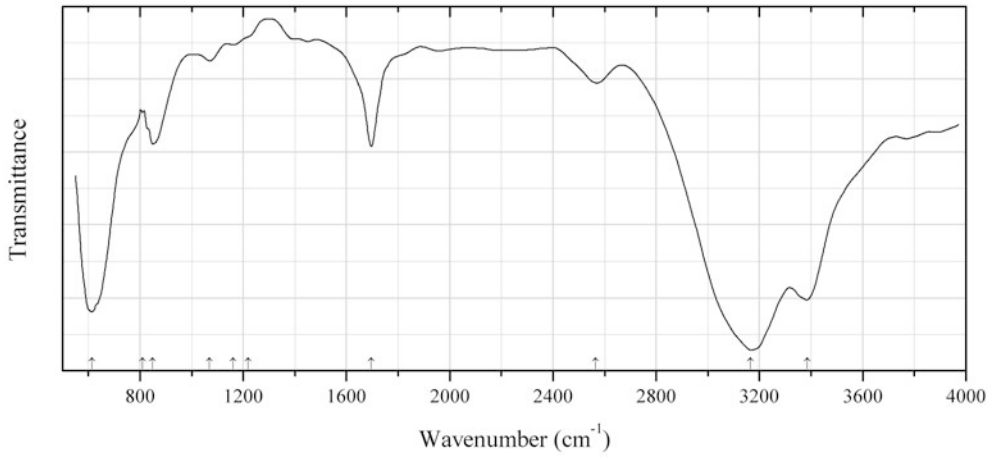

Fig. 2.466 IR spectrum of rosenbergite drawn using data from Olmi et al. (1993)

F69 Rosenbergite $AlF_3 \cdot 3H_2O$ (Fig. 2.466)
Locality: Le Cetine mine, Chiusdino, Siena province, Tuscany, Italy (type locality).
Description: Radiating tufts of slender tetragonal crystals from the association with gypsum, fluorite, elpasolite, ralstonite and onoratoite. Holotype sample. Tetragonal, space group *P*4/*n*, = 7.715(1), *c* = 3.648(1) Å, *Z* = 2. D_{meas} = 2.10(1) g/cm^3, D_{calc} = 2.111 g/cm^3. Optically uniaxial (−), ε = 1.403 (1), ω = 1.427(1). The empirical formula is $Al_{1.02}F_{2.98}H_{5.98}O_{3.03}$. The strongest lines of the powder X-ray diffraction pattern [*d*, Å (*I*, %) (*hkl*)] are: 5.47 (100) (110), 2.439 (72) (130), 2.027 (70) (131), 1.775 (78) (012), 1.725 (85) (240), 1.306 (70) (142).
Kind of sample preparation and/or method of registration of the spectrum: KBr microdisc. Transmission.
Source: Olmi et al. (1993).
Wavenumbers (cm^{-1}): 3385s, 3165s, 2565, 1696, 1161w, 1218sh, 1070w, 849, 809sh, 613s.
Note: The wavenumbers were determined by us based on spectral curve analysis of the published spectrum.

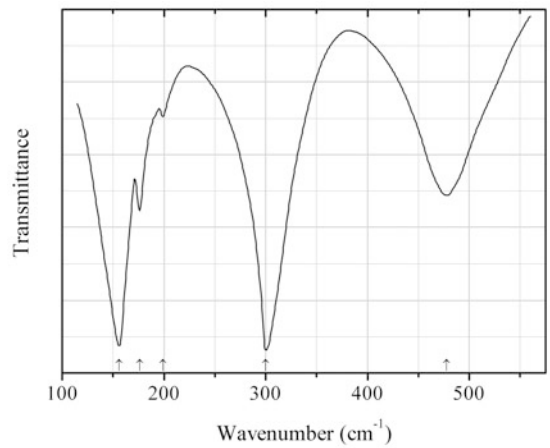

Fig. 2.467 IR spectrum of parascandolaite drawn using data from Nakagawa et al. (1967)

F70 Parascandolaite $KMgF_3$ (Fig. 2.467)

Locality: Synthetic.
Description: Prepared in the reaction between $MgCl_2$ and KHF_2 at 1200 °C in the argon atmosphere.
Kind of sample preparation and/or method of registration of the spectrum: Nujol mull. Transmission.
Source: Nakagawa et al. (1967).
Wavenumbers (cm^{-1}): 478, 300s, 199w, 176, 156s.
Note: The wavenumbers were partly determined by us based on spectral curve analysis of the published spectrum.

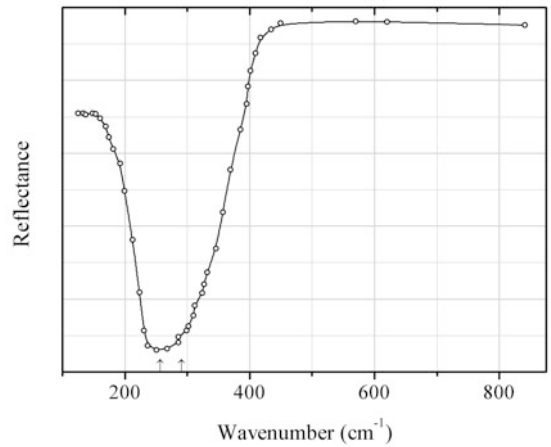

Fig. 2.468 IR spectrum of strontiofluorite drawn using data from Kaiser et al. (1962)

F71 Strontiofluorite SrF_2 (Fig. 2.468)
Locality: Synthetic.
Kind of sample preparation and/or method of registration of the spectrum: Reflection of powdered sample.
Source: Kaiser et al. (1962).
Wavenumbers (cm^{-1}): 291sh, 257.

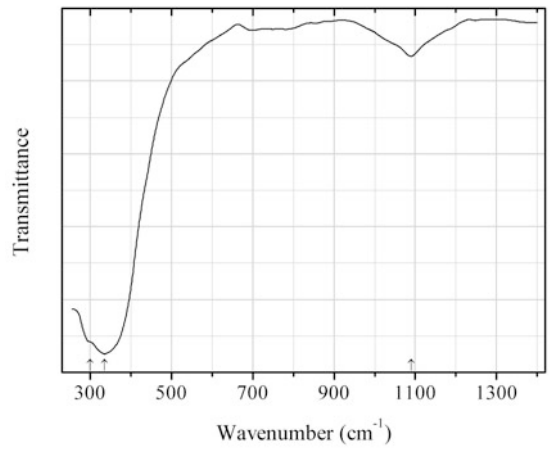

Fig. 2.469 IR spectrum of gagarinite-(Ce) drawn using data from Jambor et al. (1996)

F72 Gagarinite-(Ce) ("Zajacite-(Ce)") $Na(Ca,REE)(Ce,Ca)F_6$ (Fig. 2.469)
Locality: Strange Lake *REE* deposit, Strange Lake complex (Lac Birson complex), near the Québec-Labrador border, Canada (type locality).
Description: Anhedral grains in granite. Holotype sample. Trigonal, space group *P*-3, a = 6.099(1), c = 11.064(2) Å. D_{meas} = 4.44(1) g/cm^3. Optically uniaxial (+), ω = 1.483(1), ε = 1.503(1). The empirical formula is $Na_{0.90}REE_{1.12}Ca_{0.92}F_6$, wherein Ce is the predominant *REE*. The strongest lines of the powder X-ray diffraction pattern [d, Å (I, %) (hkl)] are: 5.29 (70) (100), 3.036 (100) (110, 103), 2.146 (70) (203), 1.757 (80) (300, 213), 1.152 (40) (410), 0.9189 (40) (513).
Kind of sample preparation and/or method of registration of the spectrum: Transmission. Kind of sample preparation is not indicated.
Source: Jambor et al. (1996).
Wavenumbers (cm^{-1}): 1090w, 335s, 299sh.
Note: The wavenumbers were partly determined by us based on spectral curve analysis of the published spectrum. The band at 1090 cm^{-1} may correspond to OH groups substituting F.

F73 Zavaritskite BiOF
Locality: Synthetic.
Description: Synthesized in the reaction between BiF_3 and Bi_2O_3 at 650 °C.
Kind of sample preparation and/or method of registration of the spectrum: KI and polyethylene discs (in the ranges from 300 to 600 and from 100 to 300 cm^{-1} respectively). Transmission.
Source: Rulmont (1972).
Wavenumbers (cm^{-1}): 565, 340–360, 145–155, 109.
Note: For the IR spectrum of zavaritskite see also Chaudhuri et al. (1991).

F74 Bararite $(NH_4)_2SiF_6$
Locality: Unknown.
Description: No data.
Kind of sample preparation and/or method of registration of the spectrum: KBr disc. Absorption.
Source: Peng and Liu (1982).
Wavenumbers (cm^{-1}): 3465sh, 3335w, 3140s, 3015w, 2800w, 1427s, 1395s, 1190w, 1095w, 740s, 480s.
Note: The sample used may contain an admixture of cryptohalite.

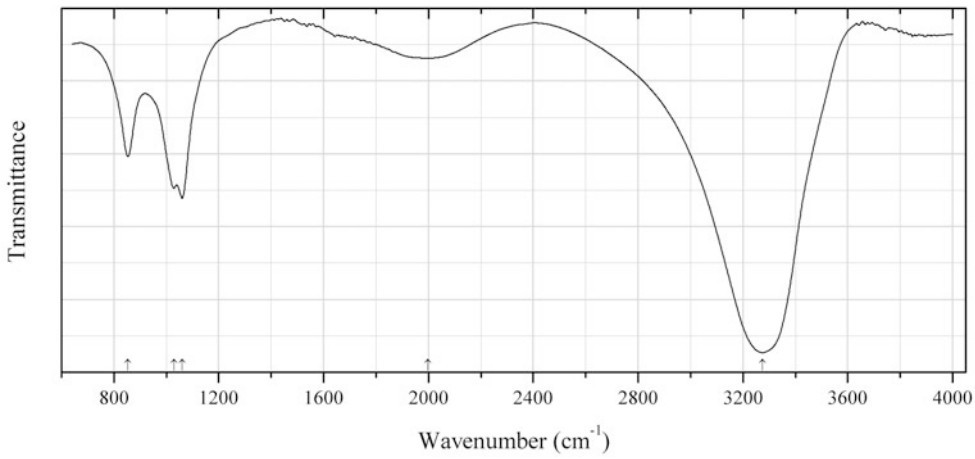

Fig. 2.470 IR spectrum of barlowite drawn using data from Elliott et al. (2014a)

F75 Barlowite $Cu_4BrF(OH)_6$ (Fig. 2.470)
Locality: Great Australia mine, Cloncurry, Queensland, Australia (type locality).
Description: Blue, thin platy, hexagonal crystals in a cuprite-quartz-goethite matrix. The associated minerals are gerhardtite and brochantite. Holotype sample. Hexagonal, space group $P6_3/mmc$, a = 6.6786(2), c = 9.2744(3) Å,, V = 358.251(19) Å^3, Z = 2. D_{meas} = 2.39(3) g/cm^3, D_{calc} = 4.21 g/cm^3. Optically uniaxial (−), ω = 1.840(4)–1.845(4), ε = 1.833(4)–1.840(4). The empirical formula is (electron microprobe): $Cu_{4.00}F_{1.11}Br_{0.95}Cl_{0.09}(OH)_{5.85}$. The strongest lines of the powder X-ray diffraction pattern [d, Å (I, %) (hkl)] are: 5.790 (100) (010), 2.889 (40) (020), 2.707 (55) (112), 2.452 (40) (022), 1.668 (30) (220).
Kind of sample preparation and/or method of registration of the spectrum: Transmittance of a powdered sample. A diamond-anvil cell was used.
Source: Elliott et al. (2014a).
Wavenumbers (cm^{-1}): 3275s, 1998w, 1060, 1029, 853.
Note: The wavenumbers were partly determined by us based on spectral curve analysis of the published spectrum. The broad band in the range from 1800 to 2200 cm^{-1} corresponds to a very strong hydrogen bond formed by acidic OH group. The calculated bond-valence sum on Br is equal to 0.378 v.u.

2.7 Chloridofluorides

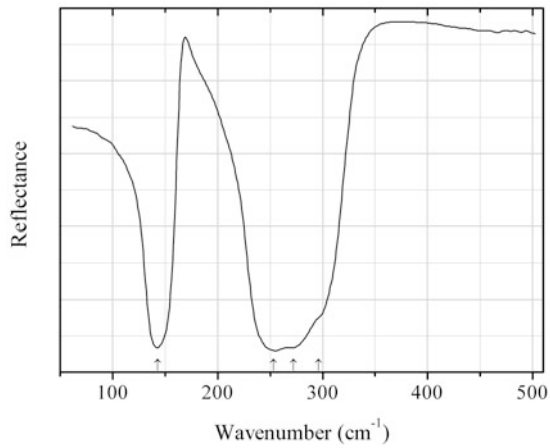

Fig. 2.471 IR spectrum of strontium fluorochloride drawn using data from Sieskind et al. (2000)

FCl1 Strontium fluorochloride SrClF (Fig. 2.471)
Locality: Synthetic.
Description: Single crystals (platelets) grown by slowly cooling a molten mixture of SrF_2 and $SrCl_2$ at the cooling rate of about 3 K/h.
Kind of sample preparation and/or method of registration of the spectrum: Reflection.
Source: Sieskind et al. (2000).
Wavenumbers (cm^{-1}): 296sh, 272sh, 253s, 143s.
Note: The wavenumbers were determined by us based on spectral curve analysis of the published spectrum.

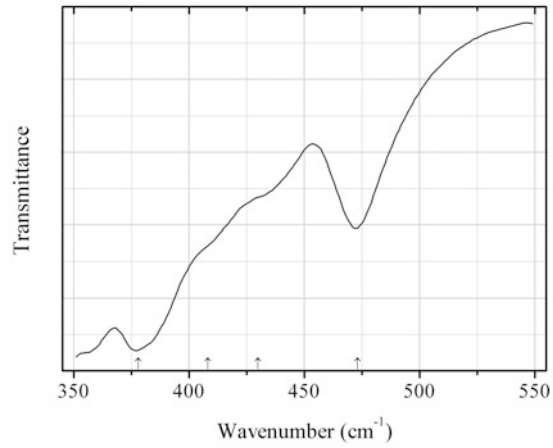

Fig. 2.472 IR spectrum of strontium fluorochloride drawn using data from Sieskind et al. (2000)

FCl2 Strontium fluorochloride SrClF (Fig. 2.472)
Locality: Synthetic.
Description: Single crystals (platelets) grown by slowly cooling a molten mixture of SrF_2 and $SrCl_2$ at the cooling rate of about 3 K/h.
Kind of sample preparation and/or method of registration of the spectrum: Absorbance in the two-phonon range.
Source: Sieskind et al. (2000).
Wavenumbers (cm^{-1}): 473, 430sh, 408sh, 378s.
Note: The wavenumbers were determined by us based on spectral curve analysis of the published spectrum.

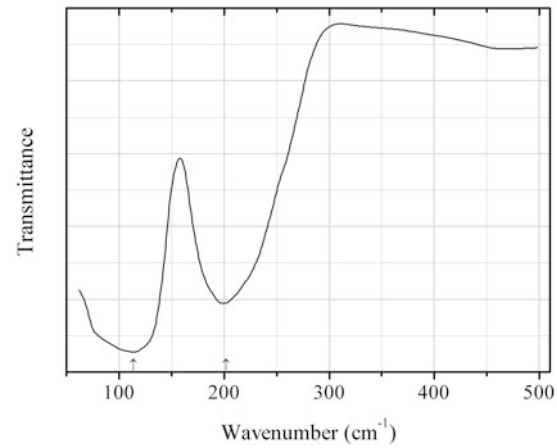

Fig. 2.473 IR spectrum of matlockite drawn using data from Sieskind et al. (2000)

FCl3 Matlockite PbFCl (Fig. 2.473)
Locality: Synthetic.
Description: Single crystals grown by slowly cooling a molten mixture of $PbCl_2$ and PbF_2.

Kind of sample preparation and/or method of registration of the spectrum: The IR reflectance spectrum was measured for a single crystals with [001] orientation.
Source: Sieskind et al. (2000).
Wavenumbers (cm^{-1}): 202, 114s.

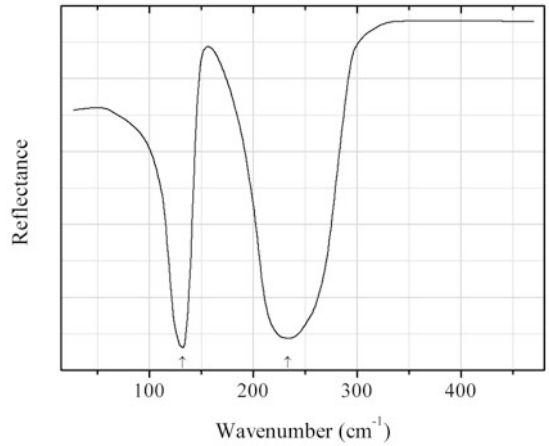

Fig. 2.474 IR spectrum of zhangpeishanite drawn using data from Sieskind et al. (1986)

FCl4 Zhangpeishanite BaFCl (Fig. 2.474)
Locality: Synthetic.
Description: Single crystals obtained by the solid-state reaction between $BaCl_2$ and BaF_2 at 1500 K.
Kind of sample preparation and/or method of registration of the spectrum: Reflection.
Source: Sieskind et al. (1986).
Wavenumbers (cm^{-1}): 233s, 132s.
Note: The wavenumbers were determined by us based on spectral curve analysis of the published spectrum.

2.8 Silicates

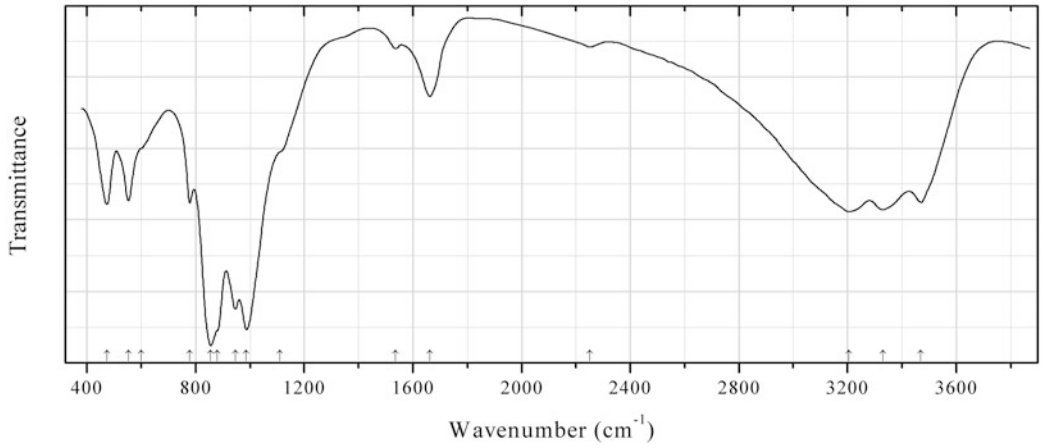

Fig. 2.475 IR spectrum of uranophane-β obtained by N.V. Chukanov

Sio118 Uranophane-β $Ca(UO_2)_2(HSiO_4)_2 \cdot 5H_2O$ (Fig. 2.475)
Locality: Bota-Burum U deposit, near Alakol lake, Almaty region, Kazakhstan.
Description: Orange-yellow crystals from the association with chistyakovaite and uramarsite. Investigated by G.A. Sidorenko. Confirmed by powder X-ray diffraction data.
Kind of sample preparation and/or method of registration of the spectrum: KBr disc. Absorption.
Wavenumbers (cm^{-1}): 3470s, 3330s, 3205s, 2250w, 1662, 1535w, 1110sh, 987s, 946s, 880sh, 855s, 778, 600sh, 552, 473.

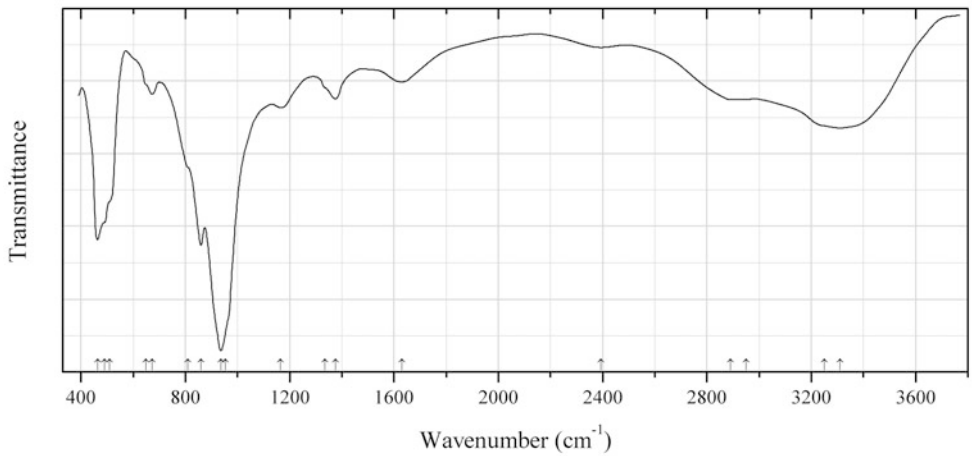

Fig. 2.476 IR spectrum of bultfonteinite obtained by N.V. Chukanov

Sio119 Bultfonteinite $Ca_2[SiO_3(OH)]F \cdot H_2O$ (Fig. 2.476)
Locality: Lakargi Mt., Upper Chegem caldera, Kabardino-Balkarian Republic, Northern Caucasus, Russia.

Description: White spherulite from the association with aklimaite, afwillite, and ettringite. Investigated by A.E. Zadov and I.V. Pekov. Identified by powder X-ray diffraction data. As-bearing variety (the content of As_2O_5 is up to 8 wt% in outer zones of individuals). Optically almost isotropic, with n = 1.594(2).
Kind of sample preparation and/or method of registration of the spectrum: KBr disc. Absorption.
Wavenumbers (cm^{-1}): 3310, 3250sh, 2950, 2890w, 2393w, 1630, 1376, 1335sh, 1165, 955sh, 937s, 860s, 810sh, 673w, 650sh, 510sh, 490sh, 464.

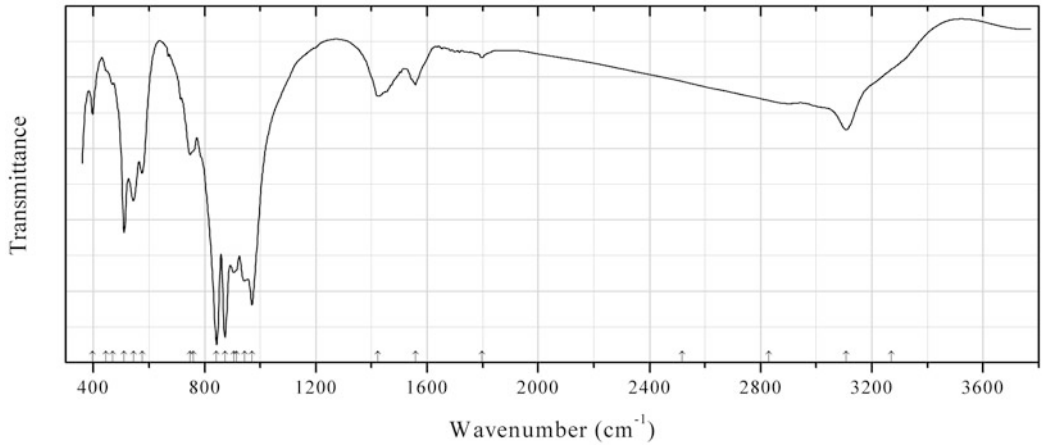

Fig. 2.477 IR spectrum of clinohedrite obtained by N.V. Chukanov

Sio120 Clinohedrite $CaZn(SiO_4)\cdot H_2O$ (Fig. 2.477)
Locality: Franklin, Sussex Co., New Jersey, USA (type locality).
Description: Colourless crusts with yellow fluorescence under UV radiation from the association with andradite and calcite. Confirmed by the IR spectrum.
Kind of sample preparation and/or method of registration of the spectrum: KBr disc. Absorption.
Wavenumbers (cm^{-1}): 3270sh, 3107, 2830, 2518w, 1798w, 1558, 1424, 970s, 945s, 915sh, 904s, 873s, 843s, 760sh, 748, 575, 544, 511, 470w, 445sh, 398.
Note: The band at 1424 cm^{-1} corresponds to the admixture of calcite.

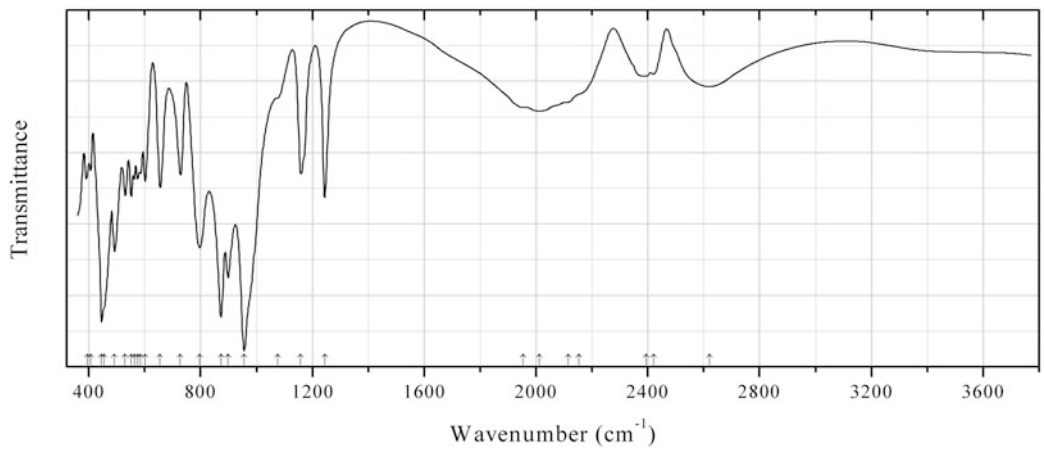

Fig. 2.478 IR spectrum of vuagnatite obtained by N.V. Chukanov

Sio121 Vuagnatite $CaAl(HSiO_4)O$ (Fig. 2.478)
Locality: Red Mountain, Mayacmas (Mayacamas) Mts., Mendocino Co., California, USA.
Description: Colourless isometric crystals. Confirmed by the IR spectrum.
Kind of sample preparation and/or method of registration of the spectrum: KBr disc. Absorption.
Wavenumbers (cm^{-1}): 2621, 2421, 2394, 2155sh, 2115, 2013, 1955, 1244, 1158, 1075sh, 955s, 898s, 873s, 797s, 727, 655, 601, 585w, 574, 562w, 552, 530, 492s, 455sh, 446s, 406, 394.
Note: No absorption maxima are observed above 2700 cm^{-1}. Consequently, vuagnatite is an acid silicate, and its formula is $CaAl(HSiO_4)O$, but not $CaAl(SiO_4)(OH)$. Structural data confirm this conclusion: in vuagnatite one Si–O bond (1.691 Å long) is elongated relative to three other Si–O bonds ranging from 1.615 to 1.640 Å (McNear et al. 1976).

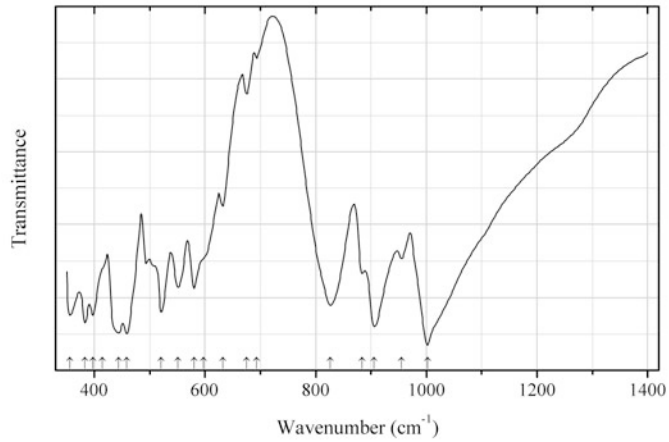

Fig. 2.479 IR spectrum of garnet Sio122 drawn using data from McMillan et al. (1989)

Sio122 Garnet Sio122 $Mg_3(MgSi)Si_3O_{12}$ (Fig. 2.479)
Locality: Synthetic.
Description: Synthesized at 20 GPa and 1800 °C.
Kind of sample preparation and/or method of registration of the spectrum: KBr disc, transmission.
Source: McMillan et al. (1989).
Wavenumbers (cm^{-1}): 1002s, 955w, 906s, 884w, 827, 693w, 675w, 632, 597sh, 580, 551, 521s, 459s, 444, 415sh, 398, 383s, 356.
Note: The wavenumbers were partly determined by us based on spectral curve analysis of the published spectrum.

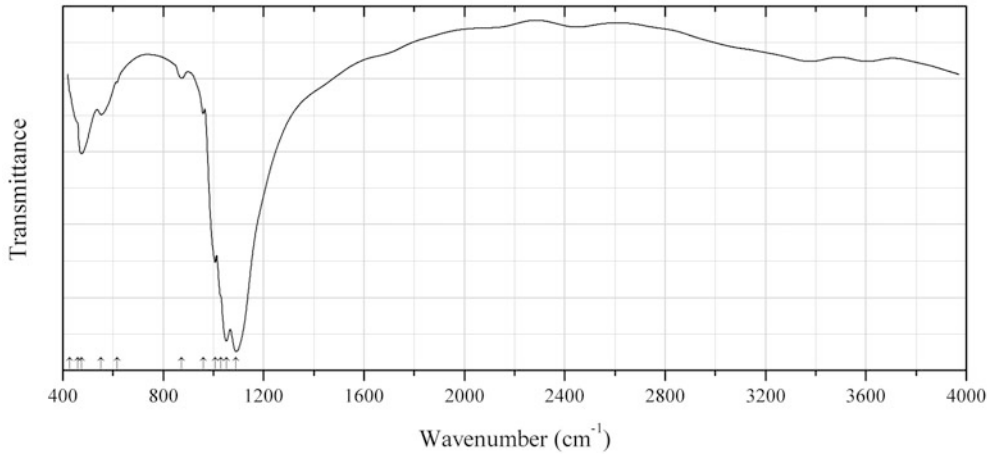

Fig. 2.480 IR spectrum of bredigite drawn using data from Mirhadi et al. (2012)

Sio123 Bredigite $(Ca,Ba)Ca_{13}Mg_2(SiO_4)_8$ (Fig. 2.480)
Locality: Synthetic.
Description: Nanocrystalline powder.
Source: Mirhadi et al. (2012).
Wavenumbers (cm^{-1}): 1090s, 1052s, 1030sh, 1007sh, 960sh, 873w, 616sh, 553, 475, 460sh, 427sh.
Note: Questionable data. The positions of the strongest bands at 1090, 1030, and 475 cm^{-1} may correspond to an amorphous phase or to a phyllosilicate, but not to a nesosilicate.

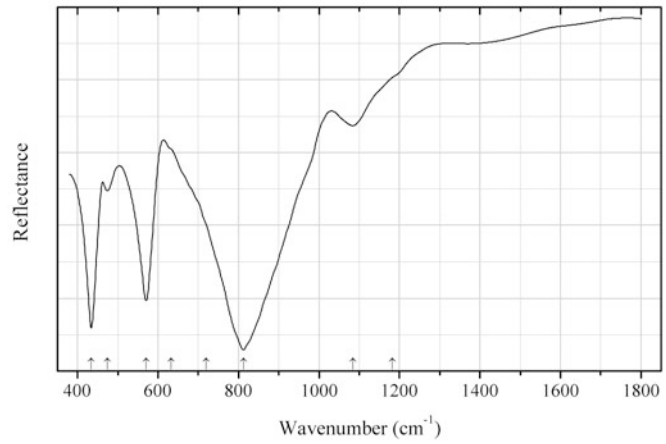

Fig. 2.481 IR spectrum of coffinite drawn using data from Clavier et al. (2014)

Sio124 Coffinite $U(SiO_4)\cdot nH_2O$ (Fig. 2.481)
Locality: Synthetic.
Description: Prepared under hydrothermal conditions. Confirmed by electron microprobe analysis.
Kind of sample preparation and/or method of registration of the spectrum: Powdered samples were deposited at the surface of an ATR crystal without any prior preparation.
Source: Clavier et al. (2014).

Wavenumbers (cm^{-1}): 1183sh, 1084w, 812s, 719sh, 633sh, 570s, 474, 434s.
Note: The wavenumbers were determined by us based on spectral curve analysis of the published spectrum. No bands of H_2O, OH or UO_2^{2+} are observed. In natural samples (Stieff et al. 1956; Abdel-Gawad and Kerr 1961) H_2O may be present as a result of metamictization.

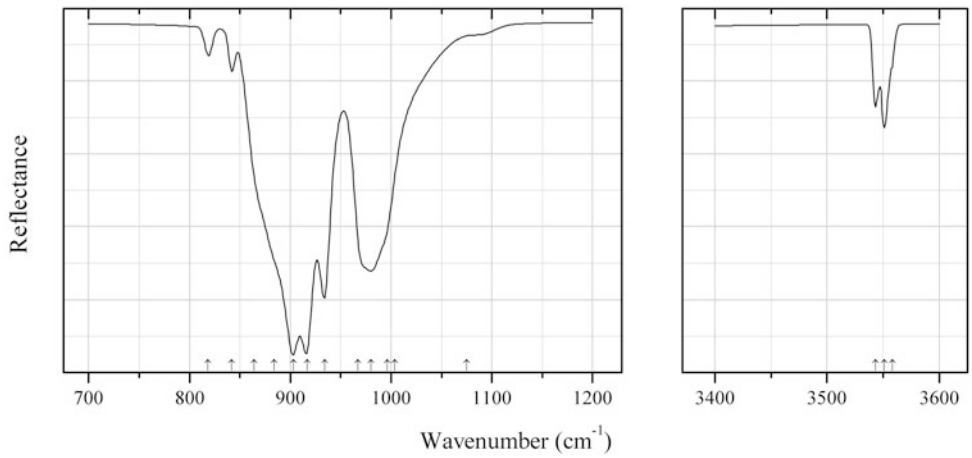

Fig. 2.482 IR spectrum of edgrewite drawn using data from Galuskin et al. (2012)

Sio125 Edgrewite $Ca_9(SiO_4)_4F_2$ (Fig. 2.482)
Locality: Lakargi Mt., Upper Chegem caldera, Kabardino-Balkarian Republic, Northern Caucasus, Russia (type locality).
Description: Colourless grains from xenolith of carbonate-silicate rock within ignimbrite. The associated minerals are bultfonteinite, hillebrandite, jennite, chegemite, as well as relics of larnite and rondorfite enclosed in a matrix of hydroxylellestadite. Holotype sample. The crystal structure is solved. Monoclinic, space group $P2_1/b11$, a = 5.0687(1), b = 11.3579(1), c = 15.4004(2) Å, α = 100.598(1)°, V = 871.47(3) $Å^3$, Z = 2. D_{calc} ≈ 2.92 g/cm^3. Optically biaxial (+), α = 1.621(2), β = 1.625(2), γ = 1.631(2), 2 V = 80(5)°.
Kind of sample preparation and/or method of registration of the spectrum: Reflectance spectra measured using infrared microscope. The reflection data were converted to standard absorption spectra using Fourier and Kramers-Krönig transformations.
Source: Galuskin et al. (2012).
Wavenumbers (cm^{-1}): 3558sh, 3551w, 3543w, 1075sh, 1004sh, 996sh, 980s, 967sh, 934s, 917s, 903s, 884sh, 864sh, 842w, 818w.
Note: The wavenumbers are indicated for the maxima of individual bands obtained as a result of the spectral curve analysis.

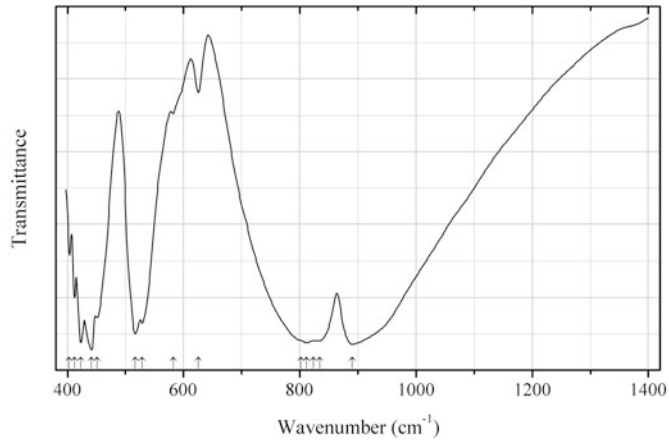

Fig. 2.483 IR spectrum of eringaite drawn using data from Wu et al. (2013)

Sio126 Eringaite $Ca_3Sc_2Si_3O_{12}$ (Fig. 2.483)
Locality: Synthetic.
Description: Ce-doped sample with Ca:Sc:Si:Ce = 2.955:2:3:0.03. Confirmed by powder X-ray diffraction data.
Kind of sample preparation and/or method of registration of the spectrum: KBr disc. Transmission.
Source: Wu et al. (2013).
Wavenumbers (cm^{-1}): 890s, 834s, 824s, 812s, 802sh, 626w, 582w, 529, 517s, 451, 441s, 423s, 412, 403.
Note: The wavenumbers were partly determined by us based on spectral curve analysis of the published spectrum.

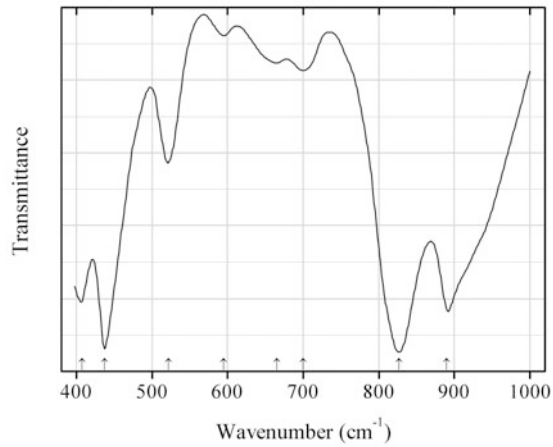

Fig. 2.484 IR spectrum of andradite drawn using data from Katerinopoulou et al. (2009)

Sio127 Andradite $Ca_3Fe^{3+}{}_2(SiO_4)_3$ (Fig. 2.484)
Locality: Maronia area, westernThrace, Greece.

Description: Dark-coloured grains from skarn. A Cr-, Ti-, and Zr-rich variety. Cubic, a = 12.0815(1) Å. The empirical formula is $(Ca_{2.99}Mn_{0.03})(Fe^{3+}{}_{0.67}Cr_{0.54}Al_{0.33}Ti_{0.29}Zr_{0.15})(Si_{2.42}Ti_{0.24}Fe_{0.18}Al_{0.14})O_{12}(OH)_{0.11}$. The Mössbauer analysis showed that the total Fe is ferric, preferentially located at the octahedral site and to a smaller extent at the tetrahedral site.
Kind of sample preparation and/or method of registration of the spectrum: KBr disc. Absorption.
Source: Katerinopoulou et al. (2009).
Wavenumbers (cm^{-1}): 890s, 827s, 700, 665, 595w, 522, 437s, 407s.

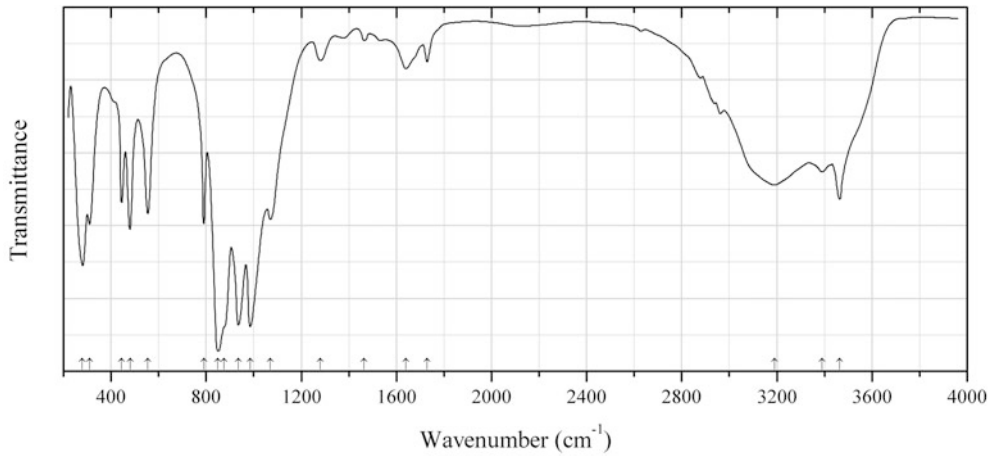

Fig. 2.485 IR spectrum of boltwoodite drawn using data from Plesko et al. (1992)

Sio128 Boltwoodite $K(UO_2)(HSiO_4)\cdot 1.5H_2O$ (Fig. 2.485)
Locality: Synthetic.
Description: Confirmed by powder X-ray diffraction data.
Kind of sample preparation and/or method of registration of the spectrum: Attenuated total reflection of powdered mineral. KBr disc. Transmission.
Source: Plesko et al. (1992).
Wavenumbers (cm^{-1}): 3465, 3390, 3190, 1730w, 1640w, 1465w, 1280w, 1070, 985s, 935s, 875sh, 850s, 790, 555, 480, 445, 310, 280s.
Note: Weak bands at 1730 and 1640 cm^{-1} correspond to bending vibrations of H_3O^+ and H_2O, respectively. Weak bands in the range from 2800 to 3000 cm^{-1} indicate possible presence of an organic matter.

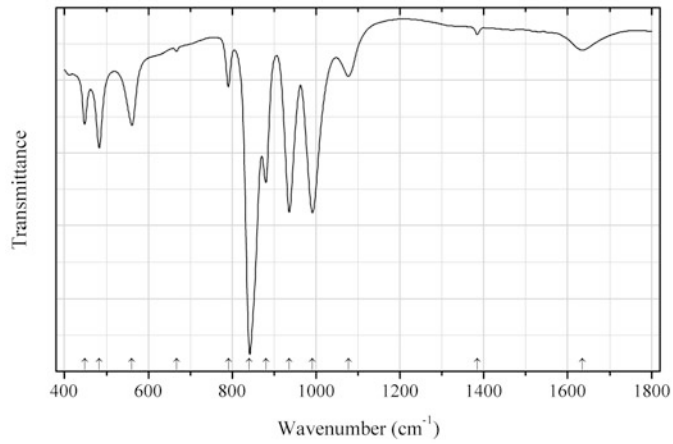

Fig. 2.486 IR spectrum of boltwoodite drawn using data from Lehmann et al. (2008)

Sio129 Boltwoodite $K(UO_2)(HSiO_4)\cdot 1.5H_2O$ (Fig. 2.486)
Locality: Synthetic.
Description: The ratio U:K:Si:H_2O determined by the ICP-MS and AAS methods is 1.1:1.1:1.0:0.8. The boltwoodite structure is confirmed by powder X-ray diffraction data.
Kind of sample preparation and/or method of registration of the spectrum: KBr disc. Absorption.
Source: Lehmann et al. (2008).
Wavenumbers (cm^{-1}): 1635w, 1384w, 1078sh, 991s, 936s, 881, 841s, 791, 667w, 561, 483, 448.
Note: Weak band at 1384 cm^{-1} corresponds to the admixture of NO_3^-; weak band at 667 cm^{-1} is atmospheric artifact.

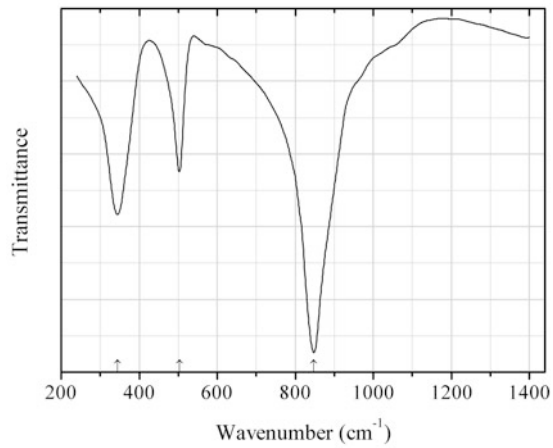

Fig. 2.487 IR spectrum of fayalite polymorph drawn using data from Jeanloz (1980)

Sio130 Fayalite polymorph γ-Fe_2SiO_4 (Fig. 2.487)
Iron(II) orthosilicate
Locality: Synthetic.
Description: Synthesized at 900 °C, 7.2 GPa. Isostructural with spinel.
Kind of sample preparation and/or method of registration of the spectrum: KBr disc. Absorption.

Source: Jeanloz (1980).
Wavenumbers (cm^{-1}): 848s, 503, 344.

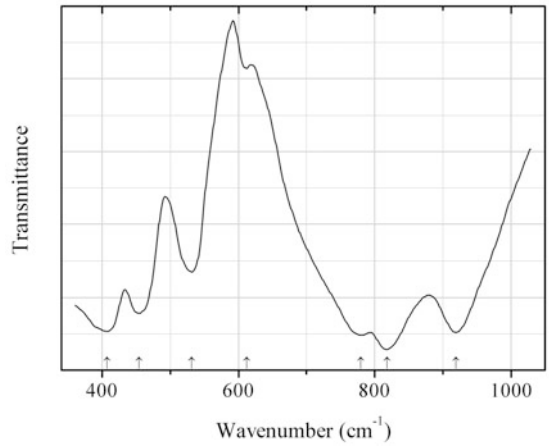

Fig. 2.488 IR spectrum of garnet Sio131 drawn using data from Nishizawa and Koizumi (1975)

Sio131 Garnet Sio131 $Ca_3Mn^{3+}{}_2(SiO_4)_3$ (Fig. 2.488)
Locality: Synthetic.
Description: Synthesized at high pressure and temperature. Cubic, a = 12.060 Å. The strongest lines of the powder X-ray diffraction pattern [d, Å (I, %) (hkl)] are: 3.015 (55) (400), 2.696 (100) (420), 2.462 (45) (422), 2.365 (20) (510), 2.202 (20) (521), 1.956 (25) (611), 1.673 (25) (640), 1.611 (60) (642).
Kind of sample preparation and/or method of registration of the spectrum: Nujol mull. Transmission.
Source: Nishizawa and Koizumi (1975).
Wavenumbers (cm^{-1}): 919s, 818s, 780s, 612w, 531, 454, 407s.
Note: The wavenumbers were partly determined by us based on spectral curve analysis of the published spectrum.

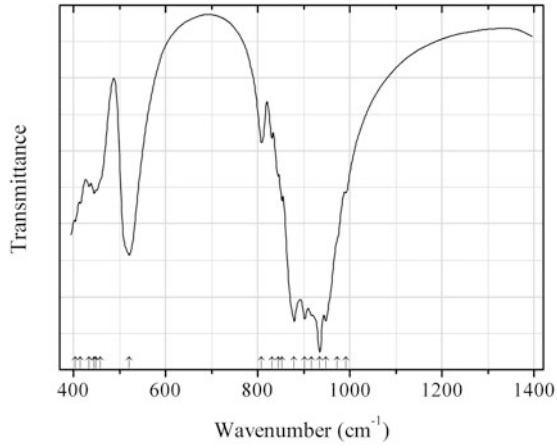

Fig. 2.489 IR spectrum of hatrurite drawn using data from Fernández-Carrasco et al. (2012)

Sio132 Hatrurite $Ca_3(SiO_4)O$ (Fig. 2.489)
Alite
Locality: Synthetic.
Description: Cement phase C_3S.
Kind of sample preparation and/or method of registration of the spectrum: Transmission. Kind of sample preparation is not indicated.
Source: Fernández-Carrasco et al. (2012).
Wavenumbers (cm^{-1}): 991, 972sh, 948s, 935s, 917sh, 902s, 879s, 853, 844, 831, 808, 521, 459sh, 449sh, 445w, 434w, 415w, 404w.
Note: The wavenumbers were partly determined by us based on spectral curve analysis of the published spectrum.

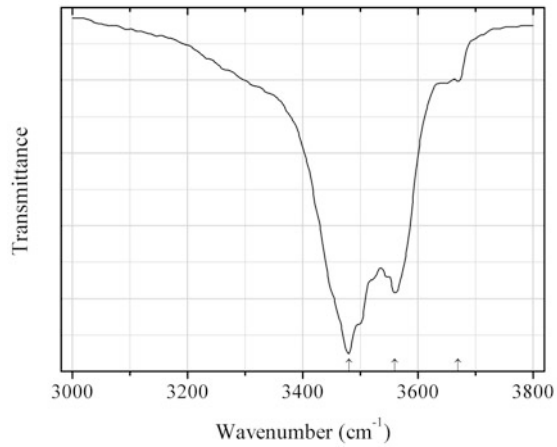

Fig. 2.490 IR spectrum of holtstamite drawn using data from Hålenius et al. (2005)

Sio133 Holtstamite $Ca_3(Al,Mn^{3+})_2(SiO_4)_2(OH)_4$ (Fig. 2.490)
Locality: Wessels mine, Hotazel, Kalahari manganese fields, Northern Cape province, South Africa (type locality).
Description: Brownish yellow grains from the association with Mn^{3+}-bearing vesuvianite, calcite, and henritermierite. Holotype sample. Tetragonal, space group $I4_1/acd$, a = 12.337 (3), c = 11.930 Å. D_{calc} = 3.25 g/cm^3. Optically uniaxial (+), ω = 1.718(2), ε = 1.746(2). The empirical formula is $Ca_{3.00}(Al_{0.96}Mn^{3+}_{0.68}Fe^{3+}_{0.37})(SiO_4)_{2.00}(OH)_{3.96}$.
Kind of sample preparation and/or method of registration of the spectrum: Absorbance using IR microscope.
Source: Hålenius et al. (2005).
Wavenumbers (cm^{-1}): 3670w, 3560, 3480s.

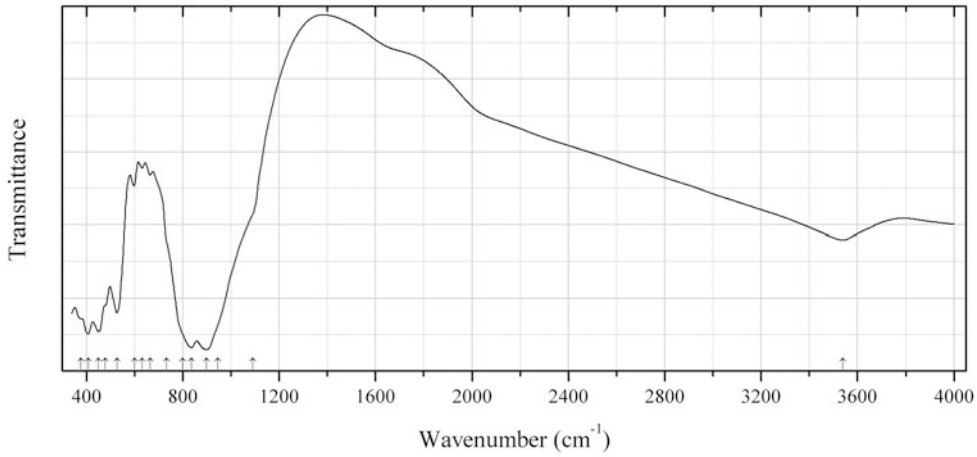

Fig. 2.491 IR spectrum of andradite (Ti,OH-bearing) drawn using data from Onuki et al. (1981)

Sio134 Andradite (Ti,OH-bearing) $Ca_3(Fe,Ti,Al,Mg)_2[(SiO_4,(OH)_4]_3$ (Fig. 2.491)
Locality: Sanbagawa terrain, Shizuoka prefecture, Japan.
Description: Anhedral grains from the association with chlorite. The empirical formula is (electron microprobe): $Ca_{3.03}(Fe^{3+}{}_{1.19}Ti_{0.56}Al_{0.25}Mg_{0.07}Mn_{0.01})(SiO_4)_{2.81}(OH)_x$. The presence of OH groups is confirmed by TGA and DTA.
Kind of sample preparation and/or method of registration of the spectrum: KBr disc. Transmission.
Source: Onuki et al. (1981).
Wavenumbers (cm^{-1}): 3540, 1092sh, 946sh, 898s, 836s, 800sh, 732sh, 665w, 632w, 600w, 527, 479sh, 450, 408, 378sh.
Note: The wavenumbers were determined by us based on spectral curve analysis of the published spectrum.

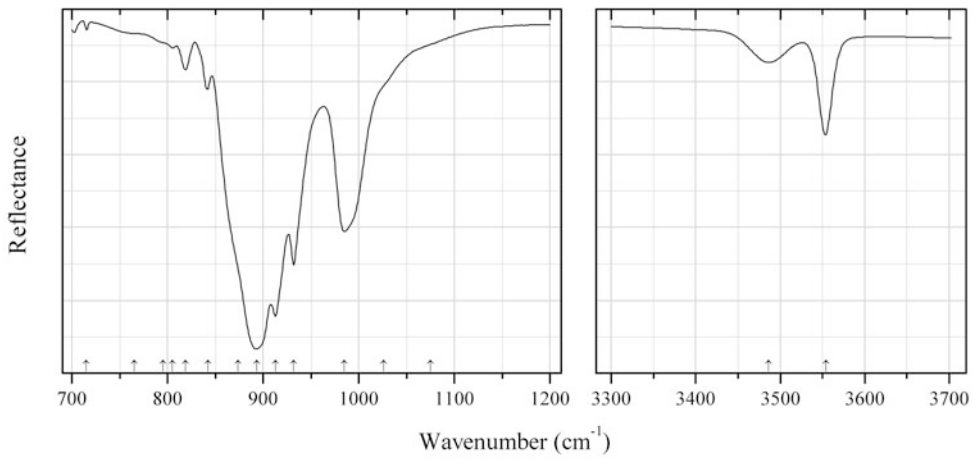

Fig. 2.492 IR spectrum of hydroxyledgrewite drawn using data from Galuskin et al. (2012)

Sio135 Hydroxyledgrewite $Ca_9(SiO_4)_4(OH)_2$ (Fig. 2.492)

Locality: Upper Chegem volcanic structure, Kabardino-Balkaria, Northern Caucasus, Russia (type locality).
Description: Colourless grains from the association with bultfonteinite, hillebrandite, jennite, and chegemite, as well as rare relics of larnite and rondorfite enclosed in a matrix of hydroxylellestadite. Holotype sample. Monoclinic, space group $P2_1/b11$, a = 5.06720(10), b = 11.35450(10), c = 15.3941 (2) Å, α = 100.5870(10)°, V = 870.63(2) Å^3, Z = 2. Optically biaxial (+), α = 1.625(2), β = 1.629(2), γ = 1.635(2), 2 V = 80(5)°.
Kind of sample preparation and/or method of registration of the spectrum: Reflection.
Source: Galuskin et al. (2012).
Wavenumbers (cm^{-1}): 3554, 3486, 1075sh, 1026sh, 985, 932s, 913s, 893s, 874sh, 842w, 819w, 805w, 795sh, 765sh, 715w.
Note: Wavenumbers are given according to drawing. In the cited paper, the wavenumbers are indicated only for the maxima of individual bands obtained as a result of the spectral curve analysis.

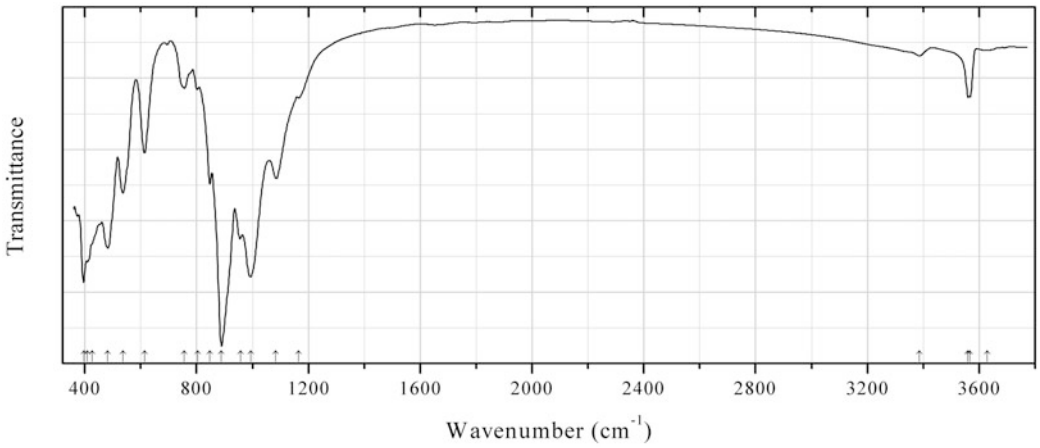

Fig. 2.493 IR spectrum of humite B-bearing obtained by N.V. Chukanov

Sio136 Humite B-bearing $(Mg,Fe)_7[(SiO_4,BO_3,B(OH)_4]_3(F,OH,O)_2$ (Fig. 2.493)
Locality: Open pit No. 97, Ilmeny Mts., Chelyabinsk region, South Urals, Russia.
Description: Orange-brown grains. Orthorhombic. The unit-cell parameters determined by A.V. Kasatkin from the single-crystal X-ray diffraction pattern are: a = 10.271(6), b = 20.854(11), c = 4.748(4) Å, V = 1017(1) Å^3. The empirical formula is (electron microprobe): $(Mg_{6.4}Fe_{0.4}Mn_{0.1}Ti_{0.05}Al_{0.05})(SiO_4)_{2.85}[BO_3,B(OH)_4]_{0.15}F_{1.5}(OH,O)_{0.5}$.
Kind of sample preparation and/or method of registration of the spectrum: KBr disc. Absorption.
Wavenumbers (cm^{-1}): 3630w, 3567, 3560, 3386w, 1165w, 1084, 993s, 957, 889s, 847, 804w, 756w, 613, 536, 482s, 425sh, 410sh, 397s.
Note: The sample can contain inclusions with clinohumite structure.

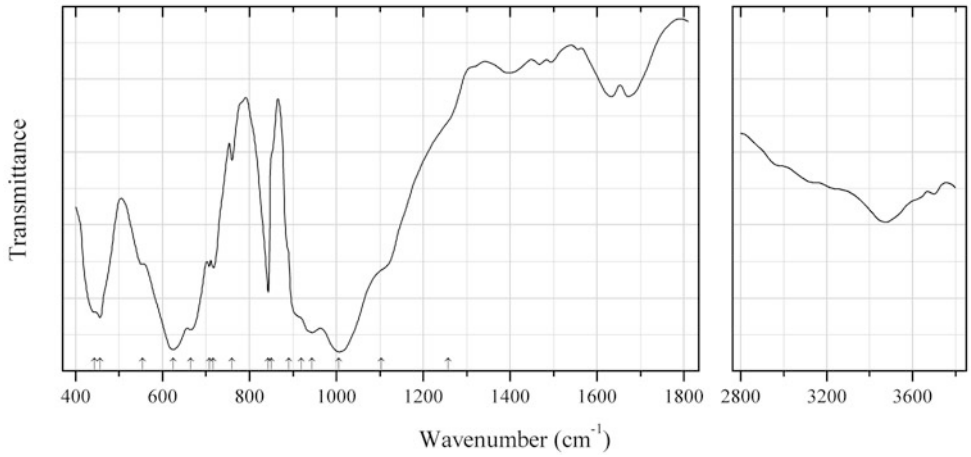

Fig. 2.494 IR spectrum of kanonaite drawn using data from Vrána et al. (1978)

Sio137 Kanonaite $Mn^{3+}AlO(SiO_4)$ (Fig. 2.494)
Locality: Kanona, Serenje, Serenje district, Central province, Zambia (type locality).
Description: Greenish black porphyroblasts in a gahnite-chlorite-coronadite-quartz shist. Holotype sample. Orthorhombic, space group *Pnnm*, a = 7.953(2), b = 8.038 23), c = 5.619(2) Å, V = 359.2(1) $Å^3$, Z = 4. D_{calc} = 3.395 g/cm^3. Optically biaxial (+), α = 1.702, β = 1.730, γ = 1.823, 2 V = 53(3)°. The empirical formula is $(Mn^{3+}_{0.76}Al_{0.23}Fe^{3+}_{0.015})Al_{1.00}Si_{0.99}O_{5.00}$. The strongest lines of the powder X-ray diffraction pattern [*d*, Å (*I*, %) (*hkl*)] are: 5.669 (100) (110), 4.590 (75) (011, 101), 3.587 + 3.567 (90) (120, 210), 2.827 (94) (220), 2.517 (90) (310, 112), 2.299 (69) (022, 311), 2.212 (83) (320, 122, 212).
Kind of sample preparation and/or method of registration of the spectrum: KBr disc. Transmission.
Source: Vrána et al. (1978).
Wavenumbers (cm^{-1}): 1257sh, 1104sh, 1006s, 944s, 919sh, 890sh, 850sh, 843s, 760, 717, 708, 665s, 624s, 554sh, 456, 444sh.
Note: The wavenumbers were determined by us based on spectral curve analysis of the published spectrum. Most bands observed above 1400 cm^{-1} correspond to water and carbonate groups in impurities.

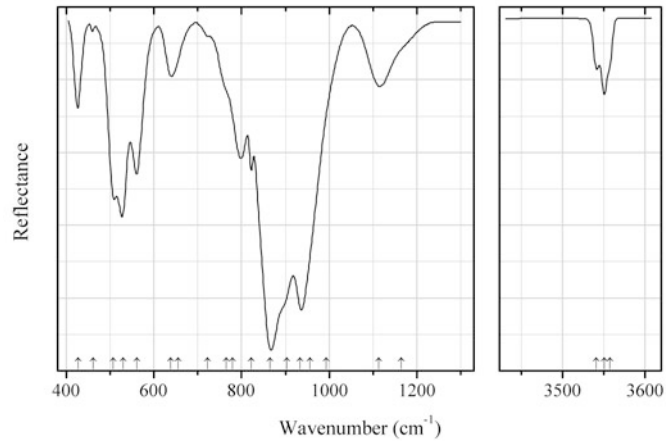

Fig. 2.495 IR spectrum of kumtyubeite drawn using data from Galuskina et al. (2009)

Sio138 Kumtyubeite $Ca_5(SiO_4)_2(F,OH)_2$ (Fig. 2.495)
Locality: Upper Chegem caldera structure, Kabardino-Balkaria, Northern Caucasus, Russia (type locality).
Description: Light-pink grains from spurrite-rondorfite-ellestadite zones of skarn. Holotype sample. Monoclinic, space group $P2_1/a$, a = 11.44637(18), b = 5.05135(8), c = 8.85234(13) Å, β = 108.8625 (7)°, V = 484.352(13) Å^3, Z = 2. Optically biaxial (−), α = 1.594(2), β = 1.605(2), γ = 1.608(2), 2 V = 44°–45°. The empirical formula is (electron microprobe): $Ca_{5.00}(Si_{1.99}Ti_{0.01})O_8[F_{1.39}(OH)_{0.61}]$.
Kind of sample preparation and/or method of registration of the spectrum: Attenuated total reflection of powdered mineral.
Source: Galuskina et al. (2009).
Wavenumbers (cm^{-1}): 3558sh, 3551, 3541, 1165sh, 1113, 993sh, 957sh, 934s, 904sh, 865s, 822, 779, 765sh, 722sh, 656sh, 638, 561, 530s, 507, 461w, 427.
Note: The wavenumbers are indicated for the maxima of individual bands obtained as a result of the spectral curve analysis.

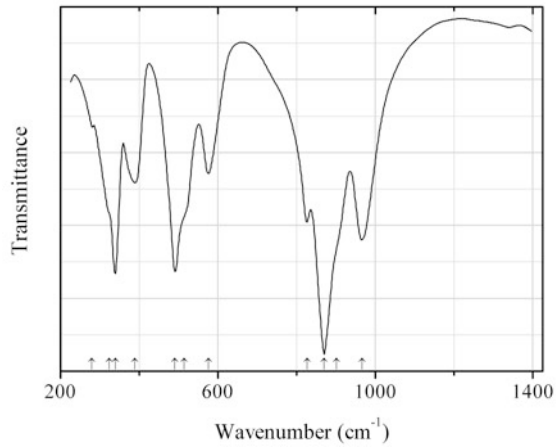

Fig. 2.496 IR spectrum of liebenbergite drawn using data from Jeanloz (1980)

Sio139 Liebenbergite $Ni_2(SiO_4)$ (Fig. 2.496)
Locality: Synthetic.
Description: Synthesized at normal pressure and 1200–750 °C at 1 °C/h cooling under Na_2WO_4 flux.
Kind of sample preparation and/or method of registration of the spectrum: KBr disc. Absorption.
Source: Jeanloz (1980).
Wavenumbers (cm^{-1}): 966, 902sh, 870s, 826, 576, 514sh, 491s, 389, 339s, 323sh, 280w.
Note: The wavenumbers were partly determined by us based on spectral curve analysis of the published spectrum.

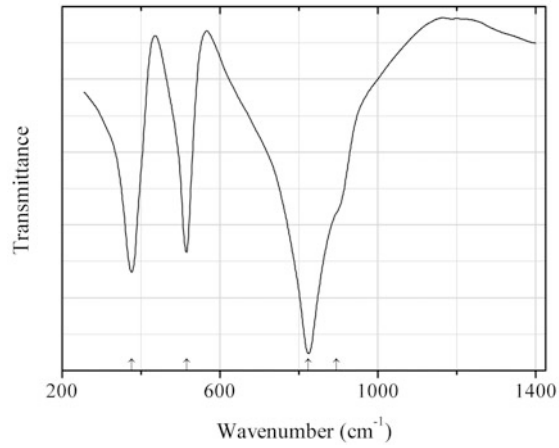

Fig. 2.497 IR spectrum of liebenbergite polymorph drawn using data from Jeanloz (1980)

Sio140 Liebenbergite polymorph γ-$Ni_2(SiO_4)$ (Fig. 2.497)
Locality: Synthetic.
Description: Synthesized 1400 °C and 5.5 GPa. γ-polymorph with the spinel-type structure.
Kind of sample preparation and/or method of registration of the spectrum: KBr disc. Absorption.
Source: Jeanloz (1980).
Wavenumbers (cm^{-1}): 895sh, 824s, 515, 376.
Note: The wavenumbers were partly determined by us based on spectral curve analysis of the published spectrum.

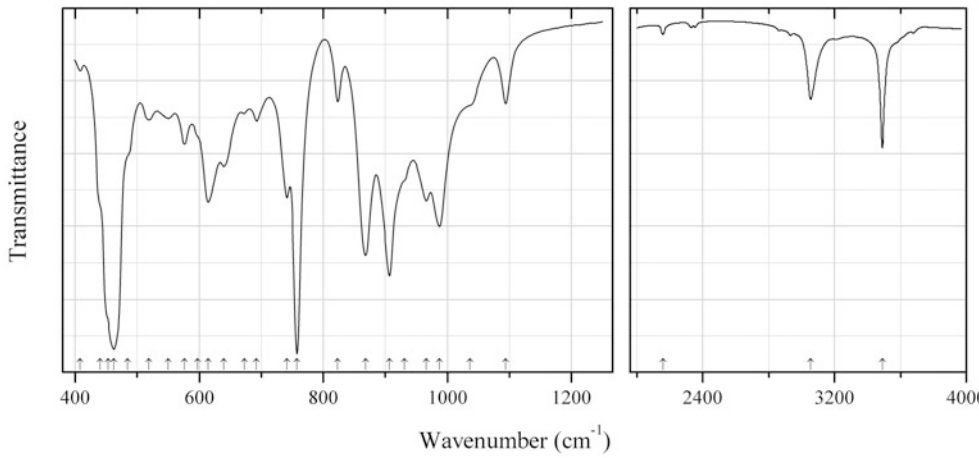

Fig. 2.498 IR spectrum of magnesiochloritoid drawn using data from Koch-Müller et al. (2002)

Sio141 Magnesiochloritoid $MgAl_2(SiO_4)O(OH)_2$ (Fig. 2.498)
Locality: Synthetic.
Description: Synthesized from oxides at high pressure and 600 °C. Triclinic, space group *P*-1.
Kind of sample preparation and/or method of registration of the spectrum: KBr disc. Absorption.

Source: Koch-Müller et al. (2002).
Wavenumbers (cm^{-1}): 3491, 3056, 2160w, 1094w, 1036sh, 987, 966, 931sh, 907s, 868s, 823, 758s, 741, 692w, 673w, 640, 615, 597sh, 576, 550w, 519w, 485sh, 463s, 453sh, 440sh, 408w.
Note: Weak bands in the ranges from 2800 to 3000 cm^{-1} and from 2300 to 2400 cm^{-1} correspond to the admixture of an organic substance and to atmospheric CO_2, respectively.

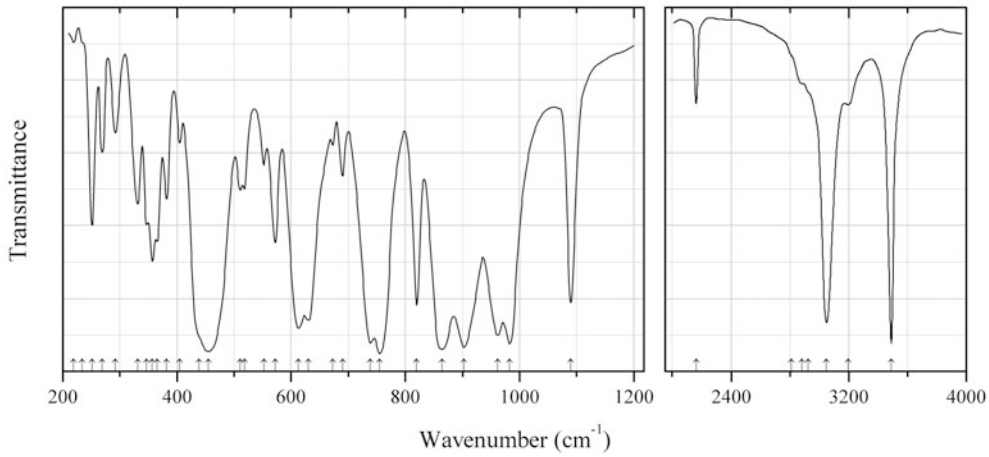

Fig. 2.499 IR spectrum of magnesiochloritoid drawn using data from Chopin et al. (1992)

Sio142 Magnesiochloritoid $MgAl_2(SiO_4)O(OH)_2$ (Fig. 2.499)
Locality: Synthetic.
Description: Magnesium end-member. Triclinic, space group *C*-1, a = 9.425(8), b = 5.444(6), c = 9.130(5) Å, α = 96.41(6)°, β = 101.10(6)°, γ = 89.97(7)°.
Kind of sample preparation and/or method of registration of the spectrum: RbI disc. Transmission.
Source: Chopin et al. (1992).
Wavenumbers (cm^{-1}): 3490s, 3195, 3050s, 2923sh, 2881sh, 2810sh, 2163, 1090, 983s, 962s, 903s, 864s, 820, 755s, 739s, 690, 673w, 630, 613s, 572, 552w, 518, 511, 455s, 439sh, 405w, 382, 365, 357, 347, 331, 292, 269, 251, 234sh, 219w.
Note: The wavenumbers were partly determined by us based on spectral curve analysis of the published spectrum.

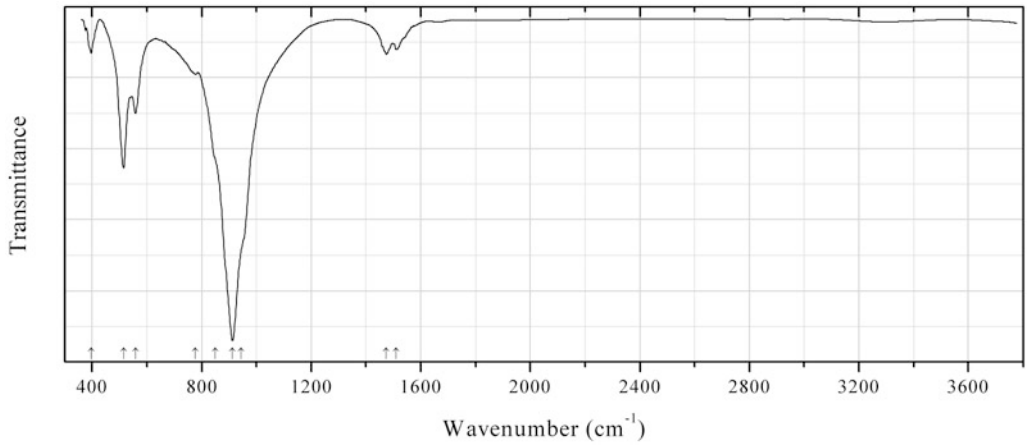

Fig. 2.500 IR spectrum of jasmundite obtained by N.V. Chukanov

Sio143 Jasmundite $Ca_{11}(SiO_4)_4O_2S$ (Fig. 2.500)
Locality: Bellerberg, near Ettringen, Eifel Mts., Rhineland-Palatinate (Rheinland-Pfalz), Germany (type locality).
Description: Dark red-brown translucent grains from metamorphosed limestone inclusion in basalt, from the association with brownmillerite, larnite, and brearleyite. The empirical formula is (electron microprobe): $(Ca_{10.8}Mg_{0.2})(SiO_4)_{4.0}S_{0.8}(O,CO_3)_{2.2}$. Confirmed by the IR spectrum.
Kind of sample preparation and/or method of registration of the spectrum: KBr disc. Absorption.
Wavenumbers (cm^{-1}): 1510, 1475, 945sh, 913s, 850sh, 777, 559, 515s, 396.

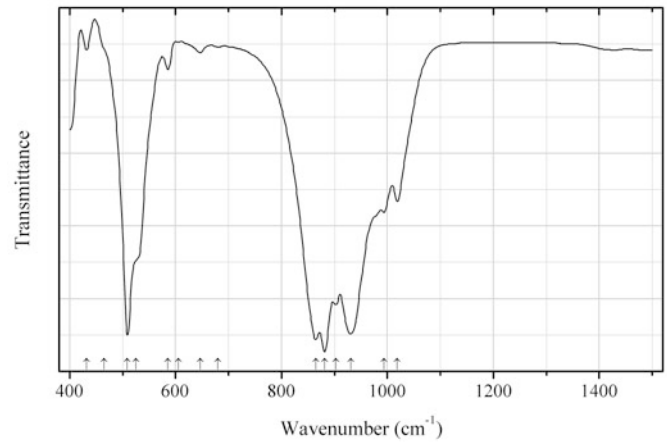

Fig. 2.501 IR spectrum of merwinite drawn using data from Kriskova et al. (2013)

Sio144 Merwinite $Ca_3Mg(SiO_4)_2$ (Fig. 2.501)
Locality: Synthetic.
Description: Prepared using the laboratory grade oxides mixed in corresponding stoichiometric proportion and fired for 20 h at 1500 °C. Confirmed by powder X-ray diffraction data.
Kind of sample preparation and/or method of registration of the spectrum: Transmission. Kind of sample preparation is not indicated.

Source: Kriskova et al. (2013).
Wavenumbers (cm^{-1}): 1019, 994, 931s, 903, 882s, 865s, 680w, 647w, 605w, 585, 525sh, 509s, 465sh, 432.
Note: The wavenumbers were determined by us based on spectral curve analysis of the published spectrum.

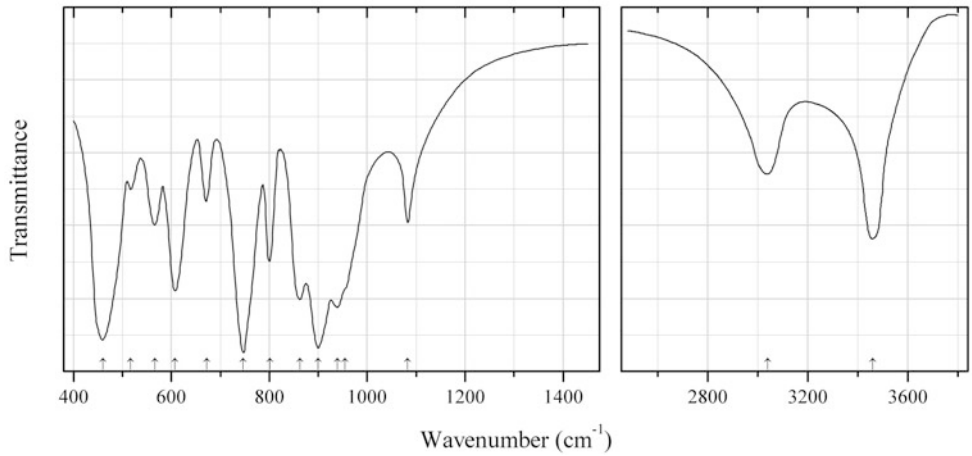

Fig. 2.502 IR spectrum of ottrélite drawn using data from Fransolet (1978)

Sio145 Ottrélite $Mn^{2+}Al_2(SiO_4)O(OH)_2$ (Fig. 2.502)
Locality: Ottré, Vielsalm, Stavelot massif, Luxembourg province, Belgium (type locality).
Description: Pistachio-green aggregate developed at the border of a quartz vein. Monoclinic, $a = 9.505$ (6), $b = 5.484(4)$, $c = 18.214(15)$ Å, $\beta = 101.77(3)°$, $V = 929(2)$ $Å^3$, $Z = 8$. $D_{meas} = 3.52(2)$ g/cm^3, $D_{calc} = 3.49$ g/cm^3. Optically biaxial (+), $\alpha = 1.709(3)$, $\beta = 1.712(3)$, $\gamma = 1.716(3)$, $2V = 60°–70°$. The empirical formula is $(Mn_{0.88}Fe^{2+}_{0.55}Mg_{0.54}Fe^{3+}_{0.03})(Al_{3.93}Fe^{3+}_{0.07})(Si_{1.97}Al_{0.03})O_{10.03}(OH)_{3.94}$.
Kind of sample preparation and/or method of registration of the spectrum: KBr disc. Transmission.
Source: Fransolet (1978).
Wavenumbers (cm^{-1}): 3460, 3040, 1083, 955sh, 939, 900s, 863s, 801, 747s, 672, 608, 566, 517, 460s.

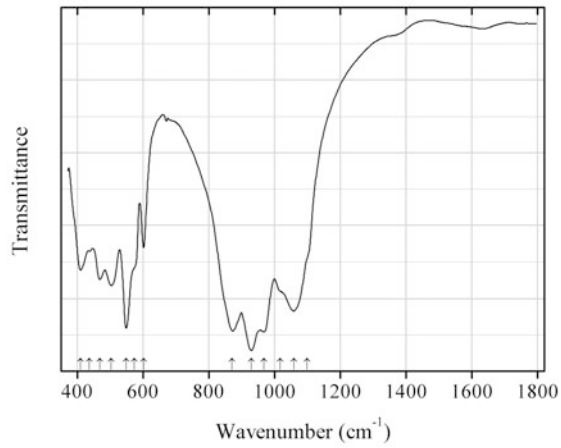

Fig. 2.503 IR spectrum of oxybritholite-(La) drawn using data from El Ouenzerfi et al. (2003)

Sio146 Oxybritholite-(La) $(La,Ca)_5(SiO_4,PO_4)_3O_{1-x}$ (Fig. 2.503)
Locality: Synthetic.
Description: Synthesized as crystalline powder by high-temperature solid-state reaction. Confirmed by powder X-ray diffraction data. The formula is ($Z = 1$): $Ca_{4.15}La_{5.38}(SiO_4)_{3.74}(PO_4)_{2.26}O_{1.31}$.
Kind of sample preparation and/or method of registration of the spectrum: Transmission. Kind of sample preparation is not indicated.
Source: El Ouenzerfi et al. (2003).
Wavenumbers (cm^{-1}): 1098sh, 1058s, 1017sh, 966s, 929s, 870s, 601, 573sh, 548s, 503, 468, 436, 409.

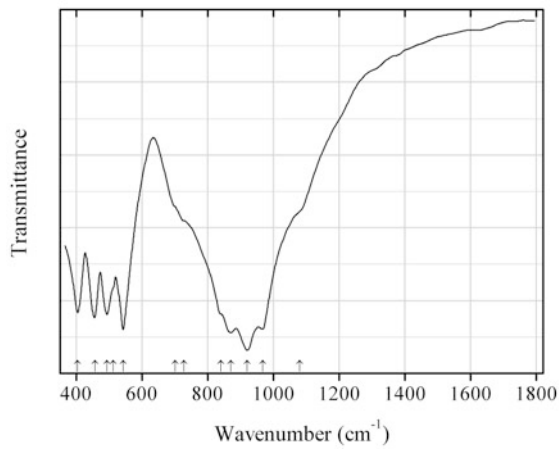

Fig. 2.504 IR spectrum of oxybritholite-(La) drawn using data from El Ouenzerfi et al. (2003)

Sio147 Oxybritholite-(La) $(La,Ca)_5(SiO_4,PO_4)_3O_{1-x}$ (Fig. 2.504)
Locality: Synthetic.
Description: Synthesized as crystalline powder by high-temperature solid-state reaction. Confirmed by powder X-ray diffraction data. The formula is ($Z = 1$): $Ca_2La_8(SiO_4)_6O_2$.
Kind of sample preparation and/or method of registration of the spectrum: Transmission. Kind of sample preparation is not indicated.

Source: El Ouenzerfi et al. (2003).
Wavenumbers (cm^{-1}): 1080sh, 966s, 920s, 870s, 840sh, 727sh, 700sh, 542s, 512sh, 493, 456, 404.
Note: The wavenumbers were partly determined by us based on spectral curve analysis of the published spectrum.

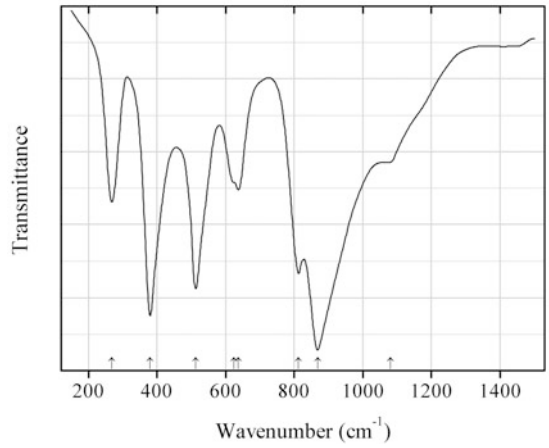

Fig. 2.505 IR spectrum of reidite drawn using data from Gucsik et al. (2004)

Sio148 Reidite $Zr(SiO_4)$ (Fig. 2.505)
Locality: Artificial.
Description: Zircon from Sri Lanka shocked at 80 GPa and containing mainly reidite phase. Identified by the IR spectrum.
Kind of sample preparation and/or method of registration of the spectrum: CsI disc. Absorption.
Source: Gucsik et al. (2004).
Wavenumbers (cm^{-1}): 1080w, 868s, 813, 637, 624sh, 513s, 380s, 268.
Note: The wavenumbers were partly determined by us based on spectral curve analysis of the published spectrum. The weak band at 1080 cm^{-1} may correspond to amorphous SiO_2.

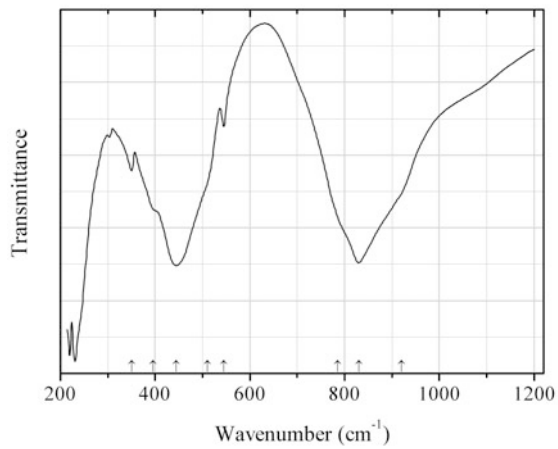

Fig. 2.506 IR spectrum of ringwoodite drawn using data from Akaogi et al. (1984)

Sio149 Ringwoodite $Mg_2(SiO_4)$ (Fig. 2.506)
Locality: Synthetic.
Description: Obtained from a reactive (poor-crystallized) forsterite at 220 kbar and 1473 K for 1 h. Confirmed by powder X-ray diffraction and optical data.
Kind of sample preparation and/or method of registration of the spectrum: KBr disc. Transmission.
Source: Akaogi et al. (1984).
Wavenumbers (cm^{-1}): 920sh, 830s, 785sh, 545w, 510sh, 445s, 395sh, 350w.

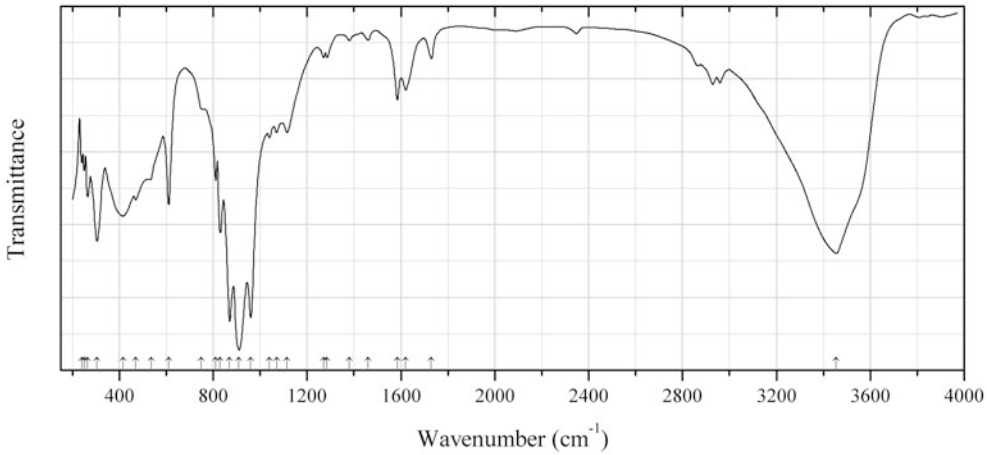

Fig. 2.507 IR spectrum of soddyite drawn using data from Plesko et al. (1992)

Sio150 Soddyite $(UO_2)_2(SiO_4)\cdot 2H_2O$ (Fig. 2.507)
Locality: Synthetic.
Description: Prepared hydrothermally. Confirmed by powder X-ray diffraction data.
Kind of sample preparation and/or method of registration of the spectrum: KBr disc. Transmission.
Source: Plesko et al. (1992).
Wavenumbers (cm^{-1}): 3455s, 1730, 1620, 1585, 1460w, 1380w, 1285w, 1270w, 1115, 1070, 1040, 960s, 910s, 870s, 830, 810, 750sh, 610, 535sh, 470, 415, 305s, 265, 250w, 240w.
Note: The bands in the range from 2800 to 3000 cm^{-1} correspond to the admixture of an organic substance.

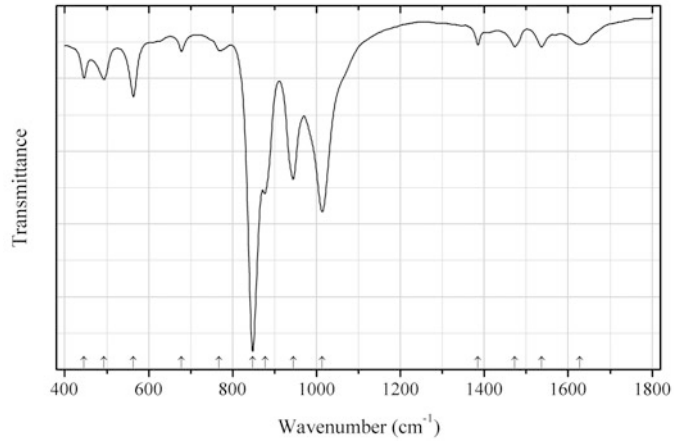

Fig. 2.508 IR spectrum of natroboltwoodite drawn using data from Lehmann et al. (2008)

Sio151 Natroboltwoodite $(H_3O)(Na,K)(UO_2)(SiO_4)\cdot H_2O$ (Fig. 2.508)
Locality: Synthetic.
Description: Synthesized hydrothermally from uranyl nitrate hexahydrate and sodium chloride at 185 °C and pH about 11.5. Characterized by inductively coupled plasma mass spectrosmetry, atomic absorption spectroscopy and powder X-ray diffraction.
Kind of sample preparation and/or method of registration of the spectrum: KBr disc. Absorption.
Source: Lehmann et al. (2008).
Wavenumbers (cm^{-1}): 1627w, 1537w, 1472w, 1384w, 1014s, 945, 878, 848s, 767w, 678w, 564, 493, 445.
Note: Measurements were carried out in the range from 7800 to 370 cm^{-1}, but in the cited paper only data for the range from 400 to 1800 cm^{-1} are given.

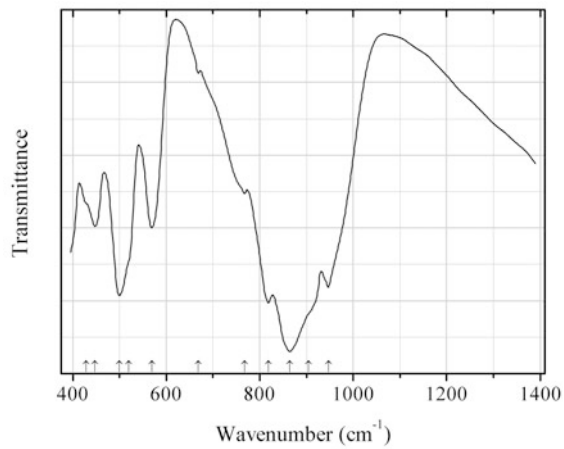

Fig. 2.509 IR spectrum of sonolite drawn using data from Pautov et al. (1990)

Sio152 Sonolite $Mn^{2+}{}_9(SiO_4)_4(OH)_2$ (Fig. 2.509)
Locality: About 8 km upriver from the settlement Inylchek, near the Trudovoe tin deposit, Inylchek range, Tien Shan Mts., Kyrgyzstan.

Description: Brownish-violet grains from the association with rhodonite, quartz, tephroite, spessartine, alleghanyite, alabandite, rhodochrosite, barite, celsian, etc. Monoclinic, a = 10.65(5), b = 4.8 (1), c = 14.3(1) Å, β = 100.3(1)°. Optically biaxial (−), α = 1.764(2), β = 1.783(2), 2 V = 70(5)°. The empirical formula is (electron microprobe, OH calculated): $(Mn_{8.71}Mg_{0.08}Fe_{0.07}Na_{0.04}Al_{0.03}Ti_{0.01})Si_{4.03}O_{16.01}[(OH)_{1.67}F_{0.36}]$. The strongest lines of the powder X-ray diffraction pattern [d, Å (I, %)] are: 2.867 (100), 2.845 (52), 2.654 (53), 2.608 (61), 2.461 (43), 1.808 (65).
Kind of sample preparation and/or method of registration of the spectrum: KBr disc. Transmission.
Source: Pautov et al. (1990).
Wavenumbers (cm^{-1}): 947s, 904sh, 864s, 819s, 768, 668w, 569, 520sh, 500s, 448, 428sh.
Note: The wavenumbers were determined by us based on spectral curve analysis of the published spectrum.

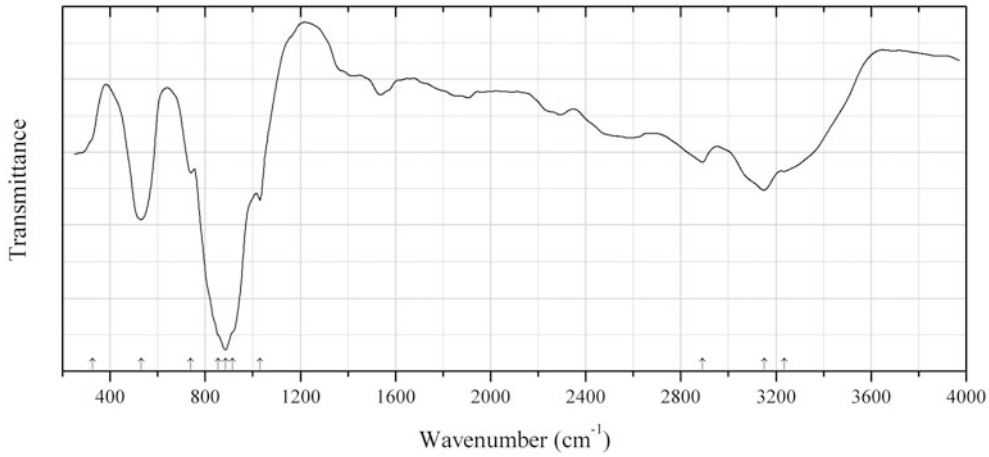

Fig. 2.510 IR spectrum of stringhamite drawn using data from Hindman (1976)

Sio153 Stringhamite $CaCu(SiO_4)\cdot H_2O$ (Fig. 2.510)
Locality: Bawana mine, at southern end of the Rocky Range, Beaver Co., Utah, USA (type locality).
Description: Blue aggregates from a diopside-magnetite skarn. The associated minerals are thaumasite, tenorite, kinoite, and calcite. Holotype sample. Monoclinic, space group $P2_1/c$, a = 5.028(5), b = 16.07(2), c = 5.303(6) Å, β = 102.58°, V = 418.2 Å^3. Optically biaxial (+), α = 1.709, β = 1.717, γ = 1.729. The empirical formula is $Ca_{0.91}Cu_{0.80}SiO_{3.80}\cdot 2.11H_2O$. The strongest lines of the powder X-ray diffraction pattern [d, Å (I, %) (hkl)] are: 8.049 (35) (020), 4.884 (21) (100), 3.928 (34) (−111), 3.618 (21) (130), 3.236 (39) (−131), 2.768 (100) (131), 2.523 (40) (141), 1.614 (23) (202).
Kind of sample preparation and/or method of registration of the spectrum: KBr disc. Transmission.
Source: Hindman (1976).
Wavenumbers (cm^{-1}): 3235, 3150, 2890, 1030, 916sh, 885s, 854sh, 740, 530s, 325sh.
Note: The wavenumbers were partly determined by us based on spectral curve analysis of the published spectrum. Numerous bands in the range from 1250 to 3000 cm^{-1} indicate partial protonation of Si–O bonds to form silanol groups.

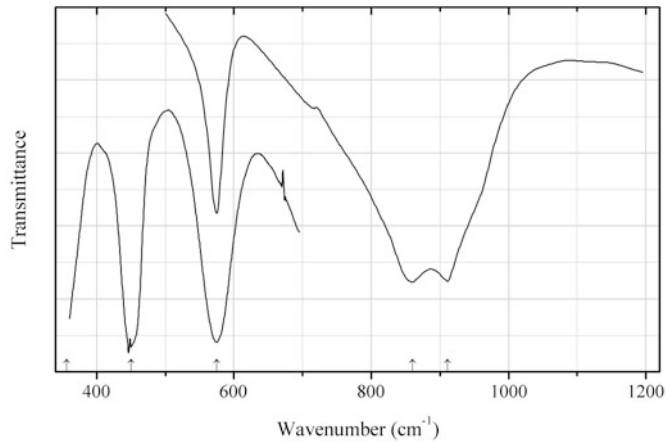

Fig. 2.511 IR spectrum of thorite drawn using data from Lahalle et al. (1986)

Sio154 Thorite $Th(SiO_4)$ (Fig. 2.511)
Locality: Synthetic.
Description: Bipyramidal crystals grown by the flux method from the solution in Li_2MoO_4–MoO_3 prepared at 1150 °C, with subsequent slow cooling up to 800 °C. Confirmed by powder X-ray diffraction data. Tetragonal, a = 7.122(4), c = 6.317(4) Å.
Kind of sample preparation and/or method of registration of the spectrum: Powder mixed with paraffin. Transmission.
Source: Lahalle et al. (1986).
Wavenumbers (cm^{-1}): 911s, 860s, 575s, 450s, 356, 332, 234s.
Note: For the IR spectrum of thorite see also Hubin and Tarte (1971).
Sio155 Huttonite $Th(SiO_4)$
Locality: Synthetic.
Kind of sample preparation and/or method of registration of the spectrum: KI disc, absorption.
Source: Hubin and Tarte (1971).
Wavenumbers (cm^{-1}): 977, 900, 865, 579, 550, 518, 488, 436, 304, 242.
Note: In the cited paper, only wavenumbers of the bands are given, without indication of their intensities.

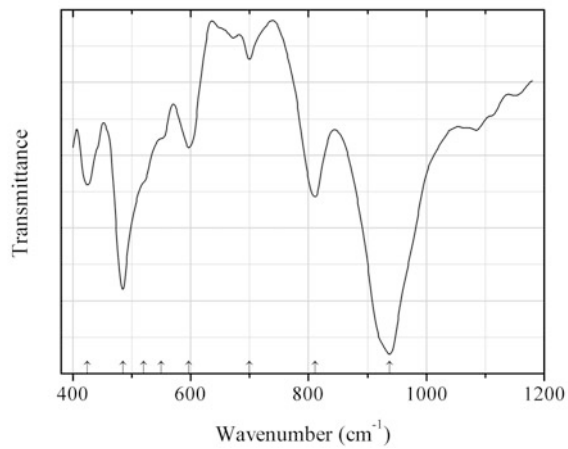

Fig. 2.512 IR spectrum of wadsleyite drawn using data from Williams et al. (1986)

Sio156 Wadsleyite $Mg_2(SiO_4)$ (Fig. 2.512)
Locality: Synthetic.
Description: β-$Mg_2(SiO_4)$ synthesized at 14.5 GPa and 1123 K for 1 h.
Kind of sample preparation and/or method of registration of the spectrum: KBr microdisc. Absorption.
Source: Williams et al. (1986).
Wavenumbers (cm^{-1}): 938s, 811, 700w, 597, 550sh, 520sh, 485s, 425.

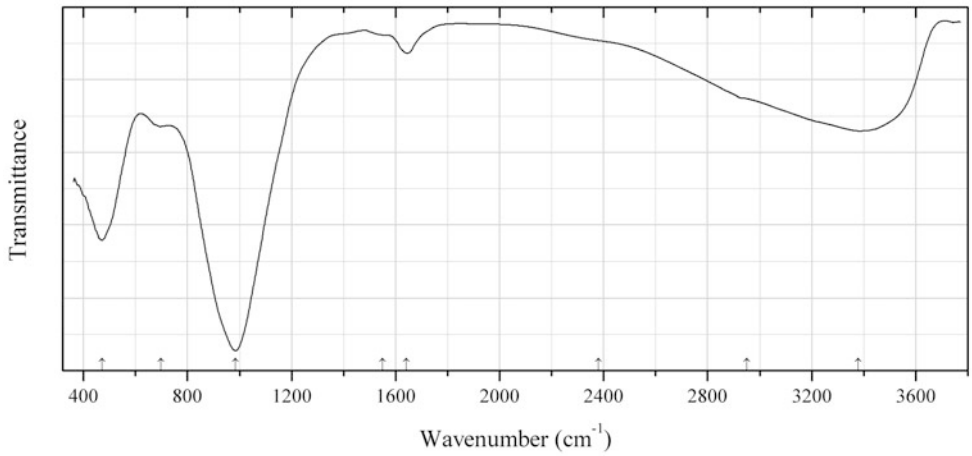

Fig. 2.513 IR spectrum of tombarthite-(Y) obtained by N.V. Chukanov

Sio157 Tombarthite-(Y) (Y,*REE*,Ca)$(HSiO_4)\cdot nH_2O$ (?) (Fig. 2.513)
Locality: Høgtveit, Evje, Setesdal, Aust-Agder, Norway (type locality).
Description: Brown grains from pegmatite. Amorphous, metamict.
Kind of sample preparation and/or method of registration of the spectrum: KBr disc. Absorption.
Wavenumbers (cm^{-1}): 3380, 2950sh, 2380sh, 1642w, 1550sh, 985s, 698w, 471s.

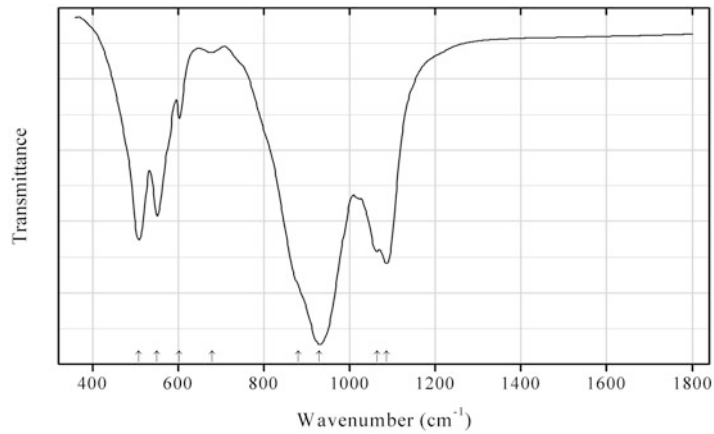

Fig. 2.514 IR spectrum of fluorcalciobritholite obtained by N.V. Chukanov

Sio158 Fluorcalciobritholite (Ca,*REE*)$_5$(SiO_4,PO_4)$_3$F (Fig. 2.514)

Locality: In den Dellen (Zieglowski) pumice quarry, 1.5 km NE of Mendig, Laacher See volcano, Eifel region, Rhineland-Palatinate (Rheinland-Palatinate), Germany.
Description: Pink prismatic crystals from sanidinite. The empirical formula is (electron microprobe): $Ca_{3.19}(Ce_{0.75}La_{0.57}Nd_{0.14}Pr_{0.04})Th_{0.20}Y_{0.10}(SiO_4)_{1.99}(PO_4)_{0.97}(SO_4)_{0.04}F_{1.0}$.
Kind of sample preparation and/or method of registration of the spectrum: KBr disc. Absorption.
Wavenumbers (cm^{-1}): 1087s, 1064s, 929s, 880sh, 678w, 602, 550, 508s.

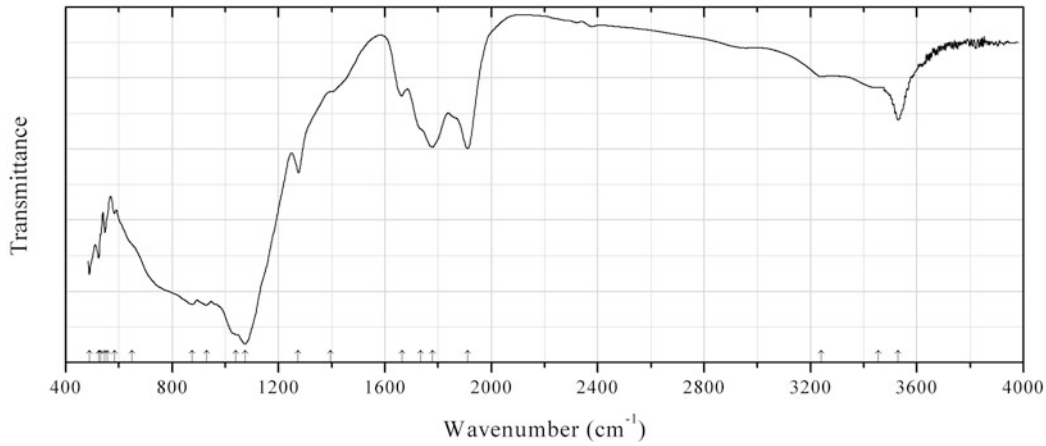

Fig. 2.515 IR spectrum of cayalsite-(Y) drawn using data from Malcherek et al. (2015)

Sio159 Cayalsite-(Y) $CaY_6Al_2Si_4O_{18}F_6$ (Fig. 2.515)
Locality: Tysfjord, Nordland, Norway (type locality).
Description: Colourless prismatic crystal from the association with yttrian fluorite, bastnäsite-(Ce), hematite and vyuntspakhkite-(Y). Cotype sample. The crystal is intergrowth of different polytypes. For the orthorhombic (space group *Pban*) MDO polytype, cayalsite-(Y)-1*O* the lattice parameters are: a = 15.993(1), b = 5.5306(3), c = 9.6590(7) Å, V = 854.35(10) $Å^3$, Z = 2. The unit-cell parameters of the monoclinic (space group *P*2/*c*) MDO polytype, cayalsite-(Y)-1 *M*, are: a = 11.0602(7), b = 5.5280 (2), c = 16.0195(9) Å, β = 118.925(3)°, V = 857.26(8) $Å^3$, Z = 2. The calculated density ranges between 4.81 and 4.86 g/cm^3. Optically biaxial (+), α = 1.730(5), β = 1.740(5), γ = 1.760(5), 2 V = 56.5(5)°. The empirical formula is (electron microprobe): $Ca_{1.03}(Y_{4.73}Dy_{0.43}Gd_{0.34}Er_{0.31}Yb_{0.22}Nd_{0.02})Al_{1.87}Si_{4.03}(O_{17.92}F_{6.08})$.
Kind of sample preparation and/or method of registration of the spectrum: Transmission of a single crystal.
Source: Malcherek et al. (2015).
Wavenumbers (cm^{-1}): 3529, 3454sh, 3240w, 1910, 1780, 1735sh, 1665w, 1395sh, 1275, 1075s, 1040sh, 930s, 875s, 650sh, 583, 557sh, 548, 532sh, 524, 490.
Note: The wavenumbers were partly determined by us based on spectral curve analysis of the published spectrum. The origin of the bands in the range 1600–2000 cm^{-1} is obscure (possibly, they are due to a contamination). The band at 3529 cm^{-1} indicates the presence of OH groups. The wavenumber of the strongest band of Si–O-stretching vibrations (1075 cm^{-1}) is anomalously high for a mineral with isolated silicate groups.

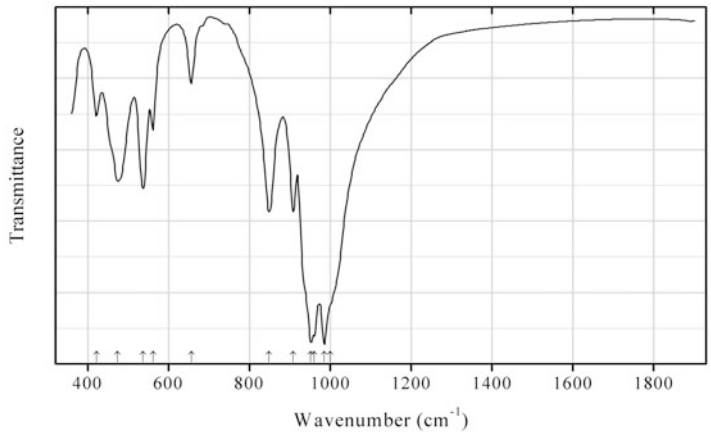

Fig. 2.516 IR spectrum of rankinite obtained by N.V. Chukanov

Sid31 Rankinite $Ca_3(Si_2O_7)$ (Fig. 2.516)
Locality: Hatrurim formation, Negev desert, southern Israel.
Description: Glassy colourless grains from the association with other Ca silicates. Identified by the powder X-ray diffraction pattern. Confirmed by the IR spectrum.
Kind of sample preparation and/or method of registration of the spectrum: KBr disc. Absorption.
Wavenumbers (cm^{-1}): 1000sh, 985s, 960s, 952s, 908, 848, 656, 561, 537, 474, 421.

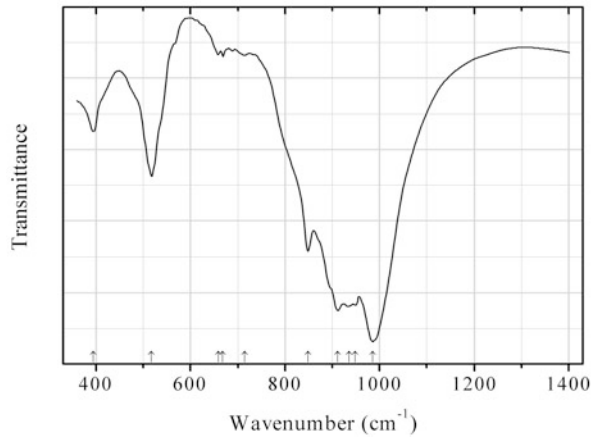

Fig. 2.517 IR spectrum of gehlenite obtained by N.V. Chukanov

Sid32 Gehlenite $Ca_2Al(SiAlO_7)$ (Fig. 2.517)
Locality: Kel'skoe plateau, South Osetia.
Description: Orange grains in calcic xenolith, in the association with hibschite. Al-deficient variety. The empirical formula is (electron microprobe): $(Ca_{1.95}Na_{0.03})(Al_{0.60}Mg_{0.25}Fe_{0.17})(Si_{1.36}Al_{0.64}O_7)$.

Kind of sample preparation and/or method of registration of the spectrum: KBr disc. Absorption.
Wavenumbers (cm^{-1}): 986s, 949s, 935s, 911s, 848s, 715w, 668w, 659w, 517, 394.

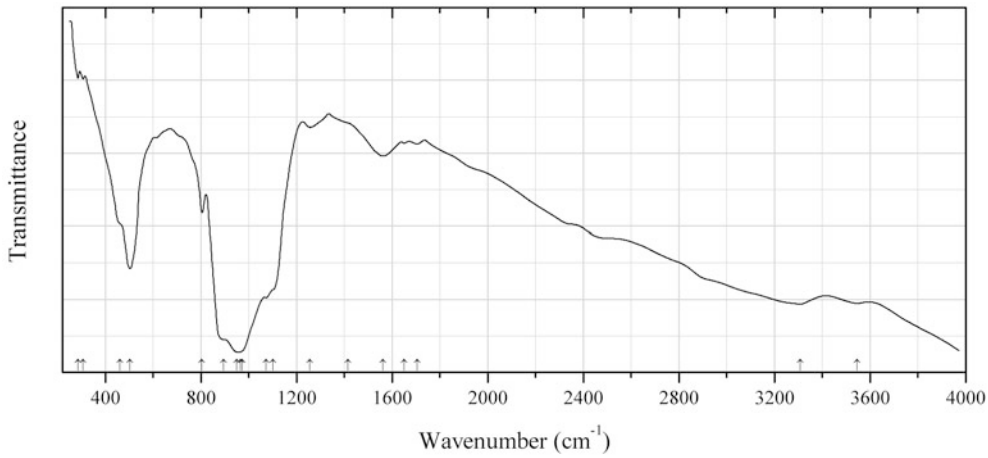

Fig. 2.518 IR spectrum of edgarbaileyite drawn using data from Roberts et al. (1990a)

Sid33 Edgarbaileyite $Hg^{+}_{6}(Si_2O_7)$ (Fig. 2.518)
Locality: Socrates mine, Sonoma County, Califomia, USA (type locality).
Description: Yellow thin crusts on fracture surfaces from the association with chalcedonic quartz, native mercury, cinirabar, and montroydite. Holotype sample. Monoclinic, space group *C*2/*m*, $a = 11.725(4)$, $b = 7.698(2)$, $c = 5.967(2)$ Å, $\beta = 112.07(3)°$, $\gamma = 115.58(5)°$, $V = 499.2(2)$ $Å^3$, $Z = 2$. $D_{meas} = 9.4(3)$ g/cm^3, $D_{calc} = 9.11$ g/cm^3. Optically biaxial. Maximum and minimum refractive indices calculated from reflectance data (at 590 nm) are 2.58 and 2.10. The empirical formula is $Hg_{6.00}Si_{2.00}O_7$. The strongest lines of the powder X-ray diffraction pattern [*d*, Å (*I*, %) (*hkl*)] are: 6.28 (20) (110), 3.160 (100) (021), 3.027 (27) (−221), 2.952 (34) (−202), 2.765 (20) (002), 2.715 (63) (400), 2.321 (24) (−421), 1.872 (36) (−602).
Kind of sample preparation and/or method of registration of the spectrum: Transmission. Kind of sample preparation is not indicated.
Source: Roberts et al. (1990a).
Wavenumbers (cm^{-1}): 3545, 3307, 1704w, 1651w, 1560, 1414sh, 1256w, 1101sh, 1072s, 974sh, 964s, 950sh, 895sh, 804, 503, 461sh, 307w, 285w.
Note: The wavenumbers were determined by us based on spectral curve analysis of the published spectrum.

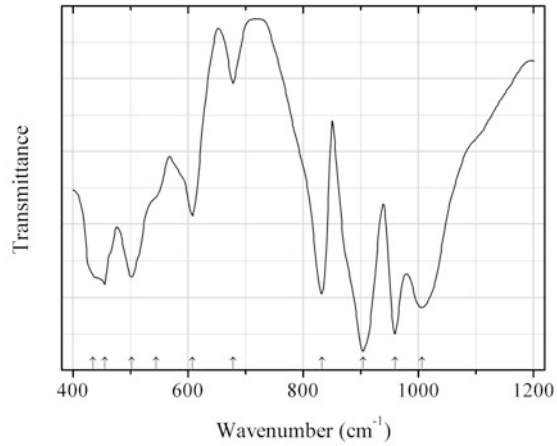

Fig. 2.519 IR spectrum of åkermanite Mn analogue drawn using data from Kimata (1986)

Sid34 Åkermanite Mn analogue $Ca_2Mn(Si_2O_7)$ (Fig. 2.519)
Locality: Synthetic.
Description: Synthesized from the melt. The empirical formula is (electron microprobe) $Ca_{2.34}Mn_{0.68}Si_{1.99}O_7$. The strongest lines of the powder X-ray diffraction pattern [*d*, Å (*I*, %)] are: 5.022 (20), 3.738 (29), 3.108 (61), 2.895 (100), 2.505 (30), 1.773 (34).
Kind of sample preparation and/or method of registration of the spectrum: KBr disc. Transmission.
Source: Kimata (1986).
Wavenumbers (cm^{-1}): 1007s, 960s, 904s, 833, 678w, 607, 544sh, 502, 455, 434sh.
Note: The band position denoted by Kimata (1986) as 696 cm^{-1} was determined by us at 678 cm^{-1} based on spectral curve analysis of the published spectrum.

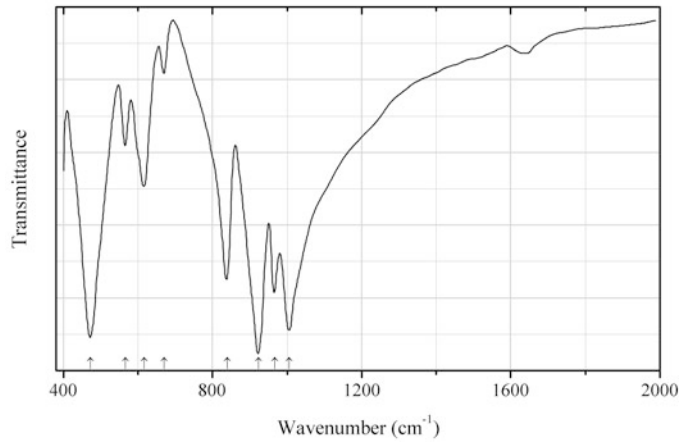

Fig. 2.520 IR spectrum of åkermanite Sr analogue drawn using data from Zhang and Wang (2012)

Sid35 Åkermanite Sr analogue $Sr_2Mg(Si_2O_7)$ (Fig. 2.520)
Locality: Synthetic.

Description: Synthesized by solid-state reaction. Confirmed by powder X-ray diffraction data.
Kind of sample preparation and/or method of registration of the spectrum: KBr disc. Transmission.
Source: Zhang and Wang (2012).
Wavenumbers (cm^{-1}): 1006s, 967, 924s, 839, 670w, 617, 566, 473s.

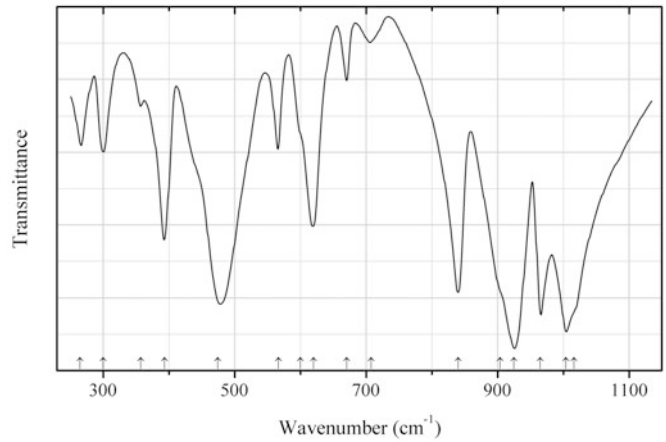

Fig. 2.521 IR spectrum of åkermanite Sr analogue drawn using data from Gabelica-Robert and Tarte (1979)

Sid36 Åkermanite Sr analogue $Sr_2Mg(Si_2O_7)$ (Fig. 2.521)
Locality: Synthetic.
Description: Synthesized by solid-state reaction.
Kind of sample preparation and/or method of registration of the spectrum: KBr disc. Transmission.
Source: Gabelica-Robert and Tarte (1979).
Wavenumbers (cm^{-1}): 1017sh, 1004s, 965s, 925s, 904sh, 840, 708w, 671, 620, 600sh, 567, 475s, 394, 358w, 300, 265.

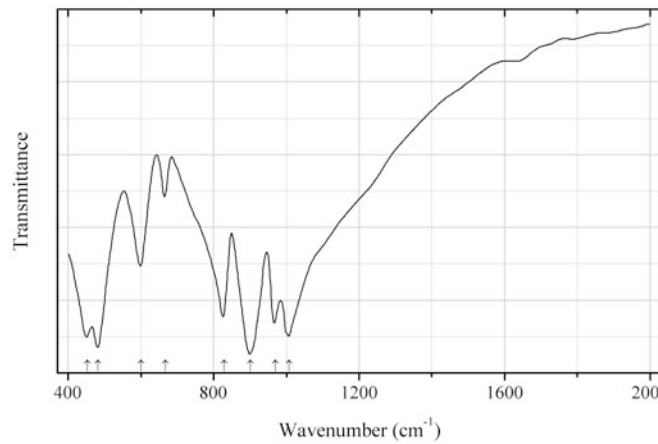

Fig. 2.522 IR spectrum of hardystonite Sr analogue drawn using data from Zhang and Wang (2012)

Sid37 Hardystonite Sr analogue $Sr_2Zn(Si_2O_7)$ (Fig. 2.522)
Locality: Synthetic.

Description: Prepared by solid state reaction between $SrCO_3$, ZnO, and H_2SiO_3. Isostructural with melilite-group minerals. Confirmed by powder X-ray diffraction data.
Kind of sample preparation and/or method of registration of the spectrum: KBr disc. Transmission.
Source: Zhang and Wang (2012).
Wavenumbers (cm^{-1}): 1007s, 969s, 901s, 828s, 667, 600, 482s, 452s.

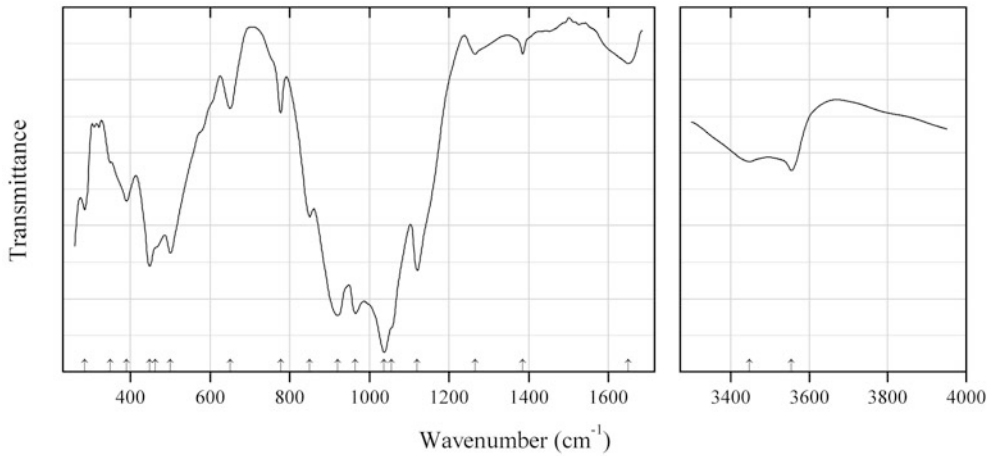

Fig. 2.523 IR spectrum of hennomartinite drawn using data from Armbruster et al. (1992)

Sid38 Hennomartinite $SrMn^{3+}{}_2(Si_2O_7)(OH)_2 \cdot 2H_2O$ (Fig. 2.523)
Locality: Wessels mine, Hotazel, Kalahari manganese fields, Northern Cape province, South Africa (type locality).
Description: Yellow-brown grains from the association with sugilite and marshallsussmanite. Holotype sample. Orthorhombic, space group *Cmcm*, $a = 6.255(1)$, $b = 9.034(2)$, $c = 13.397(2)$ Å, $Z = 4$. The empirical formula is (electron microprobe): $(Sr_{0.98}Ba_{0.01})(Mn_{2.01}Fe_{0.03})(Si_2O_7)(OH)_x \cdot nH_2O$.
Kind of sample preparation and/or method of registration of the spectrum: KBr disc. Transmission.
Source: Armbruster et al. (1992).
Wavenumbers (cm^{-1}): 3555, 3448, 1650w, 1385w, 1265w, 1120s, 1055sh, 1037s, 965s, 920s, 850, 777, 650, 500s, 463sh, 448s, 390, 349w, 285.
Note: The wavenumbers were partly determined by us based on spectral curve analysis of the published spectrum.

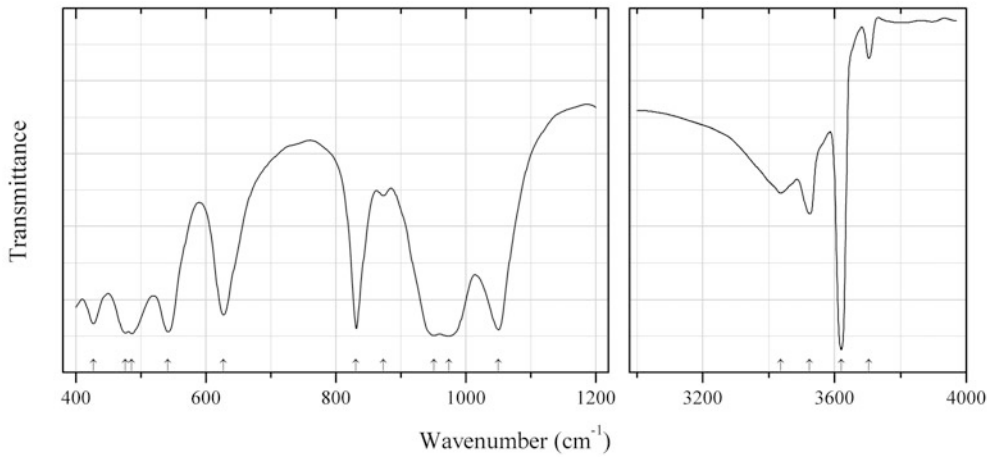

Fig. 2.524 IR spectrum of jaffeite drawn using data from Okada et al. (1994)

Sid39 Jaffeite $Ca_6Si_2O_7(OH)_6$ (Fig. 2.524)
Locality: Synthetic.
Description: Aggregate of microscopic prismatic crystals. Prepared in stirred suspension using lime and silicic acid with Ca/Si = 3.0 for 14 days at 270 °C under saturated steam pressure. Trigonal, space group *P*-3, a = 10.0291(8), c = 7.4842(11) Å. Confirmed by analytical transmission electron microscopy and powder X-ray diffraction data.
Kind of sample preparation and/or method of registration of the spectrum: KBr disc. Transmission.
Source: Okada et al. (1994).
Wavenumbers (cm^{-1}): 3704, 3620s, 3525, 3437, 1050s, 974s, 951s, 873w, 831s, 627, 542s, 486s, 476s, 427.
Note: The wavenumbers were partly determined by us based on spectral curve analysis of the published spectrum.

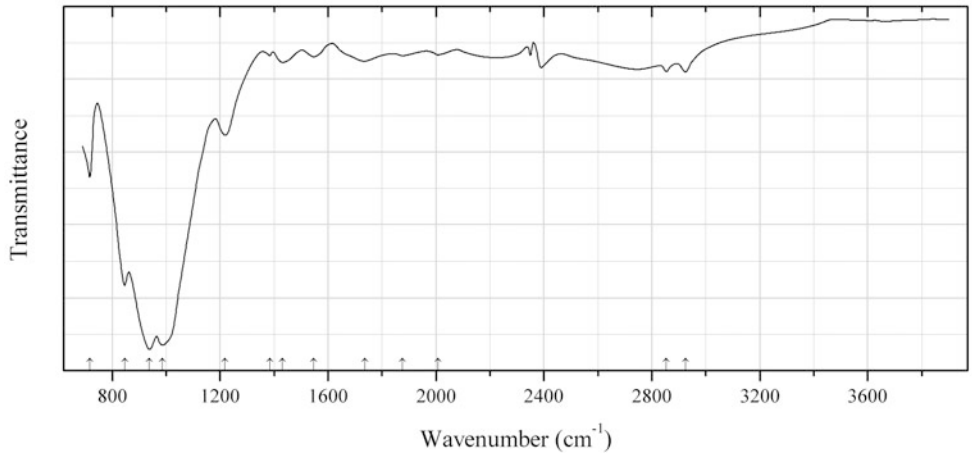

Fig. 2.525 IR spectrum of kristiansenite drawn using data from Raade et al. (2002)

Sid40 Kristiansenite $Ca_2ScSn(Si_2O_7)[Si_2O_6(OH)]$ (Fig. 2.525)

Locality: Heftetjern amazonite pegmatite, Tørdal, Telemark, Norway (type locality).
Description: Colourless crystals. Holotype sample. Triclinic (pseudo-monoclinic), space group *C*1, a = 10.028(1), b = 8.408(1), c = 13.339(2) Å, α = 90.01(1)°, β = 109.10(1)°, γ = 90.00(1)°, V = 1062.7(3) Å^3, Z = 4. D_{calc} = 3.64 g/cm^3. The mean refractive index is 1.74. The empirical formula is $(Ca_{0.96}Na_{0.04})(Sn_{0.53}Sc_{0.34}Fe_{0.07}Al_{0.02}Zn_{0.01})Si_{1.98}O_{6.34}(OH)_{0.66}$. The strongest lines of the powder X-ray diffraction pattern [*d*, Å (*I*, %) (*hkl*)] are: 5.18 (53) (1–11), 3.146 (100) (004), 3.089 (63) (−222), 2.901 (19) (221), 2.595 (34) (222), 2.142 (17) (−3–31).
Kind of sample preparation and/or method of registration of the spectrum: KBr disc. Transmission.
Source: Raade et al. (2002).
Wavenumbers (cm^{-1}): 2924w, 2854w, 2008w, 1875w, 1736w, 1547w, 1431w, 1384w, 1218, 986s, 938s, 846s, 717.
Note: The wavenumbers were partly determined by us based on spectral curve analysis of the published spectrum. The bands at 2924 and 2854 cm^{-1} correspond to the admixture of an organic substance. Other bands in the range from 1200 to 3000 cm^{-1} correspond to acid (silanol, Si–OH) groups.

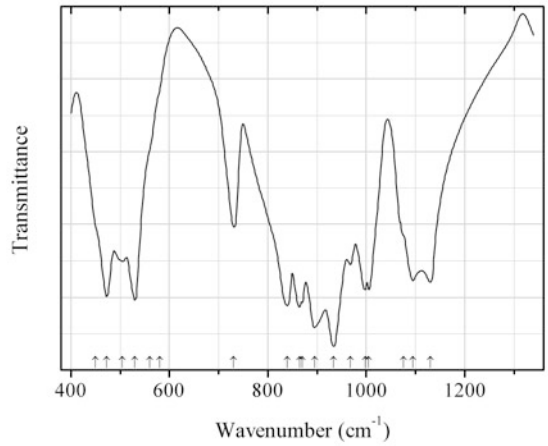

Fig. 2.526 IR spectrum of percleveite-(Ce) polymorph drawn using data from Andreev et al. (1971)

Sid42 Percleveite-(Ce) polymorph $Ce_2(Si_2O_7)$ (Fig. 2.526)
Locality: Synthetic.
Description: A monoclinic high-temperature polymorph synthesized from oxides at 1350 °C. D_{meas} = 5.00 g/cm^3.
Kind of sample preparation and/or method of registration of the spectrum: KBr disc. Transmission.
Source: Andreev et al. (1971).
Wavenumbers (cm^{-1}): 1130, 1095, 1076, 1005, 998, 968, 933s, 895s, 870sh, 865s, 840s, 730, 580sh, 560sh, 530s, 505, 473s, 450sh.

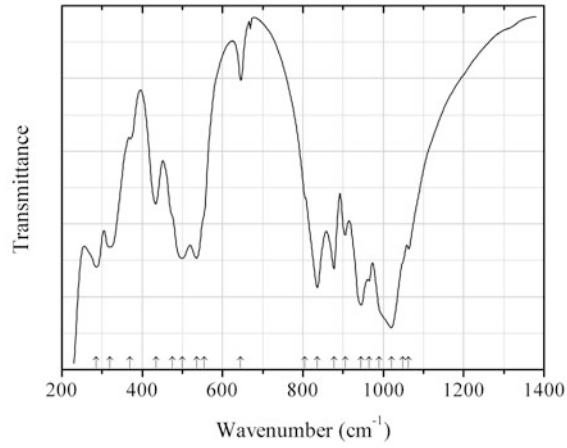

Fig. 2.527 IR spectrum of rusinovite drawn using data from Hermoneit et al. (1981)

Sid43 Rusinovite $Ca_{10}(Si_2O_7)_3Cl_2$ (Fig. 2.527)
Locality: Synthetic.
Description: Synthesized from the melt of the mixture of rankinite and $CaCl_2$ (in the ratio 2:3) by cooling to 1060 °C. Orthorhombic, a = 3.763(1), b = 34.70(1), c = 16.946(5) Å, V = 2213 Å^3. D_{meas} = 2.91 g/cm^3, D_{calc} = 2.93 g/cm^3. Confirmed by chemical analysis.
Kind of sample preparation and/or method of registration of the spectrum: KBr disc. Transmission.
Source: Hermoneit et al. (1981).
Wavenumbers (cm^{-1}): 1063, 1048sh, 1020s, 990sh, 965, 945s, 905.5, 877.5, 835.5s, 805sh, 645w, 555sh, 535, 500, 475sh, 434, 370w, 320, 285.

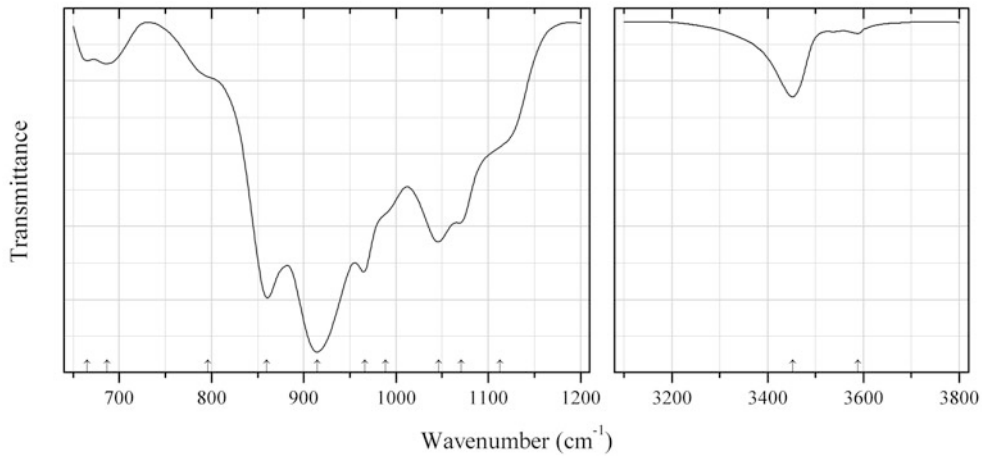

Fig. 2.528 IR spectrum of schlüterite-(Y) drawn using data from Cooper et al. (2013b)

Sid44 Schlüterite-(Y) $(Y,REE)_2Al(Si_2O_7)(OH)_2F$ (Fig. 2.528)
Locality: Stetind pegmatite, Tysfjord, Nordland, Norway (type locality).
Description: Pale pink dense, fibrous, radiating aggregates from the association with Y-rich fluorite. Holotype sample. Monoclinic, space group $P2_1/c$, a = 7.0722(2), b = 5.6198(1), c = 21.4390(4) Å,

β = 122.7756(3)°, V = 716.43(5) Å^3, Z = 4. D_{calc} = 4.644 g/cm^3. Optically biaxial (+), α = 1.755(5), β = 1.760(5), γ = 1.770(1), 2 V = 71.8(5)°. The empirical formula is (electron microprobe, OH calculated): $(Y_{0.73}Ce_{0.32}Nd_{0.30}Gd_{0.14}Dy_{0.12}La_{0.11}Sm_{0.11}Pr_{0.07}Er_{0.06}Yb_{0.05})Al_{0.99}Si_{2.01}O_7(OH)_{2.24}F_{0.76}$. The strongest lines of the powder X-ray diffraction pattern [d, Å (I, %) (hkl)] are: 4.769 (100) (012), 4.507 (36) (004), 3.289 (51) (112), 3.013 (37) (−116), 2.972 (55) (−214), 2.810 (37) (020), 2.728 (49) (−216).
Kind of sample preparation and/or method of registration of the spectrum: An IR microscope and a diamond-anvil cell were used.
Source: Cooper et al. (2013b).
Wavenumbers (cm^{-1}): 3588w, 3453, 1071, 1113sh, 1046, 989sh, 966s, 915s, 860s, 796sh, 687, 665.
Note: The wavenumbers were partly determined by us based on spectral curve analysis of the published spectrum.

Sid45 Kentrolite $Pb_2Mn^{3+}{}_2O_2(Si_2O_7)$
Locality: Långban deposit, Bergslagen ore region, Filipstad district, Värmland, Sweden (type locality).
Kind of sample preparation and/or method of registration of the spectrum: KBr disc. Absorption.
Source: Moenke (1962).
Wavenumbers (cm^{-1}): 995s, 932s, 894s, 836s, 790sh, 695, 605, 525, 505, 450, 418.

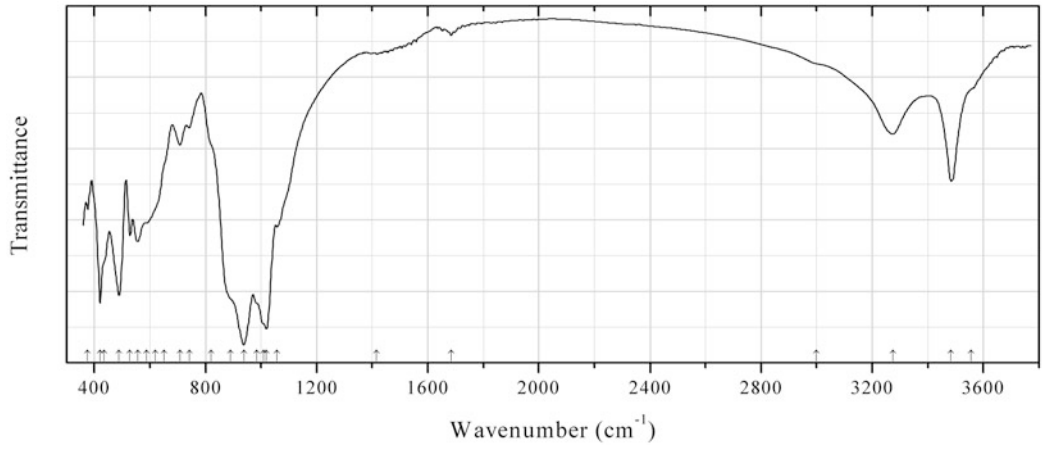

Fig. 2.529 IR spectrum of itoigawaite obtained by N.V. Chukanov

Sid46 Itoigawaite $SrAl_2Si_2O_7(OH)_2 \cdot H_2O$ (Fig. 2.529)
Locality: Oyashirazu, 15 km WSW of Itoigawa Station, Itoigawa Ohmi district, Japan (type locality).
Description: Light blue granular aggregate from jedeitite, from the association with thomsonite-Sr. The empirical formula is (electron microprobe): $(Sr_{0.98}Ca_{0.02})Al_{1.90}Si_{2.06}P_{0.02}Fe_{0.01}Mg_{0.01}(O,OH)_9 \cdot H_2O$.
Kind of sample preparation and/or method of registration of the spectrum: KBr disc. Absorption.
Wavenumbers (cm^{-1}): 3555sh, 3484, 3274, 3000sh, 1684w, 1415w, 1057, 1019s, 1010sh, 985sh, 938s, 890sh, 820sh, 742w, 708, 650sh, 620sh, 587, 556, 528, 489s, 435sh, 421s, 375.

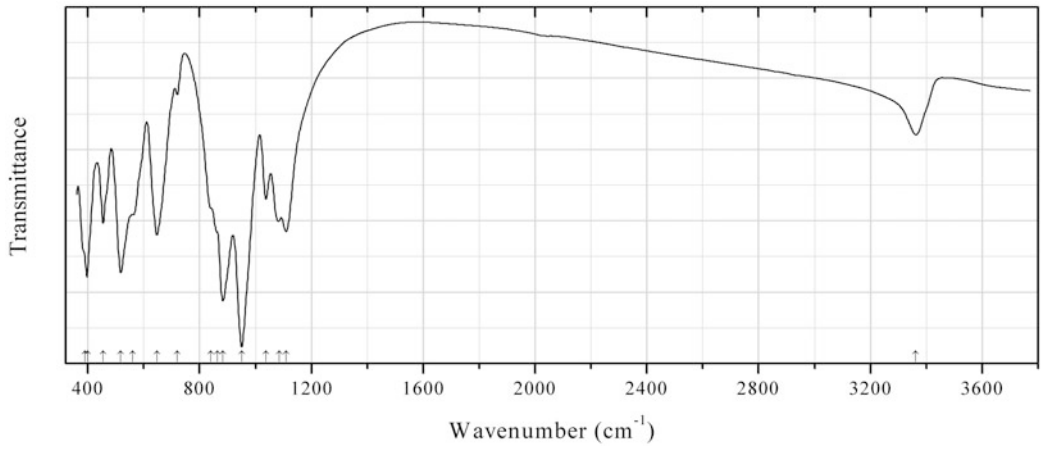

Fig. 2.530 IR spectrum of epidote obtained by N.V. Chukanov

Siod53 Epidote $Ca_2(Al_2Fe^{3+})(Si_2O_7)(SiO_4)O(OH)$ (Fig. 2.530)
Locality: Iouriren (Iourirne) mine, Akka, Tefraout, Tiznit province, Morocco.
Description: Brownish-red grains. The empirical formula is (electron microprobe): $Ca_{2.0}(Al_{2.1}Fe^{3+}_{0.8}Mn^{3+}_{0.1})Si_{3.00}O_{12}(OH)$. The strongest lines of the powder X-ray diffraction pattern [*d*, Å (*I*, %)] are: 4.02 (62), 3.494 (51), 2.905 (100), 2.823 (55), 2.602 (56), 2.406 (52).
Wavenumbers (cm^{-1}): 3363, 1109s, 1085, 1037, 950s, 883s, 865sh, 840sh, 720w, 647s, 560sh, 518s, 454, 399s, 390sh.

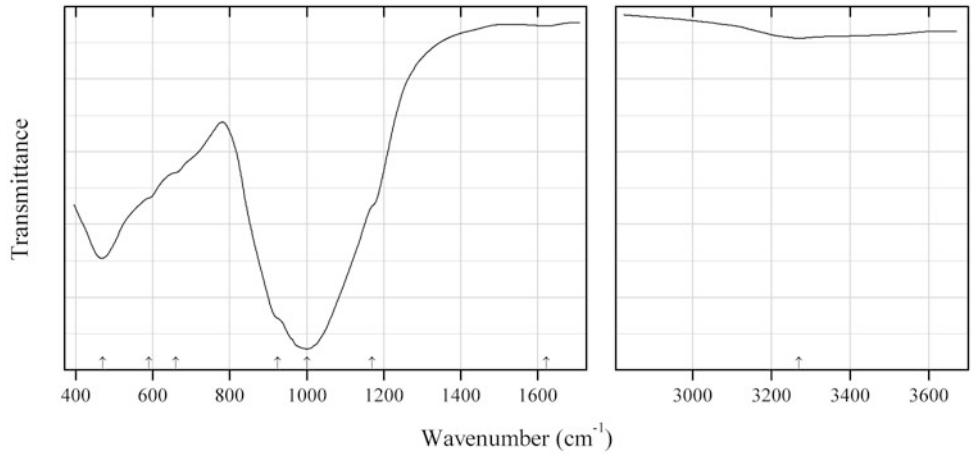

Fig. 2.531 IR spectrum of åskagenite-(Nd) drawn using data from Chukanov et al. (2010)

Siod54 Åskagenite-(Nd) $Mn^{2+}NdAl_2Fe^{3+}(Si_2O_7)(SiO_4)O_2$ (Fig. 2.531)
Locality: Åskagen deposit, near the town of Filipstad, Värmland, Sweden (type locality).
Description: Coarse prismatic crystal from the association with potassic feldspar, quartz, bastnäsite, thorite, allanite-(Nd), brookite, gadolinite-(Y), and allophane. Holotype sample. The empirical formula is $(Mn^{2+}_{0.69}Fe^{2+}_{0.26}Ca_{0.03})(Nd_{0.41}Ce_{0.30}Y_{0.12}Sm_{0.10}Pr_{0.07}La_{0.02}Yb_{0.01}Th_{0.02})(Al_{0.90}Fe^{3+}_{0.10})Al_{1.00}(Fe^{3+}_{0.60}Fe^{2+}_{0.40})Si_{2.99}O_{11}O[O_{0.63}(OH)_{0.37}]$. Amorphous, metamict. D_{meas} = 3.737(5) g/cm^3. Optically isotropic, n = 1.712(2).

Kind of sample preparation and/or method of registration of the spectrum: KBr disc. Absorption.
Source: Chukanov et al. (2010).
Wavenumbers (cm^{-1}): 3270w, 1623w, 1170sh, 1000s, 925sh, 660sh, 590sh, 469s.

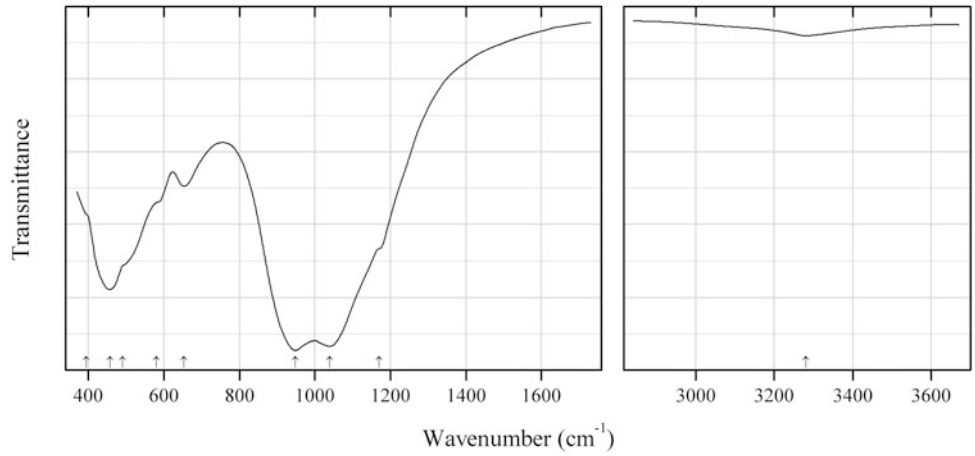

Fig. 2.532 IR spectrum of åskagenite-(Nd) drawn using data from Chukanov et al. (2010)

Siod55 Åskagenite-(Nd) $Mn^{2+}NdAl_2Fe^{3+}(Si_2O_7)(SiO_4)O_2$ (Fig. 2.532)
Locality: Åskagen deposit, near the town of Filipstad, Värmland, Sweden (type locality).
Description: Coarse prismatic crystal from the association with potassic feldspar, quartz, bastnäsite, thorite, allanite-(Nd), brookite, gadolinite-(Y), and allophane. Holotype sample heated at 600 °C during 1 h in nitrogen. Monoclinic, space group $P2_1/m$, a = 8.78(1) Å, b = 5.710(6) Å, c = 10.02(1) Å, β = 114.6(2)°; V = 456.7(8) $Å^3$, Z = 2. D_{calc} = 4.375 g/cm^3. The strongest lines of the powder X-ray diffraction pattern [d, Å (I, %) (hkl)] are: 3.50(46) (211), 3.22 (50) (−212, 201), 2.897 (100) (−301), 2.850(73) (020), 2.687(73) (120), 2.121(48) (−403), 1.630(59) (124).
Kind of sample preparation and/or method of registration of the spectrum: KBr disc. Absorption.
Source: Chukanov et al. (2010).
Wavenumbers (cm^{-1}): 3280w, 1170sh, 1040s, 948s, 654, 580sh, 490sh, 457s, 395sh.

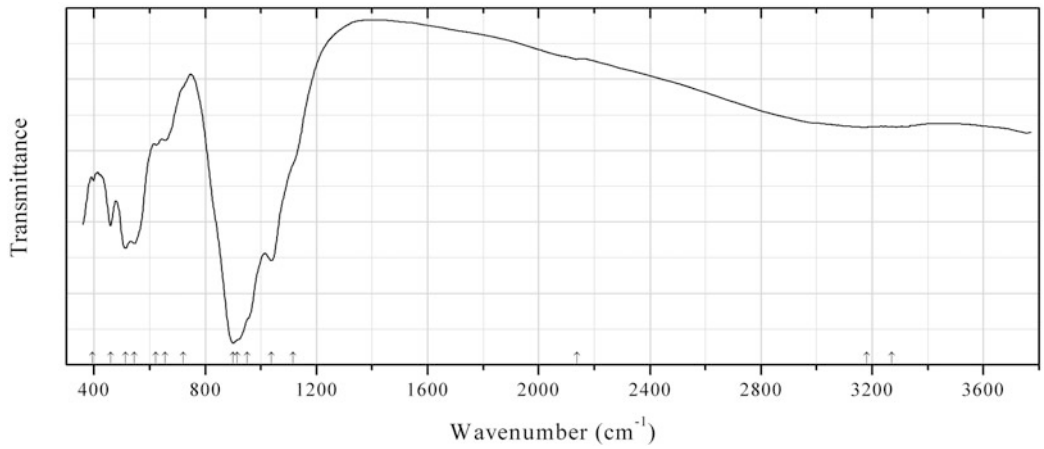

Fig. 2.533 IR spectrum of perbøeite-(Ce) obtained by N.V. Chukanov

Siod56 Perbøeite-(Ce) $CaCe_3(Al_3Fe^{2+})(Si_2O_7)(SiO_4)_3O(OH)_2$ (Fig. 2.533)
Locality: Stetind, Tysfjord, Nordland, Norway (type locality).
Description: Greenish-gray grains.
Kind of sample preparation and/or method of registration of the spectrum: KBr disc. Absorption.
Wavenumbers (cm^{-1}): 3270 (broad), 3180 (broad), 2138w, 1115sh, 1038s, 950sh, 915sh, 900s, 720sh, 655, 623, 545s, 512s, 459, 395.

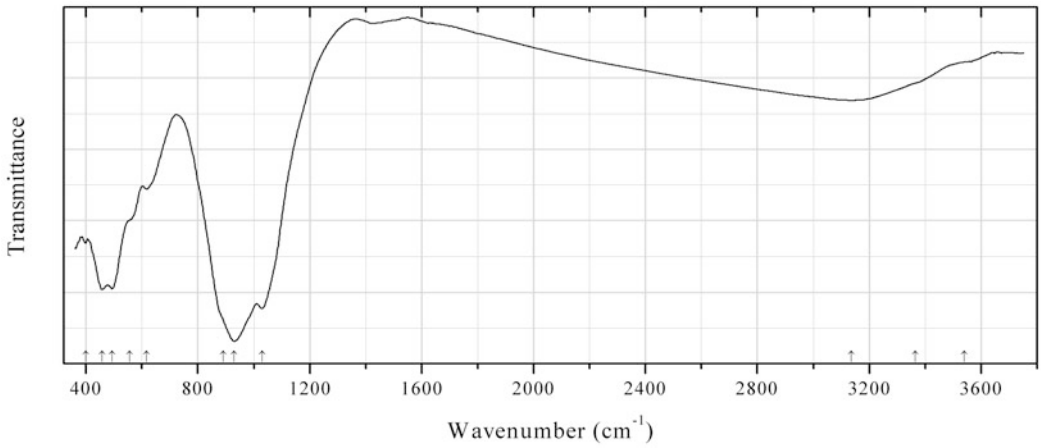

Fig. 2.534 IR spectrum of ferriallanite-(Ce) obtained by N.V. Chukanov

Siod57 Ferriallanite-(Ce) $CaCe(Fe^{3+}AlFe^{2+})(Si_2O_7)(SiO_4)O(OH)$ (Fig. 2.534)
Locality: Håkonhals quarry, Finnøy, Hamarøy, Nordland, Norway.
Description: Black grains from the association with allanite-(Ce), quartz, and feldspar. The empirical formula is (electron microprobe): $(Ca_{0.91}Mn_{0.09})[(Ce_{0.43}La_{0.25}Nd_{0.11}Pr_{0.07}\ldots)Ca_{0.08}](Fe_{1.51}Al_{1.41}Mg_{0.08})Si_3O_{12}(OH,O)$.
Kind of sample preparation and/or method of registration of the spectrum: KBr disc. Absorption.
Wavenumbers (cm^{-1}): 3540sh, 3365sh, 3136, 1029s, 930s, 890sh, 615, 555sh, 493s, 457s, 400.

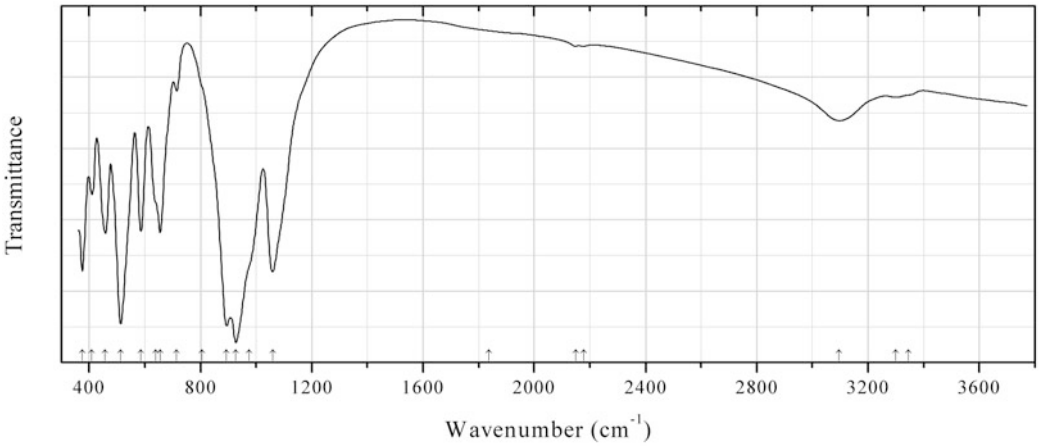

Fig. 2.535 IR spectrum of dissakisite-(Ce) obtained by N.V. Chukanov

Siod58 Dissakisite-(Ce) $CaCe(Al_2Mg)(Si_2O_7)(SiO_4)O(OH)$ (Fig. 2.535)
Locality: Trimouns talc mine, Luzenac, Ariège, Midi-Pyrénées, France.
Description: Light brown transparent crystal from the association with talc. The empirical formula is $Ca_{1.00}(Ce_{0.46}La_{0.20}Nd_{0.20}Pr_{0.09}Ca_{0.08})(Mg_{0.59}Fe_{0.35}Zn_{0.01}Al_{2.03})Si_{3.04}O_{12}(OH)$.
Kind of sample preparation and/or method of registration of the spectrum: KBr disc. Absorption.
Wavenumbers (cm^{-1}): 3345w, 3300w, 3096, 2179w, 2149w, 1837w, 1059s, 975sh, 927s, 894s, 805sh, 715w, 655, 640sh, 586, 513s, 458, 410, 376s.

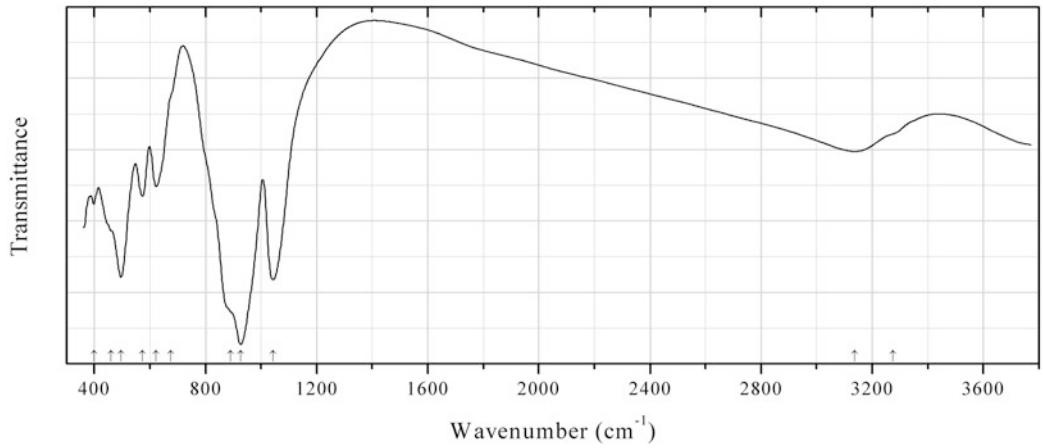

Fig. 2.536 IR spectrum of ferriallanite-(La) obtained by N.V. Chukanov

Siod59 Ferriallanite-(La) $CaLa(Fe^{3+}AlFe^{2+})(Si_2O_7)(SiO_4)O(OH)$ (Fig. 2.536)
Locality: In the Dellen (Zieglowski) pumice quarry, 1.5 km NE of Mendig, Laacher See volcano, Eifel region, Rhineland-Palatinate, Germany (type locality).
Description: Black prismatic crystal from the association with sanidine, cancrinite, and magnetite. The empirical formula is (electron microprobe): $Ca_{1.02}(La_{0.49}Ce_{0.39}Nd_{0.05}Pr_{0.03})[(Fe_{0.63}Al_{0.30}Ti_{0.07})Al(Fe_{0.68}Mn_{0.28}Mg_{0.04})](Si_{2.99}Al_{0.01})O_{12}(OH,O)$.
Kind of sample preparation and/or method of registration of the spectrum: KBr disc. Absorption.
Wavenumbers (cm^{-1}): 3275sh, 3137, 1044s, 927s, 890sh, 675sh, 622, 574, 496s, 460sh, 400.

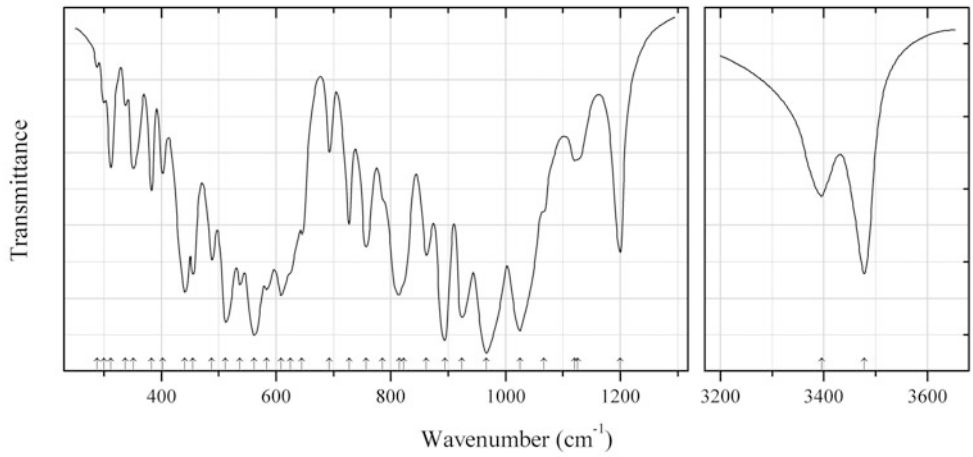

Fig. 2.537 IR spectrum of davreuxite drawn using data from Fransolet et al. (1984)

Siod60 Davreuxite $Mn^{2+}Al_6Si_4O_{17}(OH)_2$ (Fig. 2.537)
Locality: Ottré, Stavelot massif, Province of Liége, Belgium (type locality).
Description: Cream-coloured fibrous aggregates from the association with quartz, pyrophyllite, kaolinite, andalusite, ottrelite-chloritoid, sudoite, hematite, pyrophyllite, and chlorite. Monoclinic, space group $P2_1/m$, a = 9.550(2), b = 5.767(1), c = 12.077(2) Å, β = 108.02(2)°. D_{meas} = 3.30–3.38 g/cm^3, D_{calc} = 3.34 g/cm^3. Optically biaxial (−), α = 1.660(5), β = 1.684(2), γ = 1.690(2), 2 V = 48(5)°. The empirical formula is $(Mn_{0.82}Mg_{0.07}Cu_{0.06}Zn_{0.04})(Al_{5.86}Fe^{3+}_{0.09})(Si_{4.01}P_{0.03})O_{17}(OH)_2$. The strongest lines of the powder X-ray diffraction pattern [d, Å (I, %) (hkl)] are: 8.51 (30) (10–1), 5.719 (35) (10–2), 4.290 (40) (102), 3.822 (30) (003), 3.511 (100) (20–3), 3.179 (30) (30–1), 3.103 (45) (30–2), 2.870 (60) (004), 2.840 (35) (30–3), 2.130 (30) (40–4).
Kind of sample preparation and/or method of registration of the spectrum: KBr disc. Transmission.
Source: Fransolet et al. (1984).
Wavenumbers (cm^{-1}): 3478, 3396, 1200, 1126sh, 1120, 1067sh, 1025s, 967s, 924s, 894s, 862, 822sh, 815, 785sh, 757, 727, 693, 645, 625sh, 609, 583, 562s, 537, 512s, 488, 455, 441, 402, 383, 351, 337w, 312, 300w, 288w.
Note: The wavenumbers were partly determined by us based on spectral curve analysis of the published spectrum.

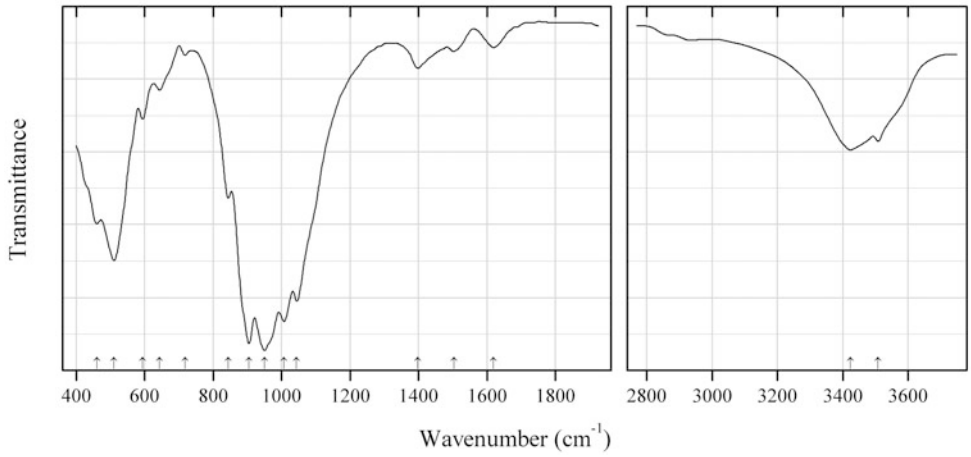

Fig. 2.538 IR spectrum of dellaite drawn using data from Zarayskiy et al. (1986)

Siod61 Dellaite $Ca_6(Si_2O_7)(SiO_4)(OH)_2$ (Fig. 2.538)
Locality: Synthetic.
Description: Aggregate of tabular and platy crystals formed (along with rustumite, spurrite, pectolite and monticellite) at the contacts of quartz with CaO + MgO in 1.0 M NaCl at 600 °C. Optically biaxial (−), α = 1.650(2), γ = 1.664(2), 2 V = 30°.
Kind of sample preparation and/or method of registration of the spectrum: Transmission. Kind of sample preparation is not indicated.
Source: Zarayskiy et al. (1986).
Wavenumbers (cm^{-1}): 3509, 3424, 1619w, 1503w, 1398w, 1044, 1007s, 950s, 904s, 844, 718w, 643w, 594, 510, 460.
Note: The wavenumbers were determined by us based on spectral curve analysis of the published spectrum.

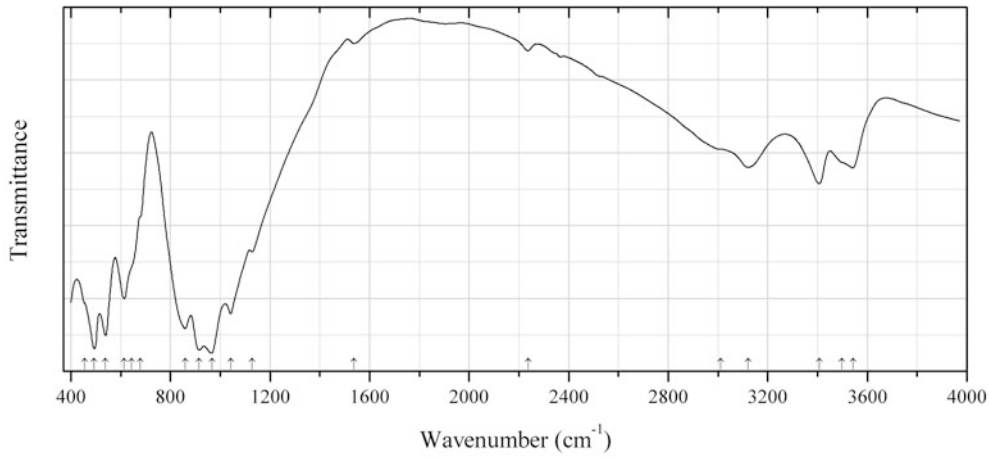

Fig. 2.539 IR spectrum of pumpellyite-(Al) drawn using data from Hatert et al. (2007)

Siod62 Pumpellyite-(Al) $Ca_2Al_3(Si_2O_7)(SiO_4)(OH)O{\cdot}H_2O$ (Fig. 2.539)
Locality: Bertrix, Ardennes Mts., Belgium (type locality).
Description: Radiating fibrous aggregates from the association with calcite, K-feldspar, and chlorite. Holotype sample. Monoclinic, space group *A*2/*m*, a = 8.818(2), b = 5.898(2), c = 19.126(6) Å, β = 97.26(3)°, V = 986.7(4) Å^3. D_{calc} = 3.24 g/cm^3. Optically biaxial (+), α = 1.678(2), β = 1.680(2), γ = 1.691(2), 2 V = 46°. The empirical formula is $(Ca_{1.99}Na_{0.01})(Al_{0.42}Fe^{2+}_{0.33}Mg_{0.24}Mn_{0.01})Al_{2.00}(SiO_4)(Si_2O_7)H_{3.58}O_3$. The strongest lines of the powder X-ray diffraction pattern [*d*, Å (*I*, %) (*hkl*)] are: 4.371 (65) (200), 3.787 (80) (202), 3.040 (70) (204), 2.912 (95) (300), 2.895 (100) (30–2), 2.731 (40) (20–6), 2.630 (35) (31–1), 2.191 (45) (40–2).
Kind of sample preparation and/or method of registration of the spectrum: KBr disc. Transmission.
Source: Hatert et al. (2007).
Wavenumbers (cm^{-1}): 3542, 3499sh, 3407, 3121, 3010sh, 2237w, 1538w, 1129, 1042s, 967s, 916s, 859s, 680sh, 644sh, 614, 539s, 494s, 455sh.
Note: The wavenumbers were partly determined by us based on spectral curve analysis of the published spectrum.

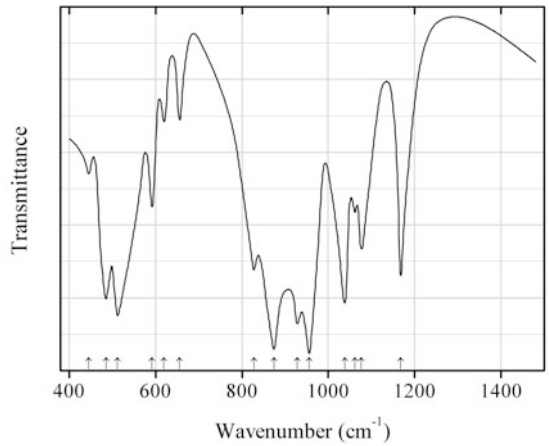

Fig. 2.540 IR spectrum of queitite drawn using data from Povarennykh et al. (1982)

Siod63 Queitite $Zn_2Pb_4(Si_2O_7)(SiO_4)(SO_4)$ (Fig. 2.540)
Locality: Tsumeb mine, Tsumeb, Namibia (type locality).
Description: Investigated by P. Keller. Confirmed by optical methods.
Kind of sample preparation and/or method of registration of the spectrum: KBr disc. Transmission.
Source: Povarennykh et al. (1982).
Wavenumbers (cm^{-1}): 1168, 1077, 1062w, 1038, 956s, 928, 874s, 828, 656w, 620w, 592, 512s, 486, 446.

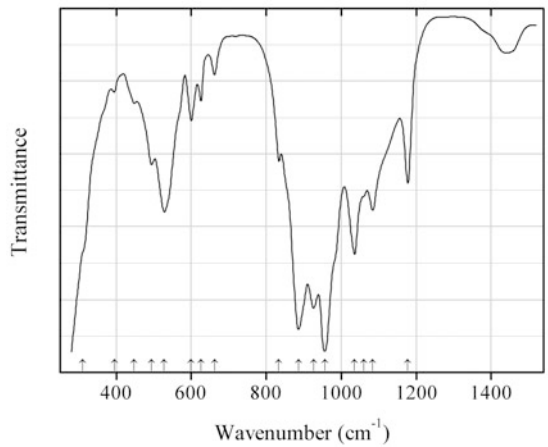

Fig. 2.541 IR spectrum of queitite drawn using data from Jackson (1990)

Siod64 Queitite $Zn_2Pb_4(Si_2O_7)(SiO_4)(SO_4)$ (Fig. 2.541)
Locality: Old mine dumps on Horner's Vein, Leadhills, Lanarkshire, UK.
Description: Dark greyish brown fibrous radiating aggregates from the association with quartz, galena, cerussite, susannite, mettheddleite, and pyromorphite. Identified by electron microprobe analysis and powder X-ray diffraction data.
Kind of sample preparation and/or method of registration of the spectrum: KBr disc. Transmission.
Source: Jackson (1990).
Wavenumbers (cm^{-1}): 1178, 1084, 1060, 1036sh, 956s, 926s, 886s, 834, 662, 626, 600, 528s, 494, 448, 395, 310sh.
Note: The absorption centered at 1442 cm^{-1} is attributed to a carbonate impurity.

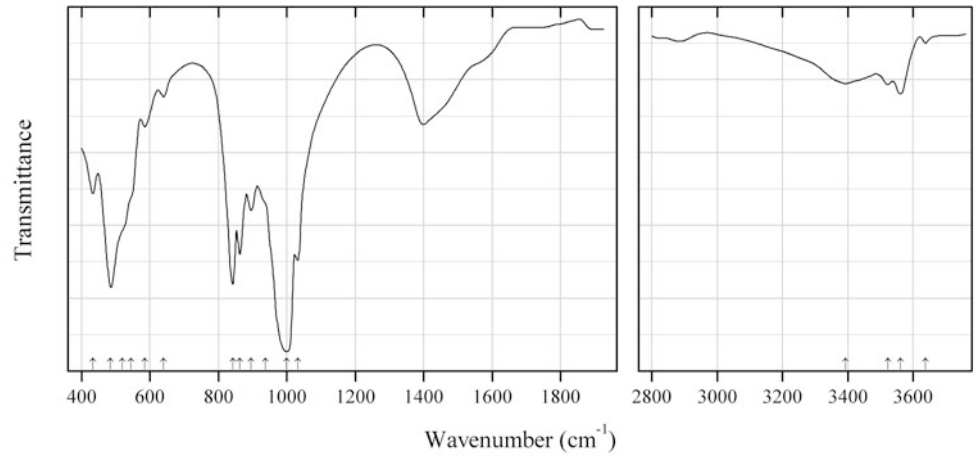

Fig. 2.542 IR spectrum of rustumite drawn using data from Zarayskiy et al. (1986)

Siod65 Rustumite $Ca_{10}(Si_2O_7)_2(SiO_4)(OH)_2Cl_2$ (Fig. 2.542)
Locality: Synthetic (type locality).
Description: Confirmed by electron microprobe analyses and powder X-ray diffraction data.
Kind of sample preparation and/or method of registration of the spectrum: Not indicated.
Source: Zarayskiy et al. (1986).
Wavenumbers (cm^{-1}): 3639w, 3561, 3523, 3393, 1032, 999s, 938sh, 896, 862, 842s, 639w, 585w, 545sh, 519sh, 485s, 433.
Note: The wavenumbers were determined by us based on spectral curve analysis of the published spectrum. The band in the range from 1300 to 1500 cm^{-1} corresponds to the admixture of a carbonate.

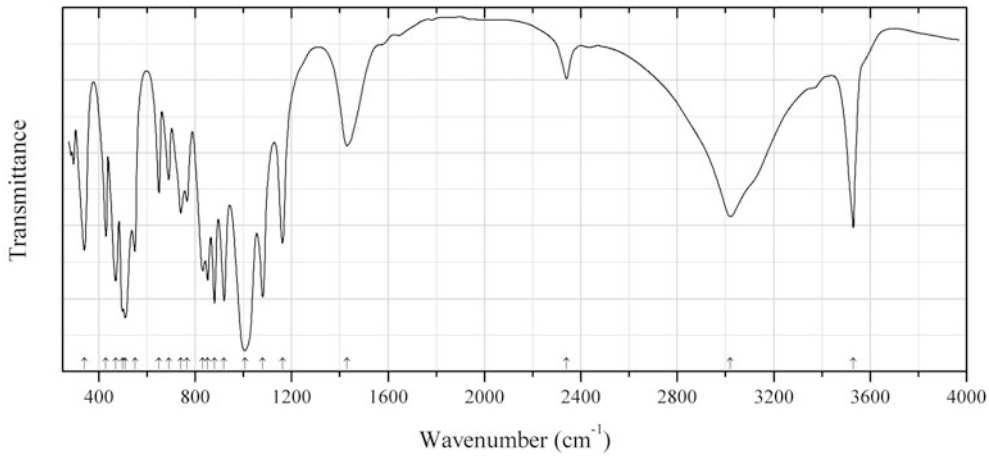

Fig. 2.543 IR spectrum of kinoite drawn using data from Kusachi et al. (2001)

Sit7 Kinoite $Ca_2Cu_2(Si_3O_{10})\cdot 2H_2O$ (Fig. 2.543)
Locality: Fuka mine, Bicchu-cho, near Takahashi city, Okayama prefecture, Honshu Island, Japan.

Description: Azure blue aggregates of flaky crystals from the association with stringhamite and calcite. Monoclinic, a = 6.989(1), b = 12.902(2), c = 5.659(1) Å, β = 96.15(2)°. D_{meas} = 3.14 g/cm^3. Optically biaxial (−), α = 1.642(2), β = 1.662(2), γ = 1.675(2). The empirical formula is: $(Ca_{2.00}Mg_{0.02})(Cu_{1.92}Fe_{0.04}Co_{0.04})Si_{2.98}O_{10}\cdot 2.25H_2O$. The strongest lines of the powder X-ray diffraction pattern [d, Å (I, %) (hkl)] are: 6.45 (38) (020), 4.73 (64) 120), 3.355 (34) (210), 3.149 (22) (−131), 3.059 (100) (220), 2.316 (45) (300).
Kind of sample preparation and/or method of registration of the spectrum: KBr disc. Transmission.
Source: Kusachi et al. (2001).
Wavenumbers (cm^{-1}): 3530, 3020, 2340w, 1430, 1162, 1080, 1006s, 920s, 880s, 852s, 832, 766, 740, 690, 650, 550, 510s, 498s, 470, 430, 340w.
Note: The band at 1430 cm^{-1} corresponds to the admixture of calcite.
Note: The wavenumbers were partly determined by us based on spectral curve analysis of the published spectrum. The band positions denoted by Kusachi et al. (2001) as 1220, 1060, and 320 cm^{-1} were determined by us at 1162, 1006, and 340 cm^{-1}, respectively.

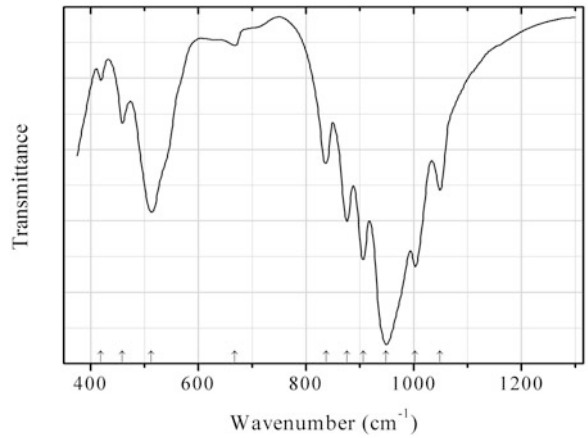

Fig. 2.544 IR spectrum of pavlovskyite obtained by N.V. Chukanov

Siot2 Pavlovskyite $Ca_8(SiO_4)_2(Si_3O_{10})$ (Fig. 2.544)
Locality: Birkhin (Ozernovskii) gabbro massif, Naryn-Kunta, Irkutsk region, eastern Siberia, Russia (type locality).
Description: Colourless grains forming rims (together with dellaite) around galuskinite veins cutting calcio-olivine skarn. Investigated by A.E. Zadov. Optically biaxial (−), α = 1.656(2), β = 1.658(2), γ = 1.660(2).
Kind of sample preparation and/or method of registration of the spectrum: KBr disc. Absorption.
Wavenumbers (cm^{-1}): 1049, 1003s, 949s, 906s, 876s, 837, 667w, 513s, 459, 419w.

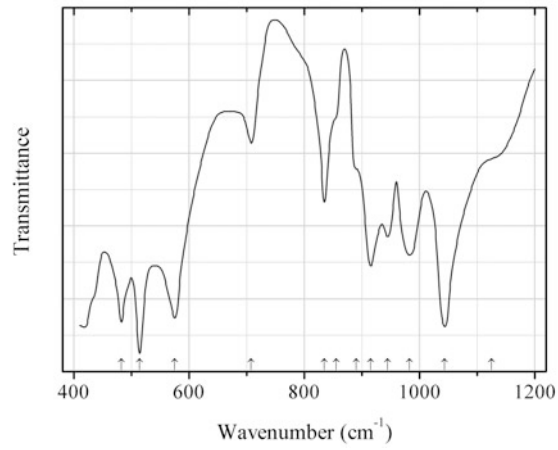

Fig. 2.545 IR spectrum of kilchoanite drawn using data from Kimata (1986)

Siot3 Kilchoanite $Ca_6(SiO_4)(Si_3O_{10})$ (Fig. 2.545)
Locality: Synthetic.
Description: Synthesized from a carbonate-silicate melt with the stoichiometry $CaCO_3$:MnO:SiO_2 = 2:1:2. Orthorhombic, a = 11.356(2), b = 5.007(1), c = 21.817(3) Å, V = 1240.4(3) $Å^3$. A Mn-rich variety. The empirical formula is (electron microprobe): $Ca_{2.32}Mn_{0.68}Si_{2.00}O_7$. The strongest lines of the powder X-ray diffraction pattern [d, Å (I, %) (hkl)] are: 3.508 (62) (114), 3.017 (100) (310), 2.849 (90) (116), 2.642 (69) (314), 2.398 (27) (217), 1.9387 (30) (226).
Kind of sample preparation and/or method of registration of the spectrum: KBr disc. Transmission.
Source: Kimata (1986).
Wavenumbers (cm^{-1}): 1125sh, 1044s, 983, 945, 915, 890sh, 855sh, 835, 708, 575s, 514s, 482s.

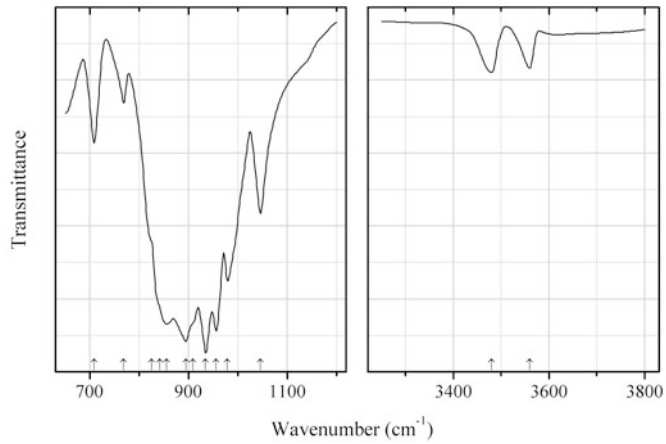

Fig. 2.546 IR spectrum of pavlovskyite drawn using data from Speakman et al. (1967)

Siot4 Pavlovskyite $Ca_8(SiO_4)_2(Si_3O_{10})$ (Fig. 2.546)
Locality: Synthetic.

Description: Imperfectly crystalline phase synthesized by a hydrothermal method. The strongest lines of the powder X-ray diffraction pattern are observed at 3.61, 3.05, 2.836, 2.691, 1.949, and 1.895 Å.
Kind of sample preparation and/or method of registration of the spectrum: KBr disc. Transmission.
Source: Speakman et al. (1967).
Wavenumbers (cm^{-1}): 3560w, 3480w, 1045, 978sh, 955s, 934s, 909sh, 894s, 855s, 841sh, 825sh, 768w, 708.
Note: The wavenumbers were partly determined by us based on spectral curve analysis of the published spectrum. The bands at 3560 and 3480 cm^{-1} correspond to an impurity (possibly, OH groups in admixed Ca-analogue of hydroxychondrodite).

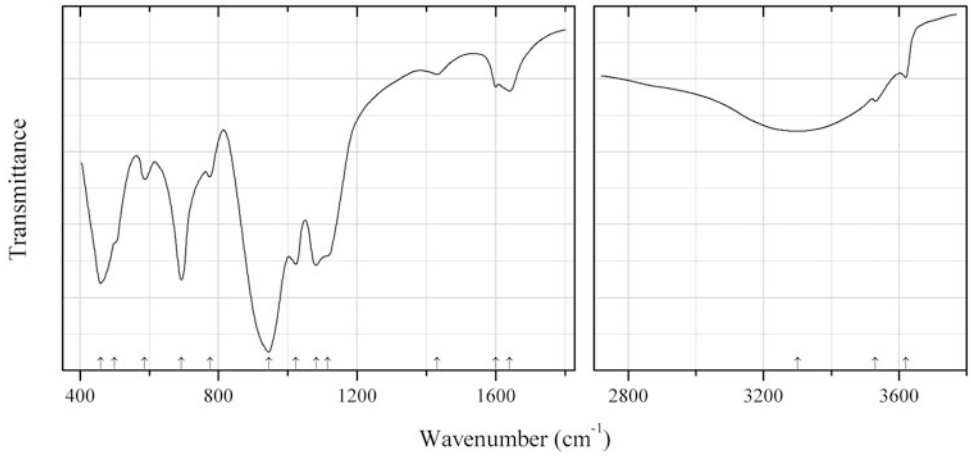

Fig. 2.547 IR spectrum of organovaite-Mn obtained by N.V. Chukanov

Sir180 Organovaite-Mn $K_2Mn(Nb,Ti)_4(Si_4O_{12})_2(O,OH)_4 \cdot 6H_2O$ (Fig. 2.547)
Locality: Pegmatite No. 61, Karnasurt Mt., Lovozero alkaline pluton, Kola peninsula, Murmansk region, Russia (type locality).
Description: Pinkish-brown crystal from the association with microcline, albite, aegirine, arfvedsonite, eudialyte, sodalite, natrolite, elpidite, cristobalite, steenstrupine-(Ce), rhabdophane-(Ce), rancieite, sauconite, and yofortierite. Holotype sample. The crystal structure is solved. Monoclinic, space group *C2/m*, $a = 14.551(2)$, $b = 14.001(2)$, $c = 15.702(3)$ Å, $\beta = 117.584(2)°$, V = 2835.3 Å ^{3}. $D_{meas} = 2.88(1)$ g/cm^3, $D_{calc} = 2.92$ g/cm^3. Optically biaxial (+), $\alpha = 1.683(2)$, $\beta = 1.692(3)$, $\gamma = 1.775(5)$. The empirical formula is $(K_{2.27}Zn_{0.62}Ca_{0.47}Na_{0.41}Ba_{0.21})(Mn^{2+}_{1.77}Fe^{2+}_{0.08})(Nb_{5.23}Ti_{2.76})(Si_{15.86}Al_{0.14}O_{48})[O_{6.03}(OH)_{1.97}] \cdot 12.79H_2O$. The strongest lines of the powder X-ray diffraction pattern [*d*, Å (*I*, %) (*hkl*)] are: 6.99 (100) (020, 002), 6.43 (25) (200, 20–2), 4.936 (28) (022), 3.227 (89) (42–2, 400, 40–4), 3.123 (68) (042, 024), 2.607 (25) (24–4, 204, 20–6), 2.520 (29) (44–2, 402, 40–4).
Kind of sample preparation and/or method of registration of the spectrum: KBr disc. Absorption.
Wavenumbers (cm^{-1}): 3620w, 3530, 3300, 1640, 1600, 1430w, 1115sh, 1082s, 1023s, 945s, 775, 693s, 587, 500sh, 460s.

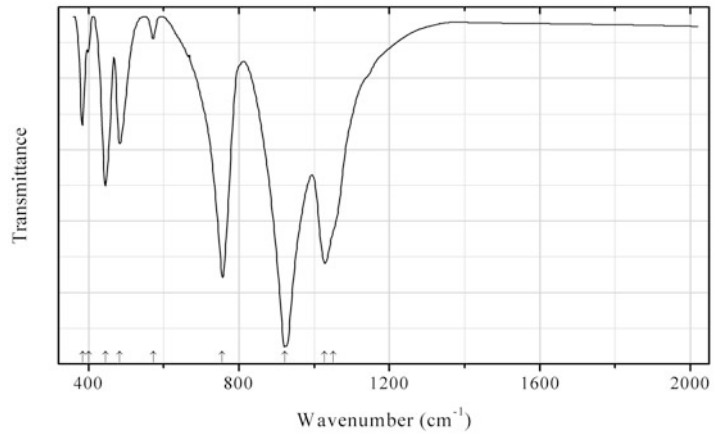

Fig. 2.548 IR spectrum of benitoite obtained by N.V. Chukanov

Sir181 Benitoite $BaTi(Si_3O_9)$ (Fig. 2.548)
Locality: California State Gem mine, San Benito Co., California, USA (type locality).
Description: Blue triangular dipyramidal crystal from the association with neptunite and joaquinite-(Ce). Confirmed by IR spectrum.
Kind of sample preparation and/or method of registration of the spectrum: KBr disc. Absorption.
Wavenumbers (cm^{-1}): 1050sh, 1028s, 921s, 756s, 572w, 483, 445, 400sh, 384.

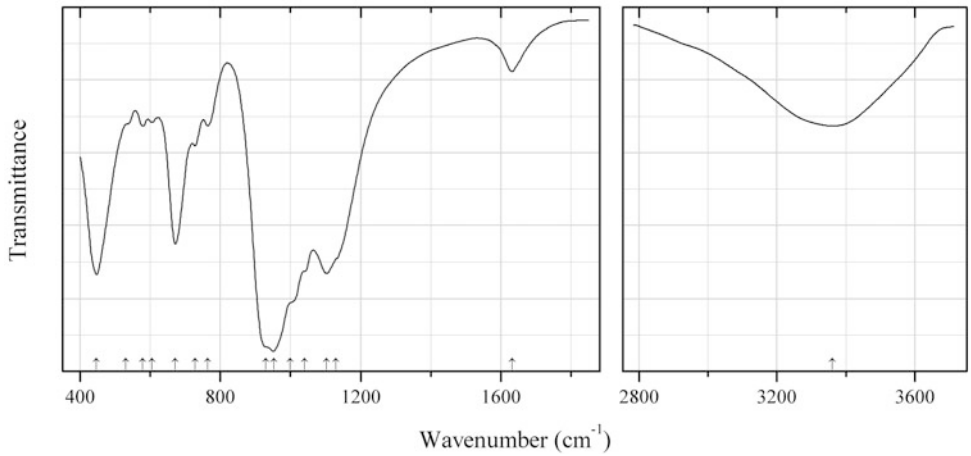

Fig. 2.549 IR spectrum of paratsepinite-Na obtained by N.V. Chukanov

Sir182 Paratsepinite-Na $(Na,Sr,Ca,K)_{2-x}(Ti,Nb)_2(Si_4O_{12})(O,OH)_2 \cdot 2H_2O$ (Fig. 2.549)
Locality: Khibinpakhkchorr Mt., Khibiny alkaline complex, Kola peninsula, Murmansk region, Russia (type locality).
Description: Colourless crystals (epitaxy on tsepinite-Na) from the association with microcline, aegirine, analcime, natrolite, catapleiite, apophyllite, labuntsovite-Mn, epididymite, fluorite, and sphalerite. Holotype sample. Monoclinic, space group $C2/m$, $a = 14.596$, $b = 14.249$, $c = 15.952$ Å, $\beta = 117.27°$, $V = 2948.9$ Å^3. Optically biaxial (+), $\alpha = 1.657(2)$, $\beta = 1.666(2)$, $\gamma = 1.765(2)$, $2V = 19°–31°$. The empirical formula is (electron microprobe): $(Na_{0.61}Sr_{0.51}Ca_{0.21}K_{0.15}Ba_{0.02})(Ti_{1.57}Nb_{0.43})$

$(Si_4O_{12})(O,OH)_2 \cdot nH_2O$. The strongest lines of the powder X-ray diffraction pattern [*d*, Å (*I*, %)] are: 7.09 (100), 3.24 (90), 3.15 (80), 3.11 (80), 2.54 (70), 2.491 (70).
Kind of sample preparation and/or method of registration of the spectrum: KBr disc. Absorption.
Wavenumbers (cm^{-1}): 3360, 1632, 1130sh, 1102s, 1040sh, 1000sh, 952s, 930sh, 764w, 728w, 671, 605w, 579w, 530sh, 447s.

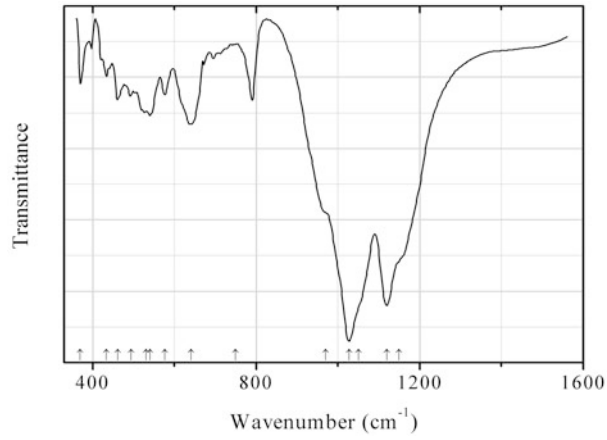

Fig. 2.550 IR spectrum of chayesite obtained by N.V. Chukanov

Sir183 Chayesite $KMg_2(Mg,Fe^{2+},Fe^{3+})_3(Si_{12}O_{30})$ (Fig. 2.550)
Locality: Bellerberg, Laacher See area, near Ettringen, Eifel Mts., Rhineland-Palatinate (Rheinland-Pfalz), Germany.
Description: Brown hexagonal zonal tabular crystal. A Fe-rich variety. The empirical formula is $K_{0.7}Mg_{2.6–3.8}Fe_{1.0–2.2}Mn_{0.2}(Si_{11.8–11.95}Al_{0.05–0.2})O_{30}$.
Kind of sample preparation and/or method of registration of the spectrum: KBr disc. Absorption.
Wavenumbers (cm^{-1}): 1150sh, 1119s, 1050sh, 1027s, 970sh, 750, 641, 576, 540, 530sh, 494, 461, 434w, 370.

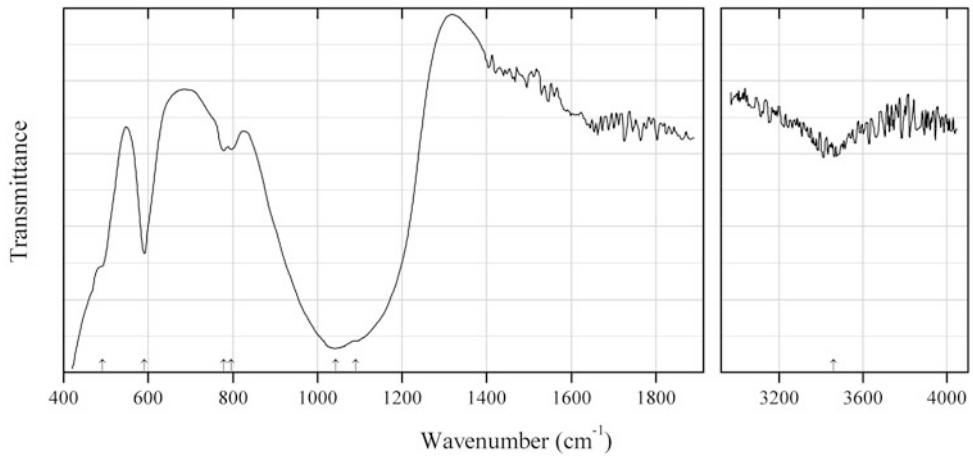

Fig. 2.551 IR spectrum of arapovite drawn using data from Agakhanov et al. (2004)

Sir185 Arapovite $U^{4+}(Ca,Na)_2K_{1-x}(Si_8O_{20})\cdot nH_2O$ (Fig. 2.551)
Locality: Dara-i Pioz glacier, Dara-i Pioz alkaline massif, Tien Shan Mts., Tajikistan (type locality).
Description: Dark-green, zones in turkestanite crystals from the association with albite, quartz, sogdianite, zektzerite, tadzhikite-(Ce), stillwellite-(Ce), and a pyrochlore-group mineral. Holotype sample. Partially metamict. The crystal structure is solved on annealed sample. Tetragonal, space group *P*4/*mcc*, a = 7.6506(4), c = 14.9318(9) Å, V = 873.9(1) Å^3, Z = 2. D_{meas} = 3.43(2) g/cm^3, D_{calc} = 3.414 g/cm^3. Optically uniaxial (−), ω = 1.615(2), ε = 1.610(2). The empirical formula is: $(U_{0.55}Th_{0.36}Pb_{0.03}Ce_{0.03}Nd_{0.03}La_{0.01}Sm_{0.01}Eu_{0.01}Dy_{0.01})(Ca_{1.29}Na_{0.73})K_{0.85}Si_8O_{20.06}\cdot 0.89H_2O$. The strongest lines of the powder X-ray diffraction pattern [*d*, Å (*I*, %) (*hkl*)] are: 7.57 (14) (010), 7.39 (12) (002), 5.34 (23) (100), 5.28 (38) (012), 3.37 (100) (120), 3.31 (58) (014), 2.640 (64) (024), 2.161 (45) (224).
Kind of sample preparation and/or method of registration of the spectrum: KBr disc. Absorption.
Source: Agakhanov et al. (2004).
Wavenumbers (cm^{-1}): 3460, 1091sh, 1043s, 797, 778, 590s, 491sh.
Notes: The bands at 797 and 778 cm^{-1} are non-typical for iraquite-group minerals and presumably are due to the admixture of quartz. Water is present as a result of metamictization.

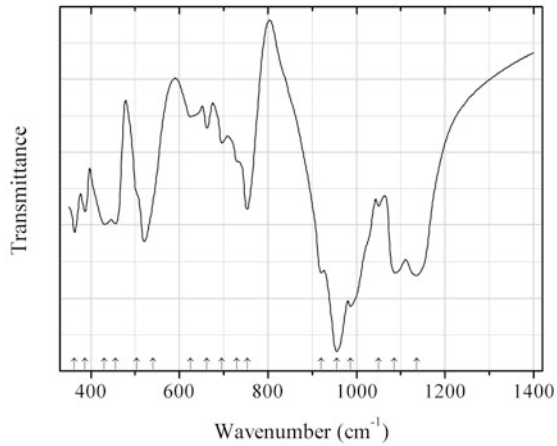

Fig. 2.552 IR spectrum of armenite drawn using data from Pouliot et al. (1984)

Sir186 Armenite $BaCa_2Al_6Si_9O_{30}\cdot 2H_2O$ (Fig. 2.552)
Locality: Rémigny, 75 km S of Rouyn-Noranda, NW Quebec, Canada.
Description: Sheaf-like aggregates of colourless prismatic crystals from the association with albite, manganiferous zoisite, and piedmontite. Hexagonal, space group *P*6*cc* or *P*6/*mcc* a = 10.732(7), c = 18.886(18) Å. D_{meas} = 2.737(12) g/cm^3, D_{calc} = 2.741 g/cm^3. For optically uniaxial (−) parts, ω = 1.556, ε = 1.550; for optically biaxial parts, α = 1.5505, β = 1.557, γ = 1.559, 2 V = 65°. The empirical formula is $(Ba_{0.89}Na_{0.10}K_{0.04})(Ca_{1.92}Sr_{0.07}Na_{0.03})Al_{3.03}(Al_3Si_9O_{30})\cdot 2[(H_2O)_{0.91}(CO_2)_{0.04}]$. The strongest lines of the powder X-ray diffraction pattern [*d*, Å (*I*, %) (*hkl*)] are: 9.29 (35) (100), 6.94 (47) (002), 4.24 (73) (112), 3.86 (98) (202), 3.40 (100) (211), 3.09 (48) (300), 2.91 (74) (114), 2.78 (71) (204), 2.68 (41) (220), 2.029 (37) (410), 1.751 (45) (226).
Kind of sample preparation and/or method of registration of the spectrum: KBr disc. Absorption.
Source: Pouliot et al. (1984).
Wavenumbers (cm^{-1}): 1136s, 1086s, 1050, 986s, 955s, 920, 753, 730sh, 696, 662w, 625w, 540, 504sh, 456, 430, 387, 363.

Note: The band positions denoted by Pouliot et al. (1984) as 556 and 530 cm^{-1} were determined by us at 456 and 430 cm^{-1}, respectively, based on spectral curve analysis of the published spectrum. For the IR spectrum of armenite see also Geiger et al. (2012).

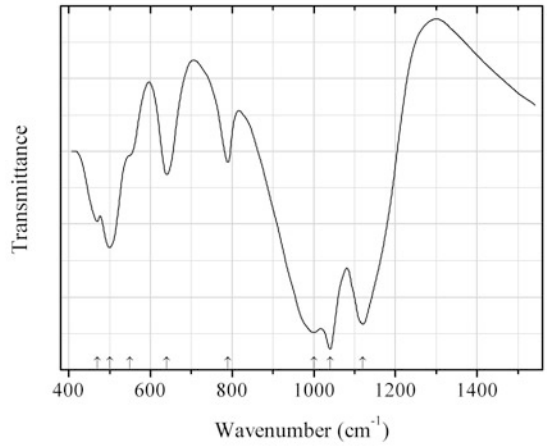

Fig. 2.553 IR spectrum of darapiosite drawn using data from Semenov et al. (1975)

Sir187 Darapiosite $K(Na,K)_2(Mn,Zr,Y)_2(Li,Zn)_3Si_{12}O_{30}$ (Fig. 2.553)
Locality: Dara-i Pioz glacier, Dara-i Pioz alkaline massif, Tien Shan Mts., Tajikistan (type locality).
Description: Holotype sample. Hexagonal, space group *P6/mcc*, a = 10.32, c = 14.39 Å. Optically uniaxial (−), ω = 1.580(2), ε = 1.575(2). The empirical formula is $K_{1.23}Na_{1.08}Ca_{0.11}$ $REE_{0.07}Mn_{1.31}Zr_{0.46}Fe_{0.26}Nb_{0.07}Li_{1.31}Zn_{1.10}Si_{12.00}O_{30}$. The strongest lines of the powder X-ray diffraction pattern [d, Å (I, %)] are: 7.09 (60), 4.43 (40), 4.13 (50), 3.75 (40), 3.26 (100), 2.93 (65), 2.76 (45), 2.56 (55).
Kind of sample preparation and/or method of registration of the spectrum: KBr disc. Absorption.
Source: Semenov et al. (1975).
Wavenumbers (cm^{-1}): 1120s, 1040s, 1000s, 790, 640, 550sh, 500s, 470.

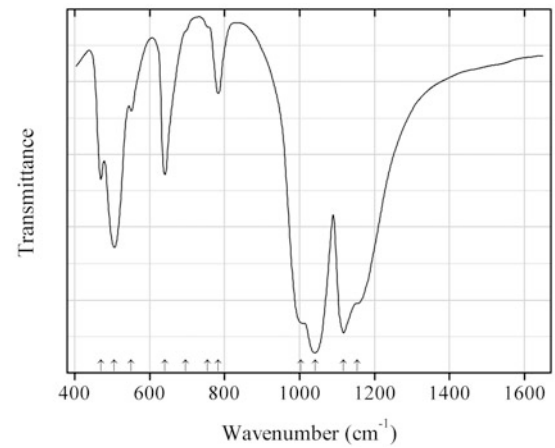

Fig. 2.554 IR spectrum of darapiosite drawn using data from Ferraris et al. (1999)

Sir188 Darapiosite $K(Na,K)_2(Mn,Zr,Y)_2(Li,Zn)_3Si_{12}O_{30}$ (Fig. 2.554)
Locality: Dara-i Pioz glacier, Dara-i Pioz alkaline massif, Tien Shan Mts., Tajikistan (type locality).
Description: The crystal structure is solved. Hexagonal, space group *P6/mcc*, a = 10.262(2), c = 14.307(1) Å, V = 1305.0(3) Å^3, Z = 2. The crystal-chemical formula is $K_{1.00}(Na_{1.22}K_{0.36}\square_{0.42})(Mn_{1.54}Zr_{0.30}Y_{0.23}Mg_{0.03})(Li_{1.53}Zn_{1.15}Fe^{2+}_{0.31})Si_{12.00}O_{30}$.
Kind of sample preparation and/or method of registration of the spectrum: KBr disc. Absorption.
Source: Ferraris et al. (1999).
Wavenumbers (cm^{-1}): 1154s, 1117s, 1041s, 1003sh, 783, 755sh, 695sh, 641, 551w, 506s, 470.

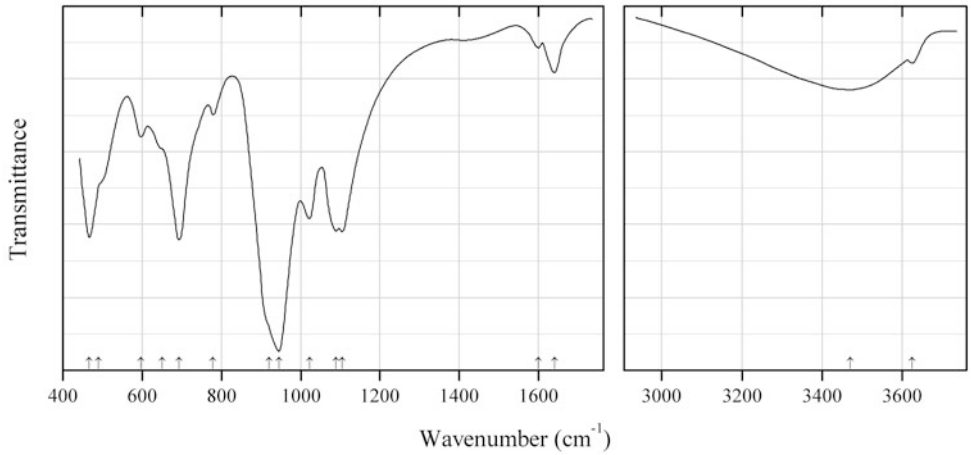

Fig. 2.555 IR spectrum of gjerdingenite-Mn drawn using data from Raade et al. (2004)

Sir189 Gjerdingenite-Mn $(K,Na)_2(Mn,Fe)(Nb,Ti)_4(Si_4O_{12})_2(O,OH)_4 \cdot 6H_2O$ (Fig. 2.555)
Locality: Gjerdingselva, Lunner, Oppland, Oslo Region, Norway (type locality).
Description: Orange-yellow prismatic crystals from miarolitic cavities of a sodic granite. Holotype sample. Monoclinic, space group *C2/m*, a = 14.563(3), b = 13.961(3), c = 7.851(2) Å, β = 117.62(3)°, V = 1414.3(6) Å^3, Z = 2. D_{calc} = 2.94 g/cm^3. Optically biaxial (+), α = 1.670(2), β = 1.685(2), γ = 1.775(5); 2 V = 52(8)°. The empirical formula is $(Na_{1.16}K_{3.07}Ba_{0.11})(Mn_{0.91}Fe_{0.70}Zn_{0.16}Mg_{0.03})(Nb_{5.92}Ti_{2.19})(Si_{15.91}Al_{0.09}O_{48})[O_{6.32}(OH)_{1.68}]\cdot 12.8H_2O$. The strongest lines of the powder X-ray diffraction pattern [d, Å (I, %) (*hkl*)] are: 6.96 (100) (020, 001), 4.94 (80) (021), 3.22 (90) (42–1, 400, 40–2), 3.10 (80) (041, 022), and 2.510 (40) (44–1, 401, 40–3, 042).
Kind of sample preparation and/or method of registration of the spectrum: KBr disc. Absorption.
Source: Raade et al. (2004).
Wavenumbers (cm^{-1}): 3625, ~3470 (broad), 1640, 1600w, 1104s, 1089s, 1022s, 945s, 920sh, 779, 693s, 650sh, 597, 490sh, 467s.

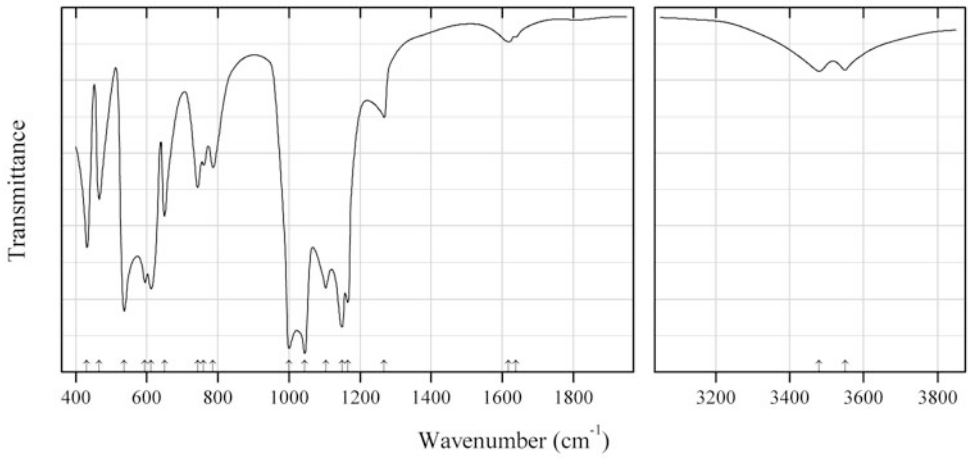

Fig. 2.556 IR spectrum of brannockite drawn using data from Povarennykh (1979)

Sir190 Brannockite $KSn_2(Li_3Si_{12})O_{30}$ (Fig. 2.556)
Locality: Not indicated.
Kind of sample preparation and/or method of registration of the spectrum: KBr disc. Absorption.
Source: Povarennykh (1979).
Wavenumbers (cm^{-1}): 3550, 3480, 1638w, 1618w, 1268, 1165s, 1149s, 1103s, 1044s, 1000s, 785, 760, 743, 650, 612s, 594s, 536s, 466, 431.
Note: The sample is contaminated with other minerals. The bands at 3550, 3480, 1638, and 1618 cm^{-1} indicate the presence of H_2O molecules. The band at 1268 cm^{-1} may correspond to B–O stretching vibrations.

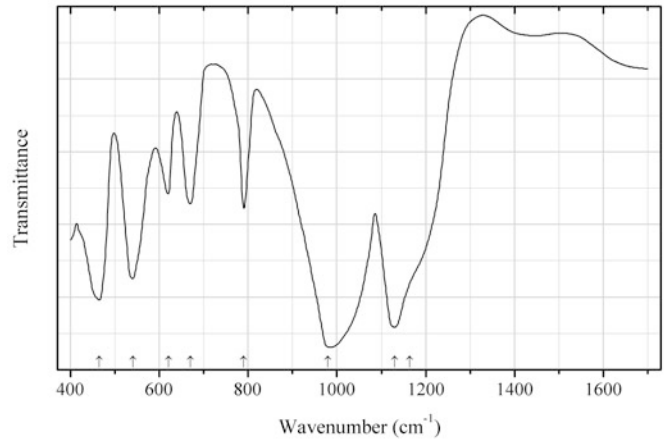

Fig. 2.557 IR spectrum of berezanskite drawn using data from Pautov and Agakhanov (1997)

Sir191 Berezanskite $KTi_2Li_3Si_{12}O_{30}$ (Fig. 2.557)
Locality: Dara-i Pioz glacier, Dara-i Pioz alkaline massif, Garm region, Tien Shan Mts., Tajikistan (type locality).
Description: White platy grains from the association with microcline, quartz, aegirine, polylithionite, sogdianite, dusmatovite, albite, reedmergnerite, kupletskite-(Cs), hyalotekite, stillwellite, etc.

Holotype sample. Hexagonal, space group *P6/mcc* (?), a = 9.903(1), c = 14.276(2) Å, Z = 2. D_{meas} = 2.66(2) g/cm^3, D_{calc} = 2.674(5) g/cm^3. Optically uniaxial (−), ω = 1.635(2), ε = 1.630(2). The empirical formula is $(K_{0.98}Na_{0.06}Ba_{0.01})(Li_{2.95}Al_{0.02})(Ti_{1.94}Nb_{0.06}Fe_{0.02})Si_{11.99}O_{30}$. The strongest lines of the powder X-ray diffraction pattern [d, Å (I, %) (*hkl*)] are: 7.15 (40) (002), 4.29 (50) (020), 4.07 (85) (112), 3.57 (80) (004), 3.16 (100) (121), 2.895 (95) (114), 2.742 (30) (024).

Kind of sample preparation and/or method of registration of the spectrum: KBr disc. Transmission.

Source: Pautov and Agakhanov (1997).

Wavenumbers (cm^{-1}): 1164sh, 1130s, 980s, 790, 670, 620, 540s, 465s.

Note: The wavenumbers were partly determined by us based on spectral curve analysis of the published spectrum.

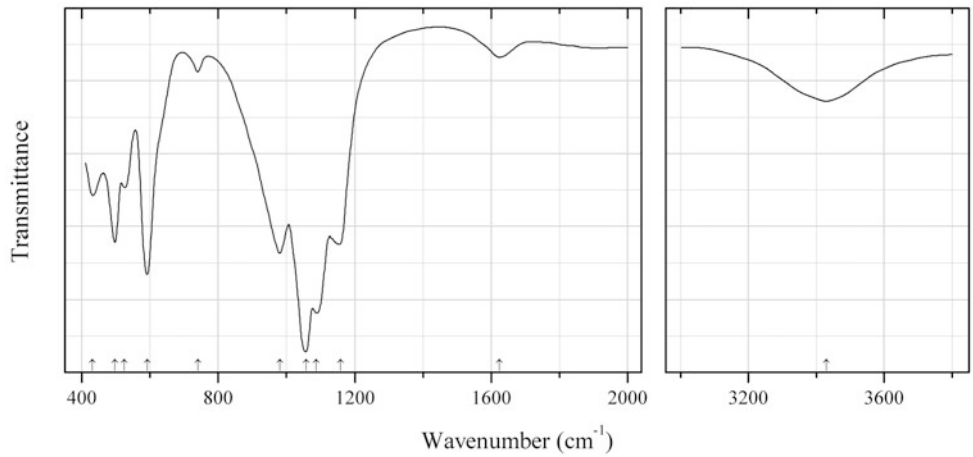

Fig. 2.558 IR spectrum of iraqite-(La) drawn using data from Povarennykh (1979)

Sir192 Iraqite-(La) $K_{1-x}(Ca,Na)_2(La,Ce,Th)Si_8O_{20}$ ($x < 0.5$) (Fig. 2.558)

Locality: Not indicated.

Description: No data.

Kind of sample preparation and/or method of registration of the spectrum: KBr disc. Transmission.

Source: Povarennykh (1979).

Wavenumbers (cm^{-1}): 3430, 1625w, 1158s, 1088s, 1057s, 980s, 740w, 592s, 525, 497s, 430.

Note: The presence of the bands of H_2O molecules at 3430 and 1625 cm^{-1} may be due to the metamict state of the mineral.

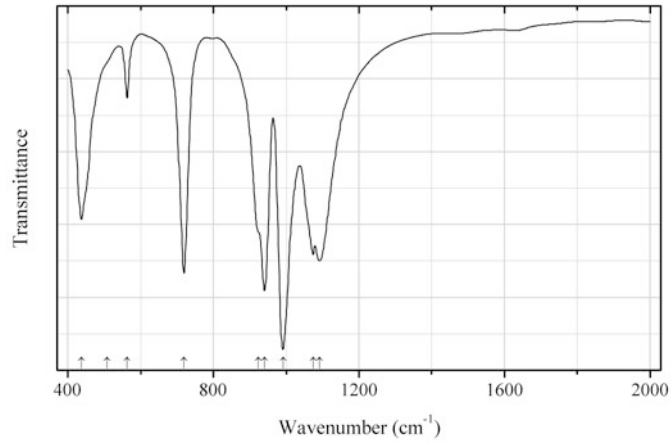

Fig. 2.559 IR spectrum of pseudowollastonite drawn using data from Rokita et al. (2014)

Sir193 Pseudowollastonite $CaSiO_3$ (Fig. 2.559)
Locality: Synthetic.
Description: A pure sample confirmed by powder X-ray diffraction data.
Kind of sample preparation and/or method of registration of the spectrum: KBr disc. Absorption.
Source: Rokita et al. (2014).
Wavenumbers (cm^{-1}): 1092s, 1074s, 992s, 941s, 923sh, 719s, 563, 507sh, 437.

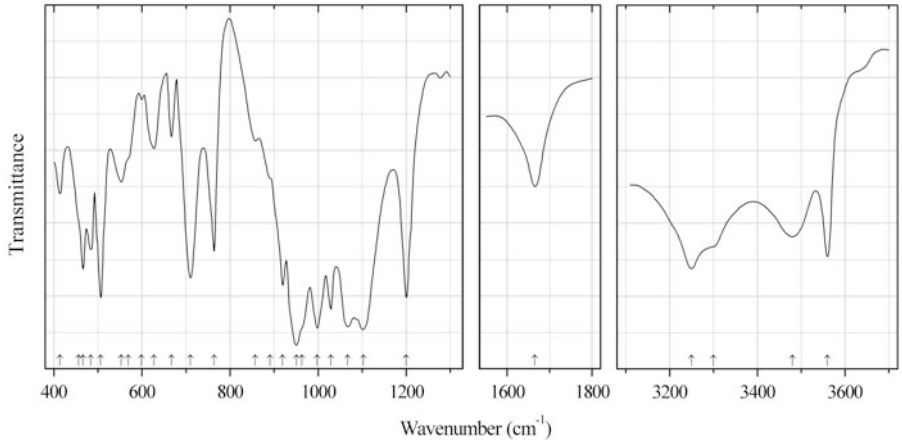

Fig. 2.560 IR spectrum of roeblingite drawn using data from Braithwaite (1985)

Sir194 Roeblingite $Ca_6Mn^{2+}Pb_2(Si_3O_9)_2(SO_4)_2(OH)_2 \cdot 4H_2O$ (Fig. 2.560)
Locality: Franklin Furnace, Sussex Co., New Jersey, USA (type locality).
Description: Specimen BM 83806 from the Natural History Museum, GB.
Kind of sample preparation and/or method of registration of the spectrum: Nujol mull between KBr plates. Transmission.
Source: Braithwaite (1985).
Wavenumbers (cm^{-1}): 3560, 3480, 3300sh, 3250, 1665, 1200s, 1103s, 1067s, 1029, 998s, 963sh, 951s, 919, 891sh, 857, 764, 710, 667, 627, 599w, 569sh, 553, 506s, 484, 466, 456sh, 414.

Note: The wavenumbers were partly determined by us based on spectral curve analysis of the published spectrum.

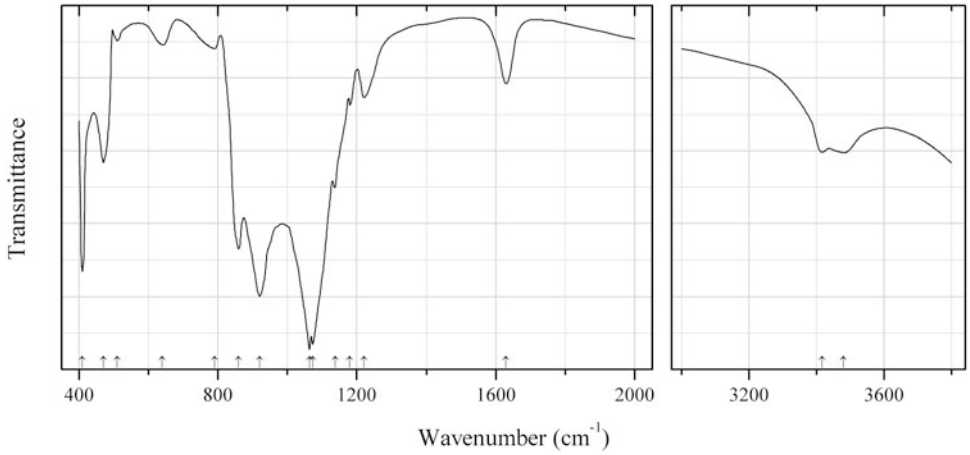

Fig. 2.561 IR spectrum of verplanckite drawn using data from Povarennykh (1979)

Sir195 Verplanckite $Ba_{12}(Mn,Fe,Ti)_6(Si_4O_{12})_3(OH,O)_2Cl_9(OH,H_2O)_7$ (Fig. 2.561)
Locality: No data.
Kind of sample preparation and/or method of registration of the spectrum: KBr disc. Transmission.
Source: Povarennykh (1979).
Wavenumbers (cm^{-1}): 3480w, 3416w, 1630, 1220w, 1180w, 1138, 1073s, 1064s, 920s, 860, 790w, 640w, 511w, 470, 410s.

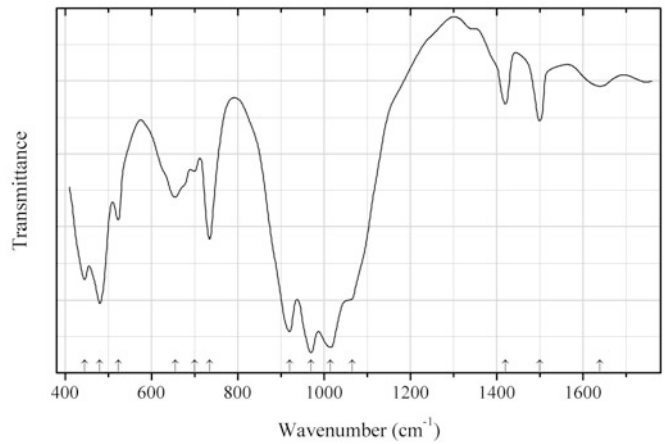

Fig. 2.562 IR spectrum of zirsilite-(Ce) drawn using data from Khomyakov et al. (2003)

Sir196 Zirsilite-(Ce) $Na_{12-x}(Ce,Na)_3Ca_6Mn_3Zr_3NbSi_{25}O_{73}(OH)_3(CO_3)\cdot H_2O$ (Fig. 2.562)
Locality: Dara-i Pioz glacier, Dara-i Pioz alkaline massif, Tien Shan Mts., Tajikistan (type locality).
Description: Creamy rhombohedral crystals from the association with quartz, microcline, aegirine, stillwellite-(Ce), ekanite, polylithionite, a pyrochlore-group mineral, calcite, fluorite, and galena.

Holotype sample. Trigonal, space group *R*3*m*, a = 14.248(2), c = 30.076(6) Å, V = 5288(4) Å^3, Z = 3. D_{meas} = 3.15(2) g/cm^3, D_{calc} = 3.10 g/cm^3. Optically uniaxial (−), ω = 1.648(2), ε = 1.637(2). The strongest lines of the powder X-ray diffraction pattern [*d*, Å (*I*, %)] are: 4.32 (51), 3.975 (37), 3.220 (100), 3.166 (56), 2.979 (95), 2.857 (66).

Kind of sample preparation and/or method of registration of the spectrum: KBr disc. Transmission.

Source: Khomyakov et al. (2003).

Wavenumbers (cm^{-1}): 1640w, 1500, 1420, 1065sh, 1015s, 970s, 920s, 735, 700w, 655, 523, 480s, 445.

Sir197 Trattnerite $Fe^{3+}{}_2(Mg_3Si_{12}O_{30})$

Locality: Stradner Kogel, Wilhelmsdorf, Bad Gleichenberg, eastern Styria, Austria (type locality).

Description: Blue-green crystals from the association with sanidine, tridymite, quartz, hematite, pyroxenes, and clinoamphibole. Holotype sample. Hexagonal, space group *P*6/*mcc*, a = 10.050(1), c = 14.338(2) Å, V = 1254.1(1) Å^3, Z = 2. D_{calc} = 2.68 g/cm^3. Optically biaxial (−), ω = 1.589(1), ε = 1.586(1). The empirical formula is (electron microprobe): $(K_{0.07}Na_{0.01})(Mg_{2.46}Fe^{3+}{}_{1.99}Fe^{2+}{}_{0.30}Mn_{0.08}Zn_{0.05}Al_{0.04}Ti_{0.01})(Si_{12.00}O_{30})$. The strongest lines of the powder X-ray diffraction pattern [*d*, Å (*I*, %) (*hkl*)] are: 8.70 (97) (100), 7.17 (100) (002), 5.535 (96) (102), 5.026 (61) (110), 3.207 (85) (211).

Kind of sample preparation and/or method of registration of the spectrum: KBr disc. Absorption.

Source: Postl et al. (2004).

Wavenumbers (cm^{-1}): 1383w, 1142s, 966s, 991sh, 790w, 630, 576, 494sh, 466sh, 427w, 366.

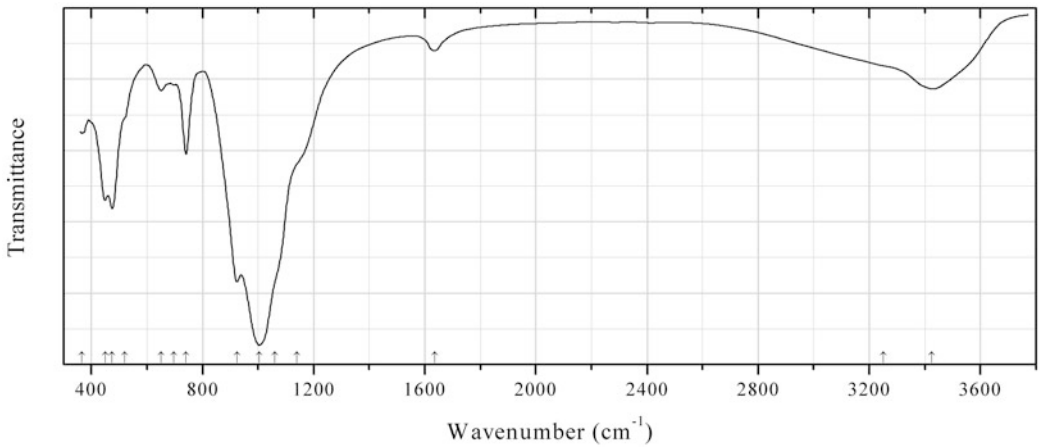

Fig. 2.563 IR spectrum of manganaqualite obtained by N.V. Chukanov

Sir198 Manganaqualite $(H_3O,Na)_{14}Ca_6Mn_2Zr_3Si_{26}O_{72}(OH)_2{\cdot}3H_2O$ (Fig. 2.563)

Locality: Kukisvumchorr Mt., Khibiny alkaline massif, Murmansk region, Kola Peninsula, Russia (type locality).

Description: Brown-orange anhedral grains from the association with aegirine, murmanite, albite, microcline, rhabdophane-(Ce), fluorite, sphalerite, andmolybdenite. Holotype sample. Trigonal, space group *R*3*m*, a = 14.1695(6), c = 31.026(1) Å, V = 5394.7(7) Å^3, Z = 3. D_{meas} = 2.67(2) g/cm^3, D_{calc} = 2.703 g/cm^3. Optically uniaxial (−), ω = 1.585(2), ε = 1.584(2). The empirical formula is $H_{36.04}(Na_{3.82}K_{0.20})(Ca_{5.65}Ce_{0.22}La_{0.14}Nd_{0.07})(Mn_{1.285}Fe_{0.48})(Zr_{2.645}Ti_{0.34})Nb_{0.31}Si_{25.41}S_{0.42}Cl_{0.23}O_{86.82}$.

The strongest lines of the powder X-ray diffraction pattern [*d*, Å (*I*, %) (*hkl*)] are: 11.44 (82) (101), 7.09

(70) (110), 6.58 (40) (104), 6.02 (44) (021), 4.371 (89) (205), 3.805(47) (303, 033), 3.376 (41) (131), 2.985 (100) (315, 128), 2.852 (92) (404).
Kind of sample preparation and/or method of registration of the spectrum: KBr disc. Absorption.
Wavenumbers (cm^{-1}): 3426, 3250sh, 1635, 1140sh, 1060sh, 1004s, 924s, 741, 696, 651, 520sh, 475s, 450s, 366.

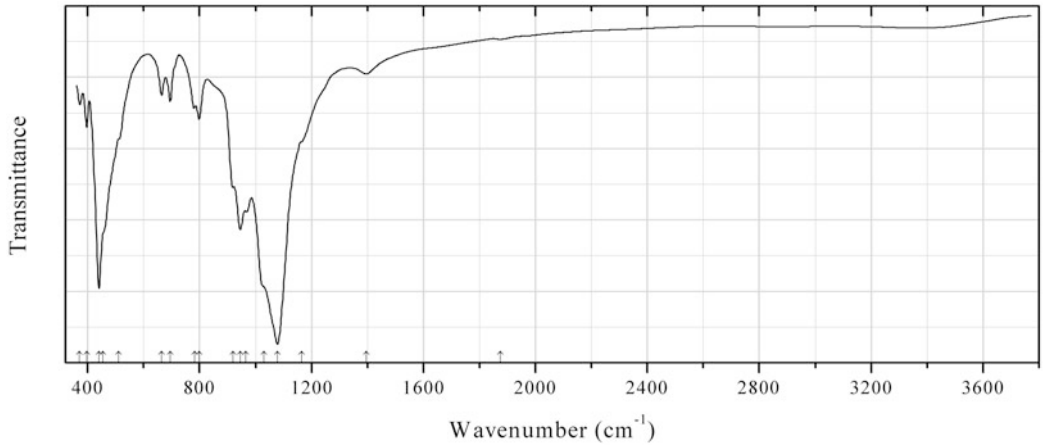

Fig. 2.564 IR spectrum of tanohataite obtained by N.V. Chukanov

Sic86 Tanohataite $HLiMn_2(Si_3O_9)$ (Fig. 2.564)
Locality: Tanohata mine, Shimohei-gun, Iwate prefecture, Tohoku region, Honshu Island, Japan (type locality).
Description: Grey fibrous aggregates from the association with quartz. Confirmed by IR spectrum and qualitative electron microprobe analysis.
Kind of sample preparation and/or method of registration of the spectrum: KBr disc. Absorption.
Wavenumbers (cm^{-1}): 1874w, 1396, 1165sh, 1078s, 1030sh, 965, 945s, 920sh, 798, 781, 695, 665, 510sh, 455sh, 440s, 398, 371.
Note: The bands at 1165, 798, 781, 510, and 455 cm^{-1}, as well as enhanced intensity of the band at 1078 cm^{-1} are due to the admixture of quartz. The band at 1396 cm^{-1} indicates the presence of H^+ cations that do not form covalent bonds with oxygen.

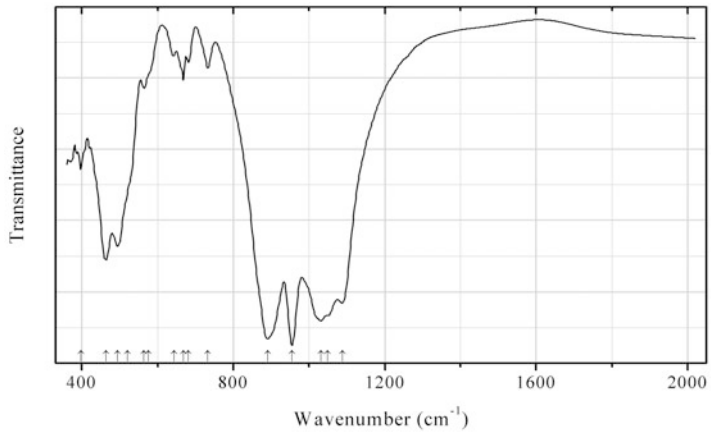

Fig. 2.565 IR spectrum of pyroxferroite obtained by N.V. Chukanov

Sic87 Pyroxferroite $(Fe^{2+},Mn^{2+})_7(Si_7O_{21})$ (Fig. 2.565)
Locality: Caspar quarry, Bellerberg, near Kottenheim, 2 km north of Mayen, Laacher See region, Eastern Eifel area, Rhineland-Palatinate (Rheinland-Pfalz), Germany.
Description: Light brown transparent crystals from a calcic xenolith in basalt. The empirical formula is (electron microprobe): $(Fe_{3.19}Mn_{2.12}Mg_{1.28}Ca_{0.42})(Si_{6.83}Fe_{0.16}Al_{0.01})O_{21}$.
Kind of sample preparation and/or method of registration of the spectrum: KBr disc. Absorption.
Wavenumbers (cm^{-1}): 1089s, 1050sh, 1031s, 955s, 890s, 733, 681w, 668, 643w, 575sh, 564, 520sh, 493s, 464s, 397.

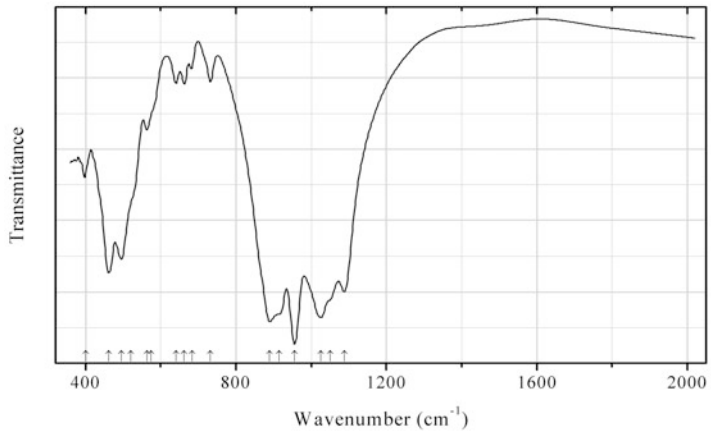

Fig. 2.566 IR spectrum of pyroxferroite obtained by N.V. Chukanov

Sic88 Pyroxferroite $(Fe^{2+},Mn^{2+})_7(Si_7O_{21})$ (Fig. 2.566)
Locality: Caspar quarry, Bellerberg, near Kottenheim, 2 km north of Mayen, Laacher See region, Eastern Eifel area, Rhineland-Palatinate (Rheinland-Pfalz), Germany.
Description: Dark brown translucent crystals from a xenolith in basalt, from the association with quartz. The empirical formula is (electron microprobe): $(Fe_{2.97}Mn_{2.74}Mg_{1.14}Ca_{0.09}Cr_{0.04})(Si_{6.99}Al_{0.01})O_{21}$.
Kind of sample preparation and/or method of registration of the spectrum: KBr disc. Absorption.
Wavenumbers (cm^{-1}): 1088s, 1050sh, 1026s, 956s, 915sh, 890s, 732, 683w, 662, 641, 575sh, 563, 520sh, 495s, 461s, 400.

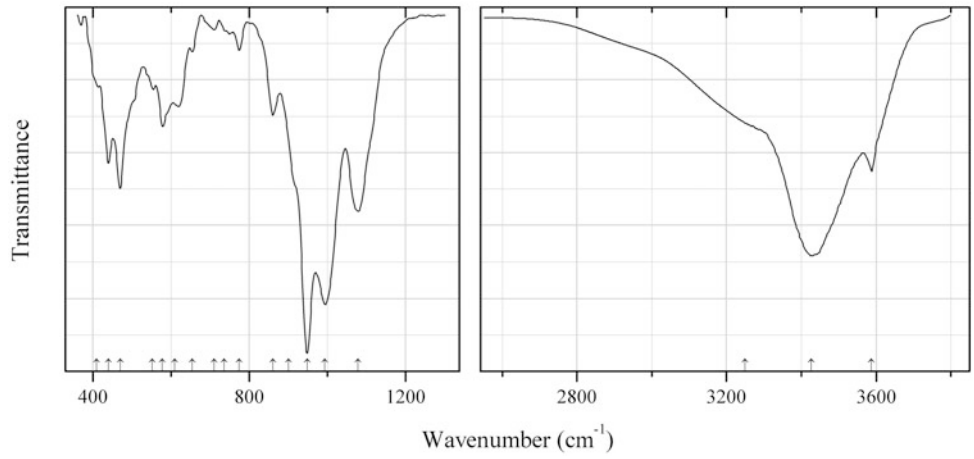

Fig. 2.567 IR spectrum of balipholite obtained by N.V. Chukanov

Sic89 Balipholite $BaLiMg_2Al_3(Si_2O_6)_2(OH)_8$ (Fig. 2.567)
Locality: Hsianhualing area, Linwu, Hunan, China (type locality).
Description: Pinkish-brown fibrous aggregate. Investigated by A.V. Kasatkin. Confirmed by electron microprobe analyses.
Kind of sample preparation and/or method of registration of the spectrum: KBr disc. Absorption.
Wavenumbers (cm^{-1}): 3587, 3427, 3250sh, 1078s, 994s, 949s, 900sh, 861, 775w, 736w, 710w, 654, 610sh, 578, 553, 470s, 440, 410sh.

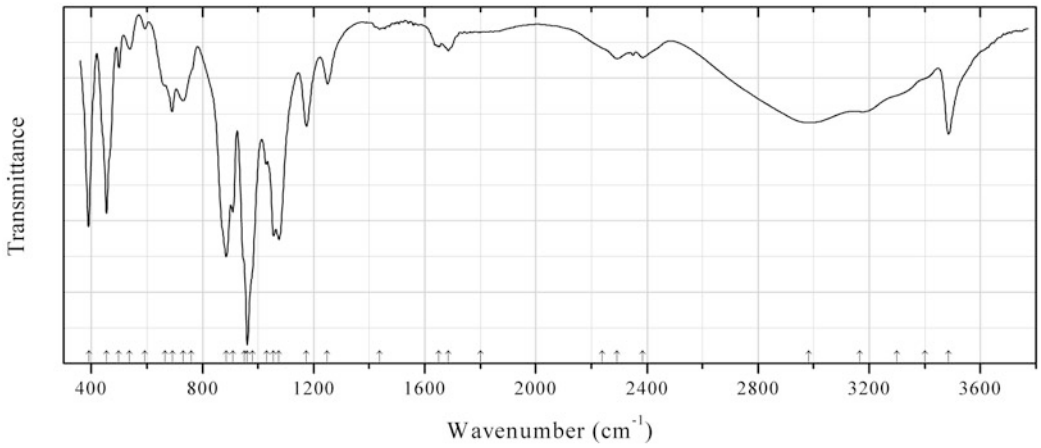

Fig. 2.568 IR spectrum of krauskopfite obtained by N.V. Chukanov

Sic90 Krauskopfite $BaSi_2O_4(OH)_2 \cdot 2H_2O$ (Fig. 2.568)
Locality: Bauman Ranch, Tulare Co., California, USA.
Description: Radial aggregates of colourless long-prismatic crystals. The empirical formula is (electron microprobe): $Ba_{1.05}Si_{1.90}Al_{0.10}O_4(OH)_2 \cdot nH_2O$.
Kind of sample preparation and/or method of registration of the spectrum: KBr disc. Absorption.

Wavenumbers (cm^{-1}): 3485, 3400sh, 3300sh, 3167, 2983, 2384, 2292, 2240sh, 1800sh, 1684, 1651w, 1437w, 1250, 1174, 1075s, 1056s, 1032, 980sh, 961s, 950sh, 909, 885s, 760sh, 730, 691, 665sh, 593w, 538w, 499, 454s, 392s.

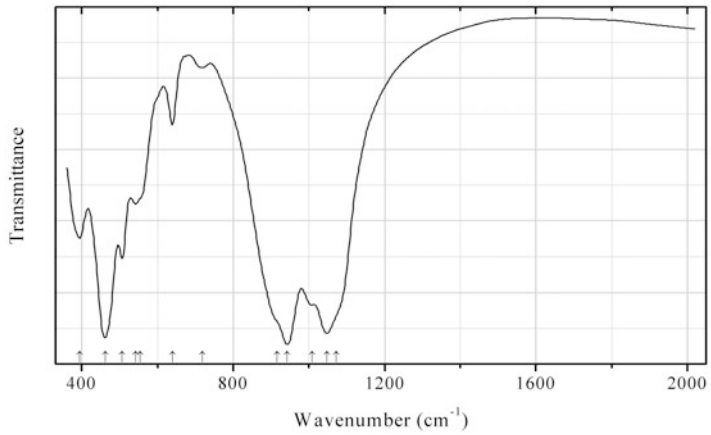

Fig. 2.569 IR spectrum of aegirine obtained by N.V. Chukanov

Sic91 Aegirine $(Na,Ca)(Fe^{3+},Mg,Fe^{2+},Mn)(Si_2O_6)$ (Fig. 2.569)
Locality: Kacharwahi, Napur district, Madya Pradesh, India.
Description: Brownish-red grains. A Na-deficient variety. The empirical formula is (electron microprobe): $(Na_{0.5}Ca_{0.3}Mn_{0.2})(Fe_{0.7}Mg_{0.2}Mn_{0.1})(Si_{1.8}Al_{0.1}Fe_{0.1}O_6)$.
Kind of sample preparation and/or method of registration of the spectrum: KBr disc. Absorption.
Wavenumbers (cm^{-1}): 1073sh, 1047s, 1009, 943s, 915sh, 718w, 639, 555sh, 542, 506, 461s, 394.

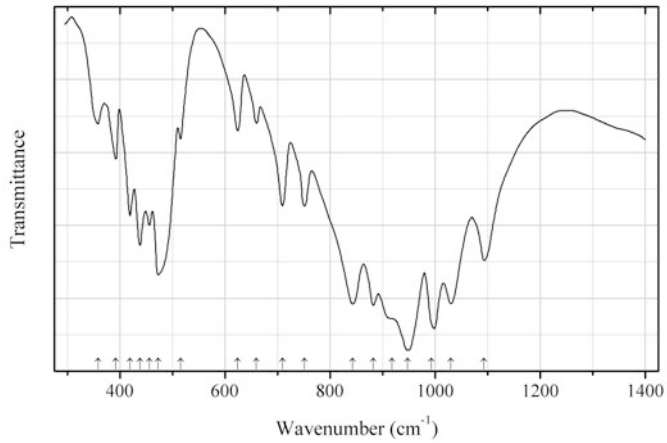

Fig. 2.570 IR spectrum of alamosite drawn using data from Furukawa et al. (1979)

Sic92 Alamosite $PbSiO_3$ (Fig. 2.570)
Locality: Synthetic
Description: Crystallized from glass. Identified by powder X-ray diffraction data.
Kind of sample preparation and/or method of registration of the spectrum: KBr disc. Transmission.
Source: Furukawa et al. (1979).

Wavenumbers (cm^{-1}): 1093, 1030s, 993s, 948s, 918sh, 882s, 843s, 751, 709, 660w, 624w, 515w, 473s, 456, 438, 419, 392, 358w.

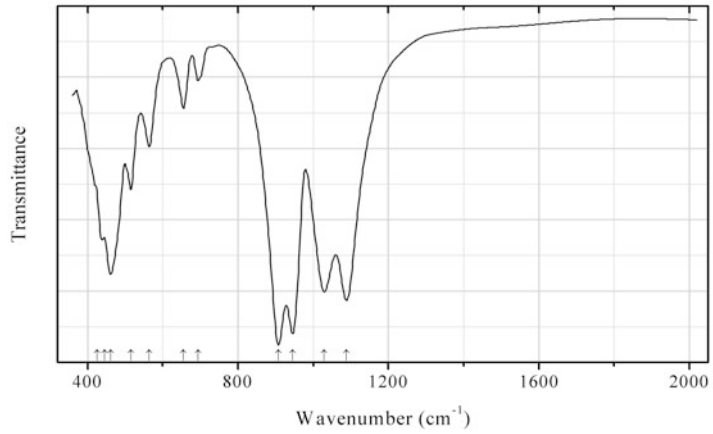

Fig. 2.571 IR spectrum of mendigite obtained by N.V. Chukanov

Sic93 Mendigite $Mn_2Mn_2MnCa(Si_3O_9)_2$ (Fig. 2.571)
Locality: In the den Dellen (Zieglowski) quarry, 1.5 km NE of Mendig, Laacher See area, Eifel region, Rhineland-Palatinate (Rheinland-Pfalz), Germany (type locality).
Description: Clusters of dark brown long-prismatic crystals from the association with sanidine, nosean, pyrochlore, rhodonite, tephroite, and magnetite. Holotype sample. The crystal structure is solved. Triclinic, space group *P*-1, $a = 7.0993(4)$, $b = 7.6370(5)$, $c = 7.7037(4)$ Å, $\alpha = 79.58(1)°$, $\beta = 61.61(1)°$, $\gamma = 76.47(1)°$, $V = 359.29(4)$ $Å^3$, $Z = 1$. Mendigite is isostructural with bustamite. $D_{calc} = 3.557$ g/cm^3. Optically biaxial (−), $\alpha = 1.7216$ (calculated), $\beta = 1.782(5)$, $\gamma = 1.796(5)$, $2V = 50(10)°$. The empirical formula is $Mn_{2.00}(Mn_{1.33}Ca_{0.67})(Mn^{2+}_{0.50}Mn^{3+}_{0.28}Fe^{3+}_{0.15}Mg_{0.07})(Ca_{0.80}Mn^{2+}_{0.20})$ $(Si_{5.57}Fe^{3+}_{0.27}Al_{0.16}O_{18})$. The strongest lines of the powder X-ray diffraction pattern [*d*, Å (*I*, %) (*hkl*)] are: 3.71 (32) (020), 3.40 (20) (002, 021), 3.199 (25) (012), 3.000 (26) (01–2, 1–20), 2.885 (100) (221, 2–11, 1–21), 2.691 (21) (222, 2–10), 2.397 (21) (02–2, 21–1, 203, 031), 1.774 (37) (412, 3–21).
Kind of sample preparation and/or method of registration of the spectrum: KBr disc. Absorption.
Wavenumbers (cm^{-1}): 1088s, 1030s, 945s, 907s, 694, 655, 564, 515, 461s, 445, 425sh.

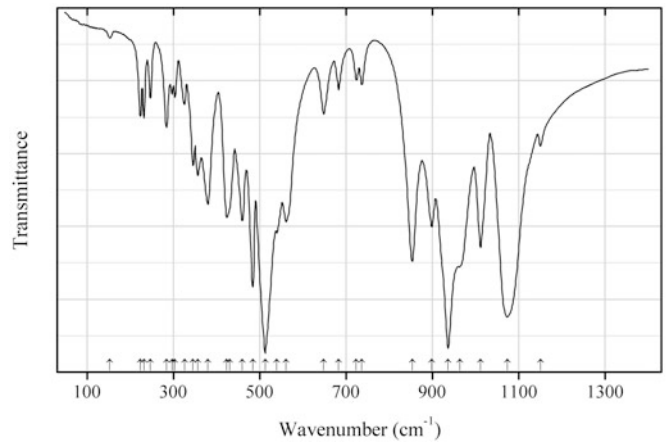

Fig. 2.572 IR spectrum of clinoenstatite drawn using data from Boffa Ballaran et al. (2001)

Sic94 Clinoenstatite $Mg_2Si_2O_6$ (Fig. 2.572)
Locality: Synthetic.
Description: Synthesized in a multi-anvil press at 9.5–10 GPa and 1050–1100 °C. Confirmed by powder X-ray diffraction data.
Kind of sample preparation and/or method of registration of the spectrum: Polyethylene disc (for the range 50–500 cm^{-1}); CsI disc (for the range 400–1500 cm^{-1}). Absorption.
Source: Boffa Ballaran et al. (2001).
Wavenumbers (cm^{-1}): 1150, 1073s, 1011, 963sh, 936s, 898, 853s, 736w, 723w, 682w, 648, 560, 539, 512s, 483s, 459, 430sh, 423, 379, 356, 345, 325, 303, 296, 283, 246, 231, 223, 152w.
Note: For the IR spectrum of clinoenstatite see also Launer (1952).
Note: The wavenumbers were determined by us based on spectral curve analysis of the published spectrum.

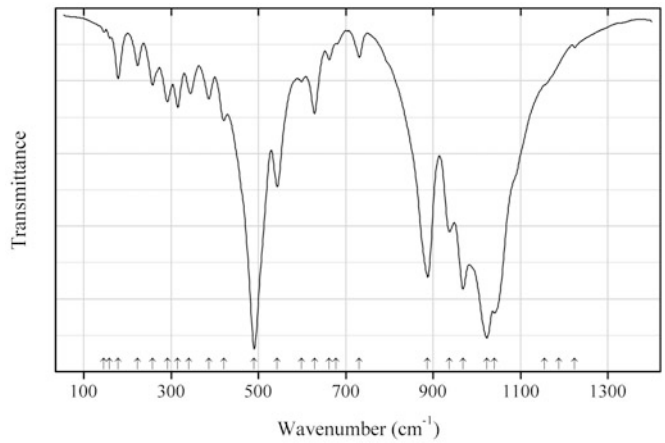

Fig. 2.573 IR spectrum of clinoferrosilite drawn using data from Boffa Ballaran et al. (2001)

Sic95 Clinoferrosilite $Fe^{2+}{}_2(Si_2O_6)$ (Fig. 2.573)
Locality: Synthetic.
Description: A purely ferrous end-member synthesized in a multi-anvil press at 9.5–10 GPa and 1050–1100 °C. Monoclinic, space group $P2_1/c$. Confirmed by powder X-ray diffraction data.
Kind of sample preparation and/or method of registration of the spectrum: Polyethylene disc (for the range 50–500 cm^{-1}); CsI disc (for the range 400–1500 cm^{-1}). Absorption.
Source: Boffa Ballaran et al. (2001).
Wavenumbers (cm^{-1}): 1224w, 1155sh, 1188sh, 1040s, 1023s, 968s, 937, 887s, 731w, 678sh, 662w, 628, 598w, 542, 490s, 420, 386w, 340w, 315w, 291w, 257w, 223w, 178w, 159w, 146w.
Note: The wavenumbers were determined by us based on spectral curve analysis of the published spectrum.

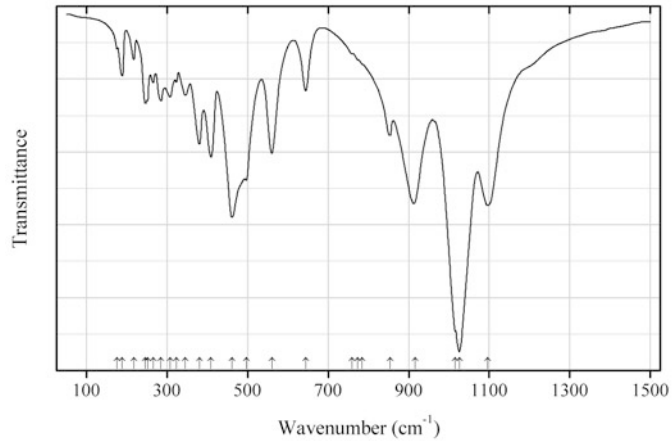

Fig. 2.574 IR spectrum of aegirine Li analogue drawn using data from Zhang et al. (2002)

Sic97 Aegirine Li analogue $LiFe^{3+}(Si_2O_6)$ (Fig. 2.574)
Locality: Synthetic.
Description: Prepared from a stoichiometric mixture of finely ground Li_2CO_3, Fe_2O_3, and SiO_2 by solid-state ceramic sintering techniques at 1223 K and ambient pressure. Characterized by powder neutron diffraction and Mössbauer measurements. Monoclinic, space group *C*2/*c*, a = 9.6641(2), b = 8.6612(3), c = 5.2924(2) Å, β = 110.12(1)°.
Kind of sample preparation and/or method of registration of the spectrum: KBr disc (in the range from 500 to 2000 cm^{-1}), CsI disc (in the range from 250 to 700 cm^{-1}), polyethylene disc (in the range from 50 to 400 cm^{-1}). Absorption.
Source: Zhang et al. (2002).
Wavenumbers (cm^{-1}): 1096s, 1026s, 1016sh, 916s, 854, 785, 774, 759, 645w, 561sh, 497, 461s, 409, 380, 345w, 323w, 307w, 285w, 265w, 251w, 246w, 217w, 188w, 175w.

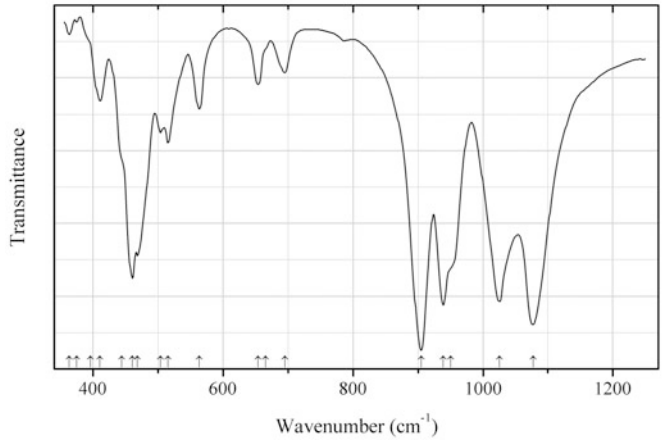

Fig. 2.575 IR spectrum of ferrobustamite drawn using data from Kazachenko et al. (2012)

Sic98 Ferrobustamite $Ca_2Ca_2(Fe,Mn,Ca)Ca(Si_3O_9)_2$ (Fig. 2.575)
Locality: Bohr quarry, Dalnegorsk, Kavalerovo mining district, Primorskiy Kray, Russia.

Description: Fibrous aggregate from the association with datolite and hedenbergite. Mn-bearing variety. The empirical formula is (Z = 6): $(Ca_{0.80–0.83}Fe_{0.09–0.10}Mn_{0.08–0.09})(Si_{1.00–1.01}O_3)$.
Kind of sample preparation and/or method of registration of the spectrum: KBr disc. Absorption.
Source: Kazachenko et al. (2012).
Wavenumbers (cm^{-1}): 1077s, 1025s, 950sh, 939s, 905s, 695, 665sh, 654, 563, 515, 504, 468s, 460s, 444sh, 410, 396sh, 375w, 363w.
Note: The wavenumbers were partly determined by us based on spectral curve analysis of the published spectrum.

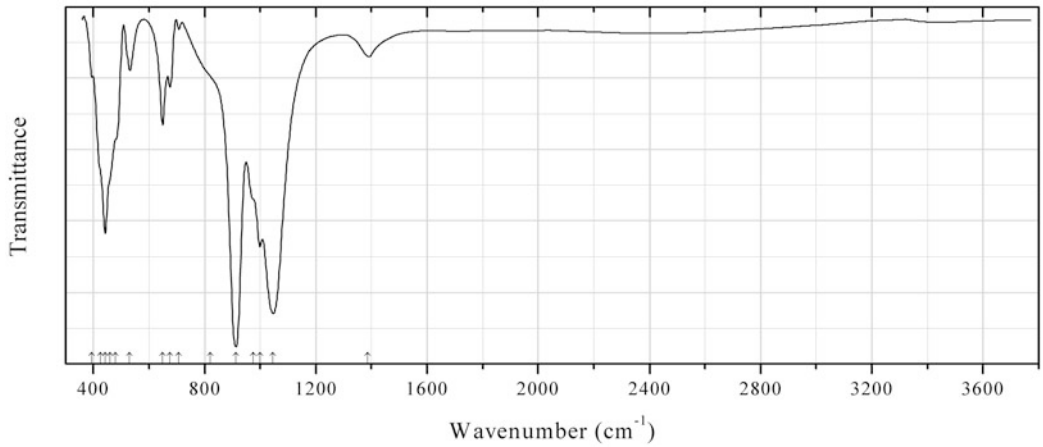

Fig. 2.576 IR spectrum of marshallsussmanite obtained by N.V. Chukanov

Sic99 Marshallsussmanite $HNaCaMn(Si_3O_9)$ (Fig. 2.576)
Locality: Wessels mine, Hotazel, Kalahari manganese fields, Northern Cape province, South Africa (type locality).
Description: Pink grains. A Mn–Ca-ordered analogue of pectolite and sérandite.
Kind of sample preparation and/or method of registration of the spectrum: KBr disc. Absorption.
Wavenumbers (cm^{-1}): 1388, 1046s, 999s, 975sh, 913s, 820sh, 707w, 675, 649, 531, 480sh, 460sh, 443s, 425sh, 395.

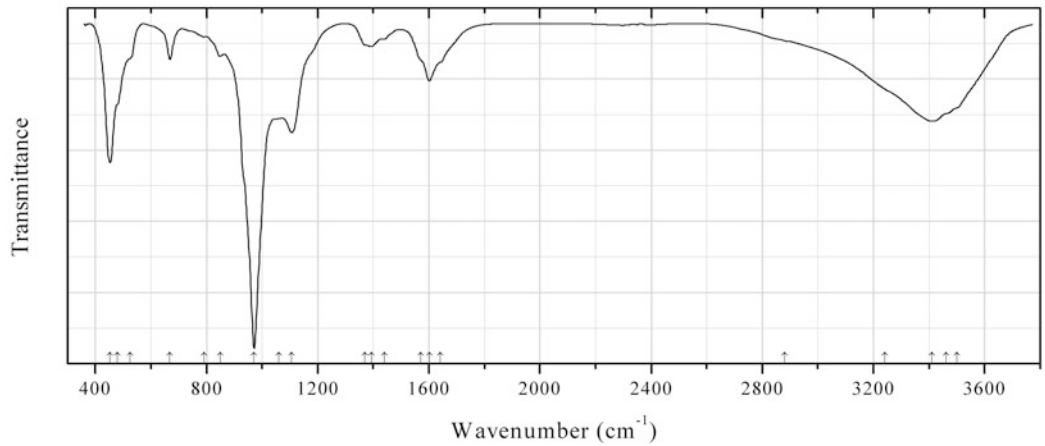

Fig. 2.577 IR spectrum of plombièrite obtained by N.V. Chukanov

Sic100 Plombièrite $Ca_5Si_6O_{16}(OH)_2 \cdot 7H_2O$ (Fig. 2.577)
Locality: Ettringer Bellerberg, near Meien, Eifel, Rheinland-Pfalz (Rhineland-Palatinate), Germany.
Description: Aggregate of white acicular crystals from the association with ettringite. Identified by IR spectrum and qualitative electron microprobe analysis.
Kind of sample preparation and/or method of registration of the spectrum: KBr disc. Absorption.
Wavenumbers (cm^{-1}): 3500sh, 3460sh, 3410, 3240sh, 2880sh, 1640sh, 1602, 1570sh, 1440sh, 1393w, 1370w, 1107, (1060), 971s, 850, 792w, 668, 525sh, 480sh, 453s.

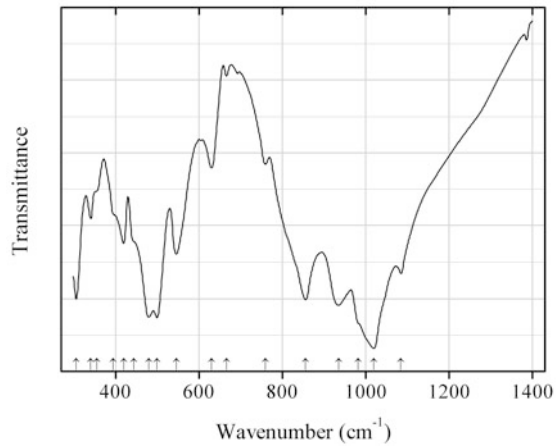

Fig. 2.578 IR spectrum of clinopyroxene $ZnSiO_3$ drawn using data from Leinenweber et al. (1989)

Sic101 Clinopyroxene $ZnSiO_3$ $ZnSiO_3$ (Fig. 2.578)
Locality: Synthetic.
Description: Synthesized at high pressure. Confirmed by the powder X-ray diffraction pattern. Monoclinic, a = 9.781(1), b = 9.179(1), c = 5.2933(9) Å, β = 111.27°.
Kind of sample preparation and/or method of registration of the spectrum: KBr disc. Absorption.
Source: Leinenweber et al. (1989).
Wavenumbers (cm^{-1}): 1085s, 1020s, 982sh, 935s, 856s, 760, 666w, 630, 546, 500s, 480s, 445sh, 420, 395sh, 356sh, 341, 306s.

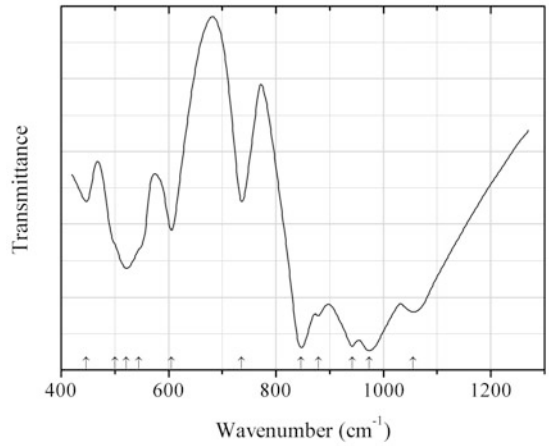

Fig. 2.579 IR spectrum of lithium metasilicate drawn using data from Lazarev and Tenisheva (1962)

Sic102 Lithium metasilicate $Li_2(SiO_3)$ (Fig. 2.579)
Locality: Syntheric.
Description: Synthesized in solid-state reaction between Li_2CO_3 and SiO_2 at 1250–1350 °C. Orthorhombic, space group $Cmc2_1$, a = 9.36, b = 5.39, c = 4.67 Å.
Kind of sample preparation and/or method of registration of the spectrum: KBr disc. Transmission.
Source: Lazarev and Tenisheva (1962).
Wavenumbers (cm^{-1}): 1055s, 973s, 942s, 879s, 847s, 736, 605, 545sh, 521, 500sh, 447.

Sic103 Fowlerite $Mn_4Zn(SiO_3)_5$
Locality: Franklin, Ogdensburg, Sussex Co., New Jersey, USA.
Kind of sample preparation and/or method of registration of the spectrum: KBr disc. Absorption.
Source: Moenke (1966).
Wavenumbers (cm^{-1}): 1625, 1447sh, 1425w, 1224sh, 1092sh, 1075sh, 1062s, 1040s, 1007sh, 957sh, 947s, 918sh, 903s, 877sh, 727, 697w, 670, 650, 604sh, 580, 568sh, 540sh, 518, 502sh, 497, 457s, 417w.
Note: The wavenumbers were determined by us based on spectral curve analysis of the published spectrum.

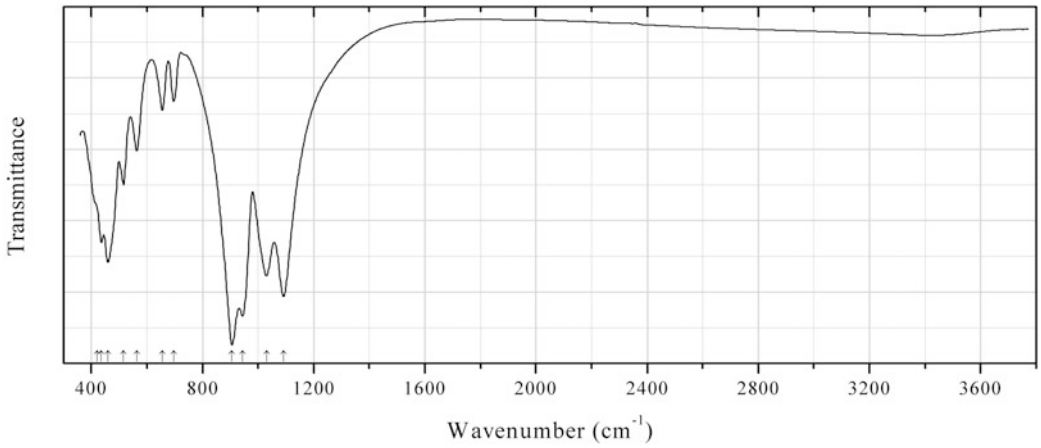

Fig. 2.580 IR spectrum of mendigite Fe analogue obtained by N.V. Chukanov

Sic104 Mendigite Fe analogue $Mn^{2+}{}_2Mn^{2+}{}_2(Fe^{3+},Fe^{2+},Mn^{2+})Ca(Si,Fe^{3+})_6O_{18}$ (Fig. 2.580)
Locality: In den Dellen pumice quarry, near Mendig, Laacher See area, Eifel Mountains, Rhineland-Palatinate (Rheinland-Pfalz), Germany.
Description: Brownish-yellow crystals from the association with christofschäferite-(Ce), orthoclase, rhodonite, bustamite, tephroite, zircon, fluorapatite, pyrophanite, jacobsite. The empirical formula is $Mn^{2+}{}_{2.00}(Mn^{2+}{}_{1.20}Ca_{0.80})(Fe^{3+}{}_{0.32}Fe^{2+}{}_{0.25}Mn^{2+}{}_{0.20}Mg_{0.17}Mn^{3+}{}_{0.06})Ca_{1.00}(Si_{5.68}Fe^{3+}{}_{0.31}Al_{0.01})O_{18}$.
Kind of sample preparation and/or method of registration of the spectrum: KBr disc. Absorption.
Wavenumbers (cm^{-1}): 1091s, 1030s, 944s, 906s, 696, 655, 563, 516, 460s, 436, 420sh.

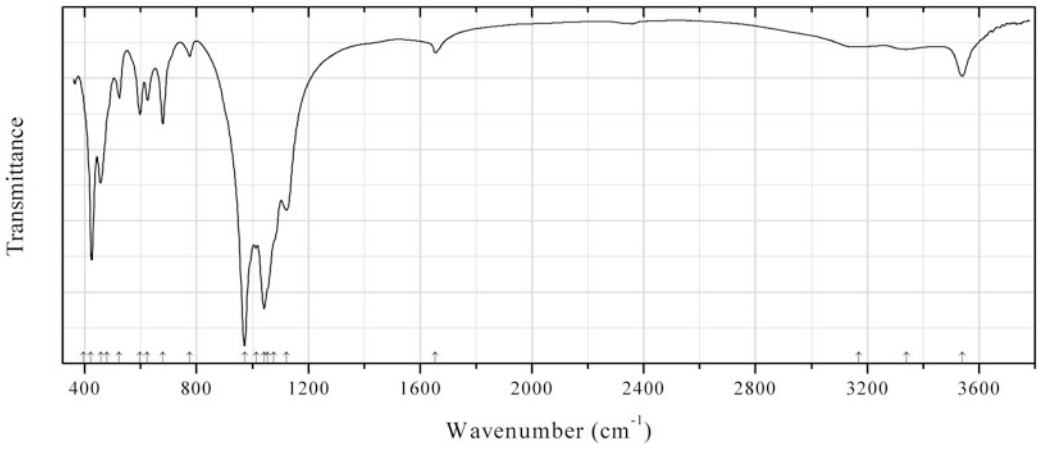

Fig. 2.581 IR spectrum of calcinaksite obtained by N.V. Chukanov

Sib119 Calcinaksite $KNaCa(Si_4O_{10})\cdot H_2O$ (Fig. 2.581)
Locality: Bellerberg volcano, between Mayen and Kottenheim, Laacher See area, Eastern Eifel region, Rhineland-Palatinate (Rheinland-Pfalz), Germany (type locality).
Description: Clusters of colourless imperfect prismatic crystals from the association with wollastonite, gehlenite, brownmillerite, Ca_2SiO_4 (presumably larnite or calcio-olivine), quartz, aragonite, calcite, jennite, tobermorite, and ettringite. Holotype sample. Triclinic, space group *P*-1, $a = 7.021(2)$, $b = 8.250(3)$, $c = 10.145(2)$ Å, $\alpha = 102.23(2)°$, $\beta = 100.34(2)°$, $\gamma = 115.09(3)°$, $V = 495.4(2)$ Å^3, $Z = 2$. $D_{meas} = 2.62(2)$ g/cm^3, $D_{calc} = 2.623$ g/cm^3. Optically biaxial (+), $\alpha = 1.542(2)$, $\beta = 1.550(2)$, $\gamma = 1.565(3)$, $2V = 75(10)°$. The empirical formula is $H_{2.11}K_{0.99}Na_{0.84}Ca_{1.04}Fe_{0.03}Si_{3.98}O_{11}$. The strongest lines of the powder X-ray diffraction pattern [*d*, Å (*I*, %)] are: 3.431 (70), 3.300 (67), 3.173 (95), 3.060 (100), 2.851 (83), 2.664 (62), 2.493 (52), 1.749 (45).
Kind of sample preparation and/or method of registration of the spectrum: KBr disc. Absorption.
Wavenumbers (cm^{-1}): 3540, 3340w, 3170w, 1654w, 1122, 1075sh, 1055sh, 1041s, 1013, 971s, 775w, 679, 624, 597, 523, 480sh, 456, 421s, 395w.

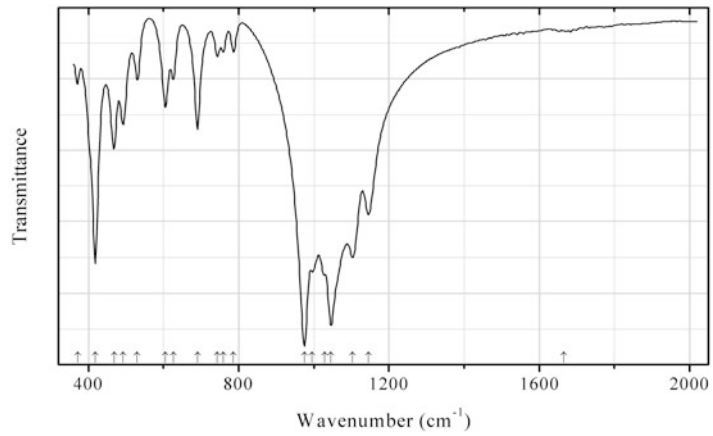

Fig. 2.582 IR spectrum of fenaksite obtained by N.V. Chukanov

Sib120 Fenaksite $KNaFe^{2+}(Si_4O_{10})$ (Fig. 2.582)

Locality: Rasvumchorr Mt., Khibiny alkaline complex, Kola peninsula, Murmansk region, Russia.
Description: Reddish-brown single-crystal grain from peralkaline pegnatite. Confirmed by the IR spectrum and qualitative electron microprobe analyses.
Kind of sample preparation and/or method of registration of the spectrum: KBr disc. Absorption.
Wavenumbers (cm^{-1}): 3615w, 1665w, 1145, 1103s, 1046s, 1030sh, 996, 975s, 786, 759, 743, 690, 626, 605, 530, 492, 468, 418s, 372.

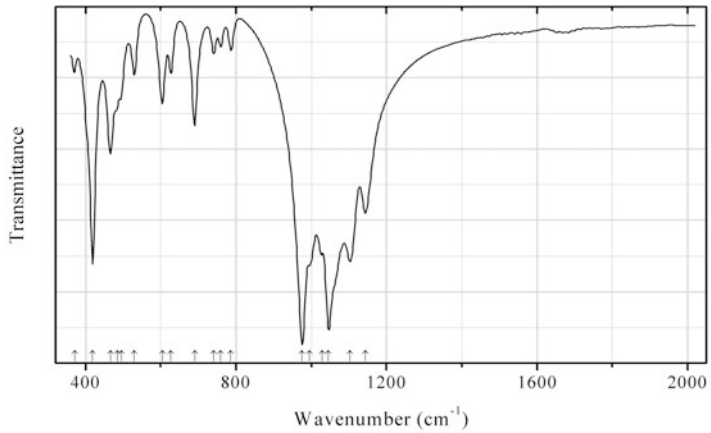

Fig. 2.583 IR spectrum of manaksite obtained by N.V. Chukanov

Sib121 Manaksite $KNaMn^{2+}Si_4O_{10}$ (Fig. 2.583)
Locality: Palitra pegmatite, Kedykverpakhk Mt., Lovozero alkaline massif, Kola peninsula, Murmansk region, Russia.
Description: Brownish-yellow crystal from the association with microcline, aegirine, arfvedsonite, nepheline, sodalite, analcime, ussingite, natrosilite, serandite, villiaumite, kazakovite, nalipoite, revdite, etc. Investigated by I.V. Pekov.
Kind of sample preparation and/or method of registration of the spectrum: KBr disc. Absorption.
Wavenumbers (cm^{-1}): 3621w, 1144, 1103s, 1046s, 1030, 996, 976s, 786w, 759w, 741w, 690, 627, 604, 529, 495sh, 485sh, 466, 419s, 372w.

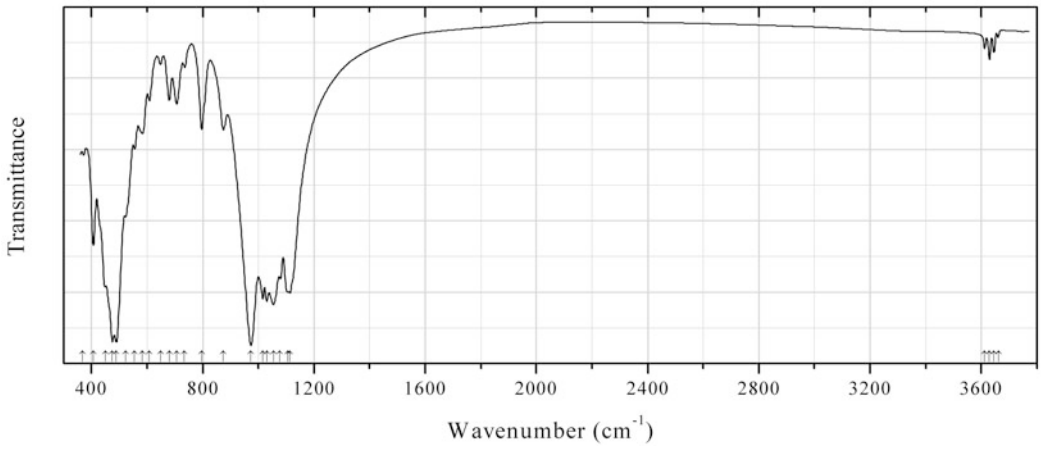

Fig. 2.584 IR spectrum of ferro-holmquistite obtained by N.V. Chukanov

Sib122 Ferro-holmquistite $\square Li_2(Fe^{2+}{}_3Al_2)(Si_8O_{22})(OH)_2$ (Fig. 2.584)
Locality: Pegmatite F, Mibra quarry, Nazareno, Minas Gerais, Brazil.
Description: Grayish-lilac parallel-fibrous aggregate from the contact zone of the pegmatite. The empirical formula is (electron microprobe): $Na_{0.06}Li_2(Fe_{1.92}Mg_{1.27}Mn_{0.06}Al_{1.75})(Si_{7.88}Al_{0.12}O_{22})(OH)_2$.
Kind of sample preparation and/or method of registration of the spectrum: KBr disc. Absorption.
Wavenumbers (cm^{-1}): 3661w, 3645w, 3629w, 3612w, 1114s, 1106s, 1076, 1054s, 1030s, 1016s, 973s, 874, 796, 734w, 706, 679, 648w, 608, 583, 555, 523, 489s, 475s, 451, 407, 368.

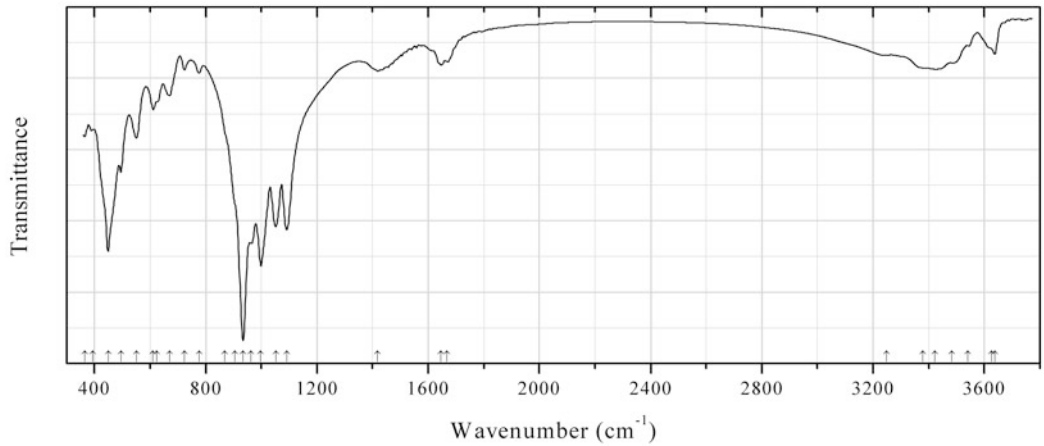

Fig. 2.585 IR spectrum of inesite obtained by N.V. Chukanov

Sib123 Inesite $Ca_2Mn^{2+}{}_7Si_{10}O_{28}(OH)_2 \cdot 5H_2O$ (Fig. 2.585)
Locality: Hale Creek mine, Mad River Rock, Coastal range, Trinity Co., California, USA.
Description: Pink crystals from the association with earlandite. Confirmed by the IR spectrum.
Kind of sample preparation and/or method of registration of the spectrum: KBr disc. Absorption.
Wavenumbers (cm^{-1}): 3637, 3625sh, 3540w, 3483, 3422, 3380sh, 3248, 1667, 1646, 1419, 1091s, 1052s, 998s, 963s, 934s, 905sh, 870sh, 776w, 724w, 671, 625sh, 611, 551, 495, 449s, 395, 365.

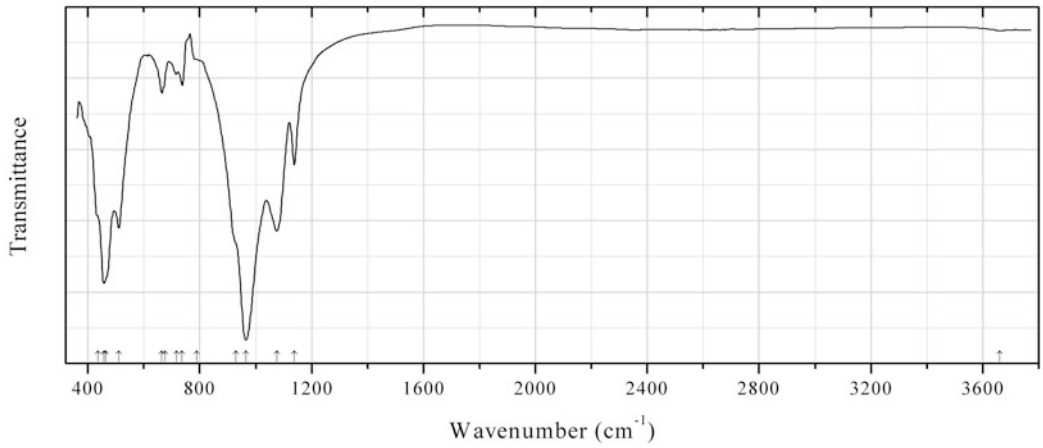

Fig. 2.586 IR spectrum of ferri-obertiite obtained by N.V. Chukanov

Sib124 Ferri-obertiite $NaNa_2(Mg_3Fe^{3+}Ti)(Si_8O_{22})O_2$ (Fig. 2.586)
Locality: Bellerberg, near Ettringen, Eifel Mts., Rhineland-Palatinate (Rheinland-Pfalz), Germany.
Description: Black prismatic crystals from calcic xenolith hosted by alkaline basalt. The empirical formula is (electron microprobe): $(Na_{0.56}K_{0.30})(Na_{1.49}Ca_{0.42}Mn_{0.09})(Mg_{1.17}Fe_{1.07}Mn_{0.76})Fe_{1.48}Ti_{0.52}(Si_{7.71}Fe^{3+}_{0.21}Al_{0.08}O_{22})(O,OH)_2$.
Kind of sample preparation and/or method of registration of the spectrum: KBr disc. Absorption.
Wavenumbers (cm^{-1}): 3660w, 1138, 1075s, 965s, 930sh, 790sh, 737, 716, 675sh, 664, 510s, 465sh, 456s, 435sh.

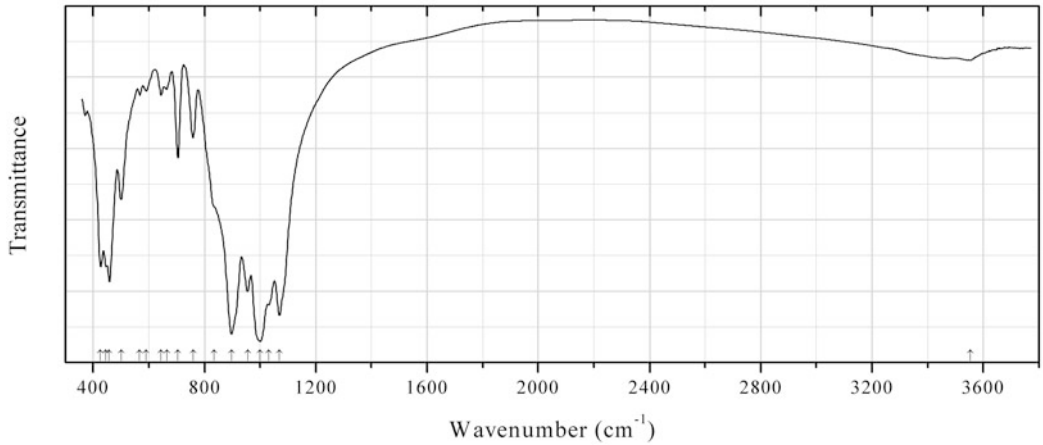

Fig. 2.587 IR spectrum of vladykinite obtained by N.V. Chukanov

Sib125 Vladykinite $Na_3Sr_4(Fe^{2+}Fe^{3+})Si_8O_{24}$ (Fig. 2.587)
Locality: Murun massif (Murunskii alkaline complex), Aldan Shield, southwest Yakutia, Siberia, Russia (type locality).
Description: Colourless grains from the association with aegirine, potassium feldspar, eudialyte, lamprophyllite, nepheline, strontianite, and K-rich vishnevite. Cotype sample.
Kind of sample preparation and/or method of registration of the spectrum: KBr disc. Absorption.
Wavenumbers (cm^{-1}): 3552w, 1070s, 1032s, 1000s, 955s, 897s, 835sh, 759, 705, 665w, 644w, 590w, 567w, 500, 458s, 445sh, 427.

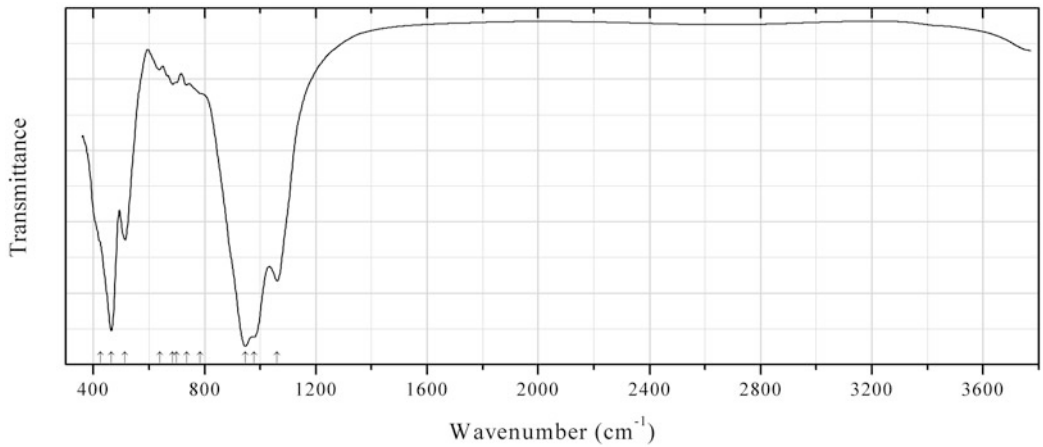

Fig. 2.588 IR spectrum of ferri-kaersutite obtained by N.V. Chukanov

Sib126 Ferri-kaersutite $NaCa_2(Mg_3TiFe^{3+})(Si_6Al_2O_{22})O_2$ (Fig. 2.588)
Locality: Rothenberg basalt quarry, Rothenberg Mt., near Mendig, Eifel Mts., Rhineland-Palatinate (Rheinland-Pfalz), Germany.
Description: Dark brown prismatic crystal from the association with augite and biotite. The empirical formula is $(Na_{0.7}K_{0.3})Ca_{2.0}(Mg_{2.7}Fe_{1.5}Ti_{0.7}Mn_{0.05}Al_{0.05})(Si_{6.3}Al_{1.7}O_{22})O_{1.4}F_{0.6}$.
Kind of sample preparation and/or method of registration of the spectrum: KBr disc. Absorption.
Wavenumbers (cm^{-1}): 1061s, 977s, 946s, 785w, 736w, 700sh, 685w, 639w, 514, 465s, 425sh.

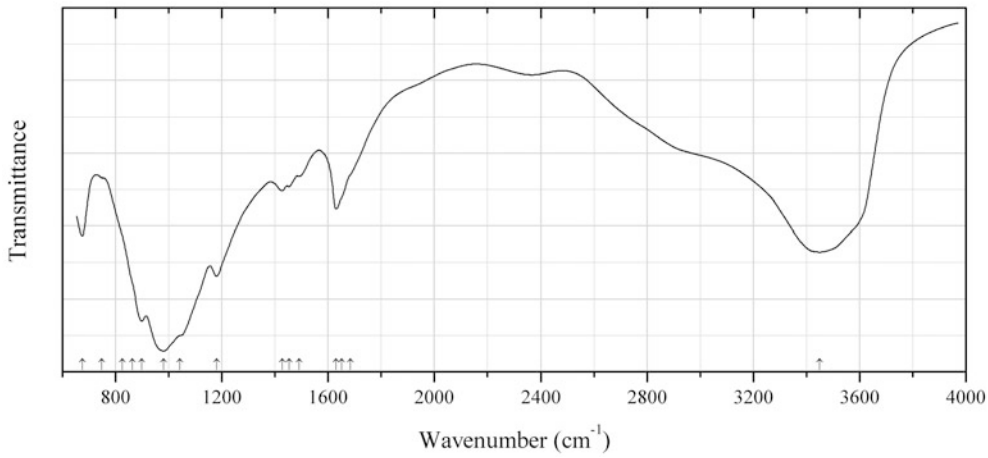

Fig. 2.589 IR spectrum of clinotobermorite drawn using data from Henmi and Kusachi (1992)

Sib129 Clinotobermorite $Ca_5[Si_6O_{16}(OH)](OH)\cdot nH_2O$ ($n \approx 5$) (Fig. 2.589)
Locality: Fuka mine, Bicchu-cho, near Takahashi city, Okayama prefecture, Honshu Island, Japan (type locality).
Description: White aggregate from the association with tobermorite, plombierite, apophyllite, and calcite. Holotype sample. Monoclinic, space group *Cc* or *C*2/*c*, $a = 11.331(9)$, $b = 7.353(7)$, $c = 22.67(2)$ Å, $\beta = 96.59(7)°$. $D_{meas} = 2.58$ g/cm^3, $D_{calc} = 2.69$ g/cm^3. The refractive indices are: $\alpha = 1.575$, $\beta = 1.580$, $\gamma = 1.585$. The empirical formula is $Ca_{5.3}Si_{6.00}(O,OH,F)_{18}\cdot nH_2O$ ($n \approx 5$). The strongest lines of the powder X-ray diffraction pattern [*d*, Å (*I*, %) (*hkl*)] are: 11.25 (100) (002), 3.745 (36) (204, 006, 11–5), 3.304 (51) (20–6, 023), 3.068 (45) (22–1), 3.012 (37) (31–4), 2.811 (41) (008, 400, 40–2), 2.794 (60) (223, 117).
Kind of sample preparation and/or method of registration of the spectrum: KBr disc. Transmission.
Source: Henmi and Kusachi (1992).
Wavenumbers (cm^{-1}): 3450s, 1683sh, 1650sh, 1630, 1491, 1453, 1428, 1180s, 1043sh, 980s, 898w, 864sh, 825sh, 748, 675.
Note: The wavenumbers were partly determined by us based on spectral curve analysis of the published spectrum.

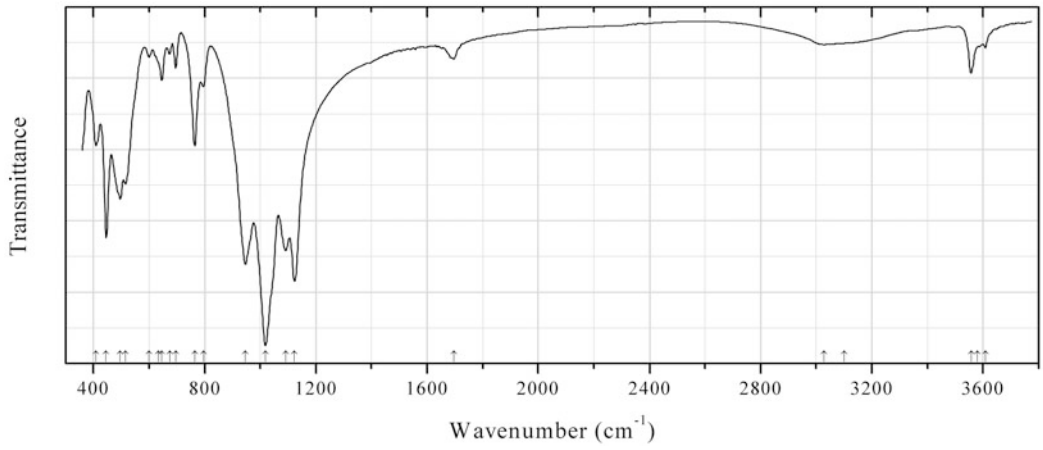

Fig. 2.590 IR spectrum of canasite obtained by N.V. Chukanov

Sib130 Canasite $K_3Na_3Ca_5(Si_{12}O_{30})(OH)_4 \cdot H_2O$ (Fig. 2.590)
Locality: Kukisvumchorr Mt., Khibiny alkaline complex, Kola peninsula, Murmansk region, Russia.
Description: Green grains from the association with pectolite and astrophyllite. Confirmed by the IR spectrum and semiquantitative electron microprobe analysis.
Kind of sample preparation and/or method of registration of the spectrum: KBr disc. Absorption.
Wavenumbers (cm^{-1}): 3609w, 3580sh, 3557, 3100sh, 3028w, 1696w, 1123s, 1091s, 1019s, 946s, 795, 764, 696, 674w, 645, 635sh, 600w, 515, 497, 446s, 409.

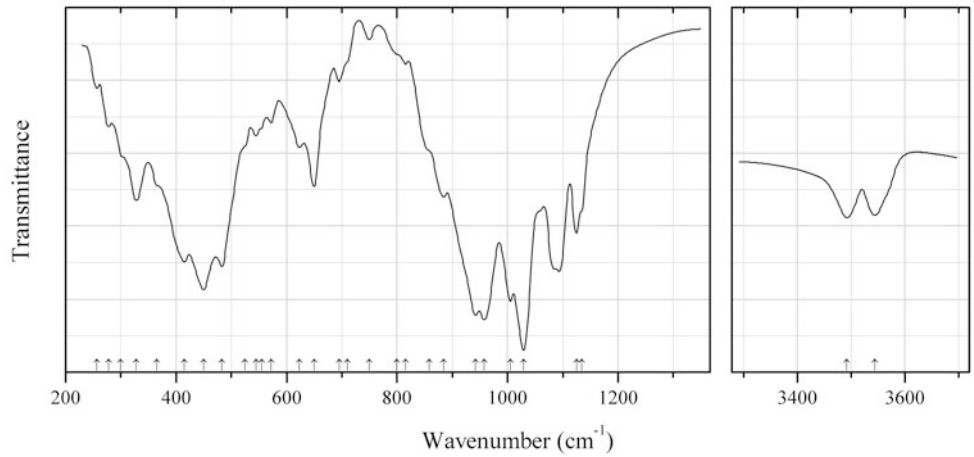

Fig. 2.591 IR spectrum of deerite drawn using data from Langer et al. (1977)

Sib131 Deerite $Fe^{2+}{}_6Fe^{3+}{}_3(Si_6O_{17})O_3(OH)_5$ (Fig. 2.591)
Locality: Laytonville quarry, Coastal range, Mendocino Co., California, USA (type locality).
Description: Black clusters from the association with stilpnomelane, quartz, garnet, alkali amphibole, and pyrite. Specimen No. 93727 from the Harvard Mineralogical Museum, Cambridge. Investigated by electron microprobe and wet chemical analysis (Agrell et al. 1965; Agrell and Gay 1970). The strongest lines of the powder X-ray diffraction pattern [*d*, Å (*I*, %) (*hkl*)] are: 9.05 (80) (110), 4.52 (17) (220), 3.224 (35) (320), 3.011 (100) (330, 160), 2.539 (41) (350), 2.258 (31) (440).

Kind of sample preparation and/or method of registration of the spectrum: KBr disc. Transmission.
Source: Langer et al. (1977).
Wavenumbers (cm^{-1}): 3544, 3492, 1135sh, 1125, 1029s, 1005s, 958s, 942s, 885, 858sh, 815w, 800sh, 750w, 710sh, 695w, 650, 623, 572w, 555sh, 545w, 525sh, 483s, 450s, 415s, 365sh, 328, 300sh, 278w, 257w.
Note: For the IR spectrum of a synthetic deerite analogue see Langer et al. (1977). See also Agrell and Gay (1970).

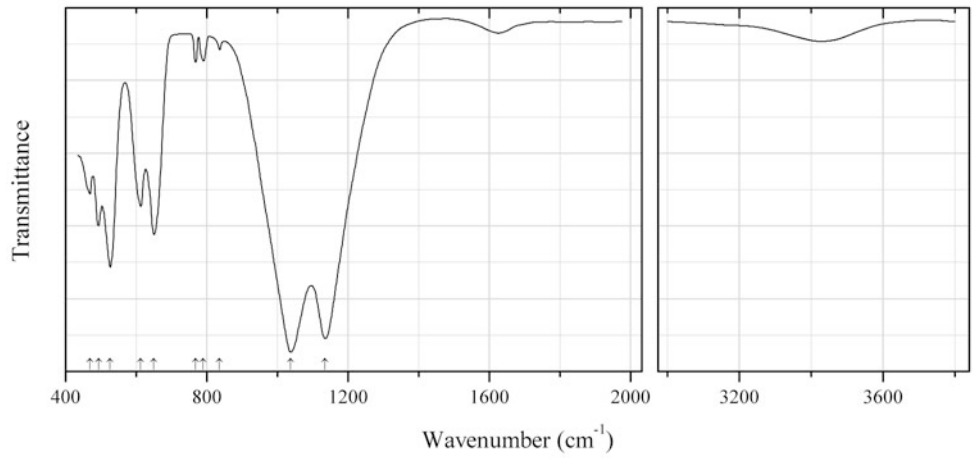

Fig. 2.592 IR spectrum of emeleusite drawn using data from Povarennykh (1979)

Sib132 Emeleusite $Na_2LiFe^{3+}(Si_6O_{15})$ (Fig. 2.592)
Locality: Not indicated.
Kind of sample preparation and/or method of registration of the spectrum: Absorption. KBr disc.
Source: Povarennykh (1979).
Wavenumbers (cm^{-1}): 1135s, 1037s, 836, 790w, 768w, 650, 613, 526, 493, 469.

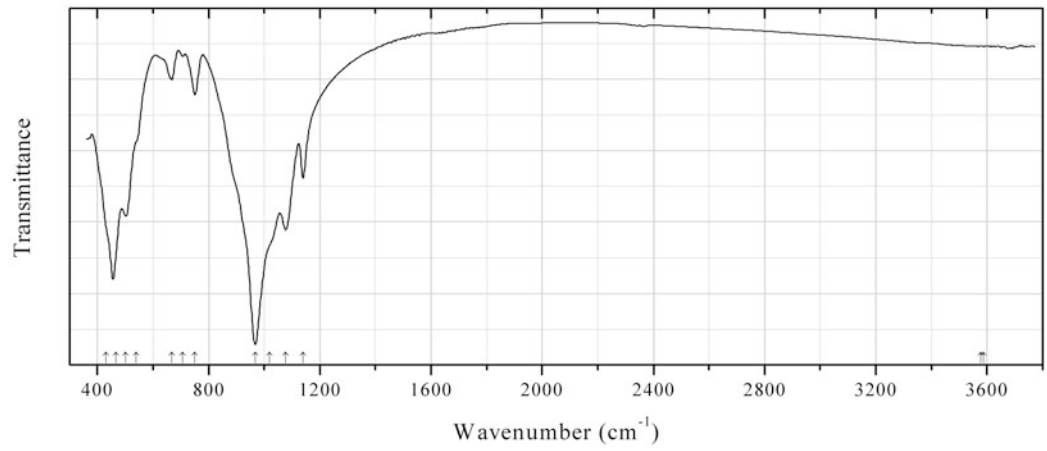

Fig. 2.593 IR spectrum of magnesio-fluoro-arfvedsonite obtained by N.V. Chukanov

Sib133 Magnesio-fluoro-arfvedsonite $NaNa_2(Mg_4Fe^{3+})(Si_8O_{22})F_2$ (Fig. 2.593)
Locality: Koklukhtiuai River valley, Lovozero alkaline complex, Kola peninsula, Murmansk region, Russia.
Description: Black prismatic crystal from peralkaline pegmatite. Investigated by I.V. Pekov. The empirical formula is $(K_{0.35}Na_{2.60}Ca_{0.10})(Mg_{2.74}Mn_{0.36}Fe_{1.69}Ti_{0.06}Li_{0.15})(Si_{7.83}Al_{0.09}Fe_{0.08}O_{22})[F_{1.42}(OH,O)_{0.58}]$.
Kind of sample preparation and/or method of registration of the spectrum: KBr disc. Absorption.
Wavenumbers (cm^{-1}): 3588w, 3577w, 1140, 1077s, 1020sh, 967s, 751, 707w, 668, 540sh, 502s, 467s, 430sh.

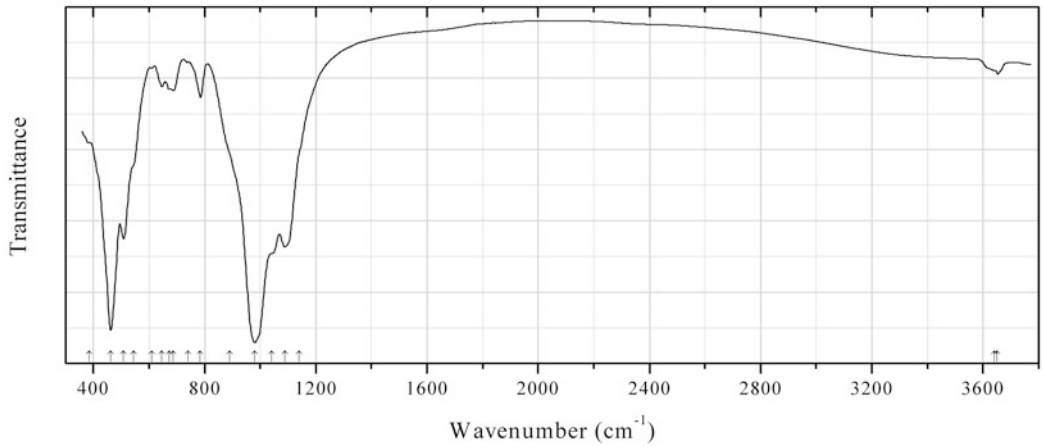

Fig. 2.594 IR spectrum of magnesioriebeckite Zn-rich variety obtained by N.V. Chukanov

Sib134 Magnesioriebeckite Zn-rich variety $\square Na_2(ZnMg_2)Fe^{3+}{}_2(Si_8O_{22})(OH)_2$ (Fig. 2.594)
Locality: "Mixed series" metamorphic complex, near Nežilovo, Pelagonian massif, Macedonia.
Description: Brownish-green crystals from the association with zincohögbomite-2*N*6*S*, barite, dolomite, quartz, Zn-rich phlogopite, spessartite, etc. The empirical formula is (electron microprobe): $Na_{0.3}(Na_{1.3}Mn_{0.4}Ca_{0.3})(Zn_{1.0}Mg_{2.1}Fe_{1.9})(Si_{7.65}Al_{0.35})(OH)_2$.
Kind of sample preparation and/or method of registration of the spectrum: KBr disc. Absorption.
Wavenumbers (cm^{-1}): 3651w, 3640sh, 1140sh, 1088s, 1040sh, 981s, 890sh, 785, 740w, 688, 672, 647, 610w, 545sh, 509s, 462s, 384.

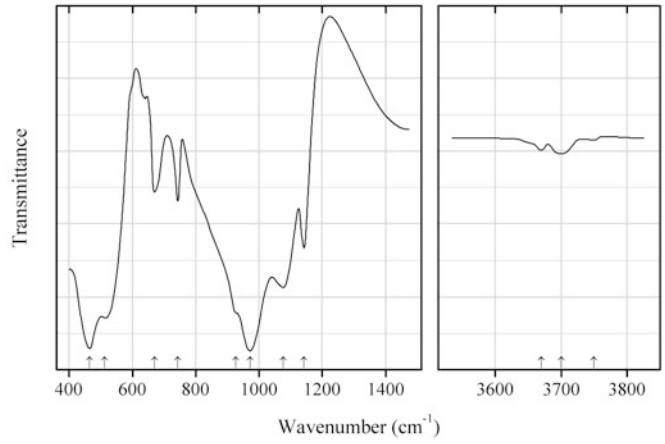

Fig. 2.595 IR spectrum of fluoro-richterite drawn using data from Bazhenov et al. (1993)

Sib135 Fluoro-richterite $Na(NaCa)Mg_5(Si_8O_{22})F_2$ (Fig. 2.595)
Locality: Ilmeny (Il'menskie) Mts., South Urals, Russia (type locality).
Description: Green prismatic crystals. Holotype or cotype sample.
Kind of sample preparation and/or method of registration of the spectrum: No data.
Source: Bazhenov et al. (1993).
Wavenumbers (cm^{-1}): 3750w, 3700w, 3670w, 1142, 1077s, 972s, 927sh, 744, 670w, 510–515s, 465s.

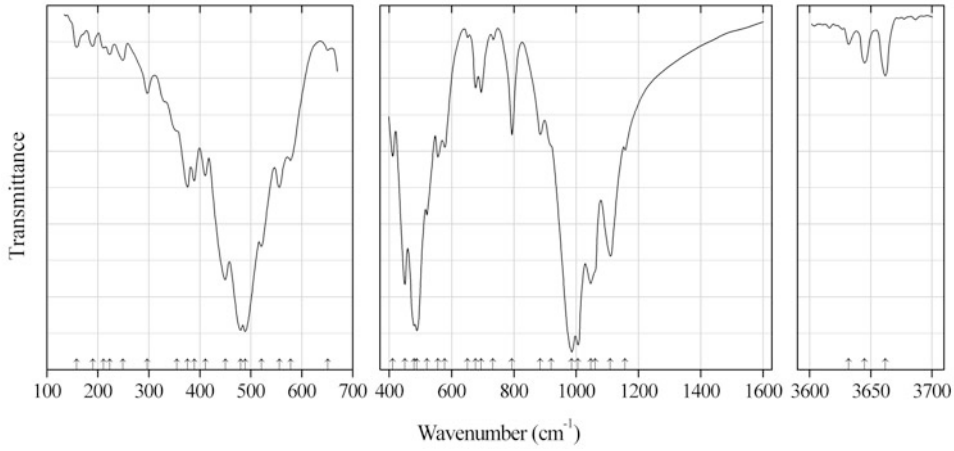

Fig. 2.596 IR spectrum of glaucophane drawn using data from Gillet et al. (1989)

Sib136 Glaucophane $\square Na_2(Mg_3Al_2)(Si_8O_{22})(OH)_2$ (Fig. 2.596)
Locality: Sesia-Lanzo zone, Western Alps.
Description: Crystals from the association with quartz. Close to the end member by composition.
Kind of sample preparation and/or method of registration of the spectrum: KBr disc. Absorption.
Source: Gillet et al. (1989).

Wavenumbers (cm^{-1}): 3662w, 3645w, 3632w, 1157, 1110, 1061sh, 1047s, 1006s, 986s, 920sh, 885, 794, 733w, 695, 677, 651w, 578, 556, 521, 489s, 480s, 450s, 411, 389, 376, 355sh, 297, 249w, 223w, 211, 190w, 158w.

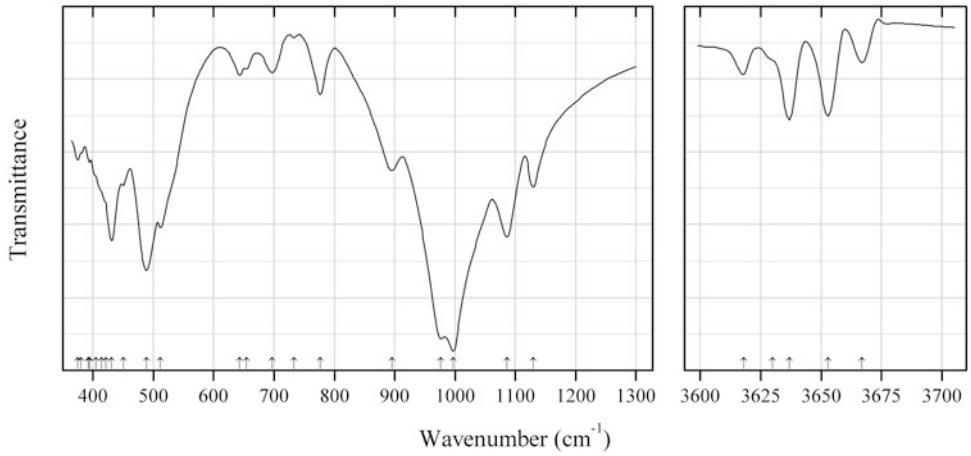

Fig. 2.597 IR spectrum of grunerite drawn using data from Apopei et al. (2011)

Sib137 Grunerite $\square Fe^{2+}_2Fe^{2+}_5(Si_8O_{22})(OH)_2$ (Fig. 2.597)
Locality: Schneeberg, Tirol, Austria.
Description: Sample No. 5848 from the collection of the "Grigore Cobâlcescu" Mineralogy and Petrography Museum of the "Alexandru Ioan Cuza"
University, Iaşi, Romania.
Kind of sample preparation and/or method of registration of the spectrum: KBr disc. Absorption.
Source: Apopei et al. (2011).
Wavenumbers (cm^{-1}): 3618w, 3630sh, 3637w, 3653w, 3667w, 1130, 1086s, 997s, 977s, 896, 777w, 733w, 697w, 654w, 643w, 512, 489s, 450, 431s, 421sh, 414sh, 405sh, 395w, 392w, 380sh, 375w.
Note: No data on the chemical composition of the sample used are given in the cited paper.

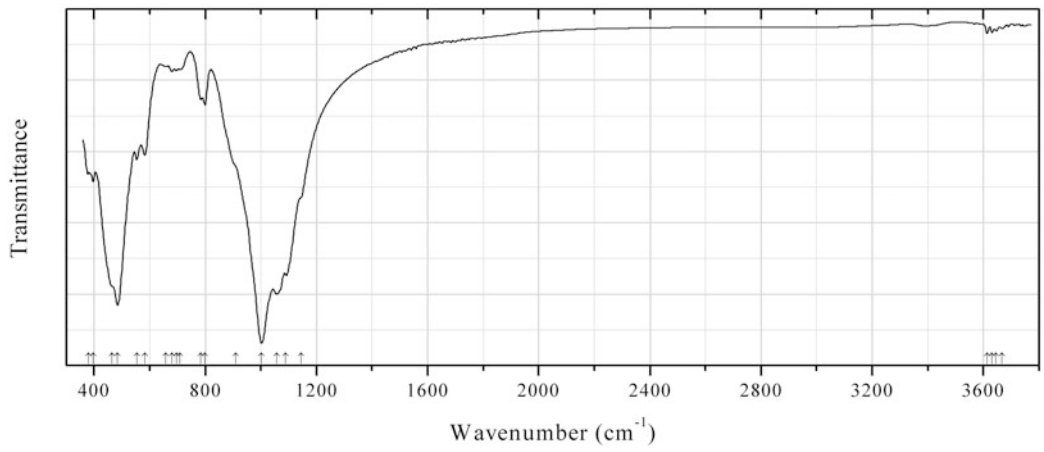

Fig. 2.598 IR spectrum of ferro-pedrizite obtained by N.V. Chukanov

Sib138 Ferro-pedrizite $NaLi_2(Fe^{2+}{}_2Al_2Li)Si_8O_{22}(OH)_2$ (Fig. 2.598)
Locality: Sangilen Upland, left side of the Sutlug Valley, Targi River Basin, Tuva Republic, Eastern Siberian Region, Russia (type locality).
Description: Dark grey-blue long-prismatic crystals from the association with quartz, albite, microcline, and spodumene, cassiterite, beryl, columbite-(Mn), fergusonite-(Y)-β, fluorapatite, schorl, trilithionite and fluorite. Holotype sample. Monoclinic, space group *C*2/*m*, $a = 9.3716(4)$, $b = 17.649(1)$, $c = 5.2800(6)$ Å, $\beta = 102.22(1)°$, $V = 853.5(1)$ Å^3, $Z = 2$. $D_{meas} = 3.13(1)$ g/cm^3, $D_{calc} = 3.135$ g/cm^3. Optically biaxial (−), $\alpha = 1.614(3)$, $\beta = 1.638(3)$, $\gamma = 1.653(3)$, $2V = 75(5)°$. The empirical formula is: $(Na_{0.55}K_{0.02})_{\Sigma 0.57}(Li_{1.85}Na_{0.11}Ca_{0.04})_{\Sigma 2.00}(Fe^{2+}{}_{1.02}Mg_{0.90}Fe^{3+}{}_{0.47}Mn_{0.07}Al_{1.86}Li_{0.68})_{\Sigma 8.00}[(Si_{7.77}Al_{0.23})_{\Sigma 8.00}O_{22}][(OH)_{1.35}F_{0.62}O_{0.03})]$. The strongest lines of the powder X-ray diffraction pattern [*d*, Å (*I*, %) (*hkl*)] are: 8.147 (52) (110), 4.420 (22) (040), 3.385 (18) (131), 3.009 (100) (310), 2.7102 (28) (330), 2.6865 (29) (151), 2.4824 (19) (20–2), 1.6236 (21) (461).
Kind of sample preparation and/or method of registration of the spectrum: KBr disc. Absorption.
Wavenumbers (cm^{-1}): 3667w, 3646w, 3630w, 3613w, 1145sh, 1089s, 1057s, 1003s, 910sh, 799, 785, 710w, 697w, 680w, 658w, 582, 553, 485s, 465sh, 398, 380.

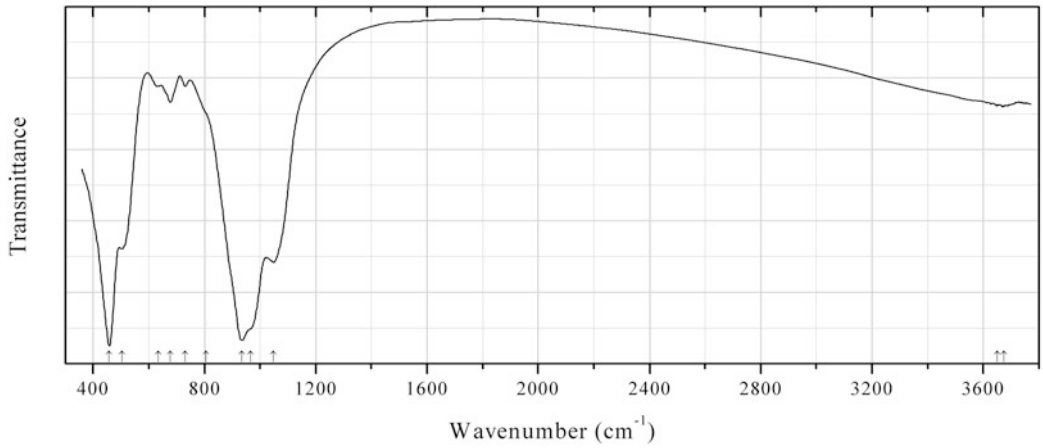

Fig. 2.599 IR spectrum of oxo-magnesio-hastingsite obtained by N.V. Chukanov

Sib139 Oxo-magnesio-hastingsite $NaCa_2Mg_2Fe^{3+}{}_3(Si_6Al_2O_{22})O_2$ (Fig. 2.599)
Locality: Radersberg, Brück-Dreis, near Daun, Eifel Mts., Germany.
Description: Dark brown rounded crystal from weathered basalt. The empirical formula is (electron microprobe): $(Na_{0.55}K_{0.44})(Ca_{1.90}Na_{0.08}Mn_{0.02})[Mg_{2.00}(Fe^{3+}{}_{1.50}Mg_{0.90}Ti_{0.40}Al_{0.19}Cr_{0.01})](Si_{5.73}Al_{2.27}O_{22})(O,OH)_2$.
Kind of sample preparation and/or method of registration of the spectrum: KBr disc. Absorption.
Wavenumbers (cm^{-1}): 3673w, 3650sh, 1049s, 965sh, 935s, 805sh, 731w, 678, 633w, 503s, 458s.

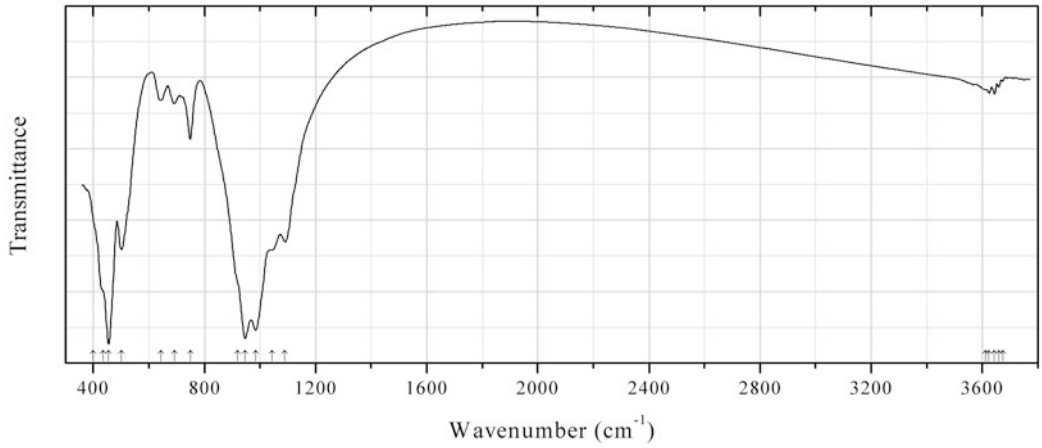

Fig. 2.600 IR spectrum of ferro-ferri-hornblende obtained by N.V. Chukanov

Sib140 Ferro-ferri-hornblende $\square Ca_2(Fe^{2+}{}_4Fe^{3+})(Si_7AlO_{22})(OH)_2$ (Fig. 2.600)
Locality: Königshainer Mts., Lausitz, Saxony, Germany.
Description: Dark green grains from granite. The empirical formula is (electron microprobe): $(\square_{0.90}K_{0.10})(Ca_{1.83}Na_{0.10}Mn_{0.07})[(Fe^{2+}{}_{2.66}Mg_{1.34})(Fe^{3+}{}_{0.60}Al_{0.37}Ti_{0.03})](Si_{6.95}Al_{1.05}O_{22})(OH)_2$.
Kind of sample preparation and/or method of registration of the spectrum: KBr disc. Absorption.
Wavenumbers (cm^{-1}): 3674w, 3659w, 3643w, 3624w, 3612sh, 1090s, 1042s, 984s, 946s, 920sh, 749, 692, 643, 501s, 455s, 435sh, 400sh.

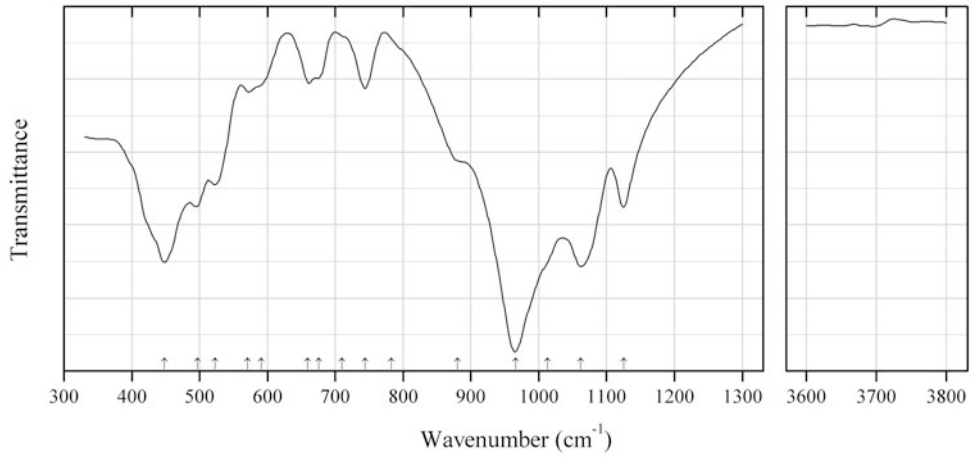

Fig. 2.601 IR spectrum of magnesio-mangani-ungarettiite drawn using data from Ishida (1989)

Sib141 Magnesio-mangani-ungarettiite $NaNa_2(Mg_2Mn^{3+}{}_3)(Si_8O_{22})O_2$ (Fig. 2.601)
Locality: Kamisugai mine, Ehime prefecture, Japan.
Description: The empirical formula is (electron microprobe): $(Na_{2.42}Ca_{0.26}K_{0.22})(Mn_{3.63}Mg_{1.15}Fe_{0.27}Ti_{0.03})Si_{8.09}O_{24}$.
Kind of sample preparation and/or method of registration of the spectrum: KBr disc. Absorption.
Source: Ishida (1989).

Wavenumbers (cm^{-1}): 1125, 1062s, 1013sh, 966s, 880, 783sh, 744w, 710w, 676w, 659w, 591sh, 571w, 523, 497, 448s.
Note: In the cited paper this sample is described under the name "kozulite". However the absence of distinct absorption bands in the range from 3600 to 3800 cm^{-1} indicates that the site *W* is predominantly occupied with O and, consequently, Mn is predominantly trivalent.

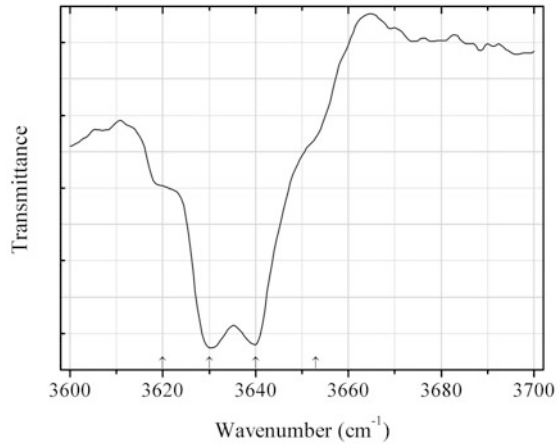

Fig. 2.602 IR spectrum of magbasite drawn using data from Welch et al. (2014)

Sib142 Magbasite $KBaFe^{3+}Mg_7(Si_8O_{22})(OH)_2F_6$ (Fig. 2.602)
Locality: Eldor carbonatite complex, Quebec, Canada.
Description: Bundles of strongly pleochroic sub-parallel crystals from the association with phlogopite, quartz, siderite, Nb-rich rutile, bafertisite, monazite-(Ce), bastnäsite-(Ce), parisite-(Ce), and fluorite. The crystal structure is solved. Orthorhombic, space group *Pmme*, a = 18.9506(3), b = 22.5045(3), c = 5.2780(1) Å, V = 2250.93(6) Å^3, Z = 4. D_{calc} = 3.326 g/cm^3. The empirical formula is $K_{0.86}Ba_{1.02}Mg_{6.50}Fe^{2+}_{0.53}Fe^{3+}_{0.90}Al_{0.19}Si_{7.90}O_{22.04}(OH)_{2.17}F_{5.79}$. The strongest lines of the powder X-ray diffraction pattern [*d*, Å (*I*, %) (*hkl*)] are: 3.628 (32) (440), 3.546 (47) (401, 421), 2.991 (68) (441), 2.848 (39) (531, 080), 2.572 (100) (461, 202), 2.416 (41) (312, 660), 2.306 (38) (042, 332, 402).
Kind of sample preparation and/or method of registration of the spectrum: KBr disc. Absorption.
Source: Welch et al. (2014).
Wavenumbers (cm^{-1}): 3653sh, 3640, 3630, 3620sh.

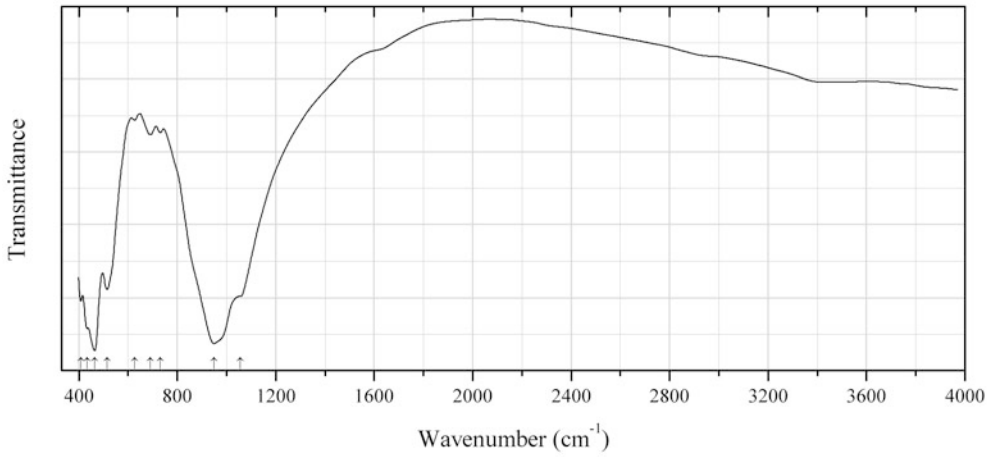

Fig. 2.603 IR spectrum of magnesio-fluoro-hastingsite drawn using data from Bojar and Walter (2006)

Sib143 Magnesio-fluoro-hastingsite $NaCa_2(Mg_4Fe^{3+})(Si_6Al_2O_{22})F_2$ (Fig. 2.603)
Locality: Dealul Uroi, Hunedoara Co., Romania (type locality).
Description: Reddish-brown crystals from trachyandesite, from the association with titaniferous hematite, augite, phlogopite, enstatite, feldspar, tridymite, titanite, fluorapatite, ilmenite, and pseudobrookite. Holotype sample. Monoclinic, space group *C*2/*m*, $a = 9.871(1)$, $b = 18.006(2)$, $c = 5.314(1)$ Å, $\beta = 105.37(1)°$, $V = 910.7(2)$ Å^3, $Z = 2$. $D_{calc} = 3.18$ g/cm^3. Optically biaxial (+), $\alpha = 1.642$, $\beta = 1.647$, $\gamma = 1.662$, $2V = 61°$. The empirical formula is $(Na_{0.50}K_{0.22}Ca_{0.17})Ca_{2.00}(Mg_{4.03}Fe^{3+}_{0.70}Al_{0.13}Ti_{0.13})(Si_{5.89}Al_{2.11}O_{22})F_{2.00}$. The strongest lines of the powder X-ray diffraction pattern [*d*, Å (*I*, %) (*hkl*)] are: 9.008 (27) (020), 8.421 (61) (110), 3.377 (44) (131), 3.271 (61) (240), 3.124 (100) (310), 2.932 (35) (221), 2.805 (28) (330), 2.700 (54) (151).
Kind of sample preparation and/or method of registration of the spectrum: KBr disc. Transmission.
Source: Bojar and Walter (2006).
Wavenumbers (cm^{-1}): 1056sh, 950s, 731w, 691w, 627w, 515s, 465s, 434s, 408s.

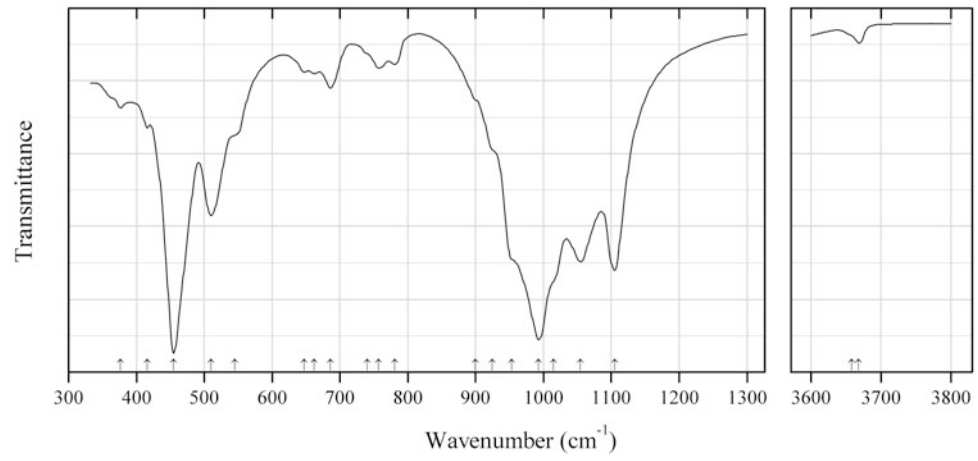

Fig. 2.604 IR spectrum of ferri-winchite manganoan variety drawn using data from Ishida (1989)

Sib144 Ferri-winchite manganoan variety □(NaCa)[(Mg,Mn^{2+})$_4$$Fe^{3+}$](Si$_8O_{22}$)(OH)$_2$ (Fig. 2.604)
Locality: Kamisugai mine, Ehime prefecture, Japan.
Description: The empirical formula is (electron microprobe): $K_{0.03}(Na_{0.91}Ca_{0.92}Mn_{0.09})[(Mg_{3.39}Mn_{0.71})(Fe^{3+}{}_{0.87}Al_{0.02}Ti_{0.01})]Si_{8.03}O_{22}(OH,O)_2$.
Kind of sample preparation and/or method of registration of the spectrum: KBr disc. Absorption.
Source: Ishida (1989).
Wavenumbers (cm^{-1}): 3668w, 3658sh, 1105s, 1054s, 1015sh, 993s, 953sh, 925sh, 900sh, 781w, 757w, 740sh, 686, 662w, 647w, 545sh, 510, 455s, 416, 376w.

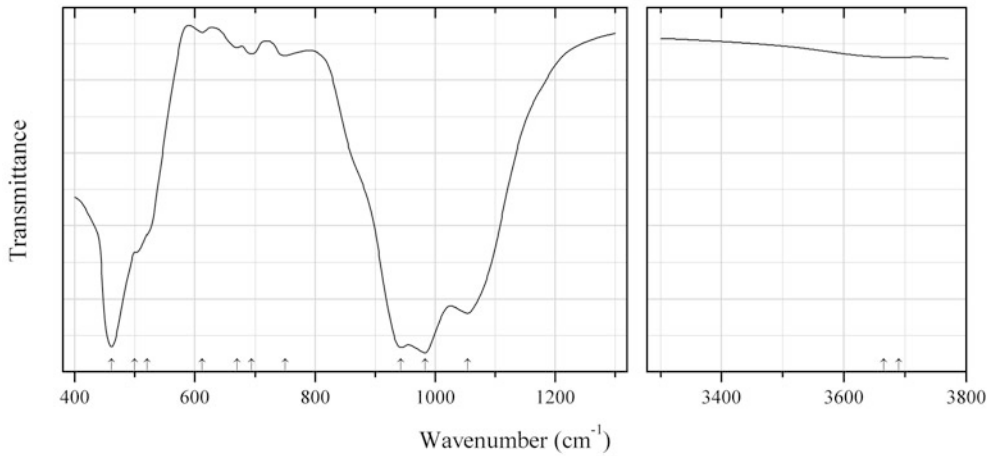

Fig. 2.605 IR spectrum of potassic-chloro-pargasite drawn using data from Chukanov et al. (2002)

Sib145 Potassic-chloro-pargasite $KCa_2(Mg_4Al)(Si_6Al_2O_{22})Cl_2$ (Fig. 2.605)
Locality: Salnye Tundry Mts., Kola Peninsula, Russia (type locality).
Description: Black grains from the association with chlorapatite, almandine, diopside, enstatite, Cl-rich biotite, potassic pargasite, marialite, and plagioclase. Holotype sample. Monoclinic, space group *C*2/*m*, a = 9.843(3), b = 18.130(5), c = 5.362(3) Å, β = 105.5(5)°, V = 922.1(6) Å^3, Z = 2. D_{meas} = 3.29(5) g/cm^3, D_{calc} = 3.35 g/cm^3. Optically biaxial (−), α = 1.675 (1), β = 1.687(1), γ = 1.690 (3), 2 V = 65(15)°. The empirical formula is (electron microprobe): $(K_{0.60}Na_{0.37})Ca_{1.89}(Mg_{2.09}Fe^{2+}{}_{1.68}Fe^{3+}{}_{0.47}Al_{0.73}Ti_{0.03})(Si_{5.99}Al_{2.01}O_{22})Cl_{1.14}(OH)_{0.86}$. The strongest lines of the powder X-ray diffraction pattern [*d*, Å (*I*, %) (*hkl*)] are: 8.42 (8) (110), 3.116 (3) (310), 2.951 (3) (−151, 221), 2.714 (10) (151), 2.562 (7) (241), 1.444 (3) (−533).
Kind of sample preparation and/or method of registration of the spectrum: KBr disc. Absorption.
Wavenumbers (cm^{-1}): 3690w, 3665w, 1054s, 983s, 943s, 750w, 694w, 670w, 612w, 520sh, 500sh, 461s.
Source: Chukanov et al. (2002).

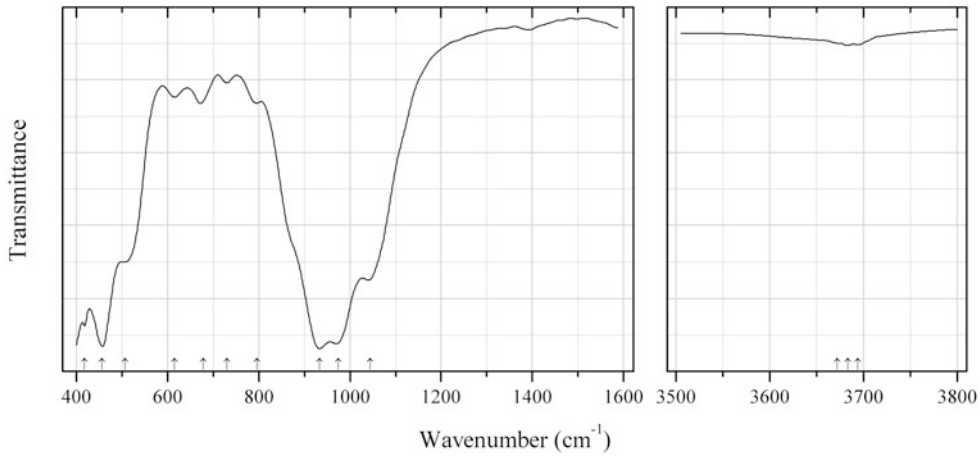

Fig. 2.606 IR spectrum of potassic-magnesio-hastingsite drawn using data from Korinevsky and Korinevsky (2006)

Sib146 Potassic-magnesio-hastingsite $KCa_2(Mg_4Fe^{3+})(Si_6Al_2O_{22})(OH)_2$ (Fig. 2.606)
Locality: Osinovy Mys (Osinovy cape), Ishkul lake, Ilmenogorsky metamorphic complex, Chelyabinsk region, South Urals, Russia (type locality).
Description: Black grains from biotite-amphibole gabbro. Cotype sample. Monoclinic, space group *C*2/*m*, a = 9.930(9), b = 718.093(4), c = 5.326(7) Å, β = 105.327(7)°, V = 922.98 Å^3. D_{meas} = 3.02 g/cm^3. Optically biaxial (−), α = 1.682(3), β = 1.695(3), γ = 1.702(3), 2 V = 58°–88°. The empirical formula is $(K_{0.53}Na_{0.47})(Ca_{1.90}Mn_{0.06}Mg_{0.03}Ba_{0.01})(Mg_{2.06}Fe^{2+}{}_{1.35}Fe^{3+}{}_{1.00}Al_{0.47}Ti_{0.19}V_{0.01})(Si_{6.03}Al_{1.97}O_{22})[(OH)_{1.93}O_{0.07}]$. The strongest lines of the powder X-ray diffraction pattern [*d*, Å (*I*, %) (*hkl*)] are: 8.480 (100) (110), 3.284 (40) (240), 2.947 (28) (221), 2.820 (28) (330), 2.714 (52) (151), 2.167 (28) (261).
Kind of sample preparation and/or method of registration of the spectrum: KBr disc. Transmission.
Source: Korinevsky and Korinevsky (2006).
Wavenumbers (cm^{-1}): 3694w, 3683w, (3672w), 1045s, 974s, 933s, 796w, 730w, 679, 616w, 507, 457s, (418s).
Note: Other weak bands with wavenumbers above 1200 cm^{-1} correspond to impurities.

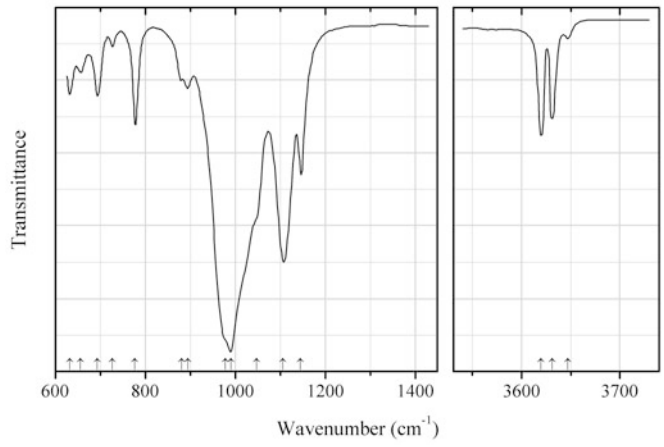

Fig. 2.607 IR spectrum of riebeckite drawn using data from Hodgson et al. (1965)

Sib147 Riebeckite $\square Na_2(Fe^{2+}{}_3Fe^{3+}{}_2)(Si_8O_{22})(OH)_2$ (Fig. 2.607)
Locality: Koegas, Bushveld Complex, Transvaal, South Africa.
Description: Crocidolite asbest. Monoclinic, space group *C*2/*m*, a = 9.80, b = 17.85, c = 5.50 Å, β = 103.83°. The approximate empirical formula is $Na_2(Fe^{2+}{}_{2.6}Mg_{0.4}Fe^{3+}{}_2)(Si_8O_{22})(OH)_2$.
Kind of sample preparation and/or method of registration of the spectrum: KBr disc. Absorption.
Source: Hodgson et al. (1965).
Wavenumbers (cm^{-1}): 3647w, 3631, 3620, 1144, 1106s, 1048sh, 991s, 978sh, 895, 881w, 777, 727w, 693, 656w, 632.

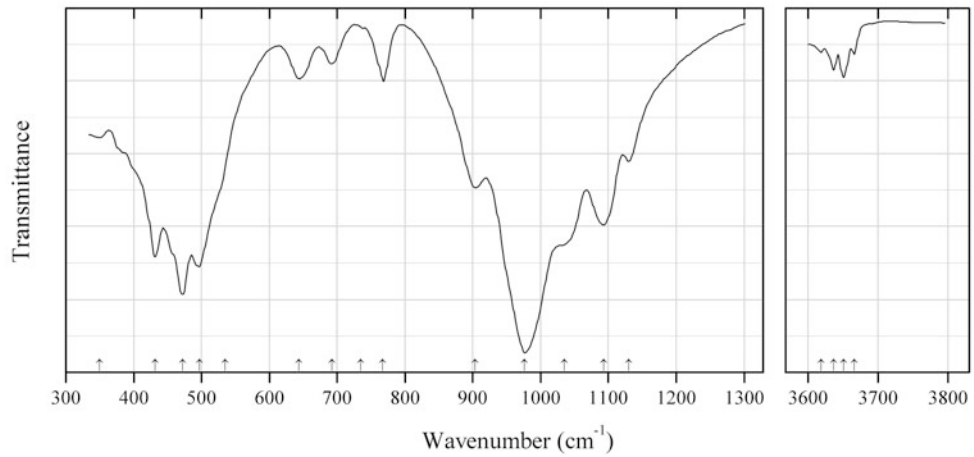

Fig. 2.608 IR spectrum of "tirodite" drawn using data from Ishida (1989)

Sib148 "Tirodite" $\square Mn_2Mg_5(Si_8O_{22})(OH)_2$ (Fig. 2.608)
Locality: Japan (exact locality is not indicated).
Description: The name "tirodite" was discredited in the new nomenclature of amphiboles (Hawthorne et al. 2012b). The empirical formula is (electron microprobe): $(Na_{0.11}K_{0.045})(Mn_{1.53}Ca_{0.35}Na_{0.12})(Mg_{3.54}Fe_{1.21}Mn_{0.23}Ti_{0.02})(Si_{7.96}Al_{0.03}Fe_{0.01}O_{22})(OH)_2$.
Kind of sample preparation and/or method of registration of the spectrum: KBr disc. Absorption.
Source: Ishida (1989).

Wavenumbers (cm^{-1}): 3666w, 3651w, 3637w, 3619w, 1130, 1093s, 1035s, 976s, 903, 767, 735w, 692w, 644, 535sh, 497s, 472s, 432s, 350

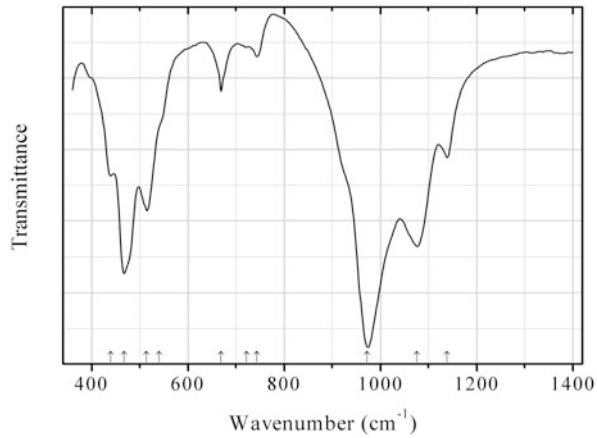

Fig. 2.609 IR spectrum of magnesio-fluoro-arfvedsonite obtained by N.V. Chukanov

Sib149 Magnesio-fluoro-arfvedsonite $NaNa_2(Mg_4Fe^{3+})(Si_8O_{22})F_2$ (Fig. 2.609)
Locality: Bellerberg, near Meien, Eifel, Rheinland-Pfalz (Rhineland-Palatinate), Germany.
Description: Orange-brown prismatic crystals from the association with aegirine-augite. The empirical formula is (electron microprobe): $(Na_{0.78}K_{0.18})(Na_{1.56}Ca_{0.44}))Mg_{4.03}Mn_{0.42}Fe_{0.48}Ti_{0.05}Cr_{0.02})(Si_{7.58}Fe_{0.27}Al_{0.15}O_{22})F_{1.97}(O,OH)_{0.03}$.
Kind of sample preparation and/or method of registration of the spectrum: KBr disc. Absorption.
Wavenumbers (cm^{-1}): 1139, 1076s, 973s, 743, 722w, 669, 540sh, 514, 467s, 440.

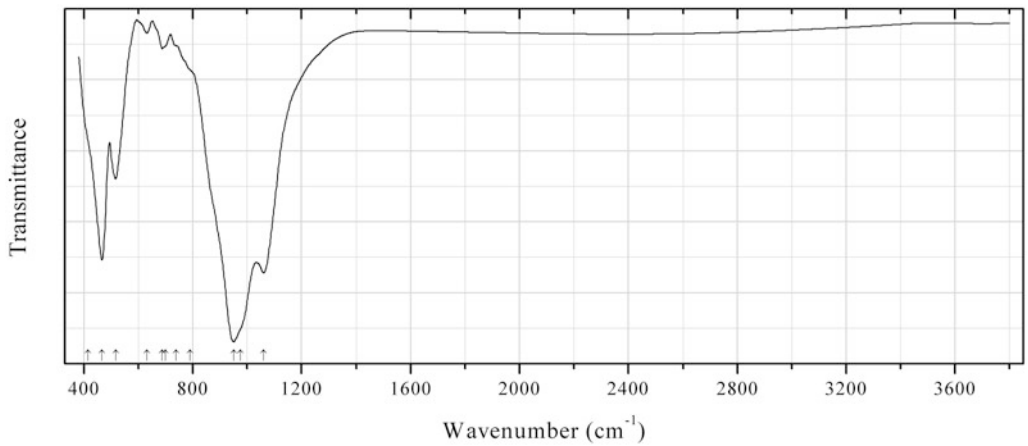

Fig. 2.610 IR spectrum of amphibole "*rootname* 4" F analogue obtained by N.V. Chukanov

Sib150 Amphibole "*rootname* 4" F analogue $NaCa_2(Mg_4Ti)(Si_5Al_3O_{22})F_2$ (Fig. 2.610)
Locality: Rothenberg basalt quarry, Rothenberg Mt., near Mendig, Eifel Mts., Rhineland-Palatinate (Rheinland-Pfalz), Germany.
Description: Orange-brown epitaxial crystalline crust on augite crystal. Monoclinic, space group *C*2/*m*, a = 9.8684(2), b = 18.046(1), c = 5.3113(1) Å, β = 105.543(3)°, V = 911.26(3) Å^3, Z = 2.

D_{calc} = 3.225 g/cm^3. The empirical formula is (electron microprobe): $(Na_{0.65}K_{0.30})(Ca_{1.95}Na_{0.05})(Mg_{3.36}Fe^{3+}_{1.02}Ti_{0.60})(Si_{5.92}Al_{2.06})O_{22}(F_{1.11}O_{0.89})$.
Kind of sample preparation and/or method of registration of the spectrum: KBr disc. Absorption.
Wavenumbers (cm^{-1}): 1060s, 975sh, 950s, 790sh, 740, 700sh, 688, 632, 517, 467s, 415sh.
Note: According to Hawthorne et al. (2012b), the subgroup of calcium amphiboles with (OH,F, Cl) > 1 *apfu* and ^{C}Ti > 0.5 *apfu* unites potentially new amphiboles with the *rootname* 4.

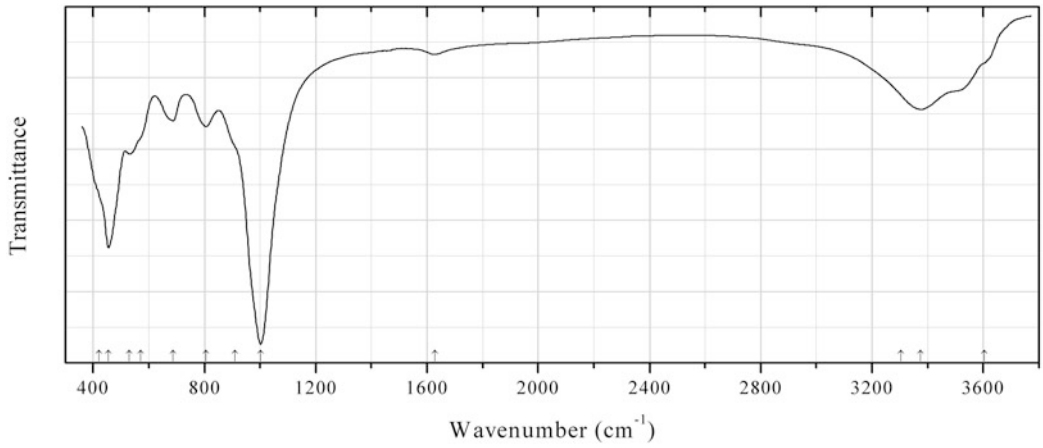

Fig. 2.611 IR spectrum of fraipontite obtained by N.V. Chukanov

Sil257 Fraipontite $(Zn,Al)_3[(Si,Al)_2O_5](OH)_4$ (Fig. 2.611)
Locality: Promezhutok cave, Kugitang-Tau ridge, Turkmenistan.
Description: White massive. Investigated by V.Yu. Karpenko. The empirical formula is (electron microprobe): $(Zn_{1.7}Al_{0.9}Mg_{0.1}Fe_{0.1}Na_{0.1})(Si_{1.4}Al_{0.6}O_5)(OH,O)_4 \cdot nH_2O$.
Kind of sample preparation and/or method of registration of the spectrum: KBr disc. Absorption.
Wavenumbers (cm^{-1}): 3605sh, 3305, 3375, 1628w, 1002s, 910sh, 805, 687, 570sh, 531, 455s, 420sh.

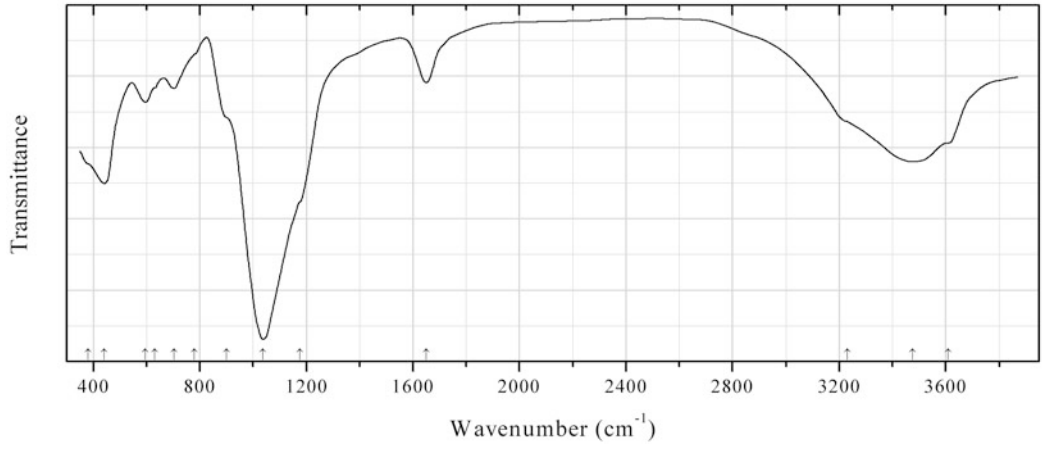

Fig. 2.612 IR spectrum of günterblassite obtained by N.V. Chukanov

Sil258 Günterblassite $(K,Ca)_{3-x}Fe[(Si,Al)_{13}O_{25}(OH,O)_4]\cdot 7H_2O$ (Fig. 2.612)
Locality: Rother Kopf Mt., near the town Gerolstein, Eifel Mountains, Rheinland-Pfalz, Germany (type locality).
Description: Flattened colourless crystals from the association with nepheline, leucite, augite, phlogopite, magnetite, perovskite, götzenite, lamprophyllite-group minerals, chabazite-K, chabazite-Ca, phillipsite-K, and calcite. Holotype sample. Orthorhombic, space group $Pnm2_1$, a = 6.528(1), b = 6.970(1), c = 37.216(5) Å; V = 1693.3(4) Å^3, Z = 2. D_{calc} = 2.17 g/cm^3, D_{meas} = 2.18(1) g/cm^3. Optically biaxial (+), α = 1.488(2), β = 1.490(2), γ = 1.493(2), 2 V = 80(5)°. The empirical formula is $Na_{0.15}K_{1.24}Ba_{0.30}Ca_{0.72}Mg_{0.16}Fe^{2+}_{0.48}[Si_{9.91}Al_{3.09}O_{25.25}(OH)_{3.75}]\cdot 7.29H_2O$. The strongest lines of the powder X-ray diffraction pattern [d, Å (I, %) (hkl)] are: 6.523 (100) (100), 6.263 (67) (101, 006), 3.244 (49) (024, 201, 1.0.10, 202), 3.062 (91) (204, 120, 121, 0.1.11, 026, 122), 2.996 (66) (1.0.11, 205, 123), 2.955 (63) (210, 211, 1.1.10, 212, 124), 2.763 (60) (1.1.11, 126, 215).
Kind of sample preparation and/or method of registration of the spectrum: KBr disc. Absorption.
Wavenumbers (cm^{-1}): 3610sh, 3475s, 3230sh, 1650, 1175sh, 1037s, 900sh, 780sh, 704, 630sh, 596, 442s, 380sh.

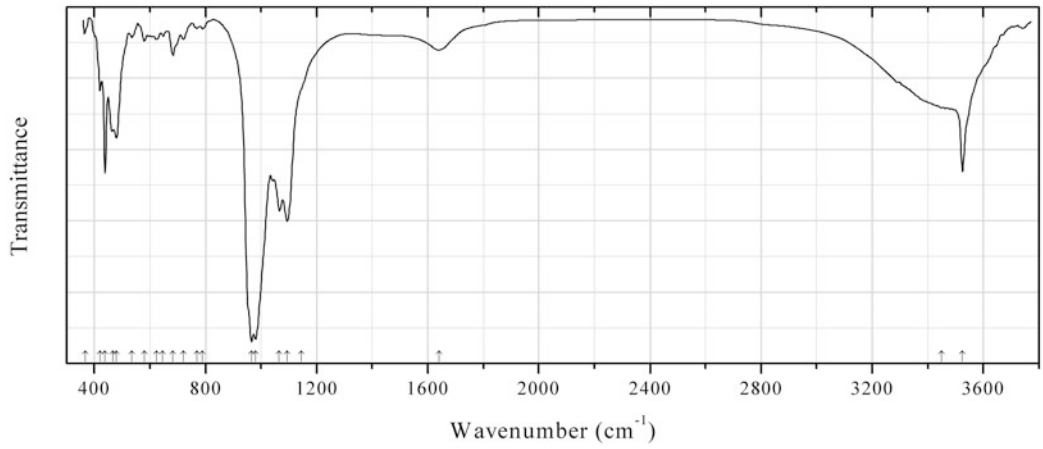

Fig. 2.613 IR spectrum of ferroceladonite obtained by N.V. Chukanov

Sil259 Ferroceladonite $KFe^{2+}Fe^{3+}(Si_4O_{10})(OH)_2$ (Fig. 2.613)
Locality: Ariskop Quarry, Aris, near Windhoek, Windhoek district, Khomas Region, Namibia.
Description: Dark bluish-green aggregate from the association with aegirine and tuperssuatsiaite. The empirical formula is (electron microprobe): $(K_{0.88}Na_{0.06}Ca_{0.03})(Fe_{1.72}Al_{0.17}Mn_{0.06}Mg_{0.04}Cr_{0.01})(Si_{3.97}Al_{0.03}O_{10})(OH)_2\cdot nH_2O$.
Kind of sample preparation and/or method of registration of the spectrum: KBr disc. Absorption.
Wavenumbers (cm^{-1}): 3525, 3450sh, 1640w, 1145sh, 1094s, 1066s, 980s, 966s, 790w, 770w, 722w, 683, 647w, 624w, 580w, 535w, 480, 467, 439, 420, 367w.

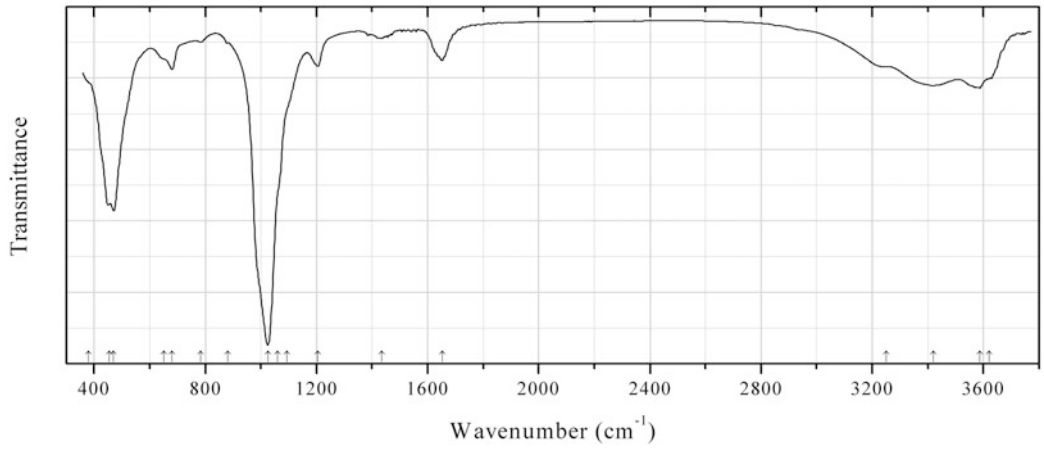

Fig. 2.614 IR spectrum of ferrosepiolite obtained by N.V. Chukanov

Sil260 Ferrosepiolite $Fe^{2+}{}_4(Si_6O_{15})(OH)_2 \cdot 6H_2O$ (Fig. 2.614)
Locality: Kedykverpakhk Mt., Lovozero alkaline complex, Kola peninsula, Murmansk region, Russia.
Description: Beige fibrous aggregate from the association with potassic feldspar, aegirine, natrolite, pyrite, and a caryochroite-like mineral. Investigated by I.V. Pekov. The empirical formula is (electron microprobe): $Na_{0.06}(Fe_{1.82}Mg_{1.68}Mn_{0.19}Al_{0.05})(Si_{6.00}O_{15})(OH)_2 \cdot nH_2O$. The strongest lines of the powder X-ray diffraction pattern [*d*, Å (*I*, %)] are: 12.1 (100), 7.49 (5), 4.405 (5), 3.750 (6), 3.381 (8), 2.540 (4).
Kind of sample preparation and/or method of registration of the spectrum: KBr disc. Absorption.
Wavenumbers (cm^{-1}): 3620sh, 3587, 3420, 3250, 1653, 1436w, 1205, 1095sh, 1060sh, 1025s, 882w, 784w, 681, 650sh, 470s, 455s, 380sh.

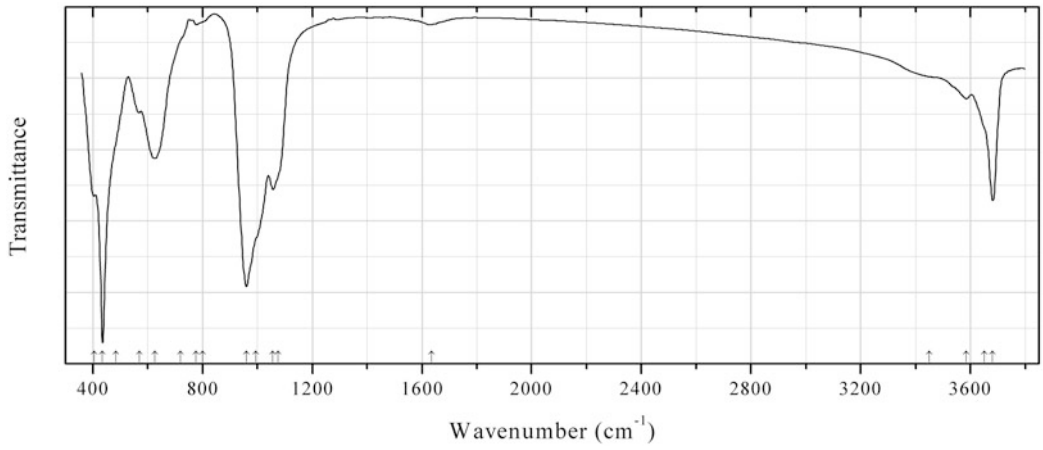

Fig. 2.615 IR spectrum of carlosturanite obtained by N.V. Chukanov

Sil261 Carlosturanite $(Mg,Fe^{2+},Ti)_{21}(Si,Al)_{12}O_{28}(OH)_{34} \cdot H_2O$ (Fig. 2.615)
Locality: Auriol mine, Sampeyre, Varaita valley, Piedmont, Italy (type locality).
Description: Greenish-brown fibrous aggregate. Confirmed by IR spectrum.
Kind of sample preparation and/or method of registration of the spectrum: KBr disc. Absorption.

Wavenumbers (cm^{-1}): 3681, 3650sh, 3585w, 3450sh, 1635w, 1075sh, 1057s, 995sh, 960s, 800sh, 777w, 720sh, 626, 570, 485sh, 436s, 406.

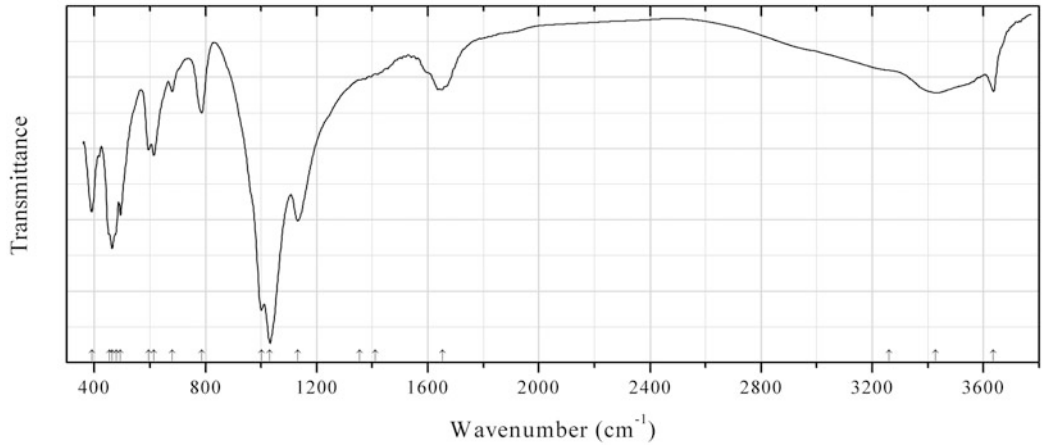

Fig. 2.616 IR spectrum of gyrolite obtained by N.V. Chukanov

Sil262 Gyrolite $NaCa_{16}(Si_{23}AlO_{60})(OH)_8 \cdot 14H_2O$ (Fig. 2.616)
Locality: Tura, Evenki autonomous area, Siberia, Russia.
Description: Light gray platelets with mica-like cleavage from the association with zeolites. A Na- and Al-deficient variety. Investigated by I.V. Pekov. The empirical formula is (electron microprobe): $Na_{0.49}Ca_{15.23}(Si_{28.80}Al_{0.20}O_{60})(OH,H_2O)_8 \cdot nH_2O$. The strongest lines of the powder X-ray diffraction pattern [*d*, Å (*I*, %)] are: 22.0 (100), 11.05 (43), 8.41 (21), 4.20 (69), 3.71 (26), 3.159 (45), 3.097 (30), 1.837 (34).
Kind of sample preparation and/or method of registration of the spectrum: KBr disc. Absorption.
Wavenumbers (cm^{-1}): 3636, 3428, 3260sh, 1652, 1410sh, 1355sh, 1132s, 1032s, 1001s, 786, 680w, 614, 595, 494, 480sh, 464s, 455sh, 392.

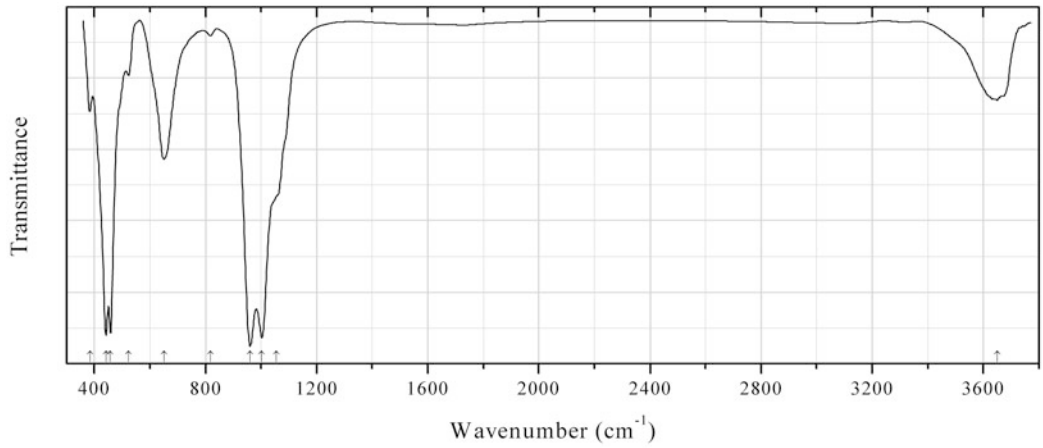

Fig. 2.617 IR spectrum of clinochlore obtained by N.V. Chukanov

Sil263 Clinochlore $(Mg,Al)_6(Si,Al)_4O_{10}(OH)_8$ (Fig. 2.617)

Locality: Bazhenovskoe (Bazhenovskoye) chrysotile asbestos deposit, Asbest, Middle Urals, Russia.
Description: Colourless platy crystals from the association with vesuvianite. A Ca-bearing variety. The empirical formula is $Ca_{0.42}(Mg_{4.46}Al_{0.96}Fe_{0.58})(Si_{3.66}Al_{0.34}O_{10})(OH)_8$.
Kind of sample preparation and/or method of registration of the spectrum: KBr disc. Absorption.
Wavenumbers (cm^{-1}): 3649, 1055sh, 1003s, 961, 817w, 650, 523w, 458s, 442s, 384.

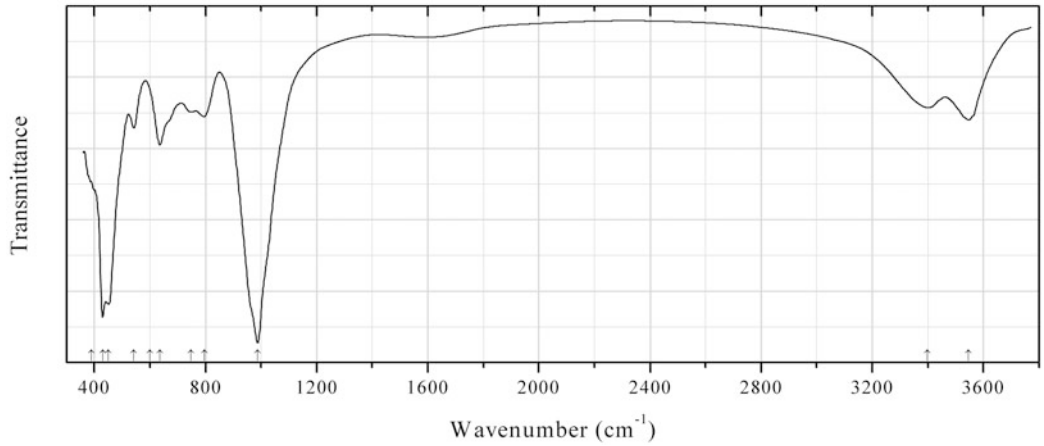

Fig. 2.618 IR spectrum of pennantite obtained by N.V. Chukanov

Sil264 Pennantite $Mn^{2+}{}_5Al(Si_3AlO_{10})(OH)_8$ (Fig. 2.618)
Locality: Molinello manganese mine, Val Graveglia, near Chiavari, Liguria, Italy.
Description: Brown scaly aggregate forming veinlet in quartz. The empirical formula is (electron microprobe): $(Mn_{2.5}Mg_{2.3}Fe_{0.1}Al_{1.1})(Si_{2.7}Al_{1.3}O_{10})(OH)_8$.
Kind of sample preparation and/or method of registration of the spectrum: KBr disc. Absorption.
Wavenumbers (cm^{-1}): 3546, 3398, 988s, 795, 748, 600sh, 636, 543, 449s, 430s, 390sh.

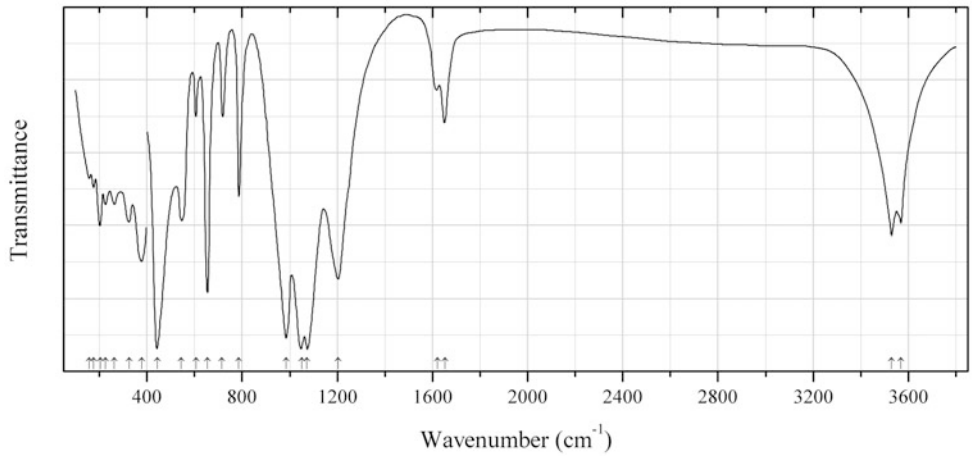

Fig. 2.619 IR spectrum of armstrongite drawn using data from Povarennykh (1976)

Sil265 Armstrongite $CaZr(Si_6O_{15})\cdot 3H_2O$ (Fig. 2.619)
Locality: Khan Bogdo massif, Gobi desert, Mongolia (type locality).

Description: Brown granular aggregate from agpaitic granite pegmatite.
Kind of sample preparation and/or method of registration of the spectrum: KBr disc. Absorption.
Source: Povarennykh (1976).
Wavenumbers (cm^{-1}): 3570, 3530, 1652, 1622, 1204s, 1073s, 1052s, 986s, 785, 714, 655s, 606, 545, 443s, 378, 325w, 264w, 226w, 204s, 176w, 158w.

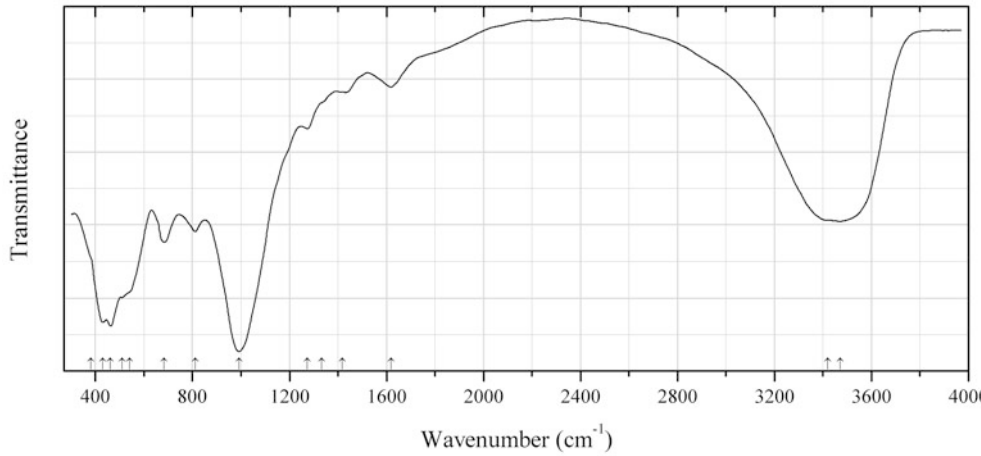

Fig. 2.620 IR spectrum of brindleyite drawn using data from Maksimovic and Bish (1978)

Sil266 Brindleyite $(Ni,Al)_3[(Si,Al)_2O_5](OH)_4$ (Fig. 2.620)
Locality: Marmara bauxite deposit, Megara, Western Attikí district, Attikí prefecture, Greece (type locality).
Description: Green coatings on limestonefrom the association with matulaite and variscite. Holotype sample. D_{calc} = 3.16 g/cm^3. The mean refractive index is 1.635(1). The approximate empirical formula is $(Ni_{1.75}Al_{1.0})(Si_{1.5}Al_{0.5})O_5(OH)_4$. The strongest lines of the powder X-ray diffraction pattern [*d*, Å (*I*, %)] are: 7.07 (100), 3.54 (81), 2.62 (18), 2.47 (18), 2.37 (18), 1.524 (17).
Kind of sample preparation and/or method of registration of the spectrum: Transmission. Kind of sample preparation is not indicated.
Source: Maksimovic and Bish (1978).
Wavenumbers (cm^{-1}): 3470, 3420sh, 1618w, 1419w, 1333sh, 1273w, 992s, 811, 683, 541sh, 509, 462s, 430s, 382sh.
Note: The wavenumbers were determined by us based on spectral curve analysis of the published spectrum.

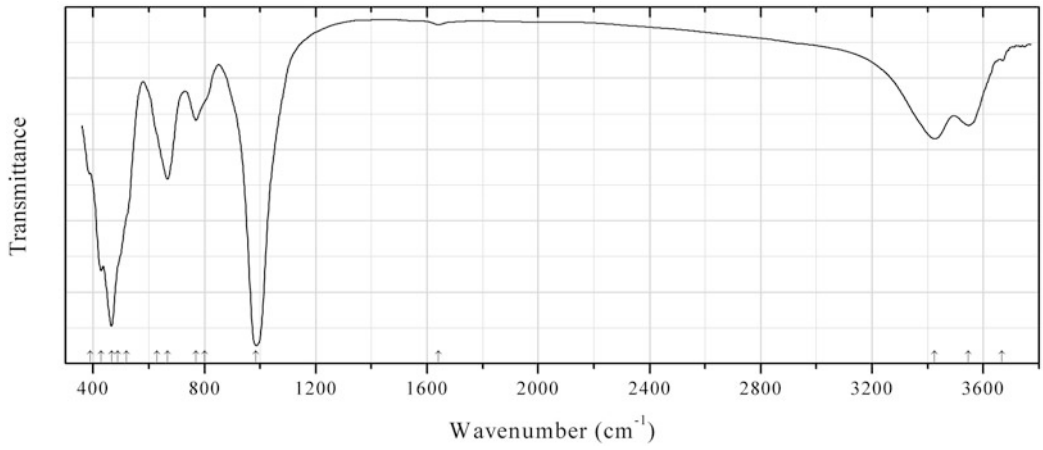

Fig. 2.621 IR spectrum of kämmererite obtained by N.V. Chukanov

Sil267 Kämmererite $Mg_4(Cr,Al)_2(Si_2Al_2O_{10})(OH)_8$ (Fig. 2.621)
Locality: Saranovskiy mine, Sarany, Perm region, Middle Urals, Russia.
Description: Black pseudomorph after uvarovite crystal from the association with Cr-bearing amesite. The empirical formula is (electron microprobe, ranges): $Na_{0–0.04}Ca_{0–0.02}Mg_{4.17–4.67}Cr_{0.85–1.21}Al_{0.28–0.32}Fe_{0.17–0.23}(Si_{2.49–2.68}Al_{1.51–1.32}O_{10})(OH,O)_8$.
Kind of sample preparation and/or method of registration of the spectrum: KBr disc. Absorption.
Wavenumbers (cm^{-1}): 3668w, 3547, 3426, 1642w, 986s, 800sh, 769, 667, 630sh, 520sh, 490sh, 466s, 429, 390sh.

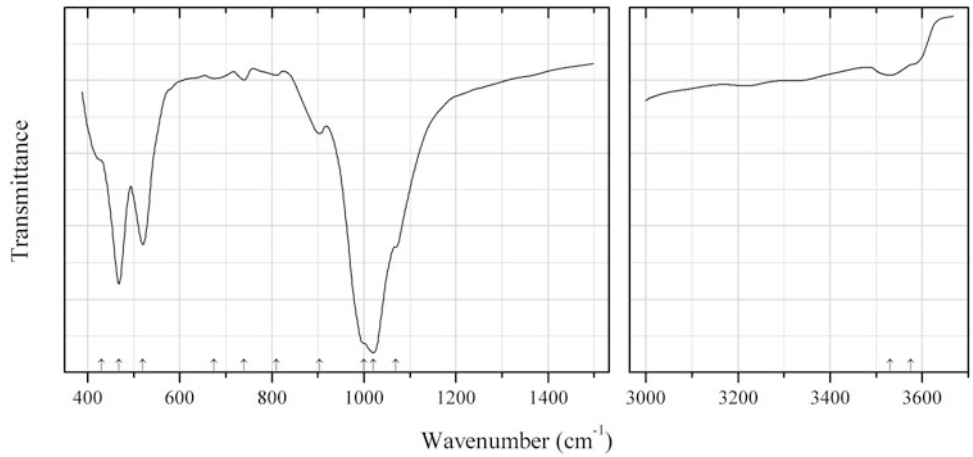

Fig. 2.622 IR spectrum of chromphyllite obtained by N.V. Chukanov

Sil268 Chromphyllite $KCr_2(Si_3AlO_{10})(OH)_2$ (Fig. 2.622)
Locality: Pereval marble quarry, Slyudyanka, Lake Baikal area, Irkutsk region, Russia.
Description: Emerald-green platelets in massive quartz. Confirmed by the IR spectrum.
Kind of sample preparation and/or method of registration of the spectrum: KBr disc. Absorption.
Wavenumbers (cm^{-1}): 3575sh, 3530, 1070sh, 1020s, 1000sh, 904, 810w, 740w, 675w, 520, 468s, 430sh.

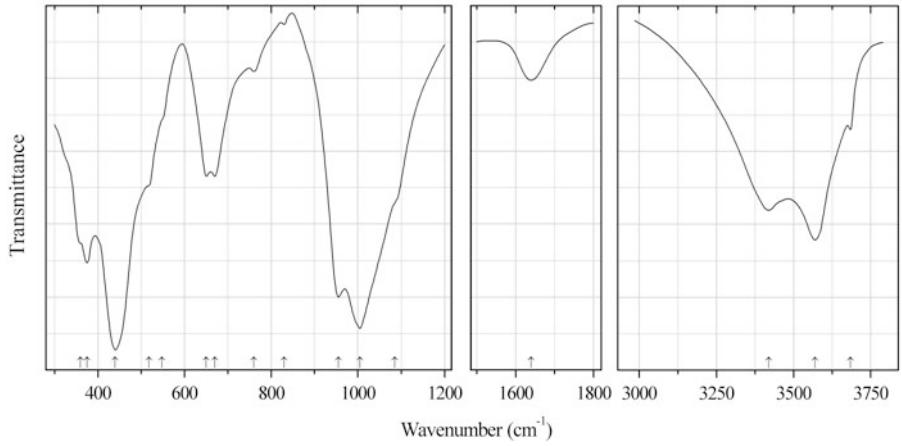

Fig. 2.623 IR spectrum of corrensite drawn using data from Bergaya et al. (1985)

Sil269 Corrensite $Ca_x(Mg,Fe,Al)_9[(Si,Al)_8O_{20}](OH)_{10}{\cdot}nH_2O$ (Fig. 2.623)
Locality: Borgotaro, Taro valley, Parma province, Emilia-Romagna, Italy.
Description: Earthy aggregate. Investigated by Brigatti and Poppi (1984, 1985). The empirical formula is $(Ca_{0.34}Na_{0.06}K_{0.01})(Mg_{7.65}Fe^{2+}_{0.55}Fe^{3+}_{0.44}Al_{0.40}Mn_{0.02}Ti_{0.06})(Si_{6.06}Al_{1.94}O_{20})(OH)_{10}{\cdot}nH_2O$.
Kind of sample preparation and/or method of registration of the spectrum: KBr disc. Transmission.
Source: Bergaya et al. (1985).
Wavenumbers (cm^{-1}): 3685, 3570s, 3420, 1640, 1085sh, 1005s, 955s, 830w, 760w, 670, 650, 548sh, 518sh, 440s, 375, 360sh.

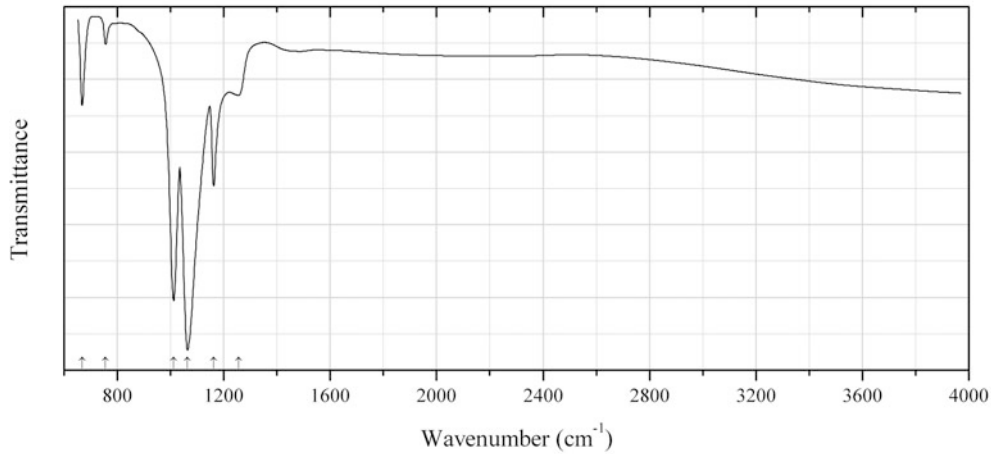

Fig. 2.624 IR spectrum of cuprorivaite drawn using data from Salvadó et al. (2005)

Sil270 Cuprorivaite $CaCu(Si_4O_{10})$ (Fig. 2.624)
Locality: Synthetic (Egyptian blue).
Description: Blue particles.
Kind of sample preparation and/or method of registration of the spectrum: Absorption. Synchrotron radiation-based Fourier transform infrared spectrum of a small particle.

Source: Salvadó et al. (2005).
Wavenumbers (cm^{-1}): 1255, 1162, 1064s, 1012s, 756w, 668.

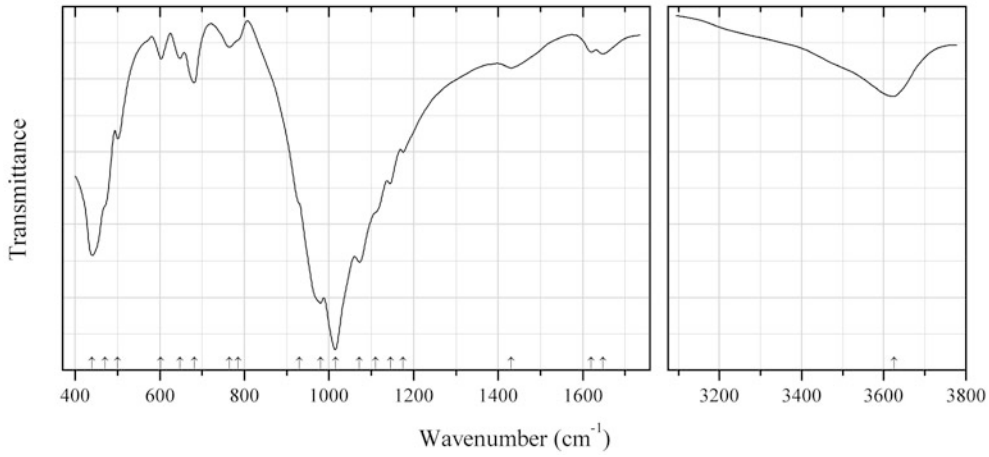

Fig. 2.625 IR spectrum of armbrusterite obtained by N.V. Chukanov

Sil271 Armbrusterite $K_5Na_6Mn^{3+}Mn^{2+}_{14}(Si_9O_{22})_4(OH)_{10}\cdot 4H_2O$ (Fig. 2.625)
Locality: Kirovskiy mine, Kukisvumchorr Mt., Khibiny alkaline complex, Kola peninsula, Murmansk region, Russia (type locality).
Description: Red-brown split crystals from the association with raite, lamprophyllite, mangan-neptunite, pectolite, vinogradovite, calcite, molybdenite, galena, sphalerite, and fluorite. The empirical formula is $K_{5.48}Na_{6.09}(Mn_{13.70}Fe_{1.22}Mg_{0.11})Si_{36.00}(O,OH)_{98}\cdot 4H_2O$.
Kind of sample preparation and/or method of registration of the spectrum: KBr disc. Absorption.
Wavenumbers (cm^{-1}): 3625, 1647w, 1620w, 1430w, 1175w, 1145, 1110sh, 1072s, 1015s, 980s, 930sh, 785sh, 765w, 681, 647w, 602w, 500, 470sh, 440s.

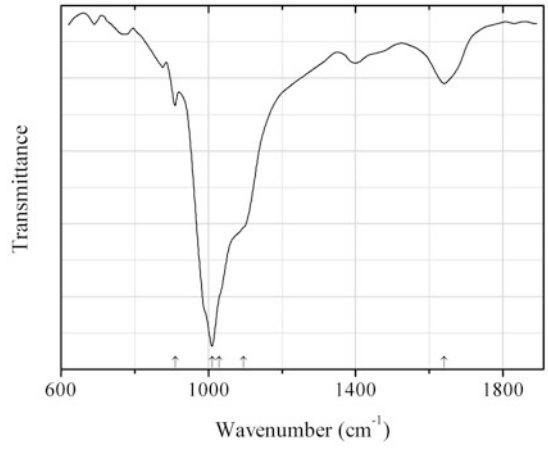

Fig. 2.626 IR spectrum of donbassite drawn using data from Merceron et al. (1988)

Sil272 Donbassite $Al_{4.33}(Si_3AlO_{10})(OH)_8$ (Fig. 2.626)
Locality: Beauvoir granite, Echassières area, Massif Central, France.

Description: Fine-grained aggregate from a vein crosscutting hydrothermally altered granite. A Li-rich variety. Confirmed by electron microprobe analysis, atomic absorption spectroscopy (for Li), and powder X-ray diffraction pattern. The empirical formula is $(Na_{0.07}K_{0.04}Ca_{0.02})(Al_{3.81}Li_{0.52}Fe_{0.01}Mg_{0.01}Mn_{0.01})(Si_{3.81}Al_{0.19}O_{10})(OH)_8 \cdot nH_2O$.
Kind of sample preparation and/or method of registration of the spectrum: KBr disc. Transmission.
Source: Merceron et al. (1988).
Wavenumbers (cm^{-1}): 3690w, 3660sh, 3645, 3620, 1640, 1095sh, 1030sh, 1010s, 910w, 535s, 470s, 420s.
Note: The band at 1640 cm^{-1} indicates the presence of H_2O molecules.

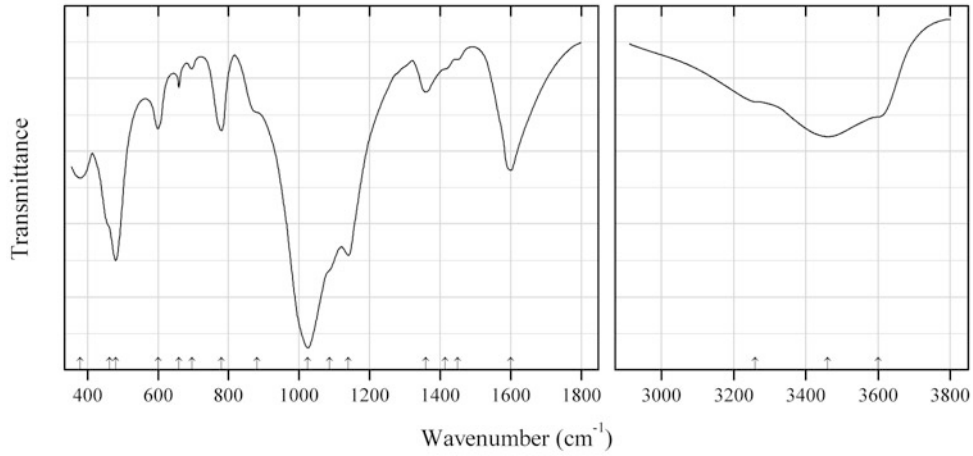

Fig. 2.627 IR spectrum of ellingsenite drawn using data from Yakovenchuk et al. (2011b)

Sil273 Ellingsenite $Na_5Ca_6Si_{18}O_{38}(OH)_{13} \cdot 6H_2O$ (Fig. 2.627)
Locality: Ariskop Quarry, Aris, near Windhoek, Windhoek district, Khomas Region, Namibia (type locality).
Description: White spherules from the association with aegirine, albite, manganoneptunite, microcline, natrolite, and polylithionite. Holotype sample. The crystal structure is solved. Triclinic, space group *P*-1, $a = 9.576(11)$, $b = 9.577(11)$, $c = 16.438(19)$ Å, $\alpha = 85.85(2)°$, $\beta = 75.23(2)°$, $\gamma = 60.142(14)°$, $V = 1262(3)$ $Å^3$, $Z = 1$. $D_{meas} = 2.32(5)$ g/cm^3, $D_{calc} = 2.38$ g/cm^3. Optically biaxial (−), $\alpha = 1.520(2)$, $\beta = 1.534(2)$, $\gamma \approx 1.536(2)$, $2V = 5°$. The empirical formula is $(Na_{4.95}K_{0.09})(Ca_{5.57}Na_{0.43})Si_{18.10}O_{38}(OH)_{13.00} \cdot 6H_2O$. The strongest lines of the powder X-ray diffraction pattern [*d*, Å (*I*, %) (*hkl*)] are: 15.50 (100) (001), 4.22 (16) (−201), 3.159 (30) (005), 3.023 (33) (−201), 2.791 (24) (−2–14), 1.827 (27) (−511).
Kind of sample preparation and/or method of registration of the spectrum: Absorption. Kind of sample preparation is not indicated.
Source: Yakovenchuk et al. (2011b).
Wavenumbers (cm^{-1}): 3600sh, 3460, 3260sh, 1600, 1450sh, 1414sh, 1360, 1140s, 1086sh, 1025s, 880sh, 780, 696w, 659w, 600, 480s, 462sh, 380.
Note: The wavenumbers were partly determined by us based on spectral curve analysis of the published spectrum. The band at 1360 cm^{-1} indicates the presence of H^+ cations formed as a result of dissociation of acid (silanol) OH groups.

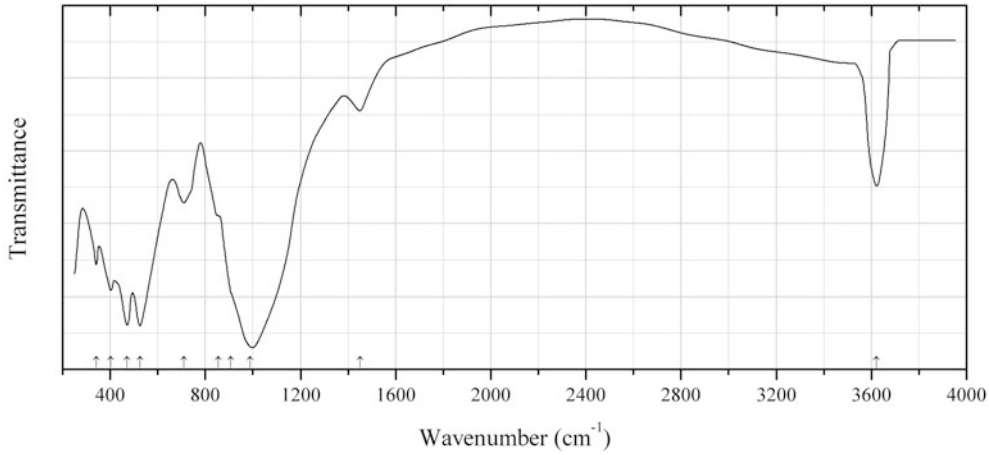

Fig. 2.628 IR spectrum of ganterite drawn using data from Graeser et al. (2003)

Sil274 Ganterite $(Ba,K,Na)(Al,Mg)_2(Si_3AlO_{10})(OH)_2$ (Fig. 2.628)
Locality: The valley Gantertal, Wasenhorn, Berisal Complex, Simplon Region, Switzerland (type locality).
Description: Light gray grains from the association with zoisite, quartz, feldspars, etc. Monoclinic, space group *C*2/c, a = 5.212(1), b = 9.046(2), c = 19.978(4) Å, β = 95.8°, V = 937.6(2) Å^3, Z = 4. D_{calc} = 3.11 g/cm^3. Optically biaxial (−), α = 1.600 (calc.), β = 1.619, γ = 1.622, 2 V = 42.5°. The empirical formula is $(Ba_{0.44}K_{0.28}Na_{0.27})(Al_{1.84}Mg_{0.09}Fe_{0.04}Ti_{0.04})(Si_{2.72}Al_{1.28}O_{10})(OH)_{1.89}$. The strongest lines of the powder X-ray diffraction pattern [*d*, Å (*I*, %) (*hkl*)] are: 4.481 (71) (110), 3.887 (76) (−113),3.737 (77) (023), 3.495 (71) (−114), 2.602 (95) (130, −131), 2.571 (100) (131, −202), 1.5054 (91) (060, 2.0.10).
Kind of sample preparation and/or method of registration of the spectrum: KBr disc. Transmission.
Source: Graeser et al. (2003).
Wavenumbers (cm^{-1}): 3622s, 1450w, 988s, 908sh, 855sh, 710, 525s, 471s, 402, 341.
Note: The wavenumbers were partly determined by us based on spectral curve analysis of the published spectrum.

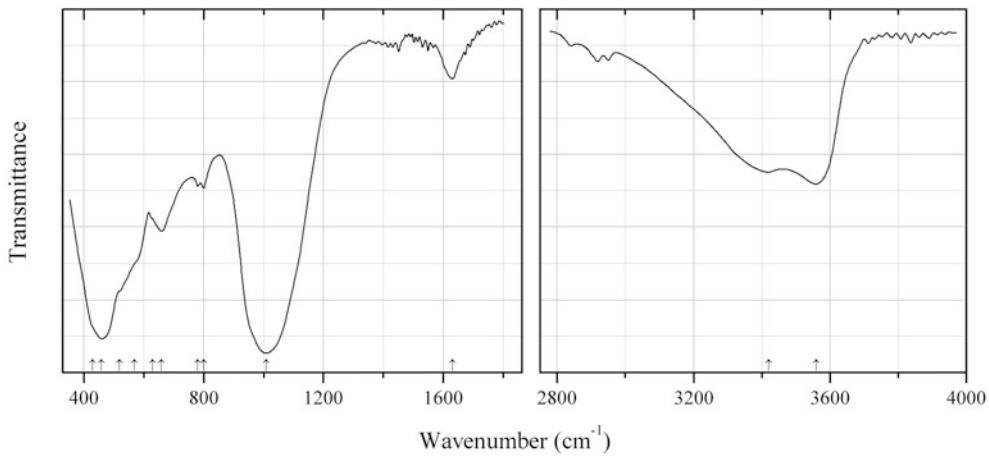

Fig. 2.629 IR spectrum of berthierine drawn using data from Hornibrook and Longstaffe (1996)

Sil275 Berthierine $(Fe^{2+},Fe^{3+},Al)_3[(Si,Al)_2O_5](OH)_4$ (Fig. 2.629)

Locality: Lower Cretaceous Clearwater Formation, east-central Alberta, Canada.
Description: Lath in oil-sand. The average empirical formula is $(Fe^{2+}_{1.01}Al_{0.82}Mg_{0.46}Fe^{3+}_{0.28}\square_{0.43})(Si_{1.74}Al_{0.26}O_5)(OH)_4$. The strongest lines of the powder X-ray diffraction pattern are observed at 14, 10, 7.1, and 3.55 Å.
Kind of sample preparation and/or method of registration of the spectrum: KBr disc. Transmission.
Source: Hornibrook and Longstaffe (1996).
Wavenumbers (cm^{-1}): 3560, 3420, 1630, 1010s, 800w, 780w, 660, 630sh, 570sh, 520, 460s, 430sh.
Note: Weak bands in the range from 2800 to 3000 cm^{-1} correspond to the admixture of organic matter. Weak bands at 780 and 800 cm^{-1} correspond to the admixture of quartz. The band at 1630 cm^{-1} indicates the presence of H_2O molecules (adsorbed water?).

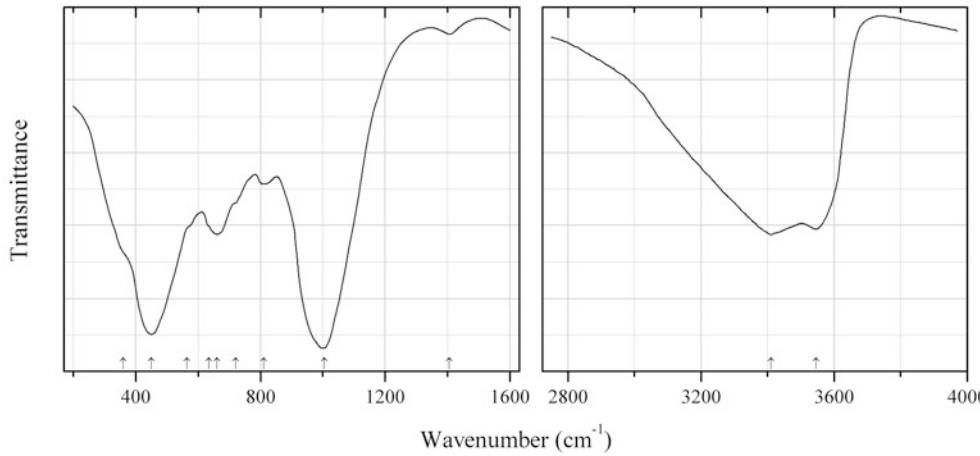

Fig. 2.630 IR spectrum of berthierine drawn using data from MacKenzie and Berezowski (1984)

Sil276 Berthierine $(Fe^{2+},Fe^{3+},Al)_3[(Si,Al)_2O_5](OH)_4$ (Fig. 2.630).
Locality: Kongeus mine, Kongsberg, Norway.
Description: Specimen BM34121 from the British Museum collection. The empirical formula is $Ca_{0.14}(Fe^{2+}_{2.30}Fe^{3+}_{1.96}Mg_{0.40}Al_{0.48})(Si_{2.98}Al_{1.02}O_{10})(OH)_{7.66}$.
Kind of sample preparation and/or method of registration of the spectrum: Transmission. Kind of sample preparation is not indicated.
Source: MacKenzie and Berezowski (1984).
Wavenumbers (cm^{-1}): 3545, 3410, 1405w, 1005s, 810w, 720sh, 660, 635sh, 565sh, 450s, 360sh.

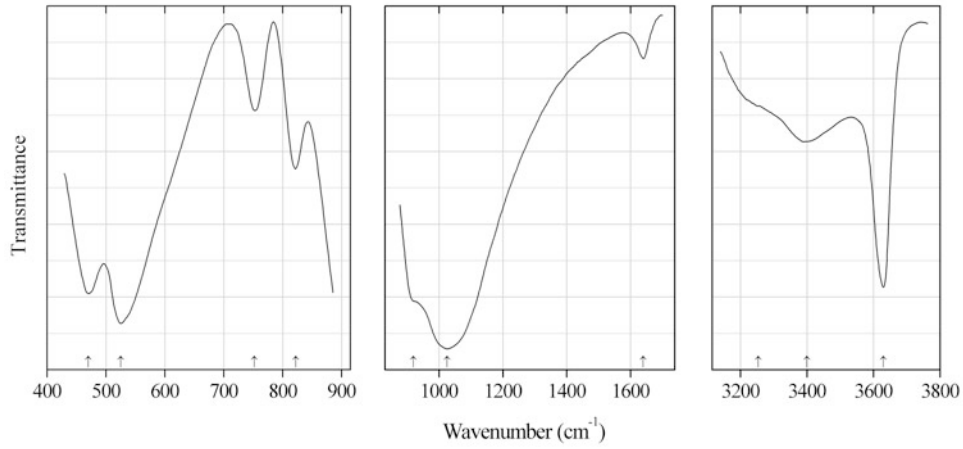

Fig. 2.631 IR spectrum of illite-1*M* drawn using data from Oinuma and Hayashi (1965)

Sil277 Illite-1*M* $K_{0.65}Al_{2.0}[Al_{0.65}Si_{3.35}O_{10}](OH)_2$ (Fig. 2.631)
Locality: Kamikita mine, Aomori Prefecture, Japan.
Kind of sample preparation and/or method of registration of the spectrum: Nujol mull. Transmission.
Source: Oinuma and Hayashi (1965).
Wavenumbers (cm^{-1}): 3630, 3400, 3254sh, 1640w, 1025s, 920sh, 822, 752w, 525s, 470s.
Note: For a detailed description of the sample see Kodama (1962).

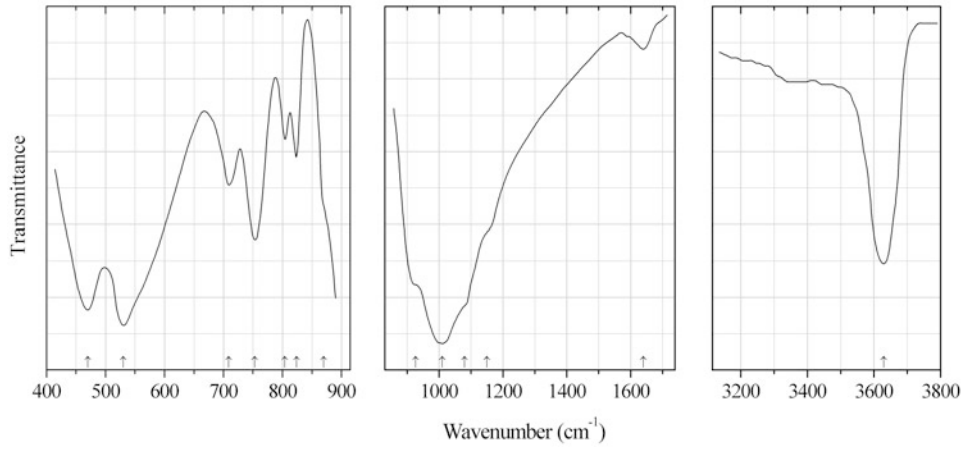

Fig. 2.632 IR spectrum of illite-2*M* drawn using data from Oinuma and Hayashi (1965)

Sil278 Illite-2*M* $K_{0.65}Al_{2.0}[Al_{0.65}Si_{3.35}O_{10}](OH)_2$ (Fig. 2.632)
Locality: Yoji pass, Ozawa-mura, Gumma Prefecture, Japan.
Kind of sample preparation and/or method of registration of the spectrum: Nujol mull. Transmission.
Source: Oinuma and Hayashi (1965).

Wavenumbers (cm^{-1}): 3630, 1640w, 1150sh, 1080sh, 1010s, 927s, 870sh, 824w, 804w, 753, 709w, 530s, 470s.
Note: For a detailed description of the sample see Kodama (1957).

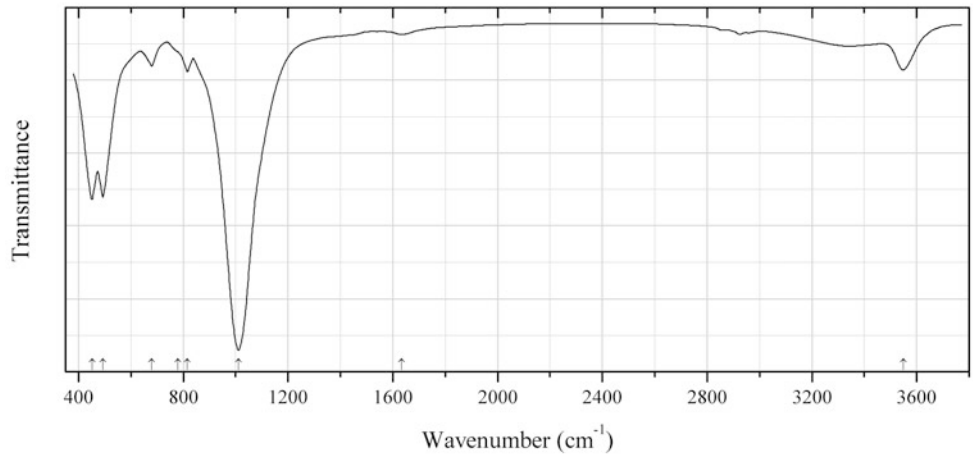

Fig. 2.633 IR spectrum of glauconite hydrated analogue drawn using data from Palchik et al. (2013)

Sil279 Glauconite hydrated analogue $K_{1-x}(Fe^{3+},Fe^{2+},Mg)_2[(Si,Fe^{3+},Al)_4O_{10}](OH)_2 \cdot nH_2O$ ($x < 0.5$) (Fig. 2.633)
Locality: The slope of the underwater Obruchev Volcano, Bottom of the Sea of Okhotsk.
Description: A variety transitional to nontronite. Described as "iron-rich nontronite", but a boad reflection between 11.05 and 11.95 Å disappears after impregnation with ethylene glycol. This disappearance casted doubt on the affiliation of the mineral to the smectite group. The empirical formula is (electron microprobe): $(K_{0.53}Ca_{0.03}Na_{0.02})(Fe_{1.63}Mg_{0.37})(Si_{3.68}Fe_{0.30}Al_{0.02}O_{10})(OH,O)_2 \cdot nH_2O$.
Kind of sample preparation and/or method of registration of the spectrum: KBr disc. Absorption.
Source: Palchik et al. (2013).
Wavenumbers (cm^{-1}): 3549s, 1633w, 1011s, 816w, 780sh, 680w, 493s, 452s.
Note: The wavenumbers were partly determined by us based on spectral curve analysis of the published spectrum.

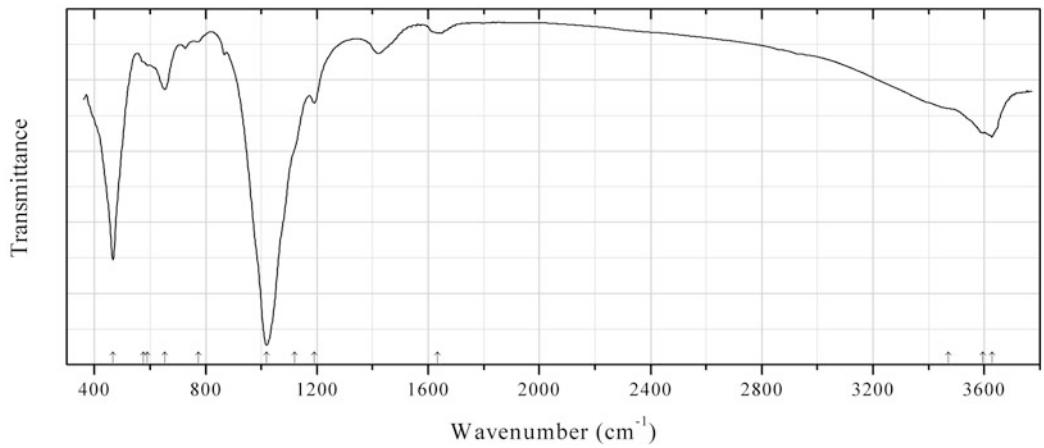

Fig. 2.634 IR spectrum of franklinphilite obtained by N.V. Chukanov

Sil280 Franklinphilite $K_4(Mn^{2+},Mg,Fe^{2+})_{48}(Si,Al)_{72}(O,OH)_{216}\cdot 6H_2O$ (Fig. 2.634)
Locality: Llyn Du Bach mine, near Moel Ysgyfarnogod, Merionethshire, North Wales, GB.
Description: Dark brown scaly aggregate forming veinlet cross-cutting manganese ore. The associated minerals are caryopilite and rhodochrosite. The empirical formula of an analogous sample is (electron microprobe; see Cotterell and Hubbard 2013): $(K_{11.58}Na_{0.20}Ca_{0.10}Ba_{0.05})(Mn_{28.95}Fe_{10.57}Mg_{8.06}Ti_{0.35}Cu_{0.30})(Si_{62.43}Al_{9.57})[(O,OH)_{198}F_{2.52}]\cdot nH_2O$. Confirmed by the powder X-ray diffraction pattern.
Kind of sample preparation and/or method of registration of the spectrum: KBr disc. Absorption.
Wavenumbers (cm^{-1}): 3627, 3594sh, 3470sh, 1634w, 1190, 1120sh, 1019s, 774w, 653, 591w, 575w, 466s.

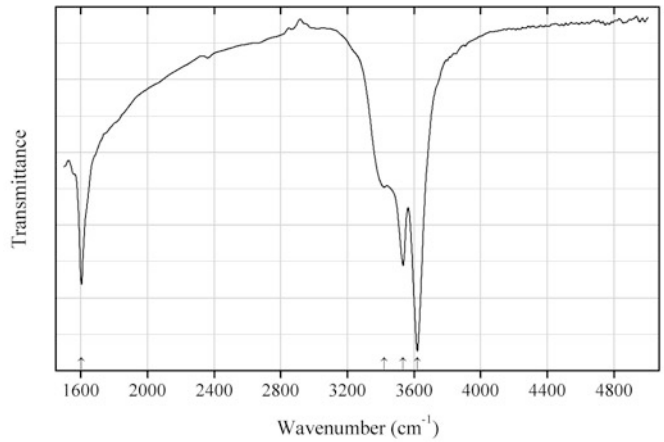

Fig. 2.635 IR spectrum of cymrite K analogue drawn using data from Fasshauer et al. (1997)

Sil281 Cymrite K analogue $K(AlSi_3O_8)\cdot H_2O$ (Fig. 2.635)
Locality: Synthetic.
Description: The crystal structure is solved. Hexagonal, space group *P6/mmm*, a = 5.3348(1), c = 7.7057(1) Å.
Kind of sample preparation and/or method of registration of the spectrum: KBr disc. Transmission.
Source: Fasshauer et al. (1997).
Wavenumbers (cm^{-1}): 3620s, 3535, 3420, 1605.

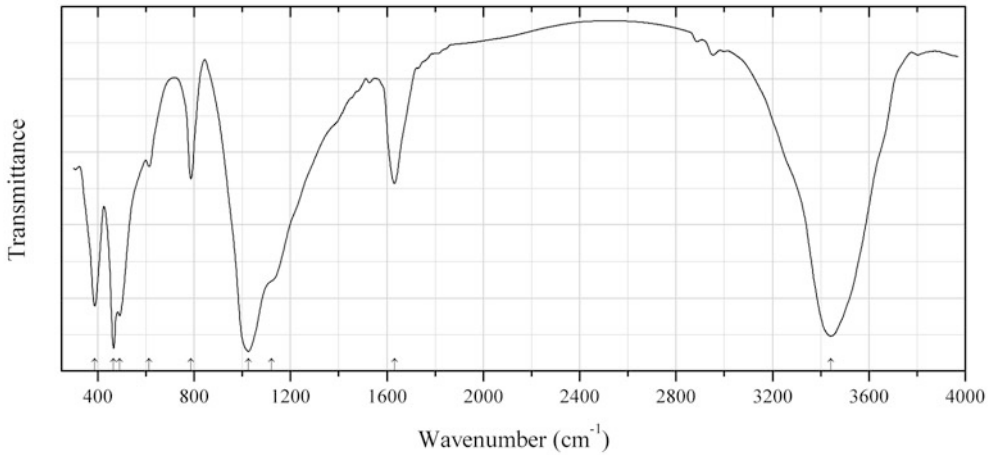

Fig. 2.636 IR spectrum of lalondeite drawn using data from McDonald and Chao (2009)

Sil282 Lalondeite $(Na,Ca)_6(Ca,Na)_3Si_{16}O_{38}(F,OH)_2 \cdot 3H_2O$ (Fig. 2.636)
Locality: Poudrette (Demix) quarry, Mont Saint-Hilaire, Rouville RCM (Rouville Co.), Montérégie, Québec, Canada (type locality).
Description: Elongate aggregates of densely packed, randomly oriented colourless crystals from the association with microcline, clinoamphibole, and narsarssukite. Holotype sample. The crystal structure is solved. Triclinic, space group *P*-1, $a = 9.589(2)$, $b = 9.613(2)$, $c = 12.115(2)$ Å, $\alpha = 96.62(2)°$, $\beta = 92.95(2)°$, $\gamma = 119.81(2)°$, $V = 954.8(1)$ Å^3, $Z = 2$. $D_{meas} = 2.50(1)$ g/cm^3, $D_{calc} = 2.51$ g/cm^3. Optically biaxial (−), $\alpha = 1.522(1)$, $\beta = 1.528(1)$, $\gamma = 1.529(1)$, $2V = 48(1)°$. The empirical formula is $Na_{5.33}Ca_{3.91}K_{0.22}Si_{16.16}O_{38}[F_{0.99}(OH)_{0.94}Cl_{0.07}] \cdot 3H_2O$. The strongest lines of the powder X-ray diffraction pattern [*d*, Å (*I*, %) (*hkl*)] are: 11.938 (90) (001), 4.142 (30) (2–20), 4.106 (30) (020, 0–21), 3.972 (40) (003, 1–22), 2.981 (2–13, 004), 2.967 (50) (−1–22, 3–11, −104, −231), 2.888 (100) (−123, 121, 2–32, −312).
Kind of sample preparation and/or method of registration of the spectrum: A single crystal of material was mounted in a low pressure diamond-anvil microsample cell.
Source: McDonald and Chao (2009).
Wavenumbers (cm^{-1}): 3443s, 1631, 1121sh, 1025s, 787, 613w, 491s, 466s, 388.

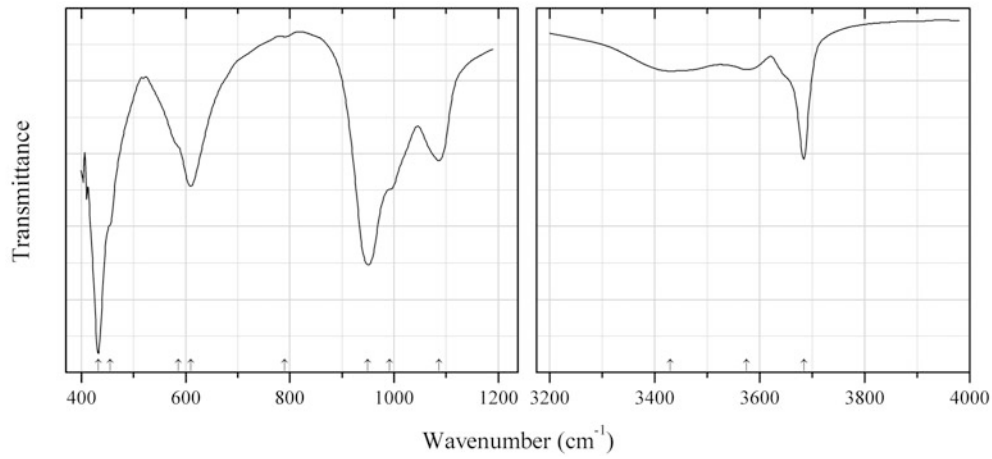

Fig. 2.637 IR spectrum of lizardite-1*T* drawn using data from Fuchs et al. (1998)

Sil283 Lizardite-1*T* $Mg_3(Si_2O_5)(OH)_4$ (Fig. 2.637)
Locality: Monte Fico, Elba, Italy.
Description: Dark-green vein of recrystallized, granoblastic lizardite is embedded in a fibrous matrix of chrysotile and minor polygonal serpentine. Previously the sample was investigated by X-ray structure refinement. The empirical formula (calculated on the basis of electron microprobe analysis and Mössbauer spectrum) is: $(Mg_{2.74}Fe^{2+}_{0.10}Fe^{3+}_{0.05}Al_{0.11})(Si_{1.94}Al_{0.05}Fe^{3+}_{0.01})O_{5.05}(OH)_{3.95}$.
Kind of sample preparation and/or method of registration of the spectrum: KBr disc. Absorption.
Source: Fuchs et al. (1998).
Wavenumbers (cm^{-1}): 3684s, 3575, 3430, 1086, 992sh, 950s, 790w, 610s, 586sh, 455sh, 432s.
Note: The band at 3430 cm^{-1} may correspond not only to O–H stretching vibrations of $Fe^{3+}\cdots OH$ fragments, but also to stretching vibrations of admixed H_2O molecules.

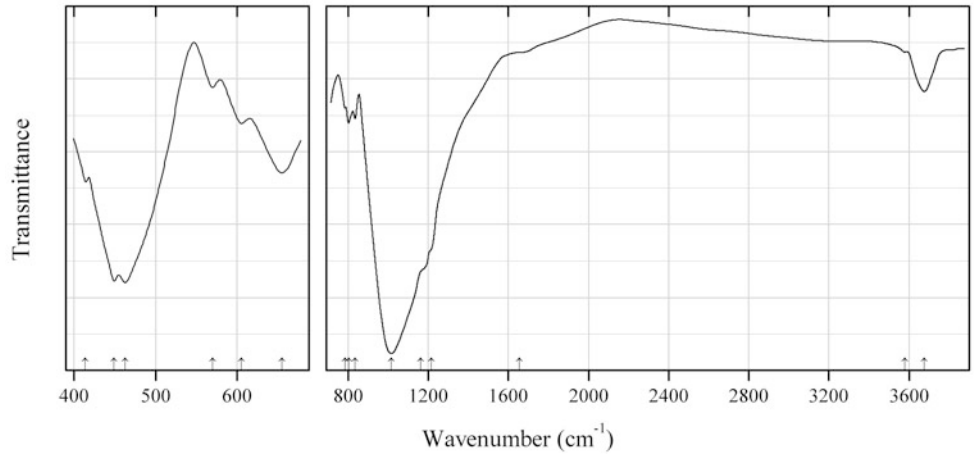

Fig. 2.638 IR spectrum of minnesotaite drawn using data from Stubičan and Roy (1961)

Sil284 Minnesotaite $Fe^{2+}_3(Si_4O_{10})(OH)_2$ (Fig. 2.638)
Locality: Synthetic.

Description: Synthesized under controlled high-temperature–high-pressure conditions. Analytical data are not presented.
Kind of sample preparation and/or method of registration of the spectrum: No data.
Source: Stubičan and Roy (1961).
Wavenumbers (cm^{-1}): 3675s, 3580w, 1655sh, 1215sh, 1164sh, 1015s, 835w, 803w, 784w, 655, 605, 570w, 463s, 449s, 414.
Note: The wavenumbers were determined by us based on spectral curve analysis of the published spectrum.

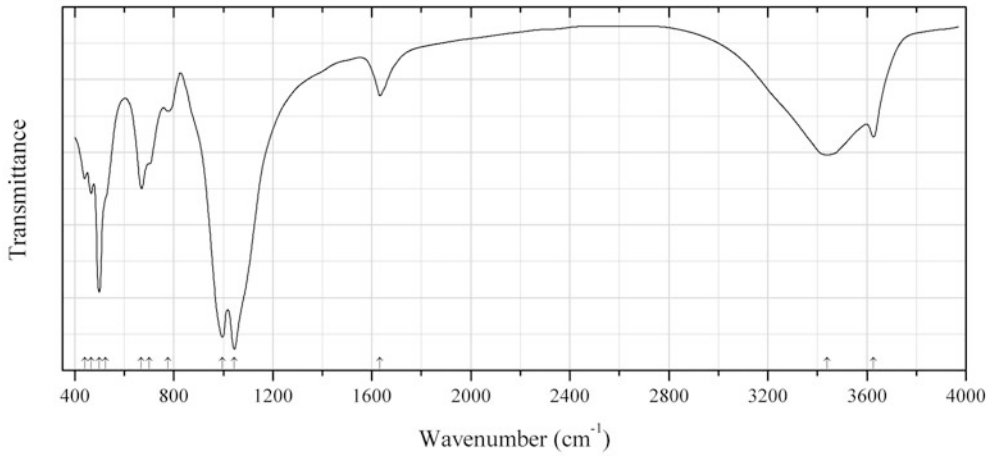

Fig. 2.639 IR spectrum of népouite drawn using data from Sufriadin et al. (2012)

Sil285 Népouite $Ni_3(Si_2O_5)(OH)_4$ (Fig. 2.639)
Locality: Petea mine, Soroako, Sulawesi Selatan Province, Sulawesi Island, Indonesia.
Description: The strongest lines of the powder X-ray diffraction pattern are observed at 7.35 and 3.67 Å. The sample contains admixture of kerolite.
Kind of sample preparation and/or method of registration of the spectrum: KBr disc. Absorption.
Source: Sufriadin et al. (2012).
Wavenumbers (cm^{-1}): 3627, 3440, 1633w, 1045s, 995s, 777w, 700sh, 669, 524sh, 499s, 466, 440.
Note: The wavenumbers were determined by us based on spectral curve analysis of the published spectrum. The bands at 3440 and 1633 cm^{-1} indicate the presence of H_2O molecules.

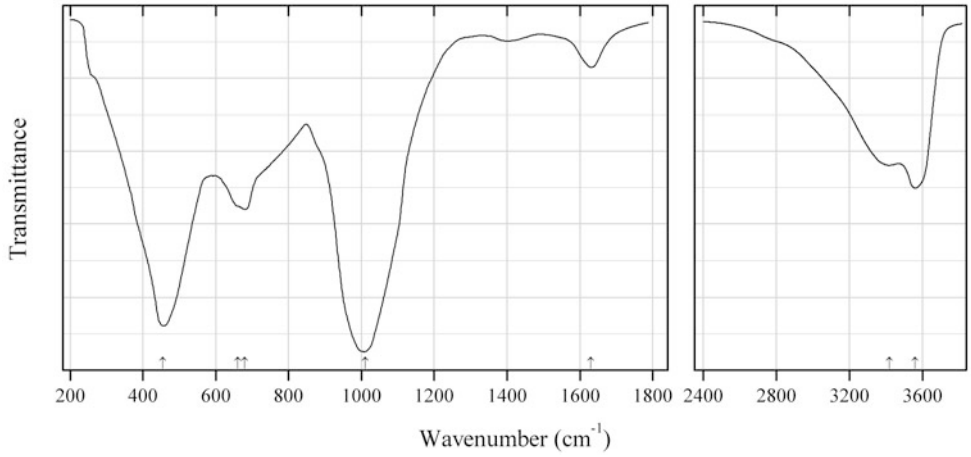

Fig. 2.640 IR spectrum of odinite drawn using data from Bailey (1988)

Sil286 Odinite $(Fe^{3+},Mg,Al,Fe^{2+})_{2-x}[(Si,Al)_2O_5](OH)_4$ (Fig. 2.640)
Locality: Reef lagoon, SW of New Caledonia.
Description: Identified by chemical composition and powder X-ray diffraction data. The sample contains impurities.
Kind of sample preparation and/or method of registration of the spectrum: KBr disc. Transmission.
Source: Bailey (1988).
Wavenumbers (cm^{-1}): 3560, 3420, 1630, 1010s, 680, 660sh, 455s.
Note: For the IR spectrum of odinite see also Hornibrook and Longstaffe (1996).

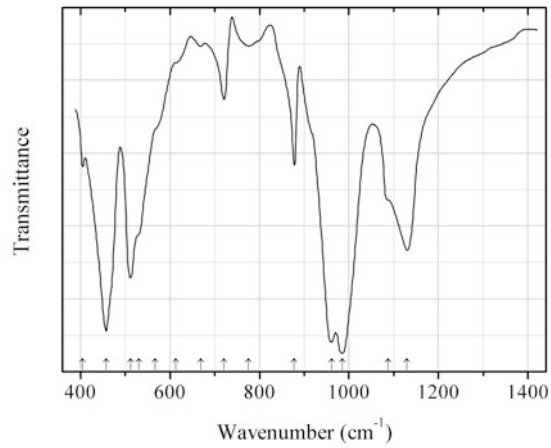

Fig. 2.641 IR spectrum of orlovite drawn using data from Agakhanov et al. (2011)

Sil287 Orlovite $KLi_2Ti(Si_4O_{10})OF$ (Fig. 2.641)
Locality: Dara-i Pioz glacier, Dara-i Pioz alkaline massif, Tien Shan Mts., Tajikistan (type locality).
Description: Colourless flaky aggregates from the association with pectolite, baratovite, faizievite, aegirine, polylithionite, leucosphenite, fluorite, etc. Holotype sample. Monoclinic, space group $C2$, $a = 5.199(3)$, $b = 9.068(7)$, $c = 10.070(4)$ Å, $\beta = 99.35(2)°$, $V = 468.4(4)$ $Å^3$, $Z = 2$. $D_{meas} = 2.91(2)$

g/cm^3, D_{calc} = 2.914 g/cm^3. Optically biaxial (−), α = 1.600(2), β = 1.620(2), γ = 1.625(2), 2 V = 50 (2)°. The empirical formula is $(K_{0.97}Rb_{0.03}Cs_{0.01})Li_{2.00}(Ti_{0.93}Nb_{0.02}Fe_{0.02}Al_{0.02})(Si_4O_{10})[O_{1.04}F_{0.94}(OH)_{0.10}$. The strongest lines of the powder X-ray diffraction pattern [d, Å (I, %) (hkl)] are: 9.96 (40) (001), 4.48 (67) (002), 3.87 (40) (111), 3.33 (100) (−121), 2.860 (35) (−113), 2.600 (28) (130), 2.570 (30) (−131), 2.400 (31) (014), 1.507 (20) (−206).

Kind of sample preparation and/or method of registration of the spectrum: KBr disc. Transmission.

Source: Agakhanov et al. (2011).

Wavenumbers (cm^{-1}): 1130s, 1087sh, 985s, 961s, 878, 776w, 721, 669w, 613sh, 567sh, 530sh, 512s, 458s, 405.

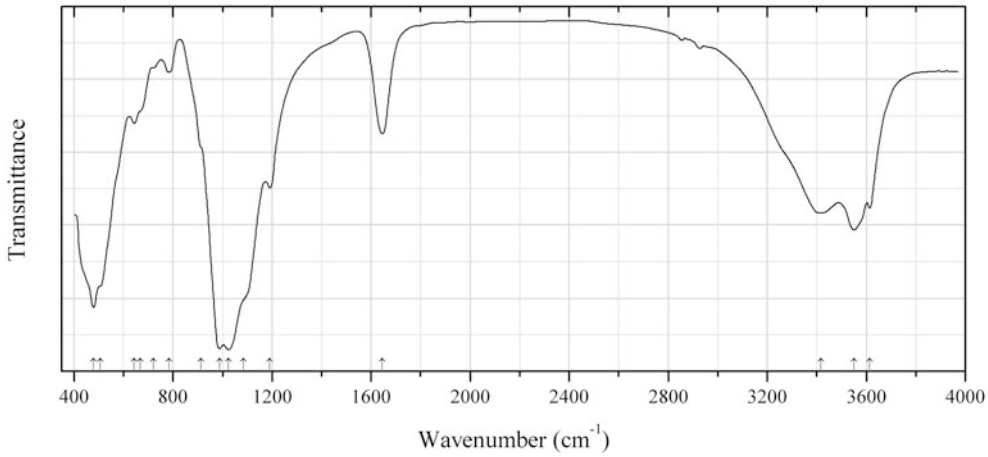

Fig. 2.642 IR spectrum of palygorskite drawn using data from García-Romero et al. (2004)

Sil288 Palygorskite $(Mg,Al)_2(Si_4O_{10})(OH)\cdot 4H_2O$ (Fig. 2.642)

Locality: Esquivias area, Madrid Basin, Spain.

Description: Micro-fibrous aggregate from the association with calcite and quartz. The empirical formula is (electron microprobe): $Na_{0.08}K_{0.05}Ca_{0.02}(Mg_{3.11}Al_{1.04}Fe^{3+}_{0.20})(Si_{7.87}Al_{0.13}O_{20})(OH)_2\cdot nH_2O$. Confirmed by powder X-ray diffraction data.

Kind of sample preparation and/or method of registration of the spectrum: KBr disc. Transmission.

Source: García-Romero et al. (2004).

Wavenumbers (cm^{-1}): 3614, 3550, 3416, 1646, 1191, 1085sh, 1025s, 988s, 912sh, 784w, 721w, 667sh, 644, 507sh, 479s.

Note: The wavenumbers were partly determined by us based on spectral curve analysis of the published spectrum.

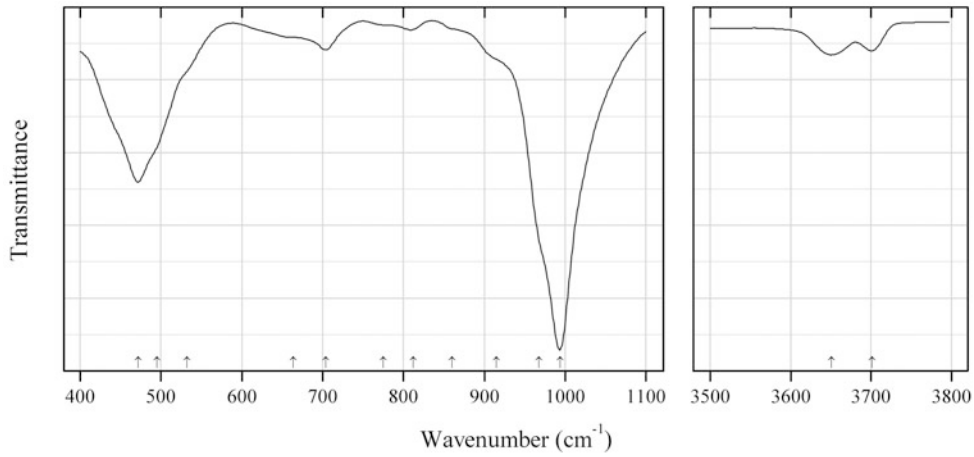

Fig. 2.643 IR spectrum of phlogopite Al-rich variety drawn using data from Papin et al. (1997)

Sil289 Phlogopite Al-rich variety $K(Mg_{2.5}Al_{0.5})(Si_{2.5}Al_{1.5})O_{10}(OH)_2$ (Fig. 2.643)
Locality: Synthetic.
Description: Synthesized from a gel under hydrothermal conditions at 600 °C and 1 kbar. Confirmed by powder X-ray diffraction data. Monoclinic, a = 5.299(1), b = 9.170(4), c = 10.317(8) Å, β = 99.94 (4)°, V = 493.8 Å^3.
Kind of sample preparation and/or method of registration of the spectrum: KBr disc. Absorption.
Source: Papin et al. (1997).
Wavenumbers (cm^{-1}): 3701w, 3651w, 994s, 968sh, 915sh, 860w, 812w, 775sh, 704, 664sh, 532sh, 495sh, 472s.
Note: The wavenumbers were partly determined by us based on spectral curve analysis of the published spectrum. In the cited paper the wavenumber 472 cm^{-1} is erroneously indicated as 482 cm^{-1}.

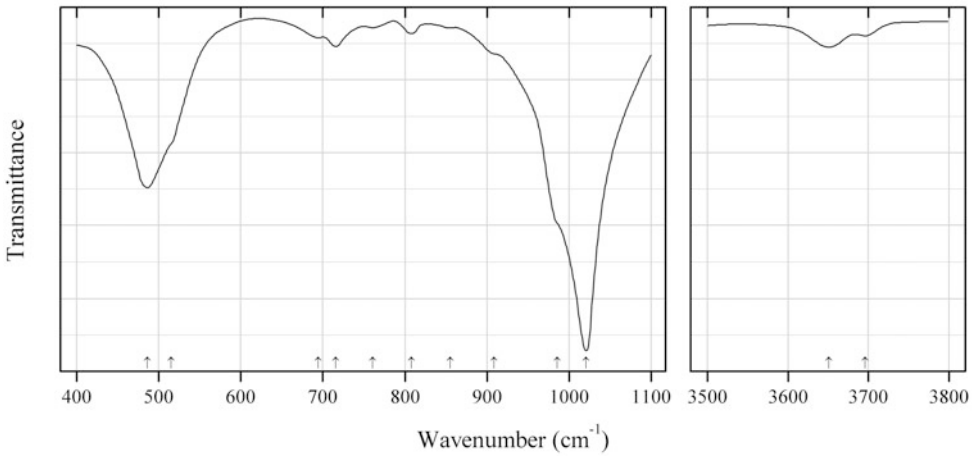

Fig. 2.644 IR spectrum of fluorphlogopite Al-rich variety drawn using data from Papin et al. (1997)

Sil290 Fluorphlogopite Al-rich variety $K(Mg_{2.5}Al_{0.5})(Si_{2.5}Al_{1.5})O_{10}(F,OH)_2$ (Fig. 2.644)
Locality: Synthetic.

Description: Synthesized from a gel under hydrothermal conditions at 600 °C and 1 kbar. The formula is $K(Mg_{2.5}Al_{0.5})(Si_{2.5}Al_{1.5})O_{10}[F_{1.4}(OH)_{0.6}]$. Confirmed by powder X-ray diffraction data. Monoclinic, a = 5.300(2), b = 9.176(4), c = 10.200(9) Å, β = 100.03(6)°, V = 488.5 Å^3.
Kind of sample preparation and/or method of registration of the spectrum: KBr disc. Absorption.
Source: Papin et al. (1997).
Wavenumbers (cm^{-1}): 3696w, 3651w, 1021s, 986sh, 909sh, 855w, 808w, 761w, 716, 694w, 515sh, 486s.
Note: The wavenumbers were partly determined by us based on spectral curve analysis of the published spectrum.

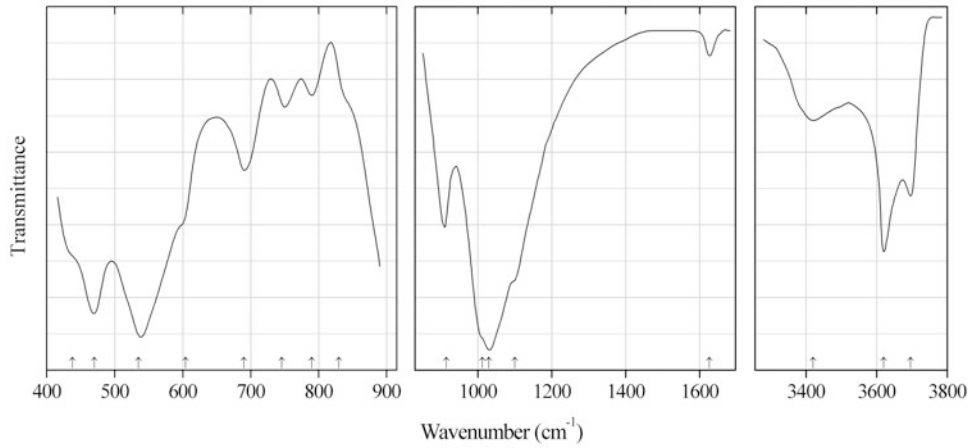

Fig. 2.645 IR spectrum of kaolinite-montmorillonite random interstratification drawn using data from Oinuma and Hayashi (1965)

Sil291 Kaolinite-montmorillonite random interstratification (Fig. 2.645)
Locality: Raimaru, Ishikawa Prefecture, Japan.
Description: Alteration product of Tertiary tuffaceous sediment. Characterized by Sudo and Hayashi (1956).
Kind of sample preparation and/or method of registration of the spectrum: Nujol mull. Transmission.
Source: Oinuma and Hayashi (1965).
Wavenumbers (cm^{-1}): 3696, 3620, 3420, 1627, 1100sh, 1030s, 1012sh, 915s, 830sh, 790w, 746w, 690, 604sh, 535s, 470s, 438sh.
Note: The wavenumbers were partly determined by us based on spectral curve analysis of the published spectrum.

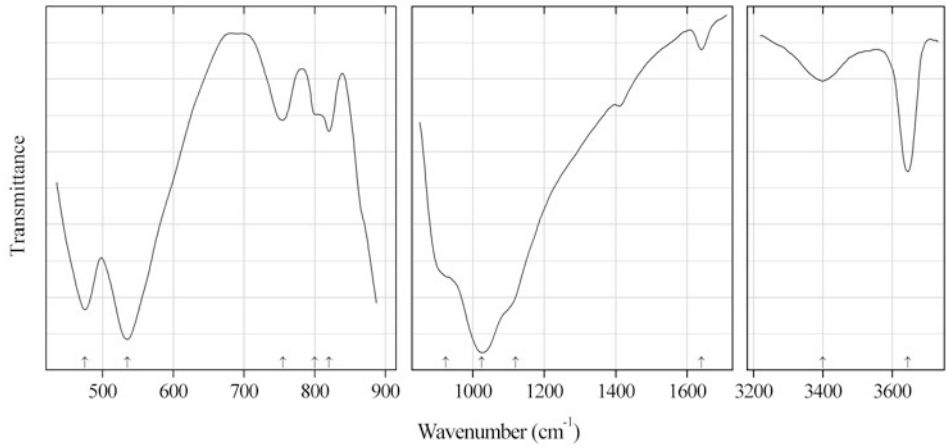

Fig. 2.646 IR spectrum of rectorite drawn using data from Oinuma and Hayashi (1965)

Sil292 Rectorite $(Na,Ca)Al_4[(Si,Al)_8O_{20}](OH)_4 \cdot 2H_2O$ (Fig. 2.646)
Locality: Yonago mine (pyrophyllite-diaspore deposit), Nagano Prefecture, Japan.
Description: A clay mineral having a 26 Å spacing due interstratification of 10 Å mica and its hydrated analogue.
Kind of sample preparation and/or method of registration of the spectrum: KBr disc (below 2000 cm^{-1}) and Nujol mull (above 3000 cm^{-1}). Transmission.
Source: Oinuma and Hayashi (1965).
Wavenumbers (cm^{-1}): 3645, 3400w, 1640w, 1120sh, 1025s, 925sh, 820w, 800sh, 755w, 535s, 475s.
Note: For a more detailed description of the sample see Shimoda and Sudo (1960). A band between 1400 and 1500 cm^{-1} may correspond to the admixture of a carbonate.

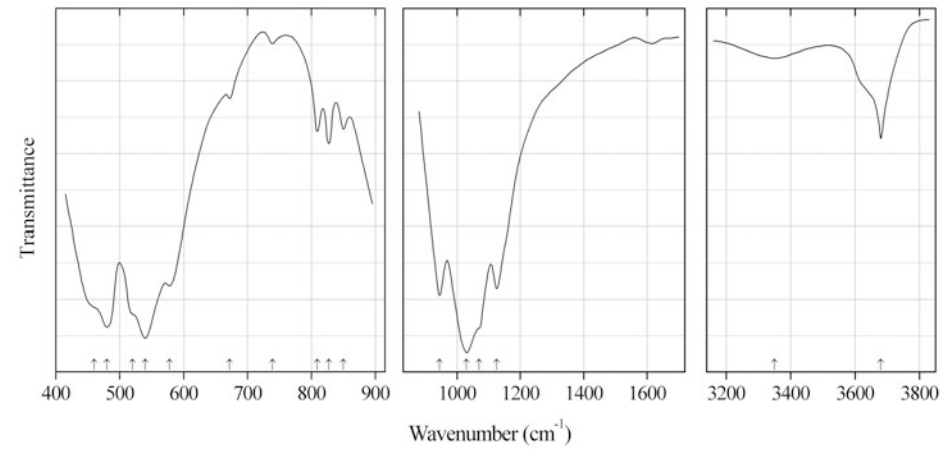

Fig. 2.647 IR spectrum of pyrophyllite-montmorillonite regular interstratification drawn using data from Oinuma and Hayashi (1965)

Sil293 Pyrophyllite-montmorillonite regular interstratification (Fig. 2.647)
Locality: Honami mine, Nagano Prefecture, Japan.

Description: Clay occurring in places along the marginal zone of a pyrophyilite deposit.
Kind of sample preparation and/or method of registration of the spectrum: KBr disc (below 2000 cm^{-1}) and Nujol mull (above 3000 cm^{-1}). Transmission.
Source: Oinuma and Hayashi (1965).
Wavenumbers (cm^{-1}): 3680, 3350w, 1125s, 1070sh, 1030s, 945s, 850w, 827w, 809w, 739w, 672, 578, 540s, 520s, 480s, 460sh.
Note: The wavenumbers were partly determined by us based on spectral curve analysis of the published spectrum. For the description of the sample see Kodama (1958).

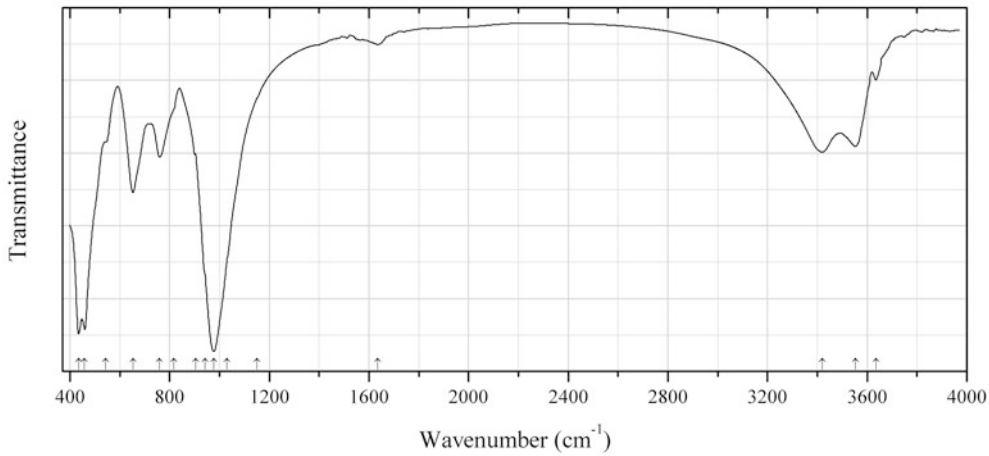

Fig. 2.648 IR spectrum of clinochlore Fe^{3+}-rich drawn using data from Kloprogge and Frost (2000)

Sil294 Clinochlore Fe^{3+}-rich $(Mg,Fe^{3+})_6(Si,Al)_4O_{10}(OH)_8$ (Fig. 2.648)
Locality: Flagstaff Hill, El Dorado Co., California, USA.
Description: A Fe^{3+}-rich variety ("ripidolite"). The empirical formula is $Ca_{0.02}(Mg_{2.24}Fe^{3+}_{1.73}Fe^{2+}_{1.51}Al_{0.30}Ti_{0.03})(Si_{2.26}Al_{1.74}O_{10})(OH,O)_8$.
Kind of sample preparation and/or method of registration of the spectrum: KBr disc. Absorption.
Source: Kloprogge and Frost (2000).
Wavenumbers (cm^{-1}): 3635w, 3553, 3419, 1636w, 1150sh, 1030sh, 978s, 943sh, 904sh, 818sh, 760, 653, 544sh, 459s, 435s.
Note: For a more detailed description of "ripidolite" from Flagstaff Hill see Post and Plummer (1972).

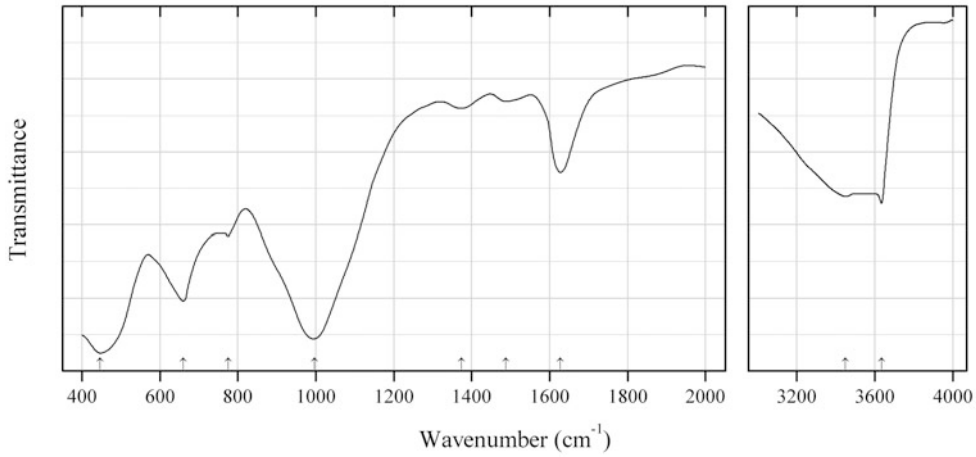

Fig. 2.649 IR spectrum of sauconite drawn using data from Yokoyama et al. (2006)

Sil295 Sauconite $Na_{0.3}Zn_3[(Si,Al)_4O_{10}](OH)_2 \cdot 4H_2O$ (Fig. 2.649)
Locality: Synthetic.
Description: Synthesized hydrothermally. Characterized by ICP-AES and powder X-ray diffraction data.
Kind of sample preparation and/or method of registration of the spectrum: KBr disc. Transmission.
Source: Yokoyama et al. (2006).
Wavenumbers (cm^{-1}): 3635, 3450, 1627, 1488w, 1374w, 996s, 775w, 660, 447s.
Note: The wavenumbers were partly determined by us based on spectral curve analysis of the published spectrum.

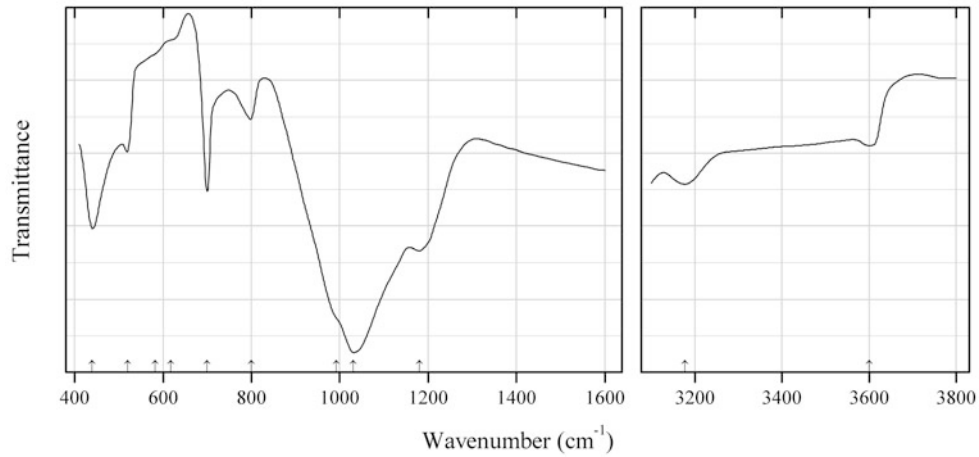

Fig. 2.650 IR spectrum of sazhinite-(Ce) drawn using data from Yes'kova et al. (1974a)

Sil296 Sazhinite-(Ce) $Na_3CeSi_6O_{15} \cdot 2H_2O$ (Fig. 2.650)
Locality: Karnasurt Mt., Lovozero alkaline complex, Kola peninsula, Murmansk region, Russia (type locality).

Description: Fine-grained aggregate from the association with natrolite, steenstrupine, neptunite, etc. Holotype sample. Orthorhombic, a = 7.35(3), b = 7.50(3), c = 15.62(6) Å. D_{meas} = 2.61 g/cm^3. Optically biaxial (+), α = 1.544(2), β = 1.528(2), γ = 1.525(2), 2 V = 47°. The empirical formula is $Na_{4.88}K_{0.35}Ca_{0.12}Mn_{0.01}Th_{0.07}REE_{1.74}Si_{10.40}Al_{0.21}P_{0.20}Ti_{0.18}Nb_{0.06}Fe_{0.04}O_x{\cdot}nH_2O$. The strongest lines of the powder X-ray diffraction pattern [d, Å (I, %) (hkl)] are: 7.25 (38) (100), 5.23 (55) (110), 3.37 (75) (022, 202), 3.23 (100) (121, 211), 2.552 (37) (124), 2.003 (38) (232, 322, 314, 225).
Kind of sample preparation and/or method of registration of the spectrum: KBr disc. Transmission.
Source: Yes'kova et al. (1974a).
Wavenumbers (cm^{-1}): 3600, 3177, 1180s, 1030s, 993sh, 800, 700, 618sh, 582sh, 520, 440s.
Note: The wavenumbers were partly determined by us based on spectral curve analysis of the published spectrum.

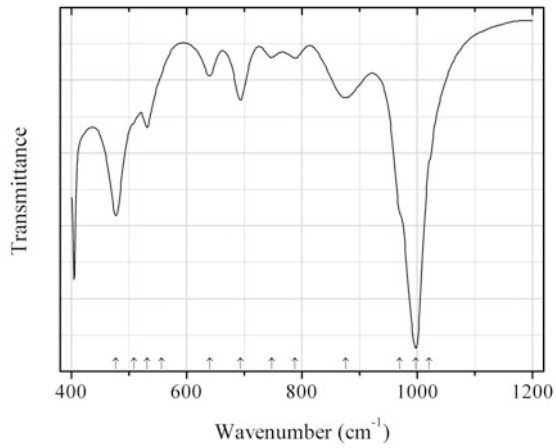

Fig. 2.651 IR spectrum of siderophyllite drawn using data from Redhammer et al. (2000)

Sil297 Siderophyllite $KFe^{2+}{}_2Al(Si_2Al_2O_{10})(OH)_2$ (Fig. 2.651)
Locality: Synthetic.
Description: Synthesized from stoichiometric gel by a hydrothermal technique. Characterized by electron microprobe analyses, Mössbauer spectroscopy, and powder X-ray diffraction data. The empirical formula is $K_{1.00}Fe^{2+}{}_{2.15}Al_{0.82}(Si_{2.19}Al_{1.81}O_{10})(OH)_2$.
Kind of sample preparation and/or method of registration of the spectrum: KBr disc. Absorption.
Source: Redhammer et al. (2000).
Wavenumbers (cm^{-1}): 3644sh, 3627, 3611sh, 3587sh, 1021sh, 998s, 970sh, 876, 788w, 748w, 693, 640w, 556sh, 531, 508sh, 477.
Note: The wavenumbers were partly determined by us based on spectral curve analysis of the published spectrum.

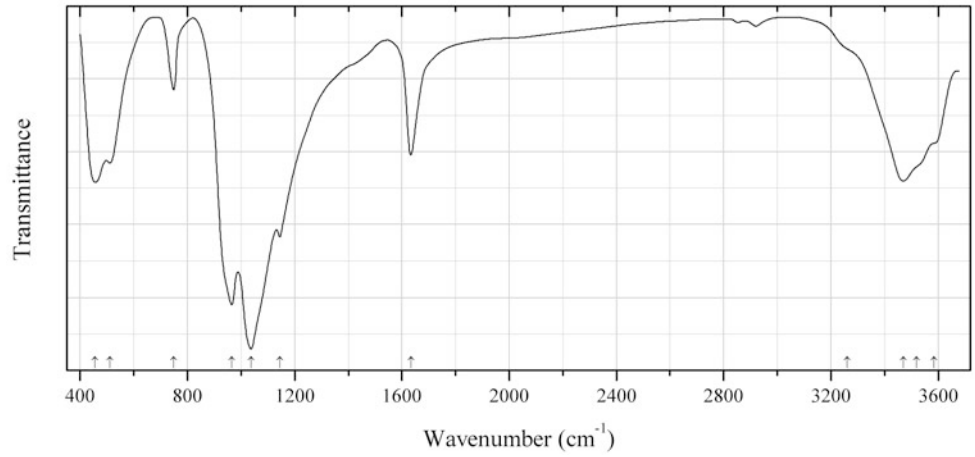

Fig. 2.652 IR spectrum of silinaite drawn using data from Alemi et al. (2013)

Sil298 Silinaite $NaLi(Si_2O_5)\cdot 2H_2O$ (Fig. 2.652)
Locality: Synthetic.
Description: Micro-rods synthesized hydrothermally from $Li_2SO_4\cdot H_2O$, $SiO_2\cdot H_2O$, and NaOH at 180 °C. Confirmed by the powder X-ray diffraction pattern.
Kind of sample preparation and/or method of registration of the spectrum: Transmission. Kind of sample preparation is not indicated.
Source: Alemi et al. (2013).
Wavenumbers (cm^{-1}): 3585sh, 3520sh, 3470, 3260sh, 1633, 1145, 1038s, 965s, 749, 510, 456.
Note: The wavenumbers were partly determined by us based on spectral curve analysis of the published spectrum.

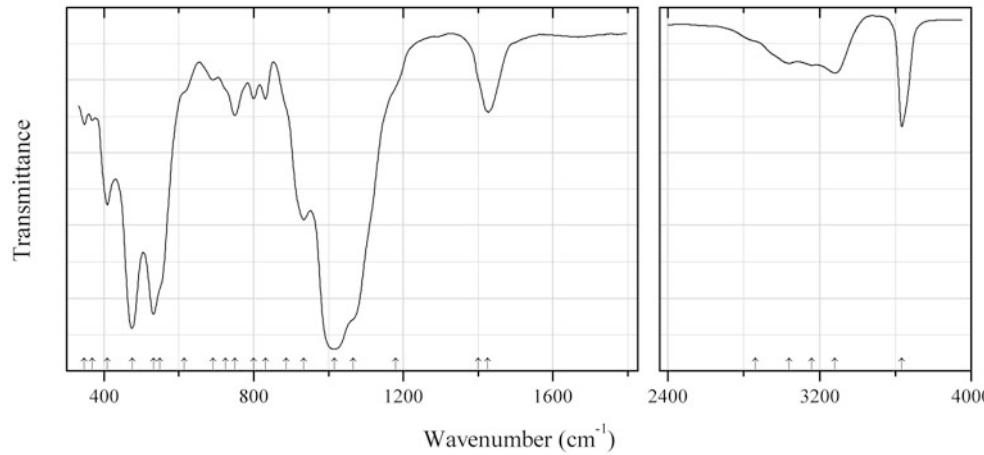

Fig. 2.653 IR spectrum of tobelite drawn using data from Higashi (1982)

Sil300 Tobelite $(NH_4)Al_2(AlSi_3O_{10})(OH)_2$ (Fig. 2.653)
Locality: Ohgidani pottery stone deposit, near Tobe, Ehime prefecture, Japan (type locality).

Description: Clayey material formed as a result of hydrothermal alteration of a biotite andesite dyke. Holotype sample. Monoclinic, space group *C*2/*m*, *a* = 5.219(4), *b* = 8.986(3), *c* = 10.447(2) Å, β = 101.31(1)°, *Z* = 2. Optically biaxial (−), α = 1.555(2), β = 1.575(2), γ = 1.581(2). The empirical formula is $[(NH_4)_{0.58}K_{0.19}Na_{0.01}](Al_{1.97}Mg_{0.05}Fe^{3+}_{0.03})(Si_{3.17}Al_{0.83}O_{10})(OH)_2$. The strongest lines of the powder X-ray diffraction pattern [*d*, Å (*I*, %) (*hkl*)] are: 10.44 (100) (001), 5.12 (70) (002), 4.486 (70) (020), 3.408 (60) (003), 3.103 (35) (112), 2.566 (45) (13–1, 004).
Kind of sample preparation and/or method of registration of the spectrum: KBr disc. Transmission.
Source: Higashi (1982).
Wavenumbers (cm^{-1}): 3635, 3280, 3160, 3040, 2860sh, 1426, 1400sh, 1179sh, 1065sh, 1015s, 934, 887sh, 832w, 800w, 750, 725sh, 691w, 615sh, 549sh, 532s, 475s, 408, 368w, 347w.
Note: The wavenumbers were partly determined by us based on spectral curve analysis of the published spectrum.

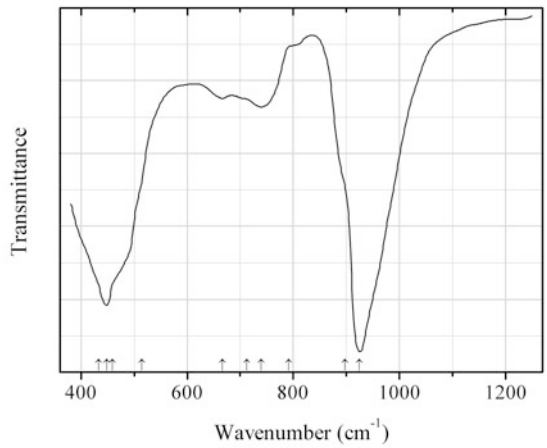

Fig. 2.654 IR spectrum of vermiculite Fe^{3+} analogue drawn using data from Ivanitsky et al. (1990)

Sil301 Vermiculite Fe^{3+}analogue $(Mg,Fe^{2+},Al)_3[(Si,Fe^{3+})_4O_{10}](OH)_2 \cdot 4H_2O$ (Fig. 2.654)
Locality: Artificial.
Description: Product of hydrothermal treatment of tetraferriphlogopite with the empirical formula $(K_{0.89}Na_{0.09}Ca_{0.03})(Fe^{2+}_{0.92}Mg_{1.65}Fe^{3+}_{0.28}Mn_{0.01})(Si_{2.93}Fe^{3+}_{1.04}Al_{0.03}O_{10})(OH)_{2.00}$ in 1 N solution of Na_2CO_3 at 570 K. Characterized by powder X-ray diffraction data. Contains admixture of tetraferriphlogopite.
Kind of sample preparation and/or method of registration of the spectrum: KBr disc. Transmission.
Source: Ivanitsky et al. (1990).
Wavenumbers (cm^{-1}): 925s, 898sh, 792sh, 740w, 712sh, 667w, 515sh, 459sh, 448s, 433sh.
Note: The wavenumbers were determined by us based on spectral curve analysis of the published spectrum.

Sil302 Nanpingite $CsAl_2(Si_3Al)O_{10}(OH)_2$
Locality: No. 31 pegmatite, Nanping, Fujian province, China (type locality).
Description: White platy grains from the association with montebrasite, quartz, and apatite. Holotype sample. Monoclinic, space group *C*2/*c*, *a* = 5.362(3), *b* = 8.86(1), *c* = 21.41(1) Å, β = 95.77(2)°, *Z* = 4. D_{meas} = 3.11(2) g/cm^3, D_{calc} = 3.19 g/cm^3. Optically biaxial (−), α = 1.551(5), β = 1.584(2),

γ = 1.588(2), 2 *V* = 46(2)°. The strongest lines of the powder X-ray diffraction pattern [*d*, Å (*I*, %) (*hkl*)] are: 2.664 (100) (008), 2.129 (85) (0.0.10), 2.122 (16) (223), 2.654 (14) (202), 1.328 (14) (067).

Kind of sample preparation and/or method of registration of the spectrum: Absorption.

Source: Yueqing et al. (1988).

Wavenumbers (cm^{-1}): 3634, (3429), (1625), 1083sh, 1018s, 911, 823w, 788w, 741w, 663w, 515s, 467s, 420.

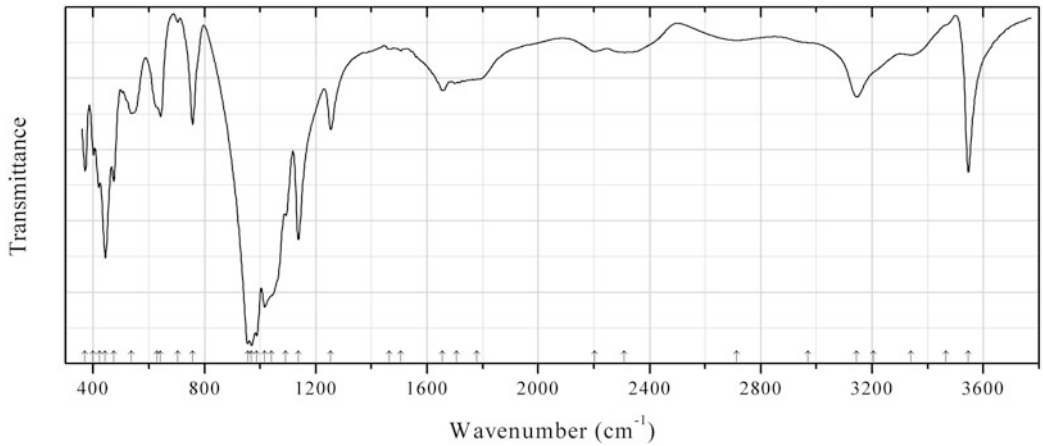

Fig. 2.655 IR spectrum of grumantite obtained by N.V. Chukanov

Sil303 Grumantite $NaSi_2O_4(OH)\cdot H_2O$ (Fig. 2.655)

Locality: Alluaiv Mt., Lovozero alkaline complex, Kola peninsula, Murmansk region, Russia (type locality).

Description: White massive aggregate from the association with ussingite, makatite, kazakovite, tisinalite, nordite-(Ce), sodalite, nepheline, potassic feldspar, arfvedsonite, aegirine, etc. Holotype sample. Orthorhombic, *a* = 15.979, *b* = 18.25, *c* = 7.169Å, *Z* = 16. D_{meas} = 2.21 g/cm^3, D_{calc} = 2.26 g/cm^3. Optically biaxial (+), α = 1.694(2), β = 1.507(2), γ = 1.523(2), 2 *V* = 85(2)°. The empirical formula is $Na_{0.98}H_{1.02}Si_2O_5\cdot 0.93H_2O$. The strongest lines of the powder X-ray diffraction pattern [*d*, Å (*I*, %)] are: 6.20 (50), 6.05 (50), 4.46 (50), 3.505 (100), 3.346 (25), 3.087 (50), 3.006 (100).

Kind of sample preparation and/or method of registration of the spectrum: KBr disc. Absorption.

Wavenumbers (cm^{-1}): 3546, 3465sh, 3340, 3205sh, 3145, 2970sh, 2714, 2310, 2202, 1780, 1706, 1655, 1505w, 1465w, 1254, 1138s, 1091, 1040sh, 1017s, 988s, 969s, 957s, 757, 705w, 642, 630sh, 538, 474, 444s, 424, 400, 371.

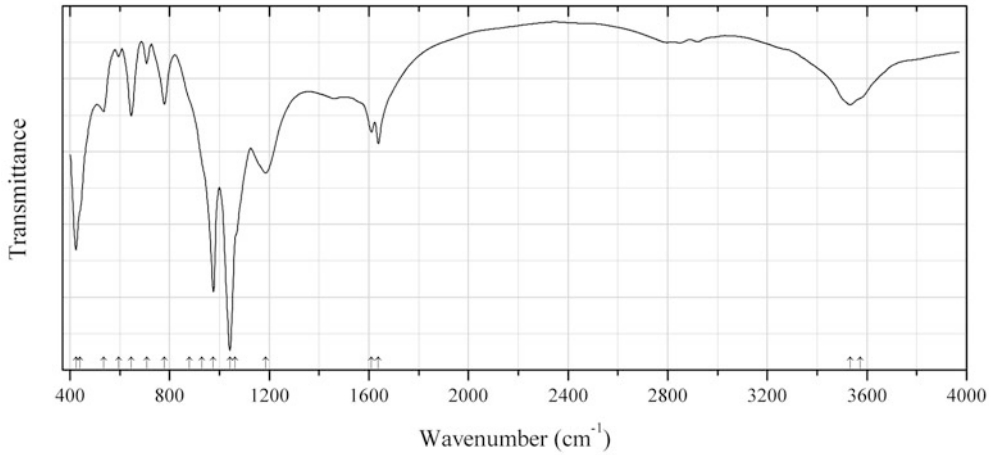

Fig. 2.656 IR spectrum of armstrongite H_2O-depleted drawn using data from Mesto et al. (2014)

Sil305 Armstrongite H_2O-depleted $CaZr(Si_6O_{15})\cdot 2H_2O$ (Fig. 2.656)
Locality: Khan Bogdo massif, Gobi desert, Mongolia (type locality).
Description: Grains from elpidite-bearing granite. The crystal structure is solved. Monoclinic, space group *C*2/*m*, a = 14.0178(7), b = 14.1289(6), c = 7.8366(3) Å, β = 109.436(3)°, V = 1463.6(1) Å^3, Z = 4. The empirical formula is $(Ca_{0.96}Ce_{0.01}Yb_{0.01})Zr_{0.99}Si_{6.00}O_{15}\cdot 2.02H_2O$.
Kind of sample preparation and/or method of registration of the spectrum: KBr disc. Absorption.
Source: Mesto et al. (2014).
Wavenumbers (cm^{-1}): 3573sh, 3533, 1638, 1610, 1186, 1064sh, 1042s, 976s, 931sh, 880sh, 779, 708w, 646, 595w, 535, 440sh, 424s.
Note: The wavenumbers were partly determined by us based on spectral curve analysis of the published spectrum. The bands in the range from 2700 to 3000 cm^{-1} correspond to very strong hydrogen bonds, which were not detected by means of X-ray structure analysis.

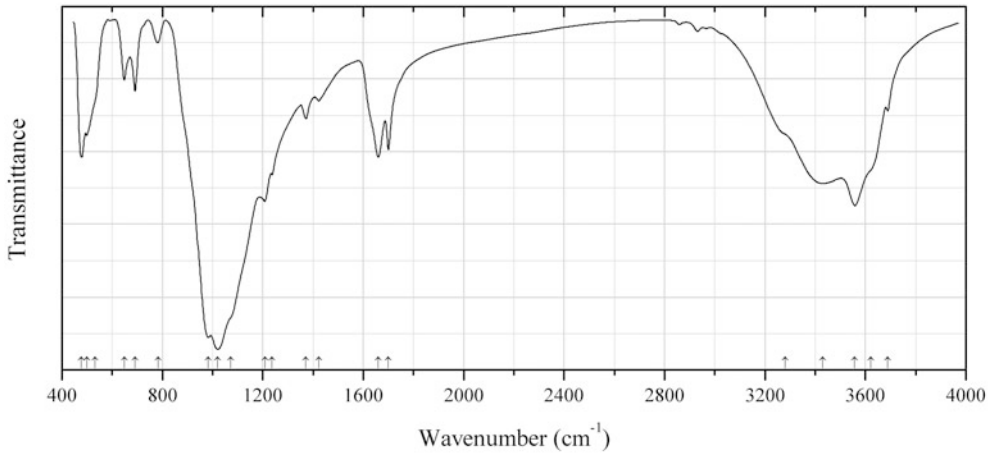

Fig. 2.657 IR spectrum of sepiolite drawn using data from Yeniyol (2014)

Sil306 Sepiolite $Mg_4Si_6O_{15}(OH)_2\cdot 6H_2O$ (Fig. 2.657)

Locality: Yenidoğan, Sivrihisar, Turkey.
Description: A well-crystallized sample with d_{110} = 12.3 Å, containing 4.39 wt% Al_2O_3 and 2.15 wt % Fe_2O_3.
Kind of sample preparation and/or method of registration of the spectrum: KBr disc. Transmission.
Source: Yeniyol (2014).
Wavenumbers (cm^{-1}): 3688w, 3622sh, 3558s, 3430, 3280sh, 1700, 1660, 1424w, 1372w, 1237, 1208, 1072sh, 1020s, 982s, 783w, 692, 649, 531sh, 499, 477.
Note: The wavenumbers were partly determined by us based on spectral curve analysis of the published spectrum. The bands in the range from 2800 to 3000 cm^{-1} (and, possibly, in the range from 1370 to 1430 cm^{-1}) correspond to the admixture of an organic substance. The bands in the range 1370–1430 cm^{-1} may also correspond to the admixture of a carbonate.

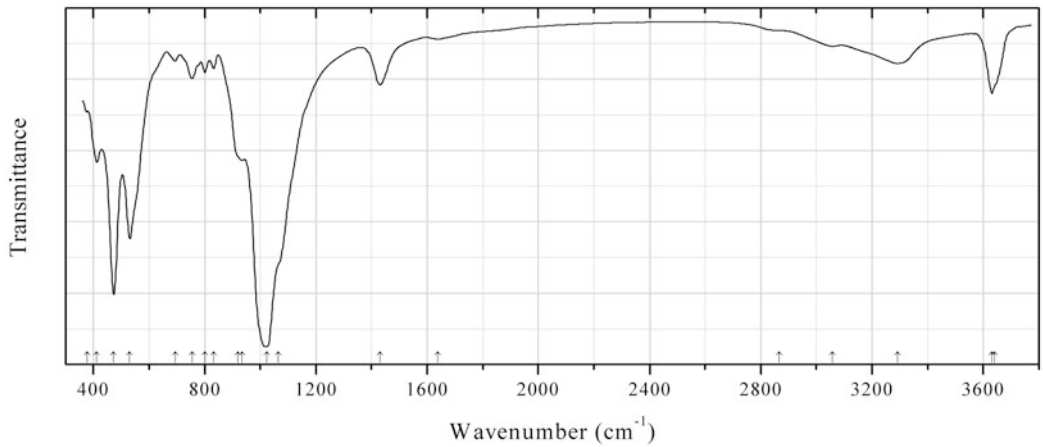

Fig. 2.658 IR spectrum of tobelite obtained by N.V. Chukanov

Sil307 Tobelite $(NH_4)Al_2(AlSi_3O_{10})(OH)_2$ (Fig. 2.658)
Locality: Five Mile Pass, Tooele Co., Utah, USA.
Description: White scales with pearly luster from the association with goethite. The empirical formula is (electron microprobe, NH_4 estimated from the IR spectrum): $(NH_4)_{0.6}K_{0.36}Na_{0.05}Al_{2.00}(Si_{3.26}Al_{2.74}O_{10})[(OH)_{1.73}O_{0.27}]\cdot nH_2O$ ($n << 1$).
Kind of sample preparation and/or method of registration of the spectrum: KBr disc. Absorption.
Wavenumbers (cm^{-1}): 3640sh, 3631, 3292, 3057, 2865w, 1639w, 1430, 1065sh, 1024s, 935, 920sh, 832, 800, 754, 694w, 531s, 473s, 412, 377.

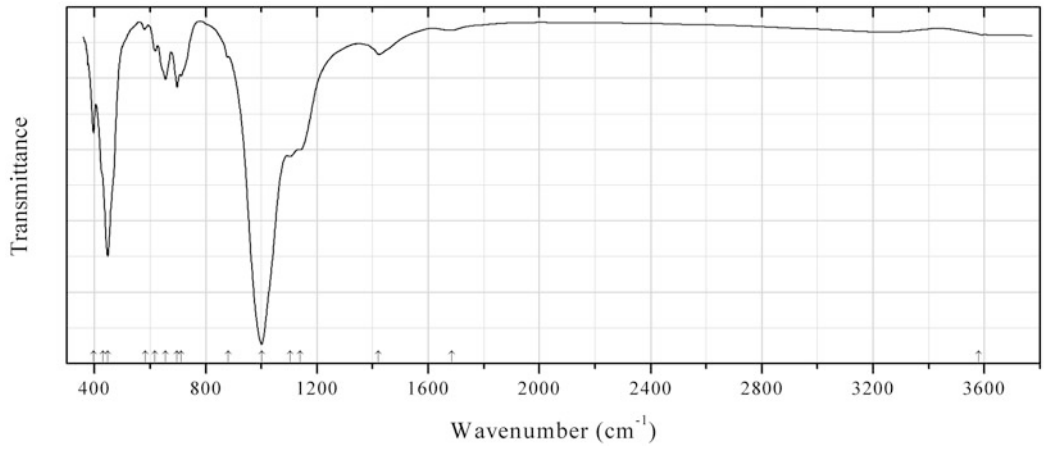

Fig. 2.659 IR spectrum of lazurite-3*C* obtained by N.V. Chukanov

Sif125 Lazurite-3*C* $Na_6Ca_2(Si_6Al_6O_{24})(S,SO_4)_2$ (Fig. 2.659)
Locality: Slyudyanka, Irkutsk region, Eastern Siberia, Russia.
Description: 3*C*-polytype of lazurite. Investigated by A.N. Sapozhnikov.
Kind of sample preparation and/or method of registration of the spectrum: KBr disc. Absorption.
Wavenumbers (cm^{-1}): (3580w), 1685w, 1422w, 1140, 1104, 1001s, 880w, 711, 697, 656, 618w, 583w, 447s, 430sh, 398.
Note: The band at 1422 cm^{-1} may correspond to the admixture of a carbonate mineral.

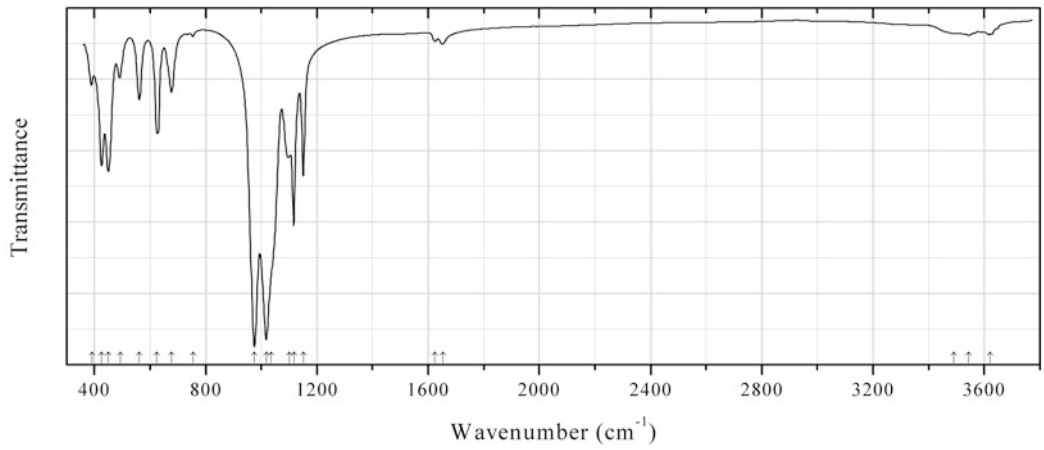

Fig. 2.660 IR spectrum of pitiglianoite obtained by N.V. Chukanov

Sif126 Pitiglianoite $K_2Na_6(Si_6Al_6O_{24})(SO_4)\cdot 2H_2O$ (Fig. 2.660)
Locality: Marchenko peak, Kukisvumchorr Mt., Khibiny alkaline complex, Kola peninsula, Murmansk region, Russia.
Description: White fibrous aggregates filling cavities in massive sodalite. The empirical formula is (electron microprobe): $K_{2.00}(Na_{5.01}K_{0.70}Ca_{0.12})(Si_{6.03}Al_{5.88}Fe_{0.09}O_{24})(SO_4)_{0.99}\cdot nH_2O$.
Kind of sample preparation and/or method of registration of the spectrum: KBr disc. Absorption.
Wavenumbers (cm^{-1}): 3620w, 3544w, 3490sh, 1652w, 1625w, 1151, 1117s, 1100, 1035sh, 1018s, 975s, 755w, 677, 625, 561, 494w, 450, 426, 391w.

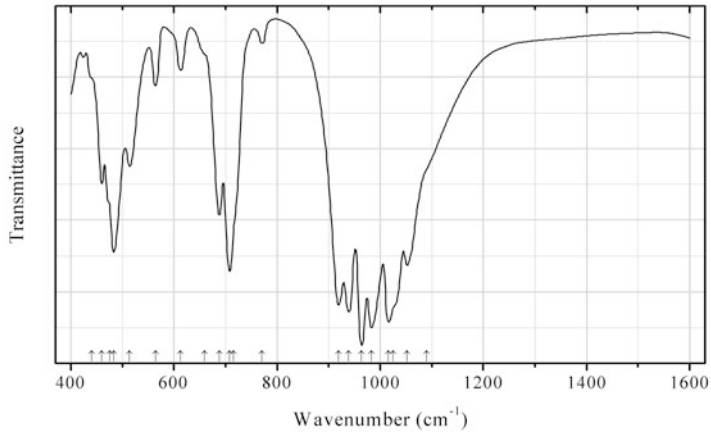

Fig. 2.661 IR spectrum of eucryptite obtained by N.V. Chukanov

Sif127 Eucryptite $Li(AlSiO_4)$ (Fig. 2.661)
Locality: Bikita mine, Bikita, east of Victoria, Zimbabwe (type locality).
Description: White coarse-grained aggregate from the association with bikitaite. Confirmed by IR spectrum.
Kind of sample preparation and/or method of registration of the spectrum: KBr disc. Absorption.
Wavenumbers (cm^{-1}): 1090sh, 1052, 1025sh, 1015s, 983s, 964s, 939s, 919s, 771w, 715sh, 708s, 688, 660sh, 613, 564, 514, 483, 475sh, 460, 440sh.

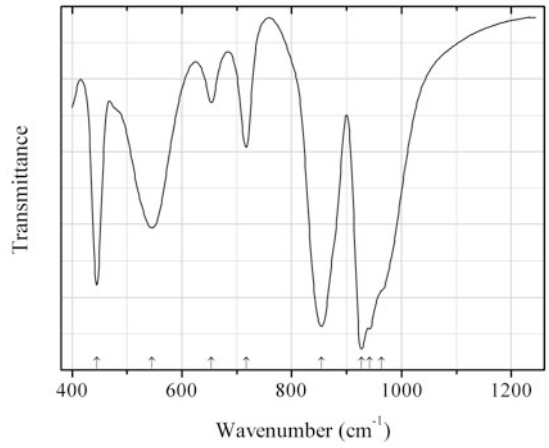

Fig. 2.662 IR spectrum of bicchulite drawn using data from Rahmoun et al. (2008)

Sif128 Bicchulite $Ca_2(Al_2SiO_6)(OH)_2$ (Fig. 2.662)
Locality: Synthetic.
Description: Synthesized hydrothermally from the melilite-type precursor compound.
Kind of sample preparation and/or method of registration of the spectrum: KBr disc. Absorption.
Source: Rahmoun et al. (2008).
Wavenumbers (cm^{-1}): 964sh, 942s, 927s, 854s, 717, 654, 545, 445s.
Note: For the method of synthesis see Gupta and Chatterjee (1978). The wavenumbers were partly determined by us based on spectral curve analysis of the published spectrum.

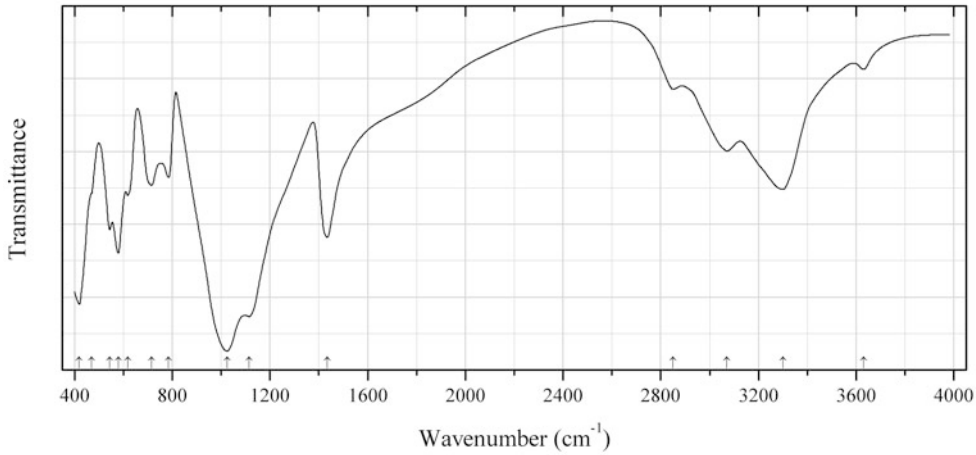

Fig. 2.663 IR spectrum of buddingtonite drawn using data from Voncken et al. (1988)

Sif129 Buddingtonite $(NH_4)(AlSi_3O_8)$ (Fig. 2.663)
Locality: Synthetic.
Description: Monoclinic, space group *C*2/*m*, a = 8.824(5), b = 13.077(8), c = 7.186(4) Å, β = 116.068(12)°, V = 744.8 Å^3, Z = 2. The strongest lines of the powder X-ray diffraction pattern [*d*, Å (*I*, %) (*hkl*)] are: 5.93 (50) (−111), 4.336 (100) (−201), 3.820 (75) (130), 3.390 (90) (220), 3.323 (60) (−202), 3.234 (90) (002).
Kind of sample preparation and/or method of registration of the spectrum: KBr disc. Absorption.
Source: Voncken et al. (1988).
Wavenumbers (cm^{-1}): 3630w, 3300s, 3070, 2850w, 1435, 1115s, 1025s, 786, 715, 618, 580, 545, 470sh, 420s.
Note: For IR spectrum of buddingtonite see also Erd et al. (1964).

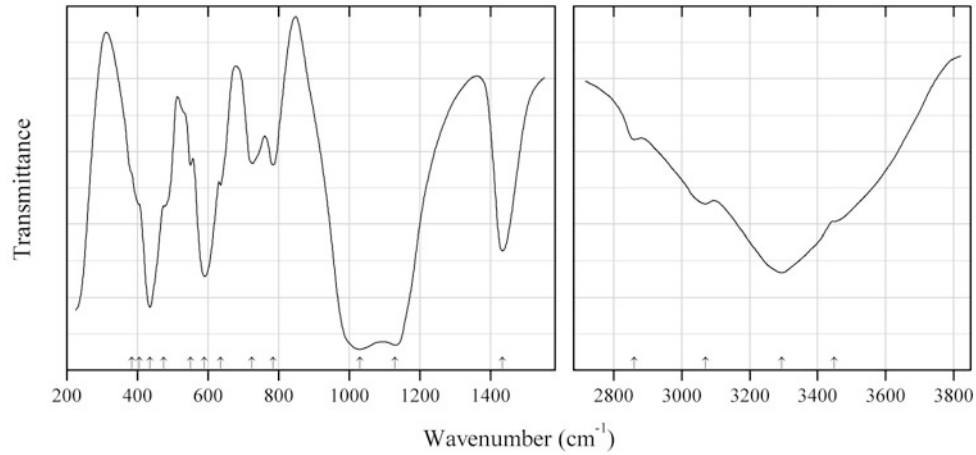

Fig. 2.664 IR spectrum of buddingtonite drawn using data from Loughnan et al. (1983)

Sif130 Buddingtonite $(NH_4)(AlSi_3O_8)$ (Fig. 2.664)
Locality: Condor oilshale deposit, near Proserpine, Queensland, Australia.

Description: Grains from the association with clay minerals, carbonates, quartz, cristobalite, and apatite. Confirmed by chemical analysis and X-ray diffraction data. The content of $(NH_4)_2O$ is 7.92 wt%. The strongest lines of the powder X-ray diffraction pattern [*d*, Å (*I*, %) (*hkl*)] are: 6.52 (87) (020), 4.33 (53) (101), 3.82 (100) (130), 3.386 (77) (220), 3.260 (55) (040), 3.226 (84) (202).
Kind of sample preparation and/or method of registration of the spectrum: Absorption. Kind of sample preparation is not indicated.
Source: Loughnan et al. (1983).
Wavenumbers (cm^{-1}): 3450sh, 3295s, 3070, 2860w, 1434, 1130s, 1030s, 785, 725, 635sh, 590s, 550, 475sh, 435s, 405sh, 385sh.
Note: For IR spectrum of buddingtonite see also Erd et al. (1964).

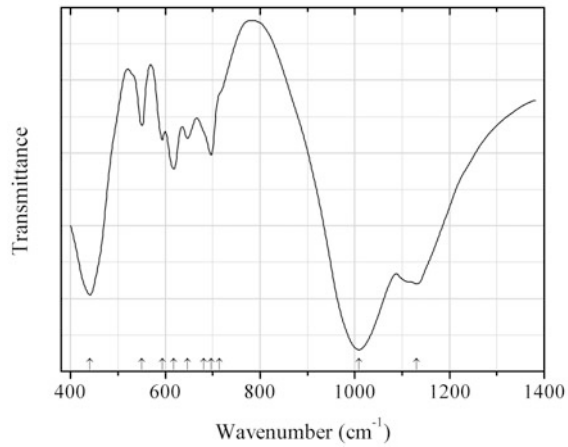

Fig. 2.665 IR spectrum of farneseite drawn using data from Cámara et al. (2005)

Sif131 Farneseite $(Na,K)_{46}Ca_{10}(Si_{42}Al_{42}O_{168})(SO_4)_{12}\cdot 3H_2O$ (Fig. 2.665)
Locality: Farnese, Viterbo province, Latium, Italy (type locality).
Description: Colourless isometric crystals from the association with sanidine with minor andradite, augite, biotite, Fe-oxides, and feldspathoids. Holotype sample. The crystal structure is solved. Farneseite is 14-layer cancrinite-group mineral with the stacking sequence is ABCABABACBACAC…, where A, B, and C represent the positions of the rings within the layers forming tetrahedral framework. Hexagonal, space group $P6_3/m$, a = 12.8784(2), c = 37.0078(12) Å, V = 5315.54(2) $Å^3$, Z = 1. D_{calc} = 2.425 g/cm^3. Optically uniaxial (+), ω = 1.499(1), ε = 1.503(1). The empirical formula is $Na_{36.43}K_{9.18}Ca_{8.75}(Si_{42.50}Al_{41.50}O_{168})(SO_4)_{11.43}Cl_{0.48}F_{0.16}\cdot 3.03H_2O$. The strongest lines of the powder X-ray diffraction pattern [*d*, Å (*I*, %) (*hkl*)] are: 3.722 (100) (300), 3.485 (65) (216), 3.119 (36) (218), 2.149 (34) (330, 4.0.11), 2.648 (32) (228, 0.0.14).
Kind of sample preparation and/or method of registration of the spectrum: Absorption. Kind of sample preparation is not indicated.
Source: Cámara et al. (2005).
Wavenumbers (cm^{-1}): 1130s, 1009s, 714sh, 697, 681sh, 647, 618, 594, 551, 441s.
Note: The wavenumbers were partly determined by us based on spectral curve analysis of the published spectrum. Unpolarised single-crystal FTIR spectrum of farneseite contains also weak bands with the following wavenumbers (cm^{-1}): 3514 (O–H stretching vibrations), 2352 (antisymmetric stretching vibrations of CO_2 molecules in channels), 1635 (H–O–H bending vibrations), and 1420 (trace amount of CO_3^{2-} groups).

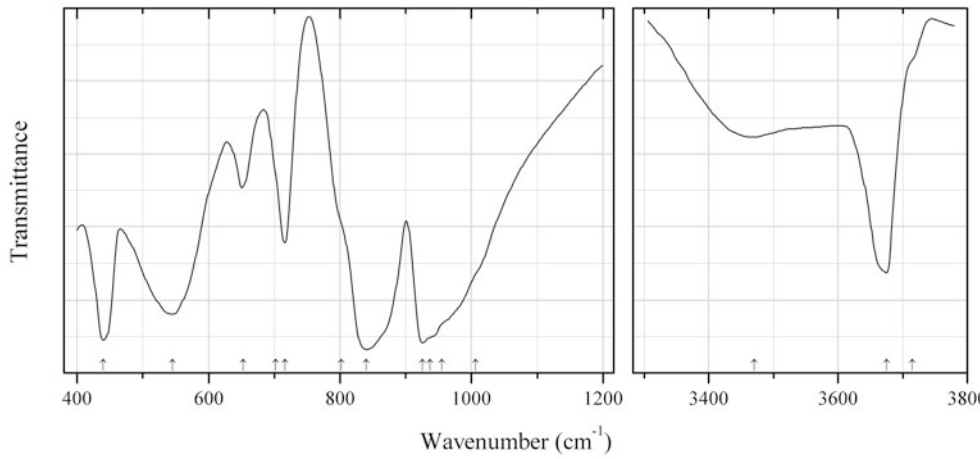

Fig. 2.666 IR spectrum of bicchulite drawn using data from Kimata and Kakefuda (1980)

Sif132 Bicchulite $Ca_2(Al_2SiO_6)(OH)_2$ (Fig. 2.666)
Locality: Synthetic.
Description: Synthesized under hydrothermal conditions.
Kind of sample preparation and/or method of registration of the spectrum: KBr disc. Transmission.
Source: Kimata and Kakefuda (1980).
Wavenumbers (cm^{-1}): 3715sh, 3675, 3470, 1006sh, 955sh, 937sh, 925s, 840s, 802sh, 716, 702sh, 653, 545s, 440s.
Note: The wavenumbers were partly determined by us based on spectral curve analysis of the published spectrum.

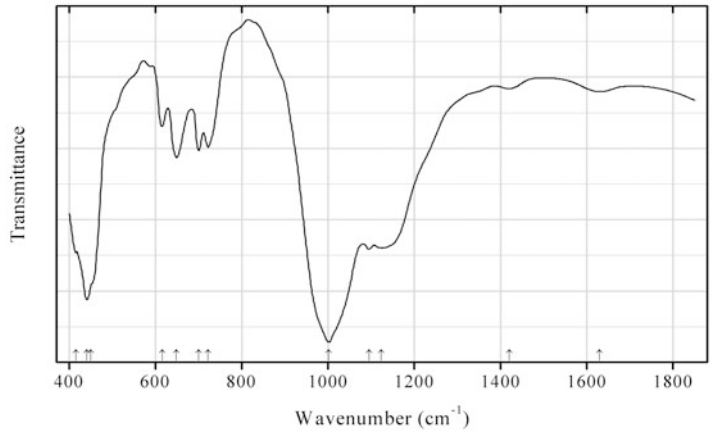

Fig. 2.667 IR spectrum of vladimirivanovite obtained by N.V. Chukanov

Sif133 Vladimirivanovite $Na_6Ca_2(Al_6Si_6O_{24})(SO_4,S_3,S_2,Cl)_2 \cdot H_2O$ (Fig. 2.667)
Locality: Tultuiskoe lazurite deposit, near Slyudyanka, Irkutsk region, Eastern Siberia, Russia (type locality).

Description: Deep blue granular aggregate from the association with lazurite. Orthorhombic (according to X-ray diffraction data obtained by A.N. Sapozhnikov). The empirical formula is (electron microprobe): $Na_{6.19}Ca_{1.65}(Si_{6.01}Al_{5.99}O_{24})S_{2.55}Cl_{0.02}(OH,CO_3)_x \cdot nH_2O$.
Kind of sample preparation and/or method of registration of the spectrum: KBr disc. Absorption.
Wavenumbers (cm^{-1}): 1630w, 1420w, 1124s, 1095s, 1002s, 722, 700, 649, 615, 450sh, 440s, 415.

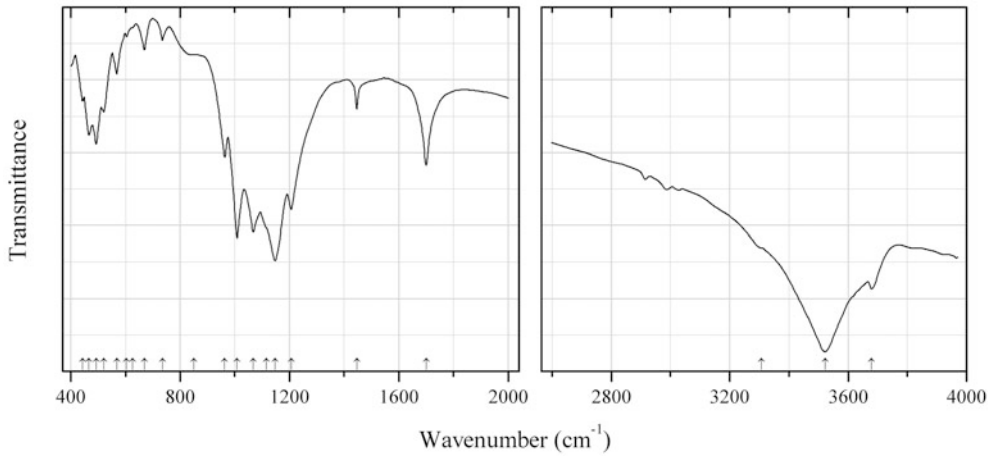

Fig. 2.668 IR spectrum of sodium copper silicate Sif134 drawn using data from Wang et al. (2005)

Sif134 Sodium copper silicate Sif134 $Na_2[Cu_2Si_4O_{11}] \cdot 2H_2O$ (Fig. 2.668)
Locality: Synthetic.
Description: Synthesized under mild hydrothermal conditions. The crystal structure of Sif134 contains double chains of SiO_4 tetrahedra that are interlinked by CuO_5 tetragonal pyramids to form a 3D framework. Triclinic, space group *P*-1, $a = 5.2254(7)$, $b = 6.4126(8)$, $c = 8.516(1)$ Å, $\alpha = 101.1(1)°$, $\beta = 94.3(1)°$, $\gamma = 102.5(1)°$, $V = 271.37(6)$ $Å^3$, $Z = 2$.
Kind of sample preparation and/or method of registration of the spectrum: KBr disc. Transmission.
Source: Wang et al. (2005).
Wavenumbers (cm^{-1}): 3680, 3522s, 3307sh, 1700, 1446, 1206s, 1147s, 1115sh, 1067s, 1008s, 963, 850sh, 735w, 669w, 625sh, 604w, 568, 521, 493, 466, 443.
Note: The wavenumbers were determined by us based on spectral curve analysis of the published spectrum.

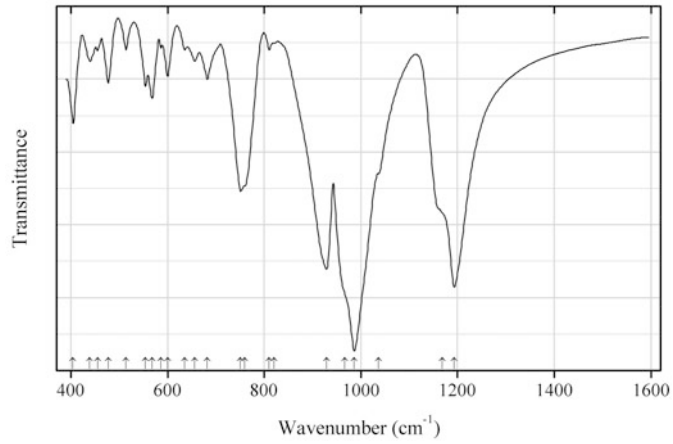

Fig. 2.669 IR spectrum of cordierite Mn^{2+} analogue drawn using data from Knorr et al. (1999)

Sif135 Cordierite Mn^{2+}analogue $Mn^{2+}{}_2Al_4Si_5O_{18}$ (Fig. 2.669)
Locality: Synthetic.
Description: Synthesized from oxides at 1225 K with subsequent recrystallization at 1370 K. The crystal structure is solved. Orthorhombic, space group *Cccm*, $a = 17.128(1)$, $b = 9.764(1)$, $c = 9.147(1)$ Å.
Kind of sample preparation and/or method of registration of the spectrum: KBr disc. Absorption.
Source: Knorr et al. (1999).
Wavenumbers (cm^{-1}): 1193s, 1168sh, 1037sh, 986s, 967sh, 929s, 820sh, 810w, 760sh, 751, 682, 656w, 635w, 600, 586w, 568, 554, 514w, 477, 455w, 439w, 404.
Note: The wavenumbers were determined by us based on spectral curve analysis of the published spectrum.

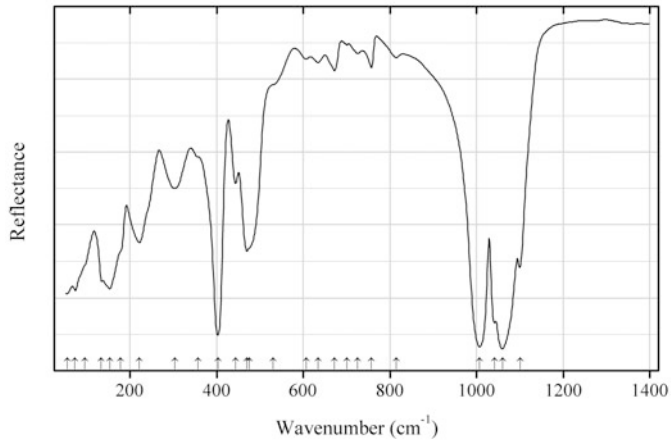

Fig. 2.670 IR spectrum of eucryptite-beta drawn using data from Zhang et al. (2003)

Sif136 Eucryptite-beta $Li(AlSiO_4)$ (Fig. 2.670)
Locality: Synthetic.
Description: Li-stuffed derivative of β-quartz. Synthesized from the mixture of powdered Li_2CO_3, Al_2O_3 and SiO_2 having a molar ratio of 1:1:2 at 1373 K for 15 h with subsequent grounding and resintering at 1573 K for 24 h. Confirmed by powder X-ray diffraction data.

Kind of sample preparation and/or method of registration of the spectrum: Reflectance spectrum obtained for a single crystal under unpolarized conditions.
Source: Zhang et al. (2003).
Wavenumbers (cm^{-1}): 1101, 1060s, 1041s, 1007s, 815w, 757w, 725w, 701w, 672w, 634w, 607w, 530sh, 476sh, 470, 444, 403s, 357sh, 303, 222, 178sh, 153s, 134, 96sh, 73, 55.
Note: The wavenumbers were determined by us based on spectral curve analysis of the published spectrum.

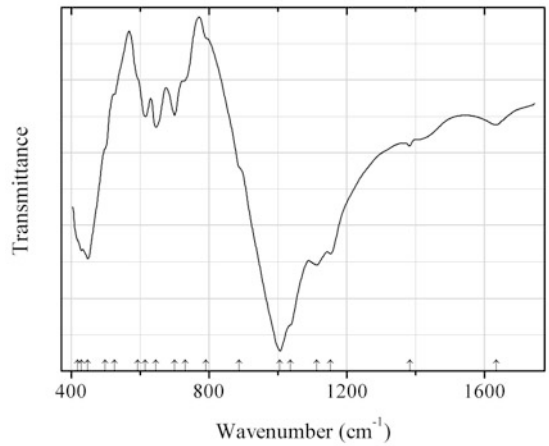

Fig. 2.671 IR spectrum of fantappièite drawn using data from Cámara et al. (2010)

Sif137 Fantappièite $[(Na,K)_{99}Ca_{33}](Si_{99}Al_{99}O_{396})(SO_4)_{33}\cdot 6H_2O$ (Fig. 2.671)
Locality: Torre Stracciacappe, Trevignano community, Rome, Latium, Italy (type locality).
Description: Colourless crystals from the association with sanidine and minor plagioclase, biotite, augitic clinopyroxene, andradite, and iron oxides. Holotype sample. Trigonal, space group *P*-3, $a = 12.8742(6)$, $c = 87.215(3)$ Å, $V = 12518.8(9)$ $Å^3$, $Z = 1$. $D_{calc} = 2.471$ g/cm^3. Optically uniaxial (−), ω = 1.5046(5), ε = 1.5027(5). The empirical formula is $(Na_{84.12}Ca_{30.00}K_{15.95}Fe_{0.19}Ti_{0.13}Mn_{0.10}Mg_{0.09})(Si_{99.36}Al_{98.64}O_{396})(SO_4)_{30.24}(CO_3)_{0.29}Cl_{0.84}F_{0.82}\cdot 5.18H_2O$. The strongest lines of the powder X-ray diffraction pattern [*d*, Å (*I*, %) (*hkl*)] are: 3.70 (100) (300), 3.60 (80) (1.0.23), 2.641 (65) (0.0.33), 6.85 (60) (0.1.10), 6.40 (55) (1.1.0).
Kind of sample preparation and/or method of registration of the spectrum: KBr disc. Transmission.
Source: Cámara et al. (2010), Bellatreccia et al. (2009a).
Wavenumbers (cm^{-1}): 1634w, 1383w, 1153s, 1113s, 1037sh, 1006s, 887sh, 790sh, 730sh, 699, 645, 614, 592sh, 524sh, 497sh, 447s, 428s, 418sh.
Note: The wavenumbers were partly determined by us based on spectral curve analysis of the published spectrum. Unpolarized light single-crystal FTIR spectrum of fantappièite contains the bands at 3622, 3580, 3406sh, 3241, 2338w, 2117, 1693sh, and 1634 cm^{-1}. The weak sharp band at 2338 cm^{-1} corresponds to antisymmetric stretching vibrations of CO_2 molecules present in structural channels.

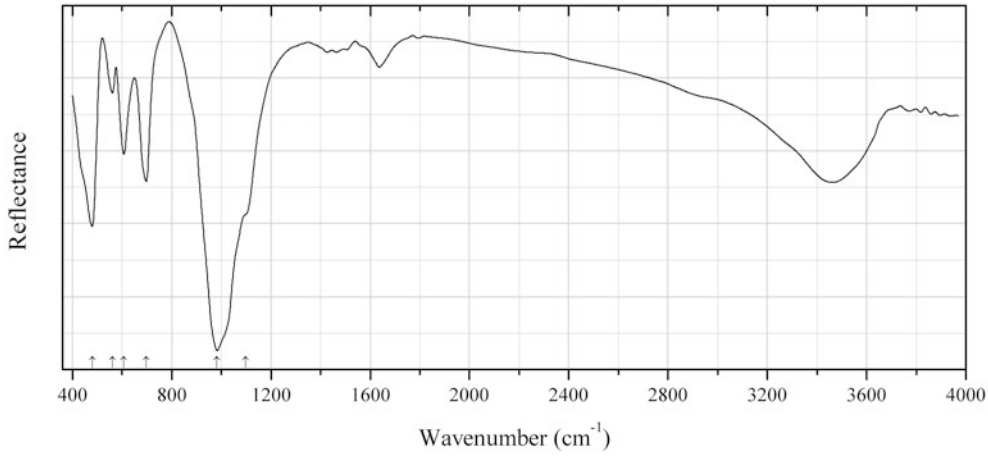

Fig. 2.672 IR spectrum of kaliophilite drawn using data from Yao et al. (2011)

Sif138 Kaliophilite $K(AlSiO_4)$ (Fig. 2.672)
Locality: Synthetic.
Description: Synthesized by fusion method using fly ash as starting material. Confirmed by powder X-ray diffraction data.
Kind of sample preparation and/or method of registration of the spectrum: Attenuated total reflection of powdered mineral. KBr disc. Transmission.
Source: Yao et al. (2011).
Wavenumbers (cm^{-1}): 1098sh, 983s, 698, 607, 561w, 480s.
Note: Additional bands (at 3463 and 1637 cm^{-1}) correspond to adsorbed water.

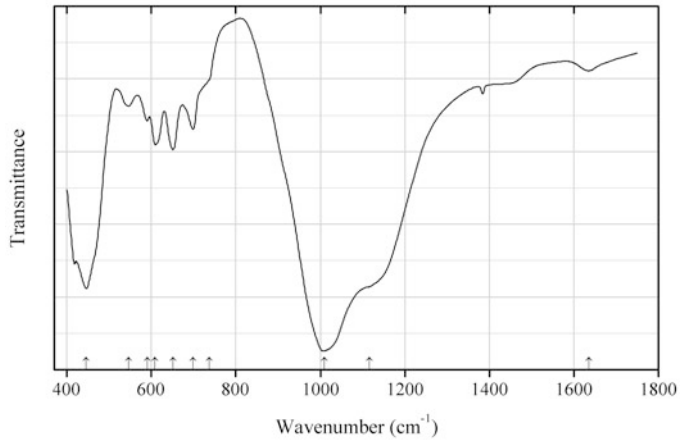

Fig. 2.673 IR spectrum of kircherite drawn using data from Cámara et al. (2012)

Sif139 Kircherite $Na_5Ca_2K(Si_6Al_6O_{24})(SO_4)_2 \cdot 0.33H_2O$ (Fig. 2.673)
Locality: Biachella valley, Sacrofano caldera, Campagnano municipality, Roma province, Latium region, Italy (type locality).
Description: Colourless tabular crystals from cavities in sanidinite. The associated minerals are sodalite, biotite, iron oxides, titanite, fluorite,, and a pyrochlore-group mineral. Holotype sample.

Trigonal, space group $R32$, a = 12.8770(7), c = 95.244(6) Å, V = 13,677(1) Å^3, Z = 18. D_{calc} = 2.457 g/cm^3. Optically uniaxial (−), ω = 1.510(2), ε = 1.502(2). The empirical formula is (Z = 1): $Na_{89.09}Ca_{31.63}K_{18.85}Fe_{0.20}Mn_{0.06}Mg_{0.05}Ti_{0.03}(Si_{108.13}Al_{107.87}O_{430})(SO_{32.58}Cl_{2.00}F_{0.53}\cdot 6.86 H_2O$. The strongest lines of the powder X-ray diffraction pattern [d, Å (I, %) (hkl)] are: 3.799 (52) (1.2.11), 3.717 (100) (300), 3.604 (53) (1.0.25), 3.584 (60) (1.2.14), 3.232 (65) (2.1.19), 3.220 (38) (220), 2.648 (100) (2.1.28, 0.0.36).

Kind of sample preparation and/or method of registration of the spectrum: KBr disc. Transmission.

Source: Cámara et al. (2012).

Wavenumbers (cm^{-1}): 1635w, 1116sh, 1009s, 737sh, 698, 651, 609, 590, 546w, 446s.

Note: Weak band at 1384 cm^{-1} corresponds to NO_3^- groups (a usual impurity in commercial KBr).

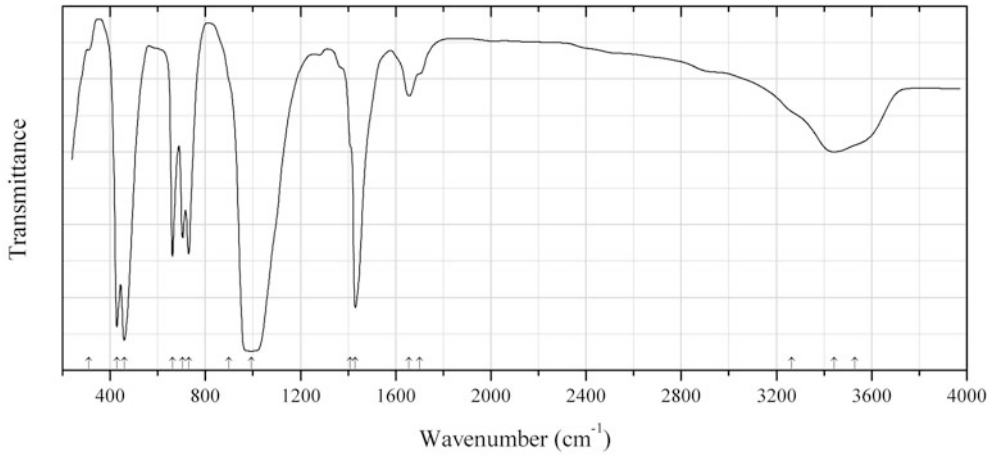

Fig. 2.674 IR spectrum of nosean CO_3-analogue drawn using data from Gesing and Buhl (1998)

Sif140 Nosean CO_3-analogue $Na_8[AlSiO_4]_6CO_3\cdot 4H_2O$ (Fig. 2.674)

Locality: Synthetic.

Description: A basic nitrite sodalite was used as a starting material for the synthesis of carbonate nosean via a high-temperature anion exchange in carbon dioxide atmosphere. Cubic, a = 8.980(1) Å.

Kind of sample preparation and/or method of registration of the spectrum: KBr disc. Transmission.

Source: Gesing and Buhl (1998).

Wavenumbers (cm^{-1}): 3530sh, 3442, 3265sh, 1700sh, 1656w, 1430s, 1410sh, 994s, 900sh, 730, 705, 662, 459s, 428s, 310w.

Note: The wavenumbers were partly determined by us based on spectral curve analysis of the published spectrum.

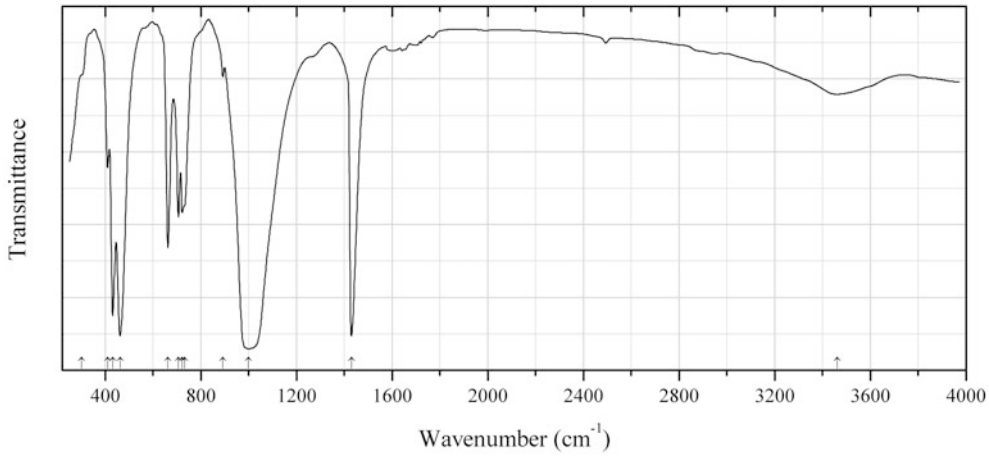

Fig. 2.675 IR spectrum of nosean anhydrous CO_3-analogue drawn using data from Gesing and Buhl (1998)

Sif141 Nosean anhydrous CO_3-analogue $Na_8[AlSiO_4]_6CO_3$ (Fig. 2.675)
Locality: Synthetic.
Description: A basic nitrite sodalite was used as a starting material for the synthesis of carbonate nosean via a high-temperature anion exchange in carbon dioxide atmosphere with subsequent dehydration. Cubic, a = 9.001(1) Å.
Kind of sample preparation and/or method of registration of the spectrum: KBr disc. Transmission.
Source: Gesing and Buhl (1998).
Wavenumbers (cm^{-1}): 3461, 1430s, 1000s, 892w, 732, 722, 705, 662, 462s, 431s, 410, 300sh.
Note: The wavenumbers were partly determined by us based on spectral curve analysis of the published spectrum.

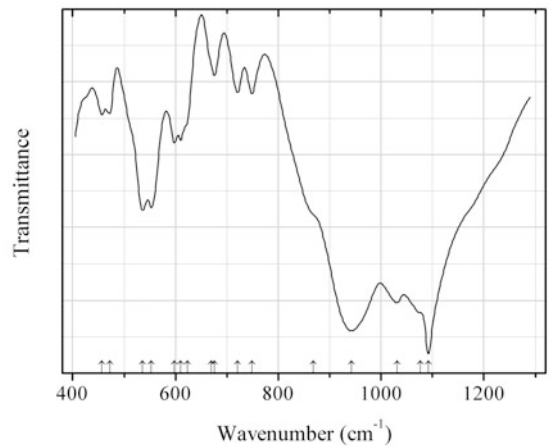

Fig. 2.676 IR spectrum of slawsonite drawn using data from Benna et al. (1995)

Sif142 Slawsonite $Sr(Si_2Al_2O_8)$ (Fig. 2.676)
Locality: Synthetic.

Description: A partly Al–Si disordered phase synthesized from a stoichiometric gel with subsequent short-time annealing at 1350 °C. Monoclinic, a = 8.394(4), b = 12.969(6), c = 14.264(7) Å, β = 115.45(9)°, V = 1402.1 Å^3.
Kind of sample preparation and/or method of registration of the spectrum: KBr disc. Absorption.
Source: Benna et al. (1995).
Wavenumbers (cm^{-1}): 1092s, 1076sh, 1031s, 943s, 868sh, 749, 721, 676w, 670sh, 623sh, 610, 598, 553, 536, 472, 457.
Note: The wavenumbers were determined by us based on spectral curve analysis of the published spectrum.

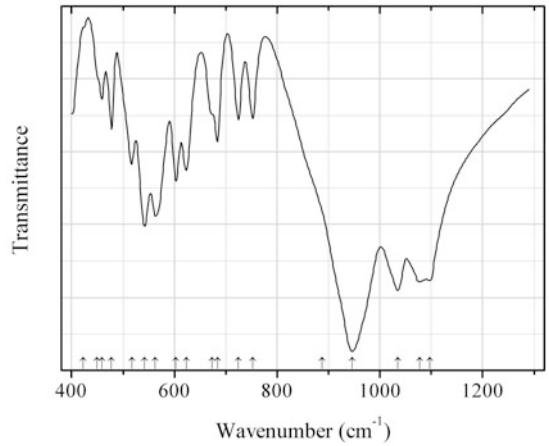

Fig. 2.677 IR spectrum of slawsonite drawn using data from Benna et al. (1995)

Sif143 Slawsonite $Sr(Si_2Al_2O_8)$ (Fig. 2.677)
Locality: Synthetic.
Description: Al–Si ordered phase obtained by annealing of a disordered metastable analogue at 1350 °C for 452 h. Monoclinic, a = 8.392(2), b = 12.980(3), c = 14.265(4) Å, β = 115.38(4)°, V = 1403.8 Å^3.
Kind of sample preparation and/or method of registration of the spectrum: KBr disc. Absorption.
Source: Benna et al. (1995).
Wavenumbers (cm^{-1}): 1097s, 1078s, 1035s, 946s, 888sh, 753, 725, 684, 674, 623, 603, 563, 542s, 517, 478, 459, 450sh, 423sh.
Note: The wavenumbers were determined by us based on spectral curve analysis of the published spectrum.

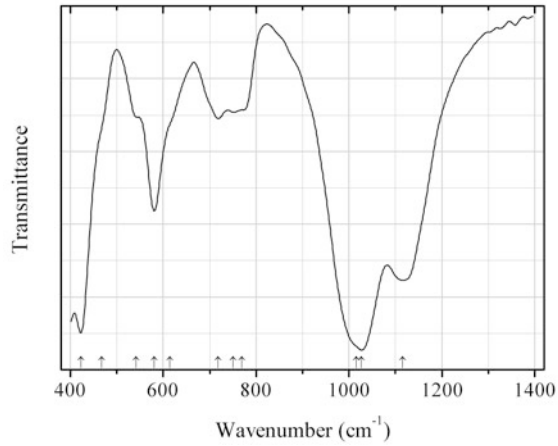

Fig. 2.678 IR spectrum of orthoclase Tl analogue drawn using data from Kyono and Kimata (2001b)

Sif144 Orthoclase Tl analogue $Tl(AlSi_3O_8)$ (Fig. 2.678)
Locality: Synthetic.
Description: Synthesized in the reaction of low-albite with $TlNO_3$ under hydrothermal conditions at 550 °C for 5 days. Characterized by electron microprobe analyses and powder X-ray diffraction data. Monoclinic, space group *C*2/*m*, a = 8.882(3), b = 13.048(2), c = 7.202(2) Å, β = 116.88(1)°, V = 744.5(4) $Å^3$, Z = 4. The empirical formula is $Tl_{0.960}Al_{1.055}Si_{2.969}O_8$.
Kind of sample preparation and/or method of registration of the spectrum: KBr disc. Transmission.
Source: Kyono and Kimata (2001b).
Wavenumbers (cm^{-1}): 1116s, 1027s, 1016sh, 769sh, 750, 718, 615sh, 581s, 542, 468sh, 423s.
Note: The wavenumbers were determined by us based on spectral curve analysis of the published spectrum.

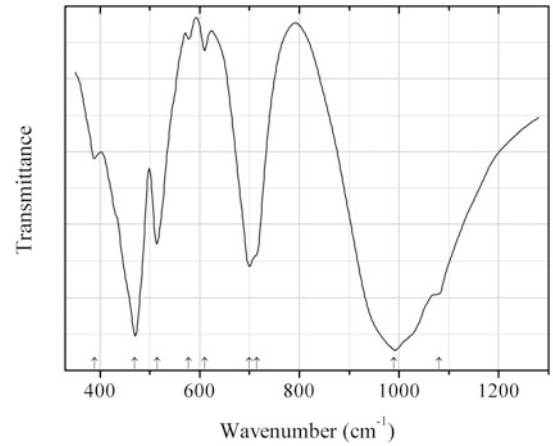

Fig. 2.679 IR spectrum of trinepheline polymorph drawn using data from Henderson and Roux (1977)

Sif145 Trinepheline polymorph $Na(AlSiO_4)$ (Fig. 2.679)
Locality: Synthetic.

Description: Synthesized hydrothermally at 600 °C. Hexagonal, a = 9.979(2), c = 8.335(2) Å, V = 718.8(3) Å^3. The empirical formula is $(Na_{0.97}K_{0.03})(AlSiO_4)$.
Kind of sample preparation and/or method of registration of the spectrum: KBr disc. Transmission.
Source: Henderson and Roux (1977).
Wavenumbers (cm^{-1}): 1080sh, 990s, 714sh, 700, 610w, 578w, 515, 470s, 389.
Note: The wavenumbers were partly determined by us based on spectral curve analysis of the published spectrum.

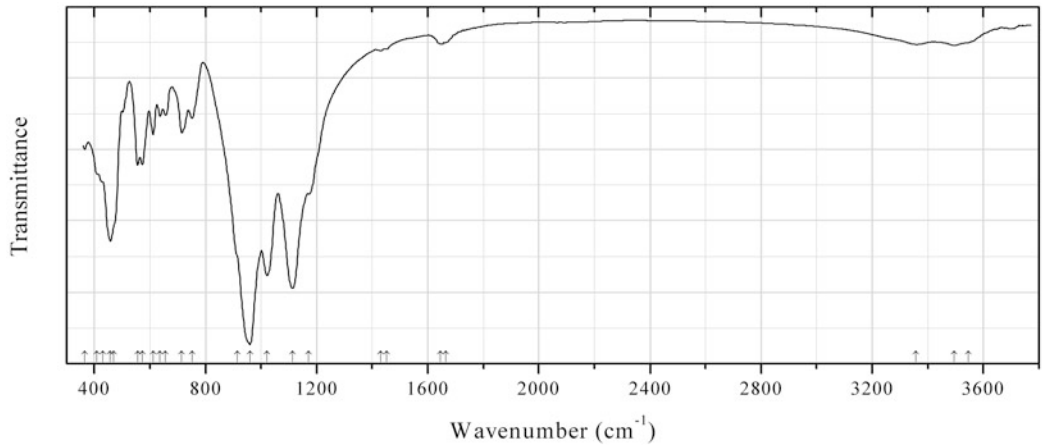

Fig. 2.680 IR spectrum of wenkite obtained by N.V. Chukanov

Sif146 Wenkite $Ba_4Ca_6(Si,Al)_{20}O_{41}(OH)_2(SO_4)_3 \cdot H_2O$ (Fig. 2.680)
Locality: Cava Mergozzoni, Candoglia, Piemonte, Italy (type locality).
Description:Colourless crystal. A Ca,S-deficient variety. The empirical formula is (electron microprobe): $(Ba_{4.0}K_{0.3})(Ca_{3.9}Sr_{0.3}Na_{0.2})(Si_{11.0}Al_{8.7}Fe_{0.3})(O,OH)_x(SO_4)_{1.9} \cdot nH_2O$.
Kind of sample preparation and/or method of registration of the spectrum: KBr disc. Absorption.
Wavenumbers (cm^{-1}): 3546sh, 3496w, 3358w, 1665sh, 1646w, 1452w, 1431w, 1171, 1113s, 1022s, 960s, 915sh, 752, 715, 657, 637, 612, 573, 556, 470sh, 458s, 430sh, 410sh, 365.

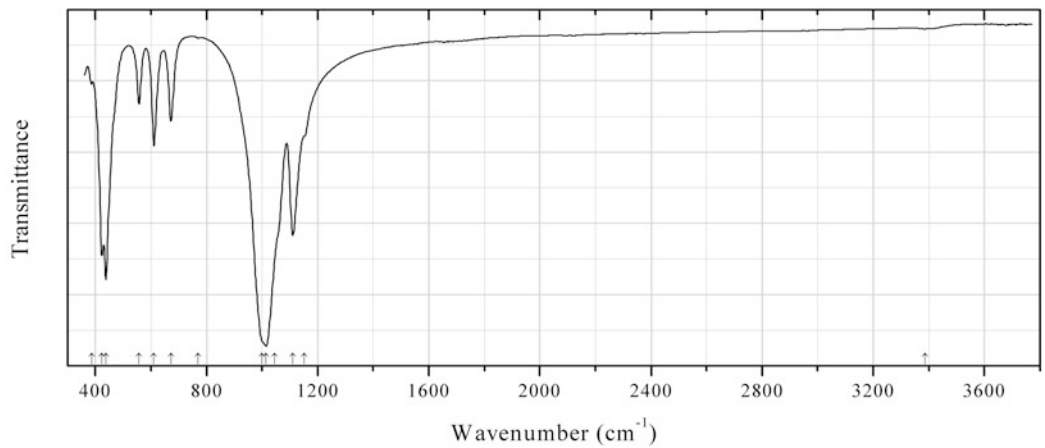

Fig. 2.681 IR spectrum of microsommite obtained by N.V. Chukanov

Sif147 Microsommite $[(Na,K)_6(SO_4)][Ca_2Cl_2][(Si_6Al_6O_{24})]$ (Fig. 2.681)

Locality: Vitiello quarry, Terzigno, Vesuvius Mt., Naples province, Campania, Italy.
Description: White short-prismatic crystals from the association with phlogopite and titanite. The empirical formula is $Na_{3.63}K_{2.35}Ca_{2.05}(Si_{6.05}Al_{5.79}Fe_{0.16}O_{24})(SO_4)_{0.88}Cl_{2.15}(OH)_{0.22}$. Confirmed by single-crystal X-ray diffraction data obtained by I.V. Pekov. Hexagonal, a = 22.244(10), c = 5.3658 (10) Å, V = 2299(2) Å^3.
Kind of sample preparation and/or method of registration of the spectrum: KBr disc. Absorption.
Wavenumbers (cm^{-1}): 3387w, 1153sh, 1111s, 1045sh, 1014s, 1000sh, 770w, 672, 611, 557, 438s, 424s, (388w).

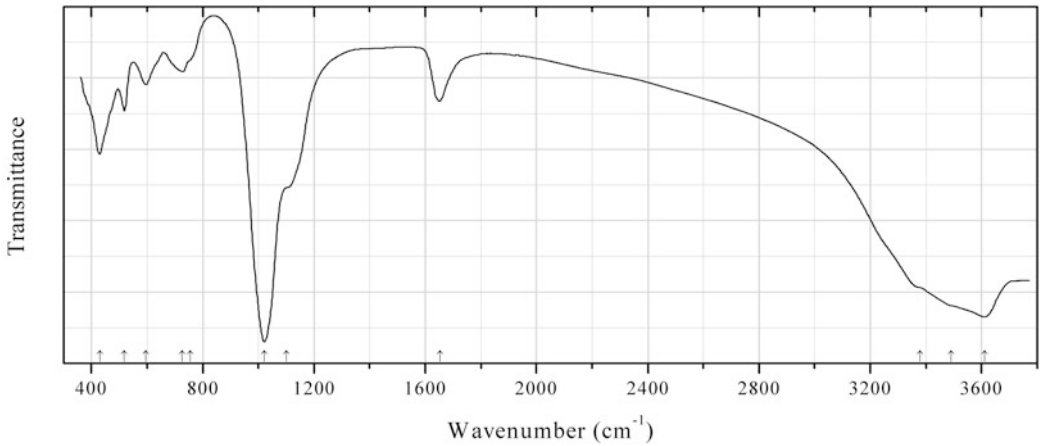

Fig. 2.682 IR spectrum of gmelinite-K obtained by N.V. Chukanov

Sif_Z104 Gmelinite-K $K_4(Si_8Al_4O_{24})\cdot 11H_2O$ (Fig. 2.682)
Locality: Aldea, Gran Canaria, Canary Islands, Spain.
Description: Epitaxy on chabazite-Ca. The associated minerals are analcime and thomsonite-Ca. The empirical formula is (electron microprobe): $(K_{1.8}Ca_{0.9}Na_{0.35})(Si_{8.05}Al_{3.8}Fe_{0.15}O_{24})\cdot nH_2O$. Confirmed by IR spectrum.
Kind of sample preparation and/or method of registration of the spectrum: KBr disc. Absorption.
Wavenumbers (cm^{-1}): 3610s, 3490sh, 3380sh, 1652, 1102sh, 1021s, 755sh, 727, 596, 518, 430s.

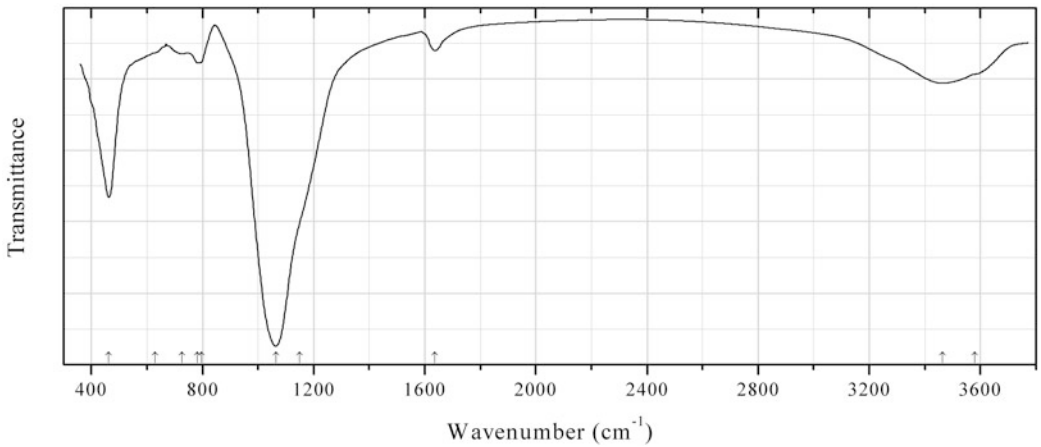

Fig. 2.683 IR spectrum of clinoptilolite-K obtained by N.V. Chukanov

Sif_Z105 Clinoptilolite-K $K_6(Si_{30}Al_6O_{72})\cdot 20H_2O$ (Fig. 2.683)
Locality: North slope of Cerro Mejillones, Mejillones Peninsula, Mejillones, Antofagasta, II Region, Chile.
Description: Random aggregate of colourless platy crystals from the association with mejillonesite, bobierrite, opal, and gypsum. The empirical formula is $H_{0.3}K_{2.5}Na_{2.2}Ca_{0.2}(Si_{30.6}Al_{5.4}O_{72})\cdot nH_2O$.
Kind of sample preparation and/or method of registration of the spectrum: KBr disc. Absorption.
Wavenumbers (cm^{-1}): 3580sh, 3464, 1637, 1150sh, 1064s, 795sh, 781, 726w, 630sh, 463s.
Note: The sample contains admixture of opal.

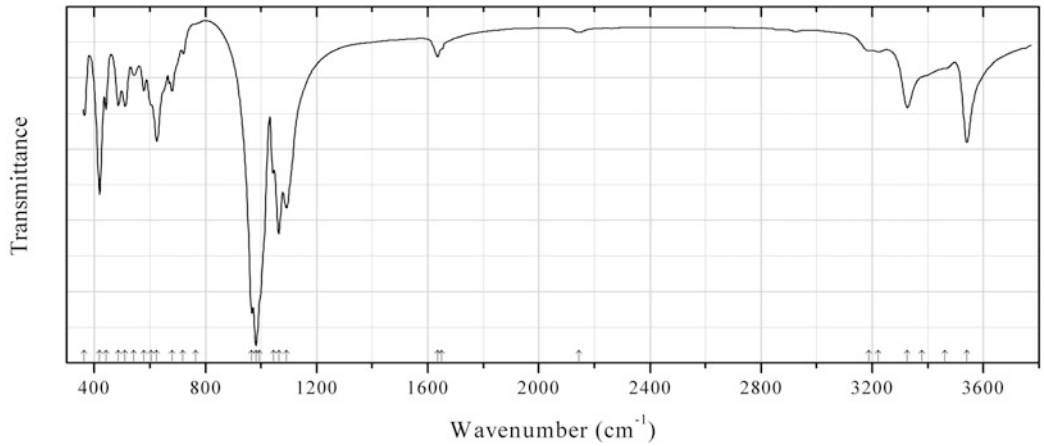

Fig. 2.684 IR spectrum of natrolite obtained by N.V. Chukanov

Sif_Z106 Natrolite $Na_2(Si_3Al_2O_{10})\cdot 2H_2O$ (Fig. 2.684)
Locality: Ariskop Quarry, Aris, near Windhoek, Windhoek district, Khomas Region, Namibia.
Description: Colourless short-prismatic crystals from the association with aegirine and ferroceladonite. A sample with complete Al–Si ordering.
Kind of sample preparation and/or method of registration of the spectrum: KBr disc. Absorption.
Wavenumbers (cm^{-1}): 3540, 3460sh, 3380sh, 3326, 3222w, 3188w, 2144w, 1650sh, 1635, 1092s, 1064s, 1045, 995sh, 982s, 966s, 765sh, 719w, 679, 625, 605sh, 578, 543, 511, 486, 442, 419s, 363.

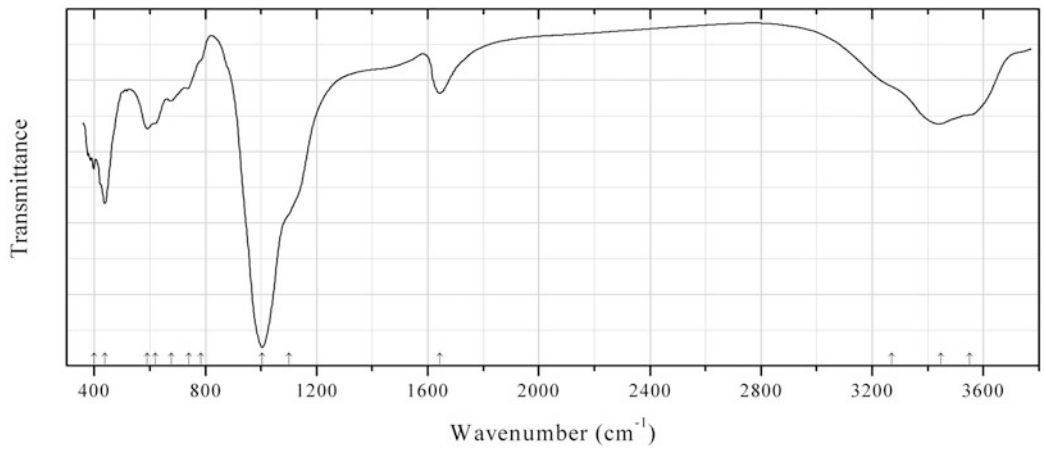

Fig. 2.685 IR spectrum of flörkeite obtained by N.V. Chukanov

Sif_Z107 Flörkeite $(K_3Ca_2Na)(Si_8Al_8O_{32})\cdot 12H_2O$ (Fig. 2.685)
Locality: Schellkopf, near Brenk, Eifel Mts., Rhineland-Palatinate (Rheinland-Pfalz), Germany.
Description: Colourless prismatic crystals from the association with kottenheimite, gonnardite, and brenkite. The empirical formula is (electron microprobe): $(K_{2.6}Ca_{1.8}Na_{0.4})(Si_{9.4}Al_{6.4}Fe_{0.2}O_{32})\cdot nH_2O$.
Kind of sample preparation and/or method of registration of the spectrum: KBr disc. Absorption.
Wavenumbers (cm^{-1}): 3550sh, 3446, 3270sh, 1643, 1100sh, 1004s, 785sh, 740, 678, 620sh, 591, 437s, 400.

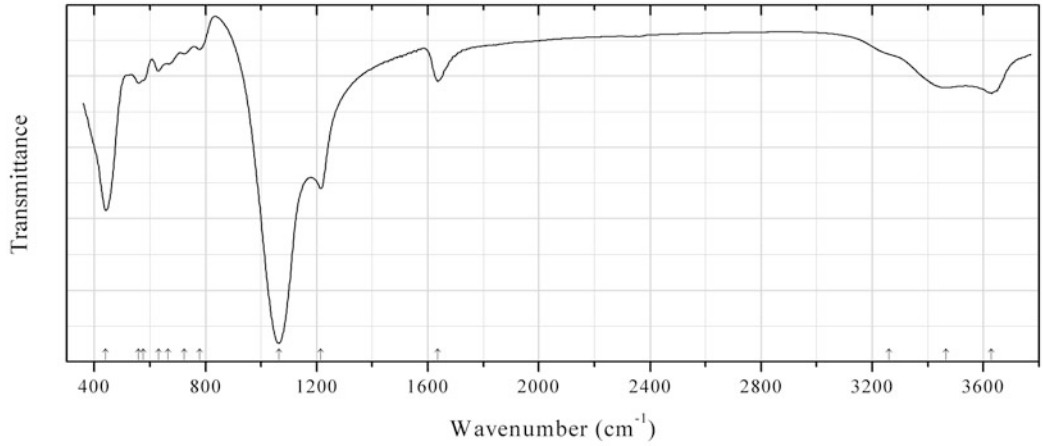

Fig. 2.686 IR spectrum of dachiardite-Ca obtained by N.V. Chukanov

Sif_Z108 Dachiardite-Ca $Ca_2(Si_{20}Al_4O_{48})\cdot 13H_2O$ (Fig. 2.686)
Locality: Austa village, near Zvezdel, Kyrdzhali region, Eastern Rhodopes, Bulgaria.
Description: Radial aggregate from the association with clinoptilolite-Ca, mordenite, and chalcedony. Investigated by I.V. Pekov. The empirical formula is (electron microprobe): $(Ca_{1.11}K_{0.65}Na_{0.17}Sr_{0.12}Ba_{0.11}Mg_{0.08})(Si_{20.28}Al_{3.64}Fe_{0.08}O_{48.03})\cdot nH_2O$. Confirmed by powder X-ray diffraction data.
Kind of sample preparation and/or method of registration of the spectrum: KBr disc. Absorption.
Wavenumbers (cm^{-1}): 3628, 3465, 3260sh, 1636, 1216s, 1064s, 780, 724, 665, 631, 575sh, 560, 441s.

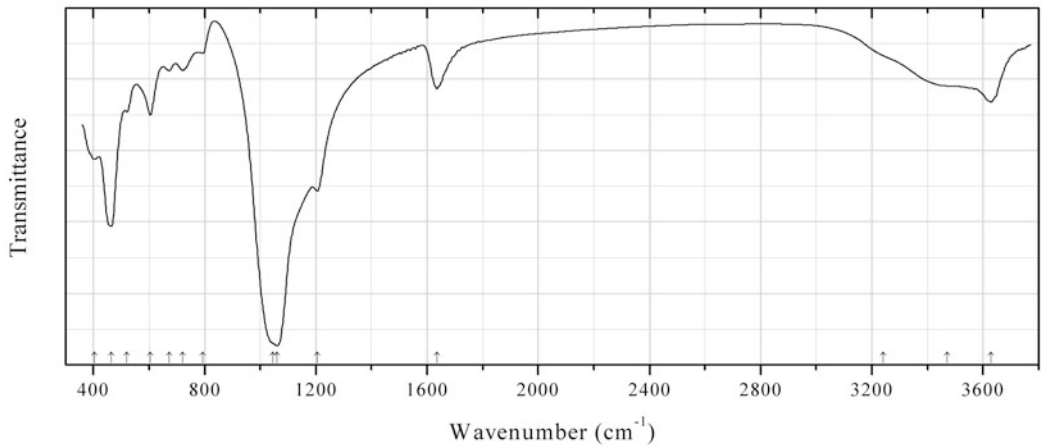

Fig. 2.687 IR spectrum of clinoptilolite-Na obtained by N.V. Chukanov

Sif_Z109 Clinoptilolite-Na $Na_6(Si_{30}Al_6O_{72})\cdot 20H_2O$ (Fig. 2.687)
Locality: Richardson Ranch, Madras, Jefferson Co., Oregon, USA.
Description: Orange split crystals. The empirical formula is $Na_{1.91}Ca_{1.62}K_{0.75}Mg_{0.31}Ba_{0.25}(Si_{28.92}Al_{7.08}O_{72})\cdot nH_2O$.
Kind of sample preparation and/or method of registration of the spectrum: KBr disc. Absorption.
Wavenumbers (cm^{-1}): 3629, 3470sh, 3240sh, 1635, 1205s, 1060s, 1045sh, 794w, 721, 672, 604, 520, 464s, 404.

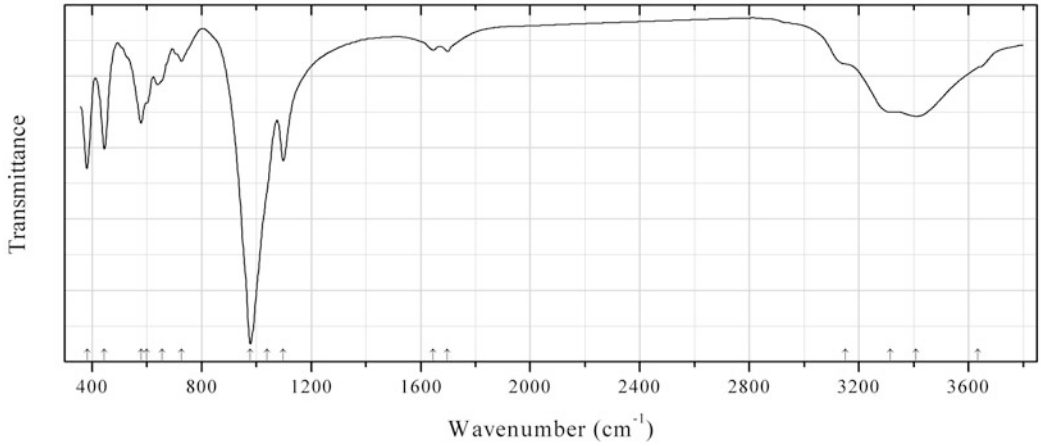

Fig. 2.688 IR spectrum of amicite obtained by N.V. Chukanov

Sif_Z110 Amicite $K_4Na_4(Al_8Si_8O_{32})\cdot 10H_2O$ (Fig. 2.688)
Locality: Marchenko Peak, Khibiny alkaline complex, Kola peninsula, Murmansk region, Russia.
Description: White split crystals from the association with gibbsite and pitiglianoite. Identified by the IR spectrum.
Kind of sample preparation and/or method of registration of the spectrum: KBr disc. Absorption.
Wavenumbers (cm^{-1}): 3635sh, 3408, 3315, 3150sh, 1698w, 1646w, 1098s, 1040sh, 978s, 726, 655sh, 600sh, 579, 445s, 384s.

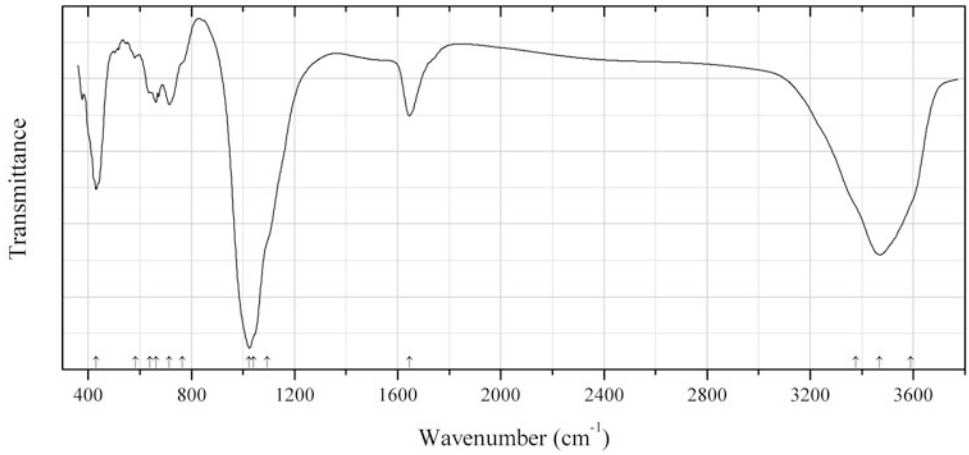

Fig. 2.689 IR spectrum of montesommaite obtained by N.V. Chukanov

Sif_Z111 Montesommaite $K_9(Si_{23}Al_9O_{64})\cdot 10H_2O$ (Fig. 2.689)
Locality: Lagno Amendolare, Sant'Anastasia, Monte Somma, Somma-Vesuvius complex, Naples province, Campania, Italy.
Description: Colourless crystals from the association with merlinoite. Visual identification.
Kind of sample preparation and/or method of registration of the spectrum: KBr disc. Absorption.
Wavenumbers (cm^{-1}): 3590sh, 3469s, 3375sh, 1645, 1095sh, 1040sh, 1024s, 765sh, 715, 663, 640sh, 584w, 431s.

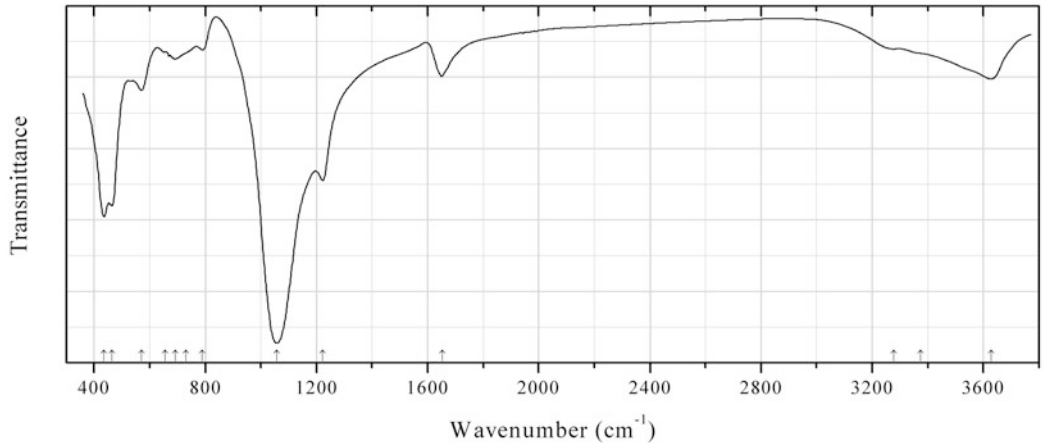

Fig. 2.690 IR spectrum of ferrierite-K obtained by N.V. Chukanov

Sif_Z112 Ferrierite-K $K_5(Si_{31}Al_5O_{72})\cdot 18H_2O$ (Fig. 2.690)
Locality: Austa village, near Zvezdel, Kyrdzhali region, Eastern Rhodopes, Bulgaria.
Description: Light gray radial aggregate from the association with chalcedony, clinoptilolite-Ca, dachiardite-Ca, and mordenite. Investigated by I.V. Pekov. The empirical formula is (electron microprobe): $(K_{1.69}Mg_{1.18}Ca_{0.27}Ba_{0.17}Na_{0.13})(Si_{30.92}Al_{5.08}O_{72})\cdot nH_2O$. The strongest lines of the powder X-ray diffraction pattern [*d*, Å (*I*, %)] are: 9.7 (100), 3.99 (5), 3.74 (3), 3.55 (3).
Kind of sample preparation and/or method of registration of the spectrum: KBr disc. Absorption.
Wavenumbers (cm^{-1}): 3629, 3375sh, 3276sh, 1652, 1223s, 1058s, 790, 730sh, 691, 655sh, 570, 464s, 436s.

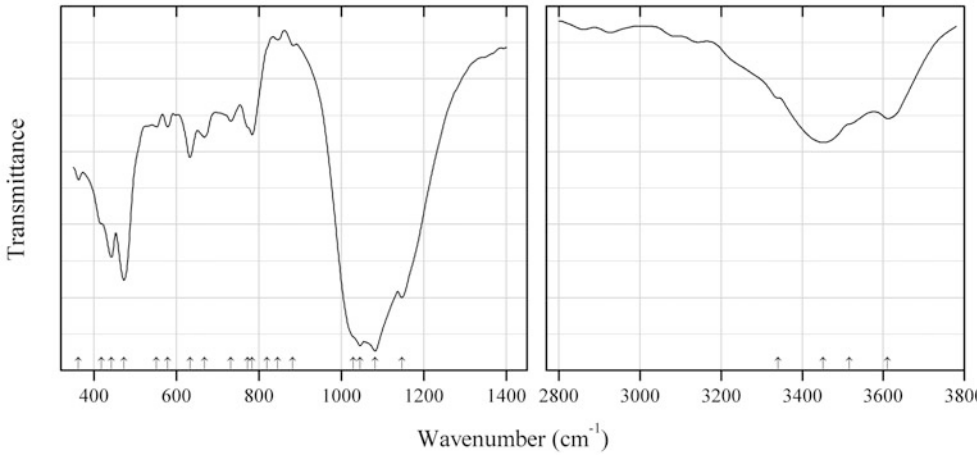

Fig. 2.691 IR spectrum of erionite-Na drawn using data from De Kimpe and Fripiat (1968)

Sif_Z114 Erionite-Na $(Na_2,Ca,K_2)_2(Al_4Si_{14}O_{36})\cdot 15H_2O$ (Fig. 2.691)
Locality: Not indicated.
Description: Confirmed by powder X-ray diffraction data and chemical analysis. The ratio Na_2O:K_2O:CaO is 9:5:12.
Kind of sample preparation and/or method of registration of the spectrum: Transmission. Kind of sample preparation is not indicated.
Source: De Kimpe and Fripiat (1968).
Wavenumbers (cm^{-1}): 3611, 3517sh, 3452, 3341sh, 1146s, 1082s, 1045s, 1029sh, 882w, 845w, 819sh, 784, 772sh, 732, 668, 633, 579, 552, 473s, 442, 418sh, 363.
Note: The wavenumbers were determined by us based on spectral curve analysis of the published spectrum.

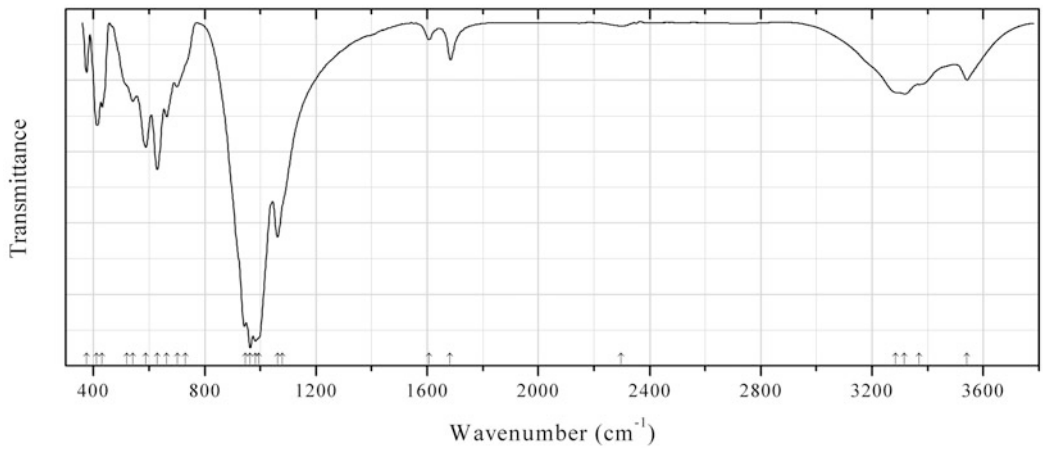

Fig. 2.692 IR spectrum of thomsonite-Sr obtained by N.V. Chukanov

Sif_Z115 Thomsonite-Sr $NaSr_2(Al_5Si_5O_{20})\cdot 6–7H_2O$ (Fig. 2.692)
Locality: Southern Yuksporlak pass, Rasvumchorr Mt., Khibiny alkaline complex, Kola peninsula, Murmansk region, Russia (type locality).

Description: White prismatic crystals from the association with microcline, aegirine, annite, astrophyllite, magnetite, fluorapatite, pyrophanite, thomsonite-Ca, etc. Investigated by I.V. Pekov.
Kind of sample preparation and/or method of registration of the spectrum: KBr disc. Absorption.
Wavenumbers (cm^{-1}): 3542, 3370, 3317, 3285sh, 2297w, 1683, 1606w, 1080sh, 1062s, 995sh, 982s, 964s, 946s, 730sh, 703, 664, 629s, 588, 541, 520sh, 431, 412, 374.

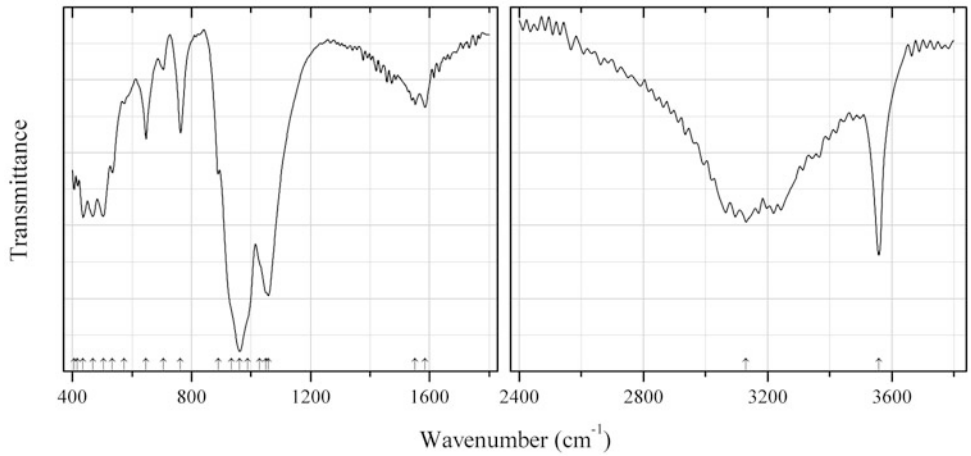

Fig. 2.693 IR spectrum of gaultite drawn using data from Ercit and Van Velthuizen (1994)

Sif_Z117 Gaultite $Na_4(Zn_2Si_7O_{18})\cdot 5H_2O$ (Fig. 2.693)
Locality: Poudrette (Demix) quarry, Mont Saint-Hilaire, Rouville RCM (Rouville Co.), Montérégie, Québec, Canada (type locality).
Description: Colourless crystals from the association with aegirine, analcime, cancrinite, catapleiite, chabazite, eudialyte, lovozerite-group minerals, makatite, microcline, nepheline, zeolites, sodalite, ussingite,villiaumite, vuonnemite, etc. Holotype sample. Orthorhombic, space group *F*2*dd*, a = 10.211(3), b = 39.88(2), c = 10.304(4) Å, V = 4196(2) $Å^3$, Z = 8. D_{meas} = 2.52(4) g/cm^3, D_{calc} = 2.52 g/cm^3. Optically biaxial (+), α = 1.520(1), β = 1.521(1), γ = 1.524(1), 2 V = 61.3(4)°. The empirical formula is $Na_{4.28}Zn_{1.88}Si_{6.99}O_{18}\cdot 5H_2O$. The strongest lines of the powder X-ray diffraction pattern [d, Å (I, %) (*hkl*)] are: 6.35 (100) (131), 4.96 (30) (080, 220), 3.240 (60) (113, 1.11.1), 3.167 (40) (262, 133), 3.140 (40) (2.10.0, 331), 2.821 (30) (173, 1.13.1).
Kind of sample preparation and/or method of registration of the spectrum: Powder infrared-absorption spectrum was obtained using a diamond-anvil microsample cell.
Source: Ercit and Van Velthuizen (1994).
Wavenumbers (cm^{-1}): 3558s, 3130, 1585, 1550, 1058s, 1050sh, 1029sh, 988sh, 962s, 934sh, 890, 763, 705w, 647, 574w, 534, 504, 468, 436, 417, 405.
Note: The wavenumbers were determined by us based on spectral curve analysis of the published spectrum.

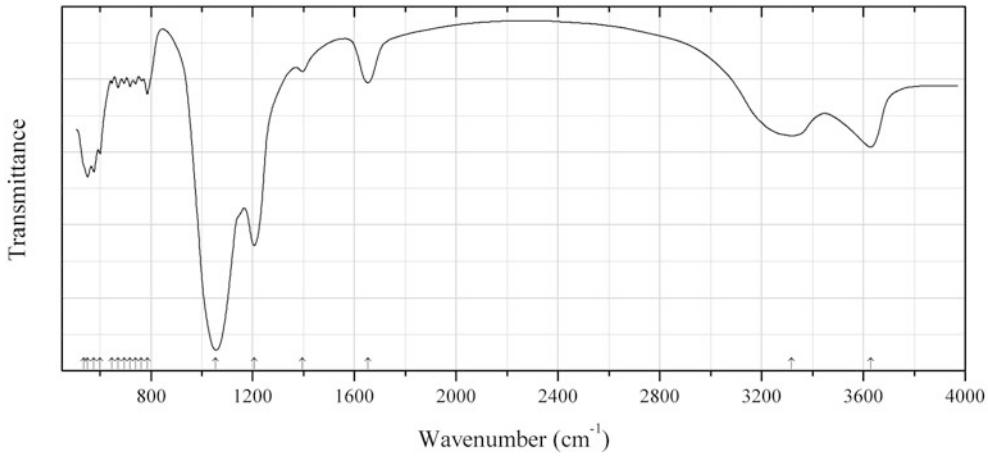

Fig. 2.694 IR spectrum of gottardiite drawn using data from Galli et al. (1996)

Sif_Z118 Gottardiite $Na_3Mg_3Ca_5(Al_{19}Si_{117}O_{272})\cdot 93H_2O$ (Fig. 2.694)
Locality: Jurassic Ferrar dolerites of Mt. Adamson, Northern Victoria Land, Antarctica (type locality).
Description: Subparallel aggregates of transparent pseudo-hexagonal lamellae from the association with other zeolites. Holotype sample. Orthorhombic, space group *Cmca*, a = 13.698(2), b = 25.213 (3), c = 22.660(2) Å. D_{meas} = 2.14(4) g/cm^3, D_{calc} = 2.16 g/cm^3. Optically biaxial (+), α = 1.480(2), β = 1.485(2), γ = 1.486(2), 2 V < 60°. The empirical formula is $(Na_{2.5}K_{0.2}Mg_{3.1}Ca_{4.8})(Al_{18.8}Si_{117.2}O_{272})\cdot 93H_2O$. The strongest lines of the powder X-ray diffraction pattern [d, Å (I, %) (*hkl*)] are: 11.34 (100) (002), 4.37 (79) (204), 4.01 (57) (153), 3.282 (68) (206, 155).
Kind of sample preparation and/or method of registration of the spectrum: KBr disc. Transmission.
Source: Galli et al. (1996).
Wavenumbers (cm^{-1}): 3629s, 3317s, 1652, 1395w, 1206s, 1055s, 786w, 763w, 740w, 718w, 695w, 670w, 646w, 600, 576, 551s, 536sh.
Note: The wavenumbers were determined by us based on spectral curve analysis of the published spectrum.

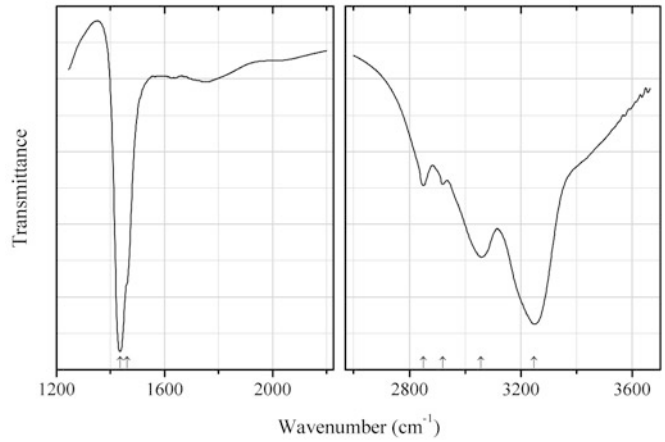

Fig. 2.695 IR spectrum of ammonioleucite drawn using data from Likhacheva et al. (2002)

Sif_Z119 Ammonioleucite $(NH_4)(AlSi_2O_6)$ (Fig. 2.695)
Locality: Ammonium-exchanged natural analcime from the basin of Nidym River, Siberian platform, Russia.
Description: Obtained in the ion-exchange reaction of pseudocubic analcime with aqueous solution of NH_4NO_3 at 140 °C. Confirmed by powder X-ray diffraction data. Tetragonal, a = 13.218, c = 13.710 Å. The empirical formula is $(NH_4)_{0.94}Al_{0.94}Si_{2.06}O_6$.
Kind of sample preparation and/or method of registration of the spectrum: KBr disc. Absorption.
Source: Likhacheva et al. (2002).
Wavenumbers (cm^{-1}): 3248s, 3057, 2920w, 2850, 1461sh, 1435s.
Note: In the cited paper this compound is described under the name "NH_4-analcime".

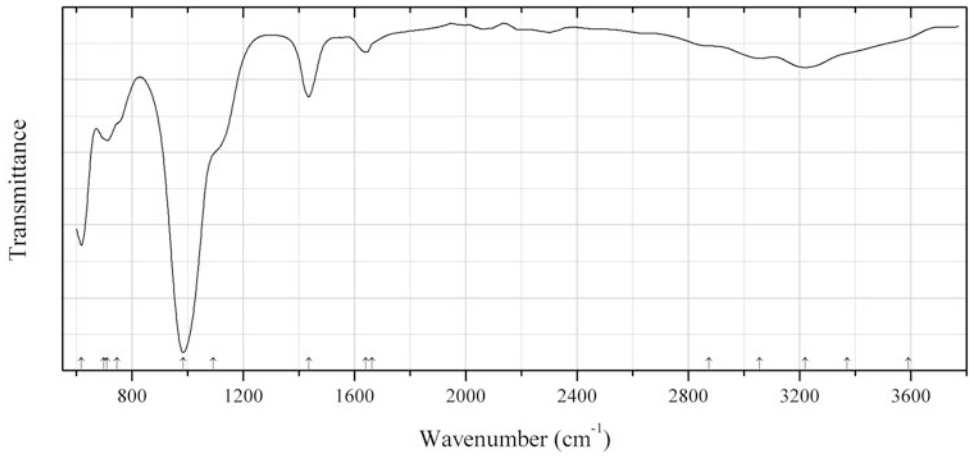

Fig. 2.696 IR spectrum of chabazite-NH_4 drawn using data from Gualtieri and Passaglia (2006)

Sif_Z120 Chabazite-NH_4 $(NH_4)_4(Si_8Al_4O_{24})\cdot nH_2O$ (Fig. 2.696)
Locality: NH_4-exchanged natural chabazite from Nova Scotia (Canada).
Description: Trigonal, space group P-3 m, a = 13.8502(1), c = 15.0313(1) Å, V = 826.288(27) $Å^3$. The empirical formula is $[(NH_4)_{3.30}Ca_{0.05}K_{0.05}](Si_{8.55}Al_{3.45}O_{24})\cdot 9.2H_2O$.
Kind of sample preparation and/or method of registration of the spectrum: KBr disc. Transmission.
Source: Gualtieri and Passaglia (2006).
Wavenumbers (cm^{-1}): 3590sh, 3370sh, 3220, 3057, 2875sh, 1662sh, 1640w, 1435, 1092sh, 983s, 746sh, 710, 699sh, 618s.
Note: The wavenumbers were determined by us based on spectral curve analysis of the published spectrum.

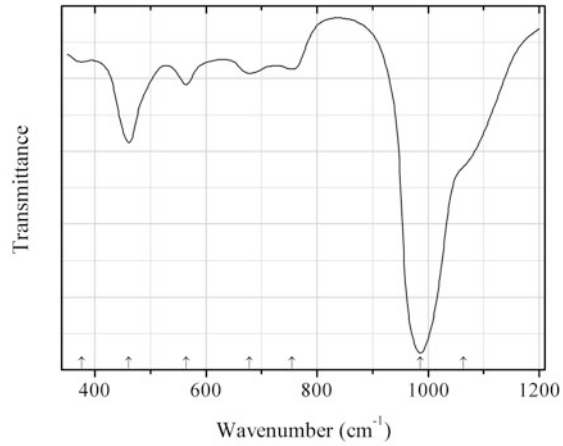

Fig. 2.697 IR spectrum of faujasite-Na drawn using data from Wright et al. (1968)

Sif_Z121 Faujasite-Na $(Na,Ca,Mg)_5[(Si,Al)_{12}O_{24}]\cdot 15H_2O$ (Fig. 2.697)
Locality: Synthetic.
Description: Synthesized from NaOH, $NaAlO_2$, and SiO_2 in the presence of water, at reflux. The composition corresponds to the formula $Na_{4.8}(Si_{7.2}Al_{4.8}O_{24})\cdot nH_2O$. Confirmed by powder X-ray diffraction data.
Kind of sample preparation and/or method of registration of the spectrum: Nujol mull. Absorption. The IR spectrum of Nujol is subtracted.
Source: Wright et al. (1968).
Wavenumbers (cm^{-1}): 1064sh, 986s, 755, 678, 564, 461, 376.
Note: The wavenumbers were determined by us based on spectral curve analysis of the published spectrum.

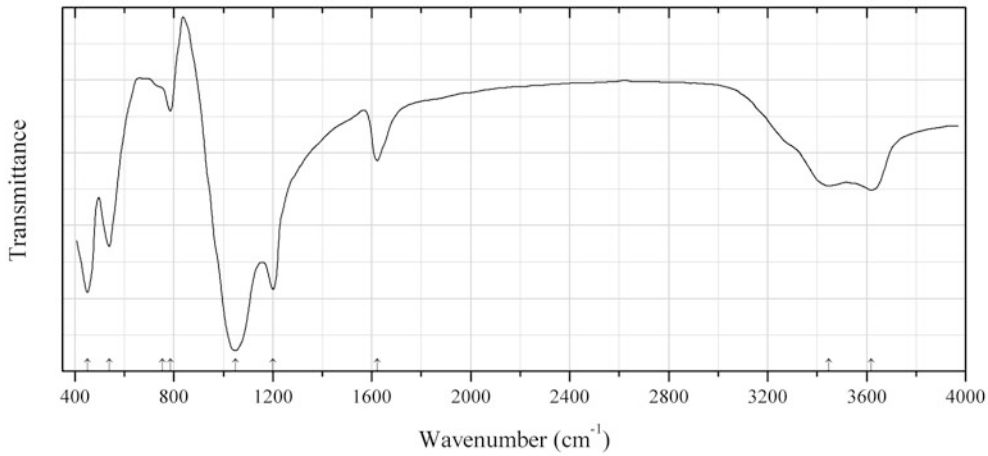

Fig. 2.698 IR spectrum of mutinaite drawn using data from Galli et al. (1997)

Sif_Z122 Mutinaite $Na_3Ca_4(Si_{85}Al_{11}O_{192})\cdot 60H_2O$ (Fig. 2.698)
Locality: Adamson Mt., Northern Victoria Land, Antarctica (type locality).

Description: Subspherical aggregates of tiny radiating lath-like crystals from the association with boggsite, tschernichite, mordenite, heulandite, lewyne, erionite, and chabazite. Holotype sample. Orthorhombic, space group *Pnma*, a = 20.223(7), b = 20.052(8), c = 13.491(5) Å. D_{meas} = 2.14(3) g/cm^3, D_{calc} = 2.17 g/cm^3. Optically biaxial (−), α = 1.485(2), β = 1.487(2), γ = 1.488(2). The empirical formula is $(Na_{2.76}K_{0.11}Ca_{3.78}Mg_{0.21})(Si_{84.91}Al_{11.20})O_{192}\cdot 60H_2O$. The strongest lines of the powder X-ray diffraction pattern [d, Å (I, %) (hkl)] are: 11.20 (84) (101, 011), 9.98 (35) (200, 020), 3.85 (100) (501, 051), 3.75 (98) (303), 3.67 (27) (133), 3.00 (32) (503).
Kind of sample preparation and/or method of registration of the spectrum: KBr disc. Transmission.
Source: Galli et al. (1997).
Wavenumbers (cm^{-1}): 3619, 3448, 1622, 1200s, 1049s, 786, 753sh, 539, 450s.
Note: The wavenumbers were determined by us based on spectral curve analysis of the published spectrum.

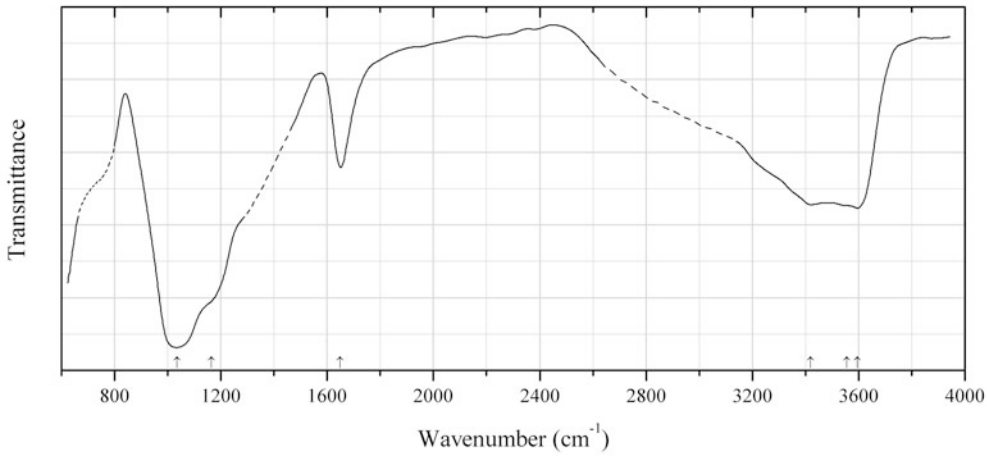

Fig. 2.699 IR spectrum of stilbite-Na drawn using data from Harada and Tomita (1967)

Sif_Z123 Stilbite-Na $Na_9(Si_{27}Al_{19}O_{72})\cdot 28H_2O$ (Fig. 2.699)
Locality: Onigajō, Kii peninsula, Mié prefecture, Japan.
Description: Nearly colourless sheaf-like aggregates from the association with heulandite and laumontite. Monoclinic, a = 13.67, b = 18.16, c = 11.31 Å, β = 129.17°. Optically biaxial (−), α = 1.482 (2), β = 1.489(2), γ = 1.496(2), 2 V = 43.2°. The empirical formula is $(Na_{3.30}Ca_{2.07}Mg_{0.57}K_{0.52})(Si_{26.55}Al_{9.57})O_{72}\cdot 28.87H_2O$. The strongest lines of the powder X-ray diffraction pattern [d, Å (I, %)] are: 9.16 (100), 4.67 (11), 4.07 (45), 3.20 (10), 3.02 (32), 3.000 (11), 2.744 (12).
Kind of sample preparation and/or method of registration of the spectrum: Nujol mull. Transmission.
Source: Harada and Tomita (1967).
Wavenumbers (cm^{-1}): 3596, 3556sh, 3420, 1648, 1165sh, 1034s.
Note: The wavenumbers were determined by us based on spectral curve analysis of the published spectrum.

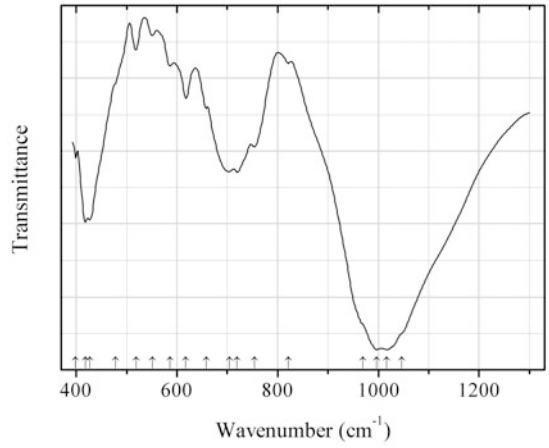

Fig. 2.700 IR spectrum of leucite Tl analogue drawn using data from Kyono et al. (1999)

Sif_Z124 Leucite Tl analogue $Tl(AlSi_2O_6)$ (Fig. 2.700)
Locality: Synthetic.
Description: Synthesized at 450 °C for 7 days by the transformation of dehydrated analcime Na $(AlSi_2O_6)$ in the presence of excess TlCl. Tetragonal, a = 13.269(2), c = 13.718(2) Å. Characterized by electron microprobe analyses and powder X-ray diffraction data. The empirical formula is $Tl_{0.929}Al_{1.013}Si_{2.008}O_6$.
Kind of sample preparation and/or method of registration of the spectrum: KBr disc. Transmission.
Source: Kyono et al. (1999).
Wavenumbers (cm^{-1}): 1046sh, 1017s, 997s, 969sh, 821w, 754, 720, 704, 658w, 618w, 586w, 551w, 519w, 478sh, 427, 418, 399.
Note: The wavenumbers were determined by us based on spectral curve analysis of the published spectrum.

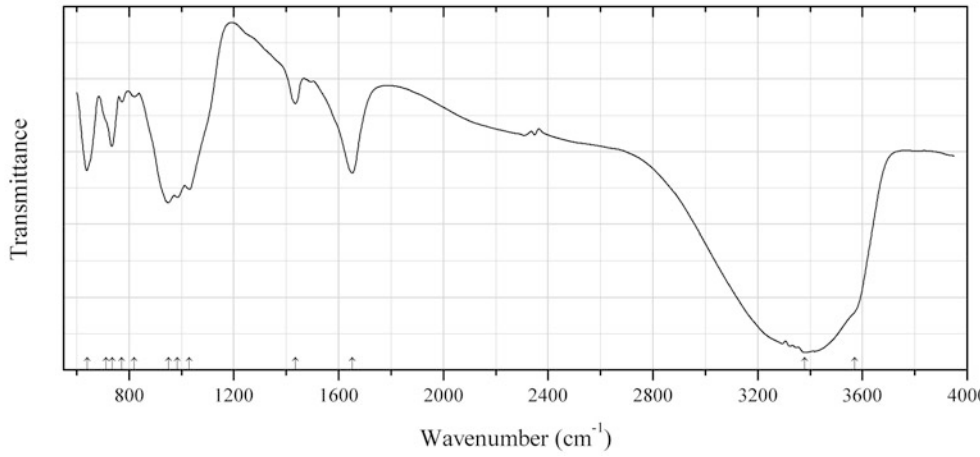

Fig. 2.701 IR spectrum of tschörtnerite drawn using data from Effenberger et al. (1998)

Sif_Z125 Tschörtnerite $Ca_4(K,Ca,Sr)_3Cu_3(Al_{12}Si_{12}O_{48})(OH)_8 \cdot nH_2O$ (n = 14–20) (Fig. 2.701)

Locality: Bellerberg, near Kottenheim, 2 km north of Mayen, Laacher See region, Eastern Eifel area, Rhineland-Palatinate (Rheinland-Pfalz), Germany (type locality).
Description: Light blue cubic crystals from the association with chalcopyrite, willhendersonite, phillipsite, gismondine, strätlingite, and bellbergite. Holotype sample. Cubic, space group *Fm*-2 m, a = 31.62(1), V = 31,614 Å^3, Z = 16. D_{meas} = 2.1(1) g/cm^3, D_{calc} = 2.10 g/cm^3. Optically isotropic, n = 1.504(2). The empirical formula is $Ca_{5.60}Sr_{1.04}K_{0.70}Ba_{0.30}Cu_{2.90}(Fe_{0.09}Al_{11.85}Si_{12.06}O_{48})(OH)_{8.44}\cdot 14.01H_2O$. Powder X-ray diffraction data are not obtained.
Kind of sample preparation and/or method of registration of the spectrum: No data.
Source: Effenberger et al. (1998).
Wavenumbers (cm^{-1}): 3570sh, 3380s, 1652, 1435, 1030s, 985s, 950s, 820w, 772w, 735, 712sh, 640.
Note: The wavenumbers were partly determined by us based on spectral curve analysis of the published spectrum.

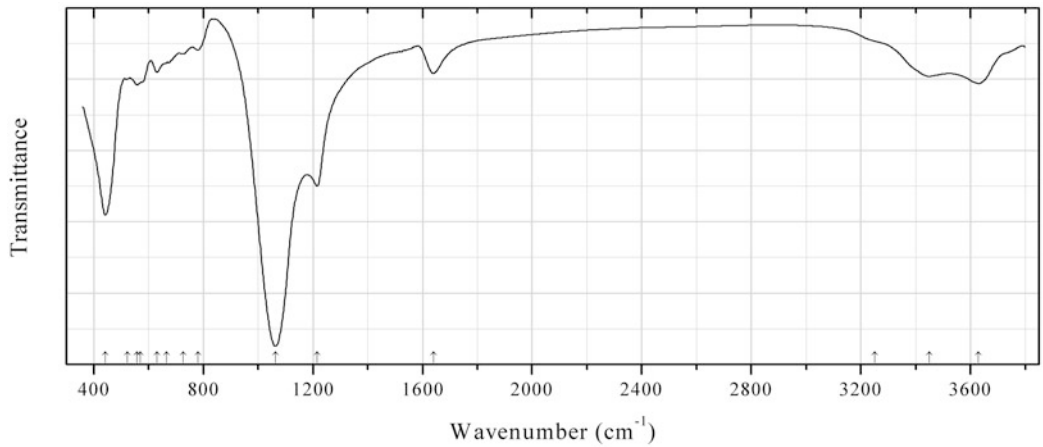

Fig. 2.702 IR spectrum of dachiardite-K obtained by N.V. Chukanov

Sif_Z126 Dachiardite-K $(K_2Ca)(Al_4Si_{20}O_{48})\cdot 13H_2O$ (Fig. 2.702)
Locality: 0.5 km east of the village of Austa, Momchilgrad municipality, Eastern Rhodopes, Bulgaria (type locality).
Description: White spherical radial aggregate from the association with chalcedony, opal, dachiardite-Ca, dachiardite-Na, ferrierite-Mg, ferrierite-K, clinoptilolite-Ca, clinoptilolite-K, mordenite, smectite, celadonite, calcite, and barite. Holotype sample. Monoclinic, space group *C*2/*m*, *Cm* or *C*2, a = 18.670(8), b = 7.511(3), c = 10.231(4) Å, β = 107.79(3)°, V = 1366(1) Å^3, Z = 1. D_{meas} = 2.18(2) g/cm^3, D_{calc} = 2.169 g/cm^3. Optically biaxial (+), α = 1.477 (calculated), β = 1.478 (2), γ = 1.481(2), 2 V = 65(10)°. The empirical formula is $H_{26.23}K_{1.71}Ca_{1.04}Ba_{0.05}Al_{3.64}Si_{20.24}O_{61}$. The strongest lines of the powder X-ray diffraction pattern [d, Å (I, %) (hkl)] are: 9.76 (24) (001), 8.85 (58) (200), 4.870 (59) (002), 3.807 (16) (202), 3.768 (20) (112, 020), 3.457 (100) (220), 2.966 (17) (−602).
Kind of sample preparation and/or method of registration of the spectrum: KBr disc. Absorption.
Wavenumbers (cm^{-1}): 3629, 3450, 3250sh, 1640w, 1215s, 1063s, 780w, 726w, 665sh, 631, 570sh, 558, 523, 442s.

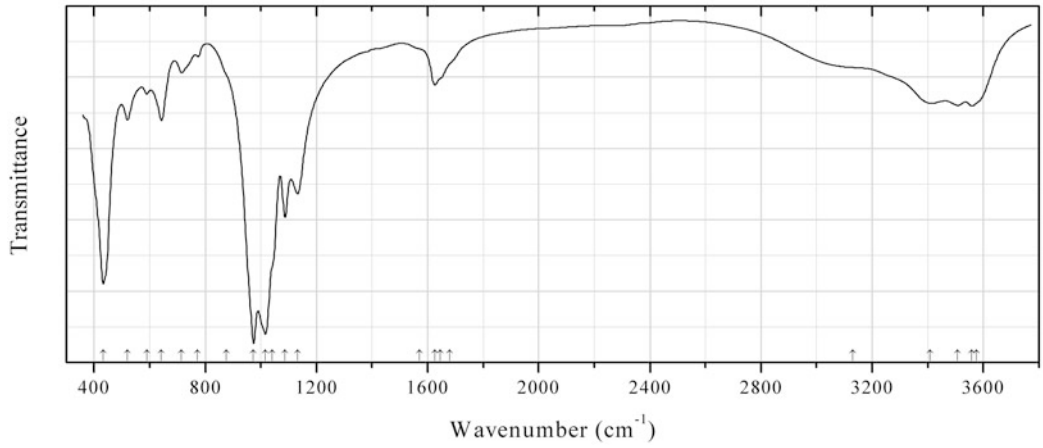

Fig. 2.703 IR spectrum of nekoite obtained by N.V. Chukanov

Si31 Nekoite $Ca_3Si_6O_{15}·7H_2O$ (Fig. 2.703)
Locality: Mina La Cotita, Inca de Oro, Copiapó province, Atacama region, Chile.
Description: Radial aggregate of colourless long-prismatic crystals from the association with apophyllite. Confirmed by IR spectrum.
Kind of sample preparation and/or method of registration of the spectrum: KBr disc. Absorption.
Wavenumbers (cm^{-1}): 3575sh, 3559, 3507, 3408, 3130sh, 1680sh, 1645sh, 1626, 1570sh, 1132s, 1087s, 1040sh, 1017s, 974s, 875sh, 773w, 715w, 642, 590w, 520, 433s.

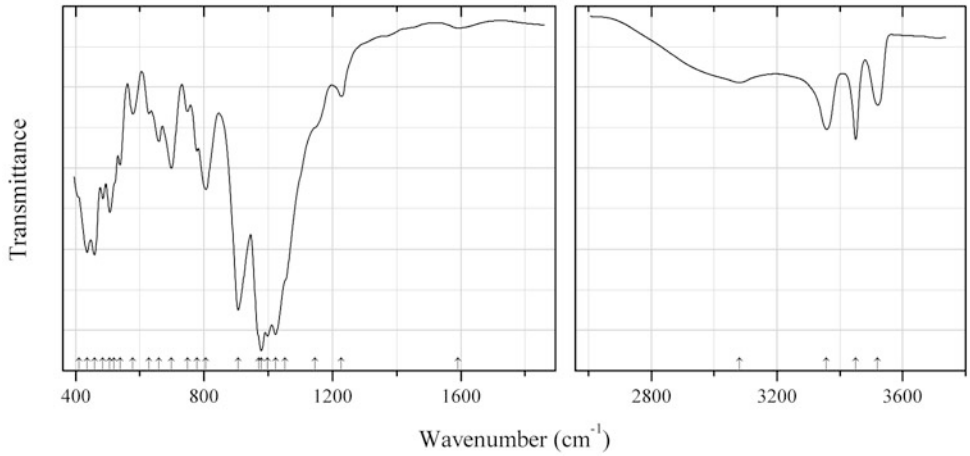

Fig. 2.704 IR spectrum of vyuntspakhkite-(Y) obtained by N.V. Chukanov

Si32 Vyuntspakhkite-(Y) $(Y,REE)_3Al_2(HSi_2O_7)(SiO_4)(HSiO_4)(OH)_3$ (Fig. 2.704)
Locality: Ploskaya Mt., Western Keivy Mts., Kola peninsula, Murmansk region, Russia (type locality).
Description: Pale yellow transparent crystals from the association with Y-rich fluorite, albite, microcline, and quartz. Confirmed by the IR spectrum and semiquantitative electron microprobe analysis.
Kind of sample preparation and/or method of registration of the spectrum: KBr disc. Absorption.

Wavenumbers (cm^{-1}): 3520, 3451, 3357, 3080, 1592w, 1228w, 1145sh, 1053sh, 1023s, 997s, 978s, 970sh, 906s, 806, 778, 748w, 698, 659, 629, 577, 538, 520sh, 506, 485, 459s, 435s, 410sh.

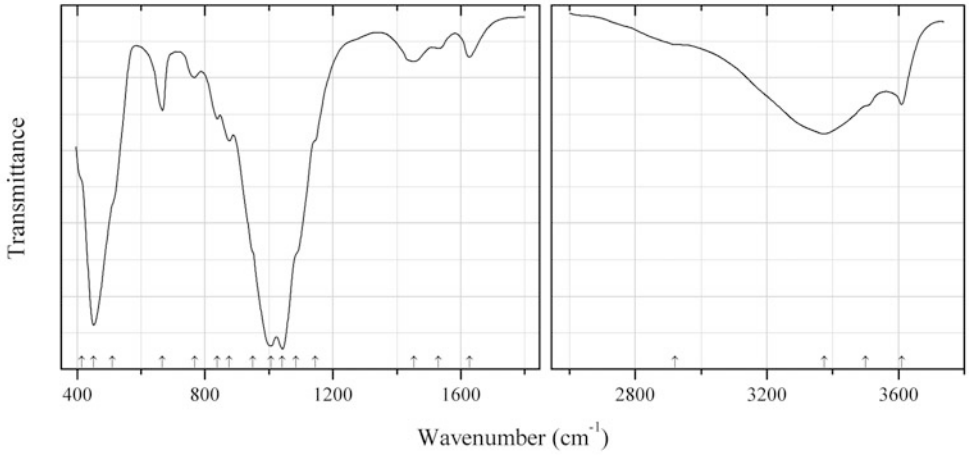

Fig. 2.705 IR spectrum of gilalite obtained by N.V. Chukanov

Si33 Gilalite $Cu_5(Si_6O_{15})(OH)_4 \cdot 5H_2O$ (?) (Fig. 2.705)
Locality: Christmas mine, Gila Co., Arizona, USA (type locality).
Description: Pale green spherulites.
Kind of sample preparation and/or method of registration of the spectrum: KBr disc. Absorption.
Wavenumbers (cm^{-1}): 3610, 3500sh, 3375, 2920sh, 1627w, 1530w, 1453w, 1145sh, 1085sh, 1042s, 1006s, 950sh, 876, 839, 768w, 667, 510sh, 452s, 415sh.
Note: Weak bands at 1530 and 1453 cm^{-1} may correspond to the admixture of a carbonate.

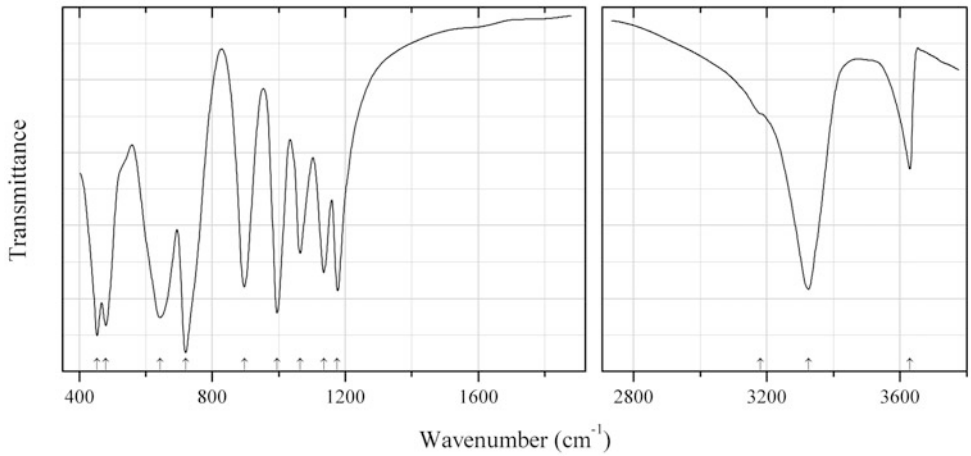

Fig. 2.706 IR spectrum of zunyite obtained by N.V. Chukanov

Si34 Zunyite $Al_{13}Si_5O_{20}(OH,F)_{18}Cl$ (Fig. 2.706)
Locality: Zuni mine, Anvil Mt., Red Mountain District, San Juan Co., Colorado, USA (type locality).

Description: Colourless octahedral crystal. Confirmed by the IR spectrum.
Kind of sample preparation and/or method of registration of the spectrum: KBr disc. Absorption.
Wavenumbers (cm^{-1}): 3630, 3325s, 3180sh, 1176, 1136, 1064, 995s, 897, 720s, 643s, 480s, 454s.
Note: For the IR spectra of zunyite and its synthetic analogue see also Hsu (1986).

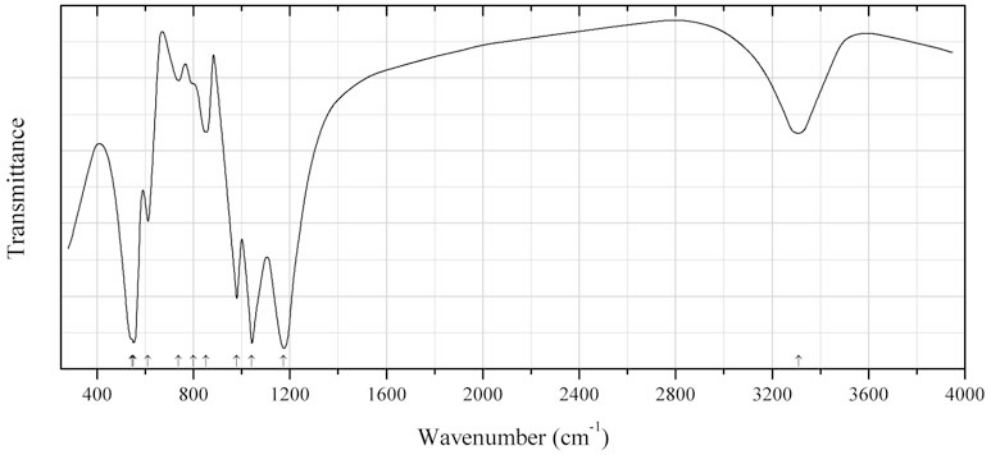

Fig. 2.707 IR spectrum of creaseyite drawn using data from Meyer et al. (1986)

Si35 Creaseyite $Pb_2Cu_2(Fe^{3+},Al)_2Si_5O_{17}\cdot 6H_2O$ (Fig. 2.707)
Locality: Oxidation zone of the Pb-Zn-Cu ore body at Black Mountain, near Aggeneys, Aggeneys Mts., South Africa.
Description: Green aggregate from the association with dioptase, chrysocolla, anglesite, linarite, beaverite, brochantite, plumbojarosite, pyromorphite, corkite, leadhillite, caledonite, atacamite, paratacamite, and diaboleite. Orthorhombic, a = 12.487–12.499, b = 21.382–21.394, c = 7.303–7.296 Å. A Fe-rich and Al-poor variety. The refractive indices are: α = 1.730, β = 1.740, γ = 1.750.
Kind of sample preparation and/or method of registration of the spectrum: KBr disc. Transmission.
Source: Meyer et al. (1986).
Wavenumbers (cm^{-1}): 3309, 1174s, 1042s, 980, 852, 799sh, 737w, 611, 552s, 546sh.
Note: The wavenumbers were determined by us based on spectral curve analysis of the published spectrum. For the IR spectrum of creaseyite see also Frost and Xi (2012a).

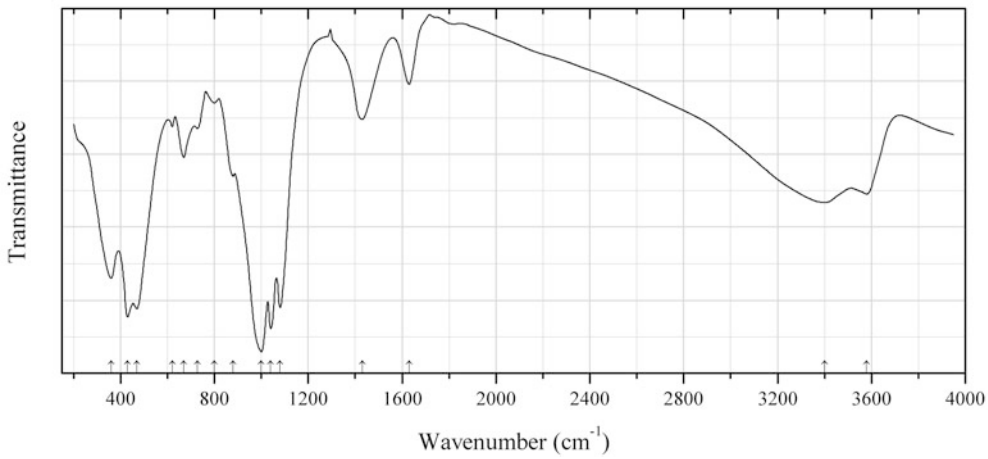

Fig. 2.708 IR spectrum of erlianite drawn using data from Feng and Yang (1986)

Si36 Erlianite $Fe^{2+}_4Fe^{3+}_2Si_6O_{15}(OH)_8$ (Fig. 2.708)
Locality: Harhada iron deposit, Inner Mongolia, China (type locality).
Description: Black aggregate of fibrous to lath-like individuals from the association with quartz, magnetite, siderite, albite, stilpnomelane, deerite, etc. Holotype sample. Orthorhombic, space group *Pmmn* or $Pm2_1n$, a = 23.20(1), b = 9.20(1), c = 13.18(1) Å, V = 2813 Å^3. D_{calc} = 3.11 g/cm^3. Optically biaxial (−), α = 1.667, β = 1.674, γ = 1.679, 2 V = 56–59°. The empirical formula is (Z = 1): $(Fe^{2+}_{19.06}Fe^{3+}_{2.19}Mg_{1.33}Mn_{0.42})(Fe^{3+}_{11.32}V_{0.68})Ti_{0.26}(Si_{34.73}Al_{0.20}Fe^{3+}_{0.81})O_{90}(OH,O)_{48}$. The strongest lines of the powder X-ray diffraction pattern [d, Å (I, %) (hkl)] are: 11.5 (100) (200, 101), 3.05 (50) (223, 130), 2.89 (60) (603, 800, 231, 621), 2.61 (60) (523, 105, 332, 224), 2.52 (50) (901, 115, 033, 531), 1.560 (50) (12.0.5, 14.2.0).
Kind of sample preparation and/or method of registration of the spectrum: Absorption. Kind of sample preparation is not indicated.
Source: Feng and Yang (1986).
Wavenumbers (cm^{-1}): 3580, 3400, 1630, 1430, 1080s, 1040s, 1000s, 880, 800w, 728, 670, 620w, 470s, 430s, 360s.
Note: The bands at 1430, 880, and 729 cm^{-1} are due to the admixture of associated siderite.

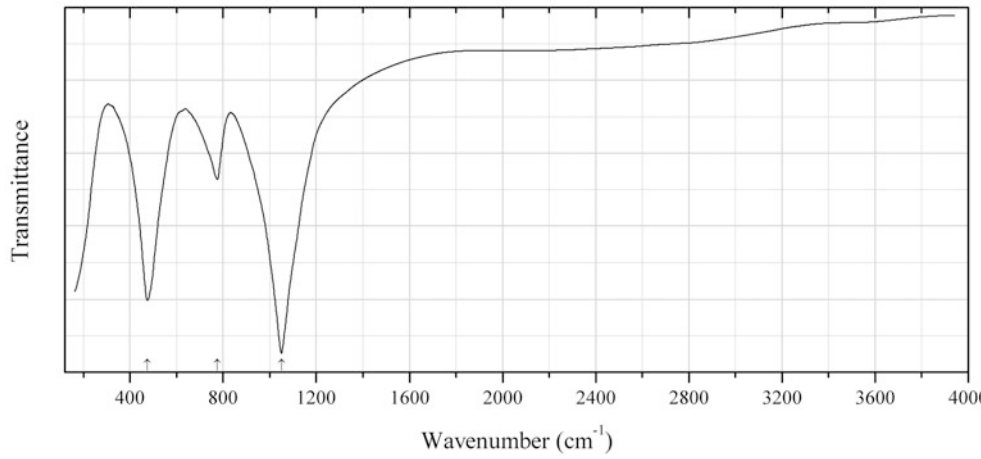

Fig. 2.709 IR spectrum of ertixiite drawn using data from Zhang et al. (1985)

Si37 Ertixiite $Na_2Si_4O_9$ (Fig. 2.709)
Locality: Altay pegmatite mine, northern Xinjiang, China (type locality).
Description: White granular aggregate from the association with topaz, apatite, clevelandite, quartz, etc. Holotype sample. Cubic, a = 5.975 Å, V = 213.3 Å^3, Z = 1. D_{meas} = 2.35 g/cm^3. D_{calc} = 2.34 g/cm^3. Optically isotropic, n = 1.502. Contains admixtures of CaO (2.7–3.0 wt%) and Al_2O_3 (1.4–1.5 wt%). The strongest lines of the powder X-ray diffraction pattern [d, Å (I, %) (hkl)] are: 3.443 (20) (111), 2.988 (20) (200), 2.674 (20) (210), 2.194 (20) (221), 1.996 (80) (221), 1.798 (100) (311).
Kind of sample preparation and/or method of registration of the spectrum: KBr disc. Absorption.
Source: Zhang et al. (1985).
Wavenumbers (cm^{-1}): 1050s, 775, 475s.

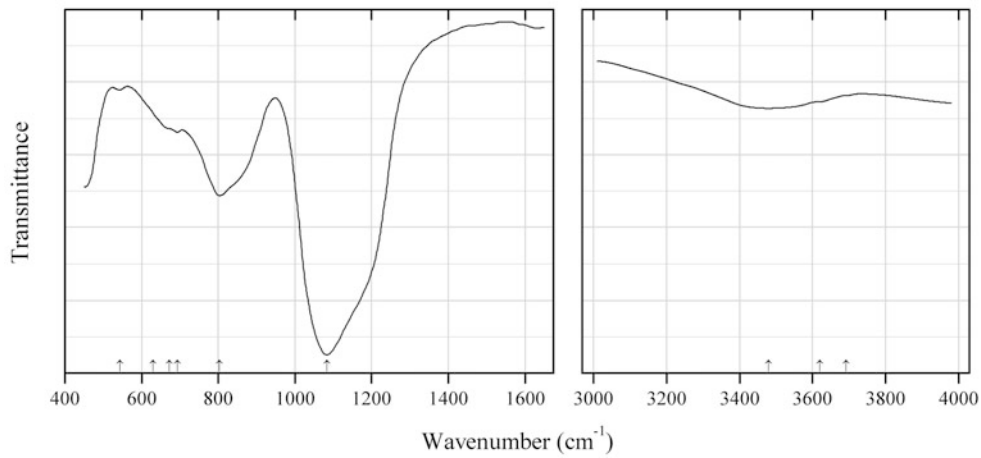

Fig. 2.710 IR spectrum of metakaolinite drawn using data from Bich et al. (2009)

Si38 Metakaolinite $Al_2Si_2O_7$ (Fig. 2.710)
Locality: Artificial.
Description: A poorly crystalline phase obtained as a result of almost complete (about 97 %) dehydroxylation of kaolinite at 650 °C for 1 h.

Kind of sample preparation and/or method of registration of the spectrum: No data.
Source: Bich et al. (2009).
Wavenumbers (cm^{-1}): 3692sh, 3620sh, 3480, 1083s, 630sh, 803, 693, 672sh, 543w.
Note: The wavenumbers were partly determined by us based on spectral curve analysis of the published spectrum. The IR spectrum of metakaolinite given in the cited paper is close to the IR spectra of opal and silica gel.

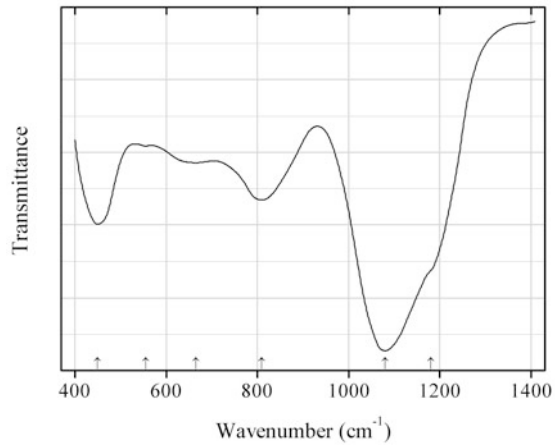

Fig. 2.711 IR spectrum of metakaolinite drawn using data from Rocha et al. (1991)

Si39 Metakaolinite $Al_2Si_2O_7$ (Fig. 2.711)
Locality: Artificial.
Description: A poorly crystalline phase obtained as a result of calcination of kaolinite at 700 °C.
Kind of sample preparation and/or method of registration of the spectrum: KBr disc. Absorption.
Source: Rocha et al. (1991).
Wavenumbers (cm^{-1}): 1180sh, 1080s, 810, 665, 555w, 450.

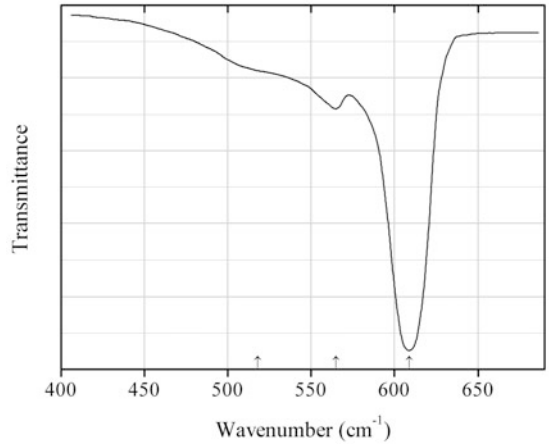

Fig. 2.712 IR spectrum of silicon drawn using data from Martin (1965)

Si40 Silicon Si (Fig. 2.712)

Locality: Synthetic.
Kind of sample preparation and/or method of registration of the spectrum: A powdered sample. Absorption.
Source: Martin (1965).
Wavenumbers (cm^{-1}): 609s, 565w, 518sh.
Note: The wavenumbers were determined by us based on spectral curve analysis of the published spectrum.

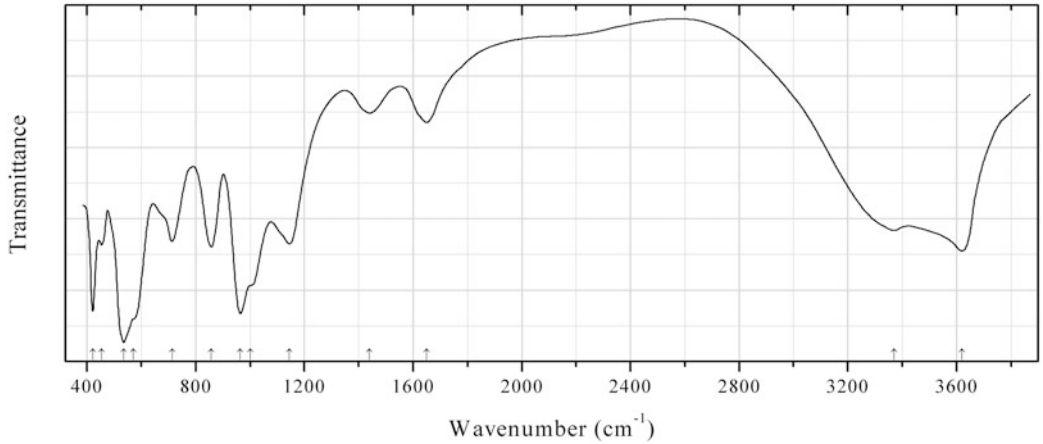

Fig. 2.713 IR spectrum of strätlingite obtained by N.V. Chukanov

Si41 Strätlingite $Ca_2Al(Si,Al)_2O_2(OH)_{10}\cdot 2.25H_2O$ (Fig. 2.713)
Locality: Bellerberg, near Kottenheim, 2 km north of Mayen, Laacher See region, Eastern Eifel area, Rhineland-Palatinate (Rheinland-Pfalz), Germany.
Description: Aggregates of colourless platelets.
Kind of sample preparation and/or method of registration of the spectrum: KBr disc. Absorption.
Wavenumbers (cm^{-1}): 3620, 3370, 1650, 1440, 1145, 1000sh, 964s, 857, 713, 570sh, 535s, 453, 421s.

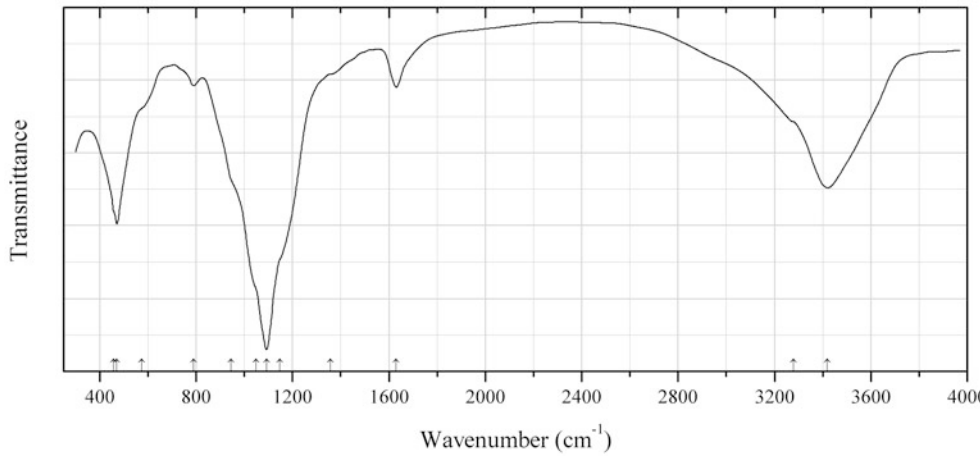

Fig. 2.714 IR spectrum of thornasite drawn using data from Ansell and Chao (1987)

Si42 Thornasite $Na_{12}Th_3(Si_8O_{19})_4 \cdot 18H_2O$ (Fig. 2.714)
Locality: Poudrette (Demix) quarry, Mont Saint-Hilaire, Rouville RCM (Rouville Co.), Montérégie, Québec, Canada (type locality).
Description: Colourless to pale green anhedral crystals from the association with yofortierite and analcime. Holotype sample. Trigonal, space group *R*3*m*, $a = 29.08(1)$, $c = 17.30(1)$ Å. $D_{meas} = 2.62(2)$ g/cm^3, $D_{calc} = 2.627$ g/cm^3. Optically uniaxial (+), $\omega = 1.510(1)$, $\varepsilon = 1.512(1)$. The strongest lines of the powder X-ray diffraction pattern [*d*, Å (*I*, %) (*hkl*)] are: 14.54 (20) (110), 8.17 (30) (012), 7.27 (100) (220), 5.09 (20) (042), 4.17 (70) (422), 3.239 (30) (262), 2.959 (20) (802), 2.890 (25) (811, 713).
Kind of sample preparation and/or method of registration of the spectrum: KBr disc. Absorption.
Source: Ansell and Chao (1987).
Wavenumbers (cm^{-1}): 3420s, 3278sh, 1630, 1357sh, 1147sh, 1092s, 1048sh, 946sh, 790w, 574sh, 471, 458sh.
Note: The wavenumbers were partly determined by us based on spectral curve analysis of the published spectrum.

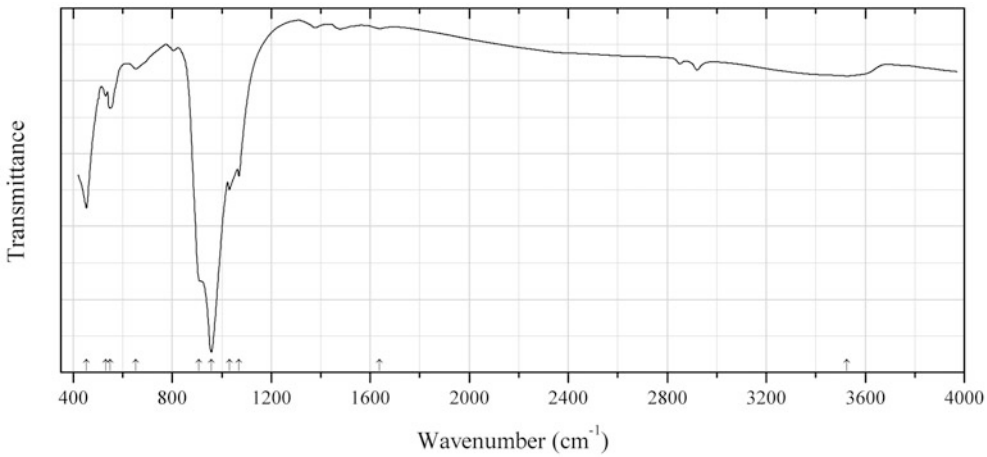

Fig. 2.715 IR spectrum of veblenite drawn using data from Cámara et al. (2013)

Si43 Veblenite $KNa(Fe^{2+}{}_5Fe^{3+}{}_4\ Mn_7)Nb_4(Si_2O_7)_2(Si_8O_{22})_2O_6(OH)_{10} \cdot 3H_2O$ (Fig. 2.715)
Locality: Ten Mile Lake, Seal Lake area, Newfoundland and Labrador, Canada (type locality).
Description: Red brown single laths and fibres from the association with niobophyllite, albite, arfvedsonite, aegirine-augite, barylite, eudidymite, neptunite, Mn-rich pectolite, pyrochlore, sphalerite, and galena. Holotype sample. Triclinic, space group *P*-1, $a = 5.3761(3)$, $b = 27.5062(11)$, $c = 18.6972(9)$ Å, $\alpha = 140.301(3)°$, $\beta = 93.033(3)°$, $\gamma = 95.664(3)°$, $V = 1720.96(14)$ Å^3. $D_{calc} = 3.046$ g/cm^3. Optically biaxial (−), $\alpha = 1.676(2)$, $\beta = 1.688(2)$, $\gamma = 1.692(2)$, $2V = 65(1)°$. The simplified crystal-chemical formula is $(K,Ba,\square)_3(\square,Na)_2(Fe^{2+},Fe^{3+},Mn)_{17}(Nb,Ti)_4(Si_2O_7)_2(Si_8O_{22})_2O_6(OH)_{10} \cdot 3H_2O$. The strongest lines of the powder X-ray diffraction pattern [*d*, Å (*I*, %) (*hkl*)] are: 16.894 (100) (010), 18.204 (23) (0–11), 4.271 (9) (1–41, 040, 120), 11.661 (8) (001), 2.721 (3) (1–95), 4.404 (3) (−1–32, 1–42), 4.056 (3) (031, 1–12; 1–52, −1–43), 3.891 (2) (003).
Kind of sample preparation and/or method of registration of the spectrum: Absorption. Kind of sample preparation is not indicated.
Source: Cámara et al. (2013).
Wavenumbers (cm^{-1}): 3525w, 1637w, 1070, 1031, 958s, 908sh, 654w, 550, 531, 453s.

Note: Weak bands in the intervals from 2800 to 3000 and from 1300 to 1500 cm^{-1} are due to the admixture of glue.

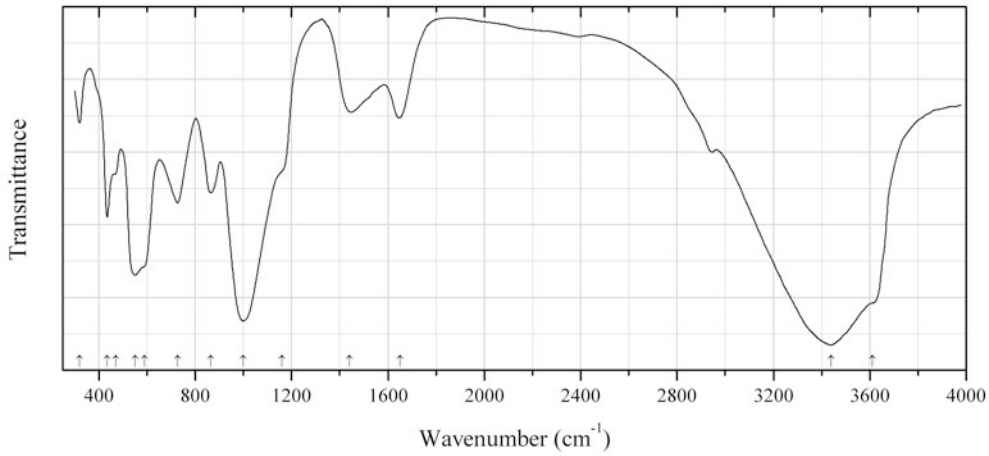

Fig. 2.716 IR spectrum of vertumnite drawn using data from Passaglia and Galli (1977)

Si44 Vertumnite $Ca_4Al_4Si_4O_6(OH)_{24}\cdot 3H_2O$ (Fig. 2.716)
Locality: Campomorto, Montalto di Castro, Viterbo, Italy (type locality).
Description: Transparent flattened crystals from the association with tobermorite. Holotype sample. Optically biaxial (+), α = 1.531(1), β = 1.535(1), γ = 1.541(1), 2 *V* = 62°. The empirical formula is $(Ca_{3.74}Sr_{0.06}K_{0.02}Na_{0.02}Ba_{0.01})Al_{4.00}(Si_{3.38}Al_{0.36}P_{0.03})O_{5.18}(OH)_{24.66}\cdot 3.09H_2O$. The strongest lines of the powder X-ray diffraction pattern [*d*, Å (*I*, %)] are: 12.51 (70), 6.275 (65), 4.275 (16), 4.187 (100), 2.873 (17).
Kind of sample preparation and/or method of registration of the spectrum: KBr disc. Transmission.
Source: Passaglia and Galli (1977).
Wavenumbers (cm^{-1}): 3610sh, 3440s, 1650, 1440, 1160sh, 1000s, 865, 727, 590sh, 550s, 470sh, 435, 320.

Si45 Mendeleevite-(Ce) $Cs_6[(Ce,REE)_{22}Ca_6](Si_{70}O_{175})(OH,F)_{14}\cdot 21H_2O$
Locality: Dara-i Pioz glacier, Dara-i Pioz alkaline massif, Tien Shan Mts., Tajikistan (type locality).
Description: Colourless cubic crystals from the association with sogdianite, stillwellite-(Ce), reedmergnerite, leucosphenite, aegirine, polylithionite, microcline, pyrochlore, turkestanite, etc. Cubic, *a* = 21.909(1) Å, *V* = 10,516.4(9) $Å^3$, *Z* = 2.
Kind of sample preparation and/or method of registration of the spectrum: KBr disc. Absorption.
Source: Pautov et al. (2013).
Wavenumbers (cm^{-1}): 3400, 1610, 1013, 978, 693, 548.

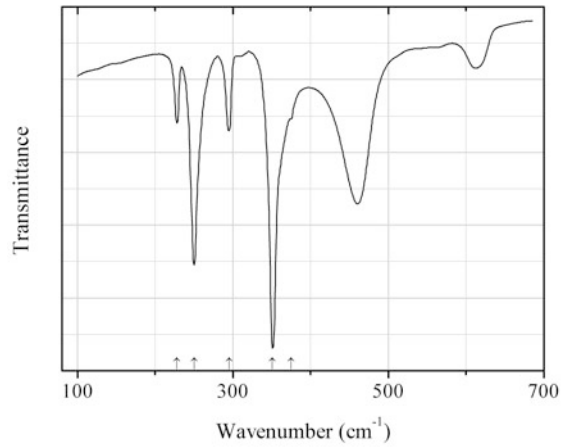

Fig. 2.717 IR spectrum of chromium disilicide drawn using data from Borghesi et al. (1990)

Si46 Chromium disilicide $CrSi_2$ (Fig. 2.717)
Locality: Synthetic.
Description: Prepared from Cr and Si evaporated in an electron gun and deposited at room temperature on oxidized Si wafer with subsequent annealing at 900 °C for 30 min.
Kind of sample preparation and/or method of registration of the spectrum: Polycrystalline film. Absorption.
Source: Borghesi et al. (1990).
Wavenumbers (cm^{-1}): 375sh, 351s, 295, 250s, 228.
Note: The bands at $\sim$600 and $\sim$450 cm^{-1} are due to vibrational modes of Si and SiO_2, respectively.

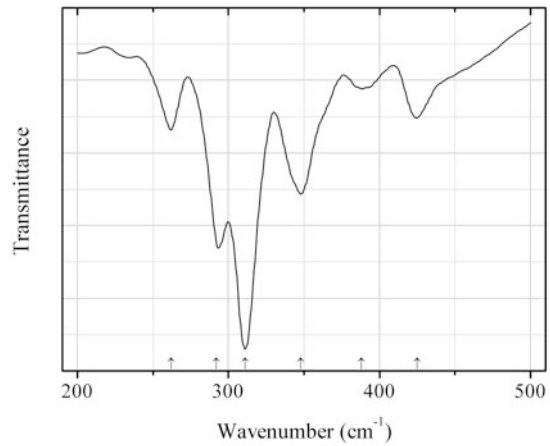

Fig. 2.718 IR spectrum of linzhiite dimorph drawn using data from Bocelli et al. (1995)

Si47 Linzhiite dimorph $FeSi_2$ (Fig. 2.718)
Locality: Synthetic.
Description: Crystals grown in closed ampoules using iodine as transporting gas. Orthorhombic, a = 9.863, b = 7.791, c = 7.833 Å.

Kind of sample preparation and/or method of registration of the spectrum: Polycrystalline film. Absorption.
Source: Bocelli et al. (1995).
Wavenumbers (cm^{-1}): 425, 388w, 348, 311s, 292s, 262.

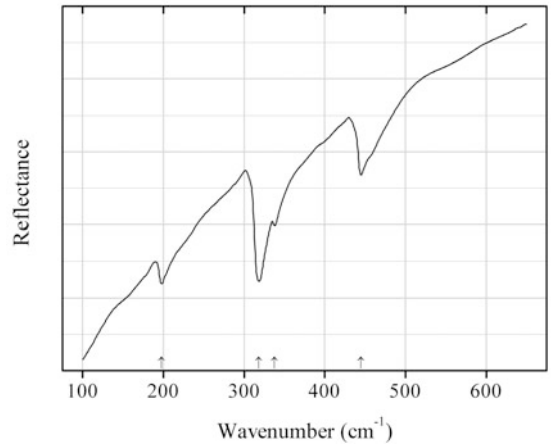

Fig. 2.719 IR spectrum of naquite drawn using data from Damascelli et al. (1997)

Si48 Naquite FeSi (Fig. 2.719)
Locality: Synthetic.
Description: Single crystals grown by the floating zone method.
Kind of sample preparation and/or method of registration of the spectrum: Single crystal. Reflection.
Source: Damascelli et al. (1997).
Wavenumbers (cm^{-1}): 445, 338, 318s, 198.

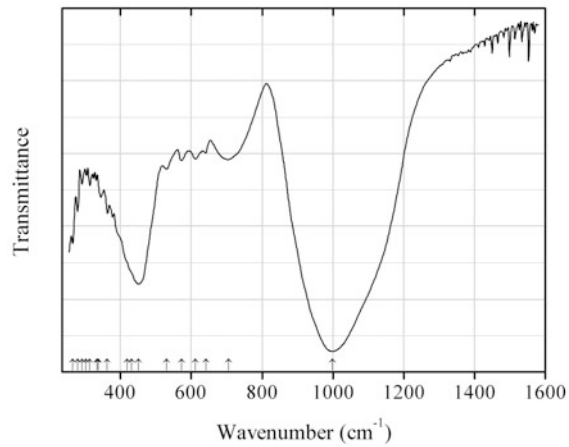

Fig. 2.720 IR spectrum of maskelynite drawn using data from Arndt et al. (1982)

Sia23 Maskelynite $(Ca,Na)[(Si,Al)_4O_8]$ (Fig. 2.720)
Labradorite glass

Locality: Manicouagan impact crater, central Quebec, Canada.
Description: Diaplectic glass with labradorite composition (Ab:An:Or = 38.7:58.2:3.1) and crystalline inclusions from shocked anorthosite containing accessory garnet, pyroxene, amphibole, etc.
Kind of sample preparation and/or method of registration of the spectrum: KBr disc. Transmission.
Source: Arndt et al. (1982).
Wavenumbers (cm^{-1}): 998s, 705, 641, 612w, 572w, 530w, 450s, 432sh, 419sh, 337, 363, 334, 313, 303, 291, 279, 265.
Note: The wavenumbers were partly determined by us based on spectral curve analysis of the published spectrum.

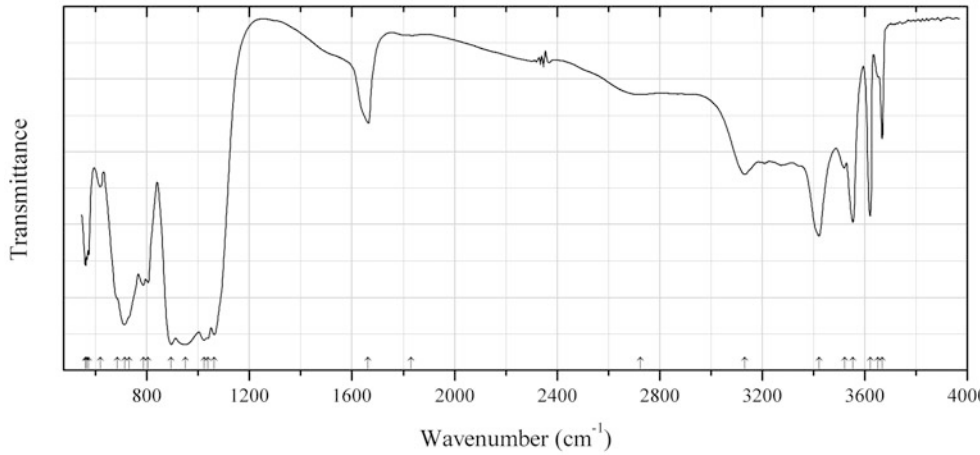

Fig. 2.721 IR spectrum of alflarsenite drawn using data from Raade et al. (2009)

BeSi65 Alflarsenite $NaCa_2Be_3Si_4O_{13}(OH)\cdot 2H_2O$ (Fig. 2.721)
Locality: Tuften larvikite quarry, Tvedalen, Larvik, Vestfold, south Norway (type locality).
Description: Pale beige aggregate from the association with calcite, analcime, and K-feldspar. Holotype sample. The crystal structure is solved. Monoclinic, space group $P2_1$, a = 7.1222(4), b = 19.8378(11), c = 9.8071(5) Å, β = 111.287(1)°, V = 1291.1(2) $Å^3$, Z = 4. D_{calc} = 2.605 g/cm^3. Optically biaxial (+), α = 1.578(1), β = 1.580(1), γ = 1.583(1). The strongest lines of the powder X-ray diffraction pattern [d, Å (I, %) (hkl)] are: 9.095 (100) (001), 6.279 (42) (−111, 110), 4.189 (32) (−122, 121), 3.972 (76) (−141, 140), 3.205 (37) (−113, 112), 2.964 (70) (−232, 230), 2.915 (92) (−133, 132), 2.757 (33) (−242, 240). Broad bands in the range 1680–3100 cm^{-1} correspond to acid OH groups.
Kind of sample preparation and/or method of registration of the spectrum: Transmission. Kind of sample preparation not indicated.
Source: Raade et al. (2009).
Wavenumbers (cm^{-1}): 3668, 3652sh, 3621, 3555, 3521w, 3422, 3131, 2725, 1830, 1663, 1062s, 1039s, 1023s, 950s, 895s, 805, 786, 730sh, 713s, 684sh, 619w, 573, 566, 561.
Note: The wavenumbers were partly determined by us based on spectral curve analysis of the published spectrum.

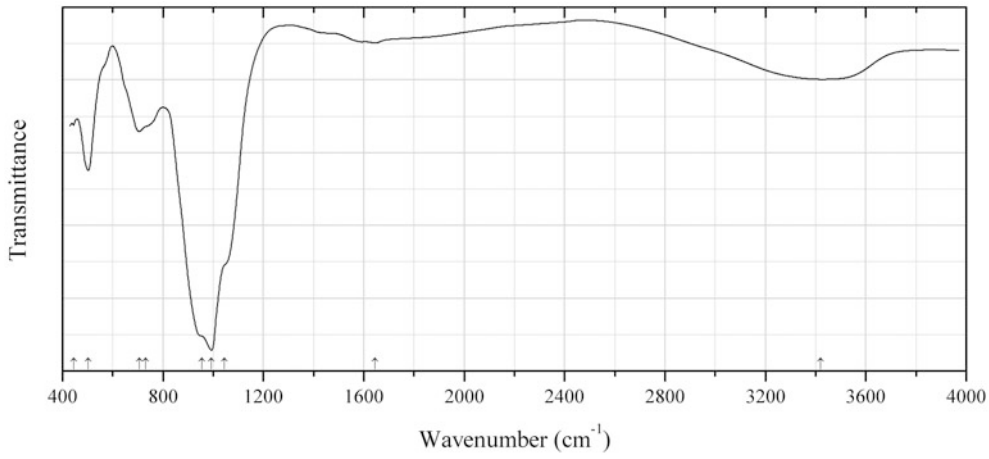

Fig. 2.722 IR spectrum of bussyite-(Ce) drawn using data from Grice et al. (2009)

BeSi66 Bussyite-(Ce) $(Ce,REE,Ca)_3(Na,H_2O)_6MnSi_9Be_5(O,OH)_{30}(F,OH)_4$ (Fig. 2.722)
Locality: Poudrette (Demix) quarry, Mont Saint-Hilaire, Rouville RCM (Rouville Co.), Montérégie, Québec, Canada (type locality).
Description: Pinkish orange crystals from the association with aegirine, albite, analcime, ancylite-(Ce), calcite, catapleiite, gonnardite, hydrotalcite, kupletskite, leucophanite, microcline, nenadkevichite, polylithionite, sérandite, and sphalerite. Holotype sample. Monoclinic, space group $C2/c$, $a = 11.654(3)$, $b = 13.916(3)$, $c = 16.583(4)$ Å, $\beta = 91.141(6)°$, $\gamma = 95.86(2)°$, $V = 2675.4(8)$ Å^3, $Z = 4$. $D_{meas} = 3.00$ g/cm^3, $D_{calc} = 3.11$ g/cm^3. Optically biaxial (−), $\alpha = 1.574(2)$, $\beta = 1.591(2)$, $\gamma = 1.597(2)$, $2V = 63(2)°$. The empirical formula is $(Ce_{0.82}Nd_{0.37}Y_{0.24}Th_{0.17}Pr_{0.10}Sm_{0.08}Gd_{0.08}Eu_{0.01})(Ca_{0.775}La_{0.225})[Na_{3.00}(H_2O)_{2.50}Ca_{0.54}K_{0.015}]$ $(Mn_{0.485}Na_{0.40}Mg_{0.01})(Si_{8.90}Be_{4.605}Al_{0.22})O_{30}[F_{2.67}(OH)_{1.33}$. The strongest lines of the powder X-ray diffraction pattern [*d*, Å (*I*, %) (*hkl*)] are: 8.120 (100) (−111), 6.959 (26) (020), 3.543 (39) (024), 3.454 (21) (−133), 2.959 (24) (−331), 2.863 (48) (331, −242), 2.749 (23) 006), 2.668 (33) (−135, 044, 402).
Kind of sample preparation and/or method of registration of the spectrum: Diamond-anvil cell microsampling.
Source: Grice et al. (2009).
Wavenumbers (cm^{-1}): 3421 (broad), 1645 (broad), 1045sh, 993s, 956sh, 730sh, 705, 503, 444.
Note: The wavenumbers were partly determined by us based on spectral curve analysis of the published spectrum.

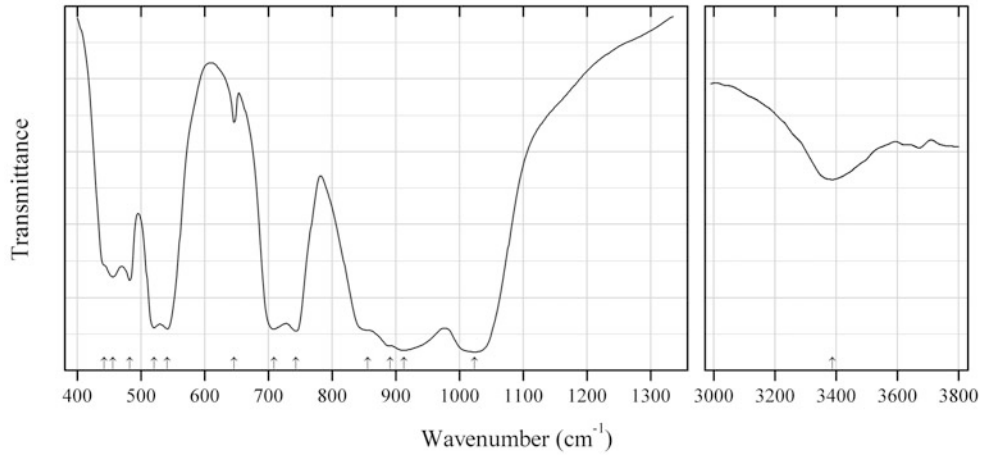

Fig. 2.723 IR spectrum of gadolinite-(Y) drawn using data from Ito and Hafner (1974)

BeSi67 Gadolinite-(Y) $Y_2Fe^{2+}Be_2(SiO_4)_2O_2$ (Fig. 2.723)
Locality: Synthetic.
Description: Synthesized from gel at 720 °C and partial pressure of H_2O about 2 kbar. Confirmed by the powder X-ray diffraction pattern and Mössbauer spectrum. Monoclinic, a = 9.920(4), b = 7.4843 (2), c = 4.7474(7) Å, β = 89.60(4)°, V = 351.7(2) Å^3.
Kind of sample preparation and/or method of registration of the spectrum: KBr disc. Transmission.
Source: Ito and Hafner (1974).
Wavenumbers (cm^{-1}): 3387, 1024s, 913s, 891sh, 856sh, 743s, 709s, 646w, 541s, 520s, 482, 456, 442sh.
Note: The wavenumbers were determined by us based on spectral curve analysis of the published spectrum. The band in the range from 3200 to 3500 cm^{-1} indicates the presence of O–H bonds (adsorbed water?).

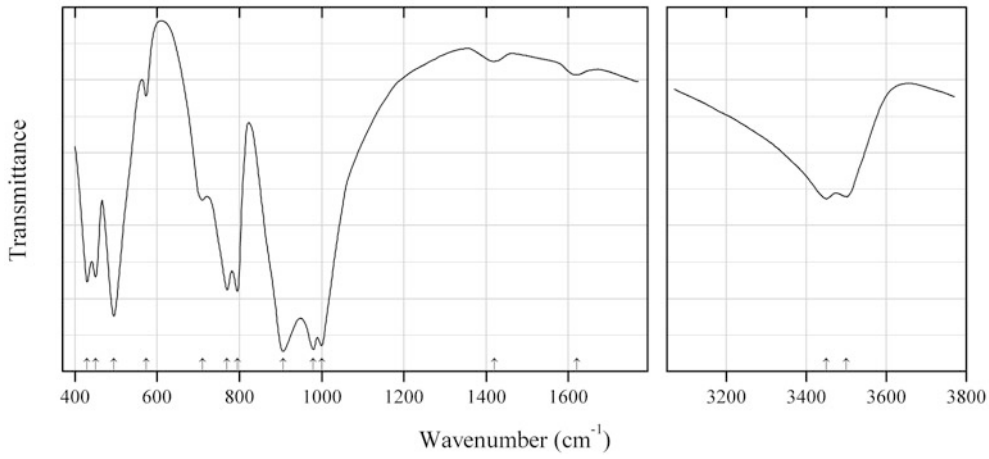

Fig. 2.724 IR spectrum of hingganite-(Yb) drawn using data from Voloshin et al. (1983a)

BeSi68 Hingganite-(Yb) $BeYb(SiO_4)(OH)$ (Fig. 2.724)

Locality: Ploskaya Mt., Western Keivy massif, Kola peninsula, Murmansk region, Russia (type locality).
Description: Spherical aggregates of fine acicular crystals from the association with plumbomicrolite, albite, quartz, and fluorite. Holotype sample. Monoclinic, space group $P2_1/a$, a = 9.888(5), b = 7.607 (3), c = 4.740(2) Å, β = 90.45(4)°, Z = 4. D_{meas} = 4.72 g/cm^3, D_{calc} = 4.83 g/cm^3. Optically biaxial (+), α = 1.725(1), β = 1.738, γ = 1.760, 2 V = 65°. The empirical formula is $(Yb_{0.45}Y_{0.20}Er_{0.11}Lu_{0.06}Ca_{0.05}Tm_{0.04}Dy_{0.03}Ho_{0.01})H_{1.08}Be_{1.13}Si_{0.96}O_5$. The strongest lines of the powder X-ray diffraction pattern [d, Å (I, %) (hkl)] are: 6.06 (70) (110), 4.76 (60) (001), 3.74 (60) (111, 11–1), 3.45 (60) (201, 20–1), 3.13 (100) (211, 21–1), 2.85 (100) (12–1), 2.572 (80) (31–1), 2.542 (80) (311), 2.206 (60) (321, 32–1), 1.977 (80) (122, 12–2).
Kind of sample preparation and/or method of registration of the spectrum: KBr disc. Absorption.
Source: Voloshin et al. (1983a).
Wavenumbers (cm^{-1}): 3500, 3450, 1620w, 1420w, 1000s, 980s, 907s, 795, 770, 710, 573w, 495s, 450, 430.

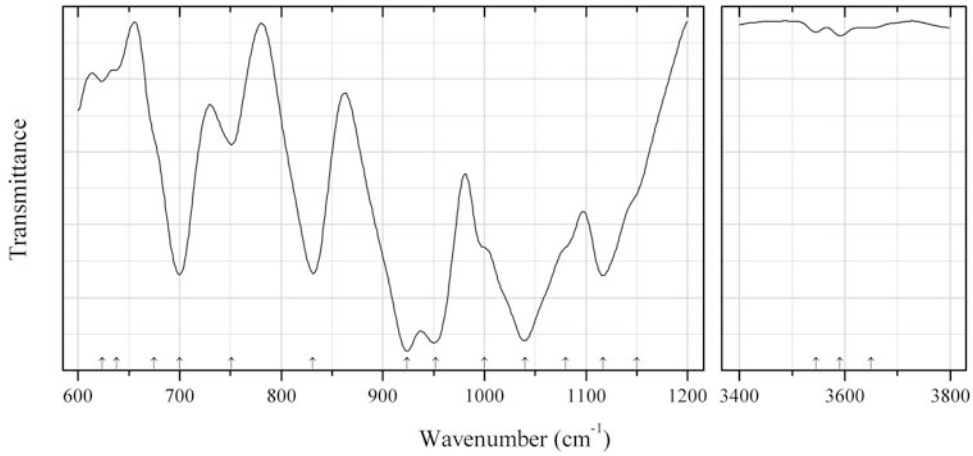

Fig. 2.725 IR spectrum of pezzottaite drawn using data from Gatta et al. (2012)

BeSi69 Pezzottaite $CsLiBe_2Al_2Si_6O_{18}$ (Fig. 2.725)
Locality: Sakavalana mine, Ambatovita, Ambatofinandrahana district, Finarantsoa province, central Madagascar (type locality).
Description: Bright pink crystal. The crystal structure is solved. Trigonal, space group R-3c, a = 15.9615(6), c = 27.8568(9) Å, V = 6146.2(4) Å^3, Z = 18. The empirical formula is $(Cs_{0.56}Rb_{0.03}K_{0.02})(Na_{0.10}Ca_{0.02})Be_{2.08}Li_{0.92}Al_{1.98}(Si_{5.94}Al_{0.06})O_{18}\cdot 0.27H_2O$.
Kind of sample preparation and/or method of registration of the spectrum: KBr disc. Transmission.
Source: Gatta et al. (2012).
Wavenumbers (cm^{-1}): 3650w, 3591w, 3545w, 1150sh, 1117, 1080sh, 1040s, 1000sh, 952s, 924s, 831, 751, 700, 675sh, 638w, 624w.
Note: The wavenumbers were partly determined by us based on spectral curve analysis of the published spectrum.

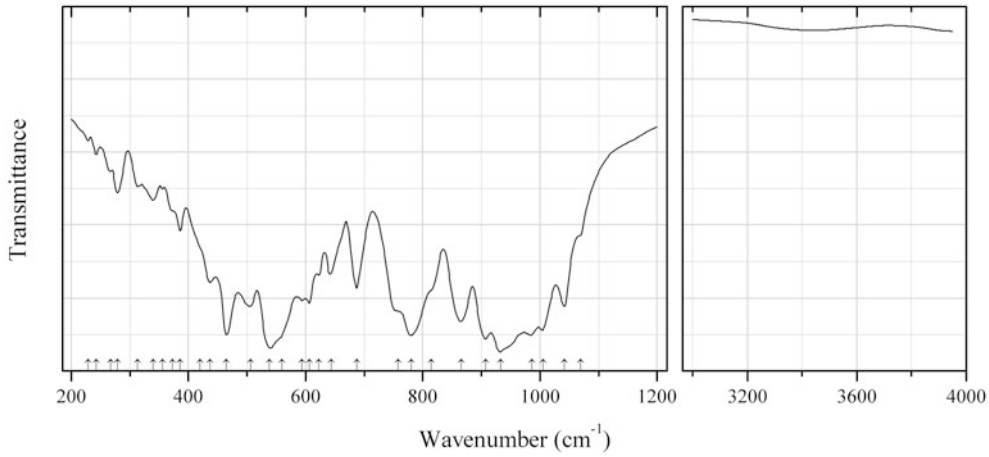

Fig. 2.726 IR spectrum of surinamite drawn using data from Hölscher et al. (1986)

BeSi70 Surinamite $Mg_3Al_3(Si_3BeAlO_{15})O$ (Fig. 2.726)
Locality: Synthetic.
Description: The pure MgAl end member obtained by spontaneous crystallization of a stoichiometric gel. Monoclinic, space group *P*2/*n*, a = 9.881(1), b = 11.311(1), c = 9.593(1) Å, β = 109.52(2)°, Z = 4. Optically biaxial, α = 1.7015(20), β = 1.7035(20), γ = 1.7055(20). Confirmed by powder X-ray diffraction data.
Kind of sample preparation and/or method of registration of the spectrum: RbI disc. Transmission.
Source: Hölscher et al. (1986).
Wavenumbers (cm^{-1}): 1070sh, 1042, 1005s, 986s, 933s, 907s, 866, 815sh, 780s, 758sh, 688, 644, 623, 606, 594, 560sh, 538s, 506, 465s, 437, 420sh, 386, 373sh, 356w, 340, 313w, 279, 267w, 243w, 229w.

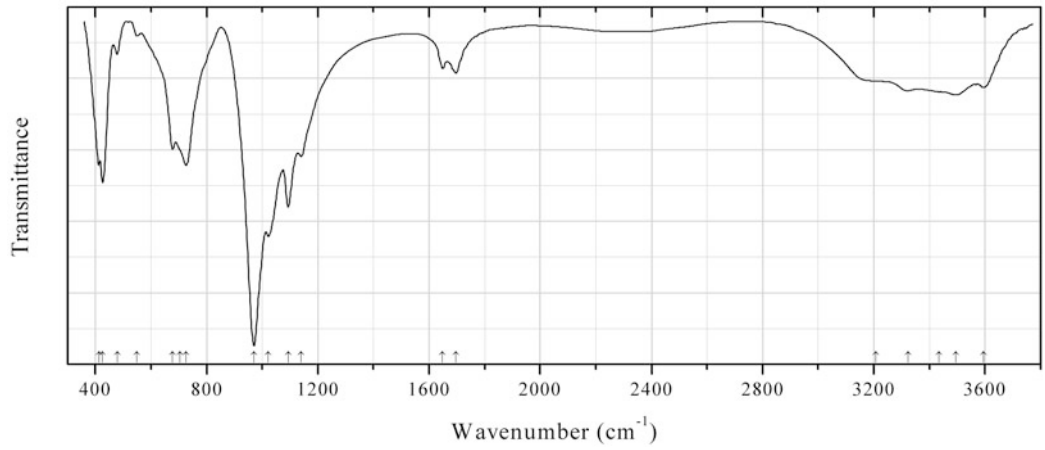

Fig. 2.727 IR spectrum of nabesite obtained by N.V. Chukanov

BeSi71 Nabesite $Na_2(BeSi_4O_{10})\cdot 4H_2O$ (Fig. 2.727)

Locality: Kvanefjeld plateau, Ilímaussaq alkaline complex, Narsaq municipality, South Greenland (type locality).
Description: White semitransparent platy crystals with perfect cleavage from the association with other zeolites.
Kind of sample preparation and/or method of registration of the spectrum: KBr disc. Absorption.
Wavenumbers (cm^{-1}): 3595, 3496, 3435sh, 3322, 3208, 1697, 1648, 1141, 1093s, 1022s, 970s, 726s, 705sh, 678, 550w, 478w, 426s, 414s.

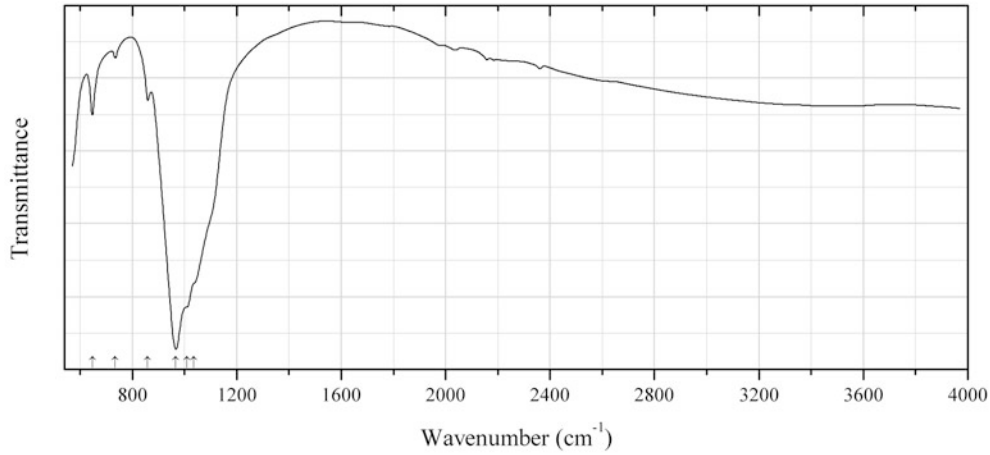

Fig. 2.728 IR spectrum of bussyite-(Y) drawn using data from Grice et al. (2015)

BeSi72 Bussyite-(Y) $(Y,REE,Ca)_3(Na,Ca)_6MnSi_9Be_5(O,OH,F)_{34}$ (Fig. 2.728)
Locality: Poudrette (Demix) quarry, Mont Saint-Hilaire, Rouville RCM (Rouville Co.), Montérégie, Québec, Canada (type locality).
Description: Dark brown crystals from the association with analcime, calcite, cappelenite-(Y), catapleiite, charmarite-2*H* and charmarite-3*T*, fluorite, helvite, kupletskite, microcline, perraultite, sérandite, and taeniolite. Holotype sample. The crystal structure is solved. Monoclinic, space group *C*2, $a = 11.545(2)$, $b = 13.840(2)$, $c = 16.504(4)$ Å, $\beta = 95.87(2)°$, $V = 2623.1(6)$ Å^3, $Z = 4$. $D_{calc} = 3.11$ g/cm^3. Optically biaxial (−), $\alpha = 1.583(2)$, $\beta = 1.593(2)$, $\gamma = 1.600(2)$, $2V = 68(2)°$. The empirical formula is $(Y_{0.874}Nd_{0.221}Ce_{0.211}Dy_{0.154}Gd_{0.142}Sm_{0.108}Er_{0.063}Pr_{0.043}La_{0.038}Yb_{0.030}Ho_{0.027}Tb_{0.022}Tm_{0.011}Eu_{0.010}Ca_{0.789}Th_{0.105})(Na_{3.449}Ca_{0.430}K_{0.022}Ba_{0.003})(Mn_{0.538}Fe_{0.072}Nb_{0.020})(Si_{8.585}Be_{5.075}Al_{0.074})[O_{24.107}(OH)_{5.893}][F_{2.386}(OH)_{1.603}Cl_{0.011}]$. The strongest lines of the powder X-ray diffraction pattern [*d*, Å (*I*, %) (*hkl*)] are: 8.049 (100) (−111), 6.924 (21) (020), 3.529 (38) (311), 3.435 (21) (−133), 3.155 (23) (−115), 2.940 (35) (−331), 2.840 (50) (331), 2.736 (30) (006), 2.651 (38) (−135), 2.629 (30) (402).
Kind of sample preparation and/or method of registration of the spectrum: Transmission. The spectrum was obtained using a diamond-anvil cell microsampling device.
Source: Grice et al. (2015).
Wavenumbers (cm^{-1}):1036sh, 1008sh, 967s, 859, 735w, 647.
Note: The only band that could be assigned to ^{IV}Be–O-stretching vibrations (at 735 cm^{-1}) is anomalously weak. Weak bands in the range from 1800 to 3000 cm^{-1} corresponds to acid OH groups.

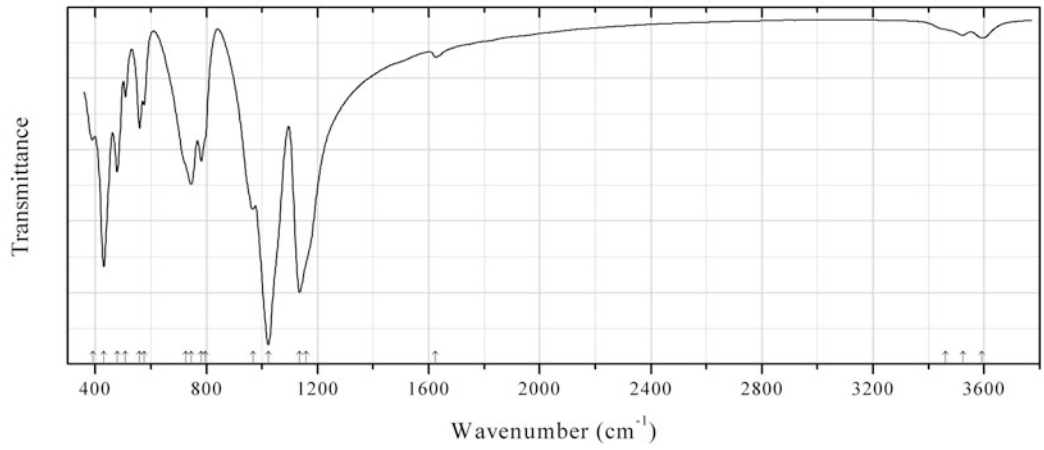

Fig. 2.729 IR spectrum of milarite Al-deficient obtained by N.V. Chukanov

BeSi73 Milarite Al-deficient $K_{2-x}Ca_2Al_{x/3}Be_3Si_{12}O_{30}{\cdot}nH_2O$ (Fig. 2.729)
Locality: José Pinto mine, Jaguaraçu, Minas Gerais, Brazil.
Description: Yellow crystals. The empirical formula is (electron microprobe): $K_{1.10}Ca_{1.68}Na_{0.15}Al_{0.36}Be_xSi_{12}O_{30}{\cdot}nH_2O$. Confirmed by powder X-ray diffraction data.
Kind of sample preparation and/or method of registration of the spectrum: KBr disc. Absorption.
Wavenumbers (cm^{-1}): 3592w, 3523w, 3460sh, 1625w, 1160sh, 1135s, 1023s, 967, 795sh, 782, 745, 725sh, 575, 560, 509w, 479, 431s, 392.

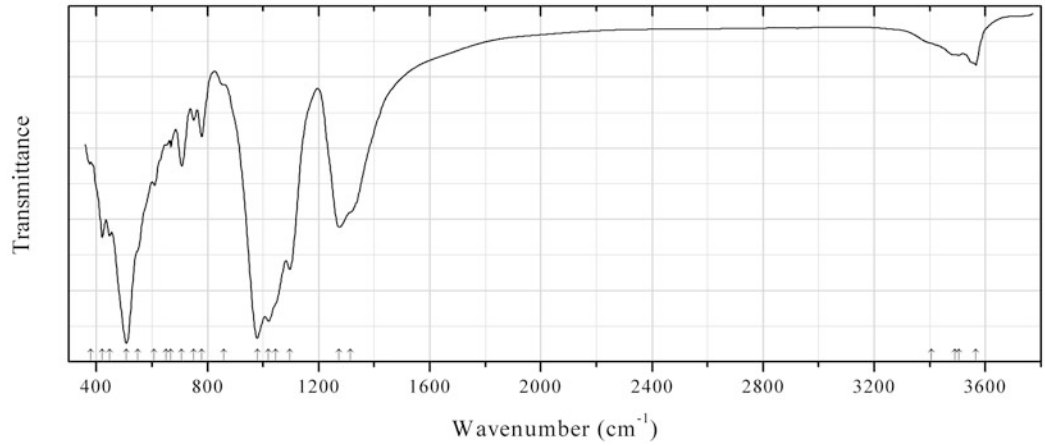

Fig. 2.730 IR spectrum of oxy-schorl obtained by N.V. Chukanov

BSi73 Oxy-schorl $Na(Fe^{2+}{}_2Al)Al_6(Si_6O_{18})(BO_3)_3(OH)_3O$ (Fig. 2.730)
Locality: Shigar valley, Skardu district, Baltistan, Pakistan.
Description: Black inner zone of tourmaline crystal (the green outer zone corresponds to rossmanite). The associated minerals are albite, quartz, and muscovite. The empirical formula is (electron microprobe): $Na_{0.99}(Fe_{1.47}Al_{1.18}Mn_{0.26}Mg_{0.03})(Al_{5.97}Ti_{0.03})(Si_6O_{18})(BO_3)_3(OH)_3(O,OH)$.
Kind of sample preparation and/or method of registration of the spectrum: KBr disc. Absorption.

Wavenumbers (cm^{-1}): 3565, 3505, 3490sh, 3405sh, 1315sh, 1274s, 1096s, 1045sh, 1019s, 979s, 858sh, 779, 750w, 707, 668w, 650sh, 608, 550sh, 508s, 448, 421, 380w.

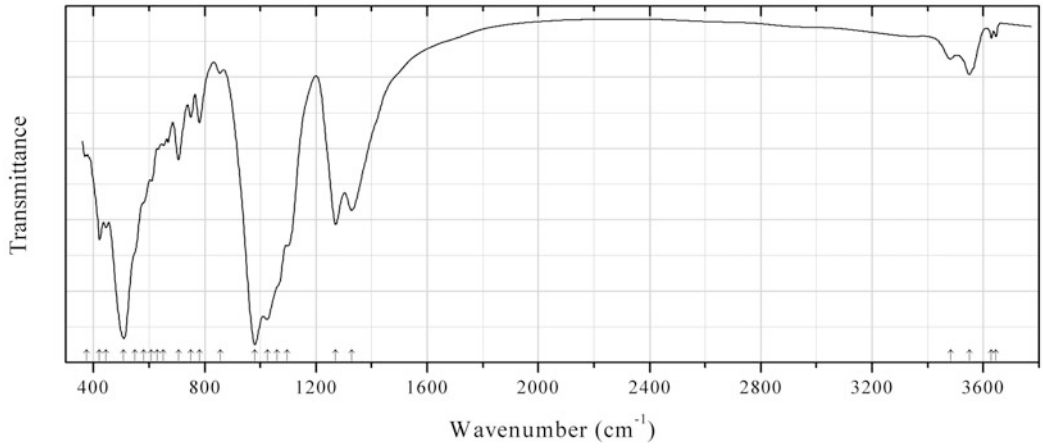

Fig. 2.731 IR spectrum of fluor-schorl obtained by N.V. Chukanov

BSi74 Fluor-schorl $NaFe^{2+}{}_3Al_6(Si_6O_{18})(BO_3)_3(OH)_3F$ (Fig. 2.731)
Locality: Lake Boga granite quarry, Victoria, Australia.
Description: Dark gray-green long-prismtic crystals.
Kind of sample preparation and/or method of registration of the spectrum: KBr disc. Absorption.
Wavenumbers (cm^{-1}): 3645w, 3628w, 3550, 3482w, 1328, 1271, 1097, 1060sh, 1025s, 980s, 856w, 781, 750w, 706, 651w, 630w, 607, 580sh, 550sh, 509s, 445, 422, 374w.

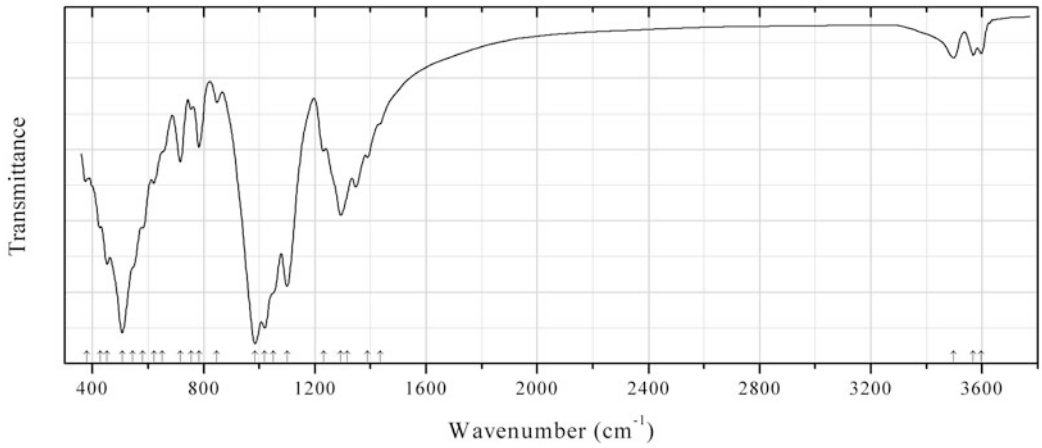

Fig. 2.732 IR spectrum of tsilaisite obtained by N.V. Chukanov

BSi75 Tsilaisite $NaMn^{2+}{}_3Al_6(Si_6O_{18})(BO_3)_3(OH)_3(OH)$ (Fig. 2.732)
Locality: Shakhdara River valley, near the former settlement Leskhoz, Khorog region, Pamir Mts., Tajikistan.
Description: Greenish-yellow crystal from the association with albite, quartz, muscovite, ixiolite, etc. The empirical formula is $Na_{0.75}(Mn_{1.3}Al_{0.9}Li_{0.8})Al_{6.0}(Si_{6.0}O_{18})(BO_3)_3(OH,O,F)_4$.

Kind of sample preparation and/or method of registration of the spectrum: KBr disc. Absorption.
Wavenumbers (cm^{-1}): 3597, 3568, 3497, 1435sh, 1390, 1317, 1293s, 1232, 1100s, 1050sh, 1020s, 985s, 848w, 783, 756w, 716, 650sh, 621, 580, 545sh, 507s, 452s, 429, 379.

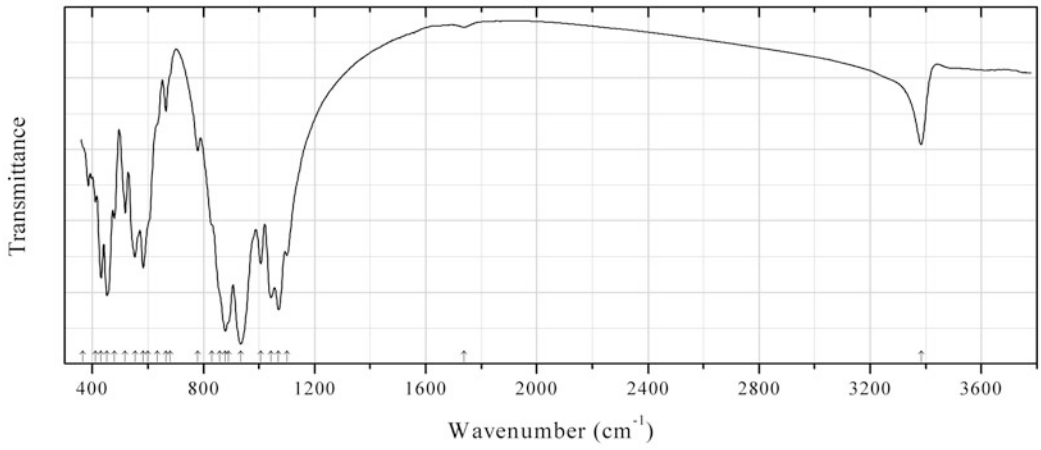

Fig. 2.733 IR spectrum of axinite-(Fe) obtained by N.V. Chukanov

BSi76 Axinite-(Fe) $Ca_2Fe^{2+}Al_2(Si_4BO_{15})(OH)$ (Fig. 2.733)
Locality: Puiva (Puyva) deposit, Subpolar Urals, Russia.
Description: Violet-brown crystal from the association with actinolite, chlorite, and quartz. The empirical formula is (electron microprobe): $Ca_{2.04}(Fe_{0.55}Mn_{0.38}Mg_{0.04})(Al_{1.89}Fe_{0.11})BSi_{4.00}O_{15}(OH)$.
Kind of sample preparation and/or method of registration of the spectrum: KBr disc. Absorption.
Wavenumbers (cm^{-1}): 3383, 1738w, 1101, 1070s, 1043s, 1006, 934s, 890sh, 878s, 860sh, 830sh, 779, 680sh, 665w, 635sh, 600sh, 583, 553, 519, 479, 453s, 431, 411, 365.

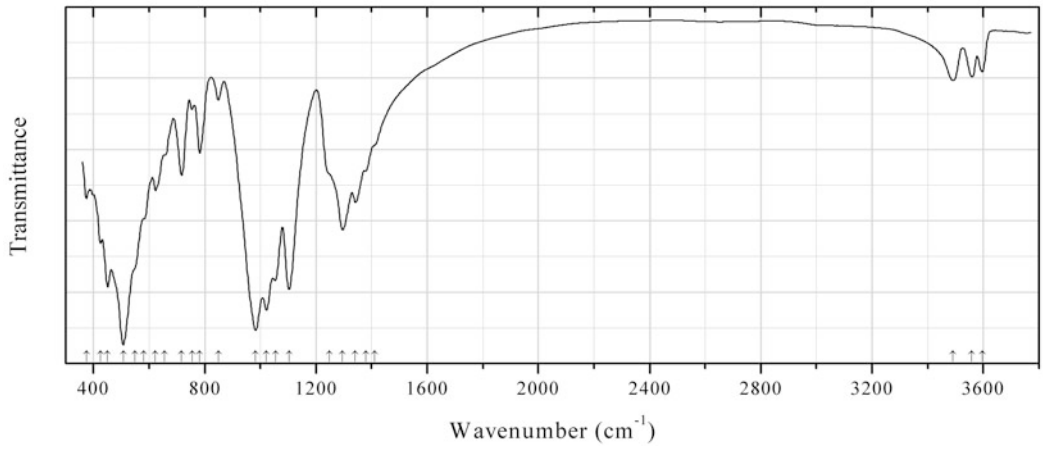

Fig. 2.734 IR spectrum of fluor-elbaite obtained by N.V. Chukanov

BSi77 Fluor-elbaite $Na(Li_{1.5}Al_{1.5})Al_6(Si_6O_{18})(BO_3)_3(OH)_3F$ (Fig. 2.734)
Locality: Ponte de Piaui, Itinga, Jequitinhonda, Minas Gerais, Brazil.

Description: Bluish-green prismtic crystal. Holotype sample. The empirical formula is $(Na_{0.79}Sr_{0.05}Ca_{0.01}K_{0.01})(Al_{0.95}Fe^{2+}_{0.79}Fe^{3+}_{0.19}Zn_{0.07}Mn_{0.06}Li_{0.94})Al_6(Si_6O_{18})(BO_3)_3(OH)_3[F_{0.71}(OH)_{0.29}]$.
Kind of sample preparation and/or method of registration of the spectrum: KBr disc. Absorption.
Wavenumbers (cm^{-1}): 3596, 3559, 3491, 1410sh, 1380sh, 1342, 1296s, 1250sh, 1103s, 1054s, 1022s, 983s, 849w, 782, 754w, 717, 655sh, 623, 580sh, 550sh, 507s, 451s, 426, 376.

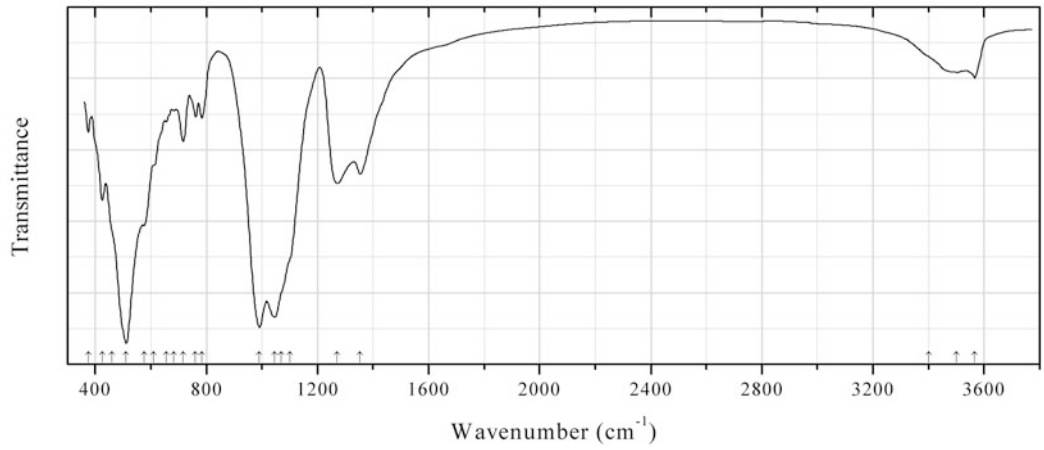

Fig. 2.735 IR spectrum of oxy-dravite obtained by N.V. Chukanov

BSi78 Oxy-dravite $Na(Al_2Mg)(Al_5Mg)(Si_6O_{18})(BO_3)_3(OH)_3O$ (Fig. 2.735)
Locality: Vico volcano, San Marino al Cimino, Latium, Italy.
Description: Gray prismatic crystals from the association with quartz and jarosite. The empirical formula is (electron microprobe): $(Na_{0.59}K_{0.01})Al_{7.26}Mg_{1.53}Fe_{0.17}Ti_{0.02}Cr_{0.01}Mn_{0.01}(Si_6O_{18})(BO_3)_3(OH)_3(O,OH)$.
Kind of sample preparation and/or method of registration of the spectrum: KBr disc. Absorption.
Wavenumbers (cm^{-1}): 3566, 3500, 3400sh, 1354, 1271, 1100sh, 1070sh, 1046s, 991s, 783, 761, 717, 682w, 655w, 611, 575, 511s, 460sh, 425, 376.

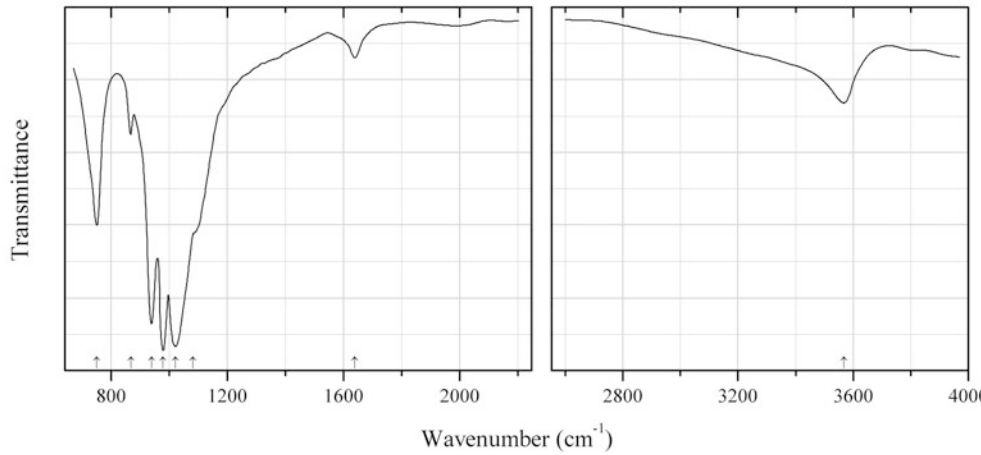

Fig. 2.736 IR spectrum of bobtraillite drawn using data from McDonald and Chao (2005)

BSi79 Bobtraillite $(Na,Ca)_{13}Sr_{11}(Zr,Y,Nb)_{14}Si_{42}B_6O_{132}(OH)_{12}\cdot 12H_2O$ (Fig. 2.736)
Locality: Poudrette quarry, Mont Saint-Hilaire, Québec, Canada (type locality).
Description: Gray to brown crystals from the association with donnayite-(Y), clinoamphibole, albite, aegirine, pyrrhotite, pyrite, annite, analcime, microcline, a white mica, titanite, clinopyroxene, and calcite. Holotype sample. Trigonal, space group *P*-3*c*1, $a = 19.720(1)$, $c = 9.9788(5)$ Å, $V = 3360.7(1)$ Å^3, $Z = 1$. $D_{calc} = 3.16$ g/cm^3. Optically uniaxial (+), $\omega = 1.627(1)$, $\varepsilon = 1.645(1)$. The empirical formula is $(Na_{11.20}Ca_{1.22})(Sr_{10.59}Ba_{0.16})(Zr_{12.69}Y_{0.63}Nb_{0.61}Hf_{0.14})Si_{41.64}B_6O_{132}(OH)_{12}\cdot 12H_2O$. The strongest lines of the powder X-ray diffraction pattern [*d*, Å (*I*, %) (*hkl*)] are: 6.46 (38) (210), 5.43 (33) (211), 3.96 (51) (212), 3.76 (49) (302), 3.13 (70) (331), 2.752 (100) (332).
Kind of sample preparation and/or method of registration of the spectrum: Low-pressure diamond-anvil microsample cell. Transmission.
Source: McDonald and Chao (2005).
Wavenumbers (cm^{-1}): 3567, 1639w, 1082, 1020s, 977s, 938s, 867, 750.
Note: The wavenumbers were determined by us based on spectral curve analysis of the published spectrum.

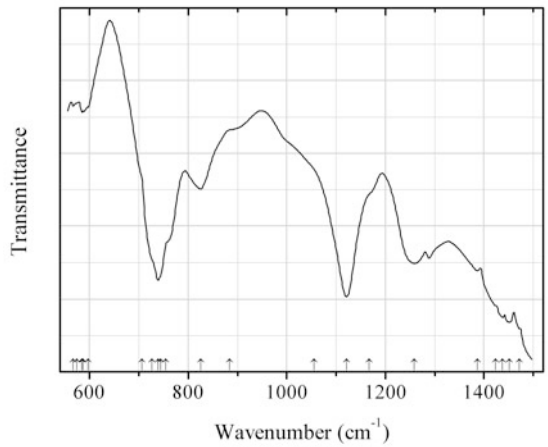

Fig. 2.737 IR spectrum of boromullite drawn using data from Lührs et al. (2012)

BSi80 Boromullite $Al_9BSi_2O_{19}$ (Fig. 2.737)
Locality: Synthetic.
Description: Synthesized from the gel containing 6.4 mol% B_2O_3, 63.9 mol% Al_2O_3, and 29.8 mol% SiO_2. Confirmed by powder X-ray diffraction data.
Kind of sample preparation and/or method of registration of the spectrum: KBr disc. Transmission.
Source: Lührs et al. (2012).
Wavenumbers (cm^{-1}): 1472sh, 1451, 1438, 1423sh, 1387, 1259, 1167sh, 1121s, 1055sh, 884sh, 825, 755sh, 744sh, 739s, 726sh, 706sh, 597sh, 587sh, 585, 574sh, 567.
Note: The wavenumbers were determined by us based on spectral curve analysis of the published spectrum. For IR spectra of synthetic low- and high-boron mullite phases see Griesser et al. (2008).

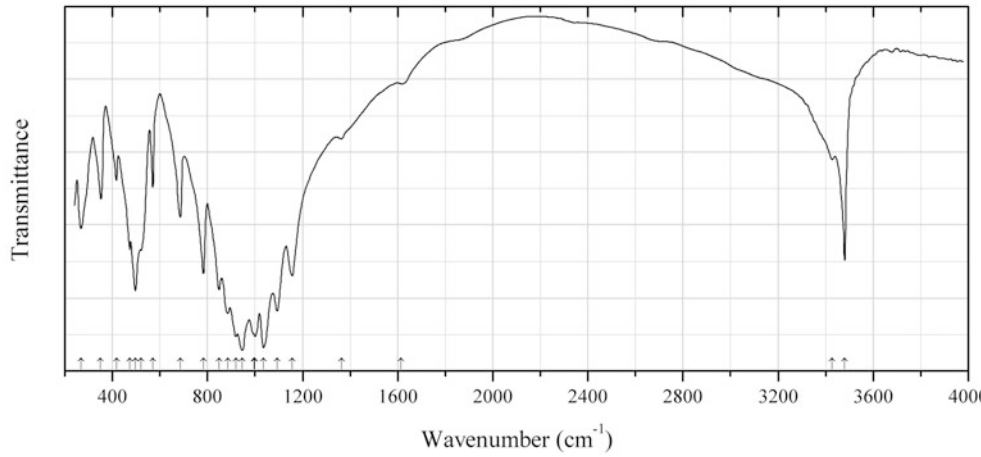

Fig. 2.738 IR spectrum of bakerite drawn using data from Kusachi et al. (1994)

BSi81 Bakerite $Ca_4B_5Si_3O_{15}(OH)_5$ (Fig. 2.738)
Locality: Fuka mine, Bicchu-cho, near Takahashi city, Okayama prefecture, Honshu Island, Japan.
Description: White aggregates forming vein in limestone together with apophyllite-(KF). Monoclinic, $a = 4.814(2)$, $b = 7.596(3)$, $c = 9.610(4)$ Å, $\beta \approx 90°$. The empirical formula calculated based on the wet chemical analysis is $Ca_{8.036}B_{9.963}Si_{6.033}O_{30.092}(OH)_{9.908}$. The strongest lines of the powder X-ray diffraction pattern [*d*, Å (*I*, %) (*hkl*)] are: 3.401 (34) (102, −102), 3.112 (100) (112, −112), 2.984 (013, 022, 120), 2.852 (78) (121, −121), 2.520 (44) (113, −113), 2.240 (43) (032, 130, 211, −211), 2.182 (38) (123, 131, −123, −131).
Kind of sample preparation and/or method of registration of the spectrum: KBr disc. Transmission.
Source: Kusachi et al. (1994).
Wavenumbers (cm^{-1}): 3480, 3427, 1615w, 1363w, 1157, 1093, 1036s, 1000s, 995sh, 947s, 920s, 885s, 849, 783, 685, 570, 521sh, 497, 473, 417, 351, 268.
Note: The wavenumbers were determined by us based on spectral curve analysis of the published spectrum.

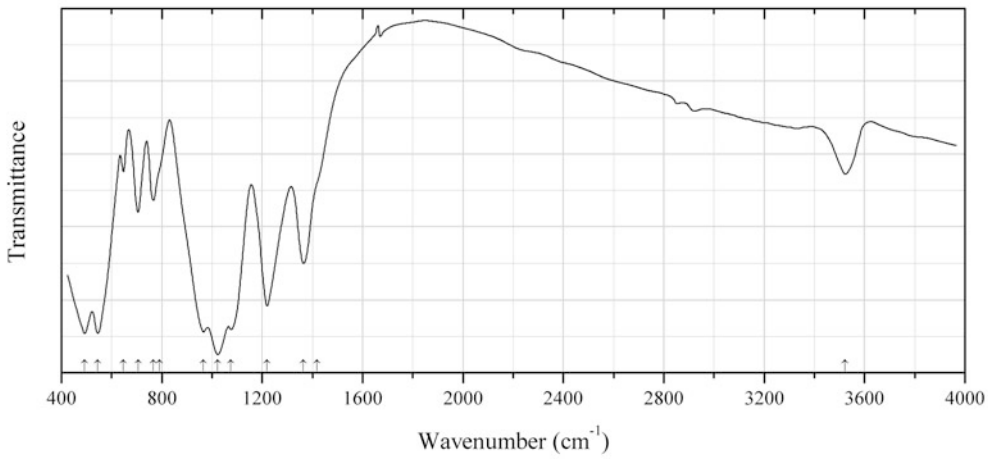

Fig. 2.739 IR spectrum of chromium-dravite drawn using data from Reznitsky et al. (2001)

BSi82 Chromium-dravite $NaMg_3Cr_6(Si_6O_{18})(BO_3)_3(OH)_3(OH)$ (Fig. 2.739)
Locality: Slyudyanka complex, Southern Lake Baikal area, Eastern Siberia, Russia.
Description: Crystals from quartz-carbonate-diopside rock, from the association with vanadium-dravite. An Al-rich, V-bearing variety. The mean ratio Cr:Al:V is 52.4:34.7:12.9 (in atomic units).
Kind of sample preparation and/or method of registration of the spectrum: KBr disc. Transmission.
Source: Reznitsky et al. (2001).
Wavenumbers (cm^{-1}): 3523, 1418sh, 1364, 1219s, 1075s, 1023s, 966s, 792sh, 765, 706, 647w, 545s, 493s.
Note: The wavenumbers were partly determined by us based on spectral curve analysis of the published spectrum. The weak bands at 2923 and 2855 cm^{-1} are due to the admixture of grease.

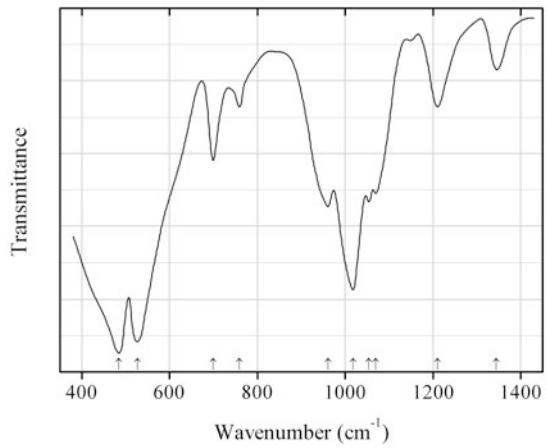

Fig. 2.740 IR spectrum of chromium-dravite obtained by N.V. Chukanov

BSi83 Chromium-dravite $NaMg_3Cr_6(Si_6O_{18})(BO_3)_3(OH)_3(OH)$ (Fig. 2.740)
Locality: Velikaya Guba U-V deposit, Zaonezhskiy peninsula, Karelia Republic, Russia (type locality).
Description: Dark green grains from the association with chromceladonite, vanadian micas, quartz, and dolomite. Holotype sample. Trigonal, *R*3*m*, a = 16.11, $b = c$ = 7.27 Å, V = 1634 $Å^3$, Z = 3. D_{meas} = 3.40 g/cm^3. Optically uniaxial (−), ω = 1.778(5), ε = 1.772(5). The empirical formula is $(Na_{0.97}Ca_{0.03})(Mg_{2.57}V_{0.22}Al_{0.16}Mn_{0.03}Ti_{0.02})(Cr_{4.71}Fe^{3+}_{1.08}Al_{0.21})[(B_{0.97}Al_{0.03})O_3][(Si_{5.81}Al_{0.19})O_{18}][(OH)_{3.77}O_{0.23}]$. The strongest lines of the powder X-ray diffraction pattern [*d*, Å (*I*, %) (*hkl*)] are: 6.57 (50), 4.31 (40), 4.05 (50), 3.58 (75), 3.04 (75), 2.62 (100), 2.079 (50).
Kind of sample preparation and/or method of registration of the spectrum: KBr disc. Absorption.
Wavenumbers (cm^{-1}): 1345, 1211, 1070s, 1054s, 1018s, 961, 759w, 699, 526s, 484s.

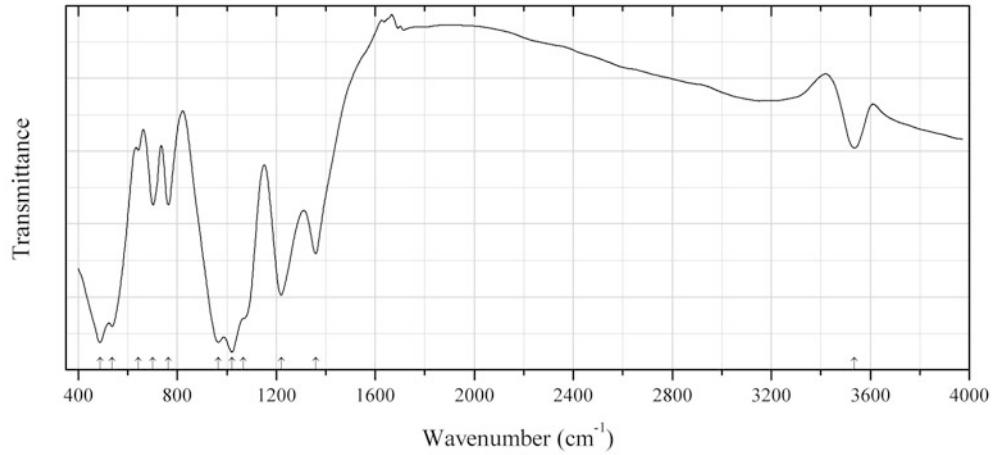

Fig. 2.741 IR spectrum of oxy-vanadium-dravite drawn using data from Reznitsky et al. (2001)

BSi84 Oxy-vanadium-dravite $NaV_3(V_4Mg_2)(Si_6O_{18})(BO_3)_3(OH)_3O$ (Fig. 2.741)
Locality: Slyudyanka complex, Southern Lake Baikal area, Eastern Siberia, Russia (type locality).
Description: Dark green prismatic crystals from the association with quartz, calcite, diopside, tremolite, Cr-bearing micas, garnets, and spinels, minerals of the series escolaite-karelianite and kosmochlor-natalyite, V-bearing titanite, anatase, etc. Holotype sample. Trigonal, space group *R*3*m*, a = 16.12(1), c = 7.39(1) Å, V = 1662(3) Å^3, Z = 3. D_{meas} = 3.32(2) g/cm^3, D_{calc} = 3.35 g/cm^3. Optically biaxial (−), ω = 1.786(5), ε = 1.729(4). The averaged empirical formula is $(Na_{0.94}K_{0.08}Ca_{0.01})(V_{5.17}Mg_{2.12}Al_{0.90}Cr_{0.60}Fe_{0.16}Ti_{0.05})(Si_{5.91}Al_{0.09})B_3O_{27}(OH)_3[O_{0.71}(OH)_{0.15}F_{0.14}]$. The strongest lines of the powder X-ray diffraction pattern [d, Å (I, %) (*hkl*)] are: 6.53 (90) (10–11), 4.03 (80) (22–40), 3.57 (70) (01–12), 3.05 (90) (41–50), 2.61 (100) (05–51), 2.07 (90) (15–62).
Kind of sample preparation and/or method of registration of the spectrum: KBr disc. Transmission.
Source: Reznitsky et al. (2001).
Wavenumbers (cm^{-1}): 3536, 1359, 1220s, 1068sh, 1021s, 966s, 764, 702, 644w, 537s, 488s.

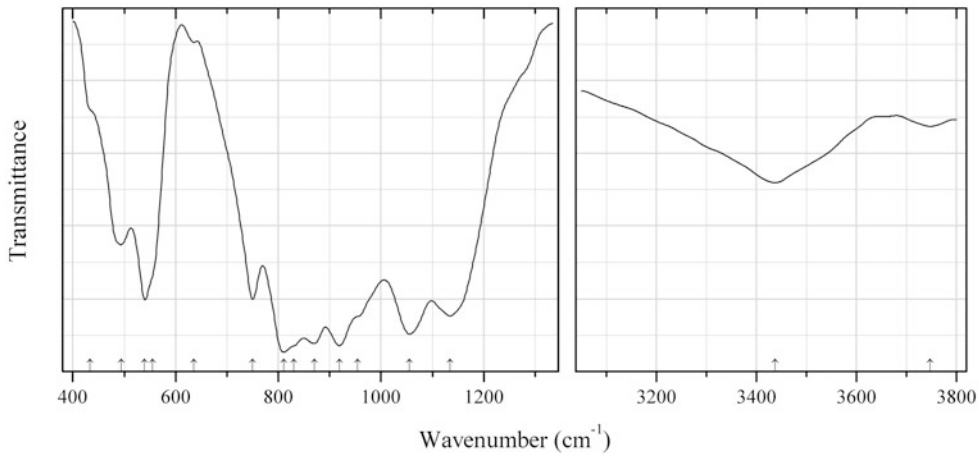

Fig. 2.742 IR spectrum of homilite drawn using data from Ito and Hafner (1974)

BSi85 Homilite $Ca_2Fe^{2+}B_2Si_2O_{10}$ (Fig. 2.742)
Locality: Langesundsfjorden, Larvik, Vestfold, Norway (type locality).
Description: Specimen No. 89603 from the Harvard University Mineralogical Museum. The specimen contains a significant amount of beryllium oxide and yttria earths.
Kind of sample preparation and/or method of registration of the spectrum: KBr disc. Transmission.
Source: Ito and Hafner (1974).
Wavenumbers (cm^{-1}): 3748, 3437, 1134, 1055s, 955sh, 919s, 871s, 830sh, 811s, 750, 635w, 555sh, 540s, 494, 434sh.
Note: The wavenumbers were determined by us based on spectral curve analysis of the published spectrum.

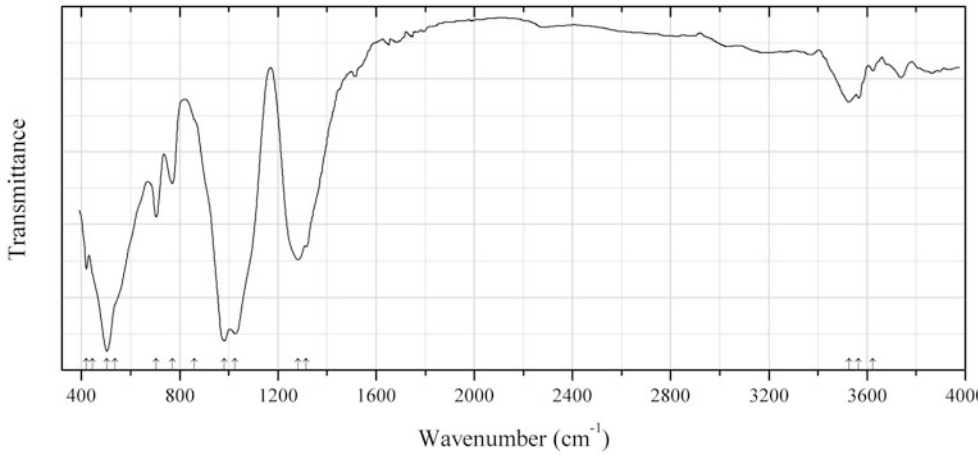

Fig. 2.743 IR spectrum of adachiite drawn using data from Nishio-Hamane et al. (2014)

BSi86 Adachiite $CaFe_3Al_6(Si_5AlO_{18})(BO_3)_3(OH)_3(OH)$ (Fig. 2.743)
Locality: Kiura mine, Saiki City, Oita Prefecture, Japan (type locality).
Description: Purple hexagonal prismatic crystals from the association with margarite, chlorite, and diaspore. Holotype sample. Trigonal, space group $R3m$, a = 15.9290(2), c = 7.1830(1) Å, V = 1578.39(4) $Å^3$, Z = 3. D_{calc} = 3.228 g/cm^3. Optically uniaxial (−), ω = 1.674 (2), ε = 1.644 (2). The empirical formula is $(Ca_{0.62}Na_{0.28}\square_{0.10})(Fe_{1.58}Al_{0.81}Mg_{0.55}Ti_{0.06})(Al_{5.81}Fe_{0.14}Mg_{0.05})(Si_{5.15}Al_{0.85}O_{18})$ $B_{3.01}O_9(OH)_3[(OH)_{0.56}O_{0.44}]$. The strongest lines of the powder X-ray diffraction pattern [d, Å (I, %) (hkl)] are: 4.9602 (34) (021), 4.2254 (40) (211), 4.0022 (65) (220), 3.4553 (34) (012), 2.9503 (31) (122), 2.9027 (33) (321), 2.5842 (100) (051), 2.0428 (52) (223, 152).
Kind of sample preparation and/or method of registration of the spectrum: KBr disc. Transmission.
Source: Nishio-Hamane et al. (2014).
Wavenumbers (cm^{-1}): 3623w, 3566, 3526, 1315sh, 1281s, 1026s, 982s, 860sh, 770, 705, 537sh, 503s, 444sh, 420.
Note: The wavenumbers were partly determined by us based on spectral curve analysis of the published spectrum.

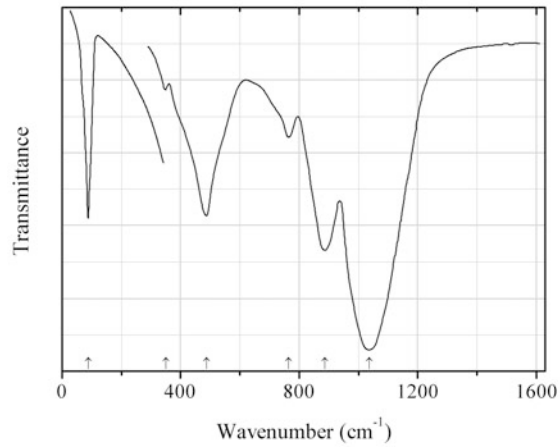

Fig. 2.744 IR spectrum of kirchhoffite drawn using data from Rulmont and Tarte (1987)

BSi87 Kirchhoffite $CsBSi_2O_6$ (Fig. 2.744)
Locality: Synthetic.
Description: Synthesized by a solid-state reaction technique. Confirmed by powder X-ray diffraction data.
Kind of sample preparation and/or method of registration of the spectrum: KBr disc (in the range from 250 to 1500 cm^{-1}) and polyethylene disc (in the range from 20 to 350 cm^{-1}). Transmission.
Source: Rulmont and Tarte (1987).
Wavenumbers (cm^{-1}): 1037s, 886, 765, 487, 350w, 88.

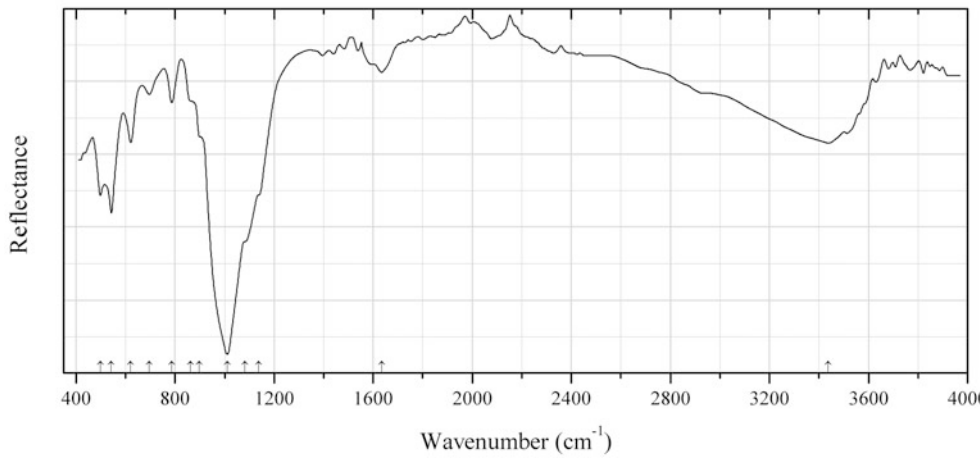

Fig. 2.745 IR spectrum of martinite drawn using data from McDonald and Chao (2007)

BSi88 Martinite $(Na,□,Ca)_{12}Ca_4(Si,S,B)_{14}B_2O_{38}(OH,Cl)_2F_2·4H_2O$ (Fig. 2.745)
Locality: Poudrette (Demix) quarry, Mont Saint-Hilaire, Rouville RCM (Rouville Co.), Montérégie, Québec, Canada (type locality).
Description: Aggregates of platy crystals from the association with aegirine, albite, erdite, eudialyte-group minerals, galena, langite, lueshite, lovozerite-group minerals, molybdenite, posnjakite, rasvumite, sérandite, sazhinite-(Ce), ussingite, villiaumite, etc. Holotype sample. Triclinic,

space group *P*-1, a = 9.5437(7), b = 9.5349(6), c = 14.0268(10) Å, α = 108.943(1)°, β = 74.154(1)°, γ = 119.780(1)°, V = 1038.1(1) Å^3, Z = 2. D_{calc} = 2.51 g/cm^3. Optically biaxial (−), α = 1.529(1), β = 1.549(1), γ = 1.551(1), 2 V = 38(1)°. The empirical formula is $(Na_{9.19}Ca_{0.82})(Ca_{3.97}Mn_{0.02}Mg_{0.01})(Si_{13.08}S_{0.46}B_{0.45}Ti_{0.01})B_2O_{38})[(OH)_{1.50}Cl_{0.50}][F_{1.84}(OH)_{0.16}]\cdot 4H_2O$. The strongest lines of the powder X-ray diffraction pattern [*d*, Å (*I*, %) (*hkl*)] are: 13.18 (100) (001), 6.58 (43) (002), 2.968 (37) (1–30), 3.29 (34) (004, −220), 2.908 (27) (3–23), 3.02 (17) (−2–11), 2.800 (17) (−212).

Kind of sample preparation and/or method of registration of the spectrum: Attenuated total reflection of a single crystal. The orientation of the crystal is not indicated.

Source: McDonald and Chao (2007).

Wavenumbers (cm^{-1}): 3437, 1634w, 1137sh, 1081sh, 1011s, 898sh, 862sh, 786, 696w, 621, 543, 498.

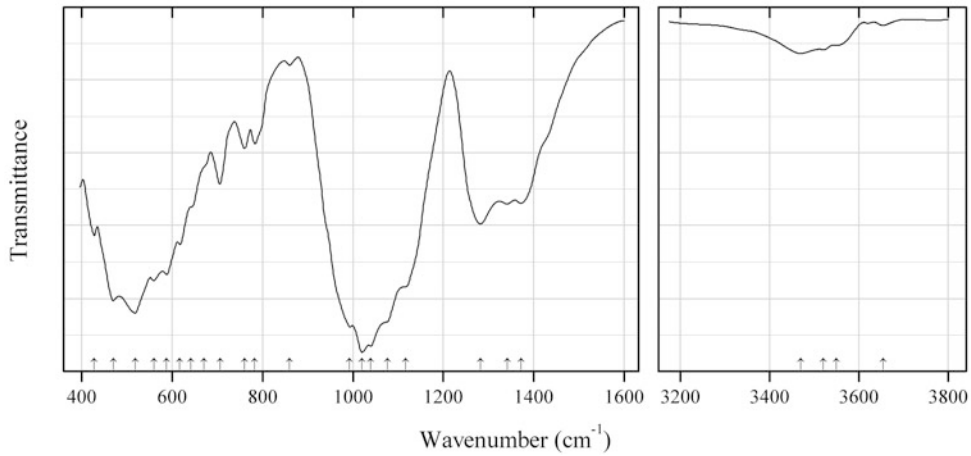

Fig. 2.746 IR spectrum of oxy-magnesio-foitite drawn using data from Osipov and Stolpovskaya (1991)

BSi89 Oxy-magnesio-foitite $\square(Mg,Al,Cr)_3Al_6(Si_6O_{18})(BO_3)_3(OH)_3(O,OH)$ (Fig. 2.746)

Locality: Sarykulboldy chrisoprase deposit, Karkaralinsk district, Karagandy region, Kazakhstan.

Description: Green acicular crystals from a quartz vein, from the association with talc. Optically uniaxial (−), ω = 1.634, ε = 1.610. The empirical formula is $(Na_{0.24}Ca_{0.01})(Mg_{1.72}Al_{0.79}Cr_{0.48}Fe^{2+}_{0.01})Al_{6.00}B_{3.00}(Si_{5.87}Al_{0.13})_{6.00}O_{27.00}(OH)_3[O_{0.64}(OH)_{0.36}]$. The strongest lines of the powder X-ray diffraction pattern [*d*, Å (*I*, %)] are: 4.60 (10), 4.22 (11), 3.98 (100), 3.46 (90), 3.12 (14), 2.950 (9).

Kind of sample preparation and/or method of registration of the spectrum: KBr disc. Transmission.

Source: Osipov and Stolpovskaya (1991).

Wavenumbers (cm^{-1}): 3654w, 3550, 3520, 3470, 1372, 1342, 1282, 1117sh, 1076sh, 1040s, 1020s, 992s, 860w, 782, 760, 706, 670sh, 641, 617, 588, 560s, 519s, 470s, 428.

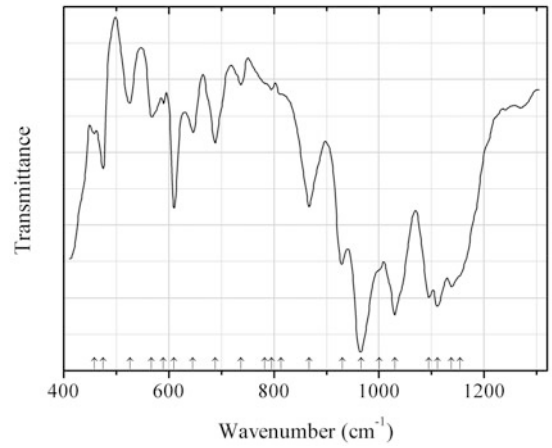

Fig. 2.747 IR spectrum of pekovite drawn using data from Pautov et al. (2004)

BSi90 Pekovite $Sr(B_2Si_2O_8)$ (Fig. 2.747)
Locality: Dara-i Pioz glacier, Dara-i Pioz alkaline massif, Tien Shan Mts., Tajikistan (type locality).
Description: Colourless grains from a pegmatitic rock consisting mainly of quartz with subordinate pectolite, aegirine, stillwellite-(Ce), polylithionite, leucosphenite, and reedmergnerite. Holotype sample. Orthorhombic, space group *Pnma*, $a = 8.155(2)$, $b = 7.919(1)$, $c = 8.921(2)$ Å, $V = 576.1(2)$ Å^3, $Z = 4$. $D_{meas} = 3.35(2)$ g/cm^3, $D_{calc} = 3.36$ g/cm^3. Optically biaxial (−), $\alpha = 1.597(2)$, $\beta = 1.627(3)$, $\gamma = 1.632(2)$, $2V = 43(3)°$. The empirical formula is $(Sr_{0.97}Ca_{0.02})B_{1.97}Si_{2.02}O_8$. The strongest lines of the powder X-ray diffraction pattern [*d*, Å (*I*, %) (*hkl*)] are: 3.62 (10) (210), 3.51 (9) (112), 2.786 (9) (103, 013, 122), 3.31 (8) (121), 1.982 (7) (232), 5.94 (6) (011), 3.01 (6) (202).
Kind of sample preparation and/or method of registration of the spectrum: KBr disc. Transmission.
Source: Pautov et al. (2004).
Wavenumbers (cm^{-1}): 1154sh, 1138, 1111s, 1095s, 1030s, 1001sh, 966s, 930, 867, 813sh, 796w, 783sh, 737w, 688, 645, 610, 590, 567, 526, 475, 458.
Note: The wavenumbers were partly determined by us based on spectral curve analysis of the published spectrum.

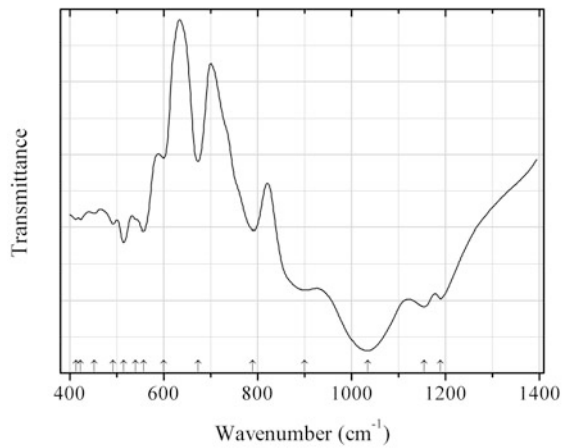

Fig. 2.748 IR spectrum of reedmergnerite K-analogue drawn using data from Mitsuyosi (1993)

BSi91 Reedmergnerite K-analogue $K(BSi_3O_8)$ (Fig. 2.748)
Locality: Synthetic.
Description: A K-analogue of reedmergnerite by the composition, structurally related to danburite. Synthesized from a stoichiometric mixture of K_2CO_3, H_3BO_3, and SiO_2 gel under hydrothermal conditions. Orthorhombic, space group *Pnam*, $a = 8.683(1)$, $b = 9.253(1)$, $c = 8.272(1)$ Å, $V = 664.4(1)$ Å^3, $Z = 4$. The crystal-chemical formula is of $K(B_{0.44}Si_{0.56})_2(B_{0.06}Si_{0.94})_2O_8$.
Kind of sample preparation and/or method of registration of the spectrum: KBr disc. Transmission.
Source: Mitsuyosi (1993).
Wavenumbers (cm^{-1}): 1190s, 1155s, 1035s, 900s, 790, 673, 600, 557, 540sh, 515, 492, 452, 423, 413.

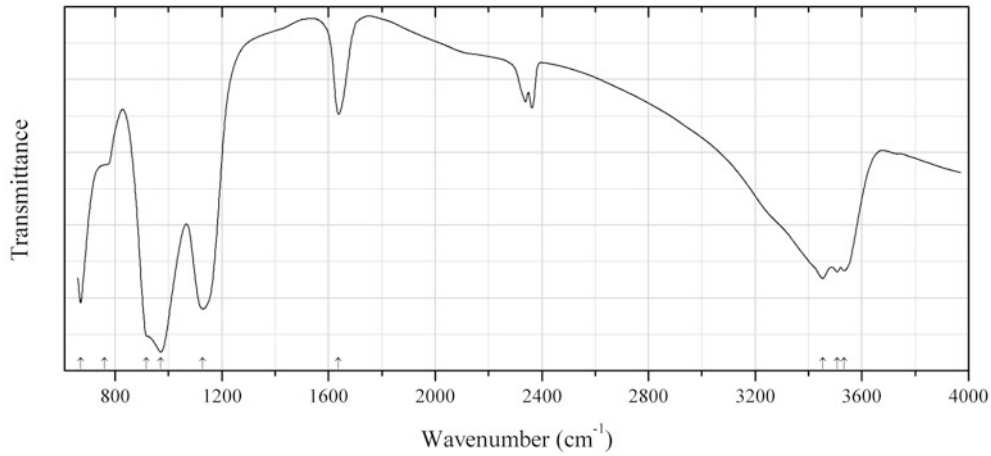

Fig. 2.749 IR spectrum of rogermitchellite drawn using data from McDonald and Chao (2010)

BSi92 Rogermitchellite $Na_6(Sr,Na)_{12}Ba_2Zr_{13}(Si,B)_{39}B_6O_{123}(OH)_{12}\cdot 9H_2O$ (Fig. 2.749)
Locality: Poudrette (Demix) quarry, Mont Saint-Hilaire, Rouville RCM (Rouville Co.), Montérégie, Québec, Canada (type locality).
Description: Colourless to grey, prismatic crystals from the association with aegirine, annite, galena, a labuntsovite-group mineral, manganoneptunite, microcline, pyrrhotite, sodalite, and zircon. Holotype sample. The crystal structure is solved. Trigonal, space group *P*-3*c*1, $a = 26.509(4)$, $c = 9.975(2)$ Å, $V = 6070.6(1)$ Å^3, $Z = 2$. $D_{calc} = 3.34$ g/cm^3. Optically uniaxial (+), $\omega = 1.640(1)$, $\varepsilon = 1.663(1)$. The empirical formula is ($Z = 1$): $Na_{12}(Sr_{21.16}Na_{1.17}Ca_{0.21})Ba_{4.00}(Zr_{25.33}Ti_{0.93})(Si_{77.02}B_{0.98})B_{12.00}O_{246}(OH)_{24}\cdot 18H_2O$. The strongest lines of the powder X-ray diffraction pattern [*d*, Å (*I*, %) (*hkl*)] are: 2.760 (100) (442), 3.761 (90) (402), 1.991 (70) (444), 3.150 (50) (441), 5.762 (40) (400), 3.924 (30) (312).
Kind of sample preparation and/or method of registration of the spectrum: A single crystal was mounted in a Spectra-Tech low-pressure diamond-anvil microsample cell. Transmission.
Source: McDonald and Chao (2010).
Wavenumbers (cm^{-1}): 3533, 3508, 3453, 1638, 1129s, 971s, 918sh, 761sh, 670.
Note: The wavenumbers were partly determined by us based on spectral curve analysis of the published spectrum. A doublet between 2300 and 2400 cm^{-1} is due to atmospheric CO_2.

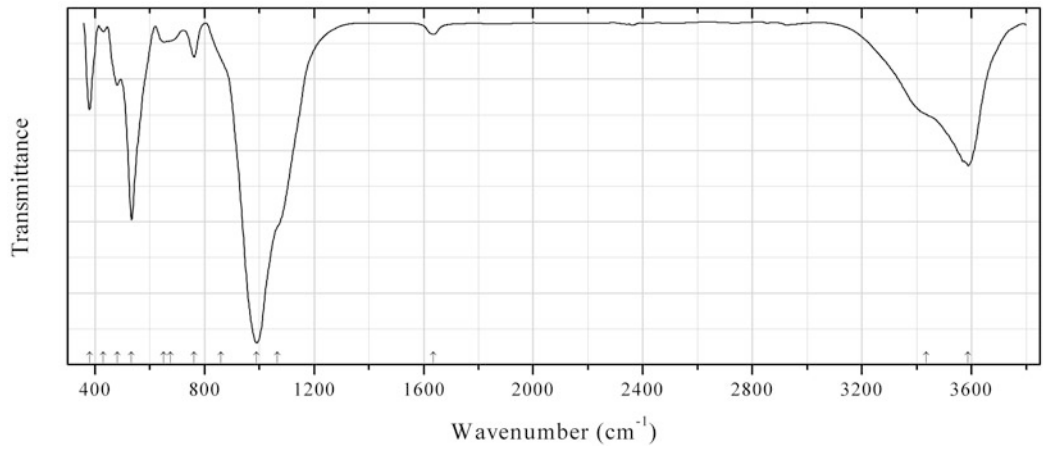

Fig. 2.750 IR spectrum of borocookeite obtained by N.V. Chukanov

BSi93 Borocookeite $LiAl_4(Si_3B)O_{10}(OH)_8$ (Fig. 2.750)
Locality: Mokhovaya pegmatite vein, Malkhan gem tourmaline deposit, Chikoy district, Chita region, Russia (type locality).
Description: Beige spherulitic crust. The associated minerals are elbaite, potassium feldspar and muscovite.
Kind of sample preparation and/or method of registration of the spectrum: KBr disc. Absorption.
Wavenumbers (cm^{-1}): 3588, 3435sh, (1636w), 1065sh, 991s, 860sh, 762, 675sh, 652w, 534s, 481, 431w, 380.
Note: For the IR spectrum of borocookeite see also Zagorsky et al. (2003).

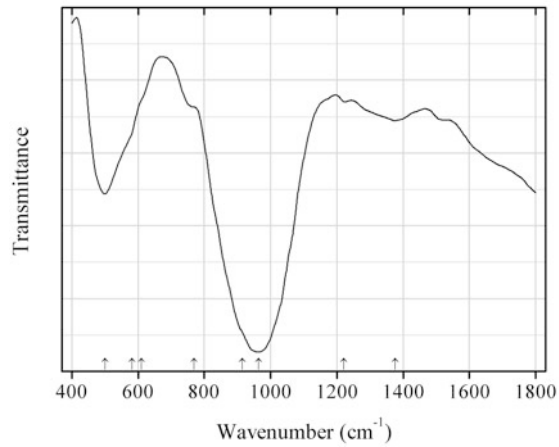

Fig. 2.751 IR spectrum of tritomite-(Ce) drawn using data from Hogarth et al. (1973)

BSi94 Tritomite-(Ce) $Ce_5(SiO_4,BO_4)_3(OH,O)$ (Fig. 2.751)
Locality: Låven, Langesundsfjord district, Larvik, Vestfold, Norway (type locality).
Description: Red brown, massive. D_{meas} = 4.20 g/cm^3. Mean refractive index is 1.763. Characterized by chemical composition.

Kind of sample preparation and/or method of registration of the spectrum: Transmission. Kind of sample preparation is not indicated.
Source: Hogarth et al. (1973).
Wavenumbers (cm^{-1}): 1377w, 1221w, 963s, 914sh, 769sh, 611sh, 582sh, 501.
Note: The wavenumbers were determined by us based on spectral curve analysis of the published spectrum.

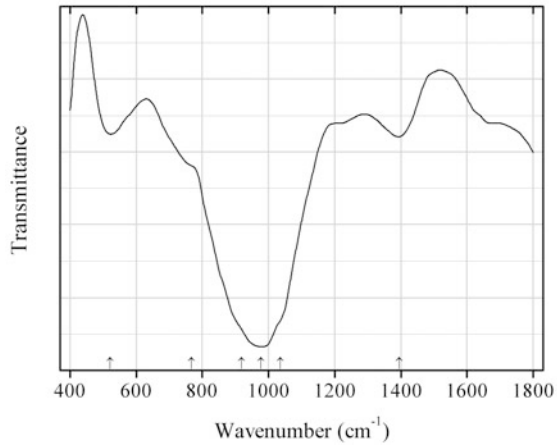

Fig. 2.752 IR spectrum of tritomite-(Y) drawn using data from Hogarth et al. (1973)

BSi95 Tritomite-(Y) ("Spencite") $Y_5(SiO_4,BO_4)_3(OH,O)$ (Fig. 2.752)
Locality: Madawaska mine (Faraday mine), Faraday township, Hastings Co., Ontario, Canada.
Description: Blackish brown massive from pegmatite. Amorphous, metamict. Recrystallizes after heating in air for 2 h at 900 °C. Annealed sample is characterized by chemical composition and by powder X-ray diffraction data for annealed sample. D_{meas} = 3.39 g/cm^3. Mean refractive index is 1.678.
Kind of sample preparation and/or method of registration of the spectrum: Transmission. Kind of sample preparation is not indicated.
Source: Hogarth et al. (1973).
Wavenumbers (cm^{-1}): 1395, 1036sh, 978s, 918sh, 768sh, 522.
Note: The wavenumbers were determined by us based on spectral curve analysis of the published spectrum.

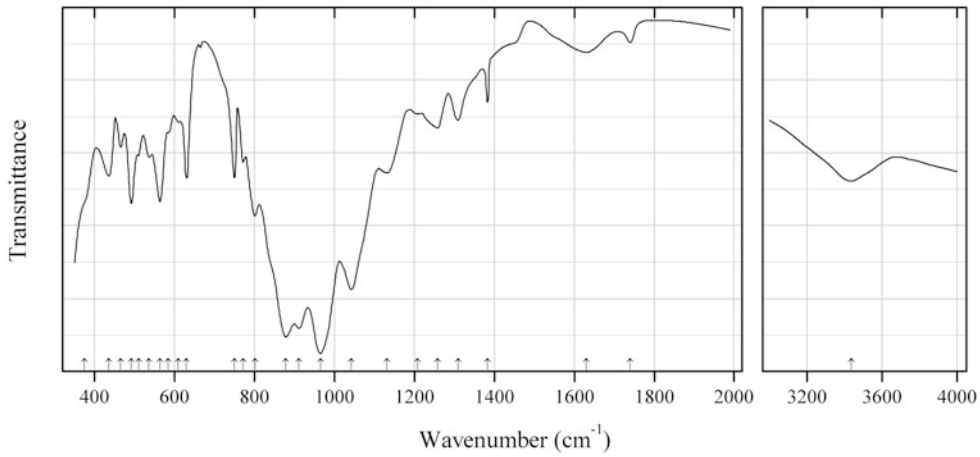

Fig. 2.753 IR spectrum of vicanite-(Ce) drawn using data from Maras et al. (1995)

BSi96 Vicanite-(Ce) $(Ca,REE,Th)_{15}Fe^{3+}(SiO_4)_3(Si_3B_3O_{18})(BO_3)(AsO_4)(AsO_3)_x(NaF_3)_{1-x}F_7 \cdot 0.2H_2O$ ($x \approx 0.4$) (Fig. 2.753)

Locality: Tre Croci, Vico volcanic complex, Vetralla, Viterbo province, Italy (type locality).

Description: Yellowish green euhedral crystals from the association with zircon, thorite, thorian uraninite, betafite, thorian hellandite, titanite, antimonian asbecasite, apatite, stillwellite-(Ce), etc. Holotype sample. Trigonal, space group $R3m$, a = 10.795(1), c = 27.336(4) Å, Z = 3. Optically uniaxial (−), ε = 1.722(2), ω = 1.757(2). The strongest lines of the powder X-ray diffraction pattern [d, Å (I, %) (hkl)] are: 7.70 (50) (012), 4.42 (50) (202), 3.13 (50) (214), 2.993 (100) (027), 2.950 (70) (303), 2.698 (50) (220), 1.839 (50) (3.0.12), 1.802 (50) (2.0.14).

Kind of sample preparation and/or method of registration of the spectrum: KBr disc. Transmission.

Source: Maras et al. (1995).

Wavenumbers (cm^{-1}): 3435, 1740w, 1631w, 1383, 1309, 1258, 1208, 1131, 1043s, 966s, 911s, 878s, 802, 772, 750, 630, 610, 585, 564, 536, 510, 492, 466, 436, 375sh.

Note: The wavenumbers were partly determined by us based on spectral curve analysis of the published spectrum. Narrow band between 1350 and 1400 cm^{-1} corresponds to the admixture of potassium nitrate in the KBr disc.

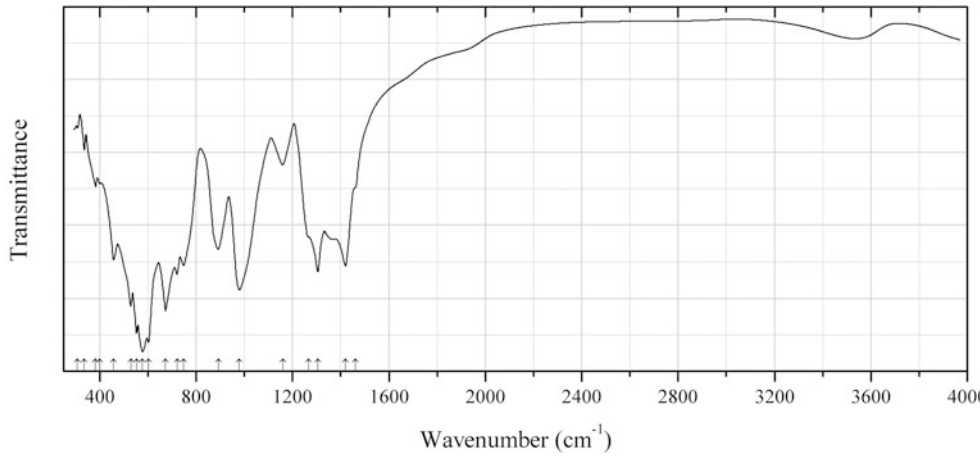

Fig. 2.754 IR spectrum of werdingite drawn using data from Werding and Schreyer (1992)

BSi97 Werdingite $Mg_2Al_{14}Si_4B_2O_{37}$ (Fig. 2.754)
Locality: Synthetic.
Description: Synthesized at 800–875 °C employing dried B_2O_3 and a fired gel of the MgAl-silicate composition. Characterized by powder X-ray diffraction data. Triclinic, a = 7.993(3), b = 8.150(2), c = 11.388(4) Å, α = 110.45(2)°, β = 110.88(2)°, γ = 84.62(2)°.
Kind of sample preparation and/or method of registration of the spectrum: RbI disc. Transmission.
Source: Werding and Schreyer (1992).
Wavenumbers (cm^{-1}): 1460sh, 1420s, 1305s, 1267sh, 1159w, 980s, 892, 748, 721, 673s, 602s, 578s, 553s, 529s, 458, 400w, 383w, 336w, 308w.
Note: The wavenumbers were partly determined by us based on spectral curve analysis of the published spectrum.

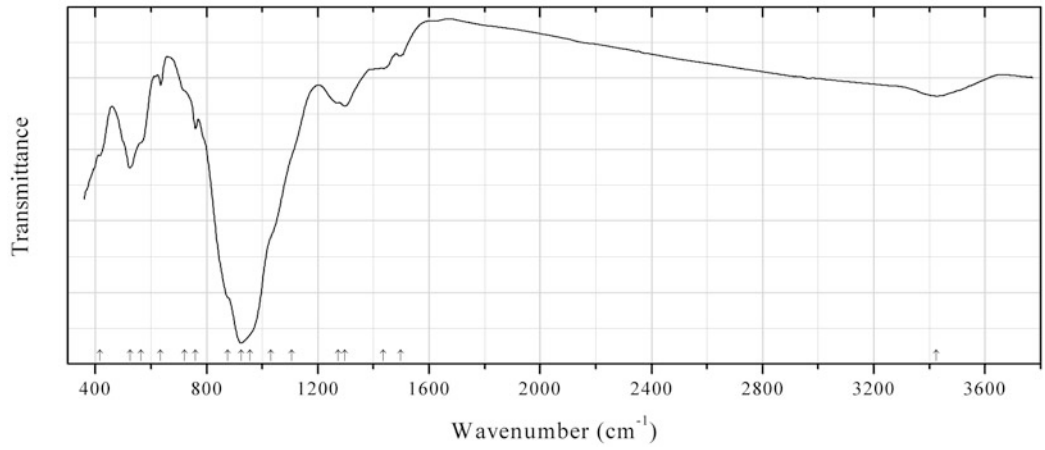

Fig. 2.755 IR spectrum of laptevite-(Ce) obtained by N.V. Chukanov

BSi98 Laptevite-(Ce) $NaFe^{2+}(REE_7Ca_5Y_3)(SiO_4)_4(Si_3B_2PO_{18})(BO_3)F_{11}$ (Fig. 2.755)
Locality: Dara-i Pioz glacier, Dara-i Pioz alkaline massif, Tien Shan Mts., Tajikistan (type locality).

Description: Brown grains from the association with calcite, bafertisite, microcline, aegirine, polylithionite, stillwellite-(Ce), etc. Confirmed by the IR spectrum and qualitative electron microprobe analyses.
Kind of sample preparation and/or method of registration of the spectrum: KBr disc. Absorption.
Wavenumbers (cm^{-1}): 3425, 1498w, 1435w, 1297, 1272, 1105sh, 1030sh, 955sh, 924s, 875sh, 760, 720sh, 635w, 565sh, 525, (416).
Note: The band at 1435 cm^{-1} may correspond to inclusions of a carbonate. The band at 3425 cm^{-1} and the absence of absorption bands in the range from 1500 to 1700 cm^{-1} indicate the presence of OH groups and the absence of H_2O molecules. In the IR spectrum of laptevite–(Ce) given in its first description (Agakhanov et al. 2013) the range above 2000 cm^{-1} is not presented; the sample used in the cited paper is strongly contaminated by carbonate (the band at 1437 cm^{-1}) and contains adsorbed water (the band at 1623 cm^{-1}).

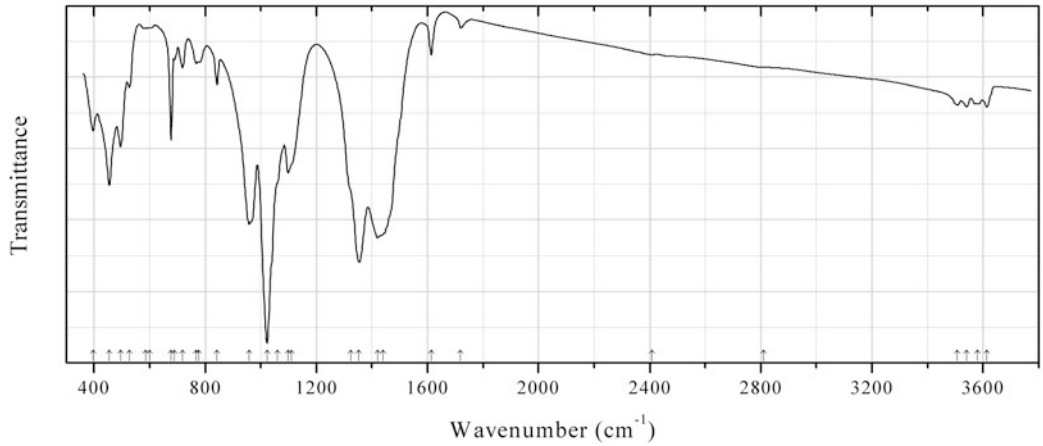

Fig. 2.756 IR spectrum of plumbotsumite obtained by N.V. Chukanov

CSi23 Plumbotsumite $Pb_{13}(Si_{10}O_{27})(CO_3)_6 \cdot 3H_2O$ (Fig. 2.756)
Locality: Blue Bell mine (Hard Luck mine), Baker, Soda Lake Mts., San Bernardino Co., California, USA.
Description: Veinlet consisting of blue platelets. The empirical formula is (electron microprobe, CO_3 calculated): $Pb_{13.15}Si_{9.7}Fe_{0.2}Al_{0.1}O_{27}(CO_3)_6 \cdot nH_2O$.
Kind of sample preparation and/or method of registration of the spectrum: KBr disc. Absorption.
Wavenumbers (cm^{-1}): 3613w, 3579w, 3541w, 3508w, 2810w, 2408w, 1719w, 1614, 1440sh, 1420s, 1354s, 1325sh, 1110sh, 1099s, 1060sh, 1023s, 958s, 843, 777, 768, 718, 690w, 677, 600w, 585w, 527, 495, 455s, 397.

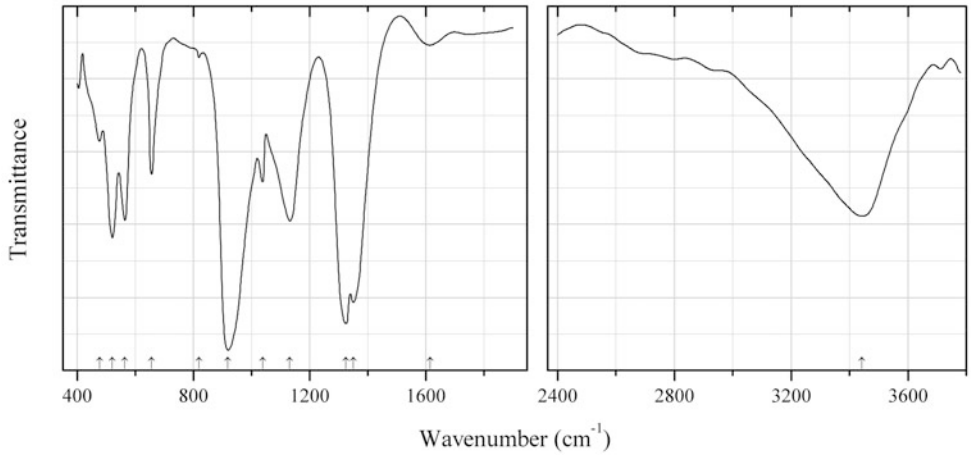

Fig. 2.757 IR spectrum of ashburtonite drawn using data from Grice et al. (1991)

CSi24 Ashburtonite $HCu_4Pb_4Si_4O_{12}(HCO_3)_4(OH)_4Cl$ (Fig. 2.757)
Locality: Anticline prospect at Ashburton Downs, Capricorn Range, about 1000 km north of Perth, Western Australia (type locality).
Description: Blue prismatic crystals from the association with diaboleite, duftite, beudantite, caledonite, plattnerite, cerussite, malachite, and brochantite. Holotype sample. The crystal structure is solved. Tetragonal, space group $I4/m$, a = 14.234(7), c = 6.103(5) Å, Z = 2. D_{calc} = 4.69 g/cm^3. Optically uniaxial (+), ω = 1.786(3), ε = 1.800(4). The strongest lines of the powder X-ray diffraction pattern [d, Å (I, %) (hkl)] are: 10.2 (100) (110), 5.644 (70) (101), 4.495 (100) (310), 3.333 (100) (321), 3.013 (90) (411), 2.805 (300) (202), 2.611 (50) (222), 2.010 (30) (710, 103, 631), 1.656 (30) (642, 503).
Kind of sample preparation and/or method of registration of the spectrum: Diamond anvil cell microsampling. Transmission.
Source: Grice et al. (1991).
Wavenumbers (cm^{-1}): 3443, 1614w, 1350s, 1325s, 1132, 1038, 918s, 820w, 656, 564, 521, 477.
Note: The wavenumbers were partly determined by us based on spectral curve analysis of the published spectrum. Typical bands of bicarbonate anion are not observed in the IR spectrum. The distances C–O are from 1.24 to 1.27 Å. The band at 1614 cm^{-1} indicates the presence of H_2O molecules. The bond-valence sum on the O5 atom belonging to the carbonate group is equal to 1.58, which may correspond to a strong hydrogen bond, but not to the group C–OH.

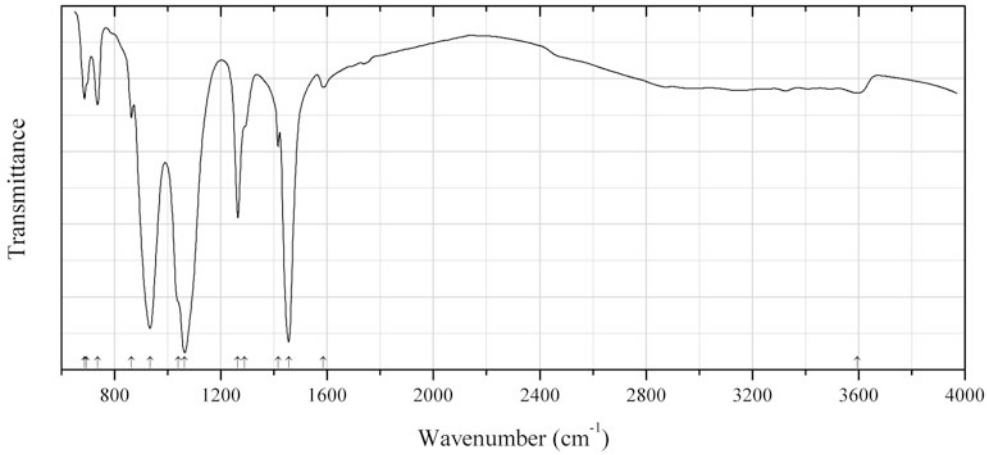

Fig. 2.758 IR spectrum of fencooperite drawn using data from Roberts et al. (2001a)

CSi25 Fencooperite $Ba_6Fe^{3+}{}_3Si_8O_{23}(CO_3)_2Cl_3{\cdot}H_2O$ (Fig. 2.758)
Locality: Trumbull Peak, Mariposa Co., California, USA (type locality).
Description: Black grains from the association with alforsite, barite, celsian, gillespite, quartz, pyrrhotite, and sanbornite. Holotype sample. Trigonal, space group $P3m1$, $a = 10.727(5)$, $c = 7085(3)$ Å, $V = 706.1(5)$ Å^3, $Z = 1$. $D_{calc} = 4.212$ g/cm^3. Optically uniaxial (−), $\omega = 1.723(4)$, $\varepsilon = 1.711(2)$. The empirical formula is $Ba_{5.89}(Fe^{3+}{}_{2.86}Al_{0.47}Mn_{0.04})(Si_{8.14}P_{0.04})O_{23.18}(CO_3)_{1.95}(Cl_{1.63}O_{1.37}){\cdot}0.97H_2O$. The strongest lines of the powder X-ray diffraction pattern [d, Å (I, %) (hkl)] are: 3.892 (100) (201), 3.148 (40) (211), 2.820 (90) (202), 2.685 (80) (220), 2.208 (40) (401), 2.136 (40) (222), 1.705 (35) (421).
Kind of sample preparation and/or method of registration of the spectrum: No data are given in the cited paper.
Source: Roberts et al. (2001a).
Wavenumbers (cm^{-1}): 3595, 1586w, 1455s, 1415w, 1290sh, 1264s, 1064s, 1039sh, 933s, 863w, 736, 694sh, 687.
Note: The wavenumbers were partly determined by us based on spectral curve analysis of the published spectrum. The band at 1264 cm^{-1} (not commented by Roberts et al. 2001a) indicates possible presence of borate groups.

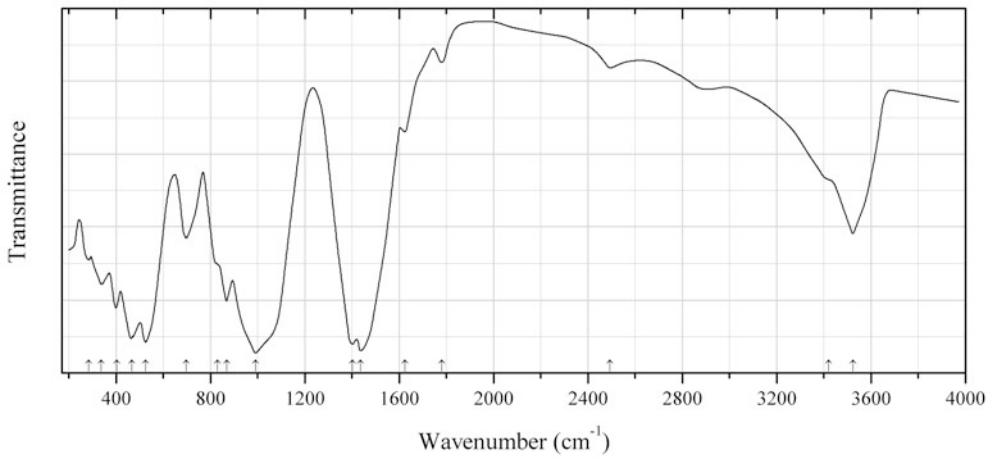

Fig. 2.759 IR spectrum of hanjiangite drawn using data from Liu et al. (2012)

CSi26 Hanjiangite $Ba_2Ca(V^{3+}Al)(Si_3AlO_{10})(OH)_2F(CO_3)_2$ (Fig. 2.759)
Locality: Shiti barium deposit, Dabashan region, southern Shaanxi, China (type locality).
Description: Green crystals and grains from the association with witherite, barite, and quartz. Holotype sample. The crystal structure is solved. Monoclinic, space group *C2*, a = 5.2050(12), b = 9.033(2), c = 32.077(8) Å, β = 93.49(8)°, V = 1505.4(8) Å^3, Z = 4. D_{meas} = 3.69 g/cm^3, D_{calc} = 3.78 g/cm^3. Optically biaxial (−), α = 1.615, β = 1.655, γ = 1.700, 2 V = 114°–115°. The empirical formula is $(Ba_{1.98}Na_{0.06}K_{0.01})(Ca_{0.76}Mg_{0.12}Y_{0.06}Sr_{0.03}La_{0.01}Nd_{0.01})(V_{1.15}Al_{0.75}Cr_{0.20}Ti_{0.12})(Si_{2.84}Al_{1.16}O_{10})$ $[(OH)_{1.25}O_{0.77})(F_{0.82}Cl_{0.01})(CO_3)_{2.05}$. The strongest lines of the powder X-ray diffraction pattern [d, Å (I, %) (hkl)] are: 15.866 (7) (002), 5.340 (91) (006), 4.010(10) (−114), 3.209 (23) (027), 2.676(100) (−1.1.10), 2.294 (29) (−137), 2.008 (11) (−228).
Kind of sample preparation and/or method of registration of the spectrum: KBr disc. Transmission.
Source: Liu et al. (2012).
Wavenumbers (cm^{-1}): 3522, 3420sh, 2494w, 1780w, 1624w, 1437s, 1402s, 991s, 868, 830sh, 697, 524s, 467s, 402, 338, 284w.
Note: The wavenumbers were partly determined by us based on spectral curve analysis of the published spectrum. The band at 1624 cm^{-1} indicates the presence of H_2O molecules.

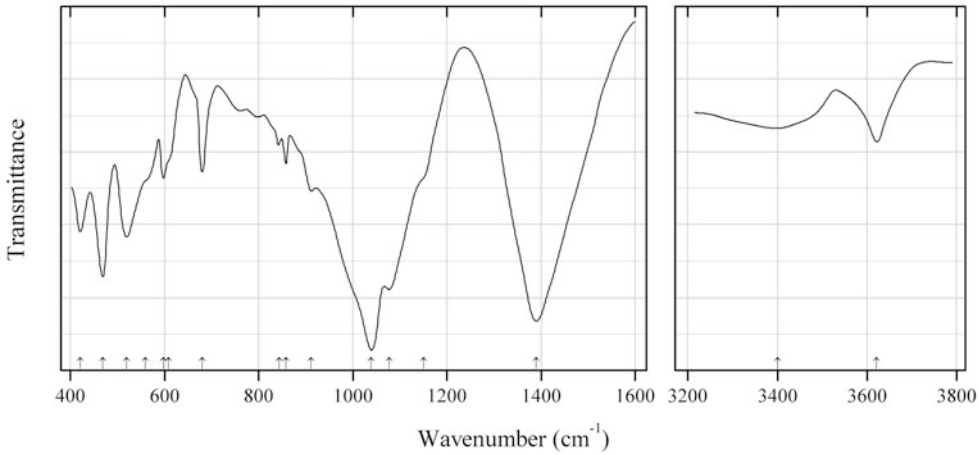

Fig. 2.760 IR spectrum of kegelite drawn using data from Braithwaite (1991)

CSi27 Kegelite $Pb_4Al_2(Si_4O_{10})(SO_4)(CO_3)_2(OH)_4$ (Fig. 2.760)
Locality: Tsumeb mine, Tsumeb, Namibia (type locality).
Kind of sample preparation and/or method of registration of the spectrum: KBr disc. Transmission.
Source: Braithwaite (1991).
Wavenumbers (cm^{-1}): 3622, 3400, 3130sh, 2440w, 1740w, 1390s, 1150sh, 1077s, 1039s, 912, 858w, 843w, 680, 608sh, 598, 560sh, 520, 469s, 421.

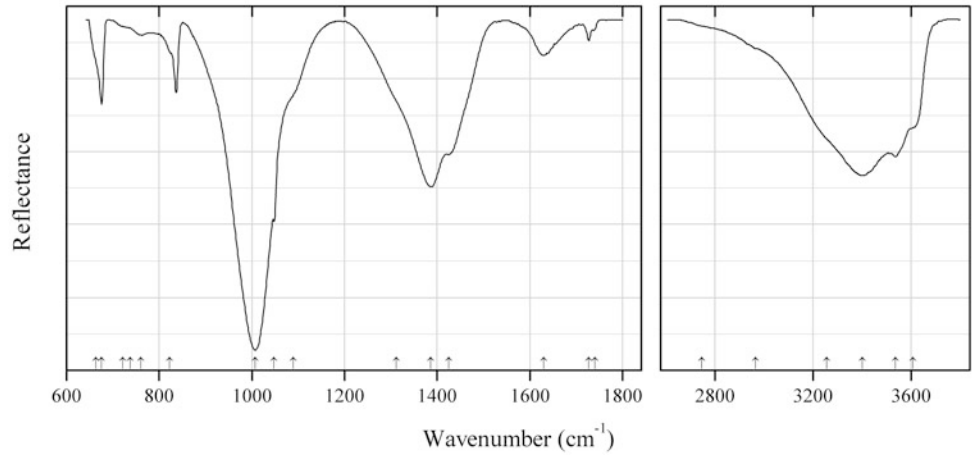

Fig. 2.761 IR spectrum of plumbotsumite drawn using data from López et al. (2013)

CSi28 Plumbotsumite $Pb_{13}(Si_{10}O_{27})(CO_3)_6 \cdot 3H_2O$ (Fig. 2.761)
Locality: St. Anthony deposit, Mammoth District, Pinal Co., Arizona, USA.
Description: Specimen No. SAB-090 from the collection of the Geology Department of the Federal University of Ouro Preto, Minas Gerais, Brazil.
Kind of sample preparation and/or method of registration of the spectrum: Attenuated total reflection of powdered mineral.
Source: López et al. (2013).
Wavenumbers (cm^{-1}): 3608sh, 3537, 3402s, 3255sh, 2964sh, 2747sh, 1741w, 1727w, 1630, 1425, 1386s, 1312sh, 1089sh, 1048, 1007s, 823sh, 760w, 737w, 722sh, 675, 664sh.
Note: In the cited paper, wavenumbers are indicated for the maxima of individual bands obtained as a result of the spectral curve analysis. The wavenumbers were determined by us based on spectral curve analysis of the published spectrum. The mineral was described with the erroneous formula $Pb_5(OH)_{10}Si_4O_8$. The bands of carbonate groups in the range 1300–1500 cm^{-1} have been erroneously assigned to Si–O vibrations.

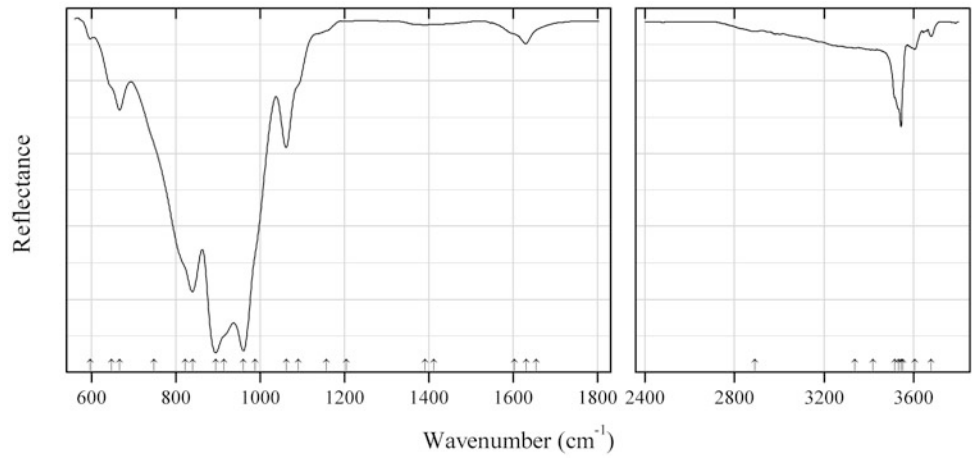

Fig. 2.762 IR spectrum of whelanite drawn using data from Frost and Xi (2012b)

CSi29 Whelanite $Cu_2Ca_6[Si_6O_{17}(OH)](CO_3)_3(OH)_3 \cdot 2H_2O$ (Fig. 2.762)
Locality: Christmas Mine, 7 km east of Hayden, Gila Co., Arizona, USA.
Description: No data.
Kind of sample preparation and/or method of registration of the spectrum: Attenuated total reflection of powdered mineral.
Source: Frost and Xi (2012b).
Wavenumbers (cm^{-1}): 3678w, 3604w, 3551sh, 3543s, 3531sh, 3516sh, 3417sh, 3337, 2891, 1655sh, 1630w, 1603sh, 1411, 1390, 1204w, 1157sh, 1090sh, 1061, 988sh, 960s, 914sh, 894s, 840s, 821sh, 748sh, 666, 646sh, 597w.
Note: In the cited paper, the wavenumbers are indicated only for the maxima of individual bands obtained as a result of the spectral curve analysis. Observed absorption maxima are not indicated. The wavenumbers were determined by us based on spectral curve analysis of the published spectrum.

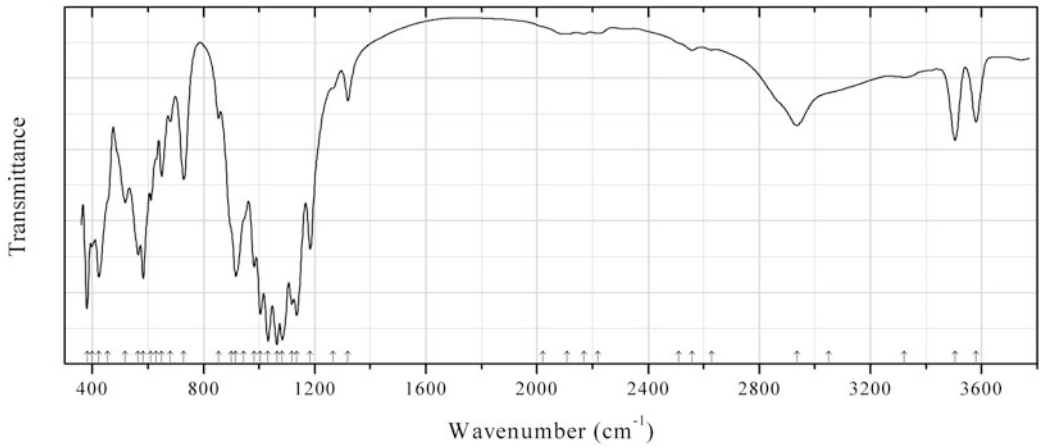

Fig. 2.763 IR spectrum of attakolite obtained by N.V. Chukanov

PSi10 Attakolite $CaMn^{2+}Al_4(HSiO_4)(PO_4)_3(OH)_4$ (Fig. 2.763)
Locality: Västanå iron mine, Skåne, Sweden (type locality).
Description: Pink fine-grained aggregate from the association with berlinite, lazulite, trolleite, etc. The empirical formula is (electron microprobe): $(Ca_{0.83}Sr_{0.15}Na_{0.01})(Mn_{0.72}Fe^{2+}_{0.17}Mg_{0.05})(Al_{3.85}Zr_{0.08}Fe_{0.06}Ti_{0.01})(HSiO_4)_{0.96}(PO_4)_{3.14}(OH)_x$.
Kind of sample preparation and/or method of registration of the spectrum: KBr disc. Absorption.
Wavenumbers (cm^{-1}): 3579, 3504, 3320w, 3050sh, 2935, 2629w, 2558w, 2510sh, 2220w, 2168w, 2107w, 2020sh, 1319w, 1265sh, 1184s, 1135s, 1118s, 1083s, 1064s, 1032s, 1004s, 982, 945sh, 916s, 900sh, 854w, 729, 681w, 649, 630sh, 611, 583s, 565, 518, 455sh, 424s, 399, 382s.

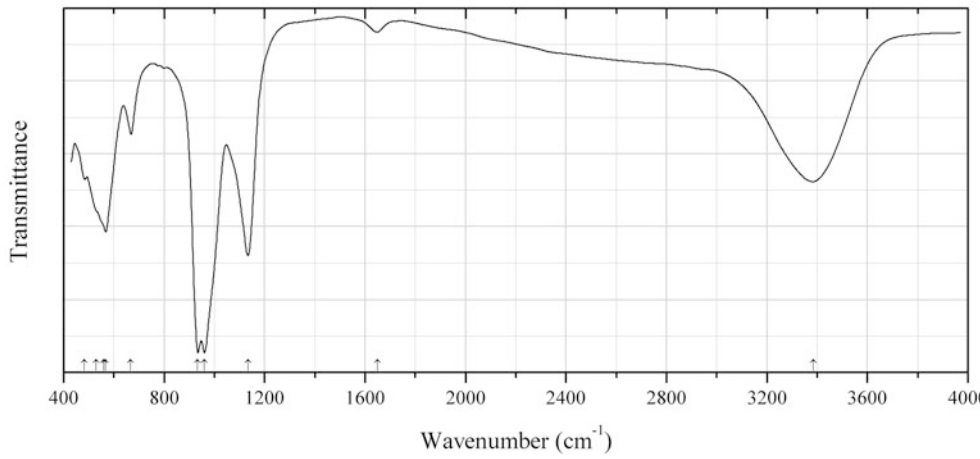

Fig. 2.764 IR spectrum of bobmeyerite drawn using data from Kampf et al. (2013b)

SSi12 Bobmeyerite $Pb_4(Al_3Cu)(Si_4O_{12})(S_{0.5}Si_{0.5}O_4)(OH)_7Cl{\cdot}3H_2O$ (Fig. 2.764)
Locality: Mammoth mine (St Anthony mine), Tiger, Pinal County, Arizona, USA (type locality).
Description: White aggregates of acicular crystals from the association with atacamite, caledonite, cerussite, connellite, diaboleite, fluorite, georgerobinsonite, hematite, leadhillite, matlockite, murdochite, phosgenite, pinalite, quartz, wulfenite, and yedlinite. Holotype sample. Orthorhombic, space group *Pnnm*, $a = 13.969(9)$, $b = 14.243(10)$, $c = 5.893(4)$ Å, $V = 1172$ Å^3, $Z = 2$. $D_{calc} = 4.381$ g/cm^3. Optically biaxial biaxial (−), $\alpha \approx \beta = 1.759(2)$, $\gamma = 1.756(2)$. The empirical formula is $Pb_{3.80}Ca_{0.04}Al_{3.04}Cu_{0.96}Cr_{0.13}Si_{4.40}S_{0.58})O_{24.43}Cl_{1.05}F_{0.52}H_{11.83}$. The strongest lines of the powder X-ray diffraction pattern [*d*, Å (*I*, %) (*hkl*)] are: 10.051 (35) (110), 5.474 (54) (011, 101), 5.011 (35) (220), 4.333 (43) (121, 211), 3.545 (34) (040, 400), 3.278 (77) (330, 231, 321), 2.9656 (88) (141, 002, 411), 2.5485 (93) (051, 222, 501), 1.873 (39) (multiple).
Kind of sample preparation and/or method of registration of the spectrum: Low-pressure diamond microsample cell. Transmission.
Source: Kampf et al. (2013b).
Wavenumbers (cm^{-1}): 3386, 1649w, 1134s, 960s, 934s, 667, 568, 560sh, 530sh, 483.
Note: The wavenumbers were partly determined by us based on spectral curve analysis of the published spectrum.

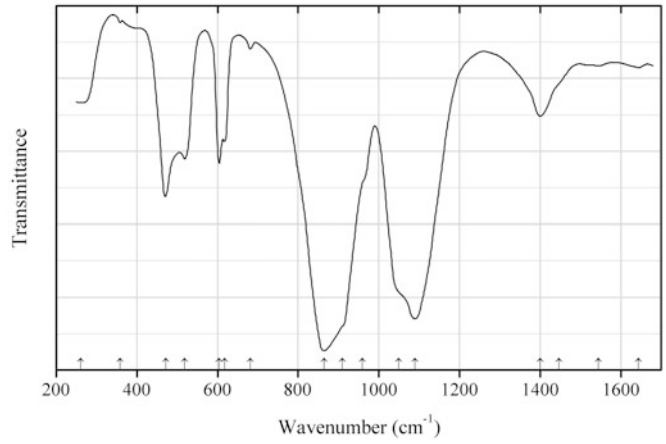

Fig. 2.765 IR spectrum of mattheddleite drawn using data from Livingstone et al. (1987)

SSi13 Mattheddleite $Pb_{10}(SiO_4)_3(SO_4)_3Cl_2$ (Fig. 2.765)
Locality: Leadhills Dod, Leadhills, Strathclyde region, UK (type locality).
Description: Colourless rosettiform aggregates from the association with quartz, lanarkite, cerussite, hydrocerussite, leadhillite, and caledonite. Holotype sample. Hexagonal, a = 9.963, c = 7.464 Å, V = 642 Å^3. D_{calc} = 6.96 g/cm^3. Optically uniaxial (−), ω = 2.017(5), ε = 1.999(5). The strongest lines of the powder X-ray diffraction pattern [d, Å (I, %) (hkl)] are: 2.988 (100) (112, 211), 4.32 (40) (200), 4.13 (40) (111), 2.877 (40) (300), 3.26 (30) (210).
Kind of sample preparation and/or method of registration of the spectrum: CsI disc. Transmission.
Source: Livingstone et al. (1987).
Wavenumbers (cm^{-1}): 1644w, 1545w, 1447sh, 1400, 1090s, 1050sh, 960sh, 910sh, 864s, 681w, 617, 604, 519, 471, 359w, ∼260.
Note: The wavenumbers were partly determined by us based on spectral curve analysis of the published spectrum. The empirical formula given in the cited paper is not charge-balanced. The bands at 1400 and 864 cm^{-1} can be assigned to CO_3^{2-} groups substituting SiO_4^{4-} and SO_4^{2-}.

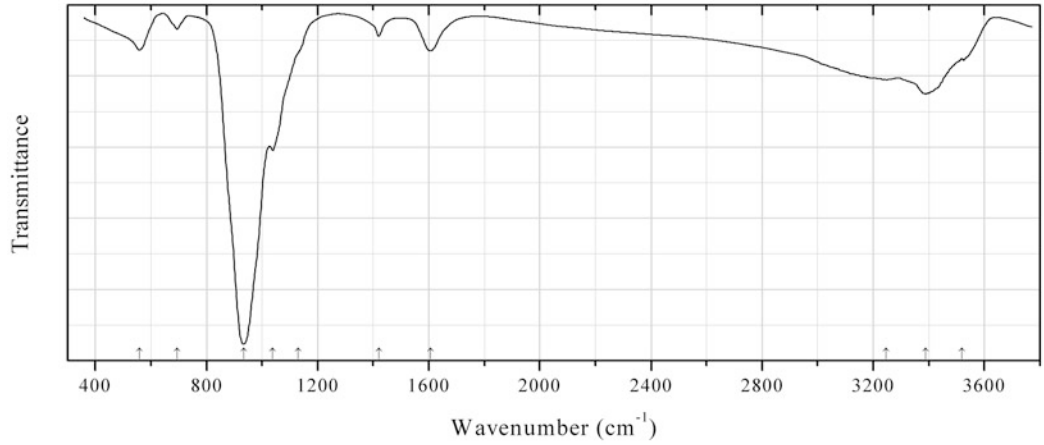

Fig. 2.766 IR spectrum of kolskyite obtained by N.V. Chukanov

TiSi273 Kolskyite $Ca\square Na_2Ti_4(Si_2O_7)_2O_4 \cdot 7H_2O$ (Fig. 2.766)
Locality: Kirovskiy mine, Kukisvumchorr Mt., Khibiny alkaline complex, Kola peninsula, Murmansk region, Russia (type locality).
Description: Beige platelets on natrolite. Holotype sample. Triclinic, space group *P*-1, $a = 5.387(1)$, $b = 7.091(1)$, $c = 15.473(3)$ Å, $\alpha = 96.580(4)°$, $\beta = 93.948(4)$, $\gamma = 89.818(4)°$, $V = 585.8(3)$ Å^3, $Z = 1$.
Kind of sample preparation and/or method of registration of the spectrum: Absorption.
Wavenumbers (cm^{-1}): 3520sh, 3389, 3246, 1607, 1420w, 1130sh, 1039, 933s, 694w, 558.

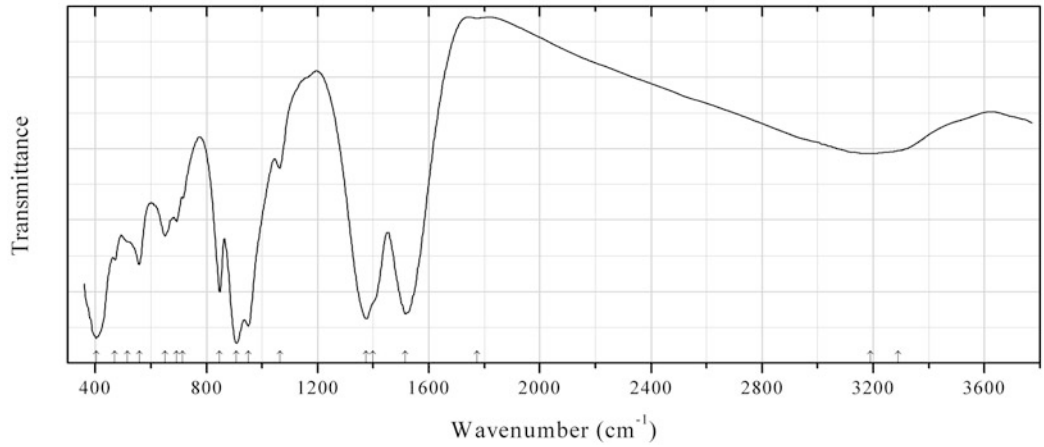

Fig. 2.767 IR spectrum of kihlmanite-(Ce) obtained by N.V. Chukanov

TiSi274 Kihlmanite-(Ce) $Ce_2Ti(SiO_4)(HCO_3)_2O_2 \cdot H_2O$ (Fig. 2.767)
Locality: Kihlman Mt., Khibiny massif, Kola peninsula, Russia (type locality).
Description: Brown prismatic crystals. Holotype sample.
Kind of sample preparation and/or method of registration of the spectrum: KBr disc. Absorption.
Wavenumbers (cm^{-1}): 3290sh, 3190, 1775w, 1516s, 1400sh, 1375s, 1064, 950s, 908s, 848, 715, 693, 651, 558, 515sh, 470, 403s.

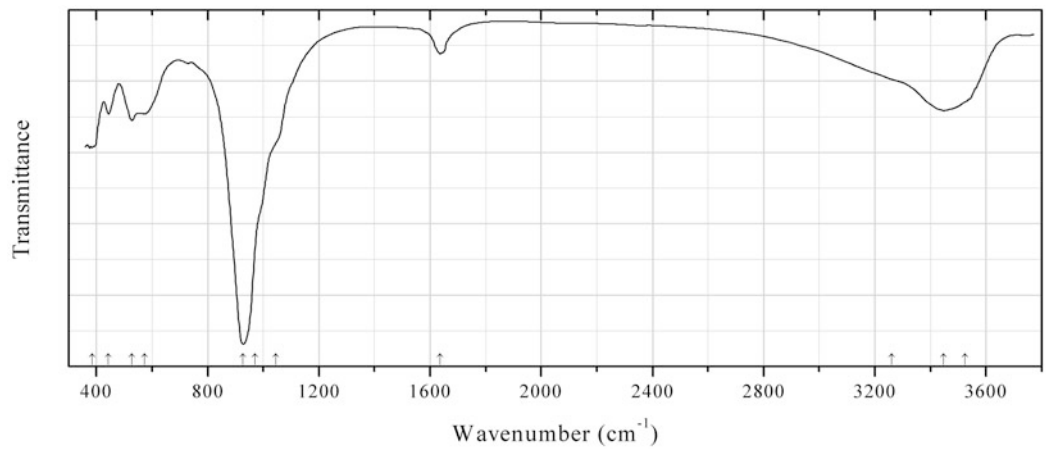

Fig. 2.768 IR spectrum of zvyaginite obtained by N.V. Chukanov

TiSi275 Zvyaginite $NaZnNb_2Ti[Si_2O_7]_2O(OH,F)_3(H_2O)_{4+x}$ ($x < 1$) (Fig. 2.768)
Locality: Malyi Punkaruaiv Mt., Lovozero alkaline complex, Murmansk region, Kola Peninsula, Russia (type locality).
Description: Lamellar crystals from the association with ussingite, microcline, aegirine, sphalerite, vigrishinite, sauconite, etc. Holotype sample. Triclinic, space group *P*-1, $a = 8.975(3)$, $b = 8.979(3)$, $c = 12.135(4)$ Å, $\alpha = 74.328(9)^o$, $\beta = 80.651(8)^o$, $\gamma = 73.959(8)^o$, $V = 900.8(6)$ Å^3, $Z = 2$. $D_{meas} = 2.88(3)$ g/cm^3, $D_{calc} = 2.94$ g/cm^3. Optically biaxial (−), $\alpha = 1.626(5)$, $\beta = 1.714(3)$, $\gamma = 1.740(5)$, $2V = 45(15)^o$. The empirical formula is $Na_{1.24}K_{0.04}Ca_{0.11}Mn_{0.16}Fe_{0.03}Zn_{0.96}Nb_{1.66}Ti_{1.25}(Si_{3.97}Al_{0.03})_{\Sigma 4}O_{15.07}(OH)_{2.10}F_{0.83}\cdot 4.64H_2O$. The strongest lines of the powder X-ray diffraction pattern [*d*, Å (*I*, %) (*hkl*)] are: 11.72 (100) (001), 5.83 (40) (002), 5.28 (53) (−1–11, 112), 4.289 (86) (200, 021), 3.896 (36) (−1–12, −201, 003, 022, 113), 2.916 (57) (310, 132, 004), 2.862 (72) (130, 312).
Kind of sample preparation and/or method of registration of the spectrum: KBr disc. Absorption.
Wavenumbers (cm^{-1}): 3525sh, 3447, 3260sh, 1636, 1045sh, 970sh, 928s, 573, 527, 444, 384.

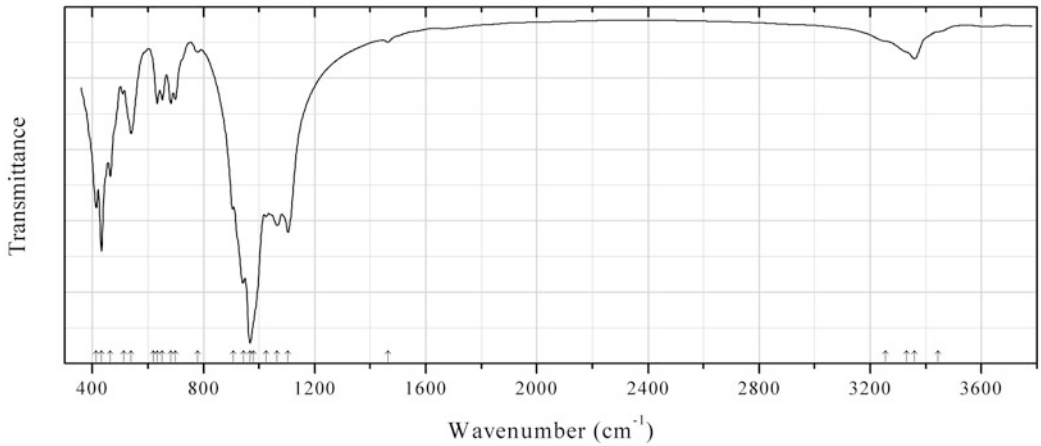

Fig. 2.769 IR spectrum of tinaksite obtained by N.V. Chukanov

TiSi276 Tinaksite $K_2Na(Ca,Mn)_2TiSi_7O_{19}(OH)$ (Fig. 2.769)
Locality: Rasvumchorr Mt., near Yuksporlak pass, Khibiny alkaline complex, Kola peninsula, Murmansk region, Russia.
Description: Yellow crystals from peralkaline pegmatite. Confirmed by electron microprobe analyses and powder X-ray diffraction data.
Kind of sample preparation and/or method of registration of the spectrum: KBr disc. Absorption.
Wavenumbers (cm^{-1}): 3445sh, 3359, 3330sh, 3255sh, 1465w, 1104s, 1066s, 1026, 980sh, 967s, 945s, 908, 779w, 620sh, 699, 682, 652, 633, 540, 512w, 465, 433s, 414.

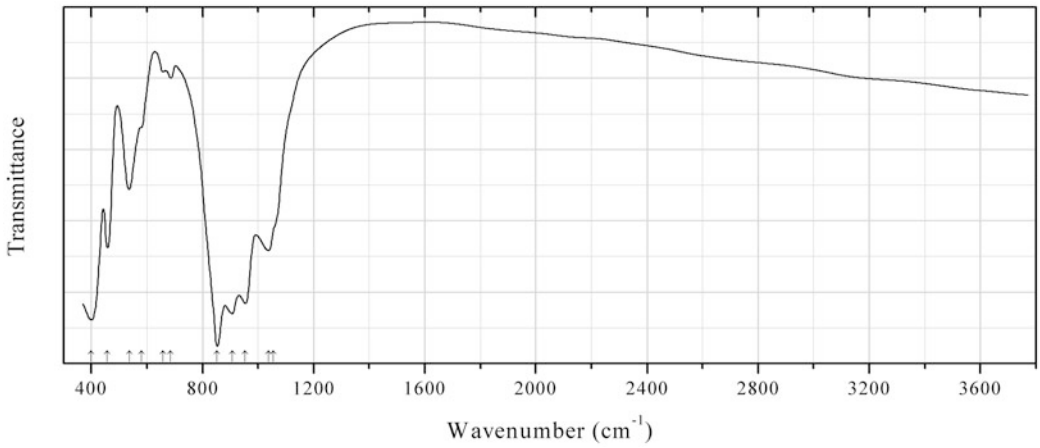

Fig. 2.770 IR spectrum of emmerichite obtained by N.V. Chukanov

TiSi277 Emmerichite $Ba_2Na(Na,Fe^{2+})_2(Fe^{3+},Mg)Ti_2(Si_2O_7)_2O_2F_2$ (Fig. 2.770)
Locality: Basalt quarry Rother Kopf, Roth, near Gerolstein, Eifel Mts., Rhineland-Palatinate (Rheinland-Pfalz), Germany (type locality).
Description: Brown lamellar crystals from the association with nepheline, leucite, augite, phlogopite, fluorapatite, götzenite, åkermanite, günterblassite, magnetite, and perovskite. Holotype sample. Monoclinic, space group *C*2/*m*, a = 19.960(1), b = 7.098(1), c = 5.4074(3) Å, β = 96.368(1)°, V = 761.37(12) Å^3, Z = 2. D_{calc} = 3.864 g/cm^3. Optically biaxial (+), α = 1.725(4), β = 1.728(4), γ = 1.759(4), 2 V = 30(10)°. The empirical formula is $Ba_{1.49}Sr_{0.27}K_{0.19}Na_{1.54}Ca_{0.31}Mn_{0.275}Mg_{0.68}Fe^{2+}_{0.59}Fe^{3+}_{0.74}Ti_{1.67}Zr_{0.04}Nb_{0.09}Si_{3.97}O_{16.36}F_{1.64}$. The strongest lines of the powder X-ray diffraction pattern [*d*, Å (*I*, %) (*hkl*)] are: 9.97 (55) (200), 3.461 (65) (510, 311, 401), 2.792 (100) (221, 511), 2.670 (56) (002, 601, 20–2), 2.140 (57) (131, 022, 621, 22–2).
Kind of sample preparation and/or method of registration of the spectrum: KBr disc. Absorption.
Wavenumbers (cm^{-1}): 1055sh, 1038s, 954s, 907s, 853s, 686w, 658w, 580sh, 536, 458s, 400s.

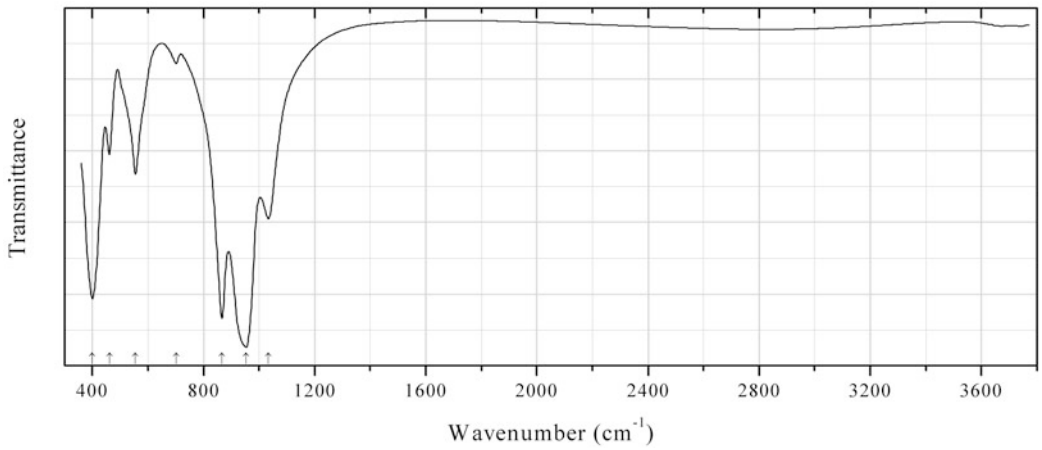

Fig. 2.771 IR spectrum of fluorlamprophyllite obtained by N.V. Chukanov

TiSi278 Fluorlamprophyllite $(Sr,Ba,K)_2Na(Na,Fe^{2+},Mn^{2+})_2TiTi_2(Si_2O_7)_2O_2(F,OH,O)_2$ (Fig. 2.771)

Locality: Alluaiv Mt., Lovozero alkaline complex, Kola peninsula, Murmansk region, Russia.
Description: Brown prismatic crystals from peralkaline pegmatite, from the association with Mn-analogue of raslakite, aegirine, and potassic feldspar. The empirical formula is (electron microprobe): $Sr_{1.0}Ba_{0.2}K_{0.1}Na_{3.3}Ca_{0.1}Mn_{0.3}Mg_{0.2}Fe_{0.2}Ti_{2.5}(Si_2O_7)_2O_2[F_{1.15}(O,OH)_{0.85}]$.
Kind of sample preparation and/or method of registration of the spectrum: KBr disc. Absorption.
Wavenumbers (cm^{-1}): 1034, 953s, 867s, 701w, 555, 461, 400s.

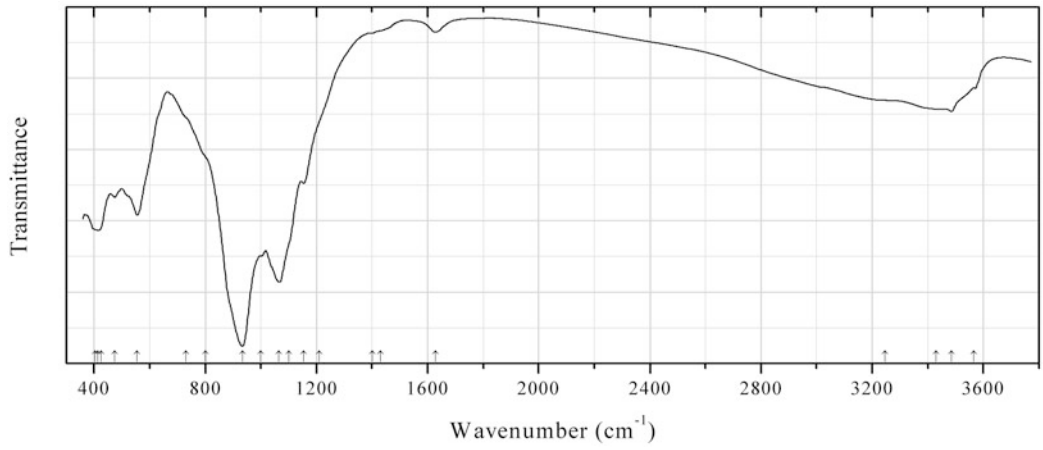

Fig. 2.772 IR spectrum of lomonosovite Cu-exchanged obtained by N.V. Chukanov

TiSi279 Lomonosovite Cu-exchanged $(Cu,Na)_3Ti_4(Si_2O_7)_2(O,OH)_4(Na_3PO_4)_{2-x}(H_2O)_y$ (Fig. 2.772)
Locality: Artificial.
Description: Obtained in the reaction of lomonosovite (a sample from the Umbozero mine, Mt. Alluaiv, Lovozero alkaline complex, Kola peninsula, Russia) with 1 N aqueous solution of $CuSO_4$ at 150 °C. Investigated by I.S. Lykova. Triclinic, space group *P*-1, a = 5.265(2), b = 7.153(3), c = 13.969(5) Å, α = 100.05(1)°, β = 96.83(1)°, γ = 91.905(10)°, V = 513.6(3) $Å^3$. The empirical formula is (electron microprobe): $\{Cu_{1.58}Na_{1.30}Ca_{0.40}\}\{Na_{1.04}Cu_{0.1}(Ti_{1.24}Mn_{0.60}Nb_{0.16})\}\{Ti_{2.00}[Si_2O_7]_2\}O_2(O,OH)_2(PO_4)_{1.78}\cdot nH_2O$.
Kind of sample preparation and/or method of registration of the spectrum: KBr disc. Absorption.
Wavenumbers (cm^{-1}): 3566w, 3485, 3430sh, 3245sh, 1629w, 1430sh, 1402w, 1210sh, 1155, 1100sh, 1066s, 1000, 933s, 800sh, 730sh, 555, 425sh, 474, 414, 405sh.

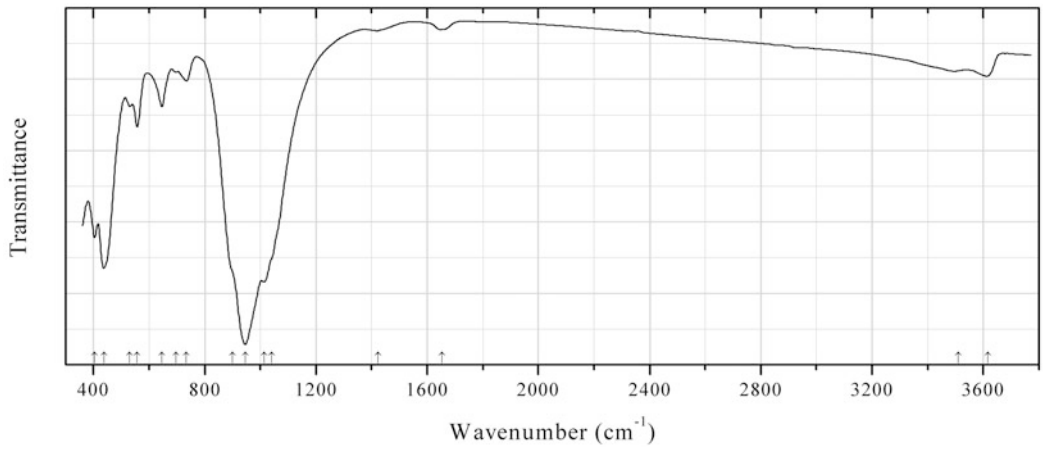

Fig. 2.773 IR spectrum of zircophyllite obtained by N.V. Chukanov

TiSi280 Zircophyllite $K_2(Na,Ca)(Mn^{2+},Fe^{2+})_7(Zr,Ti,Nb)_2Si_8O_{26}(OH)_4F$ (Fig. 2.773)
Locality: Mont Saint-Hilaire, Rouville RCM (Rouville Co.), Montérégie, Québec, Canada.
Description: Brown platy crystals with perfect cleavage from peralkaline pegmatite. The empirical formula is (electron microprobe): $K_{1.81}Na_{1.07}Ca_{0.14}[Mn_{3.25}(Fe^{2+},Fe^{3+})_{3.46}Mg_{0.12}](Zr_{0.91}Ti_{0.83}Nb_{0.27})(Si_{7.57}Al_{0.43})(O,OH,F,H_2O)_{31}$.
Kind of sample preparation and/or method of registration of the spectrum: KBr disc. Absorption.
Wavenumbers (cm^{-1}): 3617w, 3510w, 1653w, 1422w, 1040sh, 1013s, 946s, 900sh, 734w, 698w, 646, 557, 531w, 438s, 404.

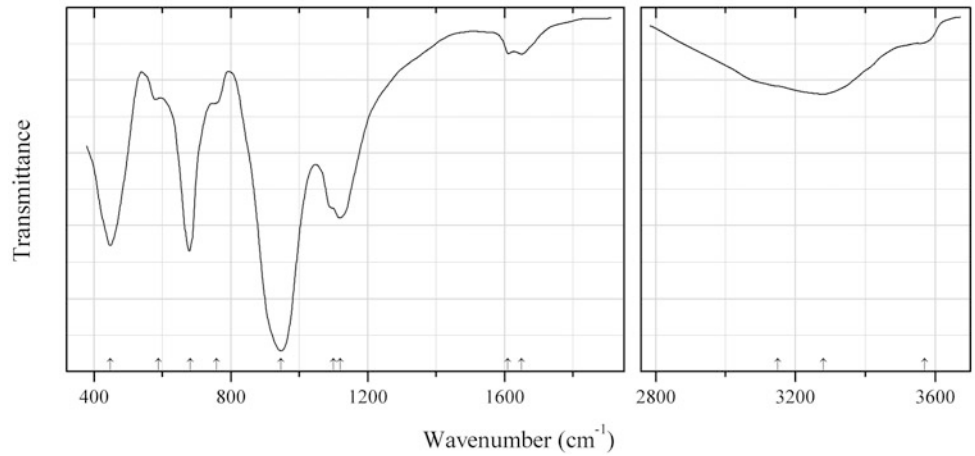

Fig. 2.774 IR spectrum of burovaite-Ca obtained by N.V. Chukanov

TiSi281 Burovaite-Ca $(Na,K)_4Ca_2(Ti,Nb)_8(Si_4O_{12})_4(OH,O)_8 \cdot 12H_2O$ (Fig. 2.774)
Locality: Eveslogchorr Mt., Khibiny alkaline complex, Kola peninsula, Murmansk region, Russia.
Description: Light beige prismatic crystals from the association with natrolite. The empirical formula is $(Na_{2.2}K_{1.3}Ba_{0.3}Sr_{0.1})Ca_{1.7}(Ti_{5.3}Nb_{2.6}Fe_{0.1})(Si_{4.00}O_{12})_4(OH,O)_8 \cdot 12H_2O$.
Kind of sample preparation and/or method of registration of the spectrum: KBr disc. Absorption.
Wavenumbers (cm^{-1}): 3570w, 3280, 3150sh, 1650w, 1610w, 1119s, 1100sh, 946s, 758w, 681s, 589w, 448s.

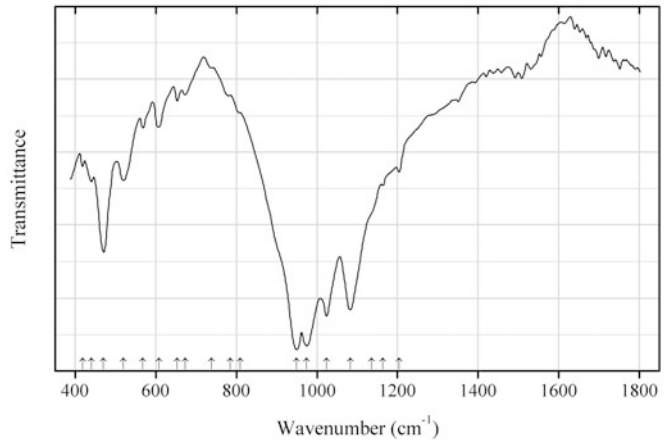

Fig. 2.775 IR spectrum of aleksandrovite drawn using data from Pautov et al. (2010)

TiSi282 Aleksandrovite $KCa_7Sn_2Li_3Si_{12}O_{36}F_2$ (Fig. 2.775)
Locality: Dara-i Pioz alkaline massif, Alaiskii ridge, Tien Shan Mts., Tajikistan.
Description: Zones in baratovite crystals, from the association with microcline, calcite, quartz, albite, aegirine-augite, fluorite, miserite, titanite, bazirite, pabstite, sogdianite, sugilite, turkestanite, and fluorapatite. Monoclinic, space group *C*2/*c*, a = 17.01(2), b = 9.751(6), c = 21.00(2) Å, β = 112.45 (8)°, V = 3219(7) Å^3, Z = 4. D_{meas} = 3.05(2) g/cm^3, D_{calc} = 3.07 g/cm^3. Optically biaxial (−), α = 1.629(2), β = 1.635(4), γ = 1.638(2). The strongest lines of the powder X-ray diffraction pattern [d, Å (I, %) (*hkl*)] are: 4.86 (21) (31–1), 3.712 (33) (312), 3.234 (100) (006), 3.206 (34) (223), 3.039 (28) (025), 2.894 (42) (314), 2.425 (42) (008), 1.950 (25) (426).
Kind of sample preparation and/or method of registration of the spectrum: KBr microdisc. Absorption.
Source: Pautov et al. (2010).
Wavenumbers (cm^{-1}): 1204w, 1164w, 1135sh, 1083s, 1024s, 974s, 950s, 809sh, 785sh, 738sh, 673w, 653w, 607w, 568w, 520, 470, 440, 418.
Note: The wavenumbers were partly determined by us based on spectral curve analysis of the published spectrum.

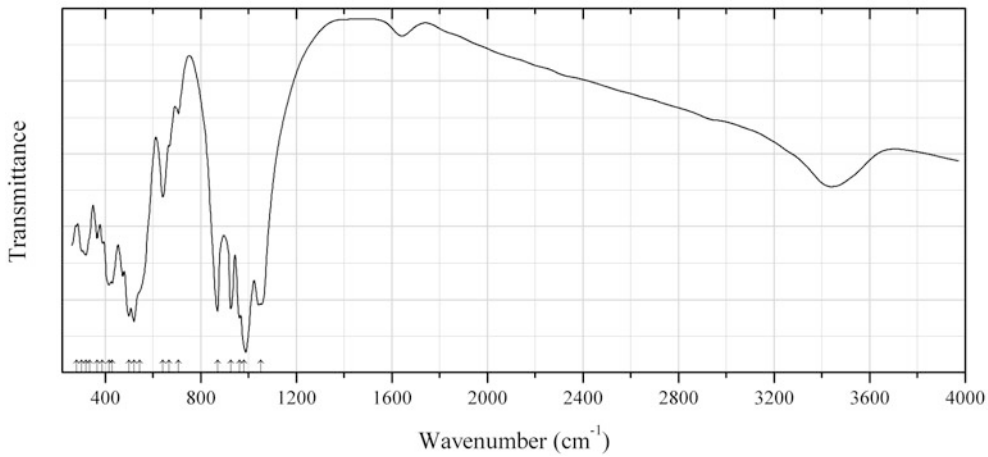

Fig. 2.776 IR spectrum of baghdadite drawn using data from Shiraga et al. (2001)

TiSi283 Baghdadite $Ca_6Zr_2(Si_2O_7)O_4$ (Fig. 2.776)
Locality: Fuka, Okayama prefecture, Honshu Island, Japan.
Description: Grayish white grains with yellowish orange luminescence under SW UV radiation, from skarn. The associated minerals are gehlenite, spurrite, tilleyite, vesuvianite, perovskite, and grandite garnet. Monoclinic, a = 10.429(2), b = 10.170(2), c = 7.365(1) Å, β = 91.01(1)°. D_{meas} = 3.36 g/cm^3, D_{calc} = 3.44 g/cm^3. Optically biaxial (−), α = 1.735, β = 1.747, γ = 1.755. The empirical formula is $(Ca_{3.03}Na_{0.01})(Zr_{0.83}Ti_{0.15})(Si_{1.99}Al_{0.01}Fe_{0.01})O_9$. The strongest lines of the powder X-ray diffraction pattern [d, Å (I, %) (hkl)] are: 7.32 (42) (110), 3.229 (60) (130), 3.035 (74) (20–2), 2.986 (100) (311, 202), 2.873 (88) (12–2, 320), 2.845 (84) (230).
Kind of sample preparation and/or method of registration of the spectrum: KBr disc. Transmission.
Source: Shiraga et al. (2001).
Wavenumbers (cm^{-1}): 1050s, 980s, 962s, 925s, 870s, 706w, 668, 640, 520s, 545sh, 500s, 429, 415, 388, 366, 334sh, 320, 302, 279.
Note: The wavenumbers were partly determined by us based on spectral curve analysis of the published spectrum. The bands at 3440 and 1640 cm^{-1} are due to the water molecules absorbed by KBr disc.

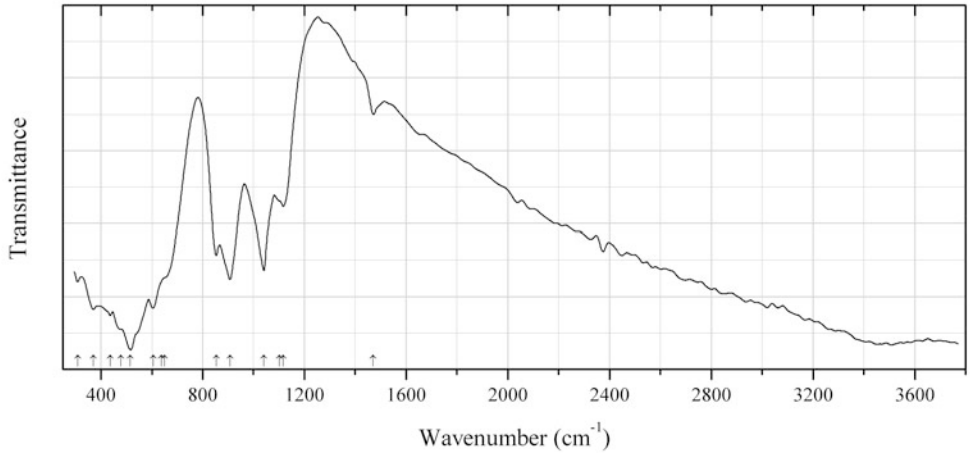

Fig. 2.777 IR spectrum of dingdaohengite-(Ce) drawn using data from Xu et al. (2008)

TiSi284 Dingdaohengite-(Ce) $(Ce,La)_4Fe^{2+}(Ti,Fe,Mg)_2Ti_2(Si_2O_7)_2O_8$ (Fig. 2.777)
Locality: Bayan Obo *REE*-Nb-Fe Mine, near Baotou city, Inner Mongolia, China (type locality).
Description: Black crystals from the association with diopside, tremolite, richterite, allanite-(Ce), magnetite, ilmenite, spinel, titanite, pyrochlore, F-rich phlogopite, fluorapatite, quartz, and fluorite. Holotype sample. Monoclinic, space group $P2_1/a$ or $C2/m$, a = 13.4656(15), b = 5.7356(6), c = 11.0977(12) Å, β = 100.636(2)°, V = 842.39(46) Å^3, Z = 2. D_{meas} = 4.83(7) g/cm^3, D_{calc} = 4.88 g/cm^3. Optically biaxial (−), α = 1.978(5), γ = 2.010(5), 2 $V \approx 60°$. The empirical formula is $(Ce_{2.13}La_{1.49}Ca_{0.48}Th_{0.01})Fe^{2+}(Ti_{0.88}Fe^{2+}_{0.47}Mg_{0.41}Fe^{3+}_{0.26}Al_{0.01})(Ti_{1.96}Nb_{0.04})(Si_2O_7)_2O_8$. The strongest lines of the powder X-ray diffraction pattern [d, Å (I, %) (hkl)] are: 3.1978 (68) (212), 3.1622 (46) (−312), 2.8702 (52) (020), 2.7524 (100) (−121), 2.7263 (98) (313), 2.5460 (54) (−304).
Kind of sample preparation and/or method of registration of the spectrum: Transmission. Kind of sample preparation is not indicated.

Source: Xu et al. (2008).
Wavenumbers (cm^{-1}): 1471w, 1117, 1102sh, 1041s, 908s, 853, 650sh, 606s, 637sh, 516s, 479sh, 436s, 370s, 308s.
Note: The wavenumbers were partly determined by us based on spectral curve analysis of the published spectrum. Apparently, the band at 1471 cm^{-1} corresponds to the admixture of carbonate.

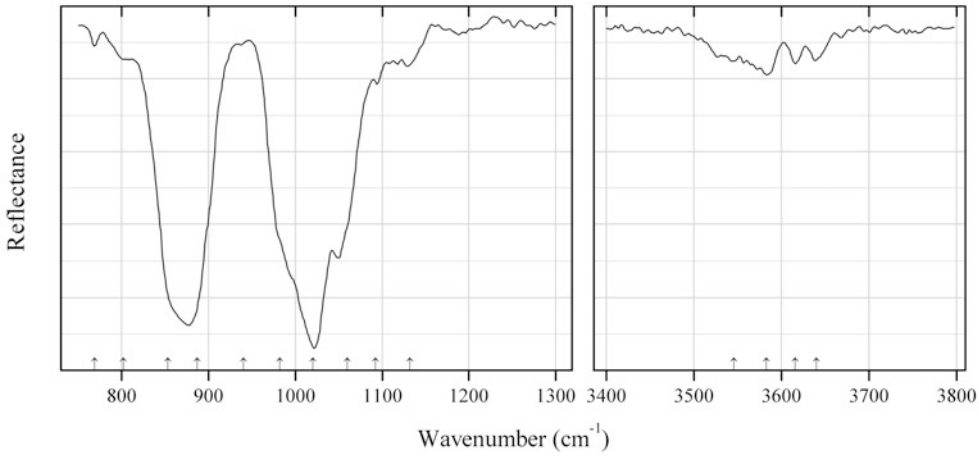

Fig. 2.778 IR spectrum of dovyrenite drawn using data from Galuskin et al. (2007)

TiSi285 Dovyrenite $Ca_6Zr(Si_2O_7)_2(OH)_4$ (Fig. 2.778)
Locality: Ioko-Dovyren (Yoko-Dovyrenskiy) layered massif, Buryatia Republic, Transbaikal Territory, Siberia, Russia (type locality).
Description: Colourless crystals from the association with pyroxene, perovskite, hydrogarnets, monticellite, vesuvianite, foshagite, brucite, calzirtite, tazheranite, baghdadite, apatite, calcite, etc.
Holotype sample. Orthorhombic, space group *Pnnm*, a = 5.666(16), b = 18.844(5), c = 3.728(11) Å, V = 398.0(2) $Å^3$, Z = 1. D_{calc} = 3.034 g/cm^3. Optically biaxial (+), α = 1.659(2), β = 1.660(2), γ = 1.676(2), 2 V = 30(5)°. The empirical formula is $(Ca_{5.73}Fe_{0.03}Mg_{0.02})(Zr_{2.98}Hf_{0.01}Ti_{0.01})[Si_4O_{13.56}(OH)_{0.44}](OH)_4$. The powder X-ray diffraction pattern of dovyrenite was not obtained experimentally.
Kind of sample preparation and/or method of registration of the spectrum: Reflectance of unpolarized IR radiation from the natural face (100).
Source: Galuskin et al. (2007).
Wavenumbers (cm^{-1}): 3640, 3616, 3583, 3546, 1132w, 1092w, 1060, 1020s, 982sh, 940w, 887s, 853sh, 802sh, 769w.
Note: The wavenumbers are indicated for the maxima of individual bands obtained as a result of the spectral curve analysis. Details of this analysis are not described.

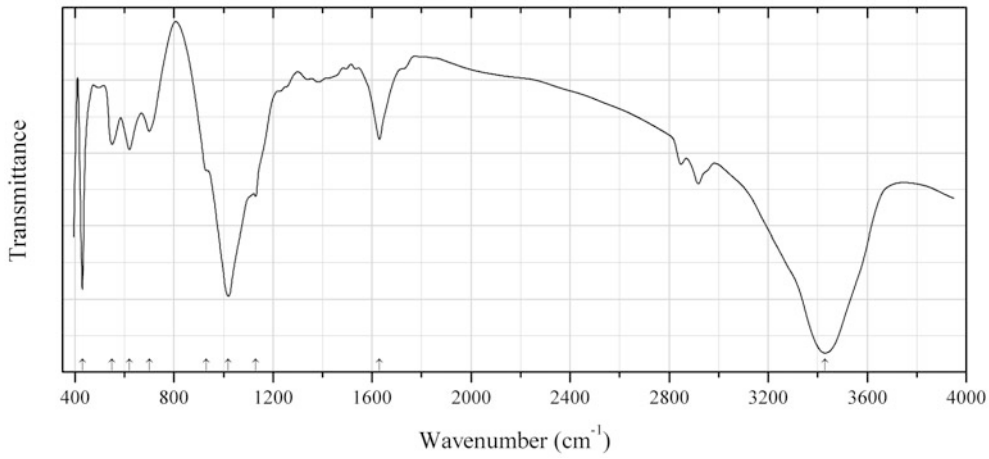

Fig. 2.779 IR spectrum of eliseevite drawn using data from Yakovenchuk et al. (2011a)

TiSi286 Eliseevite $Na_{1.5}LiTi_2[Si_4O_{10.5}(OH)_{1.5}]O_2 \cdot 2H_2O$ (Fig. 2.779)
Locality: Alluaiv Mt., Lovozero alkaline massif, Kola Peninsula, Murmansk region, Russia (type locality).
Description: Pale creamy to colorless long-prismatic crystals from the association with albite, analcime, catapleiite, chabazite-Ca, gmelinite-K, manganoneptunite, microcline, murmanite, and ussingite. Holotype sample. Monoclinic, space group *C*2/*c*, $a = 27.48(1)$, $b = 8.669(4)$, $c = 5.246(2)$ Å, $\beta = 90.782(8)°$, $V = 1249.7(9)$ Å^3, $Z = 4$. $D_{meas} = 2.68(4)$ g/cm^3, $D_{calc} = 2.706$ g/cm^3. Optically biaxial (−), $\alpha = 1.665(2)$, $\beta = 1.712(2)$, $\gamma = 1.762(5)$. The empirical formula is $(Na_{1.51}K_{0.01}Ca_{0.01})Li_{0.98}(Ti_{1.89}Nb_{0.03}Fe_{0.01}Al_{0.01})[Si_{4.00}O_{10.26}(OH)_{1.74}]O_2 \cdot 2.12H_2O$. The strongest lines of the powder X-ray diffraction pattern [*d*, Å (*I*, %) (*hkl*)] are: 13.76 (100) (200), 6.296 (60) (310), 3.577 (80) (710), 3.005 (70) (421), 2.881 (70) (910), 2.710 (50) (62–1).
Kind of sample preparation and/or method of registration of the spectrum: KBr disc. Absorption.
Source: Yakovenchuk et al. (2011a).
Wavenumbers (cm^{-1}): 3430s, 1630, 1130, 1020s, 930sh, 700, 620, 550, (430s).
Note: Weak bands in the range from 2800 to 3000 cm^{-1} correspond to the admixture of grease.

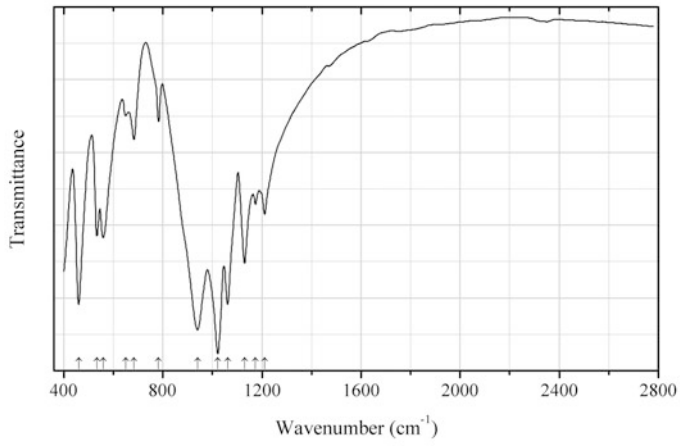

Fig. 2.780 IR spectrum of faizievite drawn using data from Agakhanov et al. (2007)

TiSi287 Faizievite $Li_6K_2Na(Ca_6Na)Ti_4(Si_6O_{18})_2(Si_{12}O_{30})F_2$ (Fig. 2.780)
Locality: Dara-i Pioz alkaline massif, Alaiskii ridge, Tien Shan Mts., Tajikistan (type locality).
Description: Colourless tabular plates from the association with pectolite, baratovite, aegirine, polylithionite, leucosphenite, fluorite, etc. Holotype sample. Triclinic, space group *P*-1, a = 9.816, b = 9.825, c = 17.309 Å, α = 99.21°, β = 94.67°, γ = 119.84°, V = 1404 Å^3, Z = 1. D_{meas} = 2.83(2) g/cm^3, D_{calc} = 2.819 g/cm^3. Optically biaxial (+), α = 1.651(2), β = 1.655(2), γ = 1.657(2), 2 V = 72 (2)°. The empirical formula is $(K_{1.98}Rb_{0.03})(Na_{0.90}\square_{0.10})(Ca_{6.16}Na_{0.63}Sr_{0.17}Ba_{0.04})(Ti_{4.00}Nb_{0.02})Li_{5.98}Si_{24}O_{66.00}(F_{1.63}O_{0.36})$. The strongest lines of the powder X-ray diffraction pattern [*d*, Å (*I*, %) (*hkl*)] are: 5.60 (9) (003), 4.25 (60) (0–21), 3.35 (100) (005), 3.14 (20) (1–32), 3.06 (90) (−1–23), 2.885 (55) (−215), 2.870 (10) (−232), 1.868 (17) (−144).
Kind of sample preparation and/or method of registration of the spectrum: No data on the kind of sample preparation and the method of registration of the IR spectrum are given by the authors.
Source: Agakhanov et al. (2007).
Wavenumbers (cm^{-1}): 1211, 1174, 1130, 1061s, 1022s, 940s, 783w, 683w, 650w, 559, 534, 460s.
Note: Original IR spectrum in the paper by Agakhanov et al. (2007) is given without scales. The wavenumbers were partly determined by us based on spectral curve analysis of the published spectrum.

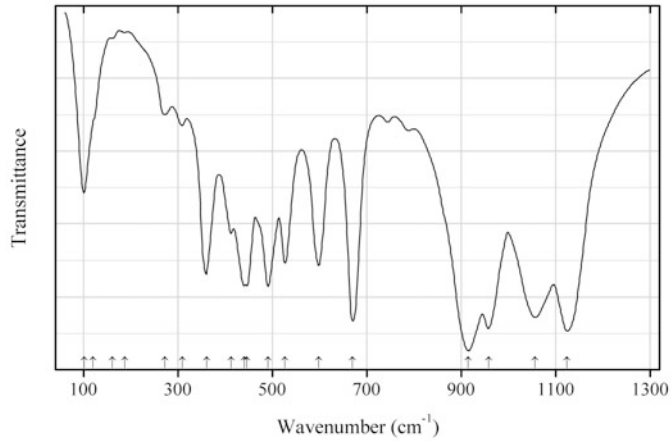

Fig. 2.781 IR spectrum of barium titanosilicate TiSi288 drawn using data from Stassen et al. (1998)

TiSi288 Barium titanosilicate TiSi288 $BaTi(Si_2O_6)O$ (Fig. 2.781)
Locality: Synthetic.
Description: Synthesized by conventional solid state reaction techniques. Monoclinic, a = 11.8831 (7), b = 10.0067(5), c = 9.9156(10) Å, β = 93.832(6)°. The strongest lines of the powder X-ray diffraction pattern [*d*, Å (*I*, %) (*hkl*)] are: 3.8231 (40) (220), 3.5194 (59) (022), 3.0899 (93) (22–2), 2.9648 (100) (400), 2.5016 (40) (040), 2.4722 (49) (004).
Kind of sample preparation and/or method of registration of the spectrum: KBr (above 250 cm^{-1}) and polyethylene discs. Absorption.
Source: Stassen et al. (1998).
Wavenumbers (cm^{-1}): 1124s, 1056s, 958s, 915s, 670s, 598, 526, 490, 446, 440, 412, 360, 309w, 272w, 187, 161, 120sh, 101.

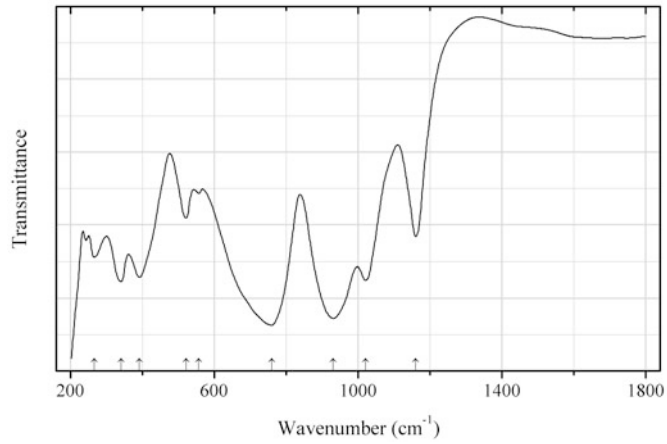

Fig. 2.782 IR spectrum of belkovite drawn using data from Voloshin et al. (1991)

TiSi289 Belkovite $Ba_3Nb_6(Si_2O_7)_2O_{12}$ (Fig. 2.782)
Locality: Vuoriyarvi alkaline-ultrabasic massif, Northern Karelia, Russia (type locality).
Description: Brown crystals from the association with magnetite, pyrochlore, phlogopite, chlorite, pyrite, pyrrothite, apatote, barite, alstonite, and nenadkevichite in dolomite-calcite carbonatite. Holotype sample. Hexagonal, space group *P*-62 *m*, $a = 8.966(3)$, $c = 7.799(3)$ Å, $Z = 1$. $D_{meas} = 4.16$ (3) g/cm^3, $D_{calc} = 4.25$ g/cm^3. Optically uniaxial (+), $\omega = 1.928(2)$, $\varepsilon = 2.002(5)$. The empirical formula is $(Ba_{2.74}K_{0.16}Na_{0.09}Ca_{0.01})(Nb_{4.41}Ti_{0.97}Fe_{0.31}Zr_{0.13}Al_{0.04}Ta_{0.01})Si_{4.12}O_{24.90}$. The strongest lines of the powder X-ray diffraction pattern [*d*, Å (*I*, %) (*hkl*)] are: 7.81 (35) (001, 010), 3.888 (51) (002, 111, 020), 3.481 (24) (012, 021), 2.937 (100) (112, 120), 2.750 (25) (022), 121), 1.948 (26) (123, 222, 040, 014).
Kind of sample preparation and/or method of registration of the spectrum: KBr disc. Absorption.
Source: Voloshin et al. (1991).
Wavenumbers (cm^{-1}): 1160, 1020, 930s, 760s, 557w, 522, 392, 340, 266.

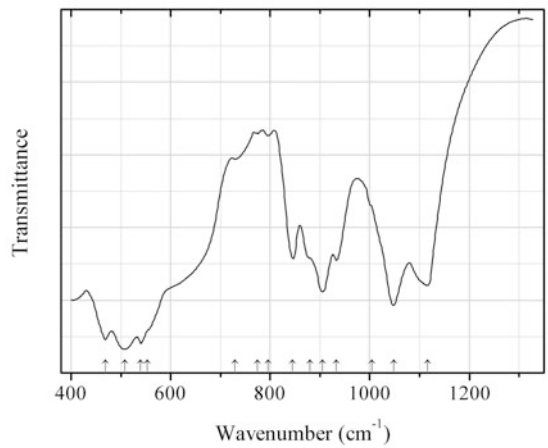

Fig. 2.783 IR spectrum of chevkinite-(Pr) Mg-analogue drawn using data from Ito and Arem (1971)

TiSi290 Chevkinite-(Pr) Mg-analogue $Pr_4Mg_2Ti_3(Si_2O_7)_2O_8$ (Fig. 2.783)

Locality: Synthetic.
Description: Synthesized from gel at 990 °C (as a compound with perrierite structure) with subsequent heating up to 1070 °C to obtain a chevkinite-type compound. Confirmed by chemical analysis and powder X-ray diffraction data. Monoclinic, space group $P2_1/a$, a = 13.376(2), b = 5.7074(7), c = 11.015(2) Å, β = 100.71(1)°. The strongest lines of the powder X-ray diffraction pattern [d, Å (I, %) (hkl)] are: 5.42 (60) (002), 3.173 (80) (311), 3.140 (60) (−312), 2.854 (60) (020), 2.744 (70) (312), 2.708 (100) (004).
Kind of sample preparation and/or method of registration of the spectrum: KBr disc. Transmission.
Source: Ito and Arem (1971).
Wavenumbers (cm^{-1}): 1116, 1048, 1004sh, 933s, 905, 880sh, 845, 796w, 775w, 729w, 553sh, 540s, 508s, 469s.
Note: The wavenumbers were partly determined by us based on spectral curve analysis of the published spectrum.

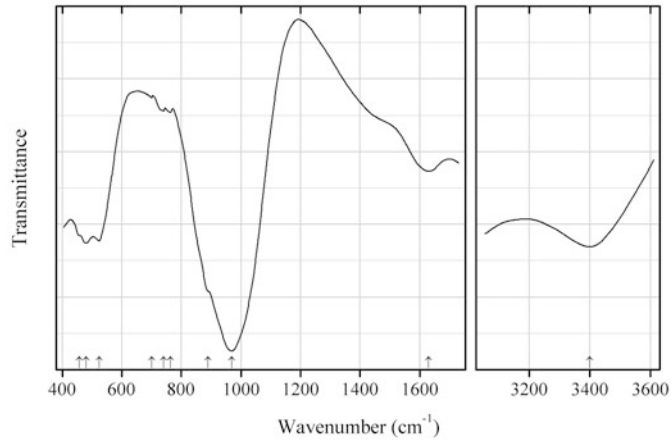

Fig. 2.784 IR spectrum of gaidonnayite Ca analogue drawn using data from Belyayevskaya et al. (1991)

TiSi291 Gaidonnayite Ca analogue $(Ca,Na,K)_{2-x}Zr(Si_3O_9)\cdot nH_2O$ (Fig. 2.784)
Locality: Mannepakhk Mt, Khibiny alkaline complex, Kola peninsula, Murmansk region, Russia.
Description: Brown pseudomorph after eudialyte from the association with feldspar, sodalite, pyroxene, lamprophyllite, and natrolite. Orthorhombic, a = 11.768, b = 12.805, c = 6.67 Å. Refractive indices are in the range from 1.68 to 1.71. The empirical formula is (ranges of components are indicated): $(Ca_{0.44–0.50}Na_{0.29–0.36}K_{0.26–0.35}Mn_{0.14–0.19}Sr_{0.04–0.05}Mg_{0.01–0.04})(Zr_{0.79–0.81}Ti_{0.09–0.11}Fe_{0.04–0.05}Al_{0–0.01})(Si_{3.00}O_9)\cdot nH_2O$. The strongest lines of the powder X-ray diffraction pattern [d, Å (I, %) (hkl)] are: 5.899 (60) (011), 3.617 (50) (221), 3.106 (100) (112), 2.942 (50–60) (400), 2.822 (50) (212), 2.208 (50) (013), 1.897 (50) (512), 1.869 (50) (360).
Kind of sample preparation and/or method of registration of the spectrum: KBr disc. Transmission.
Source: Belyayevskaya et al. (1991).
Wavenumbers (cm^{-1}): 3400, 1630, 970s, 890sh, 763w, 740w, 700w, 524s, 480s, 458sh.

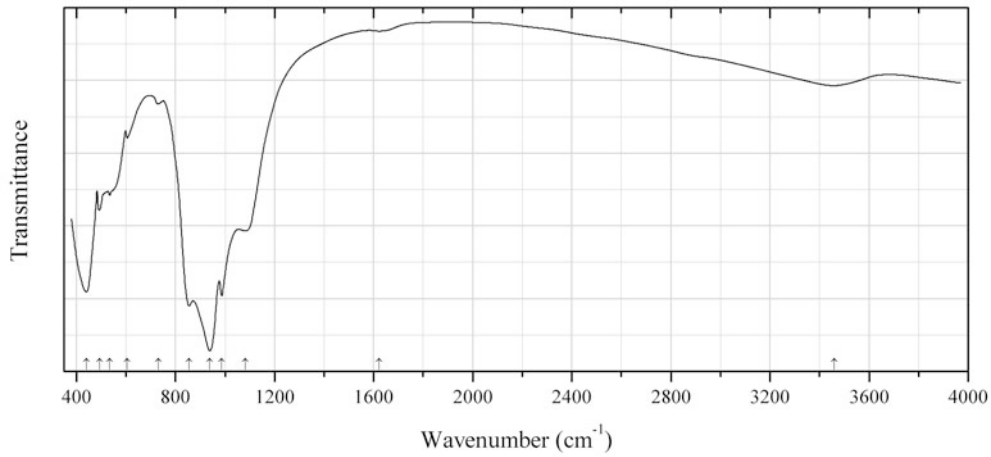

Fig. 2.785 IR spectrum of grenmarite drawn using data from Bellezza et al. (2004)

TiSi292 Grenmarite $Na_4MnZr_3(Si_2O_7)_2O_2F_2$ (Fig. 2.785)
Locality: Vesle Arøya island, Langesundsfjord district, Larvik, Vestfold, Norway (type locality).
Description: Yellowish brown, semi-parallel aggregate of elongate, flattened crystals from the association with microcline, aegirine, biotite, nepheline, albite, astrophyllite, låvenite, catapleiite, leucophanite, pyrochlore, and fluorite. Holotype sample. Monoclinic, space group $P2/c$, a = 5.608(1), b = 7.139(1), c = 18.575(5) Å, β = 102.60(2)°, V = 725.72(3) Å^3, Z = 2. D_{meas} = 3.49(1) g/cm^3, D_{calc} = 3.568 g/cm^3. Optically biaxial (+), α = 1.694, γ ≈ 1.735. The empirical formula based on 4 Si atoms is $(Na_{3.72}Ca_{0.26})(Mn_{0.48}Na_{0.29}Fe_{0.23})(Zr_{1.52}Mn_{0.46}Y_{0.02})(Zr_{0.55}Ti_{0.45})Si_{4.00}O_{15.40}F_{2.22}$. The strongest lines of the powder X-ray diffraction pattern [d, Å (I, %) (hkl)] are: 3.027 (68) (006), 2.898 (100) (121), 2.613 (26) (−204), 2.459 (24) (−125), 1.853 (24) (127).
Kind of sample preparation and/or method of registration of the spectrum: KBr disc. Transmission.
Source: Bellezza et al. (2004).
Wavenumbers (cm^{-1}): 3460, 1621w, 1082, 987s, 938s, 855s, 730w, 605w, 535, 493, 440s.
Note: The bands at 3460 and 1621 cm^{-1} indicate the presence of water molecules.

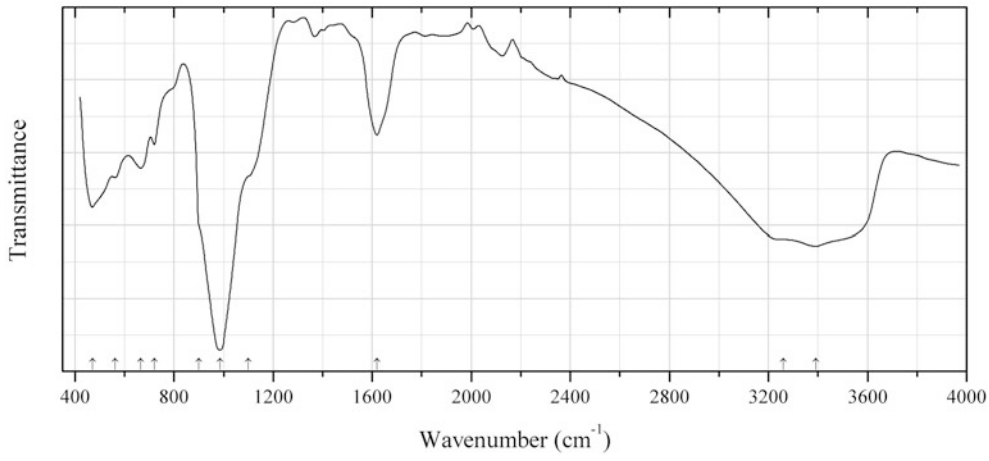

Fig. 2.786 IR spectrum of haineaultite drawn using data from McDonald and Chao (2004)

TiSi293 Haineaultite $(Na,Ca)_5Ca(Ti,Nb)_5Si_{12}O_{34}(OH,F)_8 \cdot 5H_2O$ (Fig. 2.786)
Locality: Poudrette (Demix) quarry, Mont Saint-Hilaire, Rouville RCM (Rouville Co.), Montérégie, Québec, Canada (type locality).
Description: Yellow crystals from the contact zone between peralkaline rock and marble xenolith, from the association with pectolite, vesuvianite, tainiolite, albite, fluorite, calcite, microcline, aegirine, etc. Holotype sample. The crystal structure is solved. Orthorhombic, space group *C*222, $a = 7.204(2)$, $b = 23.155(5)$, $c = 6.953(2)$ Å, $V = 1159.8(1)$ Å^3, $Z = 1$. $D_{calc} = 2.28$ g/cm^3. Optically biaxial (+), $\alpha = 1.599(1)$, $\beta = 1.610(1)$, $\gamma = 1.696(1)$, $2V = 38(1)°$. The empirical formula is $(Na_{2.41}Ca_{1.83}K_{0.71})Ca(Ti_{3.76}Nb_{0.67}Fe_{0.11}Mn_{0.06}Zr_{0.04}Mg_{0.03})(Si_{11.30}S_{0.52})O_{34}[(OH)_{7.86}F_{0.14}]\cdot 5H_2O$. The strongest lines of the powder X-ray diffraction pattern [*d*, Å (*I*, %) (*hkl*)] are: 11.564 (100) (020), 6.932 (90) (001, 110), 5.258 (40) (130), 4.446 (40) (041), 3.052 (75) (240), 2.977 (70) (042), 2.582 (40) (152, 062).
Kind of sample preparation and/or method of registration of the spectrum: Powder infrared-absorption spectrum was obtained using a diamond-anvil microsample cell.
Source: McDonald and Chao (2004).
Wavenumbers (cm^{-1}): 3392s, 3260sh, 1620, 1100sh, 985s, 900sh, 720w, 666, 562, 470s.
Note: The wavenumbers were partly determined by us based on spectral curve analysis of the published spectrum.

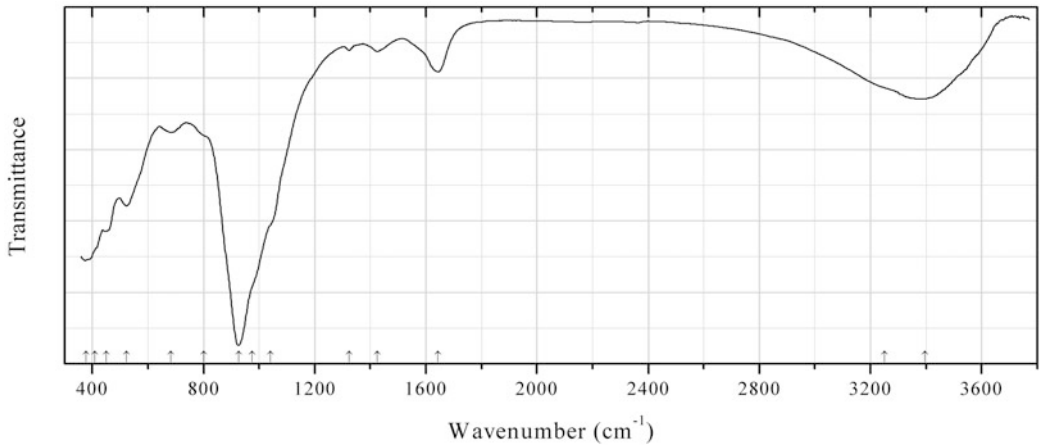

Fig. 2.787 IR spectrum of calciomurmanite obtained by N.V. Chukanov

TiSi294 Calciomurmanite $NaCa(Ti,Mg,Nb)_4[Si_2O_7]_2O_2(OH,O)_2 \cdot 4H_2O$ (Fig. 2.787)
Locality: Flora Mt., Lovozero alkaline complex, Kola peninsula, Murmansk region, Russia (type locality).
Description: Irregular aggregates of lamellar crystals from the association with microcline, aegirine, lorenzenite, fluorapatite, and calcite. Holotype sample. Triclinic, space group *P*-1, $a = 5.3470(6)$, $b = 7.0774(7)$, $c = 12.1456(13)$ Å, $\alpha = 91.827(4)°$, $\beta = 107.527(6)°$, $\gamma = 90.155(4)°$, $V = 438.03(8)$ Å^3, $Z = 1$. $D_{meas} = 2.70(3)$ g/cm^3, $D_{calc} = 2.87$ g/cm^3. Optically biaxial (−), $\alpha = 1.680(4)$, $\beta = 1.728(4)$, $\gamma = 1.743(4)$, $2V = 58(3)°$. The empirical formula is $Na_{1.34}Ca_{1.04}K_{0.05}Mg_{0.49}Mn_{0.29}Fe_{0.21}Nb_{0.36}Ti_{2.85}(Si_{3.87}Al_{0.13})_{\Sigma 4}O_{16.40}(OH)_{1.60}(PO_4)_{0.03}(H_2O)_{4.94}$. The strongest lines of the powder X-ray diffraction pattern [*d*, Å (*I*, %) (*hkl*)] are: 11.69 (100) (001), 5.87 (68) (011, 002), 4.251 (89) (−1–11, −111), 3.825 (44) (−1–12, 003, −112), 2.940 (47) (−1–21, −121), 2.900 (79) (004, 120), 2.659 (39) (−201, 0–23, −202).

Kind of sample preparation and/or method of registration of the spectrum: KBr disc. Absorption.
Wavenumbers (cm^{-1}): 3395, 3250sh, 1644, 1425w, 1324w, 1040sh, 975sh, 926s, 800sh, 682w, 523, 450, 410, 378s.

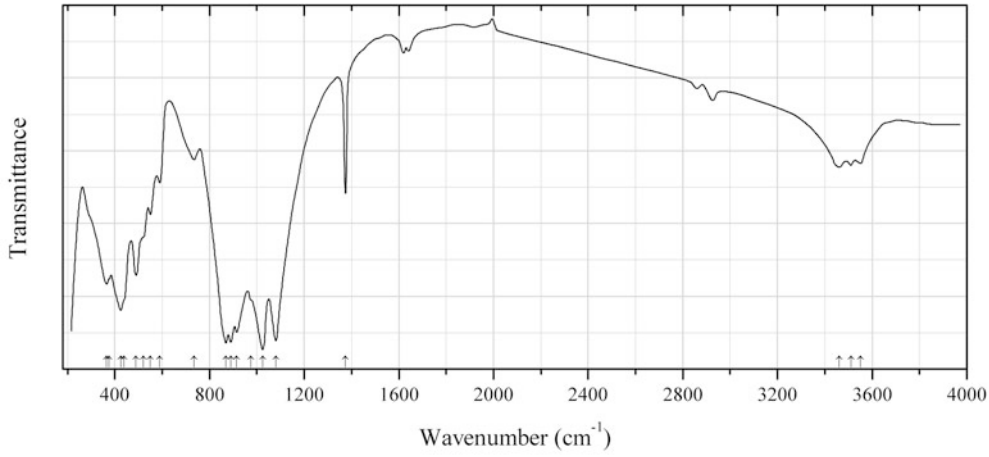

Fig. 2.788 IR spectrum of janhaugite drawn using data from Raade and Mladeck (1983)

TiSi295 Janhaugite $Na_3Mn^{2+}{}_3Ti_2(Si_2O_7)_2(O,OH,F)_4$ (Fig. 2.788)
Locality: Gjerdingselva, Lunner, Northern Oslo region, Oppland, Norway (type locality).
Description: Reddish brown sprays of long-prismatic crystals from ekerite from the association with elpidite and pyrophanite. Holotype sample. Monoclinic, space group $P2_1/n$, a = 10.668(2), b = 9.787 (4), c = 13.931(3) Å, β = 107.82(2)°, Z = 4. D_{meas} = 3.60(5) g/cm^3, D_{calc} = 3.71 g/cm^3. Optically biaxial (+), α = 1.770(4), β = 1.828(4), 2 V = 80(10)°; γ (calc) = 1.910. The empirical formula is $(Na_{2.75}Ca_{0.20}K_{0.03})(Mn_{2.43}Fe_{0.60})(Ti_{1.47}Zr_{0.38}Nb_{0.29}Ta_{0.01}Si_{3.84}O_{15.50}(OH)_{1.40}F_{1.10}$. The strongest lines of the powder X-ray diffraction pattern [d, Å (I, %) (hkl)] are: 3.202 (60) (310), 2.839 (100) (−124), 2.933 (90) (−322), 2.782 (90) (320, −105, 114, −231), 1.744 (50) (414).
Kind of sample preparation and/or method of registration of the spectrum: KI disc. Transmission.
Source: Raade and Mladeck (1983).
Wavenumbers (cm^{-1}): 3550, 3510, 3460, 1375, 1080s, 1025s, 975sh, 915s, 890s, 870s, 735w, 590w, 550, 520sh, 490, 440sh, 425s, 375sh, 365.
Note: Additional bands (cm^{-1}) correspond to the admixture of grease (2930w, 2860w), adsorbed (?) H_2O molecules (1640sh, 1620w) and NO_3^- anions (a typical admixture in KI, 1375).

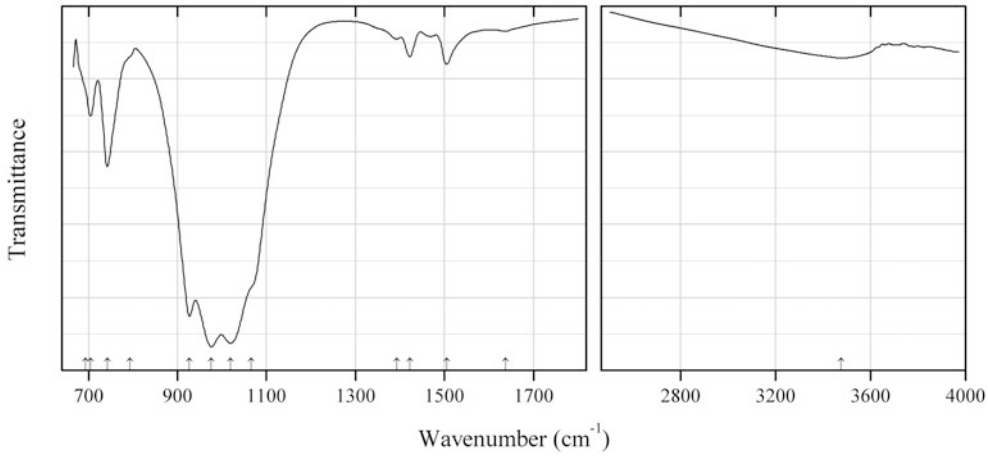

Fig. 2.789 IR spectrum of johnsenite-(Ce) drawn using data from Crice and Gault (2006)

TiSi296 Johnsenite-(Ce) $Na_{12}Ce_3Ca_6Mn_3Zr_3WSi_{25}O_{73}(CO_3)(OH)_2$ (Fig. 2.789)
Locality: Poudrette quarry, Mont Saint-Hilaire, Rouville Co., Québec, Canada (type locality).
Description: Yellow to orange skeletal crystals from the association with albite, calcite, pectolite, aegirine, fluorapophyllite, zirsilite-(Ce), dawsonite, rhodochrosite, epididymite, galena, molybdenite, etc. Holotype sample. Trigonal, space group *R*3*m*, a = 14.237(3), c = 30.03(1) Å, V = 5271(2) Å^3, Z = 3. D_{meas} = 3.24(3) g/cm^3, D_{calc} = 3.23 g/cm^3. Optically biaxial (−), ω = 1.648(1), ε = 1.637(1). The empirical formula is $Na_{11.74}[(Ce_{0.64}La_{0.33}Dy_{0.03})Sr_{0.54}Ca_{0.51}Y_{0.22}K_{0.19}][Ca(Pr_{0.24}Nd_{0.18}Gd_{0.06}Sm_{0.02})Mn_{0.44}](Mn_{2.22}Fe_{0.78})(Zr_{2.71}Ti_{0.32}Hf_{0.01})(W_{0.78}Nb_{0.21})Si_{24.97}O_{73}(CO_3)Cl_{0.75}(OH)_x$. The strongest lines of the powder X-ray diffraction pattern [*d*, Å (*I*, %) (*hkl*)] are: 11.308 (95) (101), 9.460 (81) (012), 4.295 (34) (205), 3.547 (36) (220), 3.395 (38) (131), 3.167 (75) (217), 2.968 (100) (315), 2.849 (81) (404).
Kind of sample preparation and/or method of registration of the spectrum: Diamond-anvil cell microsampling using a grain of the mineral.
Source: Crice and Gault (2006).
Wavenumbers (cm^{-1}): 3477, 1637w, 1505, 1422w, 1393w, 1066sh, 1019s, 976s, 927s, 793sh, 742, 704, 693sh.
Note: The wavenumbers were partly determined by us based on spectral curve analysis of the published spectrum. The band at 1637 cm^{-1} indicates the presence of H_2O molecules.

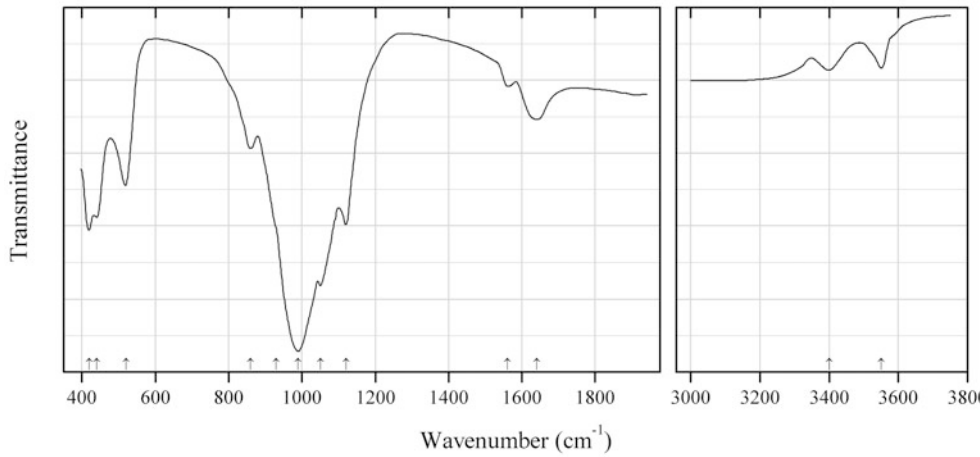

Fig. 2.790 IR spectrum of laplandite-(Ce) drawn using data from Yes'kova et al. (1974b)

TiSi297 Laplandite-(Ce) $Na_4CeTiPSi_7O_{22}{\cdot}5H_2O$ (Fig. 2.790)
Locality: Yubileinaya (Yubilee) pegmatite, Karnasurt Mt., Lovozero alkaline massif, Kola peninsula, Murmansk region, Russia (type locality).
Description: Light gray radial fibrous aggregate from the association with lomonosovite, natrolite, raite, zorite, mountainite, penkvilksite, terskite, etc. Holotype sample. Orthorhombic, space group *Pmmm*, $a = 7.27$, $b = 14.38$, $c = 22.25$ Å, $V = 2326$ Å^3. Optically biaxial (−), $\alpha = 1.568(2)$, $\beta = 1.584(2)$, $\gamma = 1.585(2)$. The strongest lines of the powder X-ray diffraction pattern [*d*, Å (*I*, %) (*hkl*)] are: 3.78 (90) (132), 3.34 (90) (212), 3.25 (70) (134, 203, 140), 3.01 (70) (204, 214, 230), 2.82 (90) (232), 1.780 (70) (346, 2.3.10).
Kind of sample preparation and/or method of registration of the spectrum: KBr disc. Transmission.
Source: Yes'kova et al. (1974b).
Wavenumbers (cm^{-1}): 3550, 3400w, 1640, 1560w, 1120, 1050s, 990s, 930sh, 860, 520, 440, 420s.

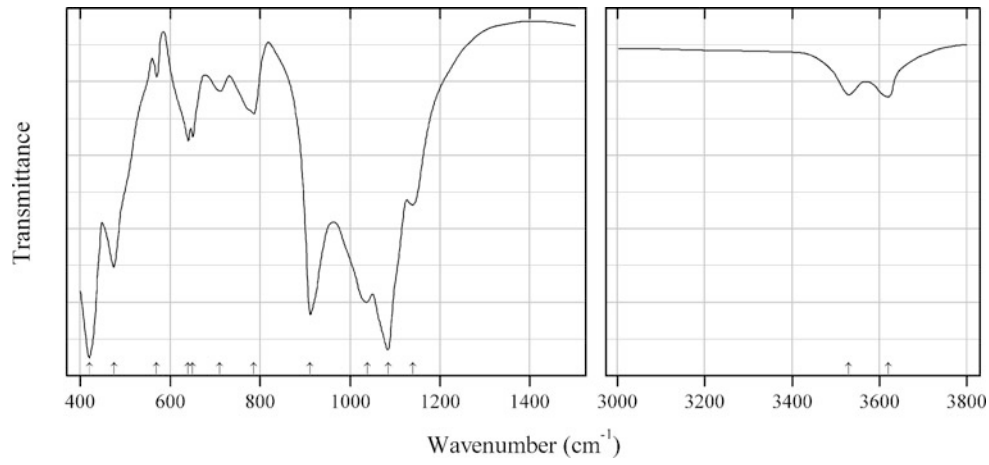

Fig. 2.791 IR spectrum of muirite drawn using data from Povarennykh (1979)

TiSi298 Muirite $Ba_{10}Ca_2Mn^{2+}TiSi_{10}O_{30}(OH,F,Cl)_{10}$ (Fig. 2.791)
Locality: Not indicated.
Description: No data.
Kind of sample preparation and/or method of registration of the spectrum: KBr disc. Absorption.
Source: Povarennykh (1979).
Wavenumbers (cm^{-1}): 3620, 3530, 1140, 1085s, 1038s, 910s, 786, 710w, 650, 640, 570w, 476s, 420s.

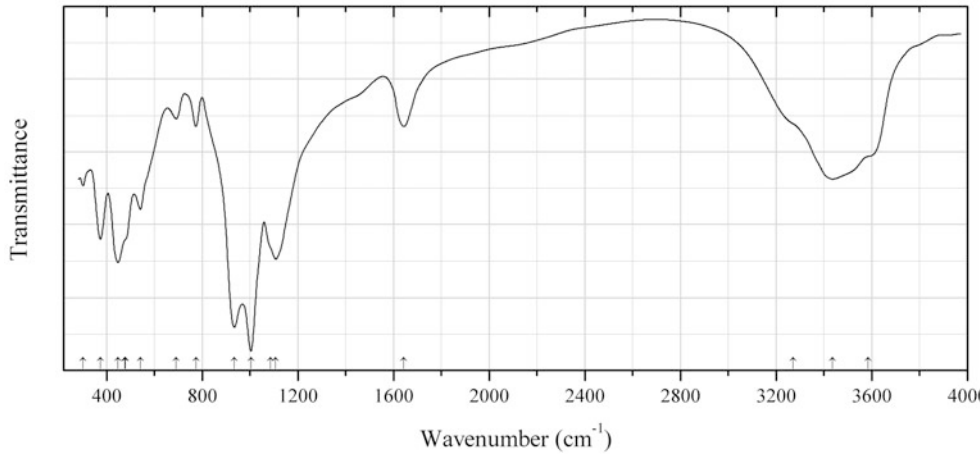

Fig. 2.792 IR spectrum of natrolemoynite drawn using data from McDonald and Chao (2001)

TiSi299 Natrolemoynite $Na_3Zr_2Si_{10}O_{26}\cdot 9H_2O$ (Fig. 2.792)
Locality: Poudrette (Demix) quarry, Mont Saint-Hilaire, Rouville RCM (Rouville Co.), Montérégie, Québec, Canada (type locality).
Description: Colourless crystals from peralkaline pegmatite. Holotype sample. The crystal structure is solved. Monoclinic, space group *C*2/*m*, *a* 10.5150(2), *b* 16.2534(4), *c* 9.1029(3) Å, β = 105.462(2) °, V = 1499.4(1) $Å^3$, Z = 2. D_{meas} = 2.47(1) g/cm^3, D_{calc} = 2.50 g/cm^3. Optically biaxial (−), α = 1.533(1), β = 1.559(1), γ = 1.567(1), 2 V = 63(1)°. The empirical formula is $(Na_{2.66}K_{0.30}Ca_{0.07}Mn_{0.02})(Zr_{1.96}Nb_{0.08}Ti_{0.05})(Si_{9.99}Al_{0.01})O_{25.79}\cdot 9H_2O$. The strongest lines of the powder X-ray diffraction pattern [*d*, Å (*I*, %) (*hkl*)] are: 8.132 (100) (020), 5.975 (40) (021), 3.974 (35) (201), 3.564 (40) (221), 3.490 (35) (−222).
Kind of sample preparation and/or method of registration of the spectrum: KBr disc. Transmission.
Source: McDonald and Chao (2001).
Wavenumbers (cm^{-1}): 3585sh, 3435, 3270sh, 1641, 1107s, 1084sh, 1004s, 934s, 773w, 691w, 541, 478sh, 477, 447s, 373, 301.
Note: The wavenumbers were partly determined by us based on spectral curve analysis of the published spectrum.

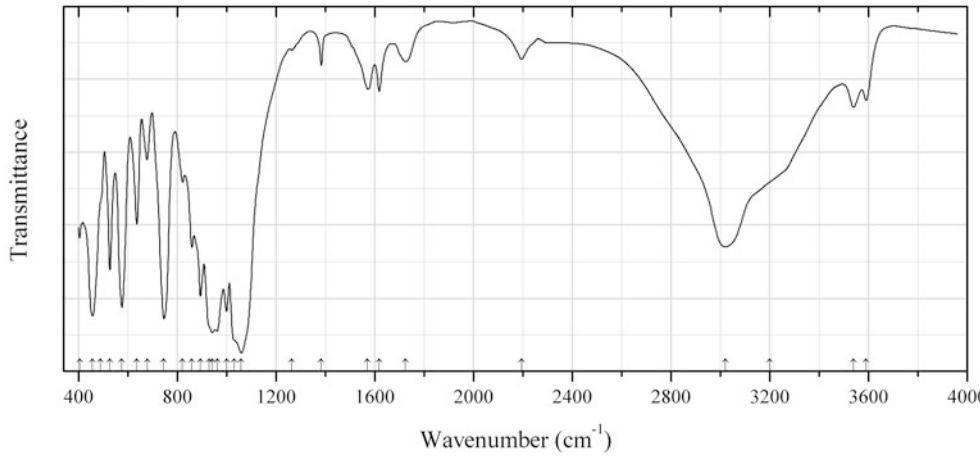

Fig. 2.793 IR spectrum of ohmilite drawn using data from Mizota et al. (1983)

TiSi300 Ohmilite $Sr_3(Ti,Fe^{3+})(Si_2O_6)_2(O,OH)\cdot 2H_2O$ (Fig. 2.793)
Locality: Ohmi, Niigata Prefecture, Central Japan (type locality).
Description: Spherulites composed of radially arranged fine needles. The crystal structure is solved. Monoclinic, space group $P2_1/m$, a = 10.979(6), b = 7.799(5), c = 7.818(4) Å, β = 100.90(3)°, V = 657.4(6) Å^3, Z = 2.
Kind of sample preparation and/or method of registration of the spectrum: Transmission. Kind of sample preparation is not indicated.
Source: Mizota et al. (1983).
Wavenumbers (cm^{-1}): 3590w, 3540w, 3200sh, 3020s, 2195w, 1725w, 1619w, 1571w, 1384w, 1264w, 1060s, 1030sh, 1000s, 962s, 942s, 930sh, 895s, 860, 822, 746s, 678, 636, 575s, 528, 490sh, 457s, 405.
Note: The band at 1384 cm^{-1} is due to NO_3^- impurity in the KBr disc.

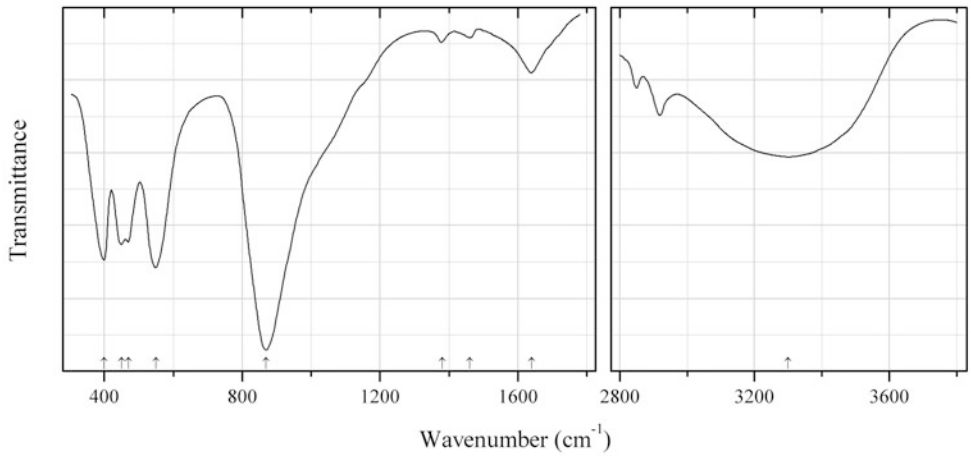

Fig. 2.794 IR spectrum of ivanyukite-Na-*C* drawn using data from Yakovenchuk et al. (2009)

TiSi301 Ivanyukite-Na-*C* $Na_2[Ti_4O_2(OH)_2(SiO_4)_3]\cdot 6H_2O$ (Fig. 2.794)

Locality: Koashva Mt., Khibiny alkaline complex, Kola peninsula, Murmansk region, Russia (type locality).

Description: Pale-orange cubic crystals from the association with microcline, vinogradovite, sazykinaite-(Y), natrolite, and djerfisherite. Holotype sample. Cubic, space group *P*-43*m*, a = 7.856 (6), Z = 1. D_{meas} = 2.60 g/cm^3, D_{calc} = 2.39 g/cm^3. Optically isotropic, n = 1.73(1). The empirical formula is $(Na_{1.17}K_{0.94}Ca_{0.03})(Ti_{3.32}Fe_{0.21}Nb_{0.15}Mn_{0.03})(Si_{2.97}Al_{0.03})O_{12.89}(OH)_{2.87}\cdot 6.01H_2O$. The strongest lines of the powder X-ray diffraction pattern [*d*, Å (*I*, %) (*hkl*)] are: 7.88 (100) (100), 4.53 (30) (111), 3.205 (80) (211), 2.774 (30) (220), 2.622 (40) (221, 300), 2.478 (40) (310), 1.960 (30) (400), 1.843 (30) (330, 411).

Kind of sample preparation and/or method of registration of the spectrum: Transmission. Kind of sample preparation is not indicated.

Source: Yakovenchuk et al. (2009).

Wavenumbers (cm^{-1}): 3300, 1640, 1460w, 1380w, 870s, 550, 470, 450, 400.

Note: The bands in the range from 2800 to 3000 cm^{-1} (and, possibly, the bands at 1460 and 1480 cm^{-1}) correspond to the admixture of an organic substance.

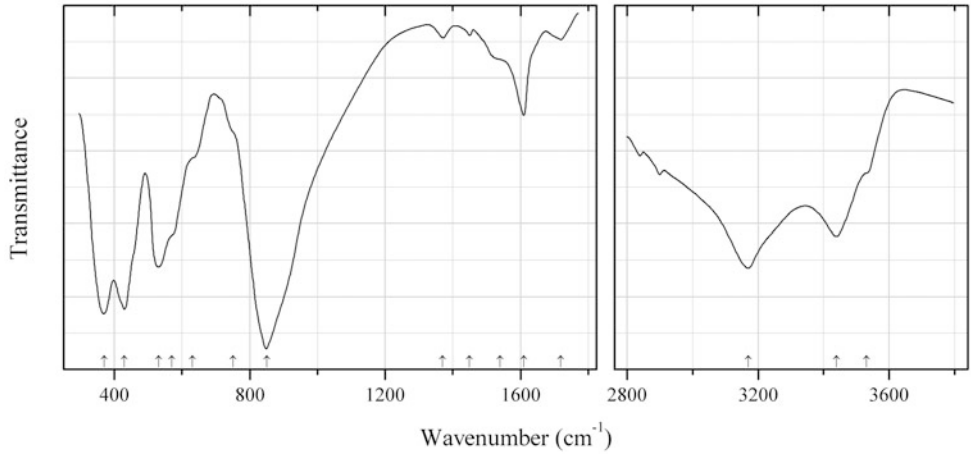

Fig. 2.795 IR spectrum of ivanyukite-Na-*T* drawn using data from Yakovenchuk et al. (2009)

TiSi302 Ivanyukite-Na-*T* $Na_3[Ti_4O_3(OH)(SiO_4)_3]\cdot 7H_2O$ (Fig. 2.795)

Locality: Koashva Mt., Khibiny alkaline complex, Kola peninsula, Murmansk region, Russia (type locality).

Description: Pale-blue pseudo-cubic crystals from the association with microcline, vinogradovite, sazykinaite-(Y), natrolite, and djerfisherite. Holotype sample. Trigonal, space group *R*3*m*, a = 10.94 (2), c = 13.97(4) Å, Z = 3. D_{meas} = 2.70 g/cm^3, D_{calc} = 2.58 g/cm^3. Optically uniaxial (+), ω = 1.76(1), ε = 1.85(9). The empirical formula is $(Na_{1.82}K_{0.95}Ca_{0.03}Ba_{0.01})(Ti_{3.68}Nb_{0.17}Fe_{0.06}Mn_{0.01})(Si_{2.99}Al_{0.01})O_{14.59}(OH)_{1.37}\cdot 7.29H_2O$. The strongest lines of the powder X-ray diffraction pattern [*d*, Å (*I*, %) (*hkl*)] are: 7.88 (100) (011), 3.277 (60) (014), 3.175 (80) (212), 2.730 (50) (220), 2.607 (70) (303), 2.471 (50) (124), 1.960 (60) (044), 1.916 (50) (135).

Kind of sample preparation and/or method of registration of the spectrum: Transmission. Kind of sample preparation is not indicated.

Source: Yakovenchuk et al. (2009).

Wavenumbers (cm^{-1}): 3530sh, 3440, 3170, 1720w, 1610, 1540sh, 1450w, 1370w, 850s, 750sh, 630sh, 570sh, 530s, 430s, 370s.

Note: The bands in the range from 2800 to 3000 cm^{-1} (and, possibly, the bands at 1720, 1540, 1450, and 1370 cm^{-1}) correspond to the admixture of an organic substance.

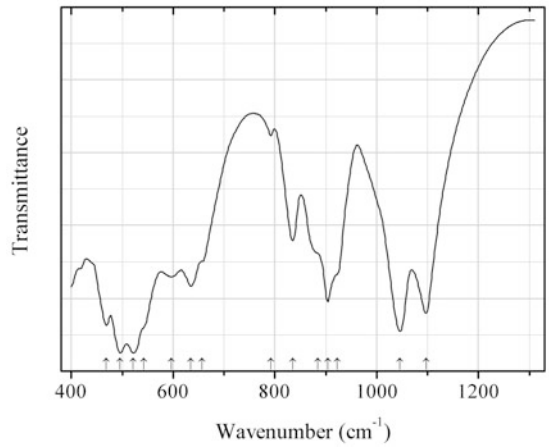

Fig. 2.796 IR spectrum of perrierite-(La) Mg analogue drawn using data from Ito and Arem (1971)

TiSi303 Perrierite-(La) Mg analogue $La_4Mg_2Ti_3Si_4O_{22}$ (Fig. 2.796)
Locality: Synthetic.
Description: Synthesized in a high-temperature solid-state reaction from evaporated solution of hydroxides of Mg, La, and Ti and silicic acid. Confirmed by powder X-ray diffraction data. Monoclinic, a = 13.786(4), b = 5.6766(9), c = 11.791(3) Å, β = 113.88(2)°, V = 834.7(4) $Å^3$.
Kind of sample preparation and/or method of registration of the spectrum: KBr disc. Absorption.
Source: Ito and Arem (1971).
Wavenumbers (cm^{-1}): 1097, 1046s, 923sh, 904, 884sh, 835, 792w, 657sh, 635, 596w, 542sh, 522s, 496s, 469s.
Note: The wavenumbers were partly determined by us based on spectral curve analysis of the published spectrum.

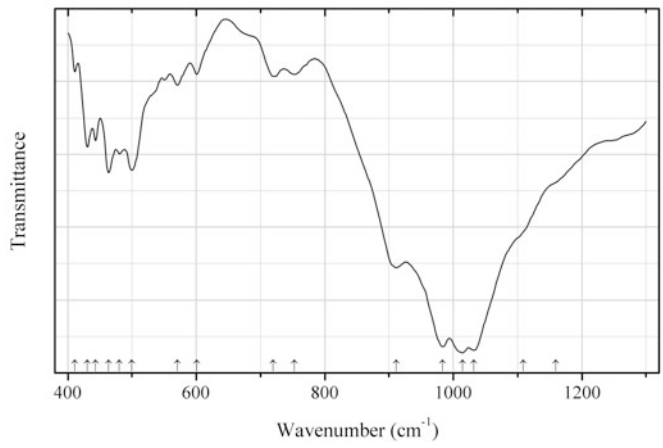

Fig. 2.797 IR spectrum of pyatenkoite-(Y) drawn using data from Khomyakov et al. (1996)

TiSi304 Pyatenkoite-(Y) $Na_5(Y,REE)TiSi_6O_{18}·6H_2O$ (Fig. 2.797)

Locality: Umbozero mine, Alluaiv Mt., Lovozero alkaline complex, Kola peninsula, Murmansk region, Russia (type locality).
Description: Colourless transparent rhombohedral crystals from peralkaline pegmatite. Holotype sample. Trigonal, space group *R*32, $a = 10.696(5)$, $c = 15.728(6)$ Å, $V = 1558(2)$ Å^3, $Z = 3$. $D_{meas} = 2.68(5)$ g/cm^3. Optically uniaxial (−), ε = 1.607(2), ω = 1.612(2). The empirical formula is $(Na_{4.70}K_{0.03})(Y_{0.50}Dy_{0.11}Gd_{0.08}Sm_{0.055}Er_{0.04}Nd_{0.03}Eu_{0.03}Tb_{0.02}Ce_{0.02}Ho_{0.01}Yb_{0.01}La_{0.005}Tm_{0.005}Th_{0.01})(Ti_{0.86}Nb_{0.17}Zr_{0.03})Si_{6.03}O_{18}\cdot 6H_2O$. The strongest lines of the powder X-ray diffraction pattern [*d*, Å (*I*, %)] are: 5.99 (60), 3.21 (100), 3.093 (40), 2.990 (85), 2.661 (40), 1.998 (55).
Kind of sample preparation and/or method of registration of the spectrum: KBr disc. Absorption.
Source: Khomyakov et al. (1996).
Wavenumbers (cm^{-1}): 1159sh, 1109sh, 1032s, 1014s, 983s, 911, 753w, 720w, 601w, 571w, 500, (480), 464, 443, 431, 411w.
Note: The bands at 1159, 1109, and 911 cm^{-1} correspond to impurities. For the IR spectrum of pure pyatenkoite-(Y) from the Kukisvumchorr Mt., Khibiny alkaline complex, Kola peninsula (not a type locality) see Chukanov (2014a).

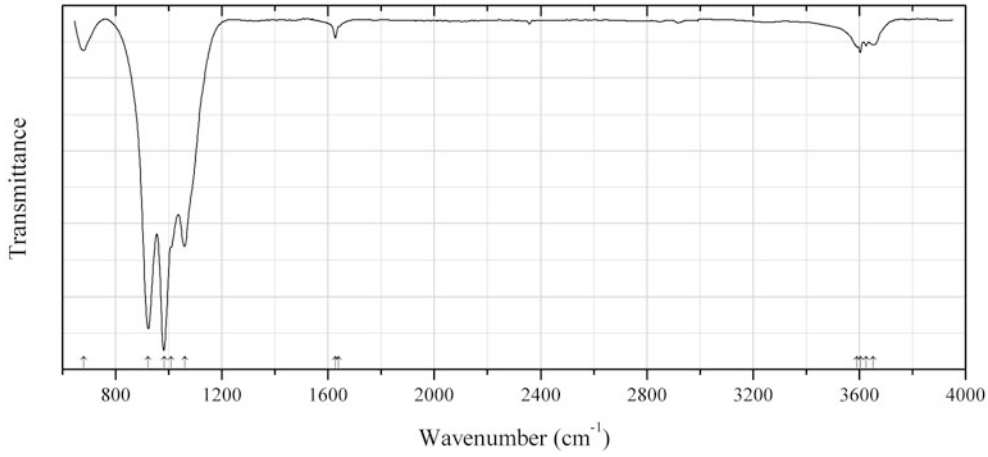

Fig. 2.798 IR spectrum of nafertisite drawn using data from Cámara et al. (2014)

TiSi305 Nafertisite $Na_3Fe^{2+}{}_{10}Ti_2(Si_6O_{17})_2O_2(OH)_6F\cdot 2H_2O$ (Fig. 2.798)
Locality: Kirovskiy mine, Kukisvumchorr Mt., Khibiny alkaline complex, Kola peninsula, Murmansk region, Russia (type locality).
Description: The crystal structure is solved. Monoclinic, space group *A*2/*m*, $a = 5.358(1)$, $b = 16.204(3)$, $c = 21.976(4)$ Å, β = 94.91(1)°, $V = 1901.0(7)$ Å^3, $Z = 2$. $D_{calc} = 3.116$ g/cm^3. The empirical formula is (electron microprobe; the content of H_2O was calculated from the structure–refinement results): $(Na_{1.39}K_{0.61})Na_{1.00}(\square_{0.92}Rb_{0.06}Cs_{0.02})(Fe^{2+}{}_{9.11}Mg_{0.46}Mn_{0.22}Al_{0.10}Na_{0.09}Ca_{0.02})(Ti_{1.90}Nb_{0.05}Mg_{0.03}Zr_{0.02})(Si_{11.81}Al_{0.19}O_{34})O_2(OH)_6(F_{0.86}O_{0.14})\cdot 1.39H_2O$. Predominantly bivalent state of iron was confirmed by Mössbauer spectroscopy.
Kind of sample preparation and/or method of registration of the spectrum: Thin film prepared by a diamond micro compression cell. Absorption.
Source: Cámara et al. (2014).
Wavenumbers (cm^{-1}): 3653w, 3626w, 3604w, 3592w, 1640sh, 1627w, 1060s, 1010sh, 983s, 923s, 679.

Note: In the single-crystal spectrum of the same nafertisite sample additional broad bands at 3400 and 3250 cm^{-1} are present.

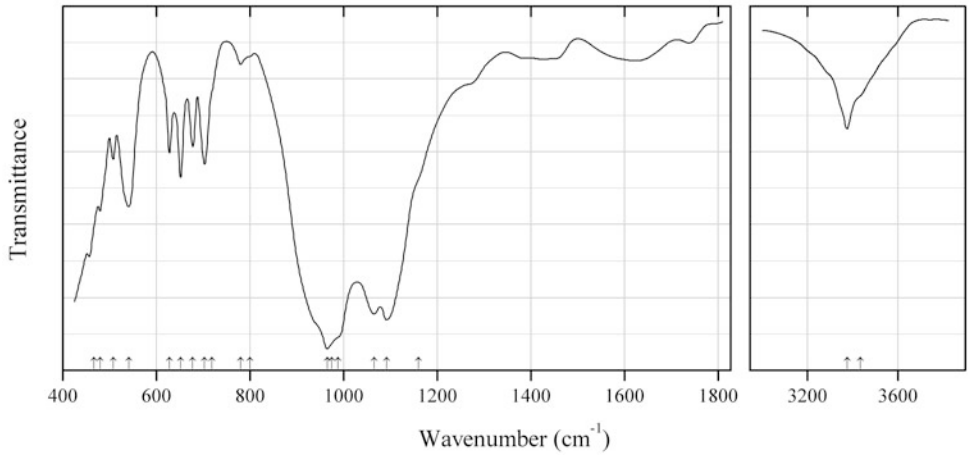

Fig. 2.799 IR spectrum of senkevichite drawn using data from Agakhanov et al. (2005)

TiSi306 Senkevichite $CsKNaCa_2Ti[Si_7O_{18}(OH)]O$ (Fig. 2.799)
Locality: Dara-i Pioz glacier, Dara-i Pioz alkaline massif, Tien Shan Mts., Tajikistan (type locality).
Description: White elongated board-like grains from the association with quartz and pectolite. Holotype sample. The crystal structure is solved. Senkevichite is a Cs-analogue of tinaksite. Triclinic, space group *P*-1, a = 10.4191(4), b = 12.2408(5), c = 7.0569(3) Å, α = 90.857(1)°, β = 99.193(1)°, γ = 91.895(1)°, Z = 2. D_{meas} = 3.12(2) g/cm^3, D_{calc} = 3.13 g/cm^3. Optically biaxial (+), α = 1.616(2), β = 1.645(2), γ = 1.683(2), 2 V = 85(2)°. The empirical formula is (electron microprobe): $Cs_{0.90}K_{1.08}Na_{1.00}(Ca_{1.65}Mn_{0.30}Fe_{0.06})(Ti_{0.93}Nb_{0.04})[Si_7O_{18}(OH)]O_{0.97}$. The strongest lines of the powder X-ray diffraction pattern [*d*, Å (*I*, %) (*hkl*)] are: 4.08 (13) (030), 3.33 (11) (11–2, 012, 3–10), 3.25 (16) (2–30), 3.14 (21) (102, 230), 3.06 (100) (20–2, 040, 2–3–1, 3–20), 2.959 (20) (1–40), 2.038 (17) (060).
Kind of sample preparation and/or method of registration of the spectrum: KBr disc. Absorption.
Source: Agakhanov et al. (2005).
Wavenumbers (cm^{-1}): 3435sh, 3375, 1160sh, 1092s, 1065s, 988sh, 965s, 975sh, 800sh, 780w, 719sh, 703, 678, 652, 628, 541s, 508, 480, 467.
Note: The wavenumbers were partly determined by us based on spectral curve analysis of the published spectrum. In the cited paper the wavenumbers 628 and 457 cm^{-1} are erroneously indicated as 638 and 467 cm^{-1}, respectively.

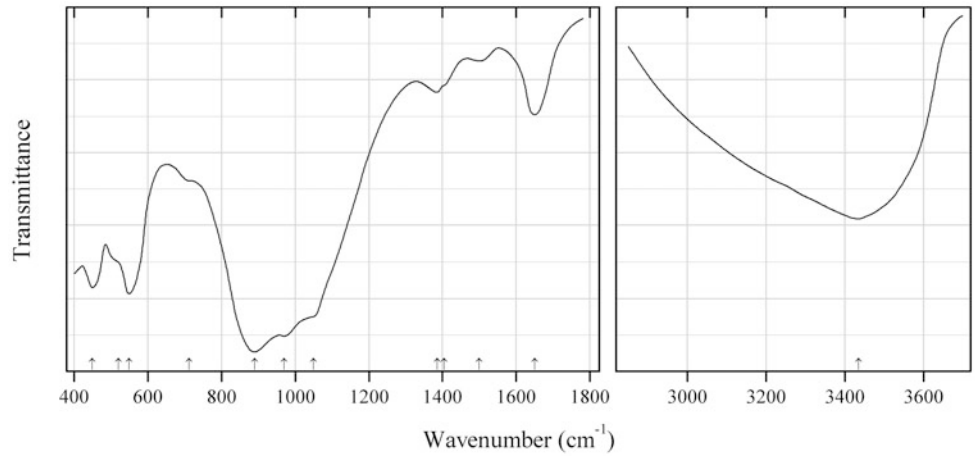

Fig. 2.800 IR spectrum of shkatulkalite drawn using data from Men'shikov et al. (1996)

TiSi307 Shkatulkalite $Na_{10}MnTi_3Nb_3(Si_2O_7)_6(OH)_2F{\cdot}12H_2O$ (Fig. 2.800)
Locality: Shkatulka pegmatite, Alluaiv Mt., Lovozero alkaline massif, Kola peninsula, Murmansk region, Russia (type locality).
Description: Aggregate of lamellae from peralkaline pegmatite. Holotype sample. Monoclinic, space group *Pm*, *P*2 or *P*2/*m*, $a = 5.468(9)$, $b = 7.18(1)$, $c = 31.1(1)$ Å, $\beta = 94.0(2)°$, $V = 1218(8)$ Å^3, $Z = 1$. $D_{meas} = 2.70(2)$ g/cm^3. Optically biaxial (+), $\alpha = 1.608(2)$, $\beta = 1.630(2)$, $\gamma = 1.660(2)$, $2V = 82(1)°$. The empirical formula is $Na_{10.38}(Mn_{0.48}Ca_{0.15}Sr_{0.09})Ti_{2.77}Nb_{3.29}(Si_{11.84}Al_{0.09}Fe^{3+}_{0.02})O_{42.03}(OH)_{1.99}F_{0.99}{\cdot}12H_2O$. The strongest lines of the powder X-ray diffraction pattern [*d*, Å (*I*, %) (*hkl*)] are: 15.56 (90) (002), 5.16 (60) (006), 3.11 (10) (019, 0.0.10), 2.850 (70) (123), 2.665 (70) (125), 2.627 (70) (0.1.11), 2.217 (60) (0.0.14), 1.795 (60) (040).
Kind of sample preparation and/or method of registration of the spectrum: KBr disc. Transmission.
Source: Men'shikov et al. (1996).
Wavenumbers (cm^{-1}): 3435s, 1650, 1500w, 1405sh, 1385w, 1050sh, 970s, 890s, 712sh, 550s, 520sh, 450s.
Note: The wavenumbers were partly determined by us based on spectral curve analysis of the published spectrum.

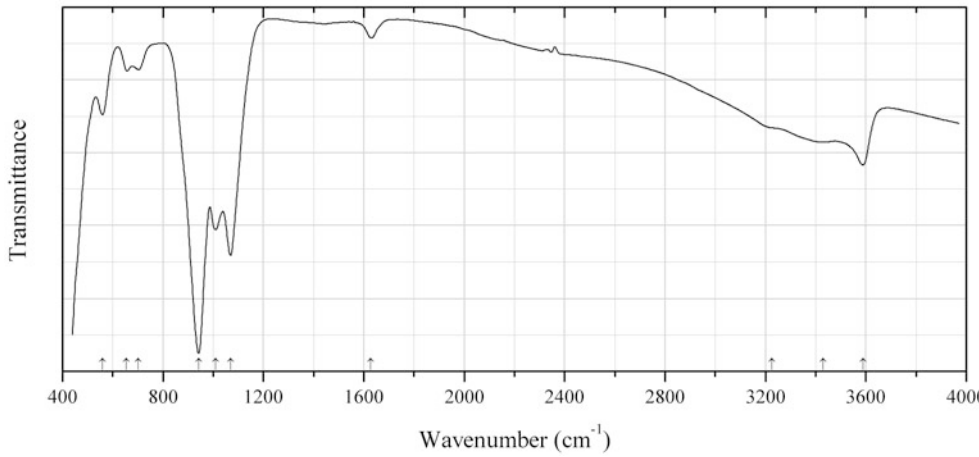

Fig. 2.801 IR spectrum of sveinbergeite drawn using data from Khomyakov et al. (2011)

TiSi308 Sveinbergeite $Ca(Fe^{2+}_6Fe^{3+})Ti_2(Si_4O_{12})_2O_2(OH)_5{\cdot}4H_2O$ (Fig. 2.801)
Locality: A syenite pegmatite at Buer, the Larvik plutonic complex, Vesterøya peninsula, Sandefjord, Oslo Region, Norway (type locality).
Description: Deep green aggregates of lamellar crystals from the association with magnesiokatophorite, aegirine, microcline, albite, calcite, fluorapatite, molybdenite, galena, etc. Holotype sample. Triclinic, space group *P*-1, a = 5.329(4), b = 11.803(8), c = 11.822(8) Å, α = 101.140(8)°, β = 98.224(8)°, γ = 102.442(8)°, V = 699.0(8) Å^3, Z = 1. D_{calc} = 3.152 g/cm^3. Optically biaxial (+), α = 1.745(2), β = 1.746(2), γ = 1.753(2), 2 V = 20(3)°. The empirical formula is $(Ca_{0.95}Na_{0.12}K_{0.14})(Fe^{2+}_{5.65}Fe^{3+}_{0.93}Mn_{0.25}Mg_{0.18})(Ti_{1.86}Nb_{0.06}Zr_{0.05}Fe^{3+}_{0.03})(Si_{7.91}Al_{0.09})O_{34.61}H_{12.34}F_{0.17}$. The strongest lines of the powder X-ray diffraction pattern [*d*, Å (*I*, %) (*hkl*)] are: 11.395 (100) (001, 010), 2.880 (38) (004), 2.640 (31) (−210, −141), 1.643 (24) (0–71), 2.492 (20) (2–11), 1.616 (15) (070), 1.573 (14) (−3–22), 2.270 (13) (−1–34), 2.757 (12) (−140, −1–32).
Kind of sample preparation and/or method of registration of the spectrum: Absorption. Kind of sample preparation is not indicated.
Source: Khomyakov et al. (2011).
Wavenumbers (cm^{-1}): 3588, 3430sh, 3225sh, 1628w, 1069s, 1009s, 942s, 702w, 655w, 560.
Note: The wavenumbers were partly determined by us based on spectral curve analysis of the published spectrum.

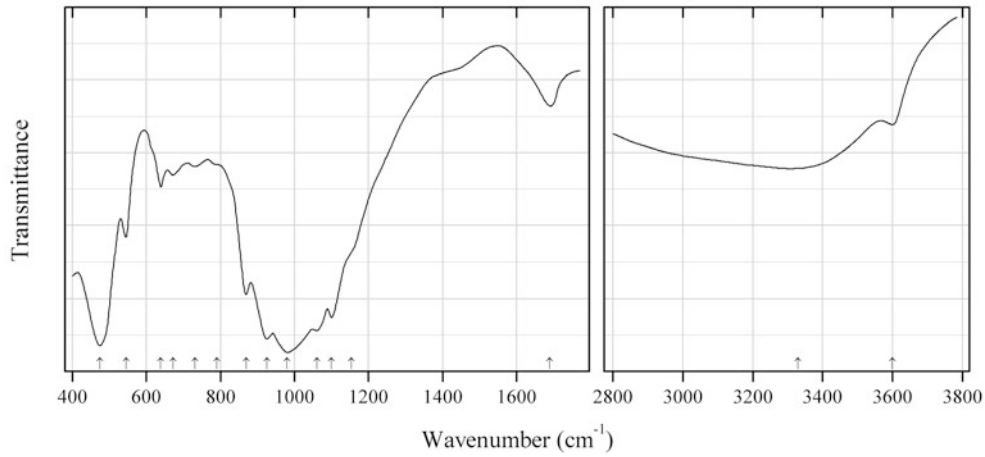

Fig. 2.802 IR spectrum of tiettaite drawn using data from Khomyakov et al. (1993)

TiSi309 Tiettaite $(Na,K)_{17}Fe^{3+}TiSi_{16}O_{29}(OH)_{30}{\cdot}2H_2O$ (Fig. 2.802)
Locality: Koashva Mt., Khibiny alkaline complex, Kola peninsula, Murmansk region, Russia (type locality).
Description: Fine-grained aggregate from the association with potassium feldspar, nepheline, sodalite, aegirine, villiaumite, natrite, rasvumite, phosinaite-(Ce), vuonnemite, etc. Holotype sample. Orthorhombic, space group *Cmcm*, *Cmc*2$_1$ or *C*2 *cm*, a = 29.77(1), b = 11.03(2), c = 17.111(5) Å, α = 99.773(5)°, β = 91.141(6)°, γ = 115.58(5)°, V = 571.6(3) Å^3, Z = 2. D_{meas} = 2.42(2) g/cm^3, D_{calc} = 2.39 g/cm^3. Optically biaxial (−), α = 1.532(2), β = 1.548(2), γ = 1.559(2), 2 V = 79(1)°. The empirical formula is $(Na_{12.51}K_{4.25}Ca_{0.11})Fe^{3+}_{1.02}Ti_{0.99}Si_{16.00}O_{29.10}(OH)_{29.80}{\cdot}1.84H_2O$. The strongest

lines of the powder X-ray diffraction pattern [*d*, Å (*I*, %) (*hkl*)] are: 13.38 (100) (110), 4.516 (75) (313), 3.220 (65) (604), 3.097 (80) (315, 623, 820), 2.975 (65) (912), 2.773 (90) (134, 913).
Kind of sample preparation and/or method of registration of the spectrum: Transmission. Kind of sample preparation is not indicated.
Source: Khomyakov et al. (1993).
Wavenumbers (cm^{-1}): 3600w, 3330 (broad), 1690w, 1154sh, 1100s, 1060s, 980s, 925s, 870s, 790sh, 731w, 672w, 638w, 545, 475s.
Note: The wavenumbers were partly determined by us based on spectral curve analysis of the published spectrum.

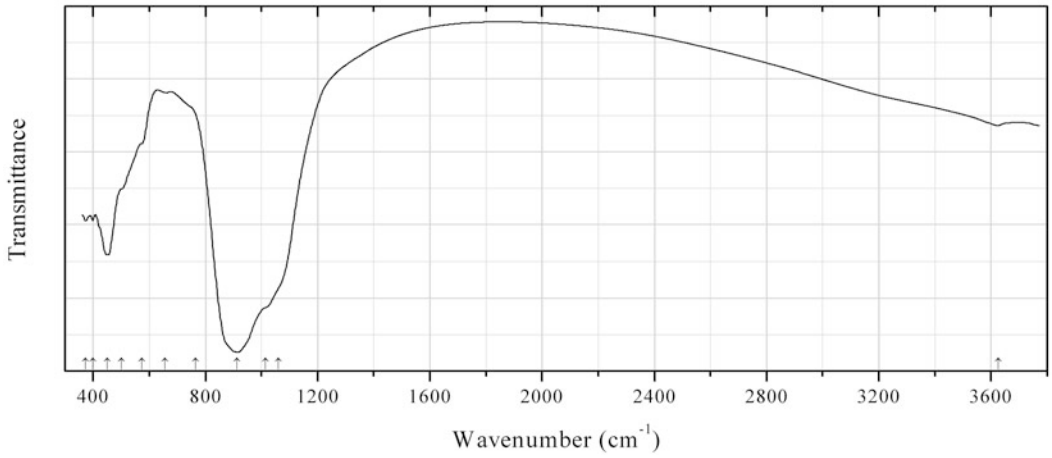

Fig. 2.803 IR spectrum of burpalite-1M_2 obtained by N.V. Chukanov

TiSi311 Burpalite-1M_2 $Na_2CaZr(Si_2O_7)F_2$ (Fig. 2.803)
Locality: Burpala (Burpalinskii) alkaline massif, Transbaikal territory, Siberia, Russia (type locality).
Description: Honey yellow grains from nepheline-bearing syenite. Holotype sample. The crystal structure is solved by A.M. Aksenov and R.K. Rastsvetaeva. Monoclinic, a = 7.2442(1); b = 10.0951 (1); c = 11.0018(1) Å, β = 108.957(1)°. D_{meas} = 3.25 g/cm^3. The empirical formula is (electron microprobe): $(Na_{1.71}Ca_{1.01}Mn_{0.10}Fe_{0.08})(Zr_{0.88}Ti_{0.11}Nb_{0.06})(Si_{2.00}O_7)F_{1.55}(O,OH)_{0.45}$.
Kind of sample preparation and/or method of registration of the spectrum: KBr disc. Absorbance.
Wavenumbers (cm^{-1}): 3626w, 1060sh, 1015sh, 912s, 765sh, 657w, 573, 500sh, 451s, 400, 373.
Note: Earlier this mineral was erroneously described as an orthorhombic analogue of lavenite (Portnov and Siderenko 1966).

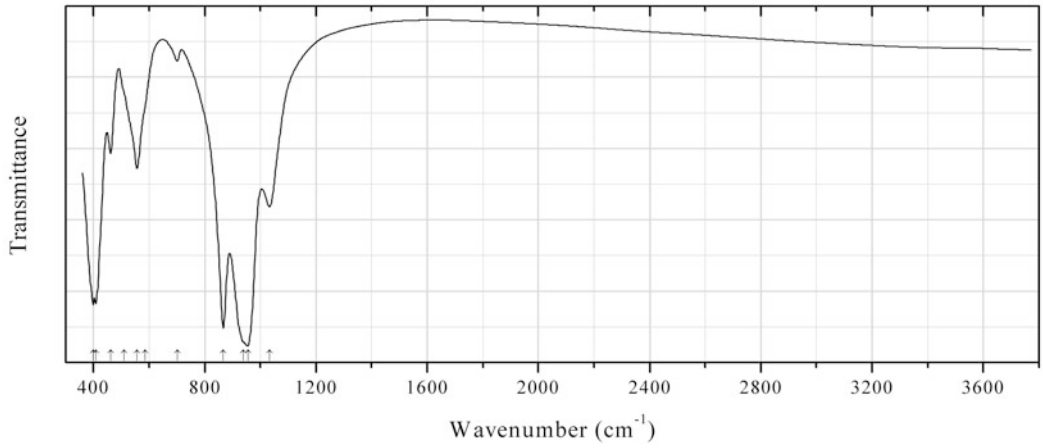

Fig. 2.804 IR spectrum of lamprophyllite obtained by N.V. Chukanov

TiSi312 Lamprophyllite $(Sr,Ba,K)_2Na(Na,Fe^{2+},Mn^{2+})_2(Ti,Fe^{3+},Mg)Ti_2(Si_2O_7)_2O_2(OH,O,F)_2$ (Fig. 2.804)
Locality: Rasvumchorr Mt., Khibiny alkaline complex, Kola peninsula, Murmansk region, Russia.
Description: Brown long-prismatic crystal from the association with delhayelite. The empirical formula is (electron microprobe): $(Sr_{0.72}Ba_{0.64}K_{0.45}Ca_{0.10}Na_{0.08})(Na_{2.58}Fe_{0.30}Mn_{0.12})(Ti_{2.67}Fe_{0.24}Mg_{0.09})(Si_{3.99}Al_{0.01}O_{14})O_2(OH,F,O)_2$.
Kind of sample preparation and/or method of registration of the spectrum: KBr disc. Absorption.
Wavenumbers (cm^{-1}): 1033, 955s, 940sh, 867s, 701w, 585sh, 556, 510sh, 462, 408s, 400s.

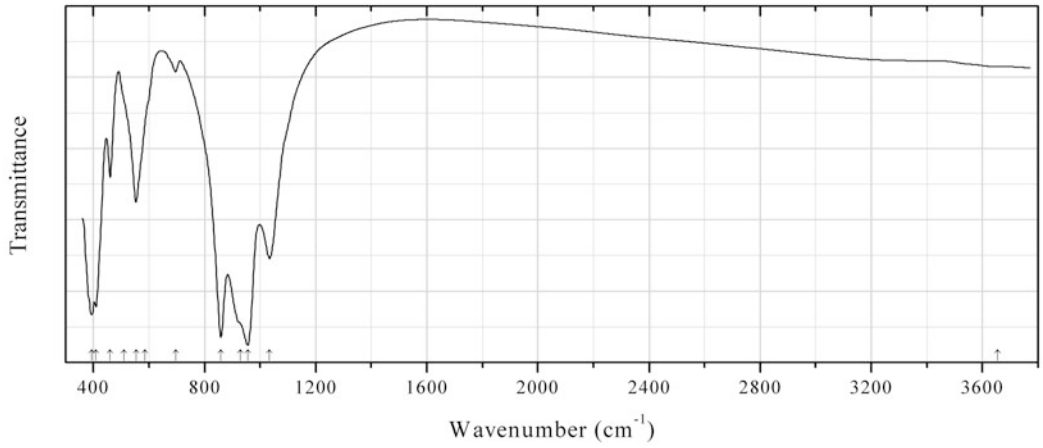

Fig. 2.805 IR spectrum of barytolamprophyllite obtained by N.V. Chukanov

TiSi313 Barytolamprophyllite $(Ba,Sr,K)_2Na(Na,Fe^{2+},Mn^{2+})_2(Ti,Fe^{3+},Mg)Ti_2(Si_2O_7)_2O_2(OH,O,F)_2$ (Fig. 2.805)
Locality: Koashva Mt., Khibiny alkaline complex, Kola peninsula, Murmansk region, Russia.
Description: Aggregate of beige platelets from the association with potassium feldspar, lemmleinite-K, and villiaumite. The empirical formula is (electron microprobe): $(Ba_{1.06}K_{0.41}Sr_{0.35}Na_{0.22}Ca_{0.03})(Na_{2.62}Mn_{0.38})(Ti_{2.72}Fe_{0.10}Nb_{0.07}Mn_{0.07}Mg_{0.04})(Si_{3.97}Al_{0.03}O_{14})O_2(OH,F,O)_2$.

Kind of sample preparation and/or method of registration of the spectrum: KBr disc. Absorption.
Wavenumbers (cm^{-1}): (3655w), 1034s, 956s, 930sh, 859s, 696w, 585sh, 553, 510sh, 460, 410s, 394s.

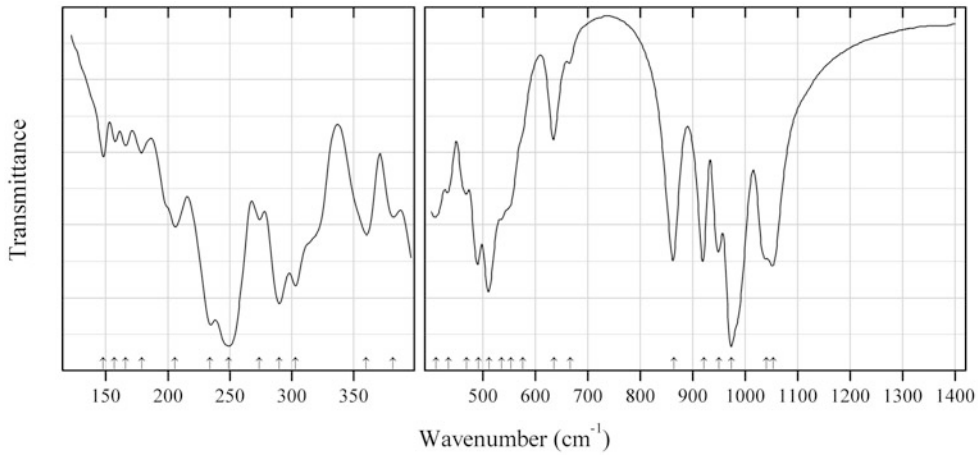

Fig. 2.806 IR spectrum of baghdadite drawn using data from Dul et al. (2015)

TiSi314 Baghdadite $Ca_3ZrSi_2O_9$ (Fig. 2.806)
Locality: Synthetic.
Description: Prepared using a powder mixture of calcium carbonate, zirconium dioxide silicon dioxide with a molar ratio of 3:1:2, at 1200 °C for 5 h with subsequent milling, pressing, and sintering at 1500 °C for 5 h. Characterized by powder X-ray diffraction data. The strongest reflections are observed at 7.3134, 3.2318, 3.0359, 2.9896, 2.8764, 2.8486, 2.4978, 1.8421, and 1.7012 Å. Monoclinic, space group $P2_1/c$. The refined unit-cell parameters are: a = 7.36025(6), b = 10.17641(4), c = 10.45135(1) Å, β ≈ 89.123°.
Kind of sample preparation and/or method of registration of the spectrum: KBr and polyethylene discs. Absorption.
Source: Dul et al. (2015).
Wavenumbers (cm^{-1}): 1053s, 1040s, 974sh, 950s, 921s, 864s, 666w, 635, 576sh, 553sh, 536sh, 512s, 491s, 469, 434, 410, 382, 360, 303, 290, 274, 249s, 234, 206, 179w, 166w, 157w, 148w.

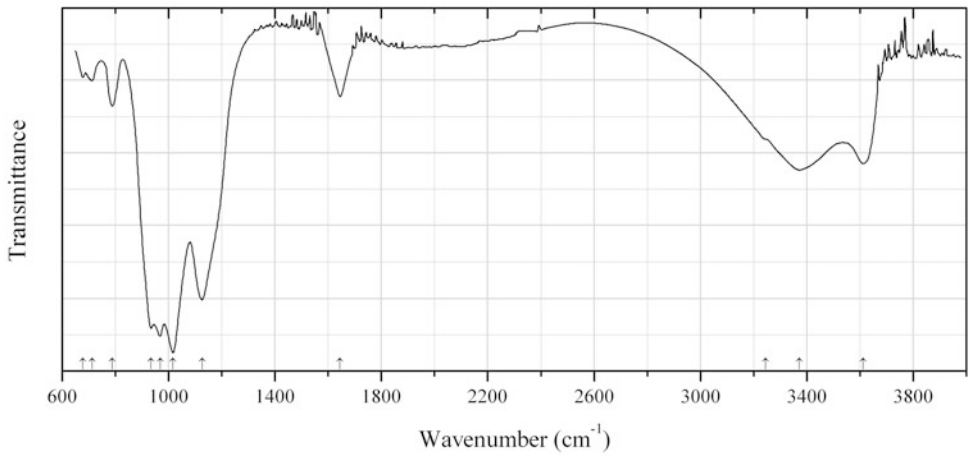

Fig. 2.807 IR spectrum of hogarthite drawn using data from McDonald et al. (2015)

TiSi315 Hogarthite $(Na,K)_2CaTi_2Si_{10}O_{26}\cdot 8H_2O$ (Fig. 2.807)
Locality: Poudrette (Demix) quarry, Mont Saint-Hilaire, Rouville RCM (Rouville Co.), Montérégie, Québec, Canada (type locality).
Description: White bladed to blocky crystals from a marble xenolith, from the association with calcite, quartz, haineaultite, labuntsovite-Mn, lemoynite, chabazite, and gmelinite-Na. Holotype sample. Monoclinic, space group *C*2/*m*, a = 10.1839(5), b = 15.8244(6), c = 9.1327(7) Å, β = 104.463(2)°, V = 1425.1(1) Å^3, Z = 2. D_{calc} = 2.40 g/cm^3. Optically biaxial (+), α = 1.567(1), β = 1.591(1), γ = 1.618(1), 2 V = 87(1)°. The empirical formula is $(Na_{0.78}K_{0.62}\square_{0.51}Ca_{0.09})Ca(Ti_{1.85}Zr_{0.09}Nb_{0.06})Si_{10.09}O_{26}\cdot 8H_2O$. The strongest lines of the powder X-ray diffraction pattern [*d*, Å (*I*, %) (*hkl*)] are: 8.835 (85) (001), 7.913 (100) (020), 6.849 (70) (−111), 4.336 (45) (−131, −112), 3.514 (80) (221), 3.426 (55) (−222, −132).
Kind of sample preparation and/or method of registration of the spectrum: Thin film obtained using a low-pressure diamond-anvil microsample cell. Transmission.
Source: McDonald et al. (2015).
Wavenumbers (cm^{-1}): 3612, 3372, 3246sh, 1645, 1126s, 1016s, 968s, 935s, 788, 712w, 678w.

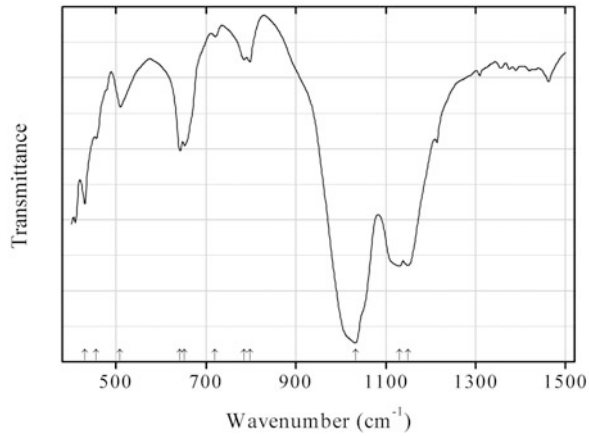

Fig. 2.808 IR spectrum of yusupovite drawn using data from Agakhanov et al. (2015)

TiSi316 Yusupovite $Na_2Zr(Si_6O_{15})\cdot 3H_2O$ (Fig. 2.808)
Locality: Dara-i Pioz glacier, Dara-i Pioz alkaline massif, Tien Shan Mts., Tajikistan (type locality).
Description: Colourless elongate grains embedded in reedmergnerite; the other associated minerals are quartz, pectolite, zeravshanite, mendeleevite-(Ce), fluorite, leucosphenite, a pyrochlore-group mineral, neptunite, telyushenkoite, moskvinite-(Y), and shibkovite. Holotype sample. The crystal structure is solved. Monoclinic, space group *C*2/*m*, a = 14.5975(4), b = 14.1100(4), c = 14.4394(4) Å, β = 90.0399(4)°, V = 2974.1(3) Å^3, Z = 8. D_{meas} = 2.69(2) g/cm^3, D_{calc} = 2.713 g/cm^3. Optically biaxial (+), α = 1.563(2), β = 1.565(2), γ = 1.577(2), 2 V = 42(3)°. The empirical formula is (electron microprobe, H_2O calculated from structure refinement): $(Na_{1.76}K_{0.12}Cs_{0.11})(Zr_{0.82}Y_{0.17}Nb_{0.02}Hf_{0.01})(Si_{6.01}O_{14.98})\cdot 2.52H_2O$. The strongest lines of the powder X-ray diffraction pattern [*d*, Å (*I*, %) (*hkl*)] are: 7.05 (100) (020), 3.24 (96) (420), 3.10 (69) (241, −241), 5.13 (53) (202, −202), 6.51 (42) (201, −201), 3.17 (34) (042).

Kind of sample preparation and/or method of registration of the spectrum: KBr disc (below 1500 cm^{-1}). Absorption.
Source: Agakhanov et al. (2015).
Wavenumbers (cm^{-1}): 3615, ~3470, ~1660sh, 1635, ~1610sh, 1150s, 1130s, 1032s, 798, 784, 720w, 652, 642, 509, 456, 430.
Note: The wavenumbers were partly determined by us based on spectral curve analysis of the published spectrum. The wavenumbers above 1600 cm^{-1} are given for the bands observed in the single-crystal IR spectrum of yusupovite.

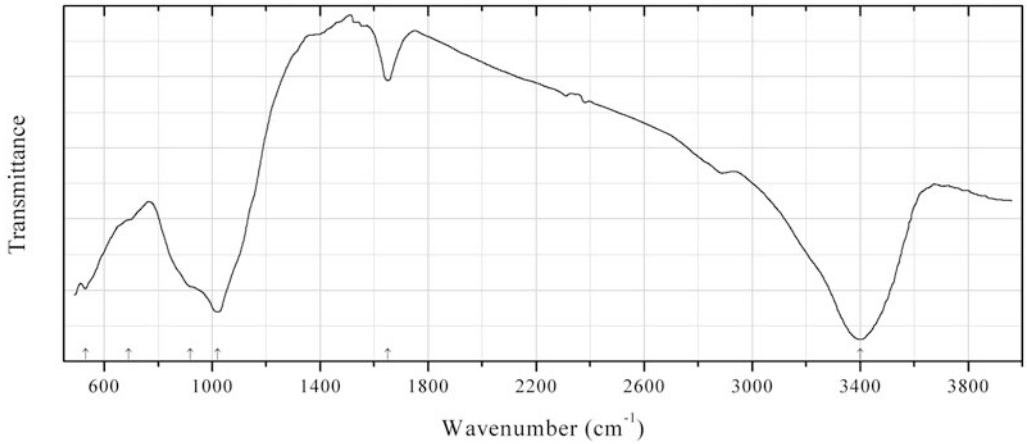

Fig. 2.809 IR spectrum of mieite-(Y) drawn using data from Miyawaki et al. (2015)

TiSi317 Mieite-(Y) $Y_4Ti(SiO_4)_2O(F,OH)_6$ (Fig. 2.809)
Locality: Souri valley, Komono, Mie Prefecture, central Japan (type locality).
Description: Amber yellow massive from the association with quartz, albite, K-feldspar, muscovite, allanite-(Ce), gadolinite-(Y), and magnesiorowlandite-(Y). Holotype sample. The raw material is significantly metamictized. Recrystallized material is orthorhombic, space group *Cmcm*, a = 14.979 (6), b = 10.548(5), c = 6.964(3) Å, V = 1100.3(8) $Å^3$, Z = 4. D_{calc} = 4.61 g/cm^3. Optically biaxial, α = 1.694(2), γ = 1.715(5). The empirical formula is (electron microprobe, H_2O calculated): $(Y_{3.13}Dy_{0.20}Gd_{0.17}Yb_{0.08}Nd_{0.08}Sm_{0.07}Er_{0.07}Th_{0.05}Tb_{0.03}Ho_{0.03}Lu_{0.03}Ce_{0.02}Tm_{0.02}U_{0.02})$ $(Ti_{0.52}Al_{0.44}Fe_{0.01})(Si_{1.92}P_{0.12})O_9[F_{3.83}(OH)_{1.91}]$. The strongest lines of the powder X-ray diffraction pattern [*d*, Å (*I*, %) (*hkl*)] are: 5.46 (58) (111), 4.26 (68) (021), 3.76 (85) (400), 3.54 (83) (002), 3.48 (82) (130), 2.68 (100) (331), 2.16 (78) (023).
Kind of sample preparation and/or method of registration of the spectrum: KBr disc. Transmission.
Source: Miyawaki et al. (2015).
Wavenumbers (cm^{-1}): 3400s, 1650, 1019s, 920sh, 690sh, 530.
Note: The wavenumbers were partly determined by us based on spectral curve analysis of the published spectrum. The bands at 3400 and 1650 cm^{-1} correspond to H_2O (water absorbed by the mineral during metamictization and/or water absorbed by the KBr disc). Weak bands in the ranges from 2800–3000 and 2300–2400 cm^{-1} may correspond to the admixture of an organic substance and to atmospheric CO_2, respectively.

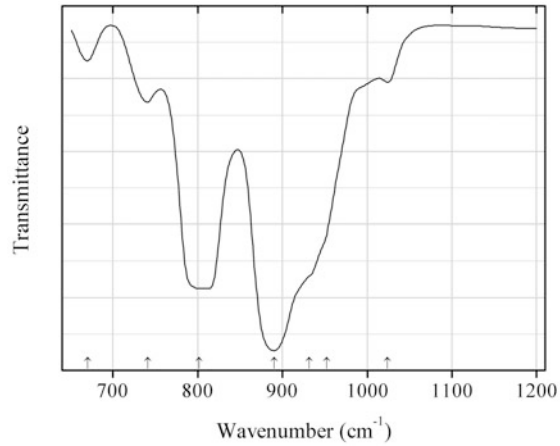

Fig. 2.810 IR spectrum of carlfrancisite drawn using data from Hawthorne et al. (2013)

AsSi9 Carlfrancisite $Mn^{2+}{}_3(Mn^{2+},Mg,Fe^{3+},Al)_{42}(AsO_3)_2(AsO_4)_4[(Si,As^{5+})O_4]_6[(As^{5+},Si)O_4]_2(OH)_{42}$ (Fig. 2.810)

Locality: Kombat mine, Grootfontein district, Otjozondjupa region, Namibia (type locality).

Description: Orange-yellow platy aggregates from the association with alleghanyite, chlorite, pyrochroite, spinel-group minerals, and ribbeite. Holotype sample. Trigonal, space group *R*-3*c*, $a = 8.2238(2)$, $c = 205.113(6)$ Å, $V = 12{,}013.5(4)$ Å^3, $Z = 6$. $D_{calc} = 3.620$ g/cm^3. Optically uniaxial (+), $\varepsilon = 1.756(2)$, $\beta = 1.758(2)$. The strongest lines of the powder X-ray diffraction pattern [*d*, Å (*I*, %) (*hkl*)] are: 4.107 (48) (−120), 3.243 (54) (0.1.56, −1.2.39), 2.918 (47) (0.2.40), 2.826 (100) (−2.2.44), 2.676 (63) (−237), 2.371 (88) (−2.3.40, −1.3.41), 1.552 (84) (−150).

Kind of sample preparation and/or method of registration of the spectrum: Thin film produced with a diamond anvil.

Source: Hawthorne et al. (2013).

Wavenumbers (cm^{-1}): 3550s, 1024w, 952sh, 932sh, 890s, ~802s (a poor-resolved triplet), 741w, 670w.

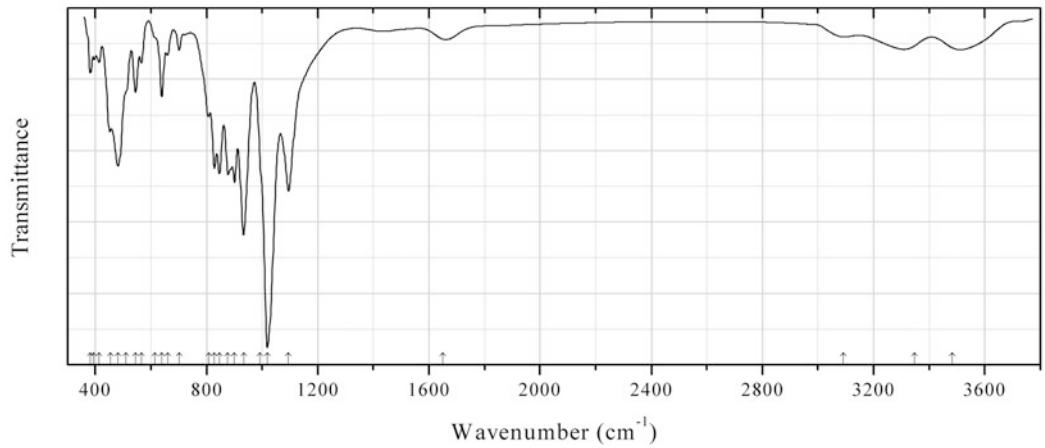

Fig. 2.811 IR spectrum of tiragalloite obtained by N.V. Chukanov

AsSi10 Tiragalloite $Mn^{2+}{}_4As^{5+}Si_3O_{12}(OH)$ (Fig. 2.811)

Locality: La Valletta mine, Colle della Valletta, Canosio, Maira Valley, Cuneo Province, Piedmont, Italy (type locality).
Description: Orange grains from the association with quartz. The empirical formula is (electron microprobe): $Mn_{4.0}Fe_{0.1}(As_{0.9}V_{0.1})Si_{3.0}O_{12}(OH,O)$.
Kind of sample preparation and/or method of registration of the spectrum: KBr disc. Absorption.
Wavenumbers (cm^{-1}): 3483, 3348, 3091w, 1650w, 1095s, 1019s, 993sh, 933s, 901s, 877, 846, 828, 808, 701w, 660w, 639, 615sh, 566w, 544, 510sh, 481, 455, 413w, 395w, 383.
Note: The band at 1650 cm^{-1} indicates possible presence of H_2O molecules.

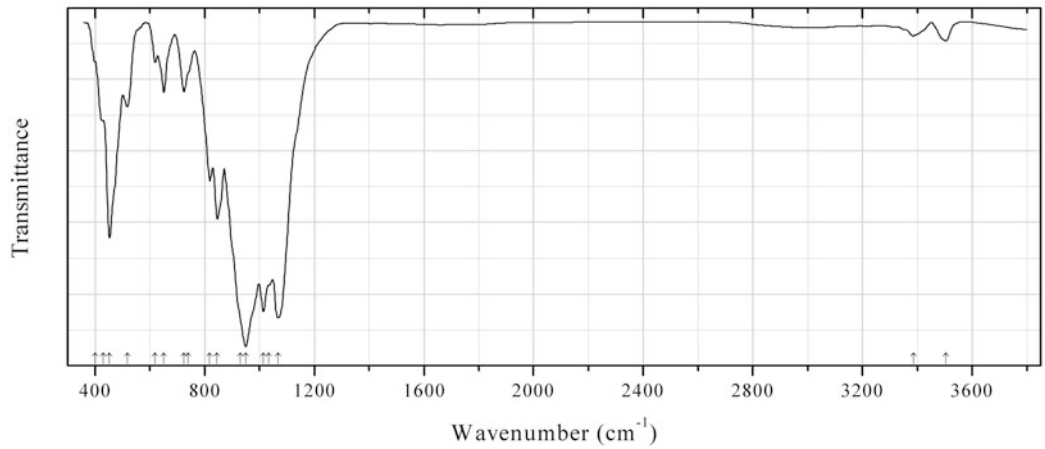

Fig. 2.812 IR spectrum of braccoite obtained by N.V. Chukanov

AsSi11 Braccoite $NaMn^{2+}{}_5[Si_5As^{5+}O_{17}(OH)](OH)$ (Fig. 2.812)
Locality: La Valetta mine, Vallone della Valetta, Maira valley, Cuneo province, Piedmont, Italy (type locality).
Description: Orange granular aggregate from the association with rhodochrosite. Confirmed by IR spectrum and qualitative electron microprobe analysis.
Kind of sample preparation and/or method of registration of the spectrum: KBr disc. Absorption.
Wavenumbers (cm^{-1}): 3504w, 3385w, 1068s, 1035sh, 1014s, 950s, 930sh, 846s, 819, 740sh, 724, 651, 620w, 518, 453s, 430sh, 400sh.

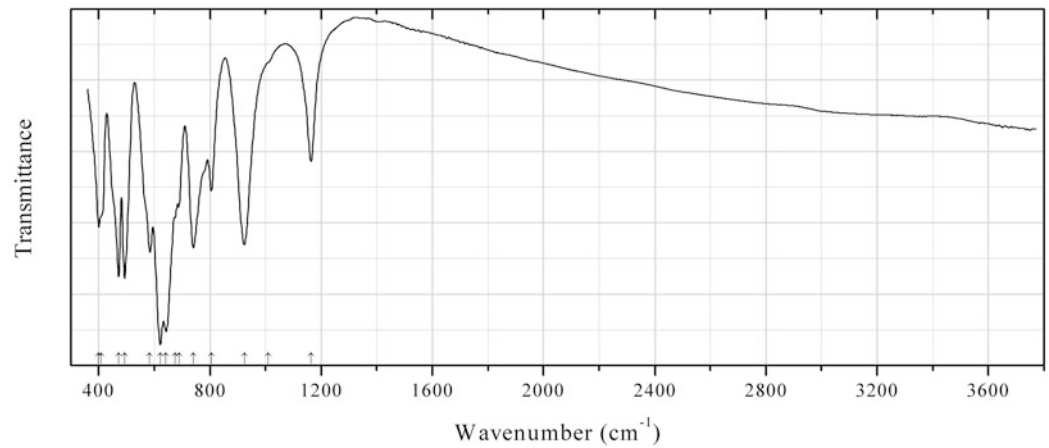

Fig. 2.813 IR spectrum of asbecasite obtained by N.V. Chukanov

AsSi12 Asbecasite $Ca_3(Be,B,Al)_2(Ti,Fe)(As,Sb)_6Si_2O_{20}$ (Fig. 2.813)
Locality: Binntal (Binn valley), Wallis (Valais), Switzerland.
Description: Yellow–beige imperfect crystals from the association with feldspar, hematite, titanite, and anatase. The empirical formula is (electron microprobe): $Ca_{3.0}(Be_xB_yAl_{0.2})(Ti_{0.8}Fe_{0.2})(As_{5.6}Sb_{0.1}Si_{0.3})Si_{2.0}O_{20}$.
Kind of sample preparation and/or method of registration of the spectrum: KBr disc. Absorption.
Wavenumbers (cm^{-1}): 1164, 1010sh, 924s, 805, 740s, 689, 675sh, 642s, 621s, 584s, 493s, 471s, 408sh, 400.

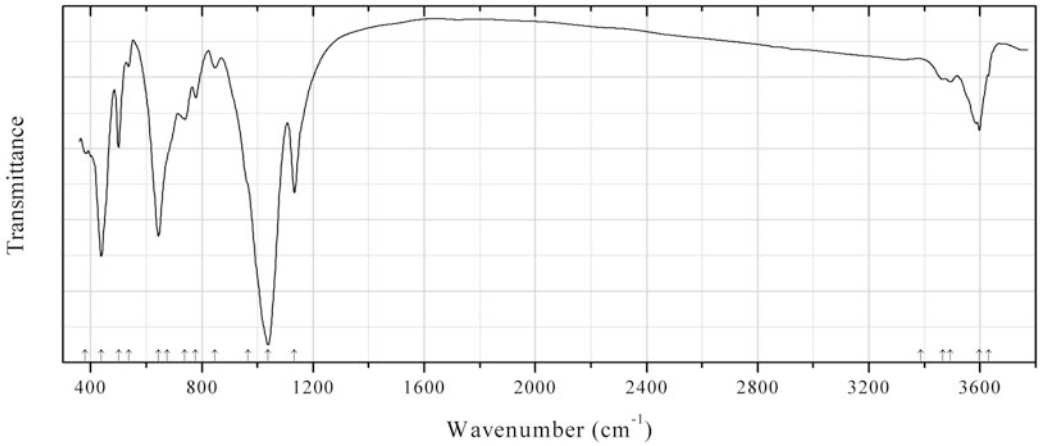

Fig. 2.814 IR spectrum of nelenite obtained by N.V. Chukanov

AsSi13 Nelenite $Mn^{2+}{}_{16}As^{3+}{}_3Si_{12}O_{36}(OH)_{17}$ (Fig. 2.814)
Locality: Huanggang mine, Chifeng, Inner Mongolia, China.
Description: Light brown tabular crystals with perfect cleavage. The empirical formula is (electron microprobe): $(Mn_{8.8}Fe_{6.4}Mg_{0.7}Al_{0.1})As^{3+}{}_{2.9}Si_{12.2}(O,OH)_{53}$.
Kind of sample preparation and/or method of registration of the spectrum: KBr disc. Absorption.
Wavenumbers (cm^{-1}): 3630sh, 3597, 3385, 3493w, 3467w, 1133s, 1038s, 965sh, 847w, 778, 739, 675sh, 643s, 536w, 500, 438s, 381.

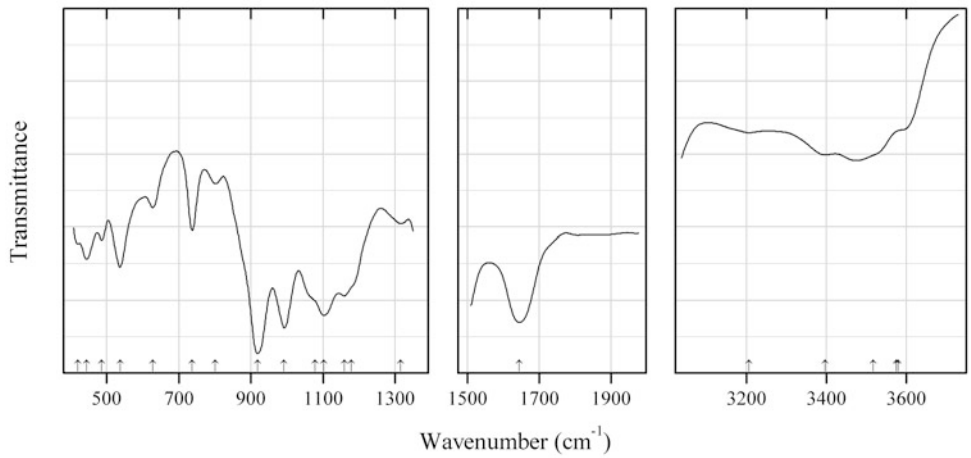

Fig. 2.815 IR spectrum of calcioursilite drawn using data from Chernikov et al. (1977)

USi6 Calcioursilite $Ca_4(UO_2)_4(Si_2O_5)_5(OH)_6 \cdot 15H_2O$ (?) (Fig. 2.815)
Locality: Oktyabr'skoe U deposit, Kyzyltyube-Sai, near Khodzhent (former Leninabad), Tajikistan (type locality).
Description: Lemon-yellow radial aggregates of flattened prismatic crystals. D = 3.034 g/cm^3. Optically biaxial (+), α = 1.548–1.552, β = 1.552–1.554, γ = 1.556–1.562. The strongest lines of the powder X-ray diffraction pattern [d, Å (I, %)] are: 10.07 (50), 9.12 (10), 4.39 (60), 3.29 (50), 3.18 (50), 3.01 (70).
Kind of sample preparation and/or method of registration of the spectrum: KBr disc. Absorption.
Source: Chernikov et al. (1977).
Wavenumbers (cm^{-1}): 3580sh, 3517sh, 3574, 3396, 3206, 1645, 1316w, 1178sh, 1159s, 1103s, 1078sh, 992s, 919s, 801w, 737, 627w, 537, 486, 444, 420.
Note: The wavenumbers were determined by us based on spectral curve analysis of the published spectrum. A questionable mineral, possibly related or identical to haiweeite. Real U:Ca ratio is between 1.5 and 2.

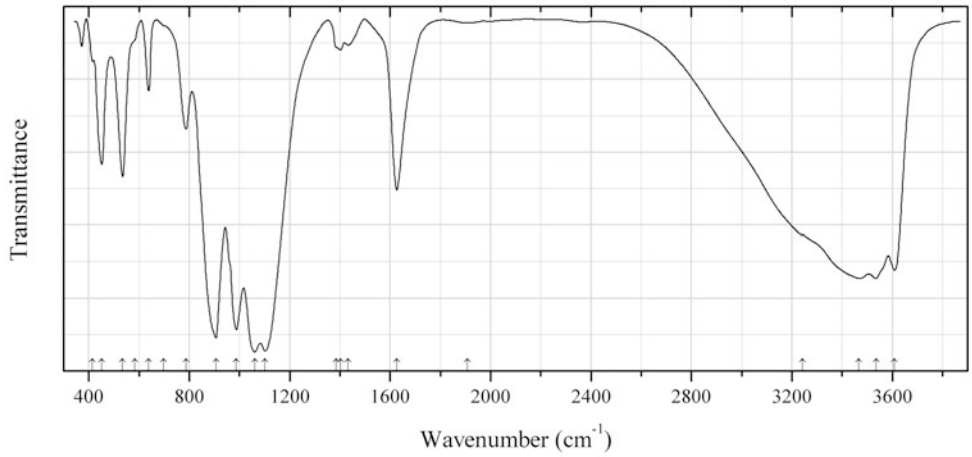

Fig. 2.816 IR spectrum of coutinhoite drawn using data from Atencio et al. (2004)

USi7 Coutinhoite $Th_xBa_{1-2x}(UO_2)_2Si_5O_{13} \cdot 3H_2O$ (Fig. 2.816)
Locality: Córrego do Urucum granitic pegmatite, Lavra Urucum, Galiléia Co., Minas Gerais, Brazil (type locality).
Description: Yellow irregular aggregate from the association with weeksite, phosphuranylite, metauranocircite, uranocircite, muscovite, and microcline. Holotype sample. Orthorhombic, space group *Cmmb*, a = 14.1676(9), b = 14.1935(9), c = 35.754(2) Å, V = 7189.7(2) Å^3, Z = 16. D_{calc} = 3.839 g/cm^3. Optically biaxial (−), α = 1.620(3), β = 1.627(3), γ = 1.629(3), 2 V = 40(5)°. The empirical formula is $(Th_{0.30}Ba_{0.19}K_{0.07}Ca_{0.04})(UO_2)_{2.00}(Si_{4.95}P_{0.08})O_{12.91} \cdot 2.86H_2O$. The strongest lines of the powder X-ray diffraction pattern [d, Å (I, %) (*hkl*)] are: 7.059 (100) (020), 5.563 (59) (024), 3.528 (86) (040), 3.287 (57) (404), 3.188 (73) (2.0.10), 2.904 (78) (2.2.10).
Kind of sample preparation and/or method of registration of the spectrum: Transmission. Kind of sample preparation is not indicated.
Source: Atencio et al. (2004).
Wavenumbers (cm^{-1}): 3609s, 3536s, 3468s, 3242sh, 1909w, 1627, 1434w, 1403w, 1386w, 1102s, 1061s, 988s, 907s, 788, 698sh, 639, 585sh, 535, 452, 415w.
Note: Weak bands at 1909 cm^{-1} and in the range 1380–1440 cm^{-1} indicate possible presence of acid groups.

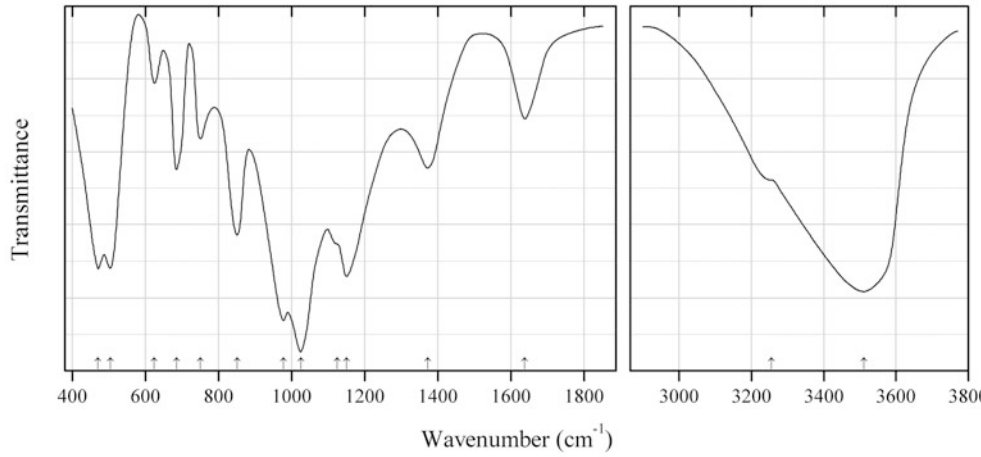

Fig. 2.817 IR spectrum of natroboltwoodite drawn using data from Chernorukov and Kortikov (2001)

USi8 Natroboltwoodite $Na(UO_2)(HSiO_4)\cdot H_2O$ (Fig. 2.817)
Locality: Synthetic.
Description: Prepared under hydrothermal conditions at the molar ratio of the reactants NaCl:$(UO_2)(NO_3)_2$:SiO_2 = 10:1:100. Monoclinic, a = 13.931(5), b = 6.943(1), c = 6.675(3) Å, β = 103.01(1)°. The strongest lines of the powder X-ray diffraction pattern [d, Å (I, %) (hkl)] are: 6.616 (100) (200), 3.355 (80) (400), 3.152 (36) (−401), 2.932 (45) (012), 2.580 (30) (411), 1.730 (30) (−622).
Kind of sample preparation and/or method of registration of the spectrum: KBr disc. Transmission.
Source: Chernorukov and Kortikov (2001).
Wavenumbers (cm^{-1}): 3511s, 3255sh, 1637, 1373, 1151s, 1125sh, 1025s, 978s, 851, 751, 685, 625w, 505s, 471s.
Note: The band position denoted by Chernorukov and Kortikov (2001) as 3225 cm^{-1} was determined by us at 3255 cm^{-1} based on spectral curve analysis of the published spectrum.

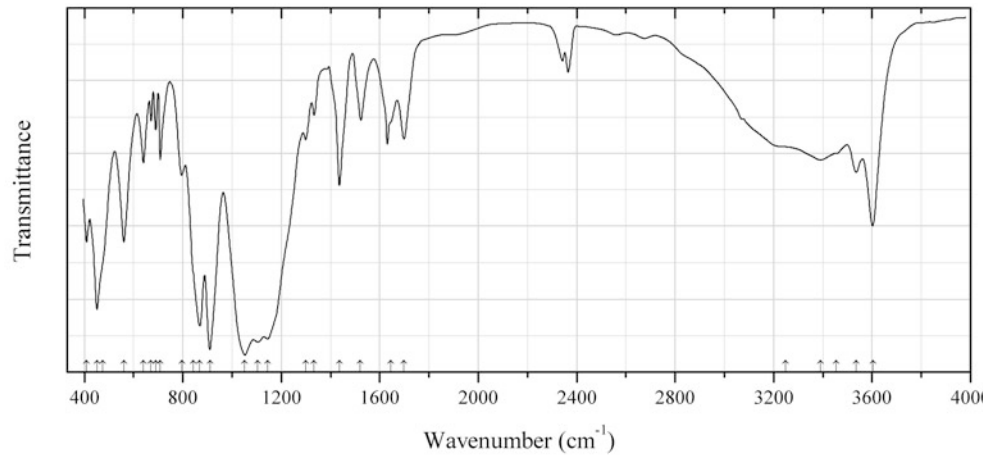

Fig. 2.818 IR spectrum of weeksite sodium analogue drawn using data from Vochten et al. (1997b)

USi9 Weeksite sodium analogue $Na_2(UO_2)_2(Si_5O_{13})\cdot 4H_2O$ (Fig. 2.818)

Locality: Synthetic.
Description: Synthesized hydrothermally from SiO_2, NaCl, and uranyl nitrate at 185 °C. Confirmed by powder X-ray diffraction data. The refined orthorhombic pseudocell parameters are: a = 7.103(2), b = 17.98(2), c = 7.084(3) Å.
Kind of sample preparation and/or method of registration of the spectrum: KBr disc. Transmission.
Source: Vochten et al. (1997b).
Wavenumbers (cm^{-1}): 3603s, 3535, 3455sh, 3391, 3250sh, 1699, 1644sh, 1633, 1521, 1436, 1333w, 1299w, 1144s, 1104s, 1052s, 910s, 867s, 842sh, 796, 708, 690w, 671w, 640, 561, 475sh, 452s, 409.
Note: The wavenumbers were determined by us based on spectral curve analysis of the published spectrum. Weak bands in the range from 2300 to 2400 cm^{-1} correspond to atmospheric CO_2.

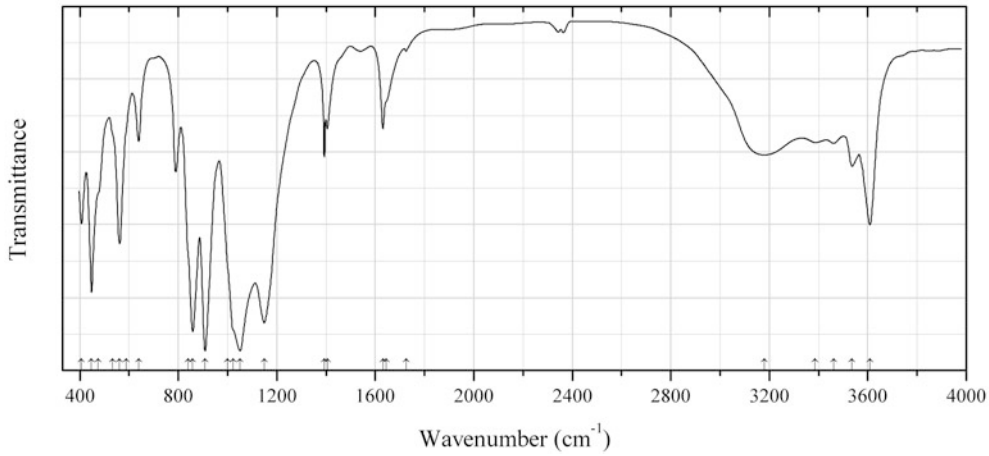

Fig. 2.819 IR spectrum of weeksite drawn using data from Vochten et al. (1997b)

USi10 Weeksite $K_2(UO_2)_2(Si_5O_{13})\cdot 4H_2O$ (Fig. 2.819)
Locality: Synthetic.
Description: Obtained from synthetic sodium weeksite analogue by ion exchange. Confirmed by powder X–ray diffraction data. The refined orthorhombic pseudocell parameters are: a = 7.112(2), b = 17.94(1), c = 7.100(2) Å.
Kind of sample preparation and/or method of registration of the spectrum: KBr disc. Transmission.
Source: Vochten et al. (1997b).
Wavenumbers (cm^{-1}): 3609s, 3536, 3462, 3387, 3179, 1725w, 1644sh, 1631, 1405, 1393, 1149s, 1050s, 1024sh, 1001sh, 909s, 859s, 840sh, 639, 588sh, 562, 534sh, 475sh, 448, 407.
Note: The wavenumbers were determined by us based on spectral curve analysis of the published spectrum. Weak bands in the range from 2300 to 2400 cm^{-1} correspond to atmospheric CO_2. The bands at 1405 and 1393 cm^{-1} may be due to impurities.

2.9 Phosphides and Phosphates (Including Carbonato-Phosphates)

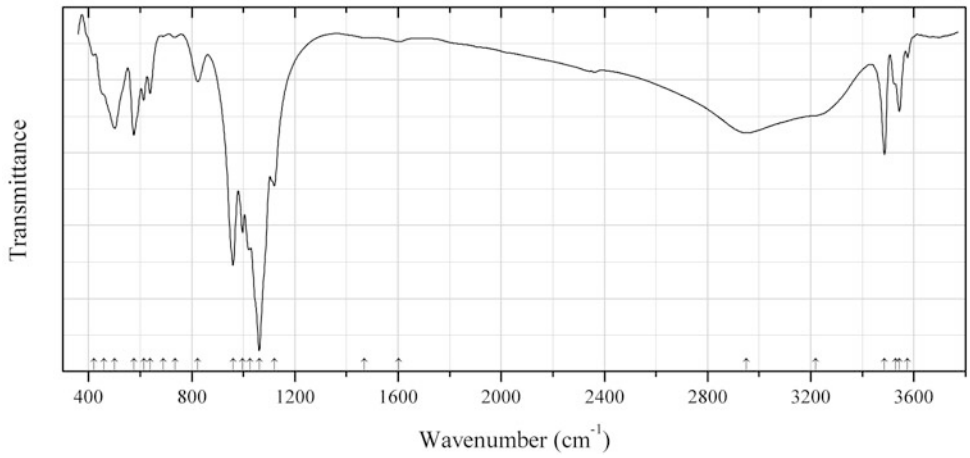

Fig. 2.820 IR spectrum of cyrilovite obtained by N.V. Chukanov

P433 Cyrilovite $NaFe^{3+}{}_3(PO_4)_2(OH)_4 \cdot 2H_2O$ (Fig. 2.820)
Locality: Eduardo pegmatite (Lavra do Eduardo), near Boa Vista creek, Conselheiro Pena municipality, Minas Gerais, Brazil.
Description: Yellow transparent crystals from the association with strengite, rockbridgeite, and albite. The empirical formula is (electron microprobe): $H_x(Na_{0.7-0.9}Ca_{0.02})(Fe_{2.86}Al_{0.16})(PO_4)_2(OH)_4 \cdot 2H_2O$.
Kind of sample preparation and/or method of registration of the spectrum: KBr disc. Absorption.
Wavenumbers (cm^{-1}): 3575w, 3543, 3528w, 3486, 3220sh, 2951, 1602w, 1470w, 1120, 1062s, 1026s, 997s, 960s, 824, 735w, 690w, 638, 614, 575, 502, 460sh, 421w.

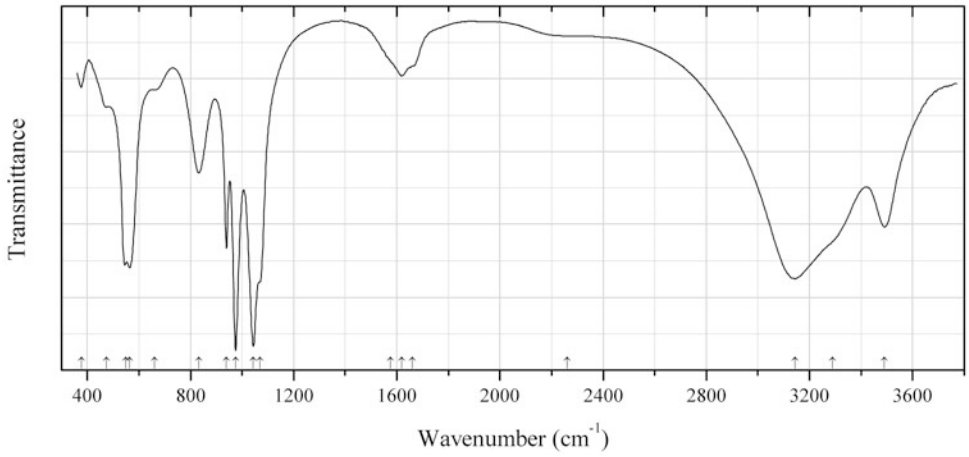

Fig. 2.821 IR spectrum of vivianite Mn-rich obtained by N.V. Chukanov

P434 Vivianite Mn-rich $(Fe^{2+},Mn^{2+})_3(PO_4)_2 \cdot 8H_2O$ (Fig. 2.821)
Locality: Cigana mine, Conselheiro Pena, Rio Doce valley, Minas Gerais, Brazil.

Description: Pale blue platy crystals from the association with triphylite and metaswitzerite. The empirical formula is (electron microprobe): $(Fe_{1.92}Mn_{0.70}Mg_{0.36})(PO_4)_{2.00}\cdot nH_2O$. Monoclinic, a = 10.145(7), b = 13.45(2), c = 4.726(4) Å, β = 104.61(10)°.
Kind of sample preparation and/or method of registration of the spectrum: KBr disc. Absorption.
Wavenumbers (cm^{-1}): 3491, 3290sh, 3144s, 2260w, 1660sh, 1618, 1575sh, 1070sh, 1044s, 975s, 939, 832, 660w, 565, 550, 475w, 378w.

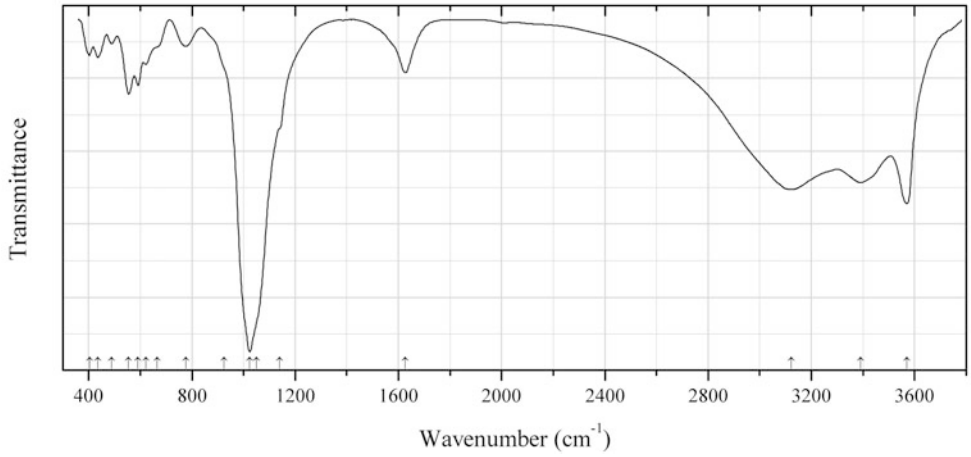

Fig. 2.822 IR spectrum of strengite obtained by N.V. Chukanov

P435 Strengite $Fe^{3+}(PO_4)\cdot 2H_2O$ (Fig. 2.822)
Locality: Eduardo pegmatite (Lavra do Eduardo), near Boa Vista creek, Conselheiro Pena municipality, Minas Gerais, Brazil.
Description: Pink transparent crystals from the association with phosphosiderite, rockbridgeite, and cyrilovite. The empirical formula is (electron microprobe): $(Fe_{0.80}Al_{0.19}Cr_{0.01})(PO_4)_{1.00}\cdot nH_2O$.
Kind of sample preparation and/or method of registration of the spectrum: KBr disc. Absorption.
Wavenumbers (cm^{-1}): 3570s, 3390s, 3122s, 1626, 1140sh, 1050sh, 1024s, 925sh, 776, 665sh, 622, 591, 555, 489w, 436, 403.

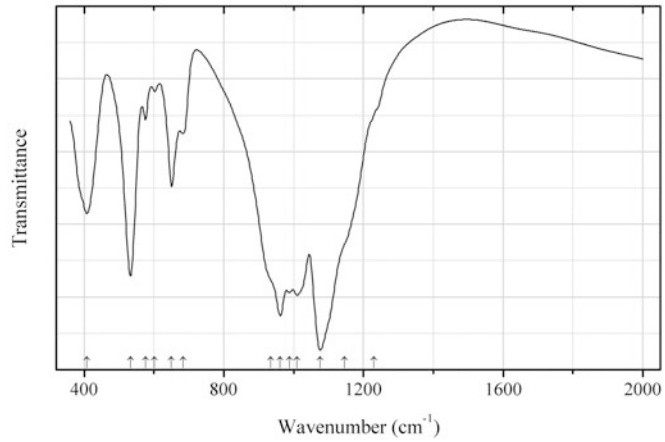

Fig. 2.823 IR spectrum of heterosite obtained by N.V. Chukanov

P436 Heterosite $Fe^{3+}(PO_4)$ (Fig. 2.823)
Locality: Boca Rica claim, Sapucaia do Norte, Galiléia, Doce valley, Minas Gerais, Brazil.
Description: Dark red massive aggregate from the association with rockbridgeite. The empirical formula is (electron microprobe): $(Fe_{0.71}Mn_{0.27}Mg_{0.03})(PO_4)$.
Kind of sample preparation and/or method of registration of the spectrum: KBr disc. Absorption.
Wavenumbers (cm^{-1}): 1230sh, 1145sh, 1076s, 1010s, 988s, 962s, 935sh, 684, 650, 602w, 576, 533s, 408.

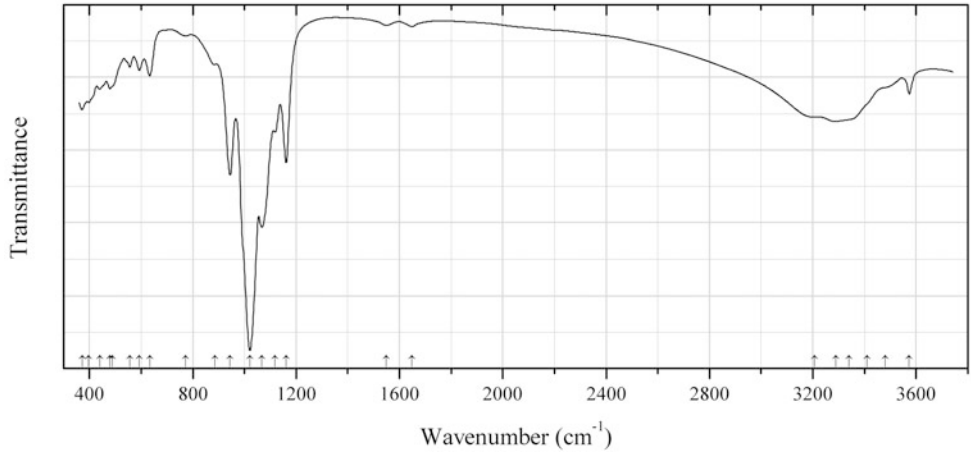

Fig. 2.824 IR spectrum of kidwellite obtained by N.V. Chukanov

P437 Kidwellite $(Fe^{3+},M^{2+})_{9+x}(PO_4)_6(OH)_{11}\cdot 3H_2O$ (Fig. 2.824)
Locality: Sapucaia (Proberil) mine, Sapucaia do Norte, Galiléia, Doce valley, Minas Gerais, Brazil.
Description: Yellow radial fibrous aggregates forming pseudomorphs after rockbridgeite, from the association with strengite. Identified by the IR spectrum.
Kind of sample preparation and/or method of registration of the spectrum: KBr disc. Absorption.
Wavenumbers (cm^{-1}): 3572, 3480sh, 3410sh, 3340sh, 3290, 3208, 1648w, 1550w, 1161s, 1117, 1067s, 1021s, 944s, 886, 772w, 633, 593, 556, 490sh, 479, 440, 398, 373.

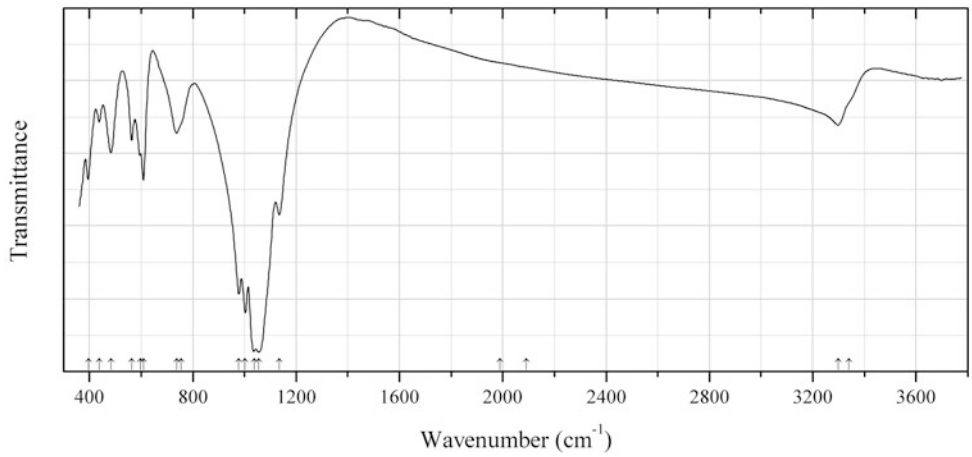

Fig. 2.825 IR spectrum of barbosalite obtained by N.V. Chukanov

P438 Barbosalite $Fe^{2+}Fe^{3+}{}_2(PO_4)_2(OH)_2$ (Fig. 2.825)
Locality: Cigana mine, Conselheiro Pena, Rio Doce valley, Minas Gerais, Brazil.
Description: Black (with blue streak) isometric crystals from the association with phosphosiderite. Confirmed by semiqualitative electron microprobe analyses.
Kind of sample preparation and/or method of registration of the spectrum: KBr disc. Absorption.
Wavenumbers (cm^{-1}): 3340sh, 3299, 2090sh, 1990sh, 1134, 1056s, 1038s, 1003s, 978s, 755sh, 737, 609, 598, 563, 483, 437w, 396.

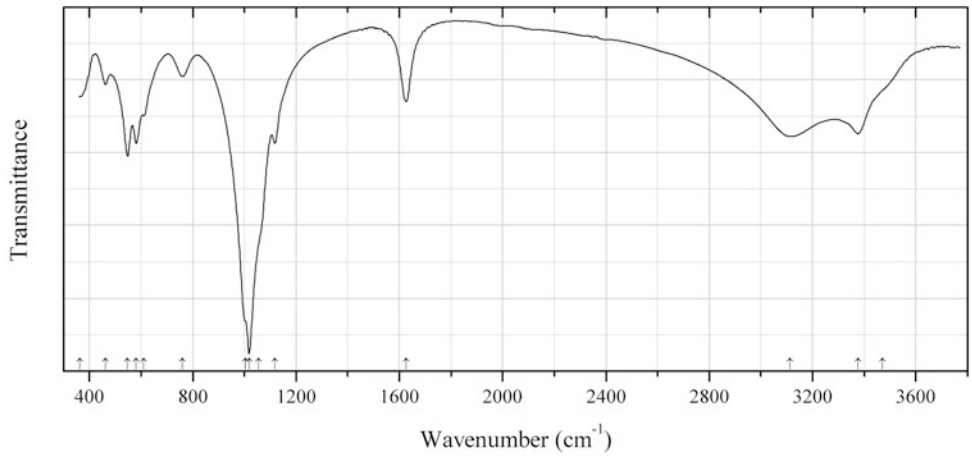

Fig. 2.826 IR spectrum of phosphosiderite obtained by N.V. Chukanov

P439 Phosphosiderite $Fe^{3+}(PO_4)\cdot 2H_2O$ (Fig. 2.826)
Locality: Cigana mine, Conselheiro Pena, Rio Doce valley, Minas Gerais, Brazil.
Description: Beige crusts from the association with barbosalite and heterosite. The empirical formula is (electron microprobe): $Fe_{1.00}(PO_4)_{1.00}\cdot nH_2O$.
Kind of sample preparation and/or method of registration of the spectrum: KBr disc. Absorption.
Wavenumbers (cm^{-1}): 3470sh, 3376, 3113, 1626, 1118, 1055sh, 1018s, 1005sh, 761w, 610, 581, 548, 462w, 364.

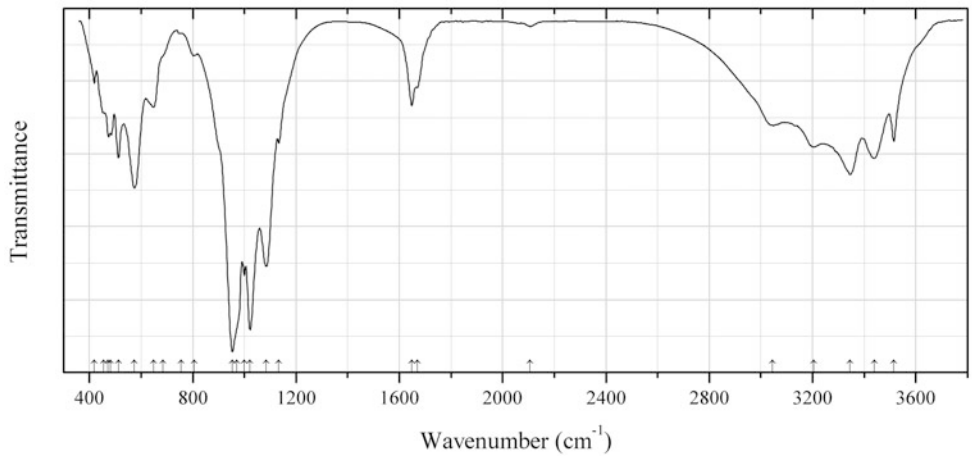

Fig. 2.827 IR spectrum of switzerite obtained by N.V. Chukanov

P440 Switzerite $Mn^{2+}{}_3(PO_4)_2 \cdot 7H_2O$ (Fig. 2.827)
Locality: Cigana mine, Conselheiro Pena, Rio Doce valley, Minas Gerais, Brazil.
Description: Aggregate of reddish-brown platelets from the association with rockbridgeite and phosphosiderite.
Kind of sample preparation and/or method of registration of the spectrum: KBr disc. Absorption.
Wavenumbers (cm^{-1}): 3515, 3440, 3346, 3205, 3045, 2106w, 1670, 1648, 1133, 1085s, 1022s, 1000s, 970sh, 953s, 806w, 754w, 685sh, 648, 574, 512, 482, 473, 455sh, 419.

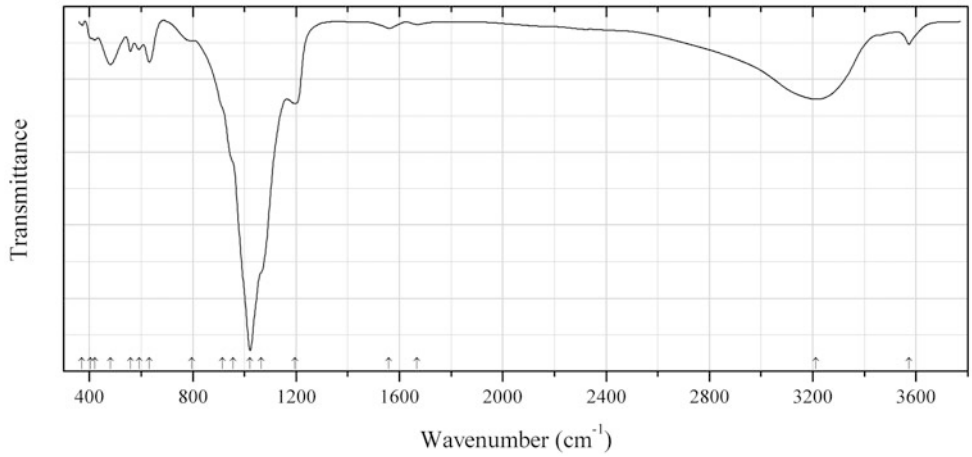

Fig. 2.828 IR spectrum of lipscombite obtained by N.V. Chukanov

P441 Lipscombite $Fe^{2+}Fe^{3+}{}_2(PO_4)_2(OH)_2$ (Fig. 2.828)
Locality: Silver Coin mine, Valmy, Edna Mountains, Humboldt Co., Nevada, USA.
Description: Brownish-green radial aggregates The empirical formula is (electron microprobe): $(Fe_{2.65}Zn_{0.20}Cu_{0.07}Mg_{0.03})(PO_4)_2(OH,H_2O)_2$.
Kind of sample preparation and/or method of registration of the spectrum: KBr disc. Absorption.
Wavenumbers (cm^{-1}): 3573, 3212, 1667w, 1558w, 1195, 1065sh, 1022s, 955sh, 915sh, 795w, 632, 593, 559, 481, 420w, 405sh, 371w.

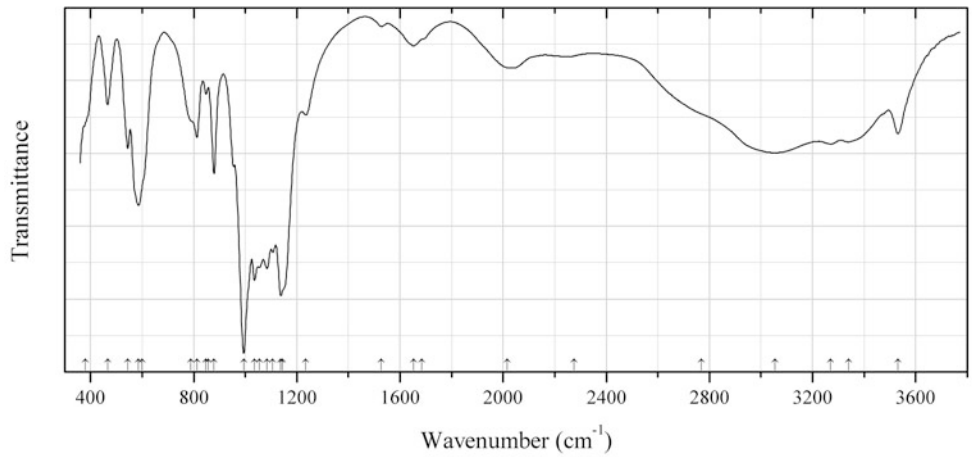

Fig. 2.829 IR spectrum of mejillonesite obtained by N.V. Chukanov

P442 Mejillonesite $NaMg_2(PO_3OH)(PO_4)(OH)\cdot H_5O_2$ (Fig. 2.829)
Locality: Paoha Island, Mono lake, Mono Co., California, USA.
Description: Colourless crystals. Identified by the IR spectrum.
Wavenumbers (cm^{-1}): 3531, 3340, 3270, 3055, 2770sh, 2275w, 2015, 1685sh, 1653w, 1527w, 1234, 1145sh, 1138s, 1107, 1084s, 1055, 1035s, 994s, 857, 879, 848w, 812, 790sh, 600sh, 586, 544, 466, 380sh.

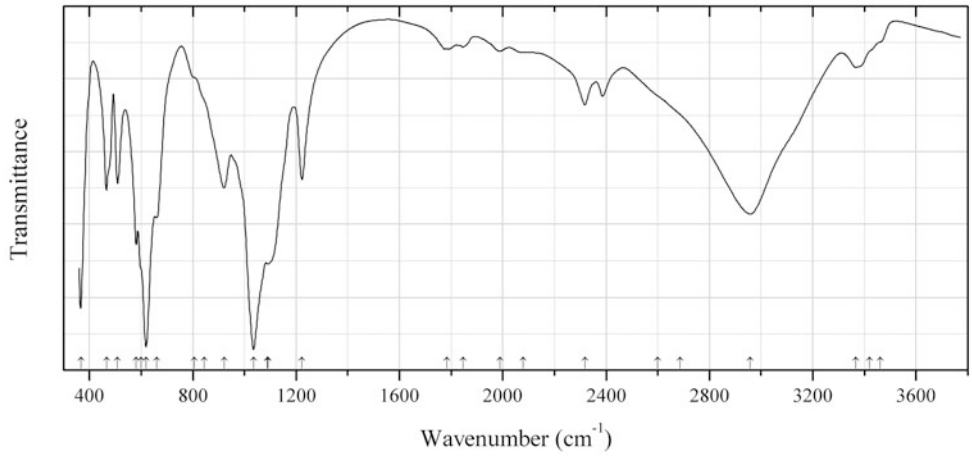

Fig. 2.830 IR spectrum of florencite-(Ce) obtained by N.V. Chukanov

P443 Florencite-(Ce) $CeAl_3(PO_4)_2(OH)_6$ (Fig. 2.830)
Locality: Svodovyi area, Grubependity Lake, Maldynyrd (Maldy-nyrd) range, Kozhim River Basin, Subpolar Urals, Komi Republic, Russia.
Description: Pink crystal from the association with quartz, xenotime-(Y), and florencite-(Sm). The empirical formula is (electron microprobe): $H_x(Ce_{0.48}La_{0.24}Nd_{0.16}Sm_{0.05}Pr_{0.04}Ca_{0.03}Sr_{0.03})Al_{2.98}[(PO_4)_{1.91}(AsO_4)_{0.09}(OH)_6$.
Kind of sample preparation and/or method of registration of the spectrum: KBr disc. Absorption.
Wavenumbers (cm^{-1}): 3460sh, 3420sh, 3366, 1090sh, 2957, 2600sh, 2686, 2318, 2080w, 1989w, 1847w, 1783w, 1223, 1091s, 1035s, 921, 845sh, 805sh, 660, 619s, 600sh, 581, 509, 466, 368w.
Note: The bands in the range from 1700 to 2600 cm^{-1} indicate the presence of acid phosphate groups.

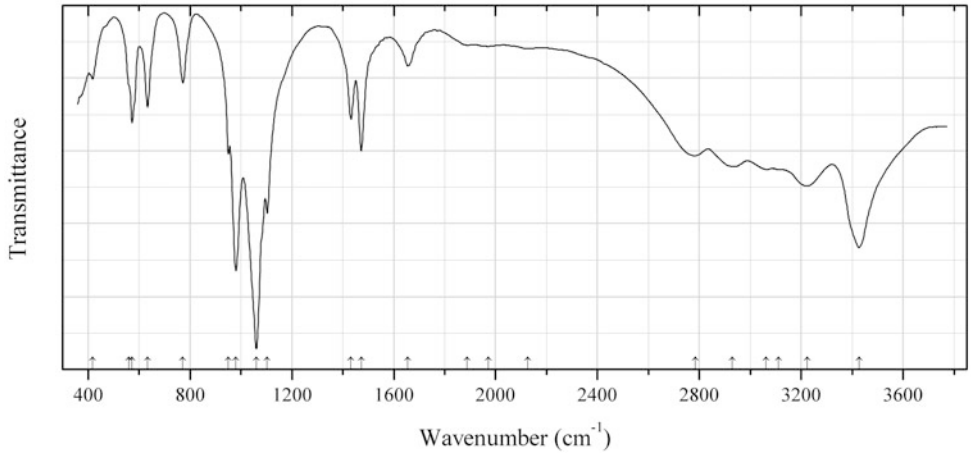

Fig. 2.831 IR spectrum of dittmarite obtained by N.V. Chukanov

P444 Dittmarite $(NH_4)Mg(PO_4)\cdot H_2O$ (Fig. 2.831)
Locality: Guano mining field at south slope of Punta de Lobos, Tarapacá region, 90 km south of Iquique, Chile.
Description: White nests. Associated minerals are witzkeite and nitratine. Identified by the IR spectrum, qualitative electron microprobe analysis and powder X-ray diffraction data.
Kind of sample preparation and/or method of registration of the spectrum: KBr disc. Absorption.
Wavenumbers (cm^{-1}): 3427s, 3223, 3112, 3063, 2929, 2784, 2127w, 1972w, 1889w, 1655, 1473, 1433, 1103s, 1061s, 980s, 951, 772, 634, 573, 560sh, 418.

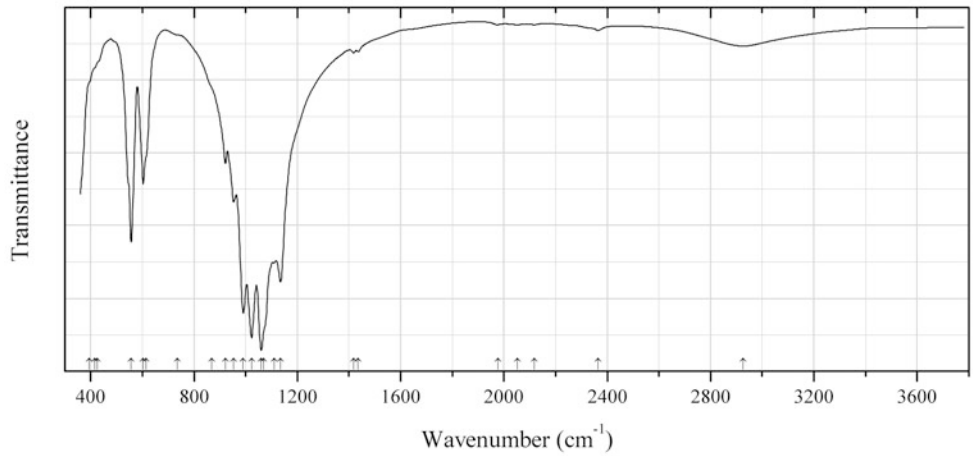

Fig. 2.832 IR spectrum of bobdownsite obtained by N.V. Chukanov

P445 Bobdownsite $Ca_9Mg(PO_3F)(PO_4)_6$ (Fig. 2.832)
Locality: Big Fish River, Yukon Territory, Canada (type locality).
Description: Colourless crystal. Cootype sample.
Kind of sample preparation and/or method of registration of the spectrum: KBr disc. Absorption.
Wavenumbers (cm^{-1}): 2927, 2364w, 2117w, 2053w, 1977w, 1435w, 1418w, 1135s, 1111, 1070sh, 1060s, 1023s, 991s, 953, 922, 870sh, 735sh, 615sh, 603, 557s, 425sh, 415sh, 395sh.

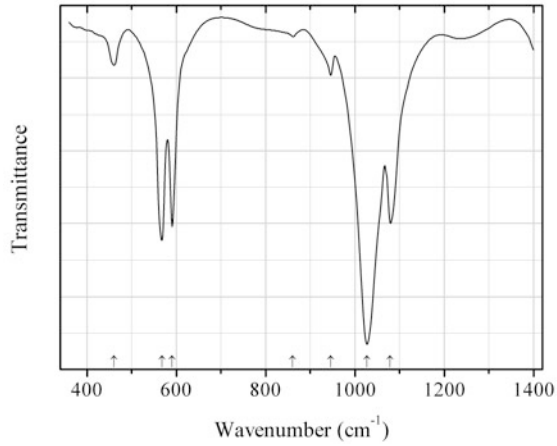

Fig. 2.833 IR spectrum of stronadelphite obtained by N.V. Chukanov

P446 Stronadelphite $Sr_5(PO_4)_3F$ (Fig. 2.833)
Locality: Kirovskiy apatite mine, Kukisvumchorr Mt., Khibiny alkaline complex, Kola peninsula, Murmansk region, Russia (type locality).
Description: Hexagonal, prismatic to acicular crystals from the association with natrolite, microcline, aegirine, pectolite, lamprophyllite, belovite-(Ce), belovite-(La), gaidonnayite, nenadkevichite, komarovite, manganokukisvumite, etc. Holotype sample. Hexagonal, space group $P6_3/m$, a = 9.845 (7), c = 7.383(4) Å, V = 619.7(7) Å^3, Z = 2. D_{calc} = 3.915 g/cm^3. Optically uniaxial (−), ω = 1.630(1), ε = 1.623(1). The empirical formula is $(Sr_{4.46}Ca_{0.33}Ba_{0.12}Na_{0.02}La_{0.02}Ce_{0.01}Th_{0.01})P_{3.01}O_{12}[F_{0.56}(OH)_{0.44}]$. The strongest lines of the powder X-ray diffraction pattern [d, Å (I, %) (hkl)] are: 3.71 (30) (002), 3.21 (40) (120, 210), 2.940 (100) (211, 121, 112), 2.823 (35) (300, 202), 2.009 (50) (222, 312, 132), 1.955 (45) (213, 123), 1.500 (30) (151, 511, 332).
Kind of sample preparation and/or method of registration of the spectrum: KBr disc. Absorption.
Wavenumbers (cm^{-1}): 1079s, 1027s, 946, 861w, 591s, 568s, 460.

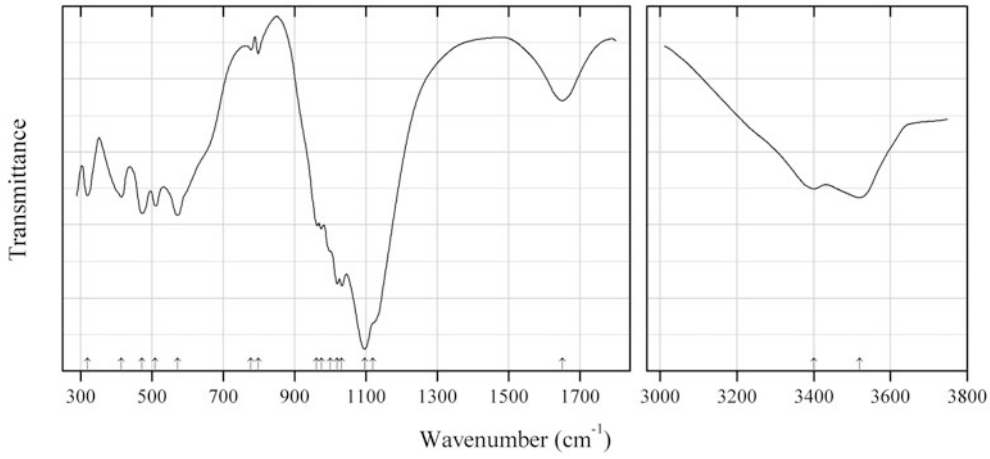

Fig. 2.834 IR spectrum of whiteite-(MnFeMg) obtained by N.V. Chukanov

P447 Whiteite-(MnFeMg) $Mn^{2+}Fe^{2+}Mg_2Al_2(PO_4)_4(OH)_2\cdot 8H_2O$ (Fig. 2.834)

Locality: Sierra Branca pegmatite, Pedra Lavrada, Paraiba, Brazil.
Description: Brownish crystals from granitic pegmatite. The empirical formula is (electron microprobe): $(Mn_{0.5}Fe_{0.3}Zn_{0.1}Ca_{0.1})Fe_{1.0}Mg_{2.0}(Al_{1.9}Fe_{0.1})(PO_4)_4(OH)_2 \cdot nH_2O$.
Kind of sample preparation and/or method of registration of the spectrum: KBr disc. Absorption.
Wavenumbers (cm^{-1}): 3520, 3400, 1650, 1119sh, 1096s, 1032s, 1020, 1000sh, 975, 962, 798, 777, 572, 510, 473, 415, 320.

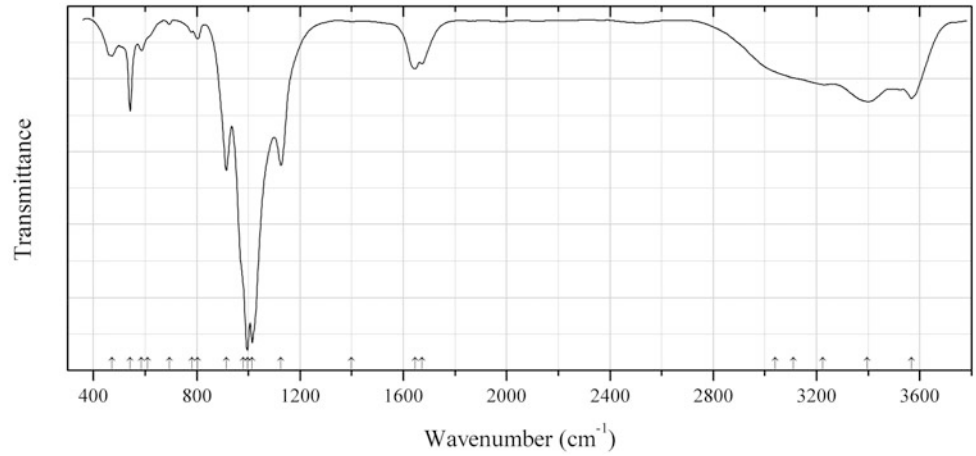

Fig. 2.835 IR spectrum of threadgoldite obtained by N.V. Chukanov

P448 Threadgoldite $Al(UO_2)_2(PO_4)_2(OH) \cdot 8H_2O$ (Fig. 2.835)
Locality: Arcu Su Linnarbu, Cogliari, Sardinia.
Description: Yellow scaly crystals from the association with meta-autunite, upalite, and quartz. The empirical formula is (electron microprobe): $Al_{0.9}Ca_{0.1}(UO_2)_{2.05}(PO_4)_{2.00}(H_2O,OH)_x$. The strongest lines of the powder X-ray diffraction pattern [*d*, Å (*I*, %)] are: 9.438 (100), 5.327 (6), 4.714 (36), 4.102 (15), 3.728 (11), 3.615 (9), 3.464 (6).
Kind of sample preparation and/or method of registration of the spectrum: KBr disc. Absorption.
Wavenumbers (cm^{-1}): 3567, 3396, 3223, 3110sh, 3040sh, 1672sh, 1645, 1400w, 1126, 1015s, 996s, 980sh, 914, 803, 782w, 695w, 610sh, 586, 542, 472.

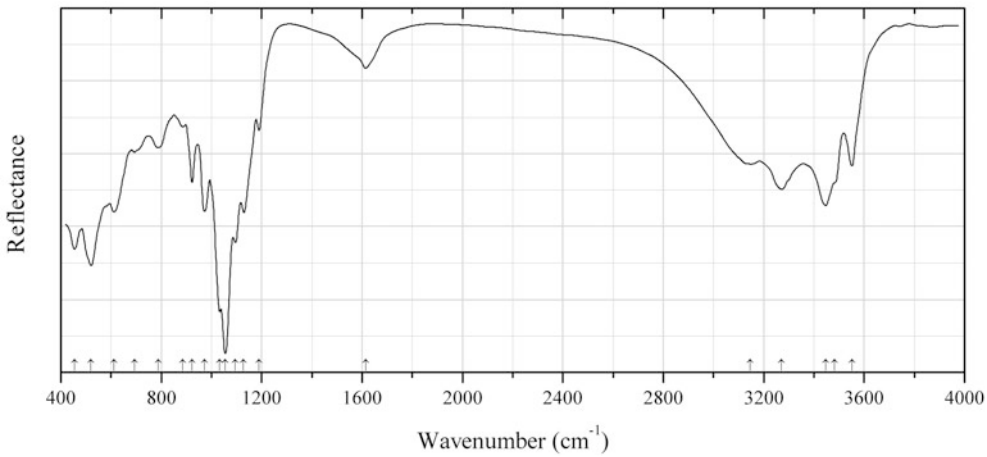

Fig. 2.836 IR spectrum of afmite drawn using data from Kampf et al. (2011)

P449 Afmite $Al_3(OH)_4(H_2O)_3(PO_4)(PO_3OH)\cdot H_2O$ (Fig. 2.836)
Locality: Fumade hamlet, near Castelnau-de-Brassac village, Tarn, France (type locality).
Description: White cockscomb aggregates from the association with matulaite and variscite. Holotype sample. Triclinic, space group *P*-1, $a = 7.386(3)$, $b = 7.716(3)$, $c = 11.345(4)$ Å, $\alpha = 99.773(5)°$, $\beta = 91.141(6)°$, $\gamma = 115.58(5)°$, $V = 571.6(3)$ Å^3, $Z = 2$. $D_{meas} = 2.39(3)$ g/cm^3, $D_{calc} = 2.391$ g/cm^3. Optically biaxial (+), $\alpha = 1.554(1)$, $\beta = 1.558(1)$, $\gamma = 1.566(1)$, 2 V = 70(5)°. The strongest lines of the powder X-ray difraction pattern [*d*, Å (*I*, %) (*hkl*)] are: 11.089 (100) (001), 3.540 (81) (0–13, −1–12), 5.484 (79) (002, 101), 2.918 (60) (−122), 3.089 (33) (−113, 201), 4.022 (30) (102, −112), 6.826 (23) (010). Typical bands of acid PO_3OH^{2-} groups (in the range 1800–2800 cm^{-1}) are absent in the IR spectrum of afmite.
Kind of sample preparation and/or method of registration of the spectrum: Attenuated total reflection of powdered mineral.
Source: Kampf et al. (2011).
Wavenumbers (cm^{-1}): 3552, 3481sh, 3448, 3270, 3145sh, 1616w, 1190w, 1128, 1095, 1056s, 1032s, 973, 923, 886w, 788, 695, 611, 520s, 454s.
Note: The wavenumbers were determined by us based on spectral curve analysis of the published spectrum.

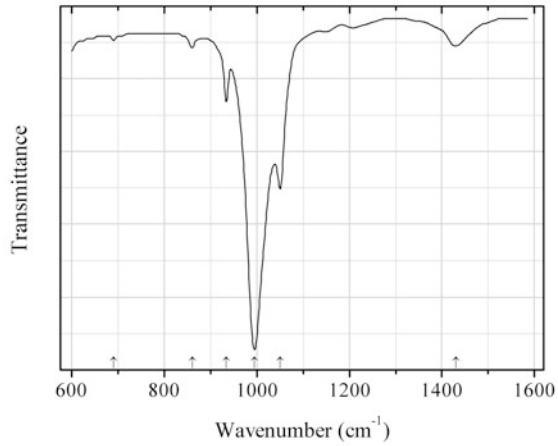

Fig. 2.837 IR spectrum of alforsite drawn using data from Yoder et al. (2012)

P450 Alforsite $Ba_5(PO_4)_3Cl$ (Fig. 2.837)
Locality: Synthetic.
Description: Confirmed by powder X-ray diffraction data. Contains 5.35 wt% CO_3^{2-}.
Kind of sample preparation and/or method of registration of the spectrum: Transmission. Kind of sample preparation is not indicated.
Source: Yoder et al. (2012).
Wavenumbers (cm^{-1}): 1430w, 1050s, 995s, 934, 860w, 690w.
Note: The wavenumbers were partly determined by us based on spectral curve analysis of the published spectrum.

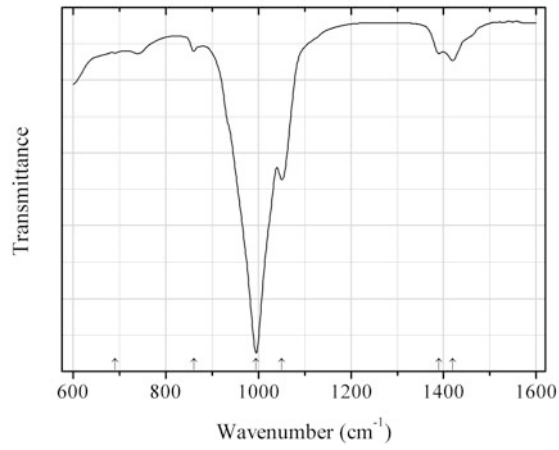

Fig. 2.838 IR spectrum of "hydroxylalforsite" drawn using data from Yoder et al. (2012)

P451 " Hydroxylalforsite " $Ba_5(PO_4)_3(OH)$ (Fig. 2.838)
Locality: Synthetic.
Description: Confirmed by powder X-ray diffraction data. The sample contains 3.9 wt% CO_3^{2-}.
Kind of sample preparation and/or method of registration of the spectrum: Transmission. Kind of sample preparation is not indicated.
Source: Yoder et al. (2012).
Wavenumbers (cm^{-1}): 1420, 1390w, 1050s, 995s, 860w, 690w.

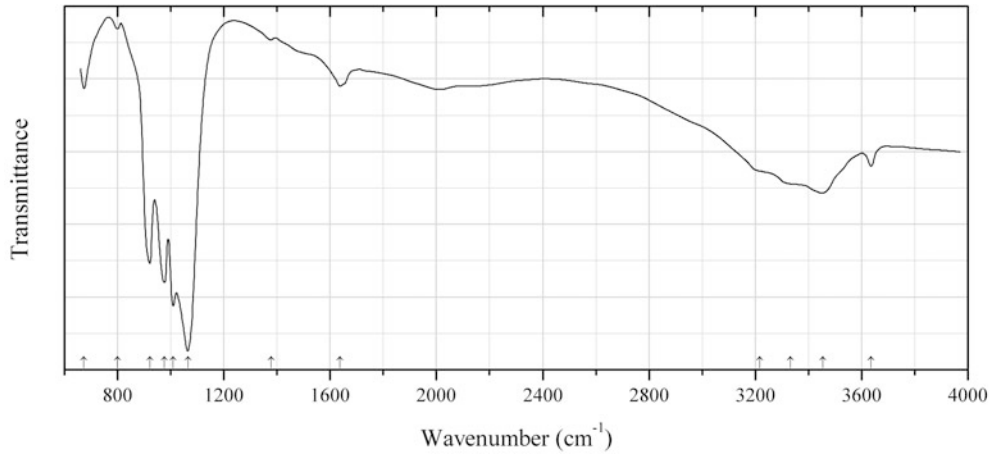

Fig. 2.839 IR spectrum of artsmithite drawn using data from Roberts et al. (2003a)

P452 Artsmithite $Hg^+_4Al(PO_4)_{2-x}(OH)_{1+3x}$ (Fig. 2.839)
Locality: Funderburk prospect, Pike Co., Arkansas, USA (type locality).
Description: White random fibrous aggregate from the association with quartz, goethite, dickite, and cinnabar. Holotype sample. Monoclinic, space group *C*2/*c*, a = 17.022(5), b = 9.074(2), c = 7.015(2) Å, β = 101.20(1)°, V = 1062.9(8) $Å^3$, Z = 4. D_{calc} = 6.40 g/cm^3. Optically biaxial (+), 2 V = 60°. The empirical formula is $Hg_{4.00}Al_{1.05}P_{1.71}O_{8.74}H_{1.78}$. The strongest lines of the powder X-ray diffraction

pattern [*d*, Å (*I*, %) (*hkl*)] are: 8.326 (100) (200), 4.739 (50) (310), 4.166 (40) (400), 2.979 (80) (202), 2.952 (50) (−402), 2.78 4(80) (600), 2.660 (75) (330), 1.755 (50) (−732, 640, −204).
Kind of sample preparation and/or method of registration of the spectrum: Absorption. For the kind of sample preparation see Roberts et al. (1994).
Source: Roberts et al. (2003a).
Wavenumbers (cm^{-1}): 3636, 3455, 3332sh, 3218sh, 1638, 1378w, 1065s, 1009s, 976, 921, 800w, 674.
Notes: The bands in the range 1700–2500 cm^{-1} and at 1378 cm^{-1} indicate the presence of acid groups (presumably HPO_4^{2-} or $H_2PO_4^-$).

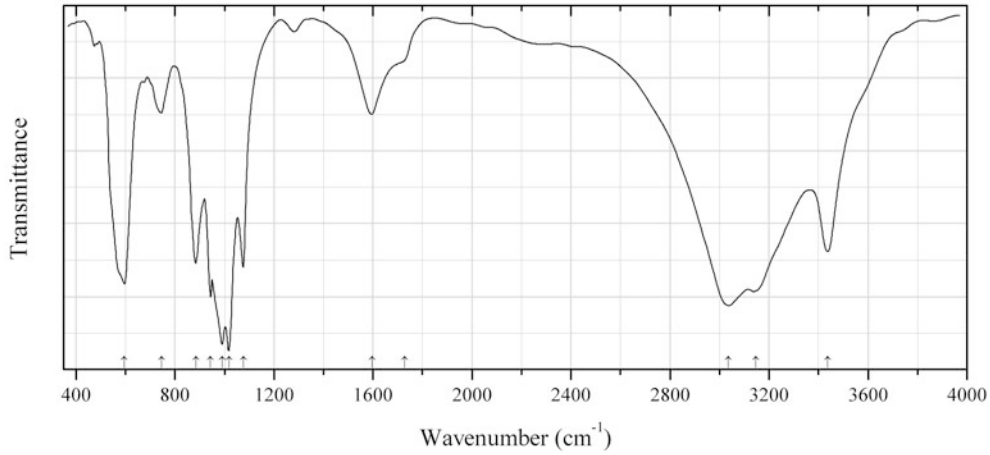

Fig. 2.840 IR spectrum of arupite drawn using data from Kullyakool et al. (2014)

P453 Arupite $Ni_3(PO_4)_2 \cdot 8H_2O$ (Fig. 2.840)
Locality: Synthesized by the wet chemical reaction between $Na_3PO_4 \cdot 12H_2O$ and $NiSO_4 \cdot 6H_2O$ at 70 °C.
Description: Pale green powder.
Kind of sample preparation and/or method of registration of the spectrum: Transmission. Kind of sample preparation is not indicated.
Source: Kullyakool et al. (2014).
Wavenumbers (cm^{-1}): 3438, 3147, 3037s, 1728sh, 1596, 1076, 1019s, 990s, 944s, 884, 746, 596s.
Note: Weak bands are not indicated. For the IR spectrum of arupite see also Kullyakool et al. (2011).

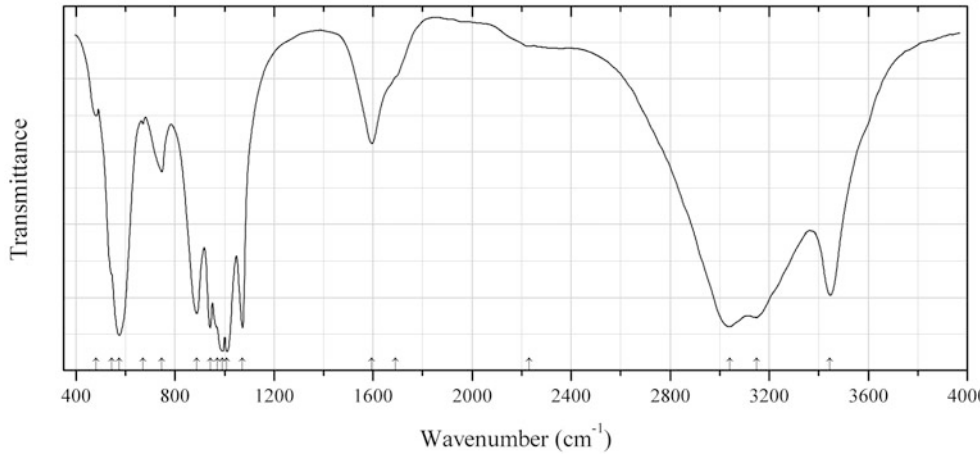

Fig. 2.841 IR spectrum of arupite drawn using data from Pechkovskii et al. (1981)

P454 Arupite $Ni_3(PO_4)_2 \cdot 8H_2O$ (Fig. 2.841)
Locality: Synthetic.
Description: Polycrystalline aggregate.
Kind of sample preparation and/or method of registration of the spectrum: KBr disc. Absorption.
Source: Pechkovskii et al. (1981).
Wavenumbers (cm^{-1}): 3445, 3150s, 3040s, 2230w, 1690sh, 1594, 1073s, 1010s, 992s, 970sh, 943s, 888, 746, 670w, 575s, 545sh, 482w, 354, 328, 314, 290sh, 284, 243, 202w, 185w.

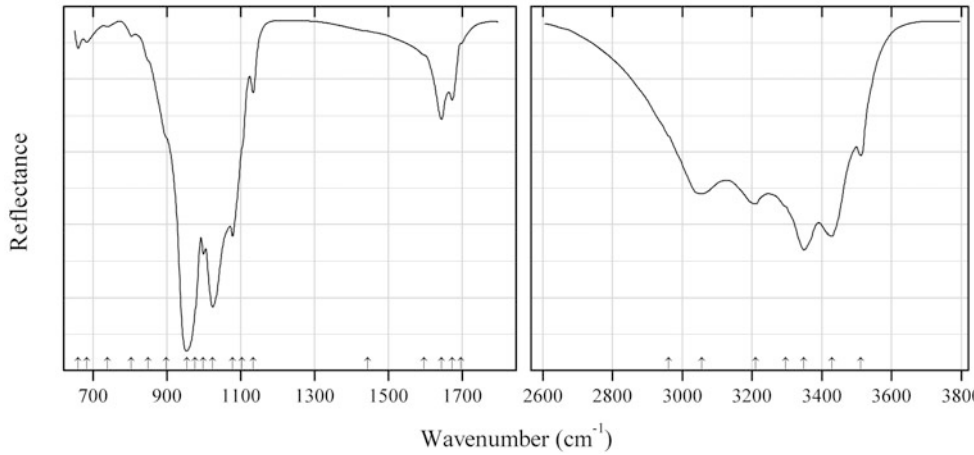

Fig. 2.842 IR spectrum of bermanite drawn using data from Frost et al. (2013c)

P455 Bermanite $Mn^{2+}Mn^{3+}{}_2(PO_4)_2(OH)_2 \cdot 4H_2O$ (Fig. 2.842)
Locality: El Criolo granitic pegmatite, Cerro Blanco pegmatite group, Eastern Pampean Ranges, Córdoba Province, Argentina.
Description: Reddish brown crystals from the association with triplite and phosphosiderite. Sample from the collection of Nelson Valenzuela (Córdoba, Argentina).
Kind of sample preparation and/or method of registration of the spectrum: Attenuated total reflection of powdered mineral.

Source: Frost et al. (2013c).
Wavenumbers (cm^{-1}): 3512, 3429s, 3348s, 3297sh, 3210, 3056, 2961sh, (1698sh), 1674, 1645, 1597sh, 1444sh, 1134w, 1103sh, 1078s, 1024s, 999s, 977sh, 954s, 898sh, 849sh, 804w, 739w, 683w, 659w.
Note: The wavenumbers were determined by us based on spectral curve analysis of the published spectrum. Bands below 650 cm^{-1} are not indicated.

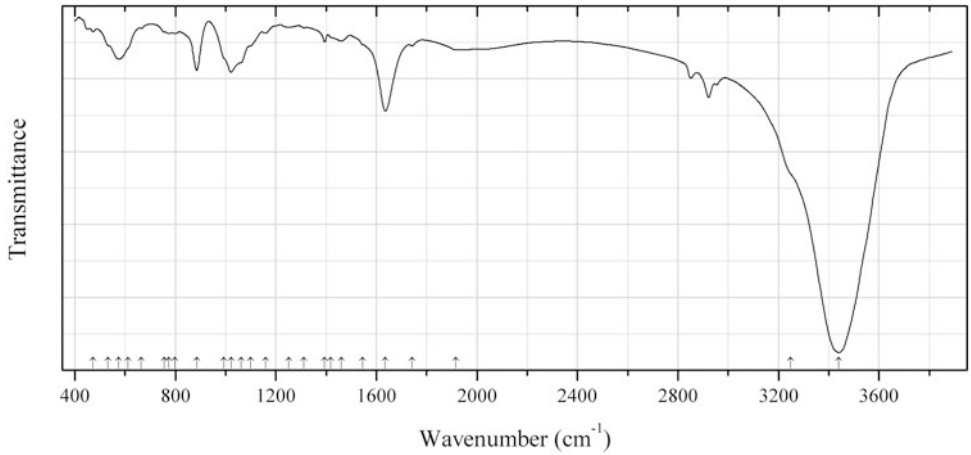

Fig. 2.843 IR spectrum of šreinite drawn using data from Sejkora and Čejka (2007)

P456 Šreinite $Pb(UO_2)_4(BiO)_3(PO_4)_2(OH)_7 \cdot 4H_2O$ (Fig. 2.843)
Locality: Horni Halže, near Měděnec, Krušne Hory (Ore Mts.), Czech Republic (type locality).
Description: Yellow crust from the association with uranosphaerite, goethite, Pb-bearing phosphuranylite, metatorbernite, bismutoferrite, kasolite, and uranophane. Holotype sample. Cubic, a = 15.5728(7), Z = 5. D_{calc} = 5.20 g/cm^3. Optically isotropic, n > 1.74. The empirical formula is $(Pb_{0.83}Ca_{0.08}Ba_{0.01}Mg_{0.01})(UO_2)_{4.10}(BiO)_{3.04}[(PO_4)_{1.15}(AsO_4)_{0.78}(SiO_4)_{0.07}](OH)_{7.02} \cdot 4H_2O$. The strongest lines of the powder X-ray diffraction pattern [d, Å (I, %) (hkl)] are: 5.513 (53) (220), 4.499 (48) (222), 4.163 (100) (321), 3.671 (77) (411, 330), 3.484 (31) (420), 3.179 (99) (422), 2.596 (54) (442, 600), 1.9776 (30) (732, 651).
Kind of sample preparation and/or method of registration of the spectrum: KBr disc. Absorption.
Source: Sejkora and Čejka (2007).
Wavenumbers (cm^{-1}): 3439s, 3247sh, 1915w, 1741w, 1635s, 1544sh, 1460w, 1419sh, 1394, 1312w, 1252w, 1158w, 1100sh, 1062sh, 1021s, 993sh, 885s, 798w, 774w, 755w, 664w, 611sh, 575s, 532sh, 472w, 450w.
Note: Presumably, anomalously strong bands at 3439 and 1635 cm^{-1} are mainly due to adsorbed water, and the bands in the range 2800–3000 cm^{-1} correspond to the admixture of grease.

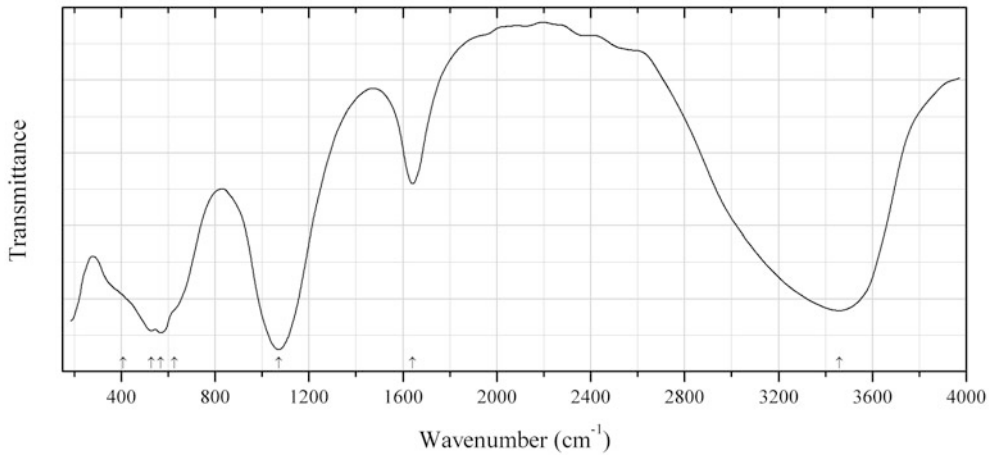

Fig. 2.844 IR spectrum of bolivarite drawn using data from García-Guinea et al. (1995)

P457 Bolivarite $Al_2(PO_4)(OH)_3 \cdot 4H_2O$ (Fig. 2.844)
Locality: Campo Lameiro, Pontevedra, Spain (type locality).
Description: Greenish yellow fracture-filling in granite. Massive, with a spherulitic texture. X-ray amorphous. D_{meas} = 2.04 g/cm^3. Optically weakly birefringent, $n \approx 1.48$. The empirical formula is $Al_2(PO_4)_{0.92}(OH)_{3.25} \cdot 4.03H_2O$.
Kind of sample preparation and/or method of registration of the spectrum: Transmission. Kind of sample preparation is not indicated.
Source: García-Guinea et al. (1995).
Wavenumbers (cm^{-1}): 3460s, 1640, 1070s, 626sh, 568s, 529s, 407sh.
Note: A questional mineral, probably related to evansite.
Note: The wavenumbers were partly determined by us based on spectral curve analysis of the published spectrum.

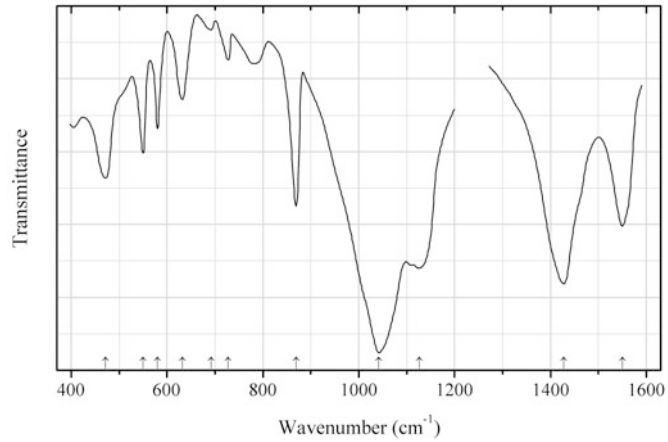

Fig. 2.845 IR spectrum of bradleyite drawn using data from Tjy et al. (1984)

P458 Bradleyite $Na_3Mg(PO_4)(CO_3)$ (Fig. 2.845)
Locality: Green River Formation, Sweetwater Co., Wyoming, USA (type locality).

Description: Monoclinic, a = 8.841(7), b = 5.117(6), c = 6.620(6) Å, β = 90.42(6)°, γ = 115.58(5)°, V = 299.6 Å^3. Optically biaxial (−), α = 1.487, β = 1.546, γ = 1.560, 2 V = 49°. The strongest lines of the powder X-ray diffraction pattern [d, Å (I, %) (hkl)] are: 3.687 (30) (111, 201), 3.344 (100) (210 + admixture of quartz), 3.309 (50) (002), 2.653 (65) (112, 202), 2.579 (50) (310, 020), 1.936 (29) (411, 320).
Kind of sample preparation and/or method of registration of the spectrum: KBr disc. Absorption.
Source: Tjy et al. (1984).
Wavenumbers (cm^{-1}): 1550s, 1428s, 1126s, 1042s, 869w, 728w, 692w, 632, 580, 550, 472.

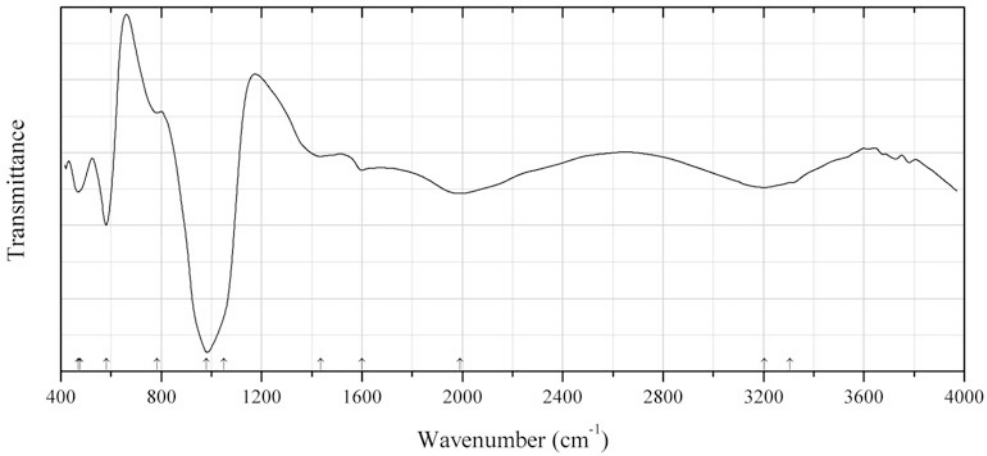

Fig. 2.846 IR spectrum of brendelite drawn using data from Krause et al. (1998b)

P459 Brendelite $(Bi,Pb)_2(Fe^{3+},Fe^{2+})(PO_4)O_2(OH)$ (Fig. 2.846)
Locality: Güldener Falk mine, near Schneeberg, Erzgebirge (Ore Mts.), Saxony, Germany (type locality).
Description: Dark brown aggregates from the association with eulytite, bismutite, and bismutoferrite. Holotype sample. Monoclinic, space group $C2/m$, a = 12.278(2), b = 3.815(1), c = 6.899(1) Å, β = 111.14(1)°, V = 301.4(1) Å^3, Z = 2. D_{calc} = 6.83 g/cm^3. Optically biaxial (−), α = 2.06, β = 2.25 (calculated), γ = 2.19, 2 V = 70(5)°. The empirical formula is $(Bi_{1.27}Pb_{0.74})(Fe^{3+}{}_{0.74}Fe^{2+}{}_{0.27})[(PO_4)_{0.95}(AsO_4)_{0.02}(VO_4)_{0.02}]O_{2.00}(OH)_{1.00}$. The strongest lines of the powder X-ray diffraction pattern [d, Å (I, %) (hkl)] are: 5.726 (54) (200), 3.372 (77) (20–2), 3.322 (37) (11–1), 3.217 (46) (002), 3.011 (100) (111), 2.863 (34) (400), 2.750 (62) (31–1).
Kind of sample preparation and/or method of registration of the spectrum: Diamond microcell. Transmission.
Source: Krause et al. (1998b).
Wavenumbers (cm^{-1}): 3305sh, 3203, 1990, 1599, 1435, 1051sh, 981, 783w, 581s, 477sh, 469.
Note: The wavenumbers were determined by us based on spectral curve analysis of the published spectrum.

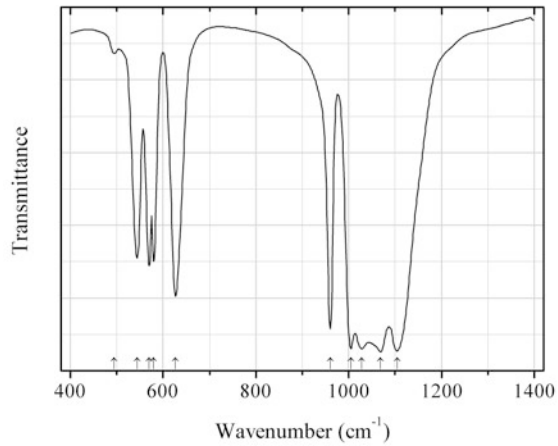

Fig. 2.847 IR spectrum of monazite-(Nd) drawn using data from Kijkowska et al. (2003)

P460 Monazite-(Nd) $Nd(PO_4)$ (Fig. 2.847)
Locality: Synthetic.
Description: Monoclinic. Prepared by crystallization from boiling phosphoric acid solution with subsequent ignition at 950 °C.
Kind of sample preparation and/or method of registration of the spectrum: Transmission. Kind of sample preparation is not indicated.
Source: Kijkowska et al. (2003).
Wavenumbers (cm^{-1}): 1105s, 1068s, 1028s, 1005s, 960, 627, 580, 570, 544, 495w.

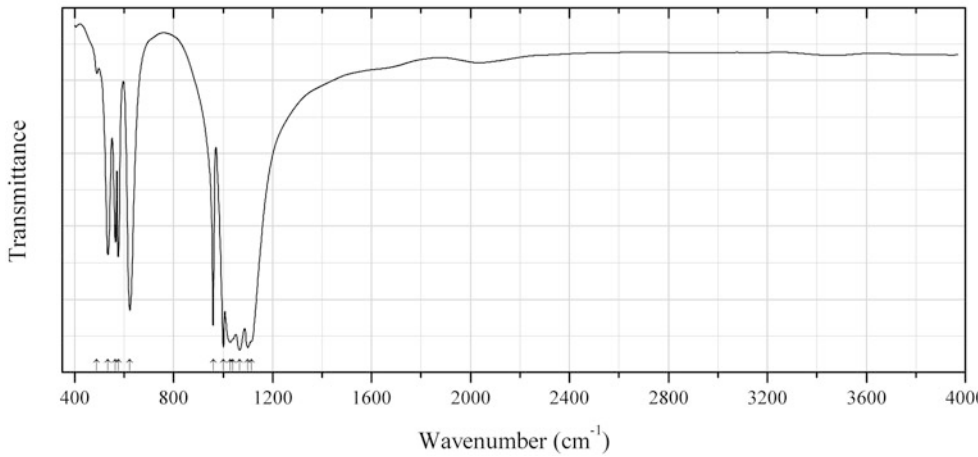

Fig. 2.848 IR spectrum of monazite-(Nd) drawn using data from Pechkovskii et al. (1981)

P461 Monazite-(Nd) $Nd(PO_4)$ (Fig. 2.848)
Locality: Synthetic.
Description: Monoclinic.
Kind of sample preparation and/or method of registration of the spectrum: KBr disc. Absorption.
Source: Pechkovskii et al. (1981).

Wavenumbers (cm^{-1}): 1114sh, 1100s, 1067s, 1040sh, 1029s, 1001s, 960, 623, 576, 565, 535, 490w, 300sh, 265, 340sh, 200, 177.

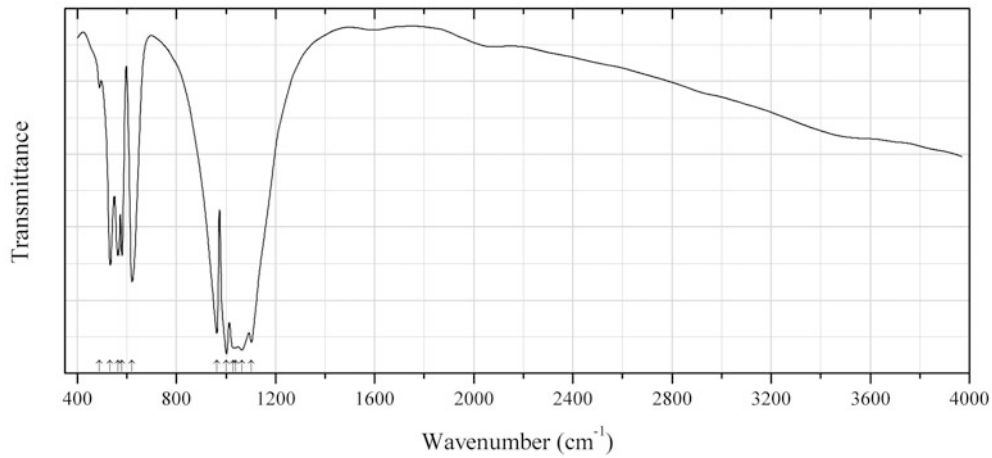

Fig. 2.849 IR spectrum of monazite-(Sm) drawn using data from Pechkovskii et al. (1981)

P463 Monazite-(Sm) $Sm(PO_4)$ (Fig. 2.849)
Locality: Synthetic.
Description: Monoclinic.
Kind of sample preparation and/or method of registration of the spectrum: KBr disc. Absorption.
Source: Pechkovskii et al. (1981).
Wavenumbers (cm^{-1}): 1102s, 1064s, 1040s, 1030s, 1002s, 963s, 621, 580, 564, 533, 490w, 390w, 300sh, 262, 250, 205, 165.

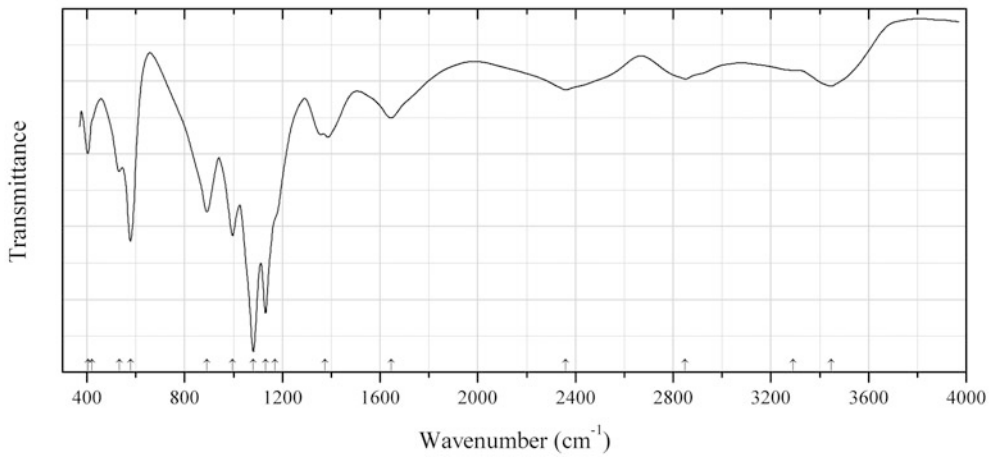

Fig. 2.850 IR spectrum of monetite drawn using data from Tortet et al. (1997)

P464 Monetite $Ca(HPO_4)$ (Fig. 2.850)
Locality: Synthetic.

Description: Investigated by neutron scattering analysis.
Kind of sample preparation and/or method of registration of the spectrum: Transmission. Kind of sample preparation is not indicated.
Source: Tortet et al. (1997).
Wavenumbers (cm^{-1}): 3447, 3290sh, 2849, 2360, 1646, 1300–1450 (broad), 1170sh, 1131s, 1081s, 996, 891, 578, 532, 420, 404.
Note: The band position denoted by Tortet et al. (1997) as 3190 cm^{-1} was determined by us at 3290 cm^{-1} based on spectral curve analysis of the published spectrum. For IR spectra of monetite see also Petrov et al. (1967), Xu et al. (1999).

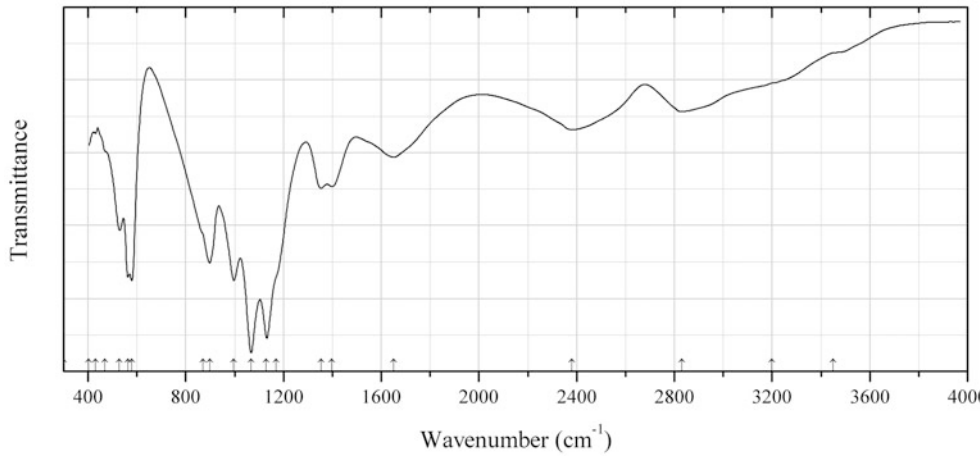

Fig. 2.851 IR spectrum of monetite drawn using data from Pechkovskii et al. (1981)

P465 Monetite $Ca(HPO_4)$ (Fig. 2.851)
Locality: Synthetic.
Kind of sample preparation and/or method of registration of the spectrum: KBr disc. Absorption.
Source: Pechkovskii et al. (1981).
Wavenumbers (cm^{-1}): 3450sh, 3200, 2830, 2380, 1650, 1398, 1354, 1170sh, 1130s, 1068s, 997s, 898, 870sh, 579s, 563, 529, 470sh, 430w, 403, 300sh, 262, 200w.

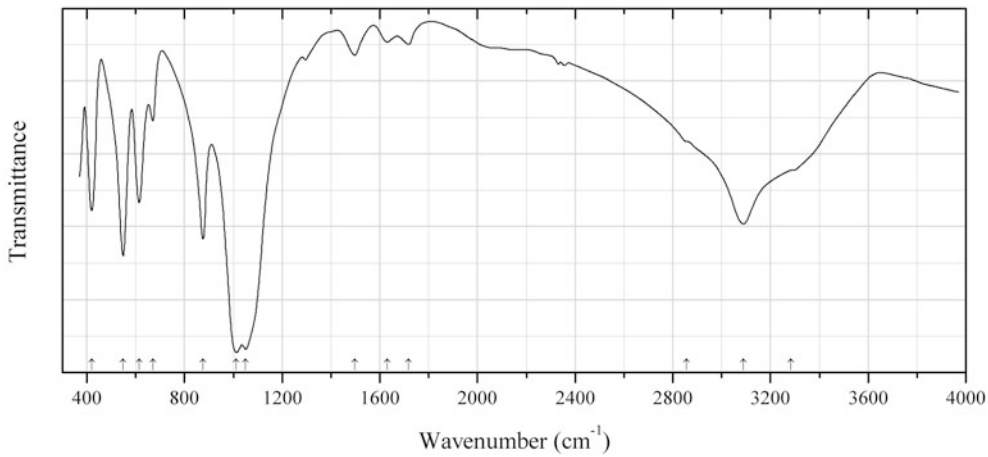

Fig. 2.852 IR spectrum of serrabrancaite drawn using data from Boonchom et al. (2008)

P466 Serrabrancaite $Mn(PO_4)\cdot H_2O$ (Fig. 2.852)
Locality: Synthetic.
Description: Nanocrystalline sample. Confirmed by powder X-ray diffraction data.
Kind of sample preparation and/or method of registration of the spectrum: KBr disc. Transmission.
Source: Boonchom et al. (2008).
Wavenumbers (cm^{-1}): 3284sh, 3090, 2857sh, 1718w, 1630w, 1498w, 1050s, 1012s, 876, 670w, 615, 548s, 420.
Note: For IR spectra of serrabrancaite see also Aranda and Bruque (1990), Aleksovska et al. (1997), Boonchom et al. (2010).

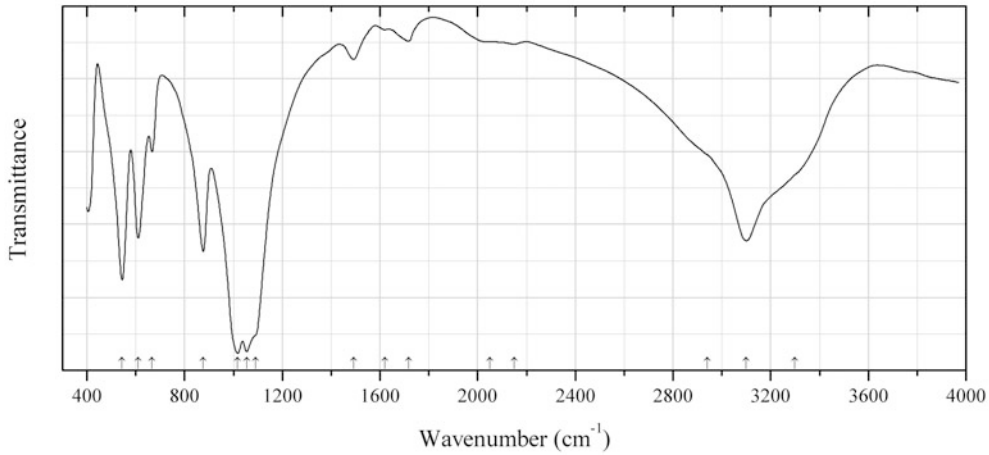

Fig. 2.853 IR spectrum of serrabrancaite drawn using data from Pechkovskii et al. (1981)

P467 Serrabrancaite $Mn(PO_4)\cdot H_2O$ (Fig. 2.853)
Locality: Synthetic.
Description: Synthesized in the reaction of MnO with 85 % orthophosphoric acid with subsequent annealing at 180 °C during 42 h and at 300 °C during 6 h.
Kind of sample preparation and/or method of registration of the spectrum: KBr disc. Transmission.
Source: Pechkovskii et al. (1981).
Wavenumbers (cm^{-1}): 3300sh, 3100, 2940sh, 2150w, 2050sh, 1717w, 1620w, 1493w, 1090sh, 1055s, 1017s, 877, 667, 610, 544s, 406, 340, 276, 230w, 206.

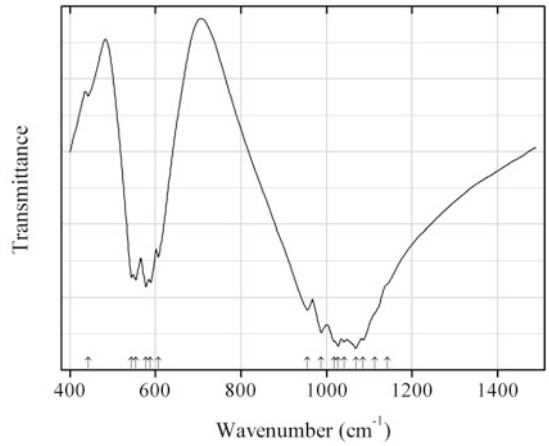

Fig. 2.854 IR spectrum of tuite polymorph drawn using data from Jillavenkatesa and Condrate (1998)

P468 Tuite polymorph α-$Ca_3(PO_4)$ (Fig. 2.854)
Locality: Synthetic.
Description: Monoclinic high-temperature polymorph, a = 12.887, b = 27.28, c = 15.219 Å, β = 126.2°. Confirmed by powder X-ray diffraction data.
Kind of sample preparation and/or method of registration of the spectrum: Absorption. Kind of sample preparation is not indicated.
Source: Jillavenkatesa and Condrate (1998).
Wavenumbers (cm^{-1}): 1142sh, 1114sh, 1086s, 1069s, 1041s, 1027s, 1018sh, 988s, 955s, 607, 588, 577, 554, 544, 443w.
Note: The wavenumbers were determined by us based on spectral curve analysis of the published spectrum.

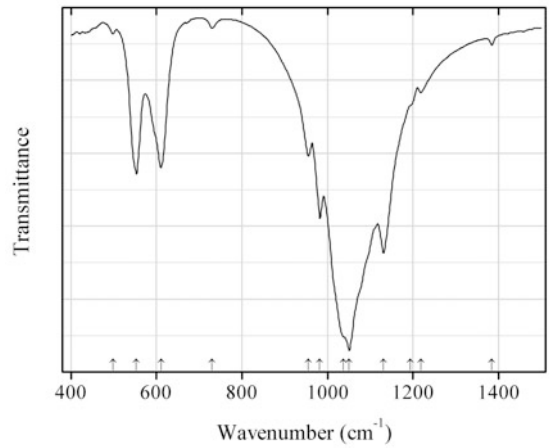

Fig. 2.855 IR spectrum of tuite polymorph drawn using data from Jillavenkatesa and Condrate (1998)

P469 Tuite polymorph β-$Ca_3(PO_4)$ (Fig. 2.855)
Locality: Synthetic.

Description: Trigonal polymorph, a = 10.439, c = 37.375 Å. Related to merrillite and whitlockite. Confirmed by powder X-ray diffraction data.
Kind of sample preparation and/or method of registration of the spectrum: Absorption. Kind of sample preparation is not indicated.
Source: Jillavenkatesa and Condrate (1998).
Wavenumbers (cm^{-1}): 1384w, 1218w, 1194sh, 1131s, 1051s, 1037sh, 982s, 955, 730w, 611, 553, 498w.
Note: For IR spectrum of β-$Ca_3(PO_4)$ see also Chabchoub and Dogguy (1993).
Note: The wavenumbers were determined by us based on spectral curve analysis of the published spectrum.

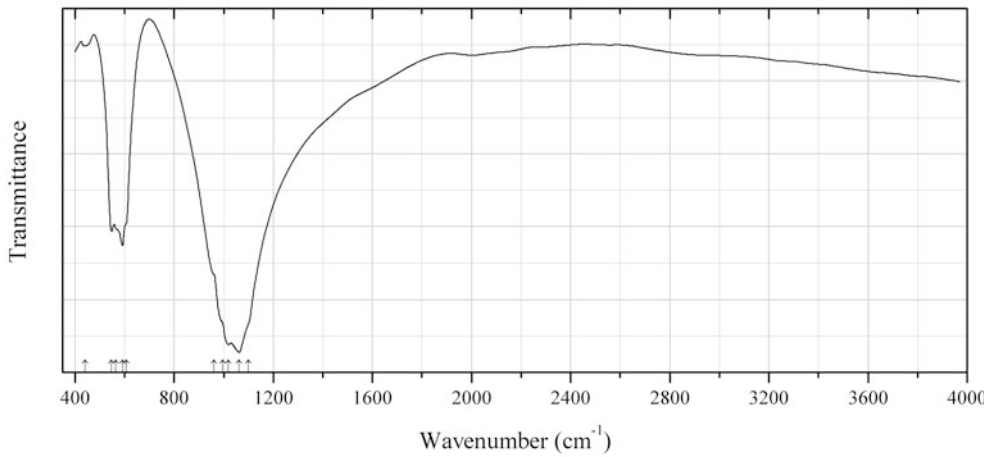

Fig. 2.856 IR spectrum of tuite polymorph drawn using data from Pechkovskii et al. (1981)

P470 Tuite polymorph α-$Ca_3(PO_4)_2$ (Fig. 2.856)
Locality: Synthetic.
Description: Monoclinic high-temperature polymorph, space group $R2_1/a$, a = 12.887, b = 27.28, c = 15.219 Å, β = 126.20°, Z = 24.
Kind of sample preparation and/or method of registration of the spectrum: KBr disc. Absorption.
Source: Pechkovskii et al. (1981).
Wavenumbers (cm^{-1}): 1100sh, 1063s, 1020s, 995sh, 960sh, 608sh, 592s, 565sh, 548s, 440w, 304s, 270s, 200s.

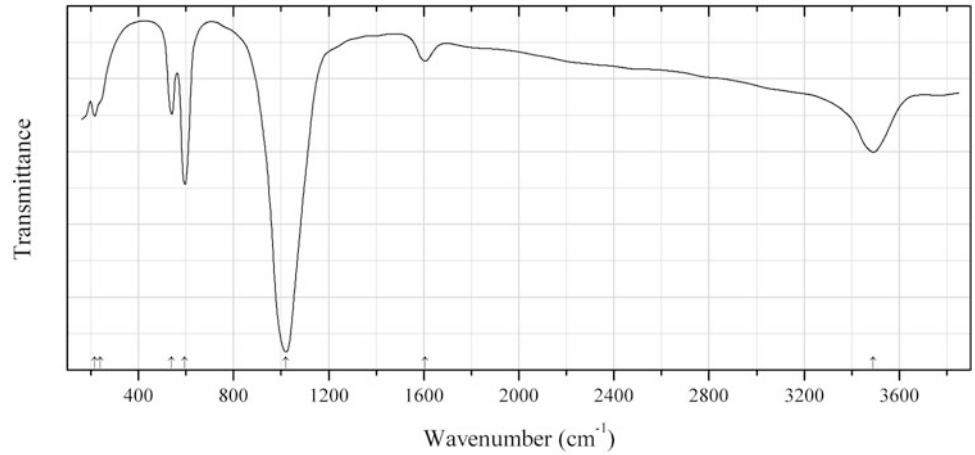

Fig. 2.857 IR spectrum of ximengite drawn using data from Jiaxin (1989)

P471 Ximengite $Bi(PO_4)$ (Fig. 2.857)
Locality: Amo Sn deposit, 420 km SW of Kunming, Ximeng Co., Yunnan province, China (type locality).
Description: White earthy aggregate from the association with waylandite and monazite. Holotype sample. Hexagonal, space group $P3_121$, a = 6.9860(16), c = 6.4753(28) Å, V = 273.68 Å^3, Z = 3. D_{calc} = 5.534 g/cm^3. The empirical formula is $Bi_{1.01}P_{0.99}O_4$. The strongest lines of the powder X-ray diffraction pattern [d, Å (I, %) (hkl)] are: 6.052 (73) (100), 4.4198 (91) (101), 3.4930 (88) (110), 3.0244 (100) (200), 2.8537 (65) (102), 2.1573 (47) (211), 1.8683 (45) (212), 1.7474 (48) (220).
Kind of sample preparation and/or method of registration of the spectrum: KBr disc. Absorption.
Source: Jiaxin (1989).
Wavenumbers (cm^{-1}): 3490, 1605w, 1020s, 595s, 540, 238sh, 216.
Note: The wavenumbers were partly determined by us based on spectral curve analysis of the published spectrum. The bands at 3490 and 1605 cm^{-1} correspond to the admixture of H_2O.

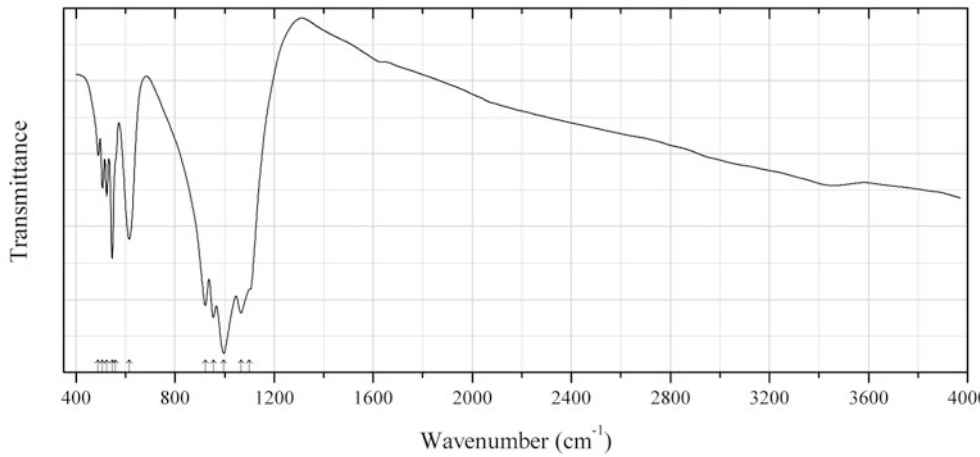

Fig. 2.858 IR spectrum of ximengite dimorph drawn using data from Pechkovskii et al. (1981)

P472 Ximengite dimorph $Bi(PO_4)$ (Fig. 2.858)

Locality: Synthetic.
Description: Monoclinic, space group $P2_1$, a = 4.88, b = 7.06, c = 4.71 Å, β = 96.3°, Z = 2. Synthesized in the reaction of bismuth nitrate with monosubstituted orthophosphate of an alkaline metal at room temperature with subsequent annealing at 1000 °C and quenching.
Kind of sample preparation and/or method of registration of the spectrum: KBr disc. Absorption.
Source: Pechkovskii et al. (1981).
Wavenumbers (cm^{-1}): 1100sh, 1066s, 997s, 956s, 923s, 615, 560sh, 546, 524, 507, 490, 333w, 240sh, 210, 182.

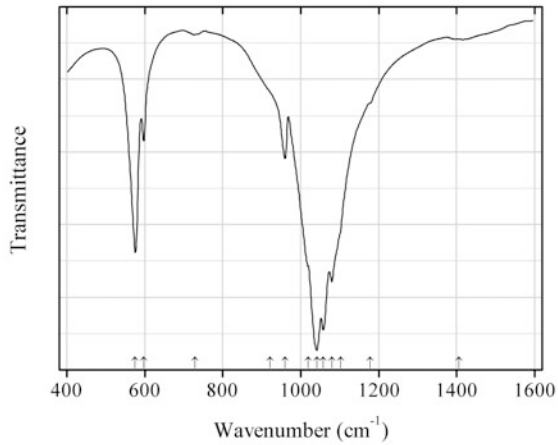

Fig. 2.859 IR spectrum of buchwaldite dimorph drawn using data from Jastrzębski et al. (2011)

P473 Buchwaldite dimorph $NaCa(PO_4)$ (Fig. 2.859)
Locality: Synthetic.
Description: Space group $Pn2_1a$.
Kind of sample preparation and/or method of registration of the spectrum: KBr disc. Absorption.
Source: Jastrzębski et al. (2011).
Wavenumbers (cm^{-1}): 1406w, 1178sh, 1102sh, 1080s, 1058s, 1041s, 1019sh, 960, 922sh, 729, 597, 575s.
Note: The wavenumbers were partly determined by us based on spectral curve analysis of the published spectrum.

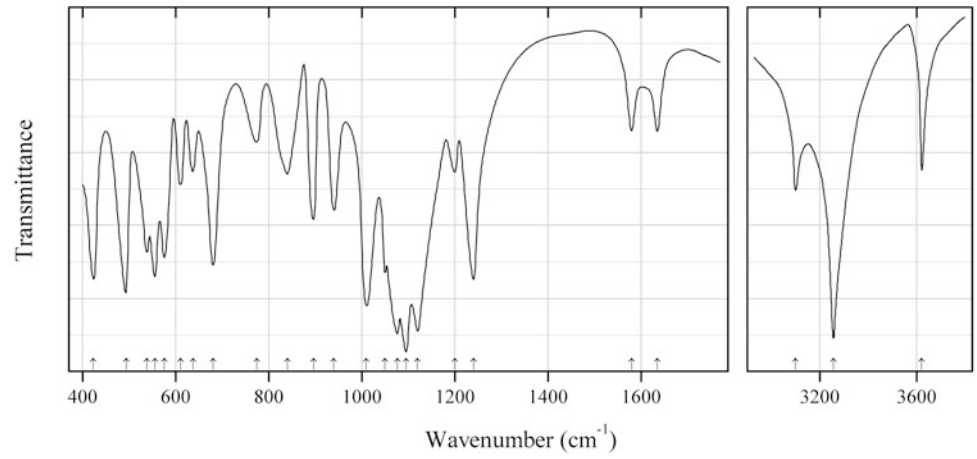

Fig. 2.860 IR spectrum of burangaite drawn using data from Povarennykh (1981b)

P474 Burangaite $NaFe^{2+}Al_5(PO_4)_4(OH)_6 \cdot 2H_2O$ (Fig. 2.860)
Locality: Buranga pegmatite, Gatumba district, Western Province, Rwanda (type locality).
Description: No data.
Kind of sample preparation and/or method of registration of the spectrum: KBr disc. Absorption.
Source: Povarennykh et al. (1981b).
Wavenumbers (cm^{-1}): 3622, 3256s, 3100, 1635, 1580, 1240s, 1200, 1120s, 1095s, 1076s, 1050, 1010s, 940, 896, 840, 774, 680, 637, 610, 575, 555s, 538, 493s, 423s.

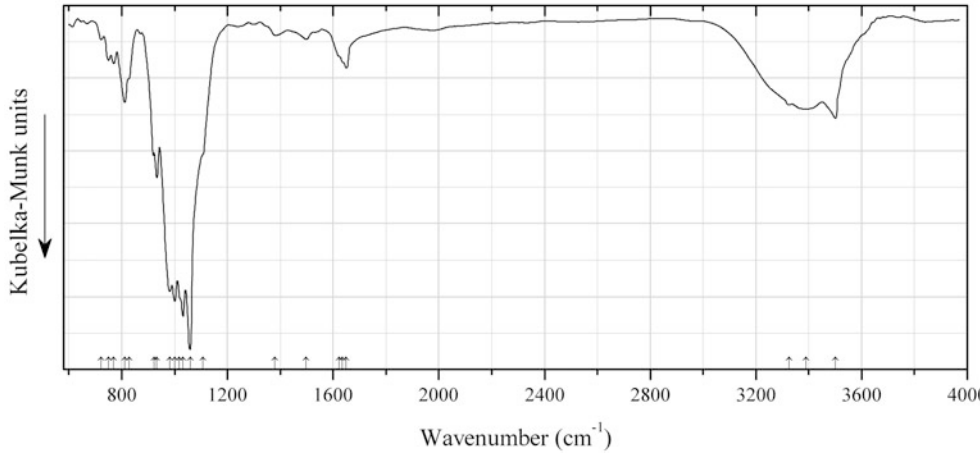

Fig. 2.861 IR spectrum of calciopetersite drawn using data from Sejkora et al. (2005)

P475 Calciopetersite $CaCu_6(PO_4)_2(HPO_4)(OH)_6 \cdot 3H_2O$ (Fig. 2.861)
Locality: An abandoned quarry located 1.5 km south of Domašov nad Bystřicí, 20 km northeast of Olomouc, northern Moravia, Czech Republic (type locality).
Description: Olive green acicular crystals from the association with chrysocolla, the Ce-dominant analogue of petersite-(Y), malachite, allophane, goethite, lepidocrocite, chalcopyrite, pyrite, covellite,

chalcocite, and quartz. Holotype sample. Hexagonal, space group $P6_3/m$, a = 13.284(4), c = 5.902(4) Å, V = 902.0(6) Å^3, Z = 2. D_{calc} = 3.332 g/cm^3. Optically uniaxial (+), ω = 1.674(5), ε ∼ 1.75. The empirical formula is $(Ca_{0.98}Y_{0.13}Ce_{0.11}Nd_{0.08}La_{0.04}K_{0.02}Dy_{0.02}Pr_{0.01}Yb_{0.01})(Cu_{5.90}Ca_{0.14})[(PO_4)_{2.06}(HPO_4)_{0.65}(AsO_4)_{0.22}(SiO_4)_{0.22}(OH)_6]\cdot 3H_2O$. The strongest lines of the powder X-ray diffraction pattern [d, Å (I, %) (hkl)] are: 11.51 (100) (100), 4.346 (88) (210), 4.140 (46) (201), 3.837 (38) (300), 3.321 (44) (220), 2.888 (53) (221), 2.877 (37) (400), 2.510 (37) (140).

Kind of sample preparation and/or method of registration of the spectrum: KBr disc. IR microscope.

Source: Sejkora et al. (2005).

Wavenumbers (cm^{-1}): 3501, 3390, 3326sh, 1650, 1635sh, 1623sh, 1498w, 1379w, 1108sh, 1059s, 1032s, 1018sh, 1001s, 982s, 933, 924sh, 829sh, 811, 770, 750, 722.

Note: Weak absorption in the range from 1900 to 2000 and at 1379 cm^{-1} may be due to vibrations of HPO_4^{2-} and H^+ respectively.

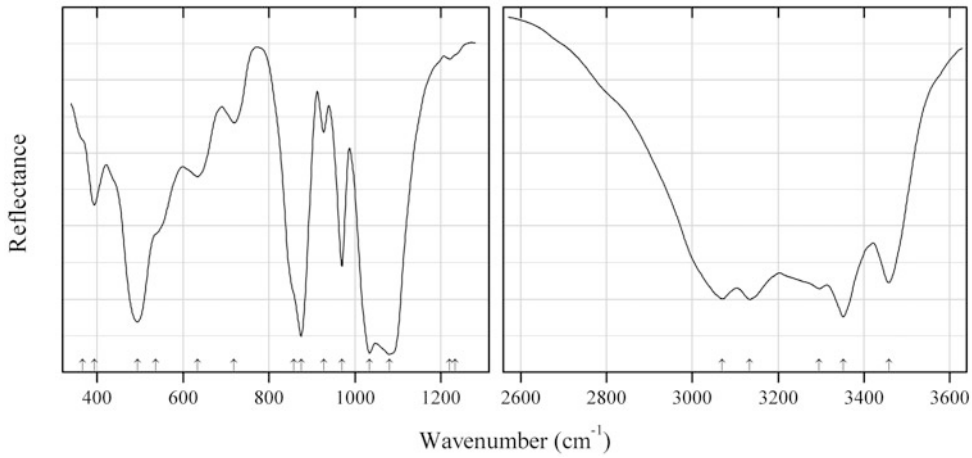

Fig. 2.862 IR spectrum of canaphite drawn using data from Sinyaev et al. (2003)

P476 Canaphite $Na_2Ca(P_2O_7)\cdot 4H_2O$ (Fig. 2.862)

Locality: Synthetic.

Description: Identified by powder X-ray diffraction data. Contains admixture of β-$Ca_2(P_2O_7)$.

Kind of sample preparation and/or method of registration of the spectrum: Attenuated total reflection of powdered mineral.

Source: Sinyaev et al. (2003).

Wavenumbers (cm^{-1}): 3459, 3352s, 3296, 3134, 3070, 1233sh, 1220w, 1080s, 1034s, 970, 927, 875s, 858sh, 719, 634, 536sh, 494s, 394, 366sh.

Note: The wavenumbers were determined by us based on spectral curve analysis of the published spectrum.

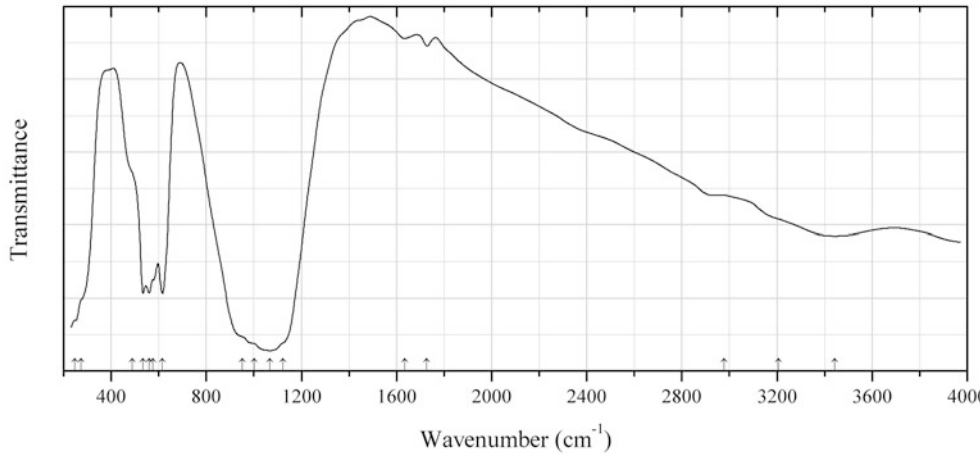

Fig. 2.863 IR spectrum of cheralite drawn using data from Bowles et al. (1980)

P477 Cheralite $CaTh(PO_4)_2$ (Fig. 2.863)
Locality: Kuttakuzhi, Travoncore, Keralia state, India (type locality).
Description: Monoclinic, space group $P2_1/n$, a = 6.7515(5), b = 6.9625(5), c = 6.4680(5) Å, β = 103.89°, V = 295.2 Å^3. D_{meas} = 2.39(3) g/cm^3, D_{calc} = 2.391 g/cm^3. The empirical formula is $(REE_{1.58}Th_{1.15}Ca_{1.03}Pb_{0.05}U_{0.15})(P_{3.67}Si_{0.33})O_{16}$. The strongest lines of the powder X-ray diffraction pattern [d, Å (I, %) (hkl)] are: 4.167 (25) (−111), 3.481 (30) (020), 3.277 (58) (200), 3.074 (100) (120), 2.8625 (65) (−112, 012), 2.177 (22) (031).
Kind of sample preparation and/or method of registration of the spectrum: KBr disc. Transmission.
Source: Bowles et al. (1980).
Wavenumbers (cm^{-1}): 3444, 3206sh, 2977sh, 1727w, 1634w, 1123sh, 1068s, 1001sh, 952sh, 616, 577, 559, 534, 490sh, 274sh, 247sh.
Note: The wavenumbers were determined by us based on spectral curve analysis of the published spectrum.

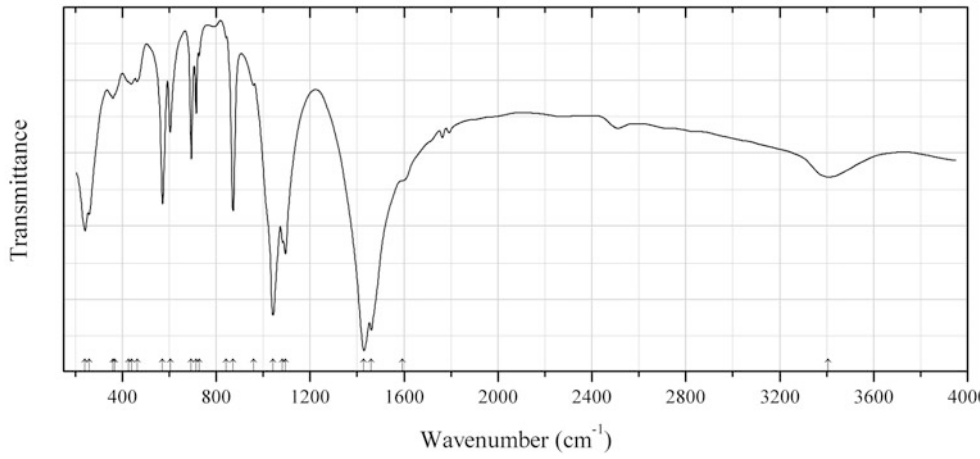

Fig. 2.864 IR spectrum of daqingshanite-(Ce) drawn using data from Appleton et al. (1992)

P478 Daqingshanite-(Ce) $Sr_3Ce(PO_4)(CO_3)_3$ (Fig. 2.864)
Locality: Nkombwa Hill carbonatite complex, northern Zambia.
Description: White crystals from dolomite matrix, from the association with barite, monazite, quartz and accessory apatite, and strontianite. The empirical formula is $(Sr_{2.69}Ba_{0.20}Ca_{0.11})(Ce_{0.50}La_{0.42}Pr_{0.07}Nd_{0.03})(PO_4)_{0.99}(CO_3)_{3-x}(OH,F)_{3x}$. The strongest lines of the powder X-ray diffraction pattern are observed at *d* values of 3.940, 3.170, 3.060, 2.520, 2.120, 2.040, and 1.948 Å.
Kind of sample preparation and/or method of registration of the spectrum: Transmission. Kind of sample preparation is not indicated.
Source: Appleton et al. (1992).
Wavenumbers (cm^{-1}): 3407, 1593sh, 1461w, 1429w, 1095s, 1083s, 1042s, 959w, 872, 842sh, 728, 715, 694, 604, 572, 463, 439w, 426sh, 368sh, 360w, 259, 241.
Note: The wavenumbers were determined by us based on spectral curve analysis of the published spectrum. The wavenumbers of absorption bands in the IR spectrum of daqingshanite-(Ce) holotype from Bayan Obo, China are (Yingchen et al. 1983): 1438s, 1094sh, 1040s, 872, 604, 570.

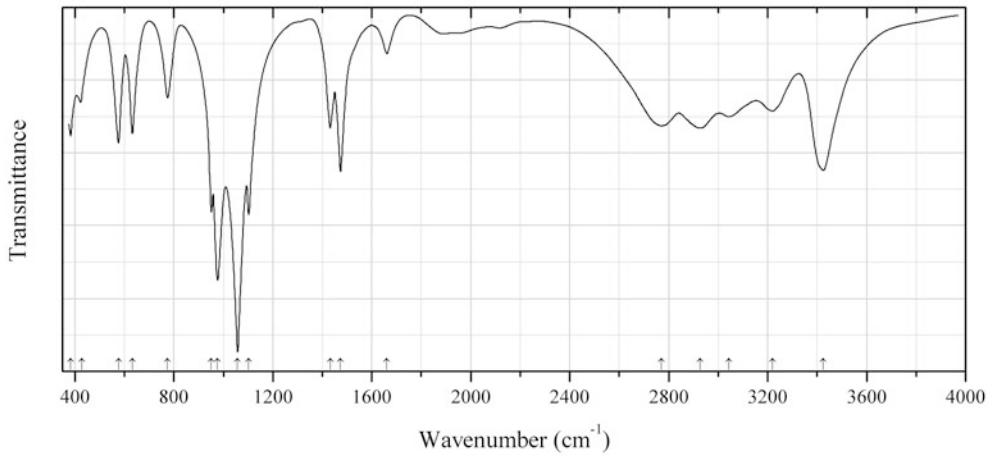

Fig. 2.865 IR spectrum of dittmarite drawn using data from Šoptrajanov et al. (2002)

P479 Dittmarite $(NH_4)Mg(PO_4)\cdot H_2O$ (Fig. 2.865)
Locality: Synthetic.
Description: Synthesized according to a method described elsewhere.
Kind of sample preparation and/or method of registration of the spectrum: KBr disc. Absorption.
Source: Šoptrajanov et al. (2002).
Wavenumbers (cm^{-1}): 3425s, 3220, 3043, 2928, 2771, 1661, 1474s, 1432, 1102s, 1058s, 977s, 952s, 775, 632, 576, 428, 382.
Note: The wavenumbers were determined by us based on spectral curve analysis of the published spectrum. According to Lai Zhnyu et al. (2012), wavenumbers in the IR spectrum of the synthetic analogue of dittmarite (cm^{-1}) are: 3500s, 3250, 2400, 1641, 1500, 1470, 1061s, 979s, 633, 576.

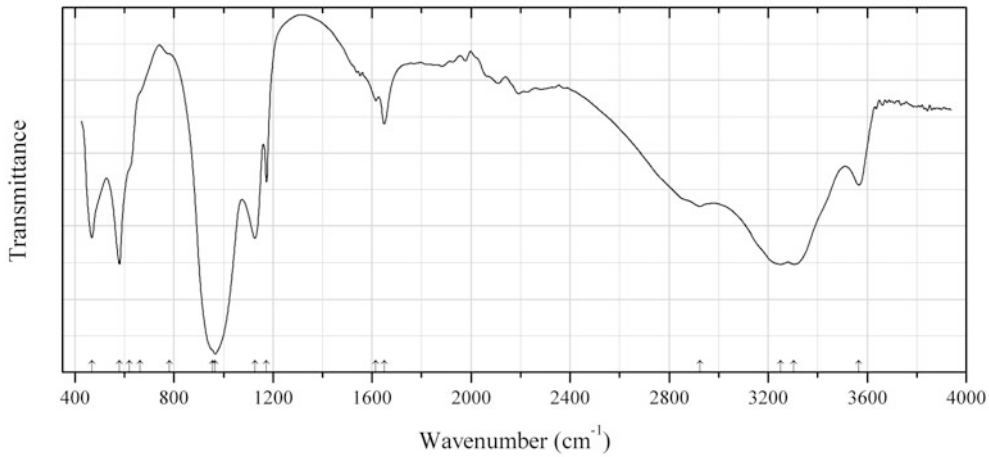

Fig. 2.866 IR spectrum of ercitite drawn using data from Fransolet et al. (2000)

P480 Ercitite $NaMn^{3+}(PO_4)(OH)\cdot 2H_2O$ (Fig. 2.866)
Locality: Tanco granitic pegmatite, at Bernic lake, southeastern Manitoba, Canada (type locality).
Description: Divergent sprays of light brown lath-like crystals from the association with altered lithiophilite, lithiophosphate, collinsite, fairfieldite, whitlockite, and other phosphates. Holotype sample. Monoclinic, space group $P2_1/n$, $a = 5.362(5)$, $b = 19.89(1)$, $c = 5.362(5)$ Å, $\beta = 108.97(8)°$, $V = 540.8(6)$ Å^3, $Z = 4$. $D_{calc} = 2.75$ g/cm^3. Optically biaxial (+), $\alpha = 1.699(2)$, $\beta = 1.715(5)$, $\gamma = 1.737(5)$, $2V = 86°$. The empirical formula is $(Na_{0.89}Ca_{0.04})(Mn^{3+}_{0.53}Fe^{3+}_{0.46}Al_{0.01})(PO_4)_{1.00}(OH)\cdot 2H_2O$. The strongest lines of the powder X-ray diffraction pattern [*d*, Å (*I*, %) (*hkl*)] are: 9.90 (100) (020), 4.920 (50) (011, 110), 3.273 (60) (14–1), 3.126 (60) (150, 051), 2.644 (80) (141), 2.542 (40) (200, 002), 2.376 (40) (17–1).
Kind of sample preparation and/or method of registration of the spectrum: Transmission. Kind of sample preparation is not indicated.
Source: Fransolet et al. (2000).
Wavenumbers (cm^{-1}): 3567, 3303s, 3250s, 2924, 1649, 1615w, 1174, 1127, 967s, 956sh, 781w, 664sh, 621sh, 580s, 468.
Note: The wavenumbers were partly determined by us based on spectral curve analysis of the published spectrum.

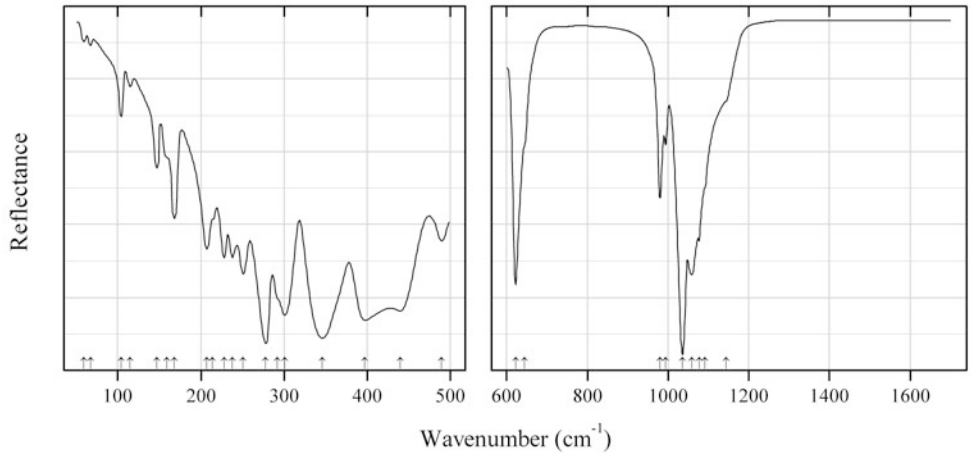

Fig. 2.867 IR spectrum of farringtonite drawn using data from Vogel et al. (2011)

P481 Farringtonite $Mg_3(PO_4)_2$ (Fig. 2.867)
Locality: Synthetic.
Kind of sample preparation and/or method of registration of the spectrum: Attenuated total reflection of powdered sample (mid IR region); polyethylene disc (far IR region).
Source: Vogel et al. (2011).
Wavenumbers (cm^{-1}): 1144sh, 1091sh, 1077, 1059s, 1036s, 994, 980, 644sh, 622s, 490w, 440, 397, 346, 301w, 292sh, 278, 251w, 238w, 228w, 214sh, 207w, 168, 159sh, 147, 115w, 104, 67w, 59w.
Note: The wavenumbers were partly determined by us based on spectral curve analysis of the published spectrum.

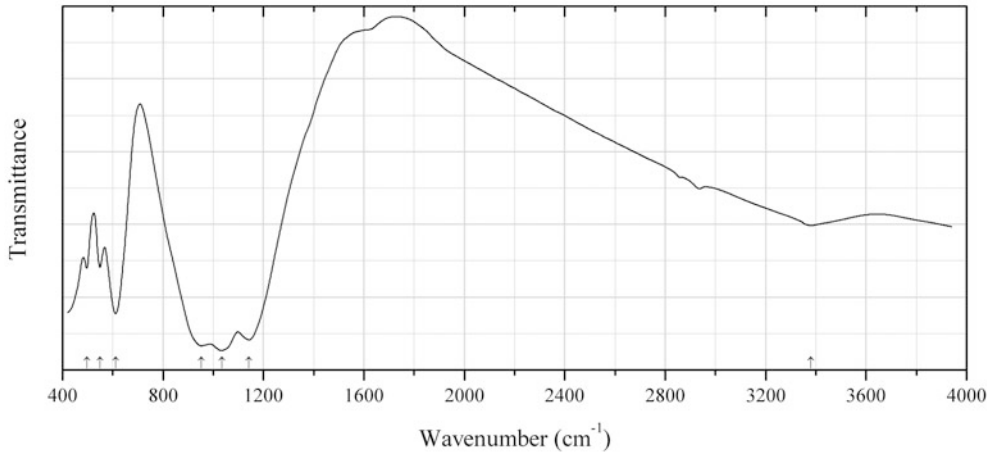

Fig. 2.868 IR spectrum of ferrorosemaryite drawn using data from Hatert et al. (2005)

P482 Ferrorosemaryite $\square NaFe^{2+}Fe^{3+}Al(PO_4)_3$ (Fig. 2.868)
Locality: The pegmatite of Rubindi-Kabilizi, 50 km west of Kigali, Gatumba pegmatitic field, Rwanda (type locality).
Description: Dark green grains from the association with scorzalite, trolleite, montebrasite, bertossaite, brazilianite, augelite, triplite, and lacroixite. Holotype sample. Monoclinic, space group $P2_1/n$,

a = 11.838(1), b = 12.347(1), c = 6.2973(6) Å, β = 114.353(6)°, V = 838.5(1). D_{calc} = 3.62 g/cm^3. Optically biaxial (−), α = 1.730(5), β = 1.758(7), γ = 1.775(5). The empirical formula is $\square_{1.00}(Na_{0.42}Mn^{2+}_{0.28}Ca_{0.04}\square_{0.26})(Fe^{2+}_{0.71}Mn^{2+}_{0.24}Fe^{3+}_{0.05})Fe^{3+}_{1.00}(Al_{0.82}Fe^{3+}_{0.16}Mg_{0.02})$ $[(P_{0.99}\square_{0.01})O_4]_3$. The strongest lines of the powder X-ray diffraction pattern [d, Å (I, %) (hkl)] are: 8.102 (30) (110), 6.167 (50) (020), 5.382 (40) (200), 4.054 (45) (220), 3.448 (65) (310), 3.011 (40) (11–2), 2.693 (75) (400), 2.677 (100) (240).

Kind of sample preparation and/or method of registration of the spectrum: KBr disc. Transmission.

Source: Hatert et al. (2005).

Wavenumbers (cm^{-1}): 3380w, 1142s, 1034s, 952s, 611, 549, 496.

Note: The band at 3380 cm^{-1} indicates possible presence of OH groups.

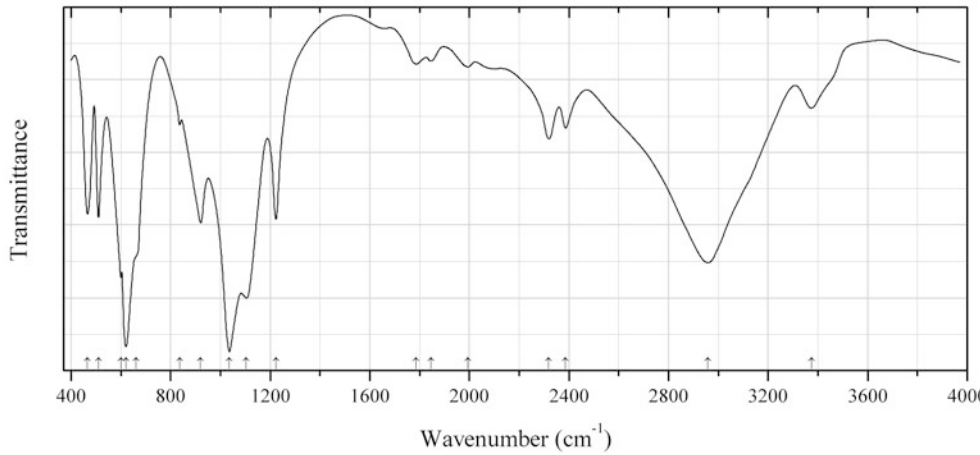

Fig. 2.869 IR spectrum of florencite-(Sm) drawn using data from Repina et al. (2010)

P483 Florencite-(Sm) $SmAl_3(PO_4)_2(OH)_6$ (Fig. 2.869)

Locality: Svodovy area, Maldynyrd Ridge, Subpolar Urals, Russia (type locality).

Description: Zones in crystals of florencite-(Ce) from the association with xenotime-(Y) and quartz. Holotype sample. Trigonal, space group R-3 m, a = 6.972(4), c = 16.182(7) Å, V = 681.2 Å^3, Z = 3. D_{meas} = 3.70 g/cm^3, D_{calc} = 3.743 g/cm^3. Optically uniaxial (+), ω = 1.704(2), ε = 1.713(2). The empirical formula is $(Sm_{0.38}Nd_{0.32}Ce_{0.10}Gd_{0.07}Pr_{0.03}La_{0.02}Eu_{0.01}Sr_{0.04}Ca_{0.03})Al_{3.04}(P_{1.91}S_{0.05}Si_{0.01})$ $O_{14}H_{5.92}$. The strongest lines of the powder X-ray diffraction pattern [d, Å (I, %) (hkl)] are: 5.65 (40) (101), 3.479 (40) (110), 2.925 (100) (113), 2.161 (50) (107), 1.881(60) (303).

Kind of sample preparation and/or method of registration of the spectrum: KBr disc. Absorption.

Source: Repina et al. (2010).

Wavenumbers (cm^{-1}): 3374, 2957, 2387, 2319, 1994w, 1845w, 1787w, 1223, 1104s, 1036s, 921, 836w, 660sh, 620s, 600, 510, 466.

Note: The bands in the range 1700–2400 cm^{-1} indicate the presence of acid groups HPO_4^{2-}.

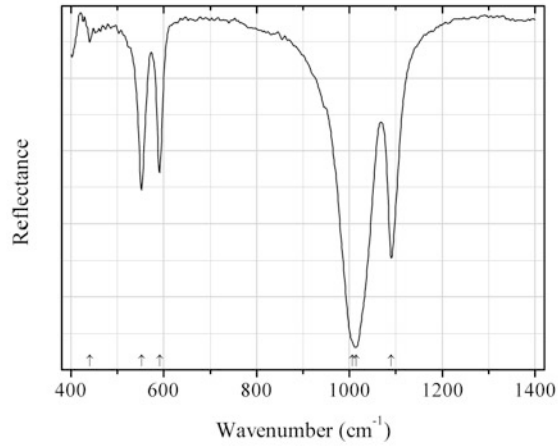

Fig. 2.870 IR spectrum of fluorphosphohedyphane drawn using data from Kampf and Housley (2011)

P484 Fluorphosphohedyphane $Ca_2Pb_3(PO_4)_3F$ (Fig. 2.870)
Locality: Blue Bell claims, 11 km west of Baker, San Bernardino Co., California, USA (type locality).
Description: Aggregate of colourless prismatic crystals from the association with cerussite, fluorite, fluorapatite, mimetite, phosphohedyphane, plumbogummite, plumbophyllite, plumbotsumite, pyromorphite, wulfenite, etc. Holotype sample. Hexagonal, space group $P6_3/m$, a = 9.6402(12), c = 7.0121(8) Å, V = 564.4(1) Å^3, Z = 2. D_{calc} = 5.445 g/cm^3. Optically uniaxial (−), ω = 1.836(5), ε = 1.824(5). The empirical formula is $Ca_{2.00}(Pb_{2.62}Ca_{0.17})P_3O_{11.91}F_{0.75}$. The strongest lines of the powder X-ray diffraction pattern [d, Å (I, %) (hkl)] are: 8.38 (22) (100), 3.974 (28) (111), 3.506 (25) (002), 2.877 (100) (121, 211), 1.878 (26) (213, 123).
Kind of sample preparation and/or method of registration of the spectrum: Attenuated total reflection of powdered mineral diluted in KBr.
Source: Kampf and Housley (2011).
Wavenumbers (cm^{-1}): 1090s, 1014s, 1007sh, 591, 552, 440w.
Note: The wavenumbers were determined by us based on spectral curve analysis of the published spectrum.

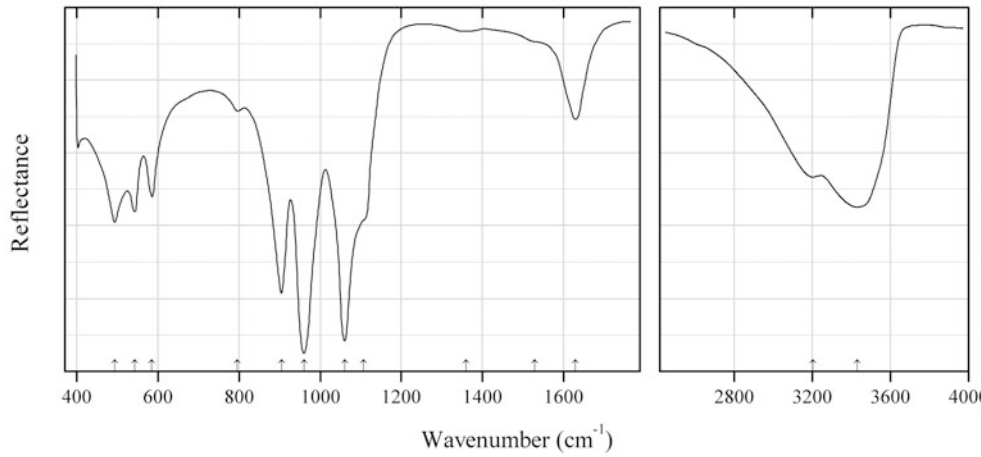

Fig. 2.871 IR spectrum of françoisite-(Nd) drawn using data from Armstrong et al. (2011)

P485 Françoisite-(Nd) $Nd(UO_2)_3(PO_4)_2O(OH)\cdot 12H_2O$ (Fig. 2.871)
Locality: Synthetic.
Description: Confirmed by thermal analysis and powder X-ray diffraction data.
Kind of sample preparation and/or method of registration of the spectrum: Attenuated total reflection of powdered sample.
Source: Armstrong et al. (2011).
Wavenumbers (cm^{-1}): 3430s, 3205, 1630, 1530sh, 1360w, 1107sh, 1060s, 960s, 905s, 796w, 585, 542, 493.

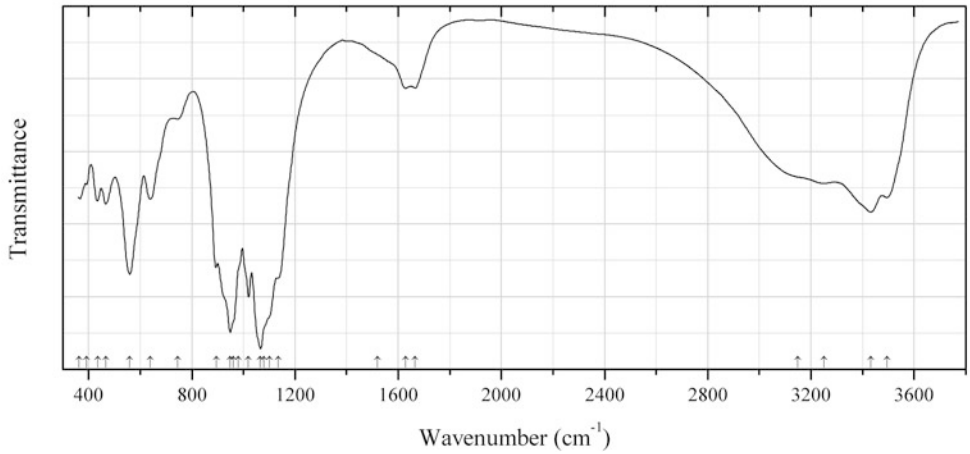

Fig. 2.872 IR spectrum of jahnsite-(NaFeMg) obtained by N.V. Chukanov

P486 Jahnsite-(NaFeMg) $NaFe^{3+}Mg_2Fe^{3+}{}_2(PO_4)_4(OH)_2\cdot 8H_2O$ (Fig. 2.872)
Locality: Tip Top pegmatite, Tip Top mine, Fourmile, Custer district, Custer Co., South Dakota, USA (type locality).
Description: Yellow-green crystals from the association with rockbridgeite, leucophosphite, mitridatite, triphylite, muscovite, quartz, and feldspar. Investigated by I.V. Pekov. The compositional ranges correspond to the following empirical formula: $(Na_{0.8}Ca_{0.2})(Fe_{0.7}Ca_{0.3})(Mg_{0.9-1.1}Mn_{1.1-0.9})(Fe_{1.9}Al_{0.1})(PO_4)_4(OH)_2\cdot 8H_2O$.
Kind of sample preparation and/or method of registration of the spectrum: KBr disc. Absorption.
Wavenumbers (cm^{-1}): 3495, 3432, 3250, 3150sh, 1665w, 1630w, 1520sh, 1135s, 1100sh, 1080sh, 1066s, 1020s, 980sh, 960sh, 949s, 895s, 745w, 638, 560, 466, 436, 391w, 364.

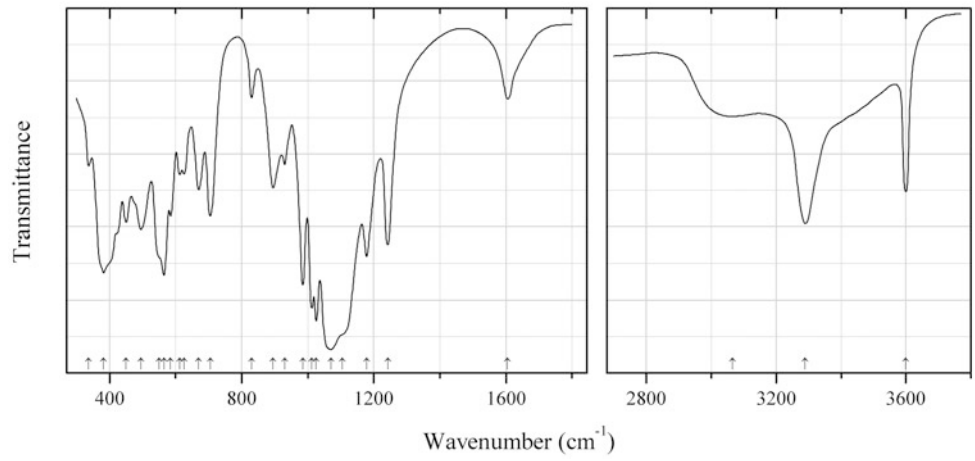

Fig. 2.873 IR spectrum of gatumbaite drawn using data from Von Knorring and Fransolet (1977)

P487 Gatumbaite $CaAl_2(PO_4)_2(OH)_2 \cdot 2H_2O$ (Fig. 2.873)
Locality: Buranga pegmatite, near Gatumba, Gisenyi province, Rwanda (type locality).
Description: White fibrous aggregates from the association with trolleite and scorzalite. Holotype sample. Monoclinic, a = 6.907(2), b = 5.095(2), c = 10.764(3) Å, β = 91.03(1)°, Z = 2. D_{meas} = 2.92 g/cm^3, D_{calc} = 2.99 g/cm^3. Optically biaxial (−), α = 1.610(2), β (estimated) = 1.63, γ = 1.639(2), 2 V = 60°–70°. The strongest lines of the powder X-ray diffraction pattern [d, Å (I, %) (hkl)] are: 4.90 (45) (100), 4.210 (100) (102), 3.207 (50) (10–3), 3.159 (50) (103), 2.772 (70) (21–1), 2.241 (100) (301), 1.921 (45) (303), 1.726 (75) (400).
Kind of sample preparation and/or method of registration of the spectrum: KI disc. Transmission.
Source: Von Knorring and Fransolet (1977).
Wavenumbers (cm^{-1}): 3600, 3290, 3065, 1605, 1242s, 1178s, 1105sh, 1070s, 1026s, 1012s, 985s, 930, 895, 830w, 705, 670, 625, 612, 585, 565s, 550sh, 495, 450, 382s, 337.

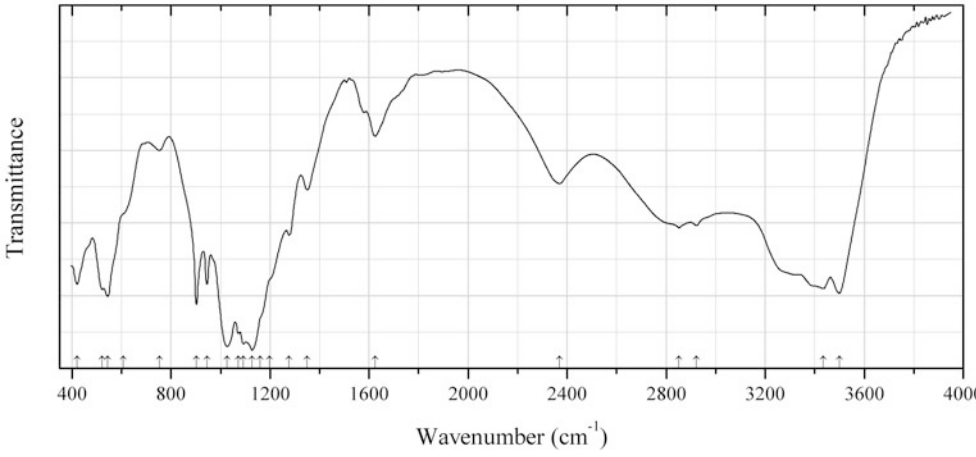

Fig. 2.874 IR spectrum of gengenbachite drawn using data from Hu et al. (2013)

P488 Gengenbachite $KFe_3(H_2PO_4)_2(HPO_4)_4 \cdot 6H_2O$ (Fig. 2.874)

Locality: Synthetic.
Description: Prepared hydrothermally at 423–393 K. The crystal structure is solved. Trigonal, space group *P*31*c*, *a* = 9.044(2), *c* = 16.706(5) Å, *V* = 1183.5(5) Å^3, *Z* = 2. D_{calc} = 2.477 g/cm^3. The empirical formula is $KH_8(Fe_{2.66}Al_{0.34})(PO_4)_6 \cdot 6H_2O$.
Kind of sample preparation and/or method of registration of the spectrum: KBr disc. Transmission.
Source: Hu et al. (2013).
Wavenumbers (cm^{-1}): 3499s, 3434s, 2369, 1624w, 1350, 1277, 1198sh, 1160sh, 1128s, 1092s, 1072s, 1026s, 945, 904s, 753w, 608sh, 544, 522w, 420.
Note: The wavenumbers were partly determined by us based on spectral curve analysis of the published spectrum. Weak sharp bands in the range from 2800 to 3000 cm^{-1} correspond to the admixture of an organic substance.

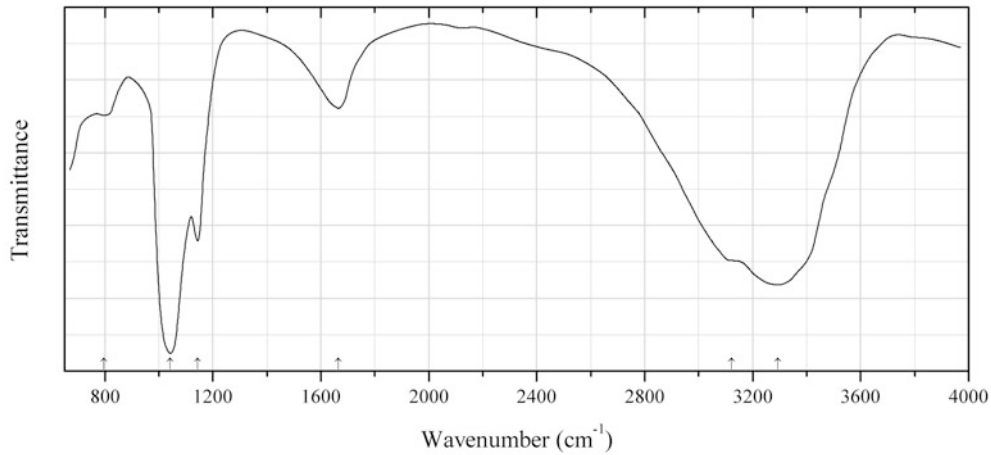

Fig. 2.875 IR spectrum of goldquarryite drawn using data from Roberts et al. (2003b)

P489 Goldquarryite (Cu, □)$Cd_2Al_3(PO_4)_4F_2(H_2O,F)_2 \cdot 10H_2O$ (Fig. 2.875)
Locality: Gold Quarry mine, Eureka Co., Nevada, USA (type locality).
Description: Blue aggregate of acicular to bladed crystals from the association with opal, CO_3-bearing fluorapatite, and hewettite. Holotype sample. Triclinic, space group *P*-1, *a* = 6.787(l), *b* = 9.082(2), *c* = 10.113(2) Å, α = 101.40(1)°, β = 104.27(1)°, γ = 102.51(1)°, *V* = 568.7(3) Å^3, *Z* = 1. D_{meas} = 2.78(1) g/cm^3, D_{calc} = 2.81 g/cm^3. Optically biaxial (+), α = 1.570, β = 1.573, γ = 1.578, 2 *V* ≈ 30°. The empirical formula is $(Cu_{0.66}Ni_{0.03}Zn_{0.01}\square_{0.30})(Cd_{2.00}Ca_{0.22}K_{0.04})(Al_{2.92}V_{0.01})(PO_4)_{3.88}F_{1.87} \cdot 12.06H_2O$. The strongest lines of the powder X-ray diffraction pattern [*d*, Å (*I*, %) (*hkl*)] are: 9.433 (100) (001), 4.726 (30) (002), 3.700 (30) (0–22), 3.173 (30b) (−1–22, −1–13, 120, 003), 3.010 (30) (−122, −212), 2.896 (30) (−2–11), 2.820 (50) (022).
Kind of sample preparation and/or method of registration of the spectrum: See Roberts et al. (1994).
Source: Roberts et al. (2003b).
Wavenumbers (cm^{-1}): 3293s, 3123sh, 1665, 1143, 1042s, 796w.

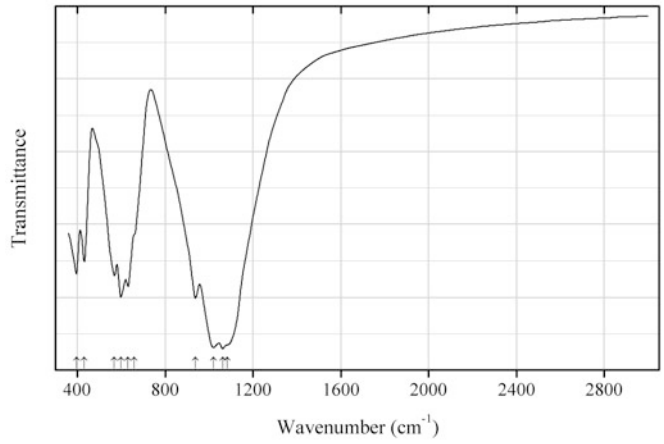

Fig. 2.876 IR spectrum of grattarolaite drawn using data from Cipriani et al. (1997)

P490 Grattarolaite $Fe^{3+}{}_3(PO_4)O_3$ (Fig. 2.876)
Locality: Santa Barbara lignite mine, Upper Arno river valley, Italy (type locality).
Description: Fine intergrowth with rodolicoite. Holotype sample. Trigonal, space group *P*3*m*, $a = 7.994(4)$, $c = 6.855(4)$ Å, $V = 379.4$ Å^3, $Z = 3$. Confirmed by electron microprobe analysis and powder X-ray diffraction data.
Kind of sample preparation and/or method of registration of the spectrum: KBr disc. Transmission.
Source: Cipriani et al. (1997).
Wavenumbers (cm^{-1}): 1082sh, 1062s, 1020s, 937s, 660sh, 631, 598s, 569, 432, 396.
Note: The wavenumbers listed above refer to the mixture of grattarolaite and rodolicoite.

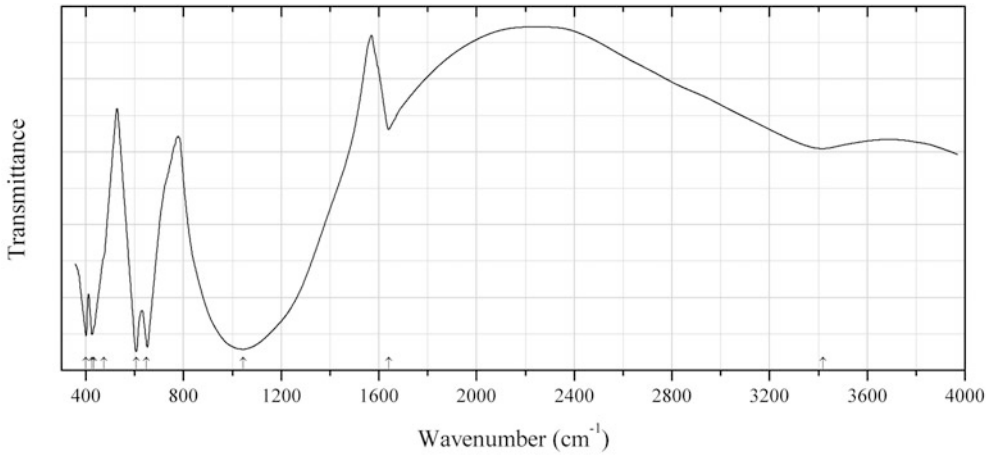

Fig. 2.877 IR spectrum of rodolicoite drawn using data from Thomas and George (2010)

P491 Rodolicoite $Fe^{3+}(PO_4)$ (Fig. 2.877)
Locality: Synthetic.
Description: Nanocrystalline. Confirmed by powder X-ray diffraction data.

Kind of sample preparation and/or method of registration of the spectrum: Transmission. Kind of sample preparation is not indicated.
Source: Thomas and George (2010).
Wavenumbers (cm^{-1}): 3420, 1640, 1045s, 648s, 608s, 474sh, 434sh, 426, 401.
Note: The bands at 3420 and 1640 cm^{-1} are due to adsorbed water.
Note: The wavenumbers were partly determined by us based on spectral curve analysis of the published spectrum.

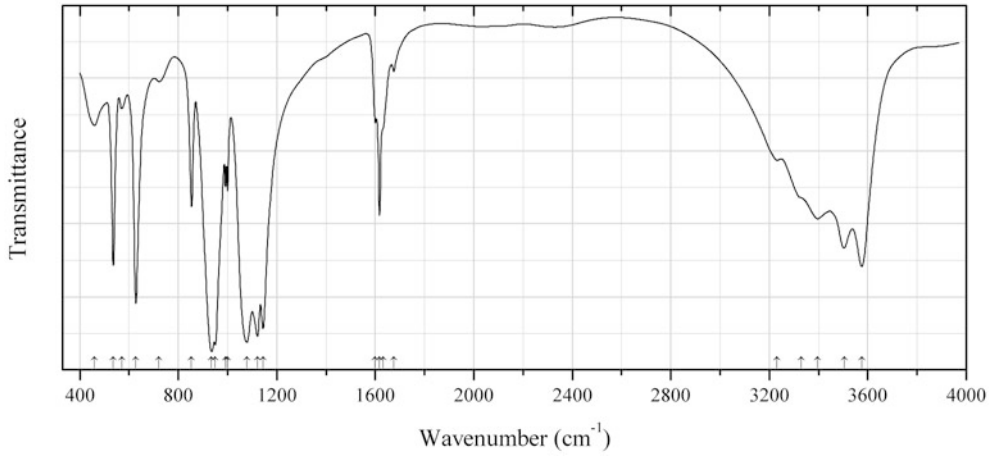

Fig. 2.878 IR spectrum of uranyl phosphate tetrahydrate drawn using data from Pechkovskii et al. (1981)

P492 Uranyl phosphate tetrahydrate $(UO_2)_3(PO_4)_2 \cdot 4H_2O$ (Fig. 2.878)
Locality: Synthetic.
Description: Synthesized in the Laboratory of Luminescence of the Institute of Applied Physical Problems, Byelorussian State University.
Kind of sample preparation and/or method of registration of the spectrum: KBr disc. Transmission.
Source: Pechkovskii et al. (1981).
Wavenumbers (cm^{-1}): 3575s, 3505s, 3395, 3330sh, 3230, 1675w, 1633sh, 1617, 1600, 1144s, 1122s, 1078s, 1000, 992w, 950s, 935s, 854, 722w, 628s, 570w, 536, 460, 286s, 250s, 218, 193w, 167.

P493 Cobalt hydroxyphosphate $Co_2(PO)_4(OH)$
Locality: Synthetic.
Description: The crystal structural is solved. Isostructural with adamite. Orthorhombic, space group *Pnnm*, a = 8.042(3), b = 8.369(2), c = 5.940(2) Å, V = 399.8 $Å^3$, Z = 4.
Kind of sample preparation and/or method of registration of the spectrum: KBr disc. Transmittance in the range from 500 to 4000 cm^{-1}.
Source: Harrison et al. (1995).
Wavenumbers (cm^{-1}): 3567, 1007s, 876.

P494 Zinc hydroxyphosphate $Zn_2(PO)_4(OH)$
Locality: Synthetic.
Description: The crystal structural is solved. Isostructural with adamite. Orthorhombic, space group *Pnnm*, a = 8.103(2), b = 8.3292(9), c = 5.9659(8) Å, V = 402.65 $Å^3$, Z = 4.

Kind of sample preparation and/or method of registration of the spectrum: KBr disc. Transmission in the range from 500 to 4000 cm^{-1}.
Source: Harrison et al. (1995).
Wavenumbers (cm^{-1}): 3561, 1020s, 868.

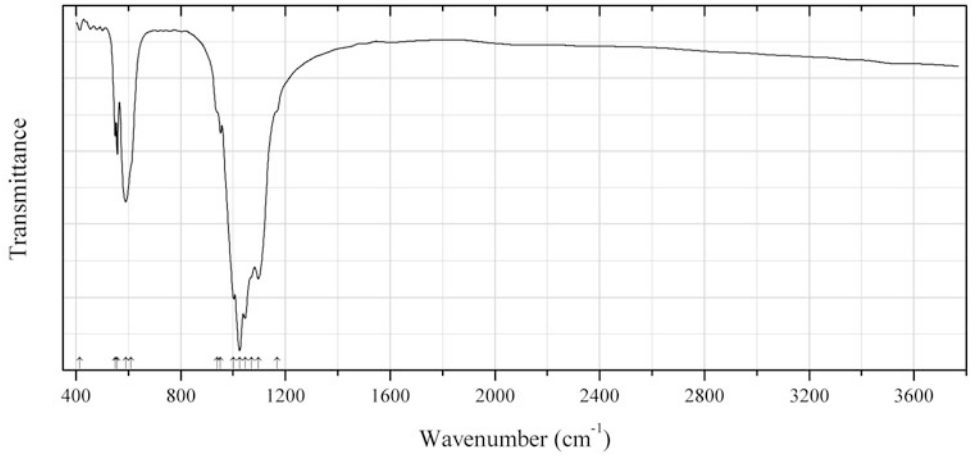

Fig. 2.879 IR spectrum of manganese(II) orthophosphate P495 drawn using data from Pechkovskii et al. (1981)

P495 Manganese(II) orthophosphate P495 α-$Mn_3(PO_4)_2$ (Fig. 2.879)
Locality: Synthetic.
Description: Monoclinic, space group $P2_1/c$, a = 8.81, b = 11.45, c = 6.27 Å, β = 99°.
Kind of sample preparation and/or method of registration of the spectrum: KBr disc. Absorption.
Source: Pechkovskii et al. (1981).
Wavenumbers (cm^{-1}): 1168sh, 1096s, 1070sh, 1046s, 1025s, 1002s, 952w, 940sh, 610sh, 590, 558, 550, 415w, 330sh, 276, 243, 202, 185.

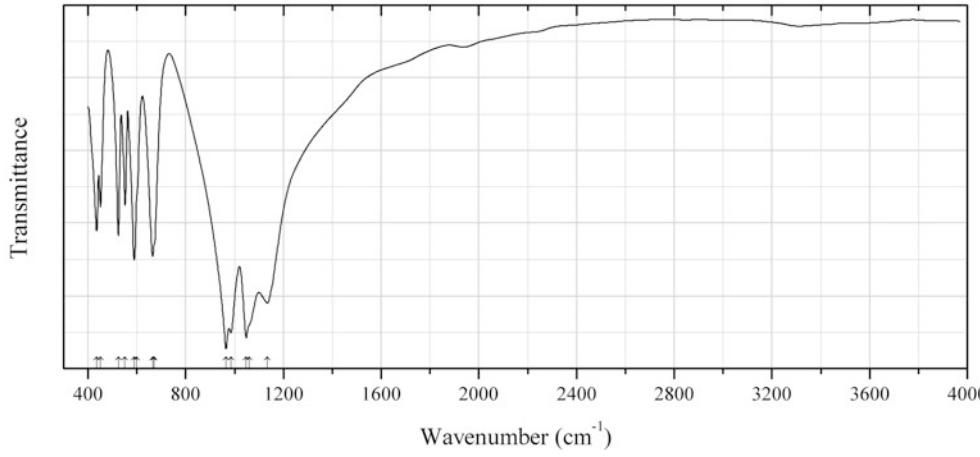

Fig. 2.880 IR spectrum of zinc orthophosphate P496 drawn using data from Pechkovskii et al. (1981)

P496 Zinc orthophosphate P496 α-$Zn_3(PO_4)_2$ (Fig. 2.880)

Locality: Synthetic.
Description: Monoclinic, space group *C2/c*, a = 8.14, b = 5.63, c = 15.04 Å, β = 105.13°.
Kind of sample preparation and/or method of registration of the spectrum: KBr disc. Absorption.
Source: Pechkovskii et al. (1981).
Wavenumbers (cm^{-1}): 1134s, 1060sh, 1048s, 985s, 965s, 670sh, 665, 600sh, 589, 552, 524, 451, 435, 350sh, 330, 250sh, 219, 183w, 161w.

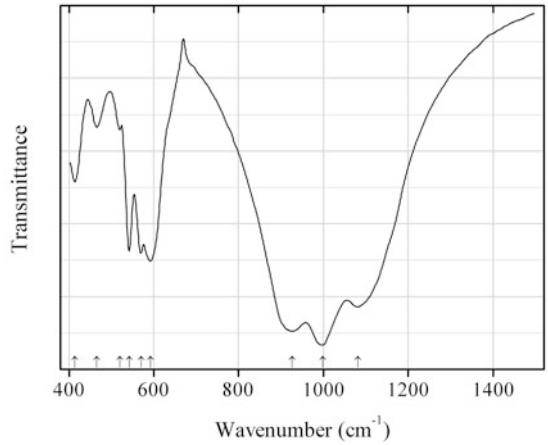

Fig. 2.881 IR spectrum of alluaudite-type phosphate P497 drawn using data from Hatert (2008)

P497 Alluaudite-type phosphate P497 $Na_{1.5}Mn_{1.5}Fe_{1.5}(PO_4)_3$ (Fig. 2.881)
Locality: Synthetic.
Description: Synthesized by the solid-state reaction in air, between 800 and 900 °C. Investigated by powder X-ray diffraction, including Rietveld refinement of the crystal structure.
Kind of sample preparation and/or method of registration of the spectrum: KBr disc. Transmission.
Source: Hatert (2008).
Wavenumbers (cm^{-1}): 1081s, 998s, 926s, 592, 570, 542, 521w, 466w, 414.

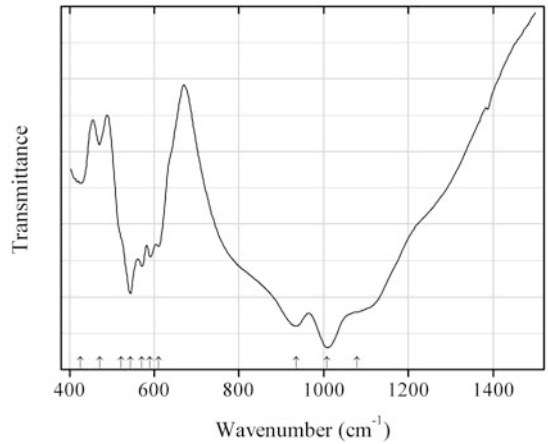

Fig. 2.882 IR spectrum of alluaudite-type phosphate P498 drawn using data from Hatert (2008)

P498 Alluaudite-type phosphate P498 $Na_{1.5}Zn_{1.5}Fe_{1.5}(PO_4)_3$ (Fig. 2.882)
Locality: Synthetic.
Description: Synthesized by the solid-state reaction in air, between 800 and 900 °C. Investigated by powder X-ray diffraction, including Rietveld refinement of the crystal structure.
Kind of sample preparation and/or method of registration of the spectrum: KBr disc. Transmission.
Source: Hatert (2008).
Wavenumbers (cm^{-1}): 1078s, 1008s, 935s, 610, 590, 571, 544s, 522sh, 471w, 426.

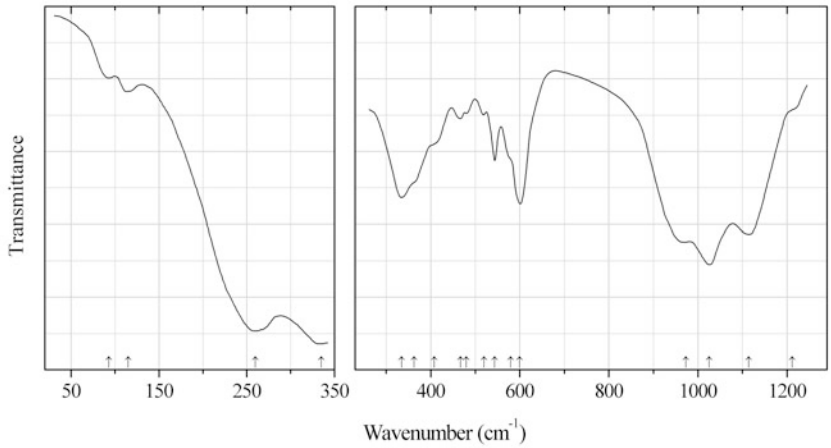

Fig. 2.883 IR spectrum of alluaudite drawn using data from Antenucci et al. (1993)

P499 Alluaudite $(Na,Ca)(Mn,Mg,Fe^{2+})(Fe^{3+},Mg)_2(PO_4)_3$ (Fig. 2.883)
Locality: Buranga pegmatite, Gatumba district, Western Province, Rwanda.
Description: A sample with the formula that is close to $NaMn^{2+}Fe^{3+}{}_2(PO_4)_3$.
Kind of sample preparation and/or method of registration of the spectrum: KBr disc. Transmission.
Source: Antenucci et al. (1993).
Wavenumbers (cm^{-1}): 1212sh, 1114s, 1025s, 973s, 600s, 580sh, 544, 520w, 480w, 467w, 408sh, 363sh, 335s, 260, 115w, 93w.
Note: The wavenumbers were partly determined by us based on spectral curve analysis of the published spectrum.

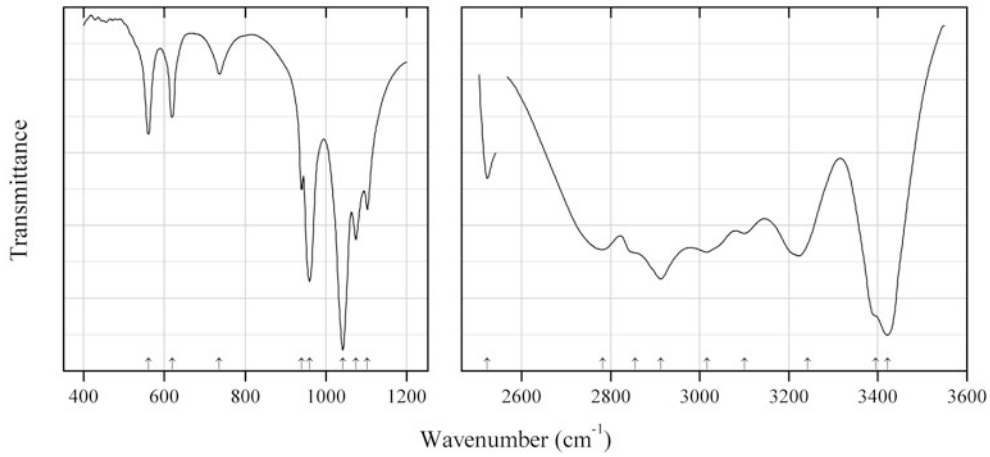

Fig. 2.884 IR spectrum of dittmarite Mn analogue drawn using data from Koleva (2005)

P500 Dittmarite Mn analogue $(NH_4)Mn(PO_4)\cdot H_2O$ (Fig. 2.884)
Locality: Synthetic.
Description: Prepared from the aqueous solution of the Mn^{2+} sulfate and $(NH_4)_2HPO_4$. Confirmed by powder X-ray diffraction data.
Kind of sample preparation and/or method of registration of the spectrum: KBr disc. Absorption.
Source: Koleva (2005, 2007).
Wavenumbers (cm^{-1}): 3422, 3395, 3243, 3100, 3016, 2913, 2855sh, 2782, 2523w, 1103, 1075, 1042s, 960s, 736w, 940, 619, 560.
Note: The wavenumbers were partly determined by us based on spectral curve analysis of the published spectrum. The band position denoted by Koleva (2005, 2007) as 3243 cm^{-1} was determined by us at 3223 cm^{-1}.

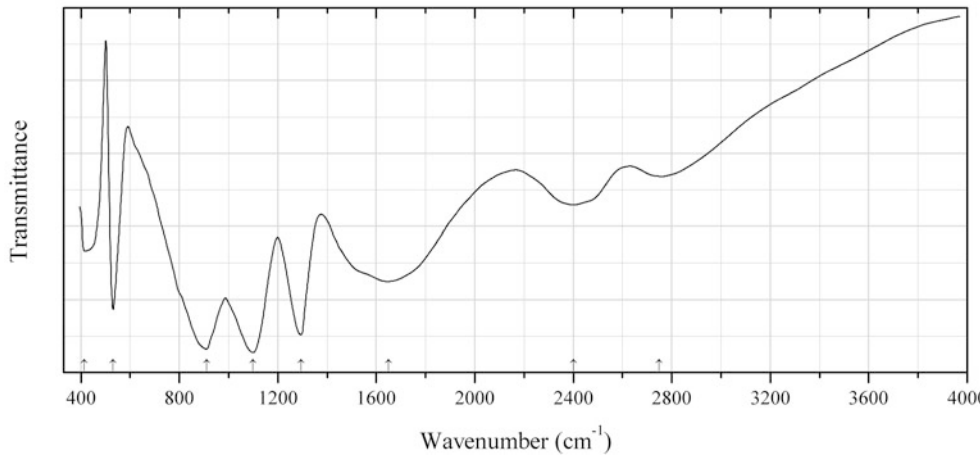

Fig. 2.885 IR spectrum of archerite drawn using data from Pechkovskii et al. (1981)

P501 Archerite $K(H_2PO_4)$ (Fig. 2.885)
Locality: Synthetic.
Description: Synthesized from acid aqueous solution.

Kind of sample preparation and/or method of registration of the spectrum: KBr disc. Absorption.
Source: Pechkovskii et al. (1981).
Wavenumbers (cm^{-1}): 2750 (broad), 2400 (broad), 1650 (broad), 1295s, 1100s, 910s, 531, 415, 365, 285w, 255w, 205, 180.

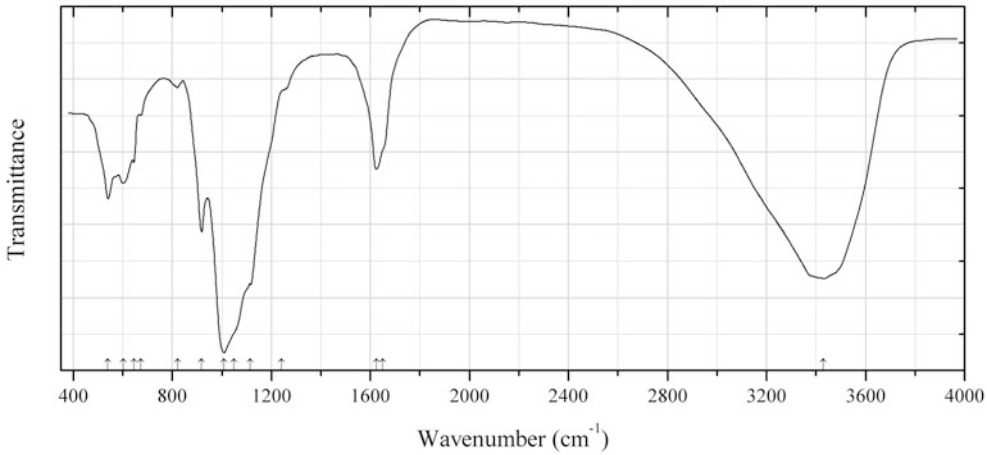

Fig. 2.886 IR spectrum of bassetite drawn using data from Vochten et al. (1984)

P502 Bassetite $Fe^{2+}(UO_2)_2(PO_4)_2 \cdot 8H_2O$ (Fig. 2.886)
Locality: Synthetic.
Description: Monoclinic, space group $P2_1/m$, $a = 6.98(4)$, $b = 17.07(4)$, $c = 7.01(7)$ Å, $\beta = 90.53(8)°$, $V = 835.2$ Å^3, $Z = 2$. The content of water corresponds to 7 H_2O molecules per formula unit. The strongest lines of the powder X-ray diffraction pattern [*d*, Å (*I*, %) (*hkl*)] are: 8.616 (100) (020), 4.9691 (70) (−101), 3.4818 (76) (−200), 2.9479 (50) (−122, −221), 2.2162 (96) (−301).
Kind of sample preparation and/or method of registration of the spectrum: KBr disc. Transmission.
Source: Vochten et al. (1984).
Wavenumbers (cm^{-1}): 3430s, 1650sh, 1624, 1240sh, 1116s, 1050sh, 1009s, 918s, 821w, 673, 645, 602, 540.
Note: The wavenumbers were determined by us based on spectral curve analysis of the published spectrum.

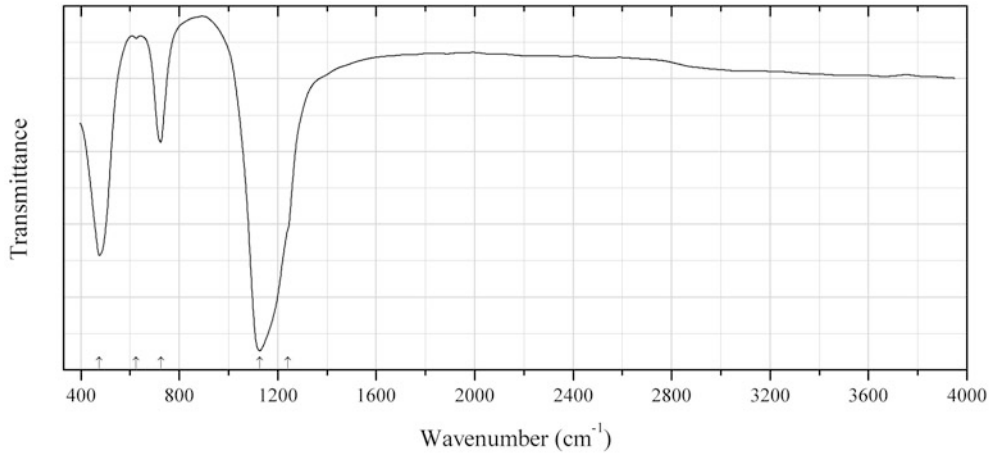

Fig. 2.887 IR spectrum of berlinite polymorph P503 drawn using data from Pechkovskii et al. (1981)

P503 Berlinite polymorph P503 $Al(PO_4)$ (Fig. 2.887)
Locality: Synthetic.
Description: Isostructural with tridymite. Synthesized in the temperature range from 600 to 800 °C.
Kind of sample preparation and/or method of registration of the spectrum: KBr disc. Absorption.
Source: Pechkovskii et al. (1981).
Wavenumbers (cm^{-1}): 1240sh, 1128s, 725, 625w, 475s, 380sh, 226w, 204sh.

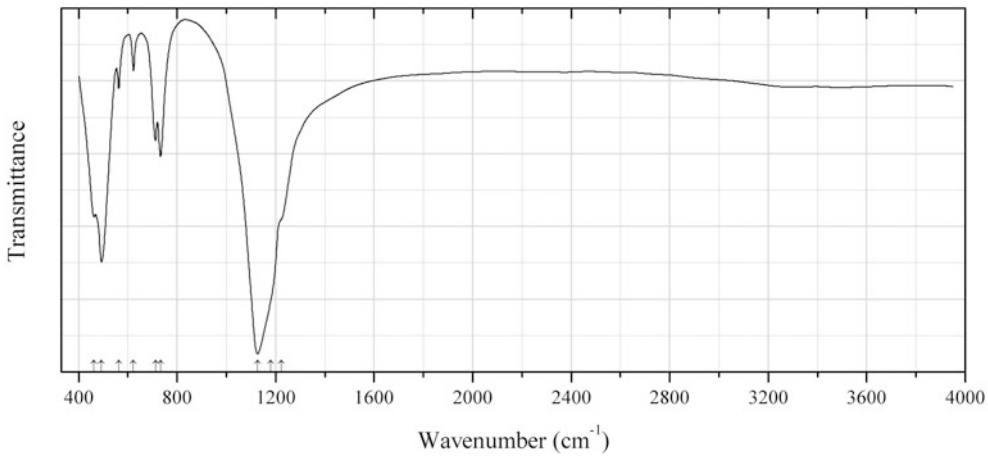

Fig. 2.888 IR spectrum of berlinite polymorph P504 drawn using data from Pechkovskii et al. (1981)

P504 Berlinite polymorph P504 $Al(PO_4)$ (Fig. 2.888)
Locality: Synthetic.
Description: Isostructural with cristobalite. Synthesized at 1100 °C.
Kind of sample preparation and/or method of registration of the spectrum: KBr disc. Absorption.
Source: Pechkovskii et al. (1981).
Wavenumbers (cm^{-1}): 1223sh, 1180sh, 1127s, 733, 712, 623w, 563w, 493s, 463, 379, 230w, 204w.

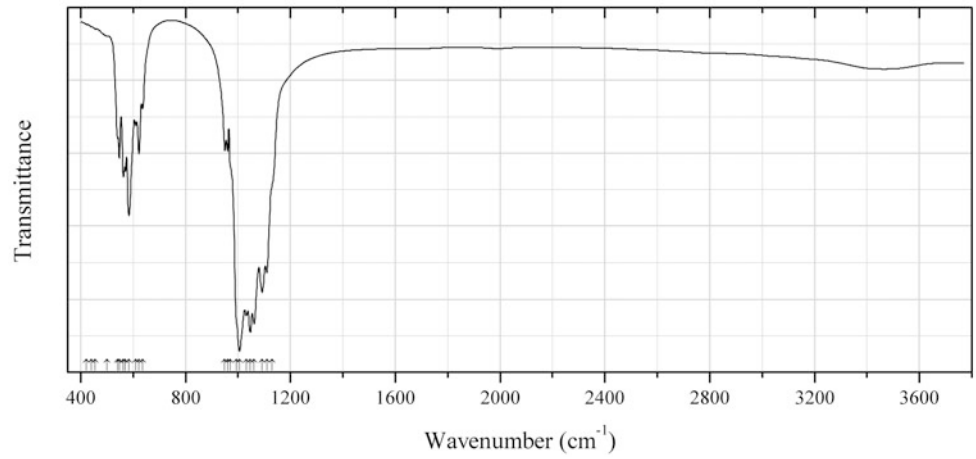

Fig. 2.889 IR spectrum of manganese(II) orthophosphate P505 drawn using data from Pechkovskii et al. (1981)

P505 Manganese(II) orthophosphate P505 β-$Mn_3(PO_4)_2$ (Fig. 2.889)
Locality: Synthetic.
Description: Synthesized by heating of a manganese(II) orthophosphate polyhydrate up to 750°–1150° with subsequent quenching. Monoclinic, space group $P2_1/c$, $a = 8.94$, $b = 10.04$, $c = 24.14$ Å, $\beta = 120.8°$, $Z = 12$.
Kind of sample preparation and/or method of registration of the spectrum: KBr disc. Absorption.
Source: Pechkovskii et al. (1981).
Wavenumbers (cm^{-1}): 1130sh, 1110s, 1092s, 1062s, 1047s, 1032s, 1006s, 995sh, 970sh, 961, 950, 636, 622, 610, 584, 570, 562, 547, 542, 500sh, 456w, 441w, 422w, 400w, 310, 250, 215, 200, 170.

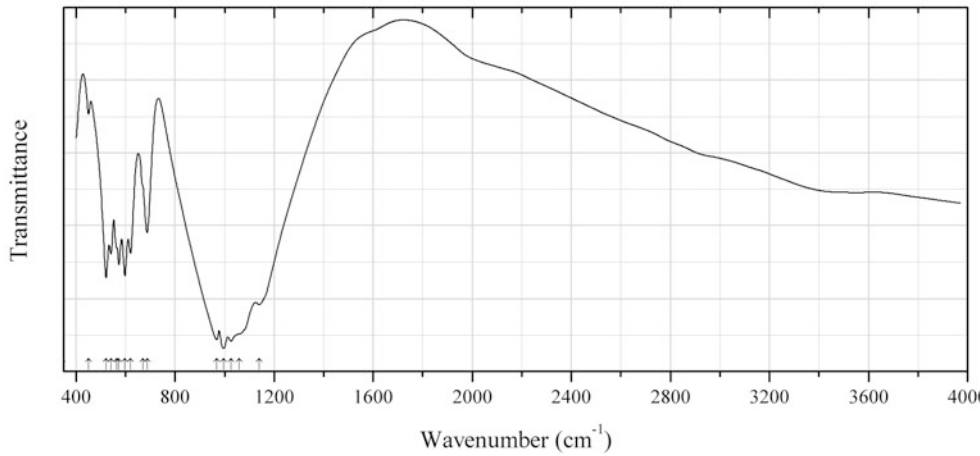

Fig. 2.890 IR spectrum of zinc orthophosphate P506 drawn using data from Pechkovskii et al. (1981)

P506 Zinc orthophosphate P506 β-$Zn_3(PO_4)_2$ (Fig. 2.890)
Locality: Synthetic.
Description: Synthesized by crystallization of the melt of zinc orthophosphate near the melting point (1062 °C) with subsequent quenching. Monoclinic, space group $P2_1/c$, $a = 9.393$, $b = 9.170$, $c = 8.686$ Å, $\beta = 125.73°$, $Z = 4$. $D_{meas} = 4.17$ g/cm^3.

Kind of sample preparation and/or method of registration of the spectrum: KBr disc. Absorption.
Source: Pechkovskii et al. (1981).
Wavenumbers (cm^{-1}): 1140s, 1060sh, 1026s, 996s, 968s, 687, 670sh, 620, 598, 573, 565, 543, 522, 452w, 400sh, 377, 345, 317, 280, 230, 190.

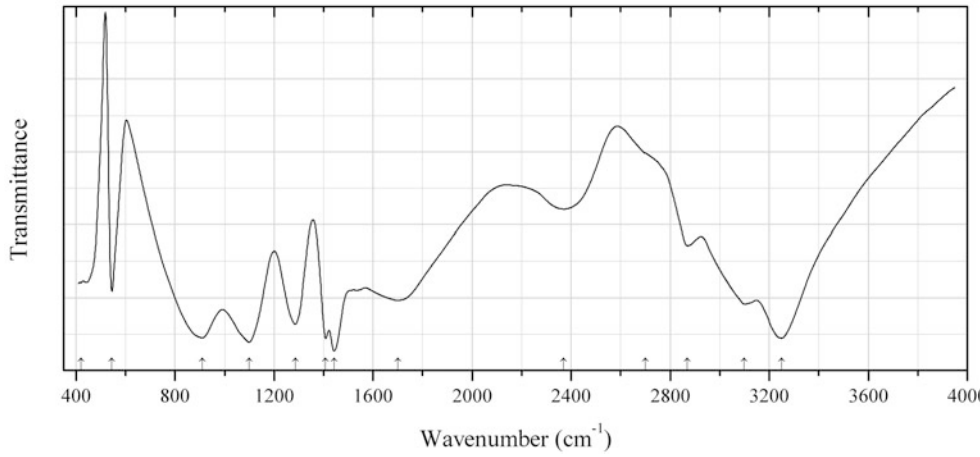

Fig. 2.891 IR spectrum of biphosphammite drawn using data from Pechkovskii et al. (1981)

P507 Biphosphammite $(NH_4)(H_2PO_4)$ (Fig. 2.891)
Locality: Synthetic.
Description: Tetragonal, space group *I*-42*d*, $a = 7.502$, $c = 7.546$ Å, $Z = 4$.
Kind of sample preparation and/or method of registration of the spectrum: KBr disc. Absorption.
Source: Pechkovskii et al. (1981).
Wavenumbers (cm^{-1}): 3250s, 3100, 2870, 2700sh, 2370, 1700, 1442s, 1407s, 1286s, 1100s, 910s, 545, 420, 287, 256, 210, 195sh, 185sh.

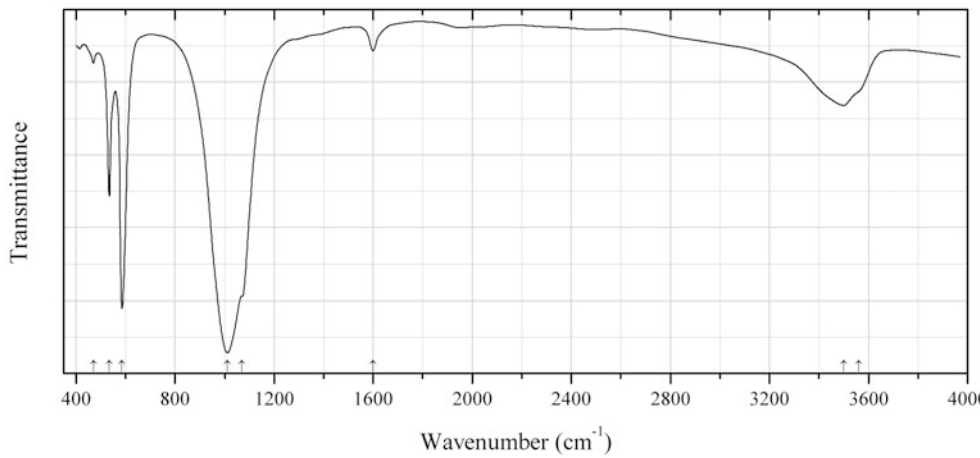

Fig. 2.892 IR spectrum of bismuth orthophosphate monohydrate drawn using data from Pechkovskii et al. (1981)

P508 Bismuth orthophosphate monohydrate $Bi(PO_4)\cdot H_2O$ (Fig. 2.892)
Locality: Synthetic.

Kind of sample preparation and/or method of registration of the spectrum: KBr disc. Absorption.
Source: Pechkovskii et al. (1981).
Wavenumbers (cm^{-1}): 3560sh, 3500, 1600w, 1070sh, 1012s, 586s, 535, 470w, 253, 186, 165.

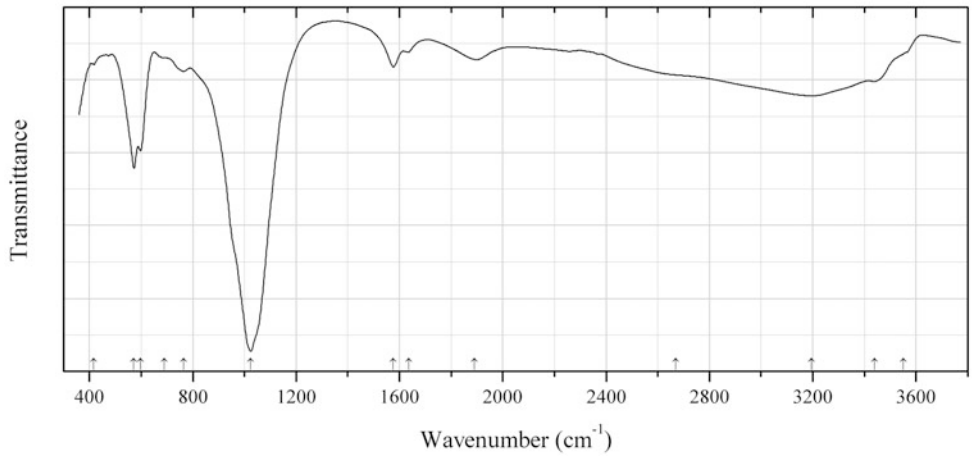

Fig. 2.893 IR spectrum of landesite obtained by N.V. Chukanov

P509 Landesite $Fe^{3+}Mn^{2+}{}_2(PO_4)_2(OH)\cdot 2H_2O$ (Fig. 2.893)
Locality: Bull Moose mine, Custer, Custer Co., South Dakota, USA.
Description: Dark brown pseudooctahedra. The empirical formula is (electron microprobe): $Fe_{1.2}Mn_{1.6}Mg_{0.2}(PO_4)_{2.0}(OH)\cdot nH_2O$.
Wavenumbers (cm^{-1}): 3550sh, 3440, 3195, 2670sh, 1891, 1635w, 1575, 1024s, 764, 690w, 597, 572s, 416w.
Note: The bands at 2670 and 1891 cm^{-1} indicate possible presence of acid groups $HPO_4{}^{2-}$.

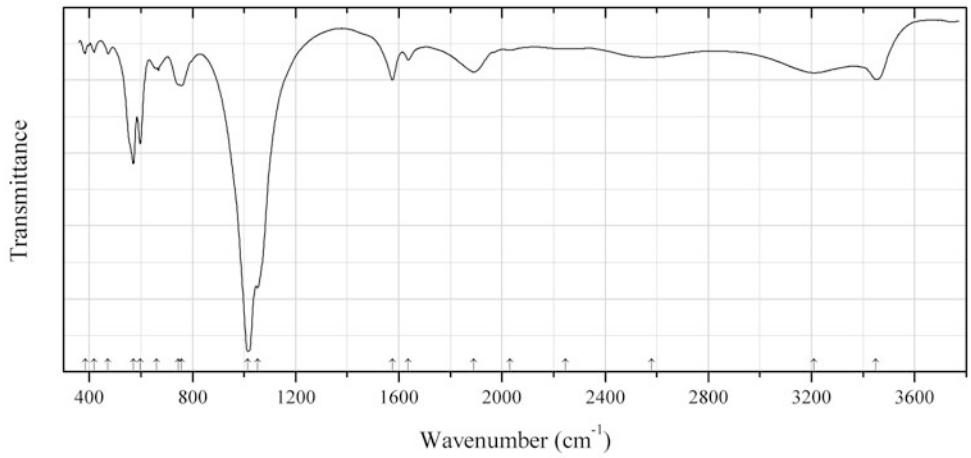

Fig. 2.894 IR spectrum of reddingite obtained by N.V. Chukanov

P510 Reddingite $Mn^{2+}Mn^{2+}{}_2(PO_4)_2\cdot 3H_2O$ (Fig. 2.894)
Locality: Hagendorf South pegmatite, Cornelia mine, Hagendorf, Waidhaus, Upper Palatinate, Bavaria, Germany.

Description: Brown pseudo-octahedral crystals. The empirical formula is (electron microprobe): $Mn_{1.85}Fe_{1.15}(PO_4)_{2.00}\cdot nH_2O$.
Kind of sample preparation and/or method of registration of the spectrum: KBr disc. Absorption.
Wavenumbers (cm^{-1}): 3450, 3209, 2580w, 2246w, 2030w, 1890, 1636w, 1575, 1053s, 1014s, 758, 745sh, 660w, 597, 570, 473w, 419w, 384w.
Note: The bands in the range of wavenumbers from 1800 to 2600 cm^{-1} indicate partial proton transfer from H_2O molecules to phosphate anions to form HPO_4^{2-}, which is a specific feature of reddingite-group minerals (Chukanov et al. 2014c; Chukanov 2014b).

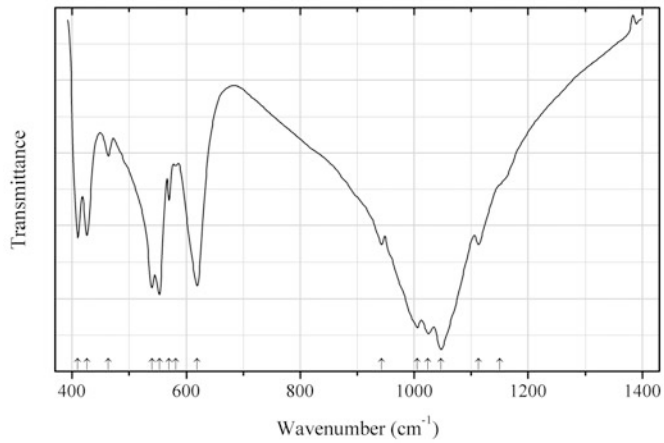

Fig. 2.895 IR spectrum of barium thorium orthophosphate drawn using data from Wallez et al. (2011)

P511 Barium thorium orthophosphate $BaTh(PO_4)_2$ (Fig. 2.895)
Locality: Synthetic.
Description: Synthesized by a wet chemistry route. Monoclinic, space group *C*2/*c*, a = 12.8053(7), b = 5.4400(3), c = 9.4636(5) Å, β = 102.247(3)°, V = 644.2(1) $Å^3$, Z = 4. D_{calc} = 4.79 g/cm^3.
Kind of sample preparation and/or method of registration of the spectrum: KBr disc. Transmission.
Source: Wallez et al. (2011).
Wavenumbers (cm^{-1}): 1150sh, 1113, 1047s, 1024s, 1005s, 943, 619, 582, 570, 553, 540, 463w, 426, 410.
Note: The wavenumbers were determined by us based on spectral curve analysis of the published spectrum.

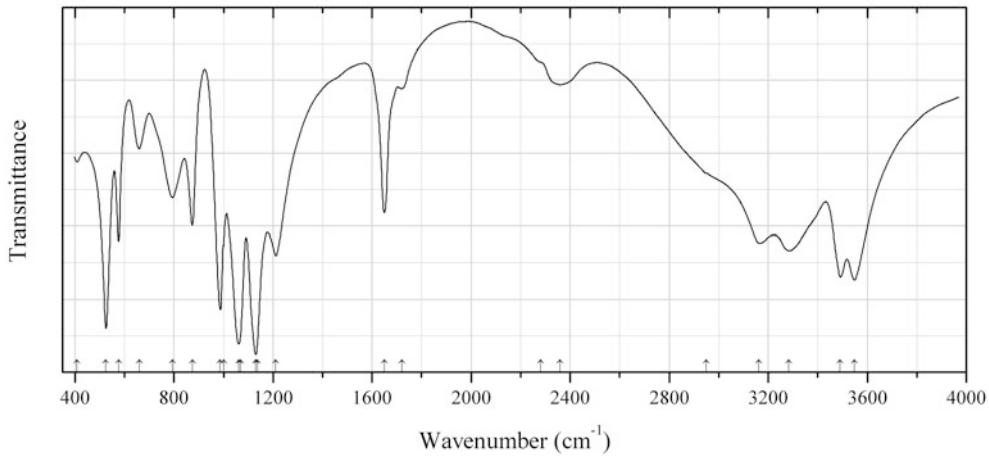

Fig. 2.896 IR spectrum of brushite drawn using data from Pechkovskii et al. (1981)

P512 Brushite $Ca(HPO_4)\cdot 2H_2O$ (Fig. 2.896)
Locality: Synthetic.
Description: Monoclinic, space group *Ia*, a = 5.812, b = 15.180, c = 6.239 Å, β = 91.141(6)°, γ = 116.42°, Z = 4. D_{calc} = 2.318 g/cm^3.
Kind of sample preparation and/or method of registration of the spectrum: KBr disc. Absorption.
Source: Pechkovskii et al. (1981).
Wavenumbers (cm^{-1}): 3548s, 3491s, 3284, 3163, 2950sh, 2360, 2280, 1720w, 1649, 1212s, 1137s, 1130sh, 1070sh, 1062s, 1000sh, 987s, 874, 795, 660, 576, 525s, 409w, 373, 312sh, 260, 234, 210, 170w.

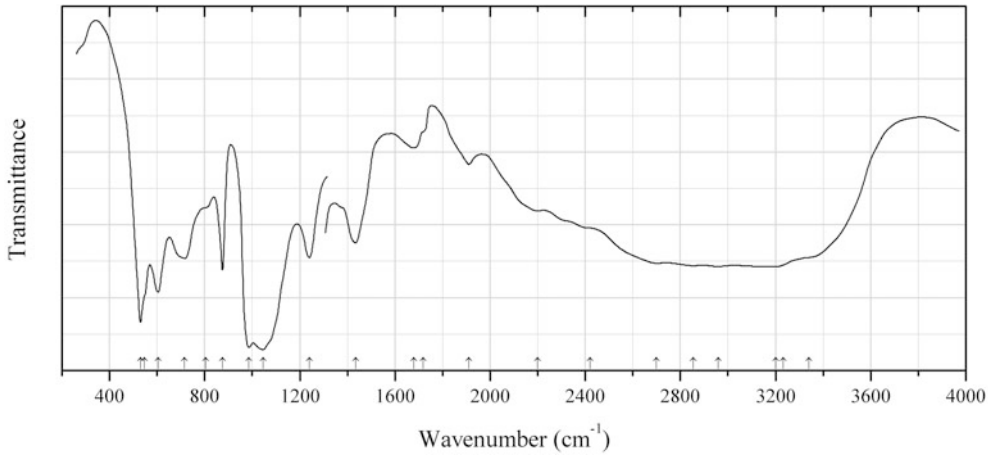

Fig. 2.897 IR spectrum of stercorite drawn using data from Keller (1971)

P513 Stercorite $(NH_4)Na(HPO_4)\cdot 4H_2O$ (Fig. 2.897)
Locality: Synthetic.
Description: Produced by Merck (the product No. 6682).

Kind of sample preparation and/or method of registration of the spectrum: KBr disc. Transmission.
Source: Keller (1971).
Wavenumbers (cm^{-1}): 3340sh, 3200, 2960, 2855, 2700, 2420, 3233sh, 2200sh, 1910, 1720sh, 1680w, 1435, 1240, 1045s, 985s, 875, 805sh, 715, 605, 548sh, 530s.

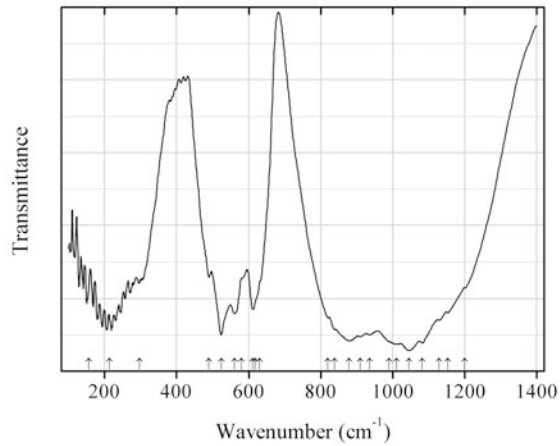

Fig. 2.898 IR spectrum of calcium neptunium orthophosphate drawn using data from Popa et al. (2010)

P514 Calcium neptunium orthophosphate $CaNp(PO_4)_2$ (Fig. 2.898)
Locality: Synthetic.
Description: Structurally related to cheralite, $CaNp(PO_4)_2$. Ca and Np are disordered
Kind of sample preparation and/or method of registration of the spectrum: KBr and polyethylene discs. Transmission.
Source: Popa et al. (2010).
Wavenumbers (cm^{-1}): (1200), (1153), (1129), 1082s, 1045s, 1011s, (990), (936), (910), 879s, (839), (820), 631sh, 618sh, 612s, 580sh, 561, 524, 490, (297), (213), (157).
Note: The wavenumbers were determined by us based on spectral curve analysis of the published spectrum.

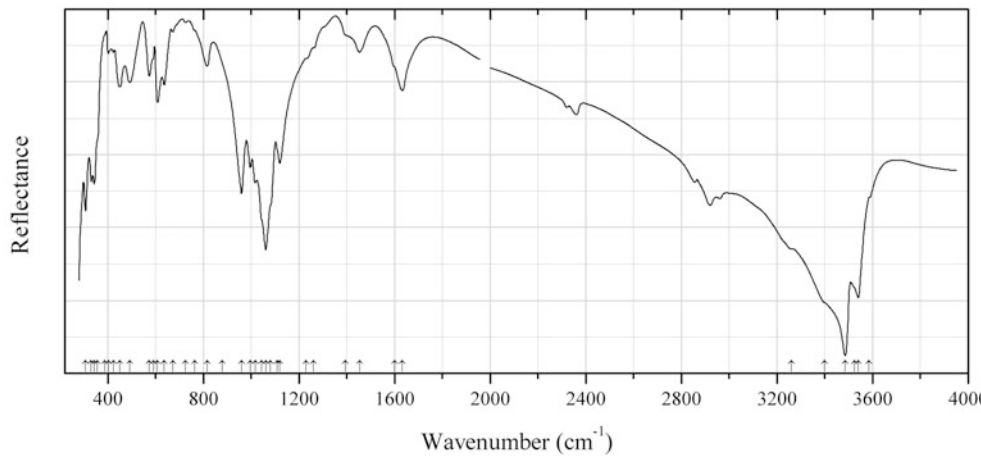

Fig. 2.899 IR spectrum of cyrilovite drawn using data from Cozzupoli et al. (1987)

P515 Cyrilovite $NaFe^{3+}{}_3(PO_4)_2(OH)_4 \cdot 2H_2O$ (Fig. 2.899)
Locality: Bosa, province of Nuoro, Sardinia, Italy.
Description: Bright yellow crust of platy crystals. Tetragonal, space group $P4_12_12$, a = 7.313(2), c = 19.315(3) Å, V = 1033.0(4) Å^3. D_{meas} = 3.096(5) g/cm^3, D_{calc} = 3.114 g/cm^3. Optically uniaxial (−), ε = 1.775, ω = 1.802. The empirical formula is $(Na_{0.92–1.05}Ca_{0.06–0.065})(Fe_{2.76–2.98}Al_{0–0.175})(PO_4)_{2.03–2.06}(OH)_{3.95–4.00} \cdot 2H_2O$. The strongest lines of the powder X-ray diffraction pattern [d, Å (I, %) (hkl)] are: 4.830 (100) (004), 3.594 (50) (201), 3.225 (30) (211), 3.178 (75) (203), 3.097 (35) (115), 2.653 (40) (205).
Kind of sample preparation and/or method of registration of the spectrum: Attenuated total reflection of powdered mineral. KBr disc. Transmission.
Source: Cozzupoli et al. (1987).
Wavenumbers (cm^{-1}): 3585sh, 3540, 3525sh, 3485s, 3400sh, 3260sh, 1632, 1600sh, 1453, 1395sh, 1260w, 1230sh, 1119, 1108sh, 1080sh, 1061s, 1044sh, 1016, 996, 960s, 880sh, 815, 763sh, 725w, 672w, 636, 607, 590sh, 573, 492, 450, (423), 402w, 388sh, 356sh, 342, 331, 307.
Note: The band positions denoted by Cozzupoli et al. (1987) as 3685, 3640, and 3625 cm^{-1} were determined by us at 3585, 3540, and 3525 cm^{-1} based on spectral curve analysis of the published spectrum. Bands in the range from 2800 to 3000 cm^{-1} correspond to the admixture of organic substance. Weak bands at 2360 and 2330 cm^{-1} are due to atmospheric CO_2. The band at 1453 cm^{-1} may correspond to the admixture of carbonate.

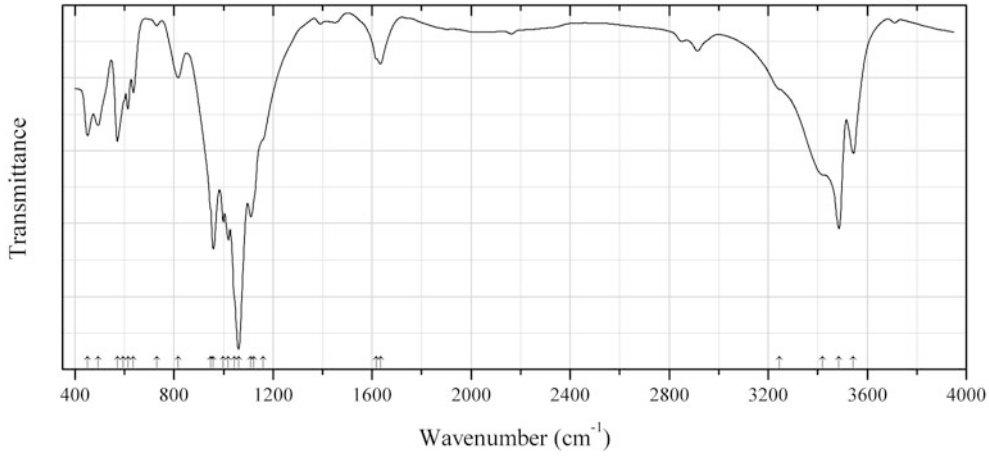

Fig. 2.900 IR spectrum of cyrilovite drawn using data from Novák et al. (2000)

P516 Cyrilovite $NaFe^{3+}{}_3(PO_4)_2(OH)_4 \cdot 2H_2O$ (Fig. 2.900)
Locality: Vyrilov (Cyrillhof) phosphate pegmatite, Velké Meziříčí, Vysočina Region, Moravia, Czech Republic (type locality).
Description: Crust of yellow to brown tabular crystals. Tetragonal, a = 7.3255(4), c = 19.328(2) Å, V = 1037.2(2) Å^3. D_{meas} = 3.085 g/cm^3, D_{calc} = 3.106–3.112 g/cm^3. Optically uniaxial (−), ε = 1.777, ω = 1.805. The empirical formula is (electron microprobe): $(Na_{0.96–0.99}Ca_{0.02–0.04})(Fe_{2.97–3.00}Al_{0.01–0.03})(PO_4)_{1.99}(OH)_{4.00} \cdot 2H_2O$. Confirmed by powder X-ray diffraction data.
Kind of sample preparation and/or method of registration of the spectrum: KBr disc. Absorption.
Source: Novák et al. (2000).
Wavenumbers (cm^{-1}): 3544, 3486s, 3420sh, 3246sh, 1634, 1616sh, 1160sh, 1122sh, 1111, 1061s, 1045sh, 1020sh, 999, 959s, 948sh, 817, 730w, 636, 614, 596sh, 571, 494, 451.
Note: Bands in the range from 2800 to 3000 cm^{-1} correspond to the admixture of organic substance.

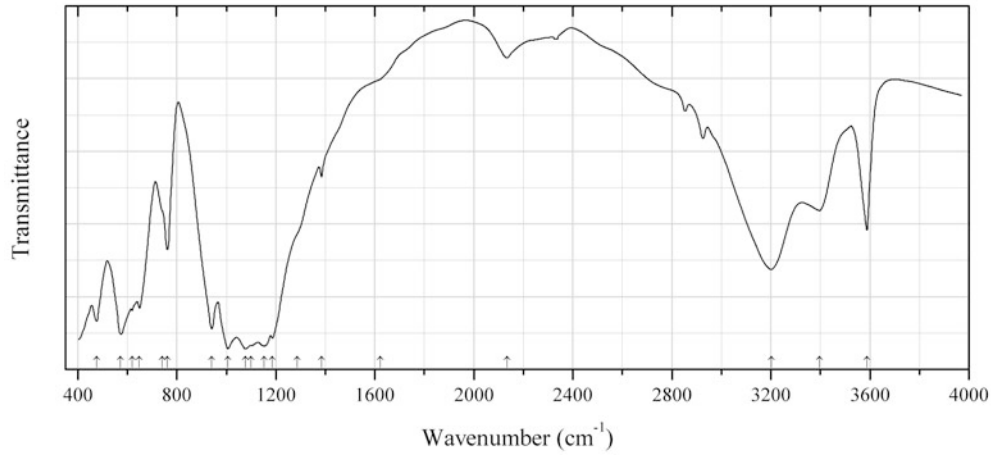

Fig. 2.901 IR spectrum of bertossaite drawn using data from Hatert et al. (2011)

P517 Bertossaite $Li_2CaAl_4(PO_4)_4(OH)_4$ (Fig. 2.901)
Locality: Buranga pegmatite, Gatumba district, Western Province, Rwanda (type locality).
Description: Xenomorphic grains included in montebrasite and associated with quartz and a phosphate of the lazulite-scorzalite series. The crystal structure is solved. Orthorhombic, space group *Imcb*, a = 11.476(1), b = 15.744(1), c = 7.228(1) Å, Z = 4. D_{calc} = 3.183 g/cm^3.
Kind of sample preparation and/or method of registration of the spectrum: KBr disc. Transmission.
Source: Hatert et al. (2011).
Wavenumbers (cm^{-1}): 3589, 3397, 3203, 2134w, 1623sh, 1385w, 1287sh, 1152s, 1186s, 1100s, 1077s, 1006s, 941s, 762, 740sh, 649, 619, 573s, 476.
Note: The wavenumbers were partly determined by us based on spectral curve analysis of the published spectrum. The bands in the range from 2800 to 3000 cm^{-1} correspond to the admixture of an organic substance.

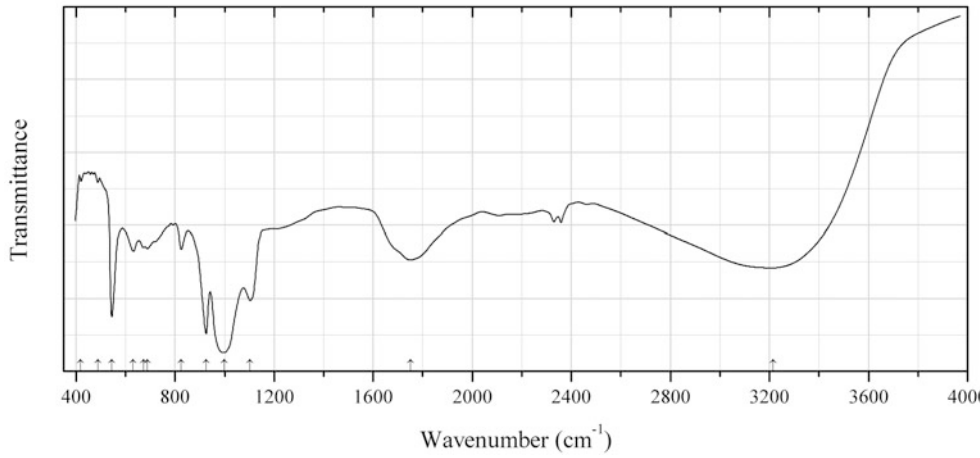

Fig. 2.902 IR spectrum of chernikovite drawn using data from Van Haverbeke et al. (1996)

P518 Chernikovite $(H_3O)(UO_2)(PO_4)\cdot 3H_2O$ (Fig. 2.902)
Locality: Synthetic.
Description: Synthesized by mixing solutions of uranyl acetate and phosphoric acid. Identified by means of chemical analysis and powder X-ray diffraction.
Kind of sample preparation and/or method of registration of the spectrum: Diffuse reflection of a powdered sample.
Source: Van Haverbeke et al. (1996).
Wavenumbers (cm^{-1}): 3215s, 1751s, 1103s, 999s, 926s, 825, 688, 672, 631, 545s, 488w, 419w.
Note: The wavenumbers were partly determined by us based on spectral curve analysis of the published spectrum. The bands in the range from 2300 to 2400 cm^{-1} may be due to atmospheric CO_2.

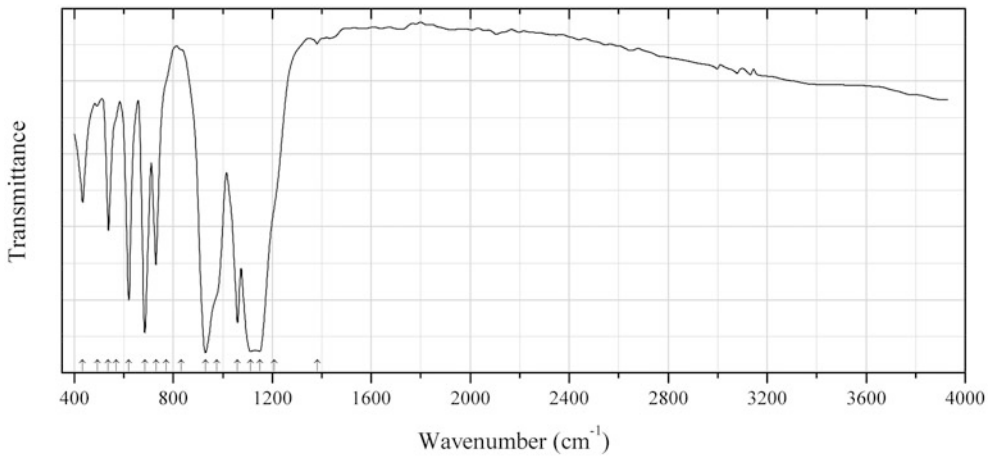

Fig. 2.903 IR spectrum of thorium oxyphosphate P519 drawn using data from Brandel et al. (2001)

P519 Thorium oxyphosphate P519 $Th_2(PO_4)_2O$ (Fig. 2.903)
Locality: Synthetic.
Description: Synthesized using a hydrothermal method. Orthorhombic, space group *Cmca*, $a = 7.177(4)$, $b = 9.225(5)$, $c = 12.858(7)$ Å, $V = 851(1)$ $Å^3$. $D_{calc} = 5.23$ g/cm^3. The strongest lines of the powder X-ray diffraction pattern [*d*, Å (*I*, %) (*hkl*)] are: 6.42 (44) (002), 4.61 (100) (020), 4.34 (62) (021), 4.25 (79) (112), 3.59 (43) (200), 3.14 (41) (023, 202), 2.79 (95) (114), 2.76 (41) (221, 131), 2.59 (42) (222, 132).
Kind of sample preparation and/or method of registration of the spectrum: KBr disc. Transmission.
Source: Brandel et al. (2001).
Wavenumbers (cm^{-1}): 1382w, 1208sh, 1149s, 1113s, 1060s, 975sh, 930s, 833sh, 772sh, 730, 685s, 620s, 570sh, 538, 493w, 434.
Note: The wavenumbers were partly determined by us based on spectral curve analysis of the published spectrum. The band position denoted by Brandel et al. (2001) as 1140 cm^{-1} was determined by us as dublet (1149 cm^{-1} and 1113 cm^{-1}).

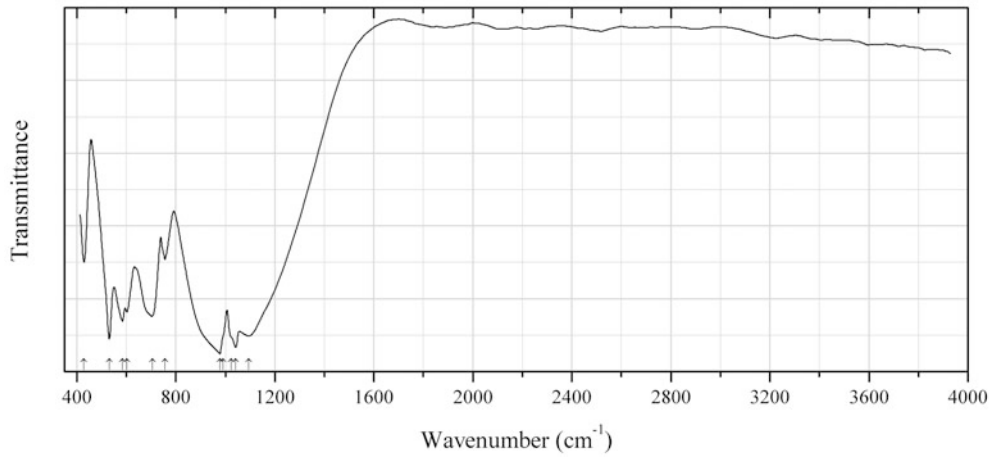

Fig. 2.904 IR spectrum of uranium oxyphosphate P520 drawn using data from Brandel et al. (2001)

P520 Uranium oxyphosphate P520 $U_2(PO_4)_2O$ (Fig. 2.904)
Locality: Synthetic.
Description: Synthesized using a hydrothermal method. Orthorhombic. For the description see Brandel et al. (1996).
Kind of sample preparation and/or method of registration of the spectrum: KBr disc. Transmission.
Source: Brandel et al. (2001).
Wavenumbers (cm^{-1}): 1094s, 1042s, 1025sh, 991sh, 978s, 756, 706, 602, 586, 532s, 429.
Note: The wavenumbers were partly determined by us based on spectral curve analysis of the published spectrum.

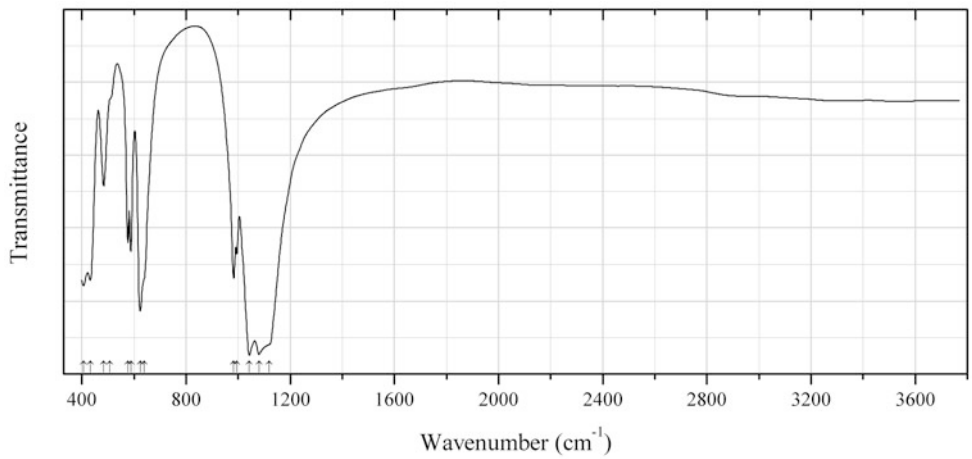

Fig. 2.905 IR spectrum of farringtonite drawn using data from Pechkovskii et al. (1981)

P521 Farringtonite $Mg_3(PO_4)_2$ (Fig. 2.905)

Locality: Synthetic.
Description: Monoclinic, space group $P2_1/n$, $a = 7.5957$, $b = 8.2305$, $c = 5.0775$ Å, $\beta = 94.05°$, $Z = 2$.
Kind of sample preparation and/or method of registration of the spectrum: KBr disc. Transmission.
Source: Pechkovskii et al. (1981).
Wavenumbers (cm^{-1}): 1120sh, 1080s, 1043s, 995, 983s, 640sh, 624s, 588, 577, 507sh, 484, 432s, 406s, 395s, 347s, 301, 292sh, 275, 250w, 225sh, 204w.

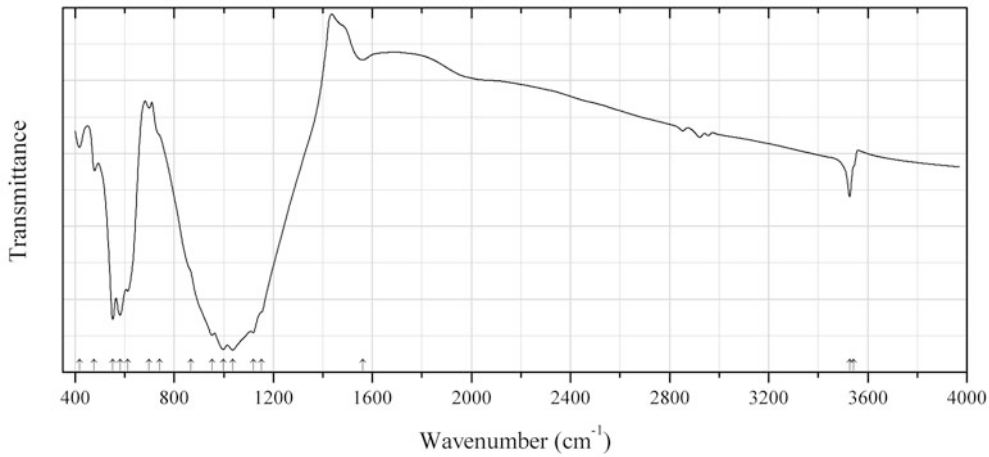

Fig. 2.906 IR spectrum of phosphate P522 drawn using data from Keller et al. (2006)

P522 Phosphate P522 $Na(Na,Mn)_7Mn_{22}(PO_4)_{18}\cdot 0.5H_2O$ (Fig. 2.906)
Fillowite-type phosphate
Locality: Synthetic.
Description: Synthesized from $NaH_2PO_4\cdot H_2O$ and MnO in the presence of water, at 800 °C. Confirmed by electron microprobe analyses. The crystal structure is solved. Trigonal, space group *R*-3, $a = 15.2741(9)$, $c = 43.334(3)$ Å, $Z = 6$.
Kind of sample preparation and/or method of registration of the spectrum: KBr disc. Transmission.
Source: Keller et al. (2006).
Wavenumbers (cm^{-1}): 3544sh, 3527, 1561w, 1152sh, 1120s, 1036s, 998s, 953s, 868sh, 741sh, 699w, 612, 581s, 552s, 477w, 417w.

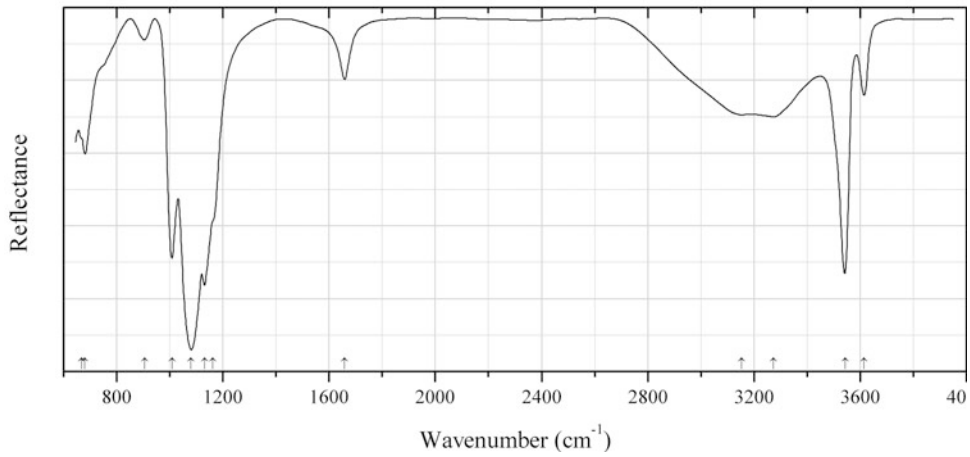

Fig. 2.907 IR spectrum of fluorowardite drawn using data from Kampf et al. (2014)

P523 Fluorowardite $NaAl_3(PO_4)_2F_2(OH)_2 \cdot 2H_2O$ (Fig. 2.907)
Locality: Silver Coin mine, Valmy, Edna Mountains, Humboldt Co., Nevada, USA (type locality).
Description: Colorless to cream-colored crystals from a complex phosphate assemblage rich in Al, Na, and F. Holotype sample. Tetragonal, space group $P4_12_12$, a = 7.077(2), c = 19.227(3) Å, V = 962.8(5) Å^3, Z = 4. D_{calc} = 2.760 g/cm^3. Optically biaxial (+), ω = 1.576(2), ε = 1.584(2). The empirical formula is $(Na_{0.87}Ca_{0.13}Mg_{0.04})(Al_{2.96}Fe^{3+}{}_{0.04})(P_{1.96}As_{0.03})O_{8.12}(OH)_{2.35}F_{1.53} \cdot 2H_2O$. The strongest lines of the powder X-ray diffraction pattern [d, Å (I, %) (hkl)] are: 4.766 (100) (004, 103), 3.099 (75) (211, 203), 3.008 (62) (115, 212), 2.834 (28) (204, 213), 2.597 (56) (205), 1.7628 (32) (400, 401), 1.6592 (29) (multiple), 1.5228 (49) (423, 2.2.10).
Kind of sample preparation and/or method of registration of the spectrum: Attenuated total reflection of powdered mineral.
Source: Kampf et al. (2014).
Wavenumbers (cm^{-1}): 3615, 3544s, 3274, 3153, 1659, 1162sh, 1131s, 1080s, 1008s, 905w, 681, 669sh.
Note: The wavenumbers were partly determined by us based on spectral curve analysis of the published spectrum.

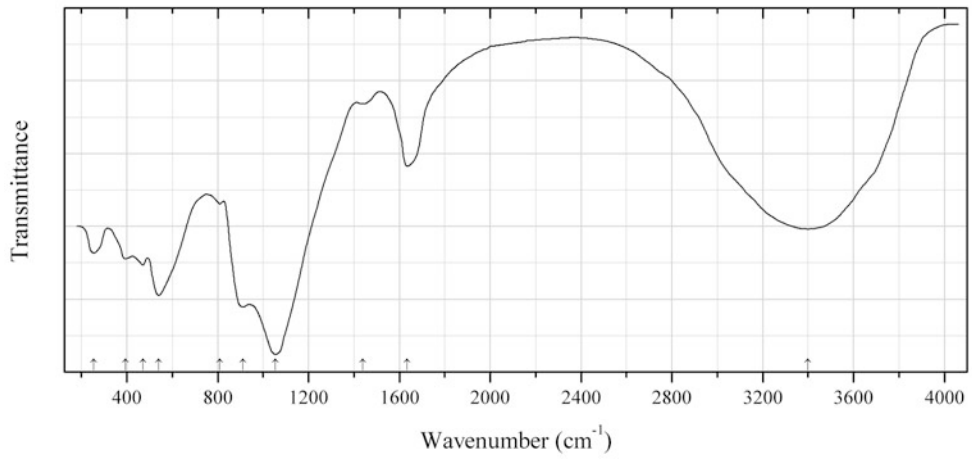

Fig. 2.908 IR spectrum of furongite drawn using data from Hunan 230 Institute, Hunan 305 Geological Team and X-ray Laboratory of Wuhan Geological Institute (1979)

P524 Furongite $Al_{13}(UO_2)_7(PO_4)_{13}(OH)_{14}\cdot 58H_2O$ (Fig. 2.908)
Locality: An uranium deposit situated in the Lower Cambrian carbonaceous shale of western Hunan province, China.
Description: Yellow massive aggregate from the association with halloysite and autunite. Triclinic, space group *P*1 or *P*-1, a = 17.87, b = 14.18, c = 12.18 Å, α = 67.8°, β = 77.5°, γ = 79.9°. D_{meas} = 2.80–2.90 g/cm^3, D_{calc} = 2.848 g/cm^3. Optically biaxial (+) or (−), α = 1.543–1.549, β = 1.564–l.567, γ = 1.570–1.575. The strongest lines of the powder X-ray diffraction pattern [*d*, Å (*I*, %)] are: 10.2 (100), 8.62 (95), 5.535 (37), 4.316 (85), 3.639 (55), 2.870 (42).
Kind of sample preparation and/or method of registration of the spectrum: Transmission. Kind of sample preparation is not indicated.
Source: Hunan 230 Institute, Hunan 305 Geological Team and X-ray Laboratory of Wuhan Geological Institute (1979).
Wavenumbers (cm^{-1}): 3400s, 1635, 1438w, 1055s, 912s, 810w, 540s, 470, 394, 255.
Note: The wavenumbers were partly determined by us based on spectral curve analysis of the published spectrum.

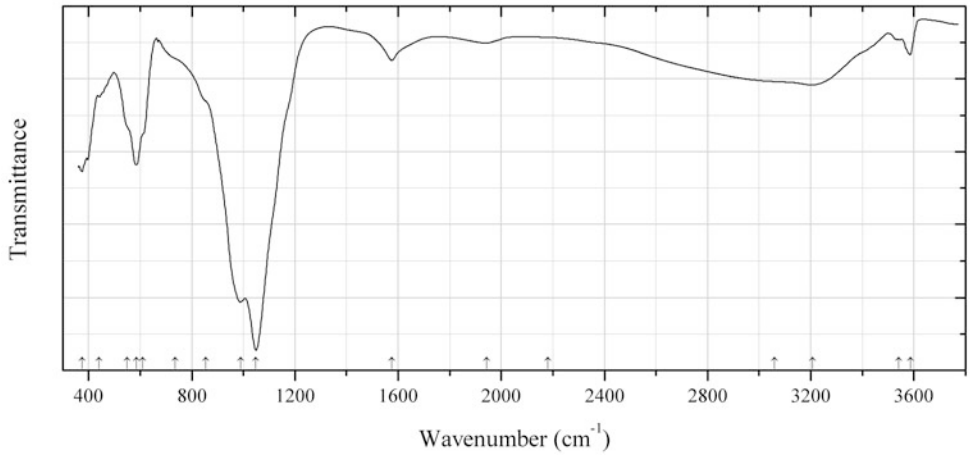

Fig. 2.909 IR spectrum of garyansellite obtained by N.V. Chukanov

P525 Garyansellite $Mg_2Fe^{3+}(PO_4)(OH)\cdot 2H_2O$ (Fig. 2.909)
Locality: Rapid Creek area, Dawson mining district, Richardson Mts., Yukon Territory, Canada (type locality).
Description: Brownish crystals. The empirical formula is (electron microprobe): $(Mg_{1.2}Fe_{0.6}Mn_{0.2})Fe^{3+}_{1.0}(PO_4)_{2.0}(H_2O,OH)_3$.
Kind of sample preparation and/or method of registration of the spectrum: KBr disc. Absorption.
Wavenumbers (cm^{-1}): 3586, 3540w, 3207, 3060sh, 2180w, 1943w, 1576, 1049s, 990s, 855sh, 735sh, 610sh, 585, 550sh, 440, 374.

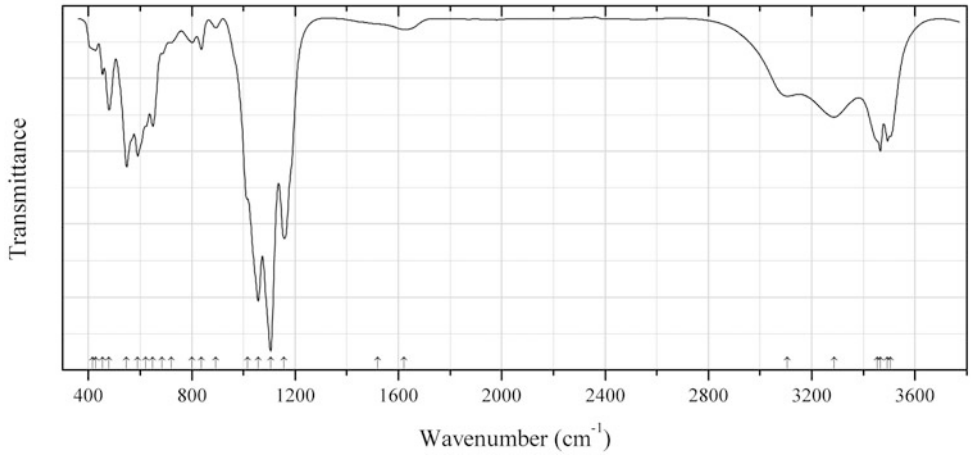

Fig. 2.910 IR spectrum of faustite obtained by N.V. Chukanov

P526 Faustite $ZnAl_6(PO_4)_4(OH)_8 \cdot 4H_2O$ (Fig. 2.910)
Locality: Kanatkazgan turquoise occurrence, 2 km SSE of Altyn-Tyube copper deposit, Karagandy region, Central Kazakhstan.
Description: Outer part of light-blue concretion. The empirical formula is (electron microprobe): $(Zn_{0.47}Cu_{0.28}Fe_{0.25})(Al_{5.47}Fe_{0.53})(PO_4)_{4.09}(OH)_x \cdot nH_2O$.
Kind of sample preparation and/or method of registration of the spectrum: KBr disc. Absorption.
Wavenumbers (cm^{-1}): 3505sh, 3493, 3465s, 3455sh, 3286, 3105, 1621w, 1520sh, 1158s, 1105s, 1057s, 1017sh, 893w, 837, 802, 720w, 686, 649, 622sh, 591s, 548s, 480, 454, 428, 415sh.

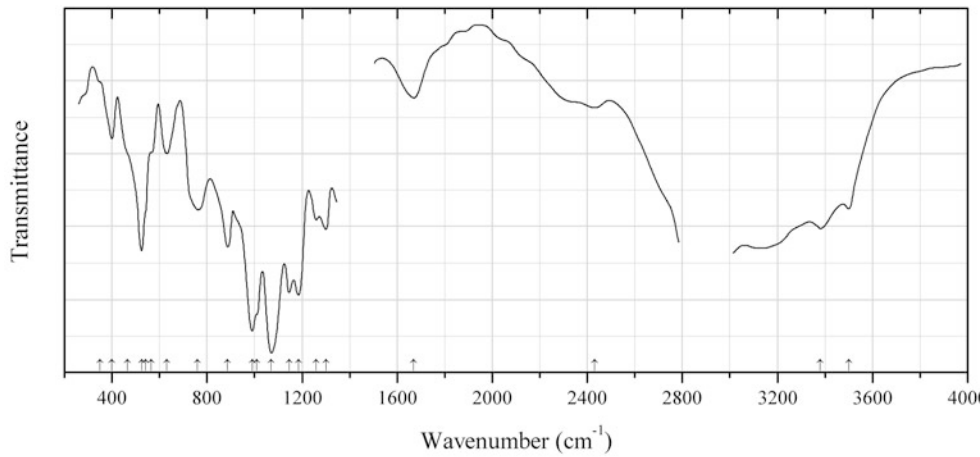

Fig. 2.911 IR spectrum of hannayite drawn using data from Keller (1971)

P527 Hannayite $(NH_4)_2Mg_3(HPO_4)_4 \cdot 8H_2O$ (Fig. 2.911)
Locality: Synthetic.
Description: Synthesized from aqueous solutions of $(NH_4)(H_2PO_4)$ and ammonium acetate below 50 °C.
Kind of sample preparation and/or method of registration of the spectrum: Suspension in mineral oil. Transmission.

Source: Keller (1971).
Wavenumbers (cm^{-1}): 3500, 3380, 2430, 1670, 1300, 1260, 1185s, 1145s, 1070s, 1009sh, 990s, 887, 760, 630, 566sh, 541sh, 525, 465sh, 400, 350sh.
Note: The wavenumbers were partly determined by us based on spectral curve analysis of the published spectrum.

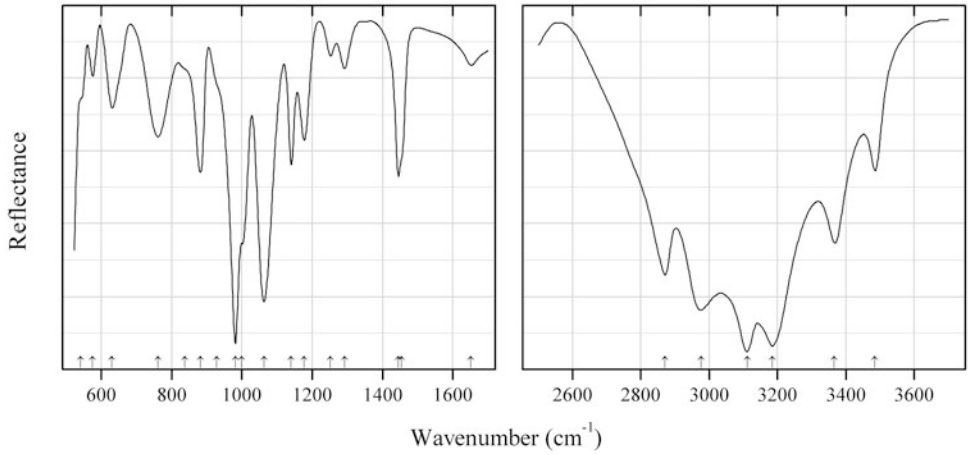

Fig. 2.912 IR spectrum of hannayite drawn using data from Frost et al. (2005b)

P528 Hannayite $(NH_4)_2Mg_3(HPO_4)_4 \cdot 8H_2O$ (Fig. 2.912)
Locality: Lava Cave, 5 km S of Skipton, Skipton, Victoria, Australia.
Description: Confirmed by the powder X-ray diffraction pattern and electron microprobe analyses.
Kind of sample preparation and/or method of registration of the spectrum: Attenuated total reflection of powdered mineral.
Source: Frost et al. (2005b).
Wavenumbers (cm^{-1}): 3485, 3366, 3185s, 3111s, 2976, 2871, 1651, 1454sh, 1445s, 1292, 1252, 1177, 1140, 1063s, 1000sh, 981s, 928sh, 882, 837sh, 761, 631, 576, 541sh.
Note: The wavenumbers are determined from the figure. In the cited paper, the wavenumbers are indicated only for the maxima of individual bands obtained as a result of the spectral curve analysis.

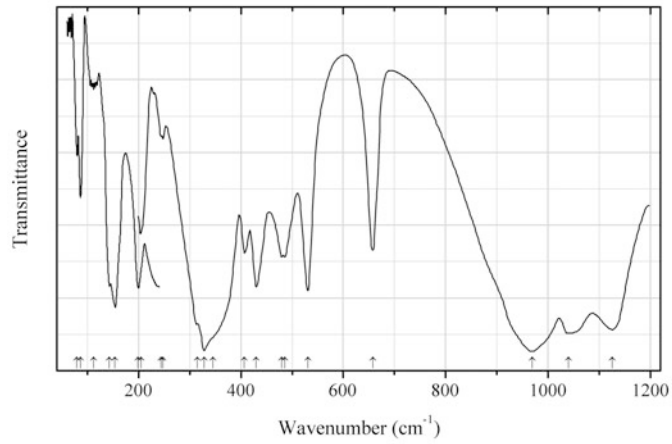

Fig. 2.913 IR spectrum of barium titanium phosphate P529 drawn using data from Paques-Ledent (1977)

P529 Barium titanium phosphate P529 $BaTi(PO_4)_2$ (Fig. 2.913)
Locality: Synthetic.
Description: Isostructural with yavapaiite. Monoclinic, $a = 8.25$, $b = 5.176$, $c = 7.713$ Å, $\beta = 94.18°$.
Kind of sample preparation and/or method of registration of the spectrum: Transmission. Kind of sample preparation is not indicated.
Source: Paques-Ledent (1977).
Wavenumbers (cm^{-1}): 1126s, 1041s, 970s, 658, 531, 486, 480, 430, 407, 345sh, 328s, 315, 248w, 244w, 205, 199, 154, 143, (112w), 86, 79.
Note: The wavenumbers were determined by us based on spectral curve analysis of the published spectrum.

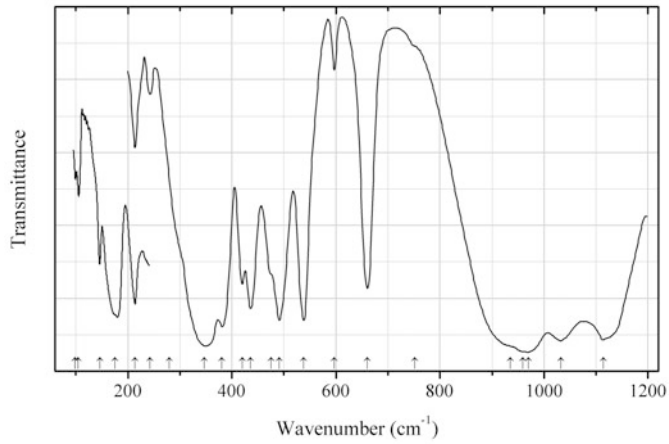

Fig. 2.914 IR spectrum of strontium titanium phosphate P530 drawn using data from Paques-Ledent (1977)

P530 Strontium titanium phosphate P530 $SrTi(PO_4)_2$ (Fig. 2.914)
Locality: Synthetic.
Description: Isostructural with yavapaiite. Monoclinic, $a = 8.146$, $b = 5.187$, $c = 7.351$ Å, $\beta = 92.95°$.
Kind of sample preparation and/or method of registration of the spectrum: Transmission. Kind of sample preparation is not indicated.
Source: Paques-Ledent (1977).
Wavenumbers (cm^{-1}): 1114s, 1033s, 970s, 960sh, 936sh, 752sh, 661s, 597w, 538s, 491s, 475sh, 436s, 420, 381, 347s, 280, 242w, 214, 175sh, 146, 105w, 99w.
Note: The wavenumbers were determined by us based on spectral curve analysis of the published spectrum.

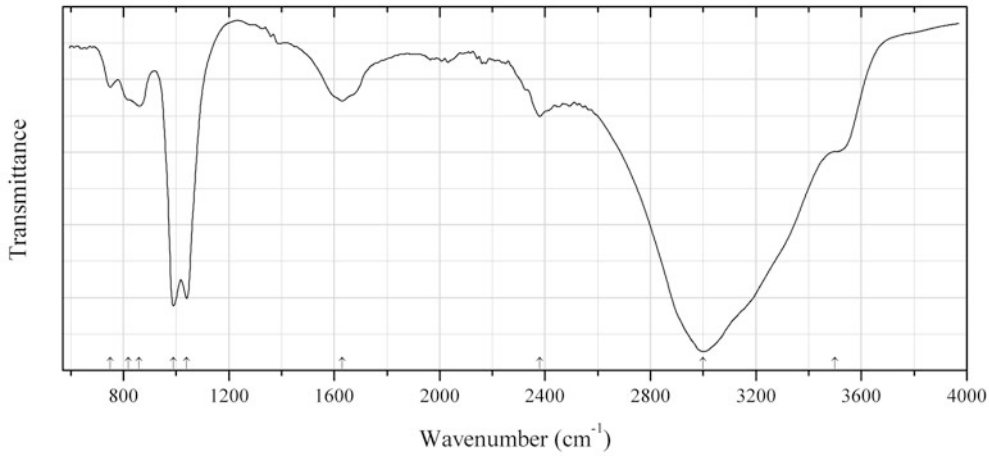

Fig. 2.915 IR spectrum of hazenite drawn using data from Yang and Sun (2004)

P531 Hazenite $KNaMg_2(PO_4)_2 \cdot 14H_2O$ (Fig. 2.915)
Locality: Biomineral formed in the laboratory by cyanobacteria.
Description: Elongate tabular crystals. The crystal structure is solved and is related to that of struvite. Orthorhombic, space group *Pnma*, $a = 25.1754(18)$, $b = 6.9316(5)$, $c = 11.2189(10)$ Å, $V = 1957.8(3)$ Å^3, $Z = 4$. $D_{calc} = 1.876$ g/cm^3. Electron microprobe analysis gives the ratio P:Mg:K:Na equal to 2.00:2.00:0.93:0.90.
Kind of sample preparation and/or method of registration of the spectrum: Absorbance of powdered sample placed as a thin film on a KBr substrate.
Source: Yang and Sun (2004).
Wavenumbers (cm^{-1}): 3500sh, 3000s, 2380w, 1630w, 1040s, 990s, 860w, 820sh, 750w.

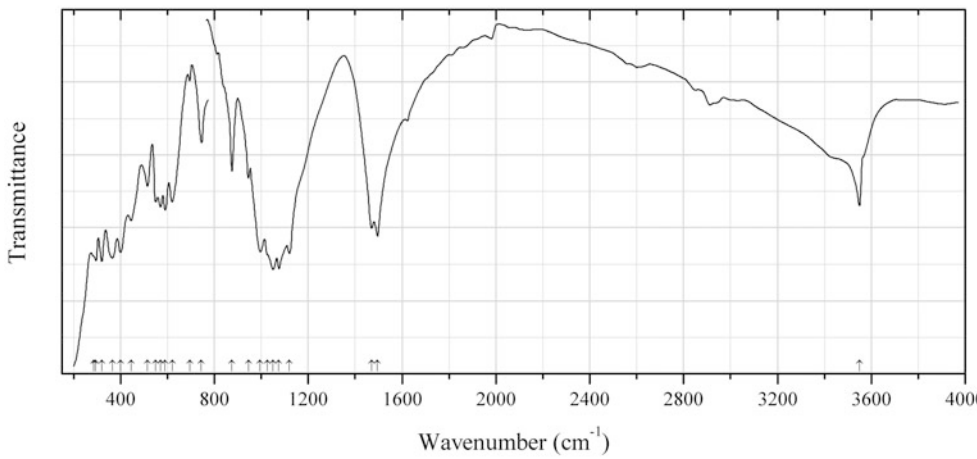

Fig. 2.916 IR spectrum of heneuite drawn using data from Raade et al. (1986)

P532 Heneuite $CaMg_5(PO_4)_3(CO_3)(OH)$ (Fig. 2.916)
Locality: Tingelstadtjern, Modum, Norway (type locality).

Description: Pale blue-green nodule from the association with serpentine, magnesite, apatite, and althausite. Holotype sample. Triclinic, space group *P*-1, $a = 6.3069(3)$, $b = 10.8386(9)$, $c = 8.6736(6)$ Å, $\alpha = 95.013(7)°$, $\beta = 93.412(7)°$, $\gamma = 101.039(7)°$, $V = 577.94(5)$ Å^3, $Z = 2$. $D_{meas} = 3.016(7)$ g/cm^3, $D_{calc} = 3.007$ g/cm^3. Optically biaxial (−), $\alpha = 1.586(2)$, $\beta = 1.620(2)$, $\gamma = 1.630(2)$. The empirical formula is $(Ca_{1.04}Na_{0.03})(Mg_{5.02}Fe_{0.03})[(PO_4)_{2.90}(AsO_4)_{0.05}](CO_3)_{1.00}(OH)_{1.07}O_{0.13}$. The strongest lines of the powder X-ray diffraction pattern [*d*, Å (*I*, %) (*hkl*)] are: 3.6738 (40) (120), 2.8756 (90) (0–32), 2.8450 (40) (0–13), 2.8363 (42) (201), 2.7894 (80) (−221), 2.7030 (100) (013).
Kind of sample preparation and/or method of registration of the spectrum: KBr disc. Transmission.
Source: Raade et al. (1986).
Wavenumbers (cm^{-1}): 3550, 1495s, 1470s, 1120s, 1075s, 1050s, 1025sh, 995s, 945, 875, 745, 695w, 620, 590, 570, 550, 515, 445, 400s, 365s, 320s, 295s, 285sh.

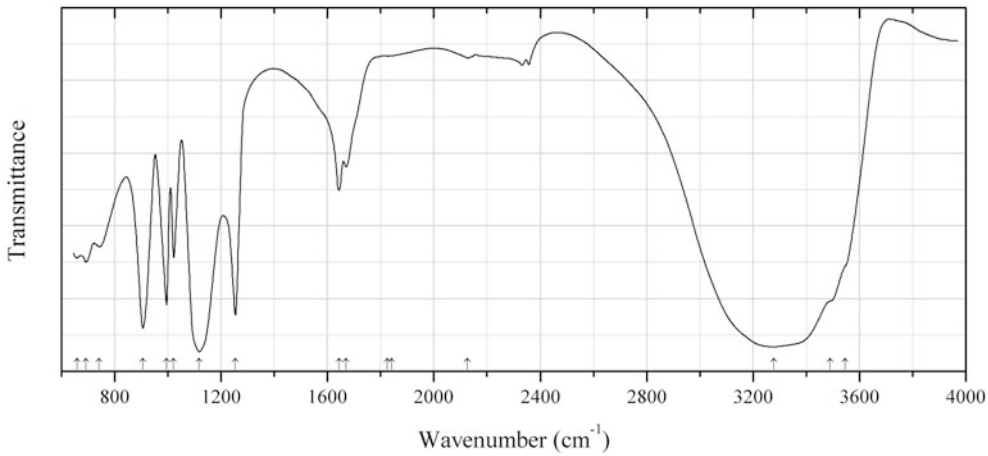

Fig. 2.917 IR spectrum of hylbrownite drawn using data from Elliott et al. (2013a)

P533 Hylbrownite $Na_3Mg(P_3O_{10})\cdot 12H_2O$ (Fig. 2.917)
Locality: Dome Rock mine, Boolcoomatta Reserve, Olary Province, South Australia, Australia (type locality).
Description: White aggregates of thin prismatic crystals from the association with conichalcite, chrysocolla, and an amorphous Cu-Mn-Co silicate. Holotype sample. Monoclinic, space group $P2_1/n$, $a = 14.722(3)$, $b = 9.240(2)$, $c = 15.052(3)$ Å, $\beta = 90.01(3)°$, $V = 2047.5(7)$ Å^3, $Z = 4$. $D_{meas} = 1.81(4)$ g/cm^3. Optically biaxial (−), $\alpha = 1.390(4)$, $\beta = 1.421(4)$, $\gamma = 1.446(4)$. The empirical formula is: $Na_{2.93}Mg_{0.99}Ca_{0.04}P_{2.99}O_{9.97}\cdot 12.03H_2O$. The strongest lines of the powder X-ray diffraction pattern [*d*, Å (*I*, %) (*hkl*)] are: 10.530 (60) (10–1, 101), 7.357 (80) (200), 6.951 (100) (11–1, 111), 4.754 (35) (10–3, 103), 3.934 (40) (022), 3.510 (45) (30–3, 303), 3.336 (35) (41–1, 411).
Kind of sample preparation and/or method of registration of the spectrum: Transmittance of powdered mineral. An IR microscope and a diamond-anvil cell were used.
Source: Eliott et al. (2013a).
Wavenumbers (cm^{-1}): 3547sh, 3490sh, 3278s, 2127w, (1842w), (1826w), 1670, 1643, 1254s, 1118s, 1022, 995s, 906s, 742, 692, 658.
Note: The wavenumbers were partly determined by us based on spectral curve analysis of the published spectrum.

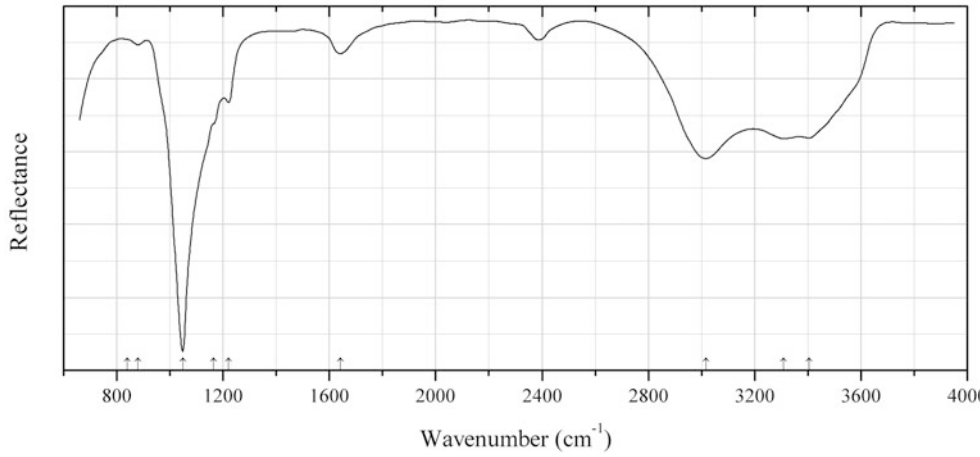

Fig. 2.918 IR spectrum of iangreyite drawn using data from Mills et al. (2011)

P534 Iangreyite $Ca_2Al_7(PO_4)_2(HPO_4)_2(OH,F)_{15}\cdot 8H_2O$ (Fig. 2.918)
Locality: Silver Coin mine, Valmy, Edna Mountains, Humboldt Co., Nevada, USA (type locality).
Description: Thin hexagonal tabular crystals from the association with meurigite-Na, plumbogummite, kidwellite, lipscombite, strengite, chalcosiderite, wardite, leucophosphite, wavellite, goethite, barite, quartz, and F-rich perhamite. Holotype sample. Trigonal, space group *P*321, a = 6.988(1), c = 16.707(3), V = 706.5(2) Å^3, Z = 1. D_{meas} = 2.46(3) g/cm^3, D_{calc} = 2.451 g/cm^3. Optically uniaxial (+), ω = 1.544(2), ε = 1.554(2). The empirical formula is: $Ca_{1.42}K_{0.22}Na_{0.09}Ba_{0.03}Sr_{0.01}Al_{6.51}Mg_{0.09}Fe_{0.02}Cu_{0.01}Zn_{0.01}P_{3.81}F_{5.24}H_{30.21}O_{33.76}$. The strongest lines of the powder X-ray diffraction pattern [*d*, Å (*I*, %) (*hkl*)] are: 16.739 (100) (001), 6.054 (18) (010), 5.687 (13) (011), 2.967 (45) (021, 113), 2.219 (19) (017), 1.896 (13) (033), 1.744 (17) (220).
Kind of sample preparation and/or method of registration of the spectrum: Attenuated total reflection of powdered mineral.
Source: Mills et al. (2011).
Wavenumbers (cm^{-1}): 3406s, 3308s, 3016s, 1641, 1220w, 1164sh, 1048s, 880, 840sh.
Note: The wavenumbers were partly determined by us based on spectral curve analysis of the published spectrum. The band position denoted by Mills et al. (2011) as 860 cm^{-1} was determined by us at 880 cm^{-1}.

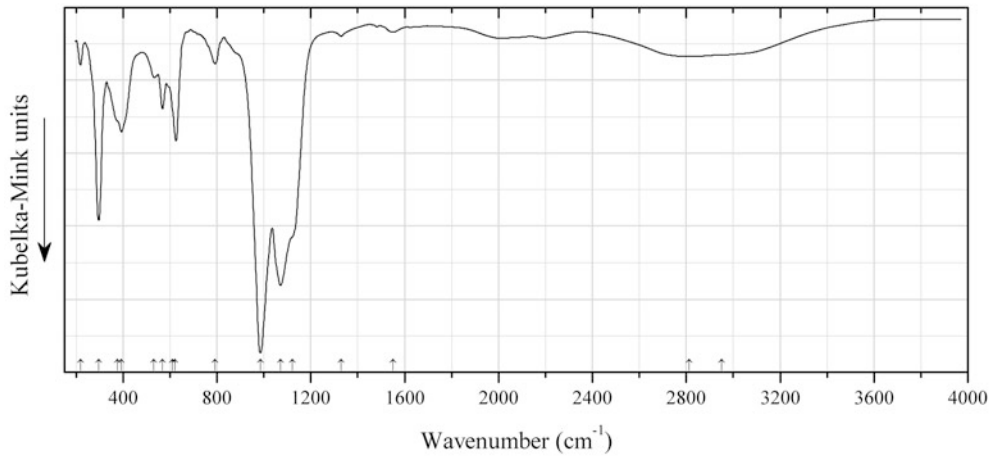

Fig. 2.919 IR spectrum of iron(III) orthophosphate monohydrate drawn using data from Marx et al. (2010)

P535 Iron(III) orthophosphate monohydrate $Fe^{3+}(PO_4)\cdot H_2O$ (Fig. 2.919)
Locality: Synthetic.
Description: Obtained from tavorite $LiFePO_4(OH)$ through a Li^+/H^+ exchange. Confirmed by different chemical analyses. The crystal structure is solved. Monoclinic, space group *C*2/*c*, $a = 6.708(2)$, $b = 7.761(2)$, $c = 7.382(2)$ Å, $\beta = 115.08(2)°$, $V = 348.1(2)$ Å^3, $Z = 2$.
Kind of sample preparation and/or method of registration of the spectrum: Attenuated total reflection of powdered sample.
Source: Marx et al. (2010).
Wavenumbers (cm^{-1}): 2952sh, 2813, 1550w, 1330w, 1121sh, 1071s, 985s, 792, 620, 611, 568, 532, 393, 376sh, 296s, 218w.
Note: The wavenumbers were determined by us based on spectral curve analysis of the published spectrum.

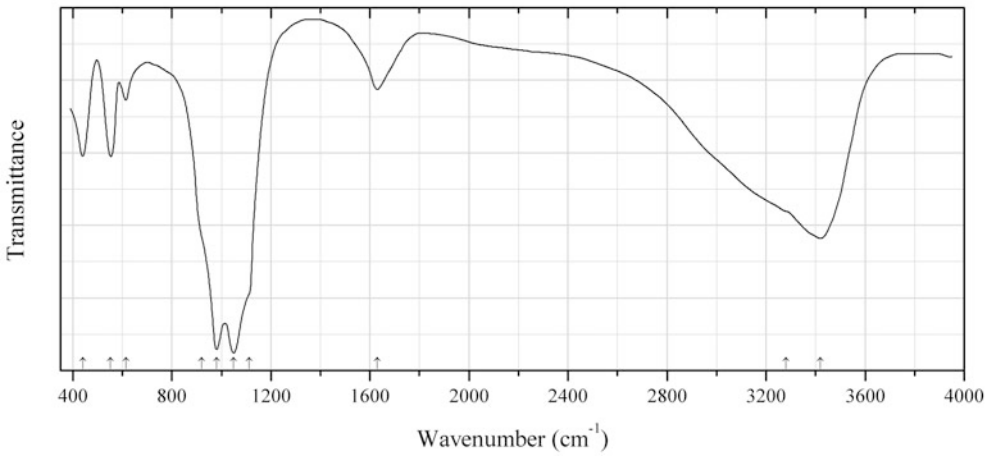

Fig. 2.920 IR spectrum of keckite drawn using data from Mücke (1983)

P536 Keckite $CaMn(Fe^{3+},Mn)_2Fe^{3+}{}_2(PO_4)_4(OH)_3\cdot 7H_2O$ (?) (Fig. 2.920)
Locality: Hagendorf South pegmatite, Cornelia mine, Hagendorf, Waidhaus, Upper Palatinate, Bavaria, Germany (type locality).
Description: No data.
Kind of sample preparation and/or method of registration of the spectrum: Transmission. Kind of sample preparation is not indicated.
Source: Mücke (1983).
Wavenumbers (cm^{-1}): 3420s, 3280sh, 1630, 1112sh, 1050s, 980s, 921sh, 614, 553, 440.
Note: The wavenumbers were partly determined by us based on spectral curve analysis of the published spectrum.

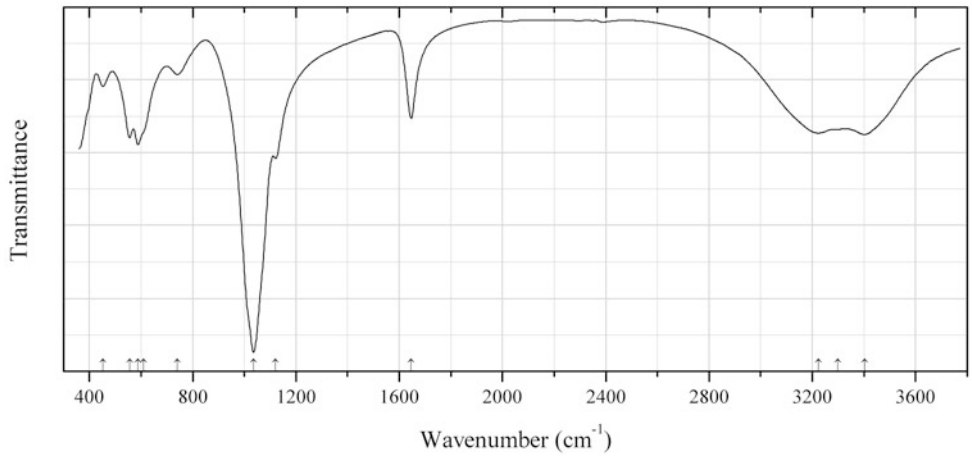

Fig. 2.921 IR spectrum of kolbeckite obtained by N.V. Chukanov

P537 Kolbeckite $Sc(PO_4)\cdot 2H_2O$ (Fig. 2.921)
Locality: Schlarbaum quarry, Klause, Bad Gleichenberg, Stiria, Austria.
Description: Greenish spherulite. The empirical formula is (electron microprobe): $(Sc_{0.93}Al_{0.05}Fe_{0.02}Cr_{0.005})(PO_4)\cdot nH_2O$. Confirmed by the IR spectrum.
Kind of sample preparation and/or method of registration of the spectrum: KBr disc. Absorption.
Wavenumbers (cm^{-1}): 3404, (3300), 3223, 1646, 1121, 1035s, 741, 610sh, 588, 556, 452.

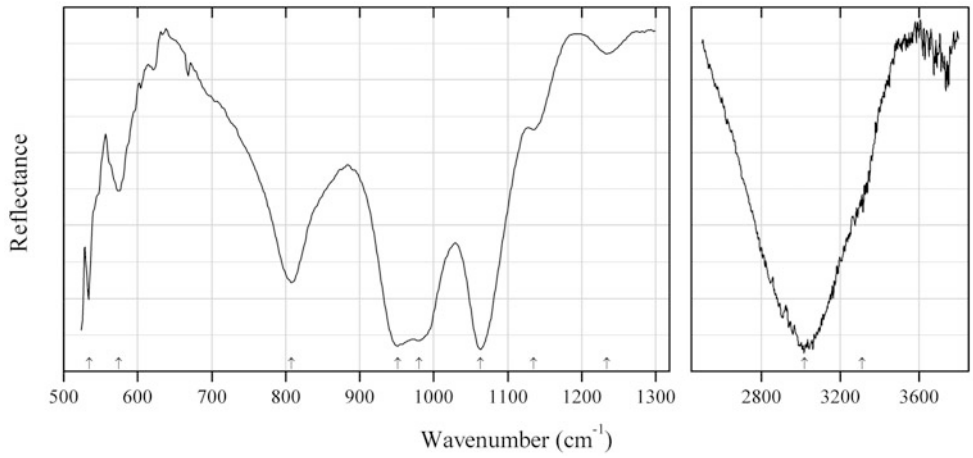

Fig. 2.922 IR spectrum of kintoreite drawn using data from Frost et al. (2006d)

P538 Kintoreite $PbFe^{3+}{}_3(PO_4)(HPO_4)(OH)_6$ (Fig. 2.922)
Locality: Not indicated.
Description: No data.
Kind of sample preparation and/or method of registration of the spectrum: Attenuated total reflection of powdered mineral.

Source: Frost et al. (2006d).
Wavenumbers (cm^{-1}): 3310sh, 3020s, 1234w, 1135, 1063s, 980s, 951s, 808, 574, (535).
Note: In the cited paper, the wavenumbers are indicated for the maxima of individual bands obtained as a result of the spectral curve analysis. Details of this analysis are not described sufficiently detailed. The wavenumbers were determined by us based on spectral curve analysis of the published spectrum.

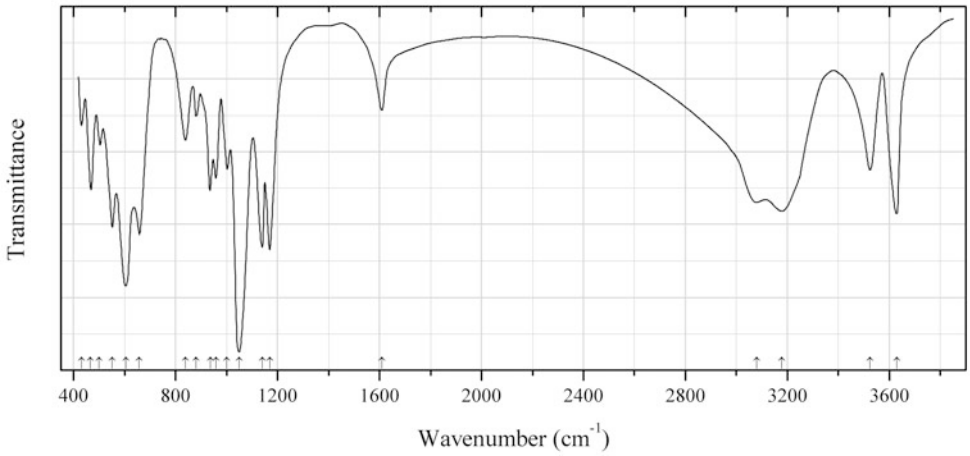

Fig. 2.923 IR spectrum of kleemanite drawn using data from Povarennykh (1981b)

P539 Kleemanite $ZnAl_2(PO_4)_2(OH)_2 \cdot 3H_2O$ (Fig. 2.923)
Locality: No data.
Kind of sample preparation and/or method of registration of the spectrum: KBr disc. Absorption.
Source: Povarennykh (1981b).
Wavenumbers (cm^{-1}): 3630s, 3525, 3177s, 3080, 1610, 1170s, 1140s, 1050s, 1000, 958, 936, 880w, 838, 658s, 605s, 552s, 500, 466, 432w.

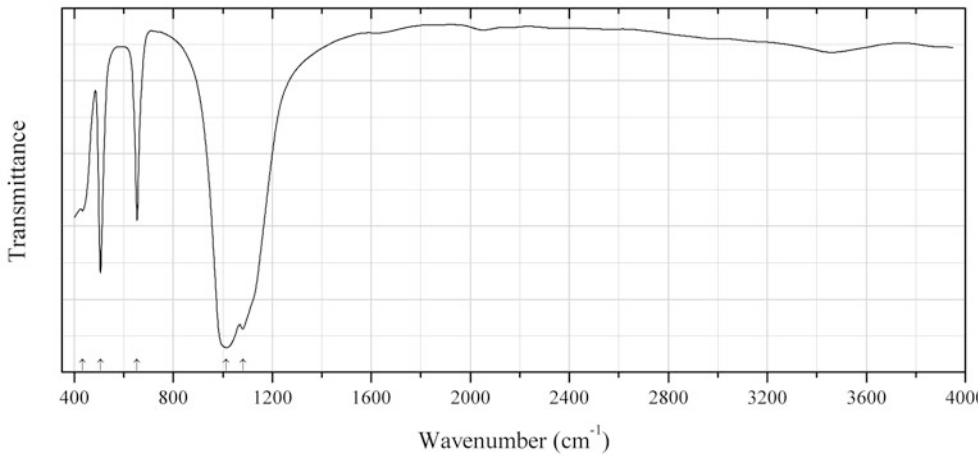

Fig. 2.924 IR spectrum of scandium orthophosphate drawn using data from Pechkovskii et al. (1981)

P540 Scandium orthophosphate $Sc(PO_4)$ (Fig. 2.924)
Locality: Synthetic.
Description: Tetragonal, space group $I4_1/amd$, a = 6.578, c = 5.796 Å, Z = 4. D_{calc} = 3.707 g/cm^3.
Kind of sample preparation and/or method of registration of the spectrum: KBr disc. Absorption.
Source: Pechkovskii et al. (1981).
Wavenumbers (cm^{-1}): 1081s, 1015s, 654, 506, 433, 362, 315sh, 285s.

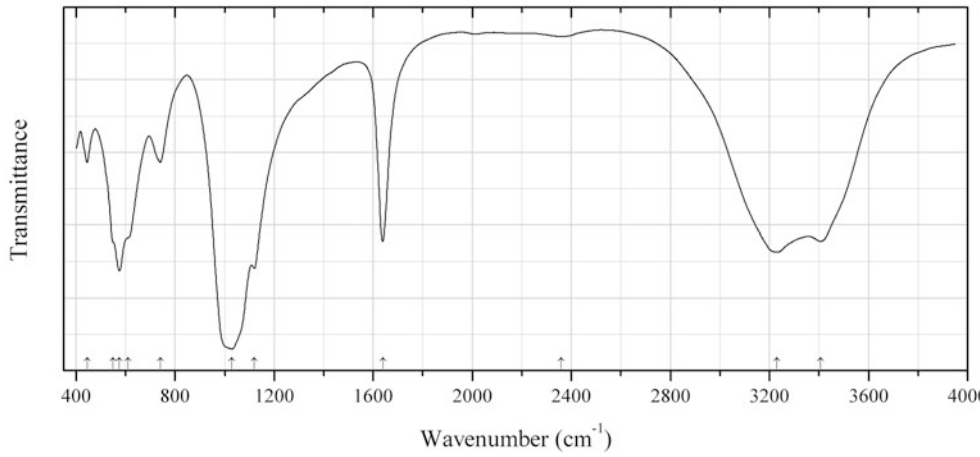

Fig. 2.925 IR spectrum of kolbeckite drawn using data from Pechkovskii et al. (1981)

P541 Kolbeckite $Sc(PO_4)\cdot 2H_2O$ (Fig. 2.925)
Locality: Synthetic.
Kind of sample preparation and/or method of registration of the spectrum: KBr disc. Absorption.
Source: Pechkovskii et al. (1981).
Wavenumbers (cm^{-1}): 3407, 3230s, 2360w, 1640s, 1120s, 1030s, 740, 610sh, 575s, 550sh, 445, 390sh, 352s, 325sh, 293s, 254sh, 205, 180.

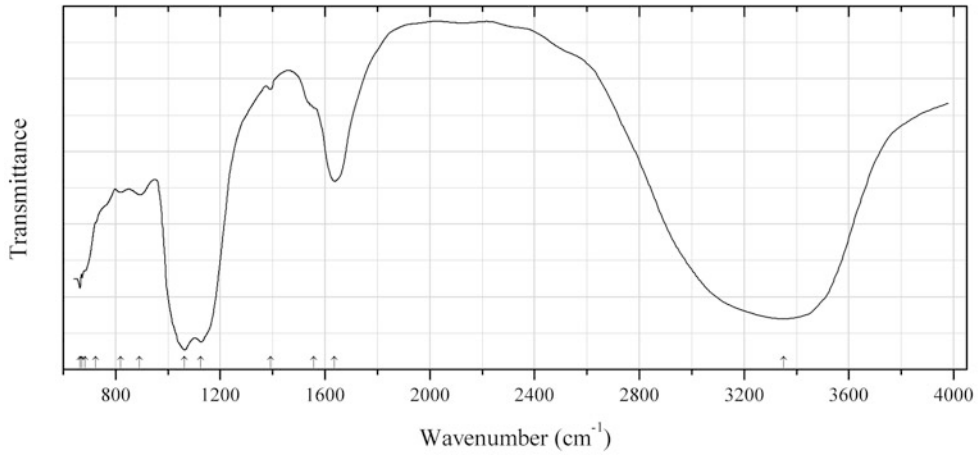

Fig. 2.926 IR spectrum of kribergite drawn using data from De Abeledo et al. (1968)

P542 Kribergite $Al_5(PO_4)_3(SO_4)(OH)_4 \cdot 4H_2O$ (Fig. 2.926)
Locality: Kristineberg mine, Skellefte ore district, Sweden (type locality).
Description: Specimen No. RM 450003 from the Mineralogical Section of the Swedish Museum of Natural History. Confirmed by powder X-ray diffraction data. The strongest reflections are observed at 11.57, 6.62, 5.85, 5.72, 5.37, and 5.02 Å.
Kind of sample preparation and/or method of registration of the spectrum: Transmission. Kind of sample preparation is not indicated.
Source: De Abeledo et al. (1968).
Wavenumbers (cm^{-1}): 3350s, 1636, 1557sh, 1391w, 1126s, 1064s, 892, 819, 725sh, 683sh, 672, 664.
Note: The wavenumbers were determined by us based on spectral curve analysis of the published spectrum.

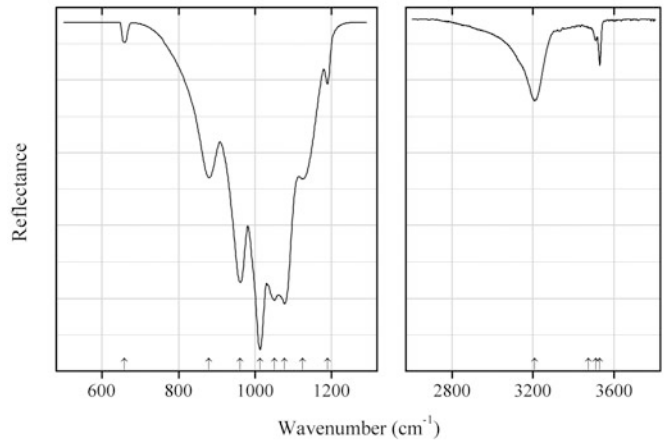

Fig. 2.927 IR spectrum of kulanite drawn using data from Frost et al. (2013b)

P543 Kulanite $BaFe^{2+}{}_2Al_2(PO_4)_3(OH)_3$ (Fig. 2.927)
Locality: Rapid Creek, Richardson Mts., Yukon Territory, Canada.
Description: Blue tabular plates. Specimen No. SAB-100 from the collection of the Geology Department of the Federal University of Ouro Preto, Minas Gerais, Brazil. Confirmed by semi-quantitative electron microprobe analysis.
Kind of sample preparation and/or method of registration of the spectrum: Attenuated total reflection of powdered mineral.
Source: Frost et al. (2013b).
Wavenumbers (cm^{-1}): 3530, 3510, 3473sh, 3208, 1189w, 1125, 1077s, 1051s, 1013s, 961s, 879, 658w.
Note: In the cited paper, wavenumbers are indicated for the maxima of individual bands obtained as a result of the spectral curve analysis. Details of this analysis are not described. The wavenumbers were determined by us based on spectral curve analysis of the published spectrum. Below 650 cm^{-1} the spectrum given in the cited paper goes off-scale.

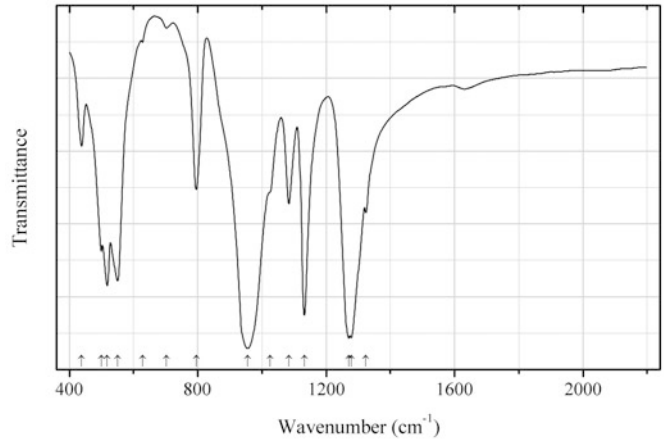

Fig. 2.928 IR spectrum of sodium cyclohexaphosphate drawn using data from Melnikova et al. (1985)

P544 Sodium cyclohexaphosphate $Na_6(P_6O_{18})$ (Fig. 2.928)
Locality: Synthetic.
Description: Obtained by dehydration of sodium cyclohexaphosphate hexahydrate at 120 °C.
Kind of sample preparation and/or method of registration of the spectrum: KBr disc. Absorption.
Source: Melnikova et al. (1985).
Wavenumbers (cm^{-1}): 1324, 1278s, 1270s, 1132s, 1084, 1025sh, 955s, 795, 702w, 628, 550s, 518s, 500, 438.

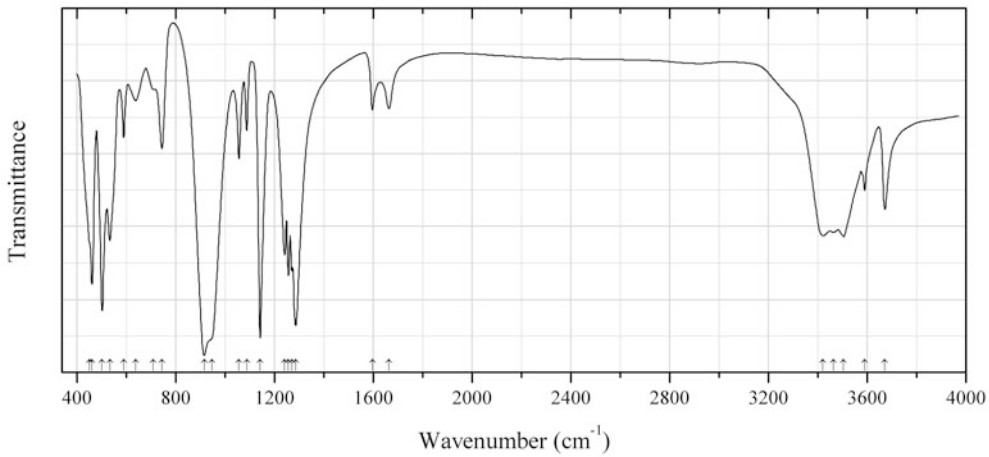

Fig. 2.929 IR spectrum of sodium cyclooctaphosphate hexahydrate drawn using data from Melnikova et al. (1985)

P545 Sodium cyclooctaphosphate hexahydrate $Na_8P_8O_{24}\cdot 6H_2O$ (Fig. 2.929)
Locality: Synthetic.
Description: Obtained in the reaction of lead cyclooctaphosphate with aqueous solution of sodium sulfide with subsequent precipitation from the solution by ethanol.

Kind of sample preparation and/or method of registration of the spectrum: KBr disc. Absorption.
Source: Melnikova et al. (1985).
Wavenumbers (cm^{-1}): 3672, 3590, 3505, 3463, 3421, 1663, 1597, 1286s, 1271, 1257, 1242, 1143s, 1088, 1057, 948sh, 916s, 745, 710, 638, 590, 534, 503s, 462s, 452sh.

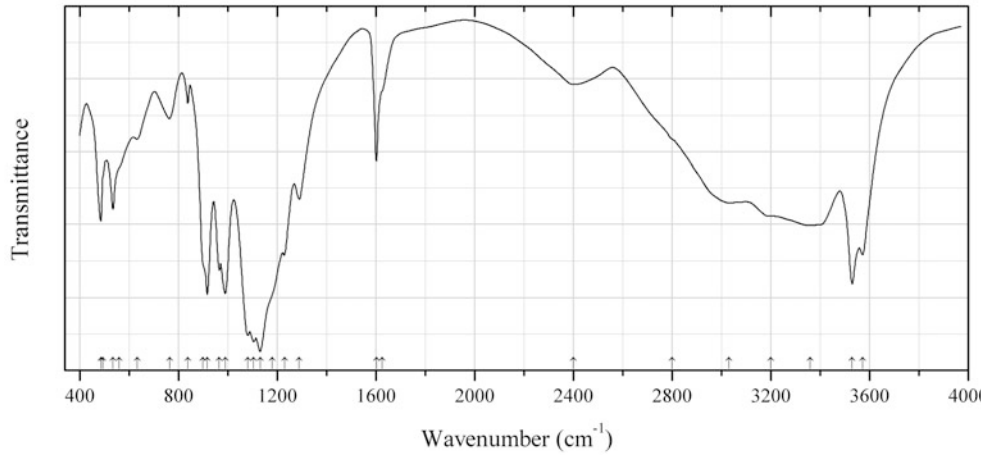

Fig. 2.930 IR spectrum of uranyl monosubstituted orthophosphate trihydrate drawn using data from Pechkovskii et al. (1981)

P546 Uranyl monosubstituted orthophosphate trihydrate $(UO_2)(H_2PO_4)_2 \cdot 3H_2O$ (Fig. 2.930)
Locality: Synthetic.
Kind of sample preparation and/or method of registration of the spectrum: KBr disc. Absorption.
Source: Pechkovskii et al. (1981).
Wavenumbers (cm^{-1}): 3572, 3530s, 3360, 3200, 3030, 2800sh, 2400, 1625sh, 1602, 1290, 1230, 1180sh, 1131s, 1105s, 1081s, 990s, 966, 917s, 900sh, 838w, 764w, 634w, 560sh, 535, 495sh, 486, 391, 351, 259, 221, 183.

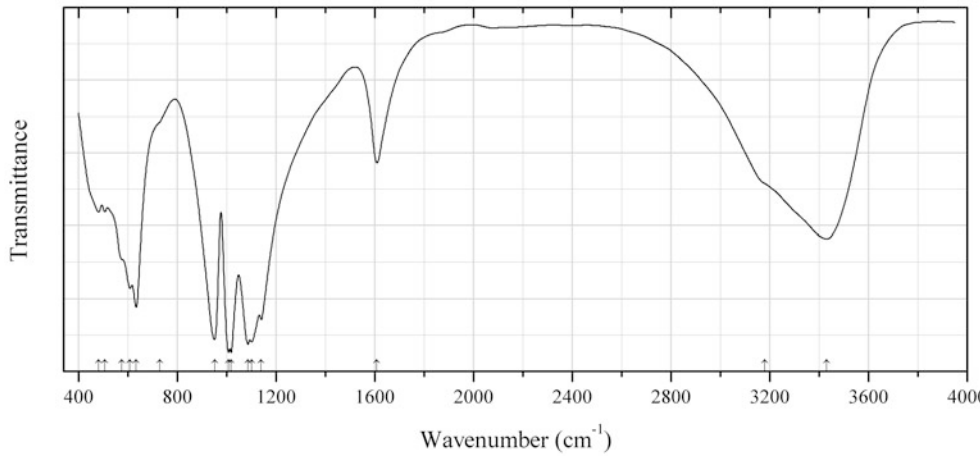

Fig. 2.931 IR spectrum of zinc orthophosphate dihydrate drawn using data from Pechkovskii et al. (1981)

P547 Zinc orthophosphate dihydrate $Zn_3(PO_4)_2 \cdot 2H_2O$ (Fig. 2.931)
Locality: Synthetic.
Description: Obtained by heating of zinc orthophosphate dehydrate at 100–170 °C up to the loss of 2 water molecules per formula unit.
Kind of sample preparation and/or method of registration of the spectrum: KBr disc. Absorption.
Source: Pechkovskii et al. (1981).
Wavenumbers (cm^{-1}): 3430s, 3180sh, 1609, 1141s, 1102s, 1087s, 1019s, 1008s, 952s, 730sh, 634s, 609, 575sh, 507, 482, 360, 320, 285, 245sh, 210, 165.

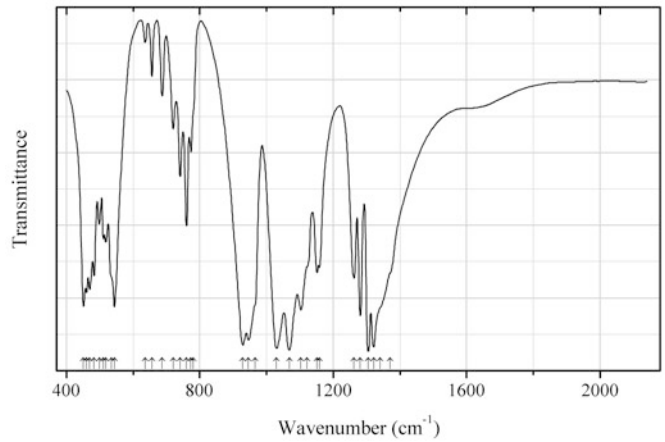

Fig. 2.932 IR spectrum of barium ultraphosphate drawn using data from Melnikova et al. (1985)

P548 Barium ultraphosphate $Ba_2P_6O_{17}$ (Fig. 2.932)
Locality: Synthetic.
Kind of sample preparation and/or method of registration of the spectrum: KBr disc. Absorption.
Source: Melnikova et al. (1985).
Wavenumbers (cm^{-1}): 1370sh, 1340sh, 1321s, 1305s, 1281, 1262, 1158, 1152, 1122sh, 1103, 1068s, 1030s, 965sh, 946s, 929s, 781sh, 773, 760, 741, 720, 687w, 656w, 636w, 544, 535sh, 518, 511, 499, 483, 470, 460, 451.

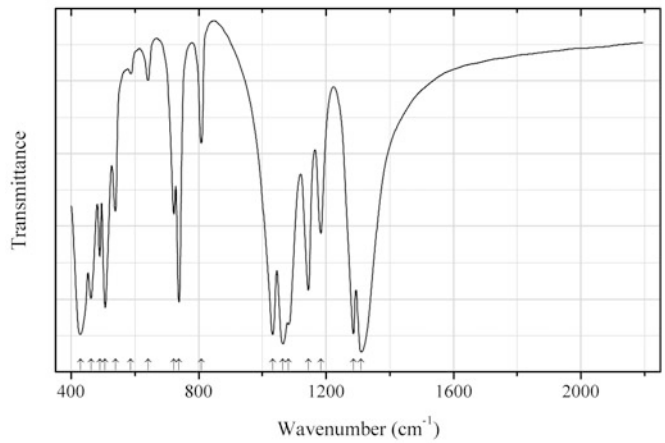

Fig. 2.933 IR spectrum of aluminium cyclotetraphosphate drawn using data from Melnikova et al. (1985)

P549 Aluminium cyclotetraphosphate $Al_4(P_4O_{12})_3$ (Fig. 2.933)
Locality: Synthetic.
Description: Cubic, space group *I*-43*d*, a = 13.71 Å, Z = 4. D_{meas} = 2.71 g/cm^3, D_{calc} = 2.76 g/cm^3.
Kind of sample preparation and/or method of registration of the spectrum: KBr disc. Absorption.
Source: Melnikova et al. (1985).
Wavenumbers (cm^{-1}): 1310s, 1286s, 1184, 1144, 1082s, 1064s, 1032s, 808, 738s, 722, 641w, 587w, 538, 506s, 489, 462, 428s.

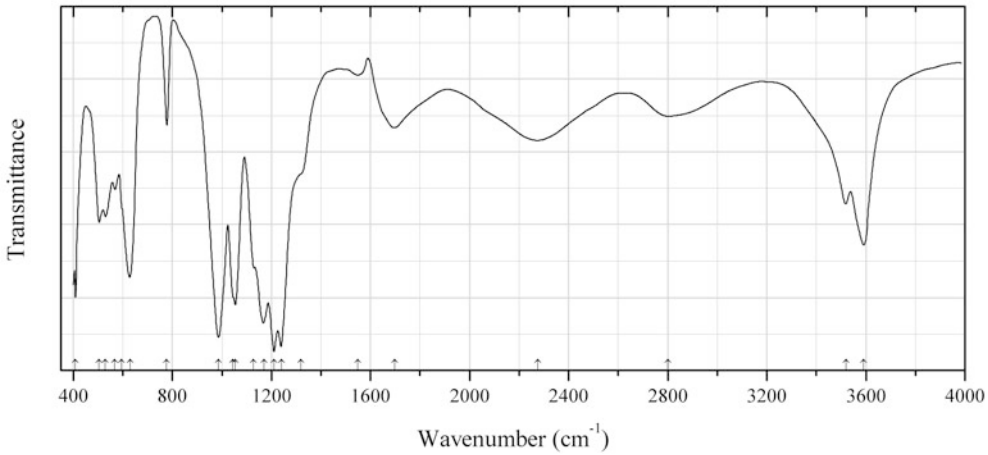

Fig. 2.934 IR spectrum of aluminium acid triphosphate dihydrate drawn using data from Melnikova et al. (1985)

P550 Aluminium acid triphosphate dihydrate $Al(H_2P_3O_{10})\cdot 2H_2O$ (Fig. 2.934)
Locality: Synthetic.
Kind of sample preparation and/or method of registration of the spectrum: KBr disc. Absorption.
Source: Melnikova et al. (1985).
Wavenumbers (cm^{-1}): 3590, 3521, 2800, 2275, 1697, 1550w, 1320sh, 1240s, 1211s, 1171s, 1128, 1054, 1045sh, 987s, 777, 630, 596sh, 568, 530, 504, 409.

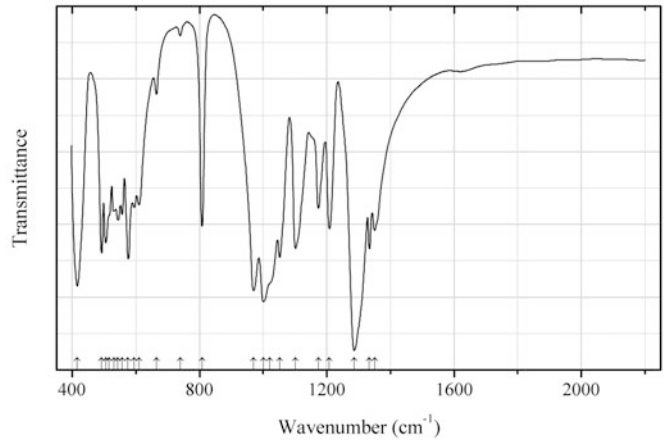

Fig. 2.935 IR spectrum of aluminium polyphosphate drawn using data from Melnikova et al. (1985)

P551 Aluminium polyphosphate $Al(PO_3)_3$ (Fig. 2.935)
Locality: Synthetic.
Kind of sample preparation and/or method of registration of the spectrum: KBr disc. Absorption.
Source: Melnikova et al. (1985).
Wavenumbers (cm^{-1}): 1351, 1334, 1286s, 1208, 1174, 1102, 1052, 1020sh, 1001s, 970s, 808, 739, 664, 609, 594, 574, 556, 543, 530, 515sh, 505, 492, 415s.

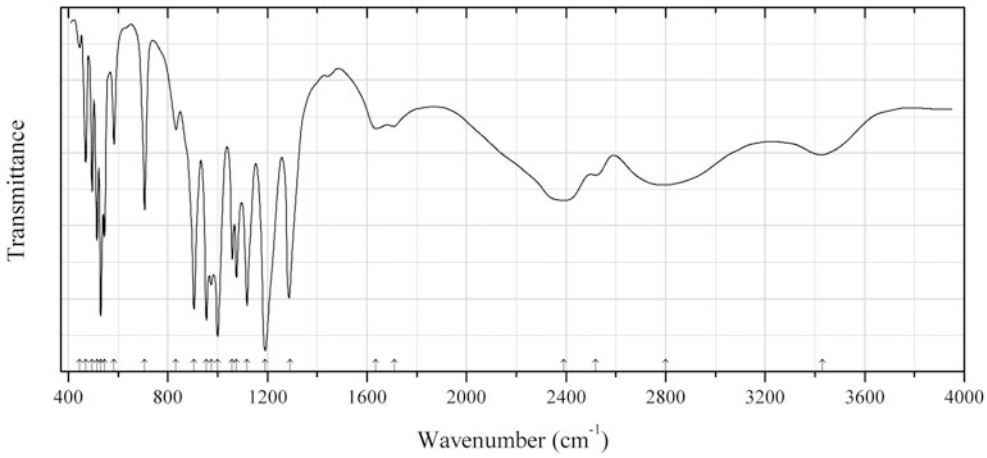

Fig. 2.936 IR spectrum of barium dihydrodiphosphate drawn using data from Melnikova et al. (1985)

P552 Barium dihydrodiphosphate $Ba(H_2P_2O_7)$ (Fig. 2.936)
Locality: The compound can be obtained in the reaction of barium oxide or hydroxide with phosphoric acid at P:Ba = 5–6 and temperature 115–125 °C during 1.5–2 days.
Kind of sample preparation and/or method of registration of the spectrum: KBr disc. Absorption.
Source: Melnikova et al. (1985).
Wavenumbers (cm^{-1}): 3430, 2800, 2520, 2390, 1710, 1635, 1292, 1191s, 1118s, 1076, 1059, 1000s, 975, 955s, 905s, 833, 706, 584, 545, 530s, 515, 496, 470, 445w.

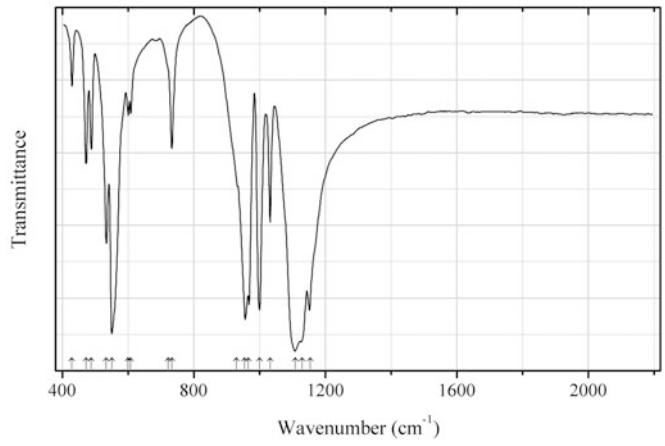

Fig. 2.937 IR spectrum of barium diphosphate drawn using data from Melnikova et al. (1985)

P553 Barium diphosphate $Ba_2(P_2O_7)$ (Fig. 2.937)
Locality: Synthetic.
Description: Orthorhombic, space group *Pnma*, $a = 9.35$, $b = 13.87$, $c = 5.61$, $Z = 4$.
Kind of sample preparation and/or method of registration of the spectrum: KBr disc. Absorption.
Source: Melnikova et al. (1985).
Wavenumbers (cm^{-1}): 1155s, 1130s, 1109s, 1033, 1000s, 967s, 955s, 930, 734, 723sh, 609w, 601w, 551s, 535, 489, 473, 430.

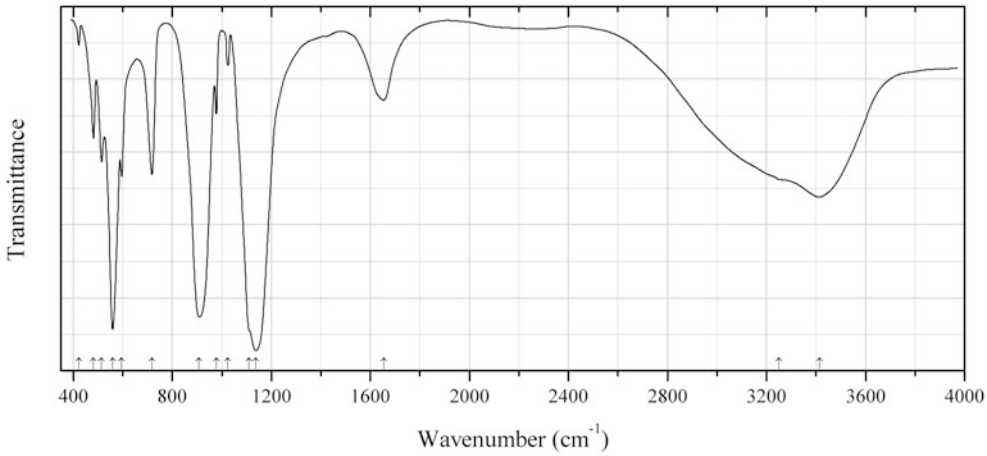

Fig. 2.938 IR spectrum of barium diphosphate dihydrate drawn using data from Melnikova et al. (1985)

P554 Barium diphosphate dihydrate $Ba_2(P_2O_7)\cdot 2H_2O$ (Fig. 2.938)
Locality: Synthetic.
Description: Synthesized from aqueous solutions of equimolar amounts of barium chloride and sodium diphosphate with subsequent crystallization of amorphous precipitate under growth solution during several hours.
Kind of sample preparation and/or method of registration of the spectrum: KBr disc. Absorption.
Source: Melnikova et al. (1985).
Wavenumbers (cm^{-1}): 3414, 3250, 1655, 1138s, 1110sh, 1025w, 978, 908s, 718, 596, 559s, 515, 482, 422w.

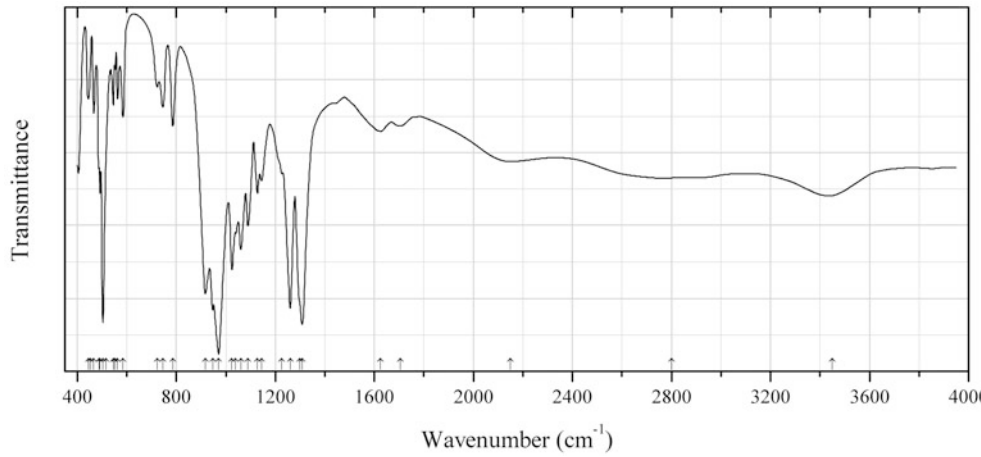

Fig. 2.939 IR spectrum of barium hydropolyphosphate drawn using data from Melnikova et al. (1985)

P555 Barium hydropolyphosphate $BaH(PO_3)_3$ (Fig. 2.939)
Locality: Synthetic.
Description: The compound can be synthesized in the reaction of barium oxide or hydroxide with phosphoric acid at the P:Ba ratio 5–6 and the temperature 160–280 °C.
Kind of sample preparation and/or method of registration of the spectrum: KBr disc. Absorption.
Source: Melnikova et al. (1985).
Wavenumbers (cm^{-1}): 3450, 2800, 2150, 1705, 1625, 1308s, 1298sh, 1260s, 1225sh, 1145, 1128, 1089, 1061, 1040, 1025, 971s, 947s, 917s, 786, 746, 723, 585, 563, 553, 546, 517, 504s, 492, 488, 467, 454, 445, 414.
Note: The bands at 3450 and 1625 cm^{-1} correspond to adsorbed water molecules.

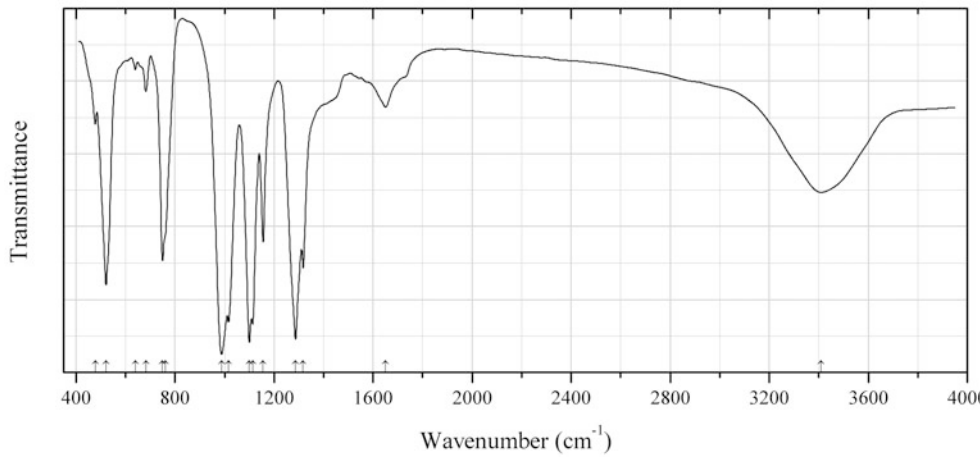

Fig. 2.940 IR spectrum of sodium cyclotriphosphate hexahydrate drawn using data from Melnikova et al. (1985)

P556 Sodium cyclotriphosphate hexahydrate $Na_3(P_3O_9)\cdot 6H_2O$ (Fig. 2.940)
Locality: Synthetic.
Description: Triclinic, space group *P*-1, $a = 9.50$, $b = 11.03$, $c = 7.98$ Å, $\alpha = 104.83°$, $\beta = 90.95°$, $\gamma = 117.98°$, $Z = 2$.

Kind of sample preparation and/or method of registration of the spectrum: KBr disc. Absorption.
Source: Melnikova et al. (1985).
Wavenumbers (cm^{-1}): 3410, 1650w, 1318, 1286s, 1156, 1114s, 1100s, 1016, 988s, 762sh, 750, 682w, 640w, 522s, 478w.

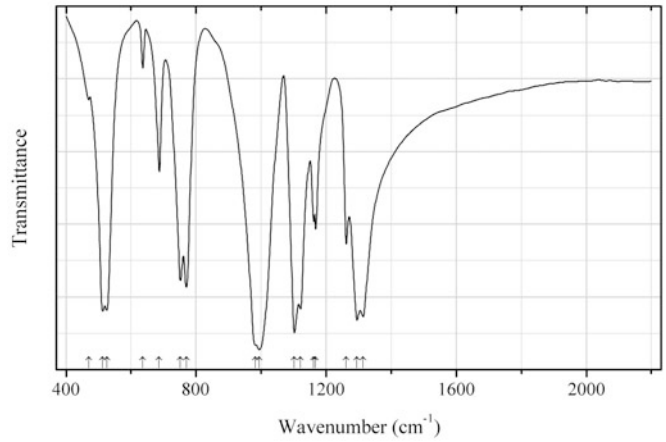

Fig. 2.941 IR spectrum of sodium cyclotriphosphate drawn using data from Melnikova et al. (1985)

P557 Sodium cyclotriphosphate $Na_3P_3O_9$ (Fig. 2.941)
Locality: Synthetic.
Description: Orthorhombic, space group *Pmcn*, a = 7.928, b = 13.214, c = 7.708 Å. D_{meas} = 2.49 g/cm^3, D_{calc} = 2.516 g/cm^3.
Kind of sample preparation and/or method of registration of the spectrum: KBr disc. Absorption.
Source: Melnikova et al. (1985).
Wavenumbers (cm^{-1}): 1314s, 1294s, 1262, 1168, 1162, 1121s, 1102s, 994s, 983s, 770, 752, 686, 636w, 525s, 513s, 470w.

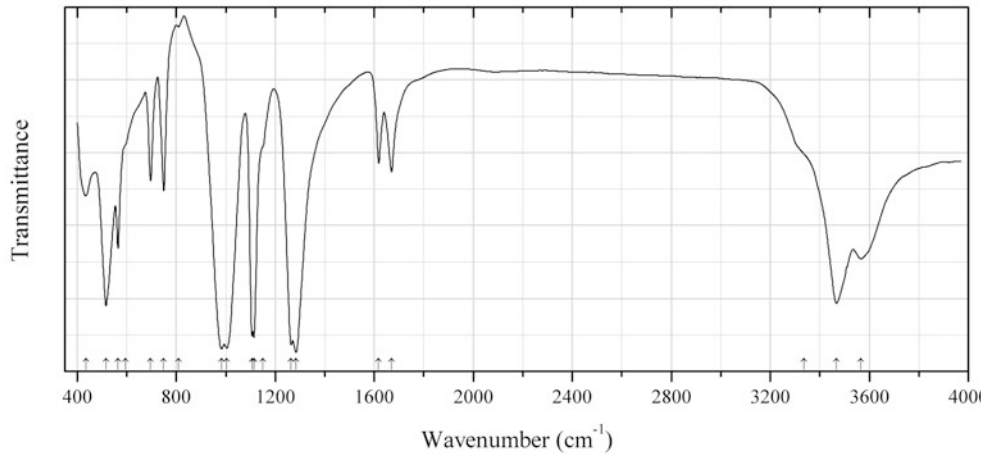

Fig. 2.942 IR spectrum of sodium cyclotetraphosphate tetrahydrate drawn using data from Melnikova et al. (1985)

P558 Sodium cyclotetraphosphate tetrahydrate $Na_4(P_4O_{12})\cdot 4H_2O$ (Fig. 2.942)
Locality: Synthetic.
Description: Monoclinic, space group $P2_1/a$, a = 9.667, b = 12.358, c = 6.170 Å, β = 92.27°, Z = 2. D_{calc} = 2.156 g/cm^3.
Kind of sample preparation and/or method of registration of the spectrum: KBr disc. Absorption.
Source: Melnikova et al. (1985).
Wavenumbers (cm^{-1}): 3567, 3467, 3335sh, 1670, 1618, 1284s, 1264s, 1150sh, 1114s, 1106s, 1005s, 983s, 810w, 750, 697, 595sh, 565, 516, 435.

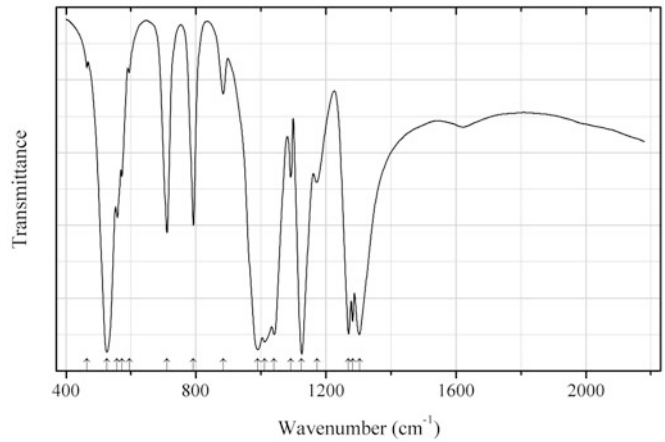

Fig. 2.943 IR spectrum of sodium cyclotetraphosphate drawn using data from Melnikova et al. (1985)

P559 Sodium cyclotetraphosphate $Na_4(P_4O_{12})$ (Fig. 2.943)
Locality: Synthetic.
Description: Orthorhombic, space group $P2_12_12_1$, a = 13.808, b = 13.633, c = 6.027 Å, Z = 4.
Kind of sample preparation and/or method of registration of the spectrum: KBr disc. Absorption.
Source: Melnikova et al. (1985).
Wavenumbers (cm^{-1}): 1303s, 1282s, 1270s, 1172, 1125s, 1092, 1041s, 1012s, 990s, 884, 792, 710, 595w, 572, 557, 525s, 464w.

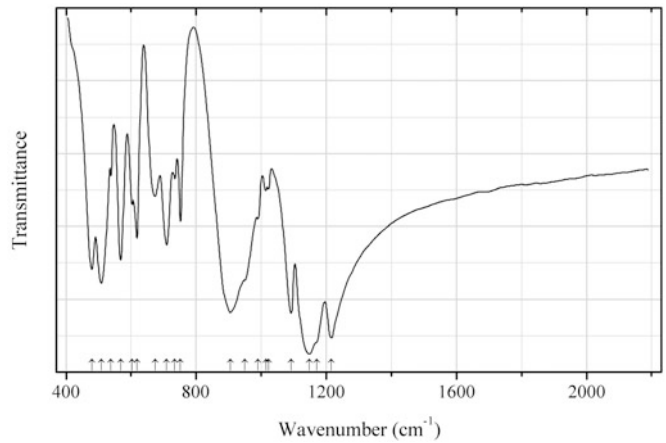

Fig. 2.944 IR spectrum of sodium triphosphate drawn using data from Melnikova et al. (1985)

P560 Sodium triphosphate $Na_5(P_3O_{10})$ (Fig. 2.944)
Locality: Synthetic.
Description: Monoclinic, space group *C*2/*c*, a = 9.61, b = 5.34, c = 19.73 Å, β = 112°, Z = 4. D_{meas} = 2.62 g/cm^3, D_{calc} = 2.60 g/cm^3.
Kind of sample preparation and/or method of registration of the spectrum: KBr disc. Absorption.
Source: Melnikova et al. (1985).
Wavenumbers (cm^{-1}): 1216s, 1171sh, 1148s, 1092s, 1022, 1015, 990w, 950sh, 905s, 752, 734, 709, 674, 618, 603, 568s, 538, 509, 479.
Note: The wavenumbers were partly determined by us based on spectral curve analysis of the published spectrum.

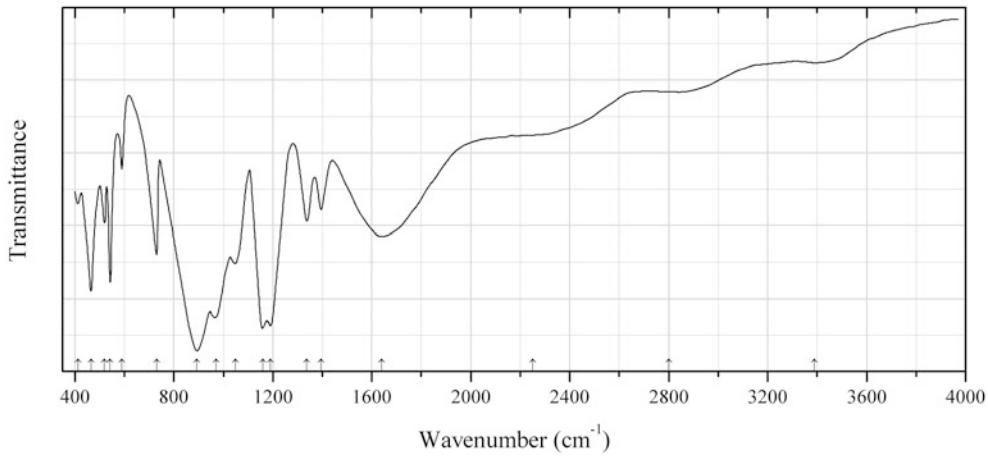

Fig. 2.945 IR spectrum of sodium dihydrodiphosphate drawn using data from Melnikova et al. (1985)

P561 Sodium dihydrodiphosphate $Na_2(H_2P_2O_7)$ (Fig. 2.945)
Locality: Synthetic.
Description: Orthorhombic, a = 12.35, b = 27.49, c = 6.86 Å. D = 2.31 g/cm^3.
Kind of sample preparation and/or method of registration of the spectrum: KBr disc. Absorption.
Source: Melnikova et al. (1985).
Wavenumbers (cm^{-1}): 3390 (broad), 2800 (broad), 2250sh, 1640 (broad), 1395, 1338, 1190s, 1160s, 1048, 970s, 892s, 730, 590, 543, 520, 465, 412w.
Note: The wavenumbers were partly determined by us based on spectral curve analysis of the published spectrum. The band positions denoted by Melnikova et al. (1985) as 2900 and 2350 cm^{-1} were determined by us at 2800 and 2250 cm^{-1}, respectively, based on spectral curve analysis of the published spectrum.

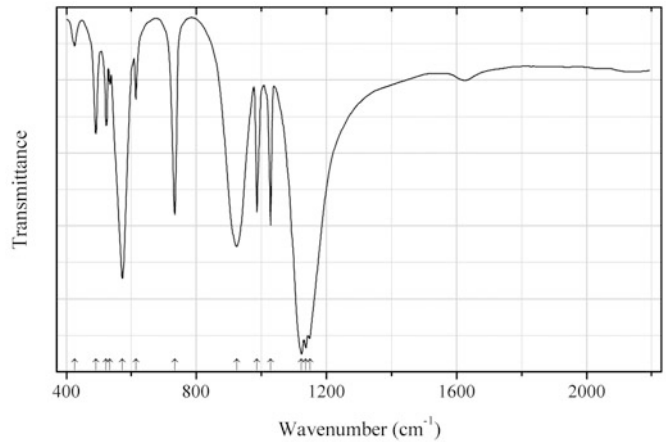

Fig. 2.946 IR spectrum of sodium diphosphate drawn using data from Melnikova et al. (1985)

P562 Sodium diphosphate $Na_4(P_2O_7)$ (Fig. 2.946)
Locality: Synthetic.
Description: Orthorhombic, space group $P2_12_12_1$, a = 9.367, b = 5.390, c = 13.480 Å, Z = 4. D_{meas} = 2.53 g/cm^3, D_{calc} = 2.595 g/cm^3.
Kind of sample preparation and/or method of registration of the spectrum: KBr disc. Absorption.
Source: Melnikova et al. (1985).
Wavenumbers (cm^{-1}): 1149s, 1137s, 1123s, 1028, 986, 924s, 733, 614w, 572s, 533w, 523, 491, 425w.

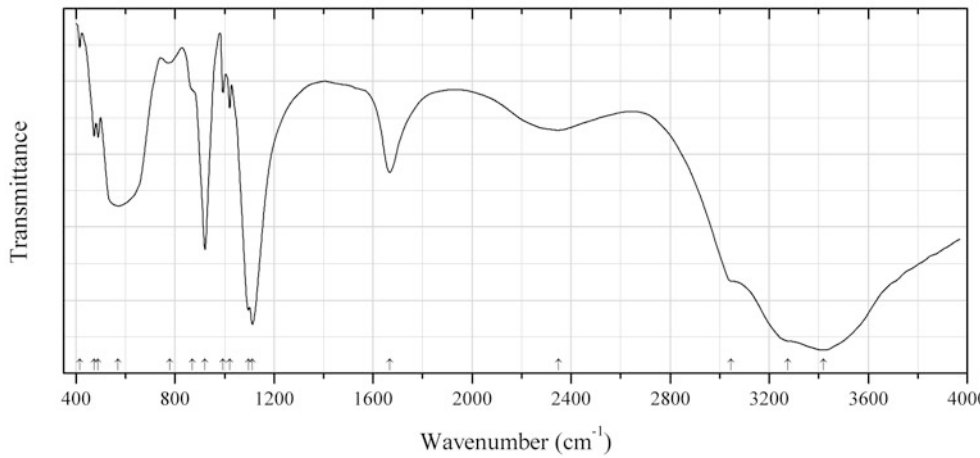

Fig. 2.947 IR spectrum of sodium diphosphate decahydrate drawn using data from Melnikova et al. (1985)

P563 Sodium diphosphate decahydrate $Na_4(P_2O_7)\cdot 10H_2O$ (Fig. 2.947)
Locality: Synthetic.
Description: Monoclinic, space group $I2/c$, a = 17.93, b = 6.96, c = 14.85 Å, β = 118.5°, Z = 4. D_{meas} = 1.817 g/cm^3, D_{calc} = 1.820 g/cm^3.

Kind of sample preparation and/or method of registration of the spectrum: KBr disc. Absorption.
Source: Melnikova et al. (1985).
Wavenumbers (cm^{-1}): 3420s, 3275sh, 3045sh, 2350, 1667, 1113s, 1096s, 1021w, 994w, 920, 870sh, 780w, 570, 490, 473, 415w.
Note: The wavenumbers were partly determined by us based on spectral curve analysis of the published spectrum.

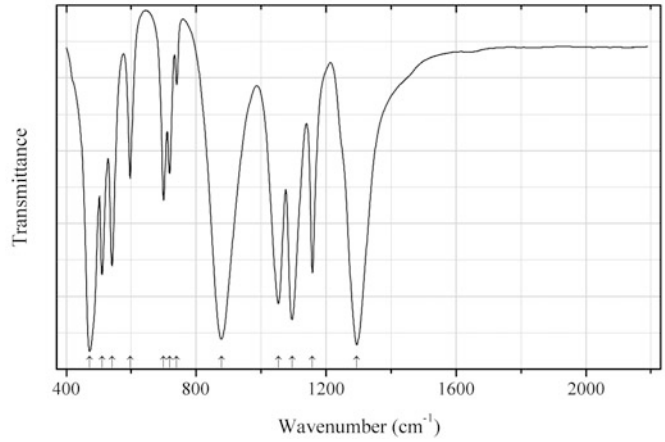

Fig. 2.948 IR spectrum of sodium polyphosphate drawn using data from Melnikova et al. (1985)

P564 Sodium polyphosphate $Na(PO_3)$ (Fig. 2.948)
Locality: Synthetic.
Description: Monoclinic, space group $P2_1/a$, a = 15.30, b = 6.96, c = 7.05 Å, β = 93.3°, Z = 12.
Kind of sample preparation and/or method of registration of the spectrum: KBr disc. Absorption.
Source: Melnikova et al. (1985).
Wavenumbers (cm^{-1}): 1295s, 1158s, 1095s, 1053s, 878s, 740w, 718, 700, 597, 541, 510, 472s.

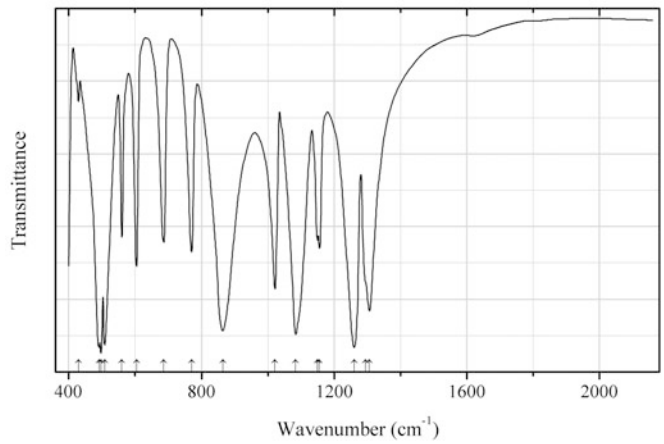

Fig. 2.949 IR spectrum of barium polyphosphate drawn using data from Melnikova et al. (1985)

P565 Barium polyphosphate $Ba(PO_3)_2$ (Fig. 2.949)
Locality: Synthetic.
Description: Orthorhombic, space group $P2_12_12_1$, a = 8.360, b = 13.44, c = 4.510 Å, Z = 4. D_{calc} = 3.87 g/cm^3.
Kind of sample preparation and/or method of registration of the spectrum: KBr disc. Absorption.
Source: Melnikova et al. (1985).
Wavenumbers (cm^{-1}): 1306s, 1294sh, 1260s, 1156, 1150, 1084s, 1022, 864s, 770, 686, 604, 560, 508s, 497s, 491s, 429w.

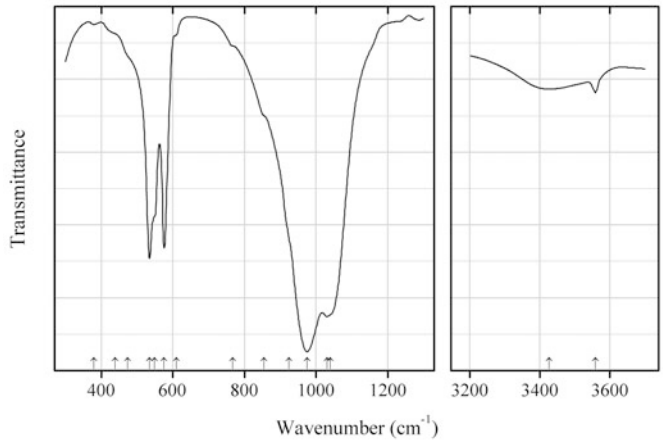

Fig. 2.950 IR spectrum of hydroxylpyromorphite drawn using data from González-Díaz and Santos (1978)

P566 Hydroxylpyromorphite $Pb_5(PO_4)_3(OH)$ (Fig. 2.950)
Locality: Synthetic.
Kind of sample preparation and/or method of registration of the spectrum: KBr disc. Transmission.
Source: González-Díaz and Santos (1978).
Wavenumbers (cm^{-1}): 3559, 3427, 1040sh, 1030s, 975s, 925sh, 855sh, 768sh, 610sh, 576, 550sh, 535, 474sh, 440sh, 380w.
Note: The wavenumbers were partly determined by us based on spectral curve analysis of the published spectrum. The band position denoted by González-Díaz and Santos (1978) as 985 cm^{-1} was determined by us at 975 cm^{-1}.

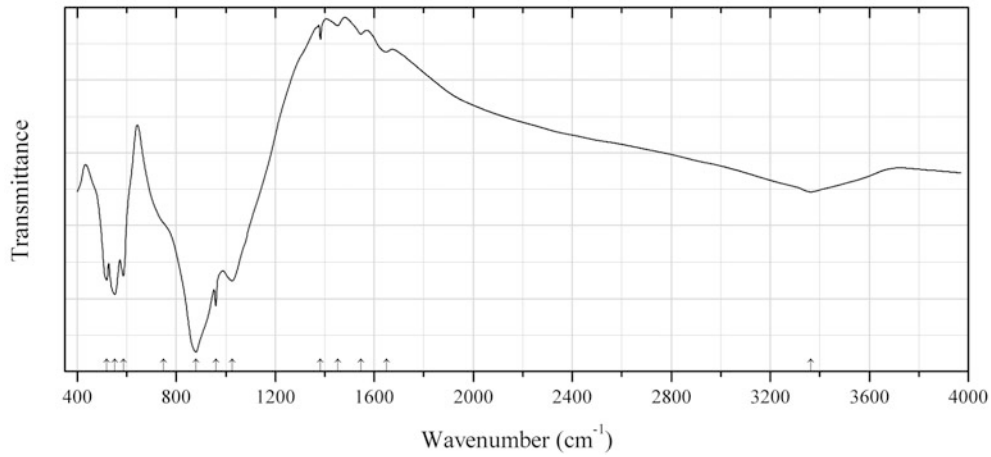

Fig. 2.951 IR spectrum of lead iron(III) phosphate hydrate drawn using data from Mills et al. (2010)

P567 Lead iron(III) phosphate hydrate $Pb_3Fe^{3+}{}_2(PO_4)_4 \cdot H_2O$ (Fig. 2.951)
Locality: Synthetic.
Description: Colourless prismatic crystals. Synthesized hydrothermally. The crystal structure is solved. Tetragonal, space group $P4_12_12$, a = 9.0440(10), c = 16.766(3) Å, V = 1371.4(3) Å^3, Z = 4. The empirical formula is $Pb_{2.88}Fe^{3+}{}_{1.90}P_{4.11}H_{1.98}O_{17}$.
Kind of sample preparation and/or method of registration of the spectrum: KBr disc. Transmission.
Source: Mills et al. (2010).
Wavenumbers (cm^{-1}): 3365, 1649, 1546w, 1452w, 1383w, 1026, 960s, 880s, 748sh, 587, 552, 519.
Note: The wavenumbers were partly determined by us based on spectral curve analysis of the published spectrum.

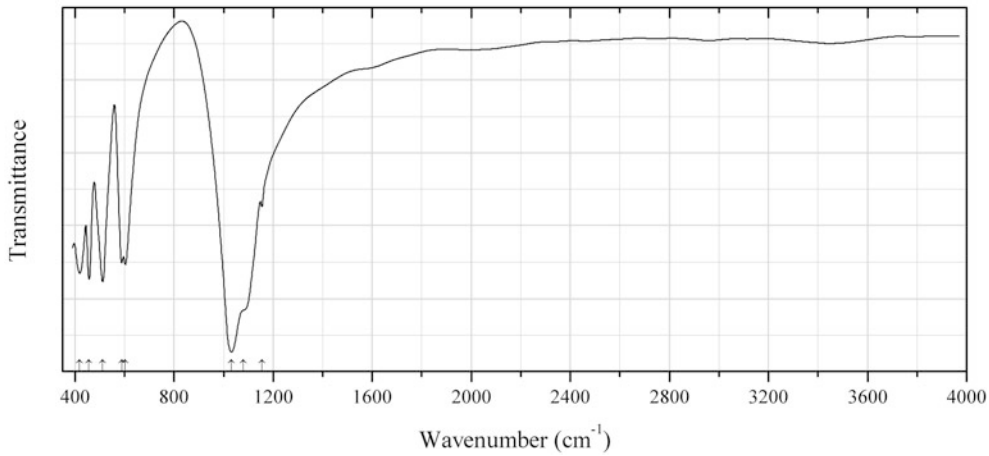

Fig. 2.952 IR spectrum of lithiophosphate dimorph drawn using data from Pechkovskii et al. (1981)

P568 Lithiophosphate dimorph γ-$Li_3(PO_4)$ (Fig. 2.952)
Locality: Synthetic.
Description: Orthorhombic, space group *Pmnb*, a = 6.12, b = 10.53, c = 4.93 Å, Z = 2. D_{meas} = 2.45 g/cm^3, D_{calc} = 2.42 g/cm^3.

Kind of sample preparation and/or method of registration of the spectrum: KBr disc. Absorption.
Source: Pechkovskii et al. (1981).
Wavenumbers (cm^{-1}): 1155w, 1080sh, 1032s, 603, 589, 512, 457, 419, 380, 355sh, 305, 230, 210sh, 181w.

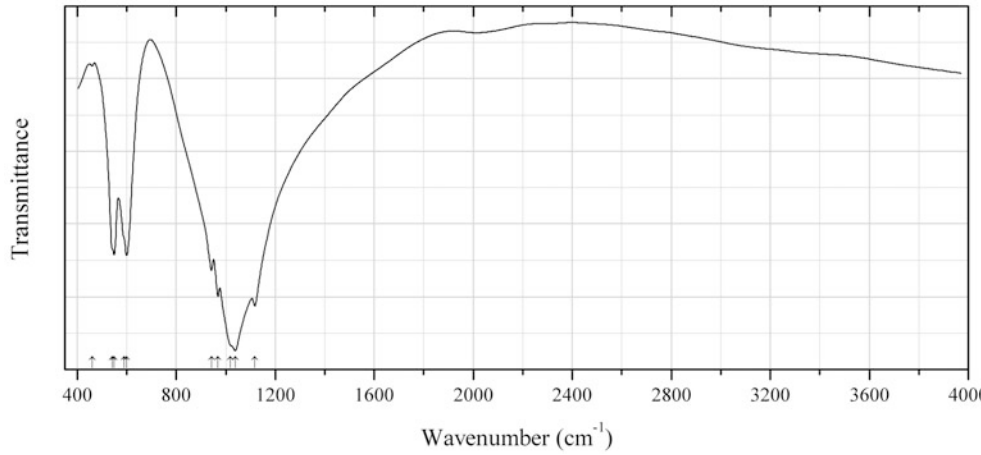

Fig. 2.953 IR spectrum of whitlockite Ca-rich analogue drawn using data from Pechkovskii et al. (1981)

P569 Whitlockite Ca-richanalogue β-$Ca_3(PO_4)_2$ (Fig. 2.953)
Locality: Synthetic.
Description: Trigonal polymorph, a = 10.439, c = 37.375 Å. Related to merrillite and whitlockite.
Kind of sample preparation and/or method of registration of the spectrum: KBr disc. Absorption.
Source: Pechkovskii et al. (1981).
Wavenumbers (cm^{-1}): 1118s, 1038s, 1020sh, 969s, 942, 600, 590sh, 549, 542sh, 460w, 308, 280, 240.
Note: For IR spectrum of β-$Ca_3(PO_4)$ see also Chabchoub and Dogguy (1993), Jillavenkatesa and Condrate (1998).

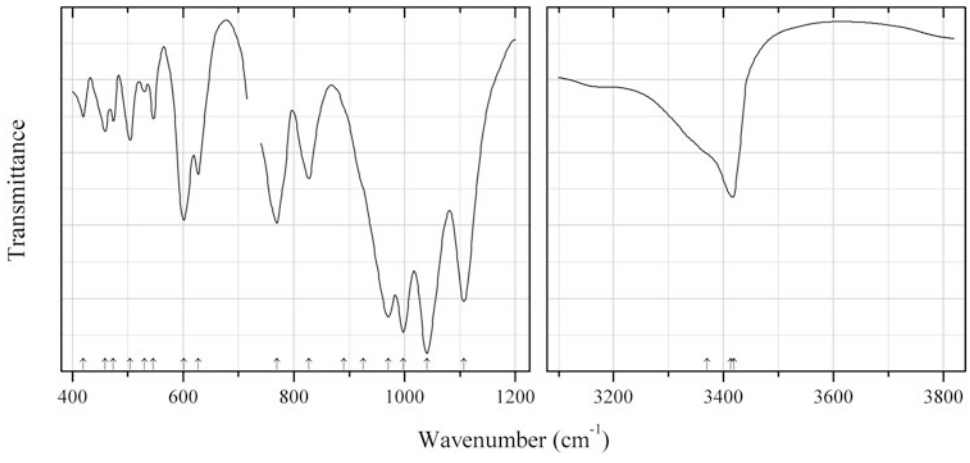

Fig. 2.954 IR spectrum of ludjibaite drawn using data from Braithwaite and Ryback (1994)

P570 Ludjibaite $Cu_5(PO_4)_2(OH)_4$ (Fig. 2.954)
Locality: Specimen No. 3816 from the Manchester Natural History Museum.
Kind of sample preparation and/or method of registration of the spectrum: Nujol mull, transmission.
Source: Braithwaite and Ryback (1994).
Wavenumbers (cm^{-1}): 3419s, 3413s, 3370sh, 1107s, 1040s, 997s, 970s, 925sh, 890sh, 827, 769s, 627, 601s, 546, 530w, 504, 474w, 459w, 419w.

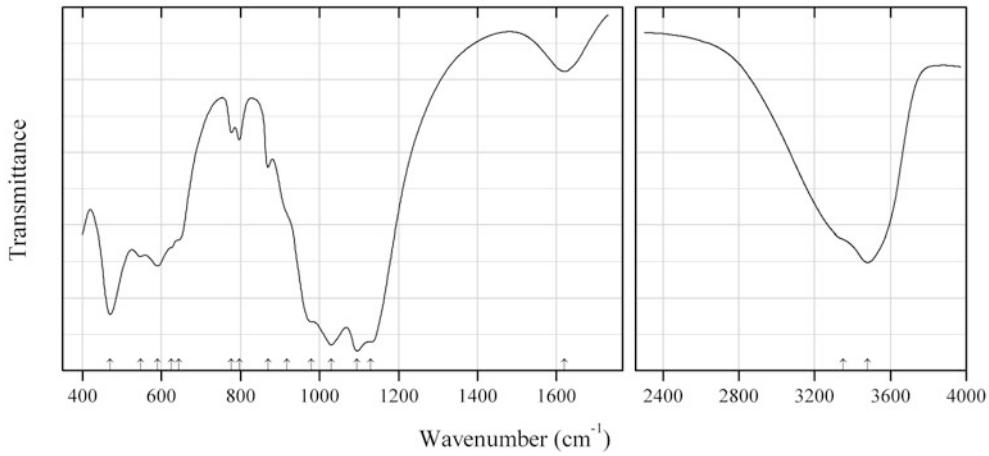

Fig. 2.955 IR spectrum of lun'okite drawn using data from Voloshin et al. (1992a)

P571 Lun'okite $MgMn^{2+}Al(PO_4)_2(OH)\cdot 4H_2O$ (Fig. 2.955)
Locality: Vasin-Myl'k Mt., Voron'i Tundras, Kola peninsula, Murmansk region, Russia (type locality).
Description: Yellowish crystals from the association with manganosegelerite, mitridatite, eosphorite, kingsmountite, gordonite, etc. Orthorhombic, space group *Pbca*, $a = 14.95$, $b = 18.71$, $c = 6.96$ Å, $V = 1946.8$ $Å^3$, $Z = 8$. $D_{meas} = 2.66$ g/cm^3.
Kind of sample preparation and/or method of registration of the spectrum: KBr disc. Absorption.
Source: Voloshin et al. (1992a).
Wavenumbers (cm^{-1}): 3480, 3350sh, 1620w, 1130sh, 1095s, 1030s, 980sh, 918sh, 870, 797w, 777w, 644sh, 625sh, 590, 547, 470s.
Note: The wavenumbers were partly determined by us based on spectral curve analysis of the published spectrum. The bands at 1095, 797, and 777 cm^{-1} may correspond to the admixture of quartz.

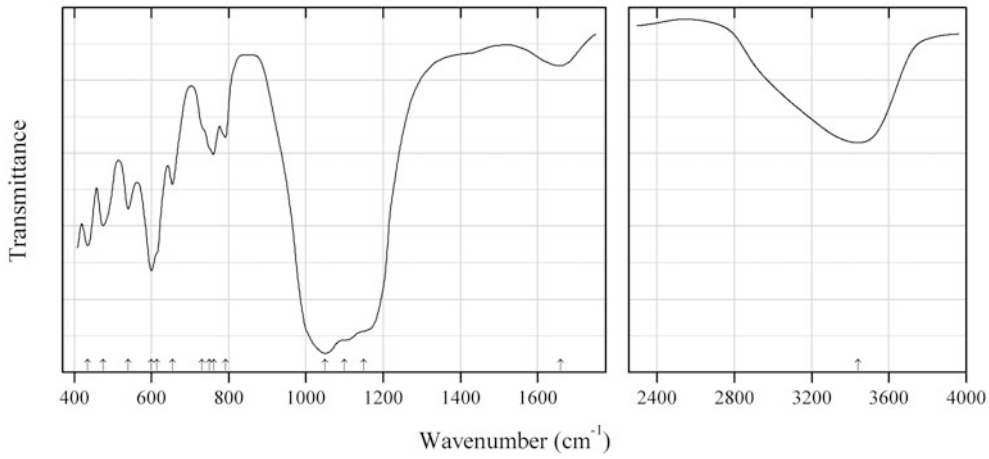

Fig. 2.956 IR spectrum of manganosegelerite drawn using data from Voloshin et al. (1992a)

P573 Manganosegelerite $Mn^{2+}{}_2Fe^{3+}(PO_4)_2(OH)\cdot 4H_2O$ (Fig. 2.956)
Locality: Vasin-Myl'k Mt., Voron'i Tundras, Kola peninsula, Murmansk region, Russia (type locality).
Description: Yellow fine-grained aggregates from the association with eosphorite, laueite, gordonite, kingsmountite, fairfieldite, lun'okite, and mitridatite. Holotype sample. Orthorhombic, space group *Pbca*, a = 14.89, b = 18.79, c = 7.408 Å, V = 2072.6 Å^3, Z = 8. D_{meas} = 2.76(3) g/cm^3, D_{calc} = 2.74 g/cm^3. Optically biaxial (+), α = 1.657(1), β = 1.568(1), γ = 1.691(2), 2 V = 75°. The empirical formula is $(Mn_{0.99}Ca_{0.39}Fe^{2+}{}_{0.33}Mg_{0.30})(Fe^{3+}{}_{0.88}Al_{0.12})(PO_4)_{2.00}(OH)_{1.02}\cdot 4.04H_2O$. The strongest lines of the powder X-ray diffraction pattern [d, Å (I, %) (hkl)] are: 9.39 (100) (020), 4.70 (50) (040), 2.97 (40) (302), 2.86 (90) (142), 2.60 (40) (412, 152), 2.019 (40) (622), 1.966 (50) (182), 1.880 (50) (661, 0.10.1).
Kind of sample preparation and/or method of registration of the spectrum: KBr disc. Transmission.
Source: Voloshin et al. (1992a).
Wavenumbers (cm^{-1}): 3440, 1660w, 1150sh, 1100sh, 1050s, 792, 761, 750sh, 730sh, 655, 615sh, 600s, 540, 475, 435.

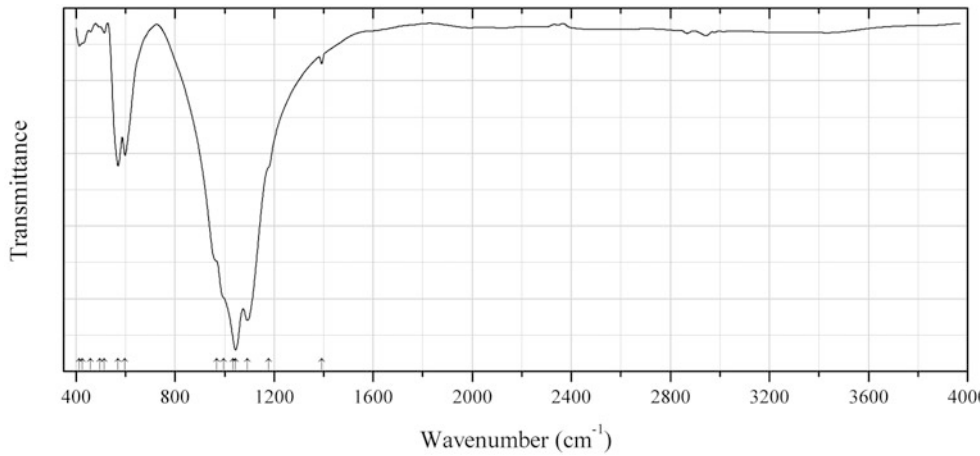

Fig. 2.957 IR spectrum of manitobaite drawn using data from Ercit et al. (2010)

P574 Manitobaite $Na_{16}Mn^{2+}{}_{25}Al_8(PO_4)_{30}$ (Fig. 2.957)
Locality: Pegmatite #22, Cross Lake, Manitoba, Canada (type locality).
Description: Crystals from the association with fluorapatite, chlorapatite, bobfergusonite, eosphorite, dickinsonite, fillowite, triploidite, goyazite, perloffite, beusite, triplite, etc. Holotype sample. Monoclinic, space group *Pc*, a = 13.4516(15), b = 12.5153(16), c = 26.661(3) Å, β = 101.579(10)°, V = 4397.1(6) Å^3, Z = 2. D_{meas} = 3.621(6) g/cm^3, D_{calc} = 3.628 g/cm^3. Optically biaxial (−), α = 1.682 (1), β = 1.681(1), γ = 1.697(1), 2 V = 78.1(6)°. The empirical formula is $Na_{15.55}Ca_{1.47}Mg_{0.88}Fe^{2+}{}_{4.19}Mn^{2+}{}_{18.78}Zn_{0.32}Al_{6.54}Fe^{3+}{}_{1.05}P_{30.08}O_{120}$. The strongest lines of the powder X-ray diffraction pattern [*d*, Å (*I*, %) (*hkl*)] are: 2.715 (100) (242), 2.730 (50) (404), 3.494 (47) (313), 3.078 (27) (−317), 2.518 (22) (−515), 2.881 (21) (−119), 6.260 (20) (020).
Kind of sample preparation and/or method of registration of the spectrum: Not indicated.
Source: Ercit et al. (2010).
Wavenumbers (cm^{-1}): 1392w, 1177sh, 1092s, 1044s, 997sh, 968sh, 1035s, 598s, 570s, 515w, 496sh, 459w, 426sh, 413w.
Note: The wavenumbers were partly determined by us based on spectral curve analysis of the published spectrum. The band position denoted by Ercit et al. (2010) as ∼1035 cm^{-1} was determined by us at 1044 cm^{-1}. The band at 1392 cm^{-1} may be due to NO_3^- impurity.

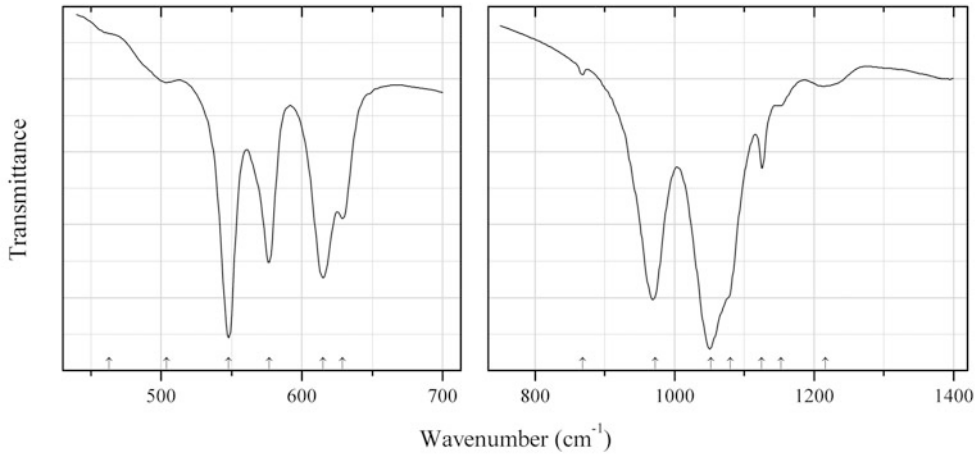

Fig. 2.958 IR spectrum of marićite drawn using data from Burba (2006)

P575 Marićite $NaFe^{2+}(PO_4)$ (Fig. 2.958)
Locality: Synthetic.
Description: Confirmed by the powder X-ray diffraction pattern and electron microprobe analysis.
Kind of sample preparation and/or method of registration of the spectrum: KBr or CsI disc. Absorption.
Source: Burba (2006).
Wavenumbers (cm^{-1}): 1216w, 1153w, 1125s, 1080sh, 1052s, 972s, 868w, 629w, 615, 577, 548s, 504w, 463sh.
Note: The wavenumbers were partly determined by us based on spectral curve analysis of the published spectrum.

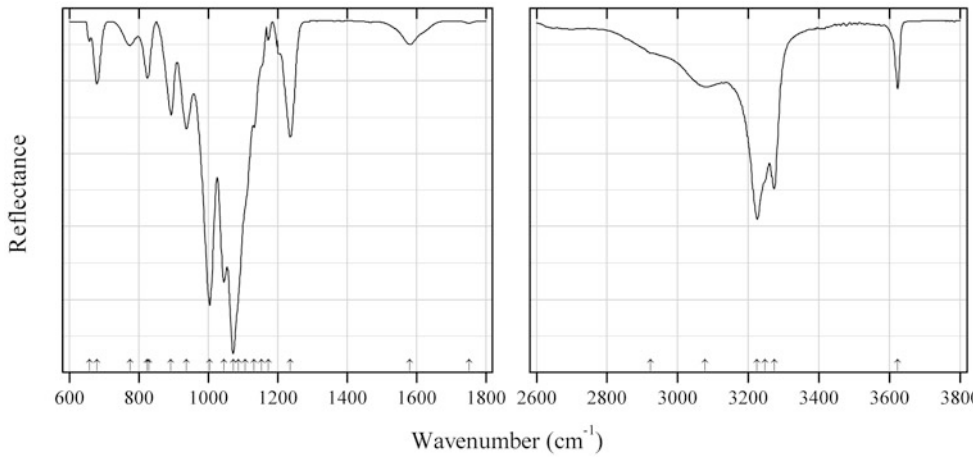

Fig. 2.959 IR spectrum of matioliite drawn using data from Scholz et al. (2013)

P576 Matioliite $NaMgAl_5(PO_4)_4(OH)_6 \cdot 2H_2O$ (Fig. 2.959)
Locality: Gentil pegmatite, Mendes Pimentel, Minas Gerais, Brazil (type locality).
Description: Blue crystals from the association with brazilianite and crandallite. Monoclinic, space group *C*2/*c*, $a = 25.075(1)$, $b = 5.0470(3)$, $c = 13.4370(7)$ Å, $\beta = 110.97(3)°$, $V = 1587.9(4)$ Å^3, $Z = 4$. Confirmed by chemical analysis.
Kind of sample preparation and/or method of registration of the spectrum: Attenuated total reflection of powdered mineral.
Source: Scholz et al. (2013).
Wavenumbers (cm^{-1}): 3624, 3274, 3248sh, 3225s, 3077, 2924, 1751w, 1581, 1236, 1173w, 1153sh, 1132, 1107sh, 1086sh, 1072s, 1045s, 1004s, 937, 892, 828sh, 824, 774w, 679, 657w.
Note: In the cited paper, wavenumbers are indicated for the maxima of individual bands obtained as a result of the spectral curve analysis. The wavenumbers were determined by us based on spectral curve analysis of the published spectrum.

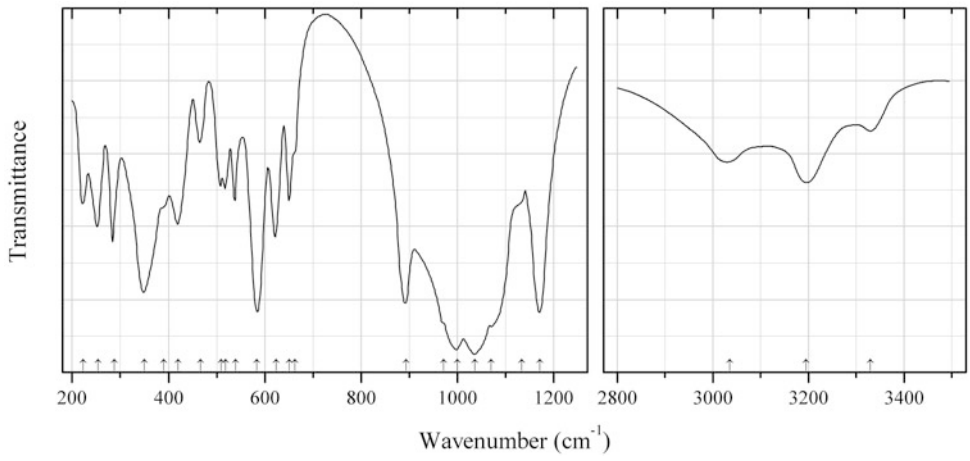

Fig. 2.960 IR spectrum of mélonjosephite drawn using data from Fransolet (1973)

P577 Mélonjosephite $CaFe^{2+}Fe^{3+}(PO_4)_2(OH)$ (Fig. 2.960)
Locality: Asgarf-South pegmatite, Tazenakht, Ouarzazate province, Souss-Massa-Draâ region, Morocco (type locality).
Description: Dark green fibrous aggregates from the association with matulaite and variscite. Holotype sample. Orthorhombic, a = 9.548, b = 10.847, c = 6.380 Å, Z = 4. D_{meas} = 3.65 g/cm^3, D_{calc} = 3.61 g/cm^3. Optically biaxial (−), α = 1.720(5), β = 1.77(1), γ = 1.80(1), 2 V = 80°–85°. The empirical formula is (Z = 1): $(Ca_{3.83}Na_{0.22}Li_{0.06})(Fe^{2+}_{3.47}Mg_{0.43}Mn^{2+}_{0.09})(Fe^{3+}_{3.91}Al_{0.06})(PO_4)_{8.04}(OH)_{3.96}$. The strongest lines of the powder X-ray diffraction pattern [d, Å (I, %) (hkl)] are: 5.42 (90) (020), 3.049 (100) (310), 2.912 (40) (112), 2.710 (90) (122), 2.624 (60) (231).
Kind of sample preparation and/or method of registration of the spectrum: KI disc. Transmission.
Source: Fransolet (1973).
Wavenumbers (cm^{-1}): 3330, 3195, 3035, 1172s, 1134sh, 1070sh, 1037s, 1000s, 971s, 894s, 663sh, 651, 624, 584s, 539, 519, 509, 467, 420, 390sh, 350s, 288, 254, 223.

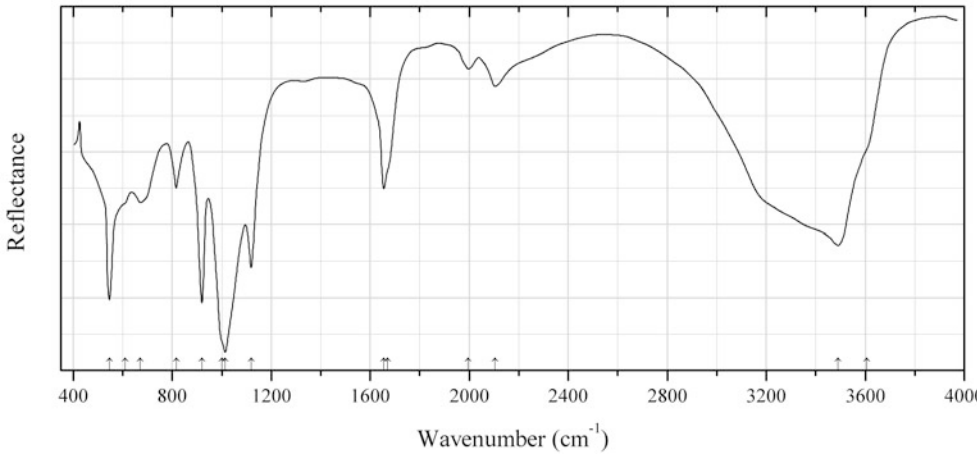

Fig. 2.961 IR spectrum of meta-ankoleite drawn using data from Van Haverbeke et al. (1996)

P578 Meta-ankoleite $K(UO_2)(PO_4)\cdot 3H_2O$ (Fig. 2.961)
Locality: Synthetic.
Description: Obtained by refluxing synthetic chernikovite several times in 1 M KCl solution. In order to obtain a phase with a higher degree of crystallinity, the product suspension in water was heated at 180 °C for 7 days. Confirmed by means of chemical analysis and X-ray diffraction.
Kind of sample preparation and/or method of registration of the spectrum: Diffuse reflection.
Source: Van Haverbeke et al. (1996).
Wavenumbers (cm^{-1}): 3606sh, 3491s, 2104w, 1996w, 1670sh, 1655, 1120s, 1014s, 1002sh, 920s, 816, 671, 610sh, 546s.
Note: The wavenumbers were partly determined by us based on spectral curve analysis of the published spectrum.

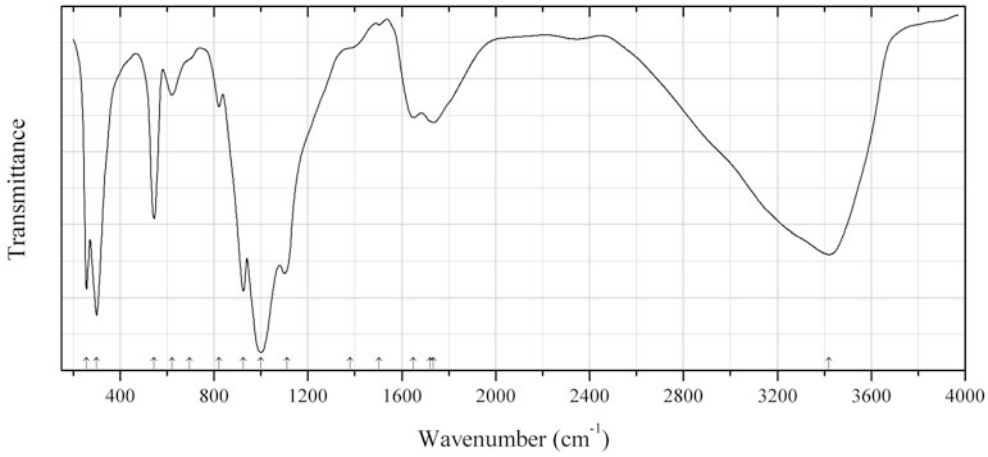

Fig. 2.962 IR spectrum of "meta-autunite-I" drawn using data from Čejka et al. (1985)

P579 "Meta-autunite-I" $Ca(UO_2)_2(PO_4)_2 \cdot 6H_2O$ (Fig. 2.962)
Locality: Synthetic.
Description: Obtained by addition of H_3PO_4 to a solution containing calcium and uranyl nitrates. Confirmed by powder X-ray diffraction data and TG analysis.
Kind of sample preparation and/or method of registration of the spectrum: KBr disc. Transmission.
Source: Čejka et al. (1985).
Wavenumbers (cm^{-1}): 3420s, 1735, 1720sh, 1650, 1502w, 1380sh, 1110s, 1000s, 925s, 821w, 696sh, 620w, 545, 300s, 257s.
Note: The wavenumbers were partly determined by us based on spectral curve analysis of the published spectrum.

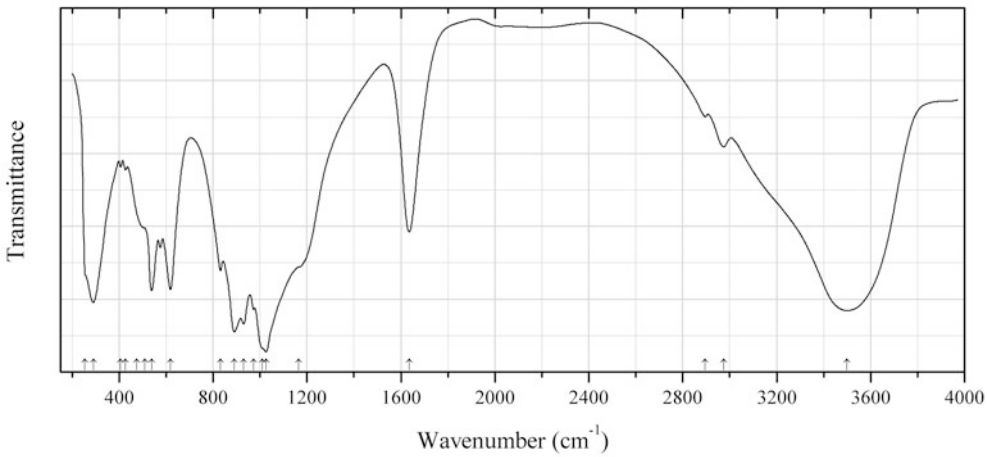

Fig. 2.963 IR spectrum of "meta-autunite-II" drawn using data from Čejka et al. (1985)

P580 "Meta-autunite-II" $Ca(UO_2)_2(PO_4)_2 \cdot 2H_2O$ (Fig. 2.963)
Locality: Synthetic.
Description: Obtained from synthetic meta-autunite by heating at 110 °C for 2 h.

Kind of sample preparation and/or method of registration of the spectrum: KBr disc. Transmission.
Source: Čejka et al. (1985).
Wavenumbers (cm^{-1}): 3500s, 2975w, 2896, 1635, 1165sh, 1025s, 1010sh, 972w, 930s, 890s, 831, 618s, 538s, 510sh, 475sh, 426w, 406w, 290s, 255sh.
Note: The wavenumbers were partly determined by us based on spectral curve analysis of the published spectrum. The band positions denoted by Čejka Jr et al. (1985) as 1125 and 475 cm^{-1} were determined by us at 1165 and 510 cm^{-1}, respectively, based on spectral curve analysis of the published spectrum.

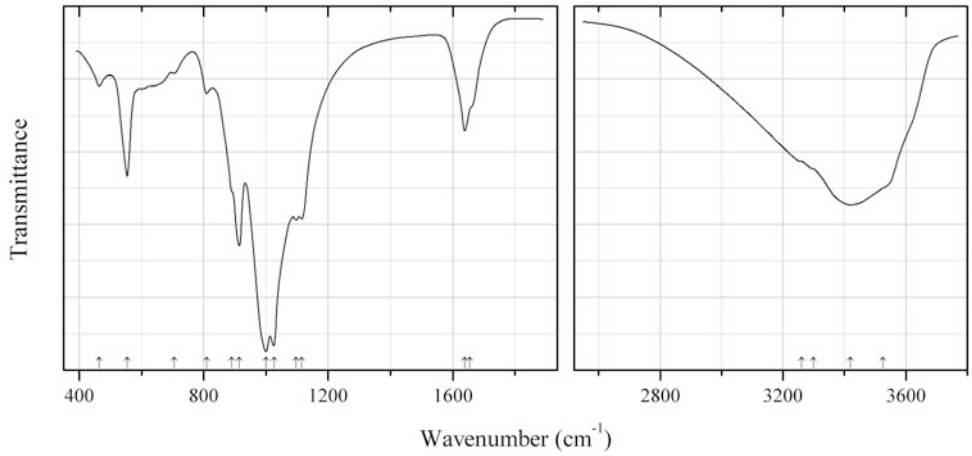

Fig. 2.964 IR spectrum of metauranocircite-I drawn using data from Barinova et al. (2003)

P581 Metauranocircite-I $Ba(UO_2)_2(PO_4)_2 \cdot 8H_2O$ (Fig. 2.964)
Locality: Bota-Burum U deposit, Alakol lake, Almaty region, Kazakhstan.
Description: Pale green platy crystals from the association with sodium uranospinite, nasturan, arsenopyrite, pyrite, and galena. Tetragonal (?). The empirical formula is $H_{0.08}(Ba_{0.83}K_{0.08}Cu_{0.05})(UO_2)_{2.00}[(PO_4)_{1.99}(AsO_4)_{0.01} \cdot 8H_2O$.
Kind of sample preparation and/or method of registration of the spectrum: KBr disc. Absorption.
Source: Barinova et al. (2003).
Wavenumbers (cm^{-1}): 3525sh, 3420s, 3300sh, 3260sh, 1655sh, 1638, 1115s, 1097s, 1026s, 1000s, 915s, 890sh, 809w, 705w, 554, 464w.
Note: The wavenumbers were partly determined by us based on spectral curve analysis of the published spectrum.

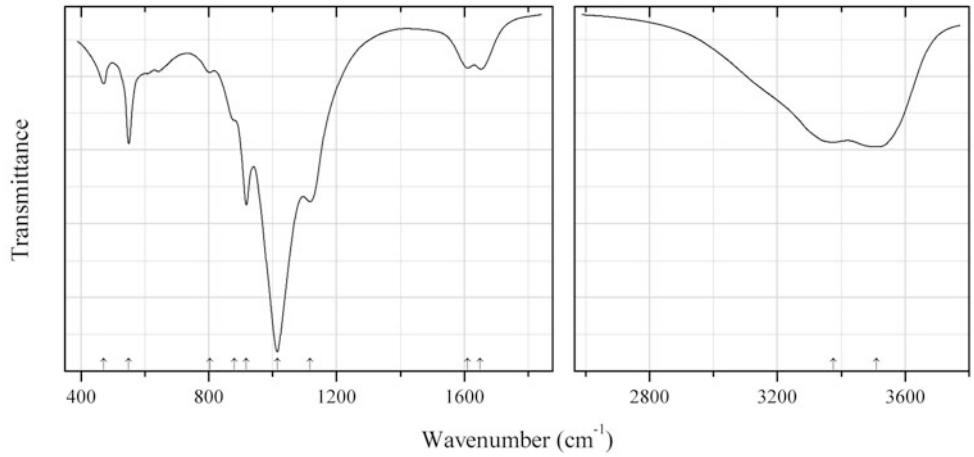

Fig. 2.965 IR spectrum of metauranocircite-II drawn using data from Barinova et al. (2003)

P582 Metauranocircite-II $Ba(UO_2)_2(PO_4)_2 \cdot 6H_2O$ (Fig. 2.965)
Locality: Bota-Burum U deposit, Alakol lake, Almaty region, Kazakhstan.
Description: Pale green platy crystals from the association with sodium uranospinite, nasturan, arsenopyrite, pyrite, and galena. A partially dehydrated sample. The crystal structure is solved. Monoclinic (pseudo-orthorhombic), space group $P2_1$, a = 6.965(3), b = 6.964(2), c = 17.65(1) Å, $\gamma \approx 90°$, V = 856.1 Å^3, Z = 2. D_{calc} = 3.78 g/cm^3. The empirical formula is $H_{0.08}(Ba_{0.83}K_{0.08}Cu_{0.05})(UO_2)_{2.00}[(PO_4)_{1.99}(AsO_4)_{0.01} \cdot 6H_2O$.
Kind of sample preparation and/or method of registration of the spectrum: KBr disc. Absorption.
Source: Barinova et al. (2003).
Wavenumbers (cm^{-1}): 3510, 3375, 1650w, 1610w, 1117s, 1015s, 918s, 880sh, 804w, 550, 472.
Note: The wavenumbers were partly determined by us based on spectral curve analysis of the published spectrum.

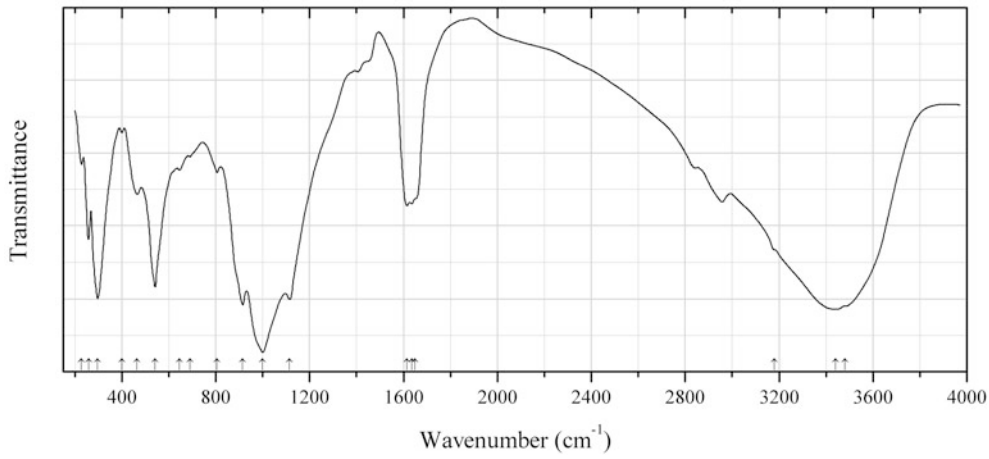

Fig. 2.966 IR spectrum of metauranocircite-I drawn using data from Čejka et al. (1984)

P583 Metauranocircite-I $Ba(UO_2)_2(PO_4)_2 \cdot 8H_2O$ (Fig. 2.966)
Locality: Bergen U deposit, Zobes-Bergen district, Vogtland, Saxony, Germany.
Description: Specimen NM 19156 from the National Museum in Prague. Space group $P2_1/n$ (?).
Kind of sample preparation and/or method of registration of the spectrum: KBr disc. Transmission.
Source: Čejka et al. (1984).
Wavenumbers (cm^{-1}): 3480sh, 3440s, 3180sh, 1650sh, 1635, 1615, 1115s, 1000s, 915s, 805w, 690w, 645w, 542s, 465w, 400w, 297s, 258, 228.

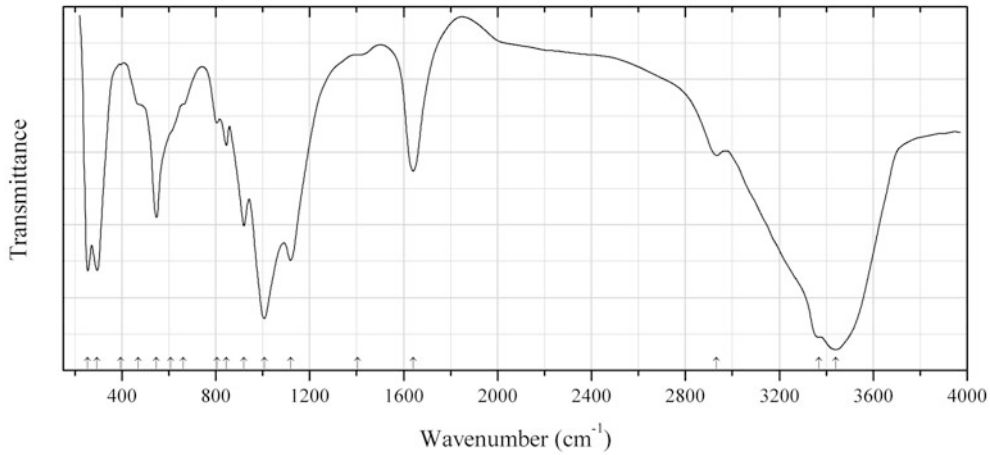

Fig. 2.967 IR spectrum of metauranocircite-II drawn using data from Čejka et al. (1984)

P584 Metauranocircite-II $Ba(UO_2)_2(PO_4)_2 \cdot 6H_2O$ (Fig. 2.967)
Locality: Not indicated.
Description: Space group $P2_1$ (?).
Kind of sample preparation and/or method of registration of the spectrum: KBr disc. Transmission.
Source: Čejka et al. (1984).
Wavenumbers (cm^{-1}): 3440s, 3370sh, 2932, 1640, 1405sh, 1118s, 1006s, 920s, 845, 805w, 662sh, 609sh, 548, 470sh, 395w, 295s, 255s.
Note: The wavenumbers were partly determined by us based on spectral curve analysis of the published spectrum.

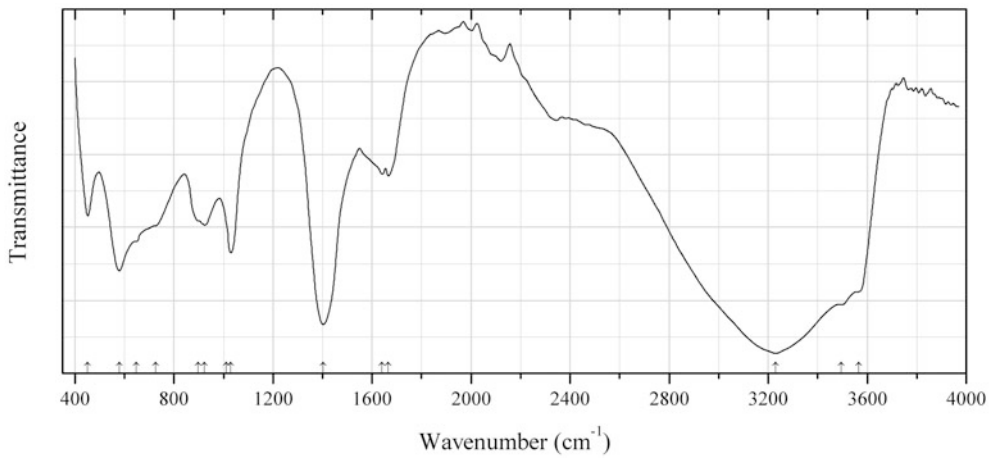

Fig. 2.968 IR spectrum of micheelsenite drawn using data from McDonald et al. (2001)

P585 Micheelsenite $(Ca,Y)_3Al(HPO_4,CO_3)(CO_3)(OH)_6 \cdot 12H_2O$ (Fig. 2.968)
Locality: Poudrette (Demix) quarry, Mont Saint-Hilaire, Rouville RCM (Rouville Co.), Montérégie, Québec, Canada (type locality).
Description: White fibrous aggregates from the association with aegirine, carbonates, and late-stage alkaline silicates. Holotype sample. Hexagonal, space group $P6_3$, a = 10.828(3), c = 10.516(4) Å, V = 1067.8(5) Å^3, Z = 2. D_{meas} = 2.15(1) g/cm^3, D_{calc} = 2.17(1) g/cm^3. Optically biaxial (−), ω = 1.532(1), ε = 1.503(1). The empirical formula is (electron microprobe): $(Ca_{1.96}Y_{1.06}Dy_{0.09}Er_{0.06}Gd_{0.03}Ho_{0.02})Al_{0.85}Si_{0.01}[(HPO_4)_{0.71}(CO_3)_{0.24}(SO_4)_{0.04}](CO_3)(OH)_6 \cdot 12H_2O$. The strongest lines of the powder X-ray diffraction pattern [*d*, Å (*I*, %) (*hkl*)] are: 9.38 (100) (100), 4.59 (70) (102), 3.77 (50) (112), 3.36 (55) (211), 2.491 (80) (213), 2.143 (65) (223, 402).
Kind of sample preparation and/or method of registration of the spectrum: An IR microscope and a diamond-anvil cell were used.
Source: McDonald et al. (2001).
Wavenumbers (cm^{-1}): 3565sh, 3495sh, 3230s, 1666, 1641, 1402s, 1030s, 1012sh, 924, 898sh, 725sh, 649sh, 579s, 452.
Note: The wavenumbers were partly determined by us based on spectral curve analysis of the published spectrum. In the IR spectrum there are no distinct signs of the presence of acid groups HPO_4^{2-}.

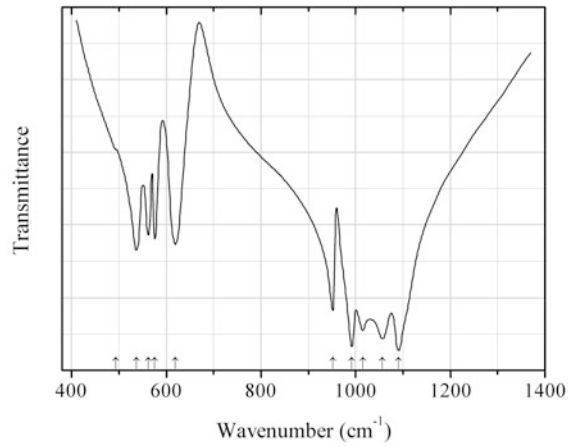

Fig. 2.969 IR spectrum of monazite-(La) drawn using data from Heuser et al. (2014)

P586 Monazite-(La) $La(PO_4)$ (Fig. 2.969)
Locality: Synthetic.
Description: Obtained in the reaction between aqueous solutions of lanthanum nitrate and phosphoric acid with subsequent calcination of the precipitate at 600 °C for 5 h. Confirmed by powder X-ray diffraction data.
Kind of sample preparation and/or method of registration of the spectrum: KBr disc. Transmission.
Source: Heuser et al. (2014).
Wavenumbers (cm^{-1}): 1091s, 1057s, 1015s, 992s, 952, 619, 576, 562, 537, 494sh.
Note: The wavenumbers were partly determined by us based on spectral curve analysis of the published spectrum.

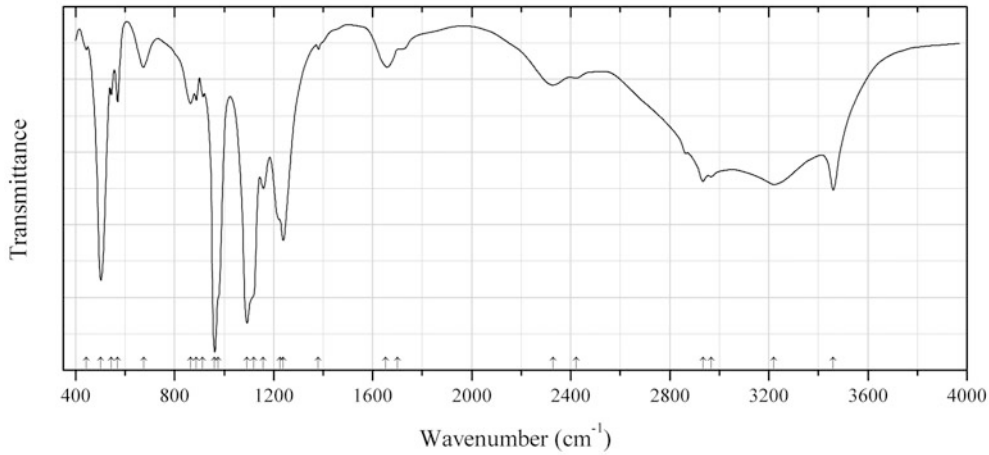

Fig. 2.970 IR spectrum of monocalcium phosphate monohydrate drawn using data from Xu et al. (1998)

P587 Monocalcium phosphate monohydrate $Ca(H_2PO_4)_2 \cdot H_2O$ (Fig. 2.970)
Locality: Synthetic.
Description: Commercial reactant obtained from Sigma (St. Louis MO).
Kind of sample preparation and/or method of registration of the spectrum: Absorption. Kind of sample preparation is not indicated.
Source: Xu et al. (1998).
Wavenumbers (cm^{-1}): 3461s, 3220s, 2967, 2934s, 2423w, 2328, 1700sh, 1653, 1381w, 1239s, 1225sh, 1158s, 1120sh, 1092s, 975sh, 962s, 914w, 888, 864, 675, 570, 545, 504–500s, 444w.
Note: The wavenumbers were partly determined by us based on spectral curve analysis of the published spectrum.

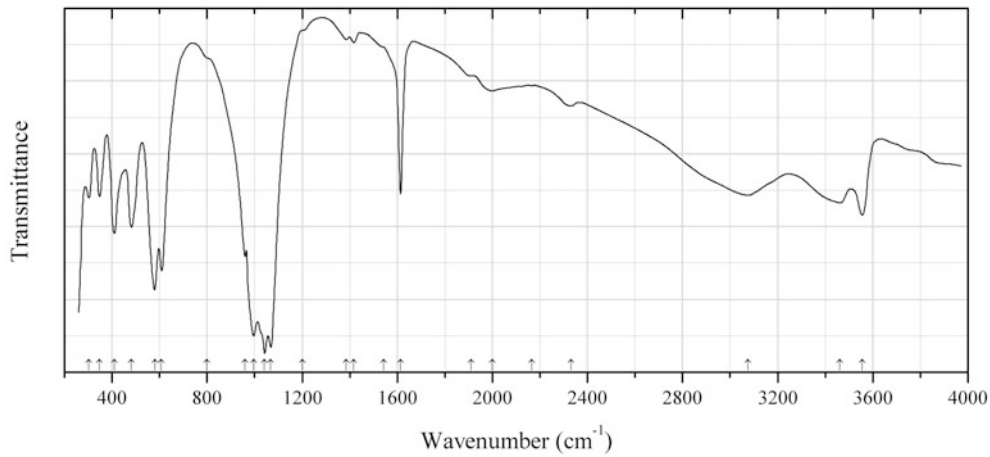

Fig. 2.971 IR spectrum of mrázekite drawn using data from Řídkošil et al. (1992)

P588 Mrázekite $Bi_2Cu_3(PO_4)_2O_2(OH)_2 \cdot 2H_2O$ (Fig. 2.971)
Locality: L'ubietová-Svätoduška, Banská Bystrica Co., Banská Bystrica region, Slovakia (type locality).

Description: Blue flattened acicular crystals from the association with libethenite, pseudomalachite, euchroite, malachite, azurite, brochantite, langite, cyanotrichite, etc. Holotype sample. Monoclinic, space group $C2/m$, $a = 12.359(6)$, $b = 6.331(4)$, $c = 9.060(4)$ Å, $\beta = 122.71(4)°$, $V = 596.55$ Å^3, $Z = 2$. D_{meas} = 4.90(2) g/cm^3, D_{calc} = 5.013 g/cm^3. The empirical formula is $Bi_{2.01}Cu_{2.96}P_{2.02}As_{0.01}O_{11.05}\cdot 1.95H_2O$. The strongest lines of the powder X-ray diffraction pattern [d, Å (I, %) (hkl)] are: 7.623 (78) (001), 5.200 (52) (200), 3.041 (100) (310), 3.014 (63) (203), 2.924 (83) (021).
Kind of sample preparation and/or method of registration of the spectrum: KBr disc. Transmission.
Source: Řídkošil et al. (1992).
Wavenumbers (cm^{-1}): 3556sh, 3460, 3076, 2330w, 2165w, 2000w, 1910sh, 1614s, 1543sh, 1418w, 1386w, 1200sh, 1068s, 1042s, 996s, 960, 800sh, 608, 580s, 482, 410, 348, 303w.

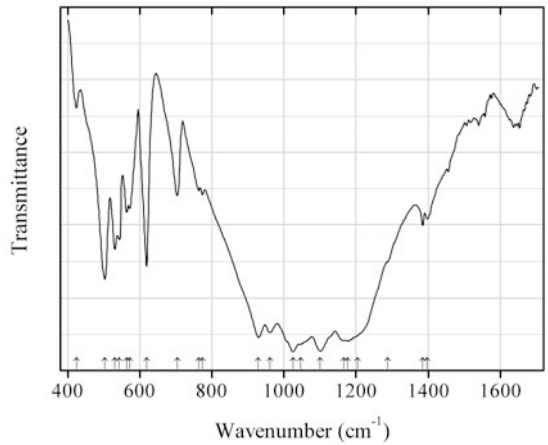

Fig. 2.972 IR spectrum of uranium orthophosphate-triphosphate drawn using data from Podor et al. (2003)

P589 Uranium orthophosphate-triphosphate $U_2(PO_4)(P_3O_{10})$ (Fig. 2.972)
Locality: Synthetic.
Description: Synthesized from UO_2 and H_3PO_4 under hydrothermal conditions, at 500 °C and 200 MPa. The crystal structure is solved. Orthorhombic, space group $Pn2_1a$, $a = 11.526(2)$, $b = 7.048(2)$, $c = 12.807(2)$ Å, $V = 1040.4(4)$ Å^3, $Z = 4$.
Kind of sample preparation and/or method of registration of the spectrum: KBr disc. Transmission.
Source: Podor et al. (2003).
Wavenumbers (cm^{-1}): 1398, 1385, 1288sh, 1205sh, 1177s, 1166sh, 1101s, 1046sh, 1025s, 961s, 929s, 774w, 763w, 704, 619, 572, 564, 544, 531, 503, 425w.
Note: The wavenumbers were partly determined by us based on spectral curve analysis of the published spectrum.

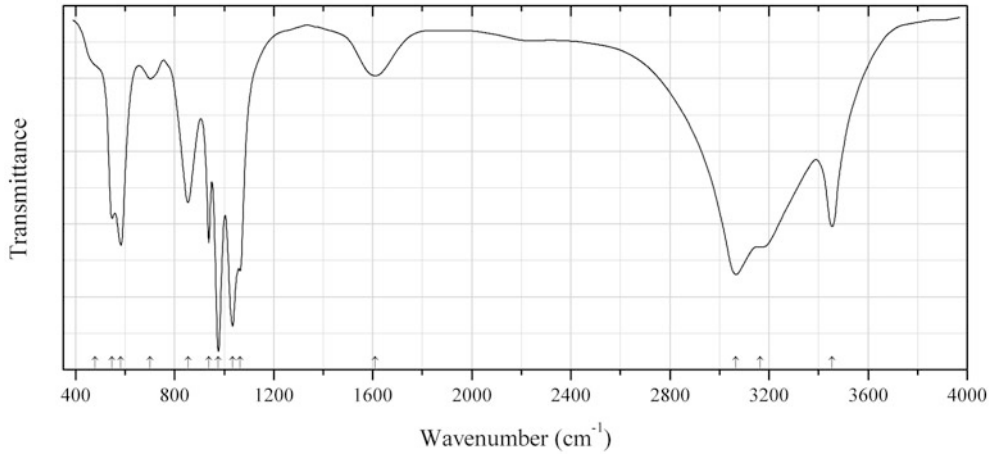

Fig. 2.973 IR spectrum of pakhomovskyite drawn using data from Kullyakool et al. (2013)

P592 Pakhomovskyite $Co_3(PO_4)_2 \cdot 8H_2O$ (Fig. 2.973)
Locality: Synthetic.
Description: Powder with the average particle size of 78.5 nm synthesized by the simple wet chemical reaction between 0.5 M $Na_3PO_4 \cdot 12H_2O$ and 0.5 M $CoSO_4 \cdot 7H_2O$ at Co/P ratio of 3:2 with subsequent heating for 24 h at 70 °C. Confirmed by powder X-ray diffraction data. Monoclinic, a = 9.916, b = 13.33, c = 3.679 Å, β = 102.30°.
Kind of sample preparation and/or method of registration of the spectrum: KBr disc. Transmission.
Source: Kullyakool et al. (2013).
Wavenumbers (cm^{-1}): 3455s, 3164sh, 3067, 1610, 1064s, 1034s, 976s, 938, 854, 701w, 583, 548, 479sh.
Note: The wavenumbers were determined by us based on spectral curve analysis of the published spectrum.

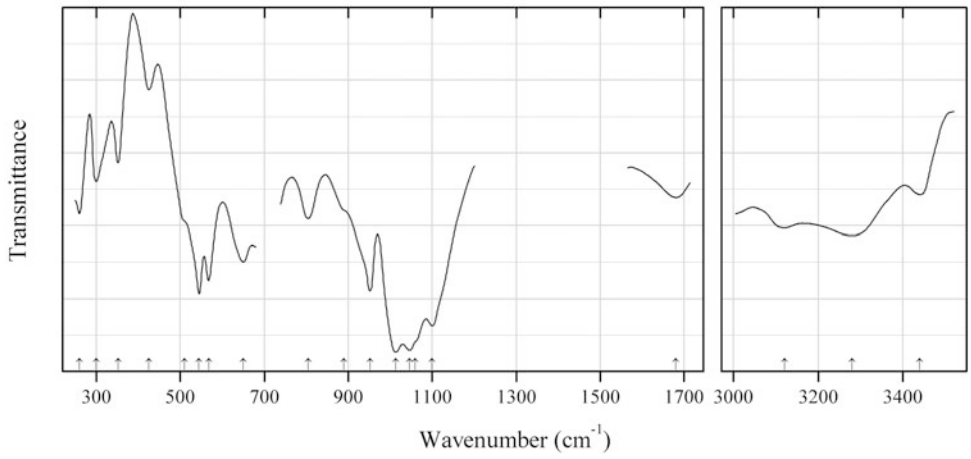

Fig. 2.974 IR spectrum of parahopeite drawn using data from Braithwaite (1988)

P593 Parahopeite $Zn_3(PO_4)_2 \cdot 4H_2O$ (Fig. 2.974)
Locality: Kabwe (Broken Hill), Zambia (type locality).
Description: Specimen No. RSWB 83-4 from R.S.W. Braithwaite collection.
Kind of sample preparation and/or method of registration of the spectrum: Nujol mull between CsI plates. Transmission.
Source: Braithwaite (1988).
Wavenumbers (cm^{-1}): 3440, 3280, 3120, 1680, 1100s, 1060sh, 1046s, 1013s, 952s, 890sh, 805, 650, 568s, 545s, 510sh, 425w, 352, 300, 260.

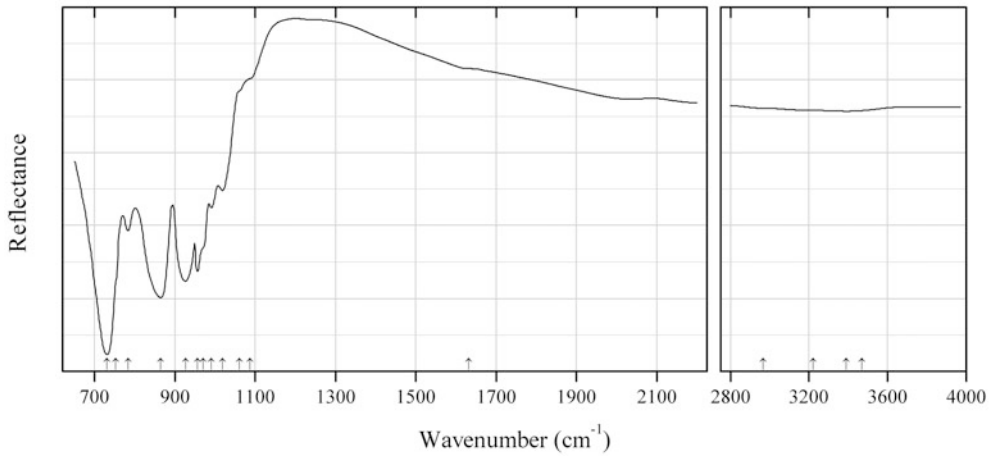

Fig. 2.975 IR spectrum of parsonsite drawn using data from Locock et al. (2005)

P594 Parsonsite $Pb_2(UO_2)(PO_4)_2$ (Fig. 2.975)
Locality: Synthetic.
Description: Yellow parallelepiped-shaped crystals synthesized under mild hydrothermal conditions. The crystal structure is solved. Triclinic, space group *P*-1, $a = 6.8432(5)$, $b = 10.4105(7)$, $c = 6.6718(4)$ Å, $\alpha = 101.418(1)°$, $\beta = 98.347(2)°$, $\gamma = 86.264(2)°$, $V = 460.64(5)$ $Å^3$, $Z = 2$. $D_{calc} = 6.304$ g/cm^3.
Kind of sample preparation and/or method of registration of the spectrum: Attenuated total reflection of powdered sample.
Source: Locock et al. (2005).
Wavenumbers (cm^{-1}): 3470sh, 3389w, 3222sh, 2965sh, 1632sh, 1087sh, 1060sh, 1018, 990, 970sh, 956, 926s, 864s, 783, 753sh, 731s.
Note: The wavenumbers were determined by us based on spectral curve analysis of the published spectrum. Possibly, in the cited paper the IR spectrum of AsO_4-analogue od parsonsite is given.

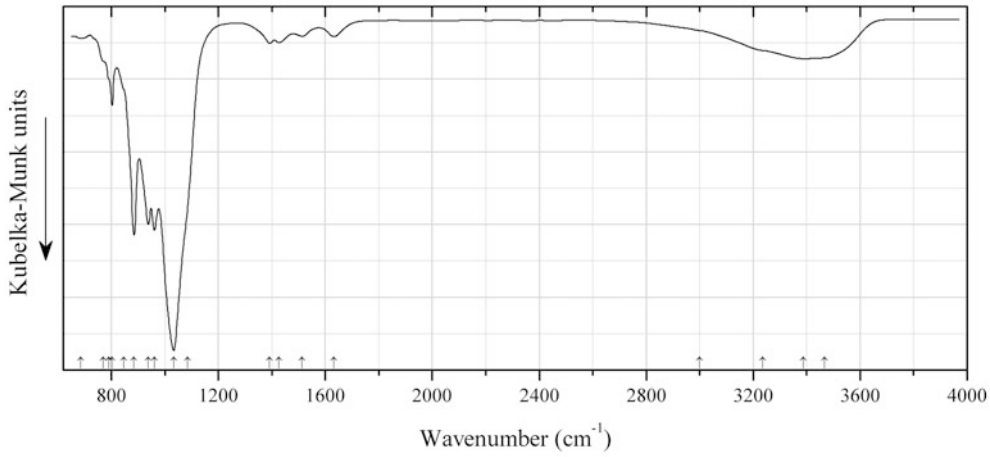

Fig. 2.976 IR spectrum of parsonsite H_2O-bearing drawn using data from Plášil et al. (2009b)

P595 Parsonsite H_2O-bearing $Pb_2(UO_2)(PO_4)_2 \cdot 2H_2O$ (Fig. 2.976)
Locality: Červené Žily vein system, Jáchymov U deposit, Krušné Hory (Ore Mts.), Western Bohemia, Czech Republic.
Description: Yellow flattened prismatic crystals. Triclinic, space group *P*-1, $a = 6.860(2)$, $b = 10.404(3)$, $c = 6.665(3)$ Å, $\alpha = 101.46(3)°$, $\beta = 98.30(3)°$, $\gamma = 86.29(2)°$, $V = 461.0(3)$ Å^3. The empirical formula is $Pb_{1.99}(UO_2)_{1.07}[(PO_4)_{1.77}(AsO_4)_{0.13}(SiO_4)_{0.03}] \cdot 1.93H_2O$. Water is determined by thermogravimetric analysis and confirmed by infrared spectroscopy. The strongest lines of the powder X-ray diffraction pattern [*d*, Å (*I*, %) (*hkl*)] are: 10.18 (27) (010), 6.78 (10) (−100), 5.10 (16) (020), 4.23 (16) (−111), 4.20 (13) (1–11), 4.15 (17) (−1–20), 3.40 (100) (030), 3.26 (31) (−2–10), 3.15 (13) (−2–11).
Kind of sample preparation and/or method of registration of the spectrum: Diffuse reflection of a mixture with KBr. An analogous KBr sample was used as a reference.
Source: Plášil et al. (2009b).
Wavenumbers (cm^{-1}): 3467sh, 3388, 3235sh, 3000sh, 1632w, 1514w, 1427w, 1392w, 1085sh, 1033s, 961s, 938s, 885s, 847sh, 803, 790sh, 770sh, 686w.
Note: The wavenumbers were partly determined by us based on spectral curve analysis of the published spectrum. In the cited paper the wavenumber 1033 cm^{-1} is erroneously indicated as 1093 cm^{-1}.

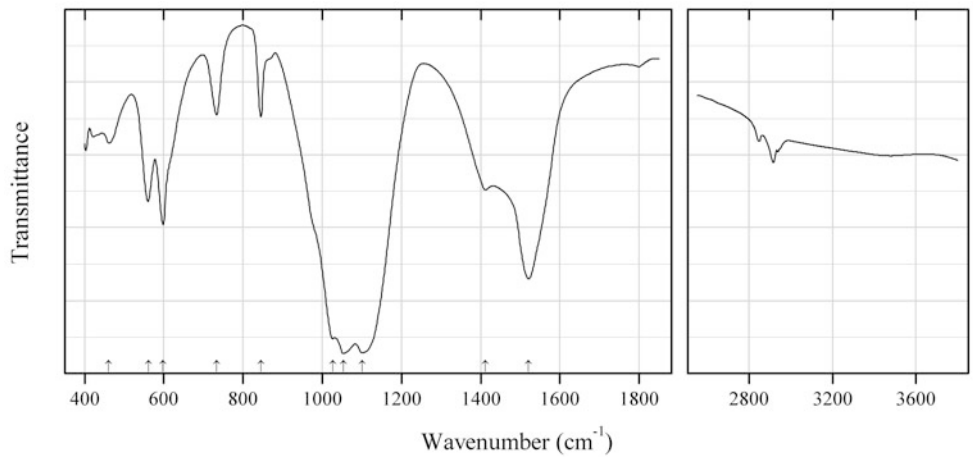

Fig. 2.977 IR spectrum of peatite-(Y) drawn using data from McDonald et al. (2013)

P596 Peatite-(Y) $Li(Y,Na,Ca,REE)_3(PO_4)_3(CO_3)(F,OH)_2$ (Fig. 2.977)
Locality: Poudrette pegmatite, Poudrette quarry, Mont Saint-Hilaire, Québec, Canada (type locality).
Description: Pseudocubic crystals from the association with albite, rhodochrosite, siderite, chabazite-Na, synchysite-(Ce), and sabinaite. Holotype sample. The crystal structure is solved. Orthorhombic, space group *P*222, a = 11.167(2), b = 11.164(2), c = 11.162(2) Å, V = 1391.7(1) $Å^3$, Z = 4. D_{calc} = 3.62(1) g/cm^3. Optically biaxial, β = 1.651(1). The empirical formula is (Z = 1): $Li_4Na_{12}(Y_{10.06}Na_{0.72}Ca_{0.62}Dy_{0.50}Er_{0.46}Yb_{0.28}Zr_{0.17}Ho_{0.11}Gd_{0.10}Tm_{0.04}Th_{0.04}Tb_{0.02})(PO)_{11.70}(CO_3)_4[F_{6.97}(OH)_{1.03}]$. The strongest lines of the powder X-ray diffraction pattern [*d*, Å (*I*, %) (*hkl*)] are: 4.56 (57) (211, 121, 112), 3.95 (57) (220, 202, 022), 3.54 (46) (310, 301, 130), 2.99 (83) (321, 312, 231), 2.63 (100) (330, 303, 033), 2.149 (42) (333).
Kind of sample preparation and/or method of registration of the spectrum: A single crystal was mounted in a low-pressure diamond-anvil microsample cell and pressed into a thin film.
Source: McDonald et al. (2013).
Wavenumbers (cm^{-1}): 1521s, 1412, 1101s, 1053s, 1026s, 845, 733, 598, 561, 461.
Note: Weak bands in the range from 2800 to 3000 cm^{-1} correspond to the admixture of an organic substance.

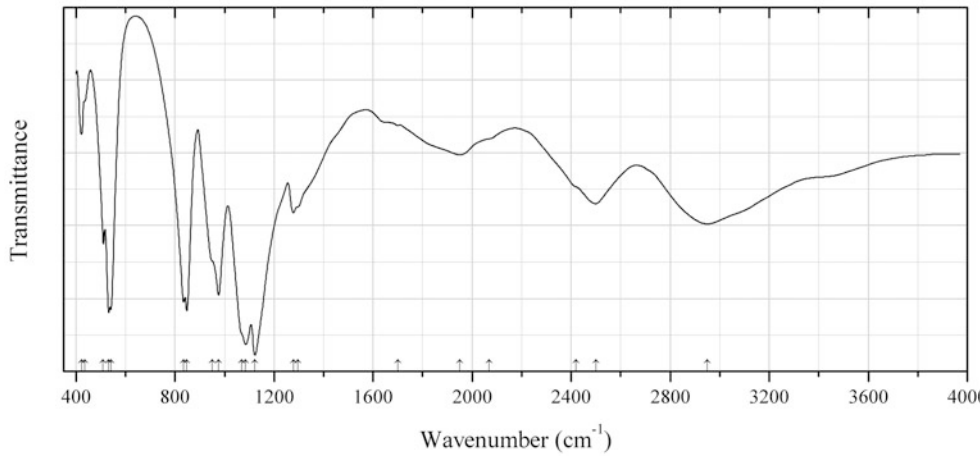

Fig. 2.978 IR spectrum of phosphammite K analogue drawn using data from Pechkovskii et al. (1981)

P597 Phosphammite K analogue $K_2(HPO_4)$ (Fig. 2.978)
Locality: Synthetic.
Kind of sample preparation and/or method of registration of the spectrum: KBr disc. Transmission.
Source: Pechkovskii et al. (1981).
Wavenumbers (cm^{-1}): 2950, 2500, 2420sh, 2070sh, 1950, 1700w, 1296sh, 1278, 1123s, 1085s, 1070sh, 976s, 950sh, 848s, 834s, 541s, 533s, 510, 435sh, 422, 405, 382sh, 221sh, 186s, 166s.

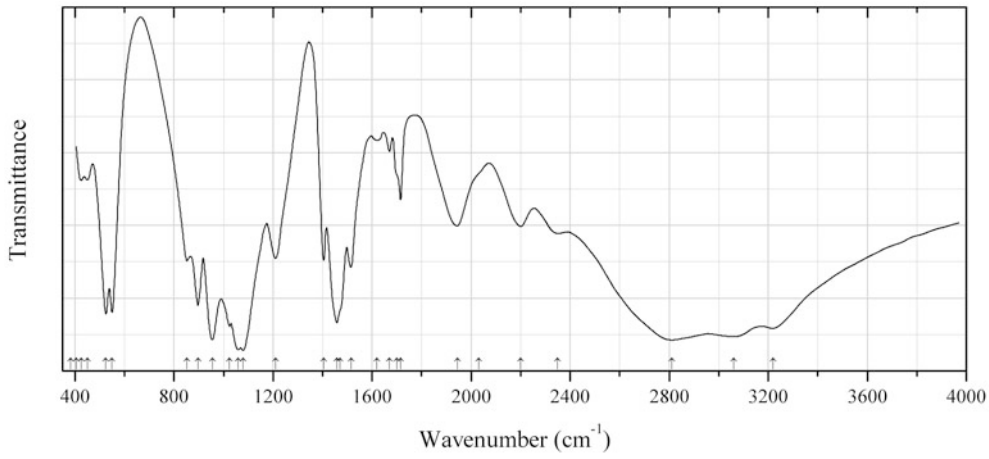

Fig. 2.979 IR spectrum of phosphammite drawn using data from Pechkovskii et al. (1981)

P598 Phosphammite $(NH_4)_2(HPO_4)$ (Fig. 2.979)
Locality: Synthetic.
Description: Monoclinic, space group $P2_1/c$, $a = 11.043$, $b = 6.700$, $c = 8.031$ Å, $\beta = 113.42°$, $Z = 4$. $D_{meas} = 1.619$ g/cm^3, $D_{calc} = 1.608$ g/cm^3.
Kind of sample preparation and/or method of registration of the spectrum: KBr disc. Transmission.
Source: Pechkovskii et al. (1981).
Wavenumbers (cm^{-1}): 3220, 3060, 2810s, 2350, 2200, 2030sh, 1945, 1715, 1700sh, 1670, 1620, 1515, 1470sh, 1458s, 1404, 1210, 1079s, 1060s, 1024, 955, 897, 852, 550, 525, 450, 425, 405, 382, 256s, 245sh, 202s, 168.

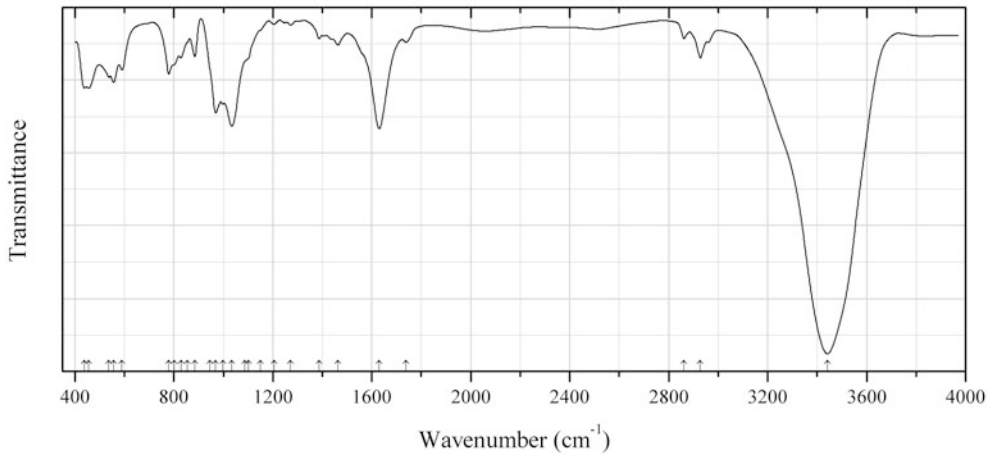

Fig. 2.980 IR spectrum of phosphowalpurgite drawn using data from Sejkora et al. (2004)

P599 Phosphowalpurgite $(UO_2)Bi_4(PO_4)_2O_4 \cdot 2H_2O$ (Fig. 2.980)
Locality: Old dumps near the As-U deposit Smrkovec, Slavovský Les Mts., near Mariánské Lázně, Czech Republic (type locality).

Description: Brownish gray flattened crystals from the association with apatite, atelestite, bismutoferrite, bismutite, eulytite, hechtsbergite, metatorbernite, mixite, petitjeanite, preisingerite, pucherite, retgersite, schumacherite, smrkovecite, and walpurgite. Holotype sample. Triclinic, space group *P*-1, $a = 7.060(3)$, $b = 10.238(4)$, $c = 5.464(3)$ Å, $\alpha = 101.22(4)°$, $\beta = 109.93(3)°$, $\gamma = 87.93(4)°$, $V = 364.0(3)$ Å^3, $Z = 1$. $D_{calc} = 6.36$ g/cm^3. The empirical formula is (electron microprobe): $[(UO_2)_{0.91}Ca_{0.08}Fe_{0.07}Cu_{0.05}Pb_{0.01})Bi_{3.91}O_{3.91}[(PO_4)_{1.50}(AsO_4)_{0.50}(SiO_4)_{0.04}(VO_4)_{0.02}]\cdot 2H_2O$. The strongest lines of the powder X-ray diffraction pattern [*d*, Å (*I*, %) (*hkl*)] are: 10.059 (100) (010), 3.346 (43) (030, 20–1), 3.251 (72) (021, 1–2–1), 3.125 (86) (210), 3.084 (95) (1–21, 2–1–1), 3.005 (52) (13–1), 2.726 (42) (220, 11–2).

Kind of sample preparation and/or method of registration of the spectrum: KBr disc. Absorption.

Source: Sejkora et al. (2004).

Wavenumbers (cm^{-1}): 3442s, 2928w, 2862w, 1739w, 1630s, 1463w, 1387w, 1271w, 1205w, 1150sh, 1102sh, 1088sh, 1035s, 998w, 969s, 946sh, 885, 855sh, 829, 802sh, 779, 591w, 557, 538, 456, 439.

Note: The bands in the range from 2800 to 3000 cm^{-1} (and, possibly, some weak bands in the range from 1200 to 1800 cm^{-1}) are due to the admixture of an organic substance. The anomaleously strong bands of H_2O molecules at 3442 and 1630 cm^{-1} may be partly due to adsorbed water.

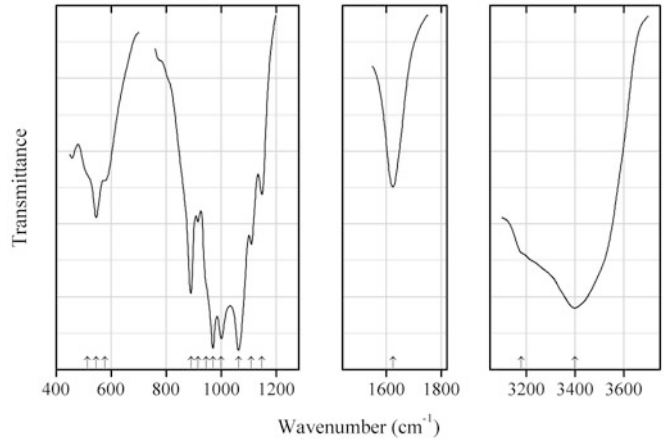

Fig. 2.981 IR spectrum of phurcalite drawn using data from Braithwaite et al. (1989)

P600 Phurcalite $Ca_2(UO_2)_3(PO_4)_2O_2\cdot 7H_2O$ (Fig. 2.981)

Locality: Merrivale quarry, Dartmoor, Devon, Southwest England, UK.

Description: Yellow blades on granite. Orthorhombic, $a = 17.44(2)$, $b = 15.87(2)$, $c = 13.56(3)$ Å. Optically biaxial (−), $\alpha = 1.670$, $\beta = 1.725$, $\gamma = 1.775$, $2V = 82(2)°$. The approximate empirical formula is $Ca_2(UO_2)_3(PO_4)_{1.85}(AsO_4)_{0.15}(OH)_4\cdot 4H_2O$. The strongest lines of the powder X-ray diffraction pattern are observed at 7.95, 4.24, 3.967, 3.378, 3.104, and 2.886 Å.

Kind of sample preparation and/or method of registration of the spectrum: Nujol mull. Transmission.

Source: Braithwaite et al. (1989).

Wavenumbers (cm^{-1}): 3400s, 3180sh, 1625, 1148, 1110, 1063s, 1000s, 970s, (945sh), 915w, 890s, 577, 545, 513sh.

Note: The wavenumbers were partly determined by us based on spectral curve analysis of the published spectrum. The band position denoted by Braithwaite et al. (1989) as 590 cm^{-1} was determined by us at 577 cm^{-1}.

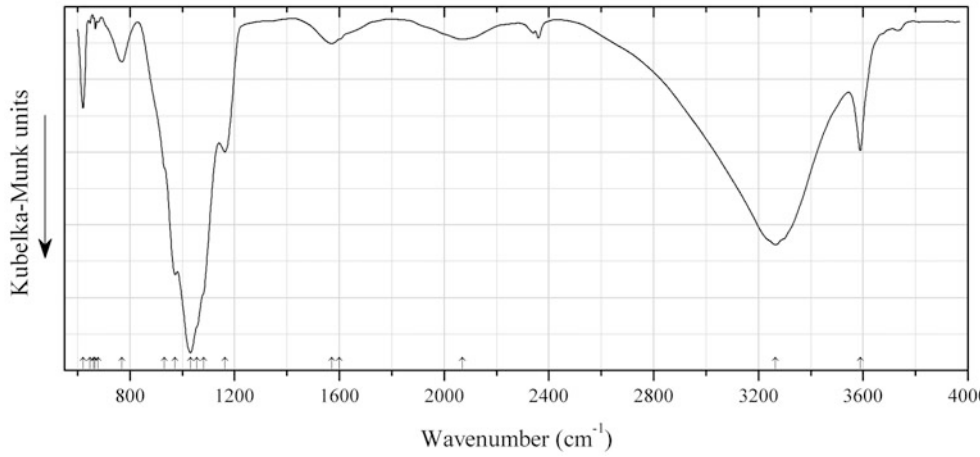

Fig. 2.982 IR spectrum of plimerite drawn using data from Sejkora et al. (2011a)

P601 Plimerite $ZnFe^{3+}{}_4(PO_4)_3(OH)_5$ (Fig. 2.982)
Locality: Huber open pit, Huber stock, Krásno, Horní Slavkov, Karlovy Vary region, Bohemia, Czech Republic (type locality).
Description: Dark green aggregate from the association with fluorapatite, isokite, kolbeckite, leucophosphite, beraunite, whitmoreite, kunatite, etc. Holotype sample. Orthorhombic, space group *Pbmm*, $a = 13.850(1)$, $b = 16.798(1)$, $c = 5.1581(3)$ Å, $V = 1200.1(2)$ Å^3, $Z = 4$. $D_{calc} = 3.65$ g/cm^3. The empirical formula is $(Zn_{1.20}Fe^{2+}{}_{0.44}Na_{0.10}Mn_{0.08}Ca_{0.06})(Fe^{3+}{}_{2.62}Al_{0.38})[(PO_4)_{2.95}(AsO_4)_{0.04}(SiO_4)_{0.01}](OH)_{3.65}$.
Kind of sample preparation and/or method of registration of the spectrum: Diffuse reflection of a powdered sample mixed with KBr.
Source: Sejkora et al. (2011a).
Wavenumbers (cm^{-1}): 3589, 3265s, 2069w, 1600sh, 1570w, 1162w, 1083sh, 1056sh, 1031s, 973s, 932sh, 769, 679w, 668w, 662w, 648w, 621.
Note: The wavenumbers were partly determined by us based on spectral curve analysis of the published spectrum. The band position denoted by Sejkora et al. (2011a) as 3228 cm^{-1} was determined by us at 3265 cm^{-1}. For the IR spectrum of plimerite see also Elliott et al. (2009).

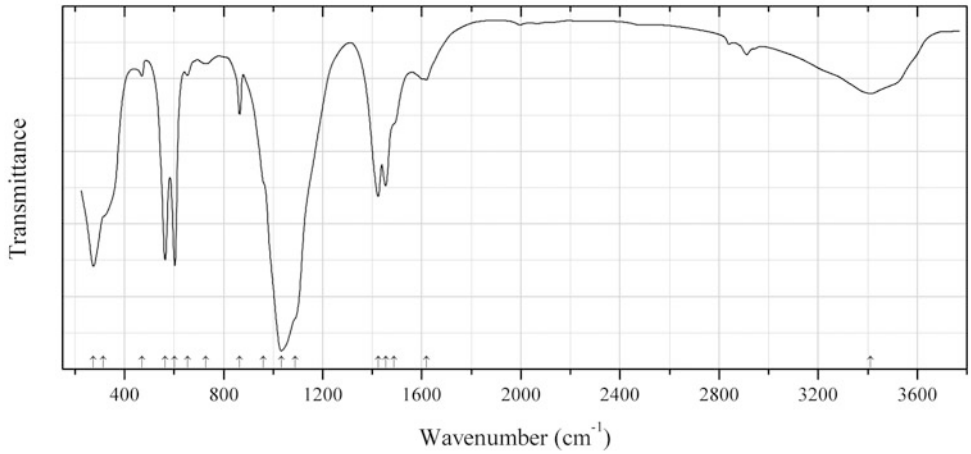

Fig. 2.983 IR spectrum of hydroxylapatite Pb,CO_3-bearing drawn using data from Livingstone (1994)

P602 Hydroxylapatite Pb,CO_3-bearing $(Ca,Pb)_5(PO_4,CO_3)_3(OH,F)$ (Fig. 2.983)
Locality: Wanlockhead, Strathclyde Region, Scotland, UK.
Description: Chalky white aggregate. Hexagonal, a = 9.472, c = 6.904 Å. The empirical formula is (Z = 1): $(Ca_{8.78}Pb_{1.22})[(PO_4)_{5.53}(CO_3)_{0.44}][(OH)_{1.70}F_{0.73}Cl_{0.13}]\cdot 1.5H_2O$. The strongest lines of the powder X-ray diffraction pattern are observed at 4.03, 3.457, 3.893, 2.800, 2.709, 2.252, 1.939, and 1.841 Å.
Kind of sample preparation and/or method of registration of the spectrum: KBr disc. Transmission.
Source: Livingstone (1994).
Wavenumbers (cm^{-1}): 3412, 1618, 1487sh, 1454, 1424, 1088sh, 1033s, 961sh, 865, 727w, 654w, 603s, 564s, 470, 313sh, 274s.
Note: The wavenumbers were partly determined by us based on spectral curve analysis of the published spectrum. Weak bands in the range from 2800 to 3000 cm^{-1} correspond to the admixture of an organic substance.

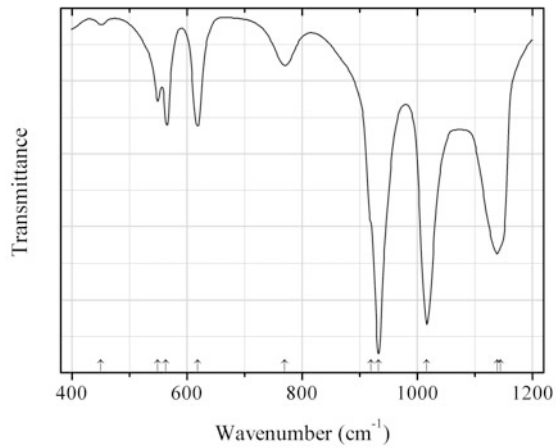

Fig. 2.984 IR spectrum of dittmarite K analogue drawn using data from Koleva (2007)

P603 Dittmarite K analogue $KMn(PO_4)\cdot H_2O$ (Fig. 2.984)
Locality: Synthetic.
Description: Prepared from aqueous solutions of $MnSO_4$ and $K_2(HPO_4)$. Isostructural with dittmarite. Orthorhombic, space group $Pmn2_1$, Z = 2.
Kind of sample preparation and/or method of registration of the spectrum: KBr disc. Absorption.
Source: Koleva (2007).
Wavenumbers (cm^{-1}): 1145sh, 1139s, 1017s, 933s, 920sh, 770, 618, 563, 549, 450w.
Note: The wavenumbers were partly determined by us based on spectral curve analysis of the published spectrum.

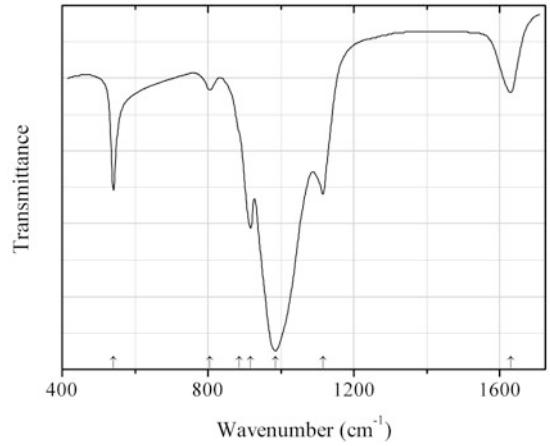

Fig. 2.985 IR spectrum of przhevalskite high-hydrous analogue drawn using data from Suleimanov et al. (2004)

P604 Przhevalskite high-hydrous analogue $Pb(UO_2)_2(PO_4)_2 \cdot 6H_2O$ (Fig. 2.985)
Locality: Synthetic.
Description: Prepared at room temperature by the reaction of crystalline $HPUO_6 \cdot 4H_2O$ and with a 0.05 M aqueous solution of lead acetate, taken in a 5-fold excess relative to the stoichiometry. Monoclinic, a = 6.765(2), b = 6.820(2), c = 16.905(5) Å, β = 91.56(4)°.
Kind of sample preparation and/or method of registration of the spectrum: Suspension in mineral oil. Transmission.
Source: Suleimanov et al. (2004).
Wavenumbers (cm^{-1}): 1630, 1115, 985s, 917s, 886sh, 805w, 541.

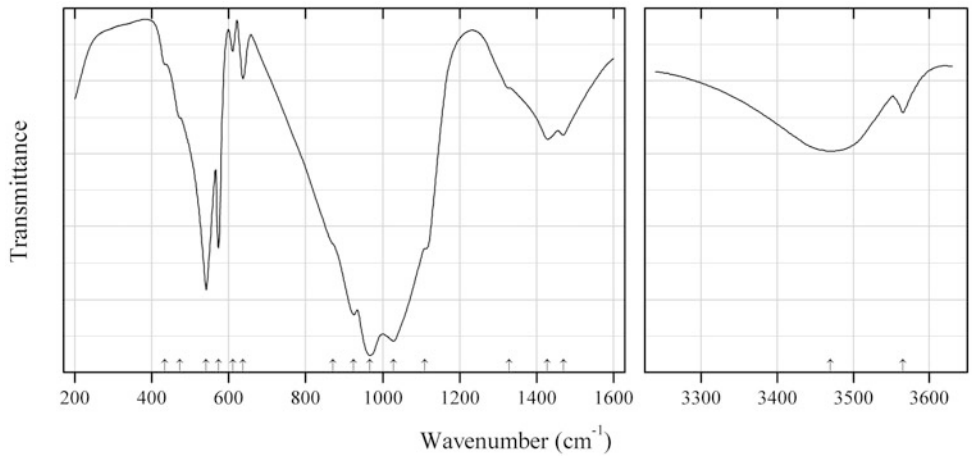

Fig. 2.986 IR spectrum of hydroxylpyromorphite drawn using data from Botto et al. (1997a)

P605 Hydroxylpyromorphite $Pb_5(PO_4)_3(OH)$ (Fig. 2.986)
Locality: Paramillos de Uspallata, Mendoza, Argentina.
Description: Short-prismatic crystals from the oxidation zone of a polymetallic vein, from the association with malachite, azurite, cerussite, Ag halogenides, Mn oxides anf goethite. Hexagonal,

a = 10.02(1), c = 7.37(1) Å. The approximate empirical formula is $(Pb_{0.96}Ba_{0.03}Ca_{0.01})[(PO_4)_{2.7}(CO_3)_{0.3}][(OH)_{1.1}Cl_{0.9}]$.

Kind of sample preparation and/or method of registration of the spectrum: KBr disc. Transmission.

Source: Botto et al. (1997a).

Wavenumbers (cm^{-1}): 3565w, 3470, 1980w, 1910w, 1840w, 1470, 1429, 1329sh, 1110sh, 1029s, 967s, 925s, 871sh, 637, 610w, 573, 541, 473sh, 434sh.

Note: The mineral is not approved by the IMA CNMNC. The band at 3470 cm^{-1} indicates possible presence of H_2O molecules.

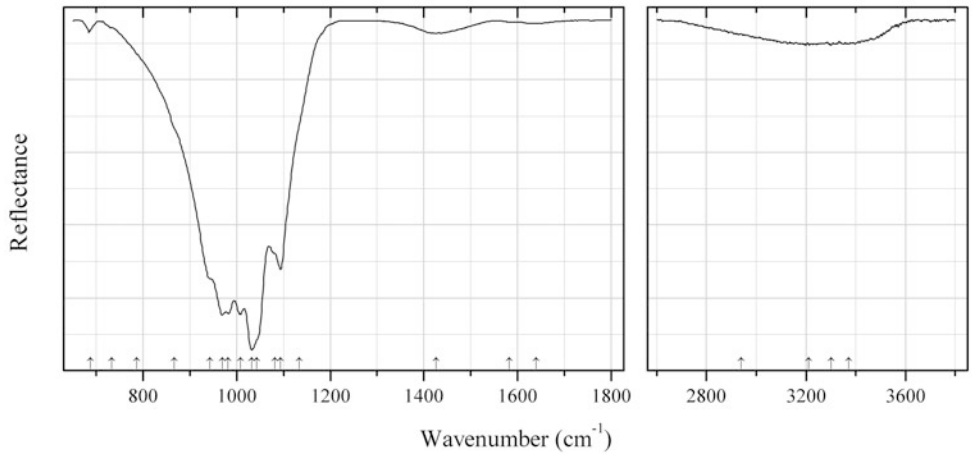

Fig. 2.987 IR spectrum of qingheiite drawn using data from Frost et al. (2013d)

P606 Qingheiite $Na_2MnMgAl(PO_4)_3$ (Fig. 2.987)

Locality: Santa Ana pegmatite, Totoral pegmatitic field, Coronel Pringles department, San Luis, Argentina.

Description: Deep green veins in beusite-lithiophilite aggregate. Specimen SAA-095 from the mineral collection of the Geology Department of the Federal University of Ouro Preto, Minas Gerais, Brazil.

Kind of sample preparation and/or method of registration of the spectrum: Attenuated total reflection of powdered mineral.

Source: Frost et al. (2013d).

Wavenumbers (cm^{-1}): 3373w, 3302w, 3212w, 2940w, 1640w, 1583w, 1427w, 1134sh, 1094, 1081sh, 1043sh, 1032s, 1008s, 982s, 969s, 943sh, 866sh, 787sh, 733sh, 687w.

Note: In the cited paper, the wavenumbers are indicated only for the maxima of individual bands obtained as a result of the spectral curve analysis. The wavenumbers were determined by us based on spectral curve analysis of the published spectrum.

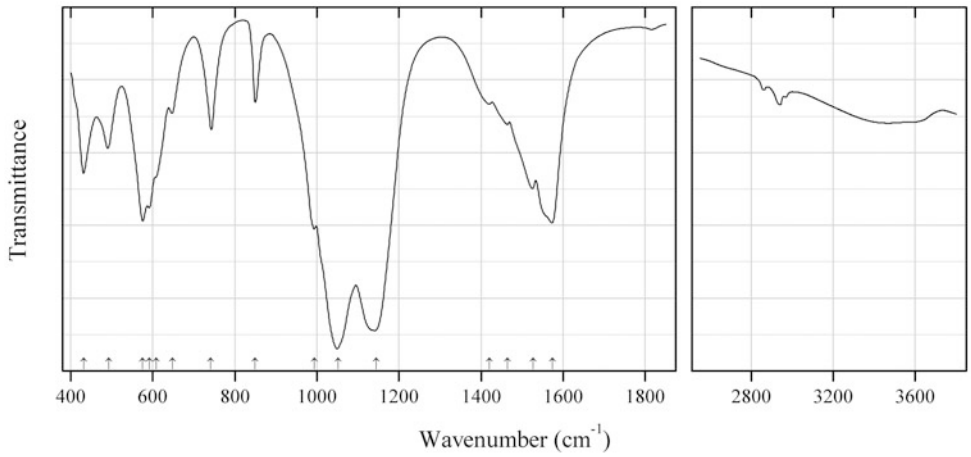

Fig. 2.988 IR spectrum of ramikite-(Y) drawn using data from McDonald et al. (2013)

P607 Ramikite-(Y) $Li_2(Na,Ca)_6(Y,Ca,REE)_3Zr_3(PO_4)_6(CO_3)_2O_2(OH,F)_2$ (Fig. 2.988)
Locality: Poudrette pegmatite, Poudrette quarry, Mont Saint-Hilaire, Québec, Canada (type locality).
Description: Rims around peatite-(Y) crystals. Associatied minerals are albite, rhodochrosite, siderite, chabazite-Na, synchysite-(Ce), and sabinaite. Holotype sample. Triclinic, space group *P*1, a = 10.9977(6), b = 10.9985(6), c = 10.9966(6) Å, α = 90.075(4)°, β = 89.984(4)°, γ = 89.969(4)°, V = 1330.1(1) Å^3, Z = 2. D_{calc} = 3.60 g/cm^3. Optically biaxial, β = 1.636(1). The empirical formula is (Z = 1): $Li_4(Na_{10.79}Ca_{1.21})(Y_{4.34}Ca_{0.99}Dy_{0.18}Er_{0.18}Yb_{0.09}La_{0.02}Ce_{0.02}Nd_{0.01})(Zr_{5.65}Hf_{0.10}Th_{0.06})[(P_{0.99}As_{0.01})O_4]_{12}(CO_3)_4O_4[(OH)_{3.03}F_{0.97}]$. The strongest lines of the powder X-ray diffraction pattern [d, Å (I, %) (hkl)] are: 11.04 (76) (0–10, 100, 00–1), 7.80 (79) (0–11, 110, 101), 6.36 (75) (11–1, 1–11, 111, 1–1–1), 3.89 (100) (0–22, 220, 202), 2.94 (98) (13–2, 12–3, 23–1), 2.59 (98) (0–33, 330, 303).
Kind of sample preparation and/or method of registration of the spectrum: A small sample was mounted in a low-pressure diamond-anvil microsample cell and pressed into a thin film.
Source: McDonald et al. (2013).
Wavenumbers (cm^{-1}): 1574, 1526, 1464, 1420w, 1144s, 1051s, 993, 849, 741, 648w, 609, 592, 575, 492, 432.
Note: Weak bands in the range from 2800 to 3000 cm^{-1} correspond to the admixture of an organic substance.

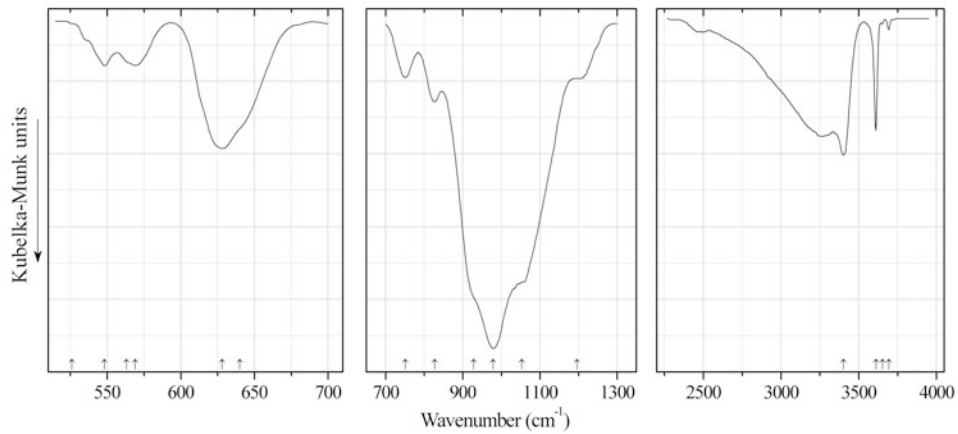

Fig. 2.989 IR spectrum of gormanite drawn using data from Frost et al. (2003) and Frost and Erickson (2005)

P608 Gormanite $Fe^{2+}{}_3Al_4(PO_4)_4(OH)_6 \cdot 2H_2O$ (Fig. 2.989)
Locality: Dawson mining district, Yukon Territory, Canada (?).
Description: The sample was analysed for phase purity by X-ray diffraction techniques and for composition by electron microprobe analyses.
Kind of sample preparation and/or method of registration of the spectrum: Attenuated total reflection of powdered mineral. The spectra were transformed using the Kubelka-Munk algorithm.
Source: Frost et al. (2003), Frost and Erickson (2005).
Wavenumbers (cm^{-1}): 3693w, 3653, 3610, 3402, 1196sh, 1053sh, 978s, 928sh, 827, 751w, 640sh, 628s, 569, 563sh, 548, 436sh, 526sh.
Note: In the cited paper, wavenumbers are indicated for the maxima of individual bands obtained as a result of the spectral curve analysis. The wavenumbers were determined by us based on spectral curve analysis of the published spectrum.

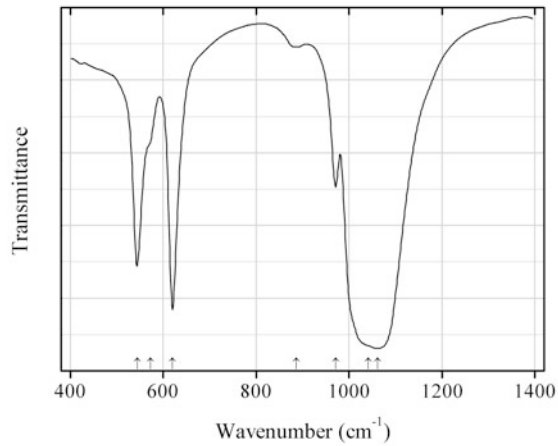

Fig. 2.990 IR spectrum of rhabdophane-(Nd) drawn using data from Kijkowska et al. (2003)

P609 Rhabdophane-(Nd) $Nd(PO_4) \cdot H_2O$ (Fig. 2.990)
Locality: Synthetic.
Description: Obtained by crystallisation from boiling phosphoric acid solution, contained water. Characterized by powder X-ray diffraction data.
Kind of sample preparation and/or method of registration of the spectrum: Transmission. Kind of sample preparation is not indicated.
Source: Kijkowska et al. (2003).
Wavenumbers (cm^{-1}): 1061s, 1042sh, 972, 887w, 620s, 573sh, 544.
Note: The wavenumbers were partly determined by us based on spectral curve analysis of the published spectrum.

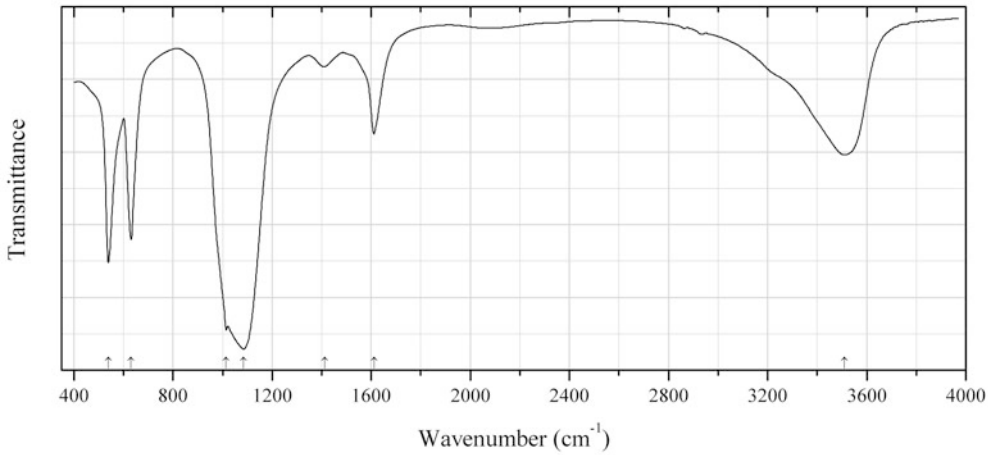

Fig. 2.991 IR spectrum of rhabdophane-(Y) drawn using data from Li et al. (2009)

P610 Rhabdophane-(Y) $Y(PO_4)\cdot H_2O$ (Fig. 2.991)
Locality: Synthetic.
Description: Synthesized hydrothermally from YCl_3 and Na_3PO_4 at pH 6 and T = 180 °C for 24 h. Characterized by powder X-ray diffraction data.
Kind of sample preparation and/or method of registration of the spectrum: KBr disc. Transmission.
Source: Li et al. (2009).
Wavenumbers (cm^{-1}): 3510, 1611, 1412w, 1085s, 1015s, 631, 539.
Note: The wavenumbers were partly determined by us based on spectral curve analysis of the published spectrum. The band at 1412 cm^{-1} may correspond to the admixture of a carbonate.

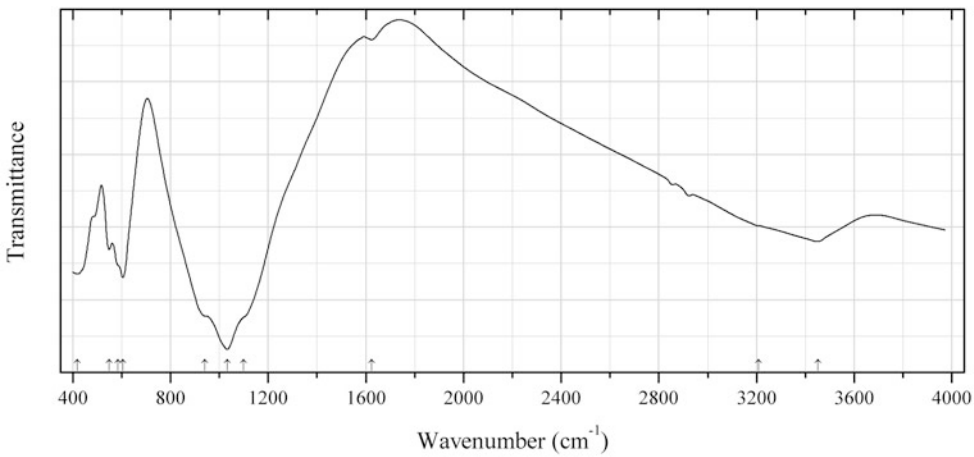

Fig. 2.992 IR spectrum of rosemaryite drawn using data from Hatert et al. (2006)

P611 Rosemaryite $NaMn^{2+}Fe^{3+}Al(PO_4)_3$ (Fig. 2.992)
Locality: Buranga pegmatite, Gatumba district, Western Province, Rwanda.

Description: The crystal structure is solved. Monoclinic, space group $P2_1/n$, a = 12.001(2), b = 12.396(1), c = 6.329(1) Å, β = 114.48(1)°, V = 856.9(2) Å^3, Z = 4. The sample was characterized by Mössbauer spectroscopy. The empirical formula is $H_{1.26}Na_{0.59}Ca_{0.10}Mg_{0.08}Mn_{1.37}Fe^{2+}_{0.15}Fe^{3+}_{1.04}Al_{0.785}P_{3.00}O_x$.
Kind of sample preparation and/or method of registration of the spectrum: KBr disc. Transmission.
Source: Hatert et al. (2006).
Wavenumbers (cm^{-1}): 3450, 3209sh, 1624w, 1101sh, 1033s, 940sh, 606s, 586sh, 549w, 419.
Note: The bands at 3450 and 1624 cm^{-1} correspond to water molecules in channels of the willeyite-type structure.

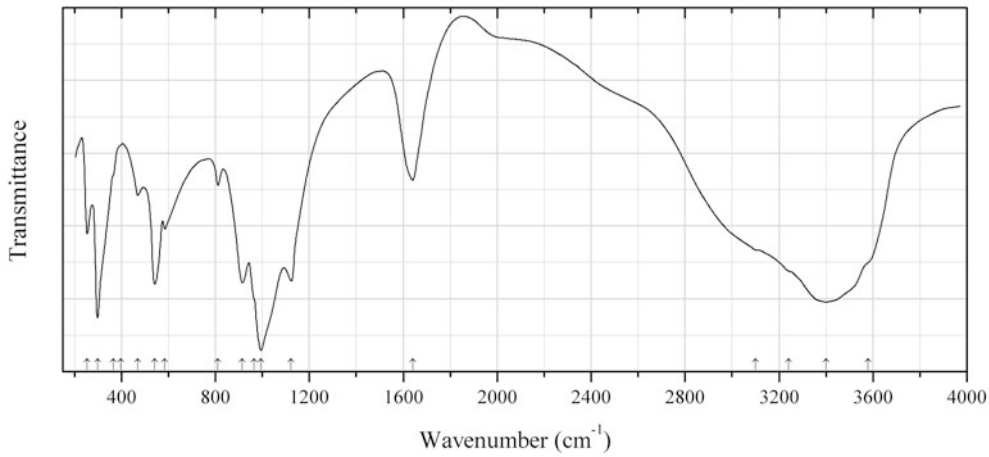

Fig. 2.993 IR spectrum of sabugalite drawn using data from Čejka et al. (1988)

P612 Sabugalite $Al(UO_2)_2(PO_4)_2F{\cdot}8H_2O$ (Fig. 2.993)
Locality: Margnac mine, Compreignac, Haute-Vienne, Limousin, France.
Description: Specimen No. 54063 from the National Museum, Prague, Czech Republic. Confirmed by powder X-ray diffraction data.
Kind of sample preparation and/or method of registration of the spectrum: KBr disc. Transmission.
Source: Čejka et al. (1988).
Wavenumbers (cm^{-1}): 3580sh, 3400s, 3240sh, 3100sh, 1640, 1123s, 995s, 965sh, 915s, 810w, 585, 542, 470w, 397sh, 365sh, 298s, 254.

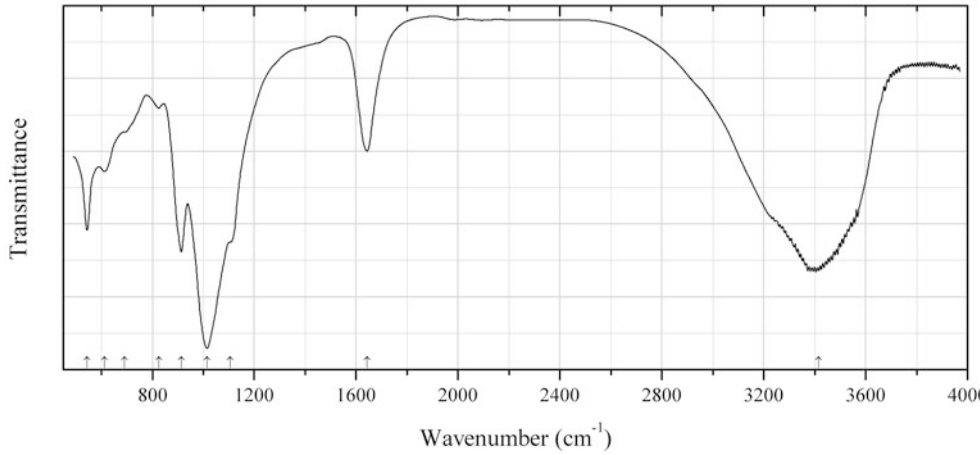

Fig. 2.994 IR spectrum of saléeite drawn using data from Vochten and Van Springel (1996)

P613 Saléeite $Mg(UO_2)_2(PO_4)_2 \cdot 10H_2O$ (Fig. 2.994)
Locality: The prospecting area Arcu su Linnarbu, Monte Arcosu, near the village Capoterra, Cagliari, Sardinia, Italy.
Description: Light yellow platy crystals. Tetragonal, space group $P2_1/c$, a = 6.982(2), c = 19.660(2) Å, Z = 2. D_{meas} = 3.242 g/cm^3. Optically biaxial (−), α = 1.572(2), β = 1.577(2), γ = 1.581(2), 2 V = 48(2)°. The empirical formula is (electron microprobe): $(Mg_{0.83}Fe_{0.16}K_{0.02})(UO_2)_{2.00}(PO_4)_{2.00} \cdot nH_2O$. The strongest lines of the powder X-ray diffraction pattern [d, Å (I, %) (hkl)] are: 3.473 (100) (114), 4.95 (50) (110), 4.91 (40) (004), 4.443 (40) (112), 2.200 (30) (118), 2.193 (30) (303), 2.178 (30) (009).
Kind of sample preparation and/or method of registration of the spectrum: KBr disc. Transmission.
Source: Vochten and Van Springel (1996).
Wavenumbers (cm^{-1}): 3416s, 1643, 1014s, 1105sh, 914s, 825w, 690sh, 613, 544.
Note: Probably, real symmetry of the mineral is monoclinic. The wavenumbers were partly determined by us based on spectral curve analysis of the published spectrum.

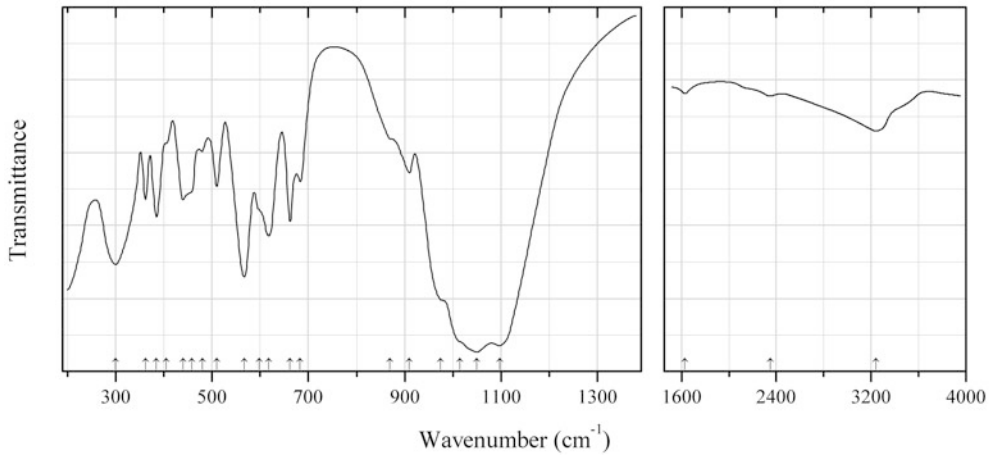

Fig. 2.995 IR spectrum of samuelsonite drawn using data from Fransolet et al. (1992)

P614 Samuelsonite $Ca_9Mn^{2+}{}_4Al_2(PO_4)_{10}(OH)_2$ (Fig. 2.995)
Locality: Buranga pegmatite, Gatumba district, Western Province, Rwanda.
Description: Fan-like aggregates of bladed crystals from the association with earlier trolleite, bertossaite, and scorzalite. Confirmed by electron microprobe and powder X-ray diffraction data. Monoclinic, space group *C*2/*m*, a = 18.621(3), b = 6.842(1), c = 14.066(2) Å, β = 112.50(2)°, V = 1655.6(3) Å^3, Z = 2. D_{meas} = 3.24(5) g/cm^3, D_{calc} = 3.22 g/cm^3. Optically biaxial (+), α = 1.648 (2), β = 1.655(2), γ = 1.667(2), 2 V = 80–85°.
Kind of sample preparation and/or method of registration of the spectrum: KBr disc. Transmission.
Source: Fransolet et al. (1992).
Wavenumbers (cm^{-1}): 3240, 2350w, 1630w, 1097s, 1050s, 1015sh, 975sh, 910w, 870sh, 683, 662, 618, 598sh, 567s, 510, 480w, 458sh, 440, 405sh, 385, 362, 300s.

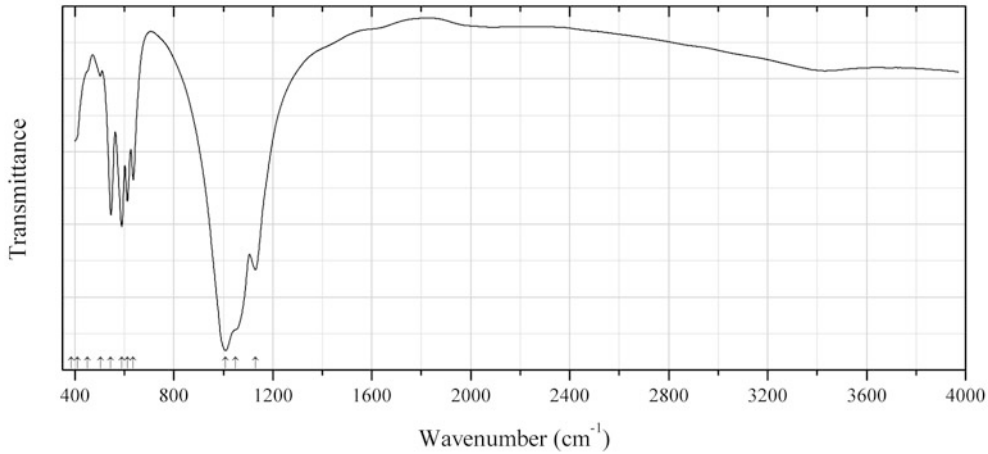

Fig. 2.996 IR spectrum of sarcopside dimorph drawn using data from Pechkovskii et al. (1981)

P615 Sarcopside dimorph $Fe^{2+}{}_3(PO_4)_2$ (Fig. 2.996)
Locality: Synthetic.
Description: Monoclinic, space group $P2_1/c$, a = 8.881, b = 11.169, c = 6.145 Å, β = 99.36°, Z = 4. D_{calc} = 3.948 g/cm^3.
Kind of sample preparation and/or method of registration of the spectrum: KBr disc. Absorption.
Source: Pechkovskii et al. (1981).
Wavenumbers (cm^{-1}): 1130s, 1050sh, 1010s, 636, 612, 590s, 545, 503w, 452sh, 410sh, 385, 324, 280, 250w, 220, 202, 180.

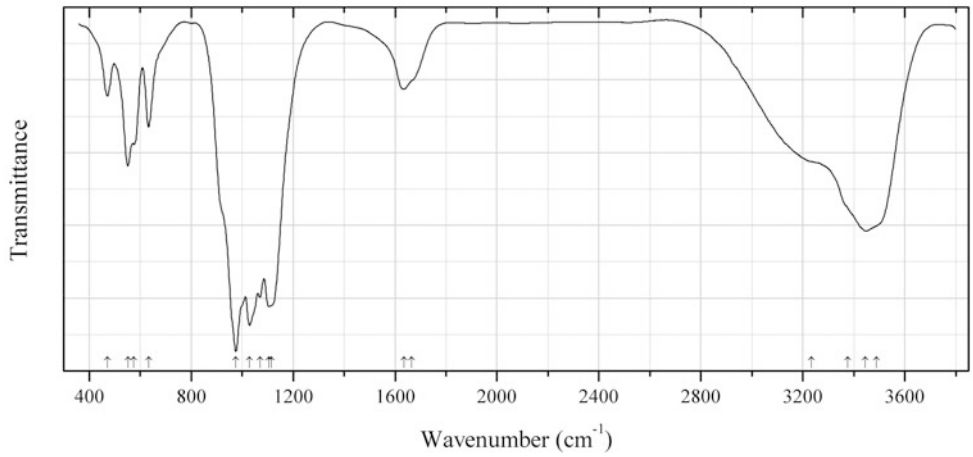

Fig. 2.997 IR spectrum of jahnsite-(CaMnMg) obtained by N.V. Chukanov

P616 Jahnsite-(CaMnMg) $CaMn^{2+}Mg_2Fe^{3+}{}_2(PO_4)_4(OH)_2 \cdot 8H_2O$ (Fig. 2.997)
Locality: The pit No. 232, Ilmeny (Il'menskie) Mts., South Urals, Russia.
Description: Light brown grains from the association with triplite, mitridatite, beraunite, fluorapatite, and other phosphates. Investigated by I.V. Pekov. Characterized by single-crystal X-ray diffraction data. Monoclinic, a = 15.12(4), b = 7.13(4), c = 10.09(3) Å, β = 110.7(3)°, V = 1018(8) $Å^3$, Z = 2. The empirical formula is $(Ca_{0.76}Mn_{0.11}Na_{0.05})Mn_{1.00}(Mg_{1.59}Mn_{0.41})(Fe_{1.85}Al_{0.04}Ti_{0.03})P_{4.12}O_{16}[(OH)_{1.82}O_{0.18}] \cdot nH_2O$.
Kind of sample preparation and/or method of registration of the spectrum: KBr disc. Absorption.
Wavenumbers (cm^{-1}): 3490sh, 3445s, 3375sh, 3235sh, 1665sh, 1636, 1115sh, 1105s, 1070s, 1029s, 975s, 633, 574, 552, 472.

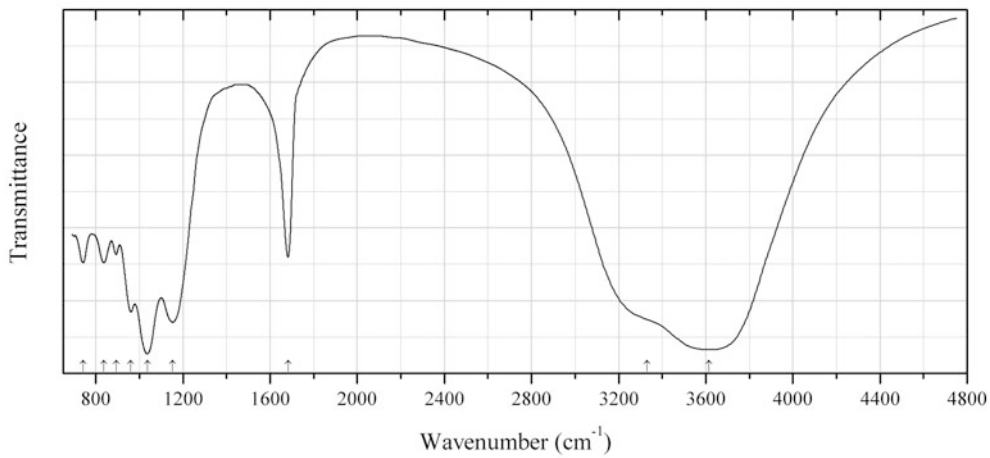

Fig. 2.998 IR spectrum of schoderite drawn using data from Hausen (1962)

P617 Schoderite $Al_2(PO_4)(VO_4) \cdot 8H_2O$ (Fig. 2.998)
Locality: VanNavSan claim, Fish Creek range, Eureka Co., Nevada, USA (type locality).

Description: Yellowish orange microcrystalline coatings associated with wavellite and vashegyite. Holotype sample. Monoclinic, $a = 11.4$, $b = 15.8$, $c = 9.2$ Å, $\beta = 79°$. Optically biaxial (+), $\alpha = 1.542$, $\beta = 1.548$, $\gamma = 1.566$, $2V = 61°$.
Kind of sample preparation and/or method of registration of the spectrum: KBr disc. Transmission.
Source: Hausen (1962).
Wavenumbers (cm^{-1}): 3614s, 3330sh, 1682, 1152s, 1037s, 961s, 894, 837, 741.
Note: The wavenumbers were determined by us based on spectral curve analysis of the published spectrum.

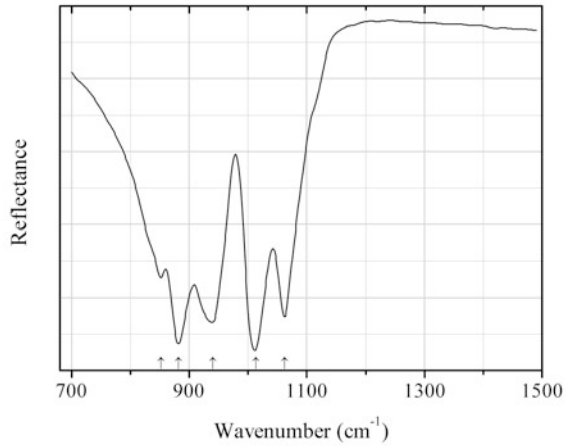

Fig. 2.999 IR spectrum of silicocarnotite drawn using data from Serena et al. (2014)

P618 Silicocarnotite $Ca_5(PO_4)_2(SiO_4)$ (Fig. 2.999)
Locality: Synthetic.
Description: Obtained by the solid state reaction between $Ca_3(PO_4)_2$ and $Ca_2(SiO_4)$ at 1500 °C for 2 h with subsequent cooling to 1200 °C at 5 °C/min. Characterized by chemical analyses and powder X-ray diffraction data.
Kind of sample preparation and/or method of registration of the spectrum: Attenuated total reflection of powdered sample.
Source: Serena et al. (2014).
Wavenumbers (cm^{-1}): 1062, 1013s, 940, 882s, 852.

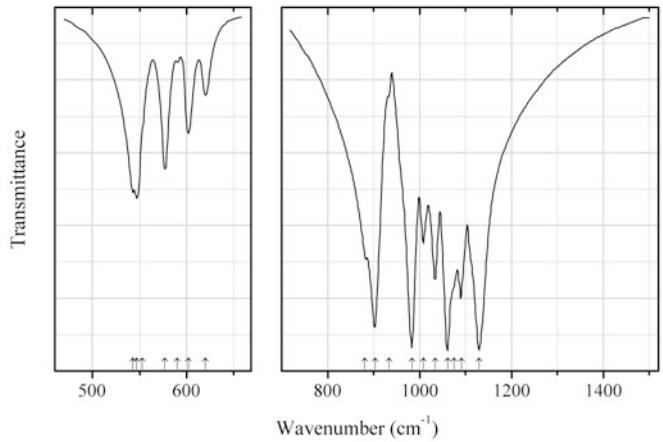

Fig. 2.1000 IR spectrum of strontiowhitlockite Fe analogue drawn using data from Belik et al. (2002)

P619 Strontiowhitlockite Fe analogue $Sr_9Fe^{3+}(PO_4)_7$ (Fig. 2.1000)
Locality: Synthetic.
Description: Synthesized by the solid state method from the mixture of $SrCO_3$, Fe_2O_3, and $NH_4(H_2PO_4)$ (added in the ratio of 9:0.5:7) at 1270–1420 K. Characterized by powder X-ray diffraction data. Monoclinic, a = 18.268(1), b = 10.6035(3), c = 8.9845(7) Å, β = 132.830(4)°, V = 1276.3(1) Å^3.
Kind of sample preparation and/or method of registration of the spectrum: KBr disc. Transmission.
Source: Belik et al. (2002).
Wavenumbers (cm^{-1}): 1130s, 1091, 1075, 1061s, 1034, 1009, 984s, 934sh, 903s, 881, 620, 602, 590w, 577, 553sh, 547, 543.

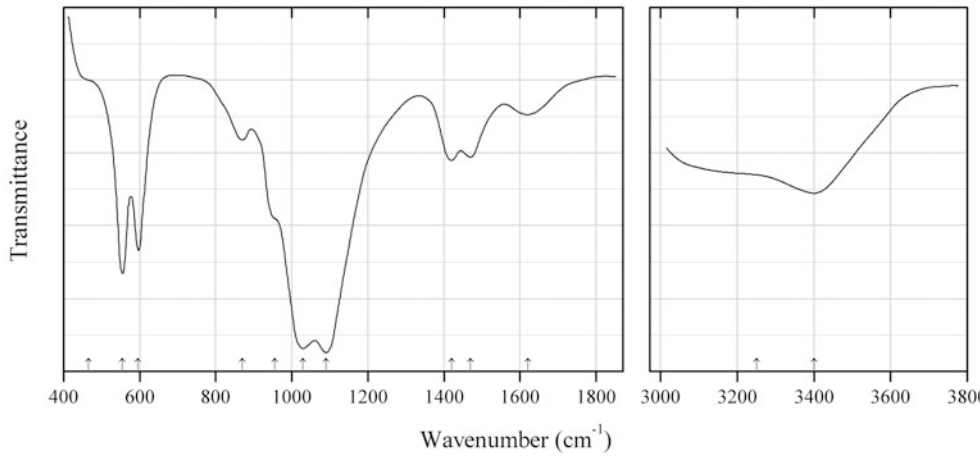

Fig. 2.1001 IR spectrum of strontiowhitlockite drawn using data from Britvin et al. (1991)

P620 Strontiowhitlockite $Sr_9Mg(HPO_4)(PO_4)_6$ (Fig. 2.1001)
Locality: Iron mine, Kovdor, Kovdor alkaline ultramafic complex, Kola peninsula, Murmansk region, Russia (type locality).
Description: White radiated aggregates from the association with dolomite, pyrite, and collinsite. Holotype sample. Hexagonal, space group $R3c$, a = 10.644(9), c = 39.54(6) Å, V = 3880 Å^3, Z = 6. D_{meas} = 3.64(2) g/cm^3, D_{calc} = 3.60 g/cm^3. Optically uniaxial (−), ω = 1.601(2), ε = 1.598(2). The empirical formula suggested by the authors of the cited paper is $(Sr_{6.96}Ca_{1.38}Ba_{0.21}Mg_{1.60}Mn^{2+}_{0.04}Fe^{2+}_{0.04})H_{0.78}P_{6.96}O_{28.00}$. However this formula does not show different crystal-chemical role of Mg and larger cations and does not contain CO_3^{2-} groups that are obviously present in the mineral. The strongest lines of the powder X-ray diffraction pattern [d, Å (I, %) (hkl)] are: 3.288 (37) (0.0.12, 214), 3.071 (29) (300), 3.004 (100) (0.2.10), 2.661 (80) (220), 1.940 (29) (238, 1.2.17), 1.783 (36) (*hkl* not indicated).
Kind of sample preparation and/or method of registration of the spectrum: KBr disc. Transmission.
Source: Britvin et al. (1991).
Wavenumbers (cm^{-1}): 3400, 3250sh, 1620w, 1470, 1420, 1090s, 1030s, 955sh, 870w, 595, 555, 465sh
Note: The wavenumbers were partly determined by us based on spectral curve analysis of the published spectrum. The bands at 3400 and 1620 cm^{-1} indicate the presence of water molecules; the bands at 1470, 1420 and, possibly, 870 cm^{-1} indicate the presence of CO_3^{2-} groups.

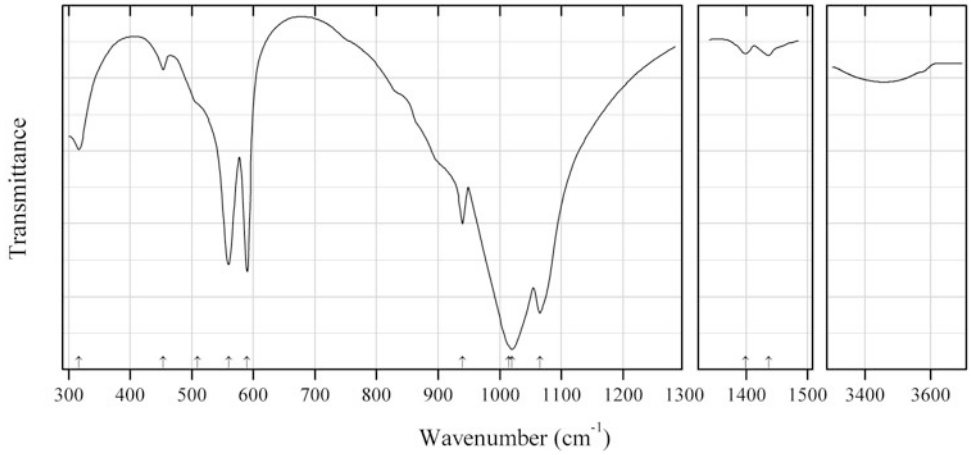

Fig. 2.1002 IR spectrum of stronadelphite Cl analogue drawn using data from González-Díaz and Santos (1978)

P621 Stronadelphite Cl analogue $Sr_5(PO_4)_3Cl$ (Fig. 2.1002)
Locality: Synthetic.
Kind of sample preparation and/or method of registration of the spectrum: KBr disc. Transmission.
Source: González-Díaz and Santos (1978).
Wavenumbers (cm^{-1}): 1437w, 1399w, 1065s, 1020s, 1015sh, 940, 589s, 560s, 509sh, 453w, 316.

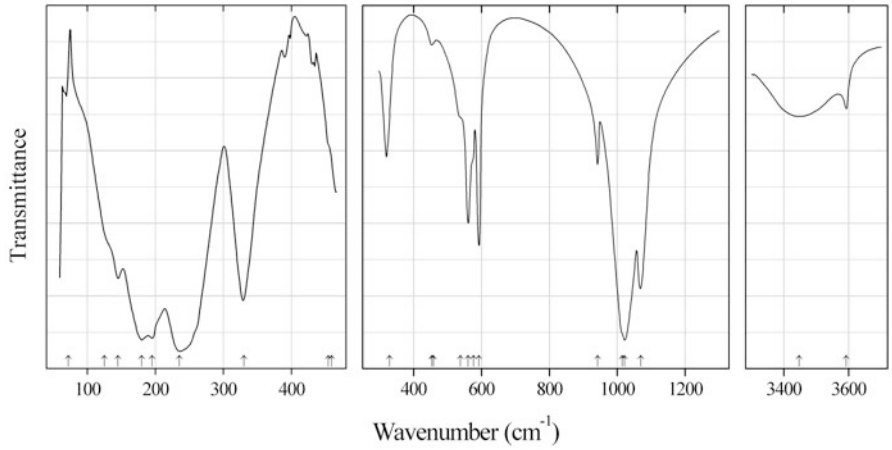

Fig. 2.1003 IR spectrum of stronadelphite OH analogue drawn using data from González-Díaz and Santos (1978)

P622 Stronadelphite OH analogue $Sr_5(PO_4)_3(OH)$ (Fig. 2.1003)
Locality: Synthetic.
Kind of sample preparation and/or method of registration of the spectrum: KBr disc. Transmission.
Source: González-Díaz and Santos (1978).
Wavenumbers (cm^{-1}): 3593w, 3448, 1070s, 1022s, 1015sh, 943, 593, 577sh, 561, 538sh, 459sh, 454w, 330, 235, 195, 180, 145, 125sh, 72w.

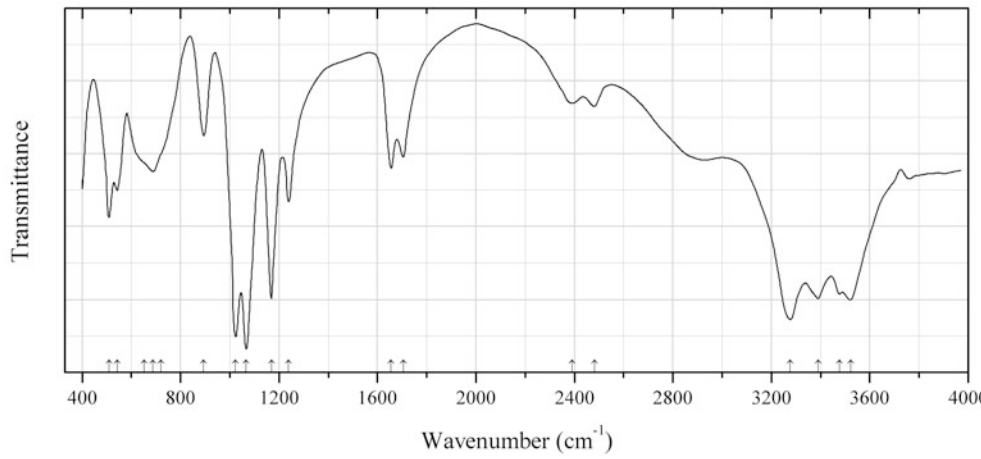

Fig. 2.1004 IR spectrum of struvite-(K) drawn using data from Chauhan et al. (2011)

P623 Struvite-(K) $KMg(PO_4)\cdot 6H_2O$ (Fig. 2.1004)
Locality: Synthetic.
Description: Crystals grown by single diffusion gel growth technique in silica hydro gel medium. Orthorhombic with unit cell parameters $a = 6.893$, $b = 6.141$, $c = 11.222$ Å. Characterized by powder X-ray diffraction data.
Kind of sample preparation and/or method of registration of the spectrum: KBr disc. Transmission.
Source: Chauhan et al. (2011).
Wavenumbers (cm^{-1}): 3522s, 3477s, 3390s, 3277s, 2481w, 2391w, 1705, 1656, 1239, 1169s, 1067s, 1024s, 894, 720sh, 688, 653sh, 543, 509.
Note: The wavenumbers were partly determined by us based on spectral curve analysis of the published spectrum.

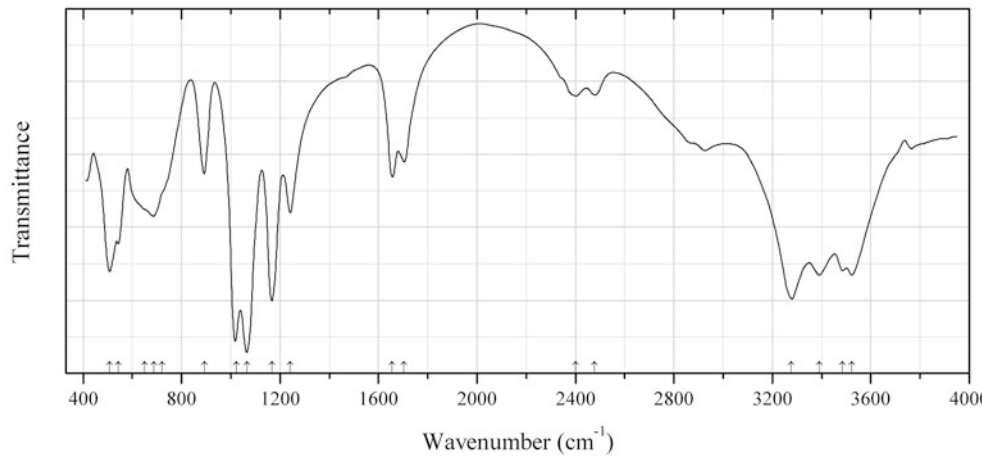

Fig. 2.1005 IR spectrum of "struvite-(Na)" drawn using data from Chauhan and Joshi (2014)

P624 "Struvite-(Na)" $NaMg(PO_4)\cdot 6H_2O$ (Fig. 2.1005)
Locality: Synthetic.
Description: Crystals grown by single diffusion gel growth technique. Orthorhombic with cell parameters as, a = 6.893, b = 6.124, c = 11.150 Å. Characterized by powder X-ray diffraction data.
Kind of sample preparation and/or method of registration of the spectrum: KBr disc. Transmission.
Source: Chauhan and Joshi (2014).
Wavenumbers (cm^{-1}): 3522s, 3485s, 3390s, 3277s, 2478w, 2401w, 1704, 1656, 1240, 1168s, 1066s, 1023s, 893, 722sh, 688, 650sh, 543, 507.
Note: The wavenumbers were partly determined by us based on spectral curve analysis of the published spectrum.

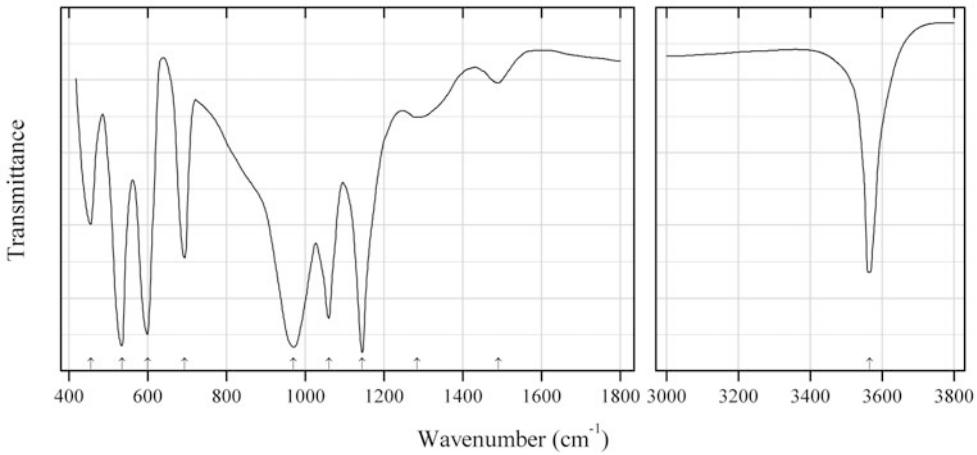

Fig. 2.1006 IR spectrum of tancoite drawn using data from Povarennykh (1981b)

P625 Tancoite $HNa_2LiAl(PO_4)_2(OH)$ (Fig. 2.1006)
Locality: Synthetic (type locality).
Description: No data.
Kind of sample preparation and/or method of registration of the spectrum: KBr disc. Transmission.
Source: Povarennykh (1981b).
Wavenumbers (cm^{-1}): 3565, 2910w, 2300w, 1490w, 1284w, 1145s, 1060s, 970s, 694, 600s, 535s, 456.
Note: The band at 3565 cm^{-1} corresponds to stretching vibrations of the OH^- group. The bands at 1490 and 1284 cm^{-1} indicate the presence of H^+ cations.

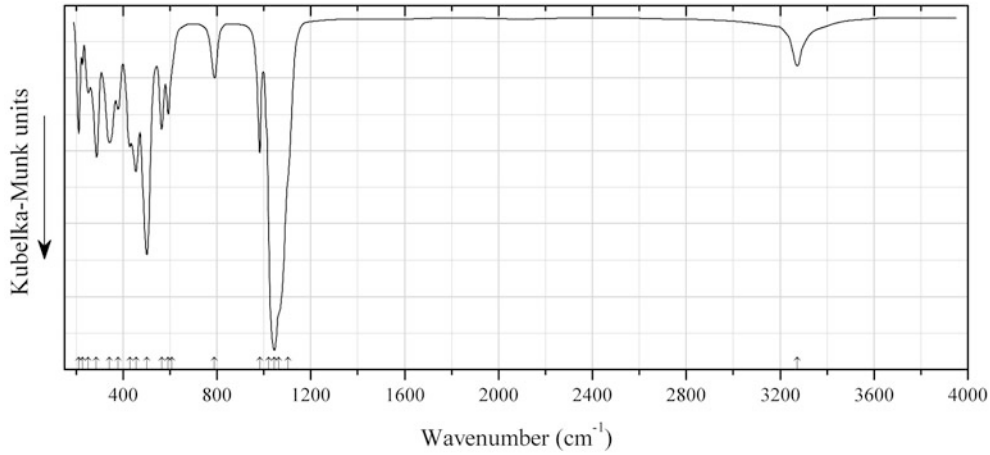

Fig. 2.1007 IR spectrum of tavorite drawn using data from Marx et al. (2010)

P626 Tavorite $LiFe^{3+}(PO_4)(OH)$ (Fig. 2.1007)
Locality: Synthetic.
Description: Synthesized hydrothermally. Confirmed by powder X-ray diffraction data and ICP-OES analyses.
Kind of sample preparation and/or method of registration of the spectrum: Diffuse reflection of powdered sample.
Source: Marx et al. (2010).
Wavenumbers (cm^{-1}): 3273w, 1103sh, 1063sh, 1045s, 1020sh, 983, 790w, 607sh, 593, 565, 501s, 455, 429, 378, 343, 287, 252w, 227w, 211.
Note: The wavenumbers were determined by us based on spectral curve analysis of the published spectrum.

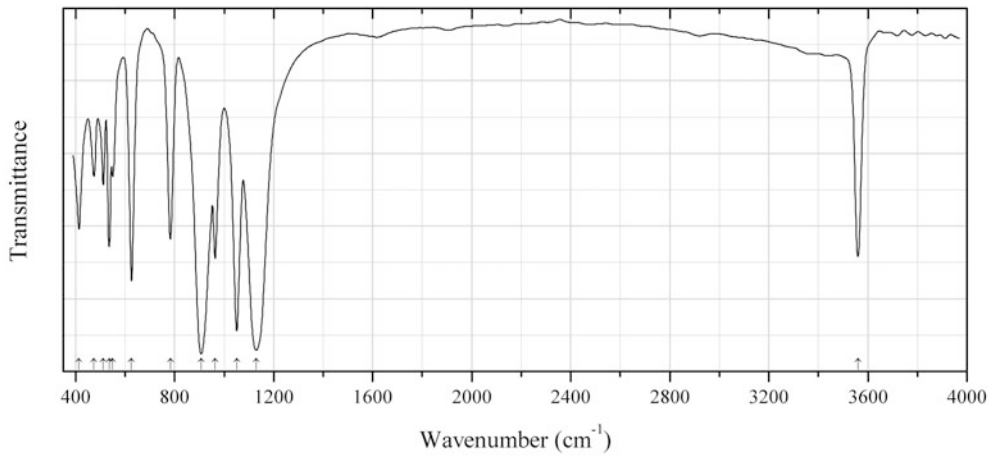

Fig. 2.1008 IR spectrum of thorium basic phosphate drawn using data from Brandel et al. (2001)

P627 Thorium basic phosphate $Th(PO_4)(OH)$ (Fig. 2.1008)
Locality: Synthetic.

Description: Synthesized hydrothermally. Orthorhombic, a = 7.177 (4), b = 9.225(5), c = 12.858(7) Å, V = 851(1) Å^3, Z = 2. Confirmed by means of electron microprobe microanalysis. The strongest lines of the powder X-ray diffraction pattern [d, Å (I, %)] are: 4.67 (100), 4.38 (57), 3.75 (33), 3.12 (30), 2.78 (43), 2.03 (31), 1.78 (31).
Kind of sample preparation and/or method of registration of the spectrum: KBr disc. Transmission.
Source: Brandel et al. (2001).
Wavenumbers (cm^{-1}): 3560, 1130s, 1052s, 964, 908s, 784, 626s, 550, 536, 512, 474, 414.

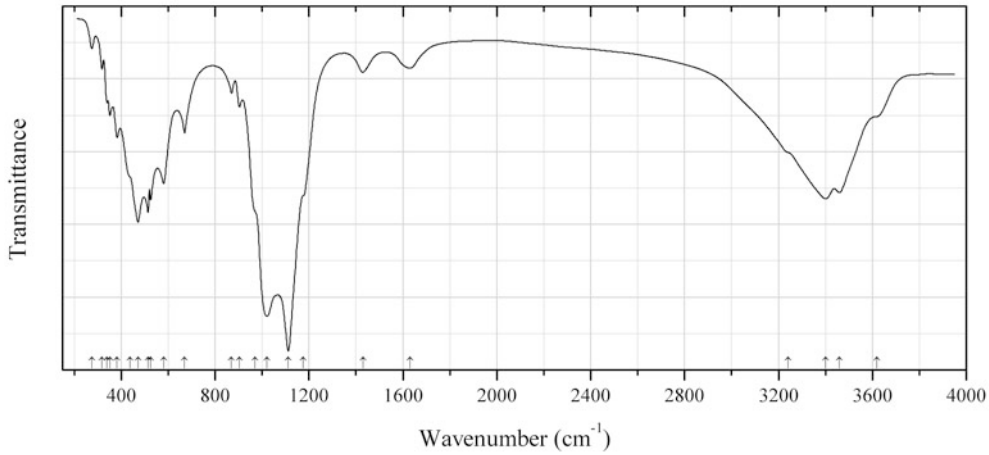

Fig. 2.1009 IR spectrum of tinsleyite drawn using data from Marincea et al. (2002)

P628 Tinsleyite $KAl_2(PO_4)_2(OH)\cdot 2H_2O$ (Fig. 2.1009)
Locality: Cioclovina Cave, Sureanu Mts., near Boşorod, Huneroada Co., Romania.
Description: Fine-grained masses from the bat guano. Characterized by electron microprobe analyses and powder X-ray diffraction data.
Kind of sample preparation and/or method of registration of the spectrum: Transmission. Kind of sample preparation is not indicated.
Source: Marincea et al. (2002).
Wavenumbers (cm^{-1}): 3620sh, 3460s, 3400s, 3240sh, 1630w, 1430w, 1175sh, 1112s, 1020s, 970sh, 904w, 870w, 670, 580, 525, 515, 472s, 438sh, 382, 352, 340w, 318w, 275w.

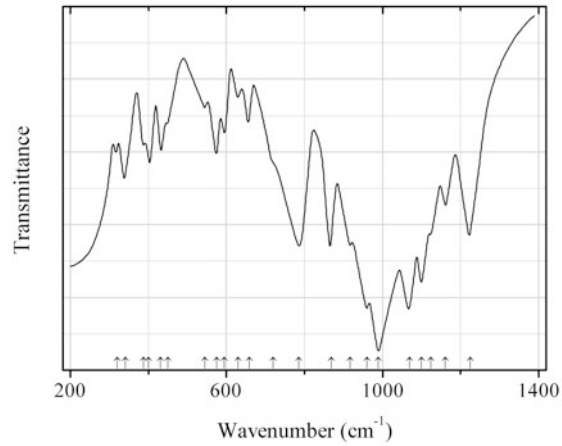

Fig. 2.1010 IR spectrum of tungsten oxyphosphate drawn using data from Kim and Condrate (1984)

P629 Tungsten oxyphosphate $W^{6+}{}_2(PO_4)_2O_3$ (Fig. 2.1010)
Locality: Synthetic.
Description: Synthesized in the solid-state reaction between WO_3 and H_3PO_4 at the temperature between 1200 and 1350 °C. Monoclinic, space group $P2_1/m$, $a \approx 7.82$, $b \approx 12.50$, $c \approx 7.75(4)$ Å, $\beta \approx 91°$. The strongest lines of the powder X-ray diffraction pattern [*d*, Å (*I*, %)] are: 4.859 (52), 4.167 (48), 3.882 (93), 3.527 (95), 3.420 (100), 3.121 (55).
Kind of sample preparation and/or method of registration of the spectrum: KBr disc. Transmission.
Source: Kim and Condrate (1984).
Wavenumbers (cm^{-1}): 1225, 1162, 1125, 1100s, 1070s, 990s, 960s, 918, 869, 785, 720sh, 659, 629w, 595, 575, 545w, 450w, 431, 400, 388, 341, 320.

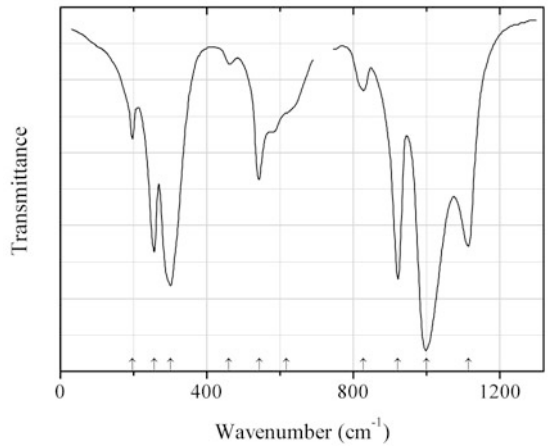

Fig. 2.1011 IR spectrum of uramphite drawn using data from Nikanovich et al. (1980)

P630 Uramphite $(NH_4)(UO_2)(PO_4)\cdot 3H_2O$ (Fig. 2.1011)
Locality: Synthetic.
Description: Confirmed by chemical analyses.
Kind of sample preparation and/or method of registration of the spectrum: Emulsion in liquid petrolatum. Transmission.
Source: Nikanovich et al. (1980).
Wavenumbers (cm^{-1}): 1115, 1000s, 922s, 828w, 618w, 543, 460w, 301s, 256, 197w.

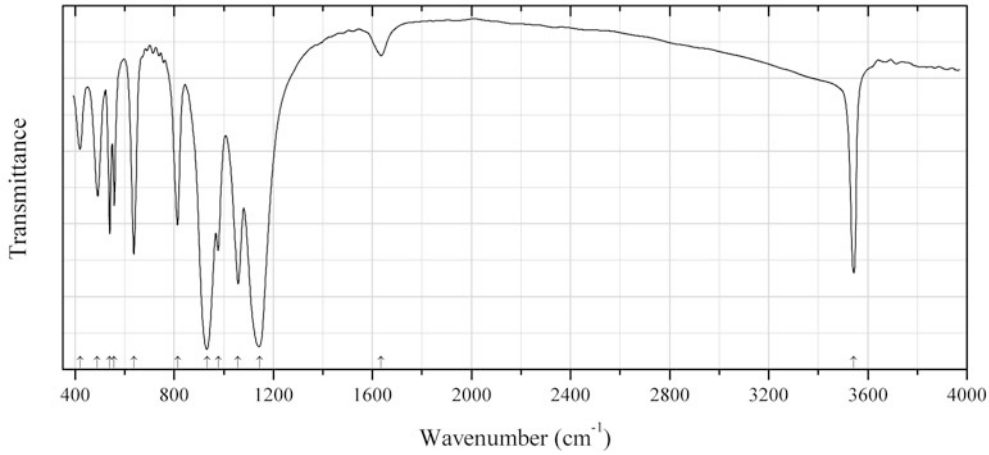

Fig. 2.1012 IR spectrum of uranium hydroxyphosphate drawn using data from Brandel et al. (2001)

P631 Uranium hydroxyphosphate $U(PO_4)(OH)$ (Fig. 2.1012)
Locality: Synthetic.
Description: Characterized by powder X-ray diffraction data.
Kind of sample preparation and/or method of registration of the spectrum: KBr disc. Transmission.
Source: Brandel et al. (2001).
Wavenumbers (cm^{-1}): 3544, 1636w, 1144s, 1058s, 978, 932s, 814, 638, 558, 540, 490, 420.
Note: The weak band at 1636 cm^{-1} indicates the presence of water molecules.

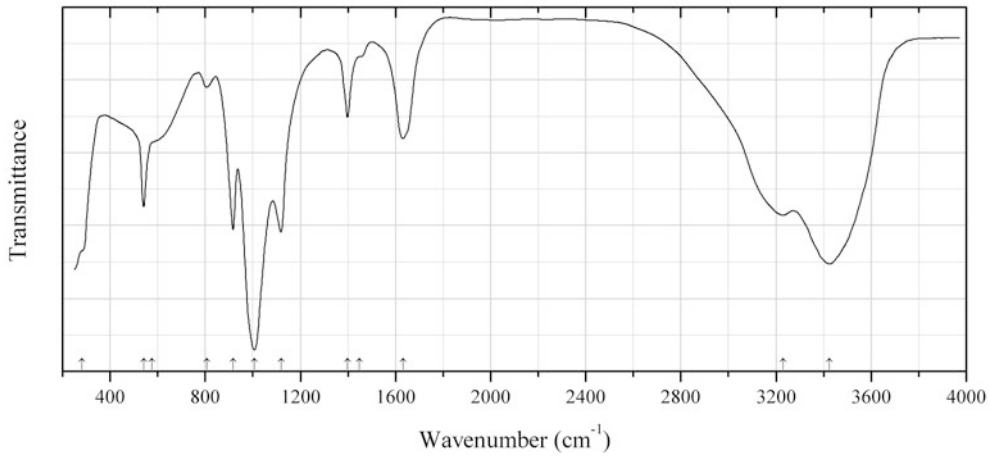

Fig. 2.1013 IR spectrum of vochtenite drawn using data from Zwaan et al. (1989)

P632 Vochtenite $Fe^{2+}Fe^{3+}(UO_2)_4(PO_4)_4(OH)\cdot 12–13H_2O$ (Fig. 2.1013)
Locality: Wheal Basset, Redruth, Cornwall, England, UK (type locality).
Description: Aggregates of brown platy crystals from the association with bassetite. Holotype sample. Monoclinic, a = 12.606, b = 19.990, c = 9.990 Å, β = 102.31°, Z = 3. D_{calc} = 3.663 g/cm^3. Optically biaxial (−), α = 1.575(2), β = 1.589(2), γ = 1.603(2). Characterized by Mössbauer

spectroscopy. The empirical formula is $(Fe^{2+}_{0.82}Mg_{0.28})Fe^{3+}_{0.90}(UO_2)_4(PO_4)_4(OH)_{0.90}\cdot 12.96H_2O$. The strongest lines of the powder X-ray diffraction pattern [*d*, Å (*I*, %) (*hkl*)] are: 9.998 (100) (020), 4.999 (30) (040), 4.892 (45) (002), 3.475 (70) (311), 3.333 (50) (060), 3.087 (40) (232), 2.205 (40) (24–4), 2.111 (45) (34–4, 47–1).

Kind of sample preparation and/or method of registration of the spectrum: KBr disc. Transmission.

Source: Zwaan et al. (1989).

Wavenumbers (cm^{-1}): 3425s, 3230, 1631, 1448sh, 1398, 1119s, 1007s, 917s, 806w, 577sh, 541, 282sh.

Note: The wavenumbers were determined by us based on spectral curve analysis of the published spectrum.

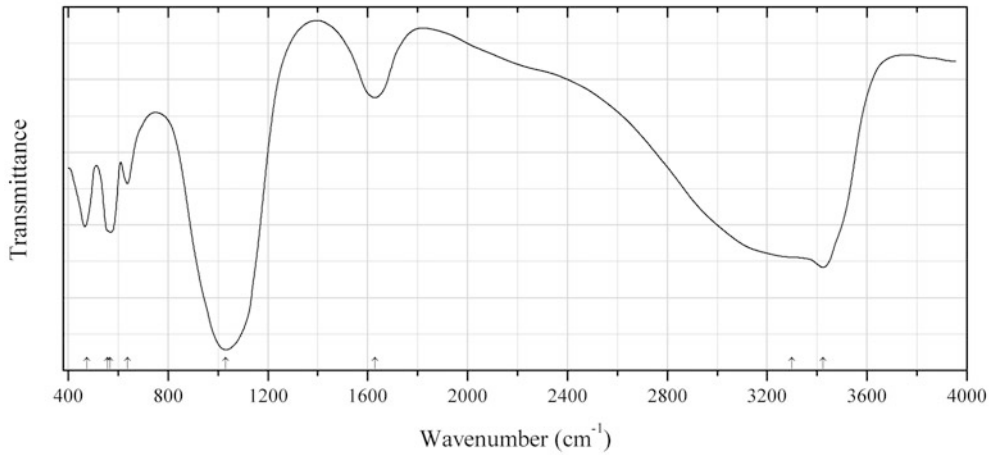

Fig. 2.1014 IR spectrum of wilhelmvierlingite drawn using data from Mücke (1983)

P633 Wilhelmvierlingite $CaMn^{2+}Fe^{3+}(PO_4)_2(OH)\cdot 2H_2O$ (Fig. 2.1014)

Locality: Hagendorf South pegmatite, Cornelia mine, Hagendorf, Waidhaus, Upper Palatinate, Bavaria, Germany (type locality).

Description: Pale yellow to brownish yellow crystals from the association with rockbridgeite. Holotype sample. Orthorhombic, a = 14.80, b = 18.70, c = 7.31 Å, Z = 8. Optically biaxial (−), α = 1.637, β = 1.664, γ = 1.692. The empirical formula is $(Ca_{0.82}Zn_{0.13})Mn_{0.99}Fe_{0.95}(PO_4)(OH)\cdot 2.33H_2O$. The strongest lines of the powder X-ray diffraction pattern [*d*, Å (*I*, %)] are: 9.34 (70), 5.00 (60), 4.67 (40), 2.86 (100), 2.58 (40), 1.98 (50), 1.96 (40).

Kind of sample preparation and/or method of registration of the spectrum: No data.

Source: Mücke (1983).

Wavenumbers (cm^{-1}): 3425s, 3300sh, 1628, 1032s, 637, 569, 557sh, 475.

Note: The wavenumbers were determined by us based on spectral curve analysis of the published spectrum.

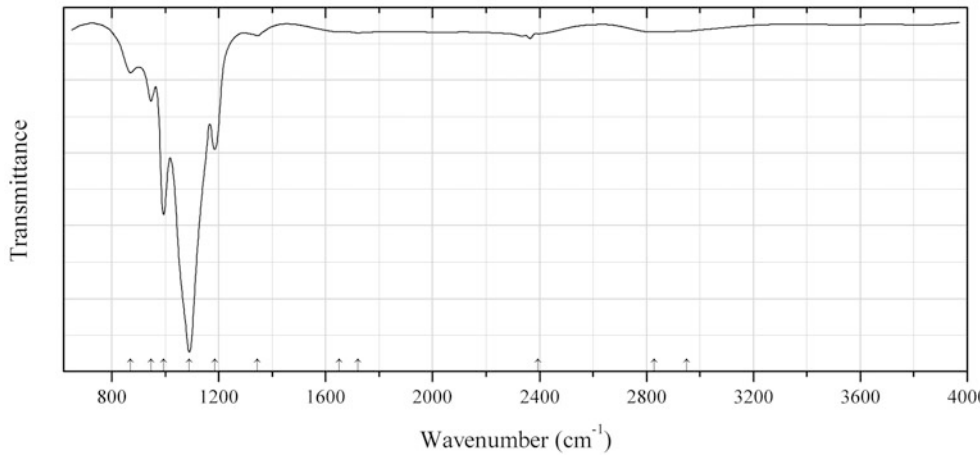

Fig. 2.1015 IR spectrum of wopmayite drawn using data from Cooper et al. (2013a)

P634 Wopmayite $Ca_6Na_3\square Mn(PO_4)_3(HPO_4)_4$ (Fig. 2.1015)
Locality: Tanco pegmatite, Tanco mine, Bernic Lake, Manitoba, Canada (type locality).
Description: Rhomb-shaped crystal from the association with rhodochrosite, quartz, whitlockite, apatite, etc. Holotype sample. The crystal structure is solved. Trigonal, space group *R*3*c*, a = 10.3926 (2), c = 37.1694(9) Å, V = 3476.7(2) Å^3, Z = 6. D_{calc} = 3.027 g/cm^3. Optically uniaxial (−), ω = 1.617 (2), ε = 1.613(2). The empirical formula is (electron microprobe): $(Ca_{7.19}Na_{1.88}Sr_{0.09})(Mn_{0.56}Mg_{0.11}Fe_{0.25}Al_{0.08})(PO_4,HPO_4)_7$. The strongest lines of the powder X-ray diffraction pattern [*d*, Å (*I*, %) (*hkl*)] are: 8.017 (31) (012), 6.421 (32) (−114), 5.166 (33) (−120), 3.425 (29) (−1.1.10), 3.186 (88) (−234), 2.858 (100) (0.2.10), 2.589 (68) (−240).
Kind of sample preparation and/or method of registration of the spectrum: An IR microscope and a diamond-anvil cell were used.
Source: Cooper et al. (2013a).
Wavenumbers (cm^{-1}): 2950sh, 2830w, 2395w, (1720w), (1651w), 1345w, 1185, 1090s, 994s, 947, 870w.
Note: The bands in the range 1300–3000 cm^{-1} indicate the presence of acid phosphate groups.

P635 Xenotime-(Yb) $Yb(PO_4)$
Locality: Synthetic.
Description: Nanoparticles synthesized by mild hydrothermal method. The formula is $Yb_{0.95}Tb_{0.05}(PO_4)$. Characterized by powder X-ray diffraction data.
Kind of sample preparation and/or method of registration of the spectrum: KBr disc. Transmission.
Source: Zhang et al. (2010).
Wavenumbers (cm^{-1}): ~3431, ~1635, ~1006, ~635, ~512.
Note: The bands at ~3431 and ~1635 cm^{-1} are due to water molecules present in the admixed amorphous phase $(Yb,Tb)PO_4{\cdot}nH_2O$.

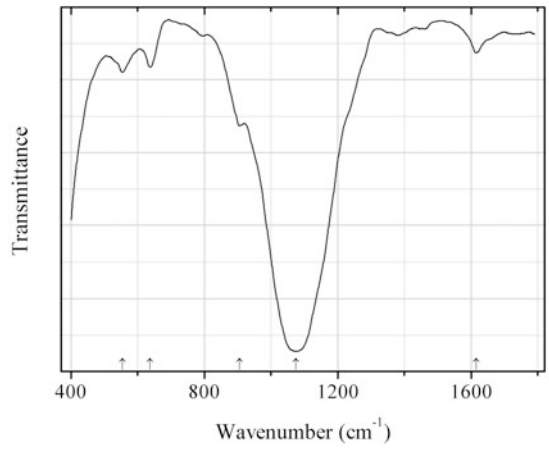

Fig. 2.1016 IR spectrum of zirconium phosphate drawn using data from Orlova et al. (2009)

P636 Zirconium phosphate $Zr_3(PO_4)_4$ (Fig. 2.1016)
Locality: Synthetic.
Description: Trigonal, space group *P*-3*c*, $a = 8.804$, $c = 23.1$ Å.
Kind of sample preparation and/or method of registration of the spectrum: Powdery film on the KBr substrate. Transmission.
Source: Orlova et al. (2009).
Wavenumbers (cm^{-1}): (1615), 1074s, 905, 637w, 554w.

P637 Torbernite $Cu(UO_2)_2(PO_4)_2 \cdot 12H_2O$
Locality: Marianské Lázně (Schönfiehl bei Marienbad), Bohemia, Czech Republic.
Kind of sample preparation and/or method of registration of the spectrum: KBr disc. Absorption.
Source: Moenke (1962).
Wavenumbers (cm^{-1}): 3570, 3430, 2940w, 1635, 1410w, 1115s, 1013s, 915s, 805, 695, 615, 550s, 465.

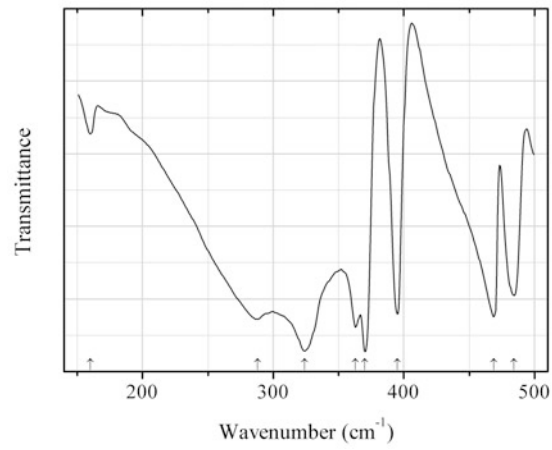

Fig. 2.1017 IR spectrum of iridium phosphide P638 drawn using data from Lutz et al. (1983)

P638 Iridium phosphide P638 IrP_2 (Fig. 2.1017)
Locality: Synthetic.
Description: Prepared by annealing stoichiometric mixture of the elements in an evacuated quartz tube at 1100 °C for 8 days. Characterized by powder X-ray diffraction data.
Kind of sample preparation and/or method of registration of the spectrum: Nujol mull. Transmission.
Source: Lutz et al. (1983).
Wavenumbers (cm^{-1}): 484, 469, 395, 370s, 363s, 324s, 288, 160w.

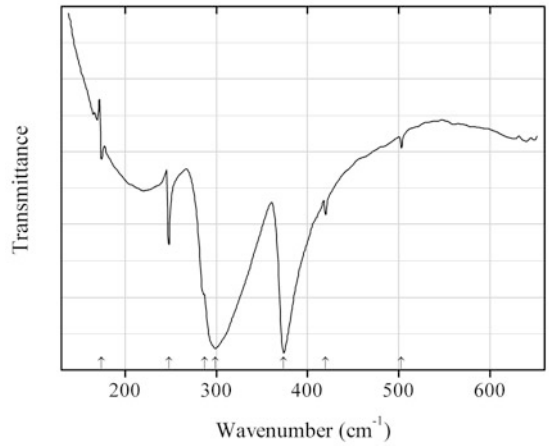

Fig. 2.1018 IR spectrum of iridium phosphide P639 drawn using data from Kliche (1991)

P639 Iridium phosphide P639 IrP_3 (Fig. 2.1018)
Locality: Synthetic.
Description: Prepared by annealing stoichiometric mixture of the pure elements in an evacuated quartz tube at 1273 K for 14 days.
Kind of sample preparation and/or method of registration of the spectrum: Polyethylene disc. Transmission.
Source: Kliche (1991).
Wavenumbers (cm^{-1}): 503w, 420w, 374s, 299s, 287sh, 248, 174w.

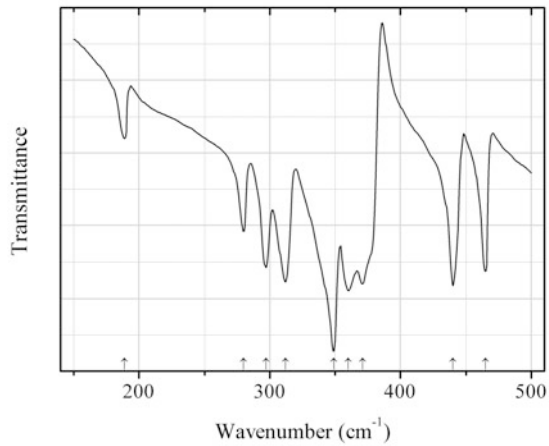

Fig. 2.1019 IR spectrum of rhodium diphosphide drawn using data from Lutz et al. (1983)

P640 Rhodium diphosphide RhP_2 (Fig. 2.1019)
Locality: Synthetic.
Description: Prepared by heating stoichiometric mixture of the elements in a closed tube at 1100 °C for 8 days. Characterized by powder X-ray diffraction data.
Kind of sample preparation and/or method of registration of the spectrum: Nujol mull. Transmission.
Source: Lutz et al. (1983).
Wavenumbers (cm^{-1}): 465, 440, 371s, 360s, 349s, 312s, 297, 280, 189w.

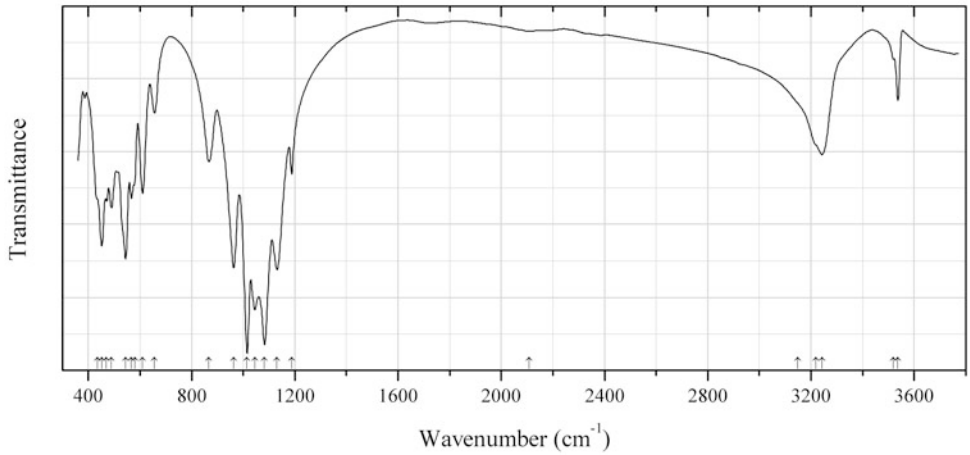

Fig. 2.1020 IR spectrum of bjarebyite obtained by N.V. Chukanov

P641 Bjarebyite $BaMn^{2+}{}_2Al_2(PO_4)_3(OH)_3$ (Fig. 2.1020)
Locality: Buranga pegmatite, Gatumba district, Western Province, Rwanda.
Description: Olive-green grains from the association with burangaite, gatumbaite, and other phosphates. The empirical formula is (electron microprobe): $(Ba_{0.98}Na_{0.02})(Mn_{1.51}Fe^{2+}{}_{0.47}Mg_{0.02})(Al_{1.84}Fe^{3+}{}_{0.14}Ti_{0.02})(PO_4)_3(OH)_3$.
Kind of sample preparation and/or method of registration of the spectrum: KBr disc. Absorption.
Wavenumbers (cm^{-1}): 3537, 3520w, 3243, 3220sh, 3150sh, 2109w, 1188, 1131s, 1083s, 1045s, 1015s, 963s, 867, 657, 610, 580sh, 567, 544s, 490, 470, 452s, 435sh.

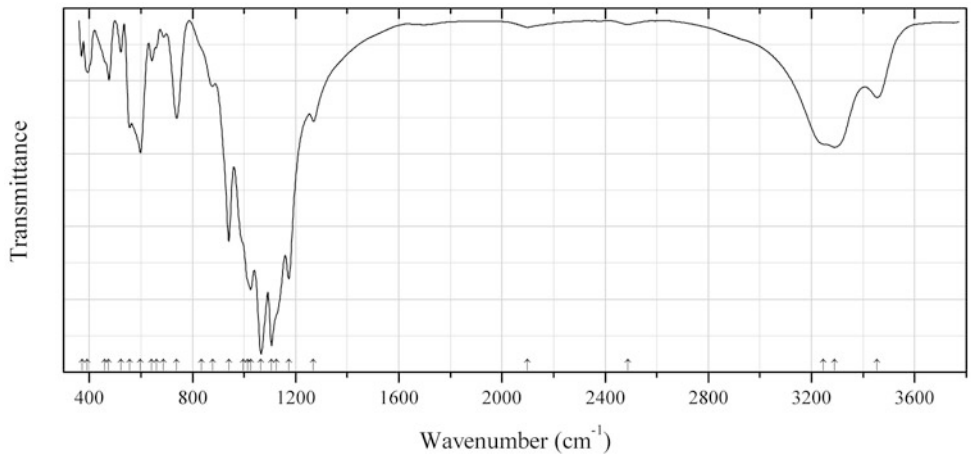

Fig. 2.1021 IR spectrum of palermoite obtained by N.V. Chukanov

P642 Palermoite $SrLi_2Al_4(PO_4)_4(OH)_4$ (Fig. 2.1021)
Locality: Palermo mine, North Groton, Grafton Co., New Hampshire, USA (type locality).
Description: Colourless prismatic crystal. The empirical formula is (electron microprobe): $(Sr_{0.93}Na_{0.08})Li_x(Al_{3.65}Fe_{0.09}Mn_{0.02}Mg_{0.02})P_{4.06}(O,OH)_{20}$.
Kind of sample preparation and/or method of registration of the spectrum: KBr disc. Absorption.
Wavenumbers (cm^{-1}): 3455, 3289, 3245sh, 2487w, 2098w, 1269, 1173s, 1125sh, 1106s, 1066s, 1025s, 1015sh, 997sh, 941s, 878, 835sh, 738, 687w, 660sh, 642, 598, 556, 522, 475, 460sh, 392, 372.

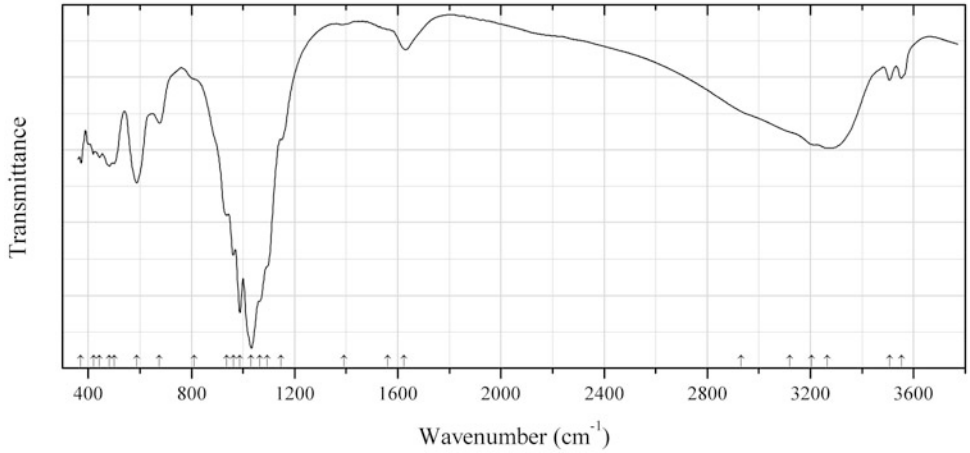

Fig. 2.1022 IR spectrum of eleonorite obtained by N.V. Chukanov

P643 Eleonorite $Fe^{3+}{}_6(PO_4)_4O(OH)_4 \cdot 6H_2O$ (Fig. 2.1022)
Locality: Rotläufchen mine, Waldgirmes, Wetzlar, Hesse, Germany.
Description: Red-brown flattened prismatic crystalsfrom the association with goethite, quartz, calcite, lepidocrocite, Mn oxides, cacoxenite, etc. Neotype sample. Monoclinic, space group *C2/c*, $a = 20.679(10)$, $b = 5.148(2)$, $c = 19.223(9)$ Å, $\beta = 93.574(9)°$, $V = 2042.5(16)$ $Å^3$, $Z = 4$. $D_{meas} = 1.92(1)$ g/cm^3, $D_{calc} = 1.931$ g/cm^3. Optically biaxial (+), $\alpha = 1.765(4)$, $\beta = 1.780(5)$, $\gamma = 1.812(6)$, $2V = 75(10)°$. The empirical formula is $(Fe^{3+}{}_{5.76}Al_{0.18}Mn^{3+}{}_{0.09})(PO_4)_{3.92}O(OH)_{4.34} \cdot 5.98H_2O$. The strongest lines of the powder X-ray diffraction pattern [*d*, Å (*I*, %) (*hkl*)] are: 10.41 (100) (200), 9.67 (38) (002), 7.30 (29) (20–2), 4.816 (31) (111, 004), 3.432 (18) (600, 114, 404, 313), 3.197 (18) (510, 51–1, 006, 31–4, 602), 3.071 (34) (314, 11–5).
Kind of sample preparation and/or method of registration of the spectrum: KBr disc. Absorption.
Wavenumbers (cm^{-1}): 3553, 3506, 3265s, 3205, 3120sh, 2930sh, 1625, 1560sh, 1392w, 1147, 1095sh, 1065sh, 1032s, 988s, 962s, 937s, 810sh, 676, 588s, 500, 482, 443, 422, 369.

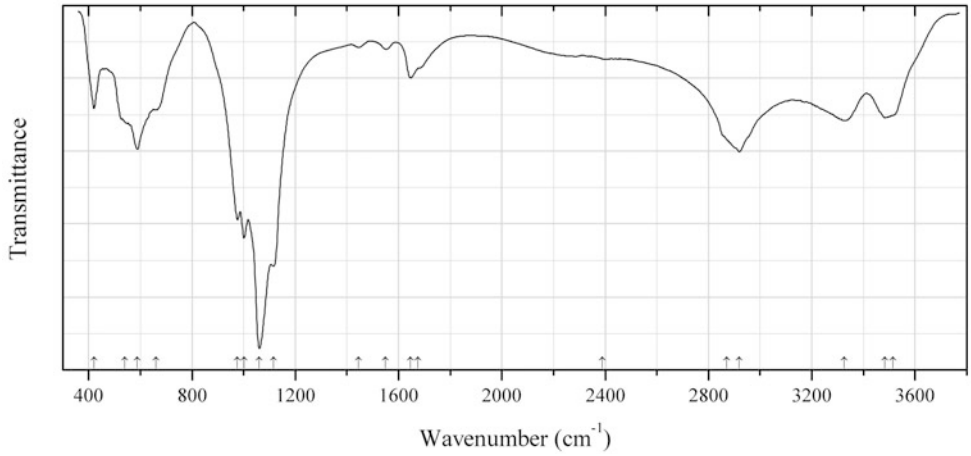

Fig. 2.1023 IR spectrum of montgomeryite obtained by N.V. Chukanov

P644 Montgomeryite $Ca_4MgAl_4(PO_4)_6(OH)_4 \cdot 12H_2O$ (Fig. 2.1023)
Locality: A stone quarry near the village Nikolskoye, Shelkandy ridge, Uiskiy district, Chelyabinsk region, Southern Urals, Russia.
Description: Colourless platy crystals from the association with apatite. Investigated by I.V. Pekov. The empirical formula is (electron microprobe): $Ca_{3.70}Mg_{1.08}Fe_{0.62}Al_{3.62}P_{5.97}O_{24}(OH)_4 \cdot nH_2O$. The strongest lines of the powder X-ray diffraction pattern [*d*, Å (*I*, %)] are: 12.13 (73), 9.30 (35), 5.55 (17), 5.12 (100), 3.135 (24), 2.958 (48), 2.894 (40), 2.619 (36).
Kind of sample preparation and/or method of registration of the spectrum: KBr disc. Absorption.
Wavenumbers (cm^{-1}): 3515sh, 3483, 3326, 2919, 2870sh, 2390sh, 1675sh, 1646, 1550w, 1445w, 1116s, 1061s, 1001s, 976s, 660sh, 589, 540sh, 421.

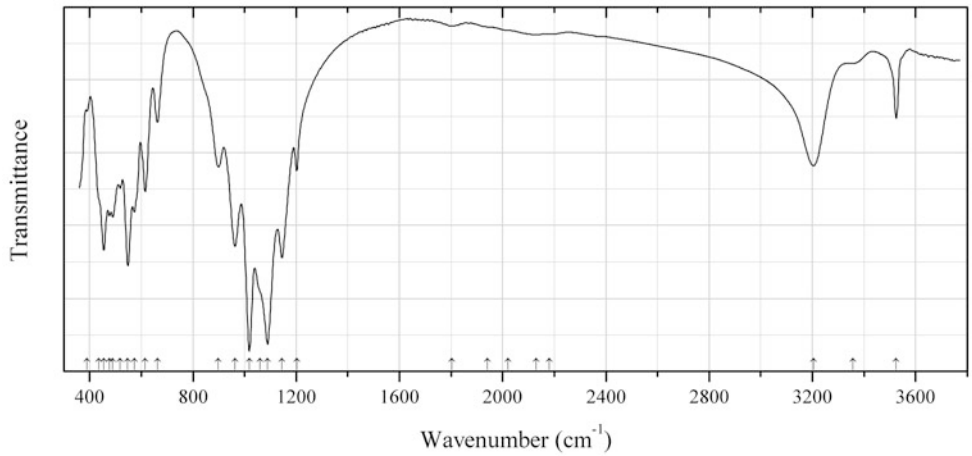

Fig. 2.1024 IR spectrum of penikisite Fe^{2+} analogue obtained by N.V. Chukanov

P645 Penikisite Fe^{2+}analogue $Ba(Fe^{2+},Mg)_2Al_2(PO_4)_3(OH)_3$ (Fig. 2.1024)
Locality: Blow river, Yukon Territory, Canada.
Description: Green crystals from the association with quartz and siderite. The empirical formula is (electron microprobe): $Ba_{1.00}(Fe^{2+}{}_{0.98}Mg_{0.92}Mn_{0.08})(Al_{1.80}Fe^{3+}{}_{0.17}Ti_{0.03})(PO_4)_{3.00}(OH)_3$.

Kind of sample preparation and/or method of registration of the spectrum: KBr disc. Absorption.
Wavenumbers (cm^{-1}): 3525, 3356w, 3204, 2180w, 2130w, 2020w, 1940w, 1803w, 1202, 1145s, 1089s, 1060sh, 1018s, 963s, 899, 662, 615, 573, 548s, 517, 489, 477, 454s, 435sh, 390w.

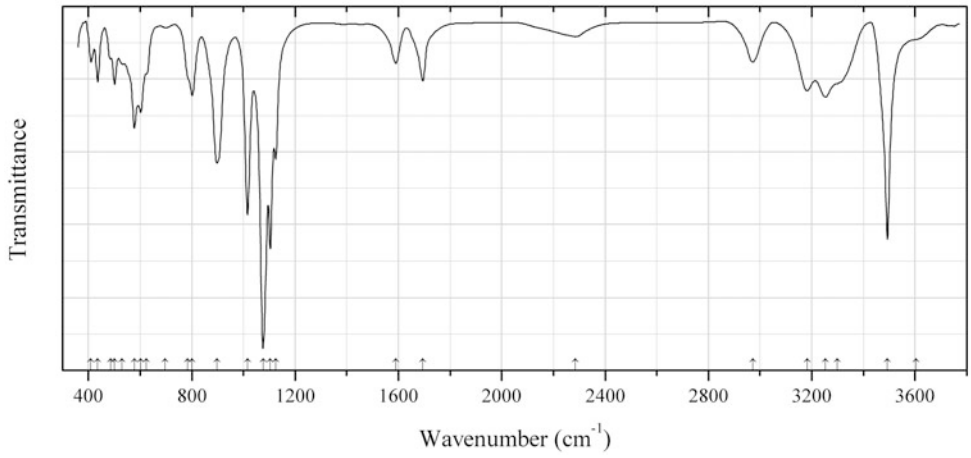

Fig. 2.1025 IR spectrum of nissonite obtained by N.V. Chukanov

P646 Nissonite $Cu_2Mg_2(PO_4)_2(OH)_2 \cdot 5H_2O$ (Fig. 2.1025)
Locality: Old Copper Prospect, Panoche valley, San Benito Co., California, USA (type locality).
Description: Blue-green crust. Confirmed by qualitative electron microprobe analysis.
Kind of sample preparation and/or method of registration of the spectrum: KBr disc. Absorption.
Wavenumbers (cm^{-1}): 3605w, 3493s, 3300sh, 3253, 3183, 2971, 2284w, 1695, 1590, 1125, 1104s, 1076s, 1016s, 897, 802, 785sh, 697w, 625sh, 602, 578, 531w, 501, 486w, 436, 410.
Note: Baseline is corrected.

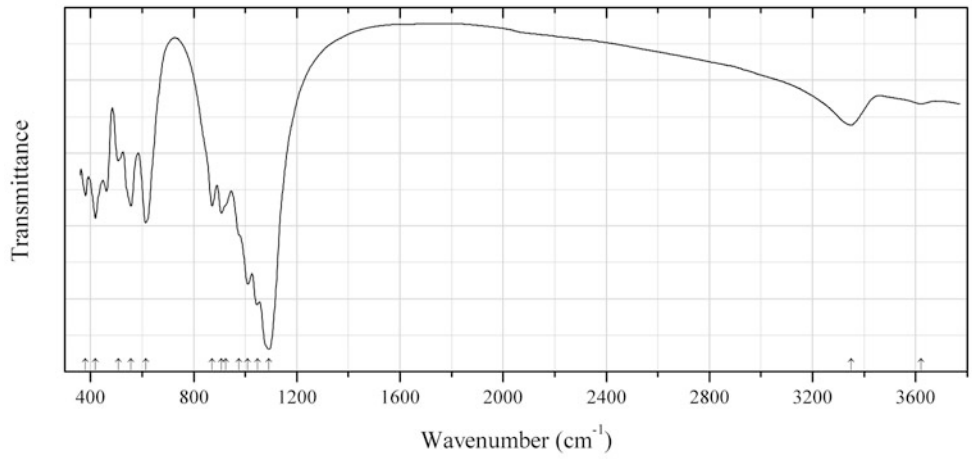

Fig. 2.1026 IR spectrum of curetonite obtained by N.V. Chukanov

P647 Curetonite $Ba(Al,Ti)(PO_4)(OH,O)F$ (Fig. 2.1026)
Locality: Redhouse barite mine, Potosi district, Osgood Mts., Humboldt Co., Nevada, USA (type locality).
Description: Green crystals from the association with barite and potassium feldspar. The empirical formula is (electron microprobe): $Ba_{1.0}(Al_{0.7}Ti_{0.15}V_{0.1})(PO_4)_{1.05}(OH,O)_xF_{1.3}$.
Kind of sample preparation and/or method of registration of the spectrum: KBr disc. Absorption.
Wavenumbers (cm^{-1}): 3620w, 3350, 1092s, 1048s, 1010s, 975sh, 925sh, 908, 872, 614s, 557, 507, 419s, 380.

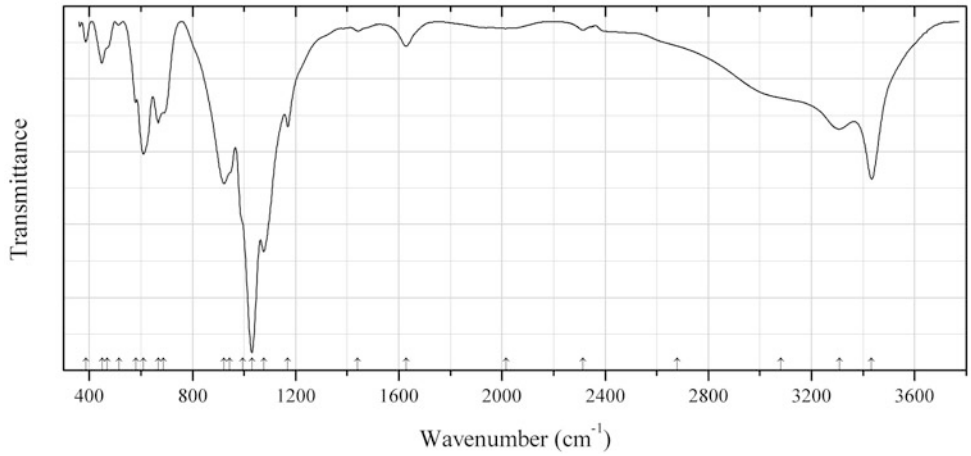

Fig. 2.1027 IR spectrum of childrenite obtained by N.V. Chukanov

P648 Childrenite $Fe^{2+}Al(PO_4)(OH)_2 \cdot H_2O$ (Fig. 2.1027)
Locality: Siglo Veinte mine, Llallagua, Rafael Bustillo province, Potosí department, Bolivia.
Description: Light brown spherulitic crusts from the association with vauxite and quartz. The empirical formula is (electron microprobe): $(Fe_{0.77}Mn_{0.15}Ca_{0.07}Mg_{0.01})(Al_{0.97}Fe_{0.03})(PO_4)_{1.02}(OH)_x \cdot nH_2O$.
Kind of sample preparation and/or method of registration of the spectrum: KBr disc. Absorption.
Wavenumbers (cm^{-1}): 3433s, 3308, 3080sh, 2680sh, (2315w), 2015w, 1628, 1441w, 1170, 1076s, 1030s, 995sh, 945sh, 922s, 688, 667, 610, 581, 515w, 470sh, 449, 388.

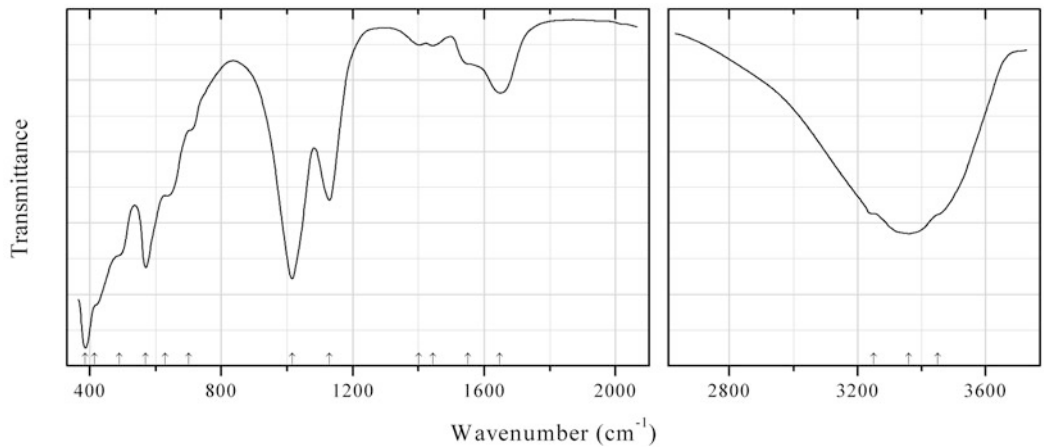

Fig. 2.1028 IR spectrum of zirconium oxyphosphate obtained by N.V. Chukanov

P649 Zirconium oxyphosphate $CaZr_8(PO_4)_2O_8 \cdot nH_2O$ (?) (Fig. 2.1028)
Locality: Iron mine, Kovdor, Kovdor alkaline ultramafic complex, Kola peninsula, Murmansk region, Russia.
Description: Pale beige pseudomorphs after catapleiite crystals from dolomite carbonatite. Characterized by electron microprobe analyses and powder X-ray diffraction data. Cubic. The empirical formula is $(Ca_{0.75}Sr_{0.1}Mn_{0.1})(Zr_{4.2}Mg_{0.4}Nb_{0.2}Fe_{0.2})[(PO_4)_{1.6}(SiO_4)_{0.4}](O,OH)_8 \cdot nH_2O$.
Kind of sample preparation and/or method of registration of the spectrum: KBr disc. Absorbtion.
Wavenumbers (cm^{-1}): 3450sh, 3360s, 3250sh, 1648, 1550sh, 1444w, 1402w, 1129, 1016s, 700sh, 630sh, 570s, 490sh, 415sh, 386s.

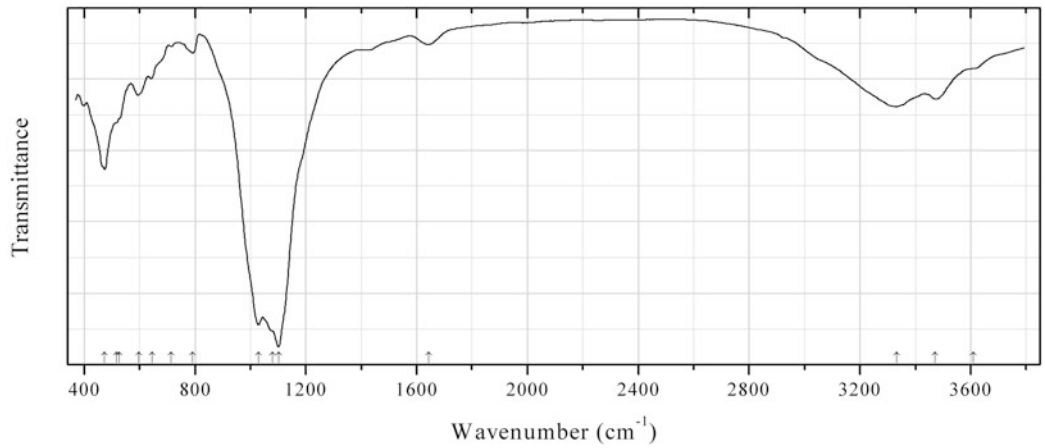

Fig. 2.1029 IR spectrum of tinsleyite obtained by N.V. Chukanov

P650 Tinsleyite $KAl_2(PO_4)_2(OH) \cdot 2H_2O$ (Fig. 2.1029)
Locality: Southern slope of Cerro Mejillones, Mejillones Peninsula, Mejillones, Antofagasta, II Region, Chile.
Description: Pale pinkish crystals from the association with a whitlockite-type mineral. The empirical formula is (electron microprobe): $(K_{0.86}Ca_{0.10}Na_{0.04})(Al_{1.36}Fe_{0.57}Mg_{0.05})(PO_4)_{2.00}(OH) \cdot 2H_2O$.
Kind of sample preparation and/or method of registration of the spectrum: KBr disc. Absorbtion.
Wavenumbers (cm^{-1}): 3610sh, 3472, 3333, 1643w, 1101s, 1081sh, 1030s, 792w, 715w, 645, 598, 528sh, 516, 474s.

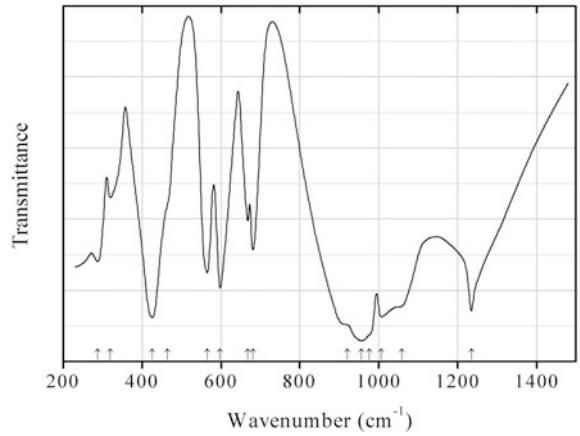

Fig. 2.1030 IR spectrum of zinc vanadyl phosphate drawn using data from Baran and Lii (1992)

P651 Zinc vanadyl phosphate $Zn_2(VO)(PO_4)_2$ (Fig. 2.1030)
Locality: Synthetic.
Description: Obtained by heating $ZnO + VO_2 + P_2O_5$ (in the molar ratio 2:1:1) in a sealed silica tube at 850 °C for 2 days. Characterized by powder X-ray diffraction data. Tetragonal, space group $I4\,cm$, $Z = 4$.
Kind of sample preparation and/or method of registration of the spectrum: KBr disc. Transmission.
Source: Baran and Lii (1992).
Wavenumbers (cm^{-1}): 1235s, 1058sh, 1007s, 976sh, 956s, 921sh, 681, 668, 598, 565, 465sh, 426s, 320, 288.

2.10 Sulfides, Sulfites, Sulfates, Carbonato-Sulfates, and Phosphato-Sulfates

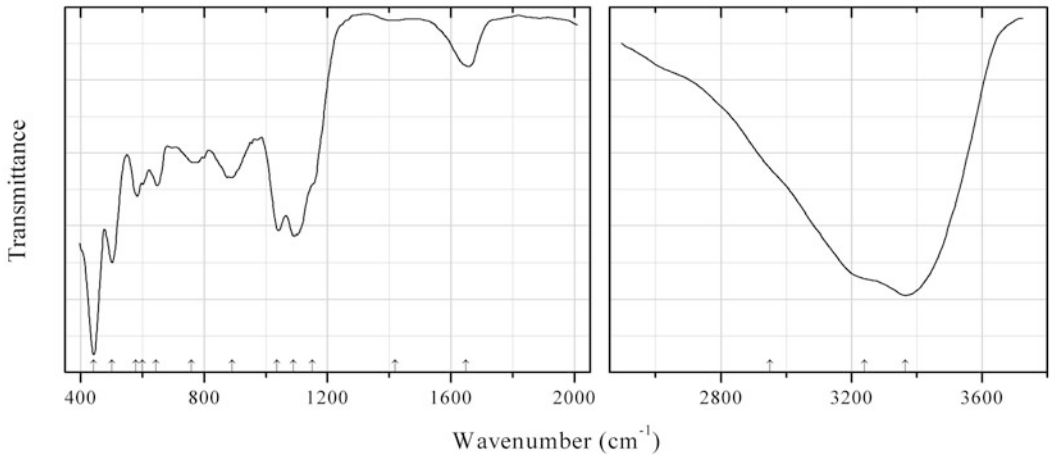

Fig. 2.1031 IR spectrum of camerolaite drawn using data from Chukanov (2014a)

S85 Camerolaite $Cu_6Al_3[Sb(OH)_6](SO_4)(OH)_{18}\cdot 2H_2O$ (Fig. 2.1031)
Locality: L'ubietová-Svätoduška, Banská Bystrica Co., Banská Bystrica region, Slovakia.

Description: Light blue acicular crystals. The empirical formula is (electron microprobe): $Cu_{6.00}(Al_{2.85}Fe_{0.09})[Sb(OH)_6]_{1.24}(SO_4)_{0.99}(OH)_y \cdot nH_2O$.
Wavenumbers (cm^{-1}): 3365s, 3240sh, 2950sh, 1648, 1420w, 1150sh, 1090s, 1037s, 890, 760, 645, 600sh, 578, 501s, 442s.
Note: This sample was described by Chukanov (2014a) as a mineral "related to camerolaite and cyanotrichite". Recent structural data (Mills et al. 2014) demonstrate that the mineral should be considered as camerolaite *ss*.

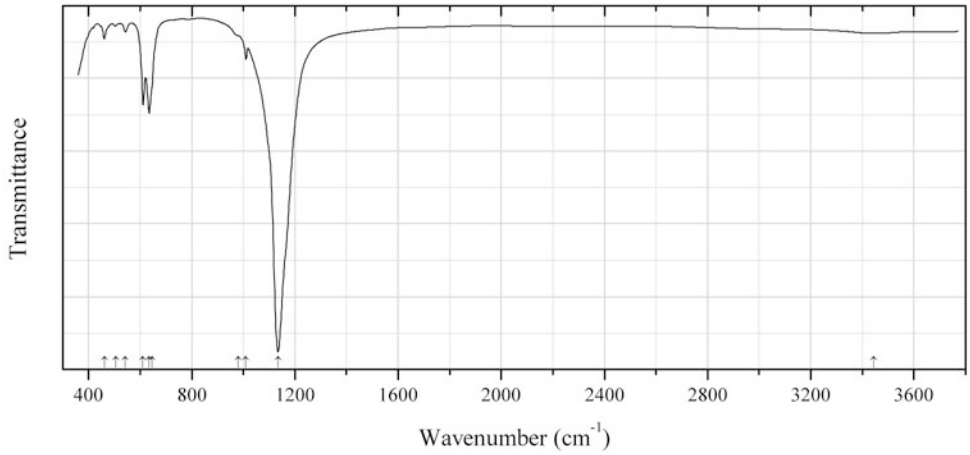

Fig. 2.1032 IR spectrum of kononovite obtained by N.V. Chukanov

S311 Kononovite $NaMg(SO_4)F$ (Fig. 2.1032)
Locality: Arsenatnaya fumarole, Second scoria cone of the Northern Breakthrough of the Great Tolbachik Fissure Eruption, Tolbachik volcano, Kamchatka peninsula, Russia (type locality).
Description: White crystals from the association with lammerite, lammerite-β, johillerite, bradaczekite, urusovite, alarsite, ericlaxmanite, kozyrevskite, hatertite, yurmarinite, popovite, euchlorine, wulffite, tilasite, svabite, aphthitalite, langbeinite, calciolangbeinite, etc. Holotype sample. Monoclinic, space group $C2/c$, $a = 6.662(2)$, $b = 8.584(3)$, $c = 7.035(2)$ Å, $\beta = 114.06(3)°$, $V = 367(1)$ $Å^3$, $Z = 4$. $D_{meas} = 2.91(1)$ g/cm^3, $D_{calc} = 2.94$ g/cm^3. Optically biaxial (+), $\alpha = 1.488(2)$, $\beta = 1.491(2)$, $\gamma = 1.496(2)$, $2V = 75(5)°$. The empirical formula is (electron microprobe): $Na_{0.99}Mg_{1.01}Zn_{0.01}S_{0.99}O_{3.97}F_{1.02}Cl_{0.01}$. The strongest lines of the powder X-ray diffraction pattern [*d*, Å (*I*, %) (*hkl*)] are: 4.766 (38) (−111), 3.233 (82) (−112), 3.210 (55) (002), 3.041 (100) (200), 2.589 (53) (130), 2.571 (38) (022).
Kind of sample preparation and/or method of registration of the spectrum: KBr disc. Absorption.
Wavenumbers (cm^{-1}): 3444w, 1135s, 1010w, 980sh, 645sh, 635, 611, 543w, 505w, 461w.

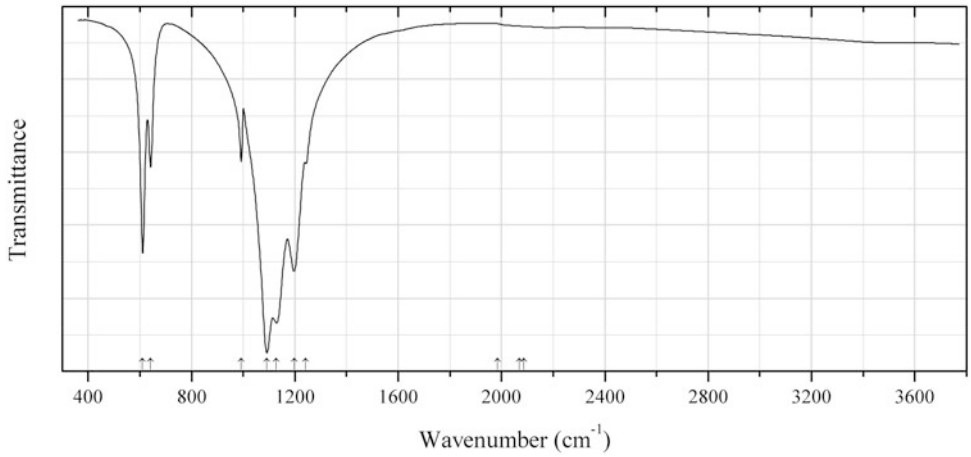

Fig. 2.1033 IR spectrum of celestine obtained by N.V. Chukanov

S312 Celestine $Sr(SO_4)$ (Fig. 2.1033)
Locality: Beineu-Kyr (Beyneu-Kyr), Tuarkyr, Turkmenistan.
Description: Pale blue transparent crystal from the association with gypsum. The empirical formula is (electron microprobe) $(Sr_{0.96}Ba_{0.02}Ca_{0.02})(SO_4)$.
Kind of sample preparation and/or method of registration of the spectrum: KBr disc. Absorption.
Wavenumbers (cm^{-1}): 2086w, 2070sh, 1984w, 1242, 1197s, 1128s, 1092s, 992, 642, 611s.

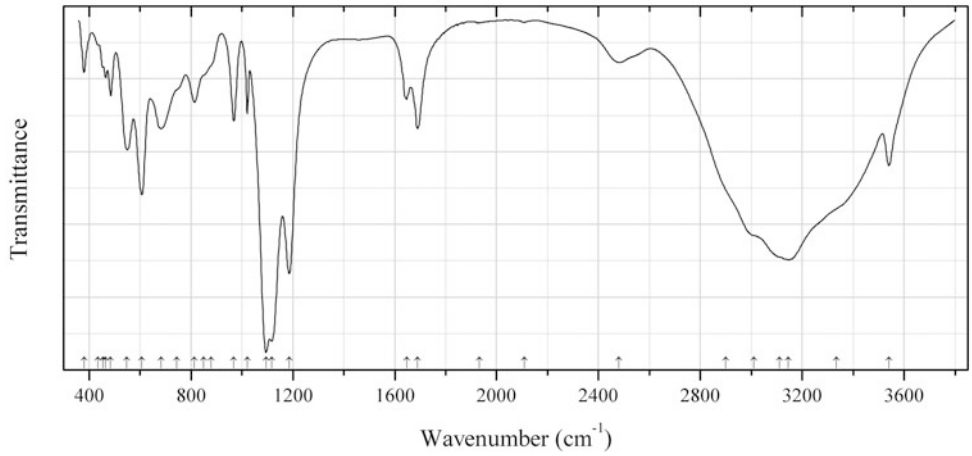

Fig. 2.1034 IR spectrum of aluminium hydroxysulfate trihydrate obtained by N.V. Chukanov

S313 Aluminium hydroxysulfate trihydrate $Al(SO_4)(OH)\cdot 3H_2O$ (Fig. 2.1034)
Locality: La Vendida copper mine (Mina La Vendida), about 5 km WNW of Sierra Gorda, Antofagasta Region, Atacama desert, Chile (type locality).
Description: Colourless platy crystals from cavities in massive aggregates of eriochalcite, Mg-rich aubertite, magnesioaubertite, belloite, and clay minerals. Holotype sample. Triclinic, space group *P*-1, a = 5.6000, b = 7.4496(8), c = 7.6709(9) Å, α = 74.7847°, β = 86.0419°, γ = 75.8103°,

V = 299.37 Å^3, Z = 2. D_{meas} = 2.11(2) g/cm^3, D_{calc} = 2.129 g/cm^3. Optically biaxial (−), α = 1.513(2), β = 1.522(2), γ = 1.526(2), 2 V = 70(5)°. The empirical formula is $Al_{0.93}(SO_4)_{0.99}(OH)_{0.81}\cdot 3.25H_2O$. The strongest lines of the powder X-ray diffraction pattern [d, Å (I, %)] are: 6.975 (100), 4.466 (18), 4.379 (19), 3.698 (18), 3.487 (20), 2.882 (17), 2.669 (54), 2.397 (40).

Kind of sample preparation and/or method of registration of the spectrum: KBr disc. Absorption.

Wavenumbers (cm^{-1}): 3540, 3335sh, 3145s, 3110sh, 3010sh, 2900sh, 2480, 2110w, 1933w, 1690, 1647, 1186s, 1117s, 1095s, 1021, 968, 880sh, 850sh, 814, 745sh, 683, 607s, 549, 485, 465, 455sh, 435sh, 382.

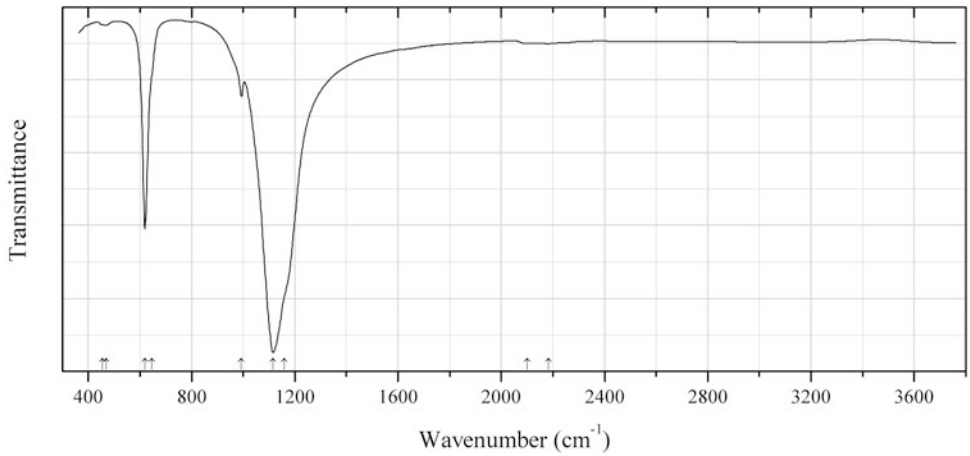

Fig. 2.1035 IR spectrum of aphthitalite obtained by N.V. Chukanov

S314 Aphthitalite $K_3Na(SO_4)_2$ (Fig. 2.1035)

Locality: Northern Breakthrough of the Main Tolbachik fracture eruption (1975–1976), Kamchatka, Russia.

Description: Colourless crystals. Investigated by I.V. Pekov. The empirical formula is $K_{3.0}Na_{1.0}(SO_4)_{2.0}$. Confirmed by single-crystal X-ray diffraction data.

Kind of sample preparation and/or method of registration of the spectrum: KBr disc. Absorption.

Wavenumbers (cm^{-1}): 2182w, 2100w, 1160sh, 1116s, 993w, 645sh, 619s, 470w, 455sh.

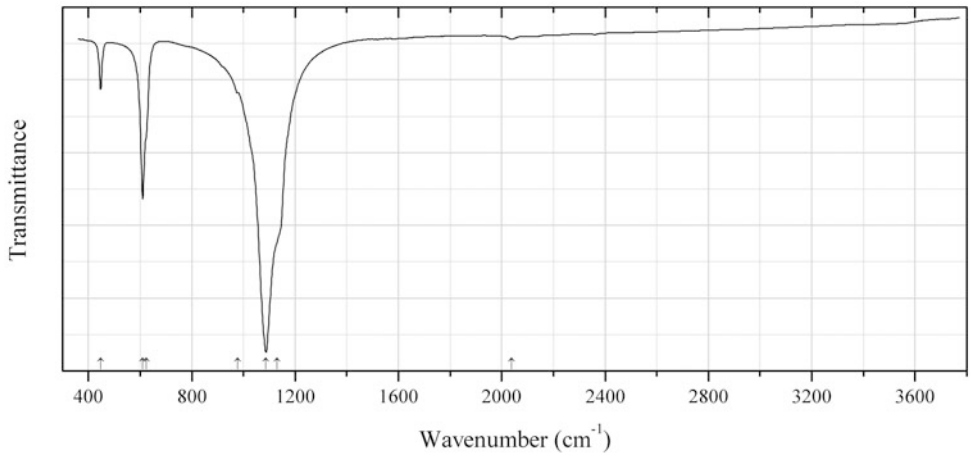

Fig. 2.1036 IR spectrum of palmierite obtained by N.V. Chukanov

S315 Palmierite $K_2Pb(SO_4)_2$ (Fig. 2.1036)
Locality: Arsenatnaya fumarole, the Second scoria cone of the Northern Breakthrough of the Great Tolbachik Fissure Eruption, Tolbachik volcano, Kamchatka peninsula, Far-Eastern Region, Russia.
Description: Aggregate of colourless crystals from the association with ericlaksmanite. Investigated by I.V. Pekov. Confirmed by the single-crystal X-ray diffraction pattern. Trigonal, a = 5.50(2), c = 20.56(6) Å. The empirical formula is (electron microprobe): $(K_{1.92}Na_{0.04}Ca_{0.02})Pb_{1.04}S_{2.00}O_{8.04}$.
Kind of sample preparation and/or method of registration of the spectrum: KBr disc. Absorption.
Wavenumbers (cm^{-1}): 2038w, 1130sh, 1087s, 978, 625sh, 610s, 447.

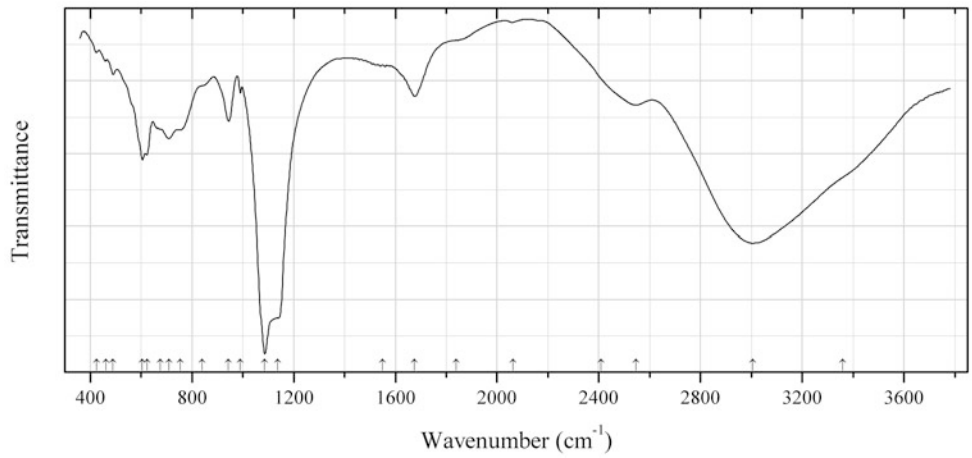

Fig. 2.1037 IR spectrum of tamarugite obtained by N.V. Chukanov

S316 Tamarugite $NaAl(SO_4)_2 \cdot 6H_2O$ (Fig. 2.1037)
Locality: La Vendida copper mine (Mina La Vendida), about 5 km WNW of Sierra Gorda, Antofagasta Region, Atacama desert, Chile (type locality).
Description: Colourless prismatic crystals from the association with jarosite, kröhnkite, and illite. Identified by morphological features and qualitative electron microprobe analysis.

Kind of sample preparation and/or method of registration of the spectrum: KBr disc. Absorption.
Wavenumbers (cm^{-1}): 3360sh, 3006s, 2547, 2410sh, 2063w, 1840sh, 1676, 1550w, 1138s, 1086s, 990w, 944, 840w, 754, 709, 675sh, 623, 605, 490w, 463w, 425w.

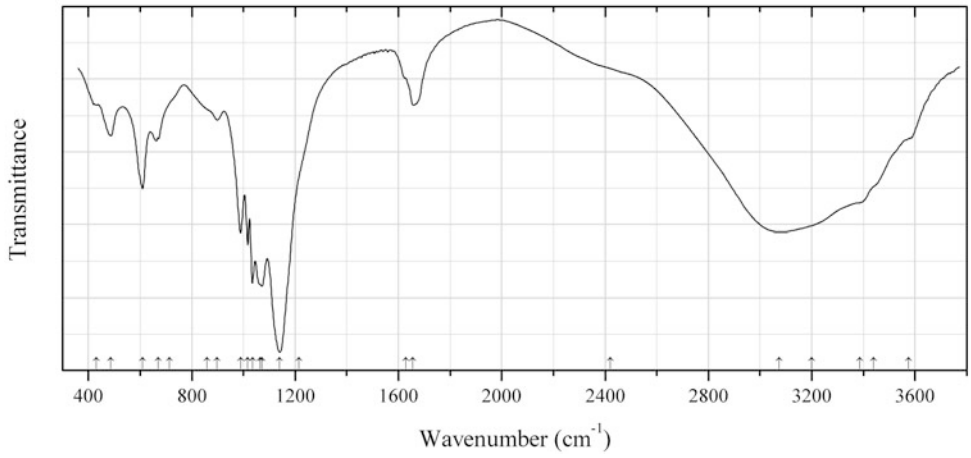

Fig. 2.1038 IR spectrum of quenstedtite obtained by N.V. Chukanov

S317 Quenstedtite $Fe^{3+}_2(SO_4)_3 \cdot 11H_2O$ (Fig. 2.1038)
Locality: Morro Mejillones, Mejillones, Antofagasta, II Region, Chile.
Description: Light violet grains with perfect cleavage from the association with chalcanthite, copiapite, römerite, anhydrite, parabutlerite, etc.
Kind of sample preparation and/or method of registration of the spectrum: KBr disc. Absorption.
Wavenumbers (cm^{-1}): 3575sh, 3440sh, 3385sh, 3200sh, 3074s, 2420sh, 1656, 1630sh, 1215sh, 1141s, 1072s, 1065sh, 1035s, 1017, 989, 899w, 860sh, 715sh, 670sh, 609, 486, 430sh.

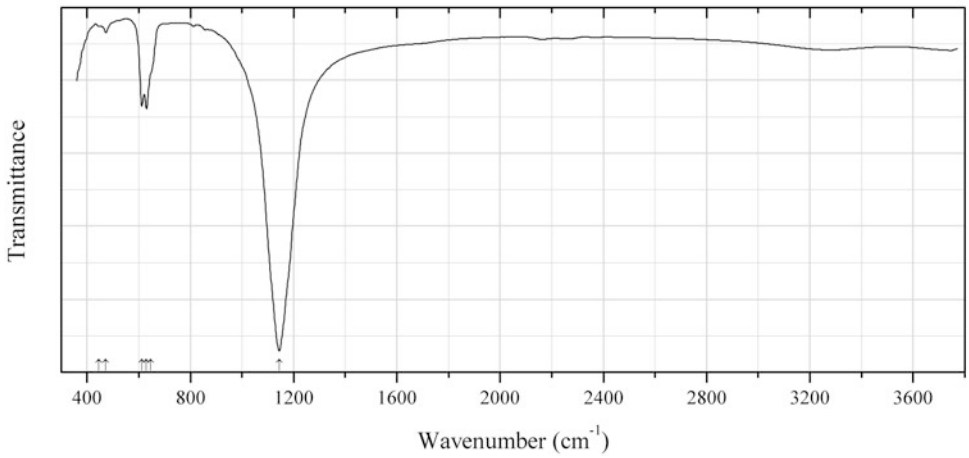

Fig. 2.1039 IR spectrum of calciolangbeinite obtained by N.V. Chukanov

S318 Calciolangbeinite $K_2Ca_2(SO_4)_3$ (Fig. 2.1039)
Locality: Yadovitaya (Poisonous) fumarole, Second scoria cone, Tolbachik volcano, Kamchatka peninsula, Kamchatka Oblast', Far-Eastern Region, Russia (type locality).
Description: Colourless crystals from the association with langbeinite, piypite, hematite, Fe- and Sb-bearing rutile, pseudobrookite, As- and Zn-bearing orthoclase, lyonsite, and chlorothionite. Holotype sample. Cubic, space group $P2_13$, a = 10.1887(2) Å, V = 1057.68(4) Å^3, Z = 4. D_{meas} = 2.68(2) g/cm^3, D_{calc} = 2.740 g/cm^3. Optically isotropic, n = 1.527(2). The empirical formula is $K_{2.01}(Ca_{1.24}Mg_{0.70}Na_{0.05}Mn_{0.02}Fe_{0.01}Al_{0.01})_{\Sigma 2.03}S_{3.00}O_{12}$. The strongest lines of the powder X-ray diffraction pattern [d, Å (I, %) (hkl)] are: 5.84 (8) (111), 4.54 (9) (120), 4.15 (27) (211), 3.218 (100) (310, 130), 2.838 (8) (230, 320), 2.736 (37) (231, 321), 2.006 (11) (431, 341), 1.658 (8) (611, 532, 352).
Kind of sample preparation and/or method of registration of the spectrum: KBr disc. Absorption.
Wavenumbers (cm^{-1}): 1144s, 645sh, 630, 612, 473w, 446w.

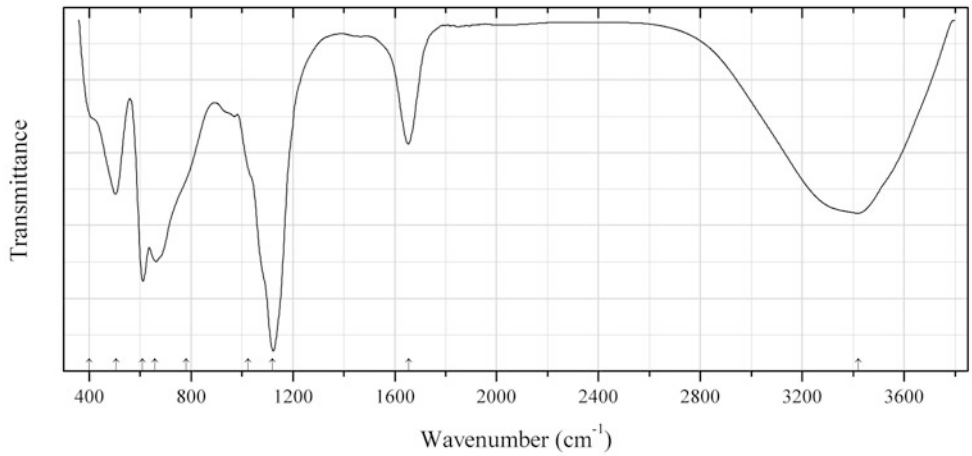

Fig. 2.1040 IR spectrum of osakaite obtained by N.V. Chukanov

S319 Osakaite $Zn_4(SO_4)(OH)_6 \cdot 5H_2O$ (Fig. 2.1040)
Locality: Friedrichssegen mine, Lahn valley, Bad Ems district, Rhineland-Palatinate (Rheinland-Pfalz), Germany.
Description: Yellow rosette-like aggregates from cavities in metallurgic slag. Identified by qualitative electron microprobe analysis and powder X-ray diffraction data obtained below 10 Å. The strongest reflections are observed at 5.50, 3.65, 2.70, and 1.55 Å.
Kind of sample preparation and/or method of registration of the spectrum: KBr disc. Absorption.
Wavenumbers (cm^{-1}): 3420s, 1655, 1120s, 1025sh, 780sh, 658s, 609s, 507s, 400.

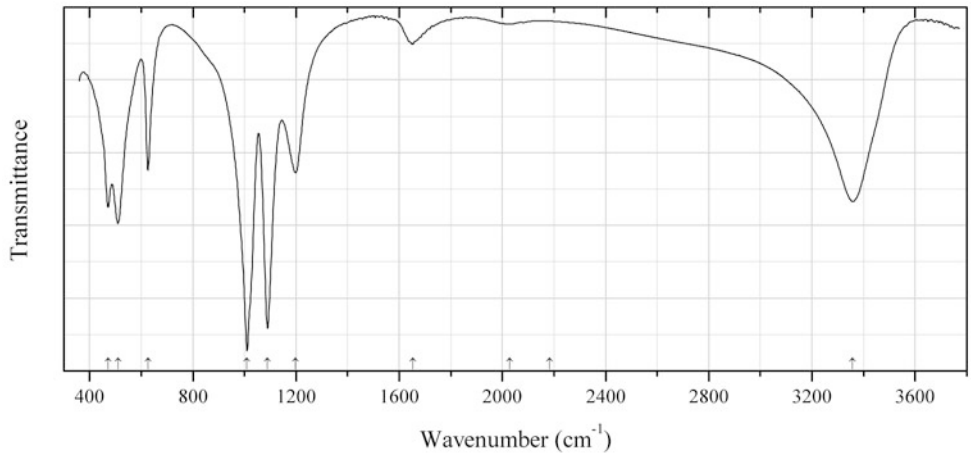

Fig. 2.1041 IR spectrum of hydroniumjarosite obtained by N.V. Chukanov

S320 Hydroniumjarosite $(H_3O)Fe^{3+}{}_3(SO_4)_2(OH)_6$ or $(H_2O)Fe^{3+}{}_3(SO_4)_2(OH)_5 \cdot H_2O$ (Fig. 2.1041)
Locality: Morro Mejillones, Mejillones, Antofagasta, II Region, Chile.
Description: Brownish-yellow transparent platy crystals from the association with destinezite, aubertite, halotrichite, and botryogen. The empirical formula is (electron microprobe): $Na_{0.02}Fe_{3.03}(SO_4)_2(OH,H_2O)_n$.
Kind of sample preparation and/or method of registration of the spectrum: KBr disc. Absorption.
Wavenumbers (cm^{-1}): 3358s, 2184w, 2028w, 1653w, 1198, 1090s, 1010s, 626, 510s, 471.
Note: The asymmetric band at 1653 cm^{-1} indicates the presence of H_2O molecules.

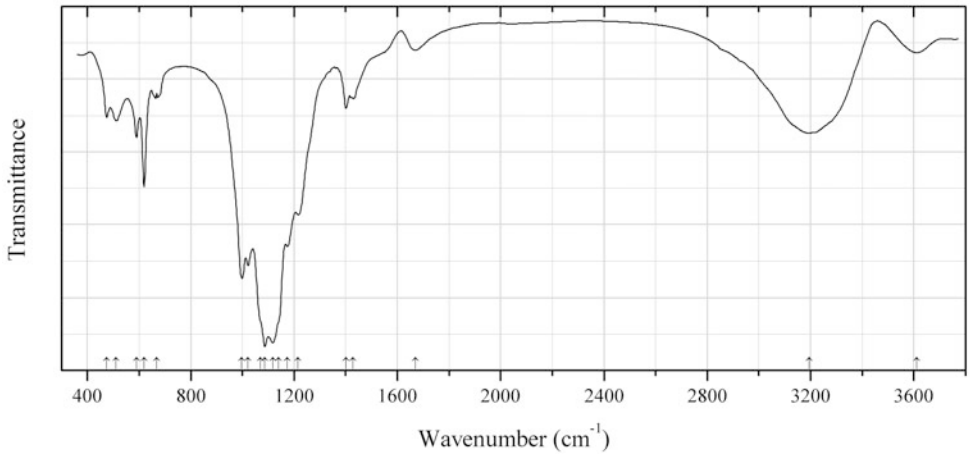

Fig. 2.1042 IR spectrum of goldichite obtained by N.V. Chukanov

S321 Goldichite $KFe^{3+}(SO_4)_2 \cdot 4H_2O$ (Fig. 2.1042)
Locality: United Verde Extension mine, Jerome, Verde district, Black Hills, Yavapai Co., Arizona, USA.
Description: Brown grains. Identified by IR spectrum.
Kind of sample preparation and/or method of registration of the spectrum: KBr disc. Absorption.

Wavenumbers (cm^{-1}): 3612w, 3194, 1670w, 1427, 1401, 1215, 1173, 1140sh, 1118s, 1087s, 1070sh, 1022s, 998s, 667w, 619, 590, 511, 475.
Note: The bands at 1427 and 1401 cm^{-1} indicate possible presence of NH_4^+ cations substituting K^+.

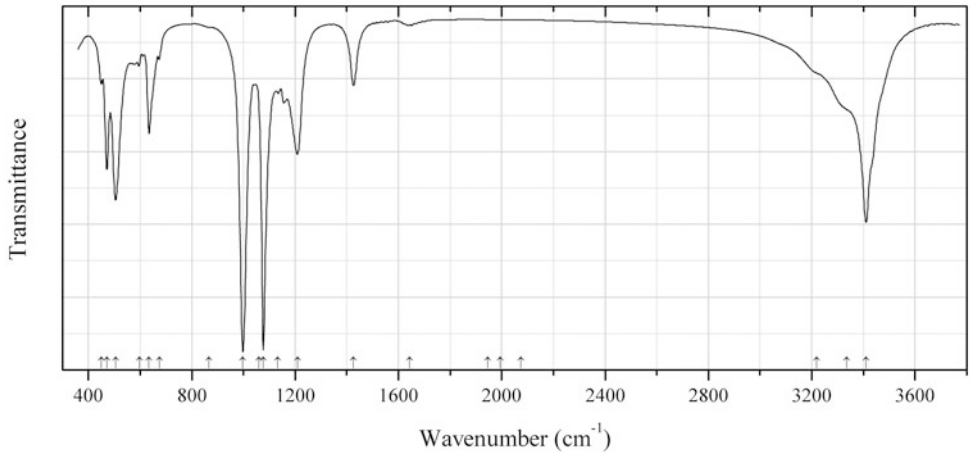

Fig. 2.1043 IR spectrum of ammoniojarosite obtained by N.V. Chukanov

S322 Ammoniojarosite $(NH_4)Fe^{3+}{}_3(SO_4)_2(OH)_6$ (Fig. 2.1043)
Locality: Coal mine Pécs-Vasas, Pécs, Mecsek Mts., Baranya Co., Hungary.
Description: Yellow powdery aggregate. The empirical formula is $(NH_4)_{0.63}(H_2O,H_3O)_x(Fe_{2.88}Al_{0.19})(SO_4)_{2.00}(OH,H_2O)_6$.
Kind of sample preparation and/or method of registration of the spectrum: KBr disc. Absorption.
Wavenumbers (cm^{-1}): 3410s, 3335sh, 3220sh, 2073w, 1995w, 1945w, 1643w, 1426, 1209, 1160, 1133, 1077s, 997s, 866w, 675w, 635, 597w, 505s, 471, 450w.

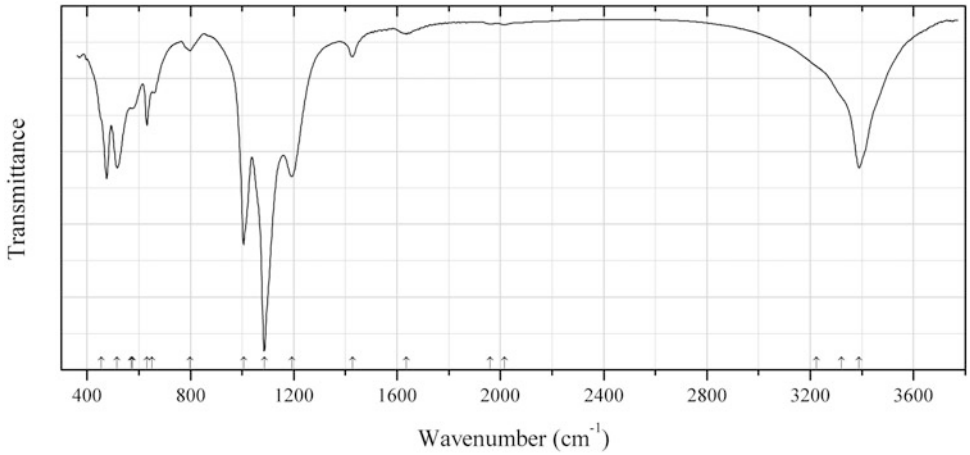

Fig. 2.1044 IR spectrum of jarosite NH_4-bearing variety obtained by N.V. Chukanov

S323 Jarosite NH_4-bearing variety $(K,NH_4)Fe_3{}^{3+}(SO_4)_2(OH)_6$ (Fig. 2.1044)
Locality: Anna mine, Alsdorf, near Aachen, Germany.

Description: Yellow fine-grained aggregate on anhydrite. The empirical formula is (electron microprobe): $K_{0.7}(NH_4,H_2O)_{0.3}(Fe_{2.8}Al_{0.2})(SO_4)_2(OH,H_2O)_6$.
Kind of sample preparation and/or method of registration of the spectrum: KBr disc. Absorption.
Wavenumbers (cm^{-1}): 3389s, 3320sh, 3225sh, 2016w, 1961w, 1636w, 1427, 1192s, 1086s, 1006s, 798w, 652, 631, 571, 516s, 576s, 455sh.
Note: The band at 1636 cm^{-1} indicates the presence of H_2O molecules.

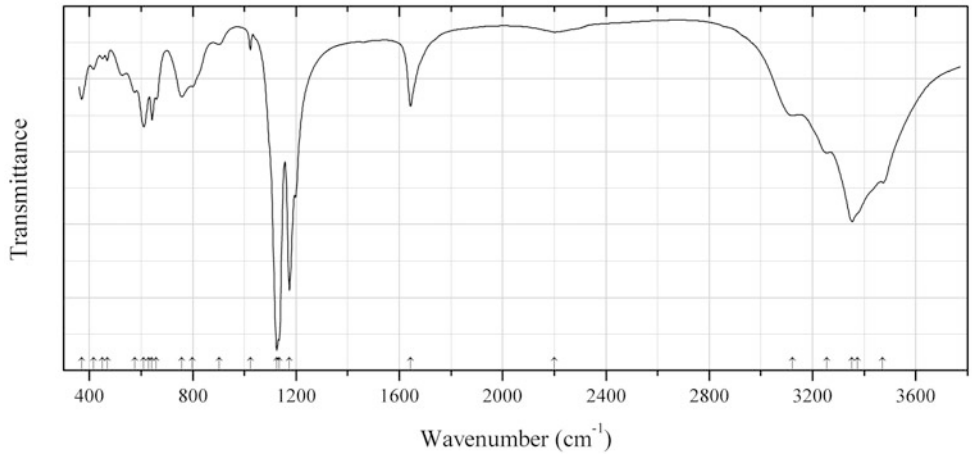

Fig. 2.1045 IR spectrum of kainite obtained by N.V. Chukanov

S324 Kainite $KMg(SO_4)Cl{\cdot}3H_2O$ (Fig. 2.1045)
Locality: Glavnaya Tenoritovaya (Major Tenorite) fumarole, Second scoria cone of the Northern Breakthrough of the Great Tolbachik Fissure Eruption, Tolbachik volcano, Kamchatka Peninsula, Far-Eastern Region, Russia.
Description: White powdery aggregate from the association with belloite, avdoninite, chlorothionite, sylvite, carnallite, sanguite, chrysothallite, etc. Investigated by I.V. Pekov. The empirical formula is (electron microprobe): $K_{0.90}Mg_{1.11}Mn_{0.01}S_{0.98}O_4Cl_{1.02}{\cdot}nH_2O$.
Kind of sample preparation and/or method of registration of the spectrum: KBr disc. Absorption.
Wavenumbers (cm^{-1}): 3472, 3375sh, 3353s, 3256, 3122, 2200w, 1644, 1174s, 1134s, 1125s, 1023w, 902w, 798, 758, 658, 642, 611, 575, 629, 469w, 450w, 415w, 371.

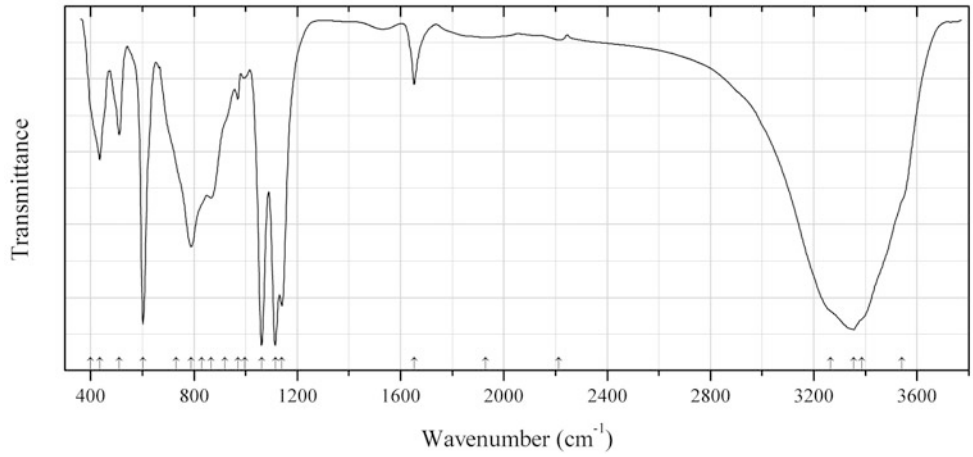

Fig. 2.1046 IR spectrum of posnjakite obtained by N.V. Chukanov

S325 Posnjakite $Cu_4(SO_4)(OH)_6 \cdot H_2O$ (Fig. 2.1046)
Locality: Marie mine, Wilnsdorf, Siegerland, North Rhine–Westphalia, Germany.
Description: Blue crystals. Identified by the IR spectrum.
Kind of sample preparation and/or method of registration of the spectrum: KBr disc. Absorption.
Wavenumbers (cm^{-1}): 3540sh, 3385sh, 3355s, 3265sh, 2212w, (1930w), 1652, 1140s, 1115s, 1062s, 996w, 970, 920sh, 867, 830sh, 789, 730sh, 602s, 510, 435, 400sh.

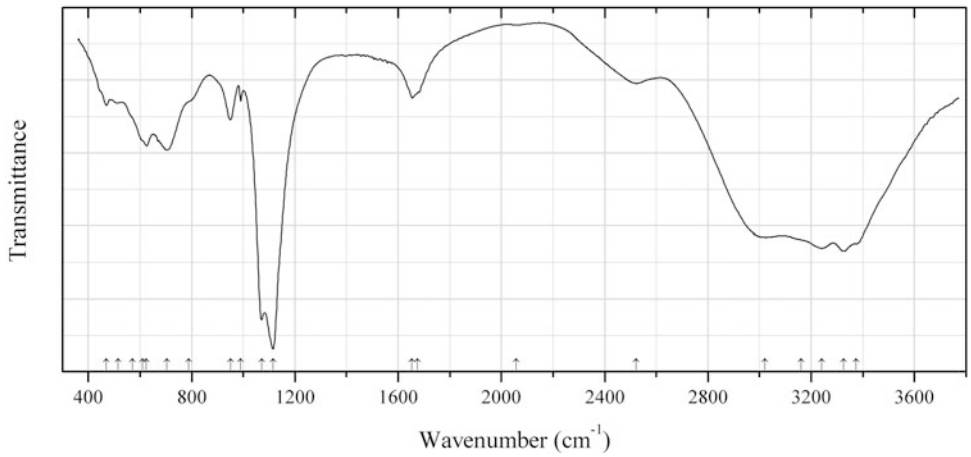

Fig. 2.1047 IR spectrum of magnesioaubertite obtained by N.V. Chukanov

S326 Magnesioaubertite $MgAl(SO_4)_2Cl \cdot 14H_2O$ (Fig. 2.1047)
Locality: La Fossa crater, Vulcano island, Lipari, Eolie (Aeolian) islands, Messina province, Sicily, Italy.
Description: Pale blue granular aggregate from the association with pickeringite. The empirical formula is (electron microprobe, ranges): $(Mg_{0.51–0.62}Cu_{0.35–0.46}Fe_{0.05})Al_{0.96–0.98}(SO_4)_{2.00}Cl_{0.90–0.96}(OH)_x \cdot nH_2O$.
Kind of sample preparation and/or method of registration of the spectrum: KBr disc. Absorption.

Wavenumbers (cm^{-1}): 3375s, 3325s, 3242s, 3160sh, 3020s, 2522, 2058w, 1675sh, 1654, 1115s, 1071s, 990, 950, 790sh, 705, 625, 610sh, 570sh, 515w, 470w.

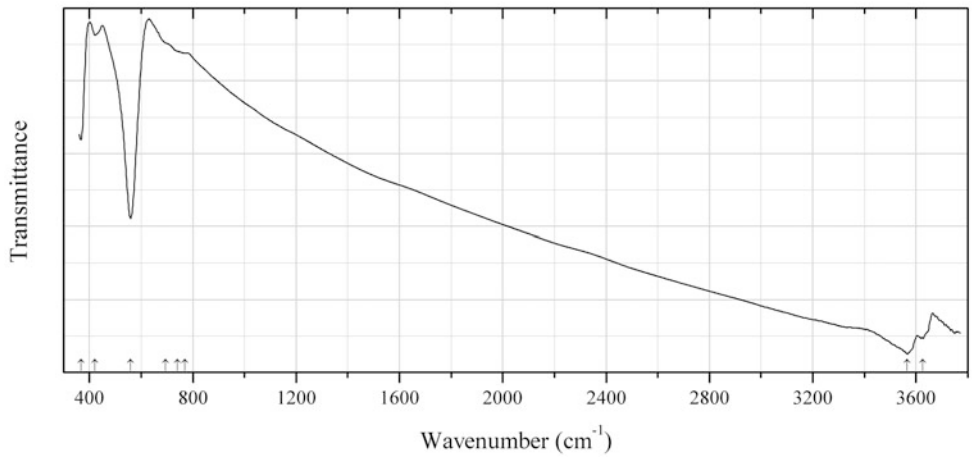

Fig. 2.1048 IR spectrum of haapalaite obtained by N.V. Chukanov

S327 Haapalaite $4(FeS)\cdot 3[(Mg,Fe)(OH)_2]$ (Fig. 2.1048)
Locality: Otamo dolomite quarry, Siikainen, Finland (type locality).
Description: Plack hexagonal platy crystals from the association with dolomite, brucite, and tochilinite. Investigated by I.V. Pekov. The empirical formula is (electron microprobe, OH calculated): $Fe_{2.94}Cu_{0.06}S_4\cdot Mg_{2.155}Fe_{0.875}(OH)_{6.05}$.
Wavenumbers (cm^{-1}): 3625, 3566, 770w, 740sh, 695sh, 559s, 421w, 367.

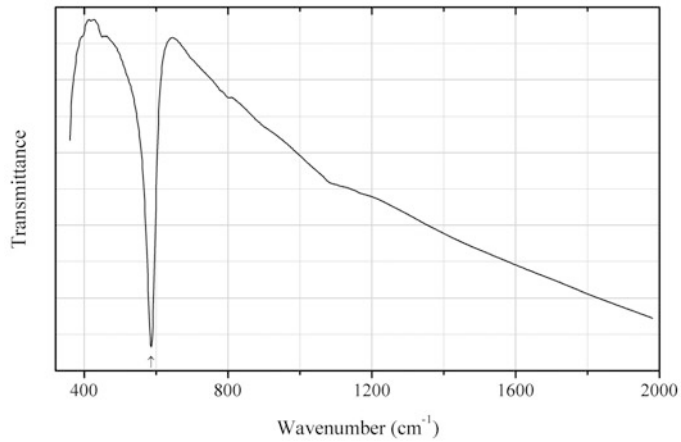

Fig. 2.1049 IR spectrum of kermesite obtained by N.V. Chukanov

S328 Kermesite Sb_2OS_2 (Fig. 2.1049)
Locality: Pezinok antimony mine, Malé Karpaty Mts., Slovakia.
Description: Clusters of dark red acicular crystals from the association with stibnite.
Kind of sample preparation and/or method of registration of the spectrum: KBr disc. Absorption.
Wavenumbers (cm^{-1}): 586s.

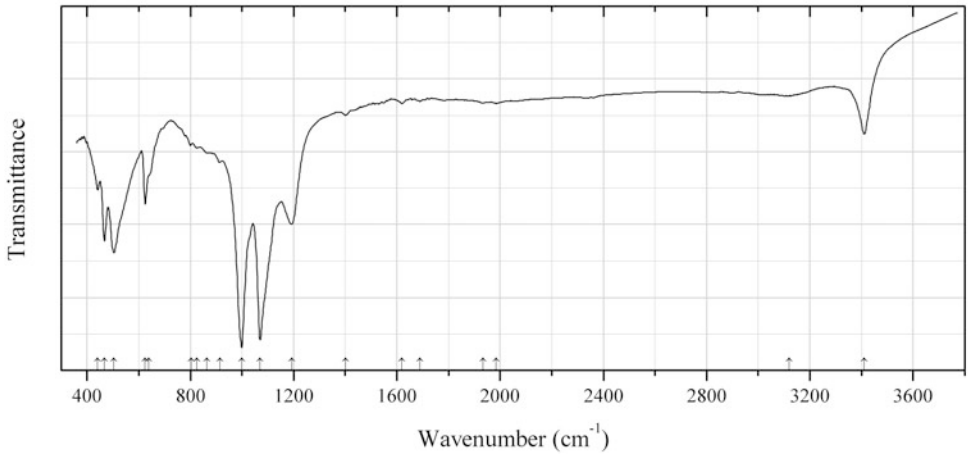

Fig. 2.1050 IR spectrum of dorallcharite obtained by N.V. Chukanov

S329 Dorallcharite $TlFe^{3+}{}_3(SO_4)_2(OH)_6$ (Fig. 2.1050)
Locality: Crven Dol, Allchar, Roszdan, Republic of Macedonia (type locality).
Description: Yellow fine-grained aggregate from the association with realgar, lorandite, and gypsum. The empirical formula is $[Tl_{0.8}K_{0.1}(H_2O,NH_4)_x](Fe_{2.9}Al_{0.1})[(SO_4)_{1.9}(AsO_4)_{0.1}](OH,H_2O)_6$. The strongest lines of the powder X-ray diffraction pattern [*d*, Å (*I*, %)] are: 5.96 (100), 3.67 (37), 3.11 (96), 2.986 (67), 2.593 (64), 1.991 (15), 1.837 (20).
Kind of sample preparation and/or method of registration of the spectrum: KBr disc. Absorption.
Wavenumbers (cm^{-1}): 3411, 3120w, 1985w, 1935w, 1690w, 1620w, 1402w, 1192, 1070s, 999s, 915w, 865sh, 825w, 803w, 640sh, 625, 504s, 467, 441.
Note: The weak bands at 3120 and 1402 cm^{-1} indicate the presence of NH_4^+; the weak band at 1620 cm^{-1} indicates the presence of H_2O.

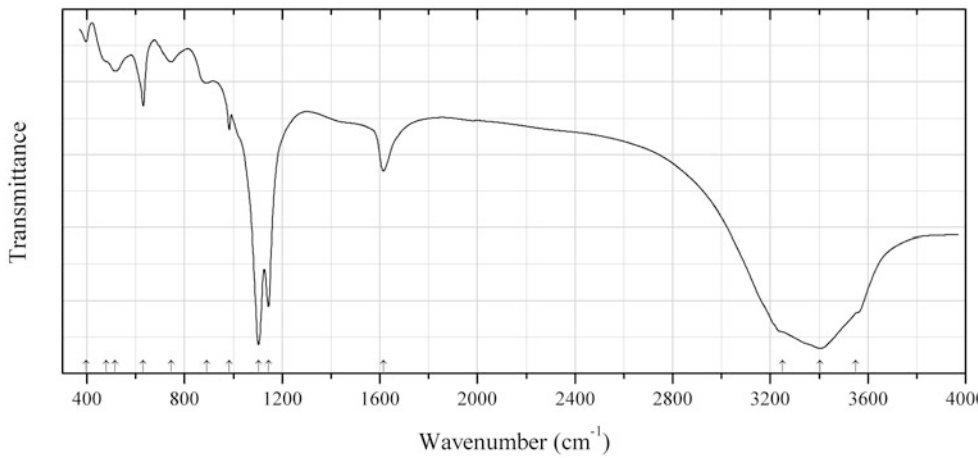

Fig. 2.1051 IR spectrum of zincmelanterite obtained by N.V. Chukanov

S330 Zincmelanterite $Zn(SO_4)\cdot 7H_2O$ (Fig. 2.1051)
Locality: Kropbach quarry, Münstertal, Schwerzwald (Black Forest) Mts., Baden-Württemberg, Germany.

Description: White crust. Confirmed by semiquantitative electron microprobe analyses.
Kind of sample preparation and/or method of registration of the spectrum: KBr disc. Absorption.
Wavenumbers (cm^{-1}): 3550sh, 3403s, 3250sh, 1615, 1144s, 1103s, 984, 890, 745, 631, 516, 480sh, 397w.

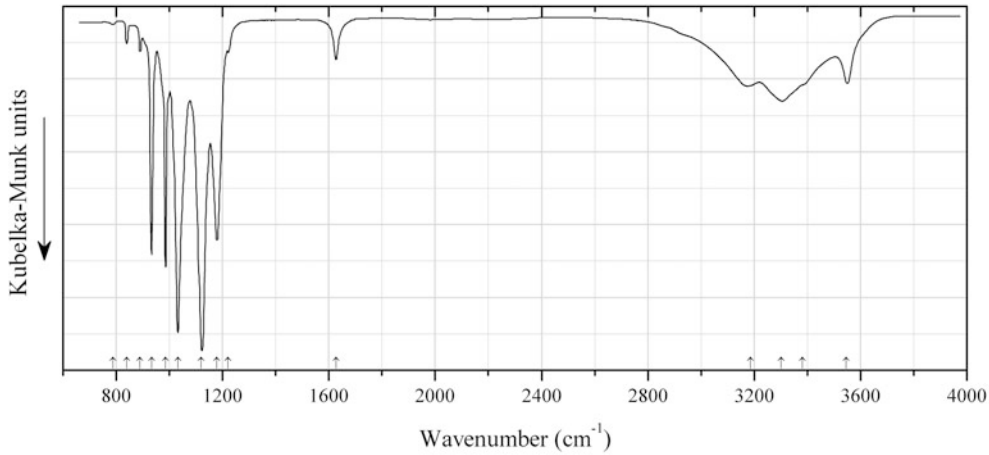

Fig. 2.1052 IR spectrum of adolfpateraite drawn using data from Plášil et al. (2012b)

S332 Adolfpateraite $K(UO_2)(SO_4)(OH)\cdot H_2O$ (Fig. 2.1052)
Locality: Svomost mine, Jáchymov ore district, Krušné Hory Mts. (Ore Mts.), Czech Republic (type locality).
Description: Greenish yellow crystalline aggregate from the association with quartz and gypsum. Holotype sample. Monoclinic, space group $P2_1/c$, a = 8.0462(1), b = 7.9256(1), c = 11.3206(2) Å, β = 107.726(2)°, V = 687.65(2) $Å^3$, Z = 4. D_{calc} = 4.24 g/cm^3. Optically biaxial, α = 1.597(2), γ = 1.659(2). The empirical formula is (H_2O calculated): $K_{0.94}(UO_2)_{1.00}(SO_4)_{1.02}(OH)_{0.90}\cdot H_2O$. The strongest lines of the powder X-ray diffraction pattern [d, Å (I, %) (hkl)] are: 7.658 (76) (100), 5.386 (100) (002), 5.218 (85) (−102), 3.718 (46) (021), 3.700 (37) (−202).
Kind of sample preparation and/or method of registration of the spectrum: A few crystals were mixed with KBr without using pressure. Micro-diffuse-reflectance method (DRIFTS).
Source: Plášil et al. (2012b).
Wavenumbers (cm^{-1}): 3546, 3381sh, 3302, 3187, 1627, 1221sh, 1179s, 1119s, 1032s, 985s, 933s, 890w, 840w, 787w.
Note: The wavenumbers were partly determined by us based on spectral curve analysis of the published spectrum.

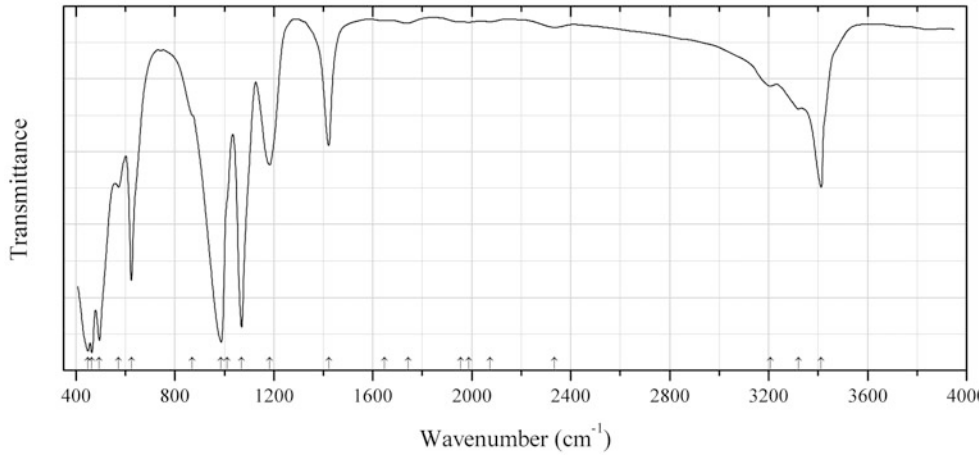

Fig. 2.1053 IR spectrum of ammoniojarosite drawn using data from Basciano and Peterson (2007a)

S333 Ammoniojarosite $(NH_4)Fe^{3+}{}_3(SO_4)_2(OH)_6$ (Fig. 2.1053)
Locality: Synthetic.
Description: End-member sample. Trigonal, space group *R*-3 *m*, $a = 7.3177(3)$, $c = 17.534(1)$ Å. The strongest lines of the powder X-ray difraction pattern [*d*, Å (*I*, %) (*hkl*)] are: 5.963 (13.5) (101), 5,87 (30.5) (003), 5.144 (100) (012), 3.119 (74.5) (021), 3.105 (95) (113), 2.935 (16) (006), 2.338 (32.5) (107), 1.988 (29) (033), 1.829 (26.5) (220).
Kind of sample preparation and/or method of registration of the spectrum: Fine powder. Absorption.
Source: Basciano and Petersen (2007a).
Wavenumbers (cm^{-1}): 3412, 3320, 3207w, 2335w, 2074w, 1988w, 1955sh, 1743w, 1647w, 1423, 1184, 1070s, 1012sh, 987s, 871sh, 624, 573sh, 495s, 464s, 449s.
Note: See also Basciano and Peterson (2007b).

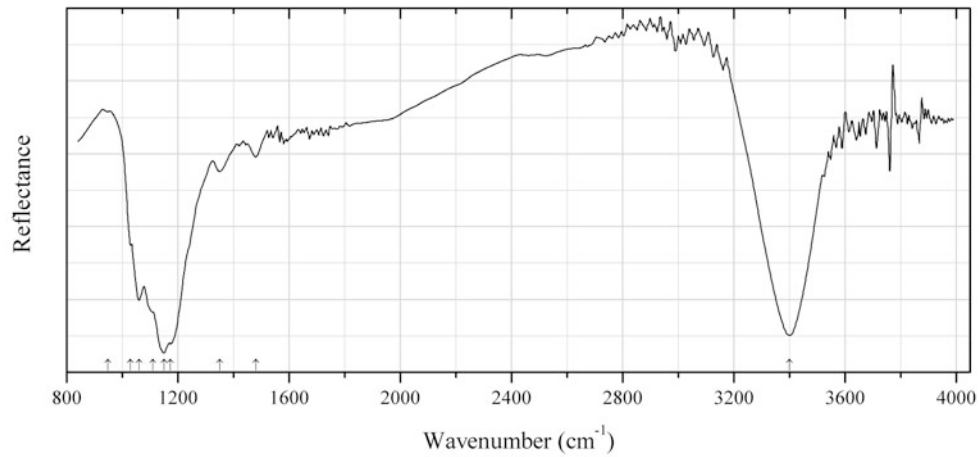

Fig. 2.1054 IR spectrum of beaverite-(Zn) drawn using data from Sato et al. (2008)

S334 Beaverite-(Zn) $PbFe^{3+}{}_2(SO_4)_2(OH)_6$ (Fig. 2.1054)
Locality: Mikawa mine, Mikawa, Aga-machi, Higashikanbara-gun, Niigata prefecture, Japan (type locality).

Description: Dark brown massive from the association with quartz, orthoclase, galena, sphalerite, pyrite, anglesite, beaverite-(Cu), and osarizawaite. Trigonal, space group *R*-3 *m*, *a* = 7.3028(2), *c* = 17.0517(4) Å, *V* = 787.56(4) Å^3. D_{calc} = 4.25 g/cm^3. The empirical formula is $Pb_{0.95}(Fe_{1.88}Al_{0.10})(Zn_{0.83}Cu_{0.30})(SO_4)_2[(OH)_{5.36}O_{0.38}]$.
Kind of sample preparation and/or method of registration of the spectrum: Reflection. Kind of sample preparation is not indicated.
Source: Sato et al. (2008).
Wavenumbers (cm^{-1}): 3400s, 1480w, 1350w, 1174s, 1150s, 1110sh, 1060s, 1030, 948w.
Note: The wavenumbers were partly determined by us based on spectral curve analysis of the published spectrum.

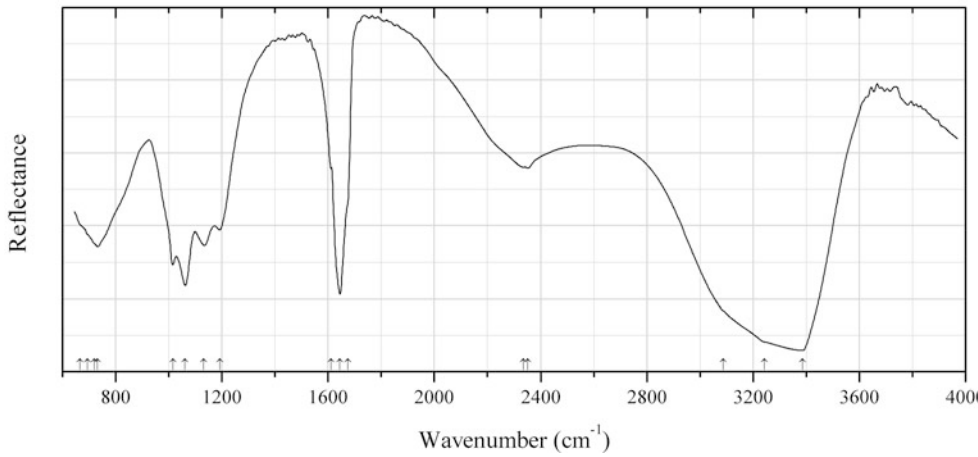

Fig. 2.1055 IR spectrum of běhounekite drawn using data from Plášil et al. (2011b)

S335 Běhounekite $U(SO_4)_2 \cdot 4H_2O$ (Fig. 2.1055)
Locality: Geschieber vein, Svornost mine, Jáchymov (St. Joachimsthal) ore district, Western Bohemia, Czech Republic (type locality).
Description: Green short-prismatic crystals from the association with kaatialaite, arsenolite, claudetite, and gypsum. Holotype sample. Orthorhombic, space group *Pnma*, *a* = 14.6464(3), *b* = 11.0786(3), *c* = 5.6910(14) Å, *V* = 923.43(4) Å^3, *Z* = 4. D_{calc} = 3.62 g/cm^3. Optically biaxial (+), α = 1.590(2), β = 1.618(4), γ = 1.659(2). The empirical formula is $(U_{0.99}Y_{0.03})(SO_4)_{1.97} \cdot 4H_2O$. The strongest lines of the powder X-ray diffraction pattern [*d*, Å (*I*, %) (*hkl*)] are: 7.330 (100) (200), 6.112 (54) (210), 5.538 (21) (020), 4.787 (42) (111), 3.663 (17) (400), 3.478 (20) (410), 3.080 (41) (321).
Kind of sample preparation and/or method of registration of the spectrum: Diffuse reflection (DRIFTS) of a powdered sample.
Source: Plášil et al. (2011b).
Wavenumbers (cm^{-1}): 3387s, 3243sh, 3088sh, 2352, 2335, 1674sh, 1645s, 1610sh, 1192, 1131, 1061, 1016, 732s, 719sh, 693sh, 665sh.
Note: The wavenumbers were partly determined by us based on spectral curve analysis of the published spectrum. The empirical formula is not charge-balanced. Broad band between 2100 and 2500 cm^{-1} (overlapping with the bands of atmospheric CO_2) corresponds to very strong hydrogen bonds (possibly, those formed by the acid sulfate groups).

S336 Bieberite $Co(SO_4) \cdot 7H_2O$

Locality: Herrengrund, near Neusohl, Hungary.
Kind of sample preparation and/or method of registration of the spectrum: KBr disc. Absorption.
Source: Moenke (1966).
Wavenumbers (cm^{-1}): 3490sh, 3400s, 3300sh, 1686, 1665, 1638, 1140sh, 1120s, 1008w, 987w, 710sh, 635s, 500, 437.

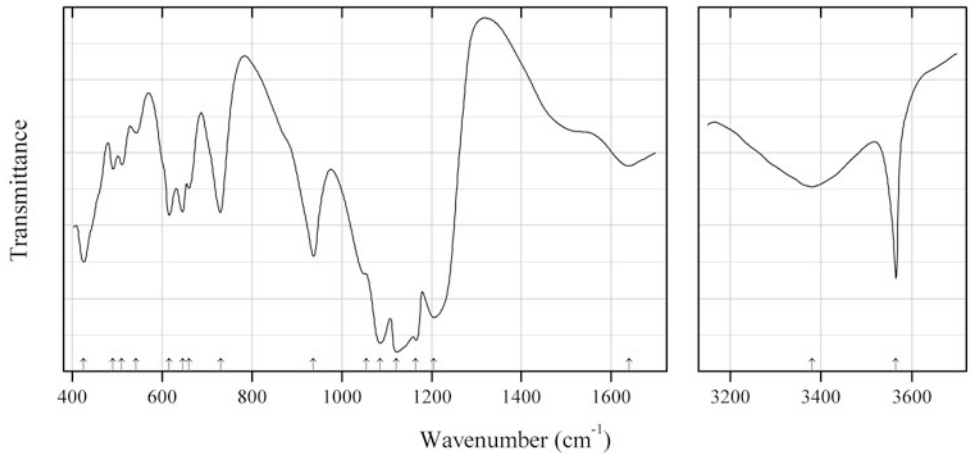

Fig. 2.1056 IR spectrum of caminite drawn using data from Apollonov et al. (1990)

S337 Caminite $Mg_7(SO_4)_5(OH)_4 \cdot H_2O$ (Fig. 2.1056)
Locality: Nepskoe K salt deposit, Nepa river basin, Irkutsk region, Eastern Siberia, Russia.
Description: Colourless grains from massive halite, from the association with anhydrite, magnesite, talc, and pyrite. The crystal structure is solved. Tetragonal, space group $I4_1/amd$, a = 5.254(2), c = 12.971(7) Å, V = 358.1 $Å^3$, Z = 2. D_{calc} = 2.77 g/cm^3. Uniaxial (−), ω = 1.562(2), ε = 1.534 (2). The strongest lines of the powder X-ray diffraction pattern [d, Å (I, %) (hkl)] are: 3.32 (100) (103), 3.21 (85) (112), 2.62 (19) (200), 2.058 (15) (213), 2.035 (15) (204), 1.644 (15) (206), 1.607 (21) (224).
Kind of sample preparation and/or method of registration of the spectrum: Not indicated (probably, KBr disc, absorption).
Source: Apollonov et al. (1990).
Wavenumbers (cm^{-1}): 3565s, 3380, 1640, 1205s, 1165s, 1122s, 1085s, 1055sh, 937s, 730, 660, 645, 615, 542w, 510w, 490w, 425s.

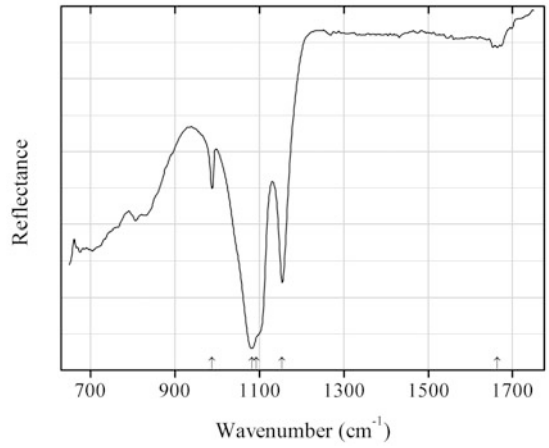

Fig. 2.1057 IR spectrum of changoite drawn using data from Kasatkin et al. (2013)

S338 Changoite $Na_2Zn(SO_4)_2 \cdot 4H_2O$ (Fig. 2.1057)
Locality: La Compañia mine, Sierra Gorda district, Antofagasta, Chile (type locality).
Description: No data.
Kind of sample preparation and/or method of registration of the spectrum: Raw grains. Reflection.
Source: Kasatkin et al. (2013).
Wavenumbers (cm^{-1}): 1664w, 1154s, 1093sh, 1082s, 988.
Note: The wavenumbers were partly determined by us based on spectral curve analysis of the published spectrum.

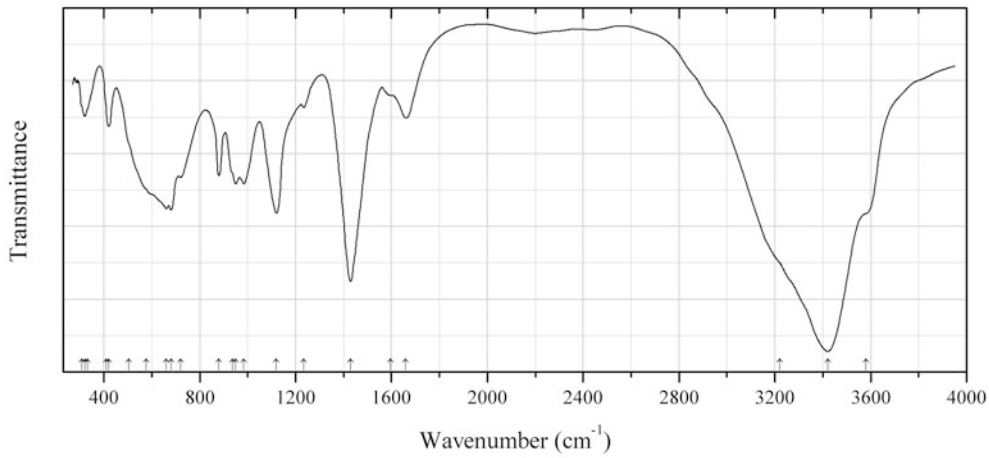

Fig. 2.1058 IR spectrum of charlesite CO_3-analogue drawn using data from Kusachi et al. (2008)

S339 Charlesite CO_3-analogue $Ca_6Al_2(SO_4)(CO_3)[B(OH)_4](OH,O)_{12} \cdot 26H_2O$ (Fig. 2.1058)
Locality: Fuka mine, Bicchu-cho, near Takahashi city, Okayama prefecture, Honshu Island, Japan.
Description: Pale brown flattened dipyramidal crystals from the association with calcite, henmilite, bultfonteinite, sillenite, and kusachiite. Hexagonal, $a = 11.097$ (5), $c = 21.22(3)$ Å. $D_{meas} = 1.84$ g/cm^3.

Optically uniaxial (−), ω = 1.498(2), ε = 1.462(2). The empirical formula is $(Ca_{5.77}Na_{0.02}K_{0.07})(Al_{1.23}Si_{0.79}Mg_{0.01}Mn_{0.01}Fe_{0.01})[(CO_3)_{1.16}(SO_4)_{0.93}][B(OH)_4]_{0.98}[(OH)_{10.62}O_{1.38}]\cdot 25.41H_2O$. The strongest lines of the powder X-ray diffraction pattern [*d*, Å (*I*, %) (*hkl*)] are: 9.67 (100) (100), 5.56 (30) (110), 3.844 (20) (114), 3.440 (18) (3.436), 2.743 (14) (304), 2.540 (18) (126), 2.185 (14) (404, 226).

Kind of sample preparation and/or method of registration of the spectrum: KBr disc. Transmission.

Source: Kusachi et al. (2008).

Wavenumbers (cm^{-1}): 3580sh, 3420s, 3220sh, 1660, 1597w, 1430s, 1234w, 1120s, 984,950, 936sh, 880, 720, 680s, 660s, 576sh, 504sh, 420, 409sh, 332sh, 320, 309sh.

Note: The wavenumbers were partly determined by us based on spectral curve analysis of the published spectrum.

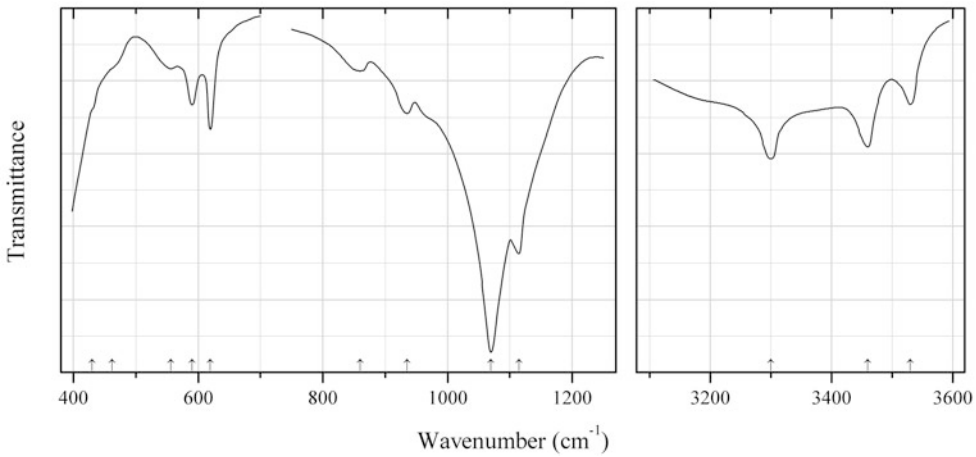

Fig. 2.1059 IR spectrum of chenite drawn using data from Paar et al. (1986)

S340 Chenite $Pb_4Cu(SO_4)_2(OH)_6$ (Fig. 2.1059)

Locality: Leadhills area, South Lanarkshire, Strathclyde, Scotland, UK (type locality).

Description: Blue crystals from the association with linarite, leadhillite, and susannite. Holotype sample. Triclinic, space group *P*1 or *P*-1, *a* = 5.791(1), *b* = 7.940(1), *c* = 7.976(1) Å, α = 112.02(1)°, β = 97.73(1)°, γ = 100.45(1)°, *V* = 326.0 Å^3, *Z* = 1. D_{meas} = 5.98(2) g/cm^3, D_{calc} = 6.044 g/cm^3. Optically biaxial (−), α = 1.871(5), β = 1.909(5), γ = 1.927(5), 2 *V* = 67(1)°. The empirical formula is $Pb_{3.98}Cu_{1.17}S_{1.98}O_{14}H_{5.82}$. The strongest lines of the powder X-ray diffraction pattern [*d*, Å (*I*, %) (*hkl*)] are: 5.55 (70) (100), 4.32 (60) (1–11), 3.60 (100) (002), 3.41 (90) (1–20), 3.30 (50) (02–2), 3.00 (50) (111), 2.80 (70) (12–2), 2.07 (60) (211, 21–3, 1–33), 1.778 (50) (3–1–2, 2–13).

Kind of sample preparation and/or method of registration of the spectrum: Suspension in mineral oil. Transmission.

Source: Paar et al. (1986).

Wavenumbers (cm^{-1}): 3530, 3460, 3300, 1115s, 1070s, 935w, 860w, 620, 590, 556w, 462sh, 430sh.

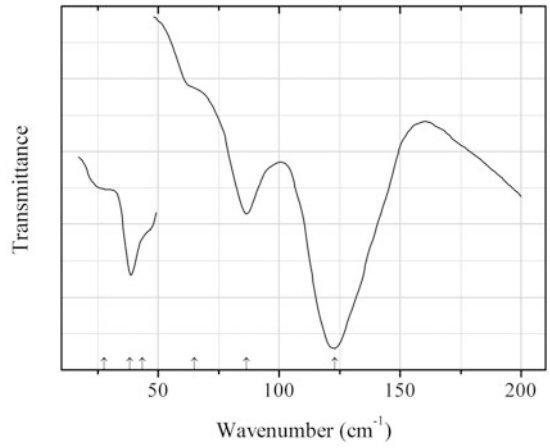

Fig. 2.1060 IR spectrum of cinnabar drawn using data from Karr and Kovach (1969)

S341 Cinnabar HgS (Fig. 2.1060)
Locality: Villabona mining area, Asturias, Spain.
Description: Phase purity was confirmed by powder X-ray diffraction.
Kind of sample preparation and/or method of registration of the spectrum: CsI disc (for the range 200–400 cm^{-1}); polyethylene disc (for the range 16.7–200 cm^{-1}). Absorption.
Source: Karr and Kovach (1969).
Wavenumbers (cm^{-1}): 340, 276, 123s, 86.5, 65sh, 43.5sh, 38.3w, 27.5sh.
Note: The wavenumbers were partly determined by us based on spectral curve analysis of the published spectrum. For IR spectra of cinnabar see also Soong and Farmer (1978), Riccius and Siemsen (1970).

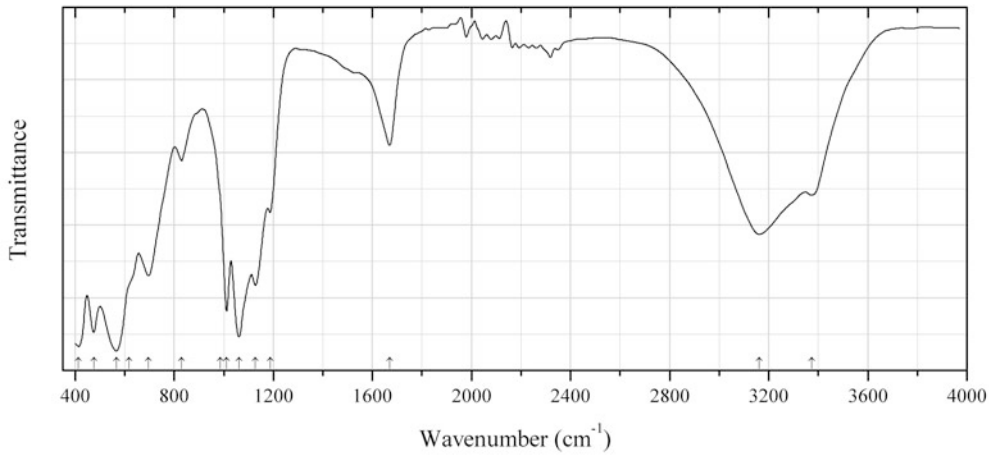

Fig. 2.1061 IR spectrum of cranswickite drawn using data from Peterson (2011)

S342 Cranswickite $Mg(SO_4)\cdot 4H_2O$ (Fig. 2.1061)
Locality: An outcrop near Calingasta, San Juan province, Argentina (type locality).
Description: Soft white vein filling in a metasedimentary rock. Associated minerals are matulaite and variscite. Holotype sample. The crystal structure is solved. Monoclinic, space group *C*2/*c*,

a = 11.9236(3), b = 5.1736(1), c = 12.1958(3) Å, β = 117.548(2)°, V = 667.0(1) Å^3, Z = 4. D_{meas} = 1.917 g/cm^3, D_{calc} = 1.918 g/cm^3. The mean refractive index is 1.465. The contents of impurities are (wt%): Mn 0.03, Ni 0.08, Zn 0.17. The strongest lines of the powder X-ray diffraction pattern [d, Å (I, %) (hkl)] are: 5.259 (100) (200), 4.603 (29) (110), 3.970 (22) (111), 3.927 (46) (11–2), 3.168 (45) (11–3), 3.118 (22) (31–1), 2.570 (23) (40–4).

Kind of sample preparation and/or method of registration of the spectrum: Transmission. Kind of sample preparation is not indicated.

Source: Peterson (2011).

Wavenumbers (cm^{-1}): 3373, 3162, 1669, 1187, 1128s, 1062s, 1012s, 986sh, 830w, 696, 617sh, 567s, 475s, 414s.

Note: The wavenumbers were determined by us based on spectral curve analysis of the published spectrum.

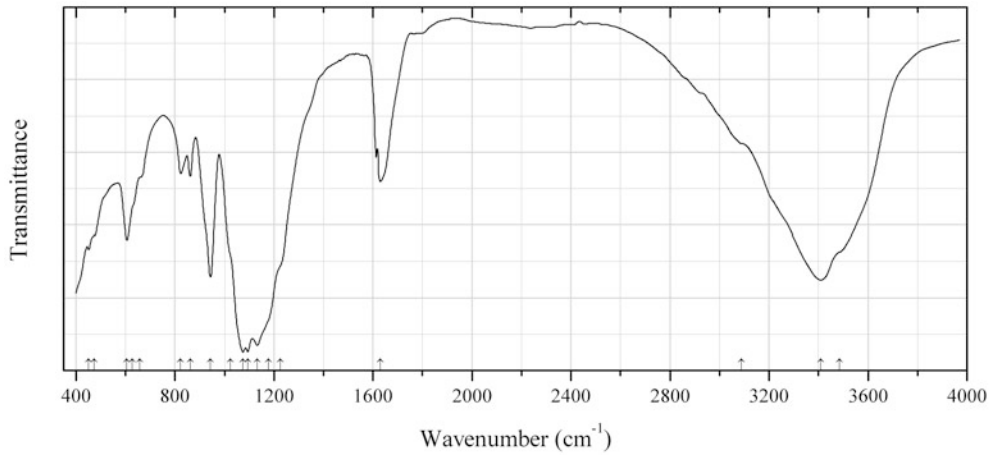

Fig. 2.1062 IR spectrum of deliensite drawn using data from Vochten et al. (1997a)

S343 Deliensite $Fe^{2+}(UO_2)_2(SO_4)_2(OH)_2 \cdot 7H_2O$ (Fig. 2.1062)

Locality: Mas d'Alary uranium deposit, Lodève, Hérault, France (type locality) .

Description: Pale yellow tabular crystals from the association with uraninite, gypsum, and pyrite. Holotype sample. Orthorhombic, space group *Pnnm* or *Pnn*2, a = 15.908(5), b = 16.274(3), c = 6.903 (1) Å, V = 1787(1) Å^3, Z = 4. D_{meas} = 3.268(7) g/cm^3, D_{calc} = 3.31 g/cm^3. Optically biaxial (−), α = 1.432 (calculated), β = 1.470(2), γ = 1.492(3), 2 V = 73(2)°. The empirical formula is $Fe_{0.909}(UO_2)_{2.081}(SO_4)_{1.949}(OH)_{2.082} \cdot 3.179H_2O$. The strongest lines of the powder X-ray diffraction pattern [d, Å (I, %) (hkl)] are: 7.95 (81) (200), 5.90 (100) (111), 4.26 (31) (031), 4.20 (37) (301), 3.94 (71) (140), 3.45 (67) (002), 3.165 (50) (202), 2.893 (41) (151), 2.596 (70) (142), 2.118 (27) (033).

Kind of sample preparation and/or method of registration of the spectrum: KBr disc. Transmission.

Source: Vochten et al. (1997a).

Wavenumbers (cm^{-1}): 3485sh, 3409s, 3090sh, 1629, 1225sh, 1177sh, 1132s, 1094s, 1075s, 1023sh, 943s, 862, 823, 658sh, 628sh, 605, 474sh, 452.

Note: The wavenumbers were partly determined by us based on spectral curve analysis of the published spectrum. The IR spectrum of deliensite from the Jáchymov ore district, Western Bohemia, Czech Republic, has been obtained by Plášil et al. (2012a) using the DRIFTS method.

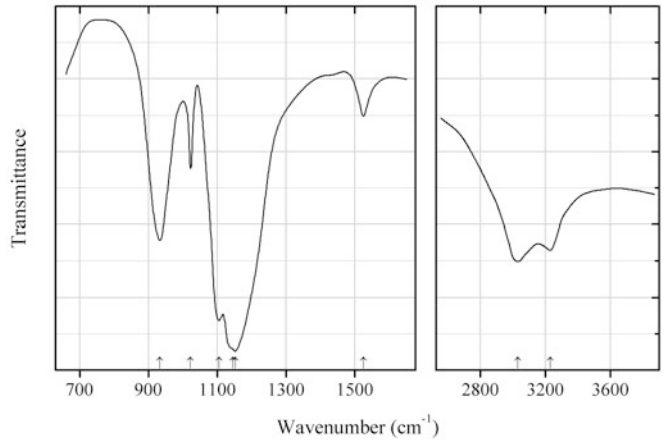

Fig. 2.1063 IR spectrum of dwornikite drawn using data from Ben-Dor and Margalith (1967)

S344 Dwornikite $Ni(SO_4)\cdot H_2O$ (Fig. 2.1063)
Locality: Synthetic.
Description: Obtained by heating of commercial nickel sulfate polyhydrate. Cobfirmed by differential thermal analysis.
Kind of sample preparation and/or method of registration of the spectrum: KBr disc. Transmission.
Source: Ben-Dor and Margalith (1967).
Wavenumbers (cm^{-1}): 3230, 3030, 1525w, 1152s, 1145sh, 1105s, 1023s, 933s.
Note: The wavenumbers were partly determined by us based on spectral curve analysis of the published spectrum.

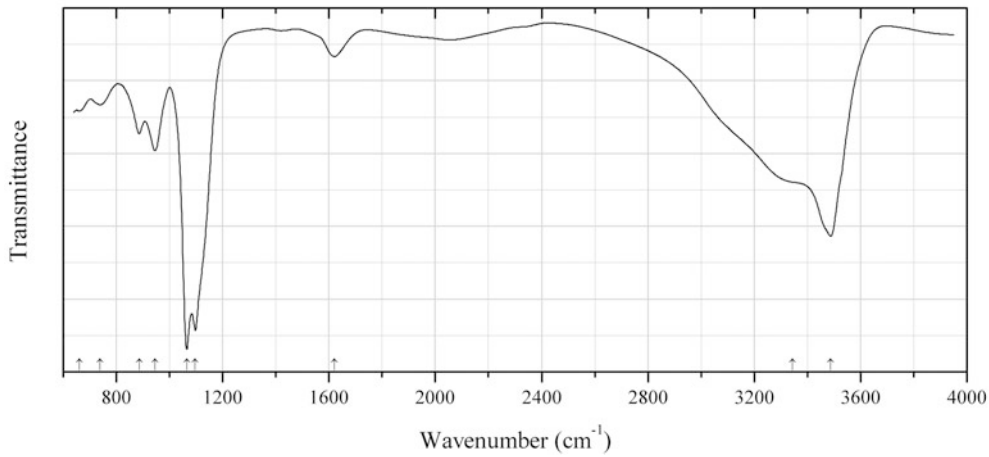

Fig. 2.1064 IR spectrum of edwardsite drawn using data from Elliott et al. (2010)

S345 Edwardsite $Cu_3Cd_2(SO_4)_2(OH)_6\cdot 4H_2O$ (Fig. 2.1064)
Locality: Block 14 Opencut, Broken Hill, New South Wales, Australia (type locality).
Description: Druse of pale blue tabular and bladed crystals from the association with niedermayrite and christelite. Holotype sample. Monoclinic, space group $P2_1/c$, a = 10.863(2), b = 13.129(3),

c = 11.169(2) Å, β = 113.04(3)°, V = 1465.9(5) Å^3, Z = 4. D_{calc} = 3.53 g/cm^3. Optically biaxial (−), α ≈ 1.74, β = 1.762(4), γ ≈ 1.77, 2 V = 62°. The empirical formula is $Cu_{2.77}Cd_{1.98}Zn_{0.22}Fe_{0.01}(SO_4)_{2.00}(OH)_{5.05}\cdot 4.06H_2O$. The strongest lines of the powder X-ray diffraction pattern [d, Å (I, %) (*hkl*)] are: 9.991 (90) (100), 5.001 (90) (200, 21–1), 4.591 (45) (20–2), 3.332 (60) (300, 032), 3.005 (30) (0–23), 2.824 (40) (−1–42), 2.769 (55) (20–4, 042, 10–4).

Kind of sample preparation and/or method of registration of the spectrum: A crystal aggregate was crushed in the diamond cell.

Source: Elliott et al. (2010).

Wavenumbers (cm^{-1}): 3488s, 3345sh, 1620w, 1097s, 1065s, 945, 886, 738, 660w.

Note: The wavenumbers were partly determined by us based on spectral curve analysis of the published spectrum.

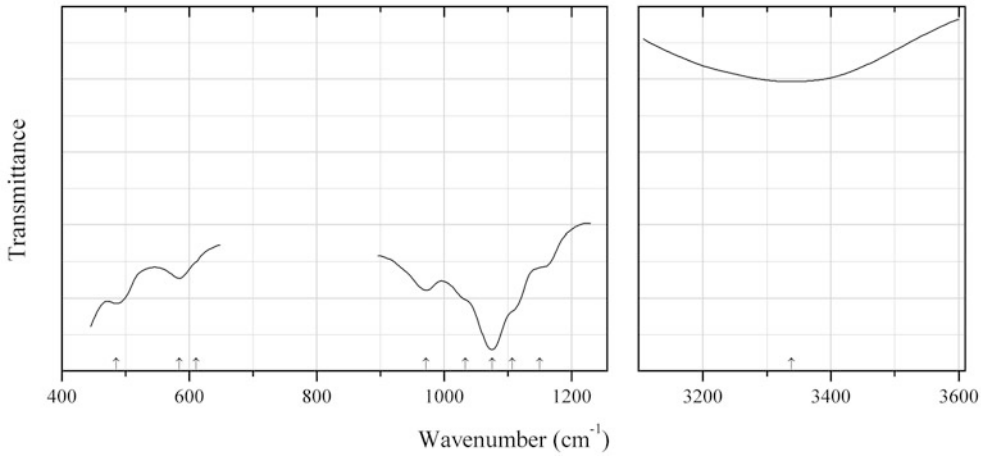

Fig. 2.1065 IR spectrum of elyite drawn using data from Paar et al. (1986)

S346 Elyite $CuPb_4(SO_4)O_2(OH)_4\cdot H_2O$ (Fig. 2.1065)

Locality: Slag locality at Meadowfoot Smelter, Wanlockhead, Dumfriesshire, Scotland, UK.

Description: Associated minerals are chenite and lanarkite.

Kind of sample preparation and/or method of registration of the spectrum: Suspension in mineral oil. Transmission.

Source: Paar et al. (1986).

Wavenumbers (cm^{-1}): 3338, 1150sh, 1107sh, 1075s, 1033sh, 971, 584, 611sh, 485.

Note: The wavenumbers were determined by us based on spectral curve analysis of the published spectrum.

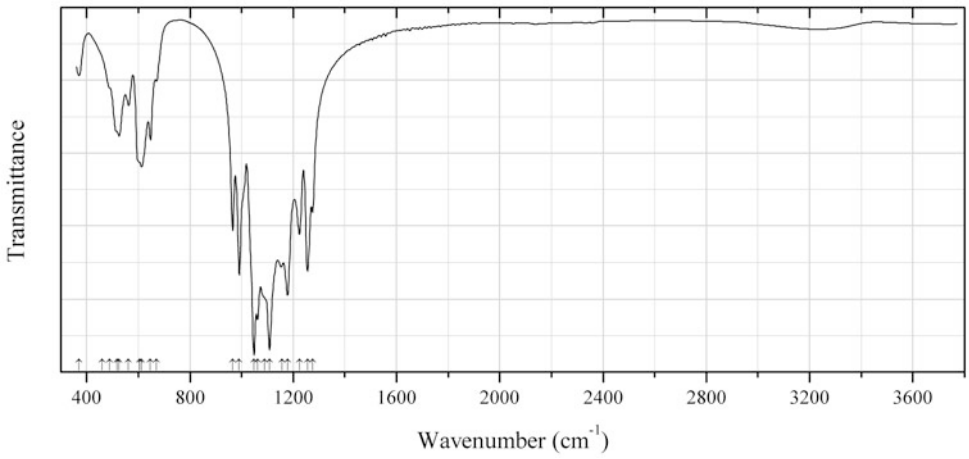

Fig. 2.1066 IR spectrum of alumoklyuchevskite obtained by N.V. Chukanov

S347 Alumoklyuchevskite $K_3Cu^{2+}{}_3Al(SO_4)_4O_2$ (Fig. 2.1066)
Locality: Fumarole "Yadovitaya" at the Second Cinder Cone, Northern Break of the Large Fissure Tolbachik Eruption, Tolbachik volcano, Kamchatka peninsula, Russia (type locality).
Description: Dark green crystalline crust from the association with langbeinite, euchlorine, fedotovite, steklite, kamchatkite, hematite, and lyonsite. Investigated by I.V. Pekov. The empirical formula is $K_{2.8}(Cu_{3.0}Zn_{0.1})(Al_{0.7}Fe^{3+}{}_{0.3})(SO_4)_4$.
Kind of sample preparation and/or method of registration of the spectrum: KBr disc. Absorption.
Wavenumbers (cm^{-1}): 1275, 1255s, 1224, 1178s, 1157s, 1108s, 1090sh, 1062s, 1048s, 991s, 966, 670w, 647, 613, 605sh, 562w, 526, 518sh, 490sh, 460w, 370w.

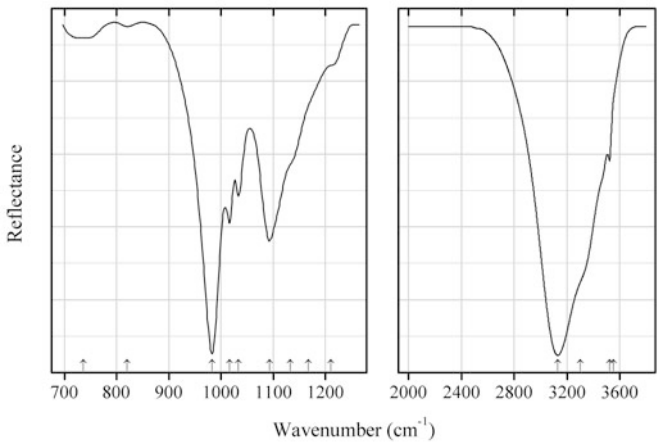

Fig. 2.1067 IR spectrum of bílinite drawn using data from Palmer et al. (2011)

S348 Bílinite $Fe^{2+}Fe^{3+}{}_2(SO_4)_4 \cdot 22H_2O$ (Fig. 2.1067)
Locality: Synthetic.
Description: Confirmed by powder X-ray diffraction data.
Kind of sample preparation and/or method of registration of the spectrum: Attenuated total reflection of powdered sample.

Source: Palmer et al. (2011).
Wavenumbers (cm^{-1}): 3552sh, 3522, 3302sh, 3130s, 1211sh, 1168sh, 1133sh, 1093s, 1033, 1017, 983s, 820w, 736w.
Note: The wavenumbers are indicated for the maxima of individual bands obtained as a result of the spectral curve analysis. Details of this analysis are not described. Observed absorption maxima are not indicated. The wavenumbers were determined by us based on spectral curve analysis of the published spectrum. Questionable data (the spectrum is very different from that of isostructural halotrichite).

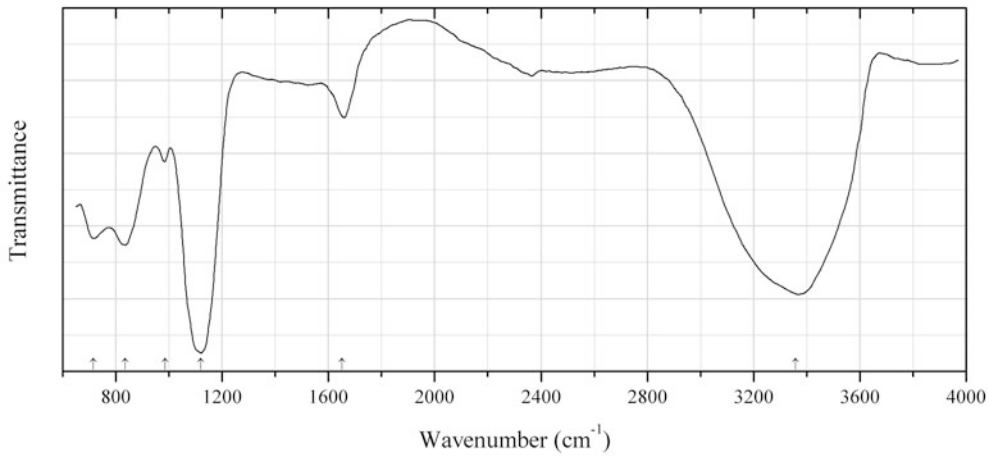

Fig. 2.1068 IR spectrum of aldridgeite drawn using data from Elliott (2010)

S349 Aldridgeite $(Cd,Ca)(Cu,Zn)_4(SO)_2(OH)_6{\cdot}3H_2O$ (Fig. 2.1068)
Locality: An occurrence at Broken Hill, New South Wales, Australia.
Description: Light blue acicular crystals from the association with niedermayrite. The crystal structure is solved. Monoclinic, space group *C*2/*c*, *a* = 22.0607(14), *b* = 6.2147(3), *c* = 21.8598(13) Å, β = 113.212(3)°, *V* = 2781.60(3) $Å^3$, *Z* = 8. The chemical composition is (wt%): CaO 2.21–5.83, CdO 7.50–13.41, CuO 30.56–44.96 and ZnO 5.41–15.12, SO_3 21.70–27.08. D_{calc} = 3.647 g/cm^3. Optically biaxial (−), α = 1.554(1), β = 1.558(1), γ = 1.566(1), 2 *V* = 70(5)°. The empirical formula is $Al_3(OH)_4(H_2O)_3(PO_4)(PO_3OH)Al_3(OH)_4(H_2O)_3(PO_4)(PO_3OH){\cdot}H_2O$. The strongest lines of the powder X-ray diffraction pattern [*d*, Å (*I*, %) (*hkl*)] are: 11.089 (100) (001), 6.826 (23) (010), 5.484 (79) (002, 101), 4.022 (30) (102, −112), 3.540 (81) (0–13, −1–12), 3.089 (33) (−113, 201), 2.918 (60) (−122).
Kind of sample preparation and/or method of registration of the spectrum: IR microscope, a diamond–anvil cell.
Source: Elliott (2010).
Wavenumbers (cm^{-1}): 3358s, 1652, 1120s, 985, 834, 716.

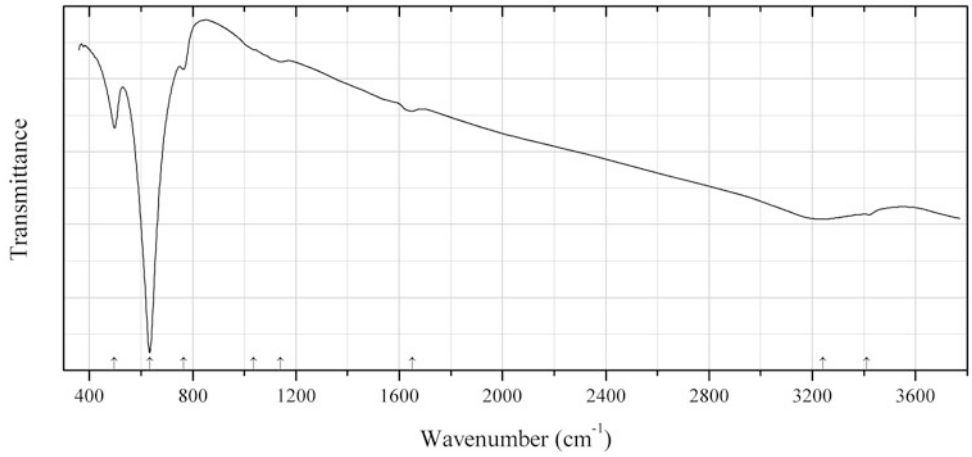

Fig. 2.1069 IR spectrum of ottensite obtained by N.V. Chukanov

S350 Ottensite $Na_3(Sb_2O_3)_3(SbS_3)\cdot 3H_2O$ (Fig. 2.1069)
Locality: Qinglong antimony deposit, Qinglong Co., Guizhou Province, China (type locality).
Description: Red-brown crust on stibnite crystals. Hexagonal, space group $P6_3$, a = 14.1758(2), c = 5.5712(1) Å, V = 969.57(3) Å^3, Z = 2. D_{calc} = 4.14 g/cm^3. The empirical formula is $(Na_{2.87}K_{0.03})(Sb_2O_3)_{3.03}(SbS_3)_{0.93}(OH)_{0.13}\cdot 3.01H_2O$. The strongest lines of the powder X-ray diffraction pattern are observed at 12.288, 4.643, 4.125, 3.406, 2.991, 2.906, 2.679, and 1.7743 Å.
Kind of sample preparation and/or method of registration of the spectrum: KBr disc. Absorption.
Wavenumbers (cm^{-1}): 3410w, 3241, 1650w, 1140w, 1035sh, 764, 633s, 497.
Note: Type material obtained from J. Hyršl. For a more detailed description see Sejkora and Hyršl (2007).

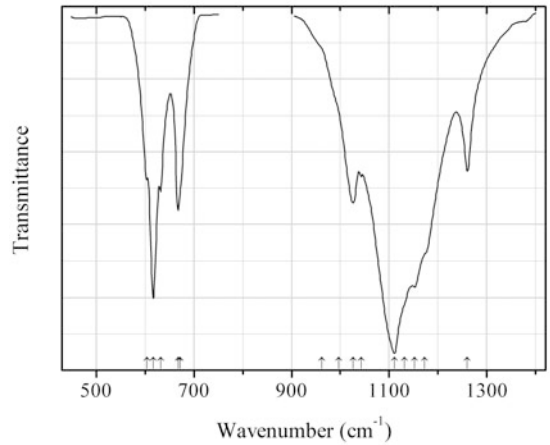

Fig. 2.1070 IR spectrum of calcium magnesium sulfate drawn using data from Smith and Seshadri (1999)

S351 Calcium magnesium sulfate ("Perkovaite") $CaMg_2(SO_4)_3$ (Fig. 2.1070)
Locality: Synthetic.

Description: Prepared by the solid-state reaction between $MgSO_4$ and $CaSO_4$ at 700 °C. Earlier this compound was found by B.V. Chesnokov on a burned dump of the Chelyabinsk coal basin, Kopeisk, South Urals, Russia and described under the name "perkovaite". For the IR spectrum of "perkovaite" see Chukanov (2014a).
Kind of sample preparation and/or method of registration of the spectrum: KBr disc. Absorption.
Source: Smith and Seshadri (1999).
Wavenumbers (cm^{-1}): 1260, 1173sh, 1152s, 1132sh, 1111s, 1043, 1026, 997sh, 962sh, 672 sh, 668, 632, 617s, 604sh.
Note: The wavenumbers were partly determined by us based on spectral curve analysis of the published spectrum.

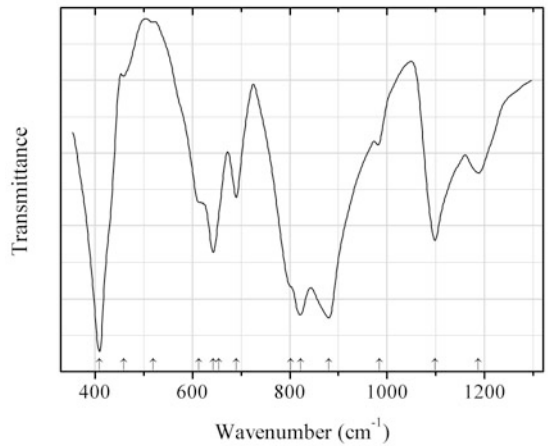

Fig. 2.1071 IR spectrum of haüyne Ca-aluminate analogue drawn using data from Henderson and Taylor (1979)

S352 Haüyne Ca-aluminate analogue $Ca_8(Al_{12}O_{24})(SO_4)_2$ (Fig. 2.1071)
Locality: Synthetic.
Description: Synthesized by the solid-state reaction. Tetragonal, pseudocubic, with the unit cell derived from the ~9 Å sodalite subcell. For the cubic pseudocell, a = 9.196 Å.
Kind of sample preparation and/or method of registration of the spectrum: Transmission. Kind of sample preparation is not indicated.
Source: Henderson and Taylor (1979).
Wavenumbers (cm^{-1}): 1187, 1098, 984w, 880s, 822s, 802sh, 690, 655sh, 643, 614sh, 520sh, 459w, 410s.
Note: The wavenumbers were partly determined by us based on spectral curve analysis of the published spectrum.

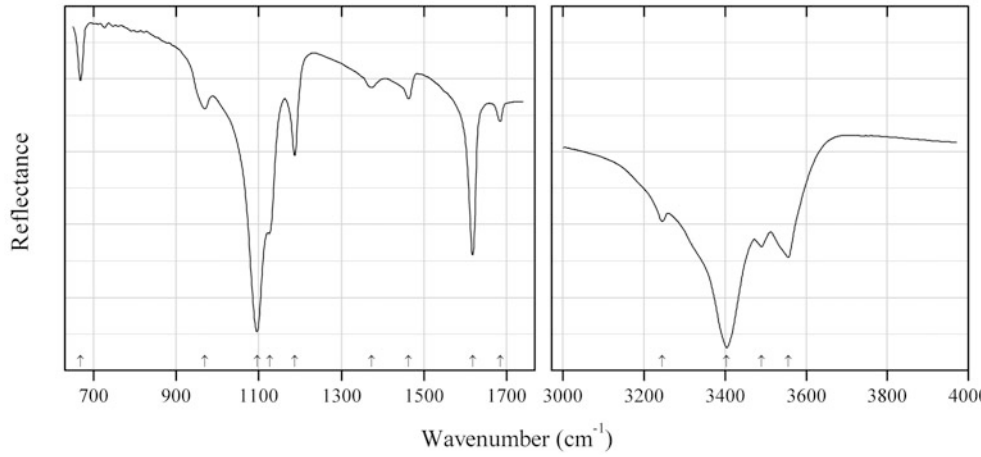

Fig. 2.1072 IR spectrum of cobaltoblödite drawn using data from Kasatkin et al. (2013)

S353 Cobaltoblödite $Na_2Co(SO_4)_2 \cdot 4H_2O$ (Fig. 2.1072)
Locality: Blue Lizard mine, White Canyon District, San Juan County, Utah, USA (type locality).
Description: Pink aggregate of anhedral grains from the association with matulaite and Mn,Co, Ni-bearing blödite, manganoblödite, chalcanthite, gypsum, sideronatrite, johannite, quartz, and feldspar. Holotype sample. Monoclinic, space group $P2_1/a$, a = 11.147(1), b = 8.268(1), c = 5.5396 (7) Å, β = 100.517(11)°, V = 501.9(1) Å^3, Z = 2. D_{meas} = 2.29(2) g/cm^3, D_{calc} = 2.347 g/cm^3. Optically biaxial (−), α = 1.498(2), β = 1.503(2), γ = 1.505(2). The empirical formula is $Na_{1.96}(Co_{0.36}Mg_{0.30}Mn_{0.17}Ni_{0.12})S_{2.02}O_8 \cdot 4H_2O$. The strongest lines of the powder X-ray diffraction pattern [d, Å (I, %) (hkl)] are: 4.551 (80) (210, 011), 4.269 (50) (−201), 3.795 (18) (−211), 3.339 (43) (310), 3.29 (100) (220, 021), 3.258 (58) (211, −121), 2.644 (21) (−401), 2.296 (22) (−122).
Kind of sample preparation and/or method of registration of the spectrum: Powdered sample. Reflection.
Source: Kasatkin et al. (2013).
Wavenumbers (cm^{-1}): 3556, 3490, 3404s, 3245, 1685w, 1618s, 1463w, 1373w, 1187, 1126sh, 1096s, 969, 668.
Note: The bands at 1463 and 1373 cm^{-1} are due to impurities; the band at 668 cm^{-1} has atmospheric origin.

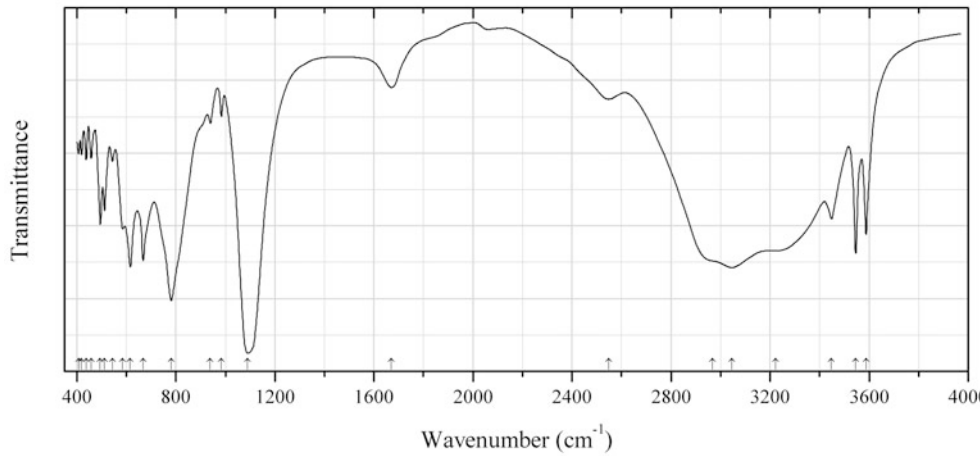

Fig. 2.1073 IR spectrum of kobyashevite drawn using data from Strandberg et al. (1995)

S354 Kobyashevite $Cu_5(SO_4)_2(OH)_6 \cdot 4H_2O$ (Fig. 2.1073)
Locality: Synthetic.
Description: Product of corrosion of copper in humide air containing SO_2. The crystal structure is solved. Triclinic, space group *P*-1, a = 6.064(2), b = 11.012(6), c = 5.490(2) Å, α = 102.68(4)°, β = 92.43(3)°, γ = 92.06(3)°, V = 357.0(5) Å^3. D_{calc} = 3.181 g/cm^3. The strongest lines of the powder X-ray diffraction pattern [*d*, Å (*I*, %) (*hkl*)] are: 10.812 (100) (010), 5.390 (47) (020), 3.591 (22) (030), 2.698 (28) (20–1), 2.649 (23) (02–2), 2.579 (26) (2–1–1), 2.424 (31) (03–2).
Kind of sample preparation and/or method of registration of the spectrum: KBr disc. Transmission.
Source: Strandberg et al. (1995).
Wavenumbers (cm^{-1}): 3588, 3546s, 3448, 3222, 3047s, 2967sh, 2548w, 1670, 1090s, 984w, 939w, 781s, 668, 616, 585, 544w, 512, 495, 458w, 438w, 419w, 407w.
Note: The wavenumbers were determined by us based on spectral curve analysis of the published spectrum.

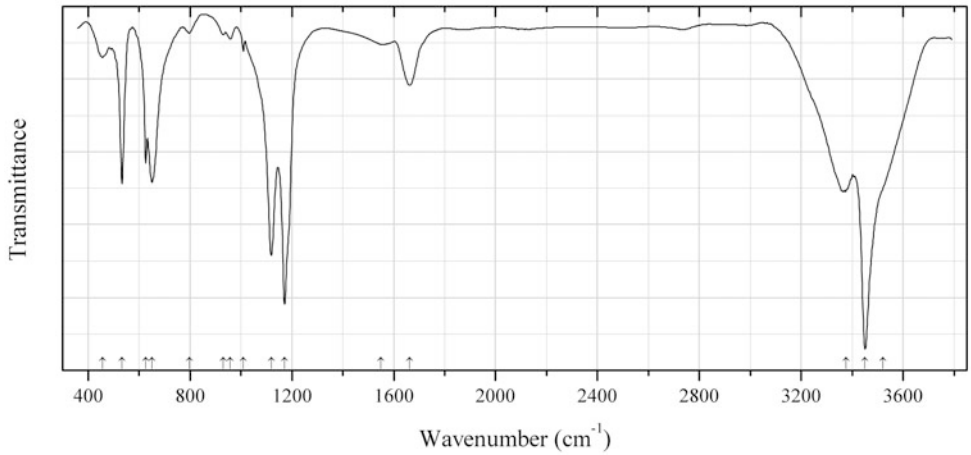

Fig. 2.1074 IR spectrum of genplesite obtained by N.V. Chukanov

S355 Genplesite $Ca_3Sn(SO_4)_2(OH)_6 \cdot 3H_2O$ (Fig. 2.1074)
Locality: No. 1 shaft, Oktyabr'sky mine, Talnakh, Norilsk area, Krasnoyarskiy Krai, Siberia, Russia (type locality).
Description: Clusters on greenalite crystal crusts lining cavities in massive chalcopyrite ore. Holotype sample. Hexagonal, space group $P6_3/mmc$, a = 8.5139(2), c = 11.1408(3) Å, V = 699.37(1) Å^3, Z = 2. D_{meas} = 2.78(1) g/cm^3, D_{calc} = 2.773 g/cm^3. Optically biaxial (−), ω = 1.597(2), ε = 1.572(2). The empirical formula is (electron microprobe): $Ca_{3.01}(Sn_{0.95}Ge_{0.03}Al_{0.01})S_{2.01}O_8(OH)_6 \cdot 3H_2O$. The strongest lines of the powder X-ray diffraction pattern [*d*, Å (*I*, %) (*hkl*)] are: 7.38 (68) (100), 4.259 (46) (110), 3.503 (15) (201), 3.383 (100) (112), 2.616 (13) (203), 2.493 (14) (212), 2.249 (14) (302), 2.130 (17) (105, 220).
Kind of sample preparation and/or method of registration of the spectrum: KBr disc. Absorption.
Wavenumbers (cm^{-1}): 3520sh, 3451s, 3375, 1663, 1550sh, 1172s, 1119s, 1010w, 959w, 932w, 798w, 651, 627, 533, 457.

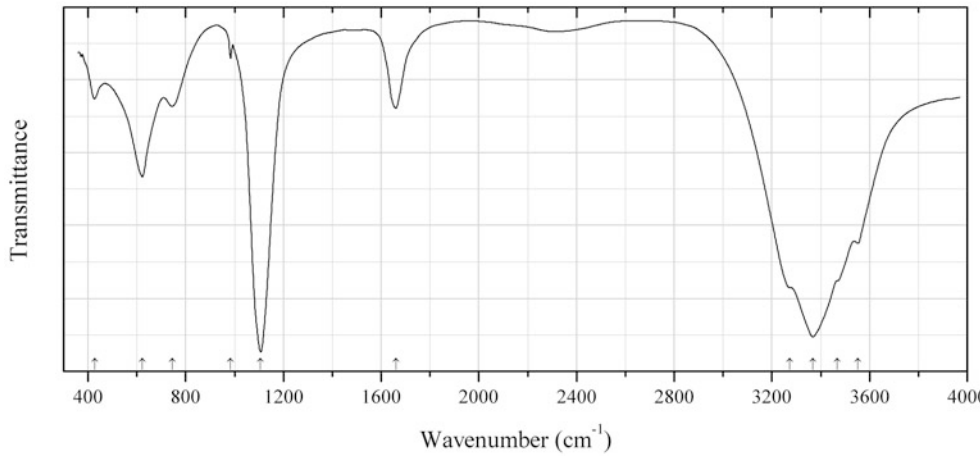

Fig. 2.1075 IR spectrum of epsomite drawn using data from Apopei et al. (2012)

S356 Epsomite $Mg(SO_4)\cdot 7H_2O$ (Fig. 2.1075)
Locality: Hondol open pit, 15 km NE of Deva city, South Apuseni Mts. (Metaliferi Mts.), Romania.
Description: Identified by Raman and IR spectra.
Kind of sample preparation and/or method of registration of the spectrum: KBr disc. Absorption.
Source: Apopei et al. (2012).
Wavenumbers (cm^{-1}): 3552, 3468sh, 3368s, 3273sh, 1660, 1107s, 984w, 744, 623, 427.

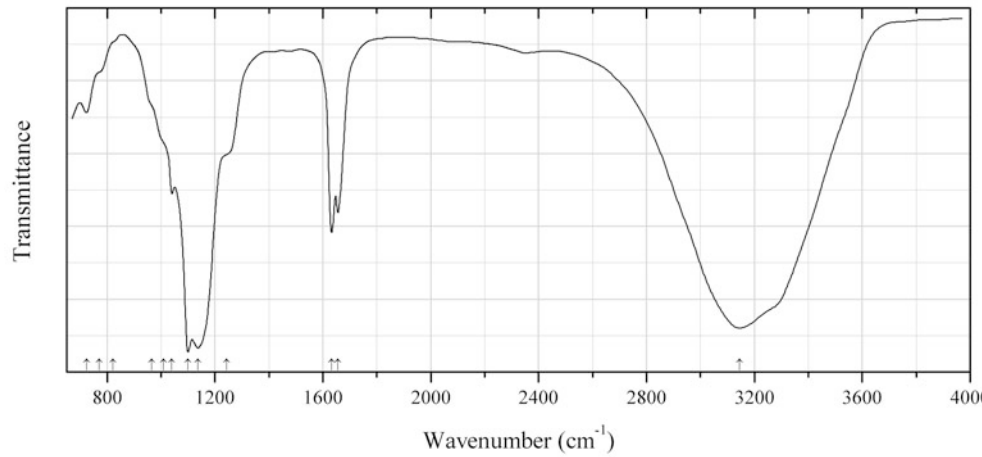

Fig. 2.1076 IR spectrum of hafnium sulfate tetrahydrate drawn using data from Adler (1965)

S357 Hafnium sulfate tetrahydrate $Hf(SO_4)_2\cdot 4H_2O$ (Fig. 2.1076)
Zircosulfate Hf analogue
Locality: Synthetic.
Description: A reagent grade chemical.
Kind of sample preparation and/or method of registration of the spectrum: KBr disc. Transmission.

Source: Adler (1965).
Wavenumbers (cm^{-1}): 3145s, 1656, 1632, 1244sh, 1136s, 1099s, 1040, 1008sh, 964sh, 822sh, 770sh, 723w.
Note: The wavenumbers were partly determined by us based on spectral curve analysis of the published spectrum.

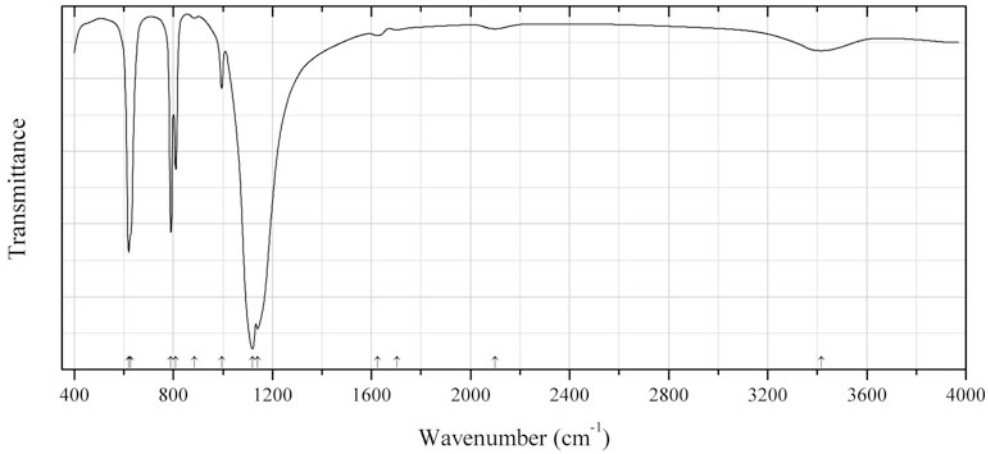

Fig. 2.1077 IR spectrum of hectorfloresite drawn using data from Ericksen et al. (1989)

S358 Hectorfloresite $Na_9(IO_3)(SO_4)_4$ (Fig. 2.1077)
Locality: Synthetic.
Kind of sample preparation and/or method of registration of the spectrum: Transmission. Kind of sample preparation is not indicated.
Source: Ericksen et al. (1989).
Wavenumbers (cm^{-1}): 3416w, 2100w, 1703w, 1625w, 1140s, 1120s, 995, 885w, 810, 790, 627sh, 620s.
Note: The wavenumbers were partly determined by us based on spectral curve analysis of the published spectrum.

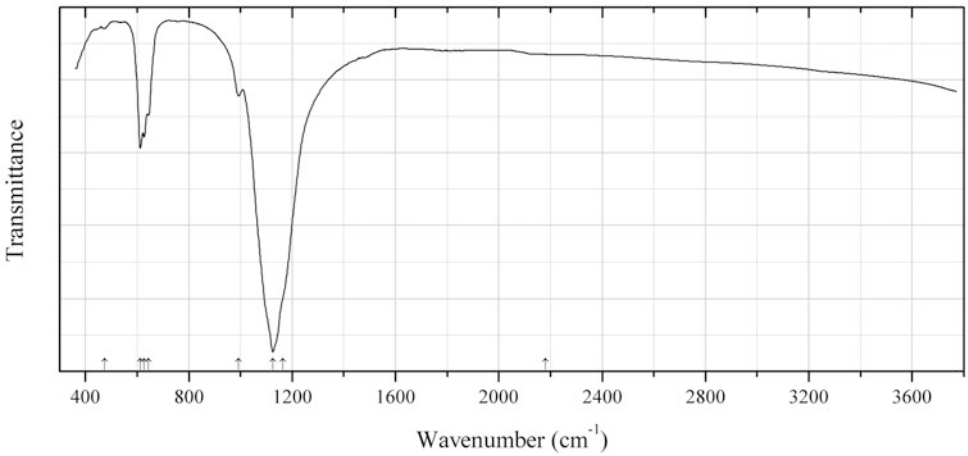

Fig. 2.1078 IR spectrum of shuvalovite obtained by N.V. Chukanov

S359 Shuvalovite $K_2(Ca_2Na)(SO_4)_3F$ (Fig. 2.1078)
Locality: Arsenatnaya fumarole, Second scoria cone of the Northern Breakthrough of the Great Tolbachik Fissure Eruption, Tolbachik volcano, Kamchatka peninsula, Russia (type locality).
Description: Colourless crystals from the association with hematite, tenorite, calciolangbeinite, langbeinite, aphthitalite, anhydrite, steklite, arcanite, krasheninnikovite, euchlorine, wulffite, alumoklyuchevskite, klyuchevskite, fluorite fluoborite, lammerite, lammerite-β, tilasite, svabite, bradaczekite, johillerite, urusovite, etc. Holotype sample. Orthorhombic, space group *Pnma*, a = 13.2383(4), b = 10.3023(3), c = 8.9909(4) Å, V = 1226.22(7) Å^3, Z = 4. D_{calc} = 2.641 g/cm^3. Optically biaxial (−), α = 1.493(1), β = 1.498(1), γ = 1.498 (1). The empirical formula is (electron microprobe): $Na_{1.16}K_{2.01}Ca_{1.86}S_{3.02}O_{12.03}F_{0.97}$. The strongest lines of the powder X-ray diffraction pattern [d, Å (I, %) (hkl)] are: 7.44 (27) (101), 4.245 (45) (102, 121), 3.963 (62) (301), 3.281 (100) (122), 3.210 (30) (031), 3.144 (84) (302, 321), 3.112 (67) (131, 401), 3.016 (78) (222), 2.785 (52) (420).
Kind of sample preparation and/or method of registration of the spectrum: KBr disc. Absorption.
Wavenumbers (cm^{-1}): 2180w, 1165sh, 1125s, 993, 643, 627, 612s, 474w.

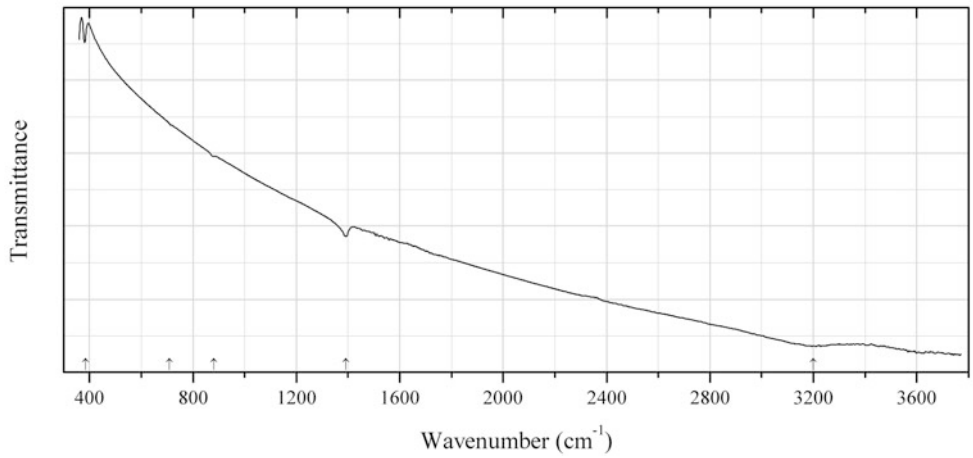

Fig. 2.1079 IR spectrum of galkhaite obtained by N.V. Chukanov

S360 Galkhaite $(Cs,Tl,NH_4,\square)(Hg,Cu,Zn)_6(As,Sb)_4S_{12}$ (Fig. 2.1079)
Locality: Khaidarkan Sb-Hg deposit, Fergana valley, Alay range, Osh region, Kyrgyzstan.
Description: Red grains in Sb-Hg ore. Investigated by I.V. Pekov. Confirmed by electron microprobe analysis and powder X-ray diffraction data.
Kind of sample preparation and/or method of registration of the spectrum: KBr disc. Absorption.
Wavenumbers (cm^{-1}): 3200, 1392, 882w, 710w, 384.
Note: The bands at 3200, 1392, and 710 cm^{-1} correspond to NH_4^+ cations.

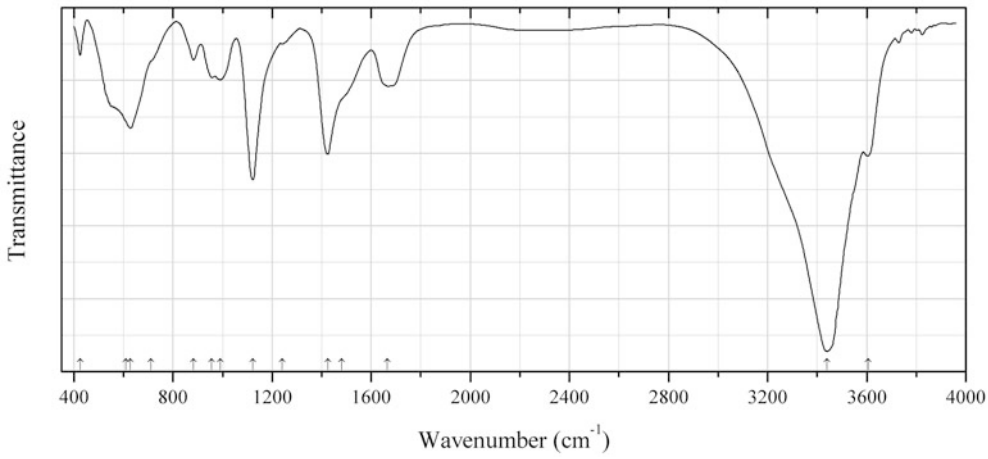

Fig. 2.1080 IR spectrum of charlesite CO_3-rich drawn using data from Kumarathasan et al. (1989)

S361 Charlesite CO_3-rich $Ca_6Al_2(SO_4,CO_3)_2[B(OH)_4]_{1+x}(OH,O)_{12}\cdot 26H_2O$ (Fig. 2.1080)
Locality: Synthetic.
Description: Synthesized from $Ca(C_4H_6O_4)$, $Na_2Al_2O_4$, Na_2SO_4, and $B(OH)_3$ at pH 12–13. Confirmed by X-ray diffraction and electron microprobe analysis.
Kind of sample preparation and/or method of registration of the spectrum: Attenuated total reflection of powdered mineral. KBr disc. Transmission.
Source: Kumarathasan et al. (1989).
Wavenumbers (cm^{-1}): 3605, 3440s, 1665, 1481sh, 1425s, 1240w, 1122s, 992, 956, 882, 710sh, 610sh, 628, 425.
Note: The wavenumbers were partly determined by us based on spectral curve analysis of the published spectrum. The band at 1425 cm^{-1} indicates the presence of carbonate anions. The bands at 992 and 956 cm^{-1} correspond to $[B(OH)_4]^-$.

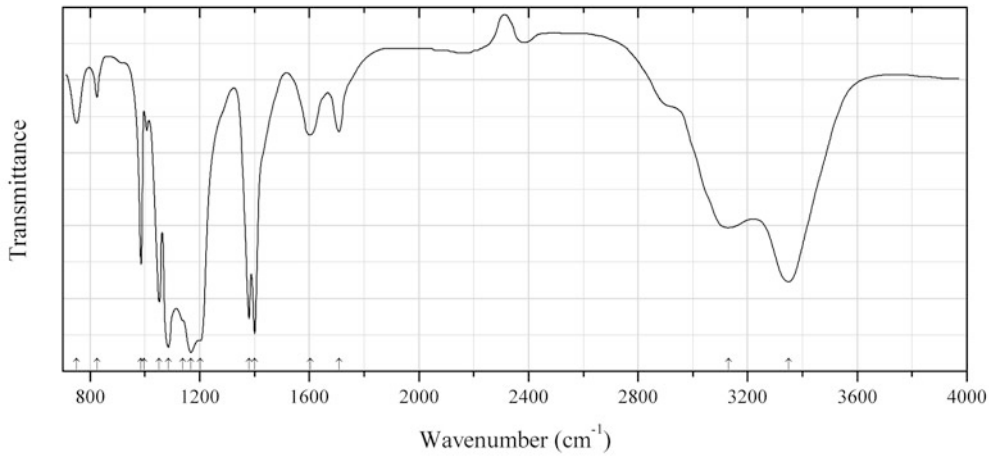

Fig. 2.1081 IR spectrum of humberstonite drawn using data from Mrose et al. (1970)

S362 Humberstonite $K_3Na_7Mg_2(SO_4)_6(NO_3)_2\cdot 6H_2O$ (Fig. 2.1081)
Locality: Oficina Alemania, Santa Catalina, Antofagasta region, Chile (type locality).

Description: White powdery aggregate. Holotype sample. Trigonal, space group *R*-3, a = 10.900(1), c = 24.410(2) Å, Z = 3. D_{meas} = 2.252 g/cm^3, D_{calc} = 2.252 g/cm^3. Optically uniaxial (−), ε = 1.436 (2), ω = 1.474(2). The strongest lines of the powder X-ray diffraction pattern [*d*, Å (*I*, %) (*hkl*)] are: 8.802 (35) (101), 8.137 (60) (003), 4.527 (35) (113), 3.393 (100) (205), 2.724 (70) (220), 2.583 (35) (223).
Kind of sample preparation and/or method of registration of the spectrum: KBr disc. Transmission.
Source: Mrose et al. (1970).
Wavenumbers (cm^{-1}): 3350, 3130, 1708, 1603, 1400s, 1380s, 1201sh, 1168s, 1138sh, 1085s, 1052s, 997w, 986, 825w, 751w.
Note: The wavenumbers were partly determined by us based on spectral curve analysis of the published spectrum.

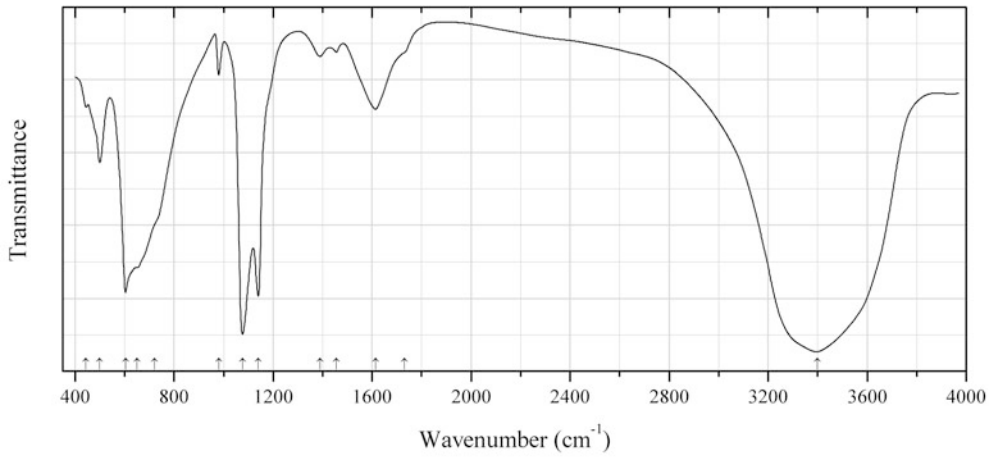

Fig. 2.1082 IR spectrum of hydrohonessite drawn using data from Bish and Livingstone (1981)

S363 Hydrohonessite $Ni_6Fe^{3+}{}_2(SO_4)(OH)_{16}\cdot 7H_2O$ (Fig. 2.1082)
Locality: Unst, Shetland, UK.
Description: Soft citron-yellow crusts on chromite. Hexagonal, a = 3.087(8), c = 33.4(3) Å. The empirical formula is $Ni_{5.55}Fe_{2.35}Mg_{0.10}(SO_4)_{1.18})(OH)_{16}\cdot nH_2O$. The strongest lines of the powder X-ray diffraction pattern are observed at 11.12, 5.58, 3.74, 2.67, 2.50, and 1.624 Å.
Kind of sample preparation and/or method of registration of the spectrum: KBr disc. Transmission.
Source: Bish and Livingstone (1981).
Wavenumbers (cm^{-1}): 3400s, 1730sh, 1615, 1456w, 1390w, 1140s, 1077s, 980w, 722sh, 650sh, 604s, 500, 444w.
Note: The wavenumbers were partly determined by us based on spectral curve analysis of the published spectrum.

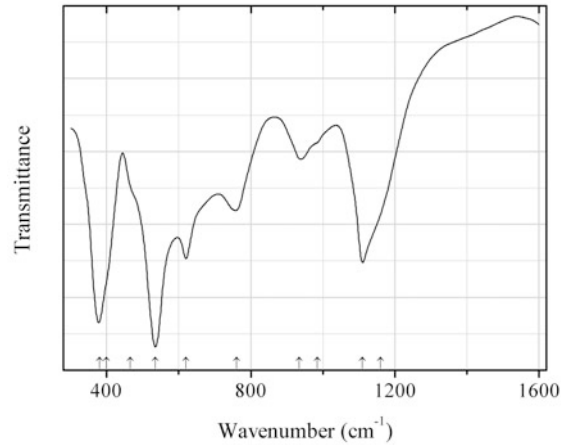

Fig. 2.1083 IR spectrum of quintinite Al,Li,SO_4-analogue drawn using data from Hernandez-Moreno et al. (1985)

S364 Quintinite Al,Li,SO_4-analogue $LiAl_2(OH)_6(SO_4)_{0.5}\cdot nH_2O$ (?) (Fig. 2.1083)
Locality: Synthetic.
Description: Confirmed by chemical analysis and powder X-ray diffraction data.
Kind of sample preparation and/or method of registration of the spectrum: KBr disc. Absorption.
Source: Hernandez-Moreno et al. (1985).
Wavenumbers (cm^{-1}): 1160sh, 1110, 985sh, 935w, 760, 620, 535s, 465sh, 400sh, 380s.
Note: The formula $Al_2Li(OH)_6(SO_4)\cdot nH_2O$ given in the cited paper isn't charge-balanced.

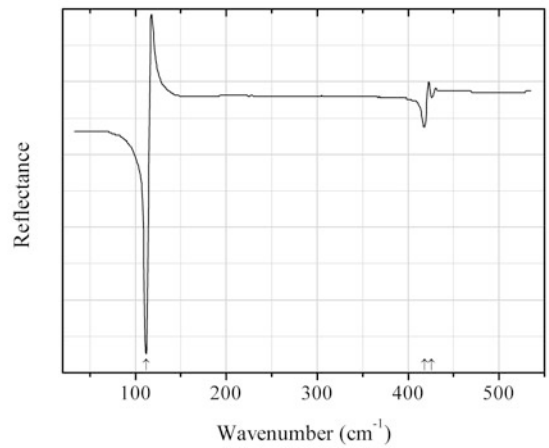

Fig. 2.1084 IR spectrum of cooperite drawn using data from Kliche (1985b)

S365 Cooperite PtS (Fig. 2.1084)
Locality: Synthetic.
Description: Obtained by thermal decomposition of PtS_2 at 800 °C during 4 h.
Kind of sample preparation and/or method of registration of the spectrum: Reflection of powdered sample.

Source: Kliche (1985b).
Wavenumbers (cm^{-1}): 426w, 418w, 112.

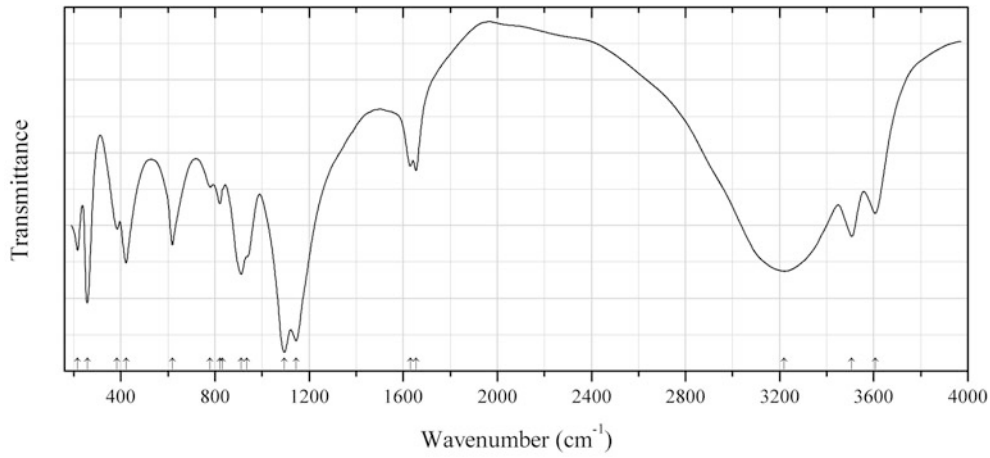

Fig. 2.1085 IR spectrum of johannite drawn using data from Čejka and Urbanec (1990)

S366 Johannite $Cu(UO_2)_2(SO_4)_2(OH)_2 \cdot 8H_2O$ (Fig. 2.1085)
Locality: Not indicated.
Kind of sample preparation and/or method of registration of the spectrum: KBr disc. Transmission.
Source: Čejka and Urbanec (1990).
Wavenumbers (cm^{-1}): 3606, 3507, 3220s, 1655, 1630, 1145s, 1096s, 936sh, 911, 832, 821, 780sh, 619, 422, 384, 257s, 216.
Note: The wavenumbers were partly determined by us based on spectral curve analysis of the published spectrum.

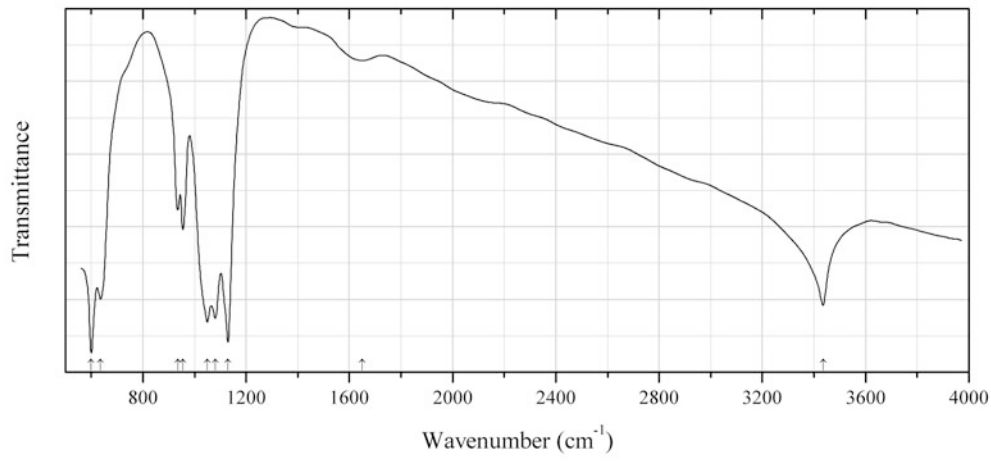

Fig. 2.1086 IR spectrum of klebelsbergite drawn using data from Nakai and Appleman (1980)

S367 Klebelsbergite $Sb^{3+}{}_4(SO_4)O_4(OH)_2$ (Fig. 2.1086)
Locality: Baia Sprie mine (formerly Felsöbánya mine), Baia Sprie, Maramureş Co., Romania (type locality).
Description: Yellow crystals radially grown on stibnite. Neotype sample. Orthorhombic, space group *Pcmb* or *Pc*21*b*, a = 11.279(2), b = 14.909(3), c = 5.7648(6) Å, Z = 4. D_{meas} = 4.62(6) g/cm^3, D_{calc} = 4.69 g/cm^3. The empirical formula is $H_{2.06}Sb_{4.07}(SO_4)_{1.00}O_{6.13}$. The strongest lines of the powder X-ray diffraction pattern [d, Å (*hkl*)] are: 6.22 (120), 3.892 (211), 3.545 (221), 3.150 (301), 3.131 (231), 2.830 (012), 2.435 (132), 1.805 (213).
Kind of sample preparation and/or method of registration of the spectrum: KBr disc. Transmission.
Source: Nakai and Appleman (1980).
Wavenumbers (cm^{-1}): 3435, 1650w, 1130s, 1080s, 1050s, 955, 935, 635, 600s.

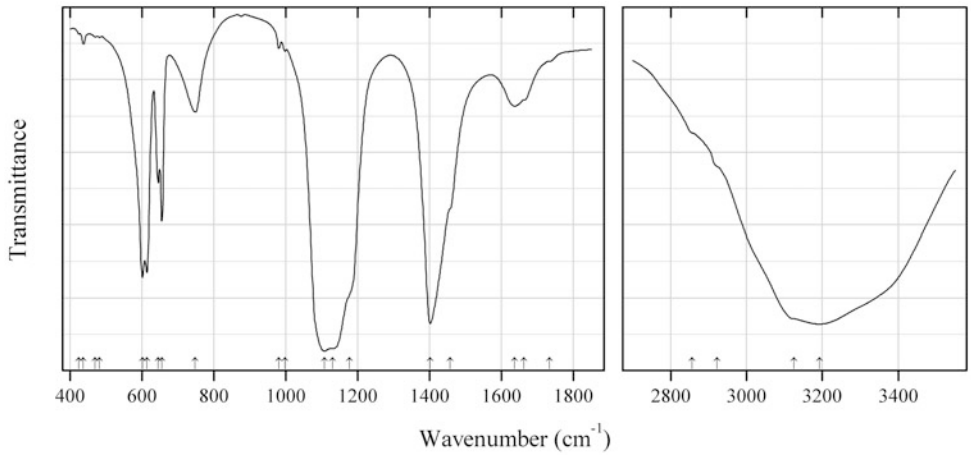

Fig. 2.1087 IR spectrum of koktaite drawn using data from Jentzsch et al. (2012a)

S368 Koktaite $(NH_4)_2Ca(SO_4)_2{\cdot}2H_2O$ (Fig. 2.1087)
Locality: Synthetic.
Kind of sample preparation and/or method of registration of the spectrum: KBr disc. Transmission.
Source: Jentzsch et al. (2012a).
Wavenumbers (cm^{-1}): 3192s, 3125sh, 2922sh, 2857sh, 1733sh, 1662sh, 1636, 1457sh, 1402s, 1177sh, 1131s, 1108s, 998w, 981w, 749, 656, 646, 614s, 602s, 483w, 471w, 438, 425w.
Note: The shoulders at 2922 and 2857 cm^{-1} correspond to the admixture of an organic substance.

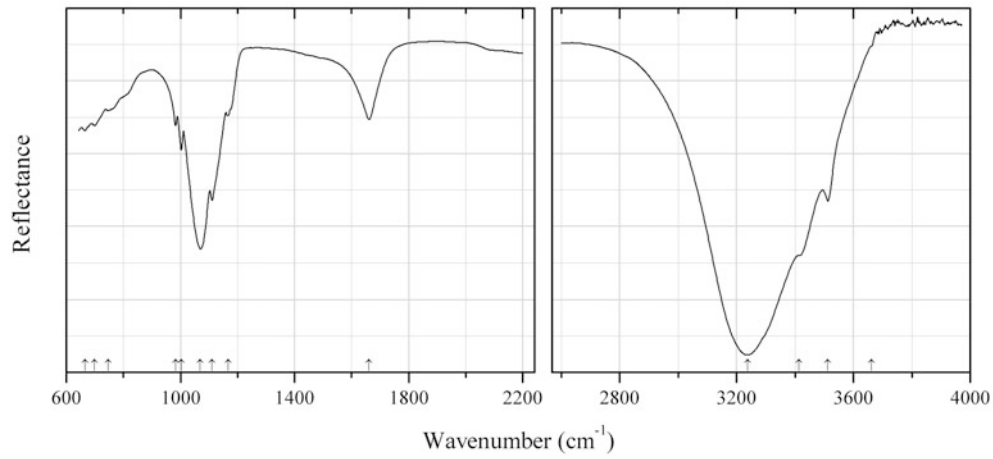

Fig. 2.1088 IR spectrum of konyaite drawn using data from Leduc (2010)

S369 Konyaite $Na_2Mg(SO_4)_2{\cdot}5H_2O$ (Fig. 2.1088)
Locality: Synthetic.
Description: Synthesized by the evaporation of the aqueous solution of $MgSO_4$ and Na_2SO_4 (with a 1:1 molar ratio) at 27 °C and 79 % relative humidity. The strongest lines of the powder X-ray diffraction pattern [*d*, Å (*I*, %) (*hkl*)] are: 4.371 (43) (111), 4.169 (41) (−131), 3.975 (100) (060), 3.929 (54) (012), 2.651 (31) (180), 2.628 (44) (−231).
Kind of sample preparation and/or method of registration of the spectrum: Attenuated total reflection of powdered sample.
Source: Leduc (2010).
Wavenumbers (cm^{-1}): 3662sh, 3512, 3414sh, 3237s, 1661, 1167w, 1111, 1070s, 1003, 983w, 746w, 699w, 665w.
Note: The band positions denoted by Leduc (2010) as 3257 and 1157 cm^{-1} were determined by us at 3237 and 1167 cm^{-1}, respectively, based on spectral curve analysis of the published spectrum.

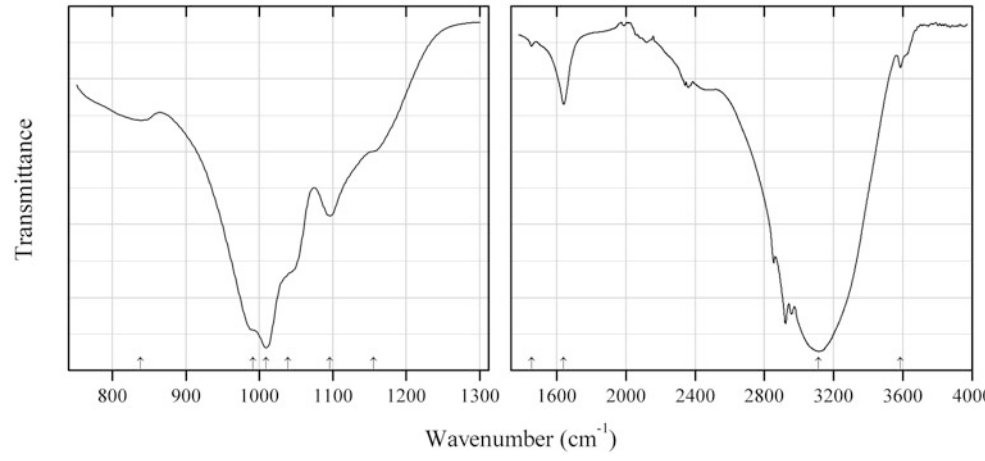

Fig. 2.1089 IR spectrum of kornelite drawn using data from Majzlan et al. (2011)

S370 Kornelite $Fe^{3+}{}_2(SO_4)_3 \cdot 7H_2O$ (?) (Fig. 2.1089)
Locality: The Iron Mountain Mine Superfund site, California, USA.
Description: Confirmed by powder X-ray diffraction вфеф. Monoclinic, a = 14.319(5), b = 20.139 (6), c = 5.429(2) Å, β = 96.78(2)°.
Kind of sample preparation and/or method of registration of the spectrum: KBr disc. Absorption.
Source: Majzlan et al. (2011).
Wavenumbers (cm^{-1}): 3586w, 3113s, 1642, 1455w, 1156sh, 1096, 1039sh, 1009s, 991sh, 838.
Note: The wavenumbers were partly determined by us based on spectral curve analysis of the published spectrum. Weak bands in the range from 2800 to 3000 cm^{-1} are due to the admixture of an organic substance.

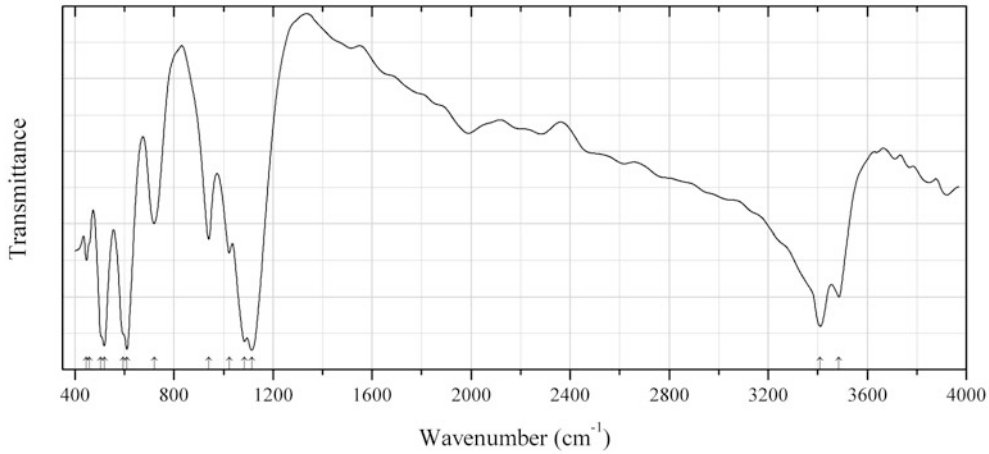

Fig. 2.1090 IR spectrum of krivovichevite drawn using data from Yakovenchuk et al. (2007)

S371 Krivovichevite $Pb_3Al(SO_4)(OH)_7$ (Fig. 2.1090)
Locality: Lepkhe-Nelm Mt., Lovozero alkaline complex, Kola peninsula, Murmansk region, Russia (type locality).
Description: Colourless equant grains from the association with natrolite, anglesite, cerussite, hydrocerussite, leadhillite, lanarkite, etc. Holotype sample. Trigonal, space group $R3c$, a = 7.693(8), c = 31.57(9) Å, V = 1618(6) Å^3, Z = 6. D_{calc} = 5.37 g/cm^3. Optically uniaxial (−), $n \approx 1.9$. The empirical formula is: $Pb_{3.04}Al_{0.94}S_{1.03}O_{3.98}(OH)_{7.08}$. The strongest lines of the powder X-ray diffraction pattern [d, Å (I, %) (hkl)] are: 3.58 (100) (201), 3.10 (60) (116), 2.591 (90) (119), 2.216 (50) (030), 2.048 (70) (036), 1.704 (80) (317).
Kind of sample preparation and/or method of registration of the spectrum: Transmission. A powdered sample. Other details of sample preparation are not indicated.
Source: Yakovenchuk et al. (2007).
Wavenumbers (cm^{-1}): 3486, 3410s, 1114s, 1084s, 1023, 940, 720, 610s, 595sh, 518s, 505sh, 458sh, 447.

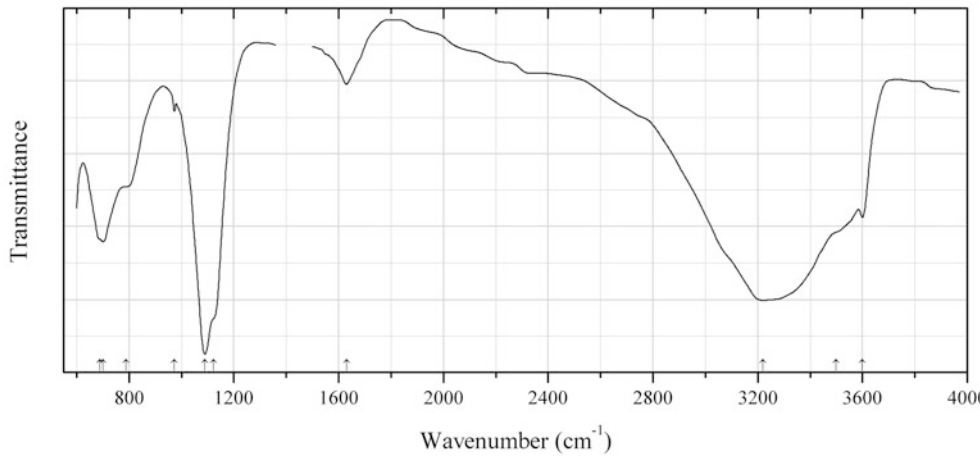

Fig. 2.1091 IR spectrum of ktenasite drawn using data from Raade et al. (1997)

S372 Ktenasite $(Cu,Zn)_5(SO_4)_2(OH)_6 \cdot 6H_2O$ (Fig. 2.1091)
Locality: Glomsrudkollen zinc mine, Modum, Norway.
Description: Green aggregates of thin platy crystals from the association with gypsum and bianchite. Monoclinic, space group $P2_1/c$, a = 5.598(3), b = 6.121(4), c = 23.762(15) Å, β = 95.55(6)°, V = 810.4 Å^3, Z = 2. D_{meas} = 2.94(1) g/cm^3, D_{calc} = 2.96 g/cm^3. Optically biaxial (−), α = 1.574(2), β = 1.615(2), γ = 1.628(2), 2 V = 59°. The empirical formula is: $H_{17.445}(Cu_{3.40}Zn_{1.455})S_{2.14}O_{20}$. The strongest lines of the powder X-ray diffraction pattern [d, Å (I, %) (hkl)] are: 11.82 (100) (002), 5.93 (85) (011, 004), 4.85 (90) (102, 013), 2.955 (50) (008, −116), 2.785 (60) (200), 2.688 (60) (120), 2.655 (50) (202).
Kind of sample preparation and/or method of registration of the spectrum: Nujol mull. Transmission.
Source: Raade et al. (1977).
Wavenumbers (cm^{-1}): 3600, 3500sh, 3220s, 1630w, 1122sh, 1090s, 973w, 788sh, 700s, 689sh.
Note: The wavenumbers were partly determined by us based on spectral curve analysis of the published spectrum.

S373 Kuzelite $Ca_4Al_2(OH)_{12}(SO_4) \cdot 6H_2O$
Locality: Maroldsweisach, northern Bavaria. Germany.
Description: White platy crystals from carbonaceous xenolith in a Tertiary basalt. Trigonal, space group R-3 or $R3$, a = 5.76(1), c = 53.66(2) Å, Z = 3. D_{meas} = 1.99(5) g/cm^3, D_{calc} = 2.014 g/cm^3. Optically uniaxial (−), ε = 1.485(5), ω = 1.504(5). The strongest lines of the powder X-ray diffraction pattern [d, Å (I, %) (hkl)] are: 8.944 (100) (006), 4.472 (70) (0.0.12), 4.003 (30) (108), 2.881 (30) (110), 2.422 (30) (1.1.12), 2.363 (40) (1.0.20), 2.236 (30) (0.0.24), 2.191 (40) (1.0.22), 2.072 (35) (1.1.18), 1.907 (30) 1.0.26), 1.827 (30) (2.0.20).
Kind of sample preparation and/or method of registration of the spectrum: Transmission. Kind of sample preparation is not indicated.
Source: Pöllmann et al. (1979).
Wavenumbers (cm^{-1}): 3650, 3600, 3100, 1650, 1150, 1105, 1095, 975, 780, 530, 415, 290.
Note: In the cited paper, the wavenumbers given in the table do not correspond to the positions of absorption bands in figure.

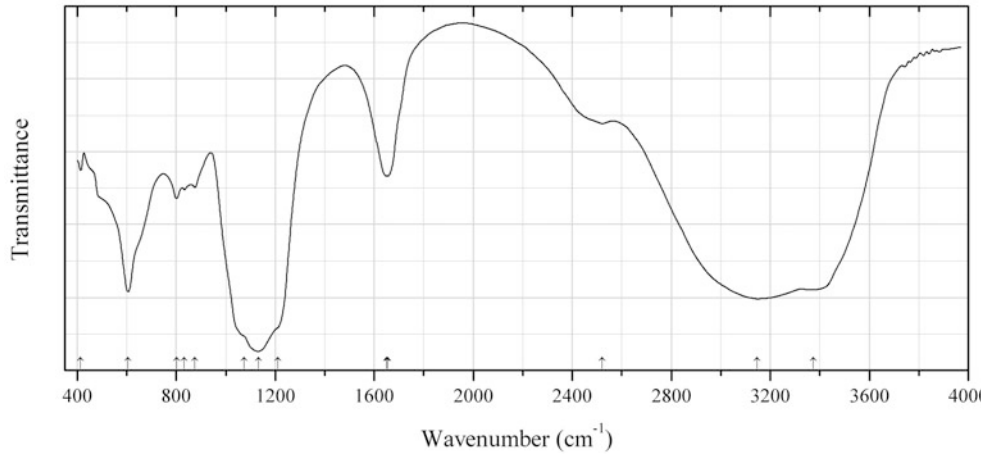

Fig. 2.1092 IR spectrum of lanmuchangite drawn using data from Daiyan et al. (2003)

S374 Lanmuchangite $TlAl(SO_4)_2 \cdot 12H_2O$ (Fig. 2.1092)
Locality: Lanmuchang Tl–Hg deposit, Xinren Co., Guizhou province, China (type locality) .
Description: Massive compact aggregate from the association with melanterite, pickeringite, potassium alum, jarosite, gypsum, sulfur, etc. Holotype sample. Cubic, space group *Pa*3, a = 12.212 (5) Å, V = 1821(2) Å^3, Z = 4. D_{meas} = 2.22 g/cm^3. Optically isotropic, n = 1.495. The empirical formula is $(Tl_{1.00}K_{0.05}Ca_{0.01}Mg_{0.01})(Al_{1.01}Si_{0.01})(SO_4)_{2.01} \cdot 11.88H_2O$. The strongest lines of the powder X-ray diffraction pattern [d, Å (I, %) (hkl)] are: 7.03 (54) (111), 6.11 (27) (200), 4.314 (100) (220), 3.676 (22) (311), 3.524 (24) (222), 3.263 (20) (321), 3.051 (22) (400), 2.801 (70) (331), 2.731 (35) (420), 2.494 (20) (422), 2.350 (21) (511), 1.932 (19) (620).
Kind of sample preparation and/or method of registration of the spectrum: KBr disc. Transmission.
Source: Daiyan et al. (2003).
Wavenumbers (cm^{-1}): 3374s, 3147s, 2522w, 1655, 1649, 1210sh, 1132s, 1075sh, 875, 833, 801, 605s, 414w.
Note: The wavenumbers were partly determined by us based on spectral curve analysis of the published spectrum.

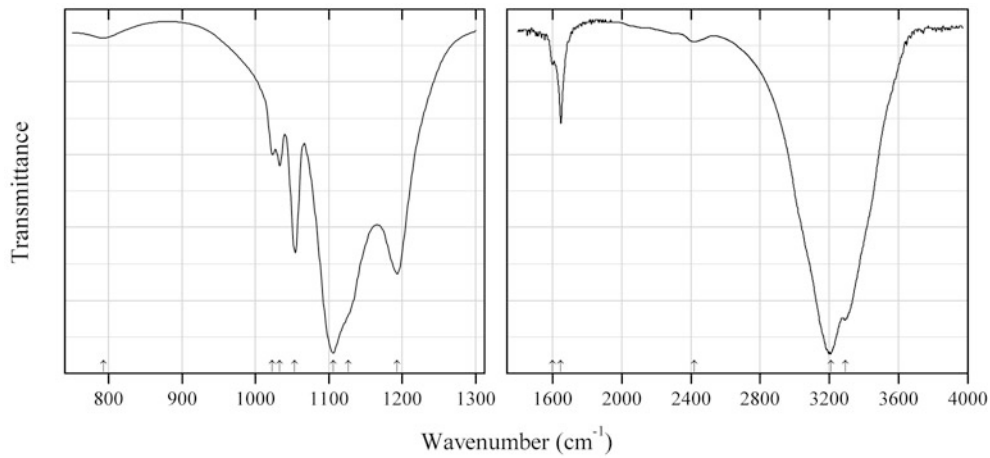

Fig. 2.1093 IR spectrum of lausenite drawn using data from Majzlan et al. (2011)

S375 Lausenite $Fe^{3+}_2(SO_4)_3 \cdot 5H_2O$ (Fig. 2.1093)
Locality: Synthetic.
Description: Monoclinic, space group $P2_1/m$, a = 10.705(1), b = 11.080(1), c = 5.5736(6) Å, β = 98.864(6)°, Z = 2.
Kind of sample preparation and/or method of registration of the spectrum: KCl disc. Transmission.
Source: Majzlan et al. (2011).
Wavenumbers (cm^{-1}): 3294s, 3210s, 2420w, 1649, 1600w, 1193s, 1127sh, 1106s, 1053, 1033, 1023, 793w.
Note: The wavenumbers were partly determined by us based on spectral curve analysis of the published spectrum.

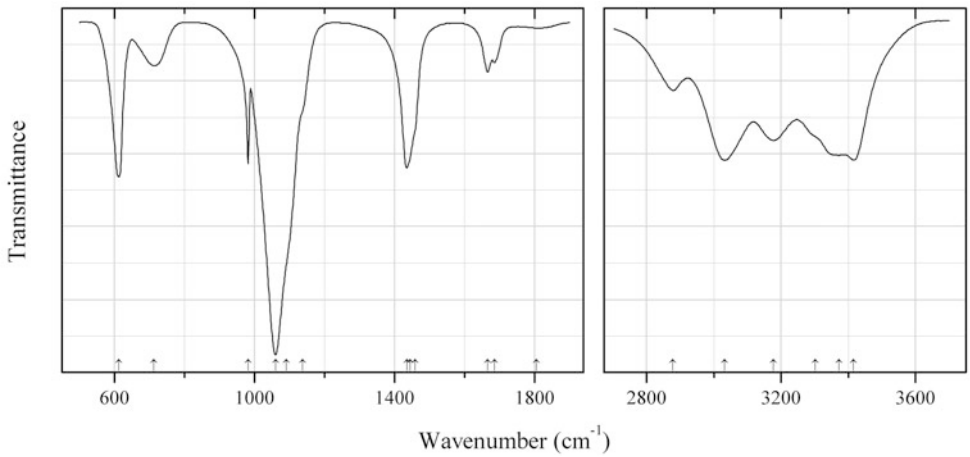

Fig. 2.1094 IR spectrum of lecontite drawn using data from Kloprogge et al. (2006)

S377 Lecontite $(NH_4)Na(SO_4) \cdot 2H_2O$ (Fig. 2.1094)
Locality: Synthetic.
Description: Synthesized at room temperature. Confirmed by Rietveld refinement of the XRD data. Orthorhombic, space group $P2_12_12_1$, a = 8.228, b = 12.852, c = 6.251 Å. D_{calc} = 1.658 g/cm^3.
Kind of sample preparation and/or method of registration of the spectrum: KBr disc. Absorption.
Source: Kloprogge et al. (2006).
Wavenumbers (cm^{-1}): 3416s, 3372s, 3302sh, 3178, 3033s, 2879, 1806w, 1686, 1666, 1459sh, 1444sh, 1435s, 1137sh, 1091sh, 1060s, 982s, 713, 612s.
Note: In the cited paper, wavenumbers are indicated for the maxima of individual bands obtained as a result of the spectral curve analysis. The wavenumbers were determined by us based on spectral curve analysis of the published spectrum.

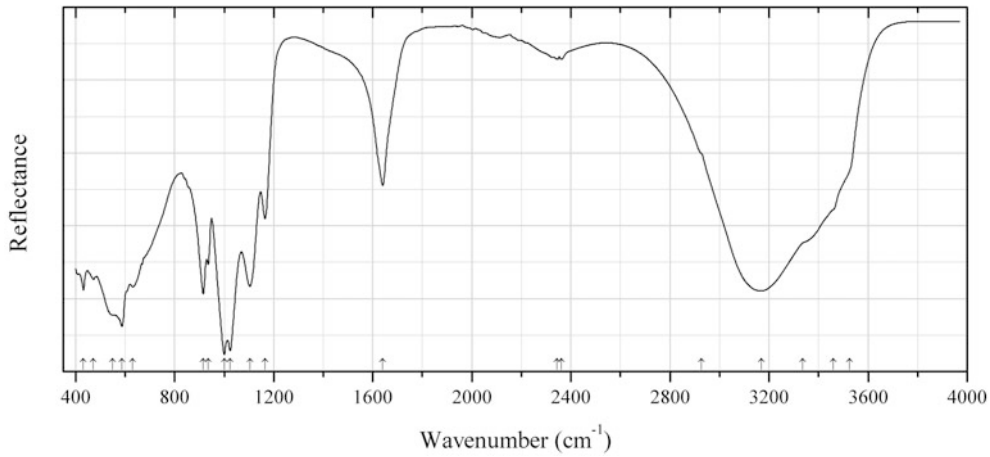

Fig. 2.1095 IR spectrum of leydetite drawn using data from Plášil et al. (2013)

S378 Leydetite $Fe^{2+}(UO_2)(SO_4)_2 \cdot 11H_2O$ (Fig. 2.1095)
Locality: Mas d'Alary, Lodève, Hérault, France (type locality).
Description: Greenish-yellow tabular crystals from the association with pyrite, uraninite, calcite, quartz, gypsum, deliensite, and unspecified clay minerals. Holotype sample. The crystal structure is solved. Monoclinic, space group *C*2/*c*, $a = 11.3203(3)$, $b = 7.7293(2)$, $c = 21.8145(8)$ Å, $\beta = 102.402(3)°$, $V = 1864.18(10)$ Å^3, $Z = 4$. $D_{calc} = 2.55$ g/cm^3. Optically biaxial, $\alpha = 1.513(2)$, $\gamma = 1.522(2)$. The empirical formula is $(Fe_{0.93}Mg_{0.07}Al_{0.04}Cu_{0.01})(U_{1.01}O_2)(S_{1.96}Si_{0.02})O_8 \cdot 11H_2O$. The strongest lines of the powder X-ray diffraction pattern [*d*, Å (*I*, %) (*hkl*)] are: 10.625 (100) (002), 6.277 (1) (−111), 5.321 (66) (004), 3.549 (5) (006), 2.663 (4) (008), 2.131 (2) (0.0.10).
Kind of sample preparation and/or method of registration of the spectrum: Attenuated total reflection of powdered mineral. KBr disc. Transmission.
Source: Plášil et al. (2013).
Wavenumbers (cm^{-1}): 3526sh, 3461sh, 3337sh, 3169s, 2927sh, 2362w, 2345w, 1641, 1166, 1104s, 1024s, 1001s, 935, 916s, 630, 588s, 550sh, 472, 432.
Note: The wavenumbers were partly determined by us based on spectral curve analysis of the published spectrum.

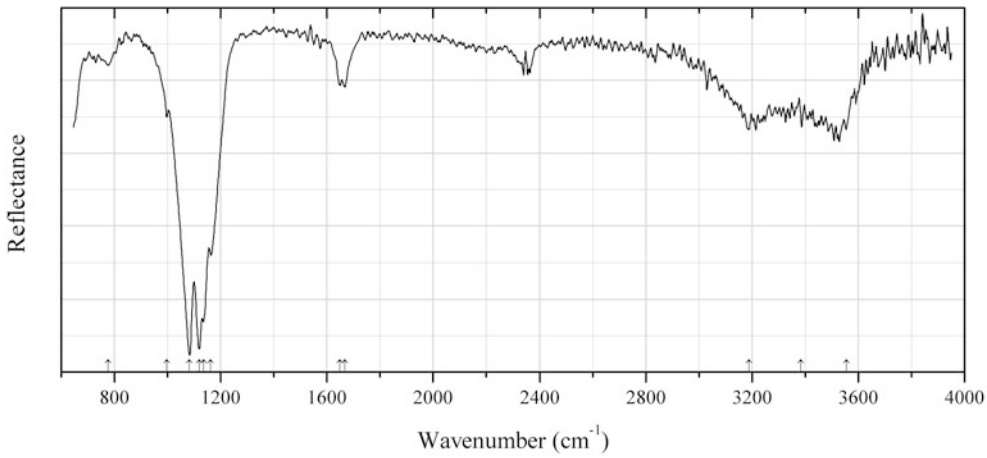

Fig. 2.1096 IR spectrum of löweite drawn using data from Leduc (2010)

S379 Löweite $Na_{12}Mg_7(SO_4)_{13}\cdot 15H_2O$ (Fig. 2.1096)
Locality: France (type locality).
Description: Confirmed by powder X-ray diffraction data.
Kind of sample preparation and/or method of registration of the spectrum: Attenuated total reflection of powdered sample.
Source: Leduc (2010).
Wavenumbers (cm^{-1}): 3555, 3384, 3189, 1667, 1649, 1163s, 1135s, 1119s, 1083s, 997, 776w.

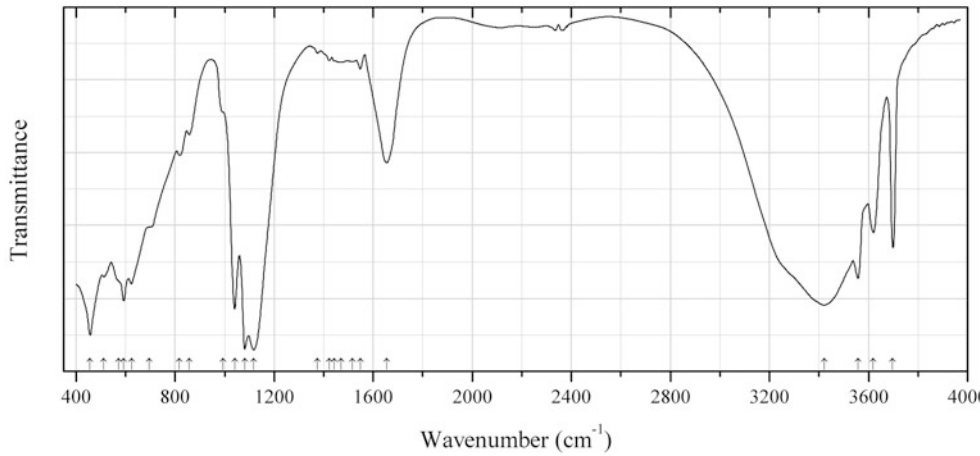

Fig. 2.1097 IR spectrum of magnesium hydroxysulfate hydrate S380 drawn using data from Fu et al. (2011)

S380 Magnesium hydroxysulfate hydrate S380 $Mg_6(SO_4)(OH)_{10}\cdot 2H_2O$ (Fig. 2.1097)
Locality: Synthetic.
Description: Aggregates of microscopic lamellar crystals. Obtained in the reaction between sodium hydroxide and magnesium sulfate solutions at 180 °C. Orthorhombic, a = 7.177(1), b = 9.804(2), c = 12.775(2) Å, V = 898.9(2) $Å^3$, Z = 4. D_{calc} = 2.476 g/cm^3.
Kind of sample preparation and/or method of registration of the spectrum: KBr disc. Transmission.
Source: Fu et al. (2011).
Wavenumbers (cm^{-1}): 3698, 3620, 3558, 3422s, 1655, 1548w, 1515w, 1470w, 1443w, 1423w, 1376w, 1118s, 1081s, 1041s, 993sh, 857w, 817w, 697sh, 624, 593s, 572sh, 512, 457s.
Note: The wavenumbers were partly determined by us based on spectral curve analysis of the published spectrum. The band position denoted by Fu et al. (2011) as 907 cm^{-1} was determined by us at 1041 cm^{-1} based on spectral curve analysis of the published spectrum.

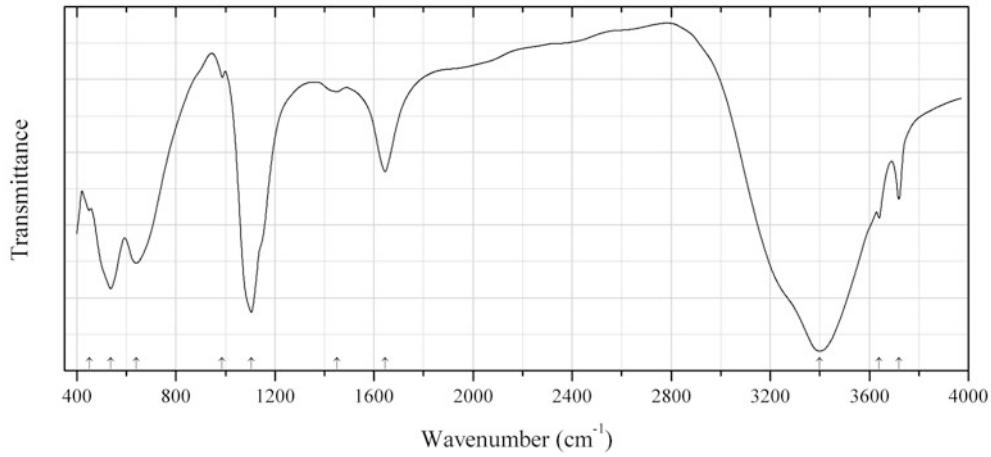

Fig. 2.1098 IR spectrum of magnesium hydroxysulfate hydrate S381 drawn using data from Runčevski et al. (2013)

S381 Magnesium hydroxysulfate hydrate S381 $Mg_6(SO_4)(OH)_{10}\cdot 7H_2O$ (Fig. 2.1098)
Locality: Synthetic.
Description: Synthesized at 20 °C from $MgSO_4\cdot 7H_2O$ and MgO in the presence of water and citric acid. Monoclinic, a = 10.260(3), b = 6.307(1), c = 15.138(3) Å, β = 103.98(2)°, Z = 4.
Kind of sample preparation and/or method of registration of the spectrum: KBr disc. Transmission.
Source: Runčevski et al. (2013).
Wavenumbers (cm^{-1}): 3720, 3640, 3400s, 1646, 1450w, 1142sh, 1105s, 987w, 640, 537s, 450.
Note: The wavenumbers were partly determined by us based on spectral curve analysis of the published spectrum.

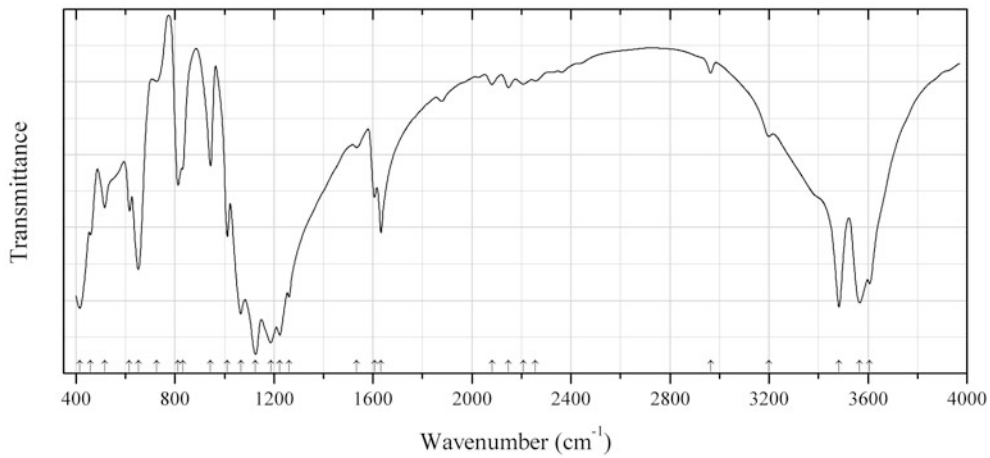

Fig. 2.1099 IR spectrum of magnesium hydroxysulfate hydrate S382 drawn using data from Tao et al. (2002)

S382 Magnesium hydroxysulfate hydrate S382 $Mg_3(SO_4)_2(OH)_2\cdot 2H_2O$ (Fig. 2.1099)
Locality: Synthetic.
Description: Synthesized from $MgSO_4$ and NaOH solutions at 160 °C for 21 days. The crystal structure is solved. Orthorhombic, space group *Pbcm*, a = 7.177(1), b = 9.804(2), c = 12.775(2) Å, Z = 4. D_{calc} = 2.476 g/cm^3. Optically biaxial (−), α = 1.554(1), β = 1.558(1), γ = 1.566(1), 2 V = 70(5)°.

Kind of sample preparation and/or method of registration of the spectrum: KBr disc. Transmission.
Source: Tao et al. (2002).
Wavenumbers (cm^{-1}): 3607s, 3567s, 3483s, 3200w, 2964w, 2257w, 2207w, 2148w, 2081w, 1880w, 1633, 1606, 1534, 1261s, 1224s, 1187s, 1126s, 1066s, 1012, 943, 831, 813, 725w, 652, 616, 516, 459, 416s.
Note: The wavenumbers were partly determined by us based on spectral curve analysis of the published spectrum.

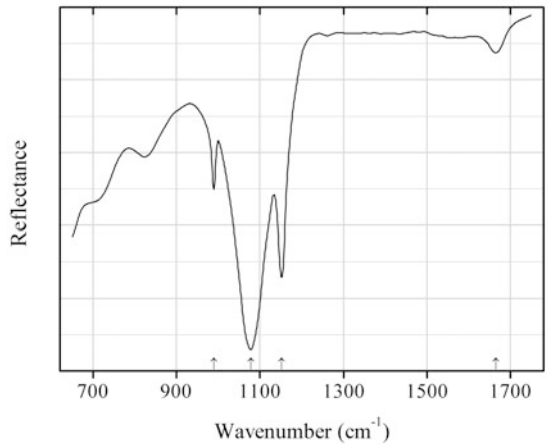

Fig. 2.1100 IR spectrum of manganoblödite drawn using data from Kasatkin et al. (2013)

S383 Manganoblödite $Na_2Mn(SO_4)_2{\cdot}4H_2O$ (Fig. 2.1100)
Locality: Blue Lizard mine, White Canyon District, San Juan County, Utah, USA (type locality).
Description: Pink aggregate of anhedral grains from the association with matulaite and Mn,Co, Ni-bearing blödite, cobaltoblödite, chalcanthite, gypsum, sideronatrite, johannite, quartz, and feldspar. Holotype sample. Monoclinic, space group $P2_1/a$, a = 11.137(2), b = 8.279(1), c = 5.5381(9) Å, β = 100.42(1)°, V = 502.20(14) $Å^3$, Z = 2. D_{meas} = 2.25(2) g/cm^3, D_{calc} = 2.338 g/cm^3. Optically biaxial (−), α = 1.493(2), β = 1.498(2), γ = 1.501(2). The empirical formula is $Na_{1.96}(Mn_{0.44}Mg_{0.29}Co_{0.14}Ni_{0.06})S_{2.03}O_8{\cdot}4H_2O$. The strongest lines of the powder X-ray diffraction pattern [d, Å (I, %) (hkl)] are: 4.556 (70) (−210, 011), 4.266 (45) (−201), 3.791 (26) (−211), 3.338 (21) (310), 3.291 (100) (220, 021), 3.256 (67) (211, −121), 2.968 (22) (−221), 2.647 (24) (−401).
Kind of sample preparation and/or method of registration of the spectrum: Powdered sample. Reflection.
Source: Kasatkin et al. (2013).
Wavenumbers (cm^{-1}): 1666w, 1152s, 1078s, 989.

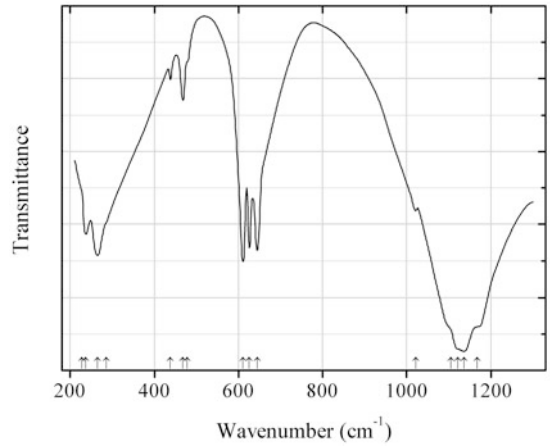

Fig. 2.1101 IR spectrum of manganolangbeinite drawn using data from Kreske and Devarajan (1982)

S384 Manganolangbeinite $K_2Mn^{2+}{}_2(SO_4)_3$ (Fig. 2.1101)
Locality: Synthetic.
Description: Obtained by slow evaporation of the 1:2 molar ratio solution of $K_2(SO_4)$ and $Mn(SO_4)$ at ~85 °C. Confirmed by powder X-ray diffraction data.
Kind of sample preparation and/or method of registration of the spectrum: Not indicated.
Source: Kreske and Devarajan (1982).
Wavenumbers (cm^{-1}): 1167sh, 1136s, 1121sh, 1105sh, 1021, 645s, 626s, 611s, 478sh, 468, 438w, (286sh), 265s, 237, 227sh, 193, 167w, 154sh, 148, (139), 129sh, 111sh, 104sh, 97, (84), 75, 67sh.
Note: The wavenumbers were partly determined by us based on spectral curve analysis of the published spectrum.

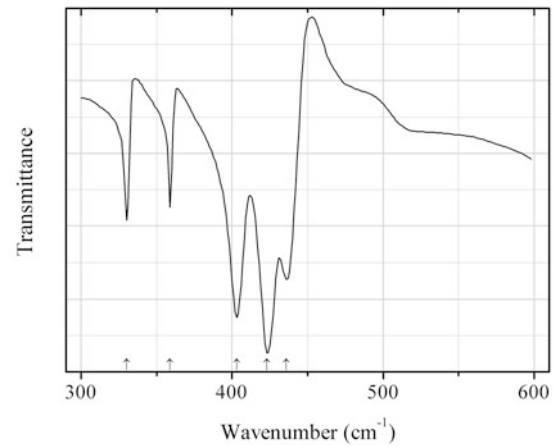

Fig. 2.1102 IR spectrum of marcasite drawn using data from Lennie and Vaughan (1992)

S385 Marcasite FeS_2 (Fig. 2.1102)
Locality: Not indicated.
Description: A sample from the Harwood Mineral Collection of the University of Manchester characterized by X-ray powder diffraction and microprobe analysis.

Kind of sample preparation and/or method of registration of the spectrum: KBr disc. Transmission.
Source: Lennie and Vaughan (1992).
Wavenumbers (cm^{-1}): 436s, 423s, 403s, 359, 330.
Note: The wavenumbers were partly determined by us based on spectral curve analysis of the published spectrum.

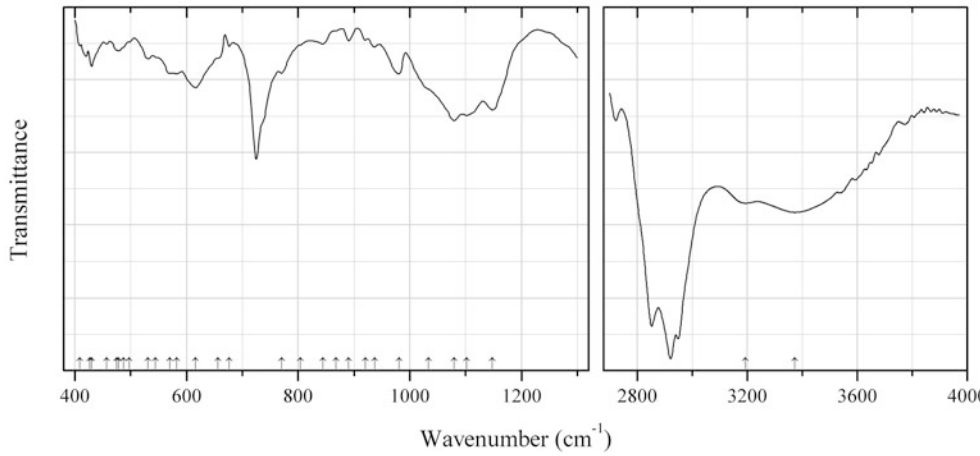

Fig. 2.1103 IR spectrum of meridianiite drawn using data from Peterson et al. (2007)

S386 Meridianiite $Mg(SO_4)\cdot 11H_2O$ (Fig. 2.1103)
Locality: A frozen pond near Ashcroft, British Columbia, Canada (type locality).
Description: White cockscomb aggregates from the association with matulaite and variscite. An ephemeral mineral stable below 2 °C. Holotype sample. Triclinic, a = 6.7459, b = 6.8173, c = 17.280 Å, α = 88.137°, β = 89.481°, γ = 62.719°.
Kind of sample preparation and/or method of registration of the spectrum: Nujol mull placed between CsI windows. Transmission.
Source: Peterson et al. (2007).
Wavenumbers (cm^{-1}): 3373s, 3194s, 1148s, 1102s, 1079s, 1033sh, 981, 937, 920, 890, 868w, 844, 804sh, 770, 676, 656sh, 616s, 582s, 570s, 545sh, 531, 497sh, 487sh, 479, 475sh, 457, 427, 430, 409.
Note: The wavenumbers were partly determined by us based on spectral curve analysis of the published spectrum. The bands in the ranges from 700 to 750 and from 2700 to 3000 cm^{-1} correspond to Nujol.

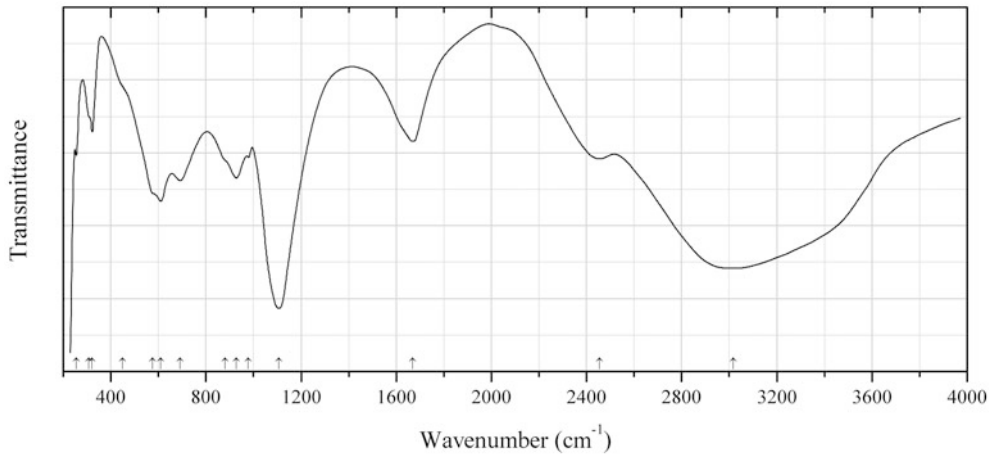

Fig. 2.1104 IR spectrum of meta-alunogen drawn using data from Hashmi et al. (1992)

S387 Meta-alunogen $Al_2(SO_4)_3 \cdot 12–16H_2O$ (?) (Fig. 2.1104)
Locality: Synthetic.
Description: Characterized using coulometry, transient ionic current and electrical conductivity.
Kind of sample preparation and/or method of registration of the spectrum: KBr disc. Transmission.
Source: Hashmi et al. (1992).
Wavenumbers (cm^{-1}): 3016s, 2454, 1670, 1107s, 979w, 928, 880sh, 692, 610s, 575sh, 450sh, 322w, 308sh, 255w.
Note: The wavenumbers were partly determined by us based on spectral curve analysis of the published spectrum.

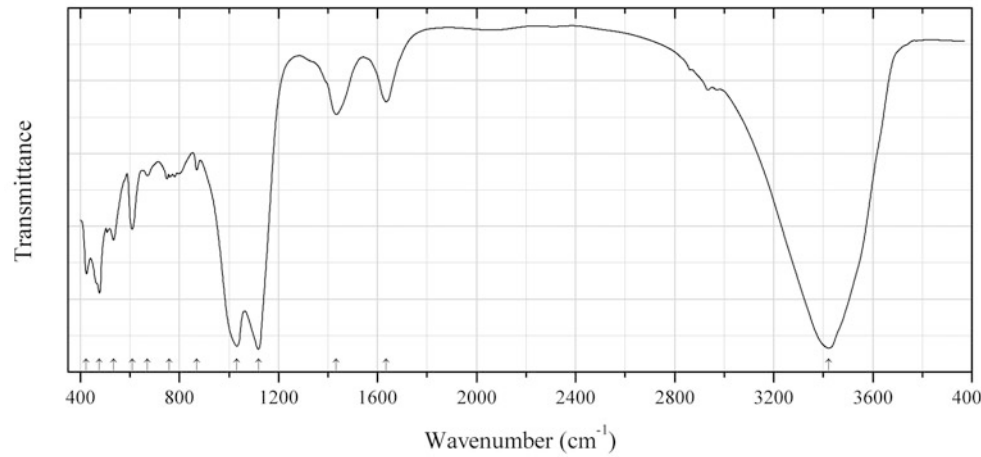

Fig. 2.1105 IR spectrum of minohlite drawn using data from Ohnishi et al. (2013)

S388 Minohlite $(Cu,Zn)_7(SO_4)_2(OH)_{10} \cdot 8H_2O$ (Fig. 2.1105)
Locality: Hirao mine at Minoh (Minoo) City, Osaka Prefecture, Japan (type locality).
Description: Blue-green rosette-like aggregates composed of hexagonal platy crystals from the association with chamosite, muscovite, smithsonite, serpierite, ramsbeckite, "limonite", and

chalcopyrite. Holotype sample. Hexagonal or trigonal, a = 8.2535(11), c = 8.1352(17) Å, V = 479.93 (16) Å^3, Z = 1. D_{calc} = 3.28 g/cm^3. The empirical formula is $(Cu_{4.43}Zn_{2.45}Fe_{0.06})(SO_4)_{1.99}(SiO_4)_{0.07}(OH)_{9.64}\cdot 7.81H_2O$. The strongest lines of the powder X-ray diffraction pattern [d, Å (I, %) (hkl)] are: 8.138 (20) (001), 4.128 (24) (110), 2.702 (100) (120), 2.564 (76) (121), 1.560 (43) (140), 1.532 (24) (141).

Kind of sample preparation and/or method of registration of the spectrum: KBr disc. Transmission.

Source: Ohnishi et al. (2013).

Wavenumbers (cm^{-1}): 3422s, 1636w, 1434w, 1119s, 1031s, 870w, 759w, 671w, 609, 534, 477s, 424.

Note: The bands in the range from 2800 to 3000 cm^{-1} correspond to the admixture of an organic substance. The bands at 1434 and 870 cm^{-1} indicate the presence of CO_3^{2-} groups in admixed smithsonite.

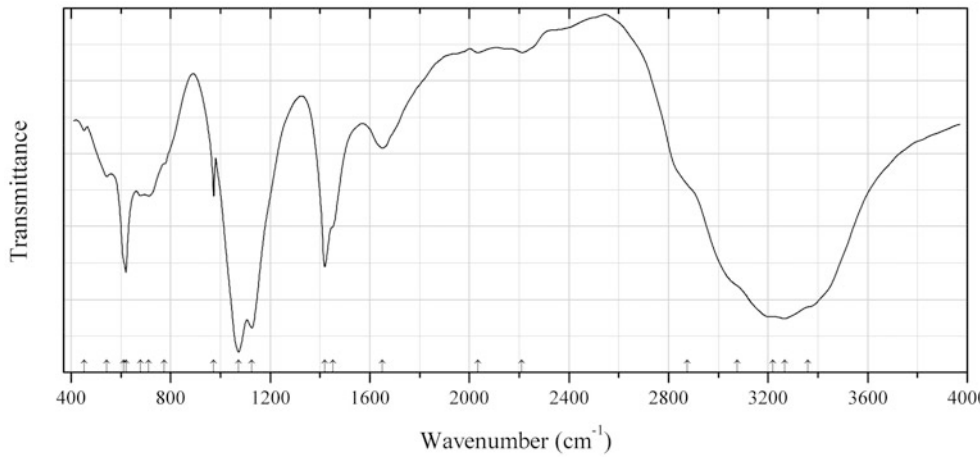

Fig. 2.1106 IR spectrum of mohrite drawn using data from Heilmann et al. (1974)

S389 Mohrite $(NH_4)_2Fe^{2+}(SO_4)_2\cdot 6H_2O$ (Fig. 2.1106)

Locality: Synthetic.

Description: Mohr salt.

Kind of sample preparation and/or method of registration of the spectrum: KBr disc. Transmission.

Source: Heilmann et al. (1974).

Wavenumbers (cm^{-1}): 3360sh, 3267s, 3220sh, 3075sh, 2875sh, 2210w, 2035w, 1650, 1451sh, 1419s, 1126s, 1073s, 973, 775sh, 712, 679, 620s, 612sh, 544, 453w.

Note: The wavenumbers were determined by us based on spectral curve analysis of the published spectrum.

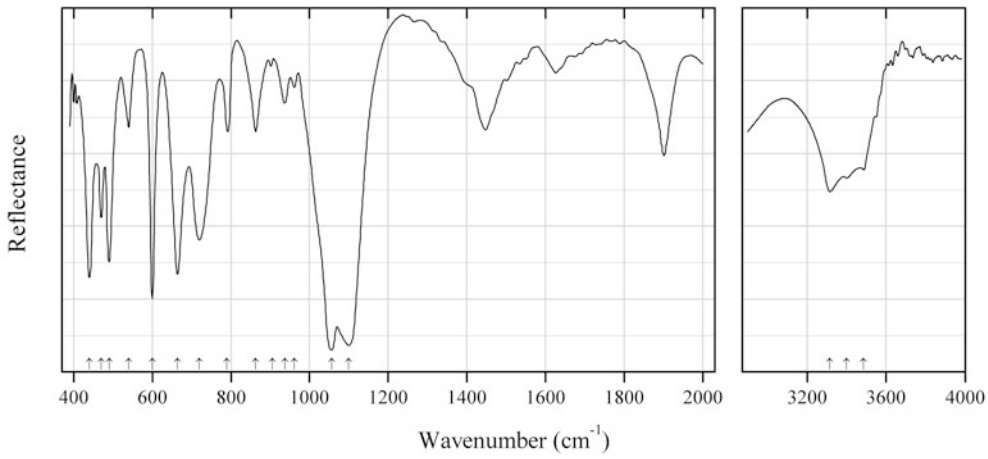

Fig. 2.1107 IR spectrum of munakataite drawn using data from Matsubara et al. (2008)

S390 Munakataite $Pb_2Cu_2(SeO_3)(SO_4)(OH)_4$ (Fig. 2.1107)
Locality: Kato mine, Munakata city, Fukuoka prefecture, Japan (type locality).
Description: Light blue coating on a fracture in a quartz vein containing Cu-Zn-Pb-Ag-Au ore minerals. Holotype sample. Monoclinic, space group $P2_1/m$, $a = 9.766(8)$, $b = 5.666(5)$, $c = 9.291(10)$ Å, $\beta = 102.40(8)°$, $V = 502.1(8)$ Å^3, $Z = 2$. $D_{calc} = 5.526$ g/cm^3. The empirical formula is $Ca_{0.01}Pb_{2.03}Cu_{1.94}(SeO_3)_{1.00}(SO_4)_{1.02}(OH)_{3.92}$. The strongest lines of the powder X-ray diffraction pattern [*d*, Å (*I*, %) (*hkl*)] are: 4.86 (44) (110), 4.47 (57) (10–2), 3.53 (39) (012, 11–2), 3.18 (100) (300), 3.14 (68) (112, 21–2).
Kind of sample preparation and/or method of registration of the spectrum: Attenuated total reflection (?).
Source: Matsubara et al. (2010).
Wavenumbers (cm^{-1}): 3486, 3400, 3315, 1100s, 1056s, 962w, 937, 905w, 863, 790, 720, 664s, 600s, 540, 490s, 470, 440s.
Note: The band positions shown by Matsubara et al. (2008) in the range above 2000 cm^{-1} are erroneous. Real border of the range is located at 2200 cm^{-1}. See for comparison Elliott (2010). The wavenumbers were partly determined by us based on spectral curve analysis of the published spectrum. The band in the range 1400–1500 cm^{-1} may correspond to a carbonate. Other bands in the range from 1300 to 2800 cm^{-1} indicate the presence of acid groups, HSO_4^- or $HSeO_3^-$. The band at 1622 cm^{-1} indicates possible presence of H_2O molecules.

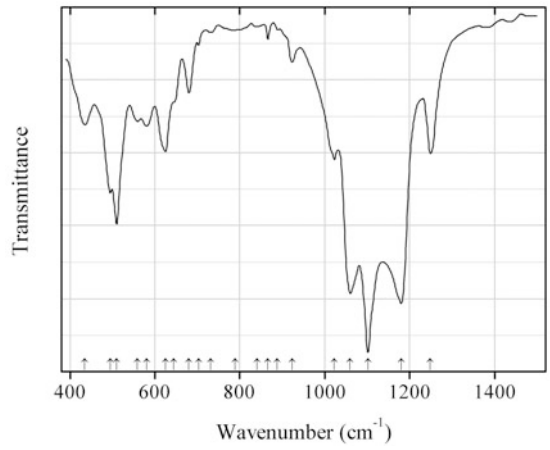

Fig. 2.1108 IR spectrum of nabokoite drawn using data from Popova et al. (1987)

S391 Nabokoite $Cu_7Te^{4+}(SO_4)_5O_4 \cdot KCl$ (Fig. 2.1108)
Locality: Second cone, Great Fissure Tolbachik volcano eruption, Kamchatka peninsula, Russia (type locality).
Description: Brown crystals from the association with euchlorine, dolerophanite, piypite, anglesite, chalcocyanite, chalcanthite, atacamite, etc. Holotype sample. Tetragonal, a = 9.84, c = 20.52 Å. D_{meas} = 4.18(5) g/cm^3. Optically uniaxial (−), ω = 1.778(3), ε = 1.773(3). The strongest lines of the powder X-ray diffraction pattern [d, Å (I, %) (hkl)] are: 10.35 (100) (002), 4.57 (40) (014), 3.421 (60) (006), 2.881 (50) (224), 2.439 (70) (226).
Kind of sample preparation and/or method of registration of the spectrum: KBr disc. Transmission.
Source: Popova et al. (1987).
Wavenumbers (cm^{-1}): 1249, 1102s, 1180s, 1060s, 1023, 923w, 888w, 866w, 840w, 789w, 732w, 703w, 680, 645sh, 625, 581, 559, 510, 495, 435.
Note: The wavenumbers were partly determined by us based on spectral curve analysis of the published spectrum.

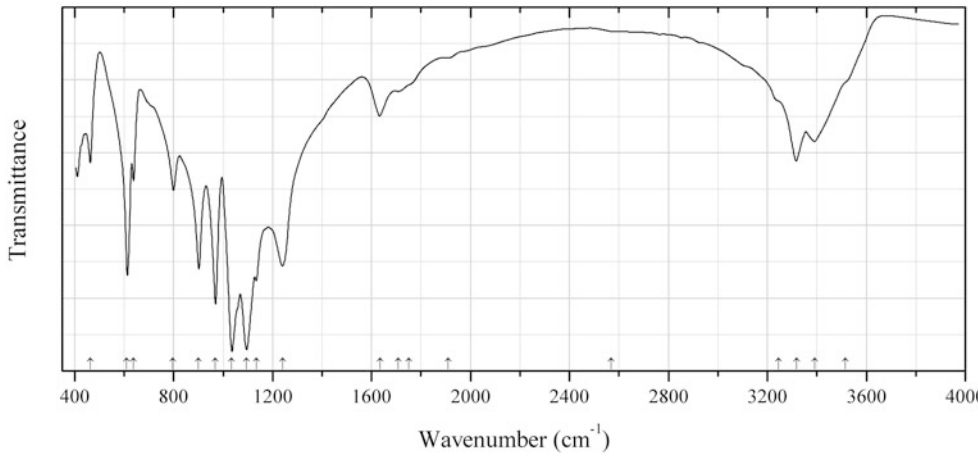

Fig. 2.1109 IR spectrum of natrochalcite Co analogue drawn using data from Krickl and Wildner (2009)

S392 Natrochalcite Co analogue $NaCo_2(SO_4)_2(OH)\cdot H_2O$ (Fig. 2.1109)
Locality: Synthetic.
Description: Synthesized under low-hydrothermal conditions.
Kind of sample preparation and/or method of registration of the spectrum: KBr microdisc. Absorption. Background spectrum was obtained on a pure KBr disc.
Source: Krickl and Wildner (2009).
Wavenumbers (cm^{-1}): 3515sh, 3391, 3318, 3246sh, 2570sh, 1910w, 1750sh, 1708w, 1635w, 1240, 1135, 1094s, 1035s, 969s, 901s, 798, 638, 611s, 463w.
Note: The wavenumbers were partly determined by us based on spectral curve analysis of the published spectrum.

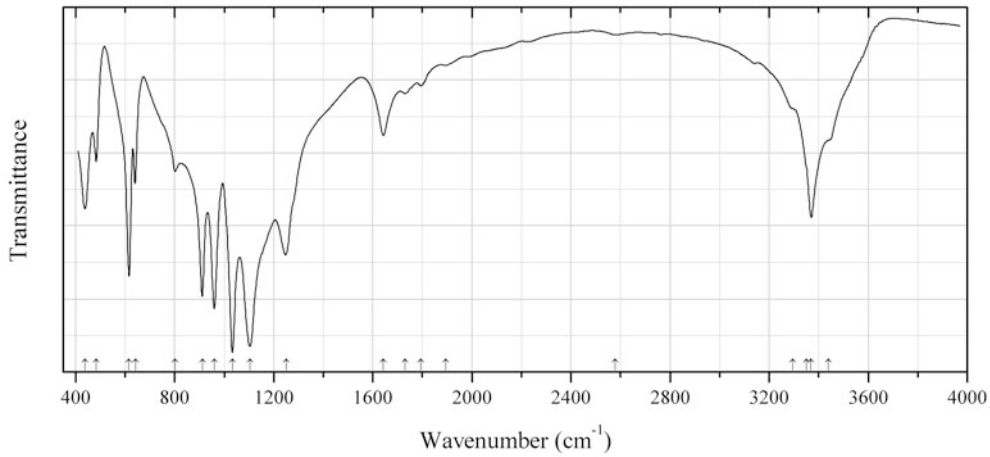

Fig. 2.1110 IR spectrum of natrochalcite Ni analogue drawn using data from Krickl and Wildner (2009)

S393 Natrochalcite Ni analogue $NaNi_2(SO_4)_2(OH)\cdot H_2O$ (Fig. 2.1110)
Locality: Synthetic.
Description: Synthesized under low-hydrothermal conditions.
Kind of sample preparation and/or method of registration of the spectrum: KBr microdisc. Absorption. Background spectra were obtained on pure KBr discs.
Source: Krickl and Wildner (2009).
Wavenumbers (cm^{-1}): 3440sh, 3370, 3351sh, 3296sh, 2580w, 1895w, 1795w, 1730w, 1643w, 1250, 1104s, 1033s, 961s, 912, 801w, 642, 616, 485w, 438.
Note: The wavenumbers were partly determined by us based on spectral curve analysis of the published spectrum.

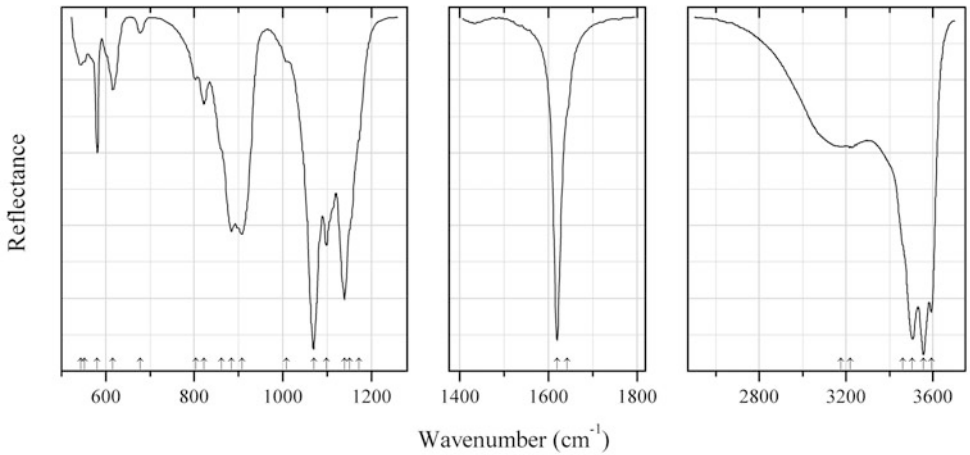

Fig. 2.1111 IR spectrum of natrozippeite drawn using data from Frost et al. (2007)

S394 Natrozippeite $Na_5(UO_2)_8(SO_4)_4O_5(OH)_3 \cdot 12H_2O$ (Fig. 2.1111)
Locality: Happy Jack Mine, White Canyon District, San Juan Co., Utah, USA. (type locality).
Description: The sample was analysed by EDX and by powder X-ray diffraction.
Kind of sample preparation and/or method of registration of the spectrum: Attenuated total reflection of powdered mineral.
Source: Frost et al. (2007).
Wavenumbers (cm^{-1}): 3594s, 3557s, 3506s, 3461sh, 3219, 3177, 1643sh, 1620s, 1172sh, 1151sh, 1139s, 1099s, 1070s, 1008w, 908s, 884s, 861sh, 822, 803w, 678w, 616, 581, 552sh, 544w.
Note: In the cited paper, the wavenumbers are indicated only for the maxima of individual bands obtained as a result of the spectral curve analysis. The wavenumbers were determined by us based on spectral curve analysis of the published spectrum.

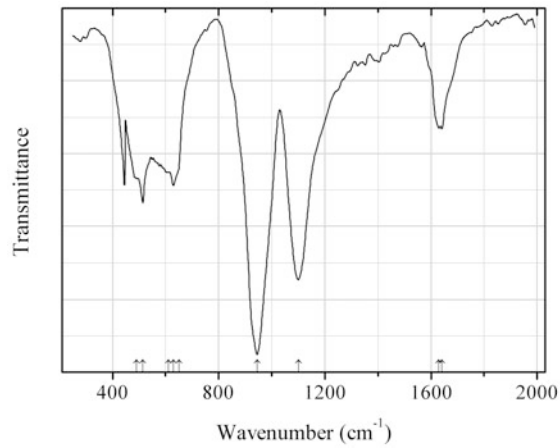

Fig. 2.1112 IR spectrum of orschallite drawn using data from Weidenthaler et al. (1993)

S395 Orschallite $Ca_3(SO_3)_2(SO_4) \cdot 12H_2O$ (Fig. 2.1112)
Locality: Hannebacher Ley, near Hannebach, Eifel volcanic area, Germany (type locality).

Description: Colourless cube-like crystals from the association with clinopyroxene, apatite, phillipsite, and calcite. Holotype sample. Trigonal, space group *R*-3*c*, $a = 11.350(1)$, $c = 28.321(2)$ Å, $V = 3159.7$ Å^3, $Z = 6$. $D_{meas} = 1.90(3)$ g/cm^3, $D_{calc} = 1.87$ g/cm^3. Optically uniaxial (+), $\omega = 1.4941(4)$, $\varepsilon = 1.4960(4)$. The strongest lines of the powder X-ray diffraction pattern [*d*, Å (*I*, %) (*hkl*)] are: 8.11 (80) (012), 5.73 (100) (104), 3.63 (60) (116), 3.28 (40) (300), 2.69 (80) (302), 2.11 (40) (229).
Kind of sample preparation and/or method of registration of the spectrum: Transmission. Kind of sample preparation is not indicated.
Source: Weidenthaler et al. (1993).
Wavenumbers (cm^{-1}): 3300, 1641, 1630, 1100s, 945s, 650sh, 630, 611sh, 514, 490sh.
Note: The wavenumbers were partly determined by us based on spectral curve analysis of the published spectrum.

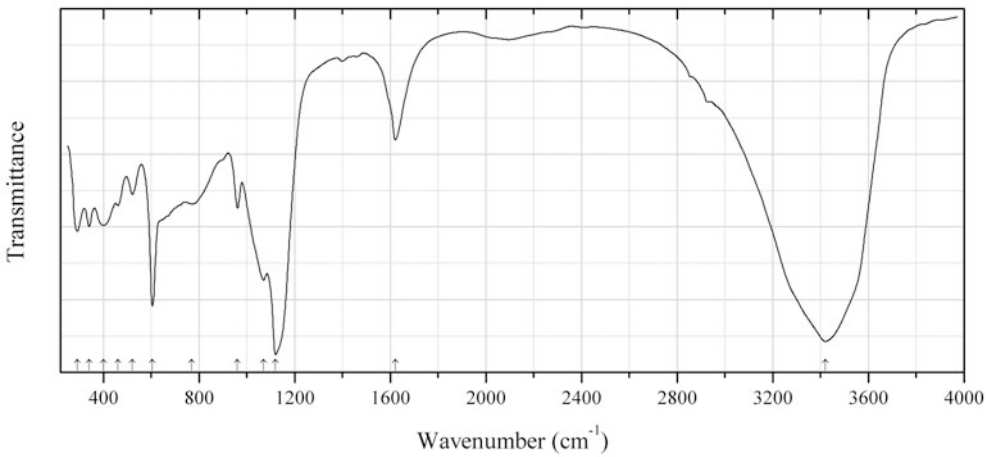

Fig. 2.1113 IR spectrum of osakaite drawn using data from Ohnishi et al. (2007c)

S396 Osakaite $Zn_4(SO_4)(OH)_6 \cdot 5H_2O$ (Fig. 2.1113)
Locality: Hirao mine, Minoo City, Osaka Prefecture, Japan (type locality).
Description: Stalactitic aggregates of colourless hexagonal platy crystals from the association with hydrozincite, smithsonite, chlorite, and "limonite". Holotype sample. Triclinic, space group *P*-1 (?), $a = 8.358(5)$, $b = 8.337(4)$, $c = 11.027(2)$ Å, $\alpha = 94.79(2)°$, $\beta = 83.16(2)°$, $\gamma = 119.61(4)°$, $V = 663.0(4)$ Å^3, $Z = 2$. $D_{meas} = 2.70(2)$ g/cm^3, $D_{calc} = 2.75$ g/cm^3. Optically biaxial (−), $\alpha = 1.532(2)$, $\beta = 1.565(2)$, $\gamma = 1.567(2)$. The empirical formula is $(Zn_{3.75}Cu_{0.24})(SO_4)_{1.01}(OH)_{5.96} \cdot 4.99H_2O$. The strongest lines of the powder X-ray diffraction pattern [*d*, Å (*I*, %) (*hkl*)] are: 10.96 (100) (001), 5.470 (16) (002), 3.642 (17) (003), 2.717 (21) (3–11), 1.574 (18) (5–33, 2–45, 5–23).
Kind of sample preparation and/or method of registration of the spectrum: KBr disc. Transmission.
Source: Ohnishi et al. (2007c).
Wavenumbers (cm^{-1}): 3420s, 1620, 1120s, 1070s, 960, 770, 605s, 520, 460, 400, 340, 290.
Note: The band position denoted by Ohnishi et al. (2007c) as 650 cm^{-1} was determined by us at 605 cm^{-1} based on spectral curve analysis of the published spectrum. For the IR spectrum of osakaite see also Eliott (2010).

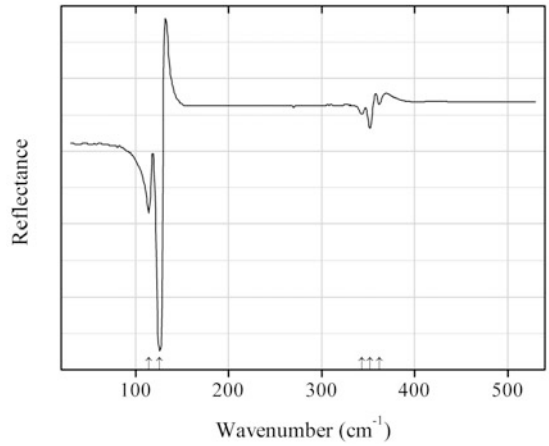

Fig. 2.1114 IR spectrum of palladium sulfide drawn using data from Kliche (1985b)

S397 Palladium sulfide PdS (Fig. 2.1114)
Locality: Synthetic.
Description: Polycrystalline aggregate obtained by annealing a stoichiometric mixture of the elements at 800 °C for 14 days. Tetragonal.
Kind of sample preparation and/or method of registration of the spectrum: Pressed disc. Reflection.
Source: Kliche (1985b).
Wavenumbers (cm^{-1}): 362w, 352w, 343w, 126s, 114.

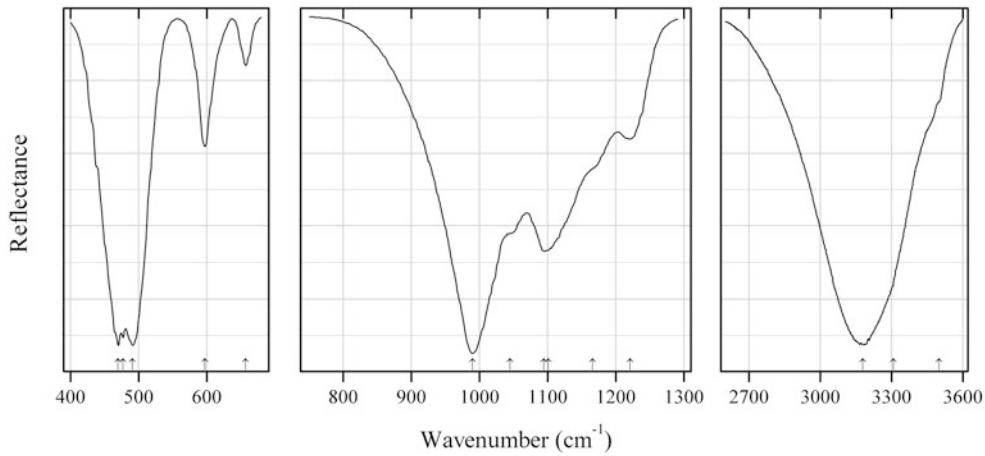

Fig. 2.1115 IR spectrum of parabutlerite drawn using data from Čejka et al. (2011)

S398 Parabutlerite $Fe^{3+}(SO_4)(OH)\cdot 2H_2O$ (Fig. 2.1115)
Locality: Alcaparrosa mine, Cerritos Bayos, Calama, El Loa Province, Antofagasta, Chile (type locality).
Description: A specimen from the mineralogical collections of the National Museum Prague, Czech Republic. Confirmed by powder X-ray diffraction data. Orthorhombic, space group *Pmnb*,

a = 7.398(2), b = 20.170(4), c = 7.230(1) Å, V = 1073.5(5) Å^3. The empirical formula is (electron microprobe): $Fe^{3+}_{1.06}(SO_4)_{1.00}(OH)_{1.18}\cdot nH_2O$.
Kind of sample preparation and/or method of registration of the spectrum: Attenuated total reflection of powdered mineral.
Source: Čejka et al. (2011).
Wavenumbers (cm^{-1}): 3498sh, 3307sh, 3178s, 1221, 1166sh, 1101sh, 1094s, 1045sh, 990s, 657, 597, 491s, 477s, 470s.
Note: In the cited paper, wavenumbers are indicated for the maxima of individual bands obtained as a result of the spectral curve analysis. The wavenumbers were determined by us based on spectral curve analysis of the published spectrum.

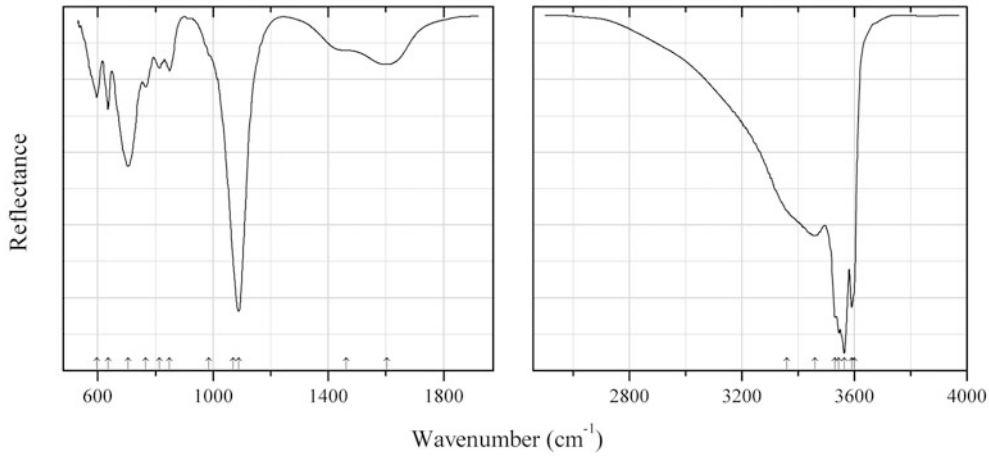

Fig. 2.1116 IR spectrum of paraotwayite drawn using data from Frost et al. (2006b)

S399 Paraotwayite $Ni(OH)_{2-x}(SO_4,CO_3)_{0.5x}$ (Fig. 2.1116)
Locality: Otway Ni deposit, Nullagine, East Pilbara Shire, Western Australia, Australia (type locality).
Description: Specimen M37166 from the Museum Victoria. Confirmed by the powder X-ray diffraction pattern.
Kind of sample preparation and/or method of registration of the spectrum: Attenuated total reflection of powdered mineral.
Source: Frost et al. (2006b).
Wavenumbers (cm^{-1}): 3600sh, 3591, 3564s, 3544, 3531, 3460, 3360sh, 1603w, 1462sh, 1089s, 1069sh, 986sh, 849w, 813w, 767, 705, 636, 597.
Note: In the cited paper, the wavenumbers are indicated only for the maxima of individual bands obtained as a result of the spectral curve analysis. The wavenumbers were determined by us based on spectral curve analysis of the published spectrum.

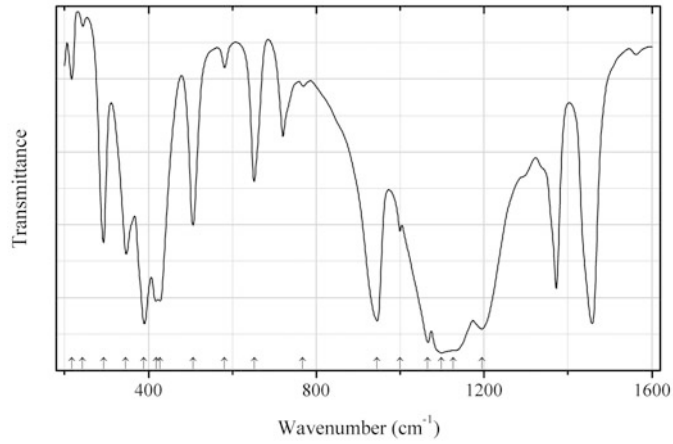

Fig. 2.1117 IR spectrum of pauflerite drawn using data from Gaubicher et al. (1997)

S400 Pauflerite β-$(VO)(SO_4)$ (Fig. 2.1117)
Locality: Synthetic.
Description: Prepared by the reduction of vanadium pentaoxide with sulfur in stoichiometric amounts, in soncentrated sulfuric acid at 140 °C for a few hours. Orthorhombic, space group *Pnma*. Condirmed by powder X-ray diffraction data.
Kind of sample preparation and/or method of registration of the spectrum: Nujol mull. Transmission.
Source: Gaubicher et al. (1997).
Wavenumbers (cm^{-1}): 1195, 1127sh, 1098s, 1066s, 1000, 945s, 768w, 652, 581w, 506, 428s, 418s, 389s, 346, 293, 243w, 217
Note: The wavenumbers were partly determined by us based on spectral curve analysis of the published spectrum. The bands with wavenumbers above 1300 cm^{-1} and at 720 cm^{-1} correspond to Nujol.

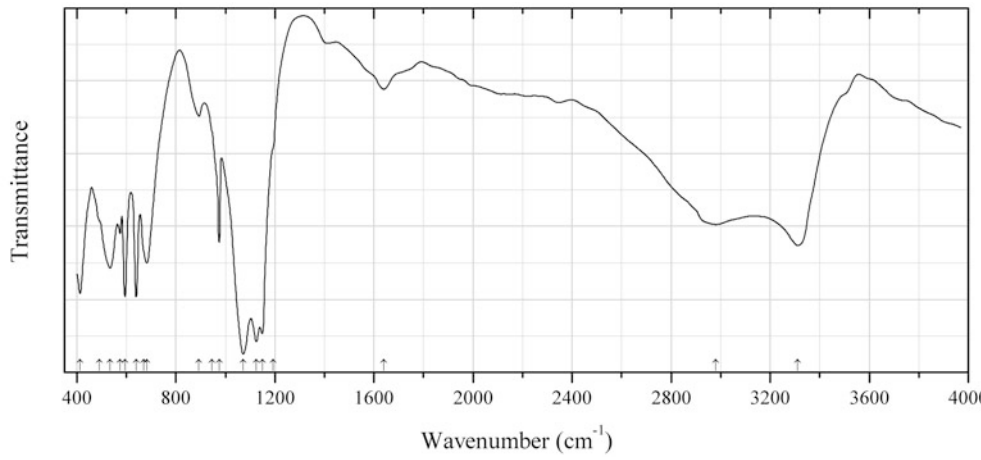

Fig. 2.1118 IR spectrum of peretaite drawn using data from Cipriani et al. (1980)

S401 Peretaite $CaSb^{3+}{}_4(SO_4)_2O_4(OH)_2 \cdot 2H_2O$ (Fig. 2.1118)
Locality: Pereta mine, Pereta, Tuscany, Italy (type locality).
Description: Colourless tabular crystals from the association with klebelsbergite, stibnite, quartz, calcite, pyrite, valentinite, kermesite, sulfur, and gypsum. Holotype sample. Monoclinic, space group *C*2/*c*, a = 24.641(2), b = 5.598(2), c = 10.180(1) Å, β = 95.95(1)°. $D_{meas} \approx 4.0$ g/cm^3, D_{calc} = 4.06 g/cm^3. Optically biaxial (+), with mean refractive index 1.841. The empirical formula is $Ca_{1.01}Sb_{4.17}S_{1.94}O_{16}H_{5.86}$. The strongest lines of the powder X-ray diffraction pattern [*d*, Å (*I*, %) (*hkl*)] are: 12.19 (100) (200), 6.12 (21) (400), 3.10 (24) (−512), 3.06 (67) (800), 2.451 (31) (10.0.0).
Kind of sample preparation and/or method of registration of the spectrum: KBr disc. Transmission.
Source: Cipriani et al. (1980).
Wavenumbers (cm^{-1}): 3310, 2980, 1640w, 1193sh, 1149s, 1125s, 1072s, 975, 946sh, 893w, 683, 670sh, 640s, 595s, 574, 535, 492sh, 413s.
Note: The wavenumbers were partly determined by us based on spectral curve analysis of the published spectrum.

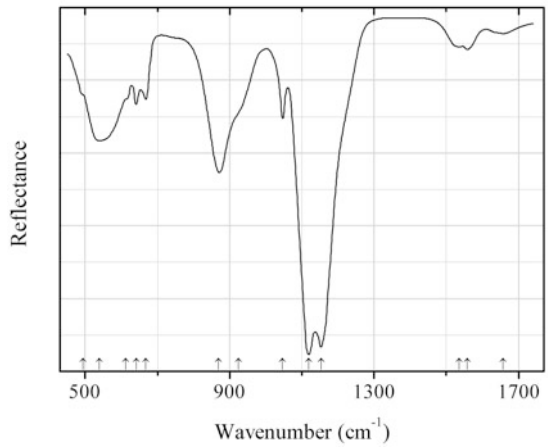

Fig. 2.1119 IR spectrum of kieserite drawn using data from Wang et al. (2008)

S402 Kieserite $Mg(SO_4) \cdot H_2O$ (Fig. 2.1119)
Locality: Syntetic.
Kind of sample preparation and/or method of registration of the spectrum: Attenuated total reflection.
Source: Wang et al. (2008).
Wavenumbers (cm^{-1}): 1658w, 1559w, 1535w, 1153s, 1119s, 1047, 925sh, 870s, 668, 641, 613sh, 540s, 494sh.
Note: The wavenumbers were determined by us based on spectral curve analysis of the published spectrum. After Moenke (1962), the wavenumbers of the IR absorption bands of kieserite are (cm^{-1}): 3390s, 3200, 1645w, 1532w, 1174s, 1135s, 1045, 900, 648, 628, 585, 537.

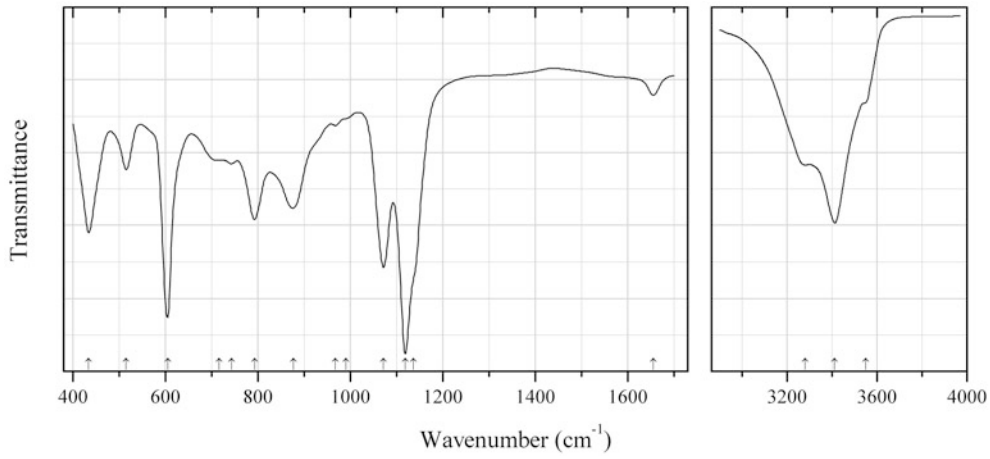

Fig. 2.1120 IR spectrum of posnjakite drawn using data from Zittlau et al. (2013)

S403 Posnjakite $Cu_4(SO_4)(OH)_6 \cdot H_2O$ (Fig. 2.1120)
Locality: Synthetic.
Description: Characterizeded by powder X-ray diffraction and calorimetric data.
Kind of sample preparation and/or method of registration of the spectrum: KBr disc. Transmission.
Source: Zittlau et al. (2013).
Wavenumbers (cm^{-1}): 3549sh, 3412s, 3282, 1655w, 1137sh, 1119s, 1072s, 991sh, 968w, 877, 793, 743w, 716sh, 605s, 515, 434.
Note: The wavenumbers were partly determined by us based on spectral curve analysis of the published spectrum.

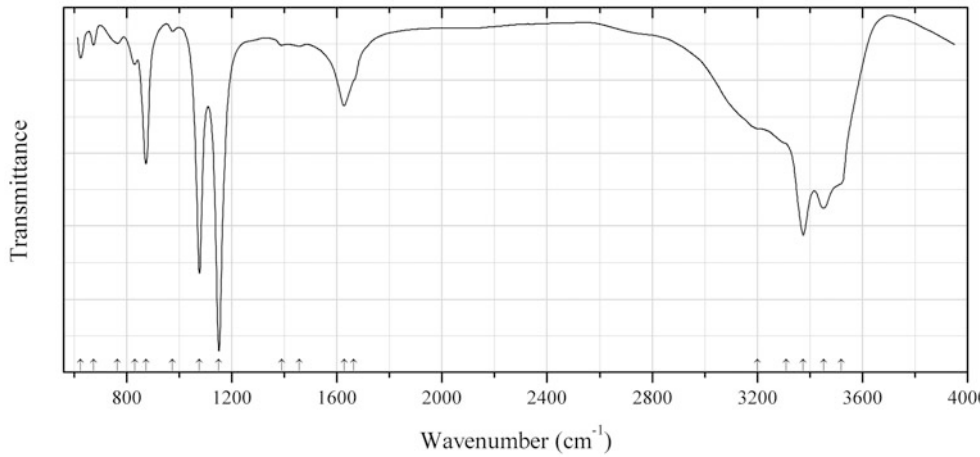

Fig. 2.1121 IR spectrum of pseudojohannite drawn using data from Brugger et al. (2006)

S404 Pseudojohannite $Cu_3(UO_2)_4(SO_4)_2O_4(OH)_2 \cdot 12H_2O$ (Fig. 2.1121)
Locality: Rovnost (Werner) shaft, Jáchymov, Bohemia, Krušné Hory Mts. (Ore Mts.), Czech Republic (type locality).

Description: Moss green, brittle aggregates from the association with johannite, uranopilite, and gypsum. Holotype sample. Triclinic, space group *P*1 or *P*-1, a = 10.0277, b = 10.8175, c = 13.3955 Å, α = 88.005°, β = 109.211°, γ = 90.864°, V = 1362.4 Å^3, Z = 2. D_{meas} = 4.31 g/cm^3, D_{calc} = 4.38 g/cm^3. Optically biaxial, n_{min} = 1.725, n_{max} = 1.740. The empirical formula is $H_{55.74}Cu_{6.52}U_{7.85}S_{4.02}O_{70}$. The strongest lines of the powder X-ray diffraction pattern [*d*, Å (*I*, %) (*hkl*)] are: 9.13 (100) (10–1), 7.09 (26) (110), 5.511 (22) 012), 4.566 (80) (−202), 3.046 (26) (30–3), 2.862 (20) (132).
Kind of sample preparation and/or method of registration of the spectrum: KBr disc. Transmission.
Source: Brugger et al. (2006).
Wavenumbers (cm^{-1}): 3520sh, 3453s, 3375s, 3310sh, 3200sh, 1665sh, 1627, 1457w, 1390w, 1151s, 1077s, 975w, 874s, 831w, 765w, 674w, 625w, 583, 497, 475.

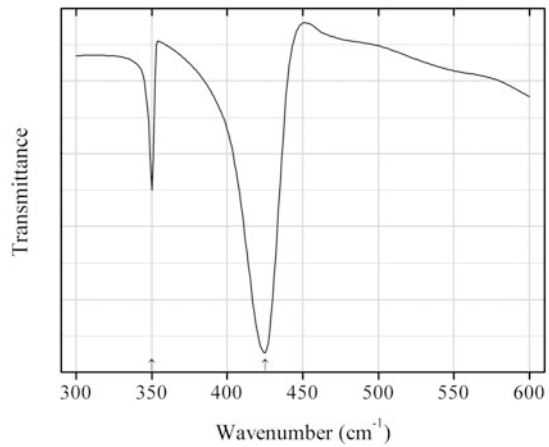

Fig. 2.1122 IR spectrum of pyrite drawn using data from Lennie and Vaughan (1992)

S405 Pyrite FeS_2 (Fig. 2.1122)
Locality: Not indicated.
Description: A natural sample characterized by powder X-ray diffraction and electron microprobe analyses.
Kind of sample preparation and/or method of registration of the spectrum: KBr disc. Transmission.
Source: Lennie and Vaughan (1992).
Wavenumbers (cm^{-1}): 425s, 350.

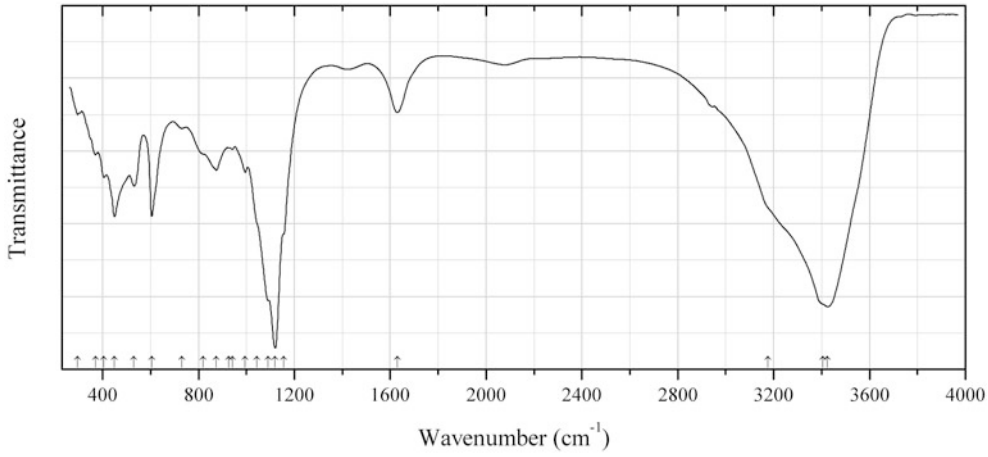

Fig. 2.1123 IR spectrum of ramsbeckite drawn using data from Ohnishi et al. (2004)

S406 Ramsbeckite $Cu_{15}(SO_4)_4(OH)_{22}\cdot 6H_2O$ (Fig. 2.1123)
Locality: Hirao mine, near the Minoo city, 17 km north of Osaka, Japan.
Description: Aggregates of euhedral crystals in the association with sphalerite, chalcopyrite, smithsonite, aurichalcite, amorphous manganese dioxide, schulenbergite, brochantite, serpierite, limonite, etc. Monoclinic, a = 16.106 (3), b = 15.568 (2), c = 7.109 (1) Å, β = 90.23(1)°, Z = 2. D_{meas} = 3.36 g/cm^3. Optically biaxial (−), α = 1.676, β = 1.704, γ = 1.707. The empirical formula is $(Cu_{9.38}Zn_{5.54}Ni_{0.03}Co_{0.03}Fe_{0.02}Mn_{0.01})[(SO_4)_{3.87}(CO_3)_{0.17}](OH)_{21.96}\cdot 6.06H_2O$. The strongest lines of the powder X-ray diffraction pattern [d, Å (I, %)] are: 7.11 (100), 3.553 (36), 3.257 (14), 1.551 (14), 2.882 (14), 2.696 (26), 2.682 (14), 2.518 (60), 2.145 (28).
Kind of sample preparation and/or method of registration of the spectrum: KBr disc. Transmission.
Source: Ohnishi et al. (2004).
Wavenumbers (cm^{-1}): 3425s, 3405sh, 3175sh, 1630, 1155sh, 1120s, 1090sh, 1044sh, 995, 941sh, 927w, 875, 820sh, 730w, 605, 530, 450, 405, 370w, 296w.
Note: The wavenumbers were partly determined by us based on spectral curve analysis of the published spectrum.

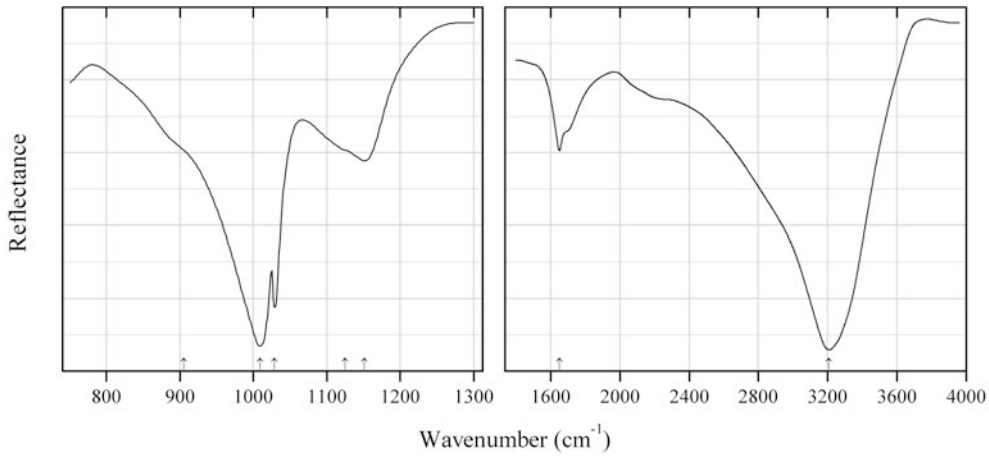

Fig. 2.1124 IR spectrum of rhomboclase drawn using data from Majzlan et al. (2011)

S407 Rhomboclase $(H_2O_5)^+Fe^{3+}(SO_4)_2 \cdot 2H_2O$ (Fig. 2.1124)
Locality: Iron Mountain mine, near Redding, northern California, USA.
Description: Characterized by powder X-ray diffraction. Orthorhombic, space group *Pnma*, $a = 9.726(3)$, $b = 18.293(9)$, $c = 5.428(3)$ Å.
Kind of sample preparation and/or method of registration of the spectrum: Attenuated total reflection of powdered mineral.
Source: Majzlan et al. (2011).
Wavenumbers (cm^{-1}): 3207s, 1651, 1151, 1125sh, 1029s, 1009s, 905sh.
Note: The wavenumbers were partly determined by us based on spectral curve analysis of the published spectrum. The IR spectrum of rhomboclase from the Iron Mountain mine is close to that of synthetic rhomboclase given in the same paper.

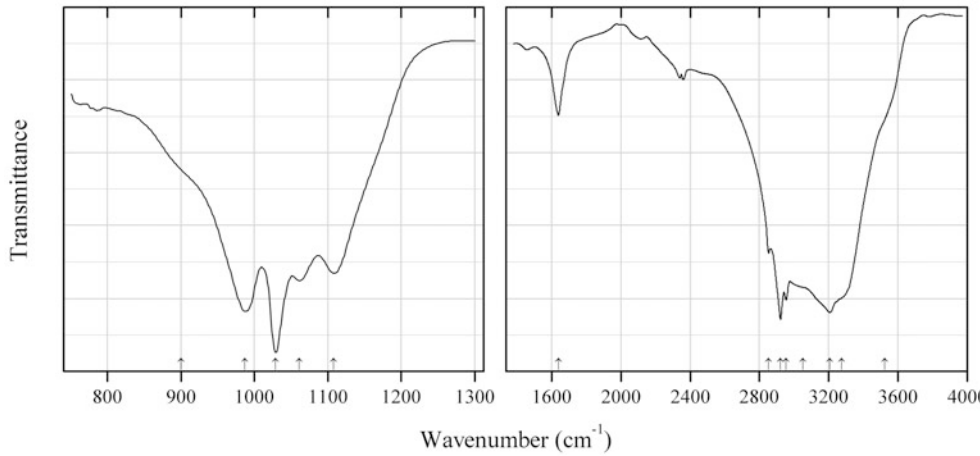

Fig. 2.1125 IR spectrum of römerite drawn using data from Majzlan et al. (2011)

S408 Römerite $Fe^{2+}Fe^{3+}{}_2(SO_4)_4 \cdot 14H_2O$ (Fig. 2.1125)
Locality: Iron Mountain mine, northern California, USA.
Description: White aggregates from the association with matulaite and variscite. Holotype sample. Triclinic, space group *P*-1, $a = 6.453(1)$, $b = 15.309(3)$, $c = 6.322(1)$ Å, $\alpha = 90.146(8)°$, $\beta = 100.932(9)°$, $\gamma = 85.86(1)°$. The sample was characterized by XANES and Mössbauer spectra.
Kind of sample preparation and/or method of registration of the spectrum: KBr disc. Absorption.
Source: Majzlan et al. (2011).
Wavenumbers (cm^{-1}): 3525sh, 3273sh, 3207s, 3050sh, 2954, 2922, 2854, 1640w, 1108, 1061, 1029s, 987s, 900sh.
Note: The wavenumbers were partly determined by us based on spectral curve analysis of the published spectrum. The bands in the range from 2800 to 3000 cm^{-1} are due to the admixture of an organic substance.

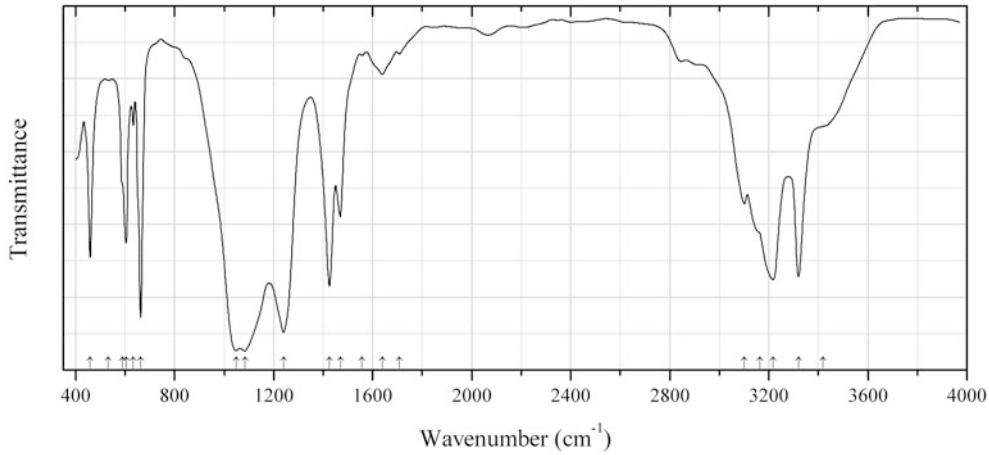

Fig. 2.1126 IR spectrum of sabieite drawn using data from Heilmann et al. (1974)

S409 Sabieite $(NH_4)Fe^{3+}(SO_4)_2$ (Fig. 2.1126)
Locality: Synthetic.
Description: Decomposition product of the Mohr salt $(NH_4)_2Fe(SO_4)_2 \cdot 6H_2O$ heated for 1 h in air at 770 K. Characterized by powder X-ray diffraction data and Mössbauer spectroscopy.
Kind of sample preparation and/or method of registration of the spectrum: KBr disc. Transmission.
Source: Heilmann et al. (1974).
Wavenumbers (cm^{-1}): 3420sh, 3320s, 3217s, 3165sh, 3102, 1708w, 1640w, 1557w, 1470, 1426, 1240s, 1084s, 1048s, 663s, 633w, 604, 589sh, 532w, 459.
Note: The wavenumbers were determined by us based on spectral curve analysis of the published spectrum.

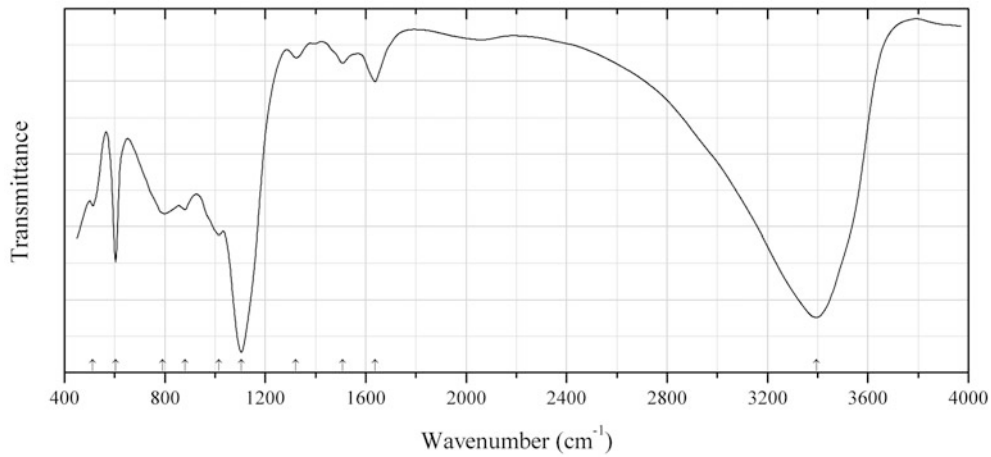

Fig. 2.1127 IR spectrum of schulenbergite drawn using data from Ohnishi et al. (2007a)

S410 Schulenbergite $(Cu,Zn)_7(SO_4)_2(OH)_{10} \cdot 3H_2O$ (Fig. 2.1127)
Locality: Hirao mine, Osaka prefecture, Japan.

Description: Greenish blue aggregates of platy crystals from the association with smithsonite, ramsbeckite, anatase, and goethite. Trigonal, a = 8.256(2), c = 7.207 (3) Å. D_{meas} = 3.18 g/cm^3, D_{calc} = 3.39 g/cm^3. Optically uniaxial (−), ω = 1.661, ε = 1.643. The empirical formula is $(Cu_{3.85}Zn_{3.13}Fe_{0.05})[(SO_4)_{1.62}(CO_3)_{0.41}(SiO_4)_{0.14}](OH)_{9.44}\cdot 3.30H_2O$. The strongest lines of the powder X-ray diffraction pattern [d, Å (I, %) (hkl)] are: 7.21 (100) (001), 3.590 (30) (002), 3.218 (28) (102), 2.704 (34) (210), 2.532 (52) (211), 2.164 (14) (212).
Kind of sample preparation and/or method of registration of the spectrum: KBr disc. Transmission.
Source: Ohnishi et al. (2007a).
Wavenumbers (cm^{-1}): 3394s, 1637, 1509w, 1321w, 1104s, 1015, 881, 792, 605, 513.

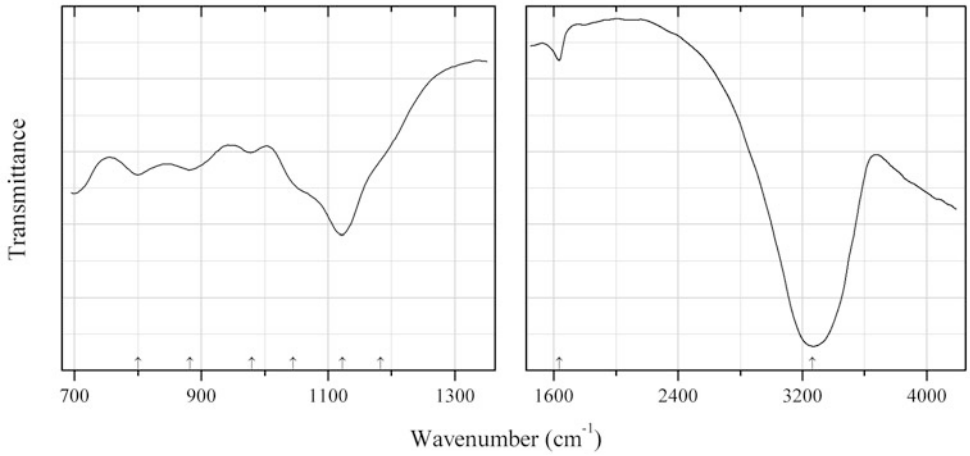

Fig. 2.1128 IR spectrum of schwertmannite drawn using data from Hyde et al. (2011)

S411 Schwertmannite $Fe^{3+}{}_8(SO_4)_2O_8(OH)_4$ (Fig. 2.1128)
Locality: Synthetic.
Description: Obtained by hydrolysis of ferric sulfate at 85 °C in deionized water for 1 h. Characterized by powder X-ray diffraction data.
Kind of sample preparation and/or method of registration of the spectrum: Absorbance of powdered sample placed on a diamond window.
Source: Hyde et al. (2011).
Wavenumbers (cm^{-1}): 3264s, 1636w, 1183sh, 1123s, 1045sh, 980, 882, 800.

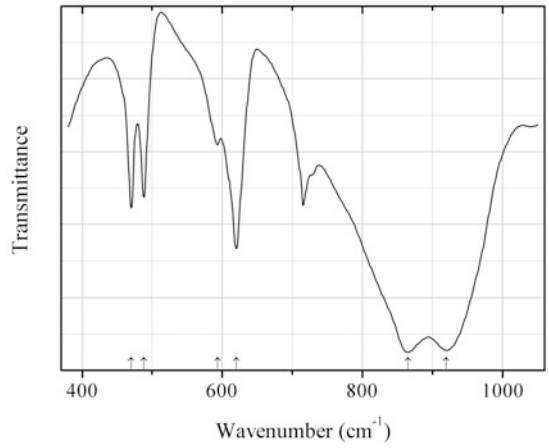

Fig. 2.1129 IR spectrum of scotlandite drawn using data from Paar et al. (1984)

S412 Scotlandite β-$Pb(SO_3)$ (Fig. 2.1129)
Locality: Susanna vein, Leadhills, Lanarkshire, Scotland, UK (type locality).
Description: Chisel-shaped and bladed crystals from the association with lanarkite, anglesite, as well as leadhillite and/or susannite. Holotype sample. Monoclinic, space group $P2_1 or P2_1/m$, $a = 4.542(2)$, $b = 5.333(2)$, $c = 6.413(2)$ Å, $\beta = 106.22(4)°$, $Z = 2$. $D_{meas} = 6.37$ g/cm^3, $D_{calc} = 6.40$ g/cm^3. Optically biaxial (+), $\alpha = 2.035$, $\beta = 2.040$, $\gamma = 2.085$, $2V = 70(5)°$. The empirical formula is $Pb_{1.06}S_{0.94}O_{2.94}$. The strongest lines of the powder X-ray diffraction pattern [*d*, Å (*I*, %) (*hkl*)] are: 3.99 (100) (011), 3.38 (70) (110), 3.25 (80) (11–1), 3.07 (40) (002), 2.66 (70) (020, 012), 2.56 (40) (11–2), 2.24 (50) (12–1, 102), 2.01 (50) (210, 022), 1.707 (40) (031), 1.538 (40) (032, 004).
Kind of sample preparation and/or method of registration of the spectrum: Nujol mull.
Source: Paar et al. (1984).
Wavenumbers (cm^{-1}): 920s, 865s, 620s, 593w, 488, 470.
Note: The wavenumbers were partly determined by us based on spectral curve analysis of the published spectrum. The band near 720 cm^{-1} corresponds to Nujol.

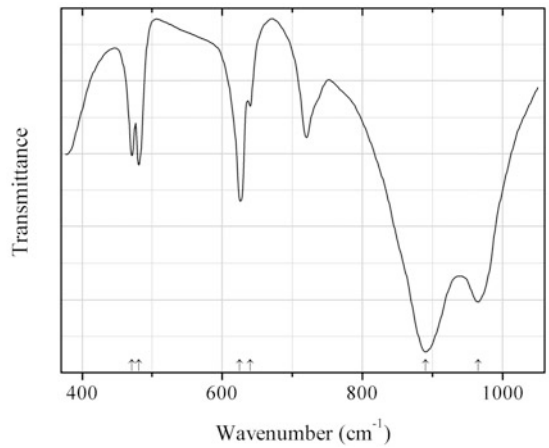

Fig. 2.1130 IR spectrum of scotlandite dimorph drawn using data from Paar et al. (1984)

S413 Scotlandite dimorph α-$Pb(SO_3)$ (Fig. 2.1130)

Locality: Synthetic.
Description: Orthorhombic.
Kind of sample preparation and/or method of registration of the spectrum: Nujol mull.
Source: Paar et al. (1984).
Wavenumbers (cm^{-1}): 965s, 890s, 640, 625s, 481, 471.
Note: The band near 720 cm^{-1} corresponds to Nujol.

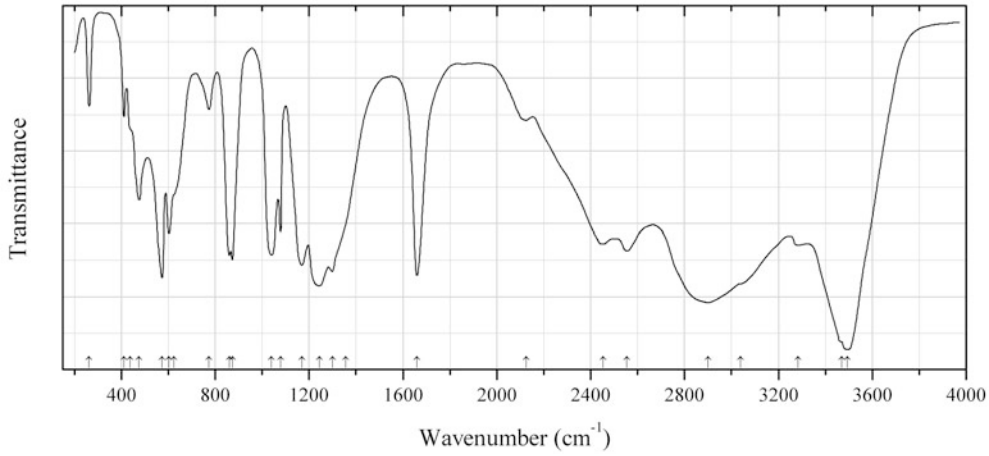

Fig. 2.1131 IR spectrum of matteuccite drawn using data from Baran et al. (1999a)

S414 Matteuccite $NaH(SO_4)\cdot H_2O$ (Fig. 2.1131)
Locality: Synthetic.
Description: Prepared by mixing Na_2SO_4 and a 96 % aqueous H_2SO_4 solution. Monoclinic, space group *Cc*.
Kind of sample preparation and/or method of registration of the spectrum: Nujol mull. Transmission.
Source: Baran et al. (1999a).
Wavenumbers (cm^{-1}): 3494s, 3470sh, 3284, 3040sh, 2900s, 2555, 2452, 2125w, 1660s, 1355sh, 1299s, 1243s, 1170s, 1078, 1040s, 873, 860sh, 773, 625sh, 603, 574s, 476, 437sh, 411, 263w.

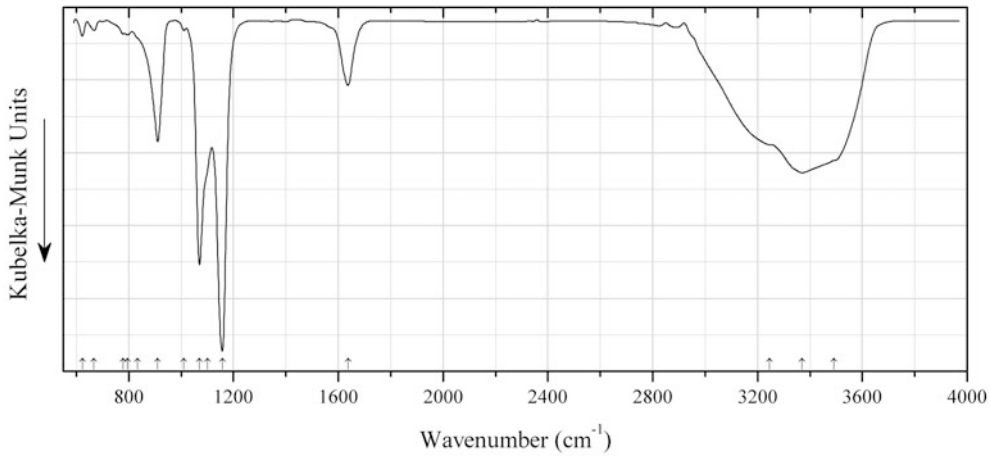

Fig. 2.1132 IR spectrum of sejkoraite-(Y) drawn using data from Plášil et al. (2011a)

S415 Sejkoraite-(Y) $Y(UO_2)_4(SO_4)_2O_3(OH)\cdot 13H_2O$ (Fig. 2.1132)
Locality: Červená vein, Jáchymov uranium deposit, Krušné Hory (Ore Mts.), Western Bohemia, Czech Republic (type locality).
Description: Aggregates consisting of yellow-orange to orange crystals from the association with pseudojohannite, rabejacite, uranopilite, zippeite, and gypsum. Holotype sample. The crystal structure is solved. Triclinic, space group *P*-1, $a = 14.0743(6)$, $b = 17.4174(7)$, $c = 17.7062(8)$ Å, $\alpha = 75.933(4)°$, $\beta = 128.001(5)°$, $\gamma = 74.419(4)°$, $V = 2777.00(19)$ Å^3, $Z = 4$. $D_{calc} = 4.04$ g/cm^3. Optically biaxial (−), $\alpha' = 1.62(2)$, $\beta' = 1.662(3)$, $\gamma' = 1.73(1)$. The empirical formula is (Z = 2): $(Y_{1.49}Dy_{0.17}Gd_{0.11}Er_{0.07}Yb_{0.05}Sm_{0.02})H_{1.54}(UO_2)_{8.19}O_8(SO_4)_{3.21}\cdot 26H_2O$. The strongest lines of the powder X-ray diffraction pattern [*d*, Å (*I*, %) (*hkl*)] are: 9.28 (100) (100), 4.64 (39) (200), 3.631 (6) (−142), 3.451 (13) (−144), 3.385 (10) (−2–42), 3.292 (9) (044), 3.904 (7) (300), 2.984 (10) (−1–42).
Kind of sample preparation and/or method of registration of the spectrum: The IR spectrum of a sample mixed with KBr powder was recorded by the DRIFTS method.
Source: Plášil et al. (2011a).
Wavenumbers (cm^{-1}): 3491sh, 3371, 3245sh, 1637, 1158s, 1100sh, 1070s, 1011w, 911, 833sh, 796w, 778w, 668w, 623w.
Note: The wavenumbers 3245 cm^{-1} and 1070 cm^{-1} were determined by us based on spectral curve analysis of the published spectrum. The bands at 796 and 778 cm^{-1} are close to those of quartz.

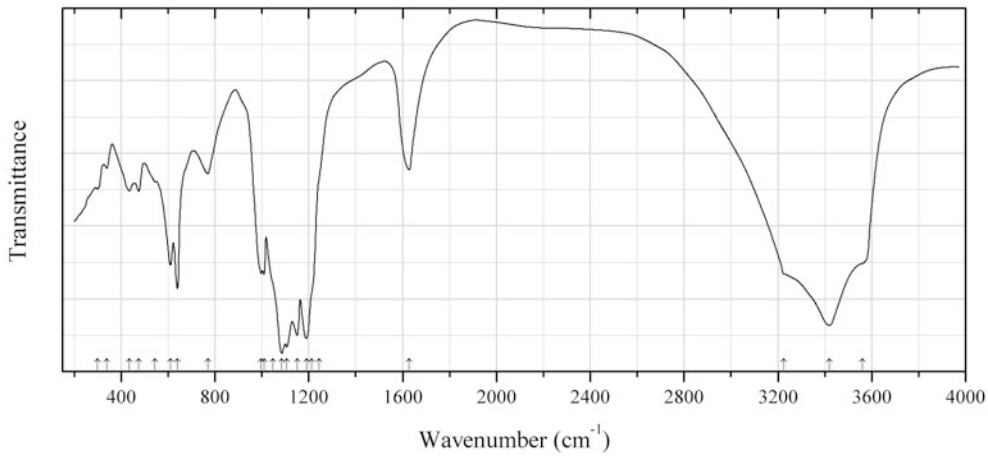

Fig. 2.1133 IR spectrum of siderotil drawn using data from Marquez Zavalia (1993)

S416 Siderotil $(Fe,Cu)(SO_4)\cdot 5H_2O$ (Fig. 2.1133)
Locality: Mina Capillitas, Catamarca, Argentina.
Description: Efflorescences associatied with gypsum, melanterite, goslarite, halotrichite, and chalcantite. Triclinic, $a = 6.26(2)$, $b = 10.62(3)$, $c = 6.08(1)$ Å, $\alpha = 97.18°$, $\beta = 109.27°$, $\gamma = 75.28°$. Optically biaxial (−), $\alpha = 1.514(3)$, $\beta = 1.524(3)$, $\gamma = 1.533(3)$. The strongest lines of the powder X-ray diffraction pattern [*d*, Å (*I*, %) (*hkl*)] are: 5.72 (70) (100), 5.07 (35) (01–1), 4.91 (100) (10–1), 3.93 (50) (02–1), 3.73 (80) (021), 2.94 (40) (22–1).

Kind of sample preparation and/or method of registration of the spectrum: Transmission. Kind of sample preparation is not indicated.
Source: Marquez Zavalia (1993).
Wavenumbers (cm^{-1}): 3560sh, 3420s, 3225sh, 1628, 1245sh, 1213sh, 1190s, 1150s, 1105s, 1085s, 1047sh, 1009, 998, 770, 640, 610, 545w, 475, 435, 339w, 299w.
Note: The wavenumbers were partly determined by us based on spectral curve analysis of the published spectrum.

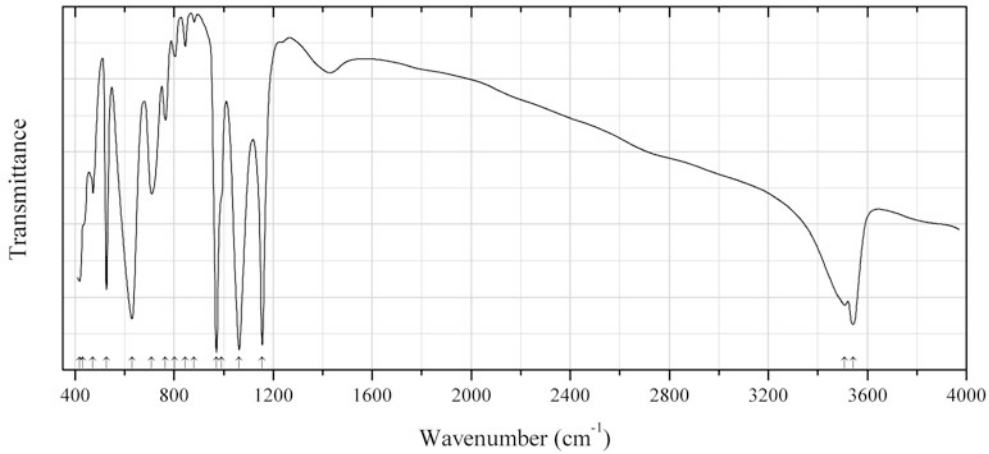

Fig. 2.1134 IR spectrum of sidpietersite drawn using data from Roberts et al. (1999)

S417 Sidpietersite $Pb^{2+}{}_4(S_2O_3)O_2(OH)_2$ (Fig. 2.1134)
Locality: Tsumeb mine, Tsumeb, Namibia (type locality).
Description: Nodular masses and crystal groups from the association with smithsonite, zincite, galena, sphalerite, quartz, and greenockite. Holotype sample. Triclinic, space group *P*-1, $a = 7.447(4)$, $b = 6.502(4)$, $c = 11.206(4)$ Å, $\alpha = 114.30(3)°$, $\beta = 89.51(4)°$, $\gamma = 89.04(6)°$, $V = 494.4(5)$ $Å^3$, $Z = 2$. $D_{calc} = 4.765$ g/cm^3. The empirical formula is $Pb_{4.09}(S^{6+}{}_{0.97}O_{2.90}S^{2-}{}_{0.97})O_{2.09}(OH)_{2.03}$. The strongest lines of the powder X-ray diffraction pattern [*d*, Å (*I*, %) (*hkl*)] are: 10.13 (100) (001), 5.93 (50) (010), 4.401 (35) (011), 3.414 (100) (003), 3.198 (80) (02–2), 2.889 (35) (02–3, 211), 2.805 (35) (−211, 01–4), 2.622 (40) (−21–3).
Kind of sample preparation and/or method of registration of the spectrum: Transmission. On the procedures for acquiring the IR spectrum of sidpietersite see Roberts et al. (1994).
Source: Roberts et al. (1999).
Wavenumbers (cm^{-1}): 3542, 3508, 1156s, 1063s, 991sh, 971s, 881w, 845w, 802w, 765, 709, 630s, 527, 472, 432sh, 418.
Note: The wavenumbers were partly determined by us based on spectral curve analysis of the published spectrum.

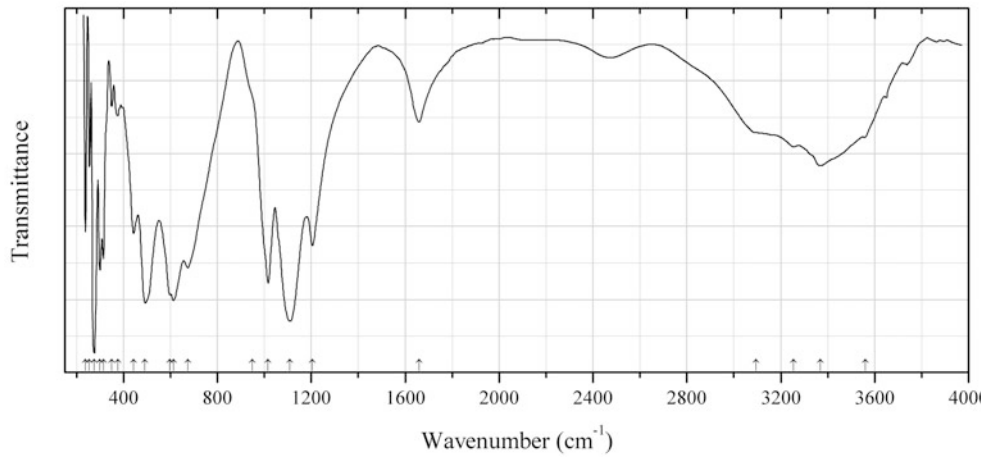

Fig. 2.1135 IR spectrum of slavíkite drawn using data from Joeckel et al. (2007)

S418 Slavíkite $(H_3O)_3Mg_6Fe_{15}(SO_4)_{21}(OH)_{18}\cdot 98H_2O$ (Fig. 2.1135)
Locality: Indian Cave Sandstone, southeastern Nebraska, USA.
Description: Aggregate of microscopic platy crystals from the association with copiapite. Confirmed by EDX spectrum and powder X-ray diffraction data.
Kind of sample preparation and/or method of registration of the spectrum: CsI disc. Transmission.
Source: Joeckel et al. (2007).
Wavenumbers (cm^{-1}): 3560sh, 3370, 3255, 3095sh, 1659, 1205, 1109s, 1015s, 950sh, 674, 613s, 598, 492s, 443, (375), (350), (315), (300), (275), (255), (238).
Note: The wavenumbers were partly determined by us based on spectral curve analysis of the published spectrum.

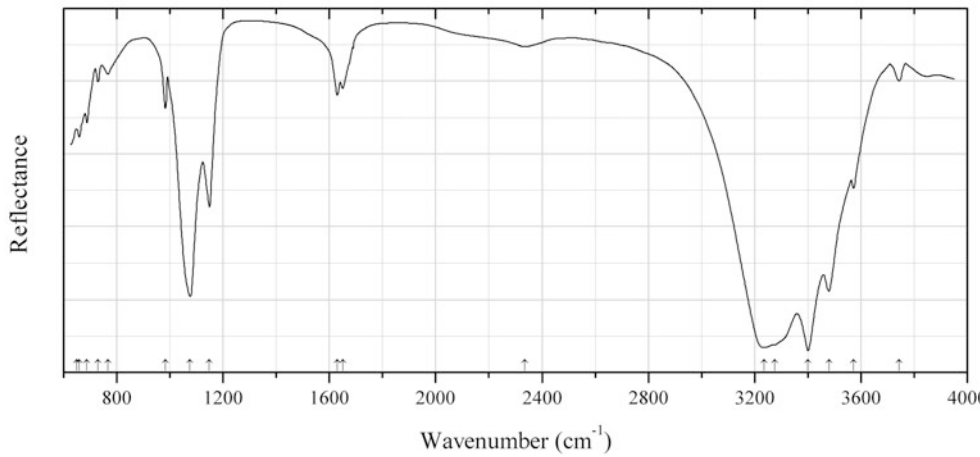

Fig. 2.1136 IR spectrum of disodium magnesium disulfate decahydrate drawn using data from Leduc (2010)

S419 Disodium magnesium disulfate decahydrate $Na_2Mg(SO_4)_2\cdot 10H_2O$ (Fig. 2.1136)
Locality: Synthetic.

Description: Obtained by evaporation of aqueous solution containing $Na_2(SO_4)$ and $Mg(SO_4)$ in stoichiometric amounts between 297 and 301 K, and 51 to 64 % relative humidity. The crystal structure is solved. Monoclinic, space group $P2_1/c$, $a = 12.4950(13)$, $b = 6.4978(7)$, $c = 9.9943(11)$ Å, $\beta = 106.362(1)°$, $V = 778.57(14)$ Å^3, $Z = 2$.
Kind of sample preparation and/or method of registration of the spectrum: Attenuated total reflection of powdered sample.
Source: Leduc (2010).
Wavenumbers (cm^{-1}): (3744w), 3573, 3480s, 3400s, 3275sh, 3236, 2335w, 1650w, 1630w, 1149, 1076s, 983, 767w, 730w, 688w, 659w, (650).
Note: The compound is compositionally related to blödite and konyaite.

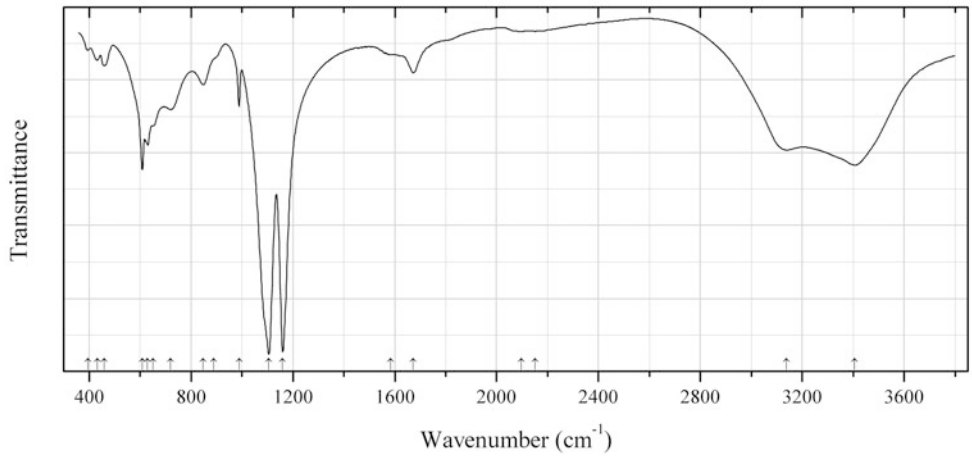

Fig. 2.1137 IR spectrum of changoite obtained by N.V. Chukanov

S420 Changoite $Na_2Zn(SO_4)_2 \cdot 4H_2O$ (Fig. 2.1137)
Locality: Namib lead mine (Deblin mine), Karibib district, Erongo region, Namibia.
Description: White coarse-grained aggregate from the association with gunningite. The empirical formula is (electron microprobe): $Na_{1.88}Zn_{1.04}Fe_{0.02}(SO_4)_2 \cdot 4H_2O$.
Kind of sample preparation and/or method of registration of the spectrum: KBr disc. Absorption.
Wavenumbers (cm^{-1}): 3406, 3137, 2150w, 2096w, 1673, 1585w, 1160s, 1106s, 989, 890sh, 848, 720, 650, 630, 609, 459, 432, 396w.

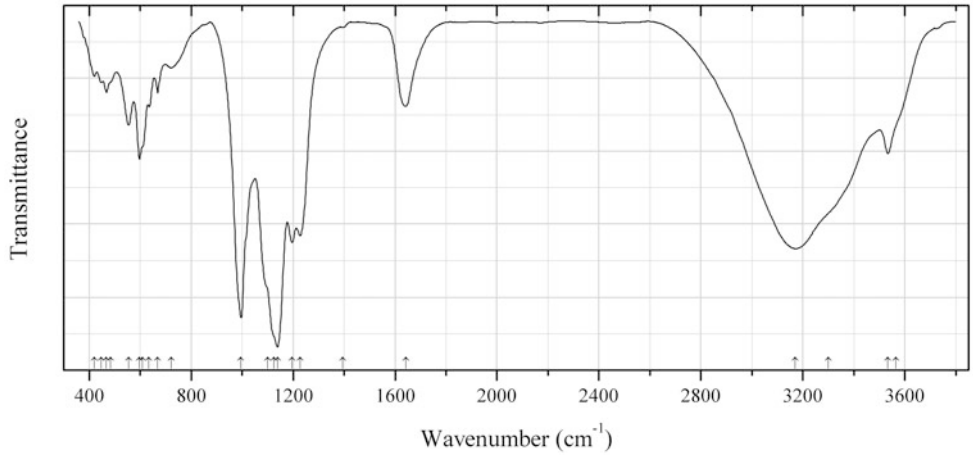

Fig. 2.1138 IR spectrum of cuprocopiapite obtained by N.V. Chukanov

S421 Cuprocopiapite $Cu^{2+}Fe^{3+}{}_4(SO_4)_6(OH)_2{\cdot}20H_2O$ (Fig. 2.1138)
Locality: Morro Mejillones, Mejillones Peninsula, Mejillones, Antofagasta, II Region, Chile.
Description: Yellow granular aggregate from the association with Cu-rich copiapite, chalcantite, and gypsum. The empirical formula is (electron microprobe): $(Cu_{0.75}Fe_{0.12}Mg_{0.07})(Fe_{3.93}Cr_{0.04}Al_{0.03})(SO_4)_{6.00}(OH)_2{\cdot}nH_2O$.
Kind of sample preparation and/or method of registration of the spectrum: KBr disc. Absorption.
Wavenumbers (cm^{-1}): 3565sh, 3534, 3300sh, 3171s, 1642, 1395w, 1228s, 1196s, 1139s, 1125sh, 1100sh, 996s, 722, 669, 635, 610sh, 598, 555, 485sh, 468, 448, 420.

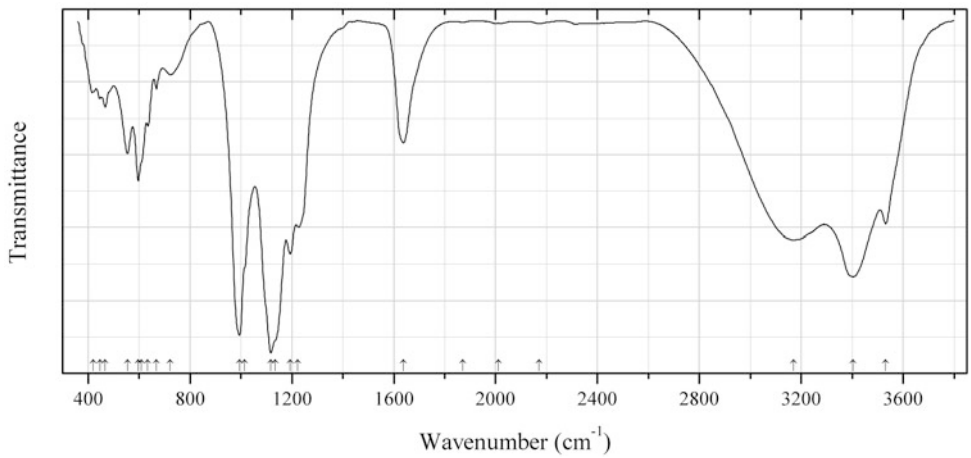

Fig. 2.1139 IR spectrum of copiapite Cu-rich obtained by N.V. Chukanov

S422 Copiapite Cu-rich $(Fe^{2+},Cu^{2+})Fe^{3+}{}_4(SO_4)_6(OH)_2{\cdot}20H_2O$ (Fig. 2.1139)
Locality: Morro Mejillones, Mejillones Peninsula, Mejillones, Antofagasta, II Region, Chile.
Description: Honey-yellow crystals from the association with cuprocopiapite, chalcantite, and gypsum. The empirical formula is (electron microprobe): $(Fe_{0.51}Cu_{0.42}Mg_{0.05}Zn_{0.02})(Fe_{3.97}Al_{0.03})(SO_4)_{6.00}(OH)_2{\cdot}nH_2O$.

Kind of sample preparation and/or method of registration of the spectrum: KBr disc. Absorption.
Wavenumbers (cm^{-1}): 3532, 3403s, 3169, 2170w, 2011w, 1871w, 1638, 1224, 1194, 1135sh, 1118s, 1015sh, 994s, 723, 668, 635, 610sh, 597, 555, 468, 448, 420.

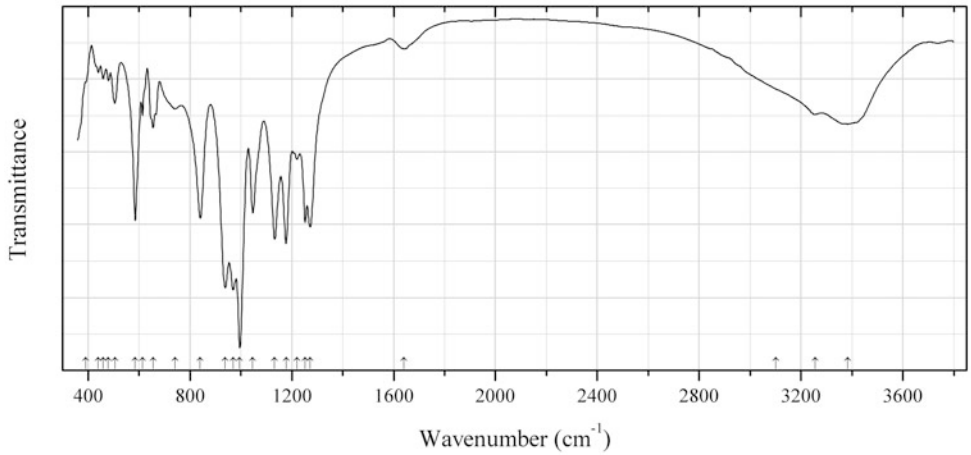

Fig. 2.1140 IR spectrum of alcaparrosaite obtained by N.V. Chukanov

S423 Alcaparrosaite $K_3Fe^{3+}Ti(SO_4)_4O{\cdot}2H_2O$ (Fig. 2.1140)
Locality: Alcaparrosa mine, Cerritos Bayos, Calama, El Loa province, Antofagasta region, Chile (type locality).
Description: Yellow equant crystals from the association with coquimbite, pertlikite, and krausite. Monoclinic, a = 7.570(8), b = 16.789(13), c = 12.163(9) Å, β = 94.1(1)°, V = 1542(2) $Å^3$ (from single-crystal X-ray diffraction data obtained by I.V. Pekov). The empirical formula is (electron microprobe): $(K_{2.84}Na_{0.04})Fe_{1.08}Ti_{1.04}(SO_4)_{4.00}O(H_2O,OH)_2$.
Kind of sample preparation and/or method of registration of the spectrum: KBr disc. Absorption.
Wavenumbers (cm^{-1}): 3383, 3256, 3100sh, 1640w, 1272, 1253, 1220w, 1178, 1133, 1047, 996s, 970s, 939s, 841, 742w, 655, 614w, 585, 505w, 480w, 459w, 440w, 390sh.

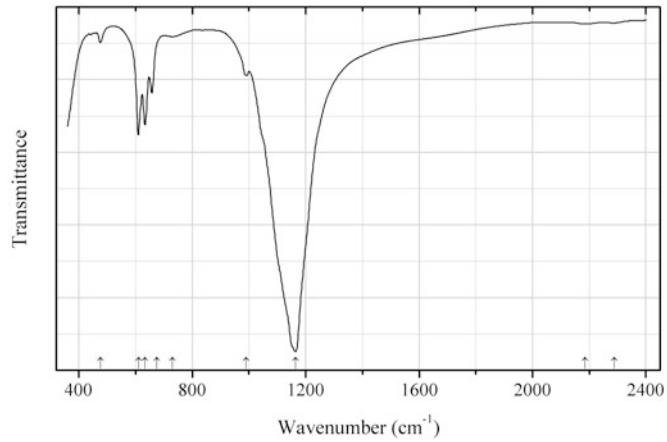

Fig. 2.1141 IR spectrum of langbeinite disordered obtained by N.V. Chukanov

S424 Langbeinite disordered $K_2Mg_2(SO_4)_3$ (Fig. 2.1141)
Locality: Tolbachik volcano, Kamchatka peninsula, Russia.
Description: White granular aggregate. A cation-disordered high-temperature variety. Investigated by I.V. Pekov. The empirical formula is (electron microprobe): $(K_{1.61}Na_{0.59}Rb_{0.04}Cs_{0.01})(Mg_{1.33}Zn_{0.27}Cu_{0.17}Ca_{0.01})(SO_3)_{3.00}$.
Kind of sample preparation and/or method of registration of the spectrum: KBr disc. Absorption.
Wavenumbers (cm^{-1}): 2290w, 2185w, 1164s, 991, 730w, 675, 634, 610, 476w.

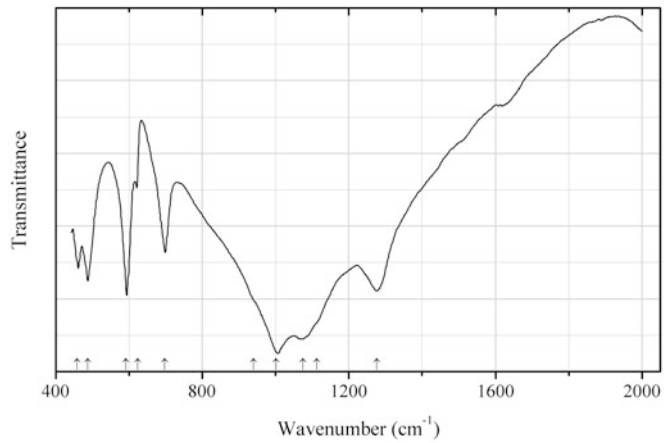

Fig. 2.1142 IR spectrum of sodium vanadium sulfate drawn using data from Boghosian et al. (1994)

S425 Sodium vanadium sulfate $NaV^{3+}(SO_4)_2$ (Fig. 2.1142)
Locality: Synthetic.
Description: Obtained on equilibrating a V_2O_5–$Na_2S_2O_7$ molten mixture (Na:V = 4.7) under 0.9 atm SO_2 in the temperature range 400–450 °C.
Kind of sample preparation and/or method of registration of the spectrum: KBr disc. Transmission.
Source: Boghosian et al. (1994).
Wavenumbers (cm^{-1}): 1276s, 1112sh, 1074s, 1002s, 940sh, 698, 624w, 592s, 487, 458.

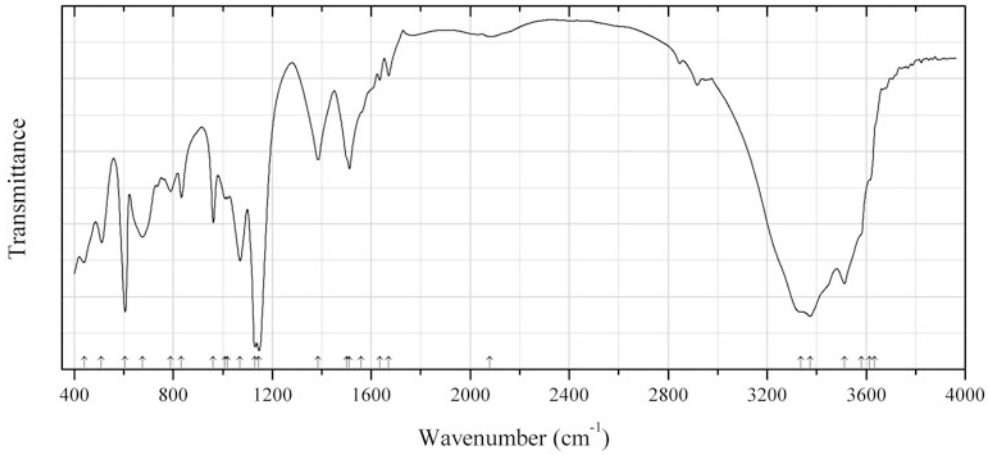

Fig. 2.1143 IR spectrum of sodium zinc basic sulfate chloride drawn using data from Jayasree et al. (2006)

S426 Sodium zinc basic sulfate chloride $NaZn_4(SO_4)Cl(OH)_6 \cdot 6H_2O$ (Fig. 2.1143)
Locality: Artificial.
Description: A product of zinc corrosion in marine water. Hexagonal, space group P_3.
Kind of sample preparation and/or method of registration of the spectrum: KBr disc. Transmission.
Source: Jayasree et al. (2006).
Wavenumbers (cm^{-1}): 3635sh, 3615sh, 3581sh, 3513s, 3373s, 3337sh, 2080w, 1670w, 1635w, 1560sh, 1512, 1500sh, 1384, 1146s, 1130s, 1070s, 1020w, 1010w, 962, 833, 789w, 675 (broad), 606s, 510w, 440w.
Note: In the cited paper the wavenumber 3337 cm^{-1} is erroneously indicated as 3377 cm^{-1}. Weak bands in the range from 2800 to 3000 cm^{-1} correspond to the admixture of an organic substance. The bands at 1512, 1384, and 833 cm^{-1} correspond to the admixture of hydrozincite.

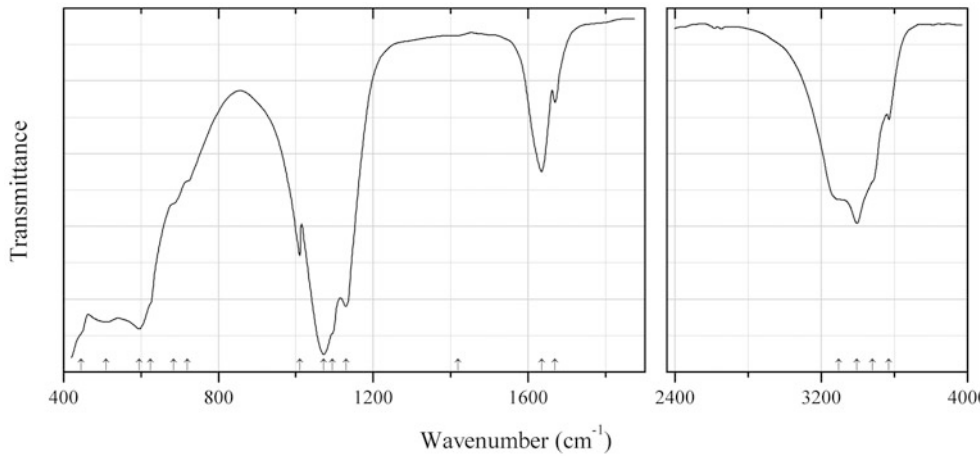

Fig. 2.1144 IR spectrum of starkeyite drawn using data from Peterson (2011)

S427 Starkeyite $Mg(SO_4)\cdot 4H_2O$ (Fig. 2.1144)
Locality: Calingasta, San Juan Province, Argentina (?).
Description: Confirmed by powder X-ray diffraction data.
Kind of sample preparation and/or method of registration of the spectrum: No data.
Source: Peterson (2011).
Wavenumbers (cm^{-1}): 3570, 3480sh, 3395s, 3295, 1670, 1635, 1420sh, 1130s, 1095sh, 1072s, 1010, 720sh, 685sh, 625sh, 595s, 510s, 445sh.
Note: The wavenumbers were determined by us based on spectral curve analysis of the published spectrum.

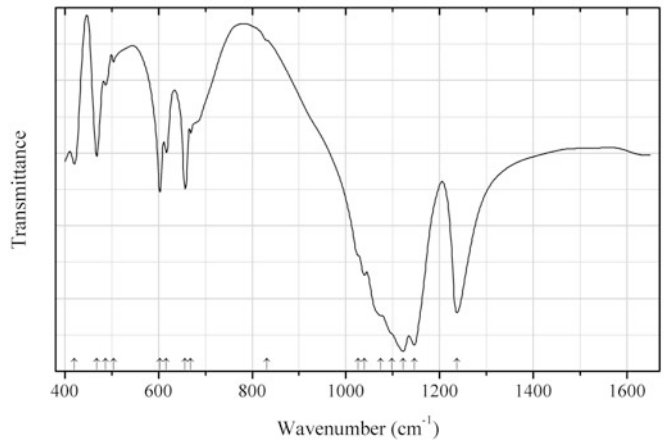

Fig. 2.1145 IR spectrum of steklite drawn using data from Aderemi and Hameed (2009)

S428 Steklite $KAl(SO_4)_2$ (Fig. 2.1145)
Locality: Synthetic.
Description: The product of calcination of $KAl(SO_4)_2\cdot 12H_2O$ at 800 °C.
Kind of sample preparation and/or method of registration of the spectrum: KBr disc. Transmission.
Source: Aderemi and Hameed (2009).
Wavenumbers (cm^{-1}): 1237s, 1146s, 1122s, 1098sh, 1074sh, 1040, 1027sh, 831sh, 669, 657, 617, 603, 504w, 487w, 468, 420.
Note: The wavenumbers were partly determined by us based on spectral curve analysis of the published spectrum.

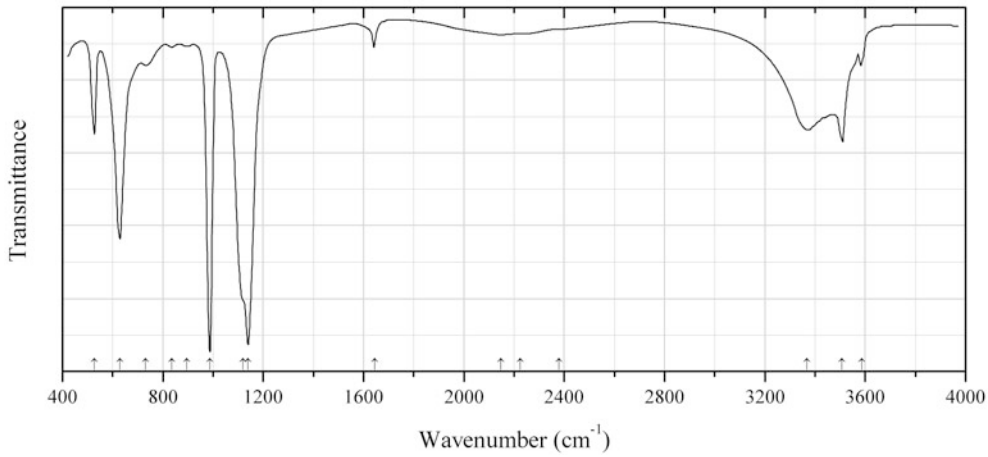

Fig. 2.1146 IR spectrum of steverustite drawn using data from Cooper et al. (2009)

S429 Steverustite $Cu^{+}Pb_5(S_2O_3)_3(OH)_5 \cdot 2H_2O$ (Fig. 2.1146)
Locality: Frongoch mine dump, Devils Bridge, Ceredigion, Wales, UK (type locality).
Description: White aggregates of fibrous to acicular crystals from the association with quartz, sphalerite, galena, covellite, cerussite, anglesite, hemimorphite, sussannite, bechererite, and caledonite. Holotype sample. Monoclinic, space group $P2_1/n$, a = 12.5631(7), b = 8.8963(5), c = 18.0132 (11) Å, β = 96.459(1)°, V = 2000.5(3) Å^3, Z = 4. D_{calc} = 5.150 g/cm^3. The empirical formula is $Pb_{4.99}Cu_{0.96}(S_2O_3)_{3.03}(OH)_{4.88} \cdot 1.67H_2O$. The strongest lines of the powder X-ray diffraction pattern [d, Å (I, %) (hkl)] are: 6.897 (80) (−111), 6.211 (60) (200), 4.794 (60) (211), 3.934 (100) (−114), 3.348 (70) (−313), 3.026 (60) (−314), 2.837 (50) (016).
Kind of sample preparation and/or method of registration of the spectrum: Absorption. Kind of sample preparation is not indicated.
Source: Cooper et al. (2009).
Wavenumbers (cm^{-1}): 3587w, 3507, 3368, 2380sh, 2225sh, 2148w (broad), 1646w, 1140s, 1120sh, 988s, 896w, 835w, 732w, 629s, 527.
Note: The wavenumbers were partly determined by us based on spectral curve analysis of the published spectrum.

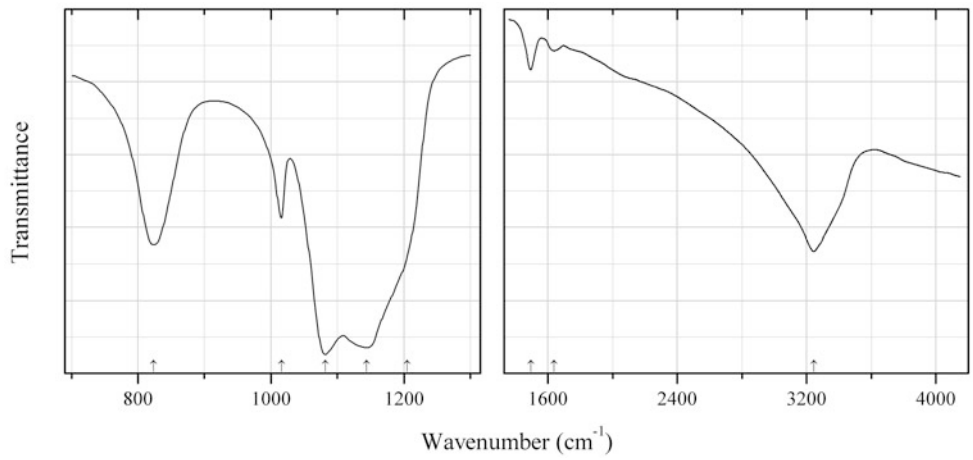

Fig. 2.1147 IR spectrum of szomolnokite drawn using data from Hyde et al. (2011)

S430 Szomolnokite $Fe(SO_4)\cdot H_2O$ (Fig. 2.1147)
Locality: Synthetic.
Description: Beige polycrystalline aggregate produced by heating the reagent ferrous sulfate at 60 °C for 24 h. Confirmed by powder X-ray diffraction data.
Kind of sample preparation and/or method of registration of the spectrum: Powdered sample placed on a diamond window. Absorption.
Source: Hyde et al. (2011).
Wavenumbers (cm^{-1}): 3244, 1636w, 1493w, 1205sh, 1144s, 1082s, 1016, 823.

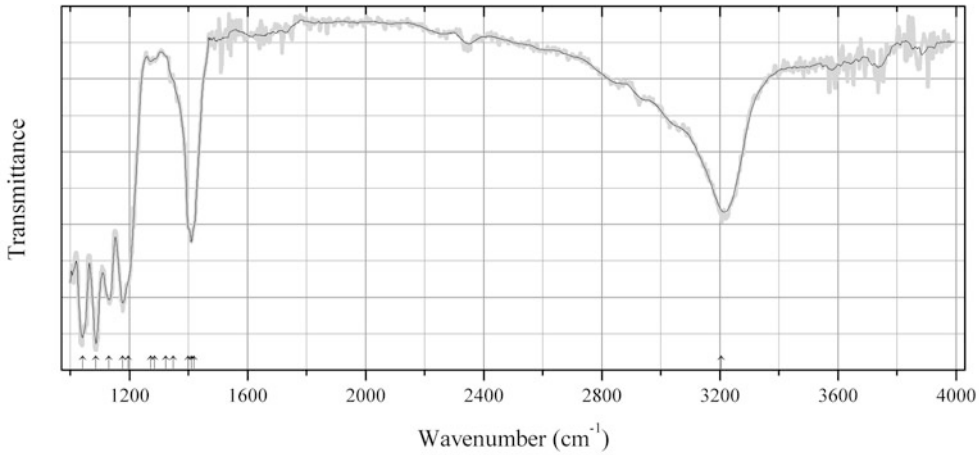

Fig. 2.1148 IR spectrum of therasiaite drawn using data from Demartin et al. (2014)

S431 Therasiaite $(NH_4)_3KNa_2Fe^{2+}Fe^{3+}(SO_4)_3Cl_5$ (Fig. 2.1148)
Locality: La Fossa crater, Vulcano island, Lipari, Eolie (Aeolian) islands, Messina province, Sicily, Italy (type locality).
Description: Brown crystals from the association with salammoniac, kremersite, and adranosite. Holotype sample. The crystal structure is solved. Monoclinic, space group *Cc*, a = 18.284(4), b = 12.073(2), c = 9.535(2) Å, β = 108.10(3)°, V = 2000.6(7) $Å^3$, Z = 4. D_{meas} = 2.41(1) g/cm^3, D_{calc} = 2.395 g/cm^3. Optically biaxial (−), α = 1.585(3), β = 1.615(3), γ = 1.630(3). The empirical formula is $(NH_4)_{2.68}K_{1.32}Na_{2.04}Fe_{1.76}Al_{0.12}Mn_{0.12}S_{2.98}O_{11.95}Cl_{5.05}$. The strongest lines of the powder X-ray diffraction pattern [d, Å (I, %) (*hkl*)] are: 2.812 (100) (−223), 2.664 (77) (−513), 3.297 (28) (33–1), 3.208 (14) (−5–12), 3.008 (12) (040), 2.942 (11) (331).
Kind of sample preparation and/or method of registration of the spectrum: No data.
Source: Demartin et al. (2014).
Wavenumbers (cm^{-1}): 3205, 1418sh, 1410, 1400sh, 1348sh, 1323sh, 1286sh, 1273w, 1196sh, 1177, 1131, 1087s, 1041s.
Note: The wavenumbers were partly determined by us based on spectral curve analysis and smoothing of the published spectrum.

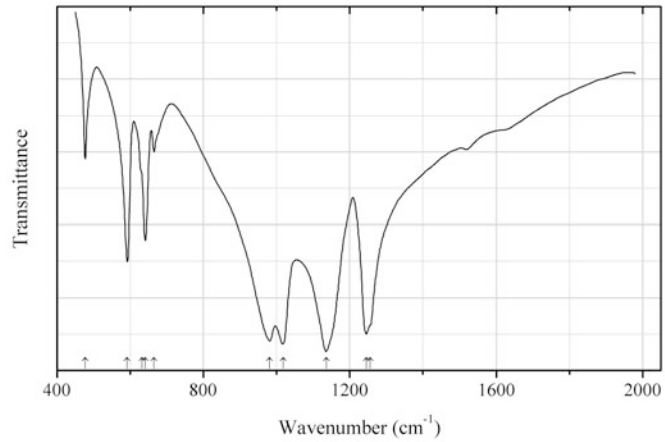

Fig. 2.1149 IR spectrum of trisodium vanadium sulfate drawn using data from Boghosian et al. (1994)

S432 Trisodium vanadium sulfate $Na_3V(SO_4)_3$ (Fig. 2.1149)
Locality: Synthetic.
Description: Dark green crystals synthesized by dissolution of V_2O_5 in $NaHSO_4$ melt at 420 °C under SO_2 atmosphere with subsequent cooling to 320 °C over a period of one week. The crystal structure is solved. Trigonal, space group *R*-3, a = 13.439(1), c = 9.091(1) Å, Z = 6. D_{calc} = 2.860 g/cm^3.
Kind of sample preparation and/or method of registration of the spectrum: KBr disc. Transmission.
Source: Boghosian et al. (1994).
Wavenumbers (cm^{-1}): 1256sh, 1245s, 1136s, 1018s, 981s, 665w, 641, 632sh, 592, 477.

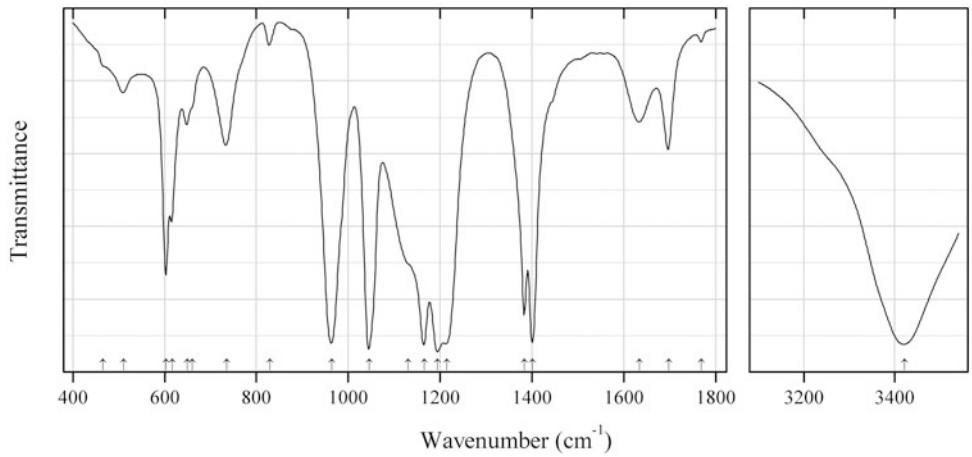

Fig. 2.1150 IR spectrum of ungemachite drawn using data from Jentzsch et al. (2012b)

S433 Ungemachite $K_3Na_8Fe^{3+}(SO_4)_6(NO_3)_2 \cdot 6H_2O$ (Fig. 2.1150)
Locality: Synthetic.
Description: Crystallized from a solution containing stoichiometric amounts of each ion. Confirmed by powder X-ray diffraction data.

Kind of sample preparation and/or method of registration of the spectrum: KBr disc. Transmission.
Source: Jentzsch et al. (2012b).
Wavenumbers (cm^{-1}): 3422s, 1769w, 1698, 1635, 1402s, 1384s, 1215s, 1195s, 1166s, 1131sh, 1046s, 964s, 829w, 735, 661sh, 649, 617, 604, 511, 466sh.

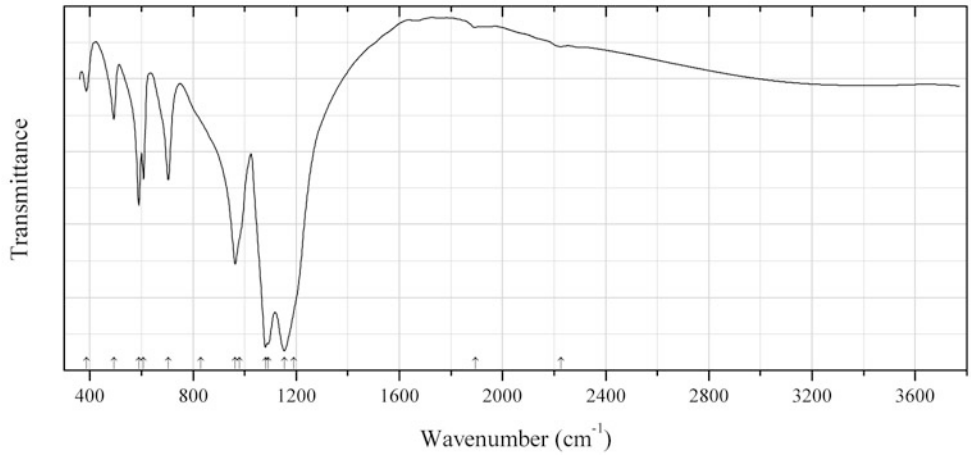

Fig. 2.1151 IR spectrum of chalcocyanite obtained by N.V. Chukanov

S434 Chalcocyanite $Cu(SO_4)$ (Fig. 2.1151)
Locality: Arsenatnaya fumarole, Second scoria cone of the Northern Breakthrough of the Great Tolbachik Fissure Eruption, Tolbachik volcano, Kamchatka peninsula, Russia.
Description: Colourless crystals from the association with euchlorine. Confirmed by powder X-ray diffraction data.
Kind of sample preparation and/or method of registration of the spectrum: KBr disc. Absorption.
Wavenumbers (cm^{-1}): 2226w, 1895w, 1190sh, 1154s, 1092s, 1081s, 980sh, 964s, 830sh, 704, 608, 590, 493, 387.

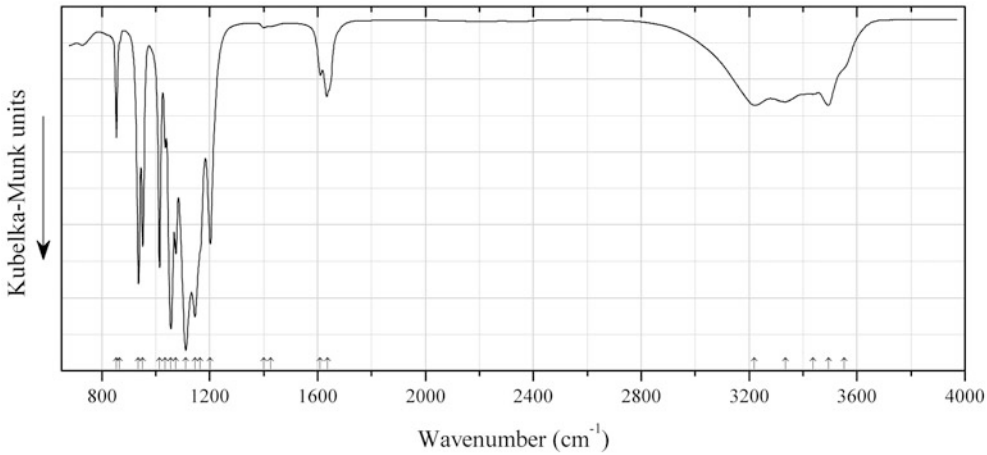

Fig. 2.1152 IR spectrum of uranyl sulfate hydrate drawn using data from Vlček et al. (2009)

S435 Uranyl sulfate hydrate $(UO_2)_2(SO_4)_2 \cdot 5H_2O$ (Fig. 2.1152)
Locality: Synthetic.
Description: Recrystallized from aqueous solution of commercial uranyl sulfate under laboratory conditions. The crystal structure is solved. Monoclinic, space group $P2_1/c$, $a = 6.7260(1)$, $b = 12.4210(2)$, $c = 16.8270(3)$ Å, $\beta = 90.781(1)°$, $V = 1405.66(4)$ Å^3, $Z = 8$. $D_{calc} = 3.84$ g/cm^3.
Kind of sample preparation and/or method of registration of the spectrum: Powder mixed with KBr. Diffuse reflection.
Source: Vlček et al. (2009).
Wavenumbers (cm^{-1}): 3552sh, 3495, 3437, 3335, 3219, 1638w, 1609w, 1427w, 1400w, 1202, 1165sh, 1145s, 1111s, 1075s, 1056s, 1035w, 1014s, 952s, 936s, 866sh, 854.

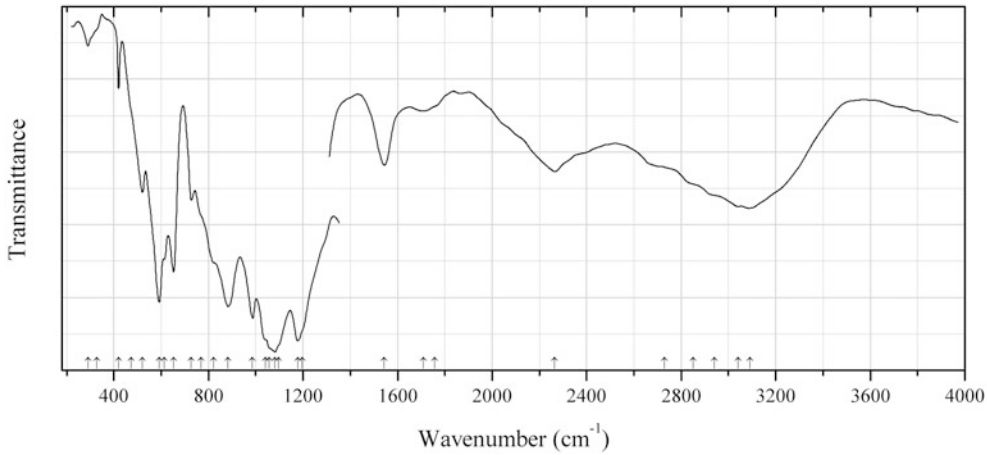

Fig. 2.1153 IR spectrum of voudourisite drawn using data from Minić et al. (1985)

S436 Voudourisite $Cd(SO_4) \cdot H_2O$ (Fig. 2.1153)
Locality: Synthetic.
Description: Product of dehydration of commercial $3CdSO_4 \cdot 8H_2O$. Confirmed by TG analysis.
Kind of sample preparation and/or method of registration of the spectrum: KBr disc. Transmission.
Source: Minić et al. (1985).
Wavenumbers (cm^{-1}): 3090, 3041, 2940sh, 2850sh, 2730sh, 2265, 1757sh, 1709, 1544, 1197sh, 1178s, 1098sh, 1082s, 1058s, 1041sh, 987s, 883, 822sh, 768sh, 727, 652, 614, 592, 520, 473sh, 420w, 328sh, 290w.
Note: The wavenumbers were determined by us based on spectral curve analysis of the published spectrum.

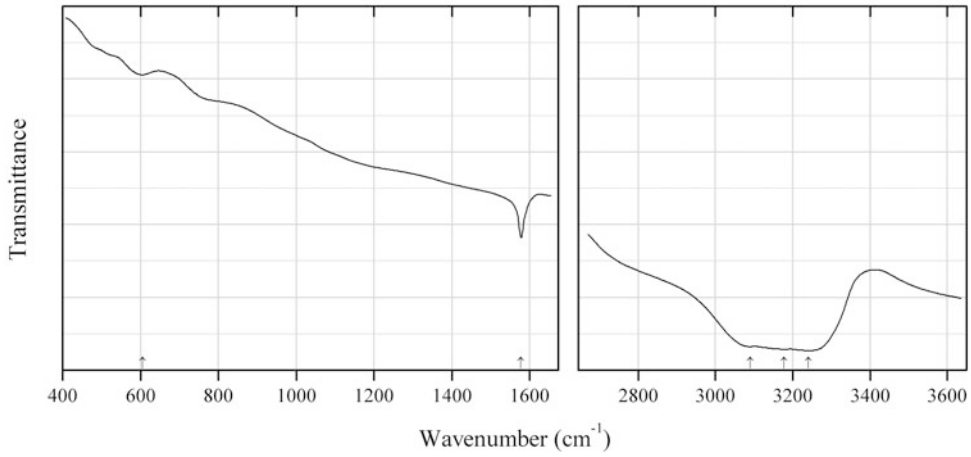

Fig. 2.1154 IR spectrum of wilhelmramsayite drawn using data from Pekov et al. (2006)

S438 Wilhelmramsayite $Cu_3FeS_3 \cdot 2H_2O$ (Fig. 2.1154)
Locality: Koashva Mt., Khibiny alkaline massif, Kola Peninsula, Russia (type locality).
Description: Dark lead-grey lamellar and tabular crystals from the association with villiaumite, thermonatrite, pectolite, aegirine, microcline, sodalite, lomonosovite, chkalovite, sphalerite, rasvumite, etc. Holotype sample. Orthorhombic, space group *Pmmm*, $a = 5.147(2)$, $b = 7.289(2)$, $c = 5.889(3)$ Å, $V = 220.9(2)$ Å^3. $D_{meas} = 2.75$ g/cm^3, $D_{calc} = 2.84$ g/cm^3. The empirical formula is $Cu_{2.91}Fe_{1.04}S_{3.00} \cdot (K_{0.03}Na_{0.02}Tl_{0.01})_{\Sigma 0.06}(H_2O)_{1.97}$. The strongest lines of the powder X-ray diffraction pattern [*d*, Å (*I*, %) (*hkl*)] are: 5.12 (40) (100), 4.21 (40) (110), 3.69 (30) (020), 3.104 (100) (021), 2.727 (50) (012), 2.292 (50) (022), 1.985 (30) (221, 003), 1.897 (70) (013), 1.828 (50) (103, 040).
Kind of sample preparation and/or method of registration of the spectrum: KBr disc. Transmission.
Source: Pekov et al. (2006).
Wavenumbers (cm^{-1}): 3240s, 3177s, 3090s, 1578, 605.
Note: The wavenumbers were partly determined by us based on spectral curve analysis of the published spectrum.

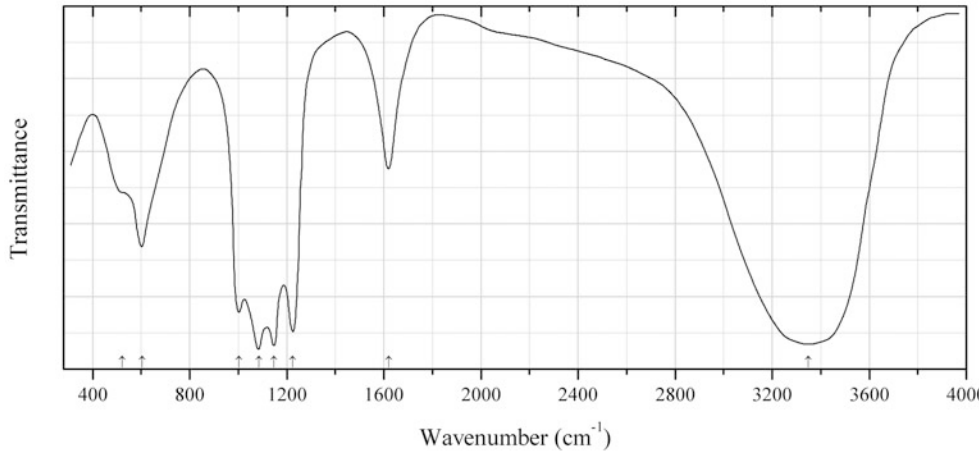

Fig. 2.1155 IR spectrum of xitieshanite drawn using data from Xilin et al. (1983)

S439 Xitieshanite $Fe^{3+}(SO_4)Cl{\cdot}6H_2O$ (Fig. 2.1155)
Locality: Xitieshan mine, Xitieshan, Da Qaidam Co., Haixi prefecture, Qinghai Province, China (type locality).
Description: Yellowish green crystals from the association with jarosite, gypsum, and native sulfur. Holotype sample. Monoclinic, space group $P2_1/a$, a = 14.102, b = 6.908, c = 10.673 Å, β = 11.266°, V = 968.9 Å^3, Z = 4. D_{meas} = 1.99 g/cm^3, D_{calc} = 2.02 g/cm^3. Optically biaxial (+), α = 1.536, β = 1.570, γ = 1.628, 2 V = 77°. In the first description of xitieshanite (Xilin et al. 1983) Cl was missing, and the following empirical formula was given: $(Na,K)_{0.01}(Fe^{3+}_{0.96}Fe^{2+}_{0.01})S_{1.01}H_{14.62}O_{11.80}$. The strongest lines of the powder X-ray diffraction pattern [d, Å (I, %) (hkl)] are: 6.67 (60) (−201), 6.09 (50) (110), 5.69 (50) (011), 4.96 (100) (002), 4.81 (100) (−211), 4.21 (50) (−112), 3.90 (90) (211).
Kind of sample preparation and/or method of registration of the spectrum: No data.
Source: Xilin et al. (1983).
Wavenumbers (cm^{-1}): 3350s, 1620, 1225s, 1148s, 1084s, 1003s, 603, 521sh.
Note: The wavenumbers were partly determined by us based on spectral curve analysis of the published spectrum.

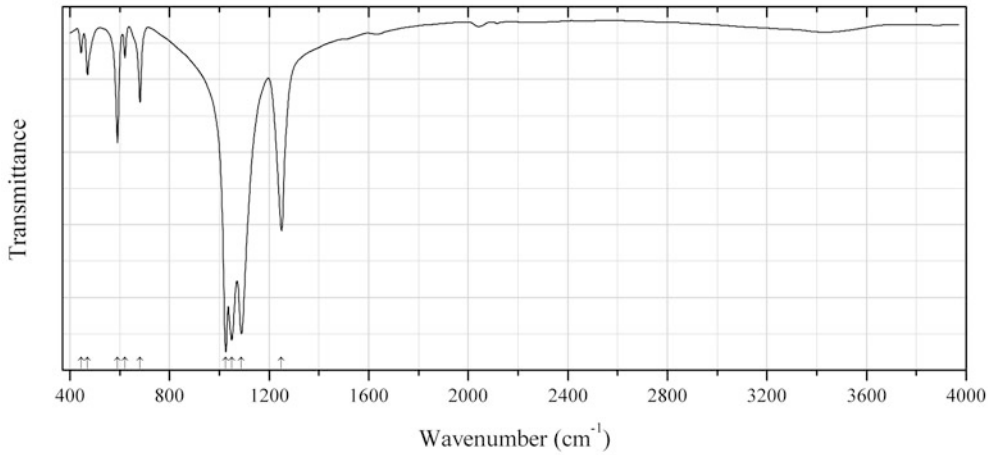

Fig. 2.1156 IR spectrum of yavapaiite drawn using data from Forray et al. (2005)

S440 Yavapaiite $KFe^{3+}(SO_4)_2$ (Fig. 2.1156)
Locality: Synthetic.
Description: Characterized by powder X-ray diffraction data. Monoclinic, a = 8.152(1), b = 5.151(1), c = 7.875(1) Å, β = 94.80°.
Kind of sample preparation and/or method of registration of the spectrum: KBr disc. Absorption.
Source: Forray et al. (2005).
Wavenumbers (cm^{-1}): 1249, 1089s, 1050s, 1026s, 682, 621w, 591, 471, 445w.
Note: Weak bands in the range from 1500 to 4000 cm^{-1} may correspond to adsorbed water.

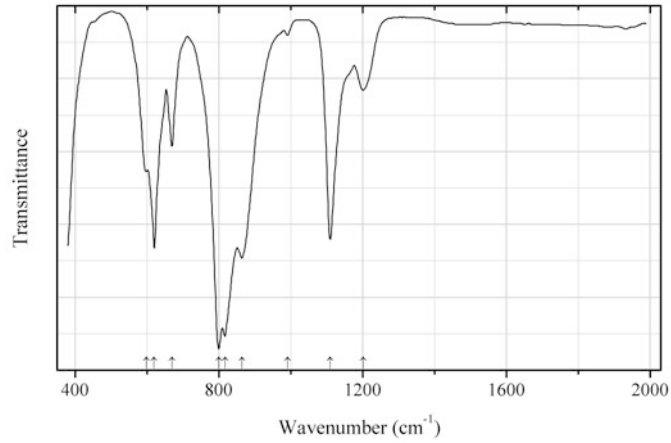

Fig. 2.1157 IR spectrum of ye'elimite drawn using data from Fernández-Carrasco et al. (2012)

S441 Ye'elimite $Ca_4Al_6O_{12}(SO_4)$ (Fig. 2.1157)
Locality: Synthetic.
Description: No data.
Kind of sample preparation and/or method of registration of the spectrum: No data.
Source: Fernández-Carrasco et al. (2012).
Wavenumbers (cm^{-1}): 1202w, 1110s, 992w, 864s, 817s, 800s, 670, 620s, 598.
Note: The wavenumbers were partly determined by us based on spectral curve analysis of the published spectrum.

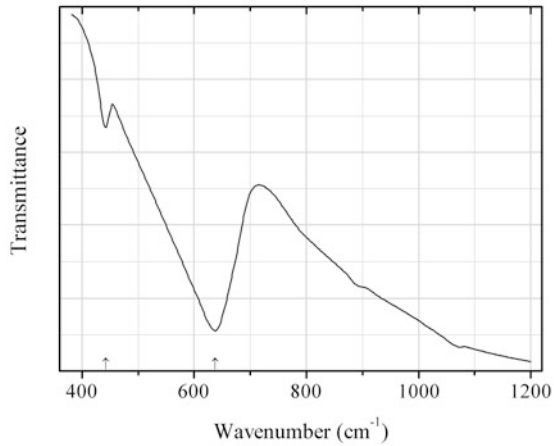

Fig. 2.1158 IR spectrum of yushkinite drawn using data from Koval'chuk, and Makeev (2007)

S442 Yushkinite $V_{1-x}S{\cdot}0.6(Mg_{1-y}Al_y)(OH)_{2+x}$ (Fig. 2.1158)
Locality: Middle Silova-Yakha river, Pai-Khoi (Pay Khoy) range, Yugorski peninsula, Nenetskiy authonomous territory, Russia (type locality).
Description: Pinkish purple with metallic lustre, massive, from the association with quartz, calcite, fluorite, sphalerite, and sulvanite. D_{meas} = 2.94(2) g/cm^3.
Kind of sample preparation and/or method of registration of the spectrum: KBr disc. Transmission.

Source: Koval'chuk and Makeev (2007).
Wavenumbers (cm^{-1}): 637s, 442.
Note: Additionally, a very broad and strong band is observed in the range from 1000 to 3000 cm^{-1}.

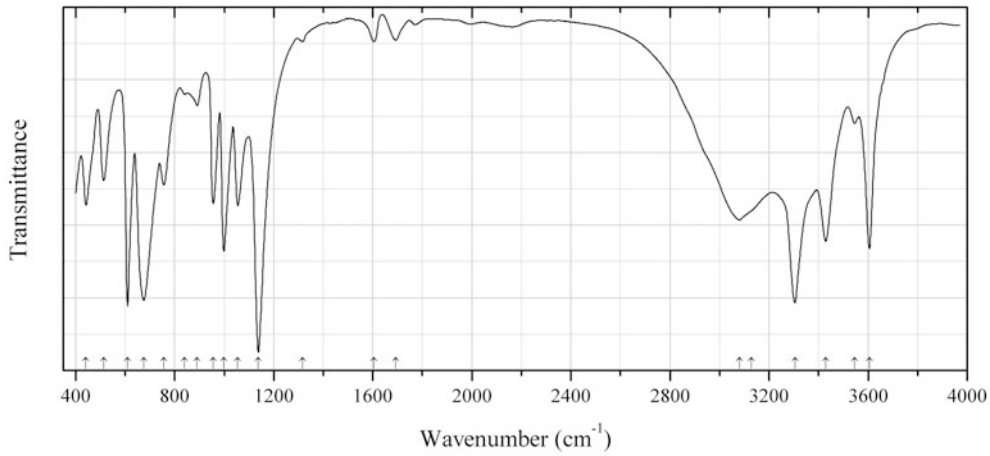

Fig. 2.1159 IR spectrum of zinc chlorohydroxysulfate hydrate drawn using data from Jayasree et al. (2006)

S443 Zinc chlorohydroxysulfate hydrate $Zn_4(SO_4)(OH)_4Cl_2 \cdot 5H_2O$ (Fig. 2.1159)
Locality: Artificial.
Description: A product of zinc corrosion in marine water. Monoclinic.
Kind of sample preparation and/or method of registration of the spectrum: KBr disc. Transmission.
Source: Jayasree et al. (2006).
Wavenumbers (cm^{-1}): 3606, 3545, 3429, 3305s, 3080, 3130, 1693w, 1605w, 1316w, 1138s, 1055, 999s, 956, 891w, 840w, 756, 675s, 610s, 513, 442.
Note: The wavenumbers were partly determined by us based on spectral curve analysis of the published spectrum.

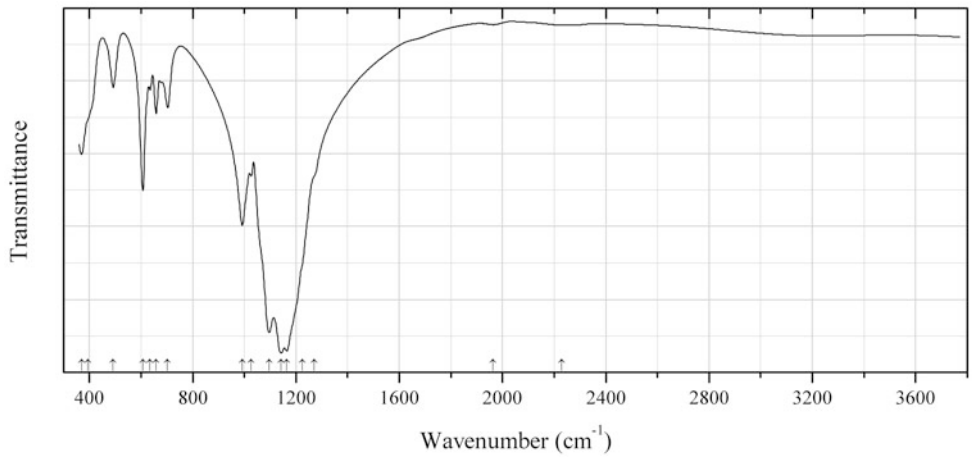

Fig. 2.1160 IR spectrum of dravertite obtained by N.V. Chukanov

S444 Dravertite $CuMg(SO_4)_2$ (Fig. 2.1160)

Locality: Arsenatnaya fumarole, Second scoria cone of the Northern Breakthrough of the Great Tolbachik Fissure Eruption, Tolbachik volcano, Kamchatka peninsula, Russia (type locality).
Description: Pale blue crust from the association with dolerophanite, euchlorine, tenorite, hematite, langbeinite, steklite, fedotovite, anhydrite, anglesite, etc. Holotype sample. Monoclinic, space group $P2_1/n$, a = 4.8141(3), b = 8.4443(5), c = 6.7731(4) Å, β = 94.598(5)°, V = 274.45(3) Å^3, Z = 2. D_{calc} = 3.508 g/cm^3. Optically biaxial (−), α = 1.624(3), β = 1.661(3), γ = 1.663(3), 2 V = 35(10)°. The empirical formula is (electron microprobe): $Mg_{0.79}Mn_{0.01}Cu_{1.14}Zn_{0.09}S_{1.99}O_8$. The strongest lines of the powder X-ray diffraction pattern [d, Å (I, %) (hkl)] are: 4.175 (68) (110), 3.666 (64) (−111), 3.579 (63) (021), 3.443 (59) (111), 2.719 (41) (−112), 2.637 (100) (022), 2.540 (22) (112), 2.430 (68) (130), 1.791 (24) (123, −231, 042).
Kind of sample preparation and/or method of registration of the spectrum: KBr disc. Absorption.
Wavenumbers (cm^{-1}): 2228w, 1963w, 1270sh, 1225sh, 1165s, 1142s, 1097s, 1025, 992s, 703, 658, 635w, 607, 492, 395sh, 370.

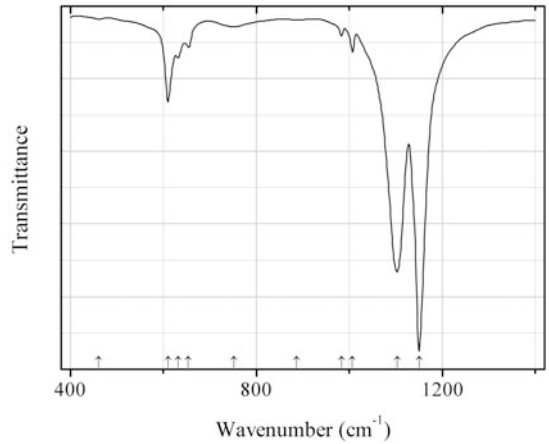

Fig. 2.1161 IR spectrum of zinkosite drawn using data from Wylde et al. (2001)

S445 Zinkosite $ZnSO_4$ (Fig. 2.1161)
Locality: Synthetic.
Description: No data.
Kind of sample preparation and/or method of registration of the spectrum: KBr disc. Transmission.
Source: Wylde et al. (2001).
Wavenumbers (cm^{-1}): 1150s, 1103s, 1007w, 983w, 886w, 752w, 654w, 632, 610, 461w.
Note: The wavenumbers were determined by us based on spectral curve analysis of the published spectrum.

S446 Bobjonesite $V^{4+}O(SO_4)\cdot 3H_2O$
Locality: Synthetic.
Description: The crystal structure is solved. Monoclinic, space group $P2_1/c$, a = 7.3850(12), b = 7.3990(7), c = 12.229(2) Å, β = 108.976(12)°, Z = 4.
Kind of sample preparation and/or method of registration of the spectrum: KBr disc. Absorption.
Source: Cevik et al. (2010).

Wavenumbers (cm^{-1}): 1730, 1650s, 1605sh, 1463w 1270sh, 1175, 1100, 1001s, 1021s, 1001s, 847, 831, 772, 736, 646, 599, 475s, 442.

S447 Chaidamuite $ZnFe^{3+}(SO_4)_2(OH)\cdot 4H_2O$
Locality: Xitieshan, Chaidamu, Qinhai Province, China.
Description: Brown granular aggregate from the association with coquimbite, copiapite, zinc-botryogen, butlerite, pyrite, etc. Holotype sample. Monoclinic, a = 9.759, b = 7.134, c = 7.335 Å, β = 106.2°, V = 490.4 $Å^3$, Z = 2. D_{meas} = 2.722 g/cm^3, D_{calc} = 2.72 g/cm^3. Optically biaxial (+), α = 1.632, β = 1.640, γ = 1.688.
Kind of sample preparation and/or method of registration of the spectrum: Absorption.
Source: Li et al. (1986).
Wavenumbers (cm^{-1}): 3381s, 1645, 1237s, 977, 653, 604, 491.

S448 Fibroferrite $Fe^{3+}(SO_4)(OH)\cdot 5H_2O$
Locality: Alcaparrosa mine, Cerritos Bayos, Calama, El Loa province, Antofagasta region, Chile.
Kind of sample preparation and/or method of registration of the spectrum: KBr disc. Absorption.
Source: Moenke (1966).
Wavenumbers (cm^{-1}): 3580s, 3410s, 1625, 1220s, 1145s, 1090s, 1005s, 780w, 730w, 675, 630, 580, 473s.

S449 Hohmannite $Fe_2^{3+}(SO_4)_2O\cdot 8H_2O$
Locality: Copiapó province, Atacama region, Chile.
Kind of sample preparation and/or method of registration of the spectrum: KBr disc. Absorption.
Source: Moenke (1966).
Wavenumbers (cm^{-1}): 3580, 3545, 3400, 1640, 1229, 1215sh, 1130s, 1085s, 1070sh, 1027s, 1008s, 1000sh, 670sh, 655, 625sh, 600, 530, 477, 420w.

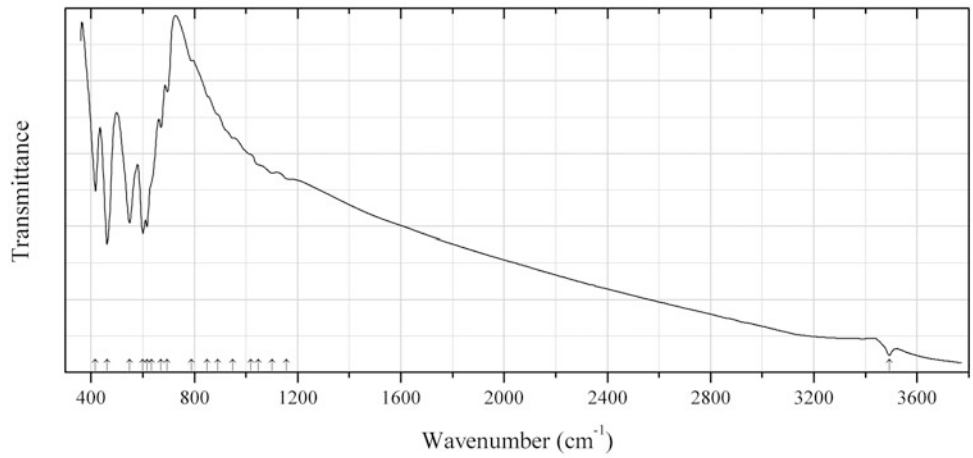

Fig. 2.1162 IR spectrum of sarabauite obtained by N.V. Chukanov

S450 Sarabauite $Sb_4S_6\cdot CaSb_6O_{10}$ (Fig. 2.1162)
Locality: Sarabau mine (Lucky Hill mine), Bau, Kuching, Sarawak, Borneo Island, Malaysia (type locality).
Description: Deep red grains from the association with quartz, calcite, wollastonite, and stibnite.

Kind of sample preparation and/or method of registration of the spectrum: KBr disc. Absorption.
Wavenumbers (cm^{-1}): 3493w, 1158w, 1100w, 1049w, 1020sh, 949w, 890sh, 850sh, 790w, 695w, 671w, 635sh, 617s, 601s, 549s, 462s, 417s.

S451 Vanthoffite $Na_6Mg(SO_4)_4$
Locality: Wilhelmshall-Ölsburg, near Gross Ilsede, Peine, Lower Saxony, Germany.
Kind of sample preparation and/or method of registration of the spectrum: KBr disc. Absorption.
Source: Moenke (1966).
Wavenumbers (cm^{-1}): 1195s, 1170s, 1138s, 1103s, 1017, 1005, 643, 627s, 610, 485w.

S452 Zincovoltaite $K_2Zn_5Fe^{3+}{}_3Al(SO_4)_{12}\cdot 18H_2O$
Locality: A Pb-Zn deposit at Xitieshan, Qinghai Province, China.
Description: Dark green granular aggregates from the association with römerite, melanterite, gypsum, quartz, pyrite, etc. Holotype sample. Cubic, space group *Fd*3*c*, a = 27.180 Å, Z = 16. D_{meas} = 2.756 g/cm^3, D_{calc} = 2.767 g/cm^3. Optically isotropic, n = 1.605(3). The strongest lines of the powder X-ray diffraction pattern [d, Å (I, %)] are: 5.54 (48), 4.26 (28), 3.53 (67), 3.39 (10), 3.13 (39), 3.03 (28), 2.84 (32).
Kind of sample preparation and/or method of registration of the spectrum: Absorption.
Source: Li et al. (1987).
Wavenumbers (cm^{-1}): 3402s, 3065s, 1686, 1138s, 1004s, 590, 442.

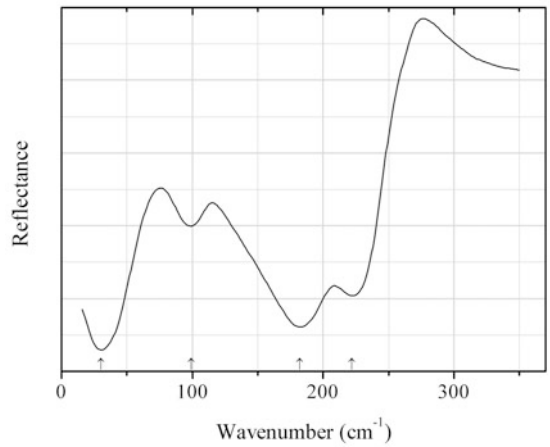

Fig. 2.1163 IR spectrum of acanthite drawn using data from Brüesch and Wullschleger (1973)

S453 Acanthite Ag_2S (Fig. 2.1163)
Locality: Synthetic.
Kind of sample preparation and/or method of registration of the spectrum: A polished polycrystalline sample. Reflection.
Source: Brüesch and Wullschleger (1973).
Wavenumbers (cm^{-1}): 222, 182s, 99, 30s.
Note: The wavenumbers were determined by us based on spectral curve analysis of the published spectrum.

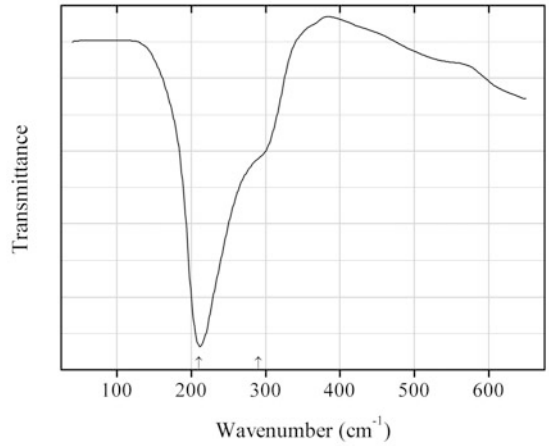

Fig. 2.1164 IR spectrum of alabandite drawn using data from Brusentsova et al. (2012)

S454 Alabandite MnS (Fig. 2.1164)
Locality: Allakh-yun, Sakha Republic (Yakutia), Siberia, Russia.
Description: Sample No. 103312 from the American Museum of Natural History.
Kind of sample preparation and/or method of registration of the spectrum: Polyethylene disc. Absorption.
Source: Brusentsova et al. (2012).
Wavenumbers (cm^{-1}): 290sh, 210.
Note: The wavenumbers were partly determined by us based on spectral curve analysis of the published spectrum.

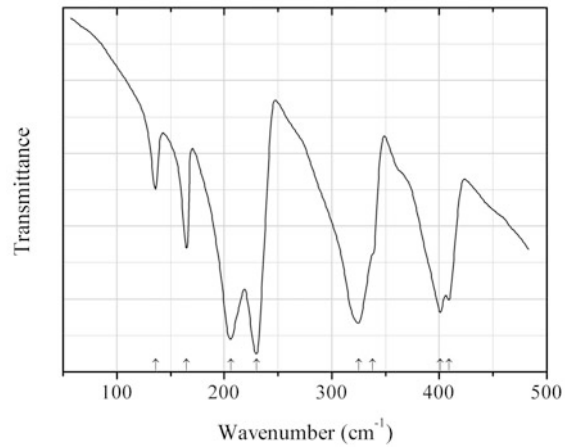

Fig. 2.1165 IR spectrum of ruthenium antimonide sulfide drawn using data from Lutz et al. (1983)

S455 Ruthenium antimonide sulfide RuSbS (Fig. 2.1165)
Locality: Synthetic.
Description: Prepared by heating stoichiometric mixture of the elements in a closed silica tube at 1000 °C. Monoclinic, space group $P2_1/m$, a = 6.183(2), b = 6.144(2), c = 6.198(2) Å, β = 111.7(2)°.

Kind of sample preparation and/or method of registration of the spectrum: Nujol mull. Transmission.
Source: Lutz et al. (1983).
Wavenumbers (cm^{-1}): 409, 401, 338sh, 325s, 230s, 206s, 165, 136.

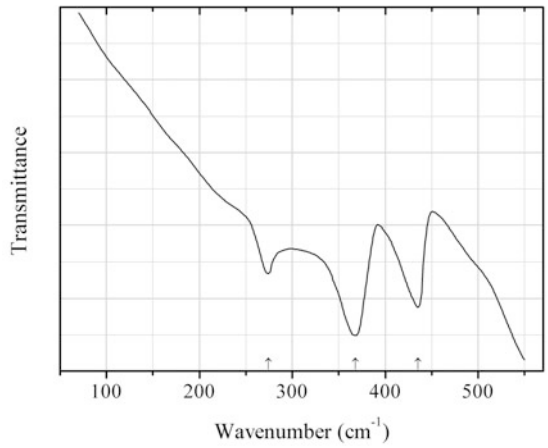

Fig. 2.1166 IR spectrum of arsenopyrite drawn using data from Lutz et al. (1983)

S456 Arsenopyrite FeAsS (Fig. 2.1166)
Locality: Synthetic.
Description: Prepared by heating stoichiometric mixture of the elements in a closed tube at 800 °C. Monoclinic, space group $P2_1/m$, a = 5.750(2), b = 5.702(1), c = 5.787(2) Å, β = 112.3(2)°.
Kind of sample preparation and/or method of registration of the spectrum: Nujol mull. Transmission.
Source: Lutz et al. (1983).
Wavenumbers (cm^{-1}): 435s, 368s, 274.
Note: For the IR spectra of arsenopyrite see also Povarennykh et al. (1973), Soong and Farmer (1978).

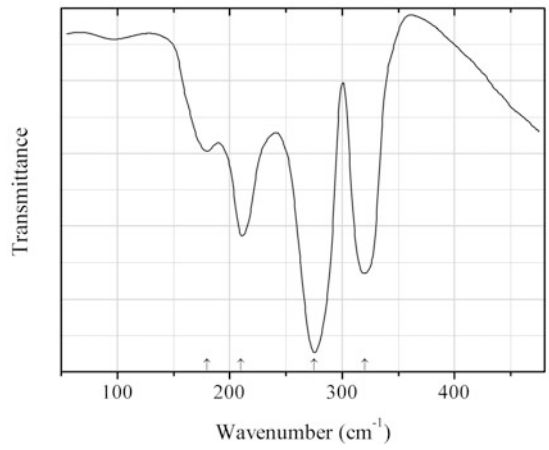

Fig. 2.1167 IR spectrum of berthierite drawn using data from Povarennykh et al. (1973)

S457 Berthierite $FeSb_2S_4$ (Fig. 2.1167)
Locality: An unknown locality near Freiberg, Saxony, Germany.
Description: No data.
Kind of sample preparation and/or method of registration of the spectrum: Nujol mull. Transmission.
Source: Povarennykh et al. (1973).
Wavenumbers (cm^{-1}): 320s, 275s, 210, 180w.

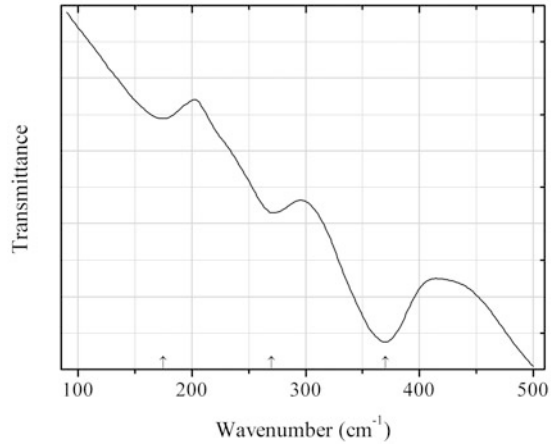

Fig. 2.1168 IR spectrum of betekhtinite drawn using data from Povarennykh et al. (1973)

S458 Betekhtinite $(Cu,Fe)_{21}Pb_2S_{15}$ (Fig. 2.1168)
Locality: Dzhezkazgan (Zhezkazgan), Karagandy region, Kazakhstan.
Description: No data.
Kind of sample preparation and/or method of registration of the spectrum: Nujol mull. Transmission.
Source: Povarennykh et al. (1973).
Wavenumbers (cm^{-1}): 370s, 270, 175.

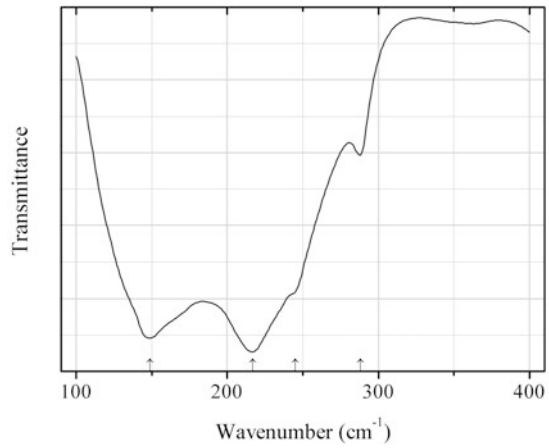

Fig. 2.1169 IR spectrum of bismuthinite drawn using data from Soong and Farmer (1978)

S459 Bismuthinite Bi_2S_3 (Fig. 2.1169)
Locality: Not indicated.
Description: Confirmed by powder X-ray diffraction data.
Kind of sample preparation and/or method of registration of the spectrum: Polyethylene disc. Absorption.
Source: Soong and Farmer (1978).
Wavenumbers (cm^{-1}): 288w, 245sh, 217s, 149s.
Note: For the IR spectrum of bismuthinite see also Petzelt and Grigas (1973).

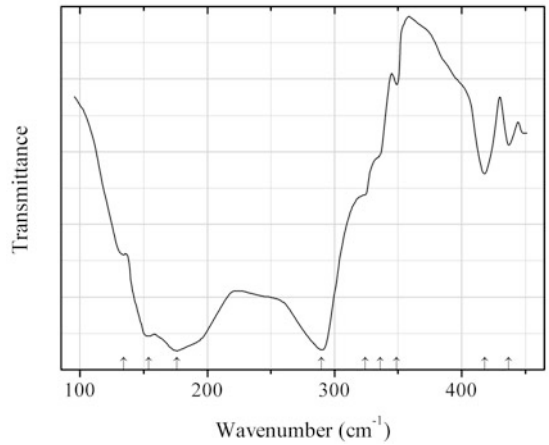

Fig. 2.1170 IR spectrum of boulangerite drawn using data from Soong and Farmer (1978)

S460 Boulangerite $Pb_5Sb_4S_{11}$ (Fig. 2.1170)
Locality: Not indicated.
Description: Confirmed by powder X-ray diffraction data.
Kind of sample preparation and/or method of registration of the spectrum: Polyethylene disc. Absorption.
Source: Soong and Farmer (1978).
Wavenumbers (cm^{-1}): 437w, 418, 349w, 336sh, 324sh, 290s, 176s, 154s, 134.

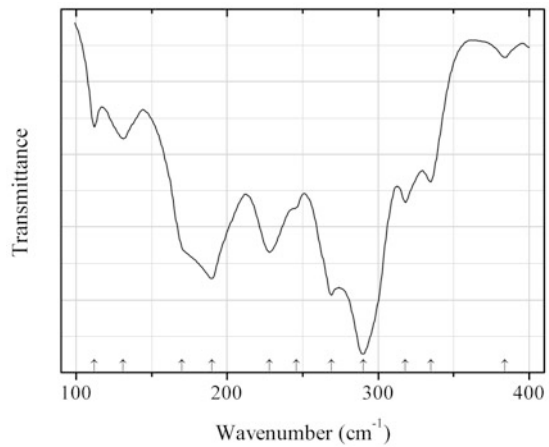

Fig. 2.1171 IR spectrum of bournonite drawn using data from Soong and Farmer (1978)

S461 Bournonite $CuPbSbS_3$ (Fig. 2.1171)
Locality: Not indicated.
Description: Confirmed by powder X-ray diffraction data.
Kind of sample preparation and/or method of registration of the spectrum: Polyethylene disc. Absorption.
Source: Soong and Farmer (1978).
Wavenumbers (cm^{-1}): 384w, 335, 318, 290s, 269s, 246sh, 228, 190s, 170sh, 131w, 112w.

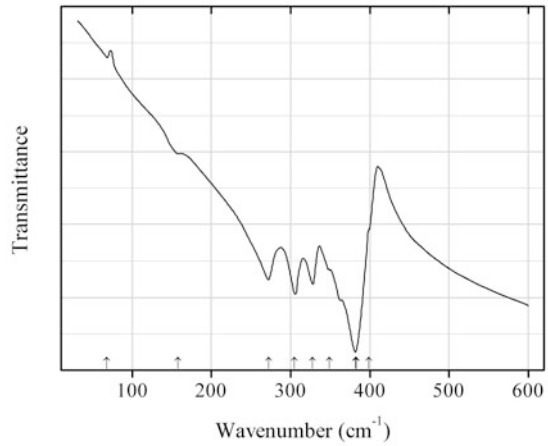

Fig. 2.1172 IR spectrum of briartite drawn using data from Himmrich and Haeuseler (1991)

S462 Briartite Cu_2FeGeS_4 (Fig. 2.1172)
Locality: Synthetic.
Description: Synthesized by solid-state reaction from stoichiometric mixture of the elements at 900 °C. Tetragonal, space group *I*-42 *m*, $a = 5.322(1)$, $c = 10.529(5)$ Å. Confirmed by powder X-ray diffraction data.
Kind of sample preparation and/or method of registration of the spectrum: Nujol mull. Transmission.
Source: Himmrich and Haeuseler (1991).
Wavenumbers (cm^{-1}): 399sh, 382s, 383sh, 349sh, 328, 305, 272, 158w, (68w).

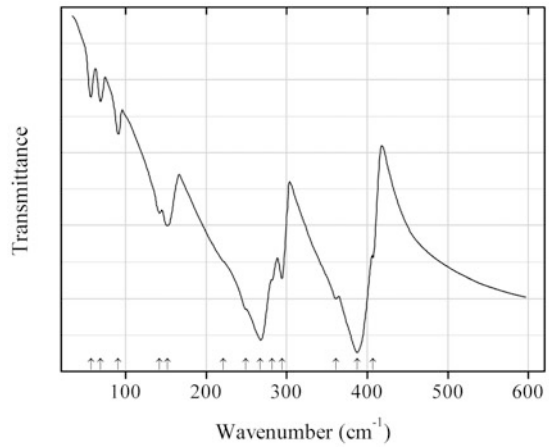

Fig. 2.1173 IR spectrum of copper cadmium germanium sulfide drawn using data from Himmrich and Haeuseler (1991)

S463 Copper cadmium germanium sulfide Cu_2CdGeS_4 (Fig. 2.1173)
Locality: Synthetic.
Description: Synthesized by solid-state reaction from stoichiometric mixture of the elements at 900 °C. Characterized by powder X-ray diffraction data. Orthorhombic, space group $Pmn2_1$, a = 7.703(1), b = 6.556(1), c = 6.299(1) Å.
Kind of sample preparation and/or method of registration of the spectrum: Nujol mull. Transmission.
Source: Himmrich and Haeuseler (1991).
Wavenumbers (cm^{-1}): 407sh, 388s, 361, 294, 282sh, 267s, 249sh, 221sh, 152, 142, 91w, 69w, 57w.

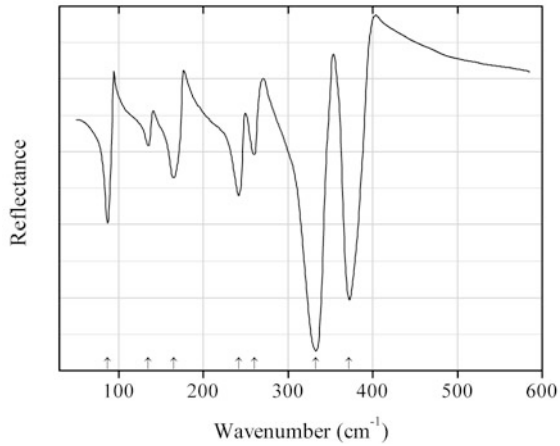

Fig. 2.1174 IR spectrum of cadmium gallium sulfide drawn using data from Haeuseler et al. (1985)

S464 Cadmium gallium sulfide $CdGa_2S_4$ (Fig. 2.1174)
Locality: Synthetic.
Description: Prepared from cadmium and gallium sulfides in closed quartz ampoule by vapour phase transport method at 600–650 °C.
Kind of sample preparation and/or method of registration of the spectrum: Hot-pressed disc. Reflection.
Source: Haeuseler et al. (1985).
Wavenumbers (cm^{-1}): 372s, 333s, 260, 242, 165, 135, 87.

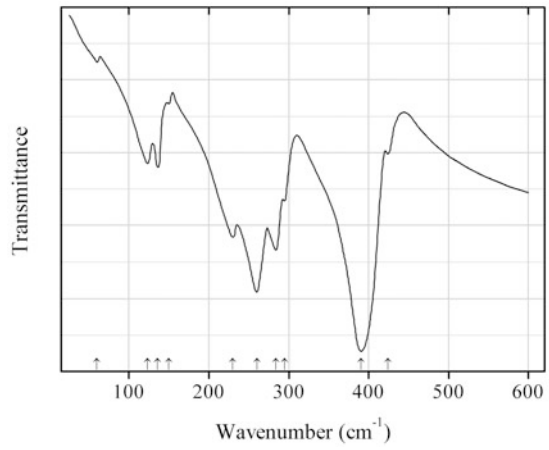

Fig. 2.1175 IR spectrum of silver cadmium germanium sulfide drawn using data from Himmrich and Haeuseler (1991)

S465 Silver cadmium germanium sulfide Ag_2CdGeS_4 (Fig. 2.1175)
Locality: Synthetic.
Description: Synthesized by solid-state reaction from stoichiometric mixture of the elements at 900 °C. Characterized by powder X-ray diffraction data. Orthorhombic, space group $Pmn2_1$, a = 8.038(1), b = 6.873(1), c = 6.589(1) Å.
Kind of sample preparation and/or method of registration of the spectrum: Nujol mull. Transmission.
Source: Himmrich and Haeuseler (1991).
Wavenumbers (cm^{-1}): 424w, 390s, 295w, 284, 260s, 230, 150sh, 136, 123, 60w.

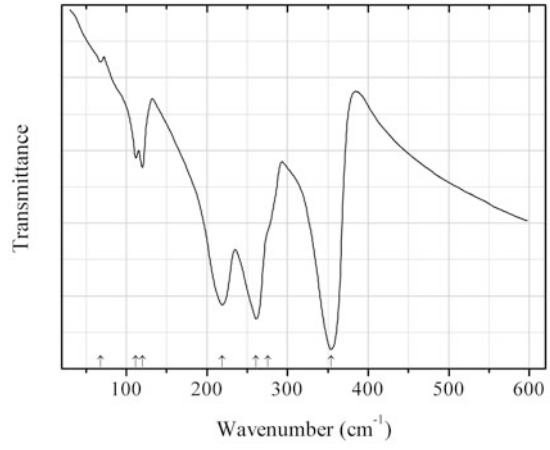

Fig. 2.1176 IR spectrum of silver cadmium tin sulfide drawn using data from Himmrich and Haeuseler (1991)

S466 Silver cadmium tin sulfide Ag_2CdSnS_4 (Fig. 2.1176)
Locality: Synthetic.
Description: Synthesized by solid-state reaction from stoichiometric mixture of the elements at 800 °C. Characterized by powder X-ray diffraction data. Orthorhombic, space group $Pmn2_1$, a = 4.114(1), b = 7.032(1), c = 6.695(1) Å.

Kind of sample preparation and/or method of registration of the spectrum: Nujol mull. Transmission.
Source: Himmrich and Haeuseler (1991).
Wavenumbers (cm^{-1}): 354s, 276sh, 261s, 219s, 120, 112, 68w.

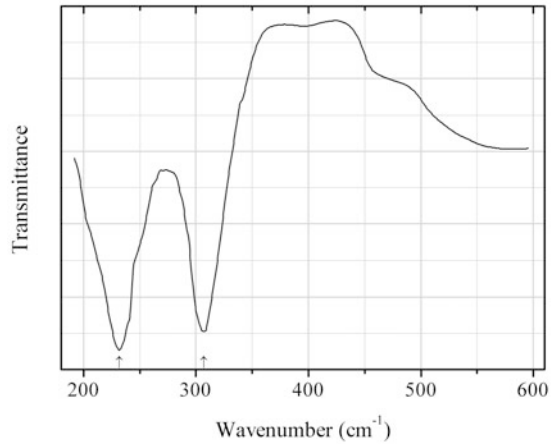

Fig. 2.1177 IR spectrum of cadmoindite drawn using data from Unger et al. (1978)

S467 Cadmoindite $CdIn_2S_4$ (Fig. 2.1177)
Locality: Synthetic.
Description: Orange-red single crystals grown by a closed-tube gas transport reaction.
Kind of sample preparation and/or method of registration of the spectrum: CsI disc. Transmission.
Source: Unger et al. (1978).
Wavenumbers (cm^{-1}): 307s, 232s.
Note: For IR spectra of cadmoindite see also Syrbu et al. (1996a, b).

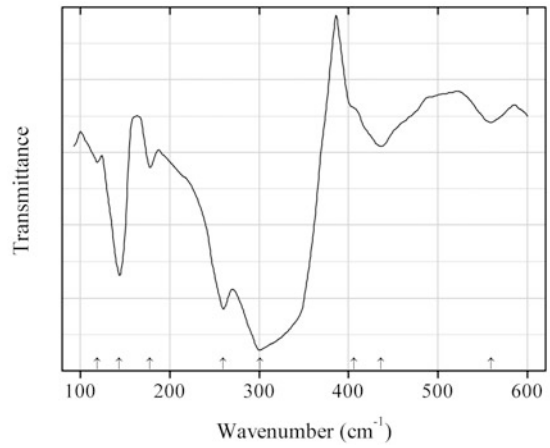

Fig. 2.1178 IR spectrum of caswellsilverite drawn using data from Unger et al. (1979)

S468 Caswellsilverite $NaCrS_2$ (Fig. 2.1178)
Locality: Synthetic.
Description: Dark red platelets. Trigonal, space group *R*-3 *m*.
Kind of sample preparation and/or method of registration of the spectrum: As grown platelet $\sim$1 cm^3 in area and $\sim$0.01 cm thick. Transmission.
Source: Unger et al. (1979).
Wavenumbers (cm^{-1}): 559, 436, 406sh, 301s, 260s, 178, 144, 119.
Note: The wavenumbers were determined by us based on spectral curve analysis of the published spectrum.

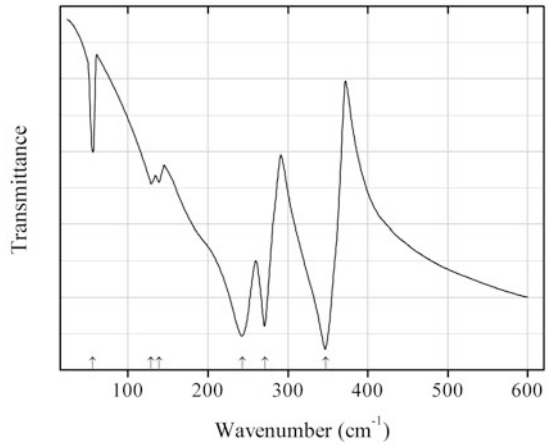

Fig. 2.1179 IR spectrum of copper cadmium tin sulfide drawn using data from Himmrich and Haeuseler (1991)

S469 Copper cadmium tin sulfide Cu_2CdSnS_4 (Fig. 2.1179)
Locality: Synthetic.
Description: Synthesized by solid-state reaction from stoichiometric mixture of the elements at 800 °C. Characterized by powder X-ray diffraction data. Tetragonal, space group *I*-42 *m*, a = 5.593(1), c = 10.840(1) Å.
Kind of sample preparation and/or method of registration of the spectrum: Nujol mull. Transmission.
Source: Himmrich and Haeuseler (1991).
Wavenumbers (cm^{-1}): 347s, 271s, 243s, 139, 129, 56.

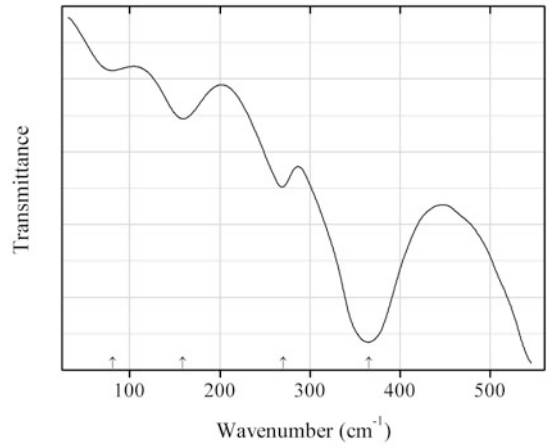

Fig. 2.1180 IR spectrum of chalcocite drawn using data from Povarennykh et al. (1973)

S470 Chalcocite Cu_2S (Fig. 2.1180)
Locality: Dzhezkazgan (Zhezkazgan), Karagandy region, Kazakhstan.
Description: No data.
Kind of sample preparation and/or method of registration of the spectrum: Nujol mull. Transmission.
Source: Povarennykh et al. (1973).
Wavenumbers (cm^{-1}): 365s, 270, 159, 81.
Note: The wavenumbers were partly determined by us based on spectral curve analysis of the published spectrum.

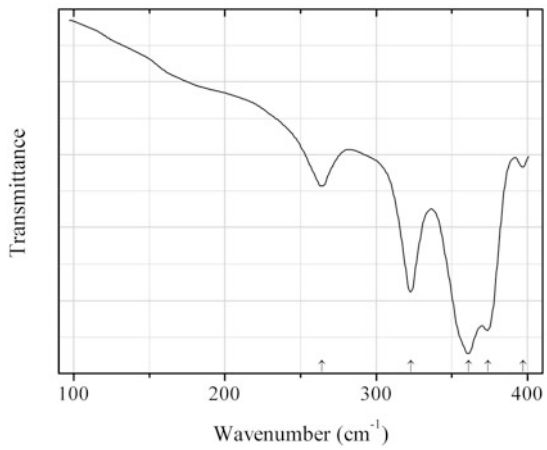

Fig. 2.1181 IR spectrum of chalcopyrite drawn using data from Soong and Farmer (1978)

S471 Chalcopyrite $CuFeS_2$ (Fig. 2.1181)
Locality: Not indicated.
Description: Confirmed by powder X-ray diffraction data.

Kind of sample preparation and/or method of registration of the spectrum: Polyethylene disc. Absorption.
Source: Soong and Farmer (1978).
Wavenumbers (cm^{-1}): 397w, 374s, 361s, 323, 264.
Note: For IR spectra of chalcopyrite see also Brusentsova et al. (2012), Povarennykh et al. (1973).

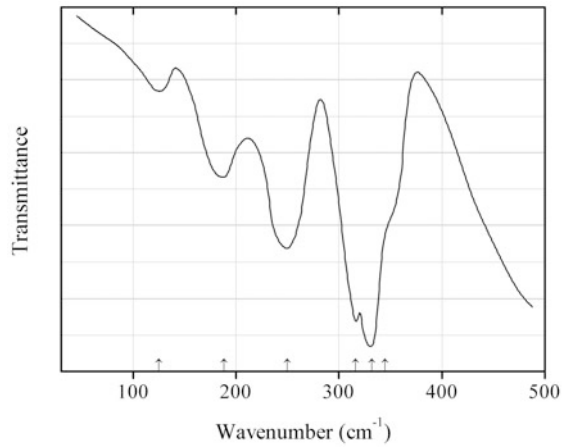

Fig. 2.1182 IR spectrum of chalcostibite drawn using data from Povarennykh et al. (1973)

S472 Chalcostibite $CuSbS_2$ (Fig. 2.1182)
Locality: An unknown locality in Harz Mts., Germany.
Description: No data.
Kind of sample preparation and/or method of registration of the spectrum: Nujol mull. Transmission.
Source: Povarennykh et al. (1973).
Wavenumbers (cm^{-1}): 345sh, 332s, 316s, 250, 188, 125w.

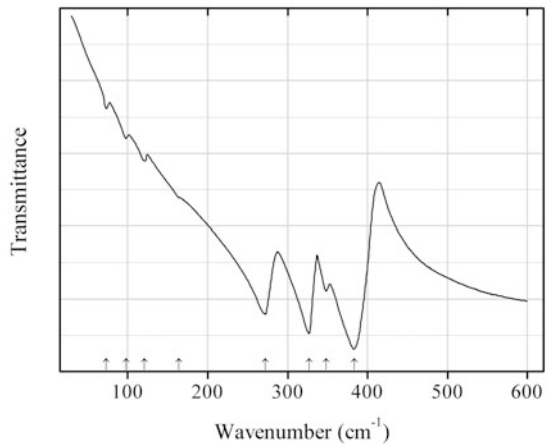

Fig. 2.1183 IR spectrum of copper cobalt germanium sulfide drawn using data from Himmrich and Haeuseler (1991)

S474 Copper cobalt germanium sulfide Cu_2CoGeS_4 (Fig. 2.1183)
Locality: Synthetic.
Description: Synthesized by solid-state reaction from stoichiometric mixture of the elements at 900 °C. Characterized by powder X-ray diffraction data. Tetragonal, space group *I*-42 *m*, a = 5.300(3), c = 10.48(1) Å.
Kind of sample preparation and/or method of registration of the spectrum: Nujol mull. Transmission.
Source: Himmrich and Haeuseler (1991).
Wavenumbers (cm^{-1}): 383s, 348, 327s, 272, 164sh, 121w, 98w, 73w.
Note: The band position denoted by Himmrich and Haeuseler (1991) as 144 cm^{-1} was determined by us at 164 cm^{-1} based on spectral curve analysis of the published spectrum.

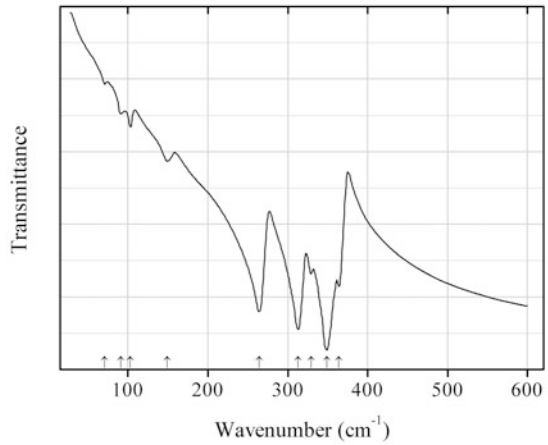

Fig. 2.1184 IR spectrum of copper cobalt tin sulfide drawn using data from Himmrich and Haeuseler (1991)

S475 Copper cobalt tin sulfide Cu_2CoSnS_4 (Fig. 2.1184)
Locality: Synthetic.
Description: Synthesized by solid-state reaction from stoichiometric mixture of the elements at 600 °C. Characterized by powder X-ray diffraction data. Tetragonal, space group *I*-42 *m*, a = 5.400(3), c = 10.793(6) Å.
Kind of sample preparation and/or method of registration of the spectrum: Nujol mull. Transmission.
Source: Himmrich and Haeuseler (1991).
Wavenumbers (cm^{-1}): 364, 349s, 329, 313s, 264s, 149w, 103w, 91w, 71w.

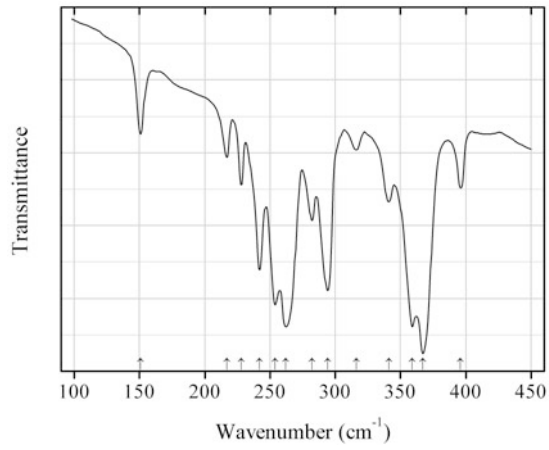

Fig. 2.1185 IR spectrum of cobaltite drawn using data from Soong and Farmer (1978)

S476 Cobaltite CoAsS (Fig. 2.1185)
Locality: Not indicated.
Description: Confirmed by powder X-ray diffraction data.
Kind of sample preparation and/or method of registration of the spectrum: Polyethylene disc. Absorption.
Source: Soong and Farmer (1978).
Wavenumbers (cm^{-1}): 396, 367s, 359s, 341, 316w, 294, 282, 262s, 254s, 242, 228, 217w, 151w.

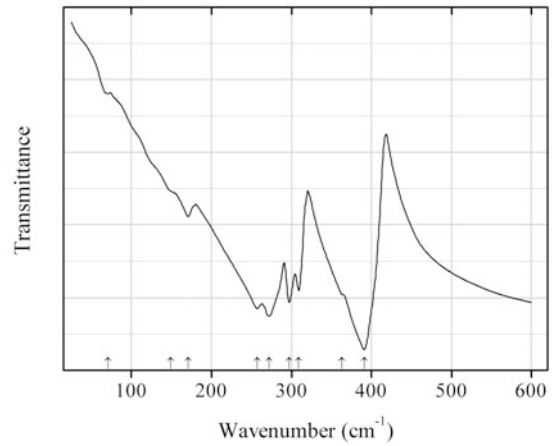

Fig. 2.1186 IR spectrum of copper manganese germanium sulfide drawn using data from Himmrich and Haeuseler (1991)

S477 Copper manganese germanium sulfide Cu_2MnGeS_4 (Fig. 2.1186)
Locality: Synthetic.
Description: Synthesized by solid-state reaction from stoichiometric mixture of the elements at 800 °C. Characterized by powder X-ray diffraction data. Orthorhombic, space group $Pmn2_1$, a = 7.609(1), b = 6.511(2), c = 6.235(2) Å.

Kind of sample preparation and/or method of registration of the spectrum: Nujol mull. Transmission.
Source: Himmrich and Haeuseler (1991).
Wavenumbers (cm^{-1}): 391s, 363sh, 309, 297s, 272s, 257s, 171w, 149sh, 71w.

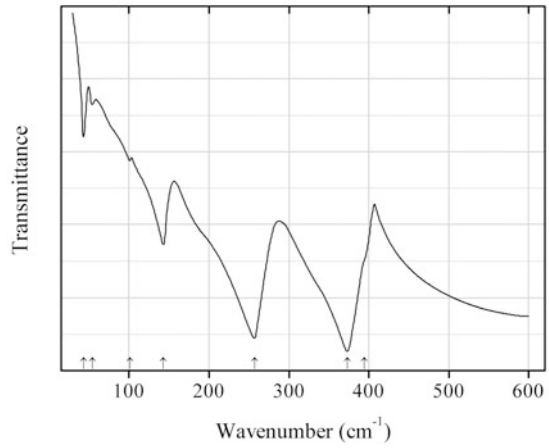

Fig. 2.1187 IR spectrum of copper mercury germanium sulfide drawn using data from Himmrich and Haeuseler (1991)

S478 Copper mercury germanium sulfide Cu_2HgGeS_4 (Fig. 2.1187)
Locality: Synthetic.
Description: Synthesized by solid-state reaction from stoichiometric mixture of the elements at 700 °C. Characterized by powder X-ray diffraction data. Tetragonal, space group *I*-42 *m*, a = 5.484(1), c = 10.536(1) Å.
Kind of sample preparation and/or method of registration of the spectrum: Nujol mull. Transmission.
Source: Himmrich and Haeuseler (1991).
Wavenumbers (cm^{-1}): 394sh, 373s, 257s, 143, 101w, 54w, 43w.

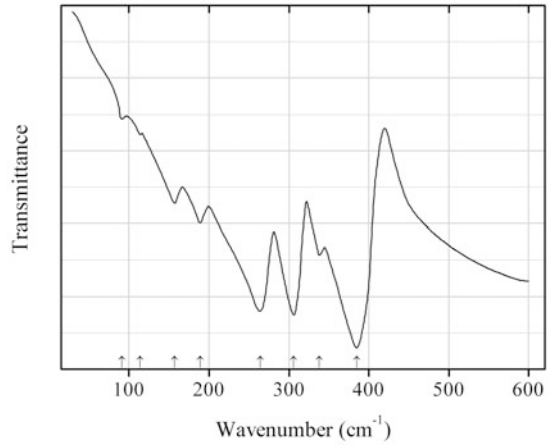

Fig. 2.1188 IR spectrum of copper zinc germanium sulfide drawn using data from Himmrich and Haeuseler (1991)

S479 Copper zinc germanium sulfide Cu_2ZnGeS_4 (Fig. 2.1188)
Locality: Synthetic.
Description: Synthesized by solid-state reaction from stoichiometric mixture of the elements at 700 °C. Characterized by powder X-ray diffraction data. Tetragonal, space group *I*-42 *m*, a = 5.344(5), c = 10.513(1) Å.
Kind of sample preparation and/or method of registration of the spectrum: Nujol mull. Transmission.
Source: Himmrich and Haeuseler (1991).
Wavenumbers (cm^{-1}): 385s, 338, 306s, 264s, 189, 157, 114w, 91w.

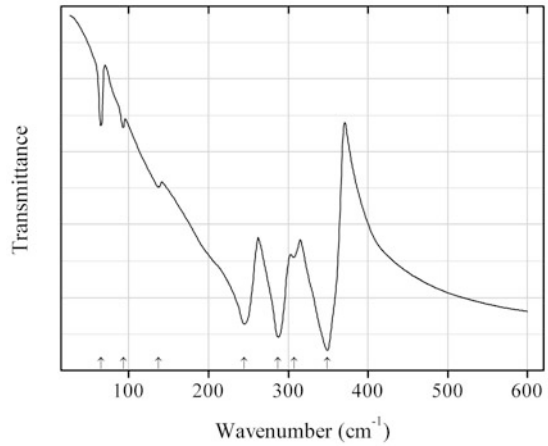

Fig. 2.1189 IR spectrum of copper manganese tin sulfide drawn using data from Himmrich and Haeuseler (1991)

S480 Copper manganese tin sulfide Cu_2MnSnS_4 (Fig. 2.1189)
Locality: Synthetic.
Description: Synthesized by solid-state reaction from stoichiometric mixture of the elements at 800 °C. Characterized by powder X-ray diffraction data. Tetragonal, space group *I*-42 *m*, a = 5.577(1), c = 10.898(2) Å.
Kind of sample preparation and/or method of registration of the spectrum: Nujol mull. Transmission.
Source: Himmrich and Haeuseler (1991).
Wavenumbers (cm^{-1}): 349s, 307, 287s, 245s, 137w, 93w, 65w.

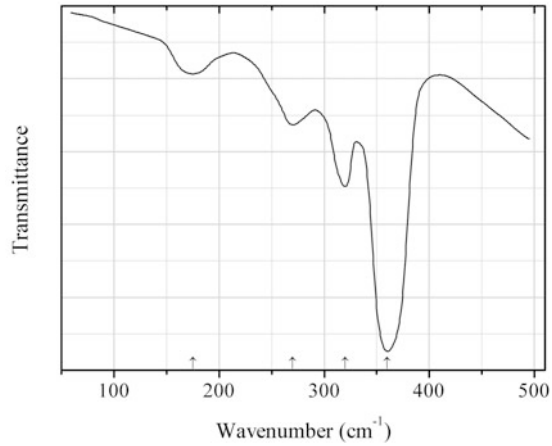

Fig. 2.1190 IR spectrum of cubanite drawn using data from Povarennykh et al. (1973)

S481 Cubanite $CuFe_2S_3$ (Fig. 2.1190)
Locality: Kaveltorp mines, Kopparberg, Ljusnarsberg, Västmanland, Sweden.
Description: No data.
Kind of sample preparation and/or method of registration of the spectrum: Nujol mull. Transmission.
Source: Povarennykh et al. (1973).
Wavenumbers (cm^{-1}): 360s, 320, 270, 175w.

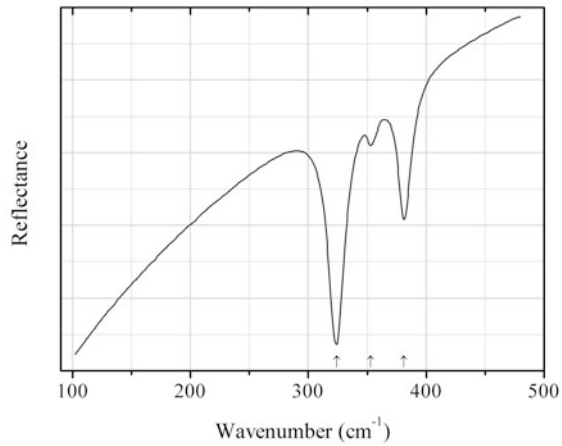

Fig. 2.1191 IR spectrum of daubréelite drawn using data from Rudolf et al. (2005)

S482 Daubréelite $FeCr_2S_4$ (Fig. 2.1191)
Locality: Synthetic.
Description: Single crystals grown using a chemical transport-reaction method with chlorine as transport agent and the ternary polycrystal as starting material. Characterized by single-crystal X-ray diffraction data.

Kind of sample preparation and/or method of registration of the spectrum: Reflection. Kind of sample preparation is not indicated.
Source: Rudolf et al. (2005).
Wavenumbers (cm^{-1}): 381, 353w, 324s.

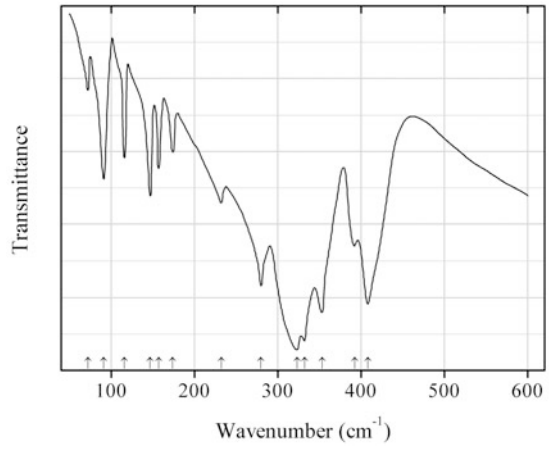

Fig. 2.1192 IR spectrum of gallium sulfide drawn using data from Julien et al. (1999)

S483 Gallium sulfide Ga_2S_3 (Fig. 2.1192)
Locality: Synthetic.
Description: No data.
Kind of sample preparation and/or method of registration of the spectrum: Powder dispersed in paraffin wax. Absorption.
Source: Julien et al. (1999).
Wavenumbers (cm^{-1}): 408s, 392, 353s, 332s, 323s, 280s, 232, 174, 157, 147, 116, 91, 72w.

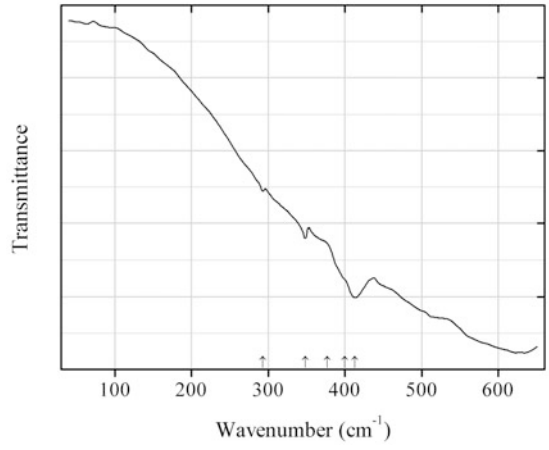

Fig. 2.1193 IR spectrum of digenite drawn using data from Brusentsova et al. (2012)

S484 Digenite $Cu_{1.8}S$ (Fig. 2.1193)

Locality: Butte mining district, Summit valley, Silver Bow Co., Montana, USA.
Description: Trigonal. The empirical formula is $Cu_{8.84}Fe_{0.16}S_{4.95}$.
Kind of sample preparation and/or method of registration of the spectrum: Polyethylene disc. Absorption.
Source: Brusentsova et al. (2012).
Wavenumbers (cm^{-1}): 413s, 400sh, 377sh, 348, 293w.

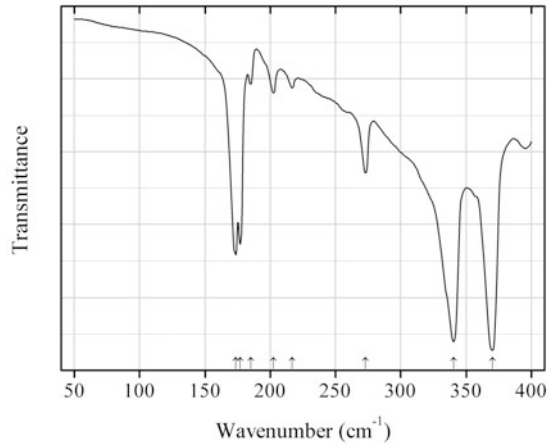

Fig. 2.1194 IR spectrum of dimorphite drawn using data from Whitfield (1971)

S485 Dimorphite As_4S_3 (Fig. 2.1194)
Locality: Synthetic.
Description: Prepared by combining stoichiometric proportions of the elements and then subliming the product under vacuum. Orthorhombic, space group *Pnma*.
Kind of sample preparation and/or method of registration of the spectrum: Powder dispersed in petroleum jelly. Absorption.
Source: Whitfield (1971).
Wavenumbers (cm^{-1}): 370s, 340.5s, 273, 217w, 202.5, 185w, 177s, 173.5s.

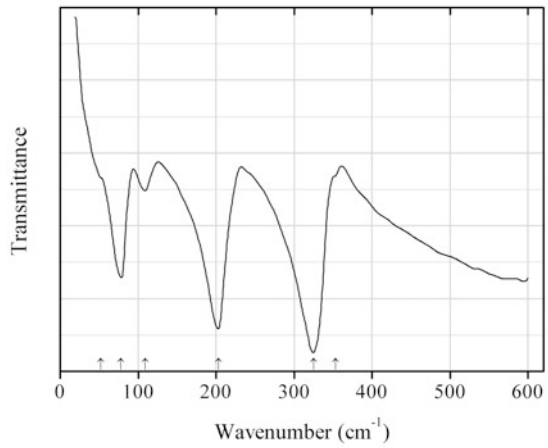

Fig. 2.1195 IR spectrum of ellisite drawn using data from Makreski et al. (2004)

S486 Ellisite Tl_3AsS_3 (Fig. 2.1195)
Locality: Synthetic.
Description: Prepared by solid-state reaction in sealed quartz tube.
Kind of sample preparation and/or method of registration of the spectrum: Nujol mull. Absorption.
Source: Makreski et al. (2004).
Wavenumbers (cm^{-1}): (353sh), 325s, 203s, 109w, 78, 52sh.

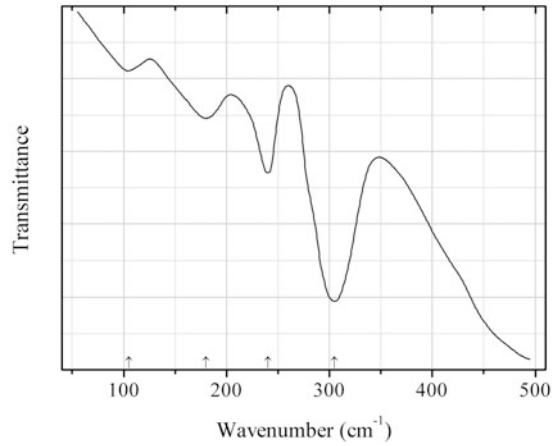

Fig. 2.1196 IR spectrum of emplectite drawn using data from Povarennykh et al. (1973)

S487 Emplectite $CuBiS_2$ (Fig. 2.1196)
Locality: Schwarzenberg district, Erzgebirge (Ore Mts.), Saxony, Germany.
Description: No data.
Kind of sample preparation and/or method of registration of the spectrum: Nujol mull. Transmission.
Source: Povarennykh et al. (1973).
Wavenumbers (cm^{-1}): 305s, 240, 180, 105w.

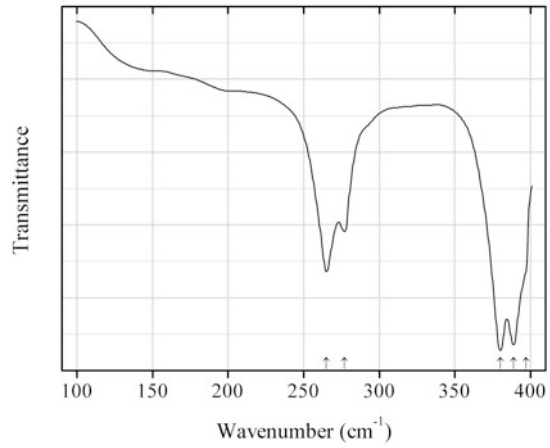

Fig. 2.1197 IR spectrum of enargite drawn using data from Soong and Farmer (1978)

S488 Enargite Cu_3AsS_4 (Fig. 2.1197)
Locality: Not indicated.
Description: No data.
Kind of sample preparation and/or method of registration of the spectrum: Polyethylene disc. Absorption.
Source: Soong and Farmer (1978).
Wavenumbers (cm^{-1}): 397sh, 389s, 380s, 277, 265.
Note: For the IR spectrum of enargite see also Povarennykh et al. (1973).

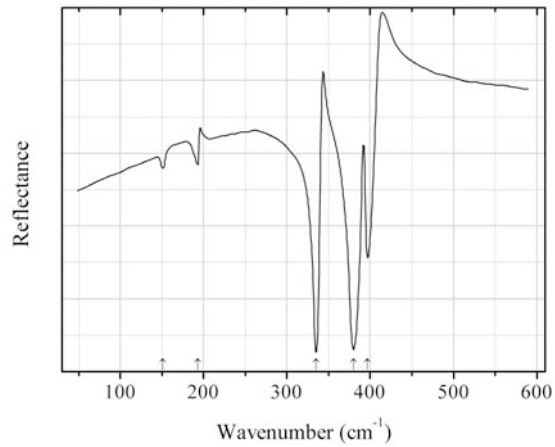

Fig. 2.1198 IR spectrum of erlichmanite drawn using data from Lutz et al. (1985)

S489 Erlichmanite OsS_2 (Fig. 2.1198)
Locality: Synthetic.
Description: Prepared by annealing stoichiometric mixture of the elements in an evacuated quartz tube at 800–900 °C for 14 days. Cubic. Characterized by powder X-ray diffraction data.
Kind of sample preparation and/or method of registration of the spectrum: A sample prepared by hot-pressing and polishing with diamond paste. Reflection.
Source: Lutz et al. (1985).
Wavenumbers (cm^{-1}): 397, 380s, 335s, 193w, 151w.

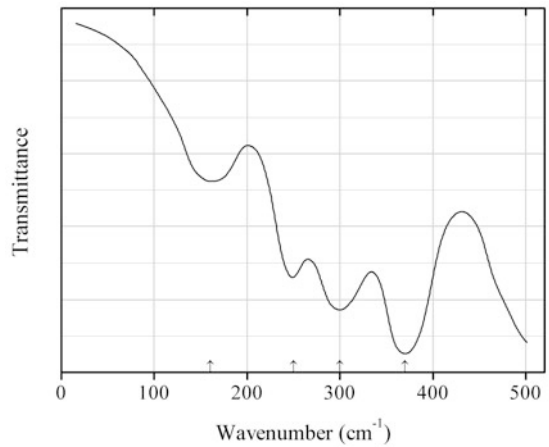

Fig. 2.1199 IR spectrum of famatinite drawn using data from Povarennykh et al. (1973)

S490 Famatinite Cu_3SbS_4 (Fig. 2.1199)
Locality: Sierra de Famatina, Argentina (type locality).
Description: No data.
Kind of sample preparation and/or method of registration of the spectrum: Nujol mull. Transmission.
Source: Povarennykh et al. (1973).
Wavenumbers (cm^{-1}): 370s, 300, 250, 160.

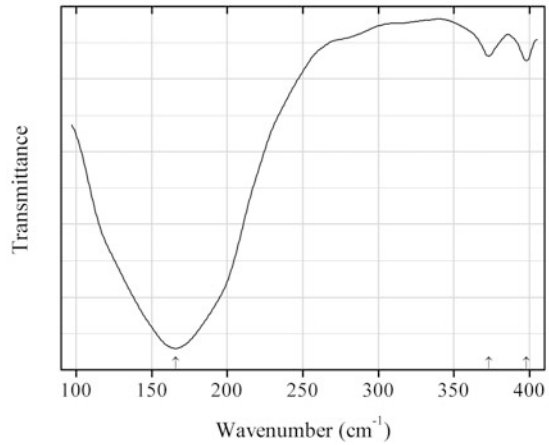

Fig. 2.1200 IR spectrum of galena drawn using data from Soong and Farmer (1978)

S491 Galena PbS (Fig. 2.1200)
Locality: Not indicated.
Description: No data.
Kind of sample preparation and/or method of registration of the spectrum: Polyethylene disc. Absorption.
Source: Soong and Farmer (1978).
Wavenumbers (cm^{-1}): 398w, 373w, 166s.
Note: For the IR spectrum of galena see also Brusentsova et al. (2012).

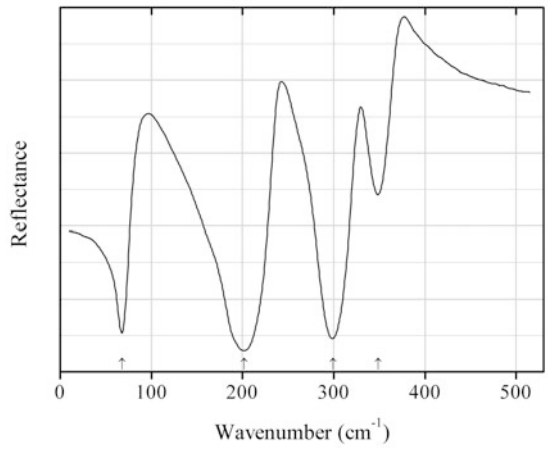

Fig. 2.1201 IR spectrum of mercury gallium indium sulfide drawn using data from Syrbu et al. (1996b)

S492 Mercury gallium indium sulfide $HgInGaS_4$ (Fig. 2.1201)
Locality: Synthetic.
Description: Single crystals with a mirror-like surface obtained by a gas-transport reaction.
Kind of sample preparation and/or method of registration of the spectrum: A single crystal. Reflection.
Source: Syrbu et al. (1996b).
Wavenumbers (cm^{-1}): 349, 299s, 202s, 68.

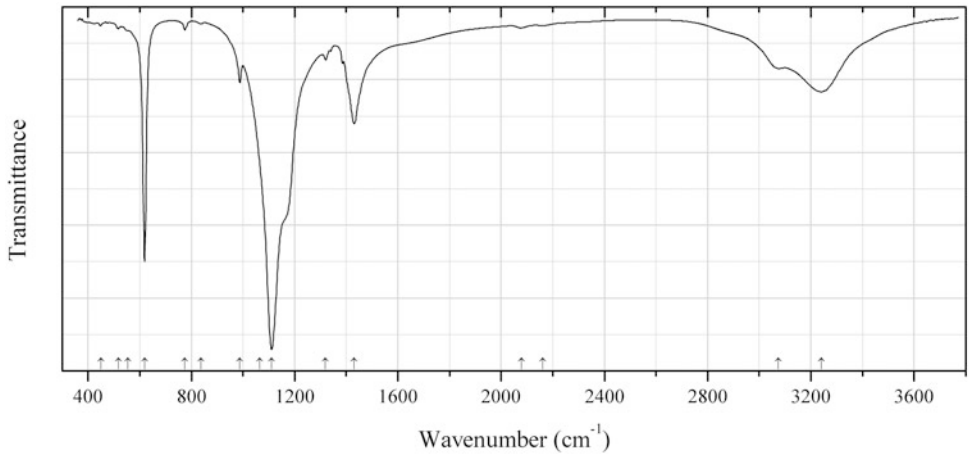

Fig. 2.1202 IR spectrum of möhnite obtained by N.V. Chukanov

S493 Möhnite $(NH_4)K_2Na(SO_4)_2$ (Fig. 2.1202)
Locality: Pabellón de Pica Mt., 1.5 km south of Chanabaya, Iquique Province, Tarapacá Region, Chile (type locality).
Description: Random aggregates and of spindle-shaped crystals from the association with salammoniac, halite, joanneumite, natroxalate, nitratine, and chanabayaite. Holotype sample. Trigonal, space group *P*-3*m*1, $a = 5.7402(3)$, $c = 7.435(1)$ Å, $V = 212.16(4)$ $Å^3$, $Z = 1$. $D_{meas} = 2.4(1)$ g/cm^3, $D_{calc} = 2.461$ g/cm^3. Optically isotropic, $\varepsilon = \omega = 1.505(2)$. The empirical formula is $(NH_4)_{0.95}Na_{0.95}K_{2.14}S_{1.99}O_8$. The strongest lines of the powder X-ray diffraction pattern [*d*, Å (*I*, %) (*hkl*)] are: 4.955 (27) (100), 4.122 (37) (101, 011), 3.708 (29) (002), 2.969 (74) (102, 012), 2.861 (100) (110), 2.474 (20) (003), 2.060 (33) (022), 1.433 (11) (220).
Kind of sample preparation and/or method of registration of the spectrum: KBr disc. Absorption.
Wavenumbers (cm^{-1}): 3240, 3074, 2162w, 2080w, 1431, 1320w, 1065sh, 1111s, 988, 837, 775, 619s, 555w, 518w, 450w.

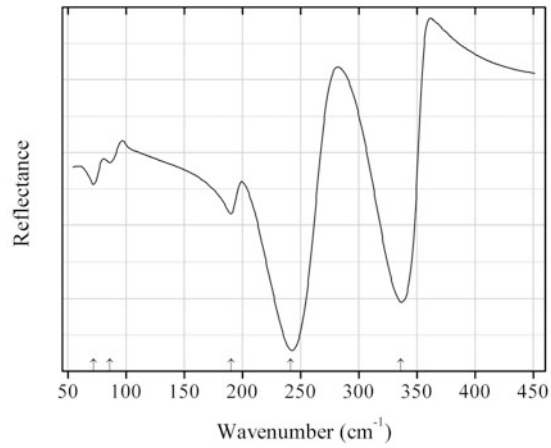

Fig. 2.1203 IR spectrum of indite drawn using data from Pauliukavets (2013)

S494 Indite $FeIn_2S_4$ (Fig. 2.1203)
Locality: Synthetic.
Description: Single crystals grown from the stoichiometric melt. Cubic, space group *Fd*3*m*.
Kind of sample preparation and/or method of registration of the spectrum: Single crystal. Reflection.
Source: Pauliukavets et al. (2013).
Wavenumbers (cm^{-1}): 336s, 241s, 190, 86w, 72w.

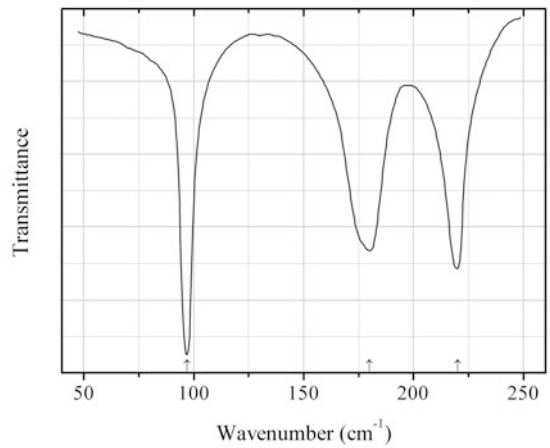

Fig. 2.1204 IR spectrum of herzenbergite drawn using data from Chamberlain et al. (1976)

S495 Herzenbergite SnS (Fig. 2.1204)
Locality: Synthetic.
Description: Single crystals prepared by the Bridgman technique. Confirmed by single-crystal and powder X-ray diffraction data. Orthorhombic, a = 3.99, b = 4.34, c = 11.20 Å.
Kind of sample preparation and/or method of registration of the spectrum: Thin single-crystal layer coplanar with c face, $E \| a$. Absorption.

Source: Chamberlain et al. (1976).
Wavenumbers (cm^{-1}): 220, 180, 97s.

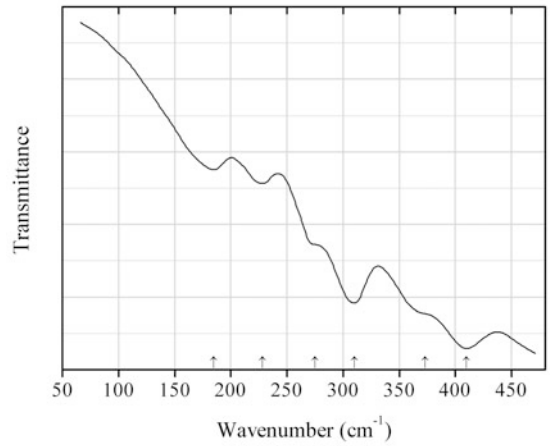

Fig. 2.1205 IR spectrum of heazlewoodite drawn using data from Plyusnina (1977)

S496 Heazlewoodite Ni_3S_2 (Fig. 2.1205)
Locality: No data.
Description: No data.
Kind of sample preparation and/or method of registration of the spectrum: Transmission. Kind of sample preparation is not indicated.
Source: Plyusnina (1977).
Wavenumbers (cm^{-1}): 410s, 373sh, 310s, 275sh, 228, 185.
Note: The wavenumbers were partly determined by us based on spectral curve analysis of the published spectrum.

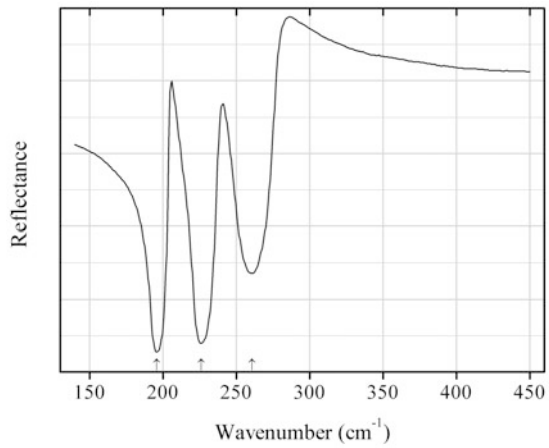

Fig. 2.1206 IR spectrum of hauerite drawn using data from Verble and Humphrey (1974)

S497 Hauerite MnS_2 (Fig. 2.1206)

Locality: Not indicated.
Description: Octahedral crystal.
Kind of sample preparation and/or method of registration of the spectrum: Reflection from the natural (111) face.
Source: Verble and Humphrey (1974).
Wavenumbers (cm^{-1}): 261, 226s, 196s.

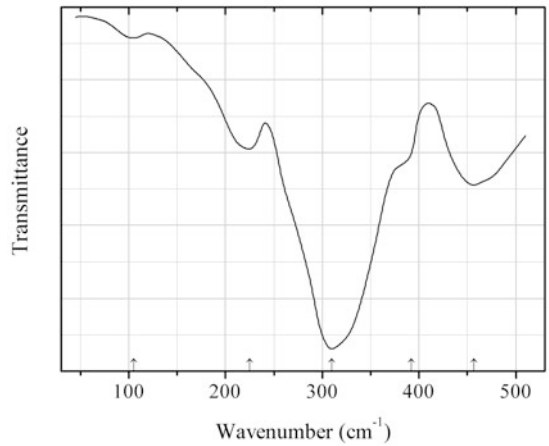

Fig. 2.1207 IR spectrum of gudmundite drawn using data from Povarennykh et al. (1973)

S498 Gudmundite FeSbS (Fig. 2.1207)
Locality: Gudmundsttorp, near Sala, Boliden, Sweden (type locality).
Description: No data.
Kind of sample preparation and/or method of registration of the spectrum: Nujol mull. Transmission.
Source: Povarennykh et al. (1973).
Wavenumbers (cm^{-1}): 457, 392, 310s, 225, 105w.

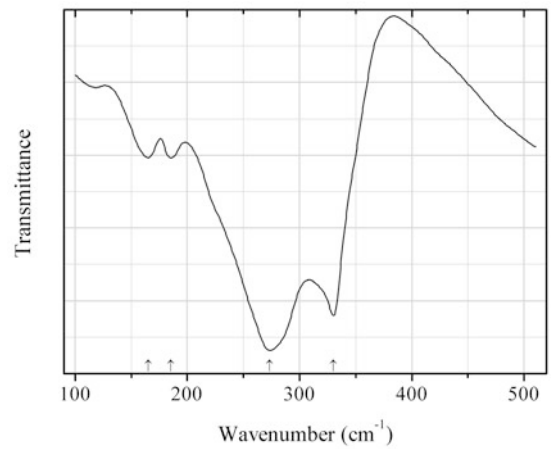

Fig. 2.1208 IR spectrum of getchellite drawn using data from Plyusnina (1977)

S499 Getchellite $SbAsS_3$ (Fig. 2.1208)
Locality: Synthetic.
Description: No data.
Kind of sample preparation and/or method of registration of the spectrum: Transmission. Kind of sample preparation is not indicated.
Source: Plyusnina (1977).
Wavenumbers (cm^{-1}): 330s, 273s, 185, 165.

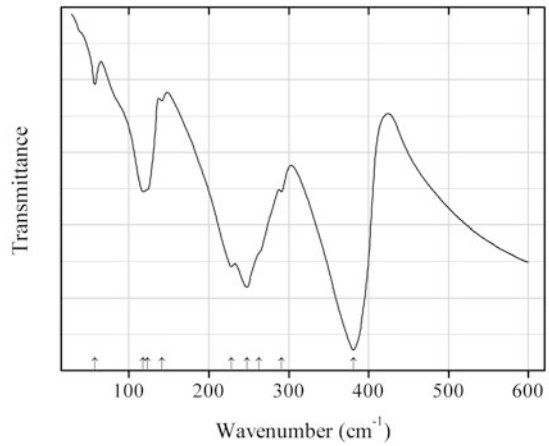

Fig. 2.1209 IR spectrum of silver mercury germanium sulfide drawn using data from Himmrich and Haeuseler (1991)

S500 Silver mercury germanium sulfide Ag_2HgGeS_4 (Fig. 2.1209)
Locality: Synthetic.
Description: Obtained from the stoichiometric mixture of the elements. Characterized by powder X-ray diffraction data.
Kind of sample preparation and/or method of registration of the spectrum: Nujol mull. Transmission.
Source: Himmrich and Haeuseler (1991).
Wavenumbers (cm^{-1}): 381s, 291w, 263sh, 248s, 228, 141w, 123sh, 118, 57w.

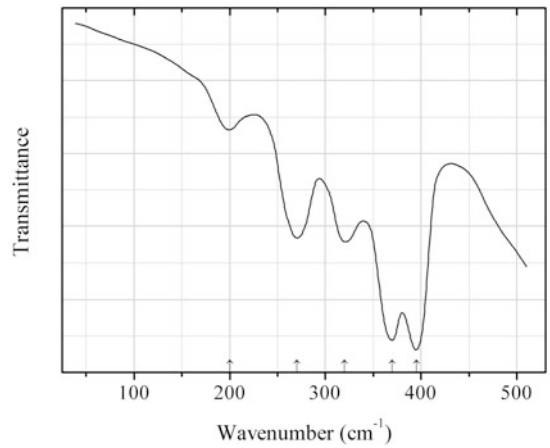

Fig. 2.1210 IR spectrum of germanite drawn using data from Povarennykh et al. (1973)

S501 Germanite $Cu_{13}Fe_2Ge_2S_{16}$ (Fig. 2.1210)
Locality: Tsumeb mine, Tsumeb, Namibia (type locality).
Description: No data.
Kind of sample preparation and/or method of registration of the spectrum: Nujol mull. Transmission.
Source: Povarennykh et al. (1973).
Wavenumbers (cm^{-1}): 395s, 370s, 320, 270, 200w.

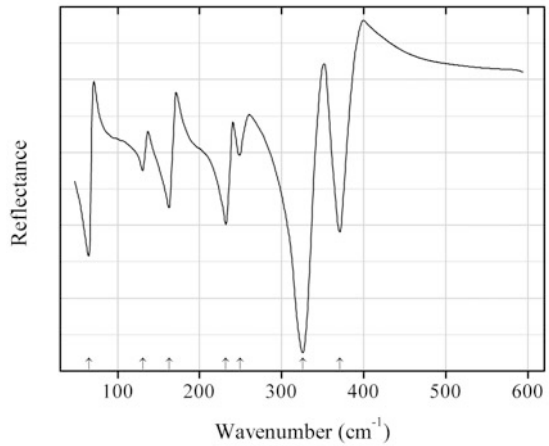

Fig. 2.1211 IR spectrum of mercury gallium sulfide drawn using data from Haeuseler et al. (1985)

S502 Mercury gallium sulfide $HgGa_2S_4$ (Fig. 2.1211)
Locality: Synthetic.
Description: Prepared by firing stoichiometric mixture of the binary chalcides in closed silica tube at 800 to 900 °C for three weeks.
Kind of sample preparation and/or method of registration of the spectrum: Hot pressed disc. Reflection.
Source: Haeuseler et al. (1985).
Wavenumbers (cm^{-1}): 371s, 326s, 249w, 232, 163, 131, 65s.

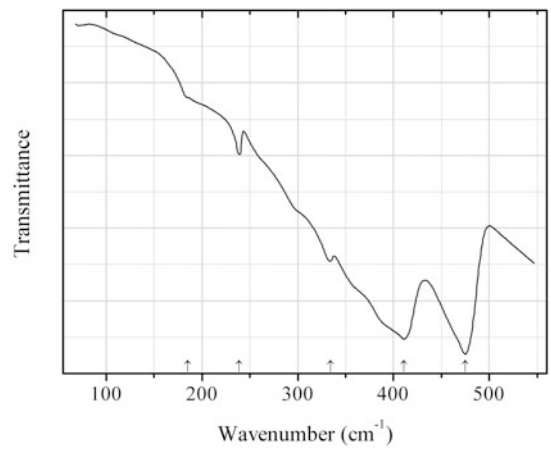

Fig. 2.1212 IR spectrum of iron phosphide sulfide drawn using data from Lutz et al. (1983)

S503 Iron phosphide sulfide FePS (Fig. 2.1212)
Locality: Synthetic.
Description: Prepared using the elements pressed to discs and heating them at 400 °C in the presence of small amounts of iodine. Characterized by powder X-ray diffraction data. Monoclinic, a = 5.617 (2), b = 5.534(2), c = 5.637(1) Å, β = 112.2(1)°.
Kind of sample preparation and/or method of registration of the spectrum: Nujol mull. Transmission.
Source: Lutz et al. (1983).
Wavenumbers (cm^{-1}): 475s, 411s, 334, 239w, 185sh.

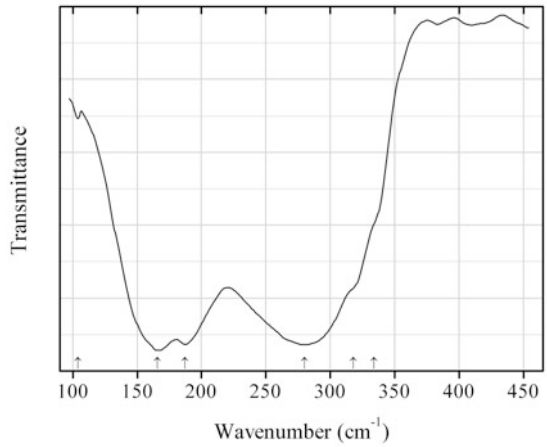

Fig. 2.1213 IR spectrum of jamesonite drawn using data from Soong and Farmer (1978)

S504 Jamesonite $Pb_4FeSb_6S_{14}$ (Fig. 2.1213)
Locality: Not indicated.
Description: No data.
Kind of sample preparation and/or method of registration of the spectrum: Polyethylene disc. Absorption.
Source: Soong and Farmer (1978).
Wavenumbers (cm^{-1}): 334sh, 318sh, 280s, 187s, 166s, 104w.
Note: For the IR spectrum of jamesonite see also Povarennykh et al. (1973).

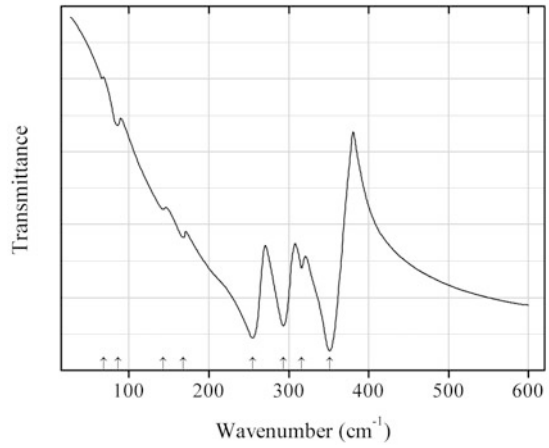

Fig. 2.1214 IR spectrum of këserite drawn using data from Himmrich and Haeuseler (1991)

S505 Këserite Cu_2ZnSnS_4 (Fig. 2.1214)
Locality: Synthetic.
Description: Obtained from the stoichiometric mixture of the elements. Characterized by powder X-ray diffraction data.
Kind of sample preparation and/or method of registration of the spectrum: Nujol mull. Transmission.
Source: Himmrich and Haeuseler (1991).
Wavenumbers (cm^{-1}): 351s, 316, 293s, 255s, 168w, 143w, 86w, 68w.

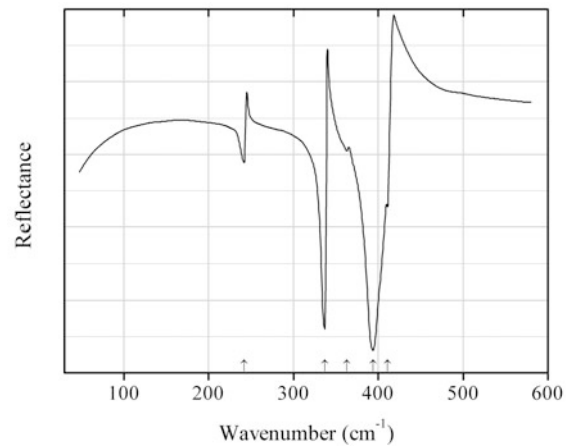

Fig. 2.1215 IR spectrum of laurite drawn using data from Lutz et al. (1985)

S506 Laurite RuS_2 (Fig. 2.1215)
Locality: Synthetic.
Description: Prepared by annealing stoichiometric mixture of the elements in an evacuated quartz tube at 800–900 °C for 14 days. Cubic. Characterized by powder X-ray diffraction data.

Kind of sample preparation and/or method of registration of the spectrum: A sample prepared by hot-pressing and polishing with diamond paste. Reflection.
Source: Lutz et al. (1985).
Wavenumbers (cm^{-1}): 411, 394s, 363w, 337s, 242.

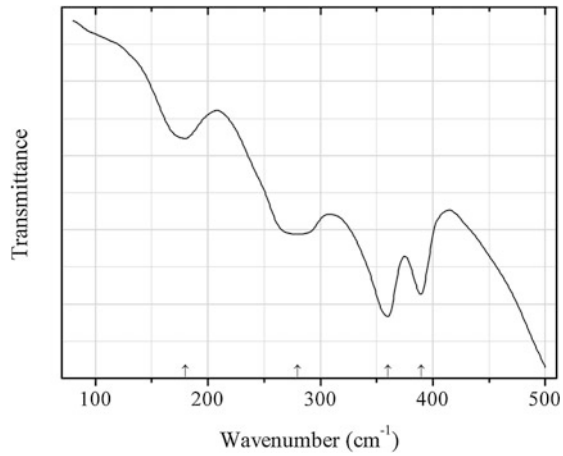

Fig. 2.1216 IR spectrum of lautite drawn using data from Povarennykh et al. (1973)

S507 Lautite CuAsS (Fig. 2.1216)
Locality: Rudolph shaft, Lauta, Marienberg district, Erzgebirge (Ore Mts.), Saxony, Germany (type locality).
Description: No data.
Kind of sample preparation and/or method of registration of the spectrum: Nujol mull. Transmission.
Source: Povarennykh et al. (1973).
Wavenumbers (cm^{-1}): 390s, 360s, 280, 180.

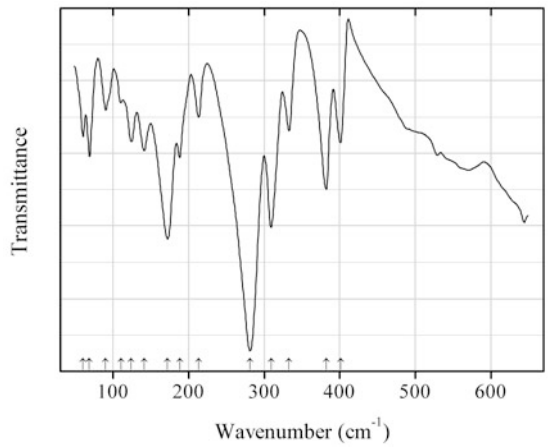

Fig. 2.1217 IR spectrum of lorándite drawn using data from Minceva-Sukarova et al. (2003)

S508 Lorándite $TlAsS_2$ (Fig. 2.1217)
Locality: Synthetic.
Description: Prepared by a solid state reaction.
Kind of sample preparation and/or method of registration of the spectrum: Nujol mull. Transmission.
Source: Minceva-Sukarova et al. (2003).
Wavenumbers (cm^{-1}): 401, 382, 333, 309s, 281s, 213, 188, 172s, 141, 124, 110w, 90w, 68.5, 60.
Note: For the IR spectrum of lorándite see also El Idrissi-Raghni et al. (1996).
Note: The wavenumbers were partly determined by us based on spectral curve analysis of the published spectrum.

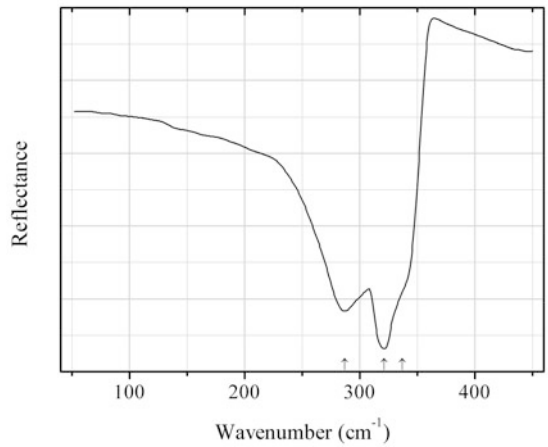

Fig. 2.1218 IR spectrum of "marmatite" drawn using data from Blagojević et al. (1991)

S509 "Marmatite" (Zn,Fe)S (Fig. 2.1218)
Locality: Synthetic.
Description: Crystals containing ~10 at.% Fe. Characterized by powder X-ray diffraction data.
Kind of sample preparation and/or method of registration of the spectrum: Reflection.
Source: Blagojević et al. (1991).
Wavenumbers (cm^{-1}): 337sh, 321s, 287s.

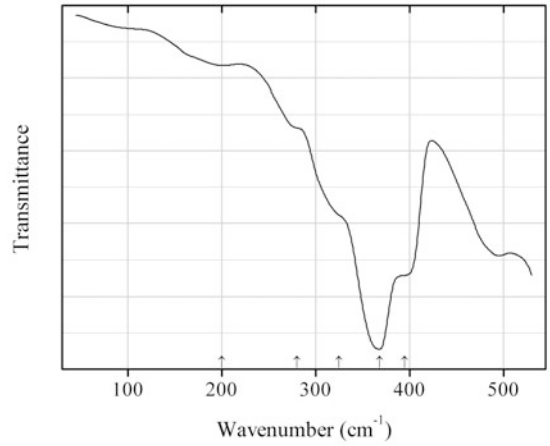

Fig. 2.1219 IR spectrum of mawsonite drawn using data from Povarennykh et al. (1973)

S510 Mawsonite $Cu_6Fe_2SnS_8$ (Fig. 2.1219)
Locality: Ikuno mine, Asago, Hyogo prefecture, Kinki region, Honshu Island, Japan.
Description: No data.
Kind of sample preparation and/or method of registration of the spectrum: Nujol mull. Transmission.
Source: Povarennykh et al. (1973).
Wavenumbers (cm^{-1}): 395sh, 368s, 325sh, 280sh, 200w.

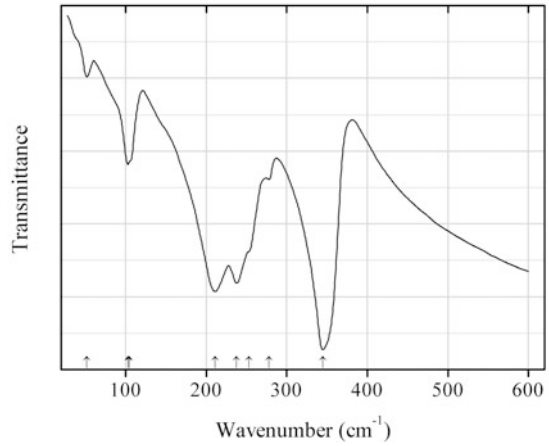

Fig. 2.1220 IR spectrum of silver mercury tin sulfide drawn using data from Himmrich and Haeuseler (1991)

S511 Silver mercury tin sulfide Ag_2HgSnS_4 (Fig. 2.1220)
Locality: Synthetic.
Description: Obtained from the stoichiometric mixture of the elements. Characterized by powder X-ray diffraction data.
Kind of sample preparation and/or method of registration of the spectrum: Nujol mull. Transmission.

Source: Himmrich and Haeuseler (1991).
Wavenumbers (cm^{-1}): 345s, 278, 253sh, 238s, 211s, 105sh, 103, 52w.

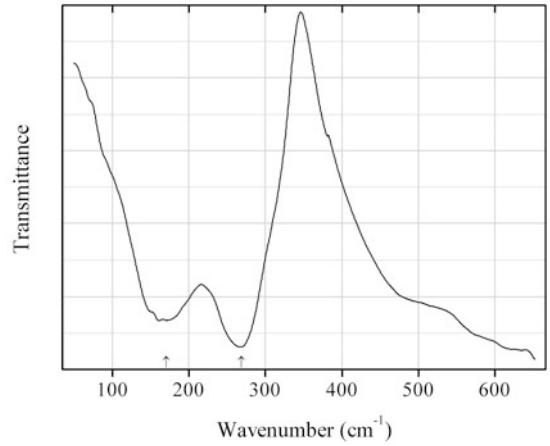

Fig. 2.1221 IR spectrum of miargyrite drawn using data from Minceva-Sukarova et al. (2003)

S512 Miargyrite $AgSbS_2$ (Fig. 2.1221)
Locality: Synthetic.
Description: Prepared by a solid state reaction.
Kind of sample preparation and/or method of registration of the spectrum: Nujol mull. Absorption.
Source: Minceva-Sukarova et al. (2003).
Wavenumbers (cm^{-1}): 269s, 171s.
Note: For the IR spectrum of miargyrite see also Golovach et al. (1976).

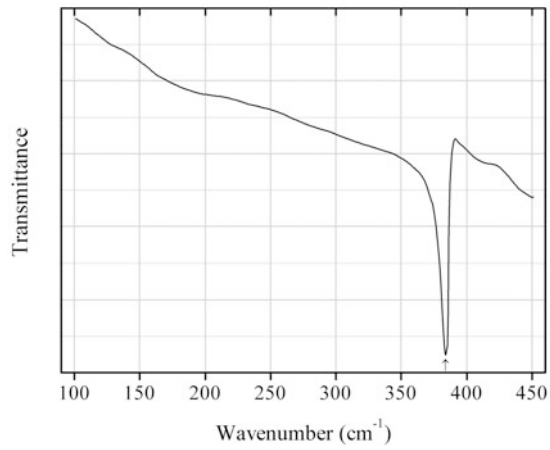

Fig. 2.1222 IR spectrum of molybdenite drawn using data from Soong and Farmer (1978)

S513 Molybdenite MoS_2 (Fig. 2.1222)
Locality: Not indicated.

Description: No data.
Kind of sample preparation and/or method of registration of the spectrum: Polyethylene disc. Absorption.
Source: Soong and Farmer (1978).
Wavenumbers (cm^{-1}): (467w), 384s.

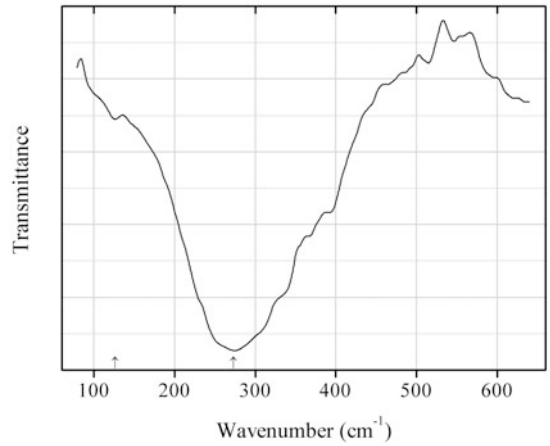

Fig. 2.1223 IR spectrum of niningerite drawn using data from Nuth et al. (1985)

S514 Niningerite MgS (Fig. 2.1223)
Locality: Synthetic.
Description: Commercial reactant containing a small admixture of MgO. Characterized by powder X-ray diffraction data.
Kind of sample preparation and/or method of registration of the spectrum: Polyethylene disc. Transmission.
Source: Nuth et al. (1985).
Wavenumbers (cm^{-1}): 273s, (126w).

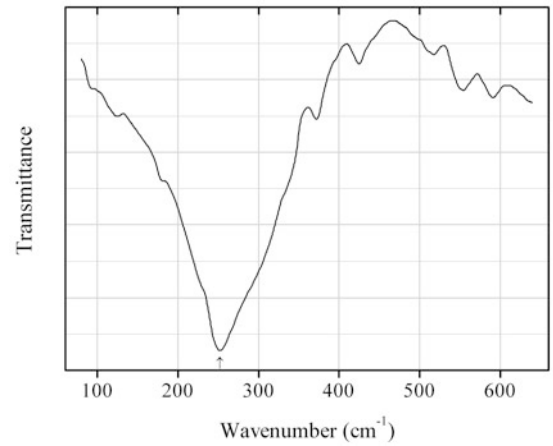

Fig. 2.1224 IR spectrum of oldhamite drawn using data from Nuth et al. (1985)

S515 Oldhamite CaS (Fig. 2.1224)
Locality: Synthetic.
Description: Commercial reactant.
Kind of sample preparation and/or method of registration of the spectrum: Polyethylene disc. Transmission.
Source: Nuth et al. (1985).
Wavenumbers (cm^{-1}): 252s.

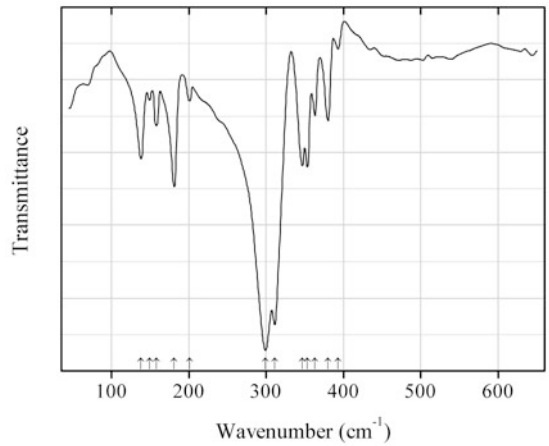

Fig. 2.1225 IR spectrum of orpiment drawn using data from Minceva-Sukarova et al. (2003)

S516 Orpiment As_2S_3 (Fig. 2.1225)
Locality: Synthetic.
Description: Prepared by a solid state reaction.
Kind of sample preparation and/or method of registration of the spectrum: Nujol mull. Absorption.
Source: Minceva-Sukarova et al. (2003).
Wavenumbers (cm^{-1}): 393w, 380, 363, 353, 347, 311s, 299s, 201w, 181, 158, 149w, 138.
Note: For the IR spectra of orpiment see also Whitfield (1971), Soong and Farmer (1978), Makreski et al. (2004).

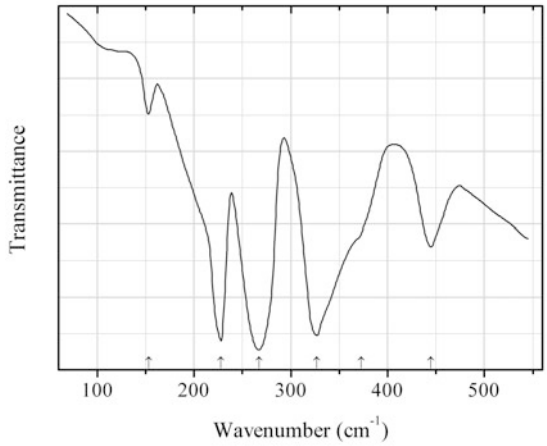

Fig. 2.1226 IR spectrum of osarsite drawn using data from Lutz et al. (1983)

S517 Osarsite OsAsS (Fig. 2.1226)
Locality: Synthetic.
Description: Prepared by heating stoichiometric mixture of the elements at 800 °C for 14 days. Characterized by powder X-ray diffraction data. Monoclinic, a = 5.933(3), b = 5.919(2), c = 6.017(2) Å, β = 112.1(2)°.
Kind of sample preparation and/or method of registration of the spectrum: Nujol mull. Transmission.
Source: Lutz et al. (1983).
Wavenumbers (cm^{-1}): 445, 373sh, 327s, 267s, 228s, 153w.

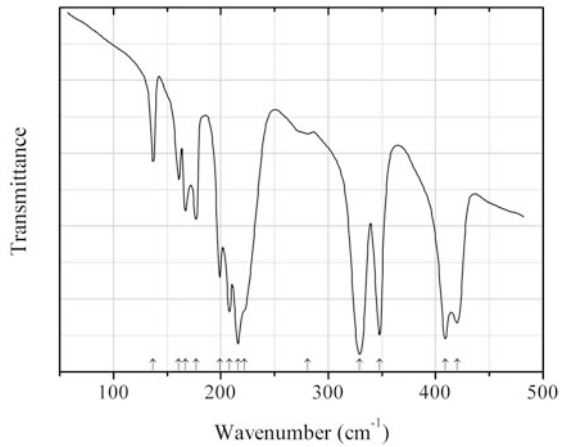

Fig. 2.1227 IR spectrum of osmium antimonide sulfide drawn using data from Lutz et al. (1983)

S518 Osmium antimonide sulfide OsSbS (Fig. 2.1227)
Locality: Synthetic.
Description: Prepared by heating stoichiometric mixture of the elements at 800 °C for 8 days. Characterized by powder X-ray diffraction data. Monoclinic, a = 6.210(1), b = 6.151(1), c = 6.227(1) Å, β = 111.7(1)°.
Kind of sample preparation and/or method of registration of the spectrum: Nujol mull. Transmission.
Source: Lutz et al. (1983).
Wavenumbers (cm^{-1}): 420s, 409s, 348s, 329s, 281w, 222sh, 216s, 208s, 199, 177, 167, 161, 137.

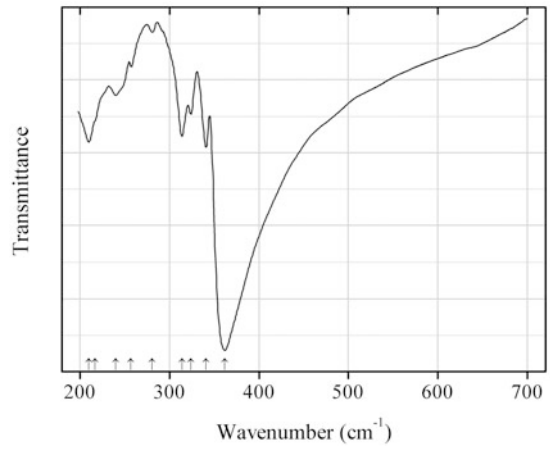

Fig. 2.1228 IR spectrum of parapierrotite drawn using data from El Idrissi-Raghni et al. (1996)

S519 Parapierrotite $TlSb_5S_8$ (Fig. 2.1228)
Locality: Synthetic.
Description: No data.
Kind of sample preparation and/or method of registration of the spectrum: Polyethylene disc. Transmission.
Source: El Idrissi-Raghni et al. (1996).
Wavenumbers (cm^{-1}): 362s, 341, 324, 314, 281w, 257w, 240, 217sh, 210.

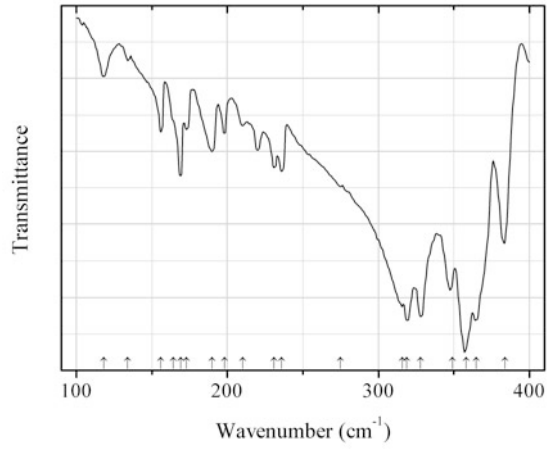

Fig. 2.1229 IR spectrum of pararealgar drawn using data from Muniz-Miranda et al. (1966)

S520 Pararealgar As_4S_4 (Fig. 2.1229)
Locality: Synthetic.

Description: The product of alteration of realgar or β-As_4S_4 under laser irradiation.
Kind of sample preparation and/or method of registration of the spectrum: Polyethylene disc. Absorption.
Source: Muniz-Miranda et al. (1996).
Wavenumbers (cm^{-1}): 384, 365sh, 358s, 349, 328s, 319s, 316sh, (275), 236, 231, 210w, 198, 190, 173, 169, 164sh, 156, 134w, 118w.
Note: The value 231 is possibly wrong (in Fig. 5 from the cited paper corresponding band is located at 220 cm^{-1}).

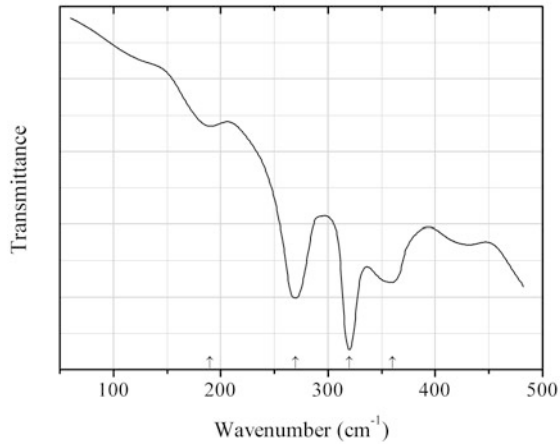

Fig. 2.1230 IR spectrum of pentlandite drawn using data from Povarennykh et al. (1973)

S521 Pentlandite $(Ni,Fe)_9S_8$ (Fig. 2.1230)
Locality: Oktyabr'skoe Cu-Ni deposit, Norilsk, Krasnoyarsk Krai, Siberia, Russia.
Description: No data.
Kind of sample preparation and/or method of registration of the spectrum: Nujol mull. Transmission.
Source: Povarennykh et al. (1973).
Wavenumbers (cm^{-1}): 360, 320s, 270s, 190w.

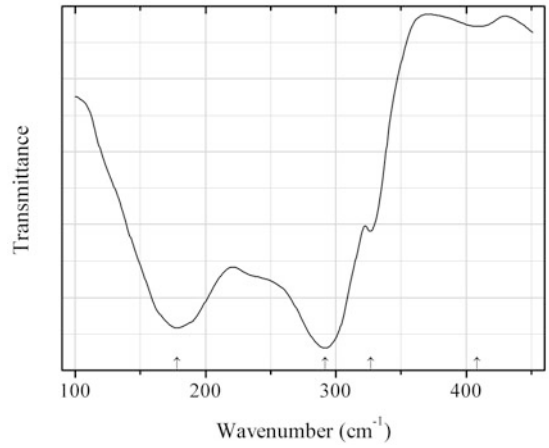

Fig. 2.1231 IR spectrum of plagionite drawn using data from Soong and Farmer (1978)

S522 Plagionite $Pb_5Sb_8S_{17}$ (Fig. 2.1231)
Locality: Not indicated.
Description: No data.
Kind of sample preparation and/or method of registration of the spectrum: Polyethylene disc. Absorption.
Source: Soong and Farmer (1978).
Wavenumbers (cm^{-1}): 408w, 327, 292s, 178s.
Note: The wavenumbers were partly determined by us based on spectral curve analysis of the published spectrum.

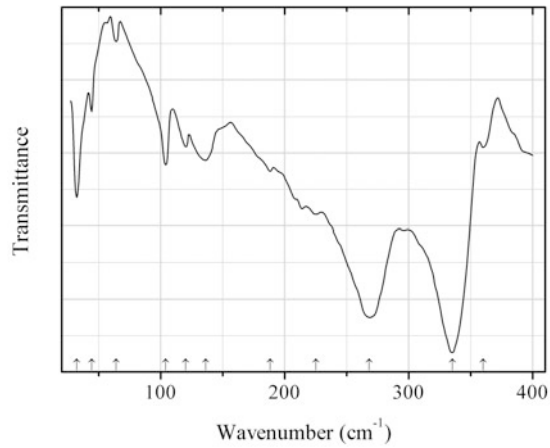

Fig. 2.1232 IR spectrum of proustite drawn using data from Byer et al. (1973)

S523 Proustite Ag_3AsS_3 (Fig. 2.1232)
Locality: Synthetic.
Description: Cylindrically shaped single crystals obtained from the Royal Radar Establishment.
Kind of sample preparation and/or method of registration of the spectrum: Nujol mull. Transmission.

Source: Byer et al. (1973).
Wavenumbers (cm^{-1}): 360w, 335s, 268s, 225, 188, 136, 120, 104, 64w, 44w, 32.
Note: For the IR spectra of proustite see also Makreski et al. (2004), Soong and Farmer (1978).

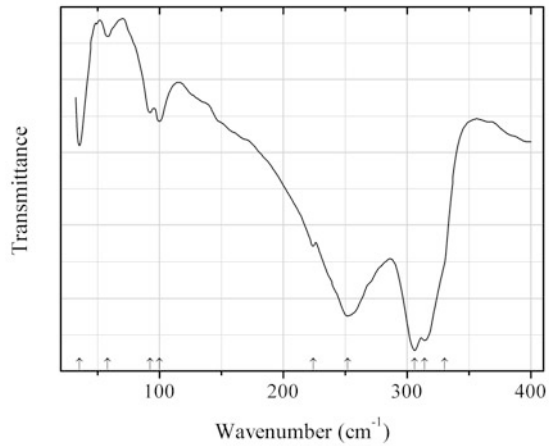

Fig. 2.1233 IR spectrum of pyrargyrite drawn using data from Byer et al. (1973)

S524 Pyrargyrite Ag_3SbS_3 (Fig. 2.1233)
Locality: Synthetic.
Description: Cylindrically shaped single crystals obtained from the Royal Radar Establishment.
Kind of sample preparation and/or method of registration of the spectrum: Nujol mull. Transmission.
Source: Byer et al. (1973).
Wavenumbers (cm^{-1}): 330sh, 314s, 306s, 252s, 224, 100, 92, 58w, 35.
Note: For the IR spectra of pyrargyrite see also Makreski et al. (2004), Soong and Farmer (1978).

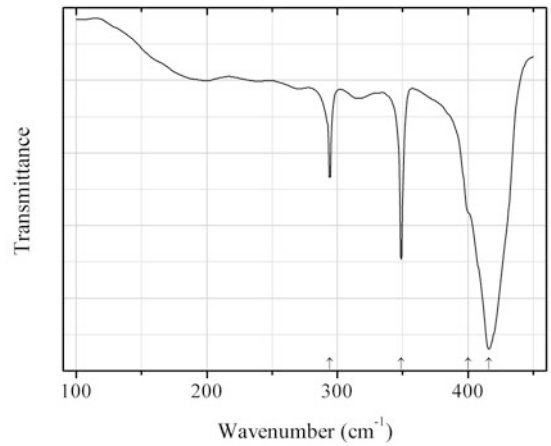

Fig. 2.1234 IR spectrum of pyrite drawn using data from Soong and Farmer (1978)

S525 Pyrite FeS_2 (Fig. 2.1234)
Locality: Not indicated.

Description: No data.
Kind of sample preparation and/or method of registration of the spectrum: Polyethylene disc. Absorption.
Source: Soong and Farmer (1978).
Wavenumbers (cm^{-1}): 416s, 400sh, 349, 294.
Note: For the IR spectrum of jamesonite see also Povarennykh et al. (1973), Brusentsova et al. (2012).

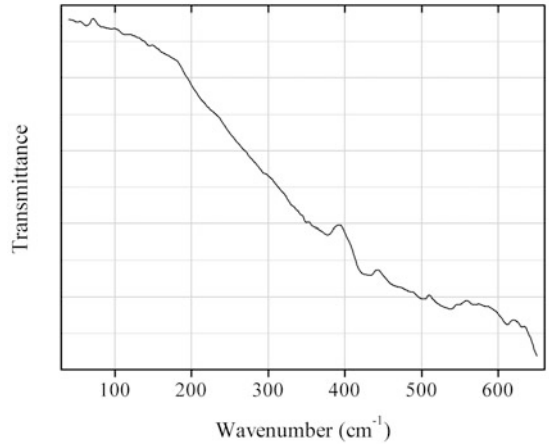

Fig. 2.1235 IR spectrum of pyrrhotite drawn using data from Brusentsova et al. (2012)

S526 Pyrrhotite Fe_7S_8 (Fig. 2.1235)
Locality: Chihuahua, Mexico.
Description: Monoclinic. The empirical formula is $Fe_{0.9}S$.
Kind of sample preparation and/or method of registration of the spectrum: Polyethylene disc. Absorption.
Source: Brusentsova et al. (2012).
Wavenumbers (cm^{-1}): The spectrum is characterized as featureless.
Note: For the IR spectrum of pyrrhotite see also Soong and Farmer (1978).

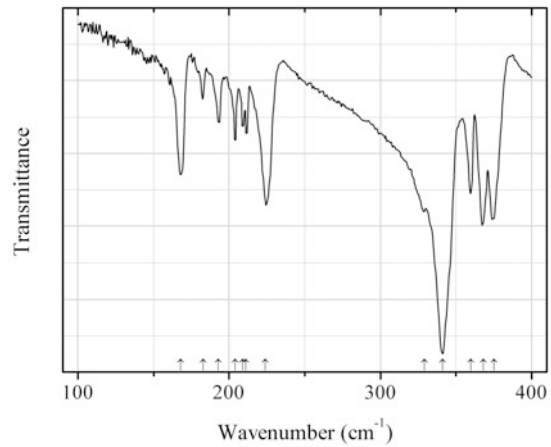

Fig. 2.1236 IR spectrum of realgar drawn using data from Muniz-Miranda et al. (1966)

S527 Realgar AsS (Fig. 2.1236)
Locality: Shiman, Hunan province, China.
Description: No data.
Kind of sample preparation and/or method of registration of the spectrum: Polyethylene disc. Absorption.
Source: Muniz-Miranda et al. (1996).
Wavenumbers (cm^{-1}): 375s, 368s, 360, 341s, 329, 224s, 211, 209, 204, 193, 183w, 168.
Note: For the IR spectrum of realgar see also Soong and Farmer (1978).

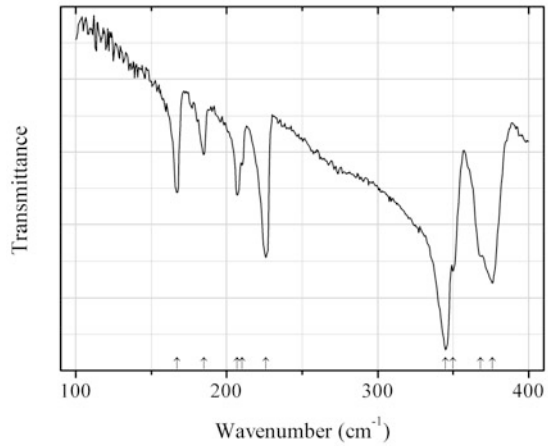

Fig. 2.1237 IR spectrum of realgar β-polymorph drawn using data from Muniz-Miranda et al. (1966)

S528 Realgar β-polymorph β-AsS (Fig. 2.1237)
Locality: Artificial.
Description: Prepared by quenching to room temperature the material obtained by heating natural realgar at 295 °C for 24 h.
Kind of sample preparation and/or method of registration of the spectrum: Polyethylene disc. Absorption.
Source: Muniz-Miranda et al. (1996).
Wavenumbers (cm^{-1}): 376s, 368sh, 350, 345s, 226, 210sh, 207, 185, 167.

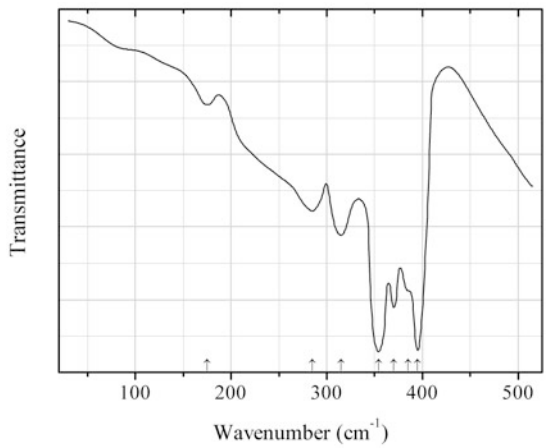

Fig. 2.1238 IR spectrum of renierite drawn using data from Povarennykh et al. (1973)

S529 Renierite $(Cu,Zn)_{11}Fe_4(Ge,As)_2S_{16}$ (Fig. 2.1238)
Locality: Tsumeb mine, Tsumeb, Namibia.
Description: No data.
Kind of sample preparation and/or method of registration of the spectrum: Nujol mull. Transmission.
Source: Povarennykh et al. (1973).
Wavenumbers (cm^{-1}): 395s, 385sh, 370s, 354s, 315, 285, 175w.
Note: For the IR spectrum of renierite see also Rama Subba Reddy et al. (2004).

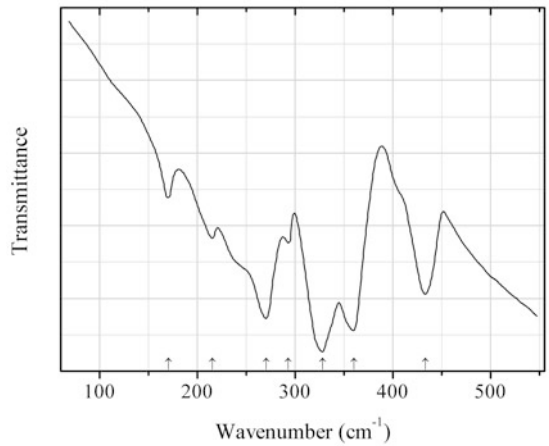

Fig. 2.1239 IR spectrum of ruarsite drawn using data from Lutz et al. (1983)

S530 Ruarsite RuAsS (Fig. 2.1239)
Locality: Synthetic.
Description: Prepared by heating stoichiometric mixture of the elements at 1000 °C for 14 days. Characterized by powder X-ray diffraction data. Monoclinic, $a = 5.934(2)$, $b = 5.913(2)$, $c = 6.016(2)$ Å, $\beta = 112.9(2)°$.
Kind of sample preparation and/or method of registration of the spectrum: Nujol mull. Transmission.
Source: Lutz et al. (1983).
Wavenumbers (cm^{-1}): 433, 360s, 328s, 293, 270s, 215w, 170w.

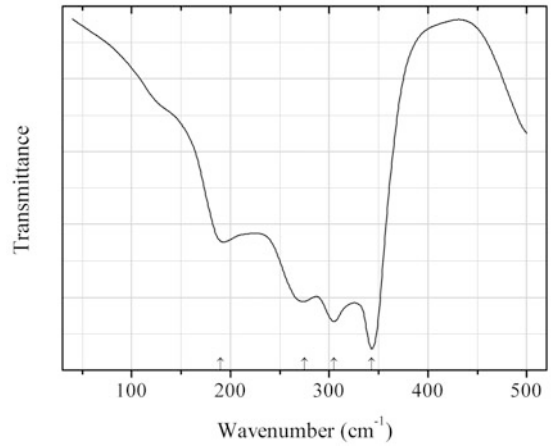

Fig. 2.1240 IR spectrum of sakuraiite drawn using data from Povarennykh et al. (1973)

S531 Sakuraiite (Cu,Zn,In,Fe,Sn)S (Fig. 2.1240)
Locality: Ikuno mine, Asago, Hyogo prefecture, Kinki region, Honshu Island, Japan.
Description: No data.
Kind of sample preparation and/or method of registration of the spectrum: Nujol mull. Transmission.
Source: Povarennykh et al. (1973).
Wavenumbers (cm^{-1}): 343s, 305, 275, 190.

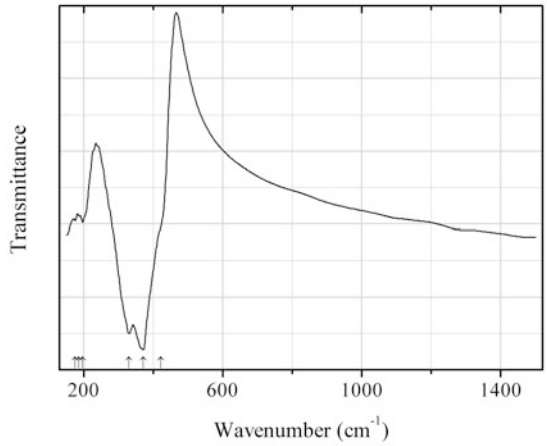

Fig. 2.1241 IR spectrum of silver gallium germanium sulfide drawn using data from Kim et al. (2008)

S532 Silver gallium germanium sulfide $AgGaGeS_4$ (Fig. 2.1241)
Locality: Synthetic.
Description: Triclinic.
Kind of sample preparation and/or method of registration of the spectrum: CsI disc. Transmission.
Source: Kim et al. (2008).
Wavenumbers (cm^{-1}): 422sh, 371s, 330s, 197, 186w, 175w.

Note: The wavenumbers were determined by us based on spectral curve analysis of the published spectrum.

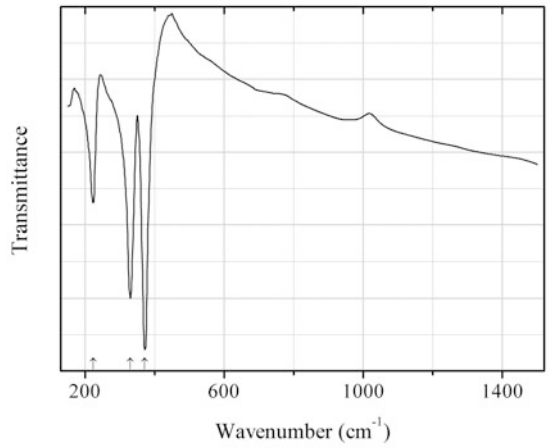

Fig. 2.1242 IR spectrum of silver gallium sulfide drawn using data from Kim et al. (2008)

S533 Silver gallium sulfide $AgGaS_2$ (Fig. 2.1242)
Locality: Synthetic.
Description: No data.
Kind of sample preparation and/or method of registration of the spectrum: CsI disc. Transmission.
Source: Kim et al. (2008).
Wavenumbers (cm^{-1}): 372s, 330s, 223.
Note: The wavenumbers were determined by us based on spectral curve analysis of the published spectrum.

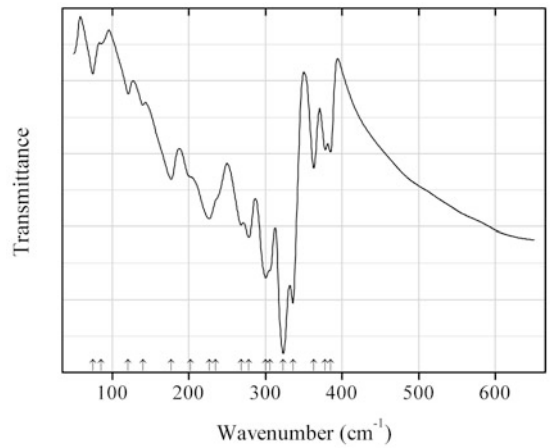

Fig. 2.1243 IR spectrum of smithite drawn using data from Minceva-Sukarova et al. (2003)

S534 Smithite $AgAsS_2$ (Fig. 2.1243)
Locality: Synthetic.

Description: Prepared by a solid state reaction.
Kind of sample preparation and/or method of registration of the spectrum: Nujol mull. Absorption.
Source: Minceva-Sukarova et al. (2003).
Wavenumbers (cm^{-1}): 385, 378, 363, 336s, 323s, 306sh, 300s, 278, 268, 235sh, 227, 202sh, 177, 140w, 121w, 86w, 75w.

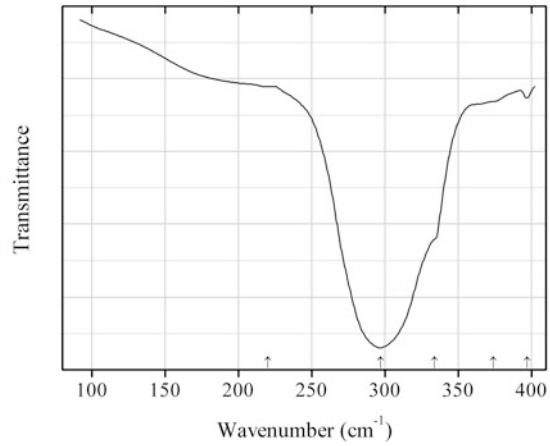

Fig. 2.1244 IR spectrum of sphalerite drawn using data from Soong and Farmer (1978)

S535 Sphalerite ZnS (Fig. 2.1244)
Locality: Not indicated.
Description: No data.
Kind of sample preparation and/or method of registration of the spectrum: Polyethylene disc. Absorption.
Source: Soong and Farmer (1978).
Wavenumbers (cm^{-1}): 397w, 374sh, 334sh, 297s, 220sh.
Note: The bands at 397 and 374 cm^{-1} were registered due to the presence of an impurity in the sample. For the IR spectrum of sphalerite see also Brusentsova et al. (2012).

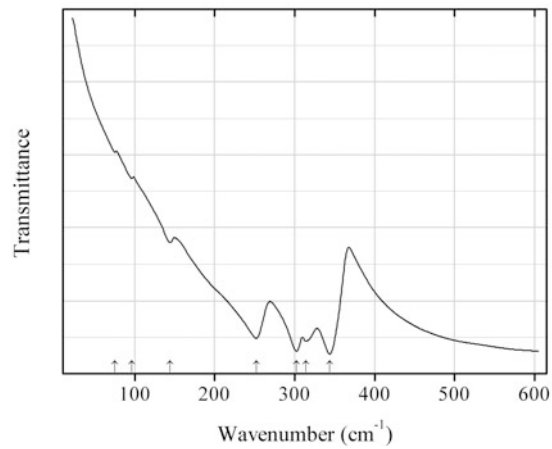

Fig. 2.1245 IR spectrum of stannite drawn using data from Himmrich and Haeuseler (1991)

S536 Stannite Cu_2FeSnS_4 (Fig. 2.1245)
Locality: Synthetic.
Description: Obtained from the stoichiometric mixture of the elements. Characterized by powder X-ray diffraction data.
Kind of sample preparation and/or method of registration of the spectrum: Nujol mull. Transmission.
Source: Himmrich and Haeuseler (1991).
Wavenumbers (cm^{-1}): 344s, 314s, 302s, 252s, 144, 96w, 75w.
Note: For the IR spectra of stannite see also Soong and Farmer (1978), Povarennykh et al. (1973).

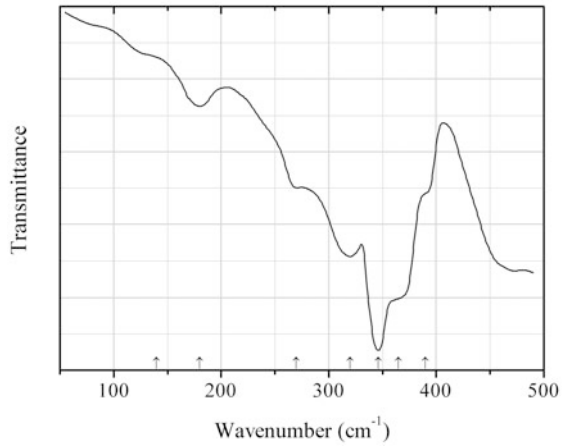

Fig. 2.1246 IR spectrum of stannoidite drawn using data from Povarennykh et al. (1973)

S537 Stannoidite $Cu_8(Fe,Cu)_3Sn_2S_{12}$ (Fig. 2.1246)
Locality: Ikuno mine, Asago, Hyogo prefecture, Kinki region, Honshu Island, Japan.
Description: No data.
Kind of sample preparation and/or method of registration of the spectrum: Nujol mull. Transmission.
Source: Povarennykh et al. (1973).
Wavenumbers (cm^{-1}): 390sh, 365sh, 346s, 320s, 270, 180, 140sh.

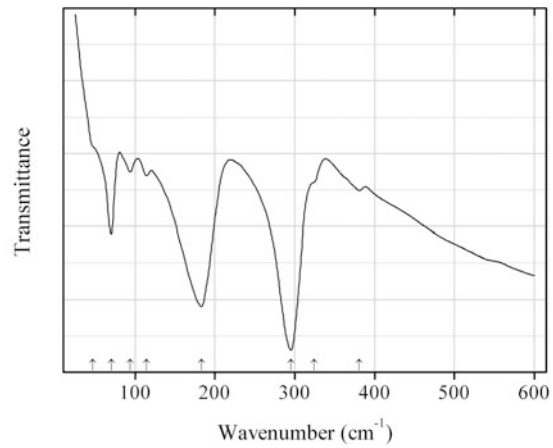

Fig. 2.1247 IR spectrum of ellisite Sb analogue drawn using data from Makreski et al. (2004)

S538 Ellisite Sb analogue Tl_3SbS_3 (Fig. 2.1247)
Locality: Synthetic.
Description: Prepared by solid-state reaction in sealed quartz tube.
Kind of sample preparation and/or method of registration of the spectrum: Nujol mull. Absorption.
Source: Makreski et al. (2004).
Wavenumbers (cm^{-1}): (381w), 324sh, 295s, 183s, 114w, 94w, 70, 47sh.

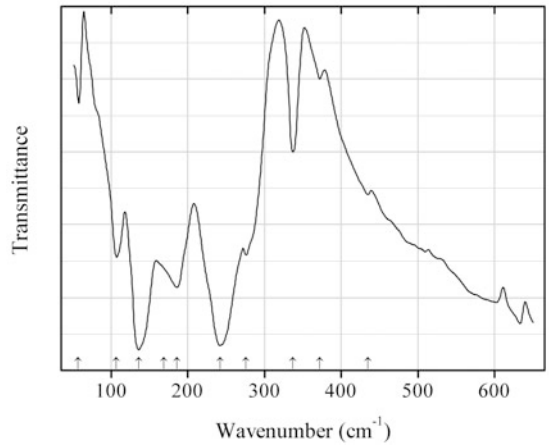

Fig. 2.1248 IR spectrum of stibnite drawn using data from Minceva-Sukarova et al. (2003)

S539 Stibnite Sb_2S_3 (Fig. 2.1248)
Locality: Synthetic.
Description: Prepared by solid state reaction.
Kind of sample preparation and/or method of registration of the spectrum: Nujol mull. Absorption.
Source: Minceva-Sukarova et al. (2003).
Wavenumbers (cm^{-1}): 435w, 372w, 337w, 276, 242s, 186, 169sh, 136s, 107, 57w.
Note: The wavenumbers were partly determined by us based on spectral curve analysis of the published spectrum. For the IR spectra of orpiment see also Soong and Farmer (1978), Makreski et al. (2004), Brusentsova (2012).

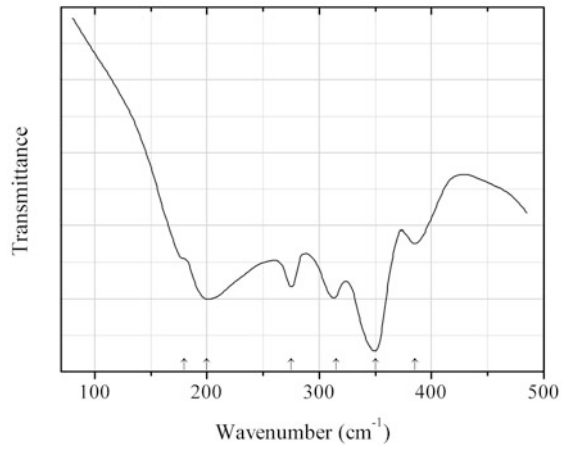

Fig. 2.1249 IR spectrum of stromeyerite drawn using data from Povarennykh et al. (1973)

S540 Stromeyerite CuAgS (Fig. 2.1249)
Locality: Sombrerete, Zacatecas, Mexico.
Description: No data.
Kind of sample preparation and/or method of registration of the spectrum: Nujol mull. Transmission.
Source: Povarennykh et al. (1973).
Wavenumbers (cm^{-1}): 385, 350s, 315, 275, 200, 180sh.

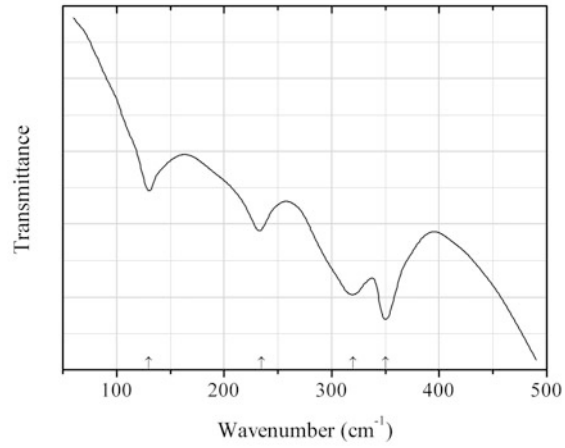

Fig. 2.1250 IR spectrum of tetradymite drawn using data from Plyusnina (1977)

S541 Tetradymite Bi_2Te_2S (Fig. 2.1250)
Locality: No data.
Description: No data.
Kind of sample preparation and/or method of registration of the spectrum: Transmission. Kind of sample preparation is not indicated.
Source: Plyusnina (1977).
Wavenumbers (cm^{-1}): 350s, 320, 235, 130.

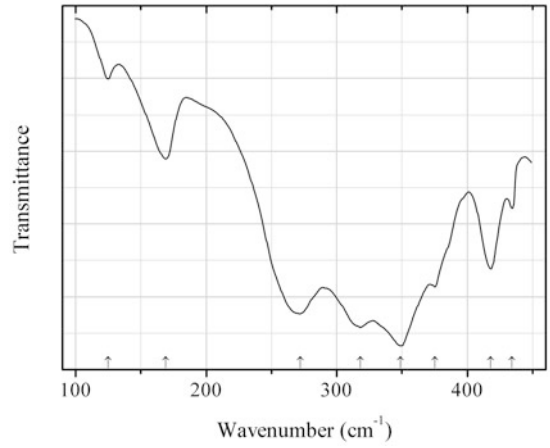

Fig. 2.1251 IR spectrum of tetrahedrite drawn using data from Soong and Farmer (1978)

S542 Tetrahedrite $Cu_6[Cu_4(Fe,Zn)_2]Sb_4S_{13}$ (Fig. 2.1251)
Locality: Not indicated.
Description: No data.
Kind of sample preparation and/or method of registration of the spectrum: Polyethylene disc. Absorption.
Source: Soong and Farmer (1978).
Wavenumbers (cm^{-1}): 434, 418, 375, 349s, 318s, 272s, 169, 125w.
Note: The bands at 418 and 348 cm^{-1} were registered due to the presence of a pyrite impurity in the sample. For the IR spectrum of tetrahedrite see also Povarennykh et al. (1973).

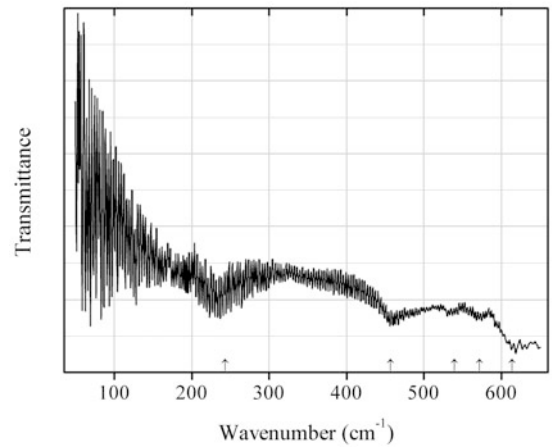

Fig. 2.1252 IR spectrum of troilite drawn using data from Kimura et al. (2005)

S543 Troilite FeS (Fig. 2.1252)
Locality: Synthetic.
Description: Commercial FeS powder.
Kind of sample preparation and/or method of registration of the spectrum: Polyethylene disc. Absorption.

Source: Kimura et al. (2005).
Wavenumbers (cm^{-1}): 614, 572, 539, 457, 243.

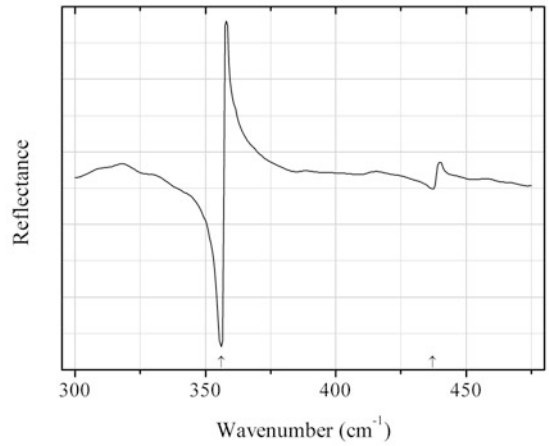

Fig. 2.1253 IR spectrum of tungstenite-2*H* drawn using data from Luttrell et al. (2006)

S544 Tungstenite-2*H* WS_2 (Fig. 2.1253)
Locality: Synthetic.
Description: Commercial reactant. Hexagonal, space group $P6_3/mmc$.
Kind of sample preparation and/or method of registration of the spectrum: Pressed disc. Reflection.
Source: Luttrell et al. (2006).
Wavenumbers (cm^{-1}): 437w, 356s.

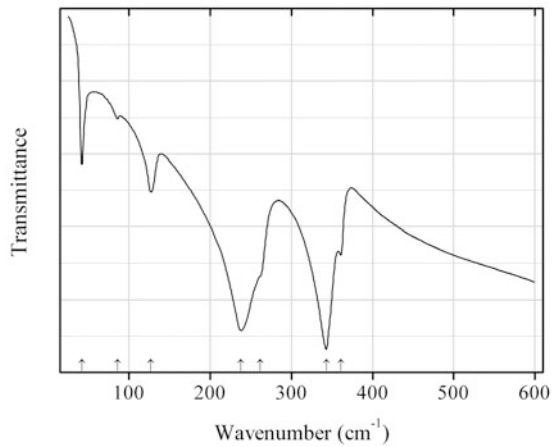

Fig. 2.1254 IR spectrum of velikite drawn using data from Himmrich and Haeuseler (1991)

S545 Velikite Cu_2HgSnS_4 (Fig. 2.1254)
Locality: Synthetic.
Description: Obtained from the stoichiometric mixture of the elements. Characterized by powder X-ray diffraction data.

Kind of sample preparation and/or method of registration of the spectrum: Nujol mull. Transmission.
Source: Himmrich and Haeuseler (1991).
Wavenumbers (cm^{-1}): 361, 343s, 262sh, 238s, 127, 86w, 42w.

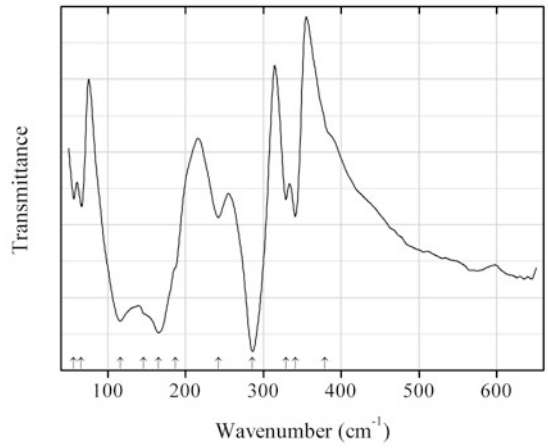

Fig. 2.1255 IR spectrum of weissbergite drawn using data from Minceva-Sukarova et al. (2003)

S546 Weissbergite $TlSbS_2$ (Fig. 2.1255)
Locality: Synthetic.
Description: Prepared by solid state reaction.
Kind of sample preparation and/or method of registration of the spectrum: Nujol mull. Absorption.
Source: Minceva-Sukarova et al. (2003).
Wavenumbers (cm^{-1}): 379sh, 341, 329, 286s, 242, 187sh, 165s, 146sh, 116s, 66, 56.

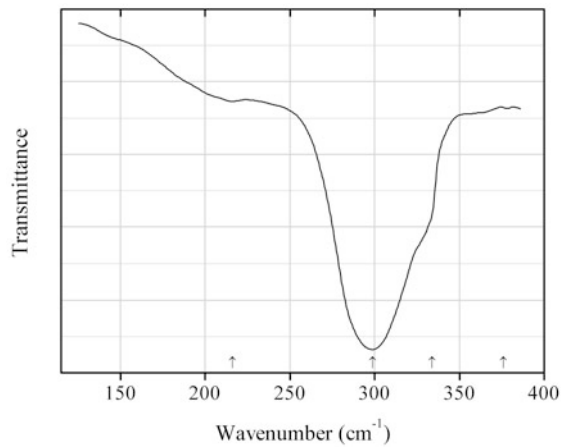

Fig. 2.1256 IR spectrum of wurtzite drawn using data from Soong and Farmer (1978)

S547 Wurtzite ZnS (Fig. 2.1256)
Locality: Not indicated.

Description: No data.
Kind of sample preparation and/or method of registration of the spectrum: Polyethylene disc. Absorption.
Source: Soong and Farmer (1978).
Wavenumbers (cm^{-1}): (376w), 334sh, 299s, 216w.
Note: For the IR spectrum of wurtzite see also Brusentsova et al. (2012).

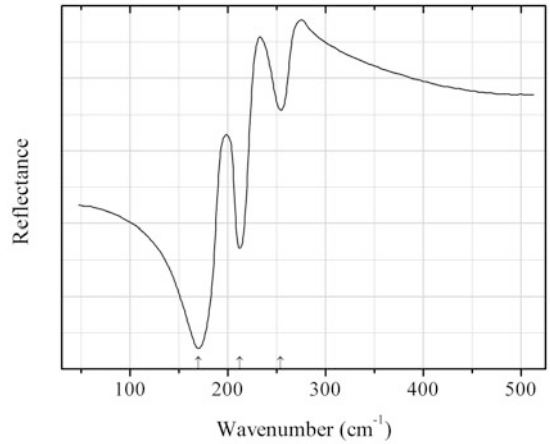

Fig. 2.1257 IR spectrum of zinc disulfide drawn using data from Anastassakis and Perry (1976)

S548 Zinc disulfide ZnS_2 (Fig. 2.1257)
Locality: Synthetic.
Description: Powdery sample. Isostructural with pyrite.
Kind of sample preparation and/or method of registration of the spectrum: Reflection.
Source: Anastassakis and Perry (1976).
Wavenumbers (cm^{-1}): 254, 212, 170s.

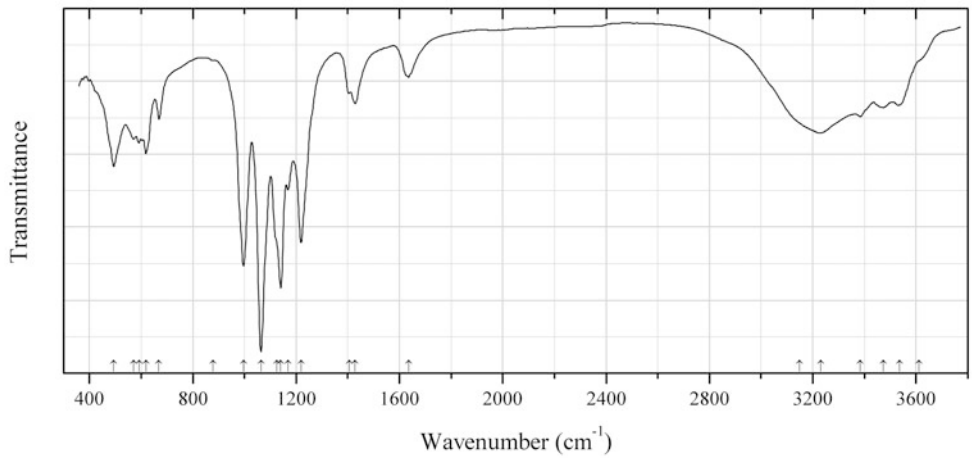

Fig. 2.1258 IR spectrum of clairite obtained by N.V. Chukanov

S549 Clairite $(NH_4)_2Fe^{3+}{}_3(SO_4)_4(OH)_3 \cdot 3H_2O$ (Fig. 2.1258)

Locality: Hilarion Mine, Agios Konstantinos (Kamariza), Lavrion District, Attikí Prefecture, Greece.
Description: Bright yellow friable aggregate of platelets from the association with goethite gypsum, chalcanthite, pyrite, chalcopyrite, and sphalerite. Investigated by I.V. Pekov. The strongest lines of the powder X-ray diffraction pattern [*d*, Å (*I*, %)] are: 17.87 (100), 8.82 (69), 8.23 (39), 7.74 (28), 7.28 (35), 4.76 (31), 4.13 (26), 3.438 (24), 3.082 (22), 3.055 (21). Confirmed by qualitative electron microprobe analyses.
Kind of sample preparation and/or method of registration of the spectrum: KBr disc. Absorption.
Wavenumbers (cm^{-1}): 3610sh, 3535, 3474, 3384, 3230, 3150sh, 1636, 1428, 1406, 1219s, 1170, 1141s, 1125sh, 1064s, 996s, 878w, 669, 619, 594, 571, 494.

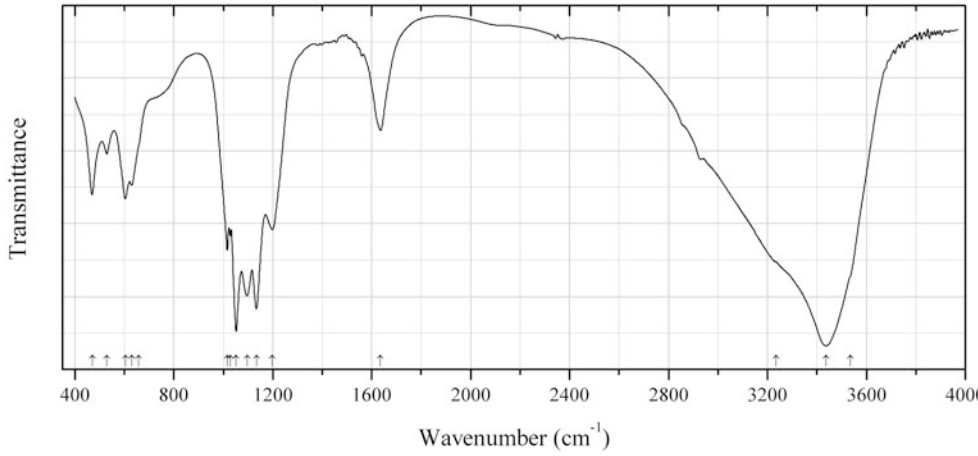

Fig. 2.1259 IR spectrum of hohmannite drawn using data from Ventruti et al. (2015)

S550 Hohmannite $Fe^{3+}{}_2(SO_4)_2O{\cdot}8H_2O$ (Fig. 2.1259)
Locality: Sierra Gorda, Antofagasta province, Antofagasta region, Chile.
Description: The crystal structure is solved. Triclinic, space group *P*-1, a = 9.1428(2), b = 10.9346 (3), c = 7.2168(2) Å, α = 90.547(1)°, β = 90.612(1)°, γ = 107.375(1)°, V = 688.46(3) Å^3, Z = 2. D_{calc} = 2.238 g/cm^3.
Kind of sample preparation and/or method of registration of the spectrum: KBr disc. Absorption.
Source: Venturi et al. (2015).
Wavenumbers (cm^{-1}): 3535sh, 3438s, 3234sh, 1636, 1198, 1134s, 1096s, 1052s, 1028, 1016, 659sh, 629, 604, 529, 470.
Note:Weak bands in the range from 2800 to 3000 cm^{-1} correspond to the admixture of an organic substance.

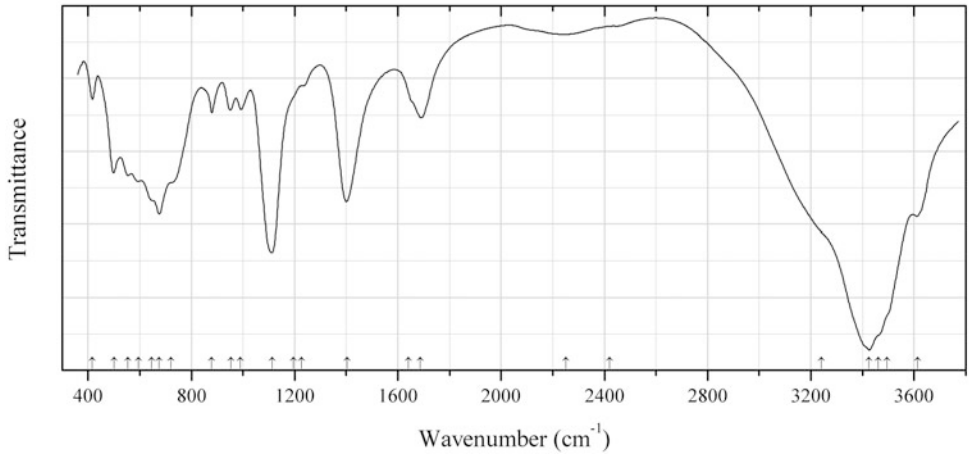

Fig. 2.1260 IR spectrum of tatarinovite obtained by N.V. Chukanov

S551 Tatarinovite $Ca_3Al(SO_4)[B(OH)_4](OH)_6 \cdot 12H_2O$ (Fig. 2.1260)
Locality: Bazhenovskoe deposit of chrysotile asbestos, city of Asbest, Sverdlovsk region, Central Urals, Russia (type locality).
Description: Colourless crystals from the association with xonotlite, diopside, and clinochlore. Cotype sample. Hexagonal, space group $P6_3$, a = 11.1110(4), c = 10.6294(6) Å, V = 1136.44(9) Å^3, Z = 2. D_{meas} = 1.79(1) g/cm^3, D_{calc} = 1.777 g/cm^3. Optically uniaxial (+), ω = 1.475(2), ε = 1.496. The empirical formula is $H_{31.41}Ca_{3.00}(Al_{0.76}Si_{0.25})(B_{0.72}S_{0.65}C_{0.59})O_{24.55}$. The crystal-chemical formula refined from single-crystal structural data is $Ca_3(Al_{0.70}Si_{0.30})\{(SO_4)_{0.34}[B(OH)_4]_{0.33}(CO_3)_{0.24}\}\{[B(OH)_4]_{0.34}(SO_4)_{0.30}(CO_3)_{0.30}[B(OH)_3]_{0.06}\}[(OH)_{5.73}O_{0.27}]\cdot 12H_2O$. The strongest lines of the powder X-ray diffraction pattern [*d*, Å (*I*, %) (*hkl*)] are: 9.63 (100) (100), 5.556 (30) (110), 4.654 (14) (102), 3.841 (21) (112), 3.441 (12) (211), 2.746 (10) (302), 2.538 (12) (213).
Kind of sample preparation and/or method of registration of the spectrum: KBr disc. Absorption.
Wavenumbers (cm^{-1}): 3614s, 3495sh, 3460sh, 3425s, 3240sh, 2420w, 2252w, 1686, 1640sh, 1403s, 1227w, 1195sh, 1114s, 991, 953, 879, 720sh, 675s, 645sh, 595, 555, 501, 417.

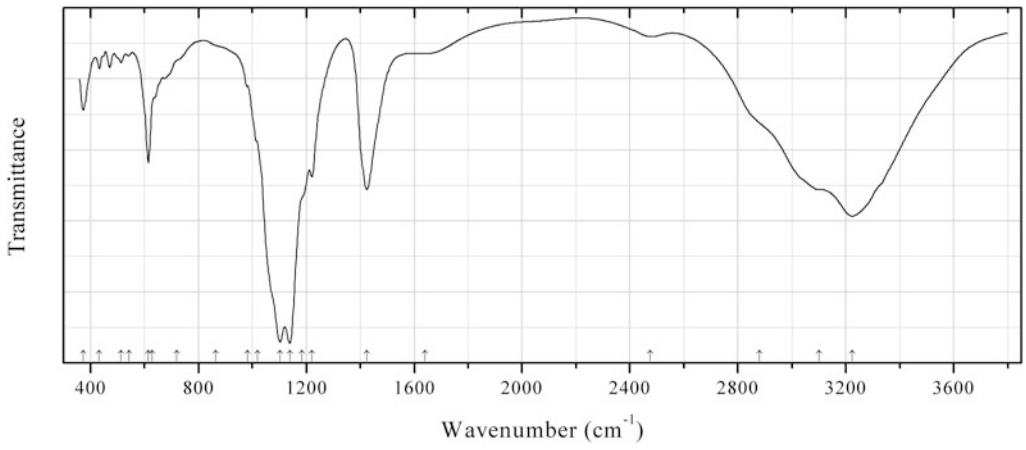

Fig. 2.1261 IR spectrum of aluminopyracmonite obtained by N.V. Chukanov

S552 Aluminopyracmonite $(NH_4)_3Al(SO_4)_3$ (Fig. 2.1261)
Locality: Pécs-Vasas, Pécs, Mecsek Mts., Baranya Co., Hungary.
Description: White crust from the association with godovikovite, chermigite, and ammonioalunite. Investigated by A.V. Kasatkin. The empirical formula is (electron microprobe, mean of 3 spot analyses): $(NH_4)_{3-x}K_{0.08}Al_{0.97}(S_{1.00}O_4)$. Confirmed by powder X-ray diffraction data.
Kind of sample preparation and/or method of registration of the spectrum: KBr disc. Absorbance.
Wavenumbers (cm^{-1}): 3225s, 3102s, 2880sh, 2475w, (~1640w), 1424s, 1221, 1185sh, 1139s, 1103s, 1020sh, 983, 865sh, 720sh, 630sh, 615, 542w, 514w, 433w, 374.
Note: The weak band at ~1650 cm^{-1} corresponds to the admixture of a hydrous sulfate. For aluminopyracmonite from its type locality (La Fossa crater, Vulcano island, Sicily, Italy) with the empirical formula $(NH_4)_{2.89}K_{0.10}Al_{1.18}Fe_{0.01}S_{2.91}O_{12}$ bands of NH_4^+ cations are located at 3208, 3048 and 1421 cm^{-1} (Demartin et al. 2013).

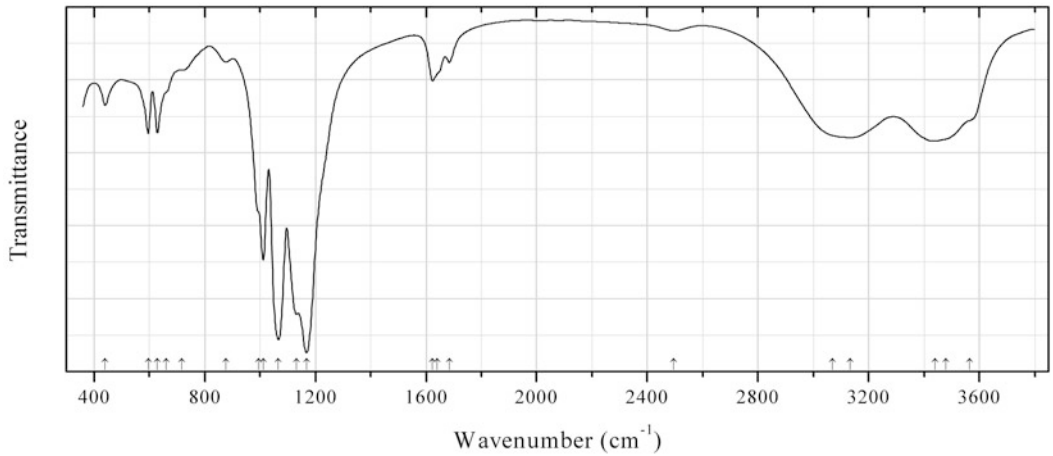

Fig. 2.1262 IR spectrum of magnesiovoltaite obtained by N.V. Chukanov

S553 Magnesiovoltaite $K_2Mg_5Fe^{3+}{}_3Al(SO_4)_{12}\cdot 18H_2O$ (Fig. 2.1262)
Locality: Alcaparrosa mine, Cerritos Bayos, Calama, El Loa province, Antofagasta region, Chile (type locality).
Description: Amber yellow crystals from the association with coquimbite and quenstedtite. Holotype sample. Cubic, space group *Fd*-3*c*, *a* = 27.1614(13). According to Mössbauer spectroscopic data, all iron is trivalent. The empirical formula is (electron microprobe): $(K_{1.9}Na_{0.1})(Mg_{4.3}Mn_{0.4}Zn_{0.2})Fe^{3+}{}_{3.2}Al_{0.9}(SO_4)_{12.0}\cdot nH_2O$.
Kind of sample preparation and/or method of registration of the spectrum: KBr disc. Absorbance.
Wavenumbers (cm^{-1}): 3565sh, 3480sh, 3441, 3134, 3070sh, 2496w, 1684, 1640sh, 1624, 1168s, 1133s, 1067s, 1011s, 995sh, 876w, 718w, 660sh, 629, 596, 440.

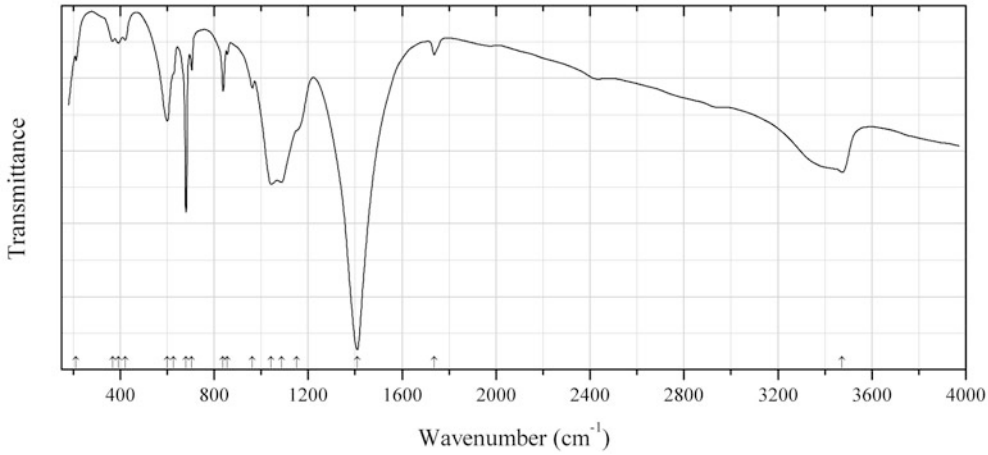

Fig. 2.1263 IR spectrum of leadhillite drawn using data from Russell et al. (1984)

SC15 Leadhillite $Pb_4(SO_4)(CO_3)_2(OH)_2$ (Fig. 2.1263)
Locality: Leadhills, Lanarkshire, Scotland, UK (type locality).
Description: Pale yellow. Biaxial.
Kind of sample preparation and/or method of registration of the spectrum: CsI disc. Transmission.
Source: Russell et al. (1984).
Wavenumbers (cm^{-1}): 3474, 1737w, 1409s, 1150sh, 1087s, 1042s, 963, 856w, 838, 705w, 680s, 627sh, 600, 422w, 392w, 367w, 212.

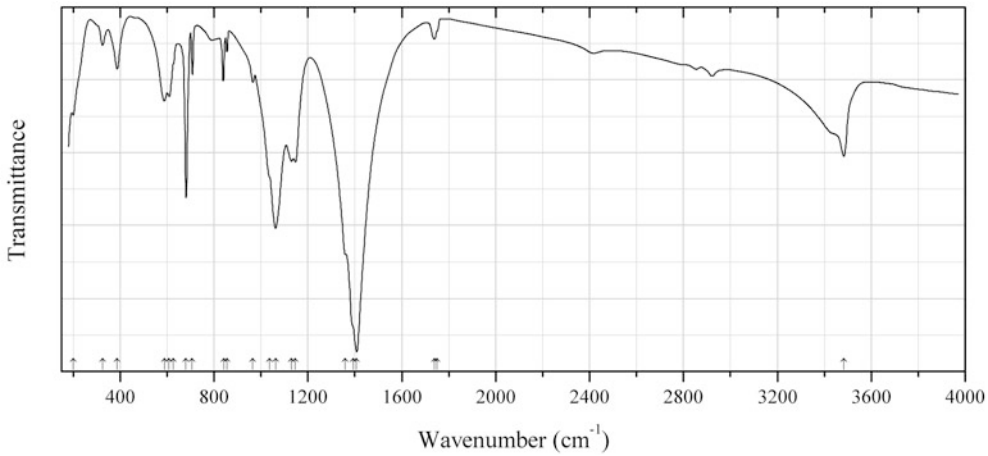

Fig. 2.1264 IR spectrum of macphersonite drawn using data from Russell et al. (1984)

SC16 Macphersonite $Pb_4(SO_4)(CO_3)_2(OH)_2$ (Fig. 2.1264)
Locality: Leadhills, Lanarkshire, Scotland, UK (type locality).
Description: Confirmed by powder X-ray diffraction data.
Kind of sample preparation and/or method of registration of the spectrum: CsI disc. Transmission.
Source: Russell et al. (1984).

Wavenumbers (cm^{-1}): 3484, 1751w, 1739w, 1408s, 1393sh, 1360sh, 1147, 1130, 1063s, 1037sh, 966w, 855w, 841, 707, 681s, 627sh, 609, 588, 387, 325w, 200.

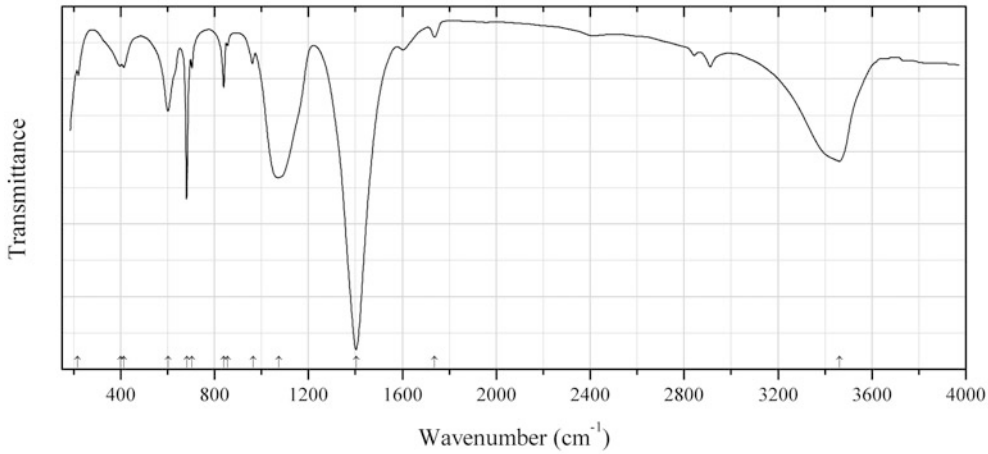

Fig. 2.1265 IR spectrum of susannite drawn using data from Russell et al. (1984)

SC17 Susannite $Pb_4(SO_4)(CO_3)_2(OH)_2$ (Fig. 2.1265)
Locality: Leadhills, Lanarkshire, Scotland, UK (type locality).
Description: Green. Uniaxial.
Kind of sample preparation and/or method of registration of the spectrum: CsI disc. Transmission.
Source: Russell et al. (1984).
Wavenumbers (cm^{-1}): 3462s, 1737w, 1404s, 1074s, 964w, 855w, 839, 704w, 682s, 602, 413, 400, 217w.

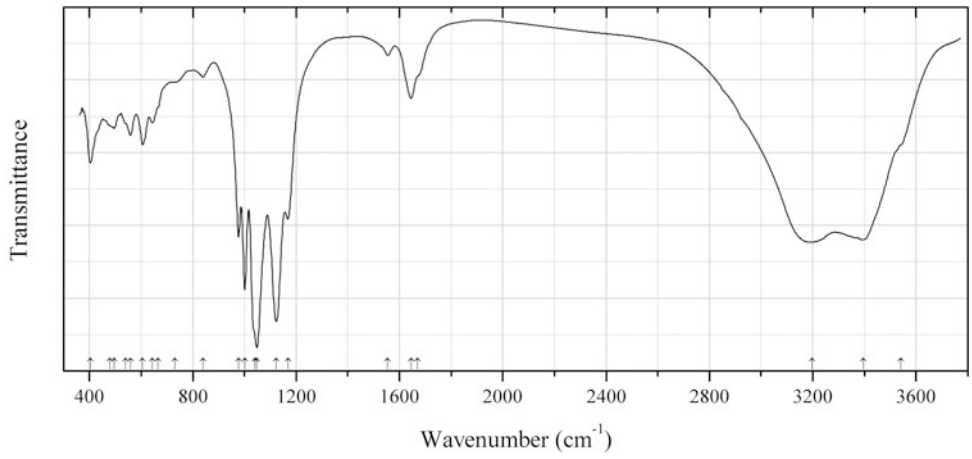

Fig. 2.1266 IR spectrum of destinezite obtained by N.V. Chukanov

SP17 Destinezite $Fe^{3+}{}_2(PO_4)(SO_4)(OH)\cdot 6H_2O$ (Fig. 2.1266)
Locality: Morro Mejillones, Mejillones peninsula, Mejillones, Antofagasta, II Region, Chile.
Description: Orange crystals from the association with gypsum. Confirmed by the IR spectrum.

Kind of sample preparation and/or method of registration of the spectrum: KBr disc. Absorption.
Wavenumbers (cm^{-1}): 3540sh, 3396s, 3197s, 1670sh, 1646, 1555w, 1168, 1123s, 1048s, 1040sh, 1001s, 977s, 839w, 730w, 665sh, 644, 606, 559, 540sh, 495, 480sh, 403.

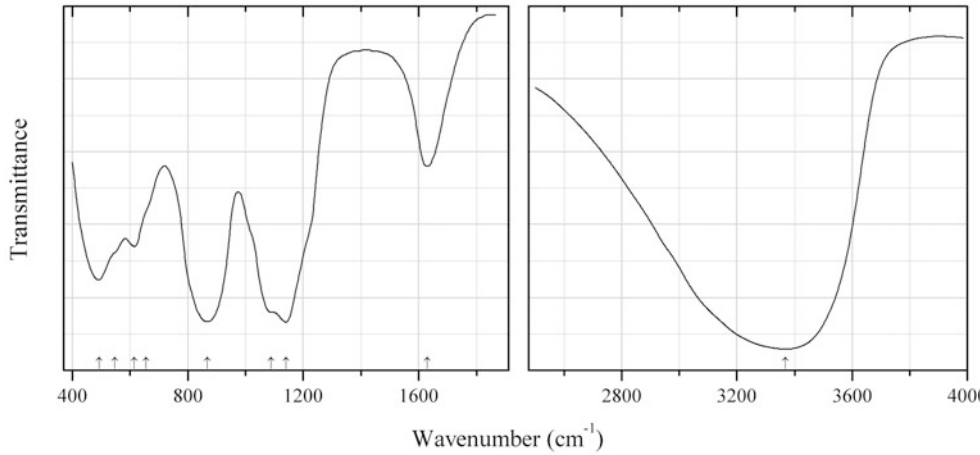

Fig. 2.1267 IR spectrum of diadochite drawn using data from Ugarte and Monhemius (1992)

SP18 Diadochite (?) $Fe^{3+}{}_2(PO_4)(SO_4)(OH)\cdot 6H_2O$ (Fig. 2.1267)
Locality: Not indicated.
Description: No data.
Kind of sample preparation and/or method of registration of the spectrum: Transmission. Kind of sample preparation is not indicated.
Source: Ugarte and Monhemius (1992).
Wavenumbers (cm^{-1}): 3368s, 1630, 1140s, 1089sh, 867s, 655sh, 615, 547sh, 494.
Note: The wavenumbers were determined by us based on spectral curve analysis of the published spectrum. In the cited paper, this sample was attributed to destinezite, but taking into account diffuse character of the spectrum, one can suppose that the matter is diadochite, i.e. amorphous analogue of destinezite.

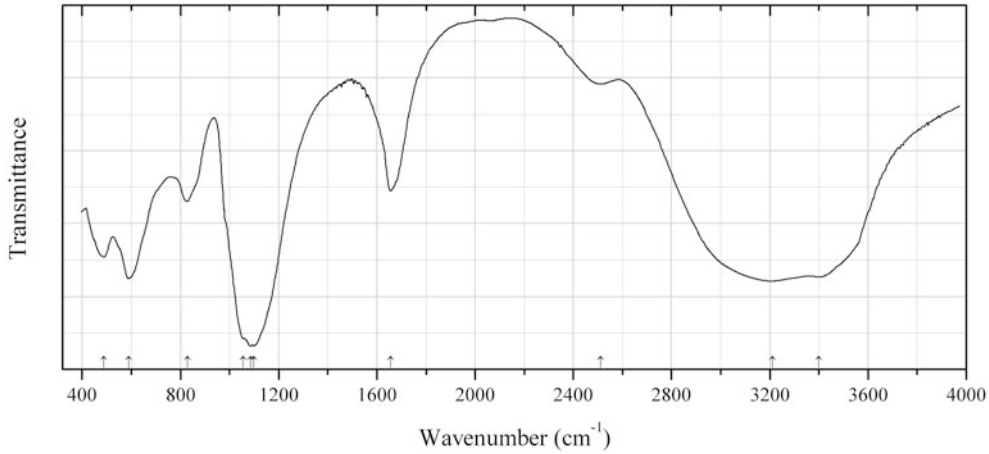

Fig. 2.1268 IR spectrum of arangasite drawn using data from Gamyanin et al. (2013)

SP19 Arangasite $Al_2(SO_4)(PO_4)F{\cdot}7.5H_2O$ (Fig. 2.1268)
Locality: Alaskitovoe deposit, Indigirka river basin, Eastern Sakha Republic (Yakutia), Russia (type locality).
Description: White compact aggregate of lamellar crystals from the oxidation zone of a cassiterite-silicate-sulfide ore body. Associated minerals are gypsum, P-bearing scorodite, jarosite, and fluellite. Holotype sample. Monoclinic, space group $P2_1$, a = 9.740(5), b = 19.31(1), c = 10.688 (5) Å, β = 98.65(8)°, V = 1987.3 Å^3. The strongest lines of the powder X-ray diffraction pattern [d, Å (I, %)] are: 10.57 (36), 9.60 (100), 7.123 (23), 5.295 (34), 4.695 (17), 4.191 (29), 3.218 (50), 2.870 (20).
Kind of sample preparation and/or method of registration of the spectrum: KBr disc. Transmission.
Source: Gamyanin et al. (2013).
Wavenumbers (cm^{-1}): 3399s, 3211s, 2510w, 1655, 1100s, 1086s, 1056s, 828, 589s, 488.
Note: The wavenumbers were partly determined by us based on spectral curve analysis of the published spectrum.

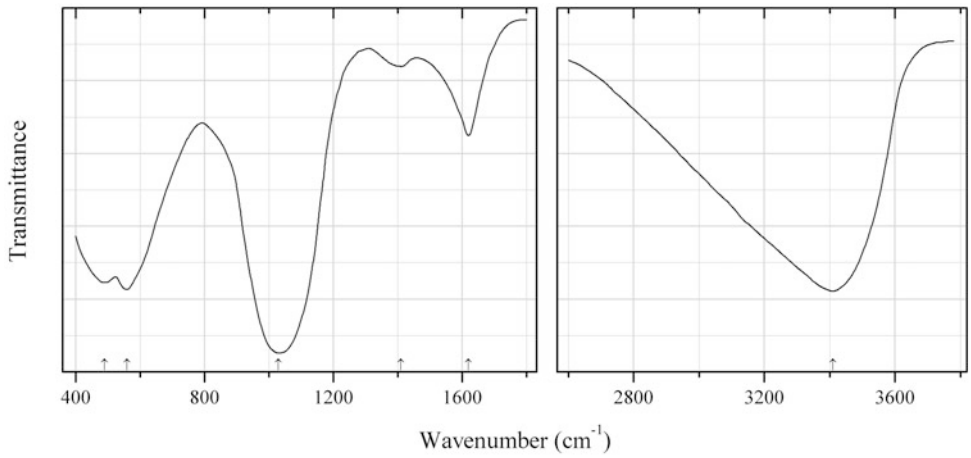

Fig. 2.1269 IR spectrum of "bořickýite" drawn using data from Čech and Povondra (1979)

SP20 "Bořickýite" $(Ca,Mg)(Fe^{3+},Al)_4(PO_4,SO_4,CO_3)_2(OH)_8{\cdot}nH_2O$ (?) (Fig. 2.1269)
Locality: Trubín, central Bohemia, Czech Republic.
Description: Specimen No. 14573 from the Department of Mineralogy of the Charles University, Prague. Reddish brown nodule. Amorphous to X-rays. The mean refractive index is between 1.625 and 1.630. Confirmed by the chemical analysis and thermal data.
Kind of sample preparation and/or method of registration of the spectrum: KBr disc. Transmission.
Source: Čech and Povondra (1979).
Wavenumbers (cm^{-1}): 3410s, 1620, 1410w, 1030s, 560s, 490s.
Note: Probably "Bořickýite" can be considered as a variety of delvauxite.

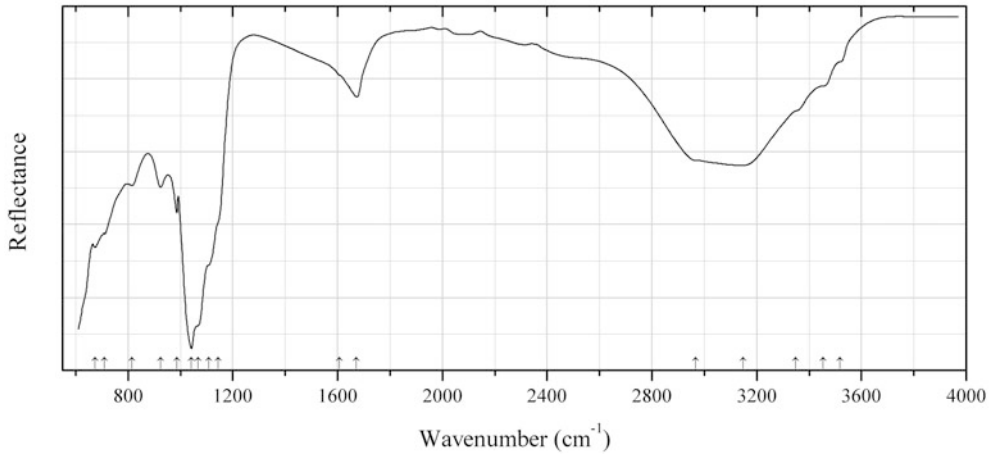

Fig. 2.1270 IR spectrum of rossiantonite drawn using data from Galli et al. (2013)

SP21 Rossiantonite $Al_3(PO_4)(SO_4)_2(OH)_2 \cdot 14H_2O$ (Fig. 2.1270)
Locality: Akopan-Dal Cin cave system, Chimanta massif, Guyana Shield, Venezuela (type locality).
Description: Colourless crystals from the association with gypsum, sanjuanite, alunite, quartz, and amorphous silica. Holotype sample. Triclinic, space group *P*-1, a = 10.3410(5), b = 10.9600(5), c = 11.1446(5) Å, α = 86.985(2)°, β = 65.727(2)°, γ = 75.064(2)°, V = 1110.5(1) Å^3, Z = 2. D_{calc} = 1.958 g/cm^3. Mean refractive index is 1.504. The empirical formula is $Al_{2.96}Fe_{0.03}P_{1.01}S_{2.00}H_{30.02}O_{28}$. The strongest lines of the powder X-ray diffraction pattern [*d*, Å (*I*, %) (*hkl*)] are: 9.12 (56) (100), 8.02 (40) (110), 7.12 (33) (011), 4.647 (100) (210), 4.006 (53) (220).
Kind of sample preparation and/or method of registration of the spectrum: Attenuated total reflection of powdered mineral.
Source: Galli et al. (2013).
Wavenumbers (cm^{-1}): 3519w, 3454sh, 3349sh, 3148, 2968sh, 1672, 1608sh, 1143sh, 1109sh, 1067sh, 1042s, 986, 925, 815w, 709sh, 674.
Note: The wavenumbers were partly determined by us based on spectral curve analysis of the published spectrum. The band position denoted by Galli et al. (2013) as 968 cm^{-1} was determined by us at 925 cm^{-1}.

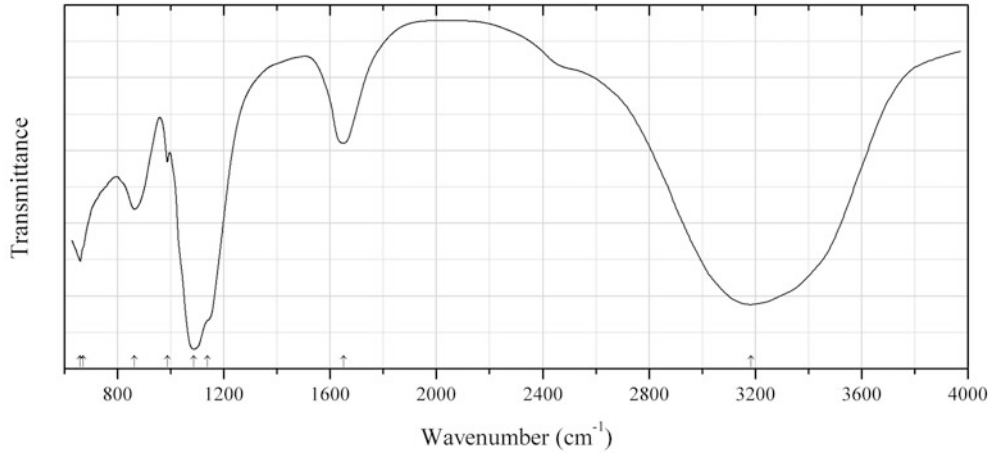

Fig. 2.1271 IR spectrum of sanjuanite drawn using data from De Abeledo et al. (1968)

SP22 Sanjuanite $Al_2(PO_4)(SO_4)(OH)\cdot 9H_2O$ (Fig. 2.1271)
Locality: 45 km SSW from San Juan City, eastern slope of Sierra Chica de Zonda, Department of Pocito, San Juan province, Argentina (type locality).
Description: White, compact masses from the association with gypsum. Holotype sample. The strongest lines of the powder X-ray diffraction pattern [*d*, Å (*I*, %)] are: 10.77 (100), 8.66 (30), 5.28 (38), 4.32 (36), 4.27 (30), 4.13 (55), 3.59 (30), 3.45 (35).
Kind of sample preparation and/or method of registration of the spectrum: KBr disc. Transmission.
Source: De Abeledo et al. (1968).
Wavenumbers (cm^{-1}): 3185s, 1650, 1139sh, 1087s, 987w, 864, 671sh, 659.
Note: The wavenumbers were determined by us based on spectral curve analysis of the published spectrum.

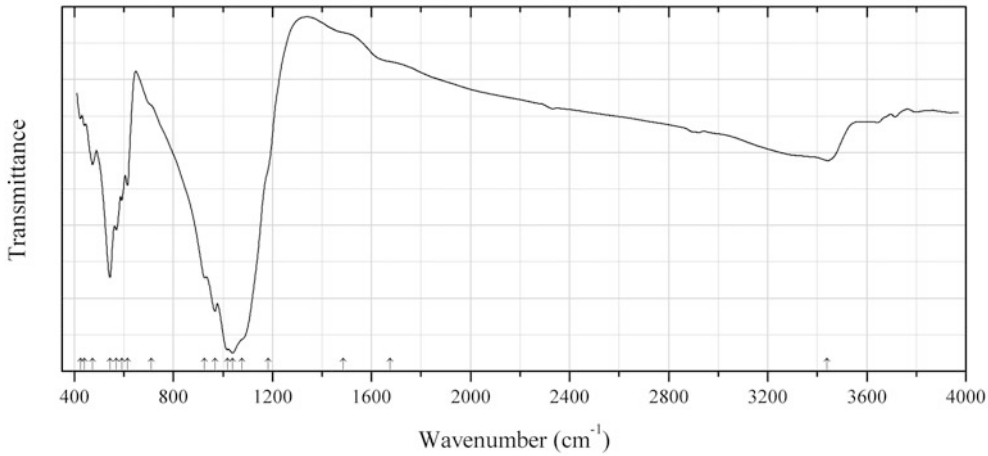

Fig. 2.1272 IR spectrum of tsumebite drawn using data from Ohnishi and Shimobayashi (2011)

SP23 Tsumebite $Pb_2Cu(PO_4)(SO_4)(OH)$ (Fig. 2.1272)
Locality: Kisamori mine, Kyowa Funaoka, near Daisen, Akita Prefecture, Japan.
Description: Emerald green nodular aggregates of platy crystals from the association with pyromorphite, quartz, limonite, and a clay mineral. Monoclinic, a = 7.850(2), b = 5.797(1), c = 8.712(2) Å, β = 111.92(2)°, V = 367.8(1) $Å^3$, Z = 2. D_{calc} = 6.23 g/cm^3. Optically biaxial (−), α = 1.554(2), β = 1.558(2), γ = 1.566(2), 2 V = 70(5)°. The empirical formula is $Pb_{2.02}(Cu_{0.99}Al_{0.01}Zn_{0.01})(PO_4)_{1.01}(SO_4)_{0.96}(OH)_{1.12}$. The strongest lines of the powder X-ray diffraction pattern [*d*, Å (*I*, %) (*hkl*)] are: 4.72 (31) (011), 3.246 (100) (−211), 2.943 (31) (−212), 2.905 (97) (−103), 2.721 (36) (112), 2.268 (38) (220).
Kind of sample preparation and/or method of registration of the spectrum: KBr disc. Transmission.
Source: Ohnishi and Shimobayashi (2011).
Wavenumbers (cm^{-1}): 3440, 1676sh, 1485sh, 1182sh, 1076sh, 1040s, 1020sh, 968s, 926s, 710sh, 615, 592, 570, 545s, 473, 441w, 425w.

Note: The wavenumbers were partly determined by us based on spectral curve analysis of the published spectrum.

SP24 Xiangjiangite $Fe^{3+}(UO_2)_4(PO_4)_2(SO_4)_2(OH)\cdot 22H_2O$
Locality: Jinyinzhai (Chenxian) mine, Suxian district, Chenzhou prefecture, Hunan province, China (type locality).
Description: Yellow powdery aggregate. Holotype sample. Pseudotetragonal, $a \approx b \approx 7.17$, $c = 22.22$ Å. $D_{meas} = 2.9–3.1$ g/cm^3. Optically biaxial (−), $\alpha = 1.558$, $\beta = 1.576$, $\gamma = 1.593$. The strongest lines of the powder X-ray diffraction pattern [*d*, Å (*I*, %)] are: 11.11 (100), 5.58 (80), 3.743 (80), 3.313 (80), 2.96 (70), 4.621 (60), 4.119 (60), 2.179 (50), 2.063 (50).
Kind of sample preparation and/or method of registration of the spectrum: Absorption.
Source: Hunan 230 Institute and X-ray Laboratory, Wuhan Geologic College (1978).
Wavenumbers (cm^{-1}): 3390s, 1617, 1044s, 923s, 613, 534, 468, 264s.

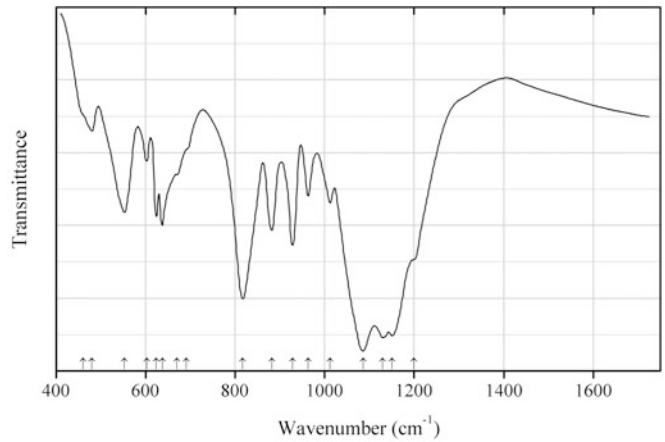

Fig. 2.1273 IR spectrum of vergasovaite obtained by N.V. Chukanov

SMo1 Vergasovaite $Cu_3(MoO_4)(SO_4)O$ (Fig. 2.1273)
Locality: Fumarole Treshchina, Second Cinder Cone, Northern Break of the Large Fissure Tolbachik Eruption, Tolbachik volcano, Kamchatka peninsula, Russia (type locality).
Description: Olive-green crystals from the association with chalcocyanite, dolerophanite, euchlorine, fedotovite, tenorite, anglesite, etc. Holotype sample. Orthorhombic, space group *Pnma*, $a = 7.421(2)$, $b = 6.754(3)$, $c = 13.624(5)$ Å, $Z = 4$. $D_{calc} = 4.32$ g/cm^3. The empirical formula is (electron microprobe): $Pb_{0.01}(Cu_{2.82}Zn_{0.10})_2[(MoO_4)_{0.79}(SO_4)_{0.20}(VO_4)_{0.04}](SO_4)O_{1.00}$. The strongest lines of the powder X-ray diffraction pattern [*d*, Å (*I*, %)] are: 3.71 (30), 3.391 (60), 3.342 (60), 3.077 (100), 2.542 (60), 2.500 (60), 2.275 (60).
Kind of sample preparation and/or method of registration of the spectrum: KBr disc. Absorption.
Wavenumbers (cm^{-1}): 1200sh, 1150s, 1130s, 1086s, 1012, 963, 928, 882, 817s, 690sh, 670sh, 637, 624, 602w, 553, 480w, 460sh.

2.11 Chlorides and Hydroxychlorides

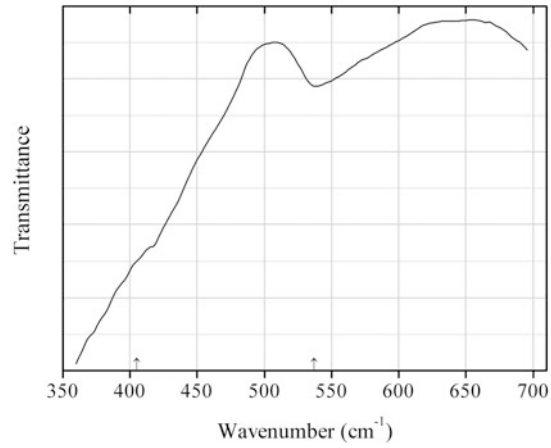

Fig. 2.1274 IR spectrum of perite obtained by N.V. Chukanov

Cl39 Perite $PbBiO_2Cl$ (Fig. 2.1274)
Locality: Kara-Oba W deposit, Betpakdala desert, Karagandy province, Central Kazakhstan.
Description: Yellow fine-grained aggregate from the association with halloysite and beyerite. Investigated by I.V. Pekov.
Kind of sample preparation and/or method of registration of the spectrum: KBr disc. Absorption.
Wavenumbers (cm^{-1}): 537, 405sh.

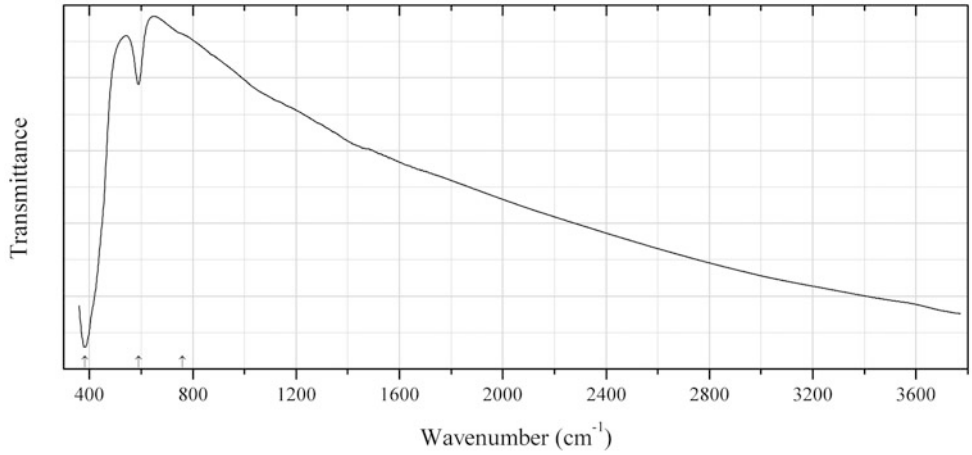

Fig. 2.1275 IR spectrum of nadorite obtained by N.V. Chukanov

Cl40 Nadorite $PbSb^{3+}O_2Cl$ (Fig. 2.1275)
Locality: Djebel Nador, Constantine, Algeria (type locality).
Description: Aggregate of brown platy crystals. Confirmed by qualitative electron microprobe analysis.
Kind of sample preparation and/or method of registration of the spectrum: KBr disc. Absorption.
Wavenumbers (cm^{-1}): 760sh, 590, 383s.

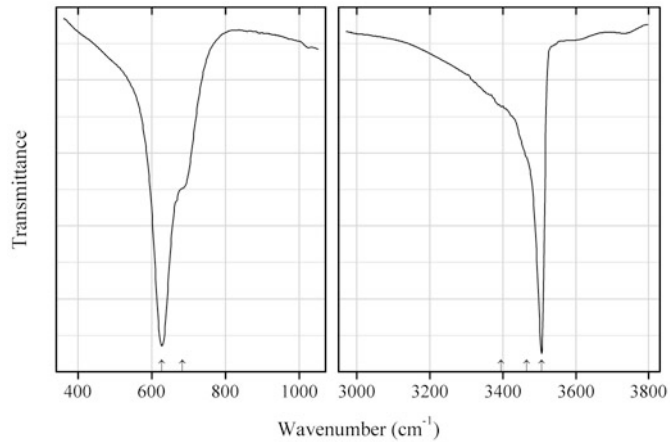

Fig. 2.1276 IR spectrum of paralaurionite obtained by N.V. Chukanov

Cl41 Paralaurionite PbCl(OH) (Fig. 2.1276)
Locality: Asunción mine, Sierra Gorda district, Antofagasta province, Antofagasta region, Chile.
Description: Colourless crystals from the association with leucostaurite. Confirmed by the IR spectrum and the single-crystal X-ray diffraction pattern.
Kind of sample preparation and/or method of registration of the spectrum: KBr disc. Absorption.
Wavenumbers (cm^{-1}): 3506s, 3465sh, 3395sh, 682sh, 627s.

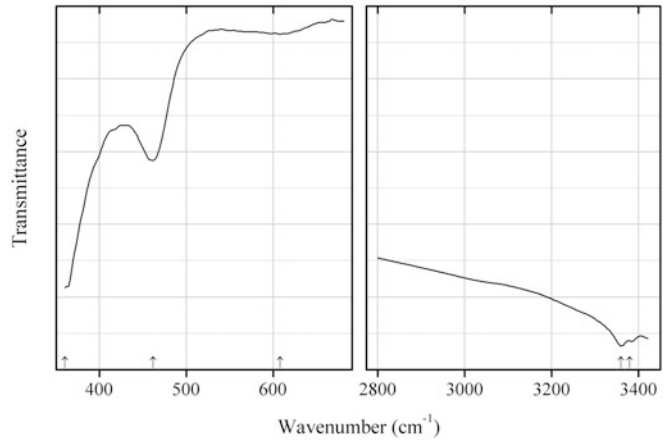

Fig. 2.1277 IR spectrum of blixite obtained by N.V. Chukanov

Cl42 Blixite $Pb_8O_5(OH)_2Cl_4$ (Fig. 2.1277)
Locality: Långban deposit, Bergslagen ore region, Filipstad district, Värmland, Sweden (type locality).
Description: Beige massive from the association with calcite, lizardite, braunite, and hausmannite.
Kind of sample preparation and/or method of registration of the spectrum: KBr disc. Absorption.
Wavenumbers (cm^{-1}): 3380, 3360, 608w, 462, (360s).

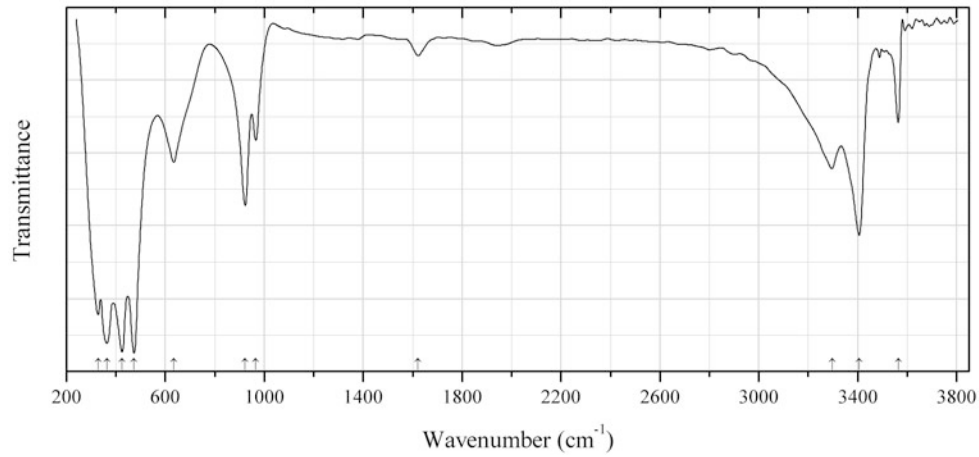

Fig. 2.1278 IR spectrum of abhurite drawn using data from Jouen et al. (2007)

Cl43 Abhurite $Sn_{21}O_6Cl_{16}(OH)_{14}$ (Fig. 2.1278)
Locality: Synthetic.
Description: Gray corrosion layer on a tin plate. Synthesized by a potentiostatic method. Identified by powder X-ray diffraction.
Kind of sample preparation and/or method of registration of the spectrum: KBr disc, transmission.
Source: Jouen et al. (2007).
Wavenumbers (cm^{-1}): 3564, 3407, 3296, 1621w, 966, 923, 634, 473s, 425s, 363s, 328s.
Note: The band at 1621 cm^{-1} indicates the presence of H_2O molecules.

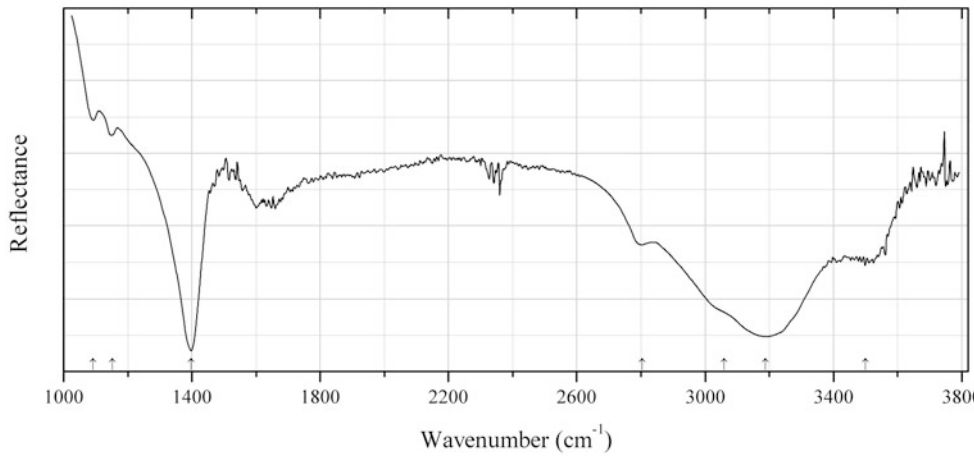

Fig. 2.1279 IR spectrum of argesite drawn using data from Demartin et al. (2012)

Cl44 Argesite $(NH_4)_7Bi_3Cl_{16}$ (Fig. 2.1279)
Locality: La Fossa crater, Vulcano island, Lipari, Eolie (Aeolian) islands, Messina province, Sicily, Italy (type locality).
Description: Pale yellow crystals from the association with bismuthinite, adranosite, brontesite, demicheleite-(Br), demicheleite-(Cl), and panichiite. Holotype sample. Trigonal, space group *R*-3*c*,

a = 13.093(1), c = 102.682(1) Å, V = 15245(2) Å^3, Z = 18. D_{meas} = 2.88(1) g/cm^3, D_{calc} = 2.763 g/cm^3. Optically uniaxial (−), ω = 1.731(2), ε = 1.725(2). The empirical formula is $[(NH_4)_{6.29}K_{0.91}Tl_{0.06}]Bi_{2.93}(Cl_{13.33}Br_{2.37}I_{0.11})$. The strongest lines of the powder X-ray diffraction pattern [d, Å (I, %) (hkl)] are: 3.164 (100) (0.3.18), 3.808 (44) (−2.2.20), 2.742 (78) (−2.4.21), 6.14 (16) (−126), 1.906 (16) (0.0.–54), 1.686 (13) (−5.6.34).

Kind of sample preparation and/or method of registration of the spectrum: Transmission. Kind of sample preparation is not indicated.

Source: Demartin et al. (2012).

Wavenumbers (cm^{-1}): 3500, 3188s, 3060sh, 2803, 1397s, 1152w, 1092w.

Note: The wavenumbers were partly determined by us based on spectral curve analysis of the published spectrum. Multiple weak narrow bands in the ranges 3400–3600 and 1500–1700 cm^{-1} correspond to absorbed atmospheric water.

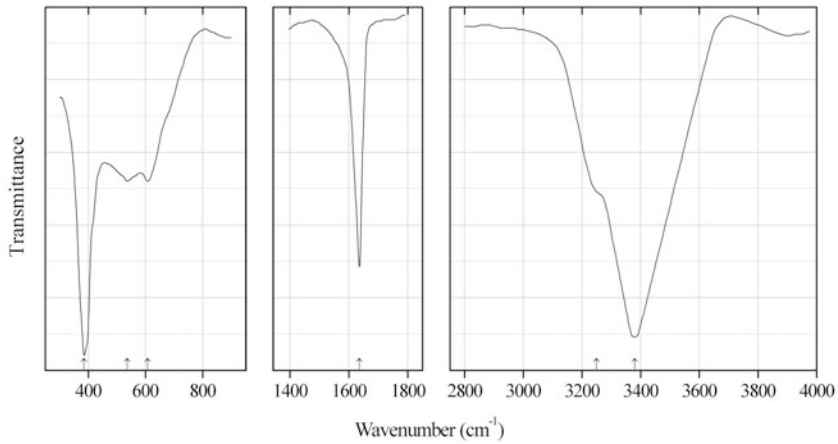

Fig. 2.1280 IR spectrum of bischofite drawn using data from Kirsh et al. (1987)

Cl45 Bischofite $MgCl_2 \cdot 6H_2O$ (Fig. 2.1280)

Locality: Synthetic.

Kind of sample preparation and/or method of registration of the spectrum: CsCl disc, absorption.

Source: Kirsh et al. (1987).

Wavenumbers (cm^{-1}): 3380s, 3250sh, 1636, 608, 537, 385s.

Note: After Moenke (1962), the wavenumbers the IR absorption bands of bischofite are (cm^{-1}): 3420s, 3235s, 1630, 612, 470.

Cl46 Carnallite $KMgCl_3 \cdot 6H_2O$

Locality: Synthetic.

Description:Produced by Kaliwerk Werra, Merkers, Rhön, Germany.

Kind of sample preparation and/or method of registration of the spectrum: KBr disc. Absorption.

Source: Moenke (1966).

Wavenumbers (cm^{-1}): 3415s, 3235s, 1638s, 615, 468.

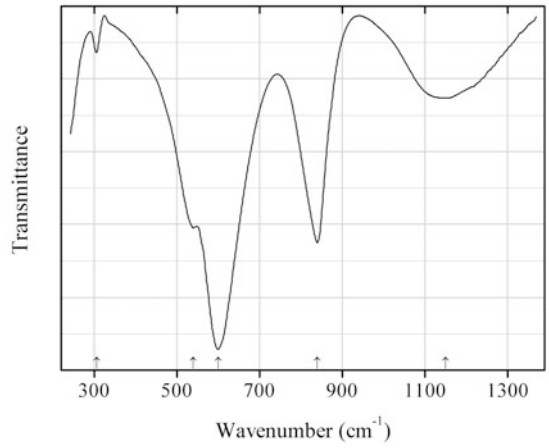

Fig. 2.1281 IR spectrum of chloraluminite drawn using data from Stefov et al. (1992)

Cl47 Chloraluminite $AlCl_3 \cdot 6H_2O$ (Fig. 2.1281)
Locality: Synthetic.
Description: A commercial product (Riedel, Hannover) recrystallized from water before use.
Kind of sample preparation and/or method of registration of the spectrum: KBr disc. Transmission.
Source: Stefov et al. (1992).
Wavenumbers (cm^{-1}): 1150, 840, 600s, 540, 306w.
Note: The wavenumbers were partly determined by us based on spectral curve analysis of the published spectrum. Additionally, IR spectrum of chloraluminite contains a strong broad band with a maximum at 3450–3460 cm^{-1} and a weak band with a maximum at 1630–1640 cm^{-1} (Isupov et al. 2000).

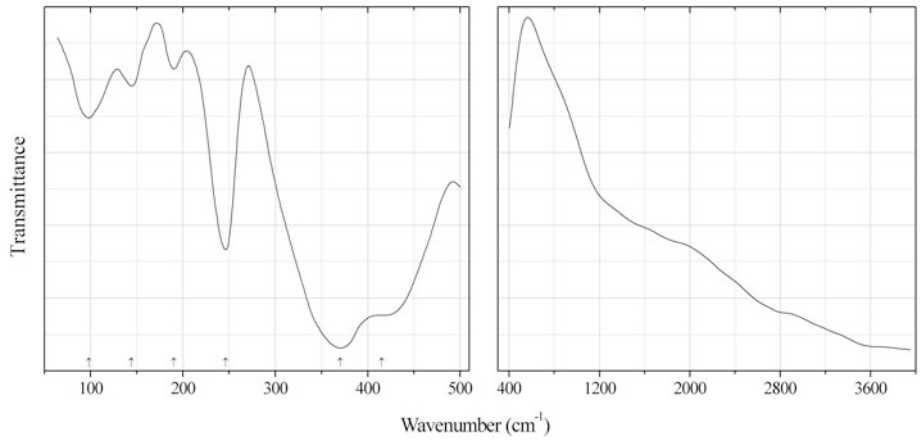

Fig. 2.1282 IR spectrum of eglestonite drawn using data from Vershkovskaya et al. (1979)

Cl48 Eglestonite $(Hg_2)^{2+}{}_3OCl_3(OH)$ (Fig. 2.1282)
Locality: Ruziobnok Hg deposit, central Tajikistan.

Description: Bright yellow veinlet from the association with dickite and cinnabar. Cubic, space group *Ia3d*. The strongest lines of the powder X-ray diffraction pattern [*d*, Å (*I*, %)] are: 4.00 (30), 3.26 (80), 2.54 (80), 1.893 (100), 1.711 (35), 1.335 (30).
Kind of sample preparation and/or method of registration of the spectrum: Precipitate on KBr plate. Absorption.
Source: Vershkovskaya et al. (1979).
Wavenumbers (cm^{-1}): 415sh, 370s, 246s, 190, 144, 98.
Note: The wavenumbers were partly determined by us based on spectral curve analysis of the published spectrum. As noted by Mereiter et al. (1992), "routine powder IR spectroscopy failed to detect a significant amount of bonded H in the case of eglestonite". However diffuse absorption in the range from 1000 to 4000 cm^{-1} may correspond to O–H-stretching vibrations.

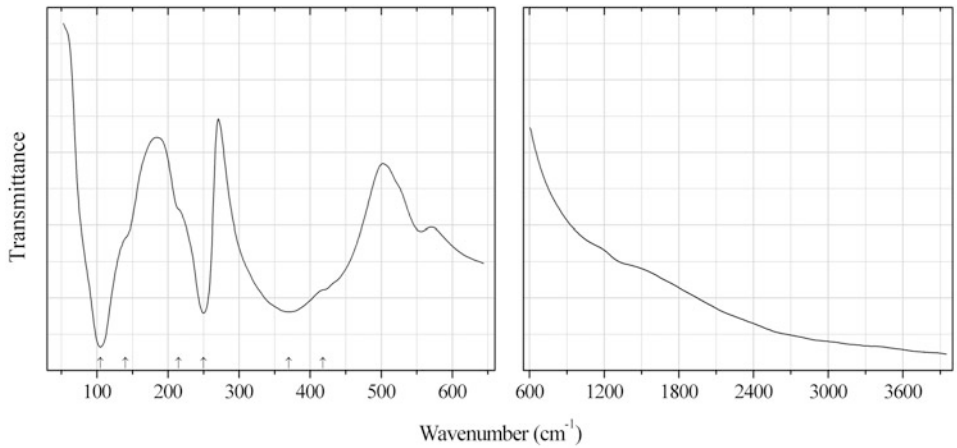

Fig. 2.1283 IR spectrum of eglestonite drawn using data from Kovaleva and Vasiliev (1987)

Cl49 Eglestonite $(Hg_2)^{2+}{}_3OCl_3(OH)$ (Fig. 2.1283)
Locality: Khaidarkan Sb-Hg deposit, Fergana valley, Alai range, Osh region, Kyrgyzstan.
Description: No data.
Kind of sample preparation and/or method of registration of the spectrum: Suspension in perfluorinated mineral oil deposited on polyethylene substrate. Absorption.
Source: Kovaleva and Vasiliev (1987).
Wavenumbers (cm^{-1}): 418sh, 370s, 250s, 215sh, 140sh, 105s.
Note: The wavenumbers were partly determined by us based on spectral curve analysis of the published spectrum. Diffuse absorption in the range from 1000 to 4000 cm^{-1} may correspond to O–H stretching vibrations. Weak band in the range from 500 to 600 cm^{-1} corresponds to perfluorinated mineral oil.

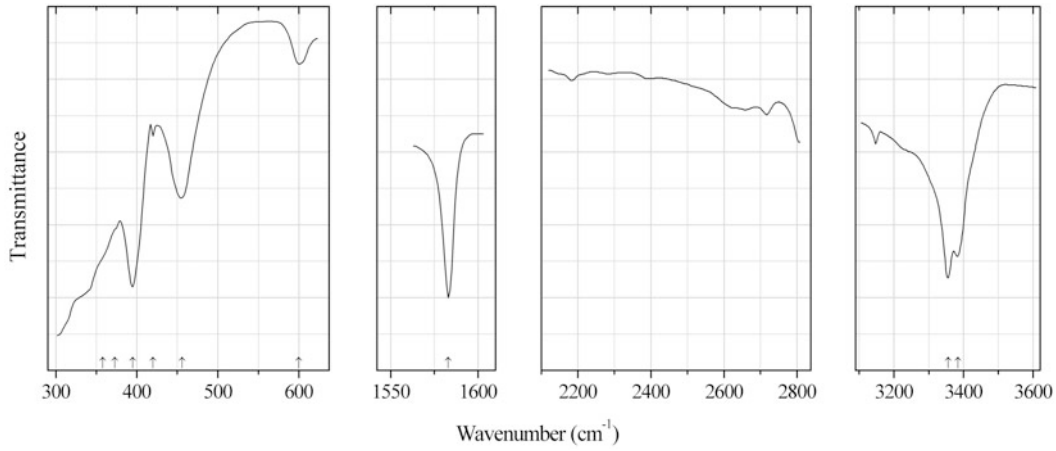

Fig. 2.1284 IR spectrum of erythrosiderite drawn using data from Falk et al. (1975)

Cl50 Erythrosiderite $K_2Fe^{3+}Cl_5 \cdot H_2O$ (Fig. 2.1284)
Locality: Synthetic.
Description: Obtained by slow evaporation of mixed aqueous solutions of $FeCl_3$ and KCl, acidified with HCl, at about 40 °C. Confirmed by chemical analysis.
Kind of sample preparation and/or method of registration of the spectrum: Suspension in Nujol. Transmission.
Source: Falk et al. (1975).
Wavenumbers (cm^{-1}): 3384s, 3356s, 1583s, 600w, 456, 420w (artefact), 395s, 373sh, 358sh.
Note: The wavenumbers were partly determined by us based on spectral curve analysis of the published spectrum.

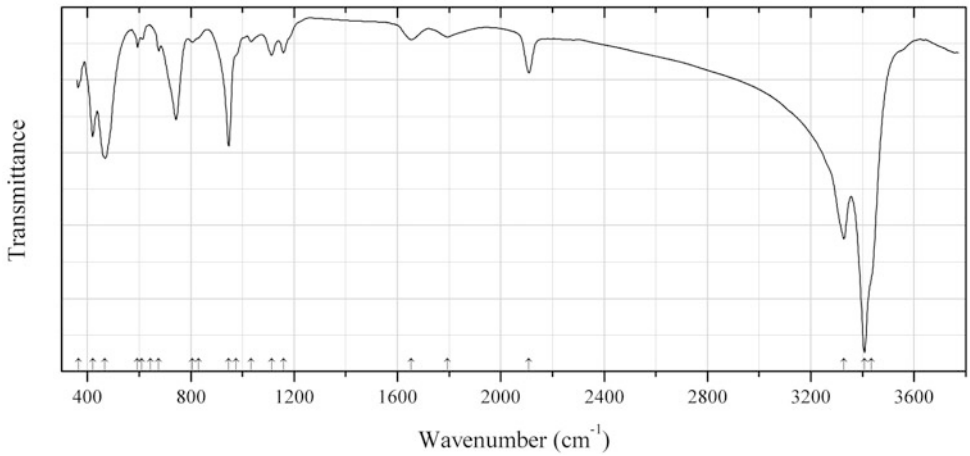

Fig. 2.1285 IR spectrum of tondiite obtained by N.V. Chukanov

Cl51 Tondiite $Cu_3MgCl_2(OH)_6$ (Fig. 2.1285)
Locality: Santo Domingo mine, Arica province, Chile.

Description: Green crystals. The empirical formula is (electron microprobe): $Cu_{3.35}Mg_{0.65}Cl_{1.85}(OH)_{6.15}$. Confirmed by powder X-ray diffraction data.
Kind of sample preparation and/or method of registration of the spectrum: KBr disc. Absorption.
Wavenumbers (cm^{-1}): 3435sh, 3408s, 3328s, 2109, 1793w, 1654w, 1159, 1113, 1034w, 975sh, 947s, 830sh, 806w, 643, 676w, 611w, 594w, 468s, 420, 365.
Note: The bands in the ranges from 1000 to 1200 and from 590 to 680 cm^{-1} indicate possible contamination with a sulfate.

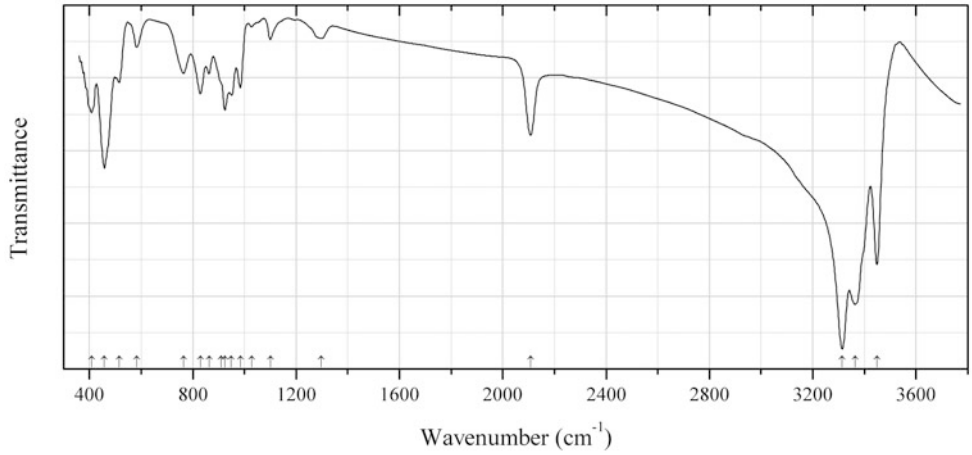

Fig. 2.1286 IR spectrum of leverettite obtained by N.V. Chukanov

Cl52 Leverettite $Cu_3CoCl_2(OH)_6$ (Fig. 2.1286)
Locality: Torrecillas mine, Salar Grande, Iquique province, Chile (type locality).
Description: Green prismatic crystals. Investigated by A.V. Kasatkin. The empirical formula is (electron microprobe): $Cu_{3.14}Co_{0.67}Ni_{0.15}Mn_{0.04}Cl_{1.77}(OH)_x$.
Kind of sample preparation and/or method of registration of the spectrum: KBr disc. Absorption.
Wavenumbers (cm^{-1}): 3448s, 3364s, 3314s, 2107, 1298w, 1100w, 1029w, 984, 949, 924, 910sh, 863, 829, 764, 583w, 515, 458s, 408.

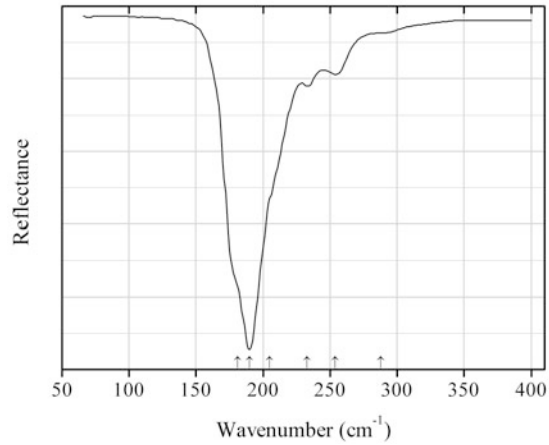

Fig. 2.1287 IR spectrum of halite drawn using data from Herron et al. (2008)

Cl53 Halite NaCl (Fig. 2.1287)
Locality: Green River formation, Sweetwater Co., Wyoming, USA.
Kind of sample preparation and/or method of registration of the spectrum: Diffuse reflection of a powdered sample in polyethylene medium.
Source: Herron et al. (2008).
Wavenumbers (cm^{-1}): 288sh, 254w, 233w, 205sh, 190s, 181sh.
Note: The wavenumbers were determined by us based on spectral curve analysis of the published spectrum.

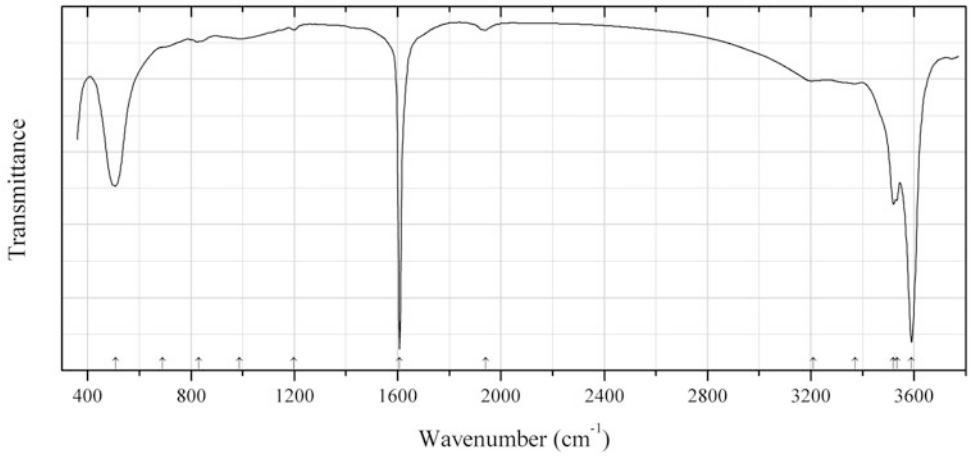

Fig. 2.1288 IR spectrum of cryobostryxite obtained by N.V. Chukanov

Cl54 Cryobostryxite $KZnCl_3 \cdot 2H_2O$ (Fig. 2.1288)
Locality: Northern fumarole field, First scoria cone of the Northern Breakthrough of the Great Tolbachik Fissure Eruption, Tolbachik volcano, Kamchatka peninsula, Far-Eastern Region, Russia (type locality).
Description: Colourless anthodites from the association with sellaite, fluorite, anhydrite, hematite, ralstonite, sofiite, halite, cotunnite, challacolloite, flinteite, zincomenite, chubarovite, gypsum, and halite. Holotype sample. Monoclinic, space group $P2_1/c$, a = 6.2795(3), b = 10.1397(3), c = 12.0829 (7) Å, β = 107.732(5)°, V = 732.79(6) $Å^3$, Z = 4. D_{meas} = 2.30(2) g/cm^3, D_{calc} = 2.301 g/cm^3. Optically biaxial (+), α = 1.522(2), β = 1.530(2), γ = 1.576(2), 2 V = 30(15)°. The empirical formula is $(K_{0.96}Tl_{0.05})_{\Sigma 1.01}Zn_{1.00}Cl_{2.99} \cdot 1.91H_2O$. The strongest lines of the powder X-ray diffraction pattern [d, Å (I, %) (hkl)] are: 7.62 (30) (011), 5.986 (43) (100), 5.766 (35) (002), 3.907 (33) (−121), 3.062 (100) (−202, 023), 2.996 (24) (−211, 200), 2.853 (27) (−114).
Kind of sample preparation and/or method of registration of the spectrum: KBr disc. Absorption.
Wavenumbers (cm^{-1}): 3590s, 3533s, 3520s, 3372, 3210, 1942w, 1607s, 1198w, 988w, 830w, 690w, 508s.

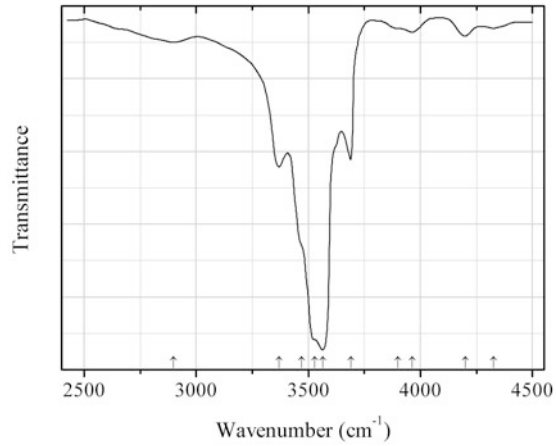

Fig. 2.1289 IR spectrum of hibbingite drawn using data from Saini-Eidukat et al. (1994)

Cl55 Hibbingite $Fe^{2+}{}_2(OH)_3Cl$ (Fig. 2.1289)
Locality: Duluth Complex, near Hibbing, Minnesota, Canada (type locality).
Description: Vein filling in partially serpentinized troctolitic rock. Holotype sample. Orthorhombic, a = 6.31(6), b = 9.20(4), c = 7.10(7) Å, V = 412.17 Å^3, Z = 4. D_{calc} = 3.04 g/cm^3. The empirical formula is $(Fe_{1.72}Mg_{0.21}Mn_{0.06})Si_{0.01}(OH)_{3.00}[Cl_{0.87}(OH)_{0.12}$. The strongest lines of the powder X-ray diffraction pattern are observed at 7.08, 5.68, 5.07, 4.60, 4.20, 3.70, 3.55, 2.93, 2.37, 2.30, 2.14, 1.90, and 1.65 Å.
Kind of sample preparation and/or method of registration of the spectrum: Absorbance of a grain using IR microscope.
Source: Saini-Eidukat et al. (1994).
Wavenumbers (cm^{-1}): 4325w, 4200w, 3965w, 3900w, 3690, 3564s, 3530sh, 3470sh, 3370, 2900w.
Note: The wavenumbers were determined by us based on spectral curve analysis of the published spectrum.

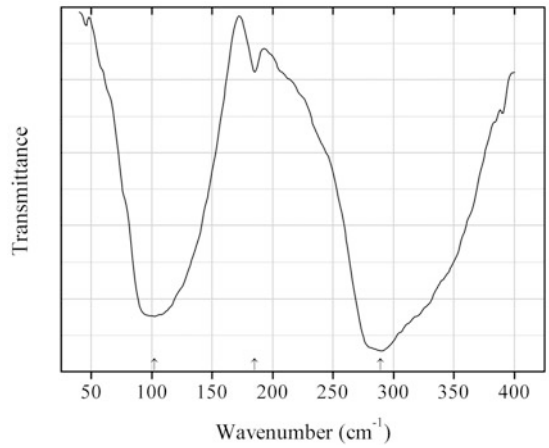

Fig. 2.1290 IR spectrum of bismoclite drawn using data from Davies (1973)

Cl56 Bismoclite BiOCl (Fig. 2.1290)

Locality: Synthetic.
Kind of sample preparation and/or method of registration of the spectrum: Nujol mull. Transmission.
Source: Davies (1973).
Wavenumbers (cm^{-1}): 289s, 185w, 102s.
Note: In the IR spectrum of synthetic BiOCl Rulmont (1972) indicates additional band at 524 cm^{-1}.

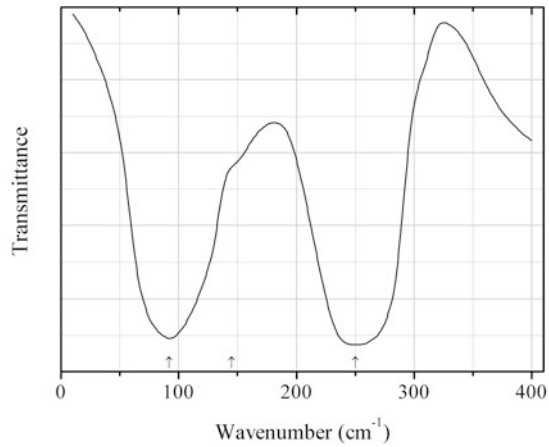

Fig. 2.1291 IR spectrum of calomel drawn using data from Ōsaka (1971)

Cl57 Calomel HgCl (Fig. 2.1291)
Locality: Synthetic.
Description: Commercial reactant (Wako Pure Chemical Industries).
Kind of sample preparation and/or method of registration of the spectrum: Nujol mull. Transmission.
Source: Ōsaka (1971).
Wavenumbers (cm^{-1}): 250s, 145sh, 92s.
Note: The wavenumbers were determined by us based on spectral curve analysis of the published spectrum.

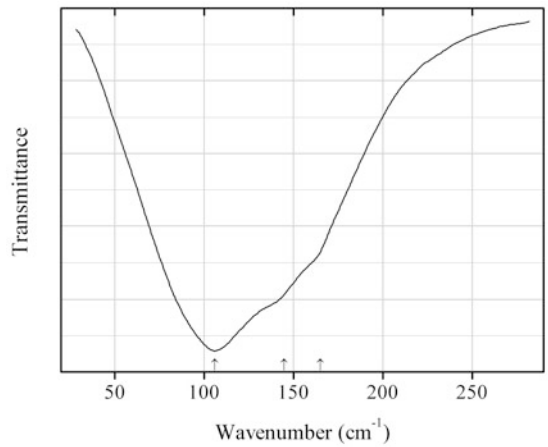

Fig. 2.1292 IR spectrum of chlorargyrite drawn using data from Bottger and Geddes (1967)

Cl58 Chlorargyrite AgCl (Fig. 2.1292)
Locality: Synthetic.
Description: Film prepared by evaporation and precipitation onto polyethylene substrate.
Kind of sample preparation and/or method of registration of the spectrum: Transmission.
Source: Bottger and Geddes (1967).
Wavenumbers (cm^{-1}): 165sh, 145sh, 106s.

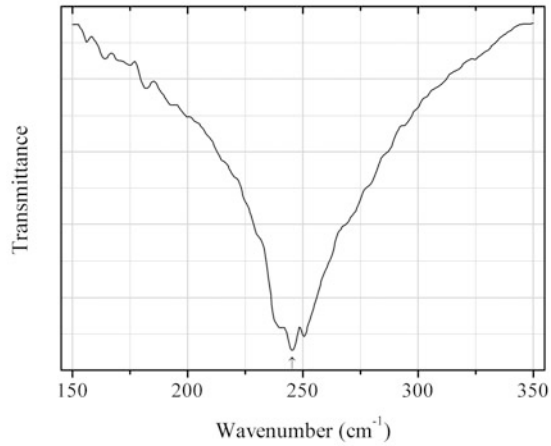

Fig. 2.1293 IR spectrum of chloromagnesite drawn using data from Di Noto and Bresadola (1996)

Cl59 Chloromagnesite $MgCl_2$ (Fig. 2.1293)
Locality: Synthetic.
Description: Commercial reactant. Confirmed by the powder X-ray diffraction pattern.
Kind of sample preparation and/or method of registration of the spectrum: Attenuated total reflection of powdered sample.
Source: Di Noto and Bresadola (1996).
Wavenumber (cm^{-1}): 245.5.
Note: The wavenumber was determined by us based on spectral curve analysis of the published spectrum.

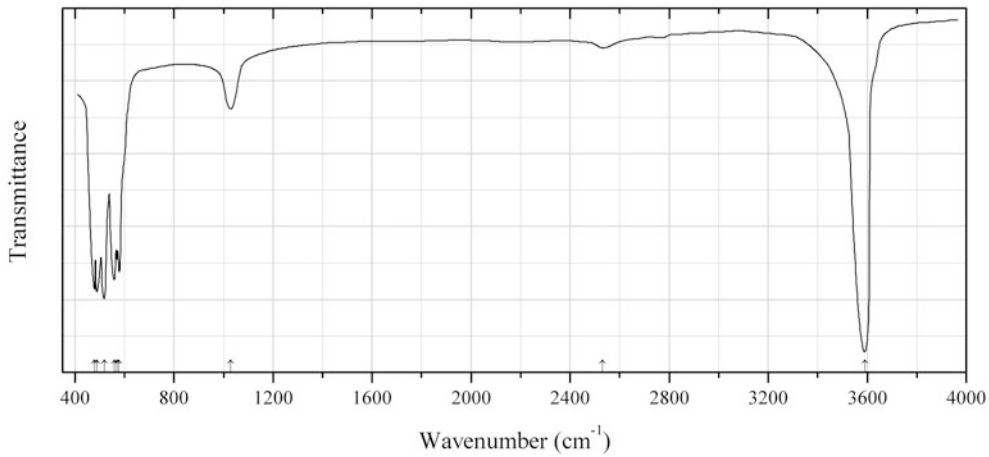

Fig. 2.1294 IR spectrum of kempite drawn using data from Mockenhaupt (2006)

Cl60 Kempite $Mn^{2+}{}_2Cl(OH)_3$ (Fig. 2.1294)
Locality: Synthetic.
Description: The crystal structure is solved. Orthorhombic, space group *Pnma*, a = 6.5002(2), b = 7.1239(3), c = 9.5310(3) Å, V = 441.35(3) Å^3, Z = 4. D_{calc} = 2.955 g/cm^3.
Kind of sample preparation and/or method of registration of the spectrum: KBr disc. Transmission.
Source: Mockenhaupt (2006).
Wavenumbers (cm^{-1}): 3591s, 2530w, 1029w, 578s, 569, 559s, 518s, 488s, 479s.
Note: The band position denoted by Mockenhaupt (2006) as 548 cm^{-1} was determined by us at 518 cm^{-1} based on spectral curve analysis of the published spectrum.

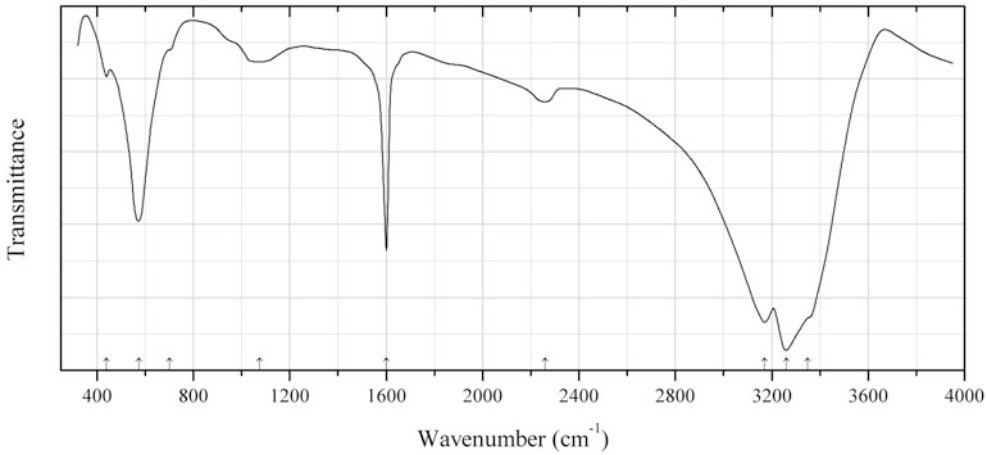

Fig. 2.1295 IR spectrum of mitscherlichite drawn using data from Thomas et al. (1974)

Cl61 Mitscherlichite $K_2CuCl_4{\cdot}2H_2O$ (Fig. 2.1295)
Locality: Synthetic.
Description: Turquois crystals obtained by allowing an aqueous solution of stoichiometric quantities of KC1 and $CuC1_2{\cdot}2H_2O$ to evaporate at room temperature. Confirmed by powder X-ray diffraction data.
Kind of sample preparation and/or method of registration of the spectrum: KBr disc. Transmission.
Source: Thomas et al. (1974).
Wavenumbers (cm^{-1}): 3350sh, 3260s, 3170s, 2260w, 1601s, 1075w, 700sh, 573s, 440w.

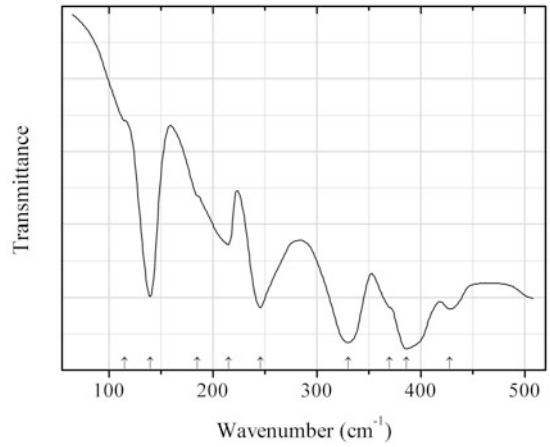

Fig. 2.1296 IR spectrum of molysite drawn using data from Kanesaka et al. (1986)

Cl62 Molysite $FeCl_3$ (Fig. 2.1296)
Locality: Synthetic.
Description: A sample purified in vacuum by means of sublimation of the commercially obtained compound.
Kind of sample preparation and/or method of registration of the spectrum: Nujol mull. Absorption.
Source: Kanesaka et al. (1986).
Wavenumbers (cm^{-1}): 428, 386s, 370sh, 330s, 246, 215, 185sh, 140, 115w.

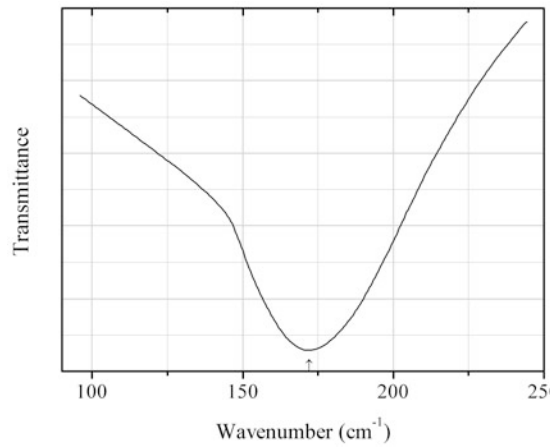

Fig. 2.1297 IR spectrum of nantokite drawn using data from Plendl et al. (1966)

Cl63 Nantokite CuCl (Fig. 2.1297)
Locality: Synthetic.
Kind of sample preparation and/or method of registration of the spectrum: Thin film sublimed on quartz plate and covered with paraffin.
Source: Plendl et al. (1966).
Wavenumbers (cm^{-1}): 172.

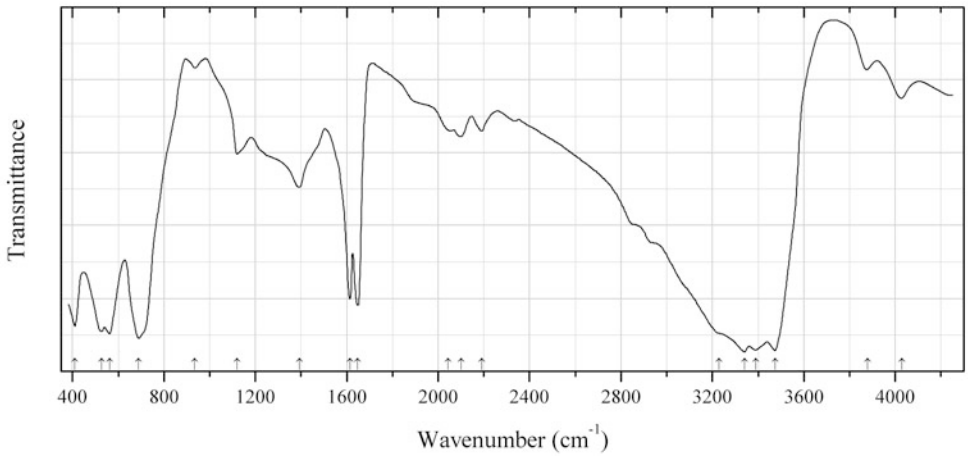

Fig. 2.1298 IR spectrum of barium chloride dihydrate drawn using data from Venkatesh and Neelakantan (1966)

Cl64 Barium chloride dihydrate $BaCl_2 \cdot 2H_2O$ (Fig. 2.1298)
Locality: Synthetic.
Description: Obtained by the slow evaporation of a saturated aqueous solution of commercial $BaCl_2 \cdot 2H_2O$. Monoclinic, space group $P2_1/n$.
Kind of sample preparation and/or method of registration of the spectrum: KBr disc. Transmission.
Source: Venkatesh and Neelakantan (1966).
Wavenumbers (cm^{-1}): 4030w, 3880w, 3475s, 3390s, 3340s, 3230sh, 2190w, 2100w, 2045w, 1647, 1614, 1394, 1120, 935w, 690s, 563s, 528s, 410s.

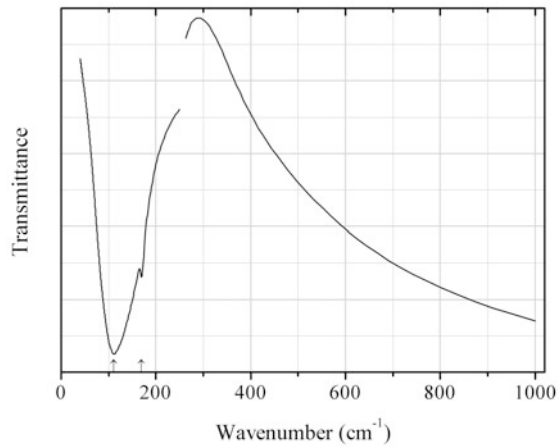

Fig. 2.1299 IR spectrum of cotunnite drawn using data from Hadni et al. (1968)

Cl65 Cotunnite $PbCl_2$ (Fig. 2.1299)
Locality: Synthetic.
Description: Orthorhombic, space group *Pnam*.
Kind of sample preparation and/or method of registration of the spectrum: Nujol mull. Transmission.

Source: Hadni et al. (1968).
Wavenumbers (cm^{-1}): 169, 111s.

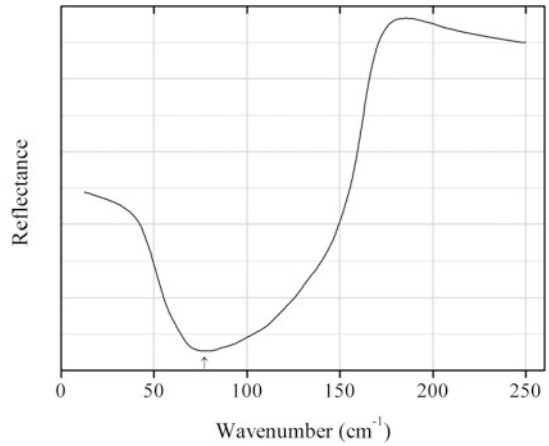

Fig. 2.1300 IR spectrum of lafossaite drawn using data from Claudel et al. (1968)

Cl66 Lafossaite TlCl (Fig. 2.1300)
Locality: Synthetic.
Description: Cubic polymorph of TlCl.
Kind of sample preparation and/or method of registration of the spectrum: Reflection.
Source: Claudel et al. (1968).
Wavenumbers (cm^{-1}): 77.
Note: The wavenumber was determined by us based on spectral curve analysis of the published spectrum.

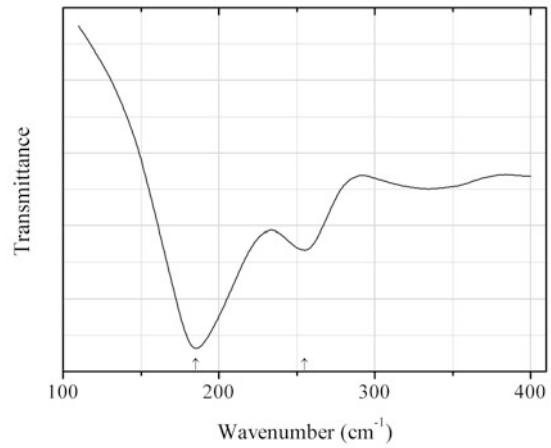

Fig. 2.1301 IR spectrum of scacchite drawn using data from Piseri and Pollini (1984)

Cl67 Scacchite $MnCl_2$ (Fig. 2.1301)
Locality: Synthetic.

Description: Obtained from the vapour phase at 550 °C by means of a flow system using pure elements as starting materials.
Kind of sample preparation and/or method of registration of the spectrum: Powdered sample imbedded in polyethylen. Absorption.
Source: Piseri and Pollini (1984).
Wavenumbers (cm^{-1}): 255, 185s.

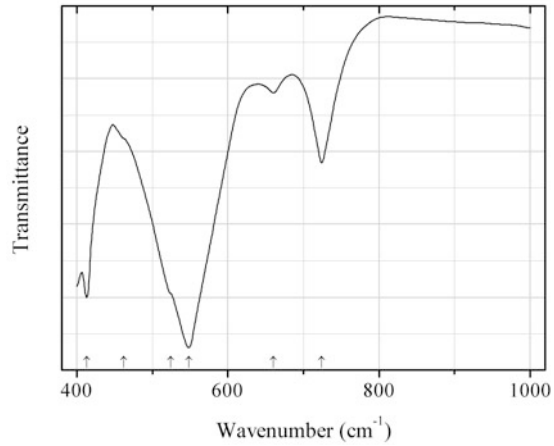

Fig. 2.1302 IR spectrum of antimony oxychloride drawn using data from Costa et al. (1990)

Cl68 Antimony oxychloride SbOCl (Fig. 2.1302)
Locality: Synthetic.
Description: Prepared following the procedure described in (Brauer 1954). The purity was confirmed by powder X-ray diffraction data.
Kind of sample preparation and/or method of registration of the spectrum: KBr disc. Absorption.
Source: Costa et al. (1990).
Wavenumbers (cm^{-1}): 724, 660w, 548s, 524sh, 462sh, 413s.

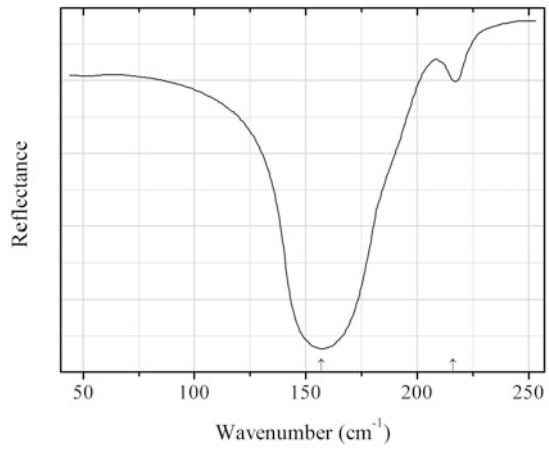

Fig. 2.1303 IR spectrum of sylvite drawn using data from Johnson and Bell (1969)

Cl69 Sylvite KCl (Fig. 2.1303)
Locality: Synthetic.
Kind of sample preparation and/or method of registration of the spectrum: Reflection of powdered sample.
Source: Johnson and Bell (1969).
Wavenumbers (cm^{-1}): 216w, 157s.
Note: The wavenumbers were determined by us based on spectral curve analysis of the published spectrum.

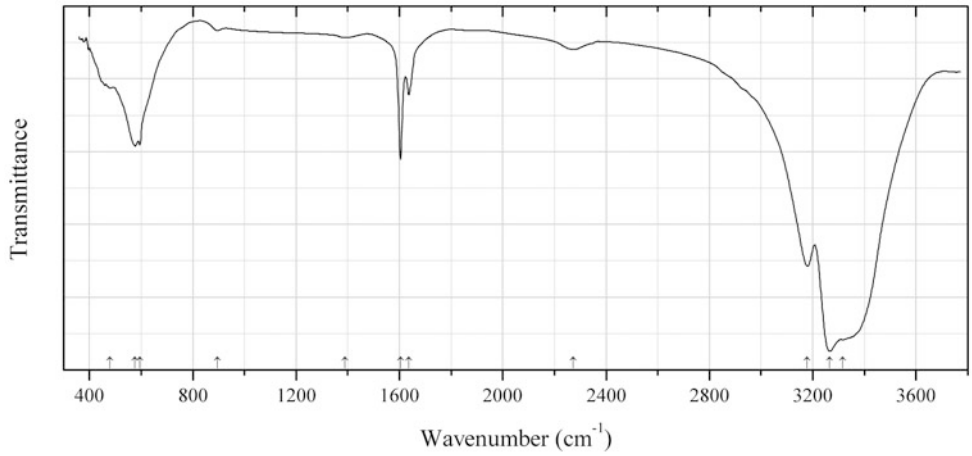

Fig. 2.1304 IR spectrum of mitscherlichite obtained by N.V. Chukanov

Cl70 Mitscherlichite $K_2CuCl_4 \cdot 2H_2O$ (Fig. 2.1304)
Locality: Tenoritovaya (Tenorite) fumarole, Second scoria cone of the Northern Breakthrough of the Great Tolbachik Fissure Eruption, Tolbachik volcano, Kamchatka peninsula, Russia.
Description: Pale green grains from the association with avdoninite, romanorlovite, belloite, chlorothionite, eriochalcite, sylvite, carnallite, sanguite, etc. Investigated by I.V. Pekov. The empirical formula is (electron microprobe): $K_{2.00}Cu_{1.00}Cl_{3.97}(OH)_{0.03} \cdot nH_2O$. The strongest lines of the powder X-ray diffraction pattern [*d*, Å (*I*, %)] are: 5.43 (100), 3.96 (31), 3.33 (21), 3.166 (61), 3.074 (40), 2.825 (20), 2.714 (71), 2.636 (79).
Kind of sample preparation and/or method of registration of the spectrum: KBr disc. Absorption.
Wavenumbers (cm^{-1}): 3315s, 3266s, 3179s, 2272w, 1637, 1604, 1390w, 896w, 595, 576, 480.

2.12 Vanadates and Vanadium Oxides

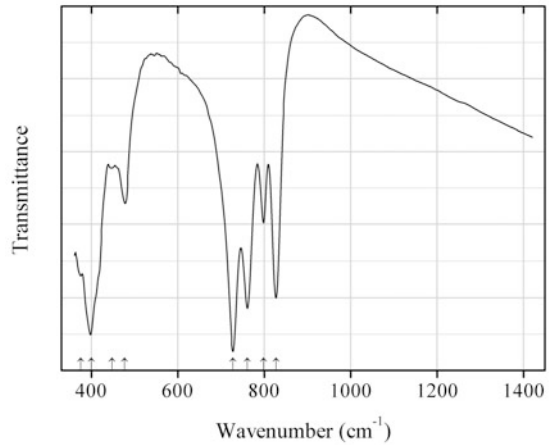

Fig. 2.1305 IR spectrum of kombatite obtained by N.V. Chukanov

V67 Kombatite $Pb_{14}O_9(VO_4)_2Cl_4$ (Fig. 2.1305)
Locality: Kombat mine, Kombat, Grootfontein district, Otjozondjupa region, Namibia (type locality).
Description: Yellow transparent grains from the association with hausmannite. The empirical formula is (electron microprobe): $Pb_{13.9}Ca_{0.15}O_{9.1}[(VO_4)_{3.9}(AsO_4)_{0.1}]Cl_{3.9}$.
Kind of sample preparation and/or method of registration of the spectrum: KBr disc. Absorption.
Wavenumbers (cm^{-1}): 827s, 799, 761s, 728s, 477, 448w, 399s, 375sh.

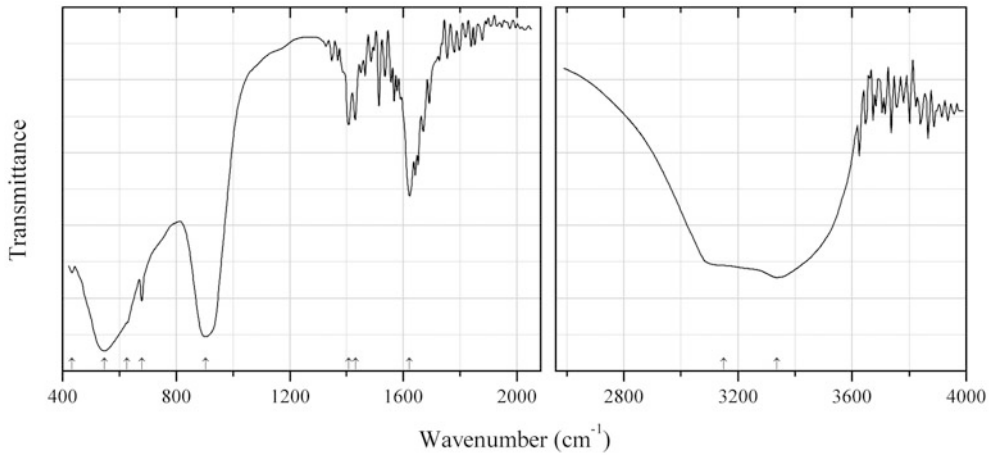

Fig. 2.1306 IR spectrum of ansermetite drawn using data from Wu et al. (2012)

V68 Ansermetite $Mn^{2+}V^{5+}{}_2O_6 \cdot 4H_2O$ (Fig. 2.1306)
Locality: Synthetic.
Description: Aggregate of microscopic road-like crystals. Confirmed by powder X-ray difraction data.
Kind of sample preparation and/or method of registration of the spectrum: Transmission. Kind of sample preparation is not indicated.

Source: Wu et al. (2012).
Wavenumbers (cm^{-1}): 3336s, 3150sh, 1621, 1431w, 1407w, 905s, 679, 627sh, 547s, 433.
Note: The wavenumbers were partly determined by us based on spectral curve analysis of the published spectrum.

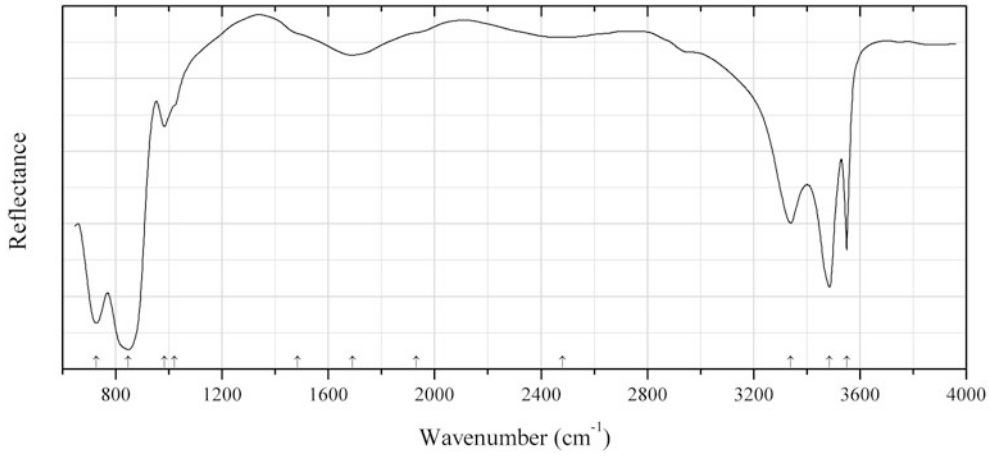

Fig. 2.1307 IR spectrum of argandite drawn using data from Brugger et al. (2011)

V69 Argandite $Mn_7(VO_4)_2(OH)_8$ (Fig. 2.1307)
Locality: A metamorphosed synsedimentary exhalative Mn deposit located underneath the Pipji glacier (Pipjigletscher) in the Turtmann valley, Central Alps, Switzerland (type locality).
Description: Orange grains from the association with pyrobelonite, reppiaite, and an unknown silico-vanadate. Holotype sample. Monoclinic, space group $P2_1/n$, a = 5.5038(2), b = 12.2665(5), c = 10.1055(5) Å, β = 95.559(4)°, V = 679.04(5) $Å^3$, Z = 2. D_{meas} = 3.71(5) g/cm^3, D_{calc} = 3.67 g/cm^3. Optically biaxial (−), α ≈ 1.74, β = 1.762(4), γ ≈ 1.77. The empirical formula is $(Mn_{6.54}Mg_{0.38}Ni_{0.04}Ca_{0.02}Zn_{0.01}Sr_{0.01})(V_{1.46}As_{0.54})O_8(OH)_{8.00}$. The strongest lines of the powder X-ray diffraction pattern [*d*, Å (*I*, %) (*hkl*)] are: 3.708 (50) (11–2, 121), 3.395 (60) (112), 3.074 (100) (131), 2.945 (50) (041, 11–3), 2.687 (70) (140, 113), 2.522 (50) (004, 20–2).
Kind of sample preparation and/or method of registration of the spectrum: Reflectance spectrum of powdered mineral.
Source: Brugger et al. (2011).
Wavenumbers (cm^{-1}): 3550, 3485s, 3340, 2480w (broad), 1930sh, 1690 (broad), 1485sh, 1022sh, 984, 848s, 728s.
Note: The wavenumbers were partly determined by us based on spectral curve analysis of the published spectrum. Taking into account strong distortion of VO_4 tetrahedra, broad bands in the range 1200–3000 cm^{-1} could be assigned to the groups HVO_4^{2-} formed as a result of proton transfer: $VO_4^{3-} + OH^- \rightarrow HVO_4^{2-} + O^{2-}$.

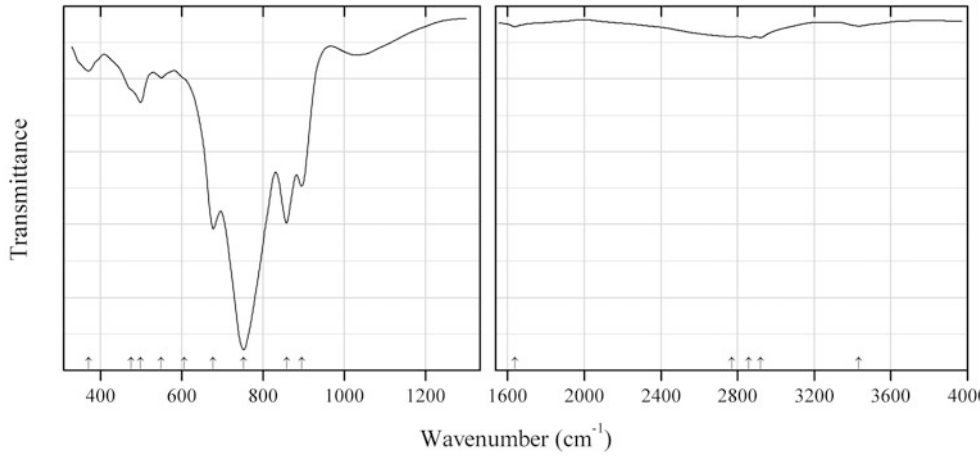

Fig. 2.1308 IR spectrum of brackebuschite drawn using data from Harlow et al. (1984)

V70 Brackebuschite $Pb_2Mn^{3+}(VO_4)_2(OH)$ (Fig. 2.1308)
Locality: Sierra de Córdoba, Argentina (type locality?).
Description: Specimen no. C78071 from the American Museum of Natural History.
Kind of sample preparation and/or method of registration of the spectrum: KBr disc. Absorption. Baseline is corrected.
Source: Harlow et al. (1984).
Wavenumbers (cm^{-1}): 3432w, 2919w, 2859w, 2770w, 1638w, 895, 858s, 752s, 678s, 607sh, 550w, 499, 476sh, 371w.
Note: The wavenumbers were determined by us based on spectral curve analysis of the published spectrum.

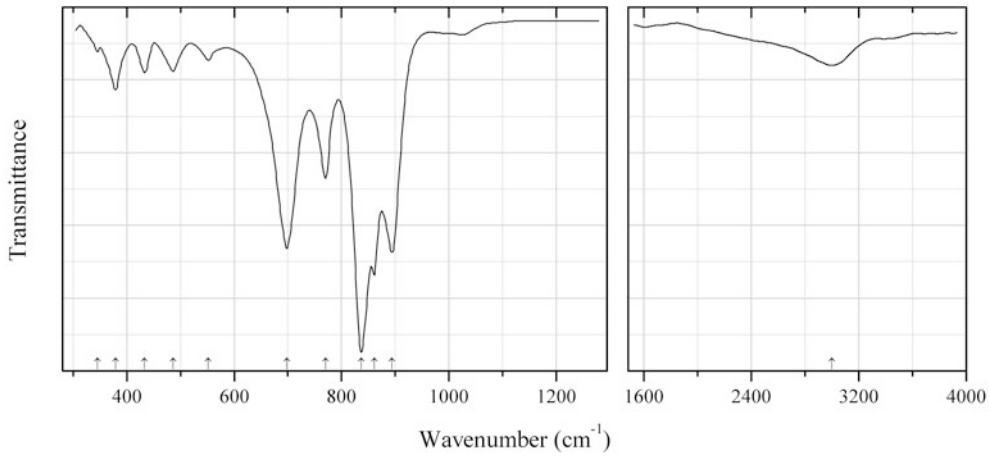

Fig. 2.1309 IR spectrum of gamagarite drawn using data from Harlow et al. (1984)

V71 Gamagarite $Ba_2Fe^{3+}(VO_4)_2(OH)$ (Fig. 2.1309)
Locality: Postmasburg district, Northern Cape Province, Republic of South Africa (type locality).
Description: Specimen no. 105142 from the American Museum of Natural History. Monoclinic, space group $P2_1/m$, a = 9.15(1), b = 6.17(1), c = 7.88(1) Å, β = 112.7(2)°, V = 410.0(11) $Å^3$, Z = 2.

The strongest lines of the powder X-ray diffraction pattern [*d*, Å (*I*, %) (*hkl*)] are: 3.309 (100) (112), 3.051 (80) (301, 212), 2.805 (80) (211), 2.349 (50) (022). Confirmed by electron microprobe analysis.
Kind of sample preparation and/or method of registration of the spectrum: KBr disc. Absorption. Baseline is corrected.
Source: Harlow et al. (1984).
Wavenumbers (cm^{-1}): 3000w, 894s, 861s, 837s, 770, 698s, 552w, 486w, 433w, 379, 345w.
Note: The wavenumbers were partly determined by us based on spectral curve analysis of the published spectrum. The band position denoted by Harlow et al. (1984) as 841 cm^{-1} was determined by us at 861 cm^{-1}.

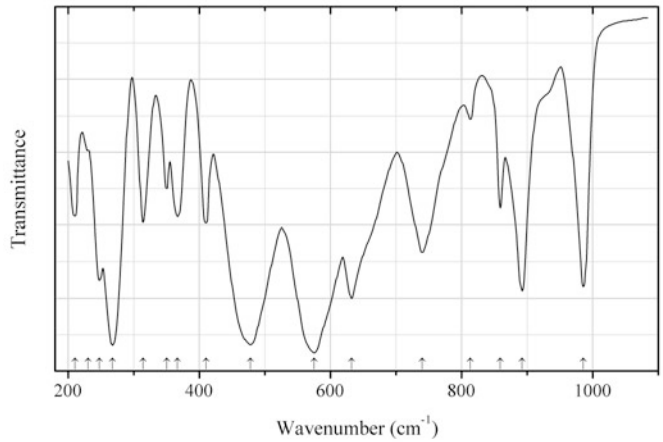

Fig. 2.1310 IR spectrum of carnotite drawn using data from Baran and Botto (1976)

V72 Carnotite $K_2(UO_2)_2(VO_4)_2 \cdot 3H_2O$ (Fig. 2.1310)
Locality: Synthetic.
Description: Synthesized in the reaction between solid V_2O_5, $(NH_4)_2V_2O_7$, and K_2CO_3. Identified by powder X-ray diffraction data.
Kind of sample preparation and/or method of registration of the spectrum: CsI disc. Transmission.
Source: Baran and Botto (1976).
Wavenumbers (cm^{-1}): 986, 892, 859, 813w, 740, 632, 575s, 478s, 410, 367, 350, 314, 268s, 248, 230sh, 210.
Note: Wavenumbers of absorption bands in the IR spectrum of natural carnotite from Walusita, Colorado, USA are (cm^{-1}; after Moenke 1962): 3440s, 1635, 1410w, 1030, 988, 900, 860, 745, 635, 580s, 480s.

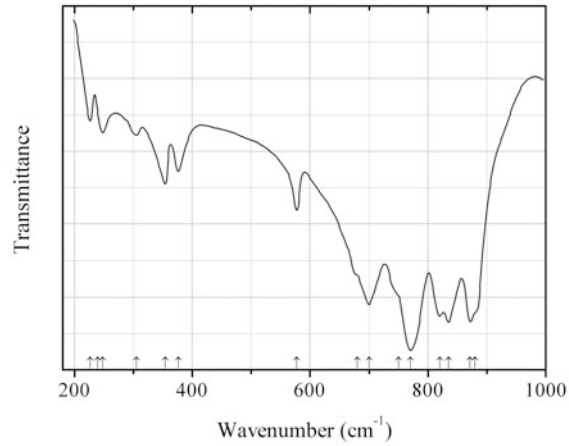

Fig. 2.1311 IR spectrum of chervetite drawn using data from Schwendt and Joniaková (1975)

V73 Chervetite $Pb_2(V_2O_7)$ (Fig. 2.1311)
Locality: Synthetic.
Description: Monoclinic, space group $P2_1/a$. Confirmed by powder X-ray diffraction data.
Kind of sample preparation and/or method of registration of the spectrum: Transmission. Kind of sample preparation is not indicated.
Source: Schwendt and Joniaková (1975).
Wavenumbers (cm^{-1}): 880sh, 872s, 835s, 820s, 771s, 750sh, 700s, 680sh, 577, 376, 354, 305w, 248w, 240w, 227w.

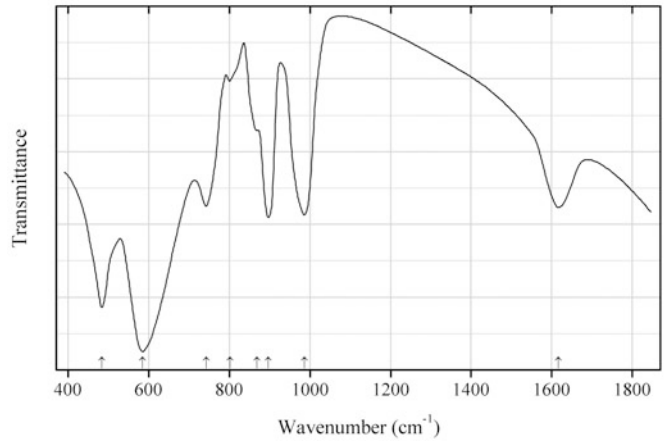

Fig. 2.1312 IR spectrum of curienite drawn using data from Suleimanov et al. (2004)

V74 Curienite $Pb(UO_2)_2(VO_4)_2 \cdot 5H_2O$ (Fig. 2.1312)
Locality: Synthetic.
Description: Synthesized from crystalline $U_2V_2O_{11}$ and saturated aqueous solution of lead nitrate under hydrothermal conditions at 180 °C. Confirmed by powder X-ray diffraction data.
Kind of sample preparation and/or method of registration of the spectrum: KBr disc. Transmission.

Source: Suleimanov et al. (2004).
Wavenumbers (cm^{-1}): 1617, 986, 897, 869w, 801w, 742, 585s, 483s.
Note: The wavenumbers were determined by us based on spectral curve analysis of the published spectrum. According to Čejka (1999), the wavenumbers in the infrared absorption spectrum of curienite are as follows (cm^{-1}): 3425, 2925w, 2852w, 2060w, 1615, 1410w, 979, 891, 804, 743, 585s, 463s, 405sh (weak bands at 2925 and 2852 cm^{-1} correspond to the admixture of grease).

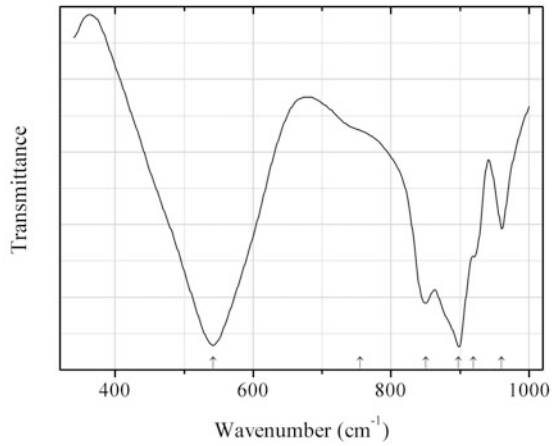

Fig. 2.1313 IR spectrum of strontium metavanadate trihydrate drawn using data from Dupuis and Lorenzelli (1969)

V75 Strontium metavanadate trihydrate $Sr(VO_3)_2 \cdot 3H_2O$ (Fig. 2.1313)
Locality: Synthetic.
Description: Synthesized in aqueous solution at pH of 7.5. Related to delrioite.
Kind of sample preparation and/or method of registration of the spectrum: CsBr disc. Transmission.
Source: Dupuis and Lorenzelli (1969).
Wavenumbers (cm^{-1}): 960, 919sh, 898s, 850, 755sh, 542s.
Note: The wavenumbers were determined by us based on spectral curve analysis of the published spectrum.

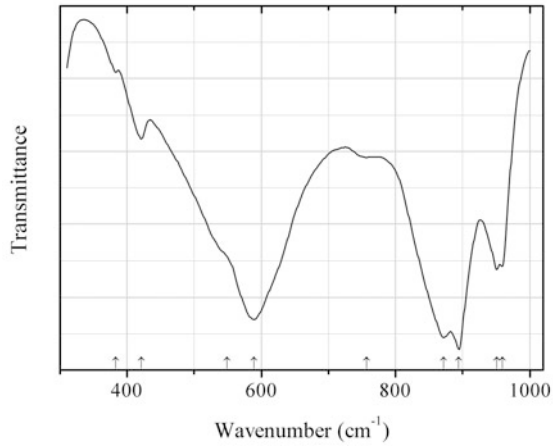

Fig. 2.1314 IR spectrum of calcium metavanadate tetrahydrate drawn using data from Dupuis and Lorenzelli (1969)

V76 Calcium metavanadate tetrahydrate $Ca(VO_3)_2{\cdot}4H_2O$ (Fig. 2.1314)
Locality: Synthetic.
Description: Synthesized in aqueous solution at pH of 7.5. Related to delrioite.
Kind of sample preparation and/or method of registration of the spectrum: CsBr disc. Transmission.
Source: Dupuis and Lorenzelli (1969).
Wavenumbers (cm^{-1}): 959, 951, 894s, 872s, 757, 589s, 549sh, 421, 383w.
Note: The wavenumbers were determined by us based on spectral curve analysis of the published spectrum.

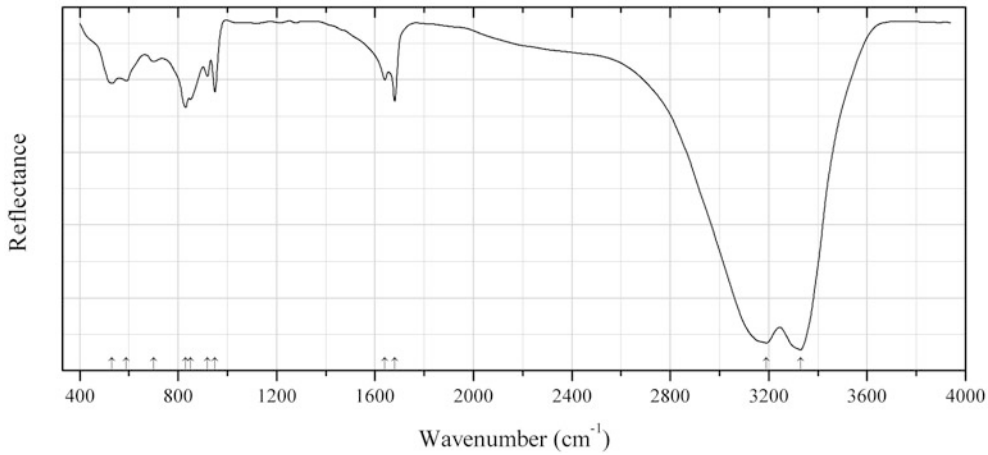

Fig. 2.1315 IR spectrum of dickthomssenite drawn using data from Hughes et al. (2001)

V77 Dickthomssenite $Mg(V_2O_6){\cdot}7H_2O$ (Fig. 2.1315)
Locality: Firefly–Pigmay mine, 16 km east of La Sal, San Juan Co., Utah, USA (type locality).
Description: Light golden brown platy crystals from the association with pascoite, sherwoodite, and native selenium. Holotype sample. Monoclinic, space group *C*2/*c*, a = 38.954(2), b = 7.2010(4), c = 16.3465(9) Å, β = 97.602(1)°, V = 4544.0(4) $Å^3$, Z = 16. D_{meas} = 1.96–2.09) g/cm^3. Optically biaxial (−), α = 1.6124(3), β = 1.6740(4), γ = 1.7104(4), 2 V = 74(1)°. The empirical formula is $(Mg_{0.94}Fe_{0.02})(V_2O_6){\cdot}nH_2O$. The strongest lines of the powder X-ray diffraction pattern [*d*, Å (*I*, %) (*hkl*)] are: 9.704 (100) (400), 8.117 (60) (002), 5.843 (100) (402), 4.061 (50) 004), 3.139 (90) (−12.0.2), 2.920 (60) (804), 2.707 (50) (006, −12.0.4).
Kind of sample preparation and/or method of registration of the spectrum: Attenuated total reflection of a single crystal.
Source: Hughes et al. (2001).
Wavenumbers (cm^{-1}): 3330s, 3190s, 1680, 1640, 950, 920, 850, 830, 700w, 590, 530.
Note: Orientation of the crystal is not indicated.

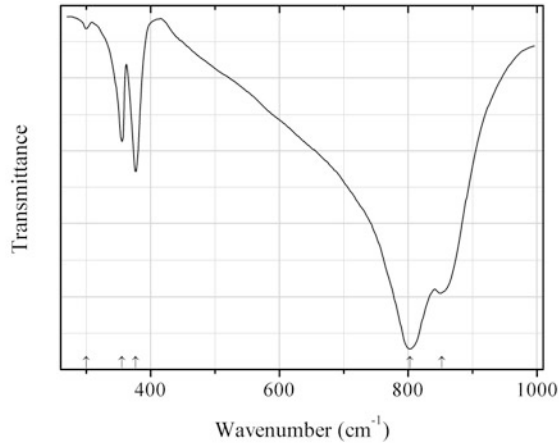

Fig. 2.1316 IR spectrum of gurimite drawn using data from Baran et al. (1972)

V78 Gurimite $Ba_2(VO_4)_2$ (Fig. 2.1316)
Locality: Synthetic.
Description: Synthesized in the solid-state reaction between V_2O_5 and $BaCO_3$.
Kind of sample preparation and/or method of registration of the spectrum: KBr or CsBr disc. Transmission.
Source: Baran et al. (1972).
Wavenumbers (cm^{-1}): 853s, 803s, 377, 355, 300w.

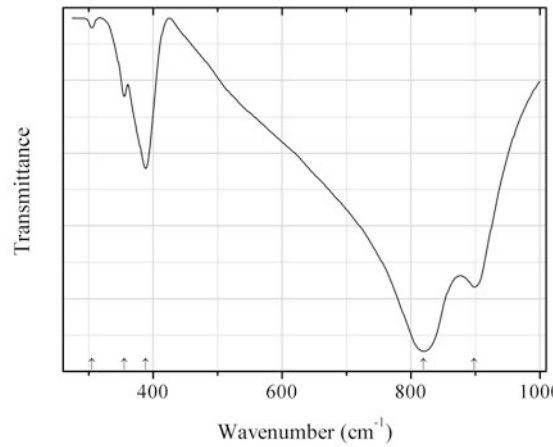

Fig. 2.1317 IR spectrum of gurimite Sr-analogue drawn using data from Baran et al. (1972)

V79 Gurimite Sr-analogue $Sr_3(VO_4)_2$ (Fig. 2.1317)
Locality: Synthetic.
Description: Synthesized in the solid-state reaction between V_2O_5 and $SrCO_3$.
Kind of sample preparation and/or method of registration of the spectrum: KBr or CsBr disc. Transmission.
Source: Baran et al. (1972).

Wavenumbers (cm^{-1}): 898s, 820s, 388, 355w, 305w.

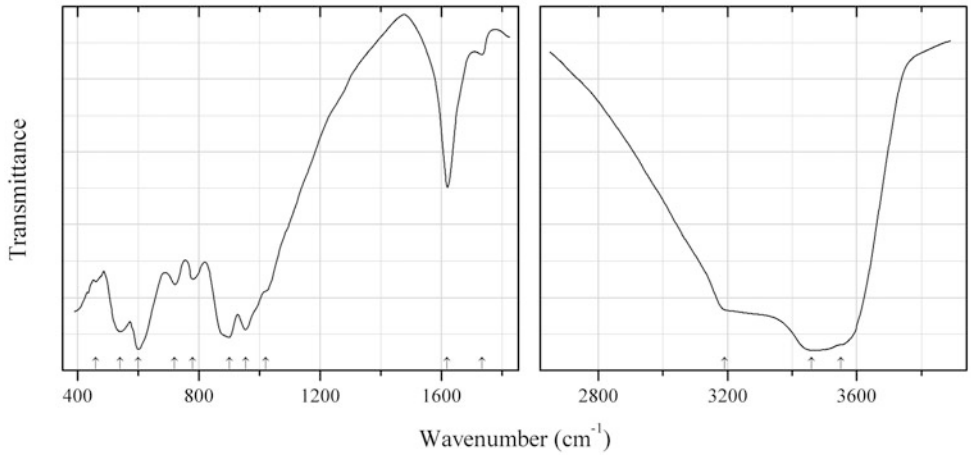

Fig. 2.1318 IR spectrum of alvanite drawn using data from Karpenko et al. (2004).

V80 Alvanite $(Zn,Ni)Al_4(VO_3)_2(OH)_{12}\cdot 2H_2O$ (Fig. 2.1318)
Locality: Kurumsak V deposit, Aksumbe, Karatau range (Kara-Tau Mts.), southern Kazakhstan (type locality).
Description: Confirned by electron microprobe analysis.
Kind of sample preparation and/or method of registration of the spectrum: KBr disc. Absorption.
Source: Karpenko et al. (2004).
Wavenumbers (cm^{-1}): 3550sh, 3460s, 3190sh, 1735w, 1620, 1020sh, 955s, 900s, 780, 720, 600s, 540s, 460w.

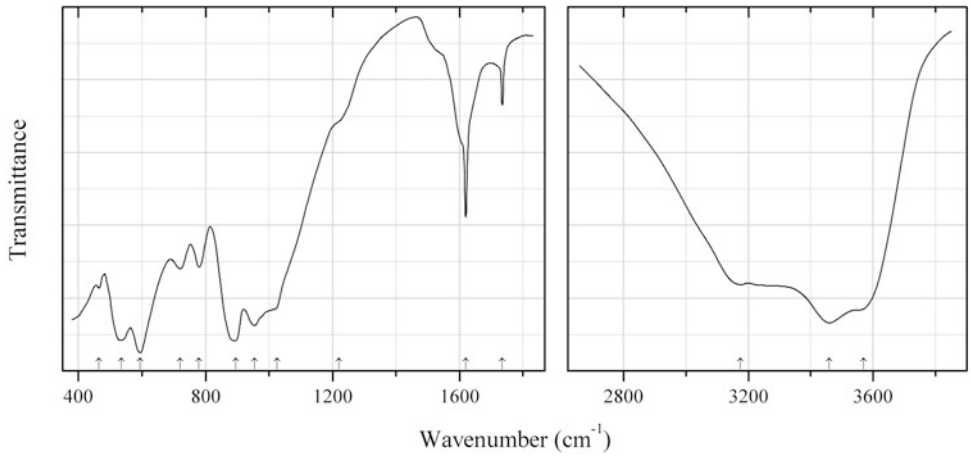

Fig. 2.1319 IR spectrum of ankinovichite drawn using data from Karpenko et al. (2004).

V81 Ankinovichite $NiAl_4(VO_3)_2(OH)_{12}\cdot 2H_2O$ (Fig. 2.1319)
Locality: Kara-Chagyr Mt., Osh region, Kara-Tau range, Kyrgyzstan (type locality).

Description: Light bluish-green elongate tabular crystals from the association with nickelalumite, kolovratite, volborthite, allophane, metatyuyamunite, roscoelite, gypsum, and tangeite. Monoclinic, space group $P2_1/n$, a = 17.8098(8), b = 5.1228(8), c = 8.8665(4) Å, β = 92.141(1)°, V = 808.4(2) Å^3, Z = 2. D_{meas} = 2.48(2) g/cm^3, D_{calc} = 2.476 g/cm^3. Optically biaxial (−), α = 1.653(2), β = 1.677(2), γ = 1.706(3), 2 V = 86(2)°. The empirical formula is $(Ni_{0.68}Zn_{0.17}Cu_{0.02}Fe_{0.01})_{0.88}Al_4(VO_3)_{1.88}Si_{0.06}(OH)_{12.12}\cdot 2.67H_2O$. The strongest lines of the powder X-ray diffraction pattern [d, Å (I, %) (*hkl*)] are: 8.89 (100) (200), 7.83 (100) (101), 3.354 (40) (012), 3.266 (50) (501), 1.970 (80) (422), 1.904 (70) (−621), 1.680 (40) (820), 1.481 (80) (−615).
Kind of sample preparation and/or method of registration of the spectrum: KBr disc. Absorption.
Source: Karpenko et al. (2004).
Wavenumbers (cm^{-1}): 3570sh, 3460s, 3175s, 1735, 1620, 1220sh, 1025sh, 955, 895s, 780, 720, 595s, 535s, 465.

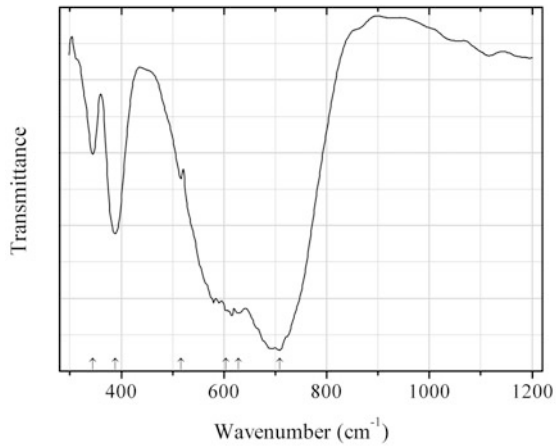

Fig. 2.1320 IR spectrum of chromium antimony vanadate V82 drawn using data from Filipek and Dąbrowska (2007)

V82 Chromium antimony vanadate V82 $CrSbVO_6$(Fig. 2.1320)
Locality: Synthetic.
Description: Synthesized from a stoichiometric mixture of oxides in a solid-state reaction. Tetragonal, a = 4.5719(12), c = 3.0282(8) Å, Z = 2. The strongest lines of the powder X-ray diffraction pattern are observed at 3.233, 2.526, 2.285, 2.210, 2.044, 1.694, 1.617, 1.514, and 1.446 Å.
Kind of sample preparation and/or method of registration of the spectrum: KBr disc. Transmission.
Source: Filipek and Dąbrowska (2007).
Wavenumbers (cm^{-1}): 708s, 628s, 604sh, 516sh, 388, 344.

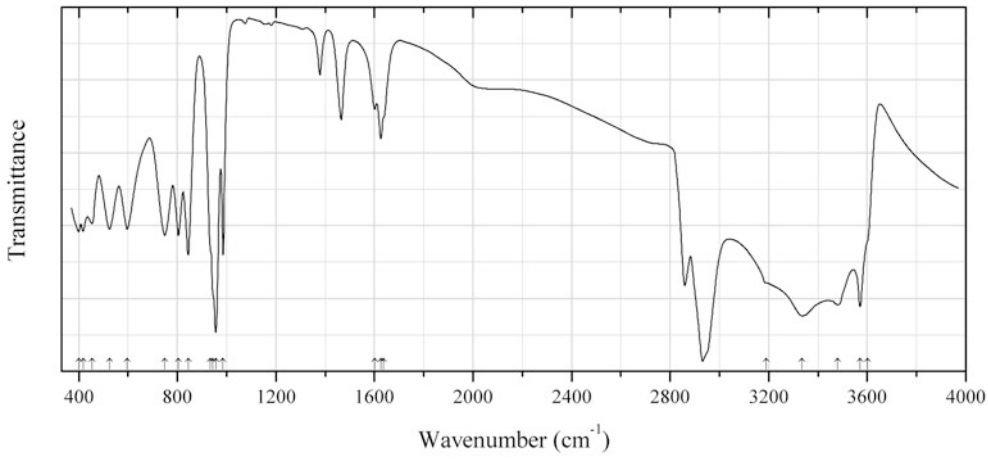

Fig. 2.1321 IR spectrum of potassium sodium decavanadate V83 drawn using data from Krasil'nikov et al. (2010)

V83 Potassium sodium decavanadate V83 $K_4Na_2V_{10}O_{28}\cdot 10H_2O$ (Fig. 2.1321)
Locality: Synthetic.
Description: Synthesized in the reaction between $Na(VO_3)$ and $K(H_2AsO_4)$ in aqueous solution. Triclinic, space group *P*-1, a = 8.5925(2), b = 10.3602(2), c = 10.9852(3) Å, α = 69.230(2)°, β = 87.123(2)°, γ = 66.185(2)°, V = 831.6 Å^3, Z = 1. Confirmed by chemical and thermal analyses.
Kind of sample preparation and/or method of registration of the spectrum: Transmission. Kind of sample preparation is not indicated.
Source: Krasil'nikov et al. (2010).
Wavenumbers (cm^{-1}): 3602sh, 3571s, 3480s, 3336sh, 3190sh, 1637sh, 1626, 1601, 986s, 956s, 945sh, 935sh, 844s, 804, 750, 596, 526, 454, 418s, 400.
Note: Bands in the ranges from 2800 to 3000 and from 1300 to 1500 cm^{-1} may be due to mineral oil used as immersion medium.

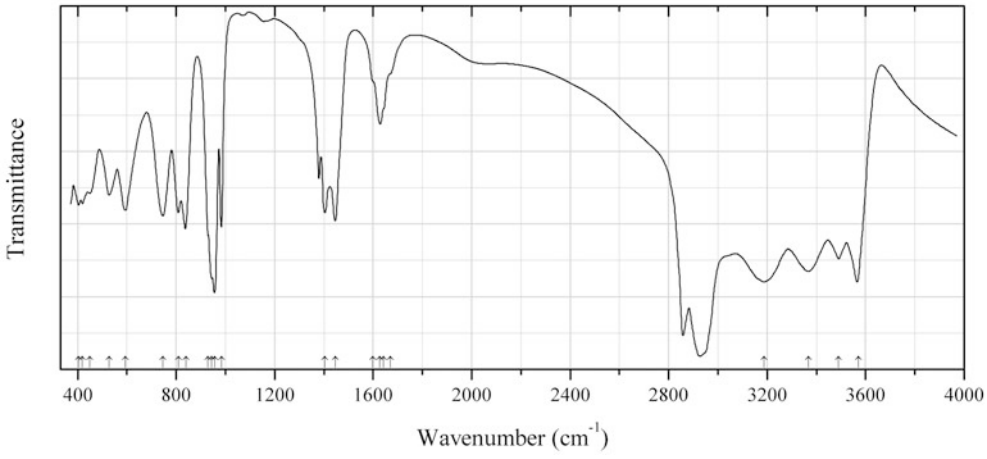

Fig. 2.1322 IR spectrum of ammonium sodium decavanadate V84 drawn using data from Krasil'nikov et al. (2010)

V84 Ammonium sodium decavanadate V84 $(NH_4)_4Na_2V_{10}O_{28}\cdot 10H_2O$ (Fig. 2.1322)

Locality: Synthetic.
Description: Synthesized in the reaction between $Na(VO_3)$ and $(NH_4)(H_2AsO_4)$ in aqueous solution. Triclinic, space group *P*-1, $a = 8.501(2)$, $b = 10.426(2)$, $c = 11.282(2)$ Å, $\alpha = 68.46(3)°$, $\beta = 87.30(3)°$, $\gamma = 67.14(3)°$, $V = 851.7$ Å^3, $Z = 1$. Confirmed by chemical and thermal analyses.
Kind of sample preparation and/or method of registration of the spectrum: Transmission. Kind of sample preparation is not indicated.
Source: Krasil'nikov et al. (2010).
Wavenumbers (cm^{-1}): 3570s, 3491s, 3368s, 3187s, 1670sh, 1642sh, 1628, 1600sh, 1446s, 1404s, 984s, 956s, 944w, 930sh, 839s, 809, 747, 594, 527, 450, 420, 403.
Note: Bands in the ranges from 2800 to 3000 cm^{-1} and (partially) from 1300 to 1500 cm^{-1} may be due to mineral oil used as immersion medium.

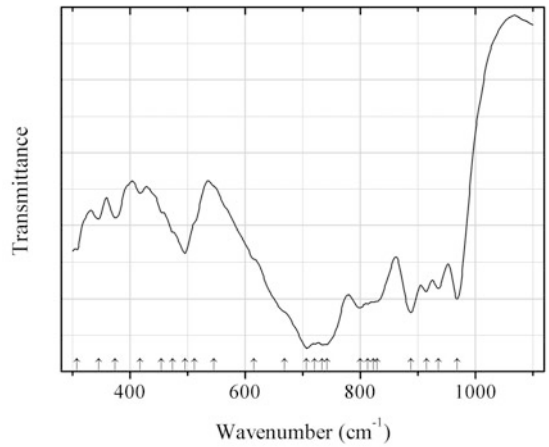

Fig. 2.1323 IR spectrum of howardevansite-type vanadate V85 drawn using data from Blonska-Tabero (2012)

V85 Howardevansite-type vanadate V85 β-$Cu_3Fe_4V_6O_{24}$ (Fig. 2.1323)
Locality: Synthetic.
Description: Synthesized by a solid-state reaction. Structurally related to howardevansite. Confirmed by powder X-ray diffraction data.
Kind of sample preparation and/or method of registration of the spectrum: KBr disc. Transmission.
Source: Blonska-Tabero (2012).
Wavenumbers (cm^{-1}): 969s, 936, 915, 888s, 830, 823, 813, 800s, 742s, 734s, 721s, 707s, 668sh, 615sh, 545sh, 512sh, 495, 474sh, 454, 417w, 374, 345, 307.
Note: The wavenumbers were determined by us based on spectral curve analysis of the published spectrum.

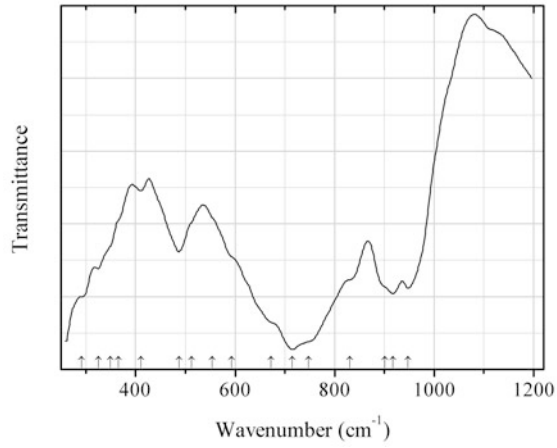

Fig. 2.1324 IR spectrum of howardevansite-type vanadate V86 drawn using data from Blonska-Tabero (2008)

V86 Howardevansite-type vanadate V86 $Zn_3Fe_4V_6O_{24}$ (Fig. 2.1324)
Locality: Synthetic.
Description: Synthesized by a solid-state reaction. Structurally related to howardevansite. Confirmed by powder X-ray diffraction data.
Kind of sample preparation and/or method of registration of the spectrum: KBr disc. Transmission.
Source: Blonska-Tabero (2008).
Wavenumbers (cm^{-1}): 947s, 917s, 901sh, 831sh, 748sh, 715s, 672sh, 593sh, 554sh, 512sh, 487, 411w, 365sh, 349sh, 325, 291sh.
Note: The wavenumbers were determined by us based on spectral curve analysis of the published spectrum.

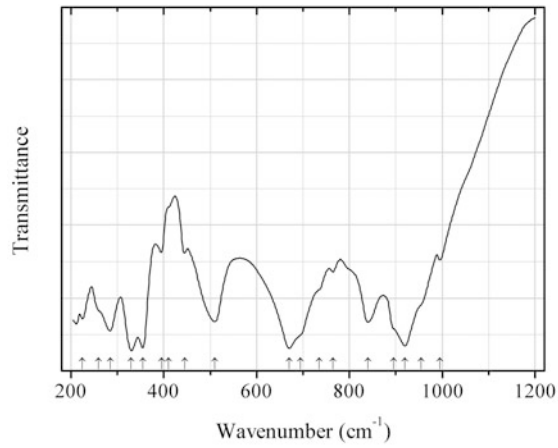

Fig. 2.1325 IR spectrum of iron(III) orthovanadate V87 drawn using data from Kurzawa (1992)

V87 Iron(III) orthovanadate V87 $Fe^{3+}(VO_4)$ (Fig. 2.1325)
Locality: Synthetic.

Kind of sample preparation and/or method of registration of the spectrum: CsI disc. Transmission.
Source: Kurzawa (1992).
Wavenumbers (cm^{-1}): 995w, 955sh, 920s, 895sh, 840, 765w, 735sh, 695sh, 670s, 510, 445w, 410sh, 395w, 355s, 330s, 285, 260sh, 225.

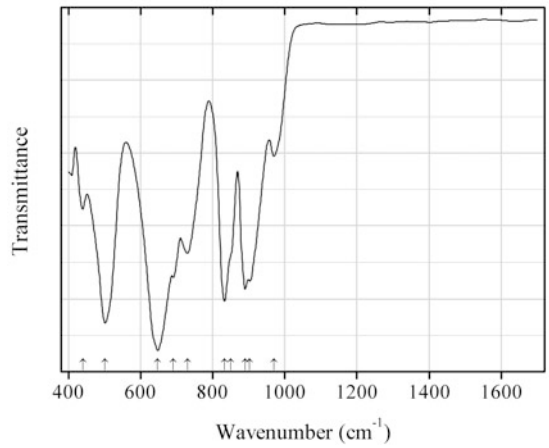

Fig. 2.1326 IR spectrum of iron(III) orthovanadate V88 drawn using data from Lehnen et al. (2014)

V88 Iron(III) orthovanadate V88 $Fe^{3+}(VO_4)$ (Fig. 2.1326)
Locality: Synthetic.
Description: Nanorods. Triclinic (JCPDS 38-1372). Confirmed by powder X-ray diffraction and Mössbauer spectroscopy data.
Kind of sample preparation and/or method of registration of the spectrum: Transmission. Kind of sample preparation is not indicated.
Source: Lehnen et al. (2014).
Wavenumbers (cm^{-1}): 970w, 903, 890, 850sh, 833, 730, 691w, 648s, 502s, 440w.
Note: The wavenumbers were partly determined by us based on spectral curve analysis of the published spectrum.

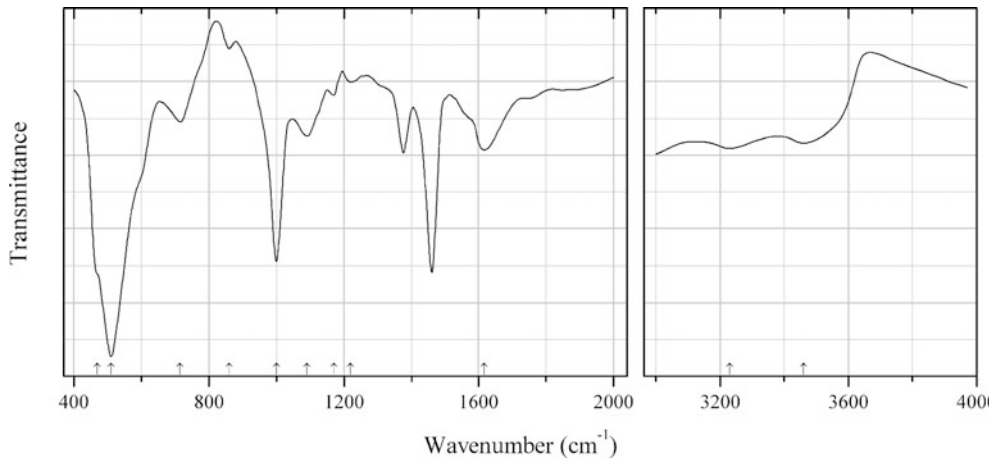

Fig. 2.1327 IR spectrum of kazakhstanite drawn using data from Ankinovitch et al. (1989)

V89 Kazakhstanite $Fe^{3+}{}_5V^{4+}{}_3V^{5+}{}_{12}O_{39}(OH)_9 \cdot 9H_2O$ (?) (Fig. 2.1327)
Locality: Balasauskandyk V deposit, Karatau range (Kara-Tau Mts.), southern Kazakhstan (type locality).
Description: Black spherulites from cavities in vanadium shist. Holotype sample. Monoclinic, space group *P*2/*c* or *Cc*, *a* = 11.84(1), *b* = 3.650(4), *c* = 21.27(1) Å, β = 100.0(1)°. D_{calc} = 3.52 g/cm^3. The strongest lines of the powder X-ray diffraction pattern [*d*, Å (*I*, %) (*hkl*)] are: 10.51 (100) (002), 3.484 (60) (110, 006), 2.915 (30) (400), 2.756 (30) (−115, −404), 2.606 (40) (311, 115).
Kind of sample preparation and/or method of registration of the spectrum: Nujol mull. Transmission.
Source: Ankinovitch et al. (1989).
Wavenumbers (cm^{-1}): 3460, 3230, 1616, 1220w, 1170w, 1091, 1000s, 860w, 715, 510s, 470sh.
Note: The wavenumbers were partly determined by us based on spectral curve analysis of the published spectrum. Bands in the range from 1300 to 1500 cm^{-1} correspond to Nujol.

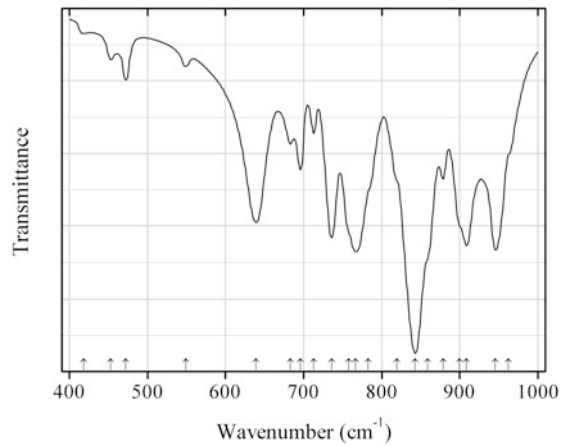

Fig. 2.1328 IR spectrum of lanthanum uranyl vanadate drawn using data from Mer et al. (2012)

V90 Lanthanum uranyl vanadate $[La(UO_2)V_2O_7][(UO_2)(VO_4)]$ (Fig. 2.1328)
Locality: Synthetic.
Description: Obtained by the solid state reaction between lanthanum chloride, U_3O_8, and V_2O at 800 °C. The crystal structure is solved. Orthorhombic, space group $P2_12_12_1$, *a* = 6.9470(2), *b* = 7.0934(2), *c* = 25.7464(6) Å, *V* = 1268.73(5) Å^3, *Z* = 4.
Kind of sample preparation and/or method of registration of the spectrum: KBr disc. Absorption.
Source: Mer et al. (2012).
Wavenumbers (cm^{-1}): 963sh, 946s, 909s, 900sh, 879, 859sh, 843s, 820sh, 783sh, 767s, 758sh, 736s, 713s, 696, 683, 639, 549w, 472w, 453w, 418w.

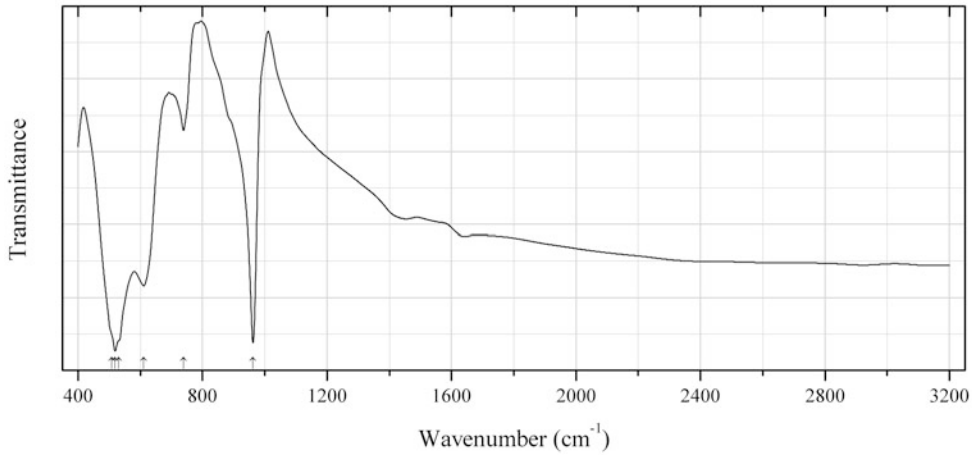

Fig. 2.1329 IR spectrum of lead chlorovanadate drawn using data from Şahin A (2004)

V91 Lead chlorovanadate $PbVO_3Cl$ (Fig. 2.1329)
Locality: Synthetic.
Description: Needle-shaped yellow crystals. Synthesized by a hydrothermal method from a reaction mixture of $NaVO_3$ and $PbCl_2$ at 170 °C for 3 days. Orthorhombic, space group *Pnma*, a = 10.022(2), b = 5.2875(11), c = 7.1714(14) Å, V = 380.00(13) Å^3, Z = 3. D_{calc} = 4.058 g/cm^3.
Kind of sample preparation and/or method of registration of the spectrum: A powder sample in the form of a disc. Transmission.
Source: Şahin (2014).
Wavenumbers (cm^{-1}): 962s, 739, 611, 530sh, 519s, 508sh.
Note: The wavenumbers were partly determined by us based on spectral curve analysis of the published spectrum.

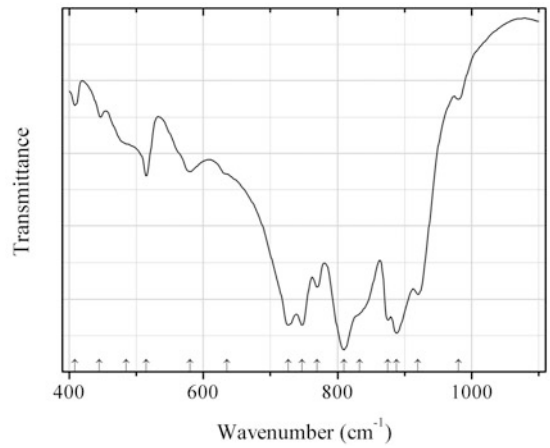

Fig. 2.1330 IR spectrum of lead uranyl divanadate drawn using data from Obbade et al. (2004)

V92 Lead uranyl divanadate $Pb(UO_2)(V_2O_7)$ (Fig. 2.1330)
Locality: Synthetic.

Description: Synthesized by a high temperature solid-state reaction. The crystal structure is solved. Monoclinic, space group $P2_1/n$, 6.9212(9), b = 9.6523(13), c = 11.7881(16) Å, β = 91.74(1)°, V = 787.01(2) Å^3, Z = 4. D_{meas} = 5.82(3) g/cm^3, D_{calc} = 5.83(1) g/cm^3.
Kind of sample preparation and/or method of registration of the spectrum: KBr disc. Transmission.
Source: Obbade et al. (2004).
Wavenumbers (cm^{-1}): 980w, 920, 888s, 875s, 833sh, 810s, 770, 747s, 727s, 635sh, 580, 515, 485sh, 445w, 409w.
Note: The wavenumbers were partly determined by us based on spectral curve analysis of the published spectrum.

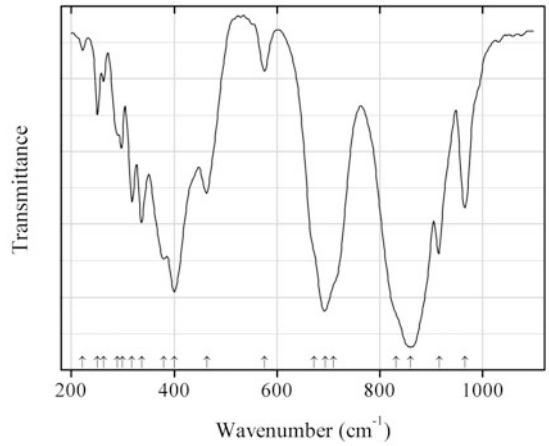

Fig. 2.1331 IR spectrum of magnesium orthovanadate drawn using data from Baran (1975)

V93 Magnesium orthovanadate $Mg_3(VO_4)_2$ (Fig. 2.1331)
Locality: Synthetic.
Description: Orthorhombic, space group *Cmca*, a = 6.053, b = 11.442, c = 8.330 Å.
Kind of sample preparation and/or method of registration of the spectrum: CsI disc. Transmission.
Source: Baran (1975).
Wavenumbers (cm^{-1}): 965, 915, 860s, 831sh, 710sh, 694s, 672sh, 576w, 464, 400s, 380s, 337, 318, 299, 289, 263w, 251w, 222w.
Note: The wavenumbers were partly determined by us based on spectral curve analysis of the published spectrum.

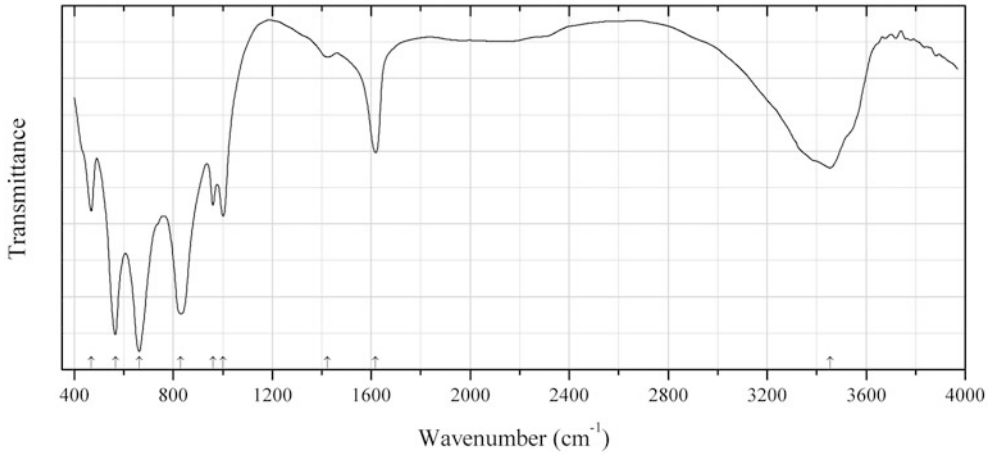

Fig. 2.1332 IR spectrum of melanovanadite drawn using data from Khan et al. (2012)

V94 Melanovanadite $CaV^{4+}{}_2V^{5+}{}_2O_{10}\cdot 5H_2O$ (Fig. 2.1332)
Locality: Synthetic.
Description: Synthesized hydrothermally and characterized by single-crystal X-ray diffraction and thermogravimetric analyses. The crystal structure is solved. Triclinic, space group *P*-1, a = 6.3232 (14), b = 6.3917(16), c = 7.9388(17) Å, α = 88.264(19)°, β = 67.428(16)°, γ = 79.433(20)°, V = 290.97(12) $Å^3$, Z = 1. D_{calc} = 2.626 g/cm^3.
Kind of sample preparation and/or method of registration of the spectrum: KBr disc. Absorption.
Source: Khan et al. (2012).
Wavenumbers (cm^{-1}): 3454, 1618, 1424w, 1002, 960, 829s, 663s, 566s, 469.

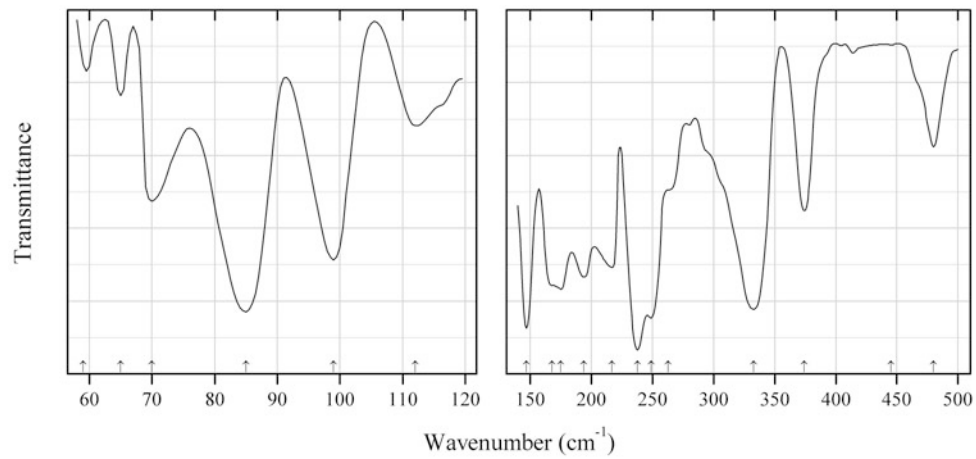

Fig. 2.1333 IR spectrum of metamunirite dimorph drawn using data from De Waal and Heyns (1992)

V95 Metamunirite dimorph α-$NaV^{5+}O_3$ (Fig. 2.1333)
Locality: Synthetic.
Description: Obtained in the reaction between V_2O_5 and Na_2CO_3 at 1173 K. Monoclinic, space group *C*2/*c*.

Kind of sample preparation and/or method of registration of the spectrum: Transmission. Kind of sample preparation is not indicated.
Source: De Waal and Heyns (1992).
Wavenumbers (cm^{-1}): 961, 941, 911, 836, 480, 445w, 374, 333s, 263sh, 249s, 238s, 217, 194, 175, 168sh, 147s, 135, 112, 99, 85s, 70, 65, 59w.
Note: The wavenumbers were partly determined by us based on spectral curve analysis of the published spectrum.

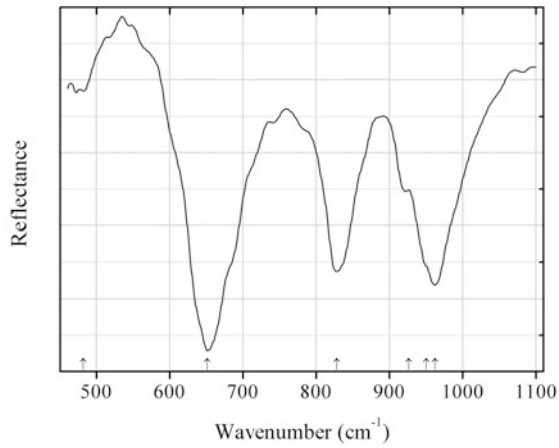

Fig. 2.1334 IR spectrum of metamunirite dimorph drawn using data from Grzechnik and McMillan (1996)

V96 Metamunirite dimorph α-$NaV^{5+}O_3$ (Fig. 2.1334)
Locality: Synthetic.
Description: Obtained in the reaction between V_2O_5 and Na_2CO_3 using Bridgman method. Monoclinic, space group *C*2/*c*. Confirmed by the powder X-ray diffraction pattern.
Kind of sample preparation and/or method of registration of the spectrum: Attenuated total reflection of a powdered mixture of α-$NaV^{5+}O_3$ with CsI.
Source: Grzechnik and McMillan (1996).
Wavenumbers (cm^{-1}): 962, 950sh, (926sh), 828s, 651s, 482w.

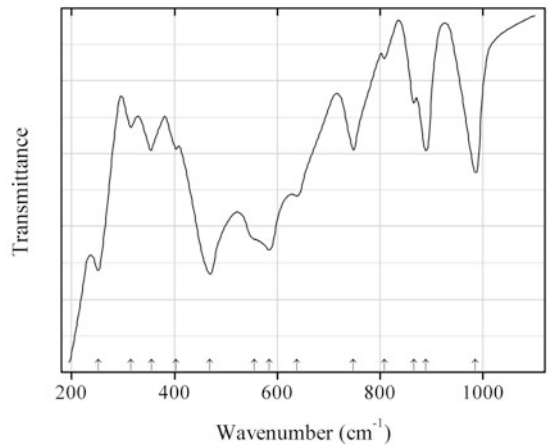

Fig. 2.1335 IR spectrum of metatyuyamunite drawn using data from Botto et al. (1989a)

V97 Metatyuyamunite $Ca(UO_2)_2(VO_4)_2 \cdot 3H_2O$ (Fig. 2.1335)
Locality: Monument #2 mine, Apache Co., Arizona, USA.
Description: A specimen from the Musée royal de l'Áfrique centrale, Tervuren, Belgium. Confirmed by powder X-ray diffraction data and electron microprobe analyses.
Kind of sample preparation and/or method of registration of the spectrum: KBr disc. Transmission.
Source: Botto et al. (1989a).
Wavenumbers (cm^{-1}): 985, 889, 865, 808w, 748, 638, 584s, 555sh, 469s, 403w, 355, 315w, 252.

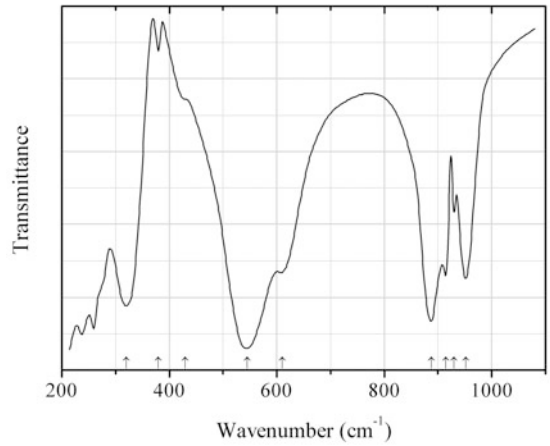

Fig. 2.1336 IR spectrum of metamunirite drawn using data from Seetharaman et al. (1983)

V98 Metamunirite β-$NaV^{5+}O_3$ (Fig. 2.1336)
Locality: Synthetic.
Description: Deep yellow powder obtained in the reaction between NH_4VO_3 and NaOH in aqueous solution with subsequent heating of precipitate at 100 °C.
Kind of sample preparation and/or method of registration of the spectrum: KBr disc. Transmission.
Source: Seetharaman et al. (1983).
Wavenumbers (cm^{-1}): 952, 930, 915, 888s, 610, 545s, 430, 380w, 320s.

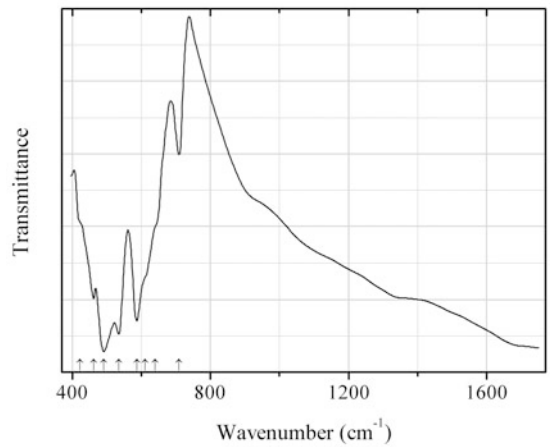

Fig. 2.1337 IR spectrum of oxyvanite drawn using data from Terukov et al. (1977)

V99 Oxyvanite $V^{3+}{}_2V^{4+}O_5$ (Fig. 2.1337)
Locality: Synthetic.
Description: Confirmed by powder X-ray diffraction data.
Kind of sample preparation and/or method of registration of the spectrum: Powder on KBr. Transmission.
Source: Terukov et al. (1977).
Wavenumbers (cm^{-1}): 710, 641sh, 612sh, 587s, 535s, 492s, 462, 422sh.
Note: The wavenumbers were partly determined by us based on spectral curve analysis of the published spectrum.

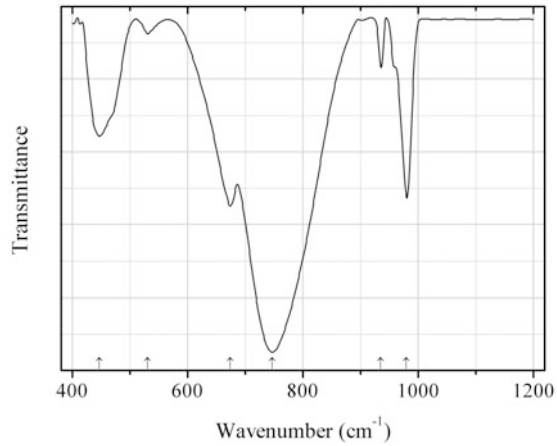

Fig. 2.1338 IR spectrum of potassium pentavanadate drawn using data from Yeon et al. (2010)

V100 Potassium pentavanadate $K_3(V_5O_{14})$ (Fig. 2.1338)
Locality: Synthetic.
Description: Prepared by a conventional solid-state method. The crystal structute is solved. Trigonal, space group $P31m$, a = 8.6970(16), c = 4.9434(19) Å, V = 323.81(15) $Å^3$, Z = 1.
Kind of sample preparation and/or method of registration of the spectrum: Transmission.
Source: Yeon et al. (2010).
Wavenumbers (cm^{-1}): 980, 935, 747s, 674, 530w, 446.

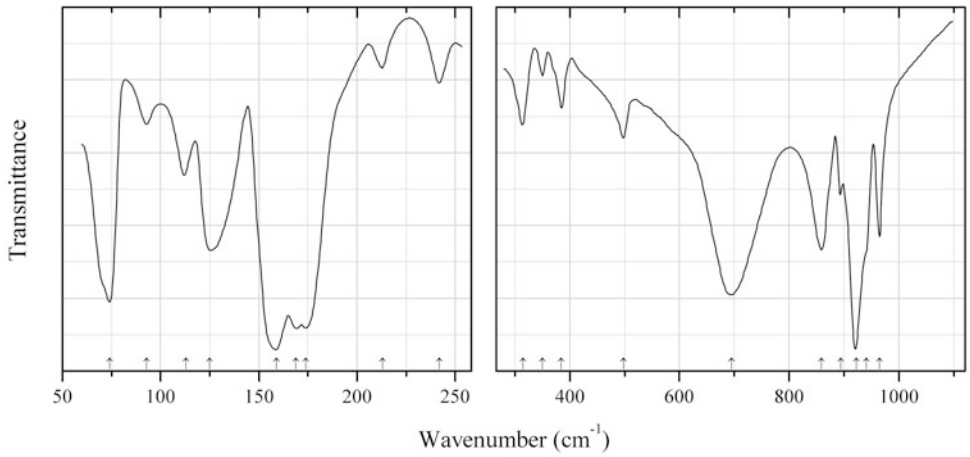

Fig. 2.1339 IR spectrum of potassium metavanadate drawn using data from Adams and Fletcher (1988)

V101 Potassium metavanadate $KV^{5+}O_3$ (Fig. 2.1339)
Locality: Synthetic.
Description: White powder prepared by the reaction in aqueous solution of potassium carbonate with vanadium (V) oxide. Orthorhombic, space group *Pbcm*, $a = 5.176(2)$, $b = 10.794(3)$, $c = 5.680(2)$ Å, $V = 317.3$ Å^3, $Z = 4$. $D_{calc} = 2.889$ g/cm^3.
Kind of sample preparation and/or method of registration of the spectrum: KBr disc. Transmission.
Source: Adams and Fletcher (1988).
Wavenumbers (cm^{-1}): 964, 940sh, 922s, 894, 859, 695s, 498, 385, 350w, 315, 242w, 213w, 174, 169, 159s, 125, 113, 93w, 74.
Note: The wavenumbers were partly determined by us based on spectral curve analysis of the published spectrum.

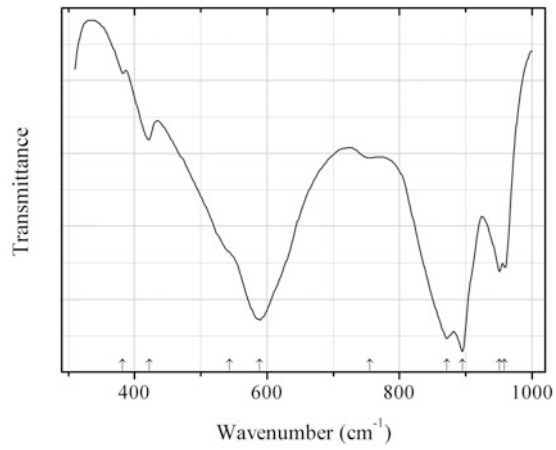

Fig. 2.1340 IR spectrum of rossite drawn using data from Dupuis and Lorenzelli (1969)

V102 Rossite $CaV^{5+}{}_2O_6 \cdot 4H_2O$ (Fig. 2.1340)

Locality: Synthetic.
Kind of sample preparation and/or method of registration of the spectrum: Suspension in mineral oil. Transmission.
Source: Dupuis and Lorenzelli (1969).
Wavenumbers (cm^{-1}): 959, 951, 895s, 872s, 755, 589s, 543sh, 422, 382w.
Note: The wavenumbers were determined by us based on spectral curve analysis of the published spectrum.

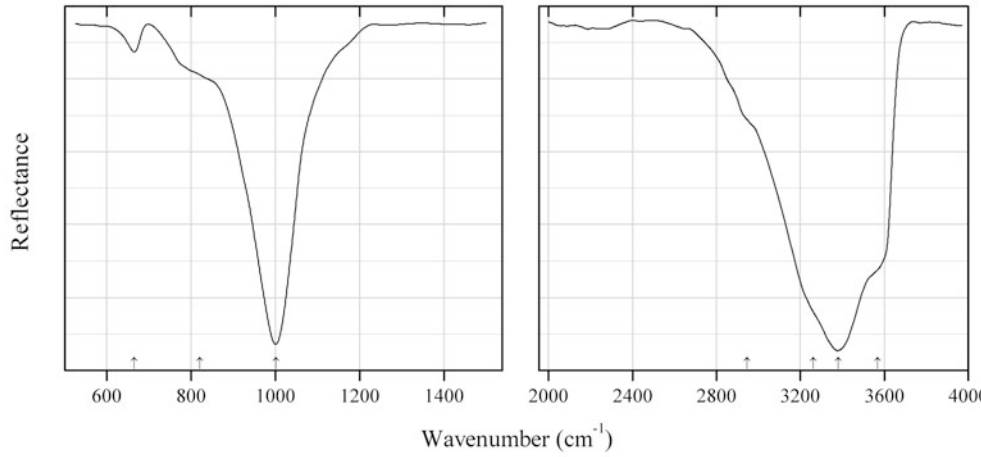

Fig. 2.1341 IR spectrum of schumacherite drawn using data from Frost et al. (2006c)

V103 Schumacherite $Bi_3(VO_4)_2O(OH)$ (Fig. 2.1341)
Locality: Synthetic (type locality).
Description: No data.
Kind of sample preparation and/or method of registration of the spectrum: Attenuated total reflection of powdered mineral.
Source: Frost et al. (2006c).
Wavenumbers (cm^{-1}): 3568sh, 3380s, 3263sh, 2945sh, 1001s, 820sh, 665w.
Note: Possibly erroneous data: the position of the strongest band near 1000 cm^{-1} corresponds to a silicate, but not to an orthovanadate.
Note: The wavenumbers were determined by us based on spectral curve analysis of the published spectrum.

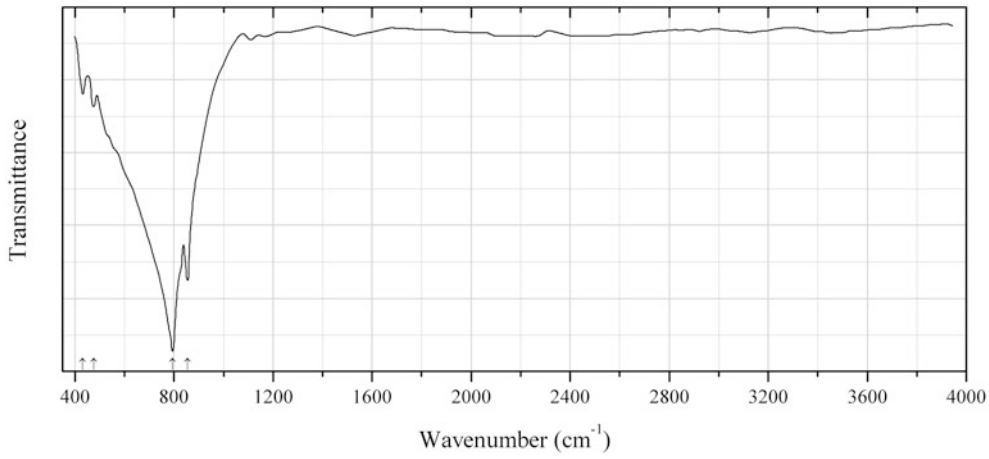

Fig. 2.1342 IR spectrum of alforsite V,F-analogue drawn using data from Kang et al. (2014)

V104 Alforsite V,F-analogue $Ba_5(VO_4)_3F$ (Fig. 2.1342)
Locality: Synthetic.
Description: Obtained in the solid-state reaction between barium ortho-vanadate and barium fluoride in a molar ratio of 3:1 at 850 °C for 1 h. Related to apatite-group minerals. Hexagonal, space group $P6_3/m$, a = 10.333(5), c = 7.697(7) Å, V = 711.7(8) Å^3, Z = 2. D_{calc} = 4.902 g/cm^3.
Kind of sample preparation and/or method of registration of the spectrum: KBr disc. Transmission.
Source: Kang et al. (2014).
Wavenumbers (cm^{-1}): 855s, 794s, 475w, 432w.

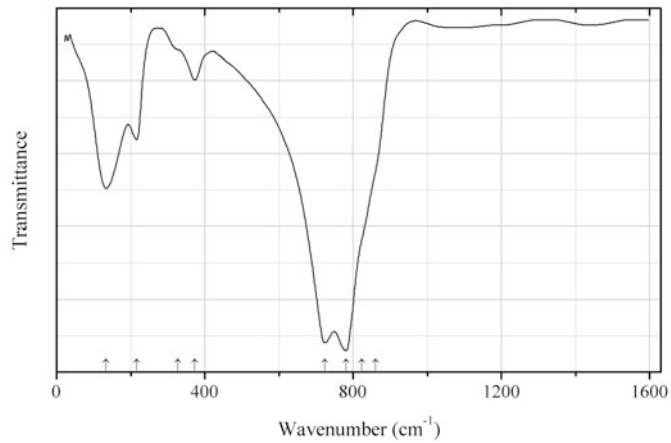

Fig. 2.1343 IR spectrum of vanadinite iodide analogue drawn using data from Zhang et al. (2007)

V105 Vanadinite iodide analogue $Pb_5(VO_4)_3I$ (Fig. 2.1343)
Locality: Synthetic.
Description: Synthesized in the solid-state reaction from the stoichiometric mixture of lead vanadate and lead iodide at 700 °C. Isostructural with vanadinite.
Kind of sample preparation and/or method of registration of the spectrum: No data.

Source: Zhang et al. (2007).
Wavenumbers (cm^{-1}): 860sh, 823sh, 781s, 724s, 373w, 327sh, 216, 133
Note: The wavenumbers were partly determined by us based on spectral curve analysis of the published spectrum.

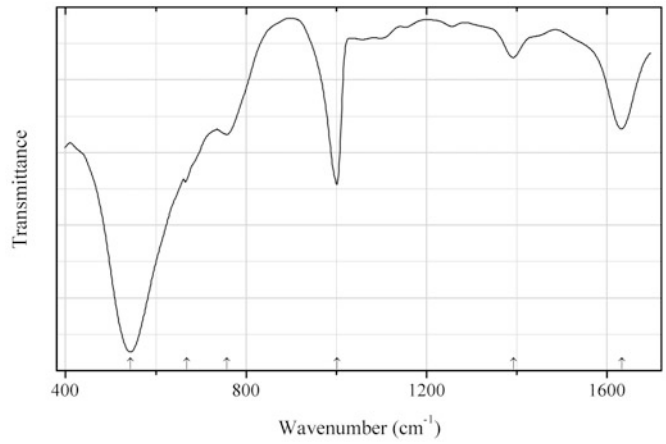

Fig. 2.1344 IR spectrum of bariandite Al-free analogue drawn using data from Menezes et al. (2009)

V106 Bariandite Al-free analogue $V_{10}O_{24}{\cdot}9H_2O$ (Fig. 2.1344)
Locality: Synthetic.
Description: Nanoparticles. Structurally related to bariandite. Characterized by powder X-ray diffraction data.
Kind of sample preparation and/or method of registration of the spectrum: KBr disc. Transmission.
Source: Menezes et al. (2009).
Wavenumbers (cm^{-1}): 1632, 1392w, 1001s, 758, (669), 544s.
Note: The wavenumbers were partly determined by us based on spectral curve analysis of the published spectrum.

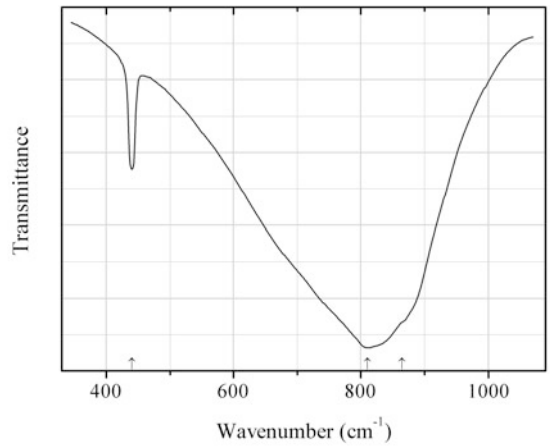

Fig. 2.1345 IR spectrum of wakefieldite-(Ce) drawn using data from Rao and Palanna (1995)

V107 Wakefieldite-(Ce) $Ce(VO_4)$ (Fig. 2.1345)
Locality: Synthetic.
Description: Obtained by heating a mixture of Ce_2O_3 and V_2O_5 in 1:1 ratio at 700 °C adopting the convential solid state ceramic technique.
Kind of sample preparation and/or method of registration of the spectrum: Nujol mull. Transmission.
Source: Rao and Palanna (1995).
Wavenumbers (cm^{-1}): 865sh, 810s, 440.

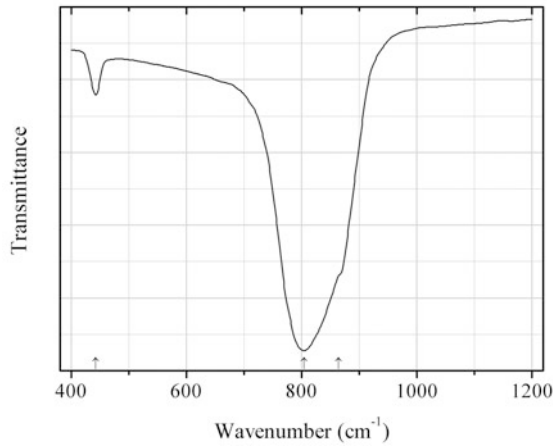

Fig. 2.1346 IR spectrum of wakefieldite-(La) drawn using data from Xie et al. (2012)

V108 Wakefieldite-(La) $La(VO_4)$ (Fig. 2.1346)
Locality: Synthetic.
Description: Nanocrystals obtained by a solution technique. Characterized by powder X-ray diffraction.
Kind of sample preparation and/or method of registration of the spectrum: KBr disc. Transmission.
Source: Xie et al. (2012)
Wavenumbers (cm^{-1}): 864sh, 804s, 442.

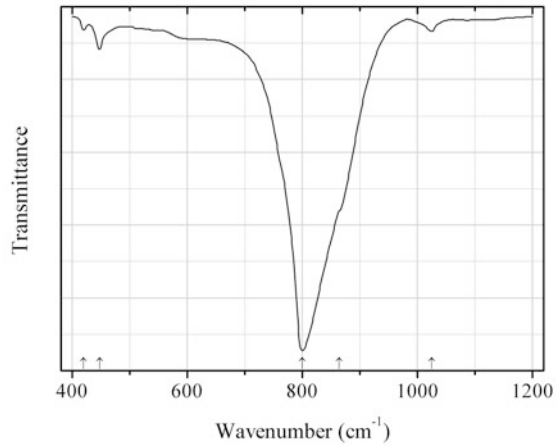

Fig. 2.1347 IR spectrum of wakefieldite-(Nd) drawn using data from Au and Zhang (1997)

V109 Wakefieldite-(Nd) $Nd(VO_4)$ (Fig. 2.1347)
Locality: Synthetic.
Description: Prepared by the citrate method. Tetragonal. The strongest lines of the powder X-ray diffraction pattern [*d*, Å (*I*, %)] are: 4.835 (30), 3.664 (100), 2.732 (75), 2.590 (20), 2.284 (16), 1.881 (55), 1.832 (16).
Kind of sample preparation and/or method of registration of the spectrum: Absorption. **Kind of sample preparation is not indicated.**
Source: Au and Zhang (1997).
Wavenumbers (cm^{-1}): 1025w, 864sh, 800s, 447, 419w.

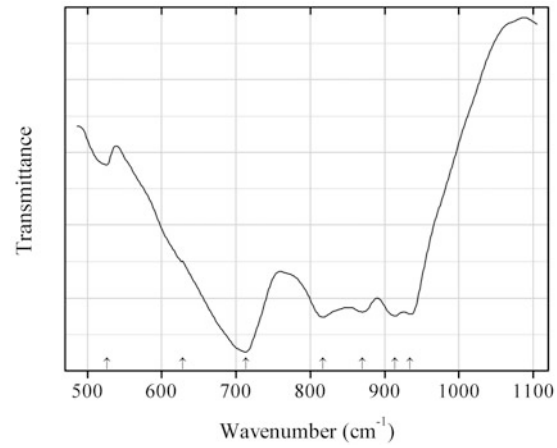

Fig. 2.1348 IR spectrum of ziesite drawn using data from De Waal and Hutter (1994)

V110 Ziesite β-$Cu_2V^{5+}{}_2O_7$ (Fig. 2.1348)
Locality: Synthetic.
Description: Synthesized using a procedure where the product is removed from the furnace at high temperature and quenched in air.
Kind of sample preparation and/or method of registration of the spectrum: KBr disc. Transmission.
Source: De Waal and Hutter (1994).
Wavenumbers (cm^{-1}): 934, 914, 870, 817, 713s, (628sh), 526w.

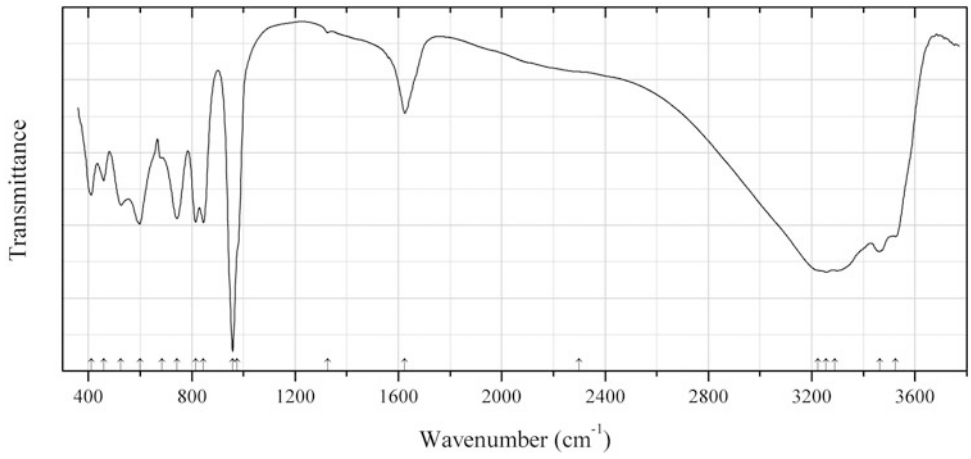

Fig. 2.1349 IR spectrum of huemulite obtained by N.V. Chukanov

V111 Huemulite $Na_4MgV^{5+}{}_{10}O_{28}\cdot 24H_2O$ (Fig. 2.1349)
Locality: Old Ni-V slag dump near the mine Kamariza, Agios Konstantinos, Lavrion, mining District, Attikí (Attika, Attica) Prefecture, Greece.
Description: Orange-yellow powdery aggregate from the association with grantsite, pascoite, and gypsum. Investigated by I.V. Pekov. The empirical formula is (electron microprobe): $Na_{4.45}Mg_{1.05}Al_{0.07}V_{8.81}Si_{0.10}\cdot nH_2O$. Confirmed by powder X-ray diffraction data.
Kind of sample preparation and/or method of registration of the spectrum: KBr disc. Absorption.
Wavenumbers (cm^{-1}): 3525sh, 3463s, 3290s, 3255s, 3225sh, 2300sh, 1624, 1326w, 975sh, 958s, 845s, 815s, 743s, 685sh, 599s, 526, 459, 411.

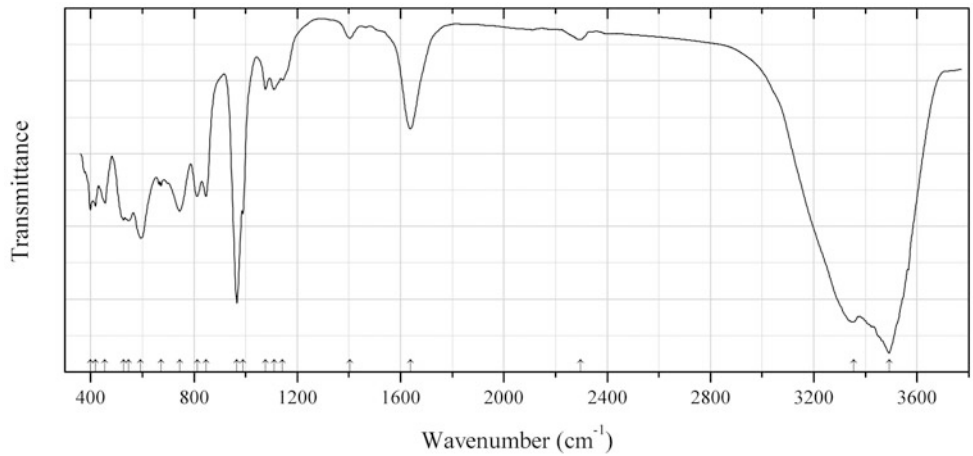

Fig. 2.1350 IR spectrum of postite obtained by N.V. Chukanov

V112 Postite $MgAl_2(V^{5+}{}_{10}O_{28})(OH)_2\cdot 27H_2O$ (Fig. 2.1350)
Locality: Vanadium Queen mine, La Sal Creek canyon, San Juan Co., Utah, USA (type locality).
Description: Yellow aggregates of acicular crystals. The empirical formula is (electron microprobe): $Mg_{1.0}(Al_{1.4}Fe^{3+}_{0.5}V^{3+}_{0.1})(V_{10}{}^{5+}O_{28})(OH)_2\cdot nH_2O$.
Kind of sample preparation and/or method of registration of the spectrum: KBr disc. Absorption.

Wavenumbers (cm^{-1}): 3492s, 3355s, 2296w, 1638, 1403w, 1143, 1110, 1076, 989s, 966s, 846, 812, 745s, 672, 593s, 546s, 527s, 456, 418, 400.

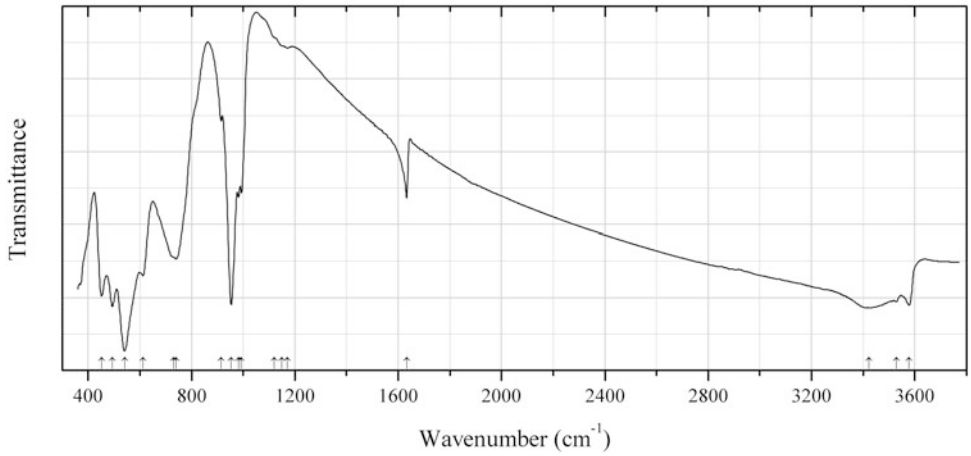

Fig. 2.1351 IR spectrum of bannermanite obtained by N.V. Chukanov

V113 Bannermanite $(Na,K)_xV^{4+}{}_xV^{5+}{}_{6-x}O_{15}$ $(0.5 < x < 0.9)$ (Fig. 2.1351)
Locality: Old Ni-V slag dump near the mine Kamariza, Agios Konstantinos, Lavrion, mining District, Attikí (Attika, Attica) Prefecture, Greece.
Description: Aggregate of prismatic crystals. Dark brown with brown-red reflections. A hydrated variety (with H_2O instead of vacancies in structural channels). The empirical formula is (electron microprobe): $Na_{0.97}(V_{5.97}Fe_{0.03})O_{15}\cdot nH_2O$. The idealized formula is $NaV^{5+}{}_5V^{4+}O_{15}\cdot H_2O$. Confirmed by single-crystal X-ray diffraction data obtained by I.V. Pekov. Monoclinic, a = 10.17, b = 3.62, c = 15.51 Å, β = 109.5°.
Kind of sample preparation and/or method of registration of the spectrum: KBr disc. Absorption.
Wavenumbers (cm^{-1}): 3578, 3528, 3423, 1633, 1172w, 1150sh, 1120sh, 993, 982, 953s, 915, 741, 730sh, 612, 541s, 494s, 452s.

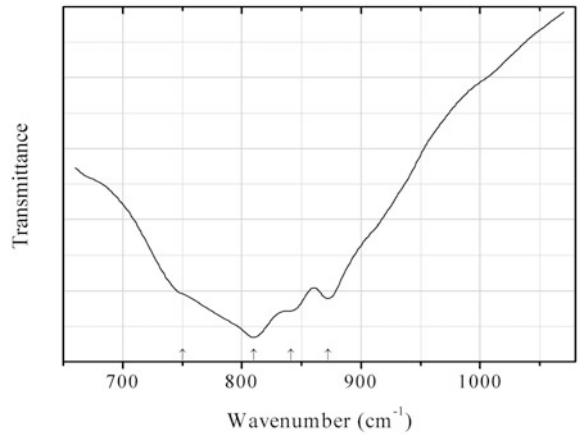

Fig. 2.1352 IR spectrum of calcium orthovanadate drawn using data from Baran and Aymonino (1969)

V114 Calcium orthovanadate $Ca_3(VO_4)_2$ (Fig. 2.1352)
Locality: Synthetic.
Description: Synthesized by solid-state reaction in the stoichiometric mixture of $CaCO_3$ and V_2O_5 at 700–800 °C during several hours. The product was grinded and annealed repeatedly at 700–800 °C during several hours. Monoclinic, space group *C*2/*c*, *Z* = 4. The strongest lines of the powder X-ray diffraction pattern [*d*, Å (*I*, %)] are: 5.49 (18), 3.552 (28), 3.334 (55), 2.975 (100), 2.855 (27), 2.710 (70), 2.608 (20), 2.005 (21).
Kind of sample preparation and/or method of registration of the spectrum: KBr disc. Transmission.
Source: Baran and Aymonino (1969).
Wavenumbers (cm^{-1}): 872, 841sh, 810s, 750sh.

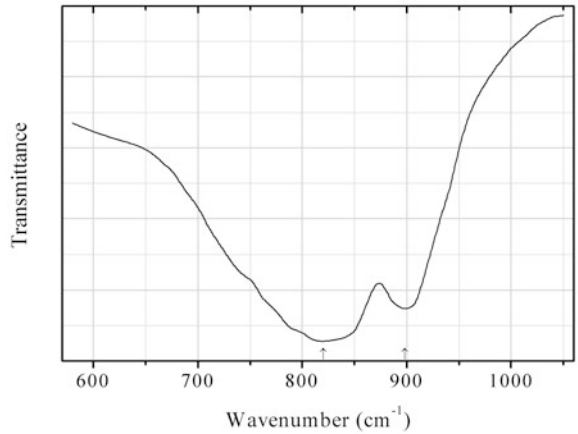

Fig. 2.1353 IR spectrum of strontium orthovanadate drawn using data from Baran and Aymonino (1969)

V115 Strontium orthovanadate $Sr_3(VO_4)_2$ (Fig. 2.1353)
Locality: Synthetic.
Description: Synthesized by solid-state reaction in the stoichiometric mixture of $SrCO_3$ and V_2O_5 at 700–800 °C during several hours. The product was grinded and annealed repeatedly at 700–800 °C during several hours. Trigonal, space group *R*5*m*, *Z* = 1.
Kind of sample preparation and/or method of registration of the spectrum: KBr disc. Transmission.
Source: Baran and Aymonino (1969).
Wavenumbers (cm^{-1}): 898, 820s.

2.13 Chromates

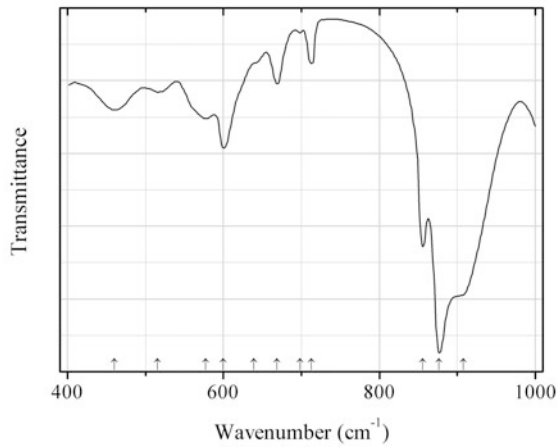

Fig. 2.1354 IR spectrum of chromatite drawn using data from Sokol et al. (2011)

Cr15 Chromatite $Ca(CrO_4)$ (Fig. 2.1354)
Locality: Nabi Musa Hill, Mottled Zone, Judean Desert, Israel.
Description: Yellow fine-grained aggregate from the association with Ca-carbonates, gypsum, afwillite, tyuyamunite, and strelkinite. The empirical formula is $Ca_{1.03}(CrO_4)_{1.82}(SO_4)_{1.09}O_{0.24}$.
Kind of sample preparation and/or method of registration of the spectrum: KBr disc. Absorption.
Source: Sokol et al. (2011).
Wavenumbers (cm^{-1}): 908s, 877s, 856, 713, 698w, 669, 639sh, 600, 577, 515, 460.
Note: The wavenumbers were partly determined by us based on spectral curve analysis of the published spectrum. The bands at 877 and 713 cm^{-1} coincide with IR absorption bands of associated calcite. The band at 699 cm^{-1} coincides with IR absorption band of associated aragonite. The bands at 669, 600, and 460 cm^{-1} are due to the admixture of gypsum.
Note: Wavenumbers in the IR spectrum of the synthetic analogue of chromatite are (Stoilova et al. 2005): 924sh, 912s, 902s, 870, 850.

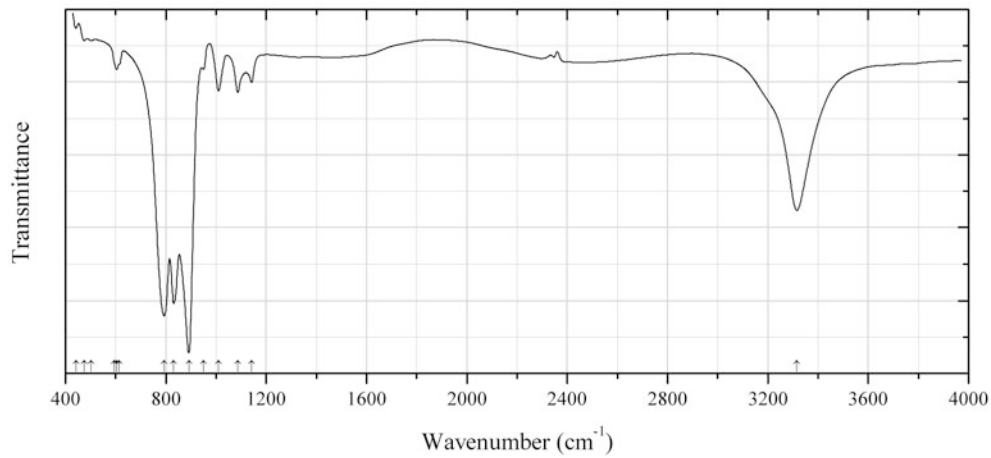

Fig. 2.1355 IR spectrum of georgerobinsonite drawn using data from Cooper et al. (2011)

Cr16 Georgerobinsonite $Pb_4(CrO_4)_2(OH)_2FCl$ (Fig. 2.1355)
Locality: Mammoth–St. Anthony mine, Tiger, Pinal Co., Arizona, USA (type locality).
Description: Intergrowths of thin tabular orange crystals from the association with caledonite, a cerchiaraite-related mineral, cerussite, diaboleite, Cr-bearing leadhillite, matlockite, murdochite, pinalite, wulfenite, and yedlinite. Holotype sample. Orthorhombic, space group *Pmmn*, $a = 7.613(2)$, $b = 11.574(3)$, $c = 6.883(2)$ Å, $V = 606.5(3)$ Å^3, $Z = 2$. $D_{calc} = 6.23$ g/cm^3. Optically biaxial (+), $\alpha \approx 2.07$, $\beta > 2.11$, $\gamma > 2.11$, $2V = 84(2)°$. The empirical formula is $Pb_{4.09}(Cr^{6+}_{1.73}S^{6+}_{0.24})O_8(OH)_{1.98}F_{0.90}Cl_{1.12}$. The strongest lines of the powder X-ray diffraction pattern [*d*, Å (*I*, %) (*hkl*)] are: 6.371 (60) (110), 3.357 (60) (031, 201), 3.308 (80) (012), 3.195 (80) (211, 220), 3.143 (60) (102), 2.131 (100) (232).
Kind of sample preparation and/or method of registration of the spectrum: Absorbance of a powdered sample.
Source: Cooper et al. (2011).
Wavenumbers (cm^{-1}): 3316s, 1142, 1087, 1011, 950w, 892s, 831s, 793s, 502, 614sh, 604w, 593sh, 474w, 442w.
Note: The wavenumbers were determined by us based on spectral curve analysis of the published spectrum.

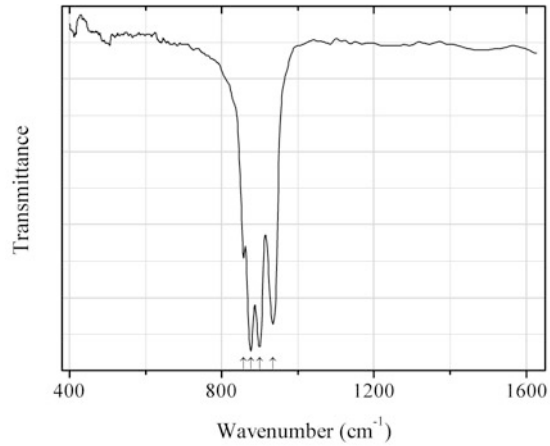

Fig. 2.1356 IR spectrum of hashemite drawn using data from Campbell (1965)

Cr17 Hashemite $Ba(CrO_4)$ (Fig. 2.1356)
Locality: Synthetic.
Kind of sample preparation and/or method of registration of the spectrum: KBr disc. Transmission.
Source: Campbell (1965).
Wavenumbers (cm^{-1}): 935s, 900s, 876s, 857.
Note: The wavenumbers were determined by us based on spectral curve analysis of the published spectrum.

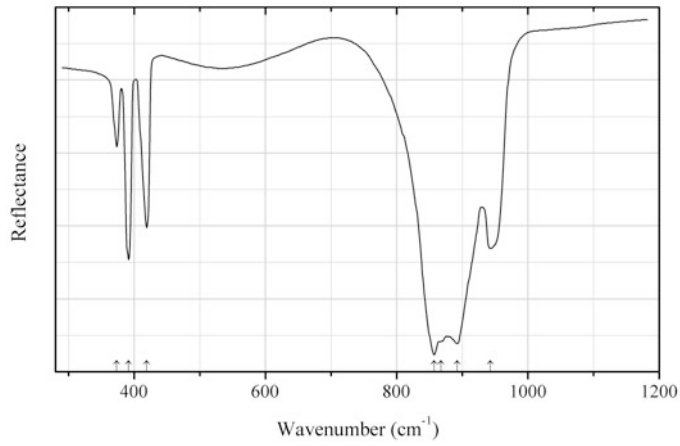

Fig. 2.1357 IR spectrum of hashemite drawn using data from Scheuermann and Schutte (1973)

Cr18 Hashemite $Ba(CrO_4)$ (Fig. 2.1357)
Locality: Synthetic.
Description: Prepared by precipitation from aqueous solutions of potassium chromate and barium chloride and dried at 150 °C. Confirmed by the powder X-ray diffraction pattern.
Kind of sample preparation and/or method of registration of the spectrum: Attenuated total reflection of powdered sample.
Source: Scheuermann and Schutte (1973).
Wavenumbers (cm^{-1}): 943s, 892s, 868sh, 857s, 419, 391, 373.

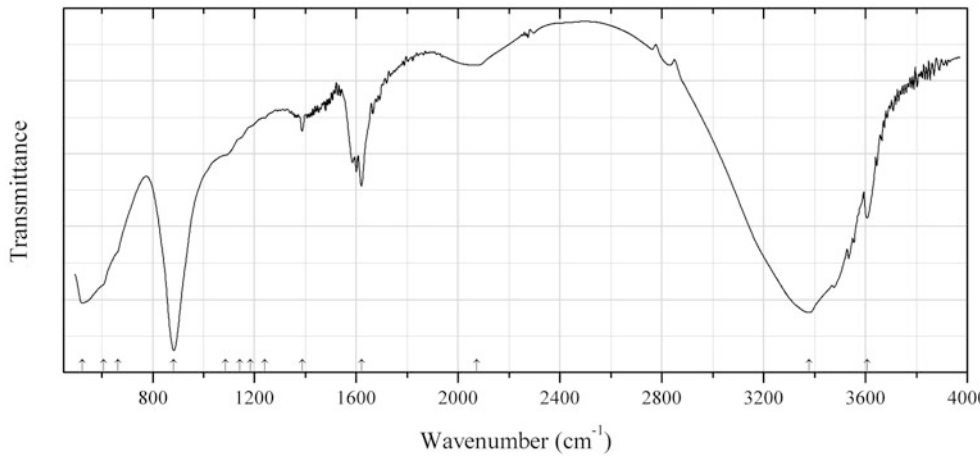

Fig. 2.1358 IR spectrum of ettringite chromate analogue drawn using data from Perkins and Palmer (2000)

Cr19 Ettringite chromate analogue $Ca_6Al_2(CrO_4)_3(OH)_{12}\cdot 26H_2O$ (Fig. 2.1358)
Locality: Synthetic.
Description: Synthesized from aqueous suspension of tricalcium aluminate and calcium chromate at *ca*. 23 °C. Condirmed by X-ray diffraction and electron microprobe analysis. The strongest lines of the powder X-ray diffraction pattern [*d*, Å (*I*, %) (*hkl*)] are: 9.938 (78) (100), 5.690 (100) (110), 5.040 (51) (112), 4.718 (45) (104), 3.908 (68) (114), 2.806 (44) (304), 2.230 (44) (226).

Kind of sample preparation and/or method of registration of the spectrum: KBr disc. Transmission.
Source: Perkins and Palmer (2000).
Wavenumbers (cm^{-1}): 3607, 3380s, 2074, 1620, 1387, 1240w, 1185sh, 1142sh, 1085sh, 883s, 663sh, 608sh, 523s.
Note: The absorptions in the range from 1300 to 1500 cm^{-1} indicate the admixture of carbonate and/or nitrate anions.
Note: The wavenumbers were partly determined by us based on spectral curve analysis of the published spectrum.

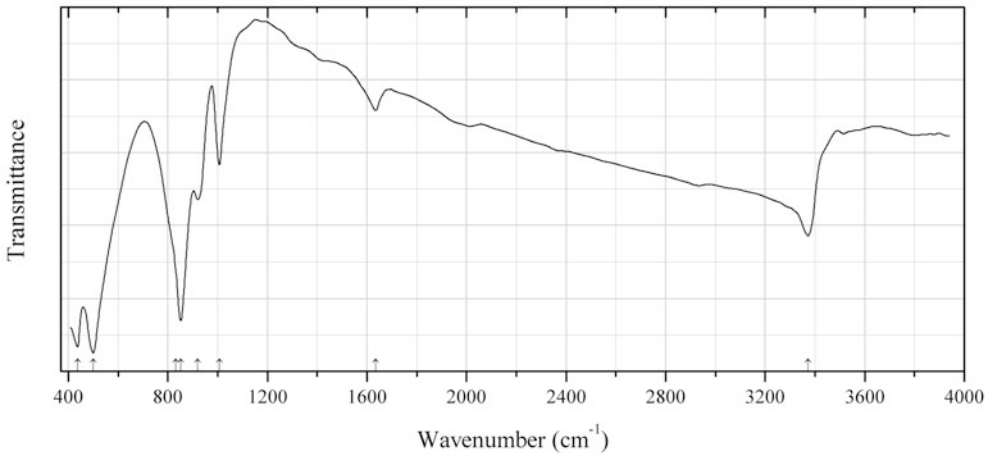

Fig. 2.1359 IR spectrum of jarosite chromate analogue drawn using data from Baron and Palmer (1996)

Cr20 Jarosite chromate analogue $KFe^{3+}{}_3(CrO_4)_2(OH)_6$ (Fig. 2.1359)
Locality: Synthetic.
Description: Prepared from the aqueous solution of $K_2(CrO_4)$ and $Fe(NO_3)_3 \cdot 9H_2O$ at 95 °C. Hexagonal, space group *R*-3, a = 7.427(6), c = 17.50(4) Å. Confirmed by electron microprobe analysis and X-ray diffraction data. The strongest lines of the powder X-ray diffraction pattern [d, Å (I, %) (hkl)] are: 5.19 (41) (012), 3.72 (25) (110), 3.17 (96) (021), 3.136 (100) (113), 2.327 (28) (122), 2.018 (35) (033), 1.857 (33) (220).
Kind of sample preparation and/or method of registration of the spectrum: Transmission. Kind of sample preparation is not indicated.
Source: Baron and Palmer (1996).
Wavenumbers (cm^{-1}): 3373, 1635w, 1007, 921, 852s, 832sh, 500s, 439s.
Note: The band at 1635 cm^{-1} indicates the presence of H_2O molecules.

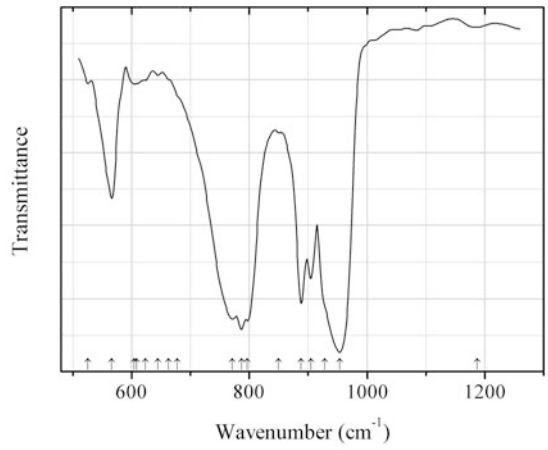

Fig. 2.1360 IR spectrum of lópezite drawn using data from Low et al. (1982)

Cr21 Lópezite $K_2Cr_2O_7$ (Fig. 2.1360)
Locality: Synthetic.
Kind of sample preparation and/or method of registration of the spectrum: Powdered sample. Absorption.
Source: Low et al. (1982).
Wavenumbers (cm^{-1}): 1187, 954s, 928sh, 905, 888, 850w, 797s, 787s, 771s, 678sh, 663sh, 645w, 623w, 609sh, 604w, 566, 526w.
Note: The wavenumbers were determined by us based on spectral curve analysis of the published spectrum.

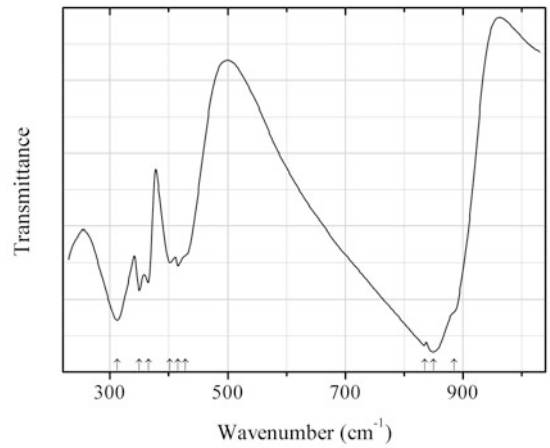

Fig. 2.1361 IR spectrum of phoenicochroite drawn using data from Roncaglia et al. (1985)

Cr22 Phoenicochroite $Pb_2(CrO_4)O$ (Fig. 2.1361)
Locality: Synthetic.

Description: Prepared by solid-state reaction of the stoichiometric mixture of PbO and Cr_2O_3 in air at 650 °C after a previous calcination at 500 °C. Confirmed by the powder X-ray diffraction pattern. Monoclinic, space group *C*2/*m*, *Z* = 4.
Kind of sample preparation and/or method of registration of the spectrum: KBr disc. Transmission.
Source: Roncaglia et al. (1985).
Wavenumbers (cm^{-1}): 885sh, 850s, 835sh, 428sh, 415, 402, 365, 350, 312s.

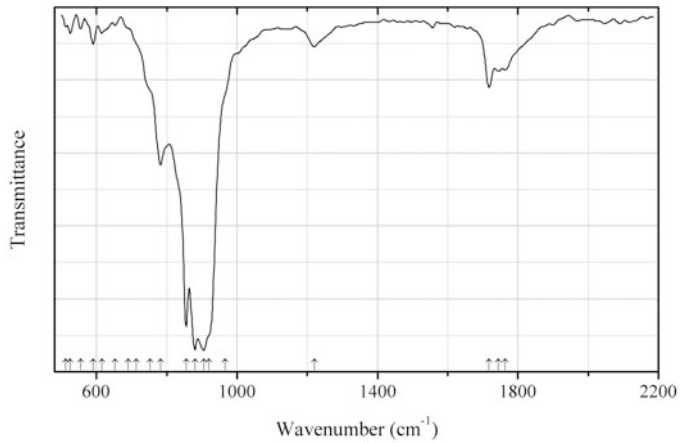

Fig. 2.1362 IR spectrum of tarapacáite drawn using data from Low et al. (1982)

Cr23 Tarapacáite $K_2(CrO_4)$ (Fig. 2.1362)
Locality: Synthetic.
Kind of sample preparation and/or method of registration of the spectrum: Absorbance of powdered sample.
Source: Low et al. (1982).
Wavenumbers (cm^{-1}): 1764w, 1745w, 1718, 1220w, 966sh, 920sh, 905s, 880s, 855s, 782, 753sh, 713sh, 690sh, 653w, 615w, 590w, 555w, 525w, 512w.
Note: The wavenumbers were determined by us based on spectral curve analysis of the published spectrum. Possibly a mixture with $K_2Cr_2O_7$. Wavenumbers of the bands in the IR absorption spectrum of pure $K_2(CrO_4)$ are: 946sh, 920sh, 892s, 855, (402) (after Moenke 1966).

2.14 Germanates

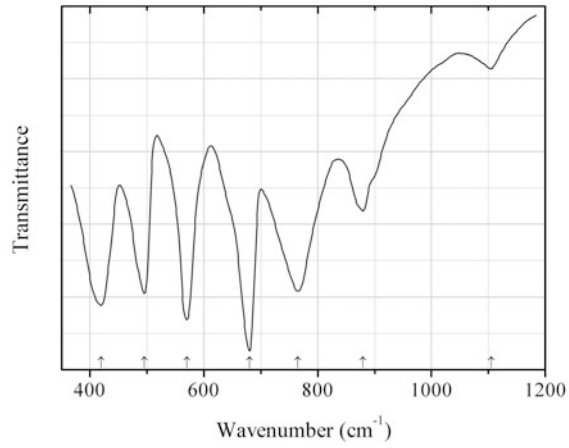

Fig. 2.1363 IR spectrum of carboirite drawn using data from Julliot et al. (1987)

Ge1 Carboirite $Fe^{2+}Al_2GeO_5(OH)_2$ (Fig. 2.1363)
Locality: Synthetic.
Description: Confirmed by powder X-ray diffraction data.
Kind of sample preparation and/or method of registration of the spectrum: KBr disc. Transmission.
Source: Julliot et al. (1987).
Wavenumbers (cm^{-1}): 3497s, 3346, 3133, 1105w, 880, 765, 680s, 570, 495, 419.

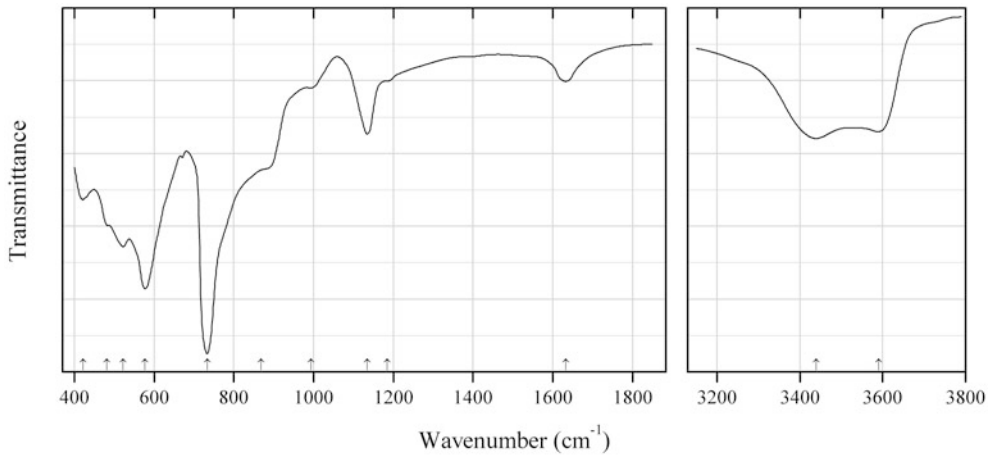

Fig. 2.1364 IR spectrum of krieselite drawn using data from Schlüter et al. (2010)

Ge2 Krieselite $Al_2(GeO_4)(F,OH)_2$ (Fig. 2.1364)
Locality: Tsumeb mine, Tsumeb, Namibia (type locality).
Description: Beige to white aggregate of fibrous crystals closely associated with quartz, wulfenite, anglesite, and graphite. Holotype sample. Orthorhombic, space group *Pbnm*, $a = 4.809(2)$, $b = 9.111(3)$,

$c = 8.536(3)$ Å, $V = 374.0(3)$ Å^3, $Z = 4$. $D_{calc} = 4.07$ g/cm^3. The calculated mean refractive index is 1.74. The empirical formula is $(Al_{1.860}Ga_{0.102}As^{3+}_{0.036}Zn_{0.020}Mg_{0.016}Fe^{3+}_{0.012}Na_{0.009}Sb^{3+}_{0.005}Ti_{0.003}Cu_{0.001})(Ge_{0.844}Al_{0.143}Si_{0.013})O_4(F_{1.103}(OH)_{0.897}$. The strongest lines of the powder X-ray diffraction pattern [*d*, Å (*I*, %) (*hkl*)] are: 3.016 (100) (112), 3.811 (78) (111), 3.315 (48) (012), 2.247 (38) (211), 2.417 (27) (023, 200).

Kind of sample preparation and/or method of registration of the spectrum: KBr disc. Absorption.

Source: Schlüter et al. (2010).

Wavenumbers (cm^{-1}): 3590, 3440, 1633w, 1185w, 1135s, 993, 869sh, 733s, 577s, 522, 482sh, 421.

2.15 Arsenic, Arsenides, Arsenites, Arsenates, and Sulfato-Arsenates

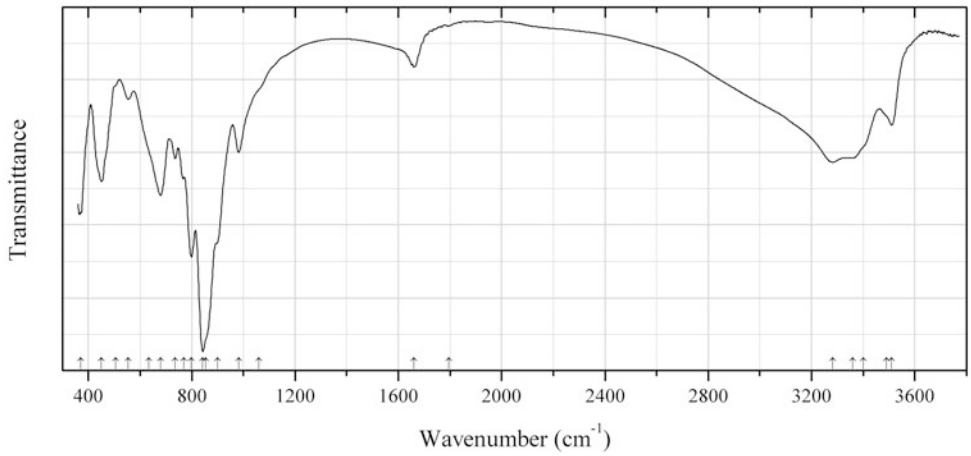

Fig. 2.1365 IR spectrum of okruschite obtained by N.V. Chukanov

As216 Okruschite $Ca_2Mn^{2+}_5Be_4(AsO_4)_6(OH)_4 \cdot 6H_2O$ (Fig. 2.1365)

Locality: Fuchs quarry, near Sailauf, Spessart Mts., Bavaria, Germany (type locality).

Description: White semitransparent split tabular crystals from the association with braunite, Mn-bearing calcite, and arseniosiderite. Holotype sample. Monoclinic, space group *C*2/*c*, a = 16.33 (4), b = 12.03(3), c = 6.93(1) Å, β = 94.84(5)°, V = 1357(4) Å^3, Z = 2. D_{meas} = 3.33(2) g/cm^3, D_{calc} = 3.340 g/cm^3. Optically biaxial (−), α = 1.671(3), β = 1.682(2), γ = 1.687(3), 2 V = 65(5)°. The empirical formula is $Ca_{1.99}(Mn_{3.09}Fe_{0.92}Mg_{0.56}Al_{0.06}Li_{0.04})Be_{4.15}(AsO_4)_{5.99}(OH)_{3.64} \cdot 6.40H_2O$. The strongest lines of the powder X-ray diffraction pattern [*d*, Å (*I*, %) (*hkl*)] are: 9.68 (39) (110), 4.95 (34) (310), 4.17 (34) (−311), 3.25 (100) (−202, 330), 3.11 (32) (−421), 2.841 (27) (240), 2.711 (26) (600), 1.726 (26) (461, −552, 004).

Kind of sample preparation and/or method of registration of the spectrum: KBr disc. Absorption.

Wavenumbers (cm^{-1}): 3510, 3490sh, 3400sh, 3360, 3282s, 1796w, 1661, 1060sh, 982, 900sh, 855sh, 843s, 798s, 769, 736, 680s, 635sh, 555w, 505sh, 450, 370s.

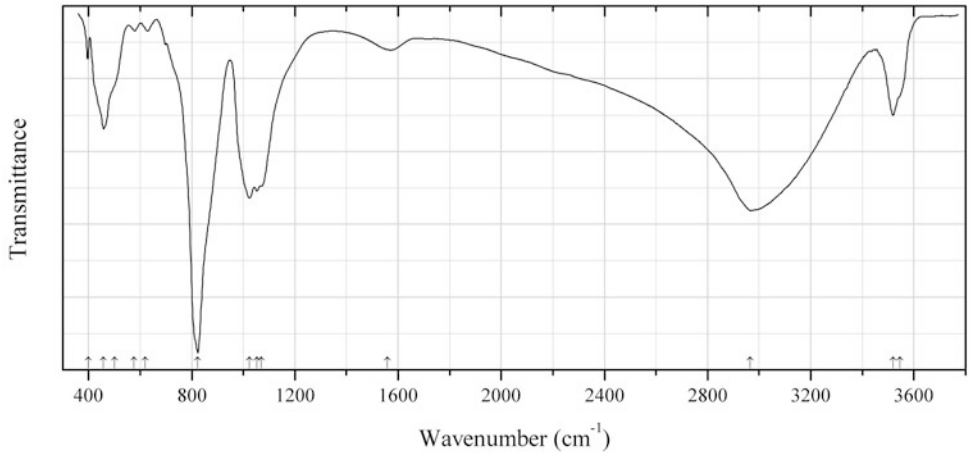

Fig. 2.1366 IR spectrum of scorodite obtained by N.V. Chukanov

As217 Scorodite $Fe^{3+}(AsO_4)\cdot 2H_2O$ (Fig. 2.1366)
Locality: Almerindo mine, Linópolis, Divino das Laranjeiras, Doce valley, Minas Gerais, Brazil.
Description: Greenish-brown crust from the association with pharmacosiderite and arsenopyrite. A PO_4-rich variety. The empirical formula is (electron microprobe): $(Fe_{0.99}Al_{0.03})[(AsO_4)_{0.78}(PO_4)_{0.22}]\cdot 2H_2O$.
Kind of sample preparation and/or method of registration of the spectrum: KBr disc. Absorption.
Wavenumbers (cm^{-1}): 3545sh, 3519, 2965s, 1558, 1070, 1053, 1023s, 823s, 619w, 575w, 500sh, 457, 399.

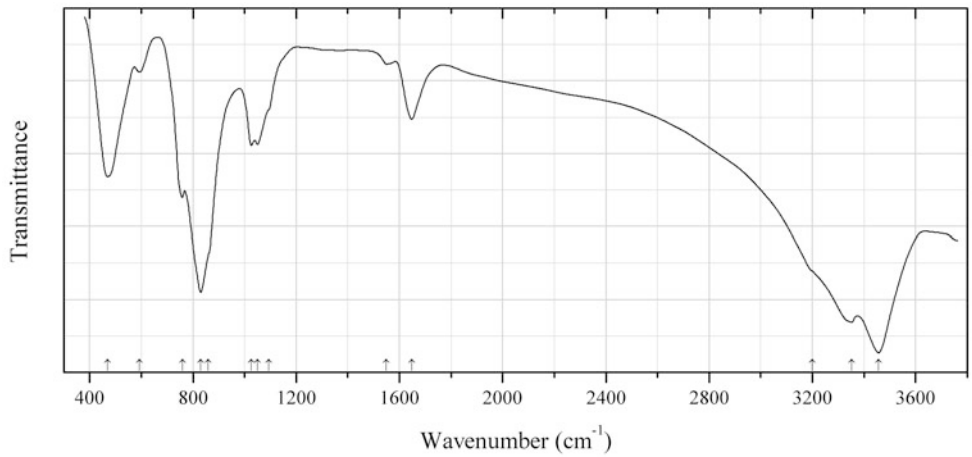

Fig. 2.1367 IR spectrum of césarferreiraite obtained by N.V. Chukanov

As218 Césarferreiraite $Fe^{2+}Fe^{3+}{}_2(AsO_4)_2(OH)_2\cdot 8H_2O$ (Fig. 2.1367)
Locality: Eduardo pegmatite mine (Lavra do Eduardo), near Boa Vista creek, Conselheiro Pena municipality, Minas Gerais, Brazil (type locality).
Description: Greenish yellow fibrous aggregate from the association with pharmacosiderite, scorodite, and earlier arsenopyrite. Holotype sample. Triclinic, space group $P\text{-}1$, a = 5.383(2), b = 10.363(3), c = 6.878(2) Å, α = 96.42(4)°, β = 109.19(3)°, γ = 102.30(2)°, V = 347.1(2) $Å^3$, Z = 1. D_{calc} = 2.934 g/cm^3.

Optically biaxial (+), n_{min} = 1.747(3), n_{max} = 1.754(3). The empirical formula is $Fe^{2+}_{0.98}Fe^{3+}_{1.96}[(AsO_4)_{1.79}(PO_4)_{0.31}](OH)_{1.52}\cdot 8.08H_2O$. The strongest lines of the powder X-ray diffraction pattern [*d*, Å (*I*, %) (*hkl*)] are: 9.85 (95) (010), 6.35 (100) (001), 3.671 (29) (−121), 3.158 (32) (1–30), 2.960 (39) (02–2), 2.884 (35) (−131), 2.680 (29) (−211), 2.540 (23) (−210).
Kind of sample preparation and/or method of registration of the spectrum: KBr disc. Absorption.
Wavenumbers (cm^{-1}): 3456s, 3352s, 3200sh, 1647, 1550w, 1095sh, 1050, 1026, 860sh, 830s, 759s, 592, 470s.

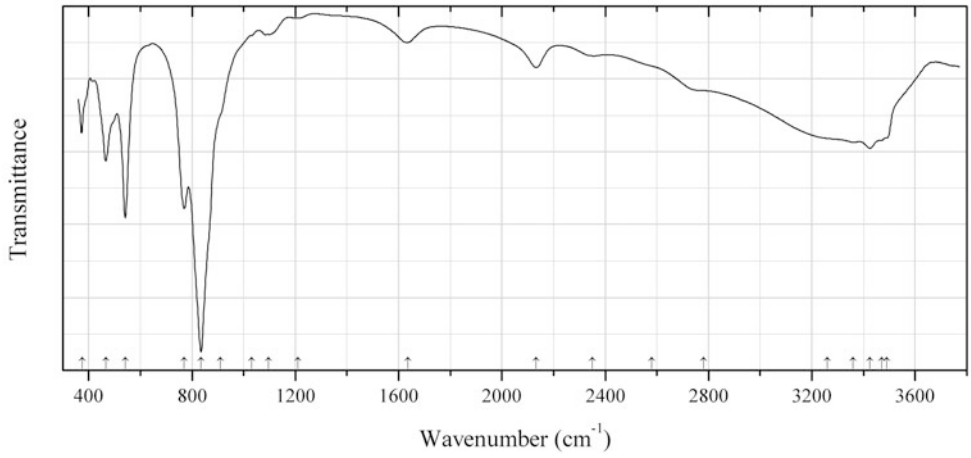

Fig. 2.1368 IR spectrum of strashimirite obtained by N.V. Chukanov

As219 Strashimirite $Cu_4(AsO_4)_2(OH)_2\cdot 2.5H_2O$ (Fig. 2.1368)
Locality: Majuba Hill mine, Antelope district, Pershing Co., Nevada, USA.
Description: Light blue crust. Confirmed by the IR spectrum.
Kind of sample preparation and/or method of registration of the spectrum: KBr disc. Absorption.
Wavenumbers (cm^{-1}): 3490, 3470, 3425, 3360, 3260sh, 2780, 2580sh, 2350w, 2133, 1635w, 1210w, 1096w, 1030sh, 910sh, 835s, 770s, 541s, 466, 374.

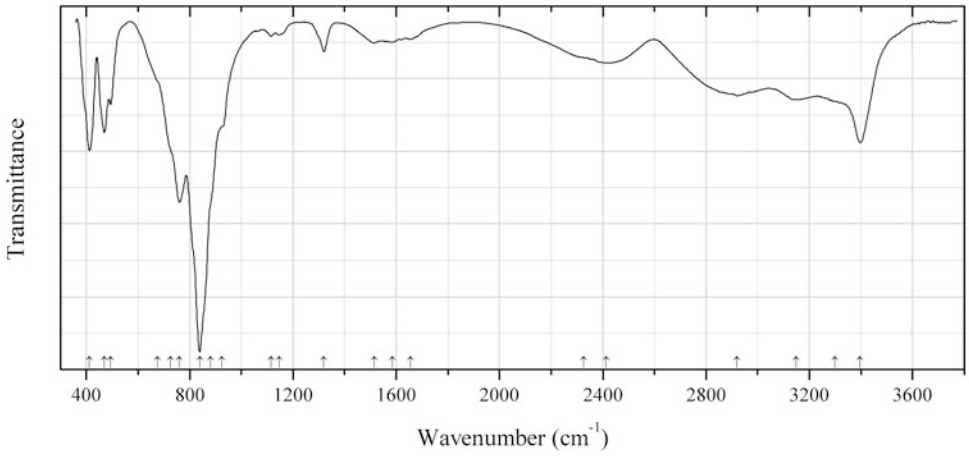

Fig. 2.1369 IR spectrum of miguelromeroite obtained by N.V. Chukanov

As220 Miguelromeroite $Mn_5(AsO_4)_2(HAsO_4)_2 \cdot 4H_2O$ (Fig. 2.1369)
Locality: Veta Negra mine, Tierra Amarilla, Copiapó Province, Chile.
Description: Pink radial aggregates from the association with other secondary arsenates. The empirical formula is (electron microprobe): $(Mn_{2.9}Mg_{0.1})(Mn_{1.2}Ca_{0.8})(AsO_4)_2(HAsO_4)_2 \cdot 4H_2O$.
Kind of sample preparation and/or method of registration of the spectrum: KBr disc. Absorption.
Wavenumbers (cm^{-1}): 3396s, 3300sh, 3150, 2920, 2412, 2325sh, 1655w, 1585w, 1516w, 1320, 1148w, 1115w, 925sh, 880sh, 839s, 761s, 725sh, 675sh, 494, 469, 412s.

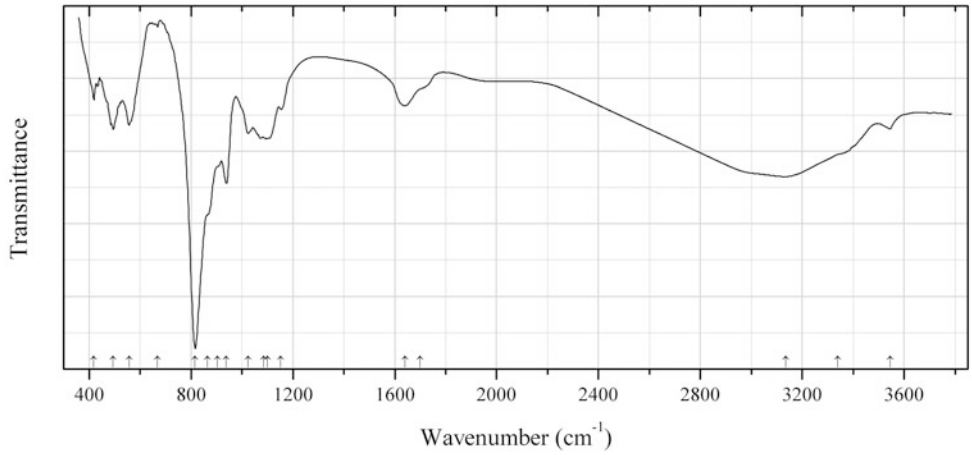

Fig. 2.1370 IR spectrum of barahonaite-(Al) obtained by N.V. Chukanov

As221 Barahonaite-(Al) $(Ca,Cu,Na,Fe,Al)_{12}Al_2(AsO_4)_8(OH,Cl)_x \cdot nH_2O$ (?) (Fig. 2.1370)
Locality: Jote mine, Pampa Larga district, Tierra Amarilla, Copiapó province, Atacama desert, Chile.
Description: Spherical aggregates of bluish-green crystals. The empirical formula is $Ca_{5.1}Cu_{4.4}Al_{4.2}Fe_{0.4}(AsO_4)_{8.0}(OH)_x \cdot nH_2O$.
Kind of sample preparation and/or method of registration of the spectrum: KBr disc. Absorption.
Wavenumbers (cm^{-1}): 3545w, 3340sh, 3135, 1700sh, 1640, 1152w, 1100, 1085, 1024, 939s, 905sh, 865sh, 816s, 668w, 557, 495, 419.

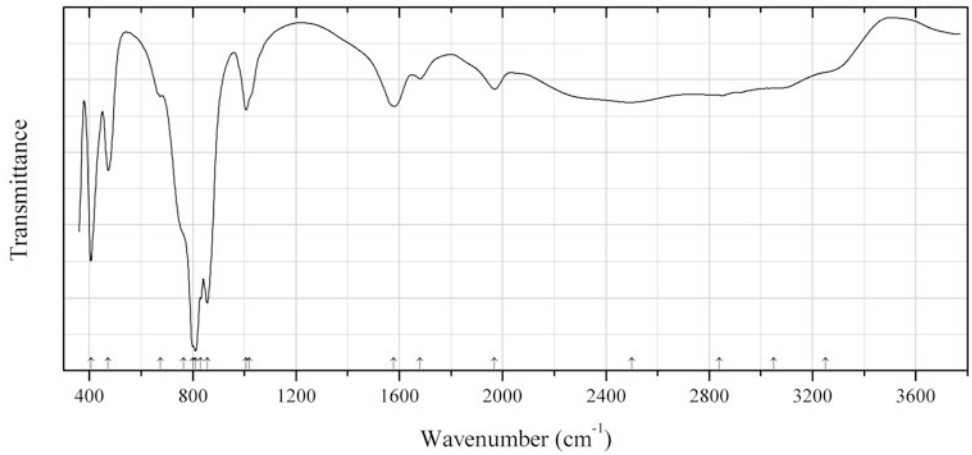

Fig. 2.1371 IR spectrum of rruffite obtained by N.V. Chukanov

As223 Rruffite $Ca_2Cu(AsO_4)_2 \cdot 2H_2O$ (Fig. 2.1371)
Locality: Jote mine, Pampa Larga district, Tierra Amarilla, Copiapó province, Atacama region, Chile.
Description: Light blue split crystals. The empirical formula is (electron microprobe): $Ca_{1.92}Cu_{0.94}Fe_{0.05}Zn_{0.04}Mg_{0.04}(AsO_4)_{2.00} \cdot nH_2O$. Confirmed by powder X-ray diffraction data.
Kind of sample preparation and/or method of registration of the spectrum: KBr disc. Absorption.
Wavenumbers (cm^{-1}): 3250sh, 3050, 2840, 2500, 1968, 1680w, 1577, 1020sh, 1007, 856s, 830sh, 811s, 802s, 765sh, 676w, 473, 406s.

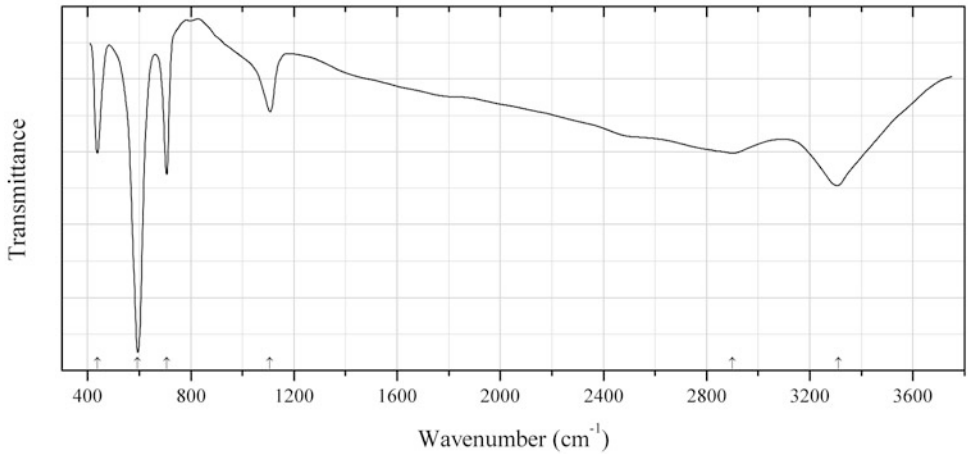

Fig. 2.1372 IR spectrum of lead acid arsenite chloride As224 drawn using data from Siidra et al. (2012)

As224 Lead acid arsenite chloride As224 $Pb_2(AsO_2OH)Cl_2$ (Fig. 2.1372)
Locality: Punta Zeza area, 3 km south of the town of Lavrion, Attiki Peninsula, Greece.
Description: Colourless, transparent prismatic crystals from cavities in ancient metallurgical slag dumped after smelting into the sea. The associated minerals are phosgenite and $Pb_5(AsO_3)Cl_7$. Monoclinic, space group $P2_1/m$, a = 6.4235(8), b = 5.5399(7), c = 9.321(1) Å, β = 90.767(2)°, V = 331.67(7) $Å^3$, Z = 2. D_{calc} = 6.09 g/cm^3. The empirical formula is (electron microprobe): $H_xPb_{2.03}(AsO_3)\ Cl_{2.00}$.
Kind of sample preparation and/or method of registration of the spectrum: KBr disc. Absorption.
Source: Siidra et al. (2012).
Wavenumbers (cm^{-1}): 3310s, 2900, 1107, 707s, 594s, 438s.

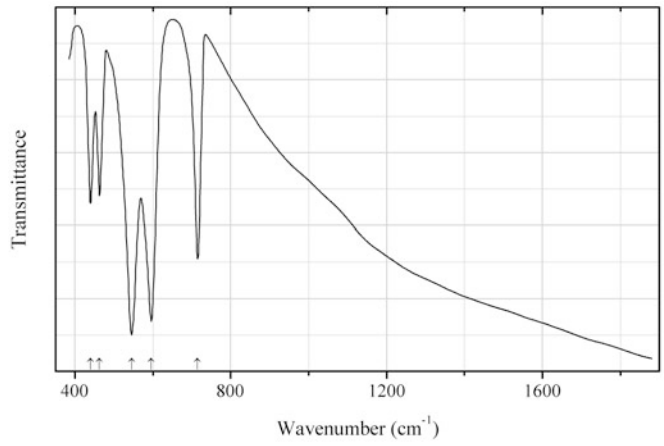

Fig. 2.1373 IR spectrum of lead arsenite chloride As225 drawn using data from Siidra et al. (2011)

As225 Lead arsenite chloride As225 $Pb_5(As^{3+}O_3)Cl_7$ (Fig. 2.1373)
Locality: Punta Zeza area, 3 km south of the town of Lavrion, Attiki Peninsula, Greece.
Description: Colourless, transparent isometric crystals from cavities in ancient metallurgical slag dumped after smelting into the sea. The associated minerals are phosgenite and $Pb_2(AsO_2OH)Cl_2$. Orthorhombic, space group *Pbcn*, $a = 16.894(2)$, $b = 10.9135(15)$, $c = 16.760(2)$ Å, $V = 3090.1(7)$ Å^3. The empirical formula is (electron microprobe): $Pb_{4.78}As^{3+}_{1.00}Cl_{7.15}O_{2.705}$.
Kind of sample preparation and/or method of registration of the spectrum: KBr disc. Absorption.
Source: Siidra et al. (2011).
Wavenumbers (cm^{-1}): 715, 596s, 545s, 463, 440.

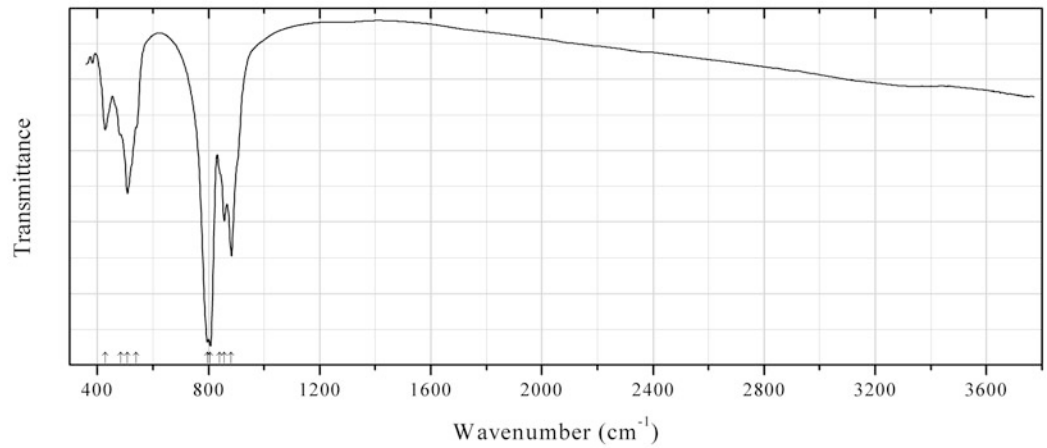

Fig. 2.1374 IR spectrum of lammerite-β obtained by N.V. Chukanov

As226 Lammerite-β $Cu_3^{2+}(AsO_4)_2$ (Fig. 2.1374)
Locality: Arsenatnaya fumarole, Second cone of the Northern Breakthrough of the Great Tolbachik Fissure Eruption, Kamchatka peninsula, Russia (type locality).
Description: Light green spherulites from the association with euchlorine, piypite, wulffite, etc. Investigated by I.V. Pekov. The empirical formula is (electron microprobe): $Cu_{3.0}(AsO_4)_{2.0}$. The

strongest lines of the powder X-ray diffraction pattern [*d*, Å (*I*, %)] are: 4.31 (25), 4.04 (30), 3.85 (27), 3.427 (47), 3.383 (23), 3.049 (26), 2.965 (29), 2.893 (41), 2.830 (100), 2.797 (69), 2.366 (20). **Kind of sample preparation and/or method of registration of the spectrum**: KBr disc. Absorption. **Wavenumbers (cm^{-1})**: 882s, 857, 840sh, 807s, 796s, 540sh, 508, 485sh, 428.

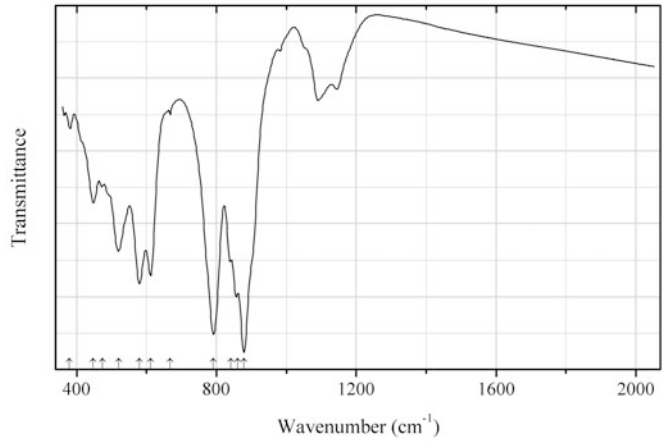

Fig. 2.1375 IR spectrum of ericlaxmanite obtained by N.V. Chukanov

As227 Ericlaxmanite $Cu_4(AsO_4)_2O$ (Fig. 2.1375)
Locality: Arsenatnaya fumarole, Second scoria cone of the Northern Breakthrough of the Great Tolbachik Fissure Eruption, Tolbachik volcano, Kamchatka peninsula, Russia (type locality).
Description: Light green crystals from the association with lammerite, lammerite-β, johillerite, bradaczekite, hatertite, urusovite, alarsite, kozyrevskite, tilasite, svabite, aphthitalite, langbeinite, calciolangbeinite, dolerophanite, hematite, tenorite, etc. Inversigated by I.V. Pekov. Triclinic, space group *P*-1, a = 6.4271(4), b = 7.6585(4), c = 8.2249(3) Å, α = 98.396(4)°, β = 112.420(5)°, γ = 98.397(5)°, V = 361.11(3) $Å^3$, Z = 2. D_{calc} = 5.036 g/cm^3. Optically biaxial (−), α = 1.870(10), β = 1.900(10), γ = 1.915(10), 2 V = 60(15)°. The empirical formula is $(Cu_{3.97}Zn_{0.06}Fe_{0.02})(As_{1.94}P_{0.02}V_{0.01}S_{0.01})O_9$. The strongest lines of the powder X-ray diffraction pattern [*d*, Å (*I*, %) (*hkl*)] are: 3.685 (100) (020, 0–12, 0–21), 3.063 (71) (−1–21, 012, 021), 2.957 (58) (0–22), 2.777 (98) (−212, −2–11), 2.201 (51) (013, 031).
Kind of sample preparation and/or method of registration of the spectrum: KBr disc. Absorption. **Wavenumbers (cm^{-1})**: 879s, 862s, 842, 792s, (667w), 612s, 580s, 520, 475w, 448, 380w.
Note: The bands in the range from 950 to 1200 cm^{-1} are due to the admixture of a sulfate.

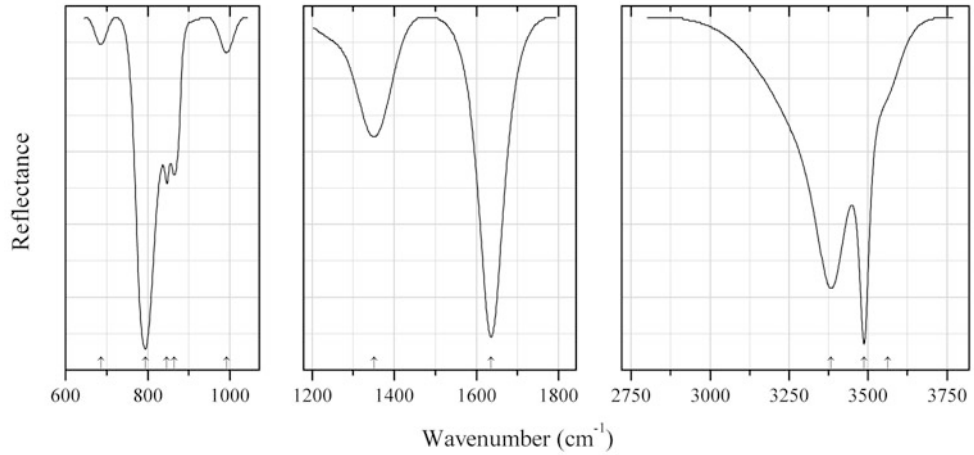

Fig. 2.1376 IR spectrum of agardite-(La) drawn using data from Frost et al. (2004)

As228 Agardite-(La) $LaCu_6^{2+}(AsO_4)_3(OH)_6{\cdot}3H_2O$ (Fig. 2.1376)
Locality: Synthetic.
Description: Powdery sample. Confirmed by powder X-ray diffraction data.
Kind of sample preparation and/or method of registration of the spectrum: Attenuated total reflection of pure sample.
Source: Frost et al. (2004).
Wavenumbers (cm^{-1}): 3563sh, 3487s, 3383, 1636, 1351, 992, 864, 847, 794s, 686.
Note: The wavenumbers were determined by us based on spectral curve analysis of the published spectrum.

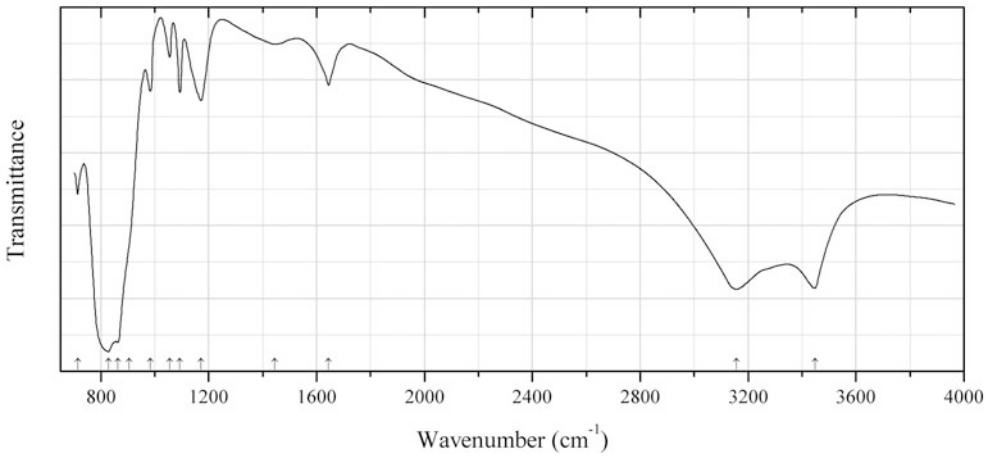

Fig. 2.1377 IR spectrum of andyrobertsite drawn using data from Cooper et al. (1999)

As229 Andyrobertsite $KCdCu_5(AsO_4)_4[As(OH)_2O_2]{\cdot}2H_2O$ (Fig. 2.1377)
Locality: Tsumeb mine, Tsumeb, Namibia (type locality).
Description: Blue lamellar crystals intimately intergrowing with calcioandyrobertsite from the association with olivenite, zincolivenite (indicated as "cuprian adamite"), and minor tennantite. Holotype sample. Monoclinic, space group $P2_1/m$, $a = 9.810(4)$, $b = 10.034(6)$, $c = 9.975(4)$ Å, $\beta = 101.84(4)°$,

V = 961.0(6) Å^3, Z = 2. D_{calc} = 4.011 g/cm^3 (for an aggregate crystal of andyrobertsite and calcioandyrobertsite in a 50:50 proportion of the end-members). Optically biaxial (−), α = 1.720(3), β = 1.749(1), γ = 1.757(1), 2 V = 50(5)°. The strongest lines of the powder X-ray difraction pattern [d, Å (I, %) (hkl)] are: 9.64 (100) (100), 3.145 (50) (130, 122), 4.46 (40) (120), 3.048 (40) (−222), 2.698 (40) (320). The empirical formulae of andyrobertsite and calcioandyrobertsite zones are $K_{1.03}(Cd_{0.61}Ca_{0.30}Mn_{0.11})(Cu_{4.85}Zn_{0.03})(AsO_4)_{4.04}[As(OH)_2O_2]\cdot 2H_2O$ and $K_{1.01}(Cd_{0.12}Ca_{0.74}Mn_{0.14})(Cu_{4.85}Zn_{0.01})(AsO_4)_{4.06}[As(OH)_2O_2]\cdot 2H_2O$ respectively. The bands in the range 980–1180 cm^{-1}, as well as low sums of analyses (95.99–97.30 wt%) indicate possible presence of SO_4^{2-} groups. Typical bands of acid groups $As(OH)_2O_2^-$ (in the wavenumber range 1800–2800 cm^{-1}) are absent or very weak.

Kind of sample preparation and/or method of registration of the spectrum: Transmittance (see Roberts et al. 1994).

Source: Cooper et al. (1999).

Wavenumbers (cm^{-1}): 3448s, 3157s, 1644, 1444w, 1171, 1093, 1055w, 983w, 904sh, 863s, 829s, 714.

Note: The wavenumbers were partly determined by us based on spectral curve analysis of the published spectrum. The band position denoted by Cooper et al. (1999) as 1023 cm^{-1} was determined by us at 1093 cm^{-1}.

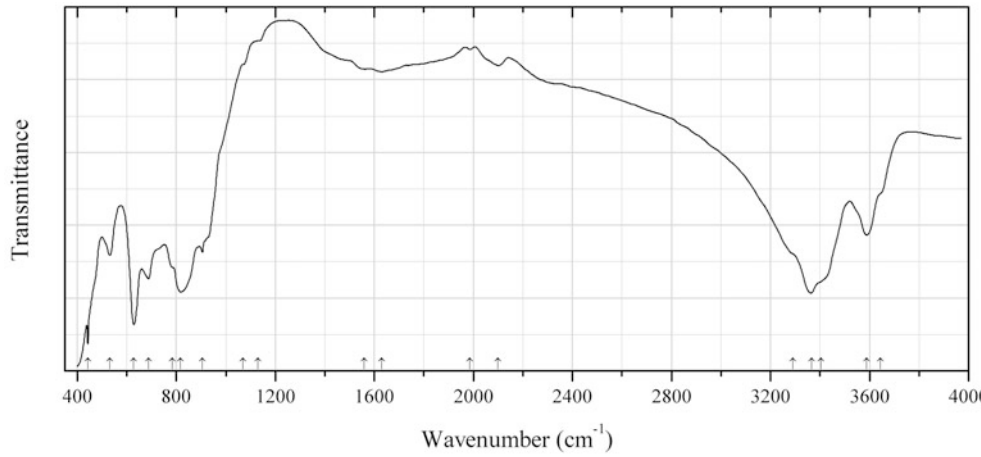

Fig. 2.1378 IR spectrum of arakiite drawn using data from Roberts et al. (2000)

As230 Arakiite $ZnMn^{2+}{}_{12}Fe^{3+}{}_2(AsO_3)(AsO_4)_2(OH)_{23}$ (Fig. 2.1378)

Locality: Långban deposit, Bergslagen ore region, Filipstad district, Värmland, Sweden (type locality).

Description: Red-brown grains from the association with hematite, calcite, and magnussonite. Holotype sample. Monoclinic, space group Cc, a = 14.248(8), b = 8.228(4), c = 24.23(1) Å, β = 93.62 (3)°, V = 2843(2) Å^3, Z = 4. D_{calc} = 3.41 g/cm^3. Optically biaxial (−), α = 1.723(4), β = 1.744(2), γ = 1.750(2), 2 V = 44(3)°. The strongest lines of the powder X-ray diffraction pattern [d, Å (I, %) (hkl)] are: 12.07 (100) (002), 6.046 (100) (004), 4.040 (90) (006), 3.148 (30) (−404, −117), 3.030 (70) (224), 2.411 (40) (424, −515), 1.552 (70) (640, −351).

Kind of sample preparation and/or method of registration of the spectrum: Transmission.

Source: Roberts et al. (2000).

Wavenumbers (cm^{-1}): 3645sh, 3589, 3405sh, 3366s, 3290sh, 2100w, 1986w, 1630w, 1560w, 1130sh, 1070sh, 906, 818s, 785sh, 687, 628s, 531, 443.
Note: The wavenumbers were partly determined by us based on spectral curve analysis of the published spectrum.

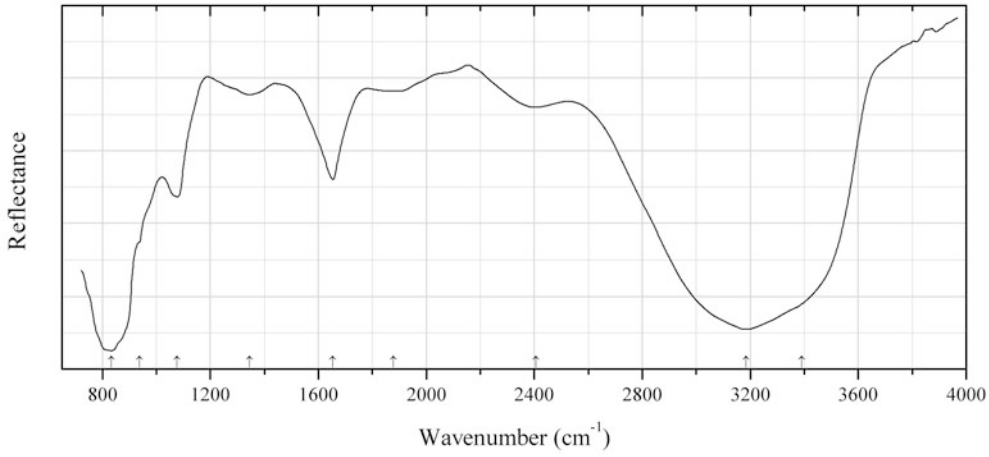

Fig. 2.1379 IR spectrum of barahonaite-(Fe) drawn using data from Viñals et al. (2008)

As231 Barahonaite-(Fe) $(Ca,Cu,Na,Fe^{3+},Al)_{12}Fe^{3+}{}_2(AsO_4)_8(OH,Cl)_x \cdot nH_2O$ (Fig. 2.1379)
Locality: Dolores prospect, near the village of Pastrana, Murcia Province, southeastern Spain (type locality).
Description: Greenish-yellow crust from the association with pharmacosiderite. Holotype sample. Monoclinic, a = 10.161(6), b = 22.39(2), c = 10.545(10) Å, β = 93.3(1)°. Optically biaxial (−), α = 1.664(2), β ≈ γ = 1.677(2). The strongest lines of the powder X-ray diffraction pattern [d, Å (I, %) (*hkl*)] are: 22.0 (100) (010), 11.2 (70) (020), 5.068 (20) (200), 3.345 (20) (023, 310), 2.763 (30) (053), 2.659 (20) (−172), 2.541 (20) (400).
Kind of sample preparation and/or method of registration of the spectrum: Attenuated total reflection of powdered mineral.
Source: Viñals et al. (2008).
Wavenumbers (cm^{-1}): 3391sh, 3184s (broad), 2405w (broad), 1878w, 1654, 1344w, 1077, 937sh, 833s.
Note: The wavenumbers were partly determined by us based on spectral curve analysis of the published spectrum.

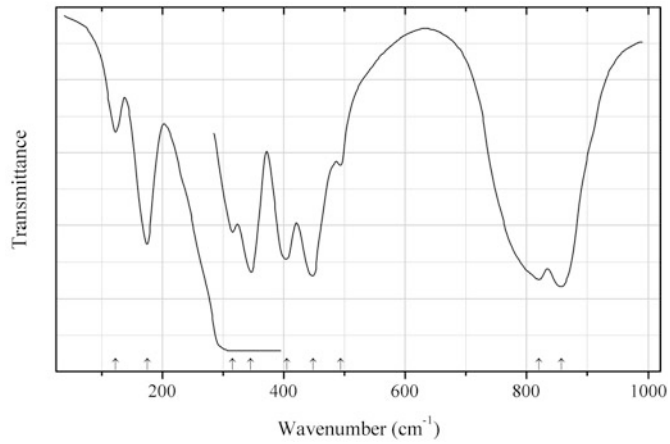

Fig. 2.1380 IR spectrum of berzeliite drawn using data from Khorari et al. (1995)

As232 Berzeliite $NaCa_2Mg_2(AsO_4)_3$ (Fig. 2.1380)
Locality: Synthetic.
Description: Confirmed by powder X-ray diffraction data.
Kind of sample preparation and/or method of registration of the spectrum: KBr disc (in the range 1500–300 cm^{-1}), polyethylene disc (in the range 350–30 cm^{-1}). Transmission.
Source: Khorari et al. (1995).
Wavenumbers (cm^{-1}): 857s, 820s, 494w, 448, 405, 345, 315, 175, 123w.

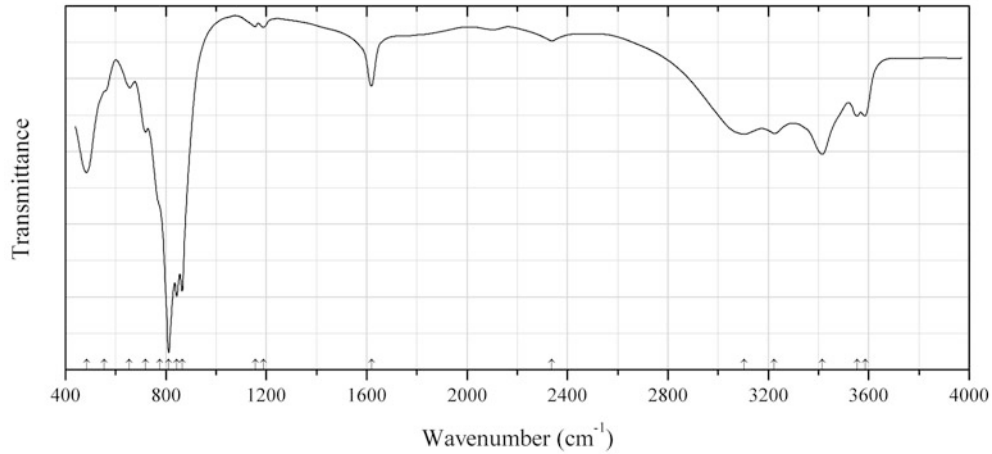

Fig. 2.1381 IR spectrum of braithwaiteite drawn using data from Paar et al. (2009)

As233 Braithwaiteite $NaCu^{2+}{}_5(Sb^{5+}Ti^{4+})(AsO_4)_4(HAsO_4)_2O_2 \cdot 8H_2O$ (Fig. 2.1381)
Locality: An epithermal Cu–Au–Ag deposit at Laurani, near Sica Sica, Bolivia (type locality).
Description: Sky-blue crystals from the association with lammerite, lavendulan (or lemanskiite), quartz, pyrite, covellite, anatase, albite–oligoclase, kaolinite, and a mineral of the chlorite group. Holotype sample. The crystal structure is solved. Triclinic, space group *P*-1, a = 7.0308(4), b = 9.8823(5), c = 10.6754(6) Å, α = 106.973(1)°, β = 104.274(1)°, γ = 93.839(1)°, V = 679.76(11) $Å^3$, Z = 1. D_{calc} = 3.753 g/cm^3. Optically biaxial (−), α = 1.698(2), β = 1.757(5), γ = 1.783(5),

2 V = 59(2)°. The empirical formula is $Na_{0.87}Cu^{2+}_{5.17}(Ti^{4+}_{0.90}Sb^{5+}_{1.15})(As_{0.98}O_4)_4(HAs_{0.98}O_4)_2O_2 \cdot 8H_2O$. The strongest lines of the powder X-ray diffraction pattern [d, Å (I, %) (hkl)] are: 9.825 (100) (001), 5.887 (50) (011), 4.635 (30) (−102), 3.354 (30) (1–22), 3.232 (30) (−2–11), 2.947 (60) (022), 2.736 (30) (−2–22).

Kind of sample preparation and/or method of registration of the spectrum: Low–pressure diamond microsample cell. Transmission.

Source: Paar et al. (2009).

Wavenumbers (cm^{-1}): 3586, 3555, 3414, 3223, 3104, 2338w, 1619, 1189w, 1156w, 865s, 843s, 812s, 776sh, 718, 655w, 555sh, 484.

Note: The wavenumbers were partly determined by us based on spectral curve analysis of the published spectrum.

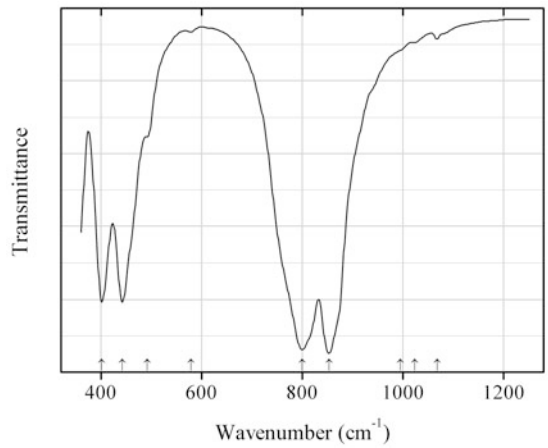

Fig. 2.1382 IR spectrum of berzeliite obtained by N.V. Chukanov

As234 Berzeliite $NaCa_2Mg_2(AsO_4)_3$ (Fig. 2.1382)

Locality: Långban deposit, Bergslagen ore region, Filipstad district, Värmland, Sweden (type locality).

Description: Yellow veinlet in skarn, in the association with braunite, hedyphane, barite, and calcite. The empirical formula is (electron microprobe) $(Ca_{2.0}Na_{1.1})(Mg_{1.35}Mn_{0.6})(AsO_4)_{3.0}$.

Kind of sample preparation and/or method of registration of the spectrum: KBr disc. Absorption.

Wavenumbers (cm^{-1}): 1068w, 1024w, 995sh, 853s, 800s, 579w, 491, 442s, 401s.

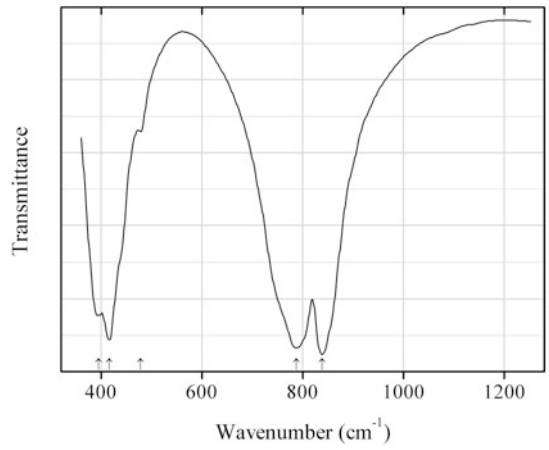

Fig. 2.1383 IR spectrum of manganberzeliite obtained by N.V. Chukanov

As235 Manganberzeliite $(NaCa_2)Mn^{2+}{}_2(AsO_4)_3$ (Fig. 2.1383)
Locality: Långban deposit, Bergslagen ore region, Filipstad district, Värmland, Sweden (type locality).
Description: Yellow veinlet in granular aggregate of tilasite. The empirical formula is (electron microprobe): $(Na_{1.0}Ca_{2.0})(Mn_{1.85}Mg_{0.15})(AsO_4)_{3.00}$.
Kind of sample preparation and/or method of registration of the spectrum: KBr disc. Absorption.
Wavenumbers (cm^{-1}): 838s, 788s, 478w, 416s, 395.

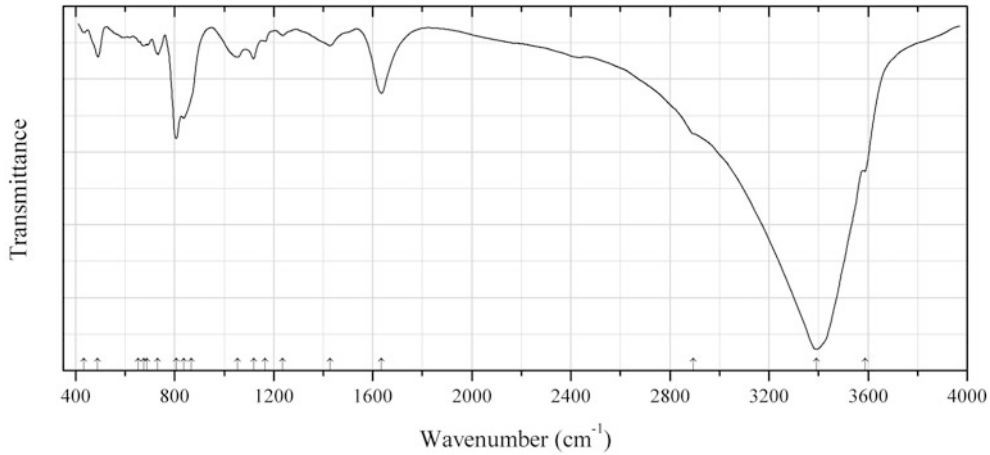

Fig. 2.1384 IR spectrum of burgessite drawn using data from Sejkora et al. (2009)

As236 Burgessite $Co_2(HAsO_4)_2 \cdot 5H_2O$ (Fig. 2.1384)
Locality: Keeley mine, South Lorrain Township, Timiskaming District, Ontario, Canada (type locality).
Description: Purplish pink radial aggregates from the association with skutterudite, cobaltite, bismuth, arsenolite, bismutoferrite, and erythrite. Holotype sample. Monolinic, space group $P2_1/n$, $a = 4.7058(12)$, $b = 9.299(3)$, $c = 12.738(4)$ Å, $\beta = 98.933(8)°$, $V = 550.6(5)$ Å^3, $Z = 2$. $D_{meas} = 2.93$ (2) g/cm^3, $D_{calc} = 2.41$ g/cm^3. Optically biaxial (+), $\alpha = 1.596(2)$, $\beta = 1.604(2)$, $\gamma = 1.628(2)$, $2V = 70$

(2)°. The empirical formula is $(Co_{1.75}Ni_{0.23}Ca_{0.02})(HAsO_4)_2 \cdot 5H_2O$. The strongest lines of the powder X-ray diffraction pattern [*d*, Å (*I*, %) (*hkl*)] are: 7.446 (100) (011), 6.267 (44) (002), 3.725 (29) (022), 3.260 (25) (12–1), 2.998 (31) (031), 2.970 (21) (014), 2.596 (23) (024).
Kind of sample preparation and/or method of registration of the spectrum: KBr disc. Absorption.
Source: Sejkora et al. (2009).
Wavenumbers (cm^{-1}): 3588sh, 3392s, 2895sh, 1635s, 1427, 1236w, 1166, 1119, 1054, 868sh, 837sh, 806s, 732, 689, 675, 654w, 490, 433.
Note: The wavenumbers were partly determined by us based on spectral curve analysis of the published spectrum. The intensities of the bands of acid O–H groups (in the range 1700–3000 cm^{-1}) are anomalously low as compared with the bands of H_2O molecules at 3392 and 1635 cm^{-1}.

As237 Calcioandyrobertsite $KCaCu_5(AsO_4)_4[As(OH)_2O_2] \cdot 2H_2O$
Locality: Tsumeb mine, Tsumeb, Namibia (type locality).
Description: Blue lamellar crystals intimately intergrowing with andyrobertsite.
Kind of sample preparation and/or method of registration of the spectrum: Transmittance (see Roberts et al. 1994).
Source: Cooper et al. (1999).
Note: For the IR spectrum of the calcioandyrobertsite-andyrobertsite intergrowth and its description see data on As229 (andyrobertsite).

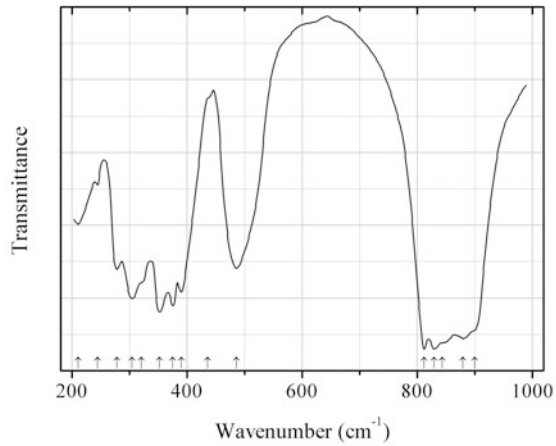

Fig. 2.1385 IR spectrum of chernovite-(Y) drawn using data from Pradhan et al. (1987)

As238 Chernovite-(Y) $Y(AsO_4)$ (Fig. 2.1385)
Locality: Synthetic.
Description: Powder. Confirmed by powder X-ray diffraction data.
Kind of sample preparation and/or method of registration of the spectrum: KBr disc. Transmission.
Source: Pradhan et al. (1987).
Wavenumbers (cm^{-1}): 900sh, 880s, 844sh, 830s, 812s, 486, 436sh, 390, 375, 352s, 320sh, 304, 278, 244w, 210w.
Note: The wavenumbers were partly determined by us based on spectral curve analysis of the published spectrum.

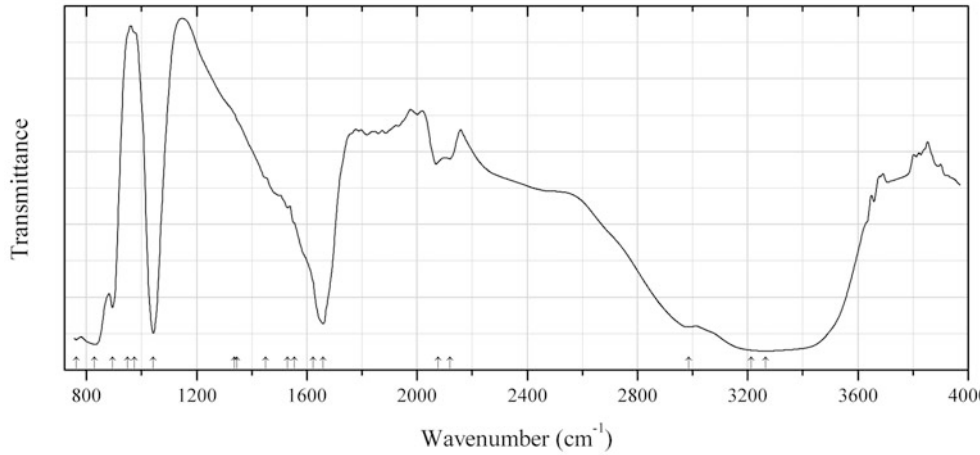

Fig. 2.1386 IR spectrum of cobaltarthurite drawn using data from Jambor et al. (2002)

As239 Cobaltarthurite $CoFe^{3+}{}_2(AsO_4)_2(OH)_2{\cdot}4H_2O$ (Fig. 2.1386)
Locality: Dolores showing, near Pastrana village, 10 km east of Mazarrón, the province of Murcia, Spain (type locality).
Description: Brown radial aggregate from the association with pharmacosiderite, olivenite, conichalcite, jarosite, and arseniosiderite. Holotype sample. Monoclinic, a = 10.27, b = 9.72, c = 5.545 Å, β = 94.46°. D_{meas} = 3.22(2) g/cm^3. Optically biaxial (+), α = 1.741, β = 1.762, γ = 1.797. The empirical formula is $(Co_{0.50}Mg_{0.12}Fe^{3+}{}_{0.11}Mn_{0.08}Cu_{0.01})Fe_2{}^{3+}[(AsO_4)_{1.95}(PO_4)_{0.04}(SO_4)_{0.01}](OH)_{1.74}{\cdot}4H_2O$. The strongest lines of the powder X-ray diffraction pattern [d, Å (I, %) (hkl)] are: 10.2 (95) (100), 7.04 (100) (110), 4.81 (65) (001), 4.24 (60) (111), 2.89 (25) (221), 2.87 (55) (−311).
Kind of sample preparation and/or method of registration of the spectrum: Uncrushed sub-parallel fibrous material mounted perpendicular to the unpolarized beam. Transmission.
Source: Jambor et al. (2002).
Wavenumbers (cm^{-1}): 3265s, 3213s, 2987, 2120w, 2076w, 1659s, 1623sh, 1554sh, 1530, 1450sh, 1345sh, 1336sh, 1042s, 973sh, 948sh, 894s, 830s, 762s.
Note: The wavenumbers were partly determined by us based on spectral curve analysis of the published spectrum. The band position denoted by Jambor et al. (2002) as 3213 cm^{-1} was determined by us at 3265 cm^{-1}.

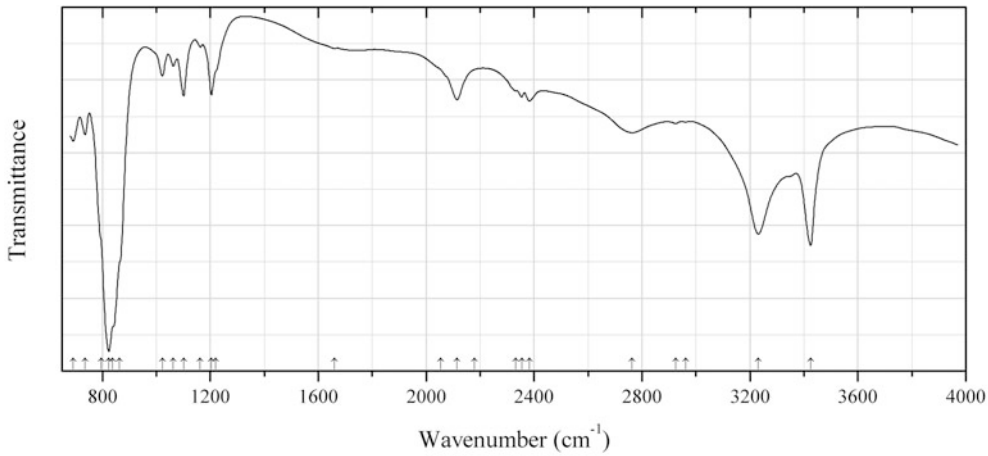

Fig. 2.1387 IR spectrum of domerockite drawn using data from Elliott et al. (2013b)

As240 Domerockite $Cu_4(AsO_4)(HAsO_4)(OH)_3 \cdot H_2O$ (Fig. 2.1387)
Locality: Dome Rock mine, Boolcoomatta Reserve, 42 km north of the railway siding of Mingary, South Australia, Australia (type locality).
Description: Aggregate of bluish green crystals from the association with conichalcite and a kaolinite-like mineral. Holotype sample. Triclinic, space group *P*-1, a = 5.378(11), b = 8.962(18) c = 9.841(2) Å, α = 75.25(3)°, β = 83.56(3)°, γ = 79.97(3)°, V = 450.5(16) Å^3, Z = 2. D_{calc} = 4.44 g/cm^3. Optically biaxial (−), α = 1.798(4), β = 1.814(4), γ = 1.817(4). The empirical formula is $(Cu_{3.94}Zn_{0.06})H_{0.91}(As_{1.97}P_{0.03}Si_{0.02}O_8(OH)_{3.00} \cdot H_2O$. The strongest lines of the powder X-ray diffraction pattern [*d*, Å (*I*, %) (*hkl*)] are: 4.716 (30) (101, 002, 111), 3.697 (25) (121), 3.605 (30) (120), 3.119 (60) (12–1), 3.073 (100) (1–2–1), 2.856 (40) (02–2, 030), 2.464 (50) (212, 1–13), 2.443 (40) (014).
Kind of sample preparation and/or method of registration of the spectrum: Diamond–anvil cell microsampling.
Source: Elliott et al. (2013b).
Wavenumbers (cm^{-1}): 3425s, 3232s, 2961w, 2925w, 2763, 2384, 2354, 2331w, 2115, 2180sh, 2054sh, 1660w, 1220sh, 1204, 1163w, 1101, 1062w, 1022, 864sh, 837sh, 824s, 796sh, 736, 692.
Note: The wavenumbers were partly determined by us based on spectral curve analysis of the published spectrum. The bands in the range from 2000 to 3000 cm^{-1} correspond to O–H stretching vibrations of acid arsenate groups.

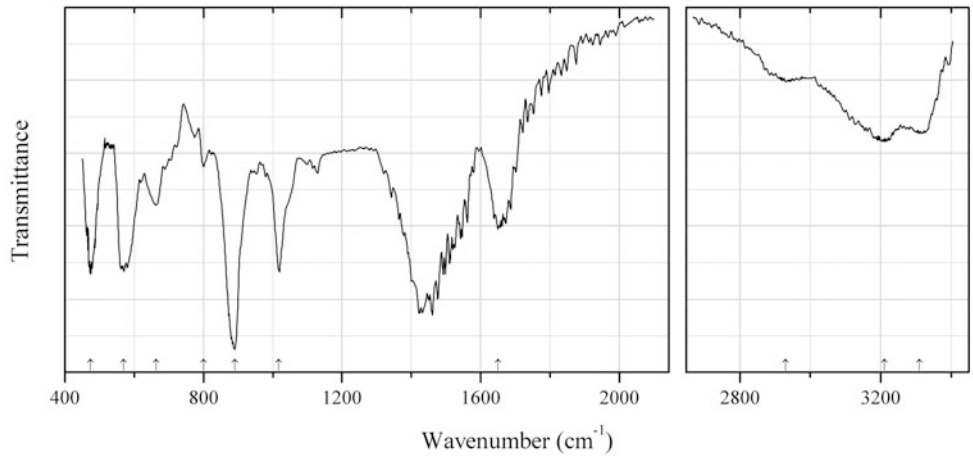

Fig. 2.1388 IR spectrum of dymkovite drawn using data from Pekov et al. (2012)

As241 Dymkovite $Ni(UO_2)_2(As^{3+}O_3)_2 \cdot 7H_2O$ (Fig. 2.1388)
Locality: Belorechenskoye deposit, Adygea Republic, Northern Caucasus, Russia (type locality).
Description: Yellow long-prismatic, lath-shaped crystals from the association with dolomite, uraninite (pitchblende), nickeline, gersdorffite, etc. Holotype sample. The crystal structure is solved. Monoclinic, space group *C*2/*m*, $a = 17.91(2)$, $b = 6.985(9)$, $c = 6.594(9)$ Å, $\beta = 99.89(2)^\circ$, $V = 813(2)$ Å^3, $Z = 2$. $D_{calc} = 3.806$ g/cm^3. Optically biaxial (−), $\alpha = 1.625(2)$, $\beta = 1.735(5)$, $\gamma = 1.745(3)$, $2V = 20(10)^\circ$. The empirical formula is $(Ni_{0.69}Mg_{0.26}Fe_{0.03}Zn_{0.03})U_{1.97}(As^{3+}_{1.88}P_{0.08})O_{9.94} \cdot 7.06H_2O$. The strongest lines of the powder X-ray diffraction pattern [*d*, Å (*I*, %) (*hkl*)] are: 8.93 (100) (200), 4.463 (34) (111, 400), 3.523 (23) (020), 3.276 (21) (220), 3.008 (26) (11–2), 2.846 (27) (112, 221, 31–2).
Kind of sample preparation and/or method of registration of the spectrum: KBr disc. Transmission.
Source: Pekov et al. (2012).
Wavenumbers (cm^{-1}): 3310, 3210, 2930, 1650s, 1017s, 890s, 800w, 663, 569s, 474s.
Note: Dymkovite is a Ni-dominant, almost arsenate-free analogue of seelite, $Mg(UO_2)_2[(As^{3+}O_3)_{1.4}(As^{5+}O_4)_{0.6}] \cdot 7H_2O$. Additional bands at 1436 and 877 cm^{-1} correspond to the admixture of dolomite.

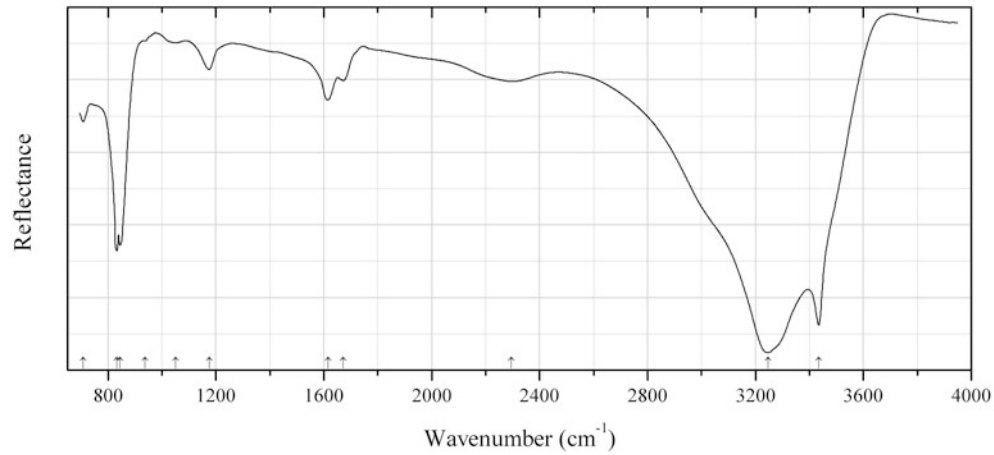

Fig. 2.1389 IR spectrum of esperanzaite drawn using data from Foord et al. (1999)

As242 Esperanzaite $NaCa_2Al_2(AsO_4)_2F_4(OH)\cdot 2H_2O$ (Fig. 2.1389)
Locality: La Esperanza mine, 60 km northeast of Durango, Zaragosa mining district, Durango State, Mexico (type locality).
Description: Blue-green botryoidal crystalline masses from the association with hematite, cassiterite, quartz, tridymite, cristobalite, opal, calcite, zeolites, mimetite, and clay minerals. Holotype sample. The crystal structure is solved. Monoclinic, space group $P2_1/m$, a = 9.687(5), b = 10.7379(6), c = 5.5523(7) Å, β = 105.32(1)°. D_{meas} = 3.24 g/cm^3, D_{calc} = 3.36 g/cm^3. Optically biaxial (−), α = 1.580(1), β = 1.588(1), γ = 1.593(1), 2 V = 74(1)°. The empirical formula is $Na_{0.68}Ca_{2.03}Al_{2.06}(AsO_4)(As_{0.94}Zn_{0.07}O_{3.87})F_{4.00}(OH)\cdot 2.13H_2O$. The strongest lines of the powder X-ray diffraction pattern [d, Å (I, %) (hkl)] are: 5.364 (80) (001, 020), 4.796 (80) (011), 3.527 (90) (220), 2.966 (100) (13–1, 31–1, 031), 2.700 (90) (221, 002, 040).
Kind of sample preparation and/or method of registration of the spectrum: Attenuated total reflection of a crushed crystal.
Source: Foord et al. (1999).
Wavenumbers (cm^{-1}): 3435s, 3246s, 2296w, 1672w, 1615, 1175, 1051w, 937w, 844s, 832s, 708.
Note: The wavenumbers were partly determined by us based on spectral curve analysis of the published spectrum. Weak bands in the range from 2000 to 2500 cm^{-1} indicate the presence of acid groups $HAsO_4^{2-}$.

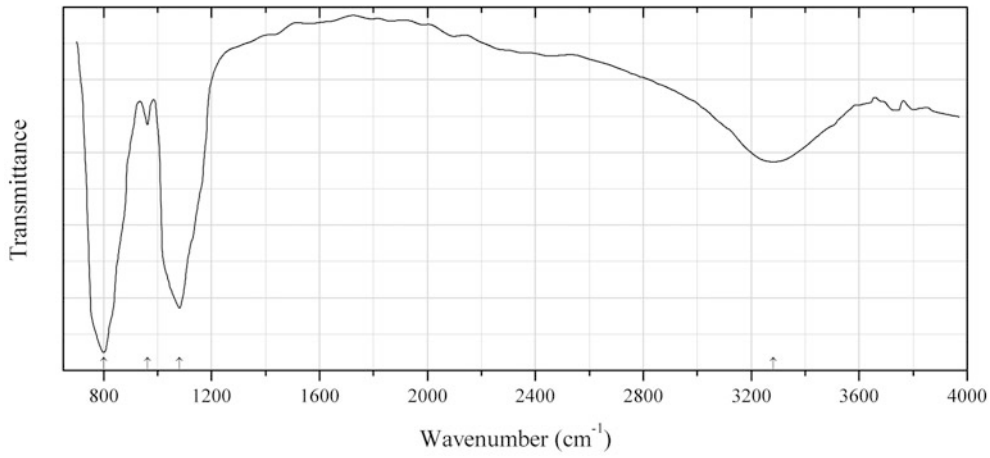

Fig. 2.1390 IR spectrum of feinglosite drawn using data from Clark et al. (1997)

As243 Feinglosite $Pb_2Zn(AsO_4)_2\cdot H_2O$ (Fig. 2.1390)
Locality: Tsumeb mine, Tsumeb, Namibia (type locality).
Description: Olive-green globular aggregate from the association with anglesite, wulfenite, and goethite. Holotype sample. Monoclinic, space group $P2_1$ or $P2_1/m$, a = 8.973(6), b = 5.955(3), c = 7.766(6) Å, β = 112.20(6)°, Z = 2. D_{calc} = 6.52 g/cm^3. The empirical formula is $H_{1.76}Pb_{2.09}(Zn_{0.68}Fe_{0.18})(As_{0.73}S_{0.25})O_9$. The strongest lines of the powder X-ray diffraction pattern [d, Å (I, %) (hkl)] are: 4.85 (50) (110), 3.246 (100) (−112), 2.988 (60) (−301), 2.769 (60) (300, 211), 2.107 (50) (−321).
Kind of sample preparation and/or method of registration of the spectrum: No data.
Source: Clark et al. (1997).
Wavenumbers (cm^{-1}): 3282, 1081s, 962, 800s.

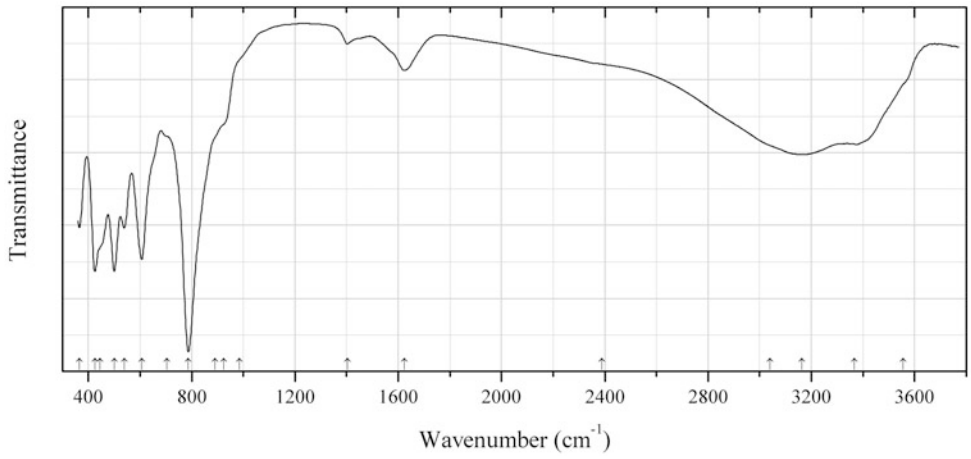

Fig. 2.1391 IR spectrum of lazarenkoite obtained by N.V. Chukanov

As244 Lazarenkoite $CaFe^{3+}As^{3+}{}_3O_7 \cdot 3H_2O$ (Fig. 2.1391)
Locality: Khovu-Aksy deposit, 80 km SW of Kyzyl, Tuva, Siberia, Russia (type locality).
Description: Orange-brown, massive. Investigated by L.I. Yakhontova. Possible contains admixture of an arsenate mineral.
Kind of sample preparation and/or method of registration of the spectrum: KBr disc. Absorption.
Wavenumbers (cm^{-1}): 3555sh, 3367, 3163, 3040sh, 2390sh, 1625, 1403w, 985sh, 925sh, 890sh, 787s, 705sh, 607, 539, 500s, 445sh, 425, 365.

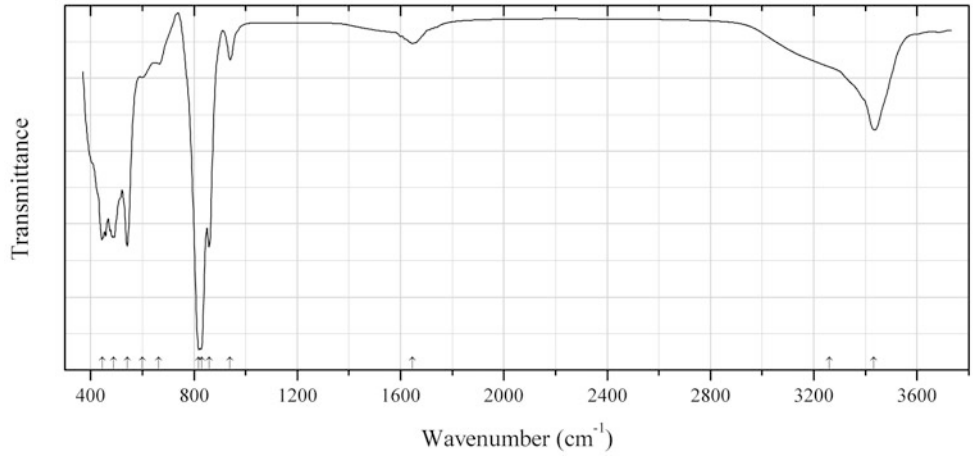

Fig. 2.1392 IR spectrum of auriacusite obtained by N.V. Chukanov

As245 Auriacusite $Cu^{2+}Fe^{3+}(AsO_4)O$ (Fig. 2.1392)
Locality: Berezovskoe gold deposit, Middle Urals, Russia.
Description: Yellow fibrous aggregate from the association with bayldonite, duftite, oxy-plumboroméite, beudantite, and goethite. Investigated by I.V. Pekov. The empirical formula is $Cu_{1.1}Fe_{1.0}(AsO_4)_{1.0}O_x$. The strongest lines of the powder X-ray diffraction pattern [*d*, Å (*I*, %)] are: 5.99 (53), 4.87 (100), 4.22 (59), 2.981 (95), 2.659 (62), 2.468 (71), 2.409 (67).
Kind of sample preparation and/or method of registration of the spectrum: KBr disc. Absorption.

Wavenumbers (cm^{-1}): 3432, 3260sh, 1645w, 940, 858s, 829s, 819s, 662w, 599w, 541s, 489, 446.
Note: The band at 3432 cm^{-1} indicates partial substitution of Fe^{3+} + O for Fe^{2+} + OH. The shoulder at 3260 cm^{-1} and the weak band at 1645 cm^{-1} correspond to adsorbed water.

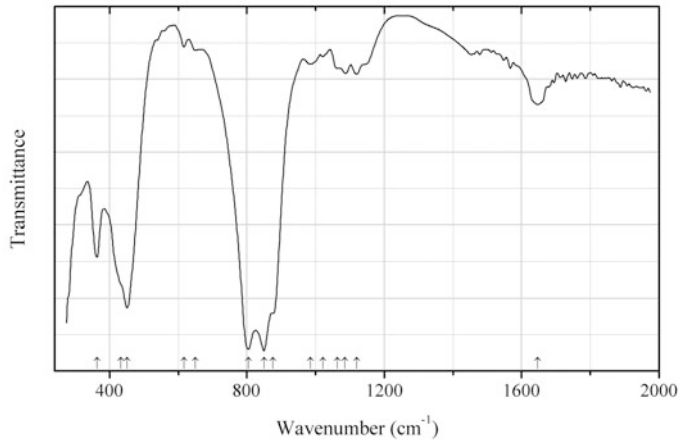

Fig. 2.1393 IR spectrum of gasparite-(Ce) drawn using data from Graeser and Schwander (1987)

As246 Gasparite-(Ce) $Ce(AsO_4)$ (Fig. 2.1393)
Locality: South-eastern slope of Pizzo Cervandone, the Penninic region of the Alps, Italy (type locality).
Description: Brown-red aggregate of microscopic crystals. Monoclinic, space group $P2_1/n$, a = 6.937 (3), b = 7.137(4), c = 6.738(6) Å, β = 104.69(5)°, V = 322.7(2) $Å^3$, Z = 4. D_{calc} = 5.63 g/cm^3. Optically biaxial (+), α = 1.810(8), β = 1.825(8), γ = 1.92(1), 2 V = 40°–45°. The empirical formula is $(Ce_{0.47}La_{0.20}Nd_{0.18}Pr_{0.06}Ca_{0.07}Th_{0.02})(As_{0.94}S_{0.03}Si_{0.03})O_4$. The strongest lines of the powder X-ray diffraction pattern [d, Å (I, %) (hkl)] are: 3.355 (77) (200), 3.156 (100) (120), 2.966 (70) (012), 2.709 (44) (−202), 2.003 (45) (212).
Kind of sample preparation and/or method of registration of the spectrum: No data.
Source: Graeser and Schwander (1987).
Wavenumbers (cm^{-1}): 1646, 1120w, 1085w, 1064sh, 1021w, 985w, 875sh, 850s, 804s, 650w, 617w, 451s, 433sh, 363.
Note: The wavenumbers were partly determined by us based on spectral curve analysis of the published spectrum. The assignment of the strong band at 451 cm^{-1} to silicate groups (Graeser and Schwander 1987) is erroneous because of the absence of strong bands above 850 cm^{-1}.

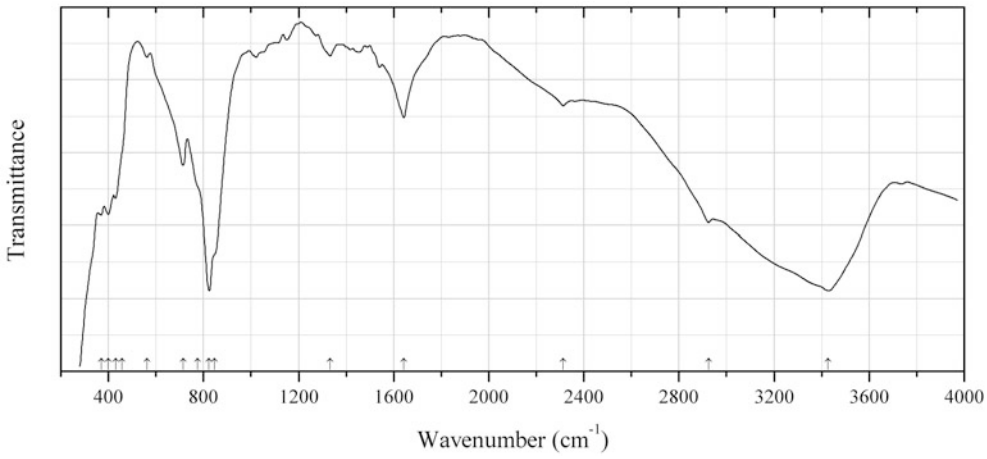

Fig. 2.1394 IR spectrum of geigerite drawn using data from Graeser et al. (1989)

As247 Geigerite $Mn^{2+}{}_5(AsO_4)_2(HAsO_4)_2 \cdot 10H_2O$ (Fig. 2.1394)
Locality: Falotta, Oberhalbstein, Canton of Grisons, Switzerland (type locality).
Description: Rose-red platy crystals from the association with brandtite, sarkinite, grischunite, bergslagite, manganberzellite, etc. Holotype sample. Triclinic, space group *P*-1, a = 7.944(1), b = 10.691(1), c = 6.770(1) Å, α = 80.97(1)°, β = 84.20(1)°, γ = 81.85(1)°, V = 560.3(1) Å^3, Z = 1. D_{meas} = 3.05(10) g/cm^3, D_{calc} = 3.00 g/cm^3. Optically biaxial (−), α = 1.601(2), β = 1.630(2), γ = 1.660(2). The strongest lines of the powder X-ray diffraction pattern [*d*, Å (*I*, %) (*hkl*)] are: 10.45 (100) (010), 7.85 (13) (100), 4.89 (12) (−101), 3.507 (21) (201), 3.340 (20) (002, 220), 3.051 (24) (01–2), 3.011 (17) (022), 2.786 (14) (230).
Kind of sample preparation and/or method of registration of the spectrum: Absorption. Kind of sample preparation is not indicated.
Source: Graeser et al. (1989).
Wavenumbers (cm^{-1}): 3428s, 2925, 2314, 1643, 1332w, 846sh, 824s, 776sh, 714, 562w, 457sh, 430, 400, 370.
Note: The wavenumbers were partly determined by us based on spectral curve analysis of the published spectrum.

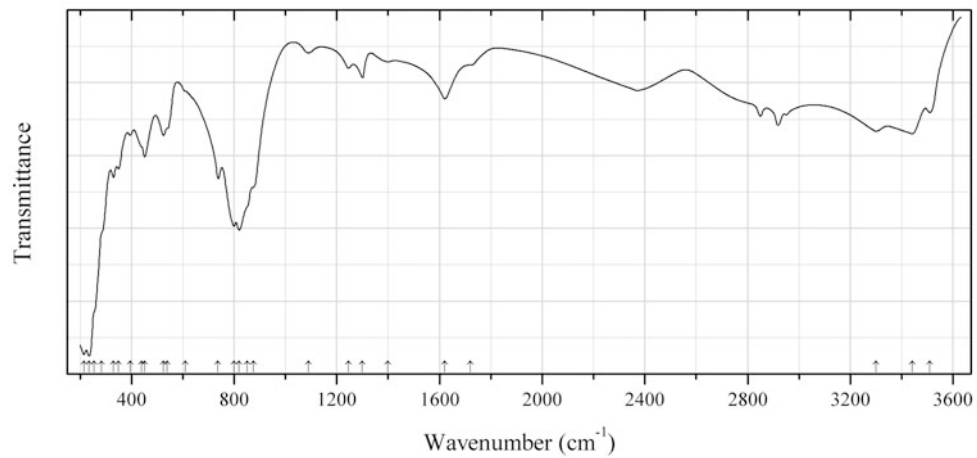

Fig. 2.1395 IR spectrum of geminite drawn using data from Sarp and Perroud (1990)

As248 Geminite $Cu^{2+}(HAsO_4)\cdot H_2O$ (Fig. 2.1395)
Locality: Cap Garonne mine, near La Pradet, Var, France (type locality).
Description: Light green crystals from the association with quartz, coveilite, tennantite, chalcanthite, lavendulan, antlerite, and brochantite. Holotype sample. Triclinic, space group *P*-1, a = 6.395(3), b = 8.110(3), c = 15.732(9) Å, α = 92.01(5)°, β = 93.87(5)°, γ = 95.02(4)°, V = 810.3(5) $Å^3$, Z = 4. D_{calc} = 3.71 g/cm^3. Optically biaxial (+), α = 1.656(2), β = 1.692(2), γ = 1.770(5), 2 V = 75(5)°. The strongest lines of the powder X-ray diffraction pattern [d, Å (I, %) (hkl)] are: 7.83 (100) (002), 4.022 (30) (020), 3.925 (60) (004), 3.850 (30) (021), 3.260 (70) (0–23), 3.107 (40) (12–2), 3.070 (70) (201), 2.815 (40) (20–3), 2.611 (50) (2–20, 006).
Kind of sample preparation and/or method of registration of the spectrum: Absorption. Kind of sample preparation is not indicated.
Source: Sarp and Perroud (1990).
Wavenumbers (cm^{-1}): 3510, 3440, 3300, 1720sh, 1620, 1400w, 1300w, 1245w, 1090w, 875sh, 850sh, 820s, 800s, 736s, 610sh, 540sh, 525, 452, 440sh, 395, 350, 330, 285sh, 255sh, 235s, 215s.
Note: The bands in the range from 2800 to 3000 cm^{-1} correspond to the admixture of an organic substance.

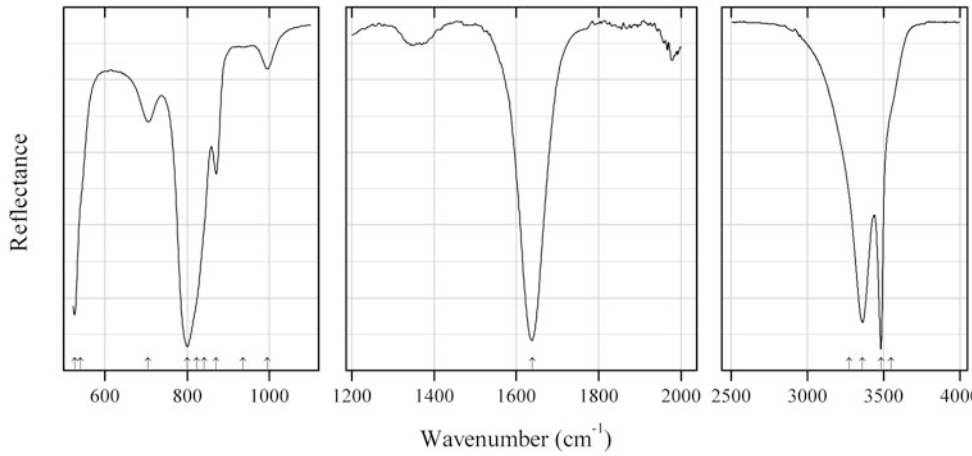

Fig. 2.1396 IR spectrum of agardite-(Y) drawn using data from Frost et al. (2006a)

As249 Agardite-(Y) $YCu_6(AsO_4)_3(OH)_6\cdot 3H_2O$ (Fig. 2.1396)
Locality: Synthetic.
Description: Synthesized from $Y(NO_3)_3$, $Cu(NO_3)_2\cdot 2.5H_2O$, and $Na_2HAsO_4\cdot 7H_2O$ in aqueous solution at 180 °C and pH 6.9. Confirmed by powder X-ray diffraction pattern.
Kind of sample preparation and/or method of registration of the spectrum: Attenuated total reflection of powdered sample.
Source: Frost et al. (2006a).
Wavenumbers (cm^{-1}): 3548sh, 3483s, 3362s, 3275sh, 1639, 995, 936w, 870, 842sh, 823sh, 800s, 705, 541sh, 527.
Note: In the cited paper the mineral is erroneously named "goudeyite". The wavenumbers are indicated for the maxima of individual bands obtained as a result of the spectral curve analysis. Details of this analysis are not described. The wavenumbers were determined by us based on spectral curve analysis of the published spectrum.

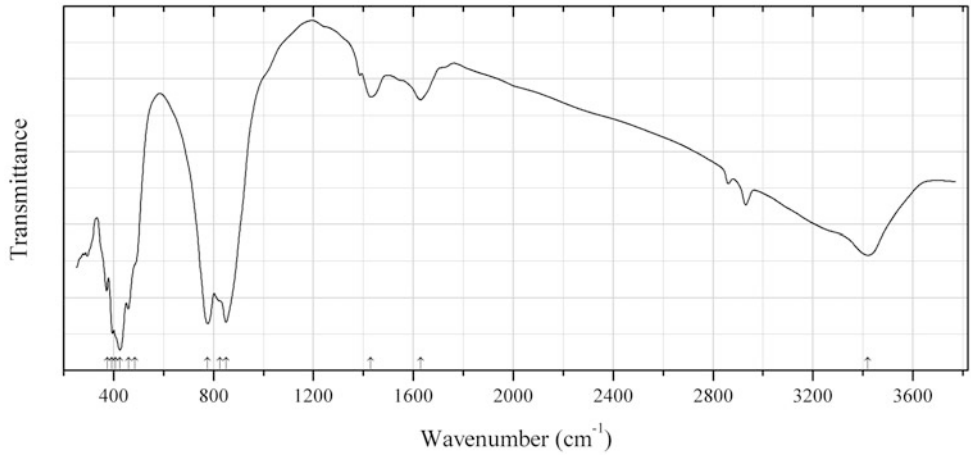

Fig. 2.1397 IR spectrum of grischunite drawn using data from Graeser et al. (1984)

As250 Grischunite $NaCa_2Mn^{2+}{}_5Fe^{3+}(AsO_4)_6 \cdot 2H_2O$ (Fig. 2.1397)
Locality: Falotta, Oberhalbstein, Canton Grisons, eastern Switzerland (type locality).
Description: Red-brown crystals from the association with brandtite, sarkinite, manganberzrliite, tilasite, and other arsenates. Holotype sample. Orthorhombic, space group *Pcab*, a = 12.913(6), b = 13.48(1), c = 12.076(6) Å. D_{meas} = 3.8(2) g/cm^3, D_{calc} = 3.99 g/cm^3. Optically biaxial (+), α = 1.784(3), β = 1.785(3), γ = 1.790(3), 2 V = 40–50°. The empirical formula is $Na_{0.72}Ca_{2.07}Mn_{5.04}Fe_{0.81}As_{6.12} \cdot nH_2O$. The strongest lines of the powder X-ray diffraction pattern [d, Å (I, %) (hkl)] are: 6.037 (30) (002), 3.617 (70) (320), 3.150 (90) (232), 3.015 (80) (004), 2.943 (60) (042), 2.838 (100) (421).
Kind of sample preparation and/or method of registration of the spectrum: Transmission. Kind of sample preparation is not indicated.
Source: Graeser et al. (1984).
Wavenumbers (cm^{-1}): 3420, 1630w, 1430w, 850s, 826sh, 777s, 486sh, 460, 426s, 408sh, 392s, 376.
Note: The wavenumbers were partly determined by us based on spectral curve analysis of the published spectrum. Despite grischunite was first described by Graeser et al. (1984) as an anhydrous mineral, the bands at 3420 and 1630 cm^{-1} together with a poor Gladstone–Dale compatibility index clearly indicate the presence of H_2O molecules. The bands in the range from 2800 to 3000 cm^{-1} correspond to the admixture of an organic substance.

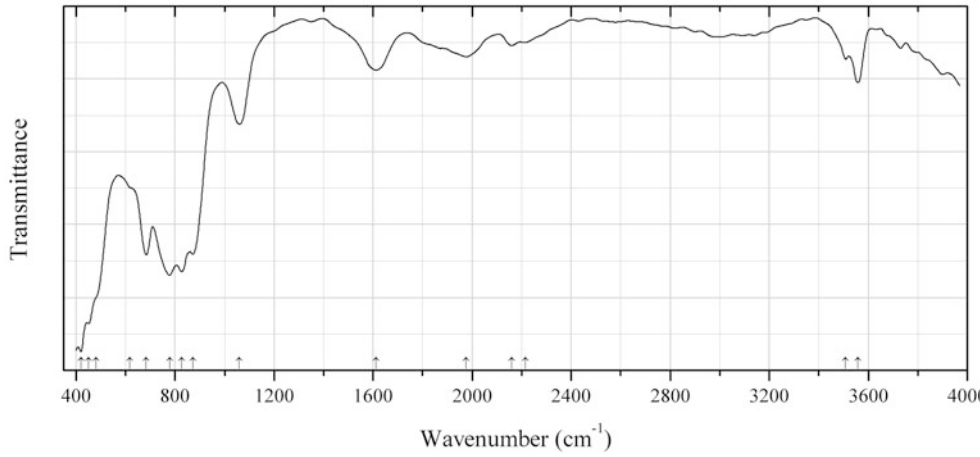

Fig. 2.1398 IR spectrum of guanacoite drawn using data from Witzke et al. (2006)

As251 Guanacoite $Cu_2Mg_3(AsO_4)_2(OH)_4 \cdot 4H_2O$ (Fig. 2.1398)
Locality: El Guanaco Mine, 93 km east of Taltal, 2nd Region, Northern Chile (type locality).
Description: Pale blue prismatic crystals in the association with arhbarite, conichalcite, olivenite, chrysocolla, brochantite, quartz, and enargite. Holotype sample. Monoclinic, space group $P2_1/c$, = 5.475(1), b = 16.865(3), c = 6.915(1) Å, β = 99.80(3)°, V = 629.2(2) Å^3, Z = 2. D_{meas} = 3.31 g/cm^3, D_{calc} = 3.30 g/cm^3. Optically biaxial (−), α = 1.664(1), β = 1.691(1), γ = 1.695 (1), 2 V = 31(1)°. The empirical formula is $Cu_{2.32}Mg_{2.64}(AsO_4)_{1.93}(OH)_{4.13} \cdot 4.15H_2O$. The strongest lines of the powder X-ray diffraction pattern [d, Å (I, %) (hkl)] are: 8.42 (100) (020), 4.322 (21) (031), 4.210 (64) (040), 3.016 (12) (051), 2.907 (10) (032).
Kind of sample preparation and/or method of registration of the spectrum: A FTIR transmittance spectrum of a powder sample was obtained using a diamond microcell.
Source: Witzke et al. (2006).
Wavenumbers (cm^{-1}): 3558, 3509, 2215w, 2160w, 1975, 1612, 1060, 872s, 827s, 778s, 684s, 617sh, 482sh, 452s, 420s.
Note: The wavenumbers were partly determined by us based on spectral curve analysis of the published spectrum. The bands in the range from 1700 to 3300 cm^{-1} indicate possible presence of acid groups $HAsO_4^{2-}$ or $H_2AsO_4^-$.

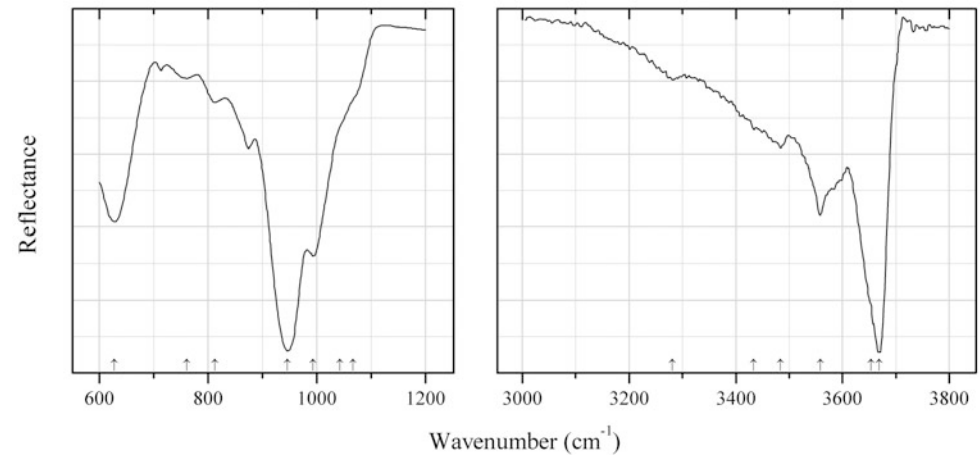

Fig. 2.1399 IR spectrum of allactite drawn using data from Frost and Weier (2006)

As252 Allactite $Mn^{2+}{}_7(AsO_4)_2(OH)_8$ (Fig. 2.1399)
Locality: Nordmark deposit, Filipstad district, Värmland, Sweden.
Description: No data are given on the appearance and physical properties for the sample used in the cited paper. EDS analysis gives 31.0 % As_2O_5 and 58.2 % MnO.
Kind of sample preparation and/or method of registration of the spectrum: Attenuated total reflection of powdered mineral.
Source: Frost and Weier (2006).
Wavenumbers (cm^{-1}): 3669s, 3653sh, 3558, 3484, 3433, 3281, 1066sh, 1042sh, 993, 946s, 812, 760w, 627.
Note: The name "Nordmarken" given for the locality by Frost and Weier (2006) is incorrect. The wavenumbers are indicated for the maxima of individual bands obtained as a result of the spectral curve analysis and do not reflect real maxima and shoulders in the spectral curve. Details of the band analysis are not described. The spectrum is questionable because the strongest bands are observed in the range from 900 to 1000 cm^{-1}, which is typical for silicates and utterly unusual for arsenates. The wavenumbers were determined by us based on spectral curve analysis of the published spectrum.

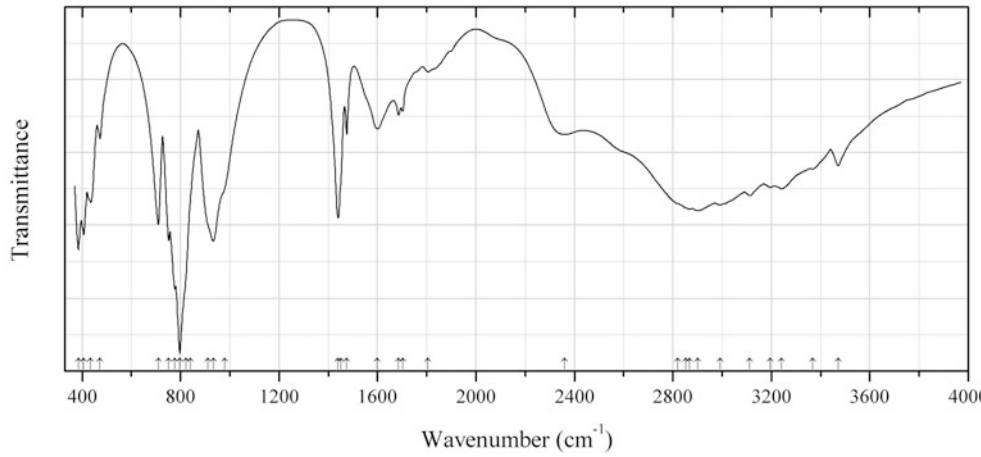

Fig. 2.1400 IR spectrum of struvite arsenate analogue drawn using data from Stefov et al. (2008)

As253 Struvite arsenate analogue $(NH_4)Mg(AsO_4)\cdot 6H_2O$ (Fig. 2.1400)
Locality: Synthetic.
Kind of sample preparation and/or method of registration of the spectrum: KBr disc. Absorption.
Source: Stefov et al. (2008).
Wavenumbers (cm^{-1}): 3472, 3367, 3242, 3195, 3112, 2992, 2900, 2869, 2854sh, 2820sh, 2360, 1805w, 1702, 1686, 1600, 1475, 1451sh, 1440s, 980sh, 935s, 910sh, 840sh, 822sh, 798s, 776s, 752s, 711s, 473, 435, 407s, 385s.
Note: The wavenumbers were partly determined by us based on spectral curve analysis of the published spectrum.

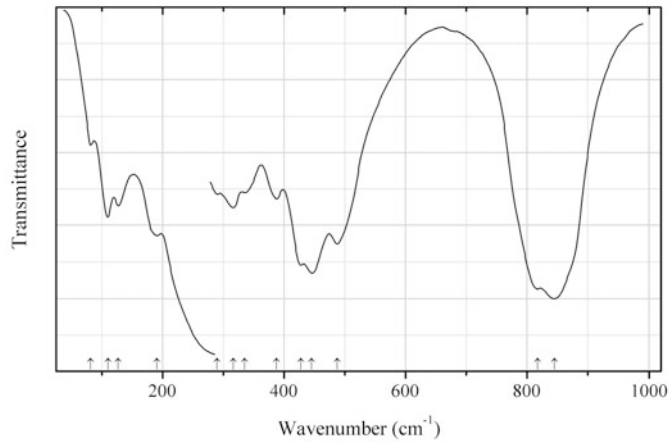

Fig. 2.1401 IR spectrum of berzeliite polymorph drawn using data from Khorari et al. (1995)

As254 Berzeliite polymorph $NaCa_2Mg_2(AsO_4)_3$ (Fig. 2.1401)
Locality: Synthetic.
Description: Confirmed by powder X-ray diffraction data.
Kind of sample preparation and/or method of registration of the spectrum: KBr disc (in the range 1500–300 cm^{-1}), polyethylene disc (in the range 350–30 cm^{-1}). Transmission.
Source: Khorari et al. (1995).
Wavenumbers (cm^{-1}): 845s, 817s, 487, 445s, 428, 388, 335, 316, 290, 191, 127, 110, 82w.

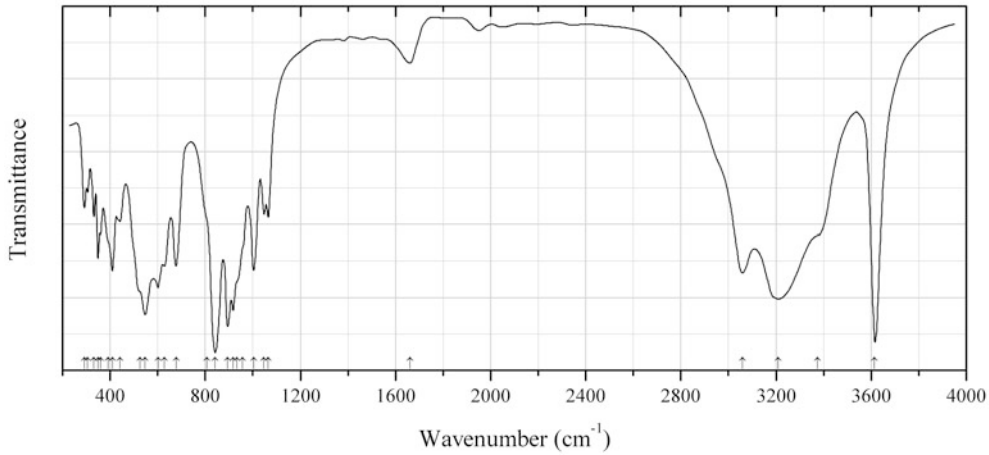

Fig. 2.1402 IR spectrum of ceruleite drawn using data from Schmetzer et al. (1976)

As255 Ceruleite $Cu_2Al_7(AsO_4)_4(OH)_{13}\cdot 11.5H_2O$ (Fig. 2.1402)
Locality: An unknown locality in Bolivia.
Description: Blue radial aggregates of microscopic prismatic crystals from the association with quartz, barite, goethite, and mansfieldite. Triclinic, a = 14.359(3), b = 14.687(3), c = 7.440(1) Å, α = 96.06(3)°, β = 93.19(4)°, γ = 91.63(4)°, V = 1556.9 $Å^3$, Z = 2. D_{meas} = 2.70 g/cm^3, D_{calc} = 2.734 g/cm^3. The strongest lines of the powder X-ray diffraction pattern [d, Å (I, %)] are: 7.296 (75), 5.926 (70), 5.650 (100), 4.760 (70), 3.545 (60), 2.650 (60).

Kind of sample preparation and/or method of registration of the spectrum: KBr disc. Transmission.
Source: Schmetzer et al. (1976).
Wavenumbers (cm^{-1}): 3615s, 3375sh, 3210s, 3060, 1660w, 1065, 1047, 1003, 957sh, 934sh, 917s, 894s, 842s, 808sh, 677, 628, 601, 547s, 526sh, 441, 409, 392sh, 360, 349, 332, 305, 292.
Note: The wavenumbers were partly determined by us based on spectral curve analysis of the published spectrum.

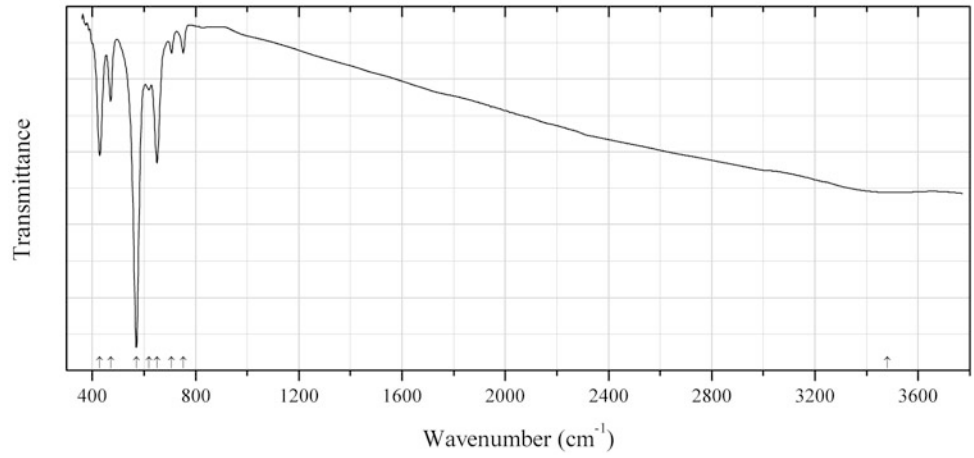

Fig. 2.1403 IR spectrum of lead copper(I) arsenite chloride As256 obtained by N.V. Chukanov

As256 Lead copper(I) arsenite chloride As256 $Pb_6Cu^+(AsO_3)_2Cl_2$ (Fig. 2.1403)
Locality: Vrissaki area, nearthe town of Lavrion, Attiki Peninsula, Greece.
Description: Colourless, transparent, hexagonal lamellar crystals from cavities in ancient metallurgical slag dumped after smelting into the sea. The associated minerals are nealite and chrysocolla. Trigonal, space group, *R*-3, $a = 9.8691(2)$, $c = 34.2028(13)$ Å, $V = 2885.01(14)$ $Å^3$, $Z = 6$. $D_{calc} = 6.219$ g/cm^3. The empirical formula is (electron microprobe): $Pb_{5.99}Cu_{0.97}Fe_{0.05}(AsO_3)_{2.01}Cl_{6.87}Br_{0.06}O_{0.02}$.
Kind of sample preparation and/or method of registration of the spectrum: KBr disc. Absorption.
Wavenumbers (cm^{-1}): (3480w), 752w, 707w, 650s, 619w, 570s, 471, 429s.

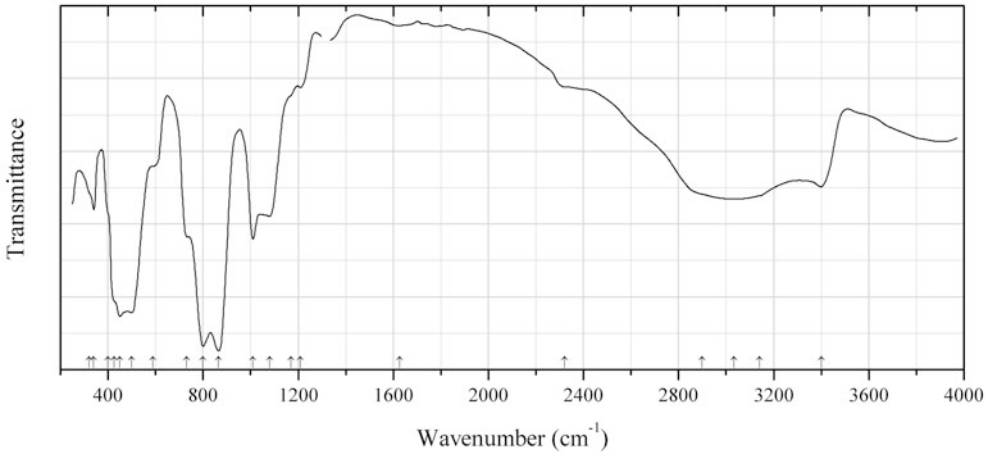

Fig. 2.1404 IR spectrum of dussertite drawn using data from Keller (1971)

As257 Dussertite $BaFe^{3+}{}_3(AsO_4)_2(OH)_5 \cdot H_2O$ (Fig. 2.1404)
Locality: Djebel Debar (Djebel Debagh), Hammam Meskoutine, Guelma, Constantine province, Algeria (type locality).
Description: Yellow-green crystals. Confirmed by powder X-ray diffraction data.
Kind of sample preparation and/or method of registration of the spectrum: Transmission. Kind of sample preparation is not indicated.
Source: Keller (1971).
Wavenumbers (cm^{-1}): 3400, 3140sh, 3033, 2900sh, 2320w, 1626w, 1210w, 1169sh, 1080, 1010, 865s, 800s, 730, 590sh, 500s, 450s, 427sh, 400sh, 340, 321sh.
Note: The wavenumbers were partly determined by us based on spectral curve analysis of the published spectrum.

As258 Eveite $Mn_2^{2+}(AsO_4)(OH)$
Locality: Långban deposit, Bergslagen ore region, Filipstad district, Värmland, Sweden (type locality).
Description: Specimen No. 390271 from the Swedish Museum of Natural History. The FTIR-spectrum of eveite obtained in the range from 3200 to 3650 cm^{-1} is characterized by one sharp absorption band at 3560 cm^{-1} and two broad and less intense bands at 3340 and 3450 cm^{-1}. In the FTIR–spectrum of the eveite dimorph sarkinite, a set of overlapping sharp absorption bands centred at 3505, 3515, 3525, and 3535 cm^{-1} are evident.
Kind of sample preparation and/or method of registration of the spectrum: Suspension in Nujol. Absorption.
Source: Hålenius and Westlund (1998).
Wavenumbers (cm^{-1}): 3560s, 3450, 3340.

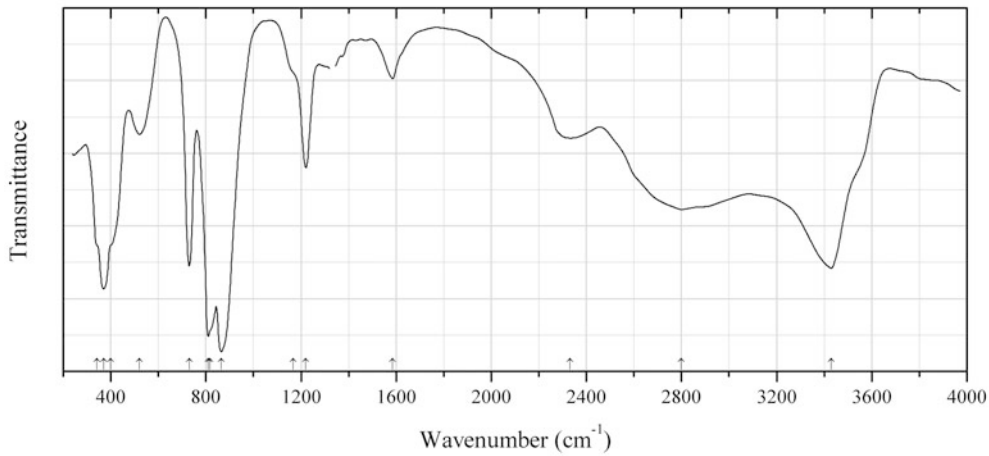

Fig. 2.1405 IR spectrum of haidingerite drawn using data from Keller (1971)

As259 Haidingerite $Ca(HAsO_4) \cdot 2H_2O$ (Fig. 2.1405)
Locality: Synthetic.
Description: Synthesized from $CaCO_3$ and $Na_2(HAsO_4) \cdot 7H_2O$ in the presence of HCl. Confirmed by optical and powder X-ray diffraction data.
Kind of sample preparation and/or method of registration of the spectrum: Suspension in mineral oil. Transmission.

Source: Keller (1971).
Wavenumbers (cm^{-1}): 3430s, 2800, 2330, 1585w, 1220, 1168sh, 865s, 818sh, 810s, 730s, 520, 400sh, 370s, 343sh.
Note: The wavenumbers were partly determined by us based on spectral curve analysis of the published spectrum. The band position denoted by Keller (1971) as 2900 cm^{-1} was determined by us at 2800 cm^{-1}.

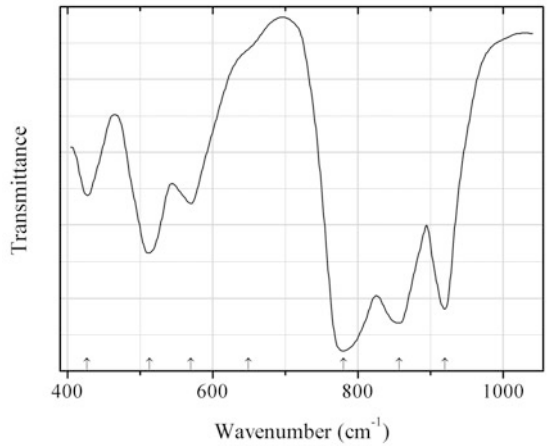

Fig. 2.1406 IR spectrum of alarsite polymorph As260 drawn using data from Chen et al. (1990)

As260 Alarsite polymorph As260 $Al(AsO_4)$ (Fig. 2.1406)
Locality: Synthetic.
Description: Framework aluminoarsenate with occluded ethylenediamine. Synthesized hydrothermally in the presence of a template ethylenediamine. Monoclinic, a = 19.953, b = 6.636, c = 10.604 Å, β = 96.88°. The strongest lines of the powder X-ray diffraction pattern [d, Å (I, %) (hkl)] are: 9.899 (100) (200), 7.681 (18) (−201), 4.939 (15) (400, 102), 4.439 (11) (202), 3.850 (12) (−402), 3.300 (18) (600), 2.7207 (12) (403).
Kind of sample preparation and/or method of registration of the spectrum: KBr disc. Transmission.
Source: Chen et al. (1990).
Wavenumbers (cm^{-1}): 920s, 857s, 780s, 649sh, 570, 513, 427.
Note: The wavenumbers were partly determined by us based on spectral curve analysis of the published spectrum. Bands of ethylenediamine observed above 1000 cm^{-1} are omitted.

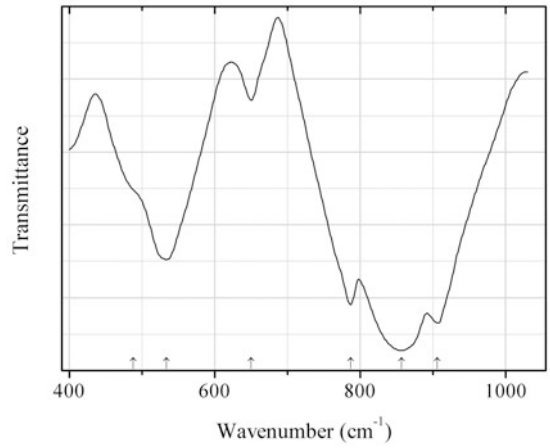

Fig. 2.1407 IR spectrum of alarsite polymorph As261 drawn using data from Chen et al. (1990)

As261 Alarsite polymorph As261 $Al(AsO_4)$ (Fig. 2.1407)
Locality: Synthetic.
Description: Framework aluminoarsenate with occluded ethylenediamine. Synthesized hydrothermally in the presence of a template ethylenediamine. Monoclinic, a = 11.777, b = 18.960, c = 5.981, β = 94.85°. The strongest lines of the powder X-ray diffraction pattern [d, Å (I, %) (hkl)] are: 9.477 (100) (020), 3.407 (47) (−301), 3.159 (15) (060), 2.9884 (7) (321, 002), 2.6928 (12) (032).
Kind of sample preparation and/or method of registration of the spectrum: KBr disc. Transmission.
Source: Chen et al. (1990).
Wavenumbers (cm^{-1}): 906s, 857s, 787s, 650, 534, 488sh.
Note: The wavenumbers were partly determined by us based on spectral curve analysis of the published spectrum. Bands of ethylenediamine observed above 1000 cm^{-1} are omitted.

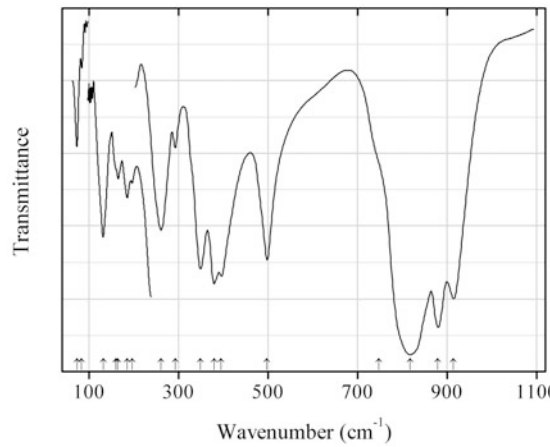

Fig. 2.1408 IR spectrum of barium zirconium arsenate As262 drawn using data from Paques-Ledent (1977)

As262 Barium zirconium arsenate As262 $BaZr(AsO_4)_2$ (Fig. 2.1408)
Locality: Synthetic.

Description: Isostructural with yavapaiite. Monoclinic, $a = 8.638$, $b = 5.495$, $c = 7.974$ Å, $\beta = 92.67°$.
Kind of sample preparation and/or method of registration of the spectrum: Transmission. Kind of sample preparation is not indicated.
Source: Paques-Ledent (1977).
Wavenumbers (cm^{-1}): 915s, 880s, 818s, 748sh, 498, 396, 380, 349, 293w, 261, 197, 186, 165, 160sh, 132, 84w, 73w.
Note: The wavenumbers were determined by us based on spectral curve analysis of the published spectrum.

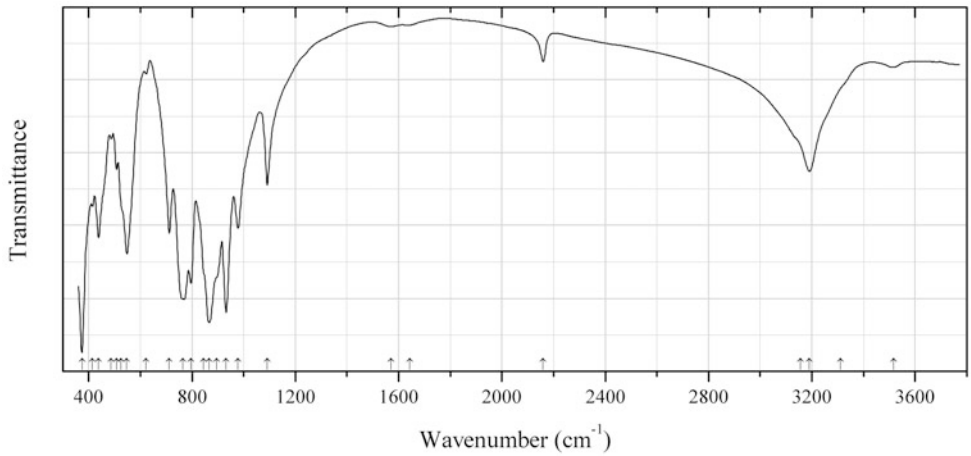

Fig. 2.1409 IR spectrum of sodium aluminium hydroxyarsenate As263 obtained by N.V. Chukanov

As263 Sodium aluminium hydroxyarsenate As263 $Na_3Al_5(AsO_4)_4O_2(OH)_2$ (Fig. 2.1409)
Locality: Synthetic.
Description: Synthesized by A.R. Kotelnikov under hydrothermal conditions. The crystal structure is investigated by O.V. Yakubovich. Orthorhombic, space group *Ibam*, $a = 7.4614(1)$, $b = 17.4677(3)$, $c = 11.2815(2)$ Å.
Kind of sample preparation and/or method of registration of the spectrum: KBr disc. Absorption.
Wavenumbers (cm^{-1}): 3517w, 3310sh, 3191, 3155sh, 2160, 1643w, 1570w, 1091, 978, 932s, 895sh, 867s, 845sh, 796, 765s, 712, 623w, 548, 525sh, 507, 487w, 438, 414, 375s.

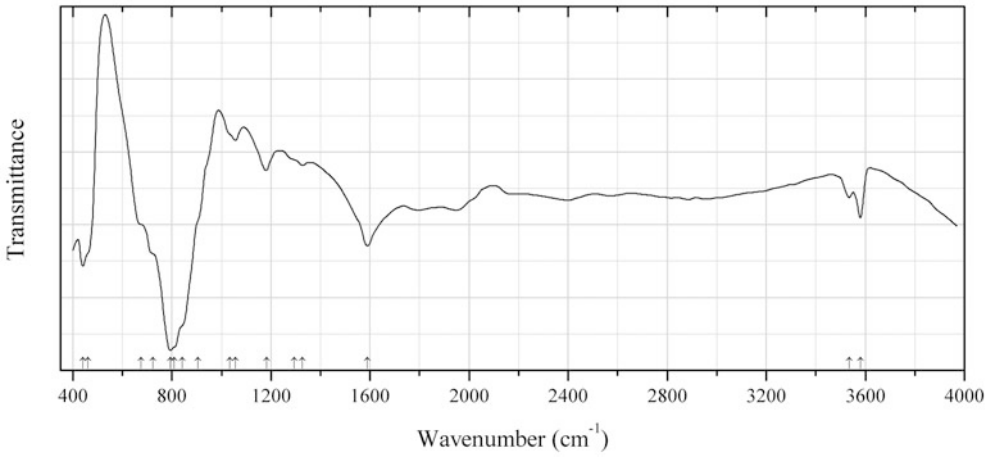

Fig. 2.1410 IR spectrum of helmutwinklerite drawn using data from Effenberger et al. (2000)

As264 Helmutwinklerite $PbZn(AsO_4)_2 \cdot 2H_2O$ (Fig. 2.1410)
Locality: No data.
Kind of sample preparation and/or method of registration of the spectrum: Diamond-anvil cell microsampling.
Source: Effenberger et al. (2000).
Wavenumbers (cm^{-1}): 3580, 3535w, 1590, 1328, 1295sh, 1182, 1056, 1035sh, 905sh, 842sh, 810sh, 794s, 723sh, 676sh, 460sh, 441s.
Note: The wavenumbers were partly determined by us based on spectral curve analysis of the published spectrum. Weak bands in the range 1700–2600 cm^{-1} indicate the presence of acid OH groups.

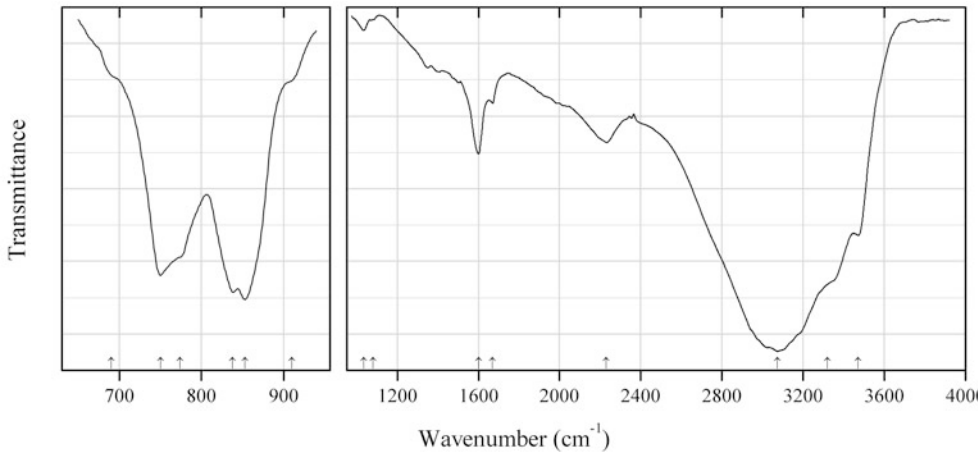

Fig. 2.1411 IR spectrum of ianbruceite drawn using data from Cooper et al. (2012)

As265 Ianbruceite $Zn_2(AsO_4)(OH) \cdot 3H_2O$ (Fig. 2.1411)
Locality: Tsumeb mine, Otjikoto (Oshikoto) region, Tsumeb, Namibia (type locality).
Description: Blue flattened aggregates from the association with köttigite, legrandite, and adamite. Holotype sample. Monoclinic, space group $P2_1/c$, a = 11.793(2), b = 9.1138(14), c = 6.8265(10) Å,

β = 103.859(9)°, V = 712.3(3) Å^3, Z = 4. D_{calc} = 3.197 g/cm^3. Optically biaxial (−), α = 1.601(2), β = 1.660(2), γ = 1.662(2), 2 V = 18(2)°. The crystal-chemical formula is $K_{0.02}(Zn_{1.93}Fe_{0.03}Al_{0.02}Mn_{0.01})(OH)_{0.96}(H_2O)(AsO_4)(H_2AsO_3)(H_2O)_{1.96}$. The strongest lines of the powder X-ray diffraction pattern [d, Å (I, %) (hkl)] are: 11.29 (100) (100), 3.143 (15) (−202), 2.922 (17) (130), 2.655 (9) (230), 2.252 (7) (222), 1.598 (8) (−152).

Kind of sample preparation and/or method of registration of the spectrum: Absorption. The spectrum was collected using an IR microscope. Kind of sample preparation is not indicated.

Source: Cooper et al. (2012).

Wavenumbers (cm^{-1}): 3471, 3320sh, 3073s, 2231, 1670w, 1600, 1080w, 1034w, 910sh, 853s, 838s, 774sh, 750s, 690sh.

Note: The wavenumbers were partly determined by us based on spectral curve analysis of the published spectrum.

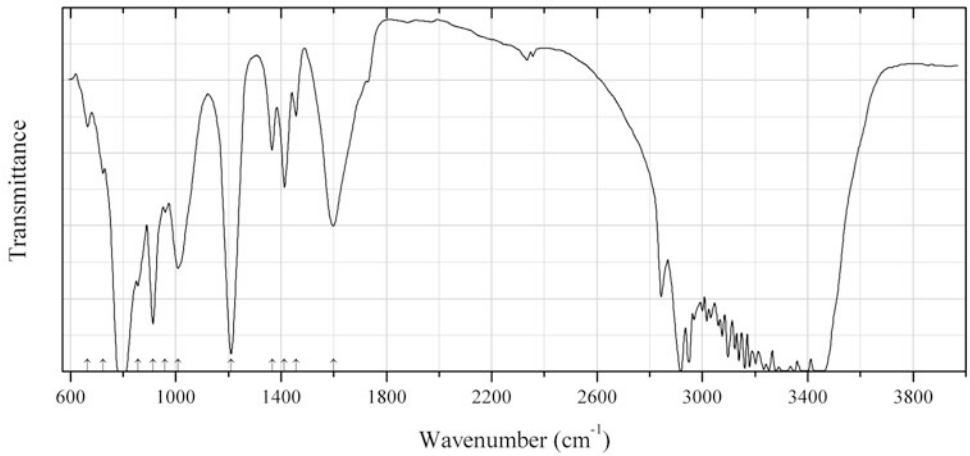

Fig. 2.1412 IR spectrum of juanitaite drawn using data from Kampf et al. (2000)

As266 Juanitaite $(Cu,Ca,Fe)_{10}Bi(AsO_4)_4(OH)_{11}\cdot 2H_2O$ (Fig. 2.1412)

Locality: Gold Hill mine, Tooele Co., Utah, USA (type locality).

Description: Green platy crystals. Holotype sample. Trtragonal, space group $P4_2/nnm$, a = 9.961(3), c = 29.29(2) Å, V = 2896(2) Å^3, Z = 4. D_{meas} = 3.61(5) g/cm^3, D_{calc} = 3.56 g/cm^3. Optically uniaxial (−), ω = 1.785(5), ε = 1.705(5). The empirical formula is $(Cu_{7.03}Ca_{2.39}Fe_{0.50})Bi_{0.99}(AsO_4)_{3.97}(OH)_{10.90}\cdot 2.22H_2O$. The strongest lines of the powder X-ray diffraction pattern [d, Å (I, %) (hkl)] are: 14.6 (100) (002), 7.04 (50) (110), 6.34 (70) (112), 5.07 (50) (114), 3.146 (60) (310, 303), 2.535 (50) (228).

Kind of sample preparation and/or method of registration of the spectrum: Absorption of unpolarized IR radiation propagating down the c axis by a single flake.

Source: Kampf et al. (2000).

Wavenumbers (cm^{-1}): ~3440s, ~1600, 1458w, 1413, 1366w, 1210s, 1009, 960, 914, 857w, ~796s, 723w, 666w.

Note: The wavenumbers were partly determined by us based on spectral curve analysis of the published spectrum.

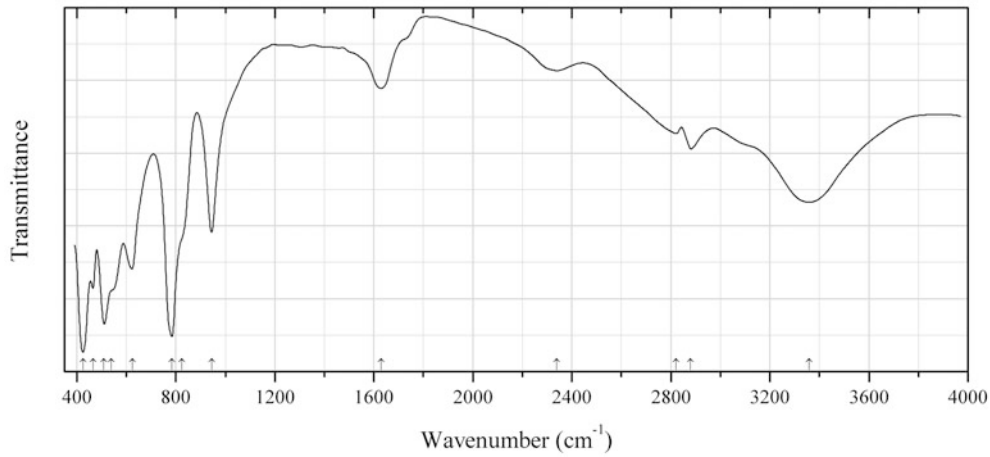

Fig. 2.1413 IR spectrum of kolfanite drawn using data from Voloshin et al. (1982)

As267 Kolfanite $Ca_2Fe^{3+}{}_3(AsO_4)_3O_2{\cdot}2H_2O$ (Fig. 2.1413)
Locality: Vasin-Myl'k Mt., Voron'i Tundry massif, Kola peninsula, Murmansk region, Russia (type locality).
Description: Red crusts from the association with apatite, mitridatite, and montebrasite. Holotype sample. Monoclinic, a = 17.86, b = 19.66, c = 11.11 Å, β = 96°, Z = 12. D_{meas} = 3.3 g/cm^3, D_{calc} = 3.75 g/cm^3. Optically biaxial (−), α = 1.810, β = 1.923, γ = 1.933. The strongest lines of the powder X-ray diffraction pattern [d, Å (I, %)] are: 8.90 (100), 5.64 (50), 3.29 (90), 2.95 (90), 2.720 (100), 2.216 (80), 1.646 (80).
Kind of sample preparation and/or method of registration of the spectrum: KBr disc. Absorption.
Source: Voloshin et al. (1982).
Wavenumbers (cm^{-1}): 3360, 2880, 2820w, 2340w, 1630, 945, 825sh, 785s, 625, 540sh, 510s, 465, 425s.
Note: The wavenumbers were partly determined by us based on spectral curve analysis of the published spectrum. A questional mineral, possibly identical to arseniosiderite.

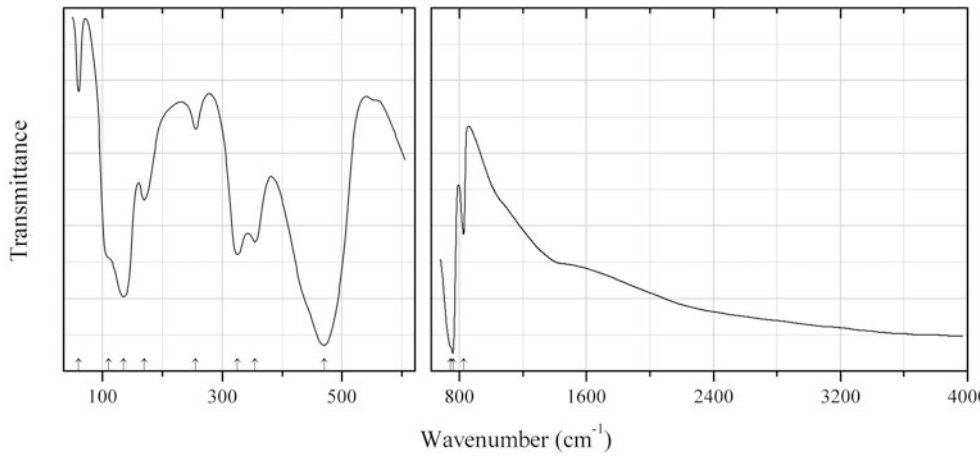

Fig. 2.1414 IR spectrum of kuznetsovite drawn using data from Kovaleva and Vasiliev (1987)

As268 Kuznetsovite $Hg^{+}{}_{2}Hg^{2+}(AsO_4)Cl$ (Fig. 2.1414)
Locality: Khaidarkan Sb-Hg deposit, Fergana valley, Alai range, Osh region, Kyrgyzstan (type locality).
Description: No data.
Kind of sample preparation and/or method of registration of the spectrum: Suspension in perfluorinated mineral oil deposited on polyethylene substrate. Absorption.
Source: Kovaleva and Vasiliev (1987).
Wavenumbers (cm^{-1}): 826, 758s, 745sh, 470s, 355, 325, 255w, 170, 135, 110sh, 60w.

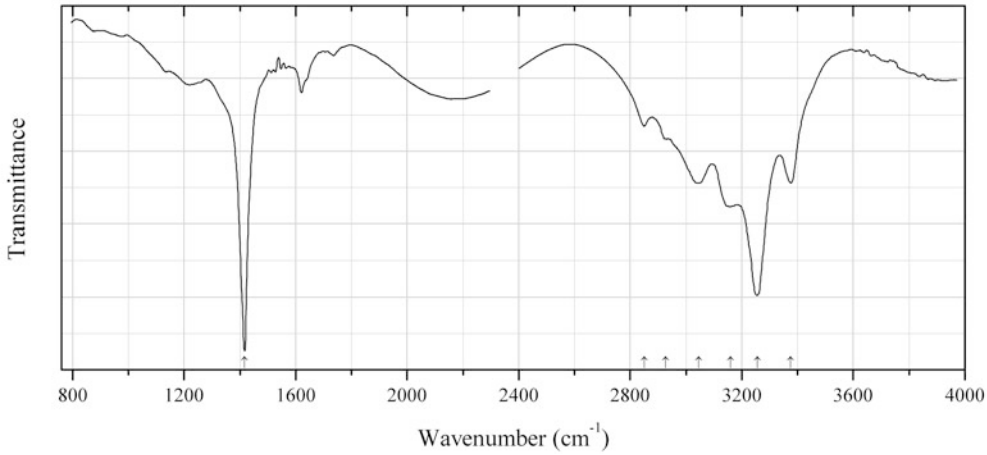

Fig. 2.1415 IR spectrum of lucabindiite drawn using data from Garavelli et al. (2013)

As269 Lucabindiite $(K,NH_4)As^{3+}{}_{4}O_6(Cl,Br)$ (Fig. 2.1415)
Locality: La Fossa crater, Vulcano island, Lipari, Eolie (Aeolian) islands, Messina province, Sicily, Italy (type locality).
Description: Colourless hexagonal platy crystals from the association with arsenolite, sal ammoniac, sulfur, and amorphous arsenic-rich sulfurite. Holotype sample. Hexagonal, space group *P6/mmma* = 5.2386(7), *c* = 9.014(2) Å, *V* = 214.23(7) $Å^3$, *Z* = 1. D_{calc} = 3.68 g/cm^3. The empirical formula is $[K_{0.51}(NH_4)_{0.49}]As_{4.00}O_{5.93}(Cl_{0.48}Br_{0.40}F_{0.19})$. The strongest lines of the powder X-ray diffraction pattern [*d*, Å (*I*, %) (*hkl*)] are: 3.20 (100) (102), 2.62 (67) (110), 4.51 (52) (002), 4.54 (30) (100), 1.97 (28) (113), 1.49 (21) (115), 1.60 (21) (212), 2.26 (19) (112).
Kind of sample preparation and/or method of registration of the spectrum: A single crystal was mounted on glass capillary. The absorbance spectrum was obtained with an IR microscope.
Source: Garavelli et al. (2013).
Wavenumbers (cm^{-1}): 3375, 3257s, 3159, 3045, 2926, 2850w, 1417s.
Note: The wavenumbers were partly determined by us based on spectral curve analysis of the published spectrum. The bands in the range from 1500 to 3100 cm^{-1} may correspond to impurities.

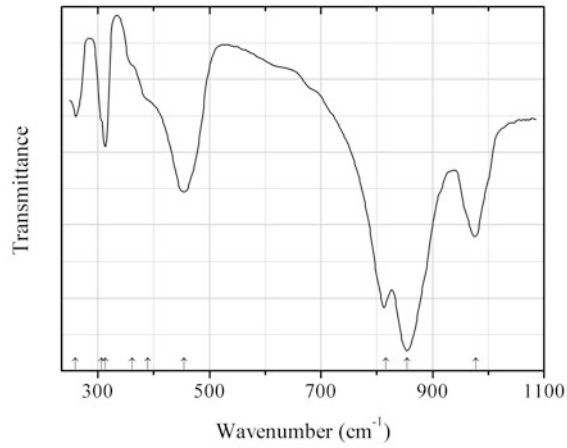

Fig. 2.1416 IR spectrum of manganese(II) diarsenate drawn using data from Botto et al. (1975)

As270 Manganese(II) diarsenate $Mn_2(As_2O_7)$ (Fig. 2.1416)
Locality: Synthetic.
Description: Obtained by the solid state reaction between As_2O_5 and $MnCO_3$ at 600 °C. Monoclinic, with the thortveitite-type structure, space group *C*2/*m*, a = 6.77(1), b = 8.78(1), c = 4.81(1) Å, β = 91.141(6)°, γ = 102.86(5)°, V = 278.85 Å^3, Z = 2. D_{meas} = 4.5(1) g/cm^3, D_{calc} = 4.43 g/cm^3. The strongest lines of the powder X-ray diffraction pattern [*d*, Å (*I*, %) (*hkl*)] are: 3.212 (100) (021), 3.038 (59) (201), 2.639 (34) (220), 1.929 (17) (−222), 1.688 (20) (132), 1.564 (17) (003).
Kind of sample preparation and/or method of registration of the spectrum: KBr disc. Transmission.
Source: Botto et al. (1975).
Wavenumbers (cm^{-1}): 978, 855s, 816s, 455, 390sh, 362sh, 313, 307sh, 260w.

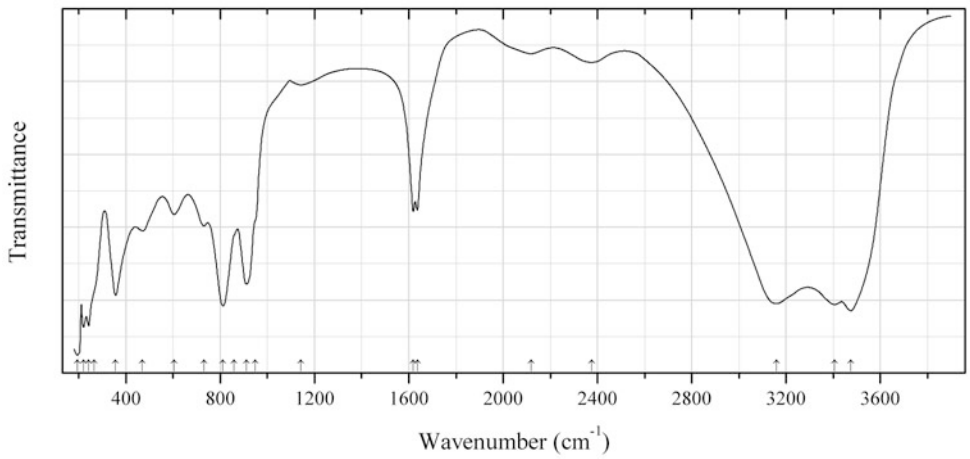

Fig. 2.1417 IR spectrum of metakahlerite Fe^{3+} analogue drawn using data from Vochten et al. (1986)

As271 Metakahlerite Fe^{3+}analogue $Fe^{3+}(UO_2)_2(AsO_4)_2(OH)\cdot 7H_2O$ (Fig. 2.1417)
Locality: Synthetic.

Description: Obtained by treating an aqueous suspension of synthetic metakahlerite with 10 % H_2O_2 for 48 h. Tetragonal, a = 20.25, c = 17.20 Å. D_{meas} = 3.19(5) g/cm^3. The empirical formula is $Fe^{3+}_{0.965}(UO_2)_{1.88}(AsO_4)_{2.025}(OH)_{0.95}\cdot 6.89H_2O$. The strongest lines of the powder X-ray diffraction pattern [d, Å (I, %) (hkl)] are: 5.925 (100) (−110), 3.407 (44) (−12–1), 3.428 (100) (−210), 2.960 (77) (102, −220), 2.535 (84) (03–2), 2.369 (44) (01–3), 1.761 (50) (21–4, 41–2).
Kind of sample preparation and/or method of registration of the spectrum: No data.
Source: Vochten et al. (1986).
Wavenumbers (cm^{-1}): 3475s, 3407s, 3160s, 2375w, 2120w, 1636, 1619, 1143w, 948sh, 912s, 859sh, 812s, 730, 604, 470, 356, 264sh, 242s, 220s, 193s.
Note: The wavenumbers were determined by us based on spectral curve analysis of the published spectrum.

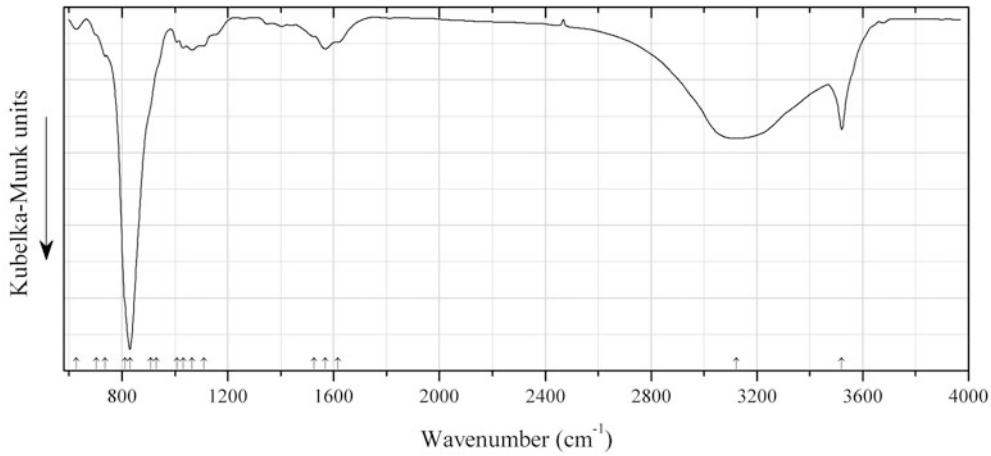

Fig. 2.1418 IR spectrum of metakirchheimerite drawn using data from Plášil et al. (2009a)

As272 Metakirchheimerite $Co(UO_2)_2(AsO_4)_2\cdot 8H_2O$ (Fig. 2.1418)
Locality: Jan Evangelista vein at the "Adit level" of the Svornost shaft, Jáchymov U deposit, Krušné Hory (Ore Mts.), Western Bohemia, Czech Republic.
Description: Aggregates of tabular pink to orange crystals from a carbonate gange containing arsenopyrite, uraninite, and skutterudite. Triclinic, space group P-1, a = 7.210(4) Å, b = 9.771(6) Å, c = 13.252(9) Å, α = 75.39(4)°, β = 83.94(6)°, γ = 81.88(6)°, V = 892(1) Å^3. The empirical formula is (electron microprobe): $Co_{0.53}Mg_{0.25}Ni_{0.08}Zn_{0.07}Fe_{0.05}Ca_{0.03})(UO_2)_{2.07}[(AsO_4)_{1.99}(PO_4)_{0.01}](H_2O, OH)_8$. The strongest lines of the powder X-ray diffraction pattern [d, Å (I, %) (hkl)] are: 11.089 (100) (001), 6.826 (23) (010), 5.484 (79) (002, 101), 4.022 (30) (102, −112), 3.540 (81) (0–13, −1–12), 3.089 (33) (−113, 201), 2.918 (60) (−122).
Kind of sample preparation and/or method of registration of the spectrum: Diffuse reflection of powdered mineral mixed with KBr.
Source: Plášil et al. (2009a).
Wavenumbers (cm^{-1}): 3521, 3123s, 1617sh, 1568, 1526sh, 1109sh, 1065, 1032w, 1007w, 930sh, 908sh, 830s, 811sh, 736, 702sh, 628w.
Note: The wavenumbers were partly determined by us based on spectral curve analysis of the published spectrum.

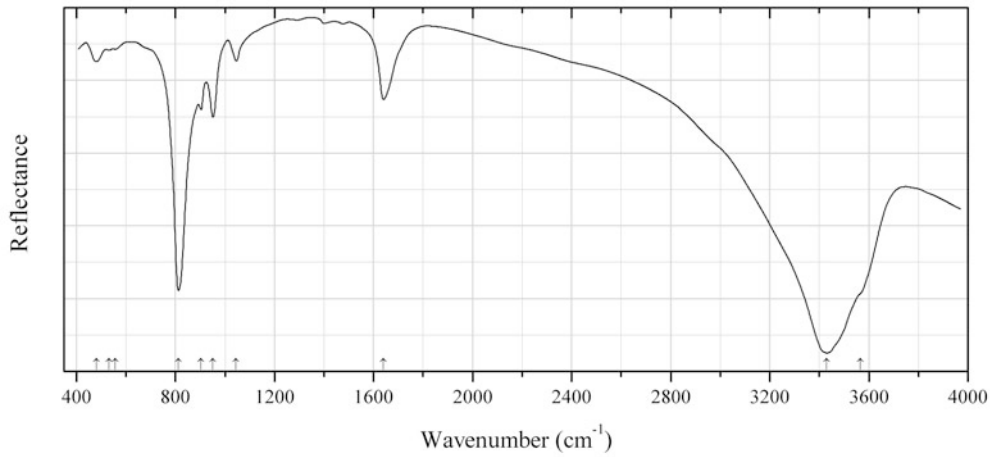

Fig. 2.1419 IR spectrum of metarauchite drawn using data from Ondruš et al. (1997)

As273 Metarauchite $Ni(UO_2)_2(AsO_4)_2 \cdot 6–8H_2O$ (Fig. 2.1419)
Locality: Jáchymov, Bohemia, Krušné Hory Mts. (Ore Mts.), Czech Republic (type locality).
Description: Yellow-green tabular crystals grown in fractures of vein material. Identified by electron microprobe and X-ray diffraction data. The strongest lines of the powder X-ray diffraction pattern [*d*, Å (*I*, %) (*hkl*)] are: 8.548 (100) (002), 4.279 (33) (004), 3.581 (5) (200), 3.424 (6) (005), 2.1396 (17) (008), 1.7124 (5) (403).
Kind of sample preparation and/or method of registration of the spectrum: Attenuated total reflection of powdered mineral. KBr disc. Transmission.
Source: Ondruš et al. (1997).
Wavenumbers (cm^{-1}): 3565, 3430s, 1641, 1045w, 951, 904, 813s, 557w, 532w, 480w.
Note: The wavenumbers were determined by us based on spectral curve analysis of the published spectrum.

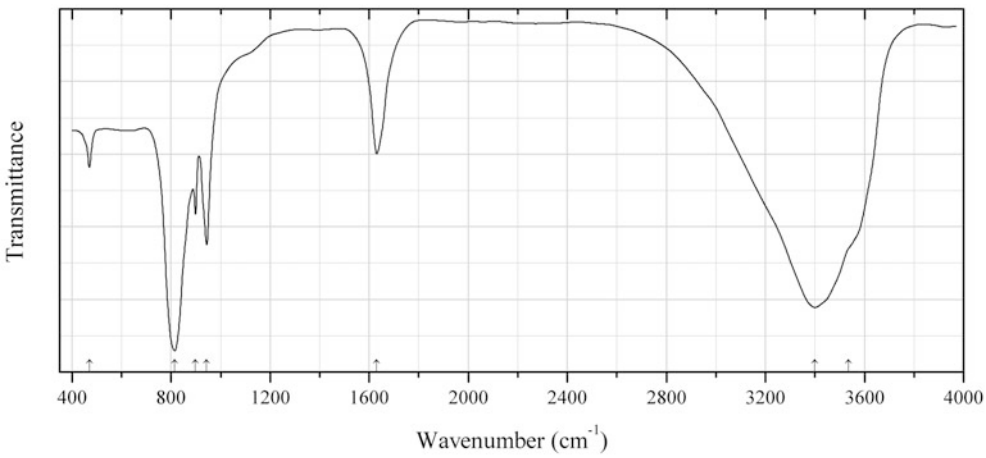

Fig. 2.1420 IR spectrum of metarauchite drawn using data from Vochten and Goeminne (1984)

As274 Metarauchite $Ni(UO_2)_2(AsO_4)_2 \cdot 6–8H_2O$ (Fig. 2.1420)

Locality: Synthetic.
Description: Tetragonal, a = 20.25, c = 17.20 Å, Z = 16. D_{meas} = 3.74 g/cm^3. The empirical formula is $Ni_{1.00}(UO_2)_{2.02}(AsO_4)_{1.98}(OH)_{0.1}\cdot 6.95H_2O$.
Kind of sample preparation and/or method of registration of the spectrum: KBr disc. Transmission.
Source: Vochten and Goeminne (1984).
Wavenumbers (cm^{-1}): 3535sh, 3400s, 1630, 944, 899, 815s, 470.
Note: The wavenumbers were partly determined by us based on spectral curve analysis of the published spectrum. The band position denoted by Vochten and Goeminne (1984) as 1650 cm^{-1} was determined by us at 1630 cm^{-1}.

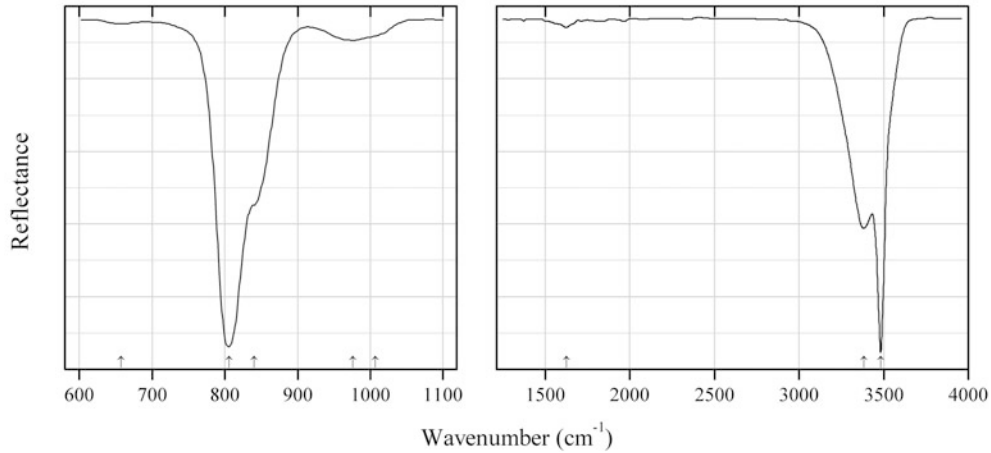

Fig. 2.1421 IR spectrum of mixite drawn using data from Frost et al. (2009c)

As275 Mixite $BiCu_6(AsO_4)_3(OH)_6\cdot 3H_2O$ (Fig. 2.1421)
Locality: As-U deposit Smrkovec, Slavovsky Les Mts., near Mariánské Lázně, Czech Republic.
Description: Confirmed by the powder X-ray diffraction pattern. Hexagonal, space group $P6_3/m$: a = 13.637(1), c = 5.910(1) Å, V = 951.8(2) Å^3. The empirical formula is $(Bi_{0.77}Ca_{0.17}Pb_{0.15})(Cu_{5.79}Fe_{0.11})[(AsO_4)_{2.17}(HAsO_4)_{0.39}(PO_4)_{0.29}(SiO_4)_{0.15}](OH)_{6.00}\cdot 3H_2O$.
Kind of sample preparation and/or method of registration of the spectrum: A mixture of powdered mineral with KBr. Micro diffuse reflection.
Source: Frost et al. (2009c).
Wavenumbers (cm^{-1}): 3483s, 3384s, 1624w, 1007sh, 976w, 840, 806s, 657.
Note: In the cited paper, the wavenumbers are indicated only for the maxima of individual bands obtained as a result of the spectral curve analysis. The wavenumbers were determined by us based on spectral curve analysis of the published spectrum.

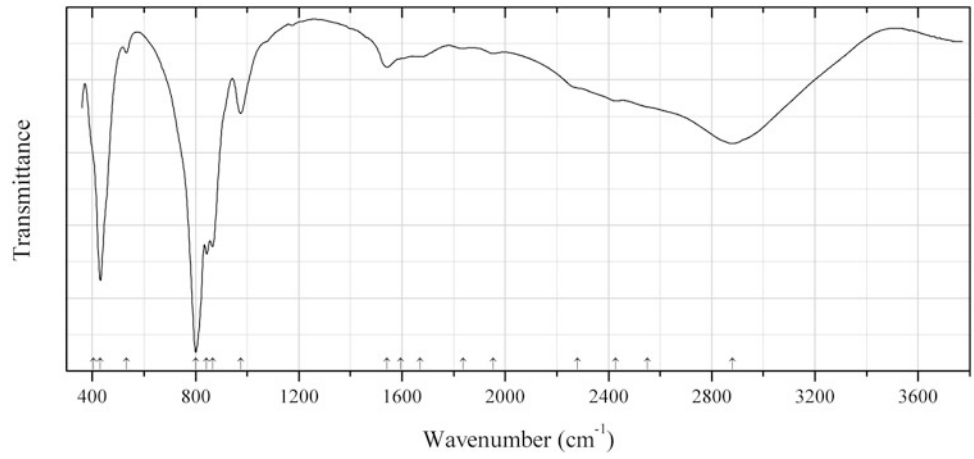

Fig. 2.1422 IR spectrum of zincroselite obtained by N.V. Chukanov

As276 Zincroselite $Ca_2Zn(AsO_4)_2 \cdot 2H_2O$ (Fig. 2.1422)
Locality: Veta Negra mine, Tierra Amarilla, Copiapó Province, Chile.
Description: Radial aggregates of colourless prismatic crystals with wendwilsonite zones. The empirical formula is (electron microprobe, ranges): $Ca_{1.9–2.1}(Zn_{0.0–0.6}Mg_{0.1–0.9}Mn_{0.0–0.4})(AsO_4)_{2.0} \cdot 2H_2O$. The strongest lines of the powder X-ray diffraction pattern are observed at 6.43, 5.10, 3.39, 3.36, 3.23, 3.16, 3.00, 2.77, 2.60, 2.33, 2.25, and 2.20 Å.
Kind of sample preparation and/or method of registration of the spectrum: KBr disc. Absorption.
Wavenumbers (cm^{-1}): 2880, 2550sh, 2428, 2280sh, 1953w, 1836w, 1670w, 1595sh, 1541, 975, 866s, 843s, 801s, 532w, 431s, 405sh.

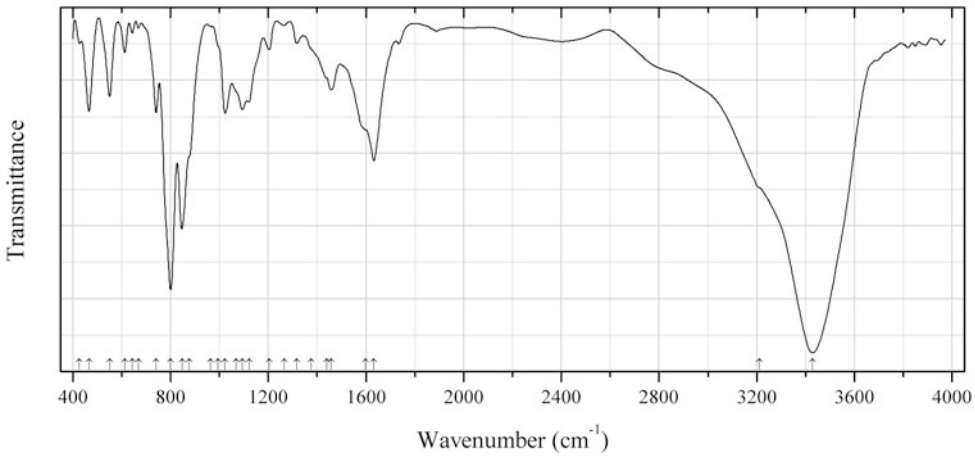

Fig. 2.1423 IR spectrum of ondrušite drawn using data from Sejkora et al. (2011b)

As277 Ondrušite $CaCu_4(AsO_4)_2(HAsO_4)_2 \cdot 10H_2O$ (Fig. 2.1423)
Locality: Jáchymov U deposit, Krušné Hory (Ore Mts.), Western Bohemia, Czech Republic (type locality).
Description: Crystalline crusts composed of fine platy to lath-shaped translucent crystals. Associatied minerals are lindackerite, geminite, lavendulan, slavkovite, strashimirite, olivenite, picropharmacolite,

and köttigite. Holotype sample. Triclinic, space group P-1, a = 6.432(1), b = 7.986(1), c = 10.827(1) Å, α = 85.75(1)°, β = 81.25(1)°, γ = 85.04(1)°, V = 546.6(1) Å^3, Z = 1. D_{meas} = 3.26 g/cm^3, D_{calc} = 3.12 g/cm^3. Optically biaxial (+), α' = 1.640(2), γ' = 1.708(2). The empirical formula is $(Ca_{0.96}Co_{0.01}Pb_{0.01})(Cu_{3.84}Mg_{0.11})[(AsO_4)_{1.73}(PO_4)_{0.05}](HAsO_4)_{2.26}\cdot 9.86H_2O$. The strongest lines of the powder X-ray diffraction pattern [d, Å (I, %) (hkl)] are: 10.671 (100) (001), 3.970 (10) (020), 3.648 (11) (02–1), 3.560 (18) (003), 3.286 (10) (022), 3.173 (13) (01–3, 200, 201), 2.922 (10) (20–1, 202), 2.736 (10) (023).

Kind of sample preparation and/or method of registration of the spectrum: KBr disc. Absorption.

Source: Sejkora et al. (2011b).

Wavenumbers (cm^{-1}): 3429s, 3210sh, 1633, 1598sh, 1458, 1439sh, 1376sh, 1318w, 1265w, 1204w, 1122, 1094, 1068sh, 1024, 996sh, 965w, 877sh, 849s, 801s, 741, 669w, 643w, 613w, 551, 467, 426.

Note: The wavenumbers were partly determined by us based on spectral curve analysis of the published spectrum.

As278 Paradamite $Zn_2(AsO_4)(OH)$

Locality: Mina Ojuela (Ojuela mine), Mapimi, Durango, Mexico (type locality).

Description: Groups of pale yellow tabular crystals. A sample from the University of Arizona Mineral Museum. Confirmed by X-ray diffraction and chemical analysis.

Kind of sample preparation and/or method of registration of the spectrum: Attenuated total reflection of powdered mineral.

Source: RRUFF (2007).

Wavenumbers (cm^{-1}): 3404, 1643, 953, 873, 823sh, 795, 781sh, 499, 472sh, 451, 430.

Note: Unlike adamite, paradamite shows O–H stretching band below 3000 cm^{-1}.

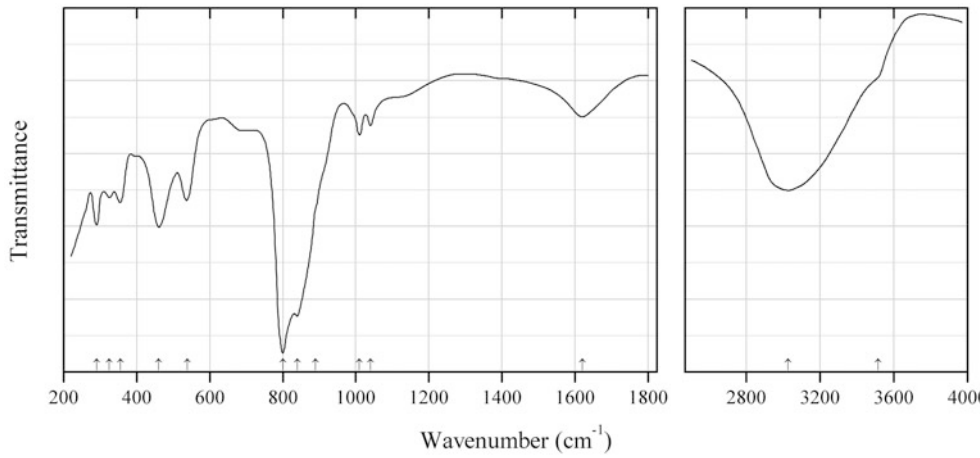

Fig. 2.1424 IR spectrum of parascorodite drawn using data from Ondruš et al. (1999)

As279 Parascorodite $Fe^{3+}(AsO_4)\cdot 2H_2O$ (Fig. 2.1424)

Locality: Kaňk, 5 km N of Kutná Hora, Bohemia, Czech Republic (type locality).

Description: Earthy yellowish-white aggregate from the association with scorodite, pitticite, bukovskýite, kaňkite, zýkaite, gypsum, and jarosite. Holotype sample. Hexagonal or trigonal, a = 8.9327(5), c = 9.9391(8) Å, V = 686.83 (8) Å^3, Z = 6. D_{meas} = 3.213(3) g/cm^3, D_{calc} = 3.212 g/cm^3. Optically biaxial (−), α = 1.554(1), β = 1.558(1), γ = 1.566(1), 2 V = 70(5)°. The empirical formula is $(Fe^{3+}_{0.98}Al_{0.01})[(AsO_4)_{0.875}(SO_4)_{0.04}(PO_4)_{0.03}(OH)_{0.17}]\cdot 2.05H_2O$. The strongest

lines of the powder X-ray diffraction pattern [*d*, Å (*I*, %) (*hkl*)] are: 4.184 (44) (012), 4.076 (100) (111), 3.053 (67) (202), 2.806 (68) (211), 2.661 (59) (113), 2.520 (54) (212), 2.2891 (44) (032).
Kind of sample preparation and/or method of registration of the spectrum: KBr disc. Transmission.
Source: Ondruš et al. (1999).
Wavenumbers (cm^{-1}): 3516sh, 3025, 1620w, 1040w, 1010w, 890sh, 840s, 800s, 538, 460, 355w, 325w, 290.

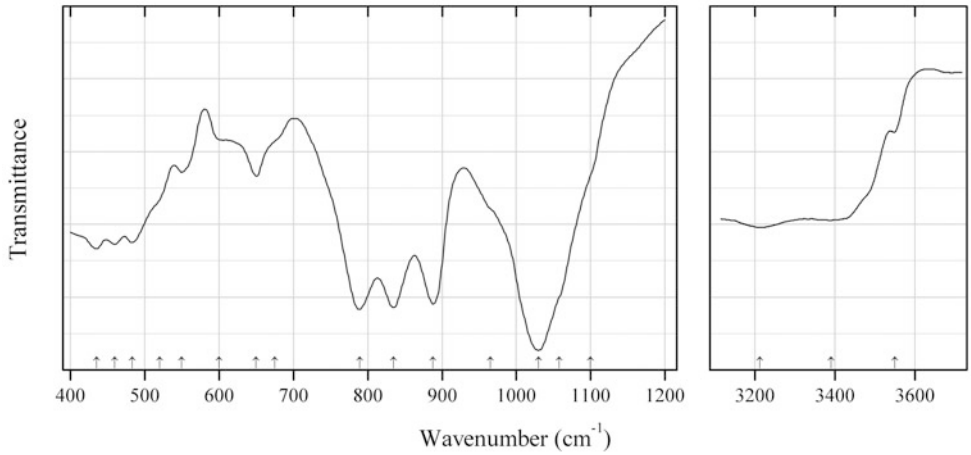

Fig. 2.1425 IR spectrum of philipsburgite drawn using data from Braithwaite and Ryback (1988)

As280 Philipsburgite $(Cu,Zn)_6(AsO_4,PO_4)_2(OH)_6 \cdot H_2O$ (Fig. 2.1425)
Locality: Black Pine mine, Philipsburg, Montana, USA (type locality).
Description: Type material (specimen NMNH 161201 from the Smithsonian Institution).
Kind of sample preparation and/or method of registration of the spectrum: Nujol mull. Transmission.
Source: Braithwaite and Ryback (1988).
Wavenumbers (cm^{-1}): 3550w, 3390, 3212, ~1640w, 1100sh, 1058sh, 1030s, 965sh, 888s, 835s, 789s, 675sh, 650w, 600sh, 550w, 520sh, 483, 460, 435.
Note: The wavenumbers were partly determined by us based on spectral curve analysis of the published spectrum.

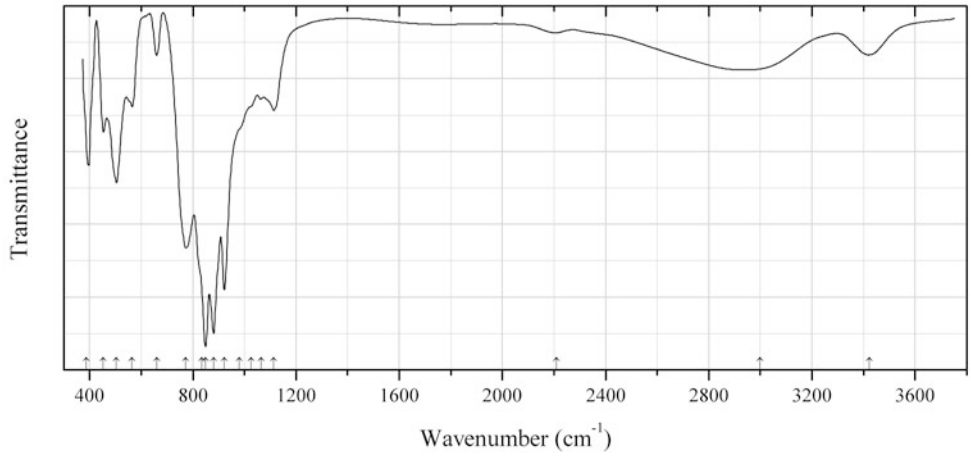

Fig. 2.1426 IR spectrum of grandaite obtained by N.V. Chukanov

As281 Grandaite $Sr_2Al(AsO_4)_2(OH)$ (Fig. 2.1426)
Locality: La Valletta mine, Vallone della Valletta, Vanosio, Maira valley, Cuneo province, Piedmont, Italy (type locality).
Description: Brownish-orange aggregate in quartz. A Ca-rich variety. The empirical formula is (electron microprobe): $(Sr_{1.05}Ca_{0.95})(Al_{0.69}Fe_{0.20}Mn_{0.11})(AsO_4)_{2.00}(OH)$.
Kind of sample preparation and/or method of registration of the spectrum: KBr disc. Absorption.
Wavenumbers (cm^{-1}): 3423, 3000, 2209w, 1114, 1065, 1025sh, 980sh, 922s, 880s, 849s, 835sh, 773s, 660, 565, 504, 453, 388.

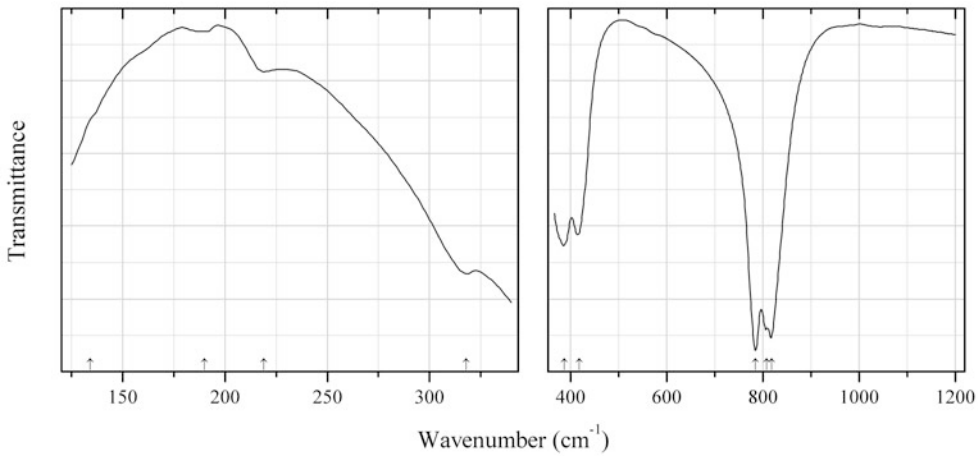

Fig. 2.1427 IR spectrum of mimetite drawn using data from Bajda (2010)

As282 Mimetite $Pb_5(AsO_4)_3Cl$ (Fig. 2.1427)
Locality: Synthetic.
Description: Powdery sample synthesized by mixing aqueous solutions of $Na_2(HAsO_4)\cdot 7H_2O$, $Pb(NO_3)_2$, and NaCl at room temperature with subsequent aging for 48 h and drying at 110 °C for 6 h. Confirmed by powder X-ray diffraction data. Hexagonal, a = 10.247(2), c = 7.448(2) Å.

Kind of sample preparation and/or method of registration of the spectrum: Absorption. Kind of sample preparation is not indicated.
Source: Bajda (2010).
Wavenumbers (cm^{-1}): 818s, 808s, 785s, 418, 387, 318, 219w, 190w, (134sh).

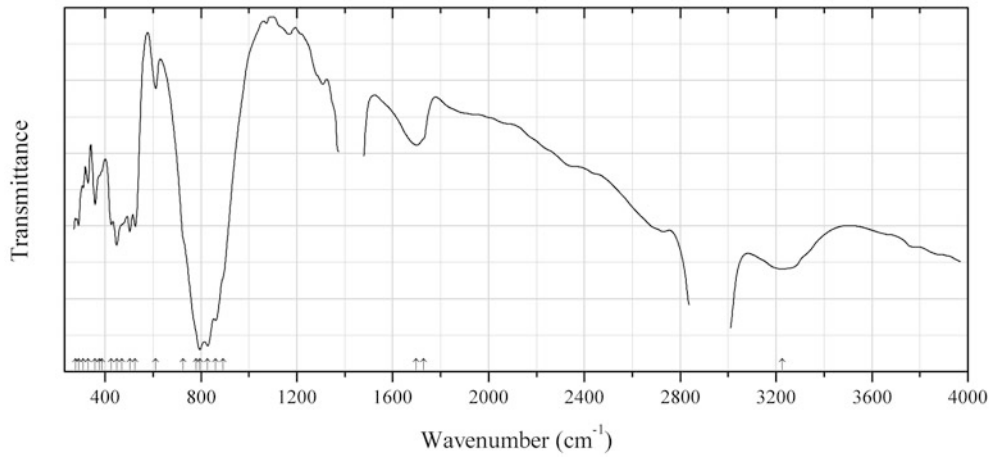

Fig. 2.1428 IR spectrum of prosperite drawn using data from Keller et al. (1982)

As283 Prosperite $Ca_2Zn_4(AsO_4)_4 \cdot H_2O$ (Fig. 2.1428)
Locality: Tsumeb mine, Tsumeb, Namibia (type locality).
Description: Crystals from the association with koritnigite and o'danielite. The crystal structure is solved. Monoclinic, space group *C*2/*c*, a = 19.238(2), b = 7.731(1), c = 9.76514) Å, β = 104.47(1)°, Z = 4. D_{calc} = 4.32 g/cm^3.
Kind of sample preparation and/or method of registration of the spectrum: Nujol mull. Transmission.
Source: Keller et al. (1982).
Wavenumbers (cm^{-1}): 3225s, 1730sh, 1699, 893sh, 861s, 828s, 796s, 780sh, 726sh, 611w, 525, 503, 470sh, 448, 426, 387sh, 375sh, 358, 328, 309, 289, 278.
Note: The wavenumbers were determined by us based on spectral curve analysis of the published spectrum.

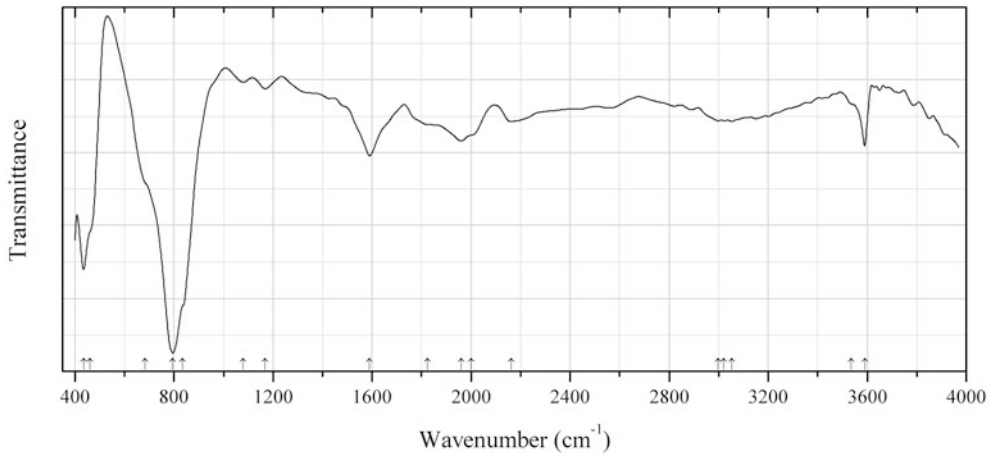

Fig. 2.1429 IR spectrum of rappoldite drawn using data from Effenberger et al. (2000)

As284 Rappoldite $PbCo_2(AsO_4)_2 \cdot 2H_2O$ (Fig. 2.1429)
Locality: Rappold mine, near Schneeberg, Saxony, Germany (type locality).
Description: red to red-brown prismatic and tabular crystals from the association with cobalt-lotharmeyerite, cobaltaustinite, scorodite, barium-pharmacosiderite, olivenite, conichalcite, erythrite, arseniosiderite, mimetite, and beudantite. Triclinic, a = 11.190(2), b = 10.548(2), c = 7.593(1) Å, α = 100.38(1)°, β = 109.59(2)°, γ = 98.96(1)°, V = 807.6 Å^3, Z = 4. D_{calc} = 5.24 g/cm^3. Optically biaxial (+), α = 1.85 (calculated), β = 1.87(2), γ = 1.90(2), 2 V = 85(5)°. The empirical formula is $(Pb_{1.01}Ca_{0.01})(Co_{0.99}Ni_{0.63}Zn_{0.35}Fe_{0.02})[(AsO_4)_{1.99}(SO_4)_{0.01}](OH)_{0.01} \cdot 1.99H_2O$. The strongest lines of the powder X-ray diffraction pattern [d, Å (I, %)] are: 4.670 (97), 3.256 (100), 3.072 (56), 2.890 (40), 2.568 (46), 1.731 (38).
Kind of sample preparation and/or method of registration of the spectrum: The spectra are obtained using a diamond microcell. No other data on the kind of sample preparation are given.
Source: Effenberger et al. (2000).
Wavenumbers (cm^{-1}): 3590, 3535sh, 3054w, 3021w, 2998w, 2163w, 2000sh, 1960, 1825sh, 1590, 1169w, 1080w, 835sh, 795s, 684sh, 460sh, 435s.
Note: The wavenumbers were partly determined by us based on spectral curve analysis of the published spectrum.

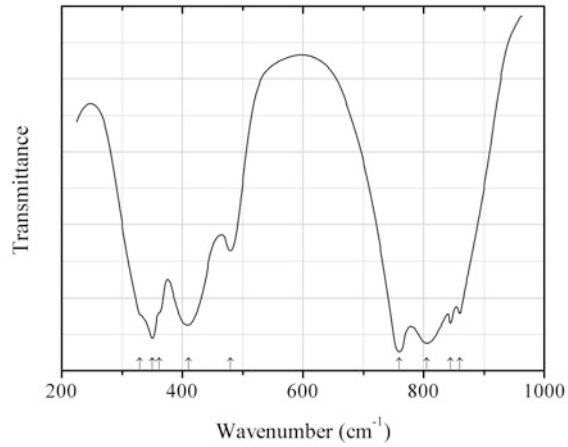

Fig. 2.1430 IR spectrum of rooseveltite drawn using data from Roncaglia et al. (1993)

As285 Rooseveltite $Bi(AsO_4)$ (Fig. 2.1430)
Locality: Synthetic.
Description: Obtained by slow addition of diluted arsenic acid to a diluted stoichiometric $Bi(NO_3)_3 \cdot 5H_2O$ solution and subsequent heating of the precipitated material at 600 °C during 12 h. The purity was checked by chemical analysis and powder X-ray diffractometry.
Kind of sample preparation and/or method of registration of the spectrum: KBr disc. Transmission.
Source: Roncaglia et al. (1993).
Wavenumbers (cm^{-1}): 845, 860, 805s, 760s, 480, 410s, 362sh, 350s, 330sh.

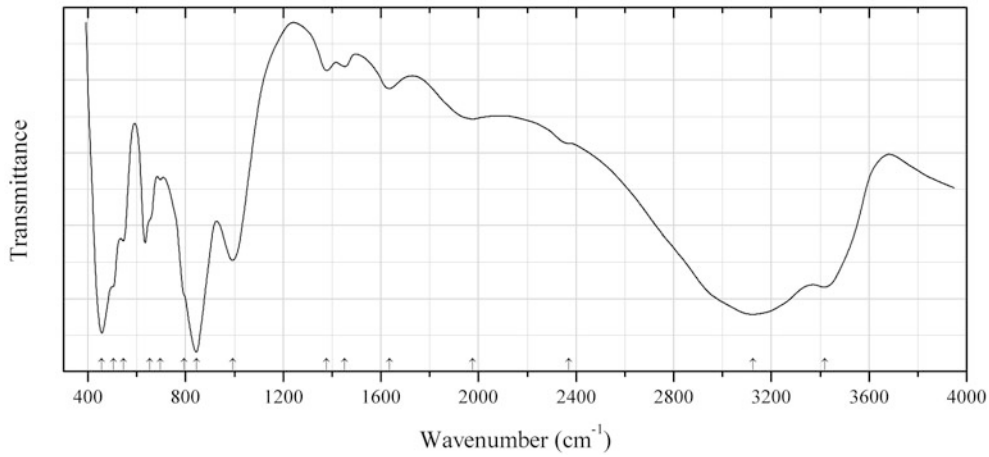

Fig. 2.1431 IR spectrum of sabelliite drawn using data from Olmi et al. (1995)

As286 Sabelliite $Cu_2Zn(AsO_4)(OH)_3$ (Fig. 2.1431)
Locality: Murvonis Mine, Domusnovas, Sardinia, Italy (type locality).
Description: Aggregates or green platy crystals from quartzitic matrix, from the association with theisite, malachite, azurite, and tetrahedrite. Holotype sample. Trigonal, space group *P*-3, a = 8.201 (1), c = 7.315(1) Å, V = 426.07(9) Å^3, Z = 3. D_{calc} = 4.65 g/cm^3. Optically uniaxial (−), ω = 1.802(2), ε = 1.797(2). The strongest lines of the powder X-ray diffraction pattern [d, Å (I, %) (hkl)] are: 2.522 (100) (121), 2.166 (88) (122), 1.805 (92) (123), 1.550 (100) (410), 1.513 (85) (124).
Kind of sample preparation and/or method of registration of the spectrum: KBr microdisc. Transmission.
Source: Olmi et al. (1995).
Wavenumbers (cm^{-1}): 3420, 3126s, 2370sh, 1977, 1636w, 1452w, 1378w, 993, 844s, 795sh, 697w, 654sh, 653, 545, 504sh, 457s.
Note: The wavenumbers were partly determined by us based on spectral curve analysis of the published spectrum. The weak peak at 1636 cm^{-1} may be attributed to water adsorbed by the KBr microdisc.

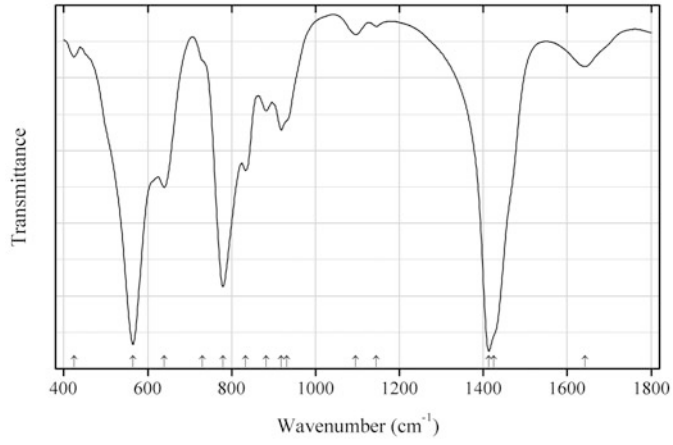

Fig. 2.1432 IR spectrum of sailaufite drawn using data from Wildner et al. (2003)

As287 Sailaufite $(Ca,Na,\square)_2Mn^{3+}{}_3(AsO_4)_2(CO_3)O_2 \cdot 3H_2O$ (Fig. 2.1432)
Locality: Fuchs quarry, Hartkoppe Hill, Sailauf, Bavaria, Germany (type locality).
Description: Dark red-brown to black tabular crystals from the association with hausmannite, arseniosiderite, kutnahorite, dolomite, quartz, and calcite. Holotype sample. The crystal structure is solved. Monoclinic, space group *Cm*, a = 11.253(1), b = 19.628(1), c = 8.932(1) Å, β = 100.05(1)°, V = 1942.6 Å^3, Z = 6. D_{calc} = 3.356 g/cm^3. The empirical formula is $(Ca_{1.35}Na_{0.42})Mn_{2.84}As_{2.13}O_{10}(CO_3)\cdot 3H_2O$. The strongest lines of the powder X-ray diffraction pattern [d, Å (I, %) (*hkl*)] are: 8.807 (100) (001), 5.654 (27) (130), 5.544 (17) (200), 2.936 (75) (003), 2.885 (19) (331), 2.816 (20) (33–2), 2.772 (36) (400), 2.514 (20) (133), 2.202 (55) (004).
Kind of sample preparation and/or method of registration of the spectrum: KBr disc. Absorption.
Source: Wildner et al. (2003).
Wavenumbers (cm^{-1}): 1642, 1425sh, 1413s, 1145w, 1096w, 931sh, 918, 882, 833, 779s, 730sh, 640, 565s, 424w.
Note: The wavenumbers were determined by us based on spectral curve analysis of the published spectrum.

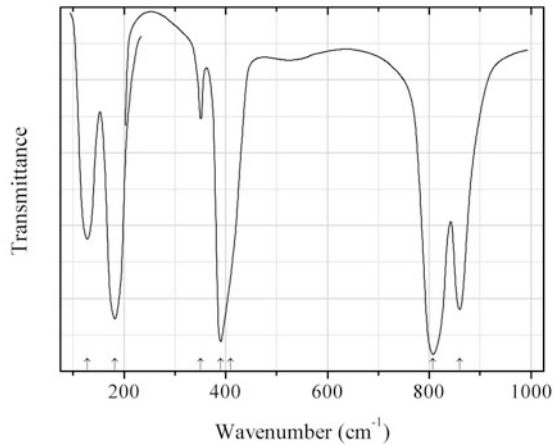

Fig. 2.1433 IR spectrum of barium ortho-arsenate drawn using data from Tarte and Thelen (1972)

As288 Barium ortho-arsenate $Ba_3(AsO_4)_2$ (Fig. 2.1433)
Locality: Synthetic.
Description: Obtained in the solid-state reaction between barium carbonate and ammonium arsenate. Trigonal.
Kind of sample preparation and/or method of registration of the spectrum: KI disc (above 200 cm^{-1}) and polyethylene disc (below 200 cm^{-1}). Transmission.
Source: Tarte and Thelen (1972).
Wavenumbers (cm^{-1}): 860s, 807s, 410sh, 390s, 351w, 182s, 128.

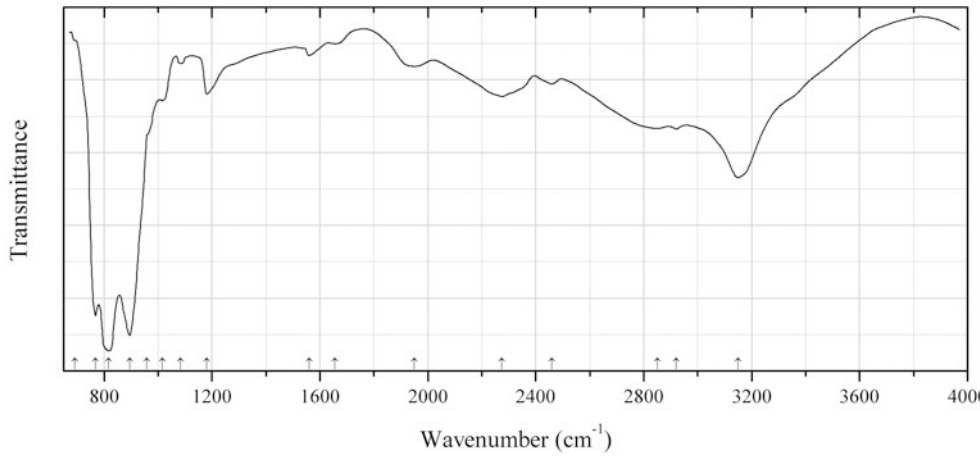

Fig. 2.1434 IR spectrum of sewardite drawn using data from Roberts et al. (2002)

As289 Sewardite $CaFe^{3+}{}_2(AsO_4)_2(OH)_2$ (Fig. 2.1434)
Locality: 31st level of the Tsumeb mine, Tsumeb, Namibia (type locality).
Description: Dark red compact aggregates from the association with tsumcorite-group minerals. Holotype sample. Orthorhombic, space group *Cccm*, a = 16.461(2), b = 7.434(1), c = 12.131(2) Å, V = 1484.5(6) Å^3, Z = 8. D_{calc} = 4.156 g/cm^3. Optically biaxial (−), α = 1.554(1), β = 1.558(1), γ = 1.566(1), 2 V = 70(5)°. The empirical formula is (electron microprobe, H_2O calculated by stoichiometry): $Ca_{0.99}(Fe^{3+}{}_{1.87}Zn_{0.10}Cu_{0.02})As^{5+}{}_{2.01}O_{8.00}[(OH)_{1.88}(H_2O)_{0.12}]$. The strongest lines of the powder X-ray diffraction pattern [d, Å (I, %) (*hkl*)] are: 4.874 (90) (202), 3.473 (50) (113), 3.389 (60) (220), 3.167 (100) (022), 3.015 (50) (510), 2.988 (50) (313), 2.919 (70) (511), 2.503 (90) (422, 314), 1.775 (50) (533, 026).
Kind of sample preparation and/or method of registration of the spectrum: Transmission. For the procedure of sample preraration see Roberts et al. (1994).
Source: Roberts et al. (2002).
Wavenumbers (cm^{-1}): 3150, 1560w, 2921, 2850, 2460w, 2275, 1950w, 1656w, 1560w?, 1181, 1084w, 1015, 958sh, 895s, 817s, 768s, 692sh.
Note: The wavenumbers were partly determined by us based on spectral curve analysis of the published spectrum. Multiple bands in the range from 1000 to 3000 cm^{-1}, as well as bond–valence calculations and the distortion of one of two AsO_4 tetrahedrons indicate the presence of acid groups formed in the reversible reaction $AsO_4^{3-} + OH^- \leftrightarrow HAsO_4^{2-} + O^{2-}$.

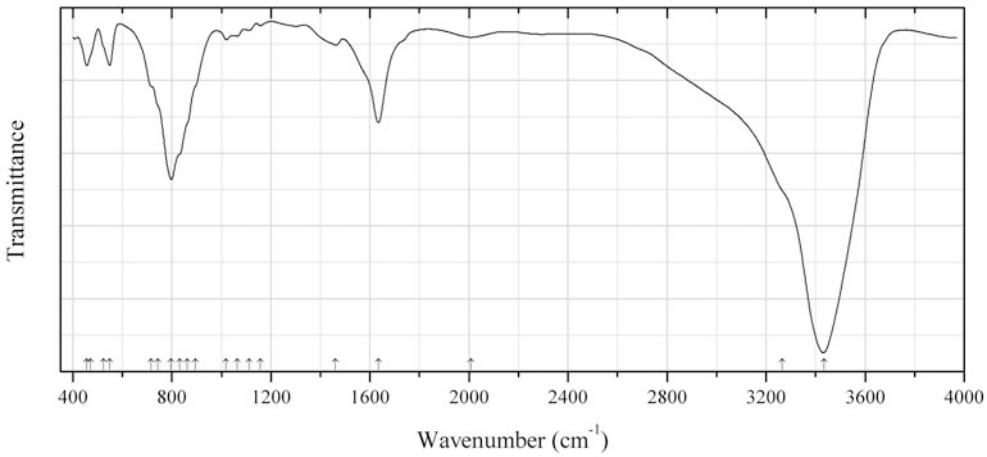

Fig. 2.1435 IR spectrum of slavkovite drawn using data from Sejkora et al. (2010b)

As290 Slavkovite $Cu_{13}(AsO_4)_6(HAsO_4)_4{\cdot}23H_2O$ (Fig. 2.1435)
Locality: Geschieber vein, Svornost mine, Jáchymov uranium deposit, Krušné Hory (Ore Mts.), Western Bohemia, Czech Republic (type locality).
Description: Aggregates of pale green crystals from the association with lavendulan, geminite, lindackerite, and ondrušite. Holotype sample. Triclinic, space group *P*-1, $a = 6.408(3)$, $b = 14.491(5)$, $c = 16.505(8)$ Å, $\alpha = 102.87(3)°$, $\beta = 101.32(5)°$, $\gamma = 97.13(3)°$, $V = 1442(1)$ Å^3, $Z = 1$. $D_{meas} = 3.05(1)$ g/cm^3, $D_{calc} = 3.05$ g/cm^3. Optically biaxial (+), $\alpha' = 1.591(2)$, $\beta' = 1.620(2)$, $\gamma' = 1.601(2)$. The empirical formula is $(Cu_{12.96}Al_{0.03}Fe_{0.04})(AsO_4)_{6.11}(HAsO_4)_{3.93}{\cdot}22.83H_2O$. The strongest lines of the powder X-ray diffraction pattern [*d*, Å (*I*, %) (*hkl*)] are: 15.70 (3) (001), 11.98 (100) (0–11), 6.992 (3) (0–21, 020), 5.992 (6) (0–22), 3.448 (5) (040), 2.967 (5) (0–35), 2.4069 (4) (1–54), 2.4002 (4) (115, −135, 0–46, 0–62)
Kind of sample preparation and/or method of registration of the spectrum: KBr disc. Absorption.
Source: Sejkora et al. (2010b).
Wavenumbers (cm^{-1}): 3434s, 3265sh, 2008, 1635, 1461w, 1158w, 1113w, 1065w, 1020w, 896sh, 863sh, 832sh, 798s, 745sh, 715sh, 549, 523sh, 470sh, 456.
Note: The wavenumbers were partly determined by us based on spectral curve analysis of the published spectrum.

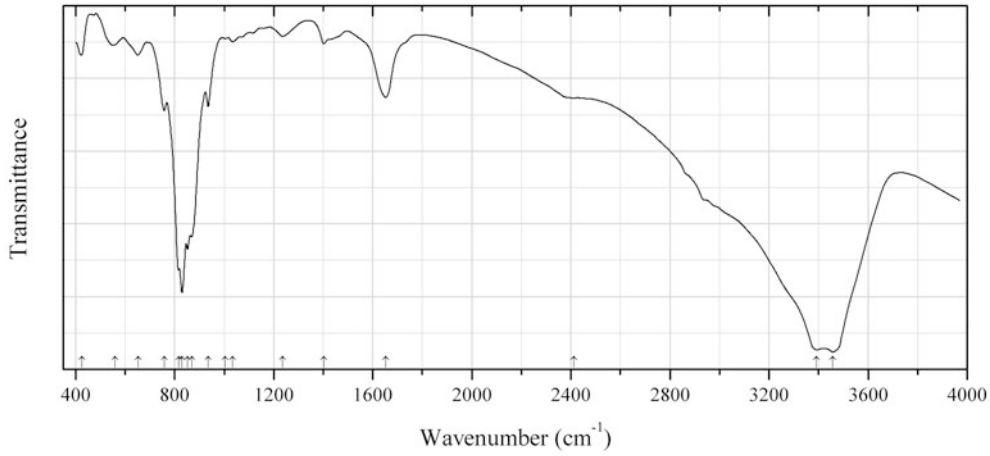

Fig. 2.1436 IR spectrum of štěpite drawn using data from Ondruš et al. (1997)

As291 Štěpite $U(HAsO_4)_2 \cdot 4H_2O$ (Fig. 2.1436)
Locality: Geschieber vein, Svornost shaft, Jáchymov uranium deposit, Krušné Hory (Ore Mts.), Western Bohemia, Czech Republic (type locality).
Description: Green crystalline crusts from the association with matulaite and variscite. The strongest lines of the powder X-ray diffraction pattern [*d*, Å (*I*, %)] are: 8.711 (28), 8.228 (100), 3.939 (27), 3.400 (44), 2.933 (34), 2.556 (21), 2.2494 (21).
Kind of sample preparation and/or method of registration of the spectrum: KBr disc. Absorption.
Source: Ondruš et al. (1997).
Wavenumbers (cm^{-1}): 3457s, 3392s, 2412, 1652, 1402w, 1236w, 1035w, 1004w, 936, 869s, 853s, 830s, 816s, 758, 653w, 559w, 425.
Note: The wavenumbers were partly determined by us based on spectral curve analysis of the published spectrum. Weak bands in the range from 2800 to 3000 cm^{-1} correspond to the admixture of an organic substance.

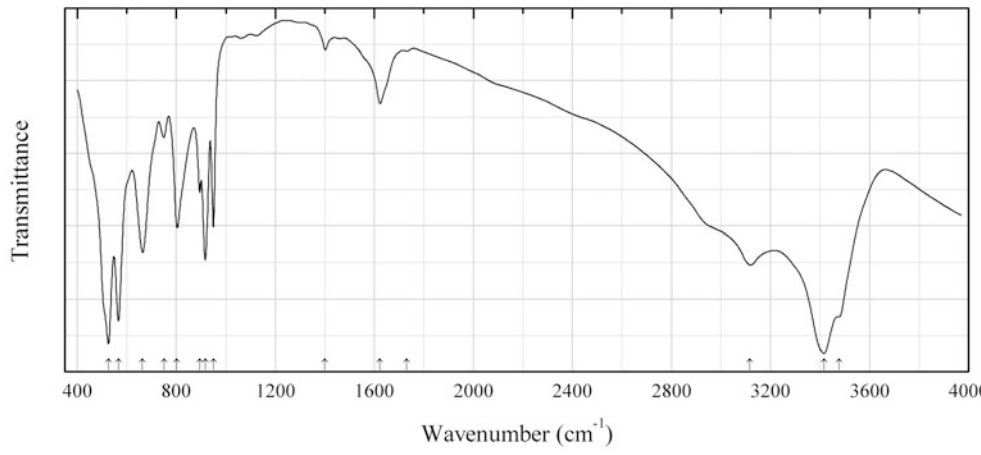

Fig. 2.1437 IR spectrum of vajdakite drawn using data from Ondruš et al. (1997)

As292 Vajdakite $(Mo^{6+}O_2)_2(As_2^{3+}O_5) \cdot 3H_2O$ (Fig. 2.1437)

Locality: Geschieber vein, Svornost shaft, 12th level, Jáchymov, Krušné Hory Mts. (Ore Mts.), Czech Republic (type locality).
Description: Aggregates of green to grey-green acicular crystals from strongly weathered arsenopyrite (löllingite)-pyrite vein, from the association with scorodite and arsenolite. Holotype sample. The crystal structure is solved. Monoclinic, space group $P2_1/c$, a = 7.0398(4), b = 12.0682 (13), c = 12.210(2) Å, β = 101.265(9)°, V = 1017.4(2) Å^3, Z = 4. D_{calc} = 3.524 g/cm^3. The empirical formula is (electron microprobe): $(MoO_2)_{1.93}(As_2O_5)_{0.95}(OH)_{0.07}\cdot 3.31H_2O$. The strongest lines of the powder X-ray diffraction pattern [d, Å (I, %) (hkl)] are: 6.915 (25) (100), 6.046 (100) (020), 3.457 (16) (200), 3.324 (59) (023, 210), 2.624 (15) (230), 2.2642 (19) (310).
Kind of sample preparation and/or method of registration of the spectrum: KBr disc. Absorption.
Source: Ondruš et al. (1997).
Wavenumbers (cm^{-1}): 3478s, 3417s, 3117, 1732, 1623w, 1401w, 951, 917s, 896, 803, 751, 664, 566s, 526s.

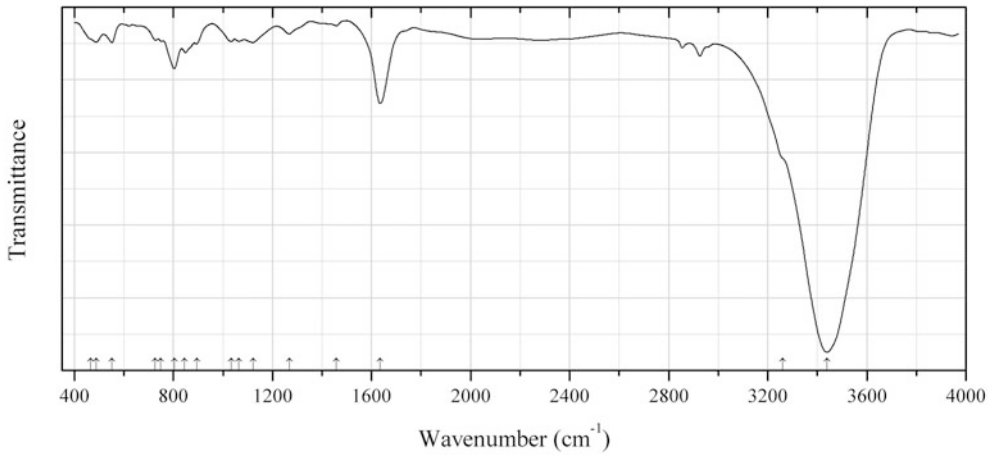

Fig. 2.1438 IR spectrum of veselovskýite drawn using data from Sejkora et al. (2010a)

As293 Veselovskýite $ZnCu_4(AsO_4)_2(HAsO_4)_2\cdot 9H_2O$ (Fig. 2.1438)
Locality: Geister vein, Mine Rovnost, Jáchymov uranium deposit, Krušné Hory (Ore Mts.), Western Bohemia, Czech Republic (type locality).
Description: Colourless to greyish white aggregates of lath-like to thin-tabular crystals from the association with strashimirite. Holotype sample. Triclinic, space group P-1, a = 6.4022(4), b = 8.0118 (4), c = 10.3665(4) Å, α = 85.491(3)°, β = 9.377(4)°, γ = 84.704(5)°, V = 519.34(4) Å^3, Z = 1. D_{calc} = 3.28 g/cm^3. Optically biaxial (+), α = 1.645(3), β = 1.68(1), γ ≈ 1.72. The empirical formula is $(Zn_{0.43}Cu_{0.24}Co_{0.13}Al_{0.05}Ni_{0.04}Mn_{0.03}Mg_{0.01}Ca_{0.01})Cu_{4.00}[(AsO_4)_{1.92}(HAsO_4)_{1.92}(PO_4)_{0.11}]\cdot 9.20H_2O$. The strongest lines of the powder X-ray diffraction pattern [d, Å (I, %) (hkl)] are: 10.185 (100) (001), 7.974 (12) (010), 3.987 (13) (020), 3.637 (15) (0–21), 3.395 (37) (003), 3.238 (15) (022), 2.910 (12) (202), 2.668 (16) (023).
Kind of sample preparation and/or method of registration of the spectrum: KBr disc. Absorption.
Source: Sejkora et al. (2010a).
Wavenumbers (cm^{-1}): 3440s, 3261sh, 1635s, 1458w, 1268, 1122, 1033, 1065, 895, 846, 805s, 750, 726, 551, 488, 465.
Note: Weak bands in the range from 2800 to 3000 cm^{-1} correspond to the admixture of an organic substance. The bands at 3440 and 1635 cm^{-1} are anomalously strong (adsorbed water?).

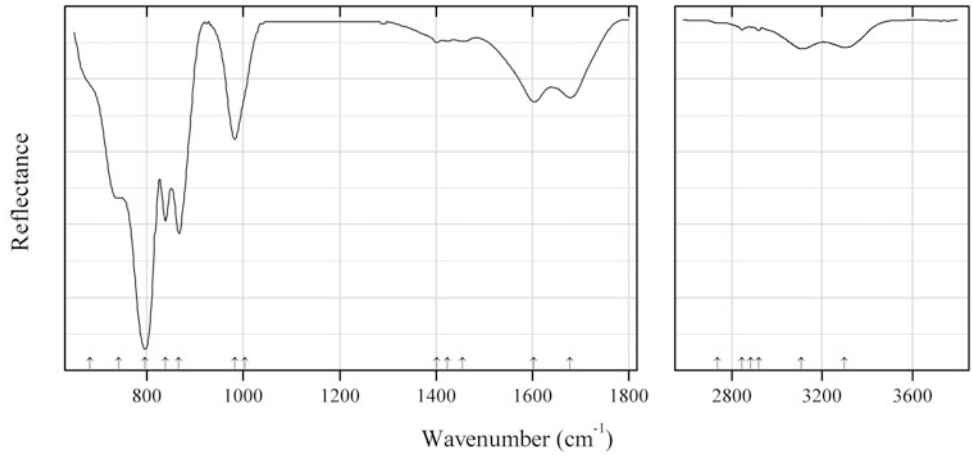

Fig. 2.1439 IR spectrum of wendwilsonite drawn using data from Frost et al. (2014b)

As294 Wendwilsonite $Ca_2Mg(AsO_4)_2 \cdot 2H_2O$ (Fig. 2.1439)
Locality: Bou Azzer district, Morocco.
Description: Short-prismatic crystals from the association with dolomite. A Co-bearing variety. Characterized by qualitative electron microprobe analysis.
Kind of sample preparation and/or method of registration of the spectrum: Attenuated total reflection of powdered mineral.
Source: Frost et al. (2014b).
Wavenumbers (cm^{-1}): 3298s, 3107s, 2918w, 2883w, 2845w, 2736w, 1678, 1603, 1455w, 1424w, 1401w, 1003sh, 982, 866, 839, 796s, 742sh, 682sh.
Note: In the cited paper, the wavenumbers are indicated only for the maxima of individual bands obtained as a result of the spectral curve analysis. Observed absorption maxima are not indicated. The wavenumbers were determined by us based on spectral curve analysis of the published spectrum.

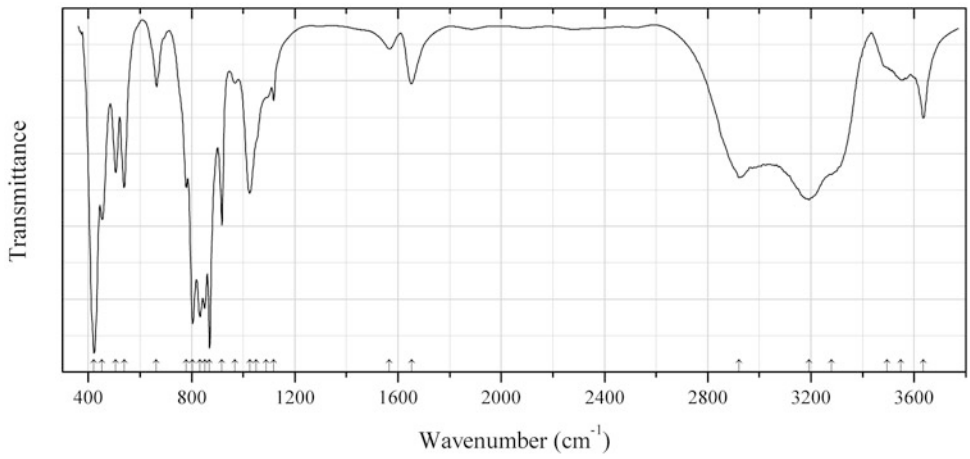

Fig. 2.1440 IR spectrum of tapiaite obtained by N.V. Chukanov

As295 Tapiaite $Ca_5Al_2(AsO_4)_4(OH)_4 \cdot 12H_2O$ (Fig. 2.1440)

Locality: Jote mine, Pampa Large district, Tierra Amarilla, Copiapó Province, Chile (type locality).
Description: Pink radiated aggregates of prismatic crystals from the association with mansfieldite and chlorargyrite. The empirical formula is (electron microprobe): $(Ca_{4.9}Fe_{0.1})(Al_{1.9}Fe_{0.2})[(AsO_4)_{3.64}(PO_4)_{0.24}](OH)_{4.2}\cdot nH_2O$. The strongest lines of the powder X-ray diffraction pattern [*d*, Å (*I*, %)] are: 7.44 (10), 4.95 (27), 4.12 (37), 3.707 (29), 2.969 (74), 2.861 (100), 2.474 (20), 2.350 (9), 2.064 (29), 2.058 (33).
Kind of sample preparation and/or method of registration of the spectrum: KBr disc. Absorption.
Wavenumbers (cm^{-1}): 3636, 3548, 3495sh, 3280sh, 3193s, 2921, 1653, 1566w, 1118, 1090sh, 1050sh, 1025s, 969w, 918s, 870s, 851s, 832s, 804s, 779, 664, 539, 506, 453s, 422s.

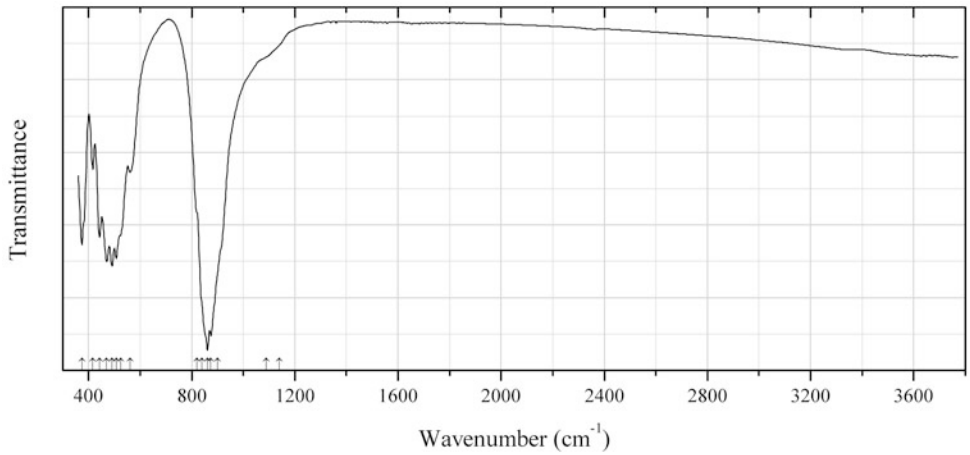

Fig. 2.1441 IR spectrum of arsenowagnerite obtained by N.V. Chukanov

As296 Arsenowagnerite $Mg_2(AsO_4)F$ (Fig. 2.1441)
Locality: Arsenatnaya fumarole, Second scoria cone of the Northern Breakthrough of the Great Tolbachik Fissure Eruption, Tolbachik volcano, Kamchatka peninsula, Russia (type locality).
Description: Pale yellow coarse tabular crystals and euhedral grains from the association with johillerite, tilasite, anhydrite, etc. Holotype sample. Monoclinic, space group $P2_1/c$, a = 9.8638(3), b = 12.9830(3), c = 12.3284(3) Å, β = 109.291(3)°, V = 1490.15(7) $Å^3$, Z = 16. D_{calc} = 3.698 g/cm^3. Optically biaxial (+), α = 1.614(2), β = 1.615(2), γ = 1.640(2), 2 V = 25(5)°. The empirical formula is (electron microprobe): $(Mg_{1.98}Cu_{0.02}Mn_{0.01}Ca_{0.01})(As_{0.99}P_{0.01})O_{4.03}F_{0.97}$. The strongest lines of the powder X-ray diffraction pattern [*d*, Å (*I*, %) (*hkl*)] are: 5.80 (41) (002), 5.31 (35) (120), 3.916 (37) (−221), 3.339 (98) (221, 023), 3.155 (65) (202), 3.043 (100) (−141), 2.940 (72) (−204), 2.879 (34) (−322), 2.787 (51) (320, −124).
Kind of sample preparation and/or method of registration of the spectrum: Attenuated total reflection of powdered mineral. KBr disc. Transmission.
Wavenumbers (cm^{-1}): 1140sh, 1090sh, 900sh, 874s, 861s, 840sh, 820sh, 561, 525sh, 507s, 491s, 470s, 443, 417, 375.

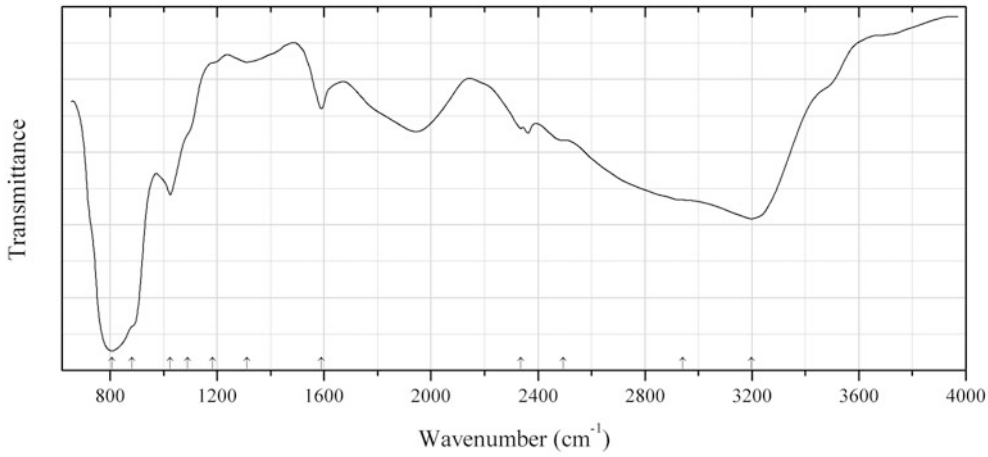

Fig. 2.1442 IR spectrum of yancowinnaite drawn using data from Elliott (2010)

As297 Yancowinnaite $PbCuAl(AsO_4)_2(OH)\cdot H_2O$ (Fig. 2.1442)
Locality: Kintore Opencut, Broken Hill, New South Wales, Australia (type locality).
Description: The empirical formula of an analogous sample is (electron microprobe): $Pb_{1.01}(Al_{0.63}Fe^{3+}_{0.32}Zn_{0.06})Cu_{1.02}(AsO_4)_{1.96}(OH)_{1.16}\cdot 0.84H_2O$. Characterized by powder X-ray diffraction data.
Kind of sample preparation and/or method of registration of the spectrum: Microsampling using a diamond-anvil cell. Transmission.
Source: Elliott et al. (2010).
Wavenumbers (cm^{-1}): 3198s, 2940sh, 2495sh, 2335, 1590, 1312w, 1183sh, 1091sh, 1025, 882sh, 808s.
Note: The wavenumbers were partly determined by us based on spectral curve analysis of the published spectrum. Weak bands between 2300 and 2400 cm^{-1} correspond to atmospheric CO_2.

As298 Yanomamite $In(AsO_4)\cdot 2H_2O$
Locality: Synthetic.
Description: Synthesized hydrothermally. Orthorhombic, space group *Pbca*, a = 10.478(1), b = 9.0998(8), c = 10.345(1) Å, Z = 8.
Kind of sample preparation and/or method of registration of the spectrum: KBr disc. Transmission.
Source: Tang et al. (2001).
Wavenumbers (cm^{-1}): 3460w, 2960s, 1530, 1260w, 830s, 635w, 580w, 500w, 470.

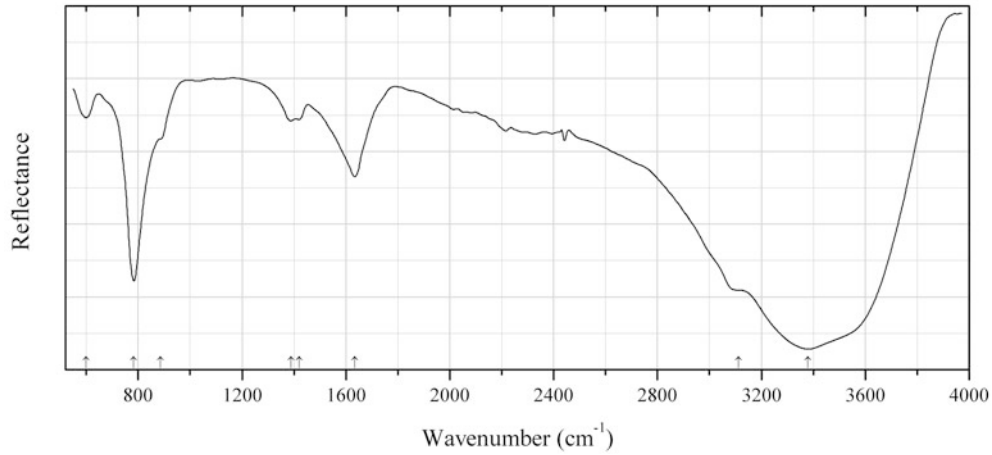

Fig. 2.1443 IR spectrum of yukonite drawn using data from Gómez and Lee (2012)

As299 Yukonite $Ca_2Fe^{3+}{}_3(AsO_4)_3(OH)_4{\cdot}4H_2O$ (?) (Fig. 2.1443)
Locality: Venus mine, Windy Arm, Tagish Lake, Carcross, Whitehorse mining district, Yukon Territory, Canada.
Description: Crystals characterized by the powder X-ray diffraction pattern.
Kind of sample preparation and/or method of registration of the spectrum: Attenuated total reflection of powdered mineral.
Source: Gómez and Lee (2012).
Wavenumbers (cm^{-1}): 3380s, 3111sh, 1634, 1419w, 1388w, 885sh, 783s, 600w.
Note: Shoulders in the range from 2800 to 3000 cm^{-1} correspond to the admixture of an organic substance.

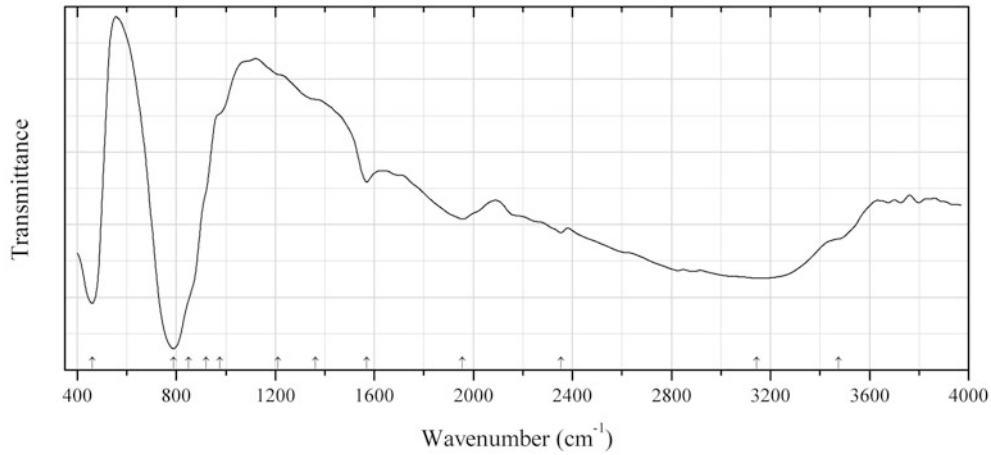

Fig. 2.1444 IR spectrum of zincgartrellite drawn using data from Effenberger et al. (2000)

As300 Zincgartrellite $PbZn_2(AsO_4)_2(H_2O,OH)_2$ (Fig. 2.1444)
Locality: Tsumeb (Tsumcorp) mine, Tsumeb, Otjikoto (Oshikoto) region, Namibia (type locality).

Description: Green-yellow rosette-like aggregates. Triclinic, space group *P*-1, a = 5.550(1), b = 5.620(1), c = 7.621(1) Å, α = 68.59(1)°, β = 69.17(1)°, γ = 69.51(1)°, V = 200.1 Å^3, Z = 1. D_{calc} = 5.29 g/cm^3. Optically biaxial (−), α = 1.91(2), β = 1.94 (calc.), γ = 1.97(2), 2 V = 87(2)°. The empirical formula is $(Pb_{0.97}Ca_{0.04})(Zn_{0.91}Fe_{0.59}Cu_{0.51}Al_{0.03})[(AsO_4)_{1.96}(SO_4)_{0.01}](OH)_{0.83}\cdot 1.31H_2O$.
Kind of sample preparation and/or method of registration of the spectrum: Transmission. A diamond-anvil microcell were used.
Source: Effenberger et al. (2000).
Wavenumbers (cm^{-1}): 3475sh, 3145, 2253, 1956, 1570, 1363sh, 1211sh, 975sh, 920sh, 849sh, 788s, 460s.
Note: The wavenumbers were partly determined by us based on spectral curve analysis of the published spectrum. The band at 1956 cm^{-1} indicates the presence of acid OH groups.

As301 Heliophyllite $Pb_6As_2O_7Cl_4$
Locality: A Pb–Zn deposit at Xitieshan, Qinghai Province, China.
Description: Greenish yellow to yellowish aggregates from the association with mimetite, cerussite, calcite, etc. Orthorhombic, a = 10.7936, b = 10.7663, c = 25.5601 Å, Z = 8. D_{meas} = 7.36 g/cm^3, D_{calc} = 7.142 g/cm^3. Optically biaxial (−). The empirical formula is $Pb_{5.92}Fe_{0.14}Ca_{0.01}As_{2.03}O_{7.09}Cl_{3.91}$. The strongest lines of the powder X-ray diffraction pattern [d, Å (I, %)] are: 3.65 (70), 3.19 (50), 2.845 (100), 2.699 (70), 2.06 (50), 1.641 (40), 1.585 (50).
Kind of sample preparation and/or method of registration of the spectrum: Absorption.
Source: Li and Chen (1985).
Wavenumbers (cm^{-1}): 842s, 700s, 606s, 388s, 323, 255.

As302 Synadelphite $Mn^{2+}{}_9(AsO_4)_2(AsO_3)(OH)_9\cdot 2H_2O$
Locality: Mossgruvan, Nordmark, near Filipstad, Värmland, Sweden.
Kind of sample preparation and/or method of registration of the spectrum: KBr disc. Absorption.
Source: Moenke (1966).
Wavenumbers (cm^{-1}): (3580), 3400, 1600w, (1435), 1080w, 950, 825sh, 810s, 780s, 720w, 642sh, 620s, 580, 530sh, 445s, 410.

As303 Yazganite $NaMgFe^{3+}{}_2(AsO_4)_3\cdot H_2O$
Locality: Erciyes volcanic complex, Kiranardi, prefecture of Kayseri, Central Anatolia Region, Turkey (type locality).
Description: Brown to black crystals from the association with hematite, tridymite, cassiterite, magnetite, orpiment, and realgar. Holotype sample. Triclinic, space group *C*2/*c*, a = 12.181(1), b = 12.807(1), c = 6.6391(5) Å, β = 112.441(9)°, V = 957.2(2) Å^3, Z = 4. D_{meas} = 4.18(2) g/cm^3, D_{calc} = 4.19 g/cm^3. Optically biaxial (−), α = 1.870(2), β = 1.897(2), γ = 1.900(2), 2 V = 35(2)°. The empirical formula is $Na_{0.99}Fe^{3+}{}_{2.05}Mg_{0.61}Mn_{0.32}Zn_{0.02}As_{2.99}O_{12}\cdot 0.88H_2O$. The strongest lines of the powder X-ray diffraction pattern [d, Å (I, %) (hkl)] are: 6.40 (20) (020), 5.630 (20) (200), 3.575 (30) (−131), 3.202 (40) (040, −112), 2.917 (35) (−312, −222), 2.780 (100) (240), 2.611 (40) (−132).
Kind of sample preparation and/or method of registration of the spectrum: Absorption.
Source: Sarp and Černý (2005).
Wavenumbers (cm^{-1}): 3400, 1630, 1110, 940, 880, 800, 745, 665, 555, 505, 400, 335.

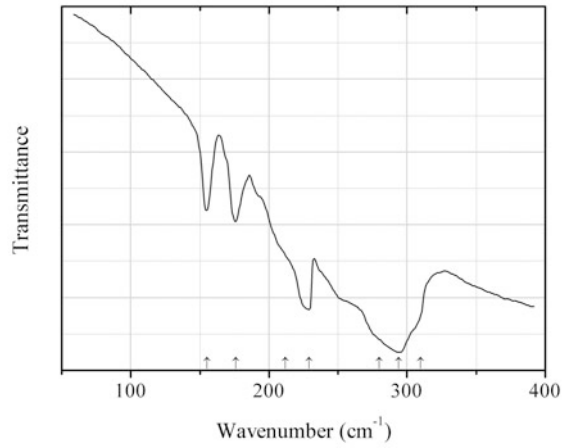

Fig. 2.1445 IR spectrum of anduoite drawn using data from Lutz et al. (1983)

As304 Anduoite $RuAs_2$ (Fig. 2.1445)
Locality: Synthetic.
Description: Prepared by heating stoichiometric mixture of the elements in a closed tube at 700 °C.
Kind of sample preparation and/or method of registration of the spectrum: Nujol mull. Transmission.
Source: Lutz et al. (1983).
Wavenumbers (cm^{-1}): 310sh, 294s, 280sh, 229s, 212sh, 176, 155.

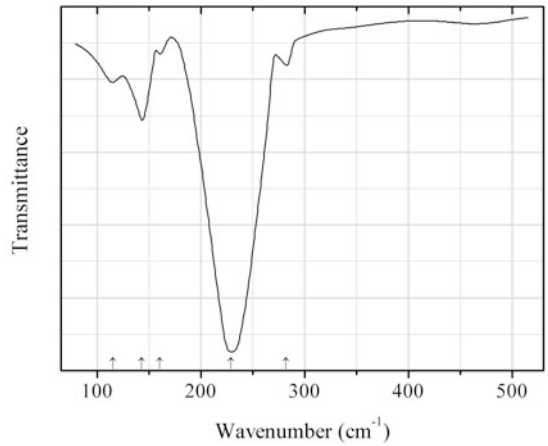

Fig. 2.1446 IR spectrum of arsenic drawn using data from Lucovsky and Knights (1974)

As305 Arsenic α-As (Fig. 2.1446)
Locality: Synthetic.
Description: Prepared by the pyrolysis of AsH_3.
Kind of sample preparation and/or method of registration of the spectrum: Transmission.
Source: Lucovsky and Knights (1974).
Wavenumbers (cm^{-1}): 282w, 229s, 160w, 143, 115.
Note: The wavenumbers were determined by us based on spectral curve analysis of the published spectrum.

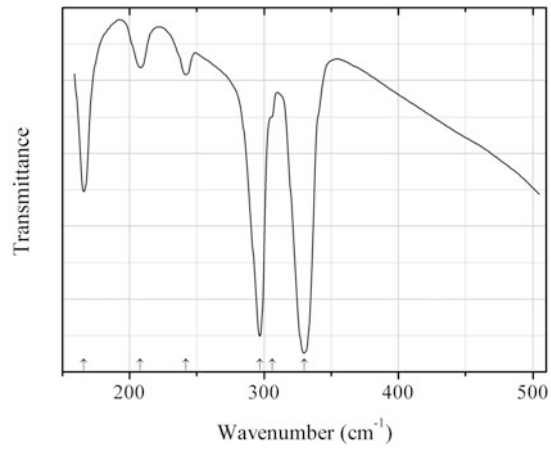

Fig. 2.1447 IR spectrum of skutterudite drawn using data from Lutz and Kliche (1981)

As306 Skutterudite $CoAs_3$ (Fig. 2.1447)
Locality: Synthetic.
Description: Prepared by heating stoichiometric mixture of the elements in a closed silica tube at 600 °C for 14 days and quenching in ice water. Confirmed by powder X-ray diffraction data.
Kind of sample preparation and/or method of registration of the spectrum: CsI disc. Transmission.
Source: Lutz and Kliche (1981).
Wavenumbers (cm^{-1}): 330s, 306sh, 297s, 242w, 208w, 166.
Note: For the IR spectrum of skutterudite see also Lutz and Kliche (1982).

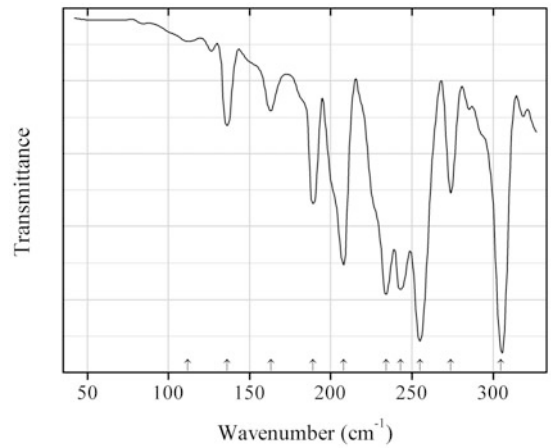

Fig. 2.1448 IR spectrum of iridarsenite drawn using data from Lutz et al. (1983)

As307 Iridarsenite $IrAs_2$ (Fig. 2.1448)
Locality: Synthetic.
Description: Prepared by annealing stoichiometric mixture of the elements in an evacuated quartz tube at 800 °C for 14 days. Characterized by powder X-ray diffraction data.
Kind of sample preparation and/or method of registration of the spectrum: Nujol mull. Transmission.

Source: Lutz et al. (1983).
Wavenumbers (cm^{-1}): 305s, 274, 255s, 243s, 234s, 208, 189, 163, 136, 112w.
Note: Apparently, the value 198 cm^{-1} is wrong. In the figure given by Lutz et al. (1983) this peak is located at 189 cm^{-1}.

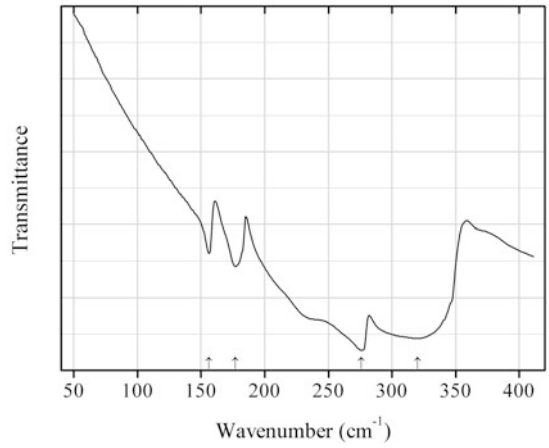

Fig. 2.1449 IR spectrum of löllingite drawn using data from Lutz et al. (1983)

As308 Löllingite $FeAs_2$ (Fig. 2.1449)
Locality: Synthetic.
Description: Prepared by annealing stoichiometric mixture of the elements in an evacuated tube at 600 °C for 20 days. Characterized by powder X-ray diffraction data.
Kind of sample preparation and/or method of registration of the spectrum: Nujol mull. Transmission.
Source: Lutz et al. (1983).
Wavenumbers (cm^{-1}): 320s, 276s, 177, 156.
Note: Apparently, the value 346 cm^{-1} is wrong. In the figure given by Lutz et al. (1983) this peak is located at 320 cm^{-1}.

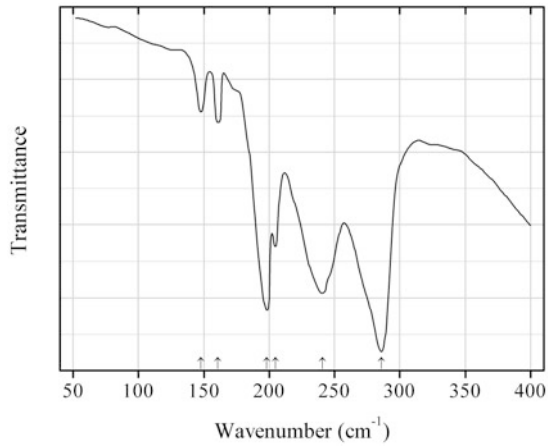

Fig. 2.1450 IR spectrum of omeiite drawn using data from Lutz et al. (1983)

As309 Omeiite $OsAs_2$ (Fig. 2.1450)
Locality: Synthetic.
Description: Prepared by heating stoichiometric mixture of the elements in a closed tube at 900 °C for 8 days.
Kind of sample preparation and/or method of registration of the spectrum: Nujol mull. Transmission.
Source: Lutz et al. (1983).
Wavenumbers (cm^{-1}): 286s, 241, 205, 198s, 161w, 148w.

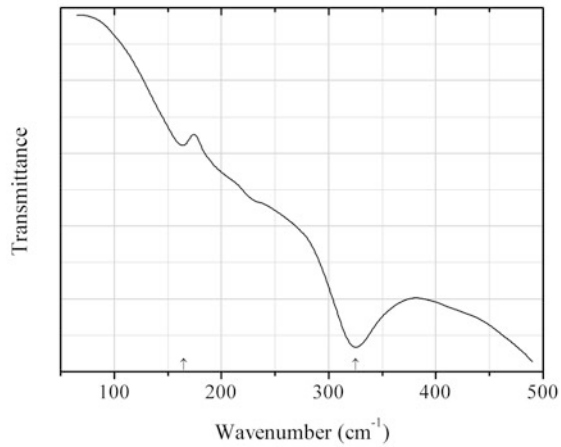

Fig. 2.1451 IR spectrum of rammelsbergite drawn using data from Plyusnina (1977)

As310 Rammelsbergite $NiAs_2$ (Fig. 2.1451)
Locality: Not indicated.
Description: No data.
Kind of sample preparation and/or method of registration of the spectrum: Transmission.
Source: Plyusnina (1977).
Wavenumbers (cm^{-1}): 325s, 165.

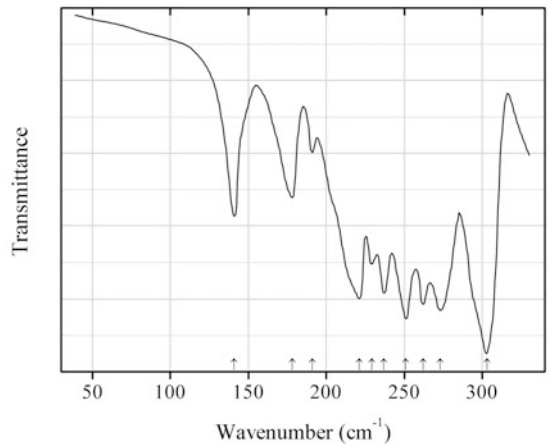

Fig. 2.1452 IR spectrum of rhodium diarsenide drawn using data from Lutz et al. (1983)

As311 Rhodium diarsenide $RhAs_2$ (Fig. 2.1452)
Locality: Synthetic.
Description: Prepared by heating stoichiometric mixture of the elements in a closed tube at 800 °C for 14 days. Characterized by powder X-ray diffraction data.
Kind of sample preparation and/or method of registration of the spectrum: Nujol mull. Transmission.
Source: Lutz et al. (1983).
Wavenumbers (cm^{-1}): 303s, 273s, 262s, 251s, 237, 229, 221, 191w, 178, 141.

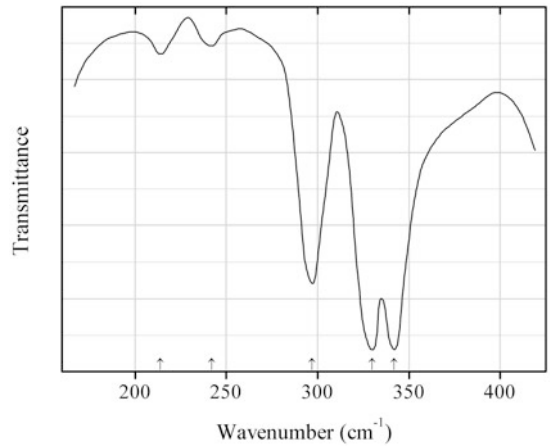

Fig. 2.1453 IR spectrum of skutterudite Sb-bearing drawn using data from Lutz and Kliche (1981)

As312 Skutterudite Sb-bearing $Co(As,Sb)_3$ (Fig. 2.1453)
Locality: Synthetic.
Description: Prepared by heating stoichiometric mixture of the elements in a closed silica tube at 600 °C for 14 days and quenching in ice water. Confirmed by powder X-ray diffraction data.
Kind of sample preparation and/or method of registration of the spectrum: CsI disc. Transmission.
Source: Lutz and Kliche (1981).
Wavenumbers (cm^{-1}): 342s, 330s, 297, 242w, 214w.

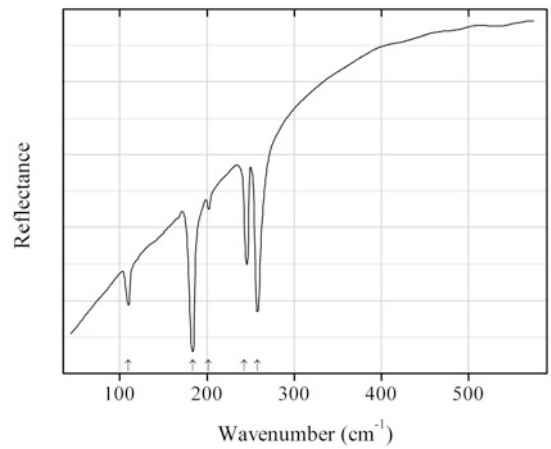

Fig. 2.1454 IR spectrum of sperrylite drawn using data from Lutz et al. (1985)

As313 Sperrylite $PtAs_2$ (Fig. 2.1454)
Locality: Synthetic.
Description: Prepared by annealing stoichiometric mixture of the elements at 600 °C for 10 days. Cubic. Characterized by powder X-ray diffraction data.
Kind of sample preparation and/or method of registration of the spectrum: A sample prepared by hot-pressing and polishing with diamond paste. Reflection.
Source: Lutz et al. (1985).
Wavenumbers (cm^{-1}): 258s, 243, 202w, 184s, 110.

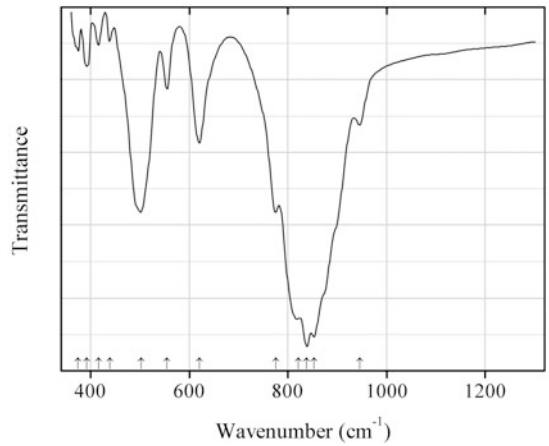

Fig. 2.1455 IR spectrum of johillerite obtained by N.V. Chukanov

As314 Johillerite $NaCuMg_3(AsO_4)_3$ (Fig. 2.1455)
Locality: Arsenatnaya fumarole, Second scoria cone of the Northern Breakthrough of the Great Tolbachik Fissure Eruption, Tolbachik volcano, Kamchatka peninsula, Russia.
Description: Violet spherulites from the association with alkaline sulfates. Investigated by I.V. Pekov. Confirmed by X-ray diffraction data and semiquantitative electron microprobe analyses. Monoclinic, a = 11.89(2), b = 12.76(1), c = 6.67(2) Å, β = 112.8(2)°, V = 933(3) $Å^3$.
Kind of sample preparation and/or method of registration of the spectrum: KBr disc. Absorption.
Wavenumbers (cm^{-1}): 945, 853s, 838s, 821s, 775s, 620, 554, 502s, 439w, 416, 392, 374.

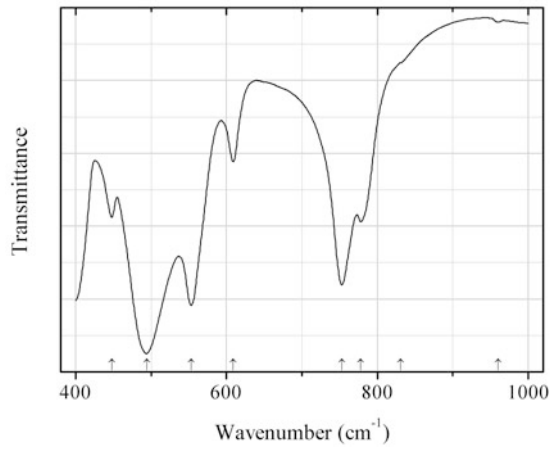

Fig. 2.1456 IR spectrum of trippkeite Ni analogue drawn using data from Đorđević et al. (2015)

As315 Trippkeite Ni analogue $NiAs_2O_4$ (Fig. 2.1456)
Locality: Synthetic.
Description: Synthesized hydrothermally from a mixture of $Ni(NO_3)_2$, As_2O_3(in the ratio 1:1) and distilled H_2O at 220 °C for 56 h with subsequent slow cooling. The crystal structure is solved. Tetragonal, space group $P4_2/mbc$, a = 8.2277(12), c = 5.6120(11) Å, V = 379.90(13) Å^3, Z = 4. D_{calc} = 4.765 g/cm^3.
Kind of sample preparation and/or method of registration of the spectrum: KBr disc. Absorption.
Source: Đorđević et al. (2015).
Wavenumbers (cm^{-1}): 960w, 831sh, 778, 753, 609, 553s, 494s, 448.
Note: The wavenumbers were partly determined by us based on spectral curve analysis of the published spectrum. The band position denoted by Đorđević et al. (2015) as 533 cm^{-1} was determined by us at 553 cm^{-1}.

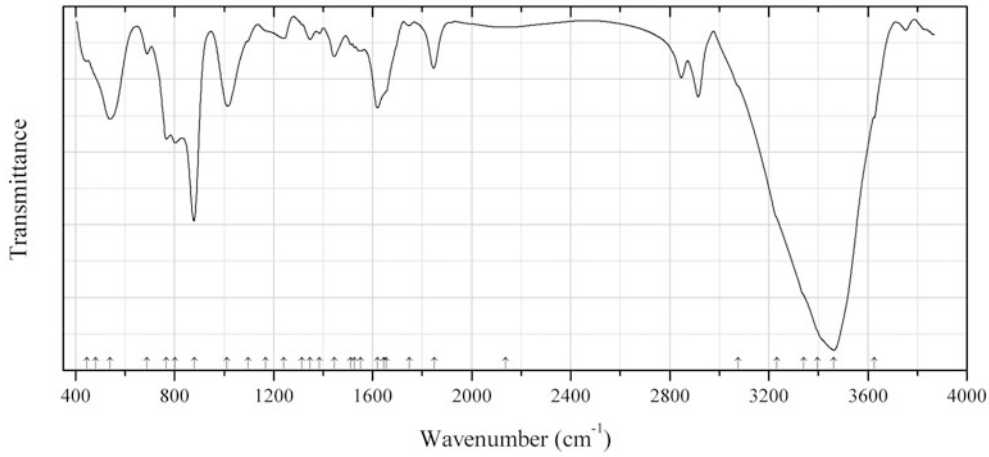

Fig. 2.1457 IR spectrum of asselbornite drawn using data from Sejkora and Čejka (2007)

UAs20 Asselbornite $Pb(UO_2)_4(BiO)_3(AsO_4)_2(OH)_7 \cdot 4H_2O$ (Fig. 2.1457)

Locality: Schneeberg, Saxony, Germany (type locality).
Description: Cubic, space group *Im*3 *m*, *I*432, *Im*3 or *I*23, a = 15.613(1) Å, V = 571.6(3) Å^3. The empirical formula is $(Pb_{0.52}Ba_{0.31}Ca_{0.08}Mg_{0.02})(UO_2)_{4.04}(BiO)_{3.08}[(AsO_4)_{1.31}(PO_4)_{0.67}(SiO_4)_{0.02}](OH)_{7.00}\cdot 4H_2O$. The strongest lines of the powder X-ray diffraction pattern [d, Å (I, %) (*hkl*)] are: 4.509 (73) (222), 4.174 (100) (321), 3.682 (84) (411, 330), 3.493 (42) (420), 3.188 (93) (422), 2.601 (63) (442, 600), 1.9812 (45) (732, 651), 1.8144 (743, 831, 750).
Kind of sample preparation and/or method of registration of the spectrum: KBr disc. Absorption.
Source: Sejkora and Čejka (2007).
Wavenumbers (cm^{-1}): 3627sh, 3463s, 3397sh, 3340sh, 3232sh, 3077sh, 2136w, 1849, 1748w, 1656sh, 1645sh, 1619, 1551w, 1527w, 1511w, 1445, 1386w, 1348, 1315sh, 1240, 1167sh, 1096sh, 1012w, 880s, 802, 767, 689, 539, 480sh, 445.
Note: The anomalously strong band at 3463 cm^{-1} may be partly due to adsorbed water.

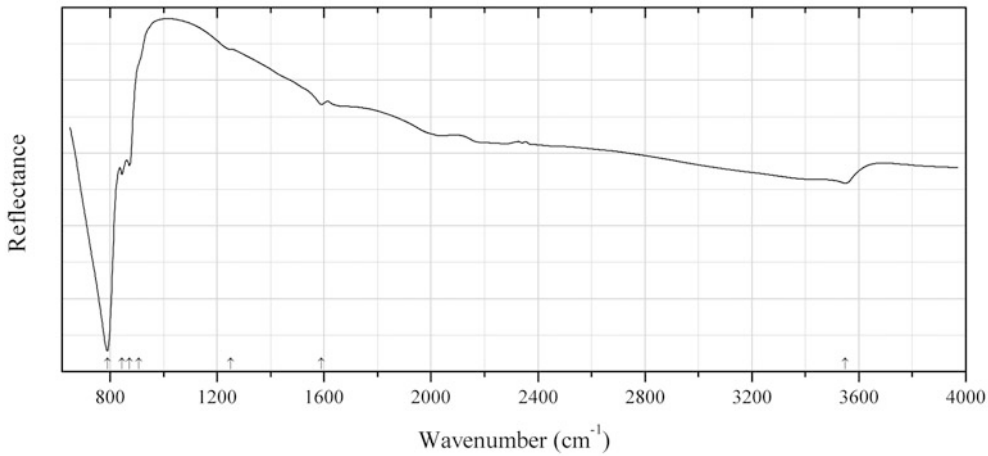

Fig. 2.1458 IR spectrum of hallimondite drawn using data from Locock et al. (2005)

UAs21 Hallimondite $Pb_2(UO_2)(AsO_4)_2\cdot nH_2O$ ($n \leq 0.5$) (Fig. 2.1458)
Locality: Synthetic.
Description: Synthesized under mild hydrothermal conditions, by the method of Walenta (1965). The crystal structure is solved. Triclinic, space group *P*-1, a = 7.1153(8), b = 10.4780(12), c = 6.8571(8) Å, α = 101.178(3)°, β = 95.711(3)°, γ = 86.651(3)°, V = 498.64(3) Å^3, Z = 2.
Kind of sample preparation and/or method of registration of the spectrum: Attenuated total reflection of powdered sample.
Source: Locock et al. (2005).
Wavenumbers (cm^{-1}): 3550, 1590w, 1250sh, 907sh, 872, 844, 790s.
Note: The wavenumbers were partly determined by us based on spectral curve analysis of the published spectrum.

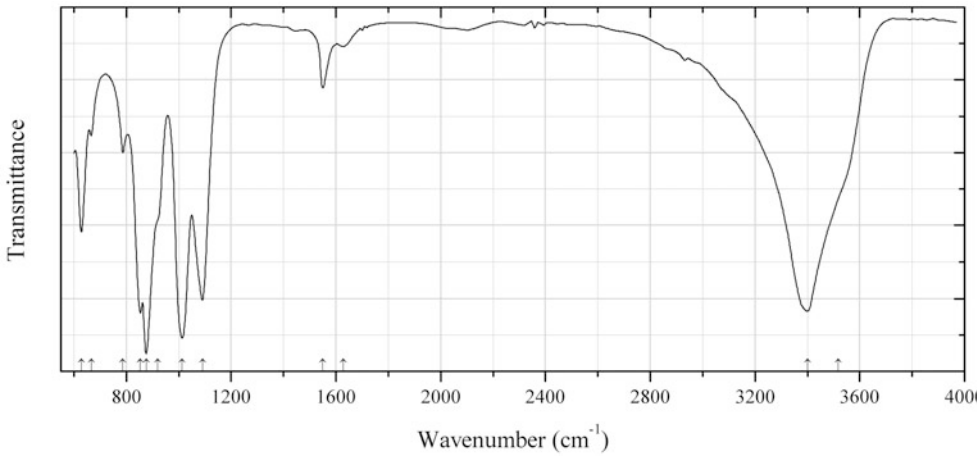

Fig. 2.1459 IR spectrum of nielsbohrite drawn using data from Walenta et al. (2009)

UAs22 Nielsbohrite $K(UO_2)_3(AsO_4)(OH)_4 \cdot H_2O$ (Fig. 2.1459)
Locality: Menzenschwand U deposit, near Menzenschwand, Kunkelbach valley, Schwarzwald (Black Forest) Mts., Baden-Württemberg, Germany (type locality).
Description: Yellow rhombohedron-like crystals from the association with hematite, pyrite, schoepite, metazeunerite, quartz, and barite. Holotype sample. Orthorhombic, space group *Cccm*, $a = 8.193(3)$, $b = 11.430(4)$, $c = 13.500(5)$ Å, $V = 1264.1(8)$ Å^3, $Z = 4$. $D_{calc} = 5.45–5.65$ g/cm^3. Optically biaxial (−), $\alpha = 1.756(2)$, $\beta = 1.764(2)$, $\gamma = 1.765(2)$, $2V = 35(5)°$. The empirical formula is $(K_{0.43}U_{0.11})(UO_2)_{3.00}(AsO_4)_{0.99}(OH,H_2O)_5$. The strongest lines of the powder X-ray diffraction pattern [*d*, Å (*I*, %) (*hkl*)] are: 6.71 (80) (110), 6.03 (100) (111), 3.78 (70) (113), 3.33 (80) (220), 2.96 (60) (024), 2.63 (50) (204), 1.942 (50) (244).
Kind of sample preparation and/or method of registration of the spectrum: crystals of 100–200 mm in diameter placed between cleaved halite plates. Transmission.
Source: Walenta et al. (2009).
Wavenumbers (cm^{-1}): 3518sh, 3400s, 1629w, 1550, 1091s, 1013s, 919sh, 876s, 854s, 787, 666w, 629.

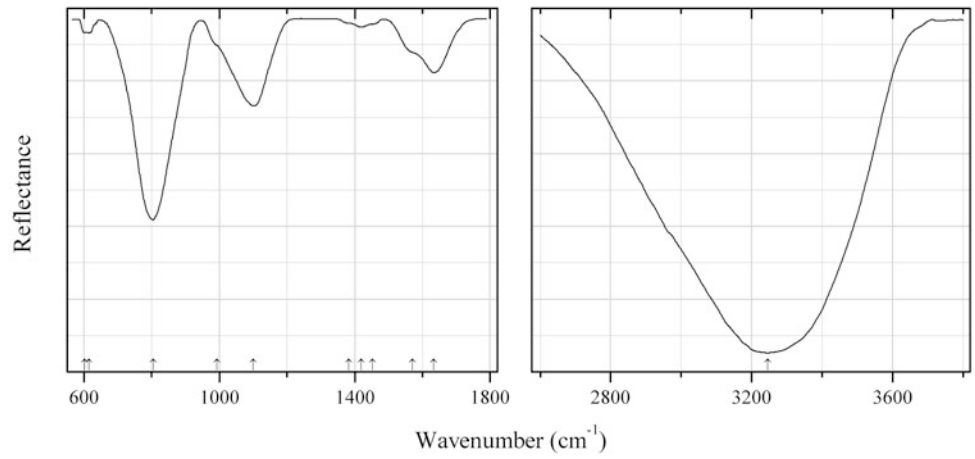

Fig. 2.1460 IR spectrum of leogangite drawn using data from Frost et al. (2011)

AsS24 Leogangite $Cu_{10}(AsO_4)_4(SO_4)(OH)_6 \cdot 8H_2O$ (Fig. 2.1460)
Locality: Vogelhalt district, Vogel Alps, Schwarzleograben, Leogang, Saalfelden, Salzburg, Austria (type locality).
Description: No data.
Kind of sample preparation and/or method of registration of the spectrum: Attenuated total reflection.
Source: Frost et al. (2011).
Wavenumbers (cm^{-1}): 3245s, 1633, 1570sh, 1453sh, 1419, 1383, 1100s, 993sh, 804s, 614w, 602w.
Note: In the cited paper, wavenumbers are indicated for the maxima of individual bands obtained as a result of the spectral curve analysis. The wavenumbers were determined by us based on spectral curve analysis of the published spectrum.

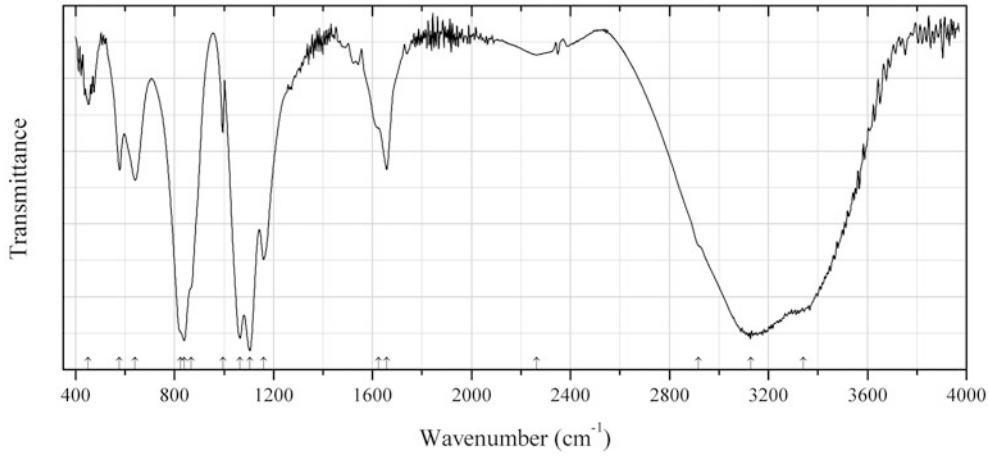

Fig. 2.1461 IR spectrum of sarmientite drawn using data from Colombo et al. (2014)

AsS25 Sarmientite $Fe^{3+}{}_2(AsO_4)(SO_4)(OH) \cdot 5H_2O$ (Fig. 2.1461)
Locality: Santa Elena mine, San Juan Province, Argentina (type locality).

Description: Pale yellowish brown, rounded mass from the association with fibroferrite, copiapite, and botryogen. The crystal structure is solved. Monoclinic, space group $P2_1/n$, a = 6.5298(1), b = 18.5228(4), c = 9.6344(3) Å, β = 97.444(2)°, V = 1155.5(5) Å^3, Z = 4. Confirmed by electron microprobe analyses.
Kind of sample preparation and/or method of registration of the spectrum: KBr disc. Transmission.
Source: Colombo et al. (2014).
Wavenumbers (cm^{-1}): 3341sh, 3130s, 2918sh, 2264w, 1658, 1625sh, 1160, 1105s, 1065s, 995, 868sh, 839s, 824sh, 640, 578, 452w.

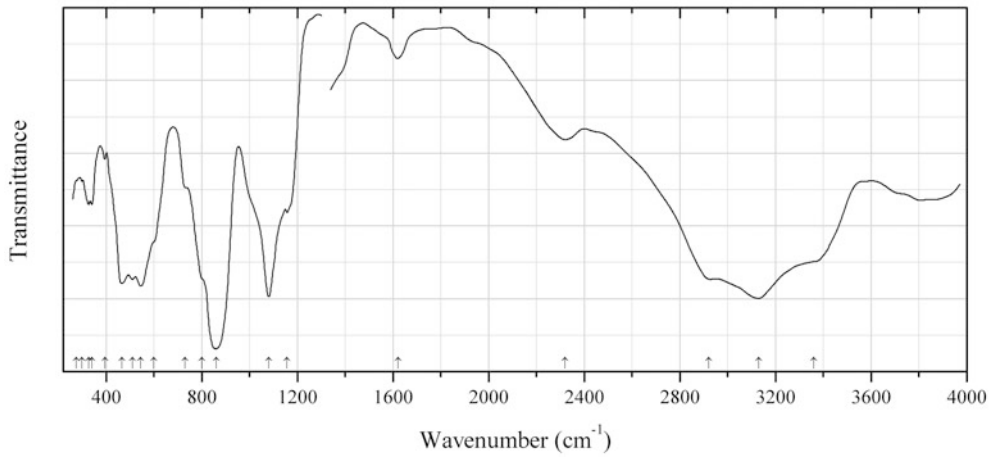

Fig. 2.1462 IR spectrum of weilerite drawn using data from Keller (1971)

AsS26 Weilerite $BaAl_3(SO_4)(AsO_4)(OH)_6$ (Fig. 2.1462)
Locality: Grube Neues Jahr (Haus Württemberg mine), Freudenstadt, near Karlsruhe, Baden-Württemberg, Germany (type locality).
Description: Yellow crusts. Characterized by optical data.
Kind of sample preparation and/or method of registration of the spectrum: No data.
Source: Keller (1971).
Wavenumbers (cm^{-1}): 3360sh, 3130s, 2920, 2320w, 1620w, 1157, 1080s, 860s, 800sh, 730w, 600sh, 545s, 511s, 465s, 394w, 340, 326, 299w, 276sh.
Note: The wavenumbers were partly determined by us based on spectral curve analysis of the published spectrum.

2.16 Antimonides and Antimonates

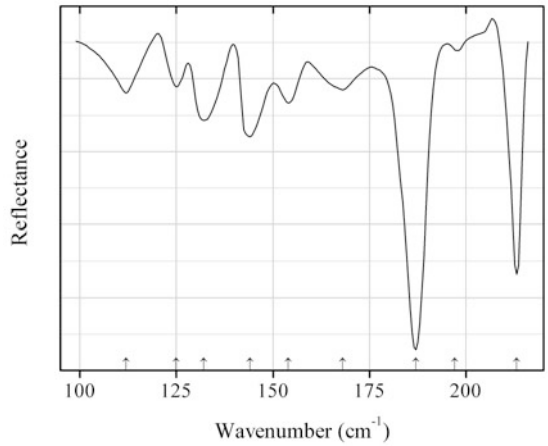

Fig. 2.1463 IR spectrum of iridium antimonide Sb1 drawn using data from Slack and Tsoukala (1994)

Sb1 Iridium antimonide Sb1 $IrSb_3$ (Fig. 2.1463)
Locality: Synthetic.
Description: Prepared by reacting Ir and Sb powders at 900 °C for 70 h. Cubic, a = 9.2503(3) Å. Characterized by powder X-ray diffraction data.
Kind of sample preparation and/or method of registration of the spectrum: Polished polycrystalline sample. Reflection.
Source: Slack and Tsoukala (1994).
Wavenumbers (cm^{-1}): 213s, 197w, 187s, 168, 154, 144, 132, 125, 112.
Note: The wavenumbers were partly determined by us based on spectral curve analysis of the published spectrum.

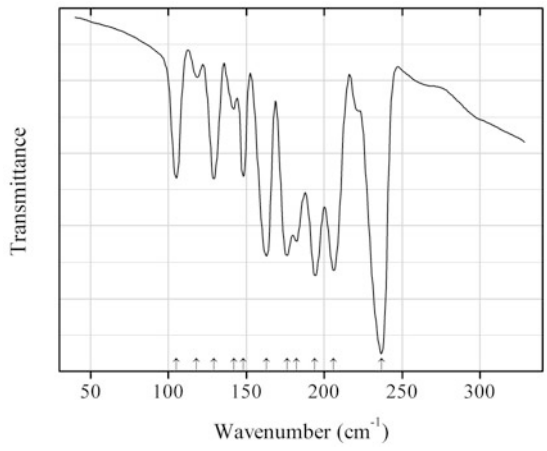

Fig. 2.1464 IR spectrum of iridium antimonide Sb2 drawn using data from Lutz et al. (1983)

Sb2 Iridium antimonide Sb2 $IrSb_2$ (Fig. 2.1464)
Locality: Synthetic.
Description: Prepared by annealing stoichiometric mixture of the elements in an evacuated quartz tube at 700 °C for 14 days. Characterized by powder X-ray diffraction data.
Kind of sample preparation and/or method of registration of the spectrum: Nujol mull. Transmission.
Source: Lutz et al. (1983).
Wavenumbers (cm^{-1}): 237s, 206, 194, 182, 176, 163, 148, 142w, 129, 118w, 105.
Note: The wavenumbers were partly determined by us based on spectral curve analysis of the published spectrum.

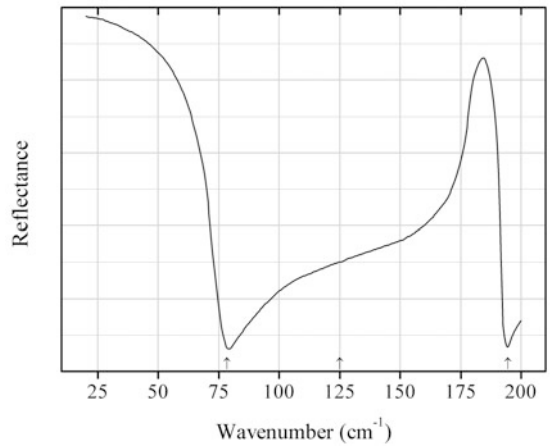

Fig. 2.1465 IR spectrum of indium antimonide drawn using data from Sanderson (1965)

Sb3 Indium antimonide InSb (Fig. 2.1465)
Locality: Synthetic.
Description: A narrow-gapsemiconductor material. Cubic.
Kind of sample preparation and/or method of registration of the spectrum: Polished polycrystalline sample. Reflection.
Source: Sanderson (1965).
Wavenumbers (cm^{-1}): 194.5s, 125sh, 78.5s.

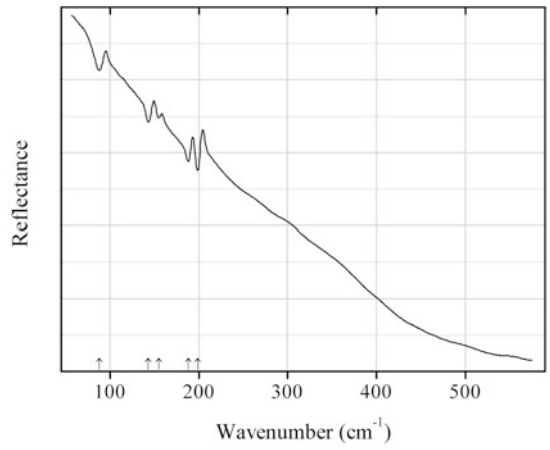

Fig. 2.1466 IR spectrum of geversite drawn using data from Lutz et al. (1985)

Sb4 Geversite $PtSb_2$ (Fig. 2.1466)
Locality: Synthetic.
Description: Prepared by annealing stoichiometric mixture of the elements in evacuated quartz tube at 600 °C for 14 days. Confirmed by powder X-ray diffraction data.
Kind of sample preparation and/or method of registration of the spectrum: Polycrystalline sample. Reflection.
Source: Lutz et al. (1985).
Wavenumbers (cm^{-1}): 199s, 188, 155w, 143, 88.

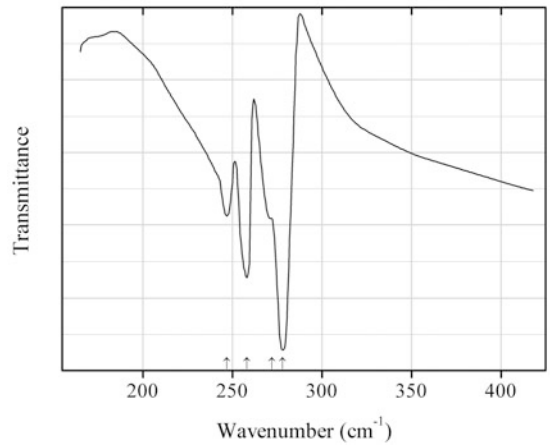

Fig. 2.1467 IR spectrum of kieftite drawn using data from Lutz and Kliche (1981)

Sb5 Kieftite $CoSb_3$ (Fig. 2.1467)
Locality: Synthetic.
Description: Prepared by heating stoichiometric mixture of the elements in a closed silica tube at 600 °C for 14 days and quenching in ice water. Confirmed by powder X-ray diffraction data.
Kind of sample preparation and/or method of registration of the spectrum: CsI disc. Transmission.

Source: Lutz and Kliche (1981).
Wavenumbers (cm^{-1}): 278s, 272sh, 258s, 247.
Note: For the IR spectrum of kieftite see also Lutz and Kliche (1982).

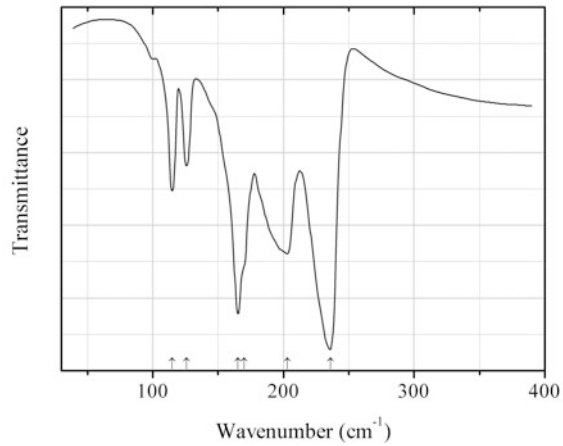

Fig. 2.1468 IR spectrum of osmium antimonide Sb6 drawn using data from Lutz et al. (1983)

Sb6 Osmium antimonide Sb6 $OsSb_2$ (Fig. 2.1468)
Locality: Synthetic.
Description: Prepared by annealing stoichiometric mixture of the elements in an evacuated quartz tube at 800 °C for 8 days. Characterized by powder X-ray diffraction data.
Kind of sample preparation and/or method of registration of the spectrum: Nujol mull. Transmission.
Source: Lutz et al. (1983).
Wavenumbers (cm^{-1}): 236s, 203, 170sh, 165s, 126, 115.

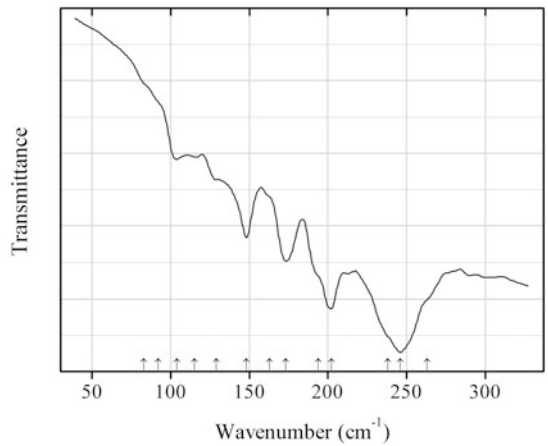

Fig. 2.1469 IR spectrum of rhodium antimonide Sb7 drawn using data from Lutz et al. (1983)

Sb7 Rhodium antimonide Sb7 $RhSb_2$ (Fig. 2.1469)
Locality: Synthetic.

Description: Prepared by heating stoichiometric mixture of the elements in a closed silica tube at 600 °C for 30 days. Cubic. Characterized by powder X-ray diffraction data.
Kind of sample preparation and/or method of registration of the spectrum: Nujol mull. Transmission.
Source: Lutz et al. (1983).
Wavenumbers (cm^{-1}): 263sh, 246s, 238sh, 202s, 194sh, 173, 163sh, 148, 129sh, 115sh, 104w, 92sh, 83sh.
Note: The wavenumbers were partly determined by us based on spectral curve analysis of the published spectrum.

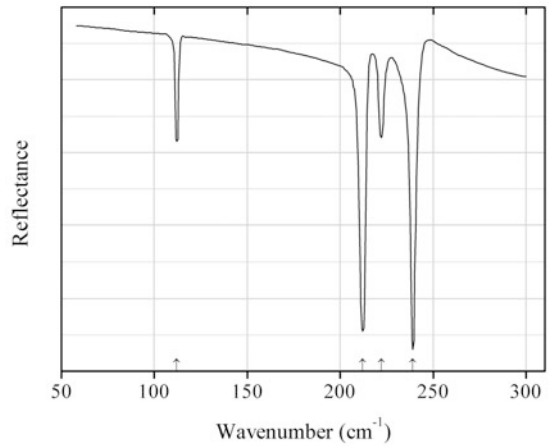

Fig. 2.1470 IR spectrum of rhodium antimonide Sb8 drawn using data from Kliche and Bauhofer (1987)

Sb8 Rhodium antimonide Sb8 $RhSb_3$ (Fig. 2.1470)
Locality: Synthetic.
Description: Prepared by heating stoichiometric mixture of the elements in a closed silica tube at 600–800 °C for 14 days. Cubic. Characterized by powder X-ray diffraction data.
Kind of sample preparation and/or method of registration of the spectrum: Hot pressed disc. Reflection.
Source: Kliche and Bauhofer (1987).
Wavenumbers (cm^{-1}): 239s, 222, 212s, 112.

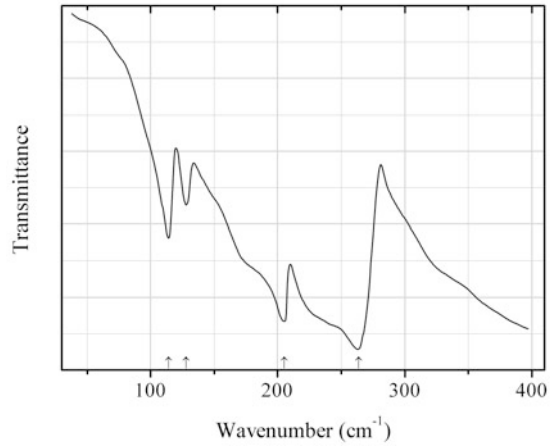

Fig. 2.1471 IR spectrum of ruthenium antimonide drawn using data from Lutz et al. (1983)

Sb9 Ruthenium antimonide $RuSb_2$ (Fig. 2.1471)
Locality: Synthetic.
Description: Prepared by heating stoichiometric mixture of the elements at 600 °C for 8 days. Characterized by powder X-ray diffraction data.
Kind of sample preparation and/or method of registration of the spectrum: Nujol mull. Transmission.
Source: Lutz et al. (1983).
Wavenumbers (cm^{-1}): 264s, 205, 128, 114.

2.17 Bromides and Bromates

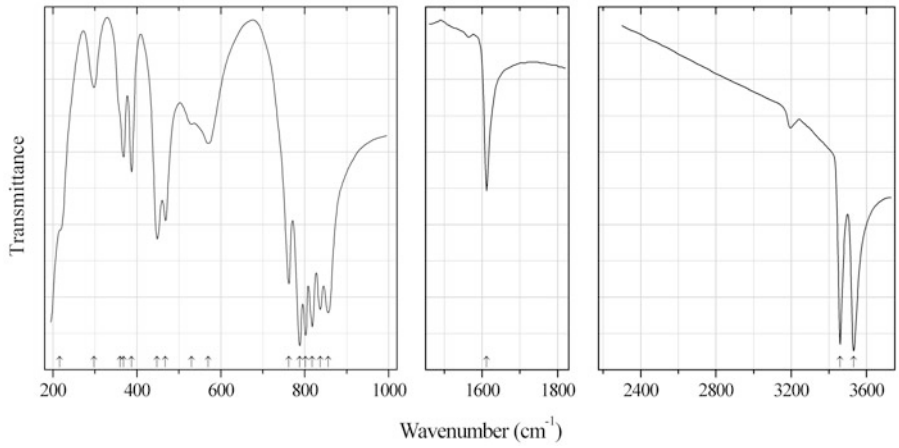

Fig. 2.1472 IR spectrum of calcium bromate monohydrate drawn using data from Alici et al. (1992)

Br1 Calcium bromate monohydrate $Ca(BrO_3)_2 \cdot H_2O$ (Fig. 2.1472)
Locality: Synthetic.

Description: Synthesized from $CaCO_3$ and $HBrO_3$ obtained as a result of ion exchange of $KBrO_3$ with Lewatit S 1080 ionite (Merck). Monoclinic, space group $P2_1/c$, a = 8.5445(7), b = 9.8900(5), c = 7.4235(6) Å, β = 96.070(5)°.
Kind of sample preparation and/or method of registration of the spectrum: Transmission. Kind of sample preparation is not indicated.
Source: Alici et al. (1992).
Wavenumbers (cm^{-1}): 3532, 3460, 1612, 856s, 837s, 818s, 802s, 788s, 762s, 570, 530, 468, 448, 387, 368, 360sh, 298w, 216sh.
Note: For the crystal structure of $Ca(BrO_3)_2 \cdot H_2O$ see Cvikl and McGrath (1970), and references therein.

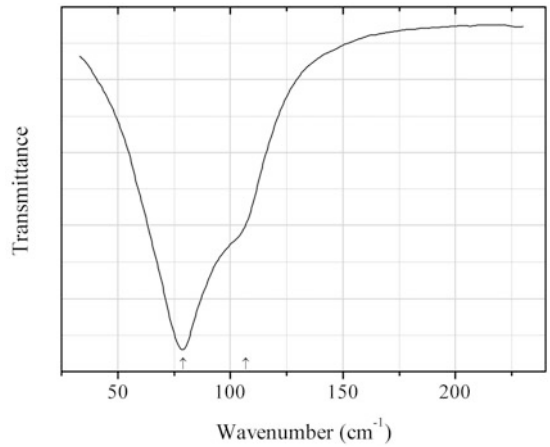

Fig. 2.1473 IR spectrum of bromargyrite drawn using data from Bottger and Geddes (1967)

Br2 Bromargyrite AgBr (Fig. 2.1473)
Locality: Synthetic.
Description: Film prepared by evaporation and precipitation onto polyethylene substrate.
Kind of sample preparation and/or method of registration of the spectrum: Transmission.
Source: Bottger and Geddes (1967).
Wavenumbers (cm^{-1}): 107sh, 79s.

2.18 Selenium, Selenites, and Selenides

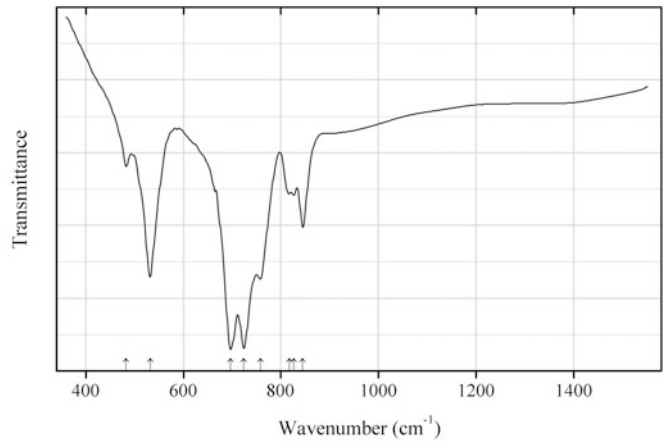

Fig. 2.1474 IR spectrum of zincomenite obtained by N.V. Chukanov

Se9 Zincomenite $Zn(SeO_3)$ (Fig. 2.1474)
Locality: Northern fumarole field, First scoria cone of the Northern Breakthrough of the Great Tolbachik Fissure Eruption, Tolbachik volcano, Kamchatka peninsula, Russia (type locality).
Description: White crystalline crusts from the association with sofiite, sellaite, fluorite, anhydrite, halite, cotunnite, challacolloite, saltonseaite, anglesite, and jakobssonite. Holotype sample. Orthorhombic, space group *Pbca*, a = 7.199(1), b = 6.238(1), c = 12.006(2) Å, V = 539.2(2) Å^3, Z = 8. D_{calc} = 4.748 g/cm^3. Optically biaxial (−), α = 1.744(5), β = 1.860(5), γ = 1.875(5). The empirical formula is (electron microprobe): $Zn_{1.02}Se_{0.99}O_3$. The strongest lines of the powder X-ray diffraction pattern [d, Å (I, %) (hkl)] are: 4.612 (26) (102), 3.601 (77) (200), 3.119 (48) (210), 3.048 (38) (113), 3.014 (100) (021, 211), 2.996 (56) (004), 2.459 (23) (023, 213).
Kind of sample preparation and/or method of registration of the spectrum: KBr disc. Absorption.
Wavenumbers (cm^{-1}): 845, 826, 818, 758, 724s, 697s, 532s, 483.

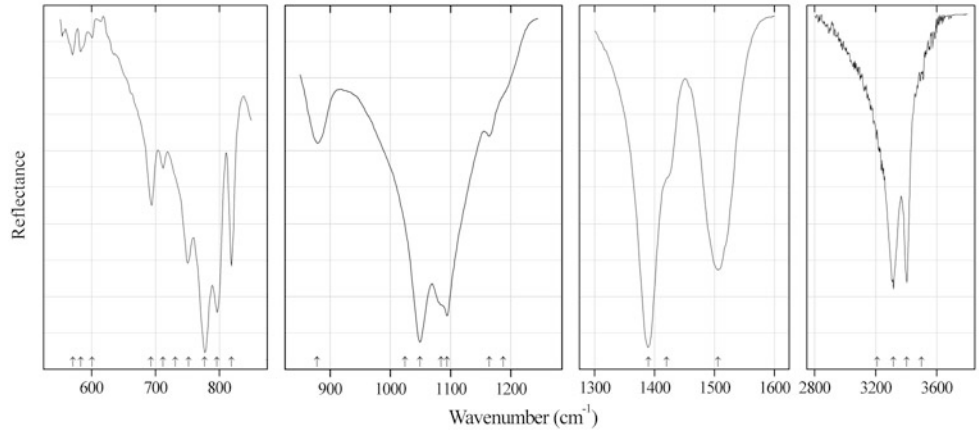

Fig. 2.1475 IR spectrum of demesmaekerite drawn using data from Frost et al. (2008a)

Se10 Demesmaekerite $Pb_2Cu_5(UO_2)_2(SeO_3)_6(OH)_6 \cdot 2H_2O$ (Fig. 2.1475)
Locality: Musonoi Cu-Co mine, near Kalwezi, Katanga Province, Democratic Republic of Congo (type locality).
Description: No data are given for the sample used.
Kind of sample preparation and/or method of registration of the spectrum: Attenuated total reflection of powdered mineral.
Source: Frost et al. (2008a).
Wavenumbers (cm^{-1}): 3501sh, 3405s, 3317s, 3211sh, 1506, 1420sh, 1390, 1187sh, 1164, 1094, 1084sh, 1049s, 1024sh, 878, 819, 796s, 777s, 752, 731sh, 712, 693, 601w, 583w, 571w.
Note: The wavenumbers correspond to individual bands determined as a result of band component analysis. IR spectrum of demesmaekerite in the range from 1600 to 2800 cm^{-1} and below 550 cm^{-1} is not given by Frost et al. (2008a). The position of the strongest band of Se–O stretching vibrations in IR spectra of most selenites, including uranyl selenites, is below 760 cm^{-1} (Chukanov, 2014a). The positions of the bands at 1164, 1084, 796, 777, and 693 cm^{-1} in the IR spectrum of demesmaekerite are close to those of quartz. The admixture of a carbonate is also not excluded. The wavenumbers were determined by us based on spectral curve analysis of the published spectrum.

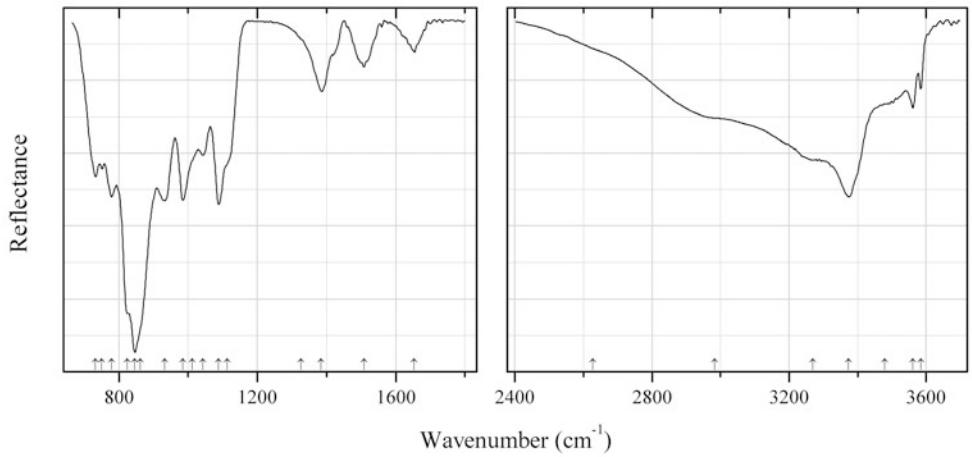

Fig. 2.1476 IR spectrum of derriksite drawn using data from Frost et al. (2014a)

Se11 Derriksite $Cu_4(UO_2)_2(SeO_3)_2(OH)_6 \cdot H_2O$ (Fig. 2.1476)
Locality: Musonoi Cu-Co mine, near Kalwezi, Katanga Province, Democratic Republic of Congo (type locality).
Description: Deep green transparent crystal. Sample SAB-098 from the collection of the Geology Department of the Federal University of Ouro Preto, Minas Gerais. Confirmed by chemical analyses.
Kind of sample preparation and/or method of registration of the spectrum: Attenuated total reflection.
Source: Frost et al. (2014a).
Wavenumbers (cm^{-1}): 3585w, 3562w, 3480sh, 3374s, 3270sh, 2983sh, 2628sh, 1654w, 1508, 1385, 1327sh, 1114sh, 1088s, 1043, 1012sh, 985s, 932s, 862sh, 846s, 825sh, 779s, 751, 732.
Note: The wavenumbers correspond to individual bands determined as a result of band component analysis. The wavenumbers were determined by us based on spectral curve analysis of the published spectrum. Questionable data: the position of the strongest band of Se–O-stretching vibrations in IR spectra of most selenites, including uranyl selenites, is below 760 cm^{-1} (Chukanov 2014a).

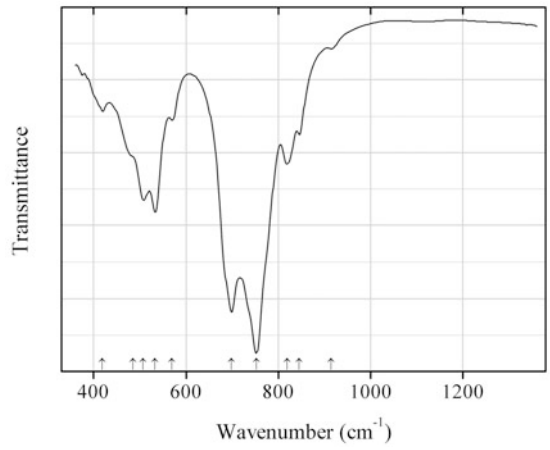

Fig. 2.1477 IR spectrum of sofiite obtained by N.V. Chukanov

Se12 Sofiite $Zn_2(SeO_3)Cl_2$ (Fig. 2.1477)
Locality: First cone of the North Breach of the Great Fissure Tolbachik volcano eruption, Kamchatka peninsula, Russia (type locality).
Description: Colourless platy crystals from the association with sellaite, fluorite, cotunnite, halite, and anhydrite. Investigated by I.V. Pekov. Identified by electron microprobe analyses.
Kind of sample preparation and/or method of registration of the spectrum: KBr disc. Absorption.
Wavenumbers (cm^{-1}): 915w, 846, 819, 753s, 699s, 570, 533, 507, 485sh, 419w.

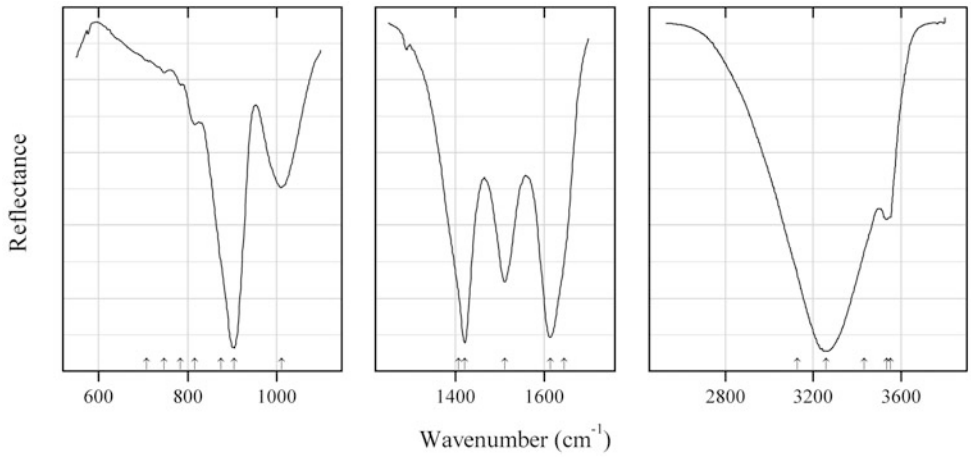

Fig. 2.1478 IR spectrum of guilleminite drawn using data from Frost et al. (2009a)

Se13 Guilleminite $Ba(UO_2)_3(SeO_3)_2O_2 \cdot 3H_2O$ (Fig. 2.1478)
Locality: Musonoi mine, Kolwezi, Katanga Copper Crescent, Democratic Republic of Congo (type locality).
Description: Type material.

Kind of sample preparation and/or method of registration of the spectrum: Attenuated total reflection of powdered mineral.
Source: Frost et al. (2009a).
Wavenumbers (cm^{-1}): 3552, 3534, 3434, 3260s, 3128sh, 1644, 1613, 1511, 1421, 1407, 1011, 904s, 874s, 816w, 784w, 747w, 708sh.
Note: The wavenumbers are indicated for the maxima of individual bands obtained as a result of the spectral curve analysis. Details of this analysis are not described. Observed absorption maxima are not indicated. The wavenumbers were determined by us based on spectral curve analysis of the published spectrum. Questionable data: the position of the strongest band of Se–O stretching vibrations in IR spectra of most selenites, including uranyl selenites, is below 760 cm^{-1} (Chukanov 2014a).

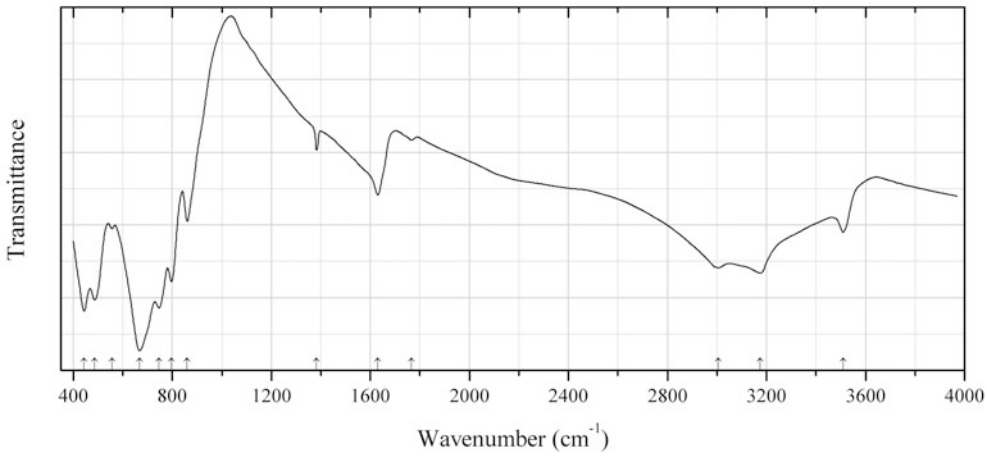

Fig. 2.1479 IR spectrum of selenite Se14 drawn using data from Johnston and Harrison (2011)

Se14 Selenite Se14 $BaCo_2(SeO_3)_3 \cdot 3H_2O$ (Fig. 2.1479)
Locality: Synthetic.
Description: The crystal structure is based on the zemannite-type framework. Hexagonal, space group $P6_3$, a = 18.0430(6), c = 7.6120(2) Å, V = 2146.08(12) $Å^3$, Z = 8.
Kind of sample preparation and/or method of registration of the spectrum: Transmission. Kind of sample preparation is not indicated.
Source: Johnston and Harrison (2011).
Wavenumbers (cm^{-1}): 3510, 3175, 3005, 1766w, 1630, 1383w, 861, 797, 746s, 668s, 556, 487s, 444s.
Note: The wavenumbers were partly determined by us based on spectral curve analysis of the published spectrum. The band at 1383 cm^{-1} may correspond to the admixture of NO_3^-.

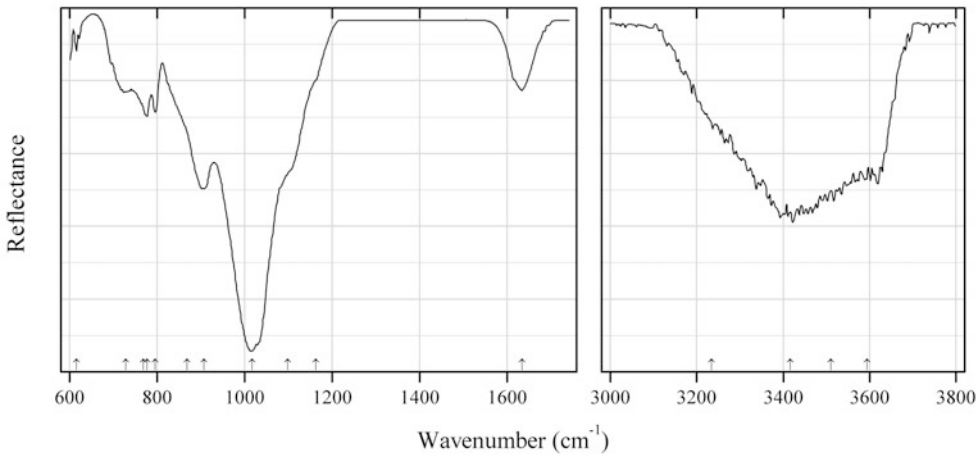

Fig. 2.1480 IR spectrum of haynesite drawn using data from Frost and Čejka (2009)

Se15 Haynesite $(UO_2)(SeO_3)_2(OH)_2 \cdot 5H_2O$ (Fig. 2.1480)
Locality: Repete Mine, Blanding, San Juan Co., Utah, USA (type locality).
Description: No data.
Kind of sample preparation and/or method of registration of the spectrum: Attenuated total reflection of powdered mineral.
Source: Frost and Čejka (2009).
Wavenumbers (cm^{-1}): 3594sh, 3510sh, 3417, 3234, 1634, 1163sh, 1099sh, 1017s, 907, 868sh, 796, 777, 768sh, 728, 615w.
Note: Frequencies are given according to drawing. In the cited paper, the wavenumbers are indicated only for the maxima of individual bands obtained as a result of the spectral curve analysis. The very strong band at 1017 cm^{-1} indicates that the sample is strongly contaminated by another (silicate?) mineral.

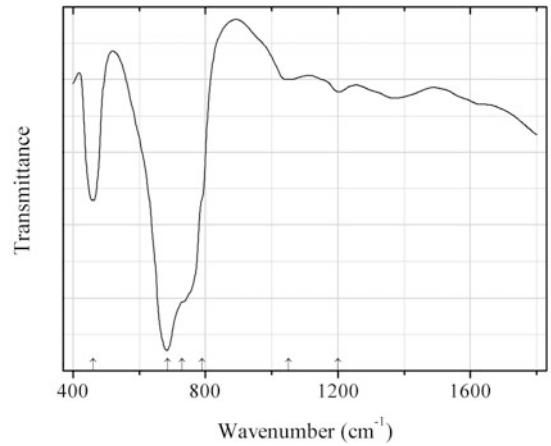

Fig. 2.1481 IR spectrum of molybdomenite drawn using data from Britvin et al. (1989)

Se16 Molybdomenite $Pb(SeO_3)$ (Fig. 2.1481)
Locality: Zaonezhskiy peninsula, South Karelia, Russia.

Description: White crystals from the association with cerussite and clausthalite. According to electron microprobe data, chemical composition is close to that of pure $Pb(SeO_3)$. Monoclinic, space group $P2_1/m$, a = 6.863(4), b = 5.519(4), c = 4.526(1) Å, β = 112.44(5)°, V = 157.7 Å^3, Z = 2. D_{calc} = 7.035 g/cm^3. The strongest lines of the powder X-ray diffraction pattern [d, Å (I, %) (hkl)] are: 4.16 (50) (001, 110), 3.406 (40) (−111), 3.325 (60) (011), 3.178 (60) (−201, 200), 3.006 (40) (101), 2.754 (100) (−211, 210), 2.258 (40) (−102), 2.082 (40) (−221, 220).
Kind of sample preparation and/or method of registration of the spectrum: Transmission. Kind of sample preparation is not indicated.
Source: Britvin et al. (1989).
Wavenumbers (cm^{-1}): 1200w, 1050w, 790sh, 730sh, 685s, 460.
Note: The bands at 1200 and 1050 cm^{-1} indicate possible presence of minor amounts of SO_4^{2-} anions.

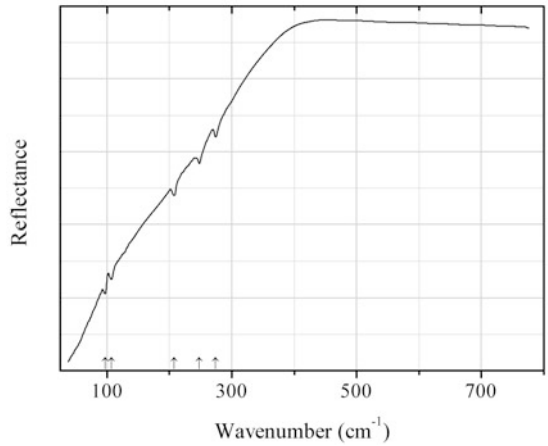

Fig. 2.1482 IR spectrum of palladium selenide drawn using data from Kliche (1985b)

Se17 Palladium selenide PdSe (Fig. 2.1482)
Locality: Synthetic.
Description: Obtained by annealing a stoichiometric mixture of the elements at 500 °C for 60 days. Tetragonal, a = 6.726, c = 6.915 Å.
Kind of sample preparation and/or method of registration of the spectrum: Pressed disc. Reflection.
Source: Kliche (1985b).
Wavenumbers (cm^{-1}): 274, 248, 208, 107, 97.

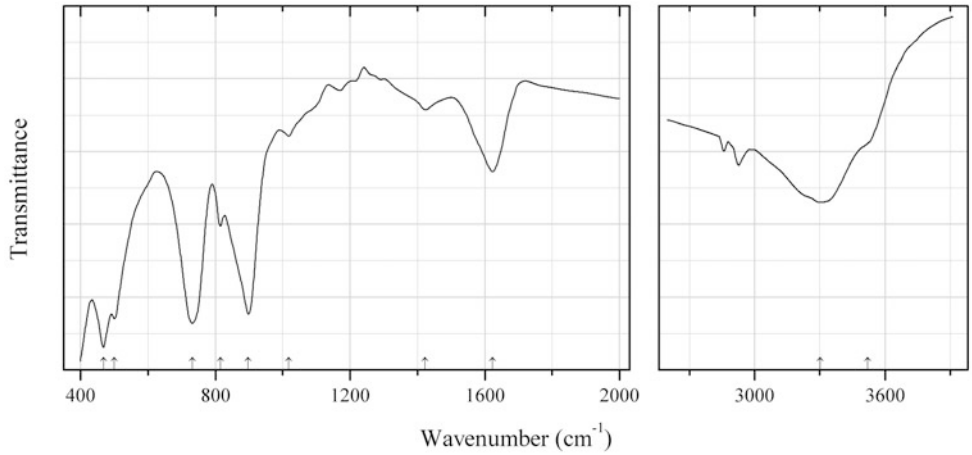

Fig. 2.1483 IR spectrum of piretite drawn using data from Vochten et al. (1996)

Se18 Piretite $Ca(UO_2)_3(SeO_3)_2(OH)_4 \cdot 4H_2O$ (Fig. 2.1483)
Locality: Shinkolobwe, Katanga (Shaba), Democratic Republic of Congo (type locality).
Description: Yellow crystals from the associarion with an orange masuyite-like U-Pb oxide on the surface of uraninite samples. Holotype sample. Orthorhombic, a = 7.010(3), b = 17.135(7), c = 17.606(4) Å, V = 2114.8(1) Å^3, Z = 4. D_{meas} = 4.00(3) g/cm^3, D_{calc} = 3.87 g/cm^3. Optically biaxial (−), α = 1.54 (calc.), β = 1.73(1), γ = 1.75(1), 2 V = 33(5)°. The empirical formula is $Ca_{0.76}(UO_2)_{3.02}(SeO_3)_{2.09}(OH)_{3.38} \cdot 3.64H_2O$. The strongest lines of the powder X-ray diffraction pattern [d, Å (I, %) (hkl)] are: 8.79 (80) (002), 8.56 (40) (020), 5.57 (20) (013), 4.43 (20) (130), 4.30 (30) (131), 3.51 (100) (200), 3.24 (40) (220), 3.093 (50) (115), 3.032 (100) (151), 1.924 (40) (237).
Kind of sample preparation and/or method of registration of the spectrum: KBr disc. Transmission.
Source: Vochten et al. (1996).
Wavenumbers (cm^{-1}): 3520sh, 3303s, 1623, 1423w, 1018, 898s, 815, 732s, 501s, 468s.
Note: In the cited paper the wavenumber 1423 cm^{-1} is erroneously indicated as 1483 cm^{-1}. The wavenumbers were partly determined by us based on spectral curve analysis of the published spectrum. Weak bands in the range from 2800 to 3000 cm^{-1} correspond to the admixture of an organic substance.

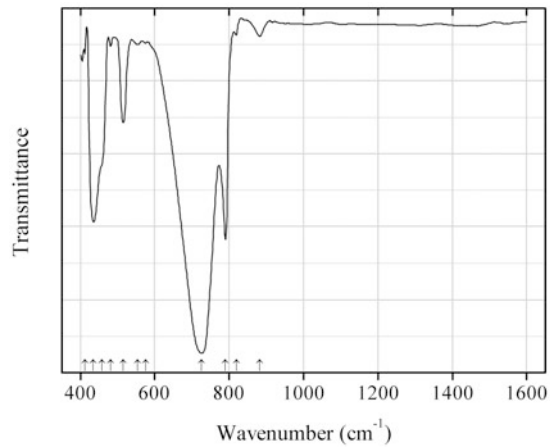

Fig. 2.1484 IR spectrum of plumboselite drawn using data from Kim et al. (2009)

Se19 Plumboselite $Pb_3(SeO_3)O_2$ (Fig. 2.1484)
Locality: Synthetic.
Description: Synthesized hydrothermally from SeO_2 and PbO in the presence of 1 M NaOH solution, at 230 °C for 2 days. Confirmed by powder X-ray diffraction. The crystal structure is solved. Orthorhombic, space group $Cmc2_1$, a = 10.5211(13), b = 10.7151(13), c = 5.7452(7) Å, V = 647.68 (14) Å^3, Z = 2. D_{calc} = 8.007 g/cm^3.
Kind of sample preparation and/or method of registration of the spectrum: Transmission. Kind of sample preparation is not indicated.
Source: Kim et al. (2009).
Wavenumbers (cm^{-1}): 882, 819, 790, 726s, 575w, 554w, 515, 481w, 457sh, 435s, 412w.
Note: The wavenumbers were partly determined by us based on spectral curve analysis of the published spectrum.

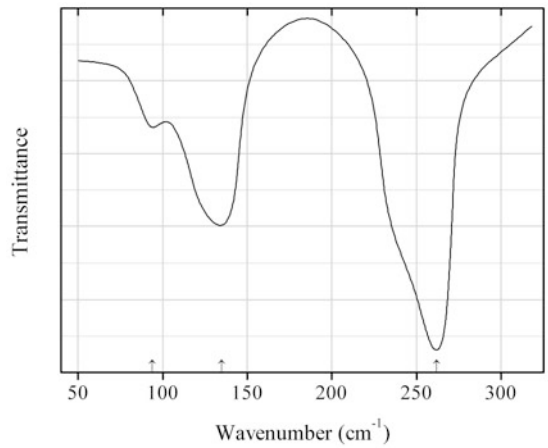

Fig. 2.1485 IR spectrum of selenium amorphous polymorph drawn using data from Lucovsky (1969)

Se20 Selenium amorphous polymorph Se (Fig. 2.1485)
Locality: Synthetic.
Kind of sample preparation and/or method of registration of the spectrum: Transmission. Kind of sample preparation is not indicated.
Source: Lucovsky (1969).
Wavenumbers (cm^{-1}): 262s, 135, 94.
Note: The wavenumbers were partly determined by us based on spectral curve analysis of the published spectrum.

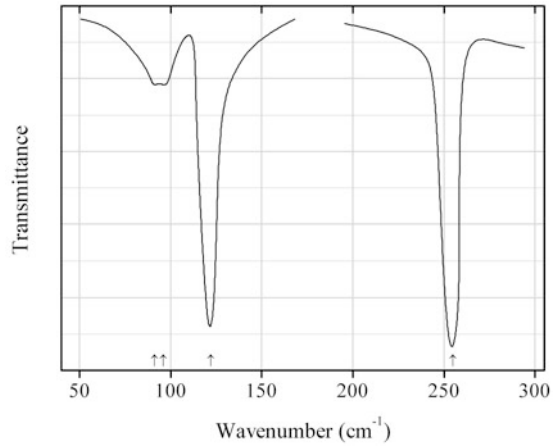

Fig. 2.1486 IR spectrum of selenium drawn using data from Lucovsky (1969)

Se21 Selenium Se (Fig. 2.1486)
Locality: Synthetic.
Kind of sample preparation and/or method of registration of the spectrum: Transmission. Kind of sample preparation is not indicated.
Source: Lucovsky (1969).
Wavenumbers (cm^{-1}): 255s, 122s, 96, 91.
Note: The wavenumbers were determined by us based on spectral curve analysis of the published spectrum.

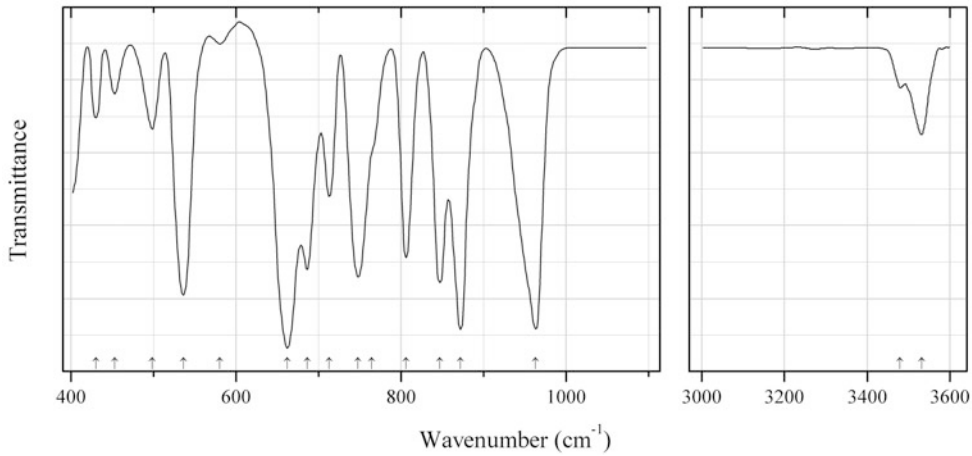

Fig. 2.1487 IR spectrum of calcium vanadyl selenite Se22 drawn using data from Yeon et al. (2012a)

Se22 Calcium vanadyl selenite Se22 $Ca_2(VO_2)_2(SeO_3)_3{\cdot}2H_2O$ (Fig. 2.1487)
Locality: Synthetic.
Description: Synthesized hydrothermally. The crystal structure is solved. Orthorhombic, space group *Pnma*, a = 7.827(4), b = 16.764(5), c = 9.679(5) Å, V = 1270.1(9) $Å^3$, Z = 4. The powder XRD pattern is in good agreement with the calculated XRD pattern from the single crystal model.
Kind of sample preparation and/or method of registration of the spectrum: No data.

Source: Yeon et al. (2012a).
Wavenumbers (cm^{-1}): 3531, 3479w, 963s, 872s, 847, 806, 764sh, 748, 713, 686w, 662s, 580w, 536s, 498, 453, 430.
Note: The wavenumbers were partly determined by us based on spectral curve analysis of the published spectrum.

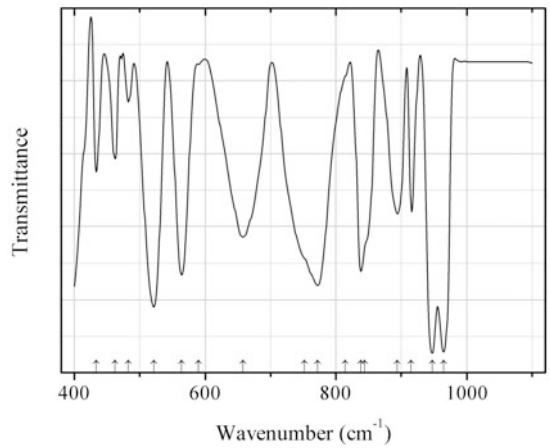

Fig. 2.1488 IR spectrum of strontium vanadyl selenite Se23 drawn using data from Yeon et al. (2012a)

Se23 Strontium vanadyl selenite Se23 $Sr_2(VO_2)_2(SeO_3)_3$ (Fig. 2.1488)
Locality: Synthetic.
Description: Synthesized hydrothermally. The crystal structure is solved. Monoclinic, space group $P2_1/c$, a = 14.739(13), b = 9.788(8), c = 8.440(7) Å, β = 96.881(11)°, V = 1208.8(18) $Å^3$, Z = 4. The powder XRD pattern is in good agreement with the calculated XRD pattern from the single crystal model.
Kind of sample preparation and/or method of registration of the spectrum: No data.
Source: Yeon et al. (2012a).
Wavenumbers (cm^{-1}): 965s, 947s, 915, 894, 844sh, 814sh, 838, 772, 752sh, 658, 590w, 564, 522s, 483w, 462, 434.
Note: The wavenumbers were partly determined by us based on spectral curve analysis of the published spectrum. The band position denoted by Yeon et al. (2012a) as 552 cm^{-1} was determined by us at 522 cm^{-1}.

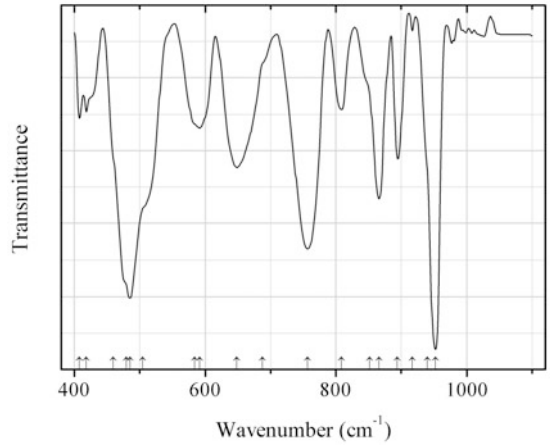

Fig. 2.1489 IR spectrum of barium vanadyl selenite Se24 drawn using data from Yeon et al. (2012a)

Se24 Barium vanadyl selenite Se24 $Ba(V_2O_5)(SeO_3)$ (Fig. 2.1489)
Locality: Synthetic.
Description: Synthesized hydrothermally. The crystal structure is solved. Orthorhombic, space group *Pnma*, a = 13.9287(7), b = 5.3787(3), c = 8.9853(5) Å, V = 673.16(6) Å^3, Z = 4. The powder XRD pattern is in good agreement with the calculated XRD pattern from the single crystal model.
Kind of sample preparation and/or method of registration of the spectrum: No data.
Source: Yeon et al. (2012a).
Wavenumbers (cm^{-1}): 952s, 940sh, 917w, 894, 866, 852sh, 808, 757s, 688sh, 648, 592, 584sh, 505sh, 485s, 480sh, 460sh, 418w, 408w.
Note: The wavenumbers were partly determined by us based on spectral curve analysis of the published spectrum.

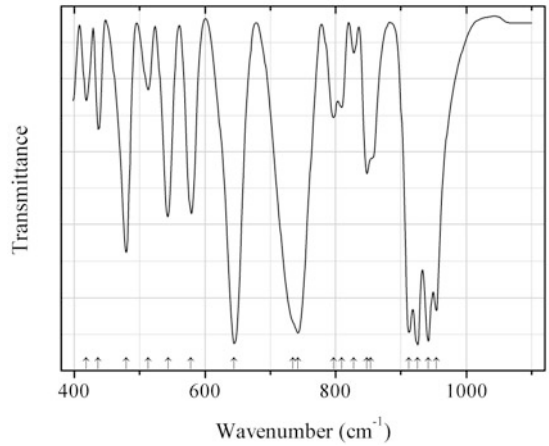

Fig. 2.1490 IR spectrum of strontium vanadyl selenite Se25 drawn using data from Yeon et al. (2012a)

Se25 Strontium vanadyl selenite Se25 $Sr_4(VO_2)_2(SeO_3)_4(Se_2O_5)$ (Fig. 2.1490)
Locality: Synthetic.

Description: Synthesized hydrothermally. The crystal structure is solved. Orthorhombic, space group *Fdd*2, $a = 25.161(3)$, $b = 12.1579(15)$, $c = 12.8592(16)$ Å, $V = 3933.7(8)$ Å^3, $Z = 8$. The powder XRD pattern is in good agreement with the calculated XRD pattern from the single crystal model.
Kind of sample preparation and/or method of registration of the spectrum: No data.
Source: Yeon et al. (2012a).
Wavenumbers (cm^{-1}): 954s, 942s, 925s, 912s, 854sh, 848, 828w, 809, 797, 742s, 735sh, 645s, 578, 544, 513w, 480, 437, 418.
Note: The wavenumbers were partly determined by us based on spectral curve analysis of the published spectrum. The band position denoted by Yeon et al. (2012a) as 457 cm^{-1} was determined by us at 437 cm^{-1}.

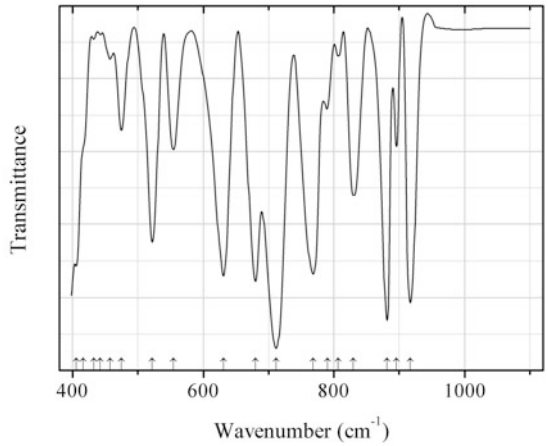

Fig. 2.1491 IR spectrum of lead vanadyl selenite Se26 drawn using data from Yeon et al. (2012a)

Se26 Lead vanadyl selenite Se26 $Pb_4(VO_2)_2(SeO_3)_4(Se_2O_5)$ (Fig. 2.1491)
Locality: Synthetic.
Description: Synthesized hydrothermally. The crystal structure is solved. Orthorhombic, space group *Fdd*2, $a = 25.029(2)$, $b = 12.2147(10)$, $c = 13.0154(10)$ Å, $V = 3979.1(6)$ Å^3, $Z = 8$. The powder XRD pattern is in good agreement with the calculated XRD pattern from the single crystal model.
Kind of sample preparation and/or method of registration of the spectrum: No data.
Source: Yeon et al. (2012a).
Wavenumbers (cm^{-1}): 917s, 896, 881s, 830, 807w, 790, 768, 712s, 680, 631, 554, 522, 475, 458w, 442w, 433w, 416sh, 406.
Note: The wavenumbers were partly determined by us based on spectral curve analysis of the published spectrum.

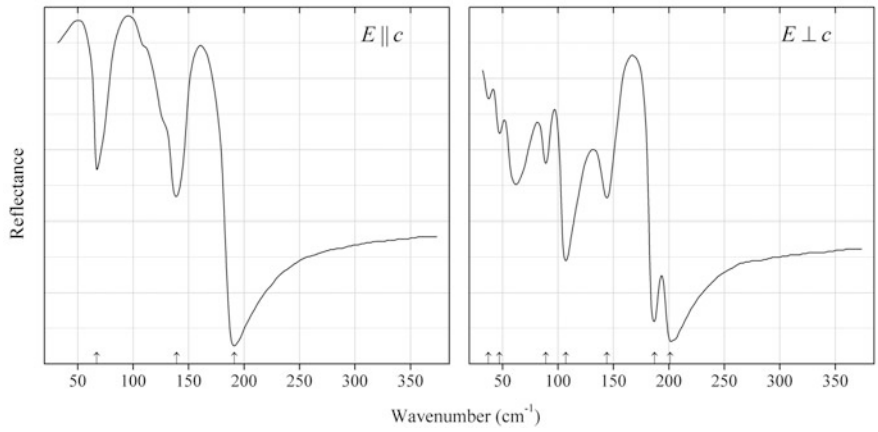

Fig. 2.1492 IR spectrum of antimonselite drawn using data from Petzelt and Grigas (1973)

Se27 Antimonselite Sb_2Se_3 (Fig. 2.1492)
Locality: Synthetic.
Description: Single crystal.
Kind of sample preparation and/or method of registration of the spectrum: Reflection from the (010) surface.
Source: Petzelt and Grigas (1973).
Wavenumbers (cm^{-1}): 191s, 139, 67 (for $E \| c$); 201s, 187, 144, 107, 89, 47w, 37w (for $E \perp c$).
Note: The wavenumbers were determined by us based on spectral curve analysis of the published spectrum.

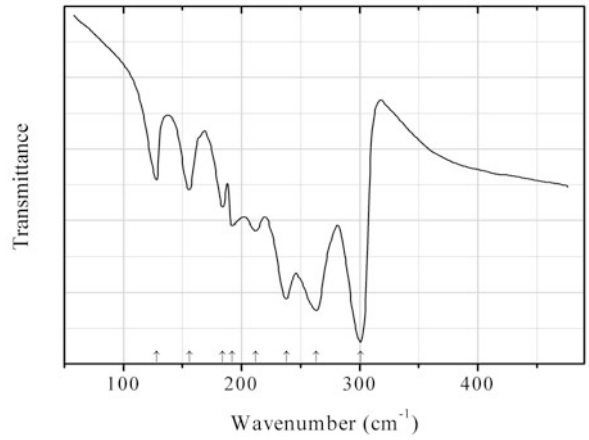

Fig. 2.1493 IR spectrum of ruthenium antimonide selenide drawn using data from Lutz et al. (1983)

Se28 Ruthenium antimonide selenide RuSbSe (Fig. 2.1493)
Locality: Synthetic.
Description: Prepared by heating stoichiometric mixture of the elements in a closed silica tube at 1000 °C. Monoclinic, space group $P2_1/m$, a = 6.358(1), b = 6.307(1), c = 6.404(1) Å, β = 113.3(1)°.
Kind of sample preparation and/or method of registration of the spectrum: Nujol mull. Transmission.

Source: Lutz et al. (1983).
Wavenumbers (cm^{-1}): 301s, 263s, 238s, 212, 192, 184, 156, 128.

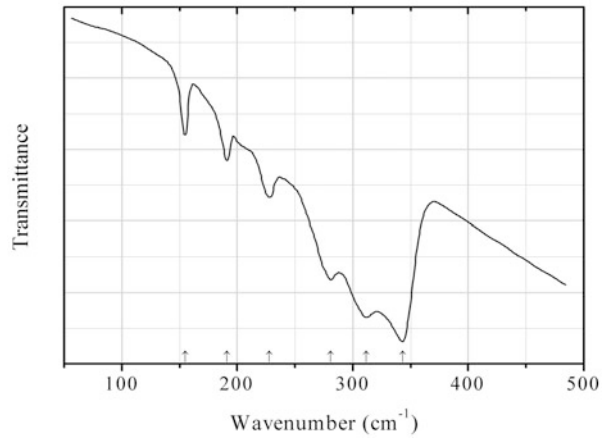

Fig. 2.1494 IR spectrum of iron arsenide selenide drawn using data from Lutz et al. (1983)

Se29 Iron arsenide selenide FeAsSe (Fig. 2.1494)
Locality: Synthetic.
Description: Prepared by heating stoichiometric mixture of the elements in a closed tube at 550 °C. Monoclinic, space group $P2_1/m$, a = 5.877(2), b = 5.871(2), c = 5.974(2) Å, β = 113.4(2)°.
Kind of sample preparation and/or method of registration of the spectrum: Nujol mull. Transmission.
Source: Lutz et al. (1983).
Wavenumbers (cm^{-1}): 343s, 312s, 281s, 228, 191, 155.

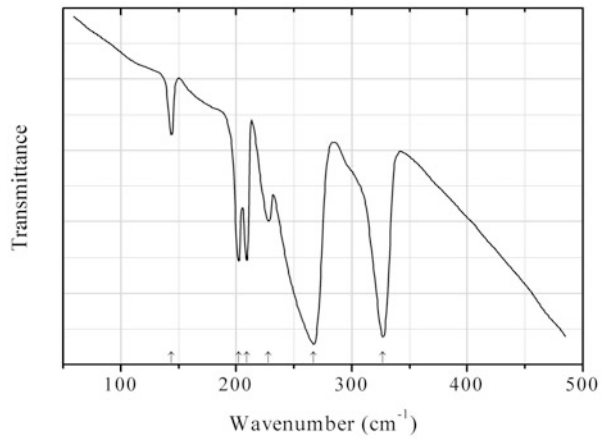

Fig. 2.1495 IR spectrum of osmium arsenide selenide drawn using data from Lutz et al. (1983)

Se30 Osmium arsenide selenide OsAsSe (Fig. 2.1495)
Locality: Synthetic.

Description: Prepared by heating stoichiometric mixture of the elements in a closed tube at 1000 °C. Monoclinic, space group $P2_1/m$, a = 6.099(2), b = 6.082(2), c = 6.199(2) Å, β = 112.5(2)°.
Kind of sample preparation and/or method of registration of the spectrum: Nujol mull. Transmission.
Source: Lutz et al. (1983).
Wavenumbers (cm^{-1}): 327s, 267s, 228, 209, 202, 144w.

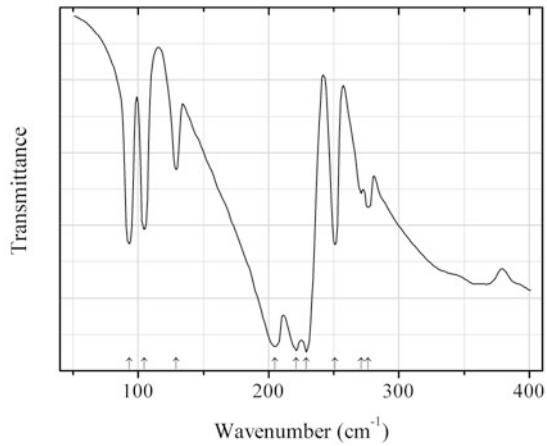

Fig. 2.1496 IR spectrum of laphamite drawn using data from Whitfield (1971)

Se31 Laphamite As_2Se_3 (Fig. 2.1496)
Locality: Synthetic.
Description: Monoclinic, a = 12.05, b = 9.89, c = 4.28 Å, β = 90.47°.
Kind of sample preparation and/or method of registration of the spectrum: Powder dispersed in petroleum jelly. Absorption.
Source: Whitfield (1971).
Wavenumbers (cm^{-1}): 276.5, 271, 251, 229s, 221s, 205s, 129, 104.5, 93.

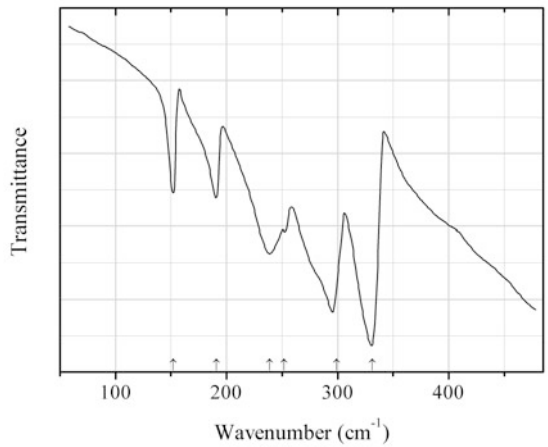

Fig. 2.1497 IR spectrum of ruthenium arsenide selenide drawn using data from Lutz et al. (1983)

Se32 Ruthenium arsenide selenide RuAsSe (Fig. 2.1497)

Locality: Synthetic.
Description: Prepared by heating stoichiometric mixture of the elements in a closed tube at 1000 °C. Monoclinic, space group $P2_1/m$, a = 6.089(1), b = 6.067(1), c = 6.165(1) Å, β = 112.5(1)°.
Kind of sample preparation and/or method of registration of the spectrum: Nujol mull. Transmission.
Source: Lutz et al. (1983).
Wavenumbers (cm^{-1}): 331s, 299s, 252, 239, 191, 152.

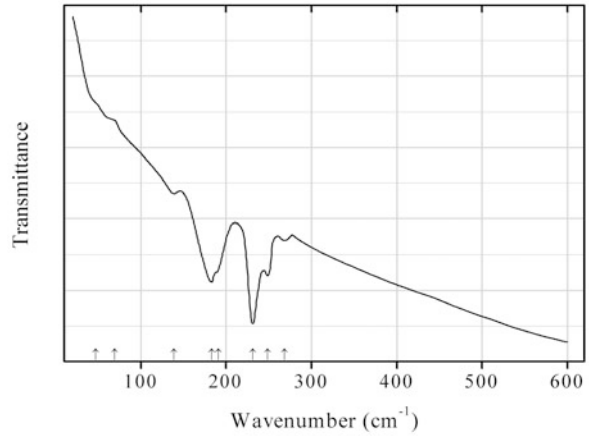

Fig. 2.1498 IR spectrum of copper cadmium tin selenide drawn using data from Himmrich and Haeuseler (1991)

Se33 Copper cadmium tin selenide $Cu_2CdSnSe_4$ (Fig. 2.1498)
Locality: Synthetic.
Description: Synthesized by the solid-state reaction from the stoichiometric mixture of the elements at 900 °C. Tetragonal, space group I-42 m, a = 5.832(1), c = 11.392(4) Å. Confirmed by powder X-ray diffraction data.
Kind of sample preparation and/or method of registration of the spectrum: Nujol mull. Transmission.
Source: Himmrich and Haeuseler (1991).
Wavenumbers (cm^{-1}): 268w, 249, 231s, 191sh, 183, 139w, 69w, 47sh.

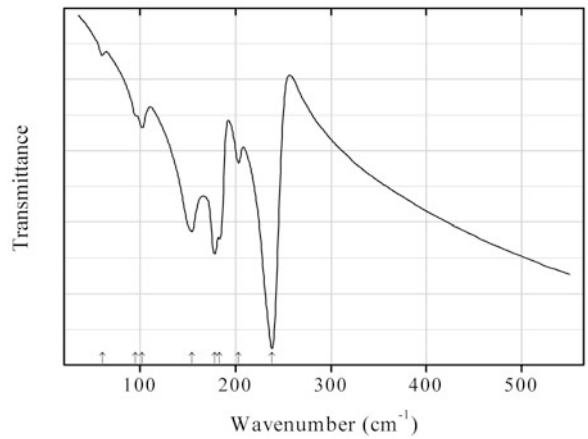

Fig. 2.1499 IR spectrum of silver cadmium tin selenide drawn using data from Himmrich and Haeuseler (1991)

Se34 Silver cadmium tin selenide $Cu_2CdSnSe_4$ (Fig. 2.1499)
Locality: Synthetic.
Description: Synthesized by the solid-state reaction from the stoichiometric mixture of the elements at 600 °C. Characterized by powder X-ray diffraction data. Orthorhombic, space group $Pmn2_1$, a = 4.274(1), b = 7.334(2), c = 6.989(2) Å.
Kind of sample preparation and/or method of registration of the spectrum: Nujol mull. Transmission.
Source: Himmrich and Haeuseler (1991).
Wavenumbers (cm^{-1}): 238s, 203w, 183, 178, 154, 102w, 95sh, 60w.

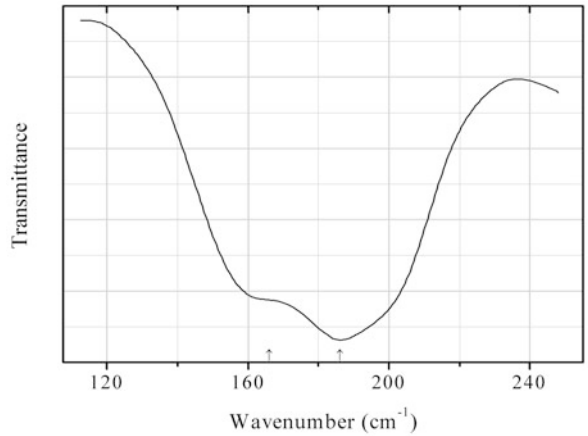

Fig. 2.1500 IR spectrum of cadmoselite drawn using data from Vasilevskiy et al. (2001)

Se35 Cadmoselite CdSe (Fig. 2.1500)
Locality: Synthetic.
Description: Nanocrystallites prepared via a wet-chemical route.
Kind of sample preparation and/or method of registration of the spectrum: Thin film. Transmission.
Source: Vasilevskiy et al. (2001).
Wavenumbers (cm^{-1}): 186, 166sh.
Note: The wavenumbers were determined by us based on spectral curve analysis of the published spectrum.

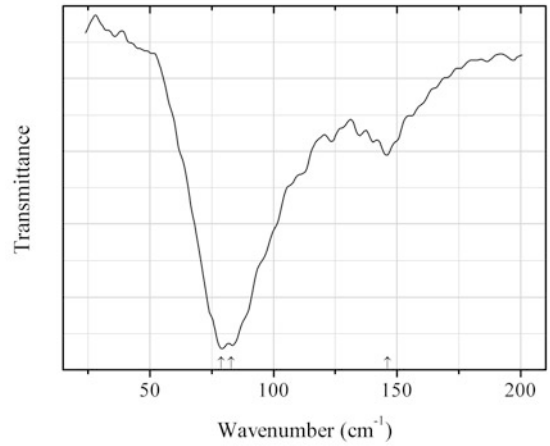

Fig. 2.1501 IR spectrum of clausthalite drawn using data from Hyun et al. (2011)

Se36 Clausthalite PbSe (Fig. 2.1501)
Locality: Synthetic.
Description: Nanorods.
Kind of sample preparation and/or method of registration of the spectrum: Absorption.
Source: Hyun et al. (2011).
Wavenumbers (cm^{-1}): 146, 83s, 79s.
Note: The wavenumbers were determined by us based on spectral curve analysis of the published spectrum.

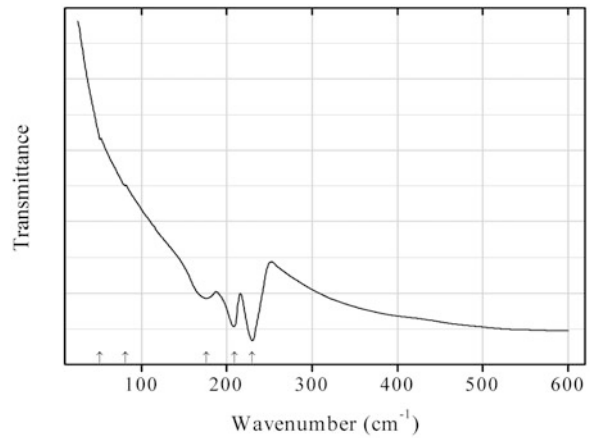

Fig. 2.1502 IR spectrum of copper manganese tin selenide drawn using data from Himmrich and Haeuseler (1991)

Se37 Copper manganese tin selenide Cu_2HgGeS_4 (Fig. 2.1502)
Locality: Synthetic.
Description: Synthesized by the solid-state reaction from the stoichiometric mixture of the elements at 550 °C. Characterized by powder X-ray diffraction data. Tetragonal, space group *I*-42 *m*, a = 5.741 (1), c = 11.420(2) Å.

Kind of sample preparation and/or method of registration of the spectrum: Nujol mull. Transmission.
Source: Himmrich and Haeuseler (1991).
Wavenumbers (cm^{-1}): 230s, 209s, 176, 81w, 51w.

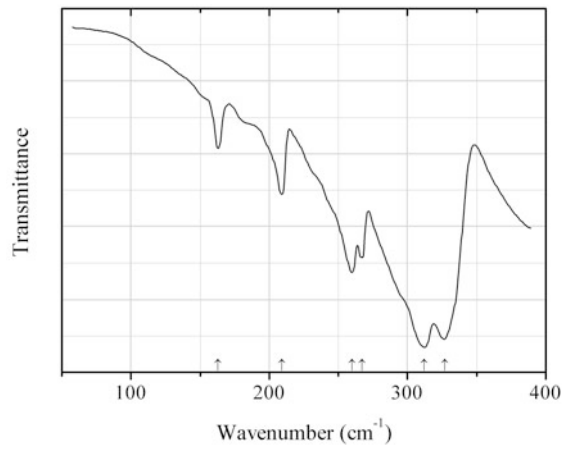

Fig. 2.1503 IR spectrum of ferroselite drawn using data from Lutz et al. (1983)

Se38 Ferroselite $FeSe_2$ (Fig. 2.1503)
Locality: Synthetic.
Description: Prepared by heating stoichiometric mixture of the elements in a closed silica tube at 400 °C for 30 days. Characterized by powder X-ray diffraction data.
Kind of sample preparation and/or method of registration of the spectrum: Nujol mull. Transmission.
Source: Lutz et al. (1983).
Wavenumbers (cm^{-1}): 327s, 312s, 267, 260, 209, 163w.

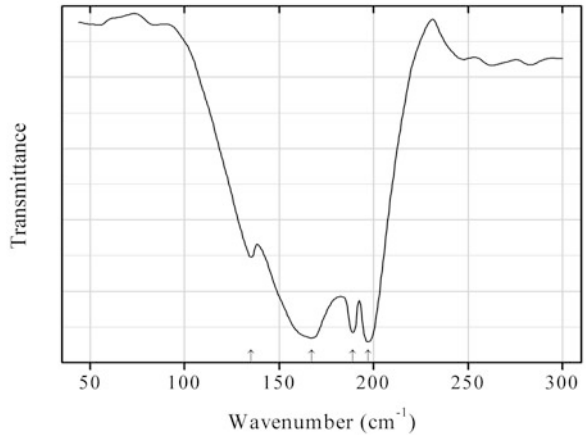

Fig. 2.1504 IR spectrum of germanium selenide drawn using data from Chamberlain et al. (1974)

Se39 Germanium selenide GeSe (Fig. 2.1504)

Locality: Synthetic.
Description: Single-crystal platelet chiped off perpendicular to the *b* direction.
Kind of sample preparation and/or method of registration of the spectrum: Transmission.
Source: Chamberlain et al. (1974).
Wavenumbers (cm^{-1}): 197s, 189s, 167s, 135.

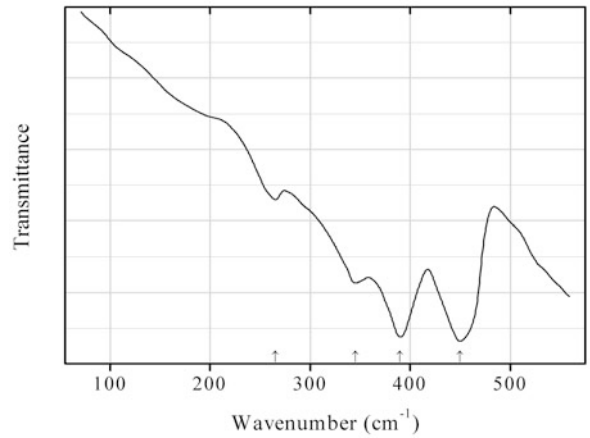

Fig. 2.1505 IR spectrum of iron phosphide selenide drawn using data from Lutz et al. (1983)

Se40 Iron phosphide selenide FePSe (Fig. 2.1505)
Locality: Synthetic.
Description: Prepared using the elements pressed to discs and heating them at 400 °C in the presence of small amounts of iodine. Monoclinic, a = 5.768(2), b = 5.707(2), c = 5.832(2) Å, β = 112.9(2)°.
Kind of sample preparation and/or method of registration of the spectrum: Nujol mull. Transmission.
Source: Lutz et al. (1983).
Wavenumbers (cm^{-1}): 450s, 390s, 345, 265w.

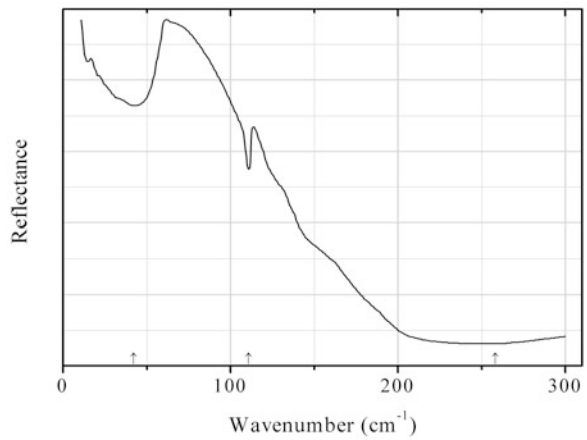

Fig. 2.1506 IR spectrum of kawazulite drawn using data from Akrap et al. (2012)

Se41 Kawazulite Bi_2Te_2Se (Fig. 2.1506)
Locality: Synthetic.
Description: Single crystals grown by the floating zone method starting from the stoichiometric ratio of metallic bismuth and chalcogenide elements.
Kind of sample preparation and/or method of registration of the spectrum: Reflectivity for light polarized in the *ab* plane.
Source: Akrap et al. (2012).
Wavenumbers (cm^{-1}): (258s) (broad), 111, 42.

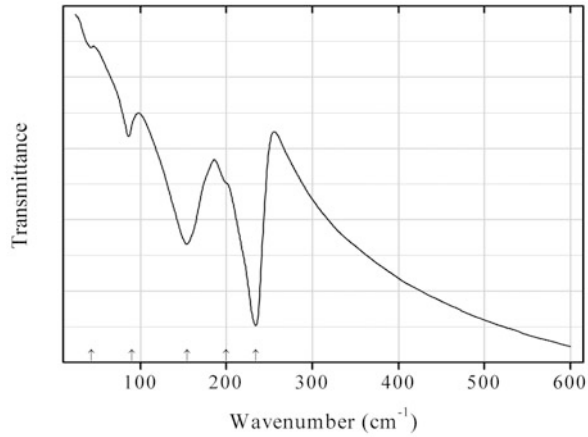

Fig. 2.1507 IR spectrum of silver mercury tin selenide drawn using data from Himmrich and Haeuseler (1991)

Se42 Silver mercury tin selenide $Ag_2HgSnSe_4$ (Fig. 2.1507)
Locality: Synthetic.
Description: Obtained from the stoichiometric mixture of the elements. Characterized by powder X-ray diffraction data.
Kind of sample preparation and/or method of registration of the spectrum: Nujol mull. Transmission.
Source: Himmrich and Haeuseler (1991).
Wavenumbers (cm^{-1}): 234s, 200sh, 154s, 90, 43w.

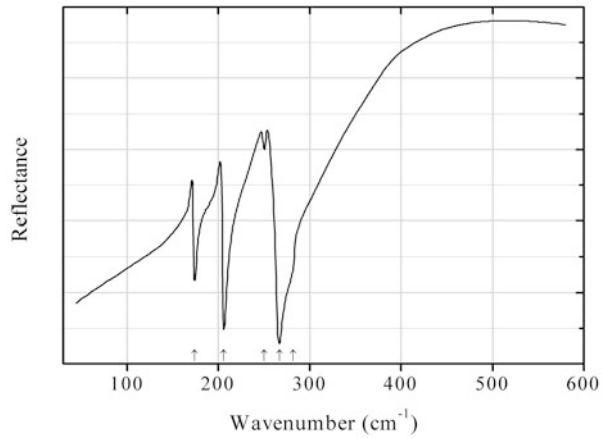

Fig. 2.1508 IR spectrum of osmium diselenide drawn using data from Lutz et al. (1985)

Se43 Osmium diselenide $OsSe_2$ (Fig. 2.1508)
Locality: Synthetic.
Description: Prepared by annealing stoichiometric mixture of the elements in an evacuated quartz tube at 800–900 °C for 14 days. Cubic. Characterized by powder X-ray diffraction data.
Kind of sample preparation and/or method of registration of the spectrum: A sample prepared by hot-pressing and polishing with diamond paste. Reflection.
Source: Lutz et al. (1985).
Wavenumbers (cm^{-1}): 282sh, 267s, 250w, 206s, 174.

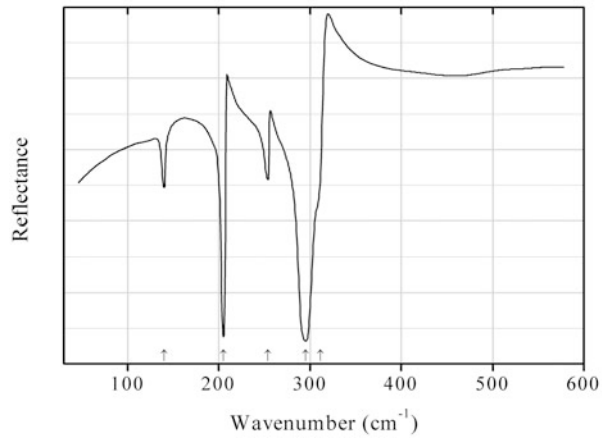

Fig. 2.1509 IR spectrum of ruthenium diselenide drawn using data from Lutz et al. (1985)

Se44 Ruthenium diselenide $RuSe_2$ (Fig. 2.1509)
Locality: Synthetic.
Description: Prepared by annealing stoichiometric mixture of the elements in an evacuated quartz tube at 800–900 °C for 14 days. Cubic. Characterized by powder X-ray diffraction data.
Kind of sample preparation and/or method of registration of the spectrum: A sample prepared by hot-pressing and polishing with diamond paste. Reflection.
Source: Lutz et al. (1985).
Wavenumbers (cm^{-1}): 311sh, 295s, 254, 205s, 140.

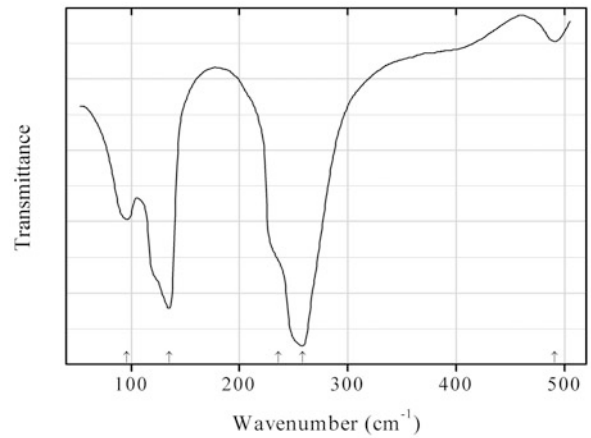

Fig. 2.1510 IR spectrum of selenium amorphous drawn using data from Nagata et al. (1981)

Se45 Selenium amorphous Se (Fig. 2.1510)
Locality: Synthetic.
Description: Characterized by powder X-ray diffraction data.
Kind of sample preparation and/or method of registration of the spectrum: A cast sample. Transmission.
Source: Nagata et al. (1981).
Wavenumbers (cm^{-1}): 491w, 258s, 236sh, 135, 96.

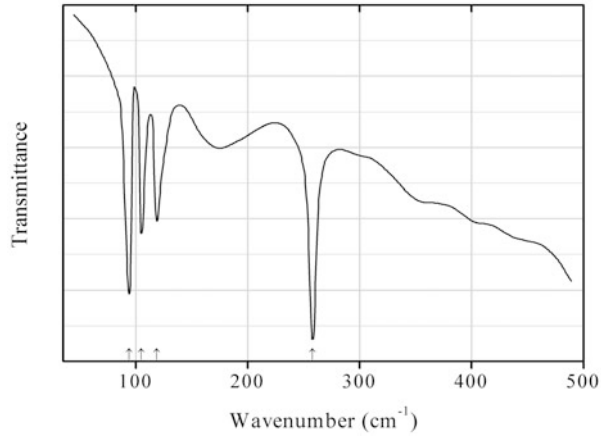

Fig. 2.1511 IR spectrum of selenium monoclinic drawn using data from Nagata et al. (1981)

Se46 Selenium monoclinic Se (Fig. 2.1511)
Locality: Synthetic.
Description: Characterized by powder X-ray diffraction data.
Kind of sample preparation and/or method of registration of the spectrum: Nujol mull. Transmission.
Source: Nagata et al. (1981).
Wavenumbers (cm^{-1}): 258s, 119, 105, 94s.

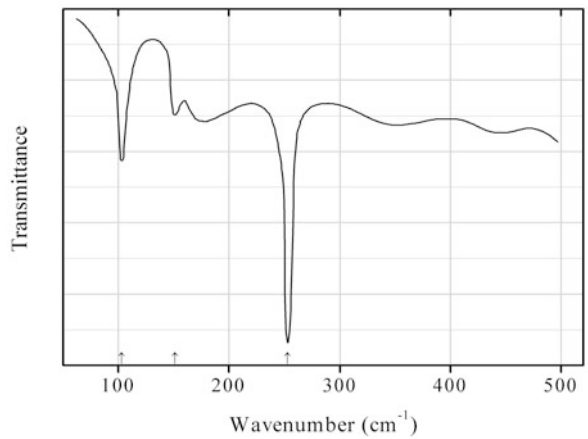

Fig. 2.1512 IR spectrum of selenium rhombohedral drawn using data from Nagata et al. (1981)

Se47 Selenium rhombohedral Se (Fig. 2.1512)
Locality: Synthetic.
Description: Characterized by powder X-ray diffraction data.
Kind of sample preparation and/or method of registration of the spectrum: Nujol mull. Transmission.
Source: Nagata et al. (1981).
Wavenumbers (cm^{-1}): 253s, 151w, 103.

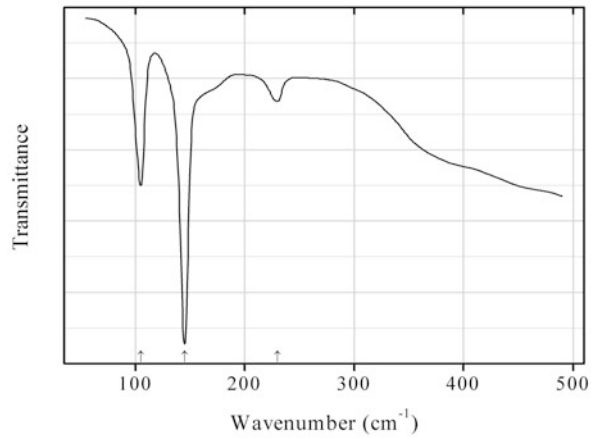

Fig. 2.1513 IR spectrum of selenium trigonal drawn using data from Nagata et al. (1981)

Se48 Selenium trigonal Se (Fig. 2.1513)
Locality: Synthetic.
Description: Characterized by powder X-ray diffraction data.
Kind of sample preparation and/or method of registration of the spectrum: Nujol mull. Transmission.
Source: Nagata et al. (1981).
Wavenumbers (cm^{-1}): 230w, 145s, 105.

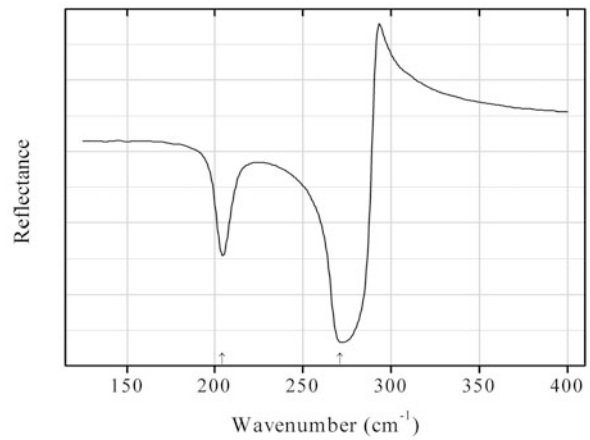

Fig. 2.1514 IR spectrum of stilleite drawn using data from Yang et al. (1999)

Se49 Stilleite ZnSe (Fig. 2.1514)
Locality: Synthetic.
Description: Layer grown on the GaAs (001) substrate.
Kind of sample preparation and/or method of registration of the spectrum: Reflection.
Source: Yang et al. (1999).
Wavenumbers (cm^{-1}): 271s, 204.

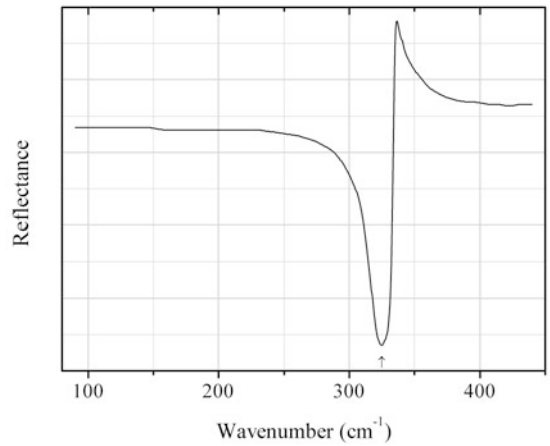

Fig. 2.1515 IR spectrum of sudovikovite drawn using data from Kliche (1985a)

Se50 Sudovikovite $PtSe_2$ (Fig. 2.1515)
Locality: Synthetic.
Description: Obtained in form of flowing polycrystalline, metallic grey powder by annealing stoichiometric mixture of the elements in evacuated quartz tube at 600–700 °C. Trigonal, $a = 3.727–3.728$, $c = 5.081–5.083$ Å. Characterized by powder X-ray diffraction data.
Kind of sample preparation and/or method of registration of the spectrum: Pressed polycrystalline disc. Reflection.
Source: Kliche (1985a).
Wavenumbers (cm^{-1}): 325.

2.19 Molybdates

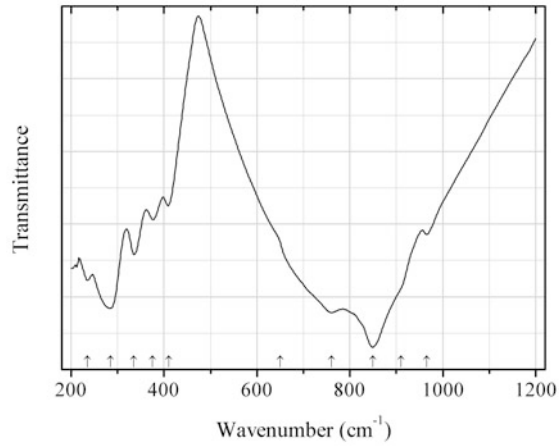

Fig. 2.1516 IR spectrum of iron(III) molybdate drawn using data from Kurzawa (1992)

Mo29 Iron(III) molybdate $Fe^{3+}{}_2(MoO_4)_3$ (Fig. 2.1516)
Locality: Synthetic.
Kind of sample preparation and/or method of registration of the spectrum: CsI disc. Transmission.
Source: Kurzawa (1992).
Wavenumbers (cm^{-1}): 965, 910sh, 850s, 760s, 650sh, 410, 375, 335, 285s, 235.

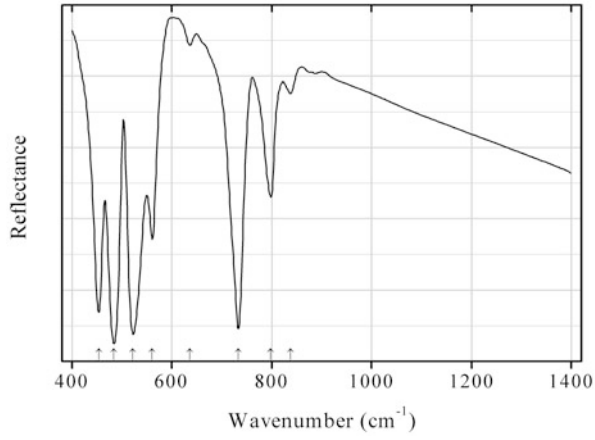

Fig. 2.1517 IR spectrum of iseite drawn using data from Das et al. (2009)

Mo30 Iseite $Mn_2Mo_3O_8$ (Fig. 2.1517)
Locality: Synthetic.
Description: Prepared by the carbothermal reduction method. The crystal structure is solved. Hexagonal, space group $P6_3mc$, a = 5.795(2), c = 10.254(2) Å. D_{meas} = 5.741 g/cm^3, D_{calc} = 5.84 g/cm^3.

Kind of sample preparation and/or method of registration of the spectrum: Attenuated total reflection of powdered mineral. KBr disc. Absorption.
Source: Das et al. (2009).
Wavenumbers (cm^{-1}): 454s, 484s, 522s, 561, 636w, 733s, 798, 838w.

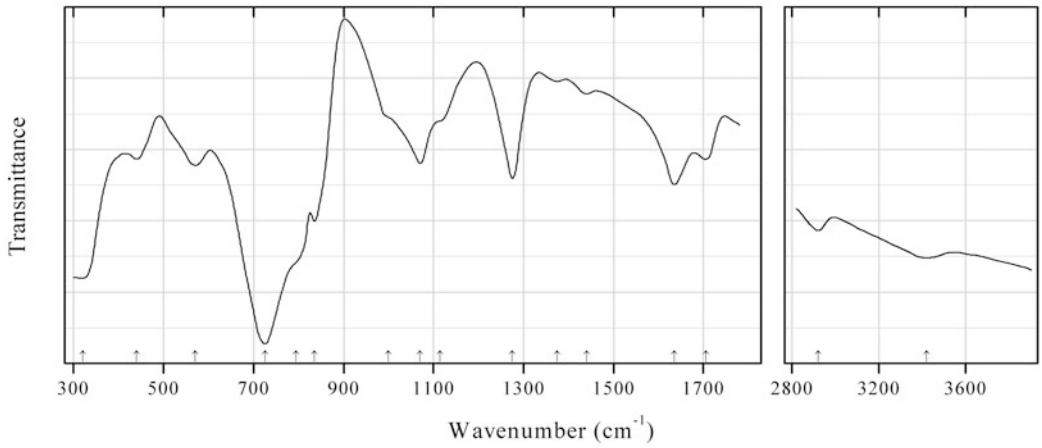

Fig. 2.1518 IR spectrum of koechlinite drawn using data from Sejkora et al. (2006b)

Mo31 Koechlinite $(BiO)_2MoO_4$ (Fig. 2.1518)
Locality: Vysoký Kámen, near Krásno, Slavkovský Les area, Czech Republic.
Description: Yellow powdery product of molybdenite alteration. Orthorhombic, a = 5.488(3), b = 16.24(1), c = 5.510(5) Å, V = 491.1 $Å^3$. D_{meas} = 2.39(3) g/cm^3, D_{calc} = 2.391 g/cm^3. Optically biaxial (−), α = 1.554(1), β = 1.558(1), γ = 1.566(1), 2 V = 70(5)°. The empirical formula is (electron microprobe): $(BiO)_{2.00}(Mo_{0.90}W_{0.06}P_{0.02}As_{0.01})O_4$.
Kind of sample preparation and/or method of registration of the spectrum: KBr disc. Transmission.
Source: Sejkora et al. (2006b).
Wavenumbers (cm^{-1}): 3420, 2920, 1705, 1635, 1440w, 1375w, 1275, 1115sh, 1070, 1000sh, 835s, 795sh, 725s, 570, 440, 320s.
Note: The bands at 3420 and 1635 cm^{-1} indicate possible presence of H_2O molecules.

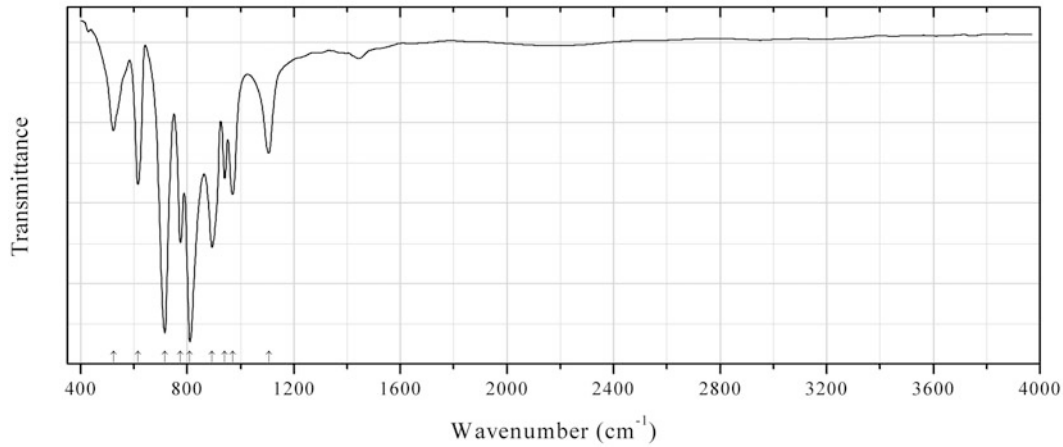

Fig. 2.1519 IR spectrum of cupromolybdite drawn using data from Liu et al. (2011)

Mo32 Cupromolybdite $Cu_3(MoO_4)_2O$ (Fig. 2.1519)
Locality: Synthetic.
Description: Nanorods obtained upon annealing $Cu_3(MoO_4)_2(OH)_2$ at 500 °C for 5 h. Confirmed by powder X-ray diffraction data.
Kind of sample preparation and/or method of registration of the spectrum: Transmission. Kind of sample preparation is not indicated.
Source: Liu et al. (2011).
Wavenumbers (cm^{-1}): 1106, 970, 941, 893, 810s, 774, 716s, 615, 523.

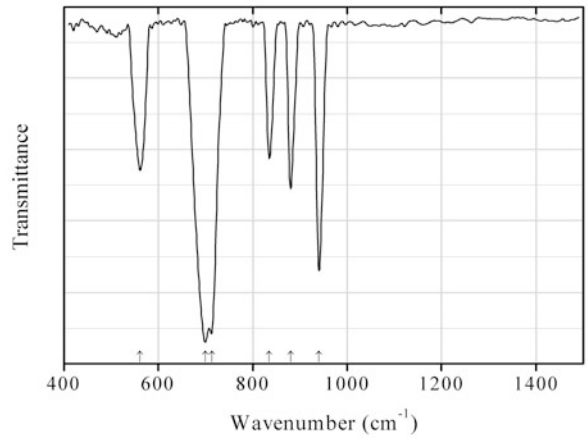

Fig. 2.1520 IR spectrum of zinc molybdate selenite drawn using data from Nguyen et al. (2011a)

Mo33 Zinc molybdate selenite $Zn_2(MoO_4)(SeO_3)$ (Fig. 2.1520)
Locality: Synthetic.
Description: Prepared in the solid-state reaction of ZnO, SeO_2, and MoO_3 in a sealed ampule at 380 °C for 24 h, then at 500 °C for 24 h, and finally at 550 °C for 48 h before being cooled to room temperature at 6 °C per 1 h. Monoclinic, space group $P2_1$, a = 5.1809(4) Å, b = 8.3238(7) Å, c = 7.1541(6) Å, β = 99.413(1)°, V = 305.2(1) $Å^3$, Z = 2.
Kind of sample preparation and/or method of registration of the spectrum: KBr disc. Transmission.
Source: Nguyen et al. (2011a).
Wavenumbers (cm^{-1}): 940s, 880, 835, 713s, 699s, 561.

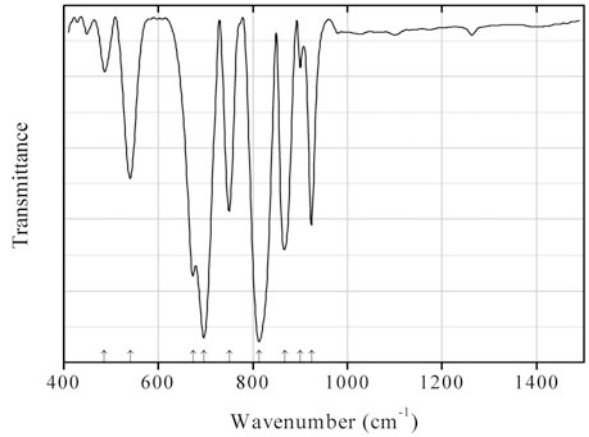

Fig. 2.1521 IR spectrum of zinc molybdate tellurite drawn using data from Nguyen et al. (2011a)

Mo34 Zinc molybdate tellurite $Zn_2(MoO_4)(TeO_3)$ (Fig. 2.1521)
Locality: Synthetic.
Description: Prepared in the reaction of ZnO, TeO_2, and MoO_3 in the presence of NH_4Cl/NH_3 1 M buffer solution at 230 °C for 2 days. The crystal structure is solved. Monoclinic, space group $P2_1$, a = 5.178(4) Å, b = 8.409(6) Å, c = 7.241(5) Å, β = 99.351(8)°, V = 311.1(4) Å^3, Z = 2.
Kind of sample preparation and/or method of registration of the spectrum: KBr disc. Transmission.
Source: Nguyen et al. (2011a).
Wavenumbers (cm^{-1}): 924, 900w, 867, 813s, 750, 697s, 673s, 541, 486w.
Note: In the cited paper the wavenumber 540.86 cm^{-1} is erroneously indicated as 640.86 cm^{-1}.

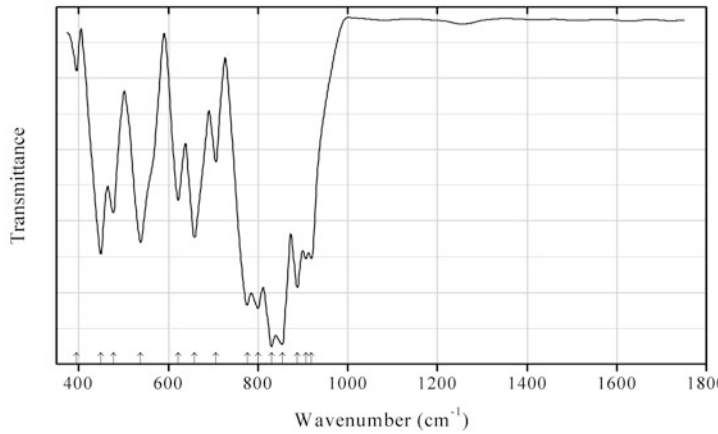

Fig. 2.1522 IR spectrum of barium tellurite dimolybdate I drawn using data from Zhang et al. (2011b)

Mo35 Barium tellurite dimolybdate I α-$BaTeMo_2O_9$ (Fig. 2.1522)
Locality: Synthetic.
Description: Synthesized in the solid-state reaction between $BaCO_3$, TeO_2, and MoO_3 in air at 580 °C for 24 h. The crystal structure is solved. Orthorhombic, space group $Pca2_1$, a = 14.8683(2) Å, b = 5.6636(1) Å, c = 17.6849(3) Å, V = 1489.21(4) Å^3, Z = 8. D_{calc} = 5.360 g/cm^3.

Kind of sample preparation and/or method of registration of the spectrum: KBr disc. Transmission.
Source: Zhang et al. (2011b).
Wavenumbers (cm^{-1}): 919, 907, 888s, 854s, 830s, 800s, 776s, 706, 658, 622, 538, 477, 449, 395w.

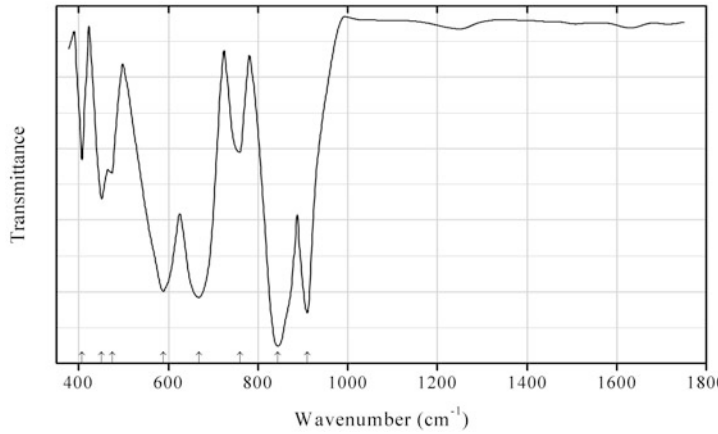

Fig. 2.1523 IR spectrum of barium tellurite dimolybdate II drawn using data from Zhang et al. (2011b)

Mo36 Barium tellurite dimolybdate II β-$BaTeMo_2O_9$ (Fig. 2.1523)
Locality: Synthetic.
Description: The crystal structure is solved. Monoclinic, space group $P2_1$, a = 5.5346(1) Å, b = 7.4562(1) Å, c = 8.8342(1) Å, β = 90.897(1)°, V = 364.517(9) $Å^3$, Z = 2. D_{calc} = 5.474 g/cm^3.
Kind of sample preparation and/or method of registration of the spectrum: KBr disc. Transmission.
Source: Zhang et al. (2011b).
Wavenumbers (cm^{-1}): 910s, 844s, 760, 668s, 588s, 474, 451, 407.

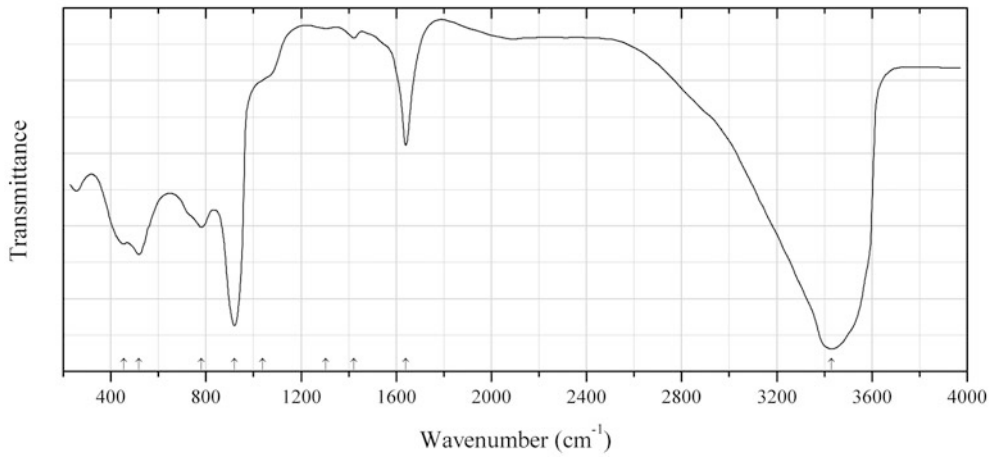

Fig. 2.1524 IR spectrum of tengchongite drawn using data from Zhangru et al. (1986)

Mo37 Tengchongite $Ca(UO_2)_6(MoO_4)_2O_5 \cdot 12H_2O$ (Fig. 2.1524)

Locality: An unknown uranium occurrence, Tengchong Co., Yunnan province, China (type locality?).
Description: Yellow tabular crystals from the association with studtite, calcurmolite, and kivuite. Holotype sample. Orthorhombic, a = 15.616(4), b = 13.043(6), c = 17.716(14) Å. D_{calc} = 4.24 g/cm^3. Optically biaxial (−), α = 1.663(2), β = 1.760(2), γ = 1.762(2), 2 V = 16°. The empirical formula is $0.93CaO \cdot 6.18UO_2 \cdot 1.89MoO_3 \cdot 11.88H_2O$. The strongest lines of the powder X-ray diffraction pattern [d, Å (I, %) (hkl)] are: 8.84 (100) (002), 5.37 (50) (013), 4.27 (50) (104), 3.38 (70) (304, 420), 3.17 (80) (413), 2.04 (40) (308).
Kind of sample preparation and/or method of registration of the spectrum: No data.
Source: Zhangru et al. (1986).
Wavenumbers (cm^{-1}): 3430s, 1640, 1422w, 1305w, 1039sh, 920s, 780, 519, 454.
Note: The wavenumbers were partly determined by us based on spectral curve analysis of the published spectrum.

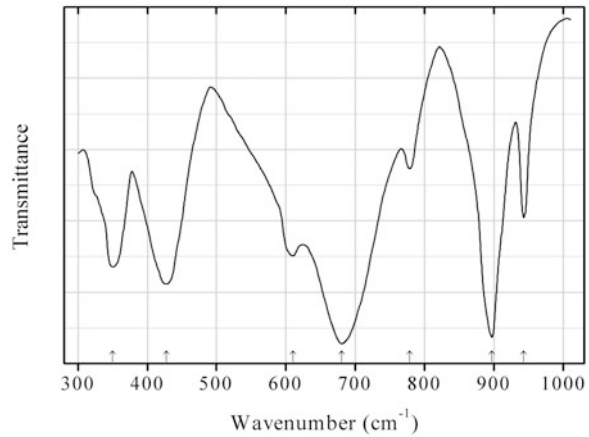

Fig. 2.1525 IR spectrum of zinc tellurite molybdate drawn using data from Botto and Baran (1980)

Mo38 Zinc tellurite molybdate $ZnTeMoO_6$ (Fig. 2.1525)
Locality: Synthetic.
Description: Synthesized by a solid-state reaction at 600 °C.
Kind of sample preparation and/or method of registration of the spectrum: KBr disc. Transmission.
Source: Botto and Baran (1980).
Wavenumbers (cm^{-1}): 943, 897s, 778w, 680s, 610, 428s, 350s.

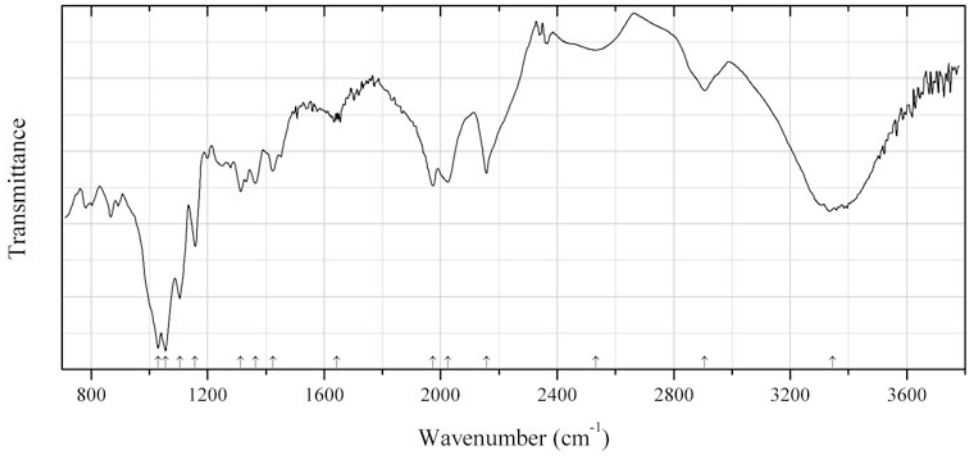

Fig. 2.1526 IR spectrum of mambertiite drawn using data from Orlandi et al. (2015)

Mo39 Mambertiite $BiMo^{5+}{}_{2.8}O_8(OH)$ (Fig. 2.1526)
Locality: Su Seinargiu, Sarroch, Cagliari, Sardinia, Italy (type locality).
Description: Pale yellow tabular crystals from the association with ferrimolybdite, muscovite, quartz, sardignaite, and wulfenite. Holotype sample. Triclinic, space group *P*-1, a = 5.854(2), b = 9.050(3), c = 7.637(3)Å, α = 112.85(1)°, β = 102.58(1)°, γ = 90.04(1)°, V = 362.3(2) Å^3, Z = 2. D_{calc} = 5.720 g/cm^3. The empirical formula is (electron microprobe): $Bi_{0.99}(Mo^{5+}_{2.74}W_{0.05})O_{7.97}(OH)_{1.03}$. The strongest lines of the powder X-ray diffraction pattern are observed at 6.80, 4.92, 3.417, 3.136, 2.850, 2.772, and 2.088 Å.
Kind of sample preparation and/or method of registration of the spectrum: Absorbance of a powdered sample prepared using a diamond compression cell.
Source: Orlandi et al. (2015).
Wavenumbers (cm^{-1}): 3345, 2907, 2532, 2157, 2024sh, 1974, 1644, 1424, 1364, 1314, 1157, 1105, 1055s, 1030s.
Note: The wavenumbers were determined by us based on spectral curve analysis of the published spectrum. The wavenumbers of the maxima of the strongest bands (at 1055 and 1030 cm^{-1}) are anomalously high for molybdates. The bands in the range from 1900 to 2600 cm^{-1} indicate the presence of the acid groups Mo^{5+}–OH.

2.20 Tellurides, Tellurites, and Tellurates

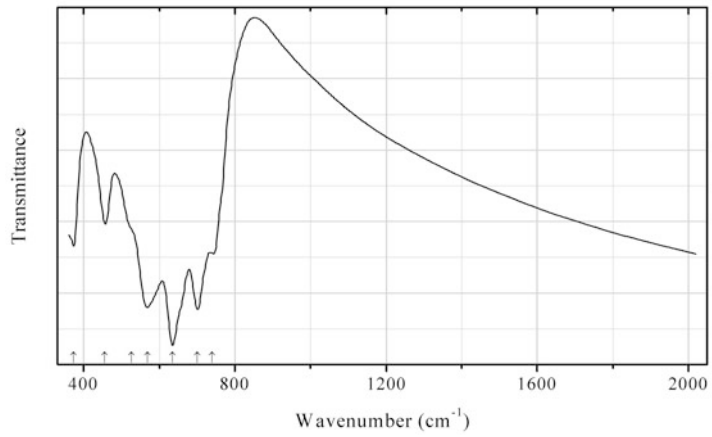

Fig. 2.1527 IR spectrum of chekhovichite obtained by N.V. Chukanov

Te11 Chekhovichite $Bi^{3+}{}_2Te^{4+}{}_4O_{11}$ (Fig. 2.1527)
Locality: Zod mine, Sotk deposit, Vardenis, Armenia (type locality).
Description: Greyish yellow grains from ancient slag.
Kind of sample preparation and/or method of registration of the spectrum: KBr disc. Absorption.
Wavenumbers (cm^{-1}): 740, 701s, 634s, 568s, 525sh, 454, 373.
Note: The spectrum of chekhovichite published earlier (Chukanov, 2014a, spectrum Te8) corresponds to a poor-crystallized glassy variety or analogue of chekhovichite.

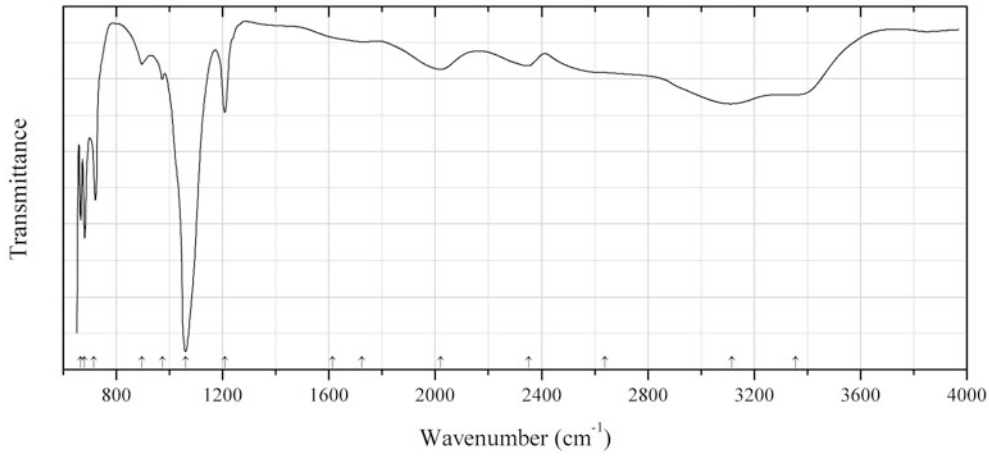

Fig. 2.1528 IR spectrum of bairdite drawn using data from Kampf et al. (2013a)

Te12 Bairdite $Pb_2Cu^{2+}{}_4Te^{6+}{}_2O_{10}(OH)_2(SO_4)\cdot H_2O$ (Fig. 2.1528)
Locality: Otto Mountain, near Baker, San Bernardino Co., California, USA (type locality).
Description: Lime green tabular crystals from the association with quartz, khinite, cerussite, goethite, and hematite. Holotype sample. Monoclinic, space group $P2_1/c$, a = 14.3126(10), b = 5.2267(3),

c = 9.4878(5) Å, β = 106.815(7)°, V = 679.41(7) Å^3, Z = 2. D_{calc} = 6.062 g/cm^3. Optically biaxial (+), α = 1.953, β = 1.966, γ = 2.039, 2 V = 47(2)°. The empirical formula is $Pb_{2.05}Ca_{0.01}Cu_{3.99}Te_{2.00}S_{0.96}O_{17.00}H_{4.16}$. The strongest lines of the powder X-ray diffraction pattern [d, Å (I, %) (hkl)] are: 4.77 (50) (110, −102), 4.522 (66) (002, 011, −111), 3.48 multiple (62) (211, −311, 012, 400), 2.999 (97) (311, −411), 2.701 (79) (−502, −113, −213), 2.614 (100) (013, 020), 1.727 multiple (−622, −415, 620, 015, 711), 1.509 (83) (−911, 033, 324).

Kind of sample preparation and/or method of registration of the spectrum: Single-crystal platelet. Absorption.

Source: Kampf et al. (2013a).

Wavenumbers (cm^{-1}): 3356, 3117, 2638sh, 2351, 2021, 1723w, 1613sh, 1208, 1060s, 973w, 896w, 716s, (681s), (666s).

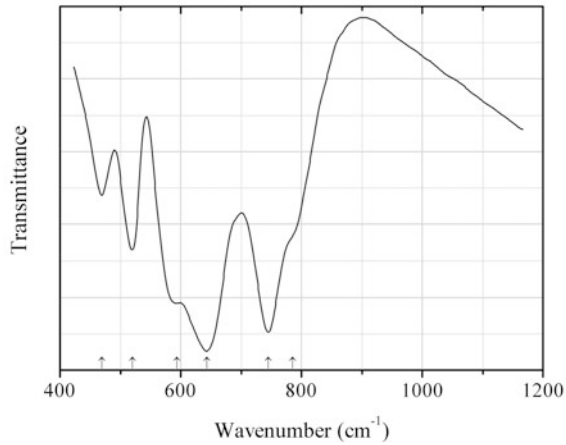

Fig. 2.1529 IR spectrum of balyakinite drawn using data from Dimitriev et al. (1983)

Te13 Balyakinite $Cu^{2+}(Te^{4+}O_3)$ (Fig. 2.1529)

Locality: Synthetic.

Description: No data.

Kind of sample preparation and/or method of registration of the spectrum: Suspension in Nujol. Absorption.

Source: Dimitriev et al. (1983).

Wavenumbers (cm^{-1}): 785sh, 745s, 644s, 594, 520, 469.

Note: The wavenumbers were determined by us based on spectral curve analysis of the published spectrum.

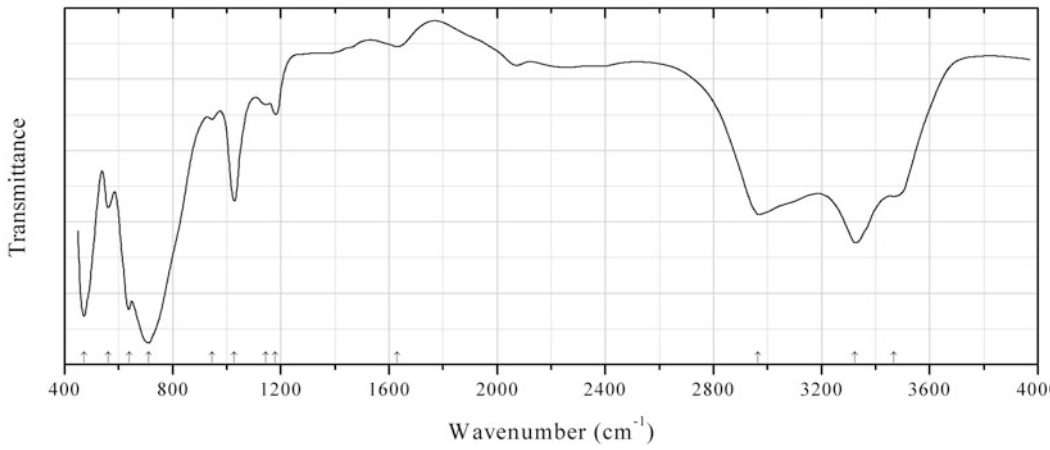

Fig. 2.1530 IR spectrum of brumadoite drawn using data from Atencio et al. (2008)

Te14 Brumadoite $Cu_3(Te^{6+}O_4)(OH)_4 \cdot 5H_2O$ (Fig. 2.1530)
Locality: Pedra Preta mine, Serra das Éguas, Brumado, Bahia, Brazil (type locality).
Description: Blue microcrystalline aggregate from the association with magnesite, mottramite, and quartz. Holotype sample. Monoclinic, space group $P2_1/m$ or $P2_1$, a = 8.629(2), b = 5.805(2), c = 7.654(2) Å, β = 103.17(2)°, V = 373.3(2) Å^3, Z = 2. D_{calc} = 4.768 g/cm^3. Mean refractive index is ~1.79. The empirical formula is $Cu_{2.90}Pb_{0.04}Ca_{0.01}(Te_{0.93}Si_{0.05})O_{3.92}(OH)_{3.84} \cdot 5.24H_2O$. The strongest lines of the powder X-ray diffraction pattern [d, Å (I, %) (hkl)] are: 8.432 (100) (100), 3.162 (66) (−202), 2.385 (27) (220), 2.291 (12) (−122), 1.916 (11) (312), 1.666 (14) (−422, 114), 1.452 (10) (323, 040), 1.450 (10) (422, 403).
Kind of sample preparation and/or method of registration of the spectrum: Transmission. Kind of sample preparation is not indicared.
Source: Atencio et al. (2008).
Wavenumbers (cm^{-1}): 3466, 3323s, 2965, 1629w, 1180, 1145w, 1028, 945w, 710s, 638s, 561, 472s.

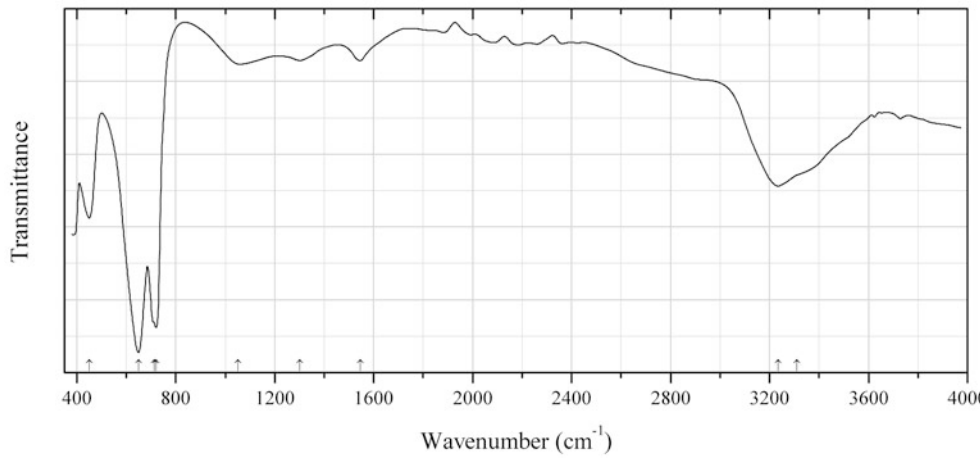

Fig. 2.1531 IR spectrum of choloalite drawn using data from Lam (1998)

Te15 Choloalite $(Pb,Ca)_3(Cu,Sb)_3Te_6O_{18}Cl$ (Fig. 2.1531)

Locality: Not indicated.
Description: Choloalite crystals were provided by the Canadian Museum of Nature. The crystal structure is solved. Cubic, space group $P4_132$, a = 12.520(2) Å.
Kind of sample preparation and/or method of registration of the spectrum: Diamond-anvil cell microsampling. A randomly-oriented powder. Transmission.
Source: Lam (1998).
Wavenumbers (cm^{-1}): 3310sh, 3235, 1546, 1301, 1052, 721s, 713sh, 650s, 451.
Note: The wavenumbers were determined by us based on spectral curve analysis of the published spectrum. The band positions denoted by Lam (1998) as 3260 and 1590 cm^{-1} were determined by us at 3235 and 1546 cm^{-1}, respectively.

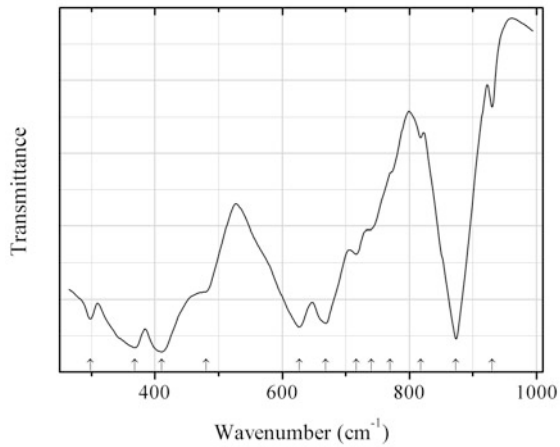

Fig. 2.1532 IR spectrum of cliffordite drawn using data from Botto and Baran (1982)

Te16 Cliffordite $UTe^{4+}{}_3O_9$ (Fig. 2.1532)
Locality: Synthetic.
Description: Synthesized in the reaction between powdered UO_3 and TeO_2 at 650 °C.
Kind of sample preparation and/or method of registration of the spectrum: KBr disc. Transmission.
Source: Botto and Baran (1982).
Wavenumbers (cm^{-1}): 930w, 873s, 818w, 770sh, 740sh, 717, 668s, 627s, 480sh, 410s, 368s, 298.

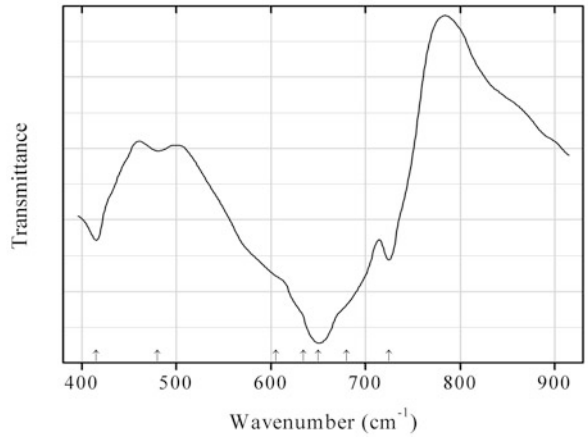

Fig. 2.1533 IR spectrum of fairbankite polymorph Te17 drawn using data from Stavrakieva et al. (1988)

Te17 Fairbankite polymorphTe17 α-Pb($Te^{4+}O_3$) (Fig. 2.1533)
Locality: Synthetic.
Description: Synthesized from the stoichiometric mixture of TeO_2 and PbO. Monoclinic, a = 27.59, b = 4.61, c = 17.97 Å, β = 112.90°. Confirmed by electron microprobe analysis and powder X-ray diffraction data.
Kind of sample preparation and/or method of registration of the spectrum: KBr disc. Absorption.
Source: Stavrakieva et al. (1988).
Wavenumbers (cm^{-1}): 725, 650sh, 680s, 634sh, 605sh, 480w, 415.
Note: The wavenumbers were partly determined by us based on spectral curve analysis of the published spectrum.

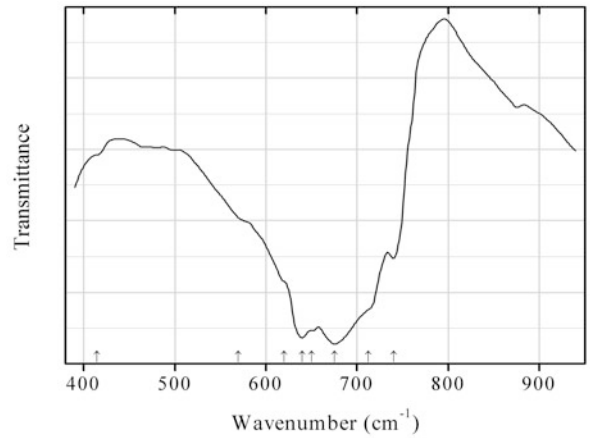

Fig. 2.1534 IR spectrum of fairbankite polymorph Te18 drawn using data from Stavrakieva et al. (1988)

Te18 Fairbankite polymorph Te18 β-Pb($Te^{4+}O_3$) (Fig. 2.1534)
Locality: Synthetic.

Description: Tetragonal, $a \approx 5.3$, $c \approx 11.9$ Å. Confirmed by electron microprobe analysis and powder X-ray diffraction data.
Kind of sample preparation and/or method of registration of the spectrum: KBr disc. Absorption.
Source: Stavrakieva et al. (1988).
Wavenumbers (cm^{-1}): 740, 712sh, 675s, 650sh, 640s, 620sh, 570sh, 415sh.
Note: The wavenumbers were partly determined by us based on spectral curve analysis of the published spectrum.

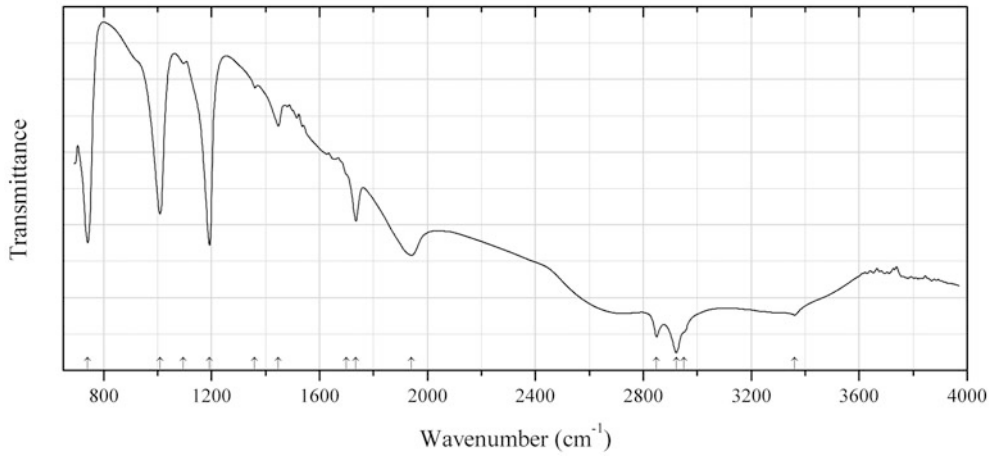

Fig. 2.1535 IR spectrum of frankhawthorneite drawn using data from Roberts et al. (1995b)

Te19 Frankhawthorneite $Cu_2(Te^{6+}O_4)(OH)_2$ (Fig. 2.1535)
Locality: Centennial Eureka mine, Juab Co., Utah, USA (type locality).
Description: Leaf green crystals from the association with mcalpineite, pyrite, hematite, acanthite, chrysocolla, connellite, enargite, hinsdalite, and svanbergite. Holotype sample. Monoclinic, space group $P2_1/n$, $a = 9.095(3)$, $b = 5.206(2)$, $c = 4.604(1)$ Å, $\beta = 98.69(2)°$, $V = 215.5(1)$ $Å^3$, $Z = 2$. $D_{calc} = 5.44$ g/cm^3. The empirical formula is $Cu_{2.03}Te^{6+}_{0.99}O_{4.00}(OH)_{2.00}$. The strongest lines of the powder X-ray diffraction pattern [*d*, Å (*I*, %) (*hkl*)] are: 4.506 (40) (110, 200), 4.337 (60) (−101), 3.838 (50) (101), 2.891 (70) (−211), 2.598 (100) (020, 321, 211), 1.834 (40) (−312), 1.713 (40) (022), 1.500 (40) (330, 231, 600).
Kind of sample preparation and/or method of registration of the spectrum: Transmission. A diamond-anvil microsample cell positioned in the microscope accessory was used. Empty diamond-anvil cell was used as a reference sample.
Source: Roberts et al. (1995b).
Wavenumbers (cm^{-1}): 3360, 2950sh, 2922, 2849, 1941, 1735, 1700sh, 1447, 1360, 1192s, 1095, 1008s, 741s.
Note: The wavenumbers were determined by us based on spectral curve analysis of the published spectrum. The bands in the range from 2800 to 3100 cm^{-1} correspond to the admixture of organic substance.

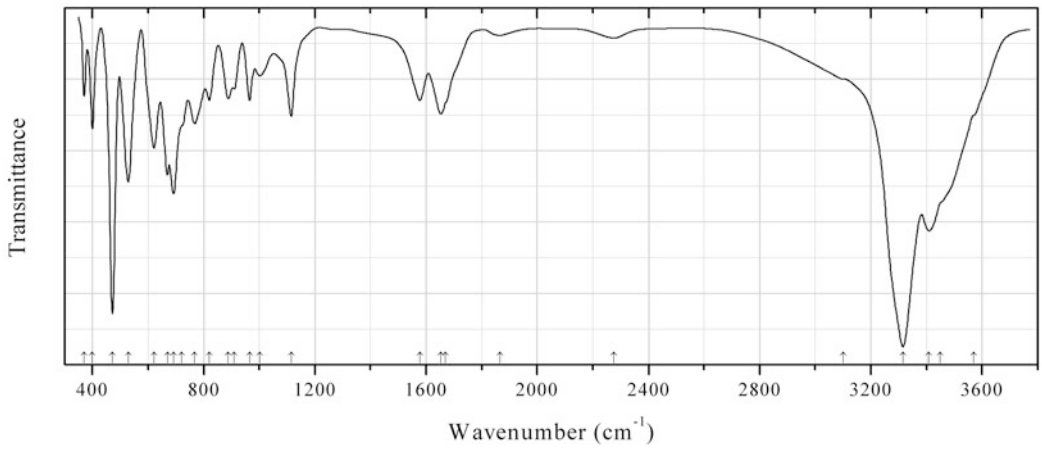

Fig. 2.1536 IR spectrum of raisaite obtained by N.V. Chukanov

Te20 Raisaite $CuMg[Te^{6+}O_4(OH)_2]\cdot 6H_2O$ (Fig. 2.1536)
Locality: Sentyabr'skoe Ag-Au occurrence, Ilirney ore district, 110 km SE of the town of Bilibino, Chukotka peninsula, North-Eastern Region, Russia (type locality).
Description: Blue crystals from the association with gypsum, paratellurite, zemannite, malachite, azurite, cerussite, anglesite, brochantite, linarite, posnjakite, chlorargyrite, gold, brucite, etc. Holotype sample. Monoclinic, space group *C*2/*c*, a = 9.9078(2), b = 10.1325(3), c = 9.8375(2) Å, β = 91.839 (2)°, V = 987.09(4) $Å^3$, Z = 4. D_{meas} = 2.82(1) g/cm^3, D_{calc} = 2.828 g/cm^3. Optically biaxial (+), α = 1.626(3), β = 1.642(5), γ = 1.665(3), 2 V = 80(10)°. The empirical formula is (electron microprobe): $Cu_{0.96}Mg_{1.11}Te_{0.99}S_{0.02}O_{4.20}(OH)_{1.80}\cdot 6H_2O$. The strongest lines of the powder X-ray diffraction pattern [d, Å (I, %) (hkl)] are: 7.088 (100) (110), 5.815 (35) (−111), 5.690 (23) (111), 4.949 (91) (200, 002), 3.310 (21) (221), 2.694 (29) (−132).
Kind of sample preparation and/or method of registration of the spectrum: KBr disc. Absorption.
Wavenumbers (cm^{-1}): 3570sh, 3450sh, 3409s, 3315s, 3100sh, 2276w, 1865w, 1670sh, 1653, 1577, 1115, 1002w, 965, 910, 889, 820, 768, 720sh, 692, 670, 621, 529, 472s, 400, 371.

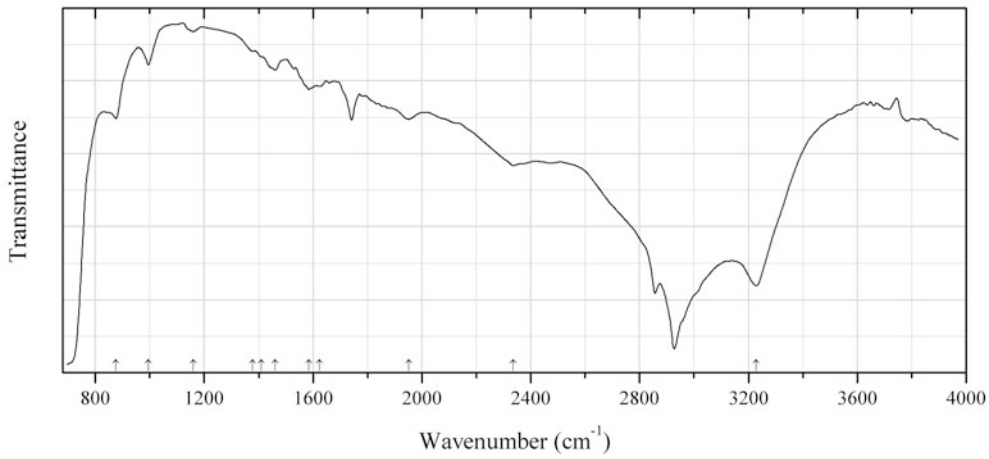

Fig. 2.1537 IR spectrum of jensenite drawn using data from Roberts et al. (1996a)

Te21 Jensenite $Cu^{2+}{}_3Te^{6+}O_6 \cdot 2H_2O$ (Fig. 2.1537)
Locality: Centennial Eureka mine, Tintic dishict, Juab Co., Utah, USA (type locality).
Description: Green crystals from the association with mcalpineite, xocomecatlite, quartz, etc. Holotype sample. Monoclinic, space group $P2_1/n$, a = 9.204(2), b = 9.170(2), c = 7.584(1) Å, β = 102.32(3)°, V = 625.3(3) Å^3, Z = 4. D_{calc} = 4.76 g/cm^3. The empirical formula is $(Cu_{2.92}Zn_{0.02})Te^{6+}{}_{1.01}O_{5.97} \cdot 2.03H_2O$. The strongest lines of the powder X-ray diffraction pattern [d, Å (I, %) (hkl)] are: 6.428 (100) (−101, 110), 3.217 (70) (−202), 2.601 (40) (202), 2.530 (50) (230), 2.144 (35) (−331), 1.750 (35) (−432).
Kind of sample preparation and/or method of registration of the spectrum: Powder infrared-absorption spectrum was obtained using a diamond-anvil microsample cell.
Source: Roberts et al. (1996a).
Wavenumbers (cm^{-1}): 3228s, 2336, 1953, 1624w, 1584, 1461, 1411sh, 1377w, 1159, 995, 876s.
Note: The wavenumbers were determined by us based on spectral curve analysis of the published spectrum. The bands at 2928, 2857, and 1742 cm^{-1} are due to the contamination by an organic substance.

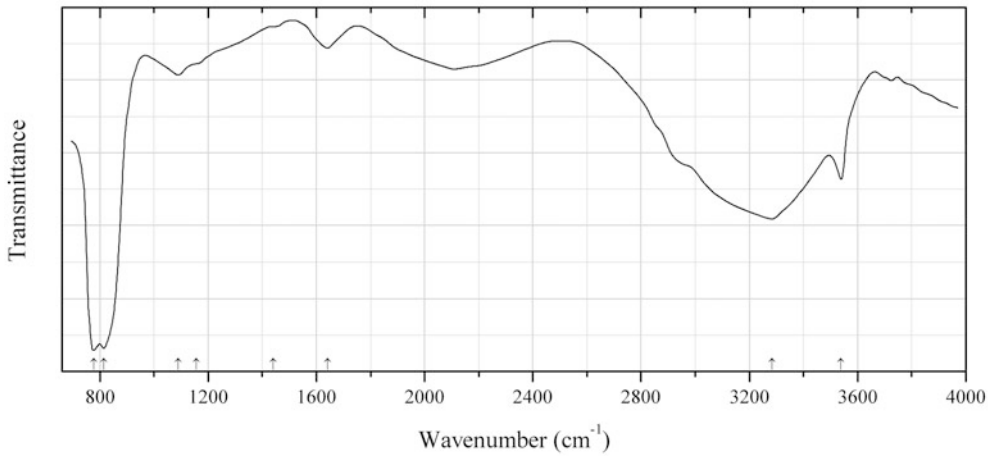

Fig. 2.1538 IR spectrum of juabite drawn using data from Roberts et al. (1997a)

Te22 Juabite $CaCu_{10}(TeO_3)_4(AsO_4)_4(OH)_2 \cdot 4H_2O$ (Fig. 2.1538)
Locality: Centennial Eureka mine, Tintic district, Juab Co., Utah, USA (type locality).
Description: Green massive from the association with enargite and beudantite. Holotype sample. Triclinic, a = 8.984(5), b = 10.079(7), c = 8.975(5) Å, α = 102.68(7)°, β = 92.45(6)°, γ = 70.45(5)°, V = 646.8(8) Å^3, Z = 2. D_{calc} = 4.59 g/cm^3. The empirical formula is $(Cu_{5.01}Pb_{0.03})(TeO_4)_{1.93}(AsO_4)_{2.07} \cdot 3.00H_2O$. The strongest lines of the powder X-ray diffraction pattern [d, Å (I, %) (hkl)] are: 9.28 (70) (010), 4.65 (70) (020), 3.097 (100) (030, −211), 3.018 (60) (212), 2.658 (50) (−301), 2.468 (50) (−22–2), 1.740 (−11–5, 521, −151).
Kind of sample preparation and/or method of registration of the spectrum: Diamond-anvil cell microsampling.
Source: Roberts et al. (1997a).
Wavenumbers (cm^{-1}): 3539, 3283s, 1642, 1440sh, 1156sh, 1089, 814s, 777s.
Note: The wavenumbers were partly determined by us based on spectral curve analysis of the published spectrum.

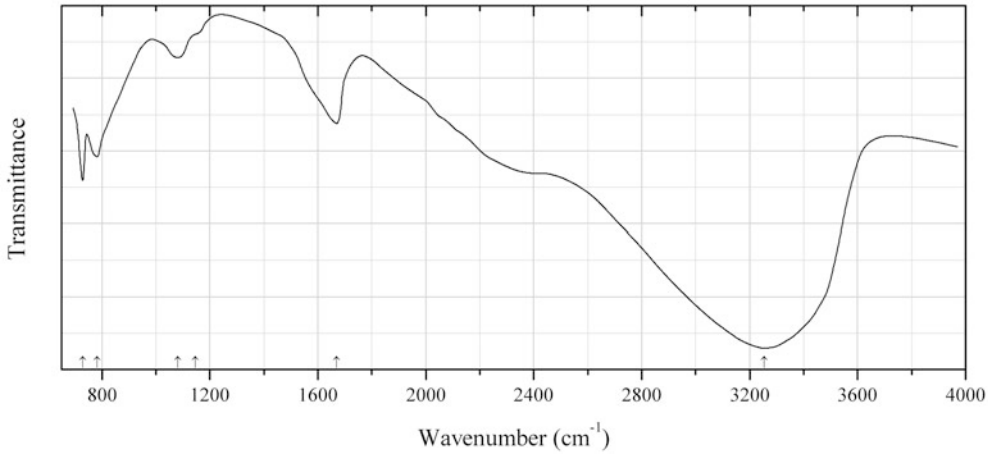

Fig. 2.1539 IR spectrum of leisingite drawn using data from Roberts et al. (1996b)

Te23 Leisingite $CuMg_2Te^{6+}{}_6 \cdot 6H_2O$ (Fig. 2.1539)
Locality: Centennial Eureka mine, Juab Co., Utah, USA (type locality).
Description: Yellow aggregates of platy crystals from the association with jensenite, cesbronite, and hematite. Holotype sample. Hexagonal, space group $P3$, $a = 5.305(1)$, $c = 9.693(6)$, $V = 236.2(2)$ Å^3, $Z = 1$. $D_{calc} = 3.41$ g/cm^3. Optically biaxial (−), $\omega = 1.803(3)$, $\varepsilon = 1.581$ (calc.). The empirical formula is: $Cu_{1.00}(Mg_{0.77}Cu_{0.56}Fe_{0.48}Zn_{0.03})Te^{6+}{}_{1.06}O_{6.02} \cdot 5.98H_2O$. The strongest lines of the powder X-ray diffraction pattern [*d*, Å (*I*, %) (*hkl*)] are: 9.70 (100) (001), 4.834 (80) (002), 4.604 (60) (100), 2.655 (60) (110), 2.556 (70) (111), 2.326 (70) (112).
Kind of sample preparation and/or method of registration of the spectrum: The procedures for acquiring the IR absorption spectrum are identical to those described by Roberts et al. (1994).
Source: Roberts et al. (1996b).
Wavenumbers (cm^{-1}): 3253s, 1670, 1146sh, 1082w, 782, 728s.
Note: The wavenumbers were partly determined by us based on spectral curve analysis of the published spectrum.

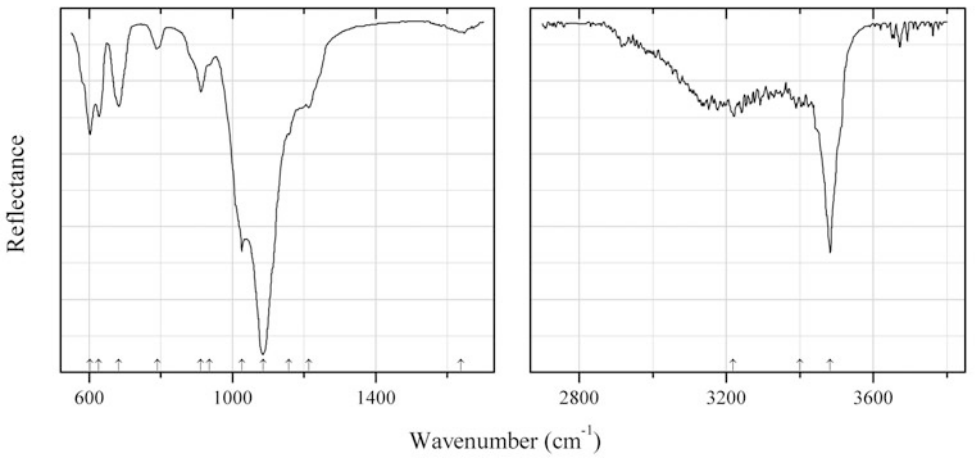

Fig. 2.1540 IR spectrum of mackayite drawn using data from Frost and Dickfos (2009)

Te24 Mackayite $Fe^{3+}Te^{4+}{}_2O_5(OH)$ (Fig. 2.1540)
Locality: Moctezuma (La Bambolla) mine, Moctezuma, Sonora, Mexico.
Description: No data.
Kind of sample preparation and/or method of registration of the spectrum: Attenuated total reflection of powdered mineral.
Source: Frost and Dickfos (2009).
Wavenumbers (cm^{-1}): 3483s, 3400, 3218, 1637w, 1213, 1157sh, 1085s, 1026, 936, 912, 790, 682w, 627w, 602.
Note: In the cited paper, wavenumbers are indicated for the maxima of individual bands obtained as a result of the spectral curve analysis. The wavenumbers were determined by us based on spectral curve analysis of the published spectrum. The bands at 1637, 1157, and 1085 cm^{-1} indicate that the sample is greatly contaminated by another mineral (opal?).

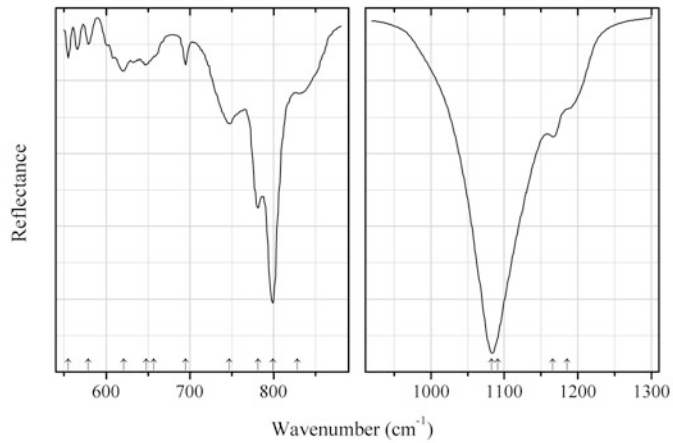

Fig. 2.1541 IR spectrum of moctezumite drawn using data from Frost et al. (2009b)

Te25 Moctezumite $Pb(UO_2)(TeO_3)_2$ (Fig. 2.1541)
Locality: Moctezuma (La Bambolla) Mine, Sonora, Mexico (type locality).
Description: No data.
Kind of sample preparation and/or method of registration of the spectrum: Attenuated total reflection of powdered mineral. KBr disc. Transmission.
Source: Frost et al. (2009b).
Wavenumbers (cm^{-1}): 1185sh, 1166w, 1091sh, 1083s, 828, 799s, 781, 747, 695w, 648w, 621w, 579w, 657w, 555w.
Note: In the cited paper, the wavenumbers are indicated only for the maxima of individual bands obtained as a result of the spectral curve analysis. The wavenumbers were determined by us based on spectral curve analysis of the published spectrum. The bands at 1083, 799, 781, and 695 cm^{-1} corresponding to quartz are erroneously attributed to moctezumite.

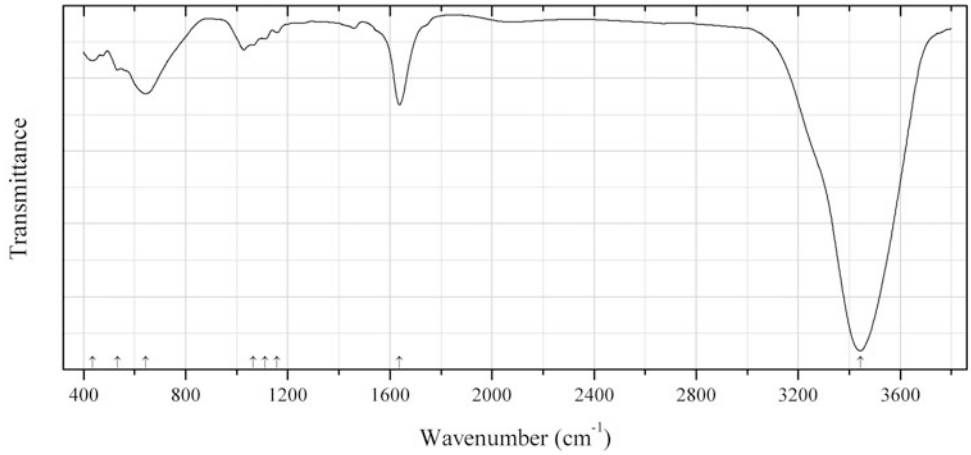

Fig. 2.1542 IR spectrum of montanite drawn using data from Sejkora et al. (2006a)

Te26 Montanite $Bi^{3+}{}_2Te^{6+}O_6 \cdot 2H_2O$ (Fig. 2.1542)
Locality: Župkov, Banská Bystrica, Vtáčnik Mts., Slovakia.
Description: Greenish to gray coatings on tetradymite. The empirical formula is $(Bi_{1.87}As_{0.01})Te_{1.07}O_{6.00} \cdot 1.97H_2O$. The strongest lines of the powder X-ray diffraction pattern [*d*, Å (*I*, %)] are: 3.513 (100), 3.205 (20), 2.800 (23), 2.606 (43), 2.092 (15), 1.9071 (39).
Kind of sample preparation and/or method of registration of the spectrum: KBr disc. Absorption.
Source: Sejkora et al. (2006a).
Wavenumbers (cm^{-1}): 3443s, 1638, 1158w, 1111, 1064sh, 643, 532, 436w.
Note: The bands at 3443 and 1638 cm^{-1} are anomalously strong (adsorbed water?).

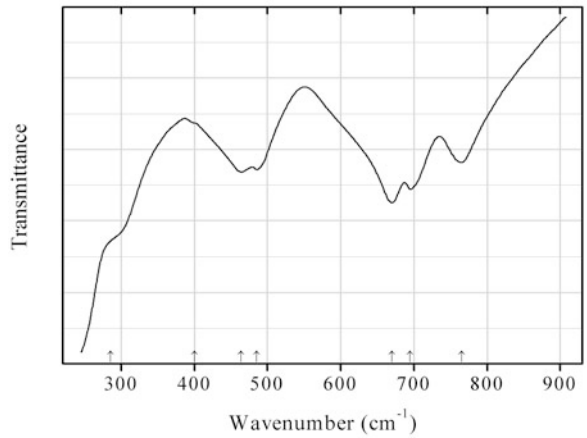

Fig. 2.1543 IR spectrum of zinc tellurite drawn using data from Bürger et al. (1992)

Te27 Zinc tellurite $Zn(Te^{4+}O_3)$ (Fig. 2.1543)
Locality: Synthetic.
Description: Synthesized by a solid-state reaction. Identified by powder X-ray diffraction data.

Kind of sample preparation and/or method of registration of the spectrum: KBr disc. Transmission.
Source: Bürger et al. (1992).
Wavenumbers (cm^{-1}): 765, 695s, 670s, 485w, 464, 400sh, 285sh.
Note: The wavenumbers were partly determined by us based on spectral curve analysis of the published spectrum.

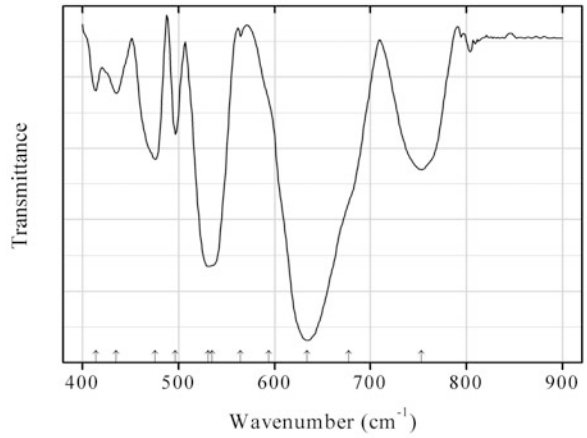

Fig. 2.1544 IR spectrum of barium magnesium tellurite-tellurate drawn using data from Yeon et al. (2012b)

Te28 Barium magnesium tellurite-tellurate $BaMgTe^{4+}Te^{6+}O_7$ (Fig. 2.1544)
Locality: Synthetic.
Description: Prepared in the solid-state reaction between $BaCO_3$, $MgCO_3$, TeO_2, and $H_2TeO_4 \cdot 2H_2O$. The crystal structure is solved. Orthorhombic, space group *Ama*2, $a = 5.558(2)$ Å, $b = 15.215(6)$ Å, $c = 7.307(3)$ Å, $V = 617.9(4)$ $Å^3$, $Z = 4$. The sample is characterized by the powder X-ray diffraction pattern.
Kind of sample preparation and/or method of registration of the spectrum: Transmission.
Source: Yeon et al. (2012b).
Wavenumbers (cm^{-1}): 753, 677sh, 634s, 594sh, 565w, 535sh, 531s, 497, 476, 435, 414.
Note: The wavenumbers were determined by us based on spectral curve analysis of the published spectrum.

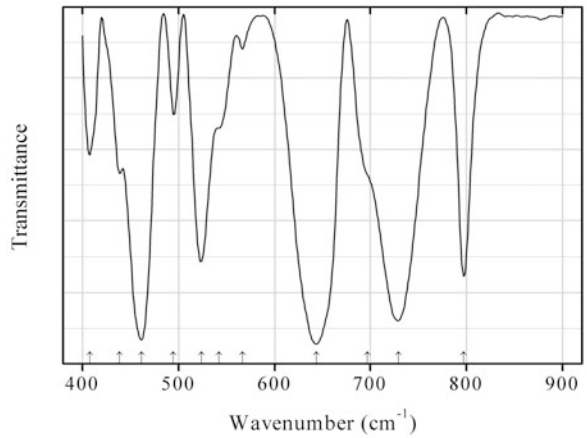

Fig. 2.1545 IR spectrum of barium zinc tellurite-tellurate drawn using data from Yeon et al. (2012b)

Te29 Barium zinc tellurite-tellurate $BaZnTe^{4+}Te^{6+}O_7$ (Fig. 2.1545)
Locality: Synthetic.
Description: Prepared in the solid-state reaction between $BaCO_3$, $ZnCO_3$, TeO_2, and $H_2TeO_4 \cdot 2H_2O$. The crystal structure is solved. Orthorhombic, space group *Ama*2, a = 5.5498(4) Å, b = 15.3161(11) Å, c = 7.3098(5) Å, V = 621.34(4) $Å^3$, Z = 4. The sample is characterized by the powder X-ray diffraction pattern.
Kind of sample preparation and/or method of registration of the spectrum: Transmission.
Source: Yeon et al. (2012b).
Wavenumbers (cm^{-1}): 797, 729, 697sh, 644s, 567w, 542, 524s, 495, 462s, 439, 408.
Note: The wavenumbers were determined by us based on spectral curve analysis of the published spectrum.

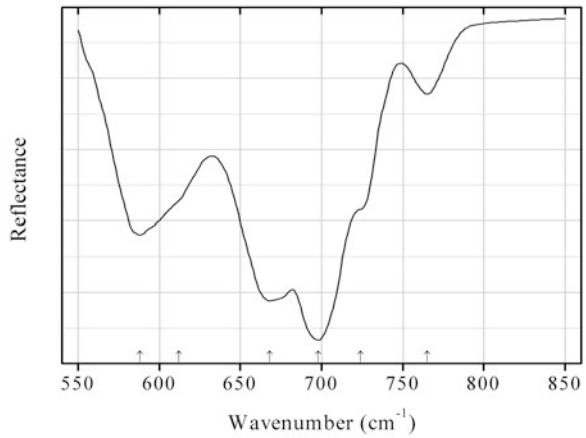

Fig. 2.1546 IR spectrum of rajite drawn using data from Frost et al. (2008c)

Te31 Rajite $CuTe^{4+}O_5$ (Fig. 2.1546)
Locality: Lone Pine Mine, Catron Co., New Mexico, USA (type locality).
Description: No data.
Kind of sample preparation and/or method of registration of the spectrum: Attenuated total reflection of powdered mineral.
Source: Frost et al. (2008c).
Wavenumbers (cm^{-1}): 765, 724sh, 698s, 668s, 612sh, 588.
Note: In the cited paper, wavenumbers are indicated for the maxima of individual bands obtained as a result of the spectral curve analysis. The wavenumbers were determined by us based on spectral curve analysis of the published spectrum.

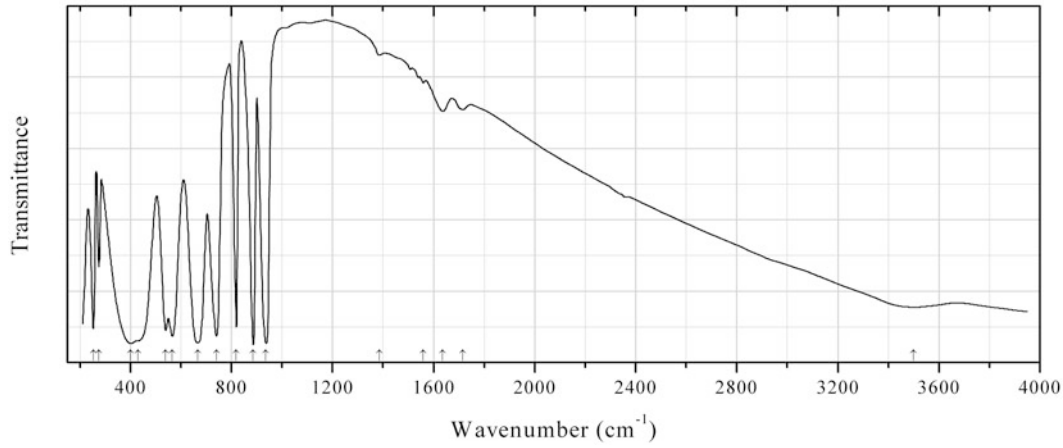

Fig. 2.1547 IR spectrum of schmitterite drawn using data from Tripathi and Namboodiri (2003)

Te32 Schmitterite $(UO_2)(TeO_3)$ (Fig. 2.1547)
Locality: Synthetic.
Description: The end product of the first step during the two-step reductive decomposition of UTe_3O_8 in Ar-8 $\%H_2$. Characterized by the powder X-ray diffraction pattern.
Kind of sample preparation and/or method of registration of the spectrum: KBr disc. Transmission.
Source: Tripathi and Namboodiri (2003).
Wavenumbers (cm^{-1}): 3500, 1716w, 1636w, 1559w, 1385w, 936s, 886s, 819s, 742s, 666s, 565s, 539s, 430, 401s, 275, 253.
Note: Most bands above 1200 cm^{-1} may relate to impurities.

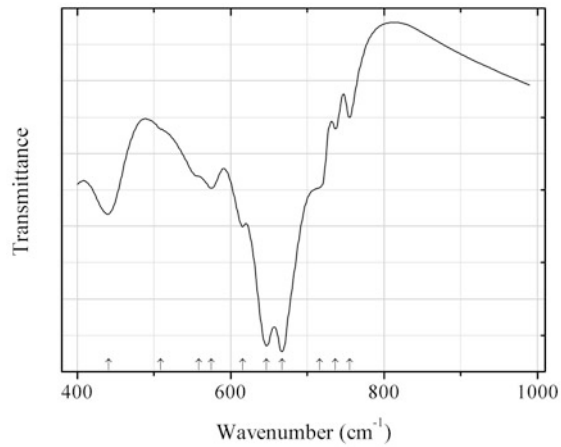

Fig. 2.1548 IR spectrum of smirnite drawn using data from Szaller et al. (2000)

Te33 Smirnite $Bi^{3+}{}_2Te^{4+}O_5$ (Fig. 2.1548)
Locality: Synthetic.

Description: Synthesized from the stoichiometric mixture of Bi_2O_3 and TeO_2 powders at 850 °C for 2 h under argon atmosphere. Confirmed by powder X-ray diffraction data. Orthorhombic, space group *Abm*2.
Kind of sample preparation and/or method of registration of the spectrum: KBr disc. Absorption.
Source: Szaller et al. (2000).
Wavenumbers (cm^{-1}): 755w, 737w, 716sh, 667s, 647s, 616, 575, 559sh, 509sh, 441.
Note: The band position denoted by Szaller et al. (2000) as 549 cm^{-1} was determined by us at 559 cm^{-1} based on spectral curve analysis of the published spectrum.

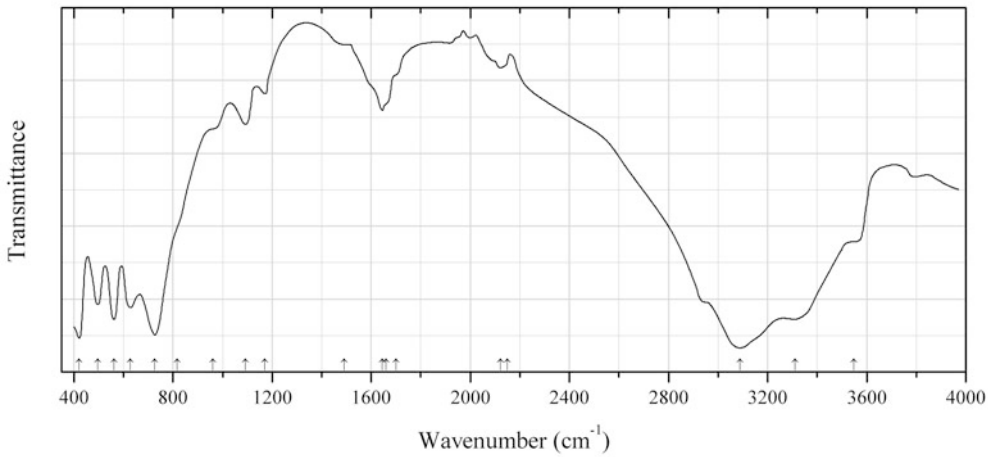

Fig. 2.1549 IR spectrum of utahite drawn using data from Roberts et al. (1997b)

Te34 Utahite $Cu_5Te_3(TeO_4)_4(OH)_8 \cdot 7H_2O$ (Fig. 2.1549)
Locality: Centennial Eureka mine, near Eureka, Tintic district, Juab Co., Utah, USA (type locality).
Description: Blue clusters from the association with cesbronite. Holotype sample. Triclinic, space group *P*1 or *P*-1, $a = 8.794(4)$, $b = 9.996(2)$, $c = 5.660(2)$ Å, $\alpha = 104.10(2)°$, $\beta = 90.07(5)°$, $\gamma = 96.34(3)°$, $V = 479.4(3)$ $Å^3$, $Z = 1$. $D_{calc} = 5.33$ g/cm^3. The empirical formula is (electron microprobe): $Cu_{4.98}Zn_{2.99}(TeO_4)_{3.98}(OH)_{7.98} \cdot 7.1H_2O$. The strongest lines of the powder X-ray diffraction pattern [*d*, Å (*I*, %) (*hkl*)] are: 9.638 (100) (010), 8.736 (50) (100), 4.841 (100) (020), 2.747 (60) (002), 2.600 (45) (−301, −31–1).
Kind of sample preparation and/or method of registration of the spectrum: See Roberts et al. (1994).
Source: Roberts et al. (1997b).
Wavenumbers (cm^{-1}): 3547sh, 3310, 3088s, 2149sh, 2123w, 1700sh, 1661sh, 1645, 1492sh, 1171w, 1092, 962sh, 818sh, 727, 628s, 562, 496, 421s.
Note: The wavenumbers were partly determined by us based on spectral curve analysis of the published spectrum.

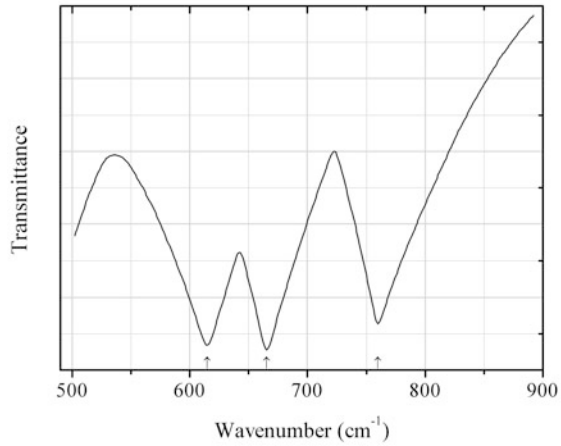

Fig. 2.1550 IR spectrum of winstanleyite drawn using data from Yamaguchi et al. (1988b)

Te35 Winstanleyite $TiTe^{4+}{}_3O_8$ (Fig. 2.1550)
Locality: Synthetic.
Description: Characterized by powder X-ray diffraction data. Cubic, $a \approx 10.96$ Å.
Kind of sample preparation and/or method of registration of the spectrum: KBr disc. Transmission.
Source: Yamaguchi et al. (1988b).
Wavenumbers (cm^{-1}): 760, 665s, 615s.

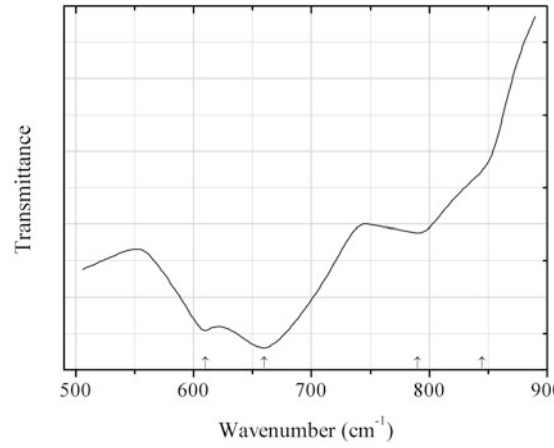

Fig. 2.1551 IR spectrum of winstanleyite dimorph drawn using data from Yamaguchi et al. (1988b)

Te36 Winstanleyite dimorph $TiTe^{4+}{}_3O_8$ (Fig. 2.1551)
Locality: Synthetic.
Description: Characterized by powder X-ray diffraction data. Hexahonal, $a = 10.764(2)$, $c = 5.142(2)$ Å.
Kind of sample preparation and/or method of registration of the spectrum: KBr disc. Transmission.
Source: Yamaguchi et al. (1988b).

Wavenumbers (cm^{-1}): 845sh, 790, 660s, 610s.
Note: The sample used contained a minor admixture of cubic $TiTe_3^{4+}O_8$ modification.

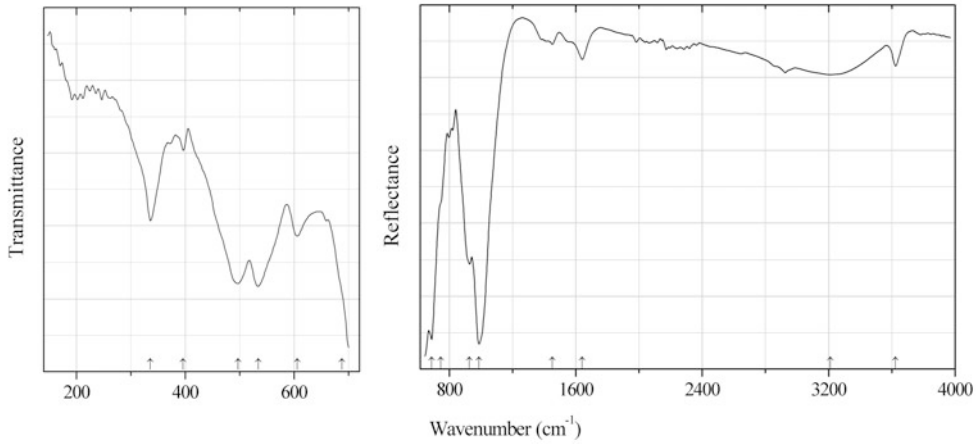

Fig. 2.1552 IR spectrum of xocolatlite drawn using data from Grundler et al. (2008)

Te37 Xocolatlite $Ca_2Mn^{4+}{}_2Te^{6+}{}_2O_{12}{\cdot}nH_2O$ (Fig. 2.1552)
Locality: Moctezuma (La Bambolla) mine, Moctezuma, Sonora, Mexico (type locality).
Description: Chocolate-brown crystalline crusts on a quartz matrix. Holotype sample. Monoclinic, space group *P*2, *P*2/*m*, or *Pm*, $a = 10.757(3)$, $b = 4.928(3)$, $c = 8.942(2)$ Å, $\beta = 102.39(3)°$, $V = 463.0(3)$ $Å^3$, $Z = 2$. $D_{calc} = 4.97$ g/cm^3. The empirical formula is (electron microprobe): $(Ca_{1.26}Mn_{0.35}Zn_{0.19}Pb_{0.12})Mn^{4+}{}_{2.00}Te^{6+}{}_{2.01}S_{0.01}O_{12.07}{\cdot}nH_2O$. The strongest lines of the powder X-ray diffraction pattern [*d*, Å (*I*, %) (*hkl*)] are: 3.267 (100) (012), 2.52 (71) (30–3), 4.361 (51) (002), 1.762 (39) (32–3), 4.924 (34) (010), 2.244 (32) (31–3), 1.455 (24) (006), 1.996 (21) (014), 1.565 (20) (611), 2.353 (18) (41–1).
Kind of sample preparation and/or method of registration of the spectrum: Polyethylene disc (transmission in the range from 100 to 700 cm^{-1}); attenuated total reflection of powdered mineral (transmission in the range from 650 to 4000 cm^{-1}).
Source: Grundler et al. (2008).
Wavenumbers (cm^{-1}): 3624w, 3212w, 1641w, 1452w, 988s, 928, 746s, 688, 606w, 534, 497, 396w, 336.

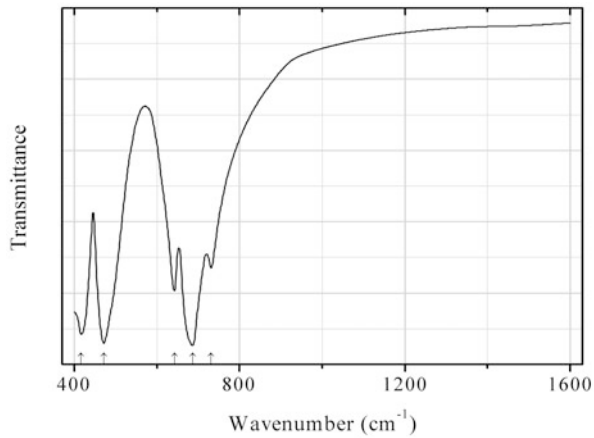

Fig. 2.1553 IR spectrum of yafsoanite drawn using data from Zhang et al. (2009)

Te38 Yafsoanite $Ca_3Te^{6+}{}_2Zn_3O_{12}$ (Fig. 2.1553)
Locality: Synthetic.
Description: Polycrystalline sample of Eu^{3+}-doped garnet-type $Ca_3Te_2(ZnO_4)_3$ synthesized by using solid-state reaction between $CaCO_3$, TeO_2, ZnO, and Eu_2O_3 up to 1100 °C for 15 h. Contains 6 mol% Eu_2O_3 relative to $CaCO_3$. Cubic, a = 12.6251(4) Å, V = 2012.35 Å^3, Z = 8.
Kind of sample preparation and/or method of registration of the spectrum: KBr disc. Transmission.
Source: Zhang et al. (2009).
Wavenumbers (cm^{-1}): 731, 686s, 642, 471s, 416s.

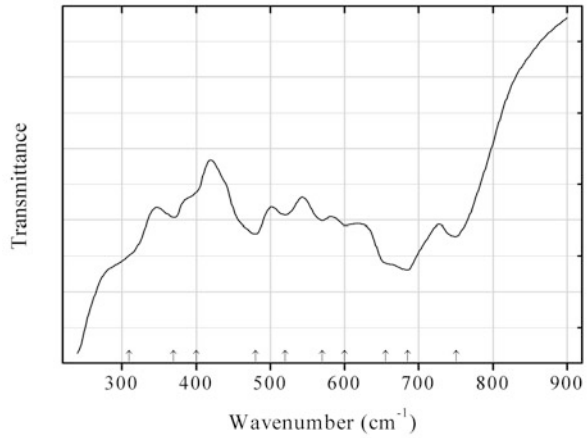

Fig. 2.1554 IR spectrum of zincospiroffite drawn using data from Bürger et al. (1992)

Te39 Zincospiroffite $Zn_2Te_3O_8$ (Fig. 2.1554)
Locality: Synthetic.
Description: Synthesized by a solid-state reaction. Identified by powder X-ray diffraction data.
Kind of sample preparation and/or method of registration of the spectrum: KBr disc. Transmission.
Source: Bürger et al. (1992).
Wavenumbers (cm^{-1}): 750s, 685s, 655sh, 600, 570, 520, 480s, 400sh, 370, 310sh.

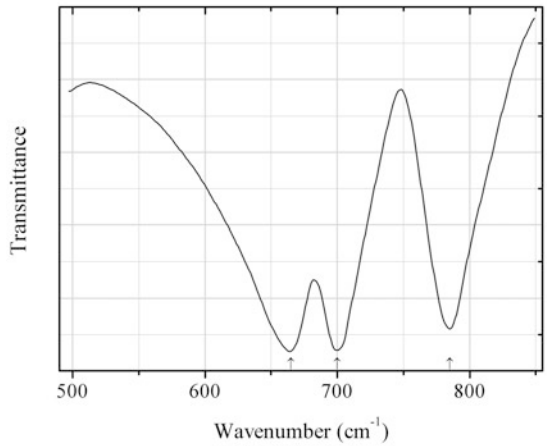

Fig. 2.1555 IR spectrum of zirconium tellurite drawn using data from Yamaguchi et al. (1988a)

Te40 Zirconium tellurite $ZrTe_3O_8$ (Fig. 2.1555)
Locality: Synthetic.
Description: Characterized by powder X-ray diffraction data. Cubic, a = 11.31.
Kind of sample preparation and/or method of registration of the spectrum: KBr disc. Transmission.
Source: Yamaguchi et al. (1988a).
Wavenumbers (cm^{-1}): 785, 700s, 665s.

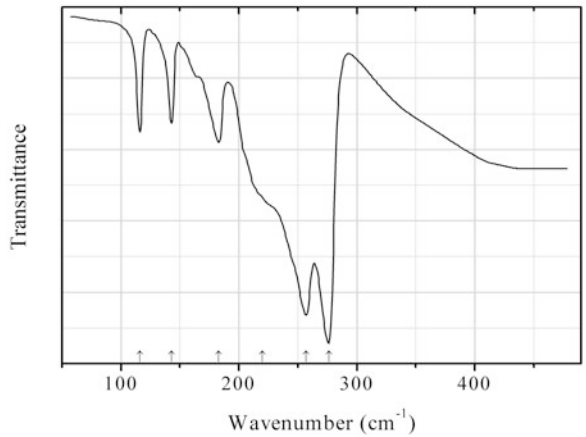

Fig. 2.1556 IR spectrum of ruthenium antimonide telluride drawn using data from Lutz et al. (1983)

Te41 Ruthenium antimonide telluride RuSbTe (Fig. 2.1556)
Locality: Synthetic.
Description: Prepared by heating stoichiometric mixture of the elements in a closed silica tube at 1000 °C. Monoclinic, space group $P2_1/m$, a = 6.543(2), b = 6.601(2), c = 6.651(3) Å, β = 114.1(2)°.
Kind of sample preparation and/or method of registration of the spectrum: Nujol mull. Transmission.
Source: Lutz et al. (1983).
Wavenumbers (cm^{-1}): 276s, 257s, 220sh, 183, 143, 116.

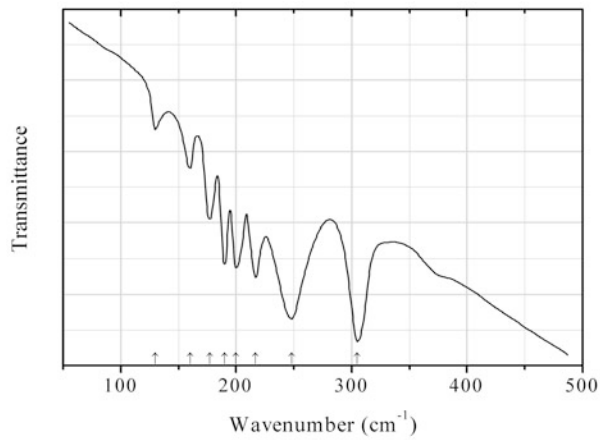

Fig. 2.1557 IR spectrum of osmium arsenide telluride drawn using data from Lutz et al. (1983)

Te42 Osmium arsenide telluride OsAsSe (Fig. 2.1557)
Locality: Synthetic.
Description: Prepared by heating stoichiometric mixture of the elements in a closed tube at 1000 °C. Monoclinic, space group $P2_1/m$, a = 6.358(2), b = 6.313(2), c = 6.415(2) Å, β = 113.1(2)°.
Kind of sample preparation and/or method of registration of the spectrum: Nujol mull. Transmission.
Source: Lutz et al. (1983).
Wavenumbers (cm^{-1}): 305s, 248s, 217, 200, 190, 177, 160, 130w.

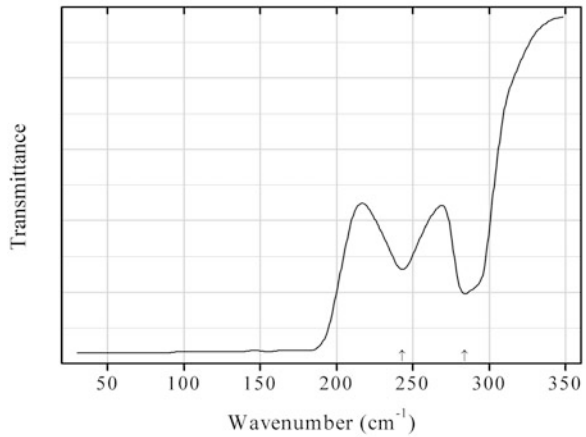

Fig. 2.1558 IR spectrum of cadmium telluride drawn using data from Stafsudd et al. (1967)

Te43 Cadmium telluride CdTe (Fig. 2.1558)
Locality: Synthetic.
Description: No data.
Kind of sample preparation and/or method of registration of the spectrum: Transmittance of a single crystal along the (111) axis.
Source: Stafsudd et al. (1967).
Wavenumbers (cm^{-1}): 284, 243.
Note: The wavenumbers were determined by us based on spectral curve analysis of the published spectrum.

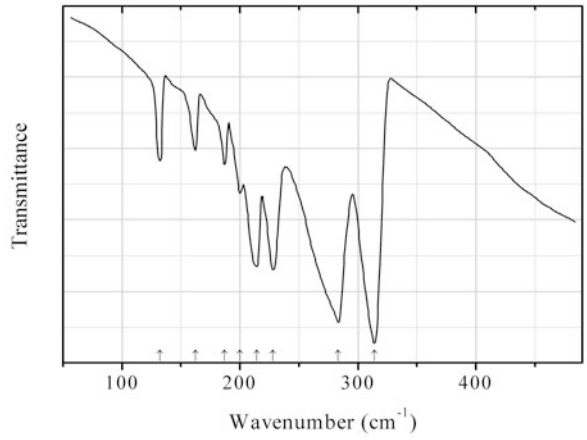

Fig. 2.1559 IR spectrum of ruthenium arsenide telluride drawn using data from Lutz et al. (1983)

Te44 Ruthenium arsenide telluride RuAsTe (Fig. 2.1559)
Locality: Synthetic.
Description: Prepared by heating stoichiometric mixture of the elements in a closed tube at 1000 °C. Monoclinic, space group $P2_1/m$, a = 6.361(1), b = 6.302(1), c = 6.410(1) Å, β = 113.5(1)°.
Kind of sample preparation and/or method of registration of the spectrum: Nujol mull. Transmission.
Source: Lutz et al. (1983).
Wavenumbers (cm^{-1}): 314s, 283s, 228, 214, 200w, 187w, 162w, 132w.

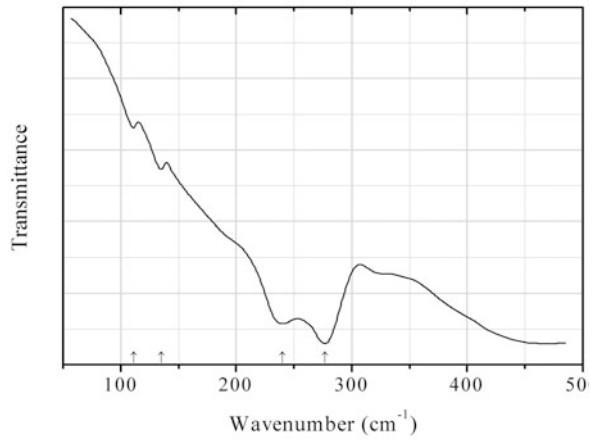

Fig. 2.1560 IR spectrum of iron antimony telluride drawn using data from Lutz et al. (1983)

Te45 Iron antimony telluride FeSbTe (Fig. 2.1560)
Locality: Synthetic.
Description: Prepared by annealing stoichiometric mixture of the elements in an evacuated quartz tube at 1000 °C for 20 days. Characterized by powder X-ray diffraction data. Monoclinic, a = 6.543 (1), b = 6.439(1), c = 6.578(2) Å, β = 113.8(1)°.

Kind of sample preparation and/or method of registration of the spectrum: Nujol mull. Transmission.
Source: Lutz et al. (1983).
Wavenumbers (cm^{-1}): 277s, 240s, 135w, 111w.

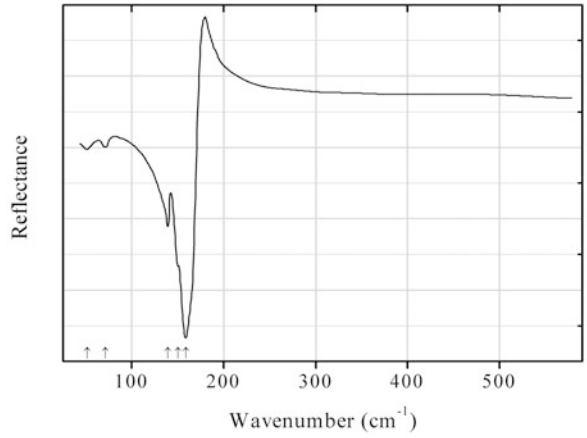

Fig. 2.1561 IR spectrum of manganese ditelluride drawn using data from Lutz et al. (1985)

Te46 Manganese ditelluride $MnTe_2$ (Fig. 2.1561)
Locality: Synthetic.
Description: Prepared by annealing stoichiometric mixture of the elements in an evacuated quartz tube at 600 °C for 14 days. Cubic. Characterized by powder X-ray diffraction data.
Kind of sample preparation and/or method of registration of the spectrum: A sample prepared by hot-pressing and polishing with diamond paste. Reflection.
Source: Lutz et al. (1985).
Wavenumbers (cm^{-1}): 159s, 150sh, 139, 71w, 51w.

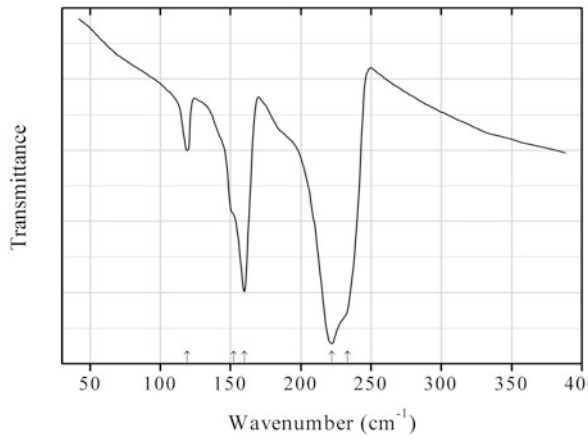

Fig. 2.1562 IR spectrum of osmium ditelluride drawn using data from Lutz et al. (1983)

Te47 Osmium ditelluride $OsTe_2$ (Fig. 2.1562)

Locality: Synthetic.
Description: Prepared by heating stoichiometric mixture of the elements in a closed silica tube at 600 °C for 21 days.
Kind of sample preparation and/or method of registration of the spectrum: Nujol mull. Transmission.
Source: Lutz et al. (1983).
Wavenumbers (cm^{-1}): 233sh, 222s, 160s, 152sh, 119.
Note: For the IR reflection spectrum of $OsTe_2$ see Luts et al. (1985).

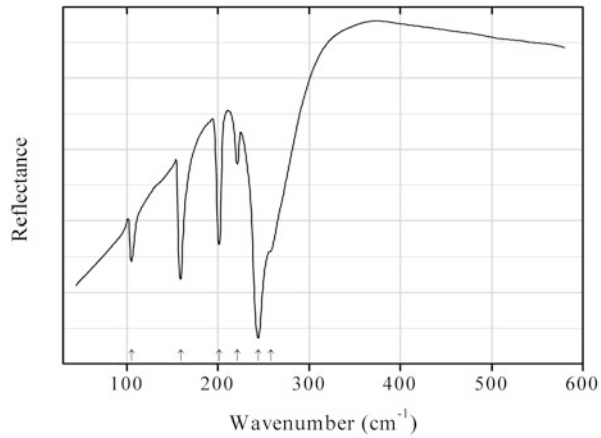

Fig. 2.1563 IR spectrum of ruthenium ditelluride drawn using data from Lutz et al. (1985)

Te48 Ruthenium ditelluride $RuTe_2$ (Fig. 2.1563)
Locality: Synthetic.
Description: Prepared by annealing stoichiometric mixture of the elements in an evacuated quartz tube at 800–900 °C for 14 days. Cubic. Characterized by powder X-ray diffraction data.
Kind of sample preparation and/or method of registration of the spectrum: A sample prepared by hot-pressing and polishing with diamond paste. Reflection.
Source: Lutz et al. (1985).
Wavenumbers (cm^{-1}): 258sh, 244s, 221w, 201, 159, 105.

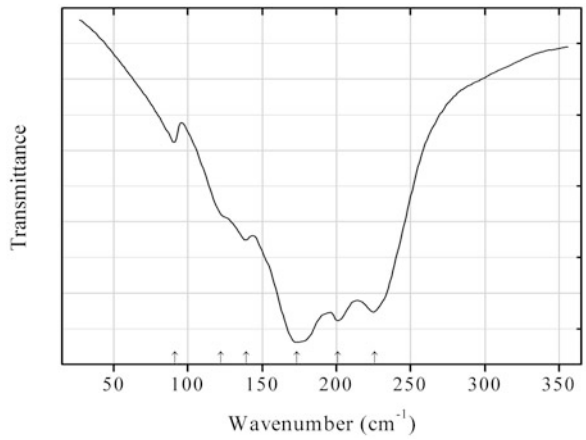

Fig. 2.1564 IR spectrum of silver gallium telluride Te49 drawn using data from Julien et al. (1996)

Te49 Silver gallium telluride Te49 $AgGa_5Te_8$ (Fig. 2.1564)
Locality: Synthetic.
Description: Prepared from Ga_2Te_3 and Ag_2Te in a sealed silica tube under vacuum which was heated slowly up to 1000 °C at a rate of 40 °C/h. Characterized by powder X-ray diffraction data. $AgGa_5Te_8$ crystallizes within the scheelite-type structure.
Kind of sample preparation and/or method of registration of the spectrum: Powder dispersed in solid paraffin wax. Absorption.
Source: Julien et al. (1996).
Wavenumbers (cm^{-1}): 226s, 201s, 173s, 139, 122sh, 91w.

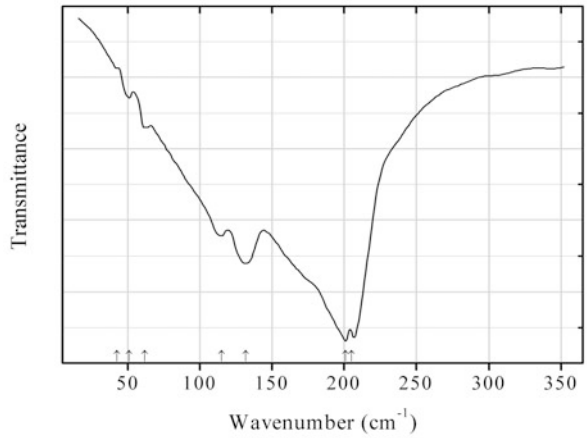

Fig. 2.1565 IR spectrum of silver gallium telluride Te50 drawn using data from Julien et al. (1996)

Te50 Silver gallium telluride Te50 $AgGaTe_2$ (Fig. 2.1565)
Locality: Synthetic.
Description: Prepared from Ga_2Te_3 and Ag_2Te in a sealed silica tube under vacuum which was heated slowly up to 1000 °C at a rate of 40 °C/h. Characterized by powder X-ray diffraction data. $AgGaTe_2$ crystallizes within the chalcopyrite-type structure.
Kind of sample preparation and/or method of registration of the spectrum: Powder dispersed in solid paraffin wax. Absorbance.
Source: Julien et al. (1996).
Wavenumbers (cm^{-1}): 205s, 201s, 132, 115, 62w, 51w, 43w.

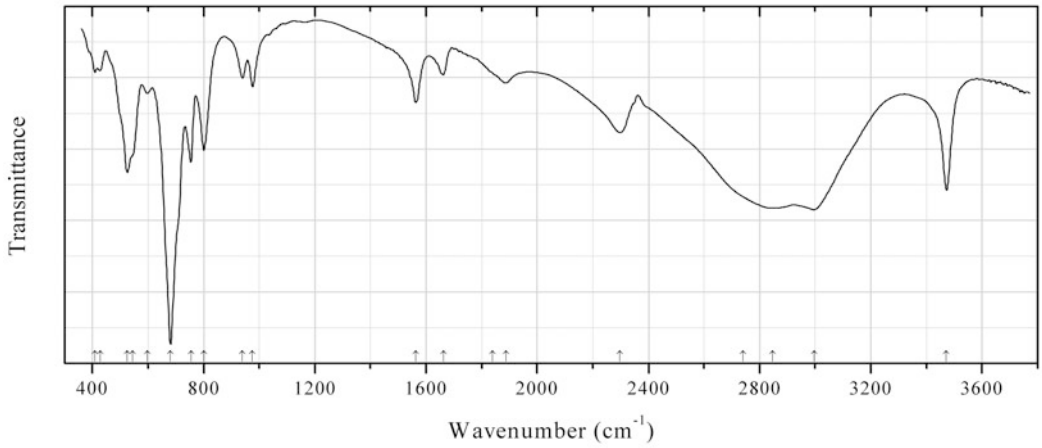

Fig. 2.1566 IR spectrum of teineite obtained by N.V. Chukanov

Te51 Teineite $Cu^{2+}(TeO_3)\cdot 2H_2O$ (Fig. 2.1566)
Locality: Gråurdfjellet, Oppdal, Norway.
Description: Deep blue crystals. The empirical formula is (electron microprobe): $Cu_{1.00}(TeO_3)_{0.96}(SO_3)_{0.04}$.
Kind of sample preparation and/or method of registration of the spectrum: KBr disc. Absorption.
Wavenumbers (cm^{-1}): 3472, 2996s, 2846s, 2740sh, 2298, 1888, 1840sh, 1662, 1563, 976, 940, 801, 754, 681s, 597, 545sh, 526, 428w, 409w.

2.21 Iodides, Iodites, and Iodates

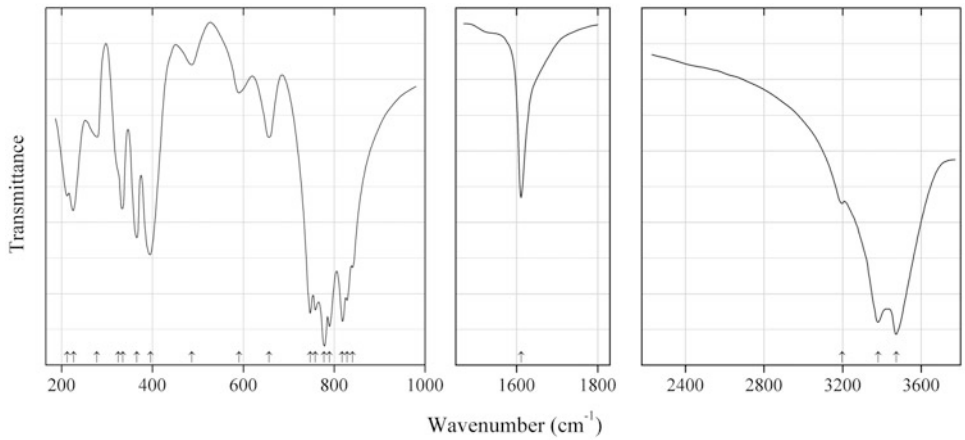

Fig. 2.1567 IR spectrum of brüggenite drawn using data from Alici et al. (1992)

I2 Brüggenite $Ca(IO_3)_2\cdot H_2O$ (Fig. 2.1567)
Locality: Synthetic.

Description: Confirmed by single-crystal X-ray diffraction data.
Kind of sample preparation and/or method of registration of the spectrum: Absorption. Kind of sample preparation is not indicated.
Source: Alici et al. (1992).
Wavenumbers (cm^{-1}): 3472s, 3380, 3197w, 1611w, 840s, 828s, 817s, 789s, 777s, 758s, 747s, 656, 590w, 486w, 395s, 365, 334, 324sh, 277, 226, 212.
Note: For IR spectrum of brüggenite see also Shitole and Saraf (2001).

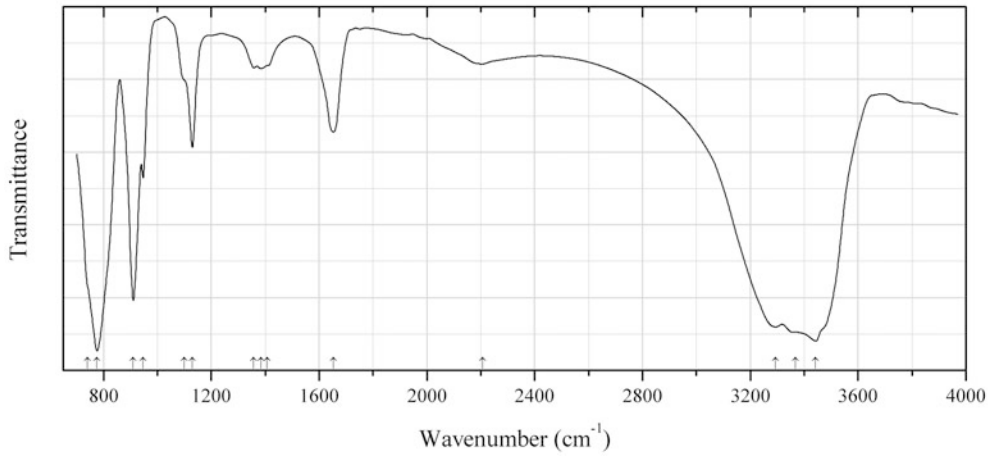

Fig. 2.1568 IR spectrum of george-ericksenite drawn using data from Cooper et al. (1998)

I3 George-ericksenite $Na_6CaMg(IO_3)_6(CrO_4)_2 \cdot 12H_2O$ (Fig. 2.1568)
Locality: Oficina Chacabuco, Sierra Gorda district, Antofagasta province, Chile (type locality).
Description: Lemon-yellow micronodules of crystals on a host rock principally composed of halite, nitratine, and niter. Holotype sample. Monoclinic, space group *C*2/*c*, a = 23.645(2), b = 10.918(1), c = 15.768(1) Å, β = 114.42(6)° V = 3707.3(6) $Å^3$, Z = 4. D_{calc} = 3.035 g/cm^3. Optically biaxial (+), α = 1.647(2), β = 1.674(2), γ = 1.704(2). The crystal-chemical formula is $Na_6CaMg(IO_3)_6[(Cr_{0.84}S_{0.16})O_4]_2 \cdot 12H_2O$. The strongest lines of the powder X-ray diffraction pattern [*d*, Å (*I*, %) (*hkl*)] are: 10.69 (100) (200), 6.36 (50) (−311), 5.65 (50) (−312), 3.590 (70) (023, 600), 3.121 (80) (223), 3.051 (80) (−623).
Kind of sample preparation and/or method of registration of the spectrum: KBr disc. Transmission.
Source: Cooper et al. (1998).
Wavenumbers (cm^{-1}): 3442s, 3367sh, 3294s, 2206w, 1653, 1408sh, 1385w, 1357w, 1130, 1100sh, 947, 909s, 776s, 740sh.
Note: The wavenumbers were partly determined by us based on spectral curve analysis of the published spectrum.

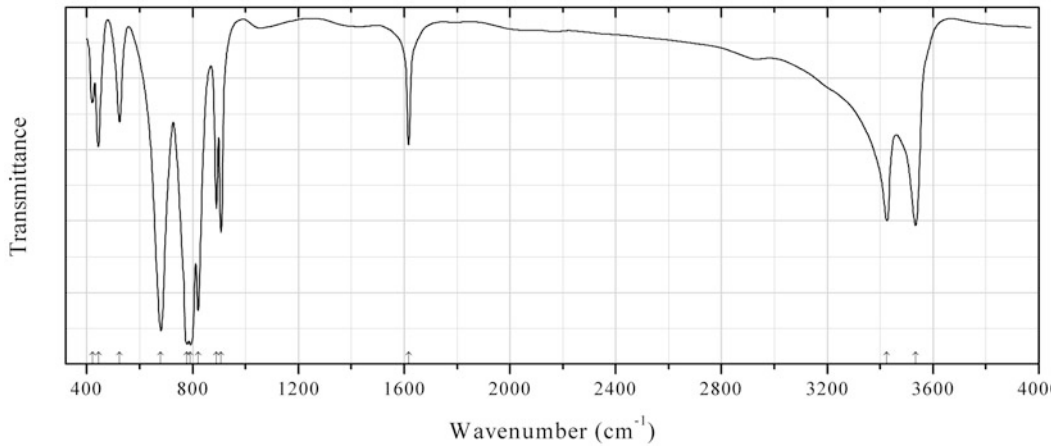

Fig. 2.1569 IR spectrum of potassium vanadyl iodate I4 drawn using data from Sun et al. (2011)

I4 Potassium vanadyl iodate I4 α-$K(VO_2)(IO_3)_2 \cdot H_2O$ (Fig. 2.1569)
Locality: Synthetic.
Description: Yellow acicular crystals. Synthesized from the mixture of K_2CO_3, V_2O_5, I_2O_5, and H_2O at 155 °C. The crystal structure is solved. Orthorhombic, space group *Pbca*, $a = 8.4998(6)$, $b = 7.2826(5)$, $c = 27.425(3)$ Å, $V = 1687.6(2)$ Å^3, $Z = 8$. Neighboring VO_6 octahedra are corner-sharing into a 1D chain with the IO_3 groups attached on both sides of the chain in a uni- or bidentate bridging fashion. $D_{calc} = 3.833$ g/cm^3.
Kind of sample preparation and/or method of registration of the spectrum: KBr disc. Transmission.
Source: Sun et al. (2011).
Wavenumbers (cm^{-1}): 3535, 3426, 1617, 908, 890, 821s, 792s, 779s, 680s, 524, 444, 421.

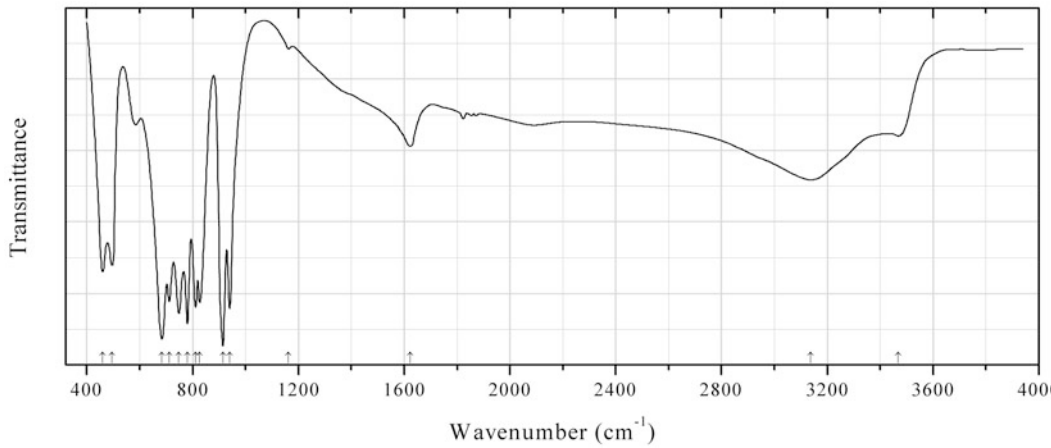

Fig. 2.1570 IR spectrum of potassium vanadyl iodate I5 drawn using data from Sun et al. (2011)

I5 Potassium vanadyl iodate I5 β-$K(VO_2)(IO_3)_2 \cdot H_2O$ (Fig. 2.1570)
Locality: Synthetic.

Description: Yellow crystals. Synthesized under hydrothermal conditions at 230 °C. The crystal structure is solved. Neighboring VO_6 octahedra are bridged by IO_3 groups into a right-handed helical chain with remaining IO_3 groups being grafted unidentately on both sides of the helical chain. Orthorhombic, space group $P2_12_12_1$, $a = 5.8083(14)$, $b = 8.793(2)$, $c = 16.785(4)$ Å, $V = 857.3(4)$ Å^3, $Z = 4$. $D_{calc} = 3.795$ g/cm^3.
Kind of sample preparation and/or method of registration of the spectrum: Transmission. Kind of sample preparation is not indicated.
Source: Sun et al. (2011).
Wavenumbers (cm^{-1}): 3468, 3137, 1623, 1163w, 940s, 915s, 827s, 811s, 780s, 748s, 712s, 684s, 495w, 460.
Note: The wavenumbers were partly determined by us based on spectral curve analysis of the published spectrum.

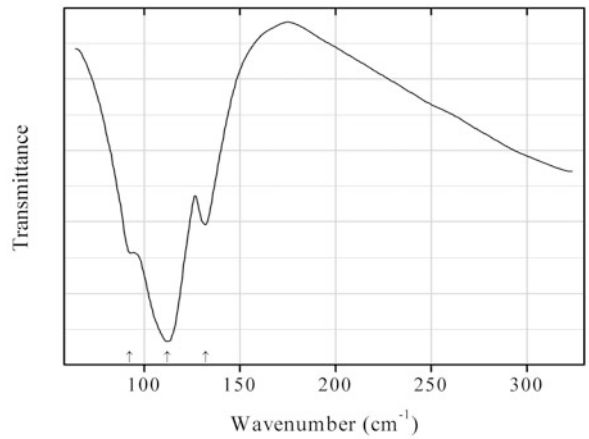

Fig. 2.1571 IR spectrum of coccinite drawn using data from Mikawa et al. (1966)

I6 Coccinite HgI_2 (Fig. 2.1571)
Locality: Synthetic.
Description: Sample purified by recrystalization from hot aqueous solution and sublimation.
Kind of sample preparation and/or method of registration of the spectrum: Nujol mull. Transmission.
Source: Mikawa et al. (1966).
Wavenumbers (cm^{-1}): 132, 112s, 92sh.
Note: For IR spectrum of synthetic HgI_2 see also Durig et al. (1969).

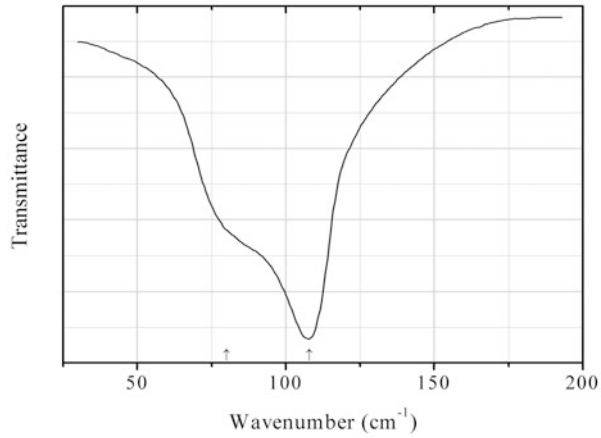

Fig. 2.1572 IR spectrum of iodargyrite drawn using data from Bottger and Geddes (1967)

I7 Iodargyrite AgI (Fig. 2.1572)
Locality: Synthetic.
Description: Hexagonal. Confirmed by powder X-ray diffraction data.
Kind of sample preparation and/or method of registration of the spectrum: Thin crystalline film with the 002 planes predominantly parallel to the polyethylene substrate. Transmission.
Source: Bottger and Geddes (1967).
Wavenumbers (cm^{-1}): 108s, 80sh.

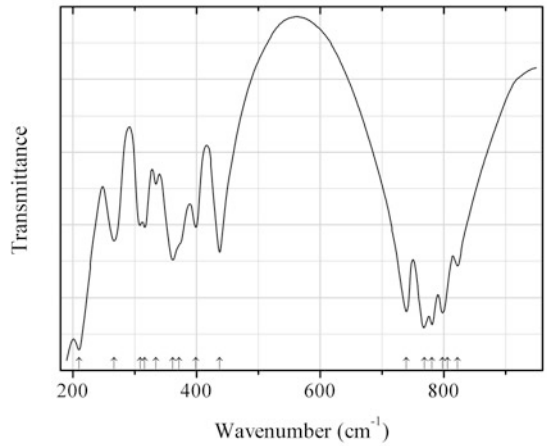

Fig. 2.1573 IR spectrum of lautarite drawn using data from Alici et al. (1992)

I8 Lautarite $Ca(IO_3)_2$ (Fig. 2.1573)
Locality: Synthetic.
Description: Confirmed by powder X-ray diffraction data.
Kind of sample preparation and/or method of registration of the spectrum: KCl disc. Transmission.
Source: Alici et al. (1992).

Wavenumbers (cm^{-1}): 823, 806sh, 798s, 781s, 769s, 740s, 438, 399, 372sh, 362, 335w, 316, 309, 267, 210s.

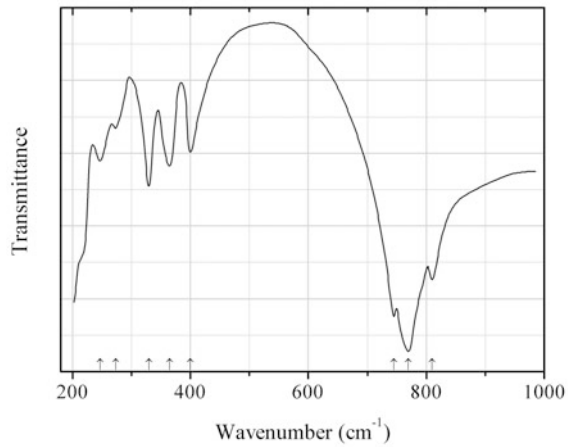

Fig. 2.1574 IR spectrum of lautarite dimorph drawn using data from Alici et al. (1992)

I9 Lautarite dimorph $Ca(IO_3)_2$ (Fig. 2.1574)
Locality: Synthetic.
Description: The powder X-ray diffraction pattern is different from that of lautarite.
Kind of sample preparation and/or method of registration of the spectrum: KCl disc. Transmission.
Source: Alici et al. (1992).
Wavenumbers (cm^{-1}): 810s, 770s, 745s, 400, 365, 330, 273w, 247.

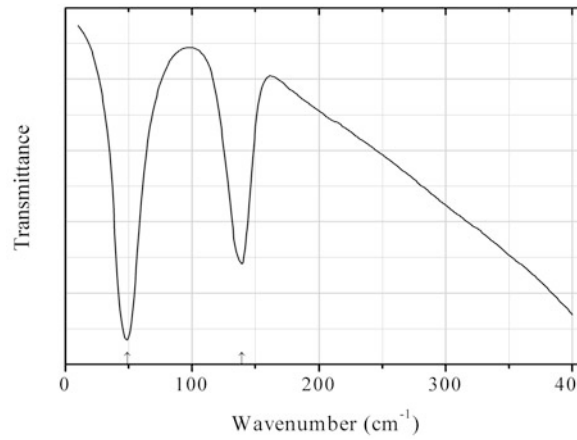

Fig. 2.1575 IR spectrum of moschelite drawn using data from Ōsaka (1971)

I10 Moschelite HgI (Fig. 2.1575)
Locality: Synthetic.
Description: Commercial reactant obtained from the Wako Pure Chemical Industries.
Kind of sample preparation and/or method of registration of the spectrum: Nujol mull.

Source: Ōsaka (1971).
Wavenumbers (cm^{-1}): 139, 49s.

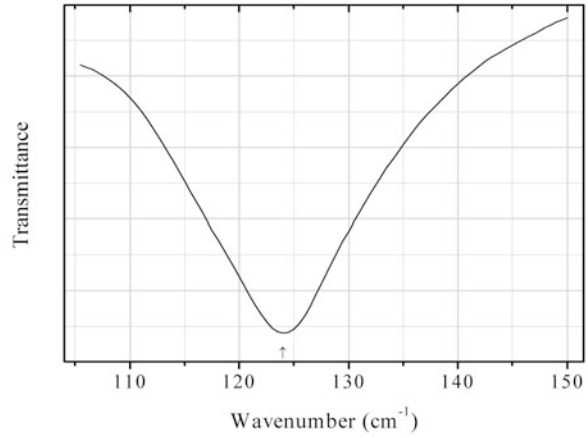

Fig. 2.1576 IR spectrum of marshite drawn using data from Plendl et al. (1966)

I11 Marshite CuI (Fig. 2.1576)
Locality: Synthetic.
Kind of sample preparation and/or method of registration of the spectrum: Thin film sublimed on quartz plate and covered with paraffin.
Source: Plendl et al. (1966).
Wavenumbers (cm^{-1}): 124.
Notes: For the IR spectrum of marshite see also Wakamura (2002).

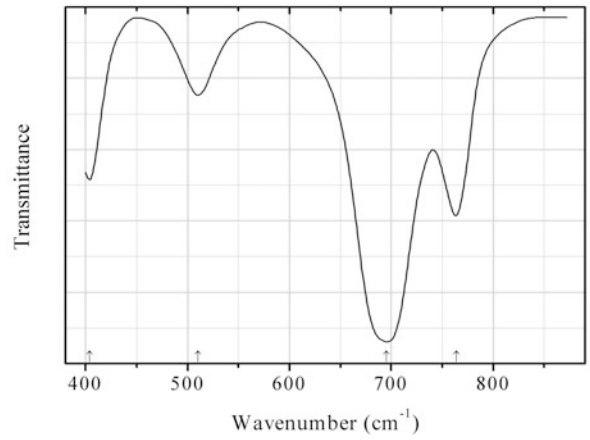

Fig. 2.1577 IR spectrum of bismuthyl iodate drawn using data from Nguyen et al. (2011b)

I12 Bismuthyl iodate $(BiO)(IO_3)$ (Fig. 2.1577)
Locality: Synthetic.
Description: Synthesized by combining $Bi(NO_3)_3 \cdot 5H_2O$, HIO_3, and 1 M HNO_3 in an autoclave at 200 °C for 1 week. The crystal structure is solved. Orthorhombic, space group $Pca2_1$, a = 5.6584(4),

b = 11.0386(8), c = 5.7476(4) Å, V = 359.00(4) Å^3. The sample is characterized by powder X-ray diffraction data.

Kind of sample preparation and/or method of registration of the spectrum: KBr disc. Transmission.

Source: Nguyen et al. (2011b).

Wavenumbers (cm^{-1}): 764, 695s, 510, 404.

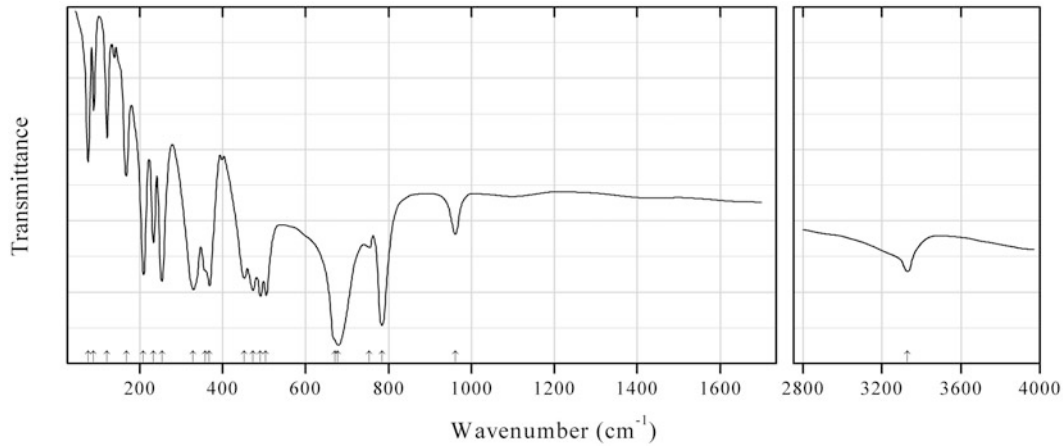

Fig. 2.1578 IR spectrum of salesite drawn using data from Nassau et al. (1973)

I13 Salesite $Cu(IO_3)(OH)$ (Fig. 2.1578)

Locality: Synthetic.

Description: Deep bluish green crystals and clusters. Confirmed by TGA and powder X-ray diffraction data.

Kind of sample preparation and/or method of registration of the spectrum: Fluorolube mull (above 1511 cm^{-1}), KBr disc (in the range from 560 to 1500 cm^{-1}), Nujol mull (below 560 cm^{-1}). Transmission.

Source: Nassau et al. (1973).

Wavenumbers (cm^{-1}): 3330, 961, 784s, 754w, 678s, 670sh, 503s, 491s, 473s, 452, 368s, 357sh, 329s, 253s, 233, 209, 167, 121, 89, 75.

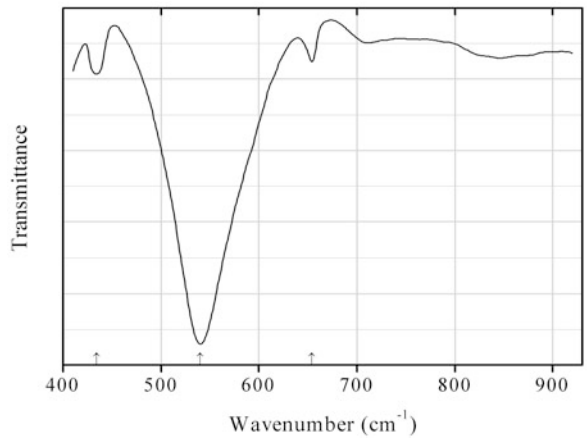

Fig. 2.1579 IR spectrum of seeligerite drawn using data from Bindi et al. (2008)

I14 Seeligerite $Pb_3(IO_4)Cl_3$ (Fig. 2.1579)
Locality: San Rafael mine, Caracoles, Sierra Gorda district, Antofagasta II Region, Antofagasta province, Chile.
Description: Specimen No. 44751/G from the mineralogical collection of the Museo di Storia Naturale, Universitá di Firenze, Italy. The crystal structure is solved. Orthorhombic, space group *Cmm*2, $a = 7.971(2)$, $b = 7.976(2)$, $c = 27.341(5)$ Å, $V = 1738.3(6)$ Å^3, $Z = 8$.
Kind of sample preparation and/or method of registration of the spectrum: Single crystal. Unpolarized radiation. Transmittance (?)
Source: Bindi et al. (2008).
Wavenumbers (cm^{-1}): 654w, 540s, 434w.

2.22 Tungstates and W-Bearing Oxides

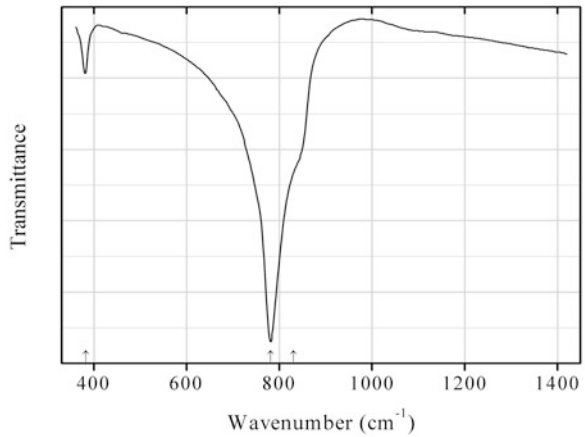

Fig. 2.1580 IR spectrum of stolzite obtained by N.V. Chukanov

W12 Stolzite $Pb(WO_4)$ (Fig. 2.1580)
Locality: Sumidouro creek, near Mariana, Minas Gerais, Brazil.
Description: Orange dipyramidal crystals on quartz. Confirmed by qualitative electron microprobe analyses.
Kind of sample preparation and/or method of registration of the spectrum: KBr disc. Absorption.
Wavenumbers (cm^{-1}): 830sh, 781s, 382w.

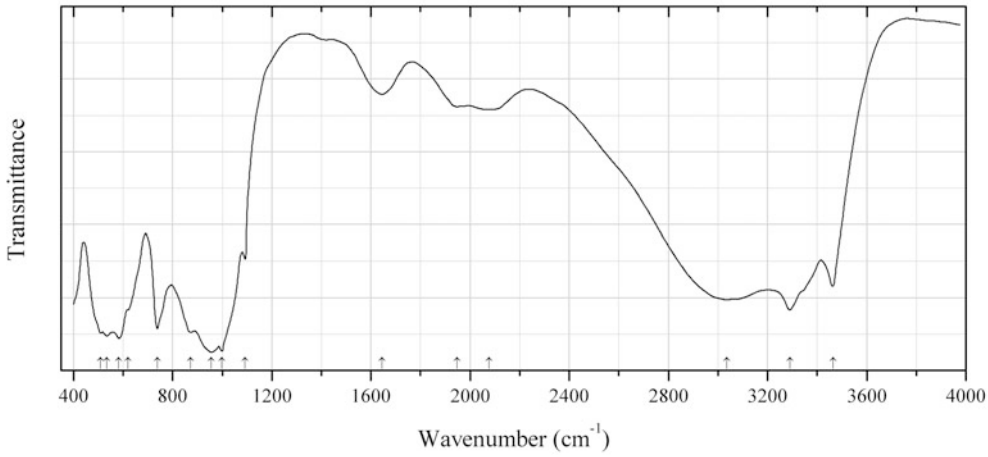

Fig. 2.1581 IR spectrum of anthoinite drawn using data from Grey et al. (2010)

W13 Anthoinite $AlWO_3(OH)_3$ (Fig. 2.1581)
Locality: Mt. Misobo Mine, Maniéma district, Katanga, Democratic Republic of the Congo (type locality).
Description: White fine-grained aggregate. The crystal structure is solved. Triclinic, space group *I*-1, $a = 8.196(1)$, $b = 9.187(1)$, $c = 11.316(1)$ Å, $\alpha = 92.82(1)°$, $\beta = 94.08(1)°$, $\gamma = 90.23(1)°$, $V = 571.6(3)$ $Å^3$, $Z = 2$. The peak at 1646 cm^{-1} is located in the region for the H–O–H bending mode of water and may be associated with H_2O molecules at the O12 site.
Kind of sample preparation and/or method of registration of the spectrum: KBr disc. Transmission.
Source: Grey et al. (2010).
Wavenumbers (cm^{-1}): 3464, 3290s, 3036s, 2076w, 1949w, 1646w, 1092, 998s, 957s, 873, 738s, 620, 583s, 534s, 509s.
Note: The wavenumbers were partly determined by us based on spectral curve analysis of the published spectrum.

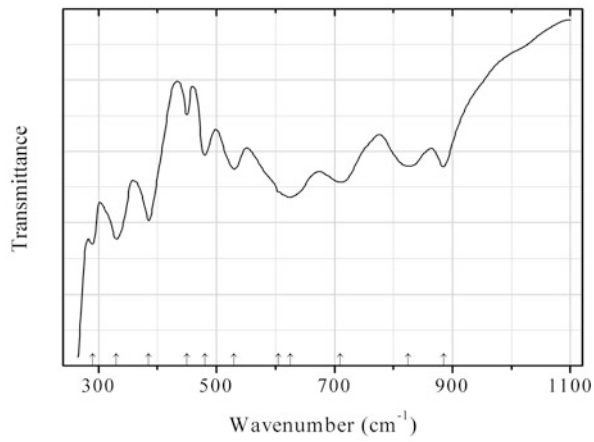

Fig. 2.1582 IR spectrum of huanzalaite drawn using data from Günter and Amberg (1989)

W14 Huanzalaite $Mg(WO_4)$ (Fig. 2.1582)
Locality: Synthetic.
Description: Isostructural with wolframite-group minerals.
Kind of sample preparation and/or method of registration of the spectrum: KBr disc. Absorption.
Source: Günter and Amberg (1989).
Wavenumbers (cm^{-1}): 885, 825, 710, 625s, (605sh), 530, 480, 450w, 385s, 330s, 290s.

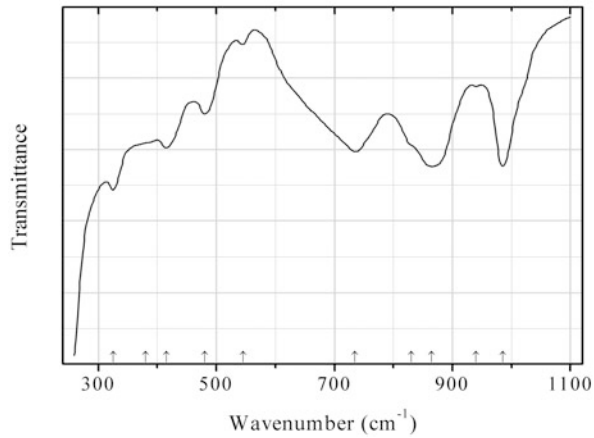

Fig. 2.1583 IR spectrum of huanzalaite dimorph drawn using data from Günter and Amberg (1989)

W15 Huanzalaite dimorph $Mg(WO_4)$ (Fig. 2.1583)
Locality: Synthetic.
Description: Prepared as a result of dehydration of $Mg(WO_4)\cdot H_2O$ above 150 °C. Triclinic, $a = 5.60$, $b = 6.58$, $c = 8.84$ Å, $\alpha = 123.2°$, $\beta = 112.7°$, $\gamma = 101.4°$, $V = 213.5$ Å^3, $Z = 4$. $D_{calc} = 8.35$ g/cm^3. The strongest lines of the powder X-ray diffraction pattern [*d*, Å (*I*, %) (*hkl*)] are: 4.648 (72) (1–10), 3.575 (57) (1–1–1), 3.188 (100) (02–2), 3.047 (40) (1–21), 2.742 (40) (1–20), 2.137 (47) (12–1, 033).
Kind of sample preparation and/or method of registration of the spectrum: KBr disc. Absorption.
Source: Günter and Amberg (1989).
Wavenumbers (cm^{-1}): 985s, 940w, 865s, 830sh, 735s, 545w, 480, 415, 380sh, 325s.

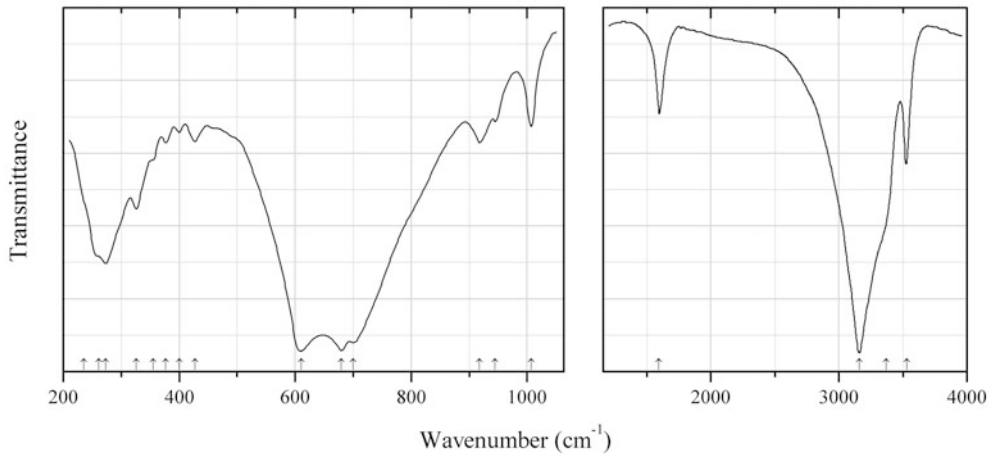

Fig. 2.1584 IR spectrum of meymacite drawn using data from Daniel et al. (1987)

W16 Meymacite $WO_3 \cdot 2H_2O$ (Fig. 2.1584)
Locality: Synthetic.
Kind of sample preparation and/or method of registration of the spectrum: Nujol or hexachlorobutadiene mull. Absorption.
Source: Daniel et al. (1987).
Wavenumbers (cm^{-1}): 3530, 3370sh, 3160s, 1595w, 1007w, 945w, 918w, 700s, 680s, 610s, 427w, 400w, 377w, 355sh, 326, 273s, 261sh, 236sh.
Note: The wavenumbers were partly determined by us based on spectral curve analysis of the published spectrum.

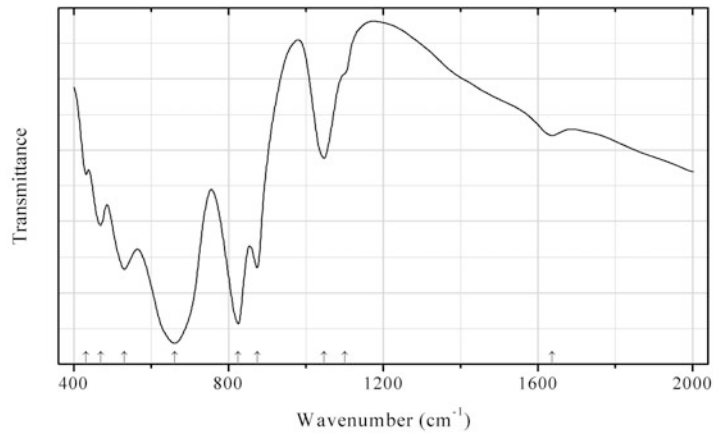

Fig. 2.1585 IR spectrum of sanmartinite drawn using data from De Oliveira et al. (2008)

W17 Sanmartinite $Zn(WO_4)$ (Fig. 2.1585)
Locality: Synthetic.
Description: Characterized by powder X-ray diffraction data.
Kind of sample preparation and/or method of registration of the spectrum: KBr disc. Transmission.

Source: De Oliveira et al. (2008).
Wavenumbers (cm^{-1}): 1637w, 1100sh, 1047w, 874, 825s, 660s, 530, 469, 432w.
Note: Absorption maxima with wavenumbers above 1000 cm^{-1} are due to impurities.

References

Abdel-Gawad AM, Kerr PF (1961) Urano-organic mineral association. Am Miner 46:402–419

Ackermann L, Cemič L, Langer K (1983) Hydrogarnet substitution in pyrope: a possible location for "water" in the mantle. Earth Planet Sci Lett 62:208–214

Adams DM, Fletcher PA (1988) Vibrational spectroscopy at high pressure: part 53. Alkali metavanadates and copper metagermanate. Spectrochim Acta A 44 (2):233–240

Aderemi BO, Hameed BH (2009) Alum as a heterogeneous catalyst for the transesterification of palm oil. Appl Catal A 370:54–58

Adler HH (1965) Examination of mass-radius effects, hydrogen bonding and v_b splitting in infrared spectra of Zr-Hf homologs. Am Miner 50:1553–1562

Agakhanov AA, Pautov LA, Karpenko VYu, Bekenova GK, Uvarova YuA (2011) Orlovite, $KLi_2TiSi_4O_{11}F$, a new mineral of the mica group. New Data Minerals 46:13–19

Agakhanov AA, Pautov LA, Karpenko VYu, Sokolova E, Abdu YA, Hawthorne FC, Pekov IV, Siidra OI (2015) Yusupovite, $Na_2Zr(Si_6O_{15})(H_2O)_3$, a new mineral species from the Darai-Pioz alkaline massif and its implications as a new microporous filter for large ions. Am Miner 100:1502–1508

Agakhanov AA, Pautov LA, Uvarova YuA, Sokolova EV, Hawthorne F, Karpenko VYu (2005) Senkevichite, $CsKNaCa_2TiO[Si_7O_{18}(OH)]$, a new mineral. New Data Minerals 40:17–22

Agakhanov AA, Pautov LA, Uvarova YuA, Sokolova EV, Hawthorne FC, Karpenko VYu (2013) Laptevite-(Ce), $NaFe^{2+}(REE_7Ca_5Y_3)(SiO_4)_4(Si_3B_2PO_{18})(BO_3)F_{11}$, a new mineral species in the vicanite group from the Dara-i Pioz alkaline massif, Tajikistan. New Data Minerals 48:5–11 (in Russian)

Agakhanov AA, Pautov LA, Uvarova YuA, Sokolova EV, Hawthorne FC, Karpenko VYu, Dusmatov VD, Semenov YeI (2004) Arapovite, (U,Th)$(Ca,Na)_2(K_{1-x}\square_x)Si_8O_{20}\cdot H_2O$ – new mineral. New Data Minerals 39:14–18

Agakhanov AA, Pautov LA, Uvarova YuA, Sokolova EV, Hawthorne FC, Karpenko VYu, Gafurov FG (2007) Faizievite, $K_2Na(Ca_6Na)Ti_4Li_6Si_{24}O_{66}F_2$ – a new mineral species. New Data Minerals 42:5–10

Agrell SO, Gay M (1970) De la deerite dans les Alpes franco-italiennes. Bull Soc Fr Minéral Cristallogr 93:263–264 (in French)

Agrell SO, Bown MG, McKie D (1965) Deerite, howieite and zussmanite, three new minerals from the Franciscan of the Laytonville district, Mendocino Co., California. Am Miner 50:278

Aines RD, Rossman GR (1984) The high temperature behavior of water and carbon dioxide in cordierite and beryl. Am Miner 69:319–327

Akaogi M, Ross NL, McMillan P, Navrotsky A (1984) The Mg_2SiO_4 polymorphs (olivine, modified spinel and spinel) – thermodynamic properties from oxide melt solution calorimetry, phase relations, and models of lattice vibrations. Am Miner 69:499–512

Akhmanova MV, Orlova LP (1966) Investigation of rare-earth carbonates by infra-red spectroscopy. Geokhimiya (Geochemistry) 5:571–578 (in Russian)

Akrap A, Tran M, Ubaldini A, Teyssier J, Giannini E, Van Der Marel D, Lerch P, Homes CC (2012) Optical properties of Bi_2Te_2Se at ambient and high pressures. Phys Rev B 86(23):235207–9

Aksenov SM, Rastsvetaeva RK, Chukanov NV, Kolitsch U (2014) Structure of calcinaksite $KNa[Ca(H_2O)][Si_4O_{10}]$, the first hydrous member of the litidionite group of silicates with $[Si_8O_{20}]^{8-}$ tubes. Acta Crystallogr B 70:768–775

Aleksovska S, Petruševski VM, Šoptrajanov B (1997) Infrared spectra of the monohydrates of manganese (III) phosphate and manganese(III) arsenate: relation to the compounds of the kieserite family. J Molec Struct 408(409):413–416

Alemi A, Joo SW, Khademinia S, Dolatyari M, Bakhtiari A, Moradi H, Saeidi S (2013) Hydrothermal synthesis and characterization of straw bundle-like lithium sodium disilicate (silinaite) micro-rods. Int Nano Lett 3(1):1–5

Alici E, Schmidt T, Lutz HD (1992) Zur Kenntnis des Calciumbromats und -iodats, Kristallstruktur, röntgenographische, IR- und Raman-spektroskopische und thermoanalytische Untersuchungen. Z anorg allg Chem 608:135–144 (in German)

Allen GC, Crofts JA, Griffiths AJ (1976) Infrared spectroscopy of the uranium/oxygen system. J Nucl Mater 62(2):273–281

N.V. Chukanov and A.D. Chervonnyi, *Infrared Spectroscopy of Minerals and Related Compounds*, Springer Mineralogy, DOI 10.1007/978-3-319-25349-7

Allen GC, Paul M (1995) Chemical characterization of transition metal spinel-type oxides by infrared spectroscopy. Appl Spectrosc 49(4):451–458

Al'Ama AG, Belokoneva EL, Dimitrova OV, Kurazhkovskaya VS, Mochenova NN (2006) Bromophosgenite: synthesis and structure solution. Zhurnal Neorganicheskoi Khimii (Russ J Inorg Chem) 51 (8):1261–1265 (in Russian)

Amayri S, Arnold T, Foerstendorf H, Geipel G, Bernhard G (2004) Spectroscopic characterization of synthetic becquerelite, $Ca[(UO_2)_6O_4(OH)_6]\cdot 8H_2O$, and swartzite, $CaMg[UO_2(CO_3)_3]\cdot 12H_2O$. Can Miner 42:953–962

Amthauer G, Rossman GR (1998) The hydrous component in andradite garnet. Am Miner 83:835–840

Anastassakis E, Perry CH (1976) Light scattering and ir measurements in XS_2 pyrite-type compounds. J Chem Phys 64(9):3604–3609

Anderson A, Chieh C, Irish DE, Tong JPK (1980) An X-ray crystallographic, Raman, and infrared spectral study of crystalline potassium uranyl carbonate, $K_4UO_2(CO_3)_3$. Can J Chem 58(16):1651–1658

Anderson AJ, Clark AH, Gray S (2001) The occurrence and origin of zabuyelite (Li_2CO_3) in spodumene-hosted fluid inclusions: Implications for the internal evolution of rare-element granitic pegmatites. Can Miner 39:1513–1527

Ando T, Kanayama A, Kobayashi S, Miyawaki R, Kishi S, Tanabe M, Kusachi I (2015) Roweite from the Fuka mine, Okayama Prefecture, Japan. J Mineral Petrol Sci 110:29–34

Andreev IF, Sokolov AN, Shebyakov AM, Tarlakov YP, Toropov NA (1971) An IR-spectroscopic study of solid solutions in the systems, $Ce_2Si_2O_7$-$Y_2Si_2O_7$ and $La_2Si_2O_7$-$Y_2Si_2O_7$. Zhurnal Prikladnoi Spektroskopii (J Appl Spectrosc) 14(2):340–343 (in Russian)

Andrieux J, Goutaudier C, Laversenne L, Jeanneau E, Miele P (2010) Synthesis, characterization, and crystal structure of a new trisodium triborate, $Na_3[B_3O_4(OH)_4]$. Inorg Chem 49:4830–4835

Andrut M, Brandstatter F, Beran A (2003) Trace hydrogen zoning in diopside. Miner Petrol 78:231–241

Andrut M, Wildner M, Beran A (2002) The crystal chemistry of birefringent natural uvarovites. Part IV. OH defect incorporation mechanisms in non-cubic garnets derived from polarized IR spectroscopy. Eur J Mineral 14:1019–1026

Ankinovitch EA, Bekenova GK, Podlipaeva NI (1989) Kazakhstanite, $Fe^{3+}{}_5V^{4+}{}_3V^{5+}{}_{12}O_{39}(OH)_9\cdot 8.55H_2O$ a new hydrous ferrovanadian mineral from carbonaceous-siliceous formation the NW Karatau (South Kazakhstan). Zapiski RMO (Proc Russ Mineral Soc) 118(5): 95–100 (in Russian)

Ansell VE, Chao GY (1987) Thornasite, a new hydrous sodium thorium silicate from Mont St-Hilaire, Quebec. Can Miner 25:181–183

Antenucci D, Miehe G, Tarte P, Schmahl WW, Fransolet A-M (1993) Combined X-ray Rietveld, infrared and Raman study of a new synthetic variety of alluaudite, $NaCdIn_2(PO_4)_3$. Eur J Mineral 5:207–213

Antonkhina TF, Savchenko NN, Sergienko VI, Ignat'eva LN, Markina IA (1992) Synthesis and physicochemical investigation of mixed alkali-metal cation hexafluorosilicates. Bull Russ Academy Sci, Division Chem Sci 41(2):193–200

Apollonov VN, Dolinina YuV, Yamnova NA, Pushcharovsky DYu, Ivanova TN (1990) Kaminite from Nepskoe K-salt deposit. Mineralogicheskiy Zhurnal (Mineral J) 12(6):79–81 (in Russian)

Apopei AI, Damian G, Buzgar N (2012) A preliminary Raman and FT-IR spectroscopic study of secondary hydrated sulfate minerals from the Hondol Open Pit (Metaliferi Mts., Romania). Roman J Miner Depos 85 (2):1–6

Apopei AI, Buzgar N, Buzatu A (2011) Raman and infrared spectroscopy of kaersutite and certain common amphiboles. Analele Stiintifice ale Universitatii "Al. I. Cuza" din Iasi Seria Geologie 57(2):35–58

Appleton JD, Bland DJ, Nancarrow PH, Styles MT, Mambwe SH, Zambezi P (1992) The occurrence of daqingshanite-(Ce) in the Nkombwa Hill carbonatite, Zambia. Mineral Mag 56:419–422

Aranda MAG, Bruque S (1990) Characterization of manganese(III) orthophosphate hydrate. Inorg Chem 29:1334–1337

Arkhipova EV, Zuev MG, Perelyaeva LA (2006) Phase relations and spectral properties of new phases in Sc_2O_3-V_2O_5-Nb_2O_5-Ta_2O_5 system. J Alloys Compd 414:48–54

Armbruster T (1985) Ar, N_2 and CO_2 in the structural cavities of cordierite, an optical and X-ray single-crystal study. Phys Chem Minerals 12:233–245

Armbruster T, Bloss FD (1982) Orientation and effects of channel H_2O and CO_2 in cordierite. Am Miner 67:284–291

Armbruster T, Oberhänsli R, Bermanec V (1992) Crystal structure of $SrMn^2[Si_2O_7](OH)_2\cdot H_2O$, a new mineral of the lawsonite type. Eur J Mineral 4:17–22

Armbruster T, Schreyer W, Hoefs J (1982) Very high CO_2 cordierite from Norwegian Lapland: mineralogy, petrology, and carbon isotopes. Contrib Mineral Petrol 81:262–267

Armstrong CR, Nash KL, Griffiths PR, Clark SB (2011) Synthesis and characterization of françoisite-(Nd): Nd $[(UO_2)_3O(OH)(PO_4)_2]\cdot 6H_2O$. Am Miner 96:417–422

Arndt J, Hummel W, Gonzalez-Cabeza I (1982) Diaplectic labradorite glass from the Manicouagan impact crater. I. Physical properties, crystallization, structural and genetic implications. Phys Chem Minerals 8:230–239

Atencio D, Andrade MB, Christy AG, Gieré R, Kartashov PM (2010) The pyrochlore supergroup of minerals: nomenclature. Can Miner 48:673–698

Atencio D, Carvalho FMS, Matioli PA (2004) Coutinhoite, a new thorium uranyl silicate hydrate, from Urucum mine, Galiléia, Minas Gerais, Brazil. Am Miner 89:721–724

Atencio D, Roberts AC, Cooper MA, Menezes Filho LAD, Coutinho JMV, Stirling JAR, Venance KE, Ball NA, Moffatt E, Chaves MLSC,

Brandão PRG, Romano AW (2012) Carlosbarbosaite, ideally $(UO_2)_2Nb_2O_6(OH)_2 \cdot 2H_2O$, a new hydrated uranyl niobate mineral with tunnels from Jaguaraçu, Minas Gerais, Brazil: description and crystal structure. Mineral Mag 76:75–90

Atencio D, Roberts AC, Matioli PA, Stirling JAR, Venance KE, Doherty W, Stanley CJ, Rowe R, Carpenter GJC, Coutinho JMV (2008) Brumadoite, a new copper tellurate hydrate, from Brumado, Bahia, Brazil. Mineral Mag 72:1201–1205

Au CT, Zhang Wei-De (1997) Oxidative dehydrogenation of propane over rare-earth orthovanadates. J Chem Soc Faraday Trans 93(6):1195–1204

Babaryk AA, Odynets IV, Khainakov S, Slobodyanika N, Garcia-Granda S (2013) $K_2Ta_4O_{11}$ (“kalitantite”): a wide band gap semiconductor synthesized in molybdate flux medium. Cryst Eng Comm 15:5539–5544

Badachhape RB, Hunter G, Mccory LD, Margrave JL (1966) Infrared absorption spectra of inorganic solids. IV. Hexafluorosilicates. Raman spectra of aqueous SiF_6^{2-}. Inorg Chem 5(5):929–931

Bailey SW (1988) Odinite, a new dioctahedral-trioctahedral Fe^{3+}-rich 1:1 clay mineral. Clay Miner 23:237–247

Bajda T (2010) Solubility of mimetite $Pb_5(AsO_4)_3Cl$ at 5–55 °C. Environ Chem 7:268–278

Bakovets VV, Levashova TM, Ratushnyak VT, Bakhturova LF (2002) Chemical vapor deposition of Y_2O_3 films using $Y(dpm)_3$. Inorg Mater 38(4):371–373

Balassone G, Bellatreccia F, Mormone A, Biagioni C, Pasero M, Petti C, Mondillo N, Fameli G (2012) Sodalite-group minerals from the Somma-Vesuvius volcanic complex, Italy: a case study of K-feldspar-rich xenoliths. Mineral Mag 76:191–212

Balassone G, Franco E, Matta CA, Puliti R (2004) Indialite in xenolithic rocks from Somma-Vesuvius volcano (Southern Italy): crystal chemistry and petrogenetic features. Am Miner 89:1–6

Balicheva TG, Roi NI (1971) IR spectra and structure of several crystalline hexahydroxyantimonates and their deutero analogs. Zhurnal Strukturnoi Khimii (J Struct Chem) 12(3):415–422 (in Russian)

Baran EJ (1975) Das Schwingungsspektrum von Magnesium-orthovanadat. Monats Chem 106:1–11 (in German)

Baran EJ, Aymonino PJ (1969) Die Infrarot-Spektren der Erdalkaliorthovanadate. Z anorg allg Chem 365:211–216 (in German)

Baran EJ, Aymonino PJ, Müller A (1972) Die Schwingungsspektren von Strontium- und Barium- Orthovanadat. J Molec Struct 11:453–457 (in German)

Baran EJ, Botto IL (1976) Das Schwingungsspektrum des synthetischen Carnotits. Monats Chem 107:633–639 (in German)

Baran EJ, Lii K-H (1992) Vibrational spectrum of $Zn_2VO(PO_4)_2$. J Raman Spectrosc 23:125–126

Baran J, Ilczyszyn MM, Marchewka MK, Ratajczak H (1999a) Vibrational studies of different modifications of the sodium hydrogen sulphate crystals. Spectrosc Lett Int J Rapid Commun 32(1):83–102

Baran EJ, Mormann T, Jeitschko W (1999b) Infrared and Raman spectra of $(Hg_2)_3(AsO_4)_2$ and $Hg_3(AsO_4)_2$. J Raman Spectrosc 30(12):1049–1051

Barinova AV, Rastsvetaeva RK, Sidorenko GA, Chukanov NV, Pushcharovskii DYu, Pasero M, Merlino S (2003) Crystal structure of metauranocircite Ba $(UO_2)_2(PO_4)_2 \cdot 6H_2O$. Doklady Akademii Nauk (Doklady Acad Sci) 389(2):203–206 (in Russian)

Baron D, Palmer CD (1996) Solubility of $KFe_3(CrO_4)_2(OH)_6$ at 4 to 35 °C. Geochim Cosmochim Acta 60(20):3815–3824

Basak D, Ghose J (1994) Infrared studies on some substituted copper chromite spinels. Spectrochim Acta A 50(4):713–718

Basciano LC, Peterson RC (2007a) The crystal structure of ammoniojarosite, $(NH_4)Fe_3(SO_4)_2(OH)_6$ and the crystal chemistry of the ammoniojarosite – hydronium jarosite solid-solution series. Mineral Mag 71:427–441

Basciano LC, Peterson RC (2007b) Jarosite – hydronium jarosite solid-solution series with full iron site occupancy: mineralogy and crystal chemistry. Am Miner 92:1465–1473

Bates JB, Quist AS (1974) Vibrational spectra of solid and molten phases of the alkali metal tetrafluoroborates. Spectrochim Acta A 31:1317–1327

Bates JB, Quist AS, Boyd GE (1971) Infrared and Raman spectra of polycrystalline $NaBF_4$. J Chem Phys 54 (1):124–126

Bauman RP, Porto SPS (1967) Lattice vibrations and structure of rare-earth fluorides. Phys Rev 161 (3):842–847

Baur WH (1972) Prediction of hydrogen bonds and hydrogen atom positions in crystalline solids. Acta Crystallogr B 28:1456–1465

Bazhenov AG, Nedosekova IL, Petersen EU (1993) Ftorrichterite $Na_2Ca(Mg,Fe)_5[Si_8O_{22}](F,OH)_2$ – a new mineral species in the amphibole group. Zapiski RMO (Proc Russ Mineral Soc) 122(3):98–102 (in Russian)

Behrens H, Müller G (1995) An infrared spectroscopic study of hydrogen feldspar ($HAlSi_3O_8$). Mineral Mag 59:15–24

Belik AA, Izumi F, Ikeda T, Okui M, Malakho AP, Morozov VA, Lazoryak BI (2002) Whitlockite-related phosphates $Sr_9A(PO_4)_7$ (A = Sc, Cr, Fe, Ga, and In): structure refinement of $Sr_9In(PO_4)_7$ with synchrotron X-Ray powder diffraction data. J Solid State Chem 168:237–244

Bell DR, Rossman GR (1992) Water in earth’s mantle: the role of nominally anhydrous minerals. Science 255:1391–1397

Bellatreccia F, Cámara F, Bindi L, Della Ventura G, Mottana A, Gunter ME, Sebastiani M (2009a) La fantappieite, nuovo minerale del gruppo cancrinite-sodalite. Il Cercapietre Notiziario Del Gruppo Mineralogico Romano 1–2:6–15 (in Italian)

Bellatreccia F, Della Ventura G, Piccinini M, Cavallo A, Brilli M (2009b) H_2O and CO_2 in minerals of the haüyne-sodalite group: an FTIR spectroscopic study. Mineral Mag 73:399–423

Bellatreccia F, Della Ventura G, Gatta GD, Guidi MC, Harley S (2012) Carbon dioxide in pollucite, a feldspathoid with the ideal composition (Cs, $Na)_{16}Al_{16}Si_{32}O_{96}{\cdot}nH_2O$. Mineral Mag 76:903–911

Bellezza M, Franzini M, Larsen AO, Merlino S, Perchiazzi N (2004) Grenmarite, a new member of the götzenite-seidozerite-rosenbuschite group from the Langesundsfjord district, Norway: definition and crystal structure. Eur J Mineral 16(6):971–978

Belokoneva EL, Al'-Ama AG, Dimitrova OV, Kurazhkovskaya VS, Stefanovich SYu (2002a) Synthesis and crystal structure of new carbonate $NaPb_2(CO_3)_2(OH)$. Kristallografiya (Crystallogr) 47(2):253–258 (in Russian)

Belokoneva EL, Kabalov YK, Al'-Ama AG, Dimitrova OV, Kurazhkovskaya VS, Stefanovich SY (2002b) New oxygen- and lead-deficient lead borate $Pb^{(I)}_{0.9}Pb^{(II)}_{0.6}[BO_{2.25}]_2 = 2Pb_{0.75}[BO_{2.25}]$ and its relation to aragonite and calcite structures. Kristallografiya (Crystallogr) 47(1):24–29 (in Russian)

Belt FR (1967) Hydrothermal ruby: infrared spectra and X-ray topography. J Appl Phys 38:2688–2689

Belyayevskaya GP, Borutskiy BYe, Marsiy IM, YeV Vlasova, Sivtsov AV, Golovanova TI, Vishnev AI (1991) Potassium-calcium gaidonnayite, $(Ca,Na,K)_2{\cdot}xZrSi_3O_9{\cdot}nH_2O$, a new mineral variety from the Khibiny block. Doklady Akademii Nauk SSSR (Doklady USSR Acad Sci) 320(5):1220–1225 (in Russian)

Ben-Dor L, Margalith R (1967) An I.R. and D.T.A. study of the hydrates of the metal sulfates of Cu^{2+}, Co^{2+}, Ni^{2+}, Cd^{2+}, Mn^{2+}, Zn^{2+}, and Mg^{2+}. Inorg Chim Acta 1 (1): 49–54

Benna P, Tribaudino M, Bruno E (1995) Al-Si Ordering in Sr-Feldspar $SrAl_2Si_2O_8$: IR, TEM and single-crystal XRD evidences. Phys Chem Minerals 22:343–350

Benramdane L, Bouatia M, Idrissi MOB, Draoui M (2008) Infrared analysis of urinary stones, using a single reflection accessory and a KBr pellet transmission. Spectrosc Lett Int J Rapid Commun 41(2):72–80

Beran A (1970a) Messung des Ultrarot-Pleochroismus von Mineralen. IX. Der Pleochroismus der OH-Streckfrequenz in Titanit. Tschermaks Miner Petr Mitt 14:1–5 (in German)

Beran A (1970b) Ultrarotspektroskopischer Nachweis von OH-Gruppen in den Mineralen der Al_2SiO_5-Modifikationen. Anzeiger – Österr Akad Wissenschaften, Math-naturwiss Klasse, S 184–185 (in German)

Beran A (1971a) Messung des Ultrarot-Pleochroismus von Mineralen. XII. Der Pleochroismus der OH-Streckfrequenz in Disthen. Tschermaks Miner Petr Mitt 16:129–135 (in German)

Beran A (1971b) Messung des Ultrarot-Pleochroismus von Mineralen. XIII. Der Pleochroismus der OH-Streckfrequenz in Axinit. Tschermaks Miner Petr Mitt 16:281–286 (in German)

Beran A (1986) A model of water allocation in alkali feldspar, derived from infrared-spectroscopic investigations. Phys Chem Minerals 13:306–310

Beran A (1987) OH groups in nominally anhydrous framework structures: an infrared spectroscopic investigation of danburite and labradorite. Phys Chem Minerals 14:441–445

Beran A (1991) Trace hydrogen in Verneuil-grown corundum and its colour varieties, an IR spectroscopic study. Eur J Mineral 3:971–975

Beran A, Gotzinger MA (1987) The quantitative IR spectroscopic determination of structural OH groups in kyanites. Miner Petrol 36:41–49

Beran A, Libowitzky E (2006) Water in natural mantle minerals II: olivine, garnet and accessory minerals. Rev Mineral Geochem 62:169–191

Beran A, Putnis A (1983) A model of the OH positions in olivine, derived from infrared-spectroscopic investigations. Phys Chem Minerals 9:57–60

Beran A, Rossman GR (1989) The water content of nepheline. Miner Petrol 40:235–240

Beran A, Rossman GR, Grew ES (1989) The hydrous component of sillimanite. Am Miner 74:812–817

Beran A, Zemann J (1969) Messung des Ultrarot-Pleochroismus von Mineralen. VIII. Der Pleochroismus der OH Streckfrequenz in Andalusit. Tschermaks Miner Petr Mitt 13:285–292 (in German)

Beran A, Zemann J (1971) Messung des Ultrarot-Pleochroismus von Mineralen. XI. Der Pleochroismus der OH-Streckfrequenz in Rutil, Anatas, Brookit und Cassiterit. Tschermaks Miner Petr Mitt 15:71–80 (in German)

Bergaya F, Brigatti MF, Fripiat JJ (1985) Contribution of infrared spectroscopy to the study of corrensite. Clays Clay Miner 33(5):458–462

Bernstein MP, Sandford SA (1999) Variations in the strength of the infrared forbidden 2328.2 cm^{-1} fundamental of solid N_2 in binary mixtures. Spectrochim Acta A 55(12):2455–2466

Berry AJ, Hermann J, O'Neill HSC, Foran GJ (2005) Fingerprinting the water site in mantle olivine. Geology 33:869–872

Berry AJ, O'Neill HSC, Hermann J, Scott DR (2007a) The infrared signature of water associated with trivalent cations in olivine. Earth Planetary Sci Lett 261:134–142

Berry AJ, Walker MA, Hermann J, O'Neill HSC, Foran GJ, Gale JD (2007b) Titanium substitution mechanisms in forsterite. Chem Geol 242:176–186

Bertoluzza A, Monti P, Battaglia MA, Bonora S (1980) Infrared and Raman spectra of orthorhombic, monoclinic and cubic metaboric acid and their relation to the "strength" of the hydrogen bond present. J Molec Struct 64:123–136

Bervas M, Yakshinskiy B, Klein LC, Amatucci GG (2006) Soft-chemistry synthesis and characterization of bismuth oxyfluorides and ammonium bismuth fluorides. J Am Ceram Soc 89(2):645–651

Bessekhouad Y, Gabes Y, Bouguelia A, Trari M (2007) The physical and photo electrochemical characterization of the crednerite $CuMnO_2$. J Mater Sci 42:6469–6476

Besson G, Drits VA (1997a) Refined relationships between chemical composition of dioctahedral fine-grained mica minerals and their infrared spectra within the OH stretching region. Part I: identification of the OH stretching bands. Clay Miner 45 (2):158–169

Besson G, Drits VA (1997b) Refined relationships between chemical composition of dioctahedral fine-grained mica minerals and their infrared spectra within the OH stretching region. Part II: the main factors affecting OH vibrations and quantitative analysis. Clays. Clay Miner 45(2):170–183

Betsch RJ, White WB (1978) Vibrational spectra of bismuth oxide and the sillenite-structure bismuth oxide derivatives. Spectrochim Acta A 34:505–514

Biagioni C, Orlandi P, Nestola F, Bianchin S (2013) Oxycalcioroméite, $Ca_2Sb_2O_6O$, from Buca della Vena mine, Apuan Alps, Tuscany, Italy: a new member of the pyrochlore supergroup. Mineral Mag 77:3027–3037

Bich Ch, Ambroise J, Péra J (2009) Influence of degree of dehydroxylation on the pozzolanic activity of metakaolin. Appl Clay Sci 44:194–200

Bilinski H, Giovanoli R, Usui A, Hanžel D (2002) Characterization of Mn oxides in cemented streambed crusts from Pinal Creek, Arizona, U.S.A., and in hot-spring deposits from Yuno-Taki Falls, Hokkaido, Japan. Am Miner 87:580–591

Bindi L, Welch MD, Bonazzi P, Pratesi G, Menchetti S (2008) The crystal structure of seeligerite, $Pb_3IO_4Cl_3$, a rare Pb-I-oxychloride from the San Rafael mine, Sierra Gorda, Chile. Mineral Mag 72:771–783

Birch WD, Kolitsch U, Witzke T, Nasdala L, Bottrill RS (2000) Petterdite, the Cr-dominant analogue of dundasite, a new mineral species from Dundas, Tasmania, Australia and Callenberg, Saxony, Germany. Can Miner 38:1467–1476

Bish DL, Livingstone A (1981) The crystal chemistry and paragenesis of honessite and hydrohonessite: the sulphate analogues of reevesite. Mineral Mag 44:339–343

Blagojević V, Gledhill GA, Hamilton A, Upadhyay SB, Nikolić PM, Pavlović MB, Raković DI (1991) Far-infrared optical properties of ZnS highly doped with Fe. Infrared Phys 31(4):387–393

Blasse G, van den Heuvel GPM (1973) Some optical properties of tantalum borate ($TaBO_4$), a compound with unusual coordinations. Phys Status Solidi A 19:111–117

Blonska-Tabero A (2008) New phase in the system $FeVO_4$-$Cd_4V_2O_9$. J Therm Anal Calorim 93:707–710

Blonska-Tabero A (2012) Phases in the subsolidus area of the system CuO-V_2O_5-Fe_2O_3. J Therm Anal Calorim 109:685–691

Blount AM, Threadgold IM, Bailey SW (1969) Refinement of the crystal structure of nacrite. Clays Clay Miner 17:185–194

Bocelli S, Guizzetti G, Marabelli F, Parravicini GB, Patrini M, Henrion W, Lange H, Tomm Y (1995) Anisotropic optical response in β-$FeSi_2$ single crystals and thin films. Mat Res Soc Symp Proc 402:349–354

Boffa Ballaran T, Carpenter MA, Ross NL (2001) Infrared powder-absorption spectroscopy of Ca-free $P2_1/c$ clinopyroxenes. Mineral Mag 65:339–350

Boghosian S, Fehrmann R, Nielsen K (1994) Synthesis and crystal structure of $Na_3V(SO_4)_3$. Spectroscopic characterization of $Na_3V(SO_4)_3$ and $NaV(SO_4)_2$. Acta Chemica Scand 48(9):724–731

Bojar H-P, Walter F (2006) Fluoro-magnesiohastingsite from Dealul Uroi (Hunedoara county, Romania): mineral data and crystal structure of a new amphibole end-member. Eur J Mineral 18:503–508

Bojar H-P, Walter F (2012) Joanneumite, IMA 2012-001. CNMNC Newsletter No. 13, June 2012, 814. Mineral Mag 76:807–817

Bojar H-P, Walter F, Baumgartner J, Färber G (2010) Ammineite, $CuCl_2(NH_3)_2$, a new species containing an ammine complex: mineral data and crystal structure. Can Miner 48:1359–1371

Bolfan-Casanova N (2005) Water in the earth's mantle. Mineral Mag 69:229–257

Bolfan-Casanova N, Keppler H, Rubie DC (2000) Water partitioning between nominally anhydrous minerals in the MgO-SiO_2-H_2O system up to 24 GPa: implications for the distribution of water in the earth's mantle. Earth Planetary Sci Lett 182:209–221

Bolfan-Casanova N, Keppler H, Rubie DC (2002) Hydroxyl in $MgSiO_3$ akimotoite: a polarized and high-pressure IR study. Am Miner 87:603–608

Bolfan-Casanova N, McCammon CA, Mackwell SJ (2006) Water in transition zone and lower mantle minerals. In: Jacobsen SD, van der Lee S (eds) Earth's deep water cycle, geophysical monograph series 168. American Geophysical Union, Washington

Bonaccorsi E, Merlino S (2005) Modular microporous minerals: cancrinite-davyne group and C-S-H phases. Rev Mineral Geochem 57:241–290

Bonadeo HA, Silberman E (1970) The vibrational spectra of sodium, potassium and ammonium fluoroborates. Spectrochim Acta A 25:2337–2343

Boonchom B, Danvirutai C, Thongkam M (2010) Non-isothermal decomposition kinetics of synthetic serrabrancaite ($MnPO_4 \cdot H_2O$) precursor in N_2 atmosphere. J Therm Anal Calorim 99:357–362

Boonchom B, Youngme S, Maensiri S, Danvirutai C (2008) Nanocrystalline serrabrancaite ($MnPO_4 \cdot H_2O$) prepared by a simple precipitation route at low temperature. J Alloys Compd 454(1-2):78–82

Borghesi A, Piaggi A, Franchini A, Guizzetti G, Nava F, Santoro G (1990) Far-infrared vibrational spectroscopy in $CrSi_2$. Europhys Lett 11(1):61–65

Boroumand F, Moser JE, van den Bergh H (1992) Quantitative diffuse reflectance and transmittance infrared spectroscopy of nondiluted powders. Appl Spectrosc 46(12):1874–1886

Bosi F, Reznitskii L, Skogby H (2012a) Oxy-chromium-dravite, $NaCr_3(Cr_4Mg_2)(Si_6O_{18})(BO_3)_3(OH)_3O$, a new mineral species of the tourmaline supergroup. Am Miner 97:2024–2030

Bosi F, Skogby H, Agrosì G, Scandale E (2012b) Tsilaisite, $NaMn_3Al_6(Si_6O_{18})(BO_3)_3(OH)_3OH$, a new

mineral species of the tourmaline supergroup from Grotta d'Oggi, San Pietro in Campo, island of Elba, Italy. Am Miner 97:989–994

Bosi F, Skogby H, Hålenius U, Reznitskii L (2013) Crystallographic and spectroscopic characterization of Fe-bearing chromo-alumino-povondraite and its relations with oxy-chromium-dravite and oxy-dravite. Am Miner 98:1557–1564

Bosi F, Skogby H, Reznitskii L, Hålenius U (2014a) Vanadio-oxy-dravite, $NaV_3(Al_4Mg_2)(Si_6O_{18})(BO_3)_3(OH)_3O$, a new mineral species of the tourmaline supergroup. Am Miner 99:218–224

Bosi F, Reznitskii L, Skogby H, Hålenius U (2014b) Vanadio-oxy-chromium-dravite, $NaV_3(Cr_4Mg_2)(Si_6O_{18})(BO_3)_3(OH)_3O$, a new mineral species of the tourmaline supergroup. Am Miner 99:1155–1162

Bosi F, Andreozzi GB, Hålenius U, Skogby H (2015) Experimental evidence for partial Fe^{2+} disorder at the *Y* and *Z* sites of tourmaline: a combined EMP, SREF, MS, IR and OAS study of schorl. Mineral Mag 79:515–528

Bottger GL, Geddes AL (1967) Infrared lattice vibrational spectra of AgCl, AgBr, and AgI. J Chem Phys 46 (8):3000–3004

Botto IL, Baran EJ (1980) Röntgenographische und spektroskopische Untersuchung einiger Telluromolybdate. Z anorg allg Chem 468(1):221–227 (in German)

Botto IL, Baran EJ (1982) Die IR-Spektren der Phasen $A^{III}_{1/2}B^{V}_{1/2}Te_3O_8$ (A = Fe, In, Sc; B = Nb, Ta) und UTe_3O_9. Z anorg allg Chem 484(1):210–214 (in German)

Botto IL, Baran EJ, Aymonino PJ, Pedregosa JC, Puelles GF (1975) Darstellung, kristallographische Daten und IR-Spektrum von Mangan(II)-diarsenat. Monats Chem 106:1559–1566 (in German)

Botto IL, Baran EJ, Deliens M (1989a) Vibrational spectrum of natural and synthetic metatyuyamunite. N Jb Miner Mh 5:212–218

Botto IL, García AC, Deliens M (1989b) Thermal and IR spectroscopic characterization of kamotoite. Collection Czechoslov Chem Commun 54:1263–1268

Botto IL, Barone VL, Castiglioni JL, Schalamuk IB (1997a) Characterization of a natural substituted pyromorphite. J Mater Sci 32:6549–6553

Botto IL, Vassallo MB, Baran EJ, Minelli G (1997b) IR spectra of VO_2 and V_2O_3. Mater Chem Phys 50:267–270

Boukili B, Holtz F, Robert J-L, Joriou M, Bény J-M, Naji M (2003) Infrared spectra of annite in the OH-stretching vibrational range. Swiss Bull Miner Petrol 83(3):331–340

Bowles JFW, Jobbins EA, Young BR (1980) A re-examination of cheralite. Mineral Mag 43:885–888

Brabers VAM, Klerk J (1974) The infrared absorption spectrum and the inversion degree of manganese ferrite. Solid State Comm 14:613–615

Braithwaite RSW (1985) Roeblingite: a revised formula from infra-red and thermal analysis data. Mineral Mag 49:756–758

Braithwaite RSW (1988) Spencerite from Kabwe, Zambia, and the infrared spectroscopy of the Kabwe zinc phosphates. Mineral Mag 52:126–129

Braithwaite RSW (1991) Kegelite: infrared spectroscopy and a structural hypothesis. Mineral Mag 55:127–134

Braithwaite RSW, Paar WH, Chisholm JE (1989) Phurcalite from Dartmoor, Southwest England, and its identity with 'nisaite' from Portugal. Mineral Mag 53:583–589

Braithwaite RSW, Ryback G (1988) Philipsburgite from the Caldbeck Fells and kipushite from Montana, and their infrared spectra. Mineral Mag 52:529–533

Braithwaite RSW, Ryback G (1994) Reichenbachite from Cornwall and Portugal. Mineral Mag 58:449–454

Brandel V, Dacheux N, Genet M (1996) Reexamination of uranium (IV) phosphate chemistry. J Solid State Chem 121(2):467–472

Brandel V, Dacheux N, Genet M, Podor R (2001) Hydrothermal synthesis and characterization of the thorium phosphate hydrogenphosphate, thorium hydroxide phosphate, and dithorium oxide phosphate. J Solid State Chem 159:139–148

Brauer G (1954) Handbuch der Prepärativen anorganischen Chemie. Verlag, Stuttgart (in German)

Brigatti MF, Poppi L (1984) 'Corrensite-like mineral' in the Taro and Ceno Valleys, Italy. Clay Miner 19:59–66

Brigatti MF, Poppi L (1985) Interlayer water and swelling properties of natural and homoionic corrensite. Clays Clay Miner 33:128–134

Brisse F, Stewart DJ, Seidl V, Knop O (1972) Pyrochlores. VIII. Studies of some 2-5 pyrochlores and related compounds and minerals. Can J Chem 50:3648–3666

Britvin SN, Burakov BE, Nikitin SA, Bogdanova AN (1989) Molybdomenite $PbSeO_3$ from selenide occurrence in southern Karelia. New Data Minerals 36:123–129 (in Russian)

Britvin SN, Pakhomovskii YaA, Bogdanova AN, Skiba VI (1991) Strontiowhitlockite, $Sr_9Mg(PO_3OH)(PO_4)_6$, a new mineral species from the Kovdor Deposit, Kola Peninsula, USSR. Can Miner 29:87–93

Bromiley FA, Ballaran TB, Zhang M (2007) An infrared investigation of the otavite-magnesite solid solution. Am Miner 92:837–843

Brooker MH, Bates JB (1971) Raman and infrared spectral studies of anhydrous Li_2CO_3 and Na_2CO_3. J Chem Phys 54:4788–4796

Brooker MH, Sunder S, Taylor P, Lopata VJ (1983) Infrared and Raman spectra and X-ray diffraction studies of solid lead(II) carbonates. Can J Chem 61:494–502

Brown BE, Bailey SW (1962) Chlorite polytypism: I. Regular and semi-random one-layer structures. Am Miner 47:819–850

Brugger J, Elliott P, Meisser N, Ansermet S (2011) Argandite, $Mn_7(VO_4)_2(OH)_8$, the V analogue of allactite from the metamorphosed Mn ores at Pipji, Turtmann Valley, Switzerland. Am Miner 96:1894–1900

Brugger J, Gieré R, Graeser S, Meisser N (1997) The crystal chemistry of roméite. Contrib Mineral Petrol 127:136–146

Brugger J, Krivovichev SV, Berlepsch P, Meisser N, Ansermet S, Armbruster T (2004) Spriggite, $Pb_3[(UO_2)_6O_8(OH)_2](H_2O)_3$, a new mineral with β-$U_3O_8$-type sheets: description and crystal structure. Am Miner 89:339–347

Brugger J, Wallwork KS, Meisser N, Pring A, Ondruš P, Čejka J (2006) Pseudojohannite from Jáchymov, Musonoï, and La Creusaz: a new member of the zippeite-group. Am Miner 91:929–936

Brunner GO, Wondratschek H, Laves F (1961) Ultrarotuntersuchungen über den Einbau von H in natürlichem Quarz. Z Elektrochem, Ber Bunsenges phys Chem 65(9):735–750 (in German)

Brusentsova T, Peale RE, Maukonen D, Figueiredo P, Harlow GE, Ebel DS, Nissinboim A, Sherman K, Lisse CM (2012) Laboratory far-infrared spectroscopy of terrestrial sulphides to support analysis of cosmic dust spectra. Mon Not Royal Astron Soc 420(3):2569–2579

Brüesch P, Wullschleger J (1973) Optical properties of α-Ag_2S and β-Ag_2S in the infrared and far-infrared. Solid State Commun 13(1):9–12

Buckley HA, Bevan JC, Brown KM, Johnson LR, Farmer VC (1978) Glauconite and celadonite: two separate mineral species. Mineral Mag 42:373–382

Buijs K, Schutte CJH (1961) The infra-red spectra and structures of Li_2CO_3 and anhydrous Na_2CO_3. Spectrochim Acta 17:927–932

Burba CM (2006) Vibrational spectroscopy of phosphate-based electrodes for lithium rechargeable batteries. Dissertation, The University of Oklahoma, Norman

Burley RA (1968) The infrared spectrum and structure of selenium dioxide. Mater Res Bull 3(9):735–744

Burns PC, Carpenter MA (1997) Phase transitions in the series boracite – trembathite – congolite: an inrared spectroscopic study. Can Miner 35:189–202

Burns PC, Roberts AC, Stirling JAR, Criddle AJ, Feinglos MN (2000) Dukeite, $Bi^{3+}{}_{24}Cr^{6+}{}_8O_{57}(OH)_6(H_2O)_3$, a new mineral from Brejaúba, Minas Gerais, Brazil: description and crystal structure. Am Miner 85:1822–1827

Burns RG, Strens RGJ (1966) Infrared study of the hydroxyl bonds in clinoamphiboles. Science 153:890–892

Busca G (1996) The use of vibrational spectroscopies in studies of heterogeneous catalysis by metal oxides: an introduction. Catal Today 27:323–352

Bushueva EB, Garanin VK, Gorbachev NS, Kudryavtseva GP (1983) Possibilities of infrared spectroscopy in the study of ilmenite. Mineralogicheskiy Zhurnal (Mineral J) 3(6):15–22 (in Russian)

Byer HH, Lloyd CB, Lefkowitz I, Deaver BS Jr (1973) Raman and far-infrared spectra of proustite (Ag_3AsS_3) and pyrargyrite (Ag_3SbS_3). Ferroelectrics 5(1):207–217

Bürger H, Kneipp K, Hobert H, Vogel W, Kozhukharov V, Neov S (1992) Glass formation, properties and structure of glasses in the TeO_2-ZnO system. J Non-Cryst Solids 151:134–142

Callegari AM, Boiocchi M, Bellatreccia F, Caprilli E, Medenbach O, Cavallo A (2011) Capranicaite, (K,□)(Ca,Na)$Al_4B_4Si_2O_{18}$: a new inosilicate from Capranica, Italy, with a peculiar topology of the periodic single chain [Si_2O_6]. Mineral Mag 75:33–43

Campbell JA (1965) Vibrational frequencies of the chromium-oxygen bond and the oxidation state of chromium. Spectrochim Acta 21:851–852

Canterford JH, Tsambourakis G, Lambert B (1984) Some observations on the properties of dypingite, $Mg_5(CO_3)_4(OH)_2{\cdot}5H_2O$, and related minerals. Mineral Mag 48:437–442

Carlson L, Schwertmann U (1980) Natural occurrence of feroxyhite (δ′-FeOOH). Clays Clay Miner 28(4):272–280

Carnall WT, Neufeldt SJ, Walker A (1965) Reactions in molten salt solutions. I. Uranate and neptunate formation in molten lithium nitrate–sodium nitrate. Inorg Chem 4(12):1808–1813

Catti M, Ferraris G, Ivaldi G (1979) Refinement of the crystal structure of anapaite, $Ca_2Fe(PO_4)_2{\cdot}4H_2O$: hydrogen bonding and relationships with the bihydrated phase. Bull Minér 102:314–318

Čech F, Povondra P (1979) A re-examination of bořickýite. Tschermaks Min Petr Mitt 26:79–86

Čejka J (1999) Infrared spectroscopy and thermal analysis of the uranyl minerals. Rev Mineral Geochem 38:521–622

Čejka J Jr, Muck A, Čejka J (1984) To the infrared spectroscopy of natural uranyl phosphates. Phys Chem Minerals 11:172–177

Čejka J Jr, Muck A, Čejka J (1985) Infrared spectra and thermal analysis of synthetic uranium micas and their deuteroanalogues. N Jb Miner Mh 3:115–126

Čejka J, Sejkora J, Plášil J, Bahfenne S, Palmer SJ, Rintoul L, Frost RL (2011) A vibrational spectroscopic study of hydrated Fe^{3+} hydroxyl-sulphates; polymorphic minerals butlerite and parabutlerite. Spectrochim Acta A 79(5):1356–1363

Čejka J, Sejkora J, Skála R, Čejka J Jr, Novotná M, Ederová J (1998) Contribution to the crystal chemistry of synthetic becquerelite, billietite and protasite. N Jb Miner Abh 174:159–180

Čejka J, Urbanec Z, Čejka J Jr, Ederová J, Muck A (1988) Thermal and infrared spectral analyses of sabugalite. J Therm Anal 33:395–399

Čejka J, Urbanec Z (1990) Secondary uranium minerals. The mineralogy, geochemistry and crystal chemistry of the secondary uranium (IV) minerals. Trans Czechoslov Academy Sci, Math Natur History Series 100, Academia, Prague

Cevik S, Şaşmaz B, Yenikaya C, Çolak F, Sari M, Büyükgüngör O (2010) Synthesis, structural, spectral, thermal and comparative biological activity studies of $[V_2O_2(SO_4)_2(H_2O)_6]$. Zhurnal Neorganicheskoi Khimii (Russ J Inorg Chem) 55(4):546–553 (in Russian)

Chabchoub S, Dogguy M (1993) Contribution a l'etude des systemes $Ca_3(PO_4)_2$-MSO_4 (M = Sr, Ba). J Therm Anal 39:359–371 (in French)

Chakhmouradian AR, Cooper MA, Medici L, Abdu YA, Shelukhina YS (2013) Anzaite-(Ce), IMA 2013-004. CNMNC Newsletter 16:2701. Mineral Mag 77:2695–2709

Chakhmouradian AR, Mitchell RH, Pankov AV, Chukanov NV (1999) Loparite and 'metaloparite' from the Burpala alkaline complex, Baikal Alkaline Province (Russia). Mineral Mag 63:519–534

Chalmers JM (2006) Anomalies, artifacts and common errors in using vibrational spectroscopy techniques. In: Handbook of vibrational spectroscopy. Wiley, Hoboken

Chamberlain JM, Nikolic PM, Merdan M, Mihailovic P (1976) Far-infrared optical properties of SnS. J Phys C Solid State Phys 9(22):L637–L642

Chamberlain JM, Sirbegović SS, Nikolić PM (1974) Far-infrared absorption in amorphous and crystalline GeSe. J Phys C 7(7):L150–L153

Chang TG, Irish DE (1973) Raman and infrared studies of hexa-, tetra-, and dihydrates of crystalline magnesium nitrate. Can J Chem 51:118–125

Chao GY, Baker J, Sabina AP, Roberts AC (1985) Doyleite, a new polymorph of $Al(OH)_3$, and its relationship to bayerite, gibbsite and nordstrandite. Can Miner 23:21–28

Chao GY, Gault RA (1997) Quintinite-2*H*, quintinite-3*T*, charmarite-2*H*, charmarite-3*T* and caresite-3*T*, a new group of carbonate minerals related to the hydrotalcite-manasseite group. Can Miner 35:1541–1549

Charoy B, de Donato P, Barres O, Pinto-Coelho C (1996) Channel occupancy in an alkali-poor beryl from Serra Branca (Goias, Brazil): spectroscopic characterization. Am Miner 81:395–403

Chaudhuri MK, Islam NS, Purkayastha S (1991) Reaction of sodium bismuthate with fluoride in an aqueous medium to give fluoro compounds of bismuth(III). J Fluor Chem 52:117–123

Chauhan CK, Joshi MJ (2014) Growth and characterization of struvite-Na crystals. J Cryst Growth 401:221–226

Chauhan CK, Vyas PM, Joshi MJ (2011) Growth and characterization of Struvite-K crystals. Cryst Res Technol 46(2):187–194

Chaussidon J (1972) The I.R. spectrum of structural hydroxyls of K-depleted biotites. Clays Clay Miner 20:59–67

Chen J, Xu R, Xu Y, Qiu J (1990) Synthesis and characterization of two aluminoarsenates with occluded ethylenediamine. J Chem Soc Dalton Trans 11:3319–3323

Chen X, Zhao Y, Chang X, Zuo J, Zang H, Xiao W (2006) Syntheses and crystal structures of two new hydrated borates, $Zn_8[(BO_3)_3O_2(OH)_3]$ and $Pb[B_5O_8(OH)]$ $1.5H_2O$. J Solid State Chem 179:3911–3918

Chernikov AA, Sidorenko GA, Valuyeva AA (1977) The new data on uranyl minerals of ursilite-weeksite group. Zapiski RMO (Proc Russ Mineral Soc) 106 (5):553–564 (in Russian)

Chernorukov NG, Knyazev AV, Knyazeva MA, Razina YuV (2003) Synthesis, structure, and physicochemical properties of $A^I_4[UO_2(CO_3)_3]\cdot nH_2O$ (A^I = Li, Na, K, NH_4). Radiokhimiya (Radiochemistry) 45(4):298–302 (in Russian)

Chernorukov NG, Kortikov VE (2001) $Na[HSiUO_6]\cdot H_2O$: synthesis, structure, and properties. Radiokhimiya (Radiochemistry) 43(3):206–208 (in Russian)

Chesnokov BV, Shcherbakova EP (1991) Mineralogiya gorelykh otvalov Chelyabinskogo ugol'nogo basseyna (opyt mineralogii tekhnogeneza) (Mineralogy of burning dumps of the Chelyabinsk coal basin (practice of mineralogy of technogenesis)). Nauka, Moscow (in Russian)

Chesnokov BV, Bazhenova LF, Bushmakin AF, Vilisov VA, Lotova EV, Mikhal TA, Nishanbaev TP, Shcherbakova EP (1991) Novyye mineraly gorelykh otvalov Chelyabinskogo ugol'nogo basseyna (soobshcheniye vtoroye), Novyye dannyye po mineralogii endogennykh mestorozhdeniy i zon tekhnogeneza Urala (New minerals from burned dumps of the Chelyabinsk coal basin (Report No. 2)), 5–14. In: New Data on Mineralogy of Endogenic Deposits and Technogenesis Zones of Urals. Ural Branch of the Academy of Sciences of the USSR, Sverdlovsk (in Russian)

Chopin C, Seidel E, Theye T, Ferraris G, Ivaldi G, Catti M (1992) Magnesiochloritoid, and the Fe-Mg series in the chloritoid group. Eur J Mineral 4:67–76

Chukanov NV (2014a) Infrared spectra of mineral species. Extended library. Springer, Dordrecht, Heidelberg, New York, London

Chukanov NV (2014b) Infrared spectroscopy of acid salts. II. Acid groups in nominally neutral and basic phosphates, arsenates and vanadates. Zapiski RMO (Proc Russ Mineral Soc) 143(2):35–44 (in Russian)

Chukanov NV, Aksenov SM, Pekov IV, Ternes B, Schüller W, Belakovskiy DI, Van KV, Blass G (2014a) Ferroindialite $(Fe^{2+},Mg)_2Al_4Si_5O_{18}$, a new beryl-group mineral from the Eifel Volcanic Region, Germany. Geol Ore Depos 56(8):637–643

Chukanov NV, Britvin SN, Möhn G, Pekov IV, Zubkova NV, Nestola F, Kasatkin AV, Dini M (2014b) Shilovite, IMA 2014-016. CNMNC Newsletter No. 21, October 2014, page 798. Mineral Mag 78:97–804

Chukanov NV, Scholz R, Zubkova NV, Pekov IV, Belakovskiy DI, Van KV, Lagoeiro L, Graça LM, Krambrock K, de Oliveira LCA, Menezes Filho LAD, Chaves MLCS, Pushcharovsky DYu (2014c) Correianevesite, $Fe^{2+}Mn^{2+}_2(PO_4)_2\cdot 3H_2O$, a new reddingite-group mineral from the Cigana mine, Conselheiro Pena, Minas Gerais, Brazil. Am Miner 99:811–816

Chukanov NV, Aksenov SM, Rastsvetaeva RK, Blass G, Varlamov DA, Pekov IV, Belakovskiy DI, Gurzhiy VV (2015a) Calcinaksite, KNaCa

$(Si_4O_{10})\cdot H_2O$, a new mineral from the Eifel volcanic area, Germany. Miner Petrol 109:397–404

Chukanov NV, Zubkova NV, Möhn G, Pekov IV, Pushcharovsky DYu, Zadov AE (2015b) Chanabayaite $Cu_2(N_3C_2H_2)_2Cl(NH_3,Cl,H_2O,\square)_4$, a new mineral containing triazolate anion. Zapiski RMO (Proc Russ Mineral Soc) 144(2):36–47 (in Russian)

Chukanov NV, Britvin SN, Möhn G, Pekov IV, Zubkova NV, Nestola F, Kasatkin AV, Dini M (2015c) Shilovite, natural copper(II) tetrammine nitrate, a new mineral species. Mineral Mag 79:613–623

Chukanov NV, Göttlicher J, Möckel S, Sofer Z, Van KV, Belakovskiy DI (2010) Åskagenite-(Nd), $Mn^{2+}NdAl_2Fe^{3+}(Si_2O_7)(SiO_4)O_2$, a new mineral of the epidote supergroup. New Data Minerals 45:17–22

Chukanov NV, Konilov AN, Zadov AE, Belakovsky DI, Pekov IV (2002) The new amphibole potassic chloropargasite $(K,Na)Ca_2(Mg,Fe^{2+})_4Al(Si_6Al_2O_{22})(Cl,OH)_2$ and conditions of its formation in the granulite complex of Sal'nye tundry massif (Kola Peninsula). Zapiski RMO (Proc Russ Mineral Soc) 131(2):58–61 (in Russian)

Chukanov NV, Pekov IV (2005) Heterosilicates with tetrahedral-octahedral frameworks: mineralogical and crystal-chemical aspects. Rev Mineral Geochem 57:105–143

Chukanov NV, Pekov IV (2012) Infrared spectroscopy of acid salts. I. Minerals of the class of silicates. Zapiski RMO (Proc Russ Mineral Soc) 141(3):129–143 (in Russian)

Chukanov NV, Pekov IV, Zadov AE, Chukanova VN, Möckel S (2003) Ferrosaponite, $Ca_{0.3}(Fe^{2+},Mg,Fe^{3+})_3(Si,Al)_4O_{10}(OH)_2\cdot 4H_2O$, a new trioctahedral smectite. Zapiski RMO (Proc Russ Mineral Soc) 132 (2):68–74 (in Russian)

Chukhrov FV, Gorshkov AI, Vitovskaya IV, Drits VA, Sivtsov AV, Rudnitskaya YeS (1980) Crystallochemical nature of Co-Ni asbolane. Izvestiya AN SSSR, seriya geologicheskaya (Bull Acad Sci USSR, ser Geol) 6:73–81 (in Russian)

Chukhrov FV, Gorshkov AI, Rudnitskaya YeS, Berezovskaya VV, Sivtsov AV (1978) On vernadite. Izvestiya AN SSSR, seriya geologicheskaya (Bull Acad Sci USSR, ser Geol) 6:5–19 (in Russian)

Chukhrov FV, Zvyagin BB, Drits VA, Gorshkov AI, Ermilova LP, Goilo EA, Rudnitskaya YeS (1979) The ferric analogue of pyrophyllite and related phases. Developments in Sedimentology. Proc VI Int Clay Conf 27:55–64

Chukhrov FV (ed) (1992a) Mineraly, Spravochnik (Minerals, Reference Book), vol IV(1). Nauka, Moscow (in Russian)

Chukhrov FV (ed) (1992b) Mineraly, Spravochnik (Minerals, Reference Book), vol IV(2). Nauka, Moscow (in Russian)

Cipriani C, Mellini M, Pratesi G, Viti C (1997) Rodolicoite and grattarolaite, two new phosphate minerals from Santa Barbara Mine, Italy. Eur J Mineral 9:1101–1106

Cipriani N, Menchetti S, Orlandi P, Sabelli C (1980) Peretaite, $CaSb_4O_4(OH)_2(SO_4)_2\cdot 2H_2O$, a new mineral from Pereta, Tuscany, Italy. Am Miner 65:936–939

Clark AM, Criddle AJ, Roberts AC, Bonardi M, Moffatt EA (1997) Feinglosite, a new mineral related to brackebuschite, from Tsumeb, Namibia. Mineral Mag 61:285–289

Claudel J, Hadni A, Strimer P, Vergnat P (1968) Spectres d'absorption et de reflexion des halogenures de thallium dans l'infrarouge lointain a basse temperature. J Phys Chem Solids 29(9):1539–1544 (in French)

Clavier N, Szenknect S, Costin DT, Mesbah A, Poinssot C, Dacheux N (2014) From thorite to coffinite: a spectroscopic study of $Th_{1-x}U_xSiO_4$ solid solutions. Spectrochim Acta A 118:302–307

Cohen-Addad C (1968) Étude structurale des hydroxystannates $CaSn(OH)_6$ et $ZnSn(OH)_6$ par diffraction neutronique, absorption infrarouge et resonance magnétique nucléaire. Bull Soc fr Minér Cristallogr 91:315–324

Coleyshaw EE, Crump G, Griffith WP (2003) Vibrational spectra of the hydrated carbonate minerals ikaite, monohydrocalcite, lansfordite and nesquehonite. Spectrochim Acta A 59:2231–2239

Colombo F, Rius J, Vallcorba O, Pannunzio Miner EV (2014) The crystal structure of sarmientite, $(AsO_4)(SO_4)(OH)\cdot 5H_2O$, solved ab initio from laboratory powder diffraction data. Mineral Mag 78:347–360

Cooper MA, Abdu YA, Ball NA, Hawthorne FC, Back ME, Tait KT, Schlüter J, Malcherek T, Pohl D, Gebhard G (2012) Ianbruceite, ideally $[Zn_2(OH)(H_2O)(AsO_4)](H_2O)_2$, a new arsenate mineral from the Tsumeb mine, Otjikoto (Oshikoto) region, Namibia: description and crystal structure. Mineral Mag 76:1119–1131

Cooper MA, Ball NA, Hawthorne FC, Paar WH, Roberts AC, Moffatt E (2011) Georgerobinsonite, $Pb_4(CrO_4)_2(OH)_2FCl$, a new chromate mineral from the Mammoth – St. Anthony mine, Tiger, Pinal County, Arizona: description and crystal structure. Can Miner 49:865–876

Cooper MA, Hawthorne FC, Abdu YA, Ball NA, Ramik RA, Tait KT (2013a) Wopmayite, ideally $Ca_6Na_3\square Mn(PO_4)_3(PO_3OH)_4$, a new phosphate mineral from the Tanco Mine, Bernic Lake, Manitoba: description and crystal structure. Can Miner 51:93–106

Cooper MA, Husdal TA, Ball NA, Abdu YA, Hawthorne FC (2013b) Schlüterite-(Y), ideally $(Y,REE)_2Al(Si_2O_7)(OH)_2F$, a new mineral species from the Stetind pegmatite, Tysfjord, Nordland, Norway: description and crystal structure. Mineral Mag 77:353–366

Cooper MA, Hawthorne FC, Moffatt E (2009) Steverustite, $Pb^{2+}{}_5(OH)_5[Cu^+(S^{6+}O_3S^{2-})_3](H_2O)_2$, a new thiosulphate mineral from the Frongoch Mine Dump, Devils Bridge, Ceredigion, Wales: description and crystal structure. Mineral Mag 73:235–250

Cooper MA, Hawthorne FC, Pinch WW, Grice JD (1999) Andyrobertsite and calcioandyrobertsite: two new mineral from the Tsumeb mine, Tsumeb, Namibia. Mineral Mag 30:181–186

Cooper MA, Hawthorne FC, Roberts AC, Grice JD, Stirling JAR, Moffatt EA (1998) Georgeericksenite, $Na_6CaMg(IO_3)_6(CrO_4)_2(H_2O)_{12}$, a new mineral from Oficina Chacabuco, Chile: description and crystal structure. Am Miner 83:390–399

Cornell RM, Schwerman U (2003) The iron oxides: structure, properties, reactions, occurences and uses. WILEY-VCH Verlag GmbH & Co. KGaA, Weinheim

Costa L, Paganetto G, Bertelli G, Camino G (1990) Thermal decomposition of antimony oxyhalides. J Therm Anal 36(3):1141–1153

Cotterell TF, Hubbard N (2013) Franklinphilite in veinlets in the lower Cambrian manganese ore bed, Harlech, Merionethshire, Wales. J Russell Soc 16:51–59

Cozzupoli D, Grubessi O, Mottana A, Zanazzi PF (1987) Cyrilovite from Italy: structure and crystal chemistry. Miner Petrol 37(1):1–14

Crice JD, Gault RA (2006) Johnsenite-(Ce): a new member of the eudialyte group from Mont Saint-Hilaire, Quebec, Canada. Can Miner 44:105–115

Crichton WA, Parise JB, Müller H, Breger J, Marshall WG, Welch MD (2012) Synthesis and structure of magnesium hydroxide fluoride, Mg(OH)F: a topological intermediate between brucite- and rutile-type structures. Mineral Mag 76:25–36

Cvikl B, McGrath JW (1970) Proton and deuteron magnetic resonance study of calcium bromate monohydrate. J Chem Phys 52(3):1560–1565

Cynn H, Hofmeister AM (1994) High-pressure spectra of lattice modes and OH vibrations in Fe-bearing wadsleyite. J Geophys Res 99:17717–17727

Cámara F, Bellatreccia F, Della Ventura G, Gunter ME, Sebactiani M, Cavallo A (2012) Kircherite, a new mineral of the cancrinite-sodalite group with a 36-layer stacking sequence: Occurrence and crystal structure. Am Miner 97:494–1504

Cámara F, Bellatreccia F, Della Ventura G, Mottana A (2005) Farneseite, a new mineral of the cancrinite – sodalite group with a 14-layer stacking sequence: occurrence and crystal structure. Eur J Mineral 17:839–846

Cámara F, Bellatreccia F, Della Ventura G, Mottana A, Bindi L, Gunter ME, Sebastiani M (2010) Fantappieite, a new mineral of the cancrinite-sodalite group with a 33-layer stacking sequence: occurrence and crystal structure. Am Miner 95:472–480

Cámara F, Sokolova E, Abdu YA, Hawthorne FC (2014) Nafertisite, $Na_3Fe^{2+}{}_{10}Ti_2(Si_6O_{17})_2O_2(OH)_6F(H_2O)_2$, from Mt. Kukisvumchorr, Khibiny alkaline massif, Kola peninsula, Russia: refinement of the crystal structure and revision of the chemical formula. Eur J Mineral 26:689–700

Cámara F, Sokolova E, Hawthorne FC, Rowe R, Grice JD, Tait KT (2013) Veblenite, $K_2\square_2Na(Fe^{2+}{}_5Fe^{3+}{}_4Mn^{2+}{}_7\square)Nb_3Ti(Si_2O_7)_2(Si_8O_{22})_2O_6(OH)_{10}(H_2O)_3$, a new mineral from Seal Lake, Newfoundland and Labrador: mineral description, crystal structure, and a new veblenite Si_8O_{22} ribbon. Mineral Mag 77:2955–2974

Dai YM, Lee WW, Lin WC, Chen CC (2013) Synthesis and photocatalytic properties of nano-crystalline In_2O_3. J Chin Chem Soc 60(12):1415–1424

Daiyan C, Guanxin W, Zhenxi Z, Yuming C (2003) Lanmuchangite, a new thallium (hydrous) sulphate from Lanmuchang, Guizhou Province, China. Chin J Geochem 22(2):185–192

Damascelli A, Schulte K, van der Marel D, Menovsky AA (1997) Infrared spectroscopic study of phonons coupled to charge excitations in FeSi. Phys Rev B 55(8): R4863–R4866

Daniel MF, Desbat B, Lassegues JC, Gerand B, Figlarz M (1987) Infrared and Raman study of WO_3 tungsten trioxides and $WO_3{\cdot}xH_2O$ tungsten trioxide hydrates. J Solid State Chem 67:235–247

Daniels P, Krosse S, Werding G, Schreyer W (1997) "Pseudosinhalite", a new hydrous MgAl-borate: synthesis, phase characterization, crystal structure, and *PT*-stability. Contrib Mineral Petrol 128:261–271

Das B, Reddy MV, Krishnamoorthi C, Tripathy S, Mahendiran R, Subba Rao GV, Chowdari BVR (2009) Carbothermal synthesis, spectral and magnetic characterization and Li-cyclability of the Mo-cluster compounds, $LiYMo_3O_8$ and $Mn_2Mo_3O_8$. Electrochim Acta 54:3360–3373

Davies JED (1973) Solid state vibrational spectroscopy-III[1]. The infrared and Raman spectra of the bismuth(III) oxide halides. J Inorg Nucl Chem 35:1531–1534

De Abeledo MEJ, Angelelli V, De Benyacar MAR (1968) Sanjuanite, a new hydrated basic sulfate-phosphate of aluminum. Am Miner 53:1–8

De Kimpe CR, Fripiat JJ (1968) Kaolinite crystallization from H-exchanged zeolites. Am Miner 53:216–230

De Oliveira EF, Castañeda C, Eeckhout SG, Gilmar MM, Kwitko RR, De Grave E, Botelho NF (2002) Infrared and Mössbauer study of Brazilian tourmalines from different geological environments. Am Miner 87:1154–1163

De Oliveira ALM, Ferreira JM, Silva MRS, Braga GS, Soledade LEB, Maurera Maria Aldeiza MA, Paskocimas CA, Lima SJG, Longo E, de Souza AG, Garcia dos Santos IM (2008) Yellow $Zn_xNi_{1-x}WO_4$ pigments obtained using a polymeric precursor method. Dyes Pigments 77:210–216

De Portilla VS, Quevedo MP, Stepanov VI (1981) The structure of bayldonite: chemical analysis, differential thermal analysis, and IR spectroscopy. Am Miner 66:148–153

De Waal SA (1970) Nickel minerals from Barberton, South Africa: III. Willemseite, a nickel-rich talc. Am Miner 55:31–42

De Waal D, Heyns AM (1992) Vibrational spectra of $NaVO_3$, KVO_3 and the solid solutions $(Na_{0.88}K_{0.12})VO_3$ and $(Na_{0.5}K_{0.5})VO_3$. Mater Res Bull 27: 129–136

De Waal D, Hutter C (1994) Vibrational spectra of two phases of copper pyrovanadate and some solid solutions of copper and magnesium pyrovanadate. Mater Res Bull 29(8):843–849

DeAngelis B, Newnham RE, White WB (1972) Factor group analysis of the vibrational spectra of crystals, a review and consolidation. Am Miner 57:255–268

Debbichi L, Marco de Lucas MC, Pierson JF, Krüger P (2012) Vibrational properties of CuO and Cu_4O_3 from first-principles calculations, and Raman and infrared spectroscopy. J Phys Chem C 116(18):10232–10237

Della Ventura G, Bellatreccia F, Bonaccorsi E (2005a) CO_2 in minerals of the cancrinite-sodalite group: pitiglianoite. Eur J Mineral 17:847–851

Della Ventura G, Iezzi G, Redhammer GJ, Hawthorne FC, Scaillet B, Novembre D (2005b) Synthesis and crystal-chemistry of alkali amphiboles in the system Na_2O-MgO-FeO-Fe_2O_3-SiO_2-H_2O as a function of f_{O2}. Am Miner 90:1375–1383

Della Ventura G, Bellatreccia F, Cámara F, Oberti R (2014) Crystal-chemistry and short-range order of fluoro-edenite and fluoro-pargasite: a combined X-ray diffraction and FTIR spectroscopic approach. Mineral Mag 78:293–310

Della Ventura G, Bellatreccia F, Cámara F, Oberti R, Lorand J-P, Parodi GC, Carlier G, Di Domenico D (2006) Carbon-bearing cordierite from Allumiere (Tolfa volcanic center, Latium, Italy): occurrence, crystal-structure and FTIR microspectroscopy. Periodico Mineralogia 75(2-3):113–126

Della Ventura G, Bellatreccia F, Parodi GC, Cámara F, Piccinini M (2007a) Single-crystal FTIR and X-ray study of vishnevite, ideally $[Na_6(SO_4)][Na_2(H_2O)_2]$ $(Si_6Al_6O_{24})$. Am Miner 92:713–721

Della Ventura G, Bellatreccia F, Rossi P (2007b) The single-crystal, polarized-light, FTIR spectrum of stoppaniite, the Fe analogue of beryl. Phys Chem Minerals 34(10):727–731

Della Ventura G, Hawthorne FC, Robert J-L, Delbove F, Welch MF, Raudsepp M (1999) Short-range order of cations in synthetic amphiboles along the richterite-pargasite join. Eur J Mineral 11:79–94

Della Ventura G, Parodi GC, Maras A, Mottana A (1992) Potassium-fluor-richterite, a new amphibole from San Vito, Monte Somma, Campania, Italy. Rend Fiz Acc Lincei 3(3):239–245

Della Ventura G, Robert J-L, Hawthorne FC (1998a) Characterization of OH-F short-range order in potassium-fluor-richterite by infrared spectroscopy in the OH-stretching region. Can Miner 36(1):181–185

Della Ventura G, Robert J-L, Hawthorne FC, Raudsepp M, Welch MD (1998b) Contrasting $^{[6]}$Al ordering in synthetic Mg- and Co-pargasite. Can Miner 36:1237–1244

Della Ventura G, Robert J-L, Raudsepp M, Hawthorne FC, Welch MD (1997) Site occupancies in synthetic monoclinic amphiboles: rietveld structure refinement and infrared spectroscopy of (nickel, magnesium, cobalt)-richterite. Am Miner 82:291–301

Demartin F, Campostrini I, Castellano C, Gramaccioli CM (2012) Argesite, $(NH_4)_7Bi_3Cl_{16}$, a new mineral from La Fossa Crater, Vulcano, Aeolian Islands, Italy: a first example of the $[Bi_2Cl_{10}]^{4-}$ anion. Am Miner 97:1446–1451

Demartin F, Castellano C, Campostrini I (2013) Aluminopyracmonite, $(NH_4)_3Al(SO_4)_3$, a new ammonium aluminium sulfate from La Fossa Crater, Vulcano, Aeolian Islands, Italy. Mineral Mag 77:443–451

Demartin F, Castellano C, Campostrini I (2014) Therasiaite, $(NH_4)_3KNa_2Fe^{2+}Fe^{3+}(SO_4)_3Cl_5$, a new sulfate chloride from La Fossa Crater, Vulcano, Aeolian islands, Italy. Mineral Mag 78:203–213

Denham P, Field GR, Morse PLR, Wilkinson GR (1970) Optical and dielectric properties and lattice dynamics of some fluorite structure ionic crystals. Proc R Soc Lond A 317:55–77

Deubener J, Sternitzke M, Müller G (1991) Feldspars MAlSi$_3$O$_8$ (M = H, Li, Ag) synthesized by low-temperature ion exchange. Am Miner 76:1620–1627

Di Noto V, Bresadola S (1996) New synthesis of a highly active δ-$MgCl_2$ for $MgCl_2$/$TiCl_4$/$AlEt_3$ catalytic systems. Macromol Chem Phys 197:3827–3835

Dimitriev Y, Dimitrov V, Arnaudov M (1983) IR spectra and structures of tellurite glasses. J Mater Sci 18 (5):1353–1358

Dimitrova OV, Yamnova NA, Kurazhkovskaya VS, Kantor AP (2004) Peculiarities of pandermite recrystallization at hydrothermal conditions. Zapiski RMO (Proc Russ Mineral Soc) 133(1):96–100 (in Russian)

Đorđević T, Karanović L (2010) A new polymorph of Ba (AsO_3OH): synthesis, crystal structure and vibrational spectra. J Solid State Chem 183(12):2835–2844

Đorđević T, Karanović L, Tillmanns E (2008) Structural and spectroscopic study of $Mg_{13.4}(OH)_6(HVO_4)_2$ $(H_{0.2}VO_4)_6$. Cryst Res Technol 43(11):1202–1209

Đorđević T, Wittwer A, Jagličić Z, Djerdj I (2015) Hydrothermal synthesis of single crystal $CoAs_2O_4$ and $NiAs_2O_4$ compounds and their magnetic properties. RSC Adv 5(24):18280–18287

Dorfman MD, Rogachev DD, Goroshchenko ZI, Mokretsova AV (1959) Fenaksite – a new mineral. Trudy Mineralogicheskogo Muzeya Akademii Nauk SSSR (Proc Mineral Museum Acad Sci USSR) 9:152–157 (in Russian)

Drits VA, Kashaev AA (1960) An X-ray study of a kaolinite single crystal. Kristallografiya (Crystallography) 5:224–227 (in Russian)

Du N, Wu H, Zhang H, Zhai C, Wu P, Wang L, Yang D (2011) Large-scale synthesis of water-soluble nanowires as versatile templates for nanotubes. Chem Commun 47(3):1006–1008

Dul K, Koleżyński A, Sitarz M, Madej D (2015) Vibrational spectra of a baghdadite synthetic analogue. Vib Spectrosc 76:1–5

Dupuis T, Lorenzelli V (1969) Etude de vanadates du vanadium(V) par analyse thermique. J Therm Anal 1 (1):15–28 (in French)

Durig JR, Lau KK, Nagarajan G, Walker M, Bragin J (1969) Vibrational spectra and molecular potential fields of mercurous chloride, bromide, and iodide. J Chem Phys 50(5):2130–2139

D'Antonio MC, Mancilla N, Wladimirsky A, Palacios D, González-Baró AC, Baran EJ (2010) Vibrational spectra of magnesium oxalates. Vib Spectrosc 53:218–221

D'Antonio MC, Torres MM, Palacios D, González-Baró AC, Baran EJ (2015) Vibrational spectra of the two hydrates of strontium oxalate. Spectrochim Acta A 137:486–489

Echigo T, Kimata M, Maruoka T (2007) Crystal-chemical and carbon-isotopic characteristics of karpatite ($C_{24}H_{12}$) from the Picacho Peak Area, San Benito County, California: evidences for the hydrothermal formation. Am Miner 92:1262–1269

Echigo T, Kimata M, Maruoka T, Shimizu M, Nishida N (2009) The crystal structure, origin, and formation of idrialite ($C_{22}H_{14}$): inferences from the microbeam and bulk analyses. Am Miner 94:1325–1332

Effenberger H, Giester G, Krause W, Bernhardt H-J (1998) Tschörtnerite, a copper-bearing zeolite from the Bellberg volcano, Eifel, Germany. Am Miner 83:607–617

Effenberger H, Krause W, Bernhardt H-J, Martin M (2000) On the symmetry of tsumcorite group minerals based on the new species rappoldite and zincgartrellite. Mineral Mag 64:1127–1144

Eggleton RA, Bailey SW (1967) Structural aspects of a dioctahedral chlorite. Am Miner 52:673–689

El Idrissi-Raghni MA, Durand J-M, Bonnet B, Hafid L, Olivier-Fourcade J, Jumas J-C (1996) Far infrared transmission study of the ternary system Sb_2S_3-As_2S_3-Tl_2S. J Alloys Compd 239(1):8–15

El Ouenzerfi R, Goutaudier C, Panczer G, Moine B, Cohen-Adad MT, Trabelsi-Ayedi M, Kbir-Ariguib N (2003) Investigation of the CaO-La_2O_3-SiO_2-P_2O_5 quaternary diagram. Synthesis, existence domain, and characterization of apatitic phosphosilicates. Solid State Ionics 156:209–222

Elderfield H, Hem JD (1973) The development of crystalline structure in aluminium hydroxide polymorphs on ageing. Mineral Mag 39:89–96

Elliott P, Brugger J, Caradoc-Davies T (2010) Description and crystal structure of a new mineral, edwardsite, $Cu_3Cd_2(SO_4)_2(OH)_6{\cdot}4H_2O$, from Broken Hill, New South Wales, Australia. Mineral Mag 74:39–53

Elliott P, Brugger J, Caradoc-Davies T, Pring A (2013a) Hylbrownite, $Na_3MgP_3O_{10}{\cdot}12H_2O$, a new triphosphate mineral from the Dome Rock Mine, South Australia: description and crystal structure. Mineral Mag 77:385–398

Elliott P, Kolitsch U, Willis AC, Libowitzky E (2013b) Description and crystal structure of domerockite, $Cu_4(AsO_4)(AsO_3OH)(OH)_3{\cdot}H_2O$, a new mineral from the Dome Rock Mine, South Australia. Mineral Mag 77:509–522

Elliott P, Cooper MA, Pring A (2014a) Barlowite, $Cu_4FBr(OH)_6$, a new mineral isostructural with claringbullite: description and crystal structure. Mineral Mag 78:1755–1762

Elliott P, Giester G, Rowe R, Pring A (2014b) Putnisite, $SrCa_4Cr^{3+}{}_8(CO_3)_8SO_4(OH)_{16}{\cdot}25H_2O$, a new mineral from Western Australia: description and crystal structure. Mineral Mag 78:131–144

Elliott P, Kolitsch U, Giester G, Libowitzky E, McCammon C, Pring A, Birch WD, Brugger J (2009) Description and crystal structure of a new mineral – plimerite, $ZnFe^{3+}{}_4(PO_4)_3(OH)_5$ – the Zn-analogue of rockbridgeite and frondelite, from Broken Hill, New South Wales, Australia. Mineral Mag 73:131–148

Elliott P (2010) Crystal chemistry of cadmium oxysalt and associated minerals from Broken Hill, New South Wales. Dissertation, University of Adelaide, Adelaide

Elton NJ, Hooper JJ (1995) Widenmannite from Cornwall, England: the second world occurrence. Mineral Mag 59:745–749

Enhessari M, Kargar Razi M, Etemad L, Parviz A, Sakhaei M (2012) Structural, optical and magnetic properties of the Fe_2TiO_5 nanopowders. J Exp Nanosci 1–10

Ercit TS, Tait KT, Cooper MA, Abdu Y, Ball NA, Anderson AJ, Černý P, Hawthorne FC (2010) Manitobaite, $Na_{16}Mn^{2+}{}_{25}Al_8(PO_4)_{30}$, a new phosphate mineral species from Cross Lake, Manitoba, Canada. Can Miner 48:1455–1463

Ercit TS, Van Velthuizen J (1994) Gaultite, a new zeolite-like mineral species from Mont Saint-Hilaire, Quebec, and its crystal structure. Can Miner 32: 855–863

Erd RC, McAllister JF, Vlisidis AC (1970) Wardsmithite, $5CaO{\cdot}MgO{\cdot}12B_2O_3{\cdot}30H_2O$, a new borate mineral from Death-Valley region, California. Am Miner 55:349–357

Erd RC, White DE, Fahey JJ, Lee DE (1964) Buddingtonite, an ammonium feldspar with zeolitic water. Am Miner 49:831–850

Ericksen GE, Evans HT Jr, Mrose ME, McGee JJ, Marinenko JW, Konnert JA (1989) Mineralogical studies of the nitrate deposits of Chile: VI. Hectorfloresite, $Na_9(IO_3)(SO_4)_4$, a new saline mineral. Am Miner 74:1207–1214

Ericksen GE, Mrose ME, Marinenko JW, McGee JJ (1986) Mineralogical studies of the nitrate deposits of Chile. V. Iquiqueite, $Na_4K_3Mg(CrO_4)B_{24}O_{39}(OH)$ $12H_2O$, a new saline mineral. Am Miner 71:830–836

Ersoy B, Dikmen S, Yildiz A, Gören R, Elitok Ö (2013) Mineralogical and physicochemical properties of talc from Emirdağ, Afyonkarahisar, Turkey. Turkish J Earth Sci 22:632–644

Escobal J, Pizarro JL, Mesa JL, Lezama L, Olazcuaga R, Arriortua MI, Rojo T (2000) A new manganese(II) phosphate templated by ethylenediamine: $(C_2H_{10}N_2)$ $[Mn_2(HPO_4)_3(H_2O)]$. Hydrothermal synthesis, crystal structure, and spectroscopic and magnetic properties. Chem Mater 12:376–382

Estep PA, Kovach JJ, Waldstein P, Karr C Jr (1972) Infrared and Raman spectroscopic studies of structural variations in minerals from Apollo 11, 12, 14, and 15 samples. Proc Third Lunar Sci Conf 3:3047–3067

Falk M, Huang C-H, Knop O (1975) Infrared studies of water in crystalline hydrates: $K_2FeCl_5{\cdot}H_2O$ (erythrosiderite) and related aquopentachloroferrates(III). Can J Chem 53:51–57

Fantini C, Tavares MC, Krambrock K, Moreira RL, Righi A (2014) Raman and infrared study of hydroxyl

sites in natural uvite, fluor-uvite, magnesio-foitite, dravite and elbaite tourmalines. Phys Chem Minerals 41(4):247–254
Farmer VC, Palmieri F (1975) The characterization of soil minerals by infrared spectroscopy. Soil Components. Springer, Berlin
Farmer VC, Russell JD (1964) The infrared spectra of layer silicates. Spectrochim Acta 20:1149–1173
Farrell DM (1977) Infrared investigation of basic double-carbonate hydrate minerals. Can Miner 15:408–413
Farrell EF, Newnham RE (1967) Electronic and vibrational absorption spectra in cordierite. Am Miner 52:380–388
Fasshauer DW, Chatterjee ND, Marler B (1997) Synthesis, structure, thermodynamic properties, and stability relations of K-cymrite, $K[AlSi_3O_8]\cdot H_2O$. Phys Chem Minerals 24:455–462
Fehér B, Szakáll S, Zajzon N, Mihály J (2015) Parádsasvárite, a new member of the malachite-rosasite group from Parádsasvár, Mátra Mountains, Hungary. Miner Petrol 109:405–411
Feng D, Wang C, Cheng W, Li G, Tian S, Liao F, Xiong M, Lin J (2009) Synthesis, crystal structure, and magnetic properties of $K_4Mn_3(HPO_4)_4(H_2PO_4)_2$. Solid State Sci 11:845–851
Feng X, Yang R (1986) Erlianite, a new vanadium - and iron-bearing silicate miner. Mineral Mag 50:285–289
Fernández J, González E, De Oñate J, López R, Navarro E (1993) IR and XRD study of the tribochemical reactions of copper sulfate with alkali halides. J Solid State Chem 107(2):314–318
Fernández-Bertrán J, Reguera E (1997) Mechanochemical reactions in alkali halide pressed disks. Solid State Ionics 93(1):139–146
Fernández-Carrasco L, Rius J (2006) Synthesis and crystal structure determination of hydrated potassium dawsonite from powder diffraction data. Eur J Mineral 18:99–104
Fernández-Carrasco L, Torrens-Martín D, Morales LM, Martínez-Ramírez S (2012) Infrared spectroscopy in the analysis of building and construction materials. In: Theophanides T (ed) Infrared spectroscopy – materials science, engineering and technology, INTECH, doi:10.5772/36186
Ferrage E, Martin F, Petit S, Pejo-Soucaille S, Micoud P, Fourty G, Ferret J, Salvi S, de Parseval P, Fotune JP (2003) Evaluation of talc morphology using FT-IR and H/D substitution. Clay Miner 38:141–150
Ferraris G, Gula A (2005) Polysomatic aspects of microporous minerals – heterophyllosilicates, palysepioles and rhodesite-related structures. Rev Mineral Geochem 57:69–104
Ferraris G, Prencipe M, Pautov LA, Sokolova EV (1999) The crystal structure of darapiosite and a comparison with Li- and Zn-bearing minerals of the milarite group. Can Miner 37:769–774
Ferrer EG, Baran EJ (1994) The infrared spectrum of VO$(OH)_2$ (synthetic duttonite). Spectrochim Acta A 50 (2):375–377
Filipek E, Dąbrowska G (2007) Synthesis and selected properties of $CrSbVO_6$ and phase relations in the V_2O_5–Cr_2O_3–α-Sb_2O_4 system in the solid state. J Mater Sci 42:4905–4915
Filipek E, Kurzawa M, Dabrowska G (2000) Initial studies on the oxide system Cr_2O_3-Sb_2O_4. J Therm Anal Calorim 60:167–171
Fischer H-H (2007) Beitrage zur Kristallchemie der Carbonate und Isonicotinate. Dissertation, Universität zu Köln (in German)
Foord EuE, Hughes JM, Cureton F, Maxwell CH, Falster AU, Sommer AJ, Hlava PF (1999) Esperanzaite, $NaCa_2Al_2(As^{5+}O_4)_2F_4(OH)\cdot 2H_2O$, a new mineral species from the La Esperanza mine, Mexico: descriptive mineralogy and atomic arrangement. Can Miner 37:67–72
Forray FL, Drouet C, Navrotsky A (2005) Thermochemistry of yavapaiite $KFe(SO_4)_2$: formation and decomposition. Geochim Cosmochim Acta 69(8):2133–2140
Fox KK, Holsinger VH, Posati LP, Pallansch MJ (1967) Composition of granules in evaporated milks stored at low temperatures. J Dairy Sci 50(7):1032–1037
Fransolet A-M (1973) La mélonjosephite $CaFe^{2+}Fe^{3+}(PO_4)_2(OH)$, une nouvelle espèce minérale. Bull Soc Fr Minér Cristallogr 96:135–142 (in French)
Fransolet A-M (1978) Données nouvelles sur l'ottrelite d'Ottré, Belgique. Bull minér 101:548–557 (in French)
Fransolet A-M, Abraham K, Sahl K (1984) Davreuxite: a reinvestigation. Am Miner 69:777–782
Fransolet A-M, Cooper MA, Černý P, Hawthorne FC, Chapman R, Grice JD (2000) The tanco pegmatite at Bernic Lake, Southeastern Manitoba. XV. Ercitite, $NaMn^{3+}PO_4(OH)(H_2O)_2$, a new phosphate mineral species. Can Miner 38:893–898
Fransolet A-M, Von Knorring O, Fontan F (1992) A new occurrence of samuelsonite in the Buranga pegmatite, Rwanda. Bull Geol Soc Finland 64:13–21
Franz G, Ackermand D, Koch E (1981) Karlite, $Mg_7(BO_3)_3(OH,Cl)_5$ a new borate mineral and associated ludwigite from the Eastern Alps. Am Miner 66:872–877
Franzini L, Pasero M, Perchiazzi N (1991) Re-discovery and re-definition of dinite, $C_{20}H_{36}$, a forgotten organic mineral from Garfagnana, northern Tuscany, Italy. Eur J Mineral 3:855–861
Friedel RA, Carlson GL (1971) Infrared spectra of ground graphite. J Phys Chem 75(8):1149–1151
Frost RL, Dickfos MJ (2009) Raman spectroscopic study of the tellurite minerals: mackayite and quetzalcoatlite. Spectrochim Acta A 72(2):445–448
Frost RL, Erickson KL, Kloprogge TJ (2005a) Vibrational spectroscopic study of the nitrate containing hydrotalcite mbobomkulite. Spectrochim Acta A 61:2919–2925
Frost R, Weier M, Martens W, Henry D, Mills S (2005b) Raman spectroscopy of newberyite, hannayite and struvite. Spectrochim Acta A 62(1):181–188
Frost RL, Erickson KL (2005) Near-infrared spectroscopic study of selected hydrated hydroxylated phosphates. Spectrochim Acta A 61(1):45–50

Frost RL, Čejka J, Dickfos MJ (2008a) Raman spectroscopic study of the uranyl selenite mineral demesmaekerite $Pb_2Cu_5(UO_2)_2(SeO_3)_6(OH)_6 \cdot 2H_2O$. J Raman Spectrosc 40:476–480

Frost RL, Dickfos MJ, Čejka J (2008b) Raman spectroscopic study of the uranyl carbonate mineral zellerite. J Raman Spectrosc 39:582–586

Frost RL, Dickfos MJ, Keeffe EC (2008c) Raman spectroscopic study of the tellurite minerals: rajite and denningite. Spectrochim Acta A 71(4):1512–1515

Frost RL, Erickson KL, Weier ML, McKinnon AR, Williams PA, Leverett P (2004) Use of infrared spectroscopy for the determination of electronegativity of rare earth elements. Appl Spectrosc 58(7):811–815

Frost RL, Erickson KL, Weier ML, Mills S (2003) Raman spectroscopy of the phosphate minerals: cacoxenite and gormanite. Asian Chem Lett 7(4):197–203

Frost RL, López A, Scholz R, Xi Y, Belotti FM (2013a) Infrared and Raman spectroscopic characterization of the carbonate mineral huanghoite – and in comparison with selected rare earth carbonates. J Molec Struct 1051:221–225

Frost RL, López A, Xi Y, Granja A, Scholz R (2013b) Vibrational spectroscopic characterization of the phosphate mineral kulanite $Ba(Fe^{2+},Mn^{2+},Mg)_2(Al,Fe^{3+})_2(PO_4)_3(OH)_3$. Spectrochim Acta A 115:22–25

Frost RL, Xi Y, Scholz R, Belotti FM (2013c) Vibrational spectroscopic characterization of the phosphate mineral bermanite – $Mn^{2+}Mn^{3+}{}_2(PO_4)_2(OH)_2 \cdot 4H_2O$. Spectrochim Acta A 105:359–364

Frost RL, Xi Y, Scholz R, López A, Moreira C, de Lena JC (2013d) Raman spectroscopic study of the mineral qingheiite $Na_2(Mn^{2+},Mg,Fe^{2+})_2(Al,Fe^{3+})(PO_4)_3$, a pegmatite phosphate mineral from Santa Ana pegmatite, Argentina. Spectrochim Acta A 114:486–490

Frost RL, Weier M (2006) Raman and infrared spectroscopy of the manganese arsenate mineral allactite. Spectrochim Acta A 65:623–627

Frost RL, Weier M, Martens WN (2006a) Raman microscopy of synthetic goudeyite $(YCu_6(AsO_4)_2(OH)_6 \cdot 3H_2O)$. Spectrochim Acta A 63(3):685–689

Frost RL, Weier ML, Martens WN, Mills SJ (2006b) The hydroxylated nickel carbonates otwayite and paraotwayite – a SEM, EDX and vibrational spectroscopic study. N Jb Miner Abh 183(1):107–116

Frost RL, Henry DA, Weier ML, Martens W (2006c) Raman spectroscopy of three polymorphs of BiVO4: clinobisvanite, dreyerite and pucherite, with comparisons to $(VO_4)^{3-}$-bearing minerals: namibite, pottsite and schumacherite. J Raman Spectrosc 37(7):722–732

Frost RL, Weier ML, Martens WN, Mills SJ (2006d) Thermo Raman spectroscopic study of kintoreite. Spectrochim Acta A 63(2):282–288

Frost RL, Xi Y (2012a) Vibrational spectroscopic study of the mineral creaseyite $Cu_2Pb_2(Fe,Al)_2(Si_5O_{17}) \cdot 6H_2O$ – a zeolite mineral? Spectrochim Acta A 94: 6–11

Frost RL, Xi Y (2012b) Whelanite $Ca_5Cu_2(OH)_2CO_3$, $Si_6O_{17} \cdot 4H_2O$ – a vibrational spectroscopic study. Spectrochim Acta A 91:319–323

Frost RL, Xi Y, Palmer SJ (2011) The structure of the mineral leogangite $Cu_{10}(OH)_6(SO_4)(AsO_4)_4 \cdot 8H_2O$ – implications for arsenic accumulation and removal. Spectrochim Acta A 82(1):221–227

Frost RL, Xi Y, Scholz R, Belotti FM, Lagoeiro LE (2012) Chemistry, Raman and infrared spectroscopic characterization of the phosphate mineral reddingite: $(Mn,Fe)_3(PO_4)_2(H_2O,OH)_3$, a mineral found in lithium-bearing pegmatite. Phys Chem Minerals 39: 803–810

Frost RL, Čejka J (2009) Near- and mid-infrared spectroscopy of the uranyl selenite mineral haynesite $(UO_2)_3(SeO_3)_2(OH)_2 \cdot 5H_2O$. Spectrochim Acta A 71:1959–1963

Frost RL, Čejka J, Ayoko GA, Weier ML (2007) Raman spectroscopic and SEM analysis of sodium zippeite. J Raman Spectrosc 38(10):1311–1319

Frost RL, Čejka J, Dickfos MJ (2009a) Raman spectroscopic study of the mineral guilleminite $Ba(UO_2)_3(SeO_3)_2(OH)_4 \cdot 3H_2O$. J Raman Spectrosc 40 (4):355–359

Frost RL, Čejka J, Dickfos MJ (2009b) Raman spectroscopic study of the uranyl tellurite mineral moctezumite $PbUO_2(TeO_3)_2$. J Raman Spectrosc 40:38–41

Frost RL, Čejka J, Sejkora J, Plášil J, Bahfenne S, Palmer SJ (2009c) Raman microscopy of the mixite mineral $BiCu_6(AsO_4)_3(OH)_6 \cdot 3H_2O$ from the Czech Republic. J Raman Spectrosc 41(5):566–570

Frost RL, Čejka J, Scholz R, López A, Theiss FL, Xi Y (2014a) Vibrational spectroscopic study of the uranyl selenite mineral derriksite $Cu_4UO_2(SeO_3)_2(OH)_6 \cdot H_2O$. Spectrochim Acta A 117:473–477

Frost RL, Scholz R, Lopez A, Belotti FM, Xi Y (2014b) Structural characterization and vibrational spectroscopy of the arsenate mineral wendwilsonite. Spectrochim Acta A 118:737–743

Fu J, Liang W, Wang H, He Z (2011) Synthesis and characterization of $MgSO_4 \cdot 5Mg(OH)_2 \cdot 2H_2O$ flake powders. J Cent South Univ Technol 18:1871–1876

Fuchs Y, Linares J, Mellini M (1998) Mössbauer and infrared spectrometry of lizardite-*1*T from Monte Fico, Elba. Phys Chem Minerals 26:111–115

Furukawa T, Brawer SA, White WB (1979) Raman and infrared spectroscopic studies of the crystalline phases in the system Pb_2SiO_4-$PbSiO_3$. J Am Ceram Soc 62 (7-8):351–356

Gabelica-Robert M, Tarte P (1979) Vibrational spectrum of akermanite-like silicates and germinates. Spectrochim Acta A 35:649–654

Galli E, Brigatti MF, Malferrari D, Sauro F, De Waele J (2013) Rossiantonite, $Al_3(PO_4)(SO_4)_2(OH)_2(H_2O)_{10} \cdot 4H_2O$, a new hydrated aluminum phosphate-sulfate mineral from Chimanta massif, Venezuela: description and crystal structure. Am Miner 98:1906–1913

Galli E, Quartieri S, Vezzalini G, Alberti A (1996) Gottardiite, a new high-silica zeolite from Antarctica: the natural counterpart of synthetic NU-87. Eur J Mineral 8:687–693

Galli E, Vezzalini G, Quartieri S, Alberti A, Franzini M (1997) Mutinaite, a new zeolite from Antarctica: the natural counterpart of ZSM-5. Zeolites 19:318–322

Galliski MA, Cooper MA, Márquez-Zavalía MF, Hawthorne FC (2010) Alfredstelznerite: a new species of calcium borate hydrate from the Santa Rosa mine, Salta, northwestern Argentina. Can Miner 48:123–128

Galuskin EV, Galuskina IO, Kusz J, Gfeller F, Armbruster T, Bailau R, Dulski M, Gazeev VM, Pertsev NN, Zadov AE, Dzierżanowski P (2015) Mayenite supergroup, part II: chlorkyuygenite from Upper Chegem, Northern Caucasus, Kabardino-Balkaria, Russia, a new microporous mineral with "zeolitic" H_2O. Eur J Mineral 27(1):113–122

Galuskin EV, Gazeev VM, Armbruster T, Zadov AE, Galuskina IO, Pertsev NN, Dzierżanowski P, Kadiyski M, Gurbanov AG, Wrzalik R, Winiarski A (2008) Lakargiite $CaZrO_3$: a new mineral of the perovskite group from the North Caucasus, Kabardino-Balkaria, Russia. Am Miner 93:1903–1910

Galuskin EV, Lazic B, Armbruster T, Galuskina IO, Pertsev NN, Gazeev VM, Włodyka R, Dulski M, Dzierżanowski P, Zadov AE, Dubrovinsky LS (2012) Edgrewite $Ca_9(SiO_4)_4F_2$ – hydroxyledgrewite $Ca_9(SiO_4)_4(OH)_2$, a new series of calcium humite-group minerals from altered xenoliths in the ignimbrite of Upper Chegem caldera, Northern Caucasus, Kabardino-Balkaria, Russia. Am Miner 97:1998–2006

Galuskin EV, Pertsev NN, Armbruster T, Kadiyski M, Zadov AE, Galuskina IO, Dzierżanowski P, Wrzalik R, Kislov EV (2007) Dovyrenite $Ca_6Zr[Si_2O_7]_2(OH)_4$ – a new mineral from skarned carbonate xenoliths in basic-ultrabasic rocks of the Ioko-Dovyren massif, Northern Baikal region, Russia. Mineralogia Polonica 38(1):15–28

Galuskina IO, Lazic B, Armbruster T, Galuskin EV, Gazeev VM, Zadov AE, Pertsev NN, Jeżak L, Wrzalik R, Gurbanov AG (2009) Kumtyubeite $Ca_5(SiO_4)_2F_2$ – a new calcium mineral of the humite group from Northern Caucasus, Kabardino-Balkaria, Russia. Am Miner 94:1361–1370

Galuskina IO, Ottolini L, Kadiyski M, Armbruster T, Galuskin EV, Dzierżanowski P, Winiarski A (2010) Pertsevite-(OH), a new mineral in the pertsevite series, $Mg_2(BO_3)_{1-x}(SiO_4)_x(F,OH)_{1-x}$ ($x < 0.5$), from the Snezhnoye deposit in Sakha-Yakutia Republic, Russia. Am Miner 95:953–958

Gamyanin GN, Zayakina NV, Galenchikova LT (2013) Arangasite, $Al_2(SO_4)(PO_4)F{\cdot}7.5H_2O$, a new mineral from Alaskitovoye deposit (Eastern Yakutia, Russia). Zapiski RMO (Proc Russ Mineral Soc) 142(5):21–30 (in Russian)

Garavelli A, Mitolo D, Pinto D, Vurro F (2013) Lucabindiite, $(K,NH_4)As_4O_6(Cl,Br)$, a new fumarole mineral from the "La Fossa" crater at Vulcano, Aeolian Islands, Italy. Am Miner 98:470–477

García-Guinea J, Chagoyen AM, Nickel EH (1995) A re-investigation of bolivarite and evansite. Can Miner 33:59–65

García-Romero E, Suárez Barrios M, Bustillo Revuelta MA (2004) Characteristics of a Mg-palygorskite in miocene rocks, Madrid basin (Spain). Clays Clay Miner 52(4):484–494

Gatta GD, Adamo I, Meven M, Lambruschi E (2012) A single-crystal neutron and X-ray diffraction study of pezzottaite, $Cs(Be_2Li)Al_2Si_6O_{18}$. Phys Chem Minerals 39(10):829–840

Gaubicher J, Chabre Y, Angenault J, Lautié A, Quarton M (1997) Lithium electrochemical intercalation in β-$VOSO_4$. J Alloys Compd 262–263:34–38

Geiger CA, Gatta GD, Xue X, McIntyre GJ (2012) A neutron/X-ray diffraction, IR, and $^1H/^{29}Si$ NMR spectroscopic investigation of armenite: behavior of extra framework Ca cations and H_2O molecules in microporous silicates. Z Kristallogr 227:411–426

Geiger CA, Langer K, Bell DR, Rossman GR, Winkler B (1991) The hydroxide component in synthetic pyrope. Am Miner 76:49–59

Gesing TM, Buhl J-C (1998) Crystal structure of a Carbonate-Nosean $Na_8[AlSiO_4]_6CO_3$. Eur J Mineral 10:71–77

Ghose S, Wan C (1979) Structural chemistry of copper and zinc minerals. VI. Bayldonite, $(Cu,Zn)_3Pb(AsO_4)_2(OH)_2$: a complex layer structure. Acta Crystallogr B 35:819–832

Ghotbi MY (2010) Synthesis and characterization of nano-sized ε-$Zn(OH)_2$ and its decomposed product, nano-zinc oxide. J Alloys Compd 494:420–422

Gies H (1983) Studies on clathrasils. III. Crystal structure of melanophlogite, a natural clathrate compound of silica. Z Kristallogr 164:247–257

Giese RF Jr, Datta P (1973) Hydroxyl orientation in kaolinite, dickite, and nacrite. Am Miner 58:471–479

Giguère PA, Falk M (1960) The infrared spectra of selenium dioxide. Spectrochim Acta 1:1–5

Giguére PA, Harvey KB (1956) On the infrared absorption of water and heavy water in condensed states. Can J Chem 34:798–808

Gillet Ph, Reynard B, Tequi C (1989) Thermodynamic properties of glaucophane new data from calorimetric and spectroscopic measurements. Phys Chem Minerals 16:659–667

Goldman DS, Rossman GR, Dollase WA (1977) Channel constituents in cordierite. Am Miner 62:1144–1157

Golovach II, Gerasimenko VS, Slivka VYu, Dov goshei NI, Golovei MI, Bogdanova AV (1976) Vitrification of and optical and photoelectrical properties of $AgAsS_2$, $AgSbS_2$, and $AgBiS_2$. Soviet Phys J 19 (3):294–298

Gonzalez-Carreño T, Fernández M, Sanz J (1988) Infrared and electron microprobe analysis of tourmalines. Phys Chem Minerals 15(5):452–460

González-Díaz PF, Santos M (1978) Infrared spectra of strontium, lead and barium apatites. Spectrochim Acta A 34:241–246

Goriletsky VI, Mitichkin AI, Belenko LE, Rebrova TP (2001) IR spectroscopy of KBr salt and crystals. Semicond Phys, Quant Electron Optoelectron 4 (2):139–141

Gotić M, Czakó-Nagy I, Popović S, Musić S (1998) Formation of nanocrystalline $NiFe_2O_4$. Philosoph Mag Lett 78(3):193–201

Gottschalk M, Andrut M (1998) Structural and chemical characterization of synthetic (Na, K)-richterite solid solutions by EMP, HRTEM, XRD and OH-valence vibrational spectroscopy. Phys Chem Minerals 25 (2):101–111

Graeser S, Hetherington CJ, Gieré R (2003) Ganterite, a new barium-dominant analogue of muscovite from the Berisal complex, Simplon region, Switzerland. Can Miner 41:1271–1280

Graeser S, Schwander H (1987) Gasparite-(Ce) and monazite-(Nd): two new minerals to the monazite group from the Alps. Schweiz Mineral Petrogr Mitt 67 (1/2):103–113

Graeser S, Schwander H, Blanchi R, Pilati T, Gramaccioli CM (1989) Geigerite, the Mn analogue of chudobaite: its description and crystal structure. Am Miner 74:676–684

Graeser S, Schwander H, Suhner B (1984) Grischunit ($CaMn_2[AsO_4]_2$), eine neue Mineralart aus den Schweizer Alpen: zur Mn-As-Mineralisation des Oberhalbstein-Gebietes (I). Schweiz Mineral Petrogr Mitt 64(1/2):1–10 (in German)

Grauby O (1993) Nature et étendue des solutions solides octaérdriques argileuses. Approche par synthèse minérale. Dissertation, Poitiers University (in French)

Greenwood NN, Earnshaw A (1997) Chemistry of the elements, 2nd edn. Butterworth-Heinemann, Oxford

Grey IE, Madsen IC, Mills SJ, Hatert F, Peterson VK, Bastow TJ (2010) A new type of cubic-stacked layer structure in anthoinite, $AlWO_3(OH)_3$. Am Miner 95:639–645

Grice JD, Ercit TS (1993) Ordering of Fe and Mg in the tourmaline crystal structure – the correct formula. N Jb Miner Abh 165(3):245–266

Grice JD, Gault RA (1998) Thomasclarkite-(Y), a new sodium – rare-earth-element bicarbonate mineral species from Mont Saint-Hilaire, Quebec. Can Miner 36:1293–1300

Grice JD, Gault RA, Chao GY (1995) Reederite-(Y), a new sodium rare-earth carbonate mineral with a unique fluorosulfate anion. Am Miner 80:1059–1064

Grice JD, Gault RA, Rowe R, Johnsen O (2006) Qaqarssukite-(Ce), a new barium-cerium fluorcarbonate mineral species from Qaqarssuk, Greenland. Can Miner 44:1137–1146

Grice JD, Gault RA, Van Velthuizen J (1996) Penobsquisite: a new borate mineral with a complex framework structure. Can Miner 34:657–665

Grice JD, Gault RA, Van Velthuizen J (1997a) Brianroulstonite: a new borate mineral with a sheet structure. Can Miner 35:751–758

Grice JD, Gault RA, Van Velthuizen J (1997b) Sheldrickite, a new sodium-calcium-fluorocarbonate mineral species from Mont Saint-Hilaire, Quebec. Can Miner 35:181–187

Grice JD, Gault RA, Van Velthuizen J, Pratt A (2002) Walkerite, a new borate mineral species in an evaporitic sequence from Sussex, New Brunswick, Canada. Can Miner 40(6):1675–1686

Grice JD, Nickel EH, Gault RA (1991) Ashburtonite, a new bicarbonate-silicate mineral from Ashburton Downs, Western Australia: description and structure determination. Am Miner 76:1701–1707

Grice JD, Rowe R, Poirier G (2015) Bussyite-(Y), a new beryllium silicate mineral species from Mont Saint-Hilaire, Quebec. Can Miner, doi:10.3749/canmin.1500005

Grice JD, Rowe R, Poirier G, Pratt A, Francis J (2009) Bussyite-(Ce), a new beryllium silicate mineral species from Mont Saint-Hilaire, Quebec. Can Miner 47:193–204

Griesser KJ, Beran A, Voll D, Schneider H (2008) Boron incorporation into mullite. Miner Petrol 92:309–320

Grundler PV, Brugger J, Meisser N, Ansermet S, Borg S, Etschmann B, Testemale D, Bolin T (2008) Xocolatlite, $Ca_2Mn^{4+}{}_2Te_2O_{12}{\cdot}H_2O$, a new tellurate related to kuranakhite: description and measurement of Te oxidation state by XANES spectroscopy. Am Miner 93:1911–1920

Grzechnik A, McMillan PF (1996) In situ high-pressure infrared spectra of α-$NaVO_3$. Solid State Commun 99 (12):869–871

Gualtieri AF, Passaglia E (2006) Rietveld structure refinement of NH_4-exchanged natural chabazite. Eur J Mineral 18:351–359

Gucsik A, Zhang M, Koeberl C, Salje EKH, Redfern SAT, Pruneda (2004) Infrared and Raman spectra of $ZrSiO_4$ experimentally shocked at high pressures. Mineral Mag 68:801–811

Gupta AK, Chatterjee ND (1978) Synthesis, composition, thermal stability, and thermodynamic properties of bicchulite, $Ca_2[Al_2SiO_6](OH)_2$. Am Miner 63:58–65

Gyrdasova OI, Krasil'nikov VN, Bazuev GV (2009) Synthesis of micro- and nanosized manganese oxides from hydrated manganese oxalates and products of their chemical modification with ethylene glycol. Zhurnal Neorganicheskoi Khimii (Russ J Inorg Chem) 54(7):1097–1102 (in Russian)

Gómez-Caballero JA, Villaseñor-Cabral MG, Santiago-Jacinto P, Ponce-Abad F (2010) Hypogene Ba-rich todorokite and associated nanometric native silver in the San Miguel Tenango Mining area, Zacatlán, Puebla. Mexico. Can Miner 48(5):1237–1253

Gómez MA, Lee K (2012) Vibrational spectroscopy of complex synthetic and industrial products. In: De Caro D (ed) Vibrational Spectroscopy, INTECH, doi: 10.5772/32982

Günter JR, Amberg M (1989) "High-temperature" magnesium tungstate, $MgWO_4$, prepared at moderate temperature. Solid State Ionics 32(33):141–146

Hadni A, Morlot G, Brehat F (1968) Spectres d'absorption dans l'infrarouge lointain de sept halogenures

anhydrés et hydratés: $BaCl_2$, $BaBr_2$, $SrBr_2$, $SrCl_2$, $PbCl_2$, $PbBr_2$ et NaI. Spectrochim Acta A 24(8):1167–1175 (in French)

Haeuseler H, Wäschenbach G, Lutz HD (1985) Directional dispersion of the phonon modes in optically uniaxial solids, far-infrared reflection spectra, dielectric and optic constants, dynamic effective ionic charges of the defect chalcopyrites $CdGa_2S_4$, $CdGa_2Se_4$, $HgGa_2S_4$, and $HgGa_2Se_4$. Phys Status Solidi B 129(2):549–558

Hansen HCB, Taylor RM (1991) Formation of synthetic analogues of double metal-hydroxy carbonate minerals under controlled pH conditions: II. The synthesis of desautelsite. Clay Miner 26:507–525

Harada K, Tomita K (1967) A sodian stilbite from Onigajō, Mié prefecture, Japan, with some experimental studies concerning the conversion of stilbite to wairakite at low water vapor pressures. Am Miner 52:1438–1450

Harlow GE, Dunn PJ, Rossman GR (1984) Gamagarite: a re-examination and comparison with brackebuschite-like minerals. Am Miner 69:803–806

Harrison WTA, Vaughey JT, Dussack LL, Jacobson AJ, Martin TE, Stucky GD (1995) Two new adamite-type phases, $Co_2(OH)PO_4$ and $Zn_2(OH)PO_4$: structure-directing effect of organic additives. J Solid State Chem 114:151–158

Hashmi SA, Rai DK, Chandra S (1992) Protonic conduction in $Al_2(SO_4)_3{\cdot}16H_2O$: coulometry, transient ionic current, infrared and electrical conductivity studies. J Mater Sci 27:175–179

Hass M (1963) Infrared lattice reflection spectra of LiCl, LiBr, KF, RbF, and CsF. J Phys Chem Solids 24 (10):1159–1164

Hatert F (2008) Crystal chemistry of the divalent cation in alluaudite-type phosphates: a structural and infrared spectral study of the $Na_{1.5}(Mn_{1-x}M^{2+}{}_x)_{1.5}Fe_{1.5}(PO_4)_3$ solid solutions ($x = 0$ to 1, $M^{2+} = Cd^{2+}$, Zn^{2+}). J Solid State Chem 181:1258–1272

Hatert F, Hermann RP, Fransolet A-M, Long GJ, Grandjean F (2006) A structural, infrared, and Mössbauer spectral study of rosemaryite, $NaMnFe^{3+}Al(PO_4)_3$. Eur J Mineral 18:775–785

Hatert F, Lefèvre P, Fransolet A-M (2011) The crystal structure of bertossaite, $CaLi_2[Al_4(PO_4)_4(OH,F)_4]$. Can Miner 49(4):1079–1087

Hatert F, Lefévre P, Fransolet A-M, Spirlet MR, Rebbouh L, Fontan F, Keller P (2005) Ferrorosemaryite, $NaFe^{2+}Fe^{3+}Al(PO_4)_3$, a new phosphate mineral from the Rubindi pegmatite, Rwanda. Eur J Mineral 17:749–759

Hatert F, Pasero M, Perchiazzi N, Theye T (2007) Pumpellyite-(Al), a new mineral from Bertrix, Belgian Ardennes. Eur J Mineral 19:247–253

Hausen DM (1962) Schoderite, a new phosphovanadate mineral from Nevada. Am Miner 47:637–648

Hawthorne FC (1995) Entropy-driven disorder in end-member amphiboles. Can Miner 33:1189–1204

Hawthorne FC, Abdu YA, Ball NA, Pinch WW (2013) Carlfrancisite: $Mn^{2+}{}_3(Mn^{2+},Mg,Fe^{3+},Al)_{42}(AsO_3)_2(AsO_4)_4[(Si,As^{5+})O_4]_6[(As^{5+},Si)O_4]_2(OH)_{42}$, a new arseno-silicate mineral from the Kombat mine, Otavi Valley, Namibia. Am Miner 98:1693–1696

Hawthorne FC, Cooper MA, Ball NA, Abdu YA, Černý P, Cámara F, Laurs BM (2012a) Billwiseite, ideally $Sb^{3+}{}_5(Nb,Ta)_3WO_{18}$, a new oxide mineral species from the Stak Nala pegmatite, Nanga Parbat-Haramosh massif, Pakistan: description and crystal structure. Can Miner 50:805–814

Hawthorne FC, Oberti R, Harlow GE, Maresch WV, Martin RF, Schumacher JC, Welch MD (2012b) IMA report: nomenclature of the amphibole supergroup. Am Miner 97:2031–2048

Hawthorne FC, Della Ventura G (2007) Short-range order in amphiboles. Rev Mineral Geochem 67:173–222

Hawthorne FC, Henry DJ (1999) Classification of the minerals of the tourmaline group. Eur J Mineral 11 (2):201–215

Healy PC, White AH (1972) Crystal structure and physical properties of anhydrous sodium copper carbonate. J Chem Soc Dalton Trans 17:1913–1917

Heilmann I, Knudsen JM, Olsen NB, Buras B, Olsen JS (1974) Studies of thermal decomposition of $(NH_4)_2Fe(SO_4)_2{\cdot}6H_2O$. Solid State Commun 15:1481–1484

Henderson CMB, Roux J (1977) Inversions in sub-potassic nephelines. Contrib Mineral Petrol 61:279–298

Henderson CMB, Taylor D (1979) Infrared spectra of aluminogermanate- and aluminate-sodalites and a re-examination of the relationship between T-O bond length, T-O-T angle and the position of the main i.r. absorption band for compounds with framework structures. Spectrochim Acta A 35:929–935

Henderson CMB, Taylor D (1982) The structural behaviour of the nepheline family: (1) Sr and Ba aluminates (MAl_2O_4). Mineral Mag 45:111–127

Henmi C, Kusachi I (1992) Clinotobermorite, $Ca_5Si_6(O,OH)_{18}{\times}5H_2O$, a new mineral from Fuka, Okayama Prefecture, Japan. Mineral Mag 56:353–358

Henry DA, Birch WD (1992) Otwayite and theophrastite from the Lord Brassey Mine, Tasmania. Mineral Mag 56:252–255

Henry DJ, Novák M, Hawthorne FC, Ertl A, Dutrow BL, Uher P, Pezzotta F (2011) Nomenclature of the tourmaline-supergroup minerals. Am Miner 96:895–913

Hermoneit B, Ziemer B, Malewski G (1981) Single crystal growth and some properties of the new compound $Ca_3Si_2O_7{\cdot}1/3CaCl_2$. J Cryst Growth 52:660–664

Hernandez-Moreno MJ, Ulibarri MA, Rendon JL, Serna CJ (1985) IR characteristics of hydrotalcite-like compounds. Phys Chem Minerals 12(1):34–38

Herron MM, Machlus M, Herron SL (2008) Log interpretation parameters determined by analysis of green river oil shale samples: initial steps. 28th oil shale symposium, Colorado School of Mines, 13–15 October, 2008, pp 1–8

Hervig RL, Fudge C, Navrotsky A (2014) Analyzing nitrogen in cordierites and other phases by SIMS.

Goldschmidt2014 Abstracts, Sacramento, California, USA, June 7th–13th, 2014, p 982

Herwig S, Hawthorne FC (2006) The topology of hydrogen bonding in brandtite, collinsite and fairfieldite. Can Miner 44:1181–1196

Heuser J, Bukaemskiy AA, Neumeier S, Neumann A, Bosbach D (2014) Raman and infrared spectroscopy of monazite-type ceramics used for nuclear waste conditioning. Prog Nucl Energy 72:149–155

Heyns AM, Range K-J, Wildenauer M (1990) The vibrational spectra of $NbBO_4$, $TaBO_4$, $NaNb_3O_8$ and $NaTa_3O_8$. Spectrochim Acta A 46(11):1621–1628

Heyward C, McMillen C, Kolis J (2012) Hydrothermal synthesis and crystal structure of two new hydrated alkaline earth metal borates $Sr_3B_6O_{11}(OH)_2$ and $Ba_3B_6O_{11}(OH)_2$. Inorg Chem 51:3956–3962

Higashi S (1982) Tobelite, a new ammonium dioctahedral mica. Mineral J (Jpn) 11(3):138–146

Hill RJ, Canterford JH, Moyle FJ (1982) New data for lansfordite. Mineral Mag 46:453–457

Himmrich M, Haeuseler H (1991) Far infrared studies on stannite and wurtzstannite type compounds. Spectrochim Acta A 47(7):933–942

Hindman JR (1976) Stringhamite, a new hydrous copper calcium silicate from Utah. Am Miner 61:189–192

Hiraishi J, Katsuhiko T, Tadao T (1979) Far infrared reflection spectra of lead (II) chloride and iodide. J Chem Phys 71(1):554–555

Hodgson AA, Freeman AG, Taylor HFW (1965) The thermal decomposition of crocidolite from Koegas, South Africa. Mineral Mag 35:5–30

Hoekstra HR, Siegel S (1973) The uranium trioxide-water system. J Inorg Nucl Chem 35:761–779

Hofmeister AM, Hoering TC, Virgo D (1987) Vibrational spectroscopy of beryllium aluminosilicates: heat capacity calculations from band assignments. Phys Chem Minerals 14:205–224

Hofmeister AM, Keppel E, Speck AK (2003) Absorption and reflection infrared spectra of MgO and other diatomic compounds. Mon Not R Astron Soc 345:16–38

Hofmeister AM, Rossman GR (1985) A model to the irradiative coloration of smoky feldspar and the inhibiting influence of water. Phys Chem Minerals 12:324–332

Hofmeister AM, Wopenka B, Locock AJ (2004) Spectroscopy and structure of hibonite, grossite, and $CaAl_2O_4$: implications for astronomical environments. Geochim Cosmochim Acta 68(21):4485–4503

Hogarth DD, Steacy HR, Semenov YeI, Proshchenko EG, Kazakova ME, Kataeva ZT (1973) New occurrences and data for spencite. Can Miner 12:66–71

Hornibrook ERC, Longstaffe FJ (1996) Berthierine from the lower cretaceous clearwater formation, Alberta, Canada. Clays Clay Miner 44(1):1–21

Hsu LC (1986) The stability relationships of zunyite under hydrothermal conditions. Mining Geol 36 (3):219–230

Hu ZB, Wang CX, Tong CQ, Huang YX, Pan Y, Mi JX (2013) Crystal structure and magnetic property of synthetic gengenbachite, $KH_8(Fe_{2.66}Al_{0.34})(PO_4)_6{\cdot}6H_2O$. Can Miner 51:223–232

Huang H, Tian N, Jin S, Zhang Y, Wang S (2014) Syntheses, characterization and nonlinear optical properties of a bismuth subcarbonate $Bi_2O_2CO_3$. Solid State Sci 30:1–5

Hubert S, Thouvenot P (1992) Luminescence of americium (III) and europium (III) in the cubic structure ThO_2. J Lumin 54:103–111

Hubin R, Tarte P (1971) Etude infrarouge des orthosilicates et des orthogermanates – IV: structures scheelite et zircon. Spectrochim Acta A 27(5):683–690 (in French)

Hughes JM, Cureton FE, Marty J, Gault RA, Guntar MA, Campana CF, Rakovan J, Sommer A, Brueseke ME (2001) Dickthomssenite, $MgV_2O_6{\cdot}7H_2O$, a new mineral species from the Firefly-Pigmay Mine, Utah: descriptive mineralogy and arrangement of atoms. Can Miner 39:1691–1700

Hunan 230 Institute and X-ray Laboratory, Wuhan Geologic College (1978) Xiangjiangite – a new uranium mineral discovered in China. Scientia Geologica Sinica 2:183–188 (in Chinese, English abstr)

Hunan 230 Institute, Hunan 305 Geological Team and X-ray Laboratory of Wuhan Geological Institute (1979) The mineralogical investigation of Furongite. Scientia Sinica 22(2):199–206

Hunt AJ, Steyer TR, Huffman DR (1973) Infrared surface modes in small NiO particles. Surface Sci 36:454–461

Hurlbut CS Jr, Erd RC (1974) Aristarainite, $Na_2O{\cdot}MgO{\cdot}6B_2O_3{\cdot}10H_2O$, a new mineral from Salta, Argentina. Am Miner 59:647–651

Husson E, Repelin Y, Brusset H, Cerez A (1979) Spectres de vibration et calcul du champ de force des antimoniates et des tantalates de structure trirutile. Spectrochim Acta A 35:1177–1187 (in French)

Hyde BC, King PL, Dyar MD, Spilde M, Ali A-MS (2011) Methods to analyze metastable and microparticulate hydrated and hydrous iron sulfate minerals. Am Miner 96:1856–1869

Hyun B-R, Bartnik AC, Weon-kyu K, Agladze NI, Wrubel JP, Sievers AJ, Murray CB, Wise FW (2011) Far-infrared absorption of PbSe nanorods. Nano Lett 11(7):2786–2790

Hålenius U, Häussermann U, Harryson H (2005) Holtstamite, $Ca_3(Al,Mn^{3+})_2(SiO_4)_{3-x}(H_4O_4)_x$, a new tetragonal hydrogarnet from Wessels Mine, South Africa. Eur J Mineral 17:375–382

Hålenius U, Westlund E (1998) Manganese valency and the colour of the $Mn_2AsO_4(OH)$ polymorphs eveite and sarkinite. Mineral Mag 62:113–119

Hölscher A, Schreyer W, Lattard D (1986) High-pressure, high-temperature stability of surinamite in the system MgO-BeO-$A1_2O_3$-SiO_2-H_2O. Contrib Mineral Petrol 92:113–127

Hölsä J, Piriou B, Räsänen M (1993) IR- and Raman-active normal vibrations of rare earth oxyfluorides, REOF; RE = Y, La, and Gd. Spectrochim Acta A 49(4):465–470

Hölsä J, Säilynoja E, Rahiala H, Valkonen J (1997) Characterization of the non-stoichiometry in

lanthanum oxyfluoride by FT-IR absorption, Raman scattering, X-ray powder diffraction and thermal analysis. Polyhedron 16(19):3421–3427

Iezzi G, Della Ventura G, Cámara F, Pedrazzi G, Robert J-L (2003a) ^{B}Na-^{B}Li solid-solution in A-site-vacant amphiboles: synthesis and cation ordering along the ferri-clinoferroholmquistite-riebeckite join. Am Miner 88:955–961

Iezzi G, Della Ventura G, Pedrazzi G, Robert J-L, Oberti R (2003b) Synthesis and characterisation of ferri-clinoferroholmquistite, $\square Li_2(Fe^{2+}{}_3Fe^{3+}{}_2)Si_8O_{22}(OH)_2$. Eur J Mineral 15(2):321–327

Iezzi G, Cámara F, Della Ventura G, Oberti R, Pedrazzi G, Robert J-L (2004a) Synthesis, crystal structure and crystal chemistry of ferri-clinoholmquistite, $\square Li_2Mg_3Fe^{3+}{}_2Si_8O_{22}(OH)_2$. Phys Chem Minerals 31(6):375–385

Iezzi G, Della Ventura G, Oberti R, Cámara F, Holtz F (2004b) Synthesis and crystal-chemistry of Na(NaMg)$Mg_5Si_8O_{22}(OH)_2$, a $P2_1/m$ amphibole. Am Miner 89:640–646

Iezzi G, Della Ventura G, Hawthorne FC, Pedrazzi G, Robert J-L, Novembre D (2005) The (Mg,Fe^{2+}) substitution in ferri-clinoholmquistite, $\square Li_2(Mg,Fe^{2+})_3Fe^{3+}{}_2O_{22}(OH)_2$. Eur J Mineral 17(5):733–740

Iezzi G, Liu Z, Della Ventura G (2009). Synthetic $^{A}Na^{B}(Na_xLi_{1-x}Mg_1)^{C}Mg_5Si_8O_{22}(OH)_2$ (with x = 0.6, 0.2 and 0) $P2_1/m$ amphiboles at high pressure: a synchrotron infrared study. Phys Chem Minerals 36 (6):343–354

Il'inchik EA (2008) Standards for X-ray photoelectron spectroscopy of boron compounds. J Appl Spectrosc 75(6):883–891

Ingrin J, Skogby H (2000) Hydrogen in nominally anhydrous upper-mantle minerals: concentration levels and implications. Eur J Mineral 12:543–570

Ishida K (1989) Infrared study of manganoan alkali-calcic amphiboles. Mineral J (Jpn) 14(6):255–265

Ishida K (1990) Infrared spectra of alkali amphiboles of the glaucophane-riebeckite series and their relation to chemical composition. Mineral J (Jpn) 15(4):147–161

Ishida K (1999) Appearance of infrared ($MgMgFe^{3+}$)-OH stretching band in heat-treated holmquistites, sodic-calcic and sodic amphiboles. Mineral J (Jpn) 21(4):157–166

Ishida K, Hawthorne FC (2001) Assignment of infrared OH-stretching bands in manganoan magnesio-arfvedsonite and richterite through heat-treatment. Am Miner 86:965–972

Ishida K, Hawthorne FC (2003) Fine structure in the infrared OH-stretching bands of holmquistite and anthophyllite. Phys Chem Minerals 30(6):330–336

Isupov VP, Chupakhina LE, Mitrofanova RP (2000) Mechanochemical synthesis of double hydroxides. J Mater Synth Process 8(3/4):251–253

Ito J, Arem JE (1971) Chevkinite and perrierite: synthesis, crystal growth and polymorphism. Am Miner 56: 307–309

Ito J, Hafner SS (1974) Synthesis and study of gadolinites. Am Miner 59:700–708

Ivanitsky VP, Mataysh IV, Plastinina MA, Sharkina EV, Pavlishin VI, Koval' VB, Samsonov VA, Taran MH (1990) Transformation of tetraferribiotite in hydrothermal solution (obtained from experimental data). Mineralogicheskiy Zhurnal (Mineral J) 12 (2):67–77 (in Russian)

Jackson B (1990) Queitite, a first Scottish occurrence. Scottish J Geol 26:57–58

Jagadale AD, Dubal DP, Lokhande CD (2012) Electrochemical behavior of potentiodynamically deposited cobalt oxyhydroxide (CoOOH) thin films for supercapacitor application. Mater Res Bull 47:672–676

Jambor JL, Roberts AC, Owens DR, Grice JD (1996) Zajacite-(Ce), a new rare-earth fluoride from the Strange Lake Deposit, Quebec-Labrador. Can Miner 34:1299–1304

Jambor JL, Viňals J, Groat LA, Raudsepp M (2002) Cobaltarthurite, $Co^{2+}Fe^{3+}{}_2(AsO_4)_2(OH)_2{\cdot}4H_2O$, a new member of the arthurite group. Can Miner 40:725–732

Janáková S, Salavcová L, Renaudin G, Ya F, Boyer D, Boutinaud P (2007) Preparation and structural investigations of sol-gel derived Eu^{3+}-doped $CaAl_2O_4$. J Phys Chem Solids 68:1147–1151

Jasperse JR, Kahan A, Plendl JN, Mitra SS (1966) Temperature dependence of infrared dispersion in ionic crystals LiF and MgO. Phys Rev 146(2):526–542

Jastrzębski W, Sitarz M, Rokita M, Bułat K (2011) Infrared spectroscopy of different phosphates structures. Spectrochim Acta A 79:722–727

Jayasree RS, Mahadevan Pillai VP, Nayar VU, Odnevall I, Keresztury G (2006) Raman and infrared spectral analysis of corrosion products on zinc $NaZn_4Cl(OH)_6SO_4{\cdot}6H_2O$ and $Zn_4Cl_2(OH)_4SO_4{\cdot}5H_2O$. Mater Chem Phys 99:474–478

Jeanloz R (1980) Infrared spectra of olivine polymorphs: α, β phase and spinel. Phys Chem Minerals 5:327–341

Jena H, Kutty KVG, Kutty TRN (2004) Ionic transport and structural investigations on $MSn(OH)_6$ (M = Ba, Ca, Mg Co, Zn, Fe, Mn) hydroxide perovskites synthesized by wet sonochemical methods. Mater Chem Phys 88(1):167–179

Jentzsch PV, Bolanz RM, Ciobotă V, Kampe B, Rösch P, Majzlan J, Popp J (2012a) Raman spectroscopic study of calcium mixed salts of atmospheric importance. Vib Spectrosc 61:206–213

Jentzsch PV, Ciobotă V, Bolanz RM, Kampe B, Rösch P, Majzlan J, Popp J (2012b) Raman and infrared spectroscopic study of synthetic ungemachite, $K_3Na_8Fe(SO_4)_6(NO_3)_2{\cdot}6H_2O$. J Molec Struct 1022:147–152

Jiaxin S (1989) A new mineral – ximengite. Chin J Geochem 8(4):385–392

Jillavenkatesa A, Condrate RA Sr (1998) The infrared and Raman spectra of β- and α-tricalcium phosphate $(Ca_3(PO_4)_2)$. Spectrosc Lett Int J Rapid Comm 31 (8):1619–1634

Xu J, Gilson DFR, Butler IS (1998) FT-Raman and high-pressure FT-infrared spectroscopic investigation

of monocalcium phosphate monohydrate, Ca $(H_2PO_4)_2{\cdot}H_2O$. Spectrochim Acta A 54:1869–1878

Joeckel RM, Wally KD, Fischbein SA, Hanson PR (2007) Sulfate mineral paragenesis in Pennsylvanian rocks and the occurrence of slavikite in Nebraska. Great Plains Res 17(1):17–33

Johnson KW, Bell EE (1969) Far-infrared optical properties of KCl and KBr. Phys Rev 187(3):1044–1052

Johnston MG, Harrison WTA (2011) New Ba*M*2 $(SeO_3)_3{\cdot}nH_2O$ (*M* = Co, Ni, Mn, Mg; $n \approx 3$) zemannite-type frameworks: single-crystal structures of $BaCo_2(SeO_3)_3{\cdot}3H_2O$, $BaMn_2(SeO_3)_3{\cdot}3H_2O$ and $BaMg_2(SeO_3)_3{\cdot}3H_2O$. Eur J Inorg Chem 2967–2974

Jones GC, Jackson B (1993) Infrared transmission spectra of carbonate ninerals. Chapman & Hall, London

Jouen S, Lefez B, Sougrati MT, Hannoyer B (2007) Fourier transform infrared spectroscopic study of abhurite $Sn_{21}O_6Cl_{16}(OH)_{14}$. Mater Chem Phys 105 (2-3):189–193

Julien C, Barnier S, Ivanov I, Guittard M, Pardo MP, Chilouet A (1999) Vibrational studies of copper thiogallate solid solutions. Mater Sci Eng B 57 (2):102–109

Julien C, Ivanov I, Khelfa A, Alapini F, Guittard M (1996) Characterization of the ternary compounds $AgGaTe_2$ and $AgGa_5Te_8$. J Mater Sci 31(12):3315–3319

Julien CM, Massot M, Poinsignon C (2004) Lattice vibrations of manganese oxides. Part I. Periodic structures. Spectrochim Acta A 60:689–700

Julliot J-Y, Volfinger M, Robert J-L (1987) Experimental study of carboirite and phases in the system GeO_2-SiO_2-Al_2O_3-FeO-H_2O at P up to 2 kbar. Miner Petrol 36:51–69

Kagi H, Nagai T, Loveday JS, Wada C, Parise JB (2003) Pressure-induced phase transformation of kalicinite ($KHCO_3$) at 2.8 GPa and local structural changes around hydrogen atoms. Am Miner 88:1446–1451

Kaiser W, Spitzer WG, Kaiser RH, Howarth LE (1962) Infrared properties of CaF_2, SrF_2, and BaF_2. Phys Rev 127(6):1950–1954

Kampf AR, Adams PM, Housley RM, Rossman GR (2014) Fluorowardite, $NaAl_3(PO_4)_2(OH)_2F_2{\cdot}2H_2O$, the fluorine analog of wardite from the Silver Coin mine, Valmy, Nevada. Am Miner 99:804–810

Kampf AR, Dunn PJ, Foord EuE (1989) Grandreefite, pseudograndreefite, laurelite, and aravaipaite: four new minerals from the Grand Reef mine, Graham County, Arizona. Am Miner 74:927–933

Kampf AR, Housley RM (2011) Fluorphosphohedyphane, $Ca_2Pb_3(PO_4)_3F$, the frst apatite supergroup mineral with essential Pb and F. Am Miner 96:423–429

Kampf AR, Mills SJ, Housley RM, Rossman GR, Marty J, Thorne B (2013a) Lead-tellurium oxysalts from Otto Mountain near Baker, California: X. Bairdite, $Pb_2Cu^{2+}{}_4Te^{6+}{}_2O_{10}(OH)_2(SO_4)(H_2O)$, a new mineral with thick HCP layers. Am Miner 98:1315–1321

Kampf AR, Pluth JJ, Chen Y-S, Roberts AC, Housley RM (2013b) Bobmeyerite, a new mineral from Tiger, Arizona, USA, structurally related to cerchiaraite and ashburtonite. Mineral Mag 77:81–91

Kampf AR, Mills SJ, Rossman GR, Steele IM, Pluth JJ, Favreau G (2011) Afmite, $Al_3(OH)_4(H_2O)_3(PO_4)(PO_3OH){\cdot}H_2O$, a new mineral from Fumade, Tarn, France: description and crystal structure. Eur J Mineral 23:269–277

Kampf AR, Wise WS, Rossman GR (2000) Juanitaite: a new mineral from Gold Hill, Utah. Miner Rec 31:301–305

Kanesaka I, Kawahara H, Yamazaki A, Kawai K (1986) The vibrational spectrum of MCl_3 (M = Al, Cr and Fe). J Molec Struct 146:41–49

Kang SY, Jeon IC, Kim K (1998) Infrared absorption enhancement at silver colloidal particles. Appl Spectrosc 52:278–283

Kang J, Yang Y, Pan S, Yu H, Zhou Z (2014) Synthesis, crystal structure and optical properties of $Ba_5V_3O_{12}F$. J Molec Struct 1056–1057:79–83

Kaposta EC (2005) Gas phase infrared photodissociation spectroscopy of mass selected cluster ions: strong hydrogen bonds and vanadium oxides. Dissertation, Free University of Berlin

Karpenko VYu, Pautov LA, Sokolova EV, Hawthorne FG, Agakhanov AA, Dikaya TV, Bekenova GK (2004) Ankinovichite – the nickel analogue of alvanite, a new mineral from Kurumsak (Kazakhstan) and Kara-Chagyr (Kyrgyzstan). Zapiski RMO (Proc Russ Mineral Soc) 133(2):59–70 (in Russian)

Karr C Jr, Kovach JJ (1969) Far-infrared spectroscopy of minerals and inorganics. Appl Spectrosc 23(3):219–223

Kasatkin AV, Nestola F, Plášil J, Marty J, Belakovskiy DI, Agakhanov AA, Mills SJ, Pedron D, Lanza A, Favaro M, Bianchin S, Lykova IS, Goliáš V, Birch WD (2013) Manganoblödite, $Na_2Mn(SO_4)_2{\cdot}4H_2O$, and cobaltoblödite, $Na_2Co(SO_4)_2{\cdot}4H_2O$: two new members of the blödite group from the Blue Lizard mine, San Juan County, Utah, USA. Mineral Mag 77:367–383

Katerinopoulou A, Katerinopoulos A, Voudouris P, Bieniok A, Musso M, Amthauer G (2009) A multi-analytical study of the crystal structure of unusual Ti-Zr-Cr-rich andradite from the Maronia skarn, Rhodope massif, western Thrace, Greece. Miner Petrol 95:113–124

Kats A (1962) Hydrogen in α-quartz. Philips Res Rep 17 (133-195):201–279

Kats A, Haven Y (1960) Infrared absorption bands in α-quartz in the 3-μ region. Phys Chem Glasses 1:99–102

Kazachenko VΦ, Perevoznikova EV, Narnov GA (2012) Accessory mineralization in skarns of Dalnegorsk ore district (Sikhote-Alin'). Zapiski RMO (Proc Russ Mineral Soc) 141(4):73–96 (in Russian)

Keester KL, White WB (1970) Crystal chemistry and properties of phases in the system SrO-PbO-O. J Solid State Chem 2:68–73

Keller P (1971) Die Kristallchemie der Phosphat- und Arsenatminerale unter besonderer Berücksichtigung der Kationen-Koordinationspolyeder und des Kristallwassers. Teil. I: Die Anionen der Phosphat- und

Arsenatminerale. N Jb Miner Mh 11:491–510 (in German)
Keller P, Hatert F, Lissner F, Schleid T, Fransolet A-M (2006) Hydrothermal synthesis and crystal structure of $Na(Na,Mn)_7Mn_{22}(PO_4)_{18}\cdot 0.5H_2O$, a new compound of fillowite structure type. Eur J Mineral 18:765–774
Keller P, Riffel H, Hess H (1982) Die Kristallstruktur von Prosperit, $Ca_2Zn_4[H_2O|(AsO_4)_4]$. Z Kristallogr 158:33–42 (in German)
Kendix E, Moscardi G, Mazzeo R, Baraldi P, Prati S, Joseph E, Capelli S (2008) Far infrared and Raman spectroscopy analysis of inorganic pigments. J Raman Spectrosc 39:1104–1112
Kendix EL, Prati S, Joseph E, Sciutto G, Mazzeo R (2009) ATR and transmission analysis of pigments by means of far infrared spectroscopy. Anal Bioanal Chem 394:1023–1032
Kermarec M, Carriat JY, Burattin P, Che M, Decarreau A (1994) FTIR identification of the supported phases produced in the preparation of silica-supported nickel catalysts. J Phys Chem 98:12008–12017
Khan MI, Aydemir K, McNeely JH, Cage B, Doedens RJ (2012) A mixed-valence vanadate as model for the nanadium mineral melanovanadite: hydrothermal synthesis, crystal structure and magnetic properties of $MgV^{V}{}_2V^{IV}{}_2O_{10}\cdot 4H_2O$. Cryst Growth Des 12:3656–3660
Khomenko VM, Langer K (2005) Carbon oxides in cordierite channels: determination of CO_2 isotopic species and CO by single crystal IR spectroscopy. Am Miner 90:1913–1917
Khomyakov AP, Cámara F, Sokolova E, Abdu Y, Hawthorne FC (2011) Sveinbergeite, $Ca(Fe^{2+}{}_6Fe^{3+})Ti_2(Si_4O_{12})_2O_2(OH)_5(H_2O)_4$, a new astrophyllite-group mineral from the Larvik Plutonic Complex, Oslo Region, Norway: description and crystal structure. Mineral Mag 75:2687–2702
Khomyakov AP, Dusmatov VD, Ferraris G, Gula A, Ivaldi G, Nechelyustov GN (2003) Zirsilite-(Ce) $(Na,\square)_{12}(Ce,Na)_3Ca_6Mn_3Zr_3Nb(Si_{25}O_{73})(OH)_3(CO)_3\cdot H_2O$ and carbokentbrooksite $(Na,\square)_{12}(Na,Ce)_3Ca_6Mn_3Zr_3Nb(Si_{25}O_{73})(OH)_3(CO_3)\cdot H_2O$ – two new eudialyte group minerals from Dara-i Pioz alkaline massif, Tajikistan. Zapiski RMO (Proc Russ Mineral Soc) 132(5):40–51 (in Russian)
Khomyakov AP, Kurova TA, Nechelyustov GN (1992) Manaksite, $NaKMnSi_4O_{10}$, a new mineral. Zapiski RMO (Proc Russ Mineral Soc) 121(1):112–115 (in Russian)
Khomyakov AP, Nechelyustov GN, Rastsvetaeva RK (1996) Pyatenkoite-(Y)$\cdot Na_5(Y,Dy,Gd)(Ti,Nb)Si_6O_{18}\cdot 6H_2O$ – a new mineral. Zapiski RMO (Proc Russ Mineral Soc) 125(4):72–78 (in Russian)
Khomyakov AP, Pavlov VP, Rogacheva DL, Zalkind OA, Martynova AV (1993) Tiettaite $(Na,K)_{17}FeTiSi_{16}O_{29}(OH)_{30}\cdot 2H_2O$ – a new mineral. Zapiski RMO (Proc Russ Mineral Soc) 122(1):121–125 (in Russian)
Khorari S, Rulmont A, Cahay R, Tarte P (1995) Structure of the complex arsenates $NaCa_2M^{2+}{}_2(AsO_4)_3$($M^{2+}$ = Mg, Ni, Co): first experimental evidence of a garnet-alluaudite reversible polymorphism. J Solid State Chem 118:267–273
Kidchob T, Malfatti L, Marongiu D, Enzo S, Innocenzi P (2009) Formation of cerium titanate, $CeTi_2O_6$, in sol-gel films studied by XRD and FAR infrared spectroscopy. J Sol-Gel Sci Technol 52(3):356–361
Kieffer SW (1979) Thermodynamics and lattice vibrations of minerals: 2. Vibrational characteristics of silicates. Rev Geophys Space Phys 17(1):20–34
Kijkowska R, Cholewka E, Duszak B (2003) X-ray diffraction and IR-absorption characteristics of lanthanide orthophosphates obtained by crystallisation from phosphoric acid solution. J Mater Sci 38:223–228
Kim SJ (1977) Janggunite, a new manganese hydroxide mineral from the Janggun mine, Bonghwa, Korea. Mineral Mag 41:519–523
Kim CY, Condrate RA Sr (1984) The vibrational spectra of crystalline $W_2O_3(PO_4)_2$ and related tungsten phosphate glasses. J Phys Chem Solids 45(11):1213–1218
Kim Y, Seo I, Martin SW, Baek J, Halasyamani PS, Arumugam N, Steinfink H (2008) Characterization of new infrared nonlinear optical material with high laser damage threshold, $Li_2Ga_2GeS_6$. Chem Mater 20 (19):6048–6052
Kim S-H, Yeon J, Halasyamani PS (2009) A noncentrosymmetric polar oxide, Pb_3SeO_5: synthesis, characterization, electronic structure calculations, and structure-property relationships. Chem Mater 21:5335–5342
Kimata M (1986) Synthetic Mn-kilchoanite – a new development in polymorphism of melilite. Mineral Mag 50:511–515
Kimata M, Kakefuda K (1980) Synthesis and thermal decomposition of Ga-bicchulite $Ca_2Ga_2SiO_6(OH)_2$. N Jb Miner Mh 9:415–427
Kimura Y, Tamura K, Koike C, Chihara H, Kaito C (2005) Laboratory production of monophase pyrrhotite grains using solid-solid reaction and their characteristic infrared spectra. Icarus 177(1):280–285
Kirsh Y, Yariv S, Shoval S (1987) Kinetic analysis of thermal dehydration and hydrolysis of $MgCl_2\cdot 6H_2O$ by DTA and TG. J Therm Anal 32:393–408
Kitamura M, Kondoh S, Morimoto N, Miller GH, Rossman GR, Putnis A (1987) Planar OH-bearing defects in mantle olivine. Nature 328:143–145
Klee WE (1966) Das Schwingungsspektrum der $B(OH)_4$-ionen im Teepleit. Z anorg allg Chem 343:58–69 (in German)
Kleppe AK, Jephcoat AP, Olijnyk H, Slesinger AE, Kohn SC, Wood BJ (2001) Raman observations of the OH stretching region in hydrous wadsleyite (β-Mg_2SiO_4) to 50 GPa. Phys Chem Minerals 28:232–241
Kliche G (1985a) Far-infrared and X-ray investigations of the mixed platinum dichalcogenides $PtS_{2-x}Se_x$, $\cdot PtSe_{2-x}Te_x$, and $PtS_{2-x}Te_x$. J Solid State Chem 56(1):26–31
Kliche G (1985b) Far-infrared reflection spectra of PdO, PdS, PdSe and PtS. Infrared Phys 25(1):381–383
Kliche G (1991) Coupled plasmon-phonon modes in CoP_3. Solid State Commun 80(1):73–77

Kliche G, Bauhofer W (1987) Infrared reflection spectra and electrical properties of the skutterudite $RhSb_3$. Mater Res Bull 22(4):551–555

Kliche G, Popovic ZV (1990) Far-infrared spectroscopic investigations on CuO. Phys Rev B 42(16):10060–10066

Kloprogge JT, Broekmans M, Duong LV, Martens WN, Hickey L, Frost RL (2006) Low temperature synthesis and characterisation of lecontite, $(NH_4)Na(SO_4)\cdot 2H_2O$. J Mater Sci 41:3535–3539

Kloprogge JT, Frost RL (1999) Fourier transform infrared and Raman spectroscopic study of the local structure of Mg-, Ni-, and Co-hydrotalcites. J Solid State Chem 146:506–515

Kloprogge JT, Frost RL (2000) Thermal decomposition of Ferrian chamosite: an infrared emission spectroscopic study. Contrib Mineral Petrol 138:59–67

Knop O, Brisse F, Castelliz L (1969) Pyrochlores. V. Thermoanalytic, X-ray, neutron, infrared, and dielectric studies of $A_2Ti_2O_7$ titanates. Can J Chem 47:971–990

Knorr K, Meschke M, Winkler B (1999) Structural and magnetic properties of $Co_2Al_4Si_5O_{18}$ and $Mn_2Al_4Si_5O_{18}$ cordierite. Phys Chem Minerals 26:521–529

Kobayashi S, Ando T, Kanayama A, Tanabe M, Kishi S, Kusachi I (2014) Calciborite from the Fuka mine, Okayama Prefecture, Japan. J Mineral Petrol Sci 109 (1):13–17

Kobayashi S, Shoji T (1983) Infrared analysis of the grossular-hydrogrossular series. Mineral J (Jpn) 11 (7):331–343

Koch A, Weber J-V (1998) Baseline correction of spectra in Fourier transform infrared: interactive drawing with Bezier curves. Appl Spectrosc 52:970–973

Koch-Müller M, Hofmeister AM, Fei Y, Liu Z (2002) High-pressure IR-spectra and the thermodynamic properties of chloritoid. Am Miner 87:609–622

Koch-Müller M, Rhede D (2010) IR-absorption coefficients for water in nominally anhydrous high-pressure minerals. Am Miner 95:770–775

Kodama H (1957) Sericite from Ozawa-mura, Gumma Prefecture. Mineral J (Jpn) 2(3):15l–161

Kodama H (1958) Mineralogical study on some pyrophyllites in Japan. Mineral J (Jpn) 2(4):236–244

Kodama H (1962) Interpretation of X-ray powder patterns of some hydromuscovites from Japan, with reference to their alkali contents. Clay Sci 1:89–99

Kohlstedt DL, Keppler H, Rubie DC (1996) Solubility of water in the α, β and γ phases of $(Mg,Fe)_2SiO_4$. Contrib Mineral Petrol 123:345–357

Kohn SC, Brooker RA, Frost DJ, Slesinger AE, Wood BJ (2002) Ordering of hydroxyl defects in hydrous wadsleyite (β-Mg_2SiO_4). Am Miner 87:293–301

Kolesov BA, Geiger GA (2000) Cordierite II: the role of CO_2 and H_2O. Am Miner 85:1265–1274

Kolesov BA, Geiger CA (2003) Molecules in the SiO_2-clathrate melanophlogite: a single-crystal Raman study. Am Miner 88:1364–1368

Koleva VG (2005) Metal-water interactions and hydrogen bonding in dittmarite-type compounds $M'M''PO_4\cdot H_2O$ ($M' = K^+$, NH_4^+; $M'' = Mn^{2+}$, Co^{2+}, Ni^{2+}). Correlations of IR spectroscopic and structural data. Spectrochim Acta A 62:1196–1202

Koleva VG (2007) Vibrational behavior of the phosphates ions in dittmarite-type compounds $M'M''PO_4\cdot H_2O$ ($M' = K^+$, NH_4^+; $M'' = Mn^{2+}$, Co^{2+}, Ni^{2+}). Spectrochim Acta A 66:413–418

Konev AA, Kartashev PM, Koneva AA, Ushchapovskaya ZF, Nartova NV (2004) Mg-deficient strontium benstonite from the ore occurrence Biraya (Siberia). Zapiski RMO (Proc Russ Mineral Soc) 133(6):65–72 (in Russian)

Konovalenko SI, Voloshin AV, Anan'ev SA, Pakhomovskii YaA, Perlina GA (1984) Tetrawickmanite from miarole pegmatites of southwest Pamir. Mineralogicheskiy Zhurnal (Mineral J) 6(1):89–92 (in Russian)

Konovalenko SI, Ananyev SA, Chukanov NV, Aksenov SM, Rastsvetaeva RK, Bakhtin AI, Nikolaev AG, Gainov RR, Vagizov FG, Sapozhnikov AN, Belakovskiy DI, Bychkova YV, Klingelhöfer G, Blumers M (1915) Ferro-pedrizite, $NaLi_2(Fe^{2+}{}_2Al_2Li)Si_8O_{22}(OH)_2$, a new mineral of the amphibole supergroup from the Sutlug pegmatite occurrence, Tyva Republic, Russia. Eur J Mineral. 27:417–426

Korinevsky VG, Korinevsky EV (2006) Potassic-magnesiohastingsite $(K,Na)Ca_2(Mg,Fe^{2+})_4(Fe^{3+},Al,Ti)[Si_6Al_2O_{22}](OH,Cl)_2$ – the new mineral species of amphiboles. Zapiski RMO (Proc Russ Mineral Soc) 135(2):49–57 (in Russian)

Koritnig S, Süsse P (1975) Meixnerit, $Mg_6Al_2(OH)_{18}\cdot 4H_2O$, ein neues Magnesium-Aluminium-Hydroxid-Mineral. Tschermaks Min Petr Mitt 22:79–87 (in German)

Kovaleva LT, Vasiliev VI (1987) New data on IR-spectroscopic studies of eglestonite, shakhovite and kuznetsovite. Geologiya i Geofizika (Geol Geophys) 2:113–116 (in Russian)

Koval'chuk NS, Makeev AB (2007) Typomorphism and parasteresis of yushkinite (Pai-Khoi anticlinorium). Zapiski RMO (Proc Russ Mineral Soc) 136(5):1–21 (in Russian)

Kovács I, O'Neill HStC, Hermann J, Hauri EH (2010) Site-specific infrared O-H absorption coeficients for water substitution into olivine. Am Miner 95:292–299

Kramer JW, Isaacs SA, Manivannan V (2009) Microwave-assisted metathesis synthesis of schoenfliesite-type $MSn(OH)_6$ (M = Mg, Ca, Zn, and Sr) materials. J Mater Sci 44:3387–3392

Krasil'nikov VN, Shtin AP, Perelyaeva LA, Baklanova IV, Tyutyunnik AP, Zubkov VG (2010) Synthesis and physicochemical study of $M_4Na_2V_{10}O_{28}\cdot 10H_2O$ (M = K, Rb, NH_4). Zhurnal Neorganicheskoi Khimii (Russ J Inorg Chem) 55 (2):167–172 (in Russian)

Krause W, Belendorff K, Bernhardt H-J, McCammon C, Effenberger H, Mikenda W (1998a) Crystal chemistry of the tsumcorite-group minerals. New data on ferrilotharmeyerite, tsumcorite, thometzekite, mounanaite, helmutwinklerite, and a redefinition of gartrellite. Eur J Mineral 10:179–206

Krause W, Bernhardt H-J, McCammon C, Effenberger H (1998b) Brendelite, $(Bi,Pb)_2Fe^{3+,2+}O_2(OH)(PO_4)$, a new mineral from Schneeberg, Germany: description and crystal structure. Miner Petrol 63:263–277

Kreske S, Devarajan V (1982) Vibrational spectra and phase transitions in ferroelectric-ferroelastic langbeinites: $K_2Mn_2(SO_4)_3$, $(NH_4)_2Cd_2(SO_4)_3$ and $Tl_2Cd_2(SO_4)_3$. J Phys C Solid State Phys 15:7333–7350

Krickl R, Wildner M (2009) Crystal chemistry of synthetic Co- and Ni-analogues of natrochalcite – the shortest known hydrogen bonds among mineral-type compounds. Part II: spectroscopic studies. Eur J Mineral 21:65–78

Kriskova L, Pontikes Y, Zhang F, Cizer Ö, Jones PT, van Balen K, Blanpain B (2013) Valorisation of stainless steel slags as a hydraulic binder. Acta Metallurgica Slovaca 19(3):176–183

Krivovichev SV, Britvin SN, Burns PC, Yakovenchuk VN (2002) Crystal structure of rimkorolgite, $Ba[Mg_5(H_2O)_7(PO_4)_4](H_2O)$, and its comparison with bakhchisaraitsevite. Eur J Mineral 14: 397–402

Kubelka P, Munk F (1931) Ein Beitrag zur Optik der Farbanstriche. Z Tech Phys (Leipzig) 12:593–601

Kudoh Y, Inoue T, Arashi H (1996) Structure and crystal chemistry of hydrous wadsleyite, $Mg_{1.75}SiH_{0.5}O_4$: possible hydrous magnesium silicate in the mantle transition zone. Phys Chem Minerals 23:461–469

Kulig W, Agmon N (2014) Both Zundel and Eigen isomers contribute to the IR spectrum of the gas-phase $H_9O_4^+$ cluster. J Phys Chem B 118:278–286

Kullyakool S, Danvirutai C, Siriwong K, Noisong P (2013) Thermal behaviour, surface properties and vibrational spectroscopic studies of the synthesized $Co_{3x}Ni_{3-3x}(PO_4)_2{\cdot}8H_2O$ ($0 \le x \le 1$). Solid State Sci 24:147–153

Kullyakool S, Danvirutai C, Siriwong K, Noisong P (2014) Determination of kinetic triplet of the synthesized $Ni_3(PO_4)_2{\cdot}8H_2O$ by non-isothermal and isothermal kinetic methods. J Therm Anal Calorim 115 (2):1497–1507

Kullyakool S, Danvirutai C, Siriwong K (2011) Synthesis and characterization of cobalt and nickel orthophosphate octahydtates. The 12th Khon Kaen Unversily Grad Res Conf PMO11-PMO11-6

Kumarathasan P, McCarthy GJ, Hassett DJ, Pflughoeft-Hassett DF (1989) Oxyanion substituted ettringites: synthesis and characterization; and their potential role in immobilization of As, B, Cr, Se and V. MRS Proceedings 178:83–104

Kurzawa M (1992) Infrared spectra of $FeVMoO_7$ and $Fe_4V_2Mo_3O_{20}$. J Mater Sci Lett 11:976–979

Kusachi I, Henmi C, Kobayashi S (1994) Chemical composition of bakerite from Fuka, Okayama Prefecture, Japan. Mineral J (Jpn) 17(3):111–117

Kusachi I, Henmi C, Kobayashi S (1995) Takedaite, a new mineral from Fuka, Okayama Prefecture, Japan. Mineral Mag 59:549–552

Kusachi I, Henmi C, Kobayashi S (1997a) Sibirskite from Fuka, Okayama Prefecture, Japan. Mineral J (Jpn) 19 (3):109–114

Kusachi I, Takeshi Y, Henmi C, Kobayashi S (1997b) Borcarite from Fuka, Okayama Prefecture, Japan. Mineral J (Jpn) 19(3):115–122

Kusachi I, Kobayashi S, Takechi Y, Nakamuta Y, Nagase T, Yokoyama K, Momma K, Miyawaki R, Shigeoka M, Matsubara S (2013) Shimazakiite-4*M* and shimazakiite-4*O*, $Ca_2B_2O_5$, two polytypes of a new mineral from Fuka, Okayama Prefecture, Japan. Mineral Mag 77:93–105

Kusachi I, Nishimura M, Shiraga K, Kobayashi S, Yamakawa J (2001) Kinoite from Fuka, Okayama Prefecture, Japan. J Mineral Petrol Sci 96:29–33

Kusachi I, Shiraga K, Kobayashi S, Yamakawa J, Takechi Y (2000) Uralborite from Fuka, Okayama Prefecture, Japan. J Mineral Petrol Sci 95(4):43–47

Kusachi I, Shiraishi N, Shimada K, Ohnishi M, Kobayashi S (2008) CO_3-rich charlesite from the Fuka mine, Okayama Prefecture, Japan. J Mineral Petrol Sci 103:47–51

Kusachi I, Takechi Y, Kobayashi S, Yamakawa J, Nakamuta Y, Lee K-H, Motomizu S (1999) Hexahydroborite from Fuka, Okayama Prefecture, Japan. Mineral J (Jpn) 21(1):9–14

Kustova GN, Obzherina KF, Batsanova LR (1968) The infrared absorption spectra of oxyfluorides of the rare earth metals. Zhurnal Prikladnoi Spektroskopii (J Appl Spectrosc) 9(3):431–435 (in Russian)

Kyono A, Kimata M (2001a) Refinement of the crystal structure of a synthetic non-stoichiometric Rb-feldspar. Mineral Mag 65:523–531

Kyono A, Kimata M (2001b) The crystal structure of synthetic $TlAlSi_3O_8$: influence of the *inert-pair effect* of thallium on the feldspar structure. Eur J Mineral 13:849–856

Kyono A, Kimata M, Shimizu M, Saito S, Nishida N, Hatta T (1999) Synthesis of thallium-leucite ($TlAlSi_2O_6$) pseudomorph after analcime. Mineral Mag 63:75–83

König R, Scholz G, Scheurell K, Heidemann D, Buchem I, Unger WES, Kemnitz E (2010) Spectroscopic characterization of crystalline AlF_3 phases. J Fluor Chem 131:91–97

Kühn R, Moenke H (1963) Ultrarotspektroskopische Charakterisierung des neuentdeckten Borminerals Fabianit $CaB_3O_5(OH)$ und seines Begleiters Howlith. Kali Steinsalz 3(12):399–401 (in German)

Lahalle MP, Krupa JC, Lepostollec M, Forgerit JP (1986) Low-temperature Raman study on $ThSiO_4$ single crystal and related infrared spectra at room temperature. J Solid State Chem 64:181–187

Lai Zhenyu, Qian Jueshi, Lu Zhongyuan, Li Qian, Zou Qiulin (2012) Rapid synthesis of dittmarite by microwave-assisted hydrothermal method. Adv Mater Sci Engin 2012, 4 pp, Article ID 968396

Lam AE (1998) An X-ray crystallographic study of the crystal structures of four tellurium oxysalt minerals: dugganite, choloalite, rodalquilarite, and graemite. Dissertation, University of British Columbia

Lan T, Fang Y, Xiong W, Kong C (2007) Automatic baseline correction of infrared spectra. Chin Opt Lett 5:613–616

Langer K, Lattard D, Schreyer W (1977) Synthesis and stability of deerite, $Fe^{2+}{}_{12}Fe^{3+}{}_{6}$ $[Si_{12}O_{40}](OH)_{10}$, and $Fe^{3+} \leftrightarrow A1^{3+}$ substitutions at 15–28 kb. Contrib Mineral Petrol 60:271–297

Lantenois S, Beny JM, Muller F, Champallier R (2007) Integration of Fe in natural and synthetic Al-pyrophyllites: an infrared spectroscopic study. Clay Miner 42:129–141

Larsen AO, Åsheim A, Berge SA (1987) Bromellite from syenite pegmatite, southern Oslo region, Norway. Can Miner 25:425–428

Last JT (1957) Infrared-absorption studies on barium titanate and related materials. Phys Rev 105(6):1740–1750

Launer PJ (1952) Regularities in the infrared absorption spectra of silicate minerals. Am Miner 37:764–784

Law AD (1981) Studies of the orthoamphiboles II. Hydroxyl spectra of anthophyllites. Bull Soc Fr Minér Cristallogr 104(4):423–430

Law AD (1982) Studies of the orthoamphiboles III, Hydroxyl spectra of gedrites. Mineral Mag 45:63–71

Law AD, Whittaker EJW (1981) Studies of the orthoamphiboles. I. The Mössbauer and infrared spectra of holmquistite. Bull Soc Fr Minér Cristallogr 104 (4):381–386

Lazarev AN, Tenisheva TF (1962) Vibrational spectra of mixed crystals in the system Li_2SiO_3-Li_2GeO_3. Optika i Spektroskopiya (Opt and Spectrosc) 13(5):708–713 (in Russian)

Le Breton N (1989) Infrared investigation of CO_2-bearing cordierites. Some implications for the study of metapelitic granulites. Contrib Mineral Petrol 103:387–396

Leduc EMS (2010) Hydrated sodium-magnesium sulfate minerals associated with inland saline systems – atomic structure, hydrogen bonding and phase stability. Dissertation, Queen's University, Kingston, Ontario

Lee M-H, Jung W-S (2013) Hydrothermal synthesis of $LaCO_3OH$ and Ln^{3+}-doped $LaCO_3OH$ powders under ambient pressure and their transformation to $La_2O_2CO_3$ and La_2O_3. Bull Korean Chem Soc 34(12):3609–3614

Lehmann S, Geipel G, Foerstendorf H, Bernhard G (2008) Syntheses and spectroscopic characterization of uranium(VI) silicate minerals. J Radioanal Nucl Chem 275(3):633–642

Lehnen T, Valldor M, Nižňanský D, Mathur S (2014) Hydrothermally grown porous $FeVO_4$ nanorods and their integration as active material in gas-sensing devices. J Mater Chem A 2:1862–1868

Leinenweber K, Navrotsky A, McMillan P, Ito E (1989) Transition enthalpies and entropies of high pressure zinc metasilicates and zinc metagermanates. Phys Chem Minerals 16:799–808

Lemaire C, Kohn SC, Brooker RA (2004) The effect of silica activity on the incorporation mechanisms of waterin synthetic forsterite: a polarised infrared spectroscopic study. Contrib Mineral Petrol 147:48–57

Lennie AR, Vaughan DJ (1992) Kinetics of the marcasite-pyrite transformation: an infrared spectroscopic study. Am Miner 77:1166–1171

Li W, Chen G (1985) The discovery of heliophyllite in China. Acta Mineralogica Sinica 3:216–220 (in Chinese, English abstr)

Li C, Hou Z, Zhang C, Yang P, Li G, Xu Z, Fan Y, Lin J (2009) Controlled synthesis of Ln^{3+} (Ln = Tb, Eu, Dy) and V^{5+} ion-doped YPO_4 nano-/microstructures with tunable luminescent colors. Chem Mater 21 (19):4598–4607

Li G, Peng C, Zhang C, Xu Z, Shang M, Yang D, Kang X, Wang W, Li C, Cheng Z, Lin J (2010) Eu^{3+}/Tb^{3+}-doped $La_2O_2CO_3/La_2O_3$ nano/microcrystals with multiform morphologies: facile synthesis, growth mechanism, and luminescence properties. Inorg Chem 49:10522–10535

Li W, Chen G, Peng Z (1986) Chaidamuite – a new zinc and ferric sulfate mineral. Acta Mineralogica Sinica 6:09–113 (in Chinese, English abstr)

Li W, Chen G, Sun S (1987) Zincovoltaite – a new sulphate mineral. Acta Mineralogica Sinica 7:307–312 (in Chinese, English abstr)

Libowitzky E, Beran A (1995) OH defects in forsterite. Phys Chem Minerals 22:387–392

Libowitzky E, Beran A (2006) The structure of hydrous species in nominally anhydrous minerals: information from polarized IR spectroscopy. Rev Mineral Geochem 62(1):29–52

Likhacheva AY, Paukshtis EA, Seryotkin YV, Shulgenko SG (2002) IR spectroscopic characterization of NH_4-analcime. Phys Chem Minerals 29:617–623

Litasov KD, Ohtani E, Kagi H, Jacobsen SD, Ghosh S (2007) Temperature dependence and mechanism of hydrogen incorporation in olivine at 12.5–14.0 GPa. Gepohys Res Lett 34:L16314

Liu J, Li G, Mao Q, Wu S, Liu Z, Su S, Xiong M, Yu X (2012) Hanjiangite, a new barium-vanadium phyllosilicate carbonate mineral from the Shiti barium deposit in the Dabashan region, China. Am Miner 97:281–290

Liu P, Liang Y, Lin X, Wang C, Yang G (2011) A general strategy to fabricate simple polyoxometalate nanostructures: electrochemistry-assisted laser ablation in liquid. ACSnano 5(6):4748–4755

Liu S, Ma R, Jiang R, Luo F (1999a) Precipitation and characterization of cerous carbonate. J Cryst Growth 206:88–92

Liu L, Wang X, Bontchev R, Ross K, Jacobson AJ (1999b) Influence of reaction conditions on the electrochemical-hydrothermal synthesis of two ammonium vanadium phosphates:$(NH_4)_2VO(HPO_4)_2{\cdot}H_2O$ and $(NH_4)_2VO(V_{0.88}P_{1.12}O_7)$. J Mater Chem 9 (7):1585–1589

Livingstone A (1987) A basic magnesium carbonate, a possible dimorph of artinite, from Unst, Shetland. Mineral Mag 51:459–462

Livingstone A (1994) An apatite high in lead from Wanlockhead, Strathclyde Region, Scotland. Mineral Mag 58:159–163

Livingstone A, Jackson B, Davidson PJ (1984) Grimaldiite, CrOOH, a second occurrence, from the Hiaca Mine, Colquechaca, Bolivia. Mineral Mag 48:560–562

Livingstone A, Ryback G, Fejer EE, Stanley CJ (1987) Mattheddleite, a new mineral of the apatite group from Leadhills, Strathclyde Region. Scott J Geol 23:1–8

Locock AJ, Burns PC, Flynn TM (2005) The role of water in the structures of synthetic hallimondite, $Pb_2[(UO_2)(AsO_4)_2](H_2O)_n$ and synthetic parsonsite, $Pb_2[(UO_2)(PO_4)_2](H_2O)_n$, $0 \le n \le 0.5$. Am Miner 90:240–246

Łodziński M, Sitarz M, Stec K, Kozanecki M, Fojud Z, Jurga S (2005) ICP, IR, Raman, NMR investigations of beryls from pegmatites of the Sudety Mts. J Mol Struct 744–747:1005–1015

Lopato LM, Red'ko VP, Veblaya TS, Kharchenko NP (1992) Infrared spectra of compounds $M_4Zr_3O_{12}$ and $M_4Hf_3O_{12}$ (M = *REE*). Neorganicheskiye Materialy (Inorg Mater) 28(10/11):2250–2252 (in Russian)

López A, Frost RL, Scholz R, Gobac ŽŽ, Xi Y (2013) Vibrational spectroscopy of the silicate mineral plumbotsumite $Pb_5(OH)_{10}Si_4O_8$ – an assessment of the molecular structure. J Molec Struct 1054:228–233

Lorenzzi JCDC (2007) Boron nitride thin films deposited by magnetron sputtering on Si_3N_4. Report from Repositório Institucional da Universidade de Aveiro, Portugal (in English)

Loughnan FC, Roberts FI, Lindner AW (1983) Buddingtonite (NH_4-feldspar) in the Condor Oilshale Deposit, Queensland, Australia. Mineral Mag 47:327–334

Low MJD, Lacroix M, Morterra C (1982) Infrared photothermal beam deflection Fourier transform spectroscopy of solids. Appl Spectrosc 36(5):582–584

Lucovsky G (1969) Comments on the structure of chalcogenide glasses from infrared spectroscopy. Mater Res Bull 4:505–514

Lucovsky G, Knights JC (1974) Infrared absorption in bulk amorphous As. Phys Rev B 10(10):4324–4330

Luo S, Lu J, Wang L, Zhu J (1993) Qilianshanite: a new boric carbonate mineral. Acta Mineralogica Sinica 13 (2):97–101 (in Chinese, English abstr)

Lührs H, Fischer RX, Schneider H (2012) Boron mullite: formation and basic characterization. Mater Res Bull 47:4031–4042

Luttrell RD, Brown S, Cao J, Musfeldt JL, Rosentsveig R, Tenne R (2006) Dynamics of bulk versus nanoscale WS_2: local strain and charging effects. Phys Rev B 73 (3):035410–035415

Lutz HD, Eckers W, Schneider G, Haeuseler H (1981) Raman and infrared spectra of barium and strontium hydroxides and hydroxide hydrates. Spectrochim Acta A 37(7):561–567

Lutz HD, Jung C, Mörtel R, Jacobs H, Stahl R (1998) Hydrogen bonding in solid hydroxides with strongly polarizing metal ions, β-$Be(OH)_2$ and ε-$Zn(OH)_2$. Spectrochim Acta A 54:893–901

Lutz HD, Kliche G (1981) Lattice vibration spectra. XXVI. Far-infared spectra of the ternary skutterudites $CoP_{3-x}As_x$, $CoAs_{3-x}Sb_x$, and $MGe_{1.5}Y_{1.5}$ (M = Co, Rh, Ir; Y = S, Se). J Solid State Chem 40:64–68

Lutz HD, Kliche G (1982) Far-infrared reflection spectra, optical and dielectric constants, effective charges, and lattice dynamics of the skutterudites CoP_3, $CoAs_3$, and $CoSb_3$. Phys Status Solidi B 112(2):549–557

Lutz HD, Schneider G, Kliche G (1983) Chalcides and pnictides of group VIII transition metals: far-infrared spectroscopic studies on compounds MX_2, *MXY,* and MY_2 with pyrite, marcasite, and arsenopyrite structure. Phys Chem Minerals 9:109–114

Lutz HD, Schneider G, Kliche G (1985) Far-infrared reflection spectra, TO- and LO-phonon frequencies, coupled and decoupled plasmon-phonon modes, dielectric constants, and effective dynamical charges of manganese, iron, and platinum group pyrite type compounds. J Phys Chem Solids 46(4):437–443

Luxon JT, Summitt R (1969) Interpretation of the infrared absorption spectra of stannic oxide and titanium dioxide (rutile) powders. J Chem Phys 50(3):1366–1370

Lyon RJP, Burns EuA (1963) Analysis of rocks and minerals by reflected infrared radiation. Econ Geol 58:274–284

MacKenzie KJD, Berezowski RM (1984) Thermal and Mössbauer studies of iron-containing hydrous silicates. V. Berthierine. Thermochim Acta 74(1-3): 291–312

Madon M, Gillet Ph, Julien Ch, Price GD (1991) A vibrational study of phase transitions among the GeO_2 polymorphs. Phys Chem Minerals 18:7–18

Majzlan J, Alpers CN, Koch CB, McCleskey RB, Myneni SCB, Neil JM (2011) Vibrational, X-ray absorption, and Mössbauer spectra of sulfate minerals from the weathered massive sulfide deposit at Iron Mountain, California. Chem Geol 284:296–305

Majzlan J, Stevens R, Boerio-Goates J, Woodfield BF, Navrotsky A, Burns PC, Crawford MK, Amos TG (2004) Thermodynamic properties, low-temperature heat-capacity anomalies, and single-crystal X-ray refinement of hydronium jarosite, $(H_3O)Fe_3(SO_4)_2(OH)_6$. Phys Chem Minerals 31:518–531

Makreski P, Jovanovski G, Minceva-Sukarova B, Soptrajanov B, Green A, Engelen B, Grzetic I (2004) Vibrational spectra of $M^I{}_3M^{III}S_3$ type synthetic minerals (M^I = Tl or Ag and M^{III} = As or Sb). Vib Spectrosc 35(1):59–65

Maksimovic Z, Bish DL (1978) Brindleyite, a nickel-rich aluminous serpentine mineral analogous to berthierine. Am Miner 63:484–489

Malcherek T, Schlüter J, Cooper M, Ball N, Husdal T (2015) Cayalsite-(Y), a new rare-earth calcium aluminium fluorosilicate with OD character. Eur J Mineral 27:683–694

Maldener J, Hösch A, Langer K, Rauch F (2003) Hydrogen in some natural garnets studied by nuclear reaction analysis and vibrational spectroscopy. Phys Chem Minerals 30(6):337–344

Mancilla N, Caliva V, D'Antonio MC, González-Baró AC, Baran EJ (2009) Vibrational spectroscopic investigation of the hydrates of manganese(II) oxalate. J Raman Spectrosc 40:915–920

Maras A, Parodi GC, della Ventura G, Ohnenstetter D (1995) Vicanite-(Ce): a new Ca-Th-REE borosilicate from the Vico volcanic district (Latium, Italy). Eur J Mineral 7:439–446

Marincea S, Dumitras D, Gibert R (2002) Tinsleyite in the "dry" Cioclovina Cave (Sureanu Mountains, Romania) the second occurrence. Eur J Mineral 14:157–164

Marquez Zavalia MF (1993) Siderotilo de Mina Cappilitas, Catamarca. Revista de la Asociación Geológica Argentina 48(2):143–146 (in Spain)

Martin DH (1965) The study of the vibrations of crystal lattices by far infra-red spectroscopy. Adv Phys 14 (53):39–99

Martin RF, Donnay G (1972) Hydroxyl in the mantle. Am Miner 57:554–570

Martin Pozas JM, Rossi G, Tazzoli V (1975) Re-examination and crystal structure analysis of litidionite. Am Miner 60:471–474

Marx N, Croguennec L, Carlier D, Bourgeois L, Kubiak P, Le Cras F, Delmas C (2010) Structural and electrochemical study of a new crystalline hydrated iron(III) phosphate $Fe(PO_4)\cdot H_2O$ obtained from $LiFePO_4(OH)$ by ion exchange. Chem Mater 22:1854–1861

Mason B, Allen RO (1973) Minor and trace elements in augite, hornblende, and pyrope megacrysts from Kakanui, New Zealand. New Zealand J Geol Geophys 16(4):935–947

Matsubara S, Mouri T, Miyawaki R, Yokoyama K, Nakahara M (2008) Munakataite, a new mineral from the Kato mine, Fukuoka, Japan. J Mineral Petrol Sci 103:327–332

Mazen SA, Abdallah MH, Sabrah BA, Hashem HAM (1992) The effect of titanium on some physical properties of $CuFe_2O_4$. Phys Status Solidi A 134:263–271

McCammon CA, Pring A, Keppler H, Sharp T (1995) A study of bernalite, $Fe(OH)_3$, using Mössbauer spectroscopy, optical spectroscopy and transmission electron microscopy. Phys Chem Minerals 22:11–20

McDevitt NT, Baun WL (1964) Infrared absorption spectroscopy in zirconia research. J Am Ceram Soc 47(12):622–624

McDevitt NT, Davidson AD (1965) Infrared study of Ag_2O in the low-frequency region. JOSA 55(2):209

McDonald AM, Back ME, Gault RA, Horváth L (2013) Peatite-(Y) and ramikite-(Y), two new Na-Li-Y±Zr phosphate-carbonate minerals from the Poudrette Pegmatite, Mont Saint-Hilaire, Quebec. Can Miner 51(4):569–596

McDonald AM, Chao GY (2001) Natrolemoynite, a new hydrated sodium zirconosilicate from Mont Saint-Hilaire, Quebec: description and structure determination. Can Miner 39:1295–1306

McDonald AM, Chao GY (2004) Haineaultite, a new hydrated sodium calcium titanosilicate from Mont Saint-Hilaire, Quebec: description, structure deter mination and genetic implications. Can Miner 42:769–780

McDonald AM, Chao GY (2005) Bobtraillite, $(Na,Ca)_{13}Sr_{11}(Zr,Y,Nb)_{14}Si_{42}B_6O_{132}(OH)_{12}\cdot 12H_2O$, a new mineral species from Mont Saint-Hilaire, Quebec: description, structure determination and relationship to benitoite and wadeite. Can Miner 43:747–758

McDonald AM, Chao GY (2007) Martinite, a new hydrated sodium calcium fluorborosilicate species from Mont Saint-Hilaire, Quebec: description, structure determination and genetic implications. Can Miner 45(5):1281–1292

McDonald AM, Chao GY (2009) Lalondeite, a new hydrated Na-Ca fluorosilicate species from Mont Saint-Hilaire, Quebec: description and crystal structure. Can Miner 47:181–191

McDonald AM, Chao GY (2010) Rogermitchellite, $Na_{12}(Sr,Na)_{24}Ba_4Zr_{26}Si_{78}(B,Si)_{12}O_{246}(OH)_{24}\cdot 18H_2O$, a new mineral species from Mont Saint-Hilaire, Quebec: description, structure determination and relationship with HFSE-bearing cyclosilicates. Can Miner 48:267–278

McDonald AM, Chao GY, Ramik RA (1991) Rouvilleite, a new sodium calcium fluorocarbonate mineral from Mont Saint-Hilaire, Quebec. Can Miner 29:107–111

McDonald AM, Petersen OV, Gault RA, Johnsen O, Niedermayr G, Brandstatter F, Giester G (2001) Micheelsenite, $(Ca,Y)_3Al(PO_3OH,CO_3)(CO_3)(OH)_6\cdot 12H_2O$, a new mineral from Mont Saint-Hilaire, Quebec, Canada and the Nanna pegmatite, Narsaarsuup Qaava, South Greenland. N Jb Miner Mh 8:37–351

McDonald AM, Tarassoff P, Chao GY (2015) Hogarthite, $(Na,K)_2CaTi_2Si_{10}O_{26}\cdot 8H_2O$, a new member of the lemoynite group from Mont Saint-Hilaire, Quebec: characterization, crystal-structure determination, and origin. Can Miner. doi:10.3749/canmin.1400079

McMillan P, Akaogi M, Ohtani E, Williams Q, Nieman R, Sato R (1989) Cation disorder in garnets along the $Mg_3Al_2Si_3O_{12}$-$Mg_4Si_4O_{12}$ join: an infrared, Raman and NMR study. Phys Chem Minerals 16:428–435

McMillan PF, Akaogi M, Sato RK, Poe B, Foley J (1991) Hydroxyl groups in β-Mg_2SiO_4. Am Miner 76:354–360

McNear E, Vincent MG, Parthé E (1976) The crystal structure of vuagnatite, $CaAl(OH)SiO_4$. Am Miner 61:831–838

Meireles AAG (2011) Ortoniobatos de iões terras raras – propriedades elétricas e óticas. Dissertação, Universidade de Aveiro (in Portuguese)

Melnikova RY, Pechkovskii VV, Dzyuba ED, Malashonok IE (1985) Atlas of infrared spectra of phosphates. Condensed phosphates, Nauka, Moscow (in Russian)

Meloche VW, Kalbus GE (1958) Anomalies in the infra-red spectra of inorganic coumpounds prepared by the potassium bromide pellet technique. J Inorg Nucl Chem 6:104–111

Mendelovici E, Villalba R, Sagarzazu A (1994) A distinctive mechanochemical transformation of manganosite into manganite by mortar dry grinding. Mater Res Bull 29(2):167–174

Menezes WG, Reis DM, Benedetti TM, Oliveira MM, Soares JF, Torresi RM, Zarbin AJG (2009) V_2O_5 nanoparticles obtained from a synthetic bariandite-like vanadium oxide: synthesis, characterization and electrochemical behavior in an ionic liquid. J Colloid Interface Sci 337:586–593

Men'shikov YuP, Khomyakov AP, Polezhaeva LI, Rastsvetaeva RK (1996) Shkatulkalite: $Na_{10}Mn Ti_3Nb_3(Si_2O_7)_6(OH)_2F{\cdot}12H_2O$ – a new mineral. Zapiski RMO (Proc Russ Mineral Soc) 125(1):120–126 (in Russian)

Mer A, Obbade S, Rivenet M, Renard C, Abraham F (2012) $[La(UO_2)V_2O_7][(UO_2)(VO_4)]$ the first lanthanum uranyl-vanadate with structure built from two types of sheets based upon the uranophane anion-topology. J Solid State Chem 185:180–186

Merceron T, Inoue A, Bouchet A, Meunier A (1988) Lithium-bearing donbassite and tosudite from Echassieres, Massif Central, France. Clays Clay Miner 36 (1):39–46

Mereiter K, Zemann J, Hewat AW (1992) Eglestonite, $[Hg_2]_3Cl_3O_2H$: confirmation of the chemical formula by neutron powder diffraction. Am Miner 77:839–842

Mernagh TP, Liu L-G (1996) Raman and infrared spectra of hydrous β-Mg_2SiO_4. Can Miner 34:1233–1240

Mesto E, Kaneva E, Schingaro E, Vladykin N, Lacalamita M, Scordari F (2014) Armstrongite from Khan Bogdo (Mongolia): crystal structure determination and implications for zeolite-like cation exchange properties. Am Miner 99:2424–2432

Meyer TQ, van der Westhuizen WA, Beukes GJ, de Bruiyn H, Schoch AE (1986) An occurrence of the hydrous lead-copper-iron silicate creaseyite in South Africa. Mineral Mag 50:346–348

Miehe G, Graetsch H (1992) Crystal structure of moganite: a new structure type for silica. Eur J Mineral 4:693–706

Mikawa Y, Jakobsen RJ, Brasch JW (1966) Far-infrared spectra of mercuric halides and their dioxane complexes. J Chem Phys 45(12):4528–4535

Miller FA, Wilkins CH (1952) Infrared spectra and characteristic frequencies of inorganic ions. Their use in qualitative analysis. Anal Chem 24(8):1253–1294

Mills SJ, Christy AG, Schnyder C, Favreau G, Price JR (2014) The crystal structure of camerolaite and structural variation in the cyanotrichite family of merotypes. Mineral Mag 78:1527–1552

Mills SJ, Kampf AR, Sejkora J, Adams PM, Birch WD, Plášil J (2011) Iangreyite: a new secondary phosphate mineral closely related to perhamite. Mineral Mag 75:327–336

Mills SJ, Kolitsch U, Miyawaki R, Hatert F, Poirier G, Kampf AR, Matsubara S, Tillmanns E (2010) $Pb_3Fe^{3+}{}_2(PO_4)_4(H_2O)$, a new octahedral-tetrahedral framework structure with double-strand chains. Eur J Mineral 22:595–604

Milton C, Dwornik EJ, Estep-Barnes PA, Finkelman RB, Pabst A, Palmer S (1978) Abelsonite, nickel porphyrin, a new mineral from the Green River Formation, Utah. Am Miner 63:930–937

Minceva-Sukarova B, Jovanovski G, Makreski P, Soptrajanov B, Griffith W, Willis R, Grzetic I (2003) Vibrational spectra of $M^IM^{III}S_2$ type synthetic minerals (M^I = Tl or Ag and M^{III} = As or Sb). J Molec Struct 651:181–189

Ming X, Ma ZS, Peng ZZ (1989) A new mineral – ankangite. Chin Sci Bull 34(7):592–596

Minić DM, Šušić MV, Mioč UB, Petranović NA (1985) Behaviour and properties of the crystallohydrate 3Cd $(SO_4){\cdot}8H_2O$ during dehydration. Mater Chem Phys 12:389–396

Mirhadi SM, Tavangarian F, Emadi R (2012) Synthesis, characterization and formation mechanism of single-phase nanostructure bredigite powder. Mater Sci Eng C 32:133–139

Mitchell RH, Chakhmouradian AR (1998) Th-rich loparite from the Khibina alkaline complex, Kola Peninsula: isomorphism and paragenesis. Mineral Mag 62:341–353

Mitsuyosi K (1993) Crystal structure of $KBSi_3O_8$ isostructural with danburite. Mineral Mag 57:157–164

Miyawaki R, Matsubara S, Yokoyama K, Shigeoka M, Momma K, Yamamoto S (2015) Mieite-(Y), $Y_4Ti(SiO_4)_2O[F,(OH)]_6$, a new mineral in a pegmatite at Souri Valley, Komono, Mie Prefecture, central Japan. J Mineral Petrol Sci 110:135–144

Mizota T, Komatsu M, Chihara K (1983) A refinement of the crystal structure of ohmilite, $Sr_3(Ti,Fe^{3+})(O,OH)(Si_2O_6)_2{\cdot}2\text{-}3H_2O$. Am Miner 68:811–817

Mockenhaupt C (2006) Strukturuntersuchungen an Amminkomplexen und Hydroxiden von Übergangsmetallen. Dissertation, Universität-Gesamthochschule-Siegen (in German)

Moenke H (1961) Beiträge zur ultrarotphotometrischen Bestimmung organischer Mineralien. Chemie der Erde 21:239–247 (in German)

Moenke H (1962) Mineralspektren I. Akademie Verlag, Berlin (in German)

Moenke H (1966) Mineralspektren II. Akademie Verlag, Berlin (in German)

Mohan C (2003) Buffers: a guide for the preparation and use of buffers in biological systems. Calbiochem®, EMD Biosciences, Inc

Momma K, Ikeda T, Nishikubo K, Takahashi N, Honma C, Takada M, Furukawa Y, Nagase T, Kudoh Y (2011) New silica clathrate minerals that are isostructural with natural gas hydrates. Nat Commun 2:196 (7 p)

Moroz T, Shcherbakova E, Kostrovsky V (2004) Vibrational spectra of kladnoite, natural analogue of phthalimide $C_6H_4(CO)_2NH$. Mitt Österr Miner Ges 149:73

Mottana A, Griffin WL (1986) Crystal chemistry of two coexisting K-richterites from St. Marcel (Val d'Aosta, Italy). Am Miner 71:1426–1433

Mrose ME, Fahey JJ, Ericksen GE (1970) Mineralogical studies of the nitrate deposits of Chile. III. Humberstonite, $K_3Na_7Mg_2(SO_4)_6(NO_3)_2{\cdot}6H_2O$, a new saline mineral. Am Miner 55:1518–1533

Muniz-Miranda M, Sbrana G, Bonazzi P, Menchetti S, Pratesi G (1996) Spectroscopic investigation and

normal mode analysis of As_4S_4 polymorphs. Spectrochim Acta A 52(11):1391–1401
Murad E (1979) Mössbauer and X-ray data on β-FeOOH (akaganéite). Clay Miner 14:273–283
Mücke A (1983) Wilhelmvierlingit, $(Ca,Zn)MnFe^{3+}[OH|(PO_4)_2]2H_2O$, ein neues Mineral von Hagendorf/Oberpfalz. Der Aufschluss 34:267–274 (in German)
Müller G (1988) Preparation of hydrogen and lithium feldspars by ion exchange. Nature 332:435–436
Nagata K, Ishibashi K, Miyamoto Y (1981) Raman and infrared spectra of rhombohedral selenium. Jpn J Appl Phys 20(3):463–469
Nakagawa T, Kihara K, Harada K (2001) The crystal structure of low melanophlogite. Am Miner 86:1506–1512
Nakagawa I, Tsuchida A, Shimanouchi T (1967) Infrared transmission spectrum and lattice vibration analysis of some perovskite fluorides. J Chem Phys 47(3):982–989
Nakai I, Appleman DE (1980) Klebelsbergite, $Sb_4O_4(OH)_2SO_4$: redefinition and synthesis. Am Miner 65:499–505
Nakamoto K (2008) Infrared and Raman spectra of inorganic and coordination compounds, theory and applications in inorganic chemistry. Wiley, New York
Nakamoto K (2009) Infrared and Raman spectra of inorganic and coordination compounds, part B, applications in coordination, organometallic, and bioinorganic chemistry. Wiley, Hoboken
Narang SN, Patel ND, Kartha VB (1994) Infrared and Raman spectral studies and normal modes of and α-B_2O_3. J Molec Struct 327:221–235
Nasdala L, Beran A, Libowitzky E, Wolf D (2001) The incorporation of hydroxyl groups and molecular water in natural zircon ($ZrSiO_4$). Am J Sci 301:831–857
Nassau K, Cooper AS, Shiever JW, Prescott BE (1973) Transition metal iodates. III. Gel growth and characterization of six cupric iodates. J Solid State Chem 8:260–273
Nazarov M, Nazarov M (2009) Infrared and terahertz spectroscopy of $Y(Ta,Nb)O_4:Eu^{3+},Tb^{3+}$ phosphors. Moldavian J Phys Sci 8(3–4):308–313
Nebel H, Epple M (2008) Continuous preparation of calcite, aragonite and vaterite, and of magnesium-substituted amorphous calcium carbonate (Mg-ACC). Z anorg allg Chem 634:1439–1443
Newnham RE (1961) A refinement of the dickite structure and some remarks on polymorphism in kaolin minerals. Mineral Mag 32:683–704
Nguyen SD, Kim S-H, Halasyamani PS (2011a) Synthesis, characterization, and structure-property relationships in two new polar oxides: $Zn_2(MoO_4)(SeO_3)$ and $Zn_2(MoO_4)(TeO_3)$. Inorg Chem 50:5215–5222
Nguyen SD, Yeon J, Kim S-H, Halasyamani PS (2011b) $BiO(IO_3)$: a new polar iodate that exhibits an Aurivillius-type $(Bi_2O_2)^{2+}$ layer and a large SHG response. J Am Chem Soc 133:12422–12425
Nikanovich MV, Umreiko DS, Sevchenko AN (1980) Vibrational spectra and structure of double phosphates of uranyl. J Appl Spectrosc 32(4):370–375
Nishio-Hamane D, Minakawa T, Yamaura J-I, Oyama T, Ohnishi M, Shimobayashi N (2014) Adachiite, a Si-poor member of the tourmaline supergroup from the Kiura mine, Oita Prefecture, Japan. J Mineral Petrol Sci 109:74–78
Nishio-Hamane D, Ohnishi M, Momma K, Shimobayashi N, Miyawaki R, Minakawa T, Inaba S (2015) Imayoshiite, $Ca_3Al(CO_3)[B(OH)_4](OH)_6 \cdot 12H_2O$, a new mineral of the ettringite group from Ise City, Mie Prefecture, Japan. Mineral Mag 79:413–423
Nishizawa H, Koizumi M (1975) Synthesis and infrared spectra of $Ca_3Mn_2Si_3O_{12}$ and $Cd_3B_2Si_3O_{12}$ (B: Al, Ga, Cr, V, Fe, Mn) garnets. Am Miner 60:84–87
Nkoumbou C, Villieras F, Barres O, Bihannic I, Pelletier M, Razafitianamaharavo A, Metang V, Yonta Ngoune C, Njopwouo D, Yvon J (2008) Physicochemical properties of talc ore from Pout-Kelle and Memel deposits (central Cameroon). Clay Miner 43:317–337
Noguera O, Merle-Méjean T, Mirgorodsky AP, Smirnov MB, Thomas P, Champarnaud-Mesjard J-C (2003) Vibrational and structural properties of glass and crystalline phases of TeO_2. J Non-Cryst Solids 330:50–60
Novák M, Ertl A, Povondra P, Vašinová Galiová M, Rossman GR, Pristacz H, Prem M, Giester G, Gadas P, Škoda R (2013) Darrellhenryite, $Na(LiAl_2)Al_6(BO_3)_3Si_6O_{18}(OH)_3O$, a new mineral from the tourmaline supergroup. Am Miner 98:1886–1892
Novák N, Sejkora J, Cooper MA (2000) Cyrilovite from Cyrilov, western Moravia, Czech Republic; new data on the type material. J Czech Geol Soc 45(1-2):101–106
Nuth JA, Moseley SH, Silverberg RF, Goebel JH, Moore WJ (1985) Laboratory infrared spectra of predicted condensates in carbon-rich stars. Astrophys J 290:L41–L43
Nyfeler D, Hoffmann C, Armbruster T, Kunz M, Libowitzky E (1997) Orthorhombic Jahn-Teller distortion and Si-OH in mozartite, $CaMn^{3+}O[SiO_3OH]$: a single-crystal X-ray, FTIR, and structure modeling study. Am Miner 82:841–848
Nyquist RA, Kagel RQ (1971) Infrared spectra of inorganic compounds (3800–45 cm^{-1}). Academic Press Inc, New York and London
Nytko EA, Shores MP, Helton JS, Nocera DG (2009) $CdCu_3(OH)_6(NO_3)_2$: an S = 1/2 kagomé antiferromagnet. Inorg Chem 48(16):7782–7786
Nytko EA (2008) Synthesis, structure, and magnetic properties of spin-1/2 kagomé antiferromagnets. Dissertation, Massachusetts Institute of Technology
Obbade S, Dion C, Saadi M, Yagoubi S, Abraham F (2004) $Pb(UO_2)(V_2O_7)$, a novel lead uranyl divanadate. J Solid State Chem 177:3909–3917
Oberti R, Cámara F, Della Ventura G, Iezzi G, Benimoff AI (2006) Parvo-mangano edenite, parvo-mangano tremolite, and the solid-solution between Ca and Mn^{2+} at the *M*4 site in amphiboles. Am Miner 91:526–532

Ohnishi M, Kobayashi S, Kusachi I, Yamakawa J, Shirakami M (2004) Ramsbeckite from the Hirao mine at Minoo, Osaka, Japan. J Mineral Petrol Sci 99:19–24

Ohnishi M, Kusachi I, Kobayashi S, Yamakawa J (2007a) Mineral chemistry of schulenbergite and its Zn-dominant analogue from the Hirao mine, Osaka, Japan. J Mineral Petrol Sci 102(4):233–239

Ohnishi M, Kusachi I, Kobayashi S, Yamakawa J, Tanabe M, Kishi S, Yasuda T (2007b) Numanoite, $Ca_4CuB_4O_6(OH)_6(CO_3)_2$, a new mineral species, the Cu analogue of borcarite from the Fuka Mine, Okayama Prefecture, Japan. Can Miner 45:307–315

Ohnishi M, Kusachi I, Kobayashi S (2007c) Osakaite, $Zn_4(SO_4)(OH)_6{\cdot}5H_2O$, a new mineral species from the Hirao Mine, Osaka, Japan. Can Miner 45:1511–1517

Ohnishi M, Shimobayashi N (2011) Tsumebite from the Kisamori mine, Akita Prefecture, Japan. J Mineral Petrol Sci 106:51–56

Ohnishi M, Shimobayashi N, Nishio-Hamane D, Shinoda K, Momma K, Ikeda T (2013) Minohlite, a new copper-zinc sulfate mineral from Minoh, Osaka, Japan. Mineral Mag 77:335–342

Ohtani E (2005) Water in the mantle. Elements 1:25–30

Oinuma K, Hayashi H (1965) Infrared study of mixed-layer clay minerals. Am Miner 50:1213–1227

Oinuma K, Hayashi H (1968) Infrared spectra of clay minerals. J Tokyo Univ General Education (Natural Sci) 9:57–98

Okada Y, Ishida H, Mitsuda T (1994) Thermal decomposition of tricalcium silicate hydrate. J Am Ceram Soc 77(9):2277–2282

Oktyabrsky RA, Shcheka SA, Lennikov AM, Afanasyeva TB (1992) The first occurrence of qandilite in Russia. Mineral Mag 56:385–389

Olmi F, Sabelli C (1991) Gysinite-(Nd), a mineral new to Italy, from Sa Duchessa, Sardinia. N Jb Miner Mh 4:185–191

Olmi F, Sabelli C (1994) Brizziite, $NaSbO_3$, a new mineral from the Cetine mine (Tuscany, Italy): description and crystal structure. Eur J Mineral 6:667–672

Olmi F, Sabelli C, Trosti-Ferroni R (1993) Rosenbergite, $AlF[F_{0.5}(H_2O)_{0.5}]_4{\cdot}H_2O$, a new mineral from the Cetine mine (Tuscany, Italy): description and crystal structure. Eur J Mineral 5:1167–1174

Olmi F, Santucci A, Trosti-Ferroni R (1995) Sabelliite, a new copper-zinc arsenate-antimonate mineral from Sardinia, Italy. Eur J Mineral 7:1325–1330

Ondruš P, Skála R, Veselovský F, Sejkora J, Vitti C (2003) Čejkaite, the triclinic polymorph of $Na_4(UO_2)(CO_3)_3$ – a new mineral from Jáchymov, Czech Republic. Am Miner 88:686–693

Ondruš P, Skála R, Viti C, Veselovský F, Novák F, Jansa J (1999) Parascorodite, $FeAsO_4{\cdot}2H_2O$ – a new mineral from Kaňk near Kutná Hora, Czech Republic. Am Miner 84:1439–1444

Ondruš P, Veselovský F, Skála R, Cisařová I, Hloušek J, Frýda J, Vavřin I, Čejka J, Gabašová A (1997) New naturally occurring phases of secondary origin from Jachymov (Joachimsthal). J Czech Geol Soc 42 (4):77–108

Onuki H, Yoshida T, Nedachi M (1981) Electron probe study of Ti-rich hydroandradites in the Sanbagawa metamorphic rocks. J Japan Assoc Min Petr Econ Geol 76:239–247

Oppermann H, Huong DQ, Zhang M, Schmidt P, Popovkin BA, Ibragimov SA, Berdonosov PS, Dolgikh VA (2001) Untersuchungen zum System $BiOCl/SeO_2$. Z anorg allg Chem 627:1347–1356 (in German)

Orlandi P, Biagioni C, Pasero M, Demartin F, Campostrini I, Merlino S (2015) Mambertiite, $BiMo^{5+}_{2.80}O_8(OH)$, a new mineral from Su Seinargiu, Sardinia, Italy: occurrence, crystal structure, and relationships with gelosaite. Eur J Mineral 27:405–415

Orlova AI, Samoilov SG, Kazantsev GN, Volgutov VY, Bykov DM, Golubev AV, Borovikova EY (2009) Investigation of zirconium phosphate $Zr_3(PO_4)_4$ during heating. Kristallografiya (Crystallogr) 54(3):464–471 (in Russian)

Ōsaka T (1971) Far-infrared absorption spectra of mercurous halides. J Chem Phys 54(3):863–867

Osipov PV, Stolpovskaya VN (1991) Basicdefect chromium-aluminum dravite – a new variety of tourmaline from Sarykulboldy massif (Kazakhstan). New Data Minerals 37:101–107 (in Russian)

Paar WH, Braithwaite RSW, Chen TT, Keller P (1984) A new mineral, scotlandite ($PbSO_3$) from Leadhills, Scotland; the first naturally occurring sulphite. Mineral Mag 48:283–288

Paar WH, Cooper MA, Hawthorne FC, Moffatt A, Gunter ME, Roberts AC, Dunn PJ (2009) Braithwaiteite, $NaCu_5(TiSb)O_2(AsO_4)_4[AsO_3(OH)]_2(H_2O)_8$, a new mineral species from Laurani, Bolivia. Can Miner 47:947–952

Paar WH, Mereiter K, Braithwaite RSW, Keller P, Dunn PJ (1986) Chenite, $Pb_4Cu(SO_4)_2(OH)_6$, a new mineral, from Leadhills, Scotland. Mineral Mag 50:129–135

Palacios D, Wladimirsky A, D'Antonio MC, González-Baró AC, Baran EJ (2011) Vibrational spectra of double oxalates of the type $M^I_2Cu(C_2O_4)_2{\cdot}2H_2O$ ($M^I = Na^+$, K^+, NH_4^+). Spectrochim Acta A 79:1145–1148

Palchik NA, Grigorieva TN, Moroz TN (2013) Composition, structure, and properties of iron-rich nontronites of different origins. Kristallografiya (Crystallogr) 58(2):283–288 (in Russian)

Palmer SJ, Reddy BJ, Frost RL (2011) Synthesis and vibrational spectroscopy of halotrichite and bilinite. Spectrochim Acta A 79:69–73

Papin A, Sergent J, Robert J-L (1997) Intersite OH-F distribution in an Al-rich synthetic phlogopite. Eur J Mineral 9:501–508

Paques-Ledent MTh (1977) $A^{II}B^{IV}(XO_4)_2$ phosphates and arsenates with yavapaiite structure I: isostructural relationship and vibrational study. J Inorg Nucl Chem 39(1):11–17

Park M, Shin I, Singh NJ, Kim KS (2007) Eigen and Zundel forms of small protonated water clusters: structures and infrared spectra. J Phys Chem A 111 (42):10692–10702

Parsons JL (1960) Vibrational spectra of orthorhombic metaboric acid. J Chem Phys 33(6):1860–1866

Parthasarathy G, Chetty TRK, Haggerty SE (2002) Thermal stability and spectroscopic studies of zemkorite: a carbonate from the Venkatampalle kimberlite of southern India. Am Miner 87:1384–1389

Passaglia E, Galli E (1977) Vertumnite, a new natural silicate. Tschermaks Min Petr Mitt 24:57–66

Passaglia E, Rinaldi R (1984) Katoite, a new member of the $Ca_3Al_2(SiO_4)_3$-$Ca_3Al_2(OH)_{12}$ series and a new nomenclature for the hydrogrossular group of minerals. Bull Minér 107:605–618

Paterakis AB (2003) The influence of conservation treatments and environmental storage factors on corrosion of copper alloys in the ancient Athenian Agora. J Am Inst Conserv 42:313–339

Pauliukavets SA (2013) Far-infrared reflection spectra of $FeIn_2S_4$ single crystals. In: 9th international youth science conference "Modern Problems of Radio Engineering and Telecommunications RT 2013", April 22–26, 2013, Sevastopol, Ukraine, p 408 (in Russian)

Paulus H, Müller G (1988) The crystal structure of a hydrogen feldspar. N Jb Miner Mh 3:481–490

Pauly H, Petersen OY (1987) Acuminite, a new Sr-fluoride from Ivigtut, South Greenland. N Jb Miner Mh 11:502–514

Pautov LA, Agakhanov AA (1997) Berezanskite, $KLi_3Ti_2Si_{12}O_{30}$, a new mineral. Zapiski RMO (Proc Russ Mineral Soc) 126(4):75–80 (in Russian)

Pautov LA, Agakhanov AA, Karpenko VYu, Gafurov FG (2010) Aleksandrovite, $KLi_3Ca_7Sn_2[Si_6O_{18}]_2F_2$ – a new tin mineral. New Data Minerals 45:5–16

Pautov LA, Agakhanov AA, Karpenko VYu, Sokolova EV, Hawthorne FC (2013) Mendeleevite-(Ce) $(Cs,\square)_6(\square,Cs)_6(\square,K)_6(REE,Ca,\square)_{30}(Si_{70}O_{175})(H_2O,OH,F,\square)_{35}$: a new mineral from the Dara-i Pioz massif, Tajikistan. Doklady Akademii Nauk (Doklady Acad Sci) 452(4):441–444 (in Russian)

Pautov LA, Agakhanov AA, Sokolova E, Hawthorne FC (2004) Maleevite, $BaB_2Si_2O_8$, and pekovite, $SrB_2Si_2O_8$, new mineral species from the Dara-I Pioz Alkaline Massif, Northern Tajikistan: description and crystal structure. Can Miner 42:107–119

Pautov LA, Bekenova GK, Karpenko VYu, Agakhanov AA (2005) Chukhrovite-(Nd), $Ca_3(Nd,Y)Al_2(SO_4)F_{13}\cdot 12H_2O$, a new mineral. New Data Minerals 40:5–10

Pautov LA, Ignatenko KI, Belakovskii DI (1990) New data on sonolite. Zapiski RMO (Proc Russ Mineral Soc) 119(2):98–101 (in Russian)

Pautov LA, Popov MP, Erokhin YV, Khiller VV, Karpenko VYu (2012) Mariinskite, $BeCr_2O_4$, a new mineral, chromium analog of chrysoberyl. Zapiski RMO (Proc Russ Mineral Soc) 141(6):43–62 (in Russian)

Pavlenko AS, Orlova LP, Akhmanova MV, Tobelko KI (1965) About thorbastnäsite, thorium fluorcarbonate. Zapiski RMO (Proc Russ Mineral Soc) 94(1):105–113 (in Russian)

Peak D, Luther GW, Sparks DL (2003) ATR-FTIR spectroscopic studies of boric acid adsorption on hydrous ferric oxide. Geochim Cosmochim Acta 67 (14):2551–2560

Pechkovskii VV, Melnikova RY, Dzyuba ED (1981) Atlas of infrared spectra of phosphates. Orthophosphates, Nauka, Moscow (in Russian)

Pekov IV, Chukanov NV, Belovitskaya YuV (1998) Khanneshite and petersenlte-(Ce) from Khibiny massif. Zapiski RMO (Proc Russ Mineral Soc) 127(2):92–100 (in Russian)

Pekov IV, Chukanov NV, Boldyreva MM, Dubinchuk VT (2006) Wilhelmramsayite, $Cu_3FeS_3\cdot 2H_2O$, a new mineral from Khibiny massif, Kola Peninsula. Zapiski RMO (Proc Russ Mineral Soc) 135(1):38–48 (in Russian)

Pekov IV, Chukanov NV, Kononkova NN, Zadov AE, Krivovichev SV (2003) Kukharenkoite-(La), $Ba_2(La,Ce)(CO_3)_3F$, a new mineral from Khibiny massif, Kola peninsula. Zapiski RMO (Proc Russ Mineral Soc) 132(3):55–64 (in Russian)

Pekov IV, Levitskiy VV, Krivovichev SV, Zolotarev AA, Chukanov NV, Bryzgalov IA, Zadov AE (2012) New nickel-uranium-arsenic mineral species from the oxidation zone of the Belorechenskoye deposit, Northern Caucasus, Russia: II. Dymkovite, $Ni(UO_2)_2(As^{3+}O_3)_2\cdot 7H_2O$, a seelite-related arsenite. Eur J Mineral 24:923–930

Peng W, Liu G (1982) Atlas of infrared spectra of minerals. Science Press, Beijing (in Chinese)

Peng X, Ichinose I (2011) Manganese oxyhydroxide and oxide nanofibers for high efficiency degradation of organic pollutants. Nanotechnology 22:015701 (7 pp)

Perkins RB, Palmer CD (2000) Solubility of $Ca_6[Al(OH)_6]_2(CrO_4)_3\cdot 26H_2O$, the chromate analog of ettringite; 5–75 °C. Appl Geochem 15:1203–1218

Pertlik F (1981) Structural investigations of synthetic fairchildite, $K_2Ca(CO_3)_2$. Z Kristallogr 157:199–205

Peters L, Rahmoun N-S, Depmeier W (2012) A series of gallium-substituted $4CaO\cdot 3Al_2O_3\cdot 3H_2O$ – cement phase analogues: X-ray powder diffraction and IR spectroscopy studies. Eur J Mineral 24:39–46

Petersen OV, Balić-Žunić T, Gault RA, Andersen T (2003) The first occurrence of ewaldite and donnayite-(Y), two rare carbonate minerals, in the Narssârssuk pegmatite, South Greenland. N Jb Miner Mh 12:543–555

Peterson RC (2011) Cranswickite $Mg(SO_4)\cdot 4H_2O$, a new mineral from Calingasta, Argentina. Am Miner 96:869–877

Peterson RC, Nelson W, Madu B, Shurvell HF (2007) Meridianiite: a new mineral species observed on Earth and predicted to exist on Mars. Am Miner 92:1756–1759

Petrakovskii GA, Udod LV, Sablina KA, Ivanov YuN, Korets AYa, Bovina AF (2005) IR and NMR spectra of crystalline and amorphous copper metaborate. Izvestiya Vysshikh Uchebnykh Zavedenii, seriya Fizika. Russ Phys J 9:73–78 (in Russian)

Petrov I, Šoptrajanov B, Fuson N, Lawson JR (1967) Infra-red investigation of dicalcium phosphates. Spectrochim Acta A 23:2637–2646

Petzelt J, Grigas J (1973) Far infrared dielectric dispersion in Sb_2S_3, Bi_2S_3 and Sb_2Se_3 single crystals. Ferroelectrics 5(1):59–68

Philip D, Aruldhas G, Ramakrishnan V (1988) Infrared and Raman spectra of aquamolybdenum (VI) oxide hydrate ($MoO_3 \cdot 2H_2O$). J Phys 30(2):129–133

Phillippi CM, Mazdiyasni KS (1971) Infrared and Raman spectra of zirconia polymorphs. J Am Ceram Soc 54 (5):254–258

Piilonen PC, McDonald AM, Grice JD, Rowe R, Gault RA, Pourier G, Cooper MA, Kolitsch U, Roberts AC, Lechner W, Palfi AG (2010) Arisite-(Ce), a new rare-earth fluorcarbonate from the Aris Phonolite, Namibia, Mont Saint-Hilaire and the Saint-Amable Sill, Quebec, Canada. Can Miner 48:661–667

Piret P, Deliens M (1980) La comblainite, $(Ni^{2+}_x,Co^{3+}_{1-x})(OH)_2(CO_3)_{(1-x)/2} \cdot yH_2O$, nouveau minéral du groupe de la pyroaurite. Bull Minér 103:113–117 (in French)

Piseri L, Pollini I (1984) Vibrational structure of d-excitons in layered manganese dihalides. J Phys C 17(25):4519–4527

Plendl JN, Hadni A, Claudel J, Henninger Y, Morlot G, Strimer P, Mansur LC (1966) Far infrared study of the copper halides at low temperatures. Appl Optics 5 (3):397–401

Plesko EP, Scheetz BE, White WB (1992) Infrared vibrational characterization and synthesis of a family of hydrous alkali uranyl silicates and hydrous uranyl silicate minerals. Am Miner 77:431–437

Plyusnina II (1977) Infrakrasnye spektry mineralov (Infrared spectra of minerals). Moscow State University, Moscow (in Russian)

Plyusnina II, Maleyev MN, Yefimova GA (1970) Infrared-spectroscopic investigation of cryptocrystalline varieties of silica. Izvestiya AN SSSR, seriya geologicheskaya. Bull Acad Sci USSR, ser Geol 9:78–83 (in Russian)

Plášil J, Dušek M, Novák M, Čejka J, Císařová I, Škoda R (2011a) Sejkoraite-(Y), a new member of the zippeite group containing trivalent cations from Jáchymov (St. Joachimsthal), Czech Republic: description and crystal structure refinement. Am Miner 96:983–991

Plášil J, Fejfarová K, Novák M, Dušek M, Škoda R, Hloušek J, Čejka J, Majzlan J, Sejkora J, Machovič V, Talla D (2011b) Běhounekite, $U(SO_4)_2(H_2O)_4$, from Jáchymov (St Joachimsthal), Czech Republic: the first natural U^{4+} sulphate. Mineral Mag 75:2739–2753

Plášil J, Hauser J, Petříček V, Meisser N, Mills SJ, Škoda R, Fejfarová K, Čejka J, Sejkora J, Hloušek J, Johannet J-M, Machovič V, Lapčák L (2012a) Crystal structure and formula revision of deliensite, $Fe[(UO_2)_2(SO_4)_2(OH)_2](H_2O)_7$. Mineral Mag 76:2837–2860

Plášil J, Hloušek J, Veselovský F, Fejfarová K, Dušek M, Škoda R, Novák M, Čejka J, Sejkora J, Ondruš P (2012b) Adolfpateraite, $K(UO_2)(SO_4)(OH)(H_2O)$, a new uranyl sulphate mineral from Jáchymov, Czech Republic. Am Miner 97:447–454

Plášil J, Kasatkin AV, Škoda R, Novák M, Kallistova A, Dušek M, Skála R, Fejfarová K, Čejka J, Meisser N, Goethals H, Machovič V, Lapčák L (2013) Leydetite, $Fe(UO_2)(SO_4)_2(H_2O)_{11}$, a new uranyl sulfate mineral from Mas d'Alary, Lodève, France. Mineral Mag 77:429–441

Plášil J, Čejka J, Sejkora J, Hloušek J, Goliáš V (2009a) New data for metakirchheimerite from Jáchymov (St. Joachimsthal), Czech Republic. J Geosci 54:373–384

Plášil J, Čejka J, Sejkora J, Škácha P (2009b) The question of water content in parsonsite: a model case-occurrence at the Červené žíly vein system, Jáchymov (St. Joachimsthal), Czech Republic. J Geosci 54:385–394

Plášil J, Čejka J, Sejkora J, Škácha P, Goliáš V, Jarka P, Laurek F, Jehlička J, Němec I, Strnad L (2010) Widenmannite, a rare uranyl lead carbonate: occurrence, formation and characterization. Mineral Mag 74:97–110

Plášil J, Škoda R, Fejfarová K, Čejka J, Kasatkin AV, Dušek M, Talla D, Lapčák L, Machovič V, Dini M (2014) Hydroniumjarosite, $(H_3O)^+Fe_3(SO_4)_2(OH)_6$, from Cerros Pintados, Chile: single-crystal X-ray diffraction and vibrational spectroscopic study. Mineral Mag 78:535–547

Plášil J, Sejkora J, Ďejka J, Škácha P, Goliáš V, Pavliček R, Hofman P (2008) Supergenni mineralizace z haldy šachty č. 16 Přibram – Háje, Supergene mineralization from the dump of the shaft No.16 Pribram – Háje (Czech Republic). Bull Miner-Petrolog Odd Nar Muz (Praha) 16/1 (in Czech)

Podor R, François M, Dacheux N (2003) Synthesis, characterization, and structure determination of the orthorhombic $U_2(PO_4)(P_3O_{10})$. J Solid State Chem 172:66–72

Pol VG, Thiyagarajan P, Calderon Moreno JM, Popa M (2009) Solvent-free fabrication of rare $LaCO_3OH$ luminescent superstructures. Inorg Chem 48:6417–6424

Pollard AM, Thomas RG, Williams PA, Just J, Bridge PJ (1991) The synthesis and composition of georgeite and its reactions to form other secondary copper(II) carbonates. Mineral Mag 55:163–166

Popa K, Wallez G, Raison PE, Bregiroux D, Apostolidis C, Lindqvist-Reis P, Konings RJM (2010) SrNp $(PO_4)_2$: an original ordered modification of cheralite. Inorg Chem 49:6904–6908

Popova VI, Popov VA, Rudashevsky NS, Glavatskikh SF, Polyakov VO, Bushmakin AF (1987) Nabokoite, $Cu_7TeO_4(SO_4)_5 \cdot KCl$, and atlasovite, $Cu_6Fe^{3+}Bi^{3+}O_4(SO_4)_5 \cdot KCl$ – new minerals of volcanic exhalations. Zapiski RMO (Proc Russ Mineral Soc) 116(3):358–367 (in Russian)

Popovici EJ, Imre-Lucaci F, Muresan L, Stefan M, Bica E, Grecu R, Indrea E (2008) Spectral investigations on niobium and rare earth activated yttrium tantalate powders. J Optoelectronics Adv Mater 10 (9):2334–2337

Popovici E-J, Nazarov M, Muresan L, Noh DY, Tudoran LB, Bica E, Indrea E (2010) Synthesis and characterisation of terbium activated yttrium tantalate phosphor. J Alloys Compd 497:201–209

Portnov AM, Siderenko GA (1977) New data on orthorhombic lavenite. Int Geol Rev 19(2):217–220
Post JL, Plummer CC (1972) The chlorite series of Flagstaff Hill area, California: a preliminary investigations. Clays Clay Miner 20:271–283
Postl W, Walter F, Ettinger K, Hauzenberger C, Bojar H-P (2004) Trattnerite, $(Fe,Mg)_2(Mg,Fe)_3[Si_{12}O_{30}]$, a new mineral of the milarite group mineral data and crystal structure. Eur J Mineral 16(2):375–380
Potter RM, Rossman GR (1979a) A magnesium analogue of chalcophanite in manganese-rich concretions from Baja, California. Am Miner 64:1227–1229
Potter RM, Rossman GR (1979b) The tetravalent manganese oxides: identification, hydration, and structural relationships by infrared spectroscopy. Am Miner 64:1199–1218
Pouliot G, Trudel P, Valiquette G, Samson P (1984) Armenite – thulite – albite veins at Rémigny, Quebec: the second occurrence of armenite. Can Miner 22:453–464
Povarennykh AS (1973) On new mineral species calcjarlite. Kontstitutsiya i Svoistva Mineralov (The constitution and properties of minerals) 7:131–135 (in Russian)
Povarennykh AS (1976) IR-absorption spectra of minerals of catapleite – elpidite – labuntsovite groups. Geologicheskiy Zhurnal (Geol J) 36(1):54–62 (in Russian)
Povarennykh AS (1978) The use of infrared spectra for the determination of minerals. Am Miner 63:956–959
Povarennykh AS (1979) Infrared spectra of cyclosilicates. Mineralogicheskiy Zhurnal (Mineral J) 1(2):3–18 (in Russian)
Povarennykh AS (1981a) Influence of the shape of atomic polyhedra on the infrared absorption spectra of minerals. Mineralogicheskiy Zhurnal (Mineral J) 6 (3):13–23 (in Russian)
Povarennykh AS (1981b) IR spectra of some rare minerals from the classes of oxides, silicates, and phosphates. Mineralogicheskiy Zhurnal (Mineral J) 3 (2):14–24 (in Russian)
Povarennykh AS, Keller P, Kristiansen R (1982) Infrared absorption spectra of swedenborgite and oueitite. Can Miner 20:601–603
Povarennykh AS, Solntseva LS, Solntsev BP (1973) Infrared absorption spectra of main copper and iron sulphides. Konstitutsiya i Svoistva Mineralov (The constitution and properties of minerals) 7:81–92 (in Russian)
Pradhan AK, Choudhary RNP (1987) Vibrational spectra of rare earth orthoniobates. Phys Status Solidi B 143: K161–K166
Pradhan AK, Choudhary RNP, Wanklyn BM (1987) Raman and infrared spectra of $YAsO_4$. Phys Status Solidi B 139:337–345
Price GH, Stuart WI (1973) Thermal decomposition of ammonium uranates. Australian Atomic Energy Commission Research Establishment Lucas Heights
Prieto AC, Dubessy AC, Cathelineau M (1991) Structure-composition relationships in trioctahedral chlorites: a vibrational spectroscopy study. Clays Clay Miner 39(5):531–539
Prost R, Dameme A, Huard E, Driard J, Leydecker JP (1989) Infrared study of structural OH in kaolinite, dickite, nacrite, and poorly crystalline kaolinite at 5 to 600 K. Clays Clay Miner 37(5):464–468
Puertas F, Blanco Varela MT, Dominguez R (1990) Characterization of Ca_2AlMnO_5. A comparative study between Ca_2AlMnO_5 and Ca_2AlFeO_5. Cem Concr Res 20:429–438
Pushcharovsky DY, Lebedeva YS, Zubkova NV, Pasero M, Bellezza M, Merlino S, Chukanov NV (2004) Crystal structure of sturmanite. Can Miner 42:723–729
Pöllmann H, Witzke T, Kohler H (1979) Kuzelite, $[Ca_4Al_2(OH)_{12}][(SO_4)\cdot 6H_2O]$, a new mineral from Maroldsweisach/Bavaria, Germany. N Jb Miner Mh 9:423–432
RRUFF (2007) Infrared spectrum for paradamite. http://rruff.info/paradamite/display=default/. Accessed 5 April 2007
Raade G (1970) Dypingite, a new hydrous basic carbonate of magnesium, from Norway. Am Miner 55:1457–1465
Raade G, Chukanov NV, Kolitsch U, Möckel S, Zadov AE, Pekov IV (2004) Gjerdingenite-Mn from Norway – a new mineral species in the labuntsovite group: descriptive data and crystal structure. Eur J Mineral 16:979–987
Raade G, Elliott CJ, Fejer EE (1977) New data on ktenasite. Mineral Mag 41:65–70
Raade G, Ferraris G, Gula A, Ivaldi G, Bernhard F (2002) Kristiansenite, a new calcium-scandium-tin sorosilicate from granite pegmatite in Tørdal, Telemark, Norway. Miner Petrol 75:89–99
Raade G, Grice JD, Cooper MA (2009) Alflarsenite, a new beryllium-silicate zeolite from a syenitic pegmatite in the Larvik plutonic complex, Oslo Region, Norway. Eur J Mineral 21:893–900
Raade G, Mladeck MH (1983) Janhaugite, $Na_3Mn_3Ti_2Si_4O_{15}(OH,F,O)_3$, a new mineral from Norway. Am Miner 68:1216–1219
Raade G, Mladeck MH, Din VK (1986) Heneuite, $CaMg_5(CO_3)(PO_4)_3(OH)$, a new mineral from Modum, Norway. N Jb Miner Mh 8:343–350
Rahmoun N-S, Peters L, Knorr K, Depmeier W (2008) Al/Si and Ca/Eu short range order in Ca/Eu-bicchulite, studied by FTIR spectroscopy. Z Kristallogr 223:441–447
Rama Subba Reddy R, Fayazuddin M, Siva Reddy G, Lakshmi Reddy S, Sambasiva Rao P, Reddy BJ, Nieto Garcia F (2004) Tetrahedral site of Fe (III) and Cu (II) in renierite. Cryst Res Technol 39(3):240–244
Rao NS, Palanna OG (1995) Electrical, thermal and infrared studies of cerium (III) orthovanadate. Bull Mater Sci 18(5):593–597
Rastsvetaeva RK, Chukanov NV, Aksenov SM (2012) Mineraly gruppy evdialita: kristallokhimiya, svoystva, genezis (Eudialyte-group minerals: crystal chemistry, properties, genesis). Nizhny Novgorod State University, Nizhny Novgorod (in Russian)

Raudsepp M, Turnock A, Hawthorne FC (1987a) Characterization of cation ordering in synthetic scandium-fluor-eckermannite, indium-fluor-eckermannite, and scandium-fluor-nyboite by Rietveld structure refinement. Am Miner 72:959–964

Raudsepp M, Turnock AC, Hawthorne FC, Sherriff BL, Hartman JS (1987b) Characterization of synthetic pargasitic amphiboles ($NaCa_2Mg_4M^{3+}Si_6Al_2O_{22}(OH,F)_2$; M^{3+} = Al, Cr, Ga, Sc, In) by infrared spectroscopy, rietveld structure refinement, and ^{27}Al, ^{29}Si, and ^{19}F MAS NMR spectroscopy. Am Miner 72:580–593

Raudsepp M, Turnock A, Hawthorne FC (1991) Amphiboles at low pressure: what grows and what doesn't. Eur J Mineral 3:983–1004

Raz S, Testeniere O, Hecker A, Weiner S, Luquet G (2002) Stable amorphous calcium carbonate is the main component of the calcium storage structures of the crustacean *Orchestia cavimana*. Biol Bull 203:269–274

Reddy JB, Frost RL, Martens WN, Wain DL, Kloprogge JT (2007) Spectroscopic characterization of Mn-rich tourmalines. Vib Spectrosc 44(1):42–49

Redhammer GJ, Beran A, Schneider J, Amthauer G, Lottermoser W (2000) Spectroscopic and structural properties of synthetic micas on the annite-siderophyllite binary: synthesis, crystal structure refinement, Mössbauer, and infrared spectroscopy. Am Miner 85:449–465

Refat MS, Elsabawy KM (2011) Infrared spectra, Raman laser, XRD, DSC/TGA and SEM investigations on the preparations of selenium metal, (Sb_2O_3, Ga_2O_3, SnO and HgO) oxides and lead carbonate with pure grade using acetamide precursors. Bull Mater Sci 34 (4):873–881

Reinecke T, Tillmans E, Bernhardt H-J (1991) Abswurmbachite, $Cu^{2+}Mn^{3+}{}_6[O_8/SiO_4]$, a new mineral of the braunite group: natural occurrence, synthesis, and crystal structure. N Jb Miner Abh 163:117–143

Repelin Y, Husson E, Dao NQ, Brusset H (1979) Etude par spectroscopies d'absorption i.r. et de diffusion Raman des composés $A^{II}B^{V}{}_2O_6$ de structure de type "blocs 1 × 2" – II. Etude du niobate de strontium $SrNb_2O_6$ et des tantalates de calcium $CaTa_2O_6$ et de baryum $BaTa_2O_6$(II). Spectrochim Acta A 35:1165–1175 (in French)

Repina SA, Popova VI, Churin EI, Belogub EV, Khiller VV (2010) Florencite-(Sm), $(Sm,Nd)Al_3(PO_4)_2(OH)_6$ – a new mineral species of the alunite-jarosite group from the Subpolar Urals. Zapiski RMO (Proc Russ Mineral Soc) 139(4):16–25 (in Russian)

Reznitskii L, Clark CM, Hawthorne FC, Grice JD, Skogby H, Hålenius U, Bosi F (2014) Chromo-alumino-povondraite, $NaCr_3(Al_4Mg_2)(Si_6O_{18})(BO_3)_3(OH)_3O$, a new mineral species of the tourmaline supergroup. Am Miner 99:1767–1773

Reznitsky LZ, Sklyarov EV, Ushchapovskaya ZF, Nartova NV, Kashaev AA, Karmanov NS, Kanakin SV, Smolin AS, Nekrasova EA (2001) Vanadiumdravite, $NaMg_3V_6[Si_6O_{18}][BO_3]_3(OH)_4$, a new mineral of the tourmaline group. Zapiski RMO (Proc Russ Mineral Soc) 130(2):59–72 (in Russian)

Riccius HD, Siemsen KJ (1970) Infrared lattice bands of trigonal and cubic mercury sulfide. J Chem Phys 52 (8):4090–4093

Řídkošil T, Šrein V, Fábry J, Hybler J, Maximov BA (1992) Mrázekite, $Bi_2Cu_3(OH)_2O_2(PO_4)_2{\cdot}2H_2O$, a new mineral species and its crystal structure. Can Miner 30:215–224

Rinnan Å, van den Berg F, Engelsen SB (2009) Review of the most common pre-processing techniques for near-infrared spectra. Trends Anal Chem 28:1201–1222

Ristić M, Popović S, Musić S (2004) Formation and properties of $Cd(OH)_2$ and CdO particles. Mater Lett 58:2494–2499

Rius J, Allmann R (1984) The superstructure of the double layer mineral wermlandite $[Mg_7(Al_{0.57},Fe^{3+}{}_{0.43})(OH)_{18}]^{2+}{\cdot}[(Ca_{0.6},Mg_{0.4})(SO_4)_2(H_2O)_{12}]^{2-}$. Z Kristallogr 168:33–144

Robert J-L, Della Ventura G, Hawthorne FC (1996) Infrared characterization of (OH, F)-pargasites. Phys Chem Minerals 23(4):307

Robert J-L, Della Ventura G, Hawthorne FC (1999) Near-infrared study of short-range disorder of OH and F in monoclinic amphiboles. Am Miner 84:86–91

Robert J-L, Kodama H (1988) Generalization of the correlations between hydroxyl-stretching wavenumbers and composition of micas in the system K_2O-MgO-Al_2O_3-SiO_2-H_2O: a single model for trioctahedral and dioctahedral micas. Am J Sci A 288:196–212

Roberts AC, Bonardi M, Erd RC, Criddle AJ, Stanley CJ, Cressey G, Angel RJ, Laflamme JHG (1990a) Edgarbaileyite, the first known silicate of mercury, from California and Texas. Miner Rec 21:215–220

Roberts AC, Ercit TS, Erd RC, Oscarson RL (1990b) Szymańskiite, $Hg^{1+}{}_{16}(Ni,Mg)_6(CO_3)_{12}(OH)_{12}(H_3O)^{1+}{}_8{\cdot}3H_2O$, a new mineral species from the Clear Creek Claim, San Benito County, California. Can Miner 28:703–707

Roberts AC, Cooper MA, Hawthorne FC, Criddle AJ, Stanley CJ, Key CL, Jambor JL (1999) Sidpietersite, $Pb^{2+}{}_4(S^{6+}O_3S^{2-})O_2(OH)_2$, a new thiosulfate-bearing mineral species from Tsumeb, Namibia. Can Miner 37:1269–1273

Roberts AC, Cooper MA, Hawthorne FC, Criddle AJ, Stirling JAR (2002) Sewardite, $CaFe^{3+}{}_2(AsO_4)_2(OH)_2$, the Ca-analogue of carminite, from Tsumeb, Namibia: description and crystal structure. Can Miner 40:1191–1198

Roberts AC, Cooper MA, Hawthorne FC, Gault RA, Grice JD, Nikischer AJ (2003a) Artsmithite, a new Hg^{1+}-Al phosphate-hydroxide from the Funderburk prospect, Pike county, Arkansas, USA. Can Miner 41:721–725

Roberts AC, Cooper MA, Hawthorne FC, Gault RA, Jensen MC, Foord EuE (2003b) Goldquarryite: a new Cd-bearing phosphate mineral from the Gold Quarry Mine, Eureka County, Nevada. Miner Rec 34:237–240

Roberts AC, Cooper MA, Hawthorne FC, Stirling JAR, Paar WH, Stanley CJ, Dunning GE, Burns PC (2003c) Vasilyevite, $(Hg_2)^{2+}{}_{10}O_6I_3Br_2Cl(CO_3)$, a new mineral species from the Clear Creek Claim, San Benito County California. Can Miner 41(5):1167–1172

Roberts AC, Cooper MA, Hawthorne FC, Grice JD, Feinglos MN (2000) Arakiite – a new Zn-bearing hematolite-like mineral from Långban, Värmland, Sweden. Mineral Mag 31:253–256

Roberts AC, Ercit TS, Criddle AJ, Jones GC, Williams RS, Cureton FF, Jensen MC (1994) Mcalpineite, $Cu_3TeO_6{\cdot}H_2O$, a new mineral from the McAlpine mine, Tuolumne County, Califomia, and from the Centennial Eureka mine, Juab County, Utah. Mineral Mag 58:417–424

Roberts AC, Ercit TS, Groat LA, Criddle AJ, Erd RC, Williams RS (1995a) Peterbaylissite, $Hg^{1+}{}_3(CO_3)(OH){\cdot}2H_2O$, a new mineral species from the Clear Creek claim, San Benito County, California. Can Miner 33:47–53

Roberts AC, Grice JD, Criddle AJ, Jensen MC, Harris DC, Moffatt EA (1995b) Frankhawthorneite, $Cu_2Te^{6+}O_4(OH)_2$, a new mineral species from the Centennial Eureka mine, Tintic District, Juab County, Utah. Can Miner 33:641–647

Roberts AC, Gault RA, Jensen MC, Criddle AJ, Moffatt EA (1997a) Juabite, $Cu_5(Te^{6+}O_4)_2(As^{5+}O_4)_2{\cdot}3H_2O$, a new mineral species from the Centennial Eureka mine, Juab County, Utah. Mineral Mag 61:139–144

Roberts AC, Stirling JA, Criddle AJ, Jensen MC, Moffatt EA, Wilson WE (1997b) Utahite, a new mineral and associated copper tellurates from the Centennial Eureka mine, Tintic District, Juab County, Utah. Miner Rec 28(3):175–179

Roberts AC, Grice JD, Dunning GE, Venance KE (2001a) Fencooperite, $Ba_6Fe^{3+}{}_3Si_8O_{23}(CO_3)_2Cl_3{\cdot}\ H_2O$, a new mineral species from Trumbull Peak, Mariposa County, California. Can Miner 39:1059–1064

Roberts AC, Groat LA, Raudsepp M, Ercit TS, Erd RC, Moffatt EA, Stirling JAR (2001b) Clearcreekite, a new polymorph of $Hg^{1+}{}_3(CO_3)(OH){\cdot}2H_2O$, from the Clear Creek Claim, San Benito County, California. Can Miner 39:779–784

Roberts AC, Grice JD, Groat LA, Criddle AJ, Gault RA, Erd RC, Moffatt EA (1996a) Jensenite, $Cu_3Te^{6+}O_6{\cdot}2H_2O$, a new mineral species from the Centennial Eureka mine, Tintic District, Juab County, Utah. Can Miner 34:49–54

Roberts AC, Groat LA, Grice JD, Gault RA, Jensen MC, Moffatt EA, Stirling JAR (1996b) Leisingite, $Cu(Mg,Cu,Fe,Zn)_2Te^{6+}O_6{\cdot}6H_2O$, a new mineral species from the Centennial Eureka mine, Juab County, Utah. Mineral Mag 60:653–657

Roberts AC, Sabina AP, Bonardi M, Jambor JL, Ramik RA, Sturman BD, Carr MJ (1986) Montroyalite, a new hydrated Sr-Al hydroxycarbonate from the Francon Quarry, Montreal Quebec. Can Miner 24:455–459

Roberts AC, Seward TM, Reusser E, Carpenter GJC, Grice JD, Clark SM, Marcus MA (2004) Eyselite, $Fe^{3+}Ge^{4+}{}_3O_7(OH)$, a new mineral species from Tsumeb, Namibia. Can Miner 42:1771–1776

Rocha J, Klinowski J, Adams JM (1991) Synthesis of zeolite Na-A from metakaolinite revisited. J Chem Soc Faraday Trans 87(18):3091–3097

Rokita M, Mozgawa W, Adamczyk A (2014) Transformation of silicate gels during heat treatment in air and in argon – spectroscopic studies. J Molec Struct 1070:125–130

Roncaglia DI, Botto IL, Baran EJ (1985) Vibrational spectrum of Pb_2CrO_5. J Mater Sci Lett 4:1427–1428

Roncaglia DI, Botto IL, Baran EJ (1993) Vibrational spectrum of synthetic rooseveltite. N Jb Miner Mh 6:249–253

Ross SD (1972) The vibrational spectra of some minerals containing tetrahedrally co-ordinated boron. Spectrochim Acta A 28:1555–1561

Rossman GR (2006) Analytical methods for measuring water in nominally anhydrous minerals. Rev Mineral Geochem 62(1):1–28

Rossman GR, Aines RD (1991) The hydrous components in garnets: grossular-hydrogrossular. Am Miner 76:1153–1164

Rouff AA, Rabe S, Nachtegaal M, Vogel F (2009) X-ray absorption fine structure study of the effect of protonation on disorder and multiple scattering in phosphate solutions and solids. J Phys Chem A 113:6895–6903

Rudolf T, Pucher K, Mayr F, Samusi D, Tsurkan V, Tidecks R, Deisenhofer J, Loidl A (2005) Phonon anomalies and charge dynamics in $Fe_{1-x}Cu_xCr_2S_4$ single crystals. Phys Rev B 72(1):014450 (8 pages)

Rulmont A (1972) Spectre infra-rouge de quelques oxyhalogénures de bismuth et de terres rares. Spectrochim Acta A 28:1287–1296 (in French)

Rulmont A, Tarte P (1987) Infrared spectrum of crystalline and glassy borosilicates $M^1BSi_2O_6$. J Mater Sci Lett 6:38–40

Runčevski T, Wu C, Yu H, Yang B, Dinnebier RE (2013) Structural characterization of a new magnesium oxysulfate hydrate cement phase and its surface reactions with atmospheric carbon dioxide. J Am Ceram Soc 96(11):3609–3616

Russell JD (1979) An infrared spectroscopic study of the interaction of nontronite and ferruginous montmorillonites with alkali metal hydroxides. Clay Miner 14:127–137

Russell JD, Fraser AR, Livingstone A (1984) The infrared absorption spectra of the three polymorphs of $PbSO_4(CO_3)_2(OH)_2$ (leadhillite, susannite, and macphersonite). Mineral Mag 48:295–297

Rémazeilles C, Refait Ph (2009) Fe(II) hydroxycarbonate $Fe_2(OH)_2CO_3$ (chukanovite) as iron corrosion product: synthesis and study by Fourier transform infrared spectroscopy. Polyhedron 28(4):749–756

Sabelli C, Vezzalini G (1987) Cetineite, a new antimony oxide-sulfide mineral from Cetine mine, Tuscany, Italy. N Jb Miner Mh 9:419–425

Şahin A (2004) Hydrothermal Synthesis and Characterization of Transition Metal Oxides. Dissertation, İzmir Institute of Technology

Saini-Eidukat B, Kucha H, Keppler H (1994) Hibbingite, γ-$Fe_2(OH)_3Cl$, a new mineral from the Duluth Complex, Minnesota, with implications for the oxidation of Fe-bearing compounds and the transport of metals. Am Miner 79:555–561

Sakamaki K, Ogasawara Y (2013) Hydroxyl in clinopyroxene and titanite in a UHP diamond-free garnet-clinopyroxene rock from the Kokchetav Massif, northern Kazakhstan. Int Geol Rev 56(2):133–149

Salvadó N, Butí S, Cotte M, Cinque G, Pradell T (2013) Shades of green in 15th century paintings: combined microanalysis of the materials using synchrotron radiation XRD, FTIR and XRF. Appl Phys A 111:47–57

Salvadó N, Butí S, Tobin MJ, Pantos E, Prag AJNW, Pradell T (2005) Advantages of the use of SR-FT-IR microspectroscopy: applications to cultural heritage. Anal Chem 77:3444–3451

Sanchez C, Livage J, Lucazeau G (1982) Infrared and Raman study of amorphous V_2O_5. J Raman Spectrosc 12(1):68–72

Sanderson RB (1965) Far infrared optical properties of indium antimonide. J Phys Chem Solids 26(5):803–810

Sarp H, Perroud P (1990) La Geminite, $Cu_2As_2O_7{\cdot}3H_2O$, un nouveau minéral de la mine de Cap Garonne, Var, France. Schweiz Mineral Petrogr Mitt 70:309–314 (in French)

Sarp H, Černý R (2005) Yazganite, $NaFe^{3+}{}_2(Mg,Mn)(AsO_4)_3{\cdot}H_2O$, a new mineral its description and crystal structure. Eur J Mineral 17(2):367–373

Sato E, Nakai I, Terada Y, Tsutsumi Y, Yokoyama K, Miyawaki R, Matsubara S (2008) Study of Zn-bearing beaverite $Pb(Fe_2Zn)(SO_4)_2(OH)_6$ obtained from Mikawa mine, Niigata Prefecture, Japan. J Mineral Petrol Sci 103:141–144

Sato M, Matsuda S (1969) Structure of vaterite and infrared spectra. Z Kristallogr 129(5,6):405–410

Scherf GWH, Brown RK (1960) Potassium derivatives of fluorene as intermediates in the preparation of C_9-substituted fluorenes I. The preparation of 9-fluorenyl potassium and the infrared spectra of fluorene and some C_9-substituted fluorenes. Can J Chem 38: 697–711

Scheuermann W, Schutte CJH (1973) Raman and infrared spectra of $BaCrO_4$ and $BaSeO_4$. J Raman Spectrosc 1 (6):605–618

Schlüter J, Geisler T, Pohl D, Stephan T (2010) Krieselite, $Al_2GeO_4(F,OH)_2$: a new mineral from the Tsumeb mine, Namibia, representing the Ge analogue of topaz. N Jb Miner Abh 187(1):33–40

Schlüter J, Pohl D, Golla-Schindler U (2008) Santarosaite, CuB_2O_4, a new mineral with disordered structure from the Santa Rosa mine, Atacama desertm, Chile. N Jb Miner Abh 185(1):27–32

Schmetzer K, Berdesinski W, Bank H, Kroužek E (1976) Neue Untersuchungen an Coeruleit. N Jb Miner Mh 9:418–426 (in German)

Schmidt BC, Gehlken P-L, Böttcher ME (2013) Vibrational spectra of $BaMn(CO_3)_2$ and a re-analysis of the Raman spectrum of $BaMg(CO_3)_2$. Eur J Mineral 25:137–144

Scholz R, Xi Y, Frost RL (2013) The molecular structure of matioliite – $NaMgAl_5(PO_4)_4(OH)_6{\cdot}2(H_2O)$ – a pegmatite mineral from Minas Gerais, Brazil. J Molec Struct 1033:265–271

Schubert G, Reck G, Jancke H, Kraus W, Patzelt C (2005) Uric acid monohydrate – a new urinary calculus phase. Urol Res 33(3):231–238

Schutte CJH, Van Rensburg DJJ (1971) Low-temperature infrared and Raman studies X. The vibrational behaviour of ammonium fluoro-borate – its phase changes and the rotational freedom of its ions. J Molec Struct 10:484–489

Schwendt P, Joniaková D (1975) Vibrational spectra of vanadium(V) compounds. II. Vibrational spectra of divanadates with nonlinear bridge VOV. Chem zvesti 29(3):381–386

Seetharaman S, Bhat HL, Narayanan PS (1983) Raman spectroscopic studies on sodium metavanadate. J Raman Spectrosc 14(6):401–405

Seguin L, Figlarz M, Cavagnat R, Lassegues J-C (1995) Infrared and Raman spectra of MoO_3 molybdenum trioxides and $MoO_3{\cdot}xH_2O$ molybdenum trioxide hydrates. Spectrochim Acta A 51:1323–1344

Sejkora J, Hawthorne FC, Cooper MA, Grice JD, Vajdak J, Jambor JL (2009) Burgessite, $Co_2(H_2O)_4[AsO_3(OH)]_2(H_2O)$, a new arsenate mineral species from the Keeley mine, South Lorrain Township, Ontario, Canada. Can Miner 47:159–164

Sejkora J, Hyršl J (2007) Ottensite – a new mineral from Qinglong Guizhou Province, China. Miner Rec 38 (1):77–81

Sejkora J, Litochleb J, Černý P, Ozdín D (2006a) Bi-Te minerálna asociácia zo Župkova (Vtáčnik, Slovenská republika). Mineralia Slovaca 36(3-4):303–315 (in Slovak)

Sejkora J, Ondruš P, Fikar M, Veselovský F, Mach Z, Gabašová A (2006b) New data on mineralogy of the Vysoký Kámen deposits near Krásno, Slavkovský les area, Czech Republic. J Czech Geol Soc 51 (1-2):43–55

Sejkora J, Novotný P, Novák M, Šrein V, Berlepsch P (2005) Calciopetersite from Domašov Nad Bystřicí, northern Moravia, Czech republic, a new mineral species of the mixite group. Can Miner 43:1393–1400

Sejkora J, Ondruš P, Novák M (2010a) Veselovskýite, triclinic $(Zn,Cu,Co)Cu_4(AsO4)_2(AsO_3OH)_2{\cdot}9H_2O$, a Zn-dominant analogue of lindackerite. N Jb Miner Abh 187(1):83–90

Sejkora J, Plášil J, Ondruš P, Veselovský F, Císařová I, Hloušek J (2010b) Slavkovite, $Cu_{13}(AsO_4)_6(AsO_3OH)_4{\cdot}23H_2O$, a new mineral species from Horní Slavkov and Jáchymov, Czech Republic: description and crystal-structure determination. Can Miner 48:1157–1170

Sejkora J, Ozdín D, Vitáloš J, Tuček P, Čejka J, Ďuďa R (2007) Schafarzikite from the type locality Pernek

(Malé Karpaty Mountains, Slovak Republic) revisited. Eur J Mineral 19:419–427

Sejkora J, Plášil J, Filip J (2011a) Plimerite from Krásno near Horní Slavkov ore district, Czech Republic. J Geosci 56:215–229

Sejkora J, Plášil J, Veselovský F, Císařová I, Hloušek J (2011b) Ondrušite, $CaCu_4(AsO_4)_2(AsO_3OH)_2 \cdot 10H_2O$, a new mineral species from the Jáchymov Ore District, Czech Republic: description and crystal-structure determination. Can Miner 49:885–897

Sejkora J, Čejka J (2007) Šreinite from Horni Halže, the Krušne hory Mountains, Czech Republic, a new mineral species, its comparison with asselbornite from Schneeberg, and new data for asselbornite. N Jb Miner Abh 184(2):197–206

Sejkora J, Čejka J, Hloušek J, Novák M, Šrein V (2004) Phosphowalpurgite, the (PO_4)-dominant analogue of walpurgite, from Smrkovec, Slavkovský Les Mountains, Czech Republic. Can Miner 42:963–972

Sejkora J, Čejka J, Kolitsch U (2008) Uranosphaerite from Horní Halže near Měděnec (Krušné hory Mountains, Czech Republic): description and vibrational characteristics. N Jb Miner Abh 185 (1):91–98

Semet MP (1973) A crystal-chemical study of synthetic magnesiohastingsite. Am Miner 58:480–494

Semenov YeI, Dusmatov VD, Khomyakov AP, Voronkov AA, Kazakova MY (1975) Darapiosite, a new mineral of the milarite group. Zapiski RMO (Proc Russ Mineral Soc) 104(5):583–585 (in Russian)

Serena S, Sainz MA, Caballero A (2014) Single-phase silicocarnotite synthesis in the subsystem $Ca_3(PO_4)_2$ -Ca_2SiO_4. Ceramics Int 40:8245–8252

Sergeev NB, Kuz'mina OV, Zvezdinskaya LV (1997) Squawcreekite $Fe^{3+}SbO_4$ from Olimpiada deposit (Enisei range) – the first finding in Russia. Doklady Akademii Nauk SSSR (Doklady USSR Acad Sci) 356 (4):525–527 (in Russian)

Shabalin BG (1982) Synthesis and IR spectra of some rare and new titanium and niobium minerals. Mineralogicheskiy Zhurnal (Mineral J) 4(5):54–61 (in Russian)

Shang X, Lu W, Yue B, Zhang L, Ni J, Iv Y, Feng Y (2009) Synthesis of three-dimensional hierarchical dendrites of $NdOHCO_3$ via a facile hydrothermal method. Cryst Growth Des 9(3):1415–1420

Shcherbakova LG, Mamsurova LG, Sukhanova GE (1979) Lanthanide titanates. Russ Chem Rev 48 (3):228–242

Shimoda S, Sudo T (1960) An interstratified mixture of mica clay minerals. Am Miner 45:1069–1077

Shiraga K, Kusachi I, Kobayashi S, Takechi Y (2002) Cahnite from Fuka, Okayama Prefecture, Japan. J Mineral Petrol Sci 97:70–73

Shiraga K, Kusachi I, Kobayashi S, Yamakawa J (2001) Baghdadite from Fuka, Okayama Prefecture, Japan. J Mineral Petrol Sci 96:43–47

Shirozu H (1980) Cation distribution, sheet thickness, and O-OH space in trioctahedral chlorites – an X-ray and infrared study. Mineral J (Jpn) 10(1):14–34

Shitole SJ, Saraf KB (2001) Growth and study of some gel grown group II single crystals of iodate. Bull Mater Sci 24(5):461–468

Sieskind M, Ayadi M, Zachmann G (1986) Infrared lattice vibration, dielectric dispersion, and lattice dynamics of BaFCl. Phys Status Solidi B 136:489–495

Sieskind M, Boulou J-C, Fettouhi A, Ayachour D (2000) Infrared modes and dielectric constants of PbFCl-type compounds. Mater Res Bul 35:1897–1905

Siidra OI, Chukanov NV, Pekov IV, Krivovichev SV, Magganas A, Katerinopoulos A, Voudouris P (2012) $Pb_2(AsO_2OH)Cl_2$, a new phase from the Lavrion ancient slags, Greece: occurrence and characterization. Mineral Mag 76:597–602

Siidra OI, Krivovichev SV, Chukanov NV, Pekov IV, Magganas A, Katerinopoulos A, Voudouris P (2011) The crystal structure of $Pb_5(As_3O_3)Cl_7$ from the historic slags of Lavrion, Greece – a novel Pb(II) chloride arsenite. Mineral Mag 75:339–348

Sinyaev VA, Levchenko LV, Shustikova ES, Griggs J (2003) Calcium phosphates coprecipitated from aqueous solutions of sodium monophosphate and diphosphate. Russ J Appl Chem 76(4):509–512

Skinner HCW, Osbaldiston GW, Wilner AN (1977) Monohydrocalcite in a guinea pig bladder stone, a novel occurrence. Am Miner 62:273–277

Skogby H (1999) Water in nominally anhydrous minerals. In: Wright K, Catlow R (eds) Microscopic properties and processes in minerals. NATO Science Series, Kluwer, Dordrecht

Slack GA, Tsoukala VG (1994) Some properties of semiconducting $IrSb_3$. J Appl Phys 76(3):1665–1671

Slonimskaya MV, Besson G, Daynyak LG, Tchoubar C, Drits VA (1986) Interpretation of the IR spectra of celadonites, glauconites in the region of OH-stretching frequencies. Clay Miner 21:377–388

Smith DH, Seshadri KS (1999) Infrared spectra of $Mg_2Ca(SO_4)_3$, $MgSO_4$, hexagonal $CaSO_4$, and orthorhombic $CaSO_4$. Spectrochim Acta A 55:795–805

Smyslova IG, Komkov AI, Pavshukov VV, Kuznetsova NV (1981) Kyzylkumite $V_2Ti_3O_9$ a new mineral from the group of complex oxides of vanadium and titanium. Zapiski RMO (Proc Russ Mineral Soc) 110(5):607–612 (in Russian)

Smyth JR, Frost DJ, Nestola F, Holl CM, Bromiley G (2006) Olivine hydration in the deep upper mantle: effects of temperature and silica activity. Geophys Res Lett 33(15):L15301

Sokol EV, Gaskova OL, Kokh SN, Kozmenko OA, Seryotkin YuV, Ye Vapnik, Murashko MN (2011) Chromatite and its Cr^{3+}- and Cr^{6+}-bearing precursor minerals from the Nabi Musa Mottled Zone complex, Judean Desert. Am Miner 96:659–674

Song Y, Moon H-S (1998) Additional data on reevesite and its Co-analogue, as a new member of the hydrotalcite group. Clay Miner 33:285–296

Soong R, Farmer VC (1978) The identification of sulphide minerals by infra-red spectroscopy. Mineral Mag 42(277):M17–M20

Šoptrajanov B, Stefov V, Kuzmanovski I, Jovanovski G, Lutz HD, Engelen B (2002) Very low H-O-H bending frequencies. IV. Fourier transform infrared spectra of synthetic dittmarite. J Molec Struct 613:7–14

Speakman K, Taylor HFW, Bennett JM, Gard JA (1967) Hydrothermal reactions of γ-dicalcium silicate. J Chem Soc A 1052–1060

Srinivasan TT, Srivastava CM, Venkataramani N, Patni MJ (1984) Infrared absorption in spinel ferrites. Bull Mater Sci 6(6):1063–1067

Stafsudd OM, Haak FA, Radisavljević K (1967) Far-infrared spectrum of Cadmium Telluride. JOSA 57(12):1475–1476

Stanley CJ, Jones GC, Hart AD, Keller P, Lloyd D (1991) Barstowite, $3PbCl_2 \cdot PbCO_3 \cdot H_2O$, a new mineral from Bounds Cliff, St Endellion, Cornwall. Mineral Mag 55:121–125

Stassen S, Tarte P, Rulmont A (1998) The barium titano-disilicate $BaTiSi_2O_7$: a structural investigation by vibrational spectroscopy and X-ray powder diffraction. Spectrochim Acta A 54:1423–1431

Stavrakieva D, IvanovaY, Pyrov J (1988) On the composition of the crystal phases in the $PbO\text{-}TeO_2$ system. J Mater Sci 23:1871–1876

Stefov V, Šoptrajanov B, Najdoski M, Engelen B, Lutz HD (2008) Infrared and Raman spectra of magnesium ammonium phosphate hexahydrate (struvite) and its isomorphous analogues. V. Spectra of protiated and partially deuterated magnesium ammonium arsenate hexahydrate (arsenstruvite). J Molec Struct 872:87–92

Stefov V, Šoptrajanov B, Petruševski V (1992) Vibrational spectra of hexaaqua complexes. II. External motions of water molecules in the spectra of $AlCl_3 \cdot 6H_2O$. J Molec Struct 267:203–208

Stieff LR, Stern TW, Sherwood AM (1956) Coffinite, a uranous silicate with hydroxyl substitution: a new mineral. Am Miner 41:675–688

Stoilova D, Georgiev M, Marinova D (2005) Infrared study of the vibrational behavior of CrO_4^{2-} guest ions matrix-isolated in metal (II) sulfates (Me = Ca, Sr, Ba, Pb). J Molec Struct 738:211–215

Strandberg H, Langer V, Johansson L-G (1995) Structure of $Cu_{2.5}(OH)_3SO_4 \cdot 2H_2O$: a novel corrosion product of copper. Acta Chemica Scand 49:5–10

Strens RGJ (1974) The common chain, ribbon, and ring silicates. In: Farmer VC (ed) Infrared spectra of minerals. Mineralogical Society Monograph Number 4. The Mineralogical Society, London

Stubičan V, Roy R (1961) Infrared spectra of layer-structure silicates. J Am Ceram Soc 44(12): 625–627

Subbotin VV, Voloshin AV, Pakhomovsky YA, Men'shikov YuP, Subbotina GF (1997) Ternovite (Mg,Ca) $Nb_4O_{11} \cdot nH_2O$ – a new mineral from carbonatites of Vuoriyarvi massif (Northern Karelia). Zapiski RMO (Proc Russ Mineral Soc) 126(3):98–104 (in Russian)

Sudo T, Hayashi H (1956) A randomly interstratified kaolin-montmorillonite in acid clay deposits in Japan. Nature 178:1115–1116

Sufriadin IA, Pramumijoyo S, Warmada IW, Nur I, Imai A, Imran AM, Kaharuddin K (2012) Thermal and infrared studies of garnierite from the Soroako nickeliferous laterite deposit, Sulawesi, Indonesia. Indonesian J Geol 7(2):77–85

Sugitani Y, Nagashima K, Fujiwara S (1966) NMR analysis of the water of crystallization in beryl. Bull Chem Soc Japan 39:672–674

Suleimanov EV, Chernorukov NG, Golubev AV (2004) Synthesis, structure, and physicochemical properties of compounds $Pb(B^VUO_6)_2 \cdot nH_2O$ (B^V = P, As, V). Radiokhimiya (Radiochemistry) 46(5):412–417 (in Russian)

Sun C-F, Hu C-L, Xu X, Yang B-P, Mao J-G (2011) Explorations of new second-order NLO materials in the potassium vanadyl iodate system. J Am Chem Soc 133:5561–5572

Syrbu NN, Bogdanash M, Moldovyan NA (1996a) Vibrational modes in $ZnAl_2S_4$ and $CdIn_2S_4$ crystals. Infrared Phys Technol 37(7):763–768

Syrbu NN, Radautsan SI, Cretu RV, Tezlevan VE, Moldoveanu NA (1996b) Far infrared and Raman optical study of $CdInGaS_4$, $CdIn_2S_4$, $HgInGaS_4$ and $CdIn_2S_2Se_2$ crystals. Cryst Res Technol 31(3):307–314

Szaller Z, Kovács L, Pöppl L (2000) Comparative study of bismuth tellurites by infrared absorption spectroscopy. J Solid State Chem 152:392–396

Szczepaniak K, Szczesniak M (1987) Matrix isolation infrared studies of nucleic acid constituents: Part 4. Guanine and 9-methylguanine monomers and their keto-enol tautomerism. J Molec Struct 156:29–42

Tang XJ, Gentiletti MJ, Lachgar A (2001) Synthesis and crystal structure of indium arsenate and phosphate dihydrates with variscite and metavariscite structure types. J Chem Crystallogr 31(1):45–50

Tang C-W, Wang C-B, Chien S-H (2008) Characterization of cobalt oxides studied by FT-IR, Raman, TPR and TG-MS. Thermochim Acta 473(1–2):68–73

Tao Y, Shiyang G, Lixia Z, Shuping X, Kaibei Yu (2002) Crystal growth and crystal structure of magnesium oxysulfate $2MgSO_4 \cdot Mg(OH)_2 \cdot 2H_2O$. J Molec Struct 616:247–252

Tarantino SC, Zema M, Maglia F, Domeneghetti MC, Carpenter MA (2005) Structural properties of $(Mn_{1-x}Fe_x)Nb_2O_6$ columbites from X-ray diffraction and IR spectroscopy. Phys Chem Minerals 32:568–577

Tarte P (1967) Infra-red spectra of inorganic aluminates and characteristic vibrational frequencies of AlO_4 tetrahedra and AlO_6 octahedra. Spectrochim Acta A 23:2127–2143

Tarte P, Rulmont A, Liégeois-Duyckaerts M, Cahay R, Winand JM (1990) Vibrational spectroscopy and solid state chemistry. Solid State Ionics 42:177–196

Tarte P, Thelen J (1972) Spectre vibrationnel des composéu type $Ba_3(XO_4)_2$ et $Sr_3(XO_4)_2$ (X^V = P, As, V, Cr, Mn). Spectrochim Acta A 28:5–14 (in French)

Taylor RM (1980) Formation and properties of Fe(II)Fe (III) hydroxyl-carbonate and its possible significance in soil formation. Clay Miner 15:369–382

Taylor P, Sunder S, Lopata VJ (1984) Structure, spectra, and stability of solid bismuth carbonates. Can J Chem 62(12):2863–2873

Taylor JCW, Weichman FL (1971) Raman effect in cuprous oxide compared with infrared absorption. Can J Phys 49(5):601–605

Taş AC (1998) Chemical preparation of the binary compounds in the calcia-alumina system by self-propagating combustion synthesis. J Am Ceram Soc 81(11):2853–2863

Terukov EI, Wagner H, Reichelt W, Oppermann H (1977) IR-spektroskopische Untersuchungen zum Halbleiter-Metall-Phasenübergang des V_3O_5. Phys Status Solidi A 44:K187–K190 (in German)

Thomas GH, Falk M, Knop O (1974) Infrared studies of water in crystalline hydrates: $K_2CuCl_4{\cdot}2H_2O$. Can J Chem 52(7):1029–1041

Thomas M, George KC (2010) Characterisation and magnetic properties of nanocrystalline $FePO_4$. Ind J Pure Appl Phys 48:104–109

Thomas S-M, Jacobsen SD, Bina CR, Reichart P, Moser M, Hauri EH, Koch-Müller M, Smyth JR, Dollinger G (2015) Quantification of water in hydrous ringwoodite. Frontiers Earth Sci. doi:10.3389/feart.2014.00038

Tilley DB, Eggleton RA (1996) The natural occurrence of eta-alumina (η-Al_2O_3) in bauxite. Clays Clay Miner 44(5):658–664

Tjy CTL, Nadezhina TN, Pobedimskaya EA, Khomyakov AP (1984) Crystal chemical characteristics of bradleyite, sidorenkite and bonshtedtite. Mineralogicheskiy Zhurnal (Mineral J) 6(5):79–84 (in Russian)

Tortet L, Gavarri JR, Nihoul G, Dianoux AJ (1997) Study of protonic mobility in $CaHPO_4{\cdot}2H_2O$ (brushite) and $CaHPO_4$ (monetite) by Infrared spectroscopy and neutron scattering. J Solid State Chem 132:6–16

Tripathi SN, Namboodiri PN (2003) New diffraction data. Structural investigations of $UTeO_4$. Powder Diffr 18 (1):42–46

Ugarte FJG, Monhemius AJ (1992) Characterisation of high-temperature arsenic-containing residues from hydrometallurgical processes. Hydrometallurgy 30:69–86

Unger WK, Farnworth B, Irwin JC, Pink H (1978) Raman and infrared spectra of $CdIn_2S_4$ and $ZnIn_2S_4$. Solid State Commun 25(11):913–915

Unger WK, Karecki D, Clayman BP, Irwin JC, Pink H (1979) Raman and far-infrared spectra of $NaCrS_2$. Solid State Commun 29(3):149–151

Unterderweide K, Engelen B, Boldt K (1994) Strong hydrogen bonds in acid selenites: correlation of infrared spectroscopic and structural data. J Molec Struct 322:233–239

Urbanec Z, Čejka J (1979a) Infrared spectra of liebigite, andersonite, voglite, and schroeckingerite. Collection Czechoslov Chem Commun 44:10–23

Urbanec Z, Čejka J (1979b) Infrared spectra of rutherfordine and sharpite. Collection Czechoslov Chem Commun 44:1–9

Van Haverbeke L, Vochten R, Van Springel K (1996) Solubility and spectrochemical characteristics of synthetic chernikovite and meta-ankoleite. Mineral Mag 60:759–766

Vandenborre MT, Husson E, Brusset H, Cerez A (1980) Spectres de vibration et calcul du champ de force des antimoniates de structure 'type $PbSb_2O_6$'. Spectrochim Acta A 36:1045–1052 (in French)

Vasilevskiy MI, Rolo AG, Artemyev MV, Filonovich SA, Gomes MJM, Rakovich YP (2001) FIR absorption in CdSe quantum dot ensembles. Phys Status Solidi B 224(2):599–604

Vedder W (1964) Correlations between infrared spectrum and chemical composition of mica. Am Miner 49:736–768

Venkatesh GM, Neelakantan P (1966) Infra-red and Raman spectra of $BaCl_2{\cdot}2H_2O$ and $BaCl_2{\cdot}2D_2O$. Proceed Indian Academy Sci A 64(1):36–43

Ventruti G, Della Ventura G, Orlando R, Scordari F (2015) Structure refinement, hydrogen-bond system and vibrational spectroscopy of hohmannite, $Fe^{3+}{}_2[O(SO_4)_2]{\cdot}8H_2O$. Mineral Mag 79:11–24

Verble JL, Humphrey FM (1974) Infrared and Raman spectra of MnS_2. Solid State Commun 15(10):1693–1697

Vershkovskaya OV, Chernitsova NM, Vlasova EV, Valueva AA, Stepanov II (1979) New data on eglestonite. Doklady Akademii Nauk SSSR (Doklady USSR Acad Sci) 248(3):715–718 (in Russian)

Verwoerd WJ (2008) Kamphaugite-(Y) from the Goudini carbonatite, south Africa. Can Miner 46:1007–1022

Vignola P, Hatert F, Bersani D, Diella V, Gentile P, Risplendente A (2012) Chukhrovite-(Ca), $Ca_{4.5}Al_2(SO_4)F_{13}{\cdot}12H_2O$, a new mineral species from the Val Cavallizza Pb-Zn-(Ag) mine, Cuasso al Monte, Varese province, Italy. Eur J Mineral 24:1069–1076

Viñals J, Jambor JL, Raudsepp M, Roberts AC, Grice JD, Kokinos M, Wise W (2008) Barahonaite-(Al) and barahonaite-(Fe), new Ca-Cu arsenate mineral species, from Murcia province, southeastern Spain, and Gold hill, Utah. Can Miner 46:205–217

Vlček V, Čejka J, Císařova I, Goliáš V, Plášil J (2009) Crystal structure of $UO_2SO_4{\cdot}2.5H_2O$: full anisotropic refinement and vibration characteristics. J Molec Struct 936:75–79

Vochten R, Blaton N, Peeters O (1997a) Deliensite, $Fe(UO_2)_2(SO_4)_2(OH)_2{\cdot}3H_2O$, a new ferrous uranyl sulfate hydroxyl hydrate from Mas D'alary Lodeve, Herault, France. Can Miner 35:1021–1025

Vochten R, Blaton N, Peeters O (1997b) Synthesis of sodium weeksite and its transformation into weeksite. N Jb Miner Mh 12:569–576

Vochten R, Blaton N, Peeters O, Deliens M (1996) Piretite, $Ca(UO_2)_3(SeO_3)_2(OH)4{\cdot}4H_2O$, a new calcium uranyl selenite from Shinkolobwe, Shaba, Zaire. Can Miner 34:1317–1322

Vochten R, Deliens M (1998) Blatonite, $UO_2CO_3{\cdot}H_2O$, a new uranyl carbonate monohydrate from San Juan county, Utah. Can Miner 36:1077–1081

Vochten R, Deliens M, Medenbach O (2001) Oswaldpeetersite, $(UO_2)_2(CO_3)(OH)_2{\cdot}4H_2O$, a new basic uranyl carbonate mineral from the Jomac Uranium Mine, San Juan County, Utah, USA. Can Miner 39:1685–1689

Vochten R, Goeminne A (1984) Synthesis, crystallographic data, solubility and electrokinetic properties of meta-zeunerite, meta-kirchheimerite and nickel-uranylarsenate. Phys Chem Minerals 11:95–100

Vochten R, De Grave E, Pelsmaekers J (1984) Mineralogical study of bassetite in relation to its oxidation. Am Miner 69:967–978

Vochten R, De Grave E, Pelsmaekers J (1986) Synthesis, crystallographic and spectroscopic data, solubility, and electrokinetic properties of metakahlerite and its Mn analogue. Am Miner 71:1037–1044

Vochten R, Van Springel K (1996) A natural ferrous substituted saleeite from Arcu su Linnarbu, Capoterra, Cagliari, Sardinia. Mineral Mag 60:647–651

Vogel C, Kohl A, Adam C (2011) Spectroscopic investigation in the mid- and far-infrared regions of phosphorus fertilizers derived from thermochemically treated sewage sludge ash. Appl Spectrosc 65(3):265–271

Voit EI, Panasenko AE, Zemnukhova LA (2009) Vibrational spectroscopic and quantum chemical study of antimony(III) oxide. J Struct Chem 50(1):60–66

Voloshin AV, Men'shikov YuP, Polezhaeva LI, Lentsi AA (1982) Kolfanite, a new mineral from granite pegmatite. Kola Peninsula. Mineralogicheskiy Zhurnal (Mineral J) 4(2):90–95 (in Russian)

Voloshin AV, Pakhomovskii YaA, Pusharovskii DYu, Nadezhina TN, Bakhchisaraitsev AYu, Kobyashev YS (1989) Strontium pyrochlore: composition and structure. New Data Minerals 36:12–24 (in Russian)

Voloshin IV, Pakhomovsky YA, Tjusheva FN (1992a) Manganosegelerite (Mn,Ca)(Mn,Fe,Mg)Fe^{3+} $(PO4)_2$ $(OH){\cdot}4H_2O$ – a new phosphate of overite group, from granite pegmatite of Kola peninsula. Zapiski RMO (Proc Russ Mineral Soc) 121(2):95–103 (in Russian)

Voloshin AV, Subbotin VV, Yakoventchuk VN, Pakhomovsky YA, Men'shikov YP, Nadezhdina TN, Pushcharovsky DY (1992b) New data on the ewaldite. Zapiski RMO (Proc Russ Mineral Soc) 121(1):55–67 (in Russian)

Voloshin AV, Subbotin VV, Pakhomovskii YaA, Bakhchisaraitsev AYu, Yamnova NA, Pushcharovskii DY (1991) Belkovite – a new barium-niobium silicate from carbonatites of the Vuoriyarvi massif (Kola Peninsula, USSR). N Jb Miner Mh 1:23–31

Voloshin AV, Subbotin VV, Yakovenchuk VN, Pakhomovskiy YA, Men'shikov YuP, Zaytsev AN (1990) Mckelveyite from carbonatites and hydrothermal metasomatites of Kola Peninsula alkaline rocks (first findings in the USSR). Zapiski RMO (Proc Russ Mineral Soc) 119(6):76–86 (in Russian)

Voloshin AV, Men'shikov YuP, Pakhomovskii YaA, Polezhaeva LI (1981) Cesstibtantite, $(Cs,Na)SbTa_4O_{12}$, a new mineral from granitic pegmatites. Zapiski RMO (Proc Russ Mineral Soc) 116(3):345–351 (in Russian)

Voloshin AV, Pakhomovskii YaA, Men'shikov YuP, Povarennykh AS, Matvinenko EN, Yakubovich OV (1983a) Hingganite-(Yb), A new mineral from amazonite pegmatite of the Kola peninsula. Doklady Akademii Nauk SSSR (Doklady USSR Acad Sci) 270 (5):1188–1192 (in Russian)

Voloshin AV, Pakhomovskii YaA, Stepanov VI, Tyusheva FN (1983b) Lithiotantite $Li(Ta,Nb)_3O_8$ – a new mineral from granite pegmatites in Eastern Kazakhstan. Mineralogicheskiy Zhurnal (Mineral J) 5 (1):91–95 (in Russian)

Von Knorring O, Fransolet A-M (1977) Gatumbaite, $CaAl_2(PO_4)_2(OH)_2{\cdot}H_2O$: a new species from Buranga pegmatite, Rwanda. N Jb Miner Mh 12:561–568

Voncken JHL, Konings RJM, Jansen JBH, Woensdregt CF (1988) Hydrothermally grown buddingtonite, an anhydrous ammonium feldspar $(NH_4AlSi_3O_8)$. Phys Chem Minerals 15:323–328

Vry JK, Brown PE, Valley JW (1990) Cordierite volatile content and the role of CO_2 in high-grade metamorphism. Am Miner 75:71–88

Vrána S, Rieder M, Podlaha J (1978) Kanonaite, $(Mn^{3+}_{0.76}Al_{0.23}Fe^{3+}_{0.02})^{[6]}Al^{[5]}[O|SiO_4]$, a new mineral isotypic with andalusite. Contrib Mineral Petrol 66:325–332

Wakamura K (2002) Observation of low energy optical phonon in far-infrared spectra of β-phase in CuI. Physica B 316:195–197

Walczak J, Filipek E, Bosacka M (1997) Reactivity of Sb_2O_3 with Fe_2O_3 in ambient air. Solid State Ionics 101–103:1363–1367

Walenta K (1965) Hallimondite, a new uranium mineral from the Michael Mine near Reichenbach (Black Forest, Germany). Am Miner 50:1143–1157

Walenta K, Hatert F, Theye T, Lissner F, Röller K (2009) Nielsbohrite, a new potassium uranyl arsenate from the uranium deposit of Menzenschwand, southern Black Forest, Germany. Eur J Mineral 21:515–520

Walker JR (1989) Polytypism of chlorite in very low grade metamorphic rocks. Am Miner 74:738–743

Walker AM, Hermann J, Berry AJ, O'Neill HSC (2007) Three water sites in upper mantle olivine and the role of titanium in the water weakening mechanism. J Geophys Res Solid Earth 112:B05211 (12 pp)

Wallez G, Bregiroux D, Popa K, Raison PE, Apostolidis C, Lindqvist-Reis P, Konings RJM, Popa AF (2011) $BaAn^{IV}(PO_4)_2$ (An^{IV} = Th, Np) – a new family of layered double phosphates. Eur J Inorg Chem 2011:110–115

Walter F, Bojar H-P, Hollerer CE, Mereiter K (2013) The crystal structure of galgenbergite-(Ce), $CaCe_2$ $(CO_3)_4{\cdot}H_2O$. Miner Petrol 107:189–199

Wang X, Liu L, Wang L, Jacobson AJ (2005) Hydrothermal synthesis and structures of the open-framework copper silicates $Na_2[Cu_2Si_4O_{11}](H_2O)_2$(CuSH-2Na), $Na_2[CuSi_3O_8]$(CuSH-3Na), $Cs_2Na_4[Cu_2Si_{12}O_{27}(OH)_2]$ $(OH)_2$(CuSH-4NaCs), and $Na_2[Cu_2Si_5O_{13}]$ $(H_2O)_3$(CuSH-6Na). Solid State Sci 7:1415–1422

Wang L, Rouse RC, Essene EJ, Peacor DR, Zhang Y (2000) Carmichaelite, a new hydroxyl-bearing titanate from Garnet Ridge, Arizona. Am Miner 85:792–800

Wang A, Freeman JJ, Arvidson R (2008) Study of two structural polymorphs of $MgSO_4 \cdot H_2O$ by Raman, IR, XRD, and humidity buffer experiments – implication for martian kieserite. In: 39th Lunar Planetary Science Conference (Lunar Planetary Science XXXIX), March 10–14, 2008, League City, Texas. LPI Contribution No. 1391, p 2172

Weidenthaler C, Tillmanns E, Hentschel G (1993) Orschallite, $Ca_3(SO_3)_2SO_4 \cdot 12H_2O$, a new calcium-sulfite-sulfate-hydrate mineral. Miner Petrol 48:167–177

Weir CE (1966) Infrared spectra of the hydrated borates. J Res Natl Bureau Stands A Phys Chem 70(2):153–164

Welch MD, Kolodziejsk W, Klinowski J (1994) A multinuclear NMR study of synthetic pargasite. Am Miner 79:261–268

Welch MD, Mitchell RH, Kampf AR, Chakhmouradian AR, Smith D, Carter M (2014) Crystal structure and topological affinities of magbasite, $KBaFe^{3+}Mg_7Si_8O_{22}(OH)_2F_6$: a trellis structure related to amphibole and carpholite. Mineral Mag 78:29–45

Werding G, Schreyer W (1992) Synthesis and stability of werdingite, a new phase in the system $MgO–Al_2O_3–B_2O_3–SiO_2$ (MABS), and another new phase in the ABS-system. Eur J Mineral 4:193–207

White WB (1967) Application of infrared spectroscopy to order-disorder problems in simple ionic solids. Mater Res Bull 2:381–394

White WB, Dachille F, Roy R (1961) High-pressure – high-temperature polymorphism of the oxides of lead. J Am Ceram Soc 44(4):170–174

Whitfield HJ (1971) The far-infrared spectra of arsenic chalcogenides. Aust J Chem 24(4):697–701

Wieczorek A, Libowitzky E, Beran A (2004) A model for the OH defect incorporation in kyanite based on polarised IR spectroscopic investigations. Schweiz Mineral Petr Mitt 84:333–343

Wildner M, Tillmanns E, Andrut M, Lorenz J (2003) Sailaufite, $(Ca,Na,\square)_2Mn_3O_2(AsO_4)_2(CO_3) \cdot 3H_2O$, a new mineral from Hartkoppe hill, Ober-Sailauf (Spessart mountains, Germany), and its relationship to mitridatite-group minerals and pararobertsite. Eur J Mineral 15:555–564

Wilkins RWT (1967) The hydroxyl-stretching region of the biotite mica spectrum. Mineral Mag 36:325–333

Wilkins RWT, Ito J (1967) Infrared spectra of some synthetic talcs. Am Miner 52:1649–1661

Wilkins RW, Mateen A, West GW (1974) The spectroscopic study of oxonium ions in minerals. Am Miner 59:811–819

Williams Q, Jeanloz R, Akaogi M (1986) Infrared vibrational spectra of beta-phase Mg_2SiO_4 and Co_2SiO_4 to pressures of 27 Gpa. Phys Chem Minerals 13:141–145

Williams Q, Hemley RJ, Kruger MB, Jeanloz R (1993) High-pressure infrared spectra of α-quartz, coesite, stishovite and silica glass. J Geophys Res 98 (B12):22,157–22,170

Wilson MJ, Jones D, Russell JD (1980) Glushinskite, a naturally occurring magnesium oxalate. Mineral Mag 43:837–840

Wilson MJ, Russell JD (1983) Melanosiderite is siliceous ferrihydrite. Mineral Mag 47:85–87

Wilson MJ, Russell JD, Tait JM, Clark DR, Fraser AR (1984) Macaulayite, a new mineral from North-East Scotland. Mineral Mag 48:127–129

Winkler B, Langer K, Johannsen PG (1989) The influence of pressure on the OH valence vibration of zoisite: an infrared spectroscopic study. Phys Chem Minerals 16:668–671

Witt K, Mecke R (1967) Ein Vergleich der IR-Spektren von 9,10-Dichlorphenanthren und Phenanthren zwischen 200 und 3200 cm^{-1}. Ber Bunsenges 71(7):668–672 (in German)

Witzke T, Kolitsch U, Krause W, Wiechowski A, Medenbach O, Kampf AR, Steele IM, Favreau G (2006) Guanacoite, $Cu_2Mg_2(Mg_{0.5}Cu_{0.5})(OH)_4(H_2O)_4(AsO_4)_2$, a new arsenate mineral species from the El Guanaco Mine, near Taltal, Chile: description and crystal structure. Eur J Mineral 18:813–821

Wood DL, Nassau K (1967) Infrared spectra of foreign molecules in beryl. J Chem Phys 47:2220–2228

Wright AC, Rupert JP, Granquist WT (1968) High- and low-silica faujasites: a substitutional series. Am Miner 53:1293–1303

Wu Y-F, Chan Y-H, Nien Y-T, Chen I-G (2013) Crystal structure and optical performance of Al^{3+} and Ce^{3+} codoped $Ca_3Sc_2Si_3O_{12}$ green phosphors for white LEDs. J Am Ceram Soc 96(1):234–240

Wu X, Wu W, Cui X, Liao S (2012) Selective self-assembly synthesis of $MnV_2O_6 \cdot 4H_2O$ with controlled morphologies and study on its thermal decomposition. J Therm Anal Calorim 109:163–169

Wunder B, Jahn S, Koch-Müller M, Speziale S (2012) The 3.65 Å phase, $MgSi(OH)_6$: structural insights from DFT-calculations and *T*-dependent IR spectroscopy. Am Miner 97:1043–1048

Wunder B, Melze S (2002) Interlayer vacancy characterization of synthetic phlogopitic micas by IR spectroscopy. Eur J Mineral 14(6):1129–1138

Wylde JJ, Allen GC, Collins IR (2001) FT-IR and Raman spectroscopic characterization of the major oilfield sulfate scale forming minerals. Appl Spectrosc 55 (9):1155–1160

Wülser P-A, Meisser N, Brugger J, Schenk K, Ansermet S, Bonin M, Bussy F (2005) Cleusonite, $(Pb,Sr)(U^{4+},U^{6+})(Fe^{2+},Zn)_2(Ti,Fe^{2+},Fe^{3+})_{18}(O,OH)_{38}$, a new mineral species of the crichtonite group from the western Swiss Alps. Eur J Mineral 17:933–942

Xie B, Lu G, Wang Y, Guo Y, Guo Y (2012) Selective synthesis of tetragonal $LaVO_4$ with different vanadium sources and its luminescence performance. J Alloys Compd 544:173–180

Xilin L, Jingliang Z, Jiaju L (1983) Xitieshanite – a new ferric sulphate mineral. Geochemistry 2(3):261–267

Xu J, Butler IS, Gilson DFR (1999) FT-Raman and high-pressure infrared spectroscopic studies of dicalcium phosphate dihydrate ($CaHPO_4{\cdot}2H_2O$) and anhydrous dicalcium phosphate ($CaHPO_4$). Spectrochim Acta A 55:2801–2809

Xu J, Yang G, Li G, Wu Z, Shen G (2008) Dingdaohengite-(Ce) from the Bayan Obo REE-Nb-Fe Mine, China: both a true polymorph of perrierite-(Ce) and a titanic analog at the *C*1 site of chevkinite subgroup. Am Miner 93:740–744

Xyla AG, Koutsoukos PG (1989) Quantitative analysis of calcium carbonate polymorphs by infrared spectroscopy. J Chem Soc Faraday Trans I 85(10):3165–3172

Yakovenchuk VN, Nikolaev AP, Selivanova EA, Pakhomovsky YA, Korchak JA, Spiridonova DV, Zalkind OA, Krivovichev SV (2009) Ivanyukite-Na-*T*, ivanyukite-Na-*C*, ivanyukite-K, and ivanyukite-Cu: new microporous titanosilicates from the Khibiny massif (Kola Peninsula, Russia) and crystal structure of ivanyukite-Na-*T*. Am Miner 94:1450–1458

Yakovenchuk VN, Pakhomovsky YA, Men'shikov YuP, Mikhailova JA, Ivanyuk GYu, Zalkind OA (2007) Krivovichevite, $Pb_3[Al(OH)_6](SO_4)(OH)$, a new mineral species from the Lovozero Alkaline Massif, Kola Peninsula, Russia. Can Miner 45:451–456

Yakovenchuk VN, Ivanyuk GYu, Krivovichev SV, Pakhomovsky YA, Selivanova EA, Korchak JA, Men'shikov YuP, Drogobuzhskaya SV, Zalkind OA (2011a) Eliseevite, $Na_{1.5}Li[Ti_2Si_4O_{12.5}(OH)_{1.5}]{\cdot}2H_2O$, a new microporous titanosilicate from the Lovozero alkaline massif (Kola Peninsula, Russia). Am Miner 96:1624–1629

Yakovenchuk VN, Ivanyuk GY, Pakhomovsky YA, Selivanova EA, Mikhailova JA (2011b) Ellingsenite, $Na_5Ca_6Si_{18}O_{38}(OH)_{13}{\cdot}6H_2O$, a new martinite-related mineral species from phonolite of the Aris alkaline complex, Namibia. Can Miner 49:1165–1173

Yakubovich OV, Massa W, Liferovivh RP, Pakhomovsky YA (2000) The crystal structure of bakhchisaraitsevite $[Na_2(H_2O)_2]\{(Mg_{4.5}Fe_{0.5})(PO_4)_4(H_2O)_5\}$, a new mineral species of hydrothermal origin from the Kovdor phoscorite-carbonatite complex, Russia. Can Miner 38:831–838

Yakubovich OV, Pekov IV, Steele IM, Massa W, Chukanov NV (2009) Alkali metals in beryl and their role in the formation of derivative structural motifs: comparative crystal chemistry of vorobyevite and pezzottaite. Kristallografiya (Crystallogr) 54(3):432–445 (in Russian)

Yamaguchi O, Ohtagaki T, Shimizu K (1988a) Formation of a continuous series of solid solutions in the system $TiTe_3O_8$-$ZrTe_3O_8$. Z anorg allg Chem 564:115–120

Yamaguchi O, Tomihisa D, Shimizu K (1988b) A new modification of $TiTe_3O_8$. J Chem Soc Dalton Trans 8:2083–2085

Yamaguchi O, Tomihisa D, Uegaki T, Shimizu K (1987) Formation and transformation of δ-Ta_2O_5 solid solution in the system Ta_2O_5-$A1_2O_3$. J Am Ceram Soc 70 (11):C-335–C-338

Yamnova NA, Borovikova EY, Dimitrova OV (2011) Crystallization, crystal-structure refinement, and IR spectroscopy of a synthetic hexahydroborite analog. Kristallografiya (Crystallogr) 56(6):1088–1093 (in Russian)

Yamnova NA, Egorov-Tismenko YK, Zubkova NV, Dimitrova OV, Kantor AP, Ye D, Xiong M (2003) Crystal structure of new synthetic calcium pentaborate $Ca[B_5O_8(OH)]{\cdot}H_2O$ and its relation to pentaborates with similar boron-oxygen radicals. Kristallografiya (Crystallogr) 48(4):608–613 (in Russian)

Yang TR, Lu CC, Chou WC, Feng ZC, Chua SJ (1999) Infrared and Raman spectroscopic study of $Zn_{1-x}Mn_xSe$ materials grown by molecular-beam epitaxy. Phys Rev B 60(23):16058–16064

Yang H, Sun HJ (2004) Crystal structure of a new phosphate compound, $Mg_2KNa(PO_4)_2{\cdot}14H_2O$. J Solid State Chem 177:2991–2997

Yang N, Yang H, Jia J, Pang X (2007) Formation and magnetic properties of nanosized $PbFe_{12}O_{19}$ particles synthesized by citrate precursor technique. J Alloys Compd 438:263–267

Yao Z, Xia M, Ye Y, Lu Z (2011) Kaliophilite from fly ash: synthesis, characterization and stability. Bull Mater Sci 34(7):1671–1674

Yariv S, Shoval S (1985) Infrared spectra of sodium salts in CsCl disks. Appl Spectrosc 39:599–604

Ye Y, Smyth JR, Jacobsen SD, Panero WR, Brown DA, Katsura T, Chang Y-Y, Townsend JP, Dera P, Tkachev S, Unterborn C, Liu Z, Goujon C (2013) Crystal structure, Raman and FTIR spectroscopy, and equations of state of OH-bearing $MgSiO_3$ akimotoite. Contrib Mineral Petrol 166:1375–1388

Yeniyol M (2014) Characterization of two forms of sepiolite and related Mg-rich clay minerals from Yenidoğan (Sivrihisar, Turkey). Clay Miner 49(1):91–108

Yeon J, Kim S-H, Halasyamani PS (2010) $A_3V_5O_{14}$ (A = K^+, Rb^+, or Tl^+): new polar oxides with a tetragonal tungsten bronze related structural topology – synthesis, structure, and functional properties. Inorg Chem 49:6986–6993

Yeon J, Kim S-H, Nguyen SD, Lee H, Halasyamani PS (2012a) New vanadium selenites: Centrosymmetric $Ca_2(VO_2)_2(SeO_3)_3(H_2O)_2$, $Sr_2(VO_2)_2(SeO_3)_3$, and $Ba(V_2O_5)(SeO_3)$, and noncentrosymmetric and polar $A_4(VO_2)_2(SeO_3)_4(Se_2O_5)$ (A = Sr^{2+} or Pb^{2+}). Inorg Chem 51:609–619

Yeon J, Kim S-H, Nguyen SD, Lee H, Halasyamani PS (2012b) Two new noncentrosymmetric (NCS) polar oxides: syntheses, characterization, and structure-property relationships in $BaMTe_2O_7$ (M = Mg^{2+} or Zn^{2+}). Inorg Chem 51:2662–2668

Yes'kova YM, Semenov YeI, Khomyakov AP, Kazakova MY, Shumyatskaya NG (1974a) Sazhinite – a new silicate of natrium and rare earths. Zapiski RMO (Proc Russ Mineral Soc) 103(3):338–341 (in Russian)

Yes'kova YM, Semenov YeI, Khomyakov AP, Kazakova MY, Sidorenko OV (1974b) Laplandite, a new

mineral. Zapiski RMO (Proc Russ Mineral Soc) 103 (5):571–575 (in Russian)

Yingchen R, Lulu X, Zhizhong P (1983) Daqingshanite—a new mineral recently discovered in China. Geochem 2(2):180–184

Yoder CH, Pasteris JD, Krol KA, Weidner VL, Schaeffer RW (2012) Synthesis, structure, and solubility of carbonated barium chlor- and hydroxylapatites. Polyedron 44:143–149

Yokoyama S, Tamura K, Hatta T, Nemoto S, Watanabe Y, Yamada H (2006) Synthesis and characterization of Zn-substituted saponite (sauconite). Clay Sci 13:75–80

Yueqing Y, Yunxiang N, Liben W, Wenying W, Yaping Z, Chenghu C (1988) Nanpingite—a new cesium mineral. Yanshi Kuangwuxue Zashi 7:49–58 (in Chinese, English abstr)

Żabiński, W. (1966) Hydrogarnets. Polska Akademia Nauk Oddział w Krakowie, Komisja Nauk Mineralogicznych, Prace mineralogiczne nr 3. Wydawnictwa Geologiczne, Warszawa (in Polish)

Zagorsky VY, Peretyazhko IS, Sapozhnikov AN, Zhukhlistov AP, Zvyagin BB (2003) Borocookeite, a new member of the chlorite group from the Malkhan gem tourmaline deposit, Central Transbaikalia, Russia. Am Miner 88:830–836

Žák L (1972) A contribution to the crystal chemistry of melanophlogite. Am Miner 57:779–796

Zarayskiy GP, Zharikov VA, Stoyanovskaya FM, Balashov VN (1986) Eksperimental'noye issledovaniye bimetasomaticheskogo skarnoobrazovaniya (The experimental study of bimetasomatic skarn formation). Nauka, Moscow (in Russian)

Zavorotynska O, Corno M, Damin A, Spoto G, Ugliengo P, Baricco M (2011) Vibrational properties of MBH_4 and MBF_4 crystals (M = Li, Na, K): a combined DFT, infrared and Raman study. J Phys Chem C 115:18890–18900

Zhan B, Cui Q, Liu W, Zhang J, Zhan F, Ning J, Zou G (2009) Well crystallized α-GaOOH nanocrystals synthesized through hydrothermal routes and their properties. Chin J Chem 27:2175–177

Zhang R, Han F, Du C (1986) Ertixiite – a new mineral from the Altay pegmatite mine, Xinjiang, China. Geochemistry 4(2):192–196

Zhang S, Huang Y, Shi L, Qiao X, Seo HJ (2009) Synthesis, luminescence and crystallographic structure of Eu^{3+}-doped garnet-type yafsoanite $Ca_3Te_2(ZnO_4)_3$. Physica B 404:4136–4141

Zhang FX, Lang M, Zhenxian Liu, Ewing RC (2011a) Phase stability of some actinides with brannerite structure at high pressures. J Solid State Chem 184 (11):2834–2839

Zhang J, Zhang Z, Zhang W, Zheng Q, Sun Y, Zhang C, Tao X (2011b) Polymorphism of $BaTeMo_2O_9$: a new polar polymorph and the phase transformation. Chem Mater 23:3752–3761

Zhang M, Maddrell ER, Abraitis PK, Salje EKH (2007) Impact of leach on lead vanado-iodoapatite $[Pb_5(VO_4)_3I]$: an infrared and Raman spectroscopic study. Mater Sci Eng B 137:149–155

Zhang M, Moxon T (2014) Infrared absorption spectroscopy of SiO_2-moganite. Am Miner 99:671–680

Zhang G, Redhammer J, Salje EKH, Mookherjee MM (2002) $LiFeSi_2O_6$ and $NaFeSi_2O_6$ at low temperatures: an infrared spectroscopic study. Phys Chem Minerals 29:609–616

Zhang ZY, Wang YH (2012) Investigation of the electronic structure and photoluminescence properties of Eu^{3+} in $Sr_2Mg_{1-x}Zn_xSi_2O_7$ ($0 \le x \le 1$). Chin Sci Bull 57(8):935–940

Zhang M, Xu H, Salje EKH, Heaney PJ (2003) Vibrational spectroscopy of beta-eucryptite ($LiAlSiO_4$): optical phonons and phase transition(s). Phys Chem Minerals 30:457–462

Zhang W, Ni Y, Huang W, Lu C, Xu Z (2010) Hydrothermal synthesis, structure study and luminescent properties of $YbPO_4$:Tb^{3+} nanoparticles. J Rare Earths 28:299–302

Zhangru C, Keding L, Falan T, Zhang Y, Xiaofa G (1986) Tengchongite, a new mineral of hydrated calcium uranyl molybdate. Kewue Tongbao 31:396–401

Zheng HL, Zhang ZC, Zhou JG, Yang SS, Zhao J (2012) Vibrational spectra of $CaGa_2O_4$, Ca_2GeO_4, $CaIn_2O_4$ and $CaSnO_3$ prepared by electrospinning. Appl Phys A 108(2):465–473

Zhigadlo ND, Zhang M, Salje EKH (2001) An infrared spectroscopic study of $Li_2B_4O_7$. J Phys Condens Matter 13:6551–6561

Zhong S-L, Xu R, Wang L, Li Y, Zhang L-F (2011) $CuSn(OH)_6$ submicrospheres: room-temperature synthesis, growth mechanism, and weak antiferromagnetic behavior. Mater Res Bull 46:2385–2391

Zittlau AH, Shi Q, Boerio-Goates J, Woodfield BF, Majzlan J (2013) Thermodynamics of the basic copper sulfates antlerite, posnjakite, and brochantite. Chemie Erde 73(1):39–50

Zolotarev AA, Dufour MS (1995) Composition, crystallostructural peculiarities and genesis of gem cordierite from the Eastern Pamirs. Zapiski RMO (Proc Russ Mineral Soc) 124(2):76–86 (in Russian)

Zvyagin BB (1967) Electron-difftaction analysis of clay mineral structures. Plenum Press, New York

Zwaan PC, Arps CES, De Grave E (1989) Vochtenite, $(Fe^{2+},Mg)Fe^{3+}[UO_2/PO_4]_4(OH)\cdot 12\text{-}13H_2O$, a new uranyl phosphate mineral from Wheal Basset, Redruth, Cornwall, England. Mineral Mag 53:473–478

Index of Minerals

N.V. Chukanov and A.D. Chervonnyi, *Infrared Spectroscopy of Minerals and Related Compounds*, Springer Mineralogy, DOI 10.1007/978-3-319-25349-7

B

C

N

Index of Synthetic Compounds

N.V. Chukanov and A.D. Chervonnyi, *Infrared Spectroscopy of Minerals and Related Compounds*, Springer Mineralogy, DOI 10.1007/978-3-319-25349-7

M

N

O

P

R

S